VOLUME 2

SURGICAL PATHOLOGY OF THE HEAD AND NECK

Third Edition

EDITED BY LEON BARNES

informa
healthcare

SURGICAL PATHOLOGY OF THE HEAD AND NECK

VOLUME 2

SURGICAL PATHOLOGY OF THE HEAD AND NECK

Third Edition

EDITED BY

LEON BARNES

University of Pittsburgh Medical Center
Presbyterian-University Hospital
Pittsburgh, Pennsylvania, USA

informa
healthcare

New York London

Informa Healthcare USA, Inc.
52 Vanderbilt Avenue
New York, NY 10017

Printed in India by Replika Press Pvt. Ltd.
10 9 8 7 6 5 4 3 2 1

International Standard Book Number-10: 1-4200-9163-8 (V1; Hardcover)
International Standard Book Number-13: 978-1-4200-9163-2 (V1; Hardcover)
International Standard Book Number-10: 1-4200-9164-6 (V2; Hardcover)
International Standard Book Number-13: 978-1-4200-9164-9 (V2; Hardcover)
International Standard Book Number-10: 1-4200-9165-4 (V3; Hardcover)
International Standard Book Number-13: 978-1-4200-9165-6 (V3; Hardcover)
International Standard Book Number-10: 0-8493-9023-0 (Set; Hardcover)
International Standard Book Number-13: 978-0-8493-9023-4 (Set; Hardcover)

Library of Congress Cataloging-in-Publication Data

Surgical pathology of the head and neck / edited by Leon Barnes. – 3rd ed.
p. ; cm.
Includes bibliographical references and index.
ISBN-13: 978-0-8493-9023-4 (hb : alk. paper)
ISBN-10: 0-8493-9023-0 (hb : alk. paper)
1. Head–Diseases–Diagnosis. 2. Neck–Diseases–Diagnosis. 3. Pathology, Surgical. 4. Head–Tumors–Diagnosis. 5. Neck–Tumors–Diagnosis. I. Barnes, Leon, 1941-
[DNLM: 1. Head–pathology. 2. Neck–pathology. 3. Head–surgery. 4. Neck–surgery. 5. Pathology, Surgical. WE 705 S961345 2008]
RC936.S87 2008
617.5'10754–dc22
2008026087

**For Corporate Sales and Reprint Permissions call 212-520-2700 or write to:
Sales Department, 52 Vanderbilt Avenue, 7th floor, New York, NY 10017.**

**Visit the Informa Web site at
www.informa.com**

**and the Informa Healthcare Web site at
www.informahealthcare.com**

Preface to Third Edition

Seven years have elapsed since the second edition of *Surgical Pathology of the Head and Neck* was published. During this interval there has been an enormous amount of new information that impacts on the daily practice of surgical pathology. Nowhere is this more evident than in the area of molecular biology and genetics. Data derived from this new discipline, once considered to be of research interest only, have revolutionized the evaluation of hematolymphoid neoplasms and are now being applied, to a lesser extent, to the assessment of mesenchymal and epithelial tumors. While immunohistochemistry has been available for almost 30 years, it has not remained static. New antibodies are constantly being developed that expand our diagnostic and prognostic capabilities.

Although these new technologies are exciting, they only supplement and do not replace the ''H&E slide,'' which is, and will continue to be, the foundation of surgical pathology and this book particularly. This edition has been revised to incorporate some of these new technologies that further our understanding of the pathobiology of disease and improve our diagnostic acumen, while at the same time retaining clinical and pathological features that are not new but remain useful and important.

Due to constraints of time and the expanse of new knowledge, it is almost impossible for a single individual to produce a book that adequately covers the pathology of the head and neck. I have been fortunate, however, to secure the aid of several new outstanding collaborators to assist in this endeavor and wish to extend to them my sincere thanks and appreciation for lending their time and expertise. In addition to new contributors, the illustrations have also been changed from black and white to color to enhance clarity and emphasize important features.

This edition has also witnessed changes in the publishing industry. The two previous editions were published by Marcel Dekker, Inc., which was subsequently acquired by Informa Healthcare, the current publisher. At Informa Healthcare, I have had the pleasure of working with many talented individuals, including Geoffrey Greenwood, Sandra Beberman, Alyssa Fried, Vanessa Sanchez, Mary Araneo, Daniel Falatko, and Joseph Stubenrauch. I am especially indebted to them for their guidance and patience.

I also wish to acknowledge the contributions of my secretary, Mrs. Donna Bowen, and my summer student, Ms. Shayna Cornell, for secretarial support and Ms. Linda Shab and Mr. Thomas Bauer for my illustrations. Lastly, this book would not have been possible without the continued unwavering support of my family, Carol, Christy, and Lori, who have endured yet another edition!

Leon Barnes

Contents

Preface to Third Edition iii
Contributors vii

Volume 1

1. **Fine Needle Aspiration of the Head and Neck 1**
   Tarik M. Elsheikh, Harsharan K. Singh, Reda S. Saad, and Jan F. Silverman

2. **Uses, Abuses, and Pitfalls of Frozen-Section Diagnoses of Diseases of the Head and Neck 95**
   Mario A. Luna

3. **Diseases of the Larynx, Hypopharynx, and Trachea 109**
   Leon Barnes

4. **Benign and Nonneoplastic Diseases of the Oral Cavity and Oropharynx 201**
   Robert A. Robinson and Steven D. Vincent

5. **Noninfectious Vesiculoerosive and Ulcerative Lesions of the Oral Mucosa 243**
   Susan Müller

6. **Premalignant Lesions of the Oral Cavity 267**
   Pieter J. Slootweg and Thijs A.W. Merkx

7. **Cancer of the Oral Cavity and Oropharynx 285**
   Samir K. El-Mofty and James S. Lewis, Jr.

8. **Diseases of the Nasal Cavity, Paranasal Sinuses, and Nasopharynx 343**
   Leon Barnes

9. **Diseases of the External Ear, Middle Ear, and Temporal Bone 423**
   Bruce M. Wenig

10. **Diseases of the Salivary Glands 475**
    John Wallace Eveson and Toshitaka Nagao

Volume 2

11. **Midfacial Destructive Diseases 649**
    Leon Barnes

12. **Tumors of the Nervous System 669**
    Beverly Y. Wang, David Zagzag, and Daisuke Nonaka

13. **Tumors and Tumor-Like Lesions of the Soft Tissues 773**
    Julie C. Fanburg-Smith, Jerzy Lasota, Aaron Auerbach, Robert D. Foss, William B. Laskin, and Mark D. Murphey

14. **Diseases of the Bones and Joints 951**
    Kristen A. Atkins and Stacey E. Mills

15. Hematolymphoid Lesions of the Head and Neck **997**
Alexander C. L. Chan and John K. C. Chan

16. Pathology of Neck Dissections **1135**
Mario A. Luna

17. The Occult Primary and Metastases to and from the Head and Neck **1147**
Mario A. Luna

18. Cysts and Cyst-like Lesions of the Oral Cavity, Jaws, and Neck **1163**
Steven D. Budnick and Leon Barnes

Volume 3

19. Odontogenic Tumors **1201**
Finn Prætorius

20. Maldevelopmental, Inflammatory, and Neoplastic Pathology in Children **1339**
Louis P. Dehner and Samir K. El-Mofty

21. Pathology of the Thyroid Gland **1385**
Lori A. Erickson and Ricardo V. Lloyd

22. Pathology of the Parathyroid Glands **1429**
Raja R. Seethala, Mohamed A. Virji, and Jennifer B. Ogilvie

23. Pathology of Selected Skin Lesions of the Head and Neck **1475**
Kim M. Hiatt, Shayestah Pashaei, and Bruce R. Smoller

24. Diseases of the Eye and Ocular Adnexa **1551**
Harry H. Brown

25. Infectious Diseases of the Head and Neck **1609**
Panna Mahadevia and Margaret Brandwein-Gensler

26. Miscellaneous Disorders of the Head and Neck **1717**
Leon Barnes

Index I-1

Contributors

Kristen A. Atkins Department of Pathology, University of Virginia Health System, Charlottesville, Virginia, U.S.A.

Aaron Auerbach Department of Hematopathology, Armed Forces Institute of Pathology, Washington D.C., U.S.A.

Leon Barnes Department of Pathology, University of Pittsburgh Medical Center, Presbyterian-University Hospital, Pittsburgh, Pennsylvania, U.S.A.

Margaret Brandwein-Gensler Department of Pathology, Albert Einstein College of Medicine, Montefiore Medical Center—Moses Division, Bronx, New York, U.S.A.

Harry H. Brown Departments of Pathology and Ophthalmology, Harvey and Bernice Jones Eye Institute, University of Arkansas for Medical Sciences, Little Rock, Arkansas, U.S.A.

Steven D. Budnick Emory University School of Medicine Atlanta, Georgia, U.S.A.

Alexander C. L. Chan Department of Pathology, Queen Elizabeth Hospital, Hong Kong

John K. C. Chan Department of Pathology, Queen Elizabeth Hospital, Hong Kong

Louis P. Dehner Lauren V. Ackerman Laboratory of Surgical Pathology, Barnes-Jewish and St. Louis Children's Hospitals, Washington University Medical Center, Department of Pathology and Immunology, St. Louis, Missouri, U.S.A.

Samir K. El-Mofty Department of Pathology and Immunology, Washington University, St. Louis, Missouri, U.S.A.

Samir K. El-Mofty Lauren V. Ackerman Laboratory of Surgical Pathology, Barnes-Jewish and St. Louis Children's Hospitals, Washington University Medical Center, Department of Pathology and Immunology, St. Louis, Missouri, U.S.A.

Tarik M. Elsheikh PA Labs, Ball Memorial Hospital, Muncie, Indiana, U.S.A.

Lori A. Erickson Mayo Clinic College of Medicine, Rochester, Minnesota, U.S.A.

John Wallace Eveson Department of Oral and Dental Science, Bristol Dental Hospital and School, Bristol, U.K.

Julie C. Fanburg-Smith Department of Orthopaedic and Soft Tissue Pathology, Armed Forces Institute of Pathology, Washington D.C., U.S.A.

Robert D. Foss Department of Oral and Maxillofacial Pathology, Armed Forces Institute of Pathology, Washington D.C., U.S.A.

Kim M. Hiatt Department of Pathology, University of Arkansas for Medical Sciences, Little Rock, Arkansas, U.S.A.

William B. Laskin Surgical Pathology, Northwestern Memorial Hospital, Feinberg School of Medicine, Northwestern University, Chicago, Illinois, U.S.A.

Jerzy Lasota Department of Orthopaedic and Soft Tissue Pathology, Armed Forces Institute of Pathology, Washington D.C., U.S.A.

James S. Lewis, Jr. Department of Pathology and Immunology, Washington University, St. Louis, Missouri, U.S.A.

Ricardo V. Lloyd Mayo Clinic College of Medicine, Rochester, Minnesota, U.S.A.

Mario A. Luna Department of Pathology, The University of Texas, M.D. Anderson Cancer Center, Houston, Texas, U.S.A.

Susan Müller Department of Pathology and Laboratory Medicine and Department of Otolaryngology-Head & Neck Surgery, Emory University School of Medicine, Atlanta, Georgia, U.S.A.

Panna Mahadevia Department of Pathology, Albert Einstein College of Medicine, Montefiore Medical Center—Moses Division, Bronx, New York, U.S.A.

Thijs A.W. Merkx Department of Oral and Maxillofacial Surgery, Radboud University Nijmegen Medical Center, Nijmegen, The Netherlands

Stacey E. Mills Department of Pathology, University of Virginia Health System, Charlottesville, Virginia, U.S.A.

Mark D. Murphey Department of Radiologic Pathology, Armed Forces Institute of Pathology, Washington D.C., U.S.A.

Toshitaka Nagao Department of Diagnostic Pathology, Tokyo Medical University, Tokyo, Japan

Daisuke Nonaka Department of Pathology, New York University School of Medicine, New York University Langone Medical Center, New York, New York, U.S.A.

Jennifer B. Ogilvie University of Pittsburgh Medical Center, Pittsburgh, Pennsylvania, U.S.A.

Shayesteh Pashaei Department of Pathology, University of Arkansas for Medical Sciences, Little Rock, Arkansas, U.S.A.

Finn Prætorius Department of Oral Pathology, University of Copenhagen, Copenhagen, Denmark

Robert A. Robinson Department of Pathology, The University of Iowa, Roy J. and Lucille A. Carver College of Medicine, Iowa City, Iowa, U.S.A.

Reda S. Saad Sunnybrook Hospital, University of Toronto, Toronto, Ontario, Canada

Raja R. Seethala University of Pittsburgh Medical Center, Pittsburgh, Pennsylvania, U.S.A.

Jan F. Silverman Department of Pathology and Laboratory Medicine, Allegheny General Hospital, and Drexel University College of Medicine, Pittsburgh, Pennsylvania, U.S.A.

Harsharan K. Singh University of North Carolina-Chapel Hill School of Medicine, Chapel Hill, North Carolina, U.S.A.

Pieter J. Slootweg Department of Pathology, Radboud University Nijmegen Medical Center, Nijmegen, The Netherlands

Bruce R. Smoller Department of Pathology, University of Arkansas for Medical Sciences, Little Rock, Arkansas, U.S.A.

Steven D. Vincent Department of Oral Pathology, Oral Radiology and Oral Medicine, The University of Iowa College of Dentistry, Iowa City, Iowa, U.S.A.

Mohamed A. Virji University of Pittsburgh Medical Center, Pittsburgh, Pennsylvania, U.S.A.

Beverly Y. Wang Departments of Pathology and Otolaryngology, New York University School of Medicine, New York University Langone Medical Center, New York, New York, U.S.A.

Bruce M. Wenig Department of Pathology and Laboratory Medicine, Beth Israel Medical Center, St. Luke's and Roosevelt Hospitals, New York, New York, U.S.A.

David Zagzag Department of Neuropathology, New York University School of Medicine, Bellevue Hospital, New York, New York, U.S.A.

Midfacial Destructive Diseases

Leon Barnes
Department of Pathology, University of Pittsburgh Medical Center, Presbyterian-University Hospital, Pittsburgh, Pennsylvania, U.S.A.

I. INTRODUCTION

The outdated phrase ''lethal midline granuloma'' has been a source of confusion ever since it was first introduced in the literature. Most clinicians use it in a generic sense to describe any patient who presents with progressive ulceration and destruction primarily of the midfacial tissues (Fig. 1). It must be emphasized, however, that it is a clinical term, much like leukoplakia, and that it cannot be equated, either clinically or pathologically, with any specific entity. The phrase is further misleading in that the diseases that cause lethal midline granuloma are not always lethal, they are not always midline, and they are not always granulomatous (Table 1). The more descriptive phrase ''midfacial destructive disease'' is, therefore, preferred.

Conditions that present as midfacial destructive disease can be grouped, for the most part, into three large categories: (*i*) infections, (*ii*) vasculitis, and (*iii*) neoplasms. Distinguishing between these diseases from a histological perspective can be easy, difficult, or absolutely impossible, depending on the size of the biopsy, the number of sections examined, the stage of the disease, and the amount of clinical information provided to the pathologist.

II. WEGENER'S GRANULOMATOSIS

A. Introduction

Wegener's granulomatosis (WG) was actually first described by Klinger, in 1931, as an atypical form of periarteritis nodosa (1). It was Wegener, however, in 1936, who recognized it as a distinct clinicopathological triad consisting of (*i*) aseptic necrotizing granulomatous inflammation and vasculitis of the upper respiratory tract and lungs, (*ii*) disseminated vasculitis involving primarily small arteries and veins, and (*iii*) necrotizing glomerulonephritis (2). Wegener was only 29 years old when he first presented his findings from three autopsies before the 29th Congress of the German Pathological Society in Breslau in 1936 (2). In 1939, he published a detailed account of these three cases, referring to them as a ''singular rhinogenic granulomatosis'' (3). It was Ringertz, in 1947, and Johnsson, in 1948, who first used the eponym ''Wegener's granulomatosis'' to describe this newly recognized disease (2,4,5).

B. Etiology

The etiology of WG continues to be an enigma. Although there are rare examples of the disease occurring in several members of the same family, there is no evidence that it is of infectious origin in the classic sense, that is, person-to-person transmission, or that it is hereditary (6,7).

Previous attempts to tissue-type patients with WG for human leukocyte antigens (HLA) using conventional microcytoxicity assays of small numbers of patients have indicated an association of the disease with HLA-B8 and HLA-DR2 (8,9). Much larger studies using highly sensitive restriction fragment-length polymorphism analysis in addition to microcytotoxicity assays have shown no association between any specific HLA and WG (10).

Current speculation centers on the role of antineutrophil cytoplasmic antibodies/autoantibodies (ANCA). Although initially thought to be an epiphenomenon, it is now apparent that they are involved in the pathogenesis of the disease (11–17).

The mere presence of ANCA, however, is not sufficient to initiate the disease. The antibodies must first react with their target antigens present in the granules of neutrophils. To do so, ANCA must either enter the cytoplasm of the neutrophil or the antigen must be externalized. The latter is currently favored. Externalization of the antigen, referred to as ''priming,'' appears to be under the control of cytokines. Cytokines can be increased by any nonspecific activation of the immune system. It is known, for instance, that the onset of WG is often preceded by a viral-like prodrome that may serve as the initial priming event. Once primed, antigens move toward the cell membrane of neutrophils where they react with ANCA, releasing free oxygen radicals and enzymes responsible for tissue destruction (18). A vicious cycle then ensues in which tissue destruction leads to the release of more cytokines and more immune activation. T lymphocytes and antiendothelial cell antibodies may also be involved, either directly or indirectly, in mediating the disease (19–21).

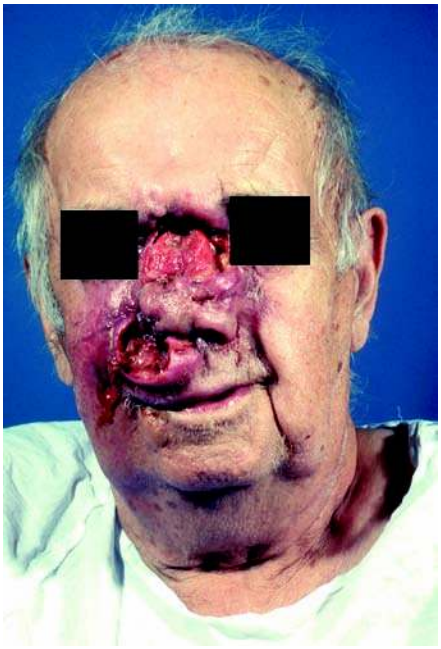

Figure 1 Patient with a neglected squamous cell carcinoma of the nasal mucosa presenting as a midfacial destructive disease.

Table 1 Partial List of Diseases That May Present as Midfacial Destructive Disease

Infections
Staphylococcus
Pseudomonas
Rhinoscleroma
Actinomycosis
Syphilis
Noma
Tuberculosis
Leprosy
Aspergillosis
Mucormycosis
Rhinosporidiosis
Vasculitis
Wegener's granulomatosis
Churg–Strauss syndrome
Polyarteritis nodosa
Systemic lupus erythematosus
Neoplasms
Natural killer (NK)/T-cell lymphoma
Other lymphomas
Carcinoma
Sarcoma
Others
Sarcoid
Cocaine abuse
Extranodal Rosai-Dorfman disease

C. Antineutrophil Cytoplasmic Antibodies/Autoantibodies

ANCA are immunoglobulin G (IgG) antibodies that were first described in 1982 by Davies et al. (22). However, it was van der Woude et al. in 1985 who first recognized their association with WG (23).

When the antibodies are tested for by indirect immunofluorescence (IIF) on cytocentrifuged, ethanol-fixed, normal neutrophils, two distinct staining patterns are recognized: cytoplasmic (C-ANCA) and perinuclear (P-ANCA). Enzyme-linked immunoabsorbant assay (ELISA) has shown the target antigen of C-ANCA to be proteinase 3 (PR3) located in the azurophilic granules of neutrophils and in the lysosomes of monocytes, and the target antigen of P-ANCA to be myeloperoxidase (MPO) (13,16,17).

WG is characteristically associated with C-ANCA in about 80% to 95% of all cases and only infrequently (about 10% of all cases) with P-ANCA (13,17). The sensitivity of the test varies with the extent, severity, and activity of disease. Patients with limited WG have a 50% to 60% C-ANCA positivity, while those with generalized disease have a 60% to 100% positivity. In 10% of WG, no ANCA will be found. A negative test, however, does not rule out WG. P-ANCA, in turn, is found most often in microscopic polyangiitis and Churg–Strauss syndrome.

In a meta-analysis of the literature on the use of C-ANCA testing for WG utilizing IIF, Rao et al. observed an average sensitivity of 66% (range 34–92%) and specificity of 98% (range 88–100%) (24).

Although ANCA are useful serological markers for the diagnosis and management of WG, microscopic polyangiitis, and Churg–Strauss syndrome, there is a growing list of other conditions that also may be associated with ANCA. Among these other conditions are a variety of rheumatic-connective tissue diseases, inflammatory bowel disease, various infections, and the use of certain drugs (such as hydralazine and propylthiouracil) (13,15). Accordingly, ANCA positivity alone, in the absence of appropriate clinical or pathological findings, should not be used to substantiate a diagnosis of WG, microscopic polyangiitis, or Churg–Strauss syndrome. The gold standard is still the tissue biopsy. Ideally, all ANCA testing by IIF should be verified with antigen-specific testing (ELISA) for PR3 and MPO. This, together with the titer of ANCA, will provide more meaningful data.

D. Clinical Features

WG is an uncommon disease with a striking proclivity for white persons (25,26). In a review of 158 patients, Hoffman et al. observed 97% to be white, 2% black, and 1% from other racial backgrounds (26). It occurs in all age groups, but tends to be infrequent in individuals younger than 10 years. In two large series consisting of 158 and 277 patients, the mean age was 41 and 53 years, respectively (26,27). The distribution between the two sexes has ranged from 1:1 to 1.4:1 in favor of males (26,27).

The disease generally starts with granulomatous inflammation and vasculitis of the upper respiratory tract and lungs, spreads in varying degrees to other organ systems, and fatally terminates, if untreated, in a necrotizing glomerulonephritis (28). In the

precyclophosphamide era, the mean survival was only five months.

Systemic complaints are often nonspecific and include malaise, night sweats, weight loss, intermittent fevers, and migrating arthralgias. The upper respiratory tract symptoms vary from an uncomplicated sinusitis and rhinorrhea to nasal mucosal ulceration with crusting, epistaxis, obstruction, and septal perforation, to a destructive, foul-smelling sinusitis involving the bony walls with or without proptosis (29,30). Progressive destruction of nasal cartilage eventually leads to a characteristic ''saddle nose'' deformity. In descending order of frequency, the maxillary, ethmoid, frontal, and sphenoid sinuses are involved, although pansinusistis is quite common.

Oral manifestations include ulcerative stomatitis and hyperplastic (''strawberry'') gingivitis with increased mobility and loss of teeth along with extraction sites that fail to heal (Fig. 2) (31). Fistulas, (oronasal, orosinus, and orocutaneous) are distinctly unusual in WG and, when present, should suggest some other disease.

Twenty to fifty percent of patients will also complain of ear problems, either at the time of diagnosis or during the course of their disease (32–35). The most common is unilateral or bilateral serous otitis media that is unresponsive to antibiotic therapy and secondary to involvement of the eustachian tube by WG. Sensorineural hearing loss caused by vasculitis of the cochlear blood vessels is the second most frequent complaint. Others consist of chronic otomastoiditis, suppurative otitis media, external otitis, cranial nerve dysfunction (especially VII), and destruction of the cartilage of the external ear. Vertigo, however, is distinctly unusual. Why the disease frequently involves the cochlear apparatus of the inner ear with sensorineural hearing loss but selectively spares the vestibular system remains a mystery. Most of the otic symptoms will either abate or at least improve following appropriate therapy.

WG also commonly involves the eye and, in addition to proptosis, may result in conjunctivitis, episcleritis, uveitis, optic nerve vasculitis, retinal artery occlusion, and nasolacrimal duct obstruction. Other rare manifestations include isolated subglottic stenosis, particularly in women, and tender, unilateral or bilateral enlargements of the parotid and submandibular glands (36–38).

Pulmonary complaints include chest pain, cough, and hemoptysis. Renal symptoms usually occur later and are heralded by proteinuria, hematuria, and red blood cell casts. Hypertension is rare.

In the study conducted by Hoffman et al. on 158 patients, the median and mean periods from the onset of symptoms to the diagnosis of WG were 4.7 and 15 months, respectively (26). The diagnosis was made within three months of onset of symptoms in 42% of patients but, in 8%, the diagnosis was not made until 5 to 16 years later. Patients in the latter group had indolent progression and mild disease.

On imaging of the chest, WG generally presents as multiple, bilateral, circumscribed nodules, with an affinity for the mid and lower lobes (Fig. 3). The nodules may cavitate, but are devoid of calcium. Hilar nodes are not enlarged, and only 10% of patients have pleural effusions (39).

With the exception of ANCA, laboratory tests in WG are nonspecific. A mild normochronic, normocytic anemia is common, as well as some degree of reactive thrombocytosis. The leukocyte count is either normal or elevated. Leukopenia, however, is not a feature of untreated WG and, if present, is indicative of some other disease, such as the angiocentric lymphomas. The erythrocyte sedimentation rate, C-reactive protein, and occasionally serum immunoglobulins are elevated. Although high titers of rheumatoid factors are common, serum complement levels are normal. Abnormalities in

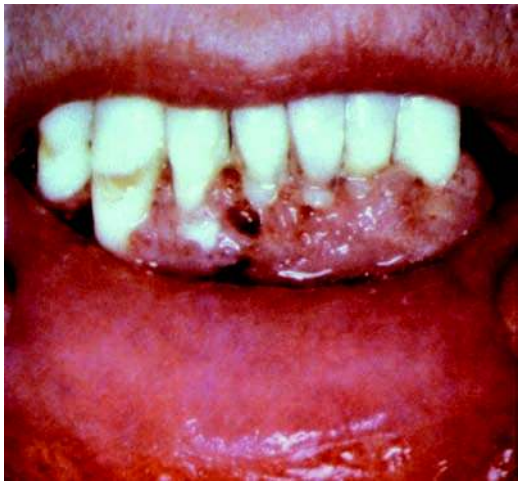

Figure 2 Wegener's granulomatosis involving the gingiva. Note the petechial hemorrhages (strawberry gingivitis).

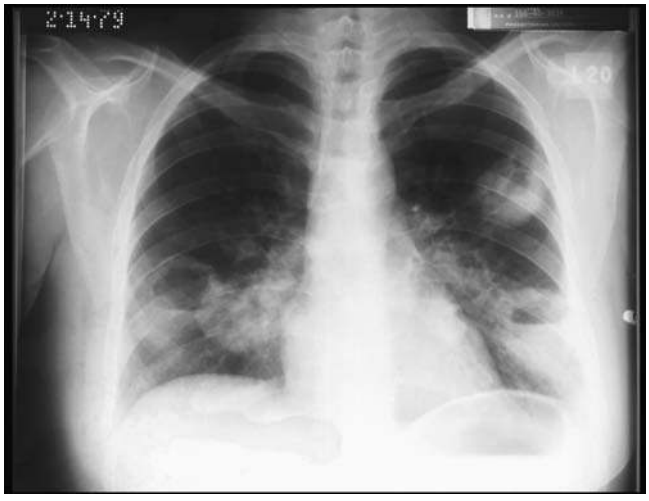

Figure 3 Wegener's granulomatosis. Image of chest shows large, circumscribed nodules of the mid- and lower-lung fields, some of which have cavitated.

Table 2 American College of Rheumatology Criteria for the Classification of Wegener's Granulomatosis (Traditional Format)

	Criterion	Definition
1.	Nasal or oral inflammation	Development of painful or painless oral ulcers or purulent or bloody nasal discharge
2.	Abnormal chest radiograph	Chest radiograph showing the presence of nodules, fixed infiltrates, or cavities
3.	Urinary sediment	Microhematuria (>5 red blood cells per high power field) or red cell casts in urine sediment
4.	Granulomatous inflammation	Histologic changes showing granulomatous inflammation on biopsy, inflammation within the wall of an artery or in the perivascular or extravascular area (artery or arteriole)

Source: From Ref. 40.

the urine sediment associated with increase in serum creatinine and urea level indicate renal disease.

The American College of Rheumatology has proposed criteria for the diagnosis of WG (Table 2) (40). According to the college proposal, a patient should be considered to have WG if at least two of the four criteria are present. The presence of any two or more criteria is associated with a sensitivity of 88% and a specificity of 92% for WG.

E. Pathology

When the diagnosis is suspected, a biopsy of the sinonasal tract is usually obtained, since it is such a readily accessible, universally involved site. For adequate biopsy, it is essential that the overlying nasal crust be removed first, followed by thorough sampling of the underlying friable tissue (Fig. 4). If the crust is not removed, the diagnosis returned by the pathologist will almost assuredly be nonspecific inflammation, necrotic debris, or granulation tissue.

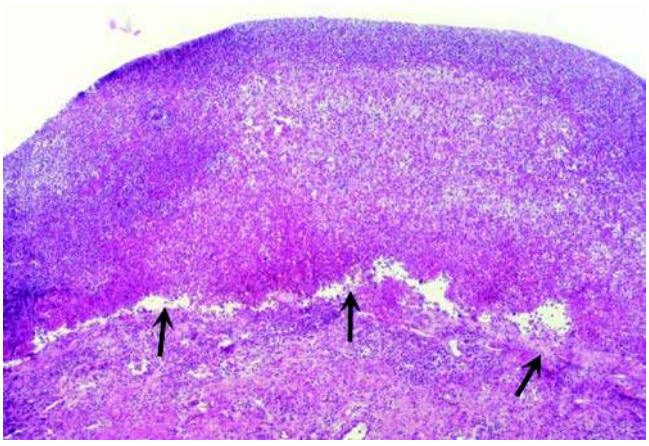

Figure 4 Nasal biopsy from a patient with Wegener's granulomatosis. Note the overlying large crust (*arrows*). This should be removed before biopsy (H&E 40×). *Abbreviation*: H&E, hematoxylin and eosin.

Table 3 Histological Findings in Wegener's Granulomatosis

Vasculitis	Necrosis	Granulomas
Fibrinoid	Fibrinoid	Scattered giant cells
Granulomatous	Microabscesses	Loosely organized granulomas
Leukocytoclastic	Granulomatous abscesses	
Acute-chronic	Geographic	
Cicatrical		

The pathological findings in WG form a diagnostic triad consisting of vasculitis, necrosis, and granulomas (41–49) (Table 3). The vasculitis characteristically involves small arteries, veins, and capillaries, and may be fibrinoid, granulomatous, leukocytoclastic, acute or chronic, or cicatricial (Fig. 5). Previously damaged vessels often show concentric fibrosis and can be accentuated by elastic stains (Fig. 5D).

Stromal necrosis manifests as swelling and fibrinoid degeneration of collagen or as scattered neutrophilic microabscesses (Figs. 6, 7). The microabscesses occasionally coalesce to form macroabscesses, or they may become surrounded by epithelioid histiocytes and multinucleated giant cells, creating a characteristic granulomatous abscess (Fig. 8). Large areas of geographic necrosis are also common. These are characterized by serpingenous, basophilic zones of necrosis, with admixed karyorrhectic nuclei surrounded by palisading histiocytes, fibroblasts, and granulation tissue (Fig. 9).

In contrast with the compact granulomas seen in sarcoid, granulomas in WG tend to be loosely aggregated; they are also free of central necrosis (Fig. 10). Widely scattered multinucleated giant cells, appearing singly or in small clusters, are also prevalent (Fig. 11). Because of the granulomatous features, all biopsies suspicious of WG should be appropriately stained to rule out fungal and mycobacterial infections.

One must also pay close attention to the character of the inflammatory cells. In WG, the inflammatory infiltrate is polymorphic, consisting of lymphocytes, histiocytes, plasma cells, eosinophils, and neutrophils. Atypical lymphoreticular cells, as seen in some angiocentric lymphomas, do not occur in WG.

The frequency of finding all three histological components of WG (vasculitis, necrosis, and granulomas) in sinonasal biopsies varies from 16% to 53% (42–45). The larger the biopsy, the greater the yield. Because of the focality of the lesions, simply cutting deeper into the paraffin block for additional sections can be, diagnostically, very rewarding.

Ulceration of the mucous membranes of the head and neck, particularly in the sinonasal tract, predisposes the patient to a variety of secondary infections that may make interpretation of biopsies very difficult. Bacteria (especially *Staphylococcus* and, to a lesser extent, *Pseudomonas* species) and fungi (*Candida* and *Aspergillus* species) are the usual culprits.

When biopsies are ''consistent with but not diagnostic of WG,'' knowledge of the status of

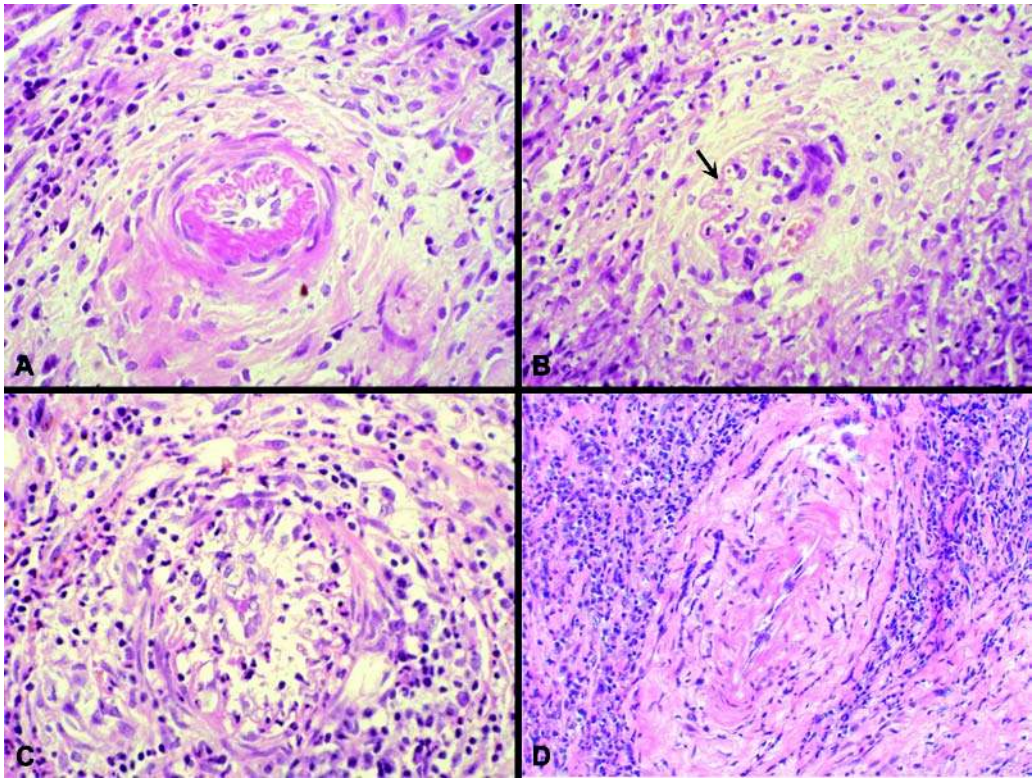

Figure 5 Blood vessels in Wegener's granulomatosis showing (**A**) fibrinoid necrosis (H&E, 200×), (**B**) granulomatous vasculitis. Note the giant cell within the vascular wall and the partially preserved internal elastic lamina (*arrow*) (H&E, 200×). (**C**) acute and chronic vasculitis with lumenal narrowing (H&E, 400×); (**D**) damaged vessel with concentric fibrosis and little, if any, ''active'' vasculitis (H&E, 700×). *Abbreviation*: H&E, hematoxylin and eosin.

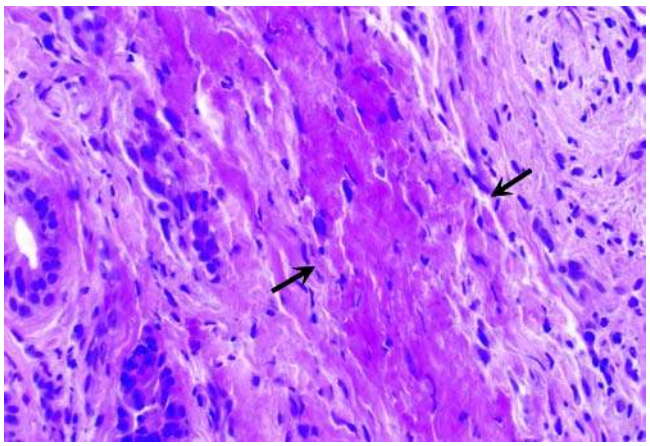

Figure 6 Nasal biopsy from a patient with Wegener's granulomatosis showing fibrinoid necrosis of collagen (*arrows*) (H&E, 100×). *Abbreviation*: H&E, hematoxylin and eosin.

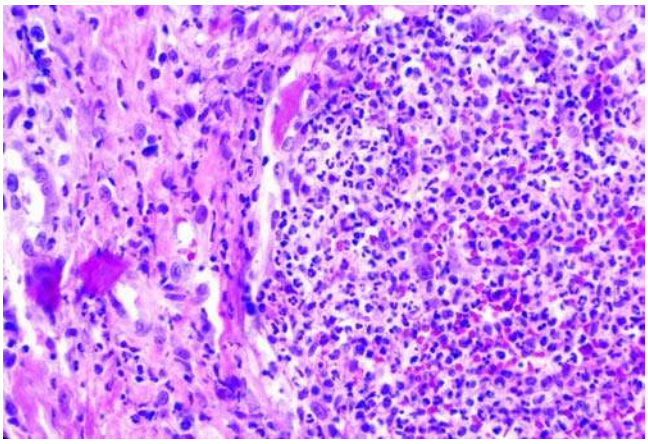

Figure 7 Neutrophilic microabscess in Wegener's granulomatosis (H&E, 200×). *Abbreviation*: H&E, hematoxylin and eosin.

ANCA in an appropriate clinical setting may be helpful in arriving at a more definitive diagnosis.

Tissue deposits of immune complexes are not seen in WG and, therefore, do not appear to play a role in the pathogenesis of the disease (50,51).

Limited Wegener's Granulomatosis

In 1966, Carrington and Liebow and, later, Cassan et al. in 1976, described a group of patients who appeared to have WG, but yet did not manifest the entire classic triad of findings (52,53). Most of their

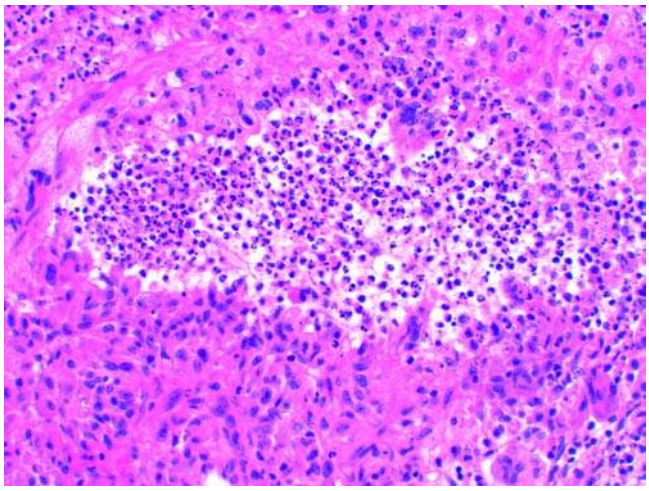

Figure 8 Granulomatous microabscess associated with Wegener's granulomatosis. Note the central collection of neutrophils surrounded by the epithelioid histiocytes and rare multinucleated giant cells (H&E, 100×). *Abbreviation*: H&E, hematoxylin and eosin.

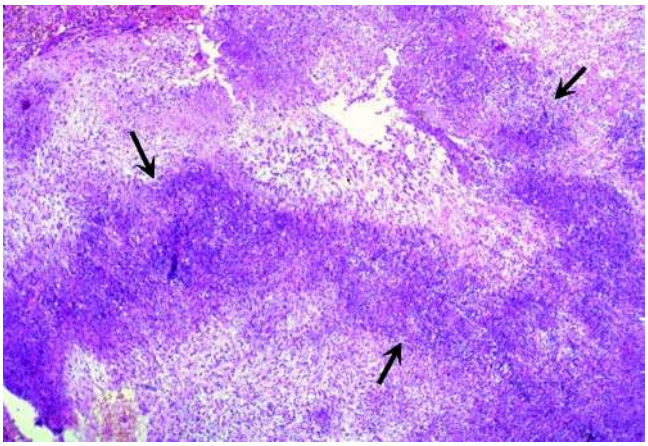

Figure 9 Geographic necrosis in Wegener's granulomatosis. The necrotic area appears purple in the photograph and has sharply defined margins (*arrows*) (H&E, 50×). *Abbreviation*: H&E, hematoxylin and eosin.

patients lacked renal involvement and were considered to have a limited form of Wegener's granulomatosis (LWG).

It is now apparent that limited and generalized WG represent a spectrum of a single disease and that individuals with LWG may eventually progress to generalized disease, or the disease may remain localized or even regress with treatment.

The ELK classification of WG proposed by DeRemee et al. is useful for staging purposes (54): *E* stands for those individuals with ear, nose, and throat involvement, *L* for lung disease, and *K* for renal involvement. According to this scheme, individuals with E, L, and EL disease would have LWG, whereas those with ELK disease would correspond to classic (generalized) WG.

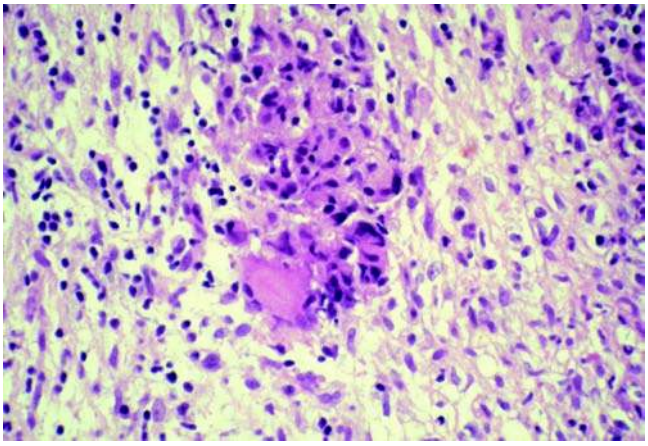

Figure 10 Loosely aggregated granuloma seen in Wegener's granulomatosis (H&E, 200×). *Abbreviation*: H&E, hematoxylin and eosin.

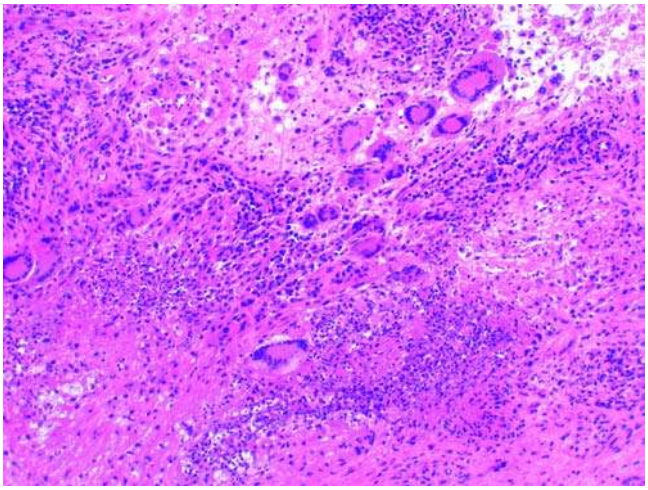

Figure 11 Widely scattered multinucleated giant cells in Wegener's granulomatosis (H&E, 100×). *Abbreviation*: H&E, hematoxylin and eosin.

In two series of 108 and 277 cases of WG, the incidence of limited disease was 58% and 29%, respectively (27,55). In the study of McDonald and DeRemee, 31 of 108 patients (29%) had disease limited entirely to the sinonasal tract (*E* disease) (55).

F. Treatment and Prognosis

Once the diagnosis and extent of disease are established, most patients are treated with a combination

of cyclophosphamide and prednisone (26,56,57). In a review of 133 patients treated with this regimen, Hoffman et al. obtained a 75% rate of complete remission. Although some patients achieved complete remission within a few months, the median time for all patients to achieve complete remission was 12 months (26). Fifty percent of patients, however, who achieved complete remission experienced one or more relapses anywhere from 3 months to 16 years after achieving complete remission. In the same study, 44% of patients had remissions of more than five consecutive years and, of this group, 13% subsequently experienced relapses. From this data, it would appear that patients with WG who experience remission, even after as long as five years or more, are not necessarily cured of disease and are at risk for recurrences throughout their life span.

WG is a life-threatening disease, with mortality rates of 20% and 28% reported in two large series of patients (26,58,59). In a study of 151 patients treated at the Mayo Clinic, 90% were alive at one year and 76% at five years (58,59). Death may be due to disease (pulmonary or renal insufficiency) or complications of therapy (infection, hemorrhagic cystitis, leukemias, and other drug-induced malignancies).

Because it is recommended that cyclophosphamide be continued for at least one year after achieving remission and because such long-term therapy is associated with significant complications, a search for alternative medications has ensued. Among these are trimethoprin-sulfamethoxazole (TS) and etanercept (60–63). The use of TS is controversial. It is not associated with significant side effects with prolonged usage but it is recommended only for those patients with limited disease (59). Patients with generalized disease or renal involvement still require cyclophosphamide and predisone. Clinicians must be aware that it may take two to eight weeks before a clinical response to TS therapy can be appreciated (39).

Tumor necrosis factor α (TNF-α) is a cytokine produced by $CD4^+$ T cells that may be an important mediator of WG (62). An antibody against TNF-α has been developed (etanercept), which offered some hope for maintenance of remission of patients with WG. Unfortunately, a large clinical trial has concluded that this drug is largely ineffective (63).

It is commonly stated that ANCAs are not influenced by infections complications and, therefore, a rise in titer of ANCA portends an exacerbation of the disease and need for increased immunosuppressive therapy. In contrast, according to Kerr et al., data derived from the National Institutes of Health indicate that changes in serial C-ANCA titers temporally correlate with a change in disease activity in only 64% of patients (64). Moreover, a rise in C-ANCA titer precedes clinical exacerbation of disease in only 24% of patients who have been in remission or have had low-grade smoldering disease. It thus appears that serial ANCA testing has only a limited role in accessing disease activity or predicting relapse.

III. MICROSCOPIC POLYANGIITIS

A. Introduction

Microscopic polyangiitis (MPA) is an ANCA-associated vasculitis that was probably first recognized by Davson et al. in 1948 (1). It is defined as a ''necrotizing vasculitis with few or no immune deposits affecting small vessels (i.e., capillaries, venules, or arterioles). Necrotizing arterites involving small and medium-sized arteries may be present. Necrotizing glomerulonephritis is very common. Pulmonary capillaritis often occurs'' (2). Since the disease involves not only arterioles/arteries but also capillaries and venules, the term ''polyangiitis'' is favored over ''polyarteritis.''

MPA is associated with P-ANCA/MPO in about 70% of cases (range 40–80%) (3–6). Rare cases have also allegedly been associated with C-ANCA/PR3 (7).

B. Clinical Features

The disease is more common in males by a ratio of 1 to 1.8:1 and occurs over a broad age range (14–92 years) with a mean/median age of about 50 to 60 years (6–9).

The kidneys, lungs, gastrointestinal tract, skin, musculoskeletal system, and nervous system bear the burden of the disease. Major signs and symptoms include fever, myalgias, arthralgias, necrotizing glomerulonephritis, renal failure, pulmonary capillaritis, hemoptysis, pulmonary hemorrhage, pleural effusions, abdominal pain, diarrhea, cutaneous purpura, and peripheral neuropathy. Depending on the series, 5% to 40% of patients also experience head and neck manifestations, particularly sore throats, mucosal ulcers, epistaxis, and sinusitis (7,9,10).

C. Pathology

The vasculitis typically involves arterioles, capillaries, and venules often with a leukocytoclastic or fibrinoid appearance. Granulomas are not seen (Figs. 12, 13).

D. Differential Diagnosis

Classic polyarteritis nodosa (PAN) and WG must be excluded (11). PAN, in contrast to MPA, involves larger blood vessels (medium size arteries) and is rarely, if ever, associated with ANCA. Other helpful features in distinguishing between these two conditions are shown in Table 4. WG more often involves the upper aerodigestive tract, rarely affects the gastrointestinal tract, exhibits granulomatous inflammation, and is associated with C-ANCA. MPA, in turn, only occasionally affects the upper aerodigestive tract, commonly involves the gastrointestinal tract, is more often associated with P-ANCA, and does not contain granulomas.

E. Treatment and Prognosis

MPA is a life-threatening disease that justifies the intensive use of corticosteroids and cytotoxic agents,

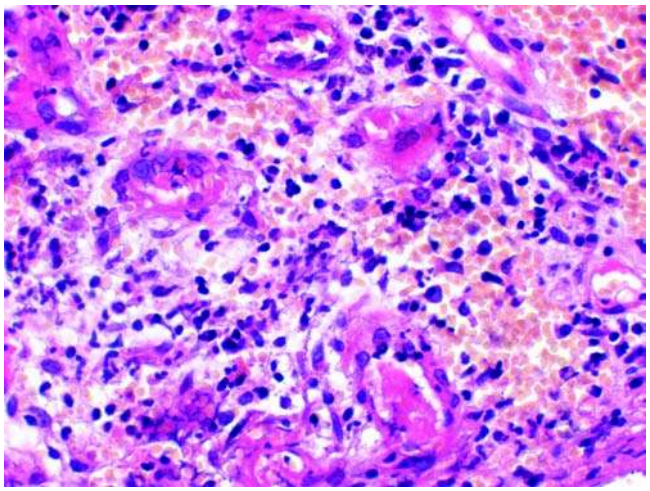

Figure 12 Microscopic polyangiitis. A cluster of capillaries exhibiting leukocytoclasis and fibrin thrombi with petechial hemorrhages (H&E, 400×). *Abbreviation*: H&E, hematoxylin and eosin.

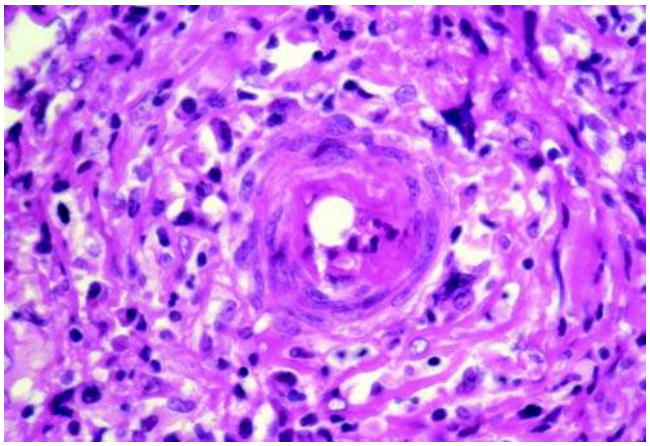

Figure 13 Microscopic polyangiitis. Arteriole with fibrinoid necrosis (H&E, 400×). *Abbreviation*: H&E, hematoxylin and eosin.

Table 4 MPA Vs. PAN

Feature	MPA	PAN
Vessel	Arterioles, venules, capillaries	Small to medium muscular arteries
ANCA	+ (P-ANCA)	−
Hepatitis B antigen	−	+
Aneurysms	−	+
Organ infarcts	−	+
Pulmonary disease	+	−
Glomerulonephritis	+	−
Peripheral neuropathy	+/−	+

Abbreviations: MPA, polyarteritis nodosa; PAN, microscopic polyangiitis; ANCA, antineutrophil cytoplasmic antibodies/autoantibodies; P-ANCA, perinuclear ANCA.

usually cyclophosphamide or azathioprine (7,12). Relapses following remission are common and occur in about one-third of patients. Mortality rates of 30% to 60% have been reported (6,8,9). Death is usually the result of active vasculitis complicated by renal failure and pulmonary hemorrhage or to treatment side effects.

IV. POLYARTERITIS NODOSA

A. Introduction

Kussmaul and Maier in 1866 are credited with the first description of PAN (1). Although they referred to the disease as ''periarteritis'' nodosa, the term ''polyarteritis'' is more appropriate because the inflammation involves all layers of the blood vessel, rather than just the periphery.

B. Clinical Features

PAN occurs in all age groups, with an average age of onset of 48 years and a gender distribution of 1:1 to 2:1 in favor of males (2–4). All ethnic groups are affected (5).

Although the etiology of the disease is unknown, most cases are thought to be related to circulating immune complexes. In support of this view is the occasional occurrence of the disease in patients with serum hepatitis B or following episodes of otitis media (6,7). Vascular lesions identical with PAN have also been seen in rheumatoid arthritis and systemic lupus erythematous.

Typically, PAN presents as a disseminated disease with a multitude of signs and symptoms, often nonspecific, that are related to tissue ischemia and visceral infarction. The skin (ulcers, petechiae, livedo reticularis), gastrointestinal tract (abdominal pain, ulcers, bleeding, vomiting), heart (infarction, cardiac failure), genitourinary tract (elevated blood pressure, hematura, albuminuria, testicular pain), and nervous system (mono- and polyneuropathy) bear the brunt of the disease. Systemic complaints such as fever, fatigue, weight loss, myalgias, and arthralgias are also common. Pulmonary involvement, however, is rare. The frequency of head and neck manifestations has ranged from 0% to 15% (5). Among the more serious are those that involve the eye, especially retinal vasculitis and detachment.

The American College of Rheumatology has suggested a list of 10 criteria for establishing the diagnosis of PAN (Table 5) (2). The presence of any 3 or more of these 10 criteria will allow one to make the diagnosis of PAN with a sensitivity of 82% and a specificity of 87% (2). Because the disease is systemic, angiography for the detection of microaneurysms and occluded blood vessels can be very helpful in confirming the diagnosis. Biopsies to document vasculitis should always be directed at clinically involved sites, for they are more likely to harbor diagnostic findings than ''blind'' biopsies (8). According to Gardner, the frequency of organ involvement in PAN is as follows: kidney, 85%; liver, 62%; gastrointestinal tract, 51%; muscle, 39%; testicle, 33%; and peripheral nerve, 32% (4).

Table 5 Criteria of the American College of Rheumatology for Classification of Polyarteritis Nodosa

Weight loss
Livedo reticularis
Testicular pain or tenderness
Myalgias, weakness, or leg tenderness
Mono- or polyneuropathy
Diastolic blood pressure greater than 90 mmHg
Elevated blood urea nitrogen or creatinine
Hepatitis B virus
Arteriographic abnormality
Biopsy of small- to medium-sized artery containing neutrophils

Source: From Ref. 2.

Limited forms of PAN have also been described, that is, the disease is confined to one organ without systemic involvement. Limited PAN most often involves the appendix, gallbladder, uterus, or testicles.

Laboratory tests are not diagnostic and include such nonspecific findings as leukocytosis, hematuria, albuminuria, elevated blood urea nitrogen and creatinine, hepatitis B antigenemia, and occasionally, cryoglobulinemia.

Strictly defined, PAN is negative for ANCA. Those cases allegedly associated with ANCA are most likely unrecognized examples of microscopic polyangiitis.

C. Pathology

Histopathologically, PAN involves small- to medium-sized muscular arteries, especially at sites of bifurcation or branching. Veins are rarely affected and then only by direct extension from nearby arterial involvement. The vessels characteristically show fibrinoid necrosis or a transmural infiltrate of neutrophils, with admixed mononuclear cells and eosinophils, which, in turn, lead to thrombosis, microaneurysms, and ischemic necrosis (Figs. 14, 15). The vascular findings are random and multifocal, at times, involving either only a part of the wall of the blood vessel or the entire circumference. It is also not uncommon to find blood vessels in both ''active'' and healed stages in the same biopsy, or lying adjacent to normal, uninvolved arteries. Granulomas are not seen.

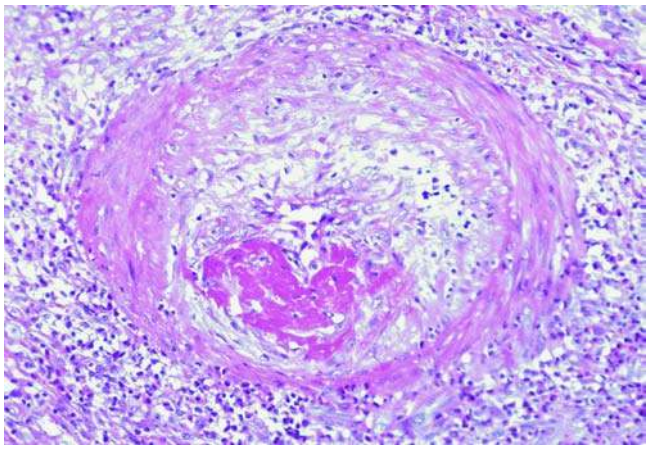

Figure 14 Polyarteritis nodosa. Medium-sized artery with fibrinoid necrosis, intimal hyperplasia, lumenal narrowing, and mild transmural and marked perivascular inflammation (H&E, 100×). *Abbreviation*: H&E, hematoxylin and eosin.

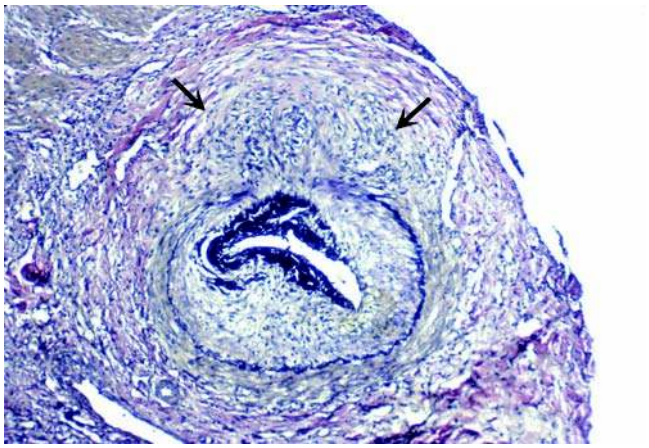

Figure 15 Polyarteritis nodosa. Damaged medium-sized artery with microaneurysm (*arrows*) (reticulin stain, 100×).

D. Treatment and Prognosis

The treatment of PAN includes corticosteroids, cytotoxic agents, or a combination of these drugs. The prognosis is closely related to the size of the largest vessel involved and the degree of end-organ damage. The five-year survival varies from 50% to 80% (4,5,9). Most deaths are due to renal failure, myocardial infarction, or cerebral vascular accident. Following remission, relapses are rare in PAN (5).

V. ALLERGIC GRANULOMATOSIS AND VASCULITIS

A. Introduction

In 1951, Churg and Strauss, two pathologists from Mt. Sinai Hospital in New York, described a new syndrome that was distinct from, but yet shared features with, WG, PAN, and the hypereosinophilic syndrome (1).

The syndrome, referred to as allergic granulomatosis and vasculitis (AGV) or Churg–Strauss syndrome, has since become well established and consists of a diagnostic triad: (*i*) asthma, which is often severe; (*ii*) systemic vasculitis that varies from granulomatous to nongranulomatous; and (*iii*) peripheral and tissue eosinophilia (2–7).

AGV is the rarest of three types of ANCA-associated vasculitides (WG, microscopic polyangiitis, and AGV), with an estimated annual incidence in the general population of one to three cases per million. If only asthmatic patients are considered, the incidence is as high as 67 cases per million (7).

B. Clinical Features

AGV occurs in all age groups with a mean age of about 50 years (range 10–86 years) and an equal gender distribution (4,8–11).

The disease characteristically evolves through three phases, each of which may last many years. The first or allergic phase consists of the onset of various atopic diseases, such as asthma and allergic rhinitis. This is followed by the eosinophilic phase in which there is peripheral as well as tissue eosinophilia producing a clinical picture resembling chronic eosinophilic pneumonia, eosinophilic gastroenteritis, eosinophilic prostatitis, and so on (4,12). The third and most life threatening is the vasculitic phase. Interestingly, with the onset of vasculitis, there is often a dramatic remission of asthma. However, these three phases of disease do not always follow one another in the order given.

Ear, nose, and throat manifestations are seen in up to 75% of patients with AGV (13,14). In fact, they are so common that it has been suggested that the syndrome should be recorded as a tetrad (rather than a triad), consisting of asthma, vasculitis, eosinophilia, and nasal disease (13). The most common features are allergic rhinitis and nasal polyps. Others include chronic rhinosinusitis, thick crusts, occasional septal perforations, serous or purulent otitis media, and sensorineural hearing loss.

Other manifestations of the disease include malaise, fever, night sweats, weight loss, myalgias, and arthralgias, Cardiac abnormalities (pericarditis, myocardial infarction, heart failure), involvement of the nervous system (peripheral neuropathy, cerebral hemorrhage, or infarction), and skin lesions (palpable purpura, erythematous maculopapular eruptions, nodules) are also common (4,15). Renal involvement, often accompanied by hypertension, is prevalent. However, in contrast to WG, the renal disease of AGV is less ''malignant'' leading to failure in no more than 10% of cases (4).

Pulmonary involvement occurs in one-third of the cases and typically presents on imaging as a transient, patchy infiltrate without an affinity for any site. Bilateral nodular infiltrates are infrequent and, in contrast with WG, rarely cavitate.

Peripheral eosinophilia, sometimes constituting up to 80% of the circulating white blood cells, is a cardinal feature of the disease. Wide and rapid fluctuations, however, are not uncommon, and if previous blood counts are not reviewed, this important finding may be overlooked. Tissue eosinophilia may occur in the absence of peripheral eosinophilia. Other laboratory abnormalities include a mild normochronic, normocytic anemia and elevation of the erythrocyte sedimentation rate. Increased levels of serum IgE are also characteristic, but circulating immune complexes with hypocomplementemia are rare (4).

ANCA have been found in 40% to 80% of patients with AGV (9–11,16). Most are of the P-ANCA/MPO type, but rare examples of C-ANCA/PR3 have also been described (11). It should be noted that ANCA associated with AGV is very sensitive to corticosteroid therapy and any prior usage of this drug may affect this test (9).

Establishing the diagnosis depends on which set of criteria are used. Some insist that the diagnosis be restricted to the original criteria and that vasculitis, eosinophilia, and extravascular granulomas must be demonstrated histologically before the diagnosis is accepted. Others believe that the syndrome can be recognized mainly on the basis of clinical findings—(*i*) asthma, (*ii*) peripheral blood eosinophilia in excess of 1.5×10^9L, and (*iii*) systemic vasculitis involving two or more extrapulmonary sites—and insist that rigid emphasis on strict histological criteria has created a false impression that the disease is rare (4). The American College of Rheumatology has proposed six criteria for establishing the diagnosis. These are listed in Table 6. According to the College, a patient will be said to have AGV if at least four of these six criteria are positive (17). The presence of any four of the six criteria yields a sensitivity of 85% and a specificity of 99.7%. The Chapel Hill Consensus Conference has defined AGV on the basis of a combination of clinical and histological features as ''an eosinophil-rich and granulomatous inflammation involving the respiratory tract, and necrotizing vasculitis affecting small- to medium-sized vessels, and associated with asthma and eosinophilia'' (18). Complicating the diagnosis is the fact that the various clinical and histopathological features noted above usually do not occur simultaneously.

C. Pathology

The vasculitis of AGV characteristically involves small- to medium-sized arteries and veins, not only in the lungs but systemic vessels as well (5,19,20). The vessels may show segmental zones of fibrinoid necrosis, with transmural infiltrate of predominantly eosinophils with few admixed lymphocytes and neutrophils, similar to that seen in classic PAN, or it may show a granulomatous vasculitis replete with multinucleated giant cells, or a combination of both patterns (Figs. 16–18). The granulomas often have centers of ischemic or fibrinoid necrosis surrounded by palisading histiocytes and multinucleated giant cells (Fig. 19). Granulomas without necrosis, however, are not uncommon. Eosinophils are prominent and tend to aggregate into eosinophilic microabscesses (Fig. 20).

Electron microscopy of biopsies obtained from the lungs and kidneys have shown no evidence of immune, electron-dense deposits (3).

Table 6 Criteria of the American College of Rheumatology for the Classification of Allergic Granulomatosis and Vasculitis

Asthma
Peripheral eosinophilia of greater than 10%
Neuropathy (mono- or polyneuropathy)
Pulmonary infiltrates, nonfixed
Paranasal sinus abnormalities (history of acute or chronic paranasal sinus pain or tenderness, or radiographic opacification of the sinuses)
Extravascular (tissue) eosinophilia

Source: From Ref. 17.

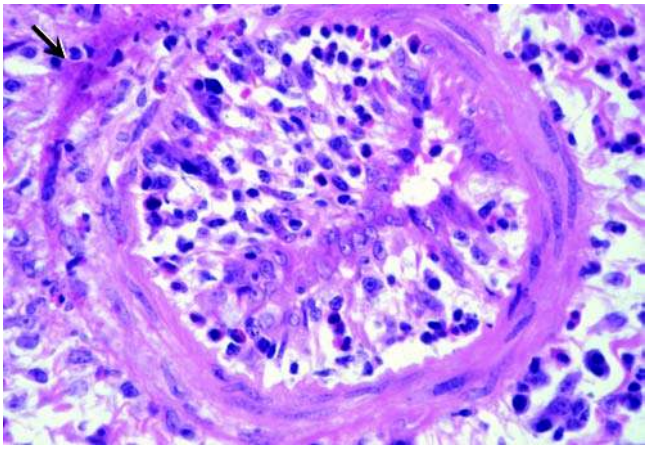

Figure 16 Allergic granulomatosis and vasculitis. Artery contains a mural infiltrate of lymphocytes and eosinophils. Note the luminal narrowing and focal, early fibrinoid necrosis (*arrow*) (H&E, 400×). *Abbreviation*: H&E, hematoxylin and eosin.

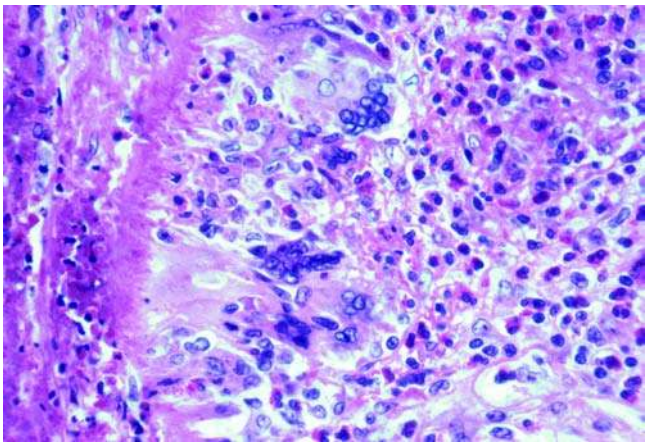

Figure 18 Higher magnification of the region identified by the arrow in Fig. 17. Note the smudgy, fibrinoid necrosis and multinucleated giant cells (H&E, 400×). *Abbreviation*: H&E, hematoxylin and eosin.

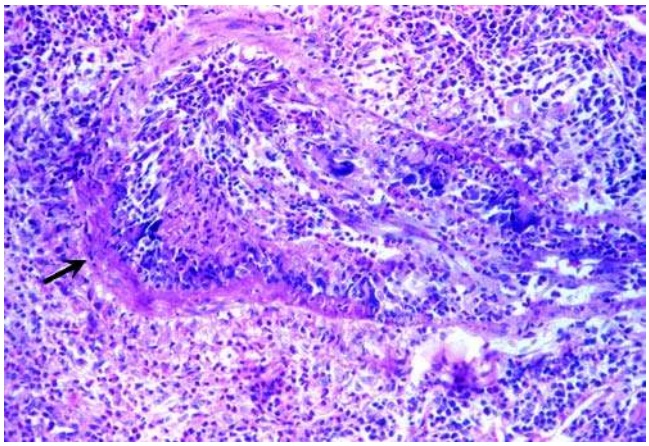

Figure 17 Allergic granulomatosis and vasculitis. Medium-sized artery with both transmural granulomatous inflammation and fibrinoid necrosis (*arrow*) (H&E, 200×). *Abbreviation*: H&E, hematoxylin and eosin.

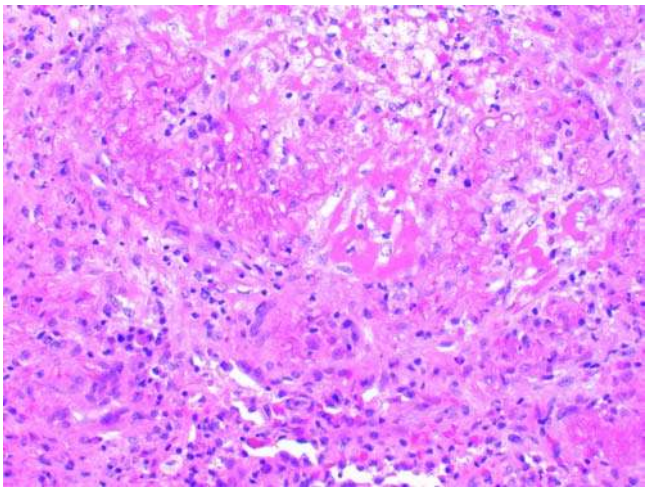

Figure 19 Allergic granulomatosis and vasculitis. Granuloma with central necrosis (H&E, 200×). *Abbreviation*: H&E, hematoxylin and eosin.

Pathologists should be aware that each of the three major histopathological features of AGV may occur in isolation or may coexist and that they may be sparse or widely distributed throughout the body. According to Lanham et al., the incidence of finding granulomas, eosinophilia, and vasculitis in biopsies is 38%, 57%, and 70%, respectively, and only 13% of biopsies will contain all the three findings together (4). Consequently, it is mandatory that all previous biopsies in patients suspected of having AGV be reviewed.

Limited Forms of Allergic Granulomatosis and Vasculitis

Patients who do not exhibit the complete clinical (systemic vasculitis, asthma, peripheral eosinophilia) or histological (vasculitis, extravascular granulomas, tissue eosinophilia) triad of findings are regarded as having a limited form of the disease analogous to LWG. Limited forms of allergic granulomatosis and vasculitis (LAGV) have been described in patients without asthma or eosinophilia (21–23). By definition, these individuals do not have systemic involvement but rather disease limited to only a few sites, especially the gastrointestinal tract (23–25). Over the course of time, some patients with LAGV may progress to the disseminated, classic form of the disease.

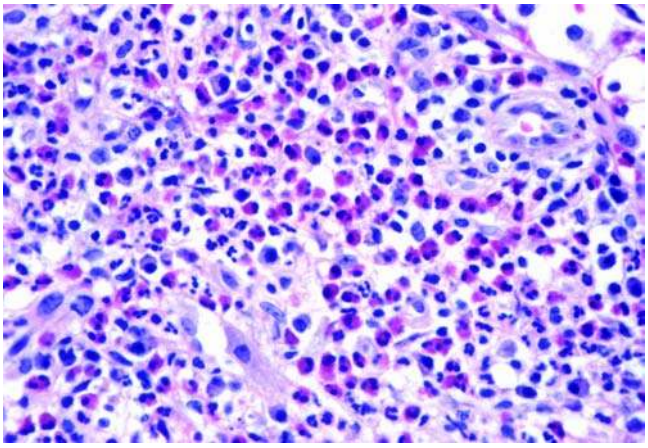

Figure 20 Allergic granulomatosis and vasculitis. Eosinophilic microabscess (H&E, 200×). *Abbreviation*: H&E, hematoxylin and eosin.

D. Treatment and Prognosis

Most patients are responsive to corticosteroids. Cytotoxic agents, however, should probably be added to the regimen in all patients who present with disease manifestations that threaten the patient's life or function of a vital organ or do not respond sufficiently to corticosteroids.

The long-term outcome and prognosis of AGV is not entirely clear. Vascular relapses are not uncommon and are listed as high as 40% in one series (7). Five-year survival rates of 62% to 75% have been recorded (4,6,26). Death is most often due to congestive heart failure or myocardial infarction and only infrequently to renal failure or cerebral/pulmonary hemorrhage (4).

VI. IDIOPATHIC MIDLINE DESTRUCTIVE DISEASE

In 1982, Tsokos et al. described 11 patients (seven women and four men) aged between 15 and 59 years (average 35 years) who presented with relentless progressive destruction of the upper respiratory tract (1). Despite repeated attempts to establish an etiology, neither infectious agents nor neoplastic infiltrates could be identified. They coined the phrase ''idiopathic midline destructive disease (IMDD)'' to describe the disorder.

Most patients presented with pansinusitis and destructive lesions of the nasal septum and hard palate. In three patients, there was ulceration through the skin of the face. In three other patients, there was extension of the sinus disease into the orbit. Some patients also had involvement of the nasopharynx, larynx, and trachea, but none had abnormalities of the lower respiratory tract or other organ systems.

Biopsies obtained from these patients showed only acute and chronic nonspecific inflammation and necrosis. The inflammatory infiltrate was composed of neutrophils, lymphocytes, histiocytes, and plasma cells, and was occasionally noted to extend into bone and cartilage. Eosinophils were inconspicuous, and multinucleated giant cells were seen in only two patients, one of which also had a well-formed granuloma. Pseudovasculitis, defined as inflammatory cells in the outer walls of small arteries and capillaries, was seen in five patients, but none of the vessels showed fibrinoid necrosis, hyalinization, or thrombosis. No atypical cells were seen.

The patients were treated with irradiation (4000–6000 rad). At last follow-up, averaging 7.3 years, eight had complete remission of their disease and three showed initial response followed by relapse or persistent residual disease. None developed disease below the clavicles.

Although I cannot be absolutely certain, but on the basis of experience gained from over three decades of looking at head and neck specimens, I am of the opinion that IMDD does not exist as a specific disease. I suspect that most, if not all, cases of alleged IMDD are probably unrecognized natural killer (NK)/T-cell lymphomas, inflammatory pseudotumors, or examples of nonrepresentative biopsies from other diseases.

VII. EXTRANODAL NK/T-CELL LYMPHOMA, NASAL TYPE

A. Introduction

There has been considerable confusion over the use of the terms ''angiocentric lymphoma,'' ''lymphomatoid granulomatosis,'' ''polymorphic reticulosis,'' ''midline malignant reticulosis,'' ''lethal midline granuloma-Stewart's type,'' and ''angiocentric immunoproliferative lesion.'' Once considered by some to be synonyms for a single lesion, it is now apparent that these terms encompass a heterogeneous group of disorders of diverse cellular lineage. Most are now recognized as extranodal NK/T-cell lymphomas, nasal type. The remaining are primarily T-cell lymphomas or T-cell rich B-cell lymphomas in which the B cells are infected with the Epstein–Barr virus (EBV) (lymphomatoid granulomatosis). The following discussion is concerned only with the extranodal NK/T-cell lymphoma, nasal type, hereafter referred to as NK/T-cell lymphoma.

The NK/T-cell lymphoma is an aggressive, predominantly extranodal lymphoma that typically presents in the nasal cavity but frequently involves contiguous sites. It is designated NK/T (rather than NK)-cell lymphoma because while most cases appear to be NK-cell neoplasms (EBV^+, $CD56^+$), rare cases show an EBV^+, $CD56^-$, cytoxic T-cell phenotype (1,2).

These lymphomas are especially common in Asia, Mexico, and Central and South America and rare in the United States (1,3–11).

B. Clinical Features

NK/T-cell lymphomas occur primarily in adults (median age about 45–55 years, range 16–86 years)

and are two to four times more common in males (4,6–8). The disease usually originates in the nasal cavity, paranasal sinuses, and/or nasopharynx, and variably involves the orbit, oral cavity, oropharynx, pharynx, and larynx. Rhinosinusitis, either unilateral or bilateral, with a purulent or bloody nasal discharge and nasal obstructions are the usual complaints. A discrete mass may be seen, but more often the lymphoma manifests as multiple mucosal ulcers which, with progressive enlargement, may destroy contiguous soft tissue, cartilage, and bone, resulting in nasal septal perforation, orbital cellulitis, and fistulas (midfacial destructive disease) (Figs. 21, 22). In contrast to WG, which often involves the ears, NK/T-cell lymphoma generally does not.

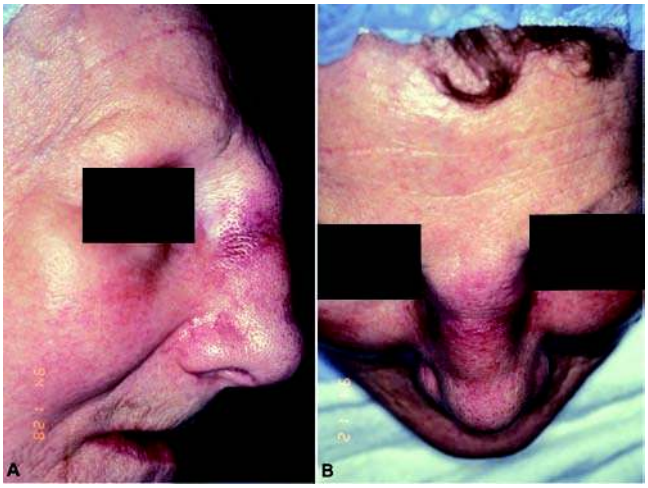

Figure 21 NK/T-cell lymphoma presenting as a cellulitis. Note the red, swollen nose and cheeks: (**A**) lateral view, (**B**) superior view.

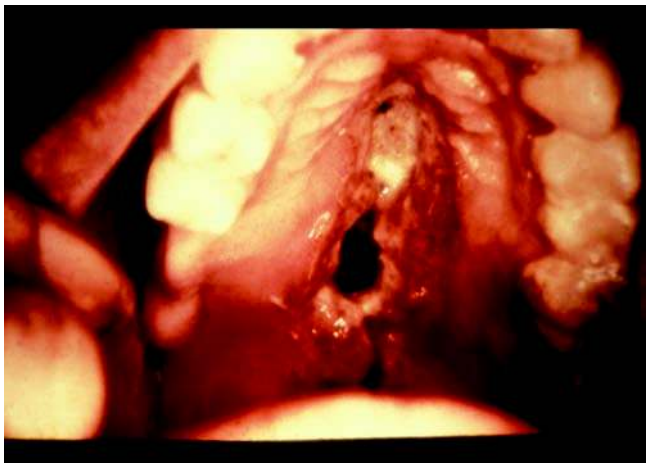

Figure 22 Intraoral view of palate showing a palatonasal fistula in a patient with NK/T-cell lymphoma. Fistulas, in general, are very unusual in Wegener's granulomatosis.

At the time of presentation, 75% to 80% are found to have local or locoregional disease with the frequency of positive cervical lymph nodes ranging from 0% to 18% (4). During the course of the disease, the lymphoma may spread systemically to other sites, especially the skin, gastrointestinal tract, liver, lymph nodes, testes, central nervous system, and bone marrow.

C. Pathology

The neoplastic cells demonstrate a broad spectrum of appearance, ranging from small cells with irregular nuclei to medium-sized cells with round to folded nuclei to large pleomorphic cells with vesicular nuclei and prominent nucleoli. A mixture of these cells is not uncommon. The lymphomatous proliferation is diffuse and often contains admixed eosinophils, plasma cells, and neutrophils, creating an aura of an ''inflammatory process'' (Figs. 23, 24). Mitoses, apoptosis, and cells with pale to clear cytoplasm are additional features (Fig. 25).

The neoplastic cells commonly invade the walls of blood vessels (angiocentric lymphoma) and may occlude their lumens with resultant ischemic necrosis (Figs. 26, 27). Spotty necrosis other than ischemic is also characteristic and is probably related to the release of cytokines (TNF) mediated by the EBV.

Some of the lymphomas are associated with exuberant pseudoepitheliomatous hyperplasia that can potentially be mistaken for squamous cell carcinoma (Fig. 28).

The diagnosis of NK/T-cell lymphoma should always be entertained in a biopsy of the sinonasal tract when there is a very prominent inflammatory infiltrate, and, especially so, if there is vascular involvement, perineural invasion, cytological atypia, prominent mitoses, increased number of cells with clear cytoplasm, and spotty stromal necrosis.

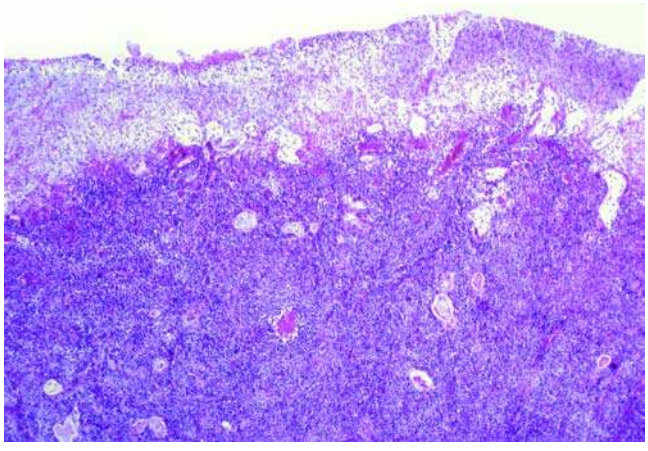

Figure 23 Sinonasal biopsy in a patient with NK/T-cell lymphoma who presented with sinusitis. Note the dense cellular infiltrate and the crust on the surface (H&E, 40×). *Abbreviation*: H&E, hematoxylin and eosin.

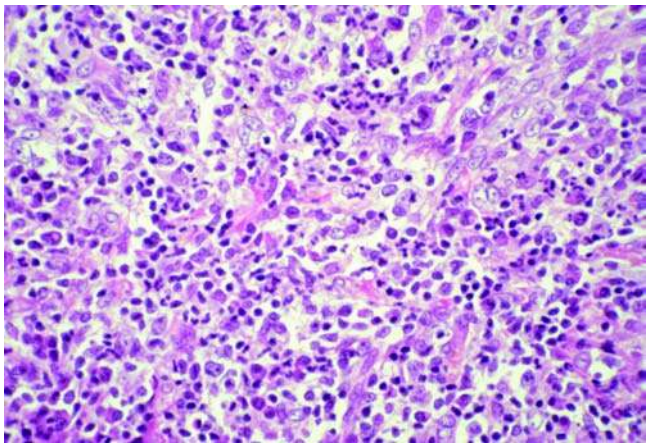

Figure 24 NK/T-cell lymphoma with admixed neutrophilis masquerading as an inflammatory lesion (H&E, 200×). *Abbreviation*: H&E, hematoxylin and eosin.

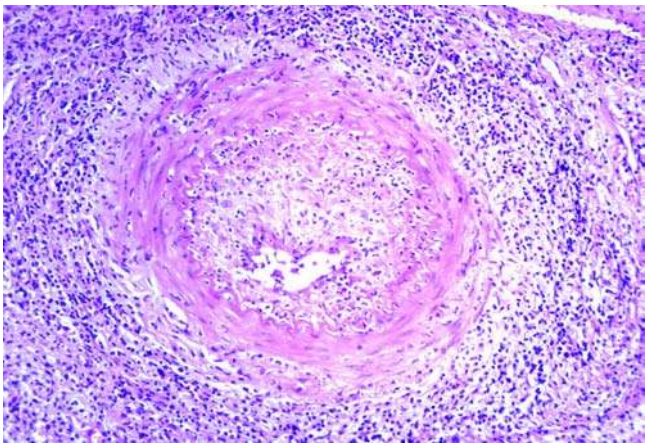

Figure 26 Sinonasal biopsy in patient with NK/T-cell lymphoma. Note the cellular infiltrate in the wall of the artery and the lumenal narrowing (H&E, 100×). *Abbreviation*: H&E, hematoxylin and eosin.

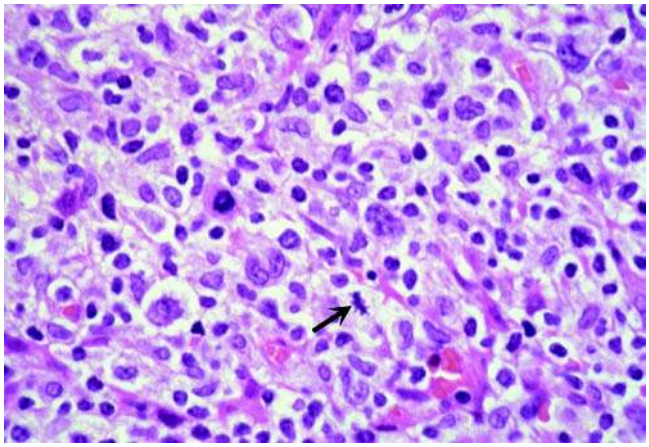

Figure 25 NK/T-cell lymphoma appearing less inflammatory. Note the clear cytoplasm, nuclear atypia, and mitosis (*arrow*) (H&E, 400×). *Abbreviation*: H&E, hematoxylin and eosin.

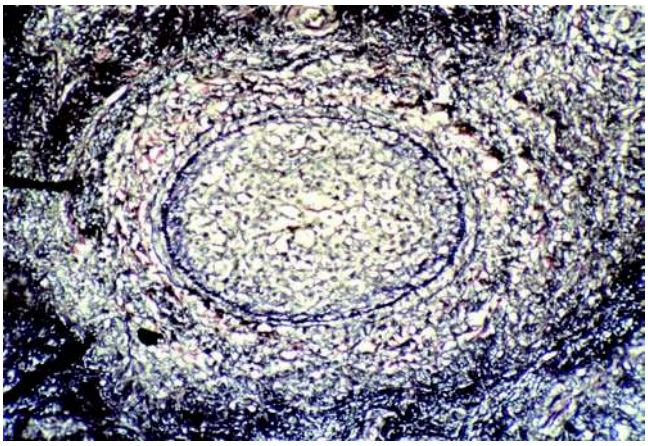

Figure 27 NK/T-cell lymphoma showing an artery totally occluded by the neoplastic cellular infiltrate (reticulin, 100×).

D. Immunohistochemistry

NK/T-cell lymphoma is almost universally positive for the EBV, which is best demonstrated by in situ hybridization (Fig. 29). The tumor cells are typically positive for CD2, CD56, CD3 cytoplasmic, TIA-1, granzyme B, and perforin and negative for CD4, CD5, CD8, CD16, and CD57. T-cell receptor genes are not rearranged.

E. Treatment and Prognosis

Radiation and/or chemotherapy is the treatment of choice. Local and systemic relapses are common even in patients achieving complete remission. A few cases may also be complicated by a hemophagocytic syndrome. The overall five-year survival is approximately 30% to 40% (4–7).

VIII. COCAINE ABUSE

A. Introduction

Cocaine, an alkaloid known chemically as benzoylmethylecgonine, is derived from the coca leaf, *Erythroxylon coca*, and cultivated primarily in South America (1,2). It has a long history of use and abuse. It was employed by the Incas thousands of years ago to reduce hunger, increase work tolerance, and promote a sense of well being. Because of its stimulating propensities, it has also been incorporated in many

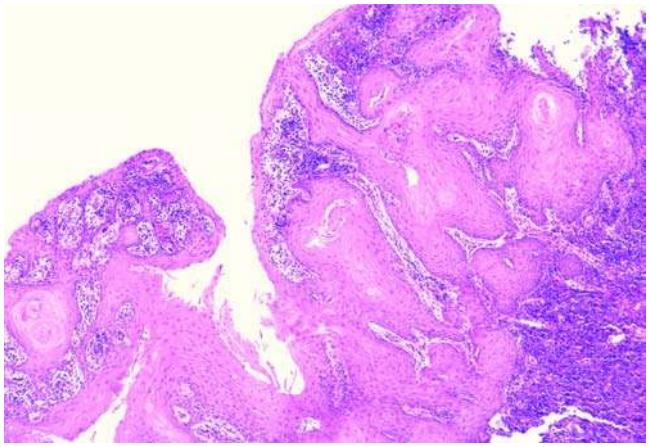

Figure 28 NK/T-cell lymphoma of the nasal cavity associated with exuberant pseudoepitheliomatous hyperplasia, which may be mistaken for carcinoma (H&E, 100×). *Abbreviation*: H&E, hematoxylin and eosin.

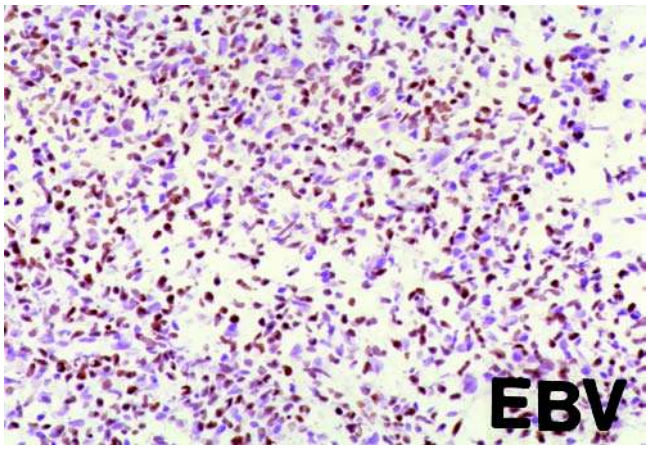

Figure 29 NK/T-cell lymphoma positive for Epstein-Barr virus (EBER, 100×).

medicinal and nonmedicinal preparations. It was even used as an ingredient in Coca Cola until 1906, when it was removed (3,4). In 1914, cocaine was classified as a narcotic, making routine use of the drug illegal (5).

Today it is used in medicine primarily for its anesthetic and vasoconstrictive properties. However, because of its intense euphoric affect, it has also become the ''recreational'' drug of choice among drug abusers.

The extent of cocaine abuse is difficult to determine. The National Institute on Drug Abuse estimated that over 22 million Americans had at least tried cocaine by 1985 (6). The National Household Survey on Drug Abuse estimated that in 1992 nearly 3.2 million Americans used cocaine on a regular basis, and the abuse continues to escalate (7).

Cocaine obtained on the black market exists basically in two forms: (*i*) a white, water soluble hydrochloride salt and (*ii*) an alkaloidal form known as ''base'' or ''crack.'' The hydrochloride salt is almost invariably diluted with adulterants, such as starch, talc, sugar, and others, with an ultimate purity of 10% to 70% (3,8,9). The abuser characteristically ''prepares'' a lump of semipurified cocaine by chopping it with a single-edged razor blade on a smooth surface. The finely pulverized cocaine is then partitioned into three or four 5-cm ''lines,'' each of which may contain about 30 mg of cocaine (8). The lines are then inhaled intranasally through a hollow instrument, such as a drinking straw. Three to four minutes later, the abuser experiences a period of euphoria, followed by a period of central nervous system depression (1).

Base or crack cocaine, in contrast, is 30% to 90% pure, usually smoked in a cigarette or pipe or heated in a water pipe and inhaled, and produces almost instantaneous euphoria. Not infrequently, the inhalation of the hot vapors or particulate matter of crack may result in thermal injury to the upper airway (10,11). Cocaine may also be abused by injecting the drug subcutaneously (''skin popping'') or directly into the peripheral veins (''mainlining'').

The plasma half-life of cocaine after administration varies from 0.5 to 1.25 hours (1,12). The average blood level for recreational use as reported by Mittleman and Wetli is 0.4 mg/L (13). For comparison, the concentration of cocaine used in medical practice ranges between 2% and 10%, and in otolaryngological surgical procedures, the maximal therapeutic dose is 80 to 200 mg, which produces a blood level of 0.2 to 0.4 mg/L (9,14).

B. Clinical Features

Chronic intranasal inhalation of cocaine produces a variety of signs and symptoms, including rhinorrhea, sniffing, nasal obstruction, rhinitis, sinusitis, congestion, ulceration, crusting, epistaxis, anosmia, septal perforation, hard palate perforation, osteocartilaginous necrosis, saddle nose deformity, pain, and rhinolalia (3,8,15–17).

At times, the nasal symptoms are often mistaken for allergic rhinitis. However, the erythematous, hemorrhagic, friable, and focally ulcerated nasal mucosa associated with cocaine addiction contrasts with the pale, boggy mucosa seen in allergies (1). In addition, the nonallergic patient with his or her lack of IgE elevation, absence of intranasal and peripheral eosinophilia, negative skin tests, and failure to respond to standard antiallergic medication should lead one to suspect other conditions, such as cocaine abuse.

The etiology of ''coke nose'' is related to multiple factors: (*i*) the anesthetic and vasoconstrictive action of the drug, (*ii*) rebound hyperemia resulting in varying degrees of nasal obstruction, (*iii*) the irritating effects of the adulterants used to dilute the cocaine, (*iv*) mucosal ulceration secondary to the instrument used to inhale the drug, (*v*) frequent nose-picking to relieve the nasal obstruction, which also contributes to

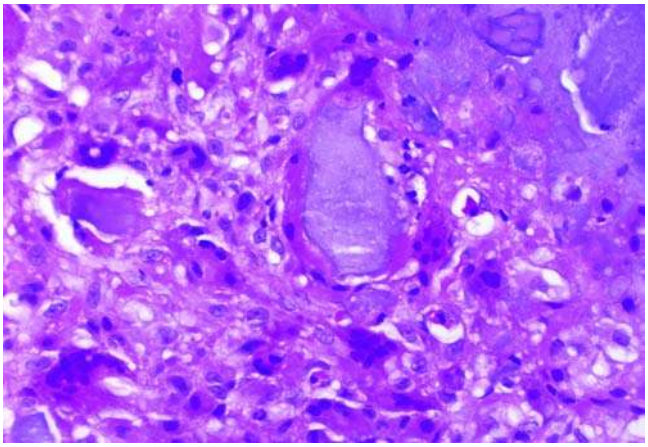

Figure 30 Nasal biopsy from a cocaine addict. Note the multinucleated giant cell reaction to the foreign material used to dilute the cocaine (H&E, 400×). *Abbreviation*: H&E, hematoxylin and eosin.

mucosal ulceration, and (*vi*) infections. As a result, a self-perpetuating cycle ensues.

C. Pathology

The histopathology of the nasal mucosa in chronic cocaine addiction shows acute and chronic nonspecific inflammation, often with mucosal ulceration and crusting. In addition, a multinucleated, foreign body giant cell reaction around the material used to dilute the cocaine is not uncommon (Fig. 30); viewing the biopsy under polarized light can be very helpful. Vasculitis is not seen, but tissue invasion by bacteria or fungi or both, is not uncommon.

D. Treatment and Prognosis

Complete abstinence from the offending drug with appropriate counseling is a prerequisite to any form of therapy. When confronted with the possibility of cocaine abuse, most patients will almost always deny the allegation initially. In this instance, urine assay for the detection of metabolites of cocaine may be rewarding. Such testing will detect any use of cocaine within a previous 48-hour period (8).

IX. DIFFERENTIAL DIAGNOSIS

Effective therapy of the various midfacial destructive diseases often requires prolonged treatment with potent medications (corticosteroids, cyclophosphamide, and others) or radiation. As a consequence, serious, sometimes life threatening, complications are not uncommon.

Distinguishing among these various diseases, which frequently have overlapping clinical and pathological manifestations, can be difficult and is often impossible on histological study alone. Knowledge of the clinical, imaging, and laboratory findings is not only desirable but also mandatory if a diagnosis is to be made with confidence.

Features that are helpful in distinguishing the ANCA-associated vasculitides (WG, microscopic polyangiitis, and AGV) are shown in Table 7. Those that are useful in separating microscopic polyangiitis and PAN are listed in Tables 4 and 7.

Table 7 Characteristic Features and Differential Diagnosis of Sinonasal Biopsies with Vasculitis and Granulomas

Wegener's granulomatosis
Vasculitis involving mainly small arteries
Giant cells/granulomas present
Micro- and granulomatoid microabscesses
Geographic zones of necrosis
Polymorphic inflammation with no cellular atypia
No asthma
Generally no tissue or peripheral eosinophilia
Upper aerodigestive tract, lungs, and kidneys are usual target sites. G-I tract and skin are uncommon sites
C-ANCA
Microscopic polyangiitis
Vasculitis involving arterioles, venules, and capillaries
No giant cells/granulomas
Polymorphic inflammation with no cellular atypia
No eosinophils
No asthma
Commonly involves skin, lungs, G-I tract, and kidneys. Upper aerodigestive tract disease is relatively uncommon
P-ANCA
See Table 4
Polyarteritis nodosa
Vasculitis involving small- to medium-sized arteries
Frequent aneurysms
No giant cells/granulomas
Prominence of neutrophils but no cellular atypia
Lungs are spared
No ANCA
See Table 4
Allergic granulomatosis and vasculitis
Vasculitis involving small- to medium-sized arteries
Giant cells/granulomas present
Tissue eosinophilia with no cellular atypia
Peripheral eosinophilia
Asthma
P-ANCA
Idiopathic midline destructive disease
No vasculitis
Giant cells/granulomas usually absent
Polymorphic inflammation with no cellular atypia
No disease below the clavicles
Extranodal NK/T-cell lymphoma
Infiltrate often appears polymorphic or inflammatory with cellular atypia
Angiocentric, angiodestructive cellular infiltrates
Spotty necrosis
No giant cells/granulomas
$CD56^{+}$ cells
No T-cell gene rearrangement
Positive for Epstein-Barr virus
At diagnosis, disease usually limited to the head and neck
No ANCA
Cocaine abuse
No vasculitis
Possible foreign body granulomas
Polymorphic inflammation with no cellular atypia
No ANCA

Abbreviation: ANCA, antineutrophil cytoplasmic antibodies/autoantibodies.

REFERENCES

II. WEGENER'S GRANULOMATOSIS

1. Klinger H. Genzformen der Pediarteritis nodosa. Frankf Z Pathol 1931; 42:455–480.
2. Wegener F. Wegener's granulomatosis. Thoughts and observations of a pathologist. Eur Arch Otorhinolaryngol 1990; 247:133–142.
3. Wegener F. Uber eine eigenartige rhinogene Granulomatose mit besonderer Beteiligung des Arteriensystems und der Nieren. Bietr Pathol Anat 1939; 109:36–68.
4. Ringertz N. En egenarted form as periarteritis nodosa (Wegener's granulomatos). Nord Med 1947; 36:2252–2253.
5. Johnsson S. A case of Wegener's granulomatosis. Acta Pathol Microbiol Scand 1948; 25:573–584.
6. Knudsen BB, Joergensen T, Munch-Jensen B. Wegener's granulomatosis in a family. A short report. Scand J Rheumatol 1988; 17:225–227.
7. Stoney PJ, Davies W, Ho SF, et al. Wegener's granulomatosis in two siblings: a family study. J Laryngol Otol 1991; 105:123–124.
8. Katz P, Alling DW, Haynes BF, et al. Association of Wegener's granulomatosis with HLA-B8. Clin Immunol Immunopathol 1979; 14:268–270.
9. Elkon KB, Sutherland DC, Rees AJ, et al. HLA antigen frequencies in systemic vasculitis: increase HLA-DR2 in Wegener's granulomatosis. Arthritis Rheum 1983; 26: 102–105.
10. Murty GE, Mains BT, Middleton D, et al. HLA antigen frequencies and Wegener's granulomatosis. Clin Otolaryngol 1991; 16:448–451.
11. Ewert BH, Jeannette JC, Falk RJ. The pathogenic role of antineutrophil cytoplasmic autoantibodies. Am J Kidney Dis 1991; 28:188–195.
12. Jennette JC, Falk RJ. Diagnostic classification of antineutrophil cytoplasmic autoantibody-associated vasculitis. Am J Kidney Dis 1991; 28:184–187.
13. Hoffman GS, Specks U. Antineutrophil cytoplasmic antibodies. Arthritis Rheum 1998; 41:1521–1537.
14. Kallenberg CGM, Rarok A, Coen A, et al. New insights into the pathogenesis of antineutrophil cytoplasmic autoantibody-associated vasculitis. Autoimmun Rev 2002; 1:61–66.
15. Gal AA, Velasquez A. Antineutrophil cytoplasmic autoantibody in the absence of Wegener's granulomatous or microscopic polyangiitis: implications for the surgical pathologist. Mod Pathol 2002; 15:197–204.
16. Savige J, Dimech W, Fritzler M, et al. Addendum to the international consensus statement on testing and reporting of antineutrophil cytoplasmic antibodies. Quality control guidelines, comments, and recommendations for testing in other autoimmune diseases. Am J Clin Pathol 2003; 120:312–318.
17. Seo P, Stone JH. The antineutrophil cytoplasmic antibody-associated vasculitides. Am J Med 2004; 117:39–50.
18. Falk RJ, Terrell RS, Charles LA, et al. Antineutrophil cytoplasmic autoantibodies induce neutrophils to degranulate and produce oxygen radicals in vivo. Proc Natl Acad Sci U S A 1990; 87:4115–4119.
19. Savage COS, Pottinger BE, Gaskin G, et al. Vascular damage in Wegener's granulomatosis and microscopic polyarteritis: presence of anti-endothelial cell antibodies and their relation to antineutrophil cytoplasmic antibodies. Clin Exp Immunol 1991; 85:14–19.
20. Bacon PA. The spectrum of Wegener's granulomatosis and disease relapse. N Engl J Med 2005; 352:330–332.
21. Bacon PA. Endothelial cell dysfunction in systemic vasculitis: new developments and therapeutic prospects. Curr Opin Rheumatol 2004; 17:49–55.
22. Davies DJ, Moran JE, Niall JF, et al. Segmental necrotizing glomerulonephritis with antineutrophil antibody: possible arbovirus aetiology? Br Med J 1982; 285:606–607.
23. Van der Woude FJ, Rasmussen N, Lobatto S, et al. Autoantibodies against neutrophils and monocytes: tool for diagnosis and marker of disease activity in Wegener's granulomatosis. Lancet 1985; 1:425–429.
24. Rao JK, Weinberger M, Oddone EZ, et al. The role of antineutrophil cytoplasmic antibody (c-ANCA) testing in the diagnosis of Wegener's granulomatosis: a literature review and meta-analysis. Ann Intern Med 1995; 123:95–932.
25. Marty GE. Wegener's granulomatosis: otorhinolaryngological manifestations. Clin Otolaryngol 1990; 15:385–393.
26. Hoffman GS, Kerr GS, Leavitt RY, et al. Wegener's granulomatosis. An analysis of 158 patients. Ann Intern Med 1992; 116:488–498.
27. Nolle B, Specks U, Ludermann J, et al. Anticytoplasmic autoantibodies: their immunodiagnostic value in Wegener's granulomatosis. Ann Intern Med 1989; 111:28–40.
28. Duna GF, Galperin C, Hoffman GS. Wegener's granulomatosis. Rheum Dis Clin North Am 1995; 21:949–986.
29. McDonald TJ, DeRemee RA, Kern EB, et al. Nasal manifestations of Wegener's granulomatosis. Laryngoscope 1974; 84:2101–2112.
30. Gubbels SP, Barkhuizen A, Hwang PH. Head and neck manifestations of Wegener's granulomatosis. Otolaryngol Clin North Am 2003; 36:685–705.
31. Handlers JP, Waterman J, Abrams AM, et al. Oral features of Wegener's granulomatosis. Arch Otolaryngol 1985; 111:267–270.
32. McCaffrey TV, McDonald TJ, Facer GW, et al. Otologic manifestations of Wegener's granulomatosis. Otolaryngol Head Neck Surg 1980; 88:586–593.
33. Kornblut AD, Wolff SM, Fauci AS. Ear disease in patients with Wegener's granulomatosis. Laryngoscope 1982; 92:713–717.
34. Illum P, Thorling K. Otological manifestations of Wegener's granulomatosis. Laryngoscope 1982; 92:801–804.
35. Macias JD, Wackym PA, McCabe BF. Early diagnosis of otologic Wegener's granulomatosis using the serologic marker C-ANCA. Ann Otol Rhinol Laryngol 1993; 102: 337–341.
36. McDonald TJ, Neel HB III, DeRemee RA. Wegener's granulomatosis of the subglottis and the upper portion of the trachea. Ann Otol Rhinol Laryngol 1982; 91:588–592.
37. Hoare TJ, Jayne D, Evans PR, et al. Wegener's granulomatosis, subglottic stenosis, and antineutrophil cytoplasm antibodies. J Laryngol Otol 1989; 103:1187–1191.
38. Specks U, Colby TV, Olsen KD, et al. Salivary gland involvement in Wegener's granulomatosis. Arch Otolaryngol Head Neck Surg 1991; 117:218–223.
39. Specks U, DeRemee RA. Granulomatous vasculitis. Wegener's granulomatosis and Churg-Strauss syndrome. Rheum Dis Clin North Am 1990; 16:377–397.
40. Leavitt RY, Fauci AS, Block DA, et al. The American College of Rheumatology 1990 Criteria for the Classification of Wegener's Granulomatosis. Arthritis Rheum 1990; 33:1101–1107.
41. Mark EJ, Matsubara O, Tan-Liu N, et al. The pulmonary biopsy in early diagnosis of Wegener's (pathergic) granulomatosis: a study based on 35 open lung biopsies. Hum Pathol 1988; 19:1065–1071.
42. Devaney KO, Travis WD, Hoffman G, et al. Interpretation of head and neck biopsies in Wegener's granulomatosis. A pathologic study of 126 biopsies in 70 patients. Am J Surg Pathol 1990; 14:555–564.
43. Lombard CM, Duncan SR, Rizk NW, et al. The diagnosis of Wegener's granulomatosis from transbronchial biopsy specimens. Hum Pathol 1990; 21:838–842.
44. Colby TV, Tazelaar HD, Specks U. Nasal biopsy in Wegener's granulomatosis. Hum Pathol 1991; 22:101–104.

45. Del Buono EA, Flint A. Diagnostic usefulness of nasal biopsy in Wegener's granulomatosis. Hum Pathol 1991; 22:107–110.
46. Travis WD, Hoffman GS, Leavitt RY, et al. Surgical pathology of the lung in Wegener's granulomatosis. Review of 87 open lung biopsies from 67 patients. Am J Surg Pathol 1991; 15:315–333.
47. Jennett JC, Falk RJ. Small-vessel vasculitis. N Engl J Med 1997; 337:1512–1523.
48. Jennett JC, Falk RJ. Do vasculitis categorization systems really matter? Curr Rheumatol Rep 2000; 2:430–438.
49. Narula N, Gupta S, Narula J. The primary vasculitides. A clinicopathologic correlation. Am J Clin Pathol 2005; 124 (suppl 1):S84–S95.
50. Gephardt GN, Shah LF, Tubbs RR, et al. Wegener's granulomatosis. Immunomicroscopic and ultrastructural study of four cases. Arch Pathol Lab Med 1990; 114: 961–965.
51. Striker LJ, Olson JL, Striker GE. Glomerular disease associated with systemic disease. In: Striker LJ, Olson JL, Striker GE, eds. The Renal Biopsy, 2nd ed. vol 8. Major Problems in Pathology Series. Philadelphia, PA: WB Saunders Co, 1990:117–164.
52. Carrington CB, Liebow AA. Limited forms of angiitis and granulomatosis of Wegener's type. Am J Med 1966; 41: 497–527.
53. Cassan SM, Coles DT, Harrison EG Jr. The concept of limited forms of Wegener's granulomatosis. Am J Med 1976; 49:366–379.
54. DeRemee RA, McDonald TJ, Harrison EG Jr., et al. Wegener's granulomatosis. Anatomic correlates, a proposed classification. Mayo Clin Proc 1976; 51:777–781.
55. McDonald TJ, DeRemee RA. Wegener's granulomatosis. Laryngoscope 1983; 93:220–231.
56. Reza MJ, Dornfeld L, Goldberg LS, et al. Wegener's granulomatosis. Long-term follow-up of patients treated with cyclophosphamide. Arthritis Rheum 1975; 18:501–506.
57. Fauci AS, Haynes BF, Katz P, et al. Wegener's granulomatosis: prospective clinical and therapeutic experience with 85 patients for 21 years. Ann Intern Med 1983; 98:76–85.
58. DeRemee RA, McDonald TJ, Weiland LH. Aspekte zur Therapie und Verlaufsbeobachtungen der Wegenerschen Granulomatose. Med Welt 1987; 38:470–473.
59. DeRemee RA. The treatment of Wegener's granulomatosis with trimethoprin/sulfamethoxazole: illusion or vision? Arthritis Rheum 1988; 31:1068–1072.
60. Leavitt RY, Hoffman GS, Fauci AS. The role of trimethoprin/sulfamethoxazole in the treatment of Wegener's granulomatosis. Arthritis Rheum 1988; 31:1073–1074.
61. McRae D, Buchanan G. Long-term sulfamethoxazole-trimethoprin in Wegener's granulomatosis. Arch Otolaryngol Head Neck Surg 1993; 119:103–105.
62. Langford CA. Treatment of ANCA-associated vasculitis. N Engl J Med 2003; 349:3–4.
63. Wegener's granulomatosis etanercept trial (WGET) research group. Etanercept standard therapy for Wegener's granulomatosis. N Engl J Med 2005; 352:351–361.
64. Kerr GS, Fleisher TA, Hallahan CW, et al. Limited prognostic vale of changes in antineutrophil cytoplasm antibody titer in patients with Wegener's granulomatosis. Arthritis Rheum 1993; 36:365–371.

III. MICROSCOPIC POLYANGIITIS

1. Davson J, Ball J, Platt R. The kidney in periarteritis nodosa. Q J Med 1948; 17:175–202.
2. Jennette JC, Falk RJ. Do vasculitis categorization systems really matter? Curr Rheumatol Rep 2000; 2:430–438.
3. Jennette JC, Falk RJ. Small-vessel vasculitis. N Engl J Med 1997; 337:1512–1537.
4. Seo P, Stone JH. The antineutrophil cytoplasmic antibody-associated vasculitides. Am J Med 2004; 117:39–50.
5. Hoffman GS, Specks U. Antineutrophil cytoplasmic antibodies. Arthritis Rheum 1998; 41:1521–1537.
6. Agard C, Mouthon L, Mahr A, et al. Microscopic polyangiitis and polyarteritis nodosa: how and when do they start? Arthritis Rheum 2003; 49:709–715.
7. Lhote F, Guillevin L. Polyarteritis nodosa, microscopic polyangiitis, and Churg-Strauss syndrome. Rheum Clin North Am 1995; 21:911–947.
8. Savage CO, Winearls CG, Evans DJ, et al. Microscopic polyarteritis: presentation, pathology and prognosis. Q J Med 1985; 220:467–483.
9. Rodgers H, Guthrie JA, Brownjohn AM, et al. Microscopic polyarteritis: clinical features and treatment. Postgrad Med J 1989; 65:515–518.
10. Kokan N, Hosomi Y, Inamoto S, et al. Microscopic polyangiitis histologically confirmed by biopsy from nasal cavity and paranasal sinuses: a case report. Rheumatol Int 2006; 26:936–938.
11. Kaufman LD, Kaplan AP. Microscopic polyarteritis. Hosp Pract 1989; 24:85–104.
12. Molloy ES, Langford CA. Advances in the treatment of small vessel vasculitis. Rheum Clin North Am 2006; 32: 157–172.

IV. POLYARTERITIS NODOSA

1. Kussmaul A, Maier R. Ueber eine bisher nicht beschriebene eigenthumliche Arterienerkrankung (periarteritis nodosa) die mit Morbus Brightii und rapid fortschreitender allgemeiner Muskellahmung einhergeht. Dtsch Arch Klin Med 1866; 1:484–518.
2. Lightfoot RW Jr., Michel BA, Bloch DA, et al. The American College of Rheumatology 1990 criteria for the classification of polyarteritis nodosa. Arthritis Rheum 1990; 33:1088–1093.
3. LeRoy CW. The systemic vasculitides. Hosp Pract 1992; 27:77–88.
4. Gardner DL. Vasculitis and vasculopathy. In: Gardner DL, ed. Pathological Basis of the Connective Tissue Diseases. Philadelphia, PA: Lea & Febiger, 1992:614–617.
5. Lhote F, Guillevin L. Polyarteritis nodosa, microscopic polyangiitis, and Churg-Strauss syndrome. Clinical aspects and treatment. Rheum Dis Clin North Am 1995; 21:911–947.
6. Sergent JS, Lockshin MD, Christian CL, et al. Vasculitis with hepatitis B antigenemia: long-term observations in nine patients. Medicine 1976; 55:1–18.
7. Sergent JS, Christian CL. Necrotizing vasculitis after acute serous otitis media. Ann Intern Med 1974; 81:195–199.
8. Albert DA, Rimon D, Silverstein MD. The diagnosis of polyarteritis nodosa. I. A literature-based decision analysis approach. Arthritis Rheum 1988; 31:1117–1127.
9. Cohen RD, Conn DL, Ilstrup DM. Clinical features, prognosis, and response to treatment in polyarteritis. Mayo Clin Proc 1980; 55:146–155.

V. ALLERGIC GRANULOMATOSIS AND VASCULITIS (CHURG-STRAUSS SYNDROME)

1. Churg J, Strauss L. Allergic granulomatosis, allergic angiitis, and periarteritis nodosa. Am J Pathol 1951; 27:277–301.
2. Chumbley LC, Harrison EG Jr., DeRemee RA. Allergic granulomatosis and angiitis (Churg-Strauss syndrome). Report and analysis of 30 cases. Mayo Clin Proc 1977; 52:477–484.

3. Koss MN, Antonovych T, Hochholzer L. Allergic granulomatosis (Churg-Strauss syndrome). Pulmonary and renal morphologic findings. Am J Surg Pathol 1981; 5:21–28.
4. Lanham JG, Elkon KB, Pusey CD, et al. Systemic vasculitis with asthma and eosinophilia; a clinical approach to the Churg-Strauss syndrome. Medicine 1984; 63:65–81.
5. Lie JT. The classification of vasculitis and a reappraisal of allergic granulomatosis and angiitis (Churg-Strauss syndrome). Mt Sinai J Med 1986; 53:429–439.
6. Lhote F, Guillevin L. Polyarteritis nodosa, microscopic polyangiitis, and Churg-Strauss syndrome. Clinical aspects and treatment. Rheum Dis Clin North Am 1995; 21: 911–947.
7. Keogh KA, Specks U. Churg-Strauss syndrome. Semin Respir Crit Care Med 2006; 27:148–157.
8. Guillevin L, Cohen P, Gayraud M, et al. Churg-Strauss syndrome. Clinical study and long-term follow-up of 96 patients. Medicine 1999; 78:26–37.
9. Keogh KA, Specks U. Churg-Strauss syndrome: Clinical presentation, antineutrophil cytoplasmic antibodies, and leukotriene receptor antagonists. Am J Med 2003; 115: 284–290.
10. Sable-Fourtassou R, Cohen P, Mahr A, et al. Antineutrophil cytoplasmic antibodies and the Churg-Strauss syndrome. Ann Intern Med 2005; 143:632–638.
11. Sinico RA, DiToma L, Maggiore U, et al. Prevalence and clinical significance of antineutrophil cytoplasmic antibodies in Churg-Strauss syndrome. Arthritis Rheum 2005; 52:2926–2935.
12. Suen KC, Burton JD. The spectrum of eosinophilic infiltration of the gastrointestinal tract and it relationship to other disorders of angiitis and granulomatosis. Hum Pathol 1979; 10:31–43.
13. Olsen KD, Neel HB III, DeRemee RA. Nasal manifestations of allergic granulomatosis and angiitis (Churg-Strauss syndrome). Otolaryngol Head Neck Surg 1980; 88:85–89.
14. Bacciu A, Bacciu S, Mercante G, et al. Ear, nose and throat manifestations of Churg-Strauss syndrome. Acta Oto-Laryngologica 2006; 126:503–509.
15. Finan MC, Winkelman RK. The cutaneous extravascular necrotizing granuloma (Churg-Strauss granuloma) and systemic disease: a review of 27 cases. Medicine 1983; 62:142–158.
16. Seo P, Stone JH. The antineutrophil cytoplasmic antibody-associated vasculitides. Am J Med 2004; 117:39–50.
17. Masi AT, Hunder GC, Lie JT, et al. The American College of Rheumatology 1990 criteria for the classification of Churg-Strauss syndrome (allergic granulomatosis and angiitis). Arthritis Rheum 1990; 33:1094–1100.
18. Jennette JC, Falk RJ, Andrassy K, et al. Nomenclature of systemic vasculitides: the proposal of the international consensus conference. Arthritis Rheum 1994; 37:187–192.
19. Lie JT. Illustrated histopathologic classification criteria for selected vasculitis syndromes. Arthritis Rheum 1990; 33:1074–1087.
20. Leavitt RY, Fauci AS. Pulmonary vasculitis. Am Rev Respir Dis 1986; 134:149–166.
21. Sasaki A, Hasewaga M, Nakazato Y, et al. Allergic granulomatosis and angiitis (Churg-Strauss syndrome). Report of an autopsy case in a nonasthmatic patient. Acta Pathol Jpn 1988; 38:781–788.
22. Lipworth BJ, Slater DN, Corrin B, et al. Allergic granulomatosis without asthma: a rare forme fruste of the Churg-Strauss syndrome. Respir Med 1989; 83:249–250.
23. Lie JT. Limited forms of Churg-Strauss syndrome. Pathol Annu 1993; 28:199–220.
24. Nissim F, Von der Valde J, Czernobilsky B. A limited form of Churg-Strauss syndrome. Ocular and cutaneous manifestations. Arch Pathol Lab Med 1982; 106:305–307.
25. Lie JT, Bayardo RJ. Isolated eosinophilic coronary arteritis and eosinophilic myocarditis. A limited form of Churg-Strauss syndrome. Arch Pathol Lab Med 1989; 113:199–201.
26. Lane SE, Watts RA, Shepstone L, et al. Primary systemic vasculitis: clinical features and mortality. Q J Med 2005; 98:97–111.

VI. IDIOPATHIC MIDLINE DESTRUCTIVE DISEASE

1. Tsokos M, Fauci AS, Costa J. Idiopathic midline destructive disease (IMDD). A subgroup of patients with the ''midline granuloma'' syndrome. Am J Clin Pathol 1982; 77:162–168.

VII. EXTRANODAL NK/T-CELL LYMPHOMA, NASAL TYPE

1. Chan JKC, Jaffe ES, Ralfkiaer E. Extranodal NK/T-cell lymphoma, nasal type. In: Jaffee ES, Harris NL, Stein H, et al., eds. World Health Organization Classification of Tumours. Pathology and Genetics. Tumours of Hematopoietic and Lymphoid Tissues. Lyon, France: IARC Press, 2001:204–207.
2. Chan ACL, Chan JKC, Cheung MMC, et al. Hematolymphoid tumours. In: Barnes L, Eveson JW, Reichart P, et al., eds. World Health Organization Classification of Tumours. Pathology and Genetics. Head and Neck Tumours. Lyon, France: IARC Press, 2005:58–64.
3. Harabuchi Y, Imai S, Wakashima J, et al. Nasal T-cell lymphoma causally associated with Epstein-Barr virus. Clinicopathologic, phenotypic and genotypic studies. Cancer 1996; 77:2137–2149.
4. Cheung MM, Chan JK, Lau WH, et al. Primary non-Hodgkin's lymphoma of the nose and nasopharynx: Clinical features, tumor immunophenotype, and treatment outcome in 113 patients. J Clin Oncol 1998; 16:70–77.
5. Quintanilla-Martinez L, Franklin JL, Guerrero I, et al. Histological and immunophenotypic profile of nasal NK/T-cell lymphomas from Peru: high prevalence of p53 overexpression. Hum Pathol 1999; 30:849–855.
6. Ko YH, Ree HJ, Kim WS, et al. Clinicopathologic and genotypic study of extranodal nasal-type natural killer/T-cell lymphoma and natural killer precursor lymphoma among Koreans. Cancer 2000; 89:2106–2116.
7. Li C-C, Tien H-F, Tang J-L, et al. Treatment outcome and pattern of failure in 77 patients with sinonasal natural killer/T-cell or T-cell lymphoma. Cancer 2004; 100:366–375.
8. Ng SB, Lai KW, Murugaya S, et al. Nasal-type extranodal natural killer/T-cell lymphomas: a clinicopathologic and genotypic study of 42 cases in Singapore. Mod Pathol 2004; 17:1097–1107.
9. Arber DA, Weiss LM, Albujar PF, et al. Nasal lymphomas in Peru. High incidence of T-cell immunophenotype and Epstein-Barr virus infection. Am J Surg Pathol 1993; 17: 392–399.
10. Aviles A, Rodriguez L, Guzman R, et al. Angiocentric T-cell lymphoma of the nose, paranasal sinuses and hard palate. Hematol Oncol 1992; 10:141–147.
11. Gaal K, Sun NCJ, Hernandez AM, et al. Sinonasal NK/T-cell lymphomas in the United States. Am J Surg Pathol 2000; 24:1511–1517.

VIII. COCAINE ABUSE

1. Snyder RD, Synyder LB. Intranasal cocaine abuse in an allergists office. Ann Allergy 1985; 54:489–492.
2. Gordon AJ, Moran DT, Jafek BW, et al. The effect of chronic cocaine abuse on human olfaction. Arch Otolaryngol Head Neck Surg 1990; 116:1415–1418.

3. Kuriloff DB, Kimmelman CP. Osteocartilaginous necrosis of the sinonasal tract following cocaine abuse. Laryngoscope 1989; 99:918–924.
4. Jaffe JH. Cocaine use in America. Natl Inst Drug Abuse Res Monogr Ser 1985; 61:133–135.
5. Isaacs SO, Martin P, Willoughby JH. ''Crack'' (an extra potent form of cocaine) abuse: a problem of the eighties. Oral Surg Oral Med Oral Pathol 1987; 63:12–16.
6. Schade CP. Smoking More Now and Enjoying it Less: The Epidemiology of Cocaine Abuse in the United States in the Late 1980's. Rockville, MD: National Institute on Drug Abuse, 1988.
7. Preliminary estimates from the 1992 National Household Survey on Drug Abuse, Advance Report No. 3. Washington, DC: Substance Abuse and Mental Health Service Administration, US Department of Health and Human Services, 1993.
8. Schwartz RH, Estroff T, Fairbanks DNF, et al. Nasal symptoms associated with cocaine abuse during adolescence. Arch Otolaryngol Head Neck Surg 1989; 115:63–64.
9. Jentzen J. Medical complications of cocaine abuse. Am J Clin Pathol 1993; 100:475–476.
10. Snyderman C, Weissman J, Tabor E, et al. Crack cocaine burns of the larynx. Arch Otolaryngol Head Neck Surg 1991; 117:792–795.
11. Reino AJ, Lawson W. Upper airway distress in crack-cocaine users. Otolaryngol Head Neck Surg 1993; 109:937–940.
12. Nolte KB, Gelman BB. Intracerebral hemorrhage associated with cocaine abuse. Arch Pathol Lab Med 1989; 113: 812–813.
13. Mittleman R, Wetli C. The Pathology of Cocaine Abuse. New York, NY: Mosby Year Book, 1991:37–70.
14. Ellenhorn M, Barceloux D. Medical Toxicology Treatment of Human Poisoning. New York, NY: Elsevier Scientific, 1988:648.
15. Becker GD, Hill S. Midline granuloma due to illicit cocaine use. Arch Otolaryngol Head Neck Surg 1988; 114:90–91.
16. Deutsch HL, Millard R Jr. A new cocaine abuse complex. Involvement of nose, septum, palate and pharynx. Arch Otolaryngol Head Neck Surg 1989; 115:235–237.
17. Mattson-Gates G, Jak AD, Hugo NE. Perforation of the hard palate associated with cocaine abuse. Ann Plast Surg 1991; 26:466–468.

12

Tumors of the Nervous System

Beverly Y. Wang
Departments of Pathology and Otolaryngology, New York University School of Medicine, New York University Langone Medical Center, New York, New York, U.S.A.

David Zagzag
Department of Neuropathology, New York University School of Medicine, Bellevue Hospital, New York, New York, U.S.A.

Daisuke Nonaka
Department of Pathology, New York University School of Medicine, New York University Langone Medical Center, New York, New York, U.S.A.

I. ORGAN OF CHIEVITZ

A. Introduction

The juxtaoral organ of Chievitz (JOC) is a normal microscopic anatomical structure that was first described in 1885 by the Danish histologist J.H. Chievitz (1). This nonneoplastic epithelial structure has been the subject of detailed monographs (2,3).

B. Embryology and Physiology

The JOC first appears in embryos measuring 7.5 to 12 mm in length (2,3). The JOC develops in the vicinity of the two lateral buccal bags of the oral cavity (sulcus buccalis), where the maxillary and mandibular walls merge (commissura buccalis). The epithelium of the commissura buccalis represents the anlage of the JOC, which gradually separates from the commissura. During its development, the organ receives its innervation from the buccal nerve. The dorsal part of the organ is related to the oral part of the medial pterygoid muscle, the middle part crosses the buccal nerve, and the oral part descends orocaudally to the place where the parotid duct penetrates the buccinator muscle.

The parenchyma begins to simultaneously develop secondary sprouts and buds, whereas the mesenchymal component becomes concentrically organized around these epithelial formations. The JOC persists throughout life, without any signs of involution.

The function of the JOC is as yet unknown, and the following hypotheses have been proposed. The parenchymal cells have abundant enzyme activity indicating a high metabolic activity (4). One study demonstrated a high activity of alkaline phosphatase, the finding being quite unique in the JOC, while the adjacent structure such as oral mucosa, parotid gland, and buccal minor salivary glands showed complete absence of activity (4). The same study also showed the resemblance of other enzyme activity patterns between the epithelium of the JOC and the duct cells of the salivary glands. In addition, genetic studies demonstrated that the development of the JOC and parotid glands were affected by the same mutation. These findings led to the speculation that the JOC represents an anlage of the parotid gland (5). However, it has been shown that the JOC has no true connection with the parotid duct or with the epithelium of the oral cavity.

The intimate relationship between parenchyma and nonmyelinated nerves, and the presence of cytoplasmic neurosecretory-like granules also suggest a possible neurosecretory function of the JOC. The JOC could represent a mechanosensor with different qualities of perception, such as deglutition, sucking, and mastication, somewhat analogous to a Pacinian corpuscle (2,6).

C. Clinical Features

The JOC is located at the angle of the mandible, bilaterally, near the buccotemporalis fascia and is intimately associated with branches of the buccal nerve (7–13). Lutman found these structures in the soft tissue on the anterior medial surfaces of 9 of 14 hemimandibulectomy specimens at a point where the ascending ramus joins the body (7). These structures were located near the medial surface of the pterygomandibular ligament deep into the minor salivary glands. Tschen and Fechner noted their presence in 14 of 25 consecutive autopsies, in three of which they could demonstrate bilaterality (8). Danforth and Baughman found these epithelial nests associated with sensory nerve fibers in 11 of 25 autopsy specimens evaluated (14). The JOC has been noted in all age groups, including newborns, stillborns, and adults (14). There is no gender predominance. The JOC rarely presents as an intraoral tumor as large as 6 cm (15–17).

D. Macroscopy

The JOC is located within the soft tissue overlying the angle of the mandible in the buccotemporal space (2,3). The JOC is not usually visualized on gross examination. When it is visualized, the JOC is a small fusiform structure, interposed between the fascia buccotemporalis and pterygoid muscles. It presents in adults as a white solid strand, resembling a nerve or a strand of connective tissue. It measures 7 to 17 mm in length and 1 to 2 mm in width, but a size as large as 6 cm has been reported (15–17).

E. Histopathology

It is important to recognize the JOC on histological examination because it has the potential to be misdiagnosed as perineural spread of carcinomas arising from this anatomic location (7–14). The JOC is not connected with the epithelium of the oral cavity or the salivary glands. The organ consists of 2 to 10 sharply circumscribed cylindrical or spherical epithelial nests. The epithelial nests resemble nonkeratinizing squamous epithelium or columnar glandular-like cells with clear cytoplasm (Fig. 1). The epithelial nests can be divided into two types (4) (Fig. 2). Type I is composed of a thick central epithelial core, from which sprouts and folds emanate. The peripheral layer of the epithelial parenchyma consists of closely packed cuboidal or columnar cells, occasionally with a basaloid appearance, whereas the central part contains whorl-like structures or concentric formations resembling Hassall's corpuscles. Some of the parenchymal sprouts display follicles filled with a metachromatic colloid mass or well-defined lumens (8). The latter structure is not stained with mucicarmine (3). Type II is an epithelial cord with a variable number of sprouts. Follicles can seldom be found in this type. Although intercellular bridges are observed in the cell nests, there is no evidence of keratin formation or keratohyalin granules. Mitoses are absent. Periodic acid-Schiff (PAS) stain shows a prominent basement membrane around the cell nests.

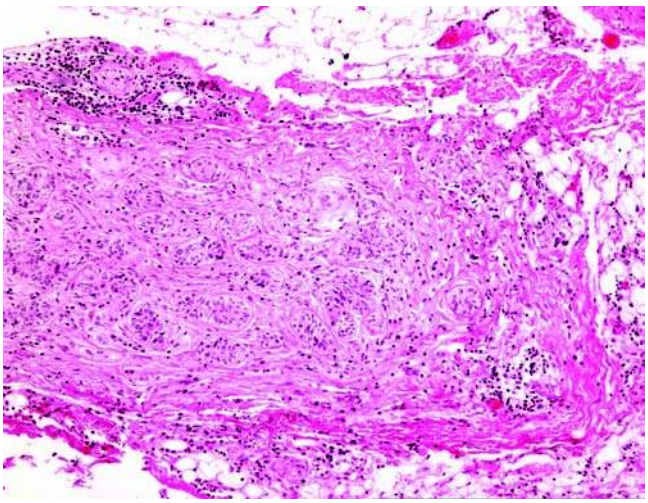

Figure 1 Cross section of a juxtaoral organ of Chievitz. Several well-circumscribed nests of epithelial cells are surrounded by loose connective tissue (H&E, 50×).

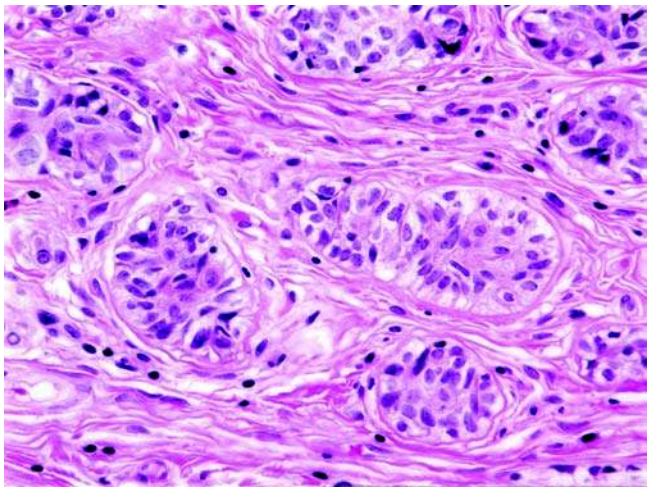

Figure 2 The inner cells have a squamoid appearance, whereas the outer layer contains basaloid cells, with palisading of their nuclei along the basement membrane (H&E, 250×).

Around this parenchyma, there is a connective tissue envelope that is divided into three parts.

1. Stratum fibrosum internum, the inner connective tissue capsule, is formed by a thin layer of connective tissue fibers and a small amount of elastic fibers.
2. Stratum nervosum, which is externally located from the stratum fibrosum internum, is a layer of a loose connective tissue that contains nerve fibers and sensory structures.
3. Stratum fibrosum externum is rich in collagenous fibers and envelops the whole organ. Within the JOC, several kinds of nerve endings, including simple arborizations, Ruffini-like or Krause-like structures, and Pacinian-type lamellar corpuscles, have been observed (6).

Scattered cells that contain melanin pigment have been described in the stroma but not in the epithelial component. They comprise S-100 +, HMB-45 + melanocytes with spindle or dendritic morphology, and CD68 + melanophages (18).

F. Ultrastructure

There are two types of parenchymal cells (2–4). Type I cells resemble keratinocytes. They are polygonal in shape with a diameter of 7 to 13 μm and contain tonofibrils, cytoplasmic granules, and inclusions. Each cell is separated by desmosomes and tight

junctions. Type II cells are less abundant and are characterized by their dendritic morphology. They contain abundant endoplasmic reticulum without tonofibrils or desmosomes. Their dendritic processes extend to the type I cells. The parenchyma is surrounded by stratum fibrosum internum with a 50-nm intervening layer of lamina basalis. The stratum fibrosum internum is composed of collagenous and elastic microfibrils. The stratum nervosum contains numerous nerve fibers with myelin as well as without myelin and different sensory structures. The cell population consists of fibroblasts, mast cells, melanin containing cells, and lymphocytes. This layer is rich in capillaries. The nerve fibers enter the stratum nervosum after penetrating the stratum fibrosum externum. The stratum fibrosum externum is formed by concentrically arranged connective tissue lamellae.

G. Immunohistochemistry

The JOC has not been immunohistochemically extensively investigated. A few reports have described the following findings (15,19,20). The epithelial component demonstrates positive reactivity for cytokeratins (CKs) such as pancytokeratin (AE1/AE3), CK8/CK18 (Cam 5.2), and CK19. It has been reported that only the inner epithelial portion expressed CK, while the outer portion did not (19,20). It is nonreactive for S-100 protein, smooth muscle actin, desmin, chromogranin, synaptophysin, neuron-specific enolase (NSE), and glial fibrillary acidic protein (GFAP) (15,19). S-100 protein and NSE demonstrate nerve fiber endings in the connective tissue stroma surrounding the epithelial component (19,20). One case report described the expression of epithelial membrane antigen (EMA) and vimentin in the epithelial component, while others reported a negative reaction to EMA (16) and positive reactions to GFAP and NSE (17).

H. Differential Diagnosis

Because the nests of squamous epithelial cells in the JOC are in close proximity to nerves, they may be confused for perineural invasion in oral carcinoma (7,10–12,14,21). Difficulty in diagnosis may arise on permanent sections or during intraoperative frozen-section diagnosis, giving rise to erroneous staging or unnecessary surgical intervention (7). The differential diagnosis includes perineural spread of carcinoma with squamoid or basaloid morphology such as squamous cell carcinoma, adenoid cystic carcinoma, or mucoepidermoid carcinoma. Differential features are listed in Table 1. The characteristic anatomical location and normal nuclear features lacking cellular atypia distinguish the JOC from carcinomas. In addition, there is no stromal desmoplastic response to the JOC, whereas invasive squamous cell carcinoma is often associated with this feature.

The JOC is mucicarmine-negative, whereas PAS stain shows a prominent basement membrane around the cell nests (14). Small dense core granules resembling neurosecretory granules have been noted on ultrastructural examination (22).

Table 1 Microscopic Features in Differentiating Between the JOC and Perineural Invasion by Carcinoma

JOC	Carcinoma
Intra- and perineural epithelium may be seen	Epithelium likely to be located in the perineural space
Basement membrane present around epithelial islands	Loss of a basement membrane except for adenoid cystic carcinoma
Central pale and outer darker basaloid cells	Less cellular organization
Retraction artifact common between parenchyma and nerves	Malignant cells more likely to abut directly on nerves
Basal parenchymal cells	Malignant cytology
Absent mitoses	Mitotic figures rarely present
Mucin-negative secretions in pseudoglandular structures	Possible mucin secretion if adenocarcinoma is present
Absence of keratin or keratohyaline granules	Keratin pearls and keratohyaline granules may be seen in keratinizing squamous cell carcinoma
Organized enveloping connective tissue layers	Occasionally more disorganized stroma
Loose and dense connective tissue stroma without inflammation	Possible desmoplastic-inflammatory stromal reaction

Abbreviation: JOC, juxtaoral organ of Chievitz.
Source: Modified from Ref. 3 (section I, "**Organ of Chievitz**").

II. NASAL GLIOMA

A. Introduction

Nasal glioma (NG, or nasal glial heterotopia) is a rare nonhereditary congenital malformation, originally reported by Reid in 1852 (1). This term implies heterotopic mature neuroglial tissue present outside the craniospinal axis, which most frequently occurs around the nose (2–4). NG is not a true neoplasm, but instead it is an abnormal embryological development with capability of autonomous growth in which there is anterior displacement of mature cerebral tissue that has lost its connection with the intracranial contents, perhaps as a consequence of sequestration of an anterior or nasofrontal encephalocele (3,4). However, the term ''nasal glioma,'' or NG, is generally accepted by head and neck surgeons, over the term ''nasal heterotopia,'' which is more appropriate for this lesion. Therefore, its continued use is probably justified, provided its true nature is explained in the surgical pathology report.

B. Clinical Features

The incidence of congenital nasal masses is 1 in every 20,000 to 40,000 live births (5). Most congenital nasofrontal masses in infancy or childhood are usually an NG, nasal encephalocele (NE), or nasal dermoid (2–11). Although NGs are often obvious at birth, some cases may remain asymptomatic and have been found in later childhood and even adulthood, with a mean age at presentation of 8.6 years (range, birth to 44 years) (3,4). The majority of NGs, however, are diagnosed and treated by two years (90%) (3).

There is neither gender prevalence nor familial occurrence. Glial heterotopias arising in the pharynx may be associated with cleft palate or choanal stenosis in about one-third of the cases. The heterotopic glial mass is situated externally on or near the bridge of the nose in 60% of cases, within the nasal cavity in 30% of cases, and in 10% both intranasal and extranasal components are present (3–25). Less frequently, glial heterotopia may present in other extracranial sites of the head and neck (''facial glioma'') such as the nasopharynx, palate, tongue, paranasal sinuses, tonsil, orbit, mandible, parapharyngeal, or face (26–33). Rare case reports have described the occurrence of glial heterotopia in the midline occipital or parietal scalp, gluteal region, and even away from the midline in the temporal region of scalp and chest wall (34).

Most NGs present as a polypoid, solid, noncompressible, nonpulsatile, and gray or purple lesion (Fig. 3) (1–3) filling one side of the nose and may cause airway obstruction. Most are solitary, but may rarely present as multiple masses (3). Intranasal lesions are often attached high on the lateral wall in the region of the middle turbinate. Extranasal lesions usually present as a smooth noncompressible subcutaneous mass on either side of the dorsum of the nose, near the inner canthus, or between the frontal nasal, ethmoid, and lacrimal bones. The overlying skin may be normal or have a blue or red discoloration. When combined, the intra- and extranasal components communicate through a defect in the nasal bone. NG lacks a connection with the cerebrospinal fluid (CSF) pathway and does not contain a fluid-filled space connected with either the ventricles or the subarachnoid spaces of the brain. The Furstenberg test (in which expansion or pulsation of the mass occurs on application of pressure to the ipsilateral jugular vein) is therefore negative in NG. Evaluation should include a complete rhinological and neurological examination.

C. Imaging

Preoperative imaging with a thin-cut axial and coronal computed tomography (CT) scan and/or multiplanner magnetic resonance imaging (MRI) is essential to rule out the potential for intracranial extension. CT and MRI reveal the presence of a soft tissue mass in or around the nose, with no associated intracranial component or any bony defect in the floor of the anterior cranial fossa (9,19). If any such communication is found, then the lesion qualifies as an encephalocele, rather than a NG, which requires different surgery. Fetal MRI can also help exclude the possibility of an encephalocele by ruling out underlying bone defects at prenatal evaluation (35,36).

D. Pathology

On gross examination, an NG appears as a polypoid, smooth, soft, gray tan, nontranslucent mass with encephaloid features. Histologically, NGs are composed of an unencapsulated disorganized mixture of neuroglial tissue and fibrovascular tissue. The large clumps or small islands of neuroglial tissue display evenly spaced astrocytes within an abundant fibrillar matrix (Fig. 4) (4,5). The neuroglial tissue is often tranversed by interlacing bands of vascularized fibroconnective tissue that merge with the collagen of the mucosal lamina propria or dermis (2,3,12–25). The relative amounts of glial and fibrous tissue vary (Fig. 5). Recurrent NG or lesions presenting in children older than 18 months tend to contain a considerable amount of fibrosis and may be misdiagnosed as a fibrotic nasal polyp or fibroma (3). Neurons are

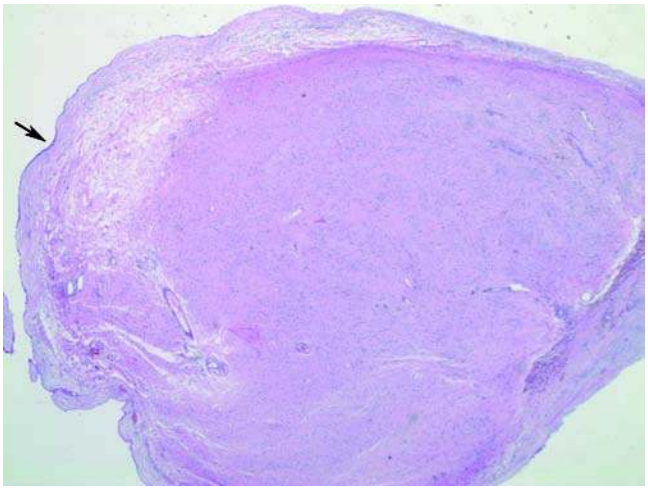

Figure 3 Low magnification of a polypoid nasal mass with an overlying nasal mucosa (*arrow*). The mass is composed of neuroglial tissue. In this case, there is no evidence of intracranial connection (H&E, 50×).

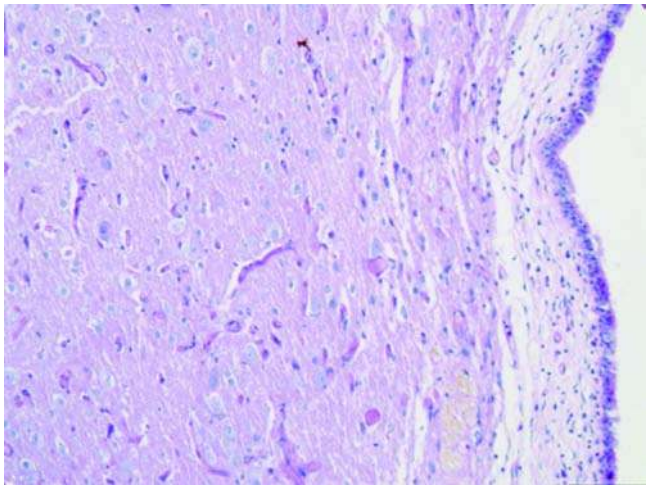

Figure 4 Higher magnification shows an intact nasal mucosa and a neuroglial component with occasional neurons without fibrosis or inflammatory cells (H&E, 200×).

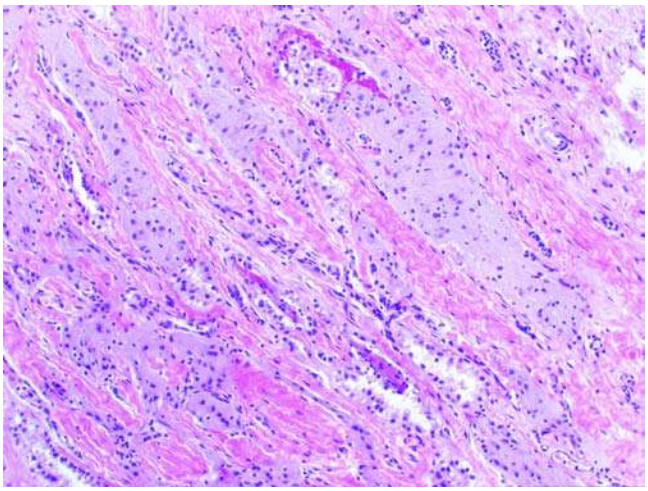

Figure 5 Nasal glioma composed of mature glial tissue in a fibrous background (H&E, 200×). *Source*: Courtesy of Dr. Leon Barnes, University of Pittsburgh School of Medicine, Pittsburgh, PA.

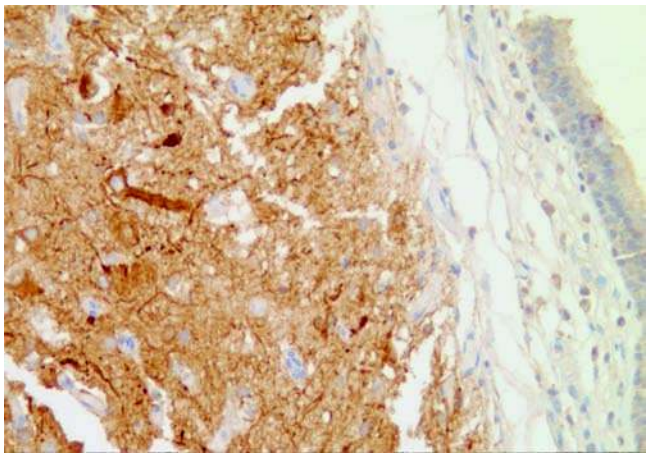

Figure 6 The glial component is positive for GFAP stain.

usually rare or absent, although in rare instances, a prominent neuronal component has been reported in NG (3,25). The cause of paucity of neurons in NG, whether owing to ischemic changes or lack of differentiation of the isolated primitive neuroectoderm, is unclear. Mitoses are absent. The astrocyte nuclei may appear enlarged or multinucleated. These ''gemistocytic'' astrocytic changes are reactive, and they should not be confused with malignancy (4,37). The presence of choroid plexus, ependyma-lined clefts, or pigmented retinal epithelium is observed in some glial heterotopias, especially those found in the palate and nasopharynx. However, tissue elements from other embryonic germ layers are absent.

Morphologically, subtle glial component on routine section can be accentuated. Phosphotungstic acid-hematoxylin staining may help identify glial fibers, but when suspected, the presence of ectopic glial tissue can be easily confirmed by demonstrating positivity for GFAP (Fig. 6), NSE, and S-100 protein (3,38,39). These stains do not, however, distinguish between ectopic glial tissue in NG and herniated brain tissue of an encephalocele. Electron microscopic examination of heterotopic glial tissue reveals features of astrocytes, such as the presence of elongated interdigitating cell processes associated with a continuous basement membrane (16,10,34,40).

E. Differential Diagnosis

The clinical differential diagnosis of NG includes a large group of benign nasofrontal congenital lesions such as NE, nasal dermoid cysts, teratomas, and hemangiomas (2,3,8,41–43). Occasionally, NG may also be mistaken for an inflammatory nasal polyp. The differentiation of NGs from NE is based on the presence of a connection between the mass and the intracranial tissue. Since both NG and NE present at birth, the diagnosis usually depends on imaging studies. However, it may be indistinguishable between two lesions, even with high-resolution CT imaging and MRI, because the connection may be very small and unapparent (5,9). CT and MRI allow visualization of the soft tissue mass, with an intracranial connection in an encephalocele (9). Histologically, although neurons are generally easily found in an encephalocele and are sparse or absent in NG, there is an overlap and the distinction between the lesions is not always possible (2,3). Furthermore, the ectopic cerebral tissue in both lesions shows reactivity for the GFAP, S-100 protein, and NSE (Fig. 6). Occasionally, NG may mimic an astrocytoma (37).

Nasal dermoid cysts or dermal sinuses represent developmental abnormalities that contain only ectodermal elements, without tissue elements from the other embryonic germ layers (2,5–11). Failure of the fonticulus nasofrontalis or foramen cecum to close allows dermal elements to invaginate through the frontonasal suture line area or between the developing nasal bones and cartilage (4). Nasal dermoids present on the dorsum of the nose with an intra- or extranasal cyst can be clinically mistaken for either NG or NE. The association of a sinus tract located at any point from the glabella to the base of the columella is characteristic. In some nasal dermoids, an intracranial connection may be seen on CT or MRI. Histologically, nasal dermoids are easily distinguished because they are lined by epidermis replete with dermal appendages and lack glial tissue (2,4,8).

Occasionally, recurrent or long-standing heterotopic glial tissue is mistaken for a fibrosed sinonasal polyp or fibroma, when there is increased fibrosis relative to the glial tissue (3,44). It should be remembered, however, that sinonasal polyps are highly unlikely occurrences in the newborn infant or even in children younger than five years. Furthermore,

sinusoidal polyps are bilateral, often multiple, and present as glistening, translucent masses that fill the nasal cavity or sinuses. Histologically, sinonasal polyps typically demonstrate stroma edema, thickening of the mucosal basement membrane, and a chronic inflammatory cell infiltrate, including eosinophils. The history of a congenital mass should suggest the possibility of heterotopic glial tissue, rather than a sinonasal polyp, and the diagnosis can be confirmed by demonstrating immunoreactivity for GFAP or S-100 protein (2).

Finally, the mere presence of respiratory epithelium (sinonasal) or ependymal-lined clefts in NGs should not be mistaken for teratoma. Because of their malignant potential, teratomas containing neuroglial tissue should be distinguished from pure NGs that have no malignant potential. Teratomas are neoplasms that arise from germ cells and are composed of tissue elements formed from all three germ layers (ectoderm, mesoderm, and endoderm) (2,45–47). Extracranial teratomas are rare and account for less than 5% of teratomas in childhood. They have been reported in the neck, nasopharynx, oropharynx, hypopharynx, face, and orbit (2). Pharyngeal teratomas are often disfiguring, with extreme malformation and associated respiratory distress or cleft lip-palate (2). Teratomas may be solid and/or cystic and are histologically classified as mature or immature, the latter containing tissue of neuroectodermal origin. Less than 5% of head and neck teratomas in children have a malignant component (2).

F. Treatment and Prognosis

The treatment of NG is surgical excision. If there is no evidence of intracranial connection, complete surgical excision is curative in most cases, a conservative extracranial approach is recommended (10,11,22,48). Recently, endoscopic surgery has been successful in removing the lesion (49,50). Deep resection margin can be assessed by frozen section of the nasal mucosa or fibrous stalk of tumor (51). The importance of imaging (CT and MRI) performed before surgery in any congenital nasofrontal mass, to exclude the possibility of an intracranial connection, cannot be overemphasized. At operation no bony defect is found in NG; but in 10% to 15% of cases, a fibrous connection may be seen to persist with the cribriform plate. NGs may recur or persist in 10% to 15% of patients, usually following incomplete excision, but there is neither any evidence of local aggressive behavior nor of any malignant potential (52).

G. Pathogenesis

NG probably results from a protrusion of forebrain secondary to faulty closure of the anterior neuropore. It therefore, can be viewed as an NE that becomes sequestrated from the brain and cranial vault early in gestation. The stalk degenerates early, obliterating a true connection to brain parenchyma (12,19), while the NE represents a herniation of brain tissue through a bony defect in the skull (2–11). This communication with the intracranial ventricular system or subarachnoid space leads to a positive Furstenberg test in some, but not all, encephaloceles (see discussion in sec. III, ''Nasal Encephalocele'').

III. NASAL ENCEPHALOCELE

A. Introduction

Meningoceles and encephaloceles are congenital herniations of meninges alone (meningocele) or meningeal-lined brain tissue (encephalocele) that connect with the intracranial ventricular system and subarachnoid space through a cranial bony defect (1–8). When they occur in the nasal cavity, the nasal encephaloceles (NEs) are virtually impossible to distinguish from nasal glioma (NG), except that the NE maintains an intracranial connection identified by imaging (Figs. 7, 8).

B. Anatomy

Encephaloceles are usually classified according to the anatomic location of the skull defect and pattern of extracranial extension. The most common location for encephalocele is occipital (75%), followed by frontal (25%) (9,10). *Frontal encephaloceles* can be divided into *Sincipital* (60%), which involve the dorsum of the nose, orbit, or forehead, and *Basal* (40%), which involve the ethmoid and sphenoid sinuses, pharynx, or orbit.

Sincipital encephaloceles appear as external nasal masses and are divided into nasofrontal, nasoethmoidal, and naso-orbital on the basis of their location. *Basal encephaloceles* are also divided into (*i*) transethmoidal, through the cribriform plate into the anterior nasal cavity; (*ii*) sphenoethmoidal, through the sphenoethmoid junction into the posterior nasal cavity; (*iii*) spheno-orbital though the superior orbital fissure or osseous fissure or osseous defect into the orbit;

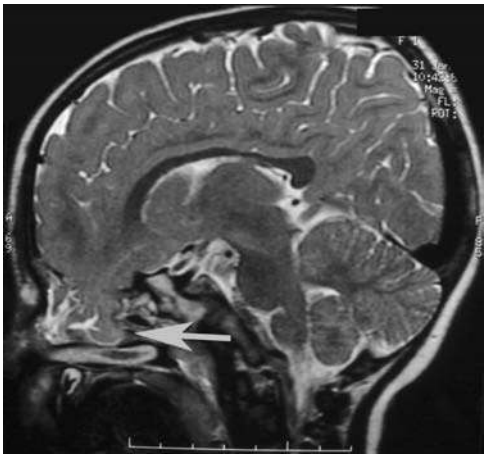

Figure 7 Sagital MRI imaging shows a protruding mass from frontal lobe downward (*arrow*).

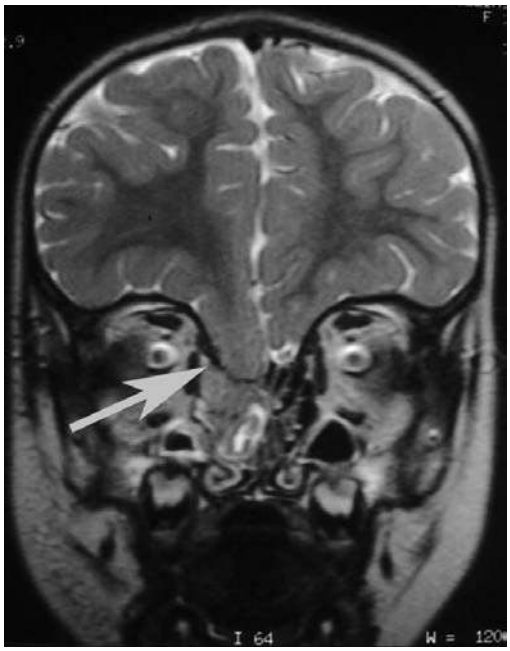

Figure 8 Coronal MRI demonstrates the herniation of the encephalocele through the frontal cribriform plate into the right nasal cavity (*arrow*).

(*iv*) transsphenoidal, through the body of the sphenoid into the nasopharynx or sphenoid sinus; and (*v*) sphenomaxillary, through the junction of the body and wing of the sphenoid into the pterygopalatine fossa, depending on the site of herniation at the skull base (10–12).

Infrequently, lateral basal sphenoid encephaloceles can be seen (12–18). They may present with unilateral decreased vision or with nonlocalizing symptoms, and on imaging, they protrude through defects in the greater wing of the sphenoid and, rarely, into the infratemporal fossa. Temporal lobe epilepsy may be associated with basal encephaloceles. Although encephaloceles that involve the cranial vault or the fronto-ethmoidal area generally present as external masses, it may be difficult to recognize basal encephaloceles that herniate internally (19–28). However, CT scan and MRI have greatly facilitated the diagnosis (13,18,27,29–31).

C. Clinical Features

Most encephaloces present at birth, although some may be diagnosed later in adulthood. While the reported incidence in the West is between 1:35,000 and 1:40,000 live births, it is estimated to be 1:5,000 live births in Southeast Asia (Thailand) (32–36).

NEs may be asymptomatic, or they may present with a nasal mass or deformity, nasal obstruction, recurrent meningitis, or rhinorrhea due to cerebrospinal fluid (CSF) leak. Some may even masquerade as nasal polyps (37). It has been reported that frontoethmoid subtype is the most common (80%), followed by the nasopharyngeal and orbital (8%), transethmoidal (8%), transsellar (3%), and interfrontal types (1%) (36). Those with the nasopharyngeal subtype commonly presented with nasal obstruction and CSF rhinorrhea. Among the frontoethmoidal encephaloceles, nasoethmoid is the commonest type, and those patients present with swelling over the bridge of the nose with significant hypertelorism and midline facial deformities (11,12,35,36). About one-third of NEs are associated with other midline facial anomalies, such as cleft palate or choanal stenosis. Patients with encephaloceles usually, but invariably, have a positive Furstenberg test, which constitutes pulsation-expansion of the mass seen on compression of the ipsilateral jugular vein.

D. Imaging

Imaging studies must be performed for any congenital frontonasal mass to exclude a skull defect with intracranial extension before surgery, which is important to help guide the appropriate surgical approach. CT and MRI together allow better visualization of a smoothly marginated soft tissue mass through a bony defect in the skull. MRI is superior for imaging brain tissue preferentially (Figs. 7, 8) (13,18,27,29–31,38).

E. Pathology

The excised lesion in a meningocele shows a cystic mass composed of loose areolar connective tissue. Whereas that of an encephalocele shows fully formed cerebral tissue with easily found neurons or disorganized islands of neuroglial tissue surrounded by collagenous septa (1–3,6). Ependyma and choroid plexus may be present. The presence of glial tissue may be confirmed by demonstrating immunoreactivity for GFAP, S-100 protein, and NSE. NE of long duration may result in excessive fibrous tissue relative to the amount of glial cells and may be associated with an absence of neurons (1,2,36).

F. Differential Diagnosis

The clinical differential diagnosis includes mainly NGs and nasal dermoids and epidermoid cysts, less often, a sinonasal polyp, and nasal chondromesenchymal hamartoma of infancy (1,21,37,39–42). NG and NE are the result of an abnormal embryological development. NG is a rare developmental abnormality without an intracranial connection. NE is a herniation of the cranial contents through a bone defect in the skull, through which it retains an intact connection with the central nervous system (CNS) (43). Exceptionally, both NG and NE may occur in the same patient (44).

The Furstenberg test is generally positive in NE because of its connection to the subarachnoid space. This test is negative in NG, most nasal dermoid cysts, and sinonasal polyps. As mentioned under the discussion for NG (see sec. II, ''Nasal Glioma''), the distinction between NE and NG cannot be made with certainty on the basis of histological examination,

and it is important to perform imaging studies (CT and MRI scans) to demonstrate the communication with the intracranial contents through a bony defect in NE. When long-standing NE results in excessive fibrous tissue relative to the amount of glial cells and is associated with an absence of neurons, the histological distinction between NG and NE may be impossible (1,2,36). Nasal dermoid cysts may also show an intracranial connection, and are often associated with a sinus tract. Histologically, the dermoid cyst lacks glial tissue and is lined by epidermis with dermal appendages.

G. Treatment

Early surgical intervention is imperative soon after diagnosis to avoid the potential risk of CSF leak and of recurrent bacterial meningitis (45–47). A frontal craniotomy approach is recommended if intracranial extension is identified on the basis of preoperative evaluation, followed by an extracranial resection, with closure of the dural defects. This approach is safer than the transnasal procedure (23,28,48,49). Nasal endoscopy, however, may be suitable for the treatment of encephloceles of the lateral wall of the sphenoid sinus (50).

The prognosis for the NE patient is generally good and is usually associated with normal intelligence and motor development. However, mental retardation, epilepsy, and ocular problems have been described in this group (51). The overall cosmetic outcome is good (35).

H. Pathogenesis

NEs develop as a result of ectopic protrusion of CNS tissue through a defect in the cranium (52,53). Theories of formation of NE include arrested closure of bone of the frontal floor and early outgrowth of neural tube preventing closure of cranial coverings (54). The transsphenoidal type may occur as part of the median facial cleft syndrome, which includes median craniofacial dysraphism (55). Not uncommon, NEs may be associated with neurofibromatosis (NF). Patients with orbitotemporal NF often have partial or complete absence of the greater wing of the sphenoid, resulting in a defect in the posterolateral wall of the orbit (36,56). Although the pathogenesis of sphenoidal encephaloceles is unknown, it is possible that lateral basal encephaloceles may result when ossification centers of the greater wing of the sphenoid fail to fuse with those of the body of the sphenoid (18).

Rare cases of NEs have also been associated with frontofacionasal dysplasia, an autosomal recessive condition (57), secondary to an abnormal chromosome translocation (58).

Although encephaloceles of the skull base are mostly congenital, they may be spontaneous or secondary to trauma (posttraumatic encephalocele). Trauma-related NEs have been described as a complication of prior sinonasal surgery (59–61), which may result in massive intracerebral hemorrhage if the encephalocele contains a frontobasal artery (62).

IV. TRAUMATIC (AMPUTATION) NEUROMA

A. Introduction

Although discussed with neurogenic tumors, the traumatic neuroma, also known as amputation neuroma, is a reactive nonneoplastic process, rather than a true neoplasm (1–5). It represents a pseudotumorous condition characterized by disorganized proliferation of axons, Schwann cells, and perineurial cells in a fibrocollagenous stroma. Following a nerve injury, either transection or crush, the proximal segment of a disrupted peripheral nerve undergoes a reparative response, while the distal segment undergoes complete degeneration of residual axons and myelin sheaths (Wallerian degeneration) (1–3,6). This condition ensues when the outgrowing axons from the proximal nerve stump are far away from the distal stump or encounter scar tissue (6). Failure to recognize a nerve injury after trauma or inadequate surgical repair with scar formation may be important factors in the development of traumatic neuroma (2).

B. Clinical Features

The two main causes of traumatic neuromas are trauma and surgery. The former occur often in young adults, while the latter is common in the elderly due to the frequency of the surgical procedures. Nerve injuries arise as a result of direct surgical cutting, fibrosis, and scarring around a nerve, which impedes dissection or excessive tension or prying on nerves. Traumatic neuroma may occur at any age. In one series, 50% of cases occurred in the third and fourth decades, with two-thirds following trauma and one-third following amputation (2). The mass may occur at any site, and, depending on the nerve involved, may be asymptomatic or may manifest with pain or tenderness, paresthesia, loss of sensation, muscle weakness, or paralysis following trauma (2). The most common symptom in this series was pain (41 cases), anesthesia (24 cases), and paralysis (17 cases), and the duration of symptoms ranged from two months to 20 years (2). On physical examination, the mass varies in size, although most are less than 2 cm in diameter.

The commonly involved locations in the head and neck are the oral cavity such as the mental foremen, lower lip, and tongue (4), and the greater auricular nerve after parotidectomy, neck dissection, and even rhytidectomy (5,7,8). Other reported locations are the pharynx (9), the maxillary division of the trigeminal nerve (10), the inferior alveolar nerve of the mandible (11), the auriculotemporal nerve, the glossopharyngeal nerve (12), and the facial nerve (13,14). These lesions can develop after injury or trauma to the dental complex or after extraction of teeth (''dental neuroma'') (3).

Traumatic neuromas of the greater auricular nerve can occur after parotidectomy, as mentioned above (7,15). It has been reported that 5.7% of patients with a new pleomorphic adenoma of the parotid gland developed a traumatic neuroma after surgery, while even more patients (9.7%) developed a traumatic neuroma after treatment for recurrent pleomorphic adenoma (15).

Rare cases of pharyngeal traumatic neuromas are associated with hoarseness, dysphagia, choking spells, intermittent aphonia, and cough (9). The common symptoms of facial traumatic neuromas include facial weakness, hearing loss, tinnitus, and vertigo or dizziness (14).

C. Macroscopy

Traumatic neuromas are circumscribed, gray-white, firm bulbous nodules without a true capsule. The nodules arise either at the proximal stump of a severed nerve or along the course of an injured nerve. No true capsule is present. They rarely exceed 5 cm in maximal dimension (6). On longitudinal section, the proximal portion of the nerve appears to splay and disappear into a firm, collagenized mass.

D. Histopathology

The traumatic neuroma consists of ill-defined, haphazard tangles of all the normal components of nerve fascicles, including regenerated axons with their investitures of myelin, Schwann cells, fibroblasts, and perineurial cells, which are admixed with collagenous fibrous tissue (Fig. 9). The stromal component may be inflamed or myxoid (6).

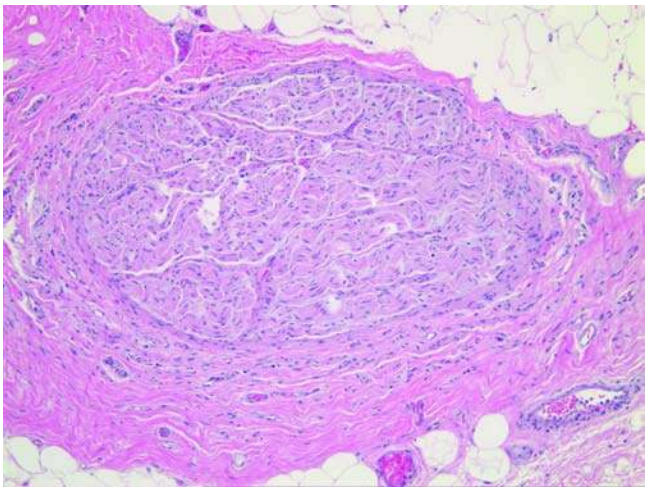

Figure 9 Ill-defined, haphazard tangles of nerve fascicles associated with reactive dense fibrous tissue (H&E, 50×).

E. Ultrastructure

The traumatic neuroma is characterized by multiple small nerve fascicles surrounded by collagen fibers. Each fascicle contains myelinated and unmyelinated axons, associated with Schwann cells (4). Small unmyelinated axons predominate. The endoneurial fibroblasts are seen at the periphery of the Schwann cells, and dense collagen fibers are observed adjacent to these fibroblasts.

F. Immunohistochemistry

The same immunoreactivities of the normal nerve elements are seen in traumatic neuroma. Axons are positive for neurofilament protein, Schwann cells express S-100 protein, fibroblasts show vimentin reaction, and perineurial cells stain for EMA (16).

G. Differential Diagnosis

Traumatic neuromas can mimic palisaded encapsulated neuromas and neurofibromas. Presence of all the elements of the nerve fascicles, along with identification of an injured nerve, distinguishes a traumatic neuroma from a neurofibroma. Palisaded encapsulated neuromas are cutaneous lesions predominantly in women, and are histologically characterized by a well circumscription and organized arrangement of nerve fascicles. Other differential diagnoses include cutaneous leiomyoma, plexiform neurofibroma (PNF), and mucosal neuroma. Immunoreaction of spindle cells to smooth muscle markers such as desmin, calponin, or caldesmon distinguishes a leiomyoma. Some traumatic neuromas may contain ganglion cells. This finding may suggest the possibility of a ganglioneuromas, which are encapsulated and found most frequently along the sympathetic ganglion chain (9). Binucleated or multinucleated ganglion cells are common in ganglioneuroma, but are rare in reactive lesions such as traumatic neuroma. Oral mucosal neuromas occur in association with multiple endocrine neoplasia (MEN) syndromes (type IIb). Mucosal neuromas are almost always multiple, and their cellular proliferation is endoneurial and orderly. Furthermore, patients with traumatic neuromas have a history of prior trauma or surgery to the involved area, and the surroundings tissue shows reactive fibrosis with or without chronic inflammation, a finding not present in mucosal neuroma.

H. Treatment and Prognosis

The treatment of symptomatic traumatic neuroma is simple excision, and the stump of the nerve ending is buried away from the surrounding scar tissue (5). The lesion may need to be excised to distinguish it from recurrent tumors in individuals previously operated on for malignant tumors or benign tumors such as pleomorphic adenoma (5,17). With adequate excision and repair, there may be recovery or improvement of sensation and motion. Traumatic neuromas may recur. The development of the traumatic neuroma can be avoided when the cut ends of traumatized

nerves are optimally approximated to facilitate orderly regeneration.

V. PERIPHERAL NERVE SHEATH TUMORS

Peripheral nerve sheath tumors can be divided into benign and malignant tumors. The benign category includes the two most common and closely related tumors, schwannoma (neurilemoma) and neurofibroma, and rare tumors such as neurothekeoma, perineurioma, granular cell tumor (GCT), and mucosal neuroma. Neurofibromas may be subdivided into localized, diffuse, and plexiform types. The term malignant peripheral nerve sheath tumor (MPNST) is used for the malignant tumor category, and it encompasses a heterogeneous group of the tumors. Although any line of the nerve sheath elements can give rise to a malignant tumor, well-differentiated tumors exhibit Schwannian features. MPNST may occur de novo, or arise in a benign peripheral nerve sheath tumor, or in a PNF in patients with von Recklinghausen's disease (NF1). Malignant transformation is extremely rare in schwannoma.

A. Schwannoma (Neurilemoma, Neurinoma)

Introduction

Schwannoma is a common benign tumor composed of neoplastic cells with the immunophenotype and ultrastructural features of Schwann cells. It is generally encapsulated, except for those arising from the sinonasal tract and nasopharynx (1–6). It can arise along the course of any nerve in the body associated with Schwann cells, including the cranial and spinal nerves with the exception of the olfactory and optic nerves, since the latter nerves lack Schwann cells, and although sensory nerves are the most frequently involved, motor and autonomic nerves may also be affected.

Clinical Features

Schwannomas can occur at any age but are most commonly seen in patients between the ages of 20 and 50 years (7–10). There is no gender predilection. Most schwannomas are solitary and arise in soft tissues. However, they may be multiple, particularly when associated with neurofibromatosis (NF)2 (2,4,6). Head and neck is the most commonly affected region, and, in fact, this location accounts approximately for 25% to 45% of the occurrence of schwannomas (7–9,11). The lateral neck is more frequently involved than any other site in the head and neck (7). The spinal roots and the cervical, sympathetic, and vagus nerves are commonly involved (6). Less frequent sites include the oral cavity, where the tongue and buccal mucosa are the preferred sites (12,13,16), paranasal sinuses (mainly the maxillary antrum and ethmoids) (17–19), nasal cavity (20), nasopharynx (1), orbit, face, forehead, scalp, jaw, parapharyngeal space (probably vagus or cervical sympathetic nerve in origin) (21), larynx (22–24), parotid gland, and other unusual sites (1,11,25–36).

Schwannomas of the larynx are uncommon and most often present in the supraglottis, particularly the aryepiglottic folds (80%) and false vocal cord, but involvement of other sites including the true vocal cord has been reported (22). Bilateral acoustic neuromas (schwannoma of the eight cranial nerves) are diagnostic of NF2 (discussed in sec. V.F, ''Neurofibromatosis 2'').

Schwannoma usually occurs as an asymptomatic mass when small, but it may rarely cause pain, tenderness, and paresthesia or site-specific symptoms (8), e.g., nasal obstruction, epistaxis, proptosis, and visual disturbances for tumors of the nasal cavity and paranasal sinuses (1,19,20,25,26); sensation of a lump, dysphagia, and phonation for tumors of the oral cavity (14) and parapharyngeal space; hoarseness, stridor, and dysphagia for the laryngeal tumor; proptosis for orbital tumors; facial paralysis, loss of hearing, and tinnitus for the tumor of the mastoid region and middle ear. Nasal or paranasal sinus tumor may present as a nasal polyp and may bleed profusely upon biopsy procedure (37). Facial nerve tumors may cause hearing loss, vertigo, otitis, media, postauricular pain, or facial nerve palsy and may present as an intraparotid mass (38,39).

Imaging

CT appearance of schwannomas are described as a well-circumscribed inhomogeneous mass because of a mixture of cellular and paucicellular histological features of schwannoma (40), although it can be homogeneous when the tumor is uniformly cellular (41). On MRI images, schwannoma is characterized by well circumscription and on T2-weighted images (T2WIs), a target pattern with peripheral hyperintense rim and central low intensity (42). The latter feature histologically corresponds to peripheral myxomatous tissue and central fibrocollagenous tissue (42). On gadopentetate dimeglumine (Gd-DTPA)-enhanced T1WIs, schwannoma can exhibit either heterogeneous or homogeneous enhancement (42).

Macroscopy

Schwannomas grossly appear as eccentric, discrete, globular, expansible masses with firm consistency (Fig. 10A, B). The tumors can vary in size from a few millimeters to more than 20 cm in diameter, but most are 1 cm to 4 cm in size (3,4,7–9). The nerve of origin can at times be seen stretched over the surface of the encapsulated schwannoma. This common finding demonstrates the expansile manner of growth of these tumors and provides the reason why the function of the nerve is generally maintained until the tumor has obtained considerable size. When the nerve of origin is small, its association with a given tumor may be difficult to demonstrate (8). The cross surface of the tumor varies from homogeneous solid myxoid gray-white to mottled red to yellow or tan color, with or without cystic spaces. Hemorrhage, either recent or old, is commonly seen.

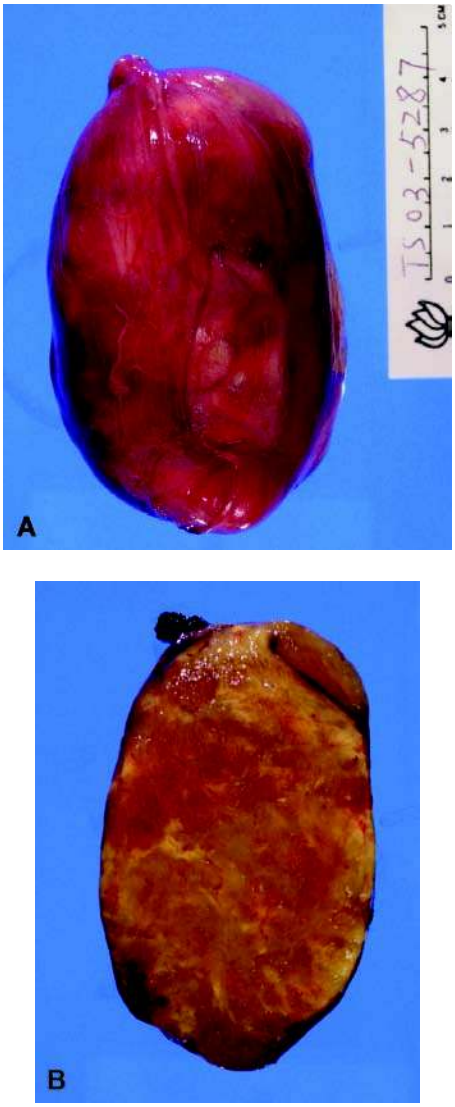

Figure 10 (**A**) Schwannoma is grossly solid, globular mass with thin fibrous capsule. (**B**) The cut surface is smooth, mucoid, and tan with patchy yellow areas due to lipid accumulation.

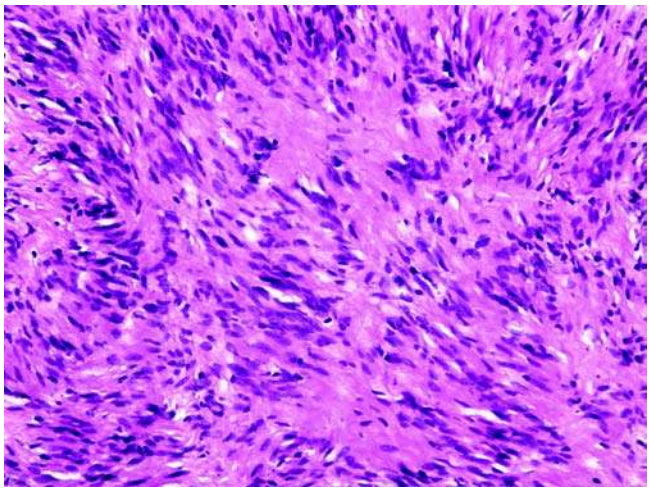

Figure 11 The compact Antoni A area features aligned, compact interlacing fascicles of spindle cells with elongated nuclei (H&E, 100×).

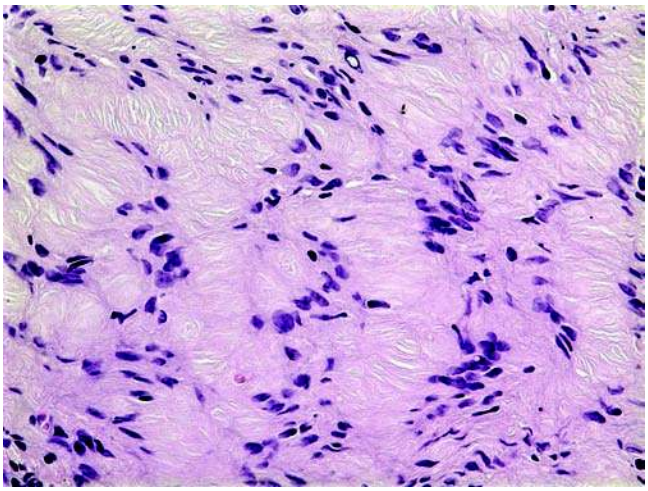

Figure 12 Verocay body is a palisaded arrangement of nuclei separated by aligned eosinophilic cell processes (H&E, 200×).

Histopathology

Schwannoma is generally sharply circumscribed by a thin fibrous capsule (3,4). A portion of or the entire tumor is composed of compactly arranged and aligned spindle cells with long wavy nuclei, moderate amount of eosinophilic cytoplasm, and indistinct cell borders. The nuclei are frequently arranged with their long axes parallel to one another. Nuclei of tumor cells may lay in a row and create a palisading pattern (3) (Fig. 11). This feature, designated as the Verocay body (Fig. 12), is neither always found in, nor diagnostic of schwannoma, and can be seen in other tumors such as leiomyoma and myoepithelioma (6). The cellular pattern described is termed ''Antoni type A'' (Fig. 11). A part of or all of a schwannoma may contain a less cellular Antoni type B pattern. The latter area is characterized by a less orderly arrangement of spindle or oval tumor cells in a loose myxoid stroma. The nuclei are round to oval and hyperchromatic. Blood vessels are typically prominent, hyalinized, and thick walled. Some of the large vessels may contain recent or organized thrombi. Foamy macrophages, hemosiderin-laden macrophages, lymphocytes, and mast cells may be found around the vessels (3,4). Long-standing and often deep-seated schwannomas demonstrate severe degenerative change represented by remote hemorrhage, stromal hyalinization, and calcification. Such tumors contain significant nuclear atypia or pleomorphism, characterized by intense

nuclear hyperchromasia and coarse chromatin, but nucleoli are inconspicuous, and mitoses are generally not found. This type of schwannoma, termed ancient schwannoma, has no prognostic implication. In the paranasal sinuses and nasopharynx the tumors tend to be unencapsulated and, when combined with hypercellularity, often raise the possibility of malignancy (1). Unlike neurofibromas, schwannomas do not contain axons and are typically separated form the nerve fibers by a capsule.

Several morphological variants of schwannoma have been described, including cellular (43–46), epithelioid (47,48), glandular (49–51), plexiform (multinodular) (52–59), melanocytic (60–70), and neuroblastoma-like (71,72). These variants may cause diagnostic difficulty; however, no prognostic association has been identified.

Cellular schwannomas are often located in the paravertebral region of the pelvis, retroperitoneum, and posterior mediastinum and are associated with a major nerve. They are rare in the head and neck with reported sites including the neck (43), paranasal sinus (73), oral cavity (13), and mandible (74). They are circumscribed or encapsulated tumors that are composed predominantly or exclusively of Antoni A areas (43–46,75). They display fascicular or whorled growth pattern with occasional nuclear palisading, but well-formed Verocay bodies are lacking (75). Mitotic activity may be seen in up to 70% of cases, but is generally low (1–4/10 HPFs), and microfoci of necrosis may be present as a solitary finding (45).

Plexiform schwannomas exhibit a plexiform pattern of growth and are not associated with NF1 or 2. (Fig. 13) Microscopically, they consist of round to oval nodules that vary in size, and each nodule is composed entirely of Antoni A component (52,54,56,57).

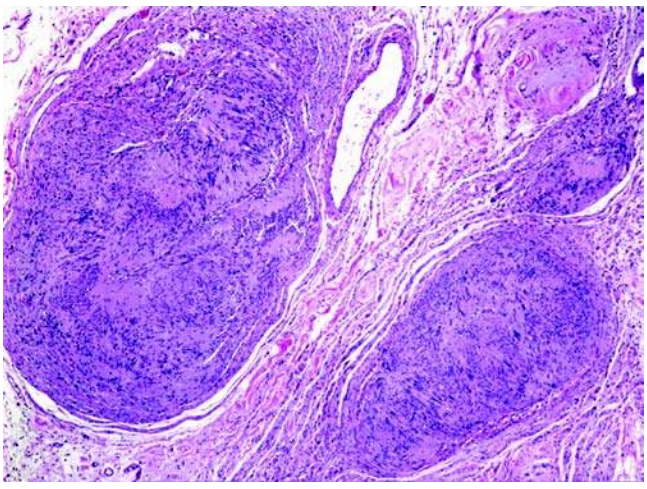

Figure 13 Plexiform schwannoma consists of round to oval nodules of varying size, each surrounded by a thin fibrous capsule. A majority of the tumor is composed of cellular Antoni A component (H&E, 100×).

Ultrastructure

The Antoni A area is composed of Schwann cells with long, slender, interdigitating cytoplasmic processes invested by a prominent, often reduplicated, continuous layer of basal lamina (76–78). These processes are connected by desmosome-like junctions. The nuclei are elongated and cigar-shaped with smooth contours, fine chromatin, and one or two small nucleoli. They are devoid of pinocytotic vesicles. The Antoni type B area is composed of Schwann cells in a large extracellular compartment. The Schwann cells have more pleomorphic nuclei with conspicuous cytoplasmic lysosomes and myelin figures.

Immunohistochemistry

Schwannoma cells are diffusely and strongly positive for S-100 protein in both nuclear and cytoplasmic pattern (4,79). Expression of CK, GFAP, and EMA is occasionally seen (79). Tumor cells are negative for synaptophysin, neurofilament, and protein gene product 9.5 (PGP 9.5). The strong reaction to lamina and collagen type IV corresponds to the presence of abundant basement membrane material (80).

Somatic Genetics

The most prominent cytogenetic feature of schwannoma is a complete or partial loss of chromosome 22 material that is seen in approximately 50% of cases. This results in the loss of heterozygosity (LOH) at one or more loci on 22q. Other cytogenetic features include loss of a sex chromosome and trisomy 7 (81). There does not appear to be any cytogenetic difference among conventional, ancient, or cellular schwannomas (81,82). A loss of chromosome 22 material is in keeping with loss of NF2 allele in molecular genetic studies of schwannomas (83–85). LOH at the NF2 locus presumably results in inactivation of the gene encoding the protein merlin (Schwannomin) (84,86).

Differential Diagnosis

Differential diagnoses include neurofibroma and benign and malignant spindle cell soft tissue tumors such as leiomyoma, leiomyosarcoma, fibrous histiocytoma, meningioma, and monophasic synovial sarcoma. The characteristic features of schwannoma, including the presence of encapsulation, the alternating Antoni A and B areas, and diffuse and strong immunostaining for S-100 protein, distinguish schwannoma from neurofibroma (4). In addition, frequent degenerative changes and hyaline thickening of vascular walls are typically seen in schwannomas and are usually absent in neurofibromas. Immunoreactivity for S-100 protein is seen in only a minority of the cells in neurofibroma. In contrast with schwannomas, which are associated with NF1 in 18% of cases (2) and rarely undergo malignant change, neurofibromas are often associated with NF1 and have a definite risk of malignant transformation when associated with NF1. Therefore, it is important

to distinguish between these two closely associated tumors in this context.

Cellular schwannoma may be mistaken for sarcoma such as MPNST, fibrosarcoma, or leiomyosarcoma. However, the increased cellularity in this variant is disproportionately high compared with the level of mitoses and atypia, and other characteristic features of schwannomas such as circumscription or encapsulation, perivascular hyalinization, and strong and diffuse immunoreactivity for S-100 protein should suggest a benign diagnosis. Cellular schwannomas can be distinguished from MPNST by the lack of geographic necrosis and much higher mitotic activity (often more than 10/10 HPFs) (45,75).

Schwannomas are histologically distinguished from leiomyomas, fibrous histiocytomas, and monomorphic synovial sarcomas by identification of the characteristic Antoni A and B patterns of proliferation and lack of immunoreactivity for muscle markers (desmin, actin, caldesmon) and CKs, respectively. Leiomyomas are not associated with nerve and generally lack the thick fibrous encapsulation. Meningiomas typically have a dual immunoreactivity for vimentin and EMA. However, in rare instances, it may not be possible to immunohistochemically distinguish between schwannomas and meningiomas, because both tumors may be positive for vimentin, EMA, and S-100 protein. In these cases, the ultrastructural demonstration of tumor cells surrounded by basal lamina may be helpful in confirming the Schwannian nature of the tumor (76–78).

Treatment and Prognosis

Gross total resection (GTR) with preservation of the nerve of origin, if possible, is considered as adequate therapy. Schwannomas are demarcated from the nerve fibers by a fibrous capsule, the feature making it possible in most instances to excise or enucleate the tumor without damage to the nerve. Total excision is usually curative. Schwannomas are slow-growing tumors, which may not cause a problem even when incomplete excision of the lesion is performed to prevent damage to the adjacent nerve. Radiation therapy is not effective in these tumors. Malignant transformation of schwannoma is exceedingly rare, and from a practical point of view, this phenomenon can be disregarded (4,43,87,88).

B. Neurofibroma

Introduction

Neurofibroma is a benign, slowly growing, relatively circumscribed but nonencapsulated nerve sheath tumor composed of a variable mixture of Schwann cells, perineurial-like cells, and fibroblasts as well as cells with intermediate features between these cells (1,2). Solitary neurofibroma is a localized neurofibroma that, by definition, occurs outside the setting of NF1 (von Recklinghausen's disease). A tumor with an identical histological pattern found in a patient with NF1 is also a neurofibroma but the adjective *solitary* cannot be used (2). Solitary neurofibroma is by far more common than NF1-associated neurofibroma. However, the diagnosis of solitary neurofibroma is always conditional, especially in young individuals, because the presence of one tumor may herald the onset of others.

Clinical Features

Patients with solitary neurofibromas are generally young, between the ages of 20 and 30 years (3). There is no gender predisposition or site predilection (1). Solitary neurofibromas present as a slow-growing, nontender mass in the skin or soft tissue (2). They are somewhat movable and firm. If solitary neurofibromas occur along the course of a peripheral nerve, the clinical symptoms are usually those related to a space-occupying lesion but can be the same as those of schwannoma. When associated with NF1, neurofibromas are multiple or segmental in distribution, superficially or deeply located, and more likely to undergo malignant transformation (1).

The head and neck is a common location for neurofibromas, which often present in the skin and subcutaneous tissue as small, sessile or pedunculated, soft tumors (4–6). However, other sites, such as those involved by schwannoma, may be involved less frequently, including the nasal cavity (7–9), paranasal sinuses (10,11), nasopharynx (7), orbit (12–14), conjunctiva (15), parapharyngeal space (16), larynx (17–21), maxilla (22,23), oral cavity (24–26), and mandible (27).

Neurofibroma of the nasal cavity and paranasal sinuses arise from the first and second division of the trigeminal nerve and autonomic plexuses and cause nasal obstruction, epistaxis, cheek swelling, pain, and proptosis (7–10).

Neurofibromas of the larynx are rare and may be solitary or an uncommon component of NF1 (17–20). They usually occur in the false vocal cord and aryepiglottic fold. They should be included in the differential diagnosis of a submucosal smooth supraglottic mass, although the tumor may also arise in the vocal cord or subglottis. Clinical findings of the laryngeal tumors include hoarseness, dysphagia, odynophagia, dysarthria, a globus sensation, and dyspnea (21).

Most orbital nerve sheath tumors affect the first division of the trigeminal nerve and present with an orbital mass, with pain or sensory loss being unusual (13). Approximately 25% of patients with orbital neurofibromas are associated with NF1.

Neurofibromas of the oral cavity present as a submucosal, nontender, discrete mass. The tongue, buccal mucosa, and vestibular area are common sites, and the posterior mandible is the most common intraosseous location (24,28).

Imaging

Cutaneous or soft tissue neurofibroma is often not imaged because it can be easily assessed clinically (29). When neurofibroma arises in association with a large nerve, a fusiform mass can be identified on MRI and CT (29). However, it is often difficult or even impossible to identify this appearance in a superficial

neurofibroma. A target pattern on MRI scans consists of a peripheral hyperintense rim and central low intensity corresponding histologically to peripheral myxomatous and fibrocollagenous tissue and can be seen in about a half of cases of neurofibromas as well as schwannomas (30). MRI cannot distinguish between neurofibromas and schwannomas, and benign nerve sheath tumors may mimic their malignant counterparts when necrosis and cystic or hemorrhagic degeneration is present.

Parapharyngeal neurofibromas in CT scans appear as well-circumscribed, moderately enhancing masses in two-thirds of cases (16).

Macroscopy

Neurofibromas are well circumscribed but not encapsulated (1). The nerve of origin is almost never seen (2). The cut surface of the tumor is homogeneously gray or gray-tan and translucent but lacks degenerative changes (1). Most often, these tumors arise from small nerves and extend into subcutaneous soft tissue, and therefore, deeper portions of the tumors are often less defined from the surrounding tissue. However, less frequently, the tumor may arise in and expand a large nerve to form a fusiform mass (localized intraneural neurofibroma), and when confined by the epineurium, a true capsule may be present (3) (Fig. 14).

Histopathology

Histologically, in contrast with schwannomas, which are encapsulated and contain a more homogenous population of cells, neurofibromas are circumscribed but not encapsulated and are composed of a mixture of varying proportions of Schwann cells, fibroblasts, axonal processes of neurons, and perineurial-like cells (1,3). Widely separated irregular spindled or stellate cells with long thin cytoplasmic processes and wavy dark staining nuclei are loosely arranged in a fibrous or myxoid matrix rich in mucopolysaccharide (31) (Fig. 15). The amount of cells and fibromyxoid stroma varies. The stroma contains mast cells, lymphocytes, and, rarely, xanthoma cells (31,32). Less frequently, neurofibromas may be cellular and composed of fascicles of Schwann cells in a uniform collagen matrix devoid of myxoid substance (1). Focal atypia or rare mitoses are not uncommon in neurofibroma or the plexiform variant. However, when seen to a marked degree, malignant transformation should be considered.

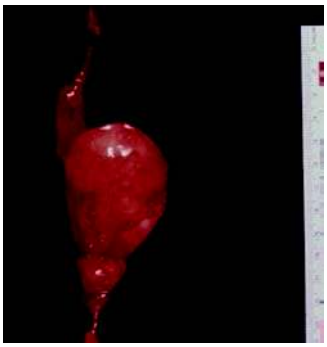

Figure 14 Localized ovoid intraneural neurofibroma with attached segment of nerve.

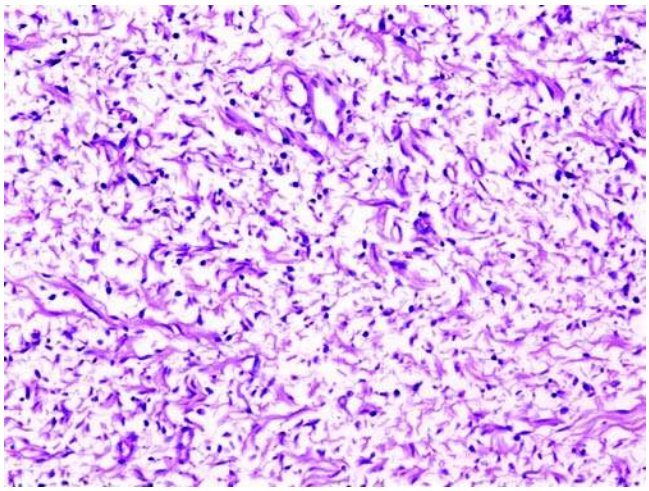

Figure 15 Neurofibroma composed of cells with thin, elongated nuclei and scant cytoplasm, embedded in a myxoid stroma (H&E, 100×).

Ultrastructure

Most cells in neurofibromas are Schwann cells (1). They are primarily found among aggregates of collagen. Schwann cells are recognized by their thin arborizing cytoplasmic processes, intermediate filaments, occasional microtubules, and continuous basement membrane (external lamina) (11,31). Pinocytic vesicles are inconspicuous. Scattered myelinated and unmyelinated nerve fibers are also seen. Perineurial-like cells are variably present, and they are characterized by long, very thin cytoplasmic processes with abundant pinocytic vesicles, and a discontinuous coat of basement membrane (1).

Immunohistochemistry

Neurofibromas demonstrate S-100 protein positivity, but the positivity is variable in a given lesion and not as striking in intensity or uniformity as in schwannoma (3,11) (Fig. 16). Neurofibromas variably stain for CD34 (33). Collagen IV stains many cells in a pericellular pattern (34).

Somatic Genetics

Chromosome studies of neurofibromas are scarce, with only a few reports of clonally abnormal karyotypes (35). Among the abnormal karyotypes, the only

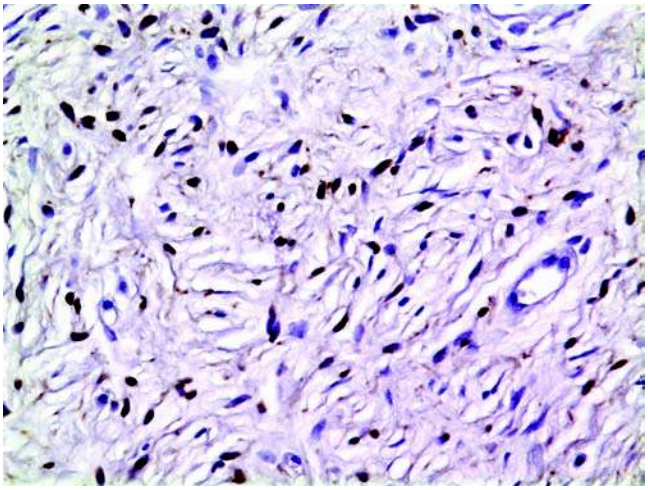

Figure 16 Neurofibroma contains numerous S-100 protein-positive cells (H&E, 200×).

recurring aberration is the monosomy 22 (35,36). 47,XY,+der(?)t(?;12)(?;q15) has been reported (37). Complex nonclonal structural aberrations can be seen. Recently (4;9)(q31;p22)-balanced reciprocal translocation has been described (35).

Differential Diagnosis

In contrast to schwannomas, which are predominantly composed of Schwann cells, neurofibromas contain a variety of cells that are associated with peripheral nerves; namely, perineurial-like cells, fibroblasts, entrapped axons, and Schwann cells (3,31,38). Furthermore, they lack a capsule, Verocay bodies, hyaline thickening of vascular walls, Antoni A and B growth patterns, and degenerative change (1). At times, however, it may be difficult to distinguish between cellular neurofibroma and schwannoma because of the presence of common features of benign nerve sheath tumors (Fig. 17). In such cases, histochemical stains to determine the presence of acid mucopolysaccharide-rich myxoid matrix in neurofibromas, which is absent in schwannoma, may be of diagnostic help. The nerve sheath origin of the tumors is confirmed by the demonstration of immunopositivity for S-100 protein, which is less striking in neurofibroma than in schwannoma (1). If special stains are not useful, then the noncommittal term ''benign nerve sheath tumor'' is appropriate.

Treatment and Prognosis

Whenever possible, simple excision is the treatment of choice (4,24). Aggressive debilitating surgery should be avoided. No recurrences requiring further surgery were found despite incomplete resection of some orbital tumors (13). Although solitary neurofibromas do not have the same incidence of malignant transformation as neurofibromas associated with NF1, the exact risk is unknown, but is probably quite small (3).

C. Plexiform Neurofibroma

Introduction

Plexiform neurofibromatosis (PNF) is a grossly and microscopically highly characteristic variant of neurofibroma, and it is generally regarded as pathognomic of NF1, although a small group of patients with a solitary PNF may lack the association (1–4). Therefore, its recognition is important. A diagnosis of PNF in a patient with no other manifestation of NF1 requires a genetic workup. PNF does not imply involvement of a nerve plexus by a neurofibroma. PNF is characterized by a network-like growth of neurofibroma involving multiple fascicles of a nerve and may include multiple diffuse masses of thickened nerves (5).

Clinical Features

PNFs generally develop early in childhood with no significant gender predominance, although they may

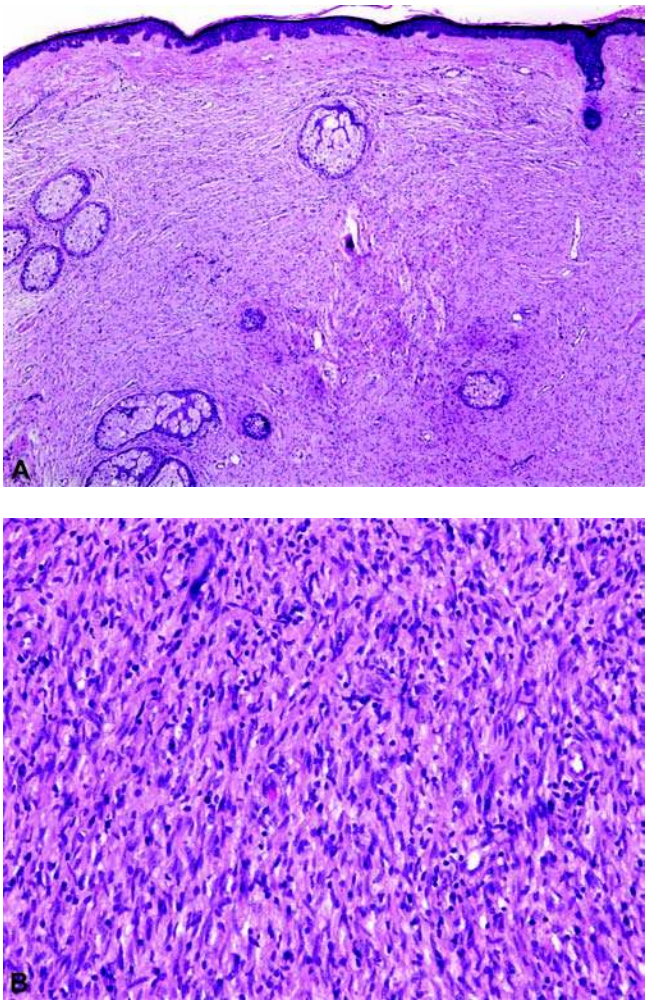

Figure 17 (**A**) Cutaneous neurofibroma. The lesion is nonencapsulated and the cells infiltrate around and between dermal appendages (H&E, 50×). (**B**) Neurofibroma with increased cellularity, ''cellular neurofibroma,'' can be mistaken for a soft tissue sarcoma (H&E, 100×).

present at older age (2,4,6). Superficial lesions are first noted as subtle enlargements of soft tissues in infancy or early childhood. The lesions, however, may exhibit rapid growth during the early years of life, leading to obvious hypertrophy or soft tissue enlargement (5). Growth of PNF can occur at anytime in life, but it appears to be particularly prominent in two periods, i.e., early childhood and during times of hormonal change including puberty and pregnancy (7).

PNF may occur at any location; however, the head and neck, back, and inguinal areas are most often involved (8,9). The head and neck is particularly common because of the rich innervation of this area. Involvement of superficial soft tissue is more frequent than deeper location. The reported incidence of head and neck manifestations in PNF varies from 14% to 55% (4,9,10). In the head and neck, the neck, scalp (11–14), face (4), tongue (15,16), lip, nose, middle ear space (4), major nerves (17–21), orbit (22,23), larynx (24–27), paranasal sinuses (28), and salivary glands (29) may be the site of tumor. PNF of the tongue usually produces unilateral macroglossia with impairment of function, and almost always occurs in children younger than three years (2,16). Otolaryngological manifestations are often an enlarging facial mass and functional impairments, the most common being hearing loss, airway obstruction, facial paresis, and impaired mastication (9).

PNFs of the head and neck may arise from cranial nerves or upper cervical nerves (5). The most common cranial nerve to give rise to PNF is the trigeminal nerve. Other commonly affected cranial nerves are nerves IX and X (8). The trigeminal PNFs usually grow into the orbit, resulting in proptosis (20,22,30,31). It is often associated with abnormality of the greater sphenoid wing. Upper trigeminal involvement leads to overgrowth of the upper eyelid and upper part of the face. Medial trigeminal nerve tumors grow along the mid-face and upper alveolar region. The lower trigeminal tumor can occur in the jaw and lower alveolar region. Tumors of the upper cervical roots can involve the skull base, scalp, or posterior auricular region and result in massive expansions of these sites (5).

Since growth of PNF occurs circumferentially around a nerve, longitudinally along a nerve, or both, PNF presents as a nodular or fusiform, poorly circumscribed mass forming tortuous cords along segments and branches of a nerve. The tumor itself usually remains within the confines of the perineurium; hence, the tortuous, enlarged nerve on palpation of tumor in soft tissue resembles a ''bag of worms'' or ''string of beads'' (6). When extensive, it may be associated with local soft tissue and skin overgrowth, referred to as ''elephantiasis neuromatosa'' (6).

Imaging

On CT scans, neurofibromas and PNFs appear as well-defined, oval, spherical, or fusiform masses, centered at the anatomical location of a cranial, spinal, autonomic, or peripheral nerve, with displacement of adjacent muscle and blood vessels (32). On IV-enhanced CT, none of the schwannomas, but approximately half of neurofibromas including PNFs, are homogenously hypodense (32). The most reliable, although not infallible, criterion of malignant nerve sheath tumors is poor definition of their margins (32).

On MRI, deep-seated PNFs exhibit a target-like appearance composed of peripheral high signal intensity on T2-weighted MRI often with a central area of low signal (33,34), while superficial PNFs tend to be asymmetric and have nontarget-like signal intensity without nodular or fascicular morphology (35). Malignancy is suspected on the basis of radiographic findings of sudden growth in a previously stable lesion or evidence of necrosis (36).

Macroscopy

PNFs consist of expanded nerves or nerve fibers that are largely replaced by the tumor (Fig. 18A, B). The enlarged tortuous nerve is confined by its perineurium; therefore, it has a nodular or fusiform appearance, with a resemblance to a bag of worms or string of beads (3,6).

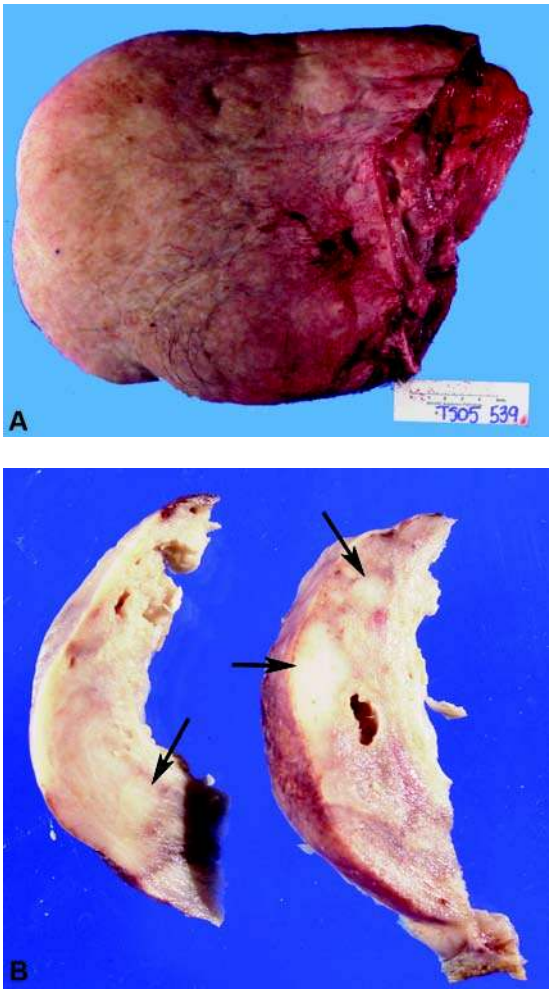

Figure 18 (**A**) Massive plexiform neurofibroma. (**B**) Cut surface of plexiform neurofibroma shows various sized and shaped nodules (*nerve arrows*), in the skin and subcutaneous tissue.

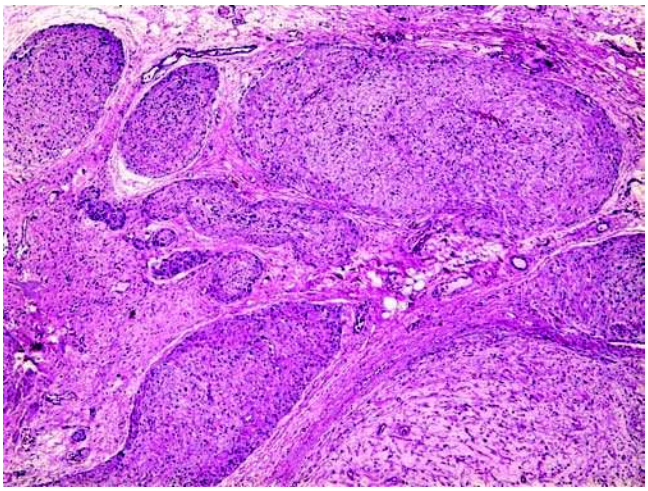

Figure 19 Tortuous enlargement of nerve fascicles, which are pale, mucoid, and paucicellular (H&E, 50×).

Histopathology

PNF consists of tortuous masses of expanded nerve fascicles (Fig. 19). At an early stage, involved fascicles are hypocellular and watery gray-blue with a hyaluronidase-sensitive mucopolysaccharide-rich matrix. The latter matrix is weakly PAS-positive and strongly Alcian blue–positive (1). Over time, the tumors grow and become more cellular with abundant collagen deposition. In addition, the cells spill out of the nerves into soft tissue, giving rise to a diffuse growth pattern.

As in other benign nerve sheath tumors, hypercellularity and variable nuclear atypia may be seen in PNF, and such lesions may be designated as atypical neurofibroma, but their presence per se is not indicative of malignancy (1,6,37). When these features are diffuse and accompanied by mitotic activity, malignant transformation should be considered (1,6).

Ultrastructure

Varying mixtures of cells are seen with predominant Schwann cells, which are surrounded by basal lamina (38).

Immunohistochemistry

PNF shows variable immunoreactivity with S-100 protein and CD57 (Leu-7) (39).

Somatic Genetics

Loss of heterozygosity (LOH) of the *NF1* gene, which is located on 17q11.2, is more common in PNFs (40–67%) than dermal neurofibromas (25–34%) (40–43).

In comparative genomic hybridization (CGH) analysis, NF1-associated neurofibromas show chromosomal imbalances (44). The gains of chromosome 17q involving chromosomal region 17q12–q22 are more frequently detected in PNF than non-NF1-associated neurofibromas in which the losses of 17q are frequent (44). The number of losses is more frequent in NF1-associated neurofibromas than in sporadic neurofibromas, indicating that inactivation of tumor suppressor genes may be more important than activation of proto-oncogenes in the development of NF1-associated neurofibroma, including PNFs.

Differential Diagnosis

In the tongue, PNF should be distinguished clinically from other causes of macroglossia, such as hemangioma, lymphangioma, amyloid, myxedema, and muscular hypertrophy. Macroglossia caused by PNF differs from these conditions in that it is unilateral, firm, noncompressible, and covered by normal mucous membrane, without a tendency to bleed at surgery. In contrast, macroglossia caused by hemangioma is usually bilateral, compressible, imparts a red color to the mucosa, and bleeds profusely at surgery.

Histologically, PNF should be distinguished from plexiform schwannoma and mucosal neuroma (45). Plexiform schwannoma is a rare nodular variant of schwannoma not associated with NF1 and without propensity for malignant transformation (45). It involves the dermis or subcutis and, except for its multinodular or plexiform architecture, has the same histological features as the usual schwannoma, but with marked cellularity dominated by Antoni type A pattern (45). In contrast to plexiform schwannoma, PNF is usually hypocellular, has a prominent myxoid matrix, and contains a disorderly array of Schwann cells, fibroblasts, perineurial-like cells, and axons (38). It is important to distinguish mucosal neuromas, a component of MEN type IIb with a risk of developing medullary thyroid carcinoma (MTC) (sec. V.H, ''Mucosal Neuroma'') from PNF associated with NF1 (1). Mucosal neuromas consist of disorganized and tortuous nerve fibers surrounded by a thickened perineurium that expresses the cellular phenotype EMA (+) and S-100 protein (–).

Malignant transformation occurs in 10% to 15% of patients with PNF associated with NF1 (1,2,46). Such malignant transformation occurs most often in deep-seated, large, centrally located PNF, with a peak incidence in the third decade of life. The detection of intranuclear p53 protein is uncommon in PNFs, but may be common in MPNST arising from PNFs (2,47). Immunohistochemically, only 2.5% of PNFs are found to demonstrate p53 expression in about 5% of the nuclei, while 80% of PNFs with associated MPNST stain for p53, with the extent of staining ranging from 1% to 25% of the tumor cells in MPNST areas (2). However, the rarity of p53 staining in the PNF regions precluded its use in predicting that those PNFs are likely to progress to MPNST (2). A recent reverse transcriptase-polymerase chain reaction (RT-PCR) study demonstrated the differential molecular profile between PNFs and MPNSTs (48). The altered genes in MPNSTs are mainly involved in cell proliferation, senescence, apoptosis, and extracellular matrix remodeling (48). Expression of matrix metalloproteinase (MMP) 13, which is related to extracellular matrix remodeling, is immunohistochemically

observed in 44% of MPNST, but is absent in NF-associated neurofibromas (49).

Treatment and Prognosis

Surgery is the therapeutic modality of choice because of the occurrence of PNF in a young age group and the doubtful effectiveness of radiation therapy (50). The management of PNF is difficult because of its tendency to grow and invade surrounding tissues and spread diffusely along the course of the nerve, resulting in frequent local recurrences (23%) (2). It appears that early surgery might prevent the development of major cosmetic and functional impairment (5). In a retrospective review of 121 patients who underwent surgery on 168 tumors, 54% did not recur after the initial surgery after a median follow-up of 6.8 years. Prognostic factors for tumor recurrence include age of less than 10 years at the time of initial surgery; head, neck, and face location; and presence of residual tumor after surgery (10).

PNF does not metastasize, but frequently recurs and may prove life threatening in strategic locations. Selective conservative surgical resection of cosmetically deforming or functionally impairing masses without resection of nerves that control important functions has been recommended (8).

There is an approximately 2% to 5% risk of a malignant transformation in PNFs (51,52). These malignant changes are very difficult to detect clinically within the mass of tissue growth.

D. Diffuse Neurofibroma

Introduction

Diffuse neurofibroma (DNF), once termed ''paraneurofibroma,'' is an uncommon, histologically distinctive variant of neurofibroma that is characterized by an infiltrative growth pattern and the presence of structures that resembles Wagner-Meissner tactile corpuscles (1,2) (Fig. 20A, B). Unlike PNF, only 10% of DNFs appear associated with NF1 (1). However, the true incidence of this association may be higher as one series reported that 61% of their cases of DNFs are associated with NF1 (3), because an unequivocal diagnosis of NF1 cannot often be established in these young patients. Unlike PNF, the incidence of malignant change in DNF is very rare (1,2,4).

Clinical Features

DNFs occur primarily in children and young adults, involves the subcutaneous tissue of the head and neck, and presents as a solitary, plaque-like elevation of the skin (1). On rare occasion, it has be reported in other sites, including the external ear canal (5), orbit (6), scalp (7), back (8,9), arm (10), ankle (11), uterine cervix (12), gallbladder (13), and stomach (14).

Imaging

CT shows diffuse infiltration of the skin and subcutaneous tissue by an ill-defined soft tissue mass that is isodense to muscle and skin (11). On MRI, the characteristic pattern is linear or reticular strands of intermediate signal intensity in the subcutaneous fat on T1-weighted imaging (8,10,11). T2-weighted imaging demonstrates high signal intensity of the linear and reticular strands of the tumor elements. The linear and reticular strands are enhanced following intravenous Gd-DTPA (8).

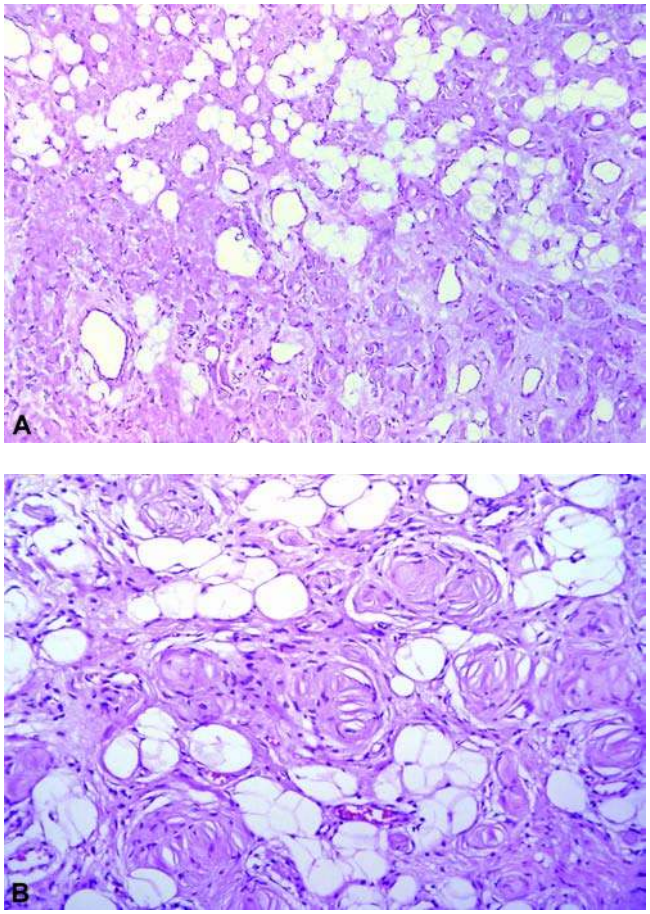

Figure 20 (**A**) Diffuse neurofibroma involving subcutaneous tissue entrapping adipocytes as it grows. It is often confused with dermatofibrosarcoma protuberans (H&E, 100×). (**B**) Diffuse neurofibroma. Higher magnification showing characteristic Wagner-Meissner bodies, which are helpful in excluding a dermatofibrosarcoma protuberans (H&E, 200×). *Source*: Courtesy of Dr. Leon Barnes, University of Pittsburgh School of Medicine, Pittsburgh, PA.

Macroscopy

DNFs are ill-defined masses, ranging in size from 0.5 to 12 cm (6,7). A glistening, gelatinous, pink-gray, homogenous, nodular mass replaces the normal subcutaneous tissue and dermis, forming soft, raised, plaque-like lesions of the skin.

Histopathology

The tumor is composed of spindle Schwann cells with round or fusiform nuclei and eosinophilic cytoplasm

within a loose matrix of fine fibrillary collagen (1,3). The Schwann cells are usually less elongated than those of conventional neurofibroma (1). Clusters of S-100 positive laminated bodies resembling Wagner-Meissner tactile corpuscles are characteristic, but not always present (3). They are predominantly localized in the vicinity of nerve fascicles entering the tumor tissue (15). In the central portion of these corpuscles, a myelinated and some unmyelinated nerve fibers are ensheathed by tactile corpuscle cells (Fig. 20A, B).

Differential Diagnosis

DNF lacks the characteristic cord-like structure confined by the perineurium that is seen in PNF and is distinguished by its highly infiltrative pattern, the presence of rounded or slightly fusiform cells that are uniformly distributed within a delicate collagenous background, and sheets of laminated bodies resembling Wagner-Meissner tactile corpuscles (1). The tumor typically insinuates itself throughout the soft tissue and envelopes rather than invades nerves or cutaneous adnexal structures. These histological features and S-100 positivity of tumor cells distinguish DNF from the spindle cell lesions that have a similar infiltrative pattern, namely, spindle cell lipoma and dermatofibrosarcoma protuberans (DFSPs) (1) (Fig. 20 A,B).

Treatment and Prognosis

Surgical excision is the treatment of choice. These lesions may be difficult to excise and may recur if not totally removed. However, unlike PNF, the incidence of malignant change in DNF is extremely unusual (1,4).

E. Neurofibromatosis 1

Introduction

Neurofibromatosis (NF) is one of a group of neurocutaneous disorders that are collectively referred to as ''phakomatoses'' (1). NF is a genetic disorder, characterized by multiple lesions, typically of diverse type, in a variety of tissues and organs (2,3). These include hyperplasias, hypoplasias, hamartomas, and benign and malignant neoplasms. The majority of lesions are neuroectodermal or mesenchymal in nature. The 1986 meeting of the Neurofibromatosis Task Force led to the acknowledgment of at least three categories of NF: (*i*) von Recklinghausen's NF or NF1, (*ii*) bilateral acoustic NF (BANF or NF2), and (*iii*) all other NFs (NF3, NF4, and NF-NOS) (4,5). The last category encompasses alternative or atypical forms of the disease. NF1 is the most common and comprises 90% of all cases of NF (3). NF1 and NF2 are clinically and genetically distinct disorders, the genes for which are located on 17q11.2 and 22q12.2, respectively (6). Both have very high rates of spontaneous mutation, resulting in 50% of cases in each disorder arising de novo (7–9). Both have essentially 100% penetrance but wide phenotypic variability (9,10). The factors modulating phenotypic variability may represent both genetic and environmental factors (11).

Clinical Features

The clinical expression of NF1 is strikingly diverse (3). About 40% of patients experience the onset of their disease before the age of one year and only 8% after the age of 25 years. The full-blown disease may not become evident until adult life. A population incidence is approximately 1 in 3000 individuals worldwide. There is an equal gender distribution, and all races may be affected. The protean manifestation of NF1 affects the peripheral nerves and skin as well as other tissues such as the central nervous system (CNS) and the skeleton (2,3). NF1 is diagnosed when two or more of the NIH diagnostic criteria listed in Table 2 are present. Multiple melanotic skin macules (''café au lait'' spots), intertriginous freckling, multiple Lisch nodules (iris melanocytic hamartomas) (12,13), and multiple cutaneous neurofibromas are highly characteristic.

Café au lait spots are usually the first clinical manifestation of NF1 and often found on the trunk, pelvis, and axilla. They increase with age and are seen in more than 95% of patients (11). They also commonly increase in number and size through puberty, subsequently fading during adulthood. Café au lait spots are hyperpigmented macules, typically ovoid in shape, about 10 to 40 mm in diameter, with relatively smooth borders.

NF1 is characterized by a high incidence of neurofibromas, which may be found in any location and first appear in childhood. Optic gliomas, spinal or peripheral neurofibromas, neurological impairment, scoliosis, and other bone abnormalities may be present (14–16). Although schwannomas may develop on any nerve in NF1 patients, bilateral acoustic neuromas are not seen. Patients with NF1 are at increased risk of a few nonnervous system neoplasms, including chronic myelogenous leukemia (17,18), juvenile xanthogranuloma (19), rhabdomyosarcoma (18,20,21), pheochromocytoma and paraganglioma (PGL) (22), gastrointestinal stromal tumor (23,24), duodenal gangliocytic paraganglioma (PGL) (25), and foregut carcinoid (26,27).

Head and neck manifestations of NF1 are frequent and have been reported in 14% to 37% of

Table 2 NIH Diagnostic Criteria for NF1

NF1 is present in a person who has ≥2 of the following signs:
≥6 café au lait macules >5 mm in greatest diameter in prepubertal individuals or <15 mm in greatest diameter after puberty.
≥2 neurofibromas of any type or ≥1 plexiform neurofibromas.
Freckling in the axial or inguinal region.
A tumor of the optic pathway.
≥2 Lisch nodules.
A distinctive osseous lesion, such as sphenoid wing dysplasia, or thinning of the cortex of the long bones (with or without pseudarthrosis).
A first-degree relative with NF1 by the above criteria.

Abbreviation: NF, neurofibromatosis.
Source: From Ref. 5 (section V.E, "**Neurofibromatosis 1**").

patients with NF1 (28–30). Nerve sheath tumors can occur anywhere, but are most often found in the midlateral neck, eyelids, and orbits. They are most common in the skin and soft tissues. However, these tumors may present in less common sites, such as the orbitotemporal region (31–35), otolaryngic tract (36–41), jaws and skull (42), and oral cavity (43). Neurofibromas, PNFs, optic pathway gliomas, and bone lesions may involve the orbit with skull and facial deformities in 5% to 20% of patients (31,32,34,35,44). In severe NF1, vision may be markedly reduced owing to the presence of ocular NF1 or functional amblyopia (32). Bony malformations, such as hypoplasia and perforating defects are typical in those with craniofacial NF1. Orbital PNFs are frequently associated with hypoplasia or dysplasia of the greater wing of the ipsilateral sphenoid bone, which may result in herniation of the dura into the orbit and manifest as a pulsating exophthalmos. The increased volume of the orbital contents due to tumor and the herniated temporal lobe may result in inferior displacement of the globe. Laryngeal or nasopharyngeal involvement is rare in NF1 and includes plexiform or localized neurofibroma of the aryepiglottic fold or supraglottis manifesting as hoarseness, dysphagia, or stridor (30,41). The oral cavity is affected in 5% of cases, with the major findings being soft tissue or intraosseous neurofibromas and macroglossia (43). At this site, neurofibromas may involve the lips, gingiva, buccal mucosa, tongue, floor of the mouth, and mucous membranes (30,32,34,37,39,42–44).

Optic glioma represents the second most common tumor seen in patients with NF1. These low-grade pilocytic astrocytomas typically arise in the optic nerve and chiasm, hypothalamus, brainstem, and cerebellum (45). A quarter to a third of the affected children develop progressive clinical signs and symptoms that require treatment.

Imaging

Skeletal abnormalities occur in 40% of patients with NF1 (3,46). Plain radiographs, CT, or MRI scans of the craniofacial and spine and paraspinal regions may be important to assess the presence of neurofibromas or other tumors that may compromise neurological function (47,48). CT and MRI scans of the orbit and brain may be necessary to confirm the diagnosis of NF1 or to determine the nature of the tumors, such as optic glioma and orbital neurofibromas, and cranial vault dysplasias. Using MRI, in 90% of children a high frequency of hyperintense signals appear on T2WIs and should not be over interpreted to indicate brain tumors (3,48). This finding is less common in adults with NF1. For visualizing bony anatomy of craniofacial structures or sphenoid wing, CT scans may be preferred. However, MRI with gadolinium enhancement is valuable and has replaced CT as the primary neuroimaging modality, especially when serial studies of eyes and brain are needed or when estimating tumor volume (3,48). MRI offers superior soft tissue contrast and provides more detailed imaging than CT of the characteristic CNS lesions (48).

Pathology

Neurofibromas are the most common tumors in NF1 and are the hallmark of the disease (1). These may be of the localized, plexiform, or diffuse types, based on their gross and histological appearance (see discussions in secs. V.B, ''Neurofibroma''–V.D.,''Diffuse Neurofibroma,'' on neurofibroma, PNF, and DNF) (1). The plexiform type of neurofibroma is seen almost exclusively in NF1 and is the most specific, whereas DNF is associated with NF1 in approximately 10% of cases (1). Although localized neurofibromas are the most common type seen in NF1, histologically they are the least characteristic, as they are identical to the solitary neurofibromas seen outside the setting of NF. Localized neurofibromas tend to be larger than solitary neurofibromas. They characteristically occur in the dermis and subcutis, but may be seen in deep soft tissue (1).

One of the most disturbing tumors in NF patients is the malignant peripheral nerve sheath tumor (MPNST). A lifetime risk for developing MPNST ranges from 8% to 13% (49). In contrast to sporadic cases, NF-associated MPNSTs occur at a significantly younger age.

Somatic Genetics

The *NF1* gene is a large gene that directs the synthesis of a protein termed ''neurofibromin,'' which is composed of 2818 amino acids. Mutations in the *NF1* gene result in loss of function of neurofibromin, a GTPase-activating protein (GAP) that helps maintain the proto-oncogene *ras* in an inactive form. Loss of neurofibromin leads to an increased *ras* activity, particularly in neurocutaneous tissues, resulting in increased proliferation and tumorigenesis (50). In addition, it appears that neurofibromin positively regulates intracellular cyclic adenosine monophosphate (cAMP) levels, which has been shown to modulate cell growth and differentiation in the brain (51).

Treatment and Prognosis

There is no treatment that alters the course of NF1. In most patients with NF1, there is an inevitable progression of the skin tumors. The neurofibromas cause significant morbidity, and their large numbers make surgical treatment impractical (52). However, surgery may be indicated for tumors associated with disabilities, for cosmetic deformities, and for large or painful tumors, or those located in critical areas impairing organ function. Recurrences may occur because of the poorly defined nature of many of these tumors (53). A more devastating complication is malignant transformation (54). Such transformation occurs most frequently in deep-seated, large central lesions. The risk of developing malignant transformation in NF1 increases in individuals who have had the disease for several years (75% of patients who develop MPNST have had NF1 for 10 years or more), and only rarely does it occur in patients who have had the disease for a period shorter than five years. The treatment of MPNST in this setting is radical surgery, but the prognosis is poor in these high-grade neoplasms with a five-year survival of less than 20% (54).

Brain tumors, whether benign or malignant, and kyphoscoliosis, with its concomitant restrictive effects on cardiopulmonary function, may also prove life threatening in NF1 patients.

The treatment and prognosis of head and neck manifestations depend on the extent of the disease and site of occurrence. For example, the treatment of orbitotemporal NF1 depends on the severity of the orbital involvement and the functional state of the eye (32).

F. Neurofibromatosis 2 (Bilateral Acoustic Neuroma)

Introduction

NF2 (bilateral acoustic neuroma) is an autosomal dominant genetic disease, distinct from NF1. It occurs in about 1:40,000 individuals, with penetrance of over 95% (1–6). Most patients present in the second to third decade (7). Offspring of a patient with NF2 have a 50% risk of developing the disease. The mutation underlying the condition is on the locus 22q12.2. The *NF2* gene encodes merlin, which may act as a regulator of growth, motility, and cellular remodeling by inhibiting the transduction of extracellular mitogenic and motogenic signals (8).

NF2 should be differentiated from NF1 because the genetic basis, spectrum of features, and overall natural history are different (3) (Table 3). NF2 should also be distinguished from sporadic, nonfamilial acoustic neuromas, which develop later in life, are not inherited, and present fewer problems in management (2).

Clinical Features

The two proposed criteria for the diagnosis of NF2 are listed in Tables 4 and 5 (9,10). Individuals with NF2 generally present with hearing loss with the development of acoustic neuromas or with other symptoms secondary to meningiomas or spinal schwannomas (11).

Table 3 Features of Neurofibromatosis Types 1 and 2 (NF1 and NF2)

	NF1	NF2
Inheritance	Autosomal dominant	Autosomal dominant
Spontaneous mutations	50%	50%
Incidence	1:3000	1:40,000
Chromosome	17q11.2	22q12.2
Gene product	Neurofibromin	Merlin
Typical presentation young	Café au lait macules during infancy or early childhood	Hearing loss of vestibular dysfunction in young adulthood or cataracts
Nerve sheath tumors	Neurofibroma, plexiform neurofibroma, MPNSTs	Schwannoma
Intracranial tumors	Optic pathway gliomas other astrocytomas/gliomas	Vestibular schwannomas, meningiomas
Spinal tumors	Nodular plexiform neurofibromas (roots)	Schwannomas (roots) ependymomas (intramedullary)
Cutaneous features	Café au lait macules, axillary/inguinal freckling, cutaneous neurofibromas, subcutaneous neurofibromas	Cutaneous schwannomas
Cognitive	LD and ADHD common, IQ mildly decreased	Normal
Skeletal	Scoliosis, short stature, pseudarthrosis, sphenoid dysplasia	None
Ophthalmologic	Lisch nodules, congenital glaucoma	Juvenile subcapsular lenticular opacities, cataracts, corneal scarring, retinal hamatomas
Other tumors	CML, pheochromocytoma	None
Other neuro manifestations	UBOs, macroencephaly	Neuropathy, areflexia
Other	Vascular abnormalities, GI bleeding, constipation	

Abbreviations: NF, neurofibromatosis; MPNST, malignant peripheral nerve sheath tumor; LD, learning disability; ADHD, attention deficit and hyperactivity disorder; CML, chronic myelogenous leukemia; UBOs, unidentified bright objects.
Source: From Ref. 11 (section V.E, "**Neurofibromatosis 1**").

Table 4 Proposed Revised Clinical Criteria for NF2

Definite NF2	Presumptive or probable NF2
Bilateral vestibular schwannomas (VS) *or* First-degree relative with NF2 *plus* 1. Unilateral VS <30 years, or 2. Any 2 of the following: meningioma, glioma, schwannoma, juvenile posterior subcapsular lenticular opacities	Unilateral VS <30 years plus at least 1 of the following: meningioma, glioma, schwannoma, juvenile posterior subcapsular lenticular opacities *or* Multiple meningiomas (>2) plus unilateral VS <30 years or 1 of the following: glioma, schwannoma, juvenile posterior subcapsular lenticular opacities

Abbreviation: VS, vestibular schwannomas.
Source: From Ref. 9 [section V.F, "**Neurofibromatosis 2 (Bilateral Acoustic Neuroma)**"].

Table 5 Manchester Clinical Diagnostic Criteria for NF2

A.	Bilateral vestibular schwannomas
B.	First-degree family relative with NF2 and unilateral vestibular schwannoma or any two[a] of: meningioma, schwannoma, glioma, neurofibroma, posterior subcapsular lenticular opacities
C.	Unilateral vestibular schwannoma and any two of: meningioma, schwannoma, glioma, neurofibroma, posterior subcapsular lenticular opacities
D.	Multiple meningiomas ($\geq$2) and unilateral vestibular schwannoma or any two of: schwannoma, glioma, neurofibroma, cataract

[a]"Any two of" refers to two individual tumors or cataract.
Source: From Ref. 1 [section V.F, "Neurofibromatosis 2 (Bilateral Acoustic Neuroma)"].

The average age of symptom onset in patients with NF2 is about 20 years, whereas the average age of diagnosis is about 28 years (1,12). The hallmark of NF2 is bilateral acoustic neuromas (vestibular schwannomas), accounting for approximately 5% of all acoustic neuromas. Bilateral acoustic neuromas are essentially universal among patients with NF2, but both acoustic neuromas are not always evident at the same time; therefore, any individual with an acoustic neuroma or a meningioma who is younger than 30 years should raise suspicion of NF2. Acoustic neuromas most commonly present with auditory symptoms [see sec. V.G, "Acoustic Neuroma (Unilateral)"].

Schwannomas arising from the dorsal spinal roots (spinal schwannomas) are also common and present in more than 80% of individuals with NF2 (13). They are generally small and asymptomatic, although they may grow large enough to compress the spinal cord or adjacent organs. These tumors radiologically resemble neurofibromas of spinal roots, with the same "dumbbell" appearance. Schwannomas can also occur from any peripheral nerve, in both superficial and deep soft tissue. They may cause pain or impaired motor or sensory function. NF2-associated schwannomas may demonstrate unusual features such as multifocality within a nerve, a nodular growth pattern, an association with peritumoral arachnoid cell proliferation, and the rare occurrence of a mixed schwannoma and meningioma phenotype (14).

Presenile posterior subcapsular or cortical lens opacities are present in 60% to 80% of patients and may precede the onset of symptoms, thus allowing for early identification of family members with the gene (2,15).

Meningiomas are often multiple and affect approximately one-half of individuals with NF2 (1,12). These occur early in life than sporadic meningiomas, and there is a female preponderance (16). Ependymomas and astrocytomas are also more prevalent in NF2 patients, with the estimated incidence of about 33% (17).

Approximately 70% of patients with NF2 have skin lesions (1,12,18). These include skin neurofibromas, café au lait spots, and rarely plexiform neurofibromatosis (PNF), but less commonly than in NF1.

In addition to bilateral acoustic neuromas seen in more than 90% of persons with the *NF2* gene, other head and neck manifestations include meningiomas of the posterior fossa and cranial nerves (19), ectopic meningioma, otological nerve sheaths tumors and deafness (20), ocular abnormalities (cataracts, retinal hamartomas, and motor deficits) (15), and neurofibroma or schwannoma of the tongue (21). In contrast to NF1, cutaneous neurofibroma and café au lait spots are fewer and less common in NF2 (19).

Imaging

MRI is the neuroimaging procedure of choice in patients with hearing impairment or abnormal brain stem auditory–evoked response (6,22,23). Gadolinium-enhanced high-resolution MRI has replaced the use of brain stem auditiometry to evaluate patients suspected of having acoustic neuromas. MRI can detect tumors as small as 1 to 2 mm in diameter on cranial and spinal nerve roots. Full spine MRI detects spinal tumors in up to 90% of patients with NF2, but only 30% have symptomatic spinal tumors (17,24).

Meningiomas are detected on MRI as enhanced areas on the meninges around the spinal cord, brain, or optic nerves. These can form confluent areas on scan. Meningiomas have more rapid growth rates than acoustic neuromas.

Pathology

Acoustic neuromas (vestibular schwannomas) have identical morphological features to schwanomas in other anatomic locations. They have a thin capsule and display two classic growth patterns (Antoni type A and B), in highly variable proportions (25,26). The Antoni type A pattern shows a compact arrangement of elongated spindle cells, with wavy nuclei, poorly defined borders, and loosely arranged fascicles having a palisading arrangement of nuclei, the Verocay body. The Antoni type B pattern is composed of a less orderly arrangement of fewer spindled tumor cells in a loose myxoid stroma. Typically, the tumor is separated from the nerve fibers by a thin capsule. Vessels with thick hyalinized walls and microcystic changes may be seen. Mitoses are rare. Acoustic neuromas in NF2 are more likely to have a lobular pattern, to be highly cellular, and contain Verocay bodies, whereas sporadic tumors are more likely to contain hyalinized vessels, recent thrombosis, and hemosiderin deposition (26).

Somatic Genetics

The *NF2* gene is located at 22q12.2 and encodes a 595 amino acid protein called merlin. The *NF2* gene contains 17 exons and has 2 splicing isoforms. A LOH via mutational inactivation and allelic loss of the *NF2* gene appears to be causal for tumorigenesis in NF2 (27–29). Merlin is conformationally regulated and exists in a closed, active state or an open, inactive state. Merlin molecules with mutations exhibit an open conformation and do not suppress cell growth (30). However, the mechanisms by which merlin acts as a tumor suppressor remain unclear (31).

Differential Diagnosis

Advances in neuroradiology have increased the clinical accuracy of distinguishing acoustic neuromas from other cerebellopontine angle lesions that present in a similar fashion. These include meningioma, cholesteatoma, and schwannomas of other cranial nerves (32). Histologically, acoustic neuromas should be distinguished from other tumors, such as leiomyoma, neurofibroma, paraganglioma (PGL), and meningoma (33). In addition to characteristic morphological features that distinguish schwannomas, such as the presence of Antoni A pattern with Verocay bodies, schwannomas are more strongly and diffusely positive for S-100 protein than are neurofibromas. Leiomyomas are distinguished by their positivity for desmin and actin. PGLs have a characteristic zellballen pattern and are positive for neuroendocrine markers (synaptophysin and chromogranin); only the supporting or sustentacular cells, not the tumor cells, are positive for S-100 protein. Meningiomas typically have a dual immunoreactivity for vimentin and EMA. However, in some cases, it may not be possible on small biopsies to immunohistochemically distinguish between acoustic neuroma and meningioma, because both may be positive for vimentin, EMA, and S-100 protein. In such cases, the ultrastructural demonstration of the basal lamina around tumor cells may help confirm the Schwann cell origin of acoustic neuroma.

Treatment and Prognosis

Acoustic neuromas have an unpredictable natural history and a highly variable growth rate. The most common disability from acoustic neuroma is bilateral severe to profound deafness. The tumors may destroy the auditory nerves and usually lead to progressive hearing loss. NF2-associated tumors are more difficult to treat than sporadic unilateral tumors because the former tumors are often multifocal in the eighth nerve complex (34). There is an increased risk in developing other intracranial and intraspinal tumors, schwannomas of other cranial nerves and spinal roots being the most common, but also meningeal and glial tumors. Although growth may be slow or only minimal in some acoustic neuromas, other may progress relentlessly and cause significant disability, and even death, by local growth into brain structures. However, there is no malignant potential. Serial MRI is useful to follow the growth of tumors accurately. Acoustic neuromas seen in NF2 are typically more aggressive than sporadic tumors.

The treatment depends on patient's age, tumor size, presence or absence of hearing and facial nerve function, and tumor growth rate (35,36). Treatment should be directed toward preserving hearing (35,36). For most tumors requiring intervention, surgery is the treatment of choice, with the optimal goal being removal of the tumor while maintaining preoperative hearing and facial function. Small acoustic neuromas in NF2 can be seen on the MRI with gadolinium enhancement, making complete surgical excision possible (2,4,36). In other situations, however, watchful waiting may often be the best management for acoustic neuromas in NF2 (2,4,34). The indication and timing of tumor resections in NF2 are dependent on the tumor extension, necessity for brain stem decompression, and on auditory function (35). In many cases hearing in the affected ear cannot be preserved.

G. Acoustic Neuroma (Unilateral)

Introduction

Acoustic Neuromas, also called vestibular schwannomas, are schwannomas that originate on the superior or inferior vestibular branches of cranial nerve VIII in the internal auditory canal and the cerebellopontine angle (1–4). They represent approximately 6% of all intracranial tumors and have an incidence of 1 per 100,000 population per year (3). They may present as a sporadic unilateral tumor or familial and bilateral tumors, the latter being the hallmark of NF2. Unilateral tumors are the most common presentation and account for 95% of all acoustic neuromas. Acoustic neuroma is the most common tumor of the cerebellopontine angle (84%).

Clinical Features

Sporadic tumors are unilateral and occur in the fourth and fifth decades, with a mean age of 50 years (5). Typically, unilateral acoustic neuromas become symptomatic after 30 years, and the most common symptom is a progressive unilateral high-frequency retrocochlear sensorineural hearing loss, which is often associated with disproportionately deficient speech discrimination (5). Sudden worsening of hearing deficit occurs commonly. Other signs and symptoms include tinnitus, dizziness, and disequilibrium (6–9), and at a late stage, headache, facial pain, numbness or tingling, facial weakness or twitching, double vision, and symptoms of brain stem compression, such as weakness of extremities, difficulty swallowing, or talking. The tumors may be large enough to cause hydrocephalus, brainstem compression, herniation, and death (8).

NF2-associated tumors account for approximately 5% of all acoustic neuromas. Patients who inherit an abnormal copy of the *NF2* tumor suppressor gene have a 95% chance of developing bilateral tumors. However, about half of the cases have no family history of NF2, and they likely represent new germline mutations that were not inherited. Schwannomas with cystic change, so-called cystic schwannomas, are clinically aggressive and can grow rapidly, and invade the surrounding cranial nerves and splay them throughout the tumors (5,10). They are more likely to have continuous growth and facial paralysis even with stereotactic radiation therapy than noncystic tumors (11,12).

Brain stem audiometry (ABR) has been used as a screening test and, when hearing levels are sufficient to obtain a response, it provides a rapid, noninvasive method to detect acoustic tumors. However, recent studies have reported sensitivity rates of only 67% to 76% for detection of intracanalicular acoustic tumors

that are smaller than 1cm (8,9,13). Therefore, the use of ABR to evaluate patients suspected of having acoustic tumors has been replaced by gadolinium-enhanced high-resolution MRI (14,15).

Acoustic neuromas can be an incidental finding on MRI images (occult acoustic neuromas), and such an incidence ranges from 0% to 2.4% (16).

Imaging

After appropriate clinical evaluation and hearing and balance testing, the definitive diagnostic test is an MRI scan with gadolinium enhancement (14,15). MRI demonstrates a smooth-bordered, round, nodular, extra-axial mass within the vestibular portion of the eighth nerve, usually beginning at the internal auditory canal, with extension to the cerebellopontine angle. The MRI characteristics of acoustic neuroma may correlate with the histological features (15). Acoustic neuromas are of low-signal intensity in the T1WIs. In the T2WIs, about half of the cases are of homogenous high-signal intensity, and such tumors are generally associated with capsular enhancement and are usually cystic tumors with high vascularity and predominantly Antoni A type tissue (15). The other half of cases are of heterogenous high-signal intensity, and these tumors are generally associated with homogeneous enhancement and mostly solid tumors with low vascularity and various tissue components. Cystic regions of the tumors do not enhance with gadolinium administration, while noncystic component enhances (5).

Pathology

Acoustic neuromas are, like conventional schwannomas, typically well circumscribed and often globular in configuration (17). A thin layer of fibrous tissue encapsulates the tumor. The parent nerve can be detected. The cut surface of the tumor is yellow and cystic degeneration is commonly seen, particularly in large tumors.

The tumor microscopically displays two growth patterns—Antoni A and B areas—that are seen in conventional schwannomas in varying proportions (18,19). Xanthoma cells, which grossly impart a yellow color to the tumor, are often present in the Antoni B component. Degenerative changes such as nuclear pleomorphism, hyperchromasia, or cystic degeneration are often found. Blood vessels in the tumor are thick and hyalinized. Immunohistochemically, they are strongly and diffusely positive for S-100 protein [see sec. V.A, ''Schwannoma (Neurilemoma, Neurinoma)''].

Somatic Genetics

Mutations within the *NF2* gene are found not only in NF2-associated schwannomas but also in sporadic unilateral tumors and cystic tumors (20,21). Such mutations have also been frequently identified in meningiomas (22) and occasionally in malignant mesotheliomas (23).

Differential Diagnosis

Acoustic neuroma should be distinguished histologically from other neoplasms, including meningioma, leiomyoma, neurofibroma, and paraganglioma (PGL), by identification of its characteristic patterns of proliferation (Antoni A and B) and diffuse, strong reactivity for S-100 protein, together with absence of reactivity with desmin, CKs, neuroendocrine markers, and in most cases, EMA (17).

Treatments and Prognosis

There is a striking variability in the natural history and growth rate of sporadic unilateral acoustic neuromas (24). Therapeutic options are based on age, symptoms, tumor size, hearing level, and rate of tumor growth (25–29). Serial MRI scanning has shown that approximately 80% of the tumors are slow growing (<2 mm/year) over decades or show no growth, whereas 20% of the tumors may progress rapidly (5 mm) (24,30–33).

There are currently four main management options available, with a combination of two or more also being used as required (25,34). These include (*i*) observation with regular clinical and radiological follow-up, (*ii*) surgery by using the operating microscope and intraoperative neurophysiological montoring, (*iii*) stereotactic radiosurgery, and (*iv*) fractionated radiotherapy (25). Not all patients are suitable for all of these methods. Accepted criteria that preclude a patient's eligibility for all methods are tumor size (>3 cm generally for surgery only), age (>70 years often not for surgery), and medical comorbidity (increased surgical risk) (25).

Earlier diagnosis and complete or partial removal by surgery or stereotatic radiosurgery has contributed to decrease morbidity, with preservation of hearing and facial movement and sensation to preoperative levels (26–29).

The explanation for the variation in tumor growth rate is unclear. There are currently no preoperative or morphological mechanisms by preoperative radiography, histopathology, or flowcytometry that can identify rapidly progressive tumors from those that have a lower rate of proliferation (30,34–36).

H. Mucosal Neuroma

Introduction

The multiple endocrine neoplasia (MEN) syndromes, defined as the association of tumors of two or more endocrine glands, are usually inherited as an autosomal dominant trait, although they may also occur in sporadic fashion (1). The major syndromes include MEN types I and II. MEN type I (Wermer's syndrome) consists of tumors or hyperplasia involving the parathyroid glands, pituitary, and pancreatic islets. Its putative gene has been mapped to chromosome 11q12. Individuals with this syndrome may develop carcinoid tumors in the foregut such as thymus, lungs, stomach and duodenum, cutaneous angiofibroma, adrenocortical hyperplasia or adenoma, and lipoma.

MEN type II encompasses three subtypes defined by the combination of tissue affected. MEN type IIa (Sipple's syndrome) consists of an association of MTC, adrenal pheochromocytoma, and parathyroid disease (1). MEN type IIb, or also referred to as MEN III by some, is characterized by the presence of multicentric MTC, bilateral pheochromocytomas, and ocular and oral neuromas as well as intestinal ganglioneuromatosis, often with a marfanoid habitus and the very rare occurrence of parathyroid disease (1–7). The third subtype is familial medullary thyroid carcinoma (FMTC). The gene for MEN IIa, IIb, and FMTC is present on chromosome 10q 11.2 and has been recognized as the *RET* proto-oncogene (1,8–13).

Clinical Features

The most consistent and distinctive feature of MEN IIb is mucosal neuromas, which are present in almost 100% of patients. There is a slight female predominance with a mean age of 22 years (7,14). Mucosal neuromas, especially oral or ocular, are noted at birth or during the first few years of life and are a constant component of this syndrome (1,15–17). They are often multiple and are believed to represent hamartomatous growth, rather than true neoplasia. The most common sites include the lips, tongue, and eyelids. Mucosal neuromas appear as small, sessile, multinodular excrescences on the vermilion of the lip, on the anterior third of the dorsal or ventral tongue, or buccal mucosa, almost invariably by eight years (1,15). Each nodule ranges from pinhead size to a few millimeters in diameter (2,18). In these patients, similar neuromas occur on the eyelid margins causing thickened and everted eyelids as well as on the palpebral and bulbar conjunctiva (16,17,19). Bilateral gray-white, prominent thickened corneal nerves are seen as a constant manifestation (17,19). Other oral sites such as gingival, palate and retrognathic or prognathic mandible, nasal cavity, larynx, pharynx, and conjunctiva may also be rarely involved (16).

The MEN IIb syndrome frequently manifests with a neck mass or diarrhea, or it may be identified during screening of individuals with affected relatives. The mucosal neuromas and a marfanoid habitus manifest at any early age, whereas the MTC and adrenal pheochromocytoma occur later in life (1,5–7). In a review of 51 patients with MEN IIb, Carney et al. found that 78% of the patients had MTC (mean age of 20 years), and 31% had pheochromocytoma, which was bilateral in two-thirds of cases (2). Of the patients with medullary carcinoma, 55% had metastatic or locally invasive tumor at diagnosis, and 18% died of metastatic tumor (2). Once the syndrome is suspected, MTC can be diagnosed by calcium-stimulated calcitonin assays earlier than by physical examination or thyroid function tests. Mucosal neuromas, which are not associated with MEN IIb, have been reported in the tongue (20), hard palate (21), conjunctiva (22), larynx (23), and bronchus (24).

Pathology

Mucosal neuromas consist of enlarged nerves within the submucosa of the affected tissue and stud the lips as well as the tip of anterior third of the tongue, at times forming confluent or sessile masses, mainly on the dorsal aspect, but also on the frenulum or ventral surface (1,2,25). The involved tortuous, highly branched and loosely arranged nerve bundles measure up to several millimeters in diameter. Histologically, sections of mucosal neuromas show subepithelial, enlarged tortuous fascicles of myelinated peripheral nerve bundles that vary in size and shape (Fig. 21A, B). The nerve bundles contain loose, mucoid endoneurial tissue and Schwann cell cords with a disorderly arrangement of axons surrounded by a thickened perineurium that expresses EMA, but is negative for S-100 protein (25,26) (Fig. 21C). Reactive fibrosis is not a feature of mucosa neuroma.

Somatic Genetics

MEN types IIa, IIb and FMTC share the common germline mutations of the *RET* proto-oncogene on chromosome 10q11.2 (12). These are generally missense mutations clustered in only a few codons of *RET*. *RET* plays a role in development and maturation of peripheral nerves and in kidney induction but also an important role in neuronal survival in the peripheral nervous system (27). It encodes a receptor tyrosine kinase, RET protein, whose ligands are persephin, artemin, neurturin, and glial cell line–derived neurotrophic factor (GDNF). All these ligands are structurally related to transforming growth factor (TGF) β (28). RET activation by the GDNF family ligands appears to occur via a unique membrane-bound multicomponent receptor complex.

Differential Diagnosis

Mucosal neuromas should be distinguished from the nonneoplastic traumatic neuroma and from the peripheral nerve sheath tumor, particularly Plexiform neurofibromatosis PNF (1,25,26). PNF is almost invariably a component of NF1 and has a predisposition to develop malignant transformation. Unlike mucosal neuromas, the plexiform neuroma and traumatic neuroma are not a component of the MEN type IIb syndrome. Patients with traumatic neuroma often have a clinical history of trauma or prior surgery. Histologically, mucosal neuromas are composed of bundles of disorganized and tortuous nerve fibers surrounded by thickened perineurium, which is EMA-positive and S-100 protein-negative, while in PNF-enlarged nerve, fascicles are seen with a loose myxoid or fibrous stroma, which is S-100 protein-positive and EMA-negative (26). Traumatic neuroma is composed of a nonencapsulated, haphazard proliferation of all elements of the nerve fascicles including axons, Schwann cells, and perineurial cells in a fibrous background. Traumatic neuromas may be positive for EMA and S-100 protein.

Treatment and Prognosis

Mucosal neuromas are often asymptomatic, benign tumors with a self-limited growth (2,7). They may be

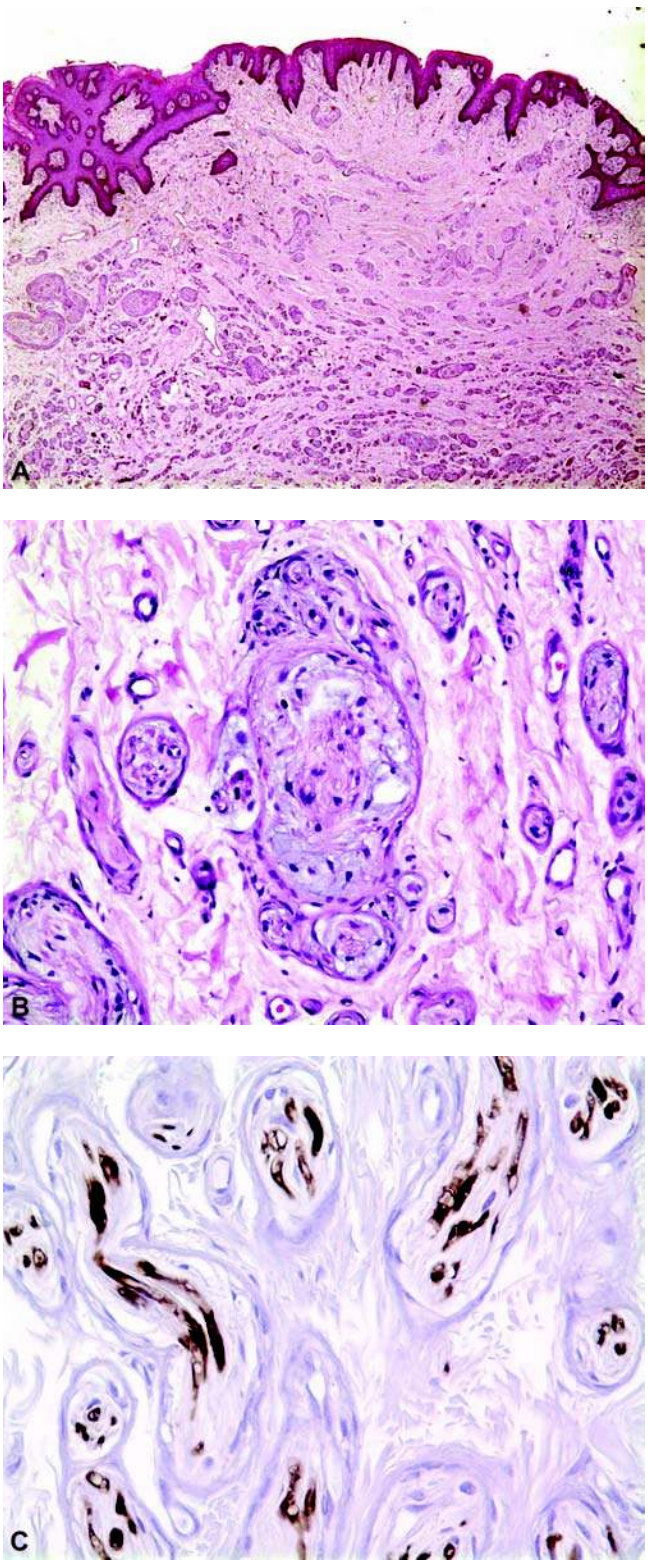

Figure 21 (**A**) Mucosal neuroma composed of various sized and shaped tortuous nerve bundles in the lamina propria (H&E, 50× *arrow*). (**B**) Nerve bundles contain increased endoneurial myxoid substance. There is no reactive fibrosis between nerve bundles (H&E, 250×). (**C**) S-100 protein immunostain highlights in the nerve bundles (H&E, 250×).

excised for cosmetic reasons. Oral surgeons should be aware of the clinical significance of the oral neuromas and refer the patient and family members for appropriate endocrine evaluation (2). The histological finding of mucosal neuromas should also initiate the search for other components of MEN IIb, especially MTC. The importance of early diagnosis and screening for MTC is emphasized, as it often pursues an aggressive course and can metastasize or cause death unless a total thyroidectomy is performed in childhood (7). Affected individuals should be periodically screened for pheochromocytoma. High calcitonin levels after total excision of medullary carcinoma suggest the presence of residual tumor or occult metastasis. When mutation is identified, the same procedure should be undertaken in all first-degree relatives (29).

I. Neurothekeoma

Introduction

Also referred to as nerve sheath myxoma, plexiform myxoma and perineurial myxoma in the literature, neurothekeoma is usually a cutaneous, multilobulated neoplasm. It can be subdivided into two histogenetically unrelated lesions; the true nerve sheath myxoma, also known as myxoid neurothekeoma, and cellular neurothekeoma. These two show different clinicopathological features. The former was originally described in 1969 by Harkin and Reed under the term ''nerve sheath myxoma,'' subsequently in 1980 by Gallagher and Helwig under the term ''neurothekeoma'' and is a myxoid tumor that exhibits Schwannian differentiation (1–4). The cellular variant was reported by Rosati et al. in 1986 (5) and is a tumor rather of fibroblastic or myofibroblastic derivation (6,7).

Clinical Features

Nerve sheath myxomas occur in adults during the third through the fifth decades, with a male to female ratio of approximately 1:2 (2,3,8). The tumors commonly involve the upper extremities and central portion of the head and neck (2,9,10), although they can occur anywhere on the body (11). In rare instances, the tumors may occur in the oral cavity, lip, tongue, palate, or external auditory canal (2,6,12–14). Neurothekeomas are not known to be associated with NF (1,2,6,9). Clinically, the lesions usually present as asymptomatic, solitary, slow-growing, skin-colored or translucent, dermal papules or nodules, measuring from 0.3 to 3.1 cm in diameter (2,6).

Cellular neurothekeomas occur in young adults with a preference for females. The forehead is the favored site. The lesions present as firm, red-brown papules or nodules, measuring from 0.5 to 3.0 cm in diameter (11).

Imaging

The literature on imaging of neurothekeoma is scarce. It has been reported that the tumor has well-defined margins, intermediate signal on T1WIs, high signal on

T2WIs, and heterogeneous mild to moderate gadolinium contrast enhancement (4,15–17). These findings are similar to those of soft tissue myxoma. The cellular neurothekeoma usually presents on CT as a well-defined expansile mass without invasion of adjacent tissue (18).

Macroscopy

Both myxoid and cellular neurothekeoma are solitary, well-circumscribed, multilobular lesions (11,19). No association with nerve is present. Myxoid neurothekeomas are gray-white and myxoid, whereas cellular neurothekeomas are gray-tan, rubbery, or hard (9).

Histopathology

The myxoid neurothekeoma is a lobulated, well-circumscribed tumor composed of predominantly spindle cells and occasionally epithelioid cells, frequently separated by collagen fibers septation and embedded in a copious myxoid matrix (Fig. 22A, B).

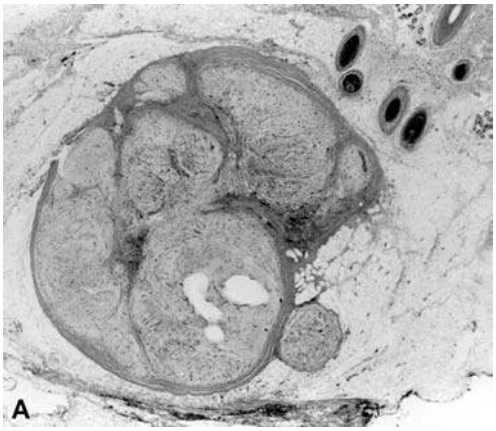

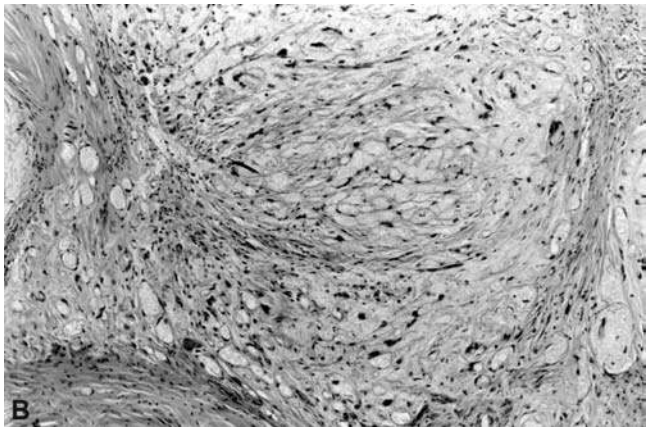

Figure 22 (**A**) The tumor is present in the reticular dermis and subcutis, and consists of well-circumscribed, multilobular, and myxoid and paucicellular tissue. The constituent lobules are demarcated by thin collagenous bands (H&E, 50×). (**B**) The tumor cells are spindle and stellate, and contain vacuolated cytoplasm, and are disposed in an abundant myxoid matrix (H&E, 100×). *Source*: Images courtesy of Dr. Jaffer Shabnum, The Mount Sinai School of Medicine, NY.

The latter matrix contains either hyaluronic (nonsulphated) acid or sulfated acid mucins (1,2,6). The spindle cells have an eosinophilic cytoplasm and ovoid nuclei with a vesicular chromatin pattern and inconspicuous nucleoli and may be arranged in nests and cords. Continuity with adjacent nerves is rarely noted (1,2,6,11). Occasional multinucleate cells may be seen. Scattered mitoses up to 8–10/10 HPF may be present (2,6) as well as mast cells.

The cellular neurothekeoma is composed of multiple, fairly well-circumscribed, highly cellular nodules partly separated by narrow collagenous bands. They may have an infiltrating pattern of growth among collagen bundles of the reticular dermis and occasionally extend into the subcutaneous tissue (20). The tumor cells are polygonal, or rarely plump and spindle-shaped, and arranged in a fascicular pattern. The cytoplasm is conspicuous and eosinophilic with rigid cytoplasmic processes and stippled chromatin pattern (5,11,20–23). As in the myxoid variant, low-grade cytological atypia and mitotic activity are common and, although worrisome, are not criteria for malignancy (20).

Ultrastructure

The spindled tumor cells in myxoid neurothekeoma have features supportive of Schwann cell origin, with folded, convoluted cytoplasmic membranes and basement-like material surrounding most cells (2,3,6, 10,11,24). The spindle cells contain variable amounts of rough endoplasmic reticulum, rounded mitochondria, and variable numbers of large membrane-bound vesicles, and these cells lack myofilaments, melanosomes, and tonofilaments (6).

Neoplastic cells of a cellular neurothekeoma contain well-developed, dilated, rough endoplasmic reticulum without basement membranes, findings suggestive of fibroblastic differentiation (11,25).

Immunohistochemistry

Myxoid neurothekeomas show a constant immunoreaction for S-100 protein, GFAP, low-affinity nerve growth factor receptor (NGFR), collagen type IV and vimentin, a variable reactivity for NSE, CD57, but no reaction for EMA (2,3,7–10,26). Cellular neurothekeomas differ from the myxoid variant in that they are usually negative for S-100 protein (5,20,23). They express collagen type IV, calponin, SMA, NK1/C3, and CD57 but generally not EMA, CK, desmin, NGFR, synaptophysin, GFAP, NSE, HMB45, CD34, or CD68 (7,8,20,22,27). PGP9.5 and S-100A6 are positive in both myxoid and cellular neurothekeomas (27,28). Positive reaction for histiocytic marker CD68 (KP1) and melanocytic marker microphthalmia transcription factor has also been reported (29,30).

Differential Diagnosis

Neurilemoma, neurofibroma, myxoma, leiomyoma, and fibrohistiocytic lesions lack the tumor cell nests and cords with distinct borders and the lobular growth typical of neurothekeoma. Furthermore, neurothekeomas

lack the palisading characteristics and alternating Antoni A and B areas of neurilemomas, and the eosinophilic neurofibrillary matrix and diffusely scattered small nerve twigs typical of neurofibromas. Myxoid neurothekeomas are distinguished from leiomyomas by their diffuse positivity for S-100 protein and absence of desmin positivity. The presence of S-100 protein positivity in neurothekeoma also excludes myxoma and fibrohistiocytic lesions. Neurothekeoma may be occasionally mistaken for a neuronevus on the basis of the nesting pattern. Junctional activity and melanin pigment are lacking, however, in all neurothekeomas (6). Ultrastructural examination of neurothekeomas may be used to demonstrate features supportive of Schwann cell origin in neurothekeomas, namely, basement membrane surrounding tumor cells and the lack of structures, such as myofilaments or melanosomes that would suggest a non-Schwann cell origin (6).

Treatment and Prognosis

Conservative, complete excision is the recommended treatment (19). In some instances, cryotherapy has been used to minimize local tissue loss (31). Both myxoid and cellular neurothekeomas behave in a benign fashion with no aggressive local growth or malignant transformation (2,6). Occasionally, they may recur after inadequate excision (2,26).

J. Perineurioma

Introduction

Perineurial cells form the outer cellular lining around the peripheral nerve fascicles and small nerves and represent the peripheral continuation of the meningeal cells in the pia-arachnoid membranes. Perineurioma encompasses a heterogeneous group of an uncommon benign tumor of perineurial cell differentiation without Schwann cell elements, and clinicopathologically can be divided into two types, i.e., intraneural perineurioma and extraneural soft tissue perineurioma (1–9). The extraneural group includes soft tissue (4,5,7,10), sclerosing (11), and reticular (6,9) variants. Tumors that show histopathological features of both perineurioma and schwannoma have also been reported (12).

Extraneural perineurioma was originally reported by Lazarus and Trombetta in 1978 on the basis of ultrastructural features of perineurial cells in a deep soft tissue tumor (1). Intraneural perineurioma is a rare lesion that was previously referred to as localized hypertrophic neuropathy, intraneural neurofibroma, and hypertrophic interstitial neuritis (13,14). There is a controversy regarding whether the intraneural perineurioma represents a neoplasm or reactive process because of repeated trauma. Reported findings such as substantial proliferative activity, occasional extensive permeation of nerve, frequent p53 expression, and clonal cytogenetic abnormalities support a neoplastic origin (2,15,8,16).

Although perineurioma is not known to be associated with NF, a case of a soft tissue perineurioma of the thigh in a patient with NF2 has been reported (17).

Clinical Features

Intraneural perineuriomas typically present in adolescence or early adulthood, with no gender predilection. Precedent history of trauma is not evident. The common manifestations include muscle weakness, which is progressive over months to years, localized muscle atrophy on physical examination, and denervation change on electromyography (18). One case of an intratemporal facial nerve perineurioma was associated with a history of gradual facial paresis of 15 years duration (18).

Soft tissue perineuriomas, including the reticular variant, commonly occur in middle-aged adults, with a mean age of 46 years, although the age range is wide (10–79 years) (5,6). There is a slight female predilection (5,10). Soft tissue perineuriomas usually present as solitary, painless superficial nodules in soft tissue of the lower extremities, upper extremities, and trunk (1,4–7,9,10). They have also been reported in the head and neck, including the neck, tongue, upper lip nostril, temple, mandible, and maxillary sinus (4,5,7,10,19).

Sclerosing perineurioma appears to be clinicopathologically different from the soft tissue variant in that there is a male gender predominance of 3:1. It commonly occurs in young adults, and sites of involvement are predominantly fingers and palms (11).

Imaging

Because of its rarity, reports of imaging findings are scarce. According to a case report of an intraneural perineurioma, high-resolution CT showed enlargement of the involved nerve, and MRI revealed strong gadolinium enhancement of the corresponding area (18).

Macroscopy

Intraneural perineuriomas show a symmetric and localized, cylindrical or tubular enlargement of the affected nerve with increased caliber. On opening the epineurium, the involved fascicles appear coarse and nodular and firm in texture (8). Most lesions measure 2 to 10 cm in length (20).

The soft tissue perineurioma is a well-circumscribed, solid, yellow to tan-white, nodular or lobulated tumor with firm or rubbery consistency (5,7,10). No encapsulation is present. The tumor ranges in size from 0.3 to 20 cm, although deep-seated tumors are larger than superficial ones (5). Some tumors may be gelatinous or myxoid on the cut surface. Hemorrhage, necrosis, and infarction are rare findings.

Histopathology

Intraneural perineurioma consists of innumerable expanded nerve fascicles surrounded by concentric, onion bulb–like spindled perineurial cell proliferation (8) (Fig. 23A). Mitoses are absent or exceedingly rare. A central degenerating axon and small amounts of Schwann cells remain in the core of each fascicle (20). A wide range of proliferative activity has been observed in these lesions, including nuclear labeling with an antibody to the proliferating cell nuclear

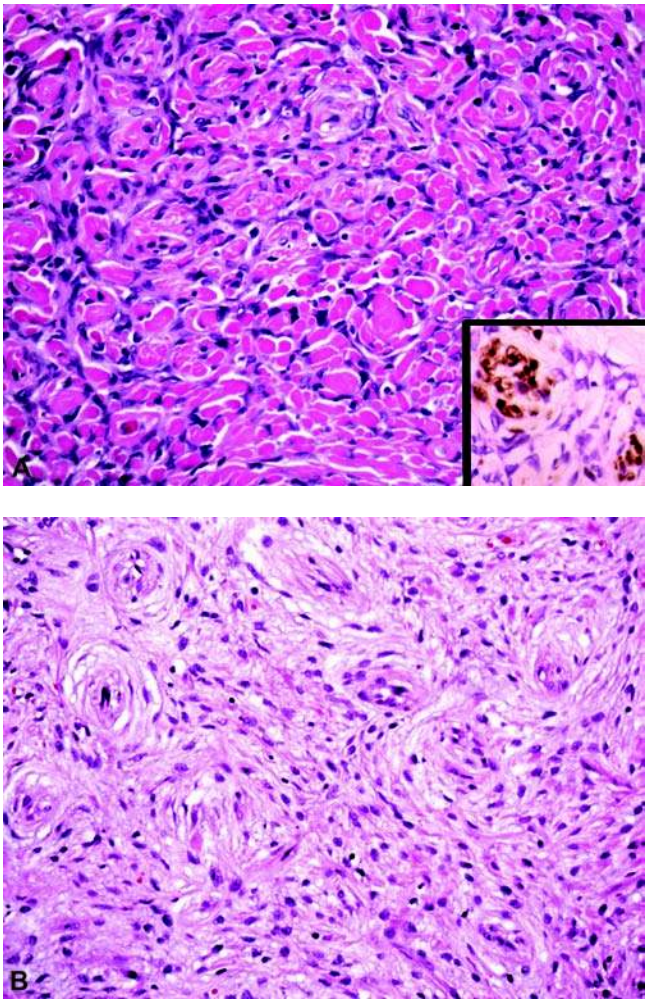

Figure 23 (**A**) Intraneural perineurioma is characterized by whorls of perineurial cells around nerve fibers, so-called pseudo-onion bulbs (H&E, 100×). EMA immunostain highlights Schwann cells (*inset*, 200×). (**B**) Bland-appearing spindle to plump cells showing the whorled arrangement (H&E, 100×).

antigen (PCNA) (mean 6%), MIB-1 (mean 7.4%), and the occasional expression of p53 (8).

The soft tissue perineurioma is composed of layers of remarkably elongated, slender, spindled-shaped cells arranged in a predominantly storiform and focally whorled architectural pattern, supported by a collagenous or myxoid stroma (Fig. 23B) (1,4,5,9). Focal areas of fascicular pattern are also commonly seen. The tumor is generally hypocellular, but hypercellular tumors or tumors with alternating hyper- and hypocellular areas also occur (5). The tumor cells have elongated, tapered, wavy nuclei, with inconspicuous nucleoli and long, delicate bipolar cytoplasmic processes. Soft tissue perineurioma may show worrisome cytological or architectural features such as scattered pleomorphic cells, marked cellularity, infarction, infiltrating growth, and mitotic figures up to 7/30 HPFs, but these are of no clinical significance (5). The reticular variant is characterized by lace-like or reticular growth pattern with delicate anastomosing and intersecting strands of cells that are set in a variably myxoid, fibrillary, or fibrous stroma (6). Cystic spaces are often present, containing fibrillary to myxoid material.

Ultrastructure

The intraneural perineurioma consists of two components, i.e., nonneoplastic axons and Scwann cells and neoplastic perineurial cells. The former component is surrounded by multiple layers of perineurial cells, which are separated by basement membrane substance and variable numbers of collagen fibrils (21,22).

The soft tissue perineurioma is composed of normal-appearing perineurial cells that are loosely organized in a myxoid or collagenous stroma (20). The tumor cells possess elongated nuclei with variably clumped, marginated chromatin, inconspicuous nucleoli, and thin, long polar cytoplasmic processes. The latter show scattered rudimentary intercellular junctions, prominent pinocytotic vesicles, sparse profiles of rough endoplasmic reticulum and intermediate filaments, and either absent or fragmented and variable basement membrane (1,3,7,10,11,23).

Immunohisochemistry

The tumor cells strongly express vimentin and EMA (Fig. 23A) and variably CD34 and lack reactivity with antibodies to S-100 protein, neurofilament protein, GFAP, desmin, and Leu-7 (4–6,10,11,15,24). Occasional immunoreaction to CK, smooth muscle actin, and claudin-1 can be seen (5,6). Tumor cells show a delicate membraneous staining pattern with EMA, laminin, and collagen type IV (11).

Somatic Genetics

A loss of chromosome 22q or the deletion of genetic material from 22q has been reported (25,26). Molecular analyses have demonstrated mutations in the NF2 gene (27,28).

Differential Diagnosis

Perineurioma is distinguished from other spindle cell tumors, such as neurofibromas, extracranial meningioma, solitary fibrous tumor, and dermatofibrosarcoma protuberans (DFSPs) not only by its immunophenotype but also by its characteristic ultrastructural features. These include the presence of intercellular junctional complexes, pinocytotic vesicles, and fragmented variable basement membrane and the lack of interdigitating cell processes (1,3,4,24). Unlike perineuriomas, neurofibromas are often cutaneous, may be associated with NF1, have a more heterogenous makeup and contain many S-100 protein-positive cells. Lack of S-100 protein and neurofilament staining in perineurioma excludes the presence of underlying nerves, especially axons or Schwann cells, both of which are common findings in neurofibroma (4). Meningiomas are also EMA-positive but are distinguished from perineurioma by the presence of

psammoma bodies, reactivity for S-100 protein, and the absence of pinocytotic vesicles on ultrastructural examination (4).

Solitary fibrous tumor is composed of bland ovoid to spindle cells with varying cellularity and a patternless pattern architecture, with ropy collagen and staghorn-like branching blood vessels, but it lacks a storiform pattern of growth and cytological features of perineurial cells. Given that solitary fibrous tumor expresses CD34 and occasionally EMA, immunohistochemistry alone may not distinguish the two entities.

When perineuriomas are cellular, they exhibit a focal storiform pattern or express CD34; the differential diagnosis includes DFSP. However, their circumscription, lack of diffuse infiltration of subcutaneous tissue, typical cellular features, and positive reaction to EMA can separate the two entities (4,5).

Treatment and Prognosis

Surgical excision is the treatment of choice. Two out of forty-three patients (5%) experienced a local recurrence in the largest series; one tumor was deep seated and the other was incompletely excised (5). Although the perienurial component and differentiation is not uncommonly seen in MPNST, perineuriomas are not known to develop malignant transformation (29).

K. Granular Cell Tumor

Introduction

GCT is a usually benign lesion of nerve sheath origin, affecting the skin, soft tissue, or mucosal sites of the upper aerodigestive tract (1–7). It was first described by Abrikossoff in 1926 (''Abrikossoff tumor'') and thought to be of primitive striated muscle origin, for which the term ''granular cell myoblastoma'' was originally proposed (1,8–10). In spite of the amount of research, the pathogenesis of the GCT is still not completely clarified. However, extensive enzyme histochemical, immunohistochemical, and ultrastructural studies have demonstrated strong evidence in support of a Schwann cell origin (11–26). More recently, genetic profiling of a GCT of the tongue demonstrated mutations in some genes related to neural alterations, also supporting a neural derivation (27).

Clinical Features

GCT is most frequently seen in the fourth to sixth decades of life (mean 38 years; range 11 months–68 years) but may occur at any age (2,28–36). It is, however, uncommon in children (28–36). It is more frequent in females by a 2:1 margin except for laryngeal GCT, which has an equal gender distribution. The tumor has been reported to occur in almost any part of the body, with a propensity to occur in the skin and subcutaneous tissue, mucous membranes of the aerodigestive tract, and breast (2,5,37–57). In a five-year review of the English literature (377 GCTs), the most common sites of origin were the subcutaneous tissue (32.6%), oral cavity (28.1%), breast (15.9%), larynx (7.6%), gastrointestinal tract (4.7%), and bronchus (3.4%) (37). The remaining involved the perineum (2.4%) and miscellaneous sites (2.9%). The head and neck is affected in 45% to 65% of GCTs and of these, 70% are located in the oral cavity (Fig. 24A–C). Common cutaneous sites in the head and neck include the forehead, nose, neck, and eyelids; the scalp is rarely involved. In the oral cavity, the tongue is the most common site, accounting for more than half of head and neck GCTs, followed by the buccal mucosa, lip, floor of the mouth, and palate (1). Other locations include the larynx, hypopharynx, oro-naso-parapharyngeal fossa, and thyroid (Fig. 25) (37,40–43,58,59).

Most GCTs are asymptomatic, solitary, smooth, firm, and painless and range in size from 1 to 5 cm, average 2 cm in diameter, often with a yellowish surface (Fig. 24A). Occasionally, GCT can present as Eagle syndrome with pain on swallowing, turning the head, or extending the tongue because of the tumor irritating the glossopharyngeal nerve (60). In 2% to 15% of cases, they may be multifocal, either synchronous or asynchronous (40,61–64).

GCT of the Larynx

Laryngeal GCT is usually seen in the third to fifth decades and has an average age of 35 years, similar to those occurring at other sites (3,4,38,39). In contrast to GCT at other sites, laryngeal GCT has no significant gender distribution, or they may be slightly more common in males (55%) (3,4). The true vocal cord is the most common site, especially the posterior one-third. The lesion is associated with slowly increasing hoarseness over a period of 2 to 10 months (3). In the series described by Compagno et al., the vocal cord was the most common site (20 cases), followed by the arytenoid (4 cases), false cord (2 cases), subglottis (2 cases), anterior commissure (2 cases), subglottis (2 cases), and postcricoid area (1 case); in five cases the exact site was not specified (3). Clinically, laryngeal GCT may be mistaken for vocal cord nodule, papilloma, or squamous carcinoma. The location on the posterior true cord, coupled with the relatively young age of patients with GCT (25–40 years), contrasts with squamous cell carcinoma, which preferentially involves the anterior half of the vocal cord and occurs in an older population (55–60 years of age or more). There is no known relation of GCT with smoking.

On examination, laryngeal GCT presents as a firm, polypoid, smooth granular papillary or cystic lesion that is often 1 cm or less in size, although it may be as large as 3 cm (3). Fixation of the vocal cord is absent. Microscopic characteristics of laryngeal GCT are similar to those described in the following discussion. Mild to severe pseudoepitheliomatous hyperplasia is often present in the overlying epithelium (65%) (3). Careful examination is necessary to distinguish from squamous cell carcinomas, since laryngeal biopsies tend to be superficial, and the potential for overdiagnosing pseudoepitheliomatous hyperplasia as squamous cell carcinoma is high. In general, pseudoepitheliomatous hyperplasia lacks nuclear atypia and pleomorphism.

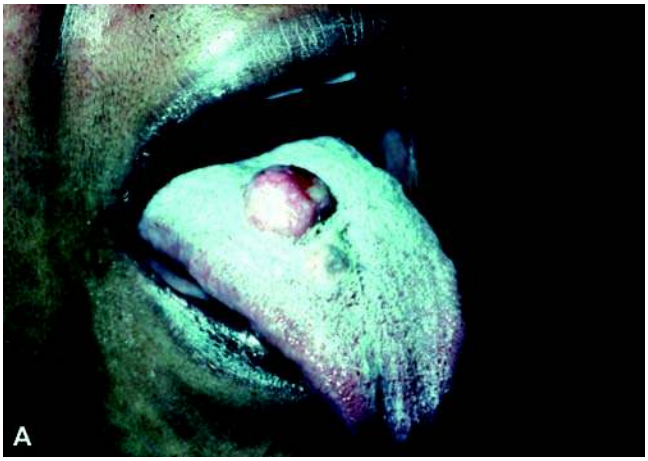

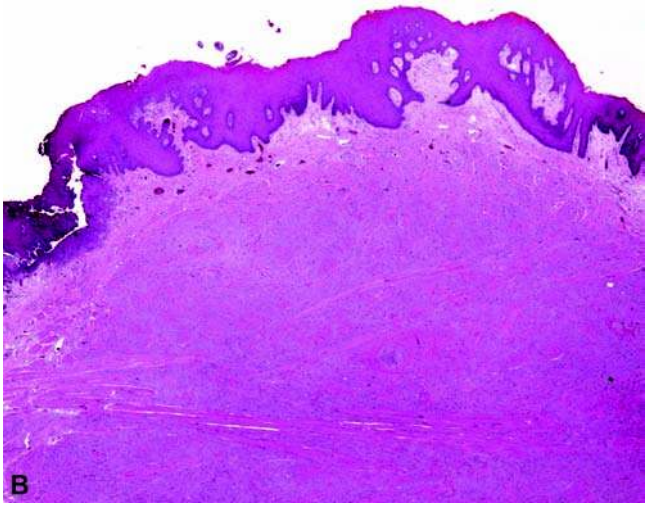

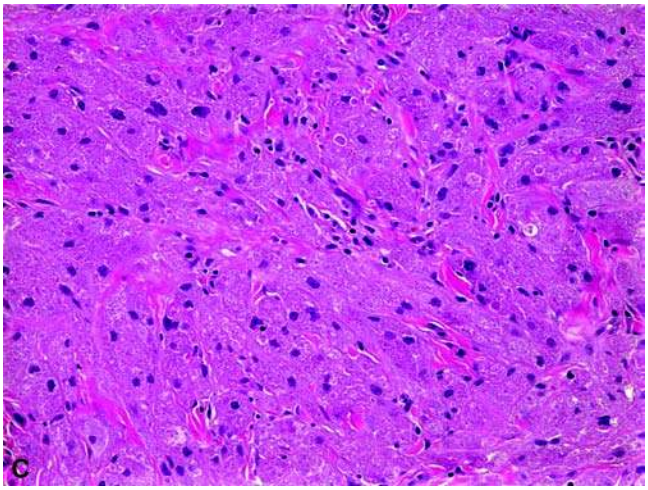

Figure 24 (**A**) A polypoid mucosal GCT of the tongue. *Source*: (A): Courtesy of Dr. M. Brandwein-Gensler, Montefiore Medical Center, New York. (**B**) Low magnification of a GCT tongue composed of diffuse sheets and lobules of eosinophilic cells. The overlying epithelium is mildly hyperlastic (H&E, 40×). (**C**) Higher magnification shows that the tumor cells are monotonous, plump to polyhedral cells with abundant granular eosinophilic cytoplasm, and indistinct cellular borders (H&E, 200×).

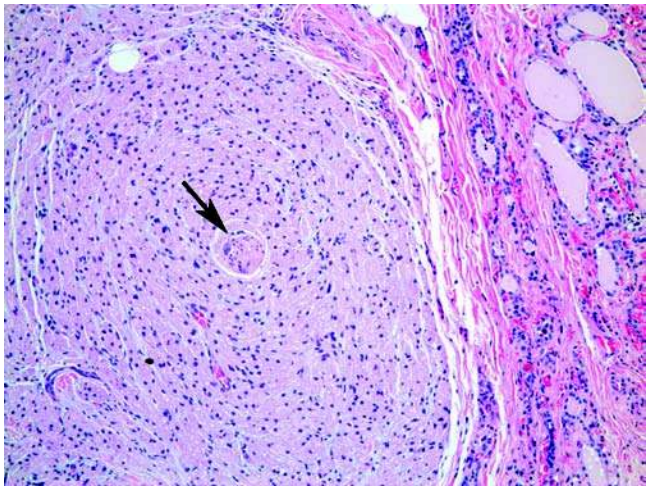

Figure 25 An intrathyroid GCT surrounding a bundle of nerve fibers (*arrow*), suggesting of Schwann cell origin (H&E, 150×).

GCT of the Tongue

About 23% of all GCTs and 81% of all oral GCTs occur in the tongue (37) (Fig. 24 A). GCTs of the tongue exhibit the same clinical and histological features as those at other sites (2,5,17,27,38–43) (Fig. 24 B–C). The most common location is the tip, followed by the dorsum, lateral border, base, and ventral surface of the tongue (2,5,37–42,65).

Pathology. On gross examination, GCTs range in size from 0.5 to 2.0 cm in diameters and are well circumscribed with a smooth, firm texture, often with no ulceration, as opposed to squamous cell carcinoma, which is often ulcerated. Histologically, GCTs are composed of large polyhedral or spindle-shaped granular cells, separated by collagen bundles, often ill defined with no obvious encapsulation. Tumor cells show acidophilic, granular cytoplasm, with poorly defined cytoplasmic borders imparting a syncytial growth pattern (Fig. 24 B–C) (2–7). The cytoplasmic granules are PAS-positive, diastase resistant, and range from being barely visible to the size of a red blood cell. The nuclei are small, central or eccentrically located, and moderately hyperchromatic, with little pleomorphism. Nucleoli are generally not prominent. Mitoses and necrosis are usually absent. The granular cells, however, may appear to ''invade'' nerve, but this feature has no significance and should not be interpreted as a sign of malignancy (2). Interstitial cells containing angulated or acicular cytoplasmic structures (angulate bodies) that are more PAS-positive than the cytoplasmic granules may be seen on close examinaiton. Pseudoepitheliomatous hyperplasia of the overlying squamous epithelium of different degrees may be seen with downward proliferation of epithelial cells, often with squamous pearl formation (3,4).

At the ultrastructural level, the small cytoplasmic granules appear as membrane-bound vesicles of Golgi origin, whereas the larger granules represent

phagolysosomes (11,12,14,18). The angulate bodies are oval membrane-enclosed structures formed by the deposition of fibrillar material within the endoplasmic reticulum. Histochemical analysis of the granules has shown the presence of glycolipid, a sialomucin-protein complex, or ribonucleic acid. Immunochemical studies have shown that the granular cells are positive for S-100 protein, peripheral nerve myelin proteins (P2 protein, PO protein, and Leu-7), HLA-DR, and vimentin and negative for desmin, actin, myoglobin, GFAP, and CK (13–18,20–26). This antigenic profile and tissue microarray genetic studies support a Schwann cell neural origin (27). One case of alleged GCT that was negative for S-100 protein has been described (66). The expression of HLA-DR by granular cells is believed to be unrelated to cellular origin, but rather, to some common immunological function (22). Expression of the macrophage-associated antigen CD68 (with monoclonal antibodies KP1, Ki-M1P, or PG-M1), cathepsin B, and α1-antitrypsin and α1-antichymotrypsin in tumor cells is related to the presence of lysosomes in the neoplastic cells and does not imply a macrophage differentiation (58–71). Immunoactivity for Ki-67 shows low proliferative activity (less than 2%). Bcl-2 is positive for majority of tumor cells, a molecule that functions as a survival factor (65,72).

Differential Diagnosis. The most important differential diagnosis of the GCT is a well-differentiated squamous cell carcinoma; others include benign muscle tumors, e.g., adult rhabdomyoma (A-RM) and, less frequently, xanthoma and other nonneural tumors that also have a granular cytoplasm (2–4,73–76).

The characteristic overlying pseudoepitheliomatous hyperplasia in a GCT may mimic a squamous cell carcinoma when a biopsy is superficial (3,4). However in GCT, the epithelial cells of the pseudoepitheliomatous hyperplasia lack cytological pleomorphism and nuclear atypia, and its epithelial tongues do not extend beyond the confines of the subjacent granular cell lesion. Although rare, bona fide examples of coexistent squamous cell carcinoma and GCT may occur, but usually in noncontiguous sites (77).

Because of its abundant eosinophilic granular cytoplasm (76), A-RM may be confused with GCT. However, the tumor cells in GCT have a syncytial growth pattern, whereas in A-RM the cells have well-delineated cell borders. Furthermore, the neoplastic cells in GCT lack the glycogen-rich cytoplasm, cross striations, vacuoles (spider cells), and crystal-like structures seen in A-RM. In GCT, the tumor cells are PAS-positive, diastase resistant, while in A-RM the glycogen-rich cytoplasm is PAS-positive, diastase sensitive. Unlike A-RM, which shows strong positivity of tumor cells for muscle markers (actin, myoglobin, and desmin) and occasionally weak S-100 positivity, most GCTs show strong, diffuse positivity for S-100 protein and are negative for muscle markers. Ultrastructurally, tumor cells in GCT are rich in cytoplasmic and phagolysosomes, whereas A-RM contains myofilaments, Z-bands, and glycogen granules. GCT may also be confused with a congenital epulis (CE) (see discussion in sec. V.K.4, ''Congenital Epulis'').

Treatment and Prognosis. Complete surgical excision is the option for treatment. Most patients are cured after a total excision of the mass. Recurrence may occur (10%), usually following inadequate excision (32). If small in size, laser surgery is useful with no consequent complications or recurrence (78).

Malignant GCT

Introduction. Although the vast majority of GCTs are benign, a few are malignant or even borderline malignant (atypical GCT) (31,44,79–92).

Malignant variants, however, are exceedingly rare, representing only about 1% to 2% of all GCTs. As of 1998, less than 90 malignant GCTs were recorded in the literature (91).

Clinical Features. Malignant GCTs occur over a broad age range (30–82 years; median about 40 years) and are two to three times more common in females (79,91).

The most common sites of occurrence are the arm, leg, and chest wall. Only 4% to 18% of all malignant GCTs occur in the head and neck, including the eyelid, larynx, buccal mucosa, tongue, and neck (85,91).

Pathology. Malignant GCTs grossly resemble their benign counterparts and have ranged in size from 0.5 to 17 cm, with median of about 4 cm (79–91).

In the past, the only accepted criterion of malignancy was metastasis. Fanburg-Smith et al. studied a series of 73 GCTs and divided them into malignant ($N = 46$), atypical ($N = 21$), and benign-multicentric ($N = 6$), using the following six criteria: (*i*) necrosis, (*ii*) spindling of the tumor cells, (*iii*) vesicular nuclei, (*iv*) increased mitotic rate (>2 mitoses/10 HPFs), (*v*) high nuclear-to-cytoplasmic ratio, and (*vi*) pleomorphism (91). If a tumor met three or more of these six criteria, it was called malignant; if it fulfilled one or two criteria, it was classified as atypical; and if it had none of these criteria or only focal pleomorphism, it was called benign.

Differential Diagnosis. Tumors that may be confused with malignant GCT include metastatic carcinoma, PGL, alveolar soft part sarcoma, and malignant muscle tumors. Malignant GCT is characterized by its eosinophilic and uniformly granular cytoplasm; absence of a rich vascular, endocrine, or organoid pattern, as in PGL or alveolar soft part sarcoma; and absence of rhabdomyoblasts or cytoplasmic glycogen (2). Immunohistochemically, GCT is distinguished from other neoplasms by its characteristically positivity for S-100 protein, NSE, and CD68 and lack of reactivity with EMA, CKs, chromogranin, and desmin (91).

Treatment and Prognosis. Surgery is the treatment of choice. Radiation is not effective. Malignant GCTs are aggressive, high-grade sarcomas (79,85,91). In the series of Fanburg-Smith, 11 of 28 (39%) patients with histologically malignant tumors (see ''Pathology'' for criteria of malignancy) with follow-up died at a median interval of three years; 8 of 28 (29%) were alive with disease at a median interval of two years; and 9 of 28 (32%) were disease free at a median follow-up of seven years. Local recurrence developed

in 32% and metastases in 50% (lymph nodes, lung, bone) (91).

As for the atypical GCT, Fanburg-Smith et al. followed up on 9 of their 21 cases and, of these, five (56%) developed local recurrence from one to eight years after diagnosis, but none developed metastasis or died of disease (91).

Immunostaining for proliferative activity (Ki-67) and p53 may have some prognostic value. Fanburgh-Smith et al. noted that 2 of 16 atypical GCTs had Ki-67 values of 10% and 20%; the remainder were 5% or less. Immunostaining for p53 (>50% of cells) was found in 4 of 18 (22%) atypical GCTs; the remaining 14 were regative for p53. Fourteen of twenty-five (56%) malignant GCTs had Ki-67 immunostaining in 10% to 50% of cells; in the remainder, less than 10% of cells were positive. In more than 50% of the cellular population, p53 was seen in 17 of 25 (68%) malignant GCTs (91). Adverse prognostic factors include malignant histological features, large size, local recurrence, metastasis, presence of necrosis, increased mitotic rate, older age, and status of p53 and Ki-67 values (91).

Congenital Epulis (Gingival GCT of the Newborn)

CE is a rare lesion that bears a remarkable histological resemblance of GCT (93–105). The histogenesis of CE is unknown (2). Despite its preference for the alveolar ridge, there is little support for an odontogenic origin. The theory of a primitive or undifferentiated mesenchymal cell origin is favored on the basis of ultrastructural and immunophenotypic analysis (95,96,103). It has been suggested that the tumor cells represent early mesodermal cells that express pericytic and myofibroblastic features that undergo cytoplasmic autophagocytosis (95).

Clinical Features. CE presents at or immediately after birth as a single, smooth or multilobulated, pink, nonulcerated tumor that varies in size from a few millimeters to 4 to 5 cm. It has a characteristic location on the labial aspect of the dental ridge and is three times more common in the upper jaws (2). It is attached to the gingiva in the incisor area by a slender pedicle or a broad sessile stalk. It is more common in females (90%), and 10% of the lesions are multiple (2).

Pathology. CE shows a similar histology to GCT but differs in that it has a prominent vascularity, especially at the pedicle, presence of scattered odontogenic epithelium, and strong phosphatase activity of cells (2). Unlike adult GCT, there is no pseudoepitheliomatous hyperplasia, and nerve bundles are less conspicuous. Ultrastructurally, membrane-bound granules or phagolysosomes are present in the cytoplasm, many of which contain collagen precursors (95), but angulate bodies are absent (93,98–102).

Immunohistochemistry. Immunophenotype shows absence of reactivity with S-100 protein in contrast to GCT, which is uniformly S-100 protein-positive, consistent with its nerve sheath origin (93,94,99,104). Similar to GCT, CE also demonstrates reactivity for macrophage markers (CD68 and Ki-MIP) (94).

Differential Diagnosis. Despite a morphological resemblance to GCT at other sites, CE is distinguished from GCT by its characteristic age of onset in infants, anatomical site on the labial alveolar ridge, female predominance, absence of pseudoepitheliomatous hyperplasia and nerve bundles on histological examination, and lack of immunoreactivity with S-100 protein.

Treatment and Prognosis. Complete surgical excision is the recommended treatment. None, however, have recurred, even after incomplete excision. Dentition is rarely impaired.

VI. MENINGIOMA

A. Introduction

Meningiomas are tumors that originate from the meningothelial arachnoidal cells, which are normally found in arachnoid villi of the meninges surrounding the brain and spinal cord (1–5). Meningiomas account for up to 30% of all primary intracranial tumors (4,6,7) and for 25% of intraspinal neoplasms (4,6). They are histologically classified according to the recommendation of the World Health Organization (WHO) (Table 6). Most meningiomas are benign lesions of WHO grade I, although some meningioma variants correspond to WHO grades II and III and are associated with a higher risk of recurrence and shorter survival times (7). Ionizing radiation is a known risk factor for intracranial meningiomas. The role of head trauma and hormonal status (endogenous and exogenous estrogens and progestins) is less certain (4,6).

B. Clinical Features

The peak age of patients with intracranial meningioma is about 45 years with a distinct female preponderance of 3:1 (1–5,16–18). Preferential sites correspond to the location of arachnoid villi from which they arise. These include the parasagittal area along the dural sinuses, lateral cerebral convexities, sphenoid ridge, cranial nerves foramina, and within the trunks or perineural sheaths of cranial nerves adjacent to the basal foramina. Symptoms and signs depend on the size and location of the masses and may be related to increased intracranial pressure or focal brain dysfunction. These include headaches, nausea, vomiting, papilledema, numbness, weakness, incoordination, focal seizures, focal neurological deficits, and visual impairment.

Table 6 Current WHO Classification of Meningiomas

- Meningioma, low grade (meningothelial, fibroblastic, transitional, psammomatous, angiomatous, microcystic, secretory, lymphoplasmacytic, metaplastic variants) (WHO grade I)
- Atypical meningioma (WHO grade II)
- Clear cell meningioma (WHO grade II)
- Chordoid meningioma (WHO grade II)
- Anaplastic meningioma (WHO grade III)
- Papillary meningioma (WHO grade III)
- Rhabdoid meningioma (WHO grade III)

Abbreviation: WHO, World Health Organization.

Meningiomas are usually solitary, although they may be multiple. Multiple meningiomas or those occurring in children or adults younger than 30 years should raise the suspicion of NF2 (16,17). Meningiomas are generally slow-growing tumors that compress rather than invade neural tissue. However, invasion of adjacent dural venous sinuses, bone, soft tissue, and muscle is sometimes seen *and* does not warrant a higher grade. However, surgical excision is more difficult when they occur. Most importantly, brain invasion is a significant finding that has a critical value in grading meningiomas. Brain invasion is defined as a breach of the pia. Perivascular extension along the Virchow-Robin spaces are of less value and does not really qualify as brain invasion.

Meningiomas exhibiting brain invasion should be considered atypical, regardless of their otherwise benign histology. Most meningiomas develop within the neuraxis; however, in 20% of patients extracranial extension secondarily involves the orbit, outer table of the calvarium, skull base, middle ear, sinonasal tract, or parapharyngeal space. In rare instances, extracranial meningiomas may be primary at these sites (18–41). Primary extracranial meningiomas are defined as those that are not connected to a meningioma arising from the neuraxis (25–28).

Orbital meningiomas arising from the optic nerve sheath are rare and represent 1% to 2% of all meningiomas (29,30). After gliomas, these are the second-most common optic nerve tumor. They occur predominantly in middle-aged women. The tumors are most often unilateral, although they may be bilateral in 5% of cases (23,29). Symptoms include visual loss, and there may be atrophy of the optic nerve. Eventually, these slow-growing neoplasms progress to blindness on the affected side.

Primary meningiomas of the paranasal sinuses or midline scalp may arise from heterotopic meningeal tissues displaced during closure of midline structures during fetal development. Sinonasal meningiomas are slow growing and may have been present for many years before presentation (26,28,31,32). Their histological features and biological behavior are similar to those of intracranial meningiomas, although patients tend to be younger males. Symptoms include progressive exophthalmos, nasal obstruction, and epistaxis.

Temporal bone and middle ear meningiomas occur as primary tumors or as extensions of intracranial posterior or middle cranial fossa tumors (33,39). Extension to these sites may occur through the tegmen tympani, medial aspect of the pyramid, jugular foramen, or internal auditory meatus (39). Meningiomas are the second-most common lesion encountered within the cerebellopontine angle (40) and rarely project into or originate from the internal auditory meatus (41). It is important to distinguish between meningiomas and acoustic neuromas preoperatively, as the choice of surgical approach may differ, depending on the tumor type. The facial, trigeminal, and acoustic nerves are susceptible as they exit through the skull base. Symptoms include deafness and tinnitus, headache, vertigo, otalgia, or facial paresis. On physical examination, a mass may be noted behind an intact tympanic membrane, or granulation tissue may be seen protruding through a perforated tympanic membrane. Raised intracranial pressure, cerebellar compression, and brain stem involvement are late signs. Carotid angiography helps distinguish clinically between a PGL and meningioma.

Parapharyngeal meningiomas may represent extracranial extension of a primary intracranial mass, tumor arising in the jugular foramen, tumor originating from arachnoidal cell clusters within the trunk or perineural sheath of cranial nerves near a neural foramen, or metastasis to cervical lymph nodes from primary intracranial meningioma (42).

C. Imaging

Imaging studies, especially CT and MRI scans (Fig. 26A–C), have proved useful in the diagnosis and management of meningiomas, e.g., in demonstrating dural sinus involvement (43,44). Some studies have attempted to examine the relationship between MRI and histopathological features in intracranial meningiomas. While tumor signals on T1WIs are found to be similar regardless of the histological subtype of the tumors, on T2WI a relationship between signals and tumor types are seen. Hypointense meningiomas are mainly fibroblastic, and hyperintense tumors are mainly syncytial, angioblastic, and partly transitional. Isointense tumors are mainly transitional, partly fibroblastic, and syncytial (45). Meningiomas are often accompanied by perifocal brain edema (46). Cystic meningiomas may show enhancement of the cyst wall (47).

D. Pathology

On gross examination, meningiomas generally appear well—demarcated; smooth or lobulated; and firm and gray-white, tan, or pink (Fig. 27A, B). Meningiomas encompass a broad spectrum of histological variants (Table 6) (2,5,48). Three basic patterns are recognized that allow ready identification of a lesion as a meningioma: (*i*) syncytial or meningothelial type, characterized by whorls and lobules of meningothelial cells with pale pink cytoplasm and indistinct cell borders, some of which appear empty owing to intranuclear cytoplasmic inclusions (Fig. 28A–D); (*ii*) fibroblastic type, characterized by interwoven fascicles of spindle-shaped meningocytes and collagen fibers; and (*iii*) transitional type, characterized by structural features of meningothelial and fibroblastic types (biphasic). These patterns have no prognostic significance. In contrast, important histological features used to grade meningiomas include brain invasion, the presence of frequent mitoses, and foci of spontaneous or geographic necrosis in the absence of preoperative embolization (49–51). However, it has not been determined what constitutes histological evidence of anaplasia or whether brain invasion alone warrants a diagnosis of malignancy (49–51). Meningiomas are considered grade I tumors when mitotic figures are rare or absent (48). ''Atypical'' meningiomas correspond to grade II,

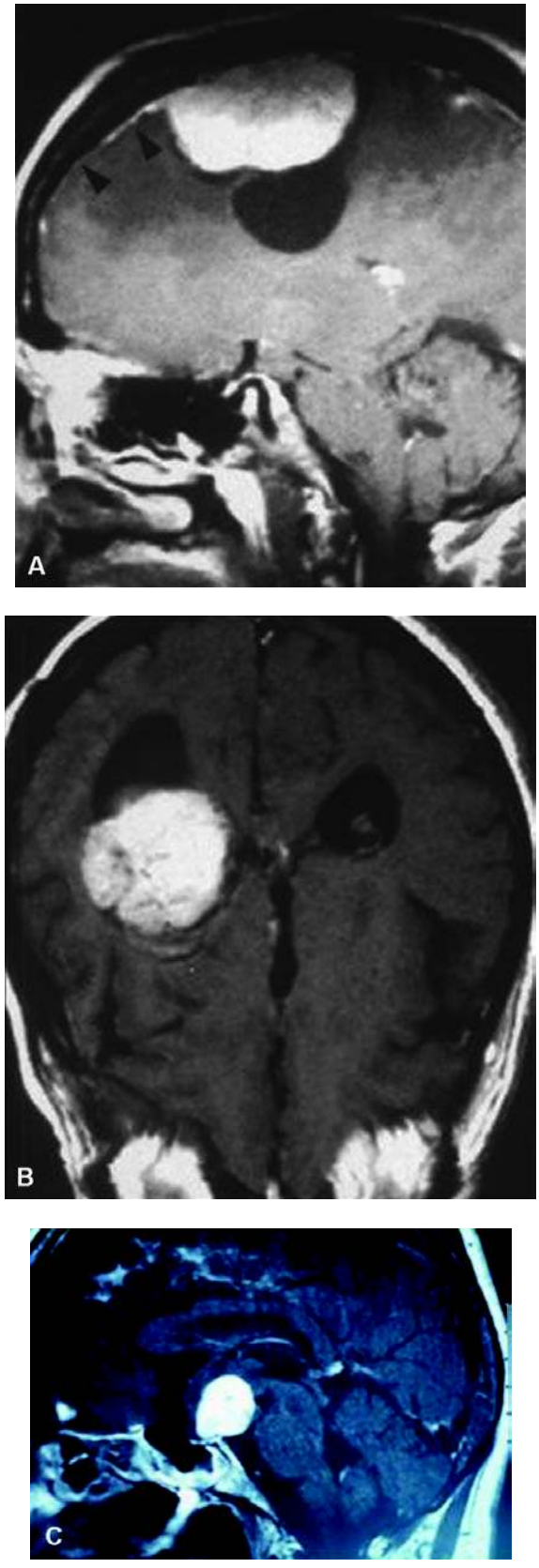

Figure 26 MRI appearances of conventional meningioma. (**A**) Convexity meningioma. (**B**) Intraventricular meningioma. (**C**) Base of the skull meningioma.

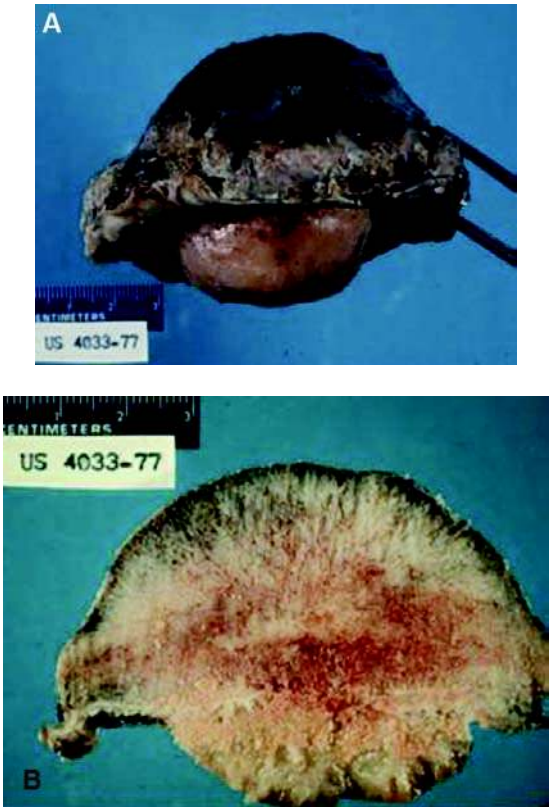

Figure 27 (**A**) Gross specimen showing the meningioma permeating the thickness of the skull. (**B**) Note the growth of the tumor both within and outside the cranial cavity.

and anaplastic meningiomas correspond to grade III tumors. Sheeting (loss of the normal whorling and/or fascicular growth pattern) and macronucleoli have also been associated with more aggressive meningiomas.

Many meningiomas may contain psammoma bodies or calcospherites (Fig. 28B). At times the psammoma bodies may be present in large numbers when the tumor is described as being ''psammomatous.'' Bone invasion is often seen. In addition, the WHO recognizes other variants, including angiomatous, microcystic, secretory (showing glandular metaplasia with acini containing PAS-positive pseudopsammoma bodies) (Fig. 29A–D), chordoid (52) (Fig. 30A–C), lymphoplasmacytic-rich lipomatous (53), and metaplastic types (3,48,54).

A few subtypes have been recognized as more aggressive forms of meningiomas. The intermediate and high-grade (II and III) examples are more aggressive. These include the clear cell and rhabdoid meningiomas (Fig. 31A, B). Clear cell meningiomas show no sex predilection, affect primarily the lumbar region and cerebellopontine angle, and despite their benign appearance, may be aggressive, particularly in intracranial examples (55). They are composed of sheets of clear, glycogen-rich, polygonal cells, forming only a few vague whorls. Hyalinization, both stromal and perivascular, is usually extensive. Mitoses are rare.

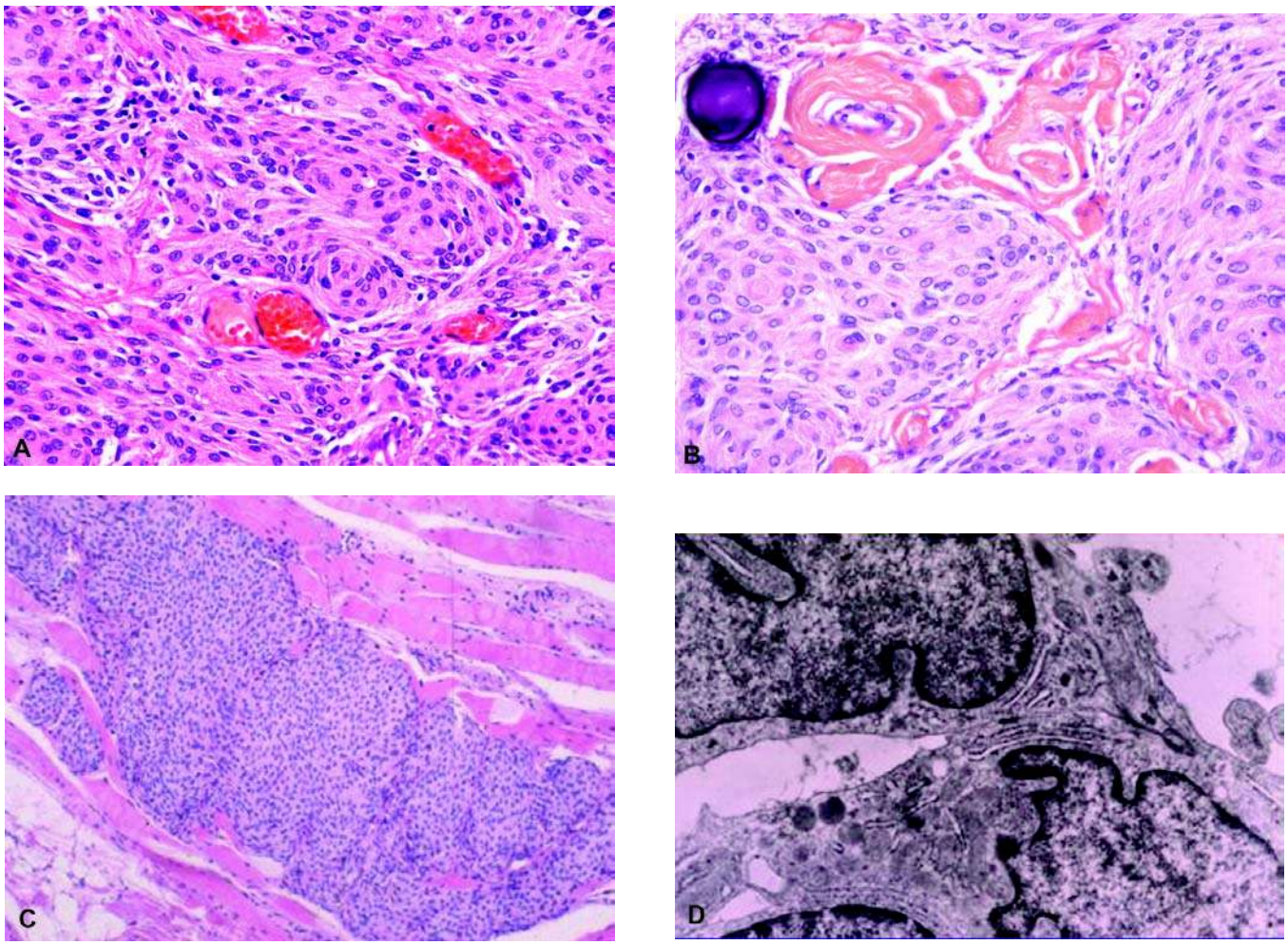

Figure 28 (**A**) H&E appearance showing the typical whorling pattern of meningothelial cells. (**B**) A laminated psammoma body (calcospherite) is seen. (**C**) Meningioma can grow in the temporalis muscle. (**D**) Ultrastructural analysis shows the typical tight junctions between tumor cells. (**A**,**C**: H&E, 100×, **B**: 200×, **D**: 1800×).

Immunohistochemistry has shown vimentin and EMA staining to be reactive in 100%. Stains for S-100 protein and CAM 5.2 are negative. Ultrastructural study shows abundant cytoplasmic glycogen, a few cytoplasmic lumina, intermediate filaments, interdigitation of cell membranes, and desmosomal junctions. The MIB-1 antigen labeling indices are variable (55).

Rhabdoid meningiomas (56,57) (Fig. 31A, B) are associated with a poor prognosis. Rhabdoid morphology is defined as sheets of loosely cohesive cells with eccentric nuclei and hyaline, paranuclear inclusions. Ultrastructurally, the latter consisted of whorls of intermediate filaments often entrapping lysosomes or other organelles. At the histological level, a conventional meningioma component is noted in most tumors. In many tumors areas of meningothelial or fibroblastic meningiomas show transition to cell groups of the rhabdoid type. In some cases, however, only rhabdoid cells are seen. Brain invasion and/or anaplasia are observed in many cases, and extracranial metastasis has been reported. In the majority, increased cell proliferation is evidenced by a high mitotic rate or an MIB-1 labeling index (LI). Many patients with rhabdoid meningiomas have recurrences, and some die from their disease. Thus, the phenotype of rhabdoid morphology is associated with aggressive biological and clinical behavior.

E. Malignant Meningiomas

Malignant meningiomas are rare and account for less than 2% of all meningiomas. Malignant meningiomas are defined by the presence of metastasis and increased number of mitotic figures (>6/10 HPF) (51) or a frankly anaplastic histology (Fig. 32).

Most of the malignant meningiomas have a high MIB-1 (Ki67) index. Among malignant meningiomas papillary meningiomas are an exceptional variant of meningioma, with high frequency in children, increased incidence of local recurrence, and potential for distant metastasis. Papillary meningiomas accounts for 1.0% to 2.5% of all meningiomas (54,58,59) and are seen in a variety of sites (58,59). They are defined by the presence of a perivascular or pseudopapillary pattern

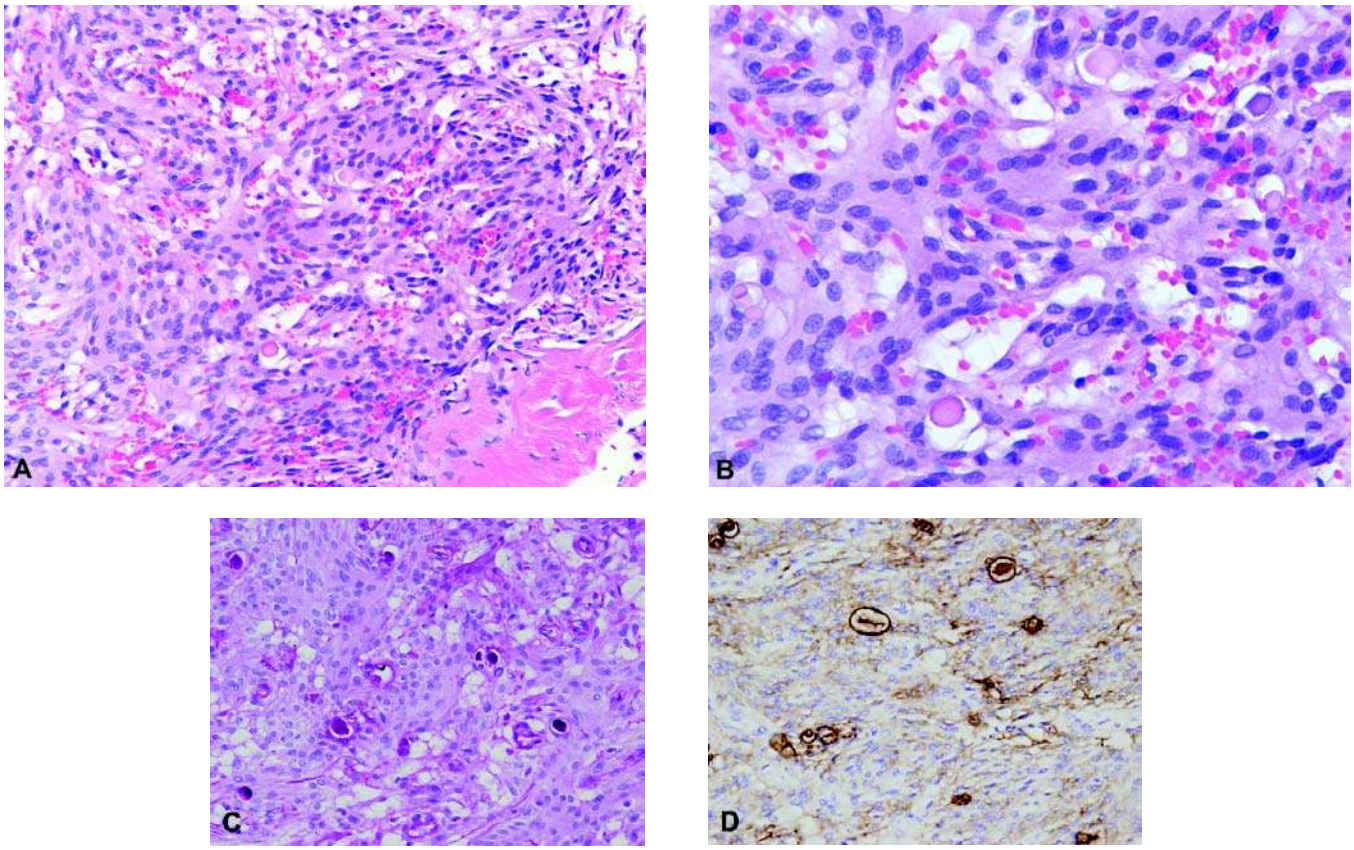

Figure 29 Secretory meningioma. (**A**,**B**) H&E stains reveal eosonophilic pseudo-psammoma bodies. **(C)** These are strongly stained by a PAS stain, (**D**) and by EMA immunostain. (**A**,**C**,**D**: H&E, 100×; **B**: 200×).

entirely or more commonly in combination with other common histological patterns of meningiomas. The tumors often show mitotic activity and bone and brain invasion. Lung is the most frequent site of extracranial metastasis. The five-year survival rate for papillary meningiomas is about 40% (58,59). Although the definition of malignant meningioma has been problematic, there is a general agreement that the presence of grossly apparent brain invasion and metastasis (cerebrospinal or extracranial) are indicators of a more aggressive biological behavior in these tumors. Meningeal sarcomas do not belong to the meningioma group and are considered grade IV lesions (Fig. 32).

F. Immunohistochemical

Immunohistochemical and electron microscopic studies show that meningiomas exhibit dual epithelial and mesenchymal differentiation (60–64). Meningiomas show immunoreactivity to EMA, vimentin, CK, and even for S-100 protein (60–63) (Fig. 29D, 30A–C). Ultrastructural study shows intermediate filaments, interdigitating of cell processes, and desmosomal intracellular junctions (Fig. 28D). Sex steroid assays in meningiomas have shown high levels of progesterone receptors (PRs) in some cases (65–68). High levels of PRs in a small group of histologically aggressive meningiomas suggested that hormonal therapy might be useful in this difficult subset of patients. However, an inverse relationship between immunoreactivity for PR with tumor grade and risk of recurrence was also reported (69). About a third of meningiomas show cytoplasmic and membranous expression of epidermal growth factor receptor (70). No difference in EGF-R reactivity between typical and aggressive meningiomas exists (70).

G. Somatic Genetics

Current data indicate that meningioma initiation is closely linked to the inactivation of one or more members of the highly conserved protein 4.1 superfamily, including the NF2 gene product merlin, protein 4.IB (DAL-1), and protein 4.1R. Mutations in the NF2 gene and loss of chromosome 22q are the most common genetic alterations associated with meningiomas. Some have also suggested a correlation between NF2 loss and histological types; e.g., the difference in NF2 gene expression between meningothelial and nonmeningothelial meningiomas has been found to be statistically significant (8). DAL-1 (differentially expressed in adenocarcinoma of the lung) located on chromosome 18p11.3 is lost in 60% of sporadic meningiomas. NF2 and DAL-1 losses are early events in meningioma tumorigenesis, suggesting that these two protein 4.1 family members are important in the

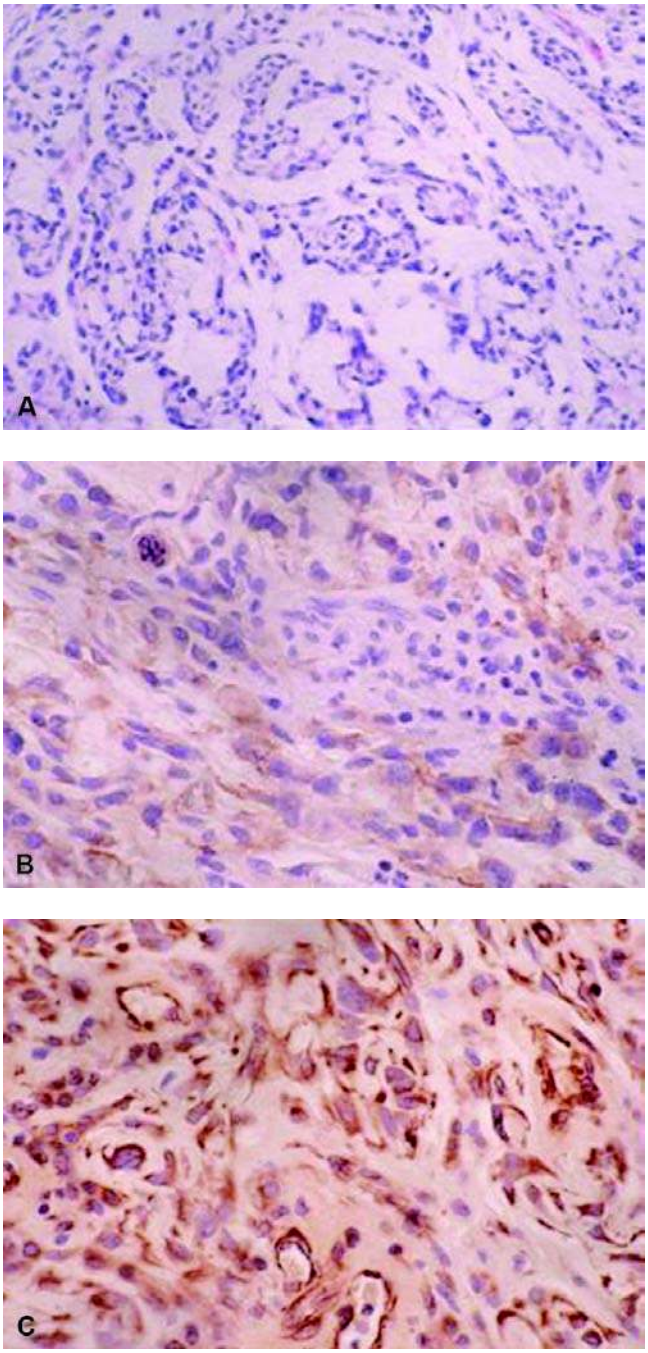

Figure 30 Chordoid mengioma. **(A)** The tumor cells form cords and are often embedded in a myxoid matrix. The tumor cells are strongly positive for **(B)** epithelial membrane antigen and **(C)** vimentin. (**A**: H&E 100×; **B**,**C**: 200×).

pathogenesis of meningiomas (9). With increase in tumor grade, additional progression-associated molecular aberrations can be found (7). These include losses on 1p, 6q, 10, 14q, and 18q as well as gains on multiple chromosomes. Even more complex genetic alterations, including frequent alteration of the CDKN2A, p14ARF, and CDKN2B tumor suppressor genes at 9p21 as well as gene amplification on 17q23 and chromosome 9p21 deletions, have all been

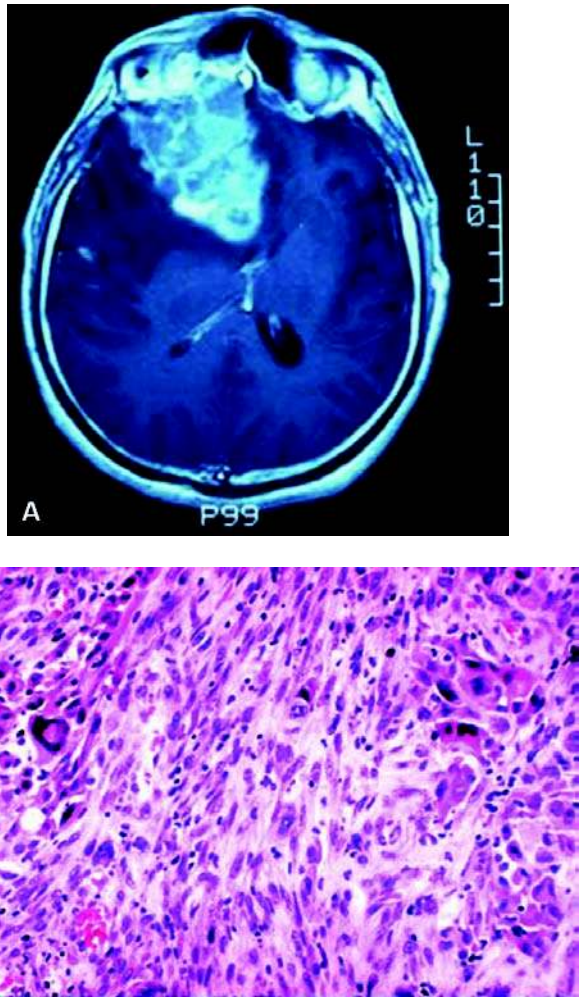

Figure 31 Rhabdoid meningioma. (**A**) MRI shows an ill-defined enhancing mass. (**B**) The tumor shows atypia and mitotic figures. (**B**: H&E, 100×).

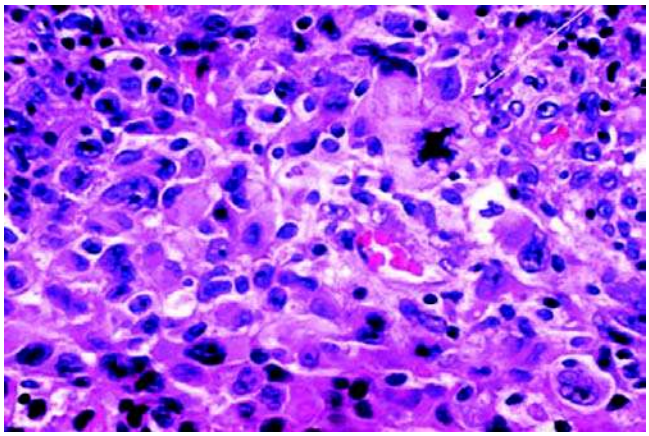

Figure 32 Meningeal sarcoma has abundant matrix and often displays atypical mitotic figures. (H&E, 250×).

described in aggressive meningioma (10–12). Despite all of these observations, many meningiomas have normal karyotype (13–15).

H. Differential Diagnosis

Although most meningiomas are readily diagnosed, the histological and immunophenotypic diversity can present difficult problems in the differential diagnosis of primary and metastatic brain tumors, especially on small biopsies. The differential diagnosis of meningiomas can be quite diverse, given the numerous histological appearances. In addition, the differential diagnosis may vary depending on the anatomical site involved. There is now general agreement based on ultrastructural and immunohistochemical characteristics that meningeal hemangiopericytoma is a separate lesion, with a metastatic potential similar to soft tissue hemangiopericytomas, rather than a variant of meningioma (71,72).

Thus, it is important to be aware of the differential diagnosis with hemangiopericytomas. Meningeal hemangiopericytomas can be distinguished from meningioma by their closely packed spindled cells having round to oval nuclei, scant cytoplasm, and a highly vascularized stroma with reticulin fibers surrounding individual tumor cells on special stains (3,63). However, anaplastic meningiomas and meningeal hemangiopericytomas can display significant morphological and immunohistochemical overlap (73). For example, hemangiopericytomas display occasional focal EMA positivity, and both hemangiopericytomas and anaplastic meningiomas can show focal CAM 5.2 expression. Hemangiopericytomas are characterized by high cellularity, branching (''staghorn'') vessels, immunoreactivity for CD34, and pericellular reticulin deposition.

However, hemangiopericytomas often show strong CD99 and Bcl-2 immunoreactivity, while anaplastic meningiomas show strong EMA but weak or focal CD99 and Bcl-2 immunoreactivity (73).

The presence of S-100 protein positivity may make the distinction of the meningothelial variant or pigmented meningioma difficult, especially from schwannomas and malignant melanoma. Immunostaining with a combination of S-100 protein and the melanocytic marker HMB45 will confirm the histological diagnosis of most melanomas; however, not all melanomas are immunopositive with HMB45.

The fibroblastic type of meningioma may be mistaken for a benign nerve sheath tumor (schwannoma or neurofibroma), fibroma, fibrosarcoma, solitary fibrous tumor or benign and malignant fibrohistiocytic neoplasms. Microcystic meningiomas can mimic pilocytic astrocytomas. The secretory and papillary variants are easily mistaken for adenocarcinoma. The differential diagnoses of a papillary meningioma include metastatic papillary adenocarcinoma, which is EMA- and CK-positive but vimentin-negative and papillary ependymoma, which is GFAP-positive. Anti-CD34 immunoreactivity is seen in solitary fibrous tumors, and anti-GFAP reacts in astrocytic tumors. Other tumors like choroids plexus papilloma may sometimes cause diagnostic confusion with papillary meningiomas. Reactivity for CK in meningiomas could also lead to a misdiagnosis of metastatic carcinoma, and the clear cell (glycogen-rich) types of meningioma may be confused with renal cell carcinoma. The chordoid variant of meningioma may be mistaken for chordoma and metaplastic variant for chondroid chordoma and mesenchymal chondrosarcoma or even osteosarcoma. The psammomatous type of meningioma may rarely be confused with a psammomatous ossifying fibroma; however, close examination reveals focal whorls of meningothelial cells in meningiomas, with a dual pattern of staining for vimentin and EMA.

On small biopsies, sinonasal meningiomas may be confused with olfactory neuroblastoma (ONB). However, the latter can be excluded by demonstrating pseudorosettes and a neurofibrillary stroma and positivity for the neuroendocrine markers synaptophysin or chromogranin. Furthermore, unlike meningioma, ONB is negative for EMA. Middle ear meningiomas may present as granulation tissue protruding through a perforated tympanic membrane and may be mistaken for PGL (''glomus tumor''), benign nerve sheath tumor, or chronic otitis media. Some meningiomas of the middle ear may histologically mimic the Zellballen pattern of a PGL. However, unlike meningioma, PGLs are positive for neuroendocrine markers, such as NSE, synaptophysin, and chromogranin.

Cutaneous meningiomas of the scalp should be differentiated from hamartomas of the scalp containing ectopic meningothelial elements (74,75). Meningiomas are composed entirely of meningothelial elements and are true neoplasms, with a potential for aggressive behavior. In contrast, meningothelial hamartomas are developmental abnormalities, composed of abnormal collections of connective tissue (vascular, adipose, and fibrous) elements intimately associated with meningiothelial cells and anastomosing vascular channels and lack any potential for aggressive behavior.

I. Treatment and Prognosis

The two most powerful prognostic factors are histological grade and extent of surgical resection. Depending on the site of involvement, surgical excision may be attempted, following imaging studies to precisely assess the extension and the relation of the tumor to surrounding structures. Management of orbital tumors is conservative, with surgery reserved for patients with blindness or severe proptosis. Meningiomas usually do not respond well to irradiation, and the use of this modality in other inoperable lesions is controversial (76). Most tumors are totally resectable (75% of cases). Meningiomas are slow-growing neoplasms and behave in a clinically benign fashion (6). The vast majority (80% or more) of surgically resected meningiomas are histologically benign and not associated with increased mortality.

However, even with seemingly complete surgical gross removal, 10% to 20% of meningiomas recur over the following 20 years, some after a prolonged period (6,77). After surgery alone, the 10-year recurrence rate is 25% in patients who had GTR and 61% in those who had less than GTR (78). This

emphasizes the need for long-term follow-up. In addition, it is now apparent that brain invasion is a critical factor for tumor recurrence. However, although local tissue invasion by intracranial meningiomas may be a sign of aggressive behavior, this finding by itself does not indicate a malignant meningioma (49). The biological behavior of meningioma is highly variable, and its correlation with microscopic features alone is not precise (79,80). Signs of clinically aggressive behavior, such as invasion, recurrence, and even metastasis, may not be associated with cytological atypia or anaplasia (2–4,78). It is often difficult to predict which of the meningiomas will behave aggressively. However, aggressive behavior may be anticipated when ''atypical'' histological features such as tumor necrosis (in the absence of preoperative embolization), increased mitotic figures (>4/10 HPF), and brain invasion are present (3,49,51). In some tumors, these atypical features are usually present at diagnosis, but in a small proportion of ordinary meningiomas, they may be observed at the time of recurrence (78,79).

Because histological features do not adequately or completely predict the biological behavior of meningiomas, several studies have attempted to elucidate the proliferative potential of these tumors (81–90). These methods include DNA content by digital cell image analysis, flow cytometry, bromodeoxyuridine (BrdU) uptake, S-phase fraction, or MIB-1 (Ki-67). Flow cytometry indicates that about 40% of meningiomas are aneuploid (86). The measurement of proliferation index may prove valuable in indicating biological aggressiveness (82–84). Meningiomas with an LI of greater than 1% as measured by BrdU labeling appeared to grow faster and recur more frequently than those with labeling indices of less than 1% (82–84). Proliferation rate in meningiomas, using the monoclonal antibody Ki-67, show less than 1% of proliferating cells in meningiomas without atypical histological features, whereas anaplastic types, and recurrent tumors, have increased scores up to 20% (88,89). Similarly, higher mitotic index and Ki-67 LI and PR negativity are predictive factors of recurrence of benign (WHO I), completely resected meningiomas, particularly when Bcl-2 positivity is associated (90). These findings suggest that DNA ploidy and immunohistological labeling of proliferating cells may have a prognostic value in predicting the biological potential of these tumors (82–84,88,89). Overall independent predicting risk factors for tumor recurrence include (*i*) brain invasion, (*ii*) mitotic index, (*iii*) subtotal tumor resection, and (*iv*) MIB-1 LI (91).

VII. PITUITARY ADENOMA

A. Introduction

The pituitary gland (hypophysis) is of dual embryological origin (1–4). The anterior lobe or adenohypophysis develops from an ectodermal invagination of the stomodeum anterior to the buccopharyngeal membrane, the Rathke's pouch. The posterior lobe or neurohypophysis is of neuroectodermal origin and develops from a downward extension of the diencephalon, the infundibulum. The Rathke's pouch epithelium appears eventually, loses its connection with the oral cavity, migrates dorsally through the tissue that subsequently becomes the sphenoid, and unites with the infundibulum to form the definitive gland in the area of the sella turcica (1–4). During its migration, small islands of primite anterior lobe tissue from the Rathke's pouch frequently become sequestered and persist in sites such as the sphenoid bone, wall of the pharynx, or in the sella turcica outside the capsule of the pituitary.

The remnant of pituitary tissue ranges from 0.2 to 9.6 mm in size and is most often found in the midline mucoperiosteum of the nasopharynx near the vomerosphenoid articulation; hence, it is referred to as the ''pharyngeal hypophysis'' (5–7). The pharyngeal pituitary has been observed to contain immunoreactivity for the anterior pituitary hormones (8). These include the adrenocorticotropic hormone (ACTH; corticotrophin), follicle-stimulating hormone (FSH), luteinizing hormone (LH), growth hormone (GH), prolactin (PRL), and thyrotropic hormone (TSH). Its ability to respond to feedback mechanisms is controversial. Although ectopic pituitary tissue usually shows little growth potential after birth, there are documented cases of true ectopic pituitary adenomas that arise in the pharyngeal pituitary or sphenoid in the presence of a normal pituitary gland (9–14). Except in pregnancy, which is associated with PRL cell hyperplasia, the normal adult pituitary gland weighs 400 to 900 mg, with a transverse measurement of 13 mm (3).

B. Clinical Features

Pituitary adenomas are benign epithelial tumors of the anterior pituitary. They account for approximately 10% of all intracranial tumors (15–18). Pituitary adenomas are divided according to size into microadenomas (those <10 mm) and macroadenomas (those ≥10 mm) (Fig. 33). Symptoms may be related to the local pressure of the tumor on adjacent structures, such as optic nerves, optic chiasma, cavernous sinus, or brain, which may result in visual disturbances, cranial nerve compromise, nausea, headache, and increased intracranial pressure. Other symptoms may be due to endocrine disturbances, including hypersection of pituitary hormones or compression of the residual normal gland or abnormal levels of target gland hormones. For example, acromegaly or gigantism may be due to hypersecretion of GH production; amenorrhea, galactorrhea, or impotence caused by hypersecretion of PRL; and Cushing's disease caused hypersecretion of ACTH. Pituitary adenomas, particularly prolactinomas, are frequently the initial manifestation in familial syndromes such as MEN I and Carney complex (19,20).

Preoperative evaluation of patients with pituitary adenomas should include assessment of serum hormonal abnormalities. About 60% to 75% of pituitary adenomas are clinically hormone producing and the remaining 25% to 40% are nonfunctioning, also referred to as ''nonsecretory or null cell'' (21–24). Most of the nonfunctional adenomas are large. They often

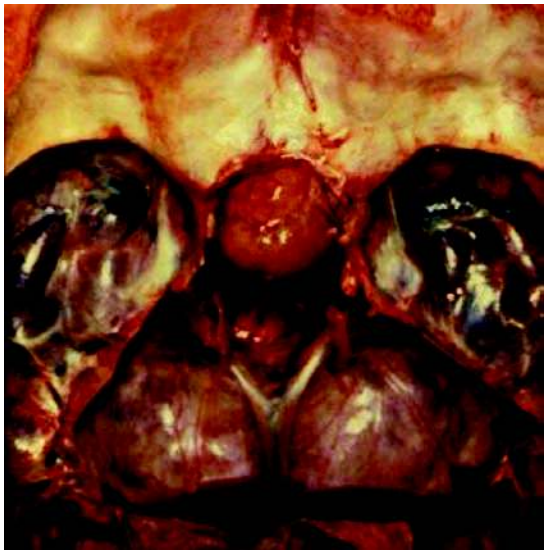

Figure 33 Incidental pituitary adenoma discovered at time of postmortem examination.

grow beyond the confines of the sella and compress the adjacent cellular structures, such as the optic chiasma, hypothalamus, and third ventricle. Rarely, they grow to a very large size and are referred to as giant pituitary adenomas (25).

Most pituitary adenomas remain intrasellar and are noninvasive; however, they may occasionally penetrate the pituitary capsule and extend beyond the sella turcica to infiltrate adjacent soft tissue or bony structures (26–40). They may invade by direct extension through dura and bone into the cranial cavity, cavernous sinuses, nasopharynx, cranial nerves, nasal cavity, and paranasal sinuses (26–40). Extension of tumor to the cavernous sinuses and along dural planes produces cranial neuropathies and facial neuralgia, which are characteristic presenting signs of invasive pituitary adenoma. Invasive pituitary adenomas have a biological behavior in between that of noninvasive pituitary adenomas and pituitary carcinoma. The presence of local invasion by pituitary tumors may be defined by imaging, studies at surgery, or on histological examination (41,42). The mere presence of local invasion by a pituitary adenoma, although a sign of local aggressive behavior, is not sufficient to designate a pituitary tumor as a carcinoma. By definition, a pituitary neoplasm is considered to be a pituitary carcinoma only when there is metastasis of the tumor to a noncontiguous focus in the brain or outside the CNS (43–61).

C. Imaging

CT and MRI (Fig. 34A–C) are essential in the preoperative evaluation of patients with pituitary adenomas for assessment of tumor size, shape, location in the sellar region, as well as ectopic sites, degrees of invasiveness, and extent of tumor (41,42). For example, MRI analysis

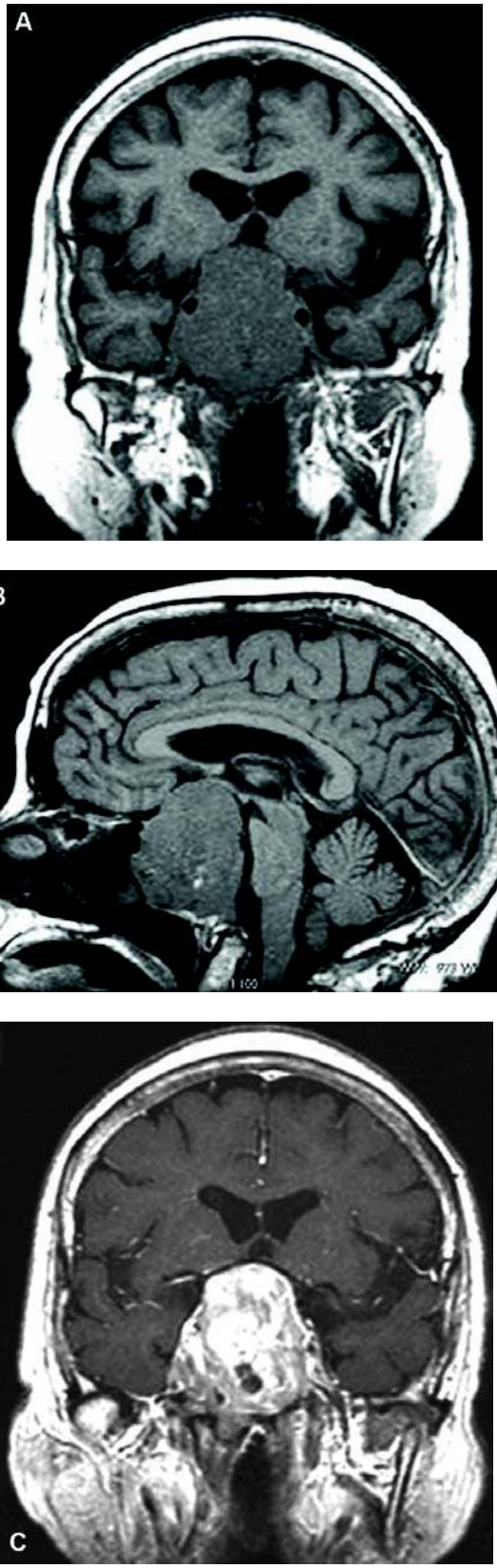

Figure 34 **A**,**B**,**C**: MRI appearance of a macroadenoma. (**A**) (Coronal) and (**B**) (Sagital). (**C**) The tumor shows a marked enhancement.

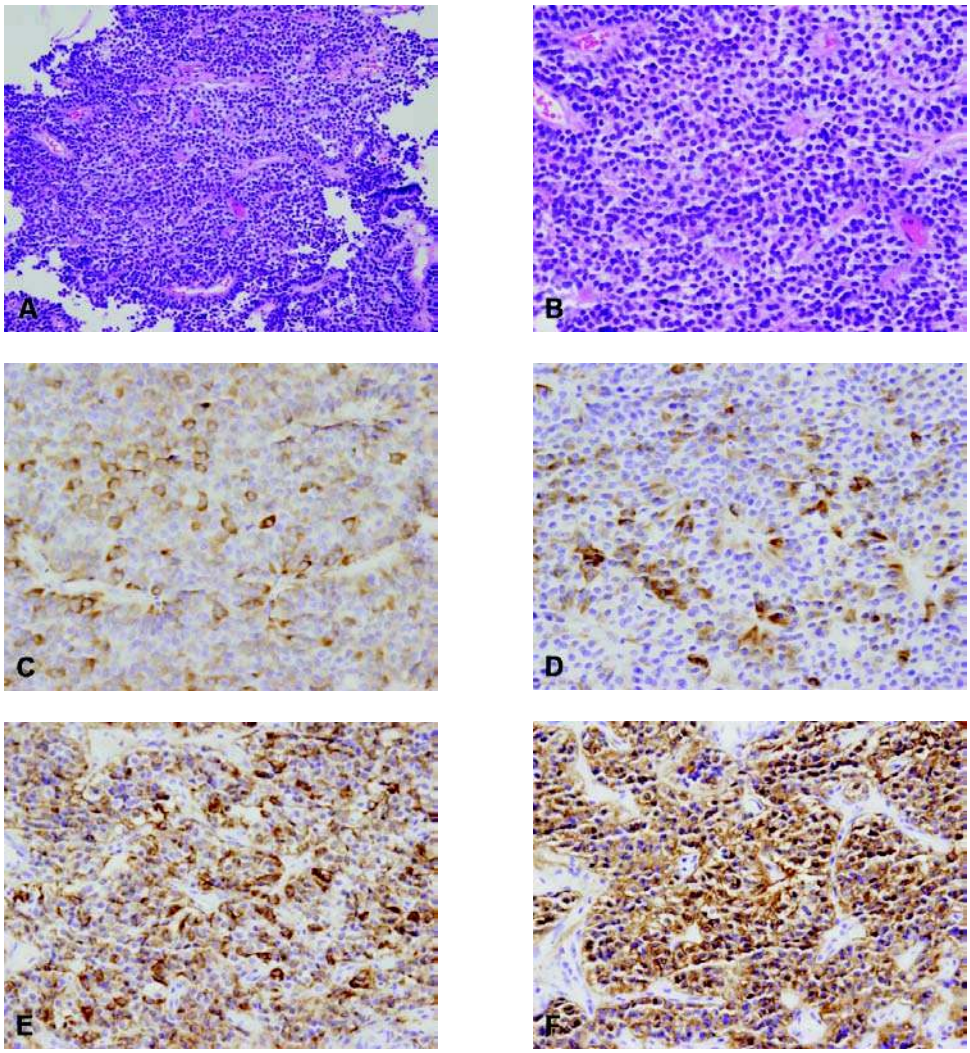

Figure 35 (**A**) H&E appearance of a typical pituitary adenoma displaying a diffuse small, round-cell infiltrate with cells arranged in suggesting a neuroendocrine pattern (**A**: H&E, 50×). (**B**) Note the perivascular distribution of the tumor cells (**B**: H&E, 200×). (**C**) The tumor cells are strongly immunoreactive for FSH, (**D**) LH (**E**) and TSH, and (**F**) Chromogranin. *Abbreviations*: FSH, follicle-stimulating hormone; LH, luteinizing hormone; TSH, thyrotropic hormone.

is important to determine if invasion of the cavernous sinus is present. An MRI sign that can predict its absence is the presence of normal pituitary gland between the adenoma and the cavernous sinus (62). Because of its higher resolution, 3-tesla MRI is superior to standard MRI for the delineation of parasellar anatomy and tumor invasion of the cavernous sinus (63). Skull films, CT scans, and MRI in individuals with invasive pituitary adenomas may show destruction of the sella and erosion of the body and wings of the sphenoid bone. A connection between the sellar and extrasellar tumor can often be demonstrated. In ectopic pituitary adenoma, MRI demonstrates a soft tissue mass isotense with gray matter onT1WIs, which enhances in a heterogenous manner (41,42). MRI is also very useful in the investigation of pituitary macroadenomas. For example, some studies have suggested that diffusion-weighted images can provide information about the consistency of macroadenomas (64). By contrast, imaging studies can have a limited impact in microadenomas, e.g., corticotropin-secreting tumors. These lesions are usually very small, located in the more central portions of the adenohypophysis, and often with signal intensity and enhancement characteristics similar to the normal pituitary parenchyma (65). Some studies have proned the use of delayed MRI 30 to 40 minutes after contrast injection to show late prominent enhancement of adenoma against a relatively dark background of the normal gland (66).

D. Pathology

The normal anterior pituitary is composed histologically of a variety of cell types (acidophilic, basophilic, and chromophobic) arranged in an acinar pattern. Reticulin stains show a fiber network that delineates

the acinar structures. In hyperplasia of the pituitary, the acinar structures are enlarged but preserved, and the reticulin fiber network is present even though distorted. By contrast, an absent or disrupted and irregular reticulin fiber network is seen in pituitary adenomas. Adenomas display a variable neuroendocrine growth pattern that is of no biological or prognostic importance that may be diffuse, papillary, trabecular, or sinusoidal (Fig. 35A, B) (15–18). Histochemical stains detecting acidophilic, basophilic, and chromophobic cells do not accurately reflect the specific hormones produced by these cells. For example, adenomas composed of acidophilic cells typically produce GH, but may produce PRL or be null-cell adenomas.

Therefore, the old tinctorial terminology applied to these cells has been replaced and the cells are now referred to by the specific hormones they produce. Most, but not all, pituitary adenomas are of one cell type and show uniform staining of the neoplastic cells. The presence of hormone production in pituitary adenomas can be confirmed by performing immunohistochemical stains using antisera to PRL, GH, LH, FSH, TSH, or ACTH (3,15,19) (Fig. 35C–E). The functional status of pituitary adenomas can be assessed not only by hormonal assays and immunohistochemistry but also by in situ hybridization (ISH) on routinely processed tissue sections (67). For example, ISH has shown the biphenotypic nature of some adenoma cells by demonstrating the production of two separate hormones within the same tumor cells, e.g., PRL and GH mRNA (67).

Several histological, immunohistochemical, and electron microscopic studies have provided abundant data about the complexity of many pituitary adenomas. For example, conclusive evidence exists regarding the marked diversity of GH-secreting adenomas. There are adenomas that secrete GH in excess, such as densely and sparsely granulated GH cell adenoma, while the mixed GH-PRL cell adenoma and the mammosomatotrope adenoma produce GH and PRL simultaneously. Densely granulated GH cell tumors may produce thyrotropin and alpha subunit as well (68). A variety of other combinations have been reported including coexpression of ACTH and PRL (69).

Among the pituitary adenomas that are hormonally active, prolactinomas are by far the most common and are usually located in lateral aspects of the adenohypophysis. Prolactinomas typically occur in young women presenting with amenorrhea and galactorrhea. A solid correlation between the PRL blood levels and MRI exists. A PRL concentration greater than 200 ng/mL practically guarantees adenoma detection, whereas with concentration less than 50 ng/mL, positive imaging findings are found in less than 50% of cases (65).

Most nonfunctioning adenomas are chromophobic and some are oncocytic on hematoxylin and eosin (H&E) stain, but here again the tinctorial property of tumor cells is not reliable in predicting the presence or type of hormone produced. The diagnosis of null-cell adenoma, which shows no immunoreactivity for anterior pituitary hormones, should be confirmed by showing immunoreactivity with general neuroendocrine markers (Fig. 36), including chromogranin A (Fig. 35F), synaptophysin, and NSE, and glutaraldehyde-fixed tissue should be submitted for ultrastructural examination for the demonstration of neurosecretory granules (Fig. 36).

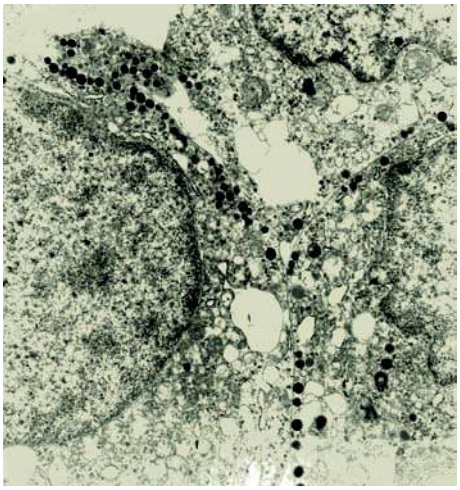

Figure 36 Ultrastructural analysis shows tumor cells containing many dense core granules.

Beside immunostains for pituitary hormones, others markers have proved to be helpful. For example, the study pattern of CK isotypes in subtypes of pituitary adenomas shows that different types of adenomas have different CK 7/20 profiles. For example, corticotrophs and sparsely granulated GH-positive adenomas are consistently CK 20–positive and CK 7–negative, whereas all other subtypes were almost always CK 20–negative (70).

The frequency of gross invasion in pituitary adenomas varies to some extent with the type of hormone produced (71). The estimated rate of gross invasion of dura and bone by pituitary adenomas of all types is 35% but ranges from 21% to 82% (71). Invasive pituitary adenomas display different growth patterns, including diffuse, papillary or trabecular, and sinusoidal types. More importantly, recurrences after therapy are more common with invasive adenomas compared with noninvasive tumors. The diagnosis of resection margins in pituitary adenomas is difficult, as these tumors may have well or poorly defined boarders.

Extrasellar adenomas presenting as tumors in head and neck sites such as the nasopharynx or nasal cavities are rare (9,14,26–40). Most present in these sites by growing through the floor of the sella into the sphenoid sinus and then protrude into the nasopharynx or nasal cavity, causing obstruction. On rare occasion, the ectopic adenoma may be associated with a normal anterior pituitary. In these cases, the pharyngeal pituitary may give rise to the tumor (9). Ectopic tumors are histologically similar to the usual

pituitary adenomas. Biopsies are frequently small and distorted; therefore, a high index of suspicion, together with knowledge of the clinical history, physical findings, and laboratory data are essential for diagnosis of extracellular tumors.

Mixed pituitary adenomas and intrasellar gangliocytomas have also been described (72–82). Tumors with both adenomatous and gangliocytic elements are rare (76).

E. Differential Diagnosis

The differential diagnosis of pituitary tumors, especially those that are nonfunctioning, includes other tumors that occur at the sellar region or at extrasellar sites (83). These include chordoma, craniopharyngioma, plasmacytoma, lymphoma, meningioma, germinoma, carcinomas, or sarcomas of the skull base, and rarely benign and malignant salivary gland like tumors of the sellar region, presumed to arise from salivary tissue (83–86). Frozen-section diagnosis may help distinguish pituitary adenoma from other tumors; however, the diagnosis may be difficult, either because of the small size of the biopsy, technical quality of the preparation, or presence of necrosis, fibrosis, or granulation tissue (87,88). Advantages of the intraoperative touch preparations over frozen sections include rapidity, better cytological detail without freezing artifacts, and preservation of the tissue for permanent histological sections, immunostaining, and electron microscopy (17,87,88). Clinicopathological and radiological correlation as well as ultrastructural or immunohistochemicals study for the presence of secretory products in pituitary adenomas may be necessary for a definitive diagnosis and to distinguish pituitary adenomas from these other neoplasms, especially in biopsies from extrasellar sites (83–86). In addition to the pituitary hormones, stains such asNSE, chromogranin, and synaptophysin are useful as general markers for neuroendocrine cells, including those of the adenohypophysis (85).

F. Treatment and Prognosis

The management of pituitary adenomas is variable. For most tumors, other than prolactinomas, transsphenoidal resection remains the mainstay of treatment. It is an effective and safe treatment for most patients with pituitary adenoma and could be considered the first-choice therapy in all cases except for prolactinomas responsive to dopamine agonists (89). Since hypothalamic secretion of dopamine inhibits PRL secretion, a dopamine agonist, such as bromocriptine, may be used for the medical management of prolactinomas (3). Although bromocriptine suppresses PRL synthesis and secretion in most patients with macroprolactinoma, most patients need long-term therapy, and additional modes of therapy including surgical resection may be necessary. The normal PRL level in men and nonlactating females is less than 25 ng/mL. Values over 200 ng/mL are usually associated with PRL-producing pituitary tumors. Selected patients with small, incidentally discovered microadenomas may be carefully followed without immediate therapy. Asymptomatic patients with microprolactinomas may be followed without medical intervention. In those with significant symptoms, such as headache, galactorrhea, or hypogonadism, bromocriptine therapy is indicated. In most patients, treatment results in reduction in serum PRL, tumor size, and galactorrhea. The PRL level returns to normal range in 50% of patients. Because the recurrence rate after surgery varies from 25% to 75% at five years, adjunctive therapy is necessary when the postoperative level of PRL rises.

Interestingly, parasellar extension of macroprolactinomas, assessed on the basis of strict MRI criteria, may predict a negative response to dopamine therapy. The responsiveness of noninvasive macroprolactinomas (over 90%) is similar to that reported in microprolactinomas, whereas invasive tumors are resistant to treatment in more than 50% of cases (90).

Dopamine agonist medications are effective as a first-line therapy for invasive giant prolactinomas because they can significantly shrink tumor volume and control the PRL level. Tumor mass vanishes in some patients after bromocriptine treatment. Thus patients with PRL-secreting microadenomas may be treated either with transsphenoidal surgery or medically with dopamine agonists. However, in patients with macroadenomas, even in the presence of chiasmatic syndrome, dopamine agonists are often proposed as primary treatment. Indeed, effects on visual disturbances are often very rapid (within a few hours or days) and tumoral shrinkage is usually very significant. In other patients with localized residual tumor, stereotactic radiosurgery is a viable option (91). Less invasive modalities, such as endoscopic transsphenoidal surgery, and stereotactic radiosurgery have shown promise as primary and adjuvant treatment modalities, respectively (92,93). Some combine intraoperative endoscopy and intraoperative MRI as an effective surgical modality for pituitary surgery (94).

Thus treatment of pituitary adenomas consists of surgery (performed in more than 99% of cases via a transphenoidal route) and radiotherapy (95), generally fractionated or, in selected cases, using stereotactic techniques such as gamma-knife, are indicated for inoperable cases or persistent disease (3,94). However, the availability of medical treatment (dopamine, agonists, somatostatin analogs, GH-receptor antagonists) has profoundly modified the indications of radiotherapy; drugs may be used as a second-line treatment, after surgery (or even as first-line treatment). Somatostatin analogs, now available in slow release form, are proposed when surgery is contraindicated or has failed to normalize GH levels.

The somatostatin analogue octreotide is more potent in suppressing GH secretion and tumor size in 75% of patients with GH-producing adenomas, but only 35% have normalization of GH levels after treatment. Preoperative octreotide therapy may improve resectability and overall cure rates. Cyproheptadine, a serotonin antagonist, is partially effective in some patients with Cushing's disease. Transphenoidal surgical resection is the primary management of

TSH-secreting adenomas and gonadotropin-secreting adenomas.

Because histological features are not reliable predictors of tumor recurrences or invasiveness, several authors have performed studies for the detection of the proliferative activity using DNA ploidy analysis or study of the proliferative rate of pituitary adenomas using antibodies to PCNA or Ki-67 (96–99). Most DNA ploidy studies show a low rate of aneuploidy in pituitary adenomas (96,97). When present, aneuploidy is usually associated with GH- and PRL-producing adenomas, but the clinical importance of these findings is unclear. Fitzgibbons et al. (96) correlated the flow of cytometric quantitation of PCNA and DNA content on nuclear suspensions from 12 paraffin-embedded pituitary macroadenomas and one pituitary carcinoma, with clinical outcome (median follow-up of 41 months). Three of these tumors (23%) were aneuploid. Of the four tumors that recurred or metastasized, only one was aneuploid. The G2 M/G G1 fluorescence ratio for PCNA was consistently higher for the three diploid tumors that recurred than for the seven nonrecurrent diploid tumors. This study indicated a low incidence of DNA aneuploidy among pituitary tumors, with no correlation between the aneuploidy and tumor aggressiveness (96).

Nagashima et al. (98) studied the proliferative potential of human pituitary tumors in situ with immunohistochemical studies of cell kinetics using BrdU and anti-BrdU antibodies to label tumor cells in the DNA synthesis phase (S-phase). Other than two cases of Nelson's syndrome in which it was more than 1%, the S-phase fraction did not correlate with patient's age, tumor size, or duration of symptoms (98). The S-phase of most pituitary adenomas is low (0.5%) and correlates with their slow growth. Higher S-phase fractions may reflect aggressive or invasive growth.

Compared with that of normal pituitary glands, Gandour-Edwards et al. reported that the proliferating index using PCNA and KI 67 was increased in intrasellar and invasive adenomas, but these markers could not be used to distinguish between them (100). In the WHO classification, the Ki-67 LI represents a major prognostic indicator for pituitary adenomas. Adenomas with more than 3% Ki-67 LI and extensive p53 immunoreactivity are classified as ''atypical adenomas.''

Pituitary Carcinoma

Pituitary carcinomas are rare, making up some 0.2% of all pituitary tumors (43). It is impossible to make an unequivocal diagnosis of pituitary carcinoma on the basis of histology alone (43,44). The diagnosis of a pituitary carcinoma requires evidence of metastatic disease, either outside the CNS or as separate noncontiguous foci within the CNS (16,43,62). Pituitary carcinomas show a greater tendency for systemic, rather than craniospinal, metastases, but in 13% both may be present (16,43,44). They may arise de novo or from a preexisting adenoma (101,102). When a macroadenoma becomes hormonally active, one should suspect malignant transformation (103).

Presenting symptoms include headache and visual field deficits, with amenorrhea and galactorrhea being less common. Most present as invasive, functional tumors associated with Cushing's or Nelson's syndrome or hyperprolactinemia; on occasion, they are nonfunctioning (16,43). CSF examination may be helpful in documenting leptomeningeal spread.

Most, but not all, pituitary carcinomas are chromophobic on histological examination. Less often, they may be basophilic or acidophilic. Nuclear pleomorphism or hyperchromasia are common (43). Some primary tumors may be cytologically bland and lack mitotic activity in the primary tumor, whereas the metastasis may show nuclear pleomorphism and mitotic activity (16,44). Thus, varying degrees of mitotic activity and MIB-1 may be seen in the primary tumor and in the metastases (43). p53 expression is frequent in primary and metastatic tumors, with a relative increase in p53 expression in metastases (43). Primary and metastatic pituitary carcinomas are mostly aneuploid (43).

As aneuploidy is common in pituitary adenomas and in virtually all pituitary carcinomas, it is of little significance in distinguishing between them. Although increased mitoses, high MIB-1 proliferative indices, and p53 immunostaining are seen in most pituitary carcinomas, their presence in a minority of invasive, but nonmetastatic, pituitary adenomas limit their use as diagnostic or prognostic indicators (43,44).

The differential diagnosis of pituitary carcinomas includes invasive pituitary adenomas and other metastatic carcinomas. Although, frank brain invasion is indicative of malignancy, it has not been used as a criterion for the diagnosis of pituitary carcinoma.

Imaging scans are of help in demonstrating the discrete, isolated nature of the metastases within the meninges or brain in pituitary carcinoma, in contrast to the direct intracranial spread in invasive pituitary adenomas. Pituitary carcinomas are distinguished from other metastatic carcinomas by the histological similarity of their metastases to the primary pituitary tumor and by immunohistochemical and ultrastructural analysis. The metastatic tumor in pituitary carcinoma should show epithelial and endocrine differentiation on H&E sections, immunoperoxidase stains, or electron microscopy and have a hormonal immunophenotype similar to that of the primary tumor (except in null-cell tumors) (44).

The treatment is usually palliative and includes radiation therapy and, for carcinomas producing PRL, dopamine agonist therapy. These patients have a poor prognosis and a poor response to radiation and chemotherapy. In the study by Pernicone et al. 80% died of metastatic disease (66% within 1 year after the diagnosis of carcinoma) and 20% were alive with metastases 9 to 18 months after diagnosis (43). Systemic metastatic sites include the liver, lung, bone, and less frequently, lymph nodes. Patients with systemic metastases have a worse prognosis compared with those with craniospinal metastases (16,43).

G. Pathogenesis

The pathogenesis of pituitary neoplasia is poorly understood. However, there is an increasing evidence that genetic alterations occur in most pituitary tumors (104–107). Analyses of X-chromosomal inactivation show that pituitary tumors are monoclonal, suggesting that one or more somatic mutations may result in the selective propagation of a single progenitor cell (107–110).

Mutation in codon 12 of the H *ras* gene in 1 of 19 pituitary tumors has also been described (108). This single *ras* mutation was found in a particularly invasive tumor in which the possibility of malignant transformation of the tumor was considered. The presence of rapid growth rate, invasion into the base of the skull and paranasal sinuses, and histological features of cellular pleomorphism with an increased number of mitoses were suggestive of a malignant pituitary neoplasm in this case. However, the absence of metastatic lesions prevented the classificastion of the tumor as a carcinoma. It is unclear what other mutations, other than Gs protein and *ras* mutations occur in pituitary tumors. It is also unknown whether a single mutation is sufficient to cause a pituitary adenoma and whether the Gs protein and *ras* mutations occurr early or late step during pituitary tumorigenesis (108).

Green et al. detected p53 tumor suppressor protein using immunohistochemistry in 23% of 31 pituitary adenomas (109). No significant association was found between the presence of apoptosis, p53 expression, and tumor type or tumor size (109).

Pit-1 nuclear-binding transcriptional factor plays a critical role in pituitary-specific activation of GH, PRL, and TSH genes. Recently Sanno et al. demonstrated the expression of Pit-1 product with high incidence in GH-, TSH-, and PRL-producing adenomas, suggesting that this transcriptional factor may have a role in the specific functional differentiation (110). However, its expression in nonfunctioning or gonadotrophic adenomas suggests the presence of other transcription factors, as yet unidentified, that may have a role in their differentiation. How Pit-1 is related to tumorigenesis or functional differentiation of pituitary adenomas is unknown. Further molecular genetic studies on the prevalence of mutations with clinical correlation may provide a better understanding of the biological characteristics of these tumors.

VIII. CRANIOPHARYNGIOMA

A. Introduction

Craniopharyngiomas are epithelial brain tumors that arise from Rathke's pouch epithelium and that account for 1% to 10% of all intracranial tumors. They represent 50% of all suprasellar masses in children and are the most common nonneuroepithelial intracerebral tumors in childhood (1–9). Craniopharyngiomas occur at a rate of 1.3:1 million person years (3). About 94% of tumors are found in the suprasellar region (4). Some tumors also involve the sella turcica or occur in the third ventricle, or rarely, within the sphenoid or nasopharynx (10–12).

The histogenesis of craniopharyngiomas is unclear. The adamantinomatous type is histologically reminiscent of adamantinoma (ameloblastoma) of the jaw and the keratinizing and calcifying odontogenic cyst (13–15). Therefore, it has been suggested that the source of origin of craniopharyngioma may be misplaced odontogenic epithelium. There is also a squamous or papillary variant of craniopharyngioma, with similarities to the Rathke's cleft cyst (1,16,17).

B. Clinical Features

Craniopharyngiomas typically occur in children and adolescents (mean age at diagnosis, 8 years; range 3–67 years), with a male to female ratio of 1.5:1 (1–9). About 50% of the patients are younger than 20 years old at diagnosis. Patients most often present with findings associated with ventricular outflow obstruction causing hydrocephalus or optic chiasm and tract compression resulting in visual dysfunction (1–9). Headache and visual field abnormalities are the most common symptoms (1–9). Symptoms of intracranial mass effect, papillary edema, and extraocular palsy of the cranial nerves may also occur. In addition, because of the hypothalamic or pituitary compression, patients may present with endocrinopathy (6,18). Pituitary gland involvement causes loss of pituitary function, which makes endocrine evaluation necessary before and after surgery. Growth failure is less frequent. The average duration of symptoms in one study was five months (2). In addition, spontaneous rupture of cystic craniopharyngiomas may occur on one or more occasions and manifests as recurrent aseptic meningitis (19). In such patients, the CSF shows neutrophilic leukocytosis, with increased protein and normal glucose levels, and may mimic that are seen in pituitary apoplexy. Characteristic multilaminar polarizable cholesterol crystals are often found in the CSF (2). Craniopharyngiomas also occur in older patients (30%) who present with a suprasellar mass, visual field deficits, headaches, and dementia (20). The majority (62%) of patients are men. Here again, headache is the most common presenting symptom. Endocrine and ophthalmic symptoms are also important. Loss of libido and amenorrhoea are seen in adults (21). While there is no significant difference in the frequency of visual field defect detected (most common bitemporal hemianopia), GH, ACTH, TSH deficiency, or diabetes insipidus between children and adults, hydrocephalus is most frequently found in children (22).

C. Radiography

The diagnostic CT and MRI characteristics of craniopharyngiomas (23–25) rely on the presence of a calcified, largely cystic, suprasellar mass. Detectable calcification seen in 50% to 80% of patients is helpful in the differential diagnosis from other brain tumors. CT is superior to MRI in the detection of calcification and enlargement of the sella turcica that is usually absent or minor (22,23). The tumor appears as an

enhancing mass that extends into the hypothalamic region with compression of the surrounding cisterns and upward displacement of the inferior portion of the third ventricle (23). On MRI, the cystic component appears as isointense to hyperintense on T1WIs and hyperintense on T2WIs (23–25). The solid tumors with prominent calcification appear hypointense on T1 and T2. FLAIR is useful in delineating cystic portions of tumor (which will be hyperintense) from loculated portions of the third ventricle or other CSF spaces (which will tend to be isointense). MRI spectroscopy demonstrating a significant lipid content may be useful (26). MRI technique is superior to CT for determining tumor extent and provided valuable information about the relationships of the tumor to surrounding structures (23). Thus, CT and MRI have complementary roles in the diagnosis and management of craniopharyngiomas (23). Finally, if performed, an angiogram reveals an avascular suprasellar mass.

D. Pathology

On gross examination, craniopharyngiomas are irregular, nodular, well-circumscribed, or encapsulated masses with a slightly yellow, firm wall displaying calcium flecks. The average tumor size is 3 to 4 cm in diameter. About 50% of tumors are largely cystic, and the remaining cases are either solid or mixed solid and cystic. The cystic tumors typically contain a dark brown or yellow fluid containing cholesterol crystal and grumous material, which has been likened to machinery oil. There are two distinct variants with some differences in clinical behavior. The squamous or papillary type is almost always seen in adults and has a more indolent course compared with the adamantinomatous type, which is more common in childhood (1,4,8, 16,17,27). The adamantinomatous type is often nodular and multicystic. In solid areas, the tumor has a distinctive prominent cloverleaf configuration of epithelial lobules composed of anastomosing trabeculae of squamous epithelium with intercellular bridges, loose aggregates of central stellate cells, and peripheral palisading rims of columnar cells resting on thin basement membranes (Fig. 37A, B) (1–8). Transition between adamantinomatous epithelium and solid nests of ordinary stratified squamous cells with keratinization, squamous pearls, and calcified masses of keratinized cells may be seen in one-third of the cases (4). Cystic areas show degenerative changes and necrosis. Cysts may be lined by both columnar basal cells resting on the basement membrane or by flattened stratified squamous epithelium, and they apparently result from degeneration of stellate squamous cells and accumulation of keratinous debris or perivascular stromal degeneration. The process of keratinization generally lacks keratohyalin granules. Typical nodules of ''wet keratin'' are composed of stacked arrays of plump, eosinophil keratinized cells with ghost nuclei (1). Dystrophic calcification occurs on these nodules of wet keratin. The necrotic cyst contents are composed of exfoliated squames, keratinous debris, and cholesterol clefts, which may be surrounded by a foreign body giant-cell reaction and chronic inflammation. The tumor often induces an intense gliosis in the adjacent brain tissue with or without Rosenthal fibers. Ultrastructurally, adamantinomatous craniopharyngiomas show characteristic features of squamous epithelium throughout, with tonofilaments and desmosomes. Basal lamina covers the palisaded epithelial cells that adjoin the stroma but not the stellate cells (2).

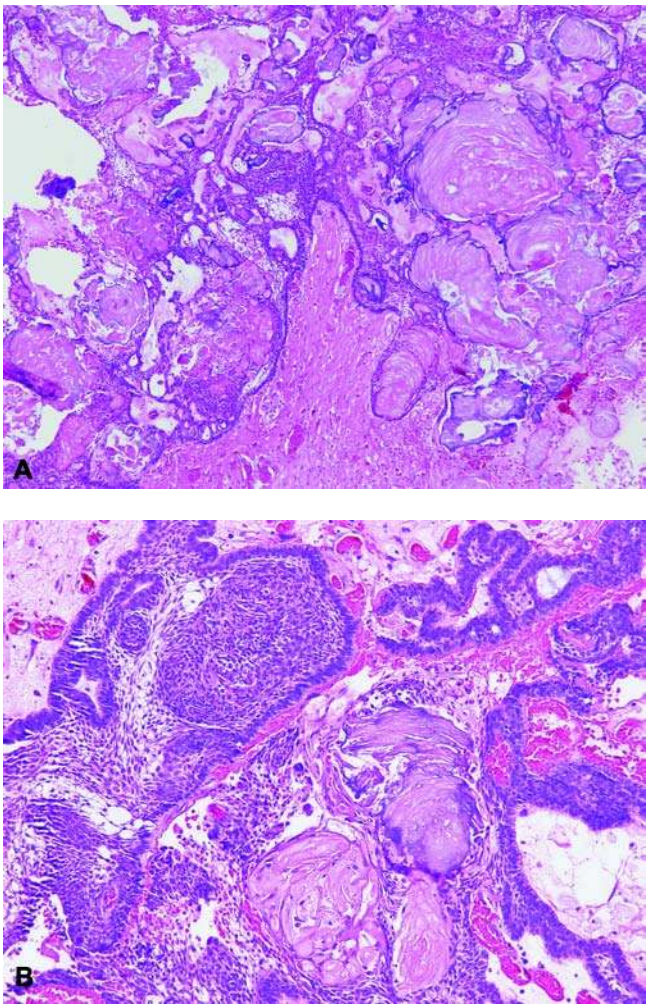

Figure 37 Craniopharyngioma, adamantinomatous type. (**A**) The epithelial component exhibits typical anastomosing trabeculae with peripheral palisading rims of columnar cells; (**B**) higher magnification shows epithelium with palisading peripheral columnar cells, calcification, nodules of "wet keratin" with ghost nuclei and microcystic degeneration. (**A**: H&E, 50×, **B**: H&E, 100×).

The papillary variant constitutes 10% of all craniopharyngiomas and differs from the classic adamantinomatous type in that it occurs almost exclusively in adults (mean age 40–45 years), often involves the third ventricle, and it is frequently solid on radiographic examination without calcification (1,16,17,25). Histologically, the tumor is encapsulated and composed of solid sheets of well-differentiated epithelial cells interrupted by papillae composed of a loose fibrovascular stroma lined by mature stratified squamous epithelium with little or no keratinization

(1,16,17). Unlike the adamantinous type, the epithelium lacks central stellate cells, palisading peripheral epithelial cells, calcification, nodules of wet keratin, microcystic degeneration, cholesterol deposition with foreign body-type giant-cell reaction, and machinery-oil-like cyst fluid. The epithelium also lacks the diffuse surface maturation and keratohyalin granules typical of epidermoid cysts (2). Rare goblet cells or ciliated cells may be seen.

E. Somatic Genetic

A possible association of aberrant reactivation of the Wnt pathway in adamantinomatous craniopharyngioma has been reported (28). β-catenin mutations are also present in craniopharyngiomas, exclusively of the adamantinomatous subtype (29,30). Since this gene product is involved with development, these results suggest that β-catenin mutations may contribute to the initiation and subsequent growth of congenital craniopharyngiomas. Chromosomal gains and losses are rare event in craniopharyngiomas (31).

F. Differential Diagnosis

The radiological differential diagnosis of a suprasellar mass extending into the hypothalamic region includes other congenital and developmental tumors, such as teratoma, germinoma, dermoid cyst, epidermoid cyst, and Rathke-cleft cyst (24). A suprasellar pituitary adenoma may occur without sellar changes seen on plain radiographs; however, CT scans would reveal abnormalities in the sella turcica. The differential diagnosis also includes Rathke cleft cysts, cystic pituitary adenoma, or other nonneoplastic cysts (32). Craniopharyngiomas typically demonstrate calcification, and approximately 90% have nodular, globular, or rim enhancement. Craniopharyngiomas are present with a wide range of appearances, but the existence of cysts, calcification, and enhancement in a suprasellar tumor strongly favors the diagnosis of craniopharyngiomas (26,33,34). The rare noncalcified cystic nonenhancing craniopharyngioma, a finding more common in adults than in children, may be impossible to distinguish from Rathke cleft cyst with imaging findings alone (35). Finally, whether diffusion-weighted imaging is useful in the differential diagnosis of an epidermoid is suspected (26).

The histological differential diagnosis includes ameloblastoma, keratinizing and calcifying odontogenic cysts, and epidermoid cysts (1,13,15). The histological similarity between craniopharyngioma and ameloblastoma is well known (13–15). Both neoplasms share gross features, such as a solid and cystic component, as well as histological and biological characteristics. However, Gorlin and Chaudhry have emphasized several differences, such as the constant cystic spaces in craniopharyngioma, owing to degeneration of stroma or epithelial cells, and the presence of foci of amorphous calcification as well as the presence of cartilage, bone, or osteoid in some of these neoplasms (14). Although ameloblastomas may also be cystic and solid, they lack calcification and metaplasia bone formation. The presence of adamantinomatous epithelium on frozen section is diagnostic of craniopharyngioma. However in its absence, a specimen from this site containing calcified or fibrous tissue, necrotic debris, or cholesterol clefts strongly suggests craniopharyngioma (2).

It may be histologically difficult to distinguish between suprasellar cystic craniopharyngiomas and epidermoid cysts, both of which are lined by stratified squamous epithelium and contain laminated masses of keratin that may form a nidus for calcification. In addition, both lesions contain fluid that can act as an irritant when leakage occurs into the subarachnoid space or after surgical exploration, causing aseptic (chemical) meningitis. In contrast with craniopharyngioma, which is most commonly seen in childhood and in adolescence, epidermoid cysts show a peak incidence in the fifth decade of life. Furthermore, epidermoid cysts lack adamantinomatous epithelium and are lined by highly organized, well-differentiated, keratinizing squamous epithelium with diffuse surface maturation, flaky keratin, and keratohyalin granules. However, a small sample from a cystic craniopharyngioma may show similar features, making the distinction impossible (4). Dermoid cysts contain hair and adnexa, which distinguish them from cystic craniopharyngioma and epidermoid cysts.

G. Treatment and Prognosis

Craniopharyngiomas are slow growing, histologically benign tumors that may show aggressive local behavior, but have no tendency for malignant transformation. These histologically benign but ''geographically malignant'' tumors are challenging to treat and require experienced clinicians from multiple disciplines, including neurosurgery, radiology, hematology or oncology, ophthalmology, endocrinology, and general pediatrics to address the multiple issues that arise with diagnosis, treatment, and long-term follow-up of affected children (36). Patients in general have high long-term survival but can have significant tumor- and treatment-associated morbidity, requiring a lifetime of medical and psychological management (6). The two treatments for craniopharyngioma are primary total resection and limited resection followed by radiotherapy. According to some, the treatment of choice in craniopharyngioma in childhood is total resection to avoid radiation therapy and recurrence (37). Surgical management of craniopharyngiomas is among the most challenging neurosurgical procedures because of their complex topographical relationship with surrounding structures such as the adherence of craniopharyngiomas to structures at the base of the brain, including important vascular and neural structures that make complete surgical resection technically challenging (38). Thus, GTR at initial surgery is the treatment of choice, the exact nature of initial resection, whether total or subtotal, has been debated (39–50). Total surgical removal of craniopharyngiomas should be attempted in children whenever possible to minimize the risk of recurrence. Only when total

resection is not possible, subtotal resection plus radiation therapy is the alternative. In case of huge tumors involving the hypothalamus, a more conservative resection should be performed, followed by possible radiotherapy (51).

The most common postoperative complications in all cases are recurrence of disease, panhypopituitarism, and diabetes insipidus (22). Thus, lifelong follow-up is crucial because of the risk of recurrence and the need for ongoing hormone replacement therapy (1–22). The rate of recurrence or regrowth of craniopharyngioma (20–50%) is associated with the presence of a residual tumor after surgery (38) and immunoreactivity to p53 (52). Some studies have suggested that the recurrence rate for the papillary type craniopharyngioma is lower than for the adamantinomatous type (27,53,54). In some studies, however, no correlation was noted between histopathological subtyping or brain invasion and recurrence (8,55). The significant clinical factors predictive of recurrence included the extent of surgical resection and tumors greater than 4 cm cystic tumors (8,55). Tumor progression and relapse are frequent and early events even in irradiated patients (56). Monitoring of cerebral imaging and clinical status is recommended in follow-up of patients with childhood craniopharyngiomas (56). Adjuvant radiation therapy for residual tumor appears to improve recurrence-free survival when subtotal resection is performed (16,49). The overall survival rate at five years is 80% (3). Survival rate appears to decrease with age (3,57). The five-year survival rate for patients younger than 20 years is greater than 90% and for patients 65 years or older, is 37% (3,57). Finally, in a study of 48 papillary craniopharyngiomas, no signifant differences between two types of craniopharyngioma relative to efficacy of radiation therapy and overall patient survival was reported (16). Thus current therapy for craniopharyngiomas is multimodal and focuses on a combination of surgical decompression, medical treatment, as well as radiotherapy (8,55,58).

IX. PARAGANGLIOMAS

A. Introduction

The paraganglionic system develops early in gestation and is of neural crest origin. It consists of two components—the adrenal medulla and a diffuse collection of extra-adrenal paraganglia. The extra-adrenal paraganglia are specialized collections of neuroendocrine cells that migrate in close association with cranial nerves, large blood vessels, and autonomic nerves and ganglia, hence the term ''paraganglia''. They range in size from those that are barely visible, such as the carotid bodies, to those that are apparent only at the microscopic level, such as the laryngeal paraganglia.

The extra-adrenal paraganglia can be further divided into sympathetic and parasympathetic types. Although they are indistinguishable at the cellular level, they differ in their anatomic distribution and secretory products. The sympathetic paraganglia are found primarily in the axial regions of the trunk along the prevertebral and paravertibral sympathetic chains and in connective tissue in or near the pelvic organs. In contrast, parasympathetic paraganglia are localized almost exclusively in the head and neck along the branches of the glossopharyngeal and vagus nerves.

Although both sympathetic and parasympathetic paraganglia produce catecholamines, clinical signs of excess production are usually associated with those that are sympathetic. Tumors associated with significant amounts of epinephrine are almost always sympathetic. Those lesions that occur in patients with hypoxemia, in contrast, are typically parasympathetic in origin. Overlaps in secretory expression, however, do occur (1).

Unlike sympathetic paragangliomas (PGLs), parasympathetic PGLs are rarely functional and less likely to be malignant (1–13% vs. 14–50%) (2).

PGLs of the head and neck are found primarily at the bifurcation of the common carotid artery, in the middle ear—temporal bone, along the course of the vagus nerve, and exceptionally, in the larynx, orbit, nasal cavity, thyroid, nasopharynx, and trachea.

B. Terminology

Tumors arising from paraganglia are uncommon, usually benign, and have been referred to by a variety of names, including chemodectomas, glomus tumors, and chromaffin and nonchromaffin PGLs. The term ''chemodectoma'' is inappropriate since not all paraganglia function as chemoreceptors. The rubric ''glomus tumor'' is unacceptable since it is often mistaken for and erroneously assumes a relationship to the tumor derived from true glomera, specialized arteriovenous shunts of the skin that regulate temperature. Dividing the tumors into chromaffin and nonchromaffin categories, once thought useful in distinguishing functional from nonfunctional tumors, has proven inadequate with discovery of nonchromaffin catecholamine-secreting tumors. The preferred terminology for tumors of the extra-adrenal paraganglia is ''paraganglioma,'' prefaced by the anatomic site of origin, for instance vagal paraganglioma (VPG). If the tumor is functional or malignant, it would be designated, e.g., as a functional VPG or a malignant VPG. Although the adrenal medulla is technically a paraganglion, similar tumors arising from this site are still regarded as pheochromocytomas rather than PGLs.

C. Imaging

CT with contrast medium and MRI with gadolinium are invaluable in defining the location, size, and extent of a PGL (3,4). The typical CT appearance of a carotid body paraganglioma (CBPG) and vagal paragranglioma (VPG) (Fig. 38) is that of a homogenous, hypervascular, well-defined soft tissue mass. If there has been hemorrhage or focal thrombosis, a heterogeneous pattern of enhancement will be seen. CT scans of jugulotympanic paragangliomas (JTPGs) may also show expansion and erosion of the jugular foramen. As the tumor expands, it may destroy the surrounding bony labyrinth and

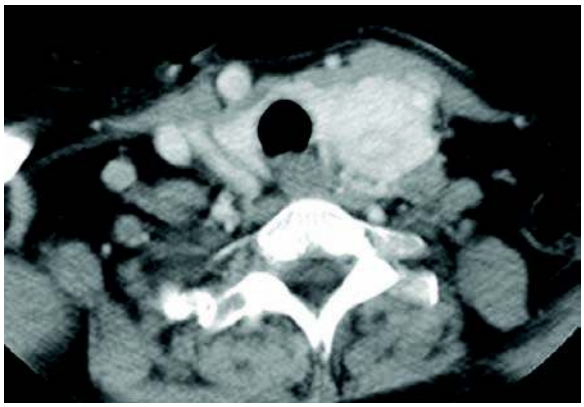

Figure 38 Computed tomography scan showing all enlarged vagal paraganglioma of the left vagus.

ossicular chain and extend into the region of the cerebellopontine angle (3).

MRI characteristics of all PGLs are similar. A well-defined hypointense mass with areas of signal void is typically seen on T1-weighted images (T1WIs). A ''salt and pepper'' pattern is commonly seen in all lesions larger than 2 cm. This pattern is usually seen on T2WIs and is due to areas of high vascularity associated with hemorrhage or slow blood perfusion. In addition to providing superior definition, MRI can also detect much smaller PGLs than CT scans.

Octreotide scintigraphy is an important adjunct. It can be used not only to confirm the diagnosis of neuroendocrine neoplasms but also to detect additional occult tumors, separate postoperative changes from residual or recurrent disease, and for screening patients at risk for familial PGLs (5).

Ultrasound has a limited role in the evaluation of PGLs of the head and neck. It is useful in the evaluation and follow-up of CBPGs and to some extent VPGs. Although noninvasive imaging has almost universally replaced angiography as the primary procedure for diagnosing PGLs, it still remains an important component in the management of these patients, especially regarding to preoperative embolization to reduce the blood supply of the tumor.

D. Pathology

PGLs are highly vascular and composed of two types of cells, chief and sustentacular, arranged in a characteristic alveolar or Zellballen pattern. The chief cells (type I cells, epithelioid cells) are more numerous and contain catecholamine-bound neurosecretory granules. The sustentacular cells (type II cells, supporting cells) are devoid of neurosecretory granules and are characteristically located at the periphery of the Zellballen (Fig. 39A–E).

The chief cells often show considerable nuclear enlargement and hyperchromatism and contain cytoplasm that varies from pink to amphophilic, which at times may also be vacuolated. Spindled-shaped chief cells are uncommon and mitoses are sparse to absent. Vascular and perineural invasion may also be seen but have no prognostic value.

E. Immunohistochemistry

The chief cells, on immunostaining, are positive for synaptophysin, chromogranin, and NSE (Fig. 39B–D). They are negative for CK, carcinoembryonic antigen, S-100 protein, and calcitonin. The sustentacular cells are positive for S-100 protein and GFAP and negative for other markers (Fig. 39E).

F. Genetics—Molecular Biology

It is commonly stated that about 10% of all PGLs of the head and neck are familial and inherited as an autosomal dominant trait, modified by genomic imprinting (6–8). There is no expression of the disease when the gene is inherited from the mother. Paternal transmission of the gene, however, results in tumors in the children even if the father is clinically unaffected. Van Schothorst et al. are of the opinion that because of skipping of generations after maternal transmission of the gene, the incidence of familial PGLs is vastly underestimated and may be as high as 50% or more of all cases (9).

Genetic linkage analyses of large families with hereditary PGLs have identified four syndromes referred to as PGL-1, PGL-2, PGL-3, and PGL-4 (10–23). To date, three of these syndromes (PGL 1, 3, and 4) have been associated with germline mutations involving subunits of the mitochondrial enzyme succinate dehydrogenase. The gene and chromosome location of each are shown in Table 7. In PGL-2, the abnormal chromosome is known but the susceptible gene remains unidentified. Each of the syndromes has characteristic features. In PGL-1, the PGLs are often multifocal (74% of cases) and none are malignant, while in PGL-3, the tumors are seldom multifocal and none are malignant. In PGL-4, 28% of the PGLs are multifocal, 33% are malignant, and there is also a higher incidence of other extra paraganglionic malignant tumors (kidney, thyroid). Patients with PGL-1 and 4 are also at risk for developing pheochromocytomas.

The incidence of finding multiple tumors in familial syndromes varies according to the thoroughness of the examination and the length of follow-up. When multiple, the tumors may appear synchronously or asynchronously.

G. Carotid Body Paragangliomas

Anatomy

Carotid body paraganglia are paired, bilateral, usually symmetrical aggregates of specialized neuroendocrine tissue that are located at the bifurcation of the common carotid artery along its posteromedial wall, either within or immediately external to the adventitia. They are anchored to the artery by a band of fibrovascular tissue referred to as the ligament of Mayer. Each measures about 2 to 7 mm in greatest dimension and weighs 3 to

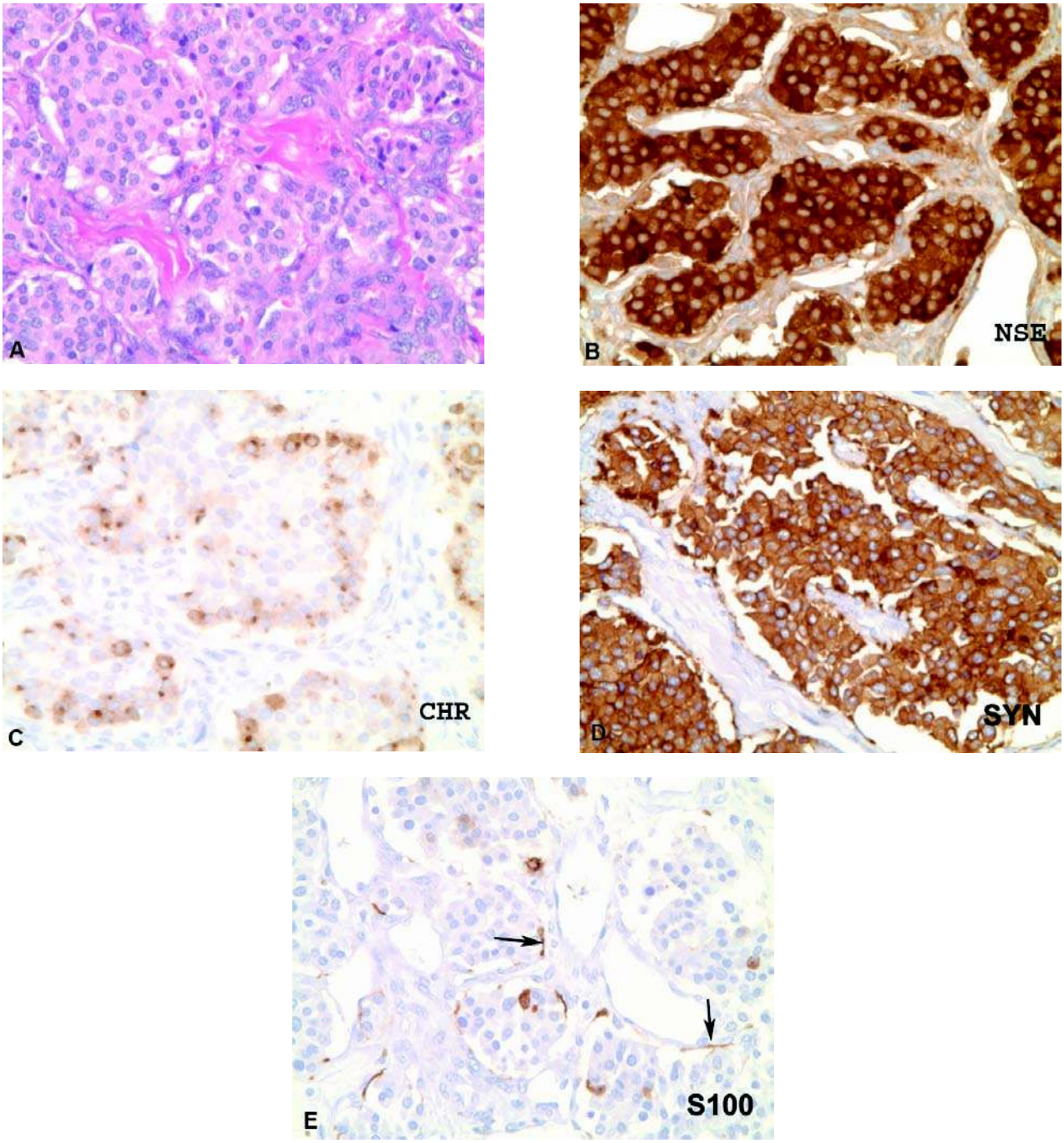

Figure 39 (**A**) The microscopic section of the paraganglioma shows polygonal epitheliod tumor cells are arranged in a distinctive compact *Zeballen* pattern (H&E, 250×). (**B**) Discrete nests of chief cells in a *Zellballen* pattern contain neuropeptides highlighted by immunohistochemical stains for Neuron-specific enolase (NSE), (**C**) Chromogranin, (**D**) Synaptophysin. (**E**, *arrows*) The supporting sustantacular cells are stained by S-100 protein, which shows elongated cellular processes.

Table 7 Genetics of Paragangliomas

Syndrome	Chromosome	Gene
PGL 1	11q 22–23	SDHD[a]
PGL 2	11q13	?
PGL 3	1q21	SDHC
PGL 4	1p36	SDHB

[a]SDH, succinate dehydrogenase, subunits D, C, and B.

16 mg (24–27). They function as chemoreceptors, sensitive to changes in oxygen tension, carbon dioxide content, and hydrogen ion concentration.

Disorders affecting the carotid bodies are infrequent and basically limited to two conditions: hyperplasia, seen in individuals who suffer from chronic hypoxic diseases or live at high altitudes, and neoplasia.

Clinical Features

Whether the CBPG or the JTPG is the most frequent PGL of the head and neck is open to debate. As a group, however, these two tumors (CBPG and JTPG) account for about 90% of all PGLs in this area of the body.

CBPGs occur mainly in adults, averaging 40 to 50 years of age, and are rare in children (28–39). The gender distribution varies according to study. In a collective review of 257 cases, Barnes and Taylor observed that 52% occurred in males and 48% in females (32). However, at altitudes above 2000 meters, females predominate by a ratio of 8.3:1 (33,40).

They typically present as a painless, slowly enlarging neck mass deep to the anterior border of the sternocleidomastoid muscle just below the angle of the mandible. Occasionally, they are associated with pain, hoarseness, dysphagia, headache, syncope, bruit, or thrill. Functional tumors with catecholamine-induced hypertension are rare (about 2–3% of all CBPGs).

Multiple-Familial CBPGs

Although typically sporadic and unilateral, at least 10% (maybe more) of CBPGs are familial and associated with one or more additional PGLs or with multiple endocrine syndromes 2A and 2B (30,41–43). According to Grufferman et al., one-third of familial CBPGs are bilateral in contrast to sporadic or non-familial tumors, which are bilateral in only 4% of cases (6). Bilateral tumors may be either synchromous or asynchromous.

A CBPG may also be a component of Carney's triad (gastric leiomyosarcoma, pulmonary chondroma, and extra-adrenal PGL) (44). Rare tumors have also been associated with a hereditary deficiency of clotting factors VII and X (45).

Angiography

Angiography reveals a highly vascular mass at the bifurcation of the common carotid artery, often with entrapment or displacement of the external and/or internal carotid arteries.

Pathology

The tumors are usually between 2 and 6 cm, firm, rubbery, well circumscribed, and surrounded by a thin, sometimes thick, fibrous capsule (Fig. 40). On cross-section, most are variegated yellow, tan, pink, or brown with areas of fibrosis and hemorrhage. A few may be more homogenous, pink, or tan.

The histopathology has been previously described (see section D "Pathology" above).

Differential Diagnosis

CBPGs are usually easily recognized. Exceptionally, they may be confused with MTC, carcinoid, melanoma, renal cell carcinoma, hemangiopericytoma, or carcinoma (46). MTC and carcinoid can be excluded by the fact that they are positive for CK, while the CBPG is negative. CBPGs are, however, positive for synaptophysin, which excludes melanoma, renal cell carcinoma, hemangiopericytoma, and carcinoma.

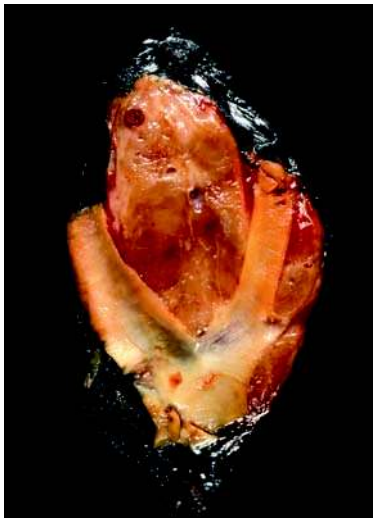

Figure 40 A cross section of a carotid body paraganglioma arising in the bifurcation of the common carotid artery, which is encased by the tumor mass. *Source*: Courtesy of Dr. L. Barnes, University of Pittsburgh School of Medicine, Pittsburgh, PA.

Treatment and Prognosis

CBPGs are slow-growing tumors, with a median growth rate of 0.83 mm/year and a median tumor doubling time of 7.13 years (47).

Surgery is the treatment of choice, often requiring that one or more branches of the carotid arterial system be sacrificed for complete removal. Preoperative embolization varies according to preference of the surgeon but is generally not indicated. Somewhere between 0% and 10% of CBPGs will recur, following removal. This is not necessarily a sign of malignancy but possible inadequate excision and regrowth.

Radiation has also been used with varying degrees of success but may be necessary for those individuals who refuse surgery, are poor operative risks, or have multiple PGLs.

Malignant CBPGs

PGLs are divided into noninvasive (circumscribed, encapsulated), locally invasive, and metastatic categories. Some locally invasive tumors may even cause death of the patient. Although clinically malignant, these tumors are still regarded as locally invasive. A tumor is considered malignant only if there is metastasis to regional lymph nodes or to more distant sites, such as the lung and bones.

The incidence of malignant (metastasizing) CBPGs ranges from 2% to 13% (32,48–50). Unfortunately, the clinical behavior cannot be predicted on the basis of routine histology. Such features as nuclear pleomorphism, mitotic activity, necrosis, and vascular-perineural invasion are unreliable prognosticators and

have been found in benign as well as malignant tumors (32). Other findings such as DNA ploidy, absence of sustentacular cells, number of expressed neuropeptides, assessment of argyrophilic nucleolar organizer regions (AgNOR), and proligerative markers (PCNA, Ki-67) show no consistent correlation with histological behaviour (32,51–58).

There is, however, preliminary evidence to suggest that patients with the PGL-4 syndrome should be followed closely, since up to one-third of these PGLs are malignant (see ''Genetics-Molecular Biology'' above).

Sporadic (nonfamilial) CBPGs are more likely to be malignant than those that are familial—12% versus 2.5% (6). Metastases may be apparent at the time of initial therapy or may not become apparent until many years later.

Surgery with or without adjuvant irradiation is used for local disease. Chemotherapy, however, is largely ineffective. The overall five-year relative survival is 59.5%. If the metastases are confined to regional lymph nodes, the five-year survival is 76.8% but decreases to 11.8% for patients with distant metastases (59,60).

H. Jugulotympanic Paragangliomas

Anatomy

PGLs are the most common tumor of the middle ear and the second most frequent tumor of the temporal bone, exceeded in the latter instance only by the acoustic neruoma. They arise from collections of paraganglion cells normally found in the adventitia of the jugular bulb, along the course of the tympanic branch of the glossopharyngeal nerve (nerve of Jacobson) and the auricular branch of the vagus nerve (nerve of Arnold), in the tympanic canaliculus and in the mucosa of the cochlear promontory (28). Their function is unknown.

The term ''tympanic paraganglioma (glomus tympanicum)'' is applied when the tumor arises from the middle ear and ''jugular paraganglioma (glomus jugulare),'' when it arises from the jugular bulb. If the precise point of origin is indeterminant, then the all-inclusive term ''jugulotympanic paraganglioma (JTPG)'' is used.

Although Otani, a pathologist, was the first to recognize a tumor of these structures (Otani's tumor), it was Rosenwaller, the surgeon who removed the tumor, who reported the case under the title ''carotid body tumor of the middle ear and mastoid'' (61).

Clinical Features

Tumors arising from the jugular bulb are more common than those of the middle ear and, in general, tend to have a worse prognosis (61,62). There is no significant lateralization of these tumors to either ear. JTPGs are three to six times more common in women and occur primarily in middle age (average 50; range 17–88 years) (63–65). A familial association has been noted in some instances. Pulsatile tinnitis and conductive hearing loss are the most common symptoms. Others include a bloody discharge, pain, and cranial nerve palsies, especially of nerves VII–XII.

On otological examination, the tumor typically presents as a blue-red mass behind an intact tympanic membrane. Exceptionally, it may secondarily involve the external auditory canal and masquerade as an inflammatory (otic) polyp.

Eight percent of patients with JTPGs have a family history of similar tumors, inherited as an autosomal dominant trait. When familial, the tumors are bilateral in 33% to 50% of cases. This is in contrast to patients with nonfamilial JTPGs who have bilateral tumors, either synchronous or asynchronous, in only 10% of cases (62–66).

Functional JTPGs are encountered in about 1% to 2% of patients, resulting in hypertension (67–72). Exceptionally, the tumor may produce hormonal peptides, such as cholecystokinin, which may explain prolonged episodes of ileus seen in some patients, following surgical removal of their tumor (73).

Pathology

The pathology is similar to that of other PGLs (see section D "Pathology" above).

Differential Diagnosis

Following surgical resection, JTPGs often show considerable crush artifact and distortion and, because of their prominent vascularity, may be confused with granulation tissue or a hemangioma. Knowing the clinical history can be very helpful; Reticulin stains are useful in accentuating the Zellballen pattern.

In contrast to granulation tissue and hemangiomas, the chief cells of a JTPG are positive for synaptophysin and negative for vascular markers (CD 31 and 34).

Treatment and Prognosis

JTPGs, like all other PGLs, are slow growing tumors with a median growth rate of 0.79 mm/year and a median tumor doubling time of 13.8 years (47). As they enlarge, they may fill the middle ear and encase the ossicles or extend through the petrous bone into the cerebellopontine angle and masquerade as an acoustic neuroma or meningioma.

Intracranial involvement occurs in 15% to 20% of JTPGs. Most of these intracranial extensions, however, are extradural and only occasionally intradural (74).

Whether surgery or radiation is the treatment of choice for JTPGs is the subject of considerable debate (75–80). It appears, however, to be the opinion of most clinicians that radiation should be relegated to a palliative therapeutic role, reserved for patients who are poor surgical candidates, those with bilateral JTPGs, those who refuse surgery, or patients with recurrent disease.

Malignant JPGLs

Although JTPGs are locally aggressive, only 1% to 6% will metastasize (28,60,65,81–84). The most common sites of dissemination, in descending order, are bones (especially the vertebral column), lung, cervical lymph nodes, and liver (84). As with CBPGs, there are no reliable features that allow one to predict behavior.

In the most comprehensive review of metastatic JTPGs, Brewis et al. noted that those tumors that metastasized had a significantly higher incidence of pain and a lower incidence of hearing loss at presentation compared with nonmetastatic tumors (84). The mean interval from diagnosis to metastasis was 4.5 years (range 0–30 years). Follow-up on 44 of 53 metastatic tumors revealed a 68% rate of death at a mean follow-up of six years two months (84). In a review of nine malignant jugular PGLs (glomus jugulare), Manolidis et al. observed a 72% five-year survival (83).

I. Vagal Paragangliomas

Anatomy

The vagus nerve (from the Latin ''vagus'' meaning wandering or meandering) arises from 8 to 10 rootlets on the lateral border of medulla and converges to form a cord on entering the jugular foramen. It is the longest cranial nerve and has a superior ganglion, which lies within the jugular foramen, and just below this, a middle ganglion. A third, much larger ganglion, known as the ganglion nodosa, lies more inferior; it is approximately 2.5 cm long and lies high in the neck, just behind the internal carotid artery (85).

Vagal paraganglia do not form a discrete ''body'' as seen at the carotid artery bifurcation but rather consist of six or seven small, dispersed aggregates of paraganglionic tissue. They may be found within (intravagal) or adjacent to (juxtavagal) the vagus nerve, usually at the level of the nodose ganglion. In rare instances, paraganglionic tissue may be found in sites just above or below the nodose ganglion. Their function in unknown but may serve as a chemoreceptor and moderator of the cardiopulmonary system.

Tumors of the vagus nerve are rare. Of those that have been reported, approximately 50% to 60% have been PGLs (Fig. 41), 20% to 35% neurilemomas, 5% to 15% neurofibromas, and 5% malignant schwannomas (85).

The VPG was first described by Stout in 1935 (86). It represents about 5% of all PGLs of the head and neck and is exceeded in frequency only by the CBPG and JTPGs.

Clinical Features

VPGs are more common in women (64%) and occur over a broad age range (19–86 years) with an average of 45 to 55 years (87–93).

They characteristically present as a slowly enlarging, asymptomatic mass at the angle of the mandible and/or as a bulge in the lateral oropharyngeal wall. As they increase in size, deficits of cranial nerves IX, X, XI, and XII and the cervical sympathetic chain are common, resulting in unilateral vocal cord dysfunction, dysphagia, hemiatrophy of the tongue, shoulder weakness, and Horner's syndrome. At the time of diagnosis, anywhere from 35% to 65% of patients will manifest one or more cranial nerve deficits. Functional tumors with catecholamine-induced hypertension, however, are distinctly uncommon, occurring in no more than 3% to 4%.

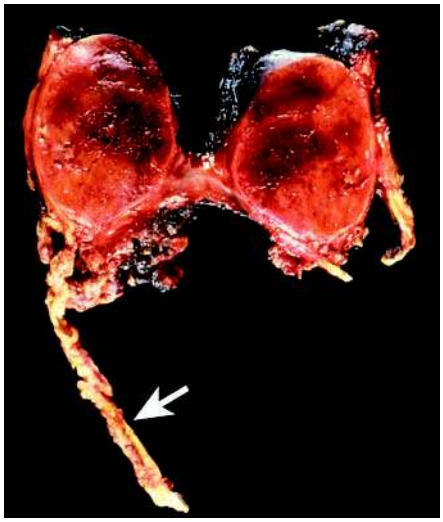

Figure 41 Vagal paraganglioma. Note attached segment of vagus nerve (*arrow*). *Source*: Courtesy of Dr. L. Barnes, University of Pittsburgh School of Medicine, Pittsburgh, PA.

In a review of 99 VPGs in which the side of origin was indicated, Zak and Lawson noted that 56% arose on the right side of the neck, 39% on the left side, and 5% were bilateral (26).

Multiple-Familal VPGs

In a review of 124 VPGs, Barnes et al. observed that 33% were associated, either sychronously or asynchronously, with additional PGLs, usually a carotid body or less frequently a JTPG (2). Seventeen present also had a family history of PGLs.

Angiography

In contrast to the CBPG, which arises at the bifurcation of the common carotid artery, VPGs are located above the bifurcation and typically displace the internal carotid artery anteriorly and medially.

Pathology

VPGs are fusiform or circular and abut directly on the base of the skull. They are usually between 2 to 6 cm and well circumscribed. In a few instances, they may be poorly defined or locally infiltrative. A portion of one or more large nerves and/or ganglion, especially the vagus, are almost invariably attached. Otherwise, they grossly and microscopically resemble the CBPG.

Differential Diagnosis

The differential diagnosis is the same as that for carotid PGL discussed above.

Treatment and Prognosis

VPGs are slowly growing tumors with an estimated median growth rate of 1 mm/year and median tumor doubling time of 8.89 years (47).

Options for treatment include surgical resection, radiation, and, in selected cases, even observation because of the slow rate of growth of the tumors (87–93). Most, however, favor surgery as the treatment of choice. Since the tumor involves the vagus nerve, it almost invariably has to be sacrificed. In those instances where the nerve is preserved, function typically remains permanently impaired. Failure to remove the nerve may also predispose the patient for future recurrence.

Radiation is usually reserved for elderly patients who are poor operative risks or for those rare unfortunate individuals who have bilateral VPGs (the larger tumor is preferentially excised, while the smaller one is irradiated).

Following surgery, 8% (range 0–10%) of VPGs will develop local recurrence (2). The tumor may recur as early as 12 months after therapy or as late as 22 years. Local reccurence is not necessarily a sign of malignancy but often inadequate excision.

Malignant VPGs

Overall, 7% of VPGs are malignant (range 0–16%) (2). In 1985, Heinrich et al. reviewed the English language literature and found only 15 VPGs that were malignant (94,95). Of these, 73% were associated with cervical lymph node metastases and 27% with distant metastases (lung, bone, liver, and brain). In all instances, the metastases were apparent either at or within four years of diagnosis. It should be noted in their review, however, that the median duration of sumptoms before diagnosis was two years (range 6 months–40 years). In one of Barnes and Taylor's cases, the malignant nature of the tumor was not recognized until four years four months after diagnosis (96). Biller et al. have described another case in which lymph node metastases occurred 10 years after diagnosis (91). It thus appears that these tumors, like PGLs in general, are unpredictable and that while the majority of those that are malignant will usually manifest as such either at or within four years of diagnosis, some may not metastasize until many years later.

In a review of 59 malignant PGLs of the head and neck (includes all sites—carotid body, jugulotympanic, vagal, etc.) on file at the National Cancer Data Base, Lee et al. observed the five-year relative survival rate to be 59.5% (60) The five-year survival rate was 76.8% for patients who had metastases limited to the regional lymph nodes as opposed to 11.8% for patients who had distant metastases. Whether chemotherapy is effective in managing patients with metastatic PGLs remains controversial.

It is not possible to predict with confidence which tumor will prove aggressive. Such features as mitoses, necrosis, nuclear pleomorphism, presence of spindle cells, and perineural-vascular invasion are unreliable prognosticators and have been found in benign as well as malignant tumors.

Barnes and Taylor studied the DNA content of 10 VPGs by image analysis and observed that abnormalities in DNA were common and could not be used to assess malignant potential (96). In this study, five tumors were diploid, four diploid-tetraploid, and one aneuploid. Two of the ten VPGs in their series were malignant (lymph node metastases) and, of these, one tumor was diploid and the other aneuploid.

Some data indicate that PGLs that contain sparse to absent sustentacular cells, express few, if any, neuropeptides and contain increased numbers of AgNOR are more likely to be aggressive. These findings, however, have shown no consistent correlation with prognosis.

There is also controversy as to whether proliferative markers (PCNA, Ki-67) have any prognostic significance. Welkoborsky et al. sutied PCNA in 36 PGLs (27 JTPGs and 9 CBPGs) and observed that recurrent tumors had an average PCNA score of 24% compared with 15% in the nonrecurrent group (58). Gjuric stidued 40 JTPGs for Ki-67 expression and observed that ''the scores for Ki-67 did not correlate with the majority of clinical parameters'' (97).

Patients with PGL-4 syndrome should be carefully evaluated and followed, since preliminary data indicate that up to one-third of these PGLs are malignant.

J. Laryngeal Paragangliomas

Anatomy

The larynx contains two pairs of paraganglia that are divided into two groups: superior and inferior. The superior group, first described in 1963 by Watzka, is between 0.1 and 0.3 mm in diameter and occurs bilaterally in the upper anterior one-third of the false vocal cord adjacent to the superior margin of the thyroid cartilage in close proximity to the superior laryngeal artery and nerve (98).

The inferior laryngeal paraganglia were described a year later in 1964 by Kleinsasser (99). They too are bilateral but larger than the superior group, averaging 0.3- to 0.4-mm in diameter. They characteristically occur between the inferior horn of the thyroid cartilage and cricoid cartilage or between the cricoid cartilage and first tracheal ring in relationship to the inferior laryngeal artery and nerve (99,100).

Aberrant and accessory paraganglia have also been described (99,101). Occasionally, paraganglia may even be found within nerves rather than adjacent to them. This is especially so regarding the recurrent laryngeal nerve (102).

Clinical Features

Laryngeal paragangliomas (LPGs) are distinctly unusual. In 1991, a critical review of the world literature revealed only 34 acceptable cases (103). By 2004, the number of acceptable cases had increased to 76 (104).

LPGs have been described in patients from 5 to 83 years (average 47 years) and are more common in females by a ratio of 3:1 (103–106). Eighty-two percent of the tumors occur in the supraglottic larynx where they characteristically present as a red-blue 0.5- to 6-cm submucosal mass in the region of the aryepiglottic fold-false vocal cord. Of the remaining cases, 15% are found in the subglottis and 3% in the glottis (103). Curiously, the tumors tend to occur more often on the right side of the larynx, with a right-to-left ratio of 2.3:1.

Most patients present with more than a complaint, the most common of which is hoarseness. Others include dysphagia, dyspnea, sore, painful throat, neck mass, hemoptysis, and a sensation of a foreign body in the throat.

Subglottic tumors may be lumenal, extralumenal, or both (dumbbell-shaped mass) and often manifest with wheezing, stridor, or dyspnea (107–109).

Functional LPGs are most unusual and probably do not exceed 3% (103).

Multiple-Familial LPGss

Although LPGs are usually solitary lesions, they may be infrequently associated with PGLs in other sites, usually a CBPG (11,103,107,110).

Angiography

The blood supply of supraglottic LPGs is derived from the superior thyroid artery, superior laryngeal artery, or a branch of the external carotid artery (103,110–112). At least one case of a subglottic LPG has been evaluated by an angiogram and, in this instance, the blood supply was via the thyrocervical trunk (113).

Pathology

The pathology is similar to that previously described (see section D "Pathology" above).

Differential Diagnosis

LPGs are often confused with the atypical carcinoid tumor (ACT) and sometimes even with MTC. It can easily be separated from the latter two tumors by the fact that LPG is negative for CK, while the ACT and MTC are positive for this marker.

Treatment and Prognosis

Surgery is the treatment of choice preferably through an external approach (105,110). Endoscopic excision should be avoided (even for small lesions) because bleeding, which may be diffuse, may be difficult to control. Preoperative angiography and embolization, in an attempt to devascularize the tumor, is not essential, since the superior thyroid artery can easily be ligated prior to resection. An elective neck dissection is not warranted. Seventeen percent of patients have developed local recurrence from 1 to 16 years after initial excision (103).

Malignant LPGs

Although commonly stated that 25% of all LPGs are malignant (114–116), a critical review of these cases has revealed that almost all of these are examples of atypical carcinoids incorrectly labeled as malignant PGLs (103).

Current studies indicate that only about 2% of all LPGs are malignant (105). Only a single acceptable case has been reported. This involved a 36-year-old woman with a PGL of the larynx that metastasized to the lumbar spine 16 years after the diagnosis (117,118).

K. Miscellaneous PGLs of the Head and Neck

PGLs in other sites of the head and neck are rare, poorly documented, and often confused with a variety of other tumors.

Orbital Paragangliomas

The normal anatomical location and microanatomy of orbital paraganglia in humans are essentially unknown (18,119). The first case of an orbital paraganglioma (OPG) was reported in 1952 by Fisher and Hazard, and since 2005, only about 35 additional possible cases have been described (119,120).

The age at presentation has ranged from 3.5 to 68 years (average 36 years) with an equal gender distribution and no significant lateralization to either orbit (121). The most common signs and symptoms are unilateral proptosis, visual disturbances, and decreased ocular mobility. At least one case has been associated with an additional PGL. The patient was diagnosed as having a right ''glomus jugulare'' at the age of 25 years and 14 years later was found to have a left OPG (121).

Surgery and/or radiation are the usual modes of therapy. If incompletely excised, the tumor may recur.

Alveolar soft part sarcoma is often mistaken for an OPG. The distinction between these two tumors is rather straight forward using a synaptophysin immunostain; the OPG is positive and the alvcolar soft part sarcoma is negative.

Sinonasal Paragangliomas

Sinonasal paragangliomas (SNPGs) have occurred in patients from 8 to 89 years (average 48 years) and are more common in females by a ratio of 1.5:1 (28,122–125).

The distribution of normal paraganglia in the sinonasal tract is largely unknown. Some, however, have found evidence of paraganglionic tissue in the pterygopalatine fossa (123,126).

SNPGs present as 1.5- to 4-cm polypoid or exophytic masses and occur most often in the region of the middle turbinate or ethmoid sinus (28,123,125). Nasal obstruction and epistaxis are the usual manifestations. There is no significant lateralization to either side of the sinonasal tract and as of to date, no familial cases have been reported (124).

The tumors may erode bone and recur if inadequately treated. According to Ketabchi et al. 5 of 28 SNPGs (17.8%) have developed recurrences and/or metastases in the brain, cervical lymph nodes and bones, and four have died of disease (125). If one assumes that brain involvement was the result of local invasion (rather than metastasis), only 2 of these 28 cases (7%) could be regarded as malignant (only accepted evidence of malignancy in PGLs is metastasis not local invasion).

The differential diagnosis is broad but primarily includes ONB, muscosal melanoma, and glomangiopericytoma. The latter two tumors can be excluded by the fact that both are negative for synaptophysin. ONB, however, is more problematic, especially since it too is synaptophysin-positive and contains sustentacular cells. ONB can be recognized by its almost

invariable connection to the cribiform plate and by the presence of a neurofibrillary matrix and rosettes (Homer–Wright and Flexner–Wintersteiner).

Thyroid Parangliomas

Although not unanimous, it is the general consensus that thyroid paragangliomas (TPGs) originate from the inferior laryngeal paraganglia and present either within the thyroid gland or adjacent to its capsule (28,127–130).

Haegert et al. are often credited for the first description of a TPG in 1974 (131). LaGuette et al., however, indicate that it might have been van Miert in 1964 (130). Only 14 TPGs have been described as of 1998 and, interestingly, all cases have occurred in females ranging in age from 9 to 73 years (average 48 years). Six tumors originated in the left lobe of the thyroid, four in the right lobe, and four in the isthmus.

The tumors have ranged from 1.5 to 10 cm and at least four extended beyond the thyroid gland to involve the larynx, trachea, mediastinum, or recurrent laryngeal nerve. Three have also been associated with CBPGs (130).

The differential diagnosis most often includes MTC. MTC, however, contains amyloid and is positive for CK, calcitonin, carcinoembryonic antigen, and thyroid transcription factor. These features are absent in TPG.

Additional PGLs

Rare examples of PGLs have also been described in the pituitary fossa, nasaopharynx, tongue, trachea, and parathyroid gland (132–136).

X. MALIGNANT PERIPHERAL NERVE SHEATH TUMOR (MALIGNANT SCHWANNOMA, NEUROFIBROSARCOMA)

A. Introduction

MPNST, also referred to as malignant schwannoma, neurogenic sarcoma, and neurofibrosarcoma, is a malignant tumor arising from or differentiating toward cells intrinsic to peripheral nerve sheath (1–9) (Fig. 42A–C). A majority of MPNSTs show some evidence of Schwann cell differentiation, and a subset of MPNSTs demonstrate features of other elements of peripheral nerve sheaths such as fibroblasts or perineurial cells, but some tumors are anaplastic without any line of evident differentiation (1,10–12). Most MPNSTs arise from neurofibromas or de novo in normal peripheral nerves (4,13). Extremely rare cases of MPNSTs arise in association with schwannoma (14), ganglioneuroma, ganglioneuroblastoma (15), or pheochromocytoma (16–18). MPNSTs often resemble nonneural soft tissue sarcomas, and a diagnosis of MPNST should be made on a basis of the following widely accepted criteria: a tumor (*i*) arises within a peripheral nerve; (*ii*) arises in transition from a benign or other malignant peripheral nerve tumor such as neurofibroma, schwannoma, ganglioneuroma/ganglioneuroblastoma, or pheochromocytoma; (*iii*) develops in a patient with NF1 (von Recklinghausen's disease) and exhibits the same histological features as

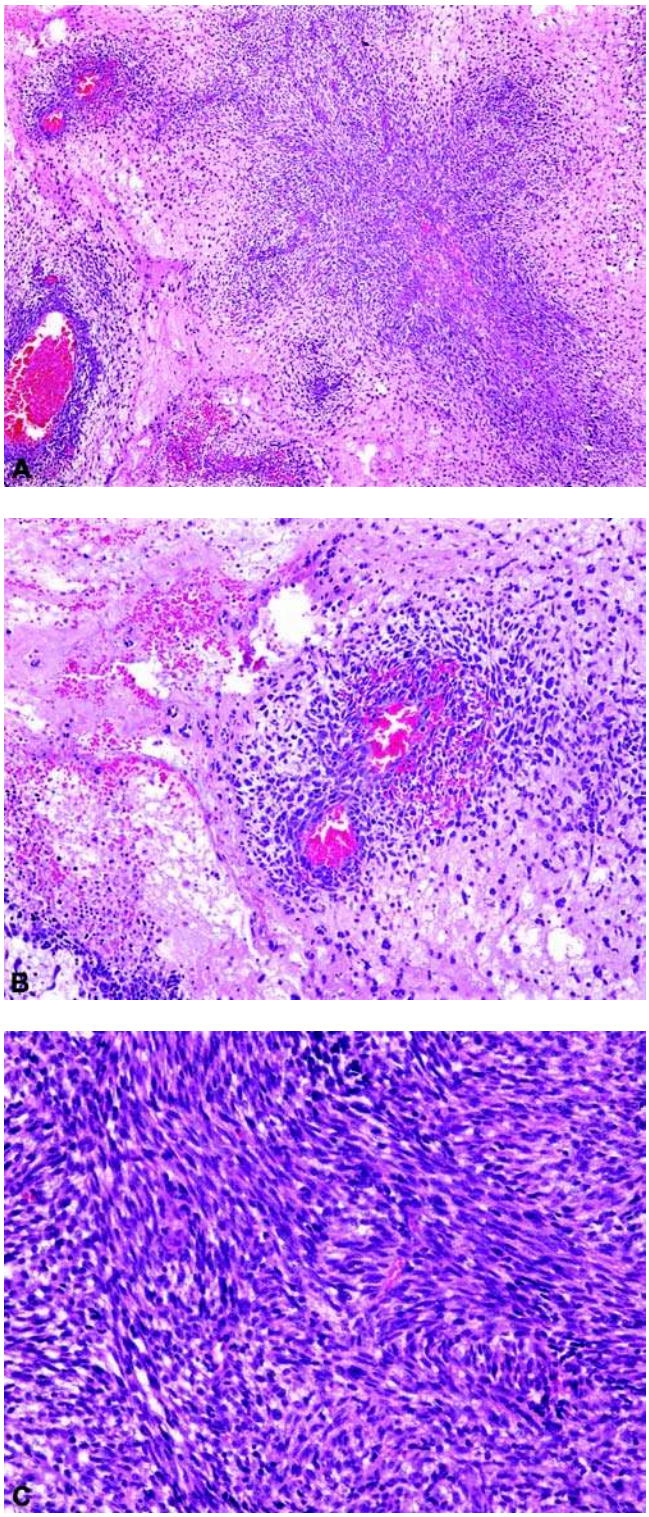

Figure 42 (**A**) Malignant peripheral nerve sheath tumor often shows alternating hypercellular and hypocellular, myxoid components (**A**: H&E, 50×). (**B**) The tumor shows diffuse necrosis with perivascular sparing of tumor cells cuffs, so-called peritheliomatous pattern (**B**: H&E, 50×). (**C**) Malignant peripheral nerve sheath tumor is generally composed of spindle cells disposed in sweeping fascicles. The spindle cells have tapered nuclei and hyperchromasia (**C**: H&E, 200×).

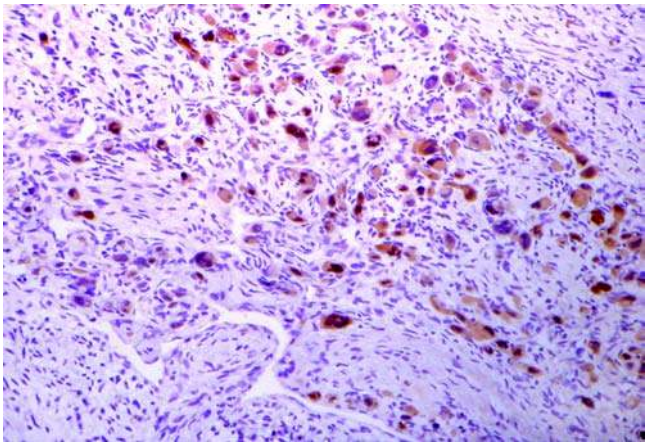

Figure 43 Malignant Triton tumor. Rhabdomyoblasts are positive for myoglobin and Schwann cells are negative (H&E, 100×). *Source*: Courtesy of Dr. L. Barnes, University of Pittsburgh School of Medicine, Pittsburgh, PA.

do a majority of MPNSTs arising from nerves; or (*iv*) develops in a patient without NF1 but exhibits the same histological features as do most MPNSTs and shows ultrastructural and immunohistochemical features of Schwann or perineurial cell differentiation. These tumors account for approximately 5% to 10% of all soft tissue sarcomas (2,12).

Several variants of MPNSTs have been described. Among these include the epithelioid MPNST (19,20), MPNST with rhabdomyoblastic differentiation (malignant Triton tumor) (Fig. 43) (21) or other mesenchymal differentiation including chondrosarcoma, osteosarcoma, and angiosarcoma (22,23), and MPNST with glands (glandular malignant schwannoma) (24). Although malignant Triton tumor can occur as a sporadic tumor, approximately half to two-thirds of reported cases occured in association with NF1 (25).

B. Clinical Features

MPNST may arise de novo or from a preexisting benign neurofibroma or PNF, especially in the setting of NF1 (1–4,7–9,26). It may also occur in areas previously exposed to ionizing radiation because of therapeutic or occupational exposure (11% of cases) with a median time from radiation to development of MPNST of approximately 15 to 18 years (27–29). Approximately 50% to 60% of MPNSTs are associated with NF1 (5,7,26,30–32). Among patients with NF1, the risk of developing MPNST is approximately 2% to 5% (4,6,7,33). Although most tumors occur in adults between the ages 20 and 50 years, patients with MPNST associated with NF1 are 10 to 15 years younger than patients without NF1 (4,13), with a median age of 28 and 40 years, respectively (4). The gender ratio is about equal in sporadic MPNSTs, whereas there is a male predominance in NF1-associated MPNSTs (1,2,31). Most tumors are associated with major nerve trunks, such as the sciatic nerve, brachial plexus, and sacral plexus, and, accordingly, common sites are the buttock, thigh, trunk, and upper arm (1,4,31).

NF1-associated MPNSTs tend to be located centrally, whereas solitary MPNSTs appear to be more widely distributed (4,31,34,35).

The head and neck is involved in 8% to 20% of cases, and the neck is the most common primary site in this region (4,36–39). The tumor has also been described in the nasal cavity (40), paranasal sinuses (36,41,42), nasopharynx (43), oral cavity (44–47), mandible (42), orbit (48–50), cranial nerves (51–53), larynx (54–56), parapharyngeal space (57), pterygomaxillary space (58), major salivary glands (47,59), and the thyroid gland (60).

MPNSTs generally present as painless, enlarging masses that are noted several months before diagnosis (2,39,42). Numbness along the distribution of the affected nerve may or may not be present (42). Tumors of the nasal cavity and paranasal sinuses may cause nasal obstruction, epistaxis, facial swelling, and proptosis (43,61). Orbital tumors typically present as a painless, palpable mass beneath the eyelid above the medial canthus. The supraorbital branch of the trigeminal nerve is usually involved, including through the superior orbital fissure to the gasserian ganglion and the trigeminal rootlets (49,50). Intracranial extension, multiple recurrences, and metastases to lungs and regional cervical lymph nodes ensue (49). Laryngeal tumors tend to be polypoid, fungating, or pedunculated, with a diameter up to 3 cm (54–56). Salivary MPNST is one of the most common primary salivary gland sarcomas, although the occurrence of the primary sarcoma itself is very rare (59). The parotid gland is the most common site, followed by the submandibular gland. The tumor presents with swelling, pain, tenderness, or paralysis in one-fourth of patients (59).

Reported cases of malignant Triton tumor in the head and neck have involved the neck, nasal cavity, paranasal sinuses, and other unusual sites such as parotid gland, thyroid gland, face, oral cavity, and infratemporal fossa (22,62–64).

C. Imaging

Tumor staging and determination of skull base involvement or intracranial spread is best evaluated by CT and MRI scans (65,66). MRI is the method of choice for evaluating the anatomical location, contour, and relation of the tumor to adjacent neural, vascular, and muscular structures. However, the imaging criteria for MPNST are not specific enough to distinguish them from other sarcomas or establish a definite diagnosis (65).

MPNST typically presents as a nonspecific soft tissue mass on imaging (67). Both bone involvement and mineralization are more common in MPNSTs than benign peripheral nerve sheath tumors and reflect the heterogeneity of the lesions seen histopathologically (67). In two reports, a significant uptake of gallium-67 citrate was seen in MPNSTs compared with minimal or no accumulation in benign nerve sheath tumors (68–70).

MPNSTs are reportedly isointense to slightly hyperintense to adjacent muscle on T1WIs and do

not demonstrate a target pattern on T2WIs (66). The tumors are inhomogeneous on T2WIs and cannot be separated from inhomogeneous benign tumors unless invasion of contiguous structure can be visualized (66). However, MPNSTs may also have well-defined margins similar to benign lesions.

D. Macroscopy

MPNSTs, particularly when arising from nerve roots or major nerves, are globoid or fusiform tumors and may be partly surrounded by epineurium. Most are surrounded by a fibrous capsule of variable thickness and are firm, fleshy, gray-tan, and often partially or extensively necrotic (12,13). The tumors generally exceed 5 cm in greatest dimension (4,13). A coexisting neurofibroma of solitary or plexiform type can be found in 81% and 41% of NF1-associated and unassociated tumors, respectively (4).

E. Histopathology

The diagnosis of MPNST should be rendered on a basis of the criteria listed in the ''Introduction.'' The tumors are highly cellular, spindle cell lesions, and resemble fibrosarcoma (2). The spindle cells have markedly irregular contours, wavy, buckled or comma-shaped nuclei, and lightly-stained, indistinct cytoplasm (1,4). Mitoses are frequently seen. Large, pleomorphic, sometimes multinucleated tumor cells can be found. The tumor cells are arranged in sweeping fascicles, but there is more variable organization than in the fibrosarcoma. Hypercellular areas alternate with hypocellular, myxoid zones (2). Perivascular crowding of tumor cells is often seen in the myxoid component. Hemangiopericytoma-type branching vessels can be found (71). Areas of geographic necrosis with or without psuedopalisading and hemorrhage may be prominent. Necrosis shows a tendency to spare the tumor cells surrounding vessels, resulting in a so-called peritheliomatous pattern.

Although most MPNSTs are high grade and conform to the above-mentioned histopathological description, low-grade tumors account for 10% to 15% of MPNSTs (4). A distinction between low-grade MPNST and neurofibromas with atypical features is often difficult. Criteria that may be helpful include (*i*) definite cell crowding, (*ii*) general nuclear enlargement (at least 3 times the size of ordinary neurofibroma nuclei), and (*iii*) hyperchromasia (1).

Approximately 20% of tumors have unusual histopathological features, which may potentially cause a diagnostic problem. About 5% of MPNSTs are characterized by epithelioid cytomorphology (epithelioid MPNSTs) (19). Epithelioid MPNST is often multinodular and is composed of nests and cords of round, eosinophilic, or amophilic epithelioid cells with vesicular nuclei and a prominent nucleolus, resembling amelanotic malignant melanoma. 15% of MPNST shows divergent differentiation such as mesenchymal or glandular differentiation (22). The mesenchymal components are generally malignant, and include rhabdomyosarcoma (malignant Triton tumor) (Fig. 43), chondrosarcoma, osteosarcoma, and angiosarcoma. The rhabdomyosarcomatous component resembles embryonal rhabdomyosarcoma, although it varies in histological appearance, and strap cells are commonly seen (21). In some cases, the myogenic differentiation is not evident on H&E stain, but it can be confirmed by immunoreactivity for skeletal muscle markers (1).

Some MPNST contain foci of malignant cartilage (chondrosarcoma) or osteoid (osteosarcoma) (22). MPNSTs with glands (glandular malignant schwannoma) are composed of a spindle cell background indistinguishable from conventional MPNSTs with a few glands that are distributed singly or in small groups and made up of well-differentiated, nonciliated cuboidal, flat, or columnar cells with clear cytoplasm and occasional goblet cells (24). The glandular elements can show squamous (1) and neuroendocrine differentiation (72).

MPNSTs with perineurial cell differentiation have been described (10,73). The perineurial component is characterized by spindle cells with long processes disposed in whorls or storiform patterns and demonstrates immunohistochemical expression for EMA but not for S-100 protein.

F. Ultrastructure

The majority of MPNSTs are undifferentiated. Some undifferentiated tumors may contain cells with features suggestive of Schwann cell differentiation, such as inconspicuous cytoplasmic processes, rudimentary cell junctions, and basement membrane material (74,75).

G. Immunohisochemistry

Approximately 40% to 80% of MPNST are positive for S-100 protein (76,77). When present, their staining is usually scattered or patchy (1). MPNSTs variably express myelin basic protein and CD57 (Leu-7) (78). This may be related to the degree of Schwann cell differentiation. Occasional MPNST may show glial fibrillary acidic protein (GFAP), EMA, or CK expression (79,80). Depending on the degree of differentiation, MPNSTs may stain for the basement membrane components such as collagen type IV and laminin (81,82). Confirmation of heterogeneous rhabdomyoblastic or glandular differentiation is readily made by immunohistochemistry (1).

H. Somatic Genetics

Patients with NF1 have germline inactivation of *NF1*. Both alleles are inactivated in neurofibromas and MPNSTs. The progression of a neurofibroma to an MPNST is associated with a number of additional chromosomal alterations. Karyotypes are complex in MPNSTs, and the most common alterations are genomic gains involving 17q, 7p, 5p, 8q, and 12q, although no pathognomic rearrangement has been identified (83). Gain of 17q material is a frequent finding that appears to be associated with poor disease outcome (84–86). A recent study showed that the topoisomerase IIα (*TOP2A*) gene on 17q21.2 might be one of the target genes for 17q amplication in MPNST and

that increased *TOP2A* expression was associated with poor clinical outcome (87). Fluorescence in situ hybridization (FISH) mapping analysis has identified a 2 Mb commonly gained or amplified region at 17q25 in MPNSTs. One of the genes included in the amplicon is *BIRC5*, which encodes an inhibitor of apoptosis. *BIRC5* is upregulated in NF1-associated MPNST, compared with PNF and dermal neurofibroma (88) and appears to be the best discriminatory information along with *MKI67* and *SPP1*, the latter two, which map to other chromosome regions (86).

I. Differential Diagnosis

A majority of MPNSTs are histologically easily recognized as a malignant tumor, and the difficulty resides in distinguishing it from other sarcomas such as fibrosarcoma, monophasic synovial sarcoma and leiomyosarcoma, and malignant melanoma. Fibrosarcoma and monophasic synovial sarcoma show a uniform fascicular growth pattern and contain fibroblast-like spindle cells. In addition, monophaisc synovial sarcomas contain hyalinized collagen bands and occasionally calcified areas (1,2). About half cases of monophasic synovial sarcoma contain cells expressing CK or EMA (89). In addition, more than 95% of synovial sarcomas are negative for S-100 protein (89–91), whereas 40% to 80% of MPNSTs express S-100 protein (76,77). Leiomyosarcomas have distinct eosinophilic cytoplasm, centrally located cigar-shaped nuclei, and perinuclear vacuoles (2) and stain positively for smooth muscle markers such as smooth muscle actin, desmin, and caldesmon (92). Fibrosarcomas lack immunoreactivity for S-100 protein and CD57 (Leu-7), and they are ultrastructurally devoid of surface basement membrane and demonstrate greater development of rough endoplasmic reticulum (1).

The distinction between MPNST and cellular neurofibroma can be made on a basis of the criteria discussed above.

Spindle cell and ordinary types of malignant melanomas can histologically resemble conventional and epithelioid MPNST, respectively. Metastatic melanomas can clinically present as a soft tissue mass, and a previous history of cutaneous melanoma is not always evident (93,94). Melanomas are not connected to a nerve, a coexistent neurofibroma, or associated with NF1 (93). A majority of malignant melanomas, including spindle cell type, show strong, diffuse immunoreactivity for S-100 protein, not to mention that ordinary malignant melanomas express a variety of melanocytic markers such as HMB45, Melan-A, tyrosinase, and microphthalmia transcription factor (95). Tumors with a microscopic appearance compatible with MPNST, but showing strong, diffuse S-100 protein immunoreaction and presence of residual lymph node structure may represent a metastatic melanoma and should initiate a search for a prior or concomitant tumor in the skin or at other sites (93). Furthermore, lymph nodes are an infrequent site for metastases in individuals with MPNST.

In the upper aerodigestive tract, MPNSTs should be distinguished from spindle cell squamous carcinoma. Spindle squamous cell carcinomas may be associated with squamous epithelial dysplasia or squamous carcinoma in situ and, although not invariably positive, reactivity of tumor cells for CK would support this diagnosis (96).

J. Treatment and Prognosis

MPNSTs are treated as high-grade sarcomas, with wide en bloc resection and local radiation therapy (37,97,98). Regional lymph node metastases rarely occur in MPNSTs, and, therefore, prophylactic lymph node dissection is not recommended (42). Chemotherapy is reserved for inoperable cases, incomplete resections, or recurrences.

The majority of MPNSTs are high-grade malignant tumors, with a high rate of metastases (1,36). The overall five-year survival of patients with MNPNST at all sites treated with surgery and with or without radiation therapy is approximately 50% (6,36). In up to 50% of patients, the tumor will recur locally, and in up to 33% of patients, metastases develop to lung and bone (6,36). In a series of 16 cases of MPNSTs in the head and neck, 66% of patients died of disease within three years, following treatment (42). Most patients had recurrence or persistence of tumor and developed metastases usually to the lungs.

The prognosis of MPNST depends on the adequacy of the surgical resection, size of the primary neoplasm, and presence or absence of NF1 (5,32,98,99). Patients with NF1-associated MPNSTs have a poorer prognosis compared with those with sporadic MPNSTs (5,30,32). Patients with malignant Triton tumors may have a worse prognosis than those with conventional MPNSTs (13,63). A subset of malignant Triton tumors of the head and neck, however, show a lower-grade histology and correlate with improved survival rate (62,100).

XI. OLFACTORY NEUROBLASTOMA

A. Introduction

ONB, first described by Berger in 1924, is a rare malignant tumor of neuroectodermal origin that originates from the olfactory neuroepithelium and accounts for approximately 3% of all intranasal tumors (1–3). The olfactory neuroepithelium extends from the roof of the nasal cavity to the midportion of the nasal septum and onto the superior turbinate (2). This epithelium is composed of sustentacular cells, sensory receptor cells, and basal cells. The basal cells are mitotically active and are presumably the progenitor of the ONB.

B. Clinical Features

ONB has a broad age range (4–14). In a recent study, the patients ranged in age from 4 to 73 years, with a mean age of 40 years and an equal sex distribution (5). About 20% of ONBs occur in the 11- to 20-year age group, and they are rare in children younger than 10 years. Unilateral nasal obstruction (71%) and epistaxis (46%) are the most common symptoms (5). Anosmia, pain, and proptosis occur in 21% of patients, each (5). ONB presents as a unilateral red-gray,

polypoid mass located high in nasal cavity and may secondarily involve the ethmoid complex, paranasal sinuses, orbit, and dura of the anterior cranial fossa (3–9). Erosion of the cribriform plate or ethmoidal roof is macroscopically present in 60% of those undergoing craniofacial resection (9). Cervical lymph nodes are involved in only 6% to 10% at presentation (10,12).

The Kadish clinical-staging system for ONB depends on whether the disease is confined to the nasal cavity (stage A) or nasal cavity and paranasal sinus(es) (stage B) or extends beyond these sites (stage C) (15). In 1997, Broich et al. performed a general review of the cases published since the discovery of the tumor in 1924 (16). Out of a total of 945 reported cases, the Kadish classification was applied to 553 cases, revealing 18% stage A, 32% stage B, and 49% stage C cases. This distribution was generally stable through the decades, and no significant changes to the proportion of Kadish stages at first diagnosis were noted in recent decades, indicating that early diagnosis is still uncommon (16).

In 1992, a study form the University of California-Los Angeles proposed a new staging system that was believed to more appropriately evaluate the most aggressive elements on ONB (5). In this classification, TI involves the nasal cavity or paranasal sinuses but not the sphenoid or the most superior ethmoidal cells. T2 involves the nasal cavity or paranasal sinuses, including the sphenoid, with erosion or extension to the cribriform plate. T3 extends to the orbit or protrudes into the anterior cranial fossa, and T4 involves the brain. With this system there was a higher correlation between stage and duration of disease-free survival, although statistical significance was not reached (5).

C. Imaging

CT and MRI scans as well as conventional radiographic techniques reveal an upper nasal soft tissue density sometimes with bone destruction and opacification of paranasal sinuses (17–22) (Fig. 44). CT shows a contrast-enhancing mass lesion and is more useful than conventional tomography in estimating extension of tumor, the associated bone destruction, secondary reaction to sinusitis, and tumoral calcification (17). CT provides the best information about local invasion into adjacent bony structures, whereas MRI allows an estimate of tumor spread into surrounding soft tissue areas, such as the anterior cranial fossa and the retromaxillary space (21). The extent of disease delineated by MRI agreed with surgical staging of the tumor in all cases studied (20). Tumors invariably involve the superior nasal cavity and then extend into the ethmoid cells (19–21). In some instances, the tumor extends to the paranasal sinuses, orbits, anterior cranial fossa, and cavernous sinus (19,20). Occasionally, skull base involvement may be missed on CT but identified correctly on MRI (20). ONBs are isointense to hyperintense with muscle on T1-weighted scans, and on T2-weighted scans, the tumor is variable in signal intensity compared with fat (20). The degree of enhancement may be minimal to moderate. In the evaluation of ONB, MRI may be more accurate than CT, and it is more useful in delineating the extent of tumor and evaluating for recurrence after craniofacial resection (19). However, the signal intensity characteristics and pattern of contrast enhancement are nonspecific for ONB and may overlap with other tumors that occur at this site (18–22).

D. Pathology

On gross examination the tumor is generally polypoid, soft, pink, tan to red-brown, and hemorrhagic (Fig. 45). Microscopically, the tumor is composed of irregular, discrete nests of lobules of small round cells slightly larger than lymphocytes often compartmentalized by prominent septa or less commonly in diffuse sheets of cells with a prominent background of capillaries but little intervening stroma (Fig. 46A–E) (3,13,23,26). The tumor cells have hyperchromatic nuclei with uniform punctate to fine chromatin

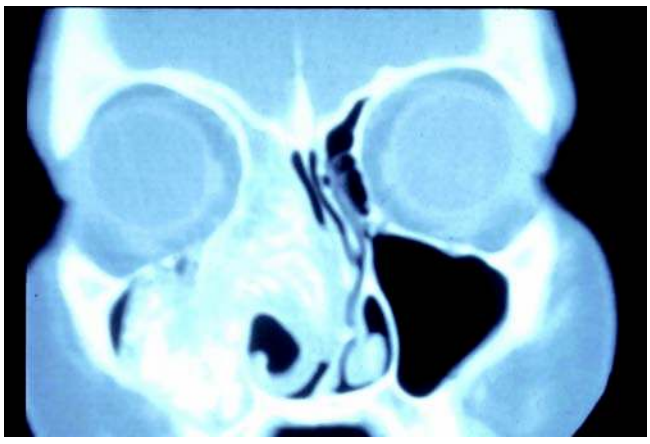

Figure 44 CT scan reveals a large tumor below the eye. *Source*: Courtesy of Dr. M. Brandwein-Gensler, Montefiore Medical Center, New York.

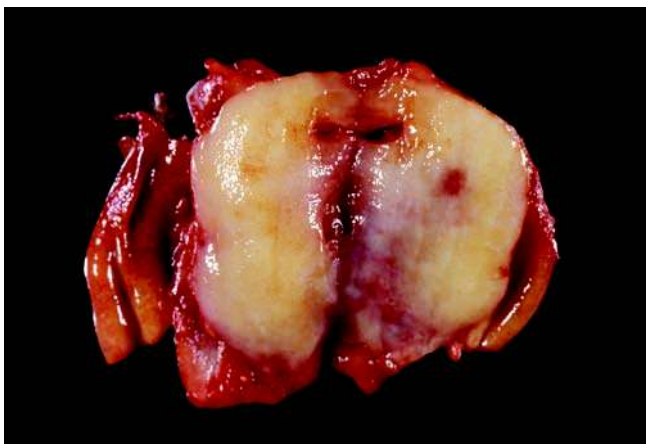

Figure 45 Olfactory neuroblastomas. Note fleshy, deceptively well-demarcated cut surface. *Source*: Courtesy of Dr. L. Barnes, University of Pittsburgh School of Medicine, Pittsburgh, PA.

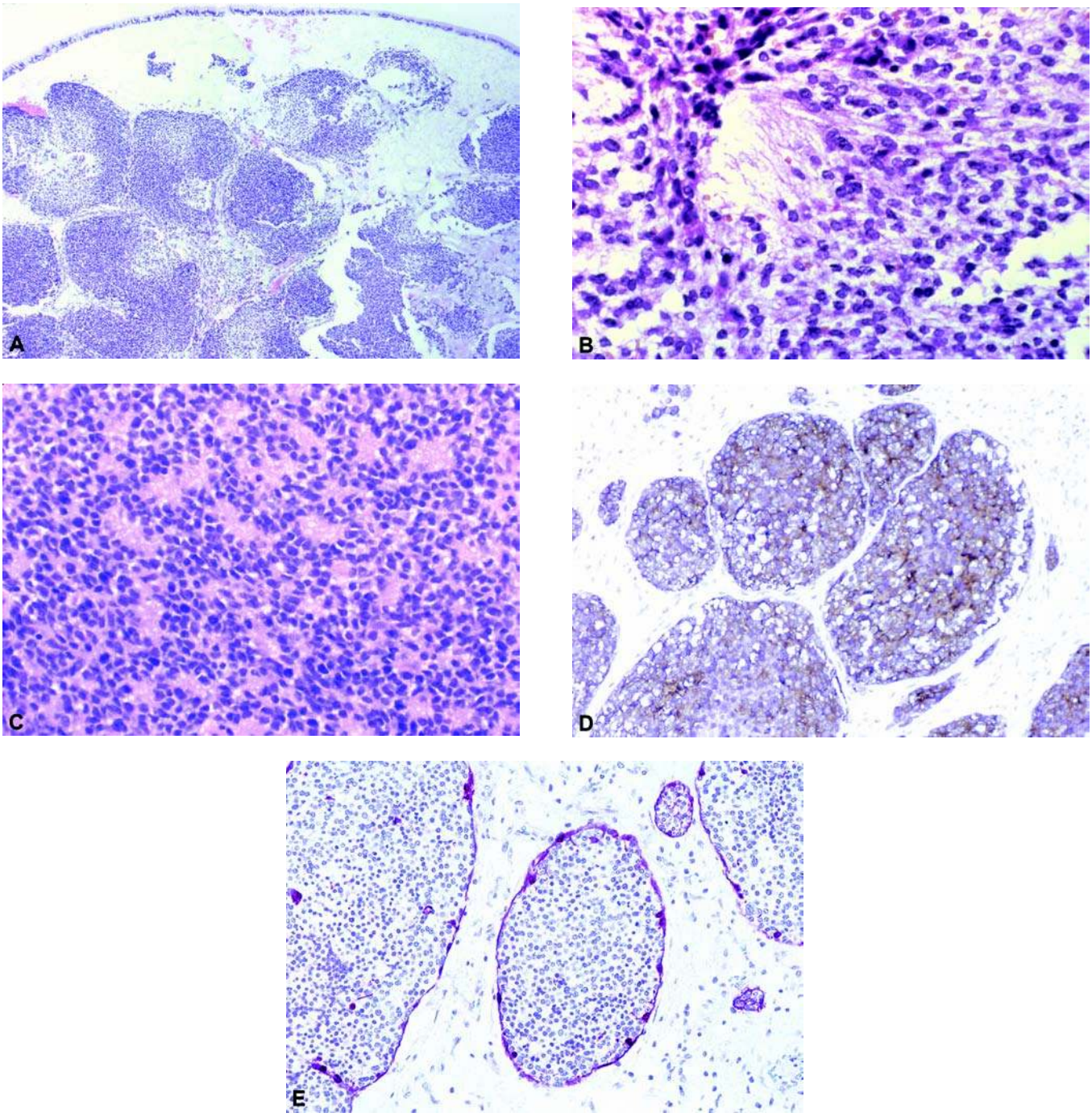

Figure 46 (**A**) Olfactory neuroblastomas. Note characteristic lobular arrangement of small round cells (**A**: H&E, 40×). The tumor is composed of uniform, small round cells. Observe the neurofibrillary matrix (**B**: H&E, 300×), and displaying prominent Homer–Wright rosettes (**C**: H&E, 200×). The tumor cells are strongly positive for synaptophysin (**D**: 200×), and the sustentacular cells are positive for S-100 protein, while the small round cells are negative (**E**: 200×). *Source*: Courtesy of Dr. Leon Barnes, University of Pittsburgh School of Medicine, Pittsburgh, PA.

distribution, small inconspicuous nucleoli, and sparse cytoplasm and are supported by a pink, delicate, neurofibrillary or edematous, well-vascularized stroma (3,13). Mitoses are absent or rare (0–2/HPF) except in high-grade tumors. Homer–Wright pseudorosettes (tumor cells surrounding a central space filled with pink fibrillar material) are seen in 30% to 50% of ONB (3,13). Flexner–Wintersteiner true rosettes (tumor cells surrounding a central lumen) are infrequent or absent (13). Necrosis, calcification, and vascular or lymphatic invasion are not uncommon. In rare instances, a few admixed ganglion cells may be seen. Cytoplasmic

Table 8 HYAMS' Grading System for Olfactory Neuroblastoma

Feature	Grade 1	Grade II	Grade III	Grade IV
Architecture	Lobular	Lobular	+/− Lobular	+/− Lobular
Mitotic activity	Absent	Present	Prominent	Marked
Nuclear pleomorphism	Absent	Moderate	Prominent	Marked
Fibrillary matrix	Prominent	Present	Minimal	Absent
Rosettes	+/− HW	+/− HW	Flexner	Absent
Necrosis	Absent	Absent	+/− Present	Common

Source: Ref. 3.

glycogen is absent and reticulin fibers surround tumor lobules rather than individual cells.

Hyams has proposed a grading system on the basis of pathological exclusion. The system includes grades (I–IV), which, according to some, correlates with prognosis (Table 8) (3). In this scheme, low-grade tumors (grades I and II) have a lobular growth pattern (3). Grade I tumors are characterized by a prominent fibrillary matrix, uniform tumor cell nuclei, and presence of Homer–Wright pseudorosettes but lack nuclear pleomorphism, mitotic activity, and necrosis (grade I). Grade II tumors show low mitotic activity (1–2/HPF) and moderate pleomorphism. In contrast, grade III to IV tumors, respectively, show prominent to marked mitotic activity, and nuclear pleomorphism, minimal to absent fibrillary matrix, focal to absent necrosis, and minimal to absent fibrillary matrix and tumor cell rosettes (3).

E. Ultrastructure

Electron microscopy and immunohistochemistry are often necessary to confirm the diagnosis of ONB (24–33). Ultrastructurally, ONB cells demonstrate uniform round nuclei and variable amounts of cytoplasmic dendritic processes containing numerous dense-core neurosecretory granules about 100 to 200 nm in diameter, in addition to neurofilaments, neurotubules, and mitochondria (25,26) (Fig. 47).

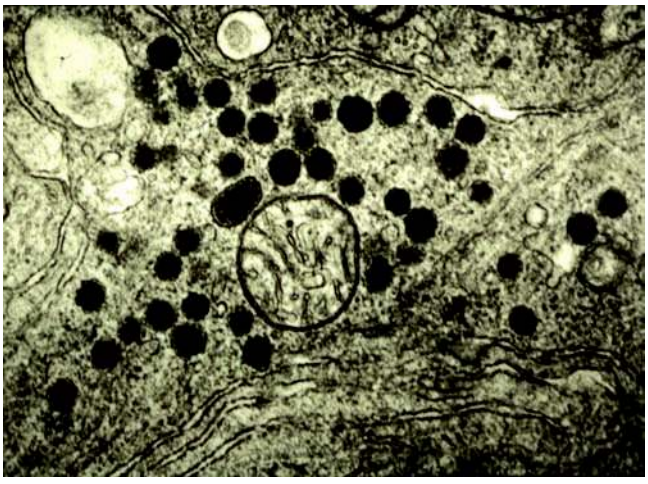

Figure 47 Ultrastructural analysis shows tumor cells containing many dense core granules.

F. Immunohistochemistry

On immunohistochemical study, consistent positive staining of tumor cells is demonstrated for NSE, and for synaptophysin or chromogranin or both in 77% to 100% of cases (9,24,25,28–32) (Fig. 46D). In some cases, tumor cells may be positive for Ber-EP4, neurofilament, or low molecular weight CK, Cam 5.2 (25–35%), but they are usually negative for CK AE1/AE3 (24,29,33). Only the supporting or sustentacicular cells, thought to be Schwann cells by electron microscopy, are positive for vimentin and S-100 protein and at times for GFAP (29). Tumor cells are invariably negative for EMA, desmin, myoglobin, vimentin, HMB45, leukocyte common antigen, and the Ewing's sarcoma (ES)/primitive neuroectodermal tumors (PNET) marker 12E7 (34–36).

G. Differential Diagnosis

The differential diagnosis of ONB is wide and includes nasopharyngeal carcinoma, sinonasal undifferentiated carcinoma (SNUC), PGL, atypical carcinoid, small cell carcinoma, malignant lymphoma, malignant melanoma, plasmacytoma, embryonal rhabdomyosarcoma, ES and related peripheral PNET, and invasive pituitary adenomas (24,29,34–37). ONB is distinguished from the other small round cell tumors that occur at this site by its characteristic morphology (pseudorosettes and neurofibrillary stroma) and ultrastructural and immunohistochemical characteristics (24–32). When rosettes are abundant, ONB may even be mistaken for adenocarcinoma.

SNUC is an aggressive tumor that is derived from Schneiderian epithelium and is distinct from ONB (Table 9) (38–41). The tumor is composed of medium-sized, polygonal cells that grow as nests, wide trabeculae, ribbons, and sheets. Tumor cells have round or oval hyperchromatic to vesicular nuclei, with moderate pleomorphism and a scant to moderate amount of eosinophilic cytoplasm. There may be accompanying dysplasia or in situ carcinoma of the overlapping epithelium. Mitoses (>10–15/10 HPF), necrosis, and vascular invasion are common. In contrast with ONB, rosettes and neurofibrillary stroma are absent, but on ultrastructural examination sparse neurosecretory granules may occasionally be seen. The tumor cells are diffusely immunoreactive for CK (AE1/AE3; 90%) and EMA (65%). Because ONB is usually negative, such positivity may help distinguish between these two tumors (39,42). In addition, ONB is

Table 9 ONB Vs. SNUC

Feature	ONB	SNUC
Age (average)	40	55–58
Site	Roof of nasal cavity	Multiple sites
Prognosis	75% 5 yr	18 mo median
Ocular-cranial nerve involvement	Occasional	Common
Anaplasia	Occasional	Common
Mitoses	Variable	Numerous
Necrosis	Occasional	Prominent
Vascular invasion	Occasional	Prominent
Neurofibrillary stroma	Common	Absent
HW rosettes	Common	Absent
Keratin	Focal at most	90%
EMA	0%	65%
NSE	100%	50%
S-100	Positive	0–15%
Synaptophysin	100%	0%
Neurosecretory granules	Numerous	Rare

Abbreviations: ONB, olfactory neuroblastoma; SNUC, sinonasal undifferentiated carcinoma.

positive for synaptophysin, whereas SNUC is negative (Fig. 46D).

ES/PNETs very rarely occur in the sinonasal region and may be mistaken for ONB. Whether ONB is a member of the ESN/PNET family of tumors has been the subject of debate. The P30/32 MIC2 (12E7) antibody, a rather specific marker for ES/PNET, is a useful method to distinguish ES/PNET from ONB and a variety of other small round cell lesions (36,37). Immunoreactivity of a small round cell malignant cytoplasm in the sinonasal tract for MIC2 (12E7) would support the diagnosis of ES/PNET rather than ONB (Table 10). ONB also is never associated with the chromosomal translocation t (11;22) (q24;q12), a finding characteristic of ES/PNET (45–47). Studies, using immunohistochemistry for expression of MIC2 antigen (antibody 12E7 or O13) and molecular techniques (RT-PCR) for the presence of the EWS/FLI1 fusion transcript, have shown that all ONB cases studied were negative (48–51). These studies have shown conclusively that ONB is not a member of the ES/PNET family.

Table 10 Differential Diagnosis of ONB Vs. ES/PNET

Features	ONB	ES/PNET
Mean age (yr)	40	>20
Gender (M:F)	1:1	1.4:1
HW rosettes	+	+
Neurofibrillary stroma	+	−
Glycogen	−	+
NSE	+	+
Synaptophysin	+	±
Neurofilament	±	±
Vimentin	−[a]	+
Cytokeratin	±	±
LCA	−	−
Desmin	−	−
S-100	−[a]	±
CD99	−	+
Neurosecretory granules (EM)	+	+
t (11;22)	−	+
Urinary catecholamines	−	−

[a]Focal, in sustentacular cells only; ±, in a proportion of cases.
Abbreviations: ONB, olfactory neuroblastoma; PNET, primitive neuroectodermal tumors; ES, Ewing's sarcoma; NSE, neuron-specific enolase; EM, electron microscopy.

H. Treatment and Prognosis

Multimodality therapy including a combination of surgery and radiation appears to provide the best disease-free and overall survival. Chemotherapy should not be used as single-modality therapy for initial treatment but may provide additional benefit when used in combination with radiation and surgery, particularly in advanced-stage disease. The literature suggests that the standard treatment of ONB is a combination of surgical resection and radiation therapy for stage A and B disease, with chemotherapy for advanced (stage C) disease (5–7,13,16,52–62). Because of the low incidence of initial cervical metastases (10%), neck dissection in a clinically negative neck is not indicated (6,14). According to Dulguerov et al., a recurrence-free status was achieved in 92% with combined craniofacial surgery and radiation therapy, compared with 14% for surgery alone and 40% for radiation alone (5).

In this study, the overall 5-year and 10-year survival, respectively, was 74% and 60%, and relapse-free survival was, respectively, 58% and 53% (5). Initial multimodality treatment in ONB is associated with long-term survival and late recurrences, and most studies indicate a five-year survival of 50% to 80% (5,10,14,16,52–56,58–62). From 14% to 68% of patients will experience local recurrences following therapy (5,7,10–14). According to Levine et al., the average time interval before recurrent disease developed was more than six years; therefore, extended follow-up is necessary (12). Sometime during the course of the disease, regional cervical lymph node metastases will develop in 10% to 25%, and distant metastases to bone, brain, and lung in 8% to 65% (4–8, 10–14,16,60,61). Distant metastases most commonly occur in bone (82%) (10).

Complete excision at initial surgery is an important prognostic factor. In the study by Dulguerov et al., adverse prognostic factors included age over 50 years at presentation, tumor recurrence, and metastases (5). Achieving local control is paramount in the success of treatment of ONB (5,7,8). According to some studies, the histological grade, low (I,II) versus high grade (III,IV), clinical stage, and DNA ploidy may be important prognostic indicators in ONB (6,62–65). Morita et al. and Lewis et al. from the Mayo Clinic found that the overall five-year survival for ONB was 67%, and that tumor grade was the only important prognostic factor (62,63). With multimodality therapy, the five-year survival for low-grade tumor was approximately 80% versus 40% for high-grade tumors (62,63). In an earlier study the five-year survival correlated with the Kadish clinical stage and was approximately 90% for clinical stage A, 71% for

state B, and 47% for stage C (6). Whether DNA ploidy is a useful, important prognostic factor has been debated (64,65). Wenig et al. studies 42 ONB by flow cytometry and observed that 14 (33%) were diploid and 28 (67%) were aneuploid or tetraploid (64). Diploid tumors were either grade I or II and aneuploid-tetraploid tumors were grade III or IV, suggesting that DNA ploidy correlates somewhat with the Hyams histological grade and may represent an additional parameter to predict prognosis.

From the study by Papadaki et al., it appears that p53 point mutation does not play an important role in the initial development of ONB (66). Their study suggests, however, that p53 wild-type overexpression may be seen in subsets of ONB likely to show local aggressive behavior and a tendency for recurrence and may be an important event in later stages of growth and progression in this tumor (66).

Van Devanter et al. found that the only cytogenetic anomaly in a case of primary ONB was the presence of trisomy 8 (67). According to these authors, trisomy 8 has not infrequently been found in other undifferentiated small round cell tumors, such as ES/PNET, Askin's tumor, and rhabdomyosarcoma, and may provide some sort of selective advantage to these tumors (67). However, further cytogenetic studies are necessary in this rare tumor to confirm the validity of this finding.

XII. MELANOTIC NEUROECTODERMAL TUMOR IN INFANCY

A. Introduction

Melanocytic neuroectodermal tumor of infancy (MNTI) is a rare neoplasm of neural crest origin affecting predominantly the craniofacial region of infants, and it is composed of a biphasic population of neuroblastic cells and pigmented epithelial cells (1–6). The lesion was first described by Krompecher in 1918 (7). It has also been referred to by a variety of terms, including ''melanotic progonoma,'' ''retinal anlage tumor,'' ''pigmented congenital epulis,'' ''melanotic ameloblastoma,'' and ''congenital melanocarcinoma,'' all of which reflect some uncertainty over its histogenesis (8). However, ultrastructural, biochemical, immunohistochemical, and cell culture studies indicate a neural crest origin (1–3,5,6,9–15). Since its first description, there have been over 350 cases reported in the literature (4).

B. Clinical Features

MNTI occurs most frequently within the first 6 months of age, with a peak incidence between the second and sixth month, and only 9% occurs at an age of more than 12 months (4). There is a slight male predominance with a male to female ratio of 1.5 to 1 (4). Approximately 93% of patients with MNTI have a mass involving craniofacial sites (3,12). The maxilla is the most common location of this tumor (61.4%) while the mandible in involved in only 6.4% (1,2,5). Other sites include the skull (8,16,17), the epididymis (18,19), the testis, the brain (20,21), and mediastinum (22). It can also present as a component of ovarian teratoma (23,24). The most common presenting symptom of the jaw tumor is a rapidly growing pigmented expansive mass, frequently involving tooth displacement (1–3). The mean duration of symptoms is 2 months, ranging from 0.5 to 5 months (1). MNTI may rarely be associated with elevated levels of α-fetoprotein (25). Rarely there are elevated serum or urine levels of vanilmandelic acid, which return to normal after excision of the tumor (26–28).

C. Imaging

The image appearance of MNTI partly depends on the location of the tumor (29). Radiographic plain films reveal predominantly osteolytic expansile bone changes caused by the rapidly growing soft tissue component of the maxillary tumor. The CT scan shows a homogenous soft tissue mass that demonstrates uniform vascular enhancement with intravenous administration of contrast material (29,30). The tumor may contain a tooth, leading to the suggestion radiologically of a dentigerous cyst or dermoid cyst. Less frequently, reactive hyperostosis at the bony margins of the maxillary or calvarial lesion may cause increased density on imaging. In such cases the differential diagnosis on imaging includes neuroblastoma, osteosarcoma, and ES (29). Although the bone changes are best seen on CT, MRI better evaluates tumor extent and tissue invasion (29). On MRI, the tumor displays homogenous isointense T1-weighted and slightly hyperintense T2-weighted signal, compared with that of muscle.

D. Macroscopy

The tumor is well-circumscribed, smooth, firm to hard, gray to blue-black, and generally ranges in size from 1 to 10 cm (mean 3.5 cm) (1,5), although tumors as large as 18 cm have been reported (31).

E. Histopathology

The MNTI is nonencapsulated and composed of alveolar nests and tubules separated by a fibrous stroma (1–3,5) (Fig. 48). The nests and tubules are populated by two distinct cell types: smaller neuroblastic cells and larger melanin-containing epithelial cells. The smaller neuroblastic cells possess small, round, hyperchromatic nuclei and scant or fibrillary cytoplasm. Maturation of neuroblastic cells to ganglion cells has been reported (32). No rosettes are present (5). The neuroblastic cells are centrally located, and surrounded and palisaded by the larger pigment-containing epithelial cells, which have less chromatic nuclei and abundant cytoplasm. Mitoses are rare, but when present as many as 7/10 HPFs can be found (5). Necrosis is usually not present.

After chemotherapy, the pigmented cells predominate in the nests, with the central portion of the nests being empty or collapsed due to depletion of the

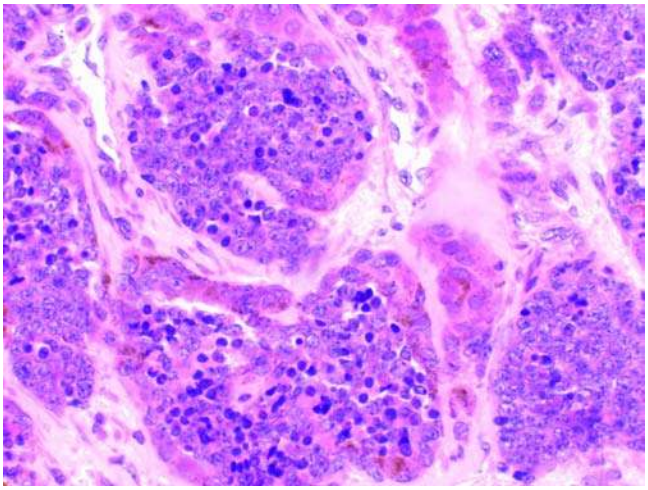

Figure 48 Small, less differentiated cells are present in the midportion of the alveolar space whereas the larger, pigmented cells are noted in the periphery (H&E, 250×). *Source*: Courtesy of Dr. Leon Barnes, University of Pittsburgh School of Medicine, Pittsburgh, PA.

neuroblastic cells (33). The stroma also becomes wider and more cellular.

F. Ultrastructure

The small cells have neurosecretory features, including dense core, membrane-bound, neurosectory granules, neurotubules, neurofilamets and cytoplasmic processes (2,3,6,11–14). The large cells demonstrate epithelial features with membrane junctional specializations such as tonofilament bundles and desmosomes, and melanocytic differentiation showing melanosomes at different stages of development.

G. Immunohistochemistry

The melanin-containing large cells are variably positive for vimentin, CK, EMA, NSE, GFAP, synaptophysin, CD57 (Leu-7), PGP 9.5, and HMB45. Immunoreactions to CD99, S-100 protein and CD56 have also been reported (1,5,10,31,34,35). The smaller cells express NSE, GFAP, PGP 9.5, CD56, and synaptophysin.

H. Somatic Genetics

MNTI does not show features of neuroblastoma, ES/peripheral neuroectodermal tumor, or desmoplastic small round cell tumor, i.e., *N-MYC* gene amplication, deletion of 1p, t(11;22)(q24;q12), and t(11;22)(p13;q12) (36). A report of cell lines derived from MNTI has described many cytogenetic structural aberrations such as der(13;21)(q10;q10) (10).

I. Differential Diagnosis

The differential diagnosis of MNTI includes small cell malignant neoplasms, such as ES/PNET, metastatic neuroblastoma, rhabdomyosarcoma, malignant lymphoma, and malignant melanoma (1,2,5). Primary malignant melanoma, especially mucosal, is extremely rare in this age group. Tumor cells of melanoma demonstrate immunoreactivity for S-100 protein and HMB45, but they are typically negative for epithelial cell markers such as CK or EMA, and other neural or neuroendocrine markers including NSE, synaptophysin, or CD57.

Neuroblastomas may rarely be pigmented, but they lack the dual cell population, and usually show diffuse reactivity for neuroendocrine markers, although they may also show positivity for CK. On occasion, MNTI may be positive for desmin and thus be confused with rhabdomyosarcomas, which are reactive not only for desmin but also for other muscle markers such as myoglobin, muscle-specific actin, myoD1, myogenin, and at times for S-100 protein and CK. MNTI, when involving the CNS, may be confused with pigmented glioma; however, its multiphenotypic nature can confirm the diagnosis of MNTI. Very rare occurrences of pigmented intraosseous odontogenic carcinoma of the maxilla, which mainly involves middle or older age groups, have been reported (9). This rare entity is distinguished from MNTI by squamous differentiation with keratinization, absence of overt neuroblastic cells, and conspicuous atypia of epithelial cells (9).

Finally, on rare occasions, immature teratomas or glial heterotopias may contain a component of MNTI (23,24,37). The teratomas containing a component of MNTI should be distinguished from pure MNTI because of their malignant potential. However, the finding of microscopic foci of MNTI in heterotopic glial tissue is of no prognostic significance. Together with its distinctive clinical and histological features, recognition of typical multiphenotypic expression should lead to an accurate diagnosis of MNTI and avoid a serious misdiagnosis (1,2).

J. Treatment and Prognosis

The clinical course is benign in most patients with MNIT; therefore, the recommended treatment is local complete excision of the tumor with negative margins (1,2,4,30,38). However, local recurrences occur in 20% of cases of MNITs, and the main locations of recurrences are maxilla and skull and brain (4). Most of the recurrences after surgical treatment occur within four weeks after the operation. Late recurrence is more common in the skull tumors, while early recurrence is more typical in the jaw tumors (4). Recurrences are frequently seen after tumor enucleation and curettage of the underlying bone, usually related to incomplete excision. 6.5% of tumors pursue malignant behaviors, which result in widespread metastases and subsequently death. The common sites of metastases are regional lymph nodes, liver, pleura, bone marrow, and pelvis (2,3,6,14,20,26,39–41). It should be noted that the potential for recurrences or metastases is unpredictable from the gross, histological, or DNA ploidy characteristics of MNTI at presentation, and there are no clinical features that distinguish between the benign form and the more aggressive variant (1,2).

The potential for malignant transformation in MNTIs further justifies the need of complete resection and close follow-up management. In patients with MNTIs in which surgical management alone is not feasible, other modalities can be selected, which include chemotherapy alone, chemotherapy with radiotherapy, chemotherapy before or after surgical treatment, radiotherapy and surgical treatment, or a combination of all (4,42).

XIII. EWING'S SARCOMA AND PRIMITIVE NEUROECTODERMAL TUMOR (PERIPHERAL NEUROEPITHELIOMA)

A. Introduction

ES/PNET are highly malignant neoplasms of neuroectodermal derivation composed of small, round, generally uniform cells with small, round, lightly stippled nuclei and glycogen-rich cytoplasm. Some of the tumor cells may be arranged in Homer–Wright rosettes and pseudorosettes (1).

Until recently, skeletal ES, extraskeletal ES, and PNET have been regarded as representing separate neoplasms. Tumors characterized by sheets of uniform primitive cells with scant cytoplasm and cytoplasmic glycogen were classified as ES, whereas tumors featuring cells with more nuclear variability, more abundant cytoplasm, and rosette formation were classified as PNET (1).

It is believed that Lücke, in 1866, was the first to recognize this tumor in the bone (2). Several well-documented cases followed. In 1921 Stout reported a tumor of the ulnar nerve characterized by undifferentiated cells and rosette formation (3). Ewing drew renewed attention to this tumor by reporting a tumor of the radius and designated it as ''diffuse endothelioma'' or ''endothelial myeloma'' (4). In 1975 Angervall and Enzinger described ES in soft tissue (extraskeletal ES) (5). The existence of extraskeletal ES was confirmed by subsequent series (6–8).

Seemayer et al. described peripheral neuroectodermal tumors, which are now called PNETs, that were not related to the nervous system (9). Jaffe et al. reported similar tumors in the bone (10). Askin et al. described the tumor under the term of ''malignant small cell tumor of the thoracopulmonary region,'' so-called Askin tumor, which was morphologically similar to PNET but with distinct clinicopathological features (11).

However, many overlapping features were also noted in skeletal ES, extraskeletal ES, PNET, and Askin tumor histopathologically, ultrastructurally, and immunohistochemically (1,12,13). Subsequently cytogenetic studies demonstrated that ES, PNET, and Askin tumor contained a common karyotypic change, i.e., t(11;22) (q24;q12), indicating a common mechanism of oncogenesis and a similar tissue of origin for these distinct clinicopathological entities (14,15). Thus the evidence supports the conclusion that ES and PNET represent a single entity in which ES represents the undifferentiated or most primitive and uncommitted member of the spectrum, whereas PNET is the more neurally differentiated counterpart, as demonstrated by morphological, ultrastructural, and immunochemical analysis (16–25).

B. Clinical Features

ES/PNET is the second most common sarcoma of bone and soft tissue in children, following rhabdomyosarcoma, and it accounts for 6% to 8% of all primary bone tumors in this age group (26,27). The etiology is unknown. These tumors rarely follow prior irradiation and chemotherapy for other malignancies in childhood (28,29). ES/PNETs show a propensity for children and adolescents. Although any age group may be affected, approximately 75% of patients are younger than 20 years, with a peak incidence in the second decade of life. There is a slight male predominance with a ratio of 1.4:1 (7,27,30–32). Occurrence is rare after the age of 40 years or before the age of 5 years (1).

Pain and a swelling or mass in the involved area are the most common symptoms. Systemic signs such as fever, anemia, leukocytosis, and increased erythrocyte sedimentation rate are also commonly seen. Pathological fracture of the involved bone is an uncommon event.

Most tumors are anatomically unassociated with nerves, ganglia, or other neural structures. ES of the bone tends to occur in the diaphysis or metaphyseal-diaphyseal portion of long bones such as the femur, tibia, humerus, and fibula, although tumors may arise in any other part of the skeleton (2,31). The pelvis and ribs are also common locations (1,33).

Soft tissues ES, referred to as extraskeletal or extraosseous ES, accounts for 4% to 7% of ESs (5,7,16,34). Extraskeletal ES has many overlapping clinical and pathological features with PNET, which also has a predisposition for soft tissues of the paraspinal tissue region, thigh, pelvis, and foot, and occur in young individuals with a mean age of 20 years (5,7,16).

Tumors of the head and neck account for approximately 8% of ES/PNET (7,35,36). In the head and neck, the skull and jaws are most often involved by ES/PNET (26,37,37,38,38,39). The mandible is affected twice as often as the maxilla (40). The tumor of the jaw commonly presents as swelling, with other manifestations including pain, loose teeth, and paresthesia (40). Less common sites in the head and neck include the nasal cavity, paranasal sinuses (41–43), particularly maxillary sinus, orbit (44–46), skull base (47,48), soft tissue of the face (49), larynx (50), pharynx (51), parapharyngeal space (52), and parotid gland (53). Rarely, ES may metastasize to the jaws from other primary sites (0.2–1.5%) (26). Primary osseous lesions are much more common than metastatic lesions in the jaws (14:1).

C. Imaging

Clinical imaging studies useful in proper staging of ES include plain radiographs, CT scans, and MRI scans (2,54–56). They may help to determine whether the tumor arises in the bone or soft tissue.

The majority of osseous tumors are located in the femur, humerus, and pelvis. On radiographs, osseous tumor may be extensive and involve the entire long bone. ES usually exhibits an osteolytic appearance

(89%), with or without bone expansion, cortical destruction, periosteal spiculated or laminated reaction (so-called onion-skin appearance), or soft tissue involvement. A pathological fracture may be present at the site of tumor. The radiographic picture, although characteristic of ES, is not specific and, especially when the tumor produces a permeative destructive appearance, may be difficult to distinguish from either osteomyelitis or other malignant tumors, such as lymphoma and metastatic carcinoma (2). Medullary involvement and subtle cortical destruction are best seen on CT scans and may be missed on plain radiographs in delineating the extent and resectability of tumor and in monitoring treatment. There is often an associated large soft tissue mass that obscures the tumor in the bone.

Imaging features of gnathic ES/PNETs are those of a poorly defined osteolytic lesion (40). An ''onion-skin'' or ''sun-ray'' periosteal reaction is rare.

Extraskeletal ES/PNET is poorly circumscribed and shows no apparent evidence of calcification prior to treatment (56,57). Tumors are of low attenuation or contain cystic areas on CT. Tumor vascularity is variable. Tumor enhancement is demonstrated in a heterogeneous fashion. On MRI images, tumors are usually hypo- or isointense compared with the muscle on T1WIs and the majority of the tumors demonstrate inhomogeneous hyperintensity relative to the muscle on T2WIs.

D. Macroscopy

The tumor is usually multilobulated, soft, friable, gray-white, and glistening with a range in size from 2 to 40 cm, with a mean of 10 cm (1,13). The tumor frequently invades bone more extensively than suspected on radiographs. Common features of ES/PNET include tumor necrosis, hemorrhage, and cyst formation. In the periosteal region the tumor may be mixed with proliferating bone and fibrous tissue. Although any part of the long bone may be involved, the medullary cavity is the most frequent site of origin. Soft tissue tumors may be surrounded by pseudocapsule. The viable tumor demonstrates a yellow-tan, fleshy appearance.

After chemotherapy, dense fibrosis, hemorrhage, and necrosis ensue without a grossly appreciable tumor component.

E. Histopathology

ES/PNET has remarkable cellularity, with little stroma, except where the lobules of the tumor are separated by strands of fibrous tissue. The tumor cells are arranged in diffuse or lobulated sheets and alveolar, angiomatoid, and a fascicular pattern. The tumor cells appear uniformly bland and undifferentiated. The mitotic index is low. The densely packed tumor cells have uniform, small, hyperchromatic, round to oval nuclei measuring 10 to 15μm in diameter, with inconspicuous nuclei, fine powdery chromatin, poorly defined vacuolated cytoplasm, and indistinct cell borders. Multinucleated giant cells are usually not present. Intracytoplasmic glycogen is present in a majority of cases and highlighted by PAS stain. However, the presence of large amounts of cytoplasmic glycogen in ES/PNET is nonspecific, as other childhood tumors also contain glycogen (31,58).

In contrast to PNET, ''pure'' ES shows no evidence of neural differentiation on routine sections, immunoshistochemistry or electron microscopy, and lacks Homer–Wright rosettes (1,13).

In the atypical or large cell variant the tumor cell nuclei are larger, with a less regular shape than that of conventional ES, and contain prominent hyperchromatin and small to medium–sized nucleoli (59). They less frequently contain cytoplasmic glycogen but more frequently form Homer–Wright rosettes and pseudorosettes (1). (Fig. 49A, B).

PNETs, in contrast to ES, form diffuse sheets, lobules, nests, or alveoli. Focal lack of cohesiveness of tumor cells may mimic that seen in rhabdomyosarcoma. Dense chromatin clumping and mitoses may be frequent in PNET (16). It is generally agreed that at least focal Homer–Wright rosette formation on histological examination, neurosecretory granules on electron microscopy, and immunoreactivity with NSE, and at least one other neuroectodermal marker (S-100 protein, Leu-7, synaptophysin, or neurofilament) is necessary for the diagnosis of PNET (16,21,60). Cytoplasmic glycogen is present in 80% and 50% of bone and soft tissue PNET, respectively (1).

A subset of ES/PNETs may show unusual morphological features that are markedly sclerosing or resemble adamantinoma or spindle cell sarcoma (61,62). Those cases may cause a diagnostic problem, and genetic confirmation may be required for a definitive diagnosis.

F. Ultrastructure

ES demonstrates densely packed uniform cells with round or oval nuclei, small nucleoli, finely dispersed chromatin, and a narrow rim of cytoplasm containing sparse organelles, rare cytoskeletal microfilaments, and pools of glycogen (6,19,20,22,63). Cell membrane densities suggestive of primitive intercellular junctions may be seen. PNET, by definition, possesses some degree of neural differentiation. Such neural differentiation may be manifested by the presence of dense-core neurosecretory granules, neuritic cell processes, synaptic-like junctions, and microtubules (16,35,63,64).

G. Immunohistochemistry

ES/PNETs show diffuse and strong immunoreaction to CD99 (MIC2) in membranous reaction and FLI1 in nuclear staining (20,61) (Fig. 49C). Vimentin is found in approximately 90% of ES/PNETs (20,35,65,66). ES/PNETs are weakly positive for low molecular weight CKs and pan-CK in 20% to 30% of ES/PNETs (20,61,63,67,68), but high molecular weight CK is

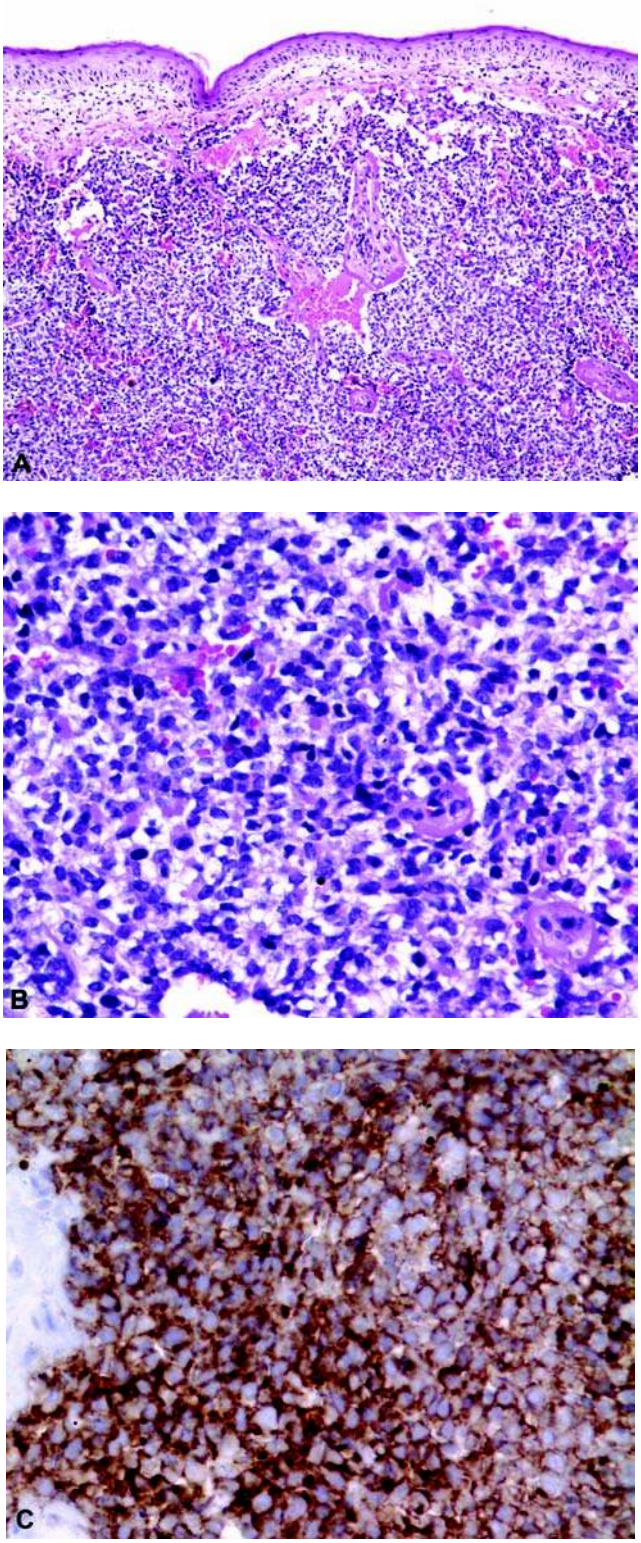

Figure 49 (**A**) Low magnification of a nasal mass composed of diffuse sheets of tumor cells with little stromal component (H&E, 50×). (**B**) The tumor cells are uniformly small and round with ill-defined, scanty, and clear to pale cytoplasm and round to oval nuclei with fine powdery chromatin (H&E, 300×). (**C**) Strong membranous CD99 immunoreactivity is characteristic of Ewing's sarcoma and primitive neuroectodermal tumor (CD 99 stain).

negative except for the tumor with adamantinoma-like morphology (61). Approximately one-quarter of cases show weak immunoreactivity for CD117 (c-kit) (61,69).

Neural markers show variable results that depend on the degree of neuroectodermal differentiation. PNETs are more commonly positive than ES. NSE reaction is found in up to 80% to 95% of PNETs (35). ES/PNETs show variable reaction to synaptophysin, CD57 (Leu-7), CD56 (NCAM), S-100 protein, neurofilament, and PGP 9.5 (20,35,60,70,71). Expression of chromogranin is uncommon (20,35).

Detection of FLI1 immunohistochemical expression, which is found in 70% of cases, also supports the diagnosis of ES/PNET (72). This marker is also expressed in lymphoblastic lymphoma and desmoplastic small round cell tumors, but is reportedly negative in other important differential diagnoses such as poorly differentiated synovial sarcomas, rhabdomyosarcoma, classic neuroblastoma, ONB, Wilms' tumor, and mesenchymal chondrosarcoma (72).

H. Somatic Genetics

Translocations involving *EWS* are a defining feature of ES/PNET. Approximately 85% of ES/PNETs are associated with the translocation t(11;22)(q24;q12), which results in the formation of the *EWS-FLI1* fusion gene (73). This fusion is commonly detected by RT-PCR and FISH (74–77). Another 10% to 15% of tumors show t(21;12)(q22;q12) that generates the *EWS-ERG* fusion, whereas the remaining 1% to 5% of tumors may harbor one of several possible translocations, each leading to a fusion gene containing a portion of the *EWS* gene and a member of ETS family of transcription factors (78).

As many as 18 types of in-frame *EWS-FLI1* chimeric transcripts have been reported. All translocations contain the trans-activating N-terminal domain of *EWS* (exons 1 to 7) and the ETS-type DNA-binding domain of *FLI1* (exon 9). The portion of the chimeric protein between these two domains is variable in size and composition, which reflects genomic breaks in one of four *EWS* introns and one of six *FLI1* introns (79,80). Approximately 85% of *EWS-FLI1* fusions are those of *EWS* exon 7 to *FLI1* exon 6 (type I) and *EWS* exon 7 to *FLI1* exon 5 (type II) (81,82). It is believed that *EWS-FLI1* as well as the other *EWS-ETS* fusion proteins functions as aberrant transcription factors (78).

Chromosomal abnormalities in ES/PNET also include both numerical and structural findings. The most common abnormalities are gains of chromosomes 8, 12, 20, and 1q, losses of 16q and 19q, and the translocation der(16)t(1;16)(q12;q11.2) (83–86).

I. Differential Diagnosis

On a purely morphological basis ES/PNET may be impossible to distinguish from the heterogeneous group of malignant small round cell tumors of childhood. These include mainly classic neuroblastoma, rhabdomyosarcoma, lymphoblastic leukemia,

malignant lymphoma, retinoblastoma, medulloblastoma, and small cell carcinoma (16,21,22,60,87–92). The diagnosis of ES/PNET has traditionally depended on the exclusion of other small cell neoplasms by light microscopy, histochemical stains, or ultrastructural studies on a basis of lack of histological and biochemical characteristics of neuroblasts, primitive skeletal muscle, epithelial cells, or lymphocytes (16,60,63). Immunophenotypic, cytogenetic, and molecular methods have greatly facilitated the differential diagnosis of these neoplasms (12,14,15,19,21,60,63,87,90–94).

ES/PNETs show varying immunopositivity for NSE and synaptophysin and are usually negative for chromogranin. Classic neuroblastomas are positive for chromogranin and show ultrastructural evidence of neurosecretory granules and neurites (10,91) (Table 10). However, they differ from ES/PNET in that they secrete catecholamines, show *N-MYC* expression, and are negative for CD99 (24,91).

Rhabdomyosarcomas are immunoreactive for muscle-specific antigens, including myogenin, myoD1, desmin, muscle-specific actin, and, less often, myoglobin (95). Occasionally, they may be focally S-100 protein- and CK-positive.

Non-Hodgkin's lymphoma can be suspected because of the undifferentiated appearance of the tumor cells. The diagnosis can be ruled out on the basis of the lobular pattern of growth and monotonous uniformity of the nuclei in ES/PNET, glycogen-rich cytoplasm, and lack of reticulin fibers in the tumor lobules (13). Lymphomas other than lymphoblastic lymphomas are usually positive for CD45 (leukocyte common antigen), and B-or T-cell markers are also expressed. Lymphoblastic leukemia/lymphoma is positive for TdT. In contrast to ES/PNET, classic neuroblastoma, central PNET (cerebellar medulloblastoma), retinoblastoma, small cell carcinoma, nonlymphoblastic lymphoma, and most rhabdomyosarcoma are negative for CD99. Although CD99 may be positive in occasional embryonal rhabdomyosarcoma and in most lymphoblastic lymphomas (12,90,93,96,97), strong diffuse CD99 immunostaining constitutes a useful positive marker for ES/PNET (73).

Cytogenetic studies and molecular methods, including Southern blot, or RT-PCR and FISH for the detection of the *EWS-FLI-1* fusion characteristic of ES/PNETs are particularly helpful in the differential diagnosis of pediatric small round cell tumors. In this heterogeneous group of tumors, only ES/PNETs demonstrate the translocation t(11;22) (q24;q12) or the *EWS-FL1-1* fusion transcripts. This cytogenetic abnormality is not seen in medulloblastoma, rhabdomyosarcoma, classic neuroblastoma, small cell carcinoma, or lymphoma and may be essential for diagnosis in difficult cases (98,99).

On occasion, ES/PNET may occur in the sinonasal region and be mistaken for ONB. Whether neuroblastoma is a member of the ES/PNET family of tumors has been long debated. However, ONB is immunonegative for CD99 and lacks the *EWS-FL1-1* fusion transcript on molecular techniques such as RT-PCR (100–103). These findings indicate that ONB is not a member of the ES/PNET family of tumors.

J. Treatment and Prognosis

ES/PNET displays an aggressive behavior with a tendency for recurrence, following resection and pronounced proclivity toward early hematogeneous metastasis to the lung, bone, and bone marrow (78). Lymph node, liver, and brain metastases are rare. Interestingly, patients with metastasis restricted to lungs seem to have a better clinical outcome compared with patients with metastasis restricted to skeletal sites or both skeletal and lung metastasis (104).

ES/PNET is currently treated by neoadjuvant chemotherapy with surgical resection followed by adjuvant chemotherapy (105). The role of radiation therapy is controversial, and many centers reserve its use for patients with positive or close margins following local resection (106). With this modality, patients can now expect 60% to 80% survival when presenting as a nonmetastatic, nonrecurrent disease, compared with about 30% a few decades ago (5,106). In those patients who do not respond well to first-line chemotherapeutic modalities or who experience a recurrence, the five-year survival rates are poor (17%) (107).

Important unfavorable prognostic factors include the presence of metastatic disease at the time of initial diagnosis, large tumor size, extensive necrosis, central axis tumors, and poor response to initial chemotherapy (108–111).

The site of the primary tumor appears to be an important prognostic factor. ES/PNET of ribs or long bones has a better prognosis than that of the pelvis, distal lesions have a better prognosis than proximal tumors, and gnathic ES/PNET has a lower mortality than ES/PNET at all other primary sites (26,38). Tumors involving cervical vertebrae are reportedly associated with a very poor prognosis (38).

Among variants of ES/PNET, atypical variant of ES appears to have a similar prognosis to that of classic ES (59), and neuroectodermal differentiation seems not to be indicative of worse prognosis (112). Patients with type I *EWS-FLI1* fusion appear to have longer disease-free survival than those with other fusion types (113). Overexpression of p53 and Ki-67 are reported to be associated with a poor outcome (114).

REFERENCES

I. ORGAN OF CHIEVITZ

1. Chievitz JH. Beitrage zur Entwickelungsgeschichte der Speicheldrusen. Arch Anat Physiol 1885; 9:401–436.
2. D'Andrea V, Malinovsky L, Biancari F, et al. The Chievitz juxtaparotid organ. G Chir 1999; 20:213–217.
3. Pantanowitz L, Balogh K. Significance of the juxtaoral organ (of Chievitz). Head Neck 2003; 25:400–405.
4. Muller E, Zenker W. Enzyme-histochemistry of the juxtaoral organ in man (''organ of Chievitz''). Histochemistry 1981; 71:279–290.
5. Gruneberg H. Exocrine glands and the Chievitz organ of some mouse mutants. J Embryol Exp Morphol 1971; 25:247–261.
6. Ide F, Mishima K, Saito I. Pacinian corpuscle in the juxtaoral organ of Chievitz. J Oral Pathol Med 2004; 33:443–444.

7. Lutman GB. Epithelial nests in intraoral sensory nerve endings simulating perineural invasion in patients with oral carcinoma. Am J Clin Pathol 1974; 61:275–284.
8. Tschen JA, Fechner RE. The juxtaoral organ of Chievitz. Am J Surg Pathol 1979; 3:147–150.
9. Ramsay AJ. Persistence of organ of Chievitz in the human. Anat Rec 1935; 63:281–293.
10. Miko T, Molnar P. The juxtaoral organ-a pitfall for pathologists. J Pathol 1981; 133:17–23.
11. Krammer EB, Zenker W. Letter: Neuroepithelial structures in the oral cavity. Am J Clin Pathol 1974; 62:571–574.
12. Lattes R. Letter: Neuroepithelial structures in the oral cavity. Am J Clin Pathol 1974; 62:570.
13. Wysocki GP, Wright BA. Intraneural and perineural epithelial structures. Head Neck Surg 1981; 4:69–71.
14. Danforth RA, Baughman RA. Chievitz's organ: a potential pitfall in oral cancer diagnosis. Oral Surg Oral Med Oral Pathol 1979; 48:31–236.
15. Vadmal MS, Rossi MB, Teichberg S, et al. Intraoral tumor of Chievitz in a child. Pediatr Dev Pathol 1998; 1:230–233.
16. Ide F, Mishima K, Saito I. Juxtaoral organ of Chievitz presenting clinically as a tumour. J Clin Pathol 2003; 56:789–790.
17. Soucy P, Cimone G, Carpenter B. An unusual intraoral mass in a child: the organ of Chievitz. J Pediatr Surg 1990; 25:1200.
18. Ide F, Mishima K, Saito I. Melanin pigmentation in the juxtaoral organ of Chievitz. Pathol Int 2003; 53:262–263.
19. Mandl L, Nerlich A, Pankratz H, et al. Das juxtaorale Organ (Chievitz-Organ)-ein sensibles Organ in der buccotemporalregion? Pathologe 1993; 14:205–209.
20. Hultenschmidt D, Vogel J, Stoll P. Das Chievitz'sche organ (juxtaorales organ): morphologische und immunohistochemische untersuchungen. Dtsch Zahn Mund Kieferheilkd Zentralbl 1991; 79:565–570.
21. Eversole LR, Leider AS. Maxillary intraosseous neuroepithelial structures resembling those seen in the organ of Chievitz. Oral Surg Oral Med Oral Pathol 1978; 46: 555–558.
22. Klacsmann PG, Taxy JB. Juxtaoral organ of Chievitz. Am J Surg Pathol 1980; 4:307–309.

II. NASAL GLIOMA

1. Reid. Uber angeborene Hirnbrucke in den Stirn und Nasengegend. Illus Med 1852; 1:133.
2. Kapadia SB, Popek EJ, Barnes L. Pediatric otorhinolaryngic pathology: diagnosis of selected lesions. Pathol Annu 1994; 29:159–209.
3. Yeoh GB, Bale PM, de Silva M. Nasal cerebral heterotopia: the so-called nasal glioma or sequestered encephalocele and its variants. Pediatric Pathol 1989; 9:531–549.
4. Penner CR, Thompson LD. Nasal glial heterotopia: A clinicopathologic and immunophenotypic analysis of 10 cases with a review of the literature. Ann Diagn Pathol 2003; 7:354–359.
5. Hughes GB, Shapiro G, Hunt W, et al. Management of the congenital nasal masses: a review. Head Neck Surg 1980; 2:222–233.
6. Myer CM, Cotton RT. Nasal obstruction in the pediatric patient. Pediatrics 1983; 72:766–777.
7. Harley EH, Pensler JM, Tomita T. Nasal midline masses in infants and children. Dermoids, encephaloceles, and gliomas. Arch Dermatol 1991; 127:362–366.
8. Paller AS, Pensler JM, Tomita T. Nasal midline masses in infants and children. Dermoids, encephaloceles, and gliomas. Arch Dermatol 1991; 127:362–366.
9. Barkovich AJ, Vandermarck P, Edwards MS, et al. Congenital nasal masses: CT and MR imaging features in 16 cases. Am J Neuroradiol 1991; 12:105–116.
10. Bradley PJ, Singh SD. Congenital nasal masses: diagnosis and management. Clin Otolaryngol 1982; 7:87–97.
11. Jaffe BF. Classification and management of anomalies of the nose. Otolaryngol Clin North Am 1981; 14:989–1004.
12. Patterson K, Kapur S, Chandra RS. ''Nasal gliomas'' and related brain heterotopias: a pathologist's perspective. Pediatr Pathol 1986; 5:353–362.
13. Azumi N, Matsuno T, Tateyama M, et al. So-called nasal glioma. Acta Pathol Jpn 1984; 34:215–220.
14. Bradley PJ, Singh SD. Nasal glioma. J Laryngol Otol 1985; 99:247–252.
15. Fletcher CD, Carpenter G, McKee PH. Nasal glioma. A rarity. Am J Dermatopathol 1986; 8:341–346.
16. Gebhart W, Hohlbrugger H, Lassmann H, et al. Nasal glioma. Int J Dermatol 1982; 21:212–215.
17. Gorenstein A, Kern EB, Facer GW, et al. Nasal gliomas. Arch Otolaryngol 1980; 106:536–540.
18. Puppala BL. Nasal glioma and encephalocele. J Neursurg 1987; 67:472–473.
19. Puppala B, Mangurten HM, McFadden J, et al. Nasal glioma. Presenting as neonatal respiratory distress. Definition of the tumor mass by MRI. Clin Pediatr 1990; 29:49–52.
20. Smith KR, Schwartz HG, Luse SA, et al. Nasal glioma: a report of five cases with electron microscopy of one. J Neurosurg 1963; 20:968–982.
21. Struass RB, Callicott JH, Hargett IR. Intranasal neuroglial heterotopia: so-called nasal glioma. Am J Dis Child 1966; 111:317–320.
22. Swift AC, Singhy SD. The presentation and management of the nasal glioma. Int J Pediatr Otorhinolaryngol 1985; 10:253–261.
23. Younus M, Coode PE. Nasal glioma and encephalocele: report of two cases. J Neurosurg 1986; 64:516–519.
24. Whitaker SR, PM. Chou SM. Nasal glioma. Arch Otolaryngol 1981; 107:550–554.
25. Mirra SS, Pearl GS, Hoffman JC, et al. Nasal glioma with prominent neuronal component: report of a case. Arch Pathol Lab Med 1981; 105:540–541.
26. Siebert RW, Seibert JJ, Angtuaco EJ. Nasopharygeal brain heterotopia – a cause of upper airway obstruction in infancy. Laryngoscope 1984; 94:818–819.
27. Madjidi A, Couly G. Heterotopic neurologial tissue of the face. Report of six cases and review of the literature. Oral Surg Oral Med Oral Pathol 1993; 76:284–288.
28. Wilkins RB, Hofmann J, Byrd WA, et al. Heterotopic brain tissue in the orbit. Arch Ophthalmol 1987; 105: 390–392.
29. Newman NJ, Miller NR, Green WR. Ectopic brain in the orbit. Ophthalmology 1986; 93:268–272.
30. Chen CY, Huang JH, Choi WM, et al. Parapharyngeal neuroglial heterotopia presenting as a growing single locular cyst: MR imaging findings. AJNR Am J Neuroradiol 2005; 26:96–99.
31. Buccoliero AM, Caldarella A, Noccioli B, et al. Brain heterotopia in pharyngeal region. A morphological and immunhistochemical study. Pathol Res Pract 2002; 198:59–63.
32. Al-Ammar AY, Al Noumas HS, Alqahtani M. A midline nasaopharyngeal heterotopic neuroglial tissue. J Laryngol Otol 2006; 120:E25.
33. Uemura T, Yoshikawa A, Onizuka T, et al. Heterotopic nasopharyngeal brain tissue associated with cleft palate. Cleft Palate Craniofac J 1999; 36:248–251.
34. McDermot MB, Glasner SD, Nielsen PL, et al. Soft tissue gliomatosis. Morphologic unity and histogenetic diversity. Am J Surg Pathol 1996; 20:148–155.

35. De Biasio P, Scarso E, Prefumo F, et al. Prenatal diagnosis of a nasal glioma in the mid trimester. Ultrasound Obstet Gynecol 2006; 27:571–573.
36. Jartti PH, Jartti AE, Karttunen AI, et al. MR of a nasal glioma in a young infant. Acta Radiol 2002; 43:141–143.
37. Amin A, Monabati A, Kumar PV, et al. Nasal glioma (neuroglial heterotopia) mimicking an astrocytoma: case report. Ear Nose Throat J 2005; 84:657–658.
38. Bozoky B, Stiller D, Ormos J. Immunohistochemical demonstration of glial fibrillary acidic protein (GFAP) in nasal gliomas. Acta Histochem 1987; 81:117–123.
39. Kindblom LG, Angervall L, Haglid K. An immunohistochemcial analysis of S100 protein in nasal glioma. Acta Pathol Microbiol Immunol Scand 1984; 92:387–389.
40. Cerda-Nicolas M, Sanchez Fernandez de Sevilla C, Lopez-Gines C, et al. Nasal glioma or nasal heterotopia? Morphological immunohistochemical and ultrastructural study of two cases. Clin Neuropathol 2002; 21:66–71.
41. Levine MR, Kellis A, Lash R. Nasal glioma masquerading as a capillary hemangioma. Ophthal Plast Reconstr Surg 1993; 9:132–134.
42. Hoeger PH, Schaefer H, Ussmueller J, et al. Nasal glioma presenting as capillary haemangioma. Eur J Pediatr 2001; 160:84–87.
43. Dasgupta NR, Bentz ML. Nasal gliomas: Identification and differentiation from hemangiomas. J Craniofac Surg 2003; 14:736–738.
44. Love GL, Riehl PA. Intranasal encephalocele masking as a nasal polyp in an adult patient. Arch Otolaryngol 1983; 109:420–421.
45. Lack EE. Extragonadal germ cell tumors of the head and neck region: review of 16 cases. Hum Pathol 1985; 16:56–64.
46. Dehner LP, Mills A, Talerman A, et al. Germ cell neoplasms of the head and neck soft tissues: a pathologic spectrum of teratomatous and endodermal sinus tumors. Hum Pathol 1990; 21:309–318.
47. Byard RW, Jimenez CL, Carpenter BF, et al. Congenital teratomas of the neck and nasopharynx: a clinical and pathologic study of 18 cases. J Paediatr Child Health 1990; 26:12–16.
48. Rahbar R, Resto VA, Robson CD, et al. Nasal glioma and encephalocele: Diagnosis and management. Laryngoscope 2003; 113:2069–2077.
49. Agirdir BV, Derin AT, Ozbilim G, et al. Endoscopic management of the intranasal glioma. J Pediatr Surg 2004; 39:1571–1573.
50. Sciarretta V, Pasquini E, Frank G, et al. Endoscopic treatment of benign tumors of the nose and paranasal sinuses: a report of 33 cases. Am J Rhinol 2006; 20:64–71.
51. Thomson HG, al-Qattan MM, Becker LE. Nasal gliomas, is dermis involvement significant? Ann Plast Surg 1995; 34:168–172.
52. Ma KH, Cheung KL. Nasal glioma. Hong Kong Med J 2006; 12:477–479.

III. NASAL ENCEPHALOCELE

1. Kapadia SB, Popek EJ, Barnes L. Pediatric otorhinolaryngic pathology: diagnosis of selected lesions. Pathol Annu 1994; 29:159–209.
2. Hyams VJ, Batsakis JG, Michaels L. Tumors of the Upper Respiratory Tract and Ear. Atlas of Tumor Pathology, 2nd Ser. Fasc 25. Washington DC: Armed Forces Institute of Pathology, 1988:251–257.
3. Janecka IP, Kapadia SB. Pediatric skull base surgery. In: Bluestone CD, Stoll SF, Kenna MA, eds. Pediatric Otolarygology. 3rd ed. Philadelphia: WB Saunders, 1995:1584–1594.
4. Adetiloye VA, Dare FO, Oyelami OA. A ten-year review of encephalocele in a teaching hospital. Int J Gynaecol Obstet 1993; 41:241–249.
5. Naidich TP, Altman NR, Braffman BH, et al. Cephaloceles and related malformations. AJNR Am J Neuroradiol 1992; 13:655–690.
6. Berry AD III, Patterson JW. Meningoceles, meningomyeloceles, and encephaloceles; a neuro-dermatopathologic study of 132 cases. J Cutan Pathol 1991; 18:164–177.
7. Docherty JG, Daly JC, Carachi R. Encephaloceles: a review 1971-1990. Eur J Pediatr Surg 1991; 1:11–13.
8. David DJ, Proudman TW. Cephaloceles: classification, pathology, and management. World J Surg 1989; 13: 349–357.
9. Blumemfeld R, Skolnik EM. Intranasal encephaloceles. Arch Otolaryngol 1965; 82:527–531.
10. Hasso AN, Miller K. Imaging of craniofacial and sinonasal anomalies. Neuroradiology J 2006; 19:413–426.
11. Rahbar R, Resto VA, Robson CD, et al. Nasal glioma and encephalocele: Diagnosis and management. Laryngoscope 2003; 113:2069–2077.
12. Suwanwela C, Sunanwela N. A morphological classification of sincipital encephalomeningoceles. J Neurosurg 1972; 36:201–211.
13. Boulanger T, Mathurin P, Dooms G, et al. Sphenopharyneal meningocephalocele: unusual clinical and radiologic features. Am J Neuroradiol 1989; 10:S80.
14. Buchfelder M, Fahlbusch R, Huk WJ, et al. Intrasphenoieal encephaloceles a clinical entity. Acta Neurochir (Wien) 1987; 89:10–15.
15. Cataltepe O, Ozcan OE. Bilateral orbital encephaloceles. An unusual cause of exophthalmos. J Clin Neuroophthalmol 1990; 10:131–134.
16. Rice JF, Eggers DM. Basal transsphenoidal encephalocele: MR findings. AJNR Am J Neuroradiol 1989; 10:S79.
17. Terry A, Patrinely JR, Anderson RL, et al. Orbital meningoencephalocele manifesting as a conjuntival mass. Am J Ophthalmol 1993; 115:46–49.
18. Kapadia SB, Janecka IP, Fernandes S, et al. Lateral basal encephalocele of the infratemporal fossa. Otolaryngol Head Neck Surg 1996; 114:116–119.
19. Choudhury AR, Taylor JC. Primary intranasal encephalocele: report of four cases. J Neurosurg 1982; 57:552–555.
20. Luyendijk W, Schmidt PH. Primary intranasal encephalocele. J Neurosurg 1983; 59:1110–1111.
21. Bagger-Sjoback D, Bergstrand G, Edner G, et al. Nasal meningocephalocele: a clinical problem. Clin Otolaryngol 1983; 8:329–335.
22. Clauser L, Baciliero U, Nordera P, et al. Frontoethmoidal meningocephalocele. A one stage correction, reconstruction, and plating by means of the micro system. J Craniofac Surg 1991; 2:2–8.
23. David DJ, Sheffield L, Simpson D, et al. Fronto-ethmoidal meningocephaloceles: morphology and treatment. Br J Plast Surg 1984; 37:271–284.
24. Losken HW, Morris WM, Earle JW. Unilateral exophthalomos caused by an anterior ethmoidal menigocephalocele. Plast Reconstr Surg 1992; 89:742–745.
25. McGarey LB, Rimsza ME, Tunnessen WW Jr. Anterior encephalocele. Am J Dis Child 1993; 147:589–590.
26. Richards CG. Frontoethmoidal meningocephalocele: a common and severe congenital abnormality in South East Asia. Arch Dis Child 1992; 67:717–719.
27. Hemmy DC, David DJ. Skeletal morphology of anterior encephaloceles defined through the use of three-dimensional reconstruction of computed tomography. Pediatr Neurosci 1985; 12:18–22.
28. Hockley AD, Goldin JW, Wake MJ. Management of anterior encephalocele. Childs Nerv Syst 1990; 6:444–446.

29. Lusk RP, Dunn VD. Magnetic resonance imaging in encephaloceles. Ann Otol Rhinol Laryngol 1986; 95:432–433.
30. Zinreich SJ, Borders JC, Eisele DW, et al. The utility of mangnetic resonance imaging in the diagnosis of intranasal meningoencephaloceles. Arch Otolaryngol Head Neck Surg 1992; 118:1253–1256.
31. Poncelet V, Dooms G, Mathurin P, et al. Contributory aspects of MRI in evaluation of basal encephaloceles. J Neuroradiol 1989; 16:214–220.
32. Lorbert J. The prognosis of occipital encephalocele. Dev Med Child Neurol (Suppl) 1966; 13:75–87.
33. Converse JM, Fleury AF. A note on frontal encephalocele. Case report with a 20-year follow-up. Plast Reconstr Surg 1972; 49:343–345.
34. Hoving EW. Nasal encephaloceles. Childs Nerv Syst 2000; 16:702–706.
35. Mahapatra AK, Suri A. Anterior encephaloceles: a study of 92 cases. Pediatr Neurosurg 2002; 36:113–118.
36. Mahapatra AK, Agrawal D. Anterior encephaloceles: a series of 103 cases over 32 years. J Clin Neurosci 2006; 13:536–539.
37. Kumar KK, Ganapathy K, Sumathi V, et al. Adult intranasal meningoencephalocele presenting as a nasal polyp. J Clin Neurosci 2005; 12:594–596.
38. Puppala B, Mangurten HH, McFadden J, et al. Nasal glioma. Presenting as neonatal respiratory distress. Definition of the tumor mass by MRI. Clin Pediatr 1990; 29:49–52.
39. Love GL, Riehl PA. Intranasal encephalocele masking as a nasal polyp in an adult patient. Arch Otolaryngol 1983; 109:420–421.
40. Charrier JB, Leboulanger N, Roger G, et al. Nasal glial heterotopia: embryological and clinical approaches. Rev Stomatol Chir Maxillofac 2006; 107:44–49.
41. Chau HN, Hopkins C, McGilligan A. A rare case of nasal glioma in the sphenoid sinus of an adult present with meningoencephalitis. Eur Arch Otorhinolaryngol 2005; 262:592–594.
42. Kim B, Park SH, Min HS, et al. Nasal chondromesenchymal hamartoma of infancy clinically mimicking meningoencephalocele. Pediatr Neurosurg 2004; 40:136–140.
43. Younus M, Coode PE. Nasal glioma and encephalocele: two separate entities. J Neurosurg 1986; 64:516–519.
44. Fujioka M, Tasaki I, Nakayama R, et al. Both nasal cerebral heterotopia and encephalocele in the same patient. Cleft Palate Craniofac J 2006; 43:112–116.
45. Kohler T, Wiedersberg H, Bollmann L. Nasal encephalocele as a cause of recurrent bacterial meningitis. Monatsschr Kinderheilkd 1991; 139:783–785.
46. Berlit P, Rakicky J, Tornow K. Primary intranasal encephalocele: a rare cause of bacterial meningitis. Acta Neurol Scand 1992; 85:404–407.
47. Hughes GB, Shapiro G, Hunt W, et al. Management of the congenital nasal masses: a review. Head Neck Surg 1980; 2:222–233.
48. David DJ, Simpson DA. Frontoethmoidal meningoencephaloceles. Clin Plast Surg 1987; 14:83–89.
49. Lello GE, Sparrow OC, Gopal R. The surgical correction of fronto-ethmoidal encephaloceles. J Craniomaxillofac Surg 1989; 17:293–298.
50. Pasquini E, Sciarretta V, Farneti G, et al. Endoscopic treatment of encephaloceles of the lateral wall of the sphenoid sinus. Minim Invasive Neurosurg 2004; 47:209–213.
51. Holmes A, Meara JG, Kolker AR, et al. Frontoethmoidal encephaloceles: Reconstruction and refinements. J Craniofac Surg 2001; 12:6–18.
52. Turgut M, Ozxan OE, Benli K, et al. Congenital nasal encephalocele: a review of 35 cases. J Craniomaxillofac Surg 1995; 23:1–5.
53. Hoving EW, Vermeij-Keers C. Frontoethmoidal encephaloceles, a study of their pathogenesis. Pediatr Neurosurg 1997; 27:246–256.
54. Marin-Padilla M. Morphogenesis of experimental encephalocele (cranioschisis occulta). J Neurol Sci 1980; 46:83–99.
55. Wexler MR, Benmeir P, Umansky F, et al. Midline cleft syndrome with sphenoethmoidal encephalocele: a case report. J Craniofac Surg 1991; 2:38–41.
56. Probst C. Multiple frontobasal meningocephalocels in neurofibromatosis. Neureofibromatosis 1989; 2:233–237.
57. Gollop TR, Kiota MM, Martins RM, et al. Frontofacionasal dysplasia: evidence of autosomal recessive inheritance. Am J Med Genet 1984; 19:301–305.
58. Jalal SM, Martin JA, Benjamin TR, et al. Unusual mosaic trisomy 13 through 13/13 translocation and monosomy 13 with a small ring. Ann Genet 1990; 33:173–175.
59. Giunta G, Piazza I. Recurrent bacterial meningitis occurring five years after closed head injury and caused by an intranasal post traumatic meningocephalocele. Postgrad Med J 1991; 67:377–379.
60. Firat AK, Firat Y. Spontaneous bilateral intrasphenoidal lateral encephaloceles: CT and MRI findings. Ear Nose Throat J 2004; 83:831–833.
61. Wolansky LJ, Chiang PK, Zurlo J, et al. Encephalocoele as a complication of intranasal sinus surgery; optimal evaluation with magnetic resonance imaging. J Laryngol Otol 1998; 112:790–792.
62. Nishizawa S, Ohta S, Yamaguchi M. Encephalocele in the ethmoid sinus presenting as a massive intracerebral hemorrhage after a ''polypectomy'': a case report. Am J Otolaryngol 2005; 26:67–70.

IV. TRAUMATIC (AMPUTATION) NEUROMA

1. Huber CC, Lewis LD. Amputation neuroma: their development and prevention. Arch Surg 1920; 1:85–113.
2. Cieslak AK, Stout AP. Traumatic and amputation neuromas. Arch Surg 1946; 53:646–651.
3. Robinson M, Slavkin HC. Dental amputation neuromas. J Am Dent Assoc 1965; 70:662–675.
4. Sist TC Jr., Greene GW. Traumatic neuroma of the oral cavity. Report of thirty-one new cases and review of the literature. Oral Surg Oral Med Oral Pathol 1981; 51:394–402.
5. Das Gupta TK, Brasfield RD. Amputation neuromas in cancer patients. N Y State J Med 1969; 69:2129–2132.
6. Scheithauer BW, Woodruff JM, Erlandson RA. Reactive lesions. In: Scheithauer BW, Woodruff JM, Erlandson RA, eds. Fascicle 24, Tumors of the Peripheral Nervous System. Washington DC: Armed Forces Institute of Pathology, 1999.
7. Hobsley M. Amputation neuroma of the great auricular nerve after parotidectomy. Br J Surg 1972; 59:735–736.
8. de Chalain T, Nahai F. Amputation neuromas of the great auricular nerve after rhytidectomy. Ann Plast Surg 1995; 35:297–299.
9. Daneshvar A. Pharyngeal traumatic neuromas and traumatic neuromas with mature ganglion cells (pseudoganglioneuromas). Am J Surg Pathol 1990; 14:565–570.
10. Gregg JM. Studies of traumatic neuralgia in the maxillofacial region: symptom complexes and response to microsurgery. J Oral Maxillofac Surg 1990; 48:135–140.
11. Chau MN, Jonsson E, Lee KM. Traumatic neuroma following sagittal mandibular osteotomy. Int J Oral Maxillofac Surg 1989; 18:95–98.
12. Waga S, Kojima T. Glossopharyngeal neuralgia of traumatic origin. Surg Neurol 1982; 17:77–79.
13. Gulya AJ, Stern NM. Facial nerve neuroma. Ann Otol Rhinol Laryngol 1993; 102:478–480.

14. Nakazawa M, Ishikawa K, Monoh K, et al. Huge facial nerve neuroma: a case report. Auris Nasus Larynx 1993; 20:309–315.
15. Gleave EN, Whittaker JS, Nicholson A. Salivary tumours–experience over thirty years. Clin Otolaryngol Allied Sci 1979; 4:247–257.
16. Chrysomali E, Papanicolaou SI, Dekker NP, et al. Benign neural tumors of the oral cavity: a comparative immunohistochemical study. Oral Surg Oral Med Oral Pathol Oral Radiol Endod 1997; 84:381–390.
17. Lee EJ, Calcaterra TC, Zuckerbraun L. Traumatic neuromas of the head and neck. Ear Nose Throat J 1998; 77:670–674, 676.

V. A. Schwannoma (Neurilemoma, Neurinoma)

1. Hasegawa SL, Mentzel T, Fletcher CD. Schwannomas of the sinonasal tract and nasopharynx. Mod Pathol 1997; 10:777–784.
2. Stout AP. The peripheral manifestations of the specific nerve sheath tumor (neurilemmoma). Am J Cancer 1935; 24:751–796.
3. Harkin JC, Reed RJ. Tumors and lesions of neurofibromatosis and other types of neurocutaneous phakomatoses. Tumors of the Peripheral Nervous System. Washington, DC: Armed Forces Institute of Pathology, 1969.
4. Scheithauer BW, Woodruff JM, Erlandson RA. Schwannoma. In: Rosai J, ed. Tumors of the Peripheral Nervous System. Washington, DC: Armed Forces Institute of Pathology, 1999.
5. Tumours of cranial and peripheral nerves, schwannomas In: Kleihues P, Cavenee WK, eds. Pathology & Genetics Tumours of the Nervous System. Lyon: IARC, 2007.
6. Weiss SW, Goldblum JR. Benign tumors of peripheral nerves. Soft Tissue Tumors. St. Louis: Mosby, 2007.
7. Das Gupta TK, Brasfield RD, Strong EW, et al. Benign solitary schwannomas (neurilemomas). Cancer 1969; 24:355–366.
8. Kragh LV, Soule EH, Masson JK. Benign and malignant neurilemmomas of the head and neck. Surg Gynecol Obstet 1960; 111:211–218.
9. Conley J, Janecka IP. Neurilemmoma of the head and neck. Trans Sect Otolaryngol Am Acad Ophthalmol Otolaryngol 1975; 80:459–464.
10. Geschickter CF. Tumors of the peripheral nerves. Am J Cancer 1935; 25:377–381.
11. Gooder P, Farrington T. Extracranial neurilemmomata of the head and neck. J Laryngol Otol 1980; 94:243–249.
12. Cherrick HM, Eversole LR. Benign neural sheath neoplasm of the oral cavity. Report of thirty-seven cases. Oral Surg Oral Med Oral Pathol 1971; 32:900–909.
13. Koizumi Y, Utsunomiya T, Yamamoto H. Cellular schwannoma in the oral mucosa. Acta Otolaryngol 2002; 122:458–462.
14. Hsu YC, Hwang CF, Hsu RF, et al. Schwannoma (neurilemmoma) of the tongue. Acta Otolaryngol 2006; 126:861–865.
15. Bildirici K, Cakli H, Kecik C, et al. Schwannoma (neurilemmoma) of the palatine tonsil. Otolaryngol Head Neck Surg 2002; 126:693–694.
16. Amir R, Altman KW, Zaheer S. Neurilemmoma of the hard palate. J Oral Maxillofac Surg 2002; 60:1069–1071.
17. Hillstrom RP, Zarbo RJ, Jacobs JR. Nerve sheath tumors of the paranasal sinuses: electron microscopy and histopathologic diagnosis. Otolaryngol Head Neck Surg 1990; 102:257–263.
18. Case records of the Massachusetts General Hospital. Weekly clinicopathological exercises. Case 14-1995. A 12-year-old boy with progressive nasal obstruction. N Engl J Med 1995; 332:1285–1291.
19. Robitaille Y, Seemayer TA, El Deiry A. Peripheral nerve tumors involving paranasal sinuses: a case report and review of the literature. Cancer 1975; 35:1254–1258.
20. Leakos M, Brown DH. Schwannomas of the nasal cavity. J Otolaryngol 1993; 22:106–107.
21. Gore DO, Rrankow R, Hanford JM. Parapharyngeal neurilemmoma. Surg Gynecol Obstet 1956; 103:193–201.
22. Taylor J, Stiefel M, Park SY. Schwannoma of the true vocal fold: a rare diagnosis. Ear Nose Throat J 2006; 85:52–53, 59.
23. Newton JR, Ruckley RW, Earl UM. Laryngeal neurilemmoma: a case report. Ear Nose Throat J 2006; 85:448–449.
24. Rosen FS, Pou AM, Quinn FB. Obstructive supraglottic schwannoma: a case report and review of the literature. Laryngoscope 2002; 112:997–1002.
25. Perzin KH, Panyu H, Wechter S. Nonepithelial tumors of the nasal cavity, paranasal sinuses and nasopharynx. A clinicopathologic study. XII: Schwann cell tumors (neurilemoma, neurofibroma, malignant schwannoma). Cancer 1982; 50:2193–2202.
26. Iwamura S, Sugiura S, Nomura Y. Schwannoma of the nasal cavity. Arch Otolaryngol 1972; 96:176–177.
27. Villanueva J, Gigoux C, Sole F. Central neurilemmoma of maxilla. A case report. Oral Surg Oral Med Oral Pathol Oral Radiol Endod 1995; 79:41–43.
28. Rootman J, Goldberg C, Robertson W. Primary orbital schwannomas. Br J Ophthalmol 1982; 66:194–204.
29. Shields JA, Kapustiak J, Arbizo V, et al. Orbital neurilemoma with extension through the superior orbital fissure. Arch Ophthalmol 1986; 104:871–873.
30. Barbosa J, Hansen LS. Solitary multilobular schwannoma of the oral cavity. J Oral Med 1984; 39:232–235.
31. Samet A, Podoshin L, Fradis M, et al. Unusual sites of schwannoma in the head and neck. J Laryngol Otol 1985; 99:523–528.
32. Hatziotis JC, Asprides H. Neurilemoma (schwannoma) of the oral cavity. Oral Surg Oral Med Oral Pathol 1967; 24:510–526.
33. Newman D, Youngs R. Neurilemmoma of the larynx. J Otolaryngol 1992; 21:72–73.
34. Takumida M, Taira T, Suzuki M, et al. Neurilemmoma of the larynx: (a case report). J Laryngol Otol 1986; 100:847–850.
35. Kumar A, Hazarika P, Kapadia RP. Neurogenic tumours of the parapharyngeal space in the paediatric age group. Int J Pediatr Otorhinolaryngol 1991; 22:195–200.
36. Aihara K, Morita A. Dumbbell-shaped hypoglossal schwannoma in an elderly woman: a clinical dilemma. Surg Neurol 2005; 63:526–528.
37. Erickson LS, Sorenson GD, McGavran MH. A Review of 140 Acoustic Neurinomas (Neurilemmoma). Laryngoscope 1965; 75:601–627.
38. Sarela AI, Bapat VN, Supe AN. Intra-parotid neurilemmomas of the facial nerve. Br J Oral Maxillofac Surg 1997; 35:71.
39. Segas JV, Kontrogiannis AD, Nomikos PN, et al. A neurilemmoma of the parotid gland: report of a case. Ear Nose Throat J 2001; 80:468–470.
40. Cohen LM, Schwartz AM, Rockoff SD. Benign schwannomas: pathologic basis for CT inhomogeneities. AJR Am J Roentgenol 1986; 147:141–143.
41. Kumar AJ, Kuhajda FP, Martinez CR, et al. Computed tomography of extracranial nerve sheath tumors with pathological correlation. J Comput Assist Tomogr 1983; 7:857–865.
42. Varma DG, Moulopoulos A, Sara AS, et al. MR imaging of extracranial nerve sheath tumors. J Comput Assist Tomogr 1992; 16:448–453.

43. Woodruff JM, Godwin TA, Erlandson RA, et al. Cellular schwannoma: a variety of schwannoma sometimes mistaken for a malignant tumor. Am J Surg Pathol 1981; 5:733–744.
44. Hajdu SI. Cellular schwannoma: a clinicopathologic, DNA flow cytometric, and proliferation marker study of 70 patients. Cancer 1996; 77:591–593.
45. Casadei GP, Scheithauer BW, Hirose T, et al. Cellular schwannoma. A clinicopathologic, DNA flow cytometric, and proliferation marker study of 70 patients. Cancer 1995; 75:1109–1119.
46. Lodding P, Kindblom LG, Angervall L, et al. Cellular schwannoma. A clinicopathologic study of 29 cases. Virchows Arch A Pathol Anat Histopathol 1990; 416:237–248.
47. DiCarlo EF, Woodruff JM, Bansal M, et al. The purely epithelioid malignant peripheral nerve sheath tumor. Am J Surg Pathol 1986; 10:478–490.
48. Kindblom LG, Meis-Kindblom JM, Havel G, et al. Benign epithelioid schwannoma. Am J Surg Pathol 1998; 22:762–770.
49. Woodruff JM. Peripheral nerve tumors showing glandular differentiation (glandular schwannomas). Cancer 1976; 37:2399–2413.
50. Woodruff JM, Christensen WN. Glandular peripheral nerve sheath tumors. Cancer 1993; 72:3618–3628.
51. Brooks JJ, Draffen RM. Benign glandular schwannoma. Arch Pathol Lab Med 1992; 116:192–195.
52. Kao GF, Laskin WB, Olsen TG. Solitary cutaneous plexiform neurilemmoma (schwannoma): a clinicopathologic, immunohistochemical, and ultrastructural study of 11 cases. Mod Pathol 1989; 2:20–26.
53. Reith JD, Goldblum JR. Multiple cutaneous plexiform schwannomas. Report of a case and review of the literature with particular reference to the association with types 1 and 2 neurofibromatosis and schwannomatosis. Arch Pathol Lab Med 1996; 120:399–401.
54. Fletcher CD, Davies SE. Benign plexiform (multinodular) schwannoma: a rare tumour unassociated with neurofibromatosis. Histopathology 1986; 10:971–980.
55. Krolls SO, McGinnis J P Jr., Quon D. Multinodular versus plexiform neurilemoma of the hard palate. Report of a case. Oral Surg Oral Med Oral Pathol 1994; 77:154–157.
56. Iwashita T, Enjoji M. Plexiform neurilemmoma: a clinicopathological and immunohistochemical analysis of 23 tumours from 20 patients. Virchows Arch A Pathol Anat Histopathol 1987; 411:305–309.
57. Woodruff JM, Marshall ML, Godwin TA, et al. Plexiform (multinodular) schwannoma. A tumor simulating the plexiform neurofibroma. Am J Surg Pathol 1983; 7:691–697.
58. Kleinman GM, Sanders FJ, Gagliardi JM. Plexiform schwannoma. Clin Neuropathol 1985; 4:265–266.
59. Val-Bernal JF, Figols J, Vazquez-Barquero A. Cutaneous plexiform schwannoma associated with neurofibromatosis type 2. Cancer 1995; 76:1181–1186.
60. Carney JA. Psammomatous melanotic schwannoma. A distinctive, heritable tumor with special associations, including cardiac myxoma and the Cushing syndrome. Am J Surg Pathol 1990; 14:206–222.
61. Di Gregorio C, Fano RA, Criscuolo M. Melanotic schwannoma: a case report. Appl Pathol 1984; 2:110–115.
62. Font RL, Truong LD. Melanotic schwannoma of soft tissues. Electron-microscopic observations and review of literature. Am J Surg Pathol 1984; 8:129–138.
63. Gregorios JB, Chou SM, Bay J. Melanotic schwannoma of the spinal cord. Neurosurgery 1982; 11:57–60.
64. Kayano H, Katayama I. Melanotic schwannoma arising in the sympathetic ganglion. Hum Pathol 1988; 19:1355–1358.
65. Killeen RM, Davy CL, Bauserman SC. Melanocytic schwannoma. Cancer 1988; 62:174–183.
66. Lowman RM, Livolsi VA. Pigmented (melanotic) schwannomas of the spinal canal. Cancer 1980; 46:391–397.
67. McGavran WL, Sypert GW, Ballinger WE. Melanotic schwannoma. Neurosurgery 1978; 2:47–51.
68. Mennemeyer RP, Hallman KO, Hammar SP, et al. Melanotic schwannoma. Clinical and ultrastructural studies of three cases with evidence of intracellular melanin synthesis. Am J Surg Pathol 1979; 3:3–10.
69. Miettinen M. Melanotic schwannoma coexpression of vimentin and glial fibrillary acidic protein. Ultrastruct Pathol 1987; 11:39–46.
70. Scully C, MacPherson SG, Reid R, et al. Melanotic nerve sheath tumour in the neck. Int J Oral Surg 1981; 10:376–379.
71. Goldblum JR, Beals TF, Weiss SW. Neuroblastoma-like neurilemoma. Am J Surg Pathol 1994; 18:266–273.
72. Fisher C, Chappell ME, Weiss SW. Neuroblastoma-like epithelioid schwannoma. Histopathology 1995; 26: 193–194.
73. Stastny JF, Frable WJ. Diagnosis of primary nerve sheath tumor of the sphenoid sinus by fine needle aspiration biopsy. A case report. Acta Cytol 1993; 37:242–246.
74. Redman RS, Guccion JG, Spector CJ, et al. Cellular schwannoma of the mandible: a case report with ultrastructural and immunohistochemical observations. J Oral Maxillofac Surg 1996; 54:339–344.
75. White W, Shiu MH, Rosenblum MK, et al. Cellular schwannoma. A clinicopathologic study of 57 patients and 58 tumors. Cancer 1990; 66:1266–1275.
76. Erlandson RA, Woodruff JM. Peripheral nerve sheath tumors: an electron microscopic study of 43 cases. Cancer 1982; 49:273–287.
77. Dickersin GR. The electron microscopic spectrum of nerve sheath tumors. Ultrastruct Pathol 1987; 11:103–146.
78. Sanguinetti C, Greco F, de Palma L, et al. The ultrastructure of schwannoma and neurofibroma of the peripheral nerves. Ital J Orthop Traumatol 1991; 17:237–246.
79. Fanburg-Smith JC, Majidi M, Miettinen M. Keratin expression in schwannoma; a study of 115 retroperitoneal and 22 peripheral schwannomas. Mod Pathol 2006; 19:115–121.
80. Haraida S, Nerlich AG, Bise K, et al. Comparison of various basement membrane components in benign and malignant peripheral nerve tumours. Virchows Arch A Pathol Anat Histopathol 1992; 421:331–338.
81. Mertens F, Dal Cin P, de Wever I, et al. Cytogenetic characterization of peripheral nerve sheath tumours: a report of the CHAMP study group. J Pathol 2000; 190:31–38.
82. Joste NE, Racz MI, Montgomery KD, et al. Clonal chromosome abnormalities in a plexiform cellular schwannoma. Cancer Genet Cytogenet 2004; 150:73–77.
83. Merel P, Hoang-Xuan K, Sanson M, et al. Predominant occurrence of somatic mutations of the NF2 gene in meningiomas and schwannomas. Genes Chromosomes Cancer 1995; 13:211–216.
84. Jacoby LB, MacCollin M, Barone R, et al. Frequency and distribution of NF2 mutations in schwannomas. Genes Chromosomes Cancer 1996; 17:45–55.
85. Irving RM, Moffat DA, Hardy DG, et al. A molecular, clinical, and immunohistochemical study of vestibular schwannoma. Otolaryngol Head Neck Surg 1997; 116:426–430.
86. Couturier J, Delattre O, Kujas M, et al. Assessment of chromosome 22 anomalies in neurinomas by combined karyotype and RFLP analyses. Cancer Genet Cytogenet 1990; 45:55–62.
87. Woodruff JM, Selig AM, Crowley K, et al. Schwannoma (neurilemoma) with malignant transformation. A rare, distinctive peripheral nerve tumor. Am J Surg Pathol 1994; 18:882–895.
88. Rasbridge SA, Browse NL, Tighe JR, et al. Malignant nerve sheath tumour arising in a benign ancient schwannoma. Histopathology 1989; 14:525–528.

V. B. Neurofibroma

1. Scheithauer BW, Woodruff JM, Erlandson RA. Neurofibroma. In: Scheithauer BW, Woodruff JM, Erlandson RA, eds. Tumors of the Peripheral Nervous System. Washington, DC: Armed Forces Institute of Pathology, 1999.
2. Harkin JC, Reed RJ. Solitary benign nerve sheath tumors. In: Harkin JC, Reed RJ, eds. Tumors of Peripheral Nervous System. Washington, DC: Armed Forces Institute of Pathology, 1969.
3. Weiss S, Goldblum J. Benign tumors of peripheral nerves. In: Weiss S, Goldblum J, eds. Soft Tissue Tumors. St. Louis: Mosby, 2001.
4. Kempf HG, Becker G, Weber BP, et al. Diagnostic and clinical outcome of neurogenic tumours in the head and neck area. ORL J Otorhinolaryngol Relat Spec 1995; 57:273–278.
5. Putney FJ, Moran JJ, Thomas GK. Neurogenic Tumors of the Head and Neck Laryngoscope 1964; 74:1037–1059.
6. Wilson JA, McLaren K, McIntyre MA, et al. Nerve-sheath tumors of the head and neck. Ear Nose Throat J 1988; 67:103–107, 110.
7. Perzin KH, Panyu H, Wechter S. Nonepithelial tumors of the nasal cavity, paranasal sinuses and nasopharynx. A clinicopathologic study. XII: Schwann cell tumors (neurilemoma, neurofibroma, malignant schwannoma). Cancer 1982; 50:2193–2202.
8. Annino DJ Jr., Domanowski GF, Vaughan CW. A rare cause of nasal obstruction: a solitary neurofibroma. Otolaryngol Head Neck Surg 1991; 104:484–488.
9. Hirao M, Gushiken T, Imokawa H, et al. Solitary neurofibroma of the nasal cavity: resection with endoscopic surgery. J Laryngol Otol 2001; 115:1012–1014.
10. Stevens DJ, Kirkham N. Neurofibromas of the paranasal sinuses. J Laryngol Otol 1988; 102:256–259.
11. Hillstrom RP, Zarbo RJ, Jacobs JR. Nerve sheath tumors of the paranasal sinuses: electron microscopy and histopathologic diagnosis. Otolaryngol Head Neck Surg 1990; 102:257–263.
12. Shields JA, Bakewell B, Augsburger JJ, et al. Classification and incidence of space-occupying lesions of the orbit. A survey of 645 biopsies. Arch Ophthalmol 1984; 102:1606–1611.
13. Rose GE, Wright JE. Isolated peripheral nerve sheath tumours of the orbit. Eye 1991; 5(Pt 6):668–673.
14. Krohel GB, Rosenberg PN, Wright JE, et al. Localized orbital neurofibromas. Am J Ophthalmol 1985; 100: 458–464.
15. Kalina PH, Bartley GB, Campbell RJ, et al. Isolated neurofibromas of the conjunctiva. Am J Ophthalmol 1991; 111:694–698.
16. Tandon DA, Bahadur S, Misra NK, et al. Parapharyngeal neurofibromas. J Laryngol Otol 1992; 106:243–246.
17. Stanley RJ, Scheithauer BW, Weiland LH, et al. Neural and neuroendocrine tumors of the larynx. Ann Otol Rhinol Laryngol 1987; 96:630–638.
18. Pearlman SJ, Friedman EA, Appel M. Neurofibroma of the larynx. Arch Otolaryngol 1950; 52:8–14.
19. Turchi R, Jemmi G. Solitary neurofibroma of the larynx. Removal by a microlaryngoscopic method. Ateneo Parmense Acta Biomed 1977; 48:27–32.
20. Mevio E, Galioto P, Scelsi M, et al. Neurofibroma of vocal cord: case report. Acta Otorhinolaryngol Belg 1990; 44:447–450.
21. Gstottner M, Galvan O, Gschwendtner A, et al. Solitary subglottic neurofibroma: a report of an unusual manifestation. Eur Arch Otorhinolaryngol 2005; 262:705–707.
22. Mori H, Kakuta S, Yamaguchi A, et al. Solitary intraosseous neurofibroma of the maxilla: report of a case. J Oral Maxillofac Surg 1993; 51:688–690.
23. Skouteris CA, Sotereanos GC. Solitary neurofibroma of the maxilla: report of a case. J Oral Maxillofac Surg 1988; 46:701–705.
24. Wright BA, Jackson D. Neural tumors of the oral cavity. A review of the spectrum of benign and malignant oral tumors of the oral cavity and jaws. Oral Surg Oral Med Oral Pathol 1980; 49:509–522.
25. Richards D. Neurofibroma of the oral cavity. Br J Oral Surg 1983; 21:36–43.
26. Zachariades N, Mezitis M, Vairaktaris E, et al. Benign neurogenic tumors of the oral cavity. Int J Oral Maxillofac Surg 1987; 16:70–76.
27. Papageorge MB, Doku HC, Lis R. Solitary neurofibroma of the mandible and infratemporal fossa in a young child. Report of a case. Oral Surg Oral Med Oral Pathol 1992; 73:407–411.
28. Ellis GL, Abrams AM, Melrose RJ. Intraosseous benign neural sheath neoplasms of the jaws. Report of seven new cases and review of the literature. Oral Surg Oral Med Oral Pathol 1977; 44:731–743.
29. Murphey MD, Smith WS, Smith SE, et al. From the archives of the AFIP. Imaging of musculoskeletal neurogenic tumors: radiologic-pathologic correlation. Radiographics 1999; 19:1253–1280.
30. Varma DG, Moulopoulos A, Sara AS, et al. MR imaging of extracranial nerve sheath tumors. J Comput Assist Tomogr 1992; 16:448–453.
31. Erlandson RA, Woodruff JM. Peripheral nerve sheath tumors: an electron microscopic study of 43 cases. Cancer 1982; 49:273–287.
32. Johnson MD, Kamso-Pratt J, Federspiel CF, et al. Mast cell and lymphoreticular infiltrates in neurofibromas. Comparison with nerve sheath tumors. Arch Pathol Lab Med 1989; 113:1263–1270.
33. Weiss SW, Nickoloff BJ. CD-34 is expressed by a distinctive cell population in peripheral nerve, nerve sheath tumors, and related lesions. Am J Surg Pathol 1993; 17:1039–1045.
34. Chanoki M, Ishii M, Fukai K, et al. Immunohistochemical localization of type I, III, IV, V, and VI collagens and laminin in neurofibroma and neurofibrosarcoma. Am J Dermatopathol 1991; 13:365–373.
35. Sawyer JR, Parr LG, Gokden N, et al. A reciprocal t(4;9) (q31;p22) in a solitary neurofibroma. Cancer Genet Cytogenet 2005; 156:172–174.
36. Krone W, Hogemann I. Cell culture studies on neurofibromatosis (von Recklinghausen). V. Monosomy 22 and other chromosomal anomalies in cultures from peripheral neurofibromas. Hum Genet 1986; 74:453–455.
37. Mertens F, Dal Cin P, De Wever I, et al. Cytogenetic characterization of peripheral nerve sheath tumours: a report of the CHAMP study group. J Pathol 2000; 190:31–38.
38. Dickersin GR. The electron microscopic spectrum of nerve sheath tumors. Ultrastruct Pathol 1987; 11:103–146.

V. C. Plexiform Neurofibroma

1. Scheithauer B, Woodruff J, Erlandson R. Neurofibroma. In: Scheithauer B, Woodruff J, Erlandson R, eds. Tumors of the Peripheral Nervous System. Washington, DC: Armed Forces Institute of Pathology, 1999.
2. McCarron KF, Goldblum JR. Plexiform neurofibroma with and without associated malignant peripheral nerve sheath tumor: a clinicopathologic and immunohistochemical analysis of 54 cases. Mod Pathol 1998; 11:612–617.
3. Harkin J, Reed R. Solitary nerve sheath tumors. In: Harkin J, Reed R, eds. Tumor of the Peripheral Nervous System. Washington, DC: Armed Forces Institute of Pathology, 1969.

4. Lin V, Daniel S, Forte V. Is a plexiform neurofibroma pathognomonic of neurofibromatosis type I? Laryngoscope 2004; 114:1410–1414.
5. Korf BR. Plexiform neurofibromas. Am J Med Genet 1999; 89:31–37.
6. Weiss S, Goldblum J. Benign Tumors of Peripheral Nerves. In: Weiss S, Goldblum J, eds. Soft Tissue Tumors. St. Louis: Mosby, 2001.
7. Dugoff L, Sujansky E. Neurofibromatosis type 1 and pregnancy. Am J Med Genet 1996; 66:7–10.
8. Krueger W, Weisberger E, Ballantyne AJ, et al. Plexiform neurofibroma of the head and neck. Am J Surg 1979; 138:517–520.
9. Sobol SE, Tewfik TL, Ortenberg J. Otolaryngologic manifestations of neurofibromatosis in children. J Otolaryngol 1997; 26:13–19.
10. Needle MN, Cnaan A, Dattilo J, et al. Prognostic signs in the surgical management of plexiform neurofibroma: the Children's Hospital of Philadelphia experience, 1974–1994. J Pediatr 1997; 131:678–682.
11. Nicol JW, Yardley MP, Parker AJ. Plexiform neurofibroma: an unusual cause of neck lump in a child. Br J Clin Pract 1994; 48:110–111.
12. Gnuechtel MM, Sales JH, Pitman KT. Plexiform neurofibroma of the retropharyngeal space: a case report. Otolaryngol Head Neck Surg 1995; 113:778–781.
13. Scott M. Massive plexiform neurofibroma of the occipital scalp. Case report. J Neurosurg 1966; 25:81–82.
14. Tseng CH, Teller WF, Zafranas A, et al. Congenital plexiform neurofibroma of the scalp. Eur Neurol 1982; 21:343–346.
15. Ayres WW, Delaney AJ, Backer MH. Congenital neurofibromatous macroglossia associated in some cases with von Recklinghausen's disease; a case report and review of the literature. Cancer 1952; 5:721–726.
16. Sahota JS, Viswanathan A, Nayak DR, et al. Giant neurofibroma of the tongue. Int J Pediatr Otorhinolaryngol 1996; 34:153–157.
17. Donner TR, Voorhies RM, Kline DG. Neural sheath tumors of major nerves. J Neurosurg 1994; 81:362–373.
18. Gholkar A, Stack JP, Isherwood I. Plexiform trigeminal neurofibroma. Clin Radiol 1988; 39:313–315.
19. Galli J, Almadori G, Paludetti G, et al. Plexiform neurofibroma of the cervical portion of the vagus nerve. J Laryngol Otol 1992; 106:643–648.
20. Boltshauser E, Stocker H, Sailer H, et al. Intracranial abnormalities associated with facial plexiform neurofibromas in neurofibromatosis type 1. Neurofibromatosis 1989; 2:274–277.
21. Tung TC, Chen YR, Chen KT, et al. Massive intratumor hemorrhage in facial plexiform neurofibroma. Head Neck 1997; 19:158–162.
22. Ferguson VM, Kyle PM. Orbital plexiform neurofibroma. Br J Ophthalmol 1993; 77:527–528.
23. Gunalp I, Gunduz K, Duruk K, et al. Neurogenic tumors of the orbit. Jpn J Ophthalmol 1994; 38:185–190.
24. Olszewski E, Dubiel-Bigaj M, Skladzien J. Plexiform neurofibroma of the larynx. A case report. Pathol Pol 1987; 38:88–92.
25. Koc C, Luxenberger W, Humer U, et al. Bilateral ventricular neurofibroma of the larynx. J Laryngol Otol 1996; 110:385–386.
26. Willcox TO, Rosenberg SI, Handler SD. Laryngeal involvement in neurofibromatosis. Ear Nose Throat J 1993; 72:811–812, 815.
27. Martin DS, Stith J, Awwad EE, et al. MR in neurofibromatosis of the larynx. AJNR Am J Neuroradiol 1995; 16:503–506.
28. Robitaille Y, Seemayer TA, El Deiry A. Peripheral nerve tumors involving paranasal sinuses: a case report and review of the literature. Cancer 1975; 35:1254–1258.
29. Tsutsumi T, Oku T, Komatsuzaki A. Solitary plexiform neurofibroma of the submandibular salivary gland. J Laryngol Otol 1996; 110:1173–1175.
30. Jackson IT, Carbonnel A, Potparic Z, et al. Orbitotemporal neurofibromatosis: classification and treatment. Plast Reconstr Surg 1993; 92:1–11.
31. Polito E, Leccisotti A, Frezzotti R. Cosmetic possibilities and problems in eyelid neurofibromas. Ophthalmic Paediatr Genet 1993; 14:43–50.
32. Chui MC, Bird BL, Rogers J. Extracranial and extraspinal nerve sheath tumors: computed tomographic evaluation. Neuroradiology 1988; 30:47–53.
33. Varma DG, Moulopoulos A, Sara AS, et al. MR imaging of extracranial nerve sheath tumors. J Comput Assist Tomogr 1992; 16:448–453.
34. Suh JS, Abenoza P, Galloway HR, et al. Peripheral (extracranial) nerve tumors: correlation of MR imaging and histologic findings. Radiology 1992; 183:341–346.
35. Lim R, Jaramillo D, Poussaint TY, et al. Superficial neurofibroma: a lesion with unique MRI characteristics in patients with neurofibromatosis type 1. AJR Am J Roentgenol 2005; 184:962–968.
36. Wise JB, Cryer JE, Belasco JB, et al. Management of head and neck plexiform neurofibromas in pediatric patients with neurofibromatosis type 1. Arch Otolaryngol Head Neck Surg 2005; 131:712–718.
37. Lin BT, Weiss LM, Medeiros LJ. Neurofibroma and cellular neurofibroma with atypia: a report of 14 tumors. Am J Surg Pathol 1997; 21:1443–1449.
38. Erlandson RA, Woodruff JM. Peripheral nerve sheath tumors: an electron microscopic study of 43 cases. Cancer 1982; 49:273–287.
39. Johnson MD, Glick AD, Davis BW. Immunohistochemical evaluation of Leu-7, myelin basic-protein, S100-protein, glial-fibrillary acidic-protein, and LN3 immunoreactivity in nerve sheath tumors and sarcomas. Arch Pathol Lab Med 1988; 112:155–160.
40. Kluwe L, Friedrich RE, Mautner VF. Allelic loss of the NF1 gene in NF1-associated plexiform neurofibromas. Cancer Genet Cytogenet 1999; 113:65–69.
41. Rasmussen SA, Overman J, Thomson SA, et al. Chromosome 17 loss-of-heterozygosity studies in benign and malignant tumors in neurofibromatosis type 1. Genes Chromosomes Cancer 2000; 28:425–431.
42. Colman SD, Williams CA, Wallace MR. Benign neurofibromas in type 1 neurofibromatosis (NF1) show somatic deletions of the NF1 gene. Nat Genet 1995; 11:90–92.
43. Serra E, Puig S, Otero D, et al. Confirmation of a double-hit model for the NF1 gene in benign neurofibromas. Am J Hum Genet 1997; 61:512–519.
44. Koga T, Iwasaki H, Ishiguro M, et al. Frequent genomic imbalances in chromosomes 17, 19, and 22q in peripheral nerve sheath tumours detected by comparative genomic hybridization analysis. J Pathol 2002; 197:98–107.
45. Woodruff JM, Marshall ML, Godwin TA, et al. Plexiform (multinodular) schwannoma. A tumor simulating the plexiform neurofibroma. Am J Surg Pathol 1983; 7:691–697.
46. Friedrich RE, Kluwe L, Funsterer C, et al. Malignant peripheral nerve sheath tumors (MPNST) in neurofibromatosis type 1 (NF1): diagnostic findings on magnetic resonance images and mutation analysis of the NF1 gene. Anticancer Res 2005; 25:1699–1702.
47. Kindblom LG, Ahlden M, Meis-Kindblom JM, et al. Immunohistochemical and molecular analysis of p53, MDM2, proliferating cell nuclear antigen and Ki67 in benign and malignant peripheral nerve sheath tumours. Virchows Arch 1995; 427:19–26.
48. Levy P, Vidaud D, Leroy K, et al. Molecular profiling of malignant peripheral nerve sheath tumors associated with

neurofibromatosis type 1, based on large-scale real-time RT-PCR. Mol Cancer 2004; 15:3–20.
49. Holtkamp N, Mautner VF, Friedrich RE, et al. Differentially expressed genes in neurofibromatosis 1-associated neurofibromas and malignant peripheral nerve sheath tumors. Acta Neuropathol (Berl) 2004; 107:159–168.
50. Greinwald J, Derkay CS, Schechter GL. Management of massive head and neck neurofibromas in children. Am J Otolaryngol 1996; 17:136–142.
51. Bader JL. Neurofibromatosis and cancer. Ann N Y Acad Sci 1986; 486:57–65.
52. Hope DG, Mulvihill JJ. Malignancy in neurofibromatosis. Adv Neurol 1981; 29:33–56.

V. D. Diffuse Neurofibroma

1. Weiss SW, Goldblum JR. Benign tumors of peripheral nerves. In: Weiss SW, Goldblum JR, eds. Soft Tissue Tumors. St. Louis: Mosby, 2001.
2. Scheithauer BW, Woodruff JM, Erlandson RA. Neurofibroma. In: Scheithauer BW, Woodruff JM, Erlandson RA, eds. Tumors of the Peripheral Nervous System. Washington, DC: Armed Forces Institute of Pathology, 1999.
3. Megahed M. Histopathological variants of neurofibroma. A study of 114 lesions. Am J Dermatopathol 1994; 16:486–495.
4. Molenaar WM, Dijkhuizen T, van Echten J, et al. Cytogenetic support for early malignant change in a diffuse neurofibroma not associated with neurofibromatosis. Cancer Genet Cytogenet 1997; 97:70–72.
5. Coakley D, Atlas MD. Diffuse neurofibroma obstructing the external auditory meatus. J Laryngol Otol 1997; 111:145–147.
6. Kapadia SB, Janecka IP, Curtin HD, et al. Diffuse neurofibroma of the orbit associated with temporal meningocele and neurofibromatosis-1. Otolaryngol Head Neck Surg 1998; 119:652–655.
7. Khan AK, Deb S, Ray DK, et al. Diffuse neurofibroma of scalp. Neurol India 2002; 50:516–517.
8. Peh WC, Shek TW, Yip DK. Magnetic resonance imaging of subcutaneous diffuse neurofibroma. Br J Radiol 1997; 70:1180–1183.
9. van Zuuren EJ, Posma AN. Diffuse neurofibroma on the lower back. J Am Acad Dermatol 2003; 48:938–940.
10. Huang GS, Huang CW, Lee HS, et al. On the AJR viewbox. Diffuse neurofibroma of the arm: MR characteristics. AJR Am J Roentgenol 2005; 184:1711–1712.
11. Beggs I, Gilmour HM, Davie RM. Diffuse neurofibroma of the ankle. Clin Radiol 1998; 53:755–759.
12. Gersell DJ, Fulling KH. Localized neurofibromatosis of the female genitourinary tract. Am J Surg Pathol 1989; 13:873–878.
13. Morizumi H, Sano T, Hirose T, et al. Neurofibroma of the gallbladder seen as a papillary polyp. Acta Pathol Jpn 1988; 38:259–268.
14. Waxman JS, Kim U, Subietas AM, et al. Diffuse neurofibroma of the pylorus: a cause of gastric outlet obstruction. Mt Sinai J Med 1989; 56:129–132.
15. Jurecka W. Tactile corpuscle-like structures in peripheral nerve sheath tumors in plastic embedded material. Am J Dermatopathol 1988; 10:74–79.

V. E. Neurofibromatosis 1

1. Scheithauer B, Woodruff J, Erlandson R. Neurofibromatosis. In: Scheithauer B, Woodruff J, Erlandson R, eds. Tumors of the Peripheral Nervous System. Washington, DC: Armed Forces Institute of Pathology, 1999.
2. Riccardi VM. Von Recklinghausen neurofibromatosis. N Engl J Med 1981; 305:1617–1627.
3. Riccardi VM. Type 1 neurofibromatosis and the pediatric patient. Curr Probl Pediatr 1992; 22:66–106.
4. Riccardi VM. Neurofibromatosis. The importance of localized or otherwise atypical forms. Arch Dermatol 1987; 123:882–883.
5. NIH Consensus Development Conference Neurofibromatosis. Conference Statement National Institutes of Health Consensus Development Conference Arch Neurol 1988; 45:575–578.
6. Barker D, Wright E, Nguyen K, et al. Gene for von Recklinghausen neurofibromatosis is in the pericentromeric region of chromosome 17. Science 1987; 236:1100–1102.
7. Lazaro C, Ravella A, Gaona A, et al. Neurofibromatosis type 1 due to germ-line mosaicism in a clinically normal father. N Engl J Med 1994; 331:1403–1407.
8. Littler M, Morton NE. Segregation analysis of peripheral neurofibromatosis (NF1). J Med Genet 1990; 27:307–310.
9. Evans DG, Huson SM, Donnai D, et al. A genetic study of type 2 neurofibromatosis in the United Kingdom. I. Prevalence, mutation rate, fitness, and confirmation of maternal transmission effect on severity. J Med Genet 1992; 29:841–846.
10. Riccardi VM, Lewis RA. Penetrance of von Recklinghausen neurofibromatosis: a distinction between predecessors and descendants. Am J Hum Genet 1988; 42:284–289.
11. Yohay K. Neurofibromatosis types 1 and 2. Neurologist 2006; 12:86–93.
12. Lubs ML, Bauer MS, Formas ME, et al. Lisch nodules in neurofibromatosis type 1. N Engl J Med 1991; 324: 1264–1266.
13. Lewis RA, Riccardi VM. Von Recklinghausen neurofibromatosis. Incidence of iris hamartomata. Ophthalmology 1981; 88:348–354.
14. Rodriguez HA, Berthrong M. Multiple primary intracranial tumors in von Recklinghausen's neurofibromatosis. Arch Neurol 1966; 14:467–475.
15. Listernick R, Charrow J, Greenwald MJ, et al. Optic gliomas in children with neurofibromatosis type 1. J Pediatr 1989; 114:788–792.
16. Crawford AH, Schorry EK. Neurofibromatosis update. J Pediatr Orthop 2006; 26:413–423.
17. Zvulunov A, Barak Y, Metzker A. Juvenile xanthogranuloma, neurofibromatosis, and juvenile chronic myelogenous leukemia. World statistical analysis. Arch Dermatol 1995; 131:904–908.
18. Matsui I, Tanimura M, Kobayashi N, et al. Neurofibromatosis type 1 and childhood cancer. Cancer 1993; 72:2746–2754.
19. Morier P, Merot Y, Paccaud D, et al. Juvenile chronic granulocytic leukemia, juvenile xanthogranulomas, and neurofibromatosis. Case report and review of the literature. J Am Acad Dermatol 1990; 22:962–965.
20. Ferrari A, Bisogno G, Macaluso A, et al. Soft-tissue sarcomas in children and adolescents with neurofibromatosis type 1. Cancer 2007; 109:1406–1412.
21. Blatt J, Jaffe R, Deutsch M, et al. Neurofibromatosis and childhood tumors. Cancer 1986; 57:1225–1229.
22. Neumann HP, Cybulla M, Shibata H, et al. New genetic causes of pheochromocytoma: current concepts and the clinical relevance. Keio J Med 2005; 54:15–21.
23. Fuller CE, Williams GT. Gastrointestinal manifestations of type 1 neurofibromatosis (von Recklinghausen's disease). Histopathology 1991; 19:1–11.
24. Miettinen M, Fetsch JF, Sobin LH, et al. Gastrointestinal stromal tumors in patients with neurofibromatosis 1: a clinicopathologic and molecular genetic study of 45 cases Am J Surg Pathol 2006; 30:90–96.
25. Scheithauer BW, Nora FE, LeChago J, et al. Duodenal gangliocytic paraganglioma. Clinicopathologic and immunocytochemical study of 11 cases. Am J Clin Pathol 1986; 86:559–565.

26. Mathew P, Roberts JA, Zwischenberger J, et al. Mediastinal atypical carcinoid and neurofibromatosis type 1. Arch Pathol Lab Med 2000; 124:319–321.
27. Hough DR, Chan A, Davidson H. Von Recklinghausen's disease associated with gastrointestinal carcinoid tumors. Cancer 1983; 51:2206–2208.
28. Davis WB, Edgerton MT, Hoffmeister SF. Neurofibromatosis of the head and neck. Plast Reconstr Surg 1954; 14:186–199.
29. White AK, Smith RJ, Bigler CR, et al. Head and neck manifestations of neurofibromatosis. Laryngoscope 1986; 96:732–737.
30. Maceri DR, Saxon KG. Neurofibromatosis of the head and neck. Head Neck Surg 1984; 6:842–850.
31. Poole MD. Experiences in the surgical treatment of craniorbital neurofibromatosis. Br J Plast Surg 1989; 42:155–162.
32. van der Meulen J. Orbital neurofibromatosis. Clin Plast Surg 1987; 14:123–135.
33. Jackson IT, Laws ER Jr., Martin RD. The surgical management of orbital neurofibromatosis. Plast Reconstr Surg 1983; 71:751–758.
34. Linder B, Campos M, Schafer M. CT and MRI of orbital abnormalities in neurofibromatosis and selected craniofacial anomalies. Radiol Clin North Am 1987; 25:787–802.
35. Huson S, Jones D, Beck L. Ophthalmic manifestations of neurofibromatosis. Br J Ophthalmol 1987; 71:235–238.
36. Holt GR. E.N.T. manifestations of Von Recklinghausen's disease. Laryngoscope 1978; 88:1617–1632.
37. Lustig LR, Jackler RK. Neurofibromatosis type I involving the external auditory canal. Otolaryngol Head Neck Surg 1996; 114:299–307.
38. Chang-Lo M. Laryngeal involvement in Von Recklinghausen's disease: a case report and review of the literature. Laryngoscope 1977; 87:435–442.
39. Heppt W, Adler D, Waldecker-Herrmann P. Laryngeal obstruction due to familial Recklinghausen's disease. Laryngorhinootologie 1991; 70:154–157.
40. Willcox TO Jr., Rosenberg SI, Handler SD. Laryngeal involvement in neurofibromatosis. Ear Nose Throat J 1993; 72:811–812, 815.
41. Martin DS, Stith J, Awwad EE, et al. MR in neurofibromatosis of the larynx. AJNR Am J Neuroradiol 1995; 16:503–506.
42. D'Ambrosio JA, Langlais RP, Young RS. Jaw and skull changes in neurofibromatosis. Oral Surg Oral Med Oral Pathol 1988; 66:391–396.
43. Geist JR, Gander DL, Stefanac SJ. Oral manifestations of neurofibromatosis types I and II. Oral Surg Oral Med Oral Pathol 1992; 73:376–382.
44. Jackson IT, Laws ER Jr., Martin RD. The surgical management of orbital neurofibromatosis. Plast Reconstr Surg 1983; 71:751–758.
45. Arun D, Gutmann DH. Recent advances in neurofibromatosis type 1. Curr Opin Neurol 2004; 17:101–105.
46. Klatte EC, Franken EA, Smith JA. The radiographic spectrum in neurofibromatosis. Semin Roentgenol 1976; 11:17–33.
47. Duffner PK, Cohen ME, Seidel FG, et al. The significance of MRI abnormalities in children with neurofibromatosis. Neurology 1989; 39:373–378.
48. Truhan AP, Filipek PA. Magnetic resonance imaging. Its role in the neuroradiologic evaluation of neurofibromatosis, tuberous sclerosis, and Sturge-Weber syndrome. Arch Dermatol 1993; 129:219–226.
49. Evans DG, Baser ME, McGaughran J, et al. Malignant peripheral nerve sheath tumours in neurofibromatosis 1. J Med Genet 2002; 39:311–314.
50. Basu TN, Gutmann DH, Fletcher JA, et al. Aberrant regulation of ras proteins in malignant tumour cells from type 1 neurofibromatosis patients. Nature 1992; 356:713–715.
51. Tong J, Hannan F, Zhu Y, et al. Neurofibromin regulates G protein-stimulated adenylyl cyclase activity. Nat Neurosci 2002; 5:95–96.
52. Adkins JC, Ravitch MM. The operative management of von Recklinghausen's neurofibromatosis in children, with special reference to lesions of the head and neck. Surgery 1977; 82:342–348.
53. Sorensen SA, Mulvihill JJ, Nielsen A. Long-term follow-up of von Recklinghausen neurofibromatosis. Survival and malignant neoplasms. N Engl J Med 1986; 314:1010–1015.
54. Guccion JG, Enzinger FM. Malignant Schwannoma associated with von Recklinghausen's neurofibromatosis. Virchows Arch A Pathol Anat Histol 1979; 383:43–57.

V. F. Neurofibromatosis 2 (Bilateral Acoustic Neuroma)

1. Evans DG, Huson SM, Donnai D, et al. A genetic study of type 2 neurofibromatosis in the United Kingdom. II. Guidelines for genetic counseling. J Med Genet 1992; 29:847–852.
2. Martuza RL, Eldridge R. Neurofibromatosis 2 (bilateral acoustic neurofibromatosis). N Engl J Med 1988; 318:684–688.
3. Riccardi VM. Molecular biology of the neurofibromatoses. Semin Dermatol 1993; 12:266–273.
4. Mulvihill JJ, Parry DM, Sherman JL, et al. NIH conference. Neurofibromatosis 1 (Recklinghausen disease) and neurofibromatosis 2 (bilateral acoustic neurofibromatosis). An update. Ann Intern Med 1990; 113:39–52.
5. Flexon PB, Nadol JB Jr., Schuknecht HF, et al. Bilateral acoustic neurofibromatosis (neurofibromatosis 2): a disorder distinct from von Recklinghausen's neurofibromatosis (neurofibromatosis 1). Ann Otol Rhinol Laryngol 1991; 100:830–834.
6. National Institutes of Health Consensus Development Conference Statement: neurofibromatosis. Bethesda, Md., USA, July 13-15, 1987 Neurofibromatosis 1988; 1:172–178.
7. Evans DG, Bourn D, Wallace A, et al. Diagnostic issues in a family with late onset type 2 neurofibromatosis. J Med Genet 1995; 32:470–474.
8. Gijtenbeek JM, Gabreels-Festen AA, Lammens M, et al. Mononeuropathy multiplex as the initial manifestation of neurofibromatosis type 2. Neurology 2001; 56:1766–1768.
9. Gutmann DH, Aylsworth A, Carey JC, et al. The diagnostic evaluation and multidisciplinary management of neurofibromatosis 1 and neurofibromatosis 2. JAMA 1997; 278:51–57.
10. Baser ME, Friedman JM, Wallace AJ, et al. Evaluation of clinical diagnostic criteria for neurofibromatosis 2. Neurology 2002; 59:1759–1765.
11. Yohay K. Neurofibromatosis types 1 and 2. Neurologist 2006; 12:86–93.
12. Parry DM, Eldridge R, Kaiser-Kupfer MI, et al. Neurofibromatosis 2 (NF2): clinical characteristics of 63 affected individuals and clinical evidence for heterogeneity. Am J Med Genet 1994; 52:450–461.
13. Mautner VF. Spinal tumors in patients with neurofibromatosis type 2: MR imaging study of frequency, multiplicity and variety. AJR Am J Roentgenol 1996; 166:1231.
14. Geddes JF, Sutcliffe JC, King TT. Mixed cranial nerve tumors in neurofibromatosis type 2. Clin Neuropathol 1995; 14:310–313.
15. Ragge NK, Baser ME, Klein J, et al. Ocular abnormalities in neurofibromatosis 2. Am J Ophthalmol 1995; 120:634–641.
16. Evans DG, Blair V, Strachan T, et al. Variation of expression of the gene for type 2 neurofibromatosis: absence

of a gender effect on vestibular schwannomas, but confirmation of a preponderance of meningiomas in females. J Laryngol Otol 1995; 109:830–835.
17. Mautner VF, Tatagiba M, Lindenau M, et al. Spinal tumors in patients with neurofibromatosis type 2: MR imaging study of frequency, multiplicity, and variety. AJR Am J Roentgenol 1995; 165:951–955.
18. Mautner VF, Lindenau M, Baser ME, et al. Skin abnormalities in neurofibromatosis 2. Arch Dermatol 1997; 133:1539–1543.
19. Costantino PD, Friedman CD, Pelzer HJ. Neurofibromatosis type II of the head and neck. Arch Otolaryngol Head Neck Surg 1989; 115:380–383.
20. Smullen S, Willcox T, Wetmore R, et al. Otologic manifestations of neurofibromatosis. Laryngoscope 1994; 104:663–665.
21. Geist JR, Gander DL, Stefanac SJ. Oral manifestations of neurofibromatosis types I and II. Oral Surg Oral Med Oral Pathol 1992; 73:376–382.
22. Selesnick SH, Jackler RK, Pitts LW. The changing clinical presentation of acoustic tumors in the MRI era. Laryngoscope 1993; 103:431–436.
23. Gillespie JE. Imaging in neurofibromatosis type 2: screening using magnetic resonance imaging. Ear Nose Throat J 1999; 78:102–109.
24. Patronas NJ, Courcoutsakis N, Bromley CM, et al. Intramedullary and spinal canal tumors in patients with neurofibromatosis 2: MR imaging findings and correlation with genotype. Radiology 2001; 218:434–442.
25. Kitamura K, Sugimoto M. Histological structures of bilateral acoustic tumors. Adv Otorhinolaryngol 1988; 42:172–176.
26. Sobel RA. Vestibular (acoustic) schwannomas: histologic features in neurofibromatosis 2 and in unilateral cases. J Neuropathol Exp Neurol 1993; 52:106–113.
27. Kluwe L, Friedrich RE, Hagel C, et al. Mutations and allelic loss of the NF2 gene in neurofibromatosis 2-associated skin tumors. J Invest Dermatol 2000; 114: 1017–1021.
28. Hung G, Faudoa R, Baser ME, et al. Neurofibromatosis 2 phenotypes and germ-line NF2 mutations determined by an RNA mismatch method and loss of heterozygosity analysis in NF2 schwannomas. Cancer Genet Cytogenet 2000; 118:167–168.
29. Lamszus K, Vahldiek F, Mautner VF, et al. Allelic losses in neurofibromatosis 2-associated meningiomas. J Neuropathol Exp Neurol 2000; 59:504–512.
30. Gutmann DH, Geist RT, Xu H, et al. Defects in neurofibromatosis 2 protein function can arise at multiple levels. Hum Mol Genet 1998; 7:335–345.
31. Yohay KH. The genetic and molecular pathogenesis of NF1 and NF2. Semin Pediatr Neurol 2006; 13:21–26.
32. Swartz JD. Lesions of the cerebellopontine angle and internal auditory canal: diagnosis and differential diagnosis. Semin Ultrasound CT MR 2004; 25:332–352.
33. Scheithauer B, Woodruff J, Erlandson R. Schwannoma. In: Scheithauer B, Woodruff J, Erlandson R, eds. Tumors of the Peripheral Nervous System. Washington, DC: Armed Forces Institute of Pathology, 1999.
34. Evans DG, Baser ME, O'Reilly B, et al. Management of the patient and family with neurofibromatosis 2: a consensus conference statement. Br J Neurosurg 2005; 19:5–12.
35. Samii M, Matthies C, Tatagiba M. Management of vestibular schwannomas (acoustic neuromas): auditory and facial nerve function after resection of 120 vestibular schwannomas in patients with neurofibromatosis 2. Neurosurgery 1997; 40:696–705.
36. McKennan KX, Bard A. Neurofibromatosis type 2: report of a family and review of current evaluation and treatment. Laryngoscope 1991; 101:109–113.

V. G. Acoustic Neuroma (Unilateral)

1. Irving RM, Moffat DA, Hardy DG, et al. A molecular, clinical, and immunohistochemical study of vestibular schwannoma. Otolaryngol Head Neck Surg 1997; 116:426–430.
2. Irving RM, Moffat DA, Hardy DG, et al. Molecular genetic analysis of the mechanism of tumorigenesis in acoustic neuroma. Arch Otolaryngol Head Neck Surg 1993; 119:1222–1228.
3. Tos M, Thomsen J. Epidemiology of acoustic neuromas. J Laryngol Otol 1984; 98:685–692.
4. Lanser MJ, Sussman SA, Frazer K. Epidemiology, pathogenesis, and genetics of acoustic tumors. Otolaryngol Clin North Am 1992; 25:499–520.
5. Neff BA, Welling DB, Akhmametyeva E, et al. The molecular biology of vestibular schwannomas: dissecting the pathogenic process at the molecular level. Otol Neurotol 2006; 27:197–208.
6. Wiegand DA, Fickel V. Acoustic neuroma–the patient's perspective: subjective assessment of symptoms, diagnosis, therapy, and outcome in 541 patients. Laryngoscope 1989; 99:179–187.
7. Jackler RK, Pitts LH. Acoustic neuroma. Neurosurg Clin N Am 1990; 1:199–223.
8. Thomsen J, Tos M. Acoustic neuroma: clinical aspects, audiovestibular assessment, diagnostic delay, and growth rate. Am J Otol 1990; 11:12–19.
9. Selesnick SH, Jackler RK. Clinical manifestations and audiologic diagnosis of acoustic neuromas. Otolaryngol Clin North Am 1992; 25:521–551.
10. Fundova P, Charabi S, Tos M, et al. Cystic vestibular schwannoma: surgical outcome. J Laryngol Otol 2000; 114:935–939.
11. Pendl G, Ganz JC, Kitz K, et al. Acoustic neurinomas with macrocysts treated with gamma knife radiosurgery. Stereotact Funct Neurosurg 1996; 66(suppl 1):103–111.
12. Shirato H, Sakamoto T, Takeichi N, et al. Fractionated stereotactic radiotherapy for vestibular schwannoma (VS): comparison between cystic-type and solid-type VS. Int J Radiat Oncol Biol Phys 2000; 48:1395–1401.
13. Chandrasekhar SS, Brackmann DE, Devgan KK. Utility of auditory brainstem response audiometry in diagnosis of acoustic neuromas. Am J Otol 1995; 16:63–67.
14. DeFilipp GJ, Buchheit WA. Magnetic resonance imaging of acoustic neuromas. Neurosurgery 1985; 16:763–765.
15. Hayashi M, Kubo O, Sato H, et al. Correlation between MR image characteristics and histological features of acoustic schwannoma. Noshuyo Byori 1996; 13:139–144.
16. Lin D, Hegarty JL, Fischbein NJ, et al. The prevalence of ''incidental'' acoustic neuroma. Arch Otolaryngol Head Neck Surg 2005; 131:241–244.
17. Burger P, Scheithauer B. Tumors of the peripheral nerve sheath. In: Burger P, Scheithauer B, eds. Tumors of the Central Nervous System. 1994, Washington, DC: Armed Forces Institute of Pathology, .
18. Nager GT. Acoustic neurinomas. Pathology and differential diagnosis. Arch Otolaryngol 1969; 89:252–279.
19. Sobel RA. Vestibular (acoustic) schwannomas: histologic features in neurofibromatosis 2 and in unilateral cases. J Neuropathol Exp Neurol 1993; 52:106–113.
20. Welling DB, Guida M, Goll F, et al. Mutational spectrum in the neurofibromatosis type 2 gene in sporadic and familial schwannomas. Hum Genet 1996; 98:189–193.
21. Jacoby LB, MacCollin M, Louis DN, et al. Exon scanning for mutation of the NF2 gene in schwannomas. Hum Mol Genet 1994; 3:413–419.
22. Merel P, Hoang-Xuan K, Sanson M, et al. Predominant occurrence of somatic mutations of the NF2 gene in

meningiomas and schwannomas. Genes Chromosomes Cancer 1995; 13:211–216.
23. Lee WC, Testa JR. Somatic genetic alterations in human malignant mesothelioma (review). Int J Oncol 1999; 14:181–188.
24. Mirz F, Jorgensen B, Fiirgaard B, et al. Investigations into the natural history of vestibular schwannomas. Clin Otolaryngol Allied Sci 1999; 24:13–18.
25. Rutherford SA, King AT. Vestibular schwannoma management: What is the 'best' option? Br J Neurosurg 2005; 19:309–316.
26. Samii M, Matthies C. Management of 1000 vestibular schwannomas (acoustic neuromas): surgical management and results with an emphasis on complications and how to avoid them. Neurosurgery 1997; 40:11–21.
27. Kondziolka D, Lunsford LD, McLaughlin MR, et al. Long-term outcomes after radiosurgery for acoustic neuromas. N Engl J Med 1998; 339:1426–1433.
28. Pitts LH, Jackler RK. Treatment of acoustic neuromas. N Engl J Med 1998; 339:1471–1473.
29. Gormley WB, Sekhar LN, Wright DC, et al. Acoustic neuromas: results of current surgical management. Neurosurgery 1997; 41:50–58.
30. Rosenberg SI, Silverstein H, Gordon MA, et al. A comparison of growth rates of acoustic neuromas: nonsurgical patients vs. subtotal resection. Otolaryngol Head Neck Surg 1993; 109:482–487.
31. Fucci MJ, Buchman CA, Brackmann DE, et al. Acoustic tumor growth: implications for treatment choices. Am J Otol 1999; 20:495–499.
32. Wiegand DA, Ojemann RG, Fickel V. Surgical treatment of acoustic neuroma (vestibular schwannoma) in the United States: report from the Acoustic Neuroma Registry. Laryngoscope 1996; 106:58–66.
33. Bederson JB, von Ammon K, Wichmann WW, et al. Conservative treatment of patients with acoustic tumors. Neurosurgery 1991; 28:646–650.
34. Flint D, Fagan P, Panarese A. Conservative management of sporadic unilateral acoustic neuromas. J Laryngol Otol 2005; 119:424–428.
35. Kesterson L, Shelton C, Dressler L, et al. Clinical behavior of acoustic tumors. A flow cytometric analysis. Arch Otolaryngol Head Neck Surg 1993; 119:269–271.
36. Welkoborsky HJ, Haibt G, Mann WJ, et al. Comparison of cytophotometric characteristics to histology and proliferation markers in acoustic neuromas. Ann Otol Rhinol Laryngol 1994; 103:49–53.

V. H. Mucosal Neuroma

1. DeLellis RA. Multiple endocrine neoplasia syndromes revisited. Clinical, morphologic, and molecular features. Lab Invest 1995; 72:494–505.
2. Carney JA, Sizemore GW, Lovestedt SA. Mucosal ganglioneuromatosis, medullary thyroid carcinoma, and pheochromocytoma: multiple endocrine neoplasia, type 2b. Oral Surg Oral Med Oral Pathol 1976; 41:739–752.
3. Schimke RN, Hartmann WH, Prout TE, et al. Syndrome of bilateral pheochromocytoma, medullary thyroid carcinoma and multiple neuromas. A possible regulatory defect in the differentiation of chromaffin tissue. N Engl J Med 1968; 279:1–7.
4. Williams ED, Pollock DJ. Multiple mucosal neuromata with endocrine tumours: a syndrome allied to von Recklinghausen's disease. J Pathol Bacteriol 1966; 91:71–80.
5. Gorlin RJ, Sedano HO, Vickers RA, et al. Multiple mucosal neuromas, pheochromocytoma and medullary carcinoma of the thyroid–a syndrome. Cancer 1968; 22:293–299.
6. Vasen HF, van der Feltz M, Raue F, et al. The natural course of multiple endocrine neoplasia type IIb. A study of 18 cases. Arch Intern Med 1992; 152:1250–1252.
7. Khairi MR, Dexter RN, Burzynski NJ, et al. Mucosal neuroma, pheochromocytoma and medullary thyroid carcinoma: multiple endocrine neoplasia type 3. Medicine (Baltimore) 1975; 54:89–112.
8. Goodfellow PJ. Mapping the inherited defects associated with multiple endocrine neoplasia type 2A, multiple endocrine neoplasia type 2B, and familial medullary thyroid carcinoma to chromosome 10 by linkage analysis. Endocrinol Metab Clin North Am 1994; 23:177–185.
9. Ponder BA. The gene causing multiple endocrine neoplasia type 2 (MEN 2). Ann Med 1994; 26:199–203.
10. Carlson KM, Dou S, Chi D, et al. Single missense mutation in the tyrosine kinase catalytic domain of the RET protooncogene is associated with multiple endocrine neoplasia type 2B. Proc Natl Acad Sci U S A 1994; 91: 1579–1583.
11. Eng C, Smith DP, Mulligan LM, et al. Point mutation within the tyrosine kinase domain of the RET proto-oncogene in multiple endocrine neoplasia type 2B and related sporadic tumours. Hum Mol Genet 1994; 3:237–241.
12. Hofstra RM, Landsvater RM, Ceccherini I, et al. A mutation in the RET proto-oncogene associated with multiple endocrine neoplasia type 2B and sporadic medullary thyroid carcinoma. Nature 1994; 367:375–376.
13. Utiger RD. Medullary thyroid carcinoma, genes, and the prevention of cancer. N Engl J Med 1994; 331:870–871.
14. Fuller CE, Williams GT. Gastrointestinal manifestations of type 1 neurofibromatosis (von Recklinghausen's disease). Histopathology 1991; 19:1–11.
15. Koppang HS, Aksdal E, Engebjerg E. Multiple endocrine neoplasia, type III. Int J Oral Maxillofac Surg 1986; 15:483–488.
16. Holloway KB, Flowers FP. Multiple endocrine neoplasia 2B (MEN 2B)/MEN 3. Dermatol Clin 1995; 13:99–103.
17. Robertson DM, Sizemore GW, Gordon H. Thickened corneal nerves as a manifestation of multiple endocrine neoplasia. Trans Sect Ophthalmol Am Acad Ophthalmol Otolaryngol 1975; 79:OP772–OP787.
18. Carney JA, Sizemore GW, Hayles AB. Multiple endocrine neoplasia, type 2b. Pathobiol Annu 1978; 8:105–153.
19. Dennehy PJ, Feldman GL, Kambouris M, et al. Relationship of familial prominent corneal nerves and lesions of the tongue resembling neuromas to multiple endocrine neoplasia type 2B. Am J Ophthalmol 1995; 120:456–461.
20. Pujol RM, Matias-Guiu X, Miralles J, et al. Multiple idiopathic mucosal neuromas: a minor form of multiple endocrine neoplasia type 2B or a new entity? J Am Acad Dermatol 1997; 37:349–352.
21. Nishihara K, Yoshida H, Onizawa K, et al. Solitary mucosal neuroma of the hard palate: a case report. Br J Oral Maxillofac Surg 2004; 42:457–459.
22. Higashide Y, Nemoto Y, Imamura T. A case of conjunctival mucosal neuroma without multiple endocrine neoplasia. Nippon Ganka Gakkai Zasshi 1997; 101:621–625.
23. Shimazaki T, Yoshida Y, Izumaru S, et al. Laryngeal solitary multiple mucosal neuromas without multiple endocrine neoplasia (MEN) type 2B. Auris Nasus Larynx 2003; 30:191–195.
24. Miura H, Kato H, Hayata Y, et al. Solitary bronchial mucosal neuroma. Chest 1989; 95:245–247.
25. Padberg BC, Holl K, Schroder S. Pathology of multiple endocrine neoplasias 2A and 2B: a review. Horm Res 1992; 38(suppl 2):24–30.
26. Cangiarella J, Jagirdar J, Adelman H, et al. Mucosal neuromas and plexiform neurofibromas: an immunocytochemical study. Pediatr Pathol 1993; 13:281–288.

27. Bordeaux MC, Forcet C, Granger L, et al. The RET proto-oncogene induces apoptosis: a novel mechanism for Hirschsprung disease. EMBO J 2000; 19:4056–4063.
28. Takahashi M. The GDNF/RET signaling pathway and human diseases. Cytokine Growth Factor Rev 2001; 12:361–373.
29. Peczkowska M, Januszewicz A. Multiple endocrine neoplasia type 2. Fam Cancer 2005; 4:25–36.

V. I. Neurothekeoma

1. Harkin JC, Reed RJ. Tumors and lesions of neurofibromatosis and other types of neurocutanoues phakomatoses. Tumors of the Peripheral Nervous System. 1969, Washington, DC: Armed Forces Institute of Pathology,
2. Pulitzer DR, Reed RJ. Nerve-sheath myxoma (perineurial myxoma). Am J Dermatopathol 1985; 7:409–421.
3. Angervall L, Kindblom LG, Haglid K. Dermal nerve sheath myxoma. A light and electron microscopic, histochemical and immunohistochemical study. Cancer 1984; 53:1752–1759.
4. Paulus W, Jellinger K, Perneczky G. Intraspinal neurothekeoma (nerve sheath myxoma). A report of two cases. Am J Clin Pathol 1991; 95:511–516.
5. Rosati LA, Fratamico FC, Eusebi V. Cellular neurothekeoma. Appl Pathol 1986; 4:186–191.
6. Gallager RL, Helwig EB. Neurothekeoma–a benign cutaneous tumor of neural origin. Am J Clin Pathol 1980; 74:759–764.
7. Laskin WB, Fetsch JF, Miettinen M. The "neurothekeoma": immunohistochemical analysis distinguishes the true nerve sheath myxoma from its mimics. Hum Pathol 2000; 31:1230–1241.
8. Argenyi ZB, LeBoit PE, Santa CD, et al. Nerve sheath myxoma (neurothekeoma) of the skin: light microscopic and immunohistochemical reappraisal of the cellular variant. J Cutan Pathol 1993; 20:294–303.
9. Fletcher CD, Chan JK, McKee PH. Dermal nerve sheath myxoma: a study of three cases. Histopathology 1986; 10:135–145.
10. Goldstein J, Lifshitz T. Myxoma of the nerve sheath. Report of three cases, observations by light and electron microscopy and histochemical analysis. Am J Dermatopathol 1985; 7:423–429.
11. Barnhill RL, Dickersin GR, Nickeleit V, et al. Studies on the cellular origin of neurothekeoma: clinical, light microscopic, immunohistochemical, and ultrastructural observations. J Am Acad Dermatol 1991; 25:80–88.
12. Mincer HH, Spears KD. Nerve sheath myxoma in the tongue. Oral Surg Oral Med Oral Pathol 1974; 37:428–430.
13. Youngs R, Kwok P, Hawke M, et al. Neurothekeoma (peripheral nerve sheath myxoma) of the external auditory canal. J Otolaryngol 1989; 18:90–93.
14. Tiffee JC, Pulitzer DR. Nerve sheath myxoma of the oral cavity: case report and review. Oral Surg Oral Med Oral Pathol Oral Radiol Endod 1996; 82:423–425.
15. O'Rourke H, Meyers SP, Katzman PJ. Neurothekeoma in the upper extremity: magnetic resonance imaging and computed tomography findings. J Comput Assist Tomogr 2005; 29:847–850.
16. Paulus W, Warmuth-Metz M, Sorensen N. Intracranial neurothekeoma (nerve-sheath myxoma). Case report. J Neurosurg 1993; 79:280–282.
17. Kaar GF, Bashir SH, N'Dow JM, et al. Neurothekeoma of the cauda equina. J Neurol Neurosurg Psychiatry 1996; 61:530–531.
18. Cohen NA, Samadi DS, Pawel BR, et al. Cellular neurothekeoma of the maxilla. Ann Otol Rhinol Laryngol 2004; 113:384–387.
19. Scheithauer BW, Woodruff JM, Erlandson RA. Miscellaneous Benign Neurogenic Tumors. In: Scheithauer BW, Woodruff JM, Erlandson RA, eds. Tumors of the Peripheral Nervous System. 1999, Washington, DC: Armed Forces Institute of Pathology, .
20. Busam KJ, Mentzel T, Colpaert C, et al. Atypical or worrisome features in cellular neurothekeoma: a study of 10 cases. Am J Surg Pathol 1998; 22:1067–1072.
21. Barnhill RL, Mihm MC Jr. Cellular neurothekeoma. A distinctive variant of neurothekeoma mimicking nevomelanocytic tumors. Am J Surg Pathol 1990; 14:113–120.
22. Calonje E, Wilson-Jones E, Smith NP, et al. Cellular 'neurothekeoma': an epithelioid variant of pilar leiomyoma? Morphological and immunohistochemical analysis of a series. Histopathology 1992; 20:397–404.
23. Tomasini C, Aloi F, Pippione M. Cellular neurothekeoma. Dermatology 1996; 192:160–163.
24. Webb JN. The histogenesis of nerve sheath myxoma: report of a case with electron microscopy. J Pathol 1979; 127:35–37.
25. Argenyi ZB, Kutzner H, Seaba MM. Ultrastructural spectrum of cutaneous nerve sheath myxoma/cellular neurothekeoma. J Cutan Pathol 1995; 22:137–145.
26. Fetsch JF, Laskin WB, Miettinen M. Nerve sheath myxoma: a clinicopathologic and immunohistochemical analysis of 57 morphologically distinctive, S-100 protein- and GFAP-positive, myxoid peripheral nerve sheath tumors with a predilection for the extremities and a high local recurrence rate. Am J Surg Pathol 2005; 29:1615–1624.
27. Wang AR, May D, Bourne P, et al. PGP9.5: a marker for cellular neurothekeoma. Am J Surg Pathol 1999; 23:1401–1407.
28. Fullen DR, Lowe L, Su LD. Antibody to S100a6 protein is a sensitive immunohistochemical marker for neurothekeoma. J Cutan Pathol 2003; 30:118–122.
29. Misago N, Satoh T, Narisawa Y. Cellular neurothekeoma with histiocytic differentiation. J Cutan Pathol 2004; 31:568–572.
30. Page RN, King R, Mihm MC, et al. Microphthalmia transcription factor and NKI/C3 expression in cellular neurothekeoma. Mod Pathol 2004; 17:230–234.
31. Breuer T, Koester M, Weidenbecher M, et al. Neurothekeoma, a rare tumour of the tongue. ORL J Otorhinolaryngol Relat Spec 1999; 61:161–164.

V. J. Perineurioma

1. Lazarus SS, Trombetta LD. Ultrastructural identification of a benign perineurial cell tumor. Cancer 1978; 41: 1823–1829.
2. Tranmer BI, Bilbao JM, Hudson AR. Perineurioma: a benign peripheral nerve tumor. Neurosurgery 1986; 19:134–138.
3. Erlandson RA. The enigmatic perineurial cell and its participation in tumors and in tumorlike entities. Ultrastruct Pathol 1991; 15:335–351.
4. Mentzel T, Dei Tos AP, Fletcher CD. Perineurioma (storiform perineurial fibroma): clinico-pathological analysis of four cases. Histopathology 1994; 25:261–267.
5. Hornick JL, Fletcher CD. Soft tissue perineurioma: clinicopathologic analysis of 81 cases including those with atypical histologic features. Am J Surg Pathol 2005; 29:845–858.
6. Graadt van Roggen JF, McMenamin ME, Belchis DA, et al. Reticular perineurioma: a distinctive variant of soft tissue perineurioma. Am J Surg Pathol 2001; 25:485–493.

7. Tsang WY, Chan JK, Chow LT, et al. Perineurioma: an uncommon soft tissue neoplasm distinct from localized hypertrophic neuropathy and neurofibroma. Am J Surg Pathol 1992; 16:756–763.
8. Emory TS, Scheithauer BW, Hirose T, et al. Intraneural perineurioma. A clonal neoplasm associated with abnormalities of chromosome 22. Am J Clin Pathol 1995; 103:696–704.
9. Michal M. Extraneural retiform perineuriomas. A report of four cases. Pathol Res Pract 1999; 195:759–763.
10. Giannini C, Scheithauer BW, Jenkins RB, et al. Soft-tissue perineurioma. Evidence for an abnormality of chromosome 22, criteria for diagnosis, and review of the literature. Am J Surg Pathol 1997; 21:164–173.
11. Fetsch JF, Miettinen M. Sclerosing perineurioma: a clinicopathologic study of 19 cases of a distinctive soft tissue lesion with a predilection for the fingers and palms of young adults. Am J Surg Pathol 1997; 21:1433–1442.
12. Michal M, Kazakov DV, Belousova I, et al. A benign neoplasm with histopathological features of both schwannoma and retiform perineurioma (benign schwannoma-perineurioma): a report of six cases of a distinctive soft tissue tumor with a predilection for the fingers. Virchows Arch 2004; 445:347–353.
13. Stanton C, Perentes E, Phillips L, et al. The immunohistochemical demonstration of early perineurial change in the development of localized hypertrophic neuropathy. Hum Pathol 1988; 19:1455–1457.
14. Iyer VG, Garretson HD, Byrd RP, et al. Localized hypertrophic mononeuropathy involving the tibial nerve. Neurosurgery 1988; 23:218–221.
15. Mitsumoto H, Wilbourn AJ, Goren H. Perineurioma as the cause of localized hypertrophic neuropathy. Muscle Nerve 1980; 3:403–412.
16. Weidenheim KM, Campbell WG Jr. Perineural cell tumor. Immunocytochemical and ultrastructural characterization. Relationship to other peripheral nerve tumors with a review of the literature. Virchows Arch A Pathol Anat Histopathol 1986; 408:375–383.
17. Pitchford CW, Schwartz HS, Atkinson JB, et al. Soft tissue perineurioma in a patient with neurofibromatosis type 2: a tumor not previously associated with the NF2 syndrome. Am J Surg Pathol 2006; 30:1624–1629.
18. Li D, Schauble B, Moll C, et al. Intratemporal facial nerve perineurioma. Laryngoscope 1996; 106:328–333.
19. Kusama K, Iwamoto A, Mikuni M, et al. A case of central perineurioma (Lazarus and Trombetta) of the mandible. J Nihon Univ Sch Dent 1981; 23:10–17.
20. Scheithauer BW, Woodruff JM, Erlandson RA. Perineurioma. In: Scheithauer BW, Woodruff JM, Erlandson RA, eds. Tumors of Peripheral Nervous System. 1999, Washington, DC: Armed Forces Institute of Pathology.
21. Bilbao JM, Khoury NJ, Hudson AR, et al. Perineurioma (localized hypertrophic neuropathy). Arch Pathol Lab Med 1984; 108:557–560.
22. Perentes E, Nakagawa Y, Ross GW, et al. Expression of epithelial membrane antigen in perineurial cells and their derivatives. An immunohistochemical study with multiple markers. Acta Neuropathol (Berl) 1987; 75:160–165.
23. Ohno T, Park P, Akai M, et al. Ultrastructural study of a perineurioma. Ultrastruct Pathol 1988; 12:495–504.
24. Ariza A, Bilbao JM, Rosai J. Immunohistochemical detection of epithelial membrane antigen in normal perineurial cells and perineurioma. Am J Surg Pathol 1988; 12: 678–683.
25. Brock JE, Perez-Atayde AR, Kozakewich HP, et al. Cytogenetic aberrations in perineurioma: variation with subtype. Am J Surg Pathol 2005; 29:1164–1169.
26. Mertens F, Dal Cin P, De Wever I, et al. Cytogenetic characterization of peripheral nerve sheath tumours: a report of the CHAMP study group. J Pathol 2000; 190: 31–38.
27. Sciot R, Cin PD, Hagemeijer A, et al. Cutaneous sclerosing perineurioma with cryptic NF2 gene deletion. Am J Surg Pathol 1999; 23:849–853.
28. Lasota J, Fetsch JF, Wozniak A, et al. The neurofibromatosis type 2 gene is mutated in perineurial cell tumors: a molecular genetic study of eight cases. Am J Pathol 2001; 158:1223–1229.
29. Hirose T, Scheithauer BW, Sano T. Perineurial malignant peripheral nerve sheath tumor (MPNST): a clinicopathologic, immunohistochemical, and ultrastructural study of seven cases. Am J Surg Pathol 1998; 22:1368–1378.

V. K. Granular Cell Tumor

1. Abrikossoff A. Uber myome ausgehened von der quergestren willkurlichen muskulatur. Virchow Arch Pathol Anat 1926; 260:215–233.
2. Enzinger FM, Weiss SW. Benign tumors of periperhal nerves. Soft Tissue Tumors, 3rd ed. St. Louis: Mosby-Year Book. 1995:821–888.
3. Campagno J. Hyams VJ, Ste-Marie P. Benign granular cell tumors of the larynx: a review of 36 cases with clinicopathologic data. Ann Otol Rhinol Laryngol 1975; 84: 308–314.
4. Hyams VJ, Batsakis JG, Michaels L. Tumors of the Upper Respiractory Tract and Ear. Atlas of Tumor Pathology, 2nd Ser. Facs 25. Washington DC: Armed Forces Institute of Pathology, 1988.
5. Lack EE, Worsham F, Callihan MD, et al. Granular cell tumor: a clinicopathologic study of 110 patients. J Surg Oncol 1980; 13:301–316.
6. Khansur T, Balducci L, Tavassoli M. Granular cell tumor. Clinical spectrum of the benign and malignant entity. Cancer 1987; 60:220–222.
7. Kershisnik M, Batsakis JG, Mackay B. Granular cell tumors. Ann Otol Rhinol Laryngol 1994; 103:416–419.
8. Strong EW, McDivitt RW, Brassfield RD. Granular cell myoblastoma. Cancer 1970; 25:415–422.
9. McSwain GR, Colpitts R, Kreutner A, et al. Granular cell myoblastoma. Surg Gynecol Obstet 1980; 150:703–710.
10. Alkek DS, Johnson WC, Graham JH. Granular cell myoblastoma: a histologic and enzymatic study. Arch Dermatol 1968; 98:543–547.
11. Fisher ER, Wechsler H. Granular cell myoblastoma – a misnomer. Electron microscopic and histochemical evidence concerning its Schwann cell derivation and nature (granular cell schwannoma). Cancer 1962; 15:936–954.
12. Sobel HJ, Schwartz R, Margret E. Light and electron-microscope study of the origin of granular cell myoblastoma. J Pathol 1973; 109:101–111.
13. Ulrich J, Heitz PU, Fisher T, et al. Granular cell tumors: Evidence for heterogenous tumor cell differentiation. An immunocytochemical study. Virchows Arch B Cell Pathol Incl Mol Pathol 1987; 53:52–57.
14. Bedetti CD, Martinez AJ, Beckford NS, et al. Granular cell tumor arising in myeliniated peripheral nerves. Light, electron microscopy and immunoperoxidase study. Virchows Arch A Pathol Anat Histopathol 1983; 402:175–183.
15. Armin A, Connelly EM, Rowden G. An ilmmunoperoxidase investigation of S-100 protein in granular cell myoblastomas. Evidence for Schwann cell deriviation. Am J Clin Pathol 1983; 79:37–44.
16. Raju GC, O'Reilly AP. Immunohistochemical study of granular cell tumor. Pathology 1987; 19:402–406.

17. Matthews JB, Mason GI. Oral granular cell myoblastoma. An immunohistochemical study. J Oral Pathol 1982; 11:343–352.
18. Miettinen M, Lehtonen E, Lehtola H, et al. Histogenesis of granular cell tumor – an immunohistochemical and ultrastructural study. J Pathol 1984; 142:221–229.
19. Mittal KR, True LD. Origin of granules in granular cell tumor. Intracellular myeliln formation with autodigestion. Arch Pathol Lab Med 1988; 112:302–303.
20. Mazur MT, Schultz JJ, Myers JL. Granular cell tumor. Immunhistochemical analysis of 21 benign tumors and one malignant tumor. Arch Pathol Lab Med 1990; 114:692–696.
21. Mukai M. Immunohistochemical localization of S-100 protein and peripheral nerve myelin proteins (P2 proteins) in granular cell tumors. Am J Pathol 1983; 112:139–146.
22. Regezi JA, Zarbo RJ, Courtney RM, et al. Immunoreactivity of granular cell lesions of skin, mucosa and jaw. Cancer 1989; 64:1455–1460.
23. Nakazato Y, Ishizeki J, Takahashi K, et al. Immunohistochemical localization of S100 protein in granular cell myoblastoma. Cancer 1982; 49:1624–1628.
24. Nathrath WB, Remberger K. Immunohistochemical study of granular cell tumours: demonstration of neuron specific enolase, S-100 protein, laminin, and alpha-1-antichmotrypsin. Virchows Arch A Pathol Anat 1986; 408:421–434.
25. Smolle J, Konrad K, Kerl H. Granular cell tumors contain myelin-associated glycoprotein. An immunohistochemical study using Leu 7 monoclonal antibody. Virchows Arch A Pathol Anat Histopathol 1985; 406:1–5.
26. Stefansson K, Wollmann, RL. S-100 protein in granular cell tumors (granular cell myoblastomas). Cancer 1982; 49:1834–1838.
27. Carinci F, Piattelli A, Rubini C, et al. Genetic profiling of granular cell myoblastoma. J Craniofac Surg 2004; 15:824–834.
28. Torsiglieri AJ, Handler SD, Uri AK. Granular cell tumors of the head and neck in children: the experience at the Children's Hospital of Philadelphia. Int J Pediatr Otorhinolaryngol 1991; 21:249–258.
29. Goldofsky E, Hirschfield LS, Abramson AL. An unusual laryngeal lesion in children: granular cell tumor. Int J Pediatr Otorhinolaryngol 1988; 15:263–267.
30. Conley SF, Milbrath MM, Beste DJ. Pediatric laryngeal granular cell tumor. J Otolaryngo 1992; 21:450–453.
31. Becelli R, Perugini M, Gasparini G, et al. Abrikossoff's tumor. J Craniofac Surg 2001; 12:78–81.
32. Brannon RB, Anand PM. Oral granular cell tumors: an analysis of 10 new pediatric and adolescent cases and review of the literature. J Clin Pediatr Dent 2004; 29:69–74.
33. Hamid AM, Alshaikhly A. Granular cell tumor of the larnx in an eight-year girl. J Laryngol Otol 1993; 107:940–941.
34. Har-El G, Shviro J, Avidor I, et al. Laryngeal granular cell tumor in children. Am J Otolaryngol 1985; 6:32–345.
35. Holland RS, Abaza N, Balsara G, et al. Granular cell tumor of the larynx in a six-year old child: case report and review of literature. Ear Nose Throat J 1998; 77:652–654, 656, 658 passim.
36. Lazar RH, Younis RT, Kluka EA, et al. Granular cell tumor of the larynx: report of two pediatric cases. Ear Nose Throat J 1992; 71:440–443.
37. Peterson LJ. Granular cell tumor: review of the literature and report of a case. Oral Surg Oral Med Oral Pathol 1974; 37:728–735.
38. Regezi JA, Batsakis JG, Courtney RM. Granular cell tumors of the head and neck. J Oral Surg 1979; 37:402–406.
39. Alessi DM, Zimmerman MC. Granular cell tumors of the head and neck. Laryngoscope 1988; 98:810–814.
40. Goodstein ML, Eisele DW, Hyams VJ, et al. Multiple synchronous granular cell tumors of the upper aerodigestive tract. Otolaryngol Head Neck Surg 1990; 103:664–668.
41. Ryan RE, McDonald TJ, Weiland LH, et al. Granular cell tumors of the tongue. Otolaryngology 1978; 86:143–146.
42. Stewart CM, Watson RE, Eversole LR, et al. Oral granular cell tumors: a clinicopathologic and immunocytochemical study. Oral Surg Oral Med Oral Pathol 1988; 65:427–435.
43. Slootweg P, de Wilde P, Vooijs P, et al. Oral granular cell lesions. An immunohistochemcal study with emphasis on intermediate-sized filaments proteins. Virchows Arch A Pathol Anat Histopathol 1983; 402:35–45.
44. Brandwein M, LeBenger J, Strauchen J, et al. Atypical granular cell tumor of the larynx: an unusually aggressive tumor clinically and microscopically. Head Neck 1990; 12:154–159.
45. Farmer RW, Scher RL. Granular cell tumor of the larynx presenting with airway obstruction. Otolaryngol Head Neck 1998; 118:874–876.
46. Cree IA, Bingham BJ, Ramesar KC. Granular cell tumour of the larynx. J Laryngol Otol 1990; 104:159–161.
47. Mukherji SK, Castillo M, Rao V, et al. Granular cell tumors of the subglottic region of the larynx: CT and MR findings. ARJ Am J Roentgenol 1995; 164:1492–1494.
48. Robb PJ, Girling A. Granular cell myoblastoma of the supraglottis. J Larygol Otol 1989; 103:328–330.
49. Solomons NB. Extensive granular cell tumor of the larynx and trachea (a case report). J Laryngol Otol 1988; 102:658–660.
50. Toncini C, Pesce C. Granular cell tumours of the esophagus and larynx. J Laryngol Otol 1985; 99:1301–1304.
51. Agarwal RK, Blitzer A, Perzin KH. Granular cell tumors of the larynx. Otolaryngol Head Neck Surg 1979; 87:807–814.
52. Holland RS, Abaza N, Balsara G, et al. Granular cell tumor of the larynx in a six-year old child. Case report and review of the literature. Ear Nose Throat J 1998; 77:652–658.
53. Damiani S, Koerner FC, Dickersin GR, et al. Granular cell tumour of the breast. Virchows Arch A Pathol Anat Histopathol 1992; 420:219–226.
54. Alvarez-Fernandez E, Carretero-Albinana L. Bronchial granular cell tumor. Presentation of three cases with tissue culture and ultrastructural study. Arch Pathol Lab Med 1987; 111:1065–1069.
55. Burton DM, Heffner DK, Patow CA. Granular cell tumors of the trachea. Laryngoscope 1992; 102:807–813.
56. Desai DP, Maddalozzo J, Holinger LD. Granular cell tumor of the trachea. Otolarygol Head Neck Surg 1999; 120:595–598.
57. David O, Jakate S. Multifocal granular cell tumor of the esophagus and proximal stomach with infiltrative pattern. A case report and review of the literature. Arch Pathol Lab Med 1999; 123:967–973.
58. Piazza C, Casirati C, Peretti G, et al. Granular cell tumor of the hypopharynx treated by endoscopic CO(2) laser excision: report of two cases. Head Neck 2000; 22:524–529.
59. Persaud R, Tudge S, Amonoo-Kuofi K, et al. Parapharyngeal granular cell tumor: a unique surgical challenge. J Laryngol Otol 2005; 119:68–70
60. Philipp K, Barnes EL, Carrau RL. Eagle syndrome produced by a granular cell tumor. Arch Otolaryngol Head Neck Surg 2001; 127:1499–1501.
61. White SW, Gallager RL, Rodman OG. Multiple granular cell tumors. J Dermatol Surg Oncol 1980; 6:57–61.
62. Seo IS, Azzarelli B, Warner TF, et al. Multiple visceral and cutaneous granular cell tumors Ultrastructural and immunocytochemical evidence of Schwann cell origin. Cancer 1984; 53:2104–2110.

63. Collins B, Jones AC. Multiple granular cell tumors of the oral cavity: report of a case and review of the literature. J Oral Maxillofac Surg 1995; 53:707–711.
64. Curtis BV, Calcaterra TC, Coulson WF. Multiple granular cell tumor: a case report and review of literature. Head Neck 1997; 19:634–637.
65. Xue JL, Fan MW, Wang SZ, et al. A clinicopathological study of 14 cases of oral granular cell tumor. Zhonghua Kou Quang Yi Xue Za Zhi 2005; 40:302–305.
66. Basile JR, Woo SB. Polypoid S-100-negative granular cell tumor of the oral cavity: a case report and review of literature. Oral Surg Oral Med Oral Pathol Oral Radiol Endod 2003; 96:70–76.
67. Tos AP, Doglioni C, Laurino L, et al. KP1 (CD68) expression in benign neural tumors. Further evidence of its low specificity as a histiocytic/myeloid marker. Histopathology 1993; 23:185–187.
68. Kaiserling E, Xiao JC, Ruck P, et al. Aberrant expression of macrophage-associated antigens (CD68 and Ki-M1P) by Schwann cells in reactive and neoplastic neural tissue. Light-and electron microscopic findings. Mod Pathol 1993; 6:463–468.
69. Kurtin PJ, Bonin DM. Immunohistochemical demonstration of the lysosome-associated glycoprotein CD68 (KP-1) in granular cell tumors and schwannomas. Hum Pathol 1994; 25:1172–1178.
70. Tsang WY, Chan JK. KP1 (CD68) staining of granular cell neoplasms: is KP1 a marker for lysosomes rather than the histioicytic lineage? Histopathology 1992; 21:84–86.
71. Pulford KA, Rigney EM, Micklem KJ, et al. KP1: a new monoclonal antibody that detects a monocyte/macrophage associated antigen in routinely processed tissue sections. J Clin Pathol 1989; 42:414–421.
72. Chrysomali E, Nikitakis NG, Tosios K, et al. Immunohistochemical evaluation of cell proliferation antigen Ki-67 and apoptosis-related proteins Bcl-2 and caspase-3 in oral granular cell tumor. Oral Surg Oral Med Oral Pathol Oral Radiol Endod 2003; 96:566–572.
73. Ritter JH, Nappi O. Oxyphilic proliferations of the respiratory tract and paranasal sinuses. Semin Diagn Pathol 1999; 16:105–116.
74. Menzel T, Wadden C, Fletcher CD. Granular cell change in smooth muscle tumours of skin and soft tissue. Histopathology 1994; 24:223–231.
75. LeBoit PE, Barr R, Burall S, et al. Primitive polypoid granular-cell tumor and other cutaneous granular cell neoplasms of apparent nonneural origin. Am J Surg Pathol 1991; 15:48–58.
76. Kapadia SB, Meis JM, Frisman DM, et al. Adult rhabdomyoma of the head and neck. Clinicopathologic and immunophenotypic study. Hum Pathol 1993; 24:608–617.
77. Goldstein A, Thaler S, Rozycki D. Granular cell myoblastoma and carcinoma of the larynx. Arch Otolaryngol 1971; 94:366–368.
78. Angiero F, Crippa R, Stefani M. Granular cell tumor in the oral cavity: report of eleven cases treated with laser surgery. Minerva Stomatol 2006; 55:423–430.
79. Jardines L, Cheung L, LiVolsi V, et al. Malignant granular cell tumors: report of a case and review of the literature. Surgery 1994; 116:49–54.
80. Klima M, Peters J. Malignant granular cell tumor. Arch Pathol Lab Med 1987; 111:1070–1073.
81. Shimamura K, Osamura RY, Ueyama Y, et al. Malignant granular cell tumor of the right sciatic nerve. Report of an autopsy case with electron microscopic, immunohistochemical, and enzyme histochemical studies. Cancer 1984; 53:524–529.
82. Steffelaar JW, Nap M, von Haelst UJ. Malignant granular cell tumor. Report of a case with special reference to carcinoembryonic antigen. Am J Surg Pathol 1982; 6:665–672.
83. Uzoaru I, Firfer B, Ray V, et al. Malignant granular cell tumor. Arch Pathol Lab Med 1992; 116:206–208.
84. Wetzel W, Leipzig B, Grunow W, et al. Malignant granular cell tumor of the tongue. Arch Otolaryngol 1982; 108:603–605.
85. Cadotte M. Malignant granular-cell myoblastoma. Cancer 1974; 33:1417–1422.
86. Parayno PP, August CZ. Malignant granular cell tumor. Report of a case with DNA ploidy analysis. Arch Pathol Lab Med 1996; 120:296–300.
87. al-Sarraf M, Loud AV, Vaitkevicius V. Malignant granular cell tumor. Arch Pathol 1971; 91:550–558.
88. Krieg AF. Malignant granular cell myoblastoma: a case report. Arch Pathol 1962; 74:251–256.
89. Mackenzie DH. Malignant granular cell myoblastoma. J Clin Pathol 1967; 20:739–742.
90. Steffelaar JW, Nap M, von Haelst UJ. Malignant granular cell tumor: a report of a case with special reference to carcinoembroynic antigen. Am J Surg Pathol 1982; 6:665–672.
91. Fanburg-Smith JC, Meis-Kindblom JM, Fante R, et al. Malignant granular cell tumor of soft tissue, diagnostic criteria and clinicopathologic correlation. Am J Surg Pathol 1998; 22:779–794.
92. Budino-Carbonero S, Navarro-Vergara P, Rodriguez-Ruiz JA, et al. Granular cell tumors: Review of the parameters determining possible malignancy. Med Oral 2003; 8:294–298.
93. Kameyama Y, Mizohata M, Takehana S, et al. Ultrastructure of congenital epulis. Virchows Arch A Pathol Anat Histopathol 1983; 401:251–260.
94. Kaiserling E, Ruck P, Xiao JC. Congenital epulis and granular cell tumor. A histologic and immunohistochemical study. Oral Surg Oral Med Oral Pathol Oral Radiol Endod 1995; 80:687–697.
95. Damm DD, Cibull ML, Geissler RH, et al. Investigation into the histogenesis of congenital epulis of the newborn. Oral Surg Oral Med Oral Pathol 1993; 76:205–212.
96. Fuhr AH, Krogh PH. Congenital epulis of the newborn. Centennial review of the literature and a report of a case. J Oral Surg 1972; 30:30–35.
97. Lack EE, Worsham GF, Callihan MD, et al. Gingival granular cell tumors of the newborn (congenital ''epulis''). A clinical and pathologic study of 21 patients. Am J Surg Pathol 1981; 5:37–46.
98. Lack EE, Perez-Atayde AR, McGill TJ, et al. Gingival granular cell tumor of the newborn (congenital 'epulis''). Ultrastructural observations relating to histogenesis. Hum Pathol 1982; 13:686–689.
99. Lifshitz MS, Flotte TJ, Greco MA. Congenital granular cell epulis, Immunohistochemical and ultrastructural observations. Cancer 1984; 53:1845–1848.
100. Monteil RA, Loubiere R, Charbit Y, et al. Gingival granular cell tumor of the newborn: immunoperoxidase investigation with anti-S-100 antiserum. Oral Surg Oral Med Oral Pathol 1987; 64:78–81.
101. Park SH, Kim TJ, Chi JG. Congenital granular cell tumor of the newborn: immunoperoxidase investigation with anti-S-100 anteiserum. Oral Surg Oral Med Oral Pathol 1987; 64:78–81.
102. Tucker MC, Rusnock EJ, Azumi N, et al. Gingival granular cell tumors of the newborn. An ultrastructural and immunohistochemical study. Arch Pathol Lab Med 1990; 114:895–898.
103. Takahashi H, Fujita S, Satoh H, et al. Immunohistochemical study of congenital gingival granular cell tumor (congenital epulis). J Oral Pathol Med 1990; 19:492–496.
104. Zarbo RJ, Lloyd RV, Beals TF, et al. Congenital gingival granular cell tumor with smooth muscle cyto differentiation. Oral Surg Oral Med Oral Pathol 1983; 56:512–520.

105. Zuker RM, Buenechea R. Congenital epulis: review of the literature and case report. J Oral Maxillofac Surg 1993; 51:1040–1043.

VI. MENINGIOMA

1. Cushing H, Eisenhardt L. Meningiomas. Their classification, Regional Behavior, Life History and Surgical End Results. Springfield, II: Charles C. Thomas, 1938.
2. Burger PC, Scheithauser BW, Vogel FS. Surgical Pathology of the Nervous System, 3rd Ser Fasc 10. Washington DC: Armed Forces Institute of Pathology, 1994:259–286.
3. Burger PC, Scheithauer BW, Vogel FS. Surgical Pathology of the Nervous System and its Coverings. 3rd ed. New York: Churchill Livingstone, 1991.
4. Kepes JJ. Meningioma–Biology, Pathology and Differential Diagnosis. New York: Masson Publishing, 1982.
5. Barnes L, Kapadia SB. The biology and pathology of skull base tumors. J Neurooncol 1994; 20:213–240.
6. Longstreth WT, Dennis LK, McGuire VM, et al. Epidemiology of intracranial meningioma. Cancer 1993; 72:639–648.
7. Riemenschneider MJ, Perry A, Reifenberger G. Histological classification and molecular genetics of meningiomas. Lancet Neurol 2006; 5:1045–1054.
8. Buccoliero AM, Castiglione F, Degl'Innocenti DR, et al. NF2 gene expression in sporadic meningiomas: relation to grades or histotypes real time-pCR study. Neuropathology 2007; 27:36–42.
9. Gutmann DH, Donahoe J, Perry A, et al. Loss of DAL-1, a protein 4.1-related tumor suppressor, is an important early event in the pathogenesis of meningiomas. Hum Mol Genet 2000; 9:1495–1500.
10. Perry A, Gutmann DH, Reifenberger G. Molecular pathogenesis of meningiomas. J Neurooncol 2004; 70:183–202.
11. Robb VA, Li W, Gascard P, et al. Identification of a third Protein 4.1 tumor suppressor, Protein 4.1R, in meningioma pathogenesis. Neurobiol Dis 2003; 13:191–202.
12. Perry A, Banerjee R, Lohse CM, et al. A role for chromosome 9p21 deletions in the malignant progression of meningiomas and the prognosis of anaplastic meningiomas. Brain Pathol 2002; 12:183–190.
13. Vagner-Capodano AM, Grisoli F, Gambarelli D, et al. Correlation between cytogenetic and histopathological findings in 75 human meningiomas. Neurosurgery 1993; 32:892–900.
14. Casartelli C, Rogatto SR, Barbieri Neto J. Karyotype evolution of human meningioma progression through malignancy. Cancer Genet Cytogenet 1989; 40:33–45.
15. Lopez-Gines C, Piquer J, Cerda-Nicolas M, et al. Meningiomas: karyotypes and histological patterns. Clin Neuropathol 1989; 8:130–133.
16. Ferrante L, Acqui M, Artico M, et al. Cerebral meningiomas in children. Childs Nerv Syst 1989; 5:83–86.
17. Deen HG, Scheithauer BW, Ebersold MJ. Clinical and pathological study of meningiomas of the first two decades of life. J Neurosurg 1982; 56:317–22.
18. Perzin KH, Pushparaj N. Nonepithelial tumors of the nasal cavity, paranasal sinuses, nasopharynx. A clinicopathologoic study. XIII: Meningiomas. Cancer 1984; 54:1860–1869.
19. Gagnon NB, Lavigne F, Mohr G, et al. Extracranial and intracranial meningiomas. J Otolaryngol 1986; 15:380–384.
20. Batsakis JG. Pathology consultation. Extracranial meningiomas. Ann Otol Rhinol Laryngol 1984; 93:282–283.
21. Kershisnik M, Callender DL, Batsakis JG. Extracranial meningiomas of the head and neck. Ann Otol Rhinol Laryngol 1993; 102:967–970.
22. Gabivov GA, Tcherekayev VA, Korshunov AG, et al. Meningiomas of the anterior skull base expanding into the orbit, paranasal sinuses, nasopharynx, and oropharynx. J Craniofac Surg 1993; 4:124–127.
23. Rose GE. Orbital meningiomas; surgery, radiotherapy or hormones? Br J Ophthalmol 1993; 77:313–314.
24. Maroon JC, Kennerdell JS, Vidovich DV, et al. Recurrent spheno-orbital meningioma. J Neurosurg 1994; 80:202–208.
25. Friedman CD, Costantino PD, Teitelbaum B, et al. Primary extracranial meningiomas of the head and neck. Laryngoscope 1990; 100:41–48.
26. El-Daly A, Pitman KT, Ferguson BJ, et al. Primary extracranial mengioma of the maxillary antrum. Skull Base Surg 1997; 7:211–215.
27. Mark WL, Sambasiva MR, Mark CH, et al. Primary ectopic meningioma of the maxillary sinus: case report and review of the literature. Head Neck 1995; 17:258–262.
28. Ho KL. Primary meningioma of the nasal cavity and paranasal sinuses. Cancer 1980; 46:1442–1447.
29. Dutton JJ. Optic nerve sheath meningiomas. Surv Ophthalmol 1992; 37:167–183.
30. Johnson TE, Weatherhead RG, Nasr AM, et al. Ectopic (extradural) meningioma of the orbit: a report of two cases in children. J Pediatr Ophthalmol Strabismus 1993; 30:43–47.
31. Taxy JB. Meningiomas of the paranasal sinuses. A report of two cases. Am J Surg Pathol 1990; 14:82–86.
32. Manni JJ. Ectopic meningioma of the maxillary sinus. J Laryngol Otol 1983; 97:657–660.
33. Nager GT, Heroy J, Hoeplinger M. Meningiomas invading the temporal bone with extension to the neck. Am J Otolaryngol 1983; 4:297–324.
34. Chang CY, Cheung SW, Jackler RK. Meningiomas presenting in the temporal bone; the pathways of spread form an intracranial site of origin. Otolaryngol Head Neck Surg 1998; 119:658–664.
35. Civantos F, Ferguson LR, Hemmati M, et al. Temporal meningiomas presenting as chronic otitis media. Am J Otol 1993; 14:403–406.
36. Fujita T, Nakagawa H, Tsuruzono K, et al. Extradural temporal meningioma directly extended to cervical bone – case report. Neurol Med Chir 1993; 33:458–462.
37. Nassif PS, Shelton C, Arriaga M. Hearing preservation following surgical removal of meningiomas affecting the temporal bone. Laryngoscope 1992; 102:1357–1362.
38. Pensak ML, Van Loveren H, Tew JM, et al. Transpetrosal access to meningiomas juxtaposing the temporal bone. Laryngoscope 1994; 104:814–820.
39. Salama N, Stafford N. Meningiomas presenting in the middle ear. Laryngoscope 1994; 104:814–820.
40. Carney AS, Ward V, Malluci CL, et al. Meningiomas involving the internal auditory canal: a diagnostic and surgical challenge. Skull Base Surg 1999; 9:87–94.
41. Zeitouni AG, Zagzag D, Cohen NL. Meningioma of the internal auditory canal. Ann Otol Rhinol Laryngol 1997; 106:657–661.
42. Mori S, Kobayashi S, Miki H, et al. Extracranial meningioma in the parapharyngeal space. Acta Pathol Jpn 1993; 43:130–134.
43. Murtagh R, Linden C. Neuroimaging of intracranial meningiomas. Neurosurg Clin N Am 1994; 5:217–233.
44. Zee CS, Chin T, Segall HD, et al. Magnetic resonance imaging of meningiomas. Semin Ultrasound CT MR 1992; 13:154–169.
45. Maiuri F, De Caro Mdel B, Esposito F, et al. Recurrences of meningiomas: predictive value of pathological features

and hormonal and growth factors. J Neurooncol 2007; 82:63–68.
46. Nakano T, Asano K, Miura H, et al. Meningiomas with brain edema: radiological characteristics on MRI and review of the literature. Clin Imaging 2002; 26:243–249.
47. Carvalho GA, Vorkapic P, Biewener G, et al. Cystic meningiomas resembling glial tumors. Surg Neurol 1997; 47:284–289.
48. Kleihues P, Burger PC, Scheithauer BW. World Health Organization Histological Typing of Tumors of the Central Nervous System. 2nd ed. New York: Springer-Verlag, 1993.
49. Perry A, Stafford SL, Scheithauer BW, et al. Meningioma grading: an analysis of histologic parameters. Am J Surg Pathol 1997; 21:1455–1465.
50. Thomas HG, Dolman CL, Berry K. Malignant meningiomas: clinical and pathological features. J Neurosurg 1981; 55:929–934.
51. Prayson RA. Malignant meningioma: a clinicopathologic study of 23 patients including MIBI and p53 immunohistochemistry. Am J Clin Pathol 1996; 105:719–726.
52. Couce ME, Aker FV, Scheithauer BW. Chordoid meningioma: a clinicopathologic study of 42 cases. Am J Surg Pathol 2000; 24:899–905.
53. Roncaroli F, Scheithauer BW, Laeng RH, et al. Lipomatous meningioma: a clinicopathologic study of 18 cases with special reference to the issue of metaplasia. Am J Surg Pathol 2001; 25:769–775.
54. Artlich A, Schmidt D. Immunohistochemical profile of meningiomas and their histological subtypes. Hum Pathol 1990; 21:843–849.
55. Zorludemir S, Scheithauer BW, Hirose T, et al. Clear cell meningioma. A clinicopathologic study of a potentially aggressive variant of meningioma. Am J Surg Pathol 1995; 19:493–505.
56. Kepes JJ, Moral LA, Wilkinson SB, et al. Rhabdoid transformation of tumor cells in meningiomas: a histologic indication of increased proliferative activity: report of four cases. Am J Surg Pathol 1998; 22:231–238.
57. Perry A, Scheithauer BW, Stafford SL, et al. "Rhabdoid" meningioma: an aggressive variant. Am J Surg Pathol 1998; 22:1482–1490.
58. Pasquier B, Gasnier F, Pasquier D, et al. Papillary mengioma. Clinicopathologic study of seven cases and review of the literature. Cancer 1986; 58:299–305.
59. Kepes JJ. Meningiomas Biology, Pathology and Differential Diagnosis. Misson: New York, 1982.
60. Meis JM, Ordonez NG, Bruner JM. Meningiomas. An immunohistochemical study of 50 cases. Arch Pathol Lab Med 1986; 110:934–937.
61. Radley MG, di Sant'Agnese PA, Eskin TA, et al. Epithelial differentiation in meningiomas. An immunohistochemical, histochemical, and ultrastructural study with review of the literature. Am J Surg Pathol 1989; 92:226–272.
62. Schnitt SJ, Vogel H. Meningiomas. Diagnostic value of immunoperoxidase staining for epithelial membrane antigen. Am J Surg Pathol 1986; 10:640–649.
63. Winek RR, Scheithauer BW, Wick MR. Meningioma, meningeal hemangiopericytoma (angioblastic meningioma), peripheral hemangiopericytoma and acoustic schwannoma. A comparative immunohistochemical study. Am J Surg Pathol 1989; 13:251–261.
64. Yamashima T, Kida S, Yamamoto S. Ultrastructural comparison of arachnoidal villi and meningiomas in man. Mod Pathol 1988; 1:224–234.
65. Lesch KP, Gross S. Estrogen receptor immunoreactivity in meningiomas. Comparison with the binding activity of estrogen, progesterone, and androgen receptors. J Neurosurg 1987; 67:237–243.
66. Lesch KP, Schott W, Engl HG, et al. Gonadal steroid receptors in meningiomas. J Neurol 1987; 234:328–333.
67. Cahill DW, Bashirelahi N, Solomon LW, et al. Estrogen and progesterone receptors in meningiomas. J Neurosurg 1984; 60:985–993.
68. Schrell UM, Fahlbusch R. Hormonal manipulation of cerebral meningiomas: In: Al-Mefy O, ed. Meningiomas, New York: Ravne Press, 1991:273–283.
69. Perry A, Cai DX, Scheithauer BW, et al. Merlin, DAL-1, and progesterone receptor expression in clinicopathologic subsets of meningioma: a correlative immunohistochemical study of 175 cases. J Neuropathol Exp Neurol 2000; 59: 872–879.
70. Jones NR, Rossi ML. Gregorioiu M, et al. Epidermal growth factor receptor expression in 72 meningiomas. Cancer 1990; 66:152–155.
71. Kabus D, Sidhu GS, Wieczorek RL, et al. Metastatic meningioma. Hemangiopericytoma or angioblastic meningioma? Am J Surg Pathol 1993; 17:1144–1150.
72. D'Amore ES, Manivel JC, Sung JH, et al. Soft tissue and meningeal hemangiopericytomas: an immunohistochemical and ultrastructural study. Hum Pathol 1990; 21:414–423.
73. Rajaram V, Brat DJ, Perry A. Anaplastic meningioma versus meningeal hemangiopericytoma: immunohistochemical and genetic markers. Hum Pathol 2004; 35:1413–1418.
74. Suster S, Rosai J. Harmartoma of the scalp with ectopic meningothelial elements. A distinctive benign soft tissue lesion that may simulate angiosarcoma. Am J Surg Pathol 1990; 14:1–11.
75. Lopez DA, Silvers DN, Helwig EB. Cutaneous meningiomas: a clinicopathologic study. Cancer 1974; 32:728–744.
76. Taylor BW, Marcus RB, Friedman WA, et al. The meningioma controversy: postoperative radiation therapy. Int J Radiat Oncol Biol Phys 1988; 15:299–304.
77. Jaaskelainen J. Seemingly complete removal of histologically benign intracranial meningioma: late recurrence rate and factors predicting recurrence in 657 patients. A multivariate analysis. Surg Neurol 1986; 26:461–469.
78. Stafford SL, Perry A, Suman VJ, et al. Primarily resected meningiomas: outcome and prognostic factors in 581 Mayo Clinic patients, 1978 through 1988. Mayo Clin Proc 1998; 73:936–942.
79. de la Monte SM, Flickinger J, Linggood RM. Histopathologic features predicting recurrence of meningiomas following subtotal resection. Am J Surg Pathol 1986; 10:836–843.
80. Mirimanoff RO, Dosoretz DE, Linggood RM, et al. Meningioma: analysis of recurrence and progression following neurosurgical resection. J Neurosurg 1985; 62:18–24.
81. Grunewald JP, Rohl FW, Kirches E, et al. Correlation of DNA content and nucleomorphometric features with World Health Organization grading of meningiomas. Mod Pathol 1998; 11:216–223.
82. Langford LA, Cooksley CS, DeMonte F. Comparison of M1B-1 (Ki67) antigen and bromodeoxyuridine proliferation indices in meningiomas. Hum Pathol 1996; 27:350–354.
83. Lee KS, Hoshino T, Rodriguez LA, et al. Bromodeoxyuridine labeling study of intracranial meningiomas: proliferative potential and recurrence. Acta Neuropathol 1990; 80:311–317.
84. Hoshino T, Nagashima T, Murovic JA, et al. Proliferative potential of human meningiomas of the brain. A cell kinetics study with bromodeoxyuridine. Cancer 1986; 58:1466–1472.
85. Salmon I, Kiss R, Levivier M, et al. Characterization of nuclear DNA content, proliferation index, and nuclear size in a series of 181 meningiomas, including benign primary, recurrent, and malignant tumors. Am J Surg Pathol 1993; 17:239–247.

86. Ironside JW, Battersby RD, Lawry J, et al. DNA in meningioma tissues and explant cell cultures; a flow cytometric study with clinicopathologic correlates. J Neurosurg 1987; 66:588–594.
87. Crone KR, Challa VR, Kute TE, et al. Relationship between flow cytometric features and clinical behavior of meningiomas. Neurosurgery 1988; 23:720–724.
88. Patsouris E, Stocker U, Kallmeyer V, et al. Relationship between Ki-67 positive cells, growth rate and histologic type of human intracranial tumors. Anticancer Res 1988; 8:537–544.
89. Roggendorf W, Schuster T, Peiffer J. Proliferative potential of meningiomas determined with the monoclonal antibody Ki-67. Acta Neuropathol (Berl) 1987; 73:361–364.
90. Maiuri F, Iaconetta G, de Divitiis O, et al. Intracranial meningiomas: correlations between MR imaging and histology. Eur J Radiol 1999; 31:69–75.
91. Kim YJ, Ketter R, Henn W, et al. Histopathologic indicators of recurrence in meningiomas: correlation with clinical and genetic parameters. Virchows Arch 2006; 449:529–538.

VII. PITUITARY ADENOMA

1. Langman J. Brian. In: Langman J, ed. Medical Embryology. Human Development- Normal and Abnormal. 3rd ed. Baltimore: Williams & Wilkins, 1975:349–351.
2. Moore KL. The nervous system: In: Wonsiewicz M, ed. The Developing Human. Philadelphia: WB Saunders, 1993:1–4.
3. Lloyd RV. Embryology and anatomy of the pituitary gland. In: Lloyd RV, ed. Major Problems in Pathology, Vol 27. Philadelphia: WB Saunders, 1993:1–4.
4. Pernicone PJ, Scheithauer BW, Horvath E, et al. Pituitary and sellar region. In: Sternberg SS, ed. Histology for Pathologists. New York: Raven Pres, 1992:279–299.
5. Boyd JD. Observations on the human pharyngeal hypophysis. J Endocrinol 1956; 14:66–77.
6. McPhie JL, Beck JS. The histologic features of human growth hormone content of the pharyngeal pituitary gland in normal and endocrinologically-disturbed patients. Clin Endocrinol 1973; 2:157–173.
7. Melchionna RH, Moore RA. The pharyngeal pituitary gland. Am J Pathol 1938; 14:763–771.
8. Ciocca DR, Puy LA, Stati AO. Identification of seven hormone-producing cell types in the human pharyngeal hypophyisis. J Clin Endocrinol Metab 1985; 60:212–216.
9. Lloyd RV, Chandler WF, Kovacs K, et al. Ectopic pituitary adenomas with normal anterior anterior pituitary glands. Am J Surg Pathol 1986; 10:546–552.
10. Lloyd RV. Ectopic adenomasIn: Lloyd RV, ed. Surgical Pathology of the Pituitary Gland. Vol 27. Major Problems in Pathology. Philadelphia: WB Saunders 1993:116–120.
11. Chessin H, Urdaneta N, Smith H, et al. Chromophobe adenoma manifesting as a nasopharyngeal mass. Arch Otolaryngol 1976; 102:631–633.
12. Warner BA, Santen RJ, Page RB. Growth hormone and prolactin secretion by a tumor of the pharyngeal pituitary. Ann Intern Med 1982; 96:65–66.
13. Burch WM, Kramer RS, Kenan PA, et al. Cushing's disease caused by an ectopic pituitary adenoma within the sphenoid sinus. N Engl J Med 1985; 312:587–588.
14. Tovi F, Hirsch M, Sacks M, et al. Ectopic pituitary adenoma of the sphenoid sinus: report of a case and review of the literature. Head Neck 1990; 12:264–268.
15. Kovacs K, Horvath E. Tumors of the pituitary gland. In: Hartman WH, Sobin LH, ed. Atlas of Tumor Pathology 2nd Seri Fasc 21. Washington, DC: Armed Forces Institute of Pathology, 1986.
16. Scheithauer BW. Surgical pathology of the pituitary: the adenomas (Part II). Pathol Annu 1984; 19:269–329, 317–374.
17. Challa VR, Marshall RB, Hopkins MB, et al. Pathobiologic study of pituitary tumors: report of 62 cases with a review of the recent literature. Hum Pathol 1985; 16:873–884.
18. Stefaneanu L, Kovics K. Light microscopic special stains and immunochemistry in the diagnosis of pituitary adenomas. In: Lloyd RV, ed. Surgical Pathology of the Pituitary Gland, Vol 27, Major Problems in Pathology. Philadelphia: WB Saunders, , 1993:34, 51.
19. O'Brien T, O'Riordan DS, Gharib H, et al. Results of treatment of pituitary disease in multiple endocrine neoplasia, type I. Neurosurgery 1996; 39:273–278.
20. Boikos SA, Stratakis CA. Carney complex: the first 20 years. Curr Opin Oncol 2007; 19:24–29.
21. Martinez AJ. The pathology of nonfunctional pituitary adenomas. Semin Diagn Pathol 1986; 3:83–94.
22. Holm R, Nesland JM, Attramadal A, et al. Null cell adenomas of the pituitary gland: an immunohistochemical study. J Pathol 1989; 158:213–217.
23. Yeh PJ, Chen JW: Pituitary tumors: surgical and medical management. Surg Oncol 1997; 6:67–92.
24. Black PM, Hsu DW, Klibanski A, et al. Hormone production in clinically nonfunctioning pituitary adenomas. J Neurosurg 1987; 66:244–250.
25. King WA, Rodts GE, Becker DP, et al. Microsurgical management of giant pituitary tumors. Skull Base Surg 1996; 6:17–26.
26. Selman WR, Laws ER, Scheithauer BW, et al. The occurrence of dural invasion in pituitary adenomas. J Neurosurg 1986; 64:402–407.
27. Anand VK, Osborne CM, Harkey HL. Infiltrative clival pituitary adenoma of ectopic origin. Otolaryngol Head Neck Surg 1993; 108:178–183.
28. Corenblum B, LeBlanc FE, Watanabe M. Acromegaly with an adenomatous pharyngeal pituitary. JAMA 1980; 243:1456–1457.
29. Luk IS, Chan JK, Chow SM, et al. Pituitary adenoma presenting as sinonasal tumor: pitfalls in diagnosis. Hum Pathol 1996; 27:605–609.
30. Kay S, Lees JK, Stout AP. Pituitary chromophobe tumors of the nasal cavity. Cancer 1950; 3:695–704.
31. Chessin H, Urdaneta N, Smith H, et al. Chromophobe adenoma manifesting as a nasopharyngeal mass. Arch Otolaryngol 1976; 102:631–633.
32. Davis JM, Weber AL. Pituitary adenoma presenting as a sphenoid sinus lesion. Ann Otol Rhinol Laryngol 1980; 89:483–484.
33. Dent JA, Rickhuss PK. Invasive pituitary adenoma presenting with nasal obstruction. J Laryngol 1989; 103:605–609.
34. Dyer EH, Civit T, Abecassis JP, et al. Functioning ectopic supradiaphragmatic pituitary adenomas. Neurosurgery 1994; 34:529–532.
35. Kikuchi K, Kowada M, Sasaki J, et al. Large pituitary adenoma of the sphenoid sinus and the nasopharynx: report of a case with ultrastrutural evaluation. Surg Neurol 1994; 42:330–334.
36. Langford L, Batsakis JG. Pituitary gland involvement of the sinonasal tract. Ann Otol Rhinol Laryngol 1995; 104:167–169.
37. Lindboe CF, Unsgard G, Myhr G, et al. ACTH and TSH producing ectopic suprasellar pituitary adenoma of the hypothalamic region: case report. Clin Neuropathol 1993; 12:138–141.
38. Nagatani T, Shibuya M, Suzuki Y, et al. Suprasellar ectopic pituitary adenoma. Acta Neurochir 1997; 139:94–95.
39. Wong K, Raisanen J, Taylor SL, et al. Pituitary adenoma as an unsuspected clival tumor. Am J Surg Pathol 1995; 19:900–903.

40. Anand VK, Osborne CM, Harkey L. Inifiltrative clival pituitary adenoma of ectopic origin. Otolaryngol Head Neck Surg 1993; 108:178–183.
41. Slonim SM, Haykal HA, Cushing GW, et al. MRI appearance of an ectopic pituitary adneoma: case report and review of the literature. Neuroradiology 1993; 35: 546–548.
42. Ishii K, Ikeda H, Takahashi S, et al. MR imaging of pituitary adenomas with sphenoid sinus invasion: characteristic MR findings indicating fibrosis. Radiat Med 1996; 14:173–178.
43. Pernicone PJ, Scheithauer BW, Sebo TJ, et al. Pituitary carcinoma: a clinicopathologic study of 15 cases. Cancer 1997; 79:804–812.
44. Pernicone PJ, Scheithauer BW. Invasive pituitary adenomas and pituitary carcinomas. In: Lloyd RV, ed. Surgical Pathology of the Pituitary Gland, Vol 27, Major Problems in Pathology. Philadelphia: WB Saunders, 1993:121–136.
45. Cai WY, Alexander JM, Hedley-Whyte ET, et al. Ras mutations in human prolactinomas and pituitary carcinomas. J Clin Endocrinol Metab 1994; 78:89–93.
46. Cartwright DM, Miller TR, Nasr AJ. Fine-needle aspiration biopsy of pituitary carcinoma with cervical lymph node metastases: a report of two cases and review of the literature. Diagn Cytopathol 1994; 11:68–73.
47. Dayan C, Guilding T, Hearing S, et al. Biochemical cure of recurrent acromegaly by resection of cervical spinal canal metastases. Clin Endocrinol (Oxf) 1996; 44:597–602.
48. Frost AR, Tenner S, Tenner M, et al. ACTH-producing pituitary carcinoma presenting as the cauda equina syndrome. Arch Pathol Lab Med 1995; 119:93–96.
49. Gollard R, Kosty M, Cheney C, et al. Prolactin-secreting pituitary carcinoma with implants in the cheek pouch and metastases to the ovaries. A case report and literature review. Cancer 1995; 76:1814–1820.
50. Greenman Y, Woolf P, Coniglio J, et al. Remission of acromegaly caused by pituitary carcinoma after surgical excision of growth hormone-secreting metastasis detected by 111-indium pentetreotide scan. J Clin Endocrinol Metab 1996; 81:1628–1633.
51. Jamjoom A, Moss T, Coakham H, et al. Cervical lymph nodes metastases from a pituitary carcinoma. Br J Neurosurg 1994; 8:87–92.
52. Kasantikul V, Boonjunwetwat D, Suwangool P. Prolactin cell carcinoma of the pituitary. J Med Assoc Thai 1993; 76:230–237.
53. Lubke D, Saeger W. Carcinomas of the pituitary: definition and review of the literature. Gen Diagn Pathol 1995; 141:81–92.
54. Mixson AJ, Friedman TC, Katz DA, et al. Thyrotropin-secreting pituitary carcinoma. J Clin Endocrinol Metab 1993; 76:529–533.
55. O'Brien DP, Phillips JP, Rawluk DR, et al. Intracranial metastases from pituitary adenoma. Br J Neurosurg 1995; 9:211–8.
56. Pei L, Melmed S, Scheithauer B, et al. H-ras mutations in human pituitary carcinoma metastases. J Clin Endocrinol Metab 1994; 78:842–846.
57. Saadeh IK, Houlston RS, Ellison DW, et al. Carcinoma of the pituitary in association with pulmonary stenosis and microcephaly. J Intern Med 1994; 235:183–184.
58. Thapar K, Kovacs K, Scheithauer BW, et al. Proliferative activity and invasiveness among pituitary adenomas and carcinomas: an analysis using the MIB-1 antibody. Neurosurgery 1996; 38:99–106.
59. Thapar K, Scheithauer BW, Kovacs K, et al. p53 expression in pituitary adenomas and carcinomas: correlation with invasiveness and tumor growth fractions. Neurosurgery 1996; 38:763–770.
60. Walker JD, Grossman A, Anderson JV, et al. Malignant prolactinoma with extracranial metastases: a report of three cases. Clin Endocrinol (Oxf) 1993; 38:411–419.
61. Scheithauer BW, Randall RV, Laws ER, et al. Prolactin cell carcinoma of the pituitary. Clinicopathologic, immunohistochemical and ultrastructural study of a case with cranial and extracranial metastases. Cancer 1985; 55:598–604.
62. Vieira JO Jr., Cukiert A, Liberman B. Evaluation of magnetic resonance imaging criteria for cavernous sinus invasion in patients with pituitary adenomas: logistic regression analysis and correlation with surgical findings. Surg Neurol 2006; 65:130–135.
63. Wolfsberger S, Ba-Ssalamah A, Pinker K, et al. Application of three-tesla magnetic resonance imaging for diagnosis and surgery of sellar lesions. J Neurosurg 2004; 100:278–286.
64. Pierallini A, Caramia F, Falcone C, et al. Pituitary macroadenomas: preoperative evaluation of consistency with diffusion-weighted MR imaging–initial experience. Radiology 2006; 239:223–231.
65. Rumboldt Z. Pituitary adenomas. Top Magn Reson Imaging 2005; 16:277–288.
66. Bonneville JF, Bonneville F, Cattin F. Magnetic resonance imaging of pituitary adenomas. Eur Radiol 2005; 15: 543–548.
67. Lloyd RV, Cano M, Chandler WF, et al. Human growth hormone and prolactin secreting pituitary adenomas analyzed by in situ hybridization. Am J Pathol 1989; 134:605–613.
68. Horvath E, Kovacs K. Pathology of acromegaly. Neuroendocrinology 2006; 83:161–165.
69. Mittelbronn M, Psaras T, Capper D, et al. ACTH- and prolactin-producing pituitary gland microadenoma with biphasic features of atypia and intermediate filament expression. Neuro Endocrinol Lett 2006; 27:89–92.
70. Coons SW, Estrada SI, Gamez R, et al. Cytokeratin CK 7 and CK 20 expression in pituitary adenomas. Endocr Pathol 2005; 16:201–210.
71. Scheithauer BW, Kovacs KT, Laws ER. Pathology of invasive pituitary tumors with special reference to functional classifications. J Neurosurg 1986; 65:733–744.
72. Bevan JS, Asa SL, Rossi ML, et al. Intrasellar gangliocytoma containing gastrin and growth hormone-releasing hormone associated with a growth hormone-secreting pituitary adenoma. Clin Endocrinol (Oxf) 1989; 30: 213–224.
73. Horvath E, Kovacs K, Scheithauer BW, et al. Pituitary adenoma with neuronal choristoma (PANCH): composite lesion or lineage infidelity? Ultrastruct Pathol 1994; 18:565–574.
74. Kamel OW, Horoupian DS, Silverberg GD. Mixed gangliocytoma-adenoma: a distinct neuroendocrine tumor of the pituitary fossa. Hum Pathol 1989; 20:1198–1203.
75. Puchner MJ, Ludecke DK, Valdueza JM, et al. Cushing's disease in a child caused by a corticotropin-releasing hormone-secreting intrasellar gangliocytoma associated with an adrenocorticotropic hormone secreting puitary adenoma. Neurosurgery 1993; 33:920–925.
76. Towfighi J, Salam MM, McLendon RE, et al. Ganglion cell-containing tumors of the pituitary gland. Arch Pathol Lab Med 1996; 120:369–377.
77. Saeger W, Puchner MJ, Ludecke DK. Combined sellar gangliocytoma and pituitary adenoma in acromegaly or Cushing's disease. A report of 3 cases. Virchows Arch 1994; 425:93–99.
78. Serebrin R, Robertson DM. Ganglioneuroma arising in the pituitary fossa: a twenty year follow up. J Neurol Neurosurg Psychiatry 1984; 47:97–98.
79. Slowik F, Fazekas I, Balint K, et al. Intrasellar hamartoma associated with pituitary adenoma. Acta Neuropathol (Berl) 1990; 80:328–333.

80. Tajika Y, Kubo O, Takeshita M, et al. An intracranial collision tumor composed of intrasellar gangliocytoma and pituitary adenoma. No Shinkei Geka 1989; 17:1181–1186.
81. Asa SL, Scheithauer BW, Bilbao JM, et al. A case for hypothalamic acromegaly: a clinicopathological study of six patients with hypothalamic gangliocytomas producing growth hormone-releasing factor. J Clin Endocrinol Metab 1984; 58:796–803.
82. Rhodes RH, Dusseau JJ, Boyd AS, et al. Intrasellar neural-adenohypophyseal choristoma: a morphological and immunocytochemical study. J Neuropathol Exp Neurol 1982; 41:267–280.
83. McKeever PE, Blaivas M, Sima AAF. Neoplasms of the sellar region. In: Lloyd RV, ed. Major Problems in Pathology, Vol 27. Philadelphia: WB Saunders, 1993:141–210.
84. Min KW. Usefulness of electron microscopy in diagnosis of ''small'' round cell tumors of the sinonasal region. Ultrastruct Pathol 1995; 19:347–363.
85. Devaney K, Wenig BM, Abbondanzo SL. Olfactory neuroblastoma and other round cell lesions of the sinonasal region. Mod Pathol 1996; 9:658–663.
86. Hampton TA, Scheithauer BW, Rojiani AM, et al. Salivary gland-like tumors of the sellar region. Am J Surg Pathol 1997; 21:424–434.
87. Lang HD, Saeger W, Ludecke DK, et al. Rapid frozen section diagnosis of pituitary tumors. Endocrinol Pathol 1990; 1:116–122.
88. Martinez AJ, Moossy J. Cytological diagnosis of pituitary adenomas. J Neuropathol Exp Neurol 1983; 42:307–311.
89. Mortini P, Losa M, Barzaghi R, et al. Results of transsphenoidal surgery in a large series of patients with pituitary adenoma. Neurosurgery 2005; 56:1222–1233.
90. Delgrange E, Duprez T, Maiter D. Influence of parasellar extension of macroprolactinomas defined by magnetic resonance imaging on their responsiveness to dopamine agonist therapy. Clin Endocrinol 2006; 64:456–462.
91. Wu ZB, Yu CJ, Su ZP, et al. Bromocriptine treatment of invasive giant prolactinomas involving the cavernous sinus: results of a long-term follow up. J Neurosurg 2006; 104:54–61.
92. Jagannathan J, Dumont AS, Jane JA Jr. Diagnosis and management of pediatric sellar lesions. Front Horm Res 2006; 34:83–104.
93. Kelley RT, Smith JL, Rodzewicz GM. Transnasal endoscopic surgery of the pituitary: modifications and results over 10 years. Laryngoscope 2006; 116:1573–1576.
94. Anand VK, Schwartz TH, Hiltzik DH, et al. Endoscopic transphenoidal pituitary surgery with real-time intraoperative magnetic resonance imaging. Am J Rhinol 2006; 20:401–405.
95. Flickinger JC, Nelson PB, Martinez AJ, et al. Radiotherapy of nonfunctional adenomas of the pituitary gland. Results with long-term follow-up. Cancer 1989; 63:2409–2414.
96. Fitzgibbons PL, Appley AJ, Turner RR, et al. Flow cytometry analysis of pituitary tumors. Correlation of nuclear antigen p105 and DNA content with clinical behavior. Cancer 1988; 62:1156–1560.
97. Anniko M, Tribukait B, Wersall J. DNA ploidy and cell phase in human pituitary tumors. Cancer 1984; 53:1708–1713.
98. Nagashima T, Murovic JA, Hoshino T, et al. The proliferative potential of human pituitary tumors in situ. J Neurosurg 1986; 64:588–593.
99. Lloyd RV. Molecular analysis of pituitary disorders. In Lloyd RV, ed. Major problems in Pathology Vol 27. Philadelphia WB, Saunders, 1993:85–93.
100. Gandour-Edwards R, Kapadia SB, Janecka IP, et al. Biological markers of invasive pituitary adenomas involving the sphenoid sinus. Mod Pathol 1995; 8:160–164.
101. Kaltsas GA, Nomikos P, Kontogeorgos G, et al. Clinical review: Diagnosis and management of pituitary carcinomas. J Clin Endocrinol Metab 2005; 90:3089–3099.
102. Scheithauer BW, Gaffey TA, Lloyd RV, et al. Pathobiology of pituitary adenomas and carcinomas. Neurosurgery 2006; 59:341–353.
103. Brown RL, Muzzafar T, Wollman R, et al. A pituitary carcinoma secreting TSH and prolactin: a non-secreting adenoma gone awry. Eur J Endocrinol 2006; 154:639–643.
104. Alexander JM, Biller BM, Bikkal H, et al. Clinically nonfunctioning pituitary tumors are monoclonal in origin. J Clin Invest 1990; 86:336–340.
105. Levy A, Lightman SL. The pathogenesis of pituitary adenomas. Clin Endocrinol 1993; 38:559–570.
106. Herman V, Fagin J, Gonsky R, et al. Clonal origin of pituitary adneomas. J Clin Endocrinol Metab 1990; 71:1427–1433.
107. Landis CA, Masters SB, Spada A, et al. Clonal origin of pituitary adenomas. J Clin Endocrinol Metab 1990; 71:1427–1433.
108. Karga HJ, Alexander JM, Hedley-Whyte ET, et al. Ras mutations in human pituitary tumors. J Clin Endocrinol Metab 1992; 74:914–919.
109. Green VL, White MC, Hipkins LJ, et al. Apoptosis and p53 suppressor gene protein expression in human anterior pituitary adenomas. Eur J Endocrinol 1997; 136:382–387.
110. Sanno N, Teramoto A, Matsuno A, et al. Expression of human Pit-1 product in the human pituitary and pituitary adenomas. Immunohistochemical studies using an antibody against synthetic human Pit-1 product. Arch Pathol Lab Med 1996; 120:73–77.

VIII. CRANIOPHARYNGIOMA

1. Alvarez M. Craniopharyngiomas. J Neurosci Nurs 2006; 38:362–368.
2. Burger PC, Scheithauer BW, eds. Tumors of the Central Nervous System. Atlas of Tumor Pathology. 2nd Ser, Fasc 6, Washington DC: Armed Forces Institute of Pathology, 1993.
3. Bunin GR, Surawicz TS, Witman PA, et al. The descriptive epidemiology of craniopharyngioma. Neurosurg Focus 1997; 15:3–e1.
4. Love JG, Marshall TM. Craniopharyngiomas. Surg Gynecol Obstet 1950; 90:591–601.
5. Petito CK, DeGirolami U, Earle KM. Craniopharyngiomas. A clinical and pathological review. Cancer 1976; 37:1944–1952.
6. Yamini B, Narayanan M. Craniopharyngiomas: an update. Expert Rev Anticancer Ther 2006; 6:85–92.
7. Rossi A, Cama A, Consales A, et al. Neuroimaging of pediatric craniopharyngiomas: a pictorial essay. J Pediatr Endocrinol Metab 2006; 19:299–319.
8. Weiner HL, Wisoff JH, Rosenberg ME, et al. Craniopharyngiomas: a clinicopathological analysis of factors predictive of recurrence and functional outcome. Neurosurgery 1994; 35:1001–1010.
9. Khafaga Y, Jenkin D, Kanaan I, et al. Craniopharyngioma in children. Int J Radiat Oncol Biol Phy 1998; 42:601–606.
10. Podoshin L, Rolan L, Altman MM, et al. ''Pharyngeal'' craniopharyngioma. J Laryngol Otol 1970; 84:93–99.
11. Byrne MN, Sessions DG. Nasopharyngeal craniopharyngioma. Case report and literature review. Ann Otol Rhinol Laryngol 1990; 99:633–639.
12. Prasad U, Kwi NK. Clinical records. Nasopharynseal craniopharyngioma. J Laryngol Otol 1975; 89:445–452.

13. Bernstein ML, Buccino JJ. The histologic similarity between craniopharyngioma and odotogenic lesions; a reapprasial. Oral Surg Oral Med Oral Pathol 1983; 56:502–511.
14. Gorlin RJ, Chaudhry AP. The ameloblasotma and craniopharyngioma; their similarities and their differences. Oral Surg Oral Med Oral Pathol 1959; 12:199–205.
15. Badger KV, Gardner DG. The relationship of adamantionomatous craniopharyngioma to ghost cell ameloblastoma of the jaws; a histologic and immunohistochemical study. J Oral Pathol Med 1997; 26:349–355.
16. Crotty TB, Scheithauer BW, Young WF, et al. Papillary craniopharyngioma: a clinicopathology study of 48 cases. J Neurol Surg 1995; 83:206–214.
17. Lopez-Carreira M, Dominguez-Franjo P, Madero S, et al. Suprasellar papillary squamous craniopharyngioma. A case report. J Neurosurg Sci 1997; 41:175–178.
18. Jane JA Jr., Laws ER. Craniopharyngioma. Pituitary 2006; 9:323–326.
19. Patrick BS, Smith RR, Bailey TO. Aseptic meningitis due to spontaneous rupture of craniopharyngioma cyst. Case report. J Neurosurg 1974; 41:387–390.
20. Russell RW, Pennybacker JB. Craniopharyngioma in the elderly. J Neurol Neurosurg Psychiatry 1961; 24:1–13.
21. Larijani B, Bastanhagh MH, Pajouhi M, et al. Presentation and outcome of 93 cases of craniopharyngioma. Eur J Cancer Care (Engl) 2004; 13:11–15.
22. Karavitaki N, Brufani C, Warner JT, et al. Craniopharyngiomas in children and adults: systematic analysis of 121 cases with long-term follow-up. Clin Endocrinol (Oxf) 2005; 62:397–409.
23. Tsuda M, Takahashi S, Higano S, et al. CT and MR imaging of craniopharyngioma. Eur Radiol 1997; 7:464–469.
24. Pusey E, Kortman KE, Flannigan BD, et al. MR of craniopharyngiomas, tumor delineation and characterization. AJR Am J Roentgenol 1987; 149:383–388.
25. Sartoretti-Schefer S, Wichmann W, Aguzzi A, et al. MR differentiation of adamantinous squamous-papillary craniopharyngiomas. AJNR Am J Neuroradiol 1997; 18:77–87.
26. Curran JG, O'Connor E. Imaging of craniopharyngioma. Childs Nerv Syst 2005; 21:635–639.
27. Adamson TE, Wiestler OD, Kleihues P, et al. Correlation with clinical and pathological features in surgically treated craniopharyngiomas. J Neurosurg 1990; 73:12–17.
28. Kato K, Nakatani Y, Kanno H, et al. Possible linkage between specific histological structures and aberrant reactivation of the Wnt pathway in adamantinomatous craniopharyngioma. J Pathol 2004; 203:814–821.
29. Oikonomou E, Barreto DC, Soares B, et al. Beta-catenin mutations in craniopharyngiomas and pituitary adenomas. J Neurooncol 2005; 73:205–209.
30. Buslei R, Nolde M, Hofmann B, et al. Common mutations of beta-catenin in adamantinomatous craniopharyngiomas but not in other tumors originating from the sellar region. Acta Neuropathol (Berl) 2005; 109:589–597.
31. Yoshimoto M, de Toledo SR, da Silva NS, et al. Comparative genomic hybridization analysis of pediatric adamantinomatous craniopharyngiomas and a review of the literature. J Neurosurg 2004; 101:85–90.
32. Osborn AG. Rathke cleft cyst. In: Diagnostic imaging: brain. Salt Lake City, Utah: Amirsys, 2004, II-2-16.
33. Byun WM, Kim OL, Kim D. MR imaging findings of Rathke's cleft cysts: significance of intracystic nodules. AJNR Am J Neuroradiol 2000; 21:485–488.
34. Shin JL, Asa SL, Woodhouse LJ, et al. Cystic lesions of the pituitary: clinicopathological features distinguishing craniopharyngioma, Rathke's cleft cyst, and arachnoid cyst. J Clin Endocrinol Metab 1999; 84:3972–3982.
35. Osborn AG, Preece MT. Intracranial cysts: radiologic-pathologic correlation and imaging approach. Radiology 2006; 239:650–664.
36. May JA, Krieger MD, Bowen I, et al. Craniopharyngioma in childhood. Adv Pediatr 2006; 53:183–209.
37. Zuccaro G. Radical resection of craniopharyngioma. Childs Nerv Syst 2005; 21:679–690.
38. Wang KC, Hong SH, Kim SK, et al. Origin of craniopharyngiomas: implication on the growth pattern. Childs Nerv Syst 2005; 21:628–634.
39. Samii M, Tatagiba M. Surgical management of craniopharyngioma: a review. Neurol Med Chir 1997; 37:141–149.
40. Fischer EG, Welch K, Belli JA, et al. Treatment of craniopharyngiomas in children: 1972-1981. J Neurosurg 1985; 62:496–501.
41. Hoffman HJ, Hendrick EB, Humphreys RP, et al. Management of craniopharyngioma in children. J Neurosurg 1977; 47:218, 227.
42. Baskin DS, Wilson CB. Surgical management of craniopharyngiomas: a review of 74 cases. J Neurosurg 1986; 65:22–27.
43. Symon L, Pell MF, Habib AH. Radical excision of craniopharyngioma by the temporal route: a review of 50 patients. Br J Neurosurg 1991; 5:539–549.
44. Tomita T, McLone DG. Radical resections of childhood craniopharyngioma by the temporal route: a review of 50 patients. Br J Neurosurg 1991; 5:539–549.
45. Yasargil MG, Curcic M, Kis M, et al. Total removal of craniopharyngiomas. Approaches and long-term results in 144 patients. J Neurosurg 1990; 73:3–11.
46. Sung DI, Chang CH, Harisiadis L, et al. Treatment results of craniopharyngiomas. Cancer 1981; 47:847–852.
47. Regine WF, Kramer S. Pediatric craniopharyngiomas: long term results of combined treatment with surgery and radiation. Int J Radiat Oncol Biol Phys 1992; 24:611–617.
48. Julow J, Lanyi F, Hajda M, et al. The radiotherapy of cystic craniopharyngioma with intracystic installation of 90Y silicate colloid. Acta Neurochir 1985; 74:94–99.
49. Caldarelli M, di Rocco C, Papacci F, et al. Management of recurrent craniopharyngioma. Acta Neurochir 1998; 140:447–454.
50. Danoff BF, Cowchock FS, Kramer S. Childhood craniopharyngioma: survival, local control, endocrine and neurologic function following radiotherapy. Int J Radiat Oncol Biol Phy 1983; 9:171–175.
51. Di Rocco C, Caldarelli M, Tamburrini G, et al. Surgical management of craniopharyngiomas–experience with a pediatric series. J Pediatr Endocrinol Metab 2006; 19:355–366.
52. Tena-Suck ML, Salinas-Lara C, Arce-Arellano RI, et al. Clinico-pathological and immunohistochemical characteristics associated to recurrence/regrowth of craniopharyngiomas. Clin Neurol Neurosurg 2006; 108:661–669.
53. Tavangar SM, Larijani B, Mahta A, et al. Craniopharyngioma: a clinicopathological study of 141 cases. Endocr Pathol 2004; 15:339–344.
54. Xu J, Zhang S, You C, et al. Microvascular density and vascular endothelial growth factor have little correlation with prognosis of craniopharyngioma. Surg Neurol 2006; 66:30–34.
55. Gupta DK, Ojha BK, Sarkar C, et al. Recurrence in craniopharyngiomas: analysis of clinical and histological features. J Clin Neuro Sci 2006; 13:438–442.
56. Muller HL, Gebhardt U, Pohl F, et al. Relapse pattern after complete resection and early progression after incomplete resection of childhood craniopharyngioma. Klin Padiatr 2006; 218:315–320.
57. Bunin GR, Surawicz TS, Witman PA, et al. The descriptive epidemiology of craniopharyngioma. Neurosurg Focus 1997; 3:e1.

58. Oskouian RJ, Samii A, Laws ER. The craniopharyngioma. Front Horm Res 2006; 34:05–126.

IX. PARAGANGLIOMA

1. Tischler AS. In: Mills SE, ed. Paraganglia in Histology for Pathologists. 3rd ed. Lippincott Williams and Wilkins, Philadelphia, 2007:1211–1233.
2. Barnes L, Tse LLY, Hunt JL, et al. Tumors of the paraganglionic system: Introduction in World Health Organization Classification of Tumors. In: Barnes L, Eveson JW, Reichart P, et al., eds. Pathology and Genetics Head and Neck Tumors. Lyon: IARC Press, 2005:361–370.
3. Rao AB, Koeller KK, Adair CF. From the archives of the AFIP. Paragangliomas of the head and neck: radiologic-pathologic correlation. Armed Forces Institute of Pathology. Radiographics 1999; 19:1605–1632.
4. Lustrin ES, Palestro C, Vaheesan K. Radiographic evaluation and assessment of paragangliomas. Otolaryngol Clin North Am 2001; 34:881–906.
5. Kwekkeboom DJ, van Urk H, Pauw BK, et al. Octreotide scintigraphy for the detection of paragangliomas. J Nucl Med 1993; 34:873–878.
6. Grufferman S, Gillman MW, Pasternak LR, et al. Familial carotid body tumors: case report and epidemiologic review. Cancer 1980; 46:2116–2122.
7. McCaffrey TV, Meyer FB, Michels VV, et al. Familial paragangliomas of the head and neck. Arch Otolaryngol Head Neck Surg 1994; 120:1211–1216.
8. van der Mey AG, Maaswinkel-Mooy PD, Cornelisse CJ, et al. Genomic imprinting in hereditary glomus tumors: evidence for new genetic theory. Lancet 1989; 2:1291–1294.
9. van Schothorst EM, Beekman M, Torremans P, et al. Paragangliomas of the head and neck region show complete loss of heterozygostiy at 11q22-q23 in chief cells and the flow-sorted DNA aneuploid fraction. Hum Pathol 1998; 29:1045–1049.
10. Heutink P, van der Mey AG, Sandkuijl LA, et al. A gene subject to genomic imprinting and responsible for hereditary paragangliomas maps to chromosome 11q23-qter. Hum Mol Genet 1992; 1:7–10.
11. Baysal BE, Ferrel RE, Willet-Brozick JE, et al. Mutations in SDHD, a mitochondrial complex II gene, in hereditary paraganglioma. Science 2000; 287:848–851.
12. Gimenez-Roqueplo AP, Favier J, Rustin P, et al. The R22X mutation of the SDHD gene in hereditary paraganglioma abolishes the enzymatic activity of complex II in the mitochondrial respiratory chain and activates the hypoxia pathway. Am J Hum Genet 2001; 69:1186–1197.
13. Baysal BE. Genetics of familial paragangliomas: past, present, and future. Otolaryngol Clin North Am 2001; 34:863–879.
14. Bikhazi PH, Messina L, Mhatre AN, et al. Molecular pathogenesis in sporadic head and neck paraganglioma. Laryngoscope 2000; 110:1346–1348.
15. Petropoulous AE, Lutje CM, Camarata PJ, et al. Genetic analysis in the diagnosis of familial paragangliomas. Laryngoscope 2000; 110:1225–1229.
16. Mariman EC, van Beersum SE, Cremers CW, et al. Fine mapping of a putatively imprint gene for familial non-chromaffin paragangliomas to chromosome 11q13.1: evidence for genetic heterogeneity. Hum Genet 1995; 95:56–62.
17. Niemann S, Steinburger D, Muller U. PGL3, a third, not maternally imprinted locus in autosomal dominant paraganglioma. Neurogenetics 1999; 2:167–170.
18. Astuti D, Latif F, Dallol A, et al. Gene mutations in the succinate dehydrogenase subunit SDHB cause susceptibility to familial pheochromocytoma and to familial paraganglioma. Am J Hum Genet 2001; 69:49–54.
19. Baysal BE, Willett-Brozick JE, Lawrence EC, et al. Prevalence of SDHB, SDHC, and SDHD germline mutations in clinic patients with head and neck paragangliomas. J Med Genet 2003; 39:178–183.
20. Lemaire M, Persu A, Hainaut P, et al. Hereditary Paraganglioma. J Intern Med 1999; 246:113–116.
21. Neumann HP, Pawlu C, Peczkowska M, et al. Distinct clinical features of paraganglioma syndromes associated with SDHB and SDHD gene mutations. JAMA 2004; 292:943–951.
22. Van Nederveen FH, Dannenberg H, Sleddens HF, et al. p53 alterations and their relationship to SDHD mutations in parasympatheric paragangliomas. Mod Pathol 2003; 16:849–856.
23. Schiavi F, Boedeker CC, Bausch B, et al. Predictors and prevalence of paraganglioma syndrome associated with mutations of the SDHC gene. JAMA 2005; 294: 2057–2063.
24. Glenner GG, Grimley PM. Tumors of the extra-adrenal paraganglion system (including chemoreceptors). In: Atlas of Tumor Pathology, Armed Forces Institute of Pathology: Washington DC, 1974.
25. Saldana MJ, Salem LE, Travezan R. High altitude hypoxia and chemodectomas. Hum Pathol 1973; 4:251–263.
26. Zak FG, Lawson W. The Paraganglionic Chemoreceptor System: Physiology, Pathology, and Clinical Medicine. New York, NY: Springer-Verlag, NY Inc, 1982.
27. Heath D, Smith P. The Pathology of the Carotid Body and Sinus. Baltimore, MD: Edward Arnold Publishers Ltds, 1985.
28. Lack EE, ed. In: Pathology of Adrenal and Extra-adrenal Paraganglia. Major Problems in Pathology. Vol 29. WB Saunders, 1994.
29. Lack EE, Cubilla AL, Woodruff JM, et al. Paragangliomas of the head and neck region. A clinical study of 69 patients. Cancer 1977; 39:397–409.
30. Granger JK, Houn HY. Head and neck paragangliomas: a clinicopathologic study with DNA flow cytometric analysis. South Med J 1990; 83:1407–1412.
31. Hodge KM, Byers RM, Peters LJ. Paragangliomas of the head and neck. Arch Otolaryngol Head Neck Surg 1988; 114:872–877.
32. Barnes L, Taylor SR. Carotid body paragangliomas. A clinicopathologic and DNA analysis of 13 tumors. Arch Otolaryngol Head Neck Surg 1990; 116:447–453.
33. Rodriguez-Cueves S, Lopez-Garza J, Labastida-Alemndaro S. Carotid body tumors in inhabitants of altitudes higher than 2000 meters above sea level. Head Neck 1998; 20:374–378.
34. Nettersville JL, Reilly KM, Robertson D, et al. Carotid body tumors: a review of 30 patients with 46 tumors. Laryngoscope 1995; 105:115–126.
35. ReMine WH, Weiland LH, Remine SG. Carotid body tumors: chemodectomas. Curr Probl Cancer 1978; 2:3–26.
36. Shamblin WR, ReMine WH, Sheps SG, et al. Carotid body tumor (chemodectoma): clinicopathologic analysis of ninety cases. Am J Surg 1971; 122:732–739.
37. Dickinson PH, Griffin SM, Guy AJ, et al. Carotid body tumor: 30 years experience. Br J Surg 1986; 73:14–16.
38. Lees CD, Levine HL, Beven EG, et al. Tumors of the carotid body: experience with 41 operative cases. Am J Surg 1981; 142:362–365.
39. Padberg FT, Cady B, Persson AV. Carotid body tumor: The Lahey Clinic experience. Am J Surg 1983; 145:526–528.
40. Jech M, Alvarado-Cobrero I, Albores-Saavedra J, et al. Genetic analysis of high altitude paragangliomas. Endocr Pathol 2006; 17:201–202.
41. McCaffery TV, Meyer FB, Michaels VV, et al. Familial paragangliomas of the head and neck. Arch Otolaryngol Head Neck Surg 1994; 120:1211–1216.

42. Sobol SM, Dailey JC. Familial multiple cervical paragangliomas: report of a kindred and review of the literature. Otolaryngol Head Neck Surg 1990; 102:382–390.
43. Larraza-Hernandez O, Albores-Saavedra J, Benavides G, et al. Multiple endocrine neoplasia, pituitary adenoma, multicentric papillary thyroid carcinoma, bilateral carotid body paraganglioma, parathyroid hyperplasia, gastric leiomymoma, and systemic amyloidosis. Am J Clin Pathol 1982; 78:527–532.
44. Carney JA. The triad of gastric epitheloid leiomysarcoma, pulmonary chondroma, and functioning extra-adrenal paraganglioma. A five-year review. Medicine 1983; 62:159–169.
45. Kroll AJ, Alexander B, Cochios F, et al. Hereditary deficiencies of clotting factors VII and X associated with carotid body tumors. N Engl J Med 1964; 270:6–13.
46. Plaza JA, Wakely PE, Moran C, et al. Sclerosing paraganglioma: report of 19 cases of an unusual variant of neuroendocrine tumor that may be mistaken for an aggressive malignant neoplasm. Am J Surg Pathol 2006; 30:7–12.
47. Jansen JC, van den Berg R, Kuiper A, et al. Estimation of growth rate in patients with head and neck paragangliomas influences the treatment proposal. Cancer 2000; 88:2811–2816.
48. Zbaren B, Lehmann W. Carotid body paraganglioma with metastases. Laryngoscope 1985; 95:450–454.
49. Strauss M, Nicholas GG, Abt AB, et al. Malignant catecholamine secreting carotid body paraganglioma. Otolaryngeal Head Neck Surg 1983; 91:315–321.
50. Pacheco-Ojeda L. Malignant carotid body tumors: report of three cases. Ann Otol Rhinol Laryngol 2001; 110:36–40.
51. Elder EE, Xu D, Hoog A, et al. KI-67 and hTERT expression can aid in the distinction between malignant and benign pheochromocytoma and paraganglioma. Mod Pathol 2003; 16:246–255.
52. Gee MS, Kliewer KE, Hinton DR. Nucleolar organizer regions in paragangliomas of the head and neck. Arch Otolaryngol Head Neck Surg 1992; 118:380–383.
53. Kliewer KE, Cochran AJ. A review of the histology, ultrastructure, immunohistology, and molecular biology of extra-adrenal paragangliomas. Arch Pathol Lab Med 1989; 113:1209–1218.
54. Kliewer KE, Wen DR, Cancilla PA, et al. Paragangliomas: assessment of prognosis by histologic, immunohistochemical, and ultrastructural techniques. Hum Pathol 1989; 20:29–39.
55. Kumaki N, Kajiwara H, Kameyama K, et al. Prediction of malignant behavior of pheochromocytomas and paragangliomas using immunohistochemical techniques. Endocr Pathol 2002; 13:149–156.
56. Linnoila RI, Lack EE, Steinberg SM, et al. Decreased expression of neuropeptides in malignant paragangliomas: an immunohistochemical study. Hum Pathol 1988; 19:41–50.
57. van Schothorst EM, Beekman M, Torremans P, et al. Paragangliomas of the head and neck region show complete loss of heterozygosity at 11q22-q23 in chief cells and the flow-sorted DNA aneuploid fraction. Hum Pathol 1998; 29:1045–1049.
58. Welkoborsky HJ, Xiao Y, Mann WJ, et al. Studies for estimating the biologic behavior and prognosis of paragangliomas of the head and neck. Skull Base Surg 1995; 5:149–156.
59. Massey V, Wallner K. Treatment of metastatic chemodectoma. Cancer 1992; 69:790–792.
60. Lee JH, Barich F, Karnell LH, et al. National cancer data base report on malignant paragangliomas of the head and neck. Cancer 2002; 94:730–737.
61. Rosenwaller H. Carotid body tumor of the middle ear and mastoid. Arch Otolaryngol 1945; 41:64–67.
62. Alford BR, Guilford FR. A comprehensive study of tumors of the glomus jugular. Laryngoscope 1962; 72:765–805.
63. Spector GJ, Ciralsky RH, Ogura JH. Glomus tumors in the head and neck: III. Analysis of clinical manifestations. Ann Otol Rhinol Laryngol 1975; 84:73–79.
64. Spector GJ, Maisal RH, Ogura JH. Glomus tumors in the middle ear. I. An analysis of 46 patients. Laryngoscope 1973; 83:1652–1672.
65. Brown JS. Glomus jugulare tumors revisited: a ten-year statistical follow-up of 231 cases. Laryngoscope 1985; 95:284–288.
66. Kamerer DB, Hirsch BE. Paragangliomas (''glomus tumors'') of the temporal bone. In: Sekhar LN, Schramm VL Jr., eds. Tumors of the Cranial Base: Diagnosis and Management. New York: Futura Publishing CO, 1987:641–654.
67. Pluta RM, Ram Z, Patronas NJ, et al. Long-term effects of radiation therapy for a catecholamine-producing glomus jugulare tumor. Case report. J Neurosurg 1994; 80: 1091–1094.
68. Kuhweide R, Lanser MJ, Fisch U. Catecholamine-secreting paragangliomas at the skull base. Skull Base Surg 1996; 6:35–45.
69. Kremer R, Michel RP, Posner B, et al. Catecholamine-secreting paraganglioma of glomus jugulare region. Am J Med Sci 1989; 297:46–48.
70. Walker PJ, Fagan PA. Catecholamine-secreting paraganglioma of the pterygopalatine fossa: case report. Am J Otol 1993; 14:306–308.
71. Cantrell RW, Kaplan MJ, Atuk NO, et al. Catecholamine-secreting infratemporal fossa paraganglioma. Ann Otol Rhinol Laryngol 1984; 93:583–588.
72. O'Leary MJ, Shelton C, Giddings NA, et al. Glomus tympanicum tumors: A clinical perspective. Laryngoscope 1991; 101:1038–1043.
73. Jackson CG, Gulya A, Knox GW, et al. A paraneoplastic syndrome associated with glomus tumors of the skull base? Early observations. Otolaryngol Head Neck Surg 1989; 100:583–587.
74. Anand VK, Leonetti JP, Al-Mefty O. Neurovascular considerations in surgery of glomus tumors with intracranial extensions. Laryngoscope 1993; 103:722–728.
75. Stewart KL. Paragangliomas of the temporal bone. Am J Otolaryngol, 1993; 14:219–226.
76. Brackman D, Kinney S, Fu K. Glomus tumor: diagnosis and management. Head Neck Surg 1987; 9:306–311.
77. van der Mey AG, Frijns JH, Cornelisse CJ, et al. Does intervention improve the natural course of glomus tumors? A series of 108 patients seen in a 32-year period. Ann Otol Rhinol Laryngol 1992; 101:635–642.
78. Gjuric M, Seidinger L, Wigard ME. Long-term results of surgery for temporal bone paraganglioma. Skull Base Surg 1996; 6:147–152.
79. Cole JM, Beiler D. Long-term result of treatment of glomus jugulare and glomus vagale tumors with radiotherapy. Laryngoscope 1994; 104:1461–1465.
80. Mendenhall WM, Parsons JT, Stringer SP, et al. Radiotherapy in the management of temporal bone chemodectoma. Skull Base Surg 1995; 5:83–91.
81. Johnstone PA, Foss RD, Desilets DJ. Malignant jugulotympanic paraganglioma. Arch Pathol Lab Med 1990; 114:976–979.
82. Bojrab DI, Bhansali SA, Zarbo RJ. Management of metastatic glomus jugulare tumors. Skull Base Surg 1992; 2:1–5.
83. Manolidis S, Shohet JA, Jackson CG, et al. Malignant glomus tumors. Laryngoscope 1999; 109:30–34.

84. Brewis C, Bottrill ID, Wharton SB, et al. Metastases from glomus jugulare tumors. J Laryngol Otol 2000; 114:17–23.
85. Green JD, Olsen KD, DeSanto LW, et al. Neoplasms of the vagus nerve. Laryngoscope 1988; 98:648–654.
86. Stout AP. Malignant tumors of peripheral nerves. Am J Cancer 1935; 25:1–36.
87. Miller RB, Boon MS, Atkins JP, et al. Vagal paraganglioma: the Jefferson experience. Ololaryngol Head Neck Surg 2000; 122:482–487.
88. Netterville JL, Jackson CG, Miller FR, et al. Vagal paraganglioma: A review of 46 patients treated during a 20-year period. Arch Otolaryrngol Head Neck Surg 1998; 124:1133–1140.
89. Urquhart AC, Johnson JT, Myers EN, et al. Glomus vagale: paragangliomas of the vagus nerve. Laryngoscope 1994; 104:440–445.
90. Erikson C, Girdhar-Gopal H, Lowry LD. Vagal paragangliomas: A report of nine cases. Am J Otolaryngol 1991; 12:278–287.
91. Biller HF, Lawson W, Som P, et al. Glomus vagale tumors. Ann Otol Rhinol Laryngol 1989; 98:21–26.
92. Lack EE, Cubilla AL, Woodruff JM. Paragangliomas of the head and neck region: A pathologic study of tumors from 71 patients. Hum Pathol 1979; 10:191–218.
93. Browne JD, Fisch U, Valavanis A. Surgical therapy of glomus vagale tumors. Skull Base Surg 1993; 3:182–192.
94. Walsh RM, Leen EJ, Gleeson MJ, et al. Malignant vagal paraganglioma. J Laryngol Otol 1997; 111:83–88.
95. Heinrich MC, Harris AE, Bell WR. Metastatic intravagal paraganglioma. Case report and review of the literature. Am J Med 1985; 78:1017–1024.
96. Barnes L, Taylor SR. Vagal paragangliomas: a clinical, pathological and DNA assessment. Clin Otolaryngol Allied Sci 1991; 16:376–382.
97. Gjuric M, Volker U, Katalinic A, et al. Prognostic Factors Including Proliferation Makers Ki-67, bax, and bcl-2 in Temporal Bone Paraganglioma. Skull Base Surg 1997; 7:175–181.
98. Watzka MA. Uber die Paraganglien in der Plica ventricularis des menschlichen Kehlkopfes. Dtsch Med Forsch 1963; 1:19–20.
99. Kleinsasser O. Das Glomus laryngicum inferior. Arch Ohrenheilk 1964; 184:214–224.
100. Zak FG, Lawson W. Glomic (paraganglionic) tissue in the larynx and capsule of the thyroid gland. Mt Sinai J Med 1972; 39:82–90.
101. Lawson W, Zak FG. The glomus bodies ('paraganglia') of the human larynx. Laryngoscope 1974; 94:98–111.
102. Dahlqvist A, Carlsoo B, Hellstrom S. Paraganglia of the human recurrent laryngeal nerve. Am J Otolaryngol 1986; 7:366–369.
103. Barnes L. Paraganglioma of the larynx. A critical review of the literature. ORL J Otorhinolaryngol Related Spec 1991; 53:220–234.
104. Myssiorek D, Rinaldo A, Barnes L, et al. Laryngeal paraganglioma: an updated critical review. Acta Otolaryngol 2004; 124:995–999.
105. Ferlito A, Barnes L, Wenig BM. Identification, classification, treatment, and prognosis of laryngeal paraganglioma. Review of the literature and eight new cases. Ann Otol Rhinol Laryngol 1994; 103:525–536.
106. Thirlwall AS, Bailey CM, Ramsay AD, et al. Laryngeal paraganglioma in a five-year-old child – the youngest case ever recorded. J Laryngol Otol 1999; 113:62–64.
107. Brandwein M, Levi G, Som P, et al. Paraganglioma of the inferior laryngeal paraganglia. A case report. Arch Otoloaryngol Head Neck Surg 1992; 118:994–996.
108. Hinojar AG, Prieto JR, Munoz E, et al. Relapsing paraganglioma of the inferior laryngeal paraganglia: case report and review of the literature. Head Neck 2002; 24:95–102.
109. Peterson KL, Fu YS, Calcaterra T. Subglottic paraganglioma. Head Neck 1997; 19:54–56.
110. Sanders KW, Abreo F, Rivera E, et al. A diagnostic and therapeutic approach to paragangliomas of the larynx. Arch Otolaryngol Head Neck Surg 2001; 127:565–569.
111. Rubin AD, Cheng SS, Bradford CR. Laryngeal paraganglioma in a patient with multiple head and neck paragangliomas. Otolaryngeal Head Neck Surg 2005; 132:520–522.
112. Del Gaudio JM, Muller S. Diagnosis and treatment of supraglottic laryngeal paraganglioma: report of a case. Head Neck 2004; 26:94–98.
113. Olofsson J, Grontoft O, Sokjer H, et al. Paraganglioma involving the larynx. ORL J Otorhinolaryngol Relat Spec 1984; 46:57–65.
114. Gallivan MV, Chun B, Rowden G, et al. Laryngeal paraganglioma. Case report with ultrastructural analysis and literature review. Am J Surg Pathol 1979; 3:85–92.
115. Smith O, Youngs R, Snell D, et al. Paraganglioma of the larynx. J Otolaryngol 1988; 17:293–301.
116. Wetmore RF, Tronzo RD, Lane RJ, et al. Nonfunctional paraganglioma of the larynx: clinical and pathological consideration. Cancer 1981; 48:2717–2723.
117. de Azevedo-Gamas A, Gloor F. A very unusual case of tumor of the larynx. Unexpected anatomopathologic diagnosis. Ann Otolaryngol Chir Cerviofac 1968; 85: 329–335.
118. Rufenacht H, Mihatsch MJ, Jundt K, et al. Gastric epitheloid leiomymomas, pulmonary chondroma, non-functioning metastasizing extra-adrenal paraganglioma and myxoma: a variant of Carney's triad. Report of a patient. Klin Wochenschr 1985; 63:282–284.
119. Sharma MC, Epari S, Gaikwad S, et al. Orbital paraganglioma: report of a case. Can J Ophthalmol 2005; 40:640–644.
120. Fischer ER, Hazard JB. Nonchromaffin paragangliomas of the orbit. Cancer 1952; 5:521–524.
121. Archer KF, Hurwitz JJ, Balogh JM, et al. Orbital nonchromaffin paraganglioma. A case report and review of the literature. Ophthalmology 1989; 96:1659–166.
122. Talbot AR. Paraganglioma of the maxillary sinus. J Laryngol Otol 1990; 104:248–251.
123. Nguyen QA, Gibbs PM, Rice DH. Malignant nasal paraganglioma: a case report and review of the literature. Otolaryngol Head Neck Surg 1995; 113:157–161.
124. Myssiorek D, Halass Y, Silver C. Laryngeal and sinonasal paragangliomas. Otolaryngol Clin North Am 2001; 34:971–982.
125. Ketabchi S, Massi D, Santoro R, et al. Paraganglioma of the nasal cavity: a case report. Eur Arch Otorhinolaryngol 2003; 260:336–340.
126. Kuhn JA, Aronoff BL. Nasal and nasopharyngeal paraganglioma. J Surg Oncol 1989; 40:38–45.
127. Mitsudo SM, Grajower MM, Balbi H, et al. Malignant paraganglioma of the thyroid gland. Arch Pathol Lab Med 1987; 111:378–380.
128. de Vries E J, Watson CG. Paragangliomas of the thyroid. Head Neck 1989; 11:462–465.
129. Brownlee RE, Shockley WW. Thyroid paraganglioma. Ann Otol Rhinol Laryngol 1992; 101:293–299.
130. LaGuette J, Matias-Guiu X, Rosai J. Thyroid paraganglioma: A clinicopathologic and immmunohistochemical study of three cases. Am J Surg Pathol 1997; 21:748–753.
131. Haegert DG, Wang NS, Farrer PA, et al. Non-chromaffin paragangliomatosis manifesting as a cold nodule. Am J Clin Pathol 1974; 61:561–570.
132. Sambaziotis D, Kontogeorgos G, Kovacs K, et al. Intrasellar paraganglioma presenting as nonfunctioning pituitary adenoma. Arch Pathol Lab Med 1999; 123:429–432.

133. Sinkre P, Lindberg G, Albores-Saavedra J. Nasopharyngeal gangliocytic paraganglioma. A case report with emphasis on histogenesis. Arch Pathol Lab Med 2001; 125:1098–1100.
134. Nielsen TO, Sejean G, Onerheim RM. Paraganglioma of the tongue. Arch Pathol Lab Med 2000; 124:877–879.
135. Liew SH, Leong AS, Tang HM. Tracheal paraganglioma: a case report with review of the literature. Cancer 1981; 47:1397–1393.
136. McCluggage WG, Cameron CH, Brooker D, et al. Paraganglioma: an unusual tumor of the parathyroid gland. J Laryngol Otol 1996; 110:196–199.

X. MALIGNANT PERIPHERAL NERVE SHEATH TUMOR (MALIGNANT SCHWANNOMA, NEUROFIBROSARCOMA)

1. Scheithauer BW, Woodruff JM, Erlandson RA. Primary malignant tumors of peripheral nerve. In: Scheithauer BW, Woodruff JM, Erlandson R, eds. Tumors of the Peripheral Nervous System. Washington, DC: Armed Forces Institute of Pathology, 1999.
2. Weiss SW, Goldblum JR. Malignant tumors of the peripheral nerves. In: Weiss SW, Goldblum JR, eds. Soft Tissue Tumors. St. Louis: Mosby, 2001.
3. Harkin JC, Reed RJ. Malignant primary nerve sheath tumors. In: Harkin JC, Reed RJ, eds. Tumors of the Peripheral Nervous System. Washington, DC: Armed Forces Institute of Pathology, 1969.
4. Ducatman BS, Scheithauer BW, Piepgras DG, et al. Malignant peripheral nerve sheath tumors. A clinicopathologic study of 120 cases. Cancer 1986; 57:2006–2021.
5. Sordillo PP, Helson L, Hajdu SI, et al. Malignant schwannoma–clinical characteristics, survival, and response to therapy. Cancer 1981; 47:2503–2509.
6. D'agostino AN, Soule EH, Miller RH. Primary malignant neoplasms of nerves (malignant neurilemomas) in patients without manifestations of multiple neurofibromatosis (von Recklinghausen's disease). Cancer 1963; 16:1003–1014.
7. D'agostino AN, Soule EH, Miller RH. Sarcomas of the peripheral nerves and somatic soft tissues associated with multiple neurofibromatosis (von Recklinghausen's disease). Cancer 1963; 16:1015–1027.
8. Trojanowski JQ, Kleinman GM, Proppe KH. Malignant tumors of nerve sheath origin. Cancer 1980; 46:1202–1212.
9. Wanebo JE, Malik JM, VandenBerg SR, et al. Malignant peripheral nerve sheath tumors. A clinicopathologic study of 28 cases. Cancer 1993; 71:1247–1253.
10. Hirose T, Sumitomo M, Kudo E, et al. Malignant peripheral nerve sheath tumor (MPNST) showing perineurial cell differentiation. Am J Surg Pathol 1989; 13: 613–620.
11. Hirose T, Sano T, Hizawa K. Heterogeneity of malignant schwannomas. Ultrastruct Pathol 1988; 12:107–116.
12. Fletcher CD. Malignant peripheral nerve sheath tumours. Curr Top Pathol 1995; 89:333–354.
13. Hruban RH, Shiu MH, Senie RT, et al. Malignant peripheral nerve sheath tumors of the buttock and lower extremity. A study of 43 cases. Cancer 1990; 66:1253–1265.
14. Woodruff JM, Selig AM, Crowley K, et al. Schwannoma (neurilemoma) with malignant transformation. A rare, distinctive peripheral nerve tumor. Am J Surg Pathol 1994; 18:882–895.
15. Ricci A, Parham DM, Woodruff JM, et al. Malignant peripheral nerve sheath tumors arising from ganglioneuromas. Am J Surg Pathol 1984; 8:19–29.
16. Miettinen M, Saari A. Pheochromocytoma combined with malignant schwannoma: unusual neoplasm of the adrenal medulla. Ultrastruct Pathol 1988; 12:513–527.
17. Min KW, Clemens A, Bell J, et al. Malignant peripheral nerve sheath tumor and pheochromocytoma. A composite tumor of the adrenal. Arch Pathol Lab Med 1988; 112:266–270.
18. Sakaguchi N, Sano K, Ito M, et al. A case of von Recklinghausen's disease with bilateral pheochromocytoma-malignant peripheral nerve sheath tumors of the adrenal and gastrointestinal autonomic nerve tumors. Am J Surg Pathol 1996; 20:889–897.
19. DiCarlo EF, Woodruff JM, Bansal M, et al. The purely epithelioid malignant peripheral nerve sheath tumor. Am J Surg Pathol 1986; 10:478–490.
20. Laskin WB, Weiss SW, Bratthauer GL. Epithelioid variant of malignant peripheral nerve sheath tumor (malignant epithelioid schwannoma). Am J Surg Pathol 1991; 15:1136–1145.
21. Woodruff JM, Chernik NL, Smith MC, et al. Peripheral nerve tumors with rhabdomyosarcomatous differentiation (malignant ''Triton'' tumors). Cancer 1973; 32:426–439.
22. Ducatman BS, Scheithauer BW. Malignant peripheral nerve sheath tumors with divergent differentiation. Cancer 1984; 54:1049–1057.
23. Brown RW, Tornos C, Evans HL. Angiosarcoma arising from malignant schwannoma in a patient with neurofibromatosis. Cancer 1992; 70:1141–1144.
24. Woodruff JM, Christensen WN. Glandular peripheral nerve sheath tumors. Cancer 1993; 72:3618–3628.
25. Woodruff JM, Perino G. Non-germ-cell or teratomatous malignant tumors showing additional rhabdomyoblastic differentiation, with emphasis on the malignant Triton tumor. Semin Diagn Pathol 1994; 11:69–81.
26. Herrera GA, de Moraes HP. Neurogenic sarcomas in patients with neurofibromatosis (von Recklinghausen's disease). Light, electron microscopy and immunohistochemistry study. Virchows Arch A Pathol Anat Histopathol 1984; 403:361–376.
27. Foley KM, Woodruff JM, Ellis FT, et al. Radiation-induced malignant and atypical peripheral nerve sheath tumors. Ann Neurol 1980; 7:311–318.
28. Ducatman BS, Scheithauer BW. Postirradiation neurofibrosarcoma. Cancer 1983; 51:1028–1033.
29. Yakulis R, Manack L, Murphy AI Jr. Postradiation malignant triton tumor. A case report and review of the literature. Arch Pathol Lab Med 1996; 120:541–548.
30. Doorn PF, Molenaar WM, Buter J, et al. Malignant peripheral nerve sheath tumors in patients with and without neurofibromatosis. Eur J Surg Oncol 1995; 21:78–82.
31. Guccion JG, Enzinger FM. Malignant schwannoma associated with von Recklinghausen's neurofibromatosis. Virchows Arch A Pathol Anat Histol 1979; 383:43–57.
32. Hope DG, Mulvihill JJ. Malignancy in neurofibromatosis. Adv Neurol 1981; 29:33–56.
33. Sorensen SA, Mulvihill JJ, Nielsen A. Long-term follow-up of von Recklinghausen neurofibromatosis. Survival and malignant neoplasms. N Engl J Med 1986; 314:1010–1015.
34. Casanova M, Ferrari A, Spreafico F, et al. Malignant peripheral nerve sheath tumors in children: a single-institution twenty-year experience. J Pediatr Hematol Oncol 1999; 21:509–513.
35. deCou JM, Rao BN, Parham DM, et al. Malignant peripheral nerve sheath tumors: the St. Jude Children's Research Hospital experience. Ann Surg Oncol 1995; 2:524–529.
36. Das Gupta TK, Brasfield RD. Solitary malignant schwannoma. Ann Surg 1970; 171:419–428.
37. Loree TR, North JH Jr., Werness BA, et al. Malignant peripheral nerve sheath tumors of the head and neck: analysis of prognostic factors. Otolaryngol Head Neck Surg 2000; 122:667–672.

38. Kempf HG, Becker G, Weber BP, et al. Diagnostic and clinical outcome of neurogenic tumours in the head and neck area. ORL J Otorhinolaryngol Relat Spec 1995; 57:273–278.
39. Vege DS, Chinoy RF, Ganesh B, et al. Malignant peripheral nerve sheath tumors of the head and neck: a clinicopathological study. J Surg Oncol 1994; 55:100–103.
40. Marvel JB, Parke RB. Malignant schwannoma of the nasal cavity. Otolaryngol Head Neck Surg 1990; 102:409–412.
41. Kameyama Y, Maeda H, Nakane S, et al. Malignant schwannoma of the maxilla in a patient without neurofibromatosis. Histopathology 1987; 11:1205–1208.
42. Bailet JW, Abemayor E, Andrews JC, et al. Malignant nerve sheath tumors of the head and neck: a combined experience from two university hospitals. Laryngoscope 1991; 101:1044–1049.
43. Perzin KH, Panyu H, Wechter S. Nonepithelial tumors of the nasal cavity, paranasal sinuses and nasopharynx. A clinicopathologic study. XII: Schwann cell tumors (neurilemoma, neurofibroma, malignant schwannoma). Cancer 1982; 50:2193–2202.
44. Neville BW, Hann J, Narang R, et al. Oral neurofibrosarcoma associated with neurofibromatosis type I. Oral Surg Oral Med Oral Pathol 1991; 72:456–461.
45. DiCerbo M, Sciubba JJ, Sordill WC, et al. Malignant schwannoma of the palate: a case report and review of the literature. J Oral Maxillofac Surg 1992; 50:1217–1221.
46. Grevers G, Rocken J. Recurrent malignant schwannoma of the lower lip: report of a case. Otolaryngol Head Neck Surg 1995; 113:138–139.
47. Martinez DP, Mitchell TE, Scott I, et al. Malignant peripheral nerve sheath tumors of the head and neck: two cases and a review of the literature. Ear Nose Throat J 2006; 85:392–396.
48. Gunalp I, Gunduz K, Duruk K, et al. Neurogenic tumors of the orbit. Jpn J Ophthalmol 1994; 38:185–190.
49. Jakobiec FA, Font RL, Zimmerman LE. Malignant peripheral nerve sheath tumors of the orbit: a clinicopathologic study of eight cases. Trans Am Ophthalmol Soc 1985; 83:332–366.
50. Lyons CJ, McNab AA, Garner A, et al. Orbital malignant peripheral nerve sheath tumours. Br J Ophthalmol 1989; 73:731–738.
51. Singh B, Shaha AR. Solitary malignant schwannoma invading the hypoglossal nerve. Ear Nose Throat J 1994; 73:842–844.
52. Hedeman LS, Lewinsky BS, Lochridge GK, et al. Primary malignant schwannoma of the Gasserian ganglion. Report of two cases. J Neurosurg 1978; 48:279–283.
53. Mrak RE, Flanigan S, Collins CL. Malignant acoustic schwannoma. Arch Pathol Lab Med 1994; 118:557–561.
54. DeLozier HL. Intrinsic malignant schwannoma of the larynx. A case report. Ann Otol Rhinol Laryngol 1982; 91:336–338.
55. Norris CM, Peale AR. Sarcoma of the larynx. Ann Otol Rhinol Laryngol 1961; 70:894–909.
56. Gorenstein A, Neel HB III, Weiland LH, et al. Sarcomas of the larynx. Arch Otolaryngol 1980; 106:8–12.
57. Elias MM, Balm AJ, Peterse JL, et al. Malignant schwannoma of the parapharyngeal space in von Recklinghausen's disease: a case report and review of the literature. J Laryngol Otol 1993; 107:848–852.
58. McGuirt WF, Browne JD. An anterolateral approach to the anterior skull base: report of a malignant schwannoma of the pterygomaxillary space. Otolaryngol Head Neck Surg 1988; 98:323–327.
59. Auclair PL, Langloss JM, Weiss SW, et al. Sarcomas and sarcomatoid neoplasms of the major salivary gland regions. A clinicopathologic and immunohistochemical study of 67 cases and review of the literature. Cancer 1986; 58:1305–1315.
60. Al Ghamdi S, Fageeh N, Dewan M. Malignant schwannoma of the thyroid gland. Otolaryngol Head Neck Surg 2000; 122:143–144.
61. Mannan AA, Singh MK, Bahadur S, et al. Solitary malignant schwannoma of the nasal cavity and paranasal sinuses: report of two rare cases. Ear Nose Throat J 2003; 82:634–636, 638, 640.
62. Victoria L, McCulloch TM, Callaghan EJ, et al. Malignant triton tumor of the head and neck: A case report and review of the literature. Head Neck 1999; 21:663–670.
63. Brooks JS, Freeman M, Enterline HT. Malignant ''Triton'' tumors. Natural history and immunohistochemistry of nine new cases with literature review. Cancer 1985; 55:2543–2549.
64. Heffner DK, Gnepp DR. Sinonasal fibrosarcomas, malignant schwannomas, and ''Triton'' tumors. A clinicopathologic study of 67 cases. Cancer 1992; 70:1089–1101.
65. Verstraete KL, Achten E, De Schepper A, et al. Nerve sheath tumors: evaluation with CT and MR imaging. J Belge Radiol 1992; 75:311–320.
66. Varma DG, Moulopoulos A, Sara AS, et al. MR imaging of extracranial nerve sheath tumors. J Comput Assist Tomogr 1992; 16:448–453.
67. Murphey MD, Smith WS, Smith SE, et al. From the archives of the AFIP. Imaging of musculoskeletal neurogenic tumors: radiologic-pathologic correlation. Radiographics 1999; 19:1253–1280.
68. Levine E, Huntrakoon M, Wetzel LH. Malignant nerve-sheath neoplasms in neurofibromatosis: distinction from benign tumors by using imaging techniques. AJR Am J Roentgenol 1987; 149:1059–1064.
69. Hammond JA, Driedger AA. Detection of malignant change in neurofibromatosis (von Recklinghausen's disease) by gallium-67 scanning. Can Med Assoc J 1978; 119:352–353.
70. Kaplan IL, Swayne LC, Baydin JA. Uptake of Ga-67 citrate in a benign neurofibroma. Clin Nucl Med 1989; 14:224.
71. Tsuneyoshi M, Daimaru Y, Enjoji M. Malignant hemangiopericytoma and other sarcomas with hemangiopericytoma-like pattern. Pathol Res Pract 1984; 178:446–453.
72. Christensen WN, Strong EW, Bains MS, et al. Neuroendocrine differentiation in the glandular peripheral nerve sheath tumor. Pathologic distinction from the biphasic synovial sarcoma with glands. Am J Surg Pathol 1988; 12:417–426.
73. Zamecnik M, Michal M. Malignant peripheral nerve sheath tumor with perineurial cell differentiation (malignant perineurioma). Pathol Int 1999; 49:69–73.
74. Chitale AR, Dickersin GR. Electron microscopy in the diagnosis of malignant schwannomas. A report of six cases. Cancer 1983; 51:1448–1461.
75. Hirose T, Hasegawa T, Kudo E, et al. Malignant peripheral nerve sheath tumors: an immunohistochemical study in relation to ultrastructural features. Hum Pathol 1992; 23:865–870.
76. Cavazzana AO, Ninfo V, Roberts J, et al. Peripheral neuroepithelioma: a light microscopic, immunocytochemical, and ultrastructural study. Mod Pathol 1992; 5:71–78.
77. Matsunou H, Shimoda T, Kakimoto S, et al. Histopathologic and immunohistochemical study of malignant tumors of peripheral nerve sheath (malignant schwannoma). Cancer 1985; 56:2269–2279.
78. Wick MR, Swanson PE, Scheithauer BW, et al. Malignant peripheral nerve sheath tumor. An immunohistochemical study of 62 cases. Am J Clin Pathol 1987; 87:425–433.
79. Gray MH, Rosenberg AE, Dickersin GR, et al. Glial fibrillary acidic protein and keratin expression by benign and malignant nerve sheath tumors. Hum Pathol 1989; 20:1089–1096.

80. Smith TA, Machen SK, Fisher C, et al. Usefulness of cytokeratin subsets for distinguishing monophasic synovial sarcoma from malignant peripheral nerve sheath tumor. Am J Clin Pathol 1999; 112:641–648.
81. Ogawa K, Oguchi M, Yamabe H, et al. Distribution of collagen type IV in soft tissue tumors. An immunohistochemical study. Cancer 1986; 58:269–277.
82. Chanoki M, Ishii M, Fukai K, et al. Immunohistochemical localization of type I, III, IV, V, and VI collagens and laminin in neurofibroma and neurofibrosarcoma. Am J Dermatopathol 1991; 13:365–373.
83. Mertens F, Dal Cin P, De Wever I, et al. Cytogenetic characterization of peripheral nerve sheath tumours: a report of the CHAMP study group. J Pathol 2000; 190:31–38.
84. Koga T, Iwasaki H, Ishiguro M, et al. Frequent genomic imbalances in chromosomes 17, 19, and 22q in peripheral nerve sheath tumours detected by comparative genomic hybridization analysis. J Pathol 2002; 197:98–107.
85. Schmidt H, Taubert H, Wurl P, et al. Cytogenetic characterization of six malignant peripheral nerve sheath tumors: comparison of karyotyping and comparative genomic hybridization. Cancer Genet Cytogenet 2001; 128:14–23.
86. Storlazzi CT, Brekke HR, Mandahl N, et al. Identification of a novel amplicon at distal 17q containing the BIRC5/SURVIVIN gene in malignant peripheral nerve sheath tumours. J Pathol 2006; 209:492–500.
87. Skotheim RI, Kallioniemi A, Bjerkhagen B, et al. Topoisomerase-II alpha is upregulated in malignant peripheral nerve sheath tumors and associated with clinical outcome. J Clin Oncol 2003; 21:4586–4591.
88. Levy P, Vidaud D, Leroy K, et al. Molecular profiling of malignant peripheral nerve sheath tumors associated with neurofibromatosis type 1, based on large-scale real-time RT-PCR. Mol Cancer 2004; 3:20.
89. Ordonez NG, Mahfouz SM, Mackay B. Synovial sarcoma: an immunohistochemical and ultrastructural study. Hum Pathol 1990; 21:733–749.
90. Fisher C, Schofield JB. S-100 protein positive synovial sarcoma. Histopathology 1991; 19:375–377.
91. Salisbury JR, Isaacson PG. Synovial sarcoma: an immunohistochemical study. J Pathol 1985; 147:49–57.
92. Watanabe K, Kusakabe T, Hoshi N, et al. h-Caldesmon in leiomyosarcoma and tumors with smooth muscle cell-like differentiation: its specific expression in the smooth muscle cell tumor. Hum Pathol 1999; 30:392–396.
93. King R, Busam K, Rosai J. Metastatic malignant melanoma resembling malignant peripheral nerve sheath tumor: report of 16 cases. Am J Surg Pathol 1999; 23:1499–1505.
94. Diaz-Cascajo C, Hoos A. Histopathologic features of malignant peripheral nerve sheath tumor are not restricted to metastatic malignant melanoma and can be found in primary malignant melanoma also. Am J Surg Pathol 2000; 24:1438–1439.
95. Miettinen M, Fernandez M, Franssila K, et al. Microphthalmia transcription factor in the immunohistochemical diagnosis of metastatic melanoma: comparison with four other melanoma markers. Am J Surg Pathol 2001; 25:205–211.
96. Zarbo RJ, Crissman JD, Venkat H, et al. Spindle-cell carcinoma of the upper aerodigestive tract mucosa. An immunohistologic and ultrastructural study of 18 biphasic tumors and comparison with seven monophasic spindle-cell tumors. Am J Surg Pathol 1986; 10:741–753.
97. Horowitz ME, Pratt CB, Webber BL, et al. Therapy for childhood soft-tissue sarcomas other than rhabdomyosarcoma: a review of 62 cases treated at a single institution. J Clin Oncol 1986; 4:559–564.
98. Raney B, Schnaufer L, Ziegler M, et al. Treatment of children with neurogenic sarcoma. Experience at the Children's Hospital of Philadelphia, 1958–1984. Cancer 1987; 59:1–5.
99. Tran LM, Mark R, Meier R, et al. Sarcomas of the head and neck. Prognostic factors and treatment strategies. Cancer 1992; 70:169–177.
100. James JA, Bali NS, Sloan P, et al. Low-grade malignant Triton tumor of the oral cavity: a case report. Oral Surg Oral Med Oral Pathol Oral Radiol Endod 2003; 95:699–704.

XI. OLFACTORY NEUROBLASTOMA

1. Berger L, Luc G, Richard D. Esthesioneuroepitheliome olfactif. Bull Assoc Fr Etude Cancer 1924; 13:410–421.
2. Nasashima T, Kimmelman CP, Snow JB. Structure of the human fetal and adult olfactory neuroepithelium. Arch Otolaryngol 1984; 110:641–646.
3. Hyams VJ, Batsakis JG, Michaels L. Tumors of the Upper Respiratory Tract and Ear. 2nd Ser, Fasc 25, Atlas of Tumor Pathology. Washington DC: Armed Forces Institute of Pathology, 1988.
4. Silva EG, Butler JJ, Mackay B, et al. Neuroblastoma and neuroendocrine carcinomes of the nasal cavity. A proposed new classificaton. Cancer 1982; 50:2388–2405.
5. Dulguerov P, Calcaterra T. Esthesioneuroblastoma: the UCLA experience. 1970–1990. Laryngoscope 1992; 102:843–849.
6. Elkon D, Hightower SI, Lim ML, et al. Esthesioneuroblastoma. Cancer 1979; 44:1087–1094.
7. O'Conner TA, McLean P, Juillard GJ, et al. Olfactory neuroblastoma. Cancer 1989; 63:2426–2428.
8. Schwab G, Michaeu C, Lee Guillou C, et al. Olfactory neuroblastoma: a report of 40 cases. Laryngoscope 1988; 98:872–876.
9. Lund VJ, Milroy C. Olfactory neuroblastoma: a clinical and pathological aspects. Rhinology 1993; 31:1–6.
10. Koka VN, Julieron M, Bourhis J, et al. Aesthesioneuroblastoma. J Laryngol Otol 1998; 112:628–633.
11. Levine PA, McLean WC, Cantrell RW. Esthesioneuroblastoma: The University of Virginia experience 1960–1985. Laryngoscope 1986; 96:742–746.
12. Levine PA, Gallagher R, Cantrell RW. Esthesioneuroblastoma: reflections of a 21-year experience. Laryngoscope 1999; 109:1539–1543.
13. Mills SE, Frierson HF Jr. Olfactory neuroblastoma. A clinicopathologic study of 21 cases. Am J Surg Pathol 1985; 9:317–327.
14. Olsen KD, DeSanto LW. Olfactory neuroblastoma. Biologic and clinical behavior. Arch Otolaryngol 1983; 109:797–802.
15. Kardish S, Goodman M, Wang CC. Olfactory neuroblastoma. A clinical analysis of 17 cases. Cancer 1976; 37: 1571–1576.
16. Broich G, Pagliari A, Ottaviani F. Esthesineuroblastoma: a general review of the cases published since the discovery of the tumor in 1924. Anticancer Res 1997; 17:2683–2706.
17. Manelfe C, Bonafe A, Fabre P, et al. Computed tomography in olfactory neuroblastoma: one case of esthesioneuroepithelioma and four cases of esthesioneuroblastoma. J Comput Assist Tomogr 1978; 2:412–420.
18. Woodhead P, Lloyd GA. Olfactory neuroblasotma: imaging by magnetic reconance, CT and conventional techniques. Clin Otolaryngol 1988; 13:387–394.
19. Schuster JJ, Phillips CD, Levine PA. MR of esthesioneuroblastoma (olfactory neuroblastoma) and appearance after cranial resection. AJNR Am J Neuroradiol 1994; 15:1169–1177.

20. Li C, Yousem DM, Hayden RE, et al. Olfactory neuroblastoma: MR evaluation. AJNR Am J Neuroradiol 1993; 14:1167–1171.
21. Kairemo KJ, Jekunen AP, Kestila MS, et al. Imaging of olfactory neuroblasotma-an analysis of 17 cases. Auris Nasus Larynx 1998; 25:173–179.
22. Derdeyn CP, Moran CJ, Wippold FJ II, et al. MRI in esthesioneuroblastoma. J Comput Assist Tomogr 1994; 18:16–21.
23. Harrison D. Surgical pathology of olfactory neuroblastoma. Head Neck Surg 1984; 7:60–64.
24. Hirose T, Scheithauer BW, Lopes MB, et al. Olfactory neuroblastoma: an immunohistochemical, ultrastructural, and flow cytometric study. Cancer 1995; 76:4–19.
25. Taxy JB, Bharani NK, Mills SE, et al. The sprectrum of olfactory neural tumors. A light-microscopic, immunohistochemical, and ultrastructural analysis. Am J Surg Pathol 1986; 10:687–695.
26. Chaudry AP, Haar JG, Koul A, et al. Olfactory neuroblastoma (esthesioneuroblastoma): a light and ultrastructural study of two cases. Cancer 1979; 44:564–579.
27. Mahooti S, Wakely PE. Cytopathologic features of olfactory neuroblastoma. Cancer 2006; 108:86–92.
28. Axe S, Kuhajda FP. Esthesioneuroblastoma. Intermediate filaments, neuroendocrine, and tissue-specific antigens. Am J Clin Pathol 1987; 88:139–145.
29. Schmidt JL, Zarbo RJ, Clark JL. Olfactory neuroblastoma: clinicopathologic and immunohistochemcial characterization of four representative cases. Laryngoscope 1990; 100:1052–1058.
30. Choi HS, Anderson PJ. Olfactory neuroblastoma: an immuno-electron microscopic study of S-100 protein positive cells. J Neuropathol Exp Neurol 1986; 45:576–587.
31. Choi HS, Anderson PJ. Immunohistochemcial diagnosis of olfactory neuroblastoma. J Neuropathol Exp Neurol 1985; 44:18–31.
32. Frierson HF, Ross GW, Mills SE, et al. Olfactory neuroblastoma. Additional immunohistochemcial characterization. Am J Clin Pathol 1990; 94:547–553.
33. Trojanowski JQ, Lee V, Pillsbury N, et al. Neuronal origin of human esthesioneuroblastoma demonstrated with antineurofilament monoclonal antibodies. N Engl J Med 1982; 307:159–161.
34. Min KW. Usefullness of electron microscopy in the diagnosis of small round cell tumors of the sinonasal region. Ultrastruct Pathol 1995; 19:347–363.
35. Wick MR, Stanley SJ, Swanson PE. Immunohistochemical diagnosis of sinonasal melanoma, carcinoma, and neuroblastoma with monoclonal antibodies HMB-45 and antisynaptophysin. Arch Pathol Lab Med 1988; 112:616–620.
36. Devaney K, Wenig BM, Abbondanzo SL. Olfactory neuroblasotma and other round cell lesions of the sinonasal region. Mod Pathol 1996; 9:658–663.
37. Fellinger EJ, Garin-Chesa P, Triche TJ, et al. Immunohistochemical analysis of Ewing's sarcoma cell surface antigen. P30/32MIC2. Am J Pathol 1991; 139:317–325.
38. Barnes L, Peel RL. Olfactory neuroblastomas versus sinonasal undifferentiated carcinoma. Head and Neck Pathology. A Text/Atlas of Differential Diagnosis. New York: Igaku-Shion, 1990:152–154.
39. Frierson HF Jr., Mills SE, Fechner RE, et al. Sinonasal undifferentiated carcinoma. An aggressive neoplasm derived from schneiderian epithelium and distinct from olfactory neuroblastoma. Am J Surg Pathol 1986; 10:771–779.
40. Houston GD, Gillies E. Sinonasal undifferentiated carcinoma. A distinctive clinicopathologic entity. Adv Anat Patol 1999; 6:317–323.
41. Lopategui JR, Gaffey MJ, Firerson HF, et al. Detection of Epstein-Barr viral RNA in sinonasal undifferentiated carcinoma from Western and Asian patients. Am J Surg Pathol 1994; 18:391–398.
42. Mills SE, Fechner RE. ''Undifferentiated'' neoplasms of the sinonasal region: differential diagnosis based on clinical, light microscopic, immunohistochemical, and ultrastructural features. Semin Diagn Pathol 1989; 6:316–328.
43. Kameya T, Shimosato Y, Adachi I, et al. Neuroendocrine carcinoma of the paranasal sinus: a morphlogical and endocrinological study. Cancer 1980; 45:330–339.
44. Rejowski JE, Campanella RS, Block LJ. Small cell carcinoma of the nose and paranasal sinuses. Otolaryngol Head Neck Surg 1982; 90:516–517.
45. Whang-Peng J, Freter CE, Knutsen T, et al. Translocatoin t(11;22), in esthesioneuroblastoma. Cancer Genet Cytogenet 1987; 29:155–157.
46. Sorenson PH, Wu JK, Berean KW, et al. Olfactory neuroblastoma is a peripheral primitive neuroectodermal tumor related to Ewing sarcoma. Proc Natl Acad Sci U S A 1996; 93:1038–1043.
47. Cavazzana AO, Navarro S, Noguera R, et al. Olfactory neuroblastoma is not a neuroblasotma but is related to primitive neuroectodermal tumor (PNET). Prog Clin Biol Res 1988; 271:463–473.
48. Nelson RS, Perlman EJ, Askin FB. Is esthesioneuroblasotma a peripheral neuroectodermal tumor? Hum Pathol 1995; 26:639–641.
49. Argani P, Perez-Ordonez B, Xiao H, et al. Olfactory neuroblastoma is not related to the Ewing family of tumors. Absence of EWS/FLI1 gene fusion and MIC2 expression. Am J Surg Pathol 1998; 22:391–398.
50. Mezzelani A, Tornielli S, Minoletti F, et al. Esthesioneuroblastoma is not a member of the primitive peripheral neuroectodermal tumor-Ewing's group. Br J Cancer 1999; 81:586–591.
51. Kumar S, Perlman E, Park S, et al. Absence of EWS/FL11 fusion in olfactory neuroblastomas indicates these tumors do not belong to the Ewing's sarcoma family. Hum Pathol 1999; 30:1356–1360.
52. Klepin HD, McMullen KP, Lesser GJ. Esthesioneuroblastoma. Curr Treat Options Oncol 2005; 6:509–518.
53. Spaulding CA, Kranyak MS, Constable WC, et al. Esthesioneuroblasotma: a comparison of two treatments eras. Int J Radiat Oncol Biol Phys 1988; 15:581–590.
54. Zappia JJ, Carroll WR, Wolf GT, et al. Olfactory neuroendocirne carcinoma of the anterior skull base: treatment results at M.D. Anderson Cancer Center. Skull Base Surg 1996; 6:1–8.
55. Austin JR, Cebru H, Kershisnik MM, et al. Olfactory neuroblasotma and neuroendocrine carcinoma of the anterior skull base: treatment results at MD Anderson Cancer Center. Skull Base Surg 1996; 6:1–8.
56. Irish J, Dasgupta R, Freeman J, et al. Outcome and analysis of the surgical management of esthesioneuroblasotma. J Otolaryngol 1997; 26:1–7.
57. Biller HF, Lawson W, Sachdev VP, et al. Esthesioneuroblastoma: surgical treatment without radiation. Laryngoscope 1990; 100:1199–1201.
58. Tandon DA, Bahadur S, Mohanti BK, et al. Olfactory neuroblastoma: results of combined therapy. Indian J Cancer 1994; 31:124–129.
59. McElroy EA, Buckner JC, Lewis JE. Chemotherapy for advanced esthesioneuroblastoma: the Mayo Clinic experience. Neurosurgery 1998; 42:1023–1027.
60. Foote RL, Morita A, Ebersold MJ, et al. Esthesioneuroblastoma: the role of adjunvant radiation therapy. Int J Radiat Oncol Biol Phys 1993; 27:835–842.
61. Eden BV, Debo RF, Larner JM, et al. Esthesioneuroblastoma. Long-term outcome and patterns of failure – the University of Virginia experience. Cancer 1994; 73:2556–2562.

62. Morita A, Ebersold MJ, Olsen KD, et al. Esthesioneuroblasotma. Prognosis and management. Neurosurgery 1993; 32:706–714.
63. Lewis JE, Morita A, Ebersold MJ. Grading and prognosis of olfactory neuroblastoma (abstr). Mod Pathol 1993; 6:82A.
64. Wenig B, Hitchcock C, Griffin J, et al. Olfactory esthesioneuroblastoma: support for a grading system based on flow cytometric and histopathologic correlation. Mod Pathol 1990; 3:65A (abstr).
65. Schwartz MR, Hicks MJ, Hicks MJ, et al. Flow cytometric analysis of olfactory neuroblastomas and high grade olfactory neuroendocirne carcinomas. Mod Pathol 1993; 6:83A.
66. Papadaki H, Kounelis S, Kapadia SB, et al. Relationship of p53 gene alterations with tumor progression and recurrence in olfactory neuroblastoma. Am J Pathol 1996; 20:71–721.
67. VanDevanter DR, George D, McNutt MA, et al. Trisomy 8 in primary esthesioneuroblastoma. Cancer Genet Cytogenet 1991; 57:133–136.

XII. MELANOTIC NEUROECTODERMAL TUMOR IN INFANCY

1. Kapadia SB, Frisman DM, Hitchcock CL, et al. Melanotic neuroectodermal tumor of infancy. Clinicopathological, immunohistochemical, and flow cytometric study. Am J Surg Pathol 1993; 17:566–573.
2. Pettinato G, Manivel JC, d'Amore ES, et al. Melanotic neuroectodermal tumor of infancy. A reexamination of a histogenetic problem based on immunohistochemical, flow cytometric, and ultrastructural study of 10 cases. Am J Surg Pathol 1991; 15:233–245.
3. Johnson RE, Scheithauer BW, Dahlin DC. Melanotic neuroectodermal tumor of infancy. A review of seven cases. Cancer 1983; 52:661–666.
4. Kruse-Losler B, Gaertner C, Burger H, et al. Melanotic neuroectodermal tumor of infancy: systematic review of the literature and presentation of a case. Oral Surg Oral Med Oral Pathol Oral Radiol Endod 2006; 102:204–216.
5. Barrett AW, Morgan M, Ramsay AD, et al. A clinicopathologic and immunohistochemical analysis of melanotic neuroectodermal tumor of infancy. Oral Surg Oral Med Oral Pathol Oral Radiol Endod 2002; 93:688–698.
6. Dehner LP, Sibley RK, Sauk JJ, et al. Malignant melanotic neuroectodermal tumor of infancy: a clinical, pathologic, ultrastructural and tissue culture study. Cancer 1979; 43:1389–1410.
7. Krompecher E. Zur Histogenese und Morphologie der Adamantinome und Sonstiger Kiefergeschwulste. Beiträge zur pathologischen Anatomie und zur allgemeinen Pathologie 1918; 64:165–197.
8. Allen MS Jr., Harrison W, Jahrsdoerfer RA. ''Retinal anlage'' tumors. Melanotic progonoma, melanotic adamantinoma, pigmented epulis, melanotic neuroectodermal tumor of infancy, benign melanotic tumor of infancy. Am J Clin Pathol 1969; 51:309–314.
9. Ijiri R, Onuma K, Ikeda M, et al. Pigmented intraosseous odontogenic carcinoma of the maxilla: a pediatric case report and differential diagnosis. Hum Pathol 2001; 32:880–884.
10. Metwaly H, Cheng J, Maruyama S, et al. Establishment and characterization of new cell lines derived from melanotic neuroectodermal tumor of infancy arising in the mandible. Pathol Int 2005; 55:331–342.
11. Claman LJ, Stetson D, Steinberg B, et al. Ultrastructural characteristics of a cell line derived from a melanotic neuroectodermal tumor of infancy. J Oral Pathol Med 1991; 20:245–249.
12. Cutler LS, Chaudhry AP, Topazian R. Melanotic neuroectodermal tumor of infancy: an ultrastructural study, literature review, and reevaluation. Cancer 1981; 48:257–270.
13. Nikai H, Ijuhnin N, Yamasaki A, et al. Ultrastructural evidence for neural crest origin of the malanotic neuroectodermal tumor of infancy. J Oral Pathol 1977; 6:221–232.
14. Navas Palacios JJ. Malignant melanotic neuroectodermal tumor: light and electron microscopic study. Cancer 1980; 46:529–536.
15. Stirling RW, Powell G, Fletcher CD. Pigmented neuroectodermal tumour of infancy: an immunohistochemical study. Histopathology 1988; 12:425–435.
16. Clarke BE, Parsons H. An embryological tumor of retinal anlage involving the skull. Cancer 1951; 4:78–85.
17. Dooling EC, Chi JG, Gilles FH. Melanotic neuroectodermal tumor of infancy: its histological similarities to fetal pineal gland. Cancer 1977; 39:1535–1541.
18. Eaton WL, Ferguson JP. A retinoblastic teratoma of the epididymis; case report. Cancer 1956; 9:718–720.
19. Frank GL, Koten JW. Melanotic hamartoma (''retinal anlage tumour'') of the epididymis. J Pathol Bacteriol 1967; 93:549–554.
20. Fowler M, Simpson DA. A malignant melanin-forming tumour of the cerebellum. J Pathol Bacteriol 1962; 84:307–311.
21. Hahn JF, Sperber EE, Netsky MG. Melanotic neuroectodermal tumors of the brain and skull. J Neuropathol Exp Neurol 1976; 35:508–519.
22. Misugi K, Okajima H, Newton WA, et al. Mediastinal origin of a melanotic progonoma or retinal anlage tumor: ultrastructural evidence for neural crest origin. Cancer 1965; 18:477–484.
23. Vajtai I, Sutak I, Varga Z. Melanotic progonoma as a component of ovarian teratoma. Histopathology 2000; 36:283–285.
24. King ME, Micha JP, Allen SL, et al. Immature teratoma of the ovary with predominant malignant retinal anlage component. A parthenogenically derived tumor. Am J Surg Pathol 1985; 9:221–231.
25. Dourov N, Mayer R, de Martelaere F, et al. Melanotic neuroectodermal tumor of infancy with high serum levels of alpha-fetoprotein. Ultrastructural study and immunological evidence of glial fibrillary protein and alpha-fetoprotein. J Oral Pathol 1987; 16:251–255.
26. De Chiara A, Van Tornout JM, Hachitanda Y, et al. Melanotic neuroectodermal tumor of infancy. A case report of paratesticular primary with lymph node involvement. Am J Pediatr Hematol Oncol 1992; 14:356–360.
27. Hoshino S, Takahashi H, Shimura T, et al. Melanotic neuroectodermal tumor of infancy in the skull associated with high serum levels of catecholamine. Case report. J Neurosurg 1994; 80:919–924.
28. Borello ED, Gorlin RJ. Melanotic neuroectodermal tumor of infancy–a neoplasm of neural crese origin. Report of a case associated with high urinary excretion of vanilmandelic acid. Cancer 1966; 19:196–206.
29. Mirich DR, Blaser SI, Harwood-Nash DC, et al. Melanotic neuroectodermal tumor of infancy: clinical, radiologic, and pathologic findings in five cases. AJNR Am J Neuroradiol 1991; 12:689–697.
30. Parizek J, Nemecek S, Cernoch Z, et al. Melanotic neuroectodermal neurocranial tumor of infancy of extra-intra- and subdural right temporal location: CT examination, surgical treatment, literature review. Neuropediatrics 1986; 17:115–123.
31. Bouckaert MM, Raubenheimer EJ. Gigantiform melanotic neuroectodermal tumor of infancy. Oral Surg Oral Med Oral Pathol Oral Radiol Endod 1998; 86:569–572.

32. Shah RV, Jambhekar NA, Rana DN, et al. Melanotic neuroectodermal tumor of infancy: report of a case with ganglionic differentiation. J Surg Oncol 1994; 55:65–68.
33. Mello RJ, Vidal AK, Fittipaldi HM, et al. Melanotic Meuroectodermal Tumor of Infancy: Clinicopathologic Study of a Case, with Emphasis on the Chemotherapeutic Effects. Int J Surg Pathol 2000; 8:247–251.
34. Nelson ZL, Newman L, Loukota RA, et al. Melanotic neuroectodermal tumour of infancy: an immunohistochemical and ultrastructural study. Br J Oral Maxillofac Surg 1995; 33:375–380.
35. Sharma MC, Mahapatra AK, Sudha K, et al. Melanotic neuroectodermal tumour of infancy: immunohistochemical and histogenetic consideration. J Assoc Physicians India 1996; 44:278–280.
36. Khoddami M, Squire J, Zielenska M, et al. Melanotic neuroectodermal tumor of infancy: a molecular genetic study. Pediatr Dev Pathol 1998; 1:295–299.
37. Lee SC, Henry MM, Gonzalez-Crussi F. Simultaneous occurrence of melanotic neuroectodermal tumor and brain heterotopia in the oropharynx. Cancer 1976; 38:249–253.
38. Gaiger de Oliveira M, Thompson LD, Chaves AC, et al. Management of melanotic neuroectodermal tumor of infancy. Ann Diagn Pathol 2004; 8:207–212.
39. Block JC, Waite DE, Dehner LP, et al. Pigmented neuroectodermal tumor of infancy. An example of rarely expressed malignant behavior. Oral Surg Oral Med Oral Pathol 1980; 49:279–285.
40. Shokry A, Briner J, Makek M. Malignant melanotic neuroectodermal tumor of infancy: a case report. Pediatr Pathol 1986; 5:217–223.
41. Hameed K, Burslem MR. A melanotic ovarian neoplasm resembling the ''retinal anlage'' tumor. Cancer 1970; 25:564–567.
42. Shaia WT, Dinardo LJ, Underhill TE, et al. Recurrent melanotic neuroectodermal tumor of infancy. Am J Otolaryngol 2002; 23:249–252.

XIII. EWING'S SARCOMA AND PRIMITIVE NEUROECTODERMAL TUMOR (PERIPHERAL NEUROEPITHELIOMA)

1. Kempson R, Fletcher C, Evans H, et al. Tumors of uncertain differentiation and those in which differentiation is nonmesenchymal. In: Kempson R, Fletcher CD, Evans HL, et al., eds. Tumors of the Soft Tissues. Washington, DC: Armed Forces Institute of Pathology, 2001.
2. Huvos A. Ewing's sarcoma. In: Huvos A, ed. Bone Tumors. Philadelphia: W.B. Saunders Company, 1979.
3. Stout A. A tumor of the ulnar nerve. Proc N Y Soc Pathol 1918; 12:2–12.
4. Ewing J. The Classic: Diffuse endothelioma of bone. Proceedings of the New York Pathological Society. Clin Orthop Relat Res 2006; 450:25–27.
5. Angervall L, Enzinger FM. Extraskeletal neoplasm resembling Ewing's sarcoma. Cancer 1975; 36:240–251.
6. Gillespie JJ, Roth LM, Wills ER, et al. Extraskeletal Ewing's sarcoma. Histologic and ultrastructural observations in three cases. Am J Surg Pathol 1979; 3:99–108.
7. Rud NP, Reiman HM, Pritchard DJ, et al. Extraosseous Ewing's sarcoma. A study of 42 cases. Cancer 1989; 64:1548–1553.
8. Soule EH, Newton W Jr., Moon TE, et al. Extraskeletal Ewing's sarcoma: a preliminary review of 26 cases encountered in the Intergroup Rhabdomyosarcoma Study. Cancer 1978; 42:259–264.
9. Seemayer TA, Thelmo WL, Bolande RP, et al. Peripheral neuroectodermal tumors. Perspect Pediatr Pathol 1975; 2:151–172.
10. Jaffe R, Santamaria M, Yunis EJ, et al. The neuroectodermal tumor of bone. Am J Surg Pathol 1984; 8:885–898.
11. Askin FB, Rosai J, Sibley RK, et al. Malignant small cell tumor of the thoracopulmonary region in childhood: a distinctive clinicopathologic entity of uncertain histogenesis. Cancer 1979; 43:2438–2451.
12. Ambros IM, Ambros PF, Strehl S, et al. MIC2 is a specific marker for Ewing's sarcoma and peripheral primitive neuroectodermal tumors. Evidence for a common histogenesis of Ewing's sarcoma and peripheral primitive neuroectodermal tumors from MIC2 expression and specific chromosome aberration. Cancer 1991; 67:1886–1893.
13. Weiss S, Goldblum J. Primitive neuroectodermal tumors and related lesions. In: Weiss S, Goldblum J, eds. Soft Tissue Tumors. St. Louis: Mosby, 2001.
14. Turc-Carel C, Aurias A, Mugneret F, et al. Chromosomes in Ewing's sarcoma. I. An evaluation of 85 cases of remarkable consistency of t(11;22)(q24;q12). Cancer Genet Cytogenet 1988; 32:229–238.
15. Whang-Peng J, Triche TJ, Knutsen T, et al. Chromosome translocation in peripheral neuroepithelioma. N Engl J Med 1984; 311:584–585.
16. Dehner LP. Primitive neuroectodermal tumor and Ewing's sarcoma. Am J Surg Pathol 1993; 17:1–13.
17. Grier HE. The Ewing family of tumors. Ewing's sarcoma and primitive neuroectodermal tumors. Pediatr Clin North Am 1997; 44:991–1004.
18. Navas-Palacios JJ, Aparicio-Duque R, Valdes MD. On the histogenesis of Ewing's sarcoma. An ultrastructural, immunohistochemical, and cytochemical study. Cancer 1984; 53:1882–1901.
19. Ushigome S, Shimoda T, Takaki K, et al. Immunocytochemical and ultrastructural studies of the histogenesis of Ewing's sarcoma and putatively related tumors. Cancer 1989; 64:52–62.
20. Brinkhuis M, Wijnaendts LC, van der Linden JC, et al. Peripheral primitive neuroectodermal tumour and extraosseous Ewing's sarcoma; a histological, immunohistochemical and DNA flow cytometric study. Virchows Arch 1995; 425:611–616.
21. Llombart-Bosch A, Contesso G, Peydro-Olaya A. Histology, immunohistochemistry, and electron microscopy of small round cell tumors of bone. Semin Diagn Pathol 1996; 13:153–170.
22. Mahoney JP, Alexander RW. Ewing's sarcoma. A light- and electron-microscopic study of 21 cases. Am J Surg Pathol 1978; 2:283–298.
23. Cavazzana AO, Miser JS, Jefferson J, et al. Experimental evidence for a neural origin of Ewing's sarcoma of bone. Am J Pathol 1987; 127:507–518.
24. Noguera R, Triche TJ, Navarro S, et al. Dynamic model of differentiation in Ewing's sarcoma cells. Comparative analysis of morphologic, immunocytochemical, and oncogene expression parameters. Lab Invest 1992; 66: 143–151.
25. Lizard-Nacol S, Lizard G, Justrabo E, et al. Immunologic characterization of Ewing's sarcoma using mesenchymal and neural markers. Am J Pathol 1989; 135:847–855.
26. Batsakis JG, Mackay B, el Naggar AK. Ewing's sarcoma and peripheral primitive neuroectodermal tumor: an interim report. Ann Otol Rhinol Laryngol 1996; 105:838–843.
27. Ushigome S, Machinami R, Sorensen P. Ewing's sarcoma/primitive neuroectodermal tumor. In: Fletcher C, Unni K, Mertens F, eds. Tumours of Soft Tissue and Bone. Lyon: IARC press, 2002.

28. Tucker MA, D'Angio GJ, Boice JD, et al. Bone sarcomas linked to radiotherapy and chemotherapy in children. N Engl J Med 1987; 317:588–593.
29. Spunt SL, Rodriguez-Galindo C, Fuller CE, et al. Ewing sarcoma-family tumors that arise after treatment of primary childhood cancer. Cancer 2006; 107:201–206.
30. Wilkins RM, Pritchard DJ, Burgert EO, et al. Ewing's sarcoma of bone. Experience with 140 patients. Cancer 1986; 58:2551–2555.
31. Kissane JM, Askin FB, Foulkes M, et al. Ewing's sarcoma of bone: clinicopathologic aspects of 303 cases from the Intergroup Ewing's Sarcoma Study. Hum Pathol 1983; 14:773–779.
32. Sneige N, Batsakis JG. Ewing's sarcoma of bone and soft tissues. Ann Otol Rhinol Laryngol 1989; 98:400–402.
33. Unni K, Inwards C, Bridge J, et al. Small cell malignancies, Ewing sarcoma. In: Unni KK, Inwards C, Bridge JA, et al, eds. Tumors of the Bones and Joints. Washington, DC: Armed Forces Institute of Pathology, 2005.
34. Lee CS, Southey MC, Slater H, et al. Primary cutaneous Ewing's sarcoma/peripheral primitive neuroectodermal tumors in childhood. A molecular, cytogenetic, and immunohistochemical study. Diagn Mol Pathol 1995; 4:174–181.
35. Cavazzana AO, Ninfo V, Roberts J, et al. Peripheral neuroepithelioma: a light microscopic, immunocytochemical, and ultrastructural study. Mod Pathol 1992; 5:71–78.
36. Jurgens H, Bier V, Harms D, et al. Malignant peripheral neuroectodermal tumors. A retrospective analysis of 42 patients. Cancer 1988; 61:349–357.
37. Jones JE, McGill T. Peripheral primitive neuroectodermal tumors of the head and neck. Arch Otolaryngol Head Neck Surg 1995; 121:1392–1395.
38. Siegal GP, Oliver WR, Reinus WR, et al. Primary Ewing's sarcoma involving the bones of the head and neck. Cancer 1987; 60:2829–2840.
39. Arafat A, Ellis GL, Adrian JC. Ewing's sarcoma of the jaws. Oral Surg Oral Med Oral Pathol 1983; 55:589–596.
40. Wood RE, Nortje CJ, Hesseling P, et al. Ewing's tumor of the jaw. Oral Surg Oral Med Oral Pathol 1990; 69:120–127.
41. Pontius KI, Sebek BA. Extraskeletal Ewing's sarcoma arising in the nasal fossa. Light-and electron-microscopic observations. Am J Clin Pathol 1981; 75:410–415.
42. Toda T, Atari E, Sadi AM, et al. Primitive neuroectodermal tumor in sinonasal region. Auris Nasus Larynx 1999; 26:83–90.
43. Harman M, Kiroglu F, Kosem M, et al. Primary Ewing's sarcoma of the paranasal sinus with intracranial extension: imaging features. Dentomaxillofac Radiol 2003; 32:343–346.
44. Choi RY, Lucarelli MJ, Imesch PD, et al. Primary orbital Ewing sarcoma in a middle-aged woman. Arch Ophthalmol 1999; 117:535–537.
45. Singh AD, Husson M, Shields CL, et al. Primitive neuroectodermal tumor of the orbit. Arch Ophthalmol 1994; 112:217–221.
46. Bansal RK, Gupta A. Primitive neuroectodermal tumour of the orbit: a case report. Indian J Ophthalmol 1995; 43:29–31.
47. Hadfield MG, Luo VY, Williams RL, et al. Ewing's sarcoma of the skull in an infant. A case report and review. Pediatr Neurosurg 1996; 25:100–104.
48. Mishra HB, Haran RP, Joseph T, et al. Primary Ewing's sarcoma of the skull. A report of two cases. Br J Neurosurg 1993; 7:683–686.
49. Lim TC, Tan WT, Lee YS. Congenital extraskeletal Ewing's sarcoma of the face: a case report. Head Neck 1994; 16:75–78.
50. Ohlms LA, McGill T, Healy GB. Malignant laryngeal tumors in children: a 15-year experience with four patients. Ann Otol Rhinol Laryngol 1994; 103:686–692.
51. O'Connell JE, Calder C, Raafat F, et al. Ewing's sarcoma of the retropharynx. J Laryngol Otol 1994; 108:363–366.
52. Ng SH, Ko SF, Cheung YC, et al. Extraskeletal Ewing's sarcoma of the parapharyngeal space. Br J Radiol 2004; 77:1046–1049.
53. Zachariades N, Koumoura F, Liapi-Avgeri G, et al. Extraskeletal Ewing's sarcoma of the parotid region: a case report with the detection of the tumour's immunophenotypical characteristics. Br J Oral Maxillofac Surg 1994; 32:328–331.
54. Eggli KD, Quiogue T, Moser RP. Ewing's sarcoma. Radiol Clin North Am 1993; 31:325–337.
55. Zelazny A, Reinus WR, Wilson AJ. Quantitative analysis of the plain radiographic appearance of Ewing's sarcoma of bone. Invest Radiol 1997; 32:59–65.
56. Ibarburen C, Haberman JJ, Zerhouni EA. Peripheral primitive neuroectodermal tumors. CT and MRI evaluation. Eur J Radiol 1996; 21:225–232.
57. Khong PL, Chan GC, Shek TW, et al. Imaging of peripheral PNET: common and uncommon locations. Clin Radiol 2002; 57:272–277.
58. Delattre O, Zucman J, Melot T, et al. The Ewing family of tumors–a subgroup of small-round-cell tumors defined by specific chimeric transcripts. N Engl J Med 1994; 331:294–299.
59. Nascimento AG, Unii KK, Pritchard DJ, et al. A clinicopathologic study of 20 cases of large-cell (atypical) Ewing's sarcoma of bone. Am J Surg Pathol 1980; 4:29–36.
60. Carter RL, al Sams SZ, Corbett RP, et al. A comparative study of immunohistochemical staining for neuron-specific enolase, protein gene product 9.5 and S-100 protein in neuroblastoma, Ewing's sarcoma and other round cell tumours in children. Histopathology 1990; 16:461–467.
61. Folpe AL, Goldblum JR, Rubin BP, et al. Morphologic and immunophenotypic diversity in Ewing family tumors: a study of 66 genetically confirmed cases. Am J Surg Pathol 2005; 29:1025–1033.
62. Bridge JA, Fidler ME, Neff JR, et al. Adamantinoma-like Ewing's sarcoma: genomic confirmation, phenotypic drift. Am J Surg Pathol 1999; 23:159–165.
63. Navarro S, Cavazzana AO, Llombart-Bosch A, et al. Comparison of Ewing's sarcoma of bone and peripheral neuroepithelioma. An immunocytochemical and ultrastructural analysis of two primitive neuroectodermal neoplasms. Arch Pathol Lab Med 1994; 118:608–615.
64. Shinoda M, Tsutsumi Y, Hata J, et al. Peripheral neuroepithelioma in childhood. Immunohistochemical demonstration of epithelial differentiation. Arch Pathol Lab Med 1988; 112:1155–1158.
65. Dierick AM, Roels H, Langlois M. The immunophenotype of Ewing's sarcoma. An immunohistochemical analysis. Pathol Res Pract 1993; 189:26–32.
66. Schmidt D, Herrmann C, Jurgens H, et al. Malignant peripheral neuroectodermal tumor and its necessary distinction from Ewing's sarcoma. A report from the Kiel Pediatric Tumor Registry. Cancer 1991; 68:2251–2259.
67. Gu M, Antonescu CR, Guiter G, et al. Cytokeratin immunoreactivity in Ewing's sarcoma: prevalence in 50 cases confirmed by molecular diagnostic studies. Am J Surg Pathol 2000; 24:410–416.
68. Collini P, Sampietro G, Bertulli R, et al. Cytokeratin immunoreactivity in 41 cases of ES/PNET confirmed by molecular diagnostic studies. Am J Surg Pathol 2001; 25:273–274.
69. Hornick JL, Fletcher CD. Immunohistochemical staining for KIT (CD117) in soft tissue sarcomas is very limited in distribution. Am J Clin Pathol 2002; 117:188–193.
70. Somers GR, Shago M, Zielenska M, et al. Primary subcutaneous primitive neuroectodermal tumor with

aggressive behavior and an unusual karyotype: case report. Pediatr Dev Pathol 2004; 7:538–545.
71. Amann G, Zoubek A, Salzer-Kuntschik M, et al. Relation of neurological marker expression and EWS gene fusion types in MIC2/CD99-positive tumors of the Ewing family. Hum Pathol 1999; 30:1058–1064.
72. Folpe AL, Hill CE, Parham DM, et al. Immunohistochemical detection of FLI-1 protein expression: a study of 132 round cell tumors with emphasis on CD99-positive mimics of Ewing's sarcoma/primitive neuroectodermal tumor. Am J Surg Pathol 2000; 24:1657–1662.
73. Khoury JD. Ewing sarcoma family of tumors. Adv Anat Pathol 2005; 12:212–220.
74. Meier VS, Kuhne T, Jundt G, et al. Molecular diagnosis of Ewing tumors: improved detection of EWS-FLI-1 and EWS-ERG chimeric transcripts and rapid determination of exon combinations. Diagn Mol Pathol 1998; 7:29–35.
75. Peter M, Gilbert E, Delattre O. A multiplex real-time pcr assay for the detection of gene fusions observed in solid tumors. Lab Invest 2001; 81:905–912.
76. Adams V, Hany MA, Schmid M, et al. Detection of t(11;22)(q24;q12) translocation breakpoint in paraffin-embedded tissue of the Ewing's sarcoma family by nested reverse transcription-polymerase chain reaction. Diagn Mol Pathol 1996; 5:107–113.
77. Hisaoka M, Tsuji S, Morimitsu Y, et al. Molecular detection of EWS-FLI1 chimeric transcripts in Ewing family tumors by nested reverse transcription-polymerase chain reaction: application to archival paraffin-embedded tumor tissues. APMIS 1999; 107:577–584.
78. Riggi N, Stamenkovic I. The Biology of Ewing sarcoma. Cancer Lett 2007 (epub ahead of print).
79. Plougastel B, Zucman J, Peter M, et al. Genomic structure of the EWS gene and its relationship to EWSR1, a site of tumor-associated chromosome translocation. Genomics 1993; 18:609–615.
80. Rossow KL, Janknecht R. The Ewing's sarcoma gene product functions as a transcriptional activator. Cancer Res 2001; 61:2690–2695.
81. Zoubek A, Pfleiderer C, Salzer-Kuntschik M, et al. Variability of EWS chimaeric transcripts in Ewing tumours: a comparison of clinical and molecular data. Br J Cancer 1994; 70:908–913.
82. Zoubek A, Dockhorn-Dworniczak B, Delattre O, et al. Does expression of different EWS chimeric transcripts define clinically distinct risk groups of Ewing tumor patients? J Clin Oncol 1996; 14:1245–1251.
83. Armengol G, Tarkkanen M, Virolainen M, et al. Recurrent gains of 1q, 8 and 12 in the Ewing family of tumours by comparative genomic hybridization. Br J Cancer 1997; 75:1403–1409.
84. Mugneret F, Lizard S, Aurias A, et al. Chromosomes in Ewing's sarcoma. II. Nonrandom additional changes, trisomy 8 and der(16)t(1;16). Cancer Genet Cytogenet 1988; 32:239–245.
85. Maurici D, Perez-Atayde A, Grier HE, et al. Frequency and implications of chromosome 8 and 12 gains in Ewing sarcoma. Cancer Genet Cytogenet 1998; 100:106–110.
86. Ozaki T, Paulussen M, Poremba C, et al. Genetic imbalances revealed by comparative genomic hybridization in Ewing tumors. Genes Chromosomes Cancer 2001; 32:164–171.
87. Mawad JK, Mackay B, Raymond AK, et al. Electron microscopy in the diagnosis of small round cell tumors of bone. Ultrastruct Pathol 1994; 18:263–268.
88. d'Amore ES, Ninfo V. Soft tissue small round cell tumors: morphological parameters. Semin Diagn Pathol 1996; 13:184–203.
89. Dickman PS, Triche TJ. Extraosseous Ewing's sarcoma versus primitive rhabdomyosarcoma: diagnostic criteria and clinical correlation. Hum Pathol 1986; 17:881–893.
90. Lumadue JA, Askin FB, Perlman EJ. MIC2 analysis of small cell carcinoma. Am J Clin Pathol 1994; 102: 692–694.
91. Pappo AS, Douglass EC, Meyer WH, et al. Use of HBA 71 and anti-beta 2-microglobulin to distinguish peripheral neuroepithelioma from neuroblastoma. Hum Pathol 1993; 24:880–885.
92. Parham DM. Immunohistochemistry of childhood sarcomas: old and new markers. Mod Pathol 1993; 6:133–138.
93. Ramani P, Rampling D, Link M. Immunocytochemical study of 12E7 in small round-cell tumours of childhood: an assessment of its sensitivity and specificity. Histopathology 1993; 23:557–561.
94. Sorensen PH, Liu XF, Delattre O, et al. Reverse transcriptase PCR amplification of EWS/FLI-1 fusion transcripts as a diagnostic test for peripheral primitive neuroectodermal tumors of childhood. Diagn Mol Pathol 1993; 2:147–157.
95. Morotti RA, Nicol KK, Parham DM, et al. An immunohistochemical algorithm to facilitate diagnosis and subtyping of rhabdomyosarcoma: the Children's Oncology Group experience. Am J Surg Pathol 2006; 30:962–968.
96. Weidner N, Tjoe J. Immunohistochemical profile of monoclonal antibody O13: antibody that recognizes glycoprotein p30/32MIC2 and is useful in diagnosing Ewing's sarcoma and peripheral neuroepithelioma. Am J Surg Pathol 1994; 18:486–494.
97. Perlman EJ, Dickman PS, Askin FB, et al. Ewing's sarcoma–routine diagnostic utilization of MIC2 analysis: a Pediatric Oncology Group/Children's Cancer Group Intergroup Study. Hum Pathol 1994; 25:304–307.
98. Whang-Peng J, Triche TJ, Knutsen T, et al. Cytogenetic characterization of selected small round cell tumors of childhood. Cancer Genet Cytogenet 1986; 21:185–208.
99. Stephenson CF, Bridge JA, Sandberg AA. Cytogenetic and pathologic aspects of Ewing's sarcoma and neuroectodermal tumors. Hum Pathol 1992; 23:1270–1277.
100. Nelson RS, Perlman EJ, Askin FB. Is esthesioneuroblastoma a peripheral neuroectodermal tumor? Hum Pathol 1995; 26:639–641.
101. Argani P, Perez-Ordonez B, Xiao H, et al. Olfactory neuroblastoma is not related to the Ewing family of tumors: absence of EWS/FLI1 gene fusion and MIC2 expression. Am J Surg Pathol 1998; 22:391–398.
102. Mezzelani A, Tornielli S, Minoletti F, et al. Esthesioneuroblastoma is not a member of the primitive peripheral neuroectodermal tumour-Ewing's group. Br J Cancer 1999; 81:586–591.
103. Kumar S, Perlman E, Pack S, et al. Absence of EWS/FLI1 fusion in olfactory neuroblastomas indicates these tumors do not belong to the Ewing's sarcoma family. Hum Pathol 1999; 30:1356–1360.
104. Paulussen M, Ahrens S, Burdach S, et al. Primary metastatic (stage IV) Ewing tumor: survival analysis of 171 patients from the EICESS studies. European Intergroup Cooperative Ewing Sarcoma Studies. Ann Oncol 1998; 9:275–281.
105. Rodriguez-Galindo C. Pharmacological management of Ewing sarcoma family of tumours. Expert Opin Pharmacother 2004; 5:1257–1270.
106. Kennedy JG, Frelinghuysen P, Hoang BH. Ewing sarcoma: current concepts in diagnosis and treatment. Curr Opin Pediatr 2003; 15:53–57.
107. Rodriguez-Galindo C, Billups CA, Kun LE, et al. Survival after recurrence of Ewing tumors: the St Jude Children's Research Hospital experience, 1979–1999. Cancer 2002; 94:561–569.

108. Cangir A, Vietti TJ, Gehan EA, et al. Ewing's sarcoma metastatic at diagnosis. Results and comparisons of two intergroup Ewing's sarcoma studies. Cancer 1990; 66:887–893.
109. Arai Y, Kun LE, Brooks MT, et al. Ewing's sarcoma: local tumor control and patterns of failure following limited-volume radiation therapy. Int J Radiat Oncol Biol Phys 1991; 21:1501–1508.
110. Baldini EH, Demetri GD, Fletcher CD, et al. Adults with Ewing's sarcoma/primitive neuroectodermal tumor: adverse effect of older age and primary extraosseous disease on outcome. Ann Surg 1999; 230:79–86.
111. Kushner BH, Meyers PA, Gerald WL, et al. Very-high-dose short-term chemotherapy for poor-risk peripheral primitive neuroectodermal tumors, including Ewing's sarcoma, in children and young adults. J Clin Oncol 1995; 13:2796–2804.
112. Parham DM, Hijazi Y, Steinberg SM, et al. Neuroectodermal differentiation in Ewing's sarcoma family of tumors does not predict tumor behavior. Hum Pathol 1999; 30:911–918.
113. de Alava E, Kawai A, Healey JH, et al. EWS-FLI1 fusion transcript structure is an independent determinant of prognosis in Ewing's sarcoma. J Clin Oncol 1998; 16:1248–1255.
114. Amir G, Issakov J, Meller I, et al. Expression of p53 gene product and cell proliferation marker Ki-67 in Ewing's sarcoma: correlation with clinical outcome. Hum Pathol 2002; 33:170–174.

13

Tumors and Tumor-Like Lesions of the Soft Tissues

Julie C. Fanburg-Smith and Jerzy Lasota
Department of Orthopaedic and Soft Tissue Pathology, Armed Forces Institute of Pathology, Washington D.C., U.S.A.

Aaron Auerbach
Department of Hematopathology, Armed Forces Institute of Pathology, Washington D.C., U.S.A.

Robert D. Foss
Department of Oral and Maxillofacial Pathology, Armed Forces Institute of Pathology, Washington D.C., U.S.A.

William B. Laskin
Surgical Pathology, Northwestern Memorial Hospital, Feinberg School of Medicine, Northwestern University, Chicago, Illinois, U.S.A.

Mark D. Murphey
Department of Radiologic Pathology, Armed Forces Institute of Pathology, Washington D.C., U.S.A.

Part I: Benign Mesenchymal Lesions and Tumors of the Head and Neck

I. INTRODUCTION

Soft tissue lesions and neoplasms in the head, neck, and oral and maxillofacial regions involve the dermis, subcutis and, skeletal muscle of the head and neck (any tissue between skin and bone). In addition, there are submucosal lesions, intra salivary gland lesions, and those of gingiva, lip, tongue, and palate. Phenotypes, or cell of origin, included in ''soft tissue'' or mesenchymal lesions include those arising from vessels, fat, skeletal muscle, smooth muscle, (myo)fibroblastic cells, and nerve sheath (the latter is covered predominantly in another chapter). There are also bone and cartilage forming tumors, mixed epithelial and mesenchymal, and tumors of uncertain phenotype.

Most soft tissue tumors are benign, with lipomas being the most common in adults and hemangiomas the most common in children. While sarcomas are exceedingly rare, compared with benign soft tissue tumors, certain sarcomas are comparatively more common than their benign counterparts, such as rhabdomyosarcoma. This sarcoma is also more common in the head and neck than other anatomic locations, particularly in children.

Tumors and tumor-like lesions of the head and neck are often different from their soft tissue counterparts in other sites. This chapter will cover benign and malignant soft tissue tumors that involve the head, neck, oral, and maxillofacial areas. It will give the most updated clinical and pathologic information about these entities, including state of the art imaging and molecular information.

The treatment for soft tissue lesions in the head and neck is generally the same as for those in other anatomic locations. Benign or reactive lesions can be locally excised, especially for diagnosis. Those with higher recurrent potential, such as fibromatosis

(desmoid), may require adjuvant therapy to control local disease, even though it is a nonmetastasizing benign lesion. Atypical or low-grade malignant tumors are treated by complete or sometimes wide excision and careful patient follow-up. Intermediate and high-grade sarcomas, grade 2-3/3, are treated by pre- and postoperative radiation followed by chemotherapy if clinically indicated, particularly in tumors greater than 5 cm or those that cannot be fully resected.

In section I (benign), head and neck soft tissue lesions include the controversial reactive to malformation to neoplastic vascular and perivascular lesions such as papillary endothelial hyperplasia (PEH), arteriovenous hemangioma (malformation), hemangioma variants, lymphangioma, and glomus tumor. Skeletal and smooth muscle lesions and tumors include focal myositis, rhabdomyoma, and leiomyoma. Adipocytic tumors include the lipoma variants. Myofibroblastic tumors range from reactive lesions such as nodular fasciitis, cranial fasciitis, proliferative fasciitis and myositis, reactive periostitis and its spectrum with bizarre parosteal osteochondromatous proliferation (BPOP) and Turret exostosis, idiopathic cervical fibrosis, fibrous hamartoma of infancy, and gingival fibromatosis (GF), to benign myofibroma, nuchal fibroma, and collagenous fibroma to benign, but aggressive tumors, such as desmoid fibromatosis. Angiofibroma (AF) is now considered by some to be related to fibromatosis, since both express nuclear β-catenin positivity. Myxoma has CD34 positive stellate cells. Specialized CD34 positive fibroblasts comprise the spectrum of solitary fibrous tumor (SFT) and hemangiopericytoma (HPC), but such cells are not seen in the myopericytic sinonasal glomangiopericytoma. Bone and cartilage forming lesions include choristoma and myositis ossificans. Ossifying fibromyxoid tumor, while still considered of unknown phenotype with a benign to uncertain biologic behavior, may be of specialized fibroblast phenotype as well. Ectomesenchymal chondromyxoid tumor (ECT) may be a variant of a mixed tumor.

In section II (malignant), the head and neck sarcomas include vascular malignancies including low-grade malignant epithelioid hemangioendothelioma and frankly malignant angiosarcoma, rhabdomyosarcoma, leiomyosarcoma, liposarcoma, the myofibroblastic malignant tumors, mixed lineage mesenchymal tumors such as malignant Triton tumor and mesenchymoma (the latter now largely an outdated term), or cartilage such as mesenchymal chondrosarcoma. Additional sarcomas include mixed epithelial and mesenchymal phenotype synovial sarcoma and malignant rhabdoid tumor and tumors still of uncertain phenotype such as alveolar soft part sarcoma.

The classification of these lesions has changed over the years as technology advances. From clinical and morphology only to imaging, ultrastructural evaluation, immunohistochemistry, and now novel genetic findings all impact the continually evolving classification of these tumors.

II. BENIGN VASCULAR AND PERIVASCULAR LESIONS

A. Papillary Endothelial Hyperplasia

Introduction

Initially considered a neoplastic process by Masson, who first described the lesion in 1923 and designated it ''vegetant intravascular hemangioendothelioma'' (1), PEH is currently recognized as a distinctive form of an organizing thrombus characterized by the formation of innumerable hyaline nodules covered by a thin layer of benign endothelial cells.

Clinical Features

PEH occurs in three distinct clinical settings. In the primary form of PEH, the lesion develops in normal vessels anywhere throughout the body. PEH engrafted on a preexisting vascular anomaly is considered a secondary form of the process. The clinical features, including location of the lesion(s), usually mirror those of the primary condition. For example, dermal-based PEH usually occurs in association with the acquired lobular capillary hemangioma, infantile capillary hemangioma, cavernous hemangioma, or lymphangioma, whereas most deep lesions arise in intramuscular angiomas (2,3). Extravascular PEH is the least frequent manifestation of the process and has origin in an extravascular thrombus (4). In this situation, the disorder has the potential to mimic a soft tissue sarcoma.

In general, the dermis of the fingers, hands, and head and neck is the most commonly affected sites in large series (5–8). Specific (noncutaneous) sites in the head and neck involved by the process include the oral cavity, particularly the lips followed by the tongue (9,10), the paranasal sinuses (11), parapharyngeal space (12), and larynx (13). Clinically, PEH presents over a wide age range but peaks in adulthood and affects females slightly more often than males (5,8,10). A prior episode of trauma is usually not elicited. The lesion typically manifests as a solitary, slow-growing, often tender dermal or subcutaneous nodule or mass with a blue to red color. Most lesions measure less than 2 cm. Multiple lesions at presentation are vanishingly rare but may raise clinical suspicion of a vascular malignancy (14).

Pathologic Findings

The morphology of the lesion is relatively consistent regardless of the clinical setting (2,3,5). At low-power magnification, a well-circumscribed collection of clotted blood (organizing thrombus) is found within the confines of a dilated vein or artery (Fig. 1) or preexisting benign vascular tumor, such as capillary hemangioma. The wall surrounding the thrombus may be fibrotic with only small remnants of native vessel, smooth muscle, or elastic tissue. The salient microscopic feature of PEH that separates it from a conventional organizing thrombus is the formation of variably sized hyaline nodules or papillae lined by a

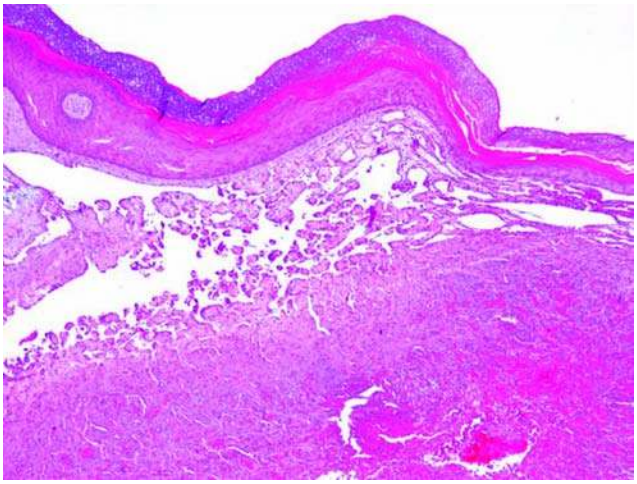

Figure 1 Low-power magnification of papillary endothelial hyperplasia demonstrates a well-circumscribed process all within a dilated vessel.

monolayer of plump, sometimes hyperchromatic but cytologically benign endothelial cells, at the periphery of the thrombus. There is no mitotic activity. Early in the evolution of PEH, endothelial cells at the interface with the thrombus dissect through the clotting blood and surround small nodules of the fibrin (Fig. 2). When fully developed, the lesion consists of innumerable, closely aggregated, nodules of eosinophilic fibrin or hyalinized collagen enveloped by a single layer by cytologically bland, mitotically inactive endothelial cells (Fig. 3). Rents in the vascular wall allow the process to focally extend into the surrounding tissue (Fig. 4).

Ultrastructure

The cells lining the matrix-rich nodules are well-differentiated endothelial cells with intracytoplasmic Weibel-Palade bodies. Cells having features of pericytic cells and undifferentiated cells are also identified beneath the endothelial surface. Basal lamina is located along the antiluminal aspect of the endothelial cell (15).

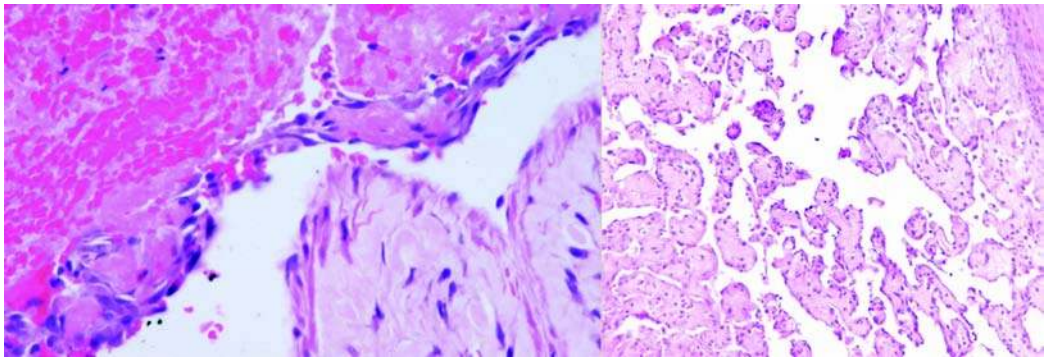

Figure 2 PEH often starts at the edge of an organizing thrombus, in an intravascular process (*left*) and can become extensive (*right*).

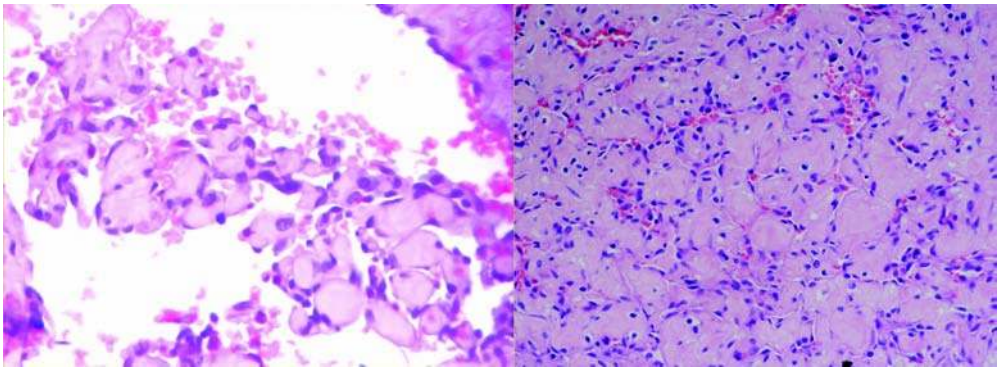

Figure 3 In the fully developed lesion, hyalinized collagenous nodules fill the lumen of a normal vessel or vessel in a preexisting vascular lesion, imparting a papillary appearance at low-power magnification. Tightly aggregated nodules of hyalinized collagen are mantled by a single layer of cytologically bland endothelial cells. This architectural pattern has the potential to mimic an angiosarcoma.

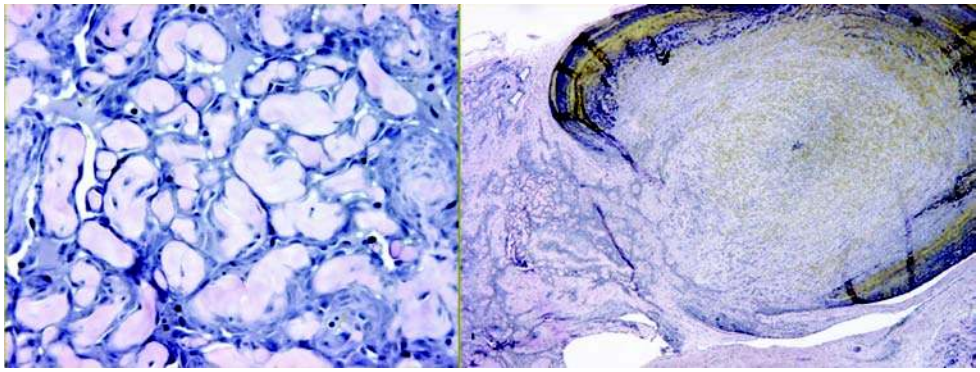

Figure 4 PEH can occasionally ''break through'' a tear in a preexisting vessel wall and become an extravascular proliferation of hyaline cores lined by benign endothelial without mitotic activity.

Immunohistochemistry

Endothelial cells express CD31 and CD34, and show variable expression of Factor VIII–related antigen in fully developed lesions (14,16). The presence of Factor XIIIa-positive cells indicates a component of dendritic cells (14).

Differential Diagnosis

The tightly aggregated, endothelial-lined collagenous nodules of fully developed PEH have the potential to resemble an angiosarcoma. This mimicry is sometimes compounded by extravascular extension of the process. PEH differs from the more ominous angiosarcoma by its smaller size, typically intravascular location, absence of infiltrative growth pattern, solid spindled or multilayer growth, marked nuclear atypia, high mitotic activity, and foci of necrosis.

Glomeruloid hemangioma (17), a reactive endothelial proliferation, exhibits an intravascular proliferation of capillary-like structures lined by bland endothelial cells. Clinically, glomeruloid hemangioma is associated with the POEMS syndrome (*p*olyneuropathy, *o*rganomengaly, *e*ndocrinopathy, *m*onoclonal gammopathy, and *s*kin changes). Microscopically, the hemangioma lacks the nodules of fibrin or collagen that typify PEH. Additionally, some of the lesional cells of glomeruloid hemangioma characteristically harbor PAS-positive, diastase-resistant eosinophilic globules of polyclonal immunoglobulin proteins.

Spindle cell hemangioma is a benign and possibly reactive process that primarily involves the extremities. Microscopically, the lesion is intravascular in about 60% of cases (18,19) and may possess cellular tufts and fibrin thrombi. In contrast to PEH, spindle cell hemangioma is more cellular, has a prominent spindle cell component, and demonstrates a more complex architecture including the presence of thin-walled cavernous spaces, sometimes with phlebolith formation.

Prognosis and Treatment

PEH is a wholly benign process that is effectively treated by a simple (local) excision. Recurrent lesions should raise suspicion of a preexisting vascular lesion (i.e., secondary PEH), and therapy should be directed toward managing the primary process.

B. Arteriovenous Hemangioma (Arteriovenous Malformation)

Introduction

The arteriovenous hemangioma or malformation (AVM) is a benign vascular lesion with a direct connection between artery and vein, without a capillary intermediate. There has been discussions as to whether this is a true neoplasm, so it is called ''arteriovenous hemangioma'' in the current WHO classification, but it is still considered a malformation. It requires clinical evidence of a bruit or radiologic evidence of shunting to confirm the histologic impression for diagnosis. The shunt is thought to be due to a failure of primitive arteriovenous channels to regress in utero (1). These can either be superficial, alternatively designated acral arteriovenous tumor (2–4) and not associated with significant arteriovenous shunting, or deeply seated (5), and associated with signs and symptoms of arteriovenous shunting. Most are deeply seated and located in skeletal muscle. Alternatively, the lesions acquired through trauma, surgery, or infection are best considered ''arteriovenous fistulas'' because there is a direct communication between the artery and the vein. As the congenital AVM occurs almost exclusively in the head and neck, it will be the focus of this discussion.

Clinical Findings

AVM requires radiologic or clinical correlation for diagnosis. The superficial AVM is a dermal-based process that occurs most often in the head and neck,

where it shows a predilection for the face, lips, and the oral cavity (2–4). The lesion presents in middle-aged individuals and affects males more often than females. The process appears as an elevated dark red or violaceous papule and is usually asymptomatic.

While the acquired arteriovenous fistula tends to be a localized lesion, the deep-seated congenital AVM is a more diffuse process involving multiple tissue planes (6). The lesion primarily affects the head and neck followed by the limbs (7). The head and neck AVM presents mostly in childhood, adolescence, or in early adulthood and shows no gender bias (1,8–11). Excluding the intracranial AVM, the majority of AVMs occur in midface structures especially the cheek, followed by the ear, nose, and upper lip and, less often, the forehead, lower lip, and submental and submandibular soft tissue (1,8,10,11). Gnathic bones are occasionally the primary site of the AVM, while other cranial bones are involved secondarily by an adjacent soft tissue AVM (1). Clinically, the lesion is present at birth and grows proportionately with the child, but typically exhibits accelerated growth at puberty or during pregnancy with the onset of hormonal changes (12), or following trauma or infection (1,13).

The deep AVM appears as a bluish mass that is warm to touch. Large lesions sometimes present with ulceration and bleeding. Auscultatory examination frequently reveals arterial pulsations or a continuous bruit or thrill over the mass. Pulsatile tinnitus is a unique and disturbing symptom of head and neck AVMs (9). Pain results from masticator muscle involvement and occurs while eating (8), or from tumors arising in the gnathic bones. Deep-seating lesions, including the acquired arteriovenous fistula, demonstrate marked arterial-to-venous ''shunting'' that results in diverse clinical findings, including reflex bradycardia when the feeding artery is compressed (Nicoladoni–Branham sign) (14), the presence of varicose veins early in life, violaceous papules on the skin overlying extremity lesions (see below), increased hair growth, or sweating over the mass (15,16). Cardiac dilatation and frank ''high-output'' heart failure are severe sequelae of large arteriovenous shunts that stimulate heart rate and cardiac output (17). Fortunately, this problem is rarely encountered with head and neck lesions (1). Many of these aforementioned clinical stigmata serve as criteria for the Schobinger staging scheme that focuses on the presenting symptomatology for statisfying patients into a clinically useful, four-tiered system (1).

Imaging

Conventional angiography identifies the ''high-flow'' hemodynamics of the AVM, and it also demonstrates enlarged arteries, veins, and ''feeder'' vessels. However, conventional angiography is an invasive procedure. Magnetic resonance (MR) imaging, including MR angiography, is a noninvasive modality that shows rapid contrast enhancement during the early arterial phase and arteriovenous shunting with early venous filling (18). Another noninvasive procedure, computed tomography (CT) angiography, allows identification of ''feeder'' vessels and assists in differentiating the ''high-flow'' AVM from the ''low-flow'' cavernous hemangioma (venous malformation) (19). These imaging studies have largely supplanted angiography as the initial imaging modality in assessment of these lesions.

MR imaging and CT highlight the enlarged vascular channels comprising the malformation and assist in determining the extent of the lesion. CT has an additional advantage in its ability to evaluate osseous involvement by the lesion. On T1-weighted MR imaging, the AVM is iso- or hypointense to muscle. The signal intensity or T2-weighted MR imaging is dependent on lesion flow. High-flow components remain low signal intensity while low-flow components are high signal intensity. Additionally, perilesional T2-weighted hyperintensity, which is due to edema and venous congestion within the malformation, can obscure the radiologic impression (20). Doppler ultrasound (US) demonstrates multiple hypoechoic serpentine channels within the lesion, identifies arterialized draining veins, and identifies the ''high-flow'' and ''low-flow'' regions of the process (21).

Pathologic Findings

AVM requires radiologic or clinical correlation for diagnosis. AVMs are variably circumscribed, nonencapsulated lesions that consist of closely aggregated, thin- and thick-walled vessels (Fig. 5). Although the proportion of thick- to thin-walled structures within the lesion varies, the thick-walled vessels usually predominate. As the lesion can harbor foci resembling cavernous or capillary hemangioma, angiographic evaluation is required for diagnosis. However, the presence of an artery juxtaposed to a thick-walled vein with a larger lumen is strong supporting

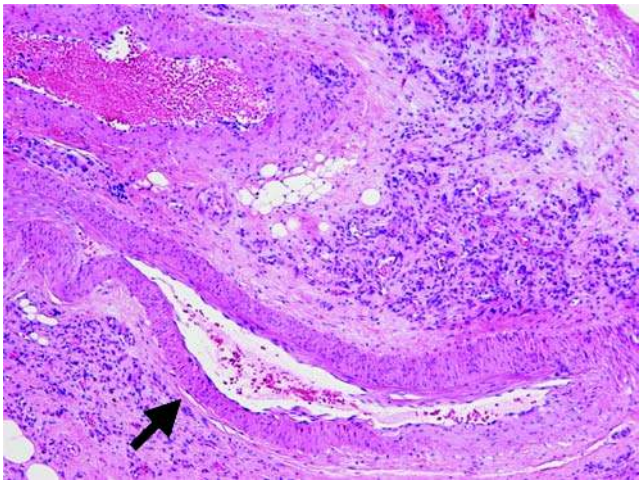

Figure 5 Low-powered magnification of an arteriovenous malformation shows an artery (*arrow*), vein, and tight congeries of capillary-sized vessels. There is often fatty overgrowth, thought to represent skeletal muscle atrophy and fatty replacement.

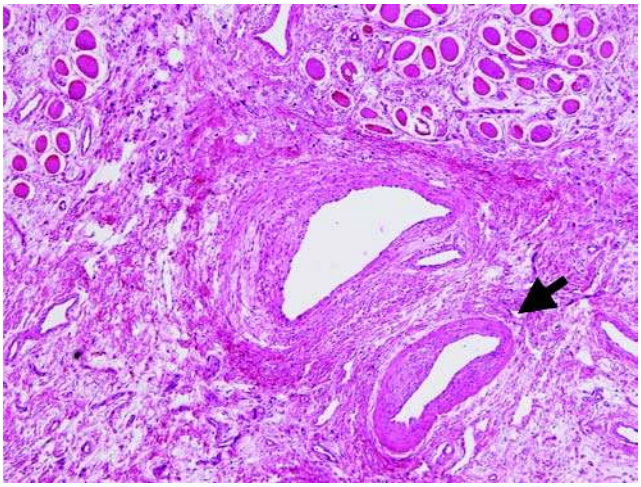

Figure 6 The one microscopic feature that supports the diagnosis of arteriovenous malformation is the presence of a thick-walled, often ''arterialized'' vein in close apposition to an artery (*arrow*). Note the usual intramuscular location.

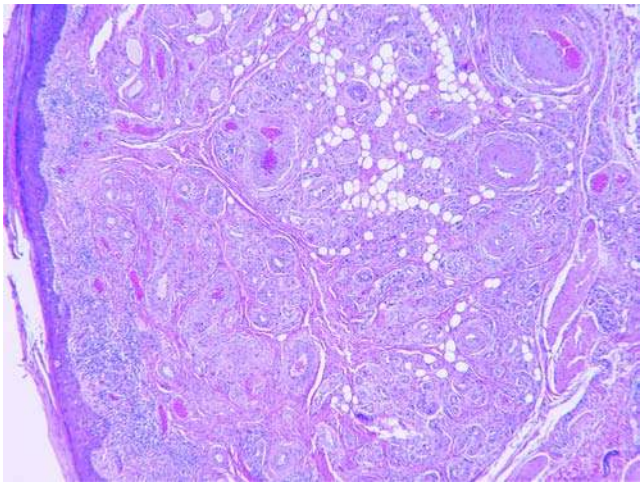

Figure 8 Superficial arteriovenous malformation consists of tightly aggregated and superficially located, thick-walled vascular structures. Elastic histochemical stain assists in identifying the arterial component of the malformation.

microscopic evidence for an AVM (Fig. 6), but this must be confirmed by imaging or clinical information. Because these venous structures demonstrate medial hypertrophy and fibrointimal hyperplasia, they resemble arteries (22); histochemical stains for elastic tissue are useful by highlighting the internal elastic membrane of arteries. The main arteriovenous shunt or ''feeding'' artery has been identified in about 25% of cases after evaluating multiple serial sections (2). The lining endothelial cells are cytologically bland, monolayered, and focally assume a ''hobnail'' appearance with their nuclei positioned toward the lumen. Organizing thrombi and phleboliths are commonly observed within the venous component (Fig. 7).

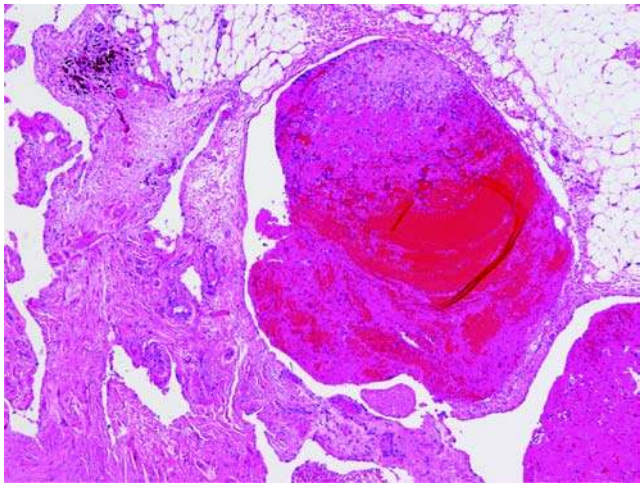

Figure 7 Area of an arteriovenous malformation resembling cavernous hemangioma and harboring a thrombosed vessel.

There is often fatty overgrowth in the intramuscular lesions, thought to be due to skeletal muscle atrophy and fatty replacement. Inflammation is a rare finding. Histochemical or S100 protein immunohistochemical stains for neuroaxons highlight scattered nerve twigs within the lesional tissue (23). The thick-walled vessels of the superficial AVM are distributed within the superficial and middle dermis, where they intermingle with native dermal structures (Fig. 8).

An overlying reactive vascular proliferation, termed acro-angiodermitis or ''pseudo-Kaposi's'' sarcoma because of its superficial resemblance to Kaposi's sarcoma (16), is sometimes encountered with deep extremity lesions. Histologically, closely aggregated, small, thick-walled vessels with plump endothelial cells arranged in a vaguely lobular pattern characterize the process. The surrounding dermal stroma is fibrotic and contains hemosiderin.

It is always best to correlate the histologic findings with a radiologic stunt or clinical bruit for complete classification.

Immunohistochemistry

CD31 and CD31 stain vessels; SMA the smooth muscle of large vessel walls. GLUT-1 and HHV8 are negative.

Differential Diagnosis

The main entity in the differential diagnosis of the AVM is the cavernous hemangioma (venous malformation). Clinically, both lesions predilect to head and neck sites and usually present in young-aged individuals. Radiologically, the AVM demonstrates ''high-flow'' hemodynamics in contrast to the ''low-flow'' characteristics of the cavernous hemangioma (7). Histologically, both lesions show significant overlap making diagnosis (without radiologic support) difficult.

However, the constituent vessels of the AVM are appreciably thicker than those of the venous malformation. Moreover, the arterial component of the AVM can be identified with an elastic stain.

The intramuscular angioma is synonymous with AVM with a deep location and a variable admixture of vessel types. Elastic stain assists in highlighting the internal elastic membrane of the arterial structures present in the AVM, but typically absent in the intramuscular angioma; the only way to truly separate these is to prove or disprove the clinical or radiologic presence of a bruit or shunt.

Angiomatosis (24), like the deep AVM, involves multiple tissue planes but, in contrast, rarely occurs in head and neck tissues. Although histologic overlap occurs, angiomatosis characteristically features large venous structures with capillary-sized vessels observed within their walls and an absence of lesional arteries.

The capillary hemangioma of infancy, like AVM, predilects to the head and neck. Radiologically, both lesions exhibit ''high-flow'' hemodynamics, but formation of phleboliths would favor the diagnosis of AVM. Clinically, the hemangioma of infancy presents earlier in life than AVM, does not grow proportionally with the child, and shows appreciable involution with age. The hemangioma of infancy appears as a noncompressible, reddish mass, whereas the AVM is a spongy, blue-colored, compressible lesion. Microscopically, the evolving hemangioma demonstrates a lobular growth pattern and is more cellular than the AVM. However, during the involuting stage of the infantile capillary hemangioma, residual vessels dilate and may simulate the vessels of AVM. The presence of arteries (confirmed by the presence of an internal elastic membrane) and intralesional nerve segments (23) supports the diagnosis of AVM. Additionally, immunohistochemical expression of GLUT-1 and/or WT-1 would strongly favor the diagnosis of infantile capillary hemangioma (25,26).

Prognosis and Treatment

AVM does not undergo spontaneous regression. Superficial variants are usually amenable to surgical excision and do not recur. Deep lesions, however, are more difficult to manage because of their size and association with malformed and ectatic vessels adjacent to the lesion that form in response to increased blood flow. Presently, these vascular tumors are treated with a combination of embolization or sclerotherapy followed by surgery and reconstruction (1,27). The major complication of embolization therapy is tissue and organ ischemia (11). Success with this combined approach is highest with low-stage (Schobinger staging scheme) lesions (1).

C. Hemangiomas

Introduction

Hemangioma is best defined as an excessive proliferation of benign endothelial cells forming vascular spaces that resemble normal blood vessels, but with too many normal vessels per unit area. There is still a pericyte around each endothelial-lined blood vessel. In contrast, vascular malformations, some of which are erroneously classified as hemangiomas, are due to abnormal vessel morphogenesis and are not proliferative lesions (1). It is often difficult to separate a vascular malformation from hemangioma, and there is much controversy over these lesions.

Although a commonly encountered pathologic process, the nature of many benign vascular disorders remains controversial as some are true neoplasms while others are regarded as malformations, hamartomatous growths or reactive endothelial hyperplasias. Nevertheless, the histologic diagnosis of benignancy in a vascular lesion is near certain when the process exhibits a zonal or lobular growth pattern and the vascular channels are composed of a monolayer of cytologically bland endothelial cells and perivascular supporting cells (i.e., pericytes or smooth muscle cells) (2). Notably, the presence of cytologic atypia alone or a seemingly infiltrative growth pattern of lesional vessels without multilayering of endothelial cells that exhibit bona fide nuclear atypia does not automatically indicate malignancy. In general, most benign vascular processes can be broadly categorized as reactive endothelial proliferations, hemangiomas (congenital or acquired), and vascular malformations (capillary, venous, lymphatic, arteriovenous, and combined).

The recent WHO histologic classification of soft tissue tumors recognizes eighteen distinct benign vascular (blood vessel and lymphatic) processes, which can be further segregated according to depth (Table 1) (3). This section will discuss five of these vascular processes that occur in the head and neck: the capillary hemangioma, cavernous hemangioma, epithelioid hemangioma, acquired ''tufted'' angioma, and intramuscular angioma. AVM and PEH are discussed separately.

Capillary hemangioma is the most common benign vascular disorder (4). The variant of capillary hemangioma with a perinatal onset, the hemangioma of infancy, is probably the most common tumor of childhood and affects up to 12% of children (5,6). The lesion is alternatively termed juvenile hemangioma, cellular capillary hemangioma, infantile hemangioendothelioma, or ''strawberry'' nevus (an appellation based primarily on its clinical appearance) (6,7). Although the proposed etiologies of this vascular process are diverse (8–12), recent molecular evidence suggests that the lesion is caused by an imbalance in angiogenic and angiostatic factors (13,14) that manifests first as a highly proliferative lesion followed by an involutionary stage characterized by accelerated apoptosis of lesional cells.

Three subtypes of capillary hemangioma that clinically present sometime after the perinatal period and are considered ''acquired'' lesions occur in the head and neck (4). The cherry hemangioma is the most common vascular tumor encountered in the dermis (15). The lesion is also known as senile hemangioma because the number of lesions increases with age so

Table 1 WHO Histologic Classification of Benign Vascular/Lymphatic Tumors

Benign Vascular/Lymphatic Tumors	ICD-O[a] code
Hemangiomas of dermis/subcutaneous tissue	
Hemangioma of infancy	9131/0
Cherry hemangioma	9120/0
Sinusoidal hemangioma	9120/0
Hobnail hemangioma	9120/0
Glomeruloid hemangioma	9120/0
Microvenular hemangioma	9120/0
Cavernous hemangioma	9120/0
Arteriovenous hemangioma	9123/0
Spindle cell hemangioma	9136/0
Tufted angioma	9161/0
Angiolymphoid hyperplasia with eosinophilia (epithelioid hemangioma)	9125/0
Lymphatic tumors of dermis/subcutaneous tissue	
Lymphangioma circumscriptum	9170/0
Progressive lymphangioma	9170/0
Hemangiomas of subcutaneous or deeper soft tissue	
Intramuscular hemangioma	9132/0
Venous hemangioma	9122/0
Synovial hemangioma	9132/0
Angiomatosis	
Lymphatic tumors of subcutaneous or deeper soft tissue	
Lymphangioma	9170/0

[a]Morphology code of the International Classification of Diseases for Oncology and the Systematized Nomenclature of Medicine
Source: From Ref. 3.

that the process becomes more apparent in older-aged adults. The acquired lobular capillary hemangioma is a rapidly growing, polypoid lesion that is traditionally known as granuloma pyogenicum (or pyogenic granuloma) because of its purported infectious origin (16) and association with trauma in some cases (17). The acquired ''tufted'' angioma, a vascular tumor characterized by slow, indolent growth, is also termed progressive capillary hemangioma or angioblastoma of Nakagawa.

So-called cavernous hemangioma is less frequently encountered than capillary hemangiomas and is usually found in deeper soft tissue. The lesion is so named for its widely dilated vascular spaces. However, many vascular lesions termed cavernous hemangioma are not true hemangiomas as previously defined, but instead represent venous malformations based on their ''low-flow'' hemodynamics, congenital onset (although the lesion typically does not clinically manifest until later in life), growth commensurate with that of the child's, and resistance to spontaneous involution (1). The remainder probably represent true capillary hemangiomas with dilated and engorged vascular spaces (1,18).

Epithelioid hemangioma or angiolymphoid hyperplasia with eosinophilia is less commonly referred to as nodular angioblastic hyperplasia with eosinophilia and lymphofolliculosis, subcutaneous angioblastic lymphoid hyperplasia with eosinophilia, and inflammatory angiomatoid nodule (19). In earlier literature, this entity was grouped first with Kimura's disease (20) and later with so-called ''histiocytoid hemangioma'' (21). Focused studies have provided convincing clinical and pathologic data indicating that Kimura's disease and epithelioid hemangioma are separate entities (22–25). It should be mentioned that the appellation ''histiocytoid'' hemangioma (21) is currently considered a collective term that refers to a variety of unrelated vascular lesions that have in common the presence of large, epithelioid endothelial cells and is not specific for any one entity. The epithelioid endothelial cell is ultrastructurally distinguished from the conventional endothelial cell by possessing an increased number of organelles and intermediate (vimentin) filaments (26,27). The nature of the epithelioid hemangioma is controversial, but a reactive vascular proliferation has been proposed for at least some examples because the tumor is frequently encountered in areas of the body with little soft tissue padding (i.e., temple, forehead, occiput scalp, and the dorsum of hands and feet), is occasionally associated with a history of prior trauma (28), and histologically shows evidence of an arteriovenous anastomosis (29) or vascular injury (28,30).

Intramuscular angioma, albeit a rare vascular lesion, is probably one of the more common deep-seated soft tissue tumors (31). The process is also known as intramuscular hemangioma and shares with angiomatosis of soft tissue the appellation intramuscular or ''infiltrating'' angiolipoma due to presence of mature fat within both the lesions. Angioma is the presently preferred nomenclature as the process is considered a vascular malformation (akin to arteriovenous or venous malformation, discussed in a separate section) owing to the presence of a variety of vessel types within the lesion.

Clinical Features

Capillary hemangioma exhibits varied clinical features depending on subtype. The hemangioma of infancy shows a marked female predominance (2–3:1 ratio) and occurs in the head or neck (>60%) including salivary gland, (4) most commonly parotid, (4) followed by the trunk (25%) and extremities (15%) (32). In the dermis, the more commonly encountered localized form of the process preferentially presents in the midcheek, lateral portion of the upper lip, and upper eyelid as a reddish-purple macule or nodule within the first two weeks of postnatal life (5). The lesion progresses rapidly to form an elevated nodule that, in many cases, has a vivid reddish-purple color and a rubbery texture (''strawberry'' nevus). Regression of the lesion may begin as early as the first few months of life, but more commonly starts by the second year of life so that over 50% of patients experience regression

by age five years and nearly all have complete involution of the process by 10 to 12 years of age (15).

Noncutaneous examples of hemangioma of infancy occur within the upper airway, where the subglottic portion of the larynx is most often the affected site (33). Infants clinically present with stridor, and occasionally the lesion results in life-threatening airway obstruction (33,34). Hemangioma of infancy has also been reported in the parotid gland (35,36) and sinonasal tract (37,38).

The hemangioma of infancy is also grouped with a variety of developmental field defects. A well-known association is the presence of cervicofacial hemangiomas (in the beard area) with hemangiomas in the upper airway or subglottis (39). Facial hemangiomas are also associated with sternal defects and malformations of certain arteries (40). A plaque-like hemangioma involving a large segment of the face heralds the presence of the PHACE (*p*osterior *f*ossa brain malformation, segmental cervicofacial *h*emangiomas, *a*rterial *a*nomalies, *c*ardiac defects and *c*oarctation of the aorta, and *e*ye anomalies) syndrome (41). Additionally, multiple hemangiomas of infancy occur with visceral hemangiomatosis (5).

The acquired lobular capillary hemangioma predilects to the head and neck and the fingers, but has a rather ubiquitous distribution (15). In the former location, the face, nasal mucosa (particularly Little's area of the anterior septum), tip of the turbinates, and oral cavity (especially gingiva, lips, and tongue) are the most often involved sites (42). Rare examples have been reported in the paranasal sinuses (43). The lesion occurs at almost any age, with peak incidence noted in children, adolescent males, and females during the reproductive years. In the latter clinical setting, the lesion is also referred to as granuloma gravidarum. Nasal lesions usually present with epistaxis or obstruction. Cutaneous lesions affect both sexes equally (44) and typically present within a period of weeks with ulceration and bleeding and involutes within a few months of onset. Multiple satellite lesions sometimes occur, (45) and rarely, the process presents in a more disseminated fashion (46). The hemangioma has also been reported in subcutaneous tissue (47) or as an intravascular process (48).

Cherry (''senile'') hemangioma generally occurs on the trunk and upper extremities and less often in the head and neck (4). The process typically presents after puberty, and the number of lesions increases with age. The hemangioma begins as an asymptomatic reddish macule and progresses to an erythematous papule that ranges in size from 2 to 10 mm.

Acquired ''tufted'' angioma manifests as multiple, dull red, indurated macules, nodules, or plaques, which are typically slow growing and occur in the face, scalp, neck, and upper trunk (49,50). Examples of ''tufted'' angioma have been reported in the oral cavity (51), face (52) and lower lip (53). Most patients are children with over 50% of cases presenting by age of five years and occasionally at birth (49). Males and females are equally affected. Although most lesions are asymptomatic, pain, hyperhidrosis, and hypertrichosis have been reported in some cases (49,54). Some degree of regression occurs within several months of onset, but complete involution is less frequently observed than with hemangioma of infancy (55). However, the lesion tends to stabilize once the child stops growing. The lesions can reach considerable size and complicate management (see below). Notably, some cases of acquired ''tufted'' angioma are complicated by the Kasabach–Merritt syndrome (56) or associated with other vascular anomalies (4).

The demographics of the cavernous hemangioma are very similar to that of the capillary hemangioma of infancy except for presentation in older-aged individuals and an almost equal male-to-female ratio (57). Unlike hemangioma of infancy, cavernous hemangioma (venous malformation) grows along with the child and typically shows no evidence of regression with age. Head and neck cavernous hemangiomas predilect to the glottic and subglottic area of the larynx (location for 90% of laryngeal hemangiomas in general), sinonasal and temporal bones, turbinates, and lateral nasal wall (43,58–61), and commonly have a polypoid macroscopic configuration when arising in mucosal sites. Cutaneous cavernous hemangioma appears as a bluish macule or nodule that may blanch and compress when pressure is applied or expand during a Valsalva maneuver. Although deeply seated cavernous hemangiomas are usually asymptomatic, lesions involving the orbital soft tissues may result in dependent exophthalmia and enophthalmia when the patient stands. Oral lesions may cause dental malalignment or impede speech if the tongue is involved. Lesions arising close to the airway are prone to cause obstructive sleep apnea (18). A variant lesion, spindle cell hemangioma (which used to be called ''spindle cell hemangioendothelioma''), has both cavernous hemangioma and kaposiform areas with epithelioid endothelial cells; it can be multiple. It was originally thought that cavernous hemangioma was found in Maffucci syndrome, but we now know that these are spindle cell hemangiomas. Maffucci syndrome thereby has multiple enchondromas, spindle cell hemangiomas, and a variety of mesenchymal and nonmesenchymal neoplasms (62). Multiple cavernous hemangiomas can be found in blue rubber bleb nevus syndrome (autosomal dominant condition characterized by cavernous hemangiomas involving the dermis, gastrointestinal tract, liver, spleen, and central nervous system) (63).

Epithelioid hemangioma presents as multiple reddish-brown nodules, papules, or plaques, sometimes arranged in a tight zosteriform configuration (64). The process occurs primarily in the preauricular area, forehead, occiput scalp, face, and less commonly on the dorsal aspect of hands and feet and in the soft tissues of the trunk and penis (28,29). Epithelioid hemangioma infrequently occurs in oral sites, particularly the tongue and lips (65–68), paranasal sinuses (69), lacrimal gland (70), orbit (71), and inner canthus of the eye (72). The tumor affects both sexes equally and occurs at any age, although most patients are young adults (28,29). The lesion is usually asymptomatic, but tenderness, pruritis, or bleeding can occasionally manifest (15).

Intramuscular angioma is a rare vascular disorder that arises within skeletal muscle. The lesion mostly affects adolescents and young adults and shows no sex predilection. The anatomic distribution of the process is wide, but the lower extremity is the single most commonly affected site, followed by the head and neck, upper limb, and trunk (31). The majority of cases in the head and neck region originate in the masseter muscle, but involvement of the trapezius, sternocleidomastoid, and temporalis muscles and the periorbital muscle group has also been reported (73). The lesion usually presents as a long-standing, slowly enlarging asymptomatic mass. Pain with exercise is sometimes the initial symptom when the lesion is extremity based.

Imaging

Radiographs may demonstrate phleboliths, which are pathognomonic of a hemangioma, in 30% to 50% of cases (most frequent in cavernous lesions) (74). CT and sonography usually reveal the serpentine vascular structures composing cavernous, venous, and arteriovenous lesions. These regions are hypoechoic on sonography, and Doppler evaluation can determine high- or low-flow components. However, in our experience, MR is the optimal imaging modality to both identify and characterize these lesions. The serpentine morphology is typically recognized, and for intramuscular lesions, fat overgrowth or atrophy is also frequent. One or both of these findings are seen in approximately 90% of intramuscular lesions. MR can also distinguish high- and low-flow components. Low-flow regions reveal low signal intensity on T1-weighting and high signal intensity on T2-weighting. In contradiction, high-flow (arteriovenous) lesions show low signal intensity on all pulse sequences. Vascular lesions may be well defined or infiltrative on imaging evaluation (Fig. 9).

While cavernous, venous and arteriovenous hemangiomas or vascular malformations typically reveal pathognomonic imaging features, capillary lesions usually show nonspecific radiologic characteristics of a soft tissue mass. This is a reflection of the small size of the vascular channels and spaces comprising the majority of these lesions. Thus, imaging will detect the lesion extent (for staging) but not reveal characteristic intrinsic features to allow diagnosis in capillary vascular lesions.

Angiography in evaluation of vascular lesions is much less common currently than in the past. MR or CT angiography and Doppler sonography have largely supplanted the use of angiography. Angiography is often limited to being performed during radiologic treatment (embolization or percutaneous) of these lesions as opposed to determining the rapidity of vascular flow (75–78).

Pathology

Hemangioma of infancy (4,7) grossly appears as solid, tan, nonencapsulated nodules that are demarcated from surrounding dermal and subcutaneous tissues. During the proliferative phase of growth, low-power microscopy demonstrates highly cellular lobules arranged in a jigsaw-like pattern and separated by thin fibrous septa (Fig. 10). Occasionally, larger ''feeding'' vessels associated with individual lobules or located at the margin of the process are identified, but these vessels usually do not become apparent until the involution phase of the process. The lobules are composed of cytologically bland, but mitotically active, short spindled cells that, in actuality, are endothelial cells and pericytes forming tightly aggregated capillary structures with poorly developed, inconspicuous lumina (Fig. 10). Mast cells are the chief inflammatory component identified in the cellular lobules.

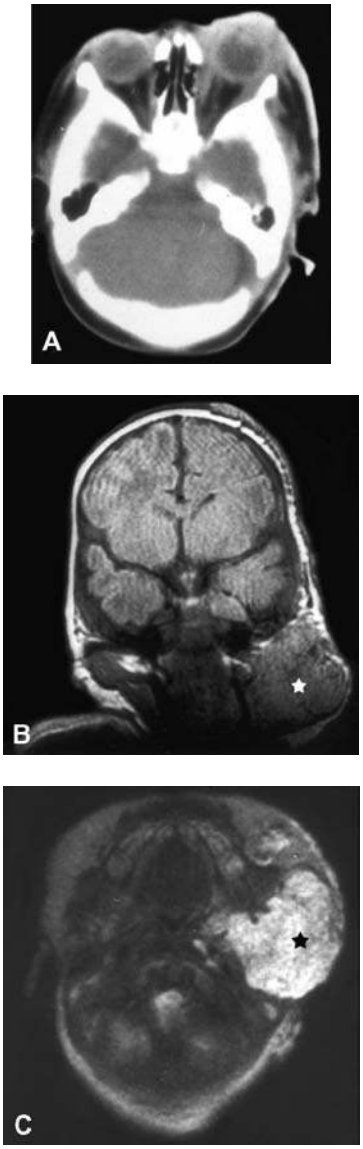

Figure 9 Capillary hemangioma of the face in an infant. CT (**A**), coronal T1-weighted MR (**B**), and axial T2-weighted MR image (**C**) show proptosis caused by a large mass (*). No serpentine vascular structure can be identified because of the capillary histology of this case. There is nonspecific high signal intensity on the T2-weighted MR image.

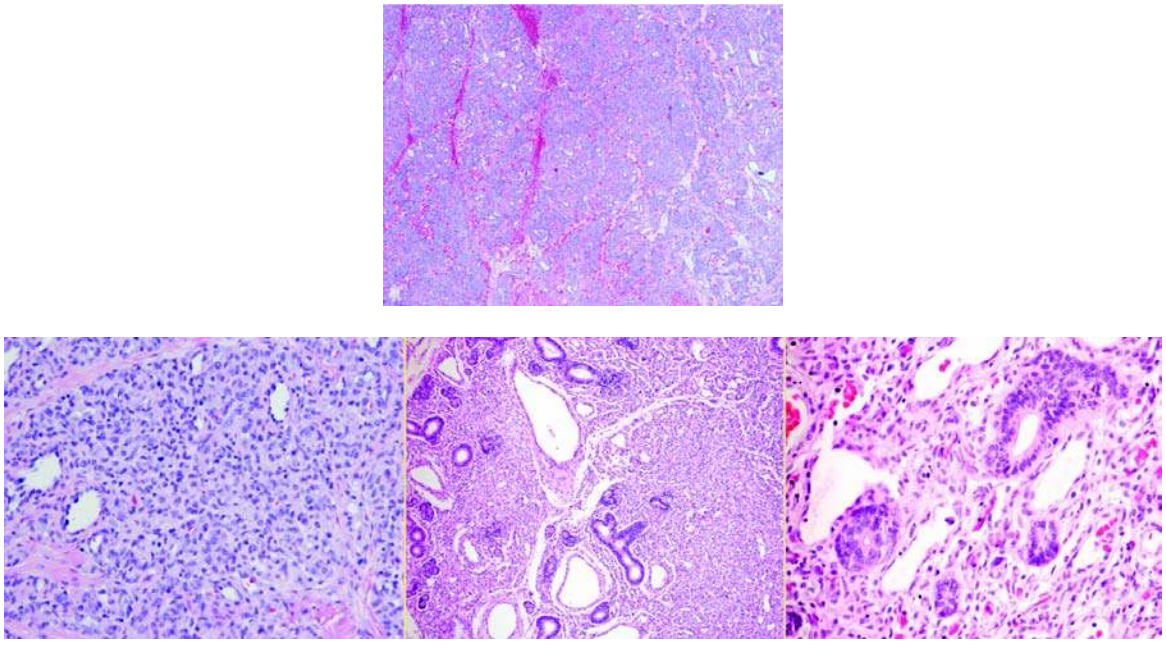

Figure 10 Low-power magnification of hemangioma of infancy demonstrates highly cellular lobules arranged in a jigsaw-like pattern (*top*). In the fully developed lesion, the lobules consist of closely aggregated vessels, most of which are poorly canalized (*bottom left*). When juvenile hemangioma occurs within the salivary gland, here parotid, it retains normal gland ducts (*bottom middle and right*).

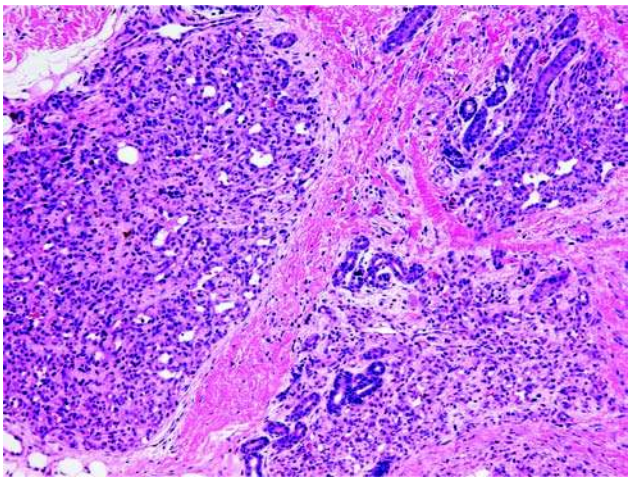

Figure 11 During the involutional stage of the hemangioma of infancy, vascular lumina becomes conspicuous and intralesional fibrous connective tissue more abundant.

With time, vascular differentiation becomes apparent as the lumens of the lesional vessels open (Fig. 11). During involution, a decrease in the number of lesional vessels and increased intralesional fibrosis result in a fibrofatty residuum with scattered capillaries and dilated veins. Ultrastructural analysis of the hemangioma of infancy confirms the presence of immature endothelial cells, pericytes, fibroblasts, and mast cells (7), as well as identifying peculiar crystalline cytoplasmic inclusions within endothelial cells (7,79).

Acquired lobular capillary hemangioma or pyogenic granuloma (4) shares similar histologic features with hemangioma of infancy but differs somewhat by its exophytic growth, surface ulceration, and resultant stromal edema and inflammatory cell infiltration by lymphocytes, plasma cells, histiocytes, and neutrophils (granulation tissue–like changes) (Fig. 12). Once the surface re-epithelializes and the aforementioned secondary changes subside, the capillary proliferation assumes a characteristic lobular architecture and is frequently delineated at its periphery and base by an epithelial ''collarette.'' Eventually, the stroma becomes increasingly more fibrotic and the vessels gradually disappear.

Cherry hemangioma microscopically consists of a well-demarcated, lobular proliferation of well-developed, thin-walled capillaries with small lumina located in the superficial dermis (Fig. 13). When the process is exophytic, the overlying epidermis typically forms a ''collarette'' at the base of the process.

Acquired ''tufted'' angioma (49,50) characteristically appears on low-power magnification as multiple, variably sized, cellular nodules scattered throughout the dermis (Fig. 14). The process is most pronounced in the middle and deep dermis, while the subcutis is usually spared. Each cellular aggregate consists of whorled arrays of cytologically bland endothelial cells and pericytes surrounding poorly canalized, capillary-sized vessels (Fig. 14, middle). The nodules have a tendency to protrude into ectatic, thin-walled vessels resulting in the formation of a cellular tuft

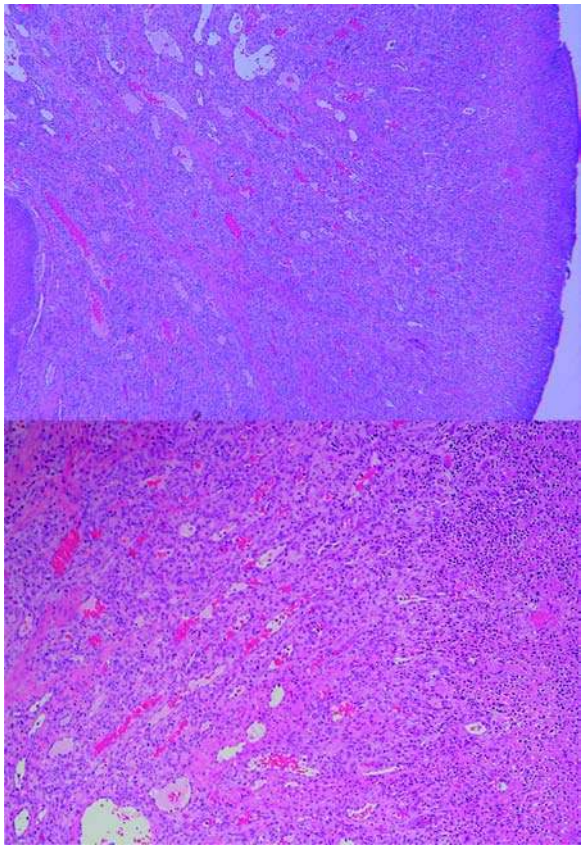

Figure 12 Acquired lobular capillary hemangioma (pyogenic granuloma) is a cellular proliferation of capillary-sized vessels, many of which have inconspicuous lumina, and is associated with an overlying ulcer (*top*) and an inflammatory infiltrate (*bottom*).

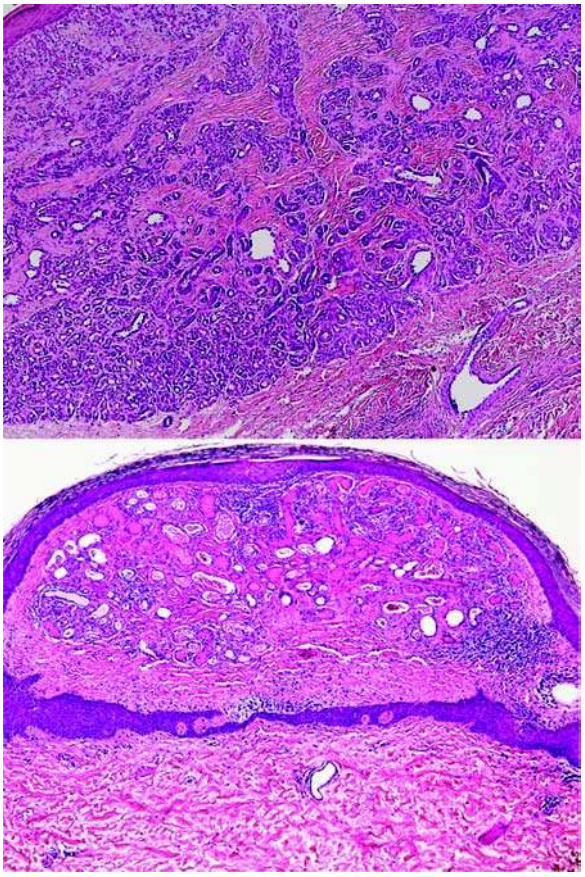

Figure 13 Cherry hemangioma (senile capillary hemangioma) is a lobular capillary vascular proliferation composed of mature vessels with open lumina (*top*). The process is commonly exophytic with epidermal extensions forming a ''collarette'' at its base (*bottom*).

within a crescent-shaped vascular space reminiscent of a kidney glomerulus (Fig. 14). Ultrastructural analysis identifies lesional cells with features of endothelial and pericytic cells. Endothelial cells sometimes have intracytoplasmic crystalloids similar to those identified in hemangioma of infancy (80).

Cavernous hemangioma is a poorly circumscribed nodular to somewhat lobular mass of multiple, dilated vascular spaces that have a thin wall and may be engorged with blood (Fig. 15). Fibrous connective tissue, sometimes with a small amount of interspersed smooth muscle, lines the vessels. Thrombosis of the vascular space is not uncommon, and phlebolith formation resulting from dystrophic calcification of an organized thrombus is a characteristic histologic finding. Chronic inflammatory cells are occasionally scattered throughout the intervening stroma. Abnormally formed vascular structures, including capillaries and/or lymphatic channels, may accompany the lesion.

At low-power magnification, epithelioid hemangioma (22,23,28,29) exhibits a vague lobular arrangement of thin-walled vessels lined by plump (epithelioid) endothelial cells (Fig. 16). In over 50% of cases, a centrally located or peripheral feeder muscular vein or artery exhibiting varying degrees of mural disruption or tumoral vessel involvement is identified (28). Lesional vessels are variably shaped and sometimes have a thin perivascular cuff of myxoid stroma. The epithelioid endothelial cell has an ample amount of eosinophilic, slightly vacuolated cytoplasm and an enlarged, vesicular nucleus harboring a small nucleolus but lacking significant cytologic atypia (Fig. 16, bottom). The cells form a monolayer lining and sometimes exhibit a ''hobnail'' appearance with the nucleus positioned toward the luminal surface of the cell. Only focally do the plump endothelial cells form small tufts or clusters. The inflammatory component of the tumor varies in density and consists of lymphocytes, often forming follicles, and eosinophils. The lymphocytic component of epithelioid hemangioma is an admixture of T- and polyclonal B-cells (4). Sometimes an epithelioid hemangioma can be florid and solid appearing, but still retains pericytes around each vessel (as an intravascular process) and lacks the myxohyaline stroma of epithelioid hemangioendothelioma. Compared with subcutaneous

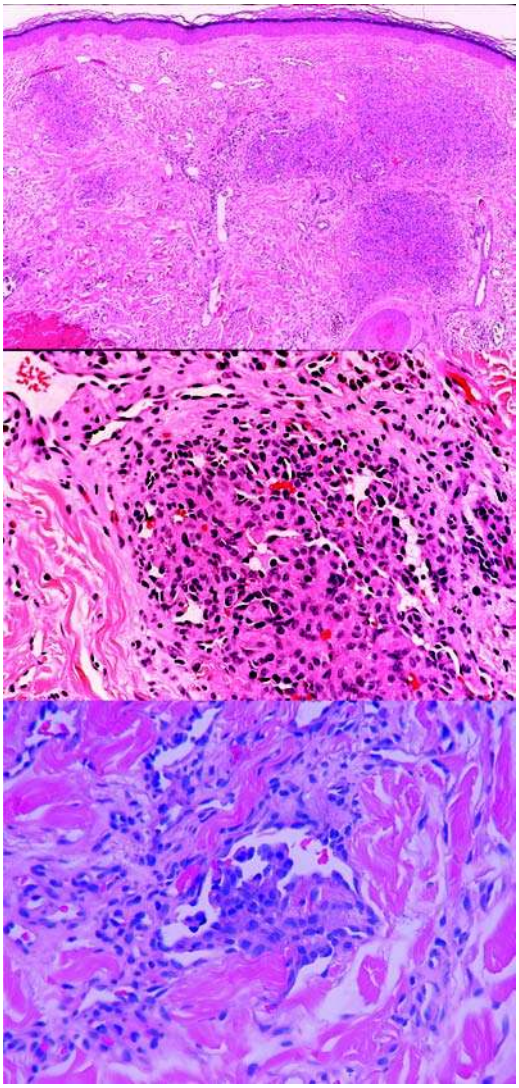

Figure 14 Acquired "tufted" angioma consists of numerous, variably sized cellular nodules localized to the mid to lower dermis (*top*). The cellular lobules are composed of short spindled cells surrounding capillary-sized vessels (*middle*). Protrusion of the cellular tuft into a dilated vascular space is a characteristic feature of the lesion (*bottom*).

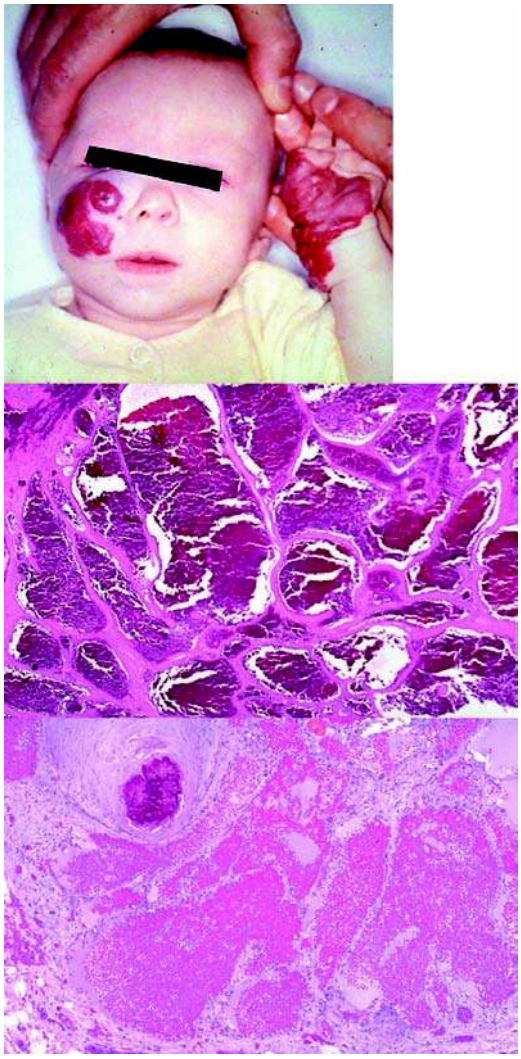

Figure 15 Cavernous hemangioma in infant face and hand. It does not regress and is composed of numerous, dilated, and typically congested thin-walled blood vessels. Thrombosed vessels, calcified phleboliths (*bottom, top left*), and mild chronic inflammation within the stroma (*bottom*) are common findings.

lesions, dermal-based epithelioid hemangiomas are less well circumscribed, exhibit a less intense inflammatory infiltrate, and are composed of vessels formed by a monolayer of endothelial cells with less pronounced epithelioid features.

Macroscopically, the intramuscular angioma (81,82) is an ill-defined intramuscular mass that typically has a variegated yellow and red cut surface owing to the presence of mature adipose tissue and blotchy foci of hemorrhage or vascular engorgement, respectively. Those with bruit or shunt are better classified as an AVM, discussed in a separate section of this chapter. Microscopically, the process exhibits an increased number of vessels within a stroma composed of fibroadipose tissue and fascicles of residual skeletal muscle (Fig. 17). The vascular morphology ranges from thin-walled capillaries, some with dilated lumens, to thick-walled muscular veins. Vessels showing morphologic features of lymphatic channels are variably present. In actuality, most cases show an admixture of these various vessels. The vessels are observed infiltrating and entrapping skeletal muscle and proliferating within adipose tissue that probably develops as a result of long-standing skeletal muscle atrophy. Less commonly, the tumor is composed primarily of capillaries, sometimes exhibiting a distinct lobular growth pattern, reminiscent of hemangioma of infancy. One report claims that 68% of head and neck intramuscular angiomas are of this capillary-predominant subtype (73). Vascular thrombosis, phlebolith formation, and stromal ossification are

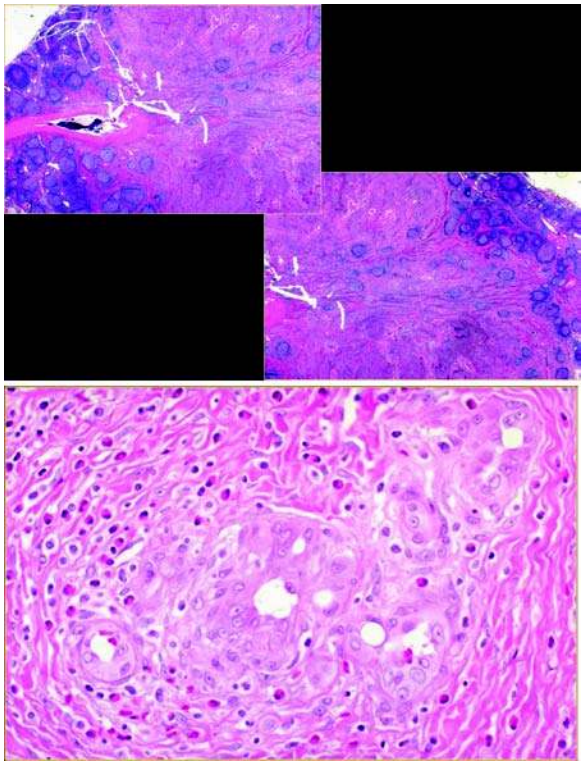

Figure 16 Low-power magnification of the epithelioid hemangioma shows a vague lobular arrangement of capillary-sized vessels and a chronic inflammatory cell infiltrate replete with lymphoid follicles. The whole lesion resembles a lymph node with a feeder vessel, usually artery (*top*). The bottom picture reveals the epithelioid or hobnail endothelial cells, some with primitive cytoplasmic lumen formation, surrounded by stroma with scattered eosinophils.

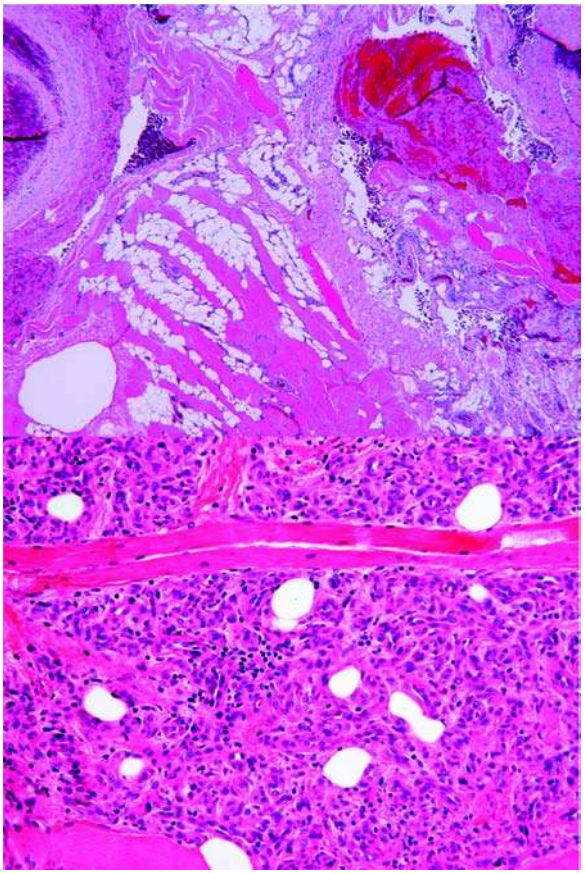

Figure 17 Vessels of the intramuscular angioma (mixed vessels) proliferate amidst fascicles of skeletal muscle and deposits of adipose tissue. A thrombosed vessel and a phlebolith are also identified. Portion of intramuscular angioma composed of capillaries with poorly developed lumina reminiscent of hemangioma of infancy (*bottom*).

additional histologic features observed in the intramuscular angioma.

Immunohistochemistry

In general, endothelial cells that line vascular structures in all these lesions show reactivity with commonly used endothelial-related antibodies including anti-factor VIII–related antigen, CD31, CD34, and anti–Ulex europeus. Muscle-specific and α-SMA highlight supporting smooth muscle cells and myopericytes.

More specifically, the lesional cells of hemangioma of infancy in all stages of development characteristically express glucose transporter protein isoform 1 (GLUT-1) (83). Additionally, WT-1 immunohistochemical expression has been reported in a limited number of infantile and acquired capillary hemangiomas but not in vascular malformations (84). Endothelial cells composing the glomerular-like structures in acquired ''tufted'' hemangioma react weakly with antibodies against factor VIII–related antigen and Ulex europeus but strongly express CD31 and CD34. α-Smooth muscle actin expression in the cellular tufts indicates a component of myopericytes (49,50).

In all benign vascular lesions, there are still pericytes around the endothelial-lined vessel, which will be positive for SMA (smooth muscle actin). Once the endothelial cell has ''invaded'' outside of vessel wall, the diagnosis of hemangioendothelioma or angiosarcoma is considered (lacking SMA-positive pericytes).

Differential Diagnosis

Three surgical pathology specimens unique to the head and neck have the potential for misdiagnosis as benign vascular tumors. First, the muscular, patulous veins located in the connective tissue of the turbinates, particularly the congested posterior turbinate vessels, constitute normal erectile tissue and should not be confused with a benign vascular tumor. Second, the vocal cord nodule occasionally harbors ectatic thin-walled vessels (telangiectatic variant) that can lead to an incorrect diagnosis of hemangioma. Recognition of this histologic variant of vocal cord nodule should allow for proper classification. Thirdly, antrochoanal polyps of the maxillary antrum

may have ectatic vessels that can mimic a hemangioma or AF (85).

Hemangioma of infancy needs separation from the cavernous hemangioma as a significant proportion of the latter are venous malformations that do not resolve spontaneously and require medical intervention. Clinically, the cavernous hemangioma does not have the striking crimson red appearance of the fully developed hemangioma of infancy. The dilated, engorged vessels lined by mitotically inactive endothelial cells of the cavernous hemangioma contrast sharply with the cellular, mitotically active hemangioma of infancy. However, the cavernous hemangioma may have overlapping microscopic features with the involuting hemangioma of infancy. Immunohistochemical expression of GLUT-1 supports the diagnosis of hemangioma of infancy (83,86).

In contrast to the hemangioma of infancy, the acquired lobular capillary hemangioma presents in an older-aged population. Microscopically, the stroma of the acquired lobular capillary hemangioma, especially early in its evolution, exhibits more edema and a greater inflammatory cell infiltrate than observed in the infantile hemangioma. Immunohistochemically, the acquired lobular capillary hemangioma is reported not to express GLUT-1 (83,87).

Hemangioma of infancy and acquired lobular capillary hemangioma must be differentiated from certain vascular malformations, particularly the nevus flammeus (''port wine stain''), which is a component of the Cobb, Sturge-Weber, and Klippel-Trenaunay-Weber syndromes and solitary angiokeratoma (12,15). Clinically, nevus flammeus presents at birth as a large, red macular lesion. In the Sturge-Weber syndrome, the lesion follows the distribution of the ophthalmic branch of the trigeminal nerve. Microscopically, nevus flammeus, unlike capillary hemangioma, is composed of widely dilated, well-developed, thin-walled vessels scattered throughout the dermis. Angiokeratoma appears as a small, dark-colored papule and can present almost anywhere including the oral cavity. Angiokeratoma consists of dilated capillary structures, some of which are thrombosed, that abut the epidermis. Both nevus flammeus and angiokeratoma lack the cellularity and lobular growth pattern of the infantile and acquired capillary hemangioma. WT-1 with and without GLUT-1 immunoexpression would support the diagnosis of infantile and acquired capillary hemangioma, respectively (83,84,86).

Granulation tissue, a common tissue response to trauma, is sometimes confused with the acquired lobular capillary hemangioma, especially in the larynx and trachea (88). In contrast to lobular arrangement of closely grouped, poorly canalized, rounded vessels of the lobular capillary hemangioma, granulation tissue is not organized in a lobular arrangement and its vessels are more elongated and typically oriented perpendicular to the mucosal surface.

Infantile variant of HPC, like hemangioma of infancy, presents early in life and commonly occurs in superficial soft tissue as a cellular, multilobular mass. This lesion is presently considered part of the morphologic spectrum of infantile myofibroma, (89) and accordingly, one may find fascicles or nodules of spindled myofibroblastic cells at least focally within the tumor. Strong GLUT-1 or diffuse SMA immunoexpression would favor the diagnosis of hemangioma of infancy or infantile HPC, respectively.

Clinically, the acquired ''tufted'' angioma enters into the differential diagnosis of hemangioma of infancy as it occasionally presents shortly after birth. However, in contrast to the vague lobular architecture of the proliferating infantile hemangioma, the acquired ''tufted'' angioma grows as distinct cellular nodules randomly scattered throughout the dermis. Characteristically, the lesional tissue protrudes into an open vascular space. The ''tufted'' angioma has the potential to mimic cutaneous angiosarcoma or Kaposi's sarcoma because of the presence of haphazardly distributed cellular nodules that simulate infiltrative growth. However, unlike the cutaneous angiosarcoma and Kaposi's sarcoma, the acquired ''tufted'' angioma presents at a much younger age and is not associated with sun damage or HIV infection, respectively. Histologically, the acquired ''tufted'' angioma lacks the growth pattern of anastomosing vascular channels dissecting through the dermis and the cytologic atypia that characterizes the aforementioned vascular malignancies.

Kaposiform hemangioendothelioma (90,91), a vascular neoplasm with low malignant potential, shares with the acquired ''tufted'' angioma a tendency to present in young children, an association with Kasabach–Merritt syndrome (92), and overlapping morphologic features. Salient microscopic differences between kaposiform hemangioendothelioma and acquired ''tufted'' angioma include fascicular growth of spindled cells with intervening slit-like spaces, presence of eosinophilic hyaline globules within the spindled element, and the infiltrative growth of ill-defined tumor nodules in the former entity.

Glomeruloid hemangioma (93), like the acquired ''tufted'' angioma, exhibits hypercellularity and a multinodular growth pattern, but demonstrates salient clinical and microscopic differences. The former is a reactive endothelial proliferation that occurs in the POEMS syndrome (*p*olyneuropathy, *o*rganomegaly, *e*ndocrinopathy, *m*onoclonal gammopathy, and *s*kin changes). Microscopically, the glomeruloid hemangioma is an intravascular proliferation of capillary-like structures lined by cytologically bland endothelial cells. Surrounding these capillaries are enlarged cells of purported endothelial cell origin that characteristically harbor PAS-positive and diastase-resistant eosinophilic globules of polyclonal immunoglobulin proteins.

Epithelioid hemangioma is differentiated from Kimura's disease by both clinical and pathologic features (22–25). Clinically, Kimura's disease usually affects young Asian males in contrast to the former that shows no sex, race, or age preference. Patients with Kimura's disease manifest lymphadenopathy, a peripheral eosinophilia, and elevated serum IgE, whereas individuals with epithelioid hemangioma do not exhibit lymphadenopathy, and only about

10% have peripheral eosinophilia. The tumoral masses of Kimura's disease are located in subcutaneous tissue, lymph nodes, and salivary gland tissue, whereas the papulonodular eruptions of epithelioid hemangioma are localized to subcutaneous or dermal tissues, sometimes with local extension into lymph node. Microscopically, the lesions of Kimura's disease have a higher concentration of lymphoid follicles and a larger number of eosinophils that form microabscesses, populate the interfollicular areas, and penetrate lymphoid follicles (folliculolysis) than observed in epithelioid hemangioma. Importantly, the numerous vessels identified in the interfollicular regions of the disorder lack the plump epithelioid endothelial cells that typify epithelioid hemangioma. Epithelioid hemangioma can be separated from epithelioid hemangioendothelioma by a proliferation of vessels, still retaining a pericyte around the endothelial cells, indicating that this is not an extravascular proliferation, as in epithelioid hemangioendothelioma. Even when florid epithelioid hemangioma will still have SMA-positive pericytes around endothelial cells, SMA will be absent in epithelioid hemangioendothelioma. Furthermore, the myxohyaline stroma of epithelioid hemangioendothelioma is notably absent in epithelioid hemangioendothelioma.

Intramuscular angioma resembles angiomatosis of soft tissue (94) by virtue of its composition by capillary and venous structures. However, angiomatosis rarely involves the head and neck and, by definition, affects a large segment of the body or multiple tissue planes (including bone) unlike the more restricted growth of intramuscular hemangioma. The presence of large, irregularly contoured veins harboring capillaries within their walls is a characteristic feature of angiomatosis.

Prognosis and Treatment

Juvenile hemangioma or infantile hemangioma (4) typically involutes during the first decade of life. Therefore, unless complications such as ulceration, obstruction of the visual fields, auditory canal, or airway intervene or undue psychologic stress develops, the patient is usually observed without medical intervention. However, as 40% to 50% of patients have residual cosmetically unappealing fibrofatty tissue, telangiectasias, or scars after involution of the hemangioma, treatment is sometimes offered at an earlier stage (95). Corticosteroids (topical and intralesional for small lesions and systemic administration for larger, more problematic hemangiomas) are usually the first line of medical therapy as this modality has a high success rate with a clinical response noted in about 90% of individuals with capillary hemangiomas (96). Laser therapy has also proven successful in treating ulcerated hemangiomas and persistent telangiectasias following involution (18). However, this technique does not seem to have any greater effect on reducing the growth of the lesion (97). α-Interferon therapy is reserved for those lesions unresponsive to steroids or requiring rapid involution because of life-threatening complications. Although it has shown a response rate of 48% (98), complications, particularly severe neurologic sequelae, hamper its use in children as the first treatment of choice (95). The acquired lobular capillary hemangioma (pyogenic granuloma) is best managed with curettage, shave excision, or laser therapy (18).

Management of the acquired ''tufted'' angioma is many times complicated by the size of the lesion. At present, no single modality is completely effective. Systemic corticosteroid administration and α-interferon have been reported to induce shrinkage of the lesions (99,100). The life-threatening complication of Kasabach–Merritt syndrome is best managed with systemic therapy, including corticosteroids, α-interferon, and vincristine (101).

Cavernous hemangioma usually does not recur after complete excision. However, in head and neck locations, a complete surgical excision may be difficult to achieve. Presently, sclerotherapy, elastic compression, surgery, and a combination approach are the mainstays of treatment (18).

Epithelioid hemangioma has a local recurrence rate of about 33% (29), which has been explained by the persistence of the underlying pathogenetic abnormality (e.g., AVM) or by the fact that the lesion may truly be a neoplastic disorder. Nevertheless, a complete (local) surgical excision is the treatment of choice for this lesion (19), if it can be achieved. These can sometimes be quite extensive and florid in head and neck locations and may locally involve a lymph node.

Intramuscular angioma has an appreciable local recurrence rate of between 30% and 50% and shows no tendency for spontaneous regression. Composition of intralesional vessels or location of the process does not seem to influence the recurrence rate, but adequacy of initial excision does (82). Therefore, wide (local) excision is the treatment of choice for the management of such lesions. Sclerotherapy, cryotherapy, and radiation have been used along with surgery for large, problematic lesions (102).

D. Lymphangioma

Introduction

The lymphangioma is a benign, localized mass of closely aggregated, dilated lymphatic channels. When occurring in the superficial dermis or submucosa, the anomaly is referred to as lymphangioma circumscriptum, whereas the term ''cavernous lymphangioma'' is used for a proliferation of large, cystically dilated lymphatic spaces. The cavernous subtype of lymphangioma with grossly visible lymphatic spaces is also known as cystic lymphangioma or cystic hygroma. The morphologic features of the above-mentioned variants of lymphangioma form a continuum and show considerable overlap. Therefore, any given lesion should be named after the predominant histologic component. In general, lymphangiomas are less commonly encountered in practice than hemangiomas.

The lymphangioma is believed to result from maldevelopment of the lymphatic system of vessels.

The exact pathogenesis of the disorder is not completely understood. Proposed causes for its development include failure of the lymphatic system to connect with the parent venous system, abnormal sequestration of lymphatic tissue, or lymphatic obstruction due to trauma, infection, or inflammation (1). Recent data demonstrating elevated levels of angiogenic-inducing factors, basic fibroblast growth factor and vascular endothelial growth factor-C, and low expression of angiogenesis inhibitors, thrombospondin-1 and pigment epithelial-derived factor, in the tumor (2–4) indicate that an imbalance in angiogenic and angiostatic mediators plays a role in the pathogenesis of the disorder.

Two additional lesions exhibiting lymphatic differentiation will be included in this discussion. The acquired progressive lymphangioma, also known as benign lymphangioendothelioma, is a benign, slow-growing, probably neoplastic process that involves the dermis and subcutis. Lymphangiomatosis is defined as a diffuse proliferation of lymphatic vessels that characteristically involves multiple tissue planes in one region of the body, including skin, soft tissue, bone, and parenchymal organs. The widespread tissue involvement by lymphangiomatosis has generated a number of alternative names for the disorder, including generalized lymphangioma, systemic cystic angiomatosis, and multiple lymphangiectasias.

Clinical and Molecular Features

Cavernous and cystic lymphangiomas (5–7) mostly present at birth or within the first two years of life, but occasionally come to clinical attention in the adult years. The sex incidence is roughly equal. Cystic lymphangioma (hygroma) develops mainly in the neck, axilla, and groin, where pliable connective tissue allows for expansion of the lesion. The cavernous subtype occurs in areas with a more restricted anatomy such as the oral cavity (particularly tongue, but also lips, mouth, and buccal region), upper trunk, limbs, and in abdominal sites.

In the fetus, cystic lymphangioma is one of a handfull of tumoral processes that can cause polyhydramnios. These lesions usually occur in the neck or axilla. Antenatal US examination in women presenting with polyhydramnios allows for early detection of the cystic lymphangioma. Such lesions identified at the time of antenatal US are frequently associated with chromosomal abnormalities (62%) including Turner syndrome (XO), trisomy 21, trisomy 18, trisomy 13, and certain nonchromosomal abnormalities such as Noonan's syndrome (8,9). Hence, chromosomal analysis of the fetus by amniocentesis or aspiration of cystic fluid contents is recommended. The presence of hydrops fetalis in this clinical setting is associated with a particularly dismal prognosis (10).

In contrast, patients diagnosed with the lesion after 30 weeks of gestation or at birth usually have a better prognosis (9). Postnatal lymphangiomas of the neck region usually arise in the posterior triangle of the neck or, less often, in the anterior triangle (beneath the angle of the jaw). Since the process has the potential to extend into the axilla, pectoral region, or mediastinum, radiologic evaluation is necessary to appreciate the full extent of the lesion. Other head and neck locations for the origin of the lymphangioma include the cheeks, lips, nose, parotid, larynx, and oral cavity, where the anterior aspect of the dorsal tongue is the most commonly affected location (6).

Clinically, patients typically present with a painless, spongy mass, which is fluctuant on palpation. Large cervicofacial lesions that involve bone have a strong tendency to cause skeletal abnormalities including skeletal hypertrophy (11) or result in feeding or airway problems. Sudden enlargement of an otherwise asymptomatic lymphangioma from infection or hemorrhage can result in rapid respiratory compromise (12). Epiglottic edema has been reported with oropharangeal lesions (13).

Lymphangioma circumscriptum (14–17) is the most common form of lymphangioma. The process presents at birth or within the first five years of life as numerous small vesicles that aggregate to form a plaque often with a verrucous surface. Lesions can be small and solitary (localized form) or large and multiple (classical form). Intralesional hemorrhage results in a violaceous appearance of the otherwise light tan to pink vesicles. The process shows a wide anatomic distribution but predilects to axillary folds, shoulders, neck, proximal extremities, tongue, and oral mucosa. Eyelids and conjunctiva are also occasionally involved (18). In rare cases, the process is associated with cavernous lymphangiomas of the mediastinum, Becker's nevus, or the Maffuci or Cobb syndrome (17).

Progressive lymphangioma (benign lymphangioendothelioma) (19,20) is a rare lymphatic-derived process that primarily affects middle-aged or older adults. The lesion presents as a slow-growing, well-demarcated dermal plaque with a pink to violaceous color. The condition most commonly arises in the extremities, but sites of involvement are diverse and include the head and neck region and oral mucosa.

Lymphangiomatosis (17,21,22) is a rare disorder with onset during the first two decades of life. Lesions occur primarily in the skin and soft tissues of the neck, trunk, and extremities. However, visceral organs, especially lungs, spleen, and liver, bones, mediastinum, and retroperitoneum are simultaneously involved in many cases. Cutaneous and soft tissue lesions appear as asymptomatic, soft, fluctuant masses, whereas visceral and osseous lesions present with symptoms referable to the particular organ or structure involved.

Imaging

US evaluation is usually the first modality employed to evaluate a lymphangioma in the antenatal setting (23,24). Lymphangiomas are typically anechoic cystic masses with thin septations. Debris and hypoechogenicity may be seen if the lesion is complicated by hemorrhage or infection. MR imaging and CT compliment the standard US examination by further evaluating the extent of the lesion. This is particularly

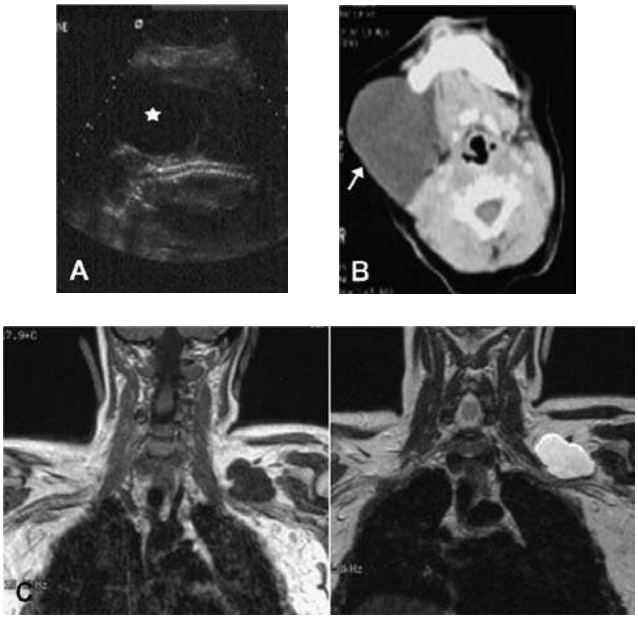

Figure 18 Three different lymphangiomas on sonography (**A**), CT (**B**), and MR images (**C**). Intrauterine sonography (**A**) shows a large anechoic neck mass (*) with septations that led to fetal demise. CT (**B**) reveals a low attenuation mass (*arrow*). MR images (**C**) demonstrate a low signal intensity mass (*arrowheads*) on T1-weighting (*left image*) and homogeneous high signal intensity on T2-weighting (*right image*). *Abbreviations*: CT, computerized tomography; MR, magnetic resonance.

important with cystic lymphangiomas of the neck because of their potential to extend into the mediastinum and compromise the airway (25,26). The MR signature of lymphangioma is that of a multiseptated cystic mass isotense to cerebrospinal fluid on both T1- and T2-weighted images. T1-weighted MR images may reveal foci of high signal intensity in up to 25% of cases reflecting hemorrhage or the fat content of chylous fluid (27). MR imaging is also an excellent technique for evaluating the lymphangioma circumscriptum (28). Both MR and CT imaging techniques as well as lymphangiography have been used to determine the extent of disease in lymphangiomatosis (24). In this disorder, radiologic evaluation of bone is crucial as lytic lesions are detected in nearly 50% of cases (Fig. 18) (29).

Pathology

Cavernous lymphangiomas are soft, compressible masses composed of thin-walled, variably sized cystic spaces filled with clear or hemorrhagic fluid. Macroscopically, visible cysts define the cystic lymphangioma (hygroma). Microscopically, the variably sized spaces have irregular, jagged contours and contain proteinaceous lymph fluid admixed with lymphocytes and a variable number of red blood cells (Fig. 19). The endothelial cells bordering the spaces are cytologically bland and form an attenuated lining (Fig. 20). The

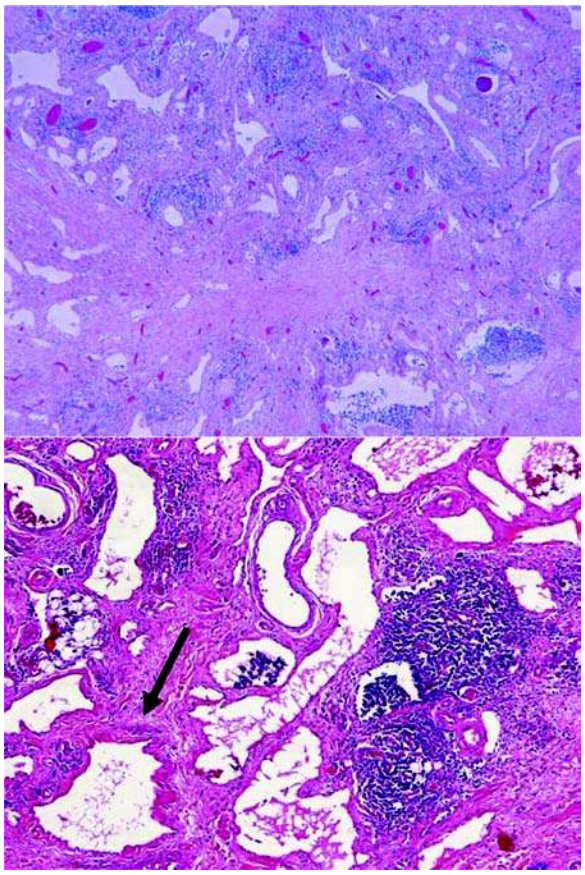

Figure 19 Cavernous lymphangioma consists of lymphatic spaces of variable size and shape. Irregularly contoured vessels contain proteinaceous fluid. A thin smooth muscle wall surrounds some of the lesional vessels (*arrow*). Lymphoid aggregates are noted in the surrounding connective tissue.

walls of the cavernous lymphatic channels are generally thin, but may have a discontinuous layer of smooth muscle (Fig. 18, bottom). Lymphatic channels possessing a thickened muscular layer may be observed in some large and deep-seated tumors (Fig. 21).

The associated stroma is collagenous and typically contains scattered aggregates of lymphocytes. In long-standing lesions subject to obstruction or infection, the inflammatory component and stromal fibrosis become more pronounced.

Lymphangioma circumscriptum (15) exhibits identical histologic features to the more deeply located cavernous/cystic lymphangioma, with the exception of its smaller size. The subepidermal component of the lesion consists of dilated lymphatic channels, which form vesicles (Fig. 22). In the classical variant, these superficial lymphatics are fed by subcutaneous lymphatic cisterns with muscular walls (15). The overlying epidermis is usually acanthotic with a hyperkeratotic surface.

The progressive lymphangioma (benign lymphangioendothelioma) (19,20) is characterized by

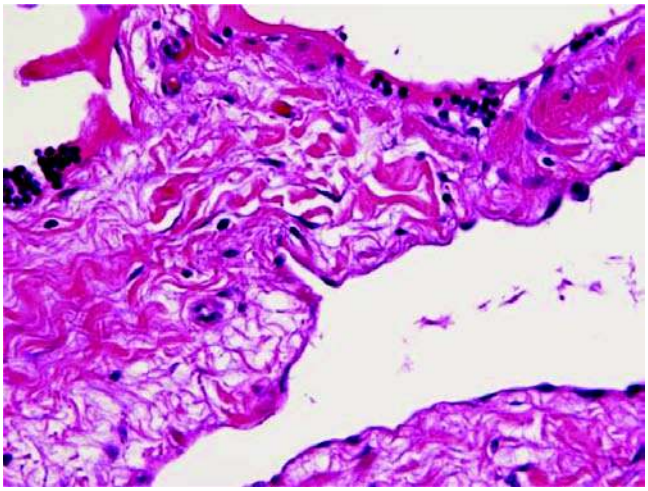

Figure 20 Lymphatic spaces have an attenuated lining of cytologically benign endothelial cells. Lymphocytes admixed with proteinaceous fluid are focally attached to the wall of a lymphatic space (*above*).

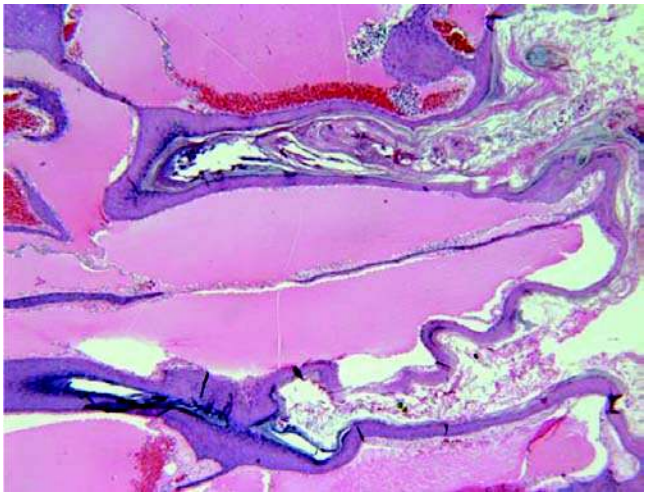

Figure 22 Cutaneous lymphangioma (lymphangioma circumscripta) consists of markedly dilated subepidermal lymphatic channels.

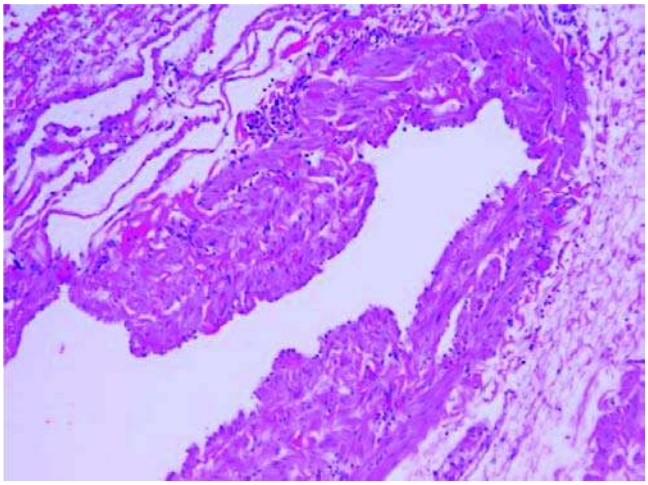

Figure 21 Lymphatic channels with a thick muscular wall are identified in large and typically deeply located cystic lymphangiomas.

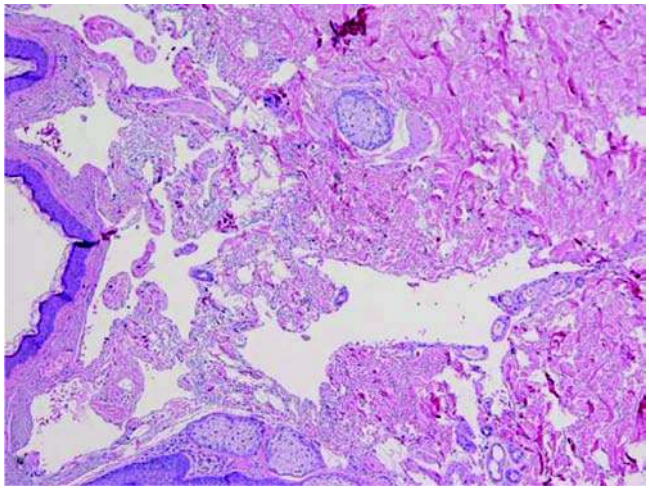

Figure 23 Progressive lymphangioma (benign lymphagioendothelioma). Lesional lymphatic vessels within the superficial dermis are irregularly contoured and dissect around adnexal structures.

dilated, irregularly contoured lymphatic spaces that infiltrate the deep dermis (Fig. 23). The spaces surround preexisting vascular and adnexal structures and demonstrate a dissecting pattern of growth through dermal collagen. As the lesional vessels extend into the deep dermis, they have a tendency to become more narrow and cleft-like. The endothelial cells are relatively more hyperchromatic and more numerous than in typical lymphangioma, but do not proliferate in multiple layers or show conspicuous cytologic atypia or mitotic activity.

Lymphangiomatosis (17,21,22) demonstrates a diffuse proliferation of numerous, predominantly empty lymphatic channels that dissect through soft tissue and sequester remnants of involved dermis, subcutis, and skeletal muscle (Fig. 24). Spaces are lined by attenuated and cytologically bland endothelial cells. Lymphoid tissue and focal deposits of hemosiderin are found in the surrounding tissues. The lesion has a reported association with kaposiform hemangioendothelioma (30).

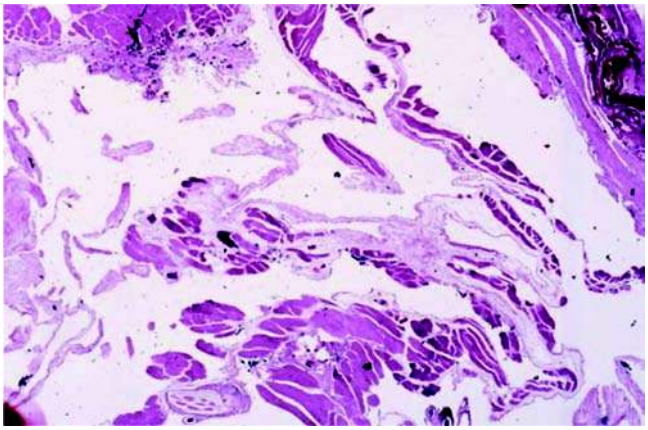

Figure 24 Lymphangiomatosis. Infiltrating lymphatic channels are dissecting around and isolating connective tissue islands composed of skeletal muscle, fibrous connective tissue, and peripheral nerve.

Immunohistochemistry

The widely used immunomarkers for endothelial cells, anti-factor VIII–related antigen, CD34, CD31, and anti–Ulex europeus, will decorate endothelial cells of lymphatic vessels, although the strength and frequency of reactivity may be less than what is observed in hemangiomatous lesions (31,32). A set of new endothelial cell markers, D2-40 (antibody directed against podoplanin) and the antibodies to the homeobox transcription factor Prox1, have shown promise in more selectively highlighting lesional cells of lymphatic tumors (33–35). Vascular endothelial growth factor receptor-3, although a sensitive marker for lymphatic-derived lesions, is also expressed in a significant minority of hemangiomas (36).

Electron Microscopy

Lymphatic vessels are ultrastructurally similar to blood vessels but differ in that they generally lack pericytes and a basal lamina (or are enveloped by a fragmented basal lamina), and the endothelia possess anchoring filaments (31). However, larger-caliber lymphatic channels may have a pericytic or smooth muscle element.

Differential Diagnosis

In the head and neck, the cystic/cavernous lymphangioma may clinically and histologically resemble the cavernous hemangioma. Radiologically, the cavernous hemangioma characteristically demonstrates phlebolith formation (calcified organized thrombi). Microscopically, the cavernous hemangioma typically lacks the lymphoid component and prominent smooth muscle investiture observed in some lymphangiomas. Moreover, the vascular spaces of cavernous hemangioma are engorged with blood or harbor thrombi (with or without dystrophic calcium).

In contrast to the cavernous/cystic lymphangioma, lymphangiomatosis is not a localized process and commonly involves bone and viscera. The extensive soft tissue and visceral involvement of lymphangiomatosis is similar to that observed in angiomatosis. However, angiomatosis (37) rarely involves the head and neck region. Microscopically, the lesional vessels of the latter do not have the infiltrative, dissecting growth pattern that typifies lymphangiomatosis and include large, irregularly contoured veins that harbor capillaries within their walls.

The major diagnostic concern with progressive lymphangioma is not to misclassify the lesion as a low-grade angiosarcoma or Kaposi's sarcoma because of its worrisome growth pattern. Angiosarcoma, in contrast to progressive lymphangioma, exhibits convincing cytologic atypia manifesting as larger cell size, nuclear hyperchromasia with abnormal chromatin patterning, multilayer growth including cellular intraluminal papillary projections, and a more complex architecture. The lesional vessels of Kaposi's sarcoma are typically smaller than those of progressive lymphangioma and tend to grow parallel to the epidermal surface. The endothelial cells exhibit mild to moderate cytologic atypia. Additional histologic features that characterize Kaposi's sarcoma include an associated spindled cell proliferation, intracellular hyaline globules, stromal plasma cells, and deposits of hemosiderin.

The ectatic vessels identified in the superficial dermis in cases of ''hobnail'' hemangioma (targetoid hemosiderotic hemangioma) (38) resemble some of the lesional vessels of progressive lymphangioma and could potentially lead to a misdiagnosis. However, the former entity features protuberant ''hobnail'' endothelial cells, and the lesional vessels within the deeper portions of the dermis are much smaller than those of progressive lymphangioma. Recent immunohistochemical evidence indicates that the ''hobnail'' hemangioma may in fact be of lymphatic origin as the cells react with anti-vascular endothelial growth factor receptor-3 and D2-40 (39,40).

Prognosis and Treatment

The cavernous lymphangioma grows at a variable rate. Complete spontaneous regression of the tumor was reported in 41% of cases and partial involution occurred in an additional 29% of patients by five years of age in one study (41). Traditionally, cavernous/cystic lymphangiomas were managed by surgical excision if no involution was noted by five years of age. Prognosis of head and neck lymphangiomas significantly depends on the stage and location of the lesion. Tumors arising in suprahyoid sites exhibit a lower rate of recurrence after surgery and a higher incidence of postoperative complications than infrahyoid lesions (9,41–45). Surgical excision of large cervicofacial lymphangiomas is complicated by facial nerve injury, infection, airway compromise, and dental caries (7). Patients with diagnosed antenatal cystic lymphangiomas resulting in airway obstruction should undergo a Cesarean section as early as possible

to avoid spontaneous labor, yet late enough to allow pulmonary maturation (46).

Alternative methods of treatment include sclerotherapy. Sclerosants commonly used for this purpose include pure ethanol and OK-432 (a biologic preparation of lyophilized powder containing *Streptococcus pyogenes* Su stain and benzylpenicillin potassium) (1). OK-432 sclerotherapy is less effective when lymphangiomas occur outside head and neck, are larger than 5 cm, or are composed primarily of microcystic spaces (47–49).

The lymphangioma circumscriptum is usually treated with surgical excision and recurs only when the deep lymphatic cisterns that ''feed'' the superficial component are not completely excised (Whimster's hypothesis) (15). Intralesional sclerotherapy coupled with limited surgical excision more effectively addresses the long-term cosmetic aspect of treating this disorder.

Surgical excision is the treatment of choice for progressive lymphangioma as local recurrence after excision is rare. Successful treatment with systemic corticosteroids has also been reported (50,51). A few cases of spontaneous regression of the lesion have been documented.

Lymphangiomatosis involving the chest and mediastinum is associated with extensive bony and visceral involvement and has a poor prognosis with high mortality (21). Surgical excision has a limited role in this condition apart from relieving symptomatology. Sclerotherapy, along with limited surgery, has been employed in some cases (52). Systemic administration of chemotherapeutic agents or α-interferon has also been tried for patients with inoperative disease with limited success (53,54).

E. Glomus Tumor

Introduction

Glomus bodies aid in body temperature regulation by functioning as an arteriovenous shunt. They consist of fibrous encapsulated vascular structures and are found in the distal digits, especially the nail beds (1). They are present at birth but do not become fully developed until early adulthood, atrophying by age 60 (1). Glomus tumor is a modified smooth muscle tumor, resembling the cells of a normal glomus body, are considered to arise in a perivascular location, and are of pericytic phenotype by immunohistochemistry (2–8). They have no clinical, histologic, or immunophenotypic resemblance to paragangliomas, which are sometimes referred to as glomus tumors. Malignant glomus tumor can occur but is exceedingly rare (9–15).

Clinical findings

Glomus tumors are rare but may be multiple in 10% of cases (16). Most glomus tumors occur in young adults, but any age may be involved, about 7% in children, some even congenital (2). These have an equal sex distribution, except subungual glomus tumors, which are more common in females (17,18). Glomus tumors generally occur in the dermis or subcutis and are found in head and neck locations in about 6% to 8% of cases (19,20), including nerve, nasal cavity (21–24), trachea (23,25–28), buccal mucosa, hard palate, gingival, tongue, lip (29), oropharynx (30,31), periodontal tissue (32), auricle (20,23,33), temporomandibular meniscus (34), and eyelid (23,35,36). Glomus tumors notoriously cause pain (2,37). The malignant glomus tumors are generally deep seated and may be painless or have symptoms associated with the organ they involve.

Radiologic Imaging

Glomus tumors typically show intermediate signal on T1 weighting and prominent high signal intensity on T2-weighted MR images. Intense enhancement may be seen following intravenous contrast administration on CT and MR imaging reflecting the vascular nature of these lesions. Doppler sonography may also demonstrate a high degree of vascularity within these lesions (38–40).

Pathologic Findings

Grossly, the typical glomus tumor is a small blue-red nodule, less than 1 cm. Histologically, glomus tumors are composed of poorly delineated nests and groups of ovoid fried egg–appearing cells with vaguely distinct cytoplasmic borders (Fig. 25). There is scant eosinophilic cytoplasm and absence of mitotic activity, atypia, or necrosis. Rarely, the tumor cells can look oncocytic or epithelioid (41,42). The stroma may be myxoid or hyalinized (Fig. 26). The cells are seen surrounding capillary-sized vessels. When a glomus tumor has enlarged vessels, it is termed ''glomangioma''(Fig. 27); associated also with spindled smooth muscle cells, transitioning from the ovoid glomus cells, it can be called ''glomangiomyoma'' (Fig. 28). Glomangiomyomatosis is extremely rare and is diagnosed by its involvement of at least three tissue planes, like angiomatosis (Fig. 29) (12,43). Symplastic glomus tumor is the term given to tumors that have striking nuclear atypia, thought to be a degenerative change, without any evidence for increased mitotic activity, deep location, large size, or necrosis. These latter features describe glomus tumors of uncertain malignant potential (Fig. 30). For the diagnosis of malignancy, glomus tumors must be greater than 2 cm and subfascial or visceral in location, have atypical mitoses, that is, show marked nuclear atypia and mitotic activity (Fig. 31). Malignant glomus tumor usually has a peripheral rim of benign glomus tumor.

Electron Microscopy

Each cell is surrounded by basal lamina and has pinocytotic vesicles and intracytoplasmic actin microfilaments (44,45).

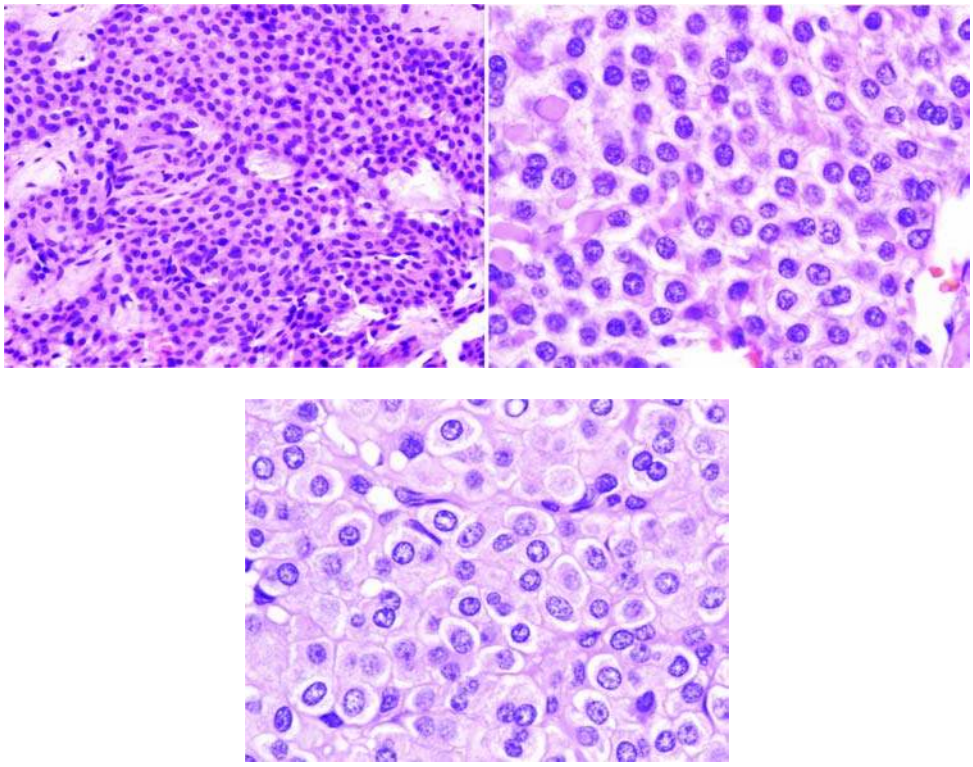

Figure 25 Glomus tumor is characterized by a uniform epithelioid sheeted population of cells that can have distinctive cytoplasmic borders, giving a "fried egg" appearance.

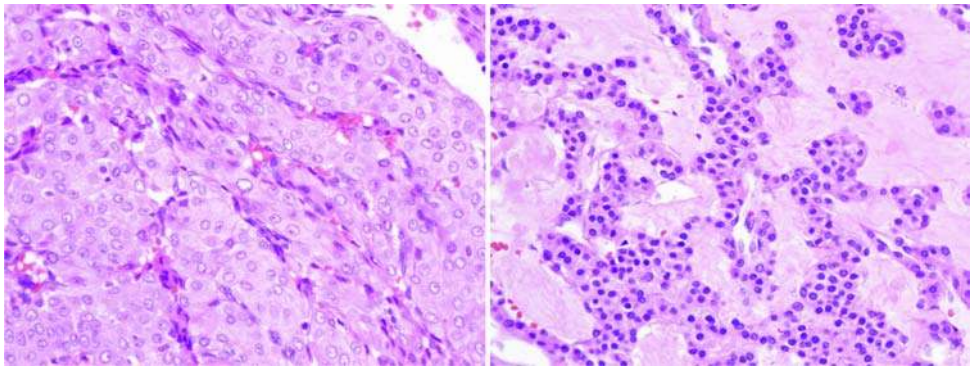

Figure 26 Occasionally, glomus can have a myopericytic appearance or a trabecular pattern of cells in a fibroid stroma. These tumors mimic eccrine spiradenoma but are keratin negative.

Immunohistochemistry

Glomus tumors are positive for SMA (Fig. 32), MSA, and collagen IV, and negative for desmin, CD34, S100 protein, synaptophysin, chromogranin, and keratin (13,46,47).

Molecular Findings

The genetic changes underlying sporadic glomus tumors are not known. However, families with multiple glomus have been reported. Although controversy exists, an autosomal dominant inheritance with incomplete penetrance and variable expressivity have been suggested (16,48,49).

Differential Diagnosis

Glomus tumor is often confused histologically with eccrine spiradenoma, an eccrine tumor that can be separated from glomus by its two-cell population and keratin reactivity (50). Other considerations may

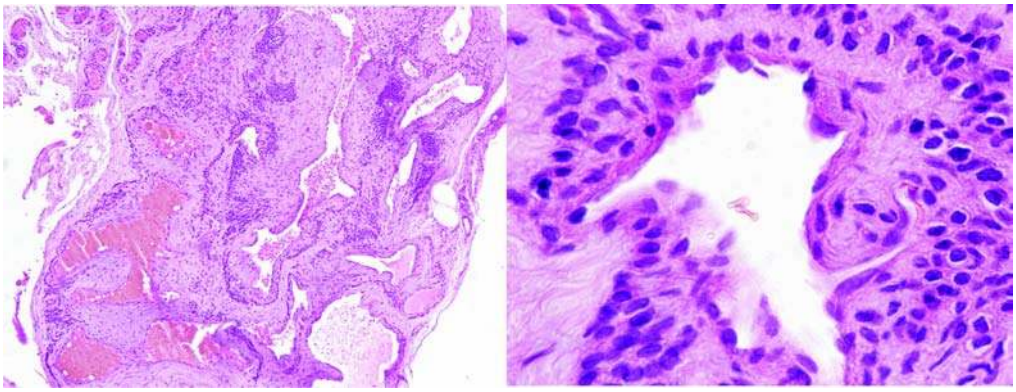

Figure 27 Glomangioma has glomus cells and dilated vessels. The glomus cells surround the vessels.

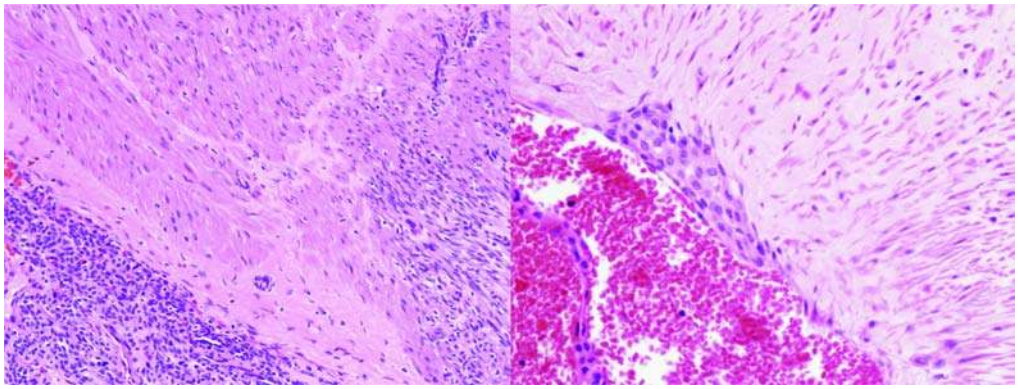

Figure 28 Glomangiomyoma shows three components: glomus cells, dilated vessels, and a smooth muscle proliferation.

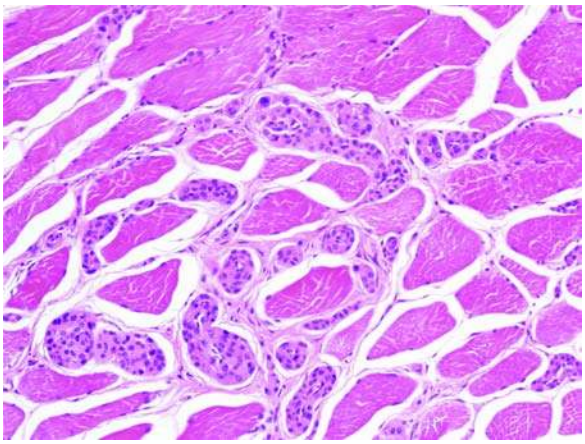

Figure 29 Glomangomatosis is seen here infiltrating skeletal muscle.

include HPC, a CD34-positive tumor, negative in glomus tumor. Myoepithelioma would be more epithelioid and have glial fibrillary acidic protein (GFAP), keratins, and S100 protein positivity, which are absent in glomus tumor. Nevi can be distinguished from glomus tumors by their S100 protein and HMB45 reactivity.

Prognosis and Treatment

Glomus tumors are generally benign, except those with uncertain malignant behavior or with truly malignant features. The latter is highly aggressive with metastasis in up to 40% of cases, resulting in patient death (9). For benign glomus tumors, excision to decrease clinical pain may be done, but recurrence is low, less than 10%. Multiple glomus tumors or glomangiomyomatosis may be left alone, once diagnosed, since they may be difficult to surgically eradicate and often do not recur.

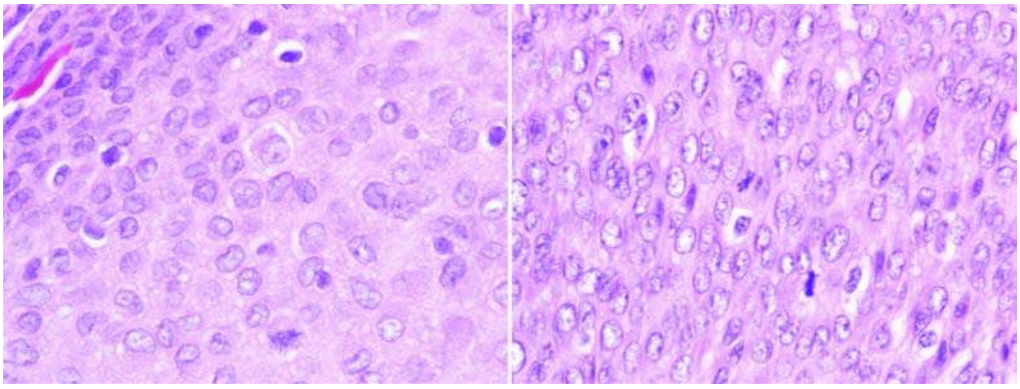

Figure 30 Atypical or uncertain potential glomus tumor has increased mitotic activity but not marked atypia. There is a peripheral cuff of "benign glomus" (left picture, *top left*).

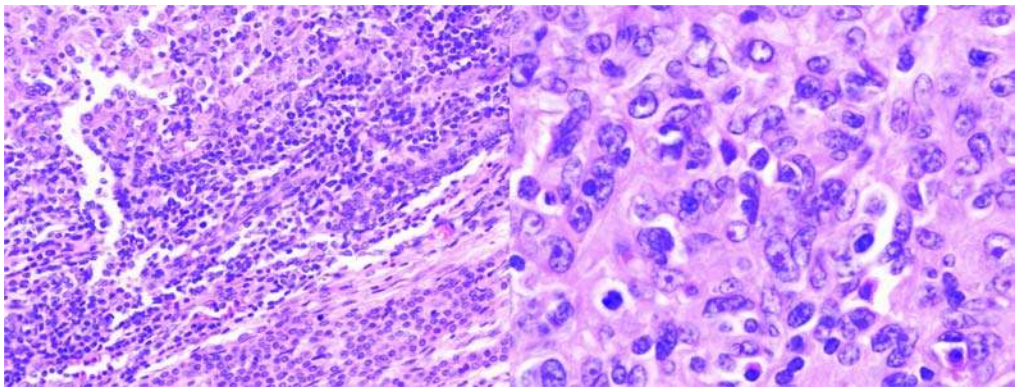

Figure 31 Malignant glomus tumor often has benign glomus tumor at its periphery (left picture, *bottom right*) and at higher magnification demonstrates marked nuclear enlargement, prominent nucleoli, and increased mitotic activity. This generally occurs in tumors that are deep and greater than 2 cm.

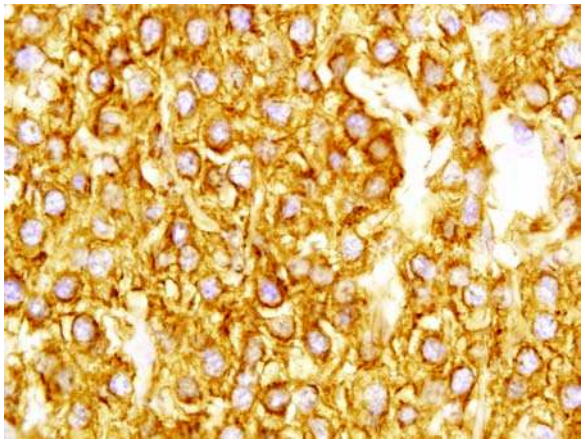

Figure 32 Smooth muscle actin (*above*) and muscle-specific actin are almost always positive in glomus tumors. They are also usually CD34 (variable) and desmin negative.

III. BENIGN SKELETAL AND SMOOTH MUSCLE LESIONS AND TUMORS

A. Focal Myositis

Definition

Focal myositis is often misunderstood because it presents as a mass simulating a tumor but acts more like an inflammatory process of skeletal muscle. Not only in the setting of focal myositis, inflammation can also involve muscle in many other disorders including infection, soft tissue tumors, and systemic inflammatory muscle diseases such as polymyositis. Focal myositis is a specific clinicopathologic entity, distinguishable from other muscle inflammatory disorders and other soft tissue tumors. First characterized by Heffner et al., focal myositis is a rare, benign pseudotumor of skeletal muscle, whose etiology is speculated but unknown (1,2).

Clinical Features

Patients with focal myositis present with an enlarging painful mass within a single muscle or muscle group. It affects men and women equally, and in a literature review of 100 cases, 6% of patients were less than 14 years of age; 80% were between 15 and 64 years of age; and 13% were over 65 years of age (3). Minimal systemic symptoms are generally the rule, although fever has been reported (4) According to a review by Yanmaz Alnigenis et al., patients present with constitutional symptoms in only 11% of cases (3).

The most common site of involvement is within muscles of the lower extremities, particularly the thigh. Although much less common in the head and neck, it has been described in the suprahyoid (5), digastric, temporal (6), and mylohyoid muscles (7,8), tongue (8–12), as well as in the esophagus (13), eyelids (14), and underneath the buccal mucosa. The most common site in the head and neck is the sternocleidomastoid muscle (2,4,15–19).

The etiology of focal myositis is still unknown. Viruses have been implicated, but no organisms have been identified. Patients do not present with trauma and no genetic link has been found.

Laboratory Studies

Initially, reports showed that white blood cell count, C-reactive protein, erythrocyte sedimentation rates, and serum creatine phosphate were normal. Subsequent studies have shown that these tests may be elevated, although most commonly, the elevations are mild (16,17). Yanmaz Alnigenis et al. reported ESR elevation in 25% and CPK increases in 24% of cases (3).

Pathology

Focal myositis presents as a poorly circumscribed pale to tan mass, which does not involve the subcutaneous tissue, fascia, or tendon. In Heffner's first description, lesional size ranged from 2 to 10 cm (1).

Under microscopic examination, the muscle fibers show variable morphology. Striated skeletal muscle fibers vary in size and shape with hypertrophic fibers intermingled with round to angular atrophic myofibers. The locations of the different sized and shaped muscle fibers are randomly distributed rather than grouped. Myofiber necrosis is usually patchy and often accompanied by phagocytosis. In addition, regenerating muscle fibers characterized by large vesicular nuclei, conspicuous nucleoli, and basophilic cytoplasm are often noted (7,19).

Lesions typically contain multifocal inflammatory infiltrates involving the perimysium with variable involvement of the endomysium (16). The inflammatory cells usually form aggregates or sheets, mostly composed of lymphocytes, but may also contain plasma cells, histiocytes, small numbers of eosinophils and neutrophils (Figs. 33–35). These infiltrates are associated with interstitial and perimysial fibrosis. Chronic lesions exhibit more fibrosis. Frank vasculitis is not found.

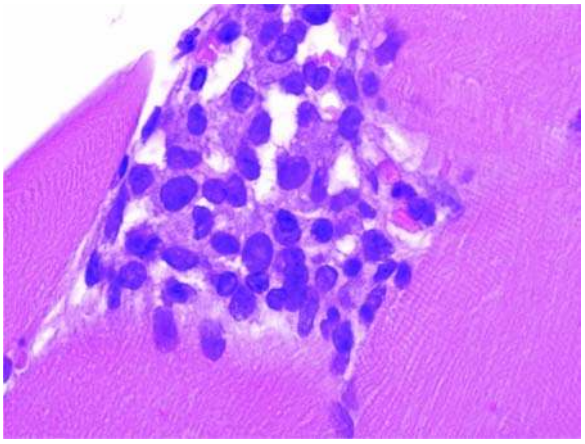

Figure 33 100× focus of inflammatory cells around skeletal muscle fibers.

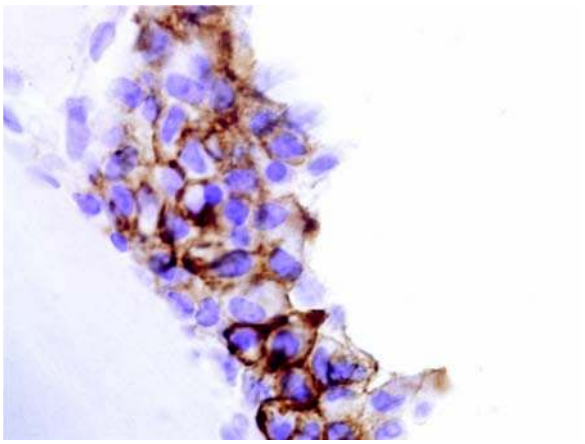

Figure 34 100× CD45. Highlights the clusters of hematopoietic cells, which are a mixture of B and T cells on further immunohistochemistry.

Nerves also appear to be affected that, according to Heffner, causes secondary denervation atrophy. Endoneurial fibrosis is often prominent, destroying nerve fibers (20). Axons may be demyelinated, swollen, or lost entirely. Many of these changes are best seen by electron microscopy.

Immunohistochemistry

Special stains and immunohistochemistry can be used to better assess the amount of fibrosis and to determine which types of inflammatory cells are present. Interstitial fibrosis is best seen with the Masson-Trichrome stain. Lymphocytes are mostly helper T cells expressing CD3 and CD4 as well as other T-cell markers. Small numbers of B cells will react with B-cell markers such as CD20. Scattered histiocytes mark with CD68. Infection should be excluded with

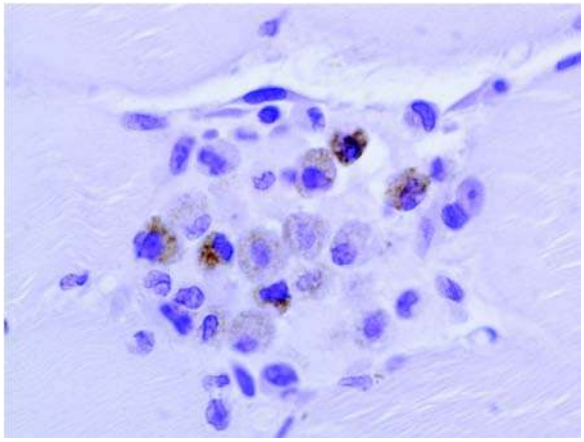

Figure 35 100× CD68. Highlights scattered histiocytes in another focus of inflammation.

the usual panel of special stains such as Brown and Brenn, Grocott methenamine silver, and Ziehl-Neelson.

Radiologic Imagery

There is only very limited radiologic literature of the imaging of focal myositis. CT and MR imaging are nonspecific with a soft tissue mass that may involve one or multiple muscle groups. There may be extensive surrounding edema suggesting an inflammatory as opposed to a neoplastic etiology (21).

Differential Diagnosis

Most commonly, focal myositis should be differentiated from inflammatory myopathies such as polymyositis and from other benign soft tissue lesions. Unlike focal myositis, polymyositis usually diffusely involves all muscles of the skeletal system and is, therefore, often easy to differentiate clinically. Histologically, the two lesions are indistinguishable. Rarely, polymyositis can present as a solitary mass mimicking focal myositis (22). High serum muscle enzyme levels and constitutional symptoms of fever and arthralgias would favor polymyositis over focal myositis.

Myositis ossificans, proliferative myositis, and nodular fasciitis are the three soft tissue proliferations most often confused with focal myositis. Unlike these soft tissue lesions, focal myositis is localized to muscle and does not involve subcutaneous tissue, fascia, or tendons. Histologically, these soft tissue lesions are distinct from focal myositis.

Focal myositis does not show the tissue culture like myofibroblasts and myxoid degeneration, mitotic rate, or fascial base that are characteristic of nodular fasciitis. Proliferative myositis is the equivalent of proliferative fasciitis, which is found in muscle. Focal myositis can be differentiated from proliferative myositis because focal myositis lacks ganglion cell–like myofibroblasts and stellate growth pattern of proliferative myositis. These ganglion-like cells of proliferative myositis usually have eccentric nuclei, prominent nucleoli, and basophilic cytoplasm. Occasionally, the regenerative myofibers of focal myositis may be mistaken for the ganglion-like cells of proliferative myositis, but myofibers are positive for desmin and the ganglion cell–like myofibroblasts are negative for desmin. Myositis ossificans differs from focal myositis in that it usually follows trauma and contains a zonal primarily intramembranous ossification, occasionally endochondral ossification, not found in focal myositis.

Treatment and Prognosis

Most often a muscle biopsy is required to establish diagnosis. Fine-needle aspirates are usually not diagnostic and should not be performed for this entity. Most lesions are self limited and will spontaneously regress (4). Therefore, excision of the mass is not necessary (23). Relapses do occur and have been documented in approximately 18% of cases in the literature (3).

B. Rhabdomyoma

Introduction

Rhabdomyomas display skeletal muscle differentiation and have a strong predilection for occurrence in the head and neck. These are distinctly uncommon tumors, representing only about 2% of all skeletal muscle tumors (1). There has been controversy as to whether these tumors represent neoplasms or hamartomas, however, current evidence, including cytogenetic confirmation of clonality and an association with disruptions of the hedgehog signaling pathway, tends to favor the former interpretation (2–4). Three histologic variants affecting the head and neck are recognized: the fetal, intermediate fetal or juvenile, and adult subtypes, any of which may be diagnosed at any patient age, but the first two are most common in young patients and the latter in adults. Collectively, the tumors of the head and neck are sometimes referred to as extracardiac rhabdomyomas to distinguish them from the tuberous sclerosis–associated cardiac rhabdomyomas of the heart. A third group of rhabdomyomas are particular to the genital region.

Clinical Features

Fetal rhabdomyomas (FRMs) present clinically as either nondescript masses of the affected site or polypoid exophytic masses. FRMs of the head and neck display a distinct male predilection of two or three to one over female patients. Despite their nomenclature, which is based on morphologic features, FRMs occur over a broad age range, from infancy to the seventh decade. The mean age at diagnosis varies between studies, but has been reported as 4.5 and 20 years of age, respectively, in separate series of cases. About half the patients are over age 15 at the time of diagnosis (5,6). Head and neck FRMs involve a wide variety of mucosal, subcutaneous, or soft tissue throughout the

Table 2 Distribution of 48 Head and Neck Fetal and Juvenile Rhabdomyomas

Site	Number of cases
Postauricular	10
Facial skin	7
Preauricular	1
Eyebrow	1
Inner canthus	1
Temple	1
Cheek	1
Nose	1
Jaw	1
Tongue	6
Neck	5
Larynx	5
Nasopharynx	5
Orbit	3
Buccal region	3
Occipital (skin)	1
Soft palate	1
Parotid	1
Parapharyngeal	1

Source: From Refs. 5, 6, and 8.

Table 3 Distribution of 64 Head and Neck Adult Rhabdomyomas

Site	Number of cases
Oral cavity	38
Floor of mouth	22
Tongue[a]	10
Soft palate	7
Palate	1
Buccal mucosa	2
Lip	1
Neck NOS[b]	11
Larynx	3
Pharynx	4
Nasopharynx	2
Face	1

[a]Includes two ''large'' base of tongue cases, extending to pharynx/larynx.
[b]Not otherwise specified.
Source: From Refs. 13–16

region, with a strong predilection for the postauricular soft tissues (Table 2) (5,7). In contrast, direct involvement of the major salivary glands is distinctly uncommon. A small portion of FRMs arise in patients with nevoid basal cell carcinoma syndrome (3,9–11). As with the FRM, the *juvenile rhabdomyoma* (JRM, intermediate FRM) is roughly twice as common in male patients as in female patients and affects a similar range of mucosal and soft tissue sites of the face. The JRM is diagnosed in somewhat older patients than the classic FRM, from adolescents through the eighth decade, but rarely in infants (5,8,12). Again, a solitary mass is the typical clinical finding. *Adult rhabdomyomas* (ARMs) display an even stronger male predilection, occurring at least three times more often in male patients. Although cases do arise in infants and children, clinically, ARMs are tumors of adults. The mean age at diagnosis is 55 to 60 years, with cases reported in the ninth decade (13,14). The majority of ARMs involve mucosal and submucosal sites in the upper aerodigestive tract, including the oral cavity, pharynx, and larynx (Table 3). Soft tissue presentation is almost always in the neck, and a few cases have been reported in the nasopharynx. Within the oral cavity, the floor of the mouth is the most common location, followed by the tongue and soft palate. The presenting sign is characteristically a nonspecific mass lesion in the affected area. Identification of the mass may be preceded by complaints of hoarseness or airway obstruction. Duration of the lesions prior to diagnosis ranges from a few weeks to several years. In contrast to the solitary presentation of FRM and JRM, a significant portion of ARMs are either multinodular or multifocal tumors, which may be synchronous or asynchronous in presentation (6,7,14,17–20). ARMs are also virtually never associated with a phacomatosis.

Imaging

CT and MR imaging are valuable adjuncts in the diagnosis and preoperative evaluation of rhabdomyomas. CT imaging reveals well-demarcated, circumscribed soft tissue mass lesion, particularly with contrast enhancement (Fig. 36). In the absence of contrast, isodense lesions may blend into adjacent skeletal muscle, falsely suggesting infiltrative growth (21). T1- and T2-weighted MR images reveal mildly hyperdense lesional tissue relative to adjacent skeletal muscle, and again, demarcation from surrounding tissues is evident. Signal intensity is homogenous across the lesion, and there may be mild enhancement with gadolinium (22,23). The multinodular or multifocal nature of ARM may be more readily apparent with such studies.

Pathology

Grossly, FRMs are circumscribed, pink, tan, red, or gray-white masses with a glistening, sometimes mucoid-appearing cut surface (1,5). They average 4 to 5 cm in diameter, but can be as large as 12 cm (5).

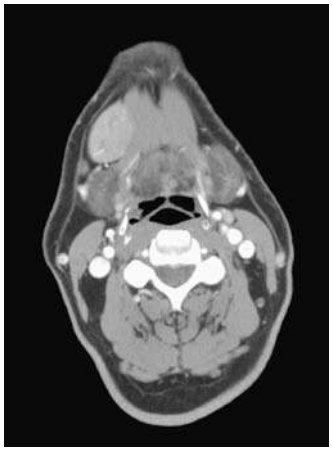

Figure 36 Axial computerized tomography of adult rhabdomyoma in the left floor of mouth demonstrates a well-circumscribed mass anterior to the submandibular gland.

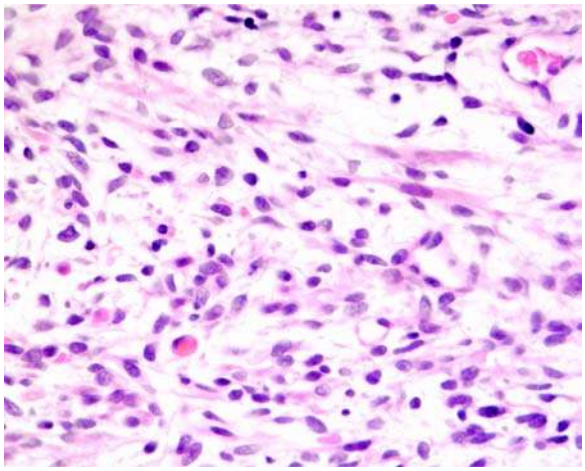

Figure 37 In the fetal rhabdomyoma, primitive mesenchymal cells are haphazardly arranged and admixed with occasional elongated cells and rhabdomyoblasts. Background is distinctly myxoid.

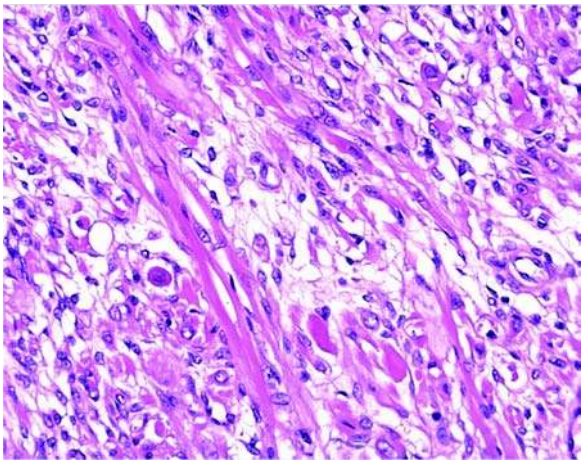

Figure 38 Juvenile rhabdomyoma demonstrates increased cellularity relative to classic fetal rhabdomyoma and displays a range of skeletal muscle differentiation varying from primitive mesenchymal cells to rhabdomyoblasts and elongated strap cells with cross striations.

Histologically, circumscription, but not encapsulation, is evident. The FRMs are composed of round to oval or spindled primitive undifferentiated mesenchymal cells. The primitive cells have hyperchromatic, sometimes angulated nuclei and minimal wispy cytoplasm. They are admixed with elongated, eosinophilic, immature skeletal muscle cells with bland nuclei, finely granular chromatin, and inconspicuous nuclei. These latter cells have narrow, tapered cytoplasmic processes with occasional cross striations and recapitulate the myotubule stage of skeletal muscle development. They are arranged into short, somewhat haphazard fascicular bundles. This admixture of cells is set in a distinctly myxoid stroma (Fig. 37). The tumors can exhibit a degree of maturation and increased cellularity at the periphery. Mitoses are generally not identified, although examples with measurable mitotic activity have been described. Nuclear atypia, increased mitotic activity, atypical mitoses, or necrosis are not features of FRMs, and their presence should raise concerns of a rhabdomyosarcoma.

The JRM, which has been histologically referred to as the cellular form of FRM, displays a significantly greater spectrum of skeletal muscle differentiation than its myxoid counterpart. Undifferentiated or primitive mesenchymal cells are present but may be inconspicuous among the abundant strap cells, round to ovoid cells, and ganglion-like rhabdomyoblasts. The strap cells may be arranged into interlacing fascicles or in a patternless fashion. These cells have abundant eosinophilic to basophilic to amphophilic cytoplasm of varying staining intensity, and glycogen accumulation can result in vacuole formation (Fig. 38). Cross striations and features of skeletal muscle differentiation in at least a portion of the more mature cells leaves little doubt of a skeletal muscle phenotype. JRMs are not circumscribed and blend into adjacent tissues, including skeletal muscle, sometime making identification of a clear margin impossible. Mitotic activity is typically limited, but some tumors contain scattered, normal mitotic figures.

ARMs are characteristically lobulated or multinodular red-brown masses on gross examination. They tend to be soft or compressible in texture. Their mean size is approximately 3 cm, but they may reach 8 or 9 cm in diameter. Microscopically, circumscription, but not encapsulation, is evident, and the tumors are composed of lobules of large polygonal cells arranged in sheets without intervening stroma. These large cells contain voluminous eosinophilic cytoplasm that may be fibrillar, granular, or display peripheral vacuolation. Exaggeration of this latter feature, due to cytoplasmic glycogen accumulation, results in the characteristic ''spider'' cell (Fig. 39). Other cytoplasmic features include irregular deposits of eosinophilic crystalline material and occasional cells with cross striations. The round to oval nuclei are either central or peripheral, with vesicular chromatin and, frequently, prominent nucleoli.

Immunohistochemistry

As would be expected, the three rhabdomyoma subtypes consistently express markers associated with skeletal muscle differentiation including muscle-specific actin, desmin, and myoglobin (5,14,15,16, 24–26). Desmin reactivity is particularly strong (Fig. 40). Although relatively few cases have been evaluated, expression of nuclear myogenin (especially skeletal muscle–specific myf4) and myo-D1 also appears to be consistent in rhabdomyomas (4,24,27). Some SMA reactivity is present in the majority of rhabdomyomas, but staining is generally more intense and uniform in the FRM. Similar results are seen with vimentin and S-100 protein stains: more uniform, intense staining in a greater percentage of FRMs

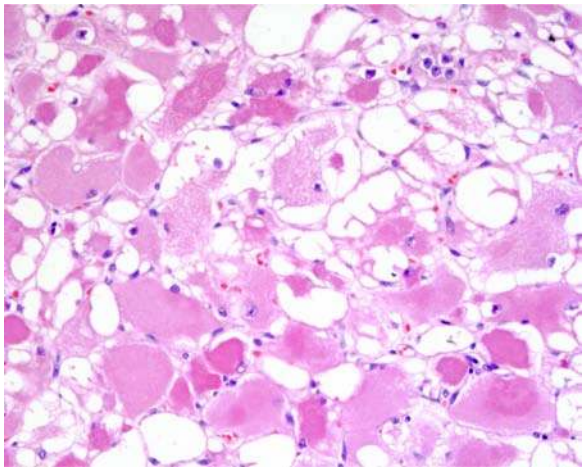

Figure 39 Characteristic microscopic appearance of adult rhabdomyoma. The tumor is composed of large polygonal cells with abundant eosinophilic cytoplasm. Prominent nuclei are evident, and many cells demonstrate peripheral cytoplasmic vacuoles, imparting a web-like appearance.

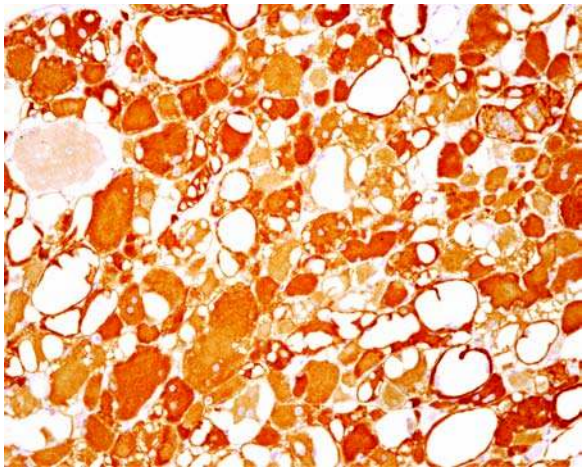

Figure 40 Strong, uniform desmin immunoreactivity is typical of adult rhabdomyoma.

than in the adult type. GFAP highlights the undifferentiated mesenchymal component in about half the cases of FRM, but fails to stain ARM. CD56 and CD57 reactivity in a minority of tumor cells has also been described (5,14,28).

Molecular Findings

Little is known about cytogenetic changes in parapharyngeal rhabdomyoma. In one case, a reciprocal translocation between chromosomes 15 and 17 has been identified as the sole abnormality. Also, a minor clone was characterized by abnormalities of the long arm of chromosome 10 (2).

Electron Microscopy

While electron microscopy currently has a limited role in the diagnosis of rhabdomyomas, ultrastructural examination does demonstrate skeletal muscle differentiation in the form of myofilaments, myofibrils, and sarcomeric formations (5,21,29). Haphazard clusters of hypertrophic Z-bands correspond to the cytoplasmic crystalline material that is sometimes seen on light microscopic examination. Additional ultrastructural features include abundant mitochondria and glycogen deposits (15,21,25,28).

Differential Diagnosis

Distinguishing FRM from embryonal rhabdomyosarcoma, particularly the botryoid variant, is the most clinically significant differential diagnostic concern. FRMs lack significant nuclear or cellular pleomorphism, mitoses, or geographic necrosis, although a few examples display scattered mitotic figures or perhaps focal ischemic necrosis. Additionally, FRMs tend to be circumscribed, lack an infiltrative growth pattern, and exhibit skeletal muscle maturation at the periphery. In contrast, embryonal rhabdomyosarcomas display cytomorphologic hallmarks of malignancy, including tumor cell necrosis, atypia, and prominent mitotic activity (28,30). Clinically, FRM and embryonal rhabdomyosarcoma have a predilection for the head and neck, but skeletal muscle tumors located in the subcutaneous tissues of the postauricular region are almost invariably FRM. The very rare neuromuscular hamartoma, a benign entity, sometimes contains primitive spindle cells like the FRM, but the presence of nerve fibers and nodular growth is usually sufficient to distinguish it from FRM (28). Separation of JRM from spindle cell rhabdomyosarcoma variants may also be problematic since both entities share similar morphologic features and mitotic rates. The margins of these tumors may be infiltrative, however, as with FRM, tumor cell necrosis and cellular pleomorphism are not features of JRM. Cautious evaluation is warranted before a definitive diagnosis is rendered. The adult spindle cell rhabdomyosarcoma variant is a morphologically high-grade tumor that also affects the head and neck. In addition to malignant spindle cells, these tumors often display sclerosing or pseudovascular growth patterns as a minor component. These latter features are not present in JRM.

Because of their distinctive histologic appearance with readily apparent skeletal muscle differentiation, ARMs rarely present a diagnostic problem. Occasionally, other tumors with large polygonal cells and abundant cytoplasm, including granular cell tumor, hibernoma, alveolar soft part sarcoma, oncocytoma, and crystal storing histiocytosis may be suggested by this appearance (14,16,28,31–33). If diagnostic concerns remain following examination of hematoxylin and eosin-stained sections, then immunohistochemical or special stains can serve to confirm skeletal muscle differentiation, which is unique to ARM in this group. The cells of both granular cell tumors and hibernomas never reach the very large

size of ARM cells. Granular cell tumors have indistinct cell borders and fine or coarsely granular amphophilic cytoplasm, with a round eosinophilc cytoplasmic inclusion of lysosomes, surrounded by a clear halo but lacking cross striations or crystalline deposits. The granules are periodic acid–Schiff (PAS) positive but diastase resistant, whereas the glycogen deposits of ARM are PAS positive and diastase labile. Unlike ARM, granular cell tumors infiltrate adjacent tissues, resulting in entrapped skeletal muscle tissue (not to be interpreted as rhabdomyoma cells) and circumferential growth around small nerves. Pseudoepitheliomatous hyperplasia of overlying epithelium is an occasional feature of granular cell tumors but not rhabdomyomas. The strong diffuse S-100- and CD68-positive staining of granular cell tumors contrasts with the skeletal muscle marker expression displayed by rhabdomyomas. Hibernomas are adipocytic tumors with variably vacuolated cytoplasm and no evidence of cross striations. These stain with S-100 stain, but not desmin or myoglobin. Oncocytomas are epithelial tumors of major or, rarely, minor salivary gland origin, composed of enlarged round to oval cells with pale, finely granular cytoplasm. The cells are typically arranged in a compact organoid pattern, rather than broad sheets as in rhabdomyoma. The distended cytoplasm is packed with mitochondria, which can be demonstrated ultrastructurally. They often stain well with phosphotungstic acid hematoxylin (PTAH), but unlike PTAH stain in rhabdomyomas, cross striations are not present. Weak or absent cytokeratin expression does not exclude the diagnosis of oncocytoma. A degree of morphologic and immunophenotypic overlap exists between ARM and alveolar soft part sarcoma, and both contain abundant eosinophilic cytoplasm and may stain with desmin, muscle-specific actin, or S-100. Alveolar soft part sarcoma usually has a distinctly alveolar growth pattern, which is not a feature of rhabdomyoma, but solid growth does occur, particularly in young patients with lesions of the tongue. A portion of the cells of alveolar soft part sarcoma will almost always contain distinctive rectangular or rhomboidal PAS-positive, diastase-resistant crystals (34). Reticulin stain can also aid in discrimination because the alveolar clusters of cells are encompassed by the reticulin, rather than single-cell staining pattern of ARM. Additionally, ARM does not react with the TFE3 stain, a diagnostic genetic-based immunohistochemical nuclear marker for alveolar soft part sarcoma. On rare occasions, low-grade B-cell neoplasms and plasma cell dyscrasias manifest with massive deposition of immunoglobulin-based crystals in reactive histiocytes. These engorged histiocytes bear some resemblance with the cells of ARM, but express histiocytic markers such as CD68 and CD163.

Treatment and Prognosis

Complete surgical removal is the treatment of choice for all types of rhabdomyoma. Recurrence is uncommon in the fetal and juvenile subtypes, accounting for less than 5% of treated cases (5,35). Reported recurrence rates for ARMs vary from 10% to 42%, which is higher than that in other variants (5,6,13). Recurrences may occur within a matter of months after initial surgery or may not be evident for many years (2,14,26). Local recurrence is presumed to result from incomplete removal of multinodular or multifocal tumors. Malignant degeneration or clinically aggressive behavior is not associated with recurrence of ARM.

C. Leiomyoma

Introduction

Leiomyoma is a benign neoplasm composed of cells exhibiting smooth muscle differentiation. Leiomyomas arising within the superficial dermis (with the exception of the so-called genital leiomyomas arising in the scrotum, vulva, or nipple of the breast) are believed to originate principally from arrector pili muscle and are termed pilar leiomyomas or piloleiomyomas. Noncutaneous leiomyomas featuring a prominent vascular component are referred to as vascular leiomyomas or angiomyomas. Owing to the fact that little or no native smooth muscle exists in the head and neck with the exception of the cervical esophagus and the circumvallate papillae and ductus lingualis of the tongue, noncutaneous smooth muscle tumors developing in this region are believed to take origin primarily from the smooth muscle forming blood vessel walls (1,2).

Clinical Findings

In general, noncutaneous head and neck leiomyomas are rare lesions. Only two leiomyomas were found by Fu and Perzin (3) in a series reviewing 256 nonepithelial neoplasms of the sinonasal tract and nasopharynx. Although the literature indicates that the vascular leiomyoma or angiomyoma is the most common leiomyoma variant found in the nasal cavity, paranasal sinuses, and oral cavity (4–6), this leiomyoma variant arises primarily in the subcutaneous tissue of the lower extremities followed by the upper extremities and only 8.5% to 13% of lesions are reported in the head and neck (4,6,7).

In large series, leiomyomas of the head and neck present mainly in the dermis, cervical esophagus (the least common site in the esophagus for smooth muscle tumors), larynx (mostly in the vestibular folds), mucosa of the sinonasal tract (mainly in the turbinates, but also in the nasal vestibule, nasal septum, and paranasal sinuses), parotid gland, and oral cavity (4–10). Leiomyomas develop more commonly in the nasal cavity than in a single paranasal sinus or in combination with the nasal cavity (5,11). In the oral cavity, the tongue, lips, cheek, and palate are the sites most often affected followed by the gingiva, floor of mouth, and mandible (9,12–14). Leiomyomas of the head and neck have also been described in the area around the submandibular gland (15), deep recesses of the neck including the carotid sheath (16), retropharyngeal space (17), tonsil (18), external auditory canal (19), orbital region (20), and thyroid gland (21).

Clinically, leiomyomas of the head and neck affect patients over a wide age range, but mainly present in the middle-aged adults. Sinonasal tract leiomyomas exhibit a female predominance, while tumors developing in the laryngeal area show a slight male bias (22,23). Sinonasal leiomyomas typically manifest as polypoid nodular masses and result in epistaxis, nasal obstruction, headache, or occasionally facial pain (3,4,11). A palpable asymptomatic mass is the most commonly reported initial manifestation of leiomyoma within the oral cavity. Difficulty in swallowing or chewing is less frequently reported presenting symptoms (9). In general, leiomyomas occurring in the more confined spaces of the head such as the sinonasal region are usually less than 2 cm in diameter at presentation, while those developing in the neck are typically larger (4,6,7).

Pilar leiomyomas are dermal-based smooth muscle tumors that predilect to the extremities. The majority of patients present in adult life and the sex distribution is roughly equal. Most large series claim a predominance of multiple over solitary lesions (24–26). Pilar leiomyomas involving the head and neck are extremely rare with most cases occurring in patients with multiple cutaneous lesions (26). Some cases of multiple cutaneous leiomyomas occur on a familial basis as an autosomal dominant disorder associated with uterine leiomyomas in women and papillary renal cell carcinoma. Germline mutations in the gene that encodes the fumarate hydratase enzyme predispose to this syndrome (27). Clinically, the lesions appear as reddish-brown to pink papules, sessile nodules, or polypoid growths usually measuring less than 1.5 cm in diameter. Multiple lesions may assume a linear or grouped pattern and are frequently painful.

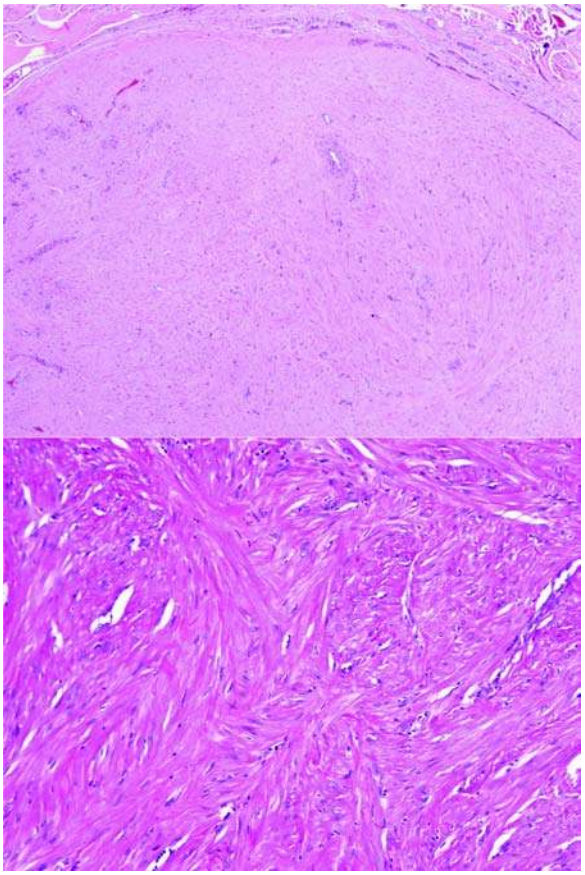

Figure 41 Well-circumscribed leiomyoma composed of intersecting fascicles of spindled cells with eosinophilic cytoplasm and thick- and thin-walled vessels (*top*). Higher magnification demonstrates the characteristic 90° orientation of adjacent smooth muscle fascicles (*bottom*).

Imaging

CT and MR imaging have both been used to evaluate sinonasal leiomyomas (28). The T2-weighted MR image exhibits a slightly hyperintense signal with marked uniform enhancement after contrast administration. CT imaging is useful for evaluating osseous involvement by the tumor. Deep-seated soft tissue lesions may demonstrate extensive calcifications (similar to uterine lesions) best depicted on radiographs or CT.

Pathologic Findings

Macroscopically, the noncutaneous leiomyoma is a well-circumscribed, spherical, firm mass. Cut section reveals a gray-white to tan whorled surface. Some tumors have a reddish-blue cut surface. Rarely, flecks of calcium are appreciated.

Microscopically, the conventional leiomyoma consists of a well-circumscribed proliferation of mature smooth muscle cells and variably sized, thick-walled vessels (Fig. 41, top). The cells are arranged in well-defined, elongated fascicles that focally intersect at 90° angles (Fig. 41, bottom). Some degree of nuclear palisading is not infrequently observed. The chief neoplastic element is a bipolar cell with brightly eosinophilic, somewhat fibrillary, cytoplasm, well-defined cytoplasmic borders, and a cytologically bland, elongated, plump nucleus with rounded or blunted ends (Fig. 42). Rarely, tumors composed chiefly of round to polygonal-shaped smooth muscle cells (epithelioid leiomyoma) occur in the head and neck (29). Dystrophic calcification, stromal hyalinization, myxoid change, or the presence of mature adipocytes (lipoleiomyoma) is feature occasionally noted in leiomyomas (5,6). Leiomyomas with degenerative atypia manifested by scattered enlarged nuclei with smudgy, ill-defined chromatin, but lacking mitotic activity and necrosis, are rarely encountered in this location.

Three histologic subtypes of the vascular leiomyoma (angiomyoma) are recognized (30). The solid variant is the most commonly encountered morphotype in the head and neck (4) and consists of intersecting smooth muscle fascicles and numerous elongated, compressed, slit-like vessels (Fig. 43). The venous subtype of angiomyoma features lesional smooth muscle cells that blend imperceptibly with the smooth muscle comprising the thick walls of

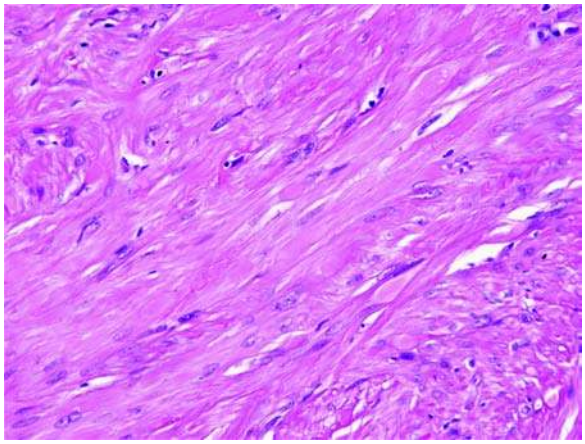

Figure 42 The cells of leiomyoma have abundant eosinophilic cytoplasm and a plump nucleus with rounded ends.

dilated venous structures. Dilated blood-filled vascular spaces lined by a thin smooth muscle sheath characterize the cavernous subtype.

Pilar leiomyomas are located primarily in the reticular dermis. The process is fairly well circumscribed and consists of fascicles of mature smooth muscle cells that grow in an interlacing or a haphazard pattern and often extend between dermal collagen bundles at the periphery (Fig. 44). In the setting of multiple leiomyomas, the growth may assume a more compact, nodular configuration (26). In rare cases, degenerative atypia is identified. However, tumors demonstrating true cytologic atypia in the form of variably sized nuclei, hyperchromasia, and an abnormal chromatin pattern coupled with any mitotic activity should be considered potentially malignant and not within the spectrum of benign leiomyoma. The overlying skin surface sometimes exhibits epidermal hyperplasia.

The Masson trichrome histochemical stain demonstrates thin, longitudinally arrayed fuchinophilic fibrils (corresponding to actin myofilaments) within the cytoplasm of the smooth muscle cell. Periodic acid–Schiff stain detects a variable amount of intracytoplasmic glycogen.

Immunohistochemistry

The tumor cells show expression of muscle-related markers including desmin, α-smooth muscle- and muscle-specific actin, h-caldesmon, and calponin (31,32). Perimembranous expression of basement membrane–related type IV collagen and laminin is also observed.

Molecular Findings

Angioleiomyoma (angiomyoma, vascular leiomyoma). Cytogenetic data are limited to four karyotypes. Although clonal chromosomal changes, including deletions of specific chromosomal regions, del(6)

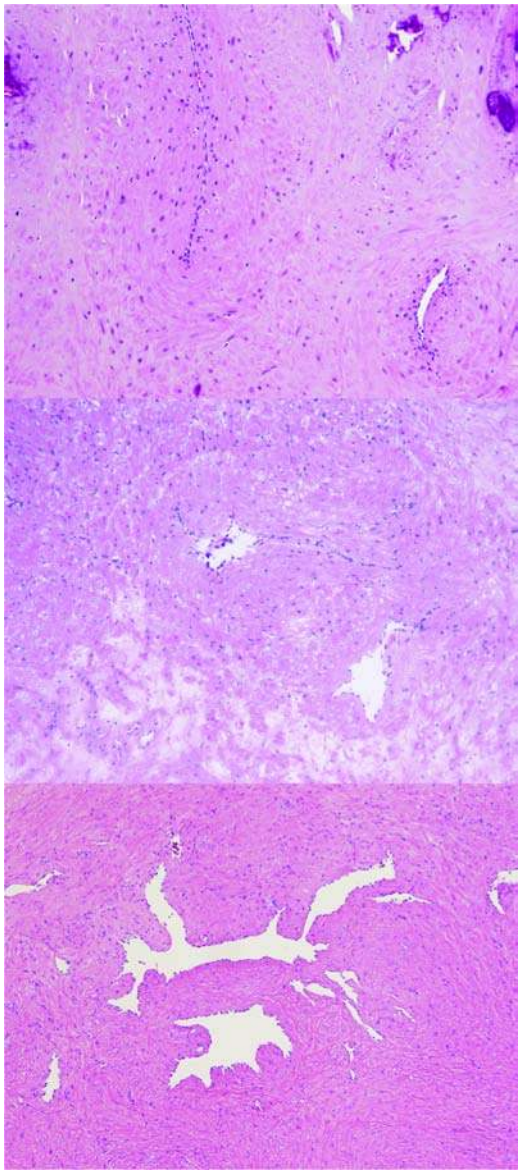

Figure 43 Angiomyomas. Solid variant featuring compressed vessels and proliferating smooth muscle cells. Small deposits of dystrophic calcium are also noted (*top*). Venous subtype of angiomyoma characterized by lesional smooth muscle merging with the smooth muscle coat of a venous structure (*middle*). Angiomyoma with open, irregularly contoured thin-walled vessels (*bottom*).

(p21p23) and del(21)(q21), monosomy of chromosome 13, and translocation t(X;10)(q22;q23.2) have been reported, no consistent or tumor-specific cytogenetic abnormality has been identified (33–35).

Esophageal leiomyomas. Deletion of the 5′ ends of the genes encoding basement membrane collagen, *COL4A5* (collagen, type IV, α-5) and *COL4A6* (collagen, type IV, α-6), reported in Alport syndrome have also been identified in esophageal leiomyomas and leiomyomatosis. This finding may suggest that both esophageal leiomyomas and leiomyomatosis are

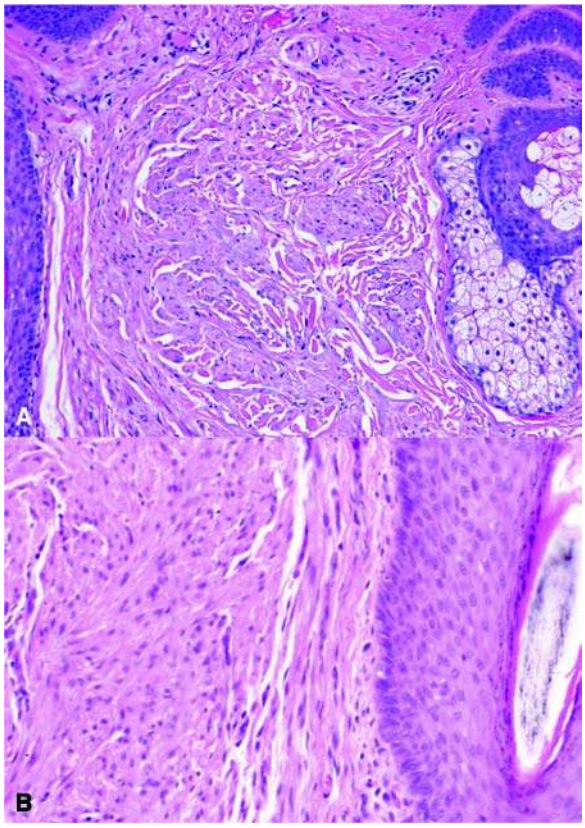

Figure 44 Cutaneous (pilar) leiomyoma features cytologically bland smooth muscle cells arranged in haphazard bundle-like fascicles within the dermis (**A** and **B**).

genetically related and driven by the same molecular mechanisms (36–39).

Electron Microscopy

Mature, well-developed smooth muscle cells have bipolar cytoplasmic processes that are filled with numerous actin and smaller numbers of myosin myofilaments. These myofilamentous bundles are characteristically arranged parallel to the surface of the cell. Additionally, scattered, longitudinally arranged, dense contractile bodies are concentrated where myofilamentous bundles bond laterally and also where they attach to the cell surface. Clusters of mitochondria, runs of rough endoplasmic reticulum, and free ribosomes also occupy the cytoplasm and concentrate near the poles of the nucleus. Basal lamina surrounds the cell membrane and subplasmalemmal pinocytotic vesicles are readily identified. The nucleus has a somewhat serrated membrane (40).

Differential Diagnosis

Well-differentiated leiomyosarcoma is the most important entity in the differential diagnosis. For noncutaneous smooth muscle tumors, the same criteria used to separate benign from malignant deep soft tissue smooth muscle tumors has been applied to sinonasal smooth muscle neoplasms (5). In general, leiomyosarcoma is favored if the tumor exhibits either cellular pleomorphism (at 10× magnification), nuclear atypia, foci of coagulative tumoral necrosis, or mitotic activity over 4 mitotic figures in 10 high-power fields (5,41). A tumor composed of bland nuclei but demonstrating mitotic activity up to 4 mitoses per 10 high-power fields should be considered a ''smooth muscle tumor of uncertain malignant potential.'' A dermal smooth muscle tumor demonstrating any degree of cellular pleomorphism (which may be focal) and mitotic activity is more appropriately classified as a cutaneous leiomyosarcoma.

The smooth muscle hamartoma exhibits some histologic overlap with pilar leiomyoma. Although most often encountered in the trunk and extremities, this lesion has been described in the head and neck (42). The smooth muscle hamartoma differs from pilar leiomyoma by its congenital onset, asymptomatic presentation as a hairy or pigmented plaque-like lesion, and microscopically by the presence of compact bundles of mature smooth muscle separated by dermal collagen (43).

Myofibroma (44) is a benign mesenchymal tumor that predilects to the head and neck and exhibits a haphazard fascicular growth pattern of plump spindled cells reminiscent of pilar leiomyoma. The lesion predilects to children within the first two years of life, but also occasionally occurs in adults (45). In contrast to the pilar leiomyoma, the cells of myofibroma have a smaller amount of cytoplasm that is less brightly eosinophilic, and nuclei that are often narrower. The myofibroma usually has a component of smaller, less differentiated cells that are associated with an intricate hemangiopericytomatous vascular network. This primitive element tends to be located toward the center of the process in infants but is more randomly distributed in adult cases. Immunohistochemically, both cellular components usually demonstrate strong expression of SMA, which in the mature spindled cell is typically concentrated toward the cell membrane (''tram-track'' pattern) because of the peripheral location of myofilaments. Unlike the leiomyoma, cells of myofibroma do not appreciably express desmin or h-caldesmon (46).

Cellular schwannoma of the head and neck (47) is usually unencapsulated and shows, at least focally, a fascicular growth pattern of spindled cells. In comparison with the leiomyoma, the cells of schwannoma possess paler, less fibrillary cytoplasm with ill-defined borders, nuclei with more irregular and buckled contours, and are arranged in less well-defined fascicles. Importantly, schwannoma shows strong and diffuse immunohistochemical expression of S-100 protein and typically lacks expression of SMA, desmin, and h-caldesmon.

A significant minority of so-called sinonasal HPCs (48) possess spindled cells arrayed in interconnected fascicles and whorls. In contrast to leiomyoma, the spindled cell of sinonasal HPC has a smaller nucleus and paler cytoplasm and is arranged in

shorter fascicles. Additionally, a glomus-like cell with a rounded, centrally located nucleus is noted about 18% of cases. Unlike the muscularized vessels of leiomyoma, the hemangiopericytomatous vessels of sinonasal HPC show conspicuous perivascular collagen deposition. Although the cells of the sinonasal HPC commonly express smooth muscle- and muscle-specific-actin, they do not express desmin.

Prognosis and Treatment

Leiomyomas, including the vascular and pilar variants, are effectively treated with conservative excision. Recurrence is rare and nondestructive but should prompt reconsideration of the lesion as a possible ''smooth muscle tumor of uncertain malignant potential.''

IV. BENIGN LIPOMATOUS TUMORS

A. Lipoma, Lipoma Variants, and Reactive Lipomatous Lesions

Introduction

Tumors and lesions of mature adipocytes can be divided into reactive, benign, and malignant. Benign tumors include classic lipoma, sometimes with metaplastic bone formation, and lipoma variants including spindle cell lipoma, chondroid lipoma, lipoblastoma, and brown fat hibernoma. The most common subtype in the head and neck and oral cavity is spindle cell lipoma (1). Angiolipoma is not usually a head and neck tumor. All lipomas are in subcutaneous or submucosal locations with rare intramuscular involvement. Multiple lipomas can occur in a posterior neck and shoulder distribution (Madelung disease) or extremity enlargement (Adiposa dolorosa) and as multiple, familial spindle cell lipomas. Newer fatty lesion entities are described.

Reactive fatty lesions include fat necrosis, silicone granuloma, and fat atrophy. These can be quite worrisome for liposarcoma, on the basis of the finding of cells that mimic atypical lipocytes or lipoblasts. Although lipoblasts are not required for the diagnosis of liposarcoma, they are frequent in true oral and head and neck liposarcomas. Another worrisome feature for liposarcoma is widened septa, which can be found in benign adipocytic processes, such as massive localized edema of the morbidly obese, which is not found in a head and neck location.

Features special to head and neck lipomas include that 15% of all lipomas involve the head or neck, salivary gland lipomas tend to occur in the parotid as a mobile, nontender mass, the buccal mucosa is the most common site for intraoral lipomas (1), hypopharyngeal lipomas may cause dysphagia or even dyspnea, and retropharyngeal lipomas may be large before detected by deglutition, respiratory problems, or obstructive sleep apnea.

Clinical and Pathology

Fat necrosis. Fat necrosis can occur in any age, in any location, not sparing head and neck locations. There is a spectrum of etiologies ranging from enzyme digestion in peripancreatic locations or hematogenous spread of pancreatic lipase and trypsin to legs, buttocks, trunk, arms, and even scalp (2) to mild trauma in all locations (3). The range of histiocytic response can be from none, during a large ischemic infarct in which there is no time for histiocytic influx, to massive histiocytic influx and therefore lipogranuloma formation, where the fat necrosis occurs multifocally in small areas (Fig. 45). Fat necrosis can look worrisome for atypia or lipoblasts, associated with liposarcoma (4). The histiocytes of fat necrosis differ from lipoblasts in liposarcoma in that they have uniform vacuoles that do not indent the nucleus. It can be found by itself, even form a mass, or can be found in the setting of a preexisting benign lipoma or even a malignant liposarcoma, both secondary to trauma of that tumor. Fat necrosis can secondarily incite fibrosis or dystrophic calcification.

Silicone granuloma. Silicone granuloma (Fig. 46) occurs where there is leakage of silicone material, generally after breast or finger joint implant, and a

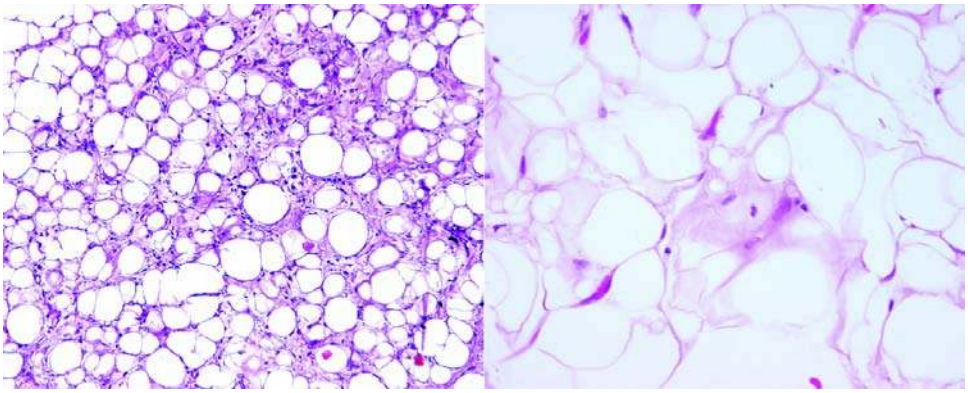

Figure 45 Fat necrosis can mimic liposarcoma because it has a busy low-power appearance but has no atypia.

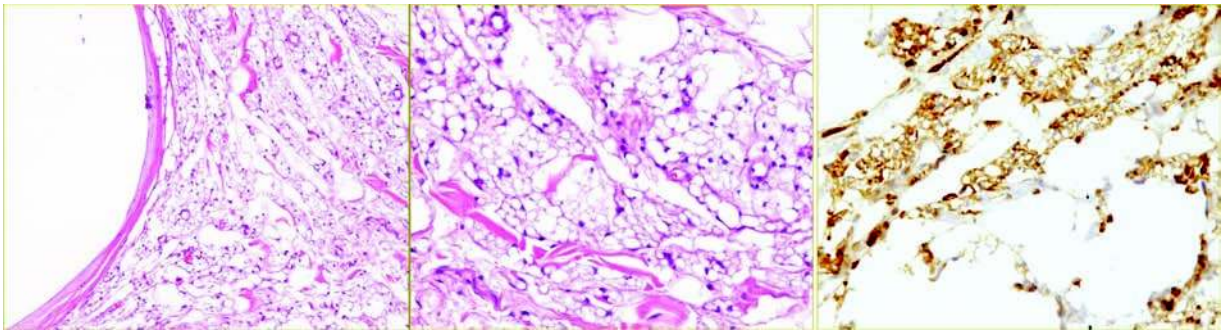

Figure 46 Silicone granuloma mimics lipoblasts as histiocytes engulf silicone material. However, these are CD163 positive and S-100 protein negative, unlike true lipoblasts.

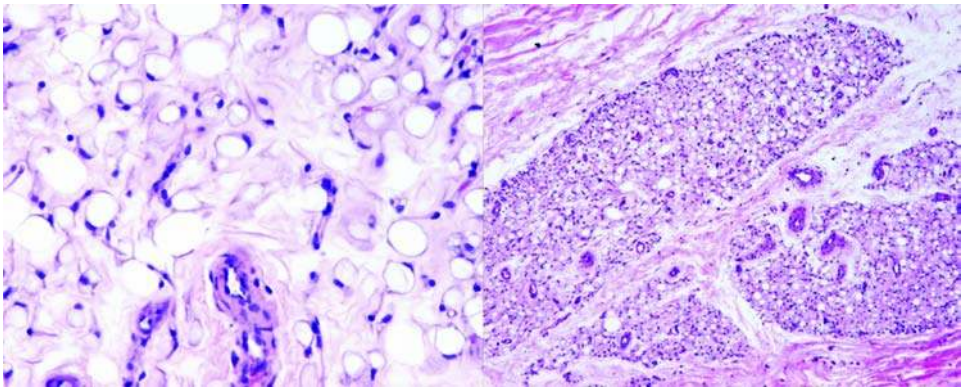

Figure 47 Fat atrophy can mimic myxoid liposarcoma, but at lower magnification, one can appreciate the normal but diminished fat lobules.

marked histiocytic response (5). The histiocytes will mimic sheets of lipoblasts (6). There will be gaping cyst-like structures where silicone material may be leached out during processing, or there may be residual small amounts of silicone that can be detected by spectrophotometry or other methods. Importantly, these histiocytes can be detected by CD163 or other histiocytic markers (7) and are negative for S-100 protein (which would be positive in mature adipocytes and in lipoblasts).

Fat atrophy. Fat atrophy (Fig. 47) occurs in settings of malnutrition or injection sites (8), often in the buttocks or other non–head and neck sites. The fatty lobules retain their structure, but the fat cell size is diminished and often resembles the monovacuolated lipoblast observed in myxoid liposarcoma. To separate this from true myxoid liposarcoma, one must know the history and see the preserved architecture at low power with absence of abundant myxoid stroma, stromal round to stellate cells, delicate y-shaped vasculature, and bivacuolated true lipoblasts at the periphery of the lobules.

Massive localized lymphedema of the morbidly obese. This entity was first described by Farshid and Weiss in 1998 (9). Massive localized lymphedema of the morbidly obese (Fig. 48) generally occurs as a pedunculous mass in the intertriginous folds of morbidly obese middle-aged females. This occurs because of compression of lymphatics and perilymphatic edema. The most common location is the inguinal area; head and neck sites are not involved. These mimic liposarcoma because there are widened fatty septa by perilymphatic fibrosis, edema, and reactive vessels at the interface between the edema and the subcutaneous fat, making the lesion appear as a large fatty tumor. These have no atypia.

Classic lipoma. Classic lipoma is a common tumor found in all anatomic sites, including head and neck and oral and maxillofacial, generally in middle-aged adults. It is usually encapsulated mature adipose tissue in a subcutaneous or submucosal location. It is a benign, nonrecurrent tumor. Rarely, when it involves skeletal muscle (Fig. 49), it can be difficult to completely excise and may locally recur (10). The head and neck cases of intramuscular lipoma have been reported in several locations including the tongue (11,12), eyelid (13,14), cheek (15), temporal muscle (16,17), and larynx (18,19). Heterologous

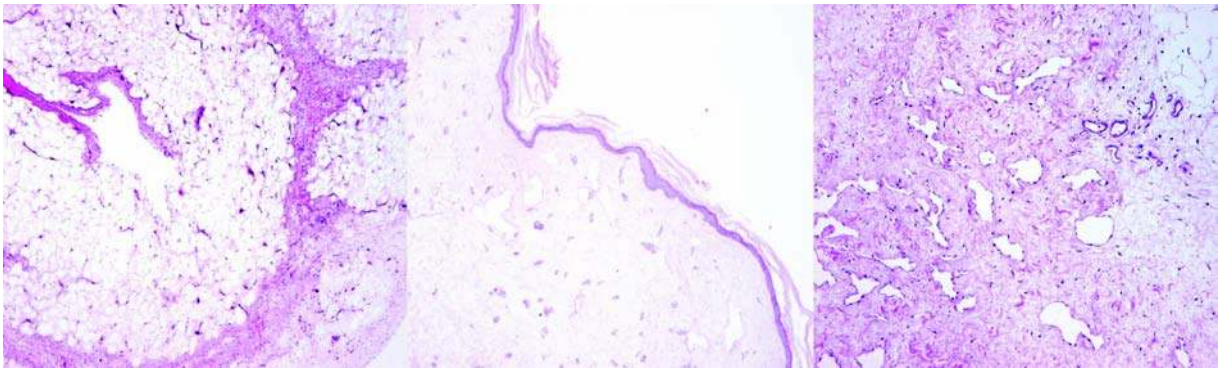

Figure 48 Massive localized lymphedema of the morbidly obese is in the differential diagnosis of fat with widened septa (often a low-power clue to liposarcoma). This is usually a non–head and neck lesion that is due to lymphatic obstruction. The features include cobblestone skin due to edema, widened septa, perilymphatic fibrosis and dilation of lymphatics, and reactive vessels at the interface between the edema and fat.

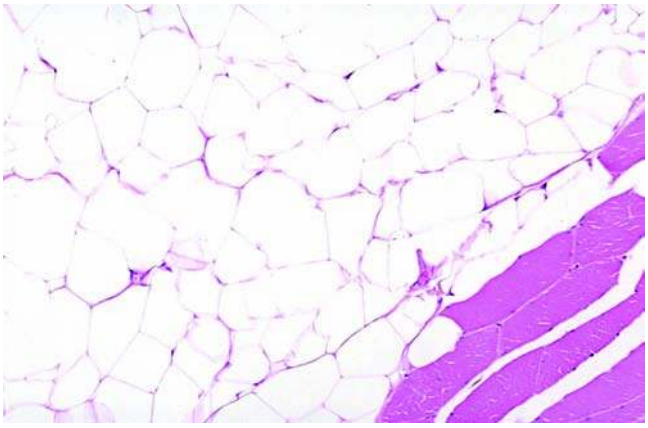

Figure 49 This is an example of intramuscular lipoma. It has a higher recurrence potential than normal submucosal or subcutaneous lipoma.

features, such as chondroid metaplasia, can be present in lipoma.

Lipomatosis. Less than 5% of patients with lipoma have multiple lipomas. Lipomatosis is a diffuse overgrowth of fat. There are many subtypes of lipomatosis including symmetrical painful enlargement of the extremities (*Adiposa dolorosa*) (20,21), symmetrical pelvic lipomatosis (22–24), and symmetrical head, neck, shoulder, and back lipomas (*Madelung disease*, Fig. 50). The latter is thought to occur more commonly in diabetic or alcoholic patients (25–27).

Spindle cell/pleomorphic lipoma. Spindle cell lipoma (Fig. 51) is the most common subtype of lipoma in the head and neck and oral cavity. It is on a spectrum with pleomorphic lipoma, and these are histologically, clinically, and genetically identical tumors, with the addition of the floret giant cell in pleomorphic lipoma (Fig. 52). The five features common to both include mature adipocytes, wavy collagen bundles, scattered mast cells, bland spindled cells, and myxoid change (28). These can occur on the face and inside the mouth, including tongue. The most common age, sex, and site are 60-year-old men in the posterior neck, back, or shoulders (29–31). In the head and neck, they have also been reported in the forehead, cheek, face, orbit, and nasolabial fold (25–27). When multiple or familial, these can be in the same symmetrical neck and shoulder distribution as Madelung disease and rarely occur below the waist (32). If one encounters a lipoma with spindle cell features below the waist, it is best

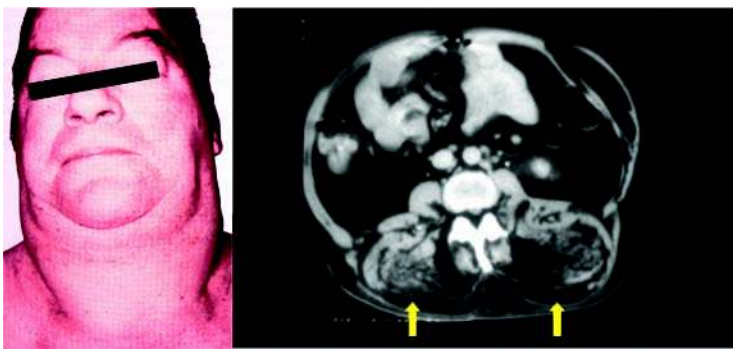

Figure 50 Madelung disease, a form of neck lipomatosis, may occur in diabetic or alcoholic patients of Mediterranean descent. A patient with Madelung-type lipomatosis. Computerized tomography reveals extensive fat infiltration of the paraspinal muscles (*arrows*).

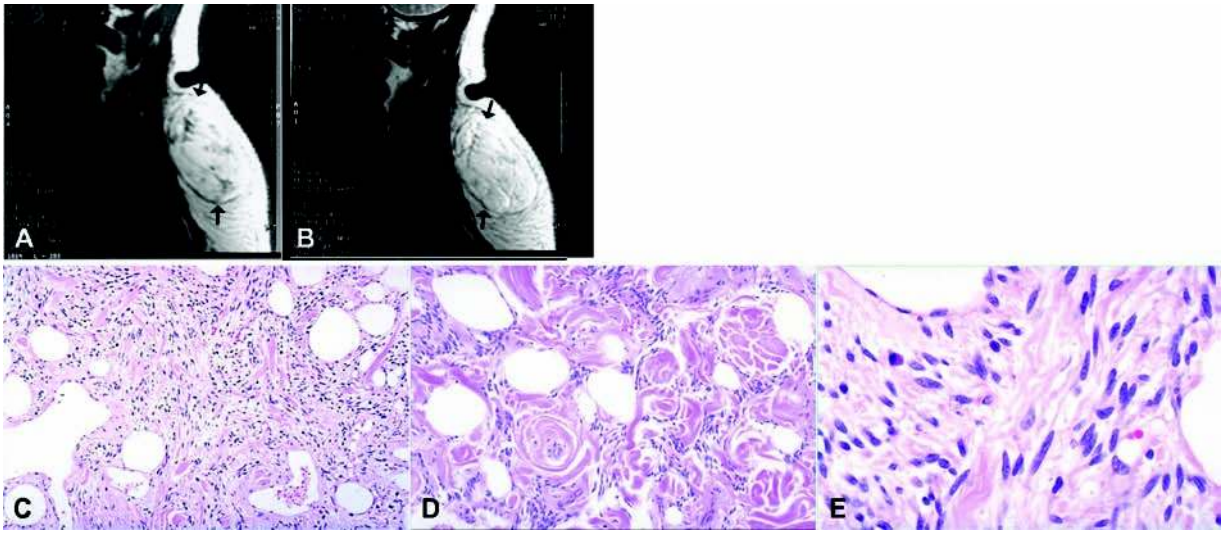

Figure 51 Spindle cell lipoma in the subcutaneous tissues of the posterior neck. Sagittal T1-weighted (**A**) and T2-weighted (**B**) magnetic resonance images show a large posterior mass (*arrows*), with the majority of tissue isointense to fat but with prominent nonlipomatous components that in a deep-seated location would suggest a well-differentiated liposarcoma. Histologically, spindle cell lipoma has five variously proportioned classic features: mature adipocytes, bland spindled cells, wavy bundles of collagen, scattered mast cells, and myxoid change **C–E**.

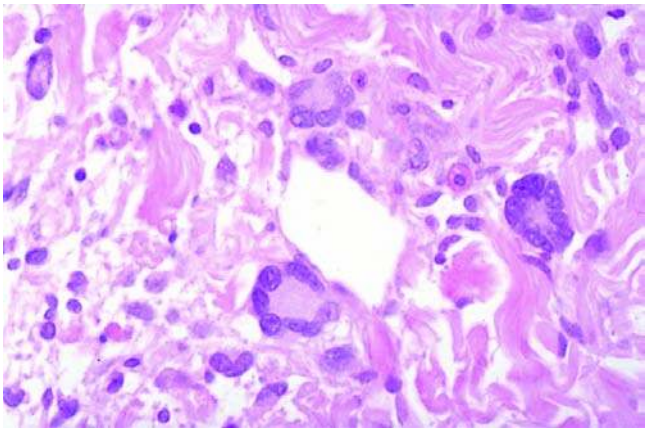

Figure 52 Pleomorphic lipoma, of the posterior neck, identical clinically and genetically to spindle cell lipoma, has all the same histologic features as spindle cell lipoma and multinucleated floret-type giant cells (nuclei to periphery of cell).

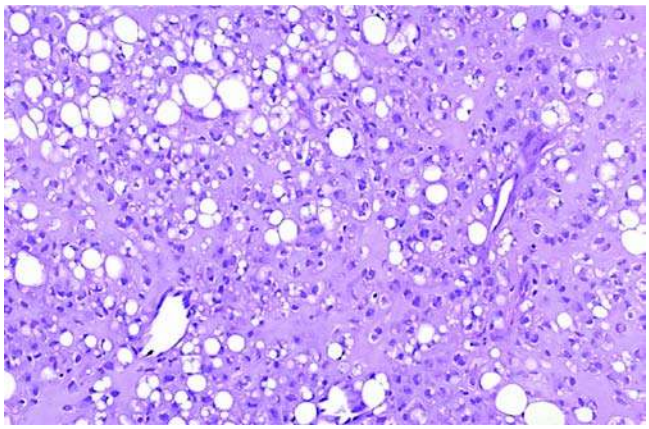

Figure 53 Chondroid lipoma of the tongue. It looks like a cross between chondrosarcoma and liposarcoma, but is benign.

diagnosed as such and not as spindle cell lipoma, as the latter refers to a distinctive clinicopathologic presentation.

Chondroid lipoma. First coined into an entity by Meis and Enzinger in 1993 (33), chondroid lipoma (Fig. 53) is now known to have a similar genetic finding as hibernoma. This tumor exhibiting chondroid matrix (34) and mimicking both chondrosarcoma and liposarcoma can rarely occur in head and neck locations, in the lower lip, soft tissue overlying the ramus of the mandible, and the submandibular region (35). It has been observed in the tongue (1).

Hibernoma. Hibernoma (Fig. 54) is a tumor composed of brown fat, generally occurring in distributions of normal brown fat, rarely in the neck. There is a subtype that is most common in the posterior neck, spindle cell hibernoma, that has all the features of spindle cell lipoma but the mature white fat is replaced by brown fat. These are never malignant, although rare normal brown fat cells can be seen in well-differentiated and myxoid liposarcomas, but once one observes brown fat comprising the lesion, it is benign (36). There are six subtypes of hibernoma: the granular variant, the pale variant, the lipoma-like variant, the myxoid variant and the spindle cell variant, and the mixed variant (37).

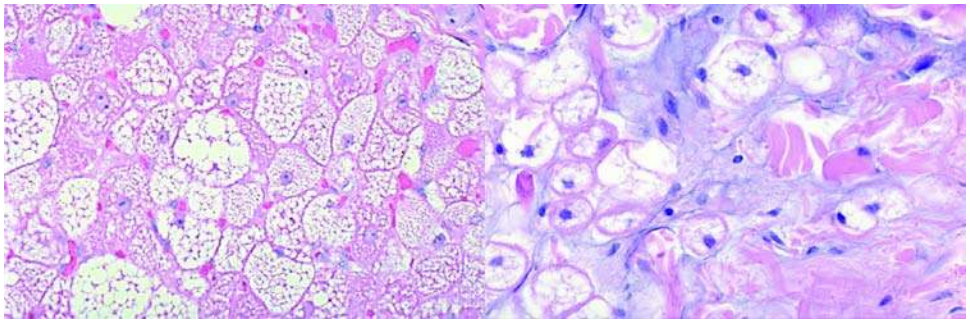

Figure 54 Hibernoma, composed of brown fat, mimics lipoblasts. A spindle cell variant of hibernoma occurs in the posterior neck.

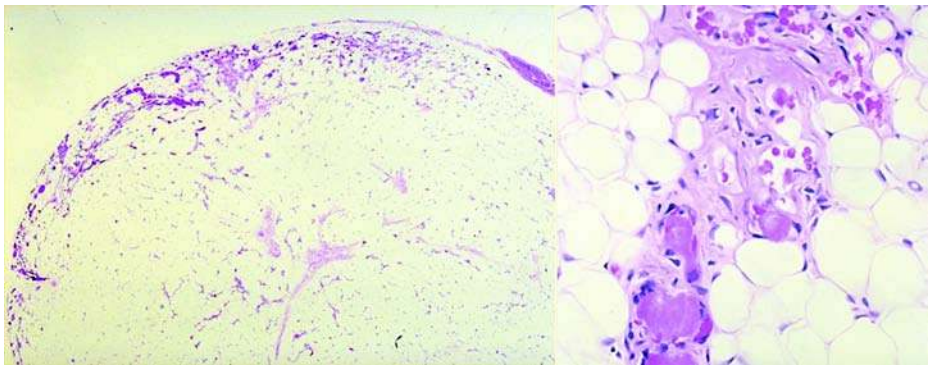

Figure 55 Angiolipoma is rare in head and neck. It can be multiple and painful. It is characterized by a peripheral proliferation of capillaries with fibrin thrombi.

Angiolipoma. Angiolipoma (Fig. 55) is extremely rare in head and neck locations (case reports in neck, buccal mucosa, hard palate, nasal cavity, parotid gland, and mandible) (38–46). This, sometimes multiple, usually trunk and extremity lesion in males, is composed of mature fat and small capillaries with fibrin thrombi and a surrounding pericytic proliferation, starting at the periphery of the fatty lobules and eventually coalescing into the center with a paucity of residual fat (47). These are one of the few painful benign soft tissue lesions (48).

Lipoblastoma. Lipoblastoma (Fig. 56) can occur in head and neck, although it is most common in the extremities (49), followed by the trunk including intra-abdominal or intrathoracic locations (50–58). It occurs in patients less than two to three years old, and it can be multiple (lipoblastomatosis) (49,59,60). When the lesion(s) mature in an older child, there are retained widened fibrous septa around lobules of mature white fat. The histologic features of lipoblastoma in young children are sheets of bland lipoblasts, myxoid change, and delicate vasculature. The lipoblasts are multivacuolated, unlike those usually found in myxoid liposarcoma, and the age of the patient helps to distinguish it from myxoid liposarcoma, the latter usually occurring in patients more than 10 years old (49,61).

Myxoid lipoma. Myxoid lipoma or myxolipoma are now better classified as a myxoid variant of spindle cell lipoma as these often have the five main histologic features of that entity, but the myxoid change predominates (62).

Fibrolipoma. Rarely are there lesions that meet this designation. More likely these are heavily collagenized and are truly Gardner or nuchal fibroma, involving posterior neck fat (63–75). Or these could be heavily collagenized spindle cell lipomas.

Angiomyolipoma. These absolutely do not occur in the head and neck; they occur in perinephric fat. These are composed of immature epithelioid smooth muscle, vessels, and fat and are part of the myomelanocytic family of tumors and therefore express desmin and HMB45 (76,77).

Myelolipoma. Generally occurring in the adrenal gland, these do not occur in the head and neck. These are composed of normal marrow elements, including megakaryocytes and other precursor cells and fat (78–80).

Atypical lipoma or atypical lipomatous tumor. Occurring mainly in the posterior neck or lateral neck, atypical lipoma (Fig. 57) is defined as a superficial or subcutaneous well-differentiated lipomatous tumor that has lipocytic atypia (81). At low magnification, histologically, there is usually a busy

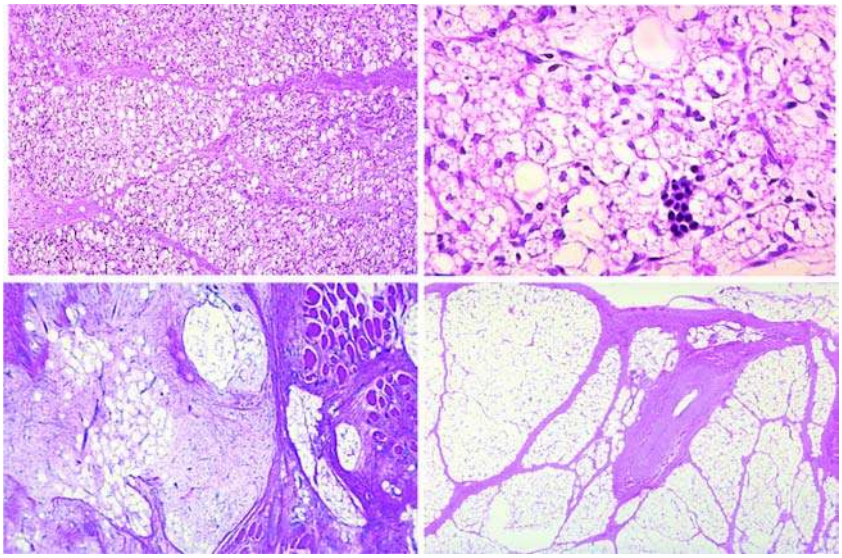

Figure 56 Lipoblastoma is a tumor of infants that has sheets of lipoblasts, separated into lobules by fibrous septa. As the lesion matures to adult-type white fat, the fibrous septa remain.

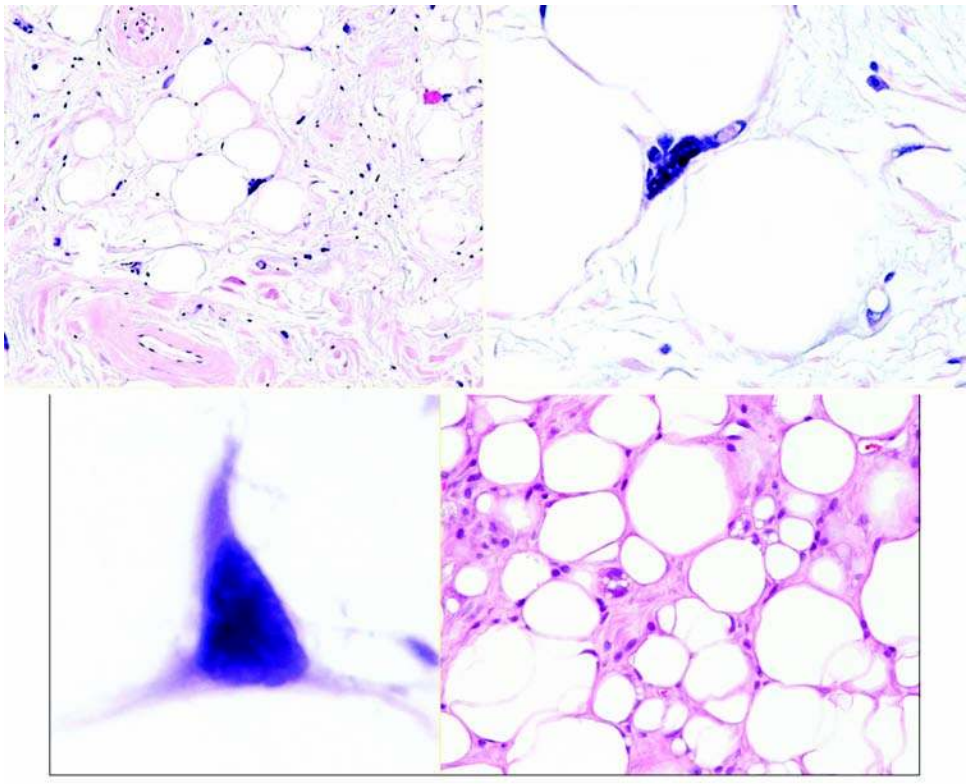

Figure 57 Atypical lipomatous tumor combines atypical lipoma, with widened septa and lipocytic atypia, and spindle cell or pleomorphic lipoma–like features. The requirement for atypical lipoma or atypical lipomatous tumor is the atypical lipocyte (*above*). Lipoblasts are not necessary for diagnosis, although often present in the head and neck well-differentiated lipomatous neoplasms.

appearance, heterogeneous cell size and shape, and widened septa. Lipoblasts do not need to be observed to make the diagnosis. The histologically identical lesion that is intramuscular or in groin or contiguous retroperitoneum is called well-differentiated liposarcoma, because it is this deeper lesion that would have the propensity to dedifferentiate and metastasize (82,83). Atypical lipoma is considered benign because

it is superficial and would not dedifferentiate or metastasize. Atypical lipomatous tumor is used synonymously by some pathologists with atypical lipoma, but reserved by others to indicate when there are both atypical lipoma and spindle cell or pleomorphic lipoma–like features (84). These tumors are frequently found in the posterior neck of patients a decade or two older than 60 when there are widened septa and lipocytic atypia outside of the acceptable range of pleomorphic lipoma's floret cells.

Hemosiderotic fibrohistiocytic lipomatous lesion. This recently described, mainly ankle lesion in middle-aged females is a fatty benign process that occurs after trauma (85–87). It does not occur in the head and neck. It is composed mainly of mature fat with spindled cells along the septa and a mixture of inflammatory cells including multinucleated histiocytes, mast cells, and other chronic inflammatory cells. The spindled cells are occasionally CD34 positive (88). These do not have a relationship with the potentially low-grade, malignant, solid, nonfatty tumor and pleomorphic hyalinizing angiectatic tumor of soft part.

Radiologic imaging

Lipomas typically reveal uniform fat on CT or MR with limited or no nonlipomatous components. A small number of thin septae (<2mm) may be seen. More prominent areas of nonlipomatous components may be seen in spindle cell lipoma or fibrolipoma, but these lesions are difficult to distinguish from well-differentiated liposarcoma by imaging. Lipomatosis reveals extensive infiltration by a diffuse lipomatous mass.

Hibernoma may reveal similar but not identical CT or MR imaging features of fat. In addition, MR imaging frequently shows prominent vascularity, a feature not seen in lipoma or liposarcoma. PET imaging usually reveals marked radionuclide activity also, in contradistinction to lipoma or well-differentiated liposarcoma.

Lipoblastoma reveals intrinsic fat by CT or MR imaging in a young child. Frequently, nonlipomatous components are prominent as well, which by imaging alone would suggest a liposarcoma, but the age of the patient eliminates this diagnosis as a realistic consideration (89–91).

Immunohistochemistry

Immunohistochemistry for fatty differentiation includes S-100 protein, which stains the lipocytes and lipoblasts, and CD34, which stains spindled cells within fatty tumors, including the spindled component of dedifferentiated liposarcoma and spindle cell lipoma.

Molecular Findings

Genetic findings for various lipomas are listed in Table 4 (92–109).

Differential Diagnosis

The differential diagnoses for reactive and benign fatty tumors are malignant fatty tumors, as outlined above in each subsection.

Table 4 Chromosomal and Molecular Genetic Aberrations Leading to Formation of Gene Fusions or Activation of Normal Genes in Benign Lipomatous Tumors

Tumor	Aberration	Affected gene
Lipoma (92–97)	t(3;12)(q27;q15)	HMGA2-LPP
	t(12;15)(q15;q24)	HMGA2-?
	t(2;12)(q35-37;q15)	HMGA2-RDC1
	t(12;13)(q15;q12)	HMGIC-LHPF
	inv(12)(p11.2;q15)	HMGA2-?
	6p23-21 rearrangements	HMGA1
	12q14-15 rearrangements	HMGA2
	13q12-14 and 13q22 deletions	
Chondroid lipoma (98)	t(11;16)(q13;p12-13)	?
Spindle cell/ pleomorphic lipoma (99)	13q and 16q deletions	?
Hibernoma (101–105)	T(9;11)(q34;q13)	?
	11q13 rearrangements, deletions	
Lipoblastoma (106–109)	8q12 rearrangements	PLAG1 HAS2-PLAG1 COL1A2-PLAG1
	t(7;8)(q22;q12)	?
	t(3;8)(q13.1;q12)	PLAG1- ?
	t(8;15)(q12;q25)	PLAG1- ?

Note: "?" in the table indicates unknown or not well characterized data.

Prognosis and Treatment

Reactive fatty lesions do not require surgical excision. Benign lipomas and their variants are usually removed because of cosmetic or mechanical reasons or for diagnosis, and their recurrence is extremely low. Atypical lipoma or atypical lipomatous tumor may locally recur, especially if incompletely excised, but do not have metastatic potential (82).

V. BENIGN (MYO)FIBROBLASTIC AND FIBROOSSEOUS LESIONS AND TUMORS

A. Nodular Fasciitis and Related Lesions Including Cranial Fasciitis

Introduction

Nodular fasciitis is the most common soft tissue pseudotumor. First described as an entity by Konwaler in 1955, it was previously recognized by pathologists since the early 1940s, but it still causes the most trouble in recognition and confusion with sarcoma of any soft tissue lesion (1,2). It occurs in the head and neck in about 20% of cases, particularly in children (3) who traumatize their forehead, and in boxers who traumatize around the ear. There are intravascular and cranial variants of nodular fasciitis, the latter occurring in children less than one year old often eroding the outer skull table.

Clinical Findings

Nodular fasciitis is a rapidly growing, sometimes tender mass that develops within a few weeks to less than two months of trauma (4–7). Both children and adults, equally in males and females, can be affected. It can actually ulcerate and bleed, when around the ear and when involving dermis (8). Most lesions occur in a deeper location and are fascial based and subcutaneous (9), but head and neck lesions can be dermal or even intramuscular. Forehead (10), periauricular (11), periorbital (12), and intraoral (13,14), particularly buccal mucosa (15,16) and lip, are common sites. Parotid, laryngeal, and nasal lesions are less common (13,17–20). Lip lesions have an intravascular proclivity. Intravascular fasciitis is a specialized intravascular organizing thrombus, occurring in veins and arteries (21,22); cranial fasciitis occurs in infants and may erode the outer skull table. The latter lesion should be separated clinically and pathologically from fibrodysplasia ossificans progressive (FOP), fibromatosis, myofibromatosis, and desmoplastic fibroma.

Imaging

Imaging of nodular fasciitis has not been extensively reported. CT and MR imaging may reveal well-defined or irregularly margined lesions, most frequently subcutaneous in location. MR imaging may demonstrate mild surrounding edema and linear extensions along the superficial fascia (fascial tail sign), a feature uncommonly seen in other deep subcutaneous lesions. Intrinsically, the imaging appearance is nonspecific, with intermediate signal intensity on T1-weighting and intermediate to high signal intensity on T2-weighting. Lesions are frequently heterogeneous, and enhancement has been reported as diffuse or peripheral in pattern (23–25). Cranial fasciitis shows similar imaging features but may additionally reveal erosion and invasion of the calvarium, suggesting a much more aggressive process (26).

Pathologic Findings

Grossly, nodular fasciitis is generally circumscribed and gray-white to yellow and can be mucoid and soft. It can be poorly delineated when growing inside and along the fascia. Intravascular fasciitis can give a plexiform growth pattern. Cranial fasciitis is rubbery firm and may also have mucoid cystic degeneration. The salient histologic features for nodular fasciitis (Fig. 58) include at least one edge being fascial based, a well-delineated growth pattern, loose storiform tissue culture–like myofibroblasts alternating with hypocellular areas of myxoid degeneration, with extravasated erythrocytes and lymphocytes (7). This latter feature is the key diagnostic feature and is always present. There may be keloidal collagen and osteoclast-type giant cells, particularly in the intravascular type. When purely intrafascial, nodular fasciitis may resemble a biopsy tract, with fibrin or myxoid change in the center, poorly delineated lesion, and reactive vessels, parallel to each other but perpendicular to the central myxoid change. Intravascular fasciitis is a specialized organizing thrombus with similar features to that of nodular fasciitis. Cranial fasciitis (Fig. 59) also has myxoid degeneration and is well delineated, but may be seen eroding the outer and sometimes inner skull tables.

Electron Microscopy

Electron microscopy (EM) is no longer used for the diagnosis of most soft tissue tumors but would show myofibroblastic features (27,28). These would include elongated cells with abundant dilated rough endoplasmic reticulum, sometimes cytoplasmic filaments with dense bodies, pinocytotic vesicles, and cell junctions. These features are found in all myofibroblastic tumors.

Immunohistochemistry

Nodular fasciitis is a histologic diagnosis, but can be identified by focal SMA positivity, occasionally muscle-specific actin and CD68 (a marker for lysosomes, mainly in histiocytes) and negativity for nuclear β-catenin, keratins, S-100 protein, desmin, and CD34 (29,30). Cytoplasmic β-catenin, or negative nuclear β-catenin, helps to separate nodular fasciitis from desmoid-type fibromatosis, which demonstrates nuclear reactivity for β-catenin (31–33).

Molecular Findings

Several cases of nodular fasciitis have been karyotyped up to now. In all cases, clonal chromosomal abnormalities have been detected. The most common, found in three cases, were translocations involving chromosome 15q (15q22, 15q25, and 15q 26). In addition, two tumors with 15q rearrangements revealed either interstitial deletion (13)(q14q21) or monosomy of chromosome 13 (34–36). Other clonal chromosomal changes identified in nodular fasciitis included rearrangements of chromosome 3q21 and translocation t(16;16)(p13.3;p11.2) (37,38). The finding of clonal chromosomal abnormalities might suggest that at least some cases of nodular fasciitis could be true neoplasms and not reactive lesions.

Differential Diagnosis

Nodular fasciitis must be separated from other benign and malignant myxoid tumors as well as other myofibroblastic tumors. For benign tumors in the differential diagnosis, the most common include fibrous histiocytoma, another benign myofibroblastic tumor with overlapping features. This is usually dermal based and has a pushing stellate periphery with plump myofibroblasts and entrapped collagen. Nodular fasciitis is usually well delineated and fascial based and has areas of myxoid degeneration, not seen in fibrous histiocytoma. Ischemic fasciitis or proliferative fasciitis has large polygonal, eccentric nuclei and abundant cytoplasm ganglion cell–like myofibroblasts, not observed in nodular fasciitis. Inflammatory myofibroblastic tumor has similar

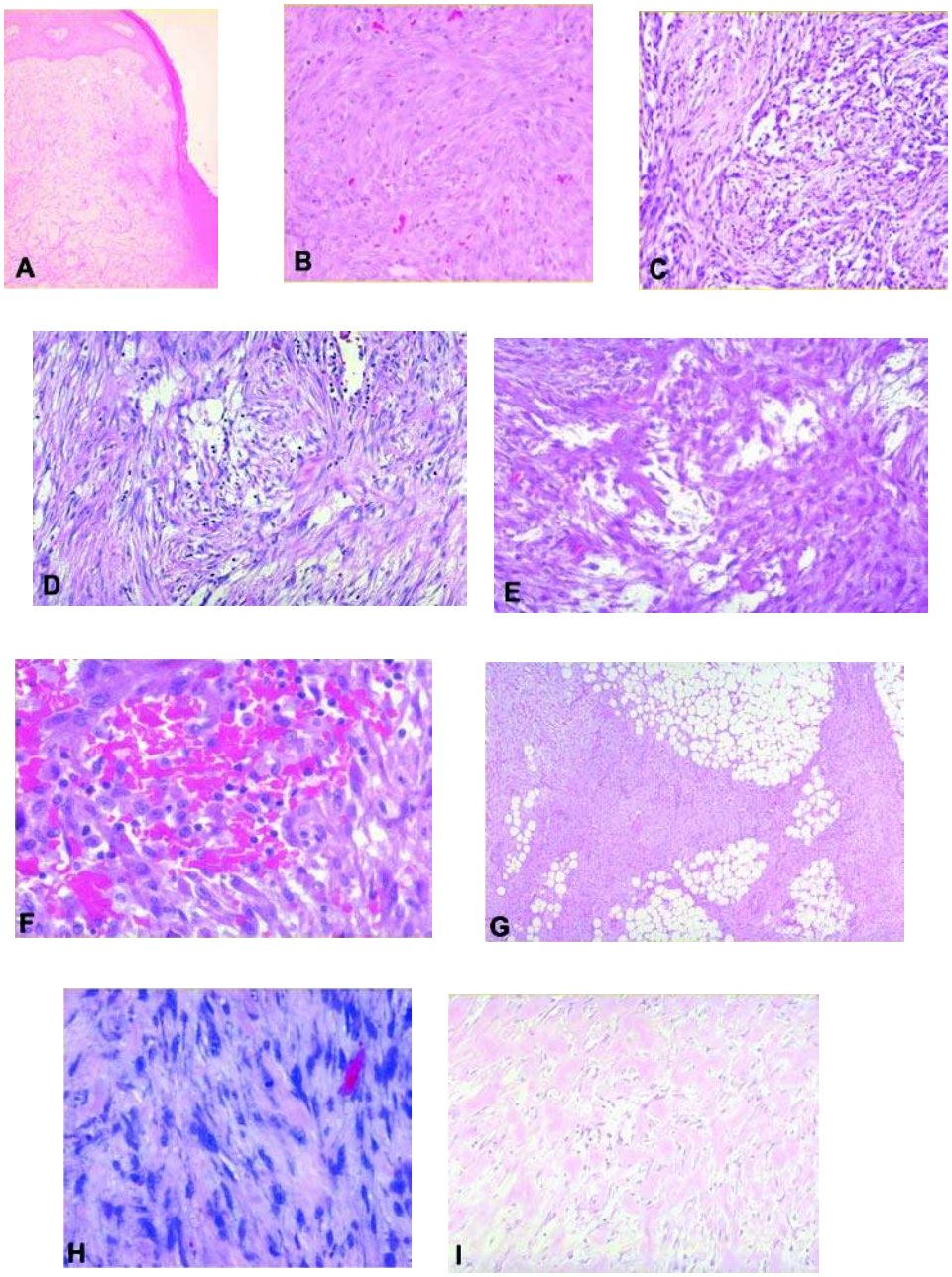

Figure 58 Nodular fasciitis is usually fascial based but can involve dermis (**A**) or mucosa in head and neck. It has alternating loose storiform myofibroblasts of variable cellularity (**B**) and myxoid change (**C–E**) with extravasated erythrocytes (**F**) and lymphocytes, the key diagnostic features. It is usually circumscribed but can be occasionally poorly delineated (**G**). Reactive atypia (**H**) keloidal collagen, (**H,I**) and normal-form mitoses may be present. Older cases have stromal hyalinization (**I**).

cells, but they are dense with admixtures of plasma cells and lymphocytes, both throughout the lesion as well as in lymphoid aggregates. Such inflammatory features are not part of nodular fasciitis. Other pseudosarcomas of internal locations like proximal aerodigestive tract are better diagnosed as pseudotumor rather than nodular fasciitis, a superficial process. Fibromatosis can be morphologically separated by its infiltrative growth pattern into fat and skeletal muscle, its purposeful direction of myofibroblasts, parallel to elongate vessels, and its perivascular hemorrhage, not intralesional hemorrhage like in nodular fasciitis, a mostly well-delineated, fascial-based lesion with reactive parallel vessels (but perpendicular to the access of myxoid change). Now, nuclear β-catenin separates fibromatosis from nodular fasciitis, even in

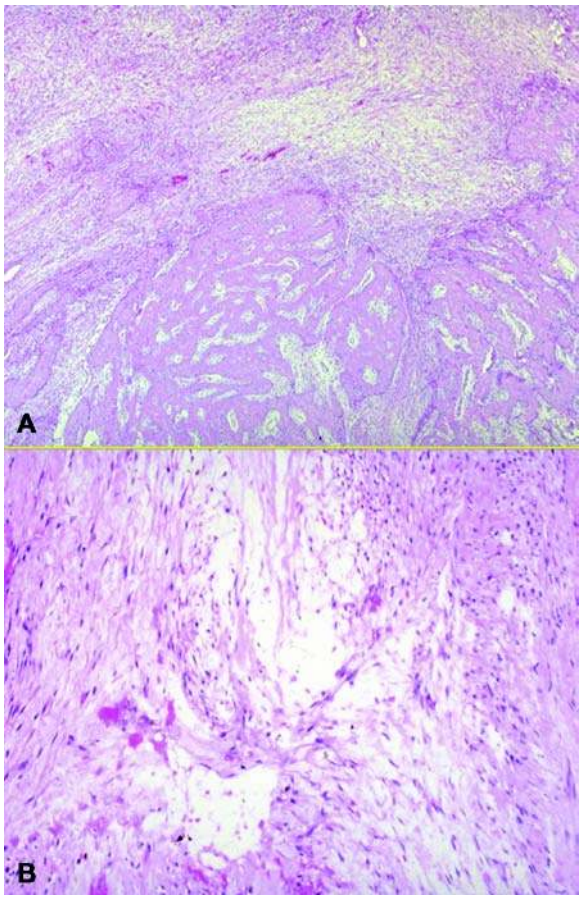

Figure 59 Cranial fasciitis often erodes outer skull table (**A**) but has the same morphologic features as nodular fasciitis, including characteristic myxoid degeneration (**B**).

cases with scant biopsy material (31–33). Myxofibrosarcoma, a low- to intermediate-grade malignancy, has myxoid lobules with prominent ropy vessels, dripping with atypical tumor cells, mitotic activity, and often pseudolipoblasts, not observed in nodular fasciitis. Intravascular fasciitis may be better recognized as an intravascular organizing thrombus. Cranial fasciitis must be separated from desmoplastic fibroma (usually a purely intraosseous lesion), fibromatosis (which is β-catenin nuclear positive, unlike nodular fasciitis), myofibromatosis (which has smooth muscle and hemangiopericytoid features), and FOP, a relentless genetically determined total-body bone forming process in young patients with first toe deviation.

Prognosis and Treatment

Nodular fasciitis is a benign, reactive lesion that only exceedingly rarely reoccurs (3), only if there is repeat trauma, particularly around the ear (8). Once the diagnosis is made by excision or incomplete excision, the lesion can be left alone (1,5,39). Cranial fasciitis is usually excised for diagnosis and may be completely excised with bone when it erodes the skull table.

B. Reactive myofibroblastic lesions, including Proliferative Fasciitis, Proliferative Myositis, and Reactive Periostitis

Introduction

These reactive pseudotumors are all less common than nodular fasciitis. However, these are important to recognize and separate from malignancy, which they can mimic. Proliferative fasciitis (1) or proliferative myositis (2) is the same lesion along fascia or in skeletal muscle, respectively. It is a reactive myofibroblastic lesion, a subcategory is atypical decubital fibroplasias (ischemic fasciitis). Ischemic fasciitis occurs over bony prominences. Reactive periostitis is a mostly osseous lesion, usually in the digits, and is on a spectrum with bizarre parosteal osteochondromatous proliferation (BPOP, Nora's lesion) and Turret exostosis (traction exostosis). These are different from subungual exostosis or other heterotopic bone formations, like fibroosseous pseudotumor and myositis ossificans. This section will be divided into (*i*) proliferative fasciitis and proliferative myositis and related lesions and (*ii*) reactive periostitis and related lesions.

Proliferative myositis/fasciitis and atypical decubital fibroplasia (ischemic fasciitis)

Clinical Findings. Proliferative myositis and fasciitis, the same lesion arising along fascia or intramuscular, respectively, occur in the elderly, with a histologically worrisome variant rarely occurring in children (3,4). There is equal gender predilection. The shoulder is the most common site, but proliferative myositis can also occur in the sternocleidomastoid and masseter muscles, as well as the mylohyoid muscle, buccinator muscle, and tongue (3,5–13). There may be discomfort with opening or closing of the jaws or stiffness of the neck. Ischemic fasciitis occurs over the bony prominences in the elderly or bedridden patients, as a specialized pressure sore, without skin erosion (14). This lesion is thought to occur due to lack of oxygen to the tissue and resultant ischemic change. It is a subcutaneous zonal lesion. It is not found in head and neck locations but is closely related to proliferative fasciitis.

Radiologic Imaging. There is limited radiologic characterization of proliferative fasciitis and myositis. Both CT and MR have been described as showing an ill-defined infiltrative soft tissue mass. The attenuation is similar to muscle on CT, low signal intensity on T1 weighting, and high signal intensity on T2 weighting (15). Ilaslan and colleagues have recently described the imaging appearance of ischemic fasciitis. MR imaging reveals poorly circumscribed replacement of the subcutaneous fat on T1 weighting. There is high signal intensity on T2-weighted MR images with peripheral edema and peripheral enhancement following contrast administration (16).

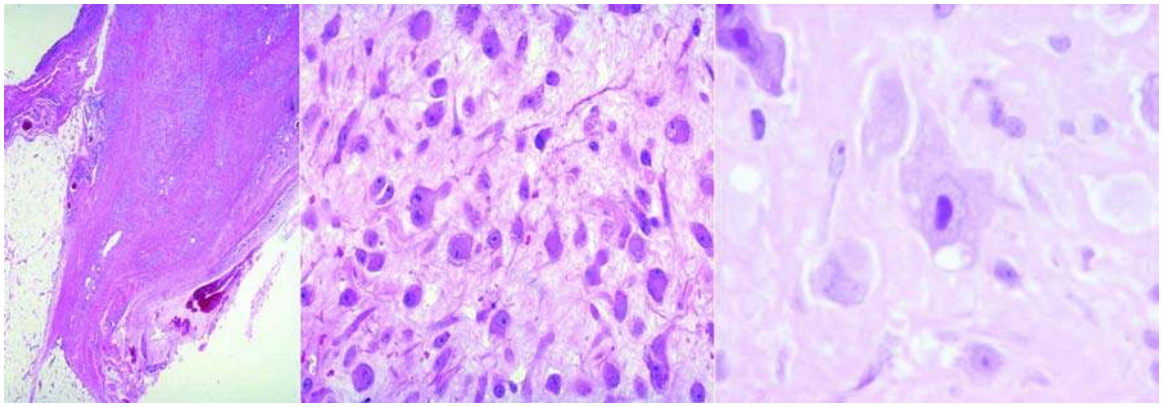

Figure 60 Proliferative fasciitis is composed of a fibromyxoid fascial lesion punctuated by ganglion cell–like myofibroblasts. The latter can mimic rhabdomyoblasts or true ganglion cells.

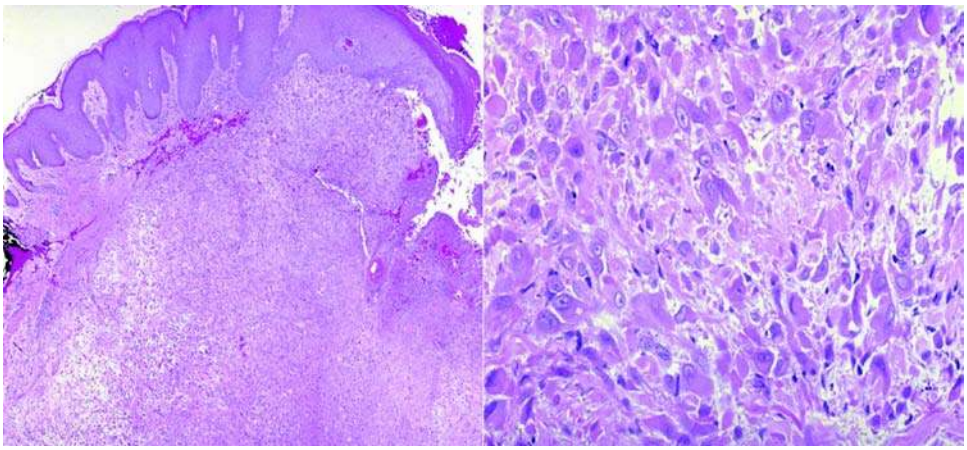

Figure 61 Proliferative fasciitis in childhood is characterized by sheets of ganglion cell–like myofibroblasts; these tumor may have focal ischemic necrosis and should be distinguished from rhabdomyosarcoma. Absent are primitive round cells, geographic necrosis, and desmin and skeletal muscle–specific marker positivity.

Pathologic Findings. Grossly, proliferative fasciitis and proliferative myositis and ischemic fasciitis are poorly delineated scarlike firm indurations of fascia, skeletal muscle, or subcutis, respectively. These are generally less than 5 cm. Microscopically, proliferative fasciitis occurs in the fascia and a poorly delineated fibromyxoid lesion, punctuated by polygonal ganglion cell–like myofibroblasts with abundant, usually stellate, amphophilic cytoplasm, an eccentric vesicular nucleus, and prominent nucleolus (Fig. 60). Mitotic activity may be present but only normal forms. The childhood form of proliferative fasciitis contains sheets of ganglion cell–like myofibroblasts (Fig. 61) and has mimicked rhabdomyosarcoma, with resultant major surgery. Focal ischemic necrosis may occasionally be present. Proliferative myositis (Fig. 62) involves skeletal muscle in a stellate or sunburst pattern, as it entraps skeletal muscle but does not replace it. It, too, has a fibromyxoid, scantly cellular spindled stroma punctuated by these large ganglion cell–like myofibroblasts. Ischemic fasciitis (Fig. 63) has a zonal growth pattern in subcutis with a central linear fibrinoid necrosis, with a fibromyxoid to myxochondroid to punctuated calcification-like stroma. The fibrin is surrounded by the ganglion cell–like myofibroblasts, which in turn are surrounded by a linear granulation tissue.

Immunohistochemistry. The ganglion cell–like myofibroblasts and stromal proliferations are positive for vimentin and occasionally actins but are negative for desmin, myoregulatory proteins (nuclear MyoD1 and skeletal muscle–specific myogenin, myf4), keratins, GFAP, CD34, S-100 protein, and HMB45 (3,4,6,17–21).

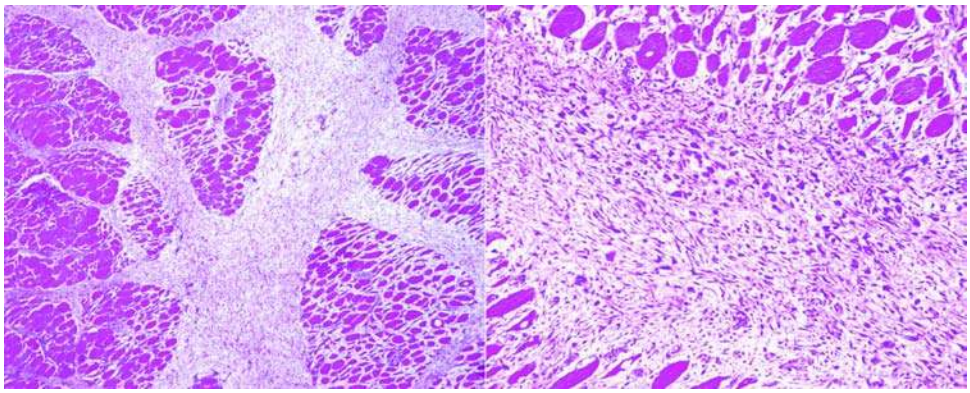

Figure 62 Proliferative myositis has a stellate growth pattern of a fibromyxoid process, also punctuated by ganglion cell–like myofibroblasts.

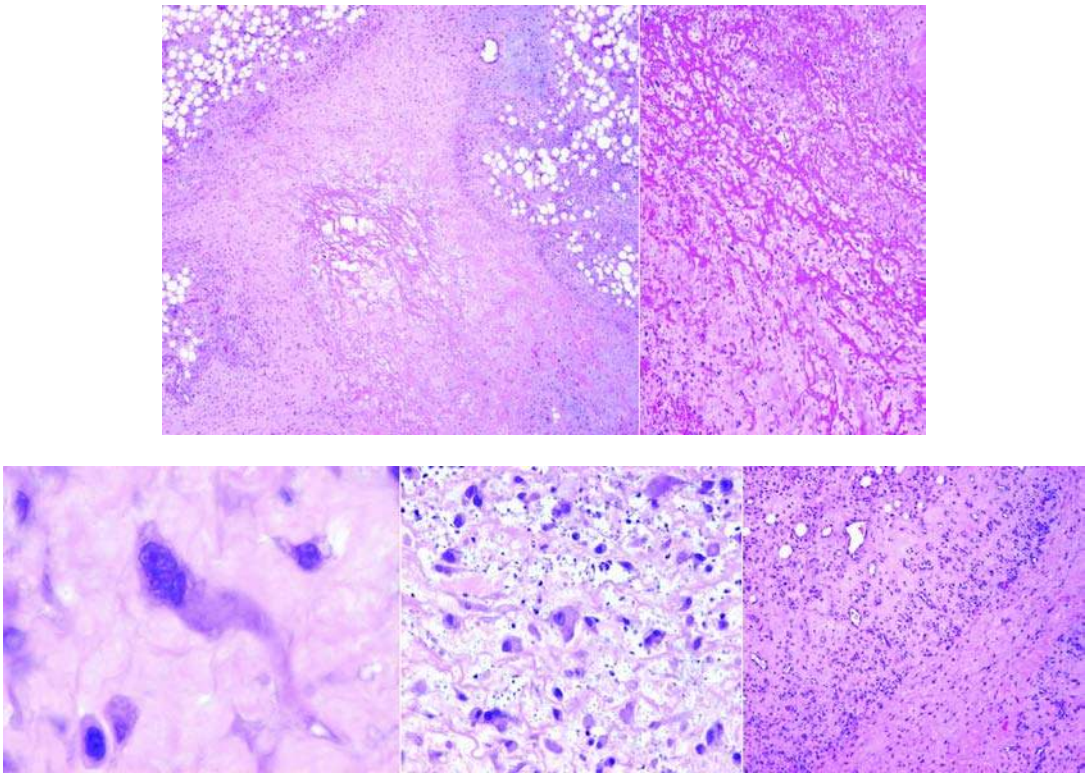

Figure 63 Atypical decubital fibroplasia (ischemic fasciitis) is a specialized pressure sore over bony prominences in the elderly or debilitated with a zonal pathology pattern: fibrinoid necrosis surrounded by ganglion cell–like myofibroblasts in a fibromyxoid stroma to punctuated calcification stroma and then linear granulation tissue.

Electron Microscopy. The ganglion cell–like myofibroblasts show features of myofibroblasts (17,22).

Molecular. The spectrum of BPOP, Turret exostosis, and reactive periostitis has a different chromosomal profile than that for subungual exostosis, but there are only a couple of cases studied (23).

Differential Diagnosis. The differential diagnosis for these lesions is broad, mostly malignant lesions, including tumors with true ganglion cells or rhabdomyoblasts. Remembering that these ganglion cell–like myofibroblasts are negative for desmin, skeletal muscle myoregulatory proteins (including MyoD1

and skeletal muscle–specific myogenin, myf4), and GFAP and the stromal cells are negative for S-100 protein, help to separate the myofibroblasts from most skeletal muscle and ganglion cell–rich neoplasms. Proliferative fasciitis of childhood, with sheets of ganglion cell–like myofibroblasts and occasionally ischemic necrosis, is often mistaken for rhabdomyosarcoma. However, true rhabdomyosarcoma has primitive round cells as well as large strap cells, abundant mitotic activity, and geographic necrosis, as well as desmin and skeletal muscle–specific marker positivity. The granulation tissue in ischemic fasciitis can be worrisome as both the fibroblastic and vascular proliferation can have reactive atypia and mimic sarcoma. Furthermore, the fibrinoid necrosis is usually misinterpreted as geographic tumor necrosis. To separate this lesion from sarcoma, one should look at the low-power zonal appearance and recognize the characteristic features of central linear fibrin, surrounded by atypical myofibroblasts and then by linear granulation tissue.

Prognosis and Treatment. Proliferative fasciitis, proliferative myositis, and atypical decubital fibroplasia (ischemic fasciitis) are all benign reactive lesions that do not require surgical excision, except for diagnosis, unless they mechanically or cosmetically bother the patient.

Reactive periostitis, BPOP, and turret exostosis

Clinical Findings. This group of reactive osseous lesions occur on the surface of bone, particularly the middle phalanges, but can occasionally occur in long bones, skull, and maxilla, including coronoid process. These are on a continuous mostly endochondral ossification process with each other and should not be confused with heterotopic ossifications of soft tissue, including myositis ossificans and fibroosseous pseudotumor of the digits, which are mostly intramembranous ossifications.

Radiologic Imaging. Radiographs of BPOP typically reveal an extensively calcified mass arising and attached to the surface of bone but without abnormality of the cortical surface. No cortical or medullary continuity with the underlying bone is seen as in an osteochondroma. CT shows similar findings, and nonmineralization components may also be apparent. On MR imaging the calcified regions show low signal intensity on all pulse sequences, while the cartilaginous regions may demonstrate high signal intensity on T2 weighting (24).

Pathologic Findings. Grossly, reactive periostitis is a firm, white, smooth periosteal new bone formation (25–39). BPOP and Turret exostosis, a traction exostosis at an insertion site, are lesions with a cartilage cap and stalk, attached to the surface of bone, but no marrow continuity with host bone. These are never more than a few centimeters in size. Microscopically, reactive periostitis is characterized by periosteal new bone formation. This is on a spectrum with BPOP and Turret, mostly in nonhead and neck locations. Reactive periosteal new bone formation could occur on any bone surface after trauma and could be resultant of a periosteal hematoma. BPOP is an osteochondroma-like lesion without marrow continuity to the marrow of the host bone and has a cartilage cap with bizarre, reactive atypical feature that is disorganized and called ''blue bone'' when it mineralizes (40–42). The Turret exostosis is maturation of the hyaline cartilage cap into organized hyaline cartilage, sometimes fibrocartilage, usually at the site of an insertion, and the stalk still is noncontiguous with host marrow cavity (43–48).

Immunohistochemistry. Immunohistochemistry does not play a role in these osseous lesions, but the cells would be positive for osteocalcin, an osteoblastic marker of cells and matrix.

Differential Diagnosis. The differential diagnosis for these lesions is a parosteal or periosteal surface osteosarcoma (49,50), separated by attention to radiologic and clinicopathologic features, particular distal location for the reactive lesions, rimming of benign new bone formation by osteoblasts, absence of a cellular stroma and longitudinal parallel slabs of woven to trabecular bone for parosteal osteosarcoma (parosteal osteosarcomas can have a similar hyaline cartilage cap), and production of malignant osteoid by atypical cartilage for periosteal osteosarcoma.

Prognosis and Treatment. These are only excised for diagnosis and for patient discomfort, mechanical or cosmetic.

C. Myositis Ossificans

Introduction

Myositis ossificans (MO) circumscripta is a reactive centripedal fibroosseous lesion that occurs mainly in the extremities and trunk (1,2). However, heterotopic bone formation can occur anywhere in soft tissue, including in the head and neck. FOP (Munchmeyer's disease) really should not be included within myositis ossificans, although it used to be referred to as myositis ossificans progressive, since it is a completely different clinicopathologic entity. MO circumscripta occurs in young adult healthy males, and FOP occurs in infants, genetically predisposed, who die at an early age because of constriction of breathing from multiple, extraskeletal, osseous lesions. However, this latter clinicopathologic entity does initiate in the posterior neck and back and will be included here for completion.

Myositis ossificans circucumscripta

Clinical Findings. In the head and neck, MO (circumscripta) generally occurs in the masseter muscle (3–5); it has also been described in the buccinator (6), digastric, medial pterygoid (7,8), temporalis (9–11), sternomastoid (12), larynx muscles (13) and platysma muscles (8), the latter following radical neck dissection. Myositis ossificans generally occurs in young patients (14–17), with a male predilection (18); there is often a history of antecedent trauma (1,19,20). The lesion rapidly arises and may be erythematous and painful in the beginning to hard and painless over the subsequent weeks. The whole lesion will mature

over six to eight weeks, and one can perform repeat imaging to watch the maturation of the lesion, to separate it from malignancy. The current belief is that a hematoma forms after trauma and for some reason, mostly intramembranous ossification takes place (i.e., fibroblasts differentiate directly to activated osteoblasts, without a cartilage intermediate, and produce bone).

Radiologic Imaging. The most important radiologic finding is that myositis ossificans has an outer shell of bone, identified on X ray, indicating that it is a zonal lesion with the most mature bone at the periphery. Myositis ossificans is also usually found only in soft tissue, without attachment to bone. Both of these features, outer shell of bone formation and soft tissue only location, distinguish myositis ossificans from parosteal osteosarcoma, which arises from the surface of bone and has central maturation of bone rather than peripheral. Radiographs of myositis ossificans demonstrate the zonal phenomenon seen pathologically with a peripheral rim of ossification representing more mature bone. However, this calcification may require two to six weeks to form and is optimally detected by CT. Lesions typically mature over the ensuing months to form a complete outer cortex and inner trabecular bone with yellow marrow when mature. Myositis ossificans is typically separate from the cortex and denser centrally, in contradistinction to parosteal osteosarcoma. Bone scintigraphy reveals marked increased radionuclide activity on all phases initially, with gradual reduction in the degree of uptake with maturation. MR imaging often simulates a more aggressive process as the peripheral rim of ossification is difficult to detect and characterize as calcification. The soft tissue mass has intermediate signal intensity on T1-weighting, high signal intensity on T2-weighting, and enhances with contrast. There is a prominent zone of irregular surrounding edema that gradually recedes toward the soft tissue mass with maturation. Mature myositis ossificans demonstrates internal yellow marrow signal characteristics on MR imaging (Fig. 64) (21,22).

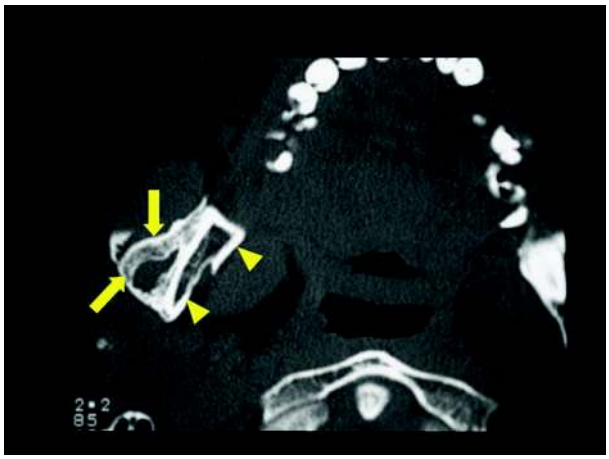

Figure 64 Young alcoholic patient with history of multiple trauma and myostis ossificans lateral to the mandible, causing limited temporomandibular joint motion. CT shows a well-corticated ossific mass (*arrows*) with marrow centrally lateral to the mandible (*arrowheads*) resulting from mature myositis ossificans.

Pathologic Findings. Grossly, myositis ossificans is a well-delineated tan mass with a soft glistening center and a firm gray-white gritty periphery. Sizes range from 2 to 12 cm but average 5 cm. Microscopically, myositis ossificans starts as a fasciitis-like stroma, often with numerous normal form mitoses and very immature osteoid in the center. The osteoid matures at the periphery of the lesion, giving the lesion a zonal distribution (Fig. 65). The central area may have cystic hemorrhage, suggesting a traumatic origin (Fig. 66). The key features of the fasciitis-like stroma are the wispy tissue culture–like myofibroblasts, sometimes plump and cellular, and the areas of myxoid degeneration with extravasated

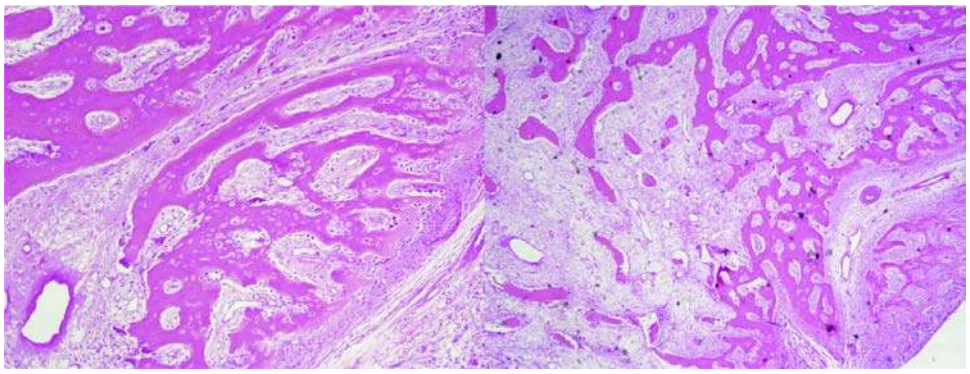

Figure 65 Myositis ossificans is a very zonal lesion with the most mature bone at the periphery.

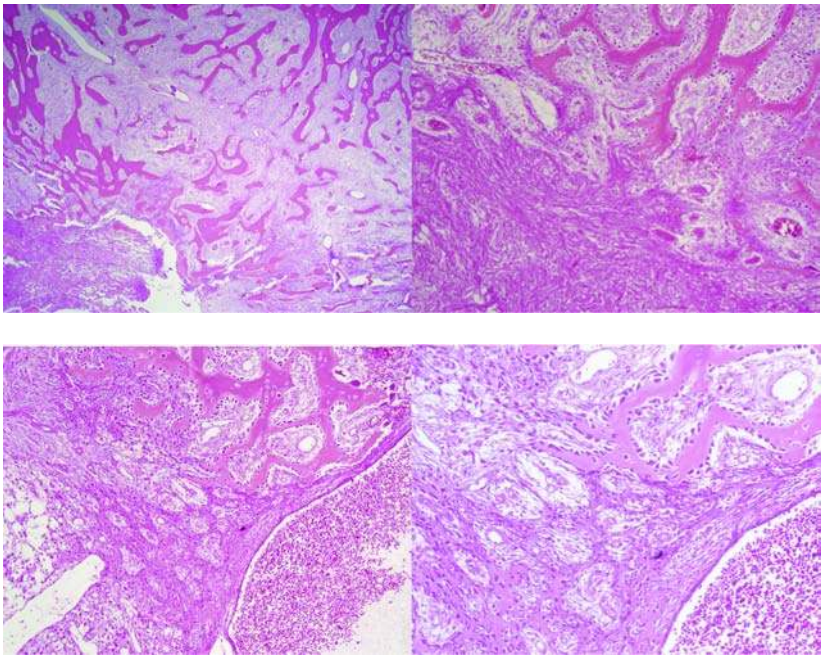

Figure 66 There is progression in myositis ossificans from the outer mature area to the central immature areas, sometimes cystic and hemorrhagic in the center, indicating that trauma has occurred. There are four components of the zonation: sometimes a central hemorrhagic area, a cellular fasciitis-like area, beginning of intramembranous ossification to very immature osteoid and then mature osteoid, rimmed by osteoblasts. The lesion can then mature to trabecular bone and the marrow can undergo fatty replacement, as the lesion resolves.

erythrocytes and lymphocytes (Fig. 67). There may also be keloidal collagen. The osteoid in the center will be lined by plump immature osteoblasts, but they blend with the background fasciitis-like stroma and can be either misinterpreted as atypical or can be hard to recognize as osteoblastic rimming and mimic osteosarcoma. If one looks at low magnification and appreciates the zonal pattern, one will also appreciate the benign sign of osteoblastic rimming (Fig. 68). The more mature bone at the periphery of the lesion may also still be woven, but have more mineralization, rimmed by more obvious osteoblasts as the stroma turns to fat, simulating fatty marrow. Over time, the peripheral bone may mature to trabecular, stress-lined bone. Cartilage may be part of the lesion, if endochondral ossification occurs, but the bone formation is usually intramembranous. As with any bone-forming lesion, radiologic correlation is required for correct diagnosis of this lesion.

Immunohistochemistry. Immunohistochemistry is not used to make the diagnosis of benign bone-forming lesions and does not distinguish benign from malignant bone-forming tumors, however, osteocalcin is a sensitive and specific marker for osteoblasts (23).

Electron Microscopy. The stromal cells are myofibroblasts with dilated rough endoplasmic reticulum and aggregates of cytoplasmic filaments occasionally associated with dense bodies (24). The bone-forming cells demonstrate evidence of osteoblastic differentiation, containing mitochondria and abundant dilated rough endoplasmic reticulum.

Differential Diagnosis. The most important of the differential diagnoses is osteosarcoma (25). Parosteal osteosarcoma, a low-grade surface osteosarcoma, has longitudinal slabs of woven to trabecular bone with a low-cellularity fibroblastic stroma and occasional mitotic activity, often with a cartilage cap. It arises from the surface of bone and is centrally more osseous and peripherally more stromal and infiltrative. Myositis ossificans, on the other hand, has a zonal, centripedal bone-forming pattern, whereby the periphery is more mature and bony and the center is less mature and more stromal; it is usually entirely within soft tissue and does not involve bone, although there may rarely be an associated periosteal new bone formation adjacent to it. Soft tissue osteosarcoma is usually high grade and has obvious malignant osteoblasts with atypical mitoses and nuclear hyperchromasia, producing ''malignant'' osteoid. Clinically, myositis ossificans is often thought to be a soft tissue tumor before it is excision (26).

Prognosis and Treatment. Myositis ossficans is a benign reactive lesion that only rarely locally recurs. The treatment of choice is to watch the lesion mature radiologically, without surgical excision, and then excise it if clinically indicated (17,27).

Fibrodysplasia ossificans progressive (myositis ossificans progressive)

Clinical Findings. This is an extremely rare disease, occurring as incomplete penetrance of an autosomal dominant mutation (28,29). The patients start at birth, with bone formation in the posterior neck and back, often in the paravertebral muscles, formation of an entire skeleton outside of their skeletons, and end up with constriction of normal respiration. There is almost always associated lateral deviation of the great toes. Patients often have severe

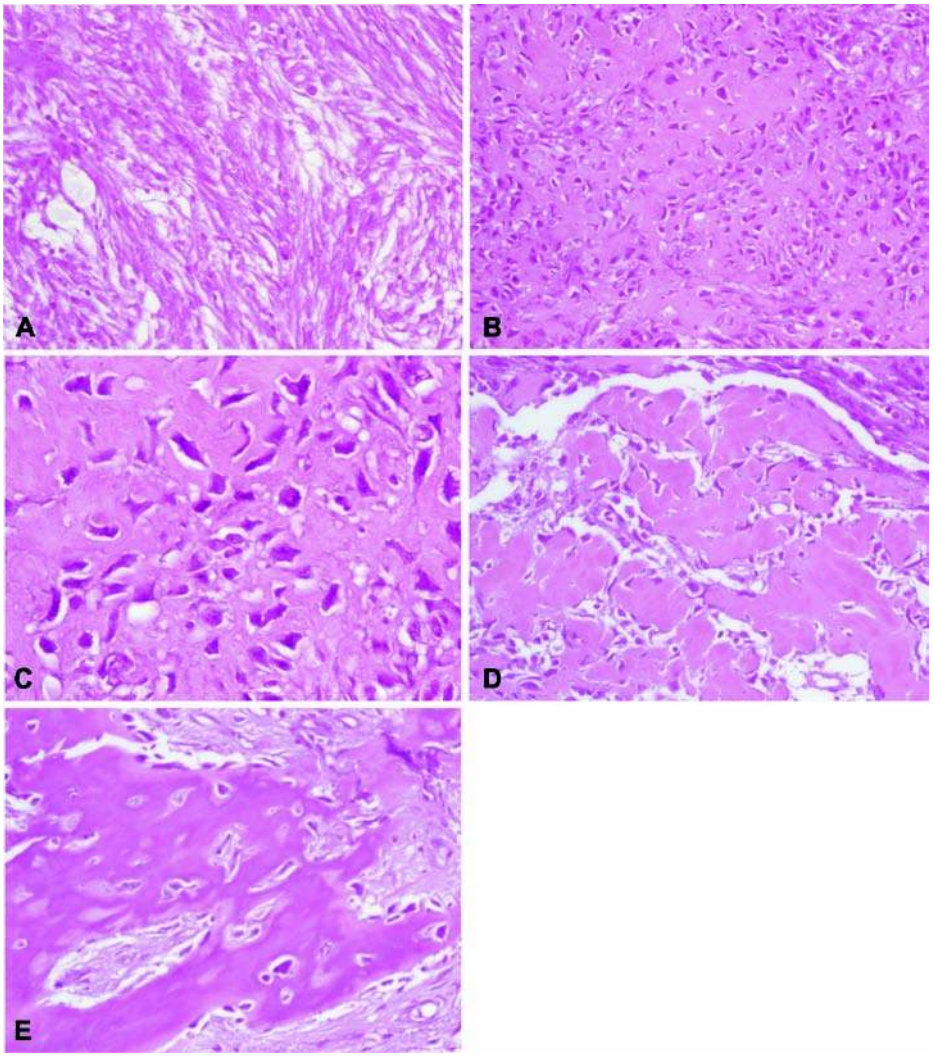

Figure 67 Progression from central fasciitis-like stroma (**A**) to intramembranous ossification and immature osteoid (**B–D**) resembling osteosarcoma to osteoblastic rimming to more interconnection and mineralization of osteoid (**E**).

difficulties with their jaws (30–32). The disease is progressive and immobilizing but can occur at different rates. For families with patients with FOP, the best website for the most updated information is http://www.ifopa.org/.

Radiologic Imaging. FOP demonstrates similar features as myositis ossificans but much more extensive and frequently beginning in the neck and upper posterior paraspinal regions. Associated osseous abnormalities include microdactyly of the great toes (typically proximal phalanx in greater than 90% of patients and often precedes soft tissue ossification) and thumbs, short, broad femoral necks, narrowed anteroposterior vertebral body dimension (cervical and lumbar), and enthesophyte formation (Fig. 69) (33).

Pathologic Findings. The lesions start off as nodular fasciitis–like lesions that ossify, similar to myositis ossificans.

Immunohistochemistry. As with myositis ossificans, this is a histologic and clinical diagnosis, but these lesions are also negative for nuclear β-catenin, separating them from fibromatosis in their early phase.

Differential Diagnosis. Early on before the bone formation, these lesions may simulate nodular fasciitis or cranial fasciitis or fibromatosis. The latter can be separated by its nuclear β-catenin positivity and morphologic features of an infiltrative, purposeful myofibroblastic proliferation with elongate vessels and perivascular hemorrhage. After bone formation, these can be separated from osteosarcoma by their benign osteoblastic rimming of bone.

Prognosis and Treatment. FOP has a poor prognosis with patients usually dying by age 20 from inability to breathe, due to immobilization by the multiple bone-forming lesions that coalesce to form bony ''plates.'' There is no effective treatment.

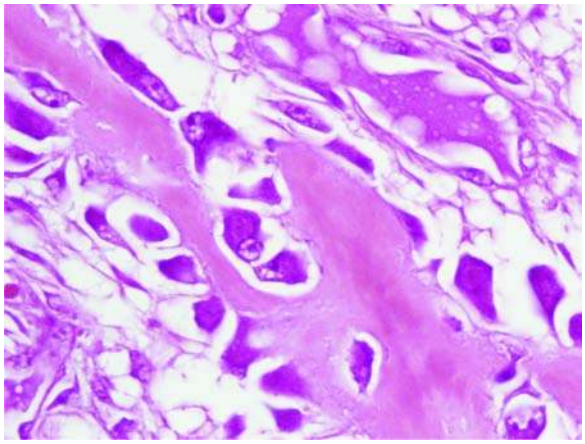

Figure 68 Low-power observation of zonation and osteoblastic rimming is a benign sign and separates myositis ossificans from malignancy.

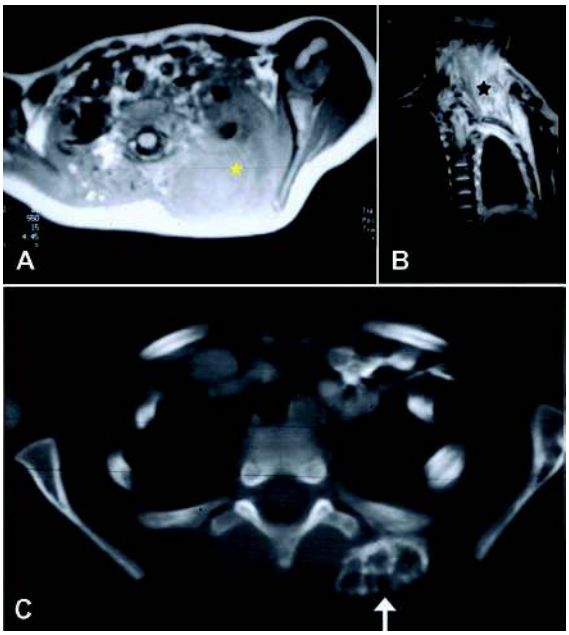

Figure 69 Fibrodysplasia ossificans progressiva developing in a young patient. Axial T1-weighted (**A**) and coronal T2-weighted (**B**) magnetic resonance images show extensive infiltration of the left neck by a large mass (*) that has high signal intensity on T2-weighting. Initial CT and radiograph (not shown) revealed no significant calcification, but subsequent CT several months (**C**) later demonstrated extensive ossification, most prominent peripherally (*arrow*).

Steroids may alleviate swelling or pain but do not alter the course of disease; chelating agents such as EDTA have been uneffective (34). Attempt at surgical excision only aggravates the field and produces more bony lesions.

D. Osseous and Cartilaginous Choristomas (Extraskeletal Osteoma and Extraskeletal Chondroma of Head and Neck)

Introduction

There is much confusion as to what is meant by ''extraskeletal osteoma.'' in the head and neck; choristomas are true extraskeletal benign osseous and cartilaginous masses in the head and neck.

The term ''osteoma'' is used by orthopedic pathologists for skull and mandibular lesions composed of hypertrophic compact cortical bone with Haversian canals and concentric lamellae and scant to absent loose stroma (not cellular). Multiple jaw or skull osteomas may be found in Gardner syndrome.

Also in the head and neck literature, ''osteoma'' is used for lesions composed of mature lamellar bone in the paranasal sinuses, facial bones, and orbit, or sometimes for external auditory meatus or tympanic bone ''enlargement.'' But these are of the outer cortex or are pedunculated and attached to bone and therefore not ''extraskeletal.'' Mostly in frontal and ethmoid sinuses, rarely in maxillary or sphenoid sinuses, this pedunculated osseous mass is almost always attached to the surface of bone. The same applies to the intraauditory lesion, and these will be covered under intraosseous lesions.

''Osteoid osteoma'' is a specific clinicopathologic entity occurring mainly in the cortex of long bones as a targetoid lesion that is painful at night, relieved by aspirin. The central nidus must be surgically removed for pain relief.

The term ''exostosis'' should be limited to long bone osteochondromas or insertion site traction (avulsion) injuries of the hands and feet proximal to middle phalanges (Turret exostosis, see BPOP above). The long bone osteochondromas are pedunculated or sessile hyaline cartilage–capped lesions with a stalk and continuous marrow space with long bone that point in a 45° angle away from a joint. Subungual exostosis is a distal digit, under the nail bed, osteochondroma-like lesion with a fibrocartilage rather than hyaline cartilage cap and has a different genetic finding than the more proximal digit lesions on a spectrum with Turret exostosis.

Any true extraskeletal bone formation is usually referred to as ''heterotopic bone'' and will generally be intramembranous and sometimes with endochondral ossification of soft tissue in a zonal, centripedal arrangement, akin to myositis ossificans.

An intraoral or dermal osseous metaplasia may be considered as an extraskeletal osteoma, although most of these are dystrophic calcifications or osseous metaplasia. This section will focus on intraoral ''osteomas.''

Osseous and cartilaginous choristomas are relatively uncommon benign developmental lesions that have a predilection for the tongue. The term choristoma refers to a tumorlike mass of histologically normal tissue in an abnormal location. These lesions have frequently been referred to as osteoma or chondromas,

but there is no evidence that these are true neoplasms and the term ''choristoma'' is preferred (1–11).

Radiologic Imaging

Osteomas are most frequent in the frontal and ethmoid region (75% of lesions) and have been observed as solitary lesions in 0.42% of all sinus radiographs. Radiographs reveal a focal area of homogeneous, markedly increased radiodensity. Similarly CT shows a region of marked high attenuation typical of osteoid matrix without medullary canal formation. On MR imaging there is low signal intensity on all pulse sequences. Lesions are attached to the cortex but show no medullary canal or cortical continuity with the underlying bone. There is no enhancement with intravenous contrast on CT or MR imaging.

Soft tissue chondromas typically reveal punctuate areas of calcification on radiographs or CT in 33% to 70% of cases. This mineralization usually reveals a punctuate ''ring and arc'' pattern suggesting a chondroid pattern. Nonmineralized regions demonstrate the high water content of hyaline cartilage with low attenuation on CT, low signal intensity on T1-weighted MR and marked high signal intensity on T2-weighted MR images.

Clinical Findings

Osseous and cartilaginous choristomas have a strong predilection for the tongue. About 85% occur on the tongue, and the majority of these are found on the dorsal posterior third near the foramen cecum. Beyond the tongue, there have been rare examples described in the buccal mucosa, vestibule, and gingiva (1,6,12–15). They are firm, exophytic nodules surfaced by intact oral mucosa. The lesion's base may be sessile or pedunculated. Depending on the lesion's size and specific location, dysphagia may be reported, but the mass itself is asymptomatic. Most cases are in adults, but the lesions occur across a broad age range, affecting patients from the first to ninth decade of life (1). Lingual osseous and cartilaginous choristomas have a strong female predilection. Over 70% of the osseous variety occurs in women.

Imaging

Because these choristomas are superficial and readily apparent on clinical examination, there is generally not a significant role for imaging studies in their diagnosis or treatment. CT examination can confirm the radiodense nature of osseous choristomas (16).

Pathologic Findings

Grossly, the samples consist of firm masses covered by oral mucosa. They are small in size and smoothly contoured. Most are 1.0 cm or less in diameter and lesions larger than 2.0 cm warrant careful microscopic examination to ensure an accurate diagnosis. Osseous choristomas are composed of dense mature bone. They appear to be simply embedded in the surrounding submucosa, without an adjacent tissue reaction. The bone may have a lobulated arrangement or be single ovoid mass. Osteoblastic rimming is not prominent, and the osteocytes are compact and unremarkable (Fig. 70). Cartilaginous choristomas are composed of mature hyaline cartilage set in fibrous tissue that resembles perichondrium. There are usually multiple lobules of cartilage. Chondrocytes vary from small to large, but lack atypia (Fig. 71). Occasionally, bone and cartilage are present in the same lesion.

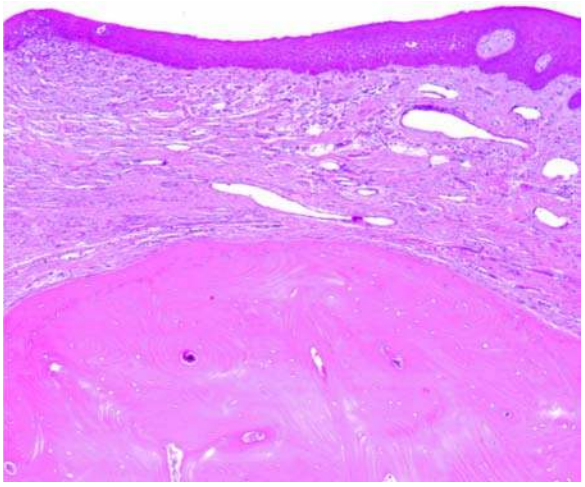

Figure 70 Osseous choristoma. The lesion consists of a dense mass of vital bone embedded in the submucosa. Overlying mucosa is intact and unremarkable.

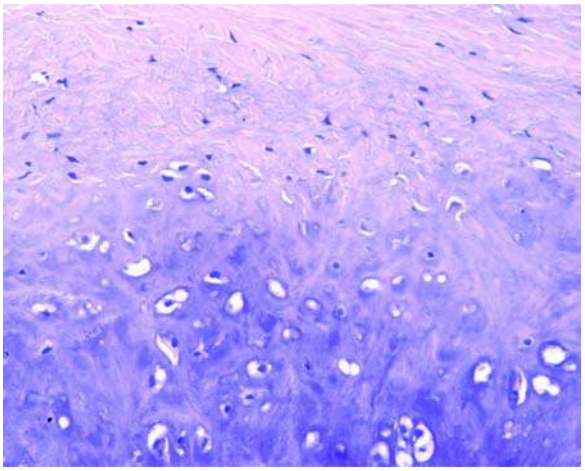

Figure 71 Cartilaginous choristoma composed of mature cartilage without atypia.

Immunohistochemistry

These choristomas can be diagnosed on the basis of histologic examination and do not require immunostains.

Differential Diagnosis

Microscopic diagnosis of these choristomas is usually not challenging, particular if appropriate clinical information is provided. It may be prudent to consider other oral lesions with osteocartilaginous differentiation, in particular the mixed tumor (pleomorphic adenoma). Choristomas may occur in areas with minor salivary gland tissue, but they do not have ductal or myoepithelial components. It is noted that, on careful examination, purported chondromas of the parapharyngeal space frequently turn out to be salivary gland mixed tumors (pleomorphic adenomas) of deep parotid lobe origin.

Prognosis and Treatment

Osseous and cartilaginous choristomas are adequately treated by local surgical excision. Recurrence is not a concern.

E. Idiopathic Cervical Fibrosis

Introduction

Idiopathic cervical fibrosis is a mass-forming fibrosclerotic process that can be considered to fall within the spectrum of idiopathic fibrosclerotic lesions involving the retroperitoneum, mediastinum, liver, and thyroid gland. The terms sclerosing cervicitis, cervical fibrosclerosis, and tumefactive fibroinflammatory lesion have been used synonymously, although the latter term also encompasses morphologically similar lesions in the sinonasal tract and face (1–11). Involvement of the head and neck is the least common presentation of this group of disorders. Cervical involvement may be isolated or occur concomitantly with other sites (11–14).

Clinical Features

Idiopathic cervical fibrosis tends to present as a mass lesion. Pain or functional deficits, such as trismus, may precede the discovery of a mass. The nature of the disease process is such that the mass is fixed to underlying or adjacent tissues with a firm texture. The clinical presentation frequently suggests a malignant or clinically aggressive neoplasm (13). This is characteristically a lesion of adults with the majority of reported examples affecting patient in the fourth and fifth decade of life, but cases have involved children or elderly patients (4,8,12,15). Men and women are equally affected. Idiopathic cervical fibrosis most often involves the soft tissue compartments of the neck. Specific sites of involvement include the lateral neck, mandibular angle, submandibular triangle, parotid region, infratemporal fossa, nasopharynx, and skull base. Similar lesions have occurred in the periorbital region, nasal cavity, paranasal sinuses, and facial soft tissue (3,4,8,10,13,15–17). Unilateral lesions are typical, but bilaterality has been reported (18). This is a diagnosis of exclusion and one must rule out a drug-related, collagen-vascular, or infectious process first.

Imaging

CT examination of idiopathic cervical fibrosis reveals an infiltrating and enhancing process that tends to diffusely involve the soft tissue structures of the neck. The process may be extensive in both the anterior-posterior and superior-inferior dimensions on CT and MR imaging. Tissue compartments and fat planes are compromised, which may lead to encasement of normal neck tissues and vital structures. There may be extrinsic compression of the airway (9). The carotid and jugular vessels when encased demonstrate only limited narrowing. Both T1- and T2-weighted images may show prominent low signal intensity. Postcontrast images reveal heterogeneous enhancement of the mass, but MR angiography suggests a relatively avascular mass (18,19).

Pathology

Grossly, idiopathic cervical fibrosis consists of a relatively well-circumscribed mass of firm, pale gray-tan tissue. Histologically, the lesions are composed of moderately to paucicellular, densely collagenous fibrous tissue containing a patchy distribution of inflammatory cells (Fig. 72). Thin walled, capillary-like vessels are interspersed throughout the fibrous tissue. The fibroblastic cells have a pattern-less or disordered arrangement and bland nuclei. The inflammatory infiltrate consists of small lymphocytes and plasma cells admixed histiocytes and less likely neutrophils or eosinophils, the latter two suggesting an alternate etiology. There is invasion, envelopment or entrapment of native blood vessels, nerve bundles, skeletal muscle, and adipose tissue by the fibroinflammatory process. It has been suggested that these fibrosclerosing lesion undergo ''maturation'' during which they become progressively more collagenous, hyalinized, and acellular (5,10). The histomorphologic features are invariably benign in appearance and the presence of cytologic atypia, increased cellularity, or significant mitotic activity, including atypical forms, supports consideration of an alternative diagnosis.

Immunohistochemistry

Immunohistochemical evaluation's primary role in diagnosis of fibroinflammatory lesions is to eliminate other entities from consideration. The fibrous component is composed of vimentin reactive cells admixed with a varying numbers of SMA positive myofibroblasts. Lymphoid markers reveal a mixed population of T and B lymphocytes along with CD68 reactive histiocytes. Kappa and lambda stains not reveal evidence of light-chain restriction in the plasma cells.

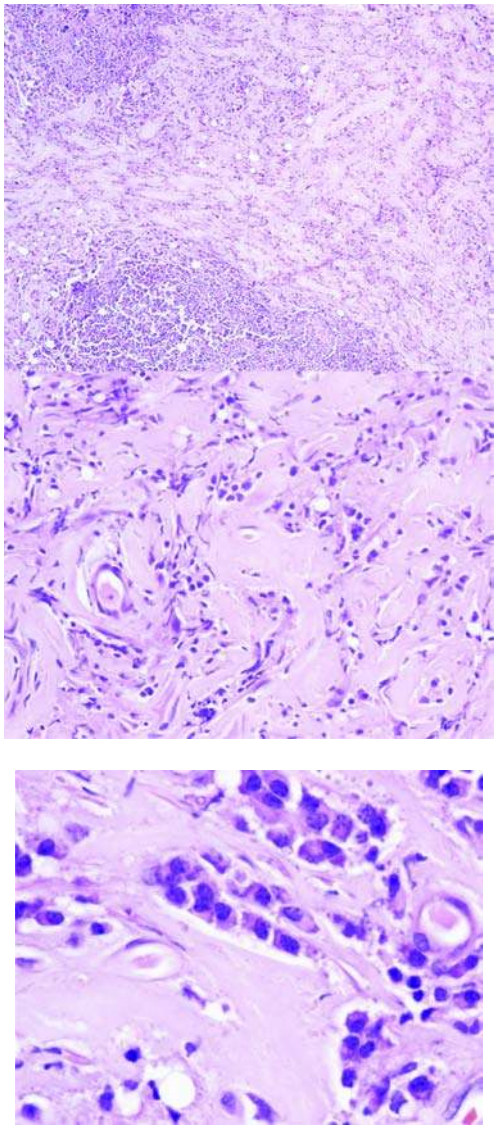

Figure 72 Idiopathic cervical fibrosis is mostly paucicellular and fibrocollagenous with scattered chronic inflammatory cells, including small lymphocytes and plasma cells. This is a diagnosis of exclusion, to rule out other etiologies, such as drugs or infection, before making this diagnosis.

Electron Microscopy

Ultrastructural examination of this fibro-inflammatory process has not been performed.

Differential Diagnosis

Idiopathic cervical fibrosis generally progresses in a benign fashion, and distinguishing it from potentially similar but clinically aggressive entities is important. Advances in immunohistochemistry and molecular pathology currently allow differentiation of a variety of conditions that may have been included under the umbrella or idiopathic fibrosclerotic disorders in the past. The differential diagnosis for fibrous and fibro-inflammatory lesion in the neck includes fibromatoses, nodular fasciitis, inflammatory myofibroblastic tumor, and low-grade myofibroblastic sarcoma (6,20–23). Nodular fasciitis is composed of moderately cellular sheets of ''tissue culture'' myofibroblasts with foci of hemorrhage or extravasated red blood cells. Entrapped tissues are uncommon, and most examples are superficial and of modest size. Fibromatoses and low-grade myofibrosarcomas are destructive lesions that invade and destroy normal tissues. They are more cellular with a better-developed fascicular growth pattern. Inflammation is not a prominent component, and SMA staining is uniform and diffuse. Inflammatory myofibroblastic tumor, in particular, warrants consideration and can be distinguished on the basis of greater cellularity, enlarged atypical cells, and a myxoid background. About half of inflammatory myofibroblastic tumors are ALK-1 positive. Additional considerations include sclerosing extranodal lymphomas and Rosai-Dorfman disease. In extranodal Rosai-Dorfman disease, the characteristic large histiocytic cells with emperipolesis can be inconspicuous relative to the fibroinflammatory component (24–26).

Treatment and Prognosis

Treatment regimens for idiopathic cervical fibrosis have included surgery, radiation, and steroids (6–8,10–13,16). Steroids are usually employed as the initial treatment of choice, but surgical excision is also utilized. The lesions usually behave in a benign fashion and respond well to steroids or surgery, but occasional examples progress in the face of conservative management (13,19). Tamoxifen has been employed for lesions that are refractory to steroids (9,14).

F. Fibrous Hamartoma of Infancy

Introduction

Fibrous hamartoma of infancy was first defined as an entity by Dr. Franz Enzinger (1). It is rare and is infrequent in the head and neck, generally occurring in a posterior or anterior axillary location in infants, before the age of one year.

Clinical Findings

Fewer than 10% of cases involve the head and neck, generally the neck, face, and scalp (2,3). It has been described in the pharynx (4). Fibrous hamartoma of infancy occurs in infants of up to two years, but 25% are discovered at birth (2,5–7). There is a predilection for males (8). It is generally a freely movable subcutaneous or dermal mass, only rarely involving skeletal muscle. The axillary folds are the most common location, followed by the shoulder, thigh, groin, back, and forearm (9). Hence, the proximal extremities are second most common.

Imaging

Fibrous harmatoma of infancy is rarely reported in the radiologic literature. In our experience, these masses are heterogeneous and may show evidence of interspersed fat on MR imaging.

Pathologic Findings

Grossly, poorly circumscribed gray-white tissue alternating with yellow fat, fibrous hamartoma of infancy is often less than 5 cm (5). Microscopically, there are three intermingled or alternating components (Fig. 73): mature fat, primitive or immature stellate to round cells in a myxoid stroma, and a hypocellular to moderately cellular spindled myofibroblastic to dense fibrous trabeculae (Fig. 74). This last component has bland uniform nuclei without mitotic activity. The primitive stellate to round cells in myxoid stroma are often oriented around small veins and also lack mitoses. The fat can be in various proportions and may be scant or abundant (Fig. 75).

Immunohistochemistry

The myofibroblastic spindled and immature primitive components may have actins but lack desmin (10). The fat can be positive for S-100 protein, as is normal fat.

Electron Microscopy

The spindled cells are myofibroblasts, and the primitive mesenchymal cells with slender cytoplasmic processes have few intracytoplasmic organelles in the loosely textured myxoid areas (11,12).

Molecular Findings

Cytogenetic analysis of fibrous hamartoma of infancy has been done twice so far. A reciprocal translocation t(2;3)(q31;q21) has been identified as the sole abnormality in one case (13). In another case, a karyotype revealed complex cytogenetic alteration involving chromosomes 6, 8, and 12, namely, t(6;12;8)(q25;q24.3;q13) translocation, as the sole abnormality (14). These cytogenetic findings might suggest that fibrous hamartoma of infancy represents a benign neoplasm.

Differential Diagnosis

The differential diagnosis would include lipofibromatosis, which generally occurs in the distal extremities

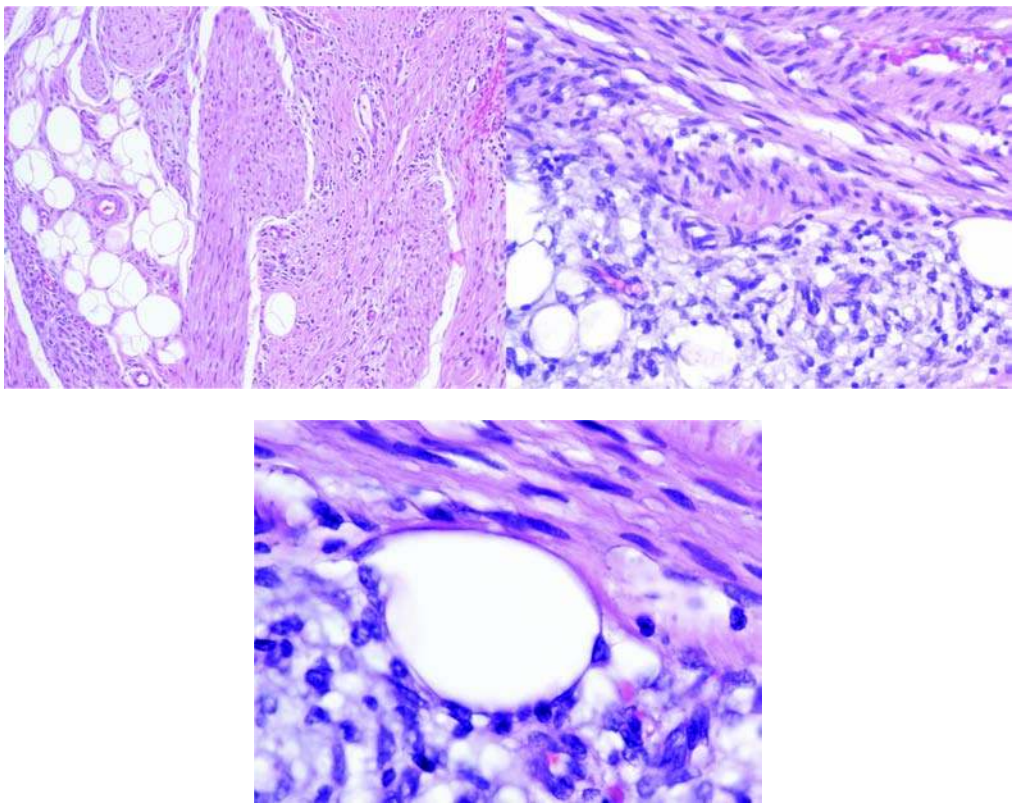

Figure 73 FHI is a lesion composed of three components of varying proportions: myxoid areas with primitive stellate to round cells, spindled myofibroblastic area, and fat. *Abbreviation:* FHI, fibrous hamartoma of infancy.

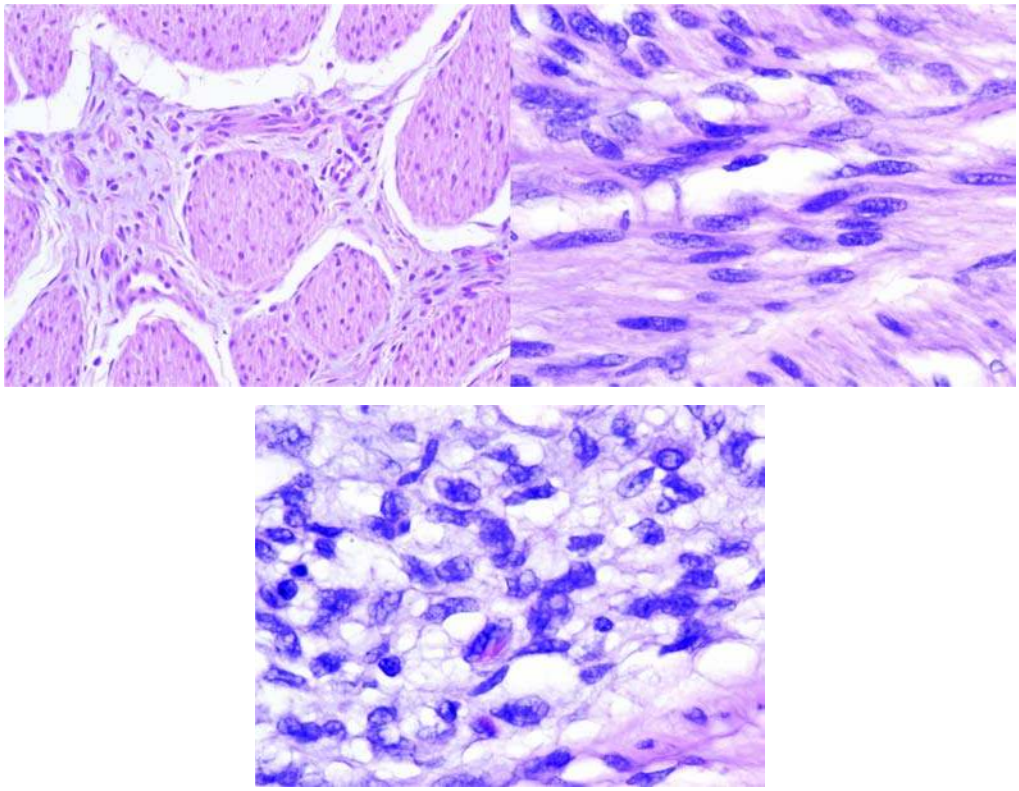

Figure 74 Recognition of the myoid and myxoid/stellate/primitive areas can be helpful to identify FHI. *Abbreviation:* FHI, fibrous hamartoma of infancy.

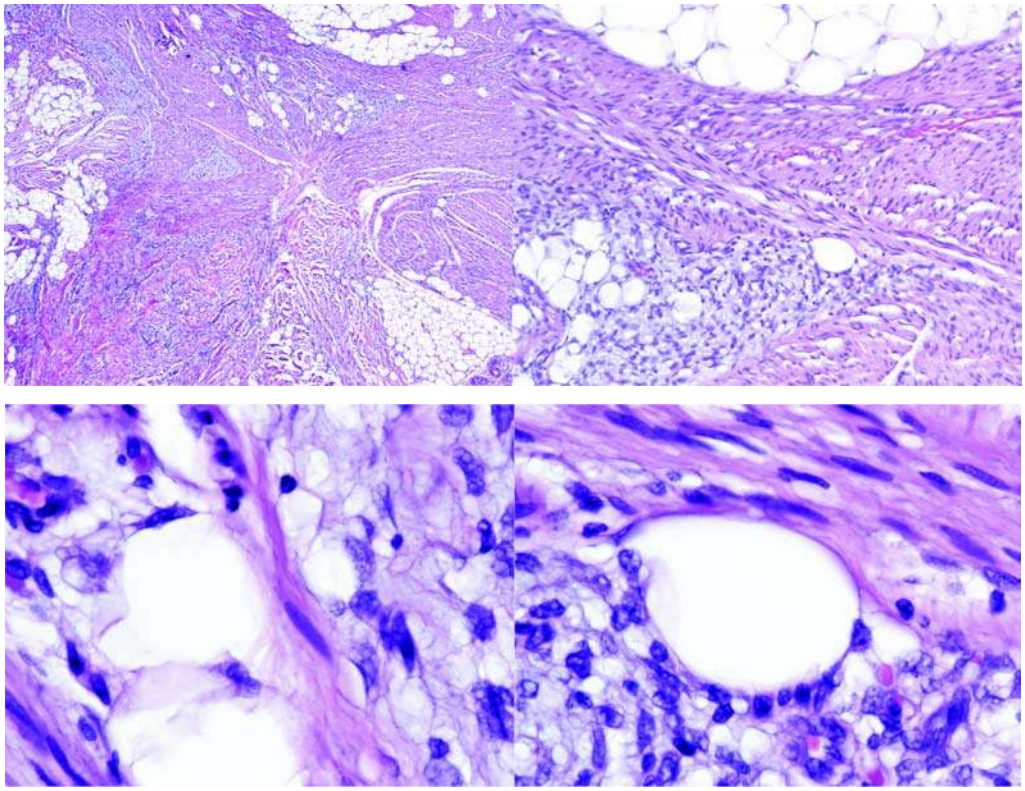

Figure 75 The fat in FHI is found in varying proportions.

and lacks an immature myxoid/stellate to round cell component (15,16). It also manifests microfat cells entrapped in the fibroblastic component, which are not observed in fibrous hamartoma of infancy. Fibromatosis would not have the other two components of fibrous hamartoma of infancy and would occur in an older age group. Small blue cell or spindled malignancy would have mitotic activity and necrosis, absent in fibrous hamartoma of infancy.

Prognosis and Treatment

This benign lesion is cured by local excision, with recurrence in about 16% of cases, which is cured by re-excision (1,5,17).

G. Fibromatosis Colli (Torticollis)

Introduction

Fibromatosis colli (FC) represent a manifestation of torticollis, or wryneck, as a mass lesion of the sternocleidomastoid muscle. The nomenclature applied to FC suffers from the use of somewhat confusing and overlapping terminology. This condition is also referred to as sternocleidomastoid tumor of infancy or pseudotumor of infancy, and at times the term congenital muscular torticollis is used synonymously (1–3). Torticollis, in general, may be congenital or acquired and result from muscular, neurogenic, infectious, neoplastic, traumatic, or psychogenic causes (4–6). The mass lesion in FC results from fibrocollagenous replacement of native sternocleidomastoid skeletal muscle tissue. Because of the presence of a mass lesion, it is distinguishable from congenital muscular torticollis, in which muscular contracture occurs in the absence of a mass. However, these entities appear to be related and represent a spectrum of the same process since in a significant portion of patients with FC, there is progression to congential muscular torticollis (1,3,6,7). FC is typically a self-limited condition that should not be included in the spectrum of aggressive extra-abdominal fibromatoses.

Clinical Features

FC is a neonatal condition that is almost always identified by the eighth week of life. Signs or symptoms are usually not present in the immediate perinatal period, but arise within a short interval, typically at two to four weeks of age. It is the most common cause of neonatal torticollis and has been estimated to occur in 0.4% of infants (8,9). Male and female patients are affected with approximately equal frequency (1,10). First-born children are more commonly affected, and in almost half of reported cases, a history of complicated delivery, such as breech birth, forceps delivery, or Cesarean section, is provided. This has led to postulation that FC is sequelae of intrauterine or perinatal trauma, although the majority of cases arise after uncomplicated deliveries (11–14). Congenital hip dysplasia is identified in over 10% of patients with FC and other developmental abnormalities, including pyloric stenosis and occurs at higher than predicted rates in this population. Patients typically present with a palpable mass in the sternocleidomastoid muscle and characteristic head tilt. Additional findings include restricted motion and plagiocephaly (1,13,15–19). The mass tends to grow rapidly for a period of weeks or a few months after which it stabilizes and remains static.

Imaging

US has emerged as the imaging modality of choice for the evaluation of FC. FC appears as a well-defined mass or an ill-defined mass enlarging the sternocleidomastoid muscle. The echogenicity is variable from hypoechoic to hyperechoic but without good through transmission. The lesions have a fusiform configuration and vary from homogeneous to heterogeneous in echogenicity (20–23). CT reveals muscle enlargement without a discrete mass. MR imaging also does not typically demonstrate a discrete soft tissue mass. The muscle is generally enlarged with diffuse abnormal signal intensity and higher signal intensity compared with muscle on T2-weighting (22,24–26). It is noted that advanced radiologic studies may not be necessary or cost effective in establishing a diagnosis of FC (1,5). Rarely, radiolucent lesions in the clavicle have been identified at the insertion of the sternocleidomastoid muscle, although radiographic studies are generally not performed on FC patients (Fig. 76) (27).

Pathology

The diagnosis of FC is most commonly made on the basis of clinical and US imaging studies. When microscopic tissue evaluation is indicated, open biopsy has largely been supplanted by fine needle aspiration biopsy. In cases where tissue becomes available, the lesion measures 1 to 2 cm in diameter and have a gray-white cut surface. The lesional tissue blends into adjacent skeletal muscle. Microscopically, there is a distinctive pattern of replacement of the sternocleidomastoid muscle by a moderately cellular myofibroblastic spindle cell proliferation without significant atypia or mitotic activity. Distributed throughout the lesion are residual muscle fibers in varying states of degeneration and atrophy (Figs. 77 and 78). Inflammatory cells and hemosiderin deposition are inconspicuous or lacking. There are no elongate vessels, and the spindled population is somewhat disorganized rather than purposeful, as in fibromatosis or desmoid. In long-standing lesions, presumably those that progress to congenital muscular torticollis, decreased cellularity and increased collagen deposition are encountered. Cytologic examination of aspiration biopsy material reveals isolated or clustered reactive-appearing myofibroblasts admixed with degenerating muscle tissue, including granular material and multinucleate cells (28–34).

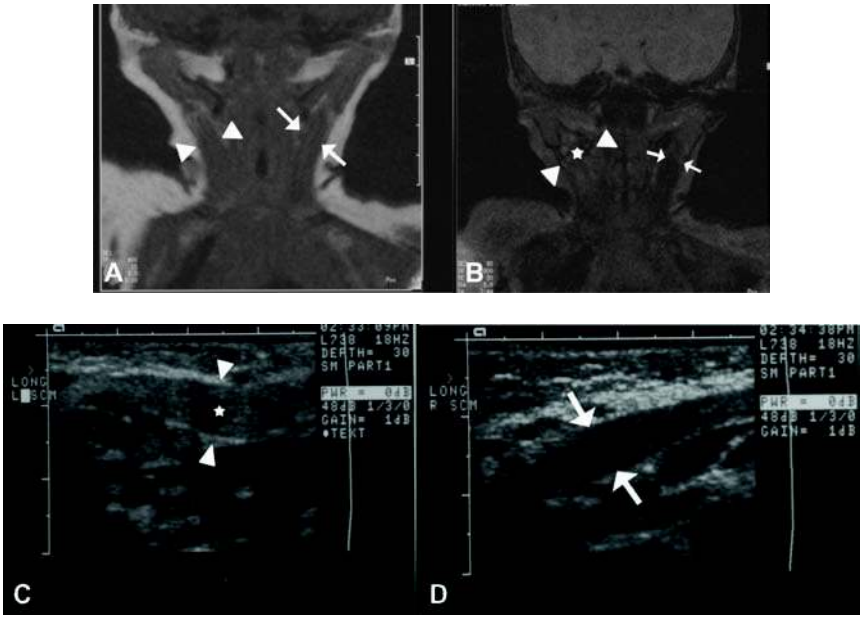

Figure 76 Ultrasonography (**A**) show diffuse enlargement of the right sternocleidomastoid muscle (between arrowheads), T2-weighting (**B**), and Coronal MR images with T1-weighting (**C,D**). There is mildly high signal on T2-weighted MR (* in **B**) and increased echogenicity on sonography (* in **C**) compared with the normal-left sternocleidomastoid muscle (between arrows in **D**).

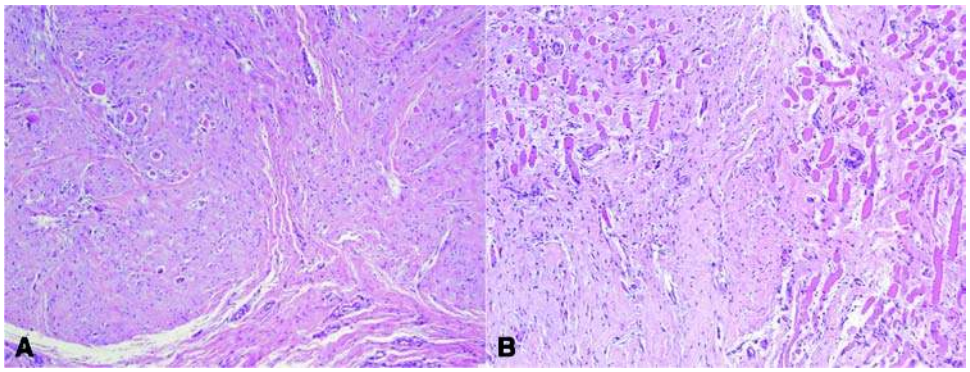

Figure 77 Fibromatosis colli, from the sternocleidomastoid muscle of an infant, demonstrates a delineated, moderately cellular myofibroblastic proliferation with entrapped muscle fibers. There is absence of parallel elongate vessels, as seen in desmoid (**A** and **B**).

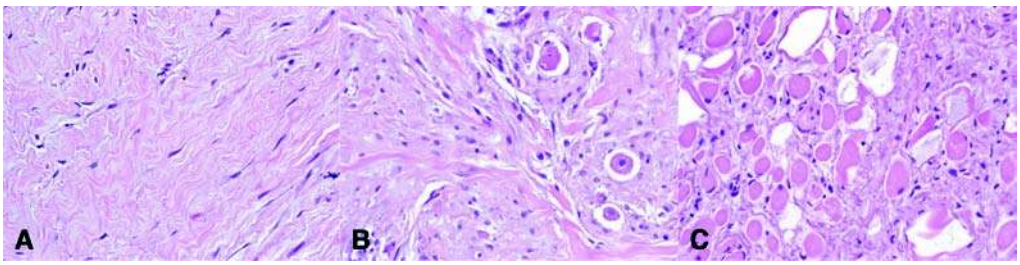

Figure 78 The cells are bland and somewhat haphazard, like a hypercellular scar (**A**), without elongate vessels, with entrapped skeletal muscle (**B),** and not overrun by tumor, as in desmoid (**C**).

Immunohistochemistry

Systematic immunohistochemical analyses of FC have not been performed, however, the constituent fibroblastic and myofibroblastic components would be expected to display immunoreactivity for vimentin and SMA. Desmin-reactive elements would be present in the residual degenerating skeletal muscle fibers only and not in the spindled cells. A single case of FC was evaluated with β-catenin and did not display nuclear reactivity (35). This supports the histomorphologic impression that FC does not fall within the spectrum of desmoid-type fibromatoses.

Electron Microscopy

Ultrastructural evaluation is not required for the diagnosis of FC, but examination reveals fibroblasts, myofibroblasts, and primitive mesenchymal cells. Proliferating or degenerating muscle cells may also be identified (36).

Molecular Findings

There is no convincing evidence of a genetic contribution to the development of FC, although affected family members and siblings have been reported (36,37).

Differential Diagnosis

If the diagnosis of FC has been established with a degree of certainty on the basis of clinical and imaging studies, the histologic differential diagnosis is limited. Desmoid-type fibromatoses are intermuscular, not intramuscular, lesions (although they infiltrate into skeletal muscle). They are characterized by elongated vessels running parallel to purposeful myofibroblasts, stromal keloidal collagen, and intralesional hemorrhage. Entrapped muscle fibers may be present at the lesion's periphery, where it infiltrates skeletal muscle, but they are not found in the body of the tumor, as in FC. FC is a completely intramuscular process, which also lacks the organization and vascular pattern of desmoid. The inflammatory cells and hemosiderin deposition that are hallmarks of reactive and posttraumatic conditions are not present to a significant degree in FC.

Treatment and Prognosis

The majority of FC cases resolve without residual cosmetic or functional deficits, and conservative management is the treatment of choice. Early intervention is recommended, with manual stretching being the primary therapeutic modality. Greater than 90% of cases resolve when addressed in this manner. Cases that do not resolve by 12 months of age, a cohort that presumably includes examples classifiable as progression to congenital muscular torticollis, may require surgical intervention. Surgical options include release (tenotomy), lengthening, or resection of the affected sternocleidomastoid muscle (1,2,5,10,12,13,17,18).

H. Gingival Fibromatosis

Introduction

GF is characterized by overgrowth of the collagenous portion of nonepithelial gingival tissue. Despite the nomenclature, GF is unrelated to the neoplastic desmoid-type fibromatoses that affect the head and neck as well as other sites in the body. GF can be considered a common phenotypic manifestation of a heterogenous group of etiologic factors. Inherited forms are collectively referred to as hereditary gingival fibromatosis (HGF) and comprise up to a third of these cases.

Clinical Features

GF may be idiopathic or familial in presentation (Table 5) (1–4). A portion of the idiopathic or nonfamilial cases result from sporadic mutations in fibromatosis-promoting genes (5). Familial or hereditary cases may be restricted to gingival enlargement or demonstrate GF in association with a variety of systemic alterations including hypertrichosis, seizure disorders, mental retardation, deafness, hypothyroidism, chondrodystrophia, growth hormone deficiency, and cherubism, either alone or in combination. Additionally, a heterogenous group of syndromes includes GF as a component. These syndromes include but are not limited to Zimmerman-Laband, Murray-Puretic-Drescher, Rutherfurd, Cowden, and Ramon (2,6). Most cases of HGF are inherited in an autosomal dominant pattern, however, autosomal recessive examples have been reported (1,7,8). Regardless of underlying genetic factors, the gingival enlargement may be either generalized or localized (3). Patients with nonhereditary, localized GF only rarely manifest hypertrichosis or other systemic alterations.

Onset of GF is typically recognized in patients before the age of 20 and coincides with the eruption of the deciduous or permanent dentition. Tooth eruption may play a role in initiation or promotion of gingival overgrowth. After onset there is a slowly progressive enlargement of the gingival tissue. The degree of enlargement can be quite significant, overgrowing or ''submerging'' associated teeth or preventing normal lip closure (Fig. 79). Once an area has been affected,

Table 5 Classification of 267 Cases of Gingival Fibromatosis

Type	Number of cases (%)
Idiopathic gingival fibromatosis	125 (47)
A. Generalized	77
B. Localized	48
Familial gingival fibromatosis	97 (36)
Gingival fibromatosis with hypertrichosis	23 (9)
Gingival fibromatosis with hypertrichosis and mental retardation or epilepsy	12 (4)
Gingival fibromatosis with mental retardation or epilepsy	10 (4)

Source: From Ref. 3

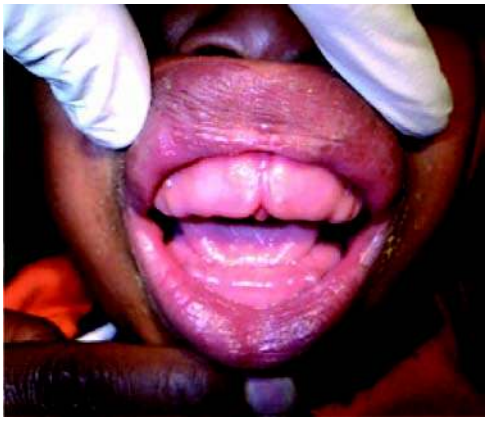

Figure 79 Four-year-old male with idiopathic (sporadic) generalized gingival fibromatosis. There is marked gingival overgrowth with severely compromised tooth eruption. *Source*: Courtesy of Dr. J Hellstein, University of Iowa School of Dentistry, Iowa City, Iowa.

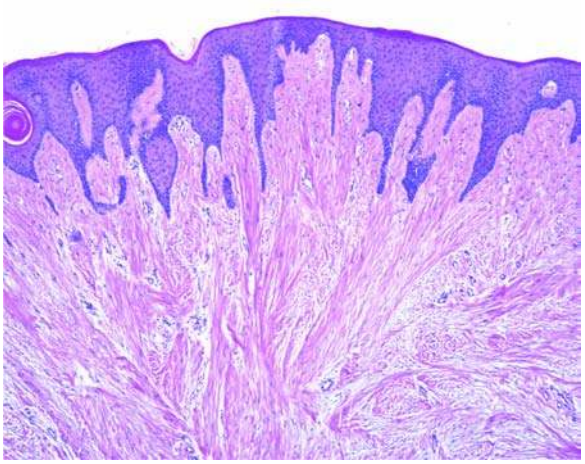

Figure 80 Gingival fibromatosis exhibiting bundles of densely collagenous fibrous tissue. The overlying surface epithelium is characterized by thin, elongated rete ridges extending into the connective tissue. Inflammatory cells are essentially absent.

subsequent tooth eruption may be compromised or misdirected. GF may be generalized or localized to one or more quadrants of the jaws. The maxilla tends to be affected more frequently and more severely, often with preferential enlargement of palatal surface. A distinctive pattern of localized GF is symmetric, bilateral enlargement of the posterior and palatal portion of the posterior maxillary alveolus, resulting in a mass lesion effect.

Clinically, affected gingiva is thick, firm, and normal in color with a smooth or finely stippled surface. As the lesions age, surface papillary projections may develop. The tissue displays little tendency to bleed, unlike inflammatory gingival hyperplasias.

Imaging

Imaging studies have only a limited role in the diagnosis of GF, but plain film radiographs may be useful in establishing the status of the affected dentition and in surgical treatment planning.

Pathology

Regardless of the form of gingival hyperplasia, the gross is a dense scar-like tissue that is firm, gray-white, and glistening. Similar to all types, the histopathologic features demonstrate coarse to fine bundles of dense collagenous tissue haphazardly arranged in all directions. Cellularity is low and consists of fibroblasts interspersed with myofibroblasts. Areas of myxoid change, and rarely, calcifications may be present. The overlying surface epithelium is mildly hyperkeratotic and hyperplastic with long, narrow, anastomosing rete ridges that extend into the connective tissue. Inflammatory cells are sparse or absent (Fig. 80).

Immunohistochemistry

Immunohistochemical staining has a limited role in the diagnosis of GF. Not unexpectedly, vimentin immunoreactivity is present in the fibroblastic cells, and SMA staining may reveal myofibroblasts in selected cases (9,10).

Electron Microscopy

Ultrastructural studies of GF have demonstrated ultrastructurally typical fibroblasts along with increased extracellular matrix production, consisting predominantly of type 1 collagen (10,11).

Molecular-Genetic Data

Inherited forms are collectively referred to as HGF and comprise up to a third of these cases (1,4,5,7,12–18).

Differential Diagnosis

Gingival hyperplasia is a relatively common oral finding that can result from a variety of inciting causes (19–22). Localized hyperplasias may be nonspecific inflammatory conditions such as inflammatory fibrous hyperplasia or morphologically distinct entities such as the pyogenic granuloma or peripheral ossifying fibroma. Periodontitis and gingivitis may result in erythematous, edematous hyperplasia that is prone to bleeding on evaluation, in contrast to the firm, normal-colored enlargement of GF. Drug-induced gingival hyperplasia is a well-recognized phenomenon that is associated with a number of systemic medications. The strongest association is with phenytoin (Dilantin), cyclosporine, and nifedipine. With other drugs, the relationship is more tenuous. Appropriate history taking and clinical

evaluation are usually sufficient to exclude GF from the differential diagnosis. Juvenile hyaline fibromatosis is an autosomal recessive connective tissue disorder in which gingival hypertrophy presents in combination with multiple cutaneous nodules, joint contractures, and osteolytic bone lesions (23–25). Rarely, neoplastic infiltrates can produce gingival enlargement. Diffuse gingival enlargement is a well-recognized, albeit uncommon, presentation of acute myelomonocytic or monocytic leukemias.

Treatment and Prognosis

Treatment of GF usually begins with conservative gingivectomy to recontour the tissue with the goal of a satisfactory cosmetic and functional result. Surgical therapy should be combined with a meticulous oral hygiene regimen. Generalized GF may recur or continue to progress after surgery, and repeated surgical intervention is not uncommon. Localized cases are less likely to recur, and clinical follow-up is recommended.

I. Fibromatosis (desmoid)

Introduction

Fibromatosis (desmoid) comprises intraabdominal, abdominal, and extraabdominal types. The latter occurs in the head and neck, particularly neck and scalp. These are separated from and have a different genetic finding than superficial fibromatoses, including palmar and plantar types.

Clinical Findings

Fibromatosis occurs mostly in children and young adults, of equal gender, and may arise in the setting of Gardner syndrome, including intestinal polyposis (familial adenomatous polyposis) (1,2), fibromas, and osteomas, but particularly when there is intraabdominal fibromatosis or multifocal fibromatosis. In the neck, these are most common in the anterolateral neck and supraclavicular regions (3–5) and also include oral (6–8), sinonasal tract (9), nasopharynx, parotid (10) and submandibular glands (11,12), pharynx (13), dura (14), orbit (15), larynx (16–19), and thyroid (20,21).

Imaging

Extraabdominal desmoids typically are centered along the superficial fascia or in an intermuscular location. Muscular involvement is common. On CT the attenuation is similar to muscle. On MR imaging there is intermediate signal intensity on T1 weighting and intermediate to high signal intensity on T2 weighting. Low signal intensity bands are frequent on T2 weighting, do not enhance and are suggestive on imaging for this diagnosis. These features correspond to more collagenized regions seen pathologically. Extension along the fascia (fascial tail sign) may also be seen. Contrast enhancement is common in the less collagenized regions. Lesion margins are often irregular or spiculated as is seen at gross pathologic examination and may suggest a more aggressive malignant process (22–25).

Pathologic Findings

Grossly, fibromatosis is a rubbery firm, whitish lesion that is infiltrative into surrounding fat and skeletal muscle. These can vary in size and reach quite large sizes. Microscopically, fibromatosis or desmoid is composed of a moderately cellular spindled, purposeful myofibroblastic proliferation, running parallel to elongate vessels. The vessels may take up an entire high-power field (Fig. 81). The nuclei are ovoid with indistinct nucleoli. Normal form mitoses may be present, but never atypical mitoses. Necrosis is not a feature of fibromatosis. Cytologic atypia is also not present, but multinucleated giant cells with overlapping hyperchromatic nuclei are occasionally observed, some may represent atrophic skeletal muscle fibers. The lesion takes over existing skeletal muscle so it is not entrapped. Keloidal collagen and perivascular

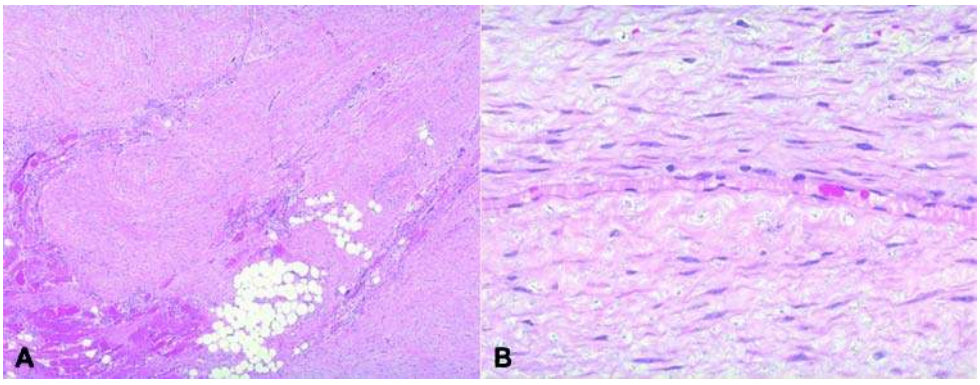

Figure 81 Fibromatosis (desmoid) is an intramuscular or deep fascial lesion that infiltrates skeletal muscle and subcutaneous fat **(A)**. It is characterized by elongate vessels with parallel purposeful myofibroblasts **(B)**.

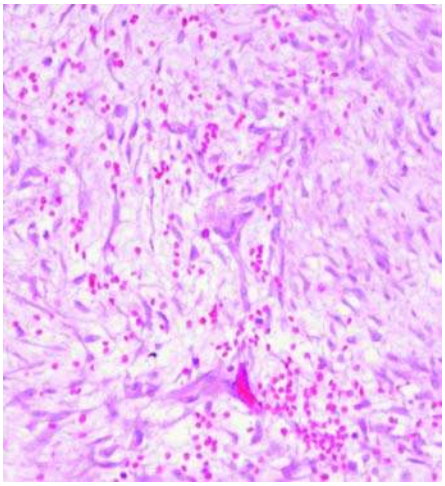

Figure 82 Fibromatosis can have myxoid change and keloidal collagen, like nodular fasciitis, but is infiltrative and has perivascular (rather than intralesional) hemorrhage.

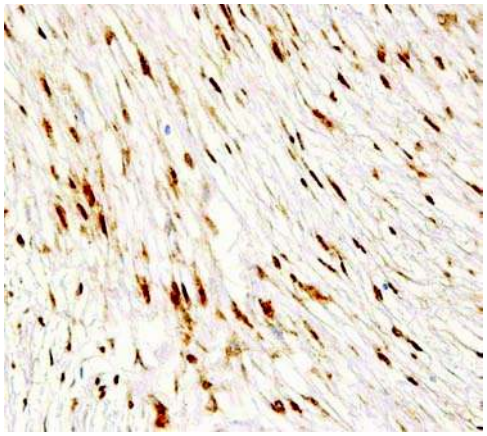

Figure 83 β-Catenin demonstrated nuclear reactivity in and specific to desmoid.

hemorrhage may be present. Some lesions, particularly scalp, breast, and intraabdominal, may have marked myxoid change and be difficult to recognize or separate from nodular fasciitis. Perivascular hemorrhage (not intralesional hemorrhage as seen in nodular fasciitis) is often present, particularly in myxoid type of desmoid (Fig. 82).

Immunohistochemistry

These are myofibroblasts and are positive occasionally for actins but are negative for desmin, S-100 protein, HMB45, keratins, and CD34. Importantly, β-catenin, a genetic-immunohistochemistry marker, shows a nuclear reactivity in fibromatosis (Fig. 83) (26–29). Desmoid can sometimes be estrogen receptor positive (30,31).

Molecular Findings

Clonal cytogenetic aberrations, including trisomies of chromosomes 8 and 20, have been reported in desmoids tumors (32). Both individual trisomies are rare in solid tumors and particularly in mesenchymal tumors, and are only known to occur in infantile fibrosarcoma (33). However, they were reported in a histologic similar to desmoid, but clinically distinct, benign fibrous lesions of bone (34). Although some studies have suggested an association between trisomy of chromosome 8 and an increased risk of recurrence, there is no consensus on this issue (32,35,36).

The *APC* (adenomatous polyposis coli) and *β-catenin* genes (*CTNNB1*) have been indicated in familial adenomatous polyposis of the colon (FAP). Normally, the APC protein interacts with β-catenin and induces its degradation. Inactivation of *APC* or activation of *CTNNB1* leads to β-catenin overexpression and pathologic signaling through the related pathways (37–40). FAP is an inherited disease characterized by colon polyposis, predisposition to develop colon cancer, and other malignancies including desmoids tumors (41).

APC, a tumor suppressor gene mapped to FAP locus on chromosome 5q21, has been shown to be frequently inactivated in desmoid tumors from FAP patients and less commonly in sporadic tumors (42–44). Germline mutations at the 3′end of *APC* gene result in a severe desmoid phenotype and overexpression of β-catenin in FAP-related desmoid tumors (45).

Also, *β-catenin*-activating mutations and a high level of protein expression were documented in sporadic desmoid tumors showing that both *APC* and *CTNNB1*, targeted by different type of mutations, play an essential role in promoting cellular proliferation by deregulation of the APC/β-catenin/Tcf pathway (44,46).

Differential Diagnosis

Fibromatosis must be separated from many benign and malignant tumors, since it is a locally aggressive, difficult to excise benign tumor. Fibrous histiocytoma is a dermal-based pushing stellate tumor composed of storiform to short fasicular more plump myofibroblsts; it lacks the infiltrative growth pattern, blandness, and elongate vessels of fibromatosis. Nodular fasciitis, difficult to separate from fibromatosis of scalp, chest, and intraabdominal, is often a fascial-based lesion, usually well delineated and has characteristic myxoid change with lesional extravasated erythrocytes and plump storiform myofibroblasts; fibromatosis has perivascular hemorrhage rather than intralesional and differs in infiltrative growth pattern, bland parallel myofibroblasts, and elongate vessels. Inflammatory myofibroblastic tumor is composed of myofibroblasts with lymphoid proliferations

and lesional inflammation with reactive myofibroblasts; these are ALK-1 positive and negative for β-catenin. More worrisome lesions, such as fibrosarcoma variants, would have higher nuclear to cytoplasmic ratios, mitotic activity, and may even exhibit necrosis, which would be negative in fibromatosis. Finally, the gold standard of nuclear β-catenin, specific to desmoid-type fibromatosis, would be negative or show only cytoplasmic reactivity (interpreted also as negative) in all other tumors.

Prognosis and Treatment

Fibromatosis or desmoid is a difficult to excise infiltrative lesion that has a high local recurrence potential (47). In the head and neck and abdomen, fibromatosis can wrap around vital structures and cause respiratory or vascular compromise or organ failure and patient death. Fibromatosis is deep and can even erode bone, particularly the skull when involving scalp, sometimes necessitating the use of radiation therapy (48,49), chemotherapy (50–52), or endocrine therapy (tamoxifen) (53,54) for surgically nonresectable lesions, despite the fact that this is a benign, nonmetastasizing tumor.

J. Angiofibroma

Introduction

AF is a benign, but locally aggressive, fibrovascular neoplasm with distinctive morphologic and clinical features. This lesion is also referred to as nasopharyngeal AF or juvenile nasopharyngeal AF in deference to involvement of the nasopharynx and occurrence in relatively young male patients. Because AFs actually originate from the posterolateral wall of the nasal cavity in the region of sphenopalatine foramen, secondarily involving the nasopharynx, the prefix ''nasopharyngeal'' is somewhat inaccurate (1–3). Additionally, because AFs are also diagnosed in adult patients, use of the term ''juvenile'' is unnecessarily limiting. From their point of origin in the posterior nasal cavity, AFs grow along the paths of least resistance almost universally involving the nasopharynx and frequently extending into the nasal cavity and paranasal sinuses. Further growth into the infratemporal fossae, cheek, orbit, oropharynx, cavernous sinus, or cranial cavity is not uncommon. AFs have a significantly higher incidence in patients with familial adenomatous polyposis and, molecular evidence suggests involvement of the β-catenin pathway in their pathogenesis (4–9).

Clinical Features

AFs are uncommon tumors, representing less than 1% of tumors involving the nasopharynx (10–14). AFs arise exclusively in male patients. Convincing evidence of lesions involving female patients is lacking and purported examples in female should be approached with a degree of skepticism. The mean age at diagnosis is approximately 15 years, and most patients are between 10 and 20 years of age; however, cases from the first or third decades of life are not uncommon (10,12,14–17). Patients classically present with nasal obstruction, periodic epistaxis, and a mass involving the nasopharynx. Epistaxis results from surface ulceration of these exophytic mass lesions. Additional presenting signs or symptoms include nasal discharge, facial asymmetry, proptosis, diplopia, exophthalmos, sinusitis, otitis media, tinnitus, rhinolalia, deafness, headache, or ansomia. Pain is uncommon.

A racial or ethnic predilection for fair-skinned and red-haired individuals has been described, with few examples reported in black patients (1,18). However, cases reported from Asia are not uncommon (13,19,20).

Imaging

Imaging studies play a substantial role in the diagnosis, staging, and management of AF. In the appropriate clinical setting, i.e., an adolescent male, the radiographic findings in AF are sufficiently specific to render incisional biopsy, with its attendant risk of severe bleeding, unnecessary. Classically, radiographic evaluation reveals a soft tissue mass in the nasopharynx associated with anterior bowing of the posterior wall of the maxillary sinus and displacement of the pterygoid plates (Holman–Miller sign). Osseous margins may be eroded, but remain distinct. Angiography also reveals virtually diagnostic features including characteristic irregular, tortuous intra-lesional vessels and tumor blush (Fig. 84). Angiography allows the identification of the feeder vessel(s), which is most commonly the internal maxillary artery. However, AF may be fed by a diverse assortment of internal or external carotid artery branches (12,21,22). Angiography also supports preoperative tumor embolization, a frequently used intervention for reducing intraoperative blood loss and improving surgical removal (14,22–24). CT and

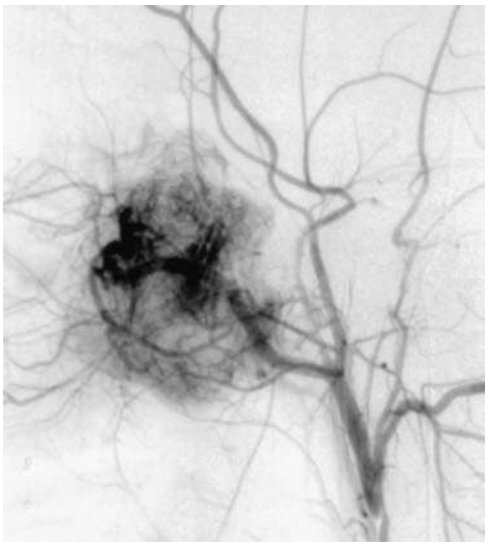

Figure 84 Angiography reveals the characteristic irregular, tortuous intralesional vessels and tumor blush of angiofibroma.

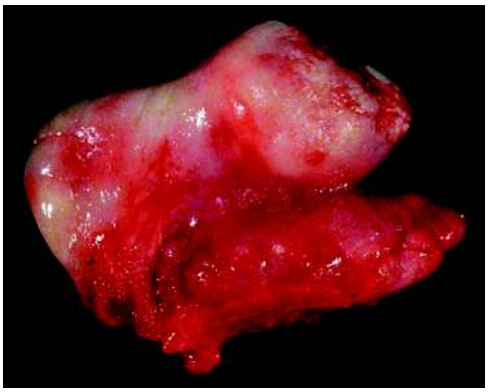

Figure 85 Grossly, angiofibromas consist of somewhat lobulated, fleshy white-tan mass. Focal surface ulceration is present, and the ragged area represents the base of the lesion.

MR imaging add greater refinement and detail to the classic radiographic findings, particularly in the region of pterygopalatine fossa and pterygoid canal. These techniques provide greater sensitivity and specificity in terms of evaluating disease extent, resulting in improved presurgical planning (2,22,25). MR imaging can also effectively demonstrate the vascular character of these tumors and obviate the need for angiography in many cases (26). Additionally, MR and CT play a role in the postoperative surveillance of AF patients (2,27).

Pathology

Grossly, AF presents as a smooth, rounded lobulated or multinodular mass with a gray-pink or gray-white cut surface (Fig. 85). Larger, gaping blood vessels may be visible on gross examination. AFs average approximately 4 cm in greatest dimension, but much larger examples may be encountered (1,10–12,17,20). Microscopic examination reveals an abundant fibrous component containing numerous blood vessels. Surface erosion or ulceration may be present, and the common presenting sign of epistaxis results from erosion into more superficial vessels. The vascular structures range from capillaries to compressed slit-like spaces to ectactic sinuses. Some vessels may focally adopt a ''staghorn'' configuration, but this feature is seldom as well developed as in HPC and related entities. The vessels are thin walled and lined by a single layer of flattened endothelium, but occasionally, thick-walled vessels with obvious smooth muscle walls are identified. Some vessels may be highlighted by readily visualized layer of pericytic cells. In the superficial portions of the tumor the vascularity may be extreme, resulting in the appearance of granulation tissue or a hemangioma. If preoperative embolization has been performed, intravascular occlusive material may be prominent and associated with areas of infarction. Between the vessels lies the fibrous tissue, representing the neoplastic portion of the AF. Because of current evidence indicating that this is neoplastic tissue, the term ''stroma'' or ''stromal cells'' may not be appropriate, despite its frequent application to this part of the AF (4,9). The fibrous tissue is composed of evenly spaced stellate and spindled fibroblastic or myofibroblastic cells set in a background of wavy, coarse, haphazardly arranged collagen bundles. Collagen may be dense and ''keloidal'' (Fig. 86). A narrow rim of pale cytoplasm may be visible surrounding nuclei that vary from pyknotic to larger vesicular forms with distinct nucleoli. A portion of enlarged binucleate or multinucleate cells or large ganglion-like cells are usually present (Fig. 87). AFs have moderate to low cellularity, and mitotic activity is always inconspicuous. Other than scattered mast cells, inflammatory cells are absent unless there is ulceration

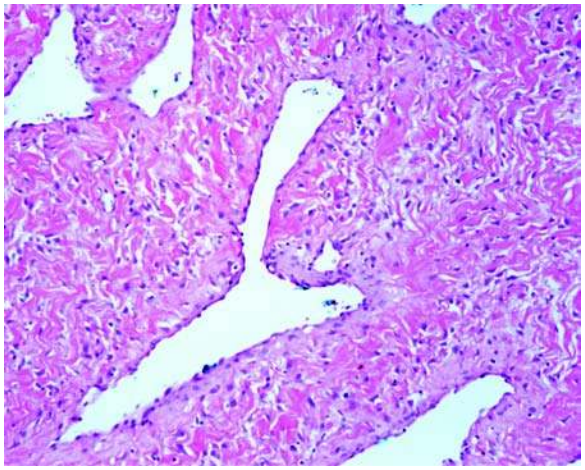

Figure 86 Angiofibroma composed of stellated and spindled fibroblastic tumor cells set in dense collagen that surrounds gaping, thin-walled vascular channels.

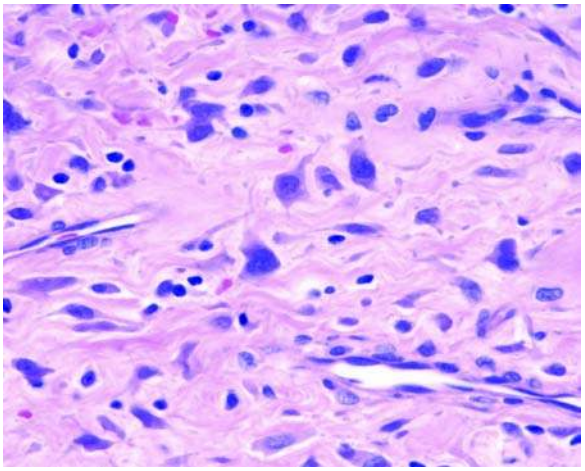

Figure 87 This microscopic field is composed predominantly of enlarged stellate tumor cells in a collagenous background. Slit-like vessels are evident, and there are scattered lymphocytes in this post-embolization example.

or an interventional procedure has been performed. Fibrosis may increase and vascularity decrease in long-standing tumors.

Immunohistochemistry

In general, the diagnosis of AF can be made without immunohistochemical evaluation; however, if performed, the fibroblastic tumor cells are consistently immunoreactive for vimentin. A minority of these cells also react with smooth muscle actin (SMA). SMA serves to highlight the vascular elements, and some of thicker-walled vessels may also stain with desmin. As expected, the endothelial cells are CD31, CD34, and factor VIII related antigen immunoreactive (11,28). Studies of androgen, estrogen, and progesterone receptor staining in AFs have yielded variable, but generally positive, results in both fibrous and endothelial cells (29–32). Nuclear β-catenin staining of the fibroblastic cells is a more recent finding in AF and is consistent with β-catenin-modulated pathogenesis (4,9). Immunohistochemical expression of a variety of growth factors, including vascular endothelial growth factor, transforming growth factor, nerve growth factor, and platelet-derived growth factors, has been reported in AFs (9,33,34).

Molecular-Genetic Data

Deregulation of the APC/β-catenin/Tcf pathway through the inactivating APC and activating CTNNB1 (β-catenin) mutations has been well documented in familial adenomatous polyposis. Although no APC alterations have been found in nasopharyngeal AF, mutational activation of β-catenin has been well documented. This might suggest that nasopharyngeal AF is an extracolonic manifestation of adenomatous polyposis (4–8). Normally, CTNNB1 co-activates the androgen receptor. Strong expression of androgen receptor in nasopharyngeal AF supports involvement of β-catenin signaling pathways in tumorigenesis. Also, a significant loss of chromosome Y in combination with a gain of chromosome X has been observed indicating that amplification of the androgen receptor is an alternative pathogenetic mechanism in nasopharyngeal AF (32,35). Comparative genomic hybridization studies revealed frequent autosomal gains suggesting possible oncogene activation through the amplification. AURKA (Aurora kinase A, previously designated STK6 or STK15, a mitotic centrosomal protein kinase) and MDM2 have been identified to be amplified in nasopharyngeal AFs (36,37).

Electron Microscopy

Ultrastructural findings are consistent with the impression of a fibroblastic or myofibroblastic tumor cell. Lobulated nuclei, intranuclear dense granules, and abundant actin-like filaments are present (38–40).

Differential Diagnosis

Correlation with radiographic findings in the appropriate clinical setting serves to limit the histologic differential diagnosis of AF to just a few possibilities. The primary considerations include sinonasal or antrochoanal polyps that may become fibrotic and contain enlarged, stellate stromal cells; however, the presence of inflammation with eosinophils, seromucinous glands, and paucicellular stroma and correlation with operative findings is sufficient to distinguish polyps from AF. Lobular capillary hemangiomas are not uncommon in the nasal cavity, but rarely involve the nasopharynx. Histologically, the lobular arrangement of capillary structures with plump endothelial cells is not seen in AF. Less likely diagnostic consideration include extra-abdominal fibromatosis, which rarely affects the sinonasal tract, tonsillar lymphangiomatous polyp, and peripheral nerve sheath tumor (1,41).

Treatment and Prognosis

AFs are benign but locally aggressive and destructive tumors with surgical removal the treatment of choice. Surgical resection is frequently preceded by angiographic embolization of selected feeder vessels, and there is evidence that preoperative embolization correlates with decreased blood loss possibly a lower recurrence rate (22,24,42,43). Open surgical approaches to AF include lateral rhinotomy, mid-face degloving, transmaxillary/transantral, infratemporal, intraoral/transoral/transpalatal resection (10,12,15,17,20,42–45). In recent decades, endonasal/endoscopic or transoral resection methods have largely superseded the open approaches, particularly for small- to medium-sized tumors (14,42,45–50). The choice of surgical technique is often predicated by tumor stage, with stage III or IV tumors potentially requiring more invasive surgical techniques. AFs are staged progressively higher as tumor extension and invasion beyond the primary nasopharyngeal location increases. A variety of staging systems for AFs have been proposed, but none have achieved universal acceptance(21,50–52). The suggested World Health Organization staging system is straightforward and provides reproducibility (Table 6) (1). Postsurgical recurrence is a primary treatment concern with AFs. Tumor recurrence, if detected, tends to arise rapidly, within 12 to 24 months. Historically, recurrence rates have been in the 20% range, but with aggressively judicious surgical management, the recurrence rate can be significantly reduced (25). It is likely that recurrence rates below 10% are achievable. Definitive control of AF with radiotherapy has been

Table 6 WHO Staging of Angiofibroma (1)

Stage	Description
Stage I	Tumor confined to the nasopharynx without bone destruction
Stage II	Tumor invades into the nasal cavity, maxillary, ethmoid, or sphenoid sinuses without bone destruction
Stage III	Tumor invades into the pterygopalatine fossa, infratemporal fossa, orbit, or parasellar region
Stage IV	Tumor with massive invasion of the cranial cavity, cavernous sinus, optic chiasm or pituitary fossa

achieved in several case series and represents a potential alternative to surgical resection (15,22,50,53). There is a well established, but limited, risk of malignant transformation in irradiated AF (54–57). Deaths due to AF have been reported, but tumor mortality would be an exceptional occurrence under current treatment regimens.

K. Myofibroma

Introduction

Myofibroma is a benign tumor composed of spindled cells exhibiting myofibroblastic differentiation, with both smooth muscle like and hemangiopericytoid areas. Stout in 1954 (1) first categorized the lesion as a congenital and multifocal subtype of fibromatosis and termed the lesion ''congenital generalized fibromatosis.'' Seventeen years later, Chung and Enzinger (2), recognizing the unique nature of the tumor including its early presentation, usual superficial location, and propensity for spontaneous resolution, renamed the tumor ''infantile myofibromatosis.'' The process was further subdivided into a superficial solitary form, a multifocal myofibromatosis (without visceral involvement), and a generalized myofibromatosis (with visceral involvement) (2–4).

Once myofibroma was established as a distinct entity and became familiar to pathologists, tumors with similar histologic features were subsequently identified in adults (5–9). Recently, investigators (9–11) documented overlapping clinicopathologic features between myofibromas occurring in adults and two mesenchymal lesions that feature a hemangiopericytomatous vascular component and exhibit myoid differentiation, myopericytoma, and glomangiopericytoma. These authors fostered the notion that the three processes are derived from a perivascular myoid cell and form a morphologic spectrum.

Due to the wide age range within which the tumor presents, the World Health Organization has eliminated the ''infantile'' modifier and simply classifies the lesion as ''myofibroma, solitary or multicentric type'' (12).

Clinical Features

Myofibroma is considered the most common fibrous tumor of infancy (13,14) with nearly 90% of cases arising within the first two years of life and over 50% of tumors presenting at, or shortly after birth (2). Chung and Enzinger (2) reported that in nearly 75% of cases of myofibroma submitted to the Armed Forces Institute of Pathology, only one lesion was clinically detected. However, a later cumulative literature survey by Wiswell et al. (15) claimed that only 47% of myofibromas were solitary. This discrepancy probably reflects failure to clinically detect all lesions in an individual and the tendency for many of the tumors to spontaneously regress.

Solitary myofibroma shows a strong male predominance (2,15) and mainly occurs within dermis, subcutaneous tissue, and less often within skeletal muscle. The head and neck is commonly involved (36%), followed by the trunk and extremities (2). The process initially exhibits rapid growth followed by a variable period of stability and, in many instances, eventual involution.

The multicentric form of the disease presents more often at birth, but tumors continue to develop for several months afterward. The condition exhibits a slight male predominance (14). Tumors arise in soft tissue (with a slight predilection for the head and neck), but osseous involvement is reported in over 50% of cases. In about one-quarter of these individuals, multiple osseous lesions are detected, with the skull virtually always involved (16). In large studies, 25% (2) and 37% (15) of individuals suffering from multicentric myofibromatosis were found to have visceral involvement with the lung representing the most often affected viscera, followed by the gastrointestinal tract, heart, kidney, pancreas, and less often, the central nervous system.

Myofibromas that occur in older-aged individuals tend more often to be solitary, superficially located, and are not known to undergo spontaneous regression (5–9), although they are thought to be reactive lesions of vessel wall (adult-type myofibroma). Rare examples of multicentric myofibromatosis (with some lesions present since birth) have been documented in adults (10,17). Patients in the fourth through sixth decades of life are mostly affected. The tumor predilects to the head and neck followed by the extremities, and typically presents as a slow-growing, asymptomatic mass.

Myofibroma of the head and neck, like in other areas of the body, clinically manifests as an asymptomatic, superficially located, firm, rubbery nodule. When located in the dermis, the lesion may occasionally ulcerate, or appear as a purplish macule owing to its rich vascularity, and as a result, it mimics a hemangioma (2). Outside of superficial head and neck soft tissue, the myofibroma has been described in the paranasal sinuses (18), nasopharynx (18), nasal cavity (19), oral cavity (20–22), tongue (18,20–23), gnathic bones (particularly, the mandible) (20,22,24,25), cranial and orbital bones (2,26–28), salivary glands (2,22), larynx (29), periorbital region (2,30), and thyroid (15). Symptoms caused by deep head and neck myofibromas generally depend upon the location of the tumor and its size. The tumor causes symptoms by compressing, but not invading, surrounding structures. Notably, rapidly growing tumors in the upper airway occasionally result in airway compromise (31).

Superficially located tumors are freely moveable, whereas deep-seated lesions tend to present as larger masses and may be fixed to surrounding tissues (2).

Radiologic Imaging

Radiographs of the soft tissue myofibroma are not very revealing, but occasionally show the presence of calcification within the lesion (2). Tumors involving the long bones present as radiolucent metaphyseal defects with well-defined, often sclerotic, borders and central calcifications (2). It is important to understand that these osseous lesions frequently involute

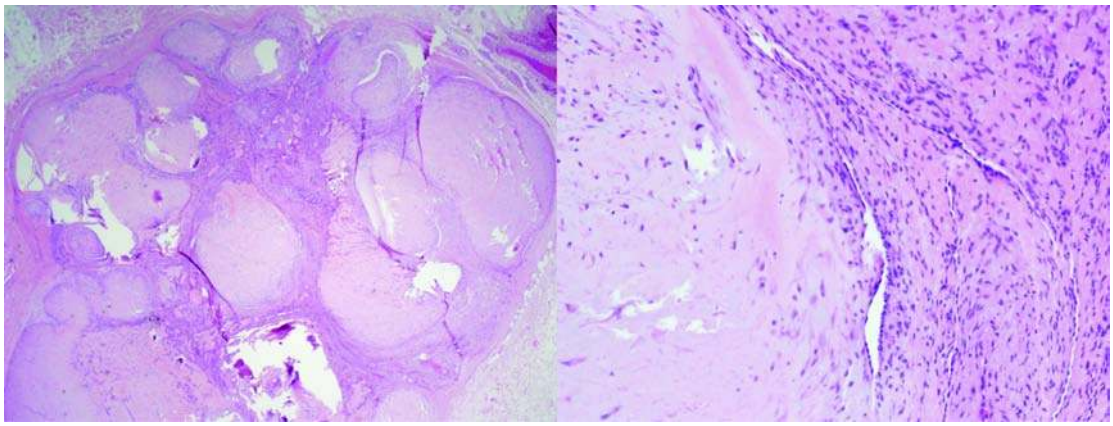

Figure 88 Well-circumscribed, unencapsulated myofibroma (*left*) with biphasic pattern of smooth muscle–like and hemangiopericytoma-like areas (*right*).

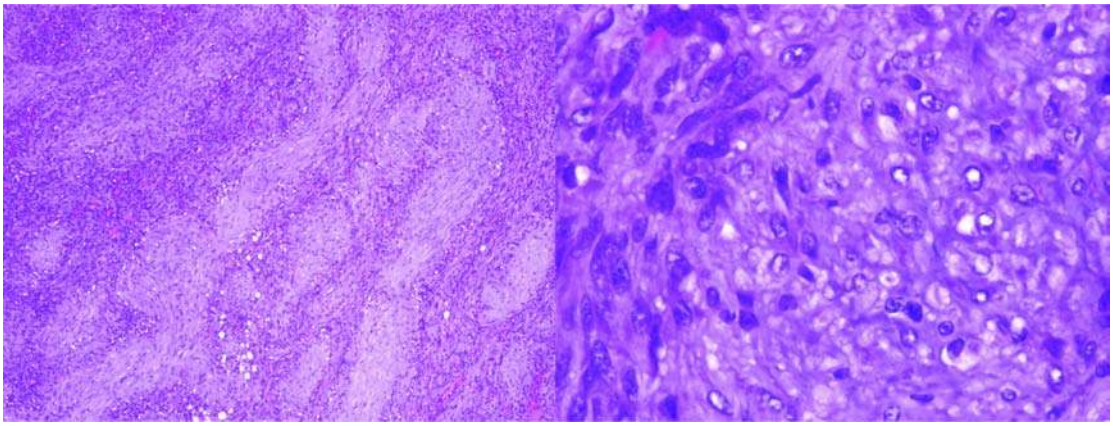

Figure 89 Infantile myofibroma exhibiting the characteristic bicellular growth pattern (*left*). Centrally located short, primitive spindled hemangiopericytoid cells (*left* on *right* picture) merging with peripheral larger smooth muscle–like myofibroblasts (*right* on *right* picture).

spontaneously and do not require treatment. Evidence of fracture may be detected on radiographs (32). US evaluation of the lesion demonstrates a mass that may contain a predominantly anechoic, necrotic center (33). Increased blood flow is sometimes demonstrated in the lesion (34,35). With computerized tomographic scans, the tumor appears isointense with muscle and may demonstrate central areas of lower attenuation and/or calcification. Foci of marked enhancement have also been reported in the lesion (36,37). MR imaging of the myofibroma typically shows nonspecific foci of moderately low to low intensity on T1-weighted imaging and foci of high intensity on T2-weighted images (37,38). Peripheral enhancement of the mass after contrast administration is suggestive of central necrosis on CT or MR imaging (39,40).

Pathologic Findings

Macroscopically, superficial tumors are usually well-circumscribed, unencapsulated nodules. Deeper lesions tend to exhibit less circumscription. The cut surface of the mass has a fibrous appearance and a light tan to brown, or reddish-purple color. The central portion of the mass may show necrosis and/or cystification. Small flecks of calcium are sometimes observed. The tumors vary in size from a few millimeters to lesions ranging from 1 cm to 7 cm.

Low-power microscopic examination reveals a smoothly contoured or lobulated nodule or, less often, a multinodular mass (Fig. 88). Large lesions presenting in infants and children characteristically display a biphasic growth pattern with a distinct zonal arrangement of the two main lesional elements (Fig. 89). The peripheral aspect of the mass consists of short fascicles, whorls, and storiform arrays of plump spindled cells with eosinophilic, slightly fibrillary cytoplasm and poorly defined cell borders (Fig. 90). The nuclei are elongated with somewhat tapered ends or have an ovoid configuration, and possess finely textured chromatin and small nucleoli. Scattered cells with mild to moderate cytologic atypia are

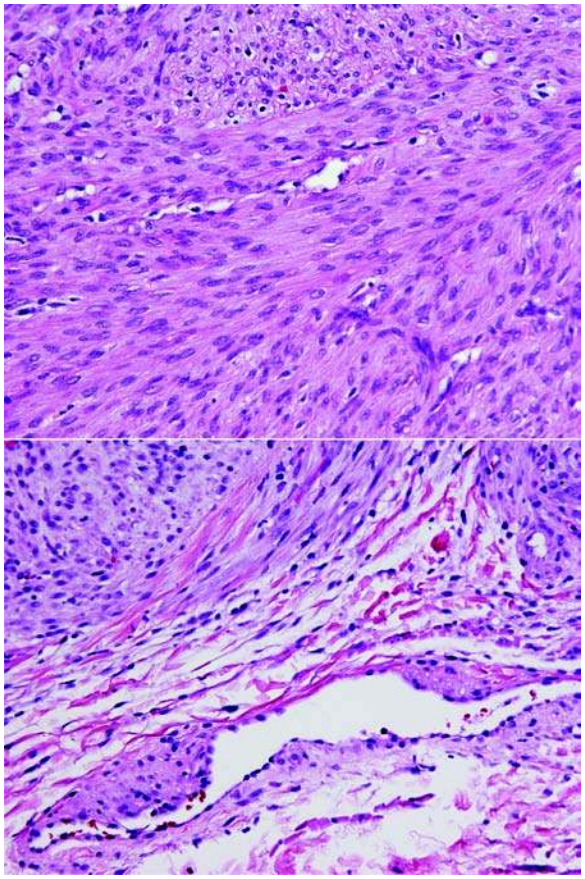

Figure 90 Peripheral portion of the infantile myofibroma composed of fascicles of plump myofibroblasts with eosinophilic cytoplasm and oval or fusiform nuclei showing bland cytologic features. Intravascular extension of tumor cells is noted at periphery of the lesion (*bottom*).

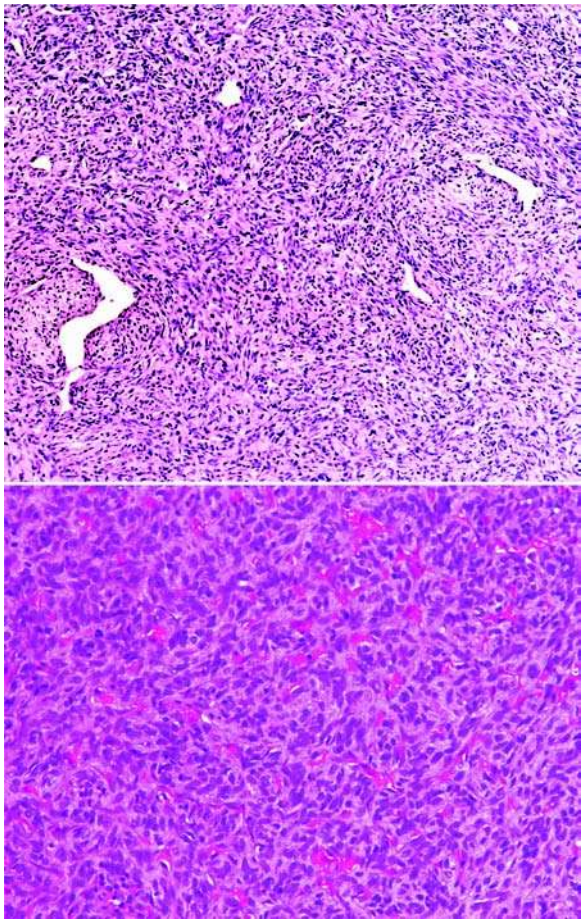

Figure 91 Low- and intermediate-power magnification of the central area of infantile myofibroma. A haphazard proliferation of small spindled cells with scanty cytoplasm grows around a myriad of capillary-sized vessels including some with irregular (hemangiopericytomatous) contours (*top*).

frequently encountered. The cells are surrounded by a collagenous or a myxohyaline stromal matrix that varies in amount. At the margin of the tumor, the spindled component demonstrates a modest degree of infiltrative growth into surrounding tissue as well as intravascular extension. The latter feature sometimes arouses false suspicion of a more ominous lesion. Osteoclast-like giant cells are occasionally identified in the spindled areas (16). The plump spindled cells show variable cytoplasmic fuchsinophilia with the trichrome histochemical stain and little or no intracytoplasmic glycogen with the periodic acidic–Schiff stain (2,41).

Toward the center of the mass, the spindled component merges with a population of less differentiated, short spindled or polyhedral-shaped cells with small, somewhat hyperchromatic nuclei and scanty cytoplasm (Fig. 91). These cells proliferate haphazardly around a myriad of irregularly contoured, thin-walled (hemangiopericytomatous) vessels. This growth pattern overlaps with that seen in the so-called ''infantile hemangiopericytoma,'' a lesion, which many investigators now believe is part of the spectrum of ''infantile myofibromatosis'' based on shared clinical, morphologic, and immunohistochemical features (42,43). Unlike the plump spindled cells at the periphery, these more primitive-appearing cells show increased mitotic activity and are prone to undergo necrosis, perhaps due to accelerated apoptosis (44), leading to cyst formation and dystrophic calcification.

Myofibromas occurring in adults often exhibit a haphazard distribution of the two main lesional elements (5,7–10). Nodules of spindled cells, some of which are paucicellular and extensively hyalinized, intermingle with cellular and highly vascular foci composed of more primitive cells, and the characteristic zonal architecture that typifies tumors presenting in infants is absent (Fig. 92). Less often, the primitive component is inconspicuous or located at the periphery of the lesion, resulting in a ''reverse zonation'' architectural pattern (2,7,9,10) (Fig. 92). Compared with the infantile form of the disease, the adult myofibroma is better circumscribed, shows less mitotic activity, and

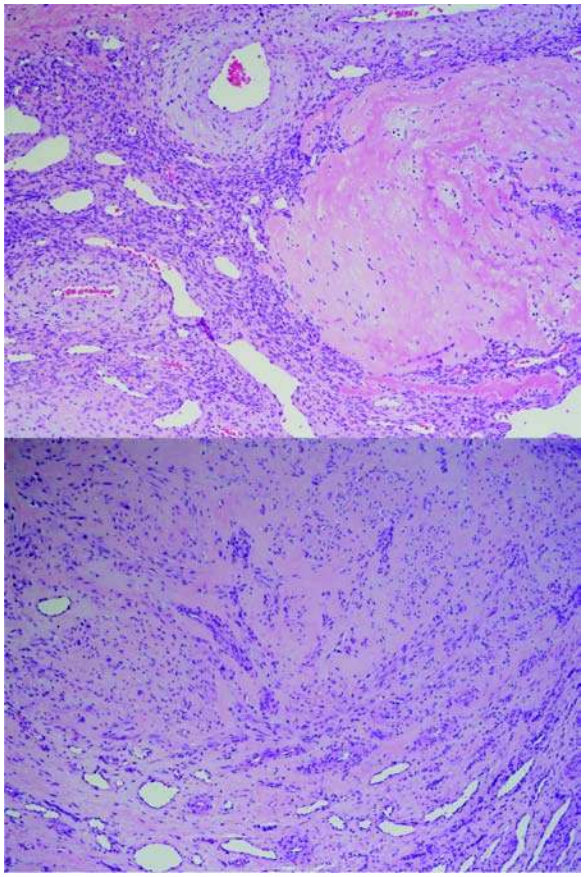

Figure 92 Adult myofibroma. Compared with the infantile variant, myofibromas occurring in older-aged patients many times are composed of a more random arrangement of primitive cells (*top*, *left*) and myxohyaline nodules of spindled myofibroblasts (*top*, *right*). An adult myofibroma with ''reverse zonation'' (*bottom*) characterized by a peripherally located primitive spindle cell component with hemangiopericytomatous blood vessels, and more centrally located myxohyaline nodules.

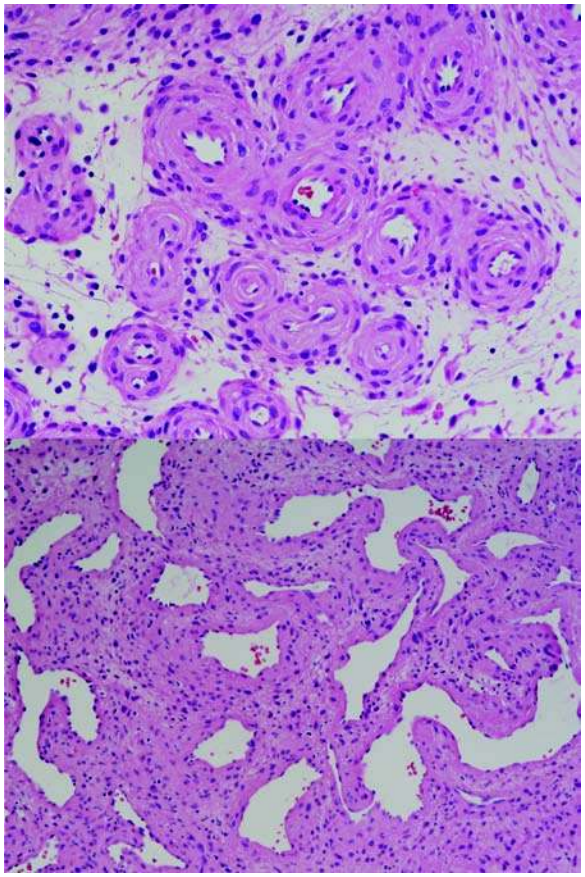

Figure 93 Perivascular myoid cell differentiation. Myopericytomatous growth (*top*) characterized by plump myoid cells encircling rounded, thin-walled vessels. Short spindled and glomus-like cells arranged around hemangiopericytomatous vessels (*bottom*) constitute histologic features of the glomangiopericytomatous pattern of perivascular myoid cell growth, resembling vascular leiomyoma.

does not undergo necrosis. Additionally, the tumors may harbor areas exhibiting myopericytomatous and/or glomangiopericytomatous growth (Fig. 93) (see sect. ''Differential Diagnosis'').

Immunohistochemical Findings

Both lesional elements express vimentin and SMA (5–10,20,22,42). In the plump spindled cells, SMA expression is typically located at the cell periphery (Fig. 94). This ''tram-track'' pattern of expression corresponds to the peripheral location of myofilamentous bundles observed ultrastructurally (5,8,9). Limited desmin expression has been reported in a few series (10,41), but most studies found an absence of desmin in tumor cells (6–9,20,22). The more primitive cellular element typically shows reduced expression of muscle actin(s). Mentzel et al. claim that the tumor cells of myofibroma usually do not express h-caldesmon (45).

Molecular Findings

Genetic data are scant, and only two different karyotypes have been reported so far (46,47). In one case, interstitial del(6)(q12q15) has been reported (46). In another case, an abnormal chromosome 9, derived from an unbalanced whole-arm translocation between chromosomes 9 and 16, has been found (47).

Familial occurrence of infantile myofibromatosis has been reported (48–52). Although autosomal recessive inheritance has been suggested in some studies (49,50), families with autosomal dominant inheritance have also been reported, suggesting possible genetic heterogeneity for infantile myofibromatosis (50–52).

Electron Microscopic Findings

The cells exhibit features of myofibroblasts with peripherally distributed actin filaments harboring dense bodies, rare micropinocytotic vesicles, and discontinuous runs of basal lamina (5,7,9,10,53). Cells

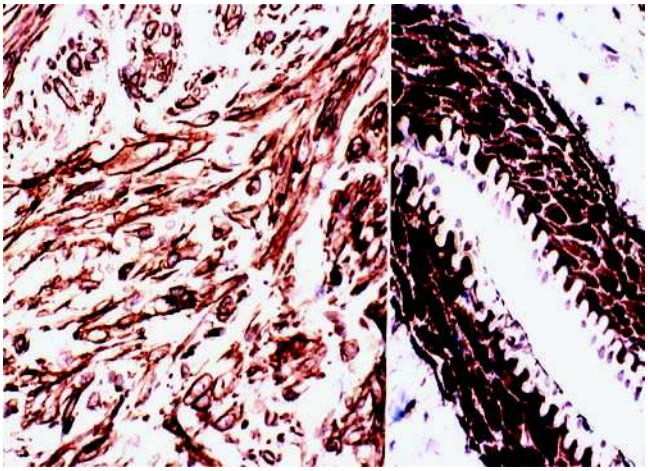

Figure 94 Immunohistochemistry. α-SMA immunoexpression in the plump spindled cells of myofibroma is found along the periphery of the cytoplasm resulting in a "tram-track" pattern (*left*). In comparison, the protein is more diffusely expressed in smooth muscle cells forming the wall of a blood vessel (*right*). These are desmin-negative lesions.

with features of fibroblasts, including an intricate network of dilated rough endoplasmic reticulin and no myofilamentous structures (7,9), and undifferentiated cells with sparse organelles are also identified (9).

Differential Diagnosis

Solitary myofibroma presenting in infancy and early childhood may be confused with a number of spindle cell myo-/fibroblastic processes. The infantile variant of fibromatosis commonly occurs in the head and neck, especially in the tongue and in the region of the mandible and mastoid, and typically presents at birth or within the first two years of life (16). Unlike most examples of myofibroma, infantile fibromatosis is typically a deep-seated lesion. Microscopically, the infantile fibromatosis lacks the biphasic pattern of growth that typifies the myofibroma, but instead is composed of fibroblasts morphologically ranging from small, primitive fibroblast-like cells with scanty cytoplasm to larger spindled cells identical to those found in the adult form of the disease. In further contrast to myofibroma, the cells of infantile fibromatosis extensively infiltrate surrounding native skeletal muscle.

FC (16) (congenital muscular torticollis) is a fibrosing process that affects the lower end of the sternocleidomastoid muscle of infants. Clinically, the lesion mimics myofibroma by appearing as a rapidly growing mass shortly after birth and disappearing by about six months of age. The characteristic head-tilt deformity (torticollis) caused by fibrous replacement of the sternocleidomastoid muscle, in many cases, becomes apparent during the child's accelerated growth phase. In comparison with the myofibroma, FC is microscopically less cellular and more highly collagenized and infiltrative.

Nodular fasciitis and cranial fasciitis (54,55) are benign tumefactions composed of proliferating myofibroblasts. Although conventional nodular fasciitis rarely occurs in infants and infrequently arises in the head and neck, the cranial fasciitis variant presents almost exclusively in infants and children and occurs in the soft tissues surrounding the cranium and, less often, in extracranial head and neck soft tissue sites. Microscopically, fasciitis-like processes share with myofibroma, relative circumscription, a cellular proliferation of spindled myofibroblast-like cells, and areas of whorled or fascicular growth. However, fasciitis-like processes feature myxoid, less collagenous areas with a more loosely arranged growth pattern of cells. Additionally, interspersed inflammatory cells and foci of hemorrhage are common histologic features of fasciitis-like processes. Importantly, necrosis or a distinct biphasic growth pattern is not found in nodular or cranial fasciitis.

Infantile fibrosarcoma (56,57) usually presents as a rapidly growing mass in extremity soft tissue. However, tumors occurring in the head and neck have also been documented (13,56). Investigators have observed histologic similarities between infantile fibrosarcoma and myofibroma, thus complicating the differential diagnosis in some cases (14,43). In general, the infantile fibrosarcoma exhibits a greater degree of invasion, higher cellularity with a prominent interlacing fascicular growth pattern, widespread cytologic atypia, and less immunohistochemical expression of SMA than does the myofibroma. If histologic overlap precludes unequivocal diagnosis, the infantile fibrosarcoma is associated with a specific 12;15 translocation (58).

The multicentric form of myofibroma must be differentiated from the rare, but clinically progressive and debilitating juvenile hyaline fibromatosis. Juvenile hyaline fibromatosis (16) is a hereditary, possibly autosomal recessive disorder associated with a high prevalence of consanguinity. The condition presents in children before four years of age with multiple superficial nodules in the head and neck, back, and extremities. In comparison with the myofibroma, juvenile hyaline fibromatosis presents later in life and frequently involves diarthrodial joints resulting in flexural contractures. Microscopically, hyaline fibromatosis is characterized by individually dispersed and corded spindled cells embedded in a hyalinized collagenous stroma, and the process lacks biphasic growth.

Myofibromas arising in adults are usually superficial and solitary, and therefore must be distinguished from myo-/fibroblastic and smooth muscle processes located primarily in the dermis and/or subcutis. Within the differential diagnosis of the adult myofibroma are two related mesenchymal lesions with a purported perivascular myoid cell derivation and shared histologic features. The myopericytoma (10,11,45), unlike the adult myofibroma, occurs primarily in the extremities and infrequently involves head and neck sites (45). Although the lesion may have areas reminiscent of myofibroma, including a hemangiopericytomatous vascular component, it is distinguished by the presence of plump spindled cells

that are arranged around numerous, closely aggregated, rounded, thin-walled blood vessels (Fig. 93). Although both lesions express SMA, the myopericytoma often expresses h-caldesmon, whereas the myofibroma does not show significant expression of this protein (45). The glomangiopericytoma, like myopericytoma, predilects to the extremities of adults (10). The characteristic histologic feature of this lesion is the presence of ovoid, glomus-like cells arranged around thin- and thick-walled hemangiopericytomatous vessels (Fig. 93). Although both tumors show overlapping histologic features with the adult myofibroma, the myopericytoma and glomangiopericytoma lack the zonal arrangement of plump spindled and small, primitive cells observed in myofibroma. Additionally, the paucicellular, hyalinized nodules identified in many examples of adult myofibroma are less commonly encountered in the myopericytoma and glomangiopericytoma (10,11). Dray et al. (11) proposed that the glomangiopericytoma-like growth pattern is part of the histologic spectrum of myopericytoma and should not be considered a separate entity. At present, any given tumor exhibiting perivascular myoid cell features microscopically should be classified according to the predominant growth pattern.

Glomangiomyoma (59) is the least commonly encountered variant of benign glomus tumor. The lesion superficially resembles the myofibroma because of its dual population of small, rounded cells and spindled myoid cells and by the presence of a prominent vascular component. The lesion generally occurs in the superficial tissues of the extremities. The tumor rarely involves the head and neck, but has been reported in the nasal cavity (60–62). Unlike the myofibroma, the glomangiomyoma is sometimes painful (60,62). Microscopically, the lesion differs from myofibroma by the presence of a glomus cell with its characteristic rounded contour, well-demarcated cell borders, and centrally placed nucleus and by a lack of a primitive cellular component. Furthermore, the vessels of glomangiomyoma are dilated (and not branching) and the spindled cell component has features of well-differentiated smooth muscle.

Vascular leiomyoma or angioleiomyoma is a well-recognized soft tissue tumor and represents the most common variant of leiomyoma reported within the oral cavity, paranasal sinuses, and nasal cavity (63–65). Unlike vascular leiomyomas arising in the extremities, those occurring in the sinonasal tract are usually painless (63). It shares with myofibroma, the presence of myoid-appearing spindled cells and a prominent vascular component. Pathologic features that distinguish the tumor from myofibroma include a monotonous proliferation of well-differentiated smooth muscle cells that immunohistochemically express desmin and h-caldesmon (along with SMA), and an absence of a biphasic growth pattern.

The nodular growth pattern of the plexiform fibrohistiocytic tumor (66) and its compliment of spindled and histiocyte-like cells may suggest a biphasic neoplasm like the myofibroma. This tumor usually arises in the superficial soft tissues of the upper extremity of children and young adults and rarely occurs in the head and neck. Microscopically, the tumor infiltrates subcutaneous tissue and even skeletal muscle. Unlike the paucicellular nodules of the adult myofibroma, the plexiform fibrohistiocytic tumor features cellular aggregates of mononuclear histiocyte-like cells and interspersed osteoclast-like giant cells. The nests are often separated by nodules and infiltrating fascicles of spindled fibroblast-like cells. Primitive cells and hemangiopericytomatous vessels that microscopically typify the myofibroma are not features of the plexiform fibrohistiocytic tumor.

Desmoid-type fibromatosis (desmoid tumor) shares with myofibroma a population of spindled myo-/fibroblastic cells. In the head and neck, the lesion mostly involves the oral cavity, especially the tongue, as well as the cheek, soft tissue around the mandible, and neck (67,68). The tumor typically occurs in children and young-aged adults. In general, the tumor presents as a much larger mass than myofibroma and originates in deeper tissues. Histologically, the monotonous spindled element of desmoid-type fibromatosis assumes an elongated, sweeping fascicular arrangement and exhibits infiltrative growth into surrounding tissues. Nuclear immunohistochemical expression of β-catenin is characteristic of desmoid-type fibromatosis and is not observed in myofibroma (69).

Low-grade myofibroblastic sarcoma is a spindled cell neoplasm that predilects to the head and neck, particularly the oral cavity (70–72). Although both the myofibroma and low-grade myofibroblastic sarcoma are composed of cells exhibiting myofibroblastic differentiation, the latter is distinguished by its typical deep location, characteristic interlacing fascicular or fasciitis-like arrangement of lesional cells, pronounced infiltrative growth into surrounding native tissue, and lack of a primitive cell component and hemangiopericytomatous vessels. Desmin immunoexpression is reported in a significant portion of low-grade myofibroblastic sarcoma, but is rarely observed in the myofibroma (71,72).

Another multinodular tumor included in the differential diagnosis of the adult myofibroma is the so-called cellular neurothekeoma (73). This enigmatic neoplasm occurs principally within the dermis of the scalp and face and upper extremities. The lesion consists of closely packed nodules of epithelioid and spindled cells with granular-appearing eosinophilic cytoplasm that proliferate within a variably myxoid stroma. In contrast to myofibroma, the nodules of cellular neurothekeoma are separated by collagen, and not by primitive cells or branching, thin-walled vessels. Cells of the cellular neurothekeoma show focal expression of SMA, but are often reactive with antibodies against microphthalmia transcription factor, NKI/C3, and PGP9.5 (74,75).

Prognosis and Treatment

Patients presenting with solitary and multicentric (nonvisceral) myofibromas in infancy and early childhood usually enjoy an excellent prognosis after simple

(local) excision. As many of the lesions undergo spontaneous regression (2,15,18), some authors advocate a policy of therapeutic abstention if the lesion is asymptomatic or if surgery could possibly result in a poor cosmetic or functional outcome (76). In large series of infantile myofibromas, recurrence rates of 9% (15) and 11%(2) have been documented. In a study of 13 children with head and neck myofibromas, Beck et al. (18) found recurrences in 4 individuals (31%) with myofibromas in locations where initial total surgical extirpation of the tumor was difficult. However, 2 of these individuals eventually experienced spontaneous regression of the tumor. Foss et al. (22) reported recurrences in 6 (2 children and 4 adults) of 32 patients (19%) with myofibromas of the oral cavity. No histologic features, including mitotic activity or intravascular growth, predict recurrent potential for any given lesion (2).

The multicentric form of the disease with visceral involvement results in substantial infant morbidity and mortality. Gastrointestinal and pulmonary complications are the chief reasons for its poor outcome (75% mortality within days or weeks of birth) (2,15). Patients suffering from this disorder less often experience spontaneous regression of their tumors. Such patients have been managed with low-dose chemotherapy, including vincristine with varying doses of either actinomycin D or methotrexate (77–79). This low-dose regiment is well tolerated with minimal long-term toxicity (79).

Myofibromas arising in adults are typically superficial, small, well-circumscribed lesions that do not spontaneously involute. Although most series claim no evidence of recurrence after simple excision (5–8), a few cases of recurrent myofibroma have surfaced in the literature (10,80). Granter et al. (10) reported recurrences in three of five adults patients, all of whom harbored multiple lesions. Nevertheless, simple (local) excision is the treatment of choice for this benign neoplasm.

L. Collagenous Fibroma (Desmoplastic Fibroblastoma)

Introduction

The collagenous fibroma is a rare, benign, paucicellular soft tissue tumor composed of fibroblasts and myofibroblasts embedded in a densely collagenous stroma. The clinicopathologic features of this morphologically distinct entity were first delineated by Evans (1) in 1995, who coined the term ''desmoplastic fibroblastoma.'' One year later, Nielsen et al. (2) argued that the designation ''collagenous fibroma'' better reflects the morphologic features of the tumor. Their premise was based on the light microscopic observation that the dense intralesional collagen is produced by the tumor cells (and not by a desmoplastic reaction to them) and on ultrastructural evidence that the main lesional cells are mature fibroblasts and myofibroblasts. In the largest series of tumors reported to date, Miettinen and Fetsch (3) suggested the term ''stellate cell fibroma'' as this nomenclature focuses on the key morphotype of the process, a stellate-shaped fibroblast-like cell.

Clinical Features

This relatively uncommon mesenchymal tumor presents in patients over a wide age range, but mostly affects adults during their fifth through seventh decades of life (1–3). The majority of patients reported in series (75%) are male (1–5). The tumor primarily arises in the subcutaneous tissue and, less often, in fascial or muscular tissues of the upper torso and extremities, including the hands, arms, shoulders, and posterior neck and upper back (nearly 65% of cases in series) (1–5), followed by the lower extremities, feet, hip, and abdominal wall (1–5). The lesion typically manifests as a slow-growing, asymptomatic, moveable mass. Rapid growth of the lesion is an exceedingly rare clinical presentation (3).

In the head and neck, soft tissues of the posterior neck represent the single most common site for the development of the collagenous fibroma (3). However, tumors have been documented in the anterior neck region (6,7), where the lesion has the potential to simulate an enlarged thyroid gland (6), as well as the parotid gland (8,9), palate (10,11), and forehead (12). In large series, the collagenous fibroma ranges in size from 1 to 20 cm in greatest dimension with most tumors measuring 2 to 5 cm at presentation (1–3).

Radiologic Findings

The radiologic features of two examples of collagenous fibroma have been reported in the literature (13,14). T1-weighted MR imaging of the lesion demonstrated a well-circumscribed heterogeneous mass with a low signal intensity compared with skeletal muscle. On T2-weighted MR imaging, both mixed signal intensity with foci of high and low signal (14) intensity (13) were observed. Shuto et al. (14) found that low signal intensity on MR imaging corresponded histologically to the densely collagenous areas of the tumor, whereas tumor foci exhibiting relatively greater cellularity demonstrated a higher T2-weighted signal intensity. In our experience of five cases, low signal intensity predominates particularly on T2 weighting. Collagenized bands are also not apparent as can be seen in fibromatosis on T2-weighted MR images.

Pathologic Findings

Macroscopically, the collagenous fibroma is a well-circumscribed firm mass with a fusiform or discoid configuration. The cut surface of the tumor has an off-white to gray-tan color. Cysts or flecks of calcium are occasionally noted. On light microscopic examination, the tumor exhibits moderately low to low cellularity and is composed of stellate- and spindle-shaped cells haphazardly arranged in a densely collagenous or fibromyxoid stroma (Fig. 95). These stellate cells are homogeneously distributed (3). The margin of the tumor is nonencapsulated and usually well demarcated, but Miettinen and Fetsch (3) noted infiltration of

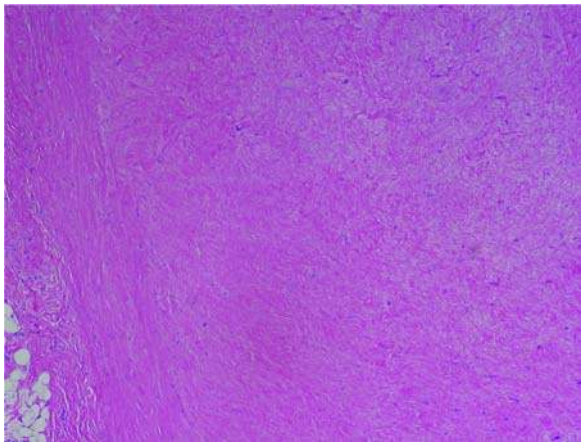

Figure 95 Low-powered magnification of collagenous fibroma shows a fairly well-demarcated, paucicellular lesion with a dense stromal collagen. The outer surface of the tumor is semicircular and has a smooth edge.

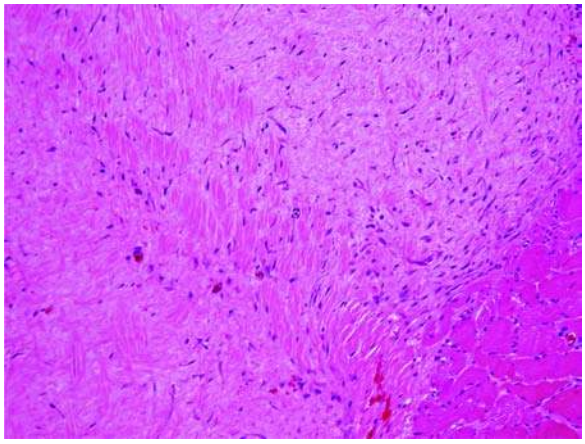

Figure 96 Occasionally these involve fat or skeletal muscle at the periphery of the tumor.

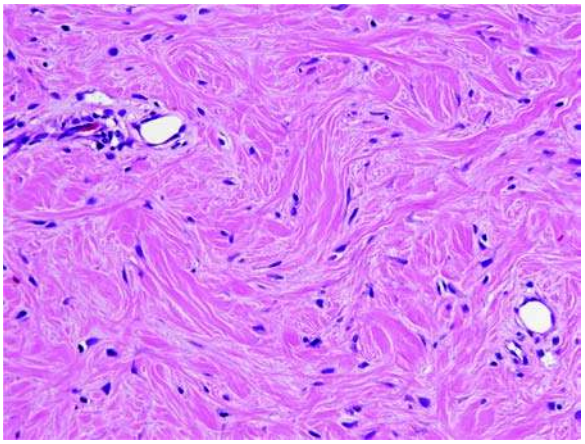

Figure 97 The vascular component is sparse and inconspicuous and the cells are uniform and bland.

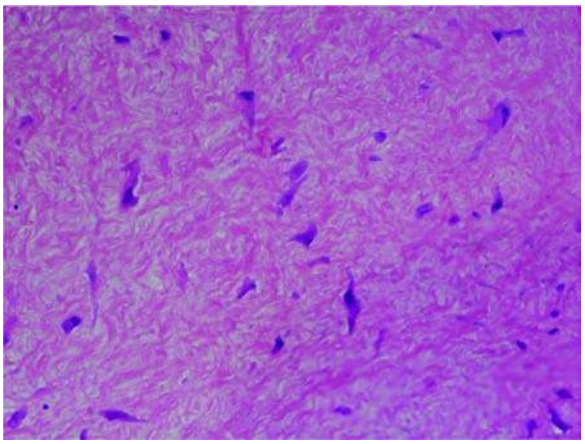

Figure 98 High-powered magnification highlights the characteristic stellate-shaped cell of the collagenous fibroma with its ovoid nucleus and small but conspicuous nucleolus.

tumor into surrounding fat or skeletal muscle in 51% and 27% of cases, respectively (Fig. 96). Occasionally, collagenous fibroma entraps fat. The vascular component is usually inconspicuous and consists of thin-walled vessels (Fig. 97). Small clusters of newly formed capillaries (3), focal perivascular hyalinization (2), foci of acute and chronic inflammation (5), and extravasated red blood cells (1–3) are additional features less often observed. Cystic degeneration sometimes occurs in larger lesions (3). Hasegawa et al. (4) described one example that contained metaplastic bone and dystrophic calcifications.

The stellate- and spindle-shaped cell comprising the tumor has scanty cytoplasm and a cytologically bland, oval, or elongated nucleus with evenly dispersed chromatin and a small eosinophilic nucleolus (Fig. 98). Floret-like multinucleated giant cells were focally observed in one documented case (4). Mitotic activity is negligible and necrosis is absent.

Immunohistochemistry

The lesional cells diffusely express vimentin and usually exhibit focal expression of muscle-specific and/or SMA (1–5). Miettinen and Fetsch (3) noted a greater degree of actin expression in tumor cells located at the periphery of the lesion. Desmin expression is typically negative, but Hasegawa et al. (4) reported one desmin-expressing tumor. Additionally, Miettinen and Fetsch (3) observed rare cells expressing keratin (cocktail of keratins AE1/3 and LP34) in 10% of tumors tested, and Nielsen et al. (2) noted diffuse, but faint,

staining with anti-S-100 protein in two examples of the lesion.

Molecular Findings

A t(2;11)(q31;q12) has been reported in two cases of collagenous fibroma and a rearrangement of the 11q12 breakpoint in a third case (15,16). These findings suggest the nonrandom association of t(2;11)(q31;q12) with collagenous fibroma. However, an identical translocation has also been described once in fibroma of tendon sheath (17).

Electron Microscopic Findings

Ultrastructural analysis of a handful of cases have demonstrated that most of the lesional cells exhibit features of fibroblasts with abundant dilated, branching rough endoplasmic reticulum and well-developed Golgi apparatus (2,5). Some cells possess subplasmalemmal actin microfilaments with interspersed dense bodies and micropinocytotic vesicles indicating myofibroblastic differentiation (2,5). Alberghini et al. (18) identified the fibronexus type of cell junction, an important ultrastructural marker of myofibroblastic differentiation, in two cases of collagenous fibroma subjected to electron microscopic evaluation.

Differential Diagnosis

A number of benign, locally aggressive, and low-grade malignant mesenchymal processes that occur in the head and neck are included in the differential diagnosis of collagenous fibroma. Fibroma of tendon sheath, with overlapping features of collagenous fibroma but separated by its heterogeneous cellularity, cleft-like spaces, and slit-like vasculature, is not found in head and neck locations. Inflammatory fibrous hyperplasia (epulis fissuratum) (19) results from ill-fitting dentures and typically affects adults in the fifth through sixth decades of life. The process usually presents as a raised to pedunculated lesion on the gingival surface of the anterior maxilla or, less often, the anterior mandible. Some examples of the process are highly collagenous and therefore can resemble the so-called inflammatory fibroma as well as the collagenous fibroma. Unlike the collagenous fibroma, this process is a site-specific lesion with a well-established etiology. Microscopically, inflammatory fibrous hyperplasia differs from collagenous fibroma by exhibiting epithelial hyperplasia, an inflammatory infiltrate, a reactive vascular component, acinar atrophy of incorporated minor salivary glands, and degenerative changes to the underlying skeletal muscle.

Nodular fasciitis (20), like the collagenous fibroma, occurs in the head and neck less frequently than in the upper extremity. The nodular fasciitis differs from collagenous fibroma by presenting in younger-aged individuals and reaching maximum size within a shorter time interval. Microscopically, the fully developed lesion is more cellular and mitotically active than the collagenous fibroma. However, in the resolving phase of the process, as interstitial collagen becomes more prominent and the cellularity decreases, histologic overlap with collagenous fibroma may ensue. Features that distinguish the nodular fasciitis from collagenous fibroma include a rich, thin-walled vascular component, cystification, hemorrhage, and focal increased cellularity in the former entity.

The sclerotic (storiform) fibroma (21,22) and the sclerotic lipoma (23,24) are two highly collagenous lesions that occur in the head and neck and have the propensity to mimic collagenous fibroma. The sclerotic (storiform) fibroma occurs as a solitary lesion or, in approximately 10% to 20% of cases, as a multifocal process associated with Cowden's syndrome (23). The lesion differs microscopically from the collagenous fibroma by its strictly dermal location and by the microscopic presence of mucinous clefts situated between thick bundles of collagen that are arrayed in a whorled to vaguely storiform pattern. Immunohistochemically, the scattered fibroblast-like cells of sclerotic fibroma express CD34, but not muscle actin (s) (25). The sclerotic lipoma occurs in regions of the body relatively devoid of soft tissues, like the digits and the scalp. These lesions, like the collagenous fibroma, are well-circumscribed, densely collagenous, and paucicellular. As a primarily lipogenic process, the sclerotic fibroma harbors residual fat, which is more randomly distributed throughout the process than in collagenous fibroma, where the fat is more often observed at the periphery of the lesion (1,3).

Nuchal-type fibroma (26,27) is a paucicellular collagenous process that occurs principally in the subcutaneous tissues of the posterior neck area and, less often, in the upper back. Rare examples of this process have been reported in the face (27). Although this lesion mainly affects young-aged adults, histologically identical lesions are found in the paraspinal area and head and neck of children and adolescents with Gardner's syndrome (Gardner-associated fibroma) (28–30). Unlike collagenous fibroma, nuchal-type fibroma has coarser bundles of collagen and frequently harbors small, closely aggregated nerve twigs reminiscent of traumatic neuroma. In further contrast to collagenous fibroma, the nuchal-type fibroma is poorly marginated and infiltrates into adjacent fat, sometimes surrounding small islands of native adipose tissue. Immunohistochemical expression of CD34 (30,31) assists in distinguishing both the nuchal-type and Gardner-associated fibroma from collagenous fibroma.

Calcifying fibrous pseudotumor (childhood fibrous tumor with psammoma bodies) (32–34) is a paucicellular, highly collagenous tumor that predilects to the extremities of young-aged individuals. The lesion infrequently arises in the soft tissues of the neck (33–39). The tumor differs from the collagenous fibroma by exhibiting fewer stellate-shaped cells, a scattered lymphoplasmacytic inflammatory infiltrate and lymphoid follicles, and foci of psammomatous and dystrophic calcifications.

Neurofibroma, at times, is extensively collagenized and as a result has the potential to mimic the collagenous fibroma. Morphologically, the cells comprising the neurofibroma are typically not stellate, but have a spindled morphology and possess tapered

nuclei with bend and buckled contours. Additionally, such collagenous variants contain a significant number of CD34-positive spindled cells (40,41), and the Schwann cell component of the process marks with S-100 protein.

SFT (42–46) and the closely related giant cell AF (47–49) are two neoplastic entities that involve the head and neck and may contain paucicellular, fibrotic areas that resemble the collagenous fibroma. These lesions are distinguished from the collagenous fibroma by their overall greater cellularity, more prominent vascular component, including hemangiopericytomatous vessels, and strong CD34 expression. The giant cell AF, a tumor that predilects to the orbital and eyelid soft tissue and has some histologic overlap with SFT, is further differentiated by the presence of multinucleated giant cells, often lining angiectatic spaces.

Soft tissue perineurioma (50–55) is a spindled cell neoplasm that typically arises in the extremities or trunk, but occasionally presents in the soft tissues of the head and neck. The histology of the tumor varies from a cellular process resembling a fibrous histiocytoma to a paucicellular lesion reminiscent of a fibroma. Unlike the collagenous fibroma, cells of the perineurioma have delicate, elongated cytoplasmic processes and their nuclei are spindled to disk shaped. The cells of the perineurioma typically grow in loose whorls and fascicles and storiform arrays. The propensity for cell processes to encircle bundles of collagen is a characteristic light microscopic feature of soft tissue perineurioma. Immunohistochemically, the perineurioma characteristically expresses epithelial membrane antigen (EMA).

Desmoid-type fibromatosis (desmoid tumor) is a highly collagenous mesenchymal tumor that, in the head and neck, mainly presents in the oral cavity, especially the tongue, as well as the cheek, soft tissue around the mandible, and neck (56,57). Unlike most examples of collagenous fibroma, the desmoid-type fibromatosis more often originates in deep muscular or fascial tissue. Although foci of hypocellularity within the process may lead to a consideration of collagenous fibroma on small biopsy, the desmoid-type fibromatosis exhibits an overall greater degree of cellularity, fasciculation, and infiltrative growth into surrounding tissues than does the collagenous fibroma.

The low-grade fibromyxoid sarcoma (58–61) is a low-grade variant of fibrosarcoma that usually presents in the deep soft tissues of the proximal extremities and trunk and infrequently involves the head and neck (58–62). Most of the tumors are larger than collagenous fibroma when first reported. Histologically, the lesion has a more complex growth pattern with myxoid foci harboring arcades of capillary-sized vessels and collagenous areas composed of spindled cells arranged in short fascicles and whorls, or located at the periphery of hyalinized collagenous nodules. In general, the tumor demonstrates greater cellularity than collagenous fibroma (especially in the myxoid areas), has a less conspicuous population of stellate-shaped cells, and shows, at least focally, a mild degree of cytologic atypia.

Prognosis and Therapy

The tumor is wholly benign. No recurrences have been documented after excision in any series (1–5). Therefore, a complete but conservative excision is adequate therapy.

M. Nuchal Fibroma

Introduction

Nuchal fibroma (NF) is a rare paucicellular collagenous, presumably nonneoplastic tumor with a strong predilection for the posterior neck, although morphologically identical lesions occur in extranuchal sites such as the face, shoulder, knee, trunk, and buttocks. Tumors outside the posterior neck are referred to as nuchal-type fibromas (1–4). Additionally, careful consideration should be given to the Gardner fibroma (Gardner-associated fibroma), particularly when nuchal-type fibromas are diagnosed in pediatric patients. Such lesions may represent the sentinel manifestation of Gardner syndrome and warrant additional clinical or radiographic evaluation (3,5–7).

Clinical Features

NFs occur in patients across a broad age range: cases have been reported in patients ranging from the first to eighth decade with a mean age at presentation of approximately 40 years. Over 80% of NFs arise in males, indicating a strong male predilection (1,2). NFs also have a strong association with diabetes mellitus and up to 44% of cases have been reported in diabetic patients (1,2,8). Other reported associations have included scleroderma, dermatofibrosarcoma protruberans, and fibromatosis (8–11), the latter particularly in the setting of Gardner syndrome. Clinically, NFs present as firm, occasionally painful, subcutaneous, or deeper mass lesions of the nuchal region. Because they blend in with adjacent tissue, they are not freely movable lesions. In rare instances, more than one discrete mass is identified (1,12).

Imaging

Radiologic imaging. CT and MR imaging may be useful in determining the extent of the lesions. CT may reveal higher attenuation as compared to muscle. On MR imaging, low signal intensity may predominate on all pulse sequences. These imaging features are related to the high collagen content of these lesions (4,8,13,14).

Pathology

Grossly, NFs are characterized as poorly circumscribed gray-white mass lesions with a firm to rubbery consistency. These range in size from 1 to 8 cm with a mean greatest dimension of approximately 3 cm. Histologically, the tumors are composed of abundant, haphazardly arranged, paucicellular collagen bundles (Fig. 99). The collagenous tissue frequently extends to entrap deposits of adipose tissue as well as underlying skeletal muscle or more superficial adnexal

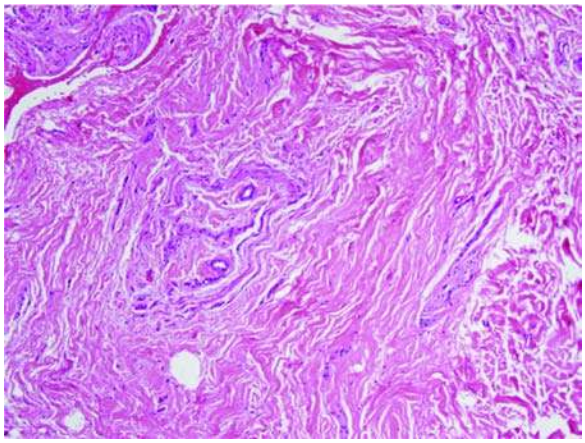

Figure 99 Nuchal fibroma is a well-delineated subcutaneous mass of dense, paucicellular fibrous tissue, with entrapped fat.

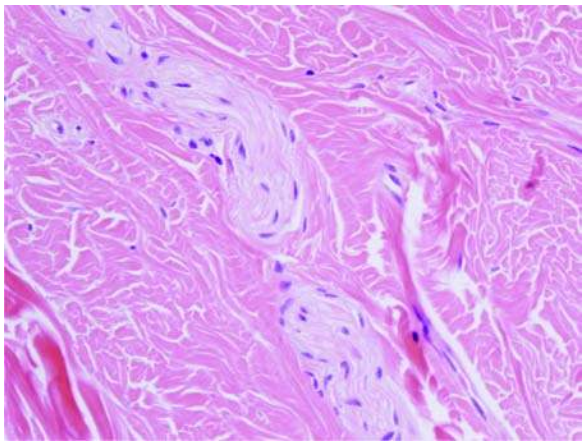

Figure 100 Nuchal fibroma often entraps normal structures, including small nerve twigs.

structures. Cross-sectioning of this tissue may lend the NF a nodular microscopic appearance. The few fibrocytes present are uniformly bland without evidence of nuclear atypia. Entrapped peripheral nerve twigs may proliferate (Fig. 100) or develop perineural fibrosis, resulting in foci reminiscent of a traumatic neuroma (2,3). A few scattered lymphocytes may be present, but inflammation is never a significant feature of NF (1).

Immunohistochemistry

NFs demonstrate consistently positive immunoreactivity with CD34, CD99, and vimentin stains (3,15). CD99 stains in a diffuse cytoplasmic pattern without the distinct membrane staining of Ewing's family tumors. S-100 protein staining can highlight entrapped neural elements as well as adipose tissue.

Electron Microscopy

Because of the paucicellular nature of the NF, electron microscopy has not played a significant role in its evaluation.

Differential Diagnosis

The clinical differential diagnosis of NF fibroma includes a variety of subcutaneous soft tissue mass forming lesions such as fibrolipoma and extraabdominal fibromatosis. Specifically, consideration can be given to pleomorphic lipoma in the nuchal region. Microscopically, lipoma, fibrolipoma, elastofibroma, fibromatosis, scar tissue, calcifying fibrous pseudotumor, collagenous fibroma (desmoplastic fibroblastoma), and nuchal fibrocartilaginous tumor all warrant consideration in the differential diagnosis (1,16). Most fibroblastic and spindle cell tumors can be excluded on the basis of the NF's lack of circumscription and paucicellularity. The elastofibroma is distinguished both by clinical location and the presence of abundant abnormal elastic fibers. Lipomatous tumors contain abundant adipose tissue relative to NF and are encapsulated or circumscribed lobulated masses. Fibromas of tendon sheath would be uncommon in this location and demonstrate greater cellularity and vascularity than would be expected in NF. Collagenous fibromas occur most commonly in the distal extremities. While these are morphologically similar they have a homogeneously more cellular stellate fibroblastic cell population and may exhibit myxoid change. The nuchal fibrocartilaginous tumor is a reactive lesion that, unlike NF, contains areas of cartilaginous differentiation. Similarly, calcifying fibrous pseudotumors are distinguished on the basis of calcifications and an inflammatory infiltrate. Extraabdominal fibromatoses are frequently infiltrative lesions but demonstrate significantly greater cellularity with purposeful myofibroblasts parallel to elongate vessels. Head and neck origin is not uncommon for extraabdominal fibromatoses; however, they are uncommon in the posterior nuchal region. On the other hand, the Gardner fibroma is morphologically identical to the NF and has a strong association with Gardner syndrome and related conditions. Judicious efforts may be warranted to exclude the possibility of Gardner syndrome when patients of any age, but particularly children, present with tumors of this type (3,5,17,18). The presence of CD34 reactivity in NF may raise the possibility of other CD34-positive tumors such as SFT, but the majority of these entities are sufficiently distinctive histologically that NF is rarely a significant diagnostic consideration. Conversely, most of the fibroblastic tumors discussed above fail to react with CD34.

Treatment and Prognosis

The treatment of NF consists of conservative surgical removal. Local recurrences do occur, but appear to be readily controlled by re-excision.

N. Solitary Fibrous Tumor/ Hemangiopericytoma

Introduction

HPC has been a highly controversial soft tissue lesion since its first description by Stout in 1942 (1). Although Stout initially believed that the tumor was derived from a pericyte, a contractile cell that resides near capillaries, it more likely has a CD34-positive fibroblastic origin and is better diagnosed as being on a spectrum with SFT. HPC was initially separated from SFT by its increased staghorn vessels with perivascular hyalinization and cellularity, whereas SFT had more collagen, less cellularity, and less staghorn vasculature. However, there are overlapping histologic features and both lesions are strongly diffusely CD34 positive, representing a specialized fibroblast. Therefore, many HPCs may be replaced by the terminology ''solitary fibrous tumor''. SFT and CD34-positive HPC occur in head and neck locations, including buccal mucosa and tongue. SFT/HPC are considered to be benign, of uncertain biologic behavior, or low-grade malignant, depending on certain histologic criteria, which are discussed below. A similar tumor occurs in the ocular region: giant cell AF, which many pathologists equate with a variant of SFT. This will briefly be discussed in the genetics section.

A different ''hemangiopericytoma'' that is specific to head and neck is the sinonasal-type HPC, which is negative for CD34 and positive for SMA, indicating a myopericytic phenotype.

''Infantile hemangiopericytoma'' is really better classified as myopericytoma(tosis), discussed elsewhere in this chapter.

A HPC-like lesion with grungy calcification and osteoclast-type giant cells can be associated with oncogenic osteomalacia (hyperphosphaturia) with marked skeletal muscle weakness and inability to ambulate; removal of the tumor improves the severe osteomalacia and symptoms (2), but this lesion is not considered a true HPC/SFT and will not be discussed in this section.

A ''hemangiopericytoma-like pattern'' means presence of staghorn vessels, some with perivascular hyalinization, which is common to several different tumors, including smooth muscle tumors, mesenchymal chondrosarcoma, and synovial sarcoma.

This section will be divided into HPC (aka SFT), a CD34-positive tumor, and sinonasal-type HPC, now better classified as glomangiopericytoma, a CD34-negative, SMA-positive myopericytic tumor.

Hemangiopericytoma/solitary fibrous tumor

Clinical Features

These occur most commonly in adults, in any anatomic area and involve the head and neck, especially tongue and buccal mucosa (3–6). The parotid gland is the most common salivary gland location, and the submandibular gland is rarely affected (7–11). In the larynx, the tumors have been predominantly supraglottic. A SFT specific to the orbit, giant cell AF, is considered in the SFT family with the addition of giant cells.

There is a female predominance, some presenting with hypoglycemia, probably from secretion of insulin-like growth factor (12,13). Only a small fraction of tumors are aggressive and the majority progress slowly.

Imaging

HPC frequently reveals a feeding high-flow vascular pedicle with intrinsic high-flow vessels as well. This has been described as ''staghorn'' appearance on angiography and MR imaging. Angiography reveals dense tumor staining, early draining views, and arteriovenous shunting. The high-flow vessels show low signal intensity on all MR pulse sequences. Enhancement is often prominent on post-contrast CT or MR imaging. The remainder (and the largest component) of the lesion demonstrates a nonspecific intrinsic imaging appearance with similar attenuation to muscle on CT, intermediate signal intensity on T1-weighted MR, and intermediate to high signal intensity on T2-weighted MR (14,15).

Pathologic Findings

On gross examination, most HPC/SFTs have a yellow to tan cut surface and sometimes prominent blood vessels can be seen. Because of this vascularity, hemorrhage may be seen, but necrosis is rare.

Histologically, gaping or slit-like branching vasculature, with perivascular hyalinization, is present. These branching vessels resemble antlers and thus have been called the ''staghorn'' pattern (Fig. 101). The endothelial cells lining the blood vessels are small and not atypical. The tumor cells are fairly small in size and relatively nondescript. The tumor cells are arranged in a haphazard pattern and the nuclei are round to oval with scant pink, spindled cytoplasm. Collagen fibers may be seen between cells and may be abundant. The margins between tumor cells are indistinct. SFT/HPC may have myxoid areas and fat, the latter called lipomatous HPC (lipomatous SFT), and have a more variable cellularity than most HPC (16–19). All HPC/SFTs have unpredictable behavior, but histologic criteria for low-grade malignant HPC/SFT include size greater than 5 cm, mitoses greater than 4/10 HPF, necrosis, hemorrhage, and cytologic atypia (Fig. 102) (20).

Immunohistochemistry

Most HPC/SFT cases are immunoreactive for CD34 and vimentin (21–26). Other endothelial markers, such as CD31, are negative in the tumor cells and stain vessels only (27). Actin, desmin, S-100 protein, and keratins are negative. CD10 can stain some fibroblastic tumors, including SFT/HPC.

Molecular Findings

Although several cytogenetic and comparative genomic hybridization (CGH) studies on SFT from head and neck and other locations have been reported, no SFT-specific recurrent genetic abnormality has been identified yet and no consistent observations have been made between SFT and HPC, despite their clinicopathologic overlap (19). At least five different translocations have been detected including t(1;16), t(4;9), t(4;15), t(6;17), t(8;12), and t(9;22) (28–33). The

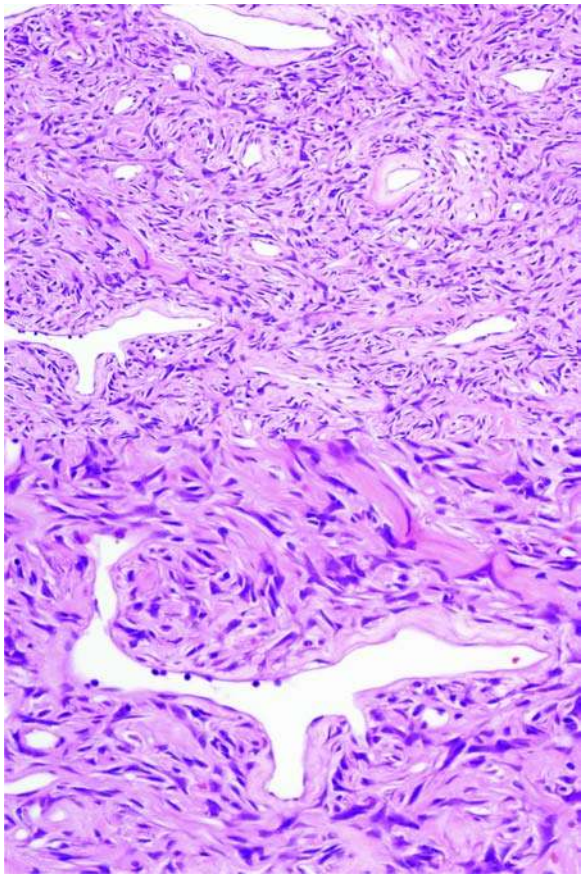

Figure 101 Hemangiopericytoma or solitary fibrous tumor, now considered a spectrum of the same tumor, has a haphazard arrangement of haphazard spindled cells and staghorn or branching vessels, often with perivascular hyalinization.

only common change in these chromosomal translocations was involvement of chromosome 4q13 in two cases (29,30). Also, trisomy 21 has been found as a sole chromosome abnormality in one case (34). Comparative genomic hybridization studies showed chromosomal gains in larger (>10 cm) SFTs, which is most likely related to tumor progression (35). Scant molecular genetic studies revealed *TP53* mutation in one of 13 analyzed SFTs and *PDGFRB* exon 18 mutation in one tumor (36,37). In the extraorbital giant cell AF, which belongs to the spectrum of SFT, the t(12;17)(q15;q23) translocation and abnormalities of chromosome 6q have each been identified once (38,39).

Electron Microscopy

The ultrastructural features of HPC resemble either undifferentiated cells or fibroblasts. Most tumors do not show specific features by electron microscopy—further evidence that HPC is not derived from a pericyte (21).

Differential Diagnosis

Because the staghorn branching pattern typical to HPC is seen at least focally in many other tumors, the differential diagnosis is quite expansive.

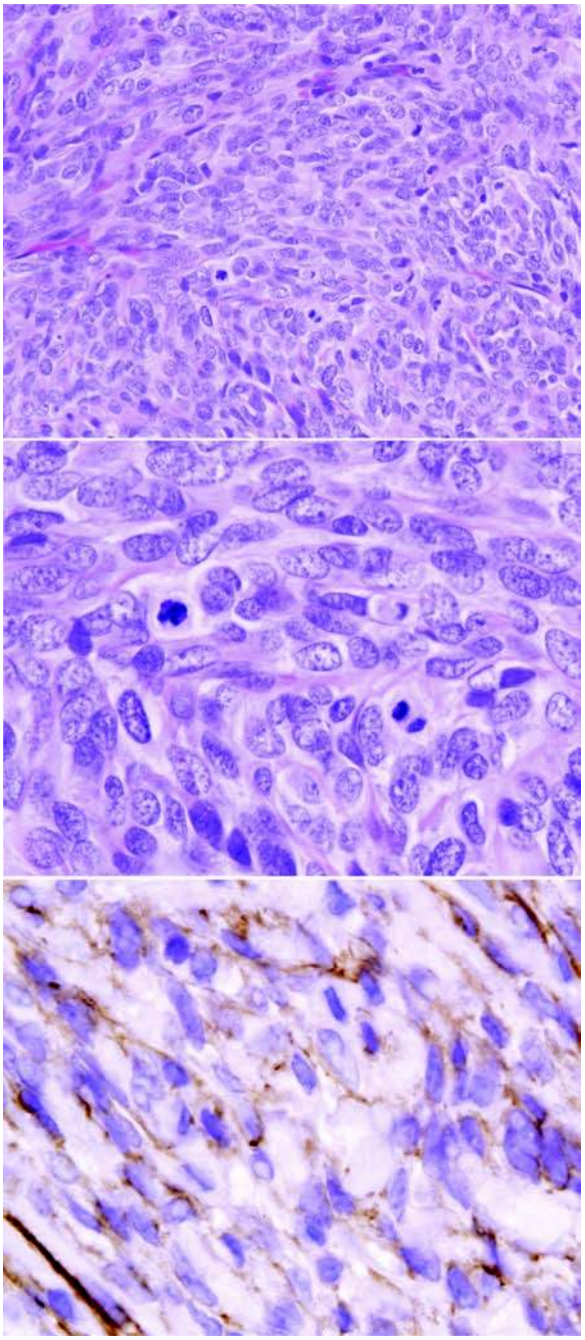

Figure 102 Malignant hemangiopericytoma or malignant solitary fibrous tumor is generally a low-grade malignant lesion characterized by size greater than 5 cm, mitoses greater than 4/10 HPF, cytologic atypia, and increased cellularity, hemorrhage, and necrosis. CD34 (*above*) will still be positive.

Cytokeratins, S-100, and HMB-45 will usually expose a carcinoma or melanoma.

Monophasic synovial sarcoma shows small, round cells and may have branching blood vessels. But the vascular pattern usually is not pervasive. Immunohistochemistry for synovial sarcoma will show CK7, keratins, and EMA, but is negative for CD34. The current gold standard for the diagnosis of

synovial sarcoma involves identification of the t(X;18) translocation (40). Mesenchymal chondrosarcoma usually exhibits a prominent hemangiopericytoid vascular pattern, but always has hyaline cartilage present and is usually S-100 protein positive. Smooth muscle tumors have different morphology, including deeply eosinophilic cytoplasm with longitudinal fibers, and are positive for SMA and desmin and negative for CD34, unlike HPC/SFT, and nerve sheath tumors would stain with S-100 protein and GFAP, unlike HPC/SFT. Endometrial stromal sarcoma can have a hemangiopericytoid vascular pattern and is positive for CD10 as well as HPC. Although CD10 can be seen in both tumors, CD34 should only be expressed in HPC and estrogen receptor is only expected in endometrial stromal sarcoma (41). Angiosarcoma can be confused with HPC because both have a vasoformative component, but angiosarcoma contains highly pleomorphic tumor cells that would be positive for CD31 and negative in HPC/SFT.

Prognosis and Treatment

The behavior of SFT/HPC cannot be predicted with certainty; many are considered borderline or of uncertain biologic behavior. In one study, Espat et al. (42) demonstrated that 3 of 25 tumors recurred and 3 of 25 were metastatic. There was a five-year survival rate in 86% of the cases. Pathologic features that suggest a low-grade malignant potential include tumor size greater than 5 cm, tumor geographic necrosis, hemorrhage, mitotic rate greater than 4/10 HPF, and nuclear pleomorphism (43,44). The treatment for all HPC/SFT is complete local resection and patient follow-up.

Sinonasal hemangiopericytoma (''glomangiopericytoma'' and myopericytoma)

Clinical Features

Sinonasal HPC occurs within the sinonasal tract. These are reclassified now as a glomangiopericytoma, a myopericytoma lesion (45).

True HPC is uncommon compared with sinonasal type of glomangiopericytoma in the nasal cavity and paranasal sinuses. Glomangiopericytoma has different morphology and a more indolent clinical picture. Glomangiopericytoma is one of the only truly distinctive tumors to the head and neck (46). It most commonly presents clinically as nasal obstruction with or without epistaxis (47). Additional symptoms include sinusitis, ocular pain, decreased visual acuity, increased tear secretion, and headache. Within the nose, many attach to the turbinates. Often, the tumor presents as a slowly enlarging painless mass, but may be painful if it grows too large or involves a nerve.

Molecular Findings

There are no genetic findings yet for glomangiopericytoma.

Pathology

Grossly, the lesions are often polypoid and may be mistaken for a benign nasal polyp. Microscopically, tumor cells are spindled to round shaped with clear to eosinophilic cytoplasm (48). The characteristic staghorn pattern of HPC is usually seen. But unlike HPC, tumor cells form short fascicles that can be storiform, whorled, or palisaded. The stroma is also usually at least focally hyalinized. Mast cells, eosinophils and extravasated red blood cells are often seen scattered in the background (Fig. 103) (49). Giant cells and myxoid stroma may occasionally be present. Malignant glomangiopericytoma is exceedingly rare (22,50). Features that would suggest malignancy include greater than four mitotic figures per 10 HPF, greater than 5 cm size, nuclear pleomorphism, and bone invasion.

Immunohistochemistry

Unlike HPC, the tumor cells of glomangiopericytoma express actin and not CD34 (22,51). Cytokeratin, CD31, desmin, h-caldesmon, and cytokeratin are also negative.

Treatment and Prognosis

Glomangiopericytoma is indolent and has a much better prognosis than HPC. The treatment of choice is complete surgical excision, with a greater than 90% five-year survival rate (22,50,52). Recurrence occurs in up to 30% of cases and may not appear until many years or decades following initial resection (22,51,53). Recurrence may occur in cases where complete surgical excision is not possible (49). Malignant sinonasal HPC, i.e., malignant glomangiopericytoma, is exceedingly rare and would also be of low malignant potential. Criteria are similar as for HPC.

O. Myxoma

Introduction

Myxoma is a benign, paucicellular tumor composed of fibroblasts, myofibroblasts, and scattered vessels emersed in a stromal matrix consisting primarily of acidic nonsulfated (stromal-type) mucin. Typically, myxomas contain only wispy collagen fibers within a mucin-rich stroma, but lesions with a relatively greater amount of collagen exist and are sometimes referred to as fibromyxomas.

The pathogenesis of myxoma formation is not fully understood, but it is believed that lesional fibroblast-like cells produce and elaborate an excessive amount of mucosubstance, primarily in the form of hyaluronic acid, into the extracellular space. In experimental models, this material inhibits the normal polymerization of the precursor protein moiety, tropocollagen, to mature type I collagen resulting in a mucinous stromal matrix relatively devoid of collagen (1).

Cardiac myxoma (2) and the myxoma that primarily arises in extremity musculature (intramuscular myxoma) (3–5) are the two most commonly encountered and recognized forms of the process. Myxomas occurring in the head and neck, however, are relatively rare. Fu and Perzin (6) found only six examples of myxoma (all intraosseous) in a study of 256 nonepithelial tumors of the nasal cavity, paranasal sinuses, and nasopharynx. Despite its rarity in head and neck tissues, three forms of myxoma are found in this

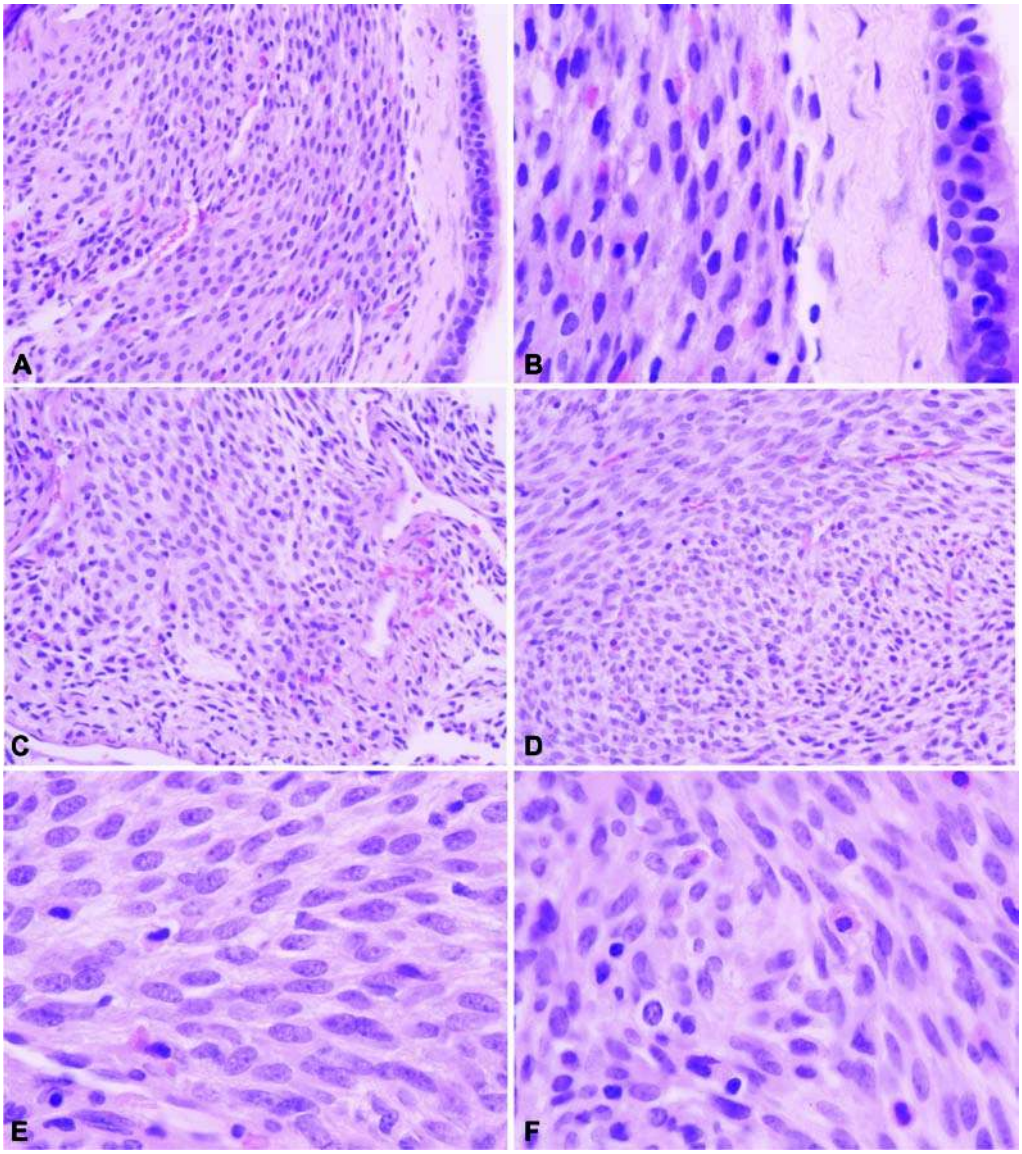

Figure 103 Sinonasal-type hemangiopericytoma, ''glomangiopericytoma,'' is found exclusively in the sinonasal tract (**A,B**) and has a hemangiopericytoma vascular pattern (**C**). The epithelioid to short spindled cells (**C,D**) are arranged in short fascicles (**E,F**) that may interlace, and there are scattered mast cells, red blood cells, or other inflammatory cells in the stroma.

region: (*i*) odontogenic myxoma, (*ii*) soft tissue myxomas, including intramuscular myxoma, and (*iii*) cutaneous or superficial angiomyxoma.

Intraosseous myxoma represents over 60% of all noncutaneous myxomas affecting the head and neck (7). The overwhelming majority of cases arise in the gnathic bones; the most common site for myxomas of bone in general. Their location in the tooth-bearing areas of the gnathic bones, the presence of odontogenic epithelial structures in some lesions (8), and the tumor's overall histologic resemblance to the normal dental papilla support an origin of the process from odontogenic mesenchyme and validate the suitability of the designation, odontogenic myxoma. A minority of tumors take origin from nongnathic bones, such as the anterior maxillary sinus wall (9).

Soft tissue myxomas are found in a variety of locations in the head and neck and are reported less often than the odontogenic myxoma (7). The origin of soft tissue myxomas in the head and neck is diverse. In deed, one must be cautious in excluding potential mimics (see section ''Differential Diagnosis''). Some true myxomas reported in the subcutaneous tissue probably represent examples of superficial angiomyxoma, whereas others originate from fascial tissue or from periosteum of bone (1).

The intramuscular variant of soft tissue myxoma is a distinct clinicopathologic entity and accounts for about 15% of nonosseous myxomas in the head and neck region (10,11). This lesion typically presents as an asymptomatic mass in deep thigh, shoulder, or buttock musculature of middle-aged adults (3–5). Rare

examples of intramuscular myxoma, sometimes occurring in multiple sites, are associated with polyostotic or, less often, monostotic fibrous dysplasia (Mazabraud's syndrome) (12,13).

Cutaneous myxoma or superficial angiomyxoma is a myxomatous process located in the dermis and subcutaneous tissues. The cutaneous myxoma has a rather wide anatomic distribution, but 17% (14) and 36% (15) of tumors are reported to involve the head and neck area in large series. Although most cutaneous myxomas are solitary, the presence of multiple small lesions occurring at an early age and in certain sites, namely, the eyelids and external ear (16,17), should raise the possibility of the Carney complex (constellation of cardiac, mammary, and cutaneous myxomas; lentigines, blue nevi with epithelioid features, and pigmented mucosal lesions; primary pigmented nodular adrenocortical disease; large-cell calcifying Sertoli cell tumor; and the psammomatous melanotic schwannoma) (17,18).

Clinical Features

Odontogenic myxoma presents over a wide age range, but has a peak incidence in the second through the fourth decades of life, and shows a female bias in most studies (19–25). The mandible is involved nearly two to three times more often than the maxilla (20,24,25) with the posterior aspect of the alveolar region of the gnathic bones representing the site of tumor origin. Compared with adults, gnathic bone myxomas represent a high proportion of odontogenic tumors in children with a 12% to 17% incidence rate quoted in some studies (23,26). The odontogenic myxoma is a slow-growing tumor that usually presents as an asymptomatic mass. Large tumors manifest symptoms including pain, paresthesia, and loosening or resorption of involved teeth (24,27). Rapidly growing odontogenic myxomas have also been described (22,28).

Sinonasal myxomas most often have their epicenter in the maxillary sinus. While many represent a sinus extension of an odontogenic myxoma arising in the posterior maxilla, a subset of these lesions demonstrate no evidence of an odontogenic origin and frequently involve the anterior maxillary sinus wall from which they purportedly arise (9). This myxoma affects patients over a wide age range, but has a peak incidence in the first two decades of life, and exhibits no gender bias. The process presents with cheek or facial swelling or, less often, as a painful mass. When symptoms of nasal congestion, epistaxis, or facial distortion occur, the tumor is more advanced and invades bony structures (29). Rare cases of myxoma developing in the sphenoid sinus have been documented in adults (7,30).

Laryngeal myxomas arise in middle-aged or older adults and show a strong male preponderance (31–36). Patients present with hoarseness or difficulty breathing, and, on occasion, emergency management is required for life-threatening airway obstruction (34). The tumor is usually located in epiglottic or supraglottic regions and usually has a polypoid configuration. Supraglottic lesions are generally asymptomatic and therefore can obtain large size before clinical detection (36).

Intramuscular myxomas involving the head and neck affect patients over a wide age range, but mostly occur in the fifth decade of life, and more commonly arise in females (3,10,11,37–48). The lesion typically presents as an asymptomatic mass or swelling. The myxoma occurs in a variety of head and neck locations, including the facial muscles and muscles of mastication, but the deep muscles of the neck are most commonly reported site.

Tse and Vander (49) in 1985 reviewed the literature regarding noncutaneous soft tissue myxomas of the head and neck region (depth of the lesion not stipulated) and found that the palate and region of the parotid were the most commonly affected sites.

Cutaneous myxoma or superficial angiomyxoma (14,15) presents over a wide age range, but mostly affects adults in the fourth through sixth decades of life, and exhibits a male predilection. The lesion occurs in three clinical settings. Most often, the process presents as a single, asymptomatic, slow-growing cutaneous papule, nodule, or polypoid mass primarily in the trunk, head and neck region, or extremities. Less commonly, multiple lesions appear, and a small proportion of these patients have the Carney complex (see above).

Radiologic Findings

MR imaging of soft tissue myxoma is frequently characteristic with very low signal intensity on T1-weighting (81–100%), marked high signal intensity on T2-weighting (100%), faint rim of adipose tissue (65–89%), and a small amount of surrounding edema (79–100%). The subtle rim of surrounding fat and edema are relatively unique for an intramuscular mass and along with intrinsic characteristics are nearly pathognomonic of the diagnosis of myxoma. These features in intramuscular myxoma are due to an incomplete pseudocapsule allowing leakage of the high water content tissue into the surrounding muscle (edema) with subsequent fat atrophy (adipose tissue). These lesions may simulate a cyst, but the intramuscular location and contrast enhancement pattern (most commonly mild and diffuse) allow differentiation from a true cyst. CT (low attenuation) and sonography (hypoechoic but not anechoic) also demonstrate the high water content of these lesions (50–53).

Pathologic Findings

Intramuscular myxoma is considered the prototypical myxoma. The tumor varies in size, but averages about 5 cm in greatest dimension. Although the lesion appears well circumscribed on cursory gross inspection, subtle infiltration into the surrounding skeletal muscle is identified on closer evaluation. Its cut surface is tan-yellow to gray, mucoid or gelatinous (Fig. 104). Small fluid-filled cysts and thin fibrous trabeculae are additional gross features. Microscopically, intramuscular myxoma is a paucicellular process composed of randomly distributed short, bipolar spindled, and stellate-shaped cells suspended in a highly myxoid stromal matrix (Fig. 105). Widely scattered, thin-walled, nonarborizing vessels are also

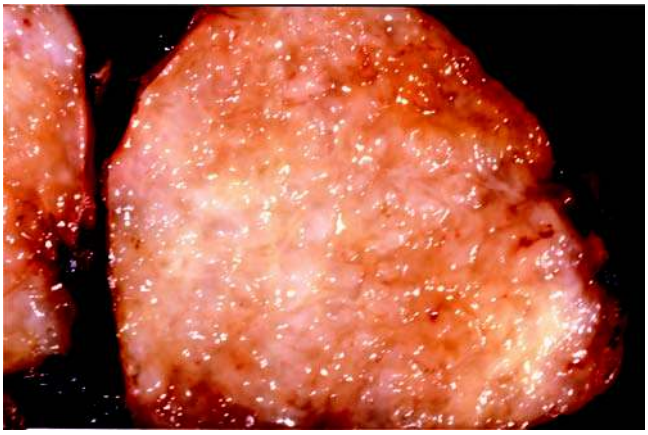

Figure 104 Cut surface of the intramuscular myxoma has a shiny, gelatinous appearance.

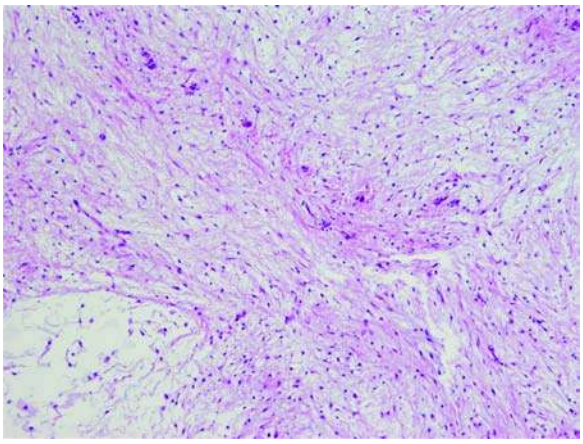

Figure 105 Low-power magnification of the intramuscular myxoma demonstrates haphazardly distributed, small spindled, and stellate cells emersed in a myxoid stroma with delicate collagen fibers and scattered thin-walled blood vessels. Note the microcyst (*lower left*).

identified in the myxomatous stroma as well as an occasional small, fluid-filled cyst. Muciphages and mast cells are additional elements commonly found within the lesion. The lesional cells have a scant amount of lightly eosinophilic, occasionally vacuolated cytoplasm. The centrally placed nucleus is oval or elongated with evenly dispersed chromatin (Fig. 106). Mitotic figures are vanishingly rare. Wispy strands of thin collagen are observed and appear to blend with the delicate cytoplasmic processes of the lesional cells. At the periphery of the process, discontinuous bands of condensed strands of wispy collagen form a fibrous pseudocapsule (Fig. 107, top), whereas in other areas, tumor infiltrates surrounding skeletal muscle, which is commonly atrophic and frequently intermixed with fat cells (Fig. 107, bottom). Tumors with areas of increased cellularity, more prominent vascularity

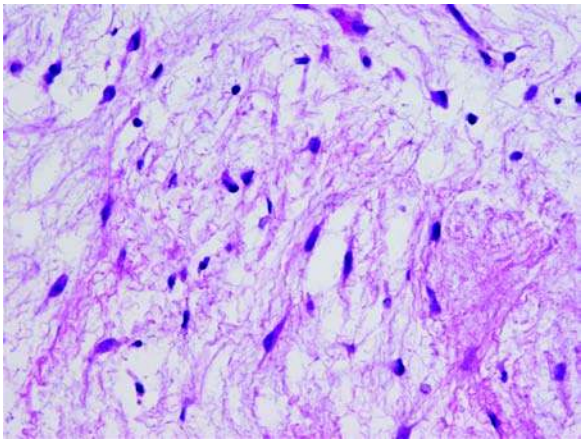

Figure 106 High-power view of the intramuscular myxoma demonstrates cytologically bland spindled and stellate cells with scanty eosinophilic cytoplasm suspended in a myxoid stromal matrix containing fine strands of collagen.

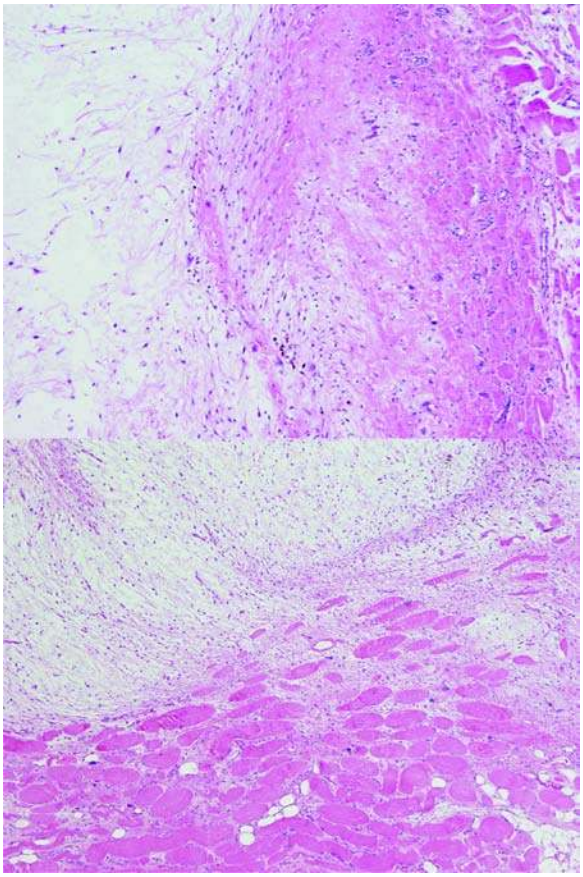

Figure 107 At the margin, condensed collagen fibers form a fibrous pseudocapsule and separate the myxoma from surrounding skeletal muscle (*top*). In other areas of the tumor, lesional tissue percolates between skeletal muscle bundles (*bottom*).

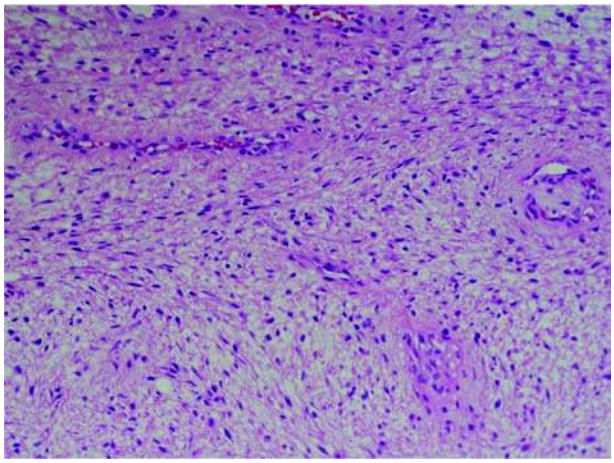

Figure 108 Cellular variant of intramuscular myxoma is characterized by a higher concentration of bland spindled and stellate tumor cells and a more prominent vascular component.

including muscularized or elongated vessels, and a higher collagen content (44,54) are termed ''cellular myxomas'' (Fig. 108). However, this variant shares with the conventional intramuscular myxoma, bland cytologic features, inconspicuous mitotic activity, and simple nonarborizing vessels.

The stromal mucin of intramuscular myxoma is strongly alcian-blue positive. This reactivity near-totally disappears after hyaluronidase pretreatment indicating a large component of hyaluronic acid (55).

Odontogenic myxoma shows histologic overlap with intramuscular myxoma with the exception of the presence of mild pleomorphism, an occasional mitotic figure, and increased vascularity in some examples (20,24) (Fig. 109). Additionally, a minority of cases reveal nests and strands of odontogenic epithelial cells, many of which exhibit conspicuous intercellular spaces, scattered throughout the lesion (Fig. 110). Infiltration of tumor between native cancellous bone is observed in some examples. Histochemical analysis including critical electrolyte concentration technique for characterizing mucosubstances has shown that the stroma consists mostly of hyaluronic acid and small amounts of chondroitin sulfate (20,56).

The superficial angiomyxoma presents as multiple angiomyxoid nodules within the dermis and subcutaneous tissue (14,15,18) (Fig. 111, top). The nodules are commonly separated from native tissue by a cleft containing mucin (Fig. 111, bottom). The process shows low to moderate cellularity and consists of bipolar spindled cells, stellate-shaped cells, and multinucleated cells with bland cytologic features emersed in a highly myxoid stroma containing wispy strands of collagen (Fig. 112). Intranuclear cytoplasmic inclusions and a smudgy nuclear chromatin are two characteristic cytologic features of the lesional cells. The vascular component varies in density and consists of simple, nonarborizing vessels (Fig. 113, top). A ''mixed'' inflammatory cell infiltrate

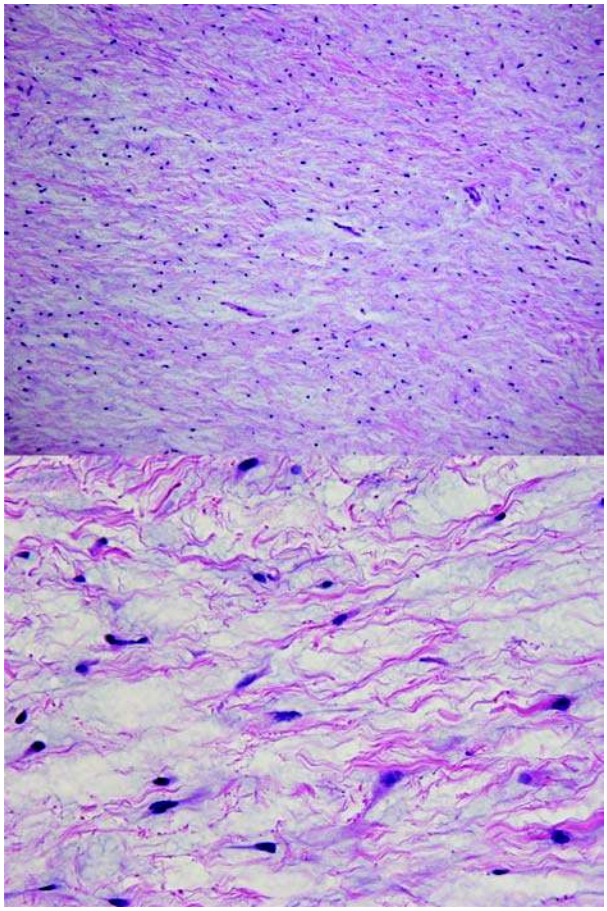

Figure 109 Low-power magnification of the odontogenic myxoma (*top*). The lesion is composed of short, cytologically benign spindled and stellate cells (*bottom*). Note microscopic similarities to intramuscular myxoma.

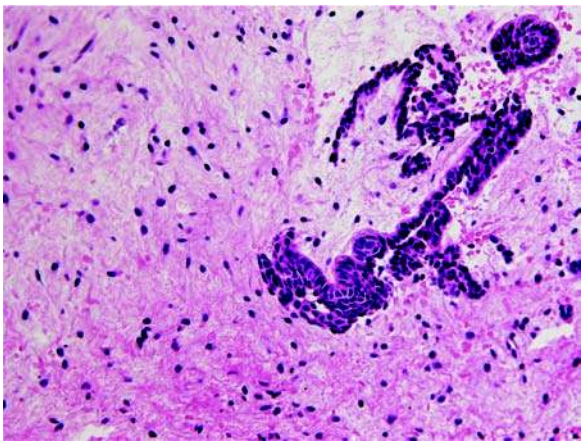

Figure 110 Nests, trabeculae, and strands of odontogenic epithelium within an odontogenic myxoma. This finding is not specific or necessary for the diagnosis.

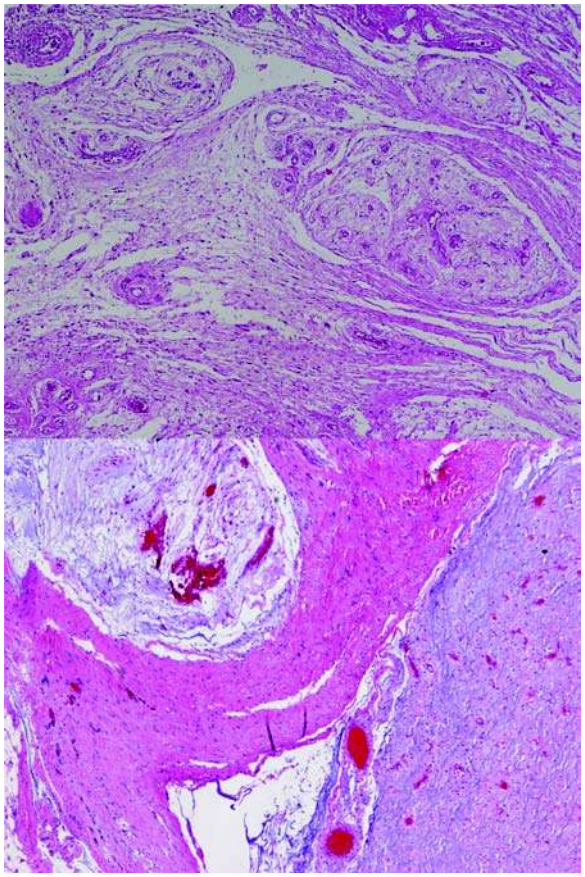

Figure 111 Superficial angiomyxoma (cutaneous myxoma) consists of variably sized, vascular myxoid nodules (*top*) separated by a clefted space from the surrounding dermis and subcutaneous tissues (*bottom*).

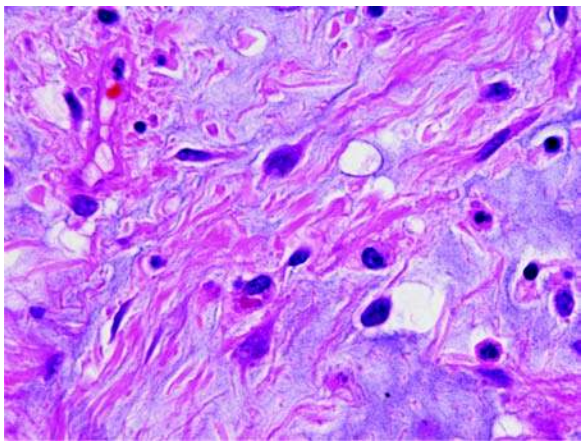

Figure 112 Short spindled and stellate tumor cells admixed with inflammatory elements. Note the characteristic smudgy quality of the nuclear chromatin.

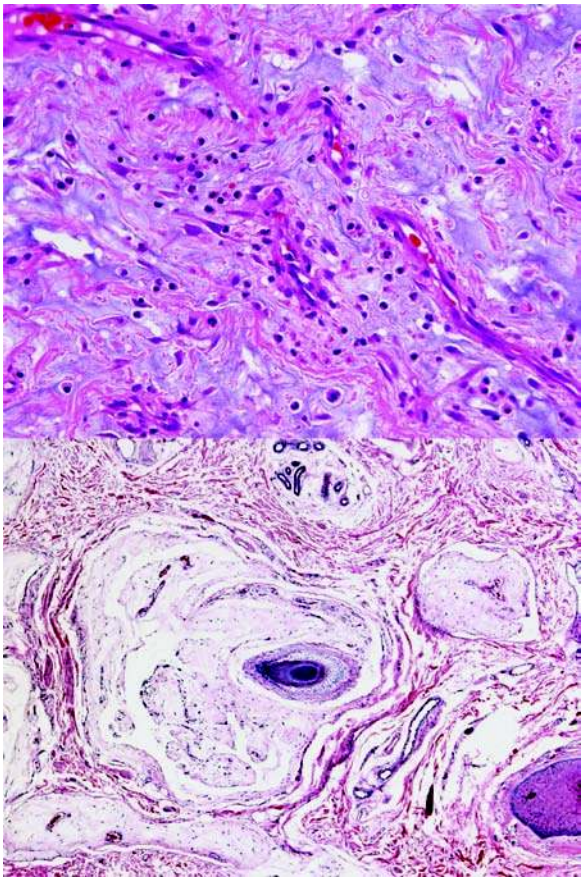

Figure 113 A variable number of non-arborizing vessels, a mixed inflammatory infiltrate (*top*), and incorporated epithelial structures (*bottom*) are additional salient microscopic features of superficial angiomyxoma (cutaneous myxoma).

of lymphocytes and acute inflammatory cells, fibrin or hemosiderin deposits, and interstitial hemorrhage are commonly identified microscopic features. Additionally, epithelial inclusions or strands of squamous or basaloid cells are found within lesional tissue in 20% to 30% of cases (Fig. 113, bottom). The stromal mucin consists primarily of hyaluronic acid.

Immunohistochemistry

The lesional cells of the intramuscular myxoma diffusely express vimentin and show variable expression of muscle actin(s) and CD34 (40,54). One report claims desmin expression in intramuscular myxomas (57). CD68 identifies muciphages within the tumor. Immunohistochemical profiling of the odontogenic myxoma shows expression of vimentin and muscle actin(s) (21,58,59). S-100 protein was reported in one study (59). The epithelial structures identified in the myxoma express keratin 19 (59). In an immunohistochemical analysis of mucosubstances present in odontogenic myxoma, Zhao et al. (60) detected chondroitin-6-sulfate (but not other sulfated mucopolysaccharides) and hyaluronic acid within the stromal matrix.

The lesional cells of the cutaneous myxoma are reported to express vimentin in large series (15,61). In a study of superficial angiomyxomas involving the genital tract, Fetsch et al. (61) found expression of CD34 in all 11 tumors, variable expression of smooth muscle and muscle-specific actins, and weak expression of S-100 protein and factor XIIIa.

Molecular Findings

Odontogenic myxoma and superficial angiomyxoma (cutaneous myxoma). Mutational inactivation and downregulation of *PRKAR1A*, a gene encoding type I regulatory subunit of protein kinase A (PKA), has been documented in several cases of sporadic odontogenic myxoma (62). Previously, *PRKAR1A* has been implicated in the familial myxoma syndrome (Carney complex); multiple superficial angiomyxomas have been reported in this syndrome. Germline mutations affecting *PRKAR1A*, an apparent tumor-suppressor gene, have been identified in a subset of patients with this disease (63,64).

Intramuscular myxoma. Molecular genetic studies have shown gain-of-function mutations in *GNAS1*, a gene encoding the α-subunit of the guanine nucleotide-binding protein, which stimulates formation of cAMP. Mutations have been reported in intramuscular myxomas with and without fibrous dysplasia. Previously, similar activating missense mutations in the 201 codon (Arg) have been identified in endocrine tumors, McCune-Albright syndrome, and isolated fibrous dysplasia of bone (65–69).

Electron Microscopy

The tumor cells of the intramuscular myxoma tumor cells show ultrastructural features of active fibroblasts with dilated rough endoplasmic reticulum containing finely granular material, well-developed Golgi complexes, and pinocytotic vesicles. Myofibroblasts with myofilamentous bundles are also identified in the intramuscular variant (40,42). Ultrastructural studies of odontogenic myxoma also demonstrate cells exhibiting fibroblastic and myofibroblastic features (8,21,58). The epithelial nests within the lesion exhibit intercellar spaces similar to those observed in the stellate reticulum of the enamel organ and are surrounded by basement membrane, which also lines intercellular vaginations of surrounding tissue (8).

Limited ultrastructural studies of cutaneous myxoma have demonstrated the presence of fibroblast-like cells with features of dermal dendritic cells, but no evidence of myofibroblasts (14,70).

Differential Diagnosis

The main concern in the differential diagnosis of the odontogenic myxoma is distinguishing two normal developmental structures: the dental follicle and papilla. In fact, Kim and Ellis (71) stated that nearly 20% of dental follicles sent to the Armed Forces Institute of Pathology were incorrectly classified with the odontogenic myxoma representing the single most common misdiagnosis rendered. Radiologically, both structures appear as small lucent defects that surround teeth. They are commonly excised along with an impacted tooth (commonly, the third molar tooth), but often separate from the tooth on extraction. Microscopically, the dental papilla is composed almost entirely of a myxoid stroma and shows a striking similarity to the odontogenic myxoma. One important gross morphologic feature of the papilla is its consistently elliptical shape. Microscopically, it is lined by palisaded cuboidal odontoblasts and usually harbors eosinophilic dentinoid material along the periphery of the myxoid tissue. The dental follicle is a more collagenous structure that exhibits focal myxoid change in nearly 75% of specimens (71). Unlike the odontogenic myxoma or fibromyxoma, the dental follicle has an epithelial lining composed of columnar, cuboidal, or squamous cells that is present in over 50% of cases (71).

The radiolucent appearance of chondromyxoid fibroma and its prominent myxoid stroma are clinicopathologic features that are shared with the odontogenic myxoma. Chondromyxoid fibroma arises principally in the metaphyseal region of the tibia, but approximately 2% of cases arise in the gnathic bones with most tumors affecting the mandible (72). Microscopically, the process differs from odontogenic myxoma by its distinctive lobular growth pattern. Furthermore, the periphery of each lobule shows accentuated cellularity including the presence of osteoclast-like giant cells and polygonal chondroblast-like cells. The cells composing the central myxoid region of the lobule are mainly stellate in shape and differ from those of odontogenic myxoma by their greater cytologic variability.

Cellular examples of odontogenic myxoma or fibromyxoma in a young-aged patient may suggest the possibility of an osteosarcoma. Radiologically, the osteosarcoma usually demonstrates cortical destruction, but early in its course, the sarcoma may only show resorption or displacement of teeth (73) similar to the radiologic features described for odontogenic myxoma. In sharp contrast to the odontogenic myxoma, the osteosarcoma microscopically exhibits higher cellularity, more cytologic atypia, increased mitotic activity and, by definition, osteoid or bone formed directly from the malignant mesenchymal component.

Myxomas presenting in the sinonasal tract require differentiation from a variety of other myxomatous processes. Mucocele of the paranasal sinuses and the ranula are composed strictly of mucinous material and a variable inflammatory infiltrate, including muciphages. The ranula is a mucus extravasation phenomenon resulting from trauma to, or obstruction of, the sublingual gland. The process usually presents as an intraoral mass emanating from the floor of the mouth, but, in some cases, it will dissect through submental, submandibular, or parapharyngeal tissues (74,75). In contrast to the myxoma, the fully developed mucocele and ranula lack a significant intralesional component of spindled and stellate-shaped cells (apart from granulation tissue that surrounds the deep or ''plunging'' ranula). Additionally, the mucosubstance of the latter has histochemical staining properties of epithelial and not stromal mucin.

In a young-aged individual, the most important lesion to exclude is embryonal rhabdomyosarcoma. Seven percent of nonmetastatic rhabdomyosarcomas (70% of which were the embryonal subtype) occurring in patients under the age of 21 years originate in the head and neck according to the Intergroup Rhabdomyosarcoma Study-IV (76). Similar to sinonasal myxoma, embryonal rhabdomyosarcoma is a highly myxoid tumor. The short, spindled rhabdomyosarcoma cells have the potential to mimic the cells composing the myxoma on cursory evaluation. However, in comparison with the cytologically bland myxoma cell, the cells of the rhabdomyosarcoma are more hyperchromatic and mitotically active, and at least some of the malignant cells have brightly eosinophilic cytoplasm harboring characteristic cross-striations. In contrast to the random growth exhibited by the cells of myxoma, the rhabdomyosarcoma cells tend to concentrate under the mucosa (cambrium layer). Immunohistochemical expression of desmin and skeletal muscle nuclear regulatory protein, myogenin (with or without MyoD1), is observed in over 90% of rhabdomyosarcomas and confirms the diagnosis (77).

Localized intraneural neurofibroma (78) is often a deeply located process that has a prominent myxoid stromal matrix. On gross examination, an appreciation for the presence of an enlarged nerve involved in the process assists in the diagnosis. The cells of the neurofibroma have irregularly contoured elongated nuclei and are characteristically apposed to bundles of collagen deposited along the course of nerve fibers within the lesion. Immunohistochemically, subsets of cells within the neurofibroma show strong expression of S-100 protein and CD34. Histochemical stains for axons such as the Bielschowsky or the neurofilament protein immunohistochemical stain frequently identify residual axons within the lesion.

Soft tissue perineurioma (79) is usually a superficially located neoplasm that primarily occurs in extremities and trunk, but occasionally is located in the head and neck. Hypocellular, predominantly myxoid variants of soft tissue perineurioma exist and, if deeply located, have the potential to mimic the intramuscular myxoma. Microscopically, the lesional cell of perineurioma has elongated, delicate cytoplasmic processes and is arrayed, at least focally, in a storiform or whorled pattern. The cells characteristically express EMA and ultrastructurally exhibit features of nonneoplastic perineurial cells including numerous pinocytotic vesicles, discontinuous external lamina, and rare cell junctions.

The low-grade myxofibrosarcoma (80–82) and the low-grade fibromyxoid sarcoma (83–85) require separation from the intramuscular myxoma, particularly the cellular variant. The low-grade myxofibrosarcoma presents in a similar age range as the intramuscular myxoma. Although the lesion can be intramuscular, the majority of tumors are located in subcutaneous or subfascial tissues. Unlike the myxoma, the myxofibrosarcoma features mono- and multinucleated cells that at least focally exhibit nuclear atypia and mitotic activity. The vascular element of the sarcoma is more highly concentrated and consists of elongated, thick-walled curvilinear or, less often, arborizing thin-walled vessels. Additionally, lesional cells of the myxofibrosarcoma have a proclivity to concentrate around these vessels. The low-grade fibromyxoid sarcoma is composed of relatively bland appearing, mitotically inactive spindled cells resembling those of myxoma. The sarcoma presents in a younger-aged individual than intramuscular myxoma and predilects to the deep soft tissue of the buttock, thigh, and shoulder and less often presents in the head and neck. Unlike the haphazard growth pattern exhibited by the myxoma, the low-grade fibromyxoid sarcoma consists of moderately cellular myxoid nodules in which lesional cells grow in a whorled or swirling pattern around arcades of thin-walled vessels as well as less cellular, collagenous regions with cells arranged in vague fascicles or grouped along the periphery of hyalinized collagenous nodules.

Laryngeal myxomas arising in the vocal cord may cause diagnostic problems with the vocal cord nodule. The vocal cord nodule is frequently encountered lesion that commonly shows myxoid change. However, the vocal cord nodule is more vascular than the myxoma and typically shows evidence of hemorrhage, including large deposits of fibrin (33).

Several myxomatous tumors that mainly affect the dermis enter into the differential diagnosis of the cutaneous myxoma. The nerve sheath myxoma (myxoid neurothekeoma) is a superficially located tumor that shares a nodular growth pattern with superficial angiomyxoma (86). Nerve sheath myxoma, however, predilects to the extremities and rarely affects the soft tissues of the head and neck. Microscopically, the nerve sheath myxoma is more cellular than the superficial angiomyxoma and each nodule is surrounded by a distinct fibrous band. The constituent spindled and epithelioid peripheral nerve sheath cells show a greater degree of orientation than the cells of the cutaneous myxoma and commonly proliferate in small syncytial nests or anastomosing, thin cord-like files. Inflammatory cells and intralesional vessels are relatively scarce. Immunohistochemically, the Schwann cells composing the tumor consistently demonstrate strong expression of S-100 protein and variable expression of GFAP.

Localized cutaneous neurofibroma is considered the most common form of neurofibroma (78). The lesion consists of short, spindled cells proliferating in a myxoid stroma. Microscopically, the process grows in a more diffuse manner within the dermis than the cutaneous angiomyxoma. Moreover, its cells possess nuclei exhibiting a greater degree of contour irregularity than the cells of cutaneous angiomyxoma. Although both lesions show variable expression of CD34, a proportion of cells in the neurofibroma show convincing expression of S-100 protein. Also, remnants of axons are occasionally identified within the lesion with histochemical or immunohistochemical stains.

Superficial angiomyxoma displays histologic overlap with a dermal-based myxomatous process termed focal cutaneous mucinosis, as well as lesions having both epithelial and mesenchymal elements including the trichogenic myxoma, fibrofolliculoma,

trichofolliculoma, and trichodiscoma. Focal cutaneous mucinosis, like superficial angiomyxoma, commonly affects the face. However, these lesions differ by being small and solitary (and not multinodular), less well circumscribed, and restricted to the dermis (61). In addition, they lack the vascularity and inflammation that typifies the superficial angiomyxoma. The fibrofolliculoma and fibrodiscoma are presently considered different developmental stages of a single, benign, ''mixed'' stromal and epithelial (appendageal) tumor (87). Multiple lesions are associated with the Birt-Hogg-Dube syndrome (88), a condition that principally affects the lung (spontaneous pneumothorax) and kidney (oncocytic renal tumors) and are not linked to the Carney complex. They exhibit histologic overlap with superficial angiomyxoma, but differ from the latter by being purely dermal in location, exhibiting evidence of sebaceous differentiation in many cases, and lacking an inflammatory component (15,87). It should be noted that some investigators have suggested that the above named adnexal tumors are interrelated lesions and best subsumed under the generic term, cutaneous myxoma (14).

Prognosis and Treatment

Odontogenic myxoma has a propensity to permeate the marrow space and thereby recur after incomplete surgical excision. Rate of recurrence for the odontogenic myxoma ranges between 10% and 33% with a reported average of about 25% (51). Recurrent disease usually manifests within two years after surgical manipulation. Conservative modes of excision such as curettage are considered adequate management of small lesions as they allow evaluation of the margin and leave the contour of the jaw intact (24,51). However, large tumors require wide excision with adequate margins particularly those originating in the maxilla as involvement of the maxillary sinus is not uncommon (51).

As the intramuscular myxoma virtually never recurs, marginal or simple (local) excision of the mass is presently considered appropriate therapy for the lesion (3,5,40,41,44,89). The cellular variant poses a small risk for nondestructive recurrence (54).

The sinonasal myxoma has the potential for destructive growth and for recurrence if incompletely excised (9). Therefore, excision with adequate margins is a recommended therapy. As many of these lesions show radiologic origin from the posterior aspect of the maxilla, partial maxillectomy is often performed as part of a wide (local) excision (30,90). Laryngeal myxomas tend to show a negligible risk of recurrence after complete (local) excision (31–34,36).

The superficial angiomyxoma has a reported recurrence rate between 33% and 39% after incomplete excision in large series (14,15,61). Recurrences are nondestructive and are associated with minimal morbidity. It is important, however, to consider the Carney complex in those patients with multiple lesions as the cardiac myxoma and the psammomatous melanotic schwannoma are the main sources of morbidity and mortality in this rare condition (18,91).

P. Ossifying Fibromyxoid Tumor

Introduction

Although these are listed here in the ''benign'' group, these are generally considered to be of uncertain to potentially low-grade malignant behavior (1). Occasionally these tumors may have osteoid, and there is controversy as to whether these become osteosarcoma or frankly malignant ossifying fibromyxoid tumors (OFMTs) (2). They are still of uncertain phenotype and many have suggested a possible nerve sheath or cartilaginous differentiation (3,4); however, there are current considerations for a specialized fibroblastic phenotype.

Clinical Findings

These most often occur in the extremities or trunk in young patients. These can also occur in the head and neck (5–11) and oral cavity (12). There is a male predilection (13). Most present as painless, subcutaneous nodules, often attached to underlying tendons, fascia, or skeletal muscle (13). OFMTs are often of long-standing duration; 80% have a partial rim of metaplastic bone at its periphery.

Radiologic Imaging

Radiographs of OFMT (Fig. 114) show a soft tissue mass with a peripheral rim of calcification that may simulate myositis ossificans. Involvement of the underlying bone with erosion and periosteal reaction may also be apparent. CT reveals the peripheral calcific rim optimally, and it is typically incomplete. On MR imaging, signal intensity of lesions are usually similar on T1 weighting to that of muscle and intermediate on T2 weighting. Unlike myositis ossificans, surrounding edema is not apparent. Nonmineralized regions usually demonstrate diffuse enhancement following contrast administration. Lesions are typically relatively well defined on CT or MR imaging. Bone scintigraphy may reveal intense radionuclide uptake owing to the calcification (13,14).

Pathologic Findings

Grossly they are generally 3 to 5 cm and are well circumscribed, multinodular, and have a fibrous pseudocapsule, with or without a partial shell of bone. They are white-tan and rubbery firm. Microscopically, OFMT is composed of lobules of round to ovoid cells embedded in a myxoid to hyalinized stroma with prominent vasculature, often with perivascular hyalinization, not found in extraskeletal myxoid chondrosarcoma. Eighty percent have an incomplete rim of metaplastic bone, rimmed by osteoblasts (Fig. 115). The tumor cells in OFMT are arranged in nests and cords and have inconspicuous nucleoli and only rare mitotic activity (Fig. 116). The cells often resemble cooked sunny-side up eggs with distinctive cytoplasmic borders embedded in their myxoid to hyalinized matrix (Fig. 117). Increased cellularity, cytologic atypia, or increased mitotic activity cause concern for worse behavior; those with true malignant osteoid

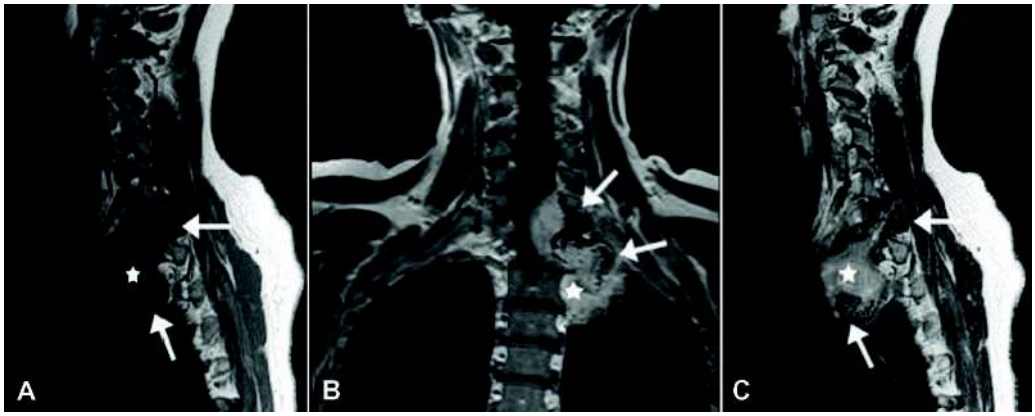

Figure 114 Ossifying fibromyoid tumor of soft parts at the base of the neck. (**A**) Sagittal T1-weighted, (**B**) coronal T1-weighted post-contrast and (**B**) sagittal T2-weighted MR images reveal the soft tissue mass (*) with diffuse contrast enhancement and intermediate signal intensity. Local area of prominent low signal intensity represents peripheral calcification (*arrows*).

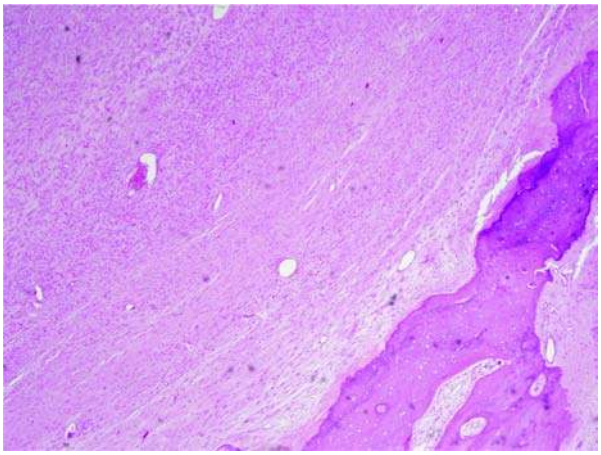

Figure 115 Ossifying fibromyxoid tumor has an incomplete rim of bone at the periphery of the lesion in 80% of cases.

(produced by atypical cells) are probably better classified as osteosarcoma.

Immunohistochemistry

The tumors are positive for vimentin and often for S-100 protein and interestingly for desmin. Leu7, GFAP, NSE, keratin, and SMA are rare in these tumors (15,16).

Molecular Findings

Cytogenetic data on the OFMT are limited. Two of three reported karyotypes revealed complex numeric and structural aberrations; the third exhibited unbalanced translocation der(6;14)(p10;q10) and an add(12)(q24.3). On the basis of these studies (16–19), common cytogenetic abnormalities specific to OFMT cannot be identified.

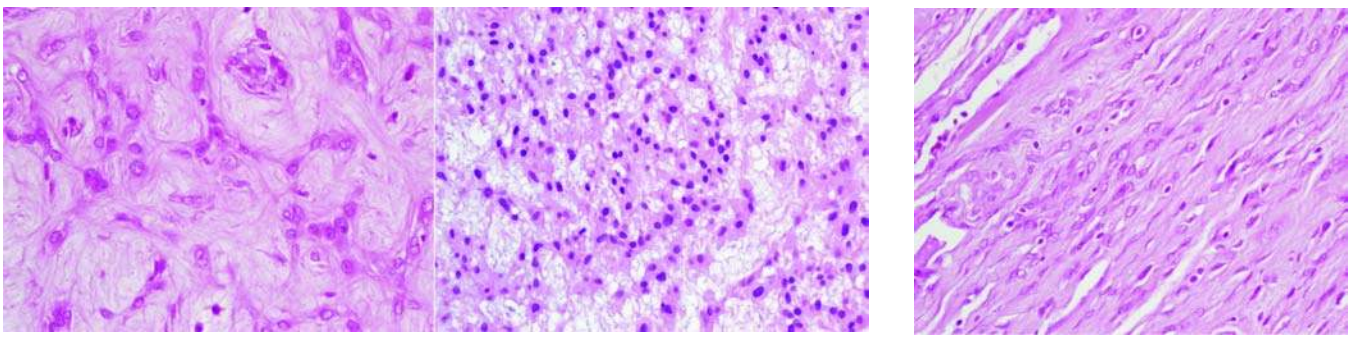

Figure 116 The ovoid to sometimes spindled cells are embedded in a fibromyxoid to myxoid stroma. They can grow in a sheet-like to trabecular to clustering to pseudoglandular pattern. Vessels are often prominent.

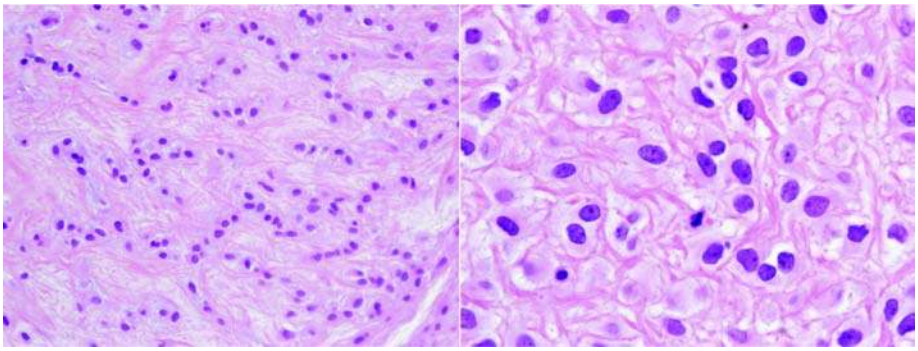

Figure 117 The nuclei are ovoid and bland with well-dispersed chromatin and distinctive cytoplasmic borders. The nuclear-to-cytoplasmic ratio is often low giving the tumor cell a "fried egg" appearance.

Electron Microscopy

The cytoplasm of these cells contains prominent rough endoplasmic reticulum with cisternal dilations, with increased mitochondria and microfilaments, often clustered in the perinuclear area (3). Ribosome-lamellar complexes are occasionally present (20). Occasionally, partial reduplication of external lamina and complex interdigitating cell processes have been observed (15,21).

Differential Diagnosis

The differential diagnosis includes other nerve sheath tumors such as epithelioid benign nerve sheath tumors, extraskeletal myxoid chondrosarcoma, and adnexal or mixed tumor. These can be separated by their lack of a bony shell, attention to uniform round egg-like nuclei with distinctive cytoplasmic borders, vascular details of OFMT and by immunohistochemistry (noting the desmin and not always strong S-100 protein reactivity for OFMT and usual absence of keratins, SMA, and GFAP).

Prognosis and Treatment

These are usually considered to be of uncertain biologic behavior due to their almost 30% recurrence potential and their exceedingly rare metastatic potential. Features such as increased cellularity or mitoses portend a worse prognosis and make them of low-grade malignant behavior (1,2,22). These should all be treated by complete (sometimes wide) surgical excision and patient follow-up.

VI. MIXED TUMOR

A. Ectomesenchymal Chondromyxoid Tumor

Introduction

ECT is a distinctive, benign soft tissue neoplasm that has a strong predilection for occurrence on the anterior dorsal tongue. The pathogenesis of this unusual tumor remains obscure. Some sources advocate inclusion of ECT in the spectrum of soft tissue myoepithelioma/mixed tumor or favor salivary gland derivation (1,2). However, the tumors consistently fail to display characteristic morphologic features of myoepitheliomas, such as plasmacytoid (hyaline) cells or focal ductal differentiation (3,4). The diagnosis of ECT is sufficiently specific that discussion as a separate entity is warranted.

Clinical Features

The ECT is an uncommon tumor, with less than 30 reported examples. In the initial description of ECT by Smith et al. (4), all patients presented with a submucosal mass lesion of the anterior tongue. Most arise on the dorsal surface, but the lateral aspect of the tongue may also be involved. Subsequent case reports and small series have supported this predilection, although one case involving the hard palate has been reported (3–12). The ECT is slow growing with a consistency varying from firm to soft. In rare cases, superficial ulceration is present, but the mucosa is usually intact. A mass lesion may be present for several years prior to diagnostic intervention. Patients range in age from the first to eighth decade of life with a median age of 32 years. Males and females are equally affected.

Imaging

ECTs are readily visualized on clinical examination and imaging studies have not played a role in their diagnosis or treatment.

Pathology

Gross examination reveals a submucosal nodule or multinodular mass lesion, pale gray to tan or yellow in color. The cut surface often has a gelatinous consistency and foci of hemorrhage may be evident. ECTs are small tumors, ranging in size from under 0.5 cm to 2.0 cm, with the majority 1.0 cm or less. Microscopically, one or more well-circumscribed

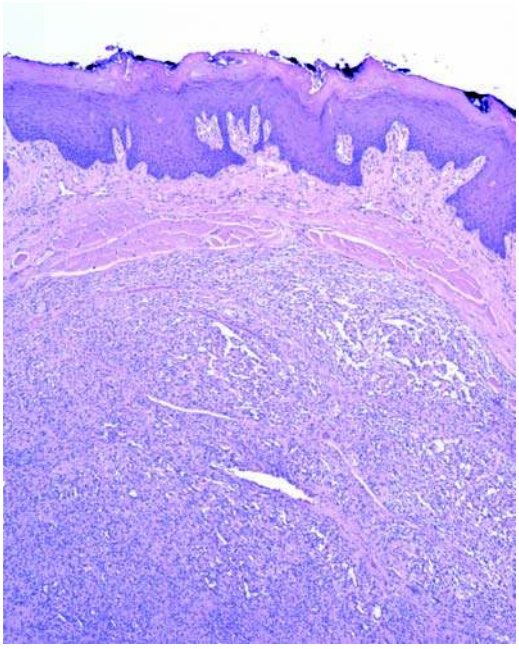

Figure 118 Ectomesenchymal chondromyxoid tumor. The unencapsulated tumor exhibits peripheral circumscription and cleft-like spaces. Skeletal muscle is present between the lesion and surface mucosa.

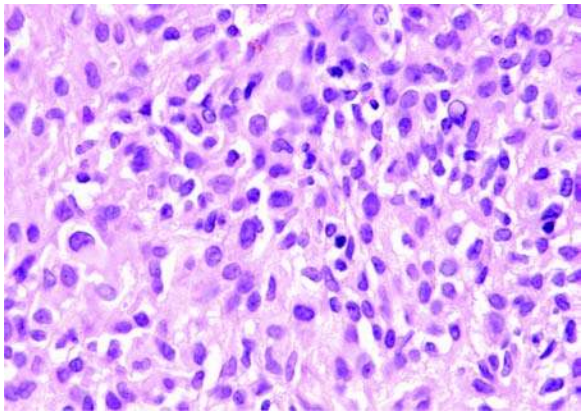

Figure 119 Ectomesenchymal chondromyxoid tumor. Sheets of cells with irregular nuclear contours, granular chromatin, and inconspicuous nucleoli. Note nuclear pseudoinclusion (*upper right*).

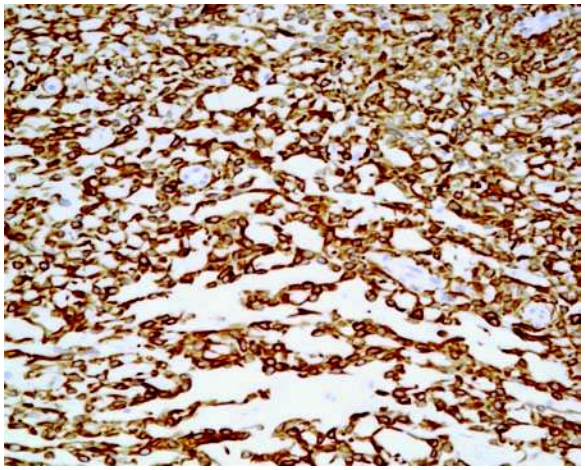

Figure 120 Ectomesenchymal chondromyxoid tumor. Strong, uniform glial fibrillary acid protein staining highlights the reticular pattern in this example.

nodules are evident. The nodules are separated by fibrous bands. The nodules compress the submucosa and musculature of the tongue with entrapped muscle fibers or nerve twigs commonly observed at the periphery (Fig. 118). These tumors are composed of admixed round, polygonal, oval, or fusiform cells arranged in sheets, cords, and strands. The sheets of cells frequently display a reticular, net-like arrangement. Cleft-like spaces or small pseudocysts are present in the majority of cases and may contain pseudopapillary projections of tumor cells. Myxoid, mucinous, or hyalinized foci may all be present in one lesion. Chondroid areas with distinct lacunae are typical, but not necessarily present in all cases. The tumor cells have moderate amounts of eosinophilic to amphophilic cytoplasm and indistinct cell borders. Cytoplasmic deposition of hemosiderin is not uncommon, especially in the peripheral cells. Nuclei are frequently irregular with indentations and pseudoinclusions, granular chromatin, and inconspicuous nucleoli (Fig. 119). Scattered mitotic figures may be identified. Foci of atypia in the form of hyperchromasia, pleomorphism, and increased cellularity are present in some ECT.

Immunohistochemistry

With one possible exception, all reported examples of ECT have expressed GFAP (Fig. 120) (2). GFAP immunostaining is usually unequivocal, but positivity varies from focal to diffuse. The majority of cases are also immunoreactive for S-100 protein. In the initial description of ECT, cytokeratin reactivity was present in 12 of 13 cases; however, subsequent published cases have largely failed to replicate this finding (4–9,12). Vimentin and Leu-7 (CD57) staining is also seen in most cases. Variable or conflicting results have been described with SMA and desmin stains. Epithelial membrane antigen stain is nonreactive.

Electron Microscopy

Ultrastructural examination of ECT reveals bilobated and concave nuclei with evenly distributed chromatin.

Basal lamina partially envelopes some, but not all, of the cells. Pinocytotic vesicles may be present. Cytoplasmic filaments have not been identified using electron microscopy (4,8).

Molecular Findings

There is no current evidence that molecular or genetic alterations play a role in the pathogenesis of ECT. Cytogenetic studies on ECTs are limited, with only a few karyotypes being reported (13). Although clonal chromosomal abnormalities, including loss of chromosome 17, have been described, the tumor-specific cytogenetic marker has not yet been identified.

Differential Diagnosis

The ECT bears some morphologic similarities to a variety of soft tissue neoplasms, including ossifying fibromyxoid tumor, extraskeletal myxoid chondrosarcoma, and neurothekeoma. Many of these entities can be excluded from consideration on clinical grounds alone as they do not tend to involve the tongue. Its small size, distinctive immunophenotype, benign appearance, and nuclear features help distinguish ECT if questions remain (8). Interestingly, because of the uniform absence of clear myoepithelial or ductal differentiation in ECT, salivary gland tumors rarely factor into the morphologic differential diagnosis. Unlike oral salivary gland tumors, minor salivary gland tissue is virtually never present in the ECT specimen. However, there are immunophenotypic similarities to the soft tissue myoepithelioma/mixed tumor spectrum of lesions (10,14). It is uncertain whether soft tissue myoepitheliomas occur in the oral cavity (with the possible exception of the ECT), but the constituent cell types, particularly plasmacytoid cells, of myoepithelioma allow differentiation of the two lesions on morphologic grounds.

Treatment and Prognosis

Conservative, complete surgical excision appears to be the treatment of choice for ECT. Many are removed in the course of excisional biopsy. Rare recurrences have been described, but re-excision resulted in elimination of lesion (4,8).

Part II: Malignant Mesenchymal Tumors of the Head and Neck

I. GRADING AND STAGING

A. Grading

Prognosis for sarcomas of the head and neck is often better than counterpart sarcomas in other anatomic locations. This may be due to the relatively small size at discovery and earlier symptoms/signs produced by head and neck primary tumors. Once a mesenchymal tumor is phenotyped and is determined to be potentially malignant, i.e., has the potential to metastasize, the tumor can be graded. Grading of sarcomas in the head and neck is exactly the same as that for sarcomas of other soft tissue sites. There have been several grading schemes utilized to determine prognosis of sarcoma, some with three and others with four tiers (1–6). Each systems measured different histologic parameters and it was very confusing for pathologists, clinicians, and patients, from one institution to another. Recently, most soft tissue pathologists have now adopted a consistent and highly reproducible grading scheme, a three-tiered system based on differentiation, mitotic activity, and necrosis, the French Federation Nationale des Centres de Lutte Contre le Cancer (FNCLCC) (5,7–10). The system is highly reproducible and correlates well with outcome. The FNCLCC is based on a total score obtained by evaluating the following three parameters, selected by multivariate analysis: differentiation, mitotic activity, and necrosis (Table 7). The subscore for each component (differentiation, mitoses, and necrosis) is added together to make a total score, which interprets the tumor as grade 1, 2, or 3 out of 3. The tissue used to create the FNCLCC score is best when previously untreated and abundant, although it is often the original biopsy material. Essentially ''differentiation'' is guided by phenotype and morphology, yielding a 3 for round cell, pleomorphic myoid tumors, or tumors of uncertain phenotype, and a 1 for well-differentiated liposarcoma (WDLS), chondrosarcoma, fibroblastic tumors, and other tumors resembling the cell of origin. The score for mitotic activity is 1 for 0–9/10 HPF (high-power field), 2 for 10–19/10HPF, and and 3 for greater or equal to 20/10 HPF. The necrosis score: none = 0, less than 50% = 1, and greater or equal to 50% of the biopsy material available = 3. The three scores are added together; total scores of 1–3 are ''low grade'' or grade 1/3, those that equal 4 or 5 are ''intermediate grade'' or grade 2/3, and a total score of 6 to 8 would be ''high grade'' or grade 3/3. Treatment is often directly related to grade, with

Table 7 FNCLCC System for Histologic Grading of Sarcoma (Usually Performed on all Available, Previously Untreated, Biopsy Material)

Differentiation score
1 = Resembles the cell of origin, such as fibro-, lipo-, chondrosarcoma.
2 = Pleomorphic liposarcoma or malignant fibrous histiocytoma (have better prognosis than myoid sarcomas)
3 = Round cell tumors and most tumors of uncertain phenotype or pleomorphic myoid sarcoma (rhabdomyosarcoma or leiomyosarcoma)

Mitotic Score
1 = 10 mitoses/10 HPF)
2 = 10–19 mitotes/10 HPF
3 = ≥20 mitoses/10 HPF

Necrosis Score
0 = No necrosis
1 = <50% necrosis
2 = ≥50% necrosis

Total Score (adding together scores for differentiation, mitoses, necrosis)
2 or 3 = Low grade (grade 1/3)
4 or 5 = Intermediate grade (grade 2/3)
6–8 = High grade (grade 3/3)

uncertain biologic behavior and low-grade malignant tumors treated by complete or sometimes wide excision and careful patient follow-up. Intermediate and high-grade sarcomas, grade 2–3/3, are treated by pre- and postoperative radiation followed by chemotherapy if clinically indicated, particularly in tumors greater than 5 cm or those that cannot be fully resected.

B. Staging

The staging for soft tissue tumors is made via a multidisciplinary approach and combines the pathologist's grade (above) with other radiologic and clinical information. Two systems that have been used for soft tissue sarcoma include Enneking's Musculoskeletal Tumor Society Staging System (Table 8) (11) and the American Joint Committee on Cancer (AJCC) system (Table 9) (12). The Enneking system is great for surgeons and it depicts the departmentalization of the tumor as well as being for both bone and soft tissue sarcoma. Yet, the new AJCC is helpful because it is a TNM system that has become standard for other tumors of these head and neck sites and other neoplasms of other anatomic sites. There is a current move toward using AJCC for sarcoma, even for pediatric sarcoma, to keep staging standardized. AJCC cannot be applied to angiosarcoma (in which poor prognosis appears independent of grade, except in oral locations, where there is better behavior) and a few other lesions in soft tissue, non–head and neck, sites. Fibromatosis or desmoid is considered a benign tumor and therefore is not graded or staged. There is separate AJCC staging for head and neck and lip and oral cavity tumors (usually epithelial neoplasms), as outlined elsewhere.

Table 8 The Enneking Staging System for Musculoskeletal Sarcoma

Stage	Grade	Site	Metastasis
IA	G1	T1	M0
IB	G1	T2	M0
IIA	G2	T1	M0
IIB	G2	T2	M0
III	G1 or G2	T1 or T2	M0

T1 = Intra-articular, superficial to deep fascia, paraosseous, intrafascial compartment
T2 = Soft tissue extension from intra-articular, deep fascial extension from superficial lesion, intraosseous or extrafascial extension from paraosseous, extrafascial compartment from intrafascial compartment

Table 9 The American Joint Committee on Cancer Sarcoma Staging: TNM System

Stage I	T1a, 1b, 2a, 2b	N0	M0	G1	Low
Stage II	T1a, 1b, 2a	N0	M0	G2-3	High
Stage III	T2b	N0	M0	G2-3	High
Stage IV	Any T	N1	M0	Any G	Low or high
Stage IV	Any T	Any N	M1	Any G	Low or high

T1 = size ≤ 5 cm
T2 = size > 5 cm
a = superficial
b = deep
NX = lymph node cannot be assessed
N0 = no regional lymph node metastasis
N1 = regional lymph node metastasis
MX = distant metastasis cannot be assessed
M0 = no distant metastases
M1 = distant metastases

II. MALIGNANT VASCULAR

A. Epithelioid Hemangioendothelioma

Introduction

Epithelioid hemangioendothelioma is a vascular neoplasm of intermediate malignant potential (between that of hemangioma and conventional angiosarcoma). The tumor is composed of an extravascular growth of epithelioid endothelial cells that demonstrate only rudimentary attempts at vascular differentiation. Initially considered a form of carcinoma, the epithelioid hemangioendothelioma involving the lung was referred to as ''intravascular bronchioloalveolar tumor'' (1), while those arising in the liver were considered variants of sclerosing cholangiocarcinoma (2). Once immunohistochemical and ultrastructural analysis confirmed the vascular nature of the tumor (3,4), the appellation epithelioid hemangioendothelioma was universally accepted (5). Angioglomoid tumor and myxoid angioblastomatosis are no longer accepted as designations for the neoplasm. The term ''histiocytoid hemangioma'' (6) is not synonymous with epithelioid hemangioendothelioma, but is used in a broader sense to group vascular lesions that have in common the presence of large, epithelioid endothelial cells.

Clinical Findings

Epithelioid hemangioendothelioma (5,7) affects nearly all age groups, but has a peak incidence during middle-age adulthood, and shows no gender bias. The tumor arises principally in somatic soft tissues, parenchyma of the liver and lung, and the bone, but a wide distribution of primary sites are documented in the literature.

The soft tissue epithelioid hemangioendothelioma most commonly arises in the extremities, the trunk, and the head and neck. In the head and neck, the soft tissues of the submandibular region are the most commonly affected sites in large series (8). However, the tumor has been reported in the oral cavity, where gingival tissue is most frequently involved (9), as well as in the nasal cavity (10), parotid gland (11,12), larynx (13), thyroid (14), craniofacial and gnathic bones (15–18), and skin (19). The majority of soft tissue epithelioid hemangioendotheliomas arise in subfascial sites and less than 10% present within the dermis (7). Over one-half of soft tissue epithelioid hemangioendotheliomas are centered around, or originate within, a vein, or less commonly, an artery (5). Therefore, thrombophlebitis or edema may be presenting signs. Although the vast majority of patients have only a solitary lesion, a small number of individuals develop multiple tumors over a prolonged period of time (7). Most patients present with an asymptomatic mass, but a significant minority of individuals experience pain most likely because of vascular occlusion by the tumor.

Imaging

Hemangioendothelioma may show a nonspecific appearance on computerized tomography (CT) or magnetic resonance (MR) imaging with a soft tissue mass alone. Serpentine vascular channels (high flow) and spaces (small component of the lesion) may be apparent in a minority of cases, suggesting the vascular etiology of this lesion. These features are optimally depicted on MR imaging as is lesion extent for staging purposes (20–22).

Pathologic Findings

On macroscopic examination, epithelioid hemangioendothelioma of soft tissue appears as a firm mass with a whitish cut surface. Those tumors that arise within a vessel resemble an organizing thrombus. The tumor has a diffusely infiltrative or nodular growth pattern with ill-defined borders on low-power microscopic examination. Tumors arising within a vessel expand the vessel, infiltrate its walls without disturbing the architecture, and exhibit a centrifugal growth pattern in the surrounding soft tissue (Fig. 121). At higher magnification, the characteristic feature of the tumor is the presence of plump epithelioid tumor cells arranged in small nests, short strands, and cords (Fig. 122). The nucleus of the cell is vesicular, has a small nucleolus, and typically shows mild cytologic atypia (Fig. 123). Mitotic activity is low.

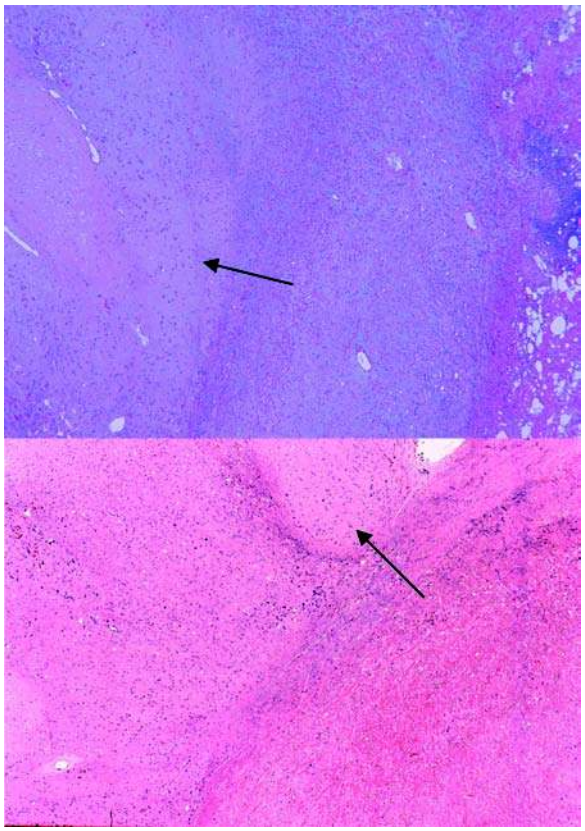

Figure 121 Epithelioid hemangioendothelioma infiltrating the wall of a vein. Arrows identify tumor within the lumen of the vessel.

The accompanying sulfated mucopolysaccharide-rich stroma has a distinctive myxohyaline or chondromyxoid appearance. Microscopic features of vascular differentiation within the lesion are often subtle and

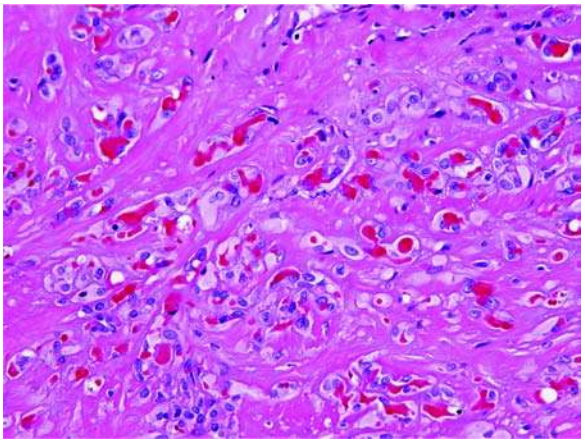

Figure 122 Epithelioid tumor cells arranged in variably sized nests and strands. Note intracytoplasmic erythrocytes.

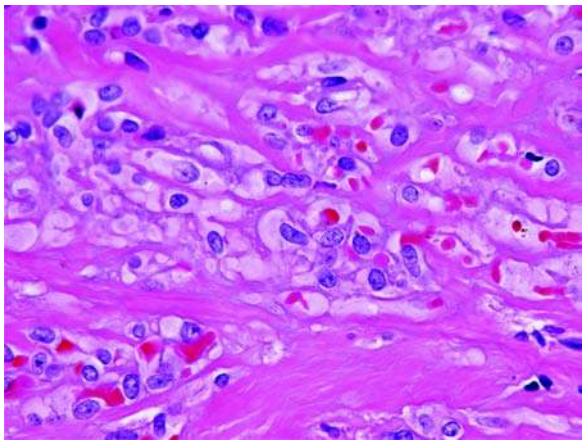

Figure 123 Cytologically, the tumor cells have lightly eosinophilic cytoplasm and a vesicular nucleus with a small nucleolus.

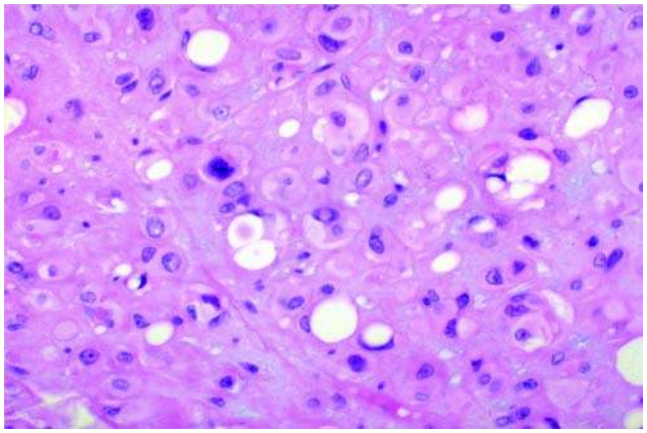

Figure 124 Rudimentary lumen formation in an epithelioid hemangioendothelioma in sheets of extravascular epithelioid endothelial cells; note the characteristic myxochondroid-appearing hyalinized cytoplasm and stroma.

mostly take the form of intracytoplasmic vacuoles containing erythrocytes or their detritus. Cells arranged in thin trabeculae occasionally separate along the long axis of the structure to form a rudimentary vascular channel, but well-developed vascular structures are rarely identified (Fig. 124). Findings of recent hemorrhage, hemosiderin deposition, chronic inflammation, and the occasional presence of osteoid (7,15,23) or osteoclast-like giant cells (the latter finding reported mostly in tumors arising in the mediastinum) (7,23,24) virtually complete the histologic spectrum of the conventional epithelioid hemangioendothelioma.

A subset of tumors (10–33%) show features reminiscent of angiosarcoma, including a disturbing degree of pleomorphism, significant mitotic activity ($\geq$2 mitoses/10 HPF), spindle cell morphology, solid growth, or necrosis (5,7,25) (Fig. 125). The term ''malignant epithelioid hemangioendothelioma'' is sometimes applied to such a tumor to convey the possibility that the neoplasm may pursue a more aggressive clinical course (25).

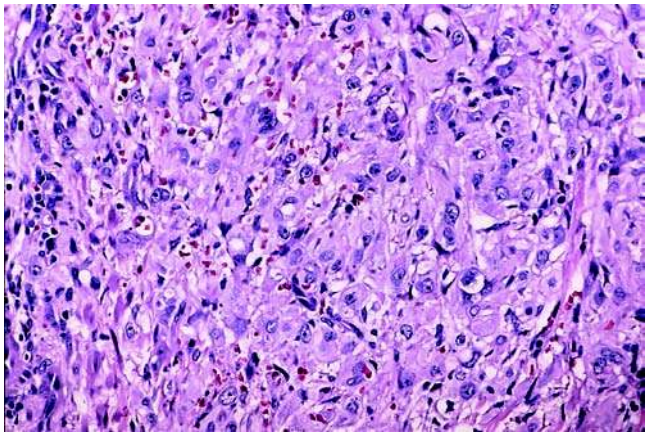

Figure 125 Epithelioid hemangioendothelioma featuring solid growth and cytologic atypia. More typical hyalinized stroma and epithelioid endothelial cells are elsewhere in this tumor.

Immunohistochemistry

Virtually all cases of epithelioid hemangioendothelioma display expression of endothelial-related markers CD31, factor VIII–related antigen, FLI1, and CD34 (7,9) (Fig. 126). Factor VIII–related antigen expression tends to be localized around the intracytoplasmic vacuoles. Keratin expression is detected in nearly one-third of tumors, but is usually focal (7,26). In one study, keratins 7 and 18 were found in 50% and 100% of epithelioid hemangioendotheliomas tested, respectively (27). Actin immunoreactivity has also been reported in lesional cells (7,9,23).

Molecular Findings

Cytogenetic data on epithelioid hemangioendothelioma are limited. Although one study identified t(1;3)(p36.3;q25) translocation in two of three analyzed tumors, suggesting that this may represent recurrent genetic aberration (28), two other studies reported t(7;22) and t(10;14) translocations, respectively, in one tumor each (29,30). Thus, genetic alterations specific for epithelioid hemangioendothelioma have not yet been determined.

Electron Microscopy

Ultrastructural features of endothelial cell differentiation include scattered Weibel–Palade bodies (rod-shaped cytoplasmic structures containing microtubules) that tend to concentrate around intracytoplasmic lumina (25), numerous pinocytotic vesicles

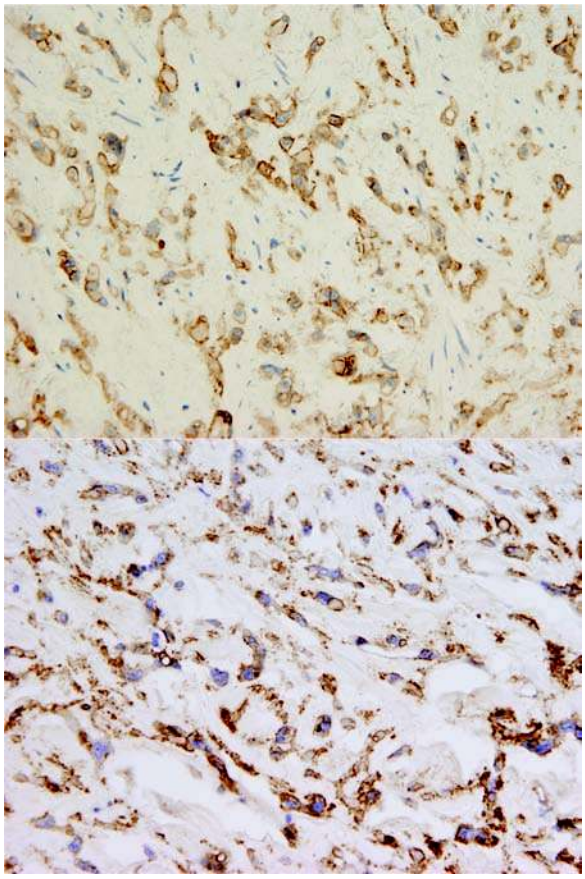

Figure 126 Tumor cells exhibit strong and diffuse membranous immunohistochemical expression of CD31 (*top*) and cytoplasmic expression of CD34 (*bottom*).

associated with the cell surface, and external basal lamina. The epithelioid appearance of the lesional cell on light microscopy is due to large aggregates of intermediate (vimentin) filaments (5).

Differential Diagnosis

In the head and neck, ''mixed'' tumors of the skin (chondroid syringoma) and salivary gland (pleomorphic adenoma) have the potential to mimic epithelioid hemangioendothelioma. Unlike epithelioid hemangioendothelioma, mixed tumors demonstrate, at least focally, evidence of epithelial differentiation such as duct formation or presence of intercellular bridges, and the cells lack intracytoplasmic lumina harboring erythrocytes. Immunohistochemical expression of keratin is stronger and more widespread in epithelial tumors than in epithelioid hemangioendothelioma, and the tumors typically express proteins associated with myoepithelial differentiation, including S-100 protein, p63, calponin, and high–molecular weight keratins. Additionally, mixed tumors lack expression of endothelial-related markers in lesional cells. Carcinomas, whether primary or metastatic, usually show a greater degree of pleomorphism and mitotic activity. Some carcinomas (e.g., metastatic lobular carcinoma of breast) may have intracytoplasmic lumina, but the content is mucin and not erythrocytes. Diffuse immunohistochemical expression of keratin or EMA and absence of endothelial-related markers assist in the differential diagnosis.

Epithelioid hemangioma (angiolymphoid hyperplasia with eosinophilia) (31–34) commonly involves preauricular, frontal, occipital, and facial soft tissues and shares with epithelioid hemangioendothelioma the presence of plump epithelioid endothelial cells. In contrast to epithelioid hemangioendothelioma, the epithelioid hemangioma features well-developed vessels that grow in a vague lobular fashion, a more pronounced inflammatory infiltrate, and a lack of a chondrohyaline stroma. In addition, a damaged native vein or artery is identified in close to one-half of cases of epithelioid hemangioma (34). Epithelioid hemangioma is an intravascular process, with an SMA-positive pericyte around each vessel, whereas epithelioid hemangioendothelioma is an extravascular proliferation of vessels, losing their surrounding pericyte. Therefore, SMA, present in epithelioid hemangioma and absent in epithelioid hemangioendothelioma, can be a helpful immunostain to separate the two lesions. Florid epithelioid hemangioma may have a solid growth pattern, but lacks the myxohyaline stroma and would continue to demonstrate SMA to delineate each vessel.

Epithelioid angiosarcoma, a neoplasm with a dismal prognosis, microscopically differs from conventional epithelioid hemangioendothelioma by exhibiting focal vasoformative areas and sheetlike growth of larger, highly pleomorphic epithelioid cells with prominent nucleoli that exhibit brisk mitotic activity. Moreover, the cells of epithelioid angiosarcoma typically show a lesser number of intracytoplasmic lumina than cells of epithelioid hemangioendothelioma. The foci of tumor demonstrating conspicuous lumen formation and the presence of large areas of necrosis and hemorrhage and the absence of myxohyaline stroma are the main features that distinguish epithelioid angiosarcoma from epithelioid hemangioendothelioma. However, some cases of epithelioid hemangioendothelioma (so-called malignant epithelioid hemangioendothelioma) may show significant histologic overlap and may be difficult to separate from angiosarcoma, but would have retained myxohyaline stroma and primitive cytoplasmic lumina. In one study, immunoexpression of c-kit (CD117) was reported in over one-half of angiosarcomas, but not in epithelioid hemangioendotheliomas (35).

Prognosis and Treatment

Epithelioid hemangioendothelioma is a frankly low-grade malignant neoplasm. Conventional forms of epithelioid hemangioendothelioma have a metastatic rate of about 20% to 30%, with the lymph nodes and lung representing most common sites for metastatic spread (7,25). Local recurrence rate of the tumor is

only about 13% (7,25). Mortality rates of 13% and 17% have been reported for soft tissue epithelioid hemangioendothelioma in large series (7,25). In general, size and histologic features of the tumor do not accurately predict the clinical course in any given case (7,25); some cases with nuclear atypia do not have worse behavior. However, histologic features ascribed to the so-called malignant epithelioid hemangioendothelioma, especially high mitotic activity or necrosis, which render the tumor to be intermediate rather than low grade, tend to predict an aggressive course (5,7,25). Conventional low-grade malignant epithelioid hemangioendothelioma requires wide (local) excision and careful patient follow-up. Adjuvant therapy may be used in higher-grade tumors per clinical recommendation.

B. Angiosarcoma

Introduction

Angiosarcoma is a frankly malignant vascular tumor with dismal prognosis, regardless of subtype or etiology; most patients die within one to two years of diagnosis (1). The only exception is angiosarcoma of the tongue (2), which is identified sooner and at a smaller size, and patients can survive their tumor. There are five subtypes of angiosarcoma: lymphedema-associated angiosarcoma (3), postmastectomy angiosarcoma (4), breast angiosarcoma, deep soft tissue angiosarcoma (usually epithelioid) comprising a quarter of tumors, and cutaneous angiosarcoma. Only the latter two occur in the head and neck.

Clinical Findings

Patients with angiosarcoma are usually elderly, with a male predilection (5–10). The scalp is the most common location for cutaneous angiosarcoma. The gingiva, buccal mucosa, hard palate, tongue, floor of mouth, tonsil, nasopharynx (11–14), larynx, sinonasal tract, and submandibular gland may be involved. Patients may have coagulopathy, anemia, persistent hematoma, or bruisability. Massive hemorrhage or even cardiac output failure from shunting may result from deep lesions. Cutaneous angiosarcoma is a bluish plaque-like lesion that can have multiple satellites (15). Occasionally, angiosarcoma can be multiple. Angiosarcoma can occur following drug administration, such as thorotrast, or postradiation or in patients with Klippel–Trenaunay syndrome (16–18). Angiosarcoma can arise from spindle cell hemangio(endothelio)ma in a Maffucci patient (19). Angiosarcoma can exceedingly rarely arise from a classic schwannoma (20).

Radiologic Imaging

Angiosarcomas frequently reveal a nonspecific imaging appearance when they involve the deep soft tissues. These highly anaplastic vasoformative lesions do not reveal sufficiently sized vascular channel or spaces to be seen at CT or MR imaging. CT attenuation is similar to muscle, while MR imaging reveals intermediate signal intensity on T1 weighting, an intermediate to high signal intensity on T2 weighting. Angiosarcoma associated with chronic lymphedema may have a more distinctive imaging appearance. The chronic lymphedema causes soft tissue enlargement with diffuse skin thickening and is apparent on imaging. Malignant transformation to angiosarcoma is suggested by a dominant nodular soft tissue mass along the skin surface.

Pathologic Findings

Grossly, angiosarcomas are bluish red and hemorrhagic, soft, spongy, and sometimes cystic or necrotic. Sizes range from 1 cm to several centimeters.

Microscopically, all angiosarcomas are composed of an extravascular proliferation of endothelial cells with cytologic atypia and mitotic activity. Some can be deceptively bland but infiltrate surrounding tissue, often dissecting collagen and involving dermis or submucosal to skeletal muscle and bone. There is usually a focal vasoformative component, even when the endothelial cells sheet out and are difficult to recognize as endothelial (Fig. 127). The usually deep epithelioid type has large epithelioid cells with prominent nucleoli and vesicular nuclei. Mitotic activity must be present for the diagnosis of angiosarcoma (Fig. 128). Sometimes atypical mitoses are found. Papillary endothelial hyperplasia or like areas can occur in angiosarcoma, with malignant endothelial cells lining hyaline papillary cores (21). Pericytes are generally absent around the infiltrating vessels, as the endothelial cells have broken outside of their normal vascular boundaries.

Immunohistochemistry

CD31 is the best vascular marker (22). CD34 is less good for angiosarcoma, but is often present. Factor

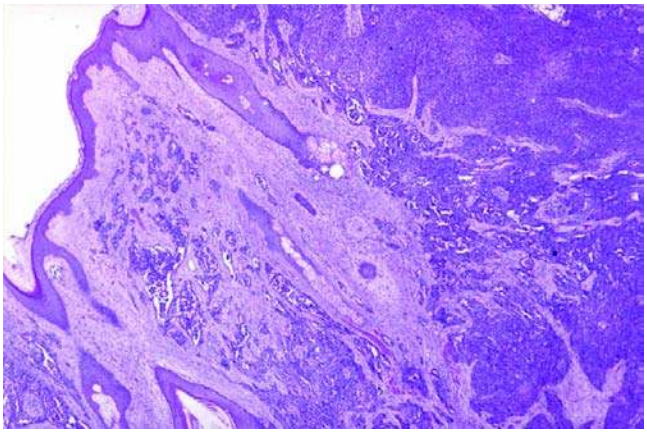

Figure 127 Angiosarcoma is a low-power infiltrating tumor that dissects tissue. Vasoformative features are always identified, even if the tumor has predominantly solid, sheetlike growth pattern.

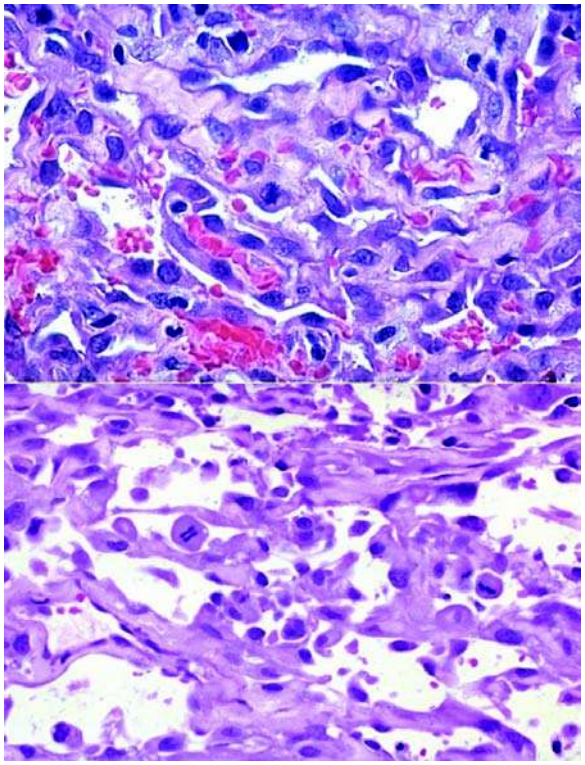

Figure 128 At higher magnification, this is an extravascular proliferation of a highly atypical endothelial cells; mitotic activity must be observed. These tumors have a dismal prognosis in other anatomic sites, regardless of grade, but in the tongue, it has a better prognosis and survival.

VIII rag has a high background and is an older stain that is not often currently used. Vascular endothelial growth factor receptor 3 (VEGFR-3) is used for lymphatic phenotype or early blood vessel phenotype and may denote a lymphangiosarcoma, which is difficult to diagnose separately from angiosarcoma. Keratins may be present, particularly in the epithelioid type (23). HHV8, a helpful genetic-immunohistochemistry marker for Kaposi sarcoma, is negative in angiosarcoma. Lack of SMA correlates with lack of pericytes around infiltrating malignant endothelial cells.

Electron Microscopy

Neoplastic cells are joined by junctional attachments and possess abundant intermediate filaments, sparse rough endoplasmic reticulum, mitochondria, or Golgi and surface-oriented pinocytotic vesicles (24,25). Weibel–Palade bodies, specific to vascular endothelium, are only rarely identified (21).

Molecular Findings

Cytogenetic studies of angiosarcomas typically have shown complex karyotypes, and no consistent recurrent chromosomal abnormalities have yet been identified. The most common genetic changes include gains of 5pter-p11, 8p12-qter, and 20pter-q12, losses of 4p, 7p15-pter, and –Y, and abnormalities involving 22q (26). Also, genetic alterations of *TP53* (tumor protein p53) has been reported and shown to affect TP53-MDM2 (mouse double-minute 2 homolog) pathway. TP53 mutational inactivation and an increase of MDM2 expression have led to upregulation of VEGF expression in up to 80% of angiosarcomas (27,28).

Differential Diagnosis

The differential diagnosis includes benign vascular tumors when vasoformative features are readily apparent and poorly differentiated neoplasms, including carcinoma, lymphoma, epithelioid sarcoma, and melanoma, and when the cells are epithelioid and arranged in sheets. CD31 reactivity and negativity for EMA, S-100 protein, and melanoma markers helps distinguish angiosarcoma from other tumor types. The infiltrative growth pattern, atypia, and mitotic activity help distinguish angiosarcoma from benign vascular tumors. Epithelioid hemangioma is still an intravascular process that will have SMA-positive pericytes around each vessel, eosinophils, and an irritated feeder artery, all of which are absent in angiosarcoma. Papillary endothelial hyperplasia is a specialized thrombus, occurring at the edge of an intravascular thrombus in a vessel or preexisting benign vascular neoplasm. When the vessel wall disrupts, it may be found outside of a vessel, but the hyline cores are surrounded by mildly hyperchromatic nuclei, and there is absence of mitotic activity. Hemangiopericytoma/solitary fibrous tumor is a CD34-positive lesion with normal, non-atypical vessels in a staghorn pattern. Kaposi sarcoma is a spindled slit-like vascular process that starts as a perivascular proliferation of endothelial cells and ends in a nodular, often pedunculated and ulcerated lesion with scattered plasma cells, many extravasated erythrocytes, and hyaline grapelike cytoplasmic inclusions (representing red blood cell breakdown products). This is positive for HHV8 and negative in angiosarcoma.

Prognosis and Treatment

The overall diagnosis of angiosarcoma is dismal with most patients succumbing to death within one to two years of diagnosis, but those in the tongue and presumably other head and neck sites, may be detected sooner at smaller sizes with overall better prognosis (10). Metastatic sites include the lung, lymph node, bone, and soft tissue. Older age and large size have been correlated with particularly poor outcome (31).

Distant metastases occur in 30% to 50% of cases, with the lungs and liver most frequently involved. Five-year survival rates of 12% to 41% have been reported; most investigators report survival rates lower than 30%. A correlation between primary tumor size and survival appears to exist; lesions

smaller than 7 cm are associated with a better prognosis.

III. MALIGNANT SKELETAL AND SMOOTH MUSCLE

A. Rhabdomyosarcoma

Introduction

Rhabdomyosarcoma (RMS) is a malignant neoplasm of skeletal muscle phenotype, which is divided into embryonal RMS (ERMS), alveolar RMS (ARMS), and pleomorphic RMS (1). Skeletal muscle differentiation can be suggested on morphology by round cells with plump eosinophilic cytoplasm and/or strap cells with cross striations and confirmed by reactivity for skeletal muscle-specific myoregulatory proteins by immunohistochemistry or by molecular studies for ARMS subtype.

Clinical Features

RMS makes up between 8% and 19% of all soft tissue sarcomas (2). These are the most common soft tissue sarcomas in children (3). They comprise the seventh most common malignancy in childhood. In population studies, more of these tumors are found in Caucasian children than in Asian or black children, and there is a very mild propensity for boys over girls (4–7). The vast majority of patients are aged between 1 and 15 years with only 10% aged between 15 and 25 years (8). However, RMSs are exceedingly rare in both neonates and in adults older than 30 years, other than pleomorphic type. Adults more commonly have ARMS, and children, ERMS.

Forty percent of RMSs are located within the head and neck, the most common site of involvement (9). RMSs of the head and neck in children are found in the nasal cavity, nasopharynx, and nasal sinuses, but many also occur in the orbit and middle ear (5). In adults, the ethmoid sinuses are the most common sites of head and neck RMSs (46% of cases), followed by the maxillary sinus, nasopharynx, and then sinonasal tract (10–12).

The Orbit

RMS is the most frequent malignant orbital neoplasm in children (13,14). Of the head and neck RMSs, about 25% arise in the orbit (15). Most occur sporadically, but they have been reported with syndromes such as Li–Fraumeni syndrome and Noonan syndrome (16,17). Most ocular RMSs arise in the soft tissues of the orbit, but they can rarely occur in the adnexa surrounding the eye and even within the eye itself. In a series of 22 orbital RMS cases, Shields et al. found that 76% were orbit, 12% conjunctiva, 3% eyelid, and 9% uveal tract (18). Patients most often present with unilateral proptosis. But, blepharoptosis edema, erythema, or a palpable mass around with conjunctiva or the eye lip may also be the initial findings. One-third of patients also have drooping of the upper eyelid, while headaches are less common, only affecting 10% of patients. Loss of central vision is relatively uncommon. Nasal bleeding or irritation most often indicates that the tumor has entered into the nasal passageway. Most tumors (75%) occur in children younger than 10 years, and more often in boys.

Although studies differ on what part of the eye sock is most commonly affected, Karcioglu et al. summarized the literature and found most tumors to be located in the superior nasal quadrant (19). On the other hand, Jones et al. found that 50% of the tumors arose centrally behind the globe (20). The tumor may spread by direct extension to the brain or hematogenously to the lungs and bones, but cervical lymph node metastasis is rare.

The Nose and Paranasal Sinuses

When RMS arises in or around the nose, patients can present with a variety of signs and symptoms, including nasal obstruction, pain, facial swelling, proptosis, numbness, and serous otitis. Sinusitis, headache, toothache, and visual problems are more common if the tumor is in the paranasal sinuses. As the disease progresses, epitaxis is often present. Of all RMSs in the head and neck, about 25% present in the nasopharynx and 10% in the paranasal sinuses (15).

One-fourth of the RMSs in this anatomic location are of the botryoid type of ERMSs. In these cases, a large gelatinous polypoid mass in found, sometimes bulging or projecting out of the nose (11). Most cases of sinonasal RMS show an alveolar histology, often of the solid variant (21).

RMSs of the nose and paranasal sinus often invade bony structures, including the orbit and skull (12,22). In aggressive cases, tumors metastasize to the lymph nodes, bone, and lungs. Bone marrow, soft tissue, liver, and brain metastases are uncommon, but can occur. Most sinonasal RMSs present at an advanced stage and carry a poor prognosis (10,21).

If the tumor resides far back in the nasopharynx, adenoid or tonsillar hyperplasia is usually first ruled out, since it is so common in children, and presents similarly. When the tumor occurs as a polypoid nasal mass, nasal polyps are in the differential diagnosis.

The Middle Ear: Mastoid

Middle ear RMS, which may arise from striated muscle in the middle ear, comprises approximately 10% of all head and neck RMSs (15). An embryonal histology is by far most common. Occurring in a young population (usually children younger than 12 years), these tumors present equally in males and females (23) and are distributed equally in both left and right ears. Patients often present with an ear mass with aural discharge (sometimes bloody) and swelling (24). The tumor most often resides in the middle ear but can extend to the external auditory canal, where it often mimics a polyp. Early on, the tumor is often mistaken for an aural polyp, otitis media, or granulation tissue, which can delay diagnosis and treatment. Neurologic findings, occurring in approximately one-third of

cases, include injury of the cranial nerves, most commonly the facial nerve, and not as often, Horner's syndrome (25,26). Tumors tend to invade bony structures throughout the skull, but can also involve the cervical lymph nodes and metastasize elsewhere (23,27). These tumors have a poor prognosis, particularly if the tumor has spread to distant sites or if there are neurologic findings (28).

The Oral Cavity: Oropharynx

Approximately one-tenth of head and neck RMSs reside in the oral cavity (15), and the soft palate and tonsil regions are the most common site within the oral cavity. Although the floor of the mouth and the gingival are very uncommon sites, these tumors are more frequently seen in the tongue, cheek, and lips (29–33). Most of these tumors present as a rapidly enlarging mass occasionally associated with pain and paresthesia.

The Hypopharynx, Larynx, and Trachea

RMSs in the hypopharynx, larynx, and trachea are extremely rare, comprising less than 2% of all RMSs of the head and neck (34–38). One of the largest literature reviews, by Dodd-o et al., identified 49 cases (39). A larger percentage of laryngeal RMSs are seen in adults as compared with RMSs elsewhere in the head and neck (39). They are most commonly seen in the mid-larynx or glottis. Barnes and Gnepp observed that most were centered on the mid-larynx or glottis (40). Like most RMSs of the head and neck, the laryngeal tumors usually show an embryonal morphologic pattern (41,42). The differential diagnosis includes spindle cell carcinoma, which is more common in these locations. Immunohistochemistry can help in this differential, with RMS expressing markers of skeletal muscle lineage such as MyoD1 and myogenin, but being nonreactive with cytokeratins. On the other hand, spindle cell carcinoma is positive for cytokeratins and negative for muscle antibodies. Although mortality is high when these cases metastasize (36,43), the overall prognosis is favorable. These tumors are responsive to combination chemoradiotherapy, allowing for excellent cure rates without the need for extensive surgery (36,44).

Pathology

Embryonal rhabdomyosarcoma. ERMS (Fig. 129), most commonly arising in the head and neck, contains cells that both look and act like embryonal skeletal muscle. Botryoid and spindle cell are both subtypes of ERMS. About three-fourths of all RMSs have an embryonal histology. In those of the head and neck, ERMSs make up an even larger proportion of the histologic subtypes, with 85% of all RMSs classified as embryonal. Most patients are children up to 10 years of age, but 25% occur in patients older than 30 years (45).

At low power, many cells in ERMS can look like dense aggregates of small to medium-sized, round

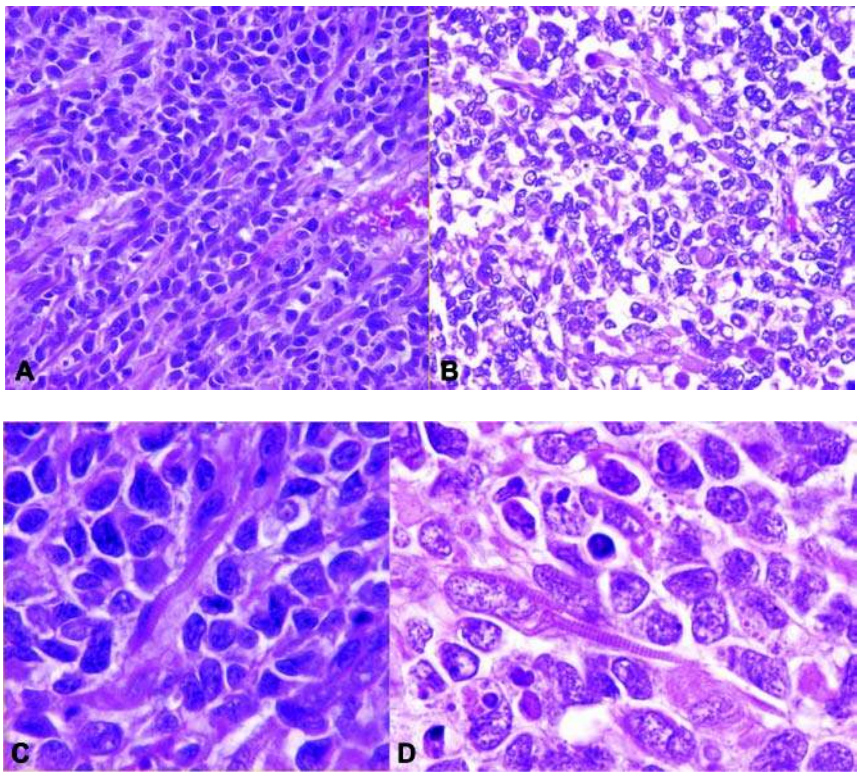

Figure 129 Embryonal rhabdomyosarcoma is composed of small round cells with abundant mitotic activity and sometimes plump small eccentric eosinophilic cytoplasm **(A,B)**. Identification of cross striations may be difficult **(C,D)**.

undifferentiated cells, similar to the rhabdomyoblasts seen in embryonal muscle. These are the most primitive cells and can be round or spindled, but they can also show nuclear atypia. If severe atypical forms and spindling are present, the tumor is better classified as a pleomorphic RMS. The more round cells resemble lymphocytes, but are generally larger in size and have more cytoplasm. Chromatin is vesicular in rare cases, but more often smooth and dense. Although nucleoli are usually inconspicuous, some cases show prominent nucleoli.

There is usually an eccentric, plump, rounded, and intensely eosinophilic cytoplasm. Scattered to more prevalent large polygonal ''strap cells'' may be observed, but cross striations are rarely seen in these cells. As the cytoplasm increases, the nucleus appears rounder and moves away from its central location to one side of the cell. This is the so-called tadpole cell, which can be multinucleated and have cross striations, observed in about one-third of cases. In patients treated with chemotherapy, the tumors will further differentiate, and ''strap cells'' and cross striations dominate within a background of necrosis and fibrosis (46). The stroma in ERMS can vary from predominant to scant and can be myxoid, edematous, or fibrotic. Cases with ample myxoid stroma can look similar to myxomas and resemble the loose stroma of embryonal muscle. Immunohistochemistry must be used to confirm phenotype.

Botryoid rhabdomyosarcoma. Botryoid RMS (Fig. 130), a variant of ERMS, accounts for about 10% of all cases of ERMS. Only 15% of botryoid RMSs preside in the head and neck, much less than other types of ERMS. Patients are younger with a mean age of seven years (3).

The term ''botryoid'' comes from the Greek word ''botry,'' meaning a bunch of grapes, which suitably describes the gross appearance of the tumor. The growth pattern of ERMS within a solid organ is limited by the tissue surrounding it. But, when these tumors form in open cavity, such as the ear, the mouth, or the vagina, their growth is unrestricted and form a polypoid mass. The tumor often bulges out from the organ in multiple grapelike nodules. This gross appearance defines the tumor. Because of this polypoid appearance, symptoms usually include obstruction.

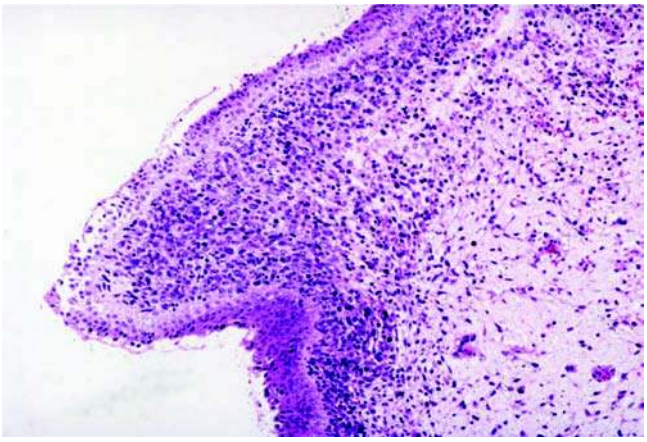

Figure 130 Botryoid embryonal rhabdomyosarcoma has a grapelike polypoid growth pattern and cambium layer of tumor cells with the rest of tumor being hypocellular.

Microscopically, these tumors only differ from conventional ERMS by abundant myxoid stroma, grapelike polypoid growth pattern, and usually a cambium layer. The cambium layer is defined as dense linear aggregates of tumor cells condensing underneath an epithelial surface. Some cases do not show a cambium layer, and in other cases it may only be focal. Cells may look deceptively banal, but mitotic figures are usually present. The cells deeper to the cambium layer and epithelial surface are usually less cellular. Thus, botryoid RMS distinguishes itself macroscopically by its polypoid grapelike nodular growth pattern and presence of a cambium layer.

Spindle cell rhabdomyosarcoma. Spindle cell RMS (Fig. 131), another variant of ERMS, is composed of

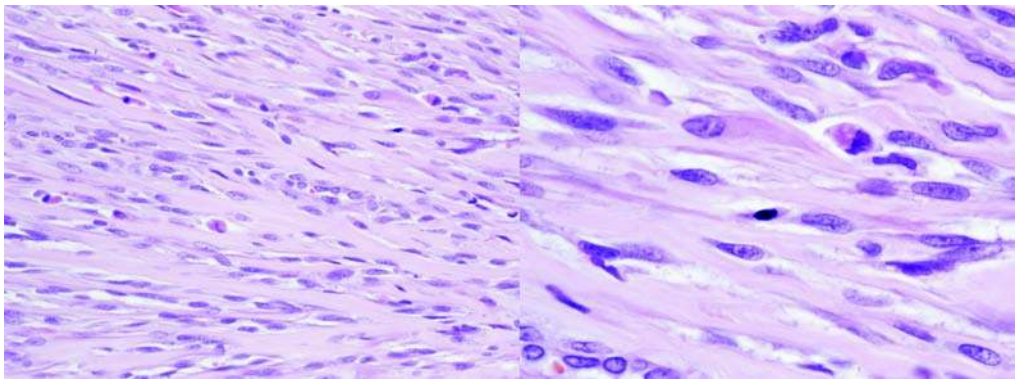

Figure 131 Spindle cell embryonal rhabdomyosarcoma is specific to head and neck sites and scrotum and can mimic other spindle cell tumors. Note the plum eosinophilic cytoplasm on some of the tumor cells, suggesting skeletal muscle phenotype.

elongated spindled cells, comprising more than half the tumor. The spindle cell variant is uncommon and makes up about 6% of ERMS (47). Most cases occur in the head and neck or in the paratesticular location and far more commonly in males. The majority occurs in children, and rarely in adults (47,48). Architecturally, the thin spindled cells form fascicles, and mitotic activity is present.

Alveolar rhabdomyosarcoma. ARMS (Fig. 132) is characterized by alveolar and solid growth of medium-sized, round tumor cells. ARMS makes up about 25% of all RMSs, and 20% of cases involve the head and neck. Most cases occur in childhood; in cases from the Intergroup RMS group, the mean age was nine years. ARMS can show one of three patterns: a typical or classic pattern, a solid pattern, and a mixed alveolar and embryonal pattern. In each of these patterns, the primary cell population is a primitive round cell, usually 10 to 15 μm in diameter. But of course, skeletal muscle differentiation must be seen by histology or confirmed by immunohistochemistry. Nuclei are hyperchromatic, with inconspicuous nucleoli and range from round to oval to spindled. These cells often look similar to lymphocytes but have more

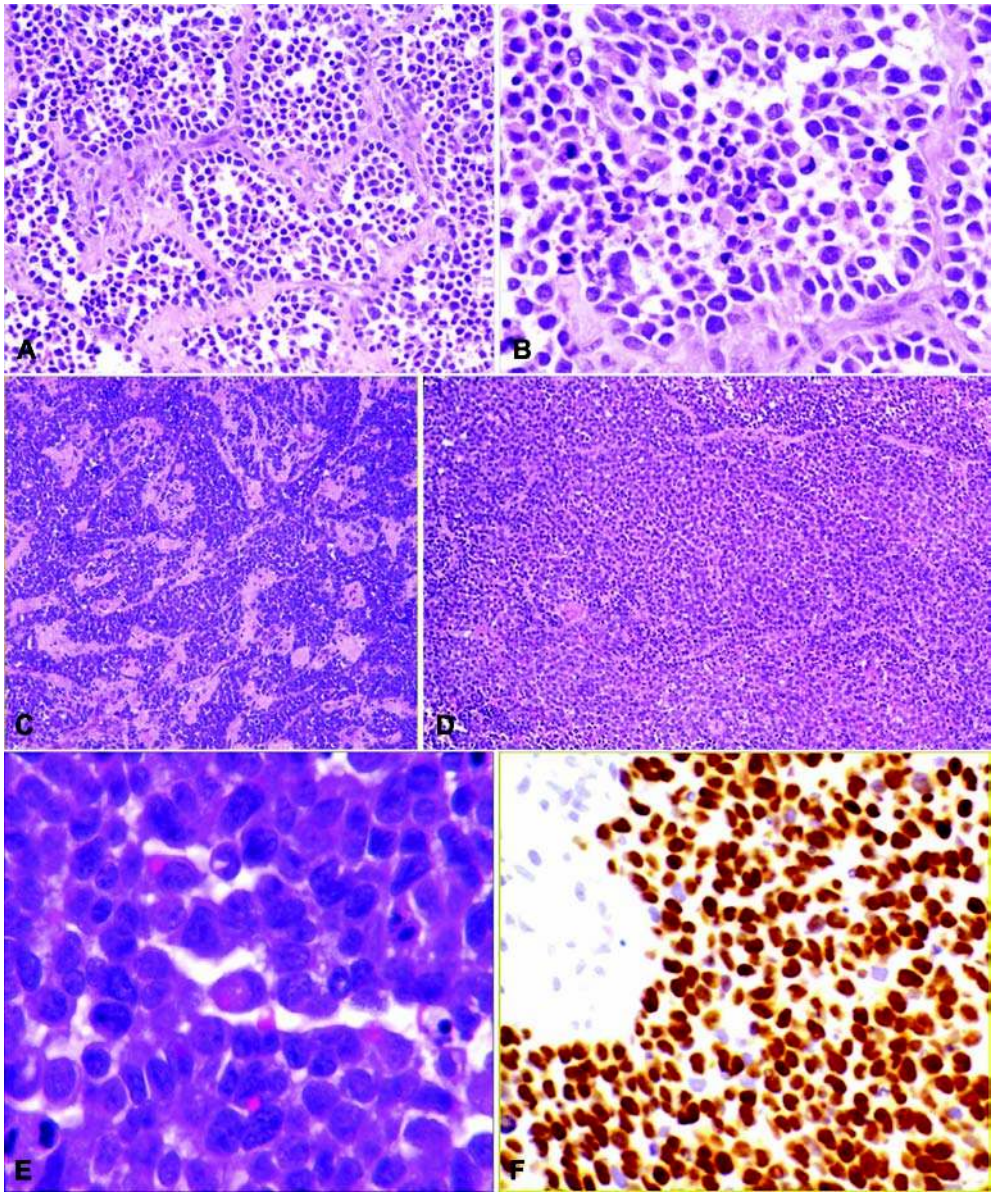

Figure 132 Alveolar RMSs can either have an alveolar pattern (**A**), with tumor clusters separated by fibrous septa (**B**), or can be ''solid type'' (**C,D**) with sheeting of medium-sized round cells; often alveolar pattern is found elsewhere in the tumor. Sometimes the plump eosinophilic cytoplasm can suggest RMS (**E**). RMS may be positive for nuclear MyoD1, a skeletal regulatory protein (**F**). Alveolar RMS has a characteristic molecular finding t(1;13) or t(2:13) that can be detected when biopsy material is small or there is solid growth patter. Alveolar RMS has a worse prognosis than embryonal RMS.

abundant cytoplasm than a lymphocyte. Some tumors may contain scattered large multinucleated giant cells.

In the typical or classical alveolar pattern, one can see, even at low power, that there are fibrovascular septae separating the tumor into nests. Toward the center of these nests, the cells are discohesive and float freely. At the periphery, the cells are attached to the fibrous septae by cytoplasmic processes. This pattern, which gives this tumor its name, mimics the lung, where open alveolar spaces are linked together by a fibrovascular architecture (49). If this ''alveolar'' pattern is seen, even focally, in a malignant tumor that shows muscle differentiation, then the tumor is best diagnosed as an ARMS.

The solid pattern of ARMS is seen when the cells are closely packed, forming sheets without an alveolar pattern (50). Most tumors contain foci of more solid tumor growth. Solid areas can range from focal to the predominant pattern. The solid variant of ARMS typically lacks the fibrovascular septae seen in the typical ARMS. Cytologically, solid variant ARMS are similar to typical ARMS. Usually, if the tumor is well sampled, a more characteristic alveolar pattern with fibrous septa is focally observed. A tumor can be classified as a mixed embryonal/alveolar pattern if both an embryonal morphology and alveolar patterns are present. Although some cases may show cells with clear cell morphology, these should not be mistaken for clear cell carcinoma or liposarcoma.

Pleomorphic rhabdomyosarcoma. Pleomorphic RMS (Fig. 133) makes up less than 5% of all cases of RMS. It is almost entirely a tumor of older individuals usually aged between 40 and 60 years, but may occasionally be seen in children (51–54). Tumor cells range in morphology from undifferentiated to polygonal to tadpole shaped to racquet shaped to round to spindle shaped. Many cells often have ample eosinophilic cytoplasm. The stroma is usually scant. Most of these look like a malignant fibrous histiocytoma with polygonal large atypical rhabdomyoblast strap cells; cross striations are difficult to identify. An alveolar histology or embryonal histology is usually not appreciable (52).

Immunohistochemistry

RMSs are positive for muscle-specific actin, desmin, and nuclear skeletal muscle-specific myoregulatory proteins, including MyoD1 and myogenin (myf4) (55). Sometimes only either MyoD1 or myf4 are present, as the tumor recapitulates embryology at various stages of skeletal muscle development, so both markers should be obtain and at least one should be present to confirm skeletal muscle phenotype (54,56). A recent study looking at 956 RMSs showed that myogenin and MyoD1 were equally sensitive, positive in 97% of cases, and highly specific (90% and 91% of cases) (57). Cytoplasmic staining of these antibodies is nonspecific, can be seen in a variety of lesions, and is interpreted as negative (58–60). CD99 can be positive in 16% of cases (61).

Myoglobin, myosin, and creatine kinase M are all markers that can be expressed in RMS, but are no longer used as they created high backgrounds (55). Vimentin is expressed in nearly all RMSs.

RMS may aberrantly express many antibodies. Scattered S-100-positive cells are seen in some cases of ERMS, and sometimes the staining is nuclear (62). The following antibodies and their percentage of expression in ERMS is detailed: CD57 (6%), CAM5.2 (5%), and CD99 (15%) (62–64).

Molecular Findings

ERMS. Cytogenetic studies have shown complex structural and numerical chromosomal changes, and no consistent structural chromosomal alteration has been identified in ERMS (65,66). However, t(2;20)(q35;p12) translocation with the break point near PAX3 have been identified in one case (67). Also, in one case, a nonrandom secondary chromosomal aberration, der(16)(1;16)(q22;q24), seen in translocation-positive ARMS, has been identified (68).

The loss of 11p15 has been indicated in the majority of ERMS (69,70). Inherited alteration of 11p15 is characteristic for Beckwith–Wiedemann syndrome, showing increased risk for cancer development, including ERMS (71). Also, in vitro studies have shown

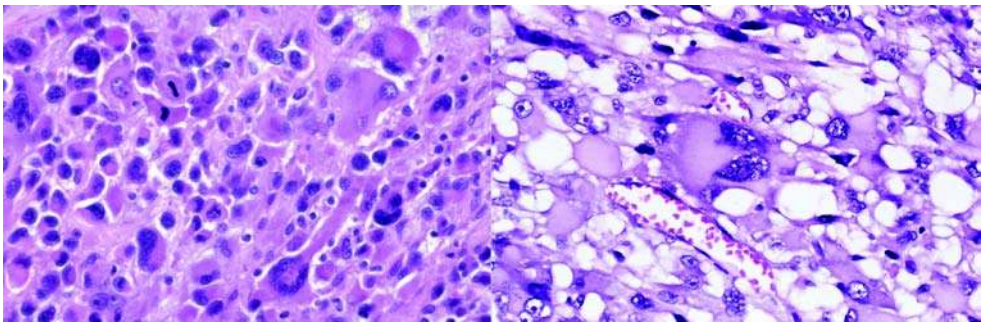

Figure 133 Pleomorphic rhabdomyosarcoma is one of the pleomorphic spindle cell sarcomas that has large strap-like cells and must be distinguished from other pleomorphic tumors by immunohistochemistry. endocrine neoplasms.

that the 11p15 region suppresses growth if introduced into ERMS cell culture (72). Thus, it is believed that inactivation of tumor suppressor gene/genes located in this region contributes to ERMS tumorigenesis.

Comparative genomic hybridization studies confirmed the presence of gains and losses, but indicated that amplifications were rare in ERMS except subset of tumors with anaplastic features (73).

Molecular genetic studies identified frequent inactivating mutations in TP53 (tumor protein p53) gene (74). TP53 is a DNA-binding protein involved in the cell cycle. Inherited alterations of TP53 have been documented in Li–Fraumeni syndrome characterized by an increased risk of developing different types of cancer, including RMS (75,76).

ARMS. Two tumor-specific chromosomal translocations, t(2;13)(q35;q14) and t(1;13)(p36;q14), are characteristic features of ARMS. The t(2;13) is most common and is found in approximately 75% of ARMS cases, while only about 10% of ARMS harbor the t(1;13) (78–82). These translocations result in fusions of the PAX3 or PAX7 genes with the FKRH gene (77–80).

PAX3 and PAX7 (mapped to 2q35 and 1p36, respectively) are highly homologous members of the PAX (paired box) transcription factor gene family. Both PAX proteins are important for normal embryonal development, and the expression of their murine homologues was documented during the development of nervous and muscular systems (81). Moreover, PAX3 loss-of-function mutations have been implicated in congenital neural and muscular anomalies in mouse (splotch mouse) and human (Waardenburg types I to III and craniofacial-deafness-hand) malformation syndromes (82–84).

FKHR (''forkhead-related'') has been mapped to 13q14 and belongs to the FOX gene subfamilies, members of which encode a transcription factor with a highly conserved DNA-binding motif related to a *Drosophila* region-specific homeotic gene forkhead (85). FKHR and other subfamily members, such as AFX and FKHRL1, play a role in insulin-signaling pathways regulating apoptosis (86,87).

PAX3-FKRH and PAX7-FKRH chimeric proteins contain highly homologous PAX3- and PAX7-derived N-terminal DNA-binding domains, which are fused to the activating, COOH-terminal domain of the FKHR gene. PAX3-FKRH chimeric protein acts as a strong transcriptional activator and shows a transforming ability when introduced into cell culture (88,89). Although murine cells with the PAX3-FKRH expression construct revealed activation of genes involved in the myogenic pathways, PAX3-FKHR transgenic mice do not develop tumors (90). When compared with wild-type PAX gene expression, PAX7-FKHR and PAX3-FKHR chimeric proteins are overexpressed because of secondary amplification of the PAX7-FKHR fusion gene and a higher transcriptional rate of PAX3-FKHR fusion gene (91–94).

Both t(2;13)and t(1;13) translocations and their gene fusion products are highly specific and sensitive genetic markers of ARMS (78). FISH and RT-PCR-based assays have been developed for routine clinical testing (95). Also, the identification of fusion type can provide important prognostic information. Tumors with PAX7-FKHR have a more limited pattern of metastatic disease and a longer disease-free survival, while ARMS with PAX3-FKHR have an adverse prognosis with more extensive metastasis (96,97).

Pleomorphic RMS. Cytogenetic data are limited, and only a few karyotypes with complex chromosome aberrations have been reported.

Imaging

There are no distinctive radiologic features of RMS. These masses are often long and fusiform, likely owing to infiltrative growth of this small round blue cell tumor. On CT the signal intensity is similar to muscle. On MR imaging, there is intermediate signal intensity on T1 weighting and intermediate to high signal intensity on T2 weighting. Mild diffuse enhancement is usually apparent following intravenous contrast administration on CT or MR imaging. Associated bone involvement with erosion and destruction is more common in orbital lesions and detected by either CT or MR imaging (98,99).

Electron Microscopy

Ultrastructurally, RMSs will show cells with a wide array of skeletal muscle differentiation. Well-formed sarcomeres show Z bands and thick (16 nm) and thin (8 nm) filaments. Myosin-ribosome complexes are also seen.

Differential Diagnosis

The differential diagnosis for RMS is very long and includes the small round cell tumors, tumors with rhabdoid morphology, as well as miscellaneous soft tissue tumors. Polyps are in the differential with botryoid RMSs.

Small round cell tumors, namely, Ewing sarcoma, neuroblastoma, lymphoma, nasopharyngeal carcinoma, and desmoplastic small round cell tumor, and Wilm tumor can mimic RMS, but the latter two do not occur in the head and neck. Ewing sarcoma can be separated from RMS by the perivascular rosette-like growth pattern and geographic necrosis with perivascular tumor sparing. The cells of Ewing sarcoma are usually round to oval with little cytoplasm and with scant stroma (100). On the other hand, the cells in RMS, have more irregular nuclei, larger size, more eosinophilic cytoplasm, and often a myxoid stroma. But some embryonal tumors will contain less cytoplasm and show cells with uniform round nuclei, indistinguishable from Ewing sarcoma. RMS will express desmin and myoregulatory skeletal muscle-specific markers that are absent in Ewing sarcoma/primitive neuroectodermal tumor (PNET). Both tumors can be positive for CD99. Each tumor also has different translocations with the t(11;22)(q12;q24) in Ewing sarcoma and t(1;13) (p36;q14) or t(2;13)(q35;q14) in ARMS.

Olfactory neuroblastoma and RMS can both occur in the nasal passageway. On H&E, cells of neuroblastoma can look like ERMS cells. However, the chromatin appears more granular in neuroblastoma, giving the cells a ''salt and pepper'' appearance. Like Ewing sarcoma, neuroblastomas often have rosettes, differentiating them from RMS. By immunohistochemistry, neuroblastoma expresses chromogranin and synaptophysin and is negative for desmin, myogenin, and MyoD1 (101).

Sometimes the eosinophilic cytoplasm in an RMS is not prominent, and lymphoma is in the differential diagnosis. Common leukocyte antigen (CD45), a marker of hematopoietic cells, is expressed in almost all lymphomas, but is not reactive in RMS. Muscle markers, such as MyoD1, are not expressed in lymphoma. Malignant melanoma also may be poorly differentiated and confused with RMS. Immunohistochemistry also easily distinguishes the two, with antibodies such as HMB-45 and other melanocytic markers selectively expressed in melanoma and not RMS. Furthermore, melanoma often occurs in older individuals, and RMS in children.

Extrarenal rhabdoid tumor and rhabdomyoma, tumors with ''rhabdoid features,'' include carcinomas, sarcomas, and melanomas. The key feature in most of these tumors is abundant hard inclusion-like eosinophilic cytoplasm. Extrarenal rhabdoid tumor can arise in the head and neck and is a malignant tumor of infants and children but expresses keratins, EMA, and often neural markers and is negative for desmin and myoregulatory skeletal muscle-specific markers (63,101–104).

Rhabdomyoma can also be in the differential diagnosis of a RMS. Both can be found in the head and neck and are skeletal muscle tumors. Particularly difficult is the distinction between fetal rhabdomyoma and RMS; mitotic activity and necrosis would favor the latter. Adult rhabdomyoma with ''spider cells'' may look similar to a spindle cell RMS. Fetal rhabdomyoma will not show mitotic figures, cytologic atypia, or necrosis. As compared with RMS, cross striations are actually more appreciable in fetal rhabdomyoma.

Polyps. Botryoid RMS must be differentiated from benign polyps. In the ear, otitis media may accumulate ample polypoid granulation tissue, which is also known as an aural polyp. Both aural polyps and RMS occur in children. Microscopically, the two lesions are usually easy to differentiate, with aural polyps containing inflammatory cells, such as plasma cells and neutrophils, and RMS containing malignant tumor cells, with mitotic activity, which express skeletal muscle markers.

When upper respiratory sinonasal polyps contain histiocytes and fibroblasts that are unusually pleomorphic, they are called sinonasal polyps with stromal atypia (105–107). Because of the atypical cells, they can be mistaken for sarcomas, although they are still clinically benign. The atypical cells cluster in a perivascular or submucosal distribution. Polyps with stromal atypia are differentiated from sarcomas by the presence of the architecture of a polyp, abundance of inflammatory cells including eosinophils, and expression of histiocyte markers such as CD163 and CD68. These polyps do not contain cells with cross striations and mitotic figures and do not immunoreact with MyoD1 or other skeletal muscle-specific markers. Additionally, in contrast to ERMS, these polyps lack a cambium layer (108).

Other tumors. Leiomyosarcoma and fibrosarcoma with a predominance of spindle cells might be mistaken for spindle cell RMS, although the former two tumors occur predominantly in older adults, and RMS is usually found in childhood. Cross striations, when they are recognizable, distinguish RMSs from these other tumors. Fibrosarcoma variants do not express skeletal muscle marker proteins such as MyodD1 or myogenin (109). Leiomyosarcoma will express desmin and muscle-specific actin, but will not express striated muscle-specific myoD1 and myogenin (52).

Alveolar soft part sarcoma (ASPS) is another soft tissue tumor that can show an alveolar pattern. These were even thought to be of skeletal muscle phenotype since they can express desmin and have cytoplasmic MyoD1; however, the latter marker is only interpreted as positive if nuclear (110). The round small to medium-sized cells of RMS are not seen in ASPS. Also, the tumor cells of alveolar sarcoma of soft parts are surrounded by thin-walled blood vessels and not the fibrovascular septae of ARMS. In addition, ASPS contains periodic acid-Schiff (PAS) diastase-positive intracytoplasmic crystalline rods and granules, unlike RMS.

Treatment and Prognosis

The prognosis of patients with RMS has drastically improved in the last 30 years. Early studies with a single modality of therapy showed a low five-year survival of 8% to 20% (111). With the introduction of triple therapy (chemotherapy, radiotherapy, and improved surgical technique), disease-free survival has improved from 20% to 70%. Surgery now functions more to debulk the tumor and to provide tissue for diagnosis and less to improve the prognosis of the patient (25,112).

Prognostic factors include the stage, location of the tumor, the histology of the tumor, the patient's age, the tumor size, and the presence of metastasis (113). Examining the tumor's site of origin, patients with head and neck tumors have a better prognosis than most other sites, and orbital tumors have the best outcomes in the head and neck (3,8,114). The five-year survival rates are 92% for the orbit, 69% for parameningeal, and 81% for other head and neck sites (3,115,116). However, between 3% and 20% of head and neck RMSs, excluding orbital tumors, will still metastasize to lymph nodes (117,118). Staging also dictates outcome. Staging is done by two methods—clinical staging (IRSV stage) or pathologic staging (IRSG group) (119). In a recent study of 331 cases, 10-year survival rates for low-risk groups were 80% and high-risk groups were 38% (120). Not surprisingly, small tumors without metastasis have a more favorable

Table 10 The Intergroup Rhabdomyosarcoma Study Group Clinical Staging System for Rhabdomyosarcoma

Group I: Localized disease with tumor completely resected and regional nodes not affected with the following: 1. Confinement to the muscle or organ of origin 2. Contiguous involvement (i.e., infiltration outside the muscle or organ of origin), as through fascial planes
Group II: Localized disease with microscopic residual disease or regional disease and no residual or microscopic residual disease and the following: 1. Grossly resected tumor with microscopic residual disease (nodes negative) 2. Completely resected regional tumor (nodes positive or negative) 3. Regional disease with grossly resected involved nodes and evidence of microscopic residual disease
Group III: Incomplete resection or biopsy sample with gross residual disease
Group IV: Metastatic disease present at onset

outcome than those that are larger or are associated with metastases.

Many studies have examined how the age of the patient and the tumor histology affects the aggressiveness of the tumor. Children almost always do better than adults when compared statistically, and this appears to be independent of other parameters, such as the stage or the site of involvement (119,121). In children, botryoid and spindle cell morphology are associated with a superior prognosis (122), while alveolar and pleomorphic variants have a much worse prognosis. Embryonal tumors usually show an intermediate prognosis (111). Children with botryoid RMS have an overall survival of more than 90%. In one series, 72% of patients with pleomorphic RMS died of disease within two years of diagnosis (52,123). In adults, prognosis is generally poor regardless of morphology, even with spindle cell RMS (48).

Clinical staging systems for RMS include the Intergroup Rhabdomyosarcoma Study Postsurgical Clinical Grouping Sytem (Table 10) (124).

B. Leiomyosarcoma

Introduction

Leiomyosarcoma is a sarcoma composed of cells exhibiting, at least focally, smooth muscle differentiation. These tumors are divided into cutaneous and noncutaneous leiomyosarcomas. Since the depth of the sarcoma affects prognosis, cutaneous leiomyosarcomas should be distinguished from tumors located strictly within the subcutis, as the latter tend to exhibit a higher rate of recurrence and metastasis than their dermal counterparts but have a better prognosis than intramuscular examples (1,2). The histologic criteria of malignancy for noncutaneous smooth muscle tumors of the head and neck region are commonly those used in evaluating deep soft tissue smooth muscle tumors (see below).

Leiomyosarcomas developing in the sinonasal tract and probably most of the oral cavity leiomyosarcomas are of vascular wall origin because the head and neck harbors little, if any, native smooth muscle with the exception of the cervical esophagus and the circumvallate papillae and the ductus lingualis of the tongue (3,4). Origin of primary cutaneous leiomyosarcoma (apart from genital tract leiomyosarcomas) is probably from either the muscular walls of vascular structures or the erector pili muscle.

Clinical Findings

Leiomyosarcoma is primarily a malignancy of the adult population and mostly arises in the uterine wall, retroperitoneum and pelvis, deep extremity soft tissue, and dermis and from the muscular walls of large vessels. Children and adolescents are less-commonly affected (5). However, a significant proportion of smooth muscle tumors in young individuals occur in the immunosuppressed and are Epstein–Barr virus-associated (6–8). This unique etiology and clinicopathologic features of this subset of smooth muscle tumors warrant a separate classification (8).

Noncutaneous leiomyosarcoma is a rare tumor in the head and neck. Fu and Perzin (9) reported that only 2.3% of 256 nonepithelial tumors of the nasal cavity, paranasal sinuses, and nasopharynx were leiomyosarcomas. Kuruvilla et al. (10) found only 9 examples of leiomyosarcoma out of 602 sinonasal tract sarcomas (1.5%) culled from the files of the Armed Forces Institute of Pathology. Leiomyosarcomas have been associated with a prior history of radiation or cyclophosphamide-based chemotherapy and with bilateral retinoblastomas (11–13).

Sinonasal leiomyosarcoma (10,14) occurs in all ages, but shows a peak in the fifth decade of life, and affects both sexes almost equally. Tumors involve both the nasal cavity and a paranasal sinus followed by the nasal cavity alone (10,15). Most common presenting clinical symptoms are stuffiness, epistaxis, and pain caused by obstruction of the airway. Rhinorrhea, swelling, and exophthalmos are less-commonly reported initial symptoms (10).

Leiomyosarcoma involving the oral cavity (16–18) presents over a wide age range, but has a bimodal peak incidence in the third, sixth, and seventh decades of life, and shows no gender predilection. Approximately 70% of reported cases in the oral cavity arise in the mandible and maxilla, whereas the remainder originate in the tongue, hard and soft palate, floor of mouth, buccal mucosa, gingival, and upper lip (16,18). Clinically, the presence of swelling or a painful mass are the two most common initial complaints followed by difficulty in chewing or swallowing.

Laryngeal leiomyosarcoma (19) occurs mostly in older adults and demonstrates a male gender bias. Tumors are generally located in the vocal folds, but no area of the larynx appears immune. Initial symptoms include hoarseness, stridor, dyspnea, and dysphagia.

Leiomyosarcoma has been reported in other noncutaneous head and neck sites, including the

major salivary glands (16,20), pharynx (16,21–23), thyroid (24), orbit (25–28), and cervical esophagus (29).

Cutaneous leiomyosarcoma (1,30–32) typically presents in the extremities of older adults mainly in the sixth decade of life. Clinically, cutaneous leiomyosarcoma ranges in appearance from small plaques or nodules to large ulcerated masses. Head and neck cutaneous leiomyosarcoma is not uncommon and more often affects males. In this region, the lesion tends to mimic an epithelial tumor or the pyogenic granuloma (30). Leiomyosarcomas arising in multiple cutaneous sites should arouse suspicion of metastatic deposits from a deep-seated primary (31).

Imaging

MR imaging and CT are frequently employed to evaluate the size and extent of the tumor as well as to depict osseous invasion. The MR imaging appearance of leiomyosarcoma is nonspecific and reveals intermediate signal intensity on T1-weighted imaging with moderate enhancement after contrast administration. The T2-weighted image demonstrates intermediate to high signal intensity (33). MRI is also useful for detecting perineural and lymph node invasion. CT reveals a large soft tissue mass with enhancement following contrast administration. Heterogeneity is frequent on both CT and MR imaging, reflecting areas of hemorrhage and necrosis that do not enhance with contrast.

Pathology

Noncutaneous leiomyosarcomas grossly form large firm masses with deceptively well-defined margins. The cut surface of the tumor may have a trabeculated and whorled appearance. Cystification is observed in large tumors. High-grade leiomyosarcomas have a lighter tan coloration and a fleshy appearance with areas of hemorrhage or necrosis. Microscopically, the sarcoma is highly cellular and composed, at least focally, of well-delineated, elongated fascicles of spindled cells with brightly eosinophilic cytoplasm (Fig. 134, top). Ninety-degree orientation of bordering fascicles is a characteristic microscopic feature (Fig. 134, bottom). High-grade tumors may show a storiform growth pattern of pleomorphic cells or possess a hemangiopericytomatous vascular component. Presence of coagulative tumoral necrosis is a characteristic marker of malignancy. Leiomyosarcomas of the head and neck infiltrate surrounding native tissues, particularly bone or cartilage, but mucosa and submucosal glands are less often involved by sarcoma (15).

The tumor cells have bipolar cytoplasmic processes with fibrillar, eosinophilic cytoplasm and well-defined cell borders (Fig. 135). The cytoplasm at the poles of the nucleus is frequently vacuolated. The cell nuclei are elongated, plump with rounded ends and show hyperchromasia and varying degrees of pleomorphism (Fig. 136). The Masson trichrome histochemical stain highlights numerous fine fuchsinophilic

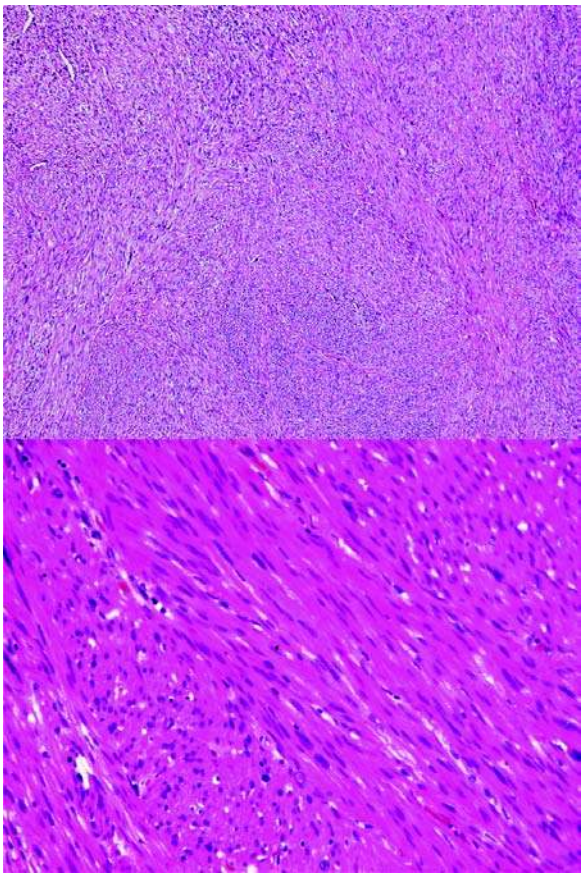

Figure 134 Highly cellular leiomyosarcoma composed of elongated fascicles of spindled cells with brightly eosinophilic cytoplasm. Note 90° orientation of adjacent fascicles (*bottom*).

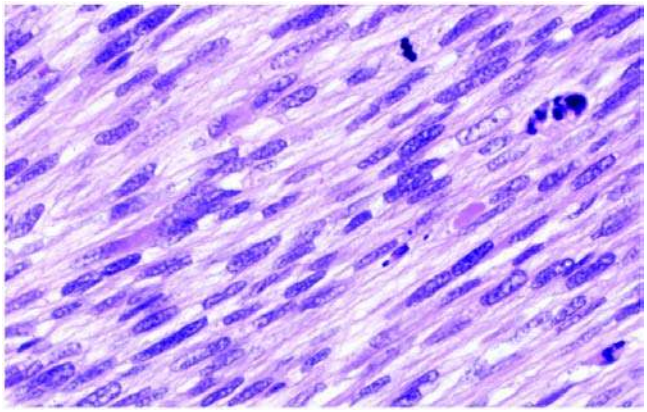

Figure 135 Spindled cells of leiomyosarcoma have well-defined cytoplasmic borders, fibrillary cytoplasm, and occasional paranuclear vacuoles.

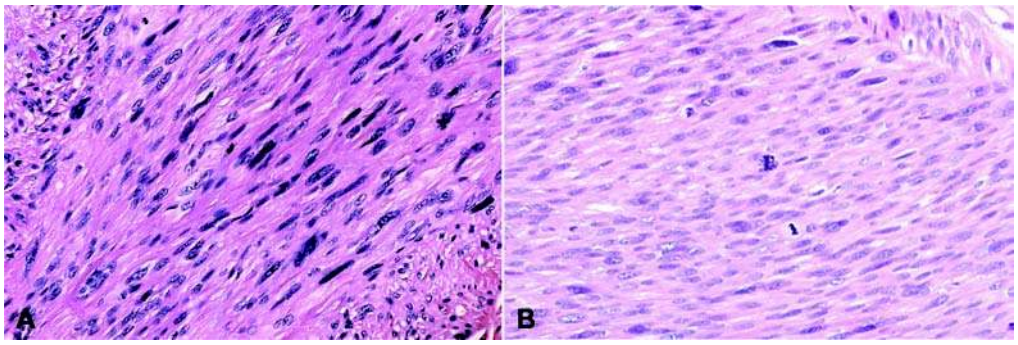

Figure 136 High-powered magnification of leiomyosarcoma showing conspicuous nuclear pleomorphism (**A**) and mitotic figures (**B**) and deeply eosinophilic cytoplasm.

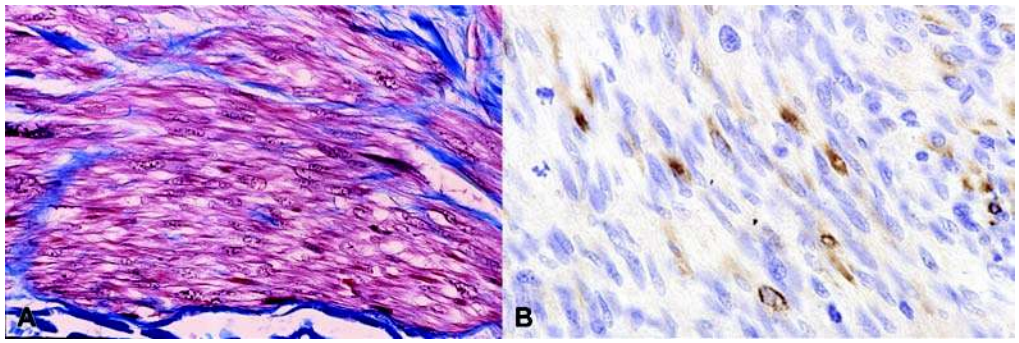

Figure 137 Masson trichrome histochemical stain (**A**) demonstrates delicate fuchsinophilic intracytoplasmic fibrils distributed throughout the tumor cell. Desmin stain shows at least focal reactivity (**B**) (together with diffuse SMA, makes the diagnosis of smooth muscle phenotype).

cytoplasmic fibrils that correspond to actin microfilaments observed ultrastructurally (Fig. 137).

The diagnosis of malignancy in a smooth muscle tumor is based on the findings of cytologic atypia manifesting as nuclear size and shape variation coupled with hyperchromasia and mitotic activity. In general, any amount of mitotic activity should indicate a potential for malignant behavior. Tumors in soft tissue, including cutaneous, subcutaneous, or intramuscular, with cytologic atypia and 1 mitosis per 50 HPF are enough for a malignant diagnosis. Additional features of coagulative tumor necrosis and not just ischemic necrosis are worrisome. A tumor exhibiting bland nuclear features and mitotic activity between 1 and 4 mitoses per 10 HPF is considered a ''smooth muscle tumor of uncertain malignant potential'' (34).

Grading of leiomyosarcoma helps predict clinical aggressiveness and is based primarily on degree of cellular differentiation, mitotic activity, and presence of necrosis. The French Federation of Cancer Centers (FNCLCC) grading system for soft tissue sarcomas is an easily applied scheme for histologically grading leiomyosarcomas on the basis of cell differentiation, mitotic activity, and necrosis (35).

Variations in the histology of a typical soft tissue leiomyosarcoma are sometimes encountered as a focal or less often a widespread phenomenon and can lead to a diagnostic dilemma. In some cases, tumor cells possess variably granular, less-fibrillar cytoplasm that, when diffuse, has the potential for mimicking a true granular cell tumor (36). A polygonal-shaped cell with well-marginated, eosinophilic cytoplasm is the predominate cell type of the epithelioid leiomyosarcoma (37–39), but this diagnosis is largely replaced by gastrointestinal stromal tumor, largely uncommon in head and neck locations. Osteoclast-like giant cells may be scattered either irregularly or in a more uniform manner throughout an otherwise conventional leiomyosarcoma (40). When extensive, their presence can lead to a diagnosis of giant-cell malignant fibrous histiocytoma. The myxoid variant of leiomyosarcoma is characterized by an overabundance of stromal mucin that results in a reticular growth pattern of individual cells as well as the presence of tumor cells in scattered small bundles or packets (41). Finally, a chronic inflammatory cell component, which tends to be more pronounced in head and neck leiomyosarcomas than those developing in other soft tissue sites

(22), may be so heavy in some examples that it masks the underlying process (42).

Rarely, a conventional leiomyosarcoma has additional sarcomatous elements (43–45). Leiomyosarcomas with an undifferentiated, high-grade sarcomatous component resembling the so-called malignant fibrous histiocytoma are considered ''dedifferentiated'' leiomyosarcomas. Biphenotypic tumors composed of leiomyosarcoma and another histogenetically distinct sarcoma such as osteosarcoma, chondrosarcoma, or RMS are also recognized, and in the past were classified as examples of ''malignant mesenchymoma,'' as discussed in a separate section. Such sarcomas are more appropriately classified in a manner that details (in some fashion) their individual components (e.g., leiomyosarcoma with foci of osteosarcoma or osteosarcomatous differentiation; biphenotypic sarcoma with leiomyosarcoma and chondrosarcoma).

Cutaneous leiomyosarcomas (1,30,31) are dermal-based lesions that demonstrate only superficial invasion of subcutaneous tissue. Tumors with a nodular growth pattern are highly cellular lesions that microscopically resemble conventional leiomyosarcomas. A unique feature observed in a significant proportion of cases is a diffuse pattern of growth (Fig. 138). The cellular element in these sarcomas tends to grow as short fascicles and bundles parallel to the epidermal surface and infiltrates native dermal collagen at the periphery of the lesion. Unlike the nodular variant, these tumors show lower cellularity and may exhibit only subtle criteria of malignancy. Foci of accentuated cellularity in the lesion are usually associated with increased mitotic activity and should be sought after to confirm the diagnosis of leiomyosarcoma (30) (Fig. 138).

Immunohistochemistry

Tumor cells exhibit strong and diffuse expression of vimentin and actin (both muscle specific and smooth muscle). Desmin shows more variable expression, but is usually positive in most cases and confirms the diagnosis as it separates the tumor from a myofibroblastic lesion (Fig. 137) (34). Calponin, h-caldesmon, and smooth muscle-myosin expression is observed in the vast majority of leiomyosarcomas (46–49). In general, expression of at least two myogenic markers is more supportive of a diagnosis of a leiomyosarcoma than expression of only one, especially the presence of SMA and desmin. High-grade dedifferentiated foci with features of malignant fibrous histiocytoma (pleomorphic sarcoma) tend to show a significant reduction in expression of myogenic markers. Rare examples of leiomyosarcoma exhibiting focal expression of keratin, EMA, S-100 protein, or CD34 have been reported (50–52).

Molecular Findings

Cytogenetic studies of leiomyosaracoma typically have shown highly complex genetic aberrations with no leiomyosarcoma-specific abnormalities being identified yet (53,54). Also, CGH studies have confirmed the complexity of genetic changes in these tumors (55). Loss of genetic material from chromosome 13, including loss of *RB1* (retinoblastoma gene), has been documented in leiomyosarcomas. Loss of *RB1* has been shown to cause abnormalities of the RB1-CCND1 (cyclin D1) pathway (56). Also, aberrations of *TP53* and *MDM2* were found in the subset of leiomyosarcomas (57,58).

Electron Microscopy

Leiomyosarcomas exhibit to some extent ultrastructural features of normal smooth muscle cells, including basal lamina and cell junction formation, subplasmalemmal micropinocytotic vesicles, and longitudinally arrayed myofilaments with dense bodies. However, the frequent absence or paucity of smooth muscle features in poorly differentiated examples makes electron microscopy not very useful for establishing histogenesis in this situation.

Differential Diagnosis

In the head and neck, sarcomatoid (spindle cell) carcinoma may harbor cellular spindled areas reminiscent of a smooth muscle tumor. These tumors occur in areas susceptible to tobacco-induced carcinogenesis, including the larynx, oral cavity, hypopharanx, and nasal cavity (59). Sarcomatoid carcinoma typically presents in mucosal-based tissues as a polypoid mass. The cellular, pleomorphic spindled element microscopically differs from leiomyosarcoma by its less

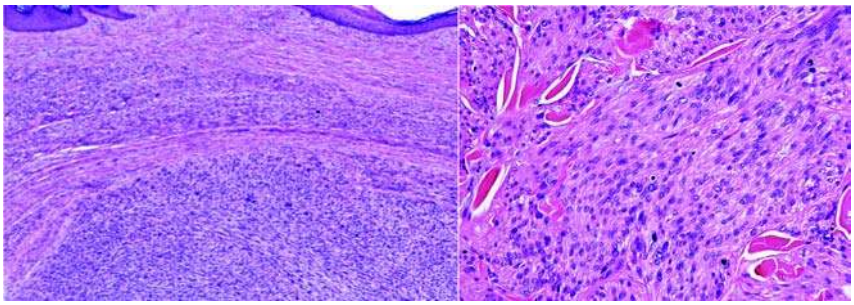

Figure 138 Cutaneous leiomyosarcoma exhibiting a haphazard growth pattern of bundles and short fascicles of spindled tumor cells within the dermis. Nuclear atypia plus 1 mitosis per 50 HPF make the diagnosis of cutaneous leiomyosarcoma. These have overall good behavior.

well-defined fascicular growth and lack of definitive cytologic features of smooth muscle differentiation. Residual squamous cell carcinoma or the presence of in situ dysplastic change supports the diagnosis. Immunohistochemically, the spindled element of sarcomatoid carcinoma may demonstrate presence of myogenic markers, actin (in less than half of tumors tested) and less often desmin (60,61), but shows variable expression of keratins in 40% to 85% of cases (62). Keratins AE1/3, 1, 18, and the EMA are reported as the most sensitive epithelial markers (61). Electron microscopic examination often detects ultrastructural evidence of epithelial differentiation such as desmosomes or tonofilaments in the spindled component.

Spindle cell melanoma (either primary or metastatic) may display a fascicular or storiform growth pattern and mimic a smooth muscle tumor. Presence of an in situ component assists in the diagnosis. Importantly, strong immunohistochemical expression of S-100 protein coupled with expression of any of the other known melanoma-related markers (i.e., HMB-45, melan-A, tyrosinase, or microphthalmia transcription factor) confirms the diagnosis of malignant melanoma. However, expression of the aforementioned melanoma-related immunomarkers is typically weak or absent in spindle cell and desmoplastic melanomas (63).

Malignant peripheral nerve sheath tumor microscopically differs from leiomyosarcoma by exhibiting areas of high cellularity interspersed with myxoid regions of lower cellularity, and by possessing cells with paler cytoplasm and less-defined cytoplasmic borders. Additionally, origin from a nerve (especially branches of the trigeminal nerve where the sarcoma commonly arises) (15) or foci of neurofibromatous growth assists in establishing the diagnosis of a malignant peripheral nerve sheath tumor. Immunohistochemically, the cells of malignant peripheral nerve sheath tumor display focal S-100 protein expression (in approximately one-half of cases), but do not demonstrate strong expression of muscle actin(s), h-caldesmon, or desmin (with the exception of a biphenotypic sarcoma with a myogenic component) (46,47).

Rare conventional fibrosarcomas or that arising in dermatofibrosarcoma protuberans (DFSP) characteristically grow in elongated fascicles that interconnect at acute angles (''herringbone'' pattern). In contrast to leiomyosarcoma, 90° orientation of apposed fascicles is not observed, and interstitial collagen is usually more abundant. The cells of fibrosarcoma have less-brightly eosinophilic cytoplasm and more slender nuclei than the constituent cells of leiomyosarcoma. Importantly, diffuse expression of myogenic markers militates against the diagnosis of fibrosarcoma. Low-grade myofibrosarcoma (myofibroblastic sarcoma) (64,65), a neoplasm exhibiting myofibroblastic differentiation that predilects to the head and neck, immunohistochemically expresses myogenic markers. However, in contrast to leiomyosarcoma, the tumor has histologic features more in keeping with fibrosarcoma, including pale spindled cells with ill-defined cytoplasmic borders and tapered nuclei, a herringbone pattern of growth in some cases, and stromal collagen.

Foci of the inflammatory myofibroblastic tumor (66,67) with a fascicular growth pattern of spindled cells that show immunoexpression of myogenic markers can mimic a smooth muscle tumor. However, the cells of inflammatory myofibroblastic tumor do not show the diffuse nuclear atypia observed in most examples of leiomyosarcomas. Additionally, the presence of characteristic paucicellular foci with dense collagen formation (fibroma-like foci) and areas showing fasciitis-like growth support the diagnosis of inflammatory myofibroblastic tumor. Immunoexpression of ALK-1 occurs in approximately 50% of cases of inflammatory myofibroblastic tumor (68), but has also been reported in rare examples of leiomyosarcoma (69).

Malignant fibrous histiocytoma (pleomorphic sarcoma) is a high-grade spindle cell lesion that should not demonstrate distinct features of cellular differentiation. The short, tight curvilinear fascicles that center on a vessel result in the characteristic storiform growth pattern observed in this sarcoma. However, a storiform architecture is also found in some high-grade leiomyosarcomas. Furthermore, some examples of malignant fibrous histiocytoma may have osteoclast-like giant cells (giant cell malignant fibrous histiocytoma) or hemangiopericytomatous vessels. In comparison with the cells of leiomyosarcoma, the cells of the malignant fibrous histiocytoma lack the brightly eosinophilic, fibrillar cytoplasm. Also, the malignant fibrous histiocytoma usually has a significant component of interstitial collagen. Immunohistochemically, the malignant fibrous histiocytoma, by definition, should not show more than focal expression of myogenic markers. As a cautionary note, dedifferentiated leiomyosarcomas may have large areas of undifferentiated sarcoma with features of malignant fibrous histiocytoma (see above).

Monophasic (fibrous type) synovial sarcoma typically has cellular areas of spindle cell growth. Unlike leiomyosarcoma, the monophasic synovial sarcoma features ropy or plaque-like deposits of collagen, cells with shorter nuclei, and less cellular pleomorphism. Although immunohistochemical expression of the myogenic marker calponin has been described in poorly differentiated examples of synovial sarcoma (70), the sarcoma typically shows expression of EMA, high- and low-molecular weight keratins, CD99, bcl-2, and CD56 (71,72). Finally, t(x;18) is the gold standard of molecular finding in synovial sarcoma, which is absent in leiomyosarcoma.

The head and neck is the second most common site (behind the genitourinary tract) for the development of the spindle cell variant of ERMS (73). Unlike leiomyosarcoma, the spindle cell RMS predilects to patients in the first two decades of life (73,74). Cells with eosinophilic cytoplasm arranged in fascicles are microscopic features that overlap with leiomyosarcoma. As cross striations are sparse in this RMS

variant, immunohistochemical expression of specific skeletal muscle markers, such as skeletal muscle nuclear regulatory proteins, MyoD1 and myogenin, assists in confirming the diagnosis.

Lastly, myoepithelioma, a tumor that occurs in the oral cavity, salivary glands, and soft tissue, may be composed almost exclusively of plump spindled cells with eosinophilic cytoplasm that immunohistochemically express SMA. In comparison with leiomyosarcoma, these tumors are usually associated with a more pronounced stromal component (collagenous or myxoid) and the lesional cells possess smaller nuclei. Immunohistochemically, the cells of the myoepithelioma express SMA and calponin but also typically express keratins, particularly high–molecular weight species, S-100 protein, glial fibrillary acidic protein, and p63 (75). Desmin is negative in myoepithelioma.

Prognosis and Treatment

In a comprehensive literature review of sinonasal leiomyosarcoma, Ulrich et al. (14) reported that the recurrence rate for the sarcoma was approximately 27% and the rate of distant metastasis was about 8%. Most recurrences were diagnosed within the first two years of initial treatment. About 18% of patients with sinonasal leiomyosarcomas succumb to disease because of direct tumor involvement of vital structures and, less often, metastatic spread. Poor prognostic factors for sinonasal leiomyosarcoma include large tumor size, extension of the sarcoma beyond the nasal cavity, and primary involvement of the orbit, pterygomaxillary fossa, posterior aspect of the paranasal sinuses, or skull base (10,18,76).

Leiomyosarcomas of the oral cavity most often metastasize to the lymph nodes or lung (16). Survival data culled from large literature reviews indicate an overall five-year survival between 45% (16) and 62% (18). Prognosis depends on the size of the tumor and its location. Leiomyosarcomas measuring 2 cm or greater in size exhibit a significantly higher rate of metastatic spread than smaller lesions (16). Location of tumor in posterior anatomic structures of the oral cavity and oropharynx, especially in the vicinity of the infratemporal fossa (i.e., mandibular condyle and posterior maxilla), where adequate surgical excision of the sarcoma is difficult, is associated with a poor outcome (18).

Marioni et al. (19) reviewed 26 immunohistochemically proven cases of leiomyosarcoma of the larynx culled from the literature and found only one patient with lymph node metastases at time of presentation. Distant metastases occurred in 15% of patients during the course of disease and most often involved the lung. Four of the 26 patients died of disease during a short 9-month follow-up interval.

In general, the primary treatment for noncutaneous head and neck leiomyosarcomas is surgical resection with a 1-cm margin of normal tissue if no radiation is used (77). Surgical resection is commonly supplemented by radiation therapy, which has shown to effectively complement surgery for local control of soft tissue sarcomas (78–80). Chemotherapy is considered ineffective treatment for leiomyosarcoma (9), but has been used along with radiation in inoperative cases for palliation (14). Lymph node dissection is not recommended for laryngeal or sinonasal leiomyosarcomas because of low yield of lymph node metastases, unless clinical lymphadenopathy is detected (23). Lymph node metastases of oral cavity leiomyosarcomas have been documented in less than 10% of reported cases (18,81).

Leiomyosarcomas arising entirely within the dermis (cutaneous leiomyosarcomas) are usually low grade and have a potential for local recurrence but an extremely low risk for metastatic spread (82). Therefore, a complete (local) excision is warranted as primary treatment. Once there is subcutaneous involvement in adults, not children, who have much better prognosis than adults, there is a 30% risk for metastasis.

IV. MALIGNANT LIPOMATOUS

A. Liposarcoma

Introduction

Liposarcomas are currently divided into three types, well differentiated/dedifferentiated (Fig. 139) (1), myxoid/round cell (Fig. 140), and pleomorphic (Fig. 141), on the basis of current molecular data. Many of the subdivisions of the WDLS have been largely replaced or dropped. Lipoma-like liposarcoma is now just WDLS. So-called sclerosing liposarcoma has been replaced by low-grade dedifferentiated liposarcoma, especially if there is greater than 10× power field of an alipogenic area. Inflammatory liposarcoma, with plasma cells and lymphocytes, is common to many liposarcomas, and the word ''inflammatory'' is no longer used (2,3). Liposarcoma with meningothelial-like whorls is probably early dedifferentiation in retroperitoneal lesions, some with metaplastic bone (4,5). ''Spindle cell liposarcoma'' is a term used for a heterogeneous group of WDLS and myxoid liposarcoma; but it is difficult to find a lesion that truly belongs to this group (6).

Dedifferentiation is important because it means that the tumor can metastasize (7,8). WDLSs, even of the retroperitoneum, can wrap around vital organs but do not metastasize without first dedifferentiating into an alipogenic spindled component.

Myxoid and round cell liposarcomas are on a spectrum with one another, as they are clinically and genetically identical, with round cell change (back-to-back cellular stromal round blue cells) portending a worse prognosis.

Pleomorphic liposarcoma can be divided into spindled malignant fibrous histiocytomas-like tumors with large, bizarre pleomorphic lipoblasts and an epithelioid-type with sheets of more mono- to bivacuolated lipoblasts, mimicking carcinomas of endocrine type (9,10).

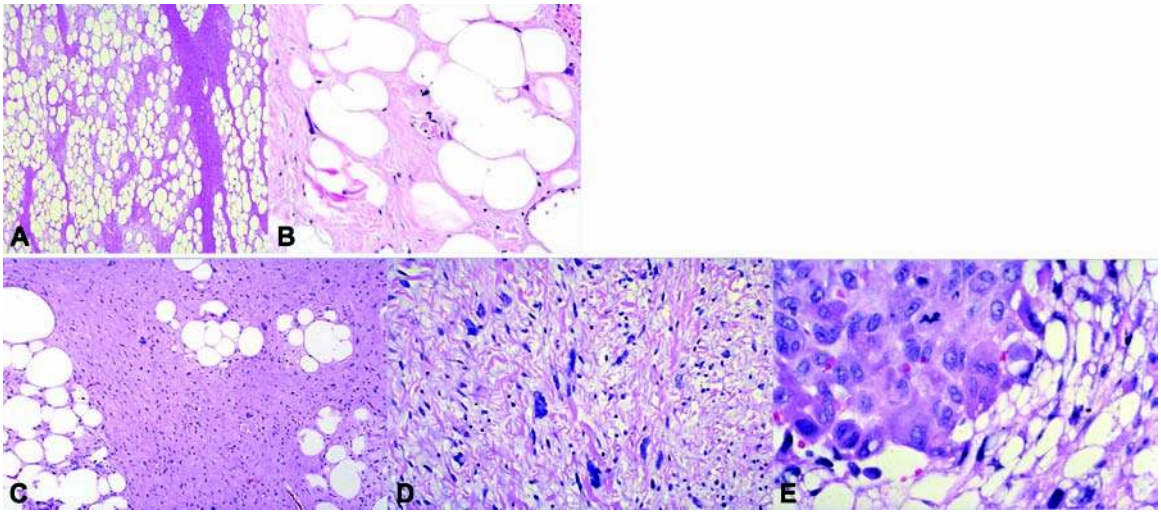

Figure 139 Liposacomas are now divided into (*i*) well differentiated (**A,B**) and dedifferentiated (**C–E**), (*ii*) myxoid and round cell, and (*iii*) pleomorphic. The former must have lipocytic atypia and be intramuscular; lipoblasts are not necessary for the diagnosis but are often found in head and neck of well-differentiated liposarcomas. Dedifferentiated liposarcoma must have at least 10× power field of an alipogenic area; this can be low to high grade.

Clinical Findings

All of the liposarcoma subtypes, except myxoid liposarcoma, occur in older adults except those found in the head and neck where they tend to occur a decade earlier (11–14). Myxoid liposarcoma notoriously occurs in young adults, mainly in the thigh or extremities. Only about 4% to 5% of liposarcomas occur in the head and neck (12–18), including the larynx and hypopharynx (11,19–28).

Imaging

The imaging appearance of liposarcoma is dependent on the histologic subtype. Similar to other soft tissue masses, MR is the optimal imaging modality for characterization and staging. WDLS typically reveals a largely lipomatous mass (>50–75% of the lesion), but, importantly, prominent nonlipomatous components are also seen. These nonlipomatous components are seen as numerous septations (often >2 mm thick or with focal nodularity) or focal globular or nodular regions. Myxoid liposarcomas most frequently demonstrate a small lipomatous component (<5–10% of tumor volume), with the other component reflecting the high water content of the lesion (low attenuation on CT, low signal intensity on T1-weighted MR, marked high signal intensity on T2-weighted MR). In a small percentage of cases, myxoid liposarcoma may not reveal intrinsic fat by imaging and simulate a cyst. However, lesion location is not that of a cyst, and sonography or postcontrast MR reveals the solid nature of the lesion requiring biopsy. Pleomorphic liposarcomas may show prominent nonspecific intrinsic appearances on CT or MR imaging. However, small focal lipomatous areas are apparent in 62% to 75% of cases, suggesting the diagnosis (29–31).

Pathologic Findings

Grossly, liposarcomas are yellow, greasy, and glistening with grossly thickened fibrous septa for well-differentiated type or gelatinous for myxoid type or white, solid and firm for dedifferentiated or pleomorphic types. The head and neck liposarcomas are generally around 5 cm and not as large as those in the retroperitoneum (27). Histologically, WDLS is intramuscular (or in the skeletal muscle of the tongue) and has lipocytic atypia. Although lipoblasts are not required for the diagnosis, they tend to be numerous in oral liposarcomas. Low-power observations include a busy appearance, heterogeneity of adipocyte size and shape, and widened septa. Myxoid liposarcoma has lobules of myxoid change, stromal stellate to round cells, which coalesce and sheet (back to back) for the round cell type, delicate plexiform or y-shaped vasculature, and mostly mono- or bivacuolated lipoblasts. The round cell liposarcomas almost always have a myxoid liposarcoma component and the round cell change comprising greater than 5% portend a worse prognosis. Pleomorphic liposarcoma, as above, can be malignant fibrous histiocytoma-like or pure sheets of lipoblasts.

Immunohistochemistry

S-100 protein can be positive in mature fat and in lipoblasts, including in the myxoid/round cell and pleomorphic liposarcoma subtypes. Spindled cells

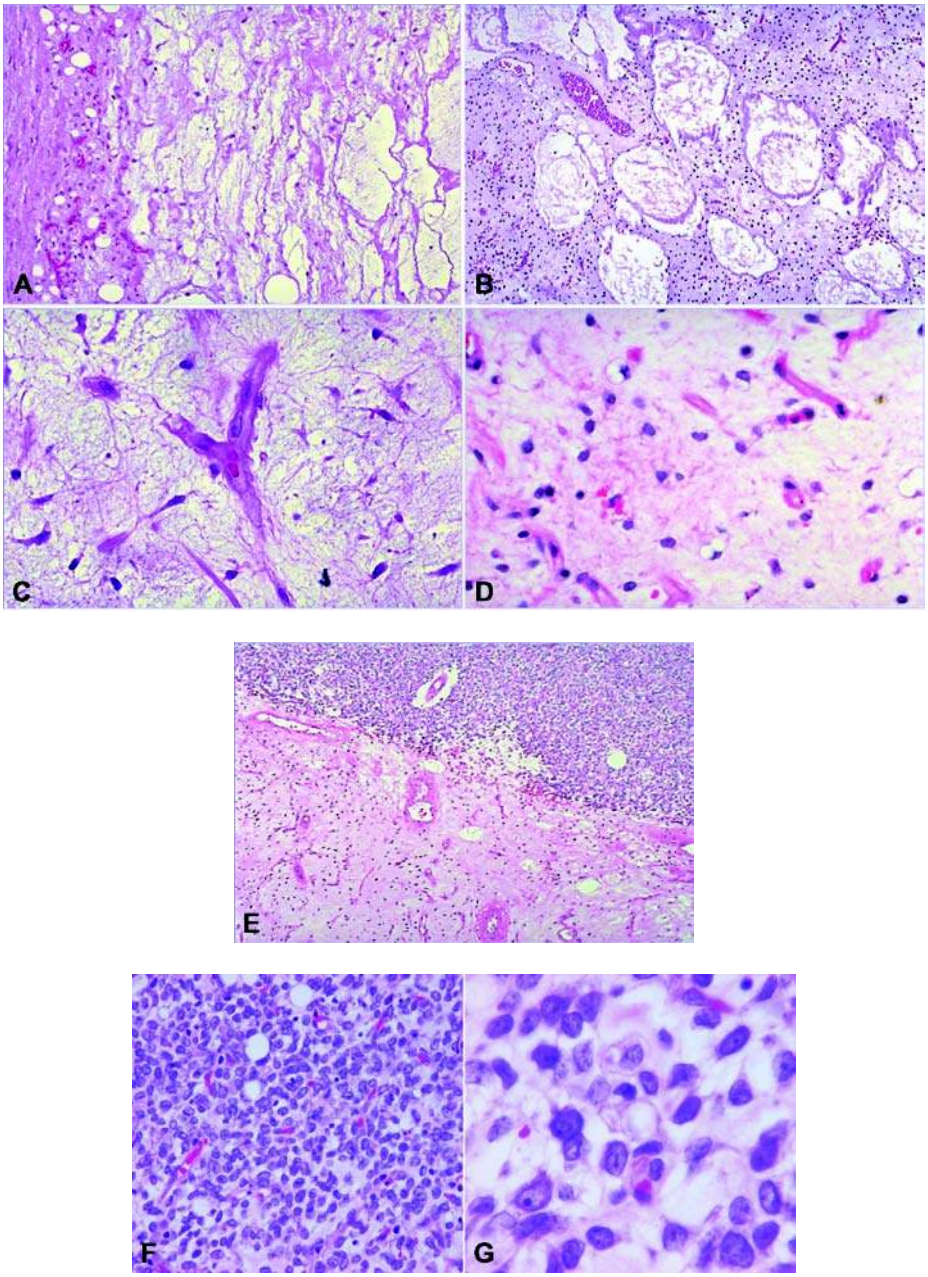

Figure 140 Myxoid liposarcoma is characterized by myxoid lobules (**A**,**B**) with delicate y-shaped vessels (**C**), mono- or bivacuolated lipoblasts (**D**), and stromal round cells, which coalesce to form the back-to-back sheets in round cell liposarcoma (**E–G**). Often a myxoid liposarcoma component is seen in round cell liposarcoma (**E**). These are on a spectrum of the same entity, with the same genetic findings; round cell morphology portends a worse prognosis.

may stain with CD34, including those in dedifferentiated liposarcoma.

Molecular Findings

Well-differentiated liposarcoma. Cytogenetic changes commonly seen in WDLS include supernumerary ring and giant marker chromosomes (32,33). Molecular genetic studies have shown that both the supernumerary ring and giant marker chromosomes are composed of amplified sequences from the 12q13–15 chromosomal region (34). Genes that are located in this region include *SAS* (sarcoma-amplified sequences), *MDM2* (murine double-minute chromosome), and *CDK4* (cyclin-dependent kinase 4). Although the exact mechanisms of WDLS tumorigenesis is not yet well known, it was hypothesized that tumor development is promoted by amplification and

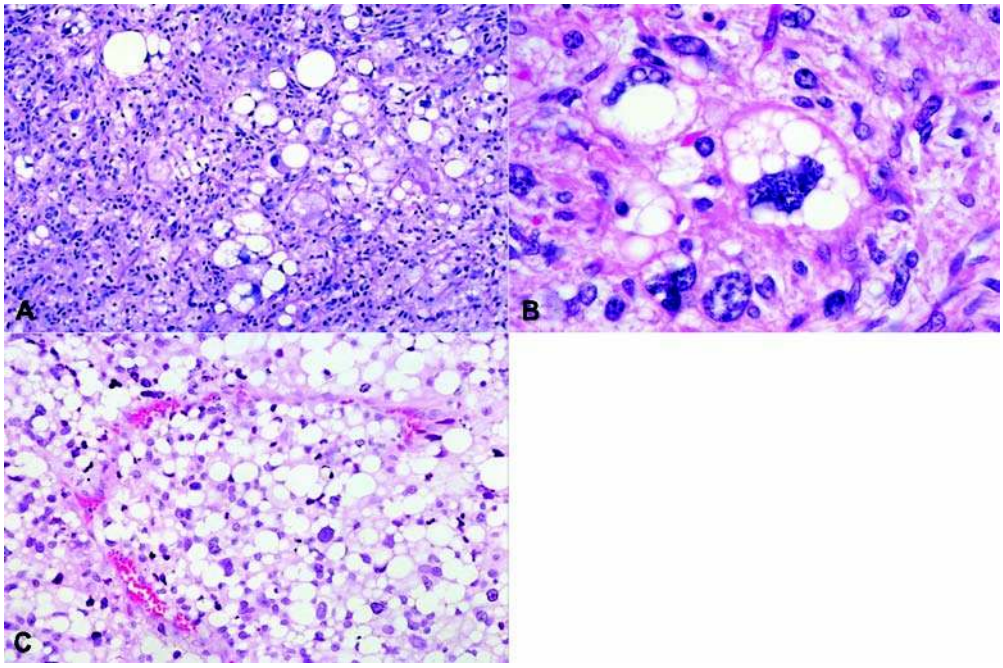

Figure 141 Pleomorphic liposarcoma can either be like a malignant fibrous histiocytoma (**A**) with bizarre pleomorphic lipoblasts (**B**) or be composed of sheets of epithelioid lipoblasts (**C**), mimicking endocrine neoplasms.

overexpression of *MDM2* and *CDK4*, proteins involved in the cell cycle regulation. On the basis of CGH and PCR (polymerase chain reaction) studies, overrepresentation of 12q13-21 and amplification of *MDM2*/*CDK4* have been suggested to be useful in separating WDLS from lipomas (35,36). Lack of MDM2 immunoreactivity in lipomas seems to confirm the diagnostic significance of this observation (37). However, use of CGH and real-time PCR testing for such diagnostic problems in everyday surgical pathology appears to be problematic.

Dedifferentiated liposarcoma. Genetics of dedifferentiated liposarcomas is poorly understood. Some studies have shown that such tumors contain ring or giant marker chromosomes and amplification of 12q14-15 (37–39).

Myxoid and round cell liposarcoma. The t(12;16)(q13;p11) translocation is a characteristic cytogenetic feature of the great majority of myxoid and round cell liposarcoma (40–42). However, a small subset of tumors is characterized by the t(12;22)(q13;q12) translocation (43,44). These translocations form *FUS-CHOP* and *EWSR1-CHOP* fusion genes, respectively (40–44). *FUS* and *EWSR1* show extensive homology, and both are the member of gene family encoding RNA-binding proteins (45). *CHOP*, also known as *DDIT3* (DNA damage-inducible transcript 3), is a member of the bZIP family of transcription factors that contains a leucine zipper motive and has been shown to be involved in adipocyte differentiation and growth arrest (46). FUS-CHOP fusion protein includes strong FUS transcriptional activation domain at full length of CHOP. This chimeric protein has been shown to inhibit preadipocytes differentiation and induce liposarcoma in transgenic mouse model (47,48). Presumably, oncogenic effect of EWS-CHOP chimeric protein is analogous to the one reported for FUS-CHOP. Although rare cases of well-differentiated and pleomorphic liposarcomas have been reported to have *FUS-CHOP* fusion transcripts, detection of such transcripts or t(12;16) and t(12;22) translocations is a diagnostic hallmark of myxoid and round cell liposarcoma (48). Both FISH and RT-PCR based assays have been developed and could be used for differential diagnosis of myxoid and round cell liposarcoma (49,50). Several different types of *FUS-CHOP* fusion transcripts resulting from the differences in the translocation break point have been identified in myxoid and round cell liposarcoma. However, unlike in other sarcomas with specific fusion genes, the type of *FUS-CHOP* fusion transcript has no prognostic value (51,52).

Pleomorphic liposarcoma. Cytogenetic studies have shown complex karyotypes with ring, double-minute, and unidentifiable marker chromosomes (53). In contrast to WDLSs, amplification of 12q13-15 region is a rare finding in pleomorphic liposarcomas (38). Also, amplification of the *MDM2* gene has been found only in a subset of cases (38,54). The presence of *FUS-CHOP* fusion transcripts in some tumors might suggest their origin from myxoid/round cell liposarcoma (55).

Electron Microscopy

Most of these liposarcomas show fatty phenotype with lipid droplets (56).

Differential Diagnosis

Malignant fatty tumors must be separated from reactive and benign fatty neoplasms, as outlined in the benign soft tissue tumor section in this chapter.

Prognosis and Treatment

Regional nodal metastases are rare. Distant metastases occur via hematogenous spread in 30% of patients, and they are associated with the more poorly differentiated round cell and pleomorphic subtypes. Fewer than 20% of myxoid tumors and 6% of well-differentiated tumors are associated with distant metastases.

Survival and local control is associated with the tumoral subtype. The five-year survival rates for liposarcomas are 85% to 100% for WDLS, 77% to 95% for myxoid liposarcomas, 21% to 45% for pleomorphic liposarcomas, and 13% to 55% for round cell liposarcomas. The incidences of local recurrence are 29% to 62% for WDLS, 33% to 57% for myxoid liposarcoma, 43% to 73% for pleomorphic liposarcoma, and 63% to 86% for round cell liposarcoma.

In the oral cavity, liposarcoma has a fairly good prognosis because the lesions are detected at a small size (57,58). Most liposarcomas of the oral cavity are well-differentiated or myxoid liposarcoma subtypes. Rarely a pleomorphic subtype can be identified. WDLSs are treated by wide local excision; myxoid liposarcomas, pleomorphic liposarcoma, and intermediate- to high-grade dedifferentiated liposarcomas are treated with adjuvant therapy (mainly radiation therapy and chemotherapy for tumors larger than 5 cm or inability to completely resect) (59–63).

V. MALIGNANT (MYO)FIBROBLASTIC, MIXED LINEAGE MESENCHYMAL, CARTILAGINOUS

A. Fibrosarcoma/Malignant Fibrous Histiocytoma

Introduction

In the past, fibrosarcoma was one of the most common soft tissue diagnoses, as any tumor with malignant spindle cells and collagen could be given this diagnosis. As other soft tissue tumors became better defined and with the onset of immunohistochemistry, we now know that many tumors originally diagnosed as fibrosarcoma would currently be better classified as another tumor such as a gastrointestinal stromal tumor, synovial sarcoma, malignant peripheral nerve sheath tumor, leiomyosarcoma, DFSP, or RMS (1–4).

Malignant tumors of fibroblastic or myofibroblastic phenotype are rarely called fibrosarcoma by itself. In fact, the term ''fibrosarcoma'' has gone out of vogue, as it has been largely replaced by other subcategories, including fibrosarcoma arising in DFSP, Evan's tumor (low-grade myxofibrosarcoma), and sclerosing epithelioid fibrosarcoma. Infantile fibrosarcoma still exists as a distinct clinicopathologic entity. Hence the terminology of fibrosarcoma is rarely used. The remaining lesions often have pleomorphism and are called ''malignant fibrous histiocytomas'' [pleomorphic sarcoma NOS (not otherwise specified)] or ''myxofibrosarcoma,'' the new terminologies for myxoid and storiform pleomorphic malignant fibrous histiocytomas, respectively.

Malignant fibrous histiocytoma, a malignant tumor composed of myofibroblasts and histiocytoid cells, is divided into (*i*) storiform pleomorphic type (pleomorphic sarcoma NOS) (5), (*ii*) myxoid malignant fibrous histiocytoma (myxofibrosarcoma) (6–8), (*iii*) inflammatory malignant fibrous histiocytoma (mainly of retroperitoneum, has additional sheets of polymorphonuclear leukocytes and histiocytes) (9–11), and (*iv*) giant cell-rich malignant fibrous histiocytoma (a multinodular tumor with the addition of osteoclast-type giant cells) (12).

Angiomatoid (malignant) fibrous histiocytoma (AFH) occurs mainly in children and young adults and has exceedingly rare metastatic potential, usually to regional lymph nodes, but the patients usually have an excellent prognosis, even with a regional lymph node metastasis (13,14). Therefore, while it is considered a borderline or intermediate category tumor and is no longer included with the malignant fibrous histiocytomas, the term ''malignant'' has been dropped from the name, but we still put this in quotation marks or parentheses to denote its rare potential It will be included here for completeness.

Imaging

Imaging of malignant fibrous histiocytoma and fibrosarcoma are indistinguishable. These lesions typically demonstrate a relatively large heterogeneous soft tissue masses with nonspecific intrinsic characteristics on ultrasonography, CT, or MR imaging. The predominant attenuation is similar to muscle on CT and intermediate in signal intensity on T1-weighted MR imaging. There is intermediate to high signal intensity on T2-weighted MR images. Areas of necrosis (low attenuation CT) and hemorrhage (high signal intensity on all MR pulse sequences) are common. No evidence of adipose tissue is seen, and masses are typically relatively well defined. Lesions demonstrate heterogeneous or peripheral nodular enhancement following administration of intravenous contrast on CT or MR imaging (6).

Infantile fibrosarcomas have similar imaging appearances but are often larger and more infiltrative. In addition, a high-flow feeding vascular pedicle as well as intrinsic high-flow vessels are often apparent. These high-flow vascular structures have a serpentine morphology and are of low signal intensity on all MR images.

Clinical Findings

Infantile fibrosarcoma makes up 12% of soft tissue tumors in infants (3). An extremely rare diagnosis after the age of two years, infantile fibrosarcoma commonly occurs (36–100%) before the patient's first birthday (15–20). It is thought to occur equally in males and females, although some believe that there is a small male predominance in infantile fibrosarcoma (15).

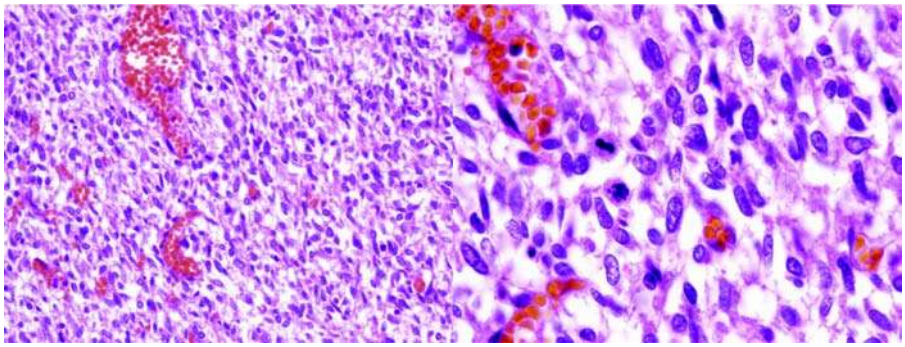

Figure 142 Infantile fibrosarcoma with a spindled appearance, more primitive than typical herringbone appearance of adults; this is rare in head and neck locations.

Infantile fibrosarcoma is locally aggressive and can involve an infant's entire extremity, but is exceedingly rare in the head and neck.

Fibrosarcoma arising in DFSP occurs mainly in adolescent males in the trunk and proximal extremities and rarely in the head and neck. Sclerosing epithelioid fibrosarcoma can occur in both soft tissue and bone in head and neck sites (21,22). Evan' tumor, low-grade fibromyxoid sarcoma (LGFMS), is generally an extremity lesion that rarely occurs in the head and neck (23). Tumors composed of myofibroblasts, i.e., fibrosarcomas (24) or malignant fibrous histiocytoma, occur in many head and neck locations (1,25–27). AFH (malignant) occurs in areas of normal lymph nodes (neck) and can follow trauma or present with symptoms suggesting cytokine release by tumor.

These myofibroblastic tumors can present as large, painless masses. The clinical symptoms usually relate to mass effect at the particular site. These tumors can produce proptosis and visual acuity when they present in the orbit. In the sinonasal tract, obstruction, epistaxis, and sinusitis are common (28).

There are no definite predisposing risk factors for fibrosarcoma. Fibrosarcoma/malignant fibrous histiocytoma can arise in patients who have been exposed to radiation, and to those with foreign body material, although much of this has been described in older literature (29–31).

Pathologic Findings

The fibrosarcoma variants are generally low grade, whereas malignant fibrous histiocytoma, with its pleomorphism and often necrosis, is generally at least intermediate grade. Fibrosarcoma arising in DFSP has a solid, firm, white appearance, distinctive from superficial, tan, softer DFSP by a line of demarcation. Evan's tumor is softer with firm areas, and sclerosing epithelioid fibrosarcoma is firm, often gritty, and white-tan. Infantile fibrosarcoma is firm and tan-white. Malignant fibrous histiocytoma varies depending on subtype, but is largely a firm to gelatinous tumor and is sometimes tan with hemorrhage and/or necrosis. AFH (malignant) is no longer included with the malignant fibrous histiocytomas, but resembles a lymph node grossly with blood-filled cystic cavities and is usually of smaller size. The tumors can vary in size from very small to quite large. Microscopically, infantile fibrosarcoma has a herringbone growth pattern of spindled myofibroblasts (Fig. 142) Zonal necrosis and hemorrhage as well as dystrophic calcifications may be present. There is little pleomorphism, but mitoses may be frequent.

Fibrosarcoma arising in DFSP (Fig. 143) is usually found in de novo lesions and is deep to the dermatofibrosarcomatous component, and there is a line of demarcation between the two elements. The fibrosarcomatous component is still of low grade, but is characterized by larger nuclear size, higher nuclear to cytoplasmic ratio, a herringbone growth pattern, less entrapped fat, and occasionally increased mitotic activity; these all impart a blue color at low power. The dermatofibrosarcomatous component has a storiform pattern, not fascicular, lower nuclear to cytoplasmic ratio, and a honeycomb and parallel pattern of fat entrapment. It appears pink on low power (20).

Sclerosing epithelioid fibrosarcoma is composed of round epithelioid cells embedded in a collagenous and sometimes osteoid-like matrix. The collagen separates cells and they can cord or nest. Mitotic activity is low but necrosis may sometimes be present (Fig. 144).

Evan's tumor (LGFMS), a polymorphogenic tumor, has lobules of myxoid change with a collagenous stroma and curvilinear vessels and fibromatosis-like and DFSP-like areas and can have hyaline rosettes surrounded by small round cells, as Evan's tumor is on a spectrum with so-called hyalinizing spindle cell tumor with giant rosettes. (8,32–34) (Fig. 145).

Storiform pleomorphic malignant fibrous histiocytoma or pleomorphic sarcoma NOS is a spindled storiform tumor with marked nuclear pleomorphism, tumor giant cells, mitotic activity, including atypical forms, and often necrosis (Fig. 146).

Myxofibrosarcoma (myxoid malignant fibrous histiocytoma) is a tumor composed of lobules of myxoid change with thick ropy vessels, dripping with tumor cells and identifiable mitotic activity. At

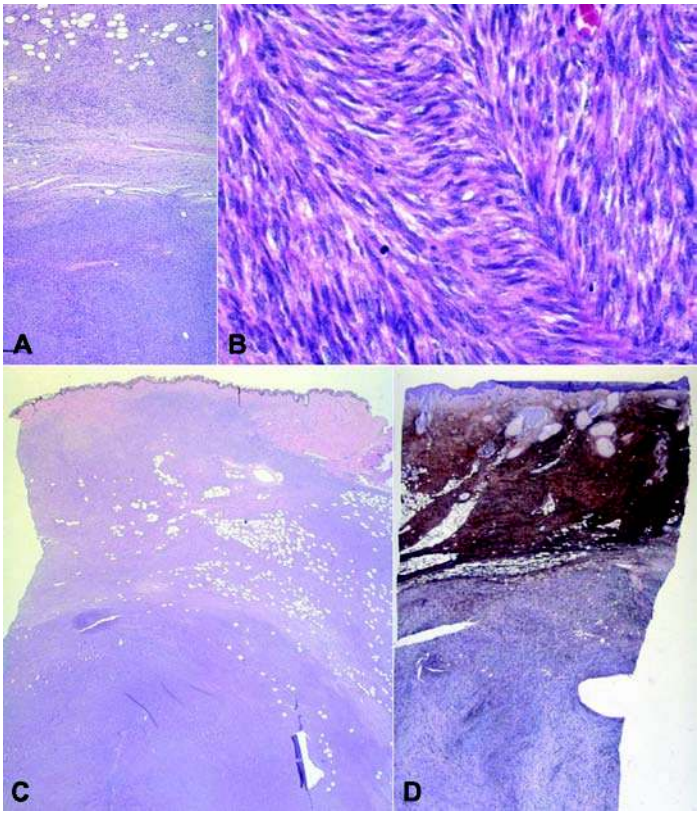

Figure 143 Fibrosarcoma arising in dermatofibrosarcoma (**A–D**) protuberans. There is a line of demarcation between the deeper, blue fibrosarcomatous component and the superficial, pink dermatofibrosarcomatous component (**A,C**). A higher magnification of the fibrosarcomatous component showing the herringbone growth pattern (**B**). Below are fibrosarcomatous transformation of dermatofibrosarcoma protuberans and the correlative CD34 (**D**), positive in the dermatofibrosarcoma protuberans component and decreased to absent in the fibrosarcomatous component.

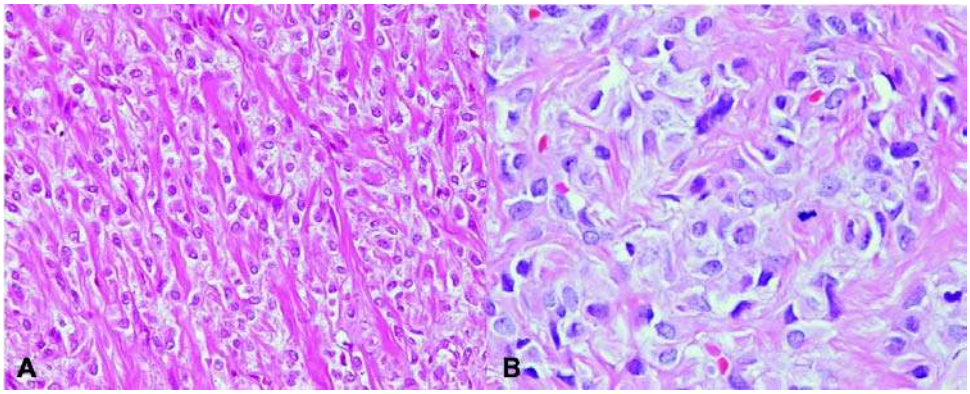

Figure 144 Sclerosing epithelioid fibrosarcoma (**A,B**), oral, is a sclerosing fibrosarcoma that is osteotrophic (likes to grow into bone) and the hyalinization can sometimes mimic osteoid.

least half of the tumor is myxoid; the other half may be solid storiform pleomorphic malignant fibrous histiocytoma. Sometime this has a bland appearance and is all myxoid. The key features are the ropy prominent vasculature and the cytologic atypia, although sometimes mild and sometimes with pseudolipoblasts containing mucopolysaccharides, and the finding of mitoses (Fig. 147).

Giant cell-rich malignant fibrous histiocytoma looks exactly like storiform pleomorphic malignant fibrous histiocytoma but is multinodular and has benign osteoclast-type giant cells as well as the atypical multinucleated cells, spindled cells, and mitotic activity with abnormal forms (Fig. 148).

Inflammatory malignant fibrous histiocytoma has sheets of polymorphonuclear leukocytes or sheets of histiocytes and large atypical, sometimes multinucleated giant cells and atypical mitoses (Fig. 149).

AFH (malignant) has four varying features: a spindled to epithelioid fibrohistiocytic component,

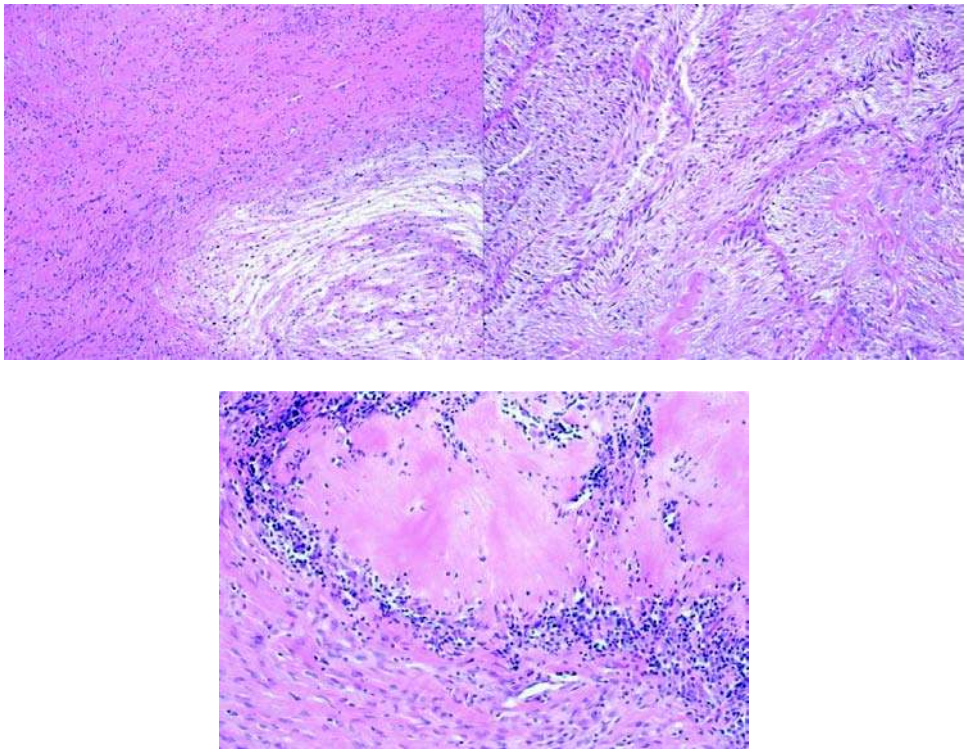

Figure 145 Low-grade fibromyxoid sarcoma (Evan's tumor) with a polymorphous morphology: collagenized myxoid areas with curvilinear vasculature alternating with dermatofibrosarcoma-like or fibromatosis-like area. Below left is a hyaline rosette (hyalinizing spindle cell tumor with giant rosettes), a tumor on the spectrum and genetically identical to Evan's tumor.

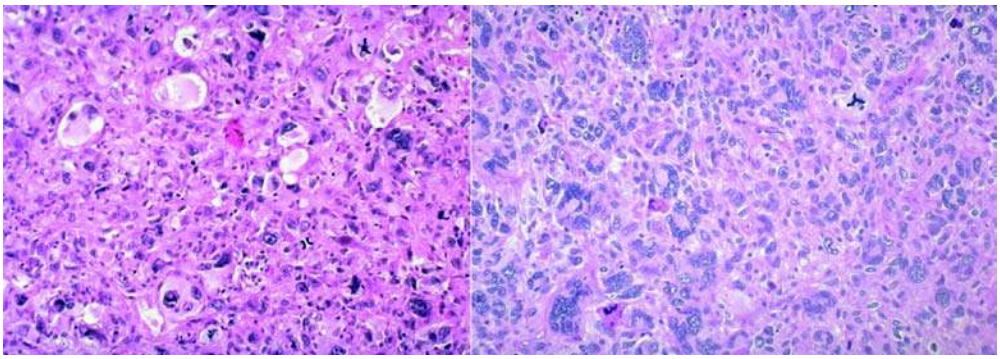

Figure 146 Storiform pleomorphic malignant fibrous histiocytoma (pleomorphic sarcoma NOS) is composed of spindled cells with tumor giant cells that are pleomorphic, mitotically activity with atypical forms and necrosis. This is a diagnosis of exclusion.

pseudovascular cystic spaces nonendothelial lined but filled with blood, a variably thick capsule, and a lymphoplasmacytic reponse with germinal center formation (Fig. 150).

Immunohistochemistry

All of these lesions are composed of myofibroblasts and may be actin- and vimentin-positive, sometimes CD68-positive and negative for S-100 protein, HMB-45, keratins, EMA, CD34, and mostly negative for desmin. Fibrosarcomatous transformation of DFSP looses or has diminished CD34 in the fibrosarcomatous component, compared with strong CD34 reactivity in the DFSP (35,36). The exception is that AFH (malignant) is a myoid tumor that is also positive for desmin in 50% of cases (14,37). In addition, AFH (malignant) can be positive for CD99 in a membrane pattern.

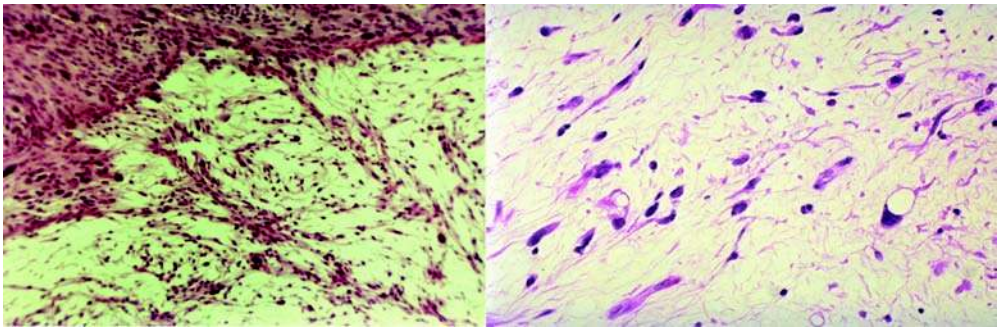

Figure 147 Myofibrosarcoma (myxoid malignant fibrous histiocytoma) is composed of lobules of myxoid change with ropy prominent vasculature dripping with atypical cells and mitotic activity. This can be found together with storiform pleomorphic type and are on a morphologic spectrum with one another. There are pseudolipoblasts in myxofibrosarcoma (*right*).

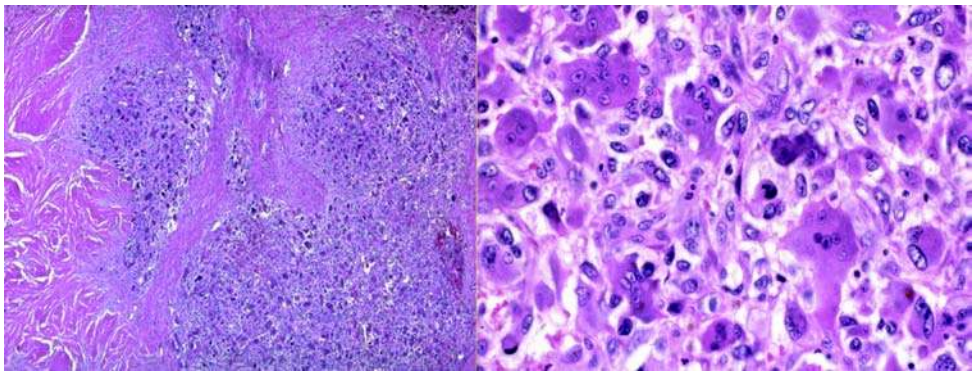

Figure 148 Giant cell-rich malignant fibrous histiocytoma is a multinodular storiform pleomorphic malignant fibrous histiocytoma with benign osteoclast-type giant cells.

Molecular Findings

Infantile fibrosarcoma. A t(12;15)(p13;q25) translocation leading to the *ETV6* and *NTRK3* gene fusion has been identified in infantile fibrosarcoma. The *ETV6-NTRK3* chimeric transcript consists of a helix-loop-helix dimerization domain of ETV6 (ETS variant gene 6, also known as TEL) fused to the protein tyrosine kinase domain of NTRK3 (neurotrophic protein kinase, receptor, type 3). The ETV6-NTRK3 oncoprotein deregulates NTRK3 signaling pathways, leading to a high constitutive expression of cyclin D1 and an aberrant cell cycle progression (38–40). An identical t(12;15) translocation associated with the *ETV-NTRK3* fusion gene has also been reported in the ''cellular'' form of congenital mesoblastic nephroma (41). The morphologic and genetic similarity between congenital mesoblastic nephroma and infantile fibrosarcoma suggests that both lesions represent a single neoplastic entity in either renal or soft tissue locations (41,42). Molecular detection of *ETV6-NTRK3* chimeric transcripts differentiates congenital fibrosarcoma from other childhood spindle cell tumors (38,39,43). However, *ETV6-NTRK3* fusion gene is not specific for this entity; an identical genetic abnormality has been described in a case of leukemia (44). This finding showed that oncogenic activation of NTRK3 and deregulations of its signaling pathways may represent a universal oncogenic mechanism seen in tumors derived from different cell lineages. Trisomies of chromosome 8, 11, 17, and 20, most likely acquired during tumor progression, represent other nonrandom genetic abnormalities characteristic of infantile fibrosarcoma (42,45).

Fibrosarcoma arising in DFSP. Supernumerary ring chromosomes containing material from chromosome 17 and 22 and t(17;22)(q22;q13) reciprocal translocations are typical cytogenetic changes seen in DFSP (46,47). Both abnormalities lead to a fusion of collagen type I α-1 (*COL1A1*) gene, localized on chromosome 17, and platelet-derived growth factor, β polypeptide (*PDGFB*) gene, localized on chromosome 22 (48). This rearrangement replaces *PDGFB* regulatory sequences with a *COL1A1* promotor, causing unregulated production of mature PDGFB and leading to autocrine growth stimulation through the PDGF receptor (48–50). The expression of COL1A1-PDGFB oncoprotein is

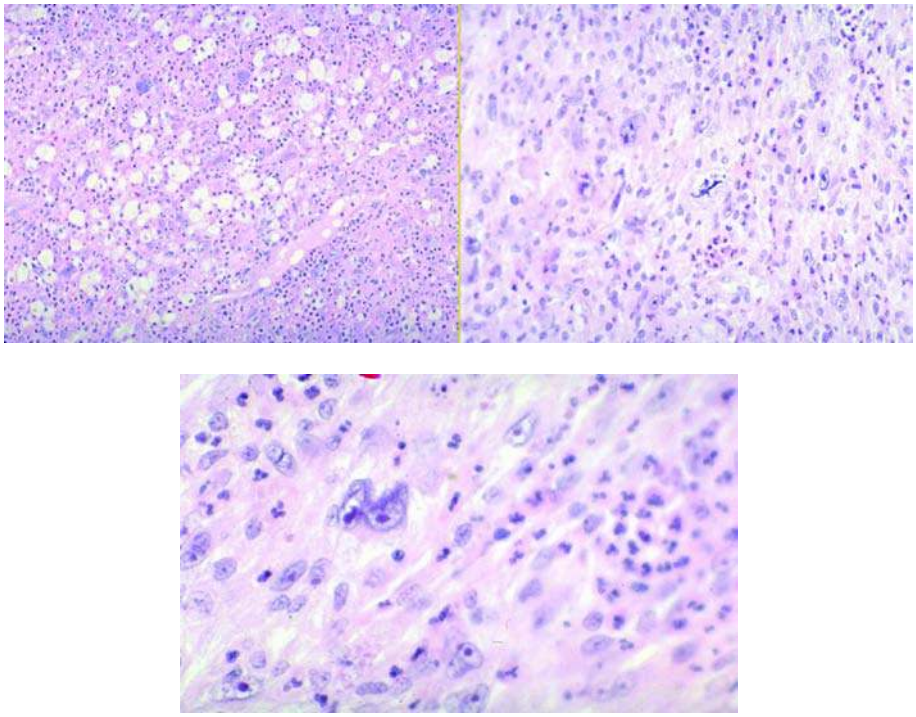

Figure 149 Inflammatory malignant fibrous histiocytoma is composed of sheets of polymorphonuclear leukocytes or histiocytes in addition to atypical pleomorphic giant cells, some resemble Reed–Sternberg cells, and atypical mitoses. These can mimic inflammatory processes and Hodgkin disease.

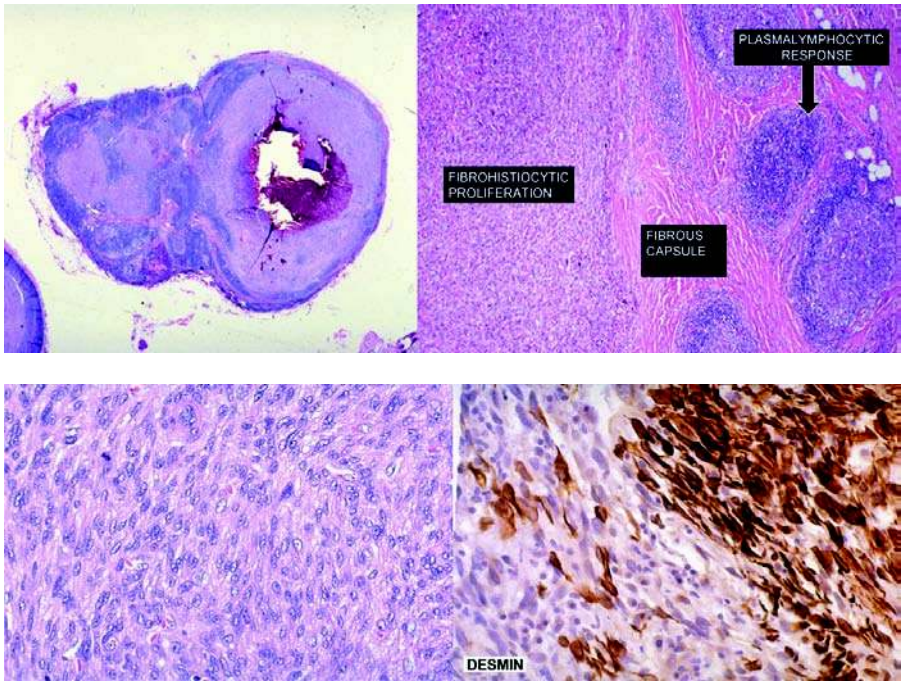

Figure 150 Angiomatoid (malignant) fibrous histiocytoma is no longer included with the malignant fibrous histiocytomas. It is desmin-positive in 50% of cases. These occur in areas of normal lymph node, including the neck, and have the following four features: a spindled to epithelioid fibrohistiocytic (myoid) component, pseudovascular spaces often filled with blood, a plasmalymphocytic response mimicking lymph node, and a fibrous pseudocapsule between the inflammatory response and the tumor.

tumorigenic in nude mice. Recent studies showed that imatinib mesylate, a tyrosine kinase inhibitor, causes growth inhibition of DFSP-derived cell cultures and mouse tumors (51). Moreover, response to the imatinib mesylate–based treatment was seen in a subset of patients with metastatic DFSP (52,53). Both FISH and RT-PCR based assays have been developed and could be used for diagnosis in problem cases (48,54,55). However, high heterogeneity in the location of *COL1A* break point requires multiple PCRs or multiplex PCR approach (48,56).

LGFMS (Evan's tumor) and sclerosing epithelioid fibrosarcoma. Cytogenetically, LGFMS is characterized by the t(7;16)(q34;p11) translocation (57). This translocation leads to the fusion between *FUS* gene located at 16p11 and *CREB3L2* (cAMP response element-binding protein 3-like 2) gene located at 7q34 (57,58). The chimeric protein consists of FUS transcriptional activation domain, which is linked to CREB3L2 basic DNA binding and leucine zipper dimerization domain and is highly expressed in LGFMS (57). Alternatively, *FUS* can be fused with *CREB3L1* as a result of t(11;16)(p11;p11) translocation reported in a subset of LGFMS. *CREB3L1* shows high homology to *CREB3L2*, and it is believed that FUS-CRAB3L1 and FUS-CRAB3L1 chimeric proteins have promoted tumorigenesis in a similar way (59). Both FISH and RT-PCR based assays have been developed and can be used in routine practice (57–59). However, *FUS-CREB3L2* fusion gene has also been identified in sclerosing epithelioid fibrosarcoma, suggesting potential relationship of this tumor to LGFMS (60).

Malignant fibrous histiocytoma. Highly heterogeneous, complex cytogenetic changes have been reported (61–63). Cytogenetic abnormalities of chromosome 19p13 and gains of 7q32 have been shown to correlate with unfavorable outcome (64,65). An amplification of 12q12-15, frequently seen in lipomatous tumors, and amplification of 8p23 have been reported in a subset of cases; *MDM2* and *MASL1* were documented to be amplified in these regions, respectively (66,67). Losses of chromosome 13, or 13q14-q21, including *RB1* gene, and *CDKN2A* (TP16) at 9p have also been reported (67–70).

AFH (malignant). Initially, the *FUS-ATF1* fusion gene has been identified in two cases of AFH (71,72). However, subsequent studies showed that *EWSR1-CREB3L1* and *EWSR1-ATF1* are the most common fusion genes in this tumor (73,74). *EWSR1-CREB3L1* has been previously reported in clear cell sarcoma of the gastrointestinal tract, while *EWSR1-ATF1* was considered a genetic hallmark of soft tissue clear cell sarcoma. Thus, identical fusions have been identified in distinct sarcomas, which may be developed from different types of mesenchymal precursor cells. Both EWSR1 and FUS form structurally similar oncogenic proteins in which strong transcriptional activation domain is fused to DNA-binding domain of transcription factors (CREB3L1 or ATF1). A prognostic significance of type of the fusion is not known; also, no correlation between the type of fusion gene and clinicopathologic features has been reported (73,74). However, RT-PCR-based detection of the fusion transcripts could be a valuable diagnostic adjunct in the distinction between AFH and other soft tissue tumors (73,74).

Electron Microscopy

All of these show features of fibroblasts and myofibroblasts. Fibroblasts usually lack myofilaments and intercellular junctions, but have prominent rough endoplasmic reticulum (30,75–78). Myofibroblasts have peripheral filament bundles. Electron microscopic data for AFH (malignant) is conflicting and inconclusive.

Differential Diagnosis

Infantile fibrosarcoma can mimic other childhood spindled lesions, including myofibroma(tosis), but is separated by atypical features and morphologic detail. For fibrosarcoma in general, other spindle cell lesions such as schwannoma, neurofibroma, leiomyosarcoma, and malignant peripheral nerve sheath tumor, can be separated by morphology and immunostains, as ''fibrosarcoma'' is negative for S-100 protein, CD34, GFAP, and desmin. RMS, which can have spindled cells, also will be highlighted by desmin and the myoregulatory proteins (myf4, myogenin, and MyoD1). Unlike fibrosarcoma, synovial sarcoma usually expresses cytokeratin and EMA. Tumors with neural differentiation, such as peripheral nerve sheath tumors, often express S-100. Peripheral nerve sheath tumors also can be seen microscopically arising from a nerve or neurofibroma, and schwannomas often have nuclei with a wavy serpentine morphology. CD34 is expressed in both solitary fibrous tumors and hemangiopericytomas, but not typically in fibrosarcomas. Hemangiopericytomas, also, do not typically form fascicles. Instead, the large open so-called staghorn blood vessels are present. It can be particularly challenging to distinguish fibrosarcoma from both fibromatosis and DFSP. Fibromatosis tends to have less pleomorphism, cellularity, and mitotic activity, but in addition are composed of myofibroblasts in a purposeful direction, parallel to elongate vessels, with open chromatin, uniform, ovoid nuclei.

DFSP can be separated from its fibrosarcoma transformation component by a monotonous storiform growth pattern, bland uniform morphology, pink low-power appearance, entrapped fat, and paucity of mitotic activity. Classically, DFSP is positive for CD34, and the fibrosarcomatous component loses its CD34 reactivity (35,79).

Sclerosing epithelioid fibrosarcoma is difficult to separate from osteosarcoma, since the collagen can mimic osteoid, other epithelial or epithelioid tumors, and, interestingly, ossifying fibromyxoid tumor. It, however, is negative for S-100 protein and GFAP and desmin, sometimes positive in the latter tumor. Osteoid in true osteosarcoma has a hard lacelike appearance with atypical osteocytes entrapped singly in the malignant osteoid matrix and is often mineralized, causing a purple-pink appearance.

Evan's tumor (LGFMS) can mimic several different tumors, including DFSP, diffuse neurofibroma, fibromatosis, and myxofibrosarcoma (low-grade myxoid malignant fibrous histiocytoma). It varies from others by its multimorphic pattern, its lack of CD34 and S-100 protein, and its curvilinear vessels rather than purposeful ones of desmoid. It is also blander and has less mitotic activity than myxofibrosarcoma and has more collagen-rich, opaque, myxoid areas than ''see through'' myxoid areas of myxofibrosarcoma. Myxofibrosarcoma additionally mimics all myxoid neoplasms, but is separated by its morphology and also lack of CD34 present in myxomas. Myxoid liposarcoma can be separated by its lobular myxoid change, delicate y-shaped vessels not dripping with tumor cells, lack of mitoses, stromal round to stellate cells, and true mono- to bivacuolated lipoblasts, mostly at the periphery of the lobules. Myxoid liposarcoma also tends to demonstrate a pulmonary alveolar-like pooling of mucoid material, not observed in myxofibrosarcoma. True lipoblasts have their fat leached out during processing, so are empty, compared with pseudolipoblasts in myxofibrosarcoma that contain mucopolysaccharides.

Storiform pleomorphic malignant fibrous histiocytoma or pleomorphic sarcoma NOS mimics all poorly differentiated malignancies and is separated by its lack of most immunostains, except vimentin, occasionally actins and CD68.

Giant cell–rich malignant fibrous histiocytoma can mimic all osteoclast giant cell–rich lesions but is more atypical with atypical mitoses than benign tumors containing giant cells. It has a multinodular growth pattern and is not entirely CD68-positive, unlike malignant tenosynovial giant cell tumor.

Inflammatory malignant fibrous histiocytoma can mimic xanthogranulomatous inflammatory processes and even Hodgkin lymphoma, but is separated by its marked atypia and atypical mitoses as well as its lack of CD15 and other inflammatory elements.

AFH (malignant) looks like a spindle cell tumor in a lymph node. It is desmin-positive but can be separated from smooth muscle tumors by its morphology and lack of cytoplasmic deep eosinophilia. Furthermore, it can be separated from CD99-positive Ewing sarcoma/PNET by prominent desmin reactivity. There may be some relationship between AFH (malignant) and fibroblastic reticulum cell sarcoma of lymphoid tissue.

Prognosis and Treatment

Fibrosarcoma variants, including those arising in DFSP, low-grade myxofibrosarcoma (Evan's tumor), and sclerosing epithelioid fibrosarcoma are generally low grade and mainly treated by complete excision and careful patient follow-up (26,80,81–85). Infantile fibrosarcoma is generally quite large but has overall good prognosis once excised. Infantile fibrosarcoma has a much better prognosis than adult fibrosarcoma (15,16,45,86,87). These patients have lower recurrence rates, less mortality, and less metastasis (15–17,83,88). In children, five-year survival rates are 85% to 95%. Local recurrence is present in fewer than 30% of cases, and distant metastases occur in approximately 5% of cases; however, distant metastases have been reported to occur as long as 20 years after initial therapy. Children older than 10 years have survival rates similar to those of adults. The treatment is most commonly surgical excision, but chemotherapy can also be used (88–91).

Storiform pleomorphic, giant cell–rich, and inflammatory malignant fibrous histiocytomas are intermediate to high-grade sarcomas that require adjuvant therapy. Myxofibrosarcoma is usually low to intermediate grade, requiring adjuvant therapy for grade 2/3 lesions, per clinical recommendation (92). AFH (malignant) is treated by surgical excision alone, sometimes excision of a regionally involved lymph node (37). The patients tend to do well, even those exceedingly rare patients with an excised pulmonary metastasis.

Prognosis is thought to be related to the grade of the tumor, the size of the tumor, high cellularity with little collagen, mitotic rate, necrosis, and positive margins (82). As with many tumors, the chance of local recurrence correlates with the completeness of excision. Depending on the study, the rate of recurrence and metastasis for patients with fibrosarcoma arising in DFSP is about double compared with DFSP alone (1,35,83,93–95). These tumors usually do not metastasize to lymph node. More commonly, they metastasize to either the bone or the pulmonary system (83). Expected five-year survival for a patient with fibrosarcomatous transformation ranges between 39% and 54% (1,81,83,96).

The overall mortality rate with malignant fibrous histiocytoma is 40% to 45%. Age appears to be correlated with mortality; one group reported a mortality rate of 72% in patients older than 60 years and a 33% mortality rate in patients aged 20 to 39 years. Local recurrence is present in 20% to 42% of cases; regional lymph node involvement occurs in 0% to 15% of cases; and distant metastases are found in 25% to 35% of cases. Recurrence usually occurs within two years of treatment. Recently, the chromosomal abnormality 19p+ has been demonstrated in malignant fibrous histiocytoma. Local recurrence is more common in tumors with 19p+. Distant metastases are more common in high-grade tumors and tumors larger than 5 cm.

B. Malignant Triton Tumor (Malignant Peripheral Nerve Sheath Tumor with Rhabdomyoblastic Differentiation)

Introduction

This tumor, first described in 1932 by Masson, is a malignant peripheral nerve sheath tumor with rhabdomyoblastic differentiation (1). It has not been intensively recently studied and many questions as to its overall comparable prognosis to malignant peripheral nerve sheath tumor, its incidence in neurofibromatosis, and others still remain (2,3).

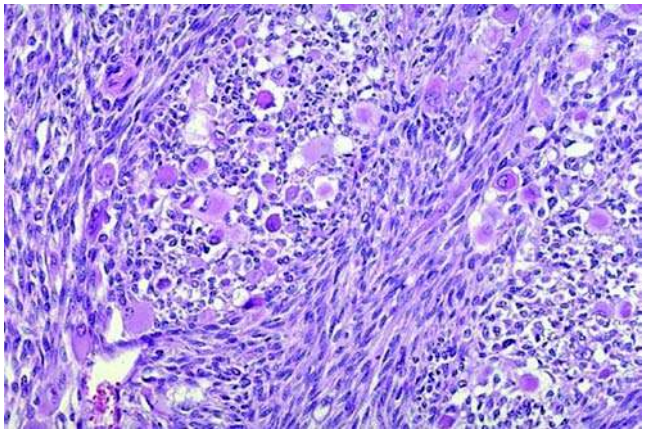

Figure 151 Malignant triton tumor is a malignant peripheral nerve sheath tumor with rhabdomyoblastic differentiation.

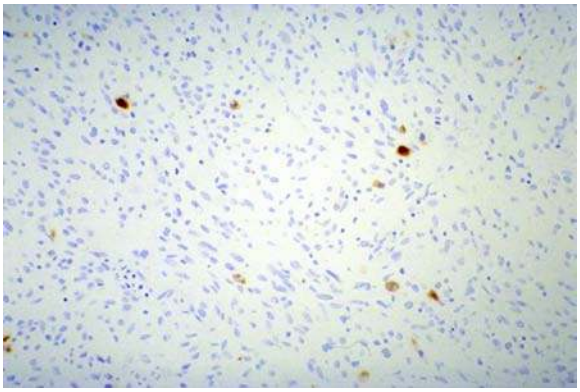

Figure 153 In malignant triton tumor, the scattered rhabdoymoblasts are positive for desmin.

Clinical Findings

One-third of malignant triton tumors occur in the head and neck (4–6), including the neck, sinonasal tract (7–11), oral cavity (12), face, parotid gland (13), maxilla (14,15), thyroid (16,17), acoustic nerve, palate, and temporal fossa (18). There is a strong association with type 1 neurofibromatosis (19–21). Tumors occurring de novo are in patients in their fourth decade, younger in patients with neurofibromatosis (22). De novo tumors arise from nerve; those in neurofibromatosis often arise from preexisting deep, often plexiform neurofibroma. There is an equal gender distribution. Rarely, this tumor has been reported to arise after radiotherapy (23–25).

Radiologic Imaging

The lesions have a similar appearance as compared to other malignant peripheral nerve sheath tumors. On CT on MR imaging, a large soft tissue mass (>5 cm) with an entering and exiting tube (representing the involved nerve) creating a fusiform shape may be seen. There is often mild irregularity at the lesion margin, and lesion growth to involve the affected nerve may also be seen. Intrinsic characteristics are nonspecific with similar attenuation to muscle on CT, intermediate signal intensity on T1-weighted MR and high signal intensity on T2-weighted MR. Areas of necrosis and hemorrhage are common causing lesion heterogeneity on CT and MR imaging (26).

Pathologic Findings

Grossly these tumor may be seen entering a nerve and may be tan, necrotic, and large. Microscopically, they are composed of spindled cells with high nuclear to cytoplasmic ratio and perivascular tumor sparing with adjacent geographic necrosis and brisk mitotic activity. The only difference between this high-grade sarcoma and malignant peripheral nerve sheath tumor are the variable amount, and varying from field to field, of rhabdomyoblasts (Fig. 151). The rhabdomyoblasts have abundant eosinophilic cytoplasm, sometimes with cross striations and will exhibit atypical changes (Fig. 152). They are positive for desmin (Fig. 153) and skeletal muscle-specific myoregulatory proteins (nuclear MyoD1 and nuclear myf4/myogenin). By cytology, the rhabdomyoblasts are round to oval and have eccentric nuclei (27). It is important to distinguish these cells from entrapped

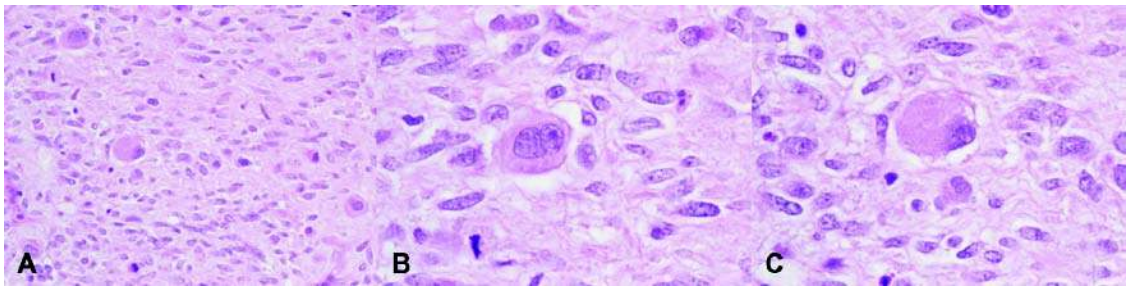

Figure 152 In malignant triton tumor(**A–C**), the rhabdomyoblasts are atypical and neoplastic (**B,C**) and are not just entrapped skeletal muscle fibers.

normal skeletal muscle fibers. A very rare variant of triton tumor has been described, which contained well-differentiated Schwann cells (28).

Immunohistochemistry

The malignant peripheral nerve sheath component may be focally positive for S-100 protein, sometimes positive for GFAP and the rhabdomyoblasts will stain for desmin and the myoregulatory proteins (nuclear Myo D1 and nuclear myf 4/myogenin) (29–31).

Molecular Findings

Cytogenetic studies of malignant triton tumors are rare, and in general, reveal complex karyotypes with structural aberrations, frequently involving the chromosomal bands or regions 1p31-36, 4q28-35, 7p22, 11q22-23, 19q13, 20q13, and 22q11-13. Similar genetic imbalances have been identified in malignant peripheral nerve sheath tumors (32–34). Although in a few cases balanced t(1;13), t(7;9) and unbalanced t(1;16) and t(14;15) translocations and isochromosome (8)(q10) have been reported as the sole karyotypic abnormalities (35–37), the triton tumor-specific genetic aberration remains elusive.

Differential Diagnosis

As mentioned, the differential diagnosis would include malignant peripheral nerve sheath tumor with entrapped normal skeletal muscle; this can be separated by the lack of atypia of the entrapped rhabdomyocytes, except when they are atrophic and have hyperchromatic multinucleation. If the rhabdomyocytes form a fascicle and are only in a very organized fashion in the tumor, this is likely entrapped skeletal muscle. Other tumors can be separated by morphology and immunohistochemistry.

Prognosis and Treatment

The overall prognosis is poor (38). There is much debate over whether malignant triton tumor has the same or worse prognosis than malignant peripheral nerve sheath tumor, but it clearly has a better prognosis when it occurs in some anatomic sites over others (19). The malignant triton tumors of the head tend to be of lower grade, less frequently associated with neurofibromatosis, and of better prognosis than those in the neck (5). In general, tumors associated with neurofibromatosis have a worse prognosis. Treatment for these high-grade sarcomas includes surgical resection and adjuvant therapy (6,39). Generally, radiation therapy and additive chemotherapy is given if tumors are greater than 5 cm or if the margins are positive.

C. Malignant Mesenchymoma

Introduction

In the 1940s, Stout first described eight cases of malignant mesenchymoma, a tumor that contained two or more sarcomatous elements that are unrelated and not expected to be seen together (1,2). Even then, pathologists realized that this definition was a simplification that needed further scrutiny. Some types of soft tissue tumors can have multiple soft tissue components, but are still not considered mesenchymomas. For example, angiomyolipoma, as is evident in its name, is a benign tumor demonstrating blood vessels, fat, and immature smooth muscle, but is not classified as a mesenchymoma. Malignant triton tumors show areas of malignant peripheral nerve sheath tumor and rhabdomyosarcomatous differentiation, but are also not placed under the rubric of mesenchymoma (3). Myofibroblastic components are not included in the definition of mesenchymoma, so dedifferentiated liposarcoma is best considered as is and not a mesenchymoma. Thus, the term ''mesenchymoma'' should be used with caution, and should only be considered if a tumor cannot be better classified.

Mesenchymoma is still accepted by the current World Health Organization classification (4). If mesenchymoma is used, then the diagnostic line should include the lines of differentiation in parentheses (5). Today most pathologists do not use the term mesenchymoma but rather list the predominant pattern of differentiation and the other soft tissue component(s). For example, a tumor could be labeled ''malignant mesenchymoma'' or ''osteosarcoma with rhabdomyoblastic differentiation.'' Most soft tissue pathologists opt to define the components.

Clinical Features

Although older studies attempted to better define epidemiologic features of patients with this diagnosis, these tumors do not form a single well-defined clinicopathologic entity. As such, these tumors show a great variety of clinical presentations. They can be found in all age groups and all locations in the body (6–17). Tumor size can range from small (<1 cm) to exceedingly large.

In some of the older medical literature, mesenchymomas consisted of 8% of all soft tissue neoplasms (18,19). But most would agree that by modern diagnostic standards and with stringent use of immunohistochemistry, this is an extremely rare diagnosis. The literature is primarily limited to a number of case reports and small series (10,20–22). Mesenchymoma has been reported in most sites of the head and neck (12–14,16,23–25). In a recent study by Adachi et al., only one of twelve mesenchymomas studies as found in the head and neck (26).

Pathology

Tumors must have several different soft tissue elements and therefore tend to be heterogeneous. One of the most commonly seen elements in a mesenchymoma are undifferentiated cells (27). However, sarcomas with areas of dedifferentiation are not generally considered mesenchymomas. A liposarcoma, which often has smooth muscle dedifferentiation, is still diagnosed as liposarcoma, and not a mesenchymoma. With immunohistochemistry, a clear lineage can now often be assigned to poorly differentiated areas.

Bone and cartilage are the soft tissue elements most frequently seen in these tumors. If a tumor

shows cartilage or bone formation plus a different soft tissue component, it might be considered a mesenchymoma (28). Yet, if the bone is clearly neoplastic (osteoid), the tumor is, by definition, an osteosarcoma. With chondroid elements, the tumor must fit into recognized chondrosarcoma variants (myxoid or mesenchymal) to be considered chondrosarcoma. If the predominant tumor is a myxoid liposarcoma, atypical lipomatous tumor, leiomyosarcoma, or RMS with metaplastic cartilaginous or osseous areas, it could either fit into the diagnostic criteria for mesenchymoma (6) or be called these predominant tumors with ''heterologous features.'' Sometimes it is difficult to discern whether the cartilage or osseous differentiation is metaplastic or malignant, so the word ''differentiation'' encompasses both processes. Leiomyosarcomas with areas of RMS also can fall under the rubric of mesenchymoma.

Imaging

The imaging appearance of mesenchymoma (benign or malignant) is typically nonspecific. CT and MR imaging may reveal components of fat, calcification, and nonspecific soft tissue.

Electron Microscopy

The ultrastructural features depend on which types of soft tissue are seen. Thus, smooth muscle, skeletal muscle (cross striations), bone, cartilage, and neural tissue, each have different features by electron microscopy (7). With the advent of immunohistochemistry and molecular, electron microscropy is rarely used for soft tissue diagnoses.

Treatment and Prognosis

Since this category tends to lump different types of tumor together and is uncommon, it is not easy to evaluate clinical outcome data. The propensity to metastasize may depend on which tissue morphology is present. Several studies have shown that the most prevalent malignant tissue component dictates prognosis (2,5,27, 38). In general, myoid sarcomas (RMS and leiomyosarcoma) have worse prognosis than other sarcomas (liposarcoma, etc.). In one recent study, there was a worse survival rate in patients with a rhabdomyosarcomatous component; but, there was no correlation with prognosis for the other mesenchymal components (26). This study also found that younger patients had a poorer outcome than older patients. Many mesenchymomas are high-grade malignant tumors with a poor prognosis (29). Unlike most of the published data, one study found mesenchymomas to be less aggressive (30). Interestingly, metastasis from a mesenchymoma may only show one of its histologic components (31). The relevance of this is undetermined.

Benign mesenchymomas. Mesenchymomas can be benign (24,32). Benign mesenchymomas have the same definition as malignant mesenchymomas: soft tissue tumors with more than one line of differentiation (33). In the benign mesenchymomas, each of the histologic components must appear benign on H&E. This is even a more rare diagnosis as benign bone and cartilage is metaplastic and benign skeletal muscle almost never found. In addition, myolipoma and lipoleiomyoma combine smooth muscle and fat into known clinicopathologic entities.

D. Mesenchymal Chondrosarcoma

Introduction

This rare chondrosarcoma subtype, first described by Lichtenstein and Bernstein in 1959, is identified by its bimorphic pattern of hyaline cartilage and a hemangiopericytoma-like round cell component (1). It occurs in intraosseous and extraskeletal locations, namely in the meninges, brain, and orbital soft tissue. It can occur in other head and neck sites, as well.

Clinical Findings

Most patients are in their second to third decade of life with an equal sex distribution. As above, the jaw (2–9), meninges (10,11), and orbit (12–16) are the most common sites. Of the jaw tumors, the maxilla and mandible are approximately equally involved (9). The patients present with long-term pain and swelling. Knott et al. looked at 13 cases in the sinonasal tract and found that patients presented with nasal obstruction (62%), epistaxis (54%), or mass effect (32%) (17). Those in the eye may experience proptosis and visual change (12,18,19).

Radiologic Imaging

Radiographs of mesenchymal chondrosarcoma reveal a soft tissue mass. Small punctuate calcification suggesting a chondroid matrix may also be apparent in 57% of cases by radiographs or CT. On MR imaging, extraskeletal mesenchymal chondrosarcoma demonstrate less water content than conventional chondrosarcoma with intermediate signal intensity on T1-weighting and intermediate to mildly high signal intensity on T2-weighting. Postcontrast images show prominent diffuse enhancement unlike conventional chondrosarcoma (mild peripheral and septal pattern) reflecting the hemangiopericytoma regions seen histologically. Areas of necrosis and hemorrhage may also be seen (20,21).

Pathologic Findings

Grossly, these tumors are gray-white, firm, defined tumors with necrosis and hemorrhage. Microscopically, these show distinctive islands of metaplastic cartilage that go from immature to hypertrophic chondrocytes and recapitulate growth plate (Fig. 154) admixed with adjacent sheets of small blue cells, with a hemangiopericytoid pattern (Fig. 155) (11,22,23). Often the cartilage mineralizes; while there is some consideration that there is morphologic overlap with small cell osteosarcoma (24,25), we believe these are undergoing endochondral ossification and these tumors can be separated from small cell osteosarcoma by SOX9 and osteocalcin.

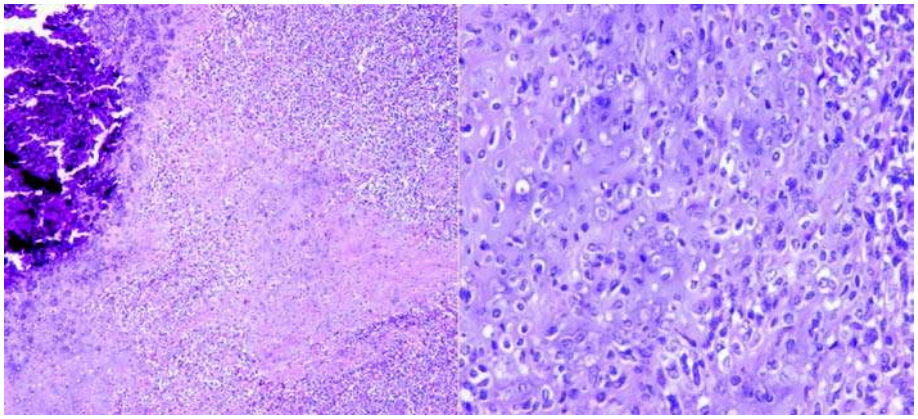

Figure 154 Mesenchymal chondrosarcoma are composed of hyaline cartilage metaplastic (*left*) and small round cells (*right*).

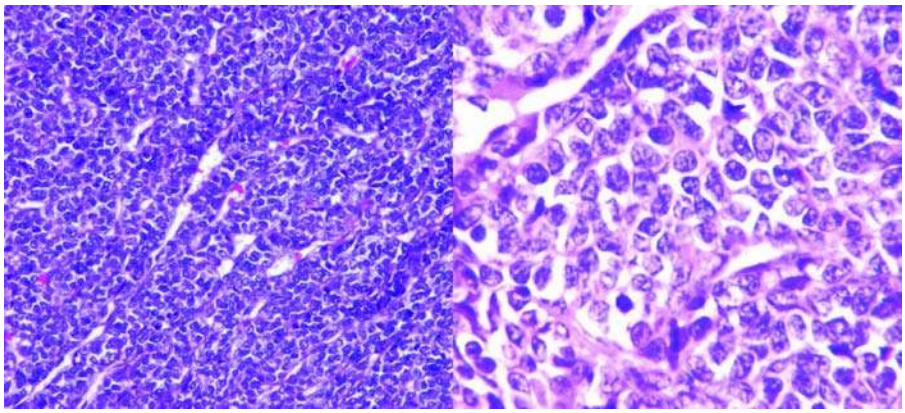

Figure 155 The small round-cell component often has a hemangiopericytoid vascular pattern.

Immunohistochemistry

The cartilage will be positive for S-100 protein and the small blue cell component positive for vimentin, Leu7, SOX9 (24,26), and CD99 (26–29).

Electron Microscopy

The cartilage shows chondrocyte-like appearance and the small cells are primitive mesenchymal cells, with little intercellular matrix, undifferentiated (30–34).

Molecular Findings

Rare cytogenetic studies of extraskeletal mesenchymal chondrosarcoma revealed either complex karyotypes or sole chromosomal abnormalities; however, no tumor-specific change has been identified yet (30,35–38,). An identical Robertsonian translocation involving chromosomes 13 and 21 [der(13;21)(q10;q10)] was detected twice and a t(4;9)(q23;q22) translocation once (36,38). Also in one case, a t(11;22)(q24;q12) translocation, commonly reported in PNET/Ewing tumor family, has been identified (37). Among other abnormalities, chromosome 8 trisomy has been found as the sole cytogenetic abnormality in one tumor (35). Extraskeletal myxoid chondrosarcoma is a completely different clinicopathologic entity, with different molecular changes (39–42).

Differential Diagnosis

The differential diagnosis includes other small round-cell tumors including small-cell osteosarcoma and PNET/Ewing sarcoma (43); these can be separated by their presence of osteoid in the former and t(11;22) for the latter. The hemangiopericytoid pattern suggests hemangiopericytoma or possibly monophasic synovial sarcoma (poorly differentiated type), both which can be separated from mesenchymal chondrosarcoma by their absence of hyaline cartilage (44). Additionally, hemangiopericytoma would be positive for CD34. Absences of keratins, especially CK7, and EMA and t(x;18) separate mesenchymal chondrosarcoma from synovial sarcoma.

Prognosis and Treatment

These are considered high-grade tumors and generally have poor prognosis, with the exception of those tumors from the jaw (6). Another study showed that tumors with a hemangiopericytoma-like pattern had a worse prognosis (9). Treatment includes resection and adjuvant therapy, as clinically indicated (45).

VI. MALIGNANT MIXED MESENCHYMAL AND EPITHELIAL PHENOTYPE

A. Synovial Sarcoma

Introduction

Synovial sarcoma is still considered under tumors of ''uncertain phenotype'' but we know that it has epithelial differentiation.

Clinical Findings

Synovial sarcoma, a tumor of young patients, is most common in non–head and neck locations, including lower extremity; but it also occurs in the head and neck in 10% of cases (1,2), particularly the neck and in parapharyngeal sites including pharynx and larynx. In the neck, synovial sarcoma is often found at the bifurcations of the carotid artery, intimately associated with the prevertebral fascia (3). Synovial sarcoma can also occur in the tongue, soft palate, trachea, and middle ear (4–8). Synovial sarcoma is a painful tumor, as it often occurs near a large nerve. Other symptoms are site specific, including hoarseness, dysphagia, dyspnea, dysphonia, otalgia, choking, hemoptysis, and weight loss. There is an equal sex distribution (2,9–15).

Radiologic Imaging

Synovial sarcoma typically reveals a large (>5 cm) heterogeneous soft tissue mass on CT or MR imaging. Areas of hemorrhage are common, which may create fluid levels and cause high signal intensity foci on T1-weighted and T2-weighted MR images. Calcification may be seen in up to 25% to 41% of cases best depicted on radiographs or CT. A lobular growth pattern (''bowl of grapes'' appearance) may also be seen. The triple sign on MR imaging (areas of low, intermediate, and high signal intensity on T2-weighting) has been reported in 35% to 57% of synovial sarcomas. Underlying bone erosion or involvement has been described in 10% to 20% of cases. Small lesions (>5 cm) may demonstrate a more homogeneous appearance on CT or MR imaging (16–19).

Pathologic Findings

Grossly, synovial sarcoma can occur near a nerve. It may be polypoid or lobular; hemorrhage may be present. Cyst formation can be observed. The tissue is often pink-gray and firm. Calcifications are not discernable grossly. Tumors range from 1 to 10 cm. Microscopically, synovial sarcoma is either biphasic

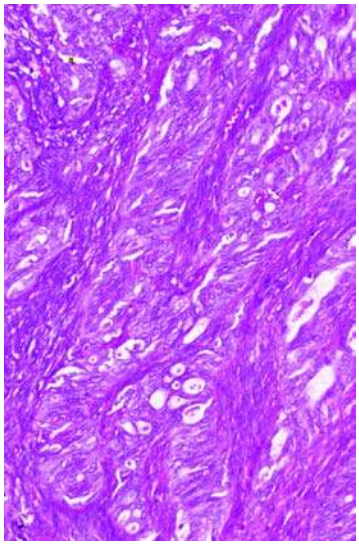

Figure 156 Biphasic synovial sarcoma with abundant epithelial component of glands and stromal spindled cells.

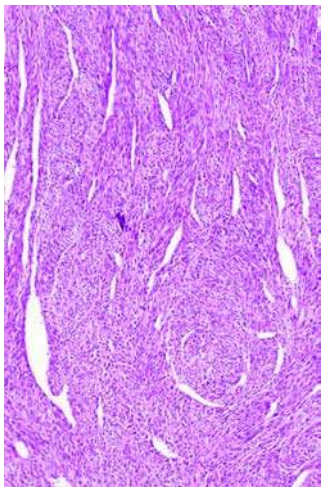

Figure 157 Monophasic synovial sarcoma demonstrating hemangiopericytoid vascular pattern.

(Fig. 156) or monophasic (Fig. 157) (9). Either type can be poorly differentiated. Biphasic synovial sarcoma is easily recognized by the spindled component and epithelial glands. The glands have varying morphologic patterns, including cribiform, interconnected, squamoid (20), columnar, or with intraluminal secretions, and are usually almost back to back with very little spindle cell component. Some cases can be mostly epithelial (21). Monophasic type is composed largely of spindled cells with uniform rather bland ovoid nuclei and a light and dark low-power appearance. The cytoplasm is often pink, giving the tumor a

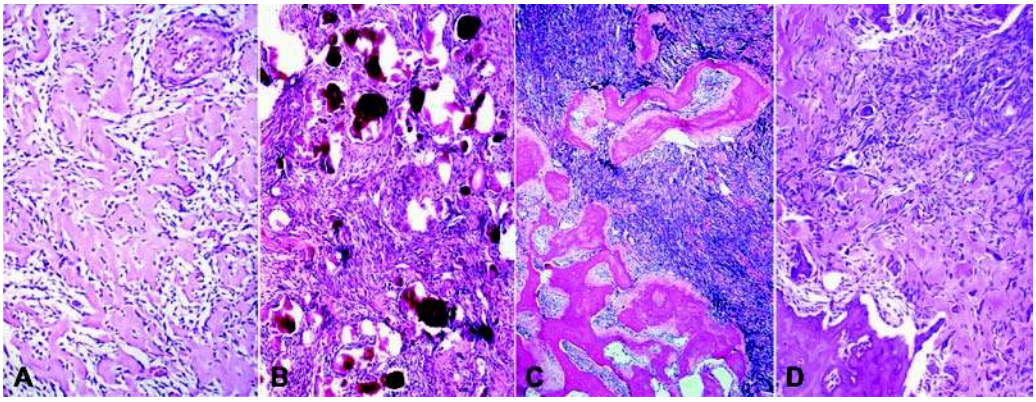

Figure 158 Stromal changes may include collagen (**A**) and psammoma-like calcifications (**B**) or bone (**C,D**) which can be detected on imaging studies.

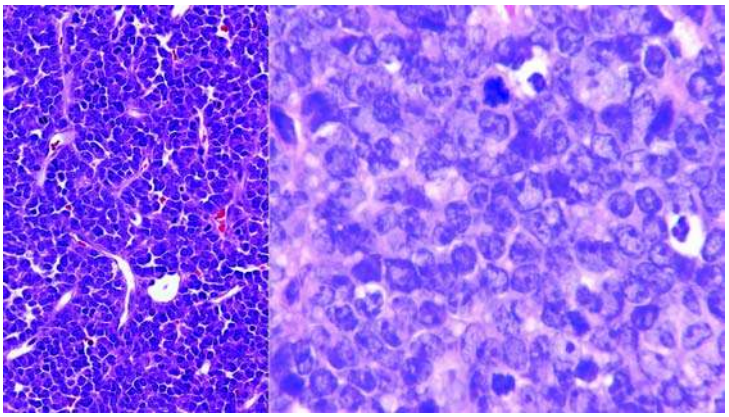

Figure 159 Poorly differentiated synovial sarcoma with epithelioid cells and high mitotic activity (>15/10HPF).

pink low-power appearance. Myxoid change can be seen (22,23), as can osteoid, bone or calcifications (Fig. 158) (24,25). There are mitoses and scattered mast cells. The stroma of either type, but more obvious in the monophasic type, can contain collagen, myxoid change, cysts, psammoma-like calcifications, or metaplastic bone. Staghorn, hemangiopericytoma-like vasculature is often present; there may be nuclear palisading of spindled cells. Poorly differentiated synovial sarcoma is of higher grade (usually grade 3 rather than grade 2), based on epithelioid or round cell morphology and increased mitotic activity (>15 mitoses/10HPF, Fig. 159) (26,27). Necrosis, particular geographic necrosis with perivascular tumor sparing, is often evident in poorly differentiated synovial sarcoma.

Immunohistochemistry

Synovial sarcoma must be positive for epithelial markers, usually pankeratin, EMA even more than keratin (Fig. 160), and CK7 in poorly differentiated tumors (28). S-100 stains residual nerve fibers in synovial sarcoma, in a ribbonlike fashion, but mostly not tumor cells. CD99 and bcl-2 are positive in synovial sarcoma, the former in a cytoplasmic membrane pattern, mimicking PNET/Ewing sarcoma (29). New markers that have been show to mark synovial sarcomas include the TEL antibody and the SYT protein (30,31).

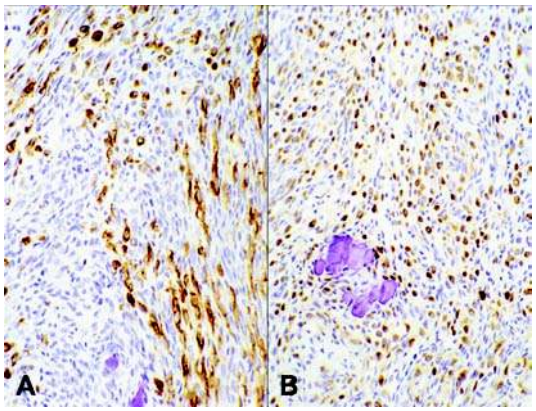

Figure 160 Immunostains on synovial sarcoma demonstrating EMA (**A**) and keratins (**B**) reactivity, respectively.

Electron Microscopy

The epithelioid cells have ovoid nuclei with narrow dense rims of chromatin and abundant cytoplasm containing mitochondria, Golgi complexes, rare paranuclear aggregates of intermediate filaments, lysosomes, smooth and rough endoplasmic reticulum occasionally in stacked arrays. They have microvilli or villous filopodia at their luminal surface, and sometimes contain electron dense mucinous material. They are connected by junctional complexes, zonulae adherens, or desmosome-like structures. The spindled cells have small nucleoli and marginated chromatin, with mitochondria and prominent Golgi but less endoplasmic reticulum than typical fibroblasts. The gland-like structures are separated from the spindled stroma by a continuous basal lamina (32–34).

Molecular Findings

The t(X;18)(p11;q11) translocation or its variants have been found in >90% of synovial sarcomas (35–37). This translocation involves the *SS18* gene (synovial sarcoma, translocation, chromosome 18), also known as *SYT*, and one of the *SSX* (synovial sarcoma X breakpoint) genes (38). Five different *SSX* genes have been identified (39), of which *SSX1* and *SSX2* are common *SS18* fusion partners (40,41), and *SS18-SSX4* fusions have been reported only in a few cases (42–45). The three fusion genes *SS18-SSX1, SS18-SSX2,* and *SS18-SSX4* account for >95% of synovial sarcomas; however negative cases might still represent rare variant translocation involving alternative gene partners. The fusion between *SS18L1* (*SS18-like gene 1*) and *SSX1* reported in one tumor confirmed the existence of genetic heterogeneity among a subset of synovial sarcomas (46). Majority of *SS18-SSX* fusions have the same junctions and heterogeneity within the fusion junctions is rare, though variant transcripts with different fusion junctions or with the insertion of additional genetic material have been described (40,41,45,47). It has been anticipated that the individual synovial sarcoma carries only one type of fusion; however, one study demonstrated in a subset of synovial sarcomas coexistence of *SS18-SSX1* and *SS18-SSX2* fusion (48). Both the normal SS18 and SSX proteins are localized in the nucleus and are involved in transcriptional regulation, with SS18 as an activator and SSX as a repressor of transcription. In the SS18-SSX fusion protein, C-terminal amino acids of SS18 are replaced by SSX transcription repression domain. Thus, it was hypothesized that SS18-SSX proteins function as ''activator-repressors'' of transcription. Also, it was suggested that SS18-SSX may cause aberrant transcriptional regulation through protein-protein interactions (37,49–51). Detection of t(X;18) translocations or *SYT-SSX* gene fusion transcripts are highly specific for the diagnosis of synovial sarcoma (37). Both FISH- and RT-PCR-based assays have been established for clinical routine testing (37,52) *SS18-SSX1* chimeric transcripts were found in biphasic tumors and their presence correlate with higher rates of proliferation and shorter metastatasis-free survival, while *SS18-SSX2* fusion transcripts were found predominantly in monophasic, spindle cell tumors, their presence being considered a favorable prognostic factor (53–56).

Differential Diagnosis

Biphasic synovial sarcoma must be distinguished from carcinosarcoma or metaplastic carcinoma. This can be done by absence of stromal mast cells and low-power light and dark appearance, a more pleomorphic spindle-cell component and the dirty necrosis of carcinoma. Low-grade malignant hemangiopericytoma is still positive for CD34 and negative for keratins and EMA; CD34 is negative in synovial sarcoma. Fibrosarcoma, now better classified as several distinct clinicopathologic entities (see section ''Fibrosarcoma/Malignant Fibrous Histiocytoma''), can readily be separated by its herringbone appearance and lack of keratins, EMA, and CK7. Spindled malignant peripheral nerve sheath tumor generally has a higher nuclear to cytoplasmic ratio than spindled monophasic synovial sarcoma, giving it a blue rather than pink low-power appearance. Although mast cells are common to both, they are more prevalent in synovial sarcoma. Malignant peripheral nerve sheath tumor is generally negative for keratins and EMA and is often positive for GFAP and focally for S-100 protein. Finally the t(x;18) gold diagnostic standard of synovial sarcoma readily separates it from all tumors above. Whenever one sees fibrous stroma with psammoma-like calcifications in it, in a young patient, one must exclude synovial sarcoma, as more characteristic, cellular areas will be found upon careful sampling, so fibrous lesions may be in the differential diagnosis as well as tumors with psammoma-like calcifications, separated by morphology, immunohistochemistry, and molecular from synovial sarcoma (25,57). Poorly differentiated synovial sarcoma often mimics Ewing sarcoma/PNET (58,59); these can be distinguished finally by the use of molecular tests.

Prognosis and Treatment

While synovial sarcoma of soft tissue has a 50% metastatic potential to lung, lymph node, and bone marrow, and is generally of intermediate-grade malignancy (grade 2/3), except poorly differentiated synovial sarcomas, which are high-grade malignant (grade 3/3); synovial sarcoma of the head and neck may have a slightly better prognosis since they are identified sooner and are thus smaller at presentation (60–62). Complete surgical excision and adjuvant therapy, as clinically recommended, are the current treatment (63,64). A total neck dissection is not performed in head and neck lesions (60,65,66). Metastases may be present at presentation or many years after initial diagnosis. Metastases from biphasic tumors may only have spindled morphology. Although controversial, there is no difference in prognosis between biphasic and monophasic types, grade for grade. Factors associated with a poor prognosis include increasing age, tumor size greater than 5 cm, and mitotic activity. Overall 5-year survival rates for synovial sarcoma of the head and neck are 36% to 51%, with a 10-year survival rate of 11.2% to 30%. Survival rates in children are 54% to 65% at five years.

B. Malignant Extrarenal Rhabdoid Tumor

Introduction

This is a controversial tumor. It is clearly recognized in the kidney as a homogeneous group of tumors with poor behavior in children less than two years. Also, in soft tissue and central nervous system (as atypical teratoid tumor), the latter often mixed with primitive round neuroectodermal tumor cells, seems to exist as an entity in infants and young children. However, tumors with rhabdoid features are common findings in many other poorly differentiated tumors, including carcinomas, synovial sarcomas, chondrosarcomas, melanomas, mesotheliomas, gastrointestinal stromal tumors, and even lymphomas, so the diagnosis of extrarenal rhabdoid tumor in adults is a diagnosis of exclusion, most being carcinomas with rhabdoid features.

Clinical Findings

Although uncommon in the head and neck (1), extrarenal rhabdoid tumor of soft tissue has been described in the neck (2) and paraspinal region (3), scalp, forehead (4), orbit (5–9), lacrimal gland (10), nasopharynx, and tongue (11) of both children and adults. In the tongue, the tumor presents with respiratory distress, in other soft tissue sites it presents with a mass or swelling (11). Some of the soft-tissue extrarenal rhabdoid tumors are associated with intracranial tumors, including small round cell tumors.

Radiologic Imaging

Imaging of extrarenal rhabdoid tumor has only rarely been reported. CT and MR imaging are ideal to evaluate lesion extent for staging. Intrinsic appearances are that of a nonspecific soft tissue tumor.

Pathologic Findings

These are firm gray-tan tumors with necrosis and may be large. Microscopically, the prototype would include sheets of large polygonal tumor cells (Fig. 161) with abundant eccentric eosinophilic cytoplasm and nuclei with large nucleoli (Fig. 162). The cytoplasm is often rounded and has a hard eosinophilic ''inclusion'' of intermediate filaments (mostly vimentin). The tumors are mitotically active, often with atypical forms, and usually demonstrate necrosis. If the necrosis is ''dirty'' with debris from acute inflammatory cells, and there are prominent eosinophilic nucleoli, it is likely that the tumor is a carcinoma or melanoma much more than a sarcoma.

Immunohistochemistry

Theoretically, these tumors are positive for keratins, EMA, vimentin, and CD99, as well as other neural markers seen in PNET/Ewing sarcoma, including synaptophysin, NSE, and sometimes focal S-100 protein. They are negative for CD34, desmin, myoregulatory proteins, and all melanoma markers. Extrarenal rhabdoid tumors show negative nuclear staining for the INI1 antibody, which corresponds to inactivation of the SNF5/INI1 tumor suppressor gene (12–16). Some studies have used this antibody to differentiate extrarenal rhabdoid tumor from other sarcomas, although synovial and epithelioid sarcomas may show variable or focal expression of the antibody (16).

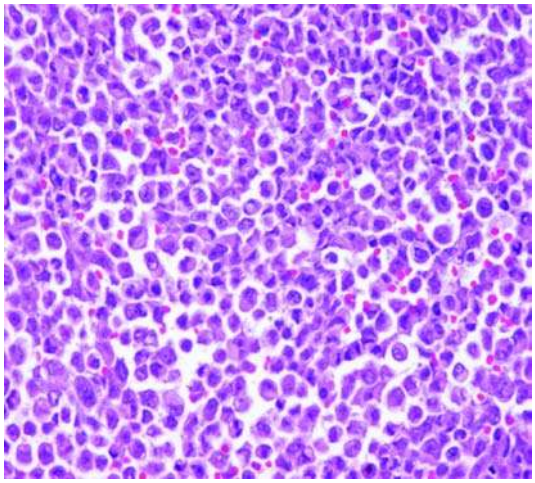

Figure 161 Rhabdoid features, seen in this extrarenal rhabdoid tumor, can be common to many tumors.

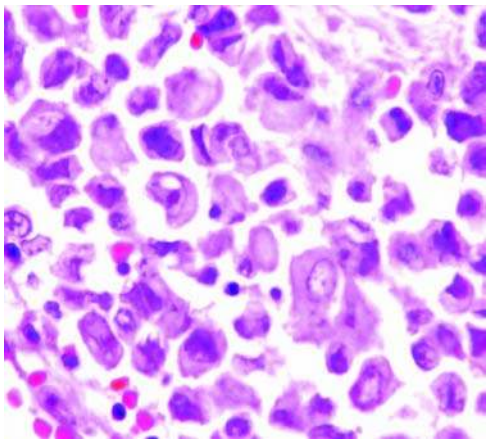

Figure 162 The features of extrarenal rhabdoid tumor or "rhabdoid features" include an eccentric eosinophilic "inclusion-like" cytoplasm, large vesicular nucleus, and prominent nucleolus. Also, there is usually abundant necrosis (not demonstrated here) that should not be "dirty."

Electron Microscopy

By electron microscopy, the paranuclear inclusions are composed of intermediate filaments whorls that may incorporate mitochondria, lipid droplets, or fragments of endoplasmic reticulum (17). There is absence of desmosomes between cells.

Molecular Findings

The *SMARCB1* gene (SWI/SNF-related, matrix-associated, actin-dependent regulator of chromatin, subfamily B, member 1, also known as hSNF5 or INI1), which encodes one of the proteins from ATP-dependent chromatin-remodeling complex, has been shown to be inactivated in extrarenal malignant rhabdoid tumor (MRT) (18). Initially, cytogenetic studies revealed monosomy of chromosome 22 and deletions or translocations involving chromosome band 22q11.2 (18–22). Subsequent molecular genetic studies identified deletions, nonsense mutations, frameshift mutations and other intragenic mutations in *SMARCB1* gene mapped to 22q11.2 (23–25). Presence of biallelic loss-of-function mutations suggested that *SMARCB1* has a tumor suppressor gene function. However, the precise mechanism by which inactivation of SMARCB1 promotes oncogenesis is still unknown. Also, constitutional loss-of-function SMARCB1 mutations were reported in the families with inherited rhabdoid tumor predisposition syndrome (26). This further supports the hypothesis that SMARCB1 acts as a tumor suppressor gene. Since biallelic loss-of-function mutations affecting *SMARCB1* have not been reported in any other soft-tissue tumors, detection of such alterations can support diagnosis of extrarenal MRT. However, this might require comprehensive genetic testing including karyotyping, FISH-, and PCR-based studies.

Differential Diagnosis

As described above, the differential diagnosis is broad. Tumors with ''dirty necrosis'' and/or prominent eosinophilic nucleoli are most likely carcinomas or melanoma; and either additional keratins (CK18) or melanoma markers such as S-100 may, respectively, separate these from extrarenal rhabdoid tumor (15,27–30). Proximal type epithelioid sarcoma can be positive for CD34, a marker that is negative in extrarenal rhabdoid tumor (31). Other tumors, such as chondrosarcoma, synovial sarcoma, and gastrointestinal stromal tumor should be distinguished by more conventional areas of tumor and immunostains.

Prognosis and Treatment

All tumors with rhabdoid features have poor prognosis, regardless of phenotype. Treatment for extrarenal rhabdoid tumor is by surgery and adjuvant therapy, with metastases to lung, liver, and lymph nodes, and only a 15% five-year survival (32,33).

VII. UNCERTAIN PHENOTYPE

A. Alveolar Soft Part Sarcoma

Introduction

ASPS occurs mainly in the buttocks and other extremity or trunk sites but can also occur in the head and neck (1), particularly in the orbit and tongue. This tumor is composed of large epithelioid cells arranged in solid nests or alveolar structures, separated by fibrous septa and thin sinusoidal vessels. This is still a tumor of uncertain phenotype. It was thought to have myoid features (2–4) because of the focal desmin found in these tumors and MyoD1, which only stains the cytoplasm and should be interpreted as negative. Only nuclear reactivity is found to be positive for this skeletal muscle-specific myoregulatory protein—MyoD1, so there is no support for a skeletal muscle phenotype in ASPS.

Clinical Findings

Typically found in non–head and neck sites (3,5,6), such as buttocks, this tumor can occur in head and neck (4,7,8) and oral sites, particularly the tongue (9–19). In the tongue, these occur primarily in children. These start off as the solid variant in young children and become more ''alveolar'' as the child is older. Even laryngeal ASPS has been reported (16,20), as well as cheek (16,21) and nasal (22). In the orbit, ASPS presents with proptosis and lid swelling. ASPS, in general, is a tumor of children and young adults, and there is a female predominance. ASPS grows slowly as a painless mass; sometimes metastasis to brain and lung are the presenting symptoms or can be found many years after disease onset (23,24).

Radiologic Imaging

ASPS often reveals relatively distinctive characteristics on MR imaging. These lesions have nonspecific intrinsic feature on CT and MR imaging with attenuation similar to muscle, intermediate signal intensity on T1-weighting and high signal intensity on T2-weighting. MR imaging reveals prominent feeding high flow serpentine vascular structures with similar channels within the lesion. Dynamic contrast enhanced CT, arteriography, and Doppler sonography may also reveal these vascular structures. Biopsy through the vascular components should be voided to limit bleeding (16,25,26).

Pathologic Findings

Grossly, ASPS is pale yellow-gray and may be soft with areas of necrosis and hemorrhage. Histologically, these can range from solid type (in the tongue of very young children) to having a more ''alveolar'' pattern (Fig. 163). The solid pattern has polygonal cells with abundant eosinophilic cytoplasm and prominent nucleoli. The ''alveolar'' pattern shows groups of tumor cells separated by fibrous septa, in an organoid pattern. The cells tend to slough off from the fibrous septa and vessels that separate the cells into alveoli and ''float'' in the center of the ''alveolus.'' The cells are characterized by large prominent nucleoli in eccentric nuclei with abundant cytoplasm, which can be eosinophilic and finely granular to clear. Cytologic atypia is rarely observed (Fig. 164). Sometimes it appears that the nuclei in ASPS have a ''bite'' taken out of it, as in a ''cookie-bite'' appearance (Fig. 165). Mitotic figures are uncommon, although vascular or lymphatic invasion at presentation (in every case) is

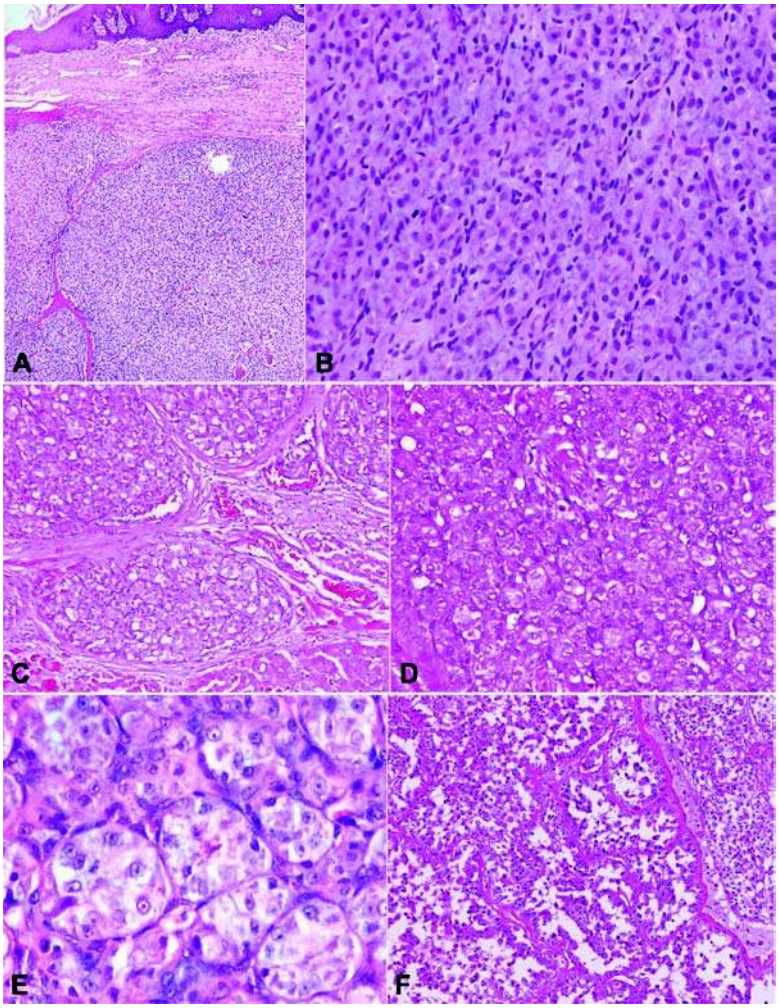

Figure 163 The spectrum of solid ASPS in infants and young children (**A,B**) to alveolar ASPS in older children (**C–E**) and adults (**F**) (sequentially). Note the solid sheetlike appearance of the solid type in the tongue to the vague nodularity to the alveolar pattern by vessels to the cells falling into the "alveoli" in the alveolar pattern.

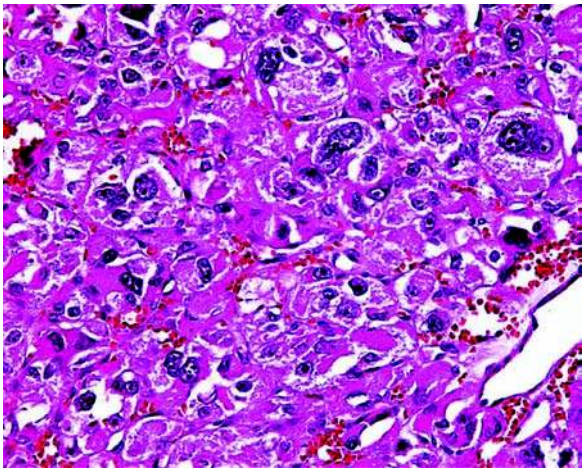

Figure 164 In rare cases, ASPS can demonstrate cytologic atypia.

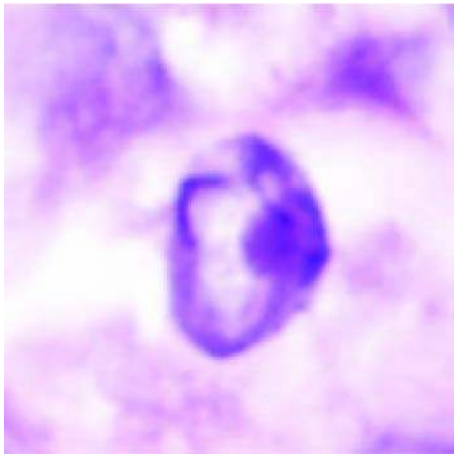

Figure 165 The nuclei in ASPS often have a "cookie bite" concave (*top of cell*) nuclear appearance.

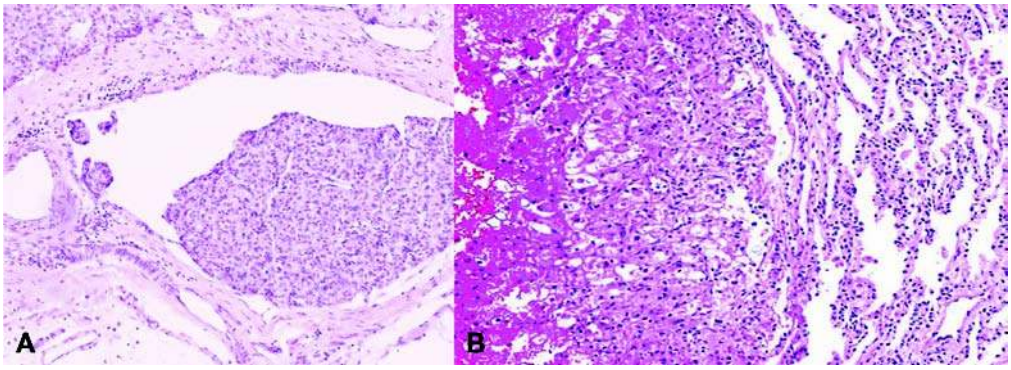

Figure 166 Intralymphatic growth is always identified in ASPS (**A**). When metastatic, it can metastasize to lung and be difficult to separate from lung parenchyma because of the alveolar pattern, but note the cells filling and the hemorrhage (**B**).

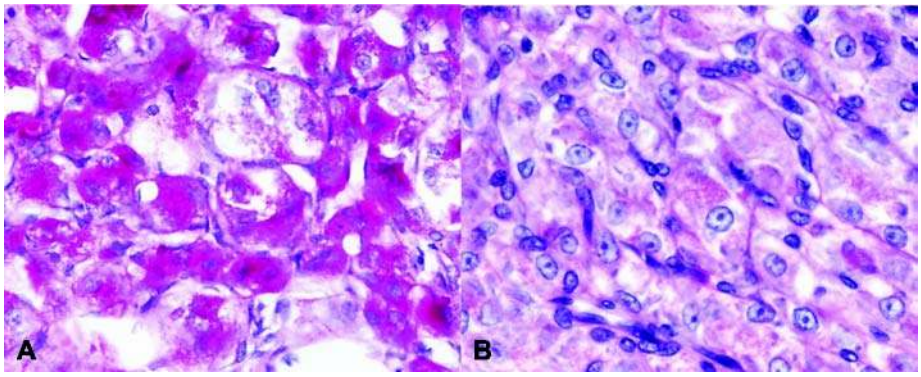

Figure 167 ASPS is characterized by PAS-positive crystals or granules, varying from abundant (**A**) to focal (**B**).

identified (Fig. 166). Metastases to lung may be hard to separate from true ''alveoli'' although the tumor is still cellular and exhibits hemorrhage (Fig. 166). On PAS stain, after diastase digestion, one can observe the cytoplasmic granular to crystalline inclusions, varying from rare to few to up to abundant (Fig. 167) (27).

Immunohistochemistry

ASPS is only identified on special stains by the PAS with diastase (-D), which demonstrates PAS-D positive granular or crystalline structures (27). Immunohistochemical stains show only consistent negativity for vimentin, unlike any other mesenchymal tumor, and consistent cytoplasmic MyoD1 (which is interpreted as negative). Desmin and S-100 protein are occasionally positive, but skeletal muscle-specific markers, including MyoD1 and myf4 myogenin, are negative (15,28,29). TFE3 is a molecular marker that can be detected by immunohistochemistry (Fig. 168).

Electron Microscopy

The nests of tumor cells are surrounded by discontinuous basal lamina; the cell membranes joined by discontinuous basal lamina. There are numerous mitochondria, prominent Golgi complexes, and abundant rough endoplasmic reticulum. The most characteristic features are the membrane bound or free rhomboid crystals with a periodicity of 10 nm. Secretory granules containing this crystalline material are also sometimes present (27,30).

Molecular Findings

A nonreciprocal t(X;17)(p11;q25) translocation has been found in ASPS (31). This translocation leads to rearrangement and fusion of *ASPL* (ASPS locus), also called ASPSCR1 (ASPS chromosome region, candidate 1), and *TFE3* (transcription factors for immunoglobulin heavy-chain enhancer 3) genes. Two variants of *ASPL-TFE3* gene fusion, involving second and third intron of *ASPL*, have been reported; however, biologic significance of the different fusion types is unknown (32). Both *ASPL-TFE3* gene fusions encode chimeric protein consisting of ASPL N-terminal region fused to TFE3 basic helix-loop-helix and leucine zipper DNA-binding domains. Expression of ASPL-TFE3 chimeric protein is believed to cause transcriptional deregulation and has been implicated as a possible tumorigenic mechanism (32–34). Detection of t(X;17)

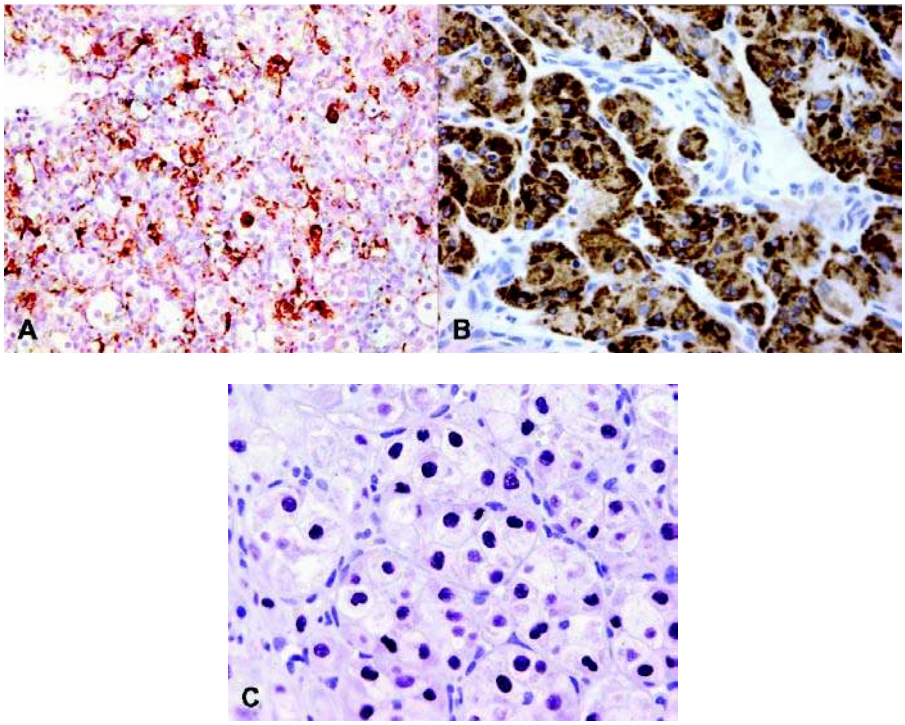

Figure 168 Immunohistochemistry for desmin (**A**) and MyoD1 (**B**), the latter which consistently stains cytoplasm, not nuclei, so is interpreted as negative, not supporting considerations of skeletal muscle phenotype. Newer genetic-based immunohistochemical marker, TFE3, is a nuclear immunohistochemical stain (**C**).

translocation or *ASPL-TFE3* fusion transcripts can be used in differential diagnosis of ASPS. However, similar but reciprocal t(X;17) (p11;q25) translocation and *ASPL-TFE3* gene fusion transcripts have been identified in the variant of childhood renal cell carcinoma. Also, *TFE3* was found to be involved in several variant translocations associated with papillary renal cell carcinomas (35–37).

Differential Diagnosis

The differential diagnosis for solid ASPS of the tongue includes rhabdomyoma, granular cell tumor, and hibernoma (the latter by morphology). Adult rhabdomyoma can be separated by its large eosinophilic cells with small nuclei and the ''spider'' like cytoplasmic features as the cytoplasm pulls away from the cell membrane. Furthermore, desmin would be diffuse and strong in rhabdomyoma, as would the skeletal muscle nuclear markers: MyoD1 and myf4 (skeletal muscle-specific myogenin). While it also has eosinophilic cytoplasm, granular cell tumor has more granularity than ASPS and contains cytoplasmic circular inclusions with halos, lysosomal material, which is absent in ASPS. Furthermore, the nuclei in benign granular cell tumor are uniform and without diffuse pleomorphism or prominent nucleoli, unlike the prominent nucleoli in ASPS. Lastly, S-100 protein is diffusely positive in granular cell tumor, a tumor of nerve sheath phenotype, and is negative in ASPS. When the lesion is completely alveolar, clear cell sarcoma may be in the differential diagnosis, but that tumor is positive for HMB45 protein, always absent in ASPS.

Prognosis and Treatment

In the tongue, solid ASPS has relative good behavior, unlike the metastatic potential for ASPS in other non–head and neck anatomic sites. Complete local excision and patient follow-up is advised. Adjuvant therapy should be used per clinical recommendation. ASPS is associated with a deceptively indolent course. Distant metastasis is present in 25% of patients at initial presentation and most commonly involves the lung, bone, and brain. Local recurrence and metastatic involvement can occur over a long period, contrary to other head and neck sarcomas. Local recurrence occurs in 20% of patients. Approximately 60% of patients who are free of metastases at initial presentation have distant metastases at some point after initial treatment. The survival rate at five years is reported to be 65%; however, when patients are monitored over time, the survival rate decreases to 38% at 10 years and 15% at 20 years.

Orbital (and tongue) ''solid type'' ASPSs are associated with a disease-free survival period longer than that of other sites in the head and neck. Children have a better overall survival rate compared with that of adults. Adjuvant radiation therapy or chemotherapy has not been shown to provide any improvement in disease control or survival.

REFERENCES

PART I

A. Papillary Endothelial Hyperplasia

1. Masson P. Hemangioendotheliome vegetant intravasculaire. Bull Soc Anat (Paris) 1923; 93:517.
2. Hashimoto H, Daimaru Y, Enjoji M. Intravascular papillary endothelial hyperplasia. A clinicopathologic study of 91 cases. Am J Dermatopathol 1983; 5:539–546.
3. Kuo T, Gomez LG. Papillary endothelial proliferation in cystic lymphangiomas. A lymphatic vessel counterpart of Masson's vegetant intravascular hemangioendothelioma. Arch Pathol Lab Med 1979; 103:306–308.
4. Pins MR, Rosenthal DI, Springfield DS, et al. Florid extravascular papillary endothelial hyperplasia (Masson's pseudoangiosarcoma) presenting as a soft-tissue sarcoma. Arch Pathol Lab Med 1993; 117:259–263.
5. Clearkin K, Enzinger F. Intravascular papillary endothelial hyperplasia. Arch Pathol Lab Med 1976; 100:441–444.
6. Kuo T, Sayers CP, Rosai J. Masson's ''vegetant intravascular hemangioendothelioma:'' a lesion often mistaken for angiosarcoma: study of seventeen cases located in the skin and soft tissues. Cancer 1976; 38:1227–1736.
7. McClatchey KD, Batsakis JG, Young SK. Intravascular angiomatosis. Oral Surg Oral Med Oral Pathol 1978; 46:70–73.
8. Amerigo J, Berry CL. Intravascular papillary endothelial hyperplasia in the skin and subcutaneous tissue. Virchows Arch A Pathol Anat Histol 1980; 387:81–90.
9. de Courten A, Kuffer R, Samson J, et al. Intravascular papillary endothelial hyperplasia of the mouth: report of six cases and literature review. Oral Dis 1999; 5: 175–178.
10. Tosios K, Koutlas IG, Papanicolaou SI. Intravascular papillary endothelial hyperplasia of the oral soft tissues: report of 18 cases and review of the literature. J Oral Maxillofac Surg 1994; 52:1263–1268.
11. Lancaster JL, Alderson DJ, Sherman IW, et al. Papillary endothelial hyperplasia (Masson' tumour) of the maxillary sinus. J Laryngol Otol 1998; 112:500–502.
12. Nishimoto K, Takaki M, Hirase H, et al. Extravascular papillary endothelial hyperplasia arising from parapharyneal space. Auris Nasus Larynx 2004; 31:305–308.
13. Sezgin S, Kotiloglu E, Kaya H, et al. Extravascular papillary endothelial hyperplasia of the larynx: a case report and review of the literature. Ear Nose Throat J 2005; 84:52–53.
14. Stewart M, Smoller BR. Multiple lesions of intravascular papillary endothelial hyperplasia (Masson's lesions). Arch Pathol Lab Med 1994; 118:315–316.
15. Kreutner A Jr., Smith RM, Trefny FA. Intravascular papillary endothelial hyperplasia: light and electron microscopic observations of a case. Cancer 1978; 42:2304–2310.
16. Hunt SJ, Santa Cruz DJ. Vascular tumors of the skin: a selective review. Semin Diagn Pathol 2004; 21:166–218.
17. Chan J, Fletcher C, Hicklin G, et al. Glomeruloid hemangioma. A distinctive cutaneous lesion of multicentric Castleman's disease associated with POEMS syndrome. Am J Surg Pathol 1990; 14:1036–1046.
18. Weiss SW, Enzinger FM. Spindle cell hemangioendotheliomas: a low grade angiosarcoma resembling a cavernous hemangioma and Kaposi's sarcoma. Am J Surg Pathol 1986; 10:521–530.
19. Perkins P, Weiss SW. Spindle cell hemangioendothelioma. An analysis of 78 cases with reassessment of its pathogenesis and biologic behavior. Am J Surg Pathol 1996; 20: 1196–1204.

B. Arteriovenous Hemangioma (Arteriovenous Malformation)

1. Kohout M, Hansen M, Pribaz JJ, et al. Arteriovenous malformations of the head and neck: natural history and management. Plast Reconstr Surg 1998; 102:643–654.
2. Girard C, Graham JH, Johnson WC. Arteriovenous hemangioma (arteriovenous shunt). A clinicopathological and histochemical study. J Cutan Pathol 1974; 1:73–87.
3. Carapeto FJ, Garcia-Perez A, Winkelmann RK. Acral arteriovenous tumor. Acta Derm Venereol 1977; 57:155–158.
4. Connelly MG. Winkelmann RK. Acral arteriovenous tumor. A clinicopathologic review. Am J Surg Pathol 1985; 9:15–21.
5. Angervall L, Nielsen JM, Stener B, et al. Concomitant arteriovenous vascular malformation in skeletal muscle: a clinical, angiographic and histologic study. Cancer 1979; 44:232–238.
6. Sako Y, Varco RL. Arteriovenous fistula: results of management of congenital and acquired forms, blood flow measurements, and observations on proximal arterial degeneration. Surgery 1970; 67:40–61.
7. Calonje E. Haemangiomas. Vascular tumors. In: Fletcher CDM, Unni KK, Mertens F, eds. Tumours of Soft Tissue and Bone. Lyon, France: IARC Press, 2002:156–158.
8. Malan E, Azzolini A. Congenital arteriovenous malformations of the face and scalp. J Cardiovasc Surg 1968; 9: 109–140.
9. Jackson IT, Carreno R, Potaric Z, et al. Hemangiomas, vascular malformations, and lymphovenous malformations: classification and methods of treatment. Plast Reconstr Surg 1993; 91:1216–1230.
10. Chen MT, Horng SY, Yeong EK, et al. Treatment of high-flow vascular malformations in the head and neck with arterial ligation followed by sclerotherapy. Ann Plast Surg 1996; 36:147–153.
11. Jeong H-S, Baek C-H, Son Y-I, et al. Treatment for extracranial arteriovenous malformations of the head and neck. Acta Otolaryngol 2006; 126:295–300.
12. Fishman SJ, Mulliken JB. Hemangiomas and vascular malformations of infancy and childhood. Pediatr Surg 1993; 40:1177–1200.
13. Mulliken JB, Glowack IJ. Hemangiomas and vascular malformations in infants and children: a classification based on endothelial characteristics. Plast Reconstr Surg 1982; 69:412–422.
14. Burchell HB. Observations on bradycardia produced by occlusion of an artery proximal to an arteriovenous fistula (Nicoladoni-Branham sign). Med Clin North Am 1958; 42:1029–1035.
15. Rusin LJ, Harrell ER. Arteriovenous fistula. Cutaneous manifestations. Arch Dermatol 1976; 112:1135–1138.
16. Marshall M, Hatfield S, Hatfield D. Arteriovenous malformation simulating Kaposi's sarcoma (pseudo-Kaposi's sarcoma). Arch Dermatol 1985; 121:99–101.
17. Holman E. Contributions to cardiovascular physiology gleaned from clinical and experimental observations of abnormal arteriovenous communication. J Cardiovasc Surg 1962; 3:48–63.
18. Chooi WK, Woodhouse N, Coley SC, et al. Pediatric head and neck lesions: assessment of vascularity by MR digital subtraction angiography. AJNR 2004; 25:1251–1255.
19. Perkins JA, Sidhu M, Manning SC, et al. Three-dimensional CT angiography imaging of vascular tumors of the head and neck. Int J Pediatr Otorhinolaryngol 2005; 69:319–325.
20. Connor SEJ, Flis C, Langdon JD. Vascular masses of the head and neck. Clin Radiol 2005; 60:856–868.

21. Yakes WF, Rossi P, Odink H. Arteriovenous malformation management. Cardiovasc Intervent Radiol 1996; 19:65–71.
22. Koutlas IG, Jessurun J. Arteriovenous hemangioma: a clinicopathological and immunohistochemical study. J Cutan Pathol 1994; 21:343–349.
23. Adegboyega PA, Qui S. Hemangioma versus vascular malformation. Presence of nerve bundle is a diagnostic clue for vascular malformation. Arch Pathol Lab Med 2005; 129:772–775.
24. Rao VK, Weiss SW. Angiomatosis of soft tissue. An analysis of the histologic features and clinical outcome in 51 cases. Am J Surg Pathol 1992; 16:764–771.
25. North PE, Waner M, Mizeracki A, et al. GLUT1: a newly discovered immunohistochemical marker for juvenile hemangiomas. Hum Pathol 2000; 31:11–22.
26. Lawley LP, Cerimele F, Weiss SW, et al. Expression of Wilms tumor 1 gene distinguishes vascular malformations from proliferative endothelial lesions. Arch Dermatol 2005; 141:1297–1300.
27. Marler JJ, Mulliken JB. Current management of hemangiomas and vascular malformations. Clin Plastic Surg 2005; 32:99–116.

C. Hemangiomas

1. Mulliken JB, Glowacki J. Hemangiomas and vascular malformations in infants and children: a classification based on endothelial characteristics. Plast Reconstr Surg 1982; 69:412–422.
2. Weiss SW. Vascular tumors: a deductive approach to diagnosis. Surg Pathol 1989; 2:185–201.
3. Fletcher CDM, Unni KK, Mertens F. WHO Classification of soft tissue tumours. In: Fletcher CDM, Unni KK, Mertens F, eds. Tumours of Soft Tissue and Bone. Lyon, France: IARC Press, 2002:10–11.
4. Childers EL, Furlong MA, Fanburg-Smith JC. Hemangioma of the salivary gland: a study of ten cases of a rarely biopsied/excised lesion. Ann Diagn Pathol 2002; 6 (6):339–344.
5. Metry D. Update on hemangiomas of infancy. Curr Opin Pediatr 2004; 16:373–377.
6. Bowers RE, Graham EA, Tomlinson KM. The natural history of strawberry nevus. Arch Dermatol 1960; 82:667–680.
7. Gonzalez-Crussi F, Reyes-Mugica M. Cellular hemangiomas of infancy (''hemangioendotheliomas''). Light microscopic, immunohistochemical, and ultrastructural observations. Am J Surg Pathol 1991; 15:769–778.
8. North PE, Waner M, Mizeracki A, et al. A unique microvascular phenotype shared by juvenile hemangiomas and human placenta. Arch Dermatol 2001; 137:559–570.
9. Boye E, Yu Y, Paranya G, et al. Clonality and altered behavior of endothelial cells from hemangiomas. J Clin Invest 2001; 107:745–752.
10. Walter JW, North PE, Waner M, et al. Somatic mutation of vascular endothelial growth factor receptors in juvenile hemangioma. Genes Chromosomes Cancer 2002; 33: 295–303.
11. Marchuk DA. Pathogenesis of hemangioma. J Clin Invest 2001; 107:665–666.
12. Bauland CG, van Steensel MAM, Steijlen PM, et al. The pathogenesis of hemangiomas: a review. Plast Reconstr Surg 2006; 117:29e–35e.
13. Folkman J, Klagsbrun M. Angiogenic factors. Science 1987; 235:442–447.
14. Klagsbrun M, D'Amore PA. Regulators of angiogenesis. Annu Rev Physiol 1991; 53:217–239.
15. Hunt SJ, Santa Cruz DJ. Vascular tumors of the skin: a selective review. Semin Diagn Pathol 2004; 21:166–218.
16. Harzell MB. Granuloma pyogenicum (botryomycosis of French authors). J Cutan Dis 1904; 22:520–525.
17. Bhaskar SM, Jacoway JR. Pyogenic granuloma. Clinical features, incidence, histology and result of treatment: report of 242 cases. J Oral Surg 1961; 24:391–398.
18. Marler JJ, Mulliken JB. Current management of hemangiomas and vascular malformations. Clin Plast Surg 2005; 32:99–116.
19. Fetsch JF. Epithelioid haemangioma. In: Fletcher CDM, Unni KK, Mertens F, eds. Tumours of Soft Tissue and Bone. Lyon, France: IARC Press, 2002:156–177.
20. Wells GC, Whimster IW. Subcutaneous angiolymphoid hyperplasia with eosinophilia. Br J Dermatol 1969; 81: 1–15.
21. Rosai J, Gold J, Landy R. The histiocytoid hemangiomas: a unifying concept embracing several previously described entities of skin, soft tissue, large vessels, bone, and heart. Hum Pathol 1979; 10:707–730.
22. Googe PB, Harris NL, Mihm MC. Kimura's disease and angiolymphoid hyperplasia with eosinophilia: two distinct histopathological entities. J Cutan Pathol 1987; 14:263–271.
23. Urabe A, Tsuneyoshi M, Enjoji M. Epithelioid hemangioma versus Kimura's disease. A comparative clinicopathologic study. Am J Surg Pathol 1987; 11:758–766.
24. Kuo TT, Shih LY, Chan HL. Kimura's disease, involvement of regional lymph nodes and distinction from angiolymphoid hyperplasia with eosinophilia. Am J Surg Pathol 1988; 12:843–854.
25. Chan JK, Hui PK, Ng CS, et al. Epithelioid haemangioma (angiolymphoid hyperplasia with eosinophilia) and Kimura's disease in Chinese. Histopathology 1989; 15:557–574.
26. Daniels DG, Schrodt R, Fliegelman MT, et al. Ultrastructural study of a case of angiolymphoid hyperplasia with eosinophilia. Arch Dermatol 1974; 109:870–872.
27. Castro C, Winkelmann RK. Angiolymphoid hyperplasia with eosinophilia in the skin. Cancer 1974; 34:1696–1705.
28. Fetsch JF, Weiss SW. Observations concerning the pathogenesis of epithelioid hemangioma (angiolymphoid hyperplasia). Mod Pathol 1991; 4:449–455.
29. Olsen TG, Helwig EB. Angiolymphoid hyperplasia with eosinophilia. A clinicopathologic study of 116 patients. J Am Acad Dermatol 1985; 12:781–796.
30. Vadlamudi G, Schinella R. Traumatic pseudoaneurysm: a possible early lesion in the spectrum of epithelioid hemangioma/angiolymphoid hyperplasia with eosinophilia. Am J Dermatopathol 1998; 20:113–117.
31. Calonje E. Haemangiomas. In: Fletcher CDM, Unni KK, Mertens F, eds. Tumours of Soft Tissue and Bone. Lyon, France: IARC Press, 2002:156–158.
32. Finn MC, Glowacki J, Mulliken JB. Congenital vascular lesions: clinical application of a new classification. J Pediatr Surg 1983; 18:894–900.
33. Brodsky L, Yoshpe N, Ruben RJ. Clinical-pathological correlates of congenital subglottic hemangiomas. Ann Otol Rhinol Laryngol Suppl 1983; 105:4–18.
34. Ferguson CF, Flake CG. Subglottic hemangioma as a cause of respiratory obstruction in infants. Ann Otol Rhinol Laryngol 1961; 70:1095–1112.
35. Batsakis JG. Vascular tumors of the salivary glands. Ann Otol Rhinol Laryngol 1986; 95:649–650.
36. Lack EE, Upton MP. Histopathologic review of salivary gland tumors in childhood. Arch Otolaryngol Head Neck Surg 1988; 114:898–906.

37. Fu YS, Perzin KH. Non-epithelial tumors of the nasal cavity, paranasal sinuses, and nasopharynx: a clinicopathologic study. I. General features and vascular tumors. Cancer 1974; 33:1275–1288.
38. Strauss M, Widome MD, Roland PS. Nasopharyneal hemangioma causing airway obstruction in infancy. Laryngoscope 1981; 91:1365–1368.
39. Orlow SJ, Isakoff MS, Blei F. Increased risk of symptomatic hemangioma of the airway in association with cutaneous hemangiomas in a ''beard'' distribution. J Pediatr 1997; 131:643–646.
40. Hersh JH, Waterfill D, Rutledge J, et al. Sternal malformation/vascular dysplasia syndrome. Am J Med Genet 1985; 21:177–186.
41. Frieden U, Reese V, Cohen D. PHACE syndrome: the association of posterior fossa brain malformations, hemangiomas, arterial anomalies, coarctation of the aorta and cardiac defects, and eye abnormalities. Arch Dermatol 1996; 132:307–311.
42. Mills SE, Cooper PH, Fechner RE. Lobular capillary hemangioma: the underlying lesion of pyogenic granuloma. A study of 73 cases from the oral and nasal mucous membranes. Am J Surg Pathol 1980; 4:470–479.
43. Sheppard LM, Mickelson SA. Hemangiomas of the nasal septum and paranasal sinuses. Henry Ford Hosp Med J 1990; 38:25–27.
44. Harris M, Desai R, Chuang T, et al. Lobular capillary hemangiomas: an epidemiologic report, with emphasis on cutaneous lesions. J Am Acad Dermatol 2000; 42: 1012–1016.
45. Taira JW, Hill TL, Everet MA. Lobular capillary hemangioma (pyogenic granuloma) with satellitosis. J Am Acad Dermatol 1992; 27:297–300.
46. Wilson BB, Greer KE, Cooper PH. Eruptive disseminated lobular capillary hemangioma (pyogenic granuloma). J Am Acad Dermatol 1989; 21:391–394.
47. Cooper P, Mills S. Subcutaneous granuloma pyogenicum. Lobular capillary hemangioma. Arch Dermatol 1982; 118:30–33.
48. Cooper P, McAllister H, Helwig E. Intravenous pyogenic granuloma. A study of 18 cases. Am J Surg Pathol 1979; 3:221–228.
49. Wilson Jones E, Orkin M. Tufted angioma (angioblastoma): a benign progressive angioma, not to be confused with Kaposi's sarcoma or low-grade angiosarcoma. J Am Acad Dermatol 1989; 20:214–225.
50. Padilla R, Orkin M, Rosai J. Acquired ''tufted'' angioma (progressive capillary hemangioma). A distinctive clinicopathologic entity related to lobular capillary hemangioma. Am J Dermatopathol 1987; 9:292–300.
51. Kleinegger CL, Hammond HL, Vincent SB, et al. Acquired tufted angioma: a unique vascular lesion not previously reported in the oral mucosa. Br J Dermatol 2000; 142: 794–799.
52. Nielsen H, Nielsen PL. Cutaneous tufted angioma as a differential diagnosis to Kaposi's sarcoma in HIV infection. AIDS 1994; 8:707–708.
53. Daley T. Acquired tufted angioma of the lower lip mucosa. J Can Dent Assoc 2000; 66:137.
54. Sumitra S, Yesudian P. Painful tufted angioma precipitated by trauma. Int J Dermatol 1994; 33:675–676.
55. Ward KA, Kennedy CT, Ashworth MT. Acquired tufted angioma frequently develops at sites other than the neck and upper trunk. Clin Exp Dermatol 1996; 21:80.
56. Alvarez-Mendoza A, Lourdes TS, Ridaura-Sanz C, et al. Histopathology of vascular lesions found in Kasabach-Merritt syndrome: review of 13 cases. Pediatr Dev Pathol 2000; 3:556–560.
57. Coffin CM, Dehner LP. Vascular tumors in children and adolescents: a clinicopathologic study of 228 tumors in 222 patients. Pathol Annu 1993; 1:97–120.
58. Ferguson GB. Hemangioma of the adult and of the infant larynx: a review of the literature and a report of two cases. Arch Otolaryngol 1944; 40:189–195.
59. Bridger GP, Nassar VH, Skinner HG. Hemangioma of the adult larynx. Arch Otolaryngol 1970; 92:493–498.
60. Jones SR, Myers EN, Barnes L. Benign neoplasms of the larynx. Otolaryngol Clin North Am 1984; 17:151–178.
61. Iwata N, Hattori K, Nakaawa T, et al. Hemangioma of the nasal cavity. A clinicopathologic study. Auris Nasus Larynx 2002; 29:335–339.
62. Fanburg JC, Meis-Kindblom JM, Rosenberg AE. Multiple enchondromas associated with spindle cell hemangioendotheliomas: an overlooked variant of Maffucci's Syndrome. Am J Surg Pathol 1995; 19(9):1029–1038.
63. Fine R, Derbes V, Clark W. Blue rubber bleb nevus. Arch Dermatol 1961; 84:144–147.
64. Dowlati B, Nabai H, Mehregan DR, et al. Zosteriform angiolymphoid hyperplasia with eosinophilia. J Dermatol 2002; 29:178–179.
65. Renshaw AA, Rosai J. Benign atypical vascular lesions of the lip. A study of 12 cases. Am J Surg Pathol 1993; 17:557–565.
66. Mariatos G, Gorgoulis VG, Laskaris G, et al. Epithelioid hemangioma (angiolymphoid hyperplasia with eosinophilia) in the oral mucosa. A case report and review of the literature. Oral Oncol 1999; 35:435–438.
67. Park Y, Chung J, Cho CG. Angiolymphoid hyperplasia with eosinophilia of the tongue: report of a case and review of the literature. Oral Oncol 2002; 38:103–106.
68. Sun ZJ, Zhang L, Zhang WF, et al. Epithelioid haemangioma in the oral mucosa: a clinicopathological study of seven cases and review of the literature. Oral Oncol 2005; 30:441–447.
69. Kurihara K, Saiki T, Takeda K, et al. Epithelioid hemangioma of the maxillary sinus: a case report. J Oral Maxillofac Surg 1995; 53:1221–1223.
70. Coombes AG, Manners RM, Ellison DW, et al. Lacrimal gland epithelioid haemangioma. Br J Ophthalmol 1997; 81:1020.
71. McEachren TM, Brownstein S, Jordan DR, et al. Epithelioid hemangioma of the orbit. Ophthalmology 2000; 107:806–810.
72. Mariatos G, Gorgoulis VG, Laskaris G, et al. Epithelioid haemangioma (angiolymphoid hyperplasia with eosinophilia) in the inner canthus. J Eur Acad Dermatol Venereol 2001; 15:90–91.
73. Rossiter JL, Hendrix RA, Tom LW, et al. Intramuscular hemangioma of the head and neck. Otolaryngol Head Neck Surg 1993; 108:18–26.
74. Connor SEJ, Flis C, Langdon JD. Vascular masses of the head and neck. Clin Radiol 2005; 60:856–868.
75. Knapp EL, Kransdorf MJ, Letson GD. Diagnostic imaging update: soft tissue sarcomas. Cancer Control 2005; 12: 22–26.
76. Chooi WK, Woodhouse N, Coley SC, et al. Pediatric head and neck lesions: assessment of vascularity by MR digital subtraction angiography. AJNR Am J Neuroradiol 2004; 25:1251–1255.
77. Griffin N, Khan N, Meirion J, et al. The radiological manifestations of intramuscular haemangiomas in adults: magnetic resonance imaging, computed tomography and ultrasound appearances. Skeletal Radiol 2007; 36: 1051–1059.
78. Murphey MD, Fairbairn KJ, Parman LM, et al. From the archives of the AFIP. Musculoskeletal angiomatous

lesions: radiologic-pathologic correlation. Radiographics 1995; 15:893–917.
79. Pasyk KA, Grabb WC, Cherry GW. Crystalloid inclusions in endothelial cells of cellular and capillary hemangiomas. Arch Dermatol 1983; 119:134–137.
80. Kumakiri M, Muramoto F, Tsukinaga T, et al. Crystalline lamellae in the endothelial cells of a type of hemangioma characterized by the proliferation of immature endothelial cells and pericytes. J Am Acad Dermatol 1983; 8:68–75.
81. Allen PW, Enzinger FM. Hemangioma of skeletal muscle. An analysis of 89 cases. Cancer 1072; 29:8–22.
82. Beham A, Fletcher CD. Intramuscular angioma: a clinicopathological analysis of 74 cases. Histopathology 1991; 18:53–59.
83. North PE, Waner M, Mizeracki A, et al. GLUT1: a newly discovered immunohistochemical marker for juvenile hemangiomas. Hum Pathol 2000; 31:11–22.
84. Lawley LP, Cerimele F, Weiss SW, et al. Expression of Wilms tumor 1 gene distinguishes vascular malformations from proliferative endothelial lesions. Arch Dermatol 2005; 141:1297–1300.
85. Batsakis JG, Sneige N. Choanal and angiomatous polyps of the sinonasal tract. Ann Otol Rhinol Laryngol 1992; 101:623–625.
86. Leon-Villapalos J, Wolfe K, Kangesu L. GLUT-1: an extra diagnositic tool to differentiate between haemangiomas and vascular malformations. Br J Plast Surg 2005; 58: 348–352.
87. Dyduch G, Okon K, Meirzynski W. Benign vascular proliferations—an immunohistochemical and comparative study. Pol J Pathol 2004; 55:59–64.
88. Fechner RE, Cooper PH, Mills SE. Pyogenic granuloma of the larynyx and trachea. A casual and pathologic misnomer for granulation tissue. Arch Otolaryngol 1981; 107: 30–32.
89. Mentzel T, Calonje E, Nascimento AG, et al. Infantile hemangiopericytoma versus infantile myofibromatosis. Study of a series suggesting a continuous spectrum of infantile myofibroblastic lesions. Am J Surg Pathol 1994; 18:922–930.
90. Zukerberg LR, Nickoloff BJ, Weiss SW. Kaposiform hemangioendothelioma of infancy and childhood. An aggressive neoplasm associated with Kasabach-Merritt syndrome and lymphangiomatosis. Am J Surg Pathol 1993; 17:321–328.
91. Lyons LL, North PE, Mac-Moune Lai F, et al. Kaposiform hemangioendothelioma; a study of 33 cases emphasizing its pathologic, immunophenotypic, and biologic uniqueness from juvenile hemangioma. Am J Surg Pathol 2004; 28:559–568.
92. Maguqiness S, Guenther L. Kasabach-Merritt syndrome. J Cutan Med Surg 2002; 6:335–339.
93. Chan JKC, Fletcher CDM, Hicklin GA, et al. Glomeruloid hemangioma. A distinctive cutaneous lesion of multicentric Castleman's disease associated with POEMS syndrome. Am J Surg Pathol 1990; 14:1036–1046.
94. Rao VK, Weiss SW. Angiomatosis of soft tissue. An analysis of the histologic features and clinical outcome in 51 cases. Am J Surg Pathol 1992; 16:764–771.
95. Werner JA, Dunne A-A, Folz BJ, et al. Current concepts in the classification, diagnosis and treatment of hemangiomas and vascular malformations of the head and neck. Eur Arch Otorhinolaryngol 2001; 258:141–149.
96. Gampper TJ, Morgan RF. Vascular anomalies: hemangiomas. Plast Reconstr Surg 2002; 110:572–585.
97. Batta K, Goodyear HM, Moss C, et al. Randomized controlled study of early pulsed dye laser treatment of uncomplicated childhood haemangiomas: results of a 1-year analysis. Lancet 2002; 360:521–527.
98. Greinwald JH, Burke DK, Bonthius DJ, et al. An update on the treatment of hemangiomas in children with interferon α-2a. Arch Otolaryngol Head Neck Surg 1999; 125:21–27.
99. Munn SE, Jackson JE, Russel Jones R. Tufted hemangiomas responding to high dose systemic steroids. Clin Exp Dermatol 1994; 19:511–514.
100. Suarez SM, Pensler JM, Paller AS. Response of deep tufted angioma to interferon alpha. J Am Acad Dermatol 1995; 33:124–126.
101. Enjolras O, Mulliken JB, Wassef M, et al. Residual lesions after Kasabach-Merritt phenomenon in 41 patients. J Am Acad Dermatol 2000; 42:225–235.
102. Giudice M, Piazza C, Bolzoni A, et al. Head and neck intramuscular haemangioma: report of two cases with unusual localization. Eur Arch Otorhinolaryngol 2003; 260:498–501.

D. Lymphangioma

1. Bloom DC, Perkins JA, Manning SC. Management of lymphatic malformation. Curr Opin Otolaryngol Head Neck Surg 2004; 12:500–504.
2. Maddalozzo J, Hughes CA, Huang L, et al. High angiogenic activity in cells isolated from cystic hygroma: role of bFGF. Arch Otolaryngol Head Neck Surg 1999; 125:45–48.
3. Huang HY, Ho CC, Huang PH, et al. Co-expression of VEGF-C and its receptors, VEGFR-2 and VEGFR-3, in endothelial cells of lymphangioma. Implication in autocrine or pararcrine regulation of lymphangioma. Lab Invest 2001; 81:1729–1734.
4. Sidle DM, Maddalozzo J, Meier JD, et al. Altered pigment epithelium-derived factor and vascular endothelial growth factor levels in lymphangioma pathogenesis and clinical recurrence. Arch Otolaryngol Head Neck Surg 2005; 131:990–995.
5. Harkins GA, Sabiston DC Jr. Lymphangioma in infancy and childhood. Surgery 1960; 47:811–822.
6. Bill AH Jr., Sumner DS. A unified concept of lymphangioma and cystic hygroma. Surg Gynecol Obstet 1965; 120:79–86.
7. Alquhtani A, Nguyen LT, Flageole H, et al. 25 years, experience with lymphangiomas in children. J Pediatr Surg 1999; 34:1164–1168.
8. Descamps PH, Jourdain O, Paillet CH. Etiology, prognosis and management of nuchal cystic hygroma: 25 new cases and literature review. Eur J Obstet Gynecol Reprod Bio 1997; 1:3–10.
9. Hamoir M, Plouin-Gaudon I, Rombauz P, et al. Lymphatic malformations of the head and neck: a retrospective review and a support for staging. Head Neck 2001; 23:326–337.
10. Fujita Y, Satoh S, Nakayama H, et al. In utero evaluation and the long-term prognosis of living infants with cystic hygroma. Fetal Diagn Ther 2001; 16:402–406.
11. Padwa BL, Hayward PG, Ferrare NF, et al. Cervicofacial lymphatic malformation: clinical course, surgical intervention, and pathogenesis of skeletal hypertrophy. Plast Reconstr Surg 1995; 95:951–960.
12. Giguere CM, Bauman NM, Smith RJ. New treatment options for lymphangioma in infants and children. Ann Otol Rhinol Laryngol 2002; 111:1066–1075.
13. Karmazyn B, Hefer T, Joachims HZ, et al. Lymphangioma: an unusual cause of pharyngeal and epiglottic edema. Otolaryngol Head Neck Surg 1997; 117:409–411.
14. Peachey RD, Lim CC, Whimster IW. Lymphangioma of skin. A review of 65 cases. Br J Dermatol 1970; 83:519–527.
15. Whimster IW. The pathology of lymphangioma circumscriptum. Br J Dermatol 1976; 94:473–486.

16. Flanagan BP, Helwig EB. Cutaneous lymphangioma. Arch Dermatol 1977; 113:24–30.
17. Sangueza OP, Kasper RC, LeBoit P, et al. Vascular tumours. In: Leboit PE, Burg G, Weedon D, et al., eds. Skin Tumours. Lyon, France: IARC Press, 2006:229–262.
18. Goble RR, Frangoulis MA. Lymphangioma circumscriptum of the eyelids and conjunctiva. Br J Ophthalmol 1009; 74:574–575.
19. Jones EW, Winkelmann RK, Zachary CB, et al. Benign lymphangioendothelioma. J Am Acad Dermatol 1990; 23:229–235.
20. Guillou L, Fletcher CD. Benign lymphangioendothelioma (acquired progressive lymphangioma): a lesion not to be confused with well-differentiated angiosarcoma and patch stage Kaposi's sarcoma: clinicopathologic analysis of a series. Am J Surg Pathol 2000; 24:1047–1057.
21. Ramani P, Shah A. Lymphangiomatosis. Histologic and immunohistochemical analysis of four cases. Am J Surg Pathol 17:329–335.
22. Gomez C, Calonje E, Ferrar DW, et al. Lymphangiomatosis of the limbs. Clinicopathologic analysis of a series with a good prognosis. Am J Surg Pathol 1995; 19:125–133.
23. Siegel MJ, Glazer HS, St Amour TE, Rosenthal DD. Lymphangiomas in children: MR imaging. Radiology 1989; 170:467–470.
24. Wunderbaldinger P, Paya K, Partik B, et al. Original Report: CT and MR imaging of generalized cystic lymphangiomatosis in pediatric patients. AJR Am J Roentgenol 2000; 174:827–832.
25. Ruano R, Aubry JP, Simon I, et al. Prenatal diagnosis of a large axillary cystic lymphangioma by three-dimensional ultrasonography and magnetic resonance imaging. J Ultrasound Med 2003; 22:419–423.
26. Perkins JA, Sidhu M, Manning SC, et al. Three-dimensional CT angiography imaging of vascular tumors of the head and neck. Int J Pediatr Otorhinolaryngol 2005; 69:319–325.
27. Imhof H, Czerny C, Hormann M, et al. Tumors and tumorlike lesions of the neck: from childhood to adult. Eur Radiol 2004; 14:L155–L165.
28. McAlvany JP, Jorizzo JL, Zanolli D, et al. Magnetic resonance imaging in the evaluation of lymphangioma circumscriptum. Arch Dermatol 1993; 692–696.
29. Kempson RL, Fletcher CDM, Evans HL, et al. Vascular tumors. In: Kempson RL, Fletcher CDM, Evans HL, et al., eds. Tumors of the Soft Tissues. 3rd series, fascicle 30. Washington, D.C.: Armed Forces Institute of Pathology, 1998:307–370.
30. Zukerberg LR, Nickoloff BJ, Weiss SW. Kaposiform hemangioendothelioma of infancy and childhood. An aggressive neoplasm associated with Kasabach-Merritt syndrome and lymphangiomatosis. Am J Surg Pathol 1993; 17:321–328.
31. Pearson JM, McWilliam LJ. A light microscopical, immunohistochemical, and ultrastructural comparison of hemangiomata and lymphangiomata. Ultrastruct Pathol 1990; 14:497–504.
32. Sauter B, Foedinger D, Sterniczky B, et al. Immunoelectron microscopic characterization of human dermal lymphatic microvascular endothelial cells. Differential expression of CD31, CD34, and type IV collagen with lymphatic endothelial cells vs. blood capillary endothelial cells in normal human skin, lymphangioma, and hemangioma in situ. J Histochem Cytochem 1998; 46:165–176.
33. Wilting J, Papoutsi M, Christ B, et al. The transcription factor Prox1 is a marker for lymphatic endothelial cells in normal and diseased human tissues. FASEB J 2002; 16:1271–1273.
34. Fukunaga M. Expression of D2-40 in lymphatic endothelium of normal tissues and in vascular tumours. Histopathology 2005; 46:396–402.
35. Galambos C, Nodit L. Identification of lymphatic endothelium in pediatric vascular tumors and malformations. Pediatr Dev Pathol 2005; 8:181–189.
36. Partanen TA, Alitalo K, Miettinen M. Lack of lymphatic vascular specificity of vascular endothelial growth factor receptor 3 in 185 vascular tumors. Cancer 1999; 86: 2406–2412.
37. Rao VK, Weiss SW. Angiomatosis of soft tissue. An analysis of the histologic features and clinical outcome in 51 cases. Am J Surg Pathol 1992; 16:764–771.
38. Santa Cruz D, Aronberg J. Targetoid hemosiderotic hemangioma. J Am Acad Dermatol 1988; 19:550–558.
39. Mentzel T, Requena L, Kaddu S, et al. Hobnail hemangioma (''targetoid hemosiderotic hemangioma''): clinicopathologic and immunohistochemical analysis of 62 cases. J Cutan Pathol 1999; 26:279–286.
40. Franke FE, Steger K, Marks A, et al. Hobnail hemangiomas (targetoid hemosiderotic hemangiomas) are true lymphangiomas. J Cutan Pathol 2004; 31:362–367.
41. Grabb WC, Dingman RO, Oneal RM, et al. Facial hamartomas in children: neurofibroma, lymphangiomas, and hemangioma. Plast Reconstr Surg 1980; 66:509–527.
42. Cohen SR, Thompson JW. Lymphangiomas of the larynx in infants and children: a survey of pediatric lymphangioma. Ann Otol Rhinol Laryngol 1986; 127:1–20.
43. Ricciardelli E, Richardson M. Cervicofacial cystic hygroma: patterns of recurrence and management of the difficult case. Arch Otolaryngol Head Neck Surg 1991; 117: 546–553.
44. de Serres L, Sie K, Richardson M. Lymphatic malformation of the head and neck: a proposal for staging. Arch Otolaryngol Head Neck Surg 1995; 121:577–582.
45. Raveh E, DeJong AL, Taylor GP. Prognostic factors in the treatment of lymphatic malformations. Arch Otolaryngol Head Neck Surg 1997; 123:1061–1065.
46. Farrell PT. Prenatal diagnosis and intrapartum management of neck masses causing airway obstruction. Paediatr Anaesth 2004; 14:48–52.
47. Giguere CM, Bauman NM, Sato Y, et al. Treatment of lymphangiomas with OK-432 (Picibanil) sclerotherapy: a prospective multi-institutional trial. Arch Otolaryngol Head Neck Surg 2002; 128:1137–1144.
48. Banieghbal B, Davies MR. Guidelines for the successful treatment of lymphangioma with OK-432. Eur J Pediatr Surg 2003; 13:103–107.
49. Hall N, Ade-Ajayi N, Brewis C, et al. Is intralesional injection of OK-432 effective in the treatment of lymphangioma in children? Surgery 2003; 133:238–242.
50. Watanabe M, Kishiyama K, Ohkawara A. Acquired progressive lymphangioma. J Am Acad Dermatol 1983; 8: 663–667.
51. Mehregan DR, Mehregan AH, Mehregan DA. Benign lymphangioendothelioma: report of 2 cases. J Cutan Pathol 1992; 19:502–505.
52. Haluk Guvenc B, Ekingen G, Tuzlaci A, et al. Diffuse neonatal abdominal lymphangiomatosis: management by limited surgical excision and sclerotherapy. Pediatr Surg Int 2005; 21:595–598.
53. Turner C, Gros S. Treatment of recurrent suprahyoid cervicofacial lymphangioma with intravenous cyclophosphamide. Am J Pediatr Hematol Oncol 1994; 16:325–328.
54. Reinhardt MA, Nelson SC, Sencer SF, et al. Treatment of childhood lymphangiomas with interferon-alpha. J Pediatr Hematol Oncol 1997; 19:232–236.

E. Glomus Tumor

1. Pepper MC, Laubenheimer R, Cripps DJ. Multiple glomus tumors. J Cutan Pathol 1977; 4:244–257.
2. Kohout E, Stout AP. The glomus tumor in children. Cancer 1961; 14:555–566.
3. Morales AR, Fine G, Pardo V, et al. The ultrastructure of smooth muscle tumors with a consideration of the possible relationship of glomangiomas, hemangiopericytomas, and cardiac myxomas. Pathol Annu 1975; 10:65–92.
4. Murad TM, von Haam E, Murthy MS. Ultrastructure of a hemangiopericytoma and a glomus tumor. Cancer 1968; 22:1239–1249.
5. Stout AP. Tumors featuring pericytes; glomus tumor and hemangiopericytoma. Lab Invest 1956; 5:217–223.
6. Tang CK, Toker C, Foris NP, et al. Glomangioma of the lung. Am J Surg Pathol 1978; 2:103–109.
7. Toker C. Glomangioma. An ultrastructural study. Cancer 1969; 23:487–492.
8. Venkatachalam MA, Greally JG. Fine structure of glomus tumor: similarity of glomus cells to smooth muscle. Cancer 1969; 23:1176–1184.
9. Folpe AL, Fanburg-Smith JC, Miettinen M, et al. Atypical and malignant glomus tumors: analysis of 52 cases, with a proposal for the reclassification of glomus tumors. Am J Surg Pathol 2001; 25:1–12.
10. Aiba M, Hirayama A, Kuramochi S. Glomangiosarcoma in a glomus tumor. An immunohistochemical and ultrastructural study. Cancer 1988; 61:1467–1471.
11. Brathwaite CD, Poppiti RJ, Jr. Malignant glomus tumor. A case report of widespread metastases in a patient with multiple glomus body hamartomas. Am J Surg Pathol 1996; 20:233–238.
12. Gould EW, Manivel JC, Albores-Saavedra J, et al. Locally infiltrative glomus tumors and glomangiosarcomas. A clinical, ultrastructural, and immunohistochemical study. Cancer 1990; 65:310–318.
13. Hiruta N, Kameda N, Tokudome T, et al. Malignant glomus tumor: a case report and review of the literature. Am J Surg Pathol 1997; 21:1096–1103.
14. Lopez-Rios F, Rodriguez-Peralto JL, Castano E, et al. Glomangiosarcoma of the lower limb: a case report with a literature review. J Cutan Pathol 1997; 24:571–574.
15. Anagnostou GD, Papademetriou DG, Toumazani MN. Subcutaneous glomus tumors. Surg Gynecol Obstet 1973; 136:945–950.
16. Tran LP, Velanovich V, Kaufmann CR. Familial multiple glomus tumors: report of a pedigree and literature review. Ann Plast Surg 1994; 32:89–91.
17. Takata H, Ikuta Y, Ishida O, et al. Treatment of subungual glomus tumour. Hand Surg 2001; 6:25–27.
18. Van Geertruyden J, Lorea P, Goldschmidt D, et al. Glomus tumours of the hand. A retrospective study of 51 cases. J Hand Surg [Br] 1996; 21:257–260.
19. Tumors and tumor-like lesions of the soft tissues. In: Barnes L, ed. Surgical Pathology of the Head and Neck, 2nd ed. New York: Marcel Dekker, Inc., 2001:901–904.
20. Yoshida GY. Glomangioma of the auricle. Otolaryngol Head Neck Surg 1995; 113:833–834.
21. Chu PG, Chang KL, Wu AY, et al. Nasal glomus tumors: report of two cases with emphasis on immunohistochemical features and differential diagnosis. Hum Pathol 1999; 30:1259–1261.
22. Hayes MM, Van der WN, Holden GP. Aggressive glomus tumor of the nasal region. Report of a case with multiple local recurrences. Arch Pathol Lab Med 1993; 117:649–652.
23. Shields JA, Eagle RC Jr., Shields CL, et al. Orbital-conjunctival glomangiomas involving two ocular rectus muscles. Am J Ophthalmol 2006; 142:511–513.
24. Gaut AW, Jay AP, Robinson RA, et al. Invasive glomus tumor of the nasal cavity. Am J Otolaryngol 2005; 26:207–209.
25. Garcia-Prats MD, Sotelo-Rodriguez MT, Ballestin C, et al. Glomus tumour of the trachea: report of a case with microscopic, ultrastructural and immunohistochemical examination and review of the literature. Histopathology 1991; 19:459–464.
26. Altinok T, Cakir E, Gulhan E, et al. Tracheal glomus tumor. J Thorac Cardiovasc Surg 2006; 132:201–202.
27. Nadrous HF, Allen MS, Bartholmai BJ, et al. Glomus tumor of the trachea: value of multidetector computed tomographic virtual bronchoscopy. Mayo Clin Proc 2004; 79:237–240.
28. Chien ST, Lee TM, Hsu JY, et al. Glomus tumor of the trachea. J Chin Med Assoc 2003; 66:551–554.
29. Moody GH, Myskow M, Musgrove C. Glomus tumor of the lip. A case report and immunohistochemical study. Oral Surg Oral Med Oral Pathol 1986; 62:312–318.
30. Ficarra G, Merrell PW, Johnston WH, et al. Intraoral solitary glomus tumor (glomangioma): case report and literature review. Oral Surg Oral Med Oral Pathol 1986; 62:306–311.
31. Gonzalez-Campora R, Villar Rodriguez JL, Vazquez RF, et al. Glomus tumour of the oropharynx. J Laryngol Otol 1995; 109:63–65.
32. Appelman HD, Helwig EB. Glomus tumors of the stomach. Cancer 1969; 23:203–213.
33. Uyar Y, Ulku CH, Koral H, et al. Glomangioma of the middle ear. Acta Otolaryngol 2004; 124:867–869.
34. Griffin CJ. A neuro-myo-arterial glomus in the temporomandibular meniscus. Med J Aust 1961; 48(1):113–116.
35. Charles NC. Multiple glomus tumors of the face and eyelid. Arch Ophthalmol 1976; 94:1283–1285.
36. Lai T, James CL, Huilgol SC, et al. Glomus tumour of the eyelid. Jpn J Ophthalmol 2004; 48:418–419.
37. Shugart RR, Soule EH, Johnson EW Jr. Glomus tumor. Surg Gynecol Obstet 1963; 117:334–340.
38. Axmann C, Feiden W, Moeller V, et al. Paravertebral glomus tumors. Skeletal Radiol 2005; 34:112–115.
39. Hermann G, Klein MJ, Springfield D, et al. Glomus tumor of the thigh: confluent with the periosteum of the femur. Skeletal Radiol 2005; 34:116–120.
40. Drape JL, Idy-Peretti I, Goettmann S, et al. Subungual glomus tumors: evaluation with MR imaging. Radiology 1995; 195:507–515.
41. Pulitzer DR, Martin PC, Reed RJ. Epithelioid glomus tumor. Hum Pathol 1995; 26:1022–1027.
42. Slater DN, Cotton DW, Azzopardi JG. Oncocytic glomus tumour: a new variant. Histopathology 1987; 11:523–531.
43. Lumley JS, Stansfeld AG. Infiltrating glomus tumour of lower limb. Br Med J 1972; 1:484–485.
44. Miettinen M, Lehto VP, Virtanen I. Glomus tumor cells: evaluation of smooth muscle and endothelial cell properties. Virchows Arch B Cell Pathol Incl Mol Pathol 1983; 43:139–149.
45. Palungwachira P, Palungwachira P, Yaguchi H. Ultrastructural study of glomus tumor. J Med Assoc Thai 2001; 84:1619–1623.
46. Porter PL, Bigler SA, McNutt M, et al. The immunophenotype of hemangiopericytomas and glomus tumors, with special reference to muscle protein expression: an immunohistochemical study and review of the literature. Mod Pathol 1991; 4:46–52.
47. Miettinen M, Paal E, Lasota J, et al. Gastrointestinal glomus tumors: a clinicopathologic, immunohistochemical, and molecular genetic study of 32 cases. Am J Surg Pathol 2002; 26:301–311.
48. Happle R, Konig A. Type 2 segmental manifestation of multiple glomus tumors: a review and reclassification of 5 case reports. Dermatology 1999; 198:270–272.

49. Mayr-Kanhauser S, Behmel A, Aberer W. Multiple glomus tumors of the skin with male-to-male transmission over four generations. J Invest Dermatol 2001; 116:475–476.
50. van den Oord JJ, Wolf-Peeters C. Perivascular spaces in eccrine spiradenoma. A clue to its histological diagnosis. Am J Dermatopathol 1995; 17:266–270.

A. Focal Myositis

1. Heffner RR Jr., Armbrustmacher VW, Earle KM. Focal myositis. Cancer 1977; 40:301–306.
2. Georgalas C, Kapoor L, Chau H, et al. Inflammatory focal myositis of the sternomastoid muscle: is there an absolute indication for biopsy? A case report and review of the literature. Eur Arch Otorhinolaryngol 2006; 263:149–151.
3. Yanmaz Alnigenis MN, Kolasinski SL, Kalovidouris AE. Focal myositis: a review of 100 previously published cases and a report of 2 new cases. Clin Exp Rheumatol 1999; 17:631.
4. Isaacson G, Chan KH, Heffner RR Jr. Focal myositis. A new cause for the pediatric neck mass. Arch Otolaryngol Head Neck Surg 1991; 117:103–105.
5. Toti P, Romano L, Villanova M, et al. Focal myositis: a polymerase chain reaction analysis for a viral etiology. Hum Pathol 1997; 28:111–113.
6. Naumann M, Toyka KV, Goebel HH, et al. Focal myositis of the temporal muscle. Muscle Nerve 1993; 16:1374–1376.
7. McCluggage WG, Mirakhur M. Focal myositis of the floor of mouth: report of two cases and review of the literature. Oral Surg Oral Med Oral Pathol Oral Radiol Endod 1996; 81:573–575.
8. Brown TF, Carr MM, Covert AA, et al. Focal myositis in the mylohyoid muscle of an adult. J Otolaryngol 2000; 29: 47–50.
9. Bamanikar S, Mathew M. Focal myositis of the tongue—a pseudotumoral lesion. Histopathology 1995; 26:291–292.
10. Azuma T, Komori A, Nagayama M. Focal myositis of the tongue. J Oral Maxillofac Surg 1987; 45:953–955.
11. Caldwell CJ, Swash M, Van der Walt JD, et al. Focal myositis: a clinicopathological study. Neuromuscul Disord 1995; 5:317–321.
12. Takita MA, Kawamoto TO, Nogami H, et al. Focal myositis of the tongue: report of a case. J Osaka Univ Dent Sch 1985; 25:161–169.
13. Chiang IP, Wang J, Tsang YM, et al. Focal myositis of esophagus: a distinct inflammatory pseudotumor mimicking esophageal malignancy. Am J Gastroenterol 1997; 92:174–175.
14. Lim KL, Robson K, Powell RJ. Focal myositis: an unusual cause of bilateral upper eyelid swellings. Postgrad Med J 1993; 69:876–878.
15. Cain AJ, Michie BA, Davis BC, et al. Focal myositis of the sternocleidomastoid muscle. J Laryngol Otol 1998; 112: 687–689.
16. Josephson GD, de Blasi H, McCormick S, et al. Focal myositis of the sternocleidomastoid muscle: a case report and review of the literature. Am J Otolaryngol 1996; 17:215–217.
17. Rivest C, Miller FW, Love LA, et al. Focal myositis presenting as pseudothrombophlebitis of the neck in a patient with mixed connective tissue disease. Arthritis Rheum 1996; 39:1254–1258.
18. Cheng N, Taylor SM, Bullock M, et al. Focal myositis of the sternocleidomastoid muscle. Otolaryngol Head Neck Surg 2005; 132:150–151.
19. Ellis GL, Brannon RB. Focal myositis of the perioral musculature. Oral Surg Oral Med Oral Pathol 1979; 48:337–341.
20. Heffner RR Jr., Barron SA. Denervating changes in focal myositis, a benign inflammatory pseudotumor. Arch Pathol Lab Med 1980; 104:261–264.
21. Kransdorf MJ, Temple HT, Sweet DE. Focal myositis. Skeletal Radiol 1998; 27:283–287.
22. Wanamaker JR, Wanamaker HH, Lavertu P. Polymyositis presenting as a neck mass. Arch Otolaryngol Head Neck Surg 1992; 118:318–320.
23. Heffner RR Jr., Barron SA. Polymyositis beginning as a focal process. Arch Neurol 1981; 38:439–442.

B. Rhabdomyoma

1. Dehner LP, Enzinger FM, Font RL. Fetal rhabdomyoma. An analysis of nine cases. Cancer 1972; 30:160–166.
2. Gibas Z, Miettinen M. Recurrent parapharyngeal rhabdomyoma. Evidence of neoplastic nature of the tumor from cytogenetic study. Am J Surg Pathol 1992; 16:721–728.
3. Tostar U, Malm CJ, Meis-Kindblom JM, et al. Deregulation of the hedgehog signalling pathway: a possible role for the PTCH and SUFU genes in human rhabdomyoma and rhabdomyosarcoma development. J Pathol 2006; 208:17–25.
4. Bjorndal SK, Godballe C, Ostergaard B, et al. Adult extracardiac rhabdomyoma: light and immunohistochemical studies of two cases in the parapharyngeal space. Head Neck 2006; 28:275–279.
5. Kapadia SB, Meis JM, Frisman DM, et al. Fetal rhabdomyoma of the head and neck: a clinicopathologic and immunophenotypic study of 24 cases. Hum Pathol 1993; 24:754–765.
6. Di Sant'Agnese PA, Knowles DM. Extracardiac rhabdomyoma: a clinicopathologic study and review of the literature. Cancer 1980; 46:780–789.
7. Fletcher CDM, Unni KK, Mertens F, eds. World Health Organization Classification of Tumours. Pathology and Genetics of Tumours of Soft Tissue and Bone. Lyon: IARC Press, 2002.
8. Crotty PL, Nakhleh RE, Dehner LP. Juvenile rhabdomyoma. An intermediate form of skeletal muscle tumor in children. Arch Pathol Lab Med 1993; 117:43–47.
9. DiSanto S, Abt AB, Boal DK, et al. Fetal rhabdomyoma and nevoid basal cell carcinoma syndrome. Pediatr Pathol 1992; 12:441–447.
10. Gorlin RJ. Nevoid basal-cell carcinoma syndrome. Medicine (Baltimore) 1987; 66:98–113.
11. Watson J, Depasquale K, Ghaderi M, et al. Nevoid basal cell carcinoma syndrome and fetal rhabdomyoma: a case study. Ear Nose Throat J 2004; 83:716–718.
12. Barnes L, Eveson JW, Reichart P, et al., eds. World Health Organization Classification of Tumours. Pathology and Genetics of Head and Neck Tumors. Lyon: IARC Press, 2005:152.
13. Corio RL, Lewis DM. Intraoral rhabdomyomas. Oral Surg Oral Med Oral Pathol 1979; 48:525–531.
14. Kapadia SB, Meis JM, Frisman DM, et al. Adult rhabdomyoma of the head and neck: a clinicopathologic and immunophenotypic study. Hum Pathol 1993; 24:608–617.
15. Cleveland DB, Chen SY, Allen CM, et al. Adult rhabdomyoma. A light microscopic, ultrastructural, virologic, and immunologic analysis. Oral Surg Oral Med Oral Pathol 1994; 77:147–153.
16. Hansen T, Katenkamp D. Rhabdomyoma of the head and neck: morphology and differential diagnosis. Virchows Arch 2005; 447:849–854.
17. Shemen L, Spiro R, Tuazon R. Multifocal adult rhabdomyomas of the head and neck. Head Neck 1992; 14: 395–400.

18. Vermeersch H, van Vugt P, Lemmerling M, et al. Bilateral recurrent adult rhabdomyomas of the pharyngeal wall. Eur Arch Otorhinolaryngol 2000; 257:24–26.
19. Golz R. Multifocal adult rhabdomyoma. Case report and literature review. Pathol Res Pract 1988; 183:512–518.
20. Liess BD, Zitsch RP III, Lane R, et al. Multifocal adult rhabdomyoma: a case report and literature review. Am J Otolaryngol 2005; 26:214–217.
21. Metheetrairut C, Brown DH, Cullen JB, et al. Pharyngeal rhabdomyoma: a clinico-pathological study. J Otolaryngol 1992; 21:257–261.
22. Liang GS, Loevner LA, Kumar P. Laryngeal rhabdomyoma involving the paraglottic space. AJR Am J Roentgenol 2000; 174:1285–1287.
23. Helmberger RC, Stringer SP, Mancuso AA. Rhabdomyoma of the pharyngeal musculature extending into the prestyloid parapharyngeal space. AJNR Am J Neuroradiol 1996; 17:1115–1118.
24. Fukuda Y, Okamura HO, Nemoto T, et al. Rhabdomyoma of the base of the tongue. J Laryngol Otol 2003; 117:503–507.
25. Helliwell TR, Sissons MC, Stoney PJ, et al. Immunochemistry and electron microscopy of head and neck rhabdomyoma. J Clin Pathol 1988; 41:1058–1063.
26. Hamper K, Renninghoff J, Schafer H. Rhabdomyoma of the larynx recurring after 12 years: immunocytochemistry and differential diagnosis. Arch Otorhinolaryngol 1989; 246:222–226.
27. Hansen T, Burg JE, Koutsimpelas D, et al. Cervical adult rhabdomyoma presenting as a rapidly growing mass in a patient with diffuse large B-cell non-Hodgkin's lymphoma. Mund Kiefer Gesichtschir 2005; 9:184–187.
28. Kempson RL, Fletcher CDM, Evans HL, et al. Tumors of the Soft Tissue. Atlas of Tumor Pathology. 3rd series, fascicle 30. Washington, D.C., Armed Forces Institute of Pathology, 2001.
29. Bozic C. Fetal rhabdomyoma of the parotid gland in an infant: histological, immunohistochemical, and ultrastructural features. Pediatr Pathol 1986; 6:139–144.
30. Gupta A, Maddalozzo J, Win HT, et al. Spindle cell rhabdomyosarcoma of the tongue in an infant: a case report with emphasis on differential diagnosis of childhood spindle cell lesions. Pathol Res Pract 2004; 200:537–543.
31. Kapadia SB, Enzinger FM, Heffner DK, et al. Crystal-storing histiocytosis associated with lymphoplasmacytic neoplasms. Report of three cases mimicking adult rhabdomyoma. Am J Surg Pathol 1993; 17:461–467.
32. Wakely P Jr. Epithelioid/granular soft tissue lesions: correlation of cytopathology and histopathology. Ann Diagn Pathol 2000; 4:316–328.
33. d'Amore ES, Ninfo V. Tumors of the soft tissues composed of large eosinophilic cells. Semin Diagn Pathol 1999; 16:178–189.
34. Fanburg-Smith JC, Miettinen M, Folpe AL, et al. Lingual alveolar soft part sarcoma; 14 cases: novel clinical and morphological observations. Histopathology 2004; 45: 526–537.
35. Valdez TA, Desai U, Volk MS. Recurrent fetal rhabdomyoma of the head and neck. Int J Pediatr Otorhinolaryngol 2006; 70:1115–1118.

C. Leiomyoma

1. Hagy DM, Halperin V, Wood C. Leiomyoma of the oral cavity. Review of the literature and report of a case. Oral Surg 1964; 17:748–755.
2. Mindell RS, Calcaterra TC, Ward PH. Leiomyosarcoma of the head and neck: a review of the literature and report of two cases. Laryngoscope 1975; 85:904–910.
3. Fu YS, Perzin KH. Nonepithelial tumors of the nasal cavity, paranasal sinuses, and nasopharynx: a clinicopathologic study. Part IV: Smooth muscle tumors (leiomyomas, leiomyosarcoma). Cancer 1975; 35:1300–1308.
4. Wang C-P, Chang Y-L, Sheen T-S. Vascular leiomyoma of the head and neck. Laryngoscope 2004; 114:661–665.
5. Huang H-Y, Antonescu CR. Sinonasal smooth muscle cell tumors. A clinicopathologic and immunohistochemical analysis of 12 cases with emphasis on the low-grade end of the spectrum. Arch Pathol Lab Med 2003; 127:297–304.
6. Hachisuga T, Hashimoto H, Enjoji M. Angioleiomyoma: a clinicopathologic reappraisal of 562 cases. Cancer 1984; 54:126–130.
7. Duhig JT, Ayer JP. Vascular leiomyoma: a study of sixty-one cases. Arch Pathol Lab Med 1959; 68:424–430.
8. Seremetis MG, Lyons WS, de Guzman VC, et al. Leiomyomata of the esophagus. An analysis of 838 cases. Cancer 1976; 38:2166–2177.
9. Wertheimer-Hatch L, Hatch GF III, Hatch KF, et al. Tumors of the oral cavity and pharynx. World J Surg 2000; 24: 395–400.
10. Hatch GF III, Wertheimer-Hatch L, Hatch KF, et al. Tumors of the esophagus. World J Surg 2000; 24:401–411.
11. Trott MS, Gewirtz A, Lavertu P, et al. Sinonasal leiomyomas. Otolaryngol Head Neck Surg 1994; 111:660–664.
12. Gutmann J, Cifuentes C, Balzarini MA, et al. Angiomyoma of the oral cavity. Oral Surg Oral Med Oral Pathol 1974; 38:269–273.
13. Epivatianos A, Trigonidis G, Papanayotou P. Vascular leiomyomas of the oral cavity. J Oral Maxillofac Surg 1985; 43:377–382.
14. Brooks JK, Nikitakis NG, Goodman NJ, et al. Clinicopathologic characterization of oral angioleiomyomas. Oral Surg Oral Med Oral Pathol Oral Radiol Endod 2002; 94:221–227.
15. Wong SK, Ahuja A, Chow J, et al. Angioleiomyomas in the submandibular region: an unusual tumor in an unusual site. Otolaryngol Head Neck Surg 2000; 122:144–145.
16. Reiner SA, Medina J, Minn KW. Vascular leiomyomas of the carotid sheath simulating a carotid body tumor. Am J Otolaryngol 1998; 19:127–129.
17. Fuse T, Yoshida S, Sakakibara A, et al. Angiomyoma of the retropharyngeal space. J Laryngol Otol 1998; 112:290–293.
18. Shetty SC, Kini U, D'Cruz MN, et al. Angioleiomyomas in the tonsil: an uncommon tumour in a rare site. Br J Oral Maxillofac Surg 2002; 40:169–171.
19. Yeh SY, Chao TK. Leiomyomas of the external auditory canal—a case report and brief review of the literature. Eur Arch Otorhinolaryngol 2005; 262:397–399.
20. Jacobiec FA, Howard GM, Rosen M, et al. Leiomyoma and leiomyosarcoma of the orbit. Am J Ophthalmol 1975; 80:1028–1042.
21. Thompson LDR, Wenig BM, Adair CF, et al. Primary smooth muscle tumors of the thyroid gland. Cancer 1997; 79:579–587.
22. Fanburg-Smith JC, Thompson LDR. Benign soft tissue tumours. In: Barnes L, Eveson JW, Reichart P, et al., eds. Head and Neck Tumours. Lyon, France: IARC Press, 2005:46–57.
23. Fanburg-Smith JC, Thompson LDR, Barnes L. Benign soft tissue tumours. In: Barnes L, Eveson JW, Reichart P, et al., eds. Head and Neck Tumours. Lyon, France: IARC Press, 2005:152–155.
24. Montgomery H, Winkelman RK. Smooth muscle tumors of the skin. Arch Dermatol 1959; 79:32–41.
25. Fisher WC, Helwig EB. Leiomyomas of the skin. Arch Dermatol 1963; 88:510–520.
26. Raj S, Calonje E, Kraus M, et al. Cutaneous pilar leiomyomas: clinicopathologic analysis of 53 lesions in 45 patients. Am J Dermatopathol 1997; 19:2–9.

27. Tomlinson IP, Alam NA, Rowan AJ, et al. Germline mutations in FH predispose to dominantly inherited uterine fibroids, skin leiomyomata and papillary renal cell cancer. Nat Genet 2002; 30:352–353.
28. Ikeda K, Kuroda M, Sakaida N, et al. Cellular leiomyoma of the nasal cavity: findings of CT and MR imaging. AJNR Am J Neuroradiol 2005; 26:1336–1338.
29. Hellquist HB, Hellquist H, Vejlens L, et al. Epithelioid leiomyoma of the larynx. Histopathology 1994; 24:155–159.
30. Morimoto N. Angiomyoma (vascular leiomyoma): a clinicopathologic study. Med J Kagoshima Univ 1973; 24: 663–683.
31. Miettinen MM, Sarlono-Rikala M, Kovatich AJ, et al. Calponin and h-caldesmon in soft tissue tumors: consistent h-caldesmon immunoreactivty in gastrointestinal stromal tumors indicates traits of smooth muscle differentiation. Mod Pathol 1999; 12:756–762.
32. Perez-Montiel MD, Plaza JA, Dominquez-Malagon H, et al. Differential expression of smooth muscle myosin, smooth muscle actin, h-caldesmon, and calponin in the diagnosis of myofibroblastic and smooth muscle lesions of skin and soft tissue. Am J Dermatopathol 2006; 28:105–111.
33. Heim S, Mandahl N, Kristoffersson U, et al. Structural chromosome aberrations in a case of angioleiomyoma. Cancer Genet Cytogenet 1986; 20:325–330.
34. Nilbert M, Mandahl N, Heim S, et al. Cytogenetic abnormalities in an angioleiomyoma. Cancer Genet Cytogenet 1989; 37:61–64.
35. Sonobe H, Ohtsuki Y, Mizobuchi H, et al. An angiomyoma with t(X; 10)(q22; q23.2). Cancer Genet Cytogenet 1996; 90:54–56.
36. Heidet L, Dahan K, Zhou J, et al. Deletions of both alpha 5 (IV) and alpha 6(IV) collagen genes in Alport syndrome and in Alport syndrome associated with smooth muscle tumours. Hum Mol Genet 1995; 4:99–108.
37. Ueki Y, Naito I, Oohashi T, et al. Topoisomerase I and II consensus sequences in a 17-kb deletion junction of the COL4A5 and COL4A6 genes and immunohistochemical analysis of esophageal leiomyomatosis associated with Alport syndrome. Am J Hum Genet 1998; 62:253–261.
38. Heidet L, Boye E, Cai Y, et al. Somatic deletion of the 5′ ends of both the COL4A5 and COL4A6 genes in a sporadic leiomyoma of the esophagus. Am J Pathol 1998; 152:673–678.
39. Segal Y, Peissel B, Renieri A, et al. LINE-1 elements at the sites of molecular rearrangements in Alport syndrome-diffuse leiomyomatosis. Am J Hum Genet 1999; 64:62–69.
40. Fawcett DW. Muscular Tissue. In: Fawcett DW, ed. Bloom and Fawcett. A textbook of histology. Philadelphia, PA: WB Saunders Company, 1986:265–310.
41. Kempson RL, Fletcher CDM, Evans HL, et al. Smooth muscle tumors. In: Kempson RL, Fletcher CDM, Evans HL, et al., eds. Tumors of the Soft Tissues. 3rd series, fascicle 30. Washington, DC: Armed Forces Institute of Pathology, 2001:239–256.
42. Knable A, Treadwell P. Pigmented plaque with hypertrichosis on the scalp on an infant. Pediatr Dermatol 1996; 13:431–433.
43. Weedon D, Williamson RM, Patterson JW. Smooth and skeletal muscle tumours. In: Leboit PE, Burg G, Weedon D, eds. Skin Tumours. Lyon, France: IARC Press, 2006:250–253.
44. Chung EB, Enzinger FM. Infantile myofibromatosis. Cancer 1981; 48:1807–1818.
45. Daimaru Y, Hashimoto H, Enjoji M. Myofibromatosis in adults (adult counterpart of infantile myofibromatosis). Am J Surg Pathol 1989; 13:859–865.
46. Mentzel T, Dei Tos AP, Sapi Z, et al. Myopericytoma of skin and soft tissues. Clinicopathologic and immunohistochemical study of 54 cases. Am J Surg Pathol 2006; 30: 104–113.
47. Hasegawa SL, Mentzel T, Fletcher CD. Schwannomas of the sinonasal tract and nasopharynx. Mod Pathol 1997; 10:777–784.
48. Thompson LD, Miettinen M, Wenig BM. Sinonasal-type hemangiopericytoma: a clinicopathologic and immunophenotypic analysis of 104 cases showing perivascular myoid differentiation. Am J Surg Pathol 2003; 27:737–749.

A. Lipoma, Lipoma Variants, and Reactive Lipomatous Lesions

1. Furlong MA, Fanburg-Smith JC, Childers EL. Lipoma of the oral and maxillofacial region: site and subclassification of 125 cases. Oral Surg Oral Med Oral Pathol Oral Radiol Endod 2004; 98:441–450.
2. Choi HJ, Kim KJ, Lee MW, et al. Pancreatic carcinoma-associated subcutaneous fat necrosis improved by palliative surgery. J Dermatol 2004; 31:584–586.
3. Tillman C, Holst R, Svedman C. Traumatic fat necrosis: a case report. Acta Derm Venereol 2003; 83:227–228.
4. Takao H, Yamahira K, Watanabe T. Encapsulated fat necrosis mimicking abdominal liposarcoma: computed tomography findings. J Comput Assist Tomogr 2004; 28:193–194.
5. Nosanchuk JS. Silicone granuloma in breast. Arch Surg 1968; 97:583–585.
6. Weiss SW. Lipomatous tumors. Monogr Pathol 1996; 38:207–239.
7. Abbondanzo SL, Young VL, Wei MQ, et al. Silicone gel-filled breast and testicular implant capsules: a histologic and immunophenotypic study. Mod Pathol 1999; 12: 706–713.
8. Di SV, Nixon JE. Skin and fat atrophy complications of local steroid injection. Pa Med 1974; 77:38.
9. Farshid G, Weiss SW. Massive localized lymphedema in the morbidly obese: a histologically distinct reactive lesion simulating liposarcoma. Am J Surg Pathol 1998; 22:1277–1283.
10. Fletcher CD, Martin-Bates E. Intramuscular and intermuscular lipoma: neglected diagnoses. Histopathology 1988; 12:275–287.
11. Garavaglia J, Gnepp DR. Intramuscular (infiltrating) lipoma of the tongue. Oral Surg Oral Med Oral Pathol 1987; 63:348–350.
12. Takeda Y. Intramuscular lipoma of the tongue: report of a rare case. Ann Dent 1989; 48:22–24.
13. Buller A, O'Donnell A, Bonshek RE, et al. Intramuscular lipoma of the eyelid: a case report. Eye 2004; 18:743–745.
14. Charles NC, Palu RN. Intramuscular lipoma of the eyelid. Ophthalmic Surg Lasers 2000; 31:340–341.
15. Piattelli A, Fioroni M, Rubini C. Intramuscular lipoma of the cheek: a case report. J Oral Maxillofac Surg 2000; 58: 817–819.
16. Ban M, Kitajima Y. Intramuscular lipoma within the temporal muscle. Int J Dermatol 2002; 41:689–690.
17. Uemura T, Suse T, Yokoyama T, et al. Intramuscular benign lipoma of the temporalis muscle. Scand J Plast Reconstr Surg Hand Surg 2002; 36:231–234.
18. Chen KT, Weinberg RA. Intramuscular lipoma of the larynx. Am J Otolaryngol 1984; 5:71–72.
19. Deschler DG, Lee K, Tami TA. Laryngeal infiltrating intramuscular lipoma. Otolaryngol Head Neck Surg 1993; 108:374–377.
20. Amine B, Leguilchard F, Benhamou CL. Dercum's disease (adiposis dolorosa): a new case-report. Joint Bone Spine 2004; 71:147–149.
21. Wortham NC, Tomlinson IP. Dercum's disease. Skinmed 2005; 4:157–162.

22. Grimmett GM, Hall MG Jr., Aird CC, et al. Pelvic lipomatosis. Am J Surg 1973; 125:347–349.
23. Heyns CF. Pelvic lipomatosis: a review of its diagnosis and management. J Urol 1991; 146:267–273.
24. Klein FA, Smith MJ, Kasenetz I. Pelvic lipomatosis: 35-year experience. J Urol 1988; 139:998–1001.
25. Dokmetas HS, Korkmaz S, Ozcelik S, et al. Madelung's disease in a patient with diabetes mellitus. Skinmed 2007; 6:247–249.
26. Luscher NJ, Prein J, Spiessl B. Lipomatosis of the neck (Madelung's neck). Ann Plast Surg 1986; 16:502–508.
27. Yang CY, Chou CW, Lin MB. Non-insulin-dependent diabetes mellitus with type I multiple symmetrical lipomatosis: a case report. Zhonghua Yi Xue Za Zhi (Taipei) 1999; 62:167–174.
28. Fletcher CD, Martin-Bates E. Spindle cell lipoma: a clinicopathological study with some original observations. Histopathology 1987; 11:803–817.
29. Angervall L, Dahl I, Kindblom LG, et al. Spindle cell lipoma. Acta Pathol Microbiol Scand [A] 1976; 84:477–487.
30. Azzopardi JG, Iocco J, Salm R. Pleomorphic lipoma: a tumour simulating liposarcoma. Histopathology 1983; 7:511–523.
31. Enzinger FM, Harvey DA. Spindle cell lipoma. Cancer 1975; 36:1852–1859.
32. Fanburg-Smith JC, Devaney KO, Miettinen M, et al. Multiple spindle cell lipomas: a report of 7 familial and 11 nonfamilial cases. Am J Surg Pathol 1998; 22:40–48.
33. Meis JM, Enzinger FM. Chondroid lipoma. A unique tumor simulating liposarcoma and myxoid chondrosarcoma. Am J Surg Pathol 1993; 17:1103–1112.
34. Kindblom LG, Meis-Kindblom JM. Chondroid lipoma: an ultrastructural and immunohistochemical analysis with further observations regarding its differentiation. Hum Pathol 1995; 26:706–715.
35. Darling MR, Daley TD. Intraoral chondroid lipoma: a case report and immunohistochemical investigation. Oral Surg Oral Med Oral Pathol Oral Radiol Endod 2005; 99: 331–333.
36. Rossouw DJ, Cinti S, Dickersin GR. Liposarcoma. An ultrastructural study of 15 cases. Am J Clin Pathol 1986; 85:649–667.
37. Furlong MA, Fanburg-Smith JC, Miettinen M. The morphologic spectrum of hibernoma: a clinicopathologic study of 170 cases. Am J Surg Pathol 2001; 25:809–814.
38. Manganaro AM, Hammond HL, Williams TP. Intraosseous angiolipoma of the mandible: a case report and review of the literature. J Oral Maxillofac Surg 1994; 52:767–769.
39. Reilly JS, Kelly DR, Royal SA. Angiolipoma of the parotid: case report and review. Laryngoscope 1988; 98:818–821.
40. Campos GM, Grandini SA, Lopes RA. Angiolipoma of the cheek. Int J Oral Surg 1980; 9:486–490.
41. Flaggert JJ III, Heldt LV, Keaton WM. Angiolipoma of the palate. Report of a case. Oral Surg Oral Med Oral Pathol 1986; 61:333–336.
42. Ida-Yonemochi H, Swelam W, Saito C, et al. Angiolipoma of the buccal mucosa: a possible role of mast cell-derived VEGF in its enhanced vascularity. J Oral Pathol Med 2005; 34:59–61.
43. Ozer E, Schuller DE. Angiolipoma of the neck. Otolaryngol Head Neck Surg 2006; 135:643–644.
44. Saydam L, Bozkurt MK, Ugur MB, et al. Angiolipoma of the neck: a case report. Ear Nose Throat J 2005; 84:375–377.
45. Shohet JA, Simpson B, Coleman JR, et al. Angiolipoma presenting as a nasal mass. Otolaryngol Head Neck Surg 1998; 118:848–849.
46. Weitzner S, Moynihan PC. Angiolipoma of the cheek in a child. Oral Surg Oral Med Oral Pathol 1978; 45:95–97.
47. Howard WR, Helwig EB. Angiolipoma. Arch Dermatol 1960; 82:924–931.
48. Dixon AY, McGregor DH, Lee SH. Angiolipomas: an ultrastructural and clinicopathological study. Hum Pathol 1981; 12:739–747.
49. Chung EB, Enzinger FM. Benign lipoblastomatosis. An analysis of 35 cases. Cancer 1973; 32:482–492.
50. Calhoun KH, Clark WD, Jones JD. Parotid lipoblastoma in an infant. Int J Pediatr Otorhinolaryngol 1987; 14:41–44.
51. Enghardt MH, Warren RC. Congenital palpebral lipoblastoma. First report of a case. Am J Dermatopathol 1990; 12:408–411.
52. Krempl GA, McGuff HS, Pulitzer DR, et al. Lipoblastoma in the parotid gland of an infant. Otolaryngol Head Neck Surg 1997; 117:S234–S237.
53. Hoehn JG, Yalamanchi BA, Pilon V. Benign lipoblastomatosis: report of a case involving the face and neck. Plast Reconstr Surg 1984; 73:455–458.
54. Shear M. Lipoblastomatosis of the cheek. Br J Oral Surg 1967; 5:173–179.
55. Adams RJ, Drwiega PJ, Rivera CA. Congenital orbital lipoblastoma: a pathologic and radiologic study. J Pediatr Ophthalmol Strabismus 1997; 34:194–196.
56. Dogan R, Kara M, Firat P, et al. An unusual tumor of the neck and mediastinum: lipoblastomatosis resulting in paraparesis. Eur J Cardiothorac Surg 2007; 31:325–327.
57. Ratan SK, Gambhir A, Mullick S, et al. Lipoblastoma of the neck. Indian J Pediatr 2000; 67:301–303.
58. Seider N, Gilboa M, Barishak YR, et al. Congenital combined orbito-nasal lipoblastoma: clinico-pathologic study. Orbit 2007; 26:125–127.
59. Collins MH, Chatten J. Lipoblastoma/lipoblastomatosis: a clinicopathologic study of 25 tumors. Am J Surg Pathol 1997; 21:1131–1137.
60. Mentzel T, Calonje E, Fletcher CD. Lipoblastoma and lipoblastomatosis: a clinicopathological study of 14 cases. Histopathology 1993; 23:527–533.
61. Kauffman SL, Stout AP. Lipoblastic tumors of children. Cancer 1959; 12:912–925.
62. Billings SD, Henley JD, Summerlin DJ, et al. Spindle cell lipoma of the oral cavity. Am J Dermatopathol 2006; 28:28–31.
63. Saitoh Y, Hama T, Ishizaka S, et al. Fibrolipoma of the parotid in a child. Am J Otolaryngol 1995; 16:433–435.
64. Baharloo F, Corhay JL, Hotermans G, et al. A case of tracheal fibrolipoma. Acta Clin Belg 1994; 49:23–25.
65. Verplancke J, Gelin G, Van den BT, et al. Esophageal fibrolipoma. J Belge Radiol 1993; 76:45.
66. Taff ML, Schwartz IS, Boglioli LR. Sudden asphyxial death due to a prolapsed esophageal fibrolipoma. Am J Forensic Med Pathol 1991; 12:85–88.
67. Kennedy KS, Wotowic PJ, St John JN. Parapharyngeal fibrolipoma. Head Neck 1990; 12:84–87.
68. Graham GS, Brannon RB, Houston GD. Fibrolipoma of the gingiva. A case report. J Periodontol 1988; 59:118–120.
69. Cole FH Jr., Hays A, Tucker C. Giant esophageal fibrolipoma: case report and review of the literature. J Tenn Med Assoc 1987; 80:267–269.
70. Kiehl RL. Oral fibrolipoma beneath complete mandibular denture. J Am Dent Assoc 1980; 100:561–562.
71. Puri ND, Vaid A, Sawhney KL. Fibrolipoma of the nasopharynx. J Indian Med Assoc 1979; 72:215–216.
72. Stewart S, Levy R, Stoopack JC. Fibrolipoma of the palate: report of two cases. N Y State Dent J 1974; 40:603–606.
73. McHenry LC, Wine CJ. Fibrolipoma of hypopharynx. Case report with 20 year follow up. J Okla State Med Assoc 1973; 66:424–425.
74. Horton JE. Lipomas of the tongue. Report of a fibrolipoma. Oral Surg Oral Med Oral Pathol 1968; 25:914–918.

75. Rose HP. Fibrolipoma of the oral cavity. Report of a case. N Y State Dent J 1967; 33:603–605.
76. Makhlouf HR, Ishak KG, Shekar R, et al. Melanoma markers in angiomyolipoma of the liver and kidney: a comparative study. Arch Pathol Lab Med 2002; 126:49–55.
77. Pea M, Bonetti F, Zamboni G, et al. Melanocyte-marker-HMB-45 is regularly expressed in angiomyolipoma of the kidney. Pathology 1991; 23:185–188.
78. O'Malley DP. Benign extramedullary myeloid proliferations. Mod Pathol 2007; 20:405–415.
79. Bishop E, Eble JN, Cheng L, et al. Adrenal myelolipomas show nonrandom X-chromosome inactivation in hematopoietic elements and fat: support for a clonal origin of myelolipomas. Am J Surg Pathol 2006; 30:838–843.
80. Daneshmand S, Quek L. Adrenal myelolipoma: diagnosis and management. Urol J 2006; 3:71–74.
81. Stewart MG, Schwartz MR, Alford BR. Atypical and malignant lipomatous lesions of the head and neck. Arch Otolaryngol Head Neck Surg 1994; 120:1151–1155.
82. Laurino L, Furlanetto A, Orvieto E, et al. Well-differentiated liposarcoma (atypical lipomatous tumors). Semin Diagn Pathol 2001; 18:258–262.
83. Dei Tos AP. Liposarcoma: new entities and evolving concepts. Ann Diagn Pathol 2000; 4:252–266.
84. Evans HL. Atypical lipomatous tumor, its variants, and its combined forms: a study of 61 cases, with a minimum follow-up of 10 years. Am J Surg Pathol 2007; 31:1–14.
85. Luzar B, Gasljevic G, Juricic V, et al. Hemosiderotic fibrohistiocytic lipomatous lesion: early pleomorphic hyalinizing angiectatic tumor? Pathol Int 2006; 56:283–286.
86. Kazakov DV, Sima R, Michal M. Hemosiderotic fibrohistiocytic lipomatous lesion: clinical correlation with venous stasis. Virchows Arch 2005; 447:103–106.
87. Guillou L, Coindre JM. Newly described adipocytic lesions. Semin Diagn Pathol 2001; 18:238–249.
88. Marshall-Taylor C, Fanburg-Smith JC. Hemosiderotic fibrohistiocytic lipomatous lesion: ten cases of a previously undescribed fatty lesion of the foot/ankle. Mod Pathol 2000; 13:1192–1199.
89. Murphey MD, Carroll JF, Flemming DJ, et al. From the archives of the AFIP: benign musculoskeletal lipomatous lesions. Radiographics 2004; 24:1433–1466.
90. Choma TJ, Kuklo TR, Islinger RB, et al. Paget's disease of bone in patients younger than 40 years. Clin Orthop Relat Res 2004; 202–204.
91. Beaman FD, Bancroft LW, Peterson JJ, et al. Imaging characteristics of cherubism. AJR Am J Roentgenol 2004; 182:1051–1054.
92. Petit MM, Swarts S, Bridge JA, et al. Expression of reciprocal fusion transcripts of the HMGIC and LPP genes in parosteal lipoma. Cancer Genet Cytogenet 1998; 106:18–23.
93. Rogalla P, Kazimierczak B, Meyer-Bolte K, et al. The t(3;12)(q27;q14-q15) with underlying HMGIC-LPP fusion is not determining an adipocytic phenotype. Genes Chromosomes Cancer 1998; 22:100–104.
94. Petit M, Mols R, Schoenmakers E, et al. LPP, the preferred fusion partner gene of *HMGIC* in lipomas, is a novel member of the LIM protein gene family. Genomics 1996; 36:118–129.
95. Petit MM, Schoenmakers EF, Huysmans C, et al. LHFP, a novel translocation partner gene of HMGIC in a lipoma, is a member of a new family of LHFP-like genes. Genomics 1999; 57:438–441.
96. Broberg K, Zhang M, Strombeck B, et al. Fusion of RDC1 with HMGA2 in lipomas as the result of chromosome aberrations involving 2q35-37and 12q13-15. Int J Oncol 2002; 21:321–326.
97. Kazmierczak B, Dal Cin P, Wanschura S, et al. Cloning and molecular characterization of part of a new gene fused to HMGIC in mesenchymal tumors. Am J Pathol 1998; 152:431–435.
98. Ballaux F, Debiec-Rychter M, De Wever I, et al. Chondroid lipoma is characterized by t(11;16)(q13;p12-13). Virchows Arch 2004; 444:208–210.
99. Sandberg AA. Updates on the cytogenetics and molecular genetics of bone and soft tissue tumors: lipoma. Cancer Genet Cytogenet 2004; 150:93–115.
100. Meloni AM, Spanier SS, Bush CH, et al. Involvement of 10q22 and 11q13 in hibernoma. Cancer Genet Cytogenet 1994; 72:59–64.
101. Martens F, Rydholm A, Brosjö O, et al. Hibernomas are characterized by rearrangements of chromosome bands 11q13-21. Int J Cancer 1994; 58:503–505.
102. Mrózek K, Karakousis CP, Bloomfield CD. Band 11q13 in nonrandomly rearranged in hibernomas. Genes Chromosomes Cancer 1994; 9:145–147.
103. Gisselsson D, Höglund M, Mertens F, et al. Hibernomas are characterized by homozygous deletions in the multiple endocrine neoplasia type I region. Metaphase fluorescence in situ hybridization reveals complex rearrangements not detected by conventional cytogenetics. Am J Pathol 1999; 155:61–66.
104. Maire G, Forus A, Foa C, et al. 11q13 alterations in two cases of hibernoma: large heterozygous deletions and rearrangement breakpoints near GARP in 11q13.5. Genes Chromosomes Cancer 2003; 37:389–395.
105. Turaga KK, Silva-Lopez E, Sanger WG, et al. A (9;11)(q34; q13) translocation in hibernoma. Cancer Genet Cytogenet 2006; 170:163–166.
106. Astrom A, D'Amore ES, Sainati L, et al. Evidence of involvement of the PLAG1 gene in lipoblastomas. Int J Oncol 2000; 16:1107–1110.
107. Hibbard MK, Kozakewich HP, Dal Cin P, et al. PLAG1 fusion oncogenes in lipoblastoma. Cancer Res 2000; 60:4869–4872.
108. Gisselsson D, Hibbard MK, Dal Cin P, et al. PLAG1 alterations in lipoblastoma: involvement in varied mesenchymal cell types and evidence for alternative oncogenic mechanisms. Am J Pathol 2001; 159:955–962.
109. Sciot R, De Wever I, Debiec-Rychter M. Lipoblastoma in a 23-year-old male: distinction from atypical lipomatous tumor using cytogenetic and fluorescence in-situ hybridization analysis. Virchows Arch 2003; 442:468–471.

A. Nodular Fasciitis and Related Lesions Including Cranial Fasciitis

1. Hutter RV, Stewart FW, Foote FW Jr. Fasciitis. A report of 70 cases with follow-up proving the benignity of the lesion. Cancer 1962; 15:992–1003.
2. Konwaler BE, Keasbey L, Kaplan L. Subcutaneous pseudosarcomatous fibromatosis (fasciitis). Am J Clin Pathol 1955; 25:241–252.
3. Shimizu S, Hashimoto H, Enjoji M. Nodular fasciitis: an analysis of 250 patients. Pathology 1984; 16:161–166.
4. Price EB Jr., Silliphant WM, Shuman R. Nodular fasciitis: a clinicopathologic analysis of 65 cases. Am J Clin Pathol 1961; 35:122–136.
5. Soule EH. Proliferative (nodular) fasciitis. Arch Pathol 1962; 73:437–444.
6. Dahl I, Jarlstedt J. Nodular fasciitis in the head and neck. A clinicopathological study of 18 cases. Acta Otolaryngol 1980; 90:152–159.

7. Bernstein KE, Lattes R. Nodular (pseudosarcomatous) fasciitis, a nonrecurrent lesion: clinicopathologic study of 134 cases. Cancer 1982; 49:1668–1678.
8. Thompson LD, Fanburg-Smith JC, Wenig BM. Nodular fasciitis of the external ear region: a clinicopathologic study of 50 cases. Ann Diagn Pathol 2001; 5:191–198.
9. Meister P, Buckmann FW, Konrad E. Extent and level of fascial involvement in 100 cases with nodular fasciitis. Virchows Arch A Pathol Anat Histol 1978; 380:177–185.
10. Handa Y, Asai T, Tomita Y. Nodular fasciitis of the forehead in a pediatric patient. Dermatol Surg 2003; 29:867–868.
11. Huang CD, Lin YH, Lee FP. Postauricular nodular fasciitis. Otolaryngol Head Neck Surg 2007; 137:164–165.
12. Font RL, Zimmerman LE. Nodular fasciitis of the eye and adnexa. A report of ten cases. Arch Ophthalmol 1966; 75:475–481.
13. Werning JT. Nodular fasciitis of the orofacial region. Oral Surg Oral Med Oral Pathol 1979; 48:441–446.
14. Dayan D, Nasrallah V, Vered M. Clinico-pathologic correlations of myofibroblastic tumors of the oral cavity: 1. Nodular fasciitis. J Oral Pathol Med 2005; 34:426–435.
15. Smith JF. Nodular fasciitis of the buccal pad. Arch Otolaryngol 1967; 86:217–218.
16. Sato M, Yanagawa T, Yoshida H, et al. Submucosal nodular fasciitis arising within the buccal area. Report of case. Int J Oral Surg 1981; 10:210–213.
17. Fischer JR, Abdul-Karim FW, Robinson RA. Intraparotid nodular fasciitis. Arch Pathol Lab Med 1989; 113:1276–1278.
18. Jones SR, Myers EN, Barnes L. Benign neoplasms of the larynx. Otolaryngol Clin North Am 1984; 17:151–178.
19. Numajiri T, Nishino K. Nodular fasciitis of the nose. Eur J Dermatol 2007; 17:542–543.
20. Saad RS, Takei H, Lipscomb J, et al. Nodular fasciitis of parotid region: a pitfall in the diagnosis of pleomorphic adenomas on fine-needle aspiration cytology. Diagn Cytopathol 2005; 33:191–194.
21. Patchefsky AS, Enzinger FM. Intravascular fasciitis: a report of 17 cases. Am J Surg Pathol 1981; 5:29–36.
22. Samaratunga H, Searle J, O'Loughlin B. Intravascular fasciitis: a case report and review of the literature. Pathology 1996; 28:8–11.
23. Kim ST, Kim HJ, Park SW, et al. Nodular fasciitis in the head and neck: CT and MR imaging findings. AJNR Am J Neuroradiol 2005; 26:2617–2623.
24. Leung LY, Shu SJ, Chan AC, et al. Nodular fasciitis: MRI appearance and literature review. Skeletal Radiol 2002; 31:9–13.
25. Wang XL, De Schepper AM, Vanhoenacker F, et al. Nodular fasciitis: correlation of MRI findings and histopathology. Skeletal Radiol 2002; 31:155–161.
26. Pagenstecher A, Emmerich B, van Velthoven V, et al. Exclusively intracranial cranial fasciitis in a child. Case report. J Neurosurg 1995; 83:744–747.
27. Wirman JA. Nodular fasciitis, a lesion of myofibroblasts: an ultrastructural study. Cancer 1976; 38:2378–2389.
28. Eyden B. The myofibroblast: a study of normal, reactive and neoplastic tissues, with an emphasis on ultrastructure. Part 2 - tumours and tumour-like lesions. J Submicrosc Cytol Pathol 2005; 37:231–296.
29. Montgomery EA, Meis JM. Nodular fasciitis. Its morphologic spectrum and immunohistochemical profile. Am J Surg Pathol 1991; 15:942–948.
30. Kayaselcuk F, Demirhan B, Kayaselcuk U, et al. Vimentin, smooth muscle actin, desmin, S-100 protein, p53, and estrogen receptor expression in elastofibroma and nodular fasciitis. Ann Diagn Pathol 2002; 6:94–99.
31. Carlson JW, Fletcher CD. Immunohistochemistry for beta-catenin in the differential diagnosis of spindle cell lesions: analysis of a series and review of the literature. Histopathology 2007; 51:509–514.
32. Hornick JL, Fletcher CD. Intraarticular nodular fasciitis—a rare lesion: clinicopathologic analysis of a series. Am J Surg Pathol 2006; 30:237–241.
33. Bhattacharya B, Dilworth HP, Iacobuzio-Donahue C, et al. Nuclear beta-catenin expression distinguishes deep fibromatosis from other benign and malignant fibroblastic and myofibroblastic lesions. Am J Surg Pathol 2005; 29:653–659.
34. Birdsall SH, Shipley JM, Summersgill BM, et al. Cytogenetic findings in a case of nodular fasciitis of the breast. Cancer Genet Cytogenet 1995; 81:166–168.
35. Sawyer JR, Sammartino G, Baker GF, et al. Clonal chromosome aberrations in a case of nodular fasciitis. Cancer Genet Cytogenet 1994; 76:154–156.
36. Velagaleti GV, Tapper JK, Panova NE, et al. Cytogenetic findings in a case of nodular fasciitis of subclavicular region. Cancer Genet Cytogenet 2003; 141:160–163.
37. Donner LR, Silva T, Dobin SM. Clonal rearrangement of 15p11.2, 16p11.2, and 16p13.3 in a case of nodular fasciitis: additional evidence favoring nodular fasciitis as a benign neoplasm and not a reactive tumefaction. Cancer Genet Cytogenet 2002; 139:138–140.
38. Weibolt VM, Buresh CJ, Roberts CA, et al. Involvement of 3q21 in nodular fasciitis. Cancer Genet Cytogenet 1998; 106:177–179.
39. Lauer DH, Enzinger FM. Cranial fasciitis of childhood. Cancer 1980; 45:401–406.

B. Reactive Myofibroblastic Lesions, Including Proliferative Fasciitis, Proliferative Myositis, and Reactive Periostitis

1. Chung EB, Enzinger FM. Proliferative fasciitis. Cancer 1975; 36:1450–1458.
2. Kern WH. Proliferative myositis; a pseudosarcomatous reaction to injury: a report of seven cases. Arch Pathol 1960; 69:209–216.
3. Enzinger FM, Dulcey F. Proliferative myositis. Report of thirty-three cases. Cancer 1967; 20:2213–2223.
4. Meis JM, Enzinger FM. Proliferative fasciitis and myositis of childhood. Am J Surg Pathol 1992; 16:364–372.
5. Choi SS, Myer CM III. Proliferative myositis of the mylohyoid muscle. Am J Otolaryngol 1990; 11:198–202.
6. Dent CD, DeBoom GW, Hamlin ML. Proliferative myositis of the head and neck. Report of a case and review of the literature. Oral Surg Oral Med Oral Pathol 1994; 78:354–358.
7. Donegan JO, Miller TH, Wirman JA. Proliferative myositis in the head and neck. Am J Otolaryngol 1983; 4:442–444.
8. Fujiwara K, Watanabe T, Katsuki T, et al. Proliferative myositis of the buccinator muscle: a case with immunohistochemical and electron microscopic analysis. Oral Surg Oral Med Oral Pathol 1987; 63:597–601.
9. Orlowski W, Freedman PD, Lumerman H. Proliferative myositis of the masseter muscle. A case report and a review of the literature. Cancer 1983; 52:904–908.
10. Scher N, Dobleman TJ, Poe DS, et al. Proliferative myositis of the masseter muscle. Laryngoscope 1987; 97:591–593.
11. Brooks JK, Scheper MA, Kramer RE, et al. Intraoral proliferative myositis: case report and literature review. Head Neck 2007; 29:416–420.
12. Georgalas C, Kapoor L, Chau H, et al. Inflammatory focal myositis of the sternomastoid muscle: is there an absolute indication for biopsy? A case report and review of the literature. Eur Arch Otorhinolaryngol 2006; 263:149–151.

13. Singh A, Philpott JM, Patel NN, et al. Proliferative myositis arising in the tongue. J Laryngol Otol 2000; 114:978–979.
14. Montgomery EA, Meis JM, Mitchell MS, et al. Atypical decubital fibroplasia. A distinctive fibroblastic pseudotumor occurring in debilitated patients. Am J Surg Pathol 1992; 16:708–715.
15. Kato K, Ehara S, Nishida J, et al. Rapid involution of proliferative fasciitis. Skeletal Radiol 2004; 33:300–302.
16. Ilaslan H, Joyce M, Bauer T, et al. Decubital ischemic fasciitis: clinical, pathologic, and MRI features of pseudosarcoma. AJR Am J Roentgenol 2006; 187:1338–1341.
17. Craver JL, McDivitt RW. Proliferative fasciitis: ultrastructural study of two cases. Arch Pathol Lab Med 1981; 105:542–545.
18. Gokel JM, Meister P, Hubner G. Proliferative myositis. A case report with fine structural analysis. Virchows Arch A Pathol Anat Histol 1975; 367:345–352.
19. Rose AG. An electron microscopic study of the giant cells in proliferative myositis. Cancer 1974; 33:1543–1547.
20. el Jabbour JN, Bennett MH, Burke MM, et al. Proliferative myositis. An immunohistochemical and ultrastructural study. Am J Surg Pathol 1991; 15:654–659.
21. Sasano H, Yamaki H, Ohashi Y, et al. Proliferative fasciitis of the forearm: case report with immunohistochemical, ultrastructural and DNA ploidy studies and a review of the literature. Pathol Int 1998; 48:486–490.
22. Lundgren L, Kindblom LG, Willems J, et al. Proliferative myositis and fasciitis. A light and electron microscopic, cytologic, DNA-cytometric and immunohistochemical study. APMIS 1992; 100:437–448.
23. Zambrano E, Nosé V, Perez-Atayde AR, et al. Distinct chromosomal rearrangements in subungual (Dupuytren) exostosis and bizarre parosteal osteochondromatous proliferation (Nora lesion). Am J Surg Pathol. 2004; 28(8): 1033–1039.
24. Dhondt E, Oudenhoven L, Khan S, et al. Nora's lesion, a distinct radiological entity? Skeletal Radiol 2006; 35: 497–502.
25. Hirao K, Sugita T, Yasunaga Y, et al. Florid reactive periostitis of the metatarsal bone: a case report. Foot Ankle Int 2005; 26:771–774.
26. Jambhekar NA, Desai SS, Puri A, et al. Florid reactive periostitis of the hands. Skeletal Radiol 2004; 33:663–665.
27. Solana J, Bosch M, Espanol I. Florid reactive periostitis of the thumb: a case report and review of the literature. Chir Main 2003; 22:99–103.
28. Sundaram M, Wang L, Rotman M, et al. Florid reactive periostitis and bizarre parosteal osteochondromatous proliferation: pre-biopsy imaging evolution, treatment and outcome. Skeletal Radiol 2001; 30:192–198.
29. Rogers GF, Brzezienski MA. Florid reactive periostitis of the middle phalanx: a case report and review of the literature. J Hand Surg [Am] 1999; 24:1014–1018.
30. Moosavi CA, Al-Nahar LA, Murphey M, et al. Fibroosseous pseudotumor of the digit: a clinicopathologic study of 43 new cases. Ann Diagn Pathol 2008; 12(1):21–28.
31. Shankman S, Desai P, Beltran J. Subperiosteal osteoid osteoma: radiographic and pathologic manifestations. Skeletal Radiol 1997; 26:457–462.
32. Howard RF, Slawski DP, Gilula LA. Florid reactive periostitis of the digit with cortical erosion: a case report and review of the literature. J Hand Surg [Am] 1996; 21: 501–505.
33. Riaz M, McCluggage WG, Bharucha H, et al. Florid reactive periostitis of the thumb. J Hand Surg [Br] 1996; 21: 276–279.
34. Loyens M, Marcinkowski I, Martens C, et al. Florid reactive periostitis. J Belge Radiol 1995; 78:175–176.
35. Yuen M, Friedman L, Orr W, et al. Proliferative periosteal processes of phalanges: a unitary hypothesis. Skeletal Radiol 1992; 21:301–303.
36. Kovach JC, Truong L, Kearns RJ, et al. Florid reactive periostitis. J Hand Surg [Am] 1986; 11:902–905.
37. Callahan DJ, Walter NE, Okoye MI. Florid reactive periostitis of the proximal phalanx. Case report. J Bone Joint Surg Am 1985; 67:968–970.
38. Jongeward RH Jr., Martel W, Louis DS, et al. Case report 304. Florid reactive periostitis proximal phalange of the left 5th finger. Skeletal Radiol 1985; 13:169–173.
39. Porter AR, Tristan TA, Rudy FR, et al. Florid reactive periostitis of the phalanges. AJR Am J Roentgenol 1985; 144:617–618.
40. Rybak LD, Abramovici L, Kenan S, et al. Cortico-medullary continuity in bizarre parosteal osteochondromatous proliferation mimicking osteochondroma on imaging. Skeletal Radiol 2007; 36:829–834.
41. Claude V, Couture C, Battin-Bertho R, et al. [Unusual parosteal osteochondromatous proliferation or Nora's tumor. A clinicopathological analysis of 4 cases]. Ann Pathol 2003; 23:258–260.
42. deLange EE, Pope TL Jr., Fechner RE, et al. Bizarre parosteal osteochondromatous proliferation vs. benign florid reactive periostitis. AJR Am J Roentgenol 1987; 148:650.
43. Kontogeorgakos VA, Lykissas MG, Mavrodontidis AN, et al. Turret exostosis of the hallux. J Foot Ankle Surg 2007; 46:130–132.
44. Mohanna PN, Moiemen NS, Frame JD. Turret exostosis of the thumb. Br J Plast Surg 2000; 53:629–631.
45. Rubin JA, Steinberg DR. Turret exostosis of the metacarpal: a case report. J Hand Surg [Am] 1996; 21:296–298.
46. Revington PJ. 'Turret exostosis' of the coronoid process. Br J Oral Maxillofac Surg 1984; 22:37–41.
47. Lee BS, Kaplan R. Turret exostosis of the phalanges. Clin Orthop Relat Res 1974; 186–189.
48. Wissinger HA, McClain EJ, Boyes JH. Turret exostosis. Ossifying hematoma of the phalanges. J Bone Joint Surg Am 1966; 48:105–110.
49. Brien EW, Zahiri CA, Mirra JM. Florid reactive periostitis ossificans of the proximal aspect of the tibia: a lesion that must be distinguished from osteosarcoma. A case report. J Bone Joint Surg Am 1999; 81:1002–1007.
50. Spjut HJ, Dorfman HD. Florid reactive periostitis of the tubular bones of the hands and feet. A benign lesion which may simulate osteosarcoma. Am J Surg Pathol 1981; 5: 423–433.

C. Myositis Ossificans

1. Norman A, Dorfman HD. Juxtacortical circumscribed myositis ossificans: evolution and radiographic features. Radiology 1970; 96:301–306.
2. Goldman AB. Myositis ossificans circumscripta: a benign lesion with a malignant differential diagnosis. AJR Am J Roentgenol 1976; 126:32–40.
3. Goodsell JO. Traumatic myositis ossificans of the masseter muscle: review of the literature and report of a case. J Oral Surg Anesth Hosp Dent Serv 1962; 20:116–122.
4. Plezia RA, Mintz SM, Calligaro P. Myositis ossificans traumatica of the masseter muscle. Report of a case. Oral Surg Oral Med Oral Pathol 1977; 44:351–357.
5. Vernale CA. Traumatic myositis ossificans of the masseter muscle. Report of two cases. Oral Surg Oral Med Oral Pathol 1968; 26:8–17.
6. Wussow GC. Myositis ossificans of the buccinator muscle. Oral Surg Oral Med Oral Pathol 1968; 26:615–618.

7. Parkash H, Goyal M. Myositis ossificans of medial pterygoid muscle. A cause for temporomandibular joint ankylosis. Oral Surg Oral Med Oral Pathol 1992; 73:27–28.
8. Shugar MA, Weber AL, Mulvaney TJ. Myositis ossificans following radical neck dissection. Ann Otol Rhinol Laryngol 1981; 90:169–171.
9. Manzano D, Silvan A, Saez J, et al. Myositis ossificans of the temporalis muscle. Case report. Med Oral Patol Oral Cir Bucal 2007; 12:E277–E280.
10. Uematsu Y, Nishibayashi H, Fujita K, et al. Myositis ossificans of the temporal muscle as a primary scalp tumor. Case report. Neurol Med Chir (Tokyo) 2005; 45:56–58.
11. Saka B, Stropahl G, Gundlach KK. Traumatic myositis ossificans (ossifying pseudotumor) of temporal muscle. Int J Oral Maxillofac Surg 2002; 31:110–111.
12. Georgalas C, Kapoor L, Chau H, et al. Inflammatory focal myositis of the sternomastoid muscle: is there an absolute indication for biopsy? A case report and review of the literature. Eur Arch Otorhinolaryngol 2006; 263:149–151.
13. Pappas DG, Johnson LA. Laryngeal myositis ossificans: a case report. Arch Otolaryngol 1965; 81:227–231.
14. Ackerman LV. Extra-osseous localized non-neoplastic bone and cartilage formation (so-called myositis ossificans): clinical and pathological confusion with malignant neoplasms. J Bone Joint Surg Am 1958; 40-A:279–298.
15. Clapton WK, James CL, Morris LL, et al. Myositis ossificans in childhood. Pathology 1992; 24:311–314.
16. Nuovo MA, Norman A, Chumas J, et al. Myositis ossificans with atypical clinical, radiographic, or pathologic findings: a review of 23 cases. Skeletal Radiol 1992; 21:87–101.
17. Sumiyoshi K, Tsuneyoshi M, Enjoji M. Myositis ossificans. A clinicopathologic study of 21 cases. Acta Pathol Jpn 1985; 35:1109–1122.
18. Dupree WB, Enzinger FM. Fibro-osseous pseudotumor of the digits. Cancer 1986; 58:2103–2109.
19. Paterson DC. Myositis ossificans circumscripta. Report of four cases without history of injury. J Bone Joint Surg Br 1970; 52:296–301.
20. Hait G, Boswick JA Jr., Stone NH. Heterotopic bone formation secondary to trauma (myositis ossificans traumatica). J Trauma 1970; 10:405–411.
21. Hagiwara H, Aida N, Machida J, et al. Contrast-enhanced MRI of an early preosseous lesion of fibrodysplasia ossificans progressiva in a 21-month-old boy. AJR Am J Roentgenol 2003; 181:1145–1147.
22. Kransdorf MJ, Meis JM, Jelinek JS. Myositis ossificans: MR appearance with radiologic-pathologic correlation. AJR Am J Roentgenol 1991; 157:1243–1248.
23. Fanburg-Smith JC, Bratthauer GL, Miettinen M. Osteocalcin and osteonectin immunoreactivity in extraskeletal osteosarcoma: a study of 28 cases. Hum Pathol 1999; 30:32–38.
24. Povysil C, Matejovsky Z. Ultrastructural evidence of myofibroblasts in pseudomalignant myositis ossificans. Virchows Arch A Pathol Anat Histol 1979; 381:189–203.
25. Ragunanthan N, Sugavanam C. Pseudomalignant myositis ossificans mimicking osteosarcoma: a case report. J Orthop Surg (Hong Kong) 2006; 14:219–221.
26. Crundwell N, O'Donnell P, Saifuddin A. Non-neoplastic conditions presenting as soft-tissue tumours. Clin Radiol 2007; 62:18–27.
27. Molloy JC, McGuirk RA. Treatment of traumatic myositis ossificans circumscripta; use of aspiration and steroids. J Trauma 1976; 16:851–857.
28. Illingworth RS. Myositis ossificans progressiva (Munchmeyer's disease). Brief review with report of two cases treated with corticosteroids and observed for 16 years. Arch Dis Child 1971; 46:264–268.
29. Letts RM. Myositis ossificans progressiva. A report of two cases with chromosome studies. Can Med Assoc J 1968; 99:856–862.
30. Marrannes J, Box I, Haspeslagh M, et al. Jaw fixation as the key to diagnosis of fibrodysplasia ossificans progressiva. JBR-BTR 2006; 89:195–197.
31. Sendur OF, Gurer G. Severe limitation in jaw movement in a patient with fibrodysplasia ossificans progressiva: a case report. Oral Surg Oral Med Oral Pathol Oral Radiol Endod 2006; 102:312–317.
32. van der Meij EH, Becking AG, van der Waal I. Fibrodysplasia ossificans progressiva. An unusual cause of restricted mandibular movement. Oral Dis 2006; 12:204–207.
33. McCarthy EF, Sundaram M. Heterotopic ossification: a review. Skeletal Radiol 2005; 34:609–619.
34. Lutwak L. Myositis ossificans progressiva. Mineral, metabolic and radioactive calcium studies of the effects of hormones. Am J Med 1964; 37:269–293.

D. Osseous and Cartilaginous Choristomas (Extraskeletal Osteoma and Extraskeletal Chondroma of Head and Neck)

1. Chou LS, Hansen LS, Daniels TE. Choristomas of the oral cavity: a review. Oral Surg Oral Med Oral Pathol 1991; 72:584–593.
2. Engel P, Cherrick HM. Extraosseous osteomas of the tongue. J Oral Med 1976; 31:99–103.
3. Landini G, Kitano M, Urago A, et al. Chondroma and osteochondroma of the tongue. Oral Surg Oral Med Oral Pathol 1989; 68:206–209.
4. Shimono M, Tsuji T, Iguchi Y, et al. Lingual osseous choristoma. Report of 2 cases. Int J Oral Surg 1984; 13:355–359.
5. Supiyaphun P, Sampatanakul P, Kerekhanjanarong V, et al. Lingual osseous choristoma: a study of eight cases and review of the literature. Ear Nose Throat J 1998; 77:316–318, 320, 325.
6. Unal T, Erturk S. Cartilaginous choristoma of the gingiva. Report of two cases; review of the literature of both gingival choristomas and intraoral chondromas. Ann Dent 1994; 53:19–27.
7. van der Wal N, van der Waal I. Osteoma or chondroma of the tongue; a clinical and postmortem study. Int J Oral Maxillofac Surg 1987; 16:713–717.
8. Vered M, Lustig JP, Buchner A. Lingual osteoma: a debatable entity. J Oral Maxillofac Surg 1998; 56:9–13.
9. Zegarelli DJ. Chondroma of the tongue. Oral Surg Oral Med Oral Pathol 1977; 43:738–745.
10. Neville BW, Damm DD, Allen CM, et al. Oral and Maxillofacial Pathology. Philadelphia: W.B. Saunders, 2002: 479–480.
11. Ishikawa M, Mizukoshi T, Notani K, et al. Osseous choristoma of the tongue. Report of two cases. Oral Surg Oral Med Oral Pathol 1993; 76:561–563.
12. Hodder SC, MacDonald DG. Osseous choristoma of buccal mucosa: report of a case. Br J Oral Maxillofac Surg 1988; 26:78–80.
13. Matsushita K, Tahara M, Sato H, et al. Cartilaginous choristoma deep in the upper midline oral vestibule. Br J Oral Maxillofac Surg 2004; 42:436–438.
14. West CB Jr., Atkins JS Jr. Choristomas of the intraoral soft tissues. Otolaryngol Head Neck Surg 1988; 99:528–530.
15. Lin CC, Chen CH, Chen YK, et al. Osseous choristoma of oral cavity—report of two cases and review of the literature. Kaohsiung J Med Sci 1998; 14:727–733.
16. Lekas MD, Sayegh R, Finkelstein SD. Osteoma of the base of the tongue. Ear Nose Throat J 1997; 76:827–828.

E. Idiopathic Cervical Fibrosis

1. Gilkeson GS, Allen NB. Retroperitoneal fibrosis. A true connective tissue disease. Rheum Dis Clin North Am 1996; 22:23–38.
2. Rice DH, Batsakis JG, Coulthard SW. Sclerosing cervicitis: homologue of sclerosing retroperitonitis and mediastinitis. Arch Surg 1975; 110:120–122.
3. Esdaile J, Murray D, Hawkins D, et al. Idiopathic fibrosis of the lateral compartment of the neck. Arch Intern Med 1980; 140:1386–1387.
4. Queen TA, Gibbs PM, Rice DH. Sclerosing cervicitis: case report and literature review. Ear Nose Throat J 1995; 74:238–240, 242.
5. Flieder DB, Suster S, Moran CA. Idiopathic fibroinflammatory (fibrosing/sclerosing) lesions of the mediastinum: a study of 30 cases with emphasis on morphologic heterogeneity. Mod Pathol 1999; 12:257–264.
6. Hostalet F, Hellin D, Ruiz JA. Tumefactive fibroinflammatory lesion of the head and neck treated with steroids: a case report. Eur Arch Otorhinolaryngol 2003; 260:229–231.
7. Said H, Razi HA, Akmal SN, et al. Tumefactive fibroinflammatory lesion of the head and neck. J Laryngol Otol 1988; 102:1064–1067.
8. Olsen KD, DeSanto LW, Wold LE, et al. Tumefactive fibroinflammatory lesions of the head and neck. Laryngoscope 1986; 96:940–944.
9. Smith M, Castillo M, Weissler M. CT findings in a case of exuberant cervical fibrosclerosis. AJR Am J Roentgenol 1992; 159:1263–1264.
10. Wold LE, Weiland LH. Tumefactive fibro-inflammatory lesions of the head and neck. Am J Surg Pathol 1983; 7:477–482.
11. Cheng AY, Davidson MJ, Perez-Ordonez B, et al. Tumefactive fibroinflammatory lesion of the nasal cavity followed by Riedel's thyroiditis. J Otolaryngol 2004; 33:315–318.
12. Husband P, Knudsen A. Idiopathic cervical and retroperitoneal fibrosis: report of a case treated with steroids. Postgrad Med J 1976; 52:788–793.
13. Laurenzo JF, Graham SM. Tumefactive fibroinflammatory lesion of the head and neck: a management strategy. Ear Nose Throat J 1995; 74:87–91, 94.
14. Savelli BA, Parshley M, Morganroth ML. Successful treatment of sclerosing cervicitis and fibrosing mediastinitis with tamoxifen. Chest 1997; 111:1137–1140.
15. Deussing EC, Daroca PJ Jr., Nemechek AJ. Sclerosing cervicitis: report of a skull base lesion with literature review. Head Neck 2003; 25:778–783.
16. Prichard AJ, Colloby P, Barton RP, et al. Tumefactive fibroinflammatory lesions of the head and neck. J Laryngol Otol 1990; 104:797–800.
17. Patel PC, Pellitteri PK, Vrabec DP, et al. Tumefactive fibroinflammatory lesion of the head and neck originating in the infratemporal fossa. Am J Otolaryngol 1998; 19:216–219.
18. Ernst RJ, Cornelius RS. MR findings of sclerosing cervicitis. AJNR Am J Neuroradiol 1995; 16:507–508.
19. Holodny AI, Kirsch CF, Hameed M, et al. Tumefactive fibroinflammatory lesion of the neck with progressive invasion of the meninges, skull base, orbit, and brain. AJNR Am J Neuroradiol 2001; 22:876–879.
20. Ritter JH, Humphrey PA, Wick MR. Malignant neoplasms capable of simulating inflammatory (myofibroblastic) pseudotumors and tumefactive fibroinflammatory lesions: pseudopseudotumors. Semin Diagn Pathol 1998; 15: 111–132.
21. Coffin CM, Dehner LP, Meis-Kindblom JM. Inflammatory myofibroblastic tumor, inflammatory fibrosarcoma, and related lesions: an historical review with differential diagnostic considerations. Semin Diagn Pathol 1998; 15:102–110.
22. Montgomery E, Goldblum JR, Fisher C. Myofibrosarcoma: a clinicopathologic study. Am J Surg Pathol 2001; 25:219–228.
23. Mentzel T, Dry S, Katenkamp D, et al. Low grade myofibroblastic sarcoma. Analysis of 18 cases in the spectrum of myofibroblastic tumors. Am J Surg Pathol 1998; 22: 1228–1238.
24. Veinot JP, Eidus L, Jabi M. Soft tissue Rosai Dorfman disease mimicking inflammatory pseudotumor: a diagnostic pitfall. Pathology 1998; 30:14–16.
25. Wenig BM, Abbondanzo SL, Childers EL, et al. Extranodal sinus histiocytosis with massive lymphadenopathy (Rosai-Dorfman disease) of the head and neck. Hum Pathol 1993; 24:483–492.
26. Montgomery EA, Meis JM, Frizzera G. Rosai-Dorfman disease of soft tissue. Am J Surg Pathol 1992; 16:122–129.

F. Fibrous Hamartoma of Infancy

1. Enzinger FM. Fibrous hamartoma of infancy. Cancer 1965; 18:241–248.
2. Paller AS, Gonzalez-Crussi F, Sherman JO. Fibrous hamartoma of infancy. Eight additional cases and a review of the literature. Arch Dermatol 1989; 125:88–91.
3. Weinberger MS, Pransky SM, Krous HF. Fibrous hamartoma of infancy presenting as a perspiring neck mass. Int J Pediatr Otorhinolaryngol 1993; 26:173–176.
4. Baarsma EA. Juvenile fibrous hamartoma of the pharynx. J Laryngol Otol 1979; 93:75–79.
5. Dickey GE, Sotelo-Avila C. Fibrous hamartoma of infancy: current review. Pediatr Dev Pathol 1999; 2:236–243.
6. Efem SE, Ekpo MD. Clinicopathological features of untreated fibrous hamartoma of infancy. J Clin Pathol 1993; 46:522–524.
7. Grynspan D, Meir K, Senger C, et al. Cutaneous changes in fibrous hamartoma of infancy. J Cutan Pathol 2007; 34:39–43.
8. Sotelo-Avila C, Bale PM. Subdermal fibrous hamartoma of infancy: pathology of 40 cases and differential diagnosis. Pediatr Pathol 1994; 14:39–52.
9. Mitchell ML, di Sant'Agnese PA, Gerber JE. Fibrous hamartoma of infancy. Hum Pathol 1982; 13:586–588.
10. Fletcher CD, Powell G, van Noorden S, et al. Fibrous hamartoma of infancy: a histochemical and immunohistochemical study. Histopathology 1988; 12:65–74.
11. Groisman G, Lichtig C. Fibrous hamartoma of infancy: an immunohistochemical and ultrastructural study. Hum Pathol 1991; 22:914–918.
12. Greco MA, Schinella RA, Vuletin JC. Fibrous hamartoma of infancy: an ultrastructural study. Hum Pathol 1984; 15: 717–723.
13. Lakshminarayanan R, Konia T, Welborn J. Fibrous hamartoma of infancy: a case report with associated cytogenetic findings. Arch Pathol Lab Med 2005; 129:520–522.
14. Rougemont AL, Fetni R, Murthy S, et al. A complex translocation (6;12;8)(q25;q24.3;q13) in a fibrous hamartoma of infancy. Cancer Genet Cytogenet 2006; 171:115–118.
15. Fetsch JF, Miettinen M, Laskin WB, et al. A clinicopathologic study of 45 pediatric soft tissue tumors with an admixture of adipose tissue and fibroblastic elements, and a proposal for classification as lipofibromatosis. Am J Surg Pathol 2000; 24:1491–1500.
16. Herrmann BW, Dehner LP, Forsen JW Jr. Lipofibromatosis presenting as a pediatric neck mass. Int J Pediatr Otorhinolaryngol 2004; 68:1545–1549.
17. Carretto E, Dall'Igna P, Alaggio R, et al. Fibrous hamartoma of infancy: an Italian multi-institutional experience. J Am Acad Dermatol 2006; 54:800–803.

G. Fibromatosis Colli (Torticollis)

1. Wei JL, Schwartz KM, Weaver AL, et al. Pseudotumor of infancy and congenital muscular torticollis: 170 cases. Laryngoscope 2001; 111:688–695.
2. Jaber MR, Goldsmith AJ. Sternocleidomastoid tumor of infancy: two cases of an interesting entity. Int J Pediatr Otorhinolaryngol 1999; 47:269–274.
3. Porter SB, Blount BW. Pseudotumor of infancy and congenital muscular torticollis. Am Fam Physician 1995; 52:1731–1736.
4. Bredenkamp JK, Maceri DR. Inflammatory torticollis in children. Arch Otolaryngol Head Neck Surg 1990; 116: 310–313.
5. Do TT. Congenital muscular torticollis: current concepts and review of treatment. Curr Opin Pediatr 2006; 18: 26–29.
6. Herman MJ. Torticollis in infants and children: common and unusual causes. Instr Course Lect 2006; 55:647–653.
7. Bredenkamp JK, Hoover LA, Berke GS, et al. Congenital muscular torticollis. A spectrum of disease. Arch Otolaryngol Head Neck Surg 1990; 116:212–216.
8. Coventry MD, Harris LE, Bianco AJ, et al. Congenital muscular torticollis (wryneck). Postgrad Med 1960; 28:383–392.
9. Blythe WR, Logan TC, Holmes DK, et al. Fibromatosis colli: a common cause of neonatal torticollis. Am Fam Physician 1996; 54:1965–1967.
10. Tatli B, Aydinli N, Caliskan M, et al. Congenital muscular torticollis: evaluation and classification. Pediatr Neurol 2006; 34:41–44.
11. Davids JR, Wenger DR, Mubarak SJ. Congenital muscular torticollis: sequela of intrauterine or perinatal compartment syndrome. J Pediatr Orthop 1993; 13:141–147.
12. Demirbilek S, Atayurt HF. Congenital muscular torticollis and sternomastoid tumor: results of nonoperative treatment. J Pediatr Surg 1999; 34:549–551.
13. Cheng JC, Tang SP, Chen TM. Sternocleidomastoid pseudotumor and congenital muscular torticollis in infants: a prospective study of 510 cases. J Pediatr 1999; 134:712–716.
14. Ho BC, Lee EH, Singh K. Epidemiology, presentation and management of congenital muscular torticollis. Singapore Med J 1999; 40:675–679.
15. Canale ST, Griffin DW, Hubbard CN. Congenital muscular torticollis. A long-term follow-up. J Bone Joint Surg Am 1982; 64:810–816.
16. Lawrence WT, Azizkhan RG. Congenital muscular torticollis: a spectrum of pathology. Ann Plast Surg 1989; 23:523–530.
17. Morrison DL, MacEwen GD. Congenital muscular torticollis: observations regarding clinical findings, associated conditions, and results of treatment. J Pediatr Orthop 1982; 2: 500–505.
18. Robin NH. Congenital muscular torticollis. Pediatr Rev 1996; 17:374–375.
19. von Heideken J, Green DW, Burke SW, et al. The relationship between developmental dysplasia of the hip and congenital muscular torticollis. J Pediatr Orthop 2006; 26:805–808.
20. Bedi DG, John SD, Swischuk LE. Fibromatosis colli of infancy: variability of sonographic appearance. J Clin Ultrasound 1998; 26:345–348.
21. Vazquez E, Enriquez G, Castellote A, et al. US, CT, and MR imaging of neck lesions in children. Radiographics 1995; 15:105–122.
22. Ablin DS, Jain K, Howell L, et al. Ultrasound and MR imaging of fibromatosis colli (sternomastoid tumor of infancy). Pediatr Radiol 1998; 28:230–233.
23. Kraus R, Han BK, Babcock DS, et al. Sonography of neck masses in children. AJR Am J Roentgenol 1986; 146: 609–613.
24. Eich GF, Hoeffel JC, Tschappeler H, et al. Fibrous tumours in children: imaging features of a heterogeneous group of disorders. Pediatr Radiol 1998; 28:500–509.
25. Entel RJ, Carolan FJ. Congenital muscular torticollis: magnetic resonance imaging and ultrasound diagnosis. J Neuroimaging 1997; 7:128–130.
26. Snitzer EL, Fultz PJ, Asselin B. Magnetic resonance imaging appearance of fibromatosis colli. Magn Reson Imaging 1997; 15:869–871.
27. Sartoris DJ, Mochizuki RM, Parker BR. Lytic clavicular lesions in fibromatosis colli. Skeletal Radiol 1983; 10:34–36.
28. Apple SK, Nieberg RK, Hirschowitz SL. Fine needle aspiration diagnosis of fibromatosis colli. A report of three cases. Acta Cytol 1997; 41:1373–1376.
29. Gonzales J, Ljung BM, Guerry T, et al. Congenital torticollis: evaluation by fine-needle aspiration biopsy. Laryngoscope 1989; 99:651–654.
30. Kurtycz DF, Logrono R, Hoerl HD, et al. Diagnosis of fibromatosis colli by fine-needle aspiration. Diagn Cytopathol 2000; 23:338–342.
31. Pereira S, Tani E, Skoog L. Diagnosis of fibromatosis colli by fine needle aspiration (FNA) cytology. Cytopathology 1999; 10:25–29.
32. Sauer T, Selmer L, Freng A. Cytologic features of fibromatosis colli of infancy. Acta Cytol 1997; 41:633–635.
33. Schwartz RA, Powers CN, Wakely PE Jr., et al. Fibromatosis colli. The utility of fine-needle aspiration in diagnosis. Arch Otolaryngol Head Neck Surg 1997; 123:301–304.
34. Wakely PE Jr., Price WG, Frable WJ. Sternomastoid tumor of infancy (fibromatosis colli): diagnosis by aspiration cytology. Mod Pathol 1989; 2:378–381.
35. Carlson JW, Fletcher CD. Immunohistochemistry for beta-catenin in the differential diagnosis of spindle cell lesions: analysis of a series and review of the literature. Histopathology 2007; 51:509–514.
36. Tang S, Liu Z, Quan X, et al. Sternocleidomastoid pseudotumor of infants and congenital muscular torticollis: fine-structure research. J Pediatr Orthop 1998; 18:214–218.
37. Macdonald D. Sternomastoid tumour and muscular torticollis. J Bone Joint Surg Br 1969; 51:432–443.

H. Gingival Fibromatosis

1. Coletta RD, Graner E. Hereditary gingival fibromatosis: a systematic review. J Periodontol 2006; 77:753–764.
2. DeAngelo S, Murphy J, Claman L, et al. Hereditary gingival fibromatosis—a review. Compend Contin Educ Dent 2007; 28:138–143.
3. Takagi M, Yamamoto H, Mega H, et al. Heterogeneity in the gingival fibromatoses. Cancer 1991; 68:2202–2212.
4. Hakkinen L, Csiszar A. Hereditary gingival fibromatosis: characteristics and novel putative pathogenic mechanisms. J Dent Res 2007; 86:25–34.
5. Johns Hopkins University BMD. Fibromatosis, Gingival, 1; GINGF. Online Mendelian Inheritance in Man, OMIM (TM) MIM Number: #135300. 2007. Available at: http://www.ncbi.nlm.nih.gov/entrez/dispomim.cgi?id=135300. Accessed August 2007.
6. Neville BW, Damm DD, Allen CM, et al. Oral & Maxillofacial Pathology. Philadelphia: W. B. Saunders, 2002.
7. Hart TC, Pallos D, Bozzo L, et al. Evidence of genetic heterogeneity for hereditary gingival fibromatosis. J Dent Res 2000; 79:1758–1764.

8. Singer SL, Goldblatt J, Hallam LA, et al. Hereditary gingival fibromatosis with a recessive mode of inheritance. Case reports. Aust Dent J 1993; 38:427–432.
9. Bitu CC, Sobral LM, Kellermann MG, et al. Heterogeneous presence of myofibroblasts in hereditary gingival fibromatosis. J Clin Periodontol 2006; 33:393–400.
10. Sakamoto R, Nitta T, Kamikawa Y, et al. Histochemical, immunohistochemical, and ultrastructural studies of gingival fibromatosis: a case report. Med Electron Microsc 2002; 35:248–254.
11. Barros SP, Merzel J, de Araujo VC, et al. Ultrastructural aspects of connective tissue in hereditary gingival fibromatosis. Oral Surg Oral Med Oral Pathol Oral Radiol Endod 2001; 92:78–82.
12. Hart TC, Zhang Y, Gorry MC, et al. A mutation in the SOS1 gene causes hereditary gingival fibromatosis type 1. Am J Hum Genet 2002; 70:943–954.
13. Hart TC, Pallos D, Bowden DW, et al. Genetic linkage of hereditary gingival fibromatosis to chromosome 2p21. Am J Hum Genet 1998; 62:876–883.
14. Jang SI, Lee EJ, Hart PS, et al. Germ line gain of function with SOS1 mutation in hereditary gingival fibromatosis. J Biol Chem 2007; 282:20245–20255.
15. Lee EJ, Jang SI, Pallos D, et al. Characterization of fibroblasts with Son of Sevenless-1 mutation. J Dent Res 2006; 85:1050–1055.
16. Tipton DA, Woodard ES III, Baber MA, et al. Role of the c-myc proto-oncogene in the proliferation of hereditary gingival fibromatosis fibroblasts. J Periodontol 2004; 75:360–369.
17. Xiao S, Bu L, Zhu L, et al. A new locus for hereditary gingival fibromatosis (GINGF2) maps to 5q13-q22. Genomics 2001; 74:180–185.
18. Ye X, Shi L, Cheng Y, et al. A novel locus for autosomal dominant hereditary gingival fibromatosis, GINGF3, maps to chromosome 2p22.3-p23.3. Clin Genet 2005; 68:239–244.
19. Anneroth G, Sigurdson A. Hyperplastic lesions of the gingiva and alveolar mucosa. A study of 175 cases. Acta Odontol Scand 1983; 41:75–86.
20. Dongari A, McDonnell HT, Langlais RP. Drug-induced gingival overgrowth. Oral Surg Oral Med Oral Pathol 1993; 76:543–548.
21. Doufexi A, Mina M, Ioannidou E. Gingival overgrowth in children: epidemiology, pathogenesis, and complications. A literature review. J Periodontol 2005; 76:3–10.
22. Esmeili T, Lozada-Nur F, Epstein J. Common benign oral soft tissue masses. Dent Clin North Am 2005; 49:223–240, x.
23. Al Malik MI, Rehbini ZA, Eltayeb AA. Oral manifestations of juvenile hyaline fibromatosis: a case report. J Clin Pediatr Dent 2005; 29:347–351.
24. Larralde M, Santos-Munoz A, Calb I, et al. Juvenile hyaline fibromatosis. Pediatr Dermatol 2001; 18:400–402.
25. Mancini GM, Stojanov L, Willemsen R, et al. Juvenile hyaline fibromatosis: clinical heterogeneity in three patients. Dermatology 1999; 198:18–25.

I. Fibromatosis (desmoid)

1. Okuno S. The enigma of desmoid tumors. Curr Treat Options Oncol 2006; 7:438–443.
2. Gurbuz AK, Giardiello FM, Petersen GM, et al. Desmoid tumours in familial adenomatous polyposis. Gut 1994; 35:377–381.
3. Conley J, Healey WV, Stout AP. Fibromatosis of the head and neck. Am J Surg 1966; 112:609–614.
4. Dehner LP, Askin FB. Tumors of fibrous tissue origin in childhood. A clinicopathologic study of cutaneous and soft tissue neoplasms in 66 children. Cancer 1976; 38:888–900.
5. Smoker WR, Lusk RP, Menezes AH. Supraclavicular fibromatosis with intraspinal extension. Ann Otol Rhinol Laryngol 1986; 95:319–320.
6. Fowler CB, Hartman KS, Brannon RB. Fibromatosis of the oral and paraoral region. Oral Surg Oral Med Oral Pathol 1994; 77:373–386.
7. Lygidakis NA, Lindenbaum RH. Oral fibromatosis in tuberous sclerosis. Oral Surg Oral Med Oral Pathol 1989; 68:725–728.
8. Takagi M, Ishikawa G. Fibromatosis of the oral cavity. Bull Tokyo Med Dent Univ 1982; 29:113–122.
9. Gnepp DR, Henley J, Weiss S, et al. Desmoid fibromatosis of the sinonasal tract and nasopharynx. A clinicopathologic study of 25 cases. Cancer 1996; 78:2572–2579.
10. Majmudar B, Winiarski N. Desmoid tumor presenting as a parotid mass. JAMA 1978; 239:337–339.
11. Shuker ST, Jabro MH. A case report of submandibular aggressive fibromatosis in a 16-month-old infant with 8-year postsurgical follow-up. J Oral Maxillofac Surg 2003; 61:951–954.
12. Roychoudhury A, Parkash H, Kumar S, et al. Infantile desmoid fibromatosis of the submandibular region. J Oral Maxillofac Surg 2002; 60:1198–1202.
13. Anderson T, Weinstein GS, Harwich J, et al. Hypopharyngeal desmoid tumor. Otolaryngol Head Neck Surg 2000; 123:279–281.
14. Dolman CL, Crichton JU, Jones EA, et al. Fibromatosis of dura presenting as infantile spasms. J Neurol Sci 1981; 49:31–39.
15. Hartstein ME, Thomas SM, Ellis LS. Orbital desmoid tumor in a pediatric patient. Ophthal Plast Reconstr Surg 2006; 22:139–141.
16. Gherman RB, Bowen E, Eggleston MK, et al. Desmoid tumor of the larynx complicating pregnancy: a case report. Am J Obstet Gynecol 1999; 180:1036–1037.
17. Mirra M, Calo S, Salviato T, et al. Aggressive fibromatosis of the larynx: report of a new case in an adult patient and review of the literature. Pathol Res Pract 2001; 197:51–55.
18. De Rosa G, Barra E, Boscaino A, et al. Fibromatosis of the larynx in the adult. J Laryngol Otol 1989; 103:1219–1221.
19. McIntosh WA, Kassner GW, Murray JF. Fibromatosis and fibrosarcoma of the larynx and pharynx in an infant. Arch Otolaryngol 1985; 111:478–480.
20. Samsi AB, Shah HK, Vaidya A, et al. Fibromatosis of thyroid gland (a case report). J Postgrad Med 1992; 38:36–37.
21. Schwarzlmuller B, Hofstadter F. [Fibromatosis of the thyroid gland region. An electron-microscopic and enzyme-histochemical study (author's transl)]. Virchows Arch A Pathol Anat Histol 1978; 377:145–155.
22. Kingston CA, Owens CM, Jeanes A, et al. Imaging of desmoid fibromatosis in pediatric patients. AJR Am J Roentgenol 2002; 178:191–199.
23. Lee JC, Thomas JM, Phillips S, et al. Aggressive fibromatosis: MRI features with pathologic correlation. AJR Am J Roentgenol 2006; 186:247–254.
24. Robbin MR, Murphey MD, Temple HT, et al. Imaging of musculoskeletal fibromatosis. Radiographics 2001; 21: 585–600.
25. Teo HE, Peh WC, Shek TW. Case 84: desmoid tumor of the abdominal wall. Radiology 2005; 236:81–84.
26. Bhattacharya B, Dilworth HP, Iacobuzio-Donahue C, et al. Nuclear beta-catenin expression distinguishes deep fibromatosis from other benign and malignant fibroblastic and myofibroblastic lesions. Am J Surg Pathol 2005; 29:653–659.
27. Carlson JW, Fletcher CD. Immunohistochemistry for beta-catenin in the differential diagnosis of spindle cell lesions: analysis of a series and review of the literature. Histopathology 2007; 51:509–514.

28. Montgomery E, Torbenson MS, Kaushal M, et al. Beta-catenin immunohistochemistry separates mesenteric fibromatosis from gastrointestinal stromal tumor and sclerosing mesenteritis. Am J Surg Pathol 2002; 26:1296–1301.
29. Saito T, Oda Y, Tanaka K, et al. Beta-catenin nuclear expression correlates with cyclin D1 overexpression in sporadic desmoid tumours. J Pathol 2001; 195:222–228.
30. Ishizuka M, Hatori M, Dohi O, et al. Expression profiles of sex steroid receptors in desmoid tumors. Tohoku J Exp Med 2006; 210:189–198.
31. Deyrup AT, Tretiakova M, Montag AG. Estrogen receptor-beta expression in extraabdominal fibromatoses: an analysis of 40 cases. Cancer 2006; 106:208–213.
32. De Wever I, Dal Cin P, Fletcher CD, et al. Cytogenetic, clinical, and morphologic correlations in 78 cases of fibromatosis: a report from the CHAMP Study Group. CHromosomes And Morphology. Mod Pathol 2000; 13:1080–1085.
33. Qi H, Dal Cin P, Hernández JM, et al. Trisomies 8 and 20 in desmoid tumors. Cancer Genet Cytogenet 1996; 92: 147–149.
34. Bridge JA, Swarts SJ, Buresh C, et al. Trisomies 8 and 20 characterize a subgroup of benign fibrous lesions arising in both soft tissue and bone. Am J Pathol 1999; 154:729–733.
35. Fletcher JA, Naeem R, Xiao S, et al. Chromosome aberrations in desmoid tumors. Trisomy 8 may be a predictor of recurrence. Cancer Genet Cytogenet 1995; 79:139–143.
36. Kouho H, Aoki T, Hisaoka M, et al. Clinicopathological and interphase cytogenetic analysis of desmoid tumours. Histopathology 1997; 31:336–341.
37. Gottardi CJ, Gumbiner BM. Adhesion signaling: how beta-catenin interacts with its partners. Curr Biol 2001; 11:R792–R794.
38. Kinzler KW, Nilbert MC, Su LK, et al. Identification of FAP locus genes from chromosome 5q21. Science 1991; 253: 661–665.
39. Nishisho I, Nakamura Y, Miyoshi Y, et al. Mutations of chromosome 5q21 genes in FAP and colorectal cancer patients. Science 1991; 253:665–669.
40. Groden J, Thliveris A, Samowitz W, et al. Identification and characterization of the familial adenomatous polyposis coli gene. Cell 1991; 66:589–600.
41. Clark SK, Neale KF, Landgrebe JC, et al. Desmoid tumours complicating familial adenomatous polyposis. Br J Surg 1999; 86:1185–1189.
42. Sen-Gupta S, van der Luijt R, Bowles LV, et al. Somatic mutation of APC gene in desmoid tumour in familial adenomatous polyposis. Lancet 1993; 342:552–553.
43. Eccles DM, van der Luijt R, Breukel C, et al. Hereditary desmoid desease due to a frameshift mutation at codon 1924 of the APC gene. Am J Hum Genet 1996; 59:1193–1201.
44. Alman BA, Li C, Pajerski ME, et al. Increased beta-catenin protein and somatic APC mutations in sporadic aggressive fibromatoses (desmoid tumors). Am J Pathol 1997; 151: 329–334.
45. Couture J, Mitri A, Lagace R, et al. A germline mutation at the extreme 3′ end of the APC gene results in a severe desmoid phenotype and is associated with overexpression of beta-catenin in the desmoid tumor. Clin Genet 2000; 57:205–212.
46. Miyoshi Y, Iwao K, Nawa G, et al. Frequent mutations in the beta-catenin gene in desmoid tumors from patients without familial adenomatous polyposis. Oncol Res 1998; 10:591–594.
47. Wang CP, Chang YL, Ko JY, et al. Desmoid tumor of the head and neck. Head Neck 2006; 28:1008–1013.
48. Ray ME, Lawrence TS. Radiation therapy for aggressive fibromatosis (desmoid tumor). J Clin Oncol 2006; 24: 3714–3715.
49. Ballo MT, Zagars GK, Pollack A. Radiation therapy in the management of desmoid tumors. Int J Radiat Oncol Biol Phys 1998; 42:1007–1014.
50. Lev D, Kotilingam D, Wei C, et al. Optimizing treatment of desmoid tumors. J Clin Oncol 2007; 25:1785–1791.
51. Patel SR, Evans HL, Benjamin RS. Combination chemotherapy in adult desmoid tumors. Cancer 1993; 72: 3244–3247.
52. Okuno SH, Edmonson JH. Combination chemotherapy for desmoid tumors. Cancer 2003; 97:1134–1135.
53. Lim CL, Walker MJ, Mehta RR, et al. Estrogen and antiestrogen binding sites in desmoid tumors. Eur J Cancer Clin Oncol 1986; 22:583–587.
54. Bauernhofer T, Stoger H, Schmid M, et al. Sequential treatment of recurrent mesenteric desmoid tumor. Cancer 1996; 77:1061–1065.

J. Angiofibroma

1. Barnes L, Eveson JW, Reichart P, et al. eds. World Health Organization Classification of Tumours. Pathology and Genetics of Head and Neck Tumors. Lyon: IARC Press, 2005.
2. Lloyd G, Howard D, Lund VJ, et al. Imaging for juvenile angiofibroma. J Laryngol Otol 2000; 114:727–730.
3. Lloyd G, Howard D, Phelps P, et al. Juvenile angiofibroma: the lessons of 20 years of modern imaging. J Laryngol Otol 1999; 113:127–134.
4. Abraham SC, Montgomery EA, Giardiello FM, et al. Frequent beta-catenin mutations in juvenile nasopharyngeal angiofibromas. Am J Pathol 2001; 158:1073–1078.
5. Ferouz AS, Mohr RM, Paul P. Juvenile nasopharyngeal angiofibroma and familial adenomatous polyposis: an association? Otolaryngol Head Neck Surg 1995; 113: 435–439.
6. Giardiello FM, Hamilton SR, Krush AJ, et al. Nasopharyngeal angiofibroma in patients with familial adenomatous polyposis. Gastroenterology 1993; 105:1550–1552.
7. Guertl B, Beham A, Zechner R, et al. Nasopharyngeal angiofibroma: an APC-gene-associated tumor? Hum Pathol 2000; 31:1411–1413.
8. Valanzano R et al. Genetic evidence that juvenile nasopharyngeal angiofibroma is an integral FAP tumour. Gut 2005; 54:1046–1047.
9. Zhang PJ, Weber R, Liang HH, et al. Growth factors and receptors in juvenile nasopharyngeal angiofibroma and nasal polyps: an immunohistochemical study. Arch Pathol Lab Med 2003; 127:1480–1484.
10. Bremer JW, Neel HB III, DeSanto LW, et al. Angiofibroma: treatment trends in 150 patients during 40 years. Laryngoscope 1986; 96:1321–1329.
11. Beham A, Fletcher CD, Kainz J, et al. Nasopharyngeal angiofibroma: an immunohistochemical study of 32 cases. Virchows Arch A Pathol Anat Histopathol 1993; 423: 281–285.
12. Neel HB III, Whicker JH, Devine KD, et al. Juvenile angiofibroma. Review of 120 cases. Am J Surg 1973; 126:547–556.
13. Liang J, Yi Z, Lianq P. The nature of juvenile nasopharyngeal angiofibroma. Otolaryngol Head Neck Surg 2000; 123:475–481.
14. Glad H et al. Juvenile nasopharyngeal angiofibromas in Denmark 1981–2003: diagnosis, incidence, and treatment. Acta Otolaryngol 2007; 127:292–299.
15. Economou TS, Abemayor E, Ward PH. Juvenile nasopharyngeal angiofibroma: an update of the UCLA experience, 1960-1985. Laryngoscope 1988; 98:170–175.

16. Witt TR, Shah JP, Sternberg SS. Juvenile nasopharyngeal angiofibroma. A 30 year clinical review. Am J Surg 1983; 146:521–525.
17. Paris J, Guelfucci B, Moulin G, et al. Diagnosis and treatment of juvenile nasopharyngeal angiofibroma. Eur Arch Otorhinolaryngol 2001; 258:120–124.
18. Sessions RB, Zarin DP, Bryan RN. Juvenile nasopharyngeal angiofibroma. Am J Dis Child 1981; 135:535–537.
19. Rao BN, Shewalkar BK. Clinical profile and multimodality approach in the management of juvenile nasopharyngeal angiofibroma. Indian J Cancer 2000; 37:133–139.
20. Tyagi I, Syal R, Goyal A. Staging and surgical approaches in large juvenile angiofibroma—study of 95 cases. Int J Pediatr Otorhinolaryngol 2006; 70:1619–1627.
21. Sessions RB, Bryan RN, Naclerio RM, et al. Radiographic staging of juvenile angiofibroma. Head Neck Surg 1981; 3:279–283.
22. Ungkanont K, Byers RM, Weber RS, et al. Juvenile nasopharyngeal angiofibroma: an update of therapeutic management. Head Neck 1996; 18:60–66.
23. Schick B, Kahle G. Radiological findings in angiofibroma. Acta Radiol 2000; 41:585–593.
24. Siniluoto TM, Luotonen JP, Tikkakoski TA, et al. Value of pre-operative embolization in surgery for nasopharyngeal angiofibroma. J Laryngol Otol 1993; 107:514–521.
25. Howard DJ, Lloyd G, Lund V. Recurrence and its avoidance in juvenile angiofibroma. Laryngoscope 2001; 111:1509–1511.
26. Lloyd GA, Phelps PD. Juvenile angiofibroma: imaging by magnetic resonance, CT and conventional techniques. Clin Otolaryngol Allied Sci 1986; 11:247–259.
27. Kania RE, Sauvaget E, Guichard JP, et al. Early postoperative CT scanning for juvenile nasopharyngeal angiofibroma: detection of residual disease. AJNR Am J Neuroradiol 2005; 26:82–88.
28. Beham A, Regauer S, Beham-Schmid C, et al. Expression of CD34-antigen in nasopharyngeal angiofibromas. Int J Pediatr Otorhinolaryngol 1998; 44:245–250.
29. Brentani MM, Butugan O, Oshima CT, et al. Multiple steroid receptors in nasopharyngeal angiofibromas. Laryngoscope 1989; 99:398–401.
30. Hwang HC, Mills SE, Patterson K, et al. Expression of androgen receptors in nasopharyngeal angiofibroma: an immunohistochemical study of 24 cases. Mod Pathol 1998; 11:1122–1126.
31. Montag AG, Tretiakova M, Richardson M. Steroid hormone receptor expression in nasopharyngeal angiofibromas. Consistent expression of estrogen receptor beta. Am J Clin Pathol 2006; 125:832–837.
32. Schick B, Rippel C, Brunner C, et al. Numerical sex chromosome aberrations in juvenile angiofibromas: genetic evidence for an androgen-dependent tumor? Oncol Rep 2003; 10:1251–1255.
33. Brieger J, Wierzbicka M, Sokolov M, et al. Vessel density, proliferation, and immunolocalization of vascular endothelial growth factor in juvenile nasopharyngeal angiofibromas. Arch Otolaryngol Head Neck Surg 2004; 130: 727–731.
34. Nagai MA, Butugan O, Logullo A, et al. Expression of growth factors, proto-oncogenes, and p53 in nasopharyngeal angiofibromas. Laryngoscope 1996; 106:190–195.
35. Brunner C, Urbschat S, Jung V, et al. Chromosomal alterations in juvenile angiofibromas. HNO 2003; 51:981–985.
36. Heinrich UR et al. Frequent chromosomal gains in recurrent juvenile nasopharyngeal angiofibroma. Cancer Genet Cytogenet 2007; 175:138–143.
37. Schick B et al. Comprehensive genomic analysis identifies MDM2 and AURKA as novel amplified genes in juvenile angiofibromas. Head Neck 2007; 29:479–487.
38. Stiller D, Katenkamp D, Kuttner K. Cellular differentiations and structural characteristics in nasopharyngeal angiofibromas. An electron-microscopic study. Virchows Arch A Pathol Anat Histol 1976; 371:273–282.
39. Taxy JB. Juvenile nasopharyngeal angiofibroma: an ultrastructural study. Cancer 1977; 39:1044–1054.
40. Hill DL. Morphology of nasopharyngeal angiofibroma. An electron microscope study. J Submicrosc Cytol 1985; 17:443–448.
41. Kardon DE, Wenig BM, Heffner DK, et al. Tonsillar lymphangiomatous polyps: a clinicopathologic series of 26 cases. Mod Pathol 2000; 13:1128–1133.
42. Mann WJ, Jecker P, Amedee RG. Juvenile angiofibromas: changing surgical concept over the last 20 years. Laryngoscope 2004; 114:291–293.
43. Petruson K, Rodriguez-Catarino M, Petruson B, et al. Juvenile nasopharyngeal angiofibroma: long-term results in preoperative embolized and non-embolized patients. Acta Otolaryngol 2002; 122:96–100.
44. Jones GC, DeSanto LW, Bremer JW, et al. Juvenile angiofibromas. Behavior and treatment of extensive and residual tumors. Arch Otolaryngol Head Neck Surg 1986; 112: 1191–1193.
45. Solomon D, Isaacson G. Transoral ''adenoidectomy' excision of juvenile nasopharyngeal angiofibromas. Ann Otol Rhinol Laryngol 2007; 116:243–247.
46. Eloy P, Watelet JB, Hatert AS, et al. Endonasal endoscopic resection of juvenile nasopharyngeal angiofibroma. Rhinology 2007; 45:24–30.
47. Enepekides DJ. Recent advances in the treatment of juvenile angiofibroma. Curr Opin Otolaryngol Head Neck Surg 2004; 12:495–499.
48. Roger G et al. Exclusively endoscopic removal of juvenile nasopharyngeal angiofibroma: trends and limits. Arch Otolaryngol Head Neck Surg 2002; 128:928–935.
49. Scholtz AW, Appenroth E, Kammen-Jolly K, et al. Juvenile nasopharyngeal angiofibroma: management and therapy. Laryngoscope 2001; 111:681–687.
50. Mendenhall WM, Werning JW, Hinerman RW, et al. Juvenile Nasopharyngeal Angiofibroma. J Hong Kong Coll Radiol 2003; 6:15–19.
51. Chandler JR, Goulding R, Moskowitz L, et al. Nasopharyngeal angiofibromas: staging and management. Ann Otol Rhinol Laryngol 1984; 93:322–329.
52. Radkowski D, McGill T, Healy GB, et al. Angiofibroma. Changes in staging and treatment. Arch Otolaryngol Head Neck Surg 1996; 122:122–129.
53. McAfee WJ, Morris CG, Amdur RJ, et al. Definitive radiotherapy for juvenile nasopharyngeal angiofibroma. Am J Clin Oncol 2006; 29:168–170.
54. Makek MS, Andrews JC, Fisch U. Malignant transformation of a nasopharyngeal angiofibroma. Laryngoscope 1989; 99:1088–1092.
55. Spagnolo DV, Papadimitriou JM, Archer M. Postirradiation malignant fibrous histiocytoma arising in juvenile nasopharyngeal angiofibroma and producing alpha-1-antitrypsin. Histopathology 1984; 8:339–352.
56. Chen KT, Bauer FW. Sarcomatous transformation of nasopharyngeal angiofibroma. Cancer 1982; 49:369–371.
57. Batsakis JG, Klopp CT, Newman W. Fibrosarcoma arising in a juvenile nasopharyngeal angiofibroma following extensive radiation therapy. Am Surg 1955; 21:786–793.

K. Myofibroma

1. Stout AP. Juvenile fibromatosis. Cancer 1954; 7:953–978.
2. Chung EB, Enzinger FM. Infantile myofibromatosis. Cancer 1981; 48:1807–1818.

3. Kauffman SL, Stout AP. Congenital mesenchymal tumors. Cancer 1965; 18:460–476.
4. Coffin CM, Neilson KA, Ingels S, et al. Congenital generalized myofibromatosis: a disseminated angiocentric myofibromatosis. Pediatr Pathol Lab Med 1995; 15:571–587.
5. Daimaru Y, Hashimoto H, Enjoji M. Myofibromatosis in adults (adult counterpart of infantile myofibromatosis). Am J Surg Pathol 1989; 13:859–865.
6. Smith KJ, Skelton HG, Barrett TL, et al. Cutaneous myofibroma. Mod Pathol 1989; 6:603–609.
7. Beham A, Badve S, Suster S, et al. Solitary myofibroma in adults: clinicopathologic analysis of a series. Histopathology 1993; 22:335–441.
8. Guitart J, Ritter JH, Wick MR. Solitary cutaneous myofibromas in adults: report of six cases and discussion of differential diagnosis. J Cutan Pathol 1996; 23:437–444.
9. Requena L, Kutzner H, Hugel H, et al. Cutaneous adult myofibroma: a vascular neoplasm. J Cutan Pathol 1996; 23:445–457.
10. Granter SR, Badizadegan K, Fletcher CDM. Myofibromatosis in adults, glomangiopericytoma, and myopericytoma. A spectrum of tumors showing perivascular myoid differentiation. Am J Surg Pathol 1998; 22:513–525.
11. Dray MS, McCarthy SW, Palmer AA, et al. Myopericytoma: a unifying term for a spectrum of tumours that show overlapping features with myofibroma. A review of 14 cases. J Clin Pathol 2006; 59:67–73.
12. Rubin BP, Bridge JA. Myofibroma/myofibromatosis. In: Fletcher CDM, Unni KK, Mertens F, eds. Tumours of Soft Tissue and Bone. Lyon, France: IARC Press, 2002:59–61.
13. Rosenberg HS, Stenback WA, Spjut JH. The fibromatosis of infancy and childhood. In: Rosenberg HS, Bolande RP, eds. Perspectives in Pediatric Pathology. Vol. 4. Chicago: Year Book Medical Publishers, Inc., 1978;269–348.
14. Coffin CM, Dehner LP. Fibroblastic-myofibroblastic tumors in children and adolescents: a clinicopathologic study of 108 examples in 103 patients. Pediatr Pathol 1991; 11:569–588.
15. Wiswell TE, Sakas EL, Stephenson SR, et al. Infantile myofibromatosis. Pediatric 1985; 76:981–984.
16. Chung EB. Pitfalls in diagnosing benign soft tissue tumors in infancy and childhood. Pathol Annu 1982; 2:323–386.
17. Giannini C, Wright A, Dyck PJ. Polyneuropathy associated with nerve angiomatosis and multiple soft tissue tumors. Am J Surg Pathol 1995; 19:1325–1332.
18. Beck JC, Devaney KO, Weatherly RA, et al. Pediatric myofibromatosis of the head and neck. Arch Otolaryngol Head Neck Surg 1999; 125:39–44.
19. Walsh RM, Leen EJ, Path MRC, et al. Solitary infantile and adult myofibromatosis of the nasal cavity: a report of two cases. J Otolaryngol 1996; 110:574–577.
20. Jones AC, Freedman PD, Kerpel SM. Oral myofibromas: a report of 13 cases and review of the literature. J Oral Maxillofac Surg 1994; 52:870–875.
21. Lingen MW, Mostof RS, Solt DB. Myofibromas of the oral cavity. Oral Surg Oral Med Oral Pathol Oral Radiol Endod 1995; 80:297–302.
22. Foss RD. Ellis GL. Myofibromas and myofibromatosis of the oral region: a clinicopathologic analysis of 79 cases. Oral Surg Oral Med Oral Pathol Oral Radiol Endod 2000; 89:57–65.
23. Slootweg PJ, Muller H. Localized infantile myofibromatosis. Report of a case originating in the mandible. J Maxillofac Surg 1984; 12:86–89.
24. Speight PM, Dayan D, CDM Fletcher. Adult and infantile myofibromatosis: a report of three cases affecting the oral cavity. J Oral Pathol Med 1991; 20:380–384.
25. Vigneswaran N, Boyd DL, Waldron CA. Solitary infantile myofibromatosis of the mandible. Report of three cases. Oral Surg Oral Med Oral Pathol 1992; 73:84–88.
26. Hidayat AA, Font RL. Juvenile fibromatosis of the periorbital region and eyelid. Arch Ophthalmol 1980; 98: 280–285.
27. Mizobuchi K, Yoshino T, Ikehara I, et al. Infantile myofibromatosis. Report of two cases. Acta Pathol Jpn 1986; 36:1411–1418.
28. Hutchinson L, Sismanis A, Ward J, et al. Infantile myofibromatosis of the temporal bone: a case report. Am J Otolaryngol 1991; 12:64–66.
29. McIntosh WA, Kassner GW, Murray JF. Fibromatosis and fibrosarcoma of the larynx and pharynx in an infant. Arch Otolaryngol 1985; 111:478–480.
30. Linder JS, Harris GJ, Segura AD. Periorbital infantile myofibromatosis. Arch Ophthalmol 1996; 114:219–222.
31. Eze N, Pitkin L, Crowley S, et al. Solitary infantile myofibroma compromising the airway. Int J Pediatr Otorhinolaryngol 2000; 53:235–244.
32. Johnson GL, Baisden BL, Fishman EK. Infantile myfibromatosis. Skeletal Radiol 1997; 26:611–614.
33. Koujok K, Ruiz RE, Hernandez RJ. Myofibromatosis: imaging characteristics. Pediatr Radiol 2005; 35:374–380.
34. Rotigliano MJ, Pollack IF, Ahdab-Barmada M, et al. Intracranial infantile myofibromatosis. J Neurosurg 1994; 81:539–543.
35. Kubota A, Imano M, Yonekura T, et al. Infantile myofibromatosis of the triceps detected by prenatal sonography. J Clin Ultrasound 1999; 27:147–150.
36. Hartig G, Koopmann C Jr., Esclamado R. Infantile myofibromatosis: a commonly misdiagnosed entity. Otolaryngol Head Neck Surg 1993; 109:753–757.
37. Hasagawa M, Kida S, Yamashima T, et al. Multicentric infantile myofibromatosis in the cranium: case report. Neurosurgery 1995; 36:1200–1203.
38. Moore JB, Waldenmaier N, Potchen EJ. Congenital generalized fibromatosis: a new management strategy provided by magnetic resonance imaging. Am J Dis Child 1987; 141:714–716.
39. Eich GF, Hoeffel J, Tschappeler H, et al. Fibrous tumors in children: imaging features of a heterogeneous group of disorders. Pediatr Radiol 1998; 28:500–509.
40. Schrodt BJ, Callen JP. A case of congenital myofibromatosis developing in an infant. Pediatrics 1999; 104:113–115.
41. Fletcher CDM, Achu P, Van Noorden S, et al. Infantile myofibromatosis: a light microscopic, histochemical and immunohistochemical study suggesting true smooth muscle differentiation. Histopathology 1987; 11:245–258.
42. Mentzel T, Calonje E, Nascimento AG, et al. Infantile hemangiopericytomas versus infantile myofibromatosis: study of a series suggesting a continuous spectrum of infantile myofibroblastic lesions. Am J Surg Pathol 1994; 18:922–930.
43. Variend S, Bax MN, Van Gorp J. Are infantile myofibromatosis, congenital fibrosarcoma and congenital haemangiopericytoma histogenetically related? Histopathology 1995; 26:57–62.
44. Fukasawa Y, Ishikura H, Takada A, et al. Massive apoptosis in infantile myofibromatosis: a putative mechanism of tumor regression. Am J Pathol 1994; 144:480–485.
45. Mentzel T, Dei Tos AP, Sapi Z, et al. Myopericytoma of skin and soft tissues. Clinicopathologic and immunohistochemical study of 54 cases. Am J Surg Pathol 2006; 30:104–113.
46. Stenman G, Nadal N, Persson S, et al. del(6)(q12q15) as the sole cytogenetic anomaly in a case of solitary infantile myofibromatosis. Oncol Rep 1999; 6:1101–1104.
47. Sirvent N, Perrin C, Lacour JP, et al. Monosomy 9q and trisomy 16q in a case of congenital solitary infantile myofibromatosis. Virchows Arch 2004; 445:537–540.
48. Chung EB, Enzinger FM. Infantile myofibromatosis. Cancer 1981; 48:1807–1818.

49. Narchi H. Four half-siblings with infantile myofibromatosis: a case for autosomal-recessive inheritance. Clin Genet 2001; 59:134–135.
50. Bracko M, Cindro L, Golouh R. Familial occurrence of infantile myofibromatosis. Am J Med Genet A 2004; 126:261–266.
51. Ikediobi NI, Iyengar V, Hwang L, et al. Infantile myofibromatosis: support for autosomal dominant inheritance. J Am Acad Dermatol 2003; 49:S148–S150.
52. Zand DJ, Huff D, Everman D, et al. Autosomal dominant inheritance of infantile myofibromatosis. Am J Med Genet A 2004; 30:261–266.
53. Benjamin SP, Mercer RD, Hawk WA. Myofibroblastic contraction in spontaneous regression of multiple congenital mesenchymal hamartomas. Cancer 1977; 40:2343–2352.
54. Lauer DH, Enzinger FM. Cranial fasciitis of childhood. Cancer 1980; 45:401–406.
55. Sarangarajan R, Dehner LP. Cranial and extracranial fasciitis of childhood: a clinicopathologic and immunohistochemical study. Hum Pathol 1999; 30:87–92.
56. Chung EB, Enzinger FM. Infantile fibrosarcoma. Cancer 1976; 38:729–738.
57. Soule EH, Pritchard DJ. Fibrosarcoma in infants and children: a review of 110 cases. Cancer 1977; 40:1711–1721.
58. Knezevich SR, McFadden DE, Tao W, et al. ETV6-NTRK3 gene fusions and trisomy 11 establish a histogenetic link between mesoblastic nephroma and congenital fibrosarcoma. Cancer Res 1998; 15:5046–5048.
59. Weiss SW, Goldblum JR. Perivascular tumors. In: Weiss SW, Goldblum JR, eds. Enzinger and Weiss's Soft Tissue Tumors. 4th ed. St. Louis, MO: Mosby, Inc.:985–1035.
60. Arens C, Dreyer T, Eistert B, et al. Glomangioma of the nasal cavity. Case report and literature review. J Otorhinolaryngol Relat Spec 1997; 59:179–181.
61. Shek TWH, Hui Y. Glomangiomyoma of the nasal cavity. Am J Otolaryngol 2001; 22:282–285.
62. Ahmed A, Sheehan AL, Dugar J. Intranasal glomangioma. Rhinology 2003; 41:58–60.
63. Wang C-P, Chang Y-L, Sheen T-S. Vascular leiomyoma of the head and neck. Laryngoscope 2004; 114:661–665.
64. Huang H-Y, Antonescu CR. Sinonasal smooth muscle cell tumors. A clinicopathologic and immunohistochemical analysis of 12 cases with emphasis on the low-grade end of the spectrum. Arch Pathol Lab Med 2003; 127:297–304.
65. Hachisuga T, Hashimoto H, Enjoji M. Angioleiomyoma: a clinicopathologic reappraisal of 562 cases. Cancer 1984; 54:126–130.
66. Enzinger FM, Zhang RY. Plexiform fibrohistiocytic tumor presenting in children and young adults. An analysis of 65 cases. Am J Surg Pathol. 1988; 12:818–826.
67. Hoos A, Lewis JJ, Urist MJ, et al. Desmoid tumors of the head and neck—a clinical study of a rare entity. Head Neck 2000; 22:814–821.
68. Fowler CB, Hartman KS, Brannon RB. Fibromatosis of the oral and paraoral region. Oral Surg Oral Med Oral Pathol 1994; 77:373–386.
69. Bhattacharya B, Dilworth HP, Iacobuzio-Donahue C, et al. Nuclear beta-catenin expression distinguishes deep fibromatosis from other benign and malignant fibroblastic and myofibroblastic lesions. Am J Surg Pathol 2005; 29:653–659.
70. Eyden BP, Christensen L, Tagore V, et al. Myofibrosarcoma of subcutaneous soft tissue of the cheek. J Submicrosc Cytol Pathol 1992; 24:307–313.
71. Smith DM, Mahmoud HH, Jenkins JJ, et al. Myofibrosarcoma of the head and neck in children. Pediatr Pathol Lab Med 1995; 15:403–418.
72. Mentzel T, Dry S, Katenkamp D, et al. Low-grade myofibroblastic sarcoma: analysis of 18 cases in the spectrum of myofibroblastic tumors. Am J Surg Pathol 1998; 22: 1228–1238.
73. Fetsch JF, Laskin WB, Hallman JR, et al. Neurothekeoma: An analysis of 178 tumors with detailed immunohistochemical data and long-term patient follow-up information. Am J Surg Pathol 2007; 31:1103–1114.
74. Wang AR, May D, Bourne P, et al. PGP9.5: a marker for cellular neurothekeoma. Am J Surg Pathol 1999; 23: 1401–1407.
75. Page RN, King R, Mihm MC Jr., Googe PB. Microphthalmia transcription factor and NKI/C3 expression in cellular neurothekeoma. Mod Pathol 2004 Feb; 17(2):230–234.
76. Loundon N, Dedieuleveult T, Ayache D, et al. Head and neck infantile myofibromatosis-a report of three cases. Int J Pediatr Otorhinolaryngol 1999; 51:181–186.
77. Michel M, Ninane J, Claus D, et al. Major malformation in a case of infantile myofibromatosis. Eur J Pediatr 1990; 149:251–252.
78. Dimson OG, Drolet BA, Southern JF, et al. Congenital generalized myofibromatosis in a neonate. Arch Derm 2000; 136:597–600.
79. Day M, Edwards AO, Weinberg A, et al. Successful therapy of a patient with infantile generalized myofibromatosis. Med Pediatr Oncol 2002; 38:371–373.
80. Gandhi MM, Nathan PC, Weitzman S, et al. Successful treatment of life-threatening generalized infantile myofibromatosis using low-dose chemotherapy. J Pediatr Hematol Oncol 2003; 25:750–754.

L. Collagenous Fibroma (Desmoplastic Fibroblastoma)

1. Evans HL. Desmoplastic fibroblastoma. A report of seven cases. Am J Surg Pathol 1995; 19:1077–1081.
2. Nielsen GP, O'Connell JX, Dickersin GR, et al. Collagenous fibroma (desmoplastic fibroblastoma): a report of seven cases. Mod Pathol 1996; 9:781–785.
3. Miettinen M, Fetsch JF. Collagenous fibroma (desmoplastic fibroblastoma): a clinicopathologic analysis of 63 cases of a distinctive soft tissue lesion with stellate-shaped fibroblasts. Hum Pathol 1998; 29:676–682.
4. Hasegawa T, Shimoda T, Hirohashi S, et al. Collagenous fibroma (desmoplastic fibroblastoma): report of four cases and review of the literature. Arch Pathol Lab Med 1998; 122:455–460.
5. Huang H-Y, Sung M-T, Eng H-L, et al. Superficial collagenous fibroma: immunohistochemical, ultrastructural, and flow cytometric study of three cases, including one pemphigus vulgaris patient with a dermal mass. APMIS 2002; 110:283–289.
6. Wilson C, Summerall J, Lubin J, et al. Collagenous fibroma (desmoplastic fibroblastoma): a unique presentation as a goiter in an 88-year-old man. Ann Diagn Pathol 2000; 4:165–169.
7. Dagli M, Eryilmaz A, Acar A, et al. Collagenous fibroma (desmoplastic fibroblastoma). Yonsei Med J 2004; 45: 941–943.
8. Fumio I, Tetsuo S, Norio H, et al. Collagenous fibroma (desmoplastic fibroblastoma) present as a parotid mass. J Oral Pathol Med 1999; 28:465–468.
9. Ide F, Shimoyama T, Horie N, et al. Collagenous fibroma (desmoplastic fibroblastoma) presenting as a parotid mass. J Oral Pathol Med 1999; 28:465–468.
10. Mesquita RA, Okuda E, Jorge WA, et al. Collagenous fibroma (desmoplastic fibroblastoma) of the palate. Oral Surg Oral Med Oral Pathol Oral Radiol Endod 2001; 91: 80–84.

11. Shimoyama T, Horie N, Ide F. Collagenous fibroma (desmoplastic fibroblastoma): a new case originating in the palate. Dentomaxillofac Radiol 2005; 43:117–119.
12. Weisberg NK, Decaudo DJ, Meland NB. Collagenous fibroma (desmoplastic fibroblastoma). J Am Acad Dermatol 1999; 41:292–294.
13. Beggs I, Salter DS, Dorfman HD. Synovial desmoplastic fibroblastoma of hip joint with bone erosion. Skeletal Radiol 1999; 28:402–406.
14. Shuto R, Kiyosue H, Hori Y, et al. CT and MR imaging of desmoplastic fibroblastoma. Eur Radiol 2002; 12: 2474–2476.
15. Sciot R, Samson I, van den Berghe H, et al. Collagenous fibroma (desmoplastic fibroblastoma): genetic link with fibroma of tendon sheath? Mod Pathol 1999; 12:565–568.
16. Bernal K, Nelson M, Neff JR, et al. Translocation (2;11)(q31; q12) is recurrent in collagenous fibroma (desmoplastic fibroblastoma). Cancer Genet Cytogenet 2004; 149:161–163.
17. Dal Cin P, Sciot R, De Smet L, et al. Translocation 2;11 in a fibroma of tendon sheath. Histopathology 1998; 32: 433–435.
18. Alberghini M, Pasquinelli G, Zanella L, et al. Desmoplastic fibroblastoma: a light and ultrastructural description of two cases. Ultrastruct Pathol 2004; 28:149–157.
19. Cutright DE. The histopathologic findings in 583 cases of epulis fissuratum. Oral Surg Oral Med Oral Pathol 1974; 37:401–411.
20. Montgomery EA, Meis JM. Nodular fasciitis. Its morphologic spectrum and immunohistochemical profile. Am J Surg Pathol 1991; 15:942–948.
21. Rapinin RP, Glitz LE. Sclerotic fibromas of the skin. J Am Acad Dermatol 1989; 20:266–271.
22. Metcalf JS, Maize JC, LeBoit PE. Circumscribed storiform collagenoma (sclerosing fibroma). Am J Dermatopathol 1991; 13:122–129.
23. Zelger BG, Zelger B, Steiner H, et al. Sclerotic lipoma; lipomas simulating sclerotic fibroma. Histopathology 1997; 31:174–181.
24. Laskin WB, Fetsch JF, Michal M, et al. Sclerotic (fibroma-like) lipoma: a distinctive lipoma variant with a predilection for the distal extremities. Am J Dermatopathol 2006; 28:308–316.
25. Hanft VN, Shea CR, McNutt NS, et al. Expression of CD34 in sclerotic ('plywood') fibromas. Am J Dermatopathol 2000; 22:17–21.
26. Balachandran K, Allen PW, MacCormac LB. Nuchal fibroma: a clinicopathologic study of nine cases. Am J Surg Pathol 1995; 19:313–317.
27. Michal M, Fetsch JF, Hes O, et al. Nuchal-type fibroma: a clinicopathologic study of 52 cases. Cancer 1999; 85: 156–163.
28. Michal M. Non-nuchal-type fibroma associated with Gardner's syndrome. A hitherto-unreported mesenchymal tumor different from fibromatosis and nuchal-type fibroma. Pathol Res Pract 2000; 196:857–860.
29. Diwan AH, Graves ED, King JA, et al. Nuchal-type fibroma in two related patients with Gardner's syndrome. Am J Surg Pathol 2000; 24:1563–1567.
30. Wehrli BM, Weiss SW, Yandow S, et al. Gardner-associated fibromas (GAF) in young patients: a distinct fibrous lesion that identifies unsuspected Gardner syndrome and risk for fibromatosis. Am J Surg Pathol 2001; 25:645–651.
31. Zamecnik M, Michal M. Nuchal-type fibroma is positive for CD34 and CD99. Am J Surg Pathol 2001; 25:970.
32. Rosenberg NS, Abdul-Karim FW. Childhood fibrous tumor with psammoma bodies. Clinicopathologic features in two cases. Arch Pathol Lab Med 1988; 112:798–800.
33. Fetsch JF, Montgomery EA, Meis JM. Calcifying fibrous pseudotumor. Am J Surg Pathol 1993; 17:502–608.
34. Nascimento AG, Ruiz R, Hornick JL, et al. Calcifying fibrous ''pseudotumour'': clinicopathologic study of 15 cases and analysis of its relationship to inflammatory myofibroblastic tumour. Int J Surg Pathol 2002; 10:189–196.
35. Sharma R, Punia RS, Sharma A, et al. Juvenile (calcifying) aponeurotic fibroma of the neck. Pediatr Surg Int 1998; 13:295–296.
36. Hill KA, Gonzalez-Crussi F, Omeroglu A, et al. Calcifying fibrous pseudotumor involving the neck of a five-week-old infant. Presence of factor XIIIa in the lesional cells. Pathol Res Pract 2000; 196:527–531.
37. Hoffmann H, Beaver ME, Maillard AA. Calcifying fibrous pseudotumor of the neck. Arch Pathol Lab Med 2000; 124:435–437.
38. Maeda A, Kawabata K, Kusuzaki K. Rapid recurrence of calcifying fibrous pseudotumor (a case report). Anticancer Res 2002; 22:1795–1797.
39. Goldstein EB, Savel RH, Sen F, et al. Calcifying fibrous pseudotumor of the neck: diagnostic challenges of a rare benign lesion. Am Surg 2005; 71:1051–1054.
40. Weiss SW, Nickoloff BJ. CD34 is expressed by a distinctive cell population in peripheral nerve, nerve sheath tumors, and related lesions. Am J Surg Pathol 1993; 17:1039–1045.
41. Chaubal A, Pauetau A, Zoltick P, et al. CD34 immunoreactivity in nervous system tumors. Acta Neuropathol 1994; 88:454–458.
42. Suster S, Nascimento A, Miettinen M, et al. Solitary fibrous tumor of soft tissue: a clinicopathologic and immunohistochemical study of 12 cases. Am J Surg Pathol 1995; 19: 1257–1265.
43. Mentzel T, Bainbridge TC, Katenkamp D. Solitary fibrous tumour: clinicopathological, immunohistochemical, and ultrastructural analysis of 12 cases arising in soft tissues, nasal cavity and nasopharynx, urinary bladder and prostate. Virchows Arch 1997; 430:445–453.
44. Nielsen GP, O'Connell JX, Dickersin GR, et al. Solitary fibrous tumor of soft tissue: a report of 15 cases, including 5 malignant examples with light microscopic, immunohistochemical, and ultrastructural data. Mod Pathol 1997; 10:1028–1037.
45. Brunnemann RB, Ro JY, Ordonez NG, et al. Extrapleural solitary fibrous tumor: a clinicopathologic study of 24 cases. Mod Pathol 1999; 12:1034–1042.
46. Hasegawa T, Matsuno Y, Shimoda T, et al. Extrathoracic solitary fibrous tumors: their histological variability and potentially aggressive behavior. Hum Pathol 1999; 30: 1464–1473.
47. Dei Tos AP, Seregard S, Calonje E, et al. Giant cell angiofibroma. A distinctive orbital tumor in adults. Am J Surg Pathol 1995; 19:1286–1293.
48. Hayashi N, Borodic G, Karesh JW, et al. Giant cell angiofibroma of the orbit and eyelid. Ophthalmology 1999; 106:1223–1229.
49. Guillou L, Gibhrad S, Coindre JM. Orbital and extraorbital giant cell angiofibroma: a giant cell-rich variant of solitary fibrous tumor? Clinicopathologic and immunohistochemical analysis of a series in favor of a unifying concept. Am J Surg Pathol 2000; 24:971–979.
50. Tsang WY, Chan JK, Chow LT, et al. Perineurioma: an uncommon soft tissue neoplasm distinct from localized hypertrophic neuropathy and neurofibroma. Am J Surg Pathol 1992; 16:756–763.
51. Mentzel T, Dei Tos AP, Fletcher CD. Perineurioma (storiform perineurial fibroma): clinico-pathological analysis of four cases. Histopathology 1994; 25:261–267.
52. Giannini C, Scheithauer BW, Jenkins RB, et al. Soft tissue perineurioma. Evidence for an abnormality of chromosome 22, criteria for diagnosis, and review of the literature. Am J Surg Pathol 1997; 21:164–173.

53. Robson AM, Calonje E. Cutaneous perineurioma: a poorly recognized tumour often misdiagnosed as epithelioid histiocytoma. Histopathology 2000; 37:332–339.
54. Hornick JL, Fletcher CDM. Soft tissue perineurioma: clinicopathologic analysis of 81 cases including those with atypical histologic features. Am J Surg Pathol 2005; 29:845–858.
55. Mentzel T, Kutzner H. Reticular and plexiform perineurioma: clinicopathological and immunohistochemical analysis of two cases and review of perineurial neoplasms of skin and soft tissues. Virchows Arch 2005; 447:677–682.
56. Hoos A, Lewis JJ, Urist MJ, et al. Desmoid tumors of the head and neck—a clinical study of a rare entity. Head Neck 2000; 22:814–821.
57. Fowler CB, Hartman KS, Brannon RB. Fibromatosis of the oral and paraoral region. Oral Surg Oral Med Oral Pathol 1994; 77:373–386.
58. Evans HL. Low-grade fibromyxoid sarcoma. A report of 12 cases. Am J Surg Pathol 1993; 17:595–600.
59. Goodlad JR, Mentzel T, Fletcher CD. Low grade fibromyxoid sarcoma: clinicopathological analysis of eleven new cases in support of a distinct entity. Histopathology 1995; 26:229–237.
60. Folpe AL, Lane KL, Pauli G, et al. Low-grade fibromyxoid sarcoma and hyalinizing spindle cell tumor with giant rosettes: a clinicopathologic study 73 cases supporting their identity and assessing the impact of high-grade areas. Am J Surg Pathol 2000; 24:1353–1360.
61. Zamecnik M, Michal M. Low-grade fibromyxoid sarcoma: a report of eight cases with histologic, immunohistochemical, and ultrastructural study. Ann Diagn Pathol 2000; 4:207–217.
62. Papadimitriou JC, Ord RA, Drachenberg CB. Head and neck fibromyxoid sarcoma: clinicopathological correlation with emphasis on peculiar ultrastructural features related to collagen processing. Ultrastruct Pathol 1997; 21:81–87.

M. Nuchal Fibroma

1. Michal M, Fetsch JF, Hes O, et al. Nuchal-type fibroma: a clinicopathologic study of 52 cases. Cancer 1999; 85: 156–163.
2. Balachandran K, Allen PW, MacCormac LB. Nuchal fibroma. A clinicopathological study of nine cases. Am J Surg Pathol 1995; 19:313–317.
3. Fletcher CDM, Unni KK, Mertens F, eds. World Health Organization Classification of Tumours. Pathology and Genetics of Tumours of Soft Tissue and Bone. Lyon: IARC Press, 2002.
4. Samadi DS, McLaughlin RB, Loevner LA, et al. Nuchal fibroma: a clinicopathological review. Ann Otol Rhinol Laryngol 2000; 109:52–55.
5. Wehrli BM, Weiss SW, Yandow S, et al. Gardner-associated fibromas (GAF) in young patients: a distinct fibrous lesion that identifies unsuspected Gardner syndrome and risk for fibromatosis. Am J Surg Pathol 2001; 25:645–651.
6. Michal M. Non-nuchal-type fibroma associated with Gardner's syndrome. A hitherto-unreported mesenchymal tumor different from fibromatosis and nuchal-type fibroma. Pathol Res Pract 2000; 196:857–860.
7. Dawes LC, La Hei ER, Tobias V, et al. Nuchal fibroma should be recognized as a new extracolonic manifestation of Gardner-variant familial adenomatous polyposis. Aust N Z J Surg 2000; 70:824–826.
8. Karonidis A, Rigby HS, Orlando A. Collagenosis nuchae: a case report of a rare and often misdiagnosed condition. J Plast Reconstr Aesthet Surg 2007; 60:320–323.
9. Banney LA, Weedon D, Muir JB. Nuchal fibroma associated with scleredema, diabetes mellitus and organic solvent exposure. Australas J Dermatol 2000; 41:39–41.
10. Diwan AH, Horenstein MG. Dermatofibrosarcoma protuberans association with nuchal-type fibroma. J Cutan Pathol 2004; 31:62–66.
11. Allen PW. Nuchal-type fibroma appearance in a desmoid fibromatosis. Am J Surg Pathol 2001; 25:828–829.
12. Lee SE, Kim YC, Kim SC. Nuchal fibroma presenting as two posterior neck masses. J Dermatol 2007; 34:262–263.
13. Tsunemi Y, Saeki H, Tamaki K. Nuchal fibroma clearly visualized by computed tomography: a case report. Int J Dermatol 2005; 44:703–704.
14. Hameed M, Benevenia J, Blacksin M, et al. Nuchal fibroma of the shoulder involving skeletal muscle: a radiographic and clinicopathological study. A case report. J Bone Joint Surg Am 1998; 80:1684–1686.
15. Zamecnik M, Michal M. Nuchal-type fibroma is positive for CD34 and CD99. Am J Surg Pathol 2001; 25:970.
16. Kempson RL, Fletcher CDM, Evans HL, et al. Tumors of the Soft Tissue. Atlas of Tumor Pathology. 3rd series, fascicle 30. Washington, DC: Armed Forces Institute of Pathology, 2001.
17. Michal M, Boudova L, Mukensnabl P. Gardner's syndrome associated fibromas. Pathol Int 2004; 54:523–526.
18. Diwan AH, Graves ED, King JA, et al. Nuchal-type fibroma in two related patients with Gardner's syndrome. Am J Surg Pathol 2000; 24:1563–1567.

N. Solitary Fibrous Tumor/ Hemangiopericytoma

1. Stout AP, Murray MR. Hemangiopericytoma: a vascular tumor featuring Zimmermann's pericytes. Ann Surg 1942; 116:26–33.
2. Folpe AL, Fanburg-Smith JC, Billings SD, et al. Most osteomalacia-associated mesenchymal tumors are a single histopathologic entity: an analysis of 32 cases and a comprehensive review of the literature. Am J Surg Pathol 2004; 28:1–30.
3. Hasegawa T, Matsuno Y, Shimoda T, et al. Extrathoracic solitary fibrous tumors: their histological variability and potentially aggressive behavior. Hum Pathol 1999; 30: 1464–1473.
4. Mentzel T, Bainbridge TC, Katenkamp D. Solitary fibrous tumour: clinicopathological, immunohistochemical, and ultrastructural analysis of 12 cases arising in soft tissues, nasal cavity and nasopharynx, urinary bladder and prostate. Virchows Arch 1997; 430:445–453.
5. Nielsen GP, O'Connell JX, Dickersin GR, et al. Solitary fibrous tumor of soft tissue: a report of 15 cases, including 5 malignant examples with light microscopic, immunohistochemical, and ultrastructural data. Mod Pathol 1997; 10:1028–1037.
6. Tanahashi J, Kashima K, Daa T, et al. Solitary fibrous tumor of the thyroid gland: report of two cases and review of the literature. Pathol Int 2006; 56:471–477.
7. Pagliaro G, Poli P, Ralza G, et al. Haemangiopericytoma of the submandibular gland (a case report). J Laryngol Otol 1988; 102:97–99.
8. Carrillo R, Rodriquez-Peralto JL, Batsakis JG, et al. Primary haemangiopericytomas of the parotid gland. J Laryngol Otol 1992; 106:659–661.
9. Massarelli G, Tanda F, Fois V, et al. Haemangiopericytoma of the parotid gland. Report of a case and review of the literature. Virchows Arch A Pathol Anat Histol 1980; 386:81–89.

10. Alawi F, Stratton D, Freedman PD. Solitary fibrous tumor of the oral soft tissues: a clinicopathologic and immunohistochemical study of 16 cases. Am J Surg Pathol 2001; 25:900–910.
11. Brunnemann RB, Ro JY, Ordonez NG, et al. Extrapleural solitary fibrous tumor: a clinicopathologic study of 24 cases. Mod Pathol 1999; 12:1034–1042.
12. Pavelic K, Spaventi S, Gluncic V, et al. The expression and role of insulin-like growth factor II in malignant hemangiopericytomas. J Mol Med 1999; 77:865–869.
13. Dotan ZA, Mor Y, Olchovsky D, et al. Solitary fibrous tumor presenting as perirenal mass associated with hypoglycemia. J Urol 1999; 162:2087–2088.
14. Lorigan JG, David CL, Evans HL, et al. The clinical and radiologic manifestations of hemangiopericytoma. AJR Am J Roentgenol 1989; 153:345–349.
15. Murphey MD, Fairbairn KJ, Parman LM, et al. From the archives of the AFIP. Musculoskeletal angiomatous lesions: radiologic-pathologic correlation. Radiographics 1995; 15:893–917.
16. Folpe AL, Devaney K, Weiss SW. Lipomatous hemangiopericytoma: a rare variant of hemangiopericytoma that may be confused with liposarcoma. Am J Surg Pathol 1999; 23:1201–1207.
17. Guillou L, Gebhard S, Coindre JM. Lipomatous hemangiopericytoma: a fat-containing variant of solitary fibrous tumor? Clinicopathologic, immunohistochemical, and ultrastructural analysis of a series in favor of a unifying concept. Hum Pathol 2000; 31:1108–1115.
18. Cameselle-Teijeiro J, Manuel LJ, Villanueva JP, et al. Lipomatous haemangiopericytoma (adipocytic variant of solitary fibrous tumour) of the thyroid. Histopathology 2003; 43:406–408.
19. Gengler C, Guillou L. Solitary fibrous tumour and haemangiopericytoma: evolution of a concept. Histopathology 2006; 48:63–74.
20. Cassarino DS, Auerbach A, Rushing EJ. Widely invasive solitary fibrous tumor of the sphenoid sinus, cavernous sinus, and pituitary fossa. Ann Diagn Pathol 2003; 7: 169–173.
21. Hasegawa T, Hirose T, Seki K, et al. Solitary fibrous tumor of the soft tissue. An immunohistochemical and ultrastructural study. Am J Clin Pathol 1996; 106:325–331.
22. Catalano PJ, Brandwein M, Shah DK, et al. Sinonasal hemangiopericytomas: a clinicopathologic and immunohistochemical study of seven cases. Head Neck 1996; 18: 42–53.
23. Schurch W, Skalli O, Lagace R, et al. Intermediate filament proteins and actin isoforms as markers for soft-tissue tumor differentiation and origin. III. Hemangiopericytomas and glomus tumors. Am J Pathol 1990; 136:771–786.
24. Nemes Z. Differentiation markers in hemangiopericytoma. Cancer 1992; 69:133–140.
25. Porter PL, Bigler SA, McNutt M, et al. The immunophenotype of hemangiopericytomas and glomus tumors, with special reference to muscle protein expression: an immunohistochemical study and review of the literature. Mod Pathol 1991; 4:46–52.
26. Middleton LP, Duray PH, Merino MJ. The histological spectrum of hemangiopericytoma: application of immunohistochemical analysis including proliferative markers to facilitate diagnosis and predict prognosis. Hum Pathol 1998; 29:636–640.
27. Miettinen M, Lindenmayer AE, Chaubal A. Endothelial cell markers CD31, CD34, and BNH9 antibody to H- and Y-antigens—evaluation of their specificity and sensitivity in the diagnosis of vascular tumors and comparison with von Willebrand factor. Mod Pathol 1994; 7:82–90.
28. de Leval L, Defraigne JO, Hermans G, et al. Malignant solitary tumor of the pleura: report of a case with cytogenetic analysis. Virchows Arch 2003; 442:388–392.
29. Debiec-Rychter M, de Wever I, Hagemeijer A, et al. Is 4q13 recurring breakpoint in solitary fibrous tumors? Cancer Genet Cytogenet 2001; 131:69–73.
30. Dal Cin P, Pauwels P, Van Den Berghe H. Solitary fibrous tumour of the pleura with t(4;15)(q13;q26). Histopathology 1999; 35:94–95.
31. Donner LR, Silva MT, Dobin SM. Solitary fibrous tumor of the pleura: a cytogenetic study. Cancer Genet Cytogenet 1999; 111:169–171.
32. Horton ES, Dobin SM, Donner LR. A clonal t(8;11)(p11.2; q24.3) as the sole abnormality in a solitary fibrous tumor of the pleura. Cancer Genet Cytogenet 2007; 172:77–79.
33. Havlik DM, Farnath DA, Bocklage T. Solitary fibrous tumor of the orbit with a t(9;22)(q31;p13). Arch Pathol Lab Med 2000; 124:756–758.
34. Dal Cin P, Sciot R, Fletcher CD, et al. Trisomy 21 in solitary fibrous tumor. Cancer Genet Cytogenet 1996; 86:58–60.
35. Miettinen MM, el-Rifai W, Sarlomo-Rikala M, et al. Tumor size-related DNA copy number changes occur in solitary fibrous tumors but not in hemangiopericytomas. Mod Pathol 1997; 10:1194–1200.
36. Morimitsu Y, Nakajima M, Hisaoka M, et al. Extrapleural solitary fibrous tumor: clinicopathologic study of 17 cases and molecular analysis of the p53 pathway. APMIS 2000; 108:617–625.
37. Rossi G, Schirosi L, Giovanardi F, et al. Pleural malignant solitary tumor with sarcomatous overgrowth showing PDGFRbeta mutation. Chest 2006; 130:581–583.
38. Qian YW, Malliah R, Lee HJ, et al. A t(12;17) in an extraorbital giant cell angiofibroma. Cancer Genet Cytogenet 2006; 165:157–160.
39. Sonobe H, Iwata J, Komatsu T, et al. A giant cell angiofibroma involving 6q. Cancer Genet Cytogenet 2000; 116:47–49.
40. Turc-Carel C, Dal Cin P, Limon J, et al. Translocation X;18 in synovial sarcoma. Cancer Genet Cytogenet 1986; 23:93.
41. Bhargava R, Shia J, Hummer AJ, et al. Distinction of endometrial stromal sarcomas from 'hemangiopericytomatous' tumors using a panel of immunohistochemical stains. Mod Pathol 2005; 18:40–47.
42. Espat NJ, Lewis JJ, Leung D, et al. Conventional hemangiopericytoma: modern analysis of outcome. Cancer 2002; 95:1746–1751.
43. Kowalski PJ, Paulino AF. Proliferation index as a prognostic marker in hemangiopericytoma of the head and neck. Head Neck 2001; 23:492–496.
44. Moriya S, Tei K, Notani K, et al. Malignant hemangiopericytoma of the head and neck: a report of 3 cases. J Oral Maxillofac Surg 2001; 59:340–345.
45. Granter SR, Badizadegan K, Fletcher CD. Myofibromatosis in adults, glomangiopericytoma, and myopericytoma: a spectrum of tumors showing perivascular myoid differentiation. Am J Surg Pathol 1998; 22:513–525.
46. Fletcher CD. Distinctive soft tissue tumors of the head and neck. Mod Pathol 2002; 15:324–330.
47. Thompson LD. Sinonasal tract glomangiopericytoma (hemangiopericytoma). Ear Nose Throat J 2004; 83:807.
48. Palacios E, Restrepo S, Mastrogiovanni L, et al. Sinonasal hemangiopericytomas: clinicopathologic and imaging findings. Ear Nose Throat J 2005; 84:99–102.
49. Thompson LD, Miettinen M, Wenig BM. Sinonasal-type hemangiopericytoma: a clinicopathologic and immunophenotypic analysis of 104 cases showing perivascular myoid differentiation. Am J Surg Pathol 2003; 27: 737–749.

50. Billings KR, Fu YS, Calcaterra TC, et al. Hemangiopericytoma of the head and neck. Am J Otolaryngol 2000; 21: 238–243.
51. Eichhorn JH, Dickersin GR, Bhan AK, et al. Sinonasal hemangiopericytoma. A reassessment with electron microscopy, immunohistochemistry, and long-term follow-up. Am J Surg Pathol 1990; 14:856–866.
52. Herve S, Abd A, I, Beautru R, et al. Management of sinonasal hemangiopericytomas. Rhinology 1999; 37:153–158.
53. Gillman G, Pavlovich JB. Sinonasal hemangiopericytoma. Otolaryngol Head Neck Surg 2004; 131:1012–1013.

O. Myxoma

1. Weiss SW, Goldblum JR. Benign soft tissue tumors and pseudotumors of miscellaneous type. In: Weiss SW, Goldblum JR, eds. Weiss and Enzinger's Soft Tissue Tumors. 4th ed. St. Louis, Mo: Mosby, Inc., 2001:1419–1481.
2. Burke AP, Virmani R. Cardiac myxomas: a clinicopathologic study. Am J Clin Pathol 1993; 100:671–680.
3. Enzinger FM. Intramuscular myxoma: a review and follow-up study of 34 cases. Am J Clin Pathol 1965; 43:104–113.
4. Ireland DCR, Soule EH, Ivins JC. Myxoma of somatic soft tissues: a report of 38 patients, 3 with multiple tumors and fibrous dysplasia of bone. Mayo Clin Proc 1973; 48:401–410.
5. Kindblom LG, Stener B, Angervall L. Intramuscular myxoma. Cancer 1974; 34:1737–1744.
6. Fu YS, Perzin KH. Non-epithelial tumors of the nasal cavity, paranasal sinuses and nasopharynx: a clinicopathologic study. VII. Myxomas. Cancer 1977; 39:195–203.
7. Andrews T, Kountakis SE, Maillard AA. Myxomas of the head and neck. Am J Otolaryngol 2000; 21:184–189.
8. Harrison JD. Odontogenic myxoma: ultrastructural and histochemical studies. J Clin Pathol 1973; 26:570–582.
9. Heffner DK. Sinonasal myxomas and fibromyxomas in children. Ear Nose Throat J 1993; 72:365–368.
10. Canalis RF, Smith GA, Konrad HR. Myxomas of the head and neck. Arch Otolaryngol 1976; 102:300–305.
11. Shugar JM, Som PM, Meyers RJ, et al. Intramuscular head and neck myxoma: report of a case and review of the literature. Laryngoscope 1987; 97:105–107.
12. Wirth WA, Leavitt D, Enzinger FM. Multiple intramuscular myxomas: another extraskeletal manifestation of fibrous dysplasia. Cancer 1971; 27:1167–1173.
13. Aoki T, Kouho H, Hisaoka M, et al. Intramuscular myxoma with fibrous dysplasia: a report of two cases with a review of the literature. Pathol Int 1995; 45:165–171.
14. Allen PW, Dymock RB, MacCormac LB. Superficial angiomyxomas with and without epithelial components. Report of 30 tumors in 28 patients. Am J Surg Pathol 1988; 12: 519–530.
15. Calonje E, Guerin D, McCormick D, et al. Superficial angiomyxoma: clinicopathologic analysis of a series of distinctive but poorly recognized cutaneous tumors with tendency for recurrence. Am J Surg Pathol 1999; 23: 910–917.
16. Ferreiro JA, Carney JA. Myxomas of the external ear and their significance. Am J Surg Pathol 1994; 18:274–280.
17. Burgdorf WHC, Carney JA. Carney complex. In: Leboit PE, Burg G, Weedon D, eds. Skin Tumours. Lyon, France: IARC Press, 2006:291–292.
18. Carney JA, Gordon H, Carpenter PC, et al. The complex of myxomas, spotty pigmentation, and endocrine overactivity. Medicine (Baltimore) 1985; 64:270–283.
19. Barros RE, Dominquez FV, Cabrini RL. Myxoma of the jaws. Oral Surg Oral Med Oral Pathol 1969; 27:225–236.
20. Slootweg PJ, Wittkampf AR. Myxoma of the jaws. An analysis of 15 cases. J Maxillofac Surg 1986; 14:46–52.
21. LoMuzio LL, Nocini P, Favia G, et al. Odontogenic myxoma of the jaws: a clinicoradiologic, immunohistochemical and ultrastructural study. Oral Surg 1996; 82:426–433.
22. Kaffe I, Naor H, Buchner A. Clinical and radiological features of odontogenic myxoma of the jaws. Dentomaxillofac Radiol 1997; 26:299–303.
23. Mosqueda-Taylor, Ledesma-Montes C, Caballero-Sandoral S, et al. Odontogenic tumors in Mexico: a collaborative retrospective study of 349 cases. Oral Surg Oral Med Oral Pathol Oral Radiol Endod 1997; 84:672–675.
24. Simon ENM, Merkx MAW, Vuhahula E, et al. Odontogenic myxoma. Int J Oral Maxillofac Surg 2004; 33:333–337.
25. Ladeinde AL, Ajayi OF, Ogunlewe MO, et al. Odontogenic tumors: a review of 319 cases in a Nigerian teaching hospital. Oral Surg Oral Med Oral Pathol Oral Radiol Endod 2005; 99:191–195.
26. Keszler A, Dominquez FV, Giannuzio G. Myxoma in childhood. An analysis of 10 cases. J Oral Maxillofac Surg 1995; 53:518–521.
27. Kangur TT, Dahlin DC, Turlington EG. Myxomatous tumours of the jaws. J Oral Surg 1975; 33:523–521.
28. Gandra R, DeAbreu E, Hipolito O, et al. Central myxoma of the mandible in a child; report of a case. J Oral Surg 1981; 39:769–771.
29. Prasannan L, Warren L, Herzog CE, et al. Sinonasal myxoma: a pediatric case. J Pediatr Hematol Oncol 2005; 27:90–92.
30. Sato H, Tomidokoro Y, Honda N. Myxoma of the sphenoidal sinus. Otolaryngol Head Neck Surg 2004; 130:378–380.
31. Chen KTK, Ballecer RA. Laryngeal myxoma. Am J Otolaryngol 1986; 7:58–59.
32. Sena T, Brady MS, Huvos AG, et al. Laryngeal myxoma. Arch Otolaryngol Head Neck Surg 1991; 117:430–432.
33. Hadley J, Gardiner Q, Dilkes M, et al. Myxoma of the larynx; a case report of the literature. J Laryngol Otol 1994; 108:811–812.
34. Kim KM, Kim SC, Jeong HJ, et al. Myxoma; like-threatening benign nonepithelial tumor of the larynx. Yonsei Med J 1997; 38:187–189.
35. Tsunoda K, Nosaka K, Housui M, et al. A rare case of laryngeal myxoma. J Laryngol Otol 1997; 111:271–273.
36. Idrees MT, Hessler R, Terris D, et al. Unusual polypoid laryngeal myxoma. Mt Sinai J Med 2005; 72:282–284.
37. Rosin RD. Intramuscular myxomas. Br J Surg 1973; 60: 122–124.
38. Feldman PS. A comparative study including ultrastructure of intramuscular myxoma and myxoid liposarcoma. Cancer 1979; 43:512–525.
39. Bedrosian SA, Goldman RL, Pearl MJ. Intramuscular myxoma of the masseter. J Oral Maxillofac Surg 1984; 42:684–686.
40. Miettinen M, Hockerstedt K, Reitamo J, et al. Intramuscular myxoma: a clinicopathologic study of twenty-three cases. Am J Clin Pathol 1985; 84:265–272.
41. Nishijima W, Tokita N, Watanabe I, et al. Intramuscular myxoma of the neck. Arch Otolaryngol 1985; 111:699–701.
42. Hashimoto H, Tsuneyoshi M, Daimaru Y, et al. Intramuscular myxoma: a clinicopathologic, immunohistochemical, and electron microscopic study. Cancer 1986; 58:740–747.
43. Orlandi A, Bianchi L, Marino B, et al. Intramuscular myxoma of the face: an unusual localization. A clinicopathological study. Dermatol Surg 1995; 21:251–254.
44. Nielsen GP, O'Connell JX, Rosenberg AE. Intramuscular myxoma: a clinicopathologic study of 51 cases with emphasis on hypercellular and hypervascular variants. Am J Surg Pathol 1998; 22:1222–1227.

45. Serrat A, Verrier A, Espeso A, et al. Intramuscular myxoma of the temporalis muscle. J Oral Maxillofac Surg 1998; 56:1206–1208.
46. Crankson SJ, Namshan M, Al Mane K, et al. Intramuscular myxoma: a rare neck mass in a child. Pediatr Radiol 2002; 32:120–122.
47. Robin C, Bastidas JA, Boguslaw B. Case report: myxoma of the temporalis muscle. Oral Surg Oral Med Oral Pathol Oral Radiol Endod 2004; 97:620–624.
48. Ozawa H, Fujii M, Tomita T, et al. Intramuscular myxoma of scalene muscle: a case report. Auris Nasus Larynx 2004; 31:319–322.
49. Tse JJ, Vander S. The soft tissue myxoma of the head and neck region—report of a case and literature review. Head Neck Surg 1985; 7:479–483.
50. Schwartz HS, Walker R. Recognizable magnetic resonance imaging characteristics of intramuscular myxoma. Orthopedics 1997; 20:431–435.
51. Murphey MD, McRae GA, Fanburg-Smith JC, et al. Imaging of soft-tissue myxoma with emphasis on CT and MR and comparison of radiologic and pathologic findings. Radiology 2002; 225:215–224.
52. Luna A, Martinez S, Bossen E. Magnetic resonance imaging of intramuscular myxoma with histological comparison and a review of the literature. Skeletal Radiol 2005; 34:19–28.
53. Bancroft LW, Kransdof MJ, Menke DM et al. Intramuscular myxoma: characteristic MR imaging features. AJR 2002; 178:1255–1259.
54. van Roggen JF, McMenamin ME, Fletcher CD. Cellular myxoma of soft tissue: a clinicopathological study of 38 cases confirming indolent clinical behaviour. Histopathology 2001; 39:287–297.
55. Kindblom LG, Angervall L. Histochemical characterization of mucosubstances in bone and soft tissue tumours. Cancer 1975; 36:985–994.
56. Harrison JD. Odontogenic myxoma: ultrastructural and histochemical studies. J Clin Pathol 1973; 26:570–582.
57. Remstein ED, Goldstein NS, Nascimento AG. Soft tissue myxoma: a histologic and immmunohistochemical analysis of 40 cases. Am J Clin Pathol 1996; 105:495 (abstr.).
58. Moshiri S, Oda D, Worthington P, et al. Odontogenic myxoma: histochemical and ultrastructural study. J Oral Pathol Med 1992; 21:401–403.
59. Lombardi T, Lock C, Samson J, et al. S100, alpha-smooth muscle actin and cytokeratin 19 immunohistochemistry in odontogenic and soft tissue myxomas. J Clin Pathol 1995; 48:759–762.
60. Zhao M, Lu Y, Takata T, et al. Immunohistochemical and histochemical characterization of the mucosubstances of odontogenic myxoma: histogenesis and differential diagnosis. Pathol Res Pract 1999; 195:391–397.
61. Fetsch JF, Laskin WB, Tavassoli FA. Superficial angiomyxoma (cutaneous myxoma). A clinicopathologic study of 17 cases arising in the genital region. Int J Gynecol Pathol 1997; 16:325–334.
62. Perdigão PF, Stergiopoulos SG, De Marco L, et al. Molecular and immunohistochemical investigation of protein kinase a regulatory subunit type 1A (PRKAR1A) in odontogenic myxomas. Genes Chromosomes Cancer 2005; 44:204–211.
63. Kirschner LS, Carney JA, Pack SD, et al. Mutations of the gene encoding the protein kinase A type I-alpha regulatory subunit in patients with the Carney complex. Nat Genet 2000; 26:89–92.
64. Kirschner LS, Sandrini F, Monbo J, et al. Genetic heterogeneity and spectrum of mutations of the PRKAR1A gene in patients with the Carney complex. Hum Mol Genet 2000; 9:3037–3046.
65. Okamoto S, Hisaoka M, Ushijima M, et al. Activating Gs (alpha) mutation in intramuscular myxomas with and without fibrous dysplasia of bone. Virchows Arch 2000; 437:133–137.
66. Yoshimoto K, Iwahana H, Fukuda A, et al. Rare mutations of the Gs alpha subunit gene in human endocrine tumors. Mutation detection by polymerase chain reaction-primer-introduced restriction analysis. Cancer 1993; 72:1386–1393.
67. Schwindinger WF, Francomano CA, Levine MA. Identification of a mutation in the gene encoding the alpha subunit of the stimulatory G protein of adenylyl cyclase in McCune-Albright syndrome. Proc Natl Acad Sci U S A 1992; 89(11):5152–5156.
68. Shenker A, Weinstein LS, Moran A, et al. Severe endocrine and nonendocrine manifestations of the McCune-Albright syndrome associated with activating mutations of stimulatory G protein GS. J Pediatr 1993; 123:509–518.
69. Shenker A, Weinstein LS, Sweet DE, et al. An activating Gs alpha mutation is present in fibrous dysplasia of bone in the McCune-Albright syndrome. J Clin Endocrinol Metab 1994; 79:750–755.
70. Murphy CM, Grau-Massanes M, Sanchez RL. Multiple cutaneous myxomas. Report of a case without other elements of Carney's complex. J Cutan Pathol 1995; 22:556–562.
71. Kim J, Ellis GL. Dental follicular tissue: misinterpretation as odontogenic tumors. J Oral Maxillofac Surg 1993; 51:762–777.
72. Sciubba JJ, Fantasia JE, Kahn LB. Nonodontogenic lesions. In: Sciubba JJ, Fantasia JE, Kahn LB, eds. Tumors and Cysts of the Jaw. Third series, fascicle 29. Washington, D.C.: Armed Forces Instiitute of Pathology, 2001:161–251.
73. Baker CG, Tishler JM. Malignant diseases of the jaws. J Can Assoc Radiol 1977; 28:129–141.
74. Batsakis JG, McClatchey KD. Cervical ranulas. Ann Otol Rhinol Laryngol 1988; 97:561–562.
75. Zhao Y-F, Jia Y, Chen X-M, et al. Clinical review of 580 ranulas. Oral Surg Oral Med Oral Pathol Oral Radiol Endod 2004; 98:281–287.
76. Crist WM, Anderson JR, Meza JL, et al. The Intergroup Rhabdomyosarcoma Study-IV: results for patients with nonmetastatic disease. J Clin Oncol 2001; 19:3091–3102.
77. Coindre JM. Immunohistochemistry in the diagnosis of soft tissue tumours. Histopathology 2003; 43:1–16.
78. Scheithauer BW, Woodruff JM, Erlandson RA. Neurofibroma. In: Scheithauer BW, Woodruff JM, Erlandson RA, eds. Tumors of the Peripheral Nervous System. Third series, fascicle 24. Washington, D.C.: Armed Forces Institute of Pathology, 1999:177–218.
79. Hornick JL, Fletcher CD. Soft tissue perineurioma: clinicopathologic analysis of 81 cases including those with atypical histologic features. Am J Surg Pathol 2005; 29:845–858.
80. Weiss SW, Enzinger FM. Myxoid variant of malignant fibrous histiocytoma. Cancer 1977; 39:1672–1685.
81. Angervall L, Kindblom L-G, Merck C. Myxofibrosarcoma. A study of 30 cases. Acta Pathol Microbiol Scand [A] 1977; 85A:127–140.
82. Mentzel T, Calonje E, Wadden C, et al. Myxofibrosarcoma. Clinicopathologic analysis of 75 cases with emphasis on the low-grade variant. Am J Surg Pathol 1996; 20:391–405.
83. Evans HL. Low-grade fibromyxoid sarcoma. A report of 12 cases. Am J Surg Pathol 1993; 17:595–600.
84. Goodlad JR, Mentzel T, Fletcher CDM. Low grade fibromyxoid sarcoma: clinicopathological analysis of eleven new cases in support of a distinct entity. Histopathology 1995; 26:229–237.
85. Folpe A, Lane KL, Aoull G, et al. Low-grade fibromyxoid sarcoma and hyalinizing spindle cell tumor with giant rosettes: a clinicopathologic study of 73 cases supporting

their identity and assessing the impact of high-grade areas. Am J Surg Pathol 2000; 24:1353–1360.
86. Fetsch JF, Laskin WB, Miettinen M. Nerve sheath myxoma: a clinicopathologic and immunohistochemical analysis of 57 morphologically distinctive, S-100 protein- and GFAP-positive, myxoid peripheral nerve sheath tumors with a predilection for the extremities and a high local recurrence rate. Am J Surg Pathol 2005; 29:1615–1624.
87. Hurt MA, Kaddu S, Kutzner H, et al. Benign tumours with follicular differentiation. Soft tissue tumours. In: Leboit PE, Burg G, Weedon D, et al. Skin Tumours. Lyon, France: IARC Press, 2006:152–159.
88. Birt AR, Hogg GR, Dube WJ. Hereditary multiple fibrofolliculomas with trichodiscomas and acrochordons. Arch Dermatol 1977; 113:1674–1677.
89. Silver WP, Harrelson JM, Scully SP. Intramuscular myxoma: a clinicopathologic study of 17 patients. Clin Orthop Relat Res 2002; 403:191–197.
90. Leiberman A, Forte V, Thorner P, et al. Maxillary myxoma in children. Int J Pediatr Otorhinolaryngol 1990; 18:277–284.
91. Carney JA. Psammomatous melanotic schwannoma. A distinctive, heritable tumor with special associations, including cardiac myxoma and the Cushing syndrome. Am J Surg Pathol 1990; 14:206–222.

P. Ossifying Fibromyxoid Tumor

1. Kilpatrick SE, Ward WG, Mozes M, et al. Atypical and malignant variants of ossifying fibromyxoid tumor. Clinicopathologic analysis of six cases. Am J Surg Pathol 1995; 19:1039–1046.
2. Yoshida H, Minamizaki T, Yumoto T, et al. Ossifying fibromyxoid tumor of soft parts. Acta Pathol Jpn 1991; 41:480–486.
3. Donner LR. Ossifying fibromyxoid tumor of soft parts: evidence supporting Schwann cell origin. Hum Pathol 1992; 23:200–202.
4. Kyriakos M. Ossifying fibromyxoid tumor. Something new to mull over. Am J Clin Pathol 1991; 95:107–111.
5. Williams SB, Ellis GL, Meis JM, et al. Ossifying fibromyxoid tumour (of soft parts) of the head and neck: a clinicopathological and immunohistochemical study of nine cases. J Laryngol Otol 1993; 107:75–80.
6. Schofield JB, Krausz T, Stamp GW, et al. Ossifying fibromyxoid tumour of soft parts: immunohistochemical and ultrastructural analysis. Histopathology 1993; 22:101–112.
7. Blum A, Back W, Naim R, et al. Ossifying fibromyxoid tumor of the nasal septum. Auris Nasus Larynx 2006; 33:325–327.
8. Mollaoglu N, Tokman B, Kahraman S, et al. An unusual presentation of ossifying fibromyxoid tumor of the mandible: a case report. J Clin Pediatr Dent 2006; 31:136–138.
9. Park DJ, Miller NR, Green WR. Ossifying fibromyxoid tumor of the orbit. Ophthal Plast Reconstr Surg 2006; 22:87–91.
10. Seykora JT, Kutcher C, van de RM, et al. Ossifying fibromyxoid tumor of soft parts presenting as a scalp cyst. J Cutan Pathol 2006; 33:569–572.
11. Al Mazrou KA, Mansoor A, Payne M, et al. Ossifying fibromyxoid tumor of the ethmoid sinus in a newborn: report of a case and literature review. Int J Pediatr Otorhinolaryngol 2004; 68:225–230.
12. Nigam S, Dhingra KK, Gulati A. Ectomesenchymal chondromyxoid tumor of the hard palate—a case report. J Oral Pathol Med 2006; 35:126–128.
13. Enzinger FM, Weiss SW, Liang CY. Ossifying fibromyxoid tumor of soft parts. A clinicopathological analysis of 59 cases. Am J Surg Pathol 1989; 13:817–827.
14. Schaffler G, Raith J, Ranner G, et al. Radiographic appearance of an ossifying fibromyxoid tumor of soft parts. Skeletal Radiol 1997; 26:615–618.
15. Miettinen M. Ossifying fibromyxoid tumor of soft parts. Additional observations of a distinctive soft tissue tumor. Am J Clin Pathol 1991; 95:142–149.
16. Motoyama T, Ogose A, Watanabe H. Ossifying fibromyxoid tumor of the retroperitoneum. Pathol Int 1996; 46: 79–83.
17. Sovani V, Velagaleti GV, Filipowicz E, et al. Ossifying fibromyxoid tumor of soft parts: report of a case with novel cytogenetic findings. Cancer Genet Cytogenet 2001; 127:1–6.
18. Nishio J, Iwasaki H, Ohjimi Y, et al. Ossifying fibromyxoid tumor of soft parts. Cytogenetic findings. Cancer Genet Cytogenet 2002; 133(2):124–128.
19. Kawashima H, Ogose A, Umezu H, et al. Ossifying fibromyxoid tumor of soft parts with clonal chromosomal aberrations. Cancer Genet Cytogenet 2007; 176:156–160.
20. Fisher C, Hedges M, Weiss SW. Ossifying fibromyxoid tumor of soft parts with stromal cyst formation and ribosome-lamella complexes. Ultrastruct Pathol 1994; 18:593–600.
21. Hirose T, Shimada S, Tani T, et al. Ossifying fibromyxoid tumor: invariable ultrastructural features and diverse immunophenotypic expression. Ultrastruct Pathol 2007; 31:233–239.
22. Folpe AL, Weiss SW. Ossifying fibromyxoid tumor of soft parts: a clinicopathologic study of 70 cases with emphasis on atypical and malignant variants. Am J Surg Pathol 2003; 27:421–431.

A. Ectomesenchymal Chondromyxoid Tumor

1. Fletcher CDM, Unni KK, Mertens F, eds. World Health Organization Classification of Tumours: Pathology and Genetics of Tumours of Soft Tissue and Bone. Lyon: IARC Press, 2002.
2. Woo VL, Angiero F, Fantasia JE. Myoepithelioma of the tongue. Oral Surg Oral Med Oral Pathol Oral Radiol Endod 2005; 99:581–589.
3. Goveas N, Ethunandan M, Cowlishaw D, et al. Ectomesenchymal chondromyxoid tumour of the tongue: unlikely to originate from myoepithelial cells. Oral Oncol 2006; 42:1026–1028.
4. Smith BC, Ellis GL, Meis-Kindblom JM, et al. Ectomesenchymal chondromyxoid tumor of the anterior tongue. Nineteen cases of a new clinicopathologic entity. Am J Surg Pathol 1995; 19:519–530.
5. Carlos R, Aguirre JM, Pineda V. Ectomesenchymal chondromyxoid tumor of the tongue. Med Oral 1999; 4:361–365.
6. de Visscher JG, Kibbelaar RE, van der Waal I. Ectomesenchymal chondromyxoid tumor of the anterior tongue. Report of two cases. Oral Oncol 2003; 39:83–86.
7. Ide F, Mishima K, Saito I. Ectomesenchymal chondromyxoid tumor of the anterior tongue with myxoglobulosislike change. Virchows Arch 2003; 442:302–303.
8. Kannan R, Damm DD, White DK, et al. Ectomesenchymal chondromyxoid tumor of the anterior tongue: a report of three cases. Oral Surg Oral Med Oral Pathol Oral Radiol Endod 1996; 82:417–422.
9. Kaplan I, Anavi Y, Calderon S. Ectomesenchymal chondromyxoid tumour of the anterior tongue. Int J Oral Maxillofac Surg 2004; 33:404–407.
10. Kilpatrick SE, Hitchcock MG, Kraus MD, et al. Mixed tumors and myoepitheliomas of soft tissue: a clinicopathologic study of 19 cases with a unifying concept. Am J Surg Pathol 1997; 21:13–22.

11. Nigam S, Dhingra KK, Gulati A. Ectomesenchymal chondromyxoid tumor of the hard palate—a case report. J Oral Pathol Med 2006; 35:126–128.
12. van der Wal JE, van der Waal I. Ectomesenchymal chondromyxoid tumor of the anterior tongue. Report of a case. J Oral Pathol Med 1996; 25:456–458.
13. Pauwels P, Dal Cin P, Roumen R, et al. Intramuscular mixed tumour with clonal chromosomal changes. Virchows Arch 1999; 434:167–171.
14. Hornick JL, Fletcher CD. Myoepithelial tumors of soft tissue: a clinicopathologic and immunohistochemical study of 101 cases with evaluation of prognostic parameters. Am J Surg Pathol 2003; 27:1183–1196.

PART II

I. GRADING AND STAGING

1. Costa J. The Grading and Staging of Soft Tissue Sarcomas in Pathology of Soft Tissue Tumors. In: Fletcher CD, McKee PH, eds. Edinburgh: Churchill Livingstone, 1990:221–238.
2. Costa J, Wesley RA, Glatstein E, et al. The grading of soft tissue sarcomas. Results of a clinicopathologic correlation in a series of 163 cases. Cancer 1984; 530–541.
3. Markhede G, Angervall L, Stener B. A multivariate analysis of the prognosis after surgical treatment of malignant soft tissue tumors. Cancer 1982; 48:1721–1733.
4. Mytre-Jensen O, Kaae S. Madsen EH, et al. Histopathological grading in soft tissue tumors. Relation to survival in 261 surgically treated patients. Acta Pathol Microbiol Imunol Scand 1983; 91(A):145–150.
5. Trojari M, Contress G, Coindre JM, et al. Soft tissue sarcomas of adults; study of pathological prognostic variables and definition of a histopathological grading system. Int J Cancer 1984; 33:37–42.
6. van Unnik JA, Coindre JM, Contesso C, et al. Grading of soft tissue sarcomas: experience of the EDRTC Soft Tissue and Bone Sarcoma Group. Eur J Cancer 1993; 29(A): 2089–2093.
7. Coindre JM, Terrier P, Blu NB, et al. Prognositic factors in adult patients with locally controlled soft tissue sarcoma. A study of 546 patients from the French Federation of Cancer Centers Sarcoma Group. J Clin Oncol 1996; 14:869–877.
8. Coindre JM, Terrier P, Guillou L, et al. Predictive value of grade for metastasis development in the main histologic types of adult soft tissue sarcomas; a study of 1240 patients from the French Federation of Cancer Centers Sarcoma Group. Cancer 2001; 91:1914–1926.
9. Coindre JM, Trojari M, Contesso G, et al. Reproducibility of a histopatholigic grading system for adult soft tissue sarcoma. Cancer 1986; 58:306–309.
10. Guillou L, Coindre JM, Bonichon F, et al. Comparative study of the National Cancer Institute and French Federation of Cancer Centers Sarcoma Group grading systems in a population of 410 adult patients with soft tissue sarcoma. J Clin Oncol 1997; 15:350–382.
11. Enneking WF, Spanier SS, Good man MA. A system for the surgical staging of musculoskeletal sarcoma. Clin Orthop 1980; 153:106.
12. AJCC cancer staging handbook, 6th ed. New York, NY: Springer-Verlag, 2002:193.

A. Epithelioid Hemangioendothelioma

1. Dail DH, Liebow AA, Gmelich JT, et al. Intravascular bronchiolo-alveolar tumor. Am J Pathol 1975; 78:6A–7A.
2. Ishak KG, Sesterhenn IA, Goodman ZD, et al: Epithelioid hemangioendothelioma of the liver: a clinicopathologic and follow-up study of 32 cases. Hum Pathol 1982; 15:839–852.
3. Corrin B, Manners B, Millard M, et al. Histogenesis of the so-called ''intravascular bronchioloalveolar tumor.'' J Pathol 1979; 128:163–167.
4. Weldon-Linne CM, Victor TA, Christ ML, et al. Angiogenic nature of ''the intravascular bronchioloalveolar tumor'' of the lung: an electron microscopic study. Arch Pathol Lab Med 1981; 165:174–179.
5. Weiss SW, Enzinger FM. Epithelioid hemangioendothelioma. A vascular tumor often mistaken for a carcinoma. Cancer 1982; 50:970–981.
6. Rosai J, Gold J, Landy R. The histiocytoid hemangiomas: a unifying concept embracing several previously described entities of skin, soft tissue, large vessels, bone, and heart. Hum Pathol 1979; 10:707–730.
7. Mentzel T, Beham A, Calonje E, et al. Epithelioid hemangioendothelioma of skin and soft tissues: clinicopathologic and immunohistochemical study of 30 cases. Am J Surg Pathol 1997; 21:363–374.
8. Ellis GL, Kratochvil FJ. Epithelioid hemangioendothelioma of the head and neck: a clinicopathologic report of twelve cases. Oral Surg Oral Med Oral Pathol 1986; 61:61–68.
9. Chi AC, Weathers DR, Folpe AL, et al. Epithelioid hemangioendothelioma of the oral cavity: Report of two cases and review of the literature. Oral Surg Oral Med Oral Pathol Oral Radiol Endod 2005; 100:717–724.
10. Tseng CC, Tsay SH, Tsai TL, et al. Epithelioid hemangioendothelioma of the nasal cavity. J Chin Med Assoc 2005; 68:45–48.
11. Pigadas N, Mohamid W, McDermott P. Epithelioid hemangioendothelioma of the parotid salivary gland. Oral Surg Oral Med Oral Pathol Oral Radiol Endod 2000; 89:730–738.
12. Falvo L, Marzullo A, Catania A, et al. Epithelioid hemangioendothelioma of the parotid salivary gland: a case report. Chir Ital 2004; 56:457–462.
13. Boscaino A, Errico ME, Orabona P, et al. Epithelioid hemangioendothelioma of the larynx. Tumori 1999; 85:515–518.
14. Siddiqui MT, Evans HL, Ro JY, et al. Epithelioid haemangioendothelioma of the thyroid gland: a case report and review of literature. Histopathol 1998; 32:473–476.
15. Lyon DB, Tang TT, Kidder TM. Epithelioid hemangioendothelioma of the orbital bones. Ophthalmology 1992; 99:1773–1778.
16. Hamakawa H, Omori T, Sumida T, et al. Intraosseous epithelioid hemangioendothelioma of the mandible: a case report with an immunohistochemical study. J Oral Pathol Med 1999; 28:233–237.
17. Koh YC, Yoo H. Epithelioid haemangioendothelioma of the sphenoid bone. J Clin Neurosci 2001; 8:63–66.
18. Ramer MA, Lumerman H, Kopp W, et al. Epithelioid hemangioendothelioma of the maxilla: case report and review of literature. Periodontal Clin Investig 2001; 23: 31–35.
19. Quante M, Patel NK, Hills, et al. Epithelioid hemangioendothelioma presenting in the skin: a clinicopathologic study of eight cases. Am J Dermatopathol 1998; 20:541–546.

20. Kleer CG, Unni KK, McLeod RA. Epithelioid hemangioendothelioma of bone. Am J Surg Pathol 1996; 20:1301–1311.
21. Nuthakki S, Fessell D, Lal N, et al. Epithelioid hemangioendothelioma mimicking a nerve sheath tumor clinically and on MR imaging. Skeletal Radiol 2007; 36:s58–s62.
22. Murphey MD, Fairbairn KJ, Parman LM, et al. From the archives of the AFIP. Musculoskeletal angiomatous lesions: radiologic-pathologic correlation. Radiographic 1995; 15:893–917.
23. Weidner N. Atypical tumor of the mediastinum: epithelioid hemangioendothelioma containing metaplastic bone and osteoclastlike giant cells. Ultrastruct Pathol 1991; 15:481–488.
24. Lamovec J, Sobel HJ, Zidar A, et al. Epithelioid hemangioendothelioma of the anterior mediastinum with osteoclast-like giant cells. Light microscopic, immunohistochemical, and electron microscopic study. Am J Clin Pathol 1990; 93: 813–817.
25. Weiss SW, Ishak KG, Dail DH, et al. Epithelioid hemangioendothelioma and related lesions. Semin Diagn Pathol 1986; 3:259–287.
26. Gray MH, Rosenberg AE, Dickersin GR, et al. Cytokeratin expression in epithelioid vascular neoplasms. Hum Pathol 1990; 21:212–217.
27. Miettinen M, Fetsch JF. Distribution of keratins in normal endothelial cells and a spectrum of vascular tumors: implications in tumor diagnosis. Hum Pathol 2000; 31: 1062–1067.
28. Mendlick M, Nelson M, Pickering D, et al. Translocation t(1;3)(p36.3q25) is a nonrandom aberration in epithelioid hemangioendothelioma. Am J Surg Pathol 2001; 25: 684–687.
29. Boudousquie AC, Lawce HC, Sherman R, et al. Complex translocation [7;22] is a nonrandom aberration in an epithelioid hemangioendothelioma. Cancer Genet Cytogenet 1996; 92:116–121.
30. He M, Das K, Blacksin M, et al. A translocation involving the placental growth factor gene is identified in a hemangioendothelioma. Cancer Genet Cytogenet 2006; 168: 150–154.
31. Olsen TG, Helwig EB. Angiolymphoid hyperplasia with eosinophilia. A clinicopathologic study of 116 patients. J Am Acad Dermatol 1985; 12:781–796.
32. Googe PB, Harris NL, Mihm MC. Kimura's disease and angiolymphoid hyperplasia with eosinophilia: two distinct histopathological entities. J Cutan Pathol 1987; 14:263–271.
33. Urabe A, Tsuneyoshi M, Enjoji. Epithelioid hemangioma versus Kimura's disease. A comparative clinicopathologic study. Am J Surg Pathol 1987; 11:758–766.
34. Fetsch JF, Weiss SW. Observations concerning the pathogenesis of epithelioid hemangioma (angiolymphoid hyperplasia). Mod Pathol 1991; 4:449–455.
35. Miettinen M, Sarlomo-Rikala M, Lasota J. KIT expression in angiosarcomas and fetal endothelial cells; lack of mutations of exon 11 and exon 17 of c-kit. Mod Pathol 2000; 13:536–541.

B. Angiosarcoma

1. Fayette J, Martin E, Piperno-Neumann S, et al. Angiosarcomas, a heterogeneous group of sarcomas with specific behavior depending on primary site: a retrospective study of 161 cases. Ann Oncol 2007; 18:2030–2036.
2. Fanburg-Smith JC, Furlong MA, Childers EL. Oral and salivary gland angiosarcoma: a clinicopathologic study of 29 cases. Mod Pathol 2003; 16:263–271.
3. d'Amore ES, Wick MR, Geisinger KR, et al. Primary malignant lymphoma arising in postmastectomy lymphedema. Another facet of the Stewart-Treves syndrome. Am J Surg Pathol 1990; 14:456–63.
4. Miettinen M, Lehto VP, Virtanen I. Postmastectomy angiosarcoma (Stewart-Treves syndrome). Light-microscopic, immunohistological, and ultrastructural characteristics of two cases. Am J Surg Pathol 1983; 7:329–339.
5. Mark RJ, Tran LM, Sercarz J, et al. Angiosarcoma of the head and neck. The UCLA experience 1955 through 1990. Arch Otolaryngol Head Neck Surg 1993; 119:973–978.
6. Panje WR, Moran WJ, Bostwick DG, et al. Angiosarcoma of the head and neck: review of 11 cases. Laryngoscope 1986; 96:1381–384.
7. Holden CA, Spittle MF, Jones EW. Angiosarcoma of the face and scalp, prognosis and treatment. Cancer 1987; 59:1046–1057.
8. Lydiatt WM, Shaha AR, Shah JP. Angiosarcoma of the head and neck. Am J Surg 1994; 168:451–454.
9. Morrison WH, Byers RM, Garden AS, et al. Cutaneous angiosarcoma of the head and neck. A therapeutic dilemma. Cancer 1995; 76:319–327.
10. Aust MR, Olsen KD, Lewis JE, et al. Angiosarcomas of the head and neck: clinical and pathologic characteristics. Ann Otol Rhinol Laryngol 1997; 106:943–951.
11. Bankaci M, Myers EN, Barnes L, et al. Angiosarcoma of the maxillary sinus: literature review and case report. Head Neck Surg 1979; 1:274–280.
12. Kurien M, Nair S, Thomas S. Angiosarcoma of the nasal cavity and maxillary antrum. J Laryngol Otol 1989; 103:874–876.
13. Kimura Y, Tanaka S, Furukawa M. Angiosarcoma of the nasal cavity. J Laryngol Otol 1992; 106:368–369.
14. Di Tommaso L, Colombo G, Miceli S, et al. Angiosarcoma of the nasal cavity. Report of a case and review of the literature. Pathologica 2007; 99:76–80.
15. Rosai J, Sumner HW, Kostianovsky M, et al. Angiosarcoma of the skin. A clinicopathologic and fine structural study. Hum Pathol 1976; 7:83–109.
16. Cafiero F, Gipponi M, Peressini A, et al. Radiation-associated angiosarcoma: diagnostic and therapeutic implications—two case reports and a review of the literature. Cancer 1996; 77:2496–2502.
17. Lipshutz GS, Brennan TV, Warren RS. Thorotrast-induced liver neoplasia: a collective review. J Am Coll Surg 2002; 195:713–78.
18. Naka N, Ohsawa M, Tomita Y, et al. Angiosarcoma in Japan. A review of 99 cases. Cancer 1995; 75:989–996.
19. Davidson TI, Kissin MW, Bradish CF, et al. Angiosarcoma arising in a patient with Maffucci syndrome. Eur J Surg Oncol 1985; 11:381–384.
20. McMenamin ME, Fletcher CD. Expanding the spectrum of malignant change in schwannomas: epithelioid malignant change, epithelioid malignant peripheral nerve sheath tumor, and epithelioid angiosarcoma: a study of 17 cases. Am J Surg Pathol 2001; 25:13–25.
21. Meis-Kindblom JM, Kindblom LG. Angiosarcoma of soft tissue: a study of 80 cases. Am J Surg Pathol 1998; 22: 683–697.
22. De Young BR, Frierson HF, Jr., Ly MN, et al. CD31 immunoreactivity in carcinomas and mesotheliomas. Am J Clin Pathol 1998; 110:374–377.
23. Al Abbadi MA, Almasri NM, Al Quran S, et al. Cytokeratin and epithelial membrane antigen expression in angiosarcomas: an immunohistochemical study of 33 cases. Arch Pathol Lab Med 2007; 131:288–292.
24. Kindblom LG, Widehn S, Meis-Kindblom JM. The role of electron microscopy in the diagnosis of pleomorphic sarcomas of soft tissue. Semin Diagn Pathol 2003; 20:72–81.
25. Fletcher CD, Beham A, Bekir S, et al. Epithelioid angiosarcoma of deep soft tissue: a distinctive tumor readily

mistaken for an epithelial neoplasm. Am J Surg Pathol 1991; 15:915–924.
26. Mitelman F, Johansson B, Martens F. Database of chromosome aberrations in cancer. Available at: http://cgap.nci.nih.gov/Chromosomes/Mitelman. 2007.
27. Naka N, Tomita Y, Nakanishi H, et al. Mutations of p53 tumor-suppressor gene in angiosarcoma. Int J Cancer 1997; 71:952–955.
28. Zietz C, Rossle M, Haas C, et al. MDM-2 oncoprotein overexpression, p53 gene mutation, and VEGF up-regulation in angiosarcomas. Am J Pathol 1998; 153:1425–1433.

A. Rhabdomyosarcoma

1. World Health Organization Classification of Tumours 1st ed. Lyon, France: IARC Press, 2002.
2. Maurer HM, Moon T, Donaldson M, et al. The intergroup rhabdomyosarcoma study: a preliminary report. Cancer 1977; 40:2015–2026.
3. Horn RC Jr., Enterline HT. Rhabdomyosarcoma: a clinicopathological study and classification of 39 cases. Cancer 1958; 11:181–199.
4. Arndt CA, Crist WM. Common musculoskeletal tumors of childhood and adolescence. N Engl J Med 1999; 341:342–352.
5. Pappo AS, Shapiro DN, Crist WM, et al. Biology and therapy of pediatric rhabdomyosarcoma. J Clin Oncol 1995; 13:2123–2139.
6. Stiller CA, McKinney PA, Bunch KJ, et al. Childhood cancer and ethnic group in Britain: a United Kingdom children's Cancer Study Group (UKCCSG) study. Br J Cancer 1991; 64:543–548.
7. Stiller CA, Parkin DM. International variations in the incidence of childhood soft-tissue sarcomas. Paediatr Perinat Epidemiol 1994; 8:107–119.
8. Crist W, Gehan EA, Ragab AH, et al. The Third Intergroup Rhabdomyosarcoma Study. J Clin Oncol 1995; 13:610–630.
9. Newton WA Jr., Soule EH, Hamoudi AB, et al. Histopathology of childhood sarcomas, Intergroup Rhabdomyosarcoma Studies I and II: clinicopathologic correlation. J Clin Oncol 1988; 6:67–75.
10. Nayar RC, Prudhomme F, Parise O Jr., et al. Rhabdomyosarcoma of the head and neck in adults: a study of 26 patients. Laryngoscope 1993; 103:1362–1366.
11. Canalis RF, Jenkens HA, Hemenway WG, et al. Nasopharyngeal rhabdomyosarcoma. A clinical perspective Arch Otolaryngol 1978; 104:122–126.
12. Feldman BA. Rhabdomyosarcoma of the head and neck. Laryngoscope 1982; 92:424–440.
13. Shields JA, Shields CL. Rhabdomyosarcoma of the orbit. Int Ophthalmol Clin 1993; 33:203–210.
14. Shields JA, Shields CL, Scartozzi R. Survey of 1264 patients with orbital tumors and simulating lesions: The 2002 Montgomery Lecture, part 1. Ophthalmology 2004; 111:997–1008.
15. Wiener ES. Head and neck rhabdomyosarcoma. Semin Pediatr Surg 1994; 3:203–206.
16. Chong DY, Demirci H, Ronan SM, et al. Orbital rhabdomyosarcoma in Li-Fraumeni syndrome. Arch Ophthalmol 2007; 125:566–569.
17. Jung A, Bechthold S, Pfluger T, et al. Orbital rhabdomyosarcoma in Noonan syndrome. J Pediatr Hematol Oncol 2003; 25:330–332.
18. Shields CL, Shields JA, Honavar SG, et al. Primary ophthalmic rhabdomyosarcoma in 33 patients. Trans Am Ophthalmol Soc 2001; 99:133–142.
19. Karcioglu ZA, Hadjistilianou D, Rozans M, et al. Orbital rhabdomyosarcoma. Cancer Control 2004; 11:328–333.
20. Jones IS, Reese AB, Kraut J. Orbital rhabdomyosarcoma. An analysis of 62 cases. Am J Ophthalmol 1966; 61:721–736.
21. Ahmed AA, Tsokos M. Sinonasal rhabdomyosarcoma in children and young adults. Int J Surg Pathol 2007; 15: 160–165.
22. Fu YS, Perzin KH. Nonepithelial tumors of the nasal cavity paranasal sinuses, and nasopharynx: a clinicopathologic study. V. Skeletal muscle tumors (rhabdomyoma and rhabdomyosarcoma). Cancer 1976; 37:364–376.
23. Jaffe BF, Fox JE, Batsakis JG. Rhabdomyosarcoma of the middle ear and mastoid. Cancer 1971; 27:29–37.
24. Holman RL. Rhabdomyosarcoma of the middle-ear region; report of a case. J Laryngol Otol 1956; 70:415–419.
25. Goepfert H, Cangir A, Lindberg R, et al. Rhabdomyosarcoma of the temporal bone. Is surgical resection necessary? Arch Otolaryngol 1979; 105:310–313.
26. Schwartz RH, Movassaghi N, Marion ED. Rhabdomyosarcoma of the middle ear: a wolf in sheep's clothing. Pediatrics 1980; 65:1131–1133.
27. Wiatrak BJ, Pensak ML. Rhabdomyosarcoma of the ear and temporal bone. Laryngoscope 1989; 99:1188–1192.
28. Leviton A, Davidson R, Gilles F. Neurologic manifestations of embryonal rhabdomyosarcoma of the middle ear cleft. J Pediatr 1972; 80:596–602.
29. Bras J, Batsakis JG, Luna MA. Rhabdomyosarcoma of the oral soft tissues. Oral Surg Oral Med Oral Pathol 1987; 64:585–596.
30. Chen SY, Thakur A, Miller AS, et al. Rhabdomyosarcoma of the oral cavity. Report of four cases. Oral Surg Oral Med Oral Pathol Oral Radiol Endod 1995; 80:192–201.
31. Meehan S, Davis V, Brahim JS. Embryonal rhabdomyosarcoma of the floor of the mouth. A case report. Oral Surg Oral Med Oral Pathol 1994; 78:603–606.
32. Peters E, Cohen M, Altini M, et al. Rhabdomyosarcoma of the oral and paraoral region. Cancer 1989; 63:963–966.
33. Wharam MD Jr., Foulkes MA, Lawrence W Jr., et al. Soft tissue sarcoma of the head and neck in childhood: nonorbital and nonparameningeal sites. A report of the Intergroup Rhabdomyosarcoma Study (IRS)-I. Cancer 1984; 53:1016–1019.
34. Canalis RF, Platz CE, Cohn AM. Laryngeal rhabdomyosarcoma. Arch Otolaryngol 1976; 102:104–107.
35. Diehn KW, Hyams VJ, Harris AE. Rhabdomyosarcoma of the larynx: a case report and review of the literature. Laryngoscope 1984; 94:201–205.
36. Gorenstein A, Neel HB III, Weiland LH, et al. Sarcomas of the larynx. Arch Otolaryngol 1980; 106:8–12.
37. Gross M, Gutjahr P. Therapy of rhabdomyosarcoma of the larynx. Int J Pediatr Otorhinolaryngol 1988; 15:93–97.
38. Ruske DR, Glassford N, Costello S, et al. Laryngeal rhabdomyosarcoma in adults. J Laryngol Otol 1998; 112:670–672.
39. Dodd-o JM, Wieneke KF, Rosman PM. Laryngeal rhabdomyosarcoma. Case report and literature review. Cancer 1987; 59:1012–1018.
40. Barnes L, Gnepp DR. Surgical Pathology of the Head and Neck. New York, NY: Marcel Dekker, 1985.
41. Da Mosto MC, Marchiori C, Rinaldo A, et al. Laryngeal pleomorphic rhabdomyosarcoma. A critical review of the literature. Ann Otol Rhinol Laryngol 1996; 105:289–294.
42. Haerr RW, Turalba CI, el Mahdi AM, et al. Alveolar rhabdomyosarcoma of the larynx: case report and literature review. Laryngoscope 1987; 97:339–344.
43. Winter LK, Lorentzen M. Rhabdomyosarcoma of the larynx. Report of two cases and a review of the literature. J Laryngol Otol 1978;92:417–24.

44. Sivanandan R, Kong CS, Kaplan MJ, et al. Laryngeal embryonal rhabdomyosarcoma: a case of cervical metastases 13 years after treatment and a 25-year review of existing literature. Arch Otolaryngol Head Neck Surg 2004; 130:1217–1222.
45. Lloyd RV, Hajdu SI, Knapper WH. Embryonal rhabdomyosarcoma in adults. Cancer 1983; 51:557–565.
46. Coffin CM, Rulon J, Smith L, et al. Pathologic features of rhabdomyosarcoma before and after treatment: a clinicopathologic and immunohistochemical analysis. Mod Pathol 1997; 10:1175–1187.
47. Cavazzana AO, Schmidt D, Ninfo V, et al. Spindle cell rhabdomyosarcoma. A prognostically favorable variant of rhabdomyosarcoma. Am J Surg Pathol 1992; 16:229–235.
48. Rubin BP, Hasserjian RP, Singer S, et al. Spindle cell rhabdomyosarcoma (so-called) in adults: report of two cases with emphasis on differential diagnosis. Am J Surg Pathol 1998; 22:459–464.
49. Parham DM, Qualman SJ, Teot L, et al. Correlation between histology and PAX/FKHR fusion status in alveolar rhabdomyosarcoma: a report from the Children's Oncology Group. Am J Surg Pathol 2007; 31:895–901.
50. Parham DM, Shapiro DN, Downing JR, et al. Solid alveolar rhabdomyosarcomas with the t(2;13). Report of two cases with diagnostic implications. Am J Surg Pathol 1994; 18:474–478.
51. Furlong MA, Fanburg-Smith JC. Pleomorphic rhabdomyosarcoma in children: four cases in the pediatric age group. Ann Diagn Pathol 2001; 5:199–206.
52. Furlong MA, Mentzel T, Fanburg-Smith JC. Pleomorphic rhabdomyosarcoma in adults: a clinicopathologic study of 38 cases with emphasis on morphologic variants and recent skeletal muscle-specific markers. Mod Pathol 2001; 14:595–603.
53. Kodet R, Newton WA Jr., Hamoudi AB, et al. Childhood rhabdomyosarcoma with anaplastic (pleomorphic) features. A report of the Intergroup Rhabdomyosarcoma Study. Am J Surg Pathol 1993; 17:443–453.
54. Wesche WA, Fletcher CD, Dias P, et al. Immunohistochemistry of MyoD1 in adult pleomorphic soft tissue sarcomas. Am J Surg Pathol 1995; 19:261–269.
55. Parham DM, Webber B, Holt H, et al. Immunohistochemical study of childhood rhabdomyosarcomas and related neoplasms. Results of an Intergroup Rhabdomyosarcoma study project. Cancer 1991; 67:3072–3080.
56. Dias P, Parham DM, Shapiro DN, et al. Myogenic regulatory protein (MyoD1) expression in childhood solid tumors: diagnostic utility in rhabdomyosarcoma. Am J Pathol 1990; 137:1283–1291.
57. Morotti RA, Nicol KK, Parham DM, et al. An immunohistochemical algorithm to facilitate diagnosis and subtyping of rhabdomyosarcoma: the Children's Oncology Group experience. Am J Surg Pathol 2006; 30:962–968.
58. Wang NP, Marx J, McNutt MA, et al. Expression of myogenic regulatory proteins (myogenin and MyoD1) in small blue round cell tumors of childhood. Am J Pathol 1995; 147:1799–1810.
59. Miettinen M. Antibody specific to muscle actins in the diagnosis and classification of soft tissue tumors. Am J Pathol 1988; 130:205–215.
60. Parham DM, Dias P, Kelly DR, et al. Desmin positivity in primitive neuroectodermal tumors of childhood. Am J Surg Pathol 1992; 16:483–492.
61. Kapadia SB, Popek EJ, Barnes L. Pediatric otorhinolaryngic pathology: diagnosis of selected lesions. Pathol Annu 1994; 29(pt 1):159–209.
62. Coindre JM, de Mascarel A, Trojani M, et al. Immunohistochemical study of rhabdomyosarcoma. Unexpected staining with S100 protein and cytokeratin. J Pathol 1988; 155:127–132.
63. Miettinen M, Rapola J. Immunohistochemical spectrum of rhabdomyosarcoma and rhabdomyosarcoma-like tumors. Expression of cytokeratin and the 68-kD neurofilament protein. Am J Surg Pathol 1989; 13:120–132.
64. Pinto A, Tallini G, Novak RW, et al. Undifferentiated rhabdomyosarcoma with lymphoid phenotype expression. Med Pediatr Oncol 1997; 28:165–170.
65. Gordon T, McManus A, Anderson J, et al. Cytogenetic abnormalities in 42 rhabdomyosarcoma: a United Kingdom Cancer Cytogenetics Group Study. Med Pediatr Oncol 2001; 36:259–267.
66. Wang-Wuu S, Soukup S, Ballard E, et al. Chromosomal analysis of sixteen human rhabdomyosarcomas. Cancer Res 1988; 48:983–987.
67. Ho RH, Johnson J, Dev VG, et al. A novel t(2;20)(q35;p12) in embryonal rhabdomyosarcoma. Cancer Genet Cytogenet 2004; 151:73–77.
68. Kapels KM, Nishio J, Zhou M, et al. Embryonal rhabdomyosarcoma with a der(16)t(1;16) translocation. Cancer Genet Cytogenet 2007; 174:68–73.
69. Koufos A, Hansen MF, Copeland NG, et al. Loss of heterozygosity in three embryonal tumours suggests a common pathogenetic mechanism. Nature 1985; 316: 330–334.
70. Scrable HJ, Witte DP, Lampkin BC, et al. Chromosomal localization of the human rhabdomyosarcoma locus by mitotic recombination mapping. Nature 1987; 329: 645–647.
71. Li M, Squire JA, Weksberg R. Molecular genetics of Wiedemann-Beckwith syndrome. Am J Med Genet 1998; 79:253–259.
72. Loh WE Jr., Scrable HJ, Livanos E, et al. Human chromosome 11 contains two different growth suppressor genes for embryonal rhabdomyosarcoma. Proc Natl Acad Sci U S A 1992; 89:1755–1759.
73. Bridge JA, Liu J, Qualman SJ, et al. Genomic gains and losses are similar in genetic and histologic subsets of rhabdomyosarcoma, whereas amplification predominates in embryonal with anaplasia and alveolar subtypes. Genes Chromosomes Cancer 2002; 33:310–321.
74. Felix CA, Kappel CC, Mitsudomi T, et al. Frequency and diversity of p53 mutations in childhood rhabdomyosarcoma. Cancer Res 1992; 52:2243–2247.
75. Diller L, Sexsmith E, Gottlieb A, et al. Germline p53 mutations are frequently detected in young children with rhabdomyosarcoma. J Clin Invest 1995; 95:1606–1611.
76. Li FP, Fraumeni JF Jr. Rhabdomyosarcoma in children: epidemiologic study and identification of a familial cancer syndrome. J Natl Cancer Inst 1969; 43:1365–1373.
77. Barr FG, Galili N, Holick J, et al. Rearrangement of the PAX3 paired box gene in the paediatric solid tumour alveolar rhabdomyosarcoma. Nat Genet 1993; 3:113–117.
78. Barr FG. Gene fusions involving PAX and FOX family members in alveolar rhabdomyosarcoma. Oncogene 2001; 20:5736–5746.
79. Davis RJ, D'Cruz CM, Lovell MA, et al. Fusion of PAX7 to FKHR by the variant t(1;13)(p36;q14) translocation in alveolar rhabdomyosarcoma. Cancer Res 1994; 54: 2869–2872.
80. Galili N, Davis RJ, Fredericks WJ, et al. Fusion of a fork head domain gene to PAX3 in the solid tumour alveolar rhabdomyosarcoma. Nat Genet 1993; 5:230–235.
81. Tremblay P, Gruss P. Pax: genes for mice and men. Pharmacol Ther 1994; 61:205–226.
82. Epstein DJ, Vekemans M, Gros P. Splotch (Sp2H), a mutation affecting development of the mouse neural

tube, shows a deletion within the paired homeodomain of Pax-3. Cell 1991; 67:767–774.
83. Tassabehji M, Read AP, Newton VE, et al. Waardenburg's syndrome patients have mutations in the human homologue of the Pax-3 paired box gene. Nature 1992; 355: 635–636.
84. Tassabehji M, Newton VE, Leverton K, et al. PAX3 gene structure and mutations: close analogies between Waardenburg syndrome and the Splotch mouse. Hum Mol Genet 1994; 3:1069–1074.
85. Kaufmann E, Knochel W. Five years on the wings of fork head. Mech Dev 1996; 57:3–20.
86. Durham SK, Suwanichkul A, Scheimann AO, et al. FKHR binds the insulin response element in the insulin-like growth factor binding protein-1 promoter. Endocrinology 1999; 140:3140–3146.
87. Guo S, Rena G, Cichy S, et al. Phosphorylation of serine 256 by protein kinase B disrupts transactivation by FKHR and mediates effects of insulin on insulin-like growth factor-binding protein-1 promoter activity through a conserved insulin response sequence. J Biol Chem 1999; 274:17184–17192.
88. Fredericks WJ, Galili N, Mukhopadhyay S, et al. The PAX3-FKHR fusion protein created by the t(2;13) translocation in alveolar rhabdomyosarcomas is a more potent transcriptional activator than PAX3. Mol Cell Biol 1995; 15:1522–1535.
89. Scheidler S, Fredericks WJ, Rauscher FJ III, et al. The hybrid PAX3-FKHR fusion protein of alveolar rhabdomyosarcoma transforms fibroblasts in culture. Proc Natl Acad Sci U S A 1996; 93:9805–9809.
90. Anderson MJ, Shelton GD, Cavenee WK, et al. Embryonic expression of the tumor-associated PAX3-FKHR fusion protein interferes with the developmental functions of Pax3. Proc Natl Acad Sci U S A 2001; 98:1589–1594.
91. Barr FG, Nauta LE, Davis RJ, et al. In vivo amplification of the PAX3-FKHR and PAX7-FKHR fusion genes in alveolar rhabdomyosarcoma. Hum Mol Genet 1996; 5:15–21.
92. Davis RJ, Barr FG. Fusion genes resulting from alternative chromosomal translocations are overexpressed by gene-specific mechanisms in alveolar rhabdomyosarcoma. Proc Natl Acad Sci U S A 1997; 94:8047–8051.
93. Fitzgerald JC, Scherr AM, Barr FG. Structural analysis of PAX7 rearrangements in alveolar rhabdomyosarcoma. Cancer Genet Cytogenet 2000; 117:37–40.
94. Weber-Hall S, McManus A, Anderson J, et al. Novel formation and amplification of the PAX7-FKHR fusion gene in a case of alveolar rhabdomyosarcoma. Genes Chromosomes Cancer 1996; 17:7–13.
95. Barr FG, Chatten J, D'Cruz CM, et al. Molecular assays for chromosomal translocations in the diagnosis of pediatric soft tissue sarcomas. JAMA 1995; 273:553–557.
96. Anderson J, Gordon T, McManus A, et al. Detection of the PAX3-FKHR fusion gene in paediatric rhabdomyosarcoma: a reproducible predictor of outcome? Br J Cancer 2001; 85:831–835.
97. Kelly KM, Womer RB, Sorensen PH, et al. Common and variant gene fusions predict distinct clinical phenotypes in rhabdomyosarcoma. J Clin Oncol 1997; 15:1831–1836.
98. Drape JL, Idy-Peretti I, Goettmann S, et al. Subungual glomus tumors: evaluation with MR imaging. Radiology 1995; 195:507–515.
99. McCarville MB, Spunt SL, Pappo AS. Rhabdomyosarcoma in pediatric patients: the good, the bad, and the unusual. AJR Am J Roentgenol 2001; 176:1563–1569.
100. Dickman PS, Triche TJ. Extraosseous Ewing's sarcoma versus primitive rhabdomyosarcoma: diagnostic criteria and clinical correlation. Hum Pathol 1986; 17:881–893.
101. Hirose T, Scheithauer BW, Lopes MB, et al. Olfactory neuroblastoma. An immunohistochemical, ultrastructural, and flow cytometric study. Cancer 1995; 76:4–19.
102. Kodet R, Newton WA Jr., Sachs N, et al. Rhabdoid tumors of soft tissues: a clinicopathologic study of 26 cases enrolled on the Intergroup Rhabdomyosarcoma Study. Hum Pathol 1991; 22:674–684.
103. Parham DM, Weeks DA, Beckwith JB. The clinicopathologic spectrum of putative extrarenal rhabdoid tumors. An analysis of 42 cases studied with immunohistochemistry or electron microscopy. Am J Surg Pathol 1994; 18: 1010–1029.
104. Kodet R, Newton WA Jr., Hamoudi AB, et al. Rhabdomyosarcomas with intermediate-filament inclusions and features of rhabdoid tumors. Light microscopic and immunohistochemical study. Am J Surg Pathol 1991; 15:257–267.
105. Compagno J, Hyams VJ, Lepore ML. Nasal polyposis with stromal atypia. Review of follow-up study of 14 cases. Arch Pathol Lab Med 1976; 100:224–226.
106. Kindblom LG, Angervall L. Nasal polyps with atypical stroma cells: a pseudosarcomatous lesion. A light and electron-microscopic and immunohistochemical investigation with implications on the type and nature of the mesenchymal cells. Acta Pathol Microbiol Immunol Scand [A] 1984; 92:65–72.
107. Nakayama M, Wenig BM, Heffner DK. Atypical stromal cells in inflammatory nasal polyps: immunohistochemical and ultrastructural analysis in defining histogenesis. Laryngoscope 1995; 105:127–134.
108. Norris HJ, Taylor HB. Polyps of the vagina. A benign lesion resembling sarcoma botryoides. Cancer 1966; 19:227–232.
109. Tallini G, Parham DM, Dias P, et al. Myogenic regulatory protein expression in adult soft tissue sarcomas. A sensitive and specific marker of skeletal muscle differentiation. Am J Pathol 1994; 144:693–701.
110. Rosai J, Dias P, Parham DM, et al. MyoD1 protein expression in alveolar soft part sarcoma as confirmatory evidence of its skeletal muscle nature. Am J Surg Pathol 1991; 15:974–981.
111. Meza JL, Anderson J, Pappo AS, et al. Analysis of prognostic factors in patients with nonmetastatic rhabdomyosarcoma treated on intergroup rhabdomyosarcoma studies III and IV: the Children's Oncology Group. J Clin Oncol 2006; 24:3844–3851.
112. Healy GB, Upton J, Black PM, et al. The role of surgery in rhabdomyosarcoma of the head and neck in children. Arch Otolaryngol Head Neck Surg 1991; 117:1185–1188.
113. Rodary C, Gehan EA, Flamant F, et al. Prognostic factors in 951 nonmetastatic rhabdomyosarcoma in children: a report from the International Rhabdomyosarcoma Workshop. Med Pediatr Oncol 1991; 19:89–95.
114. Maurer HM, Beltangady M, Gehan EA, et al. The Intergroup Rhabdomyosarcoma Study-I. A final report. Cancer 1988; 61:209–220.
115. Nakhleh RE, Swanson PE, Dehner LP. Juvenile (embryonal and alveolar) rhabdomyosarcoma of the head and neck in adults. A clinical, pathologic, and immunohistochemical study of 12 cases. Cancer 1991; 67:1019–1024.
116. Maurer HM, Gehan EA, Beltangady M, et al. The Intergroup Rhabdomyosarcoma Study-II. Cancer 1993; 71: 1904–1922.
117. Lawrence W Jr., Hays DM, Moon TE. Lymphatic metastasis with childhood rhabdomyosarcoma. Cancer 1977; 39:556–559.
118. Shimada H, Newton WA Jr., Soule EH, et al. Pathology of fatal rhabdomyosarcoma. Report from Intergroup

Rhabdomyosarcoma Study (IRS-I and IRS-II). Cancer 1987; 59:459–465.
119. Raney RB, Anderson JR, Barr FG, et al. Rhabdomyosarcoma and undifferentiated sarcoma in the first two decades of life: a selective review of intergroup rhabdomyosarcoma study group experience and rationale for Intergroup Rhabdomyosarcoma Study V. J Pediatr Hematol Oncol 2001; 23:215–220.
120. Hosoi H, Teramukai S, Matsumoto Y, et al. A review of 331 rhabdomyosarcoma cases in patients treated between 1991 and 2002 in Japan. Int J Clin Oncol 2007; 12:137–145.
121. La Quaglia MP, Heller G, Ghavimi F, et al. The effect of age at diagnosis on outcome in rhabdomyosarcoma. Cancer 1994; 73:109–117.
122. Asmar L, Gehan EA, Newton WA, et al. Agreement among and within groups of pathologists in the classification of rhabdomyosarcoma and related childhood sarcomas. Report of an international study of four pathology classifications. Cancer 1994; 74:2579–2588.
123. Gaffney EF, Dervan PA, Fletcher CD. Pleomorphic rhabdomyosarcoma in adulthood. Analysis of 11 cases with definition of diagnostic criteria. Am J Surg Pathol 1993; 17:601–609.
124. Maurer HM, Moon T, Donaldson M, et al. The intergroup rhabdomyosarcoma study: a preliminary report. Cancer 40(5):2015–2026.

B. Leiomyosarcoma

1. Fields JP, Helwig EB. Leiomyosarcoma of the skin and subcutaneous tissue. Cancer 1981; 47:156–169.
2. Hashimoto H, Daimaru Y, Tsuneyoshi M, et al. Leiomyosarcoma of the external soft tissues: a clinicopathologic, immunohistochemical, and electron microscopic study. Cancer 1986; 57:2077–2088.
3. Hagy DM, Halperin V, Wood C. Leiomyoma of the oral cavity. Review of the literature and report of a case. Oral Surg 1964; 17:748–755.
4. Mindell RS, Calcaterra TC, Ward PH. Leiomyosarcoma of nose, nasopharynx and paranasal sinuses. Ann Otol Rhinol Laryngol 1965; 74:623–630.
5. de Saint Aubain Somerhausen N, Fletcher CDM. Leiomyosarcoma of soft tissue in children. Clinicopathologic analysis of 20 cases. Am J Surg Pathol 1999; 23:755–763.
6. Chadwick EG, Connor EJ, Hanson IC, et al. Tumors of smooth-muscle origin in HIV-infected children. JAMA 1990; 263:3182–3184.
7. McClain KL, Leach CT, Jenson HB, et al. Association of Epstein-Barr virus with leiomyosarcomas in young people with AIDS. N Engl J Med 1995; 332;12–18.
8. Deyrup AT, Lee VK, Hill CE, et al. Epstein-Barr virus-associated smooth muscle tumors are distinctive mesenchymal tumors reflecting multiple infection events. A clinicopathologic and molecular analysis of 29 tumors from 19 patients. Am J Surg Pathol 2006; 30:75–82.
9. Fu Y, Perzin KH. Nonepithelial tumors of the nasal cavity, paranasal sinuses, and nasopharynx: a clinicopathologic study. IV. Smooth muscle tumors (leiomyoma, leiomyosarcoma). Cancer 1975; 35:1300–1308.
10. Kuruvilla A, Wenig BM, Humphrey DM, et al. Leiomyosarcoma of the sinonasal tract. A clinicopathologic study of nine cases. Arch Otolaryngol Head Neck Surg 1990; 116:1278–1286.
11. Folberg R, Cleasby G, Flanagan JA, et al. Orbital leiomyosarcoma after radiation therapy for bilateral retinoblastoma. Arch Opthalmol 1983; 101:1562–1565.
12. Font RL, Jurco S III, Brechner RJ. Postradiation leiomyosarcoma of the orbit complicating bilateral retinoblastoma. Arch Ophthalmol 1983; 101:1557–1561.
13. Reich DS, Palmer CA, Peters GE. Ethmoid sinus leiomyosarcoma after cyclophosphamide treatment. Otolaryngol Head Neck Surg 1995; 113:495–498.
14. Ulrich CT, Feiz-Erfan I, Spetzler RF, et al. Sinonasal leiomyosarcoma: review of literature and case report. Laryngoscope 2005; 115:2242–2248.
15. Thompson LDR, Fanburg-Smith JC. Malignant soft tissue tumours. In: Barnes L, Eveson JW, Reichart P, Sidransky D, eds. Head and Neck Tumours. Lyon, France: IARC Press, 2005:35–42.
16. Wartheimer-Hatch L, Hatch GF, Hatch KF, et al. Tumors of the oral cavity and pharynx. World J Surg 2000; 24:395–400.
17. Nikitakis NG, Lopes MA, Bailey JS, et al. Oral leiomyosarcoma: review of the literature and report of two cases with assessment of the prognostic and diagnostic significance of immunohistochemical and molecular markers. Oral Oncology 2002; 38:201–208.
18. Vilos GA, Rapidis AD, Lagogiannis GD, et al. Leiomyosarcomas of the oral tissues: clinicopathologic analysis of 50 cases. J Oral Maxillofac Surg 2005; 63:1461–1477.
19. Marioni G, Staffieri C, Marino F, et al. Leiomyosarcoma of the larynx: critical analysis of the diagnostic role played by immunohistochemistry. Am J Otolaryngol 2005; 26:201–206.
20. Kang J, Levinson JA, Hitti IF. Leiomyosarcoma of the parotid gland: a case report and review of the literature. Head Neck 1999; 21:168–171.
21. Freije JE, Gluckman JL, Biddinger PW, et al. Muscle tumors in the parapharyneal space. Head Neck 1992; 14:49–54.
22. Montgomery E, Goldblum JR, Fisher C. Leiomyosarcoma of the head and neck: a clinicopathological study. Histopathology 2002; 40:518–525.
23. Akcam T, Oysul K, Birkent H, et al. Leiomyosarcoma of the head and neck: report of two cases and review of the literature. Auris Nasus Larynx 2005; 32:209–212.
24. Thompson LDR, Wenig BM, Adair CF, et al. Primary smooth muscle tumors of the thyroid gland. Cancer 1997; 79:579–587.
25. Jakobiec FA, Howard GM, Rosen M, et al. Leiomyoma and leiomyosarcoma of the orbit. Am J Opthalmol 1975; 80:1028–1042.
26. Wojno T, Tenzel RR, Nadji M. Orbital leiomyosarcoma. Arch Ophthalmol 1983; 101:1566–1568.
27. Meekins BB, Dutton JJ, Proia AD. Primary orbital leiomyosarcoma. A case report and review of the literature. Arch Ophthalmol 1988; 106:82–86.
28. Wiechens B, Werner JA, Luttges J, et al. Primary orbital leiomyoma and leiomyosarcoma. Ophthalmologica 1999; 213:159–164.
29. Hatch GF III, Wertheimer-Hatch L, Hatch KF, et al. Tumors of the esophagus. World J Surg 2000; 24:401–411.
30. Kaddu S, Beham A, Cerroni L, et al. Cutaneous leiomyosarcoma. Am J Surg Pathol 1997; 21:979–987.
31. Dahl I, Angervall L. Cutaneous and subcutaneous leiomyosarcoma. A clinicopathologic study of 47 patients. Pathol Eur 1974; 9:307–315.
32. Snowden RT, Osborn FD, Wong FS, et al. Superficial leiomyosarcoma of the head and neck: case report and review of the literature. Ear Nose Throat J 2001; 80:449–453.
33. Tanaka H, Westesson PL, Wilbur DC. Leiomyosarcoma of the maxillary sinus: CT and MRI findings. Br J Radiol 1998; 71:221–224.
34. Kempson RL, Fletcher CDM, Evans HL, et al. Smooth Muscle Tumors. In: Kempson RL, Fletcher CDM, Evans HL, et al., eds. Tumors of the Soft Tissues. 3rd series,

fascicle 30. Washington D.C.: Armed Forces Institute of Pathology, 2001:239–256.
35. Guillou L, Coindre JM, Bonichon F, et al. Comparative study of the National Cancer Institute and the French Federation of Cancer Centers Sarcoma Group grading systems in a population of 410 of adult patients with soft tissue sarcoma. J Clin Oncol 1997; 15:350–362.
36. Nistal M, Paniagua R, Picasz ML, et al. Granular changes in vascular leiomyosarcoma. Virchows Arch a Pathol Anat Histol 1980; 386:239–248.
37. Freedman PD, Jones AC, Kerpel SM. Epithelioid leiomyosarcoma of the oral cavity: report of two cases and review of the literature. J Oral Maxillofac Surg 1993; 51:928–932.
38. Suster S. Epithelioid leiomyosarcoma of the skin and subcutaneous tissue. Clinicopathologic, immunohistochemical, and ultrastructural study of five cases. Am J Surg Pathol 1994; 18:232–240.
39. Sindwani R, Matthews TW, Venkatesan VM. Epithelioid leiomyosarcoma of the larynx. Head Neck 1998; 20: 563–567.
40. Mentzel T, Calonje E, Fletcher CD. Leiomyosarcoma with prominent osteoclast-like giant cells. Analysis of eight cases closely mimicking the so-called giant cell variant of malignant fibrous histiocytoma. Am J Surg Pathol 1994; 18:258–265.
41. Rubin BP, Fletcher CD. Myxoid leiomyosarcoma of soft tissue, an underrecognized variant. Am J Surg Pathol 2000; 24:927–936.
42. Merchant W, Calonje E, Fletcher CD. Inflammatory leiomyosarcoma: a morphological subgroup within the heterogeneous family of so-called inflammatory malignant fibrous histiocytoma. Histopathol 1995; 27:525–532.
43. Brooks JJ. The significance of double phenotypic patterns and markers in human ssarcomas: a new model of mesenchymal differentiation. Am J Pathol 1986; 125:123.
44. Hashimoto H, Daimaru Y, Tsuneyoshi M, et al. Soft tissue sarcoma with additional anaplastic components: a clinicopathologic and immunohistochemical study of 27 cases. Cancer 1990; 66:1578–1589.
45. Oda Y, Miyajima K, Kawaguchi K, et al. Pleomorphic leiomyosarcoma: clinicopathologic and immunohistochemical study with special emphasis on its distinction from ordinary leiomyosarcoma and malignant fibrous histiocytoma. Am J Surg Pathol 2001; 25:1030–1038.
46. Miettinen MM, Sarlomo-Rikala, Kovitich AJ, et al. Calponin and h-caldesmon in soft tissue tumors: consistent h-caldesmon immunoreactivity in gastrointestinal stromal tumors indicates traits of smooth muscle differentiation. Mod Pathol 1999; 12:756–762.
47. Ceballos KM, Nielsen GP, Selig MK, et al. Is anti-h-caldesmon useful for distinguishing smooth muscle and myofibroblastic tumors? Am J Clin Pathol 2000; 114:746–753.
48. Sakamoto A, Oda Y, Yamamoto H, et al. Calponin and h-caldesmon expression in atypical fibroxanthoma and superficial leiomyosarcoma. Virchows Arch 2002; 440:404–409.
49. Perez-Montiel MD, Plaza JA, Dominguez-Malagon H, et al. Differential expression of smooth muscle myosin, smooth muscle actin, h-caldesmon, and calponin in the diagnosis of myofibroblastic and smooth muscle lesions of skin and soft tissue. Am J Dermatopathol 2006; 28:105–111.
50. Miettinen M. Immunoreactivity for cytokeratin and epithelial membrane antigen in leiomyosarcoma. Arch Pathol Lab Med 1988; 112:637–640.
51. Swanson PE, Stanley MW, Scheithauer BW, et al. Primary cutaneous leiomyosarcoma. A histological and immunohistochemical study of 9 cases, with ultrastructural correlation. J Cutan Pathol 1988; 15:129–141.
52. Van de Rijn M, Rouse RV. CD34: a review. Appl Immunohistochem 1994; 2:71–80.
53. Sreekantaiah C, Davis JR, Sandberg AA. Chromosomal abnormalities in leiomyosarcoma. Am J Pathol 1993; 142:293–305.
54. Mandahl N, Fletcher CD, Dal Cin P, et al. Comparative cytogenetic study of spindle cell and pleomorphic leiomyosarcomas of soft tissues: a report from the CHAMP study group. Cancer Genet Cytogent 2000; 116:66–73.
55. El-Rifai W, Sarlomo-Rikala M, Knuutila S, et al. DNA copy number changes in development and progression in leiomyosarcomas of soft tissues. Am J Pathol 1998; 153:985–990.
56. Dei Tos AP, Maestro R, Doglioni C, et al. Tumor suppressor genes and related molecules in leiomyosarcomas. Am J Pathol 1996; 148:1037–1045.
57. Florenes VA, Maelandsmo GM, Forus A, et al. MDM2 gene amplification and transcript levels in human sarcomas: relationship to TP53 gene status. J Natl Cancer Inst 1994; 86:1297–1302.
58. Patterson H, Gill S, Fisher C, et al. Abnormalities of the p53, MDM2 and DCC genes in human leiomyosarcomas. Br J Cancer 1994; 69:1052–1058.
59. Berthelet E, Shenouda G, Black MJ, et al. Sarcomatoid carcinoma of the head and neck. Am J Surg 1994; 168:455–458.
60. Nakhleh RE, Zarbo RJ, Ewing S, et al. Myogenic differentiation in spindle cell (sarcomatoid) carcinomas of the upper aerodigestive tract. Appl Immunohistochem 1993; 1:58–68.
61. Thompson LDR, Wieneke JA, Miettinen M, et al. Spindle cell (sarcomatoid) carcinomas of the larynx. A clinicopathologic study of 187 cases. Am J Surg Pathol 2002; 26: 153–170.
62. Cardesa A, Zidar N. Spindle cell carcinoma. In: Barnes L, Eveson JW, Reichart P, et al., eds. Head and Neck Tumours. Lyon, France: IARC Press, 2005:127–128.
63. Granter SR, Weilbaecher KN, Quigley C, et al. Microphthalmia transcription factor: not a sensitive or specific marker for the diagnosis of desmoplastic melanoma and spindle cell (non-desmoplastic) melanoma. Am J Dermatopathol 2001; 23:185–189.
64. Mentzel T, Dry S, Katenkamp D, et al. Low-grade myofibroblastic sarcoma: analysis of 18 cases in the spectrum of myofibroblastic tumors. Am J Surg Pathol 1998; 22: 1228–1238.
65. Montgomery E, Goldblum J, Fisher C. Myofibrosarcoma: a clinicopathologic study. Am J Surg Pathol 2001; 25:219–228.
66. Coffin CM, Watterson J, Priest JR, et al. Extrapulmonary inflammatory myofibroblastic tumor (inflammatory pseudotumor). A clinicopathologic and immunohistochemical study of 84 cases. Am J Surg Pathol 1995; 19:859–872.
67. Wenig BM, Devaney K, Bisceglia M. Inflammatory myofibroblastic tumor of the larynx. A clinicopathologic study of eight cases simulating a malignant spindle cell neoplasm. Cancer 1995; 76:2217–2229.
68. Coffin CM, Fletcher JA. Inflammatory myofibroblastic tumour. In: Fletcher CDM, Unni KK, Mertens F. eds. Tumours of the Soft Tissue and Bone. Lyon, France: IARC Press, 2002:91–93.
69. Cessna MH, Zhou H, Sanger WG, et al. Expression of ALK1 and p80 in inflammatory myofibroblastic tumor and its mesenchymal mimics: a study of 135 cases. Mod Pathol 2002; 15:931–938.
70. Fisher C, Montgomery E, Healy V. Calponin and h-caldesmon expression in synovial sarcoma; the use of calponin in diagnosis. Histopathol 2003; 42:588–593.
71. Folpe AL, Schmidt RA, Chapman D, et al. Poorly differentiated synovial sarcoma: immunohistochemical distinction

from primitive neuroectodermal tumors and high-grade malignant peripheral nerve sheath tumors. Am J Surg Pathol 1998; 22:673–682.
72. Pelmus M, Guillou L, Hostein I, et al. Monophasic fibrous and poorly differentiated synovial sarcoma: immunohistochemical reassessment of 60 t(X;18) (SYT-SSX)-positive cases. Am J Surg Pathol 2002; 26:1434–1440.
73. Leuschner I, Newton WA Jr., Schmidt D, et al. Spindle cell variants of embryonal rhabdomyosarcoma in the paratesticular region. A report of the Intergroup Rhabdomyosarcoma Study. Am J Surg Pathol 1993; 17:221–230.
74. Cavazzana AO, Schmidt D, Ninfo V, et al. Spindle cell rhabdomyosarcoma. A prognostically favorable variant of rhabdomyosarcoma. Am J Surg Pathol 1992; 16:229–235.
75. Hornick JL, Fletcher CDM. Myoepithelial tumors of soft tissue. A clinicopathologic and immunohistochemical study of 101 cases with evaluation of prognostic parameters. Am J Surg Pathol 2003; 27:1183–1196.
76. Fusconi M, Magliulo G, Rocca CD et al. Leiomyosarcoma of the sinonasal tract: a case report and literature review. Am J Otolaryngol 2002; 23:108–111.
77. Eilber FR, Eckardt J. Surgical management of soft tissue sarcomas. Semin Oncol 1997; 24:526–533.
78. Pisters PW, Harrison LB, Leung DH, et al. Long term results of a prospective randomized trial of adjuvant brachytherapy in soft tissue sarcoma. J Clin Oncol 1996; 14: 859–868.
79. Yang JC, Chang AE, Baker AR, et al. Randomized prospective study of the benefit of adjuvant radiation therapy in the treatment of soft tissue sarcomas of the extremity. J Clin Oncol 1998; 16:197–203.
80. Suit HD, Mankin HJ, Wood WC, et al. Treatment of the patient with stage M0 soft tissue sarcoma. J Clin Oncol 1988; 6:854–862.
81. Dry SM, Jorgensen JL, Fletcher CDM. Leiomyosarcomas of the oral cavity: an unusual topographic subset easily mistaken for nonmensenchymal tumours. Histopathol 2000; 36:210–220.
82. Miettinen M, Fetsch JF. Evaluation of biological potential of smooth muscle tumours. Histopathol 2006; 48:97–105.

A. Liposarcoma

1. Henricks WH, Chu YC, Goldblum JR, et al. Dedifferentiated liposarcoma: a clinicopathological analysis of 155 cases with a proposal for an expanded definition of dedifferentiation. Am J Surg Pathol 1997; 21:271–281.
2. Argani P, Facchetti F, Inghirami G, et al. Lymphocyte-rich well-differentiated liposarcoma: report of nine cases. Am J Surg Pathol 1997; 21:884–895.
3. Kraus MD, Guillou L, Fletcher CD. Well-differentiated inflammatory liposarcoma: an uncommon and easily overlooked variant of a common sarcoma. Am J Surg Pathol 1997; 21:518–527.
4. Fanburg-Smith JC, Miettinen M. Liposarcoma with meningothelial-like whorls: a study of 17 cases of a distinctive histological pattern associated with dedifferentiated liposarcoma. Histopathology 1998; 33:414–424.
5. Nascimento AG, Kurtin PJ, Guillou L, et al. Dedifferentiated liposarcoma: a report of nine cases with a peculiar neurallike whorling pattern associated with metaplastic bone formation. Am J Surg Pathol 1998; 22:945–955.
6. Dei Tos AP, Mentzel T, Newman PL, et al. Spindle cell liposarcoma, a hitherto unrecognized variant of liposarcoma. Analysis of six cases. Am J Surg Pathol 1994; 18: 913–21.
7. McCormick D, Mentzel T, Beham A, et al. Dedifferentiated liposarcoma. Clinicopathologic analysis of 32 cases suggesting a better prognostic subgroup among pleomorphic sarcomas. Am J Surg Pathol 1994; 18:1213–1223.
8. Weiss SW, Rao VK. Well-differentiated liposarcoma (atypical lipoma) of deep soft tissue of the extremities, retroperitoneum, and miscellaneous sites. A follow-up study of 92 cases with analysis of the incidence of ''dedifferentiation''. Am J Surg Pathol 1992; 16:1051–1058.
9. Miettinen M, Enzinger FM. Epithelioid variant of pleomorphic liposarcoma: a study of 12 cases of a distinctive variant of high-grade liposarcoma. Mod Pathol 1999; 12:722–728.
10. Gebhard S, Coindre JM, Michels JJ, et al. Pleomorphic liposarcoma: clinicopathologic, immunohistochemical, and follow-up analysis of 63 cases: a study from the French Federation of Cancer Centers Sarcoma Group. Am J Surg Pathol 2002; 26:601–616.
11. Baden E, Newman R. Liposarcoma of the oropharyngeal region. Review of the literature and report of two cases. Oral Surg Oral Med Oral Pathol 1977; 44:889–902.
12. Enterline HT, Culberson JD, Rochlin DB, et al. Liposarcoma. A clinical and pathological study of 53 cases. Cancer 1960; 13:932–950.
13. Spittle MF, Newton KA, Mackenzie DH. Liposarcoma. A review of 60 cases. Br J Cancer 1970; 24:696–704.
14. Stout AP. Liposarcoma-the Malignant Tumor of Lipoblasts. Ann Surg 1944; 119:86–107.
15. Celik C, Karakousis CP, Moore R, et al. Liposarcomas: prognosis and management. J Surg Oncol 1980; 14:245–249.
16. Das Gupta TK. Tumors and tumor-like conditions of the adipose tissue. Curr Probl Surg 1970; 1–60.
17. Evans HL. Liposarcoma: a study of 55 cases with a reassessment of its classification. Am J Surg Pathol 1979; 3: 507–523.
18. Pack GT, Pierson JC. Liposarcoma; a study of 105 cases. Surgery 1954; 36:687–712.
19. Mandell DL, Brandwein MS, Woo P, et al. Upper aerodigestive tract liposarcoma: report on four cases and literature review. Laryngoscope 1999; 109:1245–1252.
20. Esclamado RM, Disher MJ, Ditto JL, et al. Laryngeal liposarcoma. Arch Otolaryngol Head Neck Surg 1994; 120: 422–426.
21. Hurtado JF, Lopez JJ, Aranda FI, et al. Primary liposarcoma of the larynx. Case report and literature review. Ann Otol Rhinol Laryngol 1994; 103:315–318.
22. Menown IB, Liew SH, Napier SS, et al. Retro-pharyngeal liposarcoma. J Laryngol Otol 1992; 106:469–471.
23. Nofal F, Thomas M. Liposarcoma in the pharynx. J Laryngol Otol 1989; 103:1080–1082.
24. Reed JM, Vick EG. Hypopharyngeal liposarcoma. Otolaryngol Head Neck Surg 1996; 114:499–500.
25. Reibel JF, Greene WM. Liposarcoma arising in the pharynx nine years after fibrolipoma excision. Otolaryngol Head Neck Surg 1995; 112:599–602.
26. Wenig BM, Weiss SW, Gnepp DR. Laryngeal and hypopharyngeal liposarcoma. A clinicopathologic study of 10 cases with a comparison to soft-tissue counterparts. Am J Surg Pathol 1990; 14:134–141.
27. Wenig BM, Heffner DK. Liposarcomas of the larynx and hypopharynx: a clinicopathologic study of eight new cases and a review of the literature. Laryngoscope 1995; 105: 747–756.
28. Peng C, Zhao X, Dong X, et al. Liposarcoma of the pleural cavity: a case report. J Thorac Cardiovasc Surg 2007; 133:1108–1109.
29. Kransdorf MJ, Bancroft LW, Peterson JJ, et al. Imaging of fatty tumors: distinction of lipoma and well-differentiated liposarcoma. Radiology 2002; 224:99–104.
30. Murphey MD, Arcara LK, Fanburg-Smith J. From the archives of the AFIP: imaging of musculoskeletal

liposarcoma with radiologic-pathologic correlation. Radiographics 2005; 25:1371–1395.
31. Peterson JJ, Kransdorf MJ, Bancroft LW, et al. Malignant fatty tumors: classification, clinical course, imaging appearance and treatment. Skeletal Radiol 2003; 32: 493–503.
32. Database chromosome aberrations in cancer. 2007. Available at: http://cgap.nci.nih.gov/Chromosomes/Mitelman
33. Stephenson CF, Berger CS, Leong SP, et al. Analysis of a giant marker chromosome in a well-differentiated liposarcoma using cytogenetics and fluorescence in situ hybridization. Cancer Genet Cytogenet 1992; 61:134–138.
34. Pedeutour F, Forus A, Coindre JM, et al. Structure of the supernumerary ring and giant rod chromosomes in adipose tissue tumors. Genes Chromosomes Cancer 1999; 24:30–41.
35. Hostein I, Pelmus M, Aurias A, et al. Evaluation of MDM2 and CDK4 amplification by real-time PCR on paraffin wax-embedded material: a potential tool for the diagnosis of atypical lipomatous tumours/well-differentiated liposarcomas. J Pathol 2004; 202:95–102.
36. Szymanska J, Virolainen M, Tarkkanen M, et al. Overrepresentation of 1q21-23 and 12q13-21 in lipoma-like liposarcomas but not in benign lipomas: a comparative genomic hybridization study. Cancer Genet Cytogenet 1997; 99:14–18.
37. Pilotti S, Della TG, Lavarino C, et al. Distinct mdm2/p53 expression patterns in liposarcoma subgroups: implications for different pathogenetic mechanisms. J Pathol 1997; 181:14–24.
38. Szymanska J, Tarkkanen M, Wiklund T, et al. Gains and losses of DNA sequences in liposarcomas evaluated by comparative genomic hybridization. Genes Chromosomes Cancer 1996; 15:89–94.
39. Meis-Kindblom JM, Sjogren H, Kindblom LG, et al. Cytogenetic and molecular genetic analyses of liposarcoma and its soft tissue simulators: recognition of new variants and differential diagnosis. Virchows Arch 2001; 439:141–151.
40. Crozat A, Aman P, Mandahl N, et al. Fusion of CHOP to a novel RNA-binding protein in human myxoid liposarcoma. Nature 1993; 363:640–644.
41. Knight JC, Renwick PJ, Cin PD, et al. Translocation t(12;16)(q13;p11) in myxoid liposarcoma and round cell liposarcoma: molecular and cytogenetic analysis. Cancer Res 1995; 55:24–27.
42. Gibas Z, Miettinen M, Limon J, et al. Cytogenetic and immunohistochemical profile of myxoid liposarcoma. Am J Clin Pathol 1995; 103:20–26.
43. Panagopoulos I, Hoglund M, Mertens F, et al. Fusion of the EWS and CHOP genes in myxoid liposarcoma. Oncogene 1996; 12:489–494.
44. Panagopoulos I, Lassen C, Isaksson M, et al. Characteristic sequence motifs at the breakpoints of the hybrid genes FUS/CHOP, EWS/CHOP and FUS/ERG in myxoid liposarcoma and acute myeloid leukemia. Oncogene 1997; 15: 1357–1362.
45. Morohoshi F, Arai K, Takahashi EI, et al. Cloning and mapping of a human RBP56 gene encoding a putative RNA binding protein similar to FUS/TLS and EWS proteins. Genomics 1996; 38:51–57.
46. Ron D, Habener JF. CHOP, a novel developmentally regulated nuclear protein that dimerizes with transcription factors C/EBP and LAP and functions as a dominant-negative inhibitor of gene transcription. Genes Dev 1992; 6: 439–53.
47. Adelmant G, Gilbert JD, Freytag SO. Human translocation liposarcoma-CCAAT/enhancer binding protein (C/EBP) homologous protein (TLS-CHOP) oncoprotein prevents adipocyte differentiation by directly interfering with C/EBPbeta function. J Biol Chem 1998; 273:15574–15581.
48. Perez-Losada J, Sanchez-Martin M, Rodriguez-Garcia MA, et al. Liposarcoma initiated by FUS/TLS-CHOP: the FUS/TLS domain plays a critical role in the pathogenesis of liposarcoma. Oncogene 2000; 19:6015–6022.
49. Willeke F, Ridder R, Mechtersheimer G, et al. Analysis of FUS-CHOP fusion transcripts in different types of soft tissue liposarcoma and their diagnostic implications. Clin Cancer Res 1998; 4:1779–1784.
50. Mezzelani A, Sozzi G, Pierotti MA, et al. Rapid differential diagnosis of myxoid liposarcoma by fluorescence in situ hybridisation on cytological preparations. Clin Mol Pathol 1996; 49:M308–M309.
51. Kuroda M, Ishida T, Horiuchi H, et al. Chimeric TLS/FUS-CHOP gene expression and the heterogeneity of its junction in human myxoid and round cell liposarcoma. Am J Pathol 1995; 147:1221–1227.
52. Antonescu CR, Tschernyavsky SJ, Decuseara R, et al. Prognostic impact of P53 status, TLS-CHOP fusion transcript structure, and histological grade in myxoid liposarcoma: a molecular and clinicopathologic study of 82 cases. Clin Cancer Res 2001; 7:3977–3987.
53. Sreekantaiah C, Karakousis CP, Leong SP, et al. Cytogenetic findings in liposarcoma correlate with histopathologic subtypes. Cancer 1992; 69:2484–2495.
54. Schneider-Stock R, Walter H, Radig K, et al. MDM2 amplification and loss of heterozygosity at Rb and p53 genes: no simultaneous alterations in the oncogenesis of liposarcomas. J Cancer Res Clin Oncol 1998; 124:532–540.
55. Weiss LM, Warhol MJ. Ultrastructural distinctions between adult pleomorphic rhabdomyosarcomas, pleomorphic liposarcomas, and pleomorphic malignant fibrous histiocytomas. Hum Pathol 1984; 15:1025–1033.
56. Fanburg-Smith JC, Furlong MA, Childers EL. Liposarcoma of the oral and salivary gland region: a clinicopathologic study of 18 cases with emphasis on specific sites, morphologic subtypes, and clinical outcome. Mod Pathol 2002; 15:1020–1031.
57. Angiero F, Sidoni A, Stefani M. Liposarcoma of the oral cavity—case reports of the pleomorphic and the dedifferentiated variants and a review of the literature. Anticancer Res 2006; 26:4857–4867.
58. Golledge J, Fisher C, Rhys-Evans PH. Head and neck liposarcoma. Cancer 1995; 76:1051–1058.
59. Kilpatrick SE, Doyon J, Choong PF, et al. The clinicopathologic spectrum of myxoid and round cell liposarcoma. A study of 95 cases. Cancer 1996; 77:1450–1458.
60. Smith TA, Easley KA, Goldblum JR. Myxoid/round cell liposarcoma of the extremities. A clinicopathologic study of 29 cases with particular attention to extent of round cell liposarcoma. Am J Surg Pathol 1996; 20:171–180.
61. Downes KA, Goldblum JR, Montgomery EA, et al. Pleomorphic liposarcoma: a clinicopathologic analysis of 19 cases. Mod Pathol 2001; 14:179–184.
62. Grosso F, Jones RL, Demetri GD, et al. Efficacy of trabectedin (ecteinascidin-743) in advanced pretreated myxoid liposarcomas: a retrospective study. Lancet Oncol 2007; 8: 595–602.

A. Fibrosarcoma/Malignant Fibrous Histiocytoma

1. Scott SM, Reiman HM, Pritchard DJ, et al. Soft tissue fibrosarcoma. A clinicopathologic study of 132 cases. Cancer 1989; 64:925–931.
2. Gutierrez JC, Perez EA, Franceschi D, et al. Outcomes for soft-tissue sarcoma in 8249 cases from a large state cancer registry. J Surg Res 2007; 141:105–114.

3. Coffin CM, Dehner LP. Fibroblastic-myofibroblastic tumors in children and adolescents: a clinicopathologic study of 108 examples in 103 patients. Pediatr Pathol 1991; 11:569–588.
4. Fisher C. The comparative roles of electron microscopy and immunohistochemistry in the diagnosis of soft tissue tumours. Histopathology 2006; 48:32–41.
5. Tos AP. Classification of pleomorphic sarcomas: where are we now? Histopathology 2006; 48:51–62.
6. Fanburg-Smith JC, Spiro IJ, Katapuram SV, et al. Infiltrative subcutaneous malignant fibrous histiocytoma: a comparative study with deep malignant fibrous histiocytoma and an observation of biologic behavior. Ann Diagn Pathol 1999; 3:1–10.
7. Billings SD, Giblen G, Fanburg-Smith JC. Superficial low-grade fibromyxoid sarcoma (Evans tumor): a clinicopathologic analysis of 19 cases with a unique observation in the pediatric population. Am J Surg Pathol 2005; 29:204–210.
8. Evans HL. Low-grade fibromyxoid sarcoma. A report of two metastasizing neoplasms having a deceptively benign appearance. Am J Clin Pathol 1987; 88:615–619.
9. Coindre JM, Hostein I, Maire G, et al. Inflammatory malignant fibrous histiocytomas and dedifferentiated liposarcomas: histological review, genomic profile, and MDM2 and CDK4 status favour a single entity. J Pathol 2004; 203:822–830.
10. Merchant W, Calonje E, Fletcher CD. Inflammatory leiomyosarcoma: a morphological subgroup within the heterogeneous family of so-called inflammatory malignant fibrous histiocytoma. Histopathology 1995; 27:525–532.
11. Merino MJ, LiVolsi VA. Inflammatory malignant fibrous histiocytoma. Am J Clin Pathol 1980; 73:276–281.
12. Singh B, Santos V, Guffin TN Jr., et al. Giant cell variant of malignant fibrous histiocytoma of the head and neck. J Laryngol Otol 1991; 105:1079–1081.
13. Lai EC, Chung KM, Chiu HF, et al. Angiomatoid fibrous histiocytoma in the neck. ANZ J Surg 2006; 76:538.
14. Fletcher CD. Angiomatoid fibrous histiocytoma. Am J Surg Pathol 1992; 16:426–427.
15. Chung EB, Enzinger FM. Infantile fibrosarcoma. Cancer 1976; 38:729–739.
16. Coffin CM, Jaszcz W, O'Shea PA, Dehner LP. So-called congenital-infantile fibrosarcoma: does it exist and what is it? Pediatr Pathol 1994; 14:133–150.
17. Iwasaki H, Enjoji M. Infantile and adult fibrosarcomas of the soft tissues. Acta Pathol Jpn 1979; 29:377–388.
18. Salloum E, Caillaud JM, Flamant F, et al. Poor prognosis infantile fibrosarcoma with pathologic features of malignant fibrous histiocytoma after local recurrence. Med Pediatr Oncol 1990; 18:295–298.
19. Soule EH, Pritchard DJ. Fibrosarcoma in infants and children: a review of 110 cases. Cancer 1977; 40:1711–1721.
20. Stout AP. Fibrosarcoma in infants and children. Cancer 1962; 15:1028–1040.
21. Meis-Kindblom JM, Kindblom LG, Enzinger FM. Sclerosing epithelioid fibrosarcoma. A variant of fibrosarcoma simulating carcinoma. Am J Surg Pathol 1995; 19:979–993.
22. Antonescu CR, Rosenblum MK, Pereira P, et al. Sclerosing epithelioid fibrosarcoma: a study of 16 cases and confirmation of a clinicopathologically distinct tumor. Am J Surg Pathol 2001; 25:699–709.
23. Fletcher CD. Recent developments in soft tissue tumors. Verh Dtsch Ges Pathol 1998; 82:33–46.
24. Leitner C, Hoffmann J, Krober S, et al. Low-grade malignant fibrosarcoma of the dental follicle of an unerupted third molar without clinical evidence of any follicular lesion. J Craniomaxillofac Surg 2007; 35:48–51.
25. Soares AB, Lins LH, Macedo AP, et al. Fibrosarcoma originating in the mandible. Med Oral Patol Oral Cir Bucal 2006; 11:E243–E246.
26. Farhood AI, Hajdu SI, Shiu MH, et al. Soft tissue sarcomas of the head and neck in adults. Am J Surg 1990; 160: 365–369.
27. Oppenheimer RW, Friedman M. Fibrosarcoma of the maxillary sinus. Ear Nose Throat J 1988; 67:193–198.
28. Plaza G, Ferrando J, Pinedo F. Sinonasal fibrosarcoma: a case report. Eur Arch Otorhinolaryngol 2006; 263:641–643.
29. Plotti F, Di DV, Zullo MA, et al. An unusual case of secondary fibrosarcoma after treatment for breast cancer. Gynecol Oncol 2006; 103:1133–1136.
30. Coia LR, Fazekas JT, Kramer S. Postirradiation sarcoma of the head and neck: a report of three late sarcomas following therapeutic irradiation for primary malignancies of the paranasal sinus, nasal cavity, and larynx. Cancer 1980; 46: 1982–1985.
31. Mark RJ, Bailet JW, Poen J, et al. Postirradiation sarcoma of the head and neck. Cancer 1993; 72:887–893.
32. Vernon SE, Bejarano PA. Low-grade fibromyxoid sarcoma: a brief review. Arch Pathol Lab Med 2006; 130:1358–1360.
33. Franchi A, Massi D, Santucci M. Hyalinizing spindle cell tumor with giant rosettes and low-grade fibromyxoid sarcoma: an immunohistochemical and ultrastructural comparative investigation. Ultrastruct Pathol 2003; 27:349–355.
34. Folpe AL, Lane KL, Paull G, et al. Low-grade fibromyxoid sarcoma and hyalinizing spindle cell tumor with giant rosettes: a clinicopathologic study of 73 cases supporting their identity and assessing the impact of high-grade areas. Am J Surg Pathol 2000; 24:1353–1360.
35. Abbott JJ, Oliveira AM, Nascimento AG. The prognostic significance of fibrosarcomatous transformation in dermatofibrosarcoma protuberans. Am J Surg Pathol 2006; 30:436–443.
36. Mentzel T, Beham A, Katenkamp D, et al. Fibrosarcomatous (''high-grade'') dermatofibrosarcoma protuberans: clinicopathologic and immunohistochemical study of a series of 41 cases with emphasis on prognostic significance. Am J Surg Pathol 1998; 22:576–587.
37. Fanburg-Smith JC, Miettinen M. Angiomatoid ''malignant'' fibrous histiocytoma: a clinicopathologic study of 158 cases and further exploration of the myoid phenotype. Hum Pathol 1999; 30:1336–1343.
38. Knezevich SR, McFadden DE, Tao W, et al. A novel ETV6-NTRK3 gene fusion in congenital fibrosarcoma. Nat Genet 1998; 18:184–187.
39. Tognon C, Garnett M, Kenward E, et al. The chimeric protein tyrosine kinase ETV6-NTRK3 requires both Ras-Erk1/2 and PI3-kinase-Akt signaling for fibroblast transformation. Cancer Res 2001; 61:8909–8916.
40. Wai DH, Knezevich SR, Lucas T, et al. The ETV6-NTRK3 gene fusion encodes a chimeric protein tyrosine kinase that transforms NIH3T3 cells. Oncogene 2000; 19:906–915.
41. Knezevich SR, Garnett MJ, Pysher TJ, et al. ETV6-NTRK3 gene fusions and trisomy 11 establish a histogenetic link between mesoblastic nephroma and congenital fibrosarcoma. Cancer Res 1998; 58:5046–5048.
42. Rubin BP, Chen CJ, Morgan TW, et al. Congenital mesoblastic nephroma t(12;15) is associated with ETV6-NTRK3 gene fusion: cytogenetic and molecular relationship to congenital (infantile) fibrosarcoma. Am J Pathol 1998; 153:1451–1458.
43. Bourgeois JM, Knezevich SR, Mathers JA, et al. Molecular detection of the ETV6-NTRK3 gene fusion differentiates congenital fibrosarcoma from other childhood spindle cell tumors. Am J Surg Pathol 2000; 24:937–946.

44. Eguchi M, Eguchi-Ishimae M, Tojo A, et al. Fusion of ETV6 to neurotrophin-3 receptor TRKC in acute myeloid leukemia with t(12;15)(p13;q25). Blood 1999; 93:1355–1363.
45. Schofield DE, Fletcher JA, Grier HE, et al. Fibrosarcoma in infants and children. Application of new techniques. Am J Surg Pathol 1994; 18:14–24.
46. Pedeutour F, Simon MP, Minoletti F, et al. Ring 22 chromosomes in dermatofibrosarcoma protuberans are low-level amplifiers of chromosome 17 and 22 sequences. Cancer Res 1995; 55:2400–2403.
47. Pedeutour F, Simon MP, Minoletti F, et al. Translocation, t(17;22)(q22;q13), in dermatofibrosarcoma protuberans: a new tumor-associated chromosome rearrangement. Cytogenet Cell Genet 1996; 72:171–174.
48. Simon MP, Pedeutour F, Sirvent N, et al. Deregulation of the platelet-derived growth factor B-chain gene via fusion with collagen gene COL1A1 in dermatofibrosarcoma protuberans and giant-cell fibroblastoma. Nat Genet 1997; 15: 95–98.
49. Greco A, Fusetti L, Villa R, et al. Transforming activity of the chimeric sequence formed by the fusion of collagen gene COL1A1 and the platelet derived growth factor b-chain gene in dermatofibrosarcoma protuberans. Oncogene 1998; 17:1313–1319.
50. Shimizu A, O'Brien KP, Sjoblom T, et al. The dermatofibrosarcoma protuberans-associated collagen type Ialpha1/platelet-derived growth factor (PDGF) B-chain fusion gene generates a transforming protein that is processed to functional PDGF-BB. Cancer Res 1999; 59: 3719–3723.
51. Sjoblom T, Shimizu A, O'Brien KP, et al. Growth inhibition of dermatofibrosarcoma protuberans tumors by the platelet-derived growth factor receptor antagonist STI571 through induction of apoptosis. Cancer Res 2001; 61: 5778–5783.
52. Maki RG, Awan RA, Dixon RH, et al. Differential sensitivity to imatinib of 2 patients with metastatic sarcoma arising from dermatofibrosarcoma protuberans. Int J Cancer 2002; 100:623–626.
53. Rubin BP, Schuetze SM, Eary JF, et al. Molecular targeting of platelet-derived growth factor B by imatinib mesylate in a patient with metastatic dermatofibrosarcoma protuberans. J Clin Oncol 2002; 20:3586–3591.
54. Navarro M, Simon MP, Migeon C, et al. COL1A1-PDGFB fusion in a ring chromosome 4 found in a dermatofibrosarcoma protuberans. Genes Chromosomes Cancer 1998; 23:263–266.
55. Wang J, Hisaoka M, Shimajiri S, et al. Detection of COL1A1-PDGFB fusion transcripts in dermatofibrosarcoma protuberans by reverse transcription-polymerase chain reaction using archival formalin-fixed, paraffin-embedded tissues. Diagn Mol Pathol 1999; 8:113–119.
56. O'Brien KP, Seroussi E, Dal Cin P, et al. Various regions within the alpha-helical domain of the COL1A1 gene are fused to the second exon of the PDGFB gene in dermatofibrosarcomas and giant-cell fibroblastomas. Genes Chromosomes Cancer 1998; 23:187–193.
57. Storlazzi CT, Mertens F, Nascimento A, et al. Fusion of the FUS and BBF2H7 genes in low grade fibromyxoid sarcoma. Hum Mol Genet 2003; 12:2349–2358.
58. Panagopoulos I, Storlazzi CT, Fletcher CD, et al. The chimeric FUS/CREB3l2 gene is specific for low-grade fibromyxoid sarcoma. Genes Chromosomes Cancer 2004; 40: 218–228.
59. Mertens F, Fletcher CD, Antonescu CR, et al. Clinicopathologic and molecular genetic characterization of low-grade fibromyxoid sarcoma, and cloning of a novel FUS/CREB3L1 fusion gene. Lab Invest 2005; 85:408–415.
60. Guillou L, Benhattar J, Gengler C, et al. Translocation-positive low-grade fibromyxoid sarcoma: clinicopathologic and molecular analysis of a series expanding the morphologic spectrum and suggesting potential relationship to sclerosing epithelioid fibrosarcoma: a study from the French Sarcoma Group. Am J Surg Pathol 2007; 31: 1387–1402.
61. Mandahl N, Heim S, Willen H, et al. Characteristic karyotypic anomalies identify subtypes of malignant fibrous histiocytoma. Genes Chromosomes Cancer 1989; 1:9–14.
62. Schmidt H, Korber S, Hinze R, et al. Detection of numerical chromosomal changes in 20 malignant fibrous histiocytomas by FISH. Int J Oncol 1998; 12:395–402.
63. Szymanska J, Tarkkanen M, Wiklund T, et al. A cytogenetic study of malignant fibrous histiocytoma. Cancer Genet Cytogenet 1995; 85:91–96.
64. Choong PF, Mandahl N, Mertens F, et al. 19p+ marker chromosome correlates with relapse in malignant fibrous histiocytoma. Genes Chromosomes Cancer 1996; 16:88–93.
65. Larramendy ML, Tarkkanen M, Blomqvist C, et al. Comparative genomic hybridization of malignant fibrous histiocytoma reveals a novel prognostic marker. Am J Pathol 1997; 151:1153–1161.
66. Hinze R, Schagdarsurengin U, Taubert H, et al. Assessment of genomic imbalances in malignant fibrous histiocytomas by comparative genomic hybridization. Int J Mol Med 1999; 3:75–79.
67. Sakabe T, Shinomiya T, Mori T, et al. Identification of a novel gene, MASL1, within an amplicon at 8p23.1 detected in malignant fibrous histiocytomas by comparative genomic hybridization. Cancer Res 1999; 59:511–515.
68. Chibon F, Mairal A, Freneaux P, et al. The RB1 gene is the target of chromosome 13 deletions in malignant fibrous histiocytoma. Cancer Res 2000; 60:6339–6345.
69. Mairal A, Terrier P, Chibon F, et al. Loss of chromosome 13 is the most frequent genomic imbalance in malignant fibrous histiocytomas. A comparative genomic hybridization analysis of a series of 30 cases. Cancer Genet Cytogenet 1999; 111:134–138.
70. Simons A, Schepens M, Jeuken J, et al. Frequent loss of 9p21 (p16(INK4A)) and other genomic imbalances in human malignant fibrous histiocytoma. Cancer Genet Cytogenet 2000; 118:89–98.
71. Raddaoui E, Donner LR, Panagopoulos I. Fusion of the FUS and ATF1 genes in a large, deep-seated angiomatoid fibrous histiocytoma. Diagn Mol Pathol 2002; 11:157–162.
72. Waters BL, Panagopoulos I, Allen EF. Genetic characterization of angiomatoid fibrous histiocytoma identifies fusion of the FUS and ATF-1 genes induced by a chromosomal translocation involving bands 12q13 and 16p11. Cancer Genet Cytogenet 2000; 121:109–116.
73. Antonescu CR, Dal Cin P, Nafa K, et al. EWSR1-CREB1 is the predominant gene fusion in angiomatoid fibrous histiocytoma. Genes Chromosomes Cancer 2007; 46: 1051–1060.
74. Hallor KH, Micci F, Meis-Kindblom JM, et al. Fusion genes in angiomatoid fibrous histiocytoma. Cancer Lett 2007; 251: 158–163.
75. Fisher C. The value of electronmicroscopy and immunohistochemistry in the diagnosis of soft tissue sarcomas: a study of 200 cases. Histopathology 1990; 16:441–454.
76. Dominguez-Malagon H, Valdez-Carrillo MC, Cano-Valdez AM. Dermatofibroma and dermatofibrosarcoma protuberans: a comparative ultrastructural study. Ultrastruct Pathol 2006; 30:283–291.
77. Suh CH, Ordonez NG, Mackay B. Fibrosarcoma: observations on the ultrastructure. Ultrastruct Pathol 1993; 17: 221–229.

78. Nakahama M, Takanashi R, Yamazaki I, et al. Primary fibrosarcoma of the liver. Immunohistochemical and electron microscopic studies. Acta Pathol Jpn 1989; 39:814–820.
79. Gu W, Ogose A, Kawashima H, et al. Congenital dermatofibrosarcoma protuberans with fibrosarcomatous and myxoid change. J Clin Pathol 2005; 58:984–986.
80. Frankenthaler R, Ayala AG, Hartwick RW, et al. Fibrosarcoma of the head and neck. Laryngoscope 1990; 100: 799–802.
81. Greager JA, Patel MK, Briele HA, et al. Soft tissue sarcomas of the adult head and neck. Cancer 1985; 56:820–824.
82. Le Vay J, O'Sullivan B, Catton C, et al. An assessment of prognostic factors in soft-tissue sarcoma of the head and neck. Arch Otolaryngol Head Neck Surg 1994; 120:981–986.
83. Mark RJ, Sercarz JA, Tran L, et al. Fibrosarcoma of the head and neck. The UCLA experience. Arch Otolaryngol Head Neck Surg 1991; 117:396–401.
84. Heffner DK, Gnepp DR. Sinonasal fibrosarcomas, malignant schwannomas, and ''Triton'' tumors. A clinicopathologic study of 67 cases. Cancer 1992; 70:1089–1101.
85. Greager JA, Reichard K, Campana JP, et al. Fibrosarcoma of the head and neck. Am J Surg 1994; 167:437–439.
86. Kim KI, Yoo SL. Infantile fibrosarcoma in the nasal cavity. Otolaryngol Head Neck Surg 1996; 114:98–102.
87. Swain RE, Sessions DG, Ogura JH. Fibrosarcoma of the head and neck in children. Laryngoscope 1976; 86:113–116.
88. Cofer BR, Vescio PJ, Wiener ES. Infantile fibrosarcoma: complete excision is the appropriate treatment. Ann Surg Oncol 1996; 3:159–161.
89. Kurkchubasche AG, Halvorson EG, Forman EN, et al. The role of preoperative chemotherapy in the treatment of infantile fibrosarcoma. J Pediatr Surg 2000; 35:880–883.
90. Kynaston JA, Malcolm AJ, Craft AW, et al. Chemotherapy in the management of infantile fibrosarcoma. Med Pediatr Oncol 1993; 21:488–493.
91. Shetty AK, Yu LC, Gardner RV, et al. Role of chemotherapy in the treatment of infantile fibrosarcoma. Med Pediatr Oncol 1999; 33:425–427.
92. Mentzel T, Calonje E, Wadden C, et al. Myxofibrosarcoma. Clinicopathologic analysis of 75 cases with emphasis on the low-grade variant. Am J Surg Pathol 1996; 20:391–405.
93. Pritchard DJ, Soule EH, Taylor WF, et al. Fibrosarcoma—a clinicopathologic and statistical study of 199 tumors of the soft tissues of the extremities and trunk. Cancer 1974; 33:888–897.
94. Wrotnowski U, Cooper PH, Shmookler BM. Fibrosarcomatous change in dermatofibrosarcoma protuberans. Am J Surg Pathol 1988; 12:287–293.
95. Wang J, Morimitsu Y, Okamoto S, et al. COL1A1-PDGFB fusion transcripts in fibrosarcomatous areas of six dermatofibrosarcomas protuberans. J Mol Diagn 2000; 2:47–52.
96. Tran LM, Mark R, Meier R, et al. Sarcomas of the head and neck. Prognostic factors and treatment strategies. Cancer 1992; 70:169–177.

B. Malignant Triton Tumor (Malignant Peripheral Nerve Sheath Tumor with Rhabdomyoblastic Differentiation)

1. Masson P. Recklinghausen's Neurofibromatosis, Sensory Neuromas and Motor Neuromas, Libman Anniversary. Vol. 2. New York, NY: International Press, 1932.
2. Ducatman BS, Scheithauer BW. Malignant peripheral nerve sheath tumors with divergent differentiation. Cancer 1984; 54:1049–1057.
3. Woodruff JM, Chernik NL, Smith MC, et al. Peripheral nerve tumors with rhabdomyosarcomatous differentiation (malignant ''Triton'' tumors). Cancer 1973; 32:426–439.
4. Sorensen KB, Godballe C, Krogdahl A. Malignant triton tumor (MTT) of the neck. Auris Nasus Larynx 2006; 33: 89–91.
5. Bhatt S, Graeme-Cook F, Joseph MP, et al. Malignant triton tumor of the head and neck. Otolaryngol Head Neck Surg 1991; 105:738–742.
6. Victoria L, McCulloch TM, Callaghan EJ, et al. Malignant triton tumor of the head and neck: A case report and review of the literature. Head Neck 1999; 21:663–670.
7. Tringali S, Philippe C, Benchemam Y, et al. Malignant triton tumor of the sinonasal tract. Rev Stomatol Chir Maxillofac 2005; 106:99–102.
8. Re M, Romeo R, Mallardi V. Paralateral-nasal malignant schwannoma with rhabdomyoblastic differentiation (Triton tumor). Report of a case. Acta Otorhinolaryngol Ital 2002; 22:245–247.
9. Kim ST, Kim CW, Han GC, et al. Malignant triton tumor of the nasal cavity. Head Neck 2001; 23:1075–1078.
10. Nicolai P, Tomenzoli D, Berlucchi M, et al. Malignant triton tumor of the ethmoid sinus and nasal cavity. Ann Otol Rhinol Laryngol 2000; 109:880–886.
11. Ben Nasr R, Ben Othman M, Gadenne C, et al. Apropos of a case of malignant schwannoma with rhabdomyoblastic components. Malignant Triton tumor. Arch Anat Cytol Pathol 1988; 36:175–177.
12. James JA, Bali NS, Sloan P, et al. Low-grade malignant Triton tumor of the oral cavity: a case report. Oral Surg Oral Med Oral Pathol Oral Radiol Endod 2003; 95:699–704.
13. Llanes F, Sanz OJ, Suarez B, et al. Triton tumor of the parotid area. Case report. Histol Histopathol 1997; 12:51–56.
14. Can Z, Saray A, Yilmaz S, et al. Malignant triton tumor of the maxilla: a patient report. Ann Plast Surg 1999; 42:96–99.
15. Shotton JC, Stafford ND, Breach NM. Malignant triton tumour of the palate—a case report. Br J Oral Maxillofac Surg 1988; 26:120–123.
16. Boos S, Meyer E, Wimmer B, et al. Malignant triton tumor of the thyroid gland. Radiat Med 1991; 9:159–161.
17. Naruse T, Koike A, Suzumura K, et al. Malignant ''triton'' tumor in the thyroid—a case report. Jpn J Surg 1991; 21: 466–470.
18. Vajramani G, Devi I, Santosh V, et al. Benign triton tumor of the trigeminal nerve. Childs Nerv Syst 1999; 15:140–144.
19. Stasik CJ, Tawfik O. Malignant peripheral nerve sheath tumor with rhabdomyosarcomatous differentiation (malignant triton tumor). Arch Pathol Lab Med 2006; 130: 1878–1881.
20. Brooks JS, Freeman M, Enterline HT. Malignant ''Triton'' tumors. Natural history and immunohistochemistry of nine new cases with literature review. Cancer 1985; 55: 2543–2549.
21. Guccion JG, Enzinger FM. Malignant Schwannoma associated with von Recklinghausen's neurofibromatosis. Virchows Arch A Pathol Anat Histol 1979; 383:43–57.
22. Ferrari A, Bisogno G, Macaluso A, et al. Soft-tissue sarcomas in children and adolescents with neurofibromatosis type 1. Cancer 2007; 109:1406–1412.
23. Ozer E, Erkilic S, Bayazit YA, et al. Malignant triton tumor of the supraclavicular region arising after radiotherapy. Auris Nasus Larynx 2002; 29:405–407.
24. Yakulis R, Manack L, Murphy AI, Jr.Postradiation malignant triton tumor. A case report and review of the literature. Arch Pathol Lab Med 1996; 120:541–548.
25. Beuvon F, Criscuolo JL, Salmon RJ, et al. Radiation-induced neurosarcoma. Clinical, histological and immunohistochemistry aspects. Bull Cancer 1991; 78:619–626.
26. Murphey MD, Smith WS, Smith SE, et al. From the archives of the AFIP. Imaging of musculoskeletal neurogenic tumors: radiologic-pathologic correlation. Radiographics 1999; 19:1253–1280.

27. Klijanienko J, Caillaud JM, Lagace R, et al. Cytohistologic correlations of 24 malignant peripheral nerve sheath tumor (MPNST) in 17 patients: the Institut Curie experience. Diagn Cytopathol 2002; 27:103–108.
28. Kurtkaya-Yapicier O, Scheithauer BW, Woodruff JM, et al. Schwannoma with rhabdomyoblastic differentiation: a unique variant of malignant triton tumor. Am J Surg Pathol 2003; 27:848–853.
29. Smirnov AV, Povisil C. Malignant triton tumor (immunomorphological research). Arkh Patol 1990; 52:39–46.
30. Dewit L, Albus-Lutter CE, de Jong AS, et al. Malignant schwannoma with a rhabdomyoblastic component, a so-called triton tumor. A clinicopathologic study. Cancer 1986; 58:1350–1356.
31. Daimaru Y, Hashimoto H, Enjoji M. Malignant ''triton'' tumors: a clinicopathologic and immunohistochemical study of nine cases. Hum Pathol 1984; 15:768–778.
32. Bridge RS, Jr. Bridge JA, Neff JR, et al. Recurrent chromosomal imbalances and structurally abnormal breakpoints within complex karyotypes of malignant peripheral nerve sheath tumour and malignant triton tumour: a cytogenetic and molecular cytogenetic study. J Clin Pathol 2004; 57:1172–1178.
33. Haddadin MH, Hawkins AL, Long P, et al. Cytogenetic study of malignant triton tumor: a case report. Cancer Genet Cytogenet 2003; 144:100–105.
34. McComb EN, McComb RD, DeBoer JM, et al. Cytogenetic analysis of a malignant triton tumor and a malignant peripheral nerve sheath tumor and a review of the literature. Cancer Genet Cytogenet 1996; 91:8–12.
35. Hennig Y, Loschke S, Katenkamp D, et al. A malignant triton tumor with an unbalanced translocation (1;13)(q10; q10) and an isochromosome (8)(q10) as the sole karyotypic abnormalities. Cancer Genet Cytogenet 2000; 118:80–82.
36. Magrini E, Pragliola A, Fantasia D, et al. Acquisition of i(8q) as an early event in malignant triton tumors. Cancer Genet Cytogenet 2004; 154:150–155.
37. Velagaleti GV, Miettinen M, Gatalica Z. Malignant peripheral nerve sheath tumor with rhabdomyoblastic differentiation (malignant triton tumor) with balanced t(7;9)(q11.2; p24) and unbalanced translocation der(16)t(1;16)(q23;q13). Cancer Genet Cytogenet 2004; 149:23–27.
38. Cano JR, Algar FJ, Alvarez A, et al. Triton tumor of the left sympathetic nerve. Interact Cardiovasc Thorac Surg 2006; 5:790–791.
39. Thoennissen NH, Schliemann C, Brunnberg U, et al. Chemotherapy in metastatic malignant triton tumor: report on two cases. Oncol Rep 2007; 18:763–767.

C. Malignant Mesenchymoma

1. Stout AP. Recent observations on mesenchymal tumours in adults and children. Can Med Assoc J 1963; 88:453–456.
2. Stout AP. Mesenchymoma, the mixed tumor of mesenchymal derivatives. Ann Surg 1948; 127:278–290.
3. Ellison DA, Corredor-Buchmann J, Parham DM, et al. Malignant triton tumor presenting as a rectal mass in an 11-month-old. Pediatr Dev Pathol 2005; 8:235–239.
4. Fletcher CD, Unni K, Mertens F. World Health Organization Classification of Tumours. Pathology and Genetics of Tumours of Soft Tissue and Bone. Lyon, France: IARC Press, 2002.
5. Enzinger F, Weiss SW. Soft tissue tumors. 2nd ed. St Louis, MO: Mostby, 1988.
6. Mrad K, Sassi S, Smida M, et al. Osteosarcoma with rhabdomyosarcomatous component or so-called malignant mesenchymoma of bone. Pathologica 2004; 96:475–478.
7. Klima M, Smith M, Spjut HJ, et al. Malignant mesenchymoma. Case report with electron microscopic study. Cancer 1975; 36:1086–1094.
8. Hayes SJ, Wells S, Harake J, et al. Fibrocartilagenous mesenchymoma of bone: the youngest reported case in a patient aged 1 year and 7 months. J Clin Pathol 2005; 58:782–783.
9. Mayer CM, Favara BE, Holton CP, et al. Malignant mesenchymoma in infants. Am J Dis Child 1974; 128:847–850.
10. Kawashima O, Kamei T, Shimizu Y, et al. Malignant mesenchymoma of the larynx. J Laryngol Otol 1990; 104:440–444.
11. Muldoon CJ. Mesenchymoma of the mandible. J Surg Oncol 1973; 5:291–295.
12. Kessler DA, Kademani D, Feldman RS, et al. Mesenchymoma: an unusual tumour of the lip. Br J Oral Maxillofac Surg 2004; 42:348–350.
13. Brannan PA, Schneider S, Grossniklaus HE, et al. Malignant mesenchymoma of the orbit: case report and review of the literature. Ophthalmology 2003; 110:314–317.
14. Ashbell TS, Baffes TG, Obillocala S, et al. Congenital malignant mesenchymoma of the face. Case report. Plast Reconstr Surg 1972; 49:348–350.
15. Small GS. Malignant mesenchymoma of the mandible. Oral Surg Oral Med Oral Pathol 1961; 14:1427–1435.
16. Sterns EE, Haust MD, Wollin DG. Malignant mesenchymoma of the mandible. Can J Surg 1969; 12:444–449.
17. Choi JE, Chung HJ, Yoo WJ, et al. Retroperitoneal malignant mesenchymoma: a case of mesenchymal mixed tumor with osteosarcoma, leiomyosarcoma, liposarcoma and fibrosarcoma. Korean J Radiol 2002; 3:264–266.
18. Gurney JG, Severson RK, Davis S, et al. Incidence of cancer in children in the United States. Sex-, race-, and 1-year age-specific rates by histologic type. Cancer 1995; 75: 2186–2195.
19. Yang JC, Glatein EJ, Rosenberg SA, et al. Cancer. Principles and Practive of Oncology. 4th ed. Philadelphia, PA: JB Lippincott, 1993.
20. Sharma TC, Huvos AG, Grabstald H. Retroperitoneal malignant mesenchymoma. J Urol 1971; 106:60–66.
21. Kalus M, Rahman F, Jenkins DE, et al. Malignant mesenchymoma of the lung. Arch Pathol 1973; 95:199–202.
22. Naka A, Matsumoto S, Shirai T, et al. Ganglioneuroblastoma associated with malignant mesenchymoma. Cancer 1975; 36:1050–1056.
23. Bittinger A, Rossberg C, Rodehuser M. Primary malignant ectomesenchymoma of the orbit. Gen Diagn Pathol 1997; 142:221–225.
24. Jones AC, Trochesset D, Freedman PD. Intraoral benign mesenchymoma: a report of 10 cases and review of the literature. Oral Surg Oral Med Oral Pathol Oral Radiol Endod 2003; 95:67–76.
25. Sakurai K, Urade M, Yasoshima H, et al. Benign mesenchymoma of the cheek: report of a case and review of the literature. Oral Surg Oral Med Oral Pathol Oral Radiol Endod 1999; 88:74–79.
26. Adachi T, Oda Y, Sakamoto A, et al. Prognostic factors in the so-called malignant mesenchymoma: a clinicopathological and immunohistochemical analysis. Oncol Rep 2003; 10:803–811.
27. Nash A, Stout AP. Malignant mesenchymomas in children. Cancer 1961; 14:524–533.
28. Orui H, Ishikawa A, Tsuchiya T, et al. Chondro-osseous differentiation in fat tissue tumors: magnetic resonance imaging with pathological correlation. Skeletal Radiol 2000; 29:459–465.
29. Brady MS, Perino G, Tallini G, et al. Malignant mesenchymoma. Cancer 1996; 77:467–473.

30. Newman PL, Fletcher CD. Malignant mesenchymoma. Clinicopathologic analysis of a series with evidence of low-grade behaviour. Am J Surg Pathol 1991; 15:607–614.
31. Heinemann MW, Lehman WL. Mediastinal mesenchymoma masquerading as liposarcoma. Cancer 1951; 4: 692–696.
32. Uramoto H, Oyama T, Yoshimatsu T, et al. Benign mesenchymoma of the mediastinum. Jpn J Thorac Cardiovasc Surg 2000; 48:814–816.
33. Chalkiadakis G, Petrakis I, Chrysos E, et al. A rare case of benign mesenchymoma of the breast in a man. Eur J Surg Oncol 1999; 25:96–97.

D. Mesenchymal Chondrosarcoma

1. Lichtenstein L, Bernstein D. Unusual benign and malignant chondroid tumors of bone: a survey of some mesenchymal cartilate tumors and malignant chondroblastic tumors, including a few multicentric ones, as well as many atypical benign chondroblastomas and chondromyxoid fibromas. Cancer 1959; 12:1142–1157.
2. Tien N, Chaisuparat R, Fernandes R, et al. Mesenchymal chondrosarcoma of the maxilla: case report and literature review. J Oral Maxillofac Surg 2007; 65:1260–1266.
3. Chidambaram A, Sanville P. Mesenchymal chondrosarcoma of the maxilla. J Laryngol Otol 2000; 114:536–539.
4. Ariyoshi Y, Shimahara M. Mesenchymal chondrosarcoma of the maxilla: report of a case. J Oral Maxillofac Surg 1999; 57:733–737.
5. Lockhart R, Menard P, Martin JP, et al. Mesenchymal chondrosarcoma of the jaws. Report of four cases. Int J Oral Maxillofac Surg 1998; 27:358–362.
6. Vencio EF, Reeve CM, Unni KK, et al. Mesenchymal chondrosarcoma of the jaw bones: clinicopathologic study of 19 cases. Cancer 1998; 82:2350–2355.
7. Zakkak TB, Flynn TR, Boguslaw B, et al. Mesenchymal chondrosarcoma of the mandible: case report and review of the literature. J Oral Maxillofac Surg 1998; 56:84–91.
8. Mateos M, Forteza G, Gay-Escoda C. Mesenchymal chondrosarcoma of the maxilla. A case report. Int J Oral Maxillofac Surg 1997; 26:210–211.
9. Takahashi K, Sato K, Kanazawa H, et al. Mesenchymal chondrosarcoma of the jaw—report of a case and review of 41 cases in the literature. Head Neck 1993; 15:459–464.
10. Rushing EJ, Armonda RA, Ansari Q, et al. Mesenchymal chondrosarcoma: a clinicopathologic and flow cytometric study of 13 cases presenting in the central nervous system. Cancer 1996; 77:1884–1891.
11. Nakashima Y, Unni KK, Shives TC, et al. Mesenchymal chondrosarcoma of bone and soft tissue. A review of 111 cases. Cancer 1986; 57:2444–2453.
12. Angotti-Neto H, Cunha LP, Oliveira AV, et al. Mesenchymal chondrosarcoma of the orbit. Ophthal Plast Reconstr Surg 2006; 22:378–382.
13. Tuncer S, Kebudi R, Peksayar G, et al. Congenital mesenchymal chondrosarcoma of the orbit: case report and review of the literature. Ophthalmology 2004; 111:1016–1022.
14. Kashyap S, Sen S, Betharia SM, et al. Mesenchymal chondrosarcoma of the orbit: a clinicopathological study. Orbit 2001; 20:63–67.
15. Khouja N, Ben Amor S, Jemel H, et al. Mesenchymal extraskeletal chondrosarcoma of the orbit. Report of a case and review of the literature. Surg Neurol 1999; 52:50–53.
16. Jacobs JL, Merriam JC, Chadburn A, et al. Mesenchymal chondrosarcoma of the orbit. Report of three new cases and review of the literature. Cancer 1994; 73:399–405.
17. Knott PD, Gannon FH, Thompson LD. Mesenchymal chondrosarcoma of the sinonasal tract: a clinicopathological study of 13 cases with a review of the literature. Laryngoscope 2003; 113:783–790.
18. Bagchi M, Husain N, Goel MM, et al. Extraskeletal mesenchymal chondrosarcoma of the orbit. Cancer 1993; 72: 2224–2226.
19. Takahashi K, Sato K, Kanazawa H, et al. Mesenchymal chondrosarcoma of the jaw—report of a case and review of 41 cases in the literature. Head Neck 1993; 15:459–464.
20. Hashimoto N, Ueda T, Joyama S, et al. Extraskeletal mesenchymal chondrosarcoma: an imaging review of ten new patients. Skeletal Radiol 2005; 34:785–792.
21. Shapeero LG, Vanel D, Couanet D, et al. Extraskeletal mesenchymal chondrosarcoma. Radiology 1993; 186: 819–826.
22. Trembath DG, Dash R, Major NM, et al. Cytopathology of mesenchymal chondrosarcomas: a report and comparison of four patients. Cancer 2003; 99:211–216.
23. Huvos AG, Rosen G, Dabska M, et al. Mesenchymal chondrosarcoma. A clinicopathologic analysis of 35 patients with emphasis on treatment. Cancer 1983; 51:1230–1237.
24. Devaney K, Vinh TN, Sweet DE. Small cell osteosarcoma of bone: an immunohistochemical study with differential diagnostic considerations. Hum Pathol 1993; 24:1211–1225.
25. Dickersin GR, Rosenberg AE. The ultrastructure of small-cell osteosarcoma, with a review of the light microscopy and differential diagnosis. Hum Pathol 1991; 22:267–275.
26. Swanson PE, Lillemoe TJ, Manivel JC, et al. Mesenchymal chondrosarcoma. An immunohistochemical study. Arch Pathol Lab Med 1990; 114:943–948.
27. Devoe K, Weidner N. Immunohistochemistry of small round-cell tumors. Semin Diagn Pathol 2000; 17:216–224.
28. Granter SR, Renshaw AA, Fletcher CD, et al. CD99 reactivity in mesenchymal chondrosarcoma. Hum Pathol 1996; 27:1273–1276.
29. Hoang MP, Suarez PA, Donner LR, et al. Mesenchymal Chondrosarcoma: a small cell neoplasm with polyphenotypic differentiation. Int J Surg Pathol 2000; 8:291–301.
30. Dobin SM, Donner LR, Speights VO Jr. Mesenchymal chondrosarcoma. A cytogenetic, immunohistochemical and ultrastructural study. Cancer Genet Cytogenet 1995; 83: 56–60.
31. Fadda M, Manunta A, Rinonapoli G, et al. Ultrastructural appearance of chondroblastoma. Int Orthop 1994; 18: 389–92.
32. Sato N, Minase T, Yoshida Y, et al. An ultrastructural study of extraskeletal mesenchymal chondrosarcoma. Acta Pathol Jpn 1984; 34:1355–63.
33. Ushigome S, Takakuwa T, Shinagawa T, et al. Ultrastructure of cartilaginous tumors and S-100 protein in the tumors. With reference to the histogenesis of chondroblastoma, chondromyxoid fibroma and mesenchymal chondrosarcoma. Acta Pathol Jpn 1984; 34:1285–300.
34. Martinez-Tello FJ, Navas-Palacios JJ. Ultrastructural study of conventional chondrosarcomas and myxoid- and mesenchymal-chondrosarcomas. Virchows Arch A Pathol Anat Histol 1982; 396:197–211.
35. Gatter KM, Olson S, Lawce H, et al. Trisomy 8 as the sole cytogenetic abnormality in a case of extraskeletal mesenchymal chondrosarcoma. Cancer Genet Cytogenet 2005; 159: 151–154.
36. Naumann S, Krallman PA, Unni KK, et al. Translocation der(13;21)(q10;q10) in skeletal and extraskeletal mesenchymal chondrosarcoma. Mod Pathol 2002; 15:572–576.
37. Sainati L, Scapinello A, Montaldi A, et al. A mesenchymal chondrosarcoma of a child with the reciprocal

translocation (11;22)(q24;q12). Cancer Genet Cytogenet 1993; 71:144–147.
38. Szymanska J, Tarkkanen M, Wiklund T, et al. Cytogenetic study of extraskeletal mesenchymal chondrosarcoma. A case report. Cancer Genet Cytogenet 1996; 86:170–173.
39. Attwooll C, Tariq M, Harris M, et al. Identification of a novel fusion gene involving hTAFII68 and CHN from a t(9;17)(q22;q11.2) translocation in an extraskeletal myxoid chondrosarcoma. Oncogene 1999; 18:7599–7601.
40. Clark J, Benjamin H, Gill S, et al. Fusion of the EWS gene to CHN, a member of the steroid/thyroid receptor gene superfamily, in a human myxoid chondrosarcoma. Oncogene 1996; 12:229–235.
41. Labelle Y, Zucman J, Stenman G, et al. Oncogenic conversion of a novel orphan nuclear receptor by chromosome translocation. Hum Mol Genet 1995; 4:2219–2226.
42. Sjogren H, Meis-Kindblom J, Kindblom LG, et al. Fusion of the EWS-related gene TAF2N to TEC in extraskeletal myxoid chondrosarcoma. Cancer Res 1999; 59:5064–5067.
43. Llombart-Bosch A, Contesso G, Peydro-Olaya A. Histology, immunohistochemistry, and electron microscopy of small round cell tumors of bone. Semin Diagn Pathol 1996; 13: 153–170.
44. Tsuneyoshi M, Daimaru Y, Enjoji M. Malignant hemangiopericytoma and other sarcomas with hemangiopericytoma-like pattern. Pathol Res Pract 1984; 178:446–453.
45. Pellitteri PK, Ferlito A, Fagan JJ, et al. Mesenchymal chondrosarcoma of the head and neck. Oral Oncol 2007; 43:970–975.

A. Synovial Sarcoma

1. Cadman NL, Soule EH, Kelly PJ. Synovial sarcoma; an analysis of 34 tumors. Cancer 1965; 18:613–127.
2. Hajdu SI, Shiu MH, Fortner JG. Tendosynovial sarcoma: a clinicopathological study of 136 cases. Cancer 1977; 39:1201–1217.
3. Golomb HM, Gorny J, Powell W, et al. Cervical synovial sarcoma at the bifurcation of the carotid artery. Cancer 1975; 35:483–489.
4. Dei Tos AP, Dal Cin P, Sciot R, et al. Synovial sarcoma of the larynx and hypopharynx. Ann Otol Rhinol Laryngol 1998; 107:1080–1085.
5. Massarelli G, Tanda F, Salis B. Synovial sarcoma of the soft palate: report of a case. Hum Pathol 1978; 9:341–345.
6. Miller LH, Santaella-Latimer L, Miller T. Synovial sarcoma of the larynx. Trans Sect Otolaryngol Am Acad Ophthalmol Otolaryngol 1975; 80:448–451.
7. Moussavi H, Ghodsi S. Synovial sarcoma of the tongue, report of a case. J Laryngol Otol 1974; 88:795–797.
8. O'Keeffe LJ, Ramsden RT, Birzgalis AR. Primary synovial sarcoma of the middle ear. J Laryngol Otol 1993; 107: 1070–1072.
9. Bergh P, Meis-Kindblom JM, Gherlinzoni F, et al. Synovial sarcoma: identification of low and high risk groups. Cancer 1999; 85:2596–2607.
10. Brodsky JT, Burt ME, Hajdu SI, et al. Tendosynovial sarcoma. Clinicopathologic features, treatment, and prognosis. Cancer 1992; 70:484–489.
11. Cagle LA, Mirra JM, Storm FK, et al. Histologic features relating to prognosis in synovial sarcoma. Cancer 1987; 59: 1810–1814.
12. Crocker DW, Stout AP. Synovial sarcoma in children. Cancer 1959; 12:1123–1133.
13. Ladenstein R, Treuner J, Koscielniak E, et al. Synovial sarcoma of childhood and adolescence. Report of the German CWS-81 study. Cancer 1993; 71:3647–3655.
14. Oda Y, Hashimoto H, Tsuneyoshi M, et al. Survival in synovial sarcoma. A multivariate study of prognostic factors with special emphasis on the comparison between early death and long-term survival. Am J Surg Pathol 1993; 17: 35–44.
15. Schmidt D, Thum P, Harms D, et al. Synovial sarcoma in children and adolescents. A report from the Kiel Pediatric Tumor Registry. Cancer 1991; 67:1667–1672.
16. Blacksin MF, Siegel JR, Benevenia J, et al. Synovial sarcoma: frequency of nonaggressive MR characteristics. J Comput Assist Tomogr 1997; 21:785–789.
17. Jones BC, Sundaram M, Kransdorf MJ. Synovial sarcoma: MR imaging findings in 34 patients. AJR Am J Roentgenol 1993; 161:827–830.
18. Murphey MD, Gibson MS, Jennings BT, et al. From the archives of the AFIP: Imaging of synovial sarcoma with radiologic-pathologic correlation. Radiographics 2006; 26:1543–1565.
19. Tateishi U, Hasegawa T, Beppu Y, et al. Synovial sarcoma of the soft tissues: prognostic significance of imaging features. J Comput Assist Tomogr 2004; 28:140–148.
20. Mirra JM, Wang S, Bhuta S. Synovial sarcoma with squamous differentiation of its mesenchymal glandular elements. A case report with light-microscopic, ultramicroscopic, and immunologic correlation. Am J Surg Pathol 1984; 8:791–796.
21. Majeste RM, Beckman EN. Synovial sarcoma with an overwhelming epithelial component. Cancer 1988; 61: 2527–2531.
22. Krane JF, Bertoni F, Fletcher CD. Myxoid synovial sarcoma: an underappreciated morphologic subset. Mod Pathol 1999; 12: 456–462.
23. Coli A, Bigotti G, Parente R, et al. Myxoid monophasic synovial sarcoma: case report of an unusual histological variant. J Exp Clin Cancer Res 2006; 25:287–291.
24. Milchgrub S, Ghandur-Mnaymneh L, Dorfman HD, et al. Synovial sarcoma with extensive osteoid and bone formation. Am J Surg Pathol 1993; 17:357–363.
25. Varela-Duran J, Enzinger FM. Calcifying synovial sarcoma. Cancer 1982; 50:345–352.
26. Folpe AL, Schmidt RA, Chapman D, et al. Poorly differentiated synovial sarcoma: immunohistochemical distinction from primitive neuroectodermal tumors and high-grade malignant peripheral nerve sheath tumors. Am J Surg Pathol 1998; 22:673–682.
27. van de RM, Barr FG, Xiong QB, et al. Poorly differentiated synovial sarcoma: an analysis of clinical, pathologic, and molecular genetic features. Am J Surg Pathol 1999; 23: 106–112.
28. Miettinen M. Keratin subsets in spindle cell sarcomas. Keratins are widespread but synovial sarcoma contains a distinctive keratin polypeptide pattern and desmoplakins. Am J Pathol 1991; 138:505–513.
29. Suster S, Fisher C, Moran CA. Expression of bcl-2 oncoprotein in benign and malignant spindle cell tumors of soft tissue, skin, serosal surfaces, and gastrointestinal tract. Am J Surg Pathol 1998; 22:863–872.
30. He R, Patel RM, Alkan S, et al. Immunostaining for SYT protein discriminates synovial sarcoma from other soft tissue tumors: analysis of 146 cases. Mod Pathol 2007; 20: 522–528.
31. Terry J, Saito T, Subramanian S, et al. TLE1 as a diagnostic immunohistochemical marker for synovial sarcoma emerging from gene expression profiling studies. Am J Surg Pathol 2007; 31:240–246.
32. Fisher C. Synovial sarcoma: ultrastructural and immunohistochemical features of epithelial differentiation in monophasic and biphasic tumors. Hum Pathol 1986; 17:996–1008.

33. Nunez-Alonso C, Gashti EN, Christ ML. Maxillofacial synovial sarcoma. Light- and electron-microscopic study of two cases. Am J Surg Pathol 1979; 3:23–30.
34. Ordonez NG, Mahfouz SM, Mackay B. Synovial sarcoma: an immunohistochemical and ultrastructural study. Hum Pathol 1990; 21:733–749.
35. Turc-Carel C, Dal Cin P, et al. Involvment of chromosome X in primary cytogenetic change in human neoplasia: Nonrandom translocation in synovial sarcoma. Proc Natl Acad Sci U.S.A. 1987; 84:1981–1985.
36. Dal Cin P, Rao U, Jani-Sait S, et al. Chromosomes in the diagnosis of soft tissue tumors. I. Synovial sarcoma. Modern Pathol 1992; 5:357–362.
37. dos Santos NR, de Bruijn DR, van Kessel AG. Molecular mechanisms underlying human synovial sarcoma development. Genes Chromosomes Cancer 2001; 30:1–14.
38. Clark AJ, Rocques PJ, Crew AJ, et al. Identification of novel genes, SYT and SSX, involved in the t(X;18)(p11.2;q11.2) translocation found in human synovial sarcoma. Nat Genet 1994; 7:502–508.
39. Gure AO, Türeci Ö, Sahin U, et al. A multigene family with several members transcribed in normal testis and human cancer. Int J Cancer 1997; 72:965–71.
40. Crew AJ, Clark J, Fisher C, et al. Fusion of SYT to two genes, SSX1 and SSX2, encoding proteins with homology to the Kruppel-associated box in human synovial sarcoma. EMBO J 1995; 14:2333–2340.
41. Fligman I, Lonardo F, Jhanwar SC, et al. Molecular diagnosis of synovial sarcoma and characterization of a variant SYT-SSX2 fusion transcript. Am J Pathol 1995; 147: 1592–1599.
42. Skytting B, Nilsson G, Brodin B, et al. A novel fusion gene, SYT-SSX4, in synovial sarcoma. J NCI 1999; 91:974–975.
43. Mancuso T, Mezzelani A, Riva C, et al. Analysis of SYT-SSX fusion transcripts and bcl-2 expression and phosphorylation status in synovial sarcoma. Lab Invest 2000; 80:805–813.
44. Tornkvist M, Brodin B, Bartolazzi A, et al. A novel type of SYT/SSX fusion: methodological and biological implications. Modern Pathol 2002; 15:679–685.
45. Brodin B, Haslam, Yang K, et al. Cloning and characterization of spliced fusion transcript variants of synovial sarcoma: SYT/SSX4, SYT/SSX4v, and SYT/SSX2v. Possible regulatory role of the fusion gene product in wild type SYT expression. Gene 2001; 268:173–182.
46. Strorlazzi CT, Mertens F, Mandahl N, et al. A novel fusion gene, SS18L1/SSX1, in synovial sarcoma. Genes Chromosmes Cancer 2003; 37:195–200.
47. Safar A, Wickert R, Nelson M, et al. Characterization of a variant SYT-SSX1 synovial sarcoma fusion transcript. Diagn Mol Pathol 1998; 7:283–287.
48. Yang K, Lui WO, Xie Y, et al. Co-existence of SYT-SSX1 and SYT-SSX2 fusions in synovial sarcomas. Oncogene 2002; 21: 4181–4190.
49. Ladanyi M. Fusions of the SYT and SSX genes in synovial sarcoma. Oncogene 2001; 20:5755–5762.
50. de Bruijn DR, Allander SV, van Dijk AH, et al. The synovial-sarcoma-associated SS18-SSX2 fusion protein induces epigenetic gene (de)regulation. Cancer Res 2006; 66:9474–9482.
51. de Bruijn DR, Nap JP, van Kessel AG. The (epi)genetics of human synovial sarcoma. Genes Chromosomes Cancer 200; 46:107–117.
52. Amary MF, Berisha F, Bernardi Fdel C, et al. Detection of SS18-SSX fusion transcripts in formalin-fixed paraffin-embedded neoplasms: analysis of conventional RT-PCR, qRT-PCR and dual color FISH as diagnostic tools for synovial sarcoma. Cancer Res 2002; 62:135–140.
53. Kawai A, Woodruff J, Healey JH, et al. SYT-SSX fusion as a determinant of morphology and prognosis in synovial sarcoma. New England J Medicine 1998; 338:153–160.
54. Nilsson G, Skytting B, Xie Y, et al. The SYT-SSX1 variant of synovial sarcoma is associated with a high rate of tumor cell proliferation and poor clinical outcome. Cancer Res 1999; 59:3180–3184.
55. Llombart-Bosch, Lopez-Guerrero JA, Peydro-Olaya A. Synovial sarcoma (SS): new perspectives supported by modern technology. Arkh Patol 2002; 64:39–47.
56. Ladanyi M, Antonescu CR, Leung DH, et al. Impact of SYT-SSX fusion type on the clinical behavior of synovial sarcoma: a multi-institutional retrospective study of 243 patients. Cancer Res 2002; 62:135–140.
57. Winnepenninckx V, De Vos R, Debiec-Rychter M, et al. Calcifying/ossifying synovial sarcoma shows t(X;18) with SSX2 involvement and mitochondrial calcifications. Histopathology 2001; 38:141–145.
58. Machen SK, Fisher C, Gautam RS, et al. Utility of cytokeratin subsets for distinguishing poorly differentiated synovial sarcoma from peripheral primitive neuroectodermal tumour. Histopathology 1998; 33:501–507.
59. Smith TA, Machen SK, Fisher C, et al. Usefulness of cytokeratin subsets for distinguishing monophasic synovial sarcoma from malignant peripheral nerve sheath tumor. Am J Clin Pathol 1999; 112:641–648.
60. Amble FR, Olsen KD, Nascimento AG, et al. Head and neck synovial cell sarcoma. Otolaryngol Head Neck Surg 1992;107:631–7.
61. Roth JA, Enzinger FM, Tannenbaum M. Synovial sarcoma of the neck: a followup study of 24 cases. Cancer 1975; 35:1243–1253.
62. Shmookler BM, Enzinger FM, Brannon RB. Orofacial synovial sarcoma: a clinicopathologic study of 11 new cases and review of the literature. Cancer 1982; 50:269–276.
63. Guadagnolo BA, Zagars GK, Ballo MT, et al. Long-term outcomes for synovial sarcoma treated with conservation surgery and radiotherapy. Int J Radiat Oncol Biol Phys 2007; 69:1173–1180.
64. Harb WJ, Luna MA, Patel SR, et al. Survival in patients with synovial sarcoma of the head and neck: association with tumor location, size, and extension. Head Neck 2007; 29:731–740.
65. Roth JA, Enzinger FM, Tannenbaum M. Synovial sarcoma of the neck: a followup study of 24 cases. Cancer 1975; 35:1243–1253.
66. Shmookler BM, Enzinger FM, Brannon RB. Orofacial synovial sarcoma: a clinicopathologic study of 11 new cases and review of the literature. Cancer 1982; 50:269–276.

B. Malignant Extrarenal Rhabdoid Tumor

1. Batsakis JG, Manning JT. Malignant rhabdoid tumor. Ann Otol Rhinol Laryngol 1988; 97:690–691.
2. Panuel M, Gentet JC, Scheiner C, et al. [Rhabdoid tumor of the neck]. Pediatrie 1992; 47:687–690.
3. Zarovnaya EL, Pallatroni HF, Hug EB, et al. Atypical teratoid/rhabdoid tumor of the spine in an adult: case report and review of the literature. J Neurooncol 2007; 84: 49–55.
4. Sola PJ, Perez-Guillermo M, Bas BA, et al. Malignant rhabdoid tumor of soft tissues: a cytopathological and immunohistochemical study. Diagn Cytopathol 1992; 8: 369–373.
5. Allen JC, Judkins AR, Rosenblum MK, et al. Atypical teratoid/rhabdoid tumor evolving from an optic pathway ganglioglioma: case study. Neuro Oncol 2006; 8:79–82.

6. Gunduz K, Shields JA, Eagle RC Jr., et al. Malignant rhabdoid tumor of the orbit. Arch Ophthalmol 1998; 116: 243–236.
7. Johnson LN, Sexton FM, Goldberg SH. Poorly differentiated primary orbital sarcoma (presumed malignant rhabdoid tumor). Radiologic and histopathologic correlation. Arch Ophthalmol 1991; 109:1275–1278.
8. Rootman J, Damji KF, Dimmick JE. Malignant rhabdoid tumor of the orbit. Ophthalmology 1989; 96:1650–1654.
9. Watanabe H, Watanabe T, Kaneko M, et al. Treatment of unresectable malignant rhabdoid tumor of the orbit with tandem high-dose chemotherapy and gamma-knife radiosurgery. Pediatr Blood Cancer 2006; 47:846–850.
10. Niffenegger JH, Jakobiec FA, Shore JW, et al. Adult extrarenal rhabdoid tumor of the lacrimal gland. Ophthalmology 1992; 99:567–574.
11. Patron M, Palacios J, Rodriguez-Peralto JL, et al. Malignant rhabdoid tumor of the tongue. A case report with immunohistochemical and ultrastructural findings. Oral Surg Oral Med Oral Pathol 1988; 65:67–70.
12. Bourdeaut F, Freneaux P, Thuille B, et al. hSNF5/INI1-deficient tumours and rhabdoid tumours are convergent but not fully overlapping entities. J Pathol 2007; 211: 323–330.
13. Haberler C, Laggner U, Slavc I, et al. Immunohistochemical analysis of INI1 protein in malignant pediatric CNS tumors: lack of INI1 in atypical teratoid/rhabdoid tumors and in a fraction of primitive neuroectodermal tumors without rhabdoid phenotype. Am J Surg Pathol 2006; 30:1462–1468.
14. Perry A, Fuller CE, Judkins AR, et al. INI1 expression is retained in composite rhabdoid tumors, including rhabdoid meningiomas. Mod Pathol 2005; 18:951–958.
15. Wagner LM, Garrett JK, Ballard ET, et al. Malignant rhabdoid tumor mimicking hepatoblastoma: a case report and literature review. Pediatr Dev Pathol 2007; 10: 409–415.
16. Hoot AC, Russo P, Judkins AR, et al. Immunohistochemical analysis of hSNF5/INI1 distinguishes renal and extrarenal malignant rhabdoid tumors from other pediatric soft tissue tumors. Am J Surg Pathol 2004; 28:1485–1491.
17. Erlandson RA, Woodruff JM. Role of electron microscopy in the evaluation of soft tissue neoplasms, with emphasis on spindle cell and pleomorphic tumors. Hum Pathol 1998; 29:1372–1381.
18. Biegel JA. Molecular genetics of atypical teratoid/rhabdoid tumor. Neurosurg Focus 2006; 20:E11.
19. Biegel JA, Rorke LB, Packer RJ, et al. Monosomy 22 in rhabdoid or atypical tumors of the brain. J Neurosurg 1990; 73:710–714.
20. Biegel JA, Burk CD, Parmiter AH, et al. Molecular analysis of a partial deletion of 22q in a central nervous system rhabdoid tumor. Genes Chromosomes Cancer 1992; 5: 104–108.
21. Biegel JA, Allen CS, Kawasaki K, et al. Narrowing the critical region for a rhabdoid tumor locus in 22q11. Genes Chromosomes Cancer 1996; 16:94–105.
22. Newsham I, Daub D, Besnard-Guerin C, et al. Molecular sublocalization and characterization of the 11;22 translocation breakpoint in a malignant rhabdoid tumor. Genomics 1994; 19:433–440.
23. Sevenet N, Sheridan E, Amram D, et al. Constitutional mutations of the hSNF5/INI1 gene predispose to a variety of cancers. Am J Hum Genet 1999; 65:1342–1348.
24. Sevenet N, Lellouch-Tubiana A, Schofield D, et al. Spectrum of hSNF5/INI1 somatic mutations in human cancer and genotype-phenotype correlations. Hum Mol Genet 1999; 8:2359–2368.
25. Versteege I, Sevenet N, Lange J, et al. Truncating mutations of hSNF5/INI1 in aggressive paediatric cancer. Nature 1998; 394:203–206.
26. Taylor MD, Gokgoz N, Andrulis IL, et al. Familial posterior fossa brain tumors of infancy secondary to germline mutation of the hSNF5 gene. Am J Hum Genet 2000; 66: 1403–1406.
27. Chang ES, Wick MR, Swanson PE, et al. Metastatic malignant melanoma with ''rhabdoid'' features. Am J Clin Pathol 1994; 102:426–431.
28. Fanburg-Smith JC, Hengge M, Hengge UR, et al. Extrarenal rhabdoid tumors of soft tissue: a clinicopathologic and immunohistochemical study of 18 cases. Ann Diagn Pathol 1998; 2:351–362.
29. Fitko R, Brainer J, Schink JC, et al. Endometrial stromal sarcoma with rhabdoid differentiation. Int J Gynecol Pathol 1990; 9:379–382.
30. Kumar S, Kumar D, Cowan DF. Transitional cell carcinoma with rhabdoid features. Am J Surg Pathol 1992; 16:515–521.
31. Miettinen M, Fanburg-Smith JC, Virolainen M, et al. Epithelioid sarcoma: an immunohistochemical analysis of 112 classical and variant cases and a discussion of the differential diagnosis. Hum Pathol 1999; 30:934–942.
32. Sotelo-Avila C, Gonzalez-Crussi F, de Mello D, et al. Renal and extrarenal rhabdoid tumors in children: a clinicopathologic study of 14 patients. Semin Diagn Pathol 1986; 3: 151–163.
33. Wick MR, Ritter JH, Dehner LP. Malignant rhabdoid tumors: a clinicopathologic review and conceptual discussion. Semin Diagn Pathol 1995; 12:233–248.

A. Alveolar Soft Part Sarcoma

1. Kanhere HA, Pai PS, Neeli SI, et al. Alveolar soft part sarcoma of the head and neck. Int J Oral Maxillofac Surg 2005; 34:268–272.
2. Foschini MP, Eusebi V. Alveolar soft-part sarcoma: a new type of rhabdomyosarcoma? Semin Diagn Pathol 1994; 11: 58–68.
3. Ordonez NG. Alveolar soft part sarcoma: a review and update. Adv Anat Pathol 1999; 6:125–139.
4. Simmons WB, Haggerty HS, Ngan B, et al. Alveolar soft part sarcoma of the head and neck. A disease of children and young adults. Int J Pediatr Otorhinolaryngol 1989; 17:139–153.
5. Kayton ML, Meyers P, Wexler LH, et al. Clinical presentation, treatment, and outcome of alveolar soft part sarcoma in children, adolescents, and young adults. J Pediatr Surg 2006; 41:187–193.
6. Szklarski W, Wasilewska A, Gruchala A, et al. Alveolar soft part sarcoma: an analysis of 8 cases. Review of the literature. Patol Pol 1991; 42:33–38.
7. Hunter BC, Devaney KO, Ferlito A, et al. Alveolar soft part sarcoma of the head and neck region. Ann Otol Rhinol Laryngol 1998; 107:810–814.
8. Spector RA, Travis LW, Smith J. Alveolar soft part sarcoma of the head and neck. Laryngoscope 1979; 89:1301–1306.
9. Bentley RP, Wake MJ, Raafat F. Alveolar soft part sarcoma of the tongue. Br J Oral Maxillofac Surg 1999; 37:451–454.
10. Caldwell JB, Fadell EJ, Hughes KW. Alveolar soft-part sarcoma of the tongue; report of case. J Oral Surg (Chic) 1956; 14:342–345.
11. Cetik F, Ozsahinoglu C, Kivanc F, et al. Alveolar soft part sarcoma of the tongue. J Laryngol Otol 1989; 103:952–954.
12. Chaudhry AP, Lin CC, Lai S, et al. Alveolar soft part sarcoma of the tongue in a female neonate. J Oral Med 1984; 39:2–7.

13. Colella G, Cianciulli S, Foresti M, et al. [A case of soft tissue alveolar sarcoma localized in the tongue]. Minerva Stomatol 1999; 48:347–352.
14. Donald PJ. Alveolar soft part sarcoma of the tongue. Head Neck Surg 1987; 9:172–178.
15. Fanburg-Smith JC, Miettinen M, Folpe AL, et al. Lingual alveolar soft part sarcoma; 14 cases: novel clinical and morphological observations. Histopathology 2004; 45: 526–537.
16. Kim HS, Lee HK, Weon YC, et al. Alveolar soft-part sarcoma of the head and neck: clinical and imaging features in five cases. AJNR Am J Neuroradiol 2005; 26: 1331–1335.
17. King VV, Fee WE, Jr. Alveolar soft part sarcoma of the tongue. Am J Otolaryngol 1983; 4:363–366.
18. Lane JE, Bowman PH, Austin MB, et al. Pathology quiz case 1. Alveolar soft part sarcoma (ASPS) of the tongue. Arch Otolaryngol Head Neck Surg 2003; 129:485–487.
19. Yoshida K, Kurauchi J, Shirasawa H, et al. Alveolar soft part sarcoma of the tongue. Report of a case. Int J Oral Maxillofac Surg 2000; 29:370–372.
20. Altug T, Inci E, Guvenc MG, et al. Alveolar soft part sarcoma of the larynx. Eur Arch Otorhinolaryngol 2007; 264:445–449.
21. Charrier JB, Esnault O, Brette MD, et al. Alveolar soft-part sarcoma of the cheek. Br J Oral Maxillofac Surg 2001; 39:394–397.
22. Rubinstein MI, Drake AF, McClatchey KD. Alveolar soft part sarcoma of the nasal cavity: report of a case and a review of the literature. Laryngoscope 1988; 98:1246–1250.
23. Master K, Berkmen YM. Pulmonary metastases 15 years after removal of an alveolar soft-part sarcoma of the tongue. Rev Interam Radiol 1979; 4:43–45.
24. Portera CA Jr., Ho V, Patel SR, et al. Alveolar soft part sarcoma: clinical course and patterns of metastasis in 70 patients treated at a single institution. Cancer 2001; 91: 585–591.
25. Castillo M, Lee YY, Yamasaki S. Infratemporal alveolar soft part sarcoma: CT, MRI and angiographic findings. Neuroradiology 1992; 34:367–369.
26. Iwamoto Y, Morimoto N, Chuman H, et al. The role of MR imaging in the diagnosis of alveolar soft part sarcoma: a report of 10 cases. Skeletal Radiol 1995; 24:267–270.
27. Carson HJ, Tojo DP, Ghosh L, et al. Primary alveolar soft part sarcoma of the tongue of an elderly man. A case report and review of the literature. Oral Surg Oral Med Oral Pathol 1993; 76:62–67.
28. do Nascimento Souza KC, Faria PR, Costa IM, et al. Oral alveolar soft-part sarcoma: review of literature and case report with immunohistochemistry study for prognostic markers. Oral Surg Oral Med Oral Pathol Oral Radiol Endod 2005; 99:64–70.
29. Matsuno Y, Mukai K, Itabashi M, et al. Alveolar soft part sarcoma. A clinicopathologic and immunohistochemical study of 12 cases. Acta Pathol Jpn 1990; 40:199–205.
30. Komori A, Takeda Y, Kakiichi T. Alveolar soft-part sarcoma of the tongue. Report of a case with electron microscopic study. Oral Surg Oral Med Oral Pathol 1984; 57: 532–539.
31. Joyama S, Ueda T, Shimizu K, et al. Chromosome rearrangement at 17q25 and xp11.2 in alveolar soft-part sarcoma: a case report and review of the literature. Cancer 1999; 86:1246–1250.
32. Ladanyi M, Lui MY, Antonescu CR, et al. The der(17)t (X;17)(p11;q25) of human alveolar soft part sarcoma fuses the TFE3 transcription factor gene to ASPL, a novel gene at 17q25. Oncogene 2001; 20:48–57.
33. Heimann P, Devalck C, Debusscher C, et al. Alveolar soft-part sarcoma: further evidence by FISH for the involvement of chromosome band 17q25. Genes Chromosomes Cancer 1998; 23:194–197.
34. Weterman MA, van Groningen JJ, den Hartog A, et al. Transformation capacities of the papillary renal cell carcinoma-associated PRCCTFE3 and TFE3PRCC fusion genes. Oncogene 2001; 20:1414–1424.
35. Clark J, Lu YJ, Sidhar SK, et al. Fusion of splicing factor genes PSF and NonO (p54nrb) to the TFE3 gene in papillary renal cell carcinoma. Oncogene 1997; 15:2233–2239.
36. Sidhar SK, Clark J, Gill S, et al. The t(X;1)(p11.2;q21.2) translocation in papillary renal cell carcinoma fuses a novel gene PRCC to the TFE3 transcription factor gene. Hum Mol Genet 1996; 5:1333–1338.
37. Weterman MA, Wilbrink M, Geurts vK. Fusion of the transcription factor TFE3 gene to a novel gene, PRCC, in t(X;1)(p11;q21)-positive papillary renal cell carcinomas. Proc Natl Acad Sci U S A 1996; 93:15294–15298.

14

Diseases of the Bones and Joints

Kristen A. Atkins and Stacey E. Mills
Department of Pathology, University of Virginia Health System, Charlottesville, Virginia, U.S.A.

I. INTRODUCTION

The craniofacial bones, trachea, and larynx are susceptible to many reactive, reparative, and neoplastic lesions seen in the rest of the axial and appendicular skeleton. However, many lesions common in the appendicular skeleton, such as giant cell tumor (GCT) and chondroblastoma, are rare in the head and neck. Conversely, tumors such as osteomas, hemangiomas, and giant cell granulomas have a propensity to occur in the craniofacial bones. A basic review of the bone, cartilage, and joint types in the head and neck follows to aid in understanding the distribution of tumors and reactive processes.

The craniofacial bones grow by both intramembranous ossification (parietal, frontal, temporal, occipital) and enchondral ossification (sphenoid, ethmoid, portions of temporal and occipital bones). All three types of cartilages are found in the head and neck. Hyaline cartilage is in joint surfaces, tracheal rings, and the larynx. Fibrocartilage is present at the insertion of tendons and elastic cartilage is found in the external auditory canal, eustachian tube, external ear, and larynx (1).

The bones are composed of cortical (compact) bone and trabecular (cancellous or medullary) bone. Cortical bone provides structural stability and is characterized by Haversian canals and their branches, Volkmann canals. These house the blood vessels and provide a rich communicating vascular system. Each Haversian canal is surrounded by lamellar bone. Trabecular bone is intramedullary and participates in mineral metabolism. It is composed of lamellar bone, which is constantly undergoing remodeling. This is best appreciated in the cement lines, which often distort the linear arrangement of the lamellar bone.

During high turnover and repair, such as in a fracture site, Paget's disease, or osteoarthritis, the initial deposition of osteoid is identified by the haphazard arrangement of the collagen fibers. Eventually, this woven bone will be replaced by lamellar bone. The parallel (lamellar) or disorganized (woven) orientation of the collagen fibers is best appreciated under polarized light.

The main cellular constituents of bone are osteoblasts (which make the osseous matrix collagen), osteocytes (cells embedded in the osseous matrix), and osteoclasts (specialized monocytes that resorb bone). The number and cytologic features of the osteoblasts and osteoclasts can give clues to the current metabolic state of the bone. When actively making osteoid, the osteoblasts are numerous and plump. When bone formation slows, the osteoblasts become flattened and attenuated. When bone remodeling or resorption is occurring, the number of osteoclasts increases.

The head and neck contain diarthrodial and synarthrodial joints. Diarthrodial joints have a synovial lining, smooth articular surfaces, and synovial fluid in the articular cavity. Diarthrodial joints in the head and neck include the temporomandibular joints, cricoarytenoid joints, and the cricothyroid joints. These joints are susceptible to the same lesions seen in the joints of long bones, although usually less frequently, such as rheumatoid arthritis (RA), gout, synovial chondromatosis, and pigmented villonodular synovitis (PVNS). Synarthrodial joints are designed for stability, and the flat bones of the skull are fused by fibrous synarthrodial joints.

As with bone lesions in other parts of the body, radiographic correlation is paramount to histologic interpretation. Particularly with the high-resolution magnetic resonance imaging (MRI) and computed tomography (CT) scans, the location (cortical, intramedullary) and extent involvement of the lesion can give great clues to the underlying pathology. Additionally, imaging studies will often give an idea of the growth rate and aggressiveness of a lesion. Those with sclerotic edges grow slowly enough for the osteoblasts to remodel the reactive bone at the edge of the lesion. Conversely, those with a ''moth-eaten'' appearance are indicative of a rapidly growing, destructive lesion. Imaging can also assess whether there is a periosteal reaction, which gives additional information regarding the aggressiveness and age of a lesion, since it takes two to three weeks for mineralization to occur and for the reaction to be seen. Some lesions such as chondroma and well-differentiated chondrosarcoma have overlapping histologic features, and imaging will weigh heavily toward the final diagnosis. Additionally, many lesions are only biopsied or are curetted, which can distort the usual hallmark features. Radiographic correlation can often greatly narrow the histologic differential diagnosis.

In this chapter, lesions of the craniofacial bones, larynx, trachea, and hyoid bones will be discussed. Each section is divided into background and current understanding of the disease process, followed by imaging characteristics and pathologic features.

II. INFLAMMATORY AND DEPOSITIONAL DISEASES OF THE JOINTS

Autoimmune diseases can affect joints in many parts of the skeleton. Most inflammatory and autoimmune diseases result in increased osteoclastic activity and inflammation resulting in excessive bone resorption. The histologic features of many rheumatologic and autoimmune diseases overlap, and the exact etiology often requires serum studies and radiographic correlation.

When the head and neck are involved, the underlying etiology is usually known. However, all joint diseases can occasionally involve the head and neck as the first presenting sign. Recognizing this will aid the pathologist in making the correct diagnosis.

A. Rheumatoid Arthritis

RA affects over 1.5 million people and as with many autoimmune diseases has a strong predilection for women (2). There is often a genetic predisposition. This multiorgan chronic autoimmune disease has a chronic waxing and waning course. Although any organ can be involved, it most frequently involves the synovium of joints, eventually leading to the destruction of involved joints and resulting in severe disabilities and deformities.

The involved synovium contains T- and B-cell lymphocytes, plasma cells, macrophages, and synovial fibroblasts. It is now believed that a great interplay of all of these cells results in joint degradation. Increased osteoclastic activity is thought to be due to receptor activation of nuclear factor kappa B ligand by activated T cells. The T cells stimulate the synovial fibroblasts to secrete cytokines that promote inflammation. Additionally, the synovial fibroblasts secrete enzymes that degrade the cartilage. B cells secrete rheumatoid factor and other autoantibodies, which can be detected in the serum. In addition to the inflamed synovium, the subchondral bone can also become chronically inflamed.

RA often affects the soft tissue, resulting in vasculitis, rheumatoid nodules, lymphadenopathy, Sjogren's syndrome, keratoconjunctivitis, iritis, scleritis, neuropathy secondary to small vessel angiitis or compression, myositis, and amyloidosis.

General Pathologic Features of RA-Associated Joint Disease

The barrage of inflammatory cells and release of cytokines, interleukins (ILs), metalloproteases, and antigens leads to the histologic findings of synovial hyperplasia, inflammation, germinal center formation, increased osteoclasts, and cartilage destruction and bone resorption. The joints in the head and neck will become edematous with a plasma cell and lymphocytic infiltrate in the synovium and underlying articular architecture (Fig. 1). The capsular tissue will form a pannus also with lymphocytes. As the bone resorbs, the articular surface of the condyle will be destroyed (3). The inflammation can extend into the surrounding periarticular tissue, leading to further joint instability.

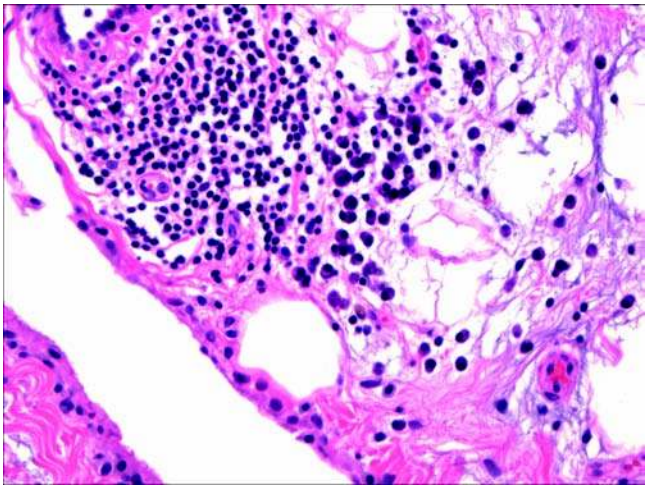

Figure 1 Typical inflammatory infiltrate in RA consists of lymphocytes and plasma cells. Germinal centers can sometimes be seen (H&E, 400×). *Abbreviations*: RA, rheumatoid arthritis; H&E, hematoxylin and eosin.

Twenty-five percent of seropositive patients develop necrotizing granulomatous nodules (rheumatoid nodules). The nodule contains a fibrinoid center with peripheral palisading histiocytes, giant cells, and lymphocytes (Fig. 2). These typically occur in the soft tissue, but occasionally can be seen in bone and cartilage (trachea, larynx, ear).

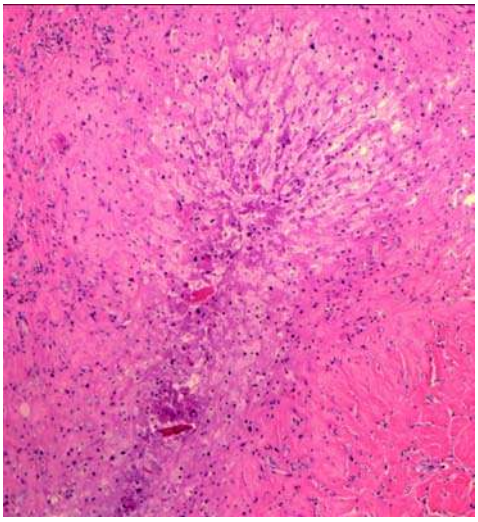

Figure 2 Rheumatoid nodule composed of histiocytes, giant cells, and lymphocytes surrounding a fibrin center (H&E, 200×). *Abbreviation*: H&E, hematoxylin and eosin.

Although the bone findings of RA are not unique to the head and neck, the clinical manifestations can be quite dramatic and are separated by site to emphasize the clinical presentations.

Larynx. The larynx contains two symmetric joints, the cricoarytenoid joints and the cricothyroid joints. The cricoarytenoid joints contribute to the movement of the true vocal cords, so when cricoarytenoid arthritis occurs, the patient may experience hoarseness, fullness in the throat, dyspnea, dysphagia, and stridor. It is estimated that 26% to 78% of patients with RA will have some laryngeal involvement, but only a quarter of these patients will have symptoms. Depending on the acuity and chronicity of involvement, laryngoscopic findings may range from a normal examination to swollen mucosa, with a decreased range in vocal cord motion, bowing of the vocal cords on inspiration, and joint deformities. Fifty-four percent to seventy-two percent will have findings on CT, such as cricoarytenoid erosion, cricoarytenoid prominence, or abnormal position of the true vocal cords. Severe ankylosis of the cricoarytenoid joints can result in significant narrowing of the airway, making the patient susceptible to acute airway obstruction. Rarely, mass lesions may form from the inflammation, simulating a malignancy (4).

Temporomandibular joint. Temporomandibular joint (TMJ) involvement is typically a late sequela of RA, although rarely it is the first presenting sign. When the TMJ is affected, it is usually bilateral. Symptoms usually include morning stiffness, decreased range of motion, crepitus, and swelling. In severe cases, erosion of the condylar head and fibrosis can lead to mandibular micronathia (5). Although not specific to RA, erosion and cysts of the mandibular condyle commonly occur (6). Voog et al. followed the changes in the TMJ by imaging and found that progression of disease correlated with serum levels of C-reactive protein, 5HT, and IL-1 soluble receptor type II (7).

Nasal septum. Rheumatoid nodules and vasculitis have been described in the septum. Rarely, spontaneous rupture of the nasal septum occurs (8,9).

Ear. RA can involve the bones of the middle ear and cause conductive hearing loss secondary to discontinuity of the ossicles and sensorineural hearing loss as a result of erosion of the cochlea (10).

B. Infectious Arthritis

It is uncommon for the craniofacial bones to develop septic arthritis. When it does occur in this area, the TMJ is the most common site of involvement and typically occurs in conjunction with a predisposing condition such as RA, diabetes, immunospression, or systemic steroid use (3). Often, it is the result of extension from external otitis or hematogenous spread from other sites (3). The most frequently identified organisms are *Staphylococcus aureus*, *Neisseria gonorrhea*, *Haemophilus influenza*, and, less commonly, *Actinomyces spp* (11).

An example of systemic bacterial infection involving the joints of the head and neck is Lyme disease. Lyme disease has numerous systemic manifestations, but, by far, arthritis is the most common late-stage disorder. It is caused by the spirochete Borrelia burgdorferi and is transmitted to humans via the Ixodes tick. The hallmark is erythema migrans, but many cases have no known antecedent rash (12). Large joints, particularly the knees, are most commonly afflicted, but occasionally patients can present with TMJ disease. If thought of and tested for, the patients can be treated with antibiotics, relieving the need for tissue confirmation. Occasionally, persistent joint effusions occur even after eradication of the organism necessitating synovectomy, suggesting the production of autoantibodies. Lyme arthritis overlaps with RA with a mixture of B- and T-cell lymphocytes, germinal centers, and collections of plasma cells (13).

C. Gout

Gout is the result of hyperuricemia and is the most common cause of arthritis in men older than 40 years (14). It is a slowly progressive disease, which eventually leads to urate deposition in the joints and/or soft tissue (particularly the helix of the ear and true and false vocal cords) called a tophus. Acute gout can mimic septic arthritis, osteoarthritis, and RA. It is typically monoarticular. The joints in the hands and feet (particularly the great toe) are the most commonly involved, followed by the wrists and knees. Acute gout is characterized by fluid accumulation in the joint. Aspirated fluid will yield needle-shaped crystals with negative birefringence. Chronic deposition of the monosodium urate crystals ultimately results in a tophus in the synovium, subchondral bone, or tendons. Chronic deposition can result in erosion of the bone and misdiagnosis on imaging.

When gout affects the joints of the head and neck, it typically is not in isolation, and patients often have synchronous involvement of the extremities. The TMJ is the most frequently involved craniofacial site (14). Occasionally, gout can exclusively involve a single joint of the head and neck without other more typical areas getting affected.

Radiologic Features

Gout is usually diagnosed before any imaging abnormalities can be detected. When radiology is employed, plain films are the most common means for assessing chronic gouty arthritis. The tophi are well circumscribed with sclerotic edges, although occasionally they can mimic neoplasms, particularly when in unusual locations (15). In this latter scenario, CT and MRI can be helpful. MRI shows heterogeneous T2-weighted images that are thought to be related to the calcium in a tophus (16). Some have advocated using CT over MRI and ultrasound as masses of 160 HU density can be detected on CT scan, which correlates to the monosodium urate crystals deposited in gout (17).

Pathologic Features

Acute gouty synovitis is typified by an acute exudate that can be mistaken for an infectious process. The

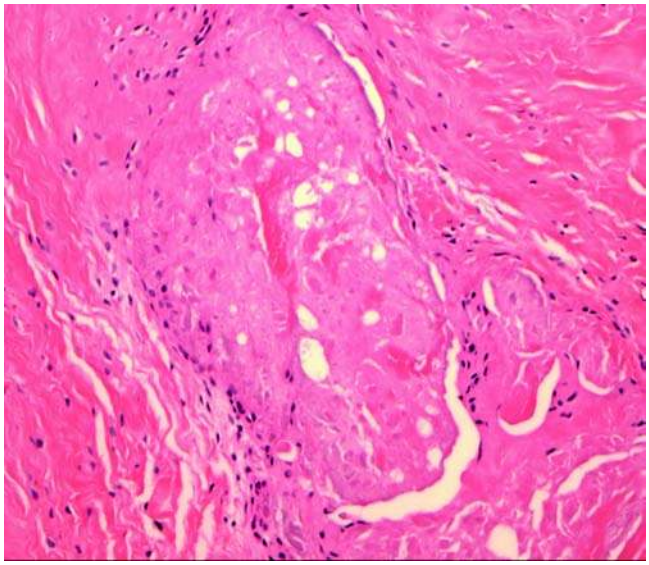

Figure 3 Gouty tophus composed of amorphous material surrounded by giant cells and histiocytes. The urate crystals often get washed away in histologic sections.

tophus of chronic gout is characterized by a foreign body giant cell reaction with amorphous eosinophilic material. Since the crystals are water soluble, routine submission for histologic sections will wash the crystals away leaving only the amorphous material, giant cells, histiocytes, and fibrosis (Fig. 3). Polarization of unstained sections, however, will often yield the needle-shaped crystals with negative birefringence (3).

D. Calcium Pyrophosphate Crystal Deposition Disease

Calcium pyrophosphate crystal deposition disease (CPCDD), also known as pseudogout or chondrocalcinosis, can mimic gout or osteoarthritis. The exact etiology is unclear but seems to be a result of overproduction of extracellular pyrophosphate (3). Crystals can be found within chondrocytes, suggesting an intracellular pathway of crystal formation (18). The knee is the most commonly affected joint, but many patients have several affected joints. Involvement of the head and neck is rare and limited to a few case reports. The TMJ seems to be the most common site of craniofacial involvement (19), followed by the inner ear (20). TMJ involvement is often characterized by destruction of the condyle. This destruction, coupled with the rarity of CPCDD, can result in misdiagnosis of a neoplasm, synovial chondromatosis, or infection requiring histologic assessment for a correct diagnosis (21,22).

Radiologic Features

There is usually a calcified intra-articular mass, with or without erosion of the cartilage and bone. The calcification is often described as fluffy or granular (23).

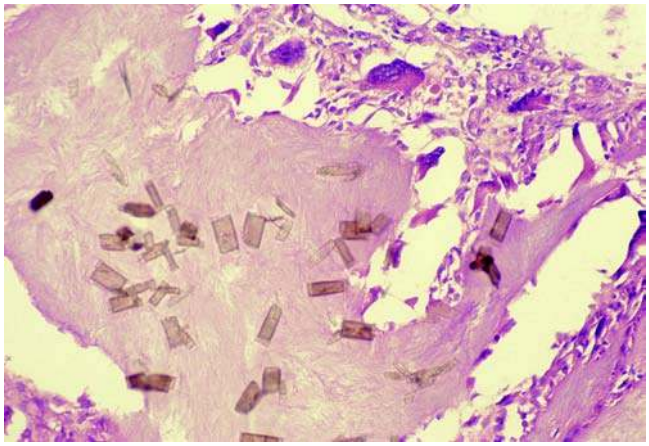

Figure 4 Rhomboid crystals of calcium pyrophosphate. The crystals can be found extracellularly and within the chondrocytes.

Pathologic Features

Grossly, joints contain a chalky white substance, which microscopically contains the weakly positively birefringent rhomboid crystals of calcium pyrophosphate (Fig. 4). Like gout, some lesions contain giant cells and histiocytes. Cartilagenous nodules are also present often with intracellular CPPD crystals (18).

E. Oxalosis

Oxalosis is a rare depositional process that results from the accumulation of oxalate from diet, chronic megadoses of vitamin C, chronic renal failure/dialysis, or an inborn error of metabolism. Deposition can occur in solid organs and in bone (24).

Radiologic Features

Primary oxalosis will result in increased bone mineral density, and the clinical course can be monitored by measuring bone mineral density (25). Secondary oxalosis can be challenging to diagnose but imaging studies usually show osteosclerosis (26).The changes overlap with other disease such as hyperparathyroid disease and renal osteodystrophy (27).

Pathologic Features

Chronic oxalosis results in the deposition of birefringent oxalate crystals, which can incite a granulomatous response (Fig. 5). The deposits can be in the trabecular bone and marrow.

F. Dystrophic Calcification and Tumoral Calcinosis

Both of these disorders are exceedingly rare in the head and neck and are limited to isolated case reports. Both entities can result in masses and, because of the

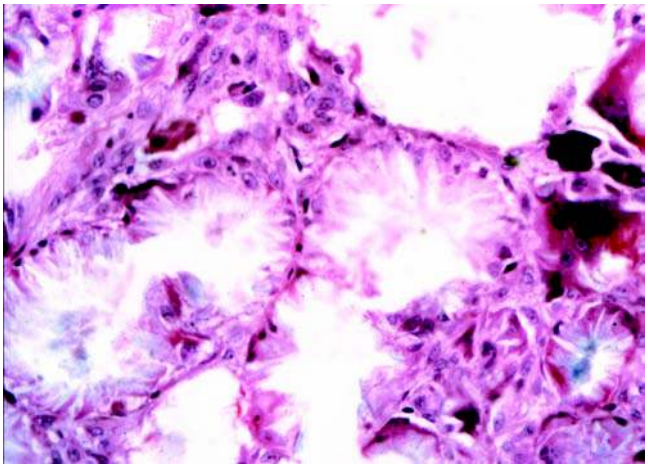

Figure 5 Starburst pattern of oxalate crystals (H&E, 400×). *Abbreviation*: H&E, hematoxylin and eosin.

unusual location, can be overinterpreted radiographically (28,29). Tumoral calcinosis can be genetic or sporadic and results in calcium deposits in or near joints (particularly the hips, shoulders, and elbows). Blood phosphate levels are often elevated.

Dystrophic calcification is calcification of damaged tissue in the absence of calcium serum level defects.

G. Synovial Chondromatosis

Synovial chondromatosis is a monoarticular cartilagenous metaplasia involving the synovium or tendon sheath, resulting in numerous cartilaginous loose bodies that ultimately calcify or ossify. Women are affected more frequently than men (30). Primary synovial chondromatosis is usually devoid of an underlying arthritis and therefore the articular surface is intact. The synovial fluid from patients with primary synovial chondromatosis has high levels of fibroblastic growth factor. Secondary synovial chondromatosis arises in the setting of inflammatory and noninflammatory arthropathies.

Synovial chondromatosis seems to develop in three stages: active intrasynovial disease devoid of loose bodies, simultaneous active intrasynovial disease with loose bodies, and, lastly, no intrasynovial disease but numerous free osteochondral loose bodies (31). Common symptoms include inflammation, pain, and decreased range of motion (32). Synovial chondromatosis can be difficult to excise, and recurrence is not an indication of malignancy.

Most cases (70%) of primary synovial chondromatosis occur in the knees, followed by the elbows, and the hips. Despite the predilection for large joints, it does occur in the head and neck, particularly the TMJ (33). TMJ synovial chondromatosis often results in preauricular mass, pain, crepitus, and restricted jaw movement and can be mistaken for a parotid mass.

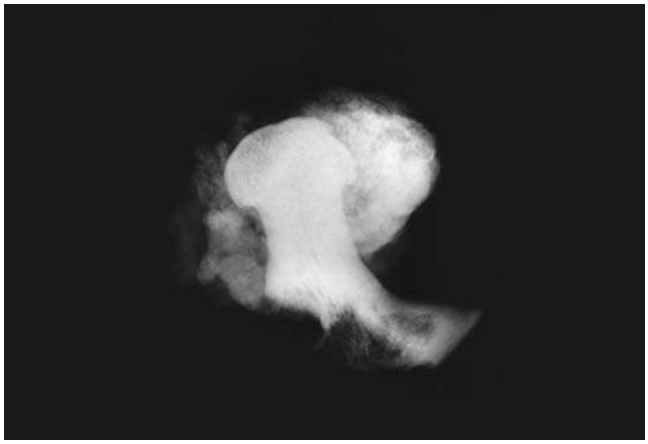

Figure 6 Plain film of synovial chondromatosis resulting in pressure erosion of the underlying bone.

Radiologic Features

Imaging features vary depending on the severity of the lesion and the degree of calcification or ossification. Intra-articular loose bodies as well as widening of the joint space and erosion of bone may be seen (Fig. 6). If the lesions have not calcified, plain films may be normal. CT scans can often highlight the loose bodies, but some studies have found MRI to be superior in identifying the lesion and assessing the extent of disease (30,34).

Pathologic Features

Grossly, the synovium is focally or diffusely involved and covered by nodules ranging from microscopic to several centimeters (Fig. 7). The number of nodules can range from 1 to 500, with most cases having fewer

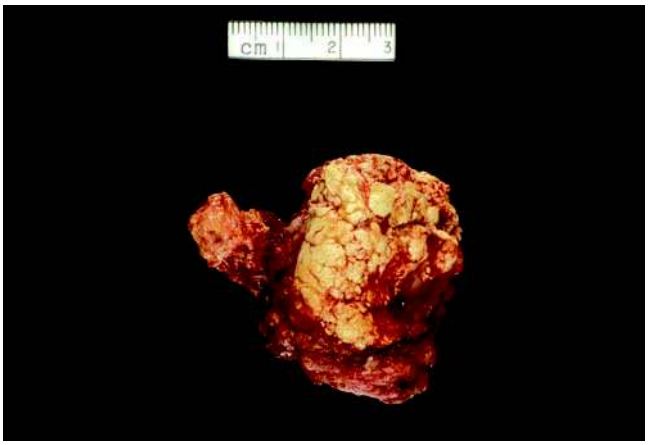

Figure 7 Resection of a left TMJ involved by extensive synovial chondromatosis. *Abbreviation*: TMJ, temporomandibular joint.

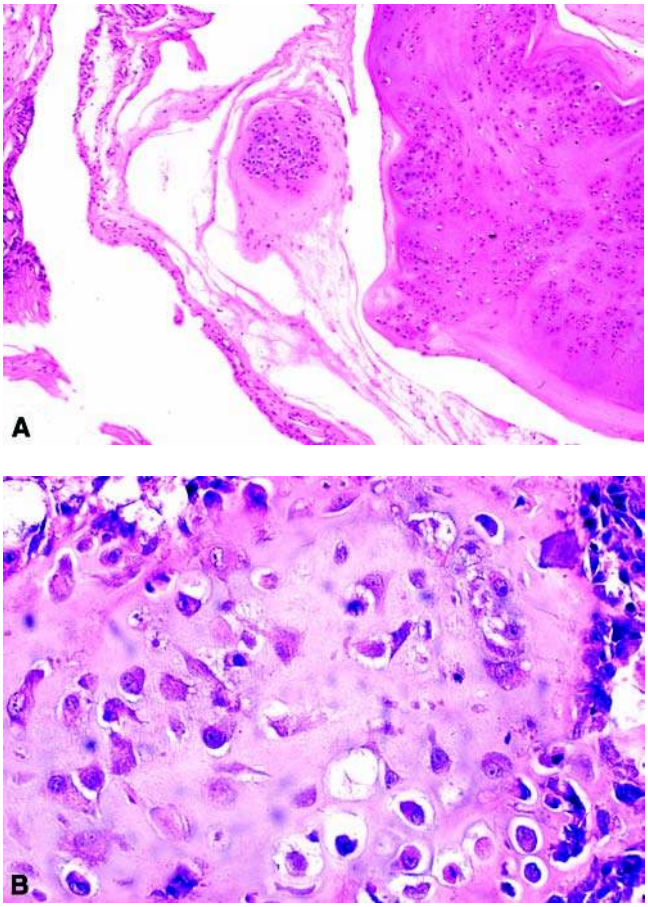

Figure 8 Histology of synovial chondromatosis demonstrating cartilaginous nodules. (**A**) Atypia is common in long-standing synovial chondromatosis. Correlation with specimen radiographs is paramount to appropriately diagnose this benign process.

than 50 (33). The nodules are composed of disorganized cartilage, commonly with some cytologic atypia (plump binucleated chondrocytes). As the nodule grows, it may detach from the synovium and ossify or calcify. Distinguishing synovial chondromatosis from chondrosarcoma can be impossible histologically and requires radiographic correlation (Fig. 8).

H. Pigmented Villonodular Synovitis

PVNS is an idiopathic, sometimes locally aggressive, process that involves the synovium and tendons. The pathogenesis is controversial. Some believe it is secondary to a chronic inflammatory process, while others think it is a neoplastic condition (35,36). It is characterized by monoarticular involvement, effusions (when in the synovium), and pain (particularly when in the tendons). It affects both genders equally and predominantly affects people in their 30s and 40s, although it can occur in all age groups. It has a predilection for the knee and hands but has been reported in the head and neck, primarily, albeit rarely, involving the TMJ. When the TMJ is involved it can form a preauricular or parotid mass (37). Some patients have undergone parotidectomy before a correct diagnosis was rendered (3). Although it is benign, it can be locally aggressive. PVNS that originates in the TMJ can spread into structures in the infratemporal fossa and the skull base (3,38). Synovectomy is the first-line treatment, followed by radiation for unresectable cases.

PVNS is divided into localized and diffuse forms. Localized PVNS is a discrete mass with smooth borders, usually less than 2 cm in greatest dimension. Eighty percent arise in the tenosynovium of the fingers (also called GCT of tendon sheath) (39). Diffuse PVNS involves the articular synovium, causing thickening of the synovial membrane. Seventy percent of diffuse PVNS occurs in the knees. The hips, ankles, elbows, and shoulders are also commonly involved. Diffuse PVNS can be challenging to excise, and recurrence is not evidence of malignancy (3).

Although PVNS is locally destructive, it is debatable whether true malignant transformation occurs. Bertoni et al. found the following features more often associated with aggressive lesions: a solid infiltrative pattern, large cells with indistinct borders, prominent nucleoli, and necrosis (40). It is important to recognize that other sarcomas have overlapping histologic features, including clear cell sarcoma, epithelioid sarcoma, and giant cell–rich carcinomas.

Radiologic Features

On plain films, early disease may show bone erosions with preservation of the joint space. As the lesion progresses, the joint capsule thickens and the joint space diminishes (41).There may be a localized intra-articular or para-articular soft tissue density. Occasionally, well-circumscribed intraosseous cysts are present secondary to the spread of PVNS along vessels into the bone (42).

By CT imaging, PVNS is a high-density mass due to the abundant hemosiderin deposition. It shows variable enhancement. CT scan will also highlight any bone erosions or cysts (41).

MRI is tauted as being the best means for determining the extent of the disese. Because of the magnetic susceptibility properties of hemosiderin, MRI shows a low signal ''blooming'' artifact (41).

Pathologic Features

PVNS is grossly nodular with red villous projections secondary to hemosiderin deposition from repeated trauma and bleeding into the delicate villi. Histologically, the nodules are composed of villi filled with mononuclear stromal cells, giant cells with intracytoplasmic iron, foamy histiocytes, fibrosis, and scant chronic inflammation (Fig. 9). Dense stromal fibrosis may develop in chronic cases.

Immunohistochemistry

The mononuclear cells express CD68. The multinucleated giant cells demonstrate an immunophenotype

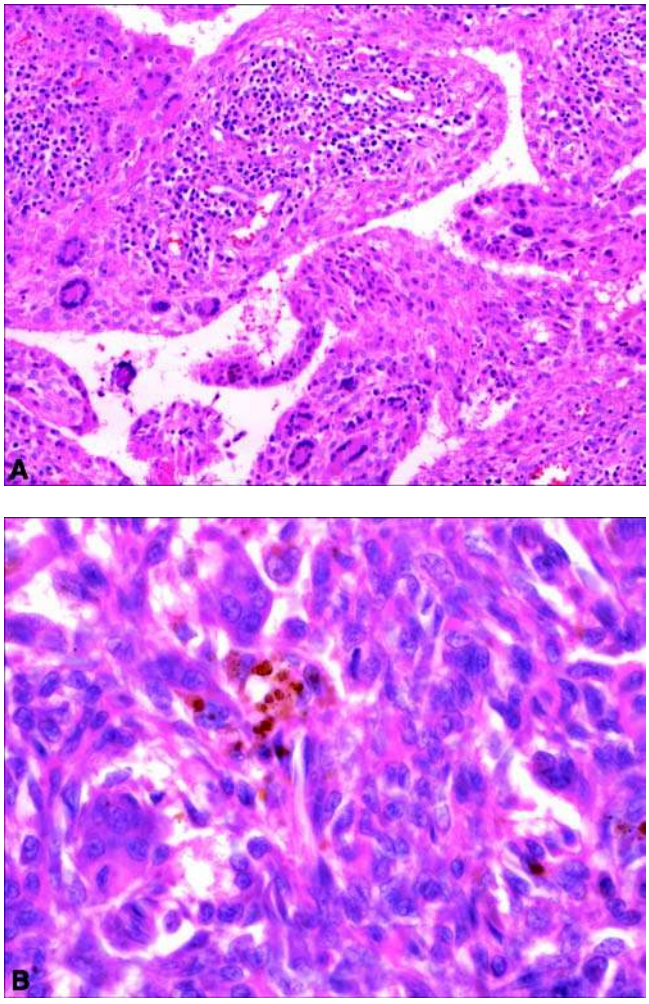

Figure 9 The papillary pattern of PVNS demonstrating the numerous multinucleated giant cells and inflammatory stroma (H&E 200×). (**A**) Hemosiderin accumulates in the giant cells and stroma because of repeated trauma and hemorrhage (H&E, 400×). *Abbreviations*: PVNS, pigmented villonodular synovitis; H&E, hematoxylin and eosin.

similar to osteoclasts and express CD51, tartrate-resistant acid phosphatase (TRAP), and calcitonin receptor (43).

I. Ganglion and Synovial Cysts

Both ganglion and synovial cysts of the bone are rare entities in the head and neck, but when they do arise, they typically involve the TMJ. Ganglion cysts are pseudocysts derived from degeneration of the joint capsule. Although benign, they can occasionally protrude from the joint space and present as preauricular masses. The clue that it is associated with the TMJ is that the mass changes position and size on movement of the jaw (44).

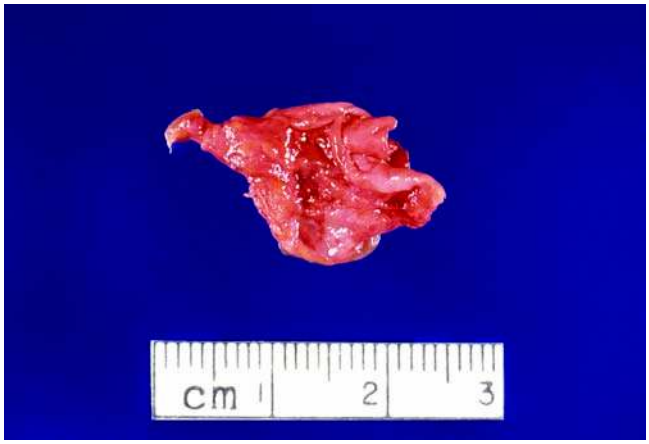

Figure 10 Collapsed multilocular ganglion cyst from theTMJ. This presented as a parotid mass. *Abbreviation*: TMJ, temporomandibular joint.

Radiologic Features

The typical findings are a uni- or multilocular mass that is para-articular or in the soft tissue. Focal bone erosion may be seen (45).

Pathologic Features

Ganglion cysts are filled with viscous to gelatinous material and are surrounded by a fibrous pseudocapsule (Fig. 10). There are no lining cells, and the cyst ''wall'' is formed by surrounding fibroblasts. Synovial cysts are radiographically and grossly similar to ganglion cysts. However, histologically, the cysts are lined by flattened synovial cells (46).

J. Dermoid Cysts

Dermoid cysts can occur in the soft tissue of the head and neck as well as in association with the nasal septum. They often present as a cyst or sinus that involves the midline of the nose between the glabella and the columella. They may extend intracranially, simulating encephaloceles, ectopic neuroglia, and teratomas (47). Occasionally, dermoid cysts in newborns and children present as frontonasal masses. These are thought to be secondary to a defect in the closure of the fonticulus nasofrontalis. Although dermoid cysts are benign, surgical excision is often necessary because of infections, osteomyelitis, nasal distortion, and intracranial involvement (47).

Radiologic Features

CT and MRI can be helpful in evaluating the extent of the lesion to assess whether anterior craniotomy is necessary (48,49).

Pathologic Features

Dermoid cysts are lined by squamous epithelium and have attached hair and sebaceous appendages (49).

III. NONNEOPLASTIC BONE AND JOINT DISEASE

A. Osteoarthritis

Degenerative joint disease is a noninflammatory process that results in abrasion, degeneration, and new bone formation of the articular surface joints. Primary osteoarthritis is a ''wear and tear'' phenomenon found in older, typically asymptomatic, individuals. Secondary osteoarthritis occurs after trauma or chronic bruxism (clenching of the jaw or teeth grinding). Secondary osteoarthritis tends to occur in younger people and is more often painful (3). Interleukin-1 and tumor necrosis factor α have been implicated in the initiation and progression of disease (50). Osteoarthritis tends to occur more frequently in women with an average ratio of 4:1 (51).

Radiologic Features

There is erosion of the articular surface of the condyle and osteophyte formation.

Pathologic Features

The condylar head is eburnated. The articular surface is uneven with ulceration and erosion as well as hyperplasia of the fibrocartilage (3). Histologically, the bone is characterized by clumping of the articular fibrocartilage and surface erosions, which may or may not be associated with fissures extending from the condylar surface to the subchondral bone. As the surface becomes denuded, exostosis may occur in an attempt at new bone formation. Alternatively, the erosion may extend into the marrow. There is usually no inflammation accompanying this severe erosive condition. Ong and Franklin reviewed the histopathology of 136 TMJ condylar head specimens and found no correlation with the symptoms and the histopathologic findings (51).

B. Osteomyelitis

Osteomyelitis can be divided into five subtypes: acute suppurative osteomyelitis, chronic suprative osteomyelitis, chronic focal sclerosing osteomyelitis, chronic diffuse sclerosing osteomyelitis, and proliferative periostitis.

Acute suppurative osteomyelitis can occur in any of the craniofacial bones but most commonly affects the jaws secondary to an odontogenic infection (52). The body of the mandible is the most frequent site of infection. The maxilla is rarely involved, probably because of the increased blood supply and thus the body's innate ability to squelch infections in this location (52). Patients usually present with excruciating pain, fever, erythema and swelling, sinus formation, purulent discharge, regional lymphadenopathy, and leukocytosis. If the acute inflammation spreads along the inferior dental canal into the pterygoid space, trismus may ensue.

The most common cause is a bacterial infection secondary to periodontal disease or an infected tooth extraction site. Other etiologies include trauma and fracture sites. Given the mixed flora in the oral cavity, it is not surprising that most infections are polymicrobial, most commonly a mixture of *Streptococcus*, *Lactobacillus*, *Klebsiella*, and *Bacteroides*. Other organisms such as *S. aureus*, *Escherichia coli*, *Veillonella parvula*, and *Peptococcus magnus* are frequently cultured (53). Rarely, viruses such as herpes virus or cytomegalovirus can result in osteomyelitis (54). As in other sites of the body, prompt treatment of osteomyelitis with antibiotics or antiviral medications is usually curative (55). However, those who are immunocompromised or those who have diabetes, anemia, malnutrition, and chronic renal failure often have a difficult time clearing the infection.

In children, osteomyelitis of the jaw is usually extension of otitis media or hematogenous spread from infections in other parts of the body (56). It is a result of infections such as actinomycosis, tuberculosis, and, less commonly today, syphylis as well as bacterial infections secondary to fractures and trauma.

It is usually a single focus but multifocal lesions can occur, particularly when viral. Typically, it is diagnostic on imaging but treated, and long-standing osteomyelitis can simulate a neoplasm. Although osteomyelitis is a reactive result of infection, long-standing osteomyelitis carries a small but real risk of ensuing malignancy. Rarely, patients develop a low-grade (well differentiated) squamous cell carcinoma in the area of chronic draining sinus (57). Even less commonly, fibrosarcomas or other sarcomas develop (58). There are contradicting findings as to whether patients who develop an infection-related malignancy do better than patients with de novo malignancies (58,59).

Radiologic Features of Acute Supprative Osteomyelitis

For acute suppurative osteomyelitis to be seen on plain films, at least 30% to 50% of the bone substance must be lost, and therefore infections may appear normal for the first week of their development (60). After 7 to 10 days, the trabeculae have undergone destruction and will be indistinct, manifesting as radiolucent areas. Occasionally, sequestra, involucra, and subperiosteal neo-osteogenesis will be seen. CT shows either unremarkable bone or slight osteolysis. MRI is more sensitive in highlighting affected bone and the extent of disease when compared with CT and plain films (61).

Pathologic Features of Acute Supprative Osteomyelitis

Acute suppurative osteomyelitis primarily affects the bone marrow and secondarily involves the trabeculae and cortex. Early changes demonstrate neutrophils in the medullary spaces. As the trabeculae become traumatized, they will appear ragged and will lose their surrounding osteoblasts. Osteonecrosis is evidenced by the loss of osteocytes from their lacunae. Overdecalcification can extinguish the osteocytes artificially. Therefore, if there is no significant inflammation or evidence of reparative bone, caution of overdiagnosis based on just necrotic bone is warranted. Bacterial colonization may be seen. Small granulomas can form

in bacterial acute osteomyelitis as well as secondary to fungal and tuberculosis.

Chronic suppurative osteomyelitis most frequently develops in the body and at an angle of the mandible. The age of occurrence ranges from 13 to 88 years, with most cases in their 50s and 60s. It can be de novo or the sequela of acute suppurative osteomyelitis (62). The latter is defined as one month in duration; therefore, it is a persistent infection despite antibiotic treatment. As with acute suppurative osteomyelitis, most present with swelling, pain, and draining fistulas. However, it is unusual for those with chronic suppurative osteomyelitis to have fever and leukocytosis (62). As with acute osteomyelitis, the lesions are typically polymicrobial. The chronic changes result in scarred, avascular tissue, resulting in an impermeable wall that surrounds a nidus of bacteria. This results in an infection prone to repeated exacerbations. Infection-induced thrombi can form, causing anoxia and tissue necrosis. If a single feeder vessel is involved, large areas of the bone may necrose, resulting in pathologic fractures, malocclusion, trismus, or loose teeth (62). Rarely, anesthesia or parathesia can occur. Some have advocated using urine concentrations of hydroxylysylpyridinoline as a means of following progression or regression of disease (63). However, surgical debridement is often necessary. Occasional resection is warranted, particularly if there is a pathologic fracture, persistent infection, or extensive bone loss.

Radiologic Features of Chronic Suppurative Osteomyelitis

Chronic suppurative osteomyelitis generally results in areas of radiolucency with interspersed radiopaque areas. Sequestra are common (52). The surrounding bone may have an increased density and the cortical bone may exhibit a periosteal reaction. As with acute suppurative osteomyelitis, MRI is usually more informative than CT scan regarding extent of the lesion and areas of active infection.

Pathologic Features of Chronic Suppurative Osteomyelitis

The marrow is fibrotic with irregular trabeculae. Osteoclasts and osteoblasts are present as a result of the bone destruction and repair. In severe lesions, sequestra and reversal lines are present. Mild lesions will show only a few lymphocytes, whereas severe lesions will have more acute and chronic inflammatory cells with abscess formation.

Chronic focal sclerosing osteomyelitis is a hyperplastic bone reaction as a result of a bacterial infection usually formed as a necrotic pulp secondary to a dental caries or cracked tooth. Most commonly, it involves the first molar in the mandible. Generally, patients present with mild pain secondary to the infected pulp. The bony trabeculae proliferate but there is no resorption leading to sclerotic bone. The involved tooth usually must be extracted. Endodontic therapy results in regression of the lesion and normalization of the periodontal ligament in 85% of cases. The 15% with residual sclerosis can be left alone unless they become symptomatic. There have been promising results with the added use of calcitonin (64).

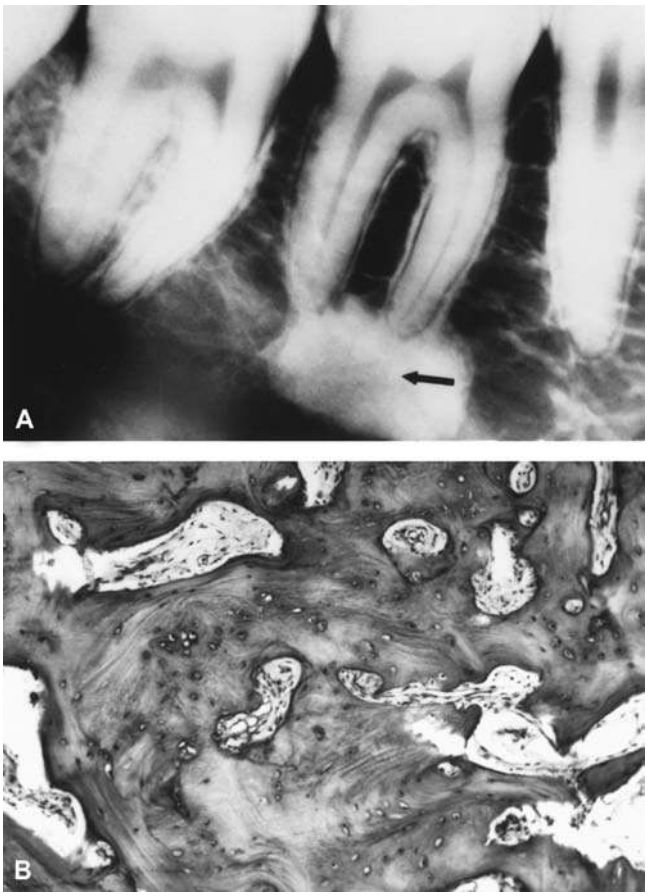

Figure 11 Chronic focal sclerosing osteomyelitis demonstrating a well-defined raiopaque mass adjacent to the apices of the mandibular first molar (**A**) Histologically, this consisted of bone, fibrous tissue, and scant inflammation (H&E, 100×). *Abbreviation*: H&E, hematoxylin and eosin.

Radiologic Features of Chronic Sclerosing Osteomyelitis

Chronic focal sclerosing osteomyelitis forms a radiopaque periapical mass of sclerotic bone. The borders may be well circumscribed or ill defined, blending into the surrounding bone (65). The periodontal ligament of the adjacent tooth is often thickened (Fig. 11A). The appearance overlaps with cementoblastoma, hypercementosis, periapical cemental dysplasia, and ossifying fibroma.

Pathologic Features of Chronic Sclerosing Osteomyelitis

The bony trabeculae are thickened and juxtaposed to one another. If stroma is present, it is usually fibrotic (Fig. 11B).

Chronic diffuse sclerosing osteomyelitis (also called nonsuppurative osteomyelitis or osteomyelitis sicca) occurs in the mandible and presents as unilateral, localized pain and swelling (66). It is often cyclical, with each exacerbation lasting one to two weeks. It can have a markedly protracted course despite therapy. It most commonly affects young

adults in their 20s, although it has been reported in most ages. Females are affected three to four times more frequently than males. It differs from the classic form of chronic osteomyelitis in that there is no acute inflammation or fistula formation (67). The cause is unclear, although there is some support that it is a result of a low-grade bacterial infection (68). Some have postulated that chronic diffuse sclerosing osteomyelitis is not an infection but rather the result of either a hyperactive immune response, painful fibro-osseous disease related to fibrous dysplasia (FD), or a response to overuse of the masseter muscles due to jaw clenching or nail biting. The result is a nonsuppurative reaction causing a periosteal and endosteal sclerosis of the mandible. Most present with pain, which is thought to be secondary to either the medullary inflammation or bone ischemia.

Radiologic Features of Chronic Diffuse Sclerosing Osteomyelitis

Chronic diffuse sclerosing osteomyelitis lesions are mixed with osteolytic and osteoblastic zones. Early lesions often demonstrate periosteal deposition of bone. The process arises in the mandible and involves the tooth-bearing areas as well as the alveolar ridge and the ascending ramus (including the condylar process). Shortening of the tooth roots is frequently observed in involved areas. Older lesions are characterized by dense sclerosis (69).

Pathologic Features of Chronic Diffuse Sclerosing Osteomyelitis

Histologic features are usually mixed and include sclerotic bone with narrowed Haversian canals in the periphery; coarse irregular trabeculae with intervening fibrotic marrow; proliferating trabeculae resembling FD embedded in a vascular, fibrotic stroma; and granulation tissue with lymphocytes, plasma cells, and osteoclasts-like giant cells but devoid of bone (70). Because of the heterogeneity of these features, any biopsy may have only a few of these findings, which are nonspecific. Correlation with imaging is paramount to the correct diagnosis (69).

Proliferative periostitis (also called periostitis ossificans) is a hyperplastic periosteal reaction to inflammation. It is the result of an infection, most commonly from a caries-induced pulpal necrosis, and inflammatory response through the buccal cortical plate that stimulates the periosteum to deposit new bone (71). The periosteum forms rows of reactive bone that are parallel to each other and expand the surface of the bone. Other stimuli include pericoronitis, periodontal defect, infected dentigerous cyst, trauma, congenital syphilis, tonsillitis, pharyngitis, parotid abscess, and tuberculosis of the mandible. Patients present with facial swelling and enlargement of the bony mandible. It can be asymptomatic or painful. It most commonly arises in the inferior border of the posterior mandible, followed by the buccal aspect and the lingual aspect. It is almost always solitary, although rare case reports of multifocal disease do exist (72). Depending on the location, it can incite restricted jaw movement. It has been described in all age groups but most commonly occurs in adolescents.

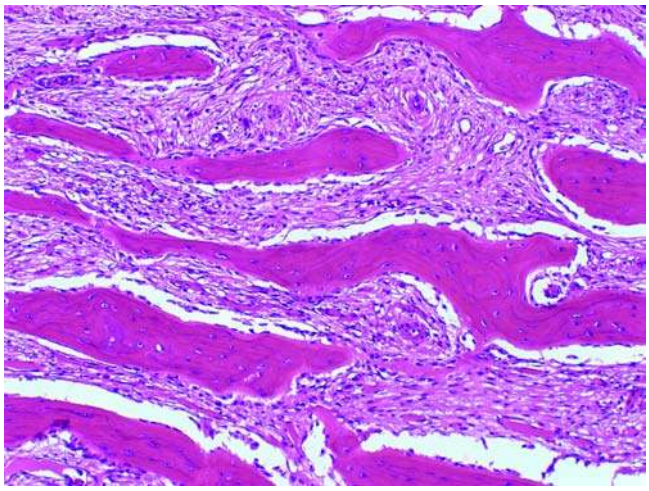

Figure 12 Proliferative periostitis is characterized by parallel, thin bony trabeculae with intervening fibrous stroma (H&E, 100×). *Abbreviation*: H&E, hematoxylin and eosin.

Nortje et al. found a slight male preponderance (1.27:1). The carious tooth needs to be extracted or treated with endodontic therapy (72). The jaw will slowly remodel and facial symmetry will be restored. Therefore, no surgical treatment of the periosteal lesion is required unless the cortical boundary is destroyed (to exclude a malignancy), the teeth move, the tooth buds are seen, or the source of inflammation cannot be identified.

Radiologic Features of Proliferative Periostitis

The prominent finding of proliferative periostitis is ''onion skinning'' or cortical duplication. The periosteal reaction can appear as a single or multiple layers. The original cortex is well defined and the lesion is well circumscribed (71).

Pathologic Features of Proliferative Periostitis

The trabecular bone is arranged in linear, parallel rows. Focally, it may be more irregular resembling FD (Fig. 12). The stroma is fibrous with only rare inflammatory cells.

C. Osteoradionecrosis

Osteoradionecrosis (ORN) occurs in 1% to 35% of patients treated with radiation for head and neck malignancies. Marx and Johnson strictly defined ORN as nonviable bone in the region of radiation that fails to heal without intervention (73,74). ORN is related to the dose of radiation (more severe when radioactive implants are used and rarely develops in doses less than 5000 cGy), dental status of the patient, and the anatomic site of the tumor (75). Radiation not only damages the pulp of the teeth but also results in the loss of saliva and therefore its anticariogenic effects. The mandible is the most commonly affected

bone in the head and neck, possibly because of its reduced blood supply and the increased amount of compact bone when compared with other craniofacial bones (76). The incidence of ORN is greatly diminished if teeth are extracted prior to radiation. Although ORN overlaps with the features of osteomyelitis, by definition it is not a primary bone infection but rather a wound-healing defect. It follows a predictable sequence of hypovascular-hypocellular-hypoxic tissue followed by a nonhealing wound that may or may not become infected. Patients with ORN develop pain and dyesthesia. Pathologic fractures, fistulas, trismus, difficulty with mastication and swallowing, or infections are the common serious complications. The dead tissue and bone usually need to be surgically removed. Treatment also includes hyperbaric oxygen therapy, analgesics, and antibiotics (76).

Radiologic Features

ORN is typified by an irregular area of radiolucent bone destruction. Areas of radiopacity are indicative of sequestrum formation. It can be impossible to differentiate ORN from recurrent or persistent carcinoma.

Pathologic Features

ORN has six stages: hyperemia, endarteritis, thrombosis, cell depletion, hypovascularity, and fibrosis. The loss of blood vessels and fibrosis begins about six months after radiation.

D. Relapsing Polychondritis

Although the cause is unknown, it is probably an autoimmune disease characterized by fluctuating inflammation of the cartilage of the ears, nose, larynx, trachea, and bronchi, which results in destruction causing distorted (''cauliflower'') or droopy ears, saddle nose deformity, and airway compromise (77). The chondritis is extremely painful and episodes last for a few days to a few weeks. The severity of the disease is variable with some experiencing symptoms several times a month and others every few years. Respiratory symptoms (dyspnea, cough, wheezing) occur in about half of the patients. Respiratory distress can occur as a result of laryngeal collapse from destruction of the tracheal and laryngeal cartilage or from airway narrowing, secondary to inflammation and fibrosis (78). Antibodies to type II collagen are often identified and titer levels seem to correlate with the activity of disease (79,80). About 30% of patients have other rheumatologic or autoimmune diseases such as RA and systemic lupus erythematosis (78,81). Relapsing polychondritis can begin at any age but most commonly affect people in their 40s. Some have found a slight increased incidence in women (81). McAdam et al. suggested that three of the six major criteria be met for the diagnosis: recurrent chondritis of bilateral auricles; chondritis of the nasal cartilage; nonerosive inflammatory polyarthritis; inflammation of ocular structures (e.g., conjunctivitis, uveitis, scleritis); laryngeal or tracheal chondritis; and choclear or vestibular damage (as evidenced by hearing loss, tinnitus, and vertigo) (78). Auricular chondritis and arthritis are the most common presenting symptoms (81). This usually develops suddenly and is characterized by diffuse involvement with a swollen, erythematous, painful pinna. About 5% to 10% of patients will develop aortic insufficiency.

Radiologic Features

Plain films will show articular cartilage damage (40%), calcification of the ears (40%), or tracheal narrowing (32%) (82). Some have advocated the use of 88 mTc methylene diphosphonate bone scintigraphy when the presentation is atypical. There is increased uptake in the cartilage of patients with relapsing polychondritis because of bone formation (83,84). CT imaging seems to be an excellent means of monitoring patients with relapsing polychondritis, as it has excellent resolution of cartilage and soft tissue. CT studies are able to highlight airway narrowing, calcified tracheal artilage, bronchiectasis and bronchial narrowing, and calcifications of the pinna and nasal cartilage (85). Behar et al. found that CT images were excellent at identifying thickening of the airway walls (86). Lee et al. found that 17 of 18 patients with relapsing polychondritis have evidence of either malacia or air trapping on expiratory CT scans (87).

Pathologic Features

When the presenting symptoms are classic, a tissue biopsy is not necessary (81). However, when the presentation is atypical or the differential diagnosis includes Wegener's granulomatosis or an infectious cause, tissue confirmation may be warranted. When the cartilage is biopsied, it usually demonstrates a loss of matrix mucopolysaccharides, resulting in a loss of the characteristic bluish hue that cartilage typically displays on hematoxylin and eosin (H&E) stain. Lymphocytes and neutrophils may be at the periphery of the cartilage. Older lesions may calcify or ossify (81).

E. Focal Osteoporotic Bone Marrow Defect

Focal osteoporotic bone marrow defect (also called focal hematopoietic hyperplasia and hematopoietic bone marrow defect) is a result of localized accumulation of marrow or fat within the jaw. There are several theories as to its pathogenesis, including ischemia, persistent embryologic marrow remnants, regeneration of trabeculae after trauma, such as extraction, and bone resorption secondary to marrow hyperplasia in response to increased blood cell demand (88–90). Most patients are asymptomatic, and it is found incidentally on dental images. Rarely patients present with pain and swelling (91).

Radiologic Features

The defects range from a few millimeters to a few centimeters, but the majority are less than 1 cm. The radiologic features are nonspecific, ranging from a poorly to a well-defined radiolucency (Fig. 13A).

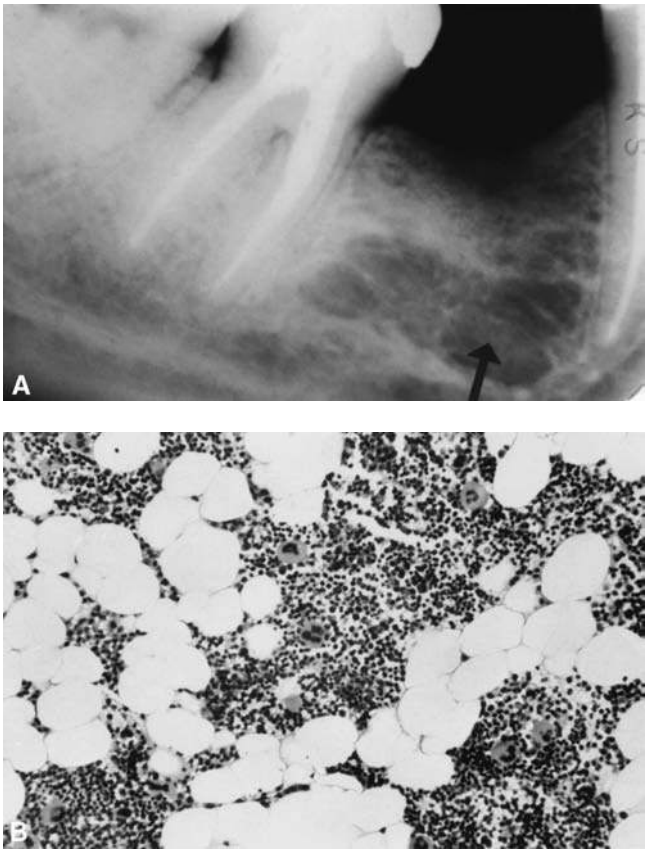

Figure 13 Focal osteoporotic–bone marrow defect characterized as a moderately defined radiolucency. (**A**) Characteristic histologic findings of focal osteoporotic–marrow defect include fatty marrow and red marrow elements (erythroid and myeloid elements) (H&E, 400×). *Abbreviation*: H&E, hematoxylin and eosin.

They can appear aggressive on plain films and be mistaken for malignancies (89). They are often in an area of previous extraction site or associated with an impacted tooth, FD, or exostosis. The most common location is the mandibular molar region (89).

Pathologic Features

Focal osteoporotic bone marrow defects are characterized by normal marrow elements (erythroid and myeloid elements with rare megakaryocytes), fatty marrow, or both (Fig. 13B). The lamellar bone is long and narrow and usually without osteoblastic rimming (88).

F. Cortical Defects of the Mandible

These depressions in the bone are subclassified into four groups: posterior lingual cortical defect (PLCD), anterior lingual cortical defect (ALSD), anterior buccal cortical defect (ABCD), and posterior buccal cortical defect (PBCD) (Table 1). Their pathogenesis is controversial. Some believe they all are secondary to pressure on the bone from a hyperplastic salivary gland, which leads to atrophy or resorption of bone and in some cases leaves residual salivary gland tissue (92). Others believe they are congenital developmental abnormalities or anatomic variants (93). Since they vary in their locations and radiographic and histologic appearances, they are discussed separately, although many of the studies in the literature combine all of the groups.

Posterior Lingual Cortical Defect

PLCD was originally described by Stafne in 1942, and these lesions often go by the eponym, Stafne cyst or Stafne defect. However, this benign lesion has a plethora of synonyms, including latent bone cyst, mandibular embryonic defect, aberrant salivary gland defect, ectopic glands of the mandible, lingual mandibular bone concavity, idiopathic bone cavity, congenital defect, or depression of the mandible containing salivary gland tissue, static bone cavity, and developmental lingual salivary gland depression.

PLCD is a solitary, static, cortical depression usually located between the angle of the mandible and the first molar, below the myohyoid line, and inferior to the mandibular canal. A less frequent location is in the ascending ramus, either along the posterior border inferior to the condylar neck or in the mandibular sulcus superior to the mandibular foramen (94). Patients are usually asymptomatic, and therefore PLCD is usually an incidental finding. It almost exclusively occurs in men in the fifth to seventh decades of life. This older age of occurrence lends some support to it being an acquired lesion rather than embryologic. However, there are case reports of PLCDs in children (93).

Radiologic features of PLCD. PLCD is a radiolucent, well-circumscribed, round or oval lesion. It ranges in size from a few millimeters to several centimeters and has a dense sclerotic edge. When

Table 1 Cortical Defects of the Mandible

	Location	Age	Gender	Histology
PLCD	Between the angle of the mandible and first molar	60–70 yr	Men (almost exclusively)	Salivary gland, lymphoid or adipose tissue
ALCD	Anterior to the 1st molar	40–50 yr	M:F, 5:1	Salivary gland, adipose tissue
ABCD	Bilateral, between the basal and alveolar parts of the mandibular body	Children	No predilection	Salivary gland, adipose tissue
PBCD	Posterior to the molars, superior to the mylohyoid line	40–50 yr	Men (almost exclusively)	Devoid of ectopic tissue

Abbreviations: PLCD, posterior lingual cortical defect; ALCD, anterior lingual cortical defect; ABCD, anterior buccal cortical defect; PBCD, posterior buccal cortical defect.

oval, the widest diameter of the defect is parallel to the inferior border of the mandible (94). The depression is open on the lingual surface with an intact corticated base, which is well appreciated on CT imaging (95). On plain films, small lesions may be difficult to discern, since a good portion of the cortical plate must be resorbed before it can be visualized.

Pathologic features of PLCD. Since these lesions are not progressive and imaging is usually diagnostic, biopsy is usually unnecessary. Occasionally, the presentation may be atypical and the differential diagnosis may include aneurysmal bone cyst (ABC), ossifying fibroma, traumatic bone cyst, and osteoporotic bone marrow defect. Grossly, PLCD is usually a well-circumscribed, single or multilobular, round-to-oval concavity or depression. Most contain salivary gland tissue, while others demonstrate fat, muscle, or lymphoid tissue. There is minimal or no reactive bone adjacent to the defect.

Anterior Lingual Cortical Defect

This variant is typically found anterior to the first molar and in the canine, the premolar, and, less frequently, in the incisor region. It too is usually asymptomatic and occurs in men five times more frequently than women (9), most commonly in the fifth and sixth decades of life.

Radiologic features of ALCD. These are round-to-oval smooth depressions with intact buccal and lingual cortical plates. As opposed to PLCD, ALCD has poorly defined radiolucent areas with no sclerotic edges and retains its normal trabecular pattern. CT scan is usually diagnostic. However, given their location, they can be confused radiographically with an odontogenic keratocyst or periapical granuloma (50).

Pathologic features of ALCD. Like the PLCD, most ALCDs contain salivary gland tissue and, less frequently, fat and connective tissue.

Anterior Buccal Cortical Defect

ABCD is a bilateral defect that, unlike PLCD and ALCD, has a propensity to occur in children. It has a prevalence of about 20%. ABCD extends from each side of the symphysis from the mental protuberance to the area of the mental foramen and in between the basal and alveolar parts of the mandibular body, usually below the level of the mental foramen (94).

Radiologic features of ABCD. Kaffe et al. found the average measurements to be 1 to 1.5 cm long, 0.3 to 0.6 cm wide, and 0.1 to 0.4 cm deep, with the long axis running parallel to the inferior border of the mandible (96).The depression regresses over time. The depth impacts the radiographic findings, and these can be radiolucent or radiopaque. The borders can be well circumscribed or poorly formed. The features overlap with ALCD, but the two entities can be differentiated by the age of the patient (ALCD occurs in adults, ABCD in children) and the nature of the lesion on subsequent films (ABCD will regress, ALCD will progress or stay static).

Pathologic features of ABCD. Because of the classic radiographic findings, biopsy is almost never needed. Occasionally there may be abnormal growth or atypical imaging findings prompting surgical intervention.

Posterior Buccal Cortical Defect

PBCD is a rare variant of the cortical defects. Kocsis et al. described four cases (out of 8282 specimens) (97). All cases occurred in men in their 40s and 50s. PBCDs are usually less than 1.5 cm and are located posterior or lateral to the molars and superior to the mylohyoid line, with their long axis oriented anteroposteriorly.

Radiologic features of PBCD. PBCD is either radiolucent or radiopaque and less than 1.5 cm. The mean measurements from the four cases described by Kocis et al. were 1.3 cm $\times$ 0.6 cm $\times$ 0.5 cm (97).

Pathologic features of PBCD. These lesions are often devoid of ectopic tissue, inflammation, or reparative changes.

G. Paget's Disease

Paget's disease or osteitis deformans is a process of impaired bone remodeling that ultimately results in disorganized bone formation. It usually occurs in adults older than 60 years, although familial chronic hyperphosphatemia may represent a variant that occurs in children (98). Up to 40% of people with Paget's disease have a family member also affected (99). The gene candidate has been isolated to chromosome arm 18q and demonstrates variable expression within individuals (100). This accounts for the familial tendency but variable severity (101). Additionally, osteoclasts and their precursors contain paramyxoviral transcripts, suggesting a virally mediated disease in genetically susceptible people (102,103). It is postulated that osteoclasts infected with the virus produce abundant IL-6 (104). Approximately 1% of patients with Paget's disease will develop an osteosarcoma. Interestingly, an osteosarcoma suppressor gene on chromosome 18q near the Paget's disease locus has been identified in sporadic osteosarcomas (105).

The marked osteoclastic activity causes massive bone resorption and, simultaneously, osteoblastic bone deposition. The acute phase results in woven bone that subsequently gets resorbed and deposited again. This disorganized bone is primed for fractures, arthritis, bone deformities, and rarely sarcomas. Although any bone can be involved, it most commonly affects the pelvis, spine, and skull. It is usually mono-ostotic but occasionally multifocal. Paget's disease can occur essentially anywhere in the head and neck, including the mandible, skull, sinuses, and, less commonly, the larynx. Depending on the location, Paget's disease of the craniofacial bones can result in auditory, vestibular, or ocular neurologic problems (106).

Radiologic Features

Early phase lesions are typified by radiolucency but late stage Paget's show dense bone with obscuring of the distinction between the cortical and cancellous bone. This feature can mimic primary and metastatic malignancies (Fig. 14).

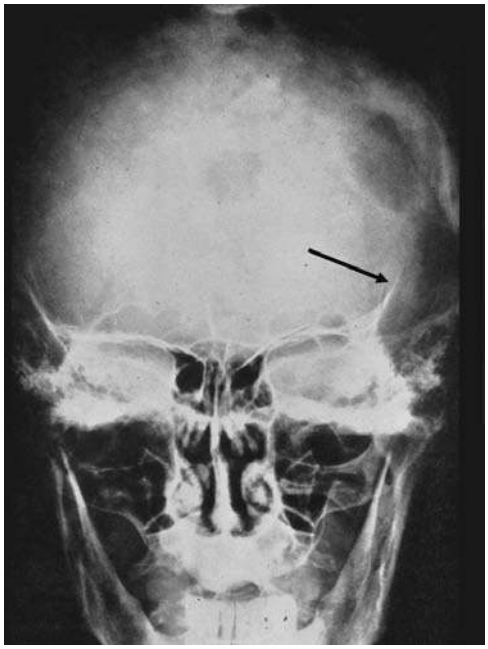

Figure 14 Plain film of Paget's disease showing the radiolucent and radiopaque lesions. The left occipital bone has developed an osteosarcoma (*arrow*).

Pathologic Features

The lesions vary depending on chronicity. Acute lesions are characterized by irregular trabeculae composed of disorganized woven bone. The trabeculae are hypercellular and lined by abundant osteoclasts with numerous nuclei. The normal fatty or hematopoietic marrow is often replaced by hypervascular, loose connective tissue. Chronic Paget's disease demonstrates thickened trabeculae (from the massive bone deposition) with increased cement lines, often best appreciated on polarization (Fig. 15).

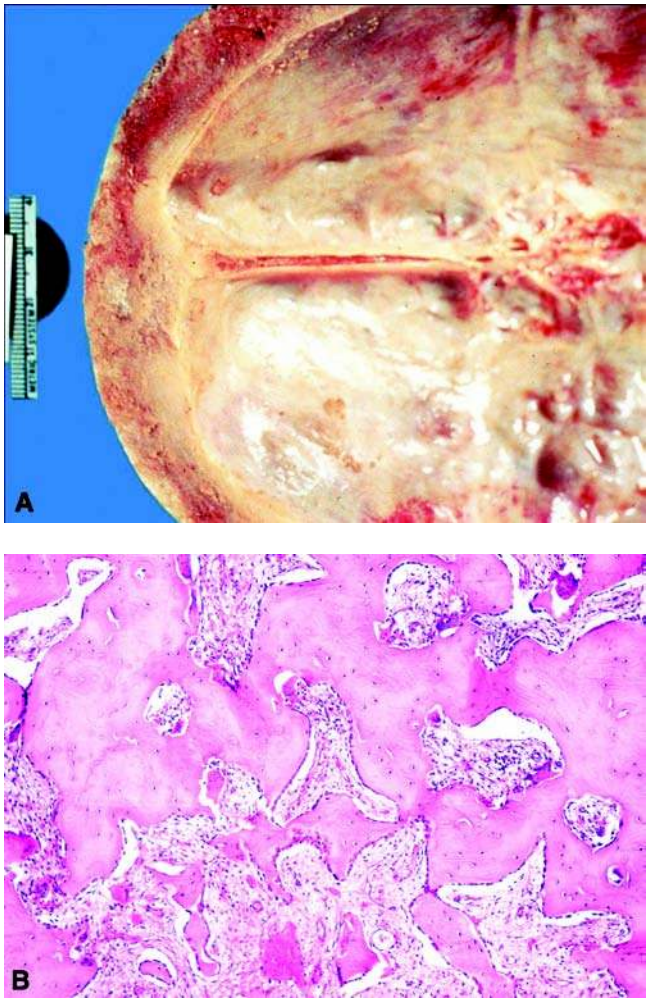

Figure 15 Cranium from a patient with Paget's disease showing the thickened bone. (**A**) Characteristic histology of late stage Paget's disease demonstrating the thickened trabeculae with increased cement lines (H&E, 200×). *Abbreviation*: H&E, hematoxylin and eosin.

H. Fibrous Dysplasia

FD is a developmental abnormality of the remodeling of primitive bone to lamellar bone. The end result is the replacement of medullary bone by irregular trabecular bone embedded in a fibrous matrix. This results in low mechanical strength leaving the site predisposed to fractures and deformities. It occurs in people younger than 30 years and is often an incidental finding on standard radiography. The most common sites of involvement are the jaw, skull, ribs, and femur. FD can involve most of the bones in the head and neck, including craniofacial bones, sinuses, and, rarely, the larynx and trachea (107,108).

Most cases are unifocal, but it can be polyostotic and affect multiple bones. Polyostotic FD can be associated with McCune Albright syndrome and Mazabraud syndrome. McCune Albright is characterized by multifocal FD, café au lait spots, endocrine abnormalities, and precocious puberty. Mazabraud syndrome is FDs associated with muscular myxomas. Patients with McCune Albright syndrome as well as some with monostotic and polyostotic FD have been found to have a G1$\acute{\alpha}$ gene mutation (GNAS1, guanine nucleotide–binding protein α-stimulating activity polypeptide 1). G1$\acute{\alpha}$ is located on chromosome 20 and has been identified in other endocrine disorders. One of the effects of this mutation is an increase in cAMP, which in turn can increase IL-6, a potent stimulator of osteoclasts (109).

FD is often an incidental finding, and the true prevalence in unknown. While many lesions can be managed without surgical intervention, some need to be excised to control pain or to treat/prevent fractures and deformities.

Monostotic Fibrous Dysplasia

This accounts for 80% of known FD cases and affects both genders equally. Although the ribs and femur are the most commonly involved bones, 10% to 20% of

monostotic FD cases occur in the head and neck. The maxilla and mandible are the most common sites of monostotic FD in the head and neck, followed by ethmoid, sphenoid, and temporal bones (110).

Polyostotic Fibrous Dyspalsia

FD is called polyostotic when it involves two or more bones. It accounts for 20% of all cases and occurs more frequently in females. Polyostotic FD has a spectrum of severity. It can be confined to one region of the body or involve essentially every bone. The bones most commonly involved in polyostotic FD are the femur, tibia, fibula, ilium, metacarpals, ribs, and humerus. Up to 50% of people with polyostotic FD have involvement of the bones in the head and neck, most commonly the maxilla and mandible.

A distinct pattern of multiple foci of FD confined to the head and neck is referred to as craniofacial FD (111). Multiple FD foci develop but are isolated to a single anatomic site. They usually involve the maxilla but can also affect the sphenoid, zygoma, frontonasal bones, and base of skull (3).

Radiologic Features

On plain films, the lesions are radiolucent with a ''ground-glass'' appearance and have a sclerotic rim. The lesions have a clear medullary predominance but obscure cancellous and cortical bone (109). Rarely, FD can have abundant cartilage, making the lesion more challenging to characterize. This occurs most commonly in a fracture site. By CT, the lesions are poorly defined, merging into adjacent bone.

Pathologic Features

Grossly, excised foci of FD are white to yellow with a gritty consistency secondary to the numerous small trabeculae. Microscopically, the lesion is characterized by fibrous stromal cells, variable amounts of collagen, and irregular trabeculae (Fig. 16A). The spindle cells are plump but bland and mitotically inactive. These cells make woven bone and produce the angulated, irregularly shaped trabeculae, commonly characterized as Chinese letters (Fig. 16B). The bone is generally not rimmed by osteoblasts; however, the presence of osteoblasts does not exclude a diagnosis of FD (112). Typically, the lesions merge smoothly into surrounding cancellous or cortical bone rather than being sharply delineated such as in ossifying fibroma (113). In the jaw, focal psammomatoid calcifications can be found, but they should not be diffuse (3). In the craniofacial bones, FD may have areas of lamellar bone, a feature not recognized in other locations (3).

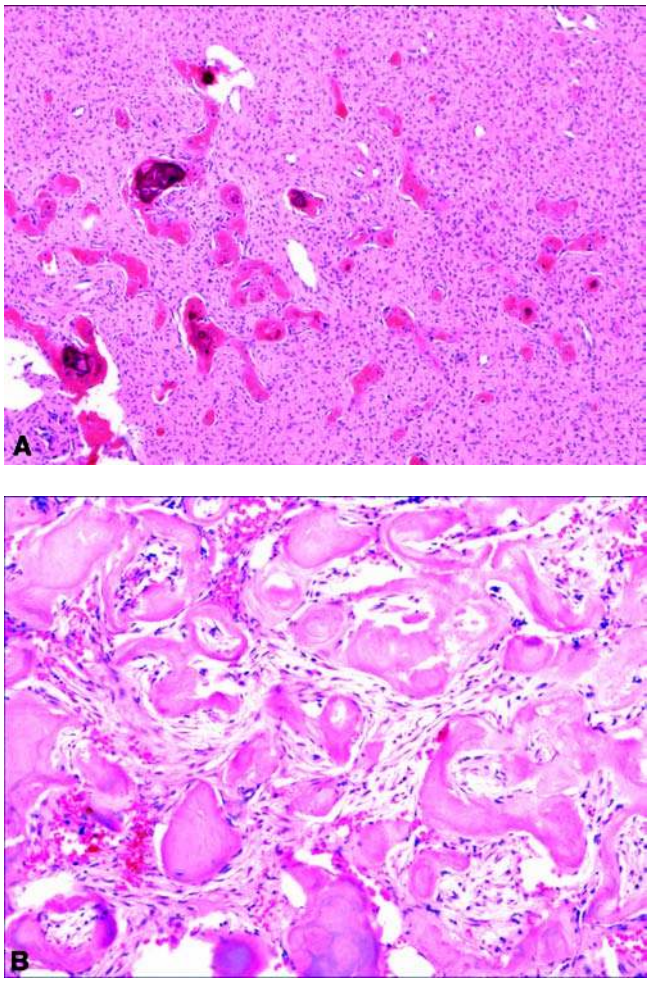

Figure 16 Low magnification of demonstrating a cellular fibrous stroma and irregular trabeculae (H&E, 100×). (**A**) High magnification of fibrous dysplasia highlighting the irregular trabeculae without osteoblastic rimming (H&E, 400×). *Abbreviations*: FD, fibrous dysplasia; H&E, hematoxylin and eosin.

I. Cemento-Osseous Dysplasia

Cemento-osseous dysplasia is a nonneoplastic condition that occurs exclusively in the tooth-bearing regions. In a study of 241 cases of cemento-osseous dysplasia Su et al. found that there was a predilection for black women with a peak incidence in the fourth and fifth decades of life (114). Cemento-osseous dysplasia is divided into three subtypes: periapical, florid (bilateral), and focal. Lesions are typically less than 2 cm, asymptomatic, and found incidentally on dental radiographs (114). Occasionally, cemento-osseous dysplasia will produce dull pain or drainage, particularly in denture-associated alveolar atrophy or in regions of prior tooth extraction (111). When florid, they are usually symmetrically bilateral or symmetric in all the four jaw quadrants. When cemento-osseous dysplasia is focal, the posterior mandible is the most common location (115).

Radiologic Features

Cemento-osseous dysplasia has a classic radiographic appearance and the diagnosis can be made without biopsy in many cases. The appearance will depend on the age of the lesion and the amount of mineralization. These can be radiolucent or radiodense or mixed with a radiolucent halo located in a tooth-bearing area (116). They are located at tooth apices or in areas of

previous extraction sites. The imaging characteristics can overlap with Paget's disease. However, Paget's disease is usually polyostotic, involving bones beside the jaw. Additionally, Paget's disease has an associated elevated serum alkaline phosphatase, which is not seen in osseous dysplasia (117).

Pathologic Features

Bone is replaced by woven bone and acellular round concretions of basophilic cementum (116). The dense mass of anastomosing trabeculae and cementum-like calcifications are embedded in a fibroblastic background. The peripheral regions often have more discernable globular cementum-like calcifications.

J. Cranial Fasciitis

Cranial fasciitis is a nonneoplastic inflammatory process similar to nodular fasciitis. It occurs almost exclusively in children, usually within the first two years of life, although case reports in adults and in patients after radiation to the skull do exist (118). It is thought to be a proliferation of fibroblasts and myofibroblasts, often with an antecedent trauma. Although it usually arises in the subcutaneous soft tissue, it commonly erodes into the skull and can extend intracranially, giving an aggressive, sarcomatous impression. It often grows quickly but usually remains less than 3 cm in greatest dimension. Cranial fasciitis almost never recurs when it is completely excised (119). Recognition of the entity is critical to avoid overtreatment (120).

Radiologic Features

Since cranial fasciitis is actually a soft tissue lesion that can erode into bone, imaging will convey a single lytic defect with an associated soft tissue component (121). By MRI, the lesion is usually isointense to skeletal muscle (122). There may be a thin sclerotic rim, although periosteal new bone formation can be seen, giving the illusion of a more aggressive process (121).

Pathologic Features

Histologically, cranial fasciitis overlaps with nodular fasciitis and has a haphazard, ''tissue culture'' arrangement of spindle cells (121). Myxoid and vascular stroma is common. Scattered inflammatory cells are seen (Fig. 17). Mitotic rate can be brisk (123).

Immunohistochemistry

The spindle cells of cranial fasciitis are positive for vimentin and smooth muscle actin and negative for S100 and CD1a, which can help differentiate it from Langerhan's cell histiocytosis (124).

K. Cherubism

Cherubism is an autosomal dominant disease with 100% penetrance in males and 70% penetrance in females. This benign fibro-osseous lesion results in painless symmetric expansion of the mandible

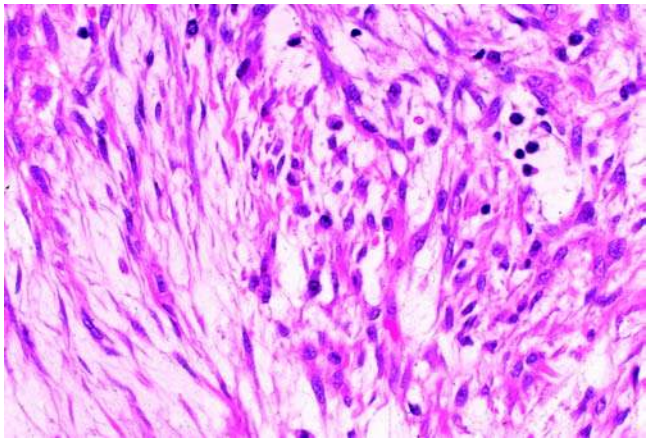

Figure 17 Cranial fasciitis demonstrating the haphazard arrangement of myofibroblasts and scattered inflammatory cells. These benign lesions can erode intracranially, giving the appearance of a malignant lesion.

(Fig. 18A). It typically affects children aged two to four years and results in maximal enlargement two years after onset. At this point it tends to remain static and in the teenage years may undergo spontaneous involution. Maxillary lesions often regress first followed by mandibular ones.

Genetic mutations in the SH3BP2 gene on chromosome 4 have been implicated. This mutation is believed to result in Msx-1 activation, which impedes the cap stage of molar development. This results in increased bone formation and deposition of fibrohistiocytic tissue. Some use a 4- or 5-point grading scale to score the severity of the disease (125). Children with cherubism have a characteristic renaissance cherub facies with rounded jaws and prominent cheeks. More severe cases result in verticle displacement of the orbital floor, resulting in laxity of the lower lids and the eyes pointing upward (''eyes-to-heaven'' appearance) (125).

Since the usual course is involution, mild cases of cherubism are often followed clinically. More severe lesions may require surgical intervention (125).

Radiologic Features

Radiographically, cherubism is characterized by bilateral, symmetric radiolucent lesions in the jaw, with thick sclerotic borders (Fig. 18B) (126). The dentition is abnormal with some tooth agenesis, root resorption, V-shaped palate, and malocclusion (125).

Pathologic Features

Histologically, cherubism is essentially identical to giant cell granuloma and is characterized by osteoclast-like giant cells embedded in a fibrous vascular stroma (see pathologic features in section ''Giant Cell Granuloma''). Hemosiderin-laden macrophages are common (125). Depending on the age of the lesion, dense sclerosis may be present. Deposition of eosinophilic amorphous material around small capillaries is a

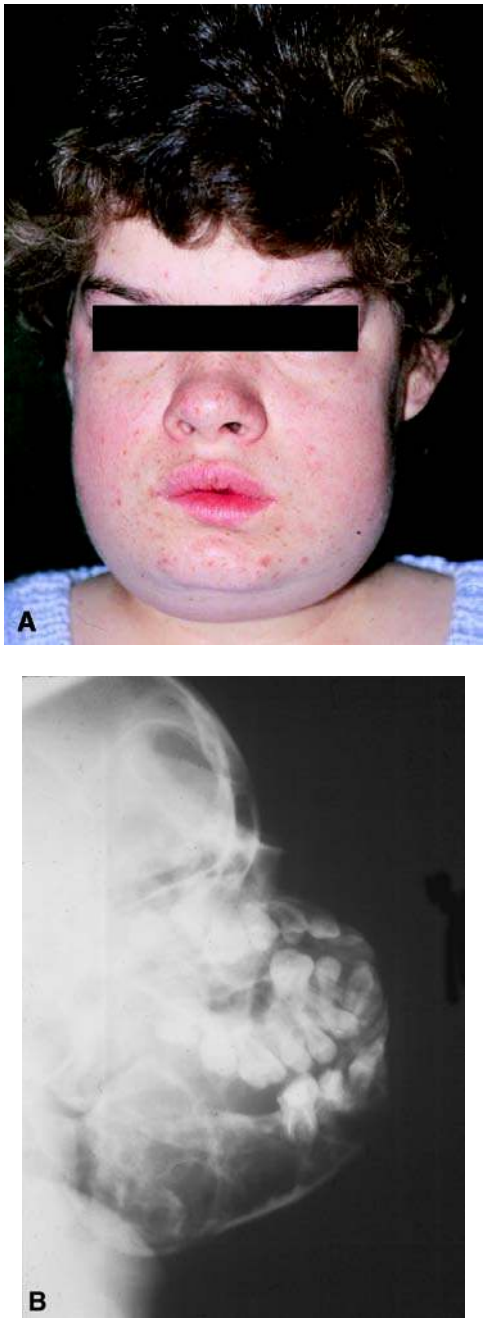

Figure 18 Patient with cherubism. Note the bilateral jaw enlargement. Plain film showing the increased bone formation in cherubism.

common finding and is considered pathonomonic for cherubism (Fig. 18) (127).

IV. NEOPLASTIC DISEASES OF THE BONE AND JOINTS, OSSEOUS AND CHONDROID

A. Exostosis and Osteoma

Exostosis simply means bony protuberance, and these commonly affect the head and neck, most frequently the palate and the lingual aspect of the mandible (near the premolars and canine areas) and the external auditory canal (128). Most consider it a reactive condition such as from dental work, buccal lacerations, and chronic immersion of the ear in cold water. While they are often asymptomatic, they can cause deformities and hearing difficulties. Lesions are often multiple.

Torus palatinus and mandibularis refer to bony protuberances of the palate and mandible, respectively. Torus palatinus occurs along the midline of the palate, varies in size, and is most commonly seen in people in their 20s. It can be idiopathic or as part of syndromes such as Primrose syndrome and chromosomal anomalies. It occurs in men and women with conflicting findings as to whether there is gender predominance (129,130). It does seem to vary among different ethnicities. In a study by Chohayeb, 448 women of a variety of ethnicities were evaluated for torus palatines; almost 70% of the participants had a torus, and it most commonly occurred in Hispanics and African-Americans (131). Genetic studies have suggested an autosomal dominant inheritance pattern (130). Torus mandibularis occurs slightly more frequently in men and may be influenced by temporomandibular disorders from jaw clenching and teeth grinding (132).

Osteomas are considered benign neoplasms that often have an associated antecedent trauma or infection (133). They have been reported in most age groups with the majority in the fourth and fifth decades of life. They rarely occur in the long bones and have a propensity for the head and neck, particularly the paranasal sinuses, external auditory canal, temporal bone and, less frequently, in the jaws (134). Those arising in the maxilla and mandible have a female predominance of 3:1, while those involving the sinuses have a male predominance of 2:1 (135).

Osteomas are classified as peripheral or exophytic when they arise from the periosteum, central when they arise from the endosteum, and extraskeletal when they arise in the soft tissue. They are usually single growths unless associated with Gardner's syndrome (colon polyps/adenocarcinoma, multiple osteomas, and epidermoid and dermoid cysts). Depending on the location, osteomas can result in deformities or malocclusion (136).

Radiologic Features

Peripheral osteomas are usually unilateral, less than 5 cm in greatest dimension, well-circumscribed pedunculated masses, which radiographically are attached to the underlying bone cortex with a broad base. The surrounding bone is usually unremarkable (i.e., no destructive changes) (136).

Pathologic Features

Histologically, they can be composed of compact lamellar bone with Haversian canals, trabeculae with marrow, or a mixture. Older lesions may be densely sclerotic. There are no reports of malignant transformation, and excision is usually curative. The differential diagnosis includes reactive new bone formation, densely ossified FD, or solid odontomas (135).

B. Osteochondroma

Osteochondroma is one of the most common bone tumors. Whether it is a true neoplasm is debatable, and some believe it to be the result of the growth of aberrant cartilage on the bone surface. It most commonly involves the metaphysis of long bones but can occur on flat bones. In the head and neck, osteochondromas have been reported in the skull, jawbones, and sinuses (137–139).

Radiologic Features

Osteochondromas have a characteristic mushroom-like growth that grows away from the nearest joint. The stalk and medullary cavity of the osteochondroma is in direct continuity with the surface and medullary cavity of the attached bone. Grossly, an osteochondroma contains a thin, even cartilaginous cap overlying the bony stalk.

Pathologic Features

Histologically, the surface of the osteochondroma is composed of periosteum from the underlying bone. The cartilaginous cap is composed of bland chondrocytes and often undergoes enchondral ossification at the base. The stalk is composed of bony trabeculae surrounded by fat or marrow. Occasionally, chondrosarcomas arise in an osteochondroma. Since these are often low-grade lesions, radiographic correlation is paramount. Features that support chondrosarcoma include a thickened cartilaginous cap (>2 cm), cystic degeneration, and invasion into the surrounding tissue. Cytologic atypia is not a helpful distinguishing feature, since this can be seen in osteochondromas.

C. Osteoid Osteoma

Osteoid osteomas are rare neoplasms that most commonly involve the long bones, although there are small case series involving the jaw, orbit, ear, and sinuses (140,141). There have been no reports of osteoid osteomas in the skull. They most commonly occur in the second decade of life with a 2:1 male to female ratio. The classic presentation of osteoid osteoma is a slowly progressive single lesion that is most painful at night and is relieved by aspirin. This is thought to be secondary to the production of prostaglandins (142). Some report excellent treatment by radiofrequency ablation (143).

Radiologic Features

It is not uncommon for pain to precede a radiographically detectable lesion. When detectable, these lesions are characterized by a well-circumscribed cortical-based mass composed of a radiolucent nidus surrounded by a dense sclerotic rim. As the lesion matures, the radiolucent central nidus may calcify and become radiopaque. The calcification begins in the center and grows outward, initially leaving a ring sequestrum (a ring of radiolucency around the central ossification) (144). The extent of the lesion is best seen on CT scan (145). Their radiographic characteristics overlap with osteoblastoma and, arbitrarily, lesions less than 1.5 cm are classified as osteoid osteoma. Other lesions that are in the differential diagnosis include intracortical abscess, osteosarcoma, eosinophilic granuloma, and metastasis (146).

Pathologic Features

Grossly, the nidus is characterized by a red, soft, granular region in an otherwise sclerotic bone. Histologically, the nidus is well delineated from the sclerotic periphery, often by a fibrovascular zone (Fig. 19A). If the nidus has not calcified or ossified, it is characterized by anastomosing thin, lacelike trabeculae lined by osteoblasts and with variable bone mineralization (Fig. 19B). The intervening stroma often has numerous osteoclasts and small thin-walled blood vessels. More

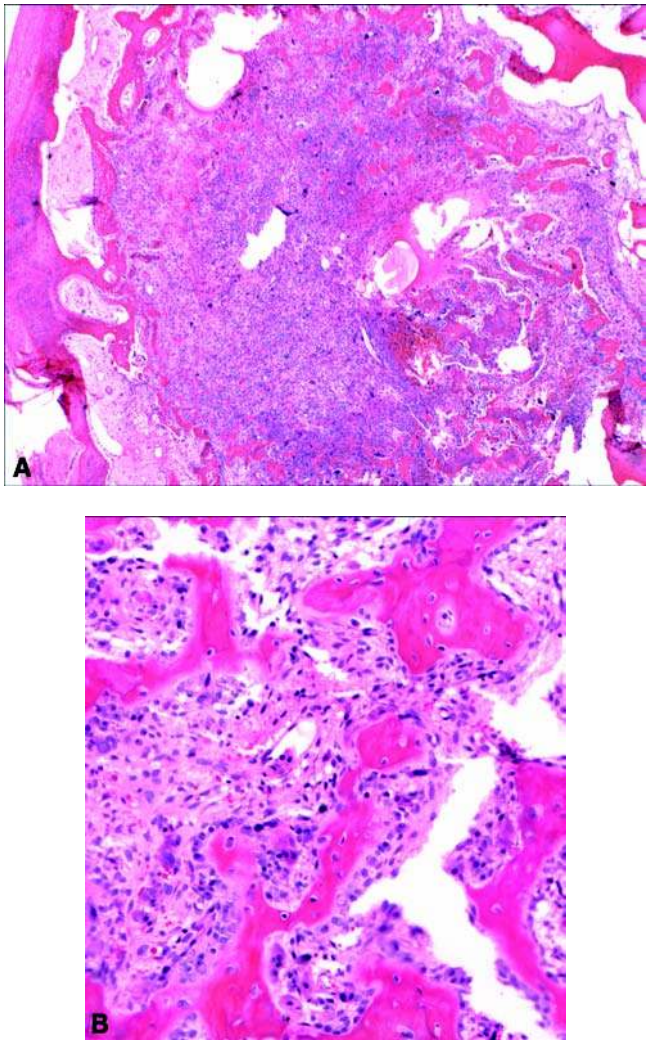

Figure 19 Osteoid osteoma is characterized by a sclerotic periphery and a cellular center/nidus (H&E, 100×). (**A**) The lacelike trabeculae of osteoid osteoma are lined by osteoblasts. The stroma is osteoclasts rich (H&E, 400×). *Abbreviation*: H&E, hematoxylin and eosin.

Table 2 Comparison of Osteoid Osteoma and Osteoblastoma

	Osteoid osteoma	Osteoblastoma
Most common location	Long bones	Spine
Most common location in the head and neck	Jaw, orbit (case reports)	Temporal, frontal, ethmoid bones
M:F	2:1	2:1
Age	< 30 yr	< 30 yr
Pain	Yes, often at night and relieved with aspirin	Not usually
Growth	Restricted	Progressive
Borders	Well circumscribed, radiolucent nidus	Well circumscribed
Size	< 1 cm	2–10 cm
Histology	Anastomosing thin trabeculae	Thin trabeculae, numerous giant cells
Radiographic features	Cortical-based with peripheral sclerosis	Medullary growth with slight peripheral sclerosis

mature lesions consist of well-mineralized trabeculae of woven bone and osteoid. Regardless of the age of the lesion, mitotic figures may be seen in the osteoblasts, but they should not be atypical. The sclerotic rim is composed of cortical or medullary lamellar bone. If only the sclerotic edge is biopsied, the sample will be nondiagnostic.

D. Osteoblastoma

Osteoblastomas share many radiographic and histologic characteristics with osteoid osteoma (Table 2). Also like osteoid osteomas, they usually occur in people younger than 30 years, and there is a male to female distribution of 2:1 (147). However, they are about one-fifth as common as osteoid osteomas (accounting for 3% of benign osseous tumors) and have a greater propensity for progressive growth. Additionally, instead of long bones, they tend to occur in the spine. Osteoblastoma rarely arises in the craniofacial bones. When it does develop in this location, it most commonly involves the temporal, frontal, and ethmoid bones (148). However, case series of osteoblastomas involving the maxilla, mandible, and occipital bones have been reported (149–151).

Radiologic Features

Osteoblastomas are medullary-based tumors, which range in size from 2 to 10 cm and are well-circumscribed, expansile, radiolucent lesions. The center usually demonstrates some stippled densities and may occasionally be sclerotic. Unlike osteoid osteoma, osteoblastoma does not usually have a dense sclerotic edge. However, older lesions can be extremely mineralized and appear radiopaque. In this scenario, CT scan and MRI can be helpful in discerning the extent of bone and soft tissue involvement (149).

Pathologic Features

The lesions are well circumscribed and red due to their high vascularity. If ossified, the lesion will be yellow and gritty.

Like osteoid osteoma, osteoblastoma does not permeate the cortical bone and is composed of a central nidus of anastomosing trabeculae lined by osteoblasts, which by definition is greater than 1.5 cm. The fibrovascular tissue is hypercellular (Fig. 20). Numerous

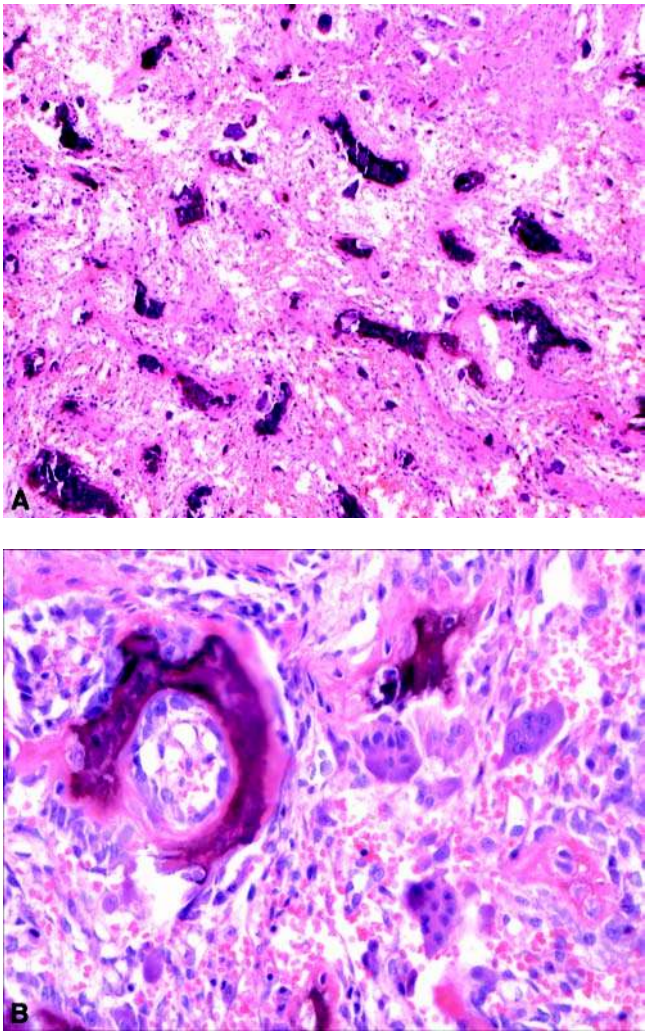

Figure 20 Osteoblastoma with hypercellular vascular stroma and irregular trabeculae (H&E, 200×). (**A**) High magnification of osteoblastoma demonstrating the irregular trabeculae with prominent osteoblastic rimming and numerous osteoclasts (note the similarity to osteoid osteoma). *Abbreviation*: H&E, hematoxylin and eosin.

Table 3 Histologic Features Helpful in Distinguishing Osteoblastoma from Osteosarcoma

	Osteoblastoma	Osteosarcoma
Cartilage Production	Never unless fractured	Yes
Tumor interface	Pushing, well-delineated margin	Infiltrative margin, uses lamellar bone as scaffolding
Stroma quantity	Prominent	Often scant
Stroma quality	Vascular, numerous osteoclasts	Zones of osteoid with little stroma
Mitoses	Focal, no atypical forms	May be focal, atypical forms common
Osteoblasts	Bland (except in bizarre osteoblastoma)	Atypical

giant cells may be seen in younger lesions, particularly around areas of hemorrhage. This can be confused with GCT, particularly on small biopsies (Fig. 20). ABC-like areas can sometimes be found (152). Although cellular, most osteoblastomas do not have cytologic atypia.

Occasionally, the histologic differential of osteoblastoma includes well-differentiated conventional osteosarcoma, and imaging may not be helpful in discerning the two processes (Table 3). Aggressive osteoblastomas may have worrisome radiographic features, and rarely well-differentiated osteosarcomas can have deceptively bland imaging characteristics. Examining the normal bone or tumor interface can be very helpful in differentiating the two lesions. Osteoblastoma typically grows in a pushing manner and has a well-defined tumor margin. Osteoblastoma abuts the normal lamellar bone, destroys it, and then replaces the bone with tumor; however, the interface remains sharp. Osteosarcoma invades the surrounding normal bone in an infiltrative manner and uses the trabeculae as ''scaffolding'' for growth of the tumor (135). Even invasion of the normal bone for more than a millimeter is a worrisome finding. Unless there is a fracture, osteoblastomas essentially never have a cartilaginous component. Therefore, if cartilage is part of the tumor, osteosarcoma should be considered. Other features helpful in discerning the two tumors include thick trabelculae with a generous amount of vascular stroma in osteoblastoma and compact tumor growth in osteosarcoma.

There is a variant called bizarre osteoblastoma in which there are scattered atypical multinucleated cells mimicking an osteosarcoma (153). However, there is usually little or no mitotic activity.

There is also a nonmetastasizing but locally destructive variant of osteoblastoma called aggressive osteoblastoma. Some have referred to this entity as a low-grade osteosarcoma or malignant osteoblastoma; however, most prefer the term ''aggressive osteoblastoma,'' given the clinical course and the histologic overlap with conventional osteoblastoma. These lesions maintain the trabeculae with prominent osteoblastic rimming, scattered osteoclasts-like giant cells, and the hypercellular fibrovascular stroma. However, aggressive osteoblastomas contain epithelioid osteoblasts, which are about twice the size of usual osteoblasts. Focal areas of ''lacelike'' osteoid may be seen but should not be prominent. In this scenario, the relationship of the lesion to the underlying cortical bone and the overall radiographic appearance is paramount in making the correct diagnosis.

E. Ossifying Fibroma

Ossifying fibroma is a general term for benign but locally aggressive fibro-osseous lesions composed of mesenchymal cells that calcify and ossify. Patients range from three-months old to elderly, with a predilection for women (154). Ossifying fibroma is distinct from FD in that they are generally well circumscribed and the trabeculae are rimmed by osteoblasts. The World Health Organization (WHO) in 1971 classified ossifying fibroma as a type of cementifying fibroma (155). To make this lesion more confusing, it is described in the literature by many names and subtypes including: cementifying fibroma, cemento-ossifying fibroma, desmo-osteoblastoma, psammo-osteoid fibroma, psammomatoid ossifying fibroma, and juvenile (aggressive) ossifying fibroma. Ossifying fibroma merely means a benign tumor with stromal, osteoid, and often cementum components.

Seventy-five percent of ossifying fibromas occur in the mandible and are amenable to local resection (156). Other sites affected include the maxilla and paranasal sinuses and rarely the temporal bone (154,157). These extramandibular locations are more challenging to resect and can result in proptosis, blindness, airway obstruction, and craniofacial deformities (158). Given the location of these tumors, it has been hypothesized that it is a result of the altered periodontum surrounding the teeth roots (159).

A subset of ossifying fibromas called aggressive psammomatoid ossifying fibroma (also called juvenile ossifying fibroma) occurs in children. This lesion has a predilection for the sinonasal region in young children (158). They can occasionally extend into the cranial cavity, resulting in marked neurologic manifestations (160).

Radiologic Features

Plain film and CT scan will show a well-circumscribed expansile mass with a thick outer surface and occasionally multiloculated, multicystic internal structure (Fig. 21). There is often peripheral calcification but no adjacent bone changes (161).

Pathologic Features

The tumors are usually well circumscribed, calcified, or gritty with areas of cystic degeneration, which are sometimes hemorrhagic (Fig. 22). They are composed of cellular and cystic stroma with lamellar and sometimes woven bone, rimmed by osteoblasts. When in the mandible, they are amenable to curettage, so a distinct bony capsule may not be appreciated.

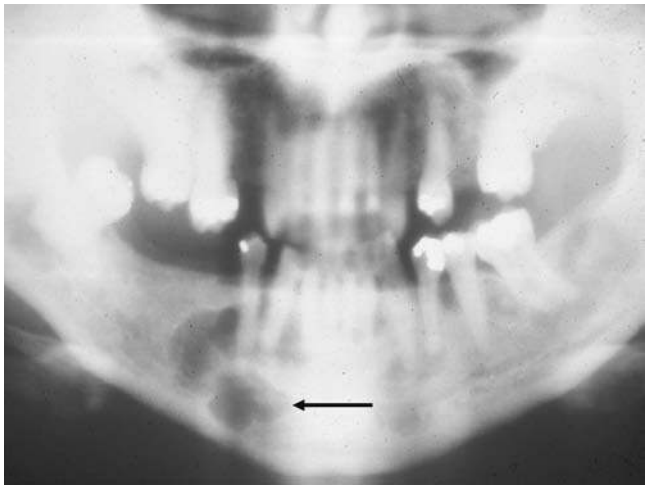

Figure 21 Plain film highlighting an ossifying fibroma. Note the well circumscribed nature of the lesion (*arrow*).

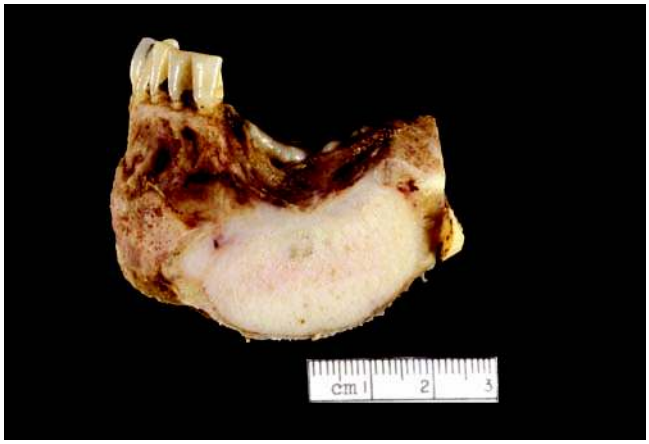

Figure 22 Central ossifying fibroma requiring partial mandibulectomy because of the large size and bone destruction.

The characteristic finding in psammomatoid ossifying fibroma is numerous lamellated ossicles resembling psammoma bodies (Fig. 23) (158). This variant can be mistaken for a sinonasal meningioma. Distinction rests on histologic features, as there is currently no reliable immunohistochemical test. Identifying cellular whorls of bland cells and syncytial growth of cells characteristic of meningioma is paramount to the diagnosis. Both psammomatoid meningioma and psammomatoid ossifying fibroma can be immunoreactive for epithelial membrane antigen, S100, vimentin, and CD10, and neither expresses cytokeratins (162).

F. Osteosarcoma

Osteosarcomas are a heterogeneous group of tumors with the commonality of osteoid matrix production.

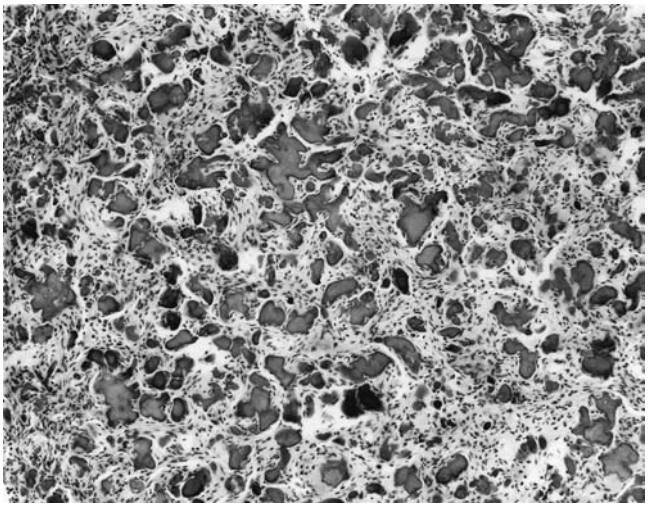

Figure 23 A classic central ossifying fibroma with round oval masses of cementum (H&E, 100×). *Abbreviation*: H&E, hematoxylin and eosin.

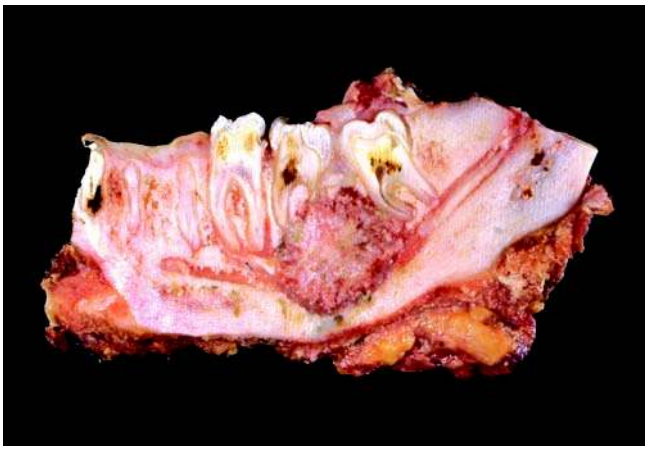

Figure 24 Resection of a mandible for a conventional osteosarcoma *Source*: Photo courtesy of L. Barnes.

Most osteosarcomas arise in children and young adults, usually in the appendicular skeleton. About 5% to 10% of osteosarcomas arise in the craniofacial bones, preferentially in the mandible and maxilla (Fig. 24) (163,164). Chromosomal anomalies, loss of heterozygosity, and gene amplifications are almost always found in osteosarcomas, although there is not one consistent finding. Syndromes are summarized in Table 4.

Gnathic Osteosarcoma

Within the craniofacial bones, the maxilla and mandible are the most frequently involved bones by osteosarcoma (165). Interestingly, in the case of osteosarcoma of the jaw, patients tend to be consistently older (in 30s and 40s) than those with osteosarcoma of the

Table 4 Select Syndromes and Associated Bone Lesions

Gardner's syndrome	Multiple osteomas
Gorham-Stout syndrome	Osteolysis (result resembles an hemangioma)
Hereditary retinoblastoma	Osteosarcoma
Langer-Giedion syndrome (a.k.a. tricho-rhino-phalyngeal syndrome with exostosis)	Exostosis
Li-Fraumeni syndrome	Osteosarcoma
Mazabraud syndrome	Fibrous dysplasia
McCune Albright syndrome	Fibrous dysplasia (polyostotic)
Paget's disease	Osteosarcoma, fibrosarcoma
Rothmund-Thompson syndrome (aka poikiloderma congenitale)	Osteosarcoma

Abbreviation: a.k.a., also known as.

appendicular skeleton. Typical complaints include swelling, loose teeth, or a change in tooth position (166). Additionally, gnathic osteosarcomas tend to be of low grade and have a more favorable prognosis (167). Some report a three-year disease-free rate of over 80% (164). This may in part be due to the ability to obtain clear margins (168). In fact, Patel et al. in a review of 44 cases of craniofacial osteosarcoma found that clear margins was the only independent factor to predict clinical outcome, which highlights the necessity of early diagnosis (164). This impact of margin status has been reproduced by others (169). Although irrefutably adjuvant chemotherapy for osteosarcomas of the long bones is beneficial to survival, its use in gnathic osteosarcomas is not as clear-cut with mixed conclusions in the literature (164).

Extragnathic Osteosarcoma

Jasnau et al. evaluated 48 patients with head and neck osteosarcomas over a 28-year period and found that in addition to margin status, an extragnathic site was a negative prognostic factor (166). Although Paget's disease, prior radiation, and conditions such as Li-Fraumeni syndrome and hereditary retinoblastoma can predispose to osteosarcoma, most cases are sporadic. Smith et al evaluated 496 cases of the head and neck osteosarcomas and found that the subtypes of osteosarcoma arising in gnathic- and skull-based osteosarcomas were similar. However, high-grade tumors were more commonly encountered in the skull and other craniofacial bones (67% high-grade histology in extragnathic sites compared with 53% in gnathic sites) (165). Metastatic potential has been reported to be greater in extragnathic sites, particularly the skull, although others have not found this correlation (164,166).

Radiologic Features

The radiographic findings can be variable. Conventional osteosarcomas are lytic, blastic, or mixed. In a review of 46 craniofacial osteosarcomas, Lee et al. found that all maxillary tumors originated from the alveolar ridge and most of the mandibular tumors began in the mandible body. As in osteosarcomas of the long bones, craniofacial osteosarcomas often exhibit cortical destruction and extension into the soft tissue. However, unlike long bone osteosarcomas, they often do not exhibit periosteal reactive bone (170). CT and MRI are often more helpful than conventional radiographs because of the numerous superimposed bones in the head and neck region. CT and MRI also aid in ascertaining the full extent of the lesion (intramedullary and soft tissue extension) and for identifying skip lesions or drop metastases (170,171).

Pathologic Features

The 2002 WHO classification scheme divides osteosarcoma into primary (with 7 subtypes) and secondary types. The primary types include conventional, parosteal, telangiectatic, small cell, low-grade central, periosteal, and high-grade surface. The secondary type encompasses syndrome and radiation-associated osteosarcomas. Conventional osteosarcoma is by far the most common type to involve the craniofacial bones followed by secondary osteosarcoma, with only case reports of parosteal osteosarcoma (172). All have ''malignant osteoid,'' although the quantity may be scant (Fig. 25). Osteoid is dense, pink, curvilinear amorphous collagen often arranged in a lacelike arrangement. Atypical osteoblasts are helpful in identifying malignant osteoid, but it is not uncommon for the malignant osteoblasts to be less anaplastic when embedded in the bone (referred to as ''normalization'' of malignant osteoid).

Conventional osteosarcoma is the most common type in the craniofacial bones (Fig. 24). It has a heterogeneous morphology, and the cells can be spindled, clear, epithelioid, plasmacytoid, or anaplastic

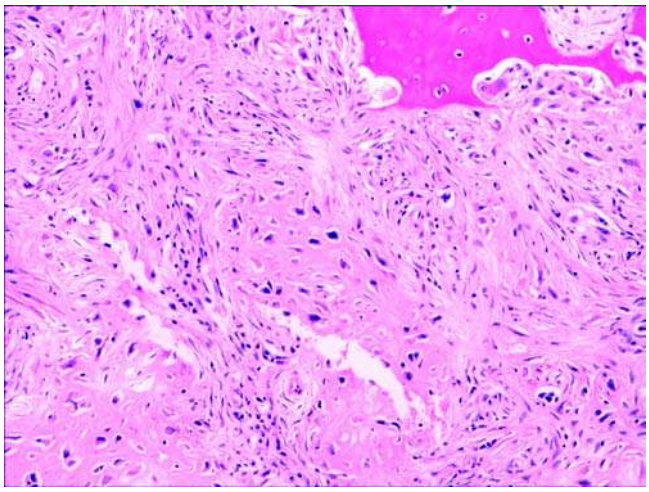

Figure 25 Conventional osteosarcoma with the typical ''malignant'' osteoid characterized by a lacelike network of mineralized new bone. Compare to the normal residual bone in the upper right-hand corner (H&E, 200×). *Abbreviation*: H&E, hematoxylin and eosin.

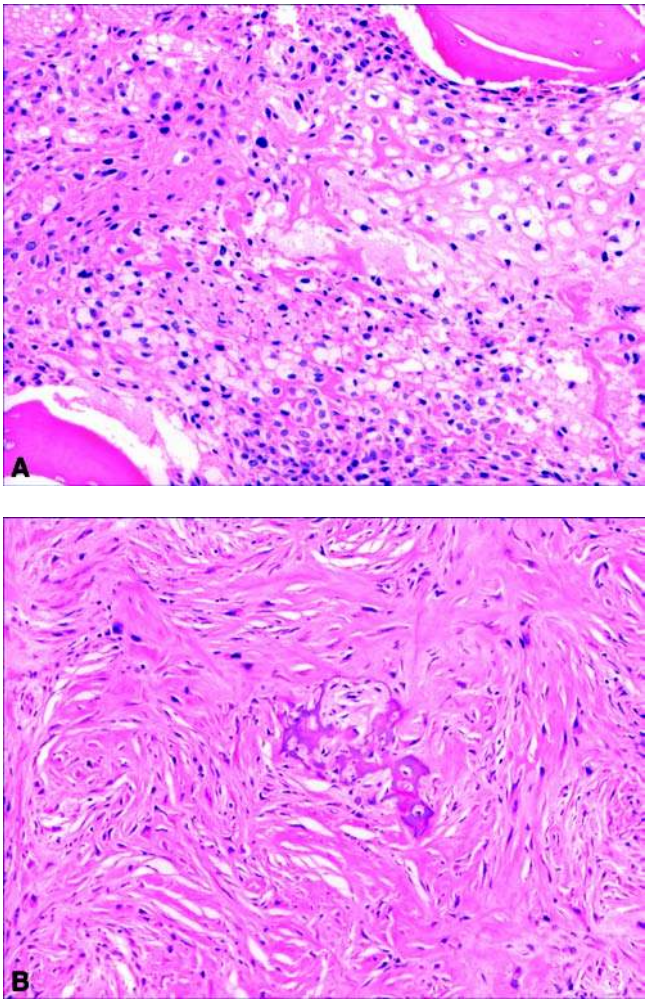

Figure 26 Chondroblastic osteosarcoma depicting both cartilaginous and osteoid components (H&E, 400×). (**A**) Fibroblastic osteosarcoma with focus of malignant osteoid (H&E, 400×). *Abbreviation*: H&E, hematoxylin and eosin.

giant cells. A mixture is often seen within the same tumor. Conventional osteosarcoma is divided into three subcategories depending on the predominant matrix formation: chondroblastic, fibroblastic, and osteoblastic (Fig. 26). There is controversial evidence as to whether there is prognostic differentiation among these subclassifications. From a diagnostic perspective, recognition of these subtypes is important for appropriate diagnosis, particularly on small biopsy samples, to avoid misclassifying a tumor as a chondrosarcoma or fibrosarcoma. In the craniofacial bones, chondroblastic osteosarcoma is the most common type followed by osteoblastic. Fibroblastic is rare except in radiation-associated osteosarcomas (see below).

Immunohistochemistry

Osteosarcoma is strongly positive for antibodies against CD30, CD68, CD117, and WT-1. Less than half will stain for EGFR and CD99. Scattered cells may express pancytokeratin, a trait that is important to remember when metastatic carcinoma is in the histologic differential diagnosis. Some p53 activity is usually appreciated. The significance is still controversial. Some have found that overexpression of p53 (> 50%) correlated with a worse prognosis in craniofacial osteosarcomas (163).

Parosteal Osteosarcoma

Parosteoal osteosarcoma (also called juxtacortical osteosarcoma) is a low-grade malignancy that arises on the cortical surface of the bone, most commonly the posterior femur. This rare variant accounts for 4% of all osteosarcomas and seldom occurs in the craniofacial bones, as reflected by few case reports in the literature (173). Regardless of the location, these osteosarcomas usually carry an excellent prognosis (174).

Radiographically, these are lobulated masses with a broad base attachment to the cortex of the involved bone. They often appear to wrap around the involved bone. Parosteal osteosarcomas are heavily mineralized with more concentrated mineralization near the bone attachment. Often they demonstrate bone spicules that blend into the soft tissue (175). About half of parosteal osteosarcomas have extensive cartilaginous differentiation. This can be so exuberant that it forms cartilaginous nodules or caps simulating an osteochondroma. As with other malignancies, CT scan and MRI can be extremely helpful in assessing the extent of disease, soft tissue extension, and satellite lesions (176). In studies of parosteal osteosarcomas of the long bones, hypervascular areas found on arteriogram often correlated to areas of dedifferentiation (177).

Pathologic features. Parosteal osteosarcoma can be deceptively bland. It is composed of bony trabeculae with interspersed hypocellular proliferations of spindle cells. Typically these exhibit only mild atypia. Cartilagenous differentiation is common, especially peripherally, and often bland. Although radiographically these can be confused with osteochondromas, histologically the presence of spindle cells and the absence of bone marrow elements should sway the pathologist away from this diagnosis. Nonossifying fibroma is also in the differential, particularly in small biopsies and when atypia is scarce. Imaging correlation is paramount in this scenario.

These tumors can dedifferentiate to a high-grade osteosarcoma, fibrosarcoma, or high-grade sarcoma not otherwise specified.

Telangiectatic Osteosarcoma

These rarely involve the craniofacial bones and are limited to rare case reports; therefore, discussion in this chapter is brief (178,179).

Radiographic features. Telangiectatic osteosarcoma is characterized by a medullary lytic mass without sclerotic edges and only minimal solid areas. There is often a wide transition zone, and occasionally matrix mineralization can be appreciated (180). Imaging characteristics overlap with ABC (181).

Pathologic features. These tumors are composed of giant cells admixed in a background of atypical spindle cells and large vessels. Low magnification will overlap with ABC, but the mononuclear cells always have some cytologic atypia.

Secondary Osteosarcoma

This group refers to osteosarcomas arising in a predisposing setting such as radiation therapy or a genetic syndrome (Fig. 14).

Radiation-Associated Osteosarcoma

Radiation-associated osteosarcomas are often of the conventional type and tend to be fibroblastic and of high grade. They usually arise at the edge of the radiation field, on average 10 to 15 years after radiation treatment (170). Although outcome varies in the literature, larger studies seem to demonstrate a trend toward worse outcome, when compared to de novo osteosarcomas of the craniofacial bones. McHugh et al. found that most patients with radiation-associated osteosarcomas died of disease within three years (163). All of their cases demonstrated high-grade histology. Despite the high-grade morphology, the high mortality rate was more often a result of locally aggressive disease rather than metastases. Additionally, they found that radiation-associated osteosarcomas have high p53 expression by immunohistochemistry more frequently than sporadic osteosarcomas.

Syndrome-Associated Osteosarcoma

Although over 50% of sarcomas arising in the setting of Paget's disease are osteosarcomas, the incidence is extremely rare, occurring in less than 0.5% of people with this condition. These osteosarcomas are usually high-grade osteoblastic or fibroblastic subtypes. Rare reports of telangiectatic and small cell osteosarcoma in the setting of Paget's disease exist (179). As discussed under Paget's disease above, there is evidence to support a genetic linkage of Paget's disease and an osteosarcoma tumor suppressor gene on chromosome 18q (182).

G. Extraosseous Osteosarcoma

This is an extremely rare variant of osteosarcoma that arises in the soft tissues, produces osteoid, and has no attachment to bone. It composes 4% of all osteosarcomas and 1.2% of all soft tissue sarcomas. By definition, it is pure osteosarcoma and is not part of a dedifferentiated sarcoma or mixed mesenchymoma (both of which can demonstrate osteosarcoma components). Most arise de novo, but up to 10% are postradiation osteosarcomas. Interestingly, these patients tend to be older than those with primary bone osteosarcomas and occur in people older than 50 years (183). Most cases occur in the soft tissues of the lower extremity and very rarely in the head and neck. Case reports exist of extraosseous osteosarcoma of the temporal region, orbit, parotid gland, tongue, larynx, and lip (184–187). Some, if not all, of these probably represent metaplastic carcinomas rather than true osteosarcomas. Wide local excision is the treatment of choice. Recurrence and metastases usually occur within two years.

Radiologic Features

Typical features of extraosseous osteosarcomas include a soft tissue mass that may be only slightly to massively mineralized. Extraosseous osteosarcomas may be well circumscribed or diffusely infiltrative with satellite nodules. Imaging is extremely important to exclude a primary osseous osteosarcoma (attachment to bone or cartilage) (183).

Pathologic Features

Grossly, the appearance will vary depending on the amount of mineralization. They can be fleshy and cystic or solid and calcified. They are identical to conventional osteosarcomas (see above). It is important to distinguish extraosseous osteosarcoma from the much more common and benign myositis ossificans. Features that support myositis ossificans are radiographic correlates such as a well-circumscribed mass with a central lucency (CT scan). Although the spindle cell component of myositis ossificans is often mitotically active, it does not harbor much cytologic atypia. Additionally, the periphery of myositis ossificans is mineralized, but malignant osteoid should not be present.

H. Cartilaginous Lesions

Although cartilaginous tumors account for less than 0.5% of all tumors of the head and neck, they are the most common mesenchymal lesions of the larynx, comprising 1% of all laryngeal tumors (188). Differentiating benign from malignant cartilaginous tumors can be extremely challenging, typically relying on imaging studies for differentiation. Often radiographic and pathologic features are inconclusive, and the diagnosis of ''low-grade cartilaginous tumor'' is the most appropriate interpretation.

I. Nasal Chondromesenchymal Hamartoma

Nasal chondromesenchymal hamartoma (also called mesenchymoma and chondroid hamartoma) is a rare tumor that typically presents as a polypoid mass in the nasal cavity and nasopharynx in children and adolescents (189). Symptoms correlate to the extent of the tumor and include nasal fullness, epistaxis, respiratory difficulty, proptosis, impaired eye movement, and hydrocephalus (190). There have only been 20 reported cases, and no malignant transformation has been described.

Radiologic Features

These lesions can appear deceptively aggressive with erosion and thinning of the bone and intracranial and intraorbital extension. Internal calcifications and cysts have been described (Fig. 27) (190).

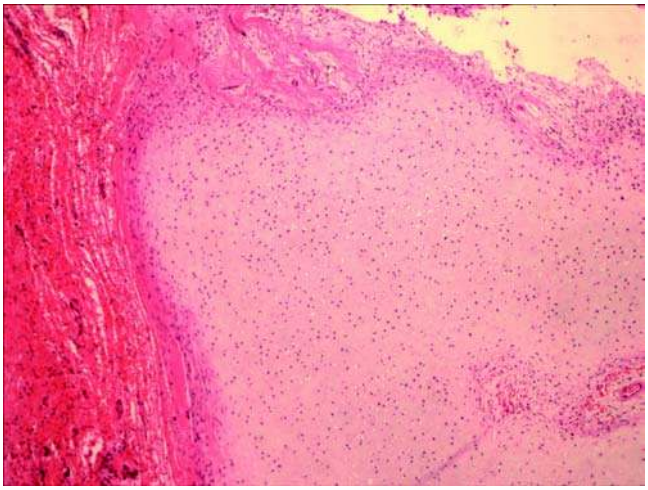

Figure 27 This chondromesenchymal hamartoma arose as a polypoid nasal mass in a 17-year-old girl. It recurred twice and she has subsequently been disease free. Chondromesenchymal hamartoma characterized by islands of cartilage embedded in a fibroblastic background (H&E, 100×). *Abbreviation*: H&E, hematoxylin and eosin.

Pathologic Features

Grossly, these tumors are pink to tan, soft to firm masses. Histologically, nasal chondromesenchymal hamartoma is characterized by islands of mature and immature hyaline cartilage with occasional binucleated chondrocytes (Fig. 28). The cartilage islands are embedded in a myxoid to cellular background with bland spindle cells, thought to be fibroblasts or myofibroblasts (191). Mitotic figures can be seen but should not be atypical (189).

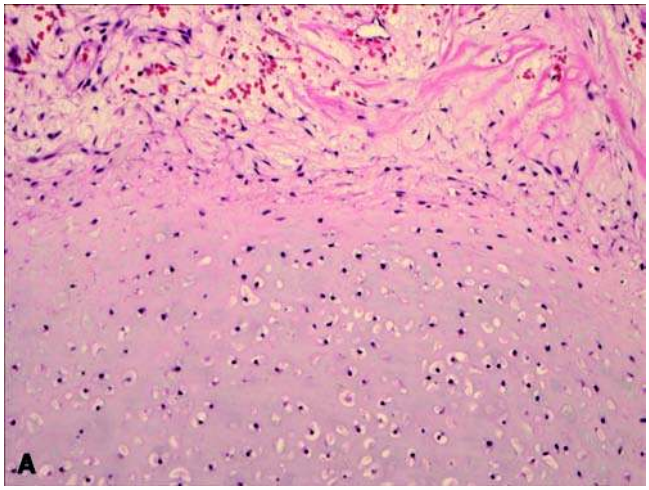

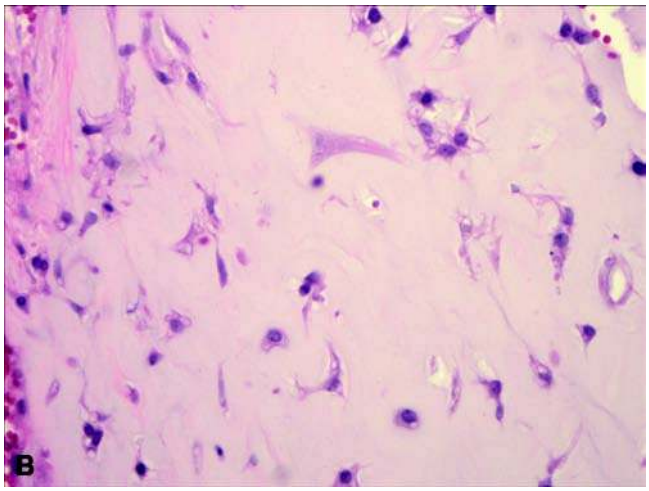

Figure 28 High magnification of chondromesenchymal hamartoma demonstrating the hyaline cartilage and occasional atypical cells [H&E; (**A**) 200×, (**B**) 400×]. *Abbreviation*: H&E, hematoxylin and eosin.

J. Chondroid Metaplasia of the Larynx

Chondroid metaplasia is a benign nonneoplastic lesion that is probably the result of trauma (192). One autopsy study found a prevalence of 2% (192). It typically occurs in the vocal cords and epiglottis and is not associated with the cartilaginous framework of the larynx (193). Most are of only a few millimeters and are asymptomatic, although hoarseness has been reported (188). When over 1 cm they may cause obstruction or hoarseness. Although nonneoplastic, they can be misdiagnosed as low-grade chondrosarcomas or benign mixed tumor (Table 5). It should also not be confused with normal laryngeal cartilage.

Table 5 Chondroid Lesions of the Head and Neck

	Location	Size	Growth pattern	Histology
Chondroid metaplasia	Vocal cords, epiglottis	$\leq$ 1 cm	Nonlobulated	Bland cartilage, indistinct borders
Chondroma	Larynx, sinonasal	Variable	Lobulated	Bland cartilage
Chondrosarcoma, low grade	Larynx, sinonasal	$>$ 1cm	Lobulated	Rare binucleation
Chondroblastoma	Temporal bone (rare in the head and neck)	$>$ 1cm (reports up to 10 cm in the temporal bone)	Lobulated, well-circumscribed	Spindled and plasmacytoid cells, osteoclast-like giant cells, chicken-wire calcification
Chondromyxoid fibroma	Mandible, maxilla (rare in the head and neck)	$>$ 1cm, usually $<$ 5 cm	Nodular	Peripheral cellularity, myxoid stroma, fine fibrous septa
Chondromesenchymal hamartoma	Sinonasal	Variable	Infiltrative	Islands of mature and immature cartilage, myxoid spindle cell stroma

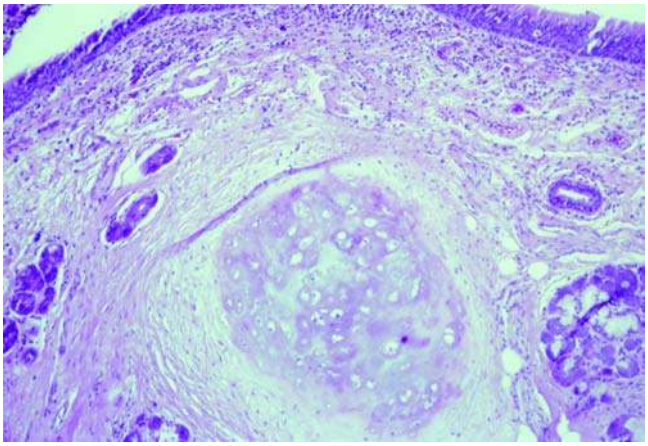

Figure 29 Incidental nodule of chondroid metaplasia of the laryngeal ventricle (H&E, 400×). *Abbreviation*: H&E, hematoxylin and eosin.

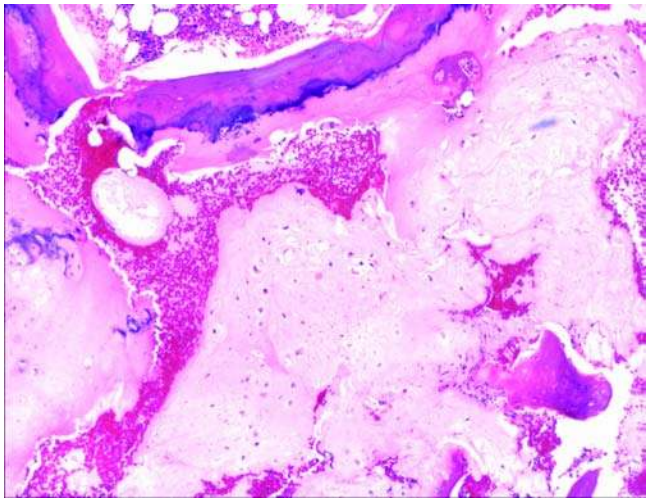

Figure 30 Chondroma demonstrating the typical bland cartilage. Differentation from low-grade chondrosarcoma can be impossible histologically.

Radiologic Features

The lesions may be single or multiple. They are nonlobulated with indistinct borders, often merging with the surrounding normal tissue (188).

Pathologic Features

Chondroid metaplasia typically has a nonlobulated growth pattern, which is distinct from most cartilaginous tumors. The lesions have poorly circumscribed borders that merge into the surrounding soft tissue (Fig. 29). The periphery often has a mucochondroid appearance (193).

K. Chondroma

Chondromas are benign neoplasms that have been rarely described in the larynx as well as the craniofacial bones. They most commonly involve the posterior lamina of the cricoid cartilage and thyroid cartilage and rarely the epiglottis (194). In these locations the most common presenting signs are difficulty in swallowing and dyspnea. In the larynx, small biopsies can be difficult to differentiate from chondrosarcoma and exuberant normal cartilage from the arytenoids (188,193).

Radiographic Features

The imaging characteristics overlap greatly with chondrosarcoma and are discussed in the following section ''Chondrosarcoma.''

Pathologic Features

Chondromas consist of bland cartilage. Differentiation of chondroma from low-grade chondrosarcoma may remain elusive, particularly when they involve the nasal cavity, sinuses, or larynx (Fig. 30) (195). When differentiation is not possible and imaging not helpful, we use the diagnosis of low-grade cartilaginous tumor. Distinction may not be of great diagnostic import, as both carry an excellent prognosis and are managed similarly (196). Both can recur but a low-grade chondrosarcoma can dedifferentiate and rarely metastasize.

L. Chondrosarcoma

Chondrosarcoma most commonly involves the pelvis, extremities, and ribs. One percent to twelve percent of chondrosarcomas occur in the head and neck region. When it does involve the head and neck, it almost exclusively involves the jaws and the hyaline cartilage of the larynx (associated with the cricoid and thyroid cartilage) (197). Less frequently, it involves the nasopharynx (198). A study of 111 laryngeal chondrosarcomas from the Armed Forces Institute of Pathology (AFIP) found a male to femal occurrence of 3.6:1 with the majority aged between 60 and 80 years (199). Koch et al. reviewed 400 cases of the head and neck chondrosarcomas from the National Cancer Database and found that laryngotracheal chondrosarcomas occurred more frequently in men (76% men) but sinonasal chondrosarcomas arose more frequently in women (65%) (197). It has been decribed after Teflon injections and radiation therapy but does not seem to be caused by smoking (199).

Surgical resection is the mainstay therapy. Recurrence is common but metastasis is rare, particularly for low-grade chondrosarcomas (193,200). Most studies quote a recurrence between 10% and 20% (197). Koch et al. found the five-year survival rate to be 87%. However, this encompasses all of the head and neck chondrosarcomas they studied and does not take grade or location into account (197). Dedifferentiated chondrosarcoma (high-grade sarcoma juxtaposed to a well-differentiated chondrosarcoma) carries a worse prognosis, although it seems to be

less aggressive than dedifferentiated chondrosarcomas of the axial skeleton (188,201).

Chondrosarcoma of the Larynx

Approximately 75% of laryngeal chondrosarcomas arise from the cricoid cartilage (particularly the posterior and posteriolateral portions), 15% to 20% arise from the thyroid cartilage, and 5% to 10% arise from the arytenoids and epiglottic cartilage. Symptoms depend on the location and include hoarseness, dysphagia, and fullness in the throat. In the Casiraghi et al. and Thompson et al. studies of laryngeal chondrosarcomas, none of the patients with low-grade or intermediate-grade chondrosarcoma died of disease (188,199). Batsakis et al. found a recurrence rate of 65% of laryngeal chondrosarcomas in their patients, but only 10% of them died as a direct result of their tumor (193).

Chondrosarcoma of the Jaw

Most chondrosarcomas of the craniofacial bones involve the jaws. The maxilla is most the frequent site (particularly the alveolar portion and the maxillary sinus) followed by the mandible. The location within the jawbones influences the signs and symptoms but includes nasal obstruction (maxillary primaries) to painless mass (more common in mandibular masses) to widened periodontal ligament space (198). Local recurrence occurs in about 20% to 35% of cases. Most are low-grade tumors and have a five-year survival of approximately 80%, with recurrence rather than metastasis being the biggest cause of mortality (197). Since chondroblastic osteosarcoma is a common type of osteosarcoma to involve the jaws, a pathologist should be extremely cautious about making a definitive diagnosis of chondrosarcoma of the jaw, particularly in younger patients and in small biopsies.

Radiologic Features

Chondrosarcoma of the head and neck can be extremely challenging to differentiate from benign cartilaginous tumors such as chondroma. Most show calcification; CT scan may be superior to plain films in identifying small calcifications. The tumors typically expand and displace the normal cartilage, but occasionally invasion and destruction of the cartilage may be discerned (Fig. 31). CT scan and MRI will assist in showing the extent of disease and the soft tissue tumor interface and aid in planning for adequate resection, but it does not necessarily aid in differentiating chondrosarcoma from chondroma (195). Some state that unless there is obvious destruction and invasion of the soft tissue, differentiation of chondroma from chondrosarcoma is impossible, radiologically (202).

Pathologic Features

Well-differentiated or grade 1 chondrosarcoma usually appears as a white, firm, lobulated mass (Fig. 32). Grade 1 chondrosarcoma is characterized by chondroid matrix with minimally atypical chondrocytes. Low-grade chondrosarcoma may be challenging or impossible to identify on the basis of histologic features alone (Table 5). In fact, Thompson and Gannon found associated chondromas in 41 of 111 laryngeal chondrosarcomas (199). Multiple chondrocytes per lacunae or binucleate chondrocytes are helpful, but not highly specific features. Grade 2 chondrosarcoma is moderately cellular with easily identified binucleate cells (Fig. 33). Mitotic figures are scarce. Grade 3 chondrosarcomas have atypia, binucleation, and easily identified mitotic figures (193). It is important to distinguish this from a chondroblastic osteosarcoma. The latter will contain osteoid (see previous discussion on osteosarcoma). Dedifferentiated chondrosarcoma by definition consists of a high-grade sarcoma juxtaposed to a well-differentiated chondrosarcoma.

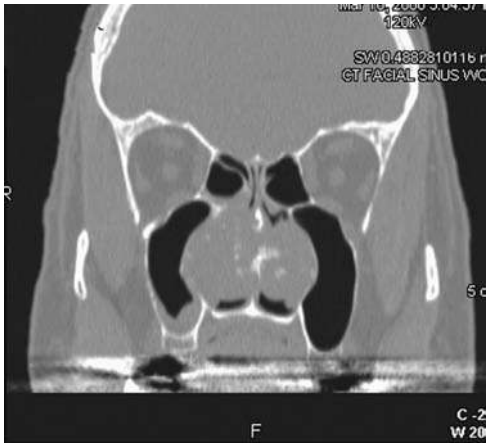

Figure 31 CT scan of a nasal cavity chondrosarcoma. Note the calcifications seen within the tumor.

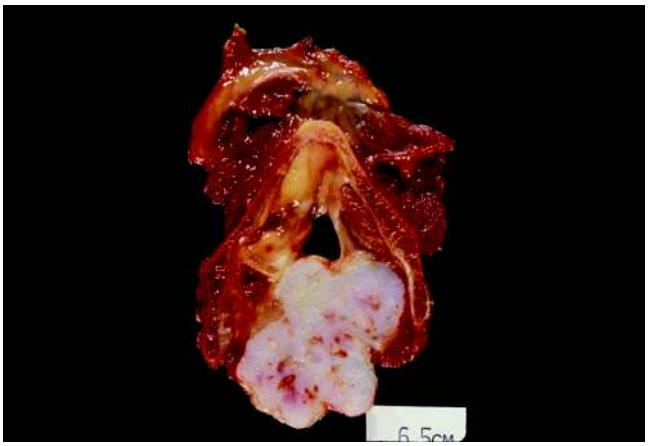

Figure 32 Section through the laryngeal glottis showing the lobulated growth pattern of chondrosarcoma of the posterior cricoid cartilage.

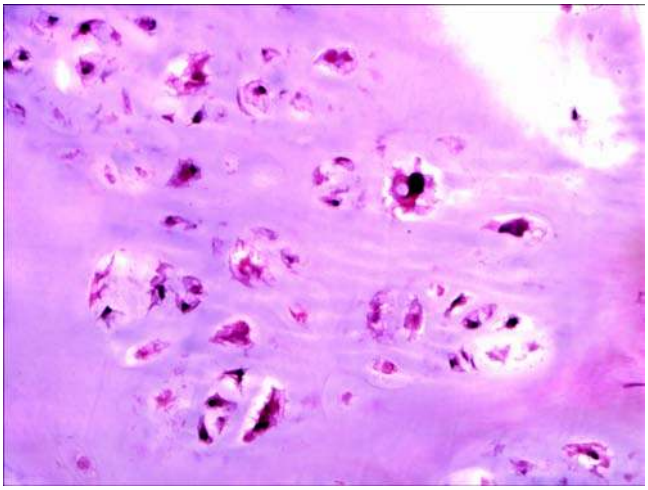

Figure 33 Grade 2 chondrosarcoma demonstrating binucleation and focal atypia (H&E, 400×). *Abbreviation*: H&E, hematoxylin and eosin.

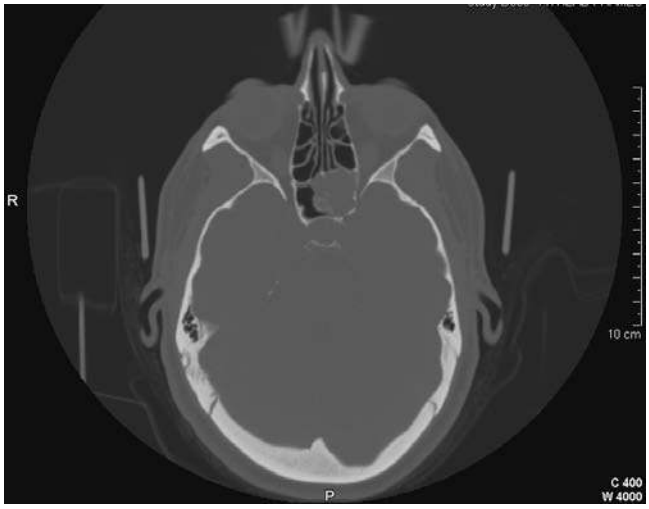

Figure 34 CT scan of a chondromyxoid fibroma involving the posterior nasal cavity and anterior sphenoid sinus. The radiologic differential diagnosis included inverted papilloma, lymohma, and chondroid neoplasms.

M. Chondromyxoid Fibroma

Chondromyxoid fibroma is a rare benign cartilaginous tumor that most commonly affects young adults (most occur between the ages of 10 and 30 years). Although it has a propensity to involve the metaphysis of long bones, particularly the tibia, essentially any bone can be involved. Approximately 2% of chondromyxoid fibromas arise in the craniofacial bones, most commonly the mandible and maxilla, followed by the nasal septum, sinuses, and skull base (203–205).

Radiologic Features

Chondromyxoid fibromas are sharply demarcated lytic lesions with scalloped margins. In flat bones, they are loculated and have irregular contours and can be locally destructive (Fig. 34) (206). Two large series found that 13% of chondromyxoid fibromas have mineralization or calcification that is found on plain films or CT scan (207,208). The cases reported in the craniofacial bones have been greater than 1 cm and less than 5 cm in greatest dimension (203). Those that arise in the skull base can be misinterpreted as chondrosarcoma or chordoma (206).

Pathologic Features

Grossly, the tumor is well circumscribed, lobulated with a blue-gray-white cut surface. Histologically, chondromyxoid fibromas are composed of nodules of myxoid or chondroid matrix with spindled to stellate bland cells and eosinophilic cytoplasm. The cell borders are usually indistinct and blend into the background matrix. The periphery of the lobule is cellular and the center is hypocellular and usually contains scattered osteoclasts-like giant cells (Fig. 35A). The large nodules are separated by narrow bands of fibrous tissue. The tumor often has a vague microlobulated architecture (Fig. 35B). ABC changes or chondroblastoma-like features are commonly found (207).

N. Chondroblastoma

Chondroblastomas are benign neoplasms with a propensity to occur in the epiphysis of long bones. They have been occasionally reported in the craniofacial bones, with 46 cases reported in the temporal bone (209,210). Most chondroblastomas occur in people aged between 5 and 25 years and occur in males twice as frequently as females. Interestingly, the reports of chondroblastoma arising in the temporal bone tend to involve an older population (third and fourth decade of life) (209). In the long bones, pain is the most common complaint. In the craniofacial bones, signs and symptoms depend on the location of the tumor but often include a nonpainful mass in the external auditory canal, tinnitus, vertigo, and hearing loss (209).

Radiologic Features

Radiographically, chondroblastomas are well-circumscribed, lobulated, osteolytic lesions with foci of calcification. They usually stay within the confines of the bone. On CT scans, chondroblastoma is a high-density mass with mild homogeneous enhancement (210). They may overlap with features of ABC but typically do not show the fluid levels seen in ABC. The caveat to this is that chondroblastomas can have ABC-like regions (211).

Pathologic Features

Chondroblastomas have a heterogeneous gross appearance and can be yellow, gray, or brown. If

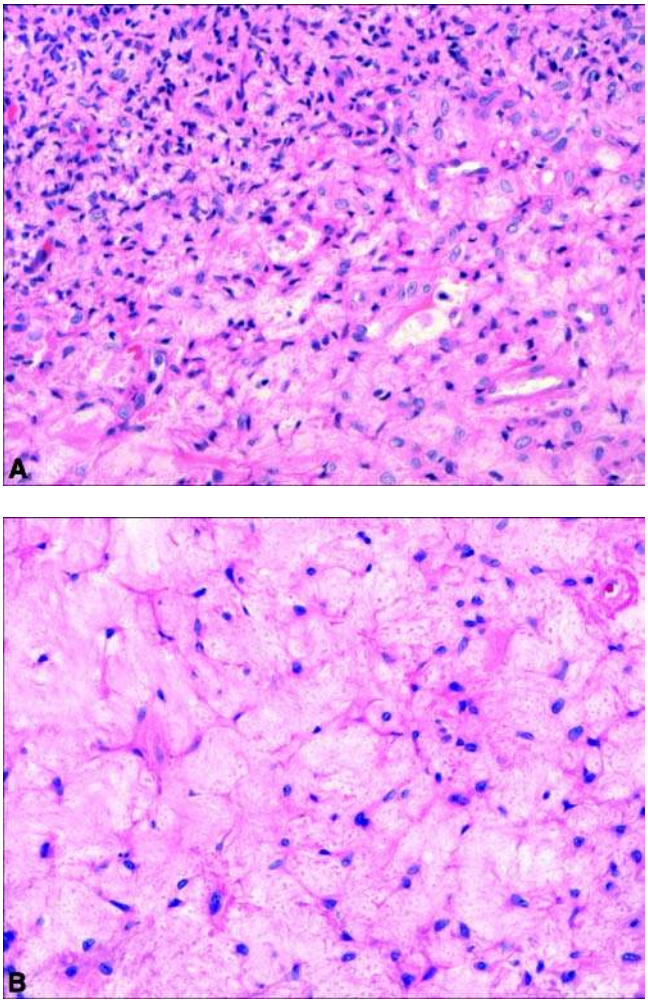

Figure 35 Chondromyxoid fibroma demonstrating the transition from a cellular periphery to a hypocellular center (H&E, 200×). (**A**) Vague micronodular pattern of chondromyxoid fibroma (H&E, 400×). *Abbreviation*: H&E, hematoxylin and eosin.

there is an ABC component, they will be red. If the chondroid component is abundant, a typical gray-blue cartilaginous hue may be appreciated. Chondroblastomas are composed of chondroblasts, which are characterized by polygonal- to spindle-shaped cells with eccentric nuclei, eosinophilic cytoplasm, and nuclear grooves (Fig. 36). The cell borders are distinct but occasional syncytial clusters are common. The cells exhibit only mild atypia and are usually mitotically inactive. Scattered osteoclasts-like giant cells are commonly found. A characteristic feature is the intercellular ''chicken-wire'' or lacelike calcification (Fig. 37). Cystic degeneration is common, and histologic features can overlap with ABC. In fact, 40% of chondroblastomas have areas of ABC.

Immunohistochemistry

The chondroblasts are positive for S100. This can be helpful in differentiating unusual cases such as PVNS with chondroid metaplasia from chondroblastoma (212).

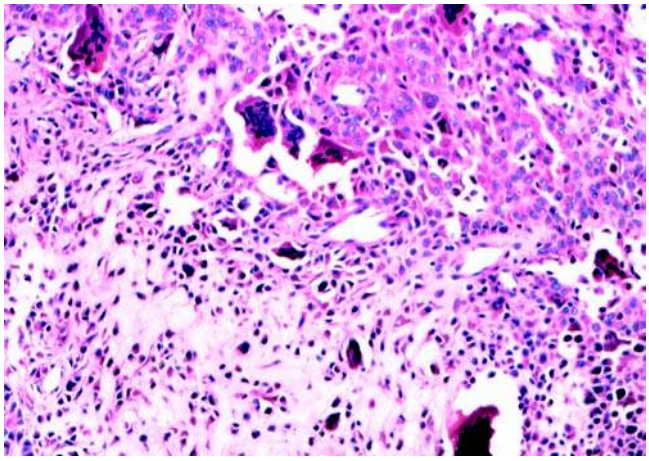

Figure 36 Chondroblastoma is characterized by polygonal and spindle-shaped cells with eccentric nuclei. Note the numerous giant cells, which can lead to an erroneous diagnosis of GCT (H&E, 200×). *Abbreviations*: GCT, giant cell tumor; H&E, hematoxylin and eosin.

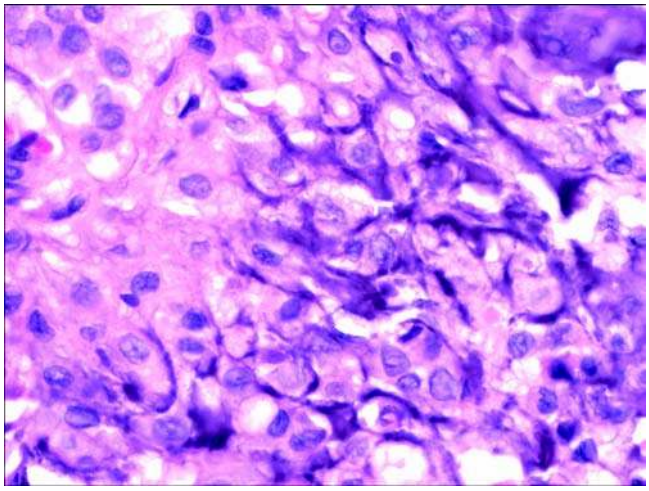

Figure 37 Chicken-wire calcification in chondroblastoma. Occasional nuclear grooves can also be seen (H&E, 400×). *Abbreviation*: H&E, hematoxylin and eosin.

O. Chordoma

Chordomas are low-grade tumors that comprise less than 5% of all bone tumors and occur almost exclusively in the axial skeleton. The majority arise in the sacrococcygeal area (50%), followed by the base of the skull (35%) and vertebral column (15%) (213,214). However, they have been reported in the nasal cavities and paranasal sinuses (215–218). Chordomas

overlap histologically and ultrastructurally with the notochord, and it is believed that they are derived from notochord embryologic remnants along the craniovertebral axis (219). Most chordomas arise in adults aged between 40 and 50 years with a slight increased incidence in men (213,220–222).

Chordomas are slow-growing tumors that often recur after resection and can metastasize to the lungs, bone, and liver. Although very slow growing, most patients will develop recurrence over a 15-year period (223). Tzortzidis et al. found a 41% five-year and a 31% 10-year recurrence-free survival in all 74 patients with either a clival- or cranial-based chordomas (224). Dedifferentiation can occur and is associated with a high mortality.

Signs and symptoms depend on the location of the tumor but often include headache, visual disturbances (particularly when intracranial), cranial neuropathies, airway obstruction, and epistaxis. Chordomas have a propensity to invade surrounding structures, and cervical chordomas can result in esophageal or tracheal compression; sacral tumors can compress the rectum or bladder.

About 5% of chordomas occur in people younger than 20 years. In this age group, the skull base is the most common location. There are mixed findings in the behavior of chordomas in children; some have reported a more aggressive course while others found a better outcome (225,226). Hoch et al. reviewed the pathology and clinical course of 73 children and adolescents with chordomas. They found a better survival in patients with conventional histology who received radiation after surgery when compared with the survival of their adult population with similar tumors and treatment. These children had over an 85% five-year survival rate. However, when the histology was poorly differentiated, the five-year survival rate was less than 20%. Most of the patients with poorly differentiated tumors were younger than 10 years (227).

Radiologic Features

Chordomas are usually midline, osteolytic tumors centered on the clivus. The radiographic features of chordoma overlap greatly with chondrosarcoma and the following CT and MRI features are true for both tumors. By CT scan, most chordomas show bone expansion and destruction and lack sclerotic edges. Dystrophic calcifications and bone sequestra are common (228). Chordomas have variable MRI characteristics and can be hypointense, isointense, or hyperintense on noncontrast T1-weighted images (Fig. 38A). Most show moderate or intense enhancement on T1-weighted images after intravenous contrast. They are usually hypo- or isointense to adjacent brain parenchyma (also on T1-weighted images). Lobule formation is commonly observed, particularly on T2-weighted images (228).

Pathologic Features

Grossly, chordomas are soft, lobulated, and gray to brown (Fig. 38B). Histologically, chordomas are

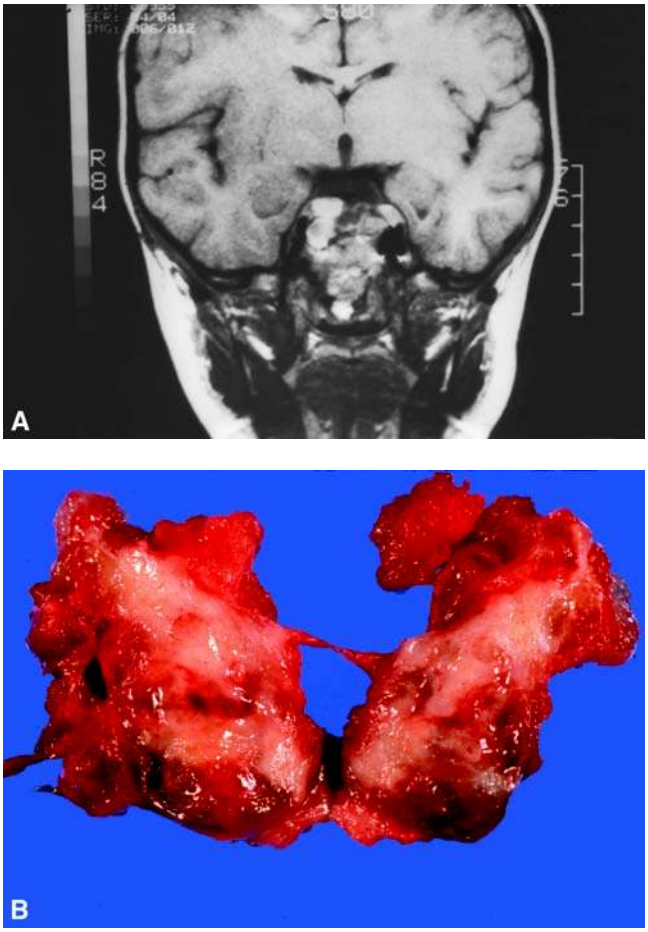

Figure 38 Coronal MRI demonstrating a chordoma in the base of the skull. (**A**) Gross resection of a chordoma. *Abbreviation*: MRI, magnetic resonance imaging.

classified in three subtypes: conventional, chondroid, and dedifferentiated. Conventional chordoma is composed of lobules separated by fibrous bands. The lobules are composed of a fibrillary to myxoid matrix with bland epithelioid to spindled cells arranged in cords, nests, and sheets (229). Many of the cells have cytoplasmic vacuoles and are referred to as physaliphorous cells (Fig. 39). Mitotic figures are scarce. Focal atypia is common and does not seem to predict behavior, and predicting the risk of metastasis or recurrence by histologic means is impossible. Triana et al. reported an association with the cadherin-catenin complex and the aggressiveness of chordomas (see the section ''Immunohistochemistry'' below) (230). The exception to this is dedifferentiation in a chordoma. Dedifferentiated chordoma is composed of spindle cells with obvious atypia and increased mitotic activity. The sarcomatous component often resembles fibrosarcoma, osteosarcoma, or high-grade sarcoma, not otherwise specified. Dedifferentiation can occur with or without radiation and may appear at initial diagnosis or many years later (231). This marked anaplasia often denotes an aggressive tumor (231).

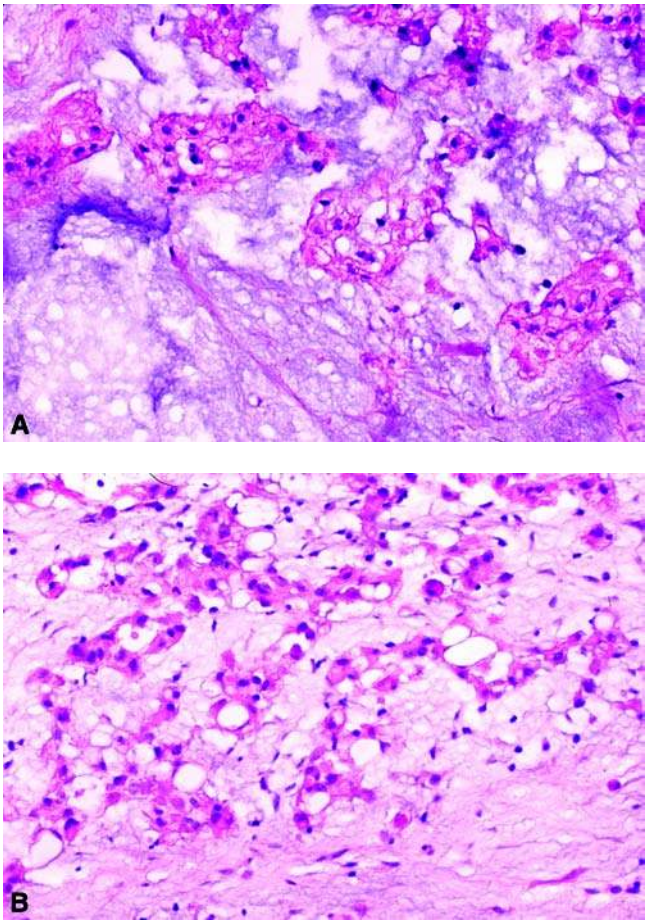

Figure 39 Chordoma characterized by myxoid stroma with islands of polygonal cells (H&E, 200×). (**A**) Classic physylliferous cells (bubbly cytoplasm) characteristic of chordoma (H&E, 200×). *Abbreviation*: H&E, hematoxylin and eosin.

Chondroid chordoma is composed of similar cells but there is a component of hyaline or hyaline-like cartilage. However, areas of usual chordoma are almost always present; the confusion is most common on biopsies when areas of classic chordoma may be absent (229). Although initially thought that patients with condroid chordomas had a significant survival advantage over those with conventional chordomas, no other studies have been able to confirm this issue. The current consensus is that the two tumors have similar survival rates.

Immunohistochemistry

Chordomas are immunoreactive for epithelial membrane antigen, S100, vimentin, and cytokeratin. Chondrosarcoma is not cytokeratin-positive and can be used in those diagnostically challenging cases (232). The mesenchymal component of a dedifferentiated chordoma may or may not express cytokeratin.

Those tumors that have upregulated N-cadherin and decreased expression of E-cadherin have been reported to have over a threefold increased risk of recurrence and over a 10-fold increased risk of dying (230).

V. NEOPLASTIC DISEASES OF THE BONE AND JOINTS, MESENCHYMAL, NONCHONDROID, AND NONOSSEOUS

A. Hemangioma

Benign vascular tumors of the bone are rare, accounting for less than 0.2% of all skull neoplasms (233). Most lesions involve the jaw, skull, and spine (234). They are usually asymptomatic and are often incidental findings in radiographs obtained for other reasons. When symptoms are present, the common complaints are spontaneous pain and tenderness to palpation/pressure (235). Although they are benign, hemangiomas can result in pathologic fractures, cord compression, and facial paralysis (236). An extremely rare condition called Gorham-Stout syndrome results in massive osteolysis and a marked proliferation of vessels that resemble hemangioma. Massive osteolysis is a sporadic, noninherited disease. The etiology is unknown but may be a result of defective osteoclast-like cells that secrete large amounts of angiogenic and osteoclastogenic factors (237). The vascular proliferation in Gorham-Stout syndrome may not be a true neoplasm. However, in biopsy specimens, the findings will be nonspecific and resemble a hemangioma.

Radiologic Features

Radiographically, hemangiomas have a nonspecific appearance. They are usually osteolytic and can be mistaken for multiple myeloma or osteosarcoma (238). Skull-based hemangiomas sometimes display a sunburst pattern on plain films, CT scan, and MRI because of the numerous bony trabeculae (235). In the spine, hemangioma has been described as a polka dot pattern, also because of the trabeculae.

Pathologic Features

Hemangiomas of the bone are either capillary or cavernous and characterized by a proliferation of vessels lined by small bland endothelial cells. Occasionally, the lining of endothelial cells will be plump but not atypical and is characteristic of an epithelioid hemangioma. If atypia is found, consideration of epithelioid hemangioendothelioma (EH) should be considered (see below). Reactive bone is frequent.

B. Epithelioid Hemangioendothelioma

EH is a low-grade vascular tumor that has such heterogeneous morphologies that its vascular nature may not be obvious histologically. It most commonly occurs in people in their 20s and 30s and affects men twice as frequently as women. Most frequently it arises in relationship to a vessel, commonly a small vein. It usually presents as a solitary mass of the deep soft tissues in the extremities. However, it has been reported in most solid organs such as the lung

(formerly called intravascular bronchioloalveolar tumor), liver (formerly called sclerosing epithelioid cholangiocarcinoma), brain, and bone. The few case reports of EH involving the craniofacial bones include the skull, temporal bone, and sphenoid sinus (239,240). About 25% to 30% of EHs will metastasize but the prognosis does seem to be impacted by grade. Additionally, multifocal disease is common and differentiating synchronous lesions versus metastasis can at times be impossible (241). Genetic studies are few but a translocation involving chromosomes 1 and 3 has been reported in a few cases (242).

Radiologic Features

These are typically lytic lesions will ill-defined borders. They can be cortical or medullary based and cortical destruction can occur. In the absence of a fracture, it is unusual to see calcification or a periosteal reaction (241).

Pathologic Features

Grossly, EH is well circumscribed with irregular borders and a red cut surface (241). The background can be myxoid, chondroid, hyalinized, or a mixture. The cells are spindled to epithelioid with eosinophilic vacuolated cytoplasm (Fig. 40). They are cytologically bland and mitotic figures are scarce. Particularly in small biopsies, the lesion can be mistaken for a reactive histiocytic process or, at the other extreme, for metastatic carcinoma (Fig. 41A). An extremely helpful feature is the identification of intracytoplasmic lumina, which may contain red blood cells.

Most EHs are cytologically bland. They portend a worse prognosis when the following features are found: mitotic figures greater than 1/10 hpf, marked cytologic atypia, necrosis, and prominent spindling of the cells. These features correspond to a malignant EH by the WHO, although all EHs regardless of their histology have malignant potential. When mitoses are greater than 2/10 hpf and there is notable atypia, epithelioid angiosarcoma is probably a better designation.

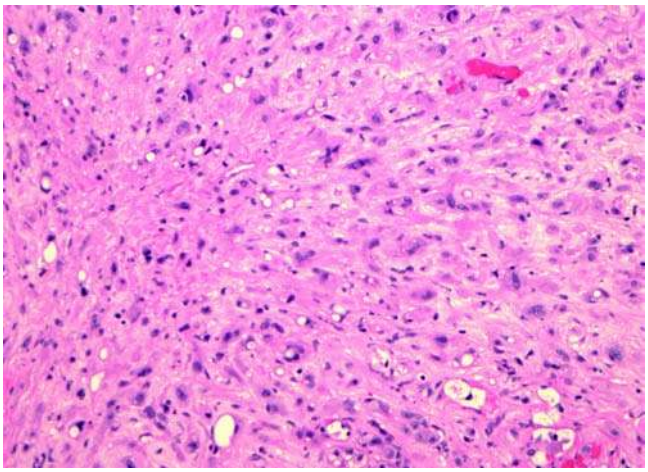

Figure 40 Epithelioid hemangioendothelioma is characterized by epithelioid and spindle cells. Occasional vacuoles can be seen (H&E, 200×). *Abbreviation*: H&E, hematoxylin and eosin.

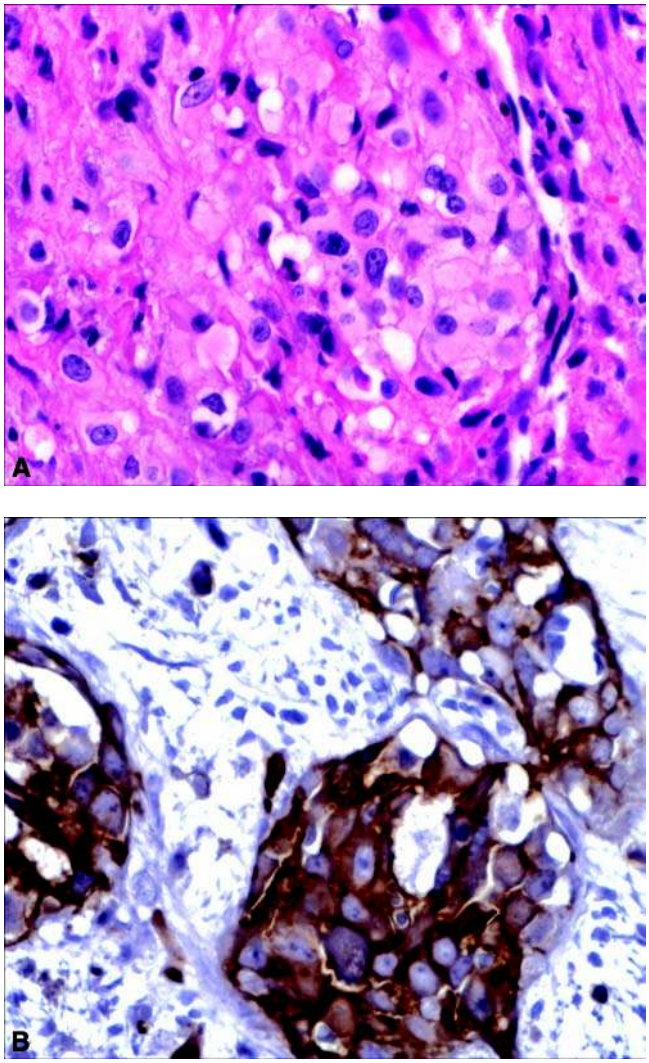

Figure 41 Epithelioid hemangioendothelioma can present histologically as a bland tumor whose vascular nature is not readily appreciated. CD31 in same case as (**A**) showing marked reactivity (400×). *Abbreviation*: H&E, hematoxylin and eosin.

C. Angiosarcoma

Angiosarcomas have been reported in numerous body sites and commonly in bone. They can be uni- or multifocal, geographically clustered (multiple foci within a single bone), or nondiscriminatory, and involve numerous bones. The most common sites in the head and neck are the skull and skin but there are reports of angiosarcoma in the nasal cavity, temporal bone, and sinuses (243–245). Angiosarcoma is a high-grade malignancy with a poor survival rate. It often metastasizes to the lung, bone, and lymph nodes. In a study from Massachusettes General Hospital of all

body site angiosarcomas, five-year survival was 60%. Poor prognostic indicators included high-grade tumors and those that arose in a field of radiation or lymphedema (246). Surgical excision is the mainstay treatment for those who develop metastatic disease, and there is no clear role for radiation or chemotherapy, although this is controversial. There are reports of successful control with recombinant IL-2 (244).

Radiologic Features

Radiographs demonstrate nonspecific findings. Angiosarcomas typically are lytic with ill-defined borders. Because of their rapid growth, they have little new bone formation.

Pathologic Features

Grossly, these tumors are hemorrhagic. The classic histology is an anastomosing network of channels filled with blood and lined by plump endothelial cells that protrude into lumina (Fig. 42). The grade of angiosarcoma is two tiered and depends on the cytologic atypia of the endothelial cells. Additionally, high-grade angiosarcomas may be predominantly solid with atypical spindled and epithelioid cells (Fig. 43). Usually some residual atypical vascular spaces can be seen but this may be elusive on small biopsies, necessitating immunohistochemistry to aid in appropriate diagnosis. When the differential diagnosis includes EH, differentiation from epithelioid angiosarcoma hinges on increased mitotic figures and cytologic atypia in epithelioid angiosarcoma.

Cytologically, angiosarcomas are composed of spindle cells in which the nucleus bulges from the cytoplasm. The nucleus is oval often with a groove. In low-grade angiosarcomas, the vascular network may be so prominent that fine needle aspiration biopsy yields only blood.

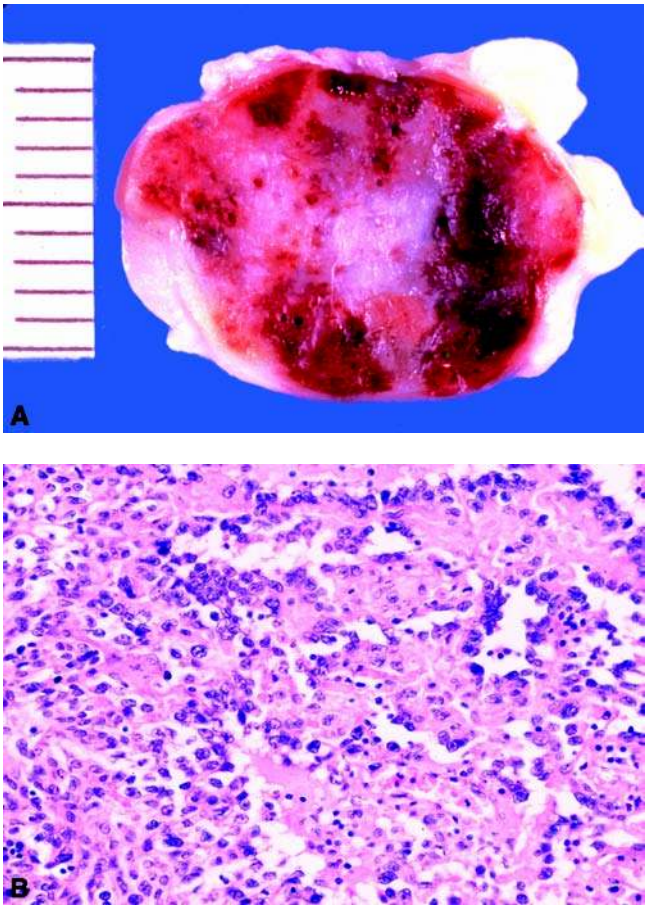

Figure 42 Gross specimen of a partial mandibulectomy for an angiosarcoma, which demonstrates a hemorrhagic cut surface. (**A**) Angiosarcoma is typified by interanastomosing vascular channels with nuclei that bulge into the lumen (H&E, 200×). *Abbreviation*: H&E, hematoxylin and eosin.

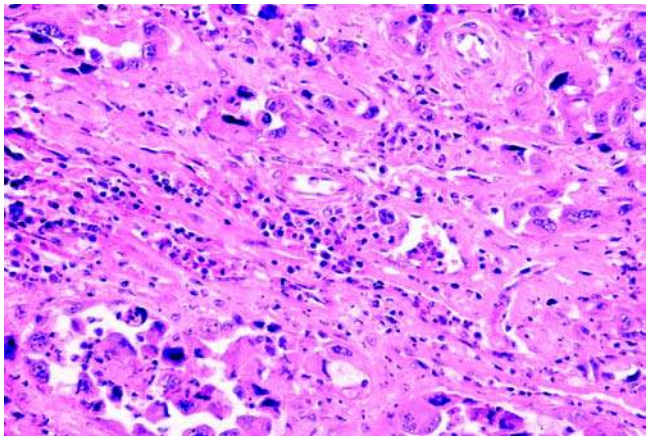

Figure 43 Epithelioid angiosarcoma can get mistaken for a metastatic carcinoma, particularly if there is focal cytokeratin positivity (H&E, 200×). *Abbreviation*: H&E, hematoxylin and eosin.

Immunohistochemistry

The spindle cells will react with vascular antibodies such as CD 31, 34, FLI-1, and factor 8 (Fig. 41B). Hemangiomas and angiosarcomas are usually negative for cytokeratins, although epithelioid angiosarcomas and EHs often have focal cytokeratin positivity.

D. Lymphangioma

Lymphangiomas most commonly occur in the soft tissues. The head and neck (nuchal cystic hygroma) is the most common location for occurrence and primary bone involvement is less common. Although typically unifocal, systemic lymphangiomatosis does occur (247). Lymphangiomas are a defect in lymphatic connection to a venous outflow tract. They are typically congenital and therefore are most commonly seen in children. Although they are benign, they can obtain large sizes, up to 15 cm, and can result in intrauterine demise or deformities.

Radiographic Features

Like hemangiomas, lymphangiomas have nonspecific findings. The lesions are usually lytic and features overlap with hemangiomas and dermoid cysts (248).

Pathologic Features

Lymphangiomas are uni- or multiloculated, usually with poorly defined borders. Lymphangiomas are composed of variably sized, irregularly shaped lymphatic channels lined by very attenuated and barely discernable endothelial cells. The vascular structures lack smooth muscle or pericytes. Scattered aggregates of lymphocytes are in the intervening walls.

Immunohistochemistry

The most specific immunohistochemical stain for lymphatics is podoplanin (249).

E. Giant Cell Tumor

GCTs of bone tend to arise in skeletally mature young adults, usually in the epiphysis of long bones (femur, tibia, and radius). They occasionally involve the hands and feet and much less commonly (less than 2% of all GCTs) arise in craniofacial bones (250–252). It is most commonly reported in the middle cranial fossa and the sphenoid and temporal bones and hyoid bone, most likely because of the endochondral growth of these bones (253). When a giant cell lesion is encountered in the head and neck, exclusion of other giant cell–rich lesions is warranted, particularly given the rarity of occurrence in this location.

Radiologic Features

The common features of a GCT are a lytic lesion in the end of a long bone that extends up to the articular cartilage. Since these tend to arise in skeletally mature people, the epiphyseal plate is closed. There is usually not a sclerotic edge and the lesion is destructive. The few case reports of GCTs of the head and neck have also been seen in mature individuals (251).

Pathologic Features

The tumors are soft and either pink or brown with variegated areas of yellow (correlating to the concentration of foam cells). Cysts are common. GCTs are often curetted, so the gross appearance may not be readily appreciable in small fragments. The classic histologic features are a hypercellular mononuclear cell proliferation with evenly distributed, interspersed multinucleated giant cells. The nuclei of the giant cells are the same as the nuclei of the background mononuclear cells (Fig. 44). Collections of foamy histiocytes are common. The mononuclear cells tend to spindle in areas of foam cells and should not be mistaken as ABC.

Grading of GCTs does not seem to correlate with predicting recurrence or aggressiveness. Recurrence is usually due to incomplete excision rather than mitotic activity or cytologic atypia. Several reports of benign metastasizing GCTs exist. These are usually solitary nodules to lung and excision is usually curative. Some hypothesize these are due to tumor emboli after surgery.

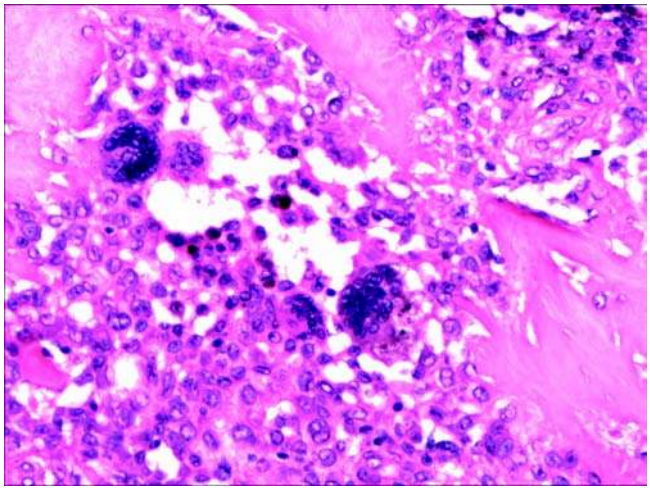

Figure 44 GCT of bone is characterized by evenly dispersed multinucleated giant cells and mononuclear stromal cells. GCT of the craniofacial bones is exceedingly rare (H&E, 400×). *Abbreviations*: GCT, giant cell tumor; H&E, hematoxylin and eosin.

Malignant GCTs have been reported but we think these may actually represent giant cell–rich osteosarcomas. Dedifferentiation of a GCT can occur as a high-grade sarcoma after treatment. Occasionally, a sarcoma is juxtaposed to a usual benign GCT (254). These behave similarly as other bone sarcomas.

Usually, GCT histologically overlaps with other lesions containing giant cells such as osteosarcoma, ABC, chondroblastoma, and ''brown tumor'' of hyperparathyroidism (Table 6). The presence of chondroid matrix should argue against a GCT. In the long bones, the location of the tumor will help significantly, as many of the lesions in the differential occur in the diaphysis or metaphysis. It is more challenging in the craniofacial bones.

F. Giant Cell Granuloma

Giant cell granuloma is a benign lesion that is thought to be a response to intraosseous hemorrhage secondary to trauma or chronic inflammation. It most commonly occurs in people younger than 30 years but reports in older individuals exist (255). It affects both genders equally (256). It usually involves the craniofacial bones, most commonly the mandible and maxilla but has also has been described in the nasal cavity, orbit, and cranial vault (Fig. 45) (255). Unlike GCTs of bone, giant cell granuloma rarely occurs in the hands and feet and long bones. However, despite the rarity in these locations, the hands are the most common extracranial sites of involvement (257).

Table 6 Distinguishing Features of Giant Cell–Rich Bone Lesions

	Age	Common location	Common location in the head and neck	Giant cells location	Giant cell morphology	Background
GCT	30s 40s	Long bones epiphysis	Case reports only	Evenly dispersed	Large, round, nuclei similar to background cells	Mononuclear cells
Giant cell granuloma	< 30	Craniofacial intracortical	Mandible, maxilla	Centered on hemorrage	Small, irregular, distinct from background cells	Fibroblastic spindle cells, areas of hemorrhage
Brown Tumor	> 30	Distal phylanges	Mandible, maxilla	Tunnel into trabeculae	Small giant cells, distinct from the background cells	Peritrabecular spindle cells
ABC	< 20	Long bones Metaphysis	Mandiible, maxilla	Haphazard arrangement	Small, distinct from background cells	Fibroblastic spindle cells, large cysts
Telangiectatic osteosarcoma	< 20	Long bones metaphysis	Case reports only	Haphazard arrangement	Small, distinct from background cells	Pleomorphic, anaplastic cells

Abbreviations: GCT, giant cell tumor; ABC, aneurysmal bone cyst.

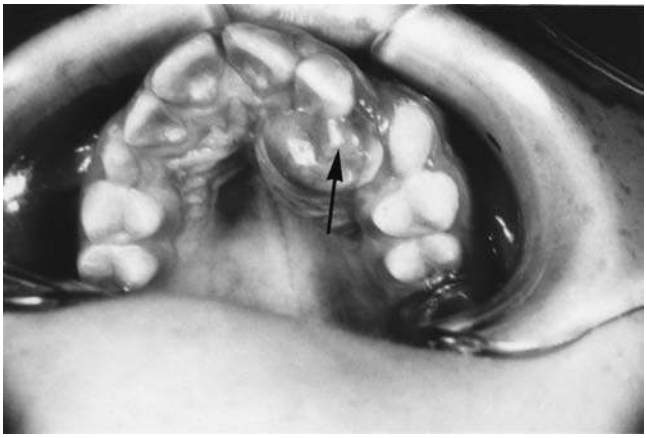

Figure 45 Giant cell granuloma involving the anterior palate gingival.

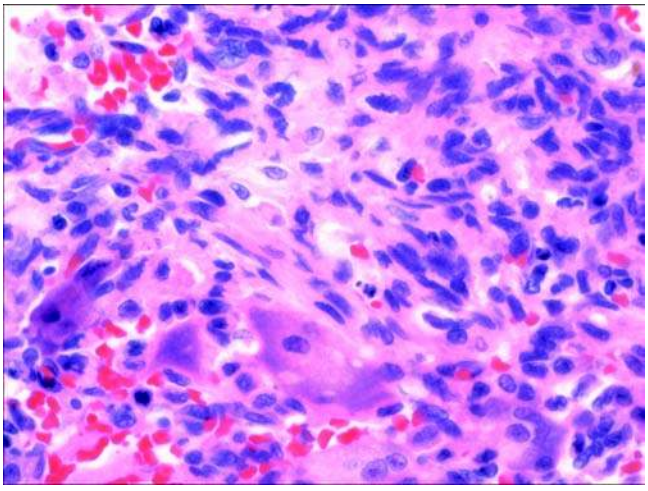

Figure 46 Giant cell reparative granuloma contain small irregularly shaped giant cells, often centered on hemorrhage (H&E, 400×). This lesion is histologically indistinguishable from "brown tumor." *Abbreviation*: H&E, hematoxylin and eosin.

Radiologic Features

Giant cell granuloma is classified as central when it is surrounded by bone and peripheral when it originates in soft tissue. It is composed of an expansile multilocular, radiolucent mass that is indistinguishable from odontogenic cysts, ABC, hyperparathyroidism, ameloblastoma, and odontogenic fibroma. It usually has a thin but intact cortex; extension into the soft tissue is extremely rare. Although it usually has a benign presentation, when it arises in the paranasal sinuses, it can be aggressive with bony destruction and occasional extension intracranially (255).

Pathologic Features

The giant cells are usually small, irregularly shaped, and centered on areas of hemorrhage (Fig. 46). It is histologically indistinguishable from brown tumor of hyperparathyroidism and correlation with serum calcium, phosphorous, and alkaline phosphatase is necessary for differentiation. The features greatly overlap with solid variants of ABC. In ABC, the giant cells are scattered throughout the lesion rather than centered on hemorrhage. However, histologic differentiation from solid ABC can be impossible (258).

G. Hyperparathyroidism

Hyperparathyroidism (excess parathyroid hormone) results in increased osteoclast activity, osteopenia, and rarely brown tumors. Primary hyperparathyroidism may be due to a parathyroid adenoma, hyperplasia, or carcinoma and results in hypercalcemia and hypophosphatemia. About 25% of patients develop bone disease, usually subclinical. Secondary hyperparathyroidism is a compensatory result of chronic renal

failure (which causes phosphate retention and hypocalcemia).

Radiologic Features

Bones of the hand are most commonly affected. The ends of the phylanges erode and there is subperiosreal cortical resorption, particularly on the radial side of the phylanges. Occasionally, a large lytic lesion will develop, simulating a bone tumor. These can be single or multiple and resemble ABCs and GCTs (259).

Pathologic Features

The tumor-like lesions are characteristically brown, which explains their synonym, brown tumor. There is marked osteoclastic activity with burrowing into the trabeculae, forming tunnels. Bone formation is also increased and results in peritrabecular fibrosis (Fig. 47). This fibrosis cuffs the trabeculae and is not evenly distributed, as would be seen in myelofibrosis. Particularly in small biopsy specimens, the differential diagnosis includes GCT, ABC, and giant cell granuloma (Table 6). The fibroblastic background and focality of the giant cells argues against GCT. It may be impossible to histologically distinguish a brown tumor from a giant cell granuloma, and correlation with serum chemistry will be necessary. If a pathologist is making the diagnosis of a central giant cell granuloma, the possibility of a brown tumor should be raised to ensure the patient has been evaluated for hyperparathyroidism.

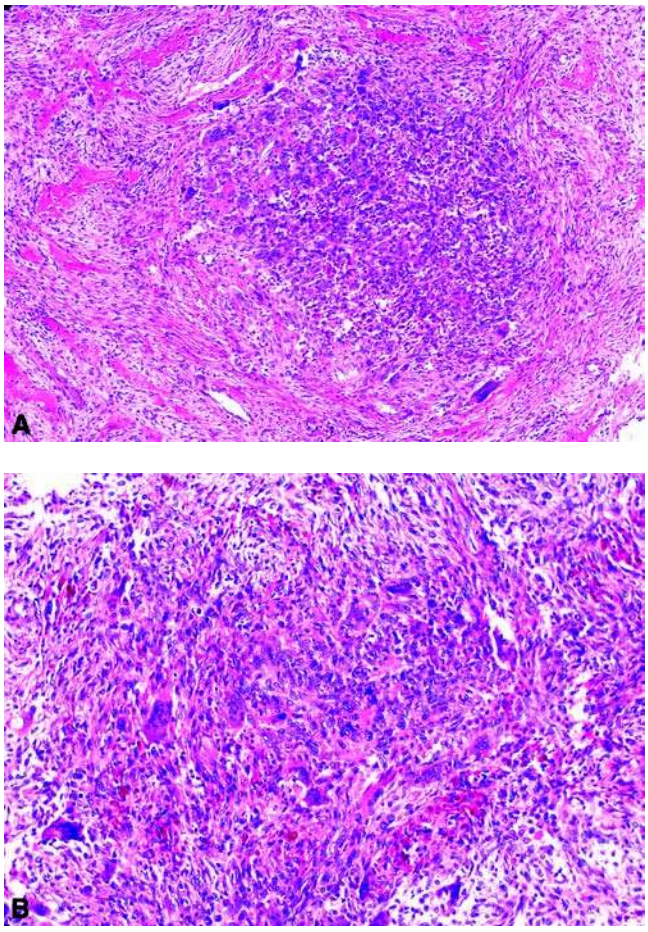

Figure 47 "Brown tumor" of hyperparathyroidism demonstrating numerous multinucleated giant cells forming vague granulomas (H&E; (**A**) 100×, (**B**) 200×). *Abbreviation*: H&E, hematoxylin and eosin.

H. Aneurysmal Bone Cyst

The etiology is unknown, but it is hypothesized that the ABC is a reactive process in response to trauma/fracture or secondary to bone neoplasms (most commonly associated with GCT, chondroblastoma, FD). They usually occur in children and young adults. Given their propensity to occur in conjunction with other bone lesions, the pathologist must search for an underlying second process or neoplasm whenever an ABC is encountered. ABCs most commonly arise in the metaphysis of the long bones. Three percent to 12% of ABCs occur in the head and neck with the mandible and maxilla being the most common sites. However, ABCs have been described in the calvarium, sphenoid and ethmoid sinuses, zygomatic arch, larynx, hyoid bone, and cervical vertebrae (260–265). Signs and symptoms depend on the location and include slowly or rapidly growing mass in the sinus or nasal cavity, soft tissue mass, headache, diplopia, proptosis, facial nerve paralysis, fracture, and spinal cord compression.

Radiologic Features

ABCs are characterized by a lytic, expansile lesion in the metaphysis that is eccentrically located. If there is soft tissue extension, there is usually a rim of new bone formation giving an "egg shell" appearance (Fig. 49). They range in size from 1 to 10 cm. The margins may be blurred, simulating a malignancy. CT and MRI will show fluid levels, a helpful feature in this lesion.

Pathologic Features

Grossly the lesions are multicystic and filled with blood or serosanguinous fluid. The lesions are characterized by large, blood-filled nonendothelialized spaces separated by septa (Fig. 48). The cysts are not true vessels and are lined by fibroblasts, histiocytes, or granulation tissue (Fig. 49). There is no surrounding wall of smooth muscle or elastin. The septa are composed of cellular, mitotically active (0–5 mitotic figures/10 hpf) but bland loosely arranged spindled cells with numerous scattered giant cells. The edges of the septa often have a thin rim of osteoid.

Although usually very cystic, approximated 5% of ABCs lack a cystic component and are referred to as solid ABC and are quite similar, if not histologically identical to giant cell granuloma.

The differential diagnosis includes other giant cell–rich lesions (Table 6) and telangiectatic osteosarcoma. The background spindle cells will aid in

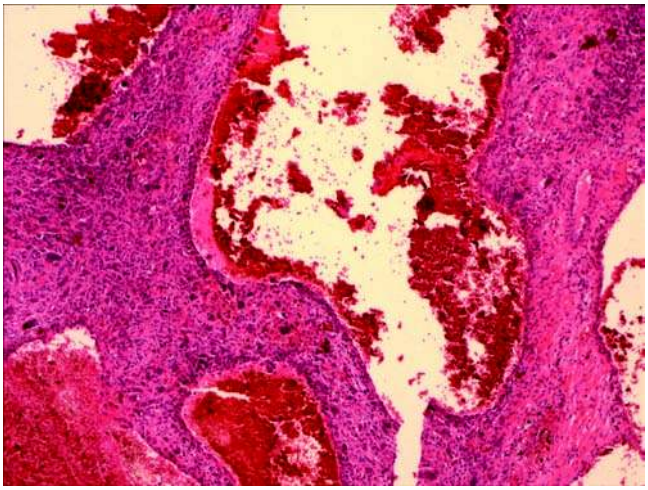

Figure 48 Low magnification of ABC demonstrating the cystic spaces filled with blood. Numerous giant cells can be seen (H&E, 100×). *Abbreviations*: ABC, aneurysmal bone cyst; H&E, hematoxylin and eosin.

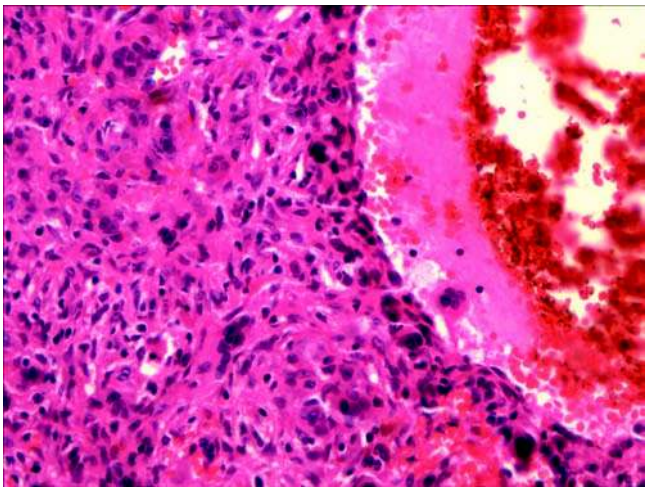

Figure 49 ABC is composed of pseudocysts. Note the compressed stroma and lack of endothelial cells. The giant cells are interspersed in a spindled stroma (H&E, 200×). *Abbreviations*: ABC, aneurysmal bone cyst; H&E, hematoxylin and eosin.

differentiating an ABC from a GCT. The lack of cytologic atypia in conjunction with imaging studies should help to sort out a telangiectatic osteosarcoma.

I. Desmoplastic Fibroma

This is the osseous counterpart of soft tissue fibromatosis or desmoid tumor and is a low-grade tumor that can be locally aggressive. This rare tumor (comprising less than 0.1% of all bone neoplasms) is predominantly discussed in case reports in the literature. Although the majority arise in the axial skeleton, about 25% arise

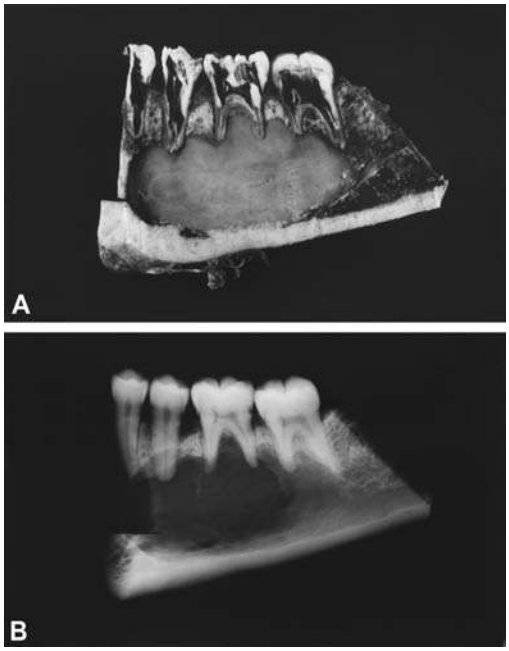

Figure 50 Desmoplastic fibroma of the mandible in a 31-year-old woman. Specimen radiograph shows a well-defined radiolucency. The excision specimen highlights the circumscribed scalloped margin of the tumor.

in the mandible, with the majority being posterior to the molar area. Desmoplatic fibroma also arises in the maxillary sinus and has only rarely been reported in the skull. It has been described in babies and the elderly, but most commonly affects people younger than 30 years (266). There is no gender predilection. When it involves the jaw, patients usually seek treatment for a painless, slow-growing mass. When the tooth root is involved, pain in the form of a toothache may occur. The pathogenesis is unclear. Surgery with cranioplasty is the current treatment of choice. If good margins are accomplished, it is extremely rare to have a recurrence (267,268).

Radiologic Features

Desmoplastic fibroma tends to be osteolytic and without mineralization (Fig. 50). Crim et al. noted ridges of intact bone in the periphery, which correlated to the uneven bone destruction (269). Pathologic fractures occur in 10% of cases. Frick et al. noted a short T2 signal pattern on MRI in 11 of 14 patients (270).

Pathologic Features

Grossly, these are white and rubbery. Histologically, they are composed of a mild-to-moderate cellular proliferation of bland spindle cells that infiltrate between bony trabeculae (Fig. 51). When it extends into soft tissue, it will wrap around surrounding structures such as nerve and individual skeletal muscle cells. Mitoses are rare and never atypical (271). Cartilaginous metaplasia has been reported (272).

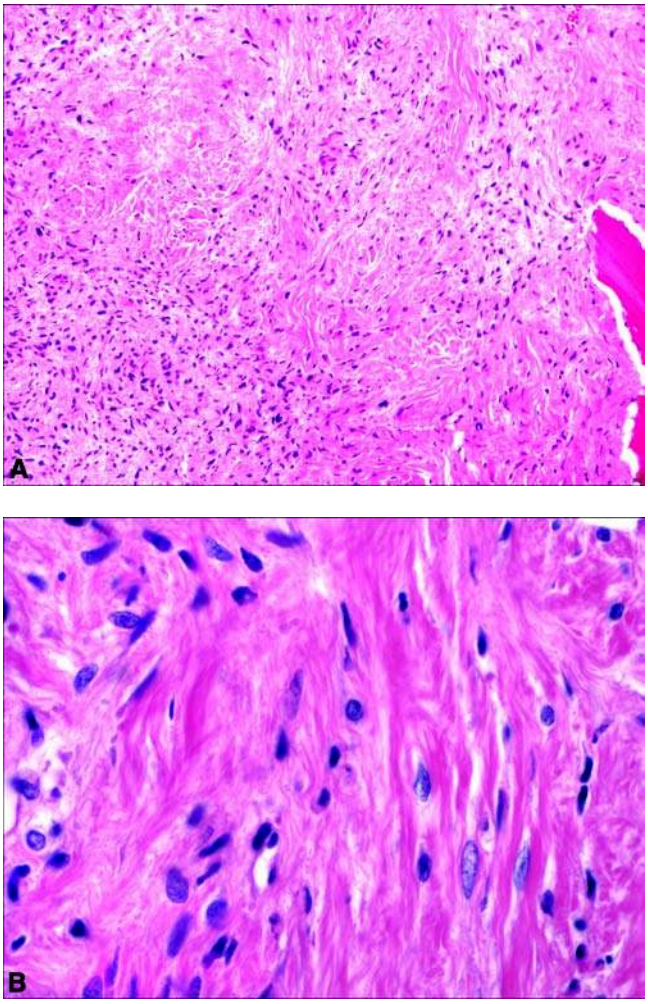

Figure 51 Low magnification of desmoplastic fibroma demonstrating cellular and hypocellular components. (**A**) High magnification showing the bland cytology.

J. Fibrosarcoma

Fibrosarcoma is the most common nonosseous sarcoma of the bone. It has been described in numerous sites but most commonly affects the metaphysis of the long bones, especially the distal femur, proximal tibia, and proximal humerus (273). Fifteen percent of all osseous fibrosarcomas arise in the head and neck with the mandible, maxilla, and skull being the most commonly affected. Fibrosarcoma tends to affect the sexes equally and occurs in people older than 30 years. The tumors are termed primary when they arise de novo and secondary when they develop in the setting of a radiation field, Paget's disease, or in areas of prior infarct. The secondary types account for 15% to 30% of all osseous fibrosarcomas, and patients tend to be older than those with primary fibrosarcoma (274,275).

Fibrosarcomas are referred to as medullary when they arise in the center of bone and periosteal when they are centered on the periphery. When periosteal, it can be difficult to decide whether the tumor is an osseous fibrosarcoma with soft tissue extension or a soft tissue fibrosarcoma invading adjacent bone. This distinction is not critical from a treatment or prognostic perspective. However, there is some suggestion that medullary fibrosarcoma is more aggressive than periosteal or soft tissue fibrosarcoma. Surgical excision is the usual treatment. Prognosis depends on the size and grade of the tumor, location (medullary versus periosteal), and margin status. The five-year survival rate for de novo head and neck fibrosarcomas ranges from 30% to 40%. Most recurrences and metastases occur within two years of diagnosis (276). Secondary fibrosarcoma has a worse prognosis regardless of the grade. One study of fibrosarcomas arising in the setting of Paget's disease found the five-year survival rate of less than 10% (179).

Radiologic Features

Fibrosarcomas are lytic, expansile lesions, often with soft tissue extension. There are no specific features that distinguish fibrosarcoma from other malignant

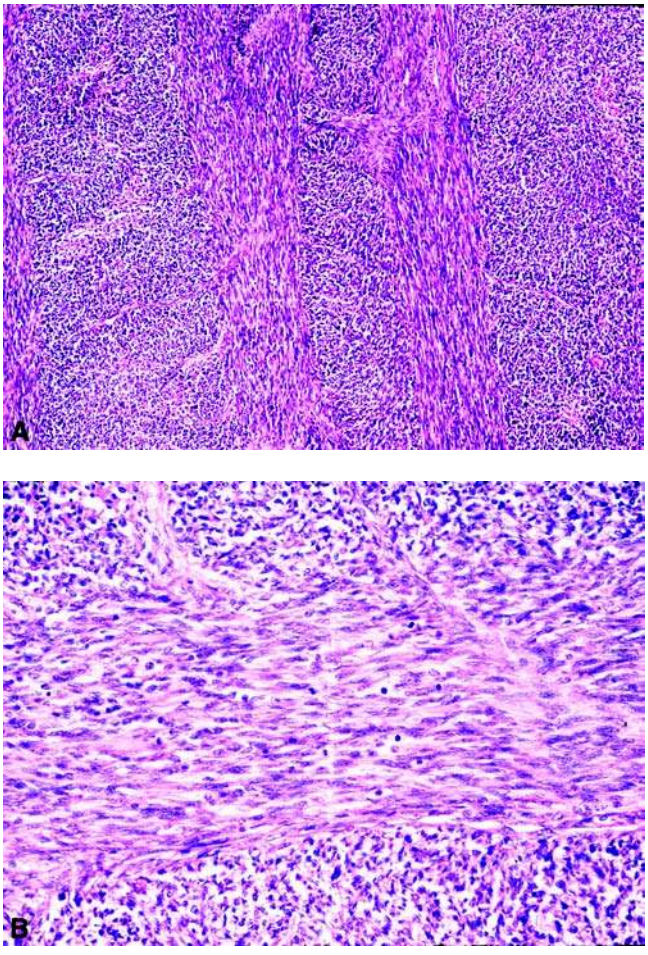

Figure 52 Fibrosarcoma displaying a herringbone pattern (H&E; (**A**) 20×, (**B**) 200×). *Abbreviation*: H&E, hematoxylin and eosin.

Table 7 Spindle Cell Lesions of the Craniofacial Bones and Differentiating Histologic Features

	Margin	Pattern	Atypia	Mitoses	Giant cells	Other
Angiosarcoma	Infiltrative	Vascular, solid when high grade	Yes	Yes	No	Anastomosing vascular spaces
Chrondromyxoid fibroma	Circubscribed, sclerotic	Nodular, cellular periphery, paucicellular centers	Yes, can be marked	No	Yes	Fibrous component small, prominent myxoid and chondroid components
Desmoplastic fibroma	Infiltrative	Parallel, haphazard, rarely herringbone or storiform	Absent	No	No	Abundant collagen, entrapped normal structures
Epithelioid hemangioendothelioma	Infiltrative	Variable. Polygonal cells, spindle cells, vascular.	Mild	Rare	No	Intracellular lumina, occasionally has myxoid stroma
Fibrosarcoma	Infiltrative	Herringbone	Present but often mild	Yes, can be atypical	Rarely	No malignant osteoid or cartilage
Ossifying fibroma	Circumscribed	Haphazard	No	No	No	Trabeculae with marked osteoblastic rimming
Osteosarcoma, fibroblastic	Infiltrative	Focal herringbone	Present	Yes, can be atypical	Usually no but can be present	Malignant osteoid

lytic tumors. Additionally, low-grade lesions may simulate a cyst and appear benign radiographically. High-grade lesions are destructive and demonstrate aggressive type periosteal new bone formation (277).

Pathologic Features

Grossly and histologically, intraosseous fibrosarcoma resembles its soft tissue counterpart. It has a white, rubbery surface. Histologically, it is characterized by a spindle cell proliferation that forms a herringbone pattern (Fig. 52). Depending on the grade, mitotic figures can be scarce to quite numerous. There is often some nuclear atypia, but even high-grade lesions may have only moderate atypia. Occasionally, there is extensive collagen deposition or a myxoid background, but there should not be any malignant osteoid or chondroid matrix.

Fibrosarcomas are graded as low or high grade. Low-grade tumors are hypocellular, bland, and have a low mitotic rate. Their features overlap with desmoplastic fibroma. However, desmoplastic fibroma should not have a herringbone pattern or atypical mitotic figures. Differentiating the two lesions on a small biopsy specimen may be impossible, and a more general diagnosis of low-grade fibrous tumor would be appropriate (Table 7). High-grade fibrosarcomas are cellular with hyperchromatic nuclei, some cytologic atypia, and a brisk mitotic rate.

K. Ewing's Sarcoma

Ewing's sarcoma is a small round blue cell tumor of childhood that frequently involves the skull base and craniofacial bones. It is described in more detail in chapter 12.

L. Eosinophilic Granuloma

The craniofacial bones are a common location for eosinophilic granuloma. For a detailed description, please see chapter 15.

REFERENCES

1. Dorfman HDBC. Bone Tumors. Baltimore: Mosby, 1998.
2. Riise T, Jacobsen BK, Gran JT, et al. Total mortality is increased in rheumatoid arthritis. A 17-year prospective study. Clin Rheumatol 2001; 20(2):123–127.
3. Franklin C. Pathology of the temporomandibular joint. Curr Diagn Pathol 2006; 12(1):31–39.
4. Chen JJ, Branstetter BF, Myers EN. Cricoarytenoid rheumatoid arthritis: an important consideration in aggressive lesions of the larynx. AJNR Am J Neuroradiol 2005; 26(4): 970–972.
5. Helenius LM, Hallikainen D, Helenius I, et al. Clinical and radiographic findings of the temporomandibular joint in patients with various rheumatic diseases. A case-control study. Oral Surg Oral Med Oral Pathol Oral Radiol Endod 2005; 99(4):455–463.
6. Goupille P, Fouquet B, Goga D, et al. The temporomandibular joint in rheumatoid arthritis: correlations between clinical and tomographic features. J Dent 1993; 21(3): 141–146.
7. Voog U, Alstergren P, Leibur E, et al. Impact of temporomandibular joint pain on activities of daily living in patients with rheumatoid arthritis. Acta Odontol Scand 2003; 61(5):278–282.

8. Willkens RF, Roth GJ, Novak A, et al. Perforation of nasal septum in rheumatic diseases. Arthritis Rheum 1976; 19(1):119–121.
9. Mathews JL, Ward JR, Samuelson CO, et al. Spontaneous nasal septal perforation in patients with rheumatoid arthritis. Clin Rheumatol 1983; 2(1):13–18.
10. Ozcan M, Karakus MF, Gunduz OH, et al. Hearing loss and middle ear involvement in rheumatoid arthritis. Rheumatol Int 2002; 22(1):16–19.
11. Hincapie JW, Tobon D, Diaz-Reyes GA. Septic arthritis of the temporomandibular joint. Otolaryngol Head Neck Surg 1999; 121(6):836–837.
12. Kudish K, Sleavin W, Hathcock L. Lyme disease trends: Delaware, 2000–2004. Del Med J 2007; 79(2):51–58.
13. Ghosh S, Seward R, Costello CE, et al. Autoantibodies from synovial lesions in chronic, antibiotic treatment-resistant Lyme arthritis bind cytokeratin-10. J Immunol 2006; 177(4):2486–2494.
14. Barthelemy I, Karanas Y, Sannajust JP, et al. Gout of the temporomandibular joint: pitfalls in diagnosis. J Craniomaxillofac Surg 2001; 29(5):307–310.
15. Gentili A. The advanced imaging of gouty tophi. Curr Rheumatol Rep 2006; 8(3):231–235.
16. Yu JS, Chung C, Recht M, et al. MR imaging of tophaceous gout. AJR Am J Roentgenol 1997; 168(2):523–527.
17. Gerster JC, Landry M, Dufresne L, et al. Imaging of tophaceous gout: computed tomography provides specific images compared with magnetic resonance imaging and ultrasonography. Ann Rheum Dis 2002; 61(1):52–54.
18. Dijkgraaf LC, Liem RS, de Bont LG, et al. Calcium pyrophosphate dihydrate crystal deposition disease: a review of the literature and a light and electron microscopic study of a case of the temporomandibular joint with numerous intracellular crystals in the chondrocytes. Osteoarthritis Cartilage 1995; 3(1):35–45.
19. Smolka W, Eggensperger N, Stauffer-Brauch EJ, et al. Calcium pyrophosphate dihydrate crystal deposition disease of the temporomandibular joint. Oral Dis 2005; 11(2):104–108.
20. Saliba I, Bouthiller A, Desrochers P, et al. Tophaceous gout and pseudogout of the middle ear and the infratemporal fossa: case report and review of the literature. J Otolaryngol 2003; 32(4):269–272.
21. Cascone P, Rivaroli A, Arangio P, et al. Chondrocalcinosis: rare localization in the temporomandibular joint. J Craniofac Surg 2006; 17(6):1189–1192.
22. Osano H, Matsumoto K, Kusama M. Calcium pyrophosphate dihydrate arthropathy with condylar destruction of the temporomandibular joint. J Oral Sci 2003; 45(4): 223–226.
23. Ishida T, Dorfman HD, Bullough PG. Tophaceous pseudogout (tumoral calcium pyrophosphate dihydrate crystal deposition disease). Hum Pathol 1995; 26(6):587–593.
24. Spiers EM, Sanders DY, Omura EF. Clinical and histologic features of primary oxalosis. J Am Acad Dermatol 1990; 22 (5 pt 2):952–956.
25. Behnke B, Kemper MJ, Kruse HP, et al. Bone mineral density in children with primary hyperoxaluria type I. Nephrol Dial Transplant 2001; 16(11):2236–2239.
26. Elmstahl B, Rausing A. A case of hyperoxaluria. Radiological aspects. Acta Radiol 1997; 38(6):1031–1034.
27. Julian BA, Faugere MC, Malluche HH. Oxalosis in bone causing a radiographical mimicry of renal osteodystrophy. Am J Kidney Dis 1987; 9(5):436–440.
28. Geirnaerdt MJ, Kroon HM, van der Heul RO, et al. Tumoral calcinosis. Skeletal Radiol 1995; 24(2):148–151.
29. Sledz K, Ortiz O, Wax M, et al. Tumoral calcinosis of the temporomandibular joint: CT and MR findings. AJNR Am J Neuroradiol 1995; 16(4):782–785.
30. Ardekian L, Faquin W, Troulis MJ, et al. Synovial chondromatosis of the temporomandibular joint: report and analysis of eleven cases. J Oral Maxillofac Surg 2005; 63(7):941–947.
31. Milgram JW. Synovial osteochondromatosis: a histopathological study of thirty cases. J Bone Joint Surg Am 1977; 59(6):792–801.
32. Martinez R, Rubin AL. Synovial chondromatosis. Curr Sports Med Rep 2003; 2(3):123–124.
33. Forssell K, Happonen RP, Forssell H. Synovial chondromatosis of the temporomandibular joint. Report of a case and review of the literature. Int J Oral Maxillofac Surg 1988; 17(4):237–241.
34. van Ingen JM, de Man K, Bakri I. CT diagnosis of synovial chondromatosis of the temporomandibular joint. Br J Oral Maxillofac Surg 1990; 28(3):164–167.
35. Granowitz SP, D'Antonio J, Mankin HL. The pathogenesis and long-term end results of pigmented villonodular synovitis. Clin Orthop Relat Res 1976(114):335–351.
36. Ray RA, Morton CC, Lipinski KK, et al. Cytogenetic evidence of clonality in a case of pigmented villonodular synovitis. Cancer 1991; 67(1):121–125.
37. Cascone P, Rinna C, Ungari C, et al. Pigmented villonodular synovitis of the temporomandibular joint. J Craniofac Surg 2005; 16(4):712–716.
38. Tosun F, Carrau RL, Weissman J. Pigmented villonodular synovitis of the temporomandibular joint: an extensive case with skull-base involvement. Am J Otolaryngol 2004; 25(3):204–207.
39. Ushijima M, Hashimoto H, Tsuneyoshi M, et al. Pigmented villonodular synovitis. A clinicopathologic study of 52 cases. Acta Pathol Jpn 1986; 36(3):317–326.
40. Bertoni F, Unni KK, Beabout JW, et al. Malignant giant cell tumor of the tendon sheaths and joints (malignant pigmented villonodular synovitis). Am J Surg Pathol 1997; 21(2):153–163.
41. Al-Nakshabandi NA, Ryan AG, Choudur H, et al. Pigmented villonodular synovitis. Clin Radiol 2004; 59(5): 414–420.
42. Curtin HD, Williams R, Gallia L, et al. Pigmented villonodular synovitis of the temporomandibular joint. Comput Radiol 1983; 7(4):257–260.
43. Neale SD, Kristelly R, Gundle R, et al. Giant cells in pigmented villo nodular synovitis express an osteoclast phenotype. J Clin Pathol 1997; 50(7):605–608.
44. Kenney JG, Smoot EC, Morgan RF, et al. Recognizing the temporomandibular joint ganglion. Ann Plast Surg 1987; 18(4):323–326.
45. Tabaddor K, Sachs D, Llena JF, et al. Ganglion cyst of the odontoid process. Case report and review of the literature. Spine 1996; 21(17):2019–2022.
46. Chang YM, Chan CP, Kung Wu SF, et al. Ganglion cyst and synovial cyst of the temporomandibular joint. Two case reports. Int J Oral Maxillofac Surg 1997; 26(3): 179–181.
47. Blake WE, Chow CW, Holmes AD, et al. Nasal dermoid sinus cysts: a retrospective review and discussion of investigation and management. Ann Plast Surg 2006; 57(5): 535–540.
48. Schlosser RJ, Faust RA, Phillips CD, et al. Three-dimensional computed tomography of congenital nasal anomalies. Int J Pediatr Otorhinolaryngol 2002; 65(2): 125–131.
49. Hedlund G. Congenital frontonasal masses: developmental anatomy, malformations, and MR imaging. Pediatr Radiol 2006; 36(7):647–662; quiz 726–727.
50. Rothe L, Collin-Osdoby P, Chen Y, et al. Human osteoclasts and osteoclast-like cells synthesize and release high basal and inflammatory stimulated levels of the potent

chemokine interleukin-8. Endocrinology 1998; 139 (10):4353–4363.
51. Ong TK, Franklin CD. A clinical and histopathological study of osteoarthrosis of the temporomandibular joint. Br J Oral Maxillofac Surg 1996; 34(2):186–192.
52. Prasad KC, Prasad SC, Mouli N, et al. Osteomyelitis in the head and neck. Acta Otolaryngol 2007; 127(2):194–205.
53. Calhoun KH, Shapiro RD, Stiernberg CM, et al. Osteomyelitis of the mandible. Arch Otolaryngol Head Neck Surg 1988; 114(10):1157–1162.
54. Meer S, Coleman H, Altini M, et al. Mandibular osteomyelitis and tooth exfoliation following zoster-CMV coinfection. Oral Surg Oral Med Oral Pathol Oral Radiol Endod 2006; 101(1):70–75.
55. Nordin U, Wannfors K, Colque-Navarro P, et al. Antibody response in patients with osteomyelitis of the mandible. Oral Surg Oral Med Oral Pathol Oral Radiol Endod 1995; 79(4):429–435.
56. Ord RA, el-Attar A. Osteomyelitis of the mandible in children–clinical presentations and review of management. Br J Oral Maxillofac Surg 1987; 25(3):204–217.
57. Saglik Y, Arikan M, Altay M, et al. Squamous cell carcinoma arising in chronic osteomyelitis. Int Orthop 2001; 25(6):389–391.
58. McGrory JE, Pritchard DJ, Unni KK, et al. Malignant lesions arising in chronic osteomyelitis. Clin Orthop Relat Res 1999(362):181–189.
59. Altay M, Arikan M, Yildiz Y, et al. Squamous cell carcinoma arising in chronic osteomyelitis in foot and ankle. Foot Ankle Int 2004; 25(11):805–809.
60. Davies HT, Carr RJ. Osteomyelitis of the mandible: a complication of routine dental extractions in alcoholics. Br J Oral Maxillofac Surg 1990; 28(3):185–188.
61. Kaneda T, Yamamoto H, Suzuki H, et al. A clinicoradiological study of maxillary osteomyelitis. J Nihon Univ Sch Dent 1989; 31(2):464–469.
62. Koorbusch GF, Fotos P, Goll KT. Retrospective assessment of osteomyelitis. Etiology, demographics, risk factors, and management in 35 cases. Oral Surg Oral Med Oral Pathol 1992; 74(2):149–154.
63. Springer IN, Wiltfang J, Dunsche A, et al. A new method of monitoring osteomyelitis. Int J Oral Maxillofac Surg 2007.
64. Jones J, Amess TR, Robinson PD. Treatment of chronic sclerosing osteomyelitis of the mandible with calcitonin: a report of two cases. Br J Oral Maxillofac Surg 2005; 43(2): 173–176.
65. Adekeye EO, Cornah J. Osteomyelitis of the jaws: a review of 141 cases. Br J Oral Maxillofac Surg 1985; 23(1): 24–35.
66. Nasir N, Aquilina K, Ryder DQ, et al. Garre's chronic diffuse sclerosing osteomyelitis of the sacrum: a rare condition mimicking malignancy. Br J Neurosurg 2006; 20(6):415–419.
67. Waldron CA, Giansanti JS, Browand BC. Sclerotic cemental masses of the jaws (so-called chronic sclerosing osteomyelitis, sclerosing osteitis, multiple enostosis, and gigantiform cementoma. Oral Surg Oral Med Oral Pathol 1975; 39(4):590–604.
68. Vienne P, Exner GU. Garre sclerosing osteomyelitis. Orthopade 1997; 26(10):902–907.
69. Jacobsson S. Diffuse sclerosing osteomyelitis of the mandible. Int J Oral Surg 1984; 13(5):363–385.
70. Jacobsson S, Heyden G. Chronic sclerosing osteomyelitis of the mandible. Histologic and histochemical findings. Oral Surg Oral Med Oral Pathol 1977; 43(3):357–364.
71. Tong AC, Ng IO, Yeung KM. Osteomyelitis with proliferative periostitis: an unusual case. Oral Surg Oral Med Oral Pathol Oral Radiol Endod 2006; 102(5):e14–e19.
72. Nortje CJ, Wood RE, Grotepass F. Periostitis ossificans versus Garre's osteomyelitis. Part II: Radiologic analysis of 93 cases in the jaws. Oral Surg Oral Med Oral Pathol 1988; 66(2):249–260.
73. Marx RE, Johnson RP. Studies in the radiobiology of osteoradionecrosis and their clinical significance. Oral Surg Oral Med Oral Pathol 1987; 64(4):379–390.
74. Marx RE. Osteoradionecrosis: a new concept of its pathophysiology. J Oral Maxillofac Surg 1983; 41(5): 283–288.
75. Curi MM, Dib LL. Osteoradionecrosis of the jaws: a retrospective study of the background factors and treatment in 104 cases. J Oral Maxillofac Surg 1997; 55(6): 540–544; (discussion 45–46).
76. Jereczek-Fossa BA, Orecchia R. Radiotherapy-induced mandibular bone complications. Cancer Treat Rev 2002; 28(1):65–74.
77. Arkin CR, Masi AT. Relapsing polychondritis: review of current status and case report. Semin Arthritis Rheum 1975; 5(1):41–62.
78. McAdam LP, O'Hanlan MA, Bluestone R, et al. Relapsing polychondritis: prospective study of 23 patients and a review of the literature. Medicine (Baltimore) 1976; 55 (3):193–215.
79. Kraus VB, Stabler T, Le ET, et al. Urinary type II collagen neoepitope as an outcome measure for relapsing polychondritis. Arthritis Rheum 2003; 48(10):2942–2948.
80. Foidart JM, Abe S, Martin GR, et al. Antibodies to type II collagen in relapsing polychondritis. N Engl J Med 1978; 299(22):1203–1207.
81. Rapini RP, Warner NB. Relapsing polychondritis. Clin Dermatol 2006; 24(6):482–485.
82. Dolan DL, Lemmon GB Jr., Teitelbaum SL, et al. Relapsing polychondritis. Analytical literature review and studies on pathogenesis. Am J Med 1966; 41(2):285–299.
83. Shi XH, Zhang FC, Chen LB, et al. The value of 99mTc methylene diphosphonate bone scintigraphy in diagnosing relapsing polychondritis. Chin Med J (Engl) 2006; 119(13): 1129–1132.
84. Imanishi Y, Mitogawa Y, Takizawa M, et al. Relapsing polychondritis diagnosed by Tc-99m MDP bone scintigraphy. Clin Nucl Med 1999; 24(7):511–513.
85. Faix LE, Branstetter BFt. Uncommon CT findings in relapsing polychondritis. AJNR Am J Neuroradiol 2005; 26(8):2134–2136.
86. Behar JV, Choi YW, Hartman TA, et al. Relapsing polychondritis affecting the lower respiratory tract. AJR Am J Roentgenol 2002; 178(1):173–177.
87. Lee KS, Ernst A, Trentham DE, et al. Relapsing polychondritis: prevalence of expiratory CT airway abnormalities. Radiology 2006; 240(2):565–573.
88. Barker BF, Jensen JL, Howell FV. Focal osteoporotic bone marrow defects of the jaws. An analysis of 197 new cases. Oral Surg Oral Med Oral Pathol 1974; 38(3):404–413.
89. Schneider LC, Mesa ML, Fraenkel D. Osteoporotic bone marrow defect: radiographic features and pathogenic factors. Oral Surg Oral Med Oral Pathol 1988; 65(1): 127–129.
90. Shankland WE, Bouquot JE. Focal osteoporotic marrow defect: report of 100 new cases with ultrasonography scans. Cranio 2004; 22(4):314–319.
91. Makek M, Lello GE. Focal osteoporotic bone marrow defects of the jaws. J Oral Maxillofac Surg 1986; 44(4): 268–273.
92. Philipsen HP, Takata T, Reichart PA, et al. Lingual and buccal mandibular bone depressions: a review based on 583 cases from a world-wide literature survey, including 69 new cases from Japan. Dentomaxillofac Radiol 2002; 31(5):281–290.

93. Campos PS, Panella J, Crusoe-Rebello IM, et al. Mandibular ramus-related Stafne's bone cavity. Dentomaxillofac Radiol 2004; 33(1):63–66.
94. Barnes L Jr., Verbin R, Appel N, et al. Diseases of the Bones and Joints. In: Barnes L, ed. Surgical Pathology of the Head and Neck. 2nd ed. New York: Marcel Dekker, 2001:1050–1121.
95. Shimizu M, Osa N, Okamura K, et al. CT analysis of the Stafne's bone defects of the mandible. Dentomaxillofac Radiol 2006; 35(2):95–102.
96. Kaffe I, Littner MM, Arensburg B. The anterior buccal mandibular depression: physical and radiologic features. Oral Surg Oral Med Oral Pathol 1990; 69(5):647–654.
97. Kocsis GS, Marcsik A, Mann RW. Idiopathic bone cavity on the posterior buccal surface of the mandible. Oral Surg Oral Med Oral Pathol 1992; 73(1):123–126.
98. Polykandriotis EP, Beutel FK, Horch RE, et al. A case of familial tumoral calcinosis in a neonate and review of the literature. Arch Orthop Trauma Surg 2004; 124(8):563–567.
99. Roodman GD. Paget's disease and osteoclast biology. Bone 1996; 19(3):209–212.
100. Cody JD, Singer FR, Roodman GD, et al. Genetic linkage of Paget disease of the bone to chromosome 18q. Am J Hum Genet 1997; 61(5):1117–1122.
101. Leach RJ, Singer FR, Cody JD, et al. Variable disease severity associated with a Paget's disease predisposition gene. J Bone Miner Res 1999; 14(suppl 2):17–20.
102. Reddy SV. Etiology of Paget's disease and osteoclast abnormalities. J Cell Biochem 2004; 93(4):688–696.
103. Mirra JM. Pathogenesis of Paget's disease based on viral etiology. Clin Orthop Relat Res 1987(217):162–170.
104. Bender IB. Paget's disease. J Endod 2003; 29(11):720–723.
105. Nellissery MJ, Padalecki SS, Brkanac Z, et al. Evidence for a novel osteosarcoma tumor-suppressor gene in the chromosome 18 region genetically linked with Paget disease of bone. Am J Hum Genet 1998; 63(3):817–824.
106. Simons RM. Paget's disease in the head and neck. Gerontology 1980; 26(3):155–159.
107. Ozek C, Gundogan H, Bilkay U, et al. Craniomaxillofacial fibrous dysplasia. J Craniofac Surg 2002; 13(3):382–389.
108. Engelking CF. Fibrous dysplasia of the trachea and larynx; report of a case. Laryngoscope 1959; 69(4):438–444.
109. DiCaprio MR, Enneking WF. Fibrous dysplasia. Pathophysiology, evaluation, and treatment. J Bone Joint Surg Am 2005; 87(8):1848–1864.
110. Yetiser S, Gonul E, Tosun F, et al. Monostotic craniofacial fibrous dysplasia: the Turkish experience. J Craniofac Surg 2006; 17(1):62–67.
111. Waldron CA. Fibro-osseous lesions of the jaws. J Oral Maxillofac Surg 1993; 51(8):828–835.
112. Song JJ, Jung HH, Lee HM, et al. Monostotic fibrous dysplasia of temporal bone: report of two cases and review of its characteristics. Acta Otolaryngol 2005; 125 (10):1126–1129.
113. Slootweg PJ, Muller H. Differential diagnosis of fibro-osseous jaw lesions. A histological investigation on 30 cases. J Craniomaxillofac Surg 1990; 18(5):210–214.
114. Su L, Weathers DR, Waldron CA. Distinguishing features of focal cemento-osseous dysplasia and cemento-ossifying fibromas. II. A clinical and radiologic spectrum of 316 cases. Oral Surg Oral Med Oral Pathol Oral Radiol Endod 1997; 84(5):540–549.
115. Summerlin DJ, Tomich CE. Focal cemento-osseous dysplasia: a clinicopathologic study of 221 cases. Oral Surg Oral Med Oral Pathol 1994; 78(5):611–620.
116. Mangala M, Ramesh DN, Surekha PS, et al. Florid cemento-osseous dysplasia: Review and report of two cases. Indian J Dent Res 2006; 17(3):131–134.
117. Wolf J, Hietanen J, Sane J. Florid cemento-osseous dysplasia (gigantiform cementoma) in a Caucasian woman. Br J Oral Maxillofac Surg 1989; 27(1):46–52.
118. Longatti P, Marton E, Bonaldi L, et al. Parasagittal cranial fasciitis after irradiation of a cerebellar medulloblastoma: case report. Neurosurgery 2004; 54(5):1263–1266; (discussion 66–67).
119. Boddie DE, Distante S, Blaiklock CT. Cranial fasciitis of childhood: an incidental finding of a lytic skull lesion. Br J Neurosurg 1997; 11(5):445–447.
120. Hunter NS, Bulas DI, Chadduck WM, et al. Cranial fasciitis of childhood. Pediatr Radiol 1993; 23(5):398–399.
121. Keyserling HF, Castillo M, Smith JK. Cranial fasciitis of childhood. AJNR Am J Neuroradiol 2003; 24(7): 1465–1467.
122. Katada T, Tsuchimochi M, Oda T, et al. Magnetic resonance imaging findings of nodular fasciitis in the mental region. Odontology 2004; 92(1):77–80.
123. Patterson JW, Moran SL, Konerding H. Cranial fasciitis. Arch Dermatol 1989; 125(5):674–678.
124. Sarangarajan R, Dehner LP. Cranial and extracranial fasciitis of childhood: a clinicopathologic and immunohistochemical study. Hum Pathol 1999; 30(1):87–92.
125. Raposo-Amaral CE, de Campos Guidi M, Warren SM, et al. Two-stage surgical treatment of severe cherubism. Ann Plast Surg 2007; 58(6):645–651.
126. Penarrocha M, Bonet J, Minguez JM, et al. Cherubism: a clinical, radiographic, and histopathologic comparison of 7 cases. J Oral Maxillofac Surg 2006; 64(6):924–930.
127. Penfold CN, McCullagh P, Eveson JW, et al. Giant cell lesions complicating fibro-osseous conditions of the jaws. Int J Oral Maxillofac Surg 1993; 22(3):158–162.
128. Antoniades DZ, Belazi M, Papanayiotou P. Concurrence of torus palatinus with palatal and buccal exostoses: case report and review of the literature. Oral Surg Oral Med Oral Pathol Oral Radiol Endod 1998; 85(5):552–557.
129. Haugen LK. Palatine and mandibular tori. A morphologic study in the current Norwegian population. Acta Odontol Scand 1992; 50(2):65–77.
130. Gorsky M, Bukai A, Shohat M. Genetic influence on the prevalence of torus palatinus. Am J Med Genet 1998; 75 (2):138–140.
131. Chohayeb AA, Volpe AR. Occurrence of torus palatinus and mandibularis among women of different ethnic groups. Am J Dent 2001; 14(5):278–280.
132. Sirirungrojying S, Kerdpon D. Relationship between oral tori and temporomandibular disorders. Int Dent J 1999; 49(2):101–104.
133. Kaplan I, Calderon S, Buchner A. Peripheral osteoma of the mandible: a study of 10 new cases and analysis of the literature. J Oral Maxillofac Surg 1994; 52(5):467–470.
134. Johann AC, de Freitas JB, de Aguiar MC, et al. Peripheral osteoma of the mandible: case report and review of the literature. J Craniomaxillofac Surg 2005; 33(4):276–281.
135. Fechner R MS. Tumors of the Bone and Joint, vol. 8. 3rd ed. Bethesda: AFIP, 1992.
136. Fenton JE, Turner J, Fagan PA. A histopathologic review of temporal bone exostoses and osteomata. Laryngoscope 1996; 106(5 pt 1):624–628.
137. Sato K, Kodera T, Kitai R, et al. Osteochondroma of the skull base: MRI and histological correlation. Neuroradiology 1996; 38(1):41–43.
138. Castillo M, Hudgins PA, Hoffman JC Jr. Lockjaw secondary to skull base osteochondroma: CT findings. J Comput Assist Tomogr 1989; 13(2):338–339.
139. Traub DJ, Marco WP, Eisenberg E, et al. Osteochondroma of the maxillary sinus: report of a case. J Oral Maxillofac Surg 1990; 48(7):752–755.

140. Bertoletti F, Capolunghi B, Bertolini G, et al. Giant osteoid osteoma of ethmoid sinus: role of functional endoscopic sinus surgery. Acta Otorhinolaryngol Ital 2004; 24(5): 297–301.
141. van der Waal I, Greebe RB, Elias EA. Benign osteoblastoma or osteoid osteoma of the maxilla. Report of a case. Int J Oral Surg 1983; 12(5):355–358.
142. Wold LE, Pritchard DJ, Bergert J, et al. Prostaglandin synthesis by osteoid osteoma and osteoblastoma. Mod Pathol 1988; 1(2):129–131.
143. Lindner NJ, Ozaki T, Roedl R, et al. Percutaneous radiofrequency ablation in osteoid osteoma. J Bone Joint Surg Br 2001; 83(3):391–396.
144. Helms CA, Jeffrey RB, Wing VW. Computed tomography and plain film appearance of a bony sequestration: significance and differential diagnosis. Skeletal Radiol 1987; 16(2):117–120.
145. Helms CA. Osteoid osteoma. The double density sign. Clin Orthop Relat Res 1987(222):167–173.
146. Yildiz Y, Bayrakci K, Altay M, et al. Osteoid osteoma: the results of surgical treatment. Int Orthop 2001; 25(2): 119–122.
147. Lucas DR, Unni KK, McLeod RA, et al. Osteoblastoma: clinicopathologic study of 306 cases. Hum Pathol 1994; 25 (2):117–134.
148. Kroon HM, Schurmans J. Osteoblastoma: clinical and radiologic findings in 98 new cases. Radiology 1990; 175 (3):783–790.
149. Moon KS, Jung S, Lee JH, et al. Benign osteoblastoma of the occipital bone: case report and literature review. Neuropathology 2006; 26(2):141–146.
150. Jones AC, Prihoda TJ, Kacher JE, et al. Osteoblastoma of the maxilla and mandible: a report of 24 cases, review of the literature, and discussion of its relationship to osteoid osteoma of the jaws. Oral Surg Oral Med Oral Pathol Oral Radiol Endod 2006; 102(5):639–650.
151. Rawal YB, Angiero F, Allen CM, et al. Gnathic osteoblastoma: clinicopathologic review of seven cases with long-term follow-up. Oral Oncol 2006; 42(2):123–130.
152. Vade A, Wilbur A, Pudlowski R, et al. Case report 566: Osteoblastoma of sacrum with secondary aneurysmal bone cyst. Skeletal Radiol 1989; 18(6):475–480.
153. Mitchell ML, Ackerman LV. Metastatic and pseudomalignant osteoblastoma: a report of two unusual cases. Skeletal Radiol 1986; 15(3):213–218.
154. Post G, Kountakis SE. Endoscopic resection of large sinonasal ossifying fibroma. Am J Otolaryngol 2005; 26(1): 54–56.
155. Pindborg JJ IK. International Histological Classification of Tumors vol. 5: World Health Organization, 1971:31–34.
156. Perez-Garcia S, Berini-Aytes L, Gay-Escoda C. Ossifying fibroma of the upper jaw: report of a case and review of the literature. Med Oral 2004; 9(4):333–339.
157. Firat Y, Firat AK, Karakas HM, et al. A case of frontal lobe abscess as a complication of frontal sinus ossifying fibroma. Dentomaxillofac Radiol 2006; 35(6):447–450.
158. Salyer KE, Barcelo CR, Por YC. Extensive neglected psammomatoid ossifying fibroma with craniofacial deformity. J Craniofac Surg 2004; 15(6):1033–1039.
159. Carlisle JE, Hammer WB. Giant central ossifying fibroma of the mandible: report of case. J Oral Surg 1979; 37(3): 206–211.
160. Hasselblatt M, Jundt G, Greiner C, et al. Juvenile psammomatoid ossifying fibroma of the neurocranium. Report of four cases. J Neurosurg 2005; 102(6):1151–1154.
161. Moon WJ, Choi S, Chung E, et al. Peripheral ossifying fibroma in the oral cavity: CT and MR findings. Dentomaxillofac Radiol 2007; 36(3):180–182.
162. Granados R, Carrillo R, Najera L, et al. Psammomatoid ossifying fibromas: immunohistochemical analysis and differential diagnosis with psammomatous meningiomas of craniofacial bones. Oral Surg Oral Med Oral Pathol Oral Radiol Endod 2006; 101(5):614–619.
163. McHugh JB, Thomas DG, Herman JM, et al. Primary versus radiation-associated craniofacial osteosarcoma: Biologic and clinicopathologic comparisons. Cancer 2006; 107(3):554–562.
164. Patel SG, Meyers P, Huvos AG, et al. Improved outcomes in patients with osteogenic sarcoma of the head and neck. Cancer 2002; 95(7):1495–1503.
165. Smith RB, Apostolakis LW, Karnell LH, et al. National Cancer Data Base report on osteosarcoma of the head and neck. Cancer 2003; 98(8):1670–1680.
166. Jasnau S, Meyer U, Potratz J, et al. Craniofacial osteosarcoma experience of the cooperative German–Austrian–Swiss osteosarcoma study group. Oral Oncol 2008; 44(3):286–294.
167. Oda D, Bavisotto LM, Schmidt RA, et al. Head and neck osteosarcoma at the University of Washington. Head Neck 1997; 19(6):513–523.
168. Bennett JH, Thomas G, Evans AW, et al. Osteosarcoma of the jaws: a 30-year retrospective review. Oral Surg Oral Med Oral Pathol Oral Radiol Endod 2000; 90(3):323–332.
169. Osteogenic sarcoma of the mandible and maxilla: a Canadian review (1980-2000). J Otolaryngol 2004; 33(3): 139–144.
170. Lee YY, Van Tassel P, Nauert C, et al. Craniofacial osteosarcomas: plain film, CT, and MR findings in 46 cases. AJR Am J Roentgenol 1988; 150(6):1397–1402.
171. Gillespy T, 3rd, Manfrini M, Ruggieri P, Spanier SS, et al. Staging of intraosseous extent of osteosarcoma: correlation of preoperative CT and MR imaging with pathologic macroslides. Radiology 1988; 167(3):765–767.
172. Hsieh ST, Guo YC, Tsai TL, et al. Parosteal osteosarcoma of the mastoid bone following radiotherapy for nasopharyngeal carcinoma. J Chin Med Assoc 2004; 67(6): 314–316.
173. Rodriguez-Arias CA, Lobato RD, Millan JM, et al. Parosteal osteosarcoma of the skull. Neurocirugia (Astur) 2001; 12(6):521–524.
174. Anthouli-Anagnostopoulou FA, Hatziolou E, Papachristou G, et al. Juxtacortical osteosarcoma. A distinct malignant bone neoplasm. Adv Clin Path 2000; 4(3):127–131.
175. Seely DR, Gates GA. Parosteal osteogenic sarcoma of the mastoid bone. Ann Otol Rhinol Laryngol 1997; 106(9): 729–732.
176. Lindell MM Jr., Shirkhoda A, Raymond AK, et al. Parosteal osteosarcoma: radiologic-pathologic correlation with emphasis on CT. AJR Am J Roentgenol 1987; 148(2): 323–328.
177. Sheth DS, Yasko AW, Raymond AK, et al. Conventional and dedifferentiated parosteal osteosarcoma. Diagnosis, treatment, and outcome. Cancer 1996; 78(10):2136–2145.
178. Chan CW, Kung TM, Ma L. Telangiectatic osteosarcoma of the mandible. Cancer 1986; 58(9):2110–2115.
179. Wick MR, Siegal GP, Unni KK, et al. Sarcomas of bone complicating osteitis deformans (Paget's disease): fifty years' experience. Am J Surg Pathol 1981; 5(1):47–59.
180. Murphey MD, wan Jaovisidha S, Temple HT, et al. Telangiectatic osteosarcoma: radiologic-pathologic comparison. Radiology 2003; 229(2):545–553.
181. Saito T, Oda Y, Kawaguchi K, et al. Five-year evolution of a telangiectatic osteosarcoma initially managed as an aneurysmal bone cyst. Skeletal Radiol 2005; 34(5):290–294.
182. Hansen MF, Nellissery MJ, Bhatia P. Common mechanisms of osteosarcoma and Paget's disease. J Bone Miner Res 1999; 14(suppl 2):39–44.

183. Ahmad SA, Patel SR, Ballo MT, et al. Extraosseous osteosarcoma: response to treatment and long-term outcome. J Clin Oncol 2002; 20(2):521–527.
184. Manning JT, Raymond AK, Batsakis JG. Extraosseous osteogenic sarcoma of the parotid gland. J Laryngol Otol 1986; 100(2):239–242.
185. Stimson PG, Valenzuela-Espinoza A, Tortoledo ME, et al. Primary osteosarcoma of the parotid gland. Oral Surg Oral Med Oral Pathol 1989; 68(1):80–86.
186. Reyes JM, Vangore SK, Putong PB, et al. Osteogenic sarcoma of the tongue. Oral Surg Oral Med Oral Pathol 1981; 51(4):421–425.
187. Bem CC, Sharpe DT. Extraskeletal osteogenic sarcoma occurring in the tongue. Br J Oral Maxillofac Surg 1988; 26(3):248–249.
188. Casiraghi O, Martinez-Madrigal F, Pineda-Daboin K, et al. Chondroid tumors of the larynx: a clinicopathologic study of 19 cases, including two dedifferentiated chondrosarcomas. Ann Diagn Pathol 2004; 8(4):189–197.
189. McDermott MB, Ponder TB, Dehner LP. Nasal chondromesenchymal hamartoma: an upper respiratory tract analogue of the chest wall mesenchymal hamartoma. Am J Surg Pathol 1998; 22(4):425–433.
190. Johnson C, Nagaraj U, Esguerra J, et al. Nasal chondromesenchymal hamartoma: radiographic and histopathologic analysis of a rare pediatric tumor. Pediatr Radiol 2007; 37(1):101–104.
191. Hsueh C, Hsueh S, Gonzalez-Crussi F, et al. Nasal chondromesenchymal hamartoma in children: report of 2 cases with review of the literature. Arch Pathol Lab Med 2001; 125(3):400–403.
192. Hill MJ, Taylor CL, Scott GB. Chondromatous metaplasia in the human larynx. Histopathology 1980; 4(2):205–214.
193. Batsakis JG, Raymond AK. Cartilage tumors of the larynx. South Med J 1988; 81(4):481–484.
194. Yang SW, Lin CY. A peculiar site of chondroma: the epiglottis. Acta Otolaryngol 2005; 125(8):906–909.
195. Baatenburg de Jong RJ, van Lent S, Hogendoorn PC. Chondroma and chondrosarcoma of the larynx. Curr Opin Otolaryngol Head Neck Surg 2004; 12(2):98–105.
196. Thome R, Thome DC, de la Cortina RA. Long-term follow-up of cartilaginous tumors of the larynx. Otolaryngol Head Neck Surg 2001; 124(6):634–640.
197. Koch BB, Karnell LH, Hoffman HT, et al. National cancer database report on chondrosarcoma of the head and neck. Head Neck 2000; 22(4):408–425.
198. Gorsky M, Epstein JB. Craniofacial osseous and chondromatous sarcomas in British Columbia—a review of 34 cases. Oral Oncol 2000; 36(1):27–31.
199. Thompson LD, Gannon FH. Chondrosarcoma of the larynx: a clinicopathologic study of 111 cases with a review of the literature. Am J Surg Pathol 2002; 26(7): 836–851.
200. Lewis JE, Olsen KD, Inwards CY. Cartilaginous tumors of the larynx: clinicopathologic review of 47 cases. Ann Otol Rhinol Laryngol 1997; 106(2):94–100.
201. Garcia RE, Gannon FH, Thompson LD. Dedifferentiated chondrosarcomas of the larynx: a report of two cases and review of the literature. Laryngoscope 2002; 112(6): 1015–1018.
202. Wang SJ, Borges A, Lufkin RB, et al. Chondroid tumors of the larynx: computed tomography findings. Am J Otolaryngol 1999; 20(6):379–382.
203. Bucci T, Dell'Aversana Orabona G, Insabato L, et al. Chondromyxoid fibroma of the zygoma: a case report. Int J Oral Maxillofac Surg 2006; 35(6):569–571.
204. Wolf DA, Chaljub G, Maggio W, et al. Intracranial chondromyxoid fibroma. Report of a case and review of the literature. Arch Pathol Lab Med 1997; 121(6):626–630.
205. Batsakis JG, Raymond AK. Chondromyxoid fibroma. Ann Otol Rhinol Laryngol 1989; 98(7 pt 1):571–572.
206. Keel SB, Bhan AK, Liebsch NJ, et al. Chondromyxoid fibroma of the skull base: a tumor which may be confused with chordoma and chondrosarcoma. A report of three cases and review of the literature. Am J Surg Pathol 1997; 21(5):577–582.
207. Wu CT, Inwards CY, O'Laughlin S, et al. Chondromyxoid fibroma of bone: a clinicopathologic review of 278 cases. Hum Pathol 1998; 29(5):438–446.
208. Yamaguchi T, Dorfman HD. Radiographic and histologic patterns of calcification in chondromyxoid fibroma. Skeletal Radiol 1998; 27(10):559–564.
209. Bian LG, Sun QF, Zhao WG, et al. Temporal bone chondroblastoma: a review. Neuropathology 2005; 25(2): 159–164.
210. Pontius A, Reder P, Ducic Y. Temporal bone chondroblastomas. Am J Otolaryngol 2003; 24(6):370–373.
211. Watanabe N, Yoshida K, Shigemi H, et al. Temporal bone chondroblastoma. Otolaryngol Head Neck Surg 1999; 121 (3):327–330.
212. Oda Y, Izumi T, Harimaya K, et al. Pigmented villonodular synovitis with chondroid metaplasia, resembling chondroblastoma of the bone: a report of three cases. Mod Pathol 2007; 20(5):545–551.
213. Heffelfinger MJ, Dahlin DC, MacCarty CS, et al. Chordomas and cartilaginous tumors at the skull base. Cancer 1973; 32(2):410–420.
214. Kaiser TE, Pritchard DJ, Unni KK. Clinicopathologic study of sacrococcygeal chordoma. Cancer 1984; 53 (11):2574–2578.
215. Lynn-Macrae A, Haines GK, 3rd, Altman KW. Primary chordoma of the lateral nasal wall: case report and review. Ear Nose Throat J 2005; 84(9):593–595.
216. Campbell WM, McDonald TJ, Unni KK, et al. Nasal and paranasal presentations of chordomas. Laryngoscope 1980; 90(4):612–618.
217. Loughran S, Badia L, Lund V. Primary chordoma of the ethmoid sinus. J Laryngol Otol 2000; 114(8):627–629.
218. Roberti F, Sekhar LN, Jones RV, et al. Intradural cranial chordoma: a rare presentation of an uncommon tumor. Surgical experience and review of the literature. J Neurosurg 2007; 106(2):270–274.
219. Pardo-Mindan FJ, Guillen FJ, Villas C, et al. A comparative ultrastructural study of chondrosarcoma, chordoid sarcoma, and chordoma. Cancer 1981; 47(11):2611–2619.
220. O'Neill P, Bell BA, Miller JD, et al. Fifty years of experience with chordomas in southeast Scotland. Neurosurgery 1985; 16(2):166–170.
221. Volpe R, Mazabraud A. A clinicopathologic review of 25 cases of chordoma (a pleomorphic and metastasizing neoplasm). Am J Surg Pathol 1983; 7(2):161–170.
222. Forsyth PA, Cascino TL, Shaw EG, et al. Intracranial chordomas: a clinicopathological and prognostic study of 51 cases. J Neurosurg 1993; 78(5):741–747.
223. Casali PG, Stacchiotti S, Sangalli C, et al. Chordoma. Curr Opin Oncol 2007; 19(4):367–370.
224. Tzortzidis F, Elahi F, Wright DC, et al. Patient outcome at long-term follow-up after aggressive microsurgical resection of cranial base chondrosarcomas. Neurosurgery 2006; 58(6):1090–1098; (discussion 90–98).
225. Coffin CM, Swanson PE, Wick MR, et al. Chordoma in childhood and adolescence. A clinicopathologic analysis of 12 cases. Arch Pathol Lab Med 1993; 117(9):927–933.
226. Wold LE, Laws ER Jr. Cranial chordomas in children and young adults. J Neurosurg 1983; 59(6):1043–1047.
227. Hoch BL, Nielsen GP, Liebsch NJ, et al. Base of skull chordomas in children and adolescents: a clinicopathologic study of 73 cases. Am J Surg Pathol 2006; 30(7):811–818.

228. Pamir MN, Ozduman K. Analysis of radiological features relative to histopathology in 42 skull-base chordomas and chondrosarcomas. Eur J Radiol 2006; 58(3):461–470.
229. Rosenberg AE, Nielsen GP, Keel SB, et al. Chondrosarcoma of the base of the skull: a clinicopathologic study of 200 cases with emphasis on its distinction from chordoma. Am J Surg Pathol 1999; 23(11):1370–1378.
230. Triana A, Sen C, Wolfe D, et al. Cadherins and catenins in clival chordomas: correlation of expression with tumor aggressiveness. Am J Surg Pathol 2005; 29(11):1422–1434.
231. Meis JM, Raymond AK, Evans HL, et al. ''Dedifferentiated'' chordoma. A clinicopathologic and immunohistochemical study of three cases. Am J Surg Pathol 1987; 11(7):516–525.
232. Wojno KJ, Hruban RH, Garin-Chesa P, et al. Chondroid chordomas and low-grade chondrosarcomas of the craniospinal axis. An immunohistochemical analysis of 17 cases. Am J Surg Pathol 1992; 16(12):1144–1152.
233. Bizzozero L, Solaining Talamonti C, et al Cavernous hemangioma of the skull. Case report and review of the literature. J Neurosurg Sci 1997; 41(4):419–421.
234. Ajja A, Oukacha N, Gazzaz M, et al. Cavernous hemangioma of the parietal bone. A case report. J Neurosurg Sci 2005; 49(4):159–162; (discussion 62).
235. Heckl S, Aschoff A, Kunze S. Cavernomas of the skull: review of the literature 1975-2000. Neurosurg Rev 2002; 25 (1–2):56–62; (discussion 66–67).
236. Curtin HD, Jensen JE, Barnes L Jr., et al. ''Ossifying'' hemangiomas of the temporal bone: evaluation with CT. Radiology 1987; 164(3):831–835.
237. Colucci S, Taraboletti G, Primo L, et al. Gorham-Stout syndrome: a monocyte-mediated cytokine propelled disease. J Bone Miner Res 2006; 21(2):207–218.
238. Khanam H, Lipper MH, Wolff CL, et al. Calvarial hemangiomas: report of two cases and review of the literature. Surg Neurol 2001; 55(1):63–67; (discussion 67).
239. Koh YC, Yoo H. Epithelioid haemangioendothelioma of the sphenoid bone. J Clin Neurosci 2001; 8(suppl 1): 63–66.
240. Joo M, Lee GJ, Koh YC, et al. Hemangioendothelioma of the sphenoid bone: a case report. J Korean Med Sci 2001; 16(2):241–244.
241. Larochelle O, Perigny M, Lagace R, et al. Best cases from the AFIP: epithelioid hemangioendothelioma of bone. Radiographics 2006; 26(1):265–270.
242. Mendlick MR, Nelson M, Pickering D, et al. Translocation t(1;3)(p36.3;q25) is a nonrandom aberration in epithelioid hemangioendothelioma. Am J Surg Pathol 2001; 25(5): 684–687.
243. Farr HW, Carandang CM, Huvos AG. Malignant vascular tumors of the head and neck. Am J Surg 1970; 120(4): 501–504.
244. Fukushima K, Dejima K, Koike S, et al. A case of angiosarcoma of the nasal cavity successfully treated with recombinant interleukin-2. Otolaryngol Head Neck Surg 2006; 134(5):886–887.
245. Scholsem M, Raket D, Flandroy P, et al. Primary temporal bone angiosarcoma: a case report. J Neurooncol 2005; 75(2):121–125.
246. Abraham JA, Hornicek FJ, Kaufman AM, et al. Treatment and outcome of 82 patients with angiosarcoma. Ann Surg Oncol 2007; 14(6):1953–1967.
247. Wallace MJ, Ross M. Bone lymphangiomatosis: treatment with percutaneous cementoplasty. Spine 2005; 30(12): E336–E339.
248. Cummings TJ, George TM, Fuchs HE, et al. The pathology of extracranial scalp and skull masses in young children. Clin Neuropathol 2004; 23(1):34–43.
249. Breiteneder-Geleff S, Soleiman A, Kowalski H, et al. Angiosarcomas express mixed endothelial phenotypes of blood and lymphatic capillaries: podoplanin as a specific marker for lymphatic endothelium. Am J Pathol 1999; 154(2):385–394.
250. Commins DJ, O'Malley S, Athanasou NA, et al. Giant cell tumour of the hyoid–first reported case. J Laryngol Otol 1999; 113(6):566–568.
251. Marioni G, Marchese-Ragona R, Guarda-Nardini L, et al. Giant cell tumour (central giant cell lesion) of the maxilla. Acta Otolaryngol 2006; 126(7):779–781.
252. Hoffman CD, Huntley TA, Wiesenfeld D, et al. Maxillary giant cell tumour associated with Paget's disease of bone. Int J Oral Maxillofac Surg 1994; 23(3):161–164.
253. do Amaral CM, Julio GL, Cardoso LA, et al. Craniofacial treatment of giant-cell tumors of the sphenoid bone. J Craniofac Surg 1994; 5(4):254–256.
254. Brien EW, Mirra JM, Kessler S, et al. Benign giant cell tumor of bone with osteosarcomatous transformation (''dedifferentiated'' primary malignant GCT): report of two cases. Skeletal Radiol 1997; 26(4):246–255.
255. Morris JM, Lane JI, Witte RJ, et al. Giant cell reparative granuloma of the nasal cavity. AJNR Am J Neuroradiol 2004; 25(7):1263–1265.
256. Ratner V, Dorfman HD. Giant-cell reparative granuloma of the hand and foot bones. Clin Orthop Relat Res 1990; (260):251–258.
257. Lorenzo JC, Dorfman HD. Giant-cell reparative granuloma of short tubular bones of the hands and feet. Am J Surg Pathol 1980; 4(6):551–563.
258. Wold LE, Dobyns JH, Swee RG, et al. Giant cell reaction (giant cell reparative granuloma) of the small bones of the hands and feet. Am J Surg Pathol 1986; 10(7):491–496.
259. Mafee MF, Yang G, Tseng A, et al. Fibro-osseous and giant cell lesions, including brown tumor of the mandible, maxilla, and other craniofacial bones. Neuroimaging Clin N Am 2003; 13(3):525–540.
260. Page EL, Peters GE. Aneurysmal bone cyst of the zygomatic arch. Head Neck 1994; 16(6):594–597.
261. Zachariades N, Vairaktaris E, Mezitis M, et al. Aneurysmal bone cyst of the jaws. Review of the literature and report of 2 cases. Int J Oral Maxillofac Surg 1986; 15(5):534–540.
262. Shadaba A, Zaidi S. Aneurysmal bone cyst of the hyoid. J Laryngol Otol 1992; 106(1):71–72.
263. Della Libera D, Redlich G, Bittesini L, et al. Aneurysmal bone cyst of the larynx presenting with hypoglottic obstruction. Arch Pathol Lab Med 2001; 125(5):673–676.
264. Schilling HE, Neal GD, Nathan M, et al. Aneurysmal bone cyst of the larynx. Am J Otolaryngol 1986; 7(5):370–374.
265. Fyrmpas G, Constantinidis J, Televantou D, et al. Primary aneurysmal bone cyst of the maxillary sinus in a child: case report and review of the literature. Eur Arch Otorhinolaryngol 2006; 263(7):695–698.
266. Fisker AV, Philipsen HP. Desmoplastic fibroma of the jaw bones. Int J Oral Surg 1976; 5(6):285–291.
267. Selfa-Moreno S, Arana-Fernandez E, Fernandez-Latorre F, et al. Desmoplastic fibroma of the skull. Case report. J Neurosurg 1995; 82(1):119–120.
268. Hufnagel TJ, Artiles C, Piepmeier J, et al. Desmoplastic fibroma of parietal bone simulating eosinophilic granuloma. Case report. J Neurosurg 1987; 67(3):449–451.
269. Crim JR, Gold RH, Mirra JM, et al. Desmoplastic fibroma of bone: radiographic analysis. Radiology 1989; 172(3):827–832.
270. Frick MA, Sundaram M, Unni KK, et al. Imaging findings in desmoplastic fibroma of bone: distinctive T2 characteristics. AJR Am J Roentgenol 2005; 184(6):1762–1767.
271. Inwards CY, Unni KK, Beabout JW, et al. Desmoplastic fibroma of bone. Cancer 1991; 68(9):1978–1983.

272. Callahan KS, Eberhardt SC, Fechner RE, et al. Desmoplastic fibroma of bone with extensive cartilaginous metaplasia. Ann Diagn Pathol 2006; 10(6):343–346.
273. Huvos AG, Higinbotham NL. Primary fibrosarcoma of bone. A clinicopathologic study of 130 patients. Cancer 1975; 35(3):837–847.
274. Weatherby RP, Dahlin DC, Ivins JC. Postradiation sarcoma of bone: review of 78 Mayo Clinic cases. Mayo Clin Proc 1981; 56(5):294–306.
275. Lustig LR, Jackler RK, Lanser MJ. Radiation-induced tumors of the temporal bone. Am J Otol 1997; 18(2): 230–235.
276. Jeffree GM, Price CH. Metastatic spread of fibrosarcoma of bone; A report on forty-nine cases, and a comparison with osteosarcoma. J Bone Joint Surg Br 1976; 58-B(4):418–425.
277. Plaza G, Ferrando J, Pinedo F. Sinonasal fibrosarcoma: a case report. Eur Arch Otorhinolaryngol 2006; 263(7): 641–643.

15

Hematolymphoid Lesions of the Head and Neck

Alexander C. L. Chan and John K. C. Chan
Department of Pathology, Queen Elizabeth Hospital, Hong Kong

I. INTRODUCTION

Myriads of reactive and neoplastic hematolymphoid conditions can affect the head and neck region, involving either nodal or extranodal sites. In this chapter, emphasis is placed on those entities that are more prevalent in the head and neck.

II. REACTIVE HEMATOLYMPHOID LESIONS OF THE HEAD AND NECK

Many lymph nodes are found in the head and neck region, especially the cervical area. These nodes can undergo enlargement as a result of reactive changes or malignancy, with the former being more common, especially in younger patients (Table 1). Among reactive lesions, most represent nonspecific reactive lymphoid hyperplasia, while specific reactive conditions are identified in only a proportion of cases. Reactive hematolymphoid lesions can also involve various extranodal sites in the head and neck region, and can mimic lymphoma clinically or histologically.

A. Nonspecific Reactive Lymphoid Hyperplasia

Lymph Node

The lymph nodes in the head and neck region commonly show nonspecific reactive lymphoid hyperplasia. The changes are often due to upper respiratory tract or systemic infection, hypersensitivity reaction (including reaction to drugs), or unknown etiology.

The normal lymph node. A lymph node normally consists of the cortex, paracortex, medullary cords, and sinuses (1). It is surrounded by a thin fibrous capsule, which is continuous with fibrous trabeculae that extend into the node alongside the sinuses. The cortex is the B-cell zone and contains lymphoid follicles; the paracortex is the T-cell zone and has a rich network of high endothelial venules (Fig. 1A–C).

In the cortex, primary and secondary lymphoid follicles are present. Primary follicle comprises small lymphocytes with round or minimally irregular nuclear outline and dense chromatin. Secondary follicle, which develops from primary follicle after exposure to antigen, consists of germinal center surrounded by mantle zone (Fig. 2A, B). Both types of follicles are formed predominantly by B cells (CD20+), supported by meshworks of follicular dendritic cells (Fig. 3). The germinal centers of secondary follicles contain follicle center B cells (consisting of a mixture of centrocytes and centroblasts), scattered intrafollicular T cells (frequently CD4+, CD10+, BCL6+, CD57+/−), and tingible-body macrophages (Fig. 2B). Centrocytes are small cells with angulated nuclei, dense chromatin, and barely visible cytoplasm, while centroblasts are large cells with round vesicular nuclei, multiple small membrane-bound nucleoli, and a thin rim of amphophilic cytoplasm (Fig. 2B). The germinal center B cells express IgG, IgA, or IgM, but not IgD. The cells in the mantle zone and primary follicles frequently coexpress IgD and IgM.

In the paracortex, there is a mixture of small lymphocytes, immunoblasts, histiocytes, S100 protein-positive antigen-presenting cells, and plasma cells (Fig. 4). Immunoblasts are large lymphoid cells with round or oval vesicular nuclei, prominent central nucleolus, and a broader rim of basophilic cytoplasm. The lymphoid cells within the paracortex are predominantly T cells expressing pan-T markers such as CD3, with CD4+ cells being often more numerous than CD8+ cells. There are also scattered B cells, many with an immunoblastic appearance. In addition, slender dendritic cells can be identified by immunostaining for cytokeratin; they probably represent a subset of fibroblastic dendritic cells (2).

The medullary cords are often packed with plasma cells. The sinuses, which connect the afferent lymphatics on the convex surface of the node to the efferent lymphatics at the hilum, frequently contain histiocytes and lymphoid cells.

Reactive lymphoid hyperplasia of lymph node. Different compartments may be affected to various degrees when lymph node undergoes reactive hyperplasia. The following terminologies can be applied when the changes do not conform to specific entities.

Reactive follicular hyperplasia is characterized by an increase in size and number of secondary lymphoid follicles (Fig. 5). Reactive follicles, in contrast to

Table 1 Causes of Enlargement of Head and Neck Lymph Nodes

Malignant	Reactive
Metastatic malignancies	Nonspecific reactive lymphoid hyperplasia
Carcinoma	Infection
Melanoma	*Viral*, e.g., Epstein-Barr virus (infectious mononucleosis), cytomegalovirus, herpes simplex virus, human herpesvirus 6, human immunodeficiency virus
Sarcoma	*Bacterial*, e.g., cat scratch disease, pyogenic infection, mycobacteria, syphilis, leprosy
Germ cell tumor	*Fungal*
Small round cell tumors of childhood, such as neuroblastoma	*Protozoan, e.g., toxoplasmosis, leishmaniasis*
Hematolymphoid neoplasms	Autoimmune diseases
Hodgkin lymphoma	e.g., rheumatoid arthritis, systemic lupus erythematosus, Sjogren syndrome
Non-Hodgkin lymphoma	Inherited diseases
Myeloid leukemia	e.g., autoimmune lymphoproliferative syndrome
Histiocytic and dendritic cell neoplasms	Unknown etiology
	e.g., progressive transformation of germinal centers, dermatopathic lymphadenopathy, Kikuchi disease, Kimura disease, Kawasaki disease, Castleman disease, Rosai–Dorfman disease, IgG4-related sclerosing disease
	Others
	e.g., amyloidosis, inflammatory pseudotumor of lymph node, extramedullary hematopoietic tumor

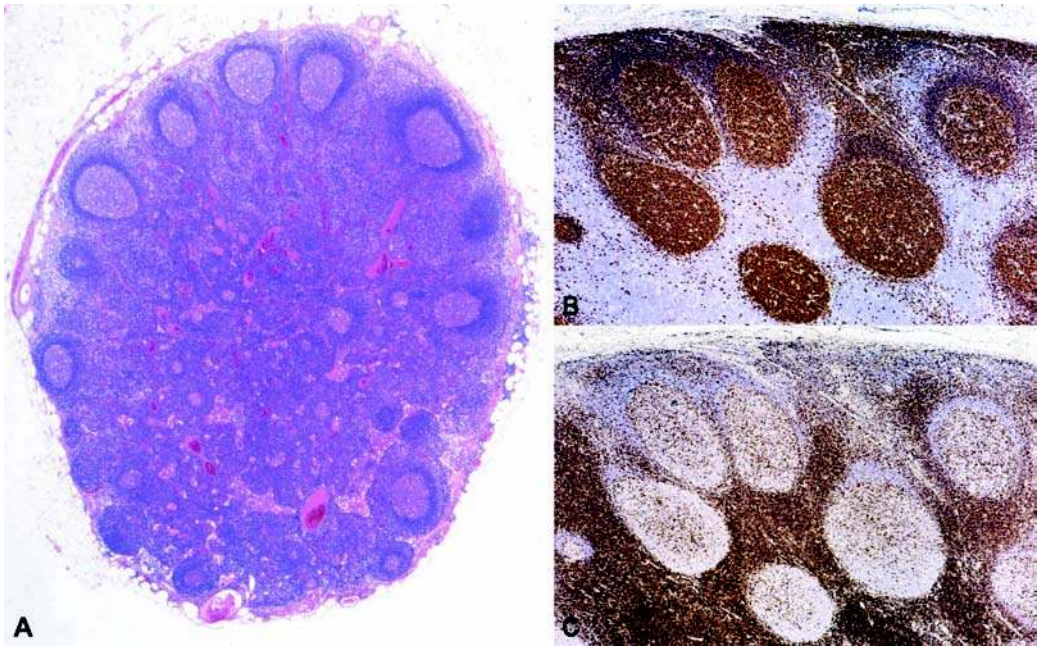

Figure 1 Normal lymph node. (**A**) The cortex comprises predominantly secondary lymphoid follicles with discrete mantles. The paracortex represents the zone between and slightly deep to the follicles. The medulla occupies the central portion of the node, consisting of dark-staining medullary cords separated by medullary sinuses. (**B**) Immunostaining for CD20 (B-lineage marker) shows that the follicles are composed mostly of B cells. Very often, there is a narrow continuous band of B cells immediately beneath the nodal capsule. (**C**) Immunostaining for CD3 (T-lineage marker) highlights the predominant population of T cells in the paracortex. Scattered T cells are also present within the lymphoid follicles.

neoplastic follicles, are not arranged in a back-to-back pattern and are surrounded by intact mantles. They have round, oval, or highly irregular contours, and characteristically show polarity, with recognizable dark and light zones (Figs. 2A and 6). Tingible-body macrophages are prominent, producing a starry-sky pattern. There is variable increase of plasma cells in the interfollicular zone. In some cases, reactive

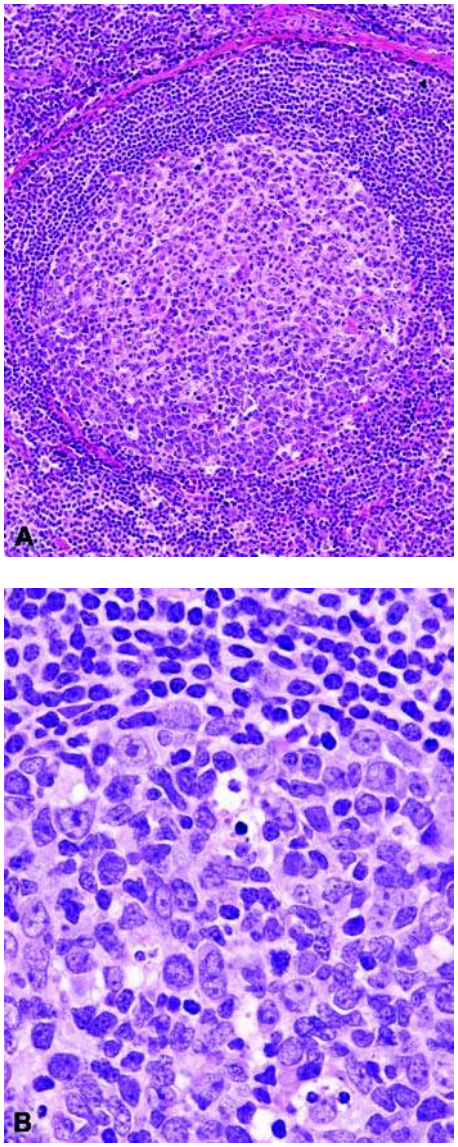

Figure 2 Normal secondary lymphoid follicle. (**A**) The germinal center is typically surrounded by a distinct mantle. It is demarcated into a light zone (*upper field*) and dark zone (*lower field*) when sectioned in the correct plane. The dark zone differs from the light zone in having a higher proportion of centroblasts. (**B**) The mantle zone comprises small lymphocytes with dark round nuclei. The predominant residents of the germinal center include centrocytes (with irregular or triangular-shaped nuclei and fairly condensed chromatin) and centroblasts (larger cells with distinct nucleoli). There are typically interspersed tingible-body macrophages with phagocytosed apoptotic bodies.

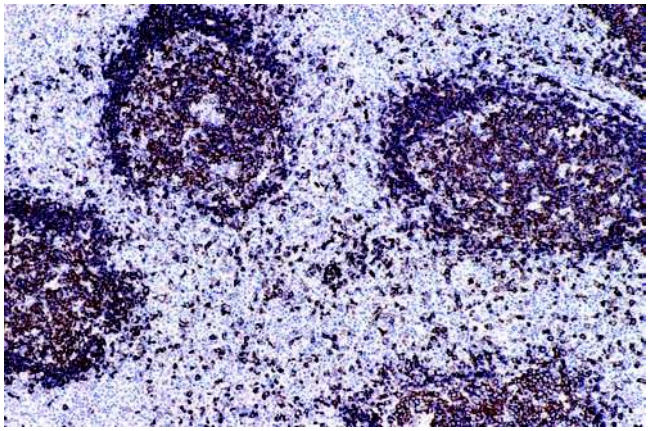

Figure 3 Reactive lymph node immunostained for CD20. The lymphoid follicles, which are rich in B cells, are well highlighted. There are usually not many CD20+ B cells in the interfollicular zone.

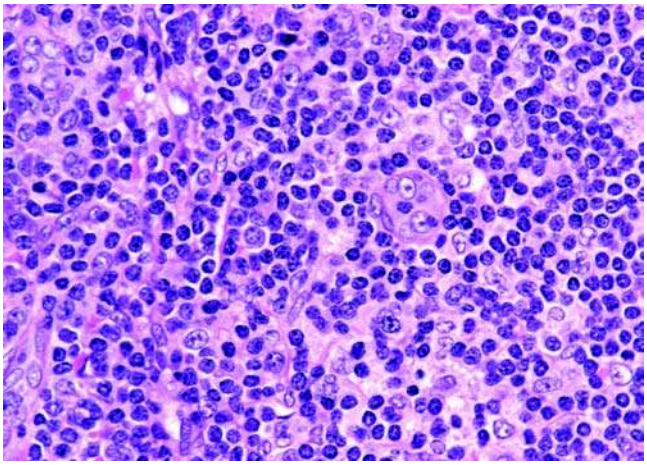

Figure 4 The normal paracortex. This zone, rich in high endothelial cells, is populated predominantly by small lymphocytes. There are scattered large cells (immunoblasts) and plasma cells.

follicular hyperplasia is accompanied by monocytoid B-cell reaction. Monocytoid B cells, which are medium-sized cells with indented or oval nuclei, fine chromatin, and a moderate amount of clear cytoplasm, typically form incomplete arcs around reactive follicles (Fig. 7A, B) (3–5). Sometimes the monocytoid B-cell population comprises larger cells with rounder nuclei, vesicular chromatin, and more prominent nucleoli (6). There can be some intermixed neutrophils and larger blastic lymphoid cells among the monocytoid B cells. Although these cells are by themselves nonspecific (6,7), they are characteristic of certain specific lymphadenopathies, such as toxoplasmosis, human immunodeficiency virus (HIV)-associated lymphadenopathy, cat scratch disease, lymphogranuloma venereum, cytomegalovirus lymphadenitis in immunocompetent hosts, and primary infection by Epstein-Barr virus (EBV) (3,4,8,9).

Reactive paracortical hyperplasia is characterized by expansion of the paracortex between reactive or atrophic lymphoid follicles (Fig. 8A). The cellular composition is similar to that seen in the normal paracortex, with

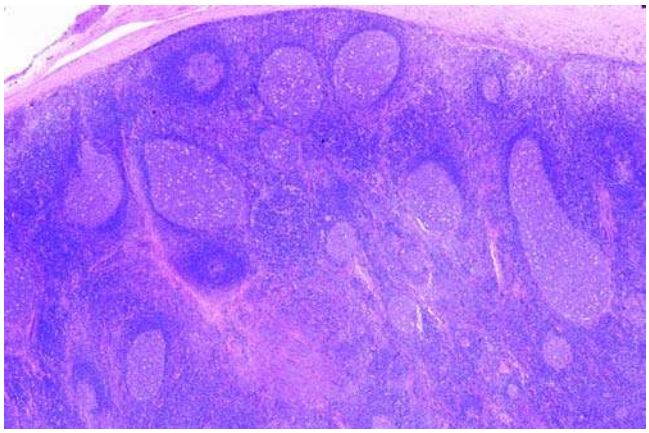

Figure 5 Reactive follicular hyperplasia of lymph node. This is characterized by an increase in the number and size of secondary lymphoid follicles. Despite this, the follicles do not show a back-to-back pattern as commonly observed in follicular lymphoma. The secondary lymphoid follicles typically have distinct mantles, show polarity (although this feature may not be evident in some follicles due to variations in the plane of sectioning), and exhibit a starry-sky pattern due to the presence of many interspersed tingible-body macrophages.

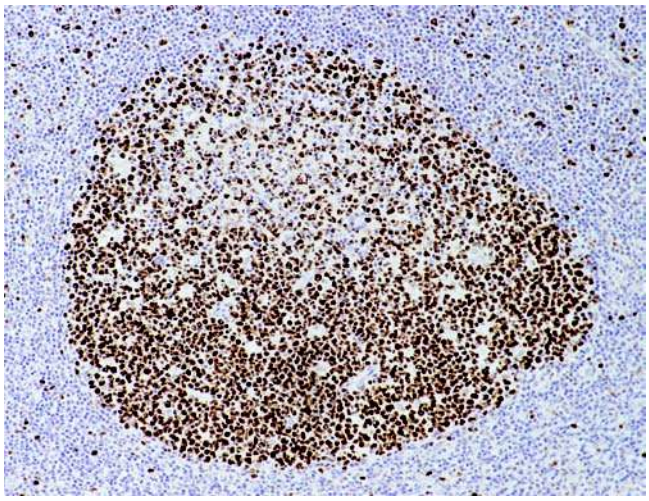

Figure 6 Reactive secondary lymphoid follicle immunostained for Ki67 (a proliferation-associated marker). The reactive follicle typically shows a very high proliferative fraction (>80%). This immunostain further highlights the polarity, with the dark zone (*lower field*) showing a higher proliferative fraction than the light zone.

lymphocytes, immunoblasts, histiocytes, S100 protein-positive antigen-presenting cells, plasma cells, and occasional eosinophils being present among a prominent network of high endothelial venules (Fig. 8B). The lymphoid cells within the paracortex are predominantly T cells, but scattered large B cells are also present

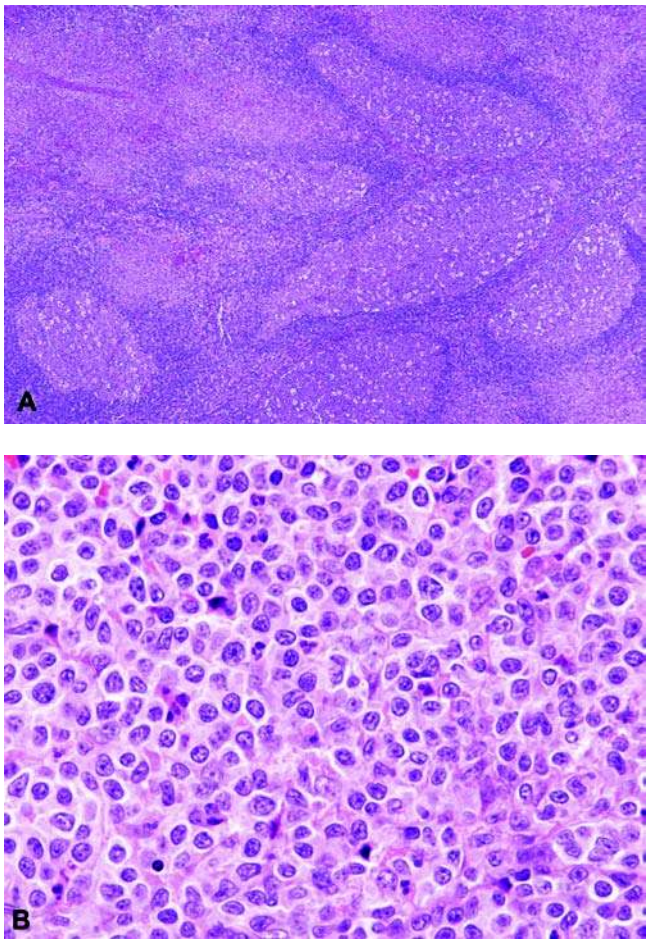

Figure 7 Reactive follicular hyperplasia of lymph node with monocytoid B-cell reaction. (**A**) Bands of pale-staining monocytoid B-cells are present adjacent to reactive lymphoid follicles. (**B**) Monocytoid B-cells are medium-sized cells with oval or slightly indented nuclei and an appreciable amount of clear to lightly eosinophilic cytoplasm.

(Fig. 9). The B cells, however, should not form broad sheets; otherwise B-cell lymphoma has to be suspected. They show polytypic immunoglobulin light chains, with a κ/λ ratio of 2–3:1. In the paracortex, there are sometimes small nodular aggregates of plasmacytoid dendritic cells (formerly known as ''plasmacytoid monocytes''), which are often accompanied by apoptotic bodies and tingible-body macrophages (Fig. 10A). These cells have eccentrically placed, medium-sized, round nuclei with moderately condensed chromatin and a moderate amount of amphophilic cytoplasm (Fig. 10B). They show a CD68+, CD123+ immunophenotype.

Sinus histiocytosis is characterized by expansion of the sinuses by bland-looking histiocytes in the sinuses. The histiocytes may show phagocytosis of red cells, white cells, or debris. Rarely, the histiocytes can assume signet-ring morphology, and have to be distinguished from metastatic carcinoma by immunohistochemistry (cytokeratin−, CD68+, CD163+) (10).

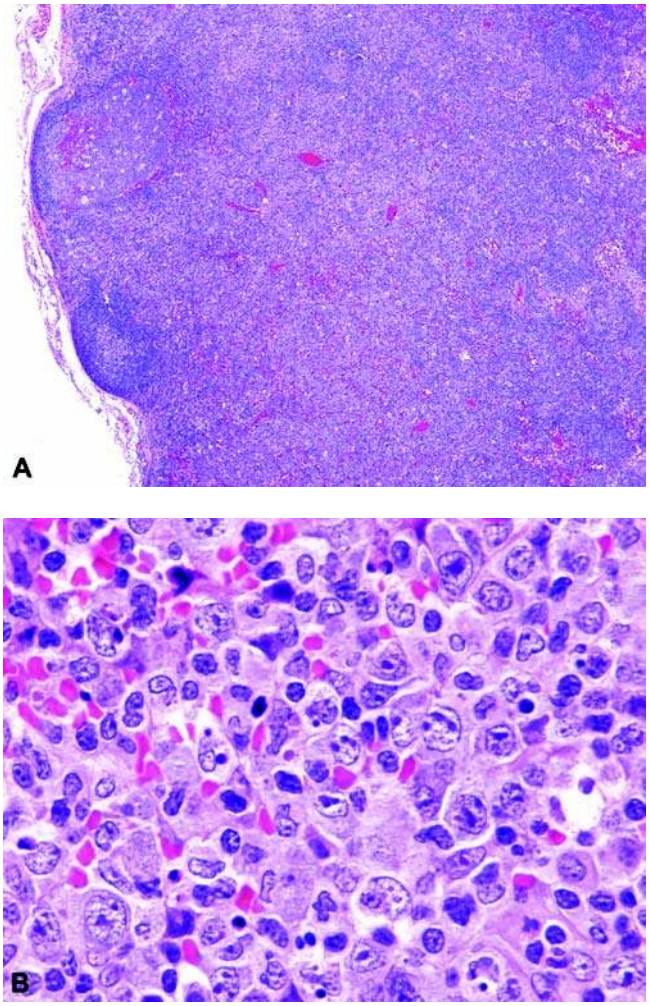

Figure 8 Reactive paracortical hyperplasia of lymph node. (**A**) The paracortex (interfollicular zone) is expanded at the expense of the lymphoid follicles. (**B**) In the paracortex, there is an increase of nonatypical immunoblasts.

Nonspecific reactive lymphoid hyperplasia refers to lymphoid reactions that show combinations of the above-mentioned changes, or do not exactly fit the above descriptions, and lacking features of specific lymphadenopathies.

Extranodal Sites in the Head and Neck

With the exception of the Waldeyer ring, the various *extranodal sites of the head and neck* (such as larynx, salivary gland, lacrimal gland, and thyroid gland) are normally devoid of organized lymphoid tissues. Nonetheless, reactive lymphoid hyperplasia, whether of specific type or nonspecific idiopathic type, can occur in these various sites. The specific types of lymphoid hyperplasia (such as lymphoepithelial sialadenitis, Kuttner tumor, IgG4-related chronic sclerosing dacryoadenitis, and HIV-associated lymphoepithelial cyst) are covered under the respective sites.

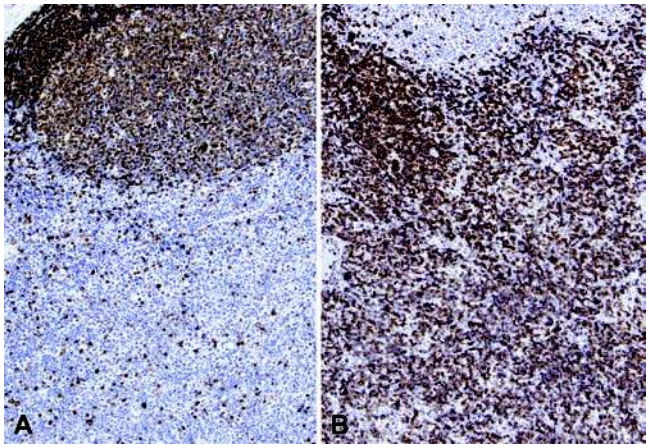

Figure 9 Reactive paracortical hyperplasia of lymph node, immunohistochemistry. CD20 highlights the B cells of the follicles, and there are only scattered CD20+ B cells in the paracortex (**A**). There are many CD3+ T cells in the paracortex (**B**).

Normal lymphoid tissues of the Waldeyer ring. The Waldeyer ring is an interrupted circle of protective lymphoid tissue at the upper ends of the respiratory and alimentary tracts. It is formed by the following: (*i*) pharyngeal tonsils of the nasopharynx (also called adenoids); (*ii*) palatine tonsils (also called faucial tonsils); (*iii*) tubal tonsils around the opening of auditory tubes; and (*iv*) lingual tonsils over the posterior surface of the tongue. Histologically, the Waldeyer ring is characterized by mass-forming lymphoid tissue covered by a folded stratified squamous epithelium or respiratory-type epithelium (Fig. 11A–C). The lymphoid tissue comprises reactive lymphoid follicles with discrete mantles, separated by interfollicular areas populated predominantly by small lymphocytes of T lineage (Fig. 11B). The small lymphocytes in mucosal sites, not uncommonly, show a ''mildly activated'' appearance, perhaps related to chronic antigen challenge, in that they are slightly larger than the typical small lymphocyte, with mild irregular nuclear foldings and slightly less condensed chromatin (Fig. 12A, B). Overlying the lymphoid follicles are large numbers of mature plasma cells and marginal zone B cells, which often infiltrate into the surface or crypt epithelium to form a ''lymphoepithelium''(Fig. 11C). The marginal zone B cells (including intraepithelial lymphoid cells) often have medium-sized, slightly indented nuclei, and a moderate amount of clear cytoplasm (Fig. 11C). In contrast to lymph nodes, sinusoids are absent.

Reactive lymphoid hyperplasia of extranodal sites. For reactive lymphoid hyperplasia of the various extranodal sites in the head and neck, the following terminologies can be applied when the clinicopathologic features do not conform to specific entities.

The prototype is *reactive follicular hyperplasia* of the palatine tonsils, although this can also occur in other extranodal sites of the head and neck. Typically, there are prominent reactive lymphoid follicles with discrete

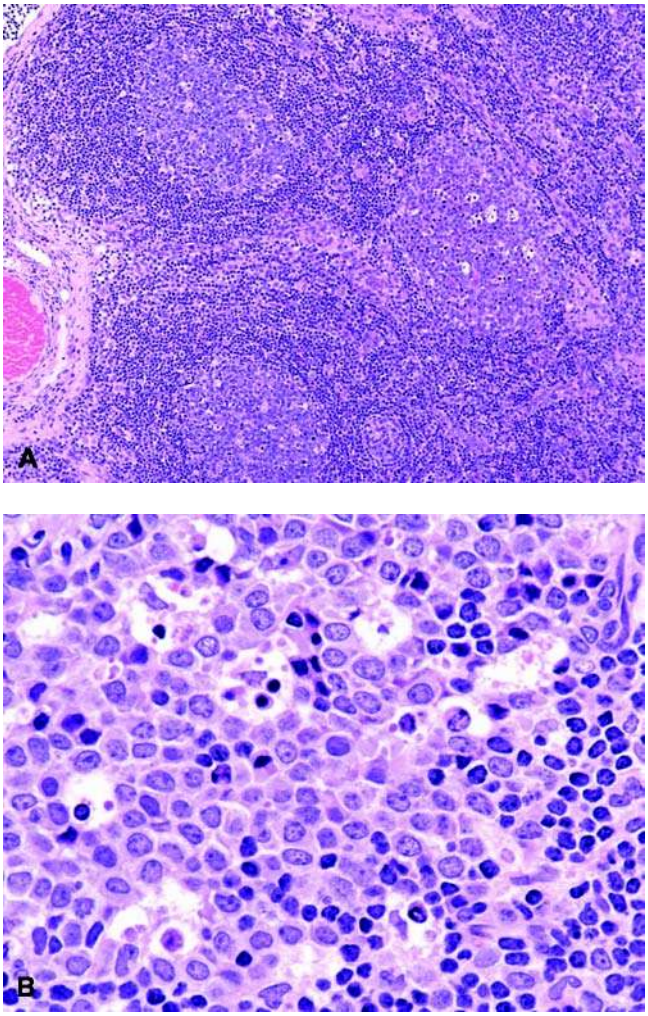

Figure 10 Plasmacytoid dendritic cell clusters in the paracortex. (**A**) Two reactive lymphoid follicles are seen in the left field. The aggregate of cells with interspersed tingible-body macrophages seen in the right field represents plasmacytoid dendritic cells. In contrast to lymphoid follicles, mantle is absent and the cells show a violaceous hue. (**B**) Plasmacytoid dendritic cells are medium-sized cells with eccentrically placed round nuclei and a moderate amount of amphophilic cytoplasm, showing a superficial resemblance to plasma cells, and hence the qualifier "plasmacytoid" in the terminology.

mantles, separated by interfollicular zones populated predominantly by small lymphocytes (Fig. 13). Variable numbers of mature plasma cells are often present, especially in the subepithelial zone. The features helpful for distinction from follicular lymphoma are discussed under the section on ''follicular lymphoma.''

In other cases, which can be termed *nonspecific reactive lymphoid hyperplasia*, the lymphoid follicles are not strikingly hyperplastic or may even be inconspicuous such that the lymphoid infiltrate may appear to be diffuse. The interfollicular zone is broadened by a lymphoid infiltrate consisting of variable numbers of small lymphocytes and activated large lymphoid cells (immunoblasts); the latter cells can be scattered singly or form large clusters (Fig. 14A, B). On immunostaining, the small lymphoid cells are predominantly of

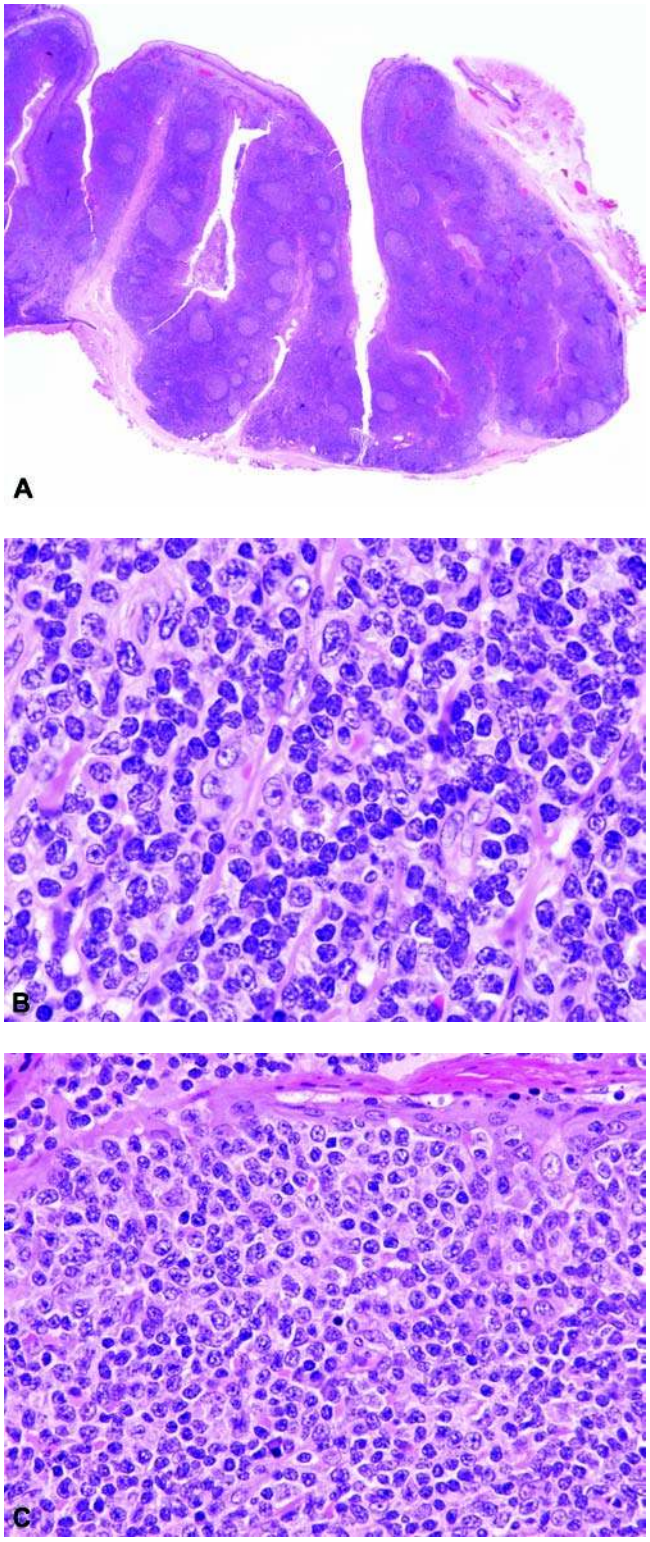

Figure 11 Reactive lymphoid hyperplasia of tonsil. (**A**) The mucosal surface is convoluted and shows deep crypts. Note the sharp base of the lymphoid band, which typically includes reactive follicles aligned uniformly like beads on a string. (**B**) The interfollicular region is populated mostly by small lymphocytes, some of which can exhibit mild nuclear enlargement and slightly more open chromatin. (**C**) Above the reactive lymphoid follicles, there are marginal zone cells with medium-sized nuclei and a moderate amount of cytoplasm. These cells infiltrate and break up the overlying stratified squamous epithelium to form a lymphoepithelium.

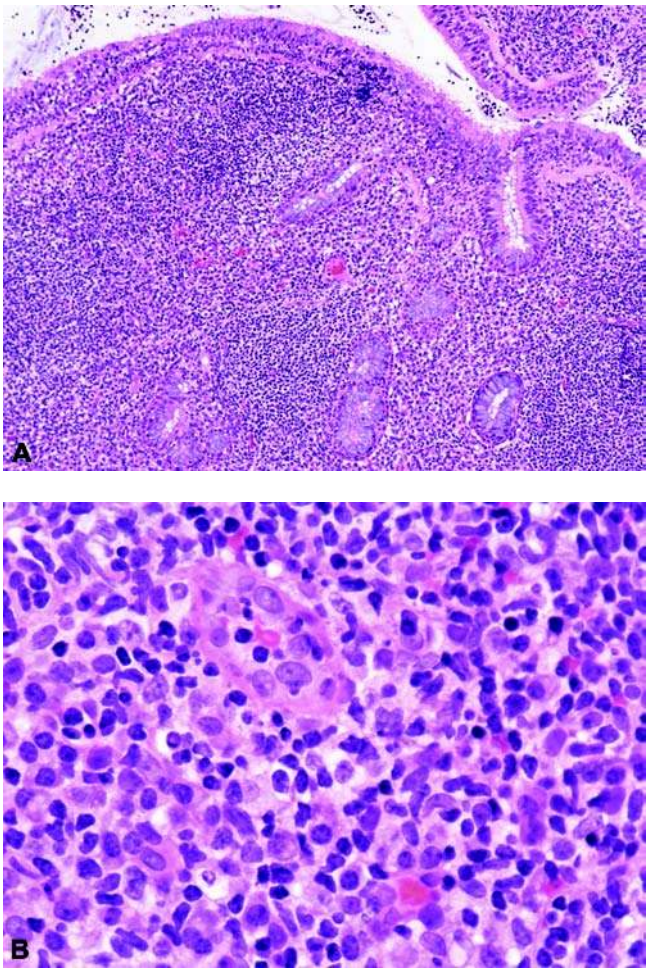

Figure 12 The normal nasopharynx. (**A**) The mucosa is covered by respiratory epithelium (although it can be covered by metaplastic stratified squamous epithelium in other cases). The stroma is typically densely populated by lymphoid cells. (**B**) The small lymphoid cells commonly exhibit a mild degree of nuclear atypia, probably reflecting some degree of activation. These cells are slightly larger than small lymphocytes, and show some nuclear foldings and slightly more open chromatin.

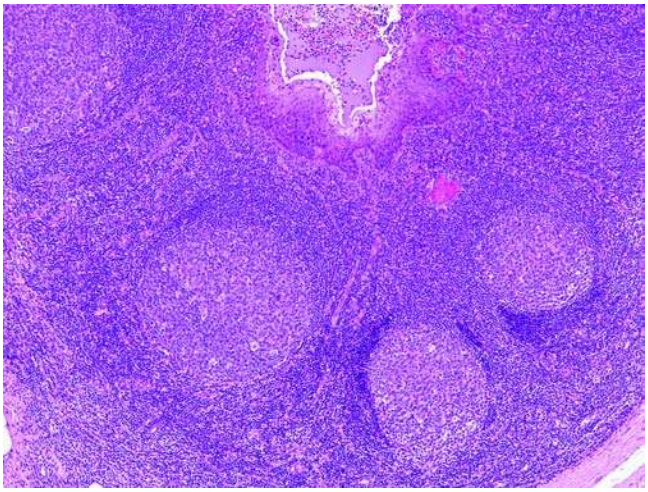

Figure 13 Reactive lymphoid hyperplasia of tonsil. There are prominent secondary lymphoid follicles.

T lineage. The large lymphoid cells can be of T or B or mixed lineage, and CD30 can be positive (Fig. 15). Distinction from malignant lymphoma can be difficult. For lesions predominated by small lymphoid cells, the main differential diagnoses are various types of low-grade B-cell lymphomas and extranodal NK/T-cell lymphoma. If the lymphoid infiltrate is destructive, causing loss or wide separation of the mucosal glands, particularly when accompanied by coagulative necrosis, extranodal NK/T-cell lymphoma has to be strongly suspected. Presence of a mild degree of atypia (such as nuclear foldings) in the small lymphoid cells is not a very helpful diagnostic pointer, because this can be seen in both reactive process and malignant lymphoma, but presence of a significant population of medium-sized cells (which may show irregular nuclear foldings or clear cytoplasm) is highly suspicious of lymphoma. Immunostaining is most helpful. Presence of diffuse dense sheets of CD20+ cells with limited numbers of admixed CD3+ T cells is supportive of a diagnosis of B-cell lymphoma, while the presence of sheets of CD3+ CD56+ cells suggests a diagnosis of extranodal NK/T-cell lymphoma, which can be further confirmed by demonstration of EBV using in situ hybridization. For infiltrates rich in large cells, lack of frank atypia in the large cells (atypia being defined by morphologic deviation from the normal immunoblast, such as giant size, irregular nuclear foldings in many cells, stippled chromatin pattern, or clear cytoplasm) and the presence of cellular differentiation (a spectrum of cells from immunoblasts to plasmablasts to immature plasma cells to mature plasma cells) would favor a reactive process. On immunostaining, the large cells are usually B cells, exhibiting CD20 immunoreactivity in a heterogeneous pattern (cells exhibiting strong, moderate, weak, as well as negative staining), which contrasts with the usually uniform strong CD20 staining in a large B-cell lymphoma. Furthermore, the large cells exhibit polytypic staining for immunoglobulin. Very often, a proportion of the large cells are CD3 positive. These findings indicate that the large cells represent a mixed population, and hence a reactive process. In the occasion that the large cells selectively stain for T-lineage markers, distinction from a peripheral T-cell lymphoma is a real problem; presence of an aberrant immunophenotype (such as loss of one or more pan-T markers) and T-cell receptor gene rearrangement would support a diagnosis of lymphoma.

B. Specific Reactive Lesions

There are specific types of reactive lymphoid hyperplasia with characteristic clinical and histologic features, involving lymph nodes and/or extranodal

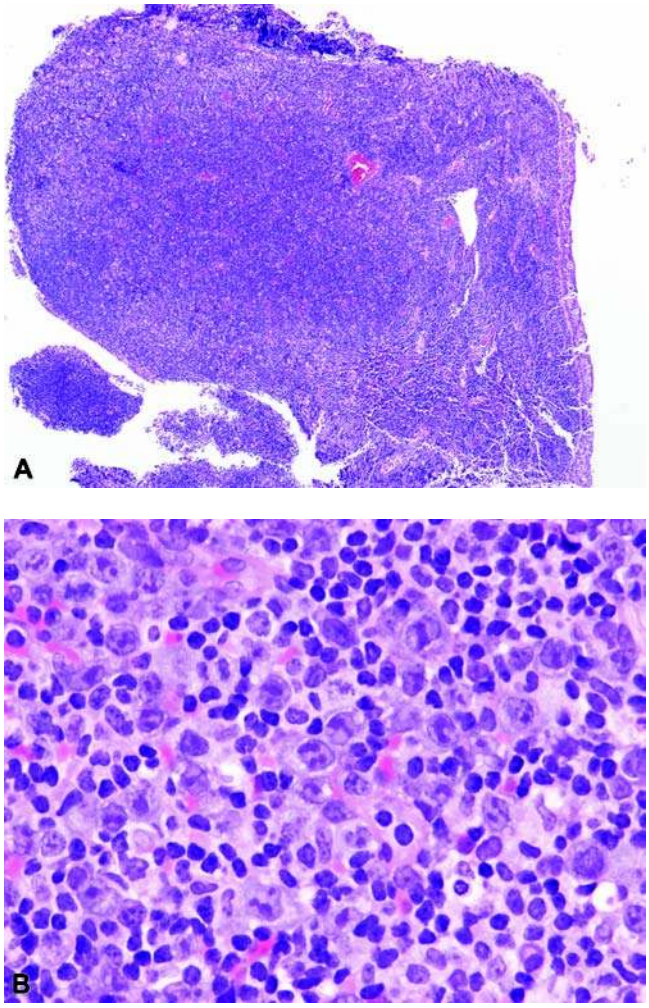

Figure 14 Reactive lymphoid hyperplasia of nasopharynx. (**A**) The mucosa is covered by intact respiratory epithelium (*right field*). Lymphoid follicles are not evident in the dense lymphoid infiltrate. (**B**) The presence of many immunoblasts among the small lymphocytes may lead to a misdiagnosis of large cell lymphoma or nasopharyngeal carcinoma.

tissues (Table 1). For example, Kimura disease can affect soft tissues, parotid gland, or lymph node, and Rosai–Dorfman disease can affect lymph node or the upper aerodigestive tract.

Progressive Transformation of Germinal Centers

Clinical features. Progressive transformation of germinal centers (PTGC) is a benign condition of unknown etiology. PTGC can occur as a focal incidental finding in up to 10% of cases of otherwise nonspecific reactive follicular hyperplasia (11). When PTGC occurs as a dominant finding, it usually affects young male patients who present with solitary enlarged lymph node, most commonly in the neck. Some may show persistent or recurrent disease (11,12).

There is a possible histogenetic relationship with nodular lymphocyte–predominant Hodgkin lymphoma,

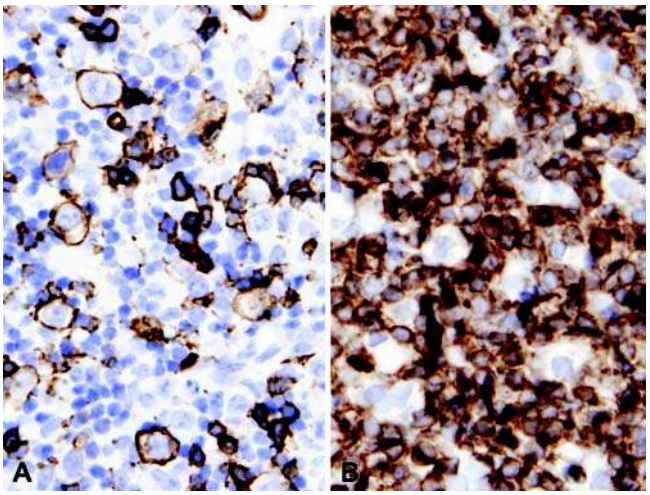

Figure 15 Reactive lymphoid hyperplasia of nasopharynx, immunohistochemistry. The large cells (immunoblasts) show heterogeneous staining for CD20, ranging from strong to weak to negative (**A**). In this example, the CD3+ cells are mostly small lymphoid cells (**B**).

in that PTGC can be seen in some patients with prior, concurrent, or subsequent nodular lymphocyte–predominant Hodgkin lymphoma (13–15). The risk of PTGC evolving to nodular lymphocyte–predominant Hodgkin lymphoma, even for florid cases, is actually very low (0–5%) (11,12,14,16).

Pathology. The lymph node shows preserved architecture and reactive follicular hyperplasia. There are scattered, large, expansile, dark-staining follicles two to four times the size of the background follicles (Fig. 16). These transformed follicles are

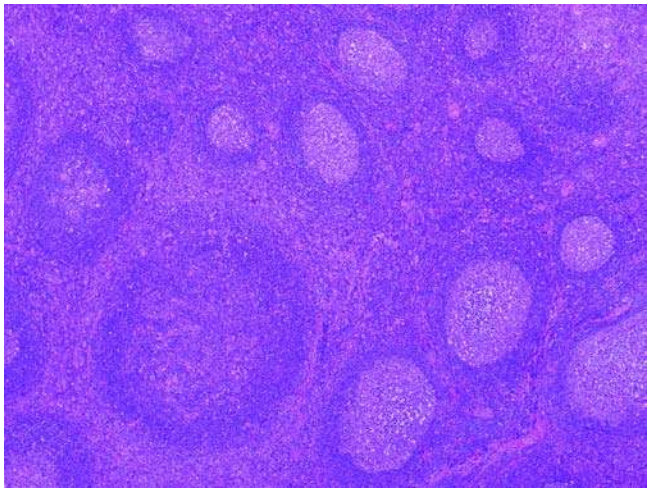

Figure 16 Progressive transformation of germinal centers, lymph node. The transformed follicle (*left field*) is typically large and dark-staining compared with the background usual-looking reactive follicles.

formed mostly by small lymphocytes, and have ill-defined, ''broken-up,'' relatively small germinal centers that can be single or multiple. Uncommonly, the transformed follicle is surrounded by a wreath of epithelioid histiocytes.

Differential diagnosis. In nonspecific reactive follicular hyperplasia, occasional lymphoid follicles can show tongues of mantle zone lymphocytes apparently intruding the germinal centers. Such follicles are often misinterpreted as progressively transformed germinal centers, but are usually merely due to tangential sectioning of the follicles.

Nodular lymphocyte–predominant Hodgkin lymphoma can be distinguished from PTGC by the following features: (*i*) clustered or extensive abnormal nodules/follicles, which are not individually interspersed among reactive follicles and (*ii*) presence of large lymphocytic/histiocytic (L&H) cells with popcorn-like nuclei.

Dermatopathic Lymphadenopathy

Clinical features. Dermatopathic lymphadenopathy is a special form of paracortical hyperplasia in which there is a prominent proliferation of interdigitating dendritic cells and Langerhans cells.

The patients usually have a chronic pruritic dermatologic condition (including mycosis fungoides) in the drainage area, but this lesion can occur in the absence of skin disease (17).

Pathology. The lymph node architecture is preserved, with marked expansion of the paracortex, which may form nodules. Characteristically, the expanded paracortex appears pale and mottled due to the pallor of the cytoplasm of the proliferated interdigitating dendritic and Langerhans cells (Fig. 17A, B). There are frequently some intermixed histiocytes with phagocytosed melanin, immunoblasts, and eosinophils. The intermingled small lymphoid cells, not uncommonly, exhibit some degree of irregular nuclear foldings. Florid examples of dermatopathic lymphadenopathy can be mistaken for Langerhans cell histiocytosis due to the abundance of dendritic cells with grooved or contorted nuclei. Features favoring the latter diagnosis include (*i*) predominantly sinusoidal rather than paracortical involvement and (*ii*) the proliferated cells exhibiting distinct ovoid contour and short or absent cell processes instead of indistinct cell borders and long dendritic cell processes (best appreciated in S100 immunostain).

Vascular Transformation of Sinuses

Clinical features. Vascular transformation of sinuses is a reactive vasoproliferative lesion of lymph node in which sinuses are converted into vascular channels of variable complexities (18). This condition appears to result from lymphovascular obstruction. The lesion is innocuous by itself, but it may indicate the presence of neoplasms in the vicinity or drainage area.

There are no distinctive clinical features. Although some patients present with lymphadenopathy, the lymph nodes are more often biopsied as part of other surgical procedures.

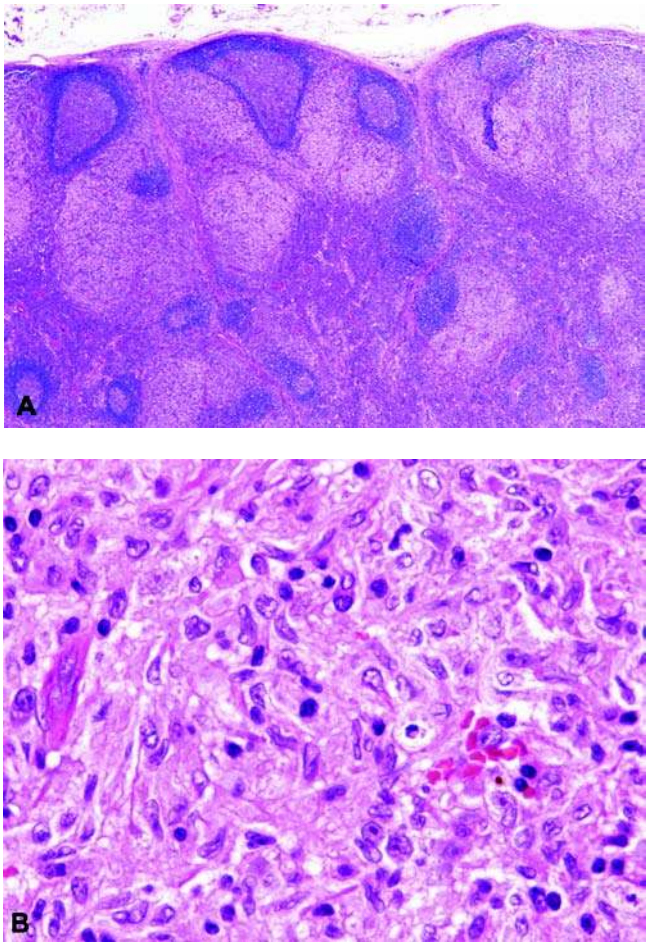

Figure 17 Dermatopathic lymphadenopathy of lymph node. (**A**) There are typically multiple pale-staining expansile foci in the paracortex, resulting in an alopecia-like appearance. (**B**) The pale foci are rich in dendritic cells with elongated, deeply grooved or contorted nuclei, pale chromatin, and abundant lightly eosinophilic cytoplasm with indistinct cell borders.

Pathology. The nodal sinuses are expanded in a diffuse or segmental fashion, with proliferated blood vessels embedded in a sclerotic stroma. The blood vessels can be rounded, slit-like sinuous, or plexiform and are lined by flat or plump endothelium. In the more cellular examples, the sinuses are packed with spindly cells that form short fascicles or haphazard arrays, interspersed with narrow branched vascular spaces (Fig. 18). The nodular spindle cell variant is characterized by the presence of single or multiple nodules with cellular composition similar to the cellular foci of vascular transformation of sinuses (19).

Differential diagnosis. The most important differential diagnosis is Kaposi sarcoma, which typically involves nodal capsule and fibrous trabeculae rather than sinuses. The well-formed, crisscrossing spindle

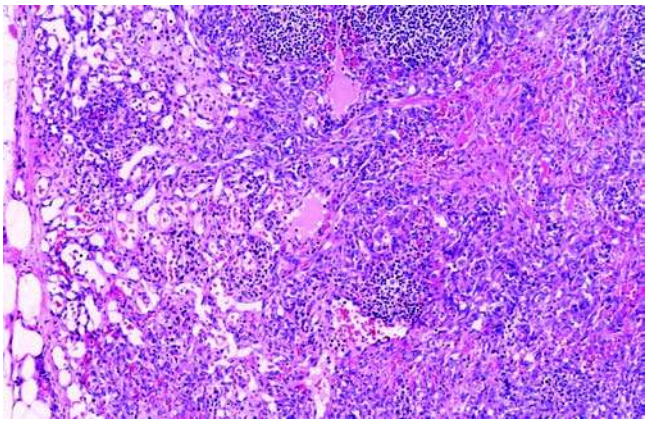

Figure 18 Vascular transformation of sinuses of lymph node. The sinuses are expanded by closely packed and complex vascular channels, resulting in a rather solid spindle cell appearance that may raise the differential diagnosis of Kaposi sarcoma (*right field*). The apparent "maturation" into better formed vascular channels toward the subcapsular sinuses (*left field*) supports a diagnosis of vascular transformation of sinuses.

cell fascicles of well-developed Kaposi sarcoma are not a feature of vascular transformation of sinuses; furthermore, the interspersed vascular slits in Kaposi sarcoma are short and nonbranching instead of irregular and branching. A diagnostically helpful feature of vascular transformation of sinuses is ''maturation'' of the cellular spindle cell foci into well-formed vascular spaces toward the nodal capsule (Fig. 18). If morphologic features are inconclusive, positive immunostaining for human herpesvirus 8 (HHV8) will provide a strong support for a diagnosis of Kaposi sarcoma.

Lymph Node Infarction

Lymph node can undergo total or subtotal infarction, either spontaneously or after fine-needle aspiration. Infarction manifests as zones of coagulative necrosis, often rimmed by histiocytes, with or without reparative fibrovascular tissue (Fig. 19A–C). While the underlying pathologic process can be reactive lymphadenopathy, lymphoma and nonhematolymphoid malignancy must be excluded (Fig. 20A, B). Thus all available tissue should be examined histologically (Fig. 20B), and the rims should be scrutinized for any residual viable tumor cells. Despite necrosis of the cells, antigens are sometimes surprisingly well preserved, such that it may be possible to use immunostaining (such as cytokeratin, S100 protein, CD20, CD3) to help determine the underlying pathology (Fig. 19B, C) (20). If there are sheets of CD20+ cells with few admixed CD3+ cells, B-cell lymphoma has to be strongly suspected. If the underlying pathology cannot be clarified, the patient should be followed up and further biopsies taken for histologic assessment as appropriate (1,21,22).

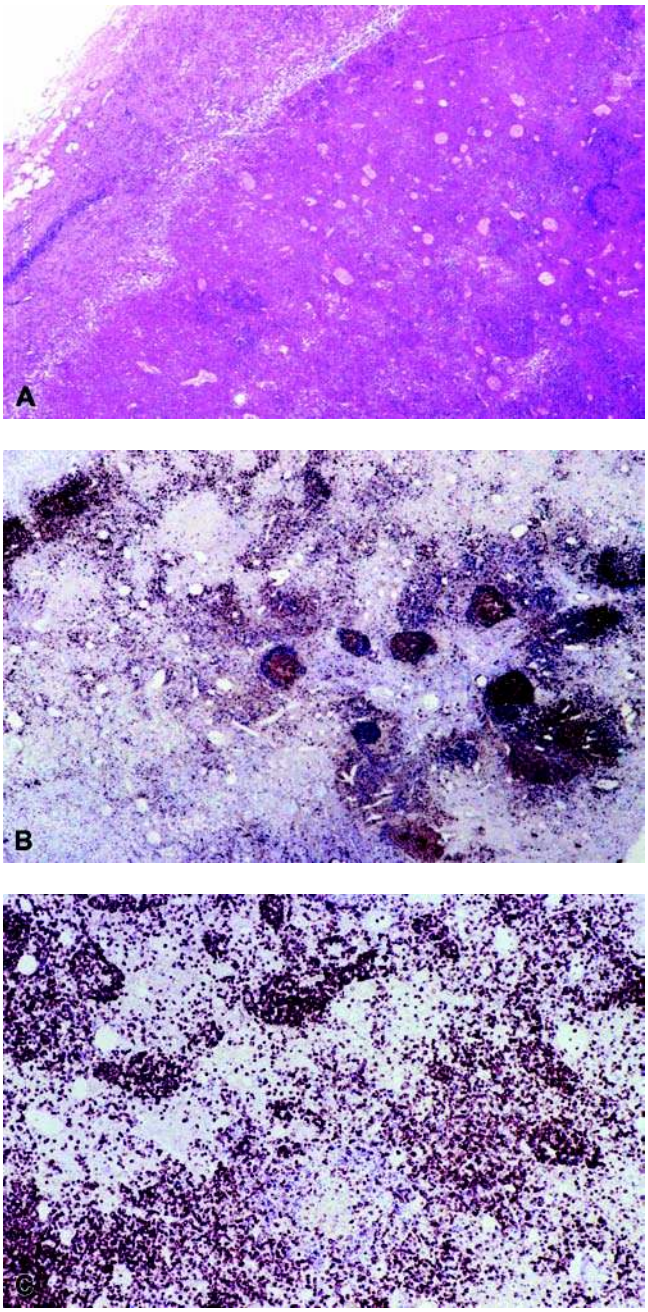

Figure 19 Infarction of reactive lymph node. (**A**) The lymph node shows total infarction. (**B**) Immunostaining for CD20 shows a normal immunoarchitecture, predominantly occurring in the form of nodules. (**C**) Immunostaining for CD3 further supports a normal immunoarchitecture, with staining in a paracortical pattern. The immunostains therefore suggest a benign process.

It is extremely important not to mistake lymph node infarction for necrotizing lymphadenitis. The former is usually characterized by unifocal rather than multifocal coagulative necrosis, with ghost shadows of cells often still being discernible. Also in contrast to the latter, it is not accompanied by

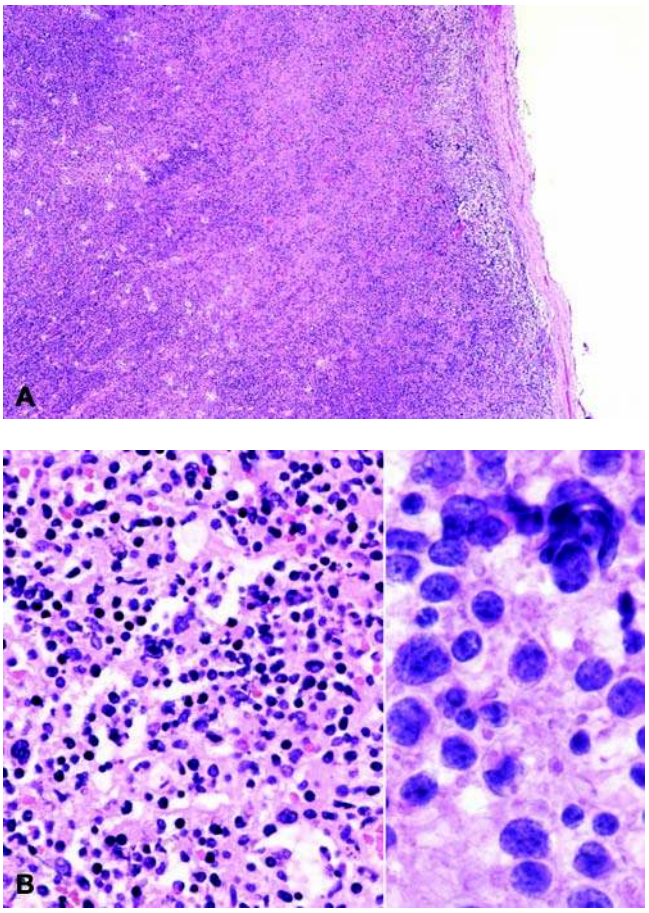

Figure 20 Infarction of lymph node involved by diffuse large B-cell lymphoma. (**A**) The lymph node shows total infarction. (**B**) The cells are so degenerated that it is impossible to tell morphologically that they were normal lymphoid cells or lymphoma cells (*left panel*). A prior fine-needle aspiration reveals many atypical large cells, supporting a diagnosis of large cell lymphoma (*right panel*).

proliferation of lymphoid cells and histiocytes in the necrotic areas.

Infectious Mononucleosis

Clinical features. Primary EBV infection is frequently asymptomatic. However, in a minority of patients, especially adolescents and young adults, the disease may present with the syndrome of infectious mononucleosis, with fever, fatigue, sore throat, lymphadenopathy (frequently cervical but may be generalized), with or without rash and hepatosplenomegaly. Atypical lymphocytes are often observed in the peripheral blood. The clinical course is self-limiting, except when it occurs in the setting of congenital or acquired immunodeficiency, wherein the disease can be progressive.

In the typical clinical setting, biopsies are not performed, and the diagnosis can be confirmed by serologic testing for EBV, e.g., heterophile antibody test (Monospot test), and antibodies to specific EBV antigens. However, in the early phase of the disease when the serologic tests may be negative or when a diagnosis of infectious mononucleosis is not suspected, biopsy of the tonsil or cervical lymph node may be undertaken to exclude malignancy.

Pathology. The histologic appearances of infectious mononucleosis, with florid immunoblastic proliferation and even sometimes presence of binucleated immunoblasts resembling Reed–Sternberg cells, can be alarming, and not infrequently lead to a misdiagnosis of large cell lymphoma (23,24). In lymph nodes, the architecture is typically incompletely effaced, with the sinuses remaining patent (Fig. 21A). Some lymphoid follicles may show germinal center necrosis. The paracortex is expanded by a lymphoid infiltrate that includes many activated lymphoid cells (Fig. 21B).

Features suggesting a diagnosis of infectious mononucleosis (or other causes of reactive immunoblastic proliferation such as other viral infections, drug reaction, postvaccination reaction, hypersensitivity) over malignant lymphoma include (*i*) young age, (*ii*) lack of frank atypia in the immunoblasts, (*iii*) presence of a spectrum of lymphoid cell differentiation both morphologically and immunophenotypically. Morphologically, the lymphoid cells show a full spectrum of maturation stages, including immunoblasts, plasmablasts, and plasma cells (Fig. 21B). On immunostaining, the immunoblasts usually consist of a mixture of B cells (showing heterogeneous staining for CD20 and polytypic immunoglobulin) and T cells (with variable numbers of large cells being CD3 positive) (25–27). In contrast, the large cells in diffuse large B-cell lymphoma (DLBCL) usually express pan-B markers with uniform intensity and/or show light-chain restriction. CD30 expression can be observed in the immunoblasts and the Reed–Sternberg like cells in infectious mononucleosis, but unlike Hodgkin lymphoma, these cells are CD15 negative (28,29). In situ hybridization shows strong nuclear staining for EBV-encoded RNAs (EBERs) in some of the immunoblasts as well as some of the smaller cells or plasmacytoid cells; the EBER-positive cells are more frequently of B-cell lineage (Fig. 21C) (26,30). Within the T-cell population, there is a slight predominance of CD8+ T cells (28). These cytotoxic CD8+ T lymphocytes may be of oligoclonal or monoclonal nature (31–33): monoclonality by itself does not equate malignancy in this situation.

Cytomegalovirus Lymphadenitis

Cytomegalovirus (CMV) infection is frequently asymptomatic, but patients may rarely present with infectious mononucleosis-like clinical features, with fever, lymphadenopathy, and atypical lymphocytosis. In immunocompetent hosts, the lymph nodes show reactive follicular hyperplasia and monocytoid B-cell hyperplasia, and small foci of necrosis may be seen within the monocytoid B-cell clusters. Cells containing viral inclusions are often scanty, being found mostly among the monocytoid B cells and occasionally in the paracortex (Fig. 22). The CMV-infected cells contain both nuclear and cytoplasmic inclusions: very large

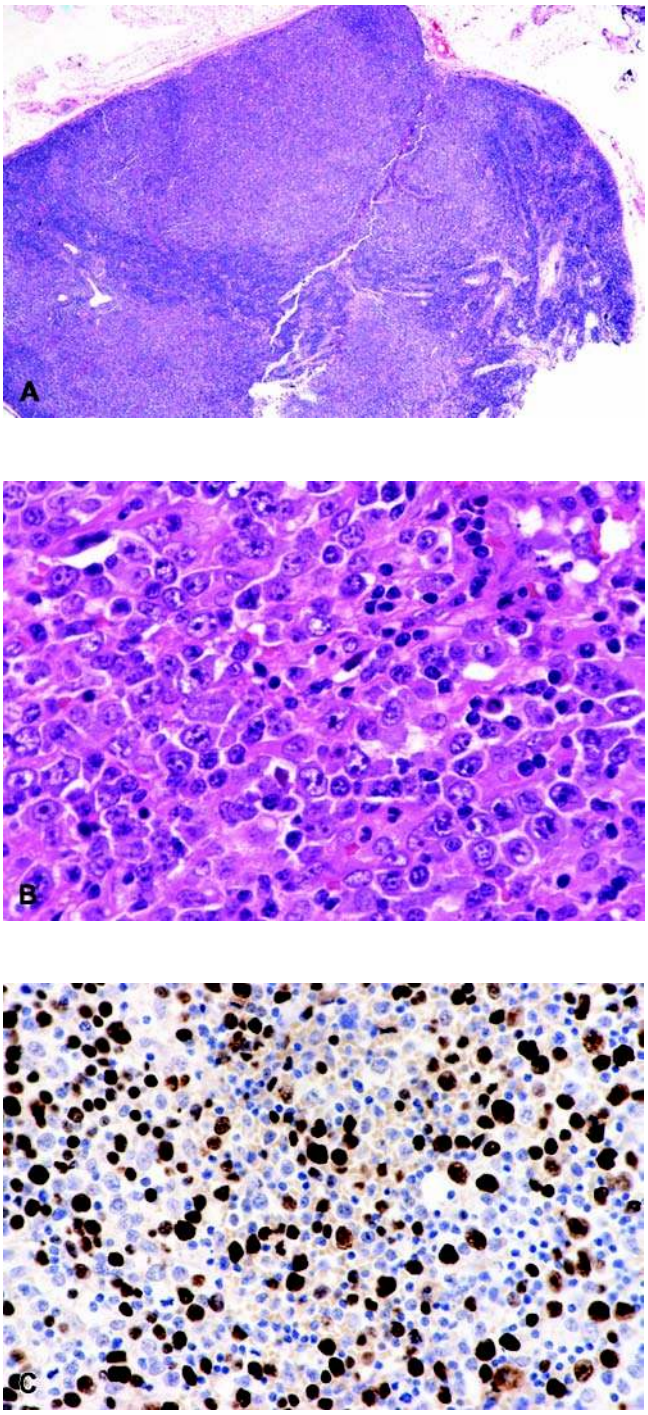

Figure 21 Infectious mononucleosis, lymph node. (**A**) Although there is extensive lymphoid proliferation, some preserved normal architecture is evident in at least some foci (dark-staining residual lymphoid tissue with recognizable sinuses). (**B**) There is an alarming increase of large lymphoid cells, but these cells lack frank nuclear atypia, and the large cells apparently exhibit a spectrum of maturation toward plasmablasts and plasma cells. (**C**) In situ hybridization for EBER reveals many positive cells, which typically include a spectrum of small, medium-sized and large cells. *Abbreviation*: EBER, EBV-encoded RNAs.

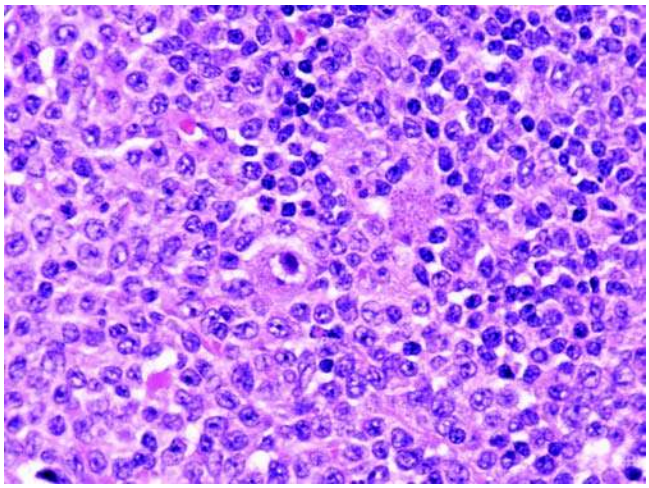

Figure 22 Cytomegalovirus infection of lymph node in immunocompetent host. Two cytomegalovirus-infected cells are seen among the monocytoid B cells. The one in the left has enlarged nucleus with nuclear inclusion as well as cytoplasmic inclusions. The one in the right shows cytoplasmic inclusions only (nucleus not included in this plane of sectioning).

single eosinophilic intranuclear inclusion in the enlarged nuclei and multiple small amphophilic cytoplasmic inclusions (Fig. 22). The CMV-infected cells can mimic Reed–Sternberg cells of classical Hodgkin lymphoma, especially since Reed–Sternberg cells can sometimes be localized predominantly within monocytoid B-cell clusters (34), and furthermore can deceptively express CD15 as in Reed–Sternberg cells (35). However, cytoplasmic inclusions should not be seen in Reed–Sternberg cells, and a diagnosis of CMV can be easily confirmed by immunohistochemistry or in situ hybridization (36).

CMV infection occurring in the setting of immunodeficiency usually represents reactivation. The involved nodes frequently show effaced nodal architecture with extensive necrosis and numerous cells containing viral inclusions. Extranodal involvement is common in this situation, with CMV retinitis (especially in patients with AIDS) and CMV involving the gastrointestinal tract frequently observed. In the head and neck region, CMV involving the oropharynx and nasal cavity has been reported in AIDS patients (37,38).

Herpes Simplex Lymphadenitis

Herpes simplex virus infection may occasionally present as fever and lymphadenitis, which can be localized or generalized. There may or may not be associated skin lesions. It can affect either immunocompetent or immunocompromised host, the latter sometimes associated with a hematolymphoid malignancy. In fact, coexisting herpes simplex virus infection and hematolymphoid malignancy (chronic lymphocytic leukemia or mantle cell lymphoma) in the same lymph node have been reported (39,40).

The involved lymph nodes show paracortical hyperplasia with proliferation of immunoblasts, predominantly of T lineage (41). Necrotic foci, sometimes associated with suppuration and histiocytic infiltrate, are frequently seen (42–46). Cells with diagnostic viral inclusions are present in variable numbers, and they are frequently found around necrotic areas and in the paracortex. These cells are often multinucleated, with ground glass nuclei, fragmented nuclear membrane, and/or intranuclear eosinophilic inclusion with clear halo. The infected cells are mostly T cells or stromal cells (41,47). The diagnosis of herpes simplex infection can be confirmed by immunohistochemistry or in situ hybridization (36).

Rarely, herpes simplex virus can cause necrotizing tonsillitis with abscess formation (48,49). Mass-forming infiltrate of CD4+, CD56+ reactive T-cells associated herpes simplex virus infection has also been reported in the nasopharynx, clinically and histologically mimicking lymphoma (50); in contrast to extranodal NK/T-cell lymphoma, CD4 is positive and EBV is negative.

Human Herpesvirus 6 Lymphadenitis

Patients with acute human herpesvirus 6 (HHV6) infection often present with fever, fatigue, skin rash, generalized lymphadenopathy, and deranged liver function (51,52). Lymph node is sometimes biopsied and the histologic features can provide the first evidence for the diagnosis, which may not be suspected clinically.

Histologically, there is marked paracortical expansion by clusters and sheets of large lymphoid cells. While these cells look superficially like usual immunoblasts, careful scrutiny shows that the nuclei contain single or multiple prominent nuclear inclusions; the inclusions can be distinguished from nucleoli in being more brightly eosinophilic and surrounded by clear haloes (Fig. 23). Eosinophilic cytoplasmic inclusions are also present. There can be many apoptotic bodies, with or without accompanying necrosis. These large lymphoid cells are mostly CD4+ T cells. The diagnosis of herpesvirus 6 infection can be confirmed by immunostaining for HHV6 gp60/110 kDa envelope glycoprotein. Ultrastructural studies demonstrate numerous viral particles in the cytoplasm and nucleus, characteristic of Herpes virus family. In lymph nodes, the presence of numerous nuclear viral inclusions is usually indicative of a diagnosis of herpesvirus-6 infection if the morphologic features do not conform to those of cytomegalovirus and herpes simplex viral inclusions.

HIV-Associated Lymphadenopathy

Clinical features and pathology. Patients with HIV infection may present with generalized lymphadenopathy in the course of the disease, and the head and neck lymph nodes are commonly involved. The histologic appearances are varied, depending on the stage of disease (53–56). In the early stage of HIV infection, the lymph node shows *explosive follicular hyperplasia*, with crowded large irregular-shaped reactive follicles featuring normal polarity and abundant tingible-body macrophages. Distinctive features of the follicles are (*i*) thin or absent mantles and (*ii*) follicle lysis (Fig. 24A). Follicle lysis manifests as the following changes in the germinal centers: hemorrhage, presence of clusters of degenerated cells, and invasion by small lymphocytes from the mantle zone (Fig. 24B). This phenomenon is believed to result from disruption of the follicular dendritic cell networks due to HIV infection of the follicular dendritic cells (57). Monocytoid B cells and polykaryocytes are frequently observed. Sometimes there can be small epithelioid granulomas, increased plasma cells, and occasional neutrophils.

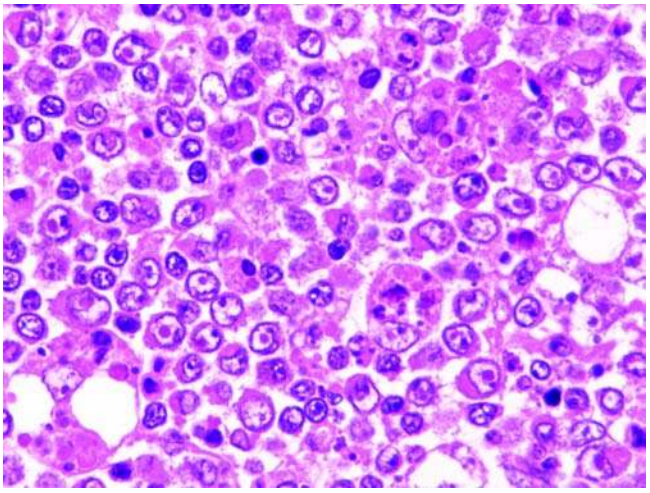

Figure 23 Human herpesvirus 6 lymphadenitis. There are many immunoblast-like cells, which actually represent virus-infected cells with prominent nuclear inclusions surrounded by clear haloes.

As the disease progresses (usually with clinical evidence of AIDS), the lymph nodes show *follicular involution with hypervascularity (hypervascular follicular hyperplasia)*. While some follicles remain hyperplastic, some become atrophic, with predominance of follicular dendritic cells and often penetration by hyalinized venules, resembling hyaline-vascular Castleman disease (Fig. 25). The interfollicular zone shows increased high endothelial venules, increased histiocytes and plasma cells, and decreased small lymphocytes. Sometimes there can be an increase of immunoblasts.

In the late stage of the disease, there is *lymphocyte depletion*, associated with fine fibrosis. These lymph nodes are frequently not enlarged and are only discovered at autopsy or incidentally in surgical excision specimens.

A small group of HIV-infected patients may present with the clinical and pathologic features of *multicentric Castleman disease* (58,59) (see subsequent section on Castleman disease). These cases are etiologically linked to HHV8, the same virus related to Kaposi sarcoma.

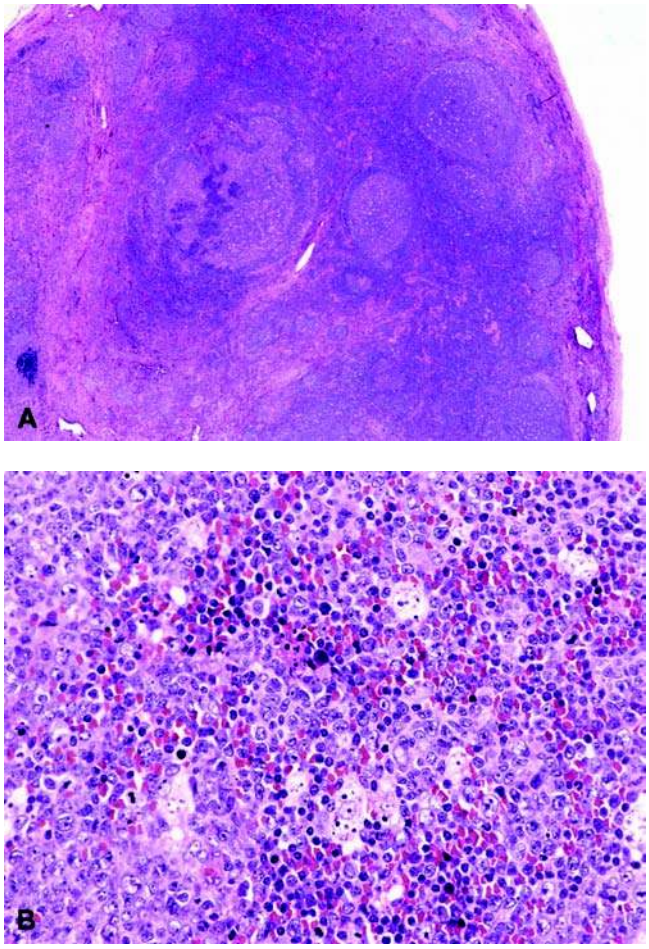

Figure 24 Explosive follicular hyperplasia of lymph node, in a patient with HIV infection. (**A**) The lymphoid follicles often have very thin or absent mantles, but they are clearly reactive because polarity and tingible-body macrophages are present. The follicle in the left field shows follicle lysis. (**B**) Follicle lysis is characterized by the presence of patches of degenerated lymphoid cells and hemorrhage in the germinal centers.

Diagnostic considerations. Although the histologic changes of HIV-associated lymphadenopathy are not specific (60,61), the constellation of histologic findings should raise the clinical suspicion, and serologic testing should be performed if clinically indicated. HIV can also be detected by immunohistochemistry (p24 protein) and in situ hybridization, mainly in the follicular dendritic cells (62–64), but such testing may have legal implications regarding patients' consent. EBV can occasionally be detected in lymph nodes from HIV-infected individuals in the follicular and extrafollicular region, and its presence is associated with increased risk of concurrent or subsequent EBV-associated lymphoma (65).

When examining lymph nodes from HIV-infected individuals, coexisting opportunistic infections (such as *Mycobacterium*, cytomegalovirus, and *Pneumocystis*) or malignancies (such as lymphoma and Kaposi sarcoma) should always be excluded.

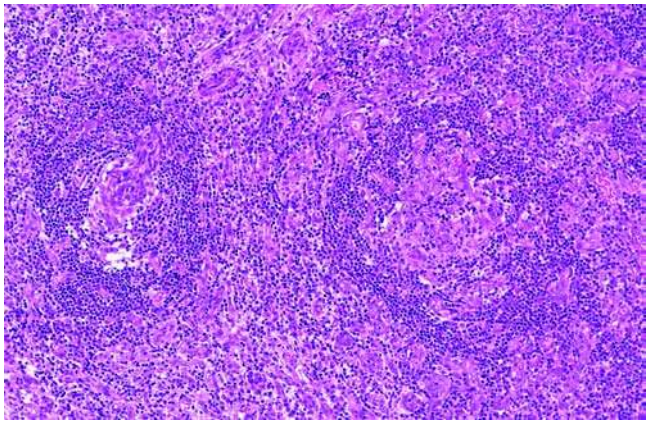

Figure 25 Follicular involution with hypervascularity, lymph node in a patient with HIV infection. The lymphoid follicles resemble those seen in hyaline-vascular Castleman disease, and the interfollicular zone shows prominent venules.

HIV-associated lymphoid hyperplasia in the head and neck extranodal sites. The Waldeyer ring in patients with HIV infection may show reactive lymphoid hyperplasia similar to changes observed in lymph nodes (66–69). In addition, multinucleated giant cells (polykaryocytes) are frequently observed adjacent to the crypts or the surface epithelium and in the interfollicular region (Fig. 26). These HIV-harboring giant cells are of histiocytic origin and show a CD68+ S100+/− immunophenotype (67–69).

In the salivary glands (especially parotid gland), HIV-infected patients may develop lymphoepithelial cyst (cystic lymphoid hyperplasia), which probably results from obstruction of the ducts by hyperplastic lymphoid tissue (70).

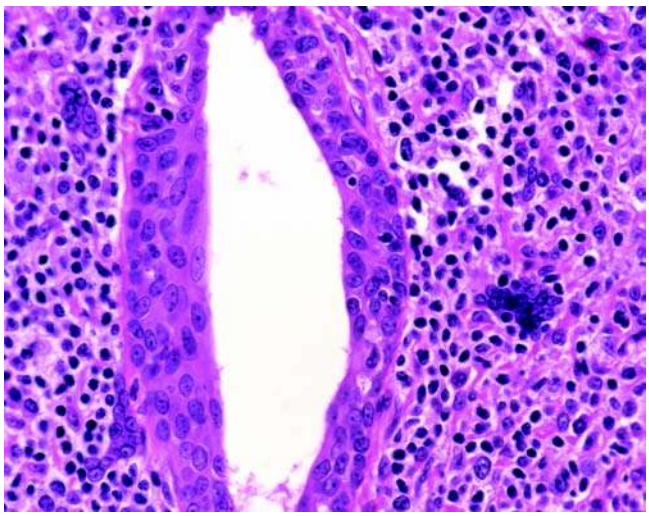

Figure 26 HIV-associated lymphoepithelial cyst. Polykaryocytes are present among the lymphoid cells.

Cat Scratch Disease

Clinical features. Cat scratch disease is the prototype of lymph nodes showing suppurative granulomas (B-cell-associated granulomas). This infection is caused mostly by the bacteria *Bartonella henselae*, but rarely by other *Bartonella* species or *Afipia felis* (71,72). Domestic cats are normal reservoirs for *B. henselae* (73), and patients frequently have recent history of contact with cats. Patients are usually children and young adults, and the lymphadenopathy develops after the detection of a skin lesion, which may go unnoticed. Although axillary lymph nodes are most commonly involved, lymph nodes in the head and neck region may also be affected.

Pathology. Histologically, the lymph node shows reactive follicular hyperplasia, monocytoid B-cell reaction, and suppurative granulomatous inflammation (Fig. 27A) (74). The suppurative granulomas are B-cell associated, in contrast to the T-cell associated granulomas in hypersensitivity reaction (including tuberculosis) (Figs. 27B and 28A) (75). They are believed to have originated from necrotic-suppurative foci within clusters of monocytoid B cells, followed by recruitment of histiocytes, which may show a palisading pattern (Fig. 28A). Multinucleated histiocytes are uncommon. Clusters of residual monocytoid B cells can be readily demonstrated in the granulomas by immunostaining for B-lineage markers, such as CD20 (Fig. 28B, C). Capsular fibrosis and inflammation are frequent. In the late phase of the disease, coalescent or stellate-shaped suppurative granulomas dominate, and the relationship with lymphoid follicles and monocytoid B cells may not be evident.

Diagnostic considerations. A definitive diagnosis of cat scratch disease requires demonstration of the microorganisms in the tissue, most commonly by silver stains such as Warthin–Starry and Dieterle, wherein the clumps of coccobacilli are highlighted in the necrotic area and in the wall of blood vessels (76,77). However, silver stains are fastidious, and the

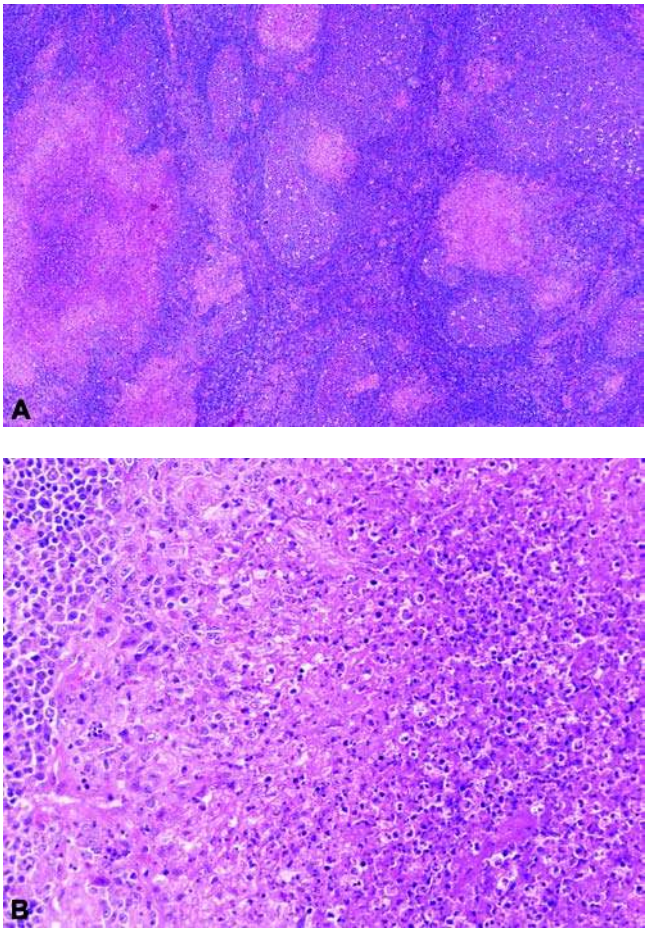

Figure 27 Cat scratch disease, lymph node. (**A**) In a background of reactive follicular hyperplasia, there are multiple suppurative granulomas. (**B**) The suppurative granulomas have necrotic centers richly infiltrated by neutrophils, and histiocytes in the peripheral portion.

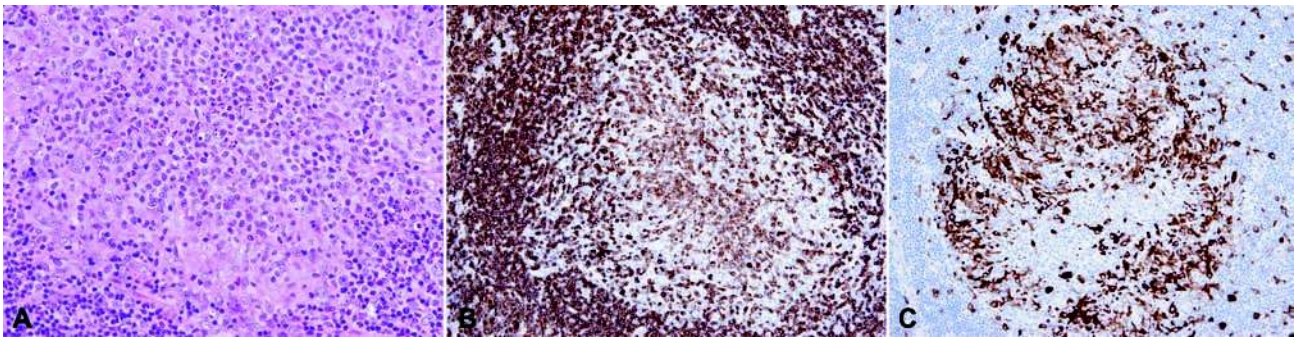

Figure 28 Cat scratch disease, lymph node. (**A**) The suppurative granulomas actually originate in areas of monocytoid B-cell hyperplasia. Some neutrophils are present among the monocytoid B cells (*upper field*), and histiocytes have begun to appear at the periphery (*lower field*). (**B**) Immunostaining for CD20 confirms presence of many B cells (monocytoid B cells) in the suppurative granulomas. (**C**) CD163+ histiocytes are located predominantly in the peripheral portion of the suppurative granulomas.

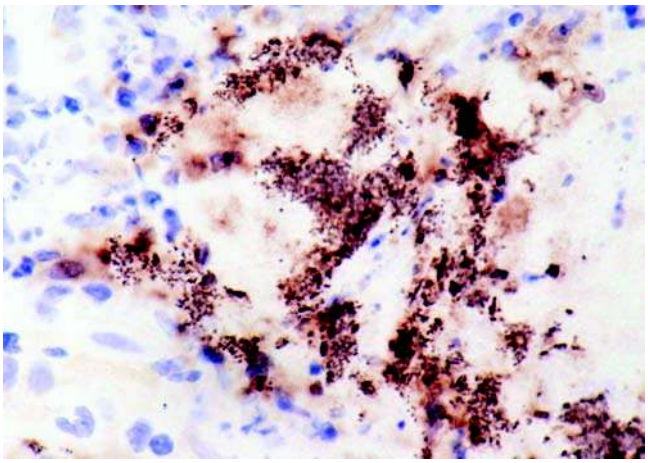

Figure 29 Cat scratch disease, lymph node. Immunostaining for *Bartonella henselae* shows clusters of coccobacilli within the suppurative granulomas.

background silver deposits can render interpretation difficult. This difficulty can be circumvented by immunostaining for *B. henselae*, with the microorganisms being much easily visualized in a clean background (Fig. 29) (78). Alternatively, the diagnosis can be confirmed by polymerase chain reaction for the microorganism (79,80).

Suppurative granulomas are not specific for cat scratch disease, but can occur in other types of infection, such as lymphogranuloma venereum (*Chlamydia trachomatis*), *Yersinia* infection, tularemia (*Francisella tularensis*), listerosis (*Listeria monocytogenes*), melioidosis (*Pseudomonas pseudomallei*), fungal infection, mycobacterial infection (especially atypical mycobacteria), and chronic granulomatous disease of childhood. These differential diagnoses can be excluded by correlating with clinical, serologic, and culture findings, or by the identification of specific organisms in the lymph node specimens.

Mycobacterial (Tuberculous) Lymphadenitis

The commonest type of mycobacterial infection is tuberculosis (*Mycobacterium tuberculosis*). With the changing epidemiology related to HIV infection and global travel, there is an overall increasing incidence of tuberculosis worldwide. Tuberculous lymphadenitis is not an uncommon presentation of the disease, and cervical nodes are most often affected. The lymph nodes may be matted together, or even show discharging sinuses in the overlying skin.

The classical histologic response is caseating granulomatous inflammation, with Langhans giant cells, epithelioid histiocytes, and lymphocytes surrounding the necrotic area. Caseation is a form of necrosis in which there is cheese-like appearance grossly, with amorphous eosinophilic material identified microscopically. Nonetheless, in some cases, the epithelioid granulomas do not exhibit necrosis. The diagnosis is confirmed by demonstration of acid-fast bacilli using Ziehl–Neelsen stain, but if negative, has to be supported by culture or polymerase chain reaction for *M. tuberculosis*.

Caseating granulomas may be observed in other infections such as fungal infection. Noncaseating epithelioid granulomas may been seen in other infective and noninfective conditions, such as sarcoidosis, associated tumors (e.g., carcinoma, seminoma, lymphoma, including Hodgkin lymphoma). Nonetheless, one should be careful in that mycobacterial infection may coexist in the same lymph node where the tumor cells are found (81).

Other than epithelioid granulomatous reaction, mycobacterial infection may also manifest as nongranulomatous histiocytic reaction, suppurative inflammation, or even spindle cell proliferation with inflammatory pseudotumor-like morphology (82). These atypical histologic patterns, however, are more commonly seen in immunocompromised patients and in nontuberculous mycobacterial infections.

Lepromatous Lymphadenitis

Patients with lepromatous leprosy can present with cervical or systemic lymphadenopathy. Histologically, the nodal parenchyma is replaced by sheets of vacuolated histiocytes that may mimic signet ring cell carcinoma. Lightly basophilic streaks or clumps are present within the vacuoles (so-called globi), and acid-fast stain (such as Fite-Faraco) will demonstrate that they are loaded with numerous bacilli (*M. leprae*) (83).

Syphilitic (Luetic) Lymphadenitis

Syphilis may present as lymphadenopathy, especially in the secondary stage where there is generalized lymphadenopathy. The enlarged lymph nodes frequently show mixed follicular and paracortical hyperplasia with prominent plasmacytosis (Fig. 30A). There can be scattered epithelioid granulomas. Capsular fibrosis, perivascular plasma cells cuffing, and obliterative endarteritis are characteristic, although not pathognomonic, features (Fig. 30B)(84). The definitive diagnosis requires confirmation of infection by the causative microorganism, *Treponema pallidum*. The spirochete can occasionally be demonstrated by silver stains such as Steiner or Warthin–Starry, but serologic testing is frequently more rewarding.

Toxoplasmic Lymphadenitis

In immunocompetent hosts, toxoplasmosis may present clinically as superficial lymphadenopathy, especially in the head and neck region. Toxoplasmic lymphadenitis may account for up to 15% of cases of reactive lymphadenopathies undergoing histologic evaluation (85). Microscopically, it is characterized by the triad of follicular hyperplasia, monocytoid B-cell reaction, and multiple small epithelioid granulomas with frequent encroachment on germinal centers (Fig. 31) (86). The granulomas are not associated with necrosis or

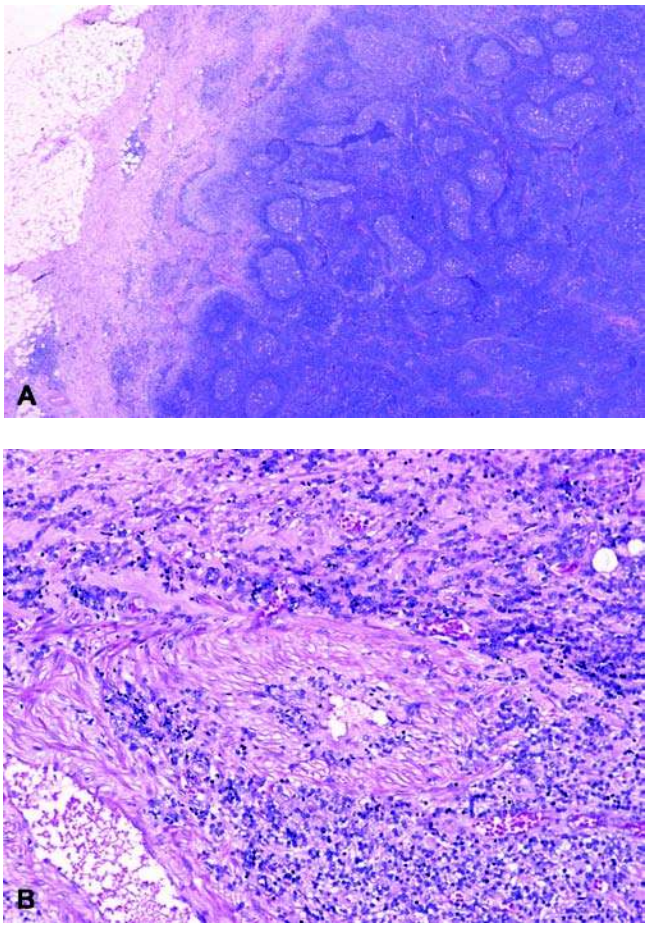

Figure 30 Syphilitic lymphadenitis. (**A**) The node shows capsular fibrosis and reactive follicular hyperplasia. (**B**) In the perinodal tissue, the veins typically show infiltration by lymphoid cells, and plasma cells are readily found.

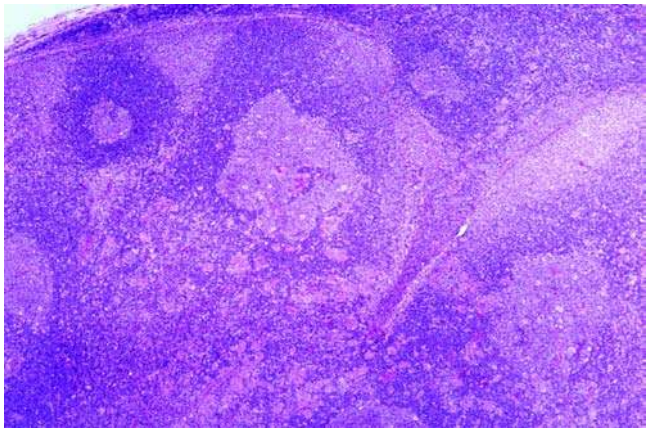

Figure 31 Toxoplasmic lymphadenitis. The node shows reactive follicular hyperplasia, small epithelioid granulomas, and monocytoid B-cell reaction.

Langhans giant cells. *Toxoplasma* cysts are rarely ever identified (87,88), but a correct diagnosis can be confirmed by serologic testing. Conflicting results have been reported on the detection of *Toxoplasma* in the lymph nodes by polymerase chain reaction, ranging from negative to frequently positive (86,89).

Other Infections

In addition to the above-mentioned specific infections, the head and neck region is often involved by various other infections. Upper respiratory tract infections of viral or bacterial origin are very common, and they may account for hyperplastic changes in the Waldeyer ring and head and neck lymph nodes. However, biopsy is seldom performed in these situations. If left untreated, *pyogenic bacterial infections* (e.g., *Streptococcus* species) can result in suppuration and abscess formation in the tonsils and lymph nodes. *Actinomyces* species, a normal commensal in the upper aerodigestive tract, may be introduced into the soft tissues by trauma or during dental surgery, resulting in suppurative inflammation (*actinomycosis*) with or without lymph node involvement. ''Sulfur granules,'' consisting of clumps of gram-positive filamentous bacteria covered by eosinophilic proteinaceous material (Splendore-Hoeppli phenomenon), can be found within the pus.

Fungal infection can be the cause of lymph node enlargement, more frequently in the immunocompromised individuals. The type of fungal organism may sometimes be identified by histochemical stains, e.g., mucicarmine stain to demonstrate the thick capsule of *Cryptococcus* and Grocott stain to identify the morphology and characteristics of budding (e.g., yeast forms of *Penicillium marneffei* show multiplication by fission); or by immunohistochemical stain, e.g., *Pneumocystis carinii*. However, culture is sometimes necessary for confirmation of the type of fungus.

Leishmaniasis, a tropical protozoan disease caused by *Leishmania* species, may affect the skin, nose, and the lymph nodes in the head and neck region. The organisms appear as Donovan bodies within histiocytes, which can be demonstrated by Giemsa stain. Detection by immunohistochemistry has also been reported (90).

Rheumatoid Arthritis

Patients with rheumatoid arthritis frequently develop lymphadenopathy during the course of the disease, and the head and neck lymph nodes may be involved. Histologically, lymph nodes typically show florid follicular hyperplasia, reactive plasmacytosis, and presence of neutrophils in sinusoids (91). However, these histologic features are nonspecific, and clinical correlation is essential for a firm diagnosis. The hyperplastic follicles sometimes may show a lower proliferative activity and fewer tingible-body macrophages compared with the usual hyperplastic follicles, and thus can mimic follicular lymphoma (92). Some CD5+ small B cells may be present in the paracortex, corresponding to the increase of such cells in the peripheral blood (93).

The lymph nodes in patients with rheumatoid arthritis are seldom biopsied unless there is clinical suspicion of infection or lymphoma. Opportunistic infections and lymphoma are common in these patients due to immunosuppressive therapy. Use of methotrexate can be associated with the development of lymphoproliferative disorders, such as DLBCL and Hodgkin lymphoma (94). Some of these methotrexate-associated lymphoproliferative disorders may respond to withdrawal of methotrexate therapy (95).

Lupus Lymphadenitis

Patients with systemic lupus erythematosus frequently develop lymphadenopathy during the course of the disease, and the head and neck lymph nodes are most commonly involved. Although necrotizing lymphadenitis is frequently described as the characteristic histologic feature (96,97), most lymph nodes from these patients show nonspecific reactive follicular hyperplasia only (98). Some of the reactive follicles have a hyaline-vascular appearance, and because of the presence of reactive plasmacytosis and some overlapping clinical features, the picture can resemble multicentric Castleman disease. For cases that show necrosis, there are overlapping histologic features with Kikuchi lymphadenitis—necrotic foci, abundant karyorrhectic debris, numerous histiocytes (some with crescentic appearance), and myeloperoxidase positivity in the histiocytes. In contrast to the latter, plasma cells and vasculitis are more common, while immunoblasts of T lineage are infrequent in the necrotizing foci of lupus lymphadenitis. Hematoxylin bodies, when present, are pathognomonic of lupus lymphadenitis; they appear as violaceous extracellular material frequently found within sinuses and around necrotic foci (Fig. 32).

Since lymphadenopathy represents part of the lupus disease process, lymph nodes are seldom biopsied unless there is clinical suspicion of infection or lymphoma, which may occur in these patients due to immunosuppression.

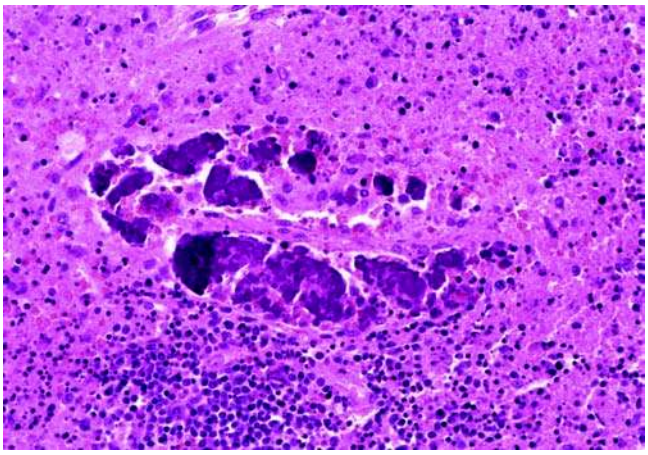

Figure 32 Lupus lymphadenitis. Hematoxylin bodies are present in areas of necrosis. They are violaceous masses of material that represent broken down nuclear material complexed with antinuclear antibodies.

Sjogren Syndrome

Sjogren syndrome is an autoimmune disorder where the patients present with dry eye and dry mouth, with or without enlargement of the salivary glands (mostly parotid gland), lacrimal glands, and the head and neck lymph nodes. Most patients are middle-aged females, and may have associated systemic symptoms, including skin rash and joint pain. Serology frequently shows elevated levels of autoantibodies SSA and SSB (Ro and La). Some patients have associated rheumatoid arthritis or systemic lupus erythematosus. Patients with Sjogren syndrome have an increased risk (44 times) of developing lymphoma compared with the general population (99), and 80% of these lymphomas are mucosa-associated lymphoid tissue (MALT) lymphomas (100).

Histologically, the reactive lymph nodes in patients with Sjogren syndrome frequently show nonspecific reactive follicular hyperplasia, which may sometimes be accompanied by monocytoid B-cell reaction (101,102). The findings in the salivary gland are described under section ''Hematolymphoid Lesions of the Salivary Gland.''

IgG4-Related Sclerosing Disease

Clinical features. IgG4 is the least common of the IgG subclasses, normally accounting for 3% to 6% of total IgG. IgG4-related sclerosing disease is a syndrome, probably autoimmune in nature, characterized by tumorlike involvement of one or more exocrine glands (most commonly pancreas, submandibular gland, and lacrimal gland) or extranodal sites by lymphoplasmacytic infiltrates and sclerosis, accompanied by increased IgG4+ plasma cells in the tissues and elevated IgG4 titer in serum (103). Lymphadenopathy, with or without synchronous or metachronous involvement of exocrine glands or other extranodal sites, is common (104). The disease is frequently systemic, although it can sometimes be localized. There is usually dramatic response to steroid therapy.

Pathology. In the head and neck extranodal sites, the orbit (particularly lacrimal gland, so-called IgG4-related chronic sclerosing dacryoadenitis) and salivary glands (particularly submandibular gland, so-called Kuttner tumor, but sometimes parotid gland) are most commonly involved (105). The pathologic changes are identical in the lacrimal and salivary glands. There is moderate to heavy infiltration of plasma cells and small lymphocytes, causing atrophy of acini. Reactive lymphoid follicles are commonly scattered throughout. There is sclerosis and broadening of the lobular septa, with variable extension into the lobules. In the late phase, sclerosis and loss of lobular acini are prominent, and the lymphoplasmacytic infiltration may become less intense. In other mucosal sites, such the nasopharyngeal mucosa, the changes may be confined to an increase of mature plasma cells, especially in the subepithelial zone. Since

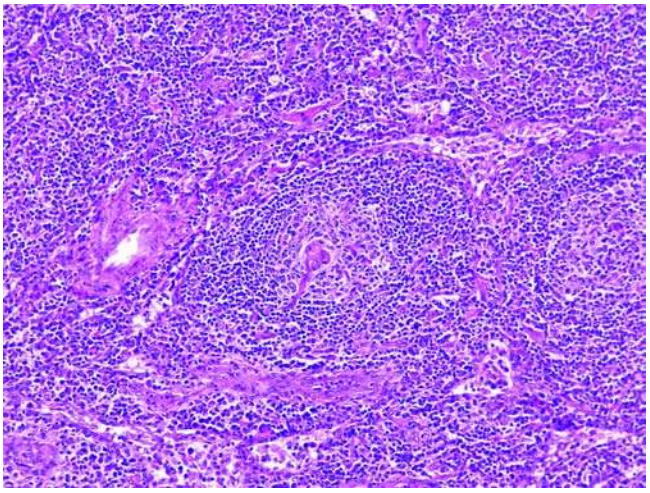

Figure 33 IgG4-related lymphadenopathy, type I. Nodal architecture is preserved. Many follicles have a hyaline-vascular appearance, and there is an increase of plasma cells.

these histologic features are not entirely specific, the diagnosis requires confirmation by immunostaining for IgG4 and IgG, wherein the number of IgG4+ cells should exceed 50 per HPF (high-power field) and the proportion of IgG4+ to IgG+ cells is >40%.

The histologic features of IgG4-related lymphadenopathy are variable (104). Type I is characterized by presence of many hyaline-vascular follicles and interfollicular plasma cells, and the sinusoids are patent; the features therefore resemble multicentric Castleman disease (Fig. 33). Type II shows features of reactive follicular hyperplasia (Fig. 34A, B). Type III shows paracortical expansion by a mixture of small lymphocytes, plasma cells, and immunoblasts, and can mimic peripheral T-cell lymphoma (Fig. 35A, B). Again the diagnosis requires confirmation by immunohistochemistry of a significant increase in IgG4+ cells (Fig. 36).

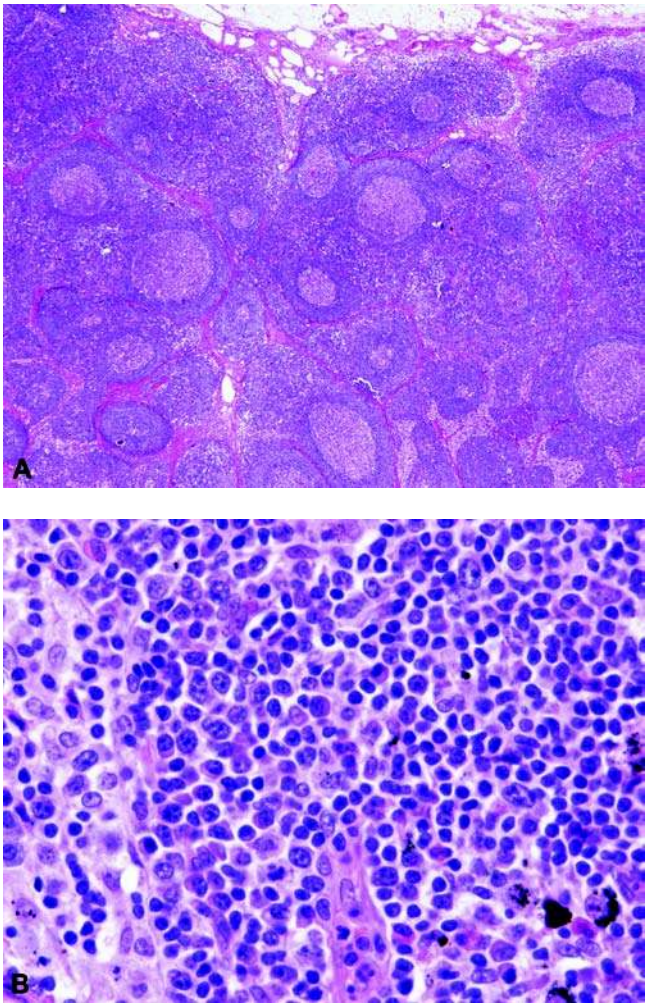

Figure 34 IgG4-related lymphadenopathy, type II. (**A**) Nodal architecture is preserved. There is usual reactive follicular hyperplasia. (**B**) The interfollicular zone shows increased plasma cells.

Kikuchi Lymphadenitis

Clinical features. Kikuchi lymphadenitis, also known as Kikuchi–Fujimoto disease or histiocytic necrotizing lymphadenitis, occurs more commonly in Oriental young adults females (106–108). Patients are usually asymptomatic except for the cervical lymphadenopathy, although some may have fever. Skin rash and generalized lymphadenopathy are uncommon features. The etiology is unknown, but possibilities include an abnormal reaction triggered by a yet-to-be identified infective organism, or a self-limiting autoimmune phenomenon. The affected lymph nodes resolve spontaneously in most patients, and the recurrence rate is less than 5% (106,107).

Pathology. The size of the affected lymph node is usually less than 2 cm. The nodal architecture is typically distorted but not effaced. At low magnification, there are multiple pale-staining, variable-sized, nonexpansile foci infiltrated by a mixture of cells, which are typically interspersed with abundant karyorrhectic debris (Fig. 37A–C). Some of these foci can be wedge shaped, with the base facing the capsular side of the node. Within the foci, there are numerous histiocytes, including ''crescentic'' histiocytes with eccentrically located moon-shaped nucleus and ingested cellular debris, and histiocytes with twisted nuclei and no phagocytosed material in the cytoplasm (Fig. 37B). Plasmacytoid dendritic cells are always present, and are recognized by their medium-sized round nuclei (Fig. 37D). Variable numbers of activated lymphoid cells (immunoblasts) are always present; while most have round or oval nuclei with prominent nucleoli, some may show irregular nuclear foldings (Fig. 37C). Plasma cells and neutrophils are typically scanty or absent.

The cell composition apparently changes with evolution of the diseases, although lesions of different

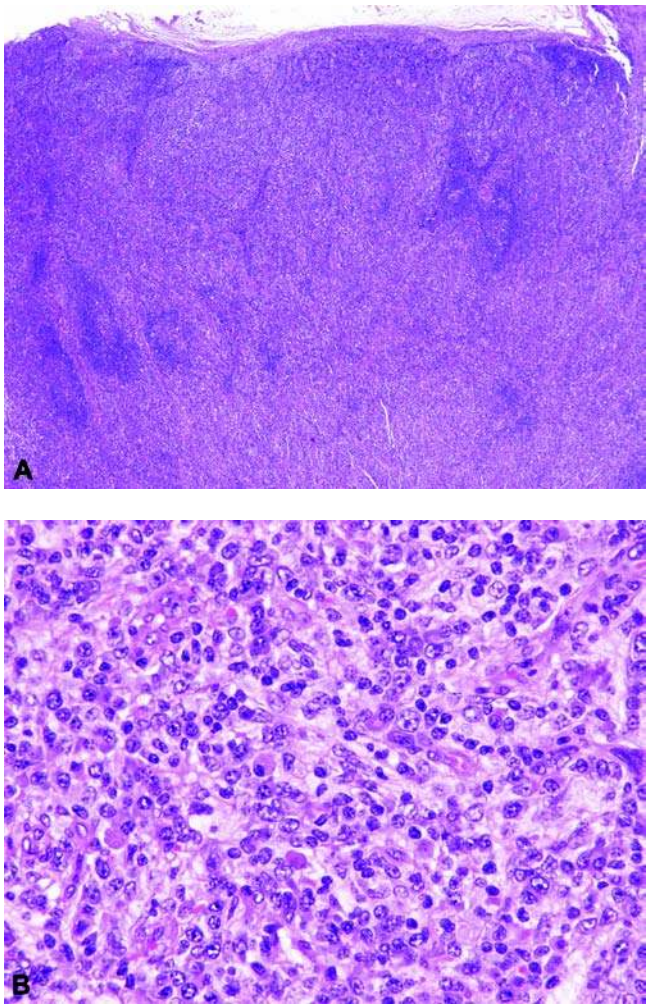

Figure 35 IgG4-related lymphadenopathy, type III. (**A**) The node shows marked paracortical expansion. (**B**) The paracortex is populated by small lymphocytes, immunoblasts, and plasma cells. High endothelial venules are also prominent.

phases are sometimes seen in the same node. The early proliferative phase is richly cellular, with an admixture of histiocytes, plasmacytoid dendritic cells, and immunoblasts. The necrotic phase is characterized by presence of coagulative necrosis. The xanthomatous phase is characterized by the accumulation of foamy histiocytes. The reparative phase features hypocellular loose vascularized tissue, and the characteristic cellular infiltrates are no longer present in these foci.

Immunohistochemistry. In the involved areas, there are three major cell populations: (*i*) CD8+ cytotoxic T cells, which may mediate the prominent apoptosis; (*ii*) plasmacytoid dendritic cells, which are CD68+, myeloperoxidase−, CD123+; and (*iii*) histiocytes, which are CD68+, myeloperoxidase+, CD123− (Fig. 38) (109–111). Identification of these distinctive cell types can aid in diagnosis of problematic cases, especially in small biopsies.

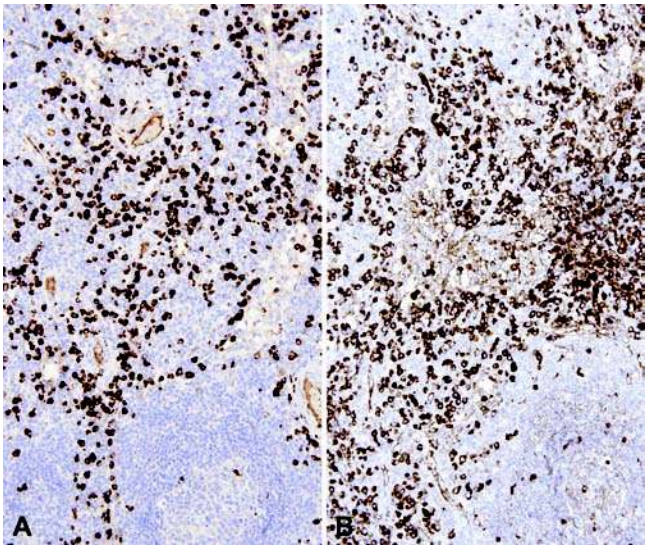

Figure 36 IgG4-related lymphoadenopathy, immunohistochemistry. (**A**) There are many IgG4+ plasma cells. (**B**) Many IgG+ cells are also present. The IgG4/IgG ratio is approximately 50% in this csae.

Differential diagnosis. Lupus lymphadenitis can show histologic features similar to Kikuchi lymphadenitis, including the presence of myeloperoxidase-positive histiocytes; clinical and serologic correlation is essential for the distinction (96). Histologic features that are more suggestive of the former include a significant plasma cell infiltrate, vasculitis, and the pathognomonic hematoxylin bodies (but which are uncommon).

Cases with numerous activated lymphoid cells and plasmacytoid dendritic cells can potentially be misdiagnosed as large cell lymphoma. The young age of the patient, the focal and segmental nature of lesions in Kikuchi lymphadenitis, abundance of karyorrhectic debris, and the presence of the characteristic cellular composition (including myeloperoxidase-positive histiocytes) should permit the correct diagnosis of Kikuchi lymphadenitis to be made. Extranodal NK/T-cell lymphoma is characterized by prominent apoptosis and necrosis, and may thus mimic Kikuchi lymphadenitis, but the lymphoid cells express CD56 and are positive for EBV by in situ hybridization.

When a case of Kikuchi disease shows prominent necrosis, infection also enters into the differential diagnosis. In contrast to infected lymph nodes, granulomas and neutrophilic infiltrate are not observed in Kikuchi disease.

Kimura Disease

Clinical features. Kimura disease is a mass-forming chronic inflammatory condition of unknown etiology, frequently involving the soft tissues, salivary glands, lymph nodes, and ocular adnexa in the head and neck region. It is more common in Orientals, but

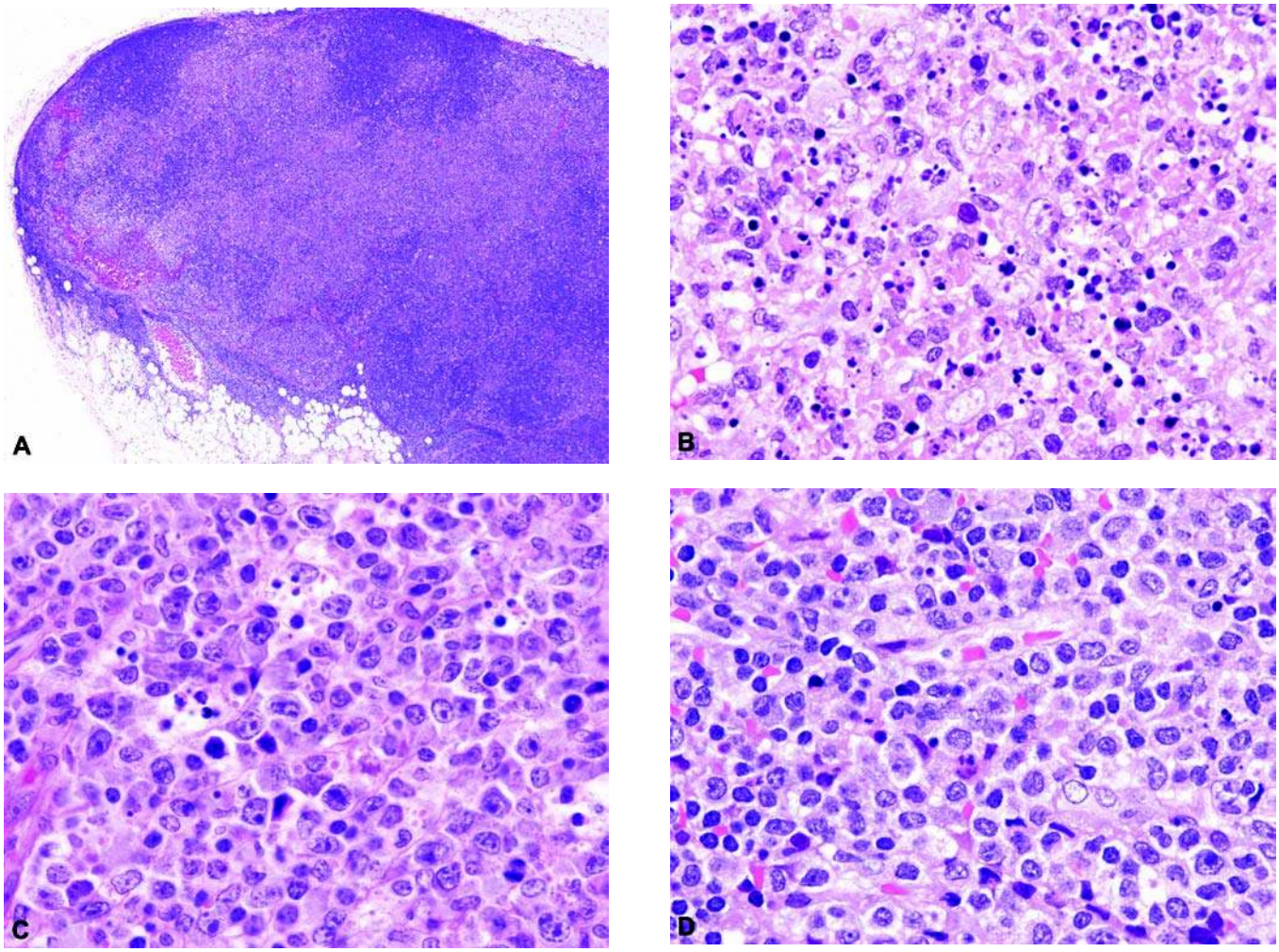

Figure 37 Kikuchi lymphadenitis. (**A**) The lymph node shows the characteristic low magnification appearance of Kikuchi lymphadenitis—presence of multiple discrete, pale-staining, nonexpansile foci. (**B**) The pale-staining foci are rich in apoptotic bodies, crescentic histiocytes, and histiocytes with twisted nuclei. (**C**) In some cases, there is an alarming number of admixed activated large lymphoid cells, raising the differential diagnosis of a large cell lymphoma. (**D**) Closer scrutiny reveals admixed plasmacytoid dendritic cells (with medium-sized round nuclei), especially in the peripheral zone of the pale-staining foci.

cases have also been reported in Westeners. The patients are usually young to middle-aged males (112–115). The blood shows elevated IgE level and eosinophilia. Occasional patients may be complicated by nephrotic syndrome due to immune complex deposition in the kidney.

Patients usually have persistent or recurrent disease, and surgery may not be required except for cosmetic or diagnostic reasons. The mass lesions may sometimes respond to steroid therapy.

Pathology. Histologically, the involved lymph nodes and extranodal tissues show marked follicular lymphoid hyperplasia and heavy eosinophilic infiltrate (Fig. 39A). The lymphoid follicles have prominent germinal centers, often with vascularization. Some may show eosinophil infiltration, eosinophil abscess formation, eosinophilic follicle lysis, or presence of scattered polykaryocytes (Fig. 39B). The interfollicular zone shows infiltration of small lymphocytes, plasma cells, eosinophils, and mast cells (Fig. 39C). Eosinophil abscesses can be formed, and there can be scattered polykaryocytes (Fig. 39C). High endothelial venules are increased, and perivenular sclerosis is common. Sclerosis is a common finding, especially in the later stage of the disease.

Differential diagnosis. In the past, Kimura disease has been confused with epithelioid hemangioma (angiolymphoid hyperplasia with eosinophilia). Although both conditions are characterized by heavy eosinophilic infiltration, vascular proliferation, and

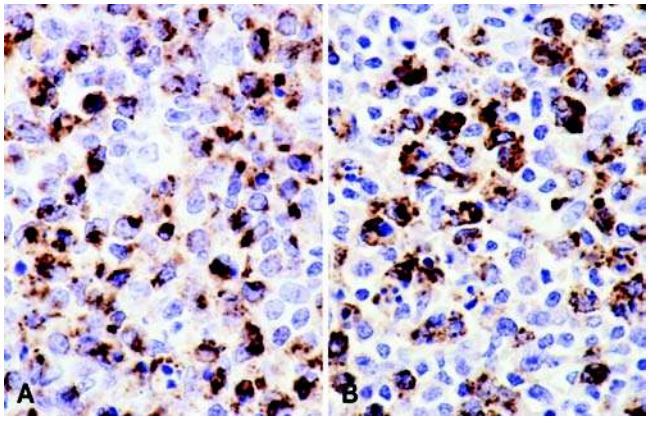

Figure 38 Kikuchi lymphadenitis, immunohistochemistry. (**A**) Both the histiocytes (with ingested debris) and plasmacytoid dendritic cells (with medium-sized round nuclei) are positive for CD68. (**B**) Typically the histiocytes are also positive for myeloperoxidase.

predilection for the head and neck region, epithelioid hemangioma occurs predominantly in the skin, is usually not associated with a heavy lymphoid infiltrate, and characterized by histiocytoid endothelial cells with abundant hyaline, sometimes vacuolated, cytoplasm (113).

With a heavy eosinophilic infiltration, other differential diagnoses may include classical Hodgkin lymphoma, Langerhans cell histiocytosis, parasitic infestation, allergy, and drug reaction. Classical Hodgkin lymphoma can be recognized by the presence of Reed–Sternberg cells in the inflammatory background, and Langerhans cell histiocytosis by the presence of compact clusters of Langerhans cells with grooved nuclei and abundant eosinophilic cytoplasm. Kimura disease can be distinguished from the other diseases with tissue eosinophilia in that there must be florid reactive follicular hyperplasia, accompanied by the characteristic germinal center changes as described above.

Kawasaki Disease

Clinical features. Kawasaki disease is an acute vasculitis that affects infants and children. It is characterized by fever, bilateral nonexudative conjunctivitis, erythema of the lips and oral mucosa, changes in the extremities, rash, and cervical lymphadenopathy (116). Coronary artery aneurysms develop in up to 25% of untreated children and may lead to ischemic heart disease or sudden death. The etiology remains unknown.

Pathology. In the affected lymph node, there are multiple foci of geographic necrosis, in which there are karyorrhectic debris and some neutrophils (Fig. 40A, B). Typically, in the nonnecrotic foci, fibrin thrombi can be found within the small blood vessels (117). Although the histologic features are not specific, the identification

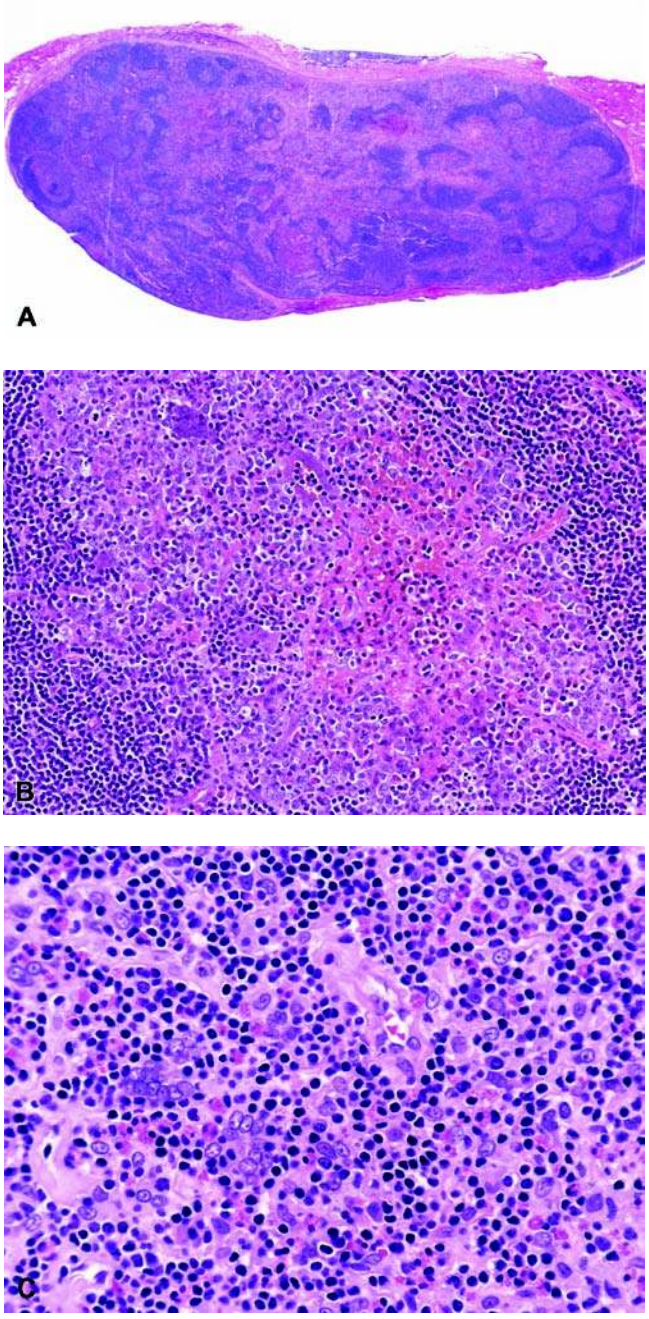

Figure 39 Kimura disease lymphadenopathy. (**A**) There is typically reactive follicular hyperplasia. Some germinal centers appear red due to eosinophil infiltration. (**B**) The germinal center shows penetration by venules and infiltration by eosinophils. A polykaryocyte is seen in the upper field. (**C**) The interfollicular zone is rich in high endothelial venules, small lymphocytes, plasma cells, and eosinophils. Polykaryocytes are also present.

of these findings should raise the suspicion of Kawasaki disease. Early diagnosis is essential because prompt treatment with intravenous immunoglobulin can lower the chance of developing the potentially fatal coronary aneurysms.

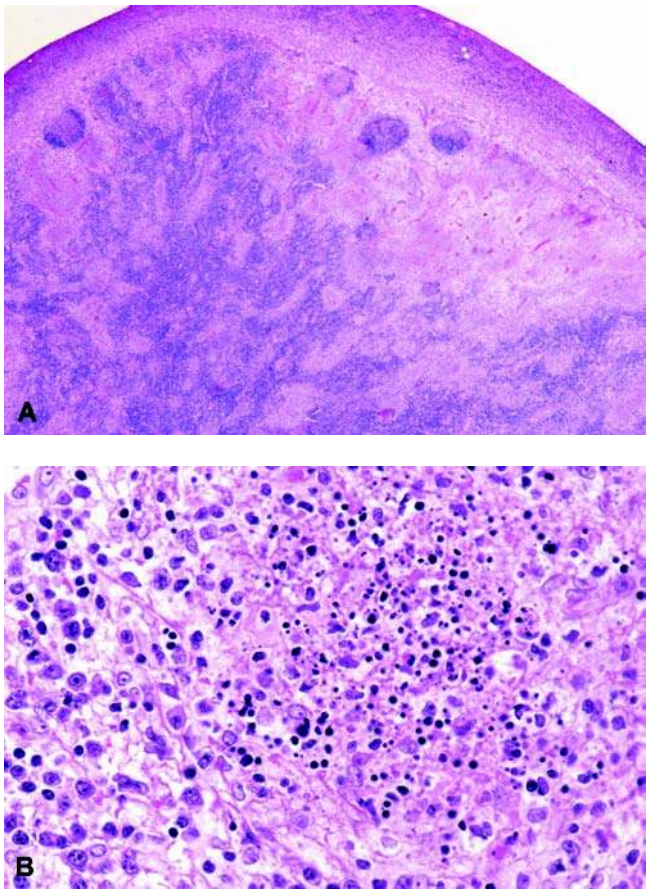

Figure 40 Kawasaki disease, lymph node. (**A**) There are multiple geographic foci of necrosis. (**B**) Apoptotic bodies and histiocytes are found in the necrotizing foci.

In contrast to lupus lymphadenitis, it occurs in much younger patients, hematoxylin bodies are absent, and serum antinuclear antibodies are negative. In contrast to Kikuchi lymphadenitis, Kawasaki disease occurs in children rather than adults, and histologically shows more extensive geographic rather than discrete focal necrosis and prominent fibrinoid thrombosis, and presence of neutrophils.

Hyaline-Vascular Castleman Disease

Clinical features. Hyaline-vascular Castleman disease is a distinctive form of lymphoid proliferation that can affect patients of a wide age range, but most often in young adults. It typically presents as a localized mass, which can reach a considerable size. Mediastinal involvement is common. In the head and neck region, cervical lymph node involvement occurs (118), and presentation at extranodal sites, e.g., nasopharynx, oropharynx, orbit, larynx, has also been reported (119–122). Rare patients may have associated paraneoplastic pemphigus. This is a totally benign condition curable by local excision, although the surgical procedure may be difficult because of profuse bleeding.

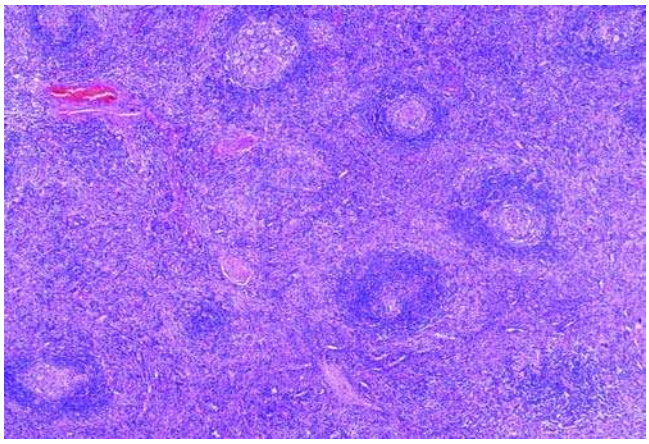

Figure 41 Hyaline-vascular Castleman disease, lymph node. Abnormal follicles are separated by a richly vascularized stroma, and sinuses are absent. Most follicles have a hyaline-vascular appearance, while occasional follicles (*upper field*) can be indistinguishable from usual reactive follicles.

Pathology. The essential diagnostic features include (*i*) abnormal hyaline-vascular follicles, (*ii*) hypervascular interfollicular zone, and (*iii*) lack of nodal sinuses within the main lesion (although sinuses may sometimes be found in the periphery of the lesion) (Fig. 41) (122).

In the typical example, the follicles have small germinal centers depleted of lymphoid cells and composed mostly of follicular dendritic cells and endothelial cells, surrounded by thick mantles with concentric disposition of the small lymphocytes (Fig. 42A–G). Some follicular dendritic cells can have enlarged hyperchromatic or bizarre nuclei (Fig. 42H). The follicles are penetrated by one or more venules with or without hyalinization, producing a lollipop-like appearance. Lymphoid follicle with multiple small discrete germinal centers sharing an expanded mantle zone is another characteristic finding, if present (Fig. 42D).

The interfollicular zone is rich in high endothelial venules and densely populated by small lymphocytes, with few large lymphoid cells or plasma cells (Fig. 43). Perivenular sclerosis can be present. There are commonly some clusters of plasmacytoid dendritic cells. Rare large bizarre cells can be found in the interfollicular zone in some cases.

In a proportion of cases, the histologic features may not be so classical. The follicles can have large germinal centers, resembling usual reactive follicles, but they can be distinguishable from the latter by the whorled arrangement of germinal center cells, lack of polarity, lower cell density, and focal presence of hyalinized venules in the germinal centers (Figs. 41 and 42E). Some follicles can be very large, being devoid of germinal centers and radially penetrated by multiple venules (Fig. 42G).

In some cases, the interfollicular zone is very broad, so-called stroma-rich variant, defined by an

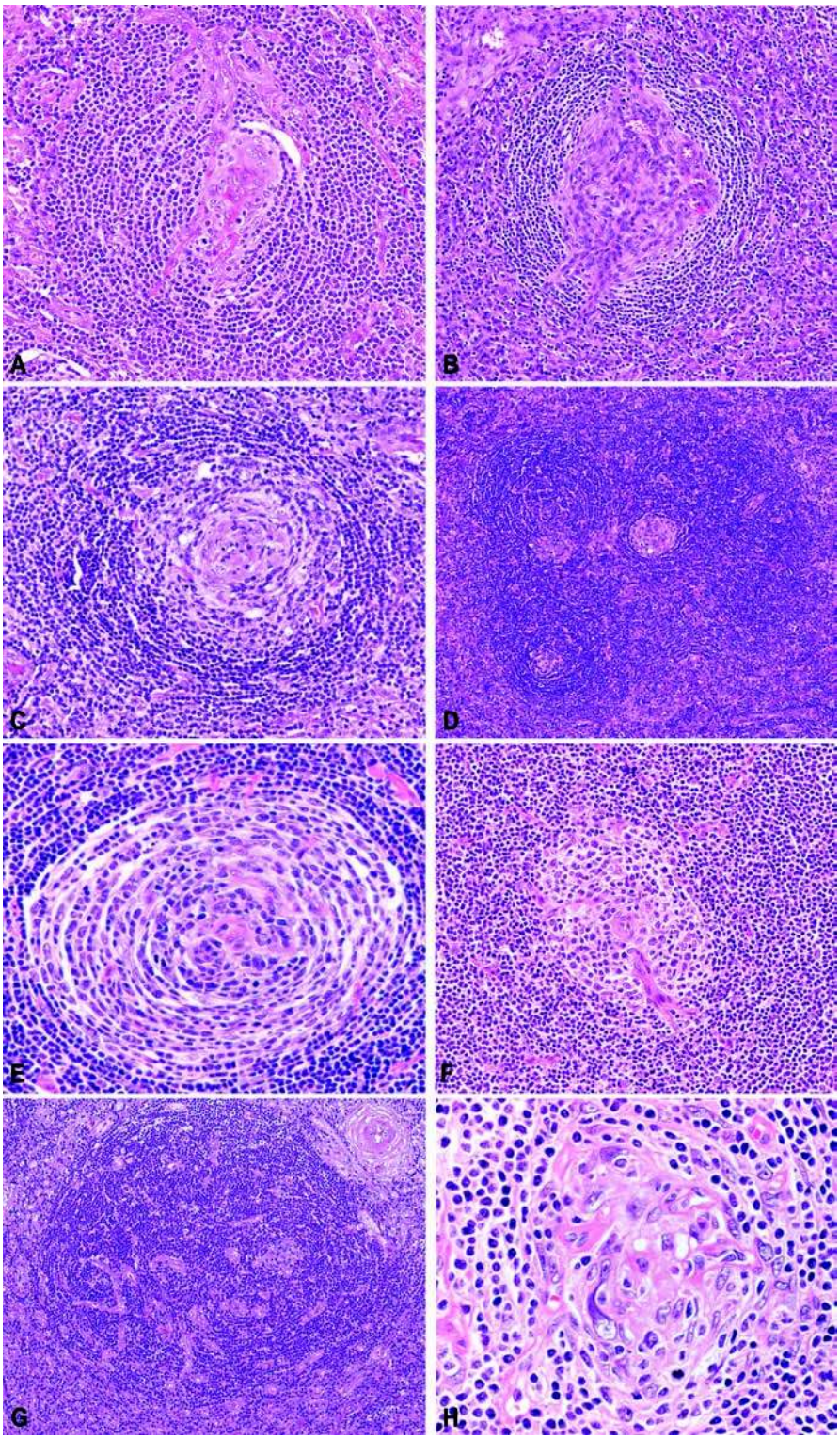

Figure 42 The morphologic spectrum of follicles in hyaline-vascular Castleman disease. (**A**) Small germinal center composed mostly of follicular dendritic cells and penetrated by multiple hyalinized venules. (**B**) Germinal center replaced by entangled blood vessels. (**C**) Whorled germinal center with lymphoid cell depletion in the central portion, and penetration by venules. (**D**) Follicle with several discrete round germinal centers, a feature practically diagnostic of hyaline-vascular Castleman disease if present. (**E**) Whorled germinal center. (**F**) Germinal center penetrated by multiple venules. The mantle may not show concentric arrangement of small lymphocytes as in this follicle. (**G**) Follicle composed exclusively of small lymphoid cells, and penetrated by multiple venules. (**H**) Follicle with occasional large bizarre cells.

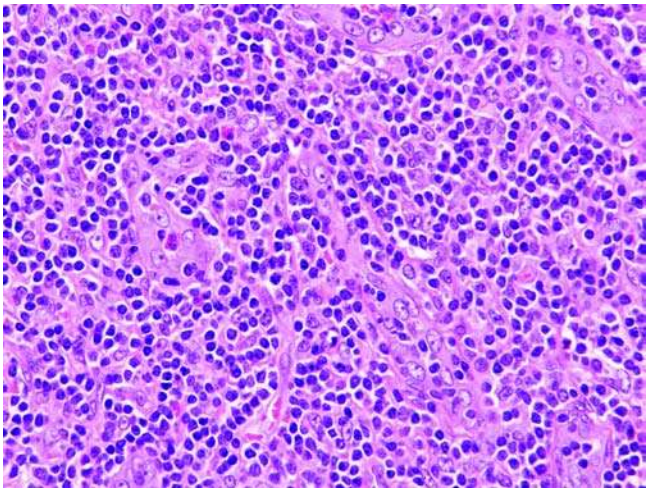

Figure 43 Hyaline-vascular Castleman disease, lymph node. The interfollicular zone consists of many high endothelial venules, admixed with small lymphocytes. There are few plasma cells and immunoblasts.

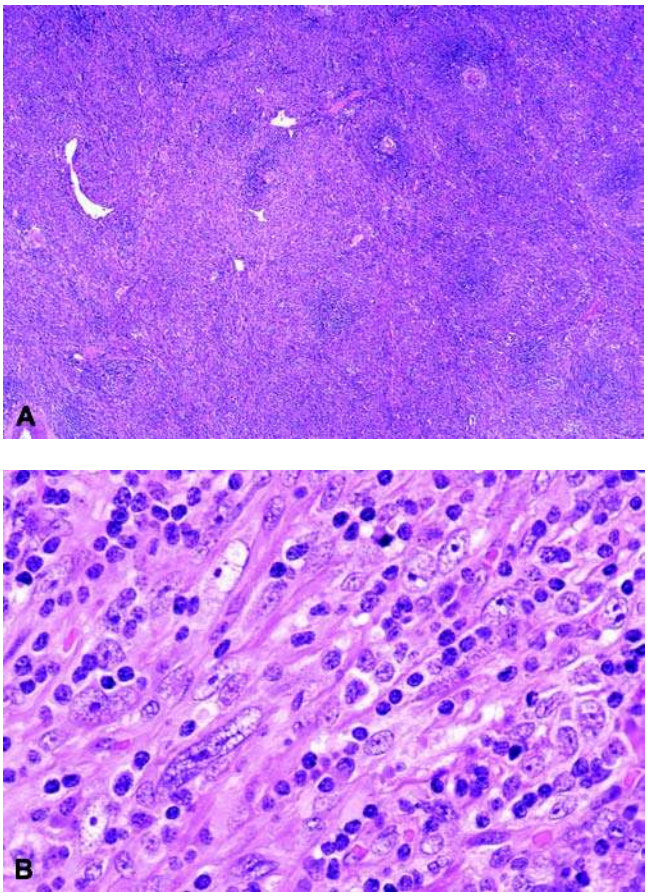

Figure 44 Hyaline-vascular Castleman disease. (**A**) Stroma-rich variant. Some hyaline-vascular follicles are seen in the right upper field, while the rest of the tissue is occupied by interfollicular tissue lacking follicles. (**B**) Stromal cell overgrowth of undetermined lineage. The spindly cells show significant nuclear atypia.

interfollicular zone occupying >50% of the lesional area, such that the diagnostic hyaline-vascular follicles are widely scattered or inconspicuous (Fig. 44A) (123). Sclerosis can be prominent, particularly in long-standing lesions. The sclerosis takes the form of extensive perivenular sclerosis merging into broad sclerotic bands or large sclerotic nodules, which can show central calcification.

Immunohistochemistry and molecular genetic data. On immunohistochemical staining, the follicles are rich in B cells (CD20+) while the interfollicular zone is rich in T cells (CD3+), which are predominantly of T-helper (CD4+) phenotype. The B cells in the mantle zones and the follicle centers show polytypic immunoglobulin light chains (124,125). Staining with CD21 or CD35 reveals abnormal follicular dendritic cell networks, which are expanded and disrupted, or appear as multiple tight concentric collections.

Immunoglobulin and T-cell receptor genes are in germ line configuration (126,127), and EBV is negative.

Associated cellular proliferations and neoplasms. Hyaline-vascular Castleman disease can be accompanied or complicated by hamartomas or tumors, such as angiolipomatous hamartoma, follicular dendritic cell sarcoma, vascular neoplasm, and various stromal cell proliferations that are sometimes difficult to classify (Fig. 44B) (128–130). Recent studies have identified cytogenetic abnormalities in rare cases of Castleman disease, indicating that the stromal cells or follicular dendritic cells may harbor cytogenetic abnormalities before the development of overt superimposed tumors (131–133).

Differential diagnosis. Hyaline-vascular follicles are not pathognomonic of hyaline-vascular Castleman disease, but similar ''burnt-out'' follicles can be seen in HIV-associated lymphadenopathy (Fig. 25), angioimmunoblastic T-cell lymphoma, or even in nonspecific reactive lymphoid hyperplasia. The rich vascularity of the interfollicular region and lack of sinuses are important additional criterion essential for diagnosis of hyaline-vascular Castleman disease.

The broad mantle zones of hyaline-vascular Castleman disease can also raise the possibility of mantle cell lymphoma. In contrast to the former, there is coalescence of the mantle zones, the lymphoid cells usually show nuclear irregularities and exhibit CD5+, cyclin D1+ immunophenotype.

Localized Plasma Cell Castleman Disease

Clinical features. Localized plasma cell Castleman disease is much less common than hyaline-vascular Castleman disease. It affects predominantly young adults, who present with a mass lesion, most commonly abdominal lymph node. There are usually

associated systemic manifestations such as fever, hypergammaglobulinemia, elevated erythrocyte sedimentary rate, anemia, and bone marrow plasmacytosis. The disease is usually curable by resection (122).

There is an increase in serum interleukin-6, which plays an important role in the pathogenesis of plasma cell Castleman disease and causation of the systemic symptoms. Monoclonal antibody against interleukin-6 has been reported to control the systemic symptoms (134).

Pathology. Histologically, the lymph node architecture is preserved. There is marked reactive follicular hyperplasia; most follicles are usual-looking, but some may have a hyaline-vascular appearance (Fig. 45A). The interfollicular zone is densely packed with normal-looking plasma cells, which extend all the way to the cortex (Fig. 45B). The plasma cells are either polytypic (60%) or monotypic (40%) (135), and clonal rearrangements of immunoglobulin gene are identified in some cases (136).

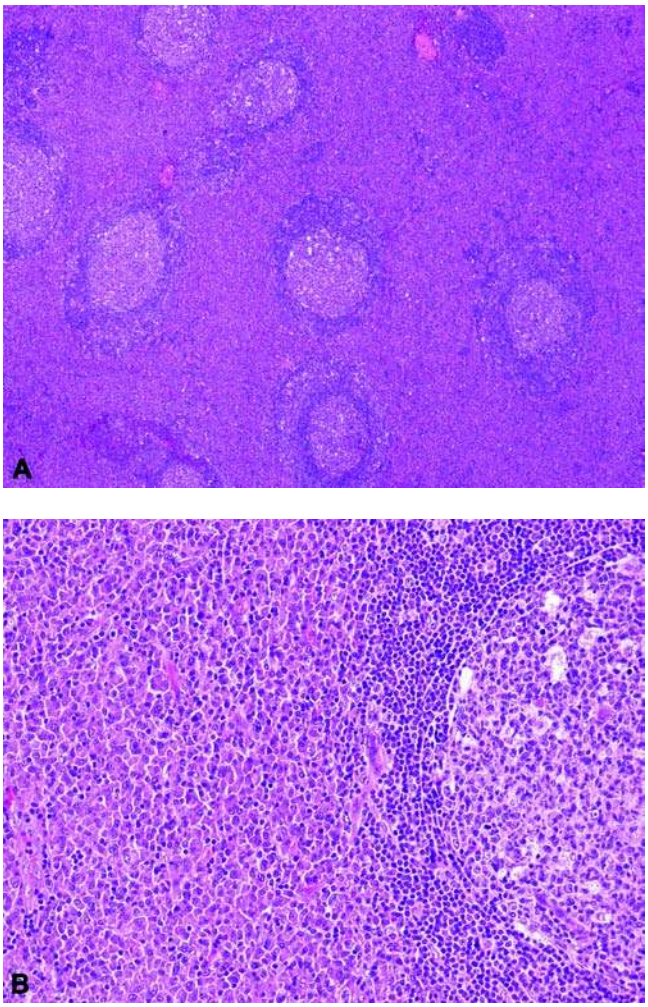

Figure 45 Plasma cell Castleman disease, lymph node. (**A**) There are usual-looking reactive lymphoid follicles. The interfollicular zone is expanded by a dense infiltrate of plasma cells. (**B**) Sheets of mature plasma cells are present between the follicles.

The morphologic appearances are nonspecific. Similar features may be seen in autoimmune diseases (such as rheumatoid arthritis or systemic lupus erythematosus), IgG4-related sclerosing disease, chronic infection (such as syphilis), HIV infection, or cancer (especially Hodgkin lymphoma) (137), and correlation with clinical findings is essential for a definitive diagnosis. Furthermore, it is always advisable to rule out a component of Hodgkin lymphoma in lymph node showing features of plasma cell Castleman disease.

The presence of monotypic plasma cells in plasma cell Castleman disease does not equate a diagnosis of plasmacytoma. Plasmacytoma is associated with destruction of normal nodal architecture and the identification of cytologically atypical plasma cells.

Multicentric Castleman Disease

Clinical features. Multicentric Castleman disease is a clinical syndrome in which the presentation is predominantly lymphadenopathic, with involvement of multiple peripheral nodes; there are systemic symptoms (e.g., fever) with evidence of multisystem involvement (e.g., bone marrow plasmacytosis, hepatosplenomegaly, proteinuria, skin rash, polyneuropathy); histologic features are usually those of plasma cell–type Castleman disease; and there are no known underlying causes (138). Patients are frequently older than those with localized Castleman disease, and the clinical features may sometimes overlap with those of autoimmune diseases. Laboratory findings include anemia, elevated erythrocyte sedimentation rate, hypergammaglobulinemia, hypoalbuminemia, and thrombocytopenia. Many signs and symptoms of multicentric Castleman disease are related to the overproduction of interleukin-6 (''interleukin-6 syndrome''). Some patients may be complicated by amyloidosis, usually the AA type.

The clinical outcome is variable, ranging from a rapidly aggressive course to a chronic course with recurrent exacerbations and remissions (138). The mortality rate is 45%, and overall median survival is 34 months. The commonest cause of death is infection. The optimal treatment remains uncertain, but many patients have benefited from steroids, chemotherapy, or anti-interleukin-6 receptor antibody therapy (139).

Primary and secondary forms of multicentric Castleman disease are identified, with the latter being associated with HIV infection, Kaposi sarcoma, plasma cell dyscrasia, malignant lymphoma, or autoimmune diseases (138). Etiologically, a proportion of cases of multicentric Castleman disease are associated with HHV8, involving either HIV-infected or HIV noninfected individuals (59,140). HHV8 is detected in 47% of primary cases, and 90% to 100% in cases associated with Kaposi sarcoma, HIV infection, POEMS syndrome, and plasmablastic lymphoma (138). The expression of viral interleukin-6 in these HHV8-associated cases partly accounts for the interleukin-6 syndrome. For cases not associated with HHV8, overproduction of human interleukin-6 may be responsible (138).

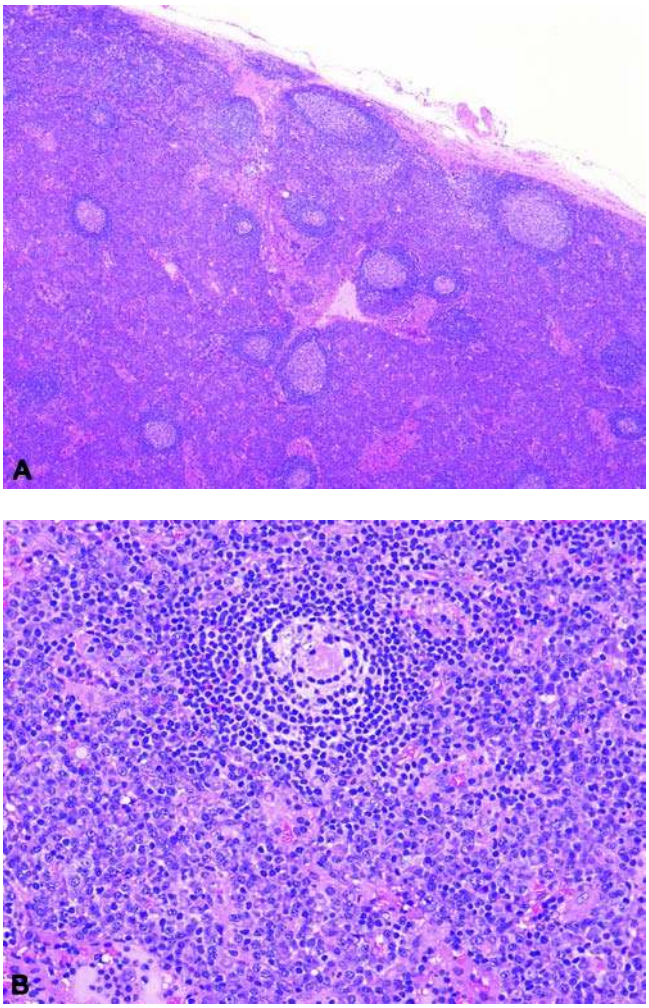

Figure 46 Multicentric Castleman disease, lymph node. (**A**) Nodal architecture is preserved, with intact sinuses. There are reactive follicles and interfollicular plasmacytosis. (**B**) Some follicles can have a hyaline-vascular appearance, and the interfollicular zone is packed with mature plasma cells.

Pathology. Histologically, the lymph nodes show features similar to those of localized plasma cell Castleman disease. The sinuses are patent. There are hyperplastic, regressed, and/or hyaline-vascular follicles in the cortex, and there is an increase of mature plasma cells in between (Fig. 46A, B). Some cases show monotypic λ-expressing plasma cells and clonal immunoglobulin gene rearrangement (138). An important differential diagnosis is IgG4-related sclerosing disease.

Some of the HHV8-associated cases may show increased plasmablasts disposed singly or in small aggregates, usually in the mantle zones of regressed follicles. This is also known as the plasmablastic variant of multicentric Castleman disease. The plasmablasts express monotypic λ light chain, but they are frequently polyclonal on molecular analysis. These cells are HHV8 positive. The disease may rarely progress to frank lymphoma—*large B-cell lymphoma arising in HVV8-associated multicentric Castleman disease* (141–143).

Since some secondary forms of multicentric Castleman disease are related to tumors (such as Kaposi sarcoma, plasmacytoma, or lymphoma), such associated lesions should be excluded when examining a lymph node of suspected multicentric Castleman disease.

Rosai–Dorfman Disease (Sinus Histiocytosis with Massive Lymphadenopathy)

Clinical features. Rosai–Dorfman disease is a reactive histiocytic proliferation of unknown etiology. Patients are frequently children and young adults, but any age may be affected. While this is predominantly a nodal disease, 40% of patients have extranodal disease with or without nodal involvement. Multiple extranodal sites may be affected in the same patient (144). Skin, nasal cavity, soft tissue, eyelid/orbit, bone, and salivary glands are commonly involved extranodal sites, but any other head and neck sites such as oral cavity, larynx, Waldeyer ring, thyroid, and ear may also be affected. Patients with head and neck disease frequently present with a cervical mass or symptoms related to the mass in the upper aerodigestive tract (e.g., nasal obstruction, sinusitis, epistaxis, facial pain, or saddle nose deformity). About 13% of patients have associated immune-mediated phenomenon such as autoantibodies against blood cells and joint disease.

Most cases of Rosai–Dorfman disease are treated by excision alone, with steroid, radiotherapy, and chemotherapy having been given in a minority of cases. In general, the prognosis is excellent, with most patients being free of disease or with stable disease. However, some patients may develop recurrent disease in the original site or other body sites.

A histologic pattern identical to Rosai–Dorfman disease has been observed as a focal phenomenon in lymph nodes from about 40% of patients with autoimmune lymphoproliferative syndrome (145).

Pathology. The lymph nodes typically show marked capsular fibrosis and striking sinusoidal distension by a distinctive type of histiocytes that are very large, with round nuclei, distinct central nucleoli, and voluminous lightly eosinophilic or pale cytoplasm (Fig. 47A, B). Some histiocytes show emperipolesis (phagocytosis), with lymphocytes or plasma cells, and sometimes neutrophils, in the cytoplasm (Fig. 47B–D). In some cases, a proportion of histiocytes can exhibit mildly atypical or irregular nuclei, and may lead to a misdiagnosis of malignancy such as histiocytic sarcoma or melanoma (Fig. 47C). Numerous plasma cells are present in the paracortex and medullary cords.

In extranodal sites, the lesion recapitulates the sinus growth in lymph node, even though sinuses are absent, with light-staining bands alternating with dark-staining bands. The light-staining bands are formed by aggregates of the distinctive Rosai–Dorfman histiocytes, while the dark-staining bands are formed by plasma cells. Emperipolesis is usually less

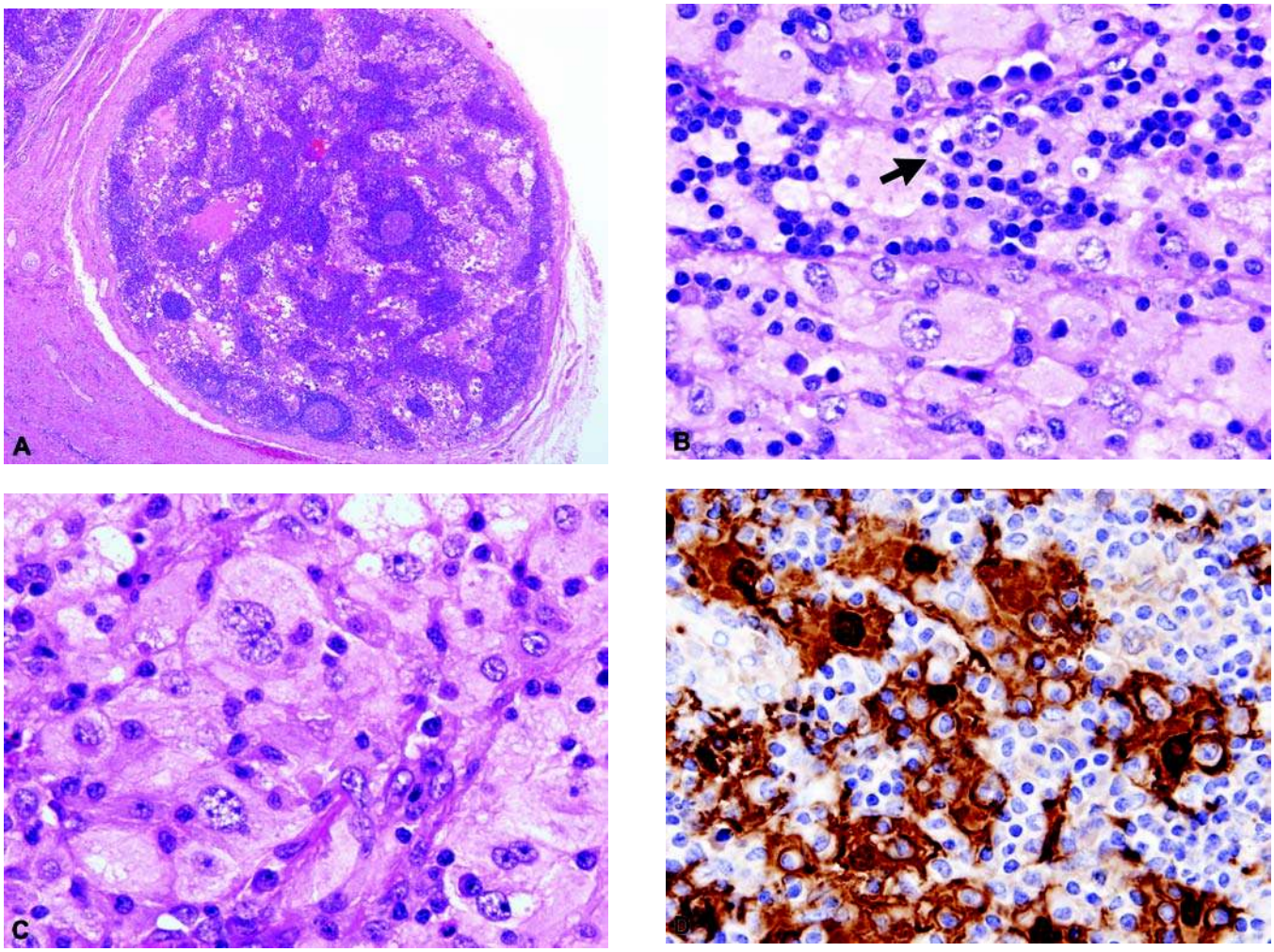

Figure 47 Rosai–Dorfman disease, lymph node. (**A**) Marked sinusoidal distension and capsular fibrosis are highly characteristic low magnification appearances of this entity. (**B**) The sinuses are packed with very large histiocytes with round nuclei, distinct nucleoli, and abundant pale-staining cytoplasm. Emperipolesis (lymphophagocytosis) is evident in some histiocytes (*arrow*). (**C**) Some histiocytes can show nuclear atypia, raising the differential diagnosis of histiocytic sarcoma. Note also the characteristic presence of many admixed plasma cells. (**D**) Immunostaining for S100 gives positive results in the nuclei as well as cell bodies of the histiocytes. The negatively stained phagocytosed cells within the positively stained cytoplasm of the histiocytes are remarkably highlighted—thus this immunostain is an excellent tool for identifying emperipolesis (lymphophagocytosis).

striking compared with lymph node. Regressive changes can be present, with decreased Rosai–Dorfman histiocytes, accumulation of foamy histiocytes, and fibrosis (Fig. 48). As a result of fibrosis and spindling of some of the Rosai–Dorfman histiocytes, the histologic picture can mimic fibrohistiocytic tumor or inflammatory pseudotumor.

Immunohistochemically, the Rosai–Dorfman histiocytes typically express S100 protein in the nuclei and cytoplasm. Since the cell bodies of the histiocytes are clearly stained up while the phagocytosed cells remain unstained, S100 protein immunostain is very helpful for highlighting emperipolesis or lymphophagocytosis (Fig. 47D). The histiocytic markers CD68 and CD163 are positive, while CD1a and langerin (CD207) are negative. Foamy histiocytes, if present, are negative for S100 protein.

Autoimmune Lymphoproliferative Syndrome

Introduction. Autoimmune lymphoproliferative syndrome is an inherited disorder of lymphocyte apoptosis, caused by germ line mutation in the Fas (*TNFRSF6*), Fas ligand (*TNFSF6*), or caspase (*CASP10* or *CASP8*) gene (146–148). The rare sporadic form of the disease results from somatic heterozygous mutation in the *TNFRSF6* gene (149). As a result of impaired lymphocyte apoptosis, lymphoid cells accumulate in the body after antigenic challenge, resulting in persistent enlargement of reticuloendothelial system. There is no increased susceptibility to infections.

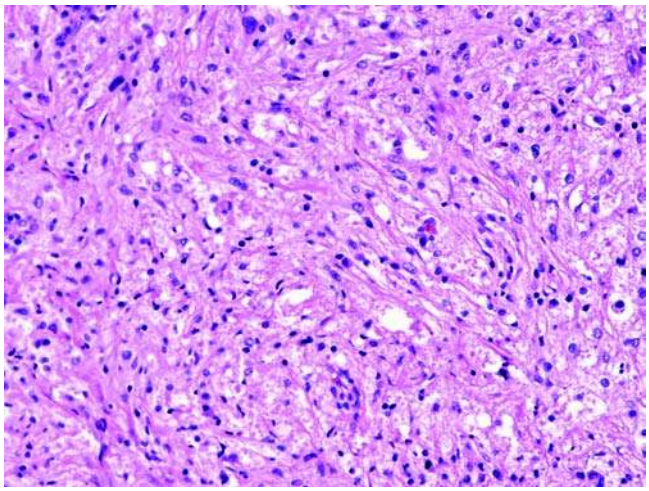

Figure 48 Rosai–Dorfman disease, soft tissue. In chronic lesions, there can be areas with cellular spindling and accumulation of foamy histiocytes, producing a xanthogranulomatous appearance.

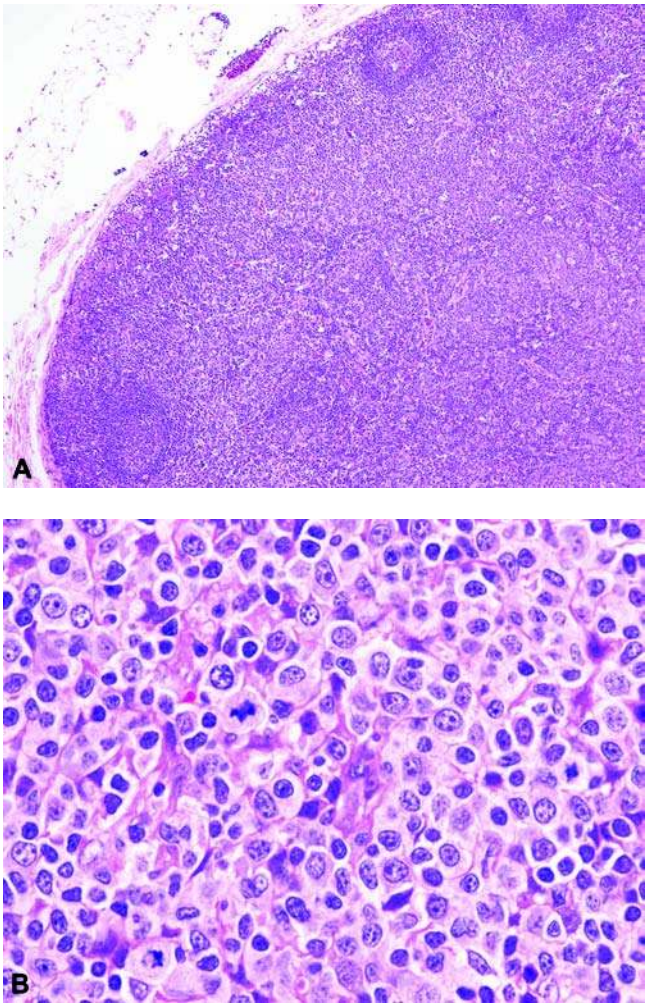

Figure 49 Autoimmune lymphoproliferative syndrome involving lymph node. (**A**) The nodal architecture is distorted but not effaced. There is marked paracortical expansion. (**B**) In the paracortex, there are many medium-sized to large lymphoid cells, and some of them have clear cytoplasm. The picture is practically indistinguishable from peripheral T-cell lymphoma.

Clinical features. Patients usually present with chronic lymphadenopathy in infancy or early childhood (mean age 2 years), which is often generalized and recurrent and sometimes massive. Splenomegaly and hepatomegaly are common. Autoimmunity is a key feature of the disease, most notably directed against blood cells, manifesting as Coombs-positive hemolytic anemia, immune-mediated thrombocytopenia, or autoimmune neutropenia. Other circulating autoantibodies are also common, such as anti-cardiolipin antibody, anti-nuclear antibody, and rheumatoid factor, associated with variable clinical manifestations of autoimmune diseases. The most characteristic finding is an increase in circulating CD4− CD8− T lymphocytes (usually accounting for 5–20% of the CD3+ cells); these double-negative cells express αβ rather than γδ T-cell receptors. There is polyclonal hypergammaglobulinemia. The patients have an increased risk of developing Hodgkin lymphoma or non-Hodgkin lymphoma (150).

Pathology. The lymph node shows reactive follicular hyperplasia, and some germinal centers may exhibit features of progressive transformation (151). There is marked paracortical expansion by a mixture of immunoblasts, plasma cells, and medium-sized clear cells (Fig. 49A, B). Some of the immunoblasts and medium-sized cells may even show irregular foldings of the nuclei. On immunostaining, a significant proportion of the paracortical T cells exhibit a CD4−, CD8−, CD45RO−, CD57+ immunophenotype (Fig. 50). The morphology and ''aberrant'' immunophenotype can therefore entice the pathologist to render erroneous diagnosis of peripheral T-cell lymphoma (T-zone lymphoma). The most important clue to the correct diagnosis is the young age of the patient—since peripheral T-cell lymphomas other than anaplastic large cell lymphomas are very rare in this age group, the possibility of autoimmune lymphoproliferative syndrome must be seriously considered.

In some patients, the lymph nodes may in addition show morphologic features of Rosai–Dorfman disease in focal areas (145).

Inflammatory Pseudotumor of Lymph Node

Introduction and clinical features. Inflammatory pseudotumor, also frequently known as inflammatory myofibroblastic tumor, refers to a tumor-forming mass consisting of a mixture of inflammatory cells and spindly fibroblasts and myofibroblasts, with variable degree of fibrosis. In the head and neck, it may involve the nasal cavity (152), larynx (153), salivary gland (154), and orbit (155); a proportion of cases express ALK due

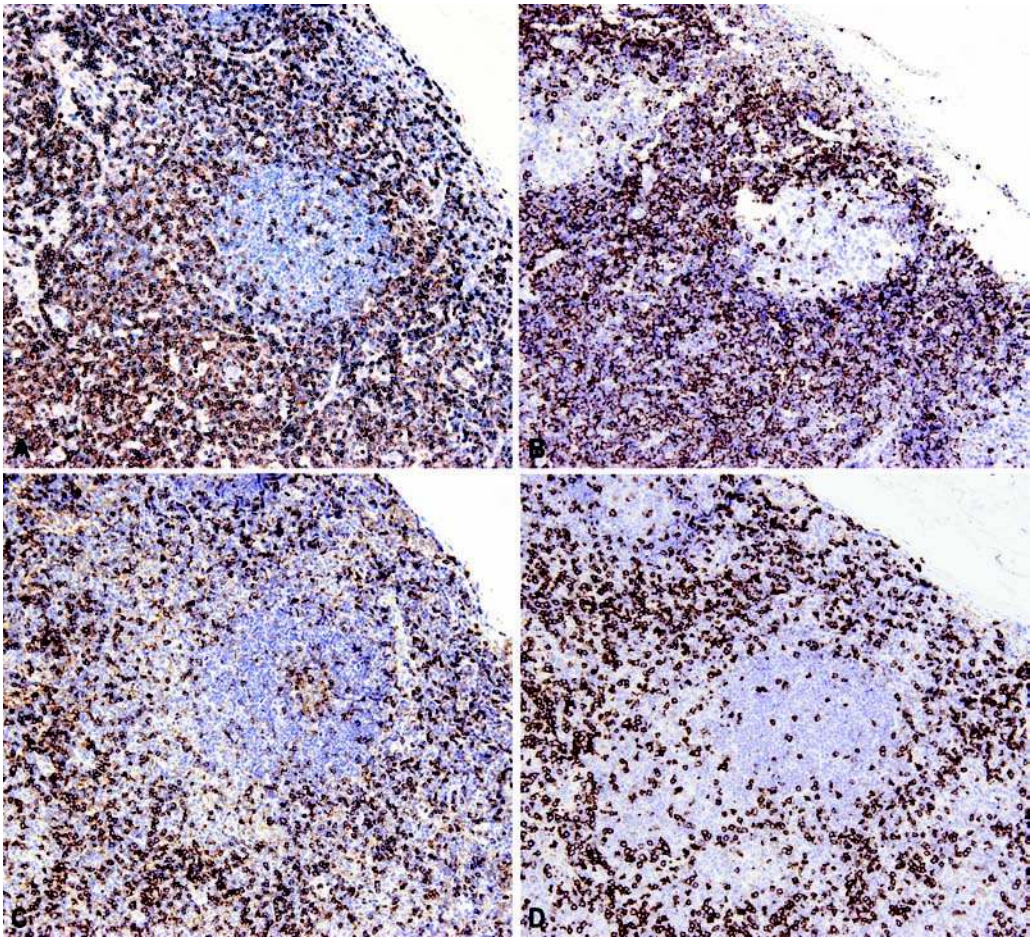

Figure 50 Autoimmune lymphoproliferative syndrome involving lymph node, immunohistochemistry. Take particular note of the lymphoid population around the lymphoid follicle. (**A**) Most cells outside the follicle are CD3+ T cells. (**B**) Many of these cells express CD57, which normally is expressed in only a minority of T cells. (**C**) Many perifollicular T cells are CD4 negative. (**D**) Many perifollicular T cells are also CD8 negative.

to the presence of *ALK* gene translocation (156–158). The entity described as inflammatory pseudotumor of lymph node appears to be a completely different entity, more related to the family of inflammatory fibrosclerosing lesions (156,157,159–161). Patients may have systemic symptoms such as fever. Inflammatory pseudotumor of lymph node frequently follows a benign course, but it may persist or relapse; some cases may respond to steroid and anti-inflammatory drugs (1).

Pathology. Inflammatory pseudotumor of lymph node is characterized by expansion of the connective tissue framework of the node (capsule, fibrous trabeculae, hilum) by a fibroinflammatory process, with fibrosis, scattered bland-looking spindly cells, vascular proliferation, and inflammatory cell infiltration (Fig. 51A, B). The inflammatory cells most frequently include lymphocytes, histiocytes, and plasma cells, but immunoblasts, eosinophils, and neutrophils can also be present. Phlebitis may be observed in the perinodal tissues. Some cases have been described to show effacement of nodal architecture by a sclerotic process with sparse inflammation (159), but it is unclear whether they truly represent the burned out phase of inflammatory pseudotumor of lymph node.

Extramedullary Hematopoietic Tumor

Introduction and clinical features. Extramedullary hematopoietic tumor is a mass-forming lesion composed of hematopoietic cells. It can involve the head and neck lymph nodes and extranodal sites such as the orbit, middle ear, nasal cavity, larynx, and thyroid (162–167). Patients usually have underlying hematologic diseases such as myeloproliferative diseases (most frequently primary myelofibrosis); it may also be iatrogenic, or secondary to therapy by granulocyte colony-stimulating factor (168).

Pathology. All three hematopoietic lineages are often present, and it is the identification of these cell types that clinches the diagnosis. Megakaryocytes,

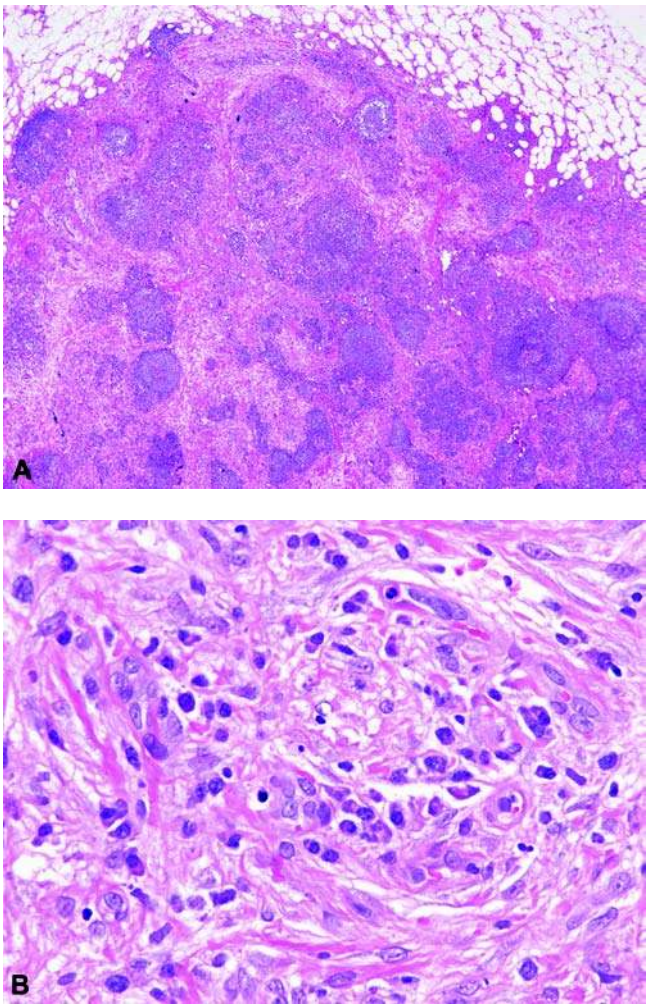

Figure 51 So-called inflammatory pseudotumor of lymph node. (**A**) The pathologic process typically involves the connective tissue framework of the node, with thickening of the capsule and fibrous trabeculae. (**B**) Bland-looking spindly cells, blood vessels, lymphocytes, and plasma cells are found in a collagenous stroma.

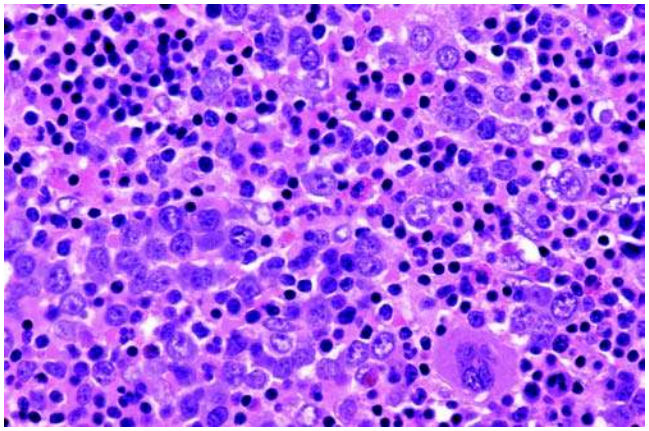

Figure 52 Extramedullary hematopoiesis in the orbit. The presence of many large cells and occasional huge "bizarre" cells can easily entice the pathologist to render a diagnosis of malignancy. The largest cell (*right lower field*) is in fact a megakaryocyte. The clusters of large cells are immature erythroblasts, and not lymphoma cells. The best clue to diagnosis is finding clusters of late normoblasts (*upper field*)—these cells differ from small lymphocytes in that the chromatin is even more condensed, and they possess a broad rim of eosinophilic to amphophilic cytoplasm.

which are giant multinucleated cells with pleomorphic nuclei and abundant eosinophilic cytoplasm, can be highlighted by immunostaining for factor VIII, CD31, and CD34. Myeloid precursors possess immature nuclei and fine cytoplasmic granules, and they express myeloperoxidase (Fig. 52). Erythroid precursors frequently occur in aggregates, and range from primitive erythroblasts to smaller normoblasts (Fig. 52). Erythroblasts have large round hyperchromatic nuclei, high nuclear-to-cytoplasmic ratio, and amphophilic cytoplasm, while the smaller normoblasts have small round dense hyperchromatic nuclei and amphophilic to eosinophilic cytoplasm. Their erythroid nature can be confirmed by immunostaining for glycophorin A. To the inexperienced, the pleomorphic megakaryocytes can be mistaken for carcinoma or histiocytic sarcoma, while the erythroid and myeloid precursors can be mistaken for lymphoma cells. The best clue to diagnosis is the presence of islands of normoblasts—the nuclei are much more hyperchromatic than those of lymphoma cells and the color of the cytoplasm approximates that of erythrocytes.

The sclerosing variant poses even greater problem in diagnosis (169). Since the hematopoietic cells are disposed in a sclerotic to myxoid background, the picture simulates sarcomas (such as sclerosing liposarcoma) or Hodgkin lymphoma (Fig. 53A, B).

Amyloidosis

Introduction. Amyloid is a special type of extracellular amorphous eosinophilic proteinaceous deposit with distinctive tinctorial characteristics. With Congo red stain, it has a salmon pink color under ordinary light and shows a diagnostic apple green birefringence under polarized light. Ultrastructural examination shows nonbranching fibrils with a diameter of 7.5 to 10 nm. The characteristic cross-β-pleated sheet conformation as demonstrated with X-ray crystallography and infrared spectroscopy is the cause for the unique staining property, irrespective of the chemical composition of the fibrils (170).

The amyloid deposit consists predominantly of fibril proteins (95%), with the P component and other glycoproteins accounting for the remaining 5%. At least 25 types of human fibril proteins have been reported to give rise to amyloid (171), and abnormal folding of the proteins is believed to be the underlying mechanism for fibril formation and amyloid deposition (170). The two commonest types of fibril proteins are AL (amyloid light chain) type derived from immunoglobulin light chain (especially λ) produced by

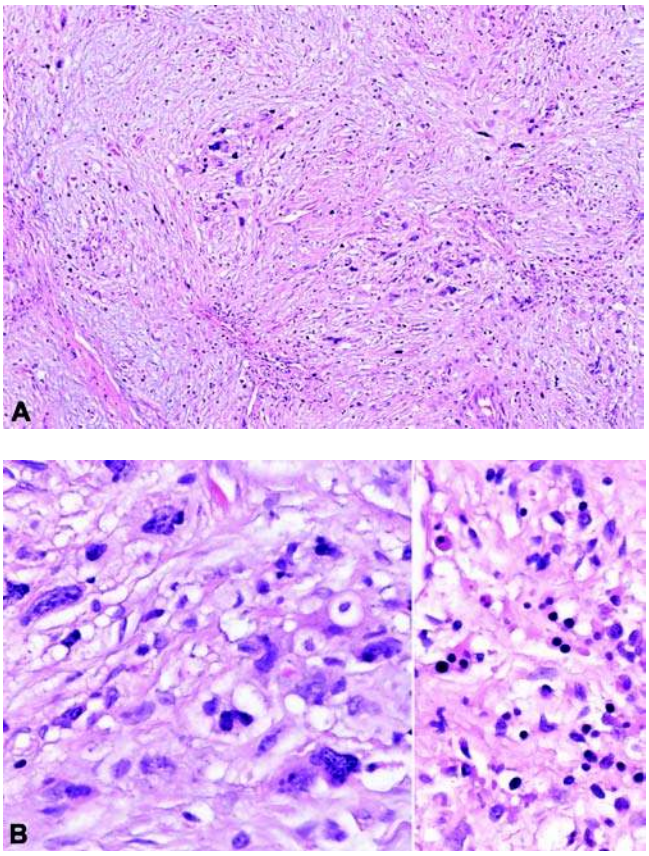

Figure 53 Sclerosing extramedullary hematopoietic tumor of the orbit. (**A**) The presence of many large atypical cells and spindly cells in a myxoid stroma results in a sarcoma-like appearance. (**B**) The megakaryocytes can look alarming if this possibility is not considered (*left panel*). Identification of late normoblasts provides the best clue to the correct diagnosis (*right panel*).

plasma cells and AA (amyloid-associated) type synthesized by the liver. Other than classifying based on the chemical composition of the amyloid protein, amyloidosis can also be classified according to clinicopathologic settings as follows:

1. Systemic amyloidosis secondary to immunocyte dyscrasia (primary amyloidosis; AL type, derived from immunoglobulin light chain)
2. Reactive systemic amyloidosis (secondary amyloidosis; AA type, derived from serum AA protein) secondary to chronic inflammation of diverse etiologies, such as tuberculosis, rheumatoid arthritis, and some tumor types (e.g., renal cell carcinoma and Hodgkin lymphoma)
3. Hemodialysis-associated systemic amyloidosis (derived from β_2-microglobulin), in chronic renal failure patients on long-term hemodialysis
4. Heredofamilial amyloidosis, such as familial Mediterranean fever (derived from serum AA protein), and familial amyloidotic polyneuropathies (derived from transthyretin)
5. Senile systemic amyloidosis (derived from transthyretin), often with significant involvement of the heart
6. Localized amyloidosis
   a. Alzheimer disease (derived from amyloid precursor protein APP)
   b. Endocrine tumor-associated, such as carcinoid, medullary thyroid carcinoma, islet cell tumor (derived from peptide hormones or prohormones)
   c. Localized amyloidosis associated with nonendocrine tumors, e.g., nasopharyngeal carcinoma, squamous cell carcinoma; the amyloid is often derived from cytokeratins
   d. Localized amyloidosis of various organs, such as larynx, Waldeyer ring, thyroid; the amyloid is often of AL type (derived from immunoglobulin light chain).

Typing of the amyloid deposit has become increasingly relevant for clinical management, since the treatment options differ for different types of amyloidosis (172,173). Typing by histochemical method (abolition of Congo red staining by potassium permanganate indicating AA-type and $A\beta_2m$-type amyloid) (174,175) has been shown to be unreliable. Immunohistochemical staining for the different fibril proteins (e.g., such as immunoglobulin light chain, AA protein, transthyretin, β_2 microglobulin) has been increasingly used for typing (173,176), but the results can be difficult to interpret and can be unpredictable (177). Clinicopathologic correlation remains essential in the final interpretation. Other methods of typing such as chemical analysis with tandem mass spectrometry are being explored (178).

Clinical features. The head and neck region may be affected in both systemic and localized forms of amyloidosis, with the tongue being the commonest involved site in systemic amyloidosis (179,180). Systemic amyloidosis is associated with organomegaly, and may result in macroglossia and goiter (181).

In contrast, localized amyloidosis most frequently occurs in the larynx (182,183), but has also been described in other head and neck sites, including the tongue, tonsil, oropharynx, lip, palate, floor of mouth, nasopharynx, nasal cavity and sinuses, parotid gland, ear, periocular and orbital tissues, thyroid, lymph node, skin, and cervical soft tissue (184–198). Patients with localized laryngeal amyloidosis most often are in the fourth to sixth decades of life, and frequently present with hoarseness of voice (182,183). The false cord is the commonest involved region, but the true cord or the rest of the larynx may also be affected, and the disease can be unilateral or bilateral (182,183,199). Macroscopically, the lesion appears as elevated, bosselated, or polypoid masses covered by intact mucosa. There is usually no serologic evidence of monoclonal gammopathy or bone marrow plasma cell dyscrasia at presentation. The treatment of choice is surgery, but local recurrence is common, including involvement of the lower respiratory tract. Subsequent systemic

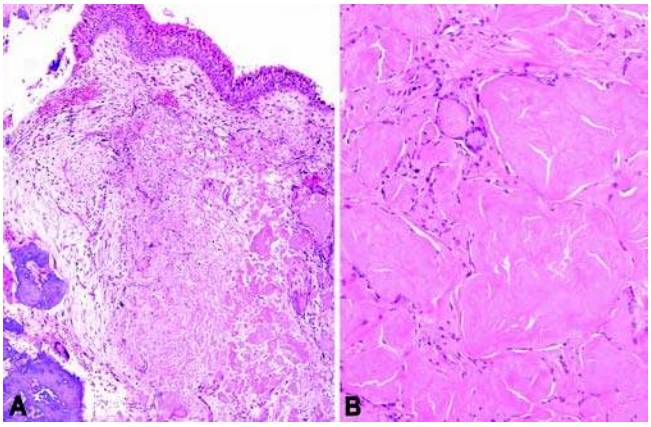

Figure 54 Amyloidosis of nasal cavity. (**A**) Beneath an intact epithelium, there are deposits of eosinophilic material consistent with amyloid. Calcification and ossification of the amyloid is evident in the left field. (**B**) Amyloid can be recognized by the blotchy staining characteristics, and the presence of occasional interspersed histiocytes, some of which are multinucleated.

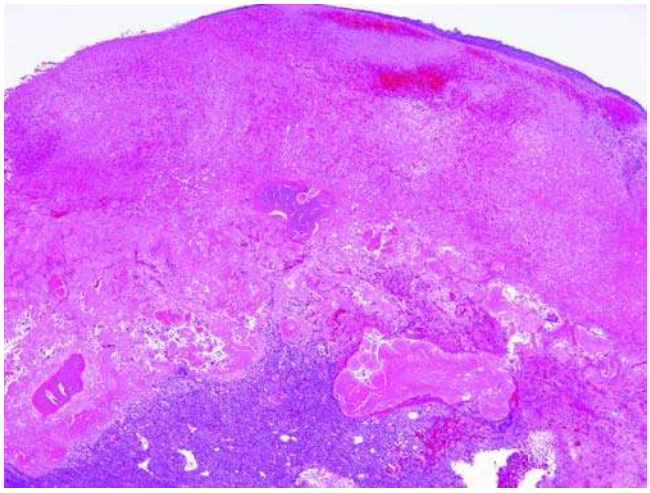

Figure 55 Plasmacytoma of the nasal cavity, complicated by amyloid deposition. The neoplastic plasma cell infiltrate is seen in the lower field.

involvement or development of multiple myeloma, however, is rare.

Patients with localized amyloidosis associated with endocrine and nonendocrine tumors present with symptoms related to the underlying tumors.

Pathology. In tissues, amyloid appears as sheets and clumps of extracellular amorphous eosinophilic material, often accompanied by deposition of similar material in blood vessel walls (Fig. 54A). Sometimes there can be calcification or ossification. The finding of focal foreign body giant cell reaction against the eosinophilic material provides a strong clue that the material represents amyloid rather than sclerosis or hyaline change (Fig. 54B). The deposit has a pink to red color with Congo red stain, and shows green birefringence under polarized light.

In the various head and neck sites, whether of systemic or localized type of amyloidosis, the subepithelial or interstitial deposition of amyloid is often accompanied by atrophy and loss of specialized tissues, such as mucosal glands. Small amounts of chronic inflammatory cells, including plasma cells, are commonly admixed with the amyloid deposits. In contrast to lymphoma and plasmacytoma, the lymphoplasmacytic cells do not show cytologic atypia and do not form sheets. On immunohistochemical staining, the lymphoid cells consist of a mixture of T and B cells. The amyloid is often shown to be of AL type, and the plasma cells in some cases can show immunoglobulin light-chain restriction (more frequently λ light chain) (182,183,200). However, these monoclonal plasma cells do not form sheets as in plasmacytoma, but their presence suggests that the amyloidosis is the result of a form of localized plasma cell dyscrasia.

Prominent amyloid deposition can also be observed in some tumors in the head and neck region, such as plasmacytoma (Fig. 55) (201–205). The presence of dense sheets of plasma cells (which may exhibit nuclear atypia) associated with tissue destruction indicates a diagnosis of coexisting plasmacytoma. Lymphomas, especially MALT lymphoma with plasmacytic differentiation may also be accompanied by tumor-forming amyloid of AL type (206). In the thyroid gland, medullary carcinoma, a calcitonin-producing neuroendocrine carcinoma, commonly shows amyloid deposition (207,208). In a small proportion of cases of nasopharyngeal carcinoma, amyloid taking the form of extracellular globules can occur among the tumor cells.

III. HEMATOLYMPHOID NEOPLASMS OF THE HEAD AND NECK: DESCRIPTION BY TUMOR TYPE

A. General Features

Hematolymphoid neoplasms are tumors of lymphoid, myeloid, or histiocytic cells. Lymphomas are subdivided into Hodgkin lymphomas and non-Hodgkin lymphomas, with the latter being more common. The classification scheme for the former has long been widely accepted, while that for non-Hodgkin lymphomas has been problematic due to the presence of several rivalry classifications in use adopting different terminologies for the same entity. The 2001 WHO classification, which originated from the 1994 REAL classification, has now been widely adopted (209,210), and recently updated (2008) (Table 2) (211).

Most lymphomas encountered in routine practice belong to the mature B-cell neoplasms category (210). The most common hematolymphoid neoplasms presenting in the head and neck region are DLBCL, follicular lymphoma, and classical Hodgkin

Table 2 2008 WHO Classification of Lymphomas and Histiocytic/Dendritic Cell Tumors

Hodgkin lymphoma
- Nodular lymphocyte–predominant Hodgkin lymphoma
- Classical Hodgkin lymphoma
  - Nodular sclerosis classical Hodgkin lymphoma
  - Mixed cellularity classical Hodgkin lymphoma
  - Lymphocyte-rich classical Hodgkin lymphoma
  - Lymphocyte-depleted classical Hodgkin lymphoma

Precursor lymphoid cell neoplasms
- B-lymphoblastic leukemia/lymphoma
- T-lymphoblastic leukemia/lymphoma

Mature B-cell neoplasms
- Chronic lymphocytic leukemia/small lymphocytic lymphoma (CLL/SLL)
- B-cell prolymphocytic leukemia
- Lymphoplasmacytic lymphoma
- Splenic B-cell marginal zone lymphoma
- *Splenic lymphoma/leukemia, unclassifiable*
  - *Splenic diffuse red pulp small B-cell lymphoma*
  - *Hairy cell leukemia variant*
- Hairy cell leukemia
- Plasmacytoma
- Extranodal marginal zone lymphoma of mucosa-associated lymphoid tissue (MALT lymphoma)
- Nodal marginal zone lymphoma
- Follicular lymphoma
- Primary cutaneous follicle center lymphoma
- Mantle cell lymphoma
- Diffuse large B-cell lymphoma (DLBCL), not otherwise specified (NOS)
- Diffuse large B-cell lymphoma, distinct subtypes:
  - Primary mediastinal (thymic) large B-cell lymphoma
  - Intravascular large B-cell lymphoma
  - Primary effusion lymphoma
  - T-cell/histiocyte-rich large B-cell lymphoma
  - Plasmablastic lymphoma
  - ALK-positive large B-cell lymphoma
  - *EBV+ diffuse large B-cell lymphoma of the elderly*
  - Diffuse large B-cell lymphoma associated with chronic inflammation
  - Primary diffuse large B-cell lymphoma of the central nervous system
  - Primary cutaneous diffuse large B-cell lymphoma, leg-type
  - Large B-cell lymphoma arising in HHV8-associated multicentric Castleman disease
- Lymphomatoid granulomatosis
- Burkitt lymphoma
- B-cell lymphoma, unclassifiable, with features intermediate between diffuse large B-cell lymphoma and Burkitt lymphoma
- B-cell lymphoma, unclassifiable, with features intermediate between diffuse large B-cell lymphoma and classical Hodgkin lymphoma

Mature T-cell and NK-cell neoplasms
- T-cell prolymphocytic leukemia
- T-cell large granular lymphocytic leukemia
- Adult T-cell leukemia/lymphoma
- Aggressive NK-cell leukemia
- *Chronic lymphoproliferative disorder of NK cells*
- EBV+ T-cell lymphoproliferative disease of childhood
  - Systemic EBV+ T-cell lymphoproliferative disease of childhood
  - Hydroa vacciniforme-like lymphoma
- Extranodal NK/T-cell lymphoma, nasal-type
- Enteropathy-associated T-cell lymphoma
- Hepatosplenic T-cell lymphoma
- Angioimmunoblastic T-cell lymphoma
- Peripheral T-cell lymphoma, not otherwise specified (NOS)
- Anaplastic large cell lymphoma, ALK+
- Anaplastic large cell lymphoma, ALK−
- Mycosis fungoides/Sézary syndrome
- Subcutaneous panniculitis-like T-cell lymphoma
- Primary cutaneous CD30-positive T-cell lymphoproliferative disorders
  - Lymphomatoid papulosis
  - Primary cutaneous anaplastic large cell lymphoma
- *Primary cutaneous CD8+ aggressive epidermotropic cytotoxic T-cell lymphoma*
- *Primary cutaneous $\gamma\delta$ T-cell lymphoma*
- Primary cutaneous CD4+ small/medium T-cell lymphoma

Immunodeficiency-associated lymphoproliferative disorders
- Lymphoproliferative diseases associated with primary immune disorders
- HIV-related lymphomas
- Posttransplant lymphoproliferative disorders
- Methotrexate-associated lymphoproliferative disorders

Histiocytic and dendritic cell neoplasms
- Histiocytic sarcoma
- Langerhans cell histiocytosis
- Langerhans cell sarcoma
- Follicular dendritic cell sarcoma
- Interdigitating dendritic cell sarcoma
- Indeterminate dendritic cell tumor
- Fibroblastic reticular cell tumor
- Disseminated juvenile xanthogranuloma
- Blastic plasmacytoid dendritic cell neoplasm (formerly "blastic NK-cell lymphoma")

Entities shown in *Italics* are provisional entities.

lymphoma for lymph nodes; and DLBCL, extranodal marginal zone lymphoma of mucosa-associated lymphoid tissue (MALT lymphoma), extranodal NK/T-cell lymphoma, and extramedullary plasmacytoma for extranodal sites. Mantle cell lymphoma, although not a common nodal lymphoma, shows frequent involvement of extranodal sites in the head and neck. The endemic form of Burkitt lymphoma shows a predilection for the jaw in children of central Africa, and the sporadic form can affect the tonsils and lymph nodes of children and young adults.

The distribution of various lymphoma types differs in different geographic populations (212). For example, follicular lymphoma is more prevalent in the United States as compared to Europe and Asia, while extranodal NK/T-cell lymphoma is more frequent in Asia, Central America, and South America (212). It is beyond the scope of this chapter to cover all

lymphoma types in details. The less common entities and those that are of little relevance to the head and neck will only be very briefly mentioned. The general features and details of the individual lymphoma entities are covered in this section, while the site-specific features will be addressed in the subsequent sections dealing with the individual anatomic locations.

B. Etiology

The etiology of most types of lymphoma is unknown, but some cases are associated with immunosuppression, e.g., posttransplant lymphoproliferative disorder (PTLD) and HIV infection (acquired immunodeficiency syndrome). Certain viruses, e.g., EBV, HHV8, human T-lymphotropic virus type 1, also play an important role in some lymphoma types. EBV is found in most cases of extranodal NK/T-cell lymphoma and lymphomas associated with immunosuppression, and in a proportion of cases of Hodgkin lymphoma and Burkitt lymphoma. The development of acquired MALT in organs where lymphoid tissue is not normally present can also be a forerunner of MALT lymphoma, and this may be the result of autoimmunity (e.g., Hashimoto thyroiditis, lymphoepithelial sialadenitis of Sjogren syndrome) or infection (e.g., *Helicobacter pylori*–associated chronic gastritis).

C. Procurement of Tissue for Pathologic Examination

Excisional biopsy is the preferred method in obtaining diagnostic material for suspected lymphoma. Although fine-needle aspiration cytology or core needle biopsy, a simple office procedure associated with minimal morbidity, is used increasingly, the obtained material is not generally suitable for the initial diagnosis of lymphoma even with application of a variety of investigation tools, such as flow cytometry and molecular analysis. Fine-needle aspiration and core needle biopsy have inherent problems in that the limited material obtained does not permit as thorough histologic assessment as in excisional biopsy, architectural features are either limited or not available, and the cellular details are sometimes suboptimal for assessment. For example, it is often impossible to distinguish grade 3 follicular lymphoma from DLBCL or to render a diagnosis of lymphoma supervening lymphoepithelial sialadenitis of the salivary gland.

Fine-needle aspiration cytology is preferably used as a screening tool for patients presenting with superficial lymphadenopathy or other mass lesions, for diagnosis of metastatic carcinoma or melanoma, and for diagnosis of recurrent lymphoma.

D. Staging

Staging by clinical examination, imaging studies, and bone marrow examination is an important step in the management of lymphoma patients. The information can guide further management and predict clinical outcome. The commonly used staging system is the Ann Arbor system (213) (Table 3); although the system was designed for Hodgkin lymphoma, it is also applied for non-Hodgkin lymphomas.

The clinical outcome depends on multiple factors, but a major independent prognostic factor is the International Prognostic Index (214,215) (Table 4). The International Prognostic Index score takes into account the patient's age, performance status, clinical stage, serum lactate dehydrogenase level, and number of involved extranodal sites.

Table 3 Staging System for Patients with Lymphoma

Stage I	Involvement of a single lymph node region (I); or Localized involvement of a single extralymphatic organ or site in the absence of any lymph node involvement (IE)
Stage II	Involvement of two or more lymph node regions on the same side of the diaphragm (II); or Localized involvement of a single extralymphatic organ or site in association with regional lymph node involvement with or without involvement of other lymph node regions on the same side of the diaphragm (IIE)
Stage III	Involvement of lymph node regions on both sides of the diaphragm (III), which also may be accompanied by extralymphatic extension in association with adjacent lymph node involvement (IIIE) or by involvement of the spleen (IIIS) or both (IIIE, IIIS)
Stage IV	Diffuse or disseminated involvement of one or more extralymphatic organs, with or without associated lymph node involvement; or Isolated extralymphatic organ involvement in the absence of adjacent regional lymph node involvement, but in conjunction with disease in distant site(s) Any involvement of the liver or bone marrow, or nodular involvement of the lung(s)

Each stage is further subclassified as either A or B according to the presence or absence of fever (unexplained fever above 38°C), night sweat, or weight loss (>10% in the 6 months prior to diagnosis).

Table 4 International Prognostic Index (IPI) Scoring System

Prognostic factors (1 score each)

- Age > 60 years
- Elevated serum lactate dehydrogenase
- Poor performance status
- High stage (III/IV)
- >1 extranodal site

Risk score			
0 1	2	3	4 5
Low	Low intermediate	High intermediate	High

The treatment options of lymphoma range from simple observation (''watch and wait'' approach), surgery (for localized disease or for ''debulking''), radiotherapy (for localized disease), chemotherapy (single agent or aggressive multiagent protocol), targeted therapy (such as anti-CD20), bone marrow transplant, or a combination. The choice depends on a number of factors, such as the lymphoma type, stage, general condition, and response to previous treatment.

E. Hodgkin Lymphomas

Classical Hodgkin Lymphoma

Introduction. Classical Hodgkin lymphoma accounts for 10% to 30% of all lymphomas (216). It is characterized by neoplastic Reed–Sternberg cells and their variants scattered in an appropriate inflammatory background. Since there is good evidence that the neoplastic cells are lymphoid cells (almost exclusively B lineage), the term ''Hodgkin lymphoma'' has replaced the original term ''Hodgkin disease.'' Four histologic subtypes are described: nodular sclerosis (the commonest), mixed cellularity, lymphocyte-rich, and lymphocyte-depleted.

Clinical features. Patients show a bimodal age distribution, with a peak in young adults (15–35 years) and another in late adulthood after the sixth decade. Classical Hodgkin lymphoma is predominantly a nodal-based disease, although extranodal presentation can also occur, such as in the Waldeyer ring (217). Peripheral lymphadenopathy is the commonest presentation. Nodular sclerosis Hodgkin lymphoma, the commonest subtype (>60% of cases), shows distinctive clinical features in frequent presentation with mediastinal involvement, sometimes accompanied by simultaneous supraclavicular or cervical lymphadenopathy. Lymphocyte-depleted Hodgkin lymphoma, the rarest subtype, occurs almost exclusively in immunocompromised patients or underdeveloped countries. B symptoms such as fever, night sweat, and weight loss may be present. 55% of patients have stage I/II disease at presentation.

Pathology. All four histologic subtypes of classical Hodgkin lymphoma are characterized by large Reed–Sternberg cells and their variants scattered singly or in aggregates in a background of reactive cells, including small lymphocytes, plasma cells, histiocytes, eosinophils, neutrophils, and/or fibroblasts (Fig. 56). There may be interspersed epithelioid granulomas or coalescing small clusters of epithelioid histiocytes (Lennert pattern). Diagnostic Reed–Sternberg cell is a large cell with bilobed or two nuclei, central inclusion-like eosinophilic nucleoli, and abundant lightly basophilic or eosinophilic cytoplasm. The mononuclear form is known as Hodgkin cell, while pyknotic tumor cells have been termed mummified cells. The lacunar cell, which apparently lies inside lacunar spaces, is another Reed–Sternberg cell variant that is characteristic of the nodular sclerosis subtype. The lacunar appearance probably results from cytoplasmic membrane retraction secondary to formalin fixation artifact. The lacunar cells are sometimes smaller than Reed–Sternberg cells and Hodgkin cells.

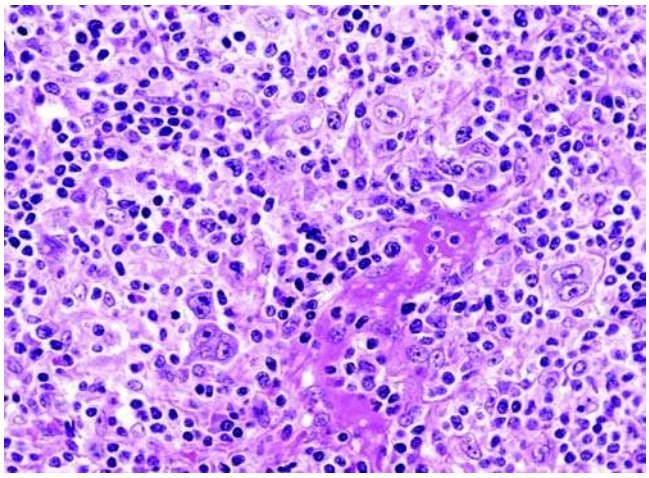

Figure 56 Classical Hodgkin lymphoma, lymph node. Diagnostic Reed–Sternberg cells and mononuclear variants are dispersed in a background of small lymphocytes and plasma cells.

Mixed Cellularity. The lymph node or extranodal tissue shows complete diffuse effacement of architecture or rarely interfollicular involvement (Fig. 57A). By definition, there are no sclerotic bands. The infiltrate typically includes readily identifiable diagnostic Reed–Sternberg cells and mononuclear variants, which are uniformly distributed throughout the involved areas (Fig. 57B). The inflammatory background is variable, but usually include small lymphocytes, histiocytes, and eosinophils.

Nodular Sclerosis. Irrespective of involved tissue, the tumor consists of nodules separated by thick bands of birefringent collagen fibers (Fig. 58A, B). Lacunar cells represent the predominant neoplastic cells. They tend to be grouped into nodular aggregates, contrasting with the uniform distribution of neoplastic cells in mixed cellularity subtype (Fig. 58C). There is a variable inflammatory cell background, such as small lymphocytes, eosinophils, and neutrophils. Cases with sheets of tumor cells have been referred to as ''syncytial variant,'' and commonly show geographic foci of coagulative necrosis (Fig. 59A–C). The term ''cellular phase'' has been used for cases without sclerosis, but with lacunar cells forming vague nodular aggregates.

The British National Lymphoma Investigation has introduced a grading system (218). Grade II is defined by (*i*) >25% of the nodules contain increased number of Reed–Sternberg cells forming sheets, i.e., showing lymphocyte depletion; (*ii*) >80% of the nodules show fibrohistiocytic type of lymphocyte depletion (Fig. 59D); or (*iii*) >25% of the nodules without lymphocyte depletion contain numerous anaplastic Reed–Sternberg cells. Grade I includes cases with none of these three features. Some, but not all, studies

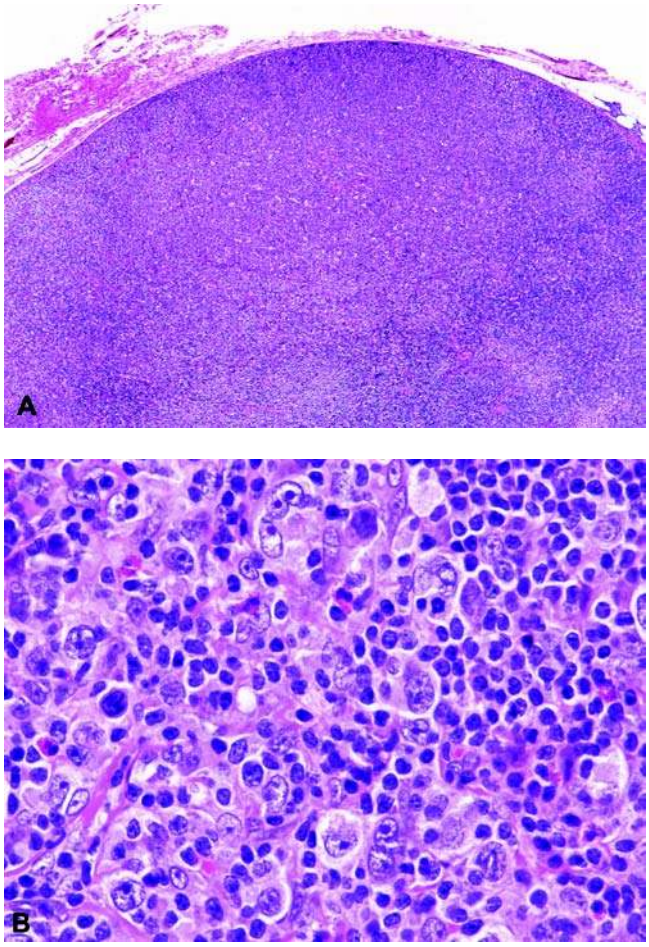

Figure 57 Mixed cellularity classical Hodgkin lymphoma, lymph node. (**A**) The lymph node architecture is diffusely effaced, with obliteration of sinuses. (**B**) Reed–Sternberg cells and variants, which are very large cells, are uniformly dispersed throughout the background of small lymphocytes, plasma cell, and eosinophils.

have shown grade II cases to represent a poor prognostic subgroup.

Lymphocyte-Rich. The lymphocyte-rich classical Hodgkin lymphoma subtype, accounting for only 4% of all Hodgkin lymphomas, was first recognized in the REAL classification (219). In the past, such cases were probably classified as lymphocyte-predominant or mixed cellularity Hodgkin lymphoma. It can occur in a nodular (more common) and a diffuse (less common) form; the boundary of the latter with mixed cellularity Hodgkin lymphoma is not always sharp and is based on a paucity of Reed–Sternberg cells and variants.

In the nodular lymphocyte–rich classical Hodgkin lymphoma, there are large nodules composed predominantly of small lymphocytes, with small germinal centers being occasionally identified in some of them (Fig. 60A, B). Reed–Sternberg cells and variants

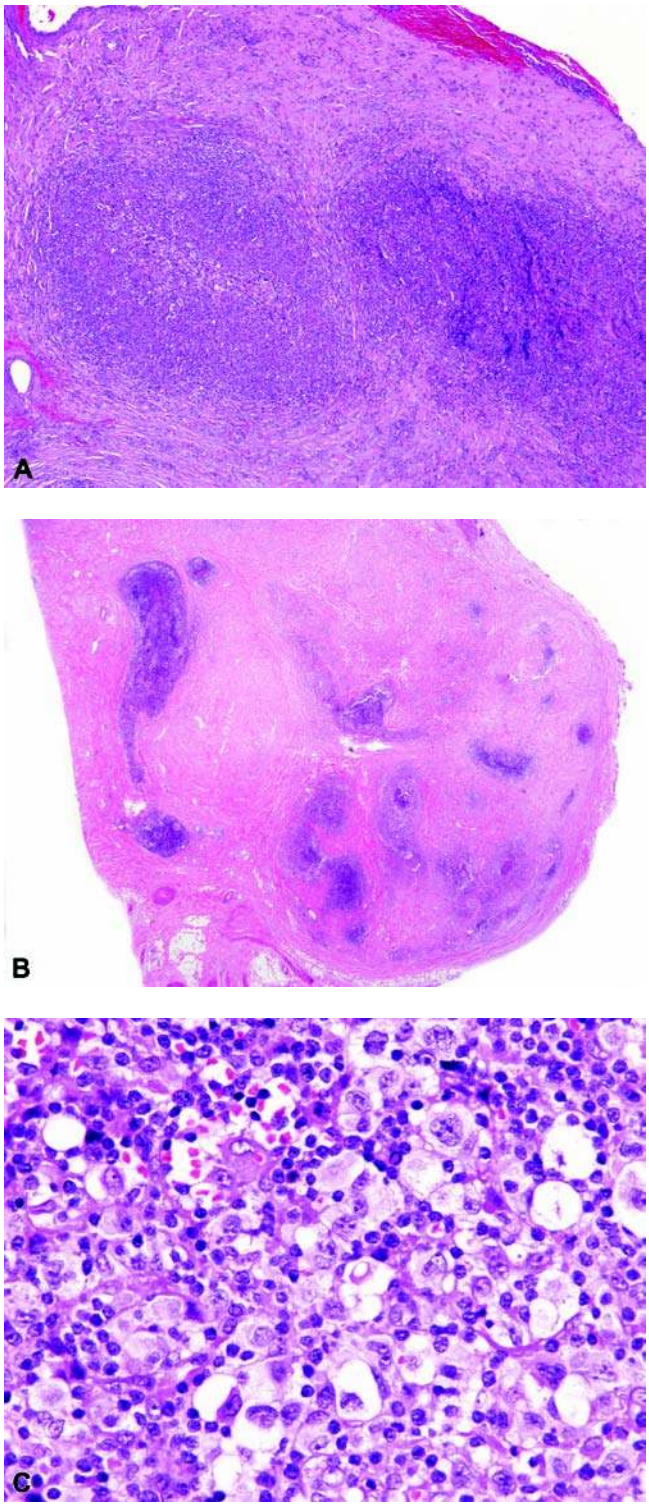

Figure 58 Nodular sclerosis classical Hodgkin lymphoma, lymph node. (**A**) Typical low magnification appearance, with broad sclerotic bands and nodule formation. (**B**) Sclerosis can be very extensive, reducing the lymphomatous component to isolated small nodules. (**C**) Lacunar cells occur in a mixed inflammatory background, and they tend to show vague nodular grouping.

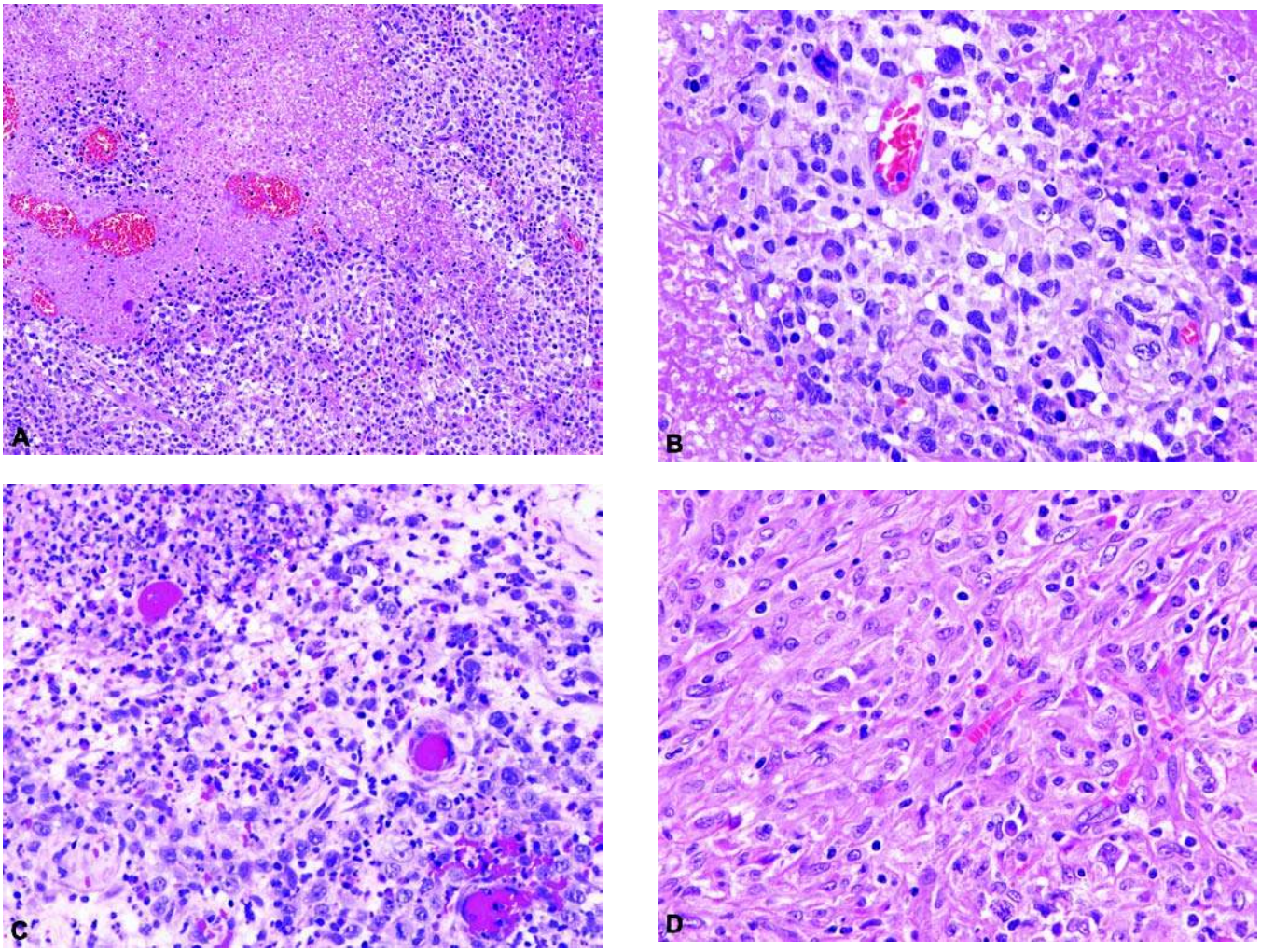

Figure 59 Nodular sclerosis classical Hodgkin lymphoma, lymph node. (**A**) Syncytial variant, characterized by sheets of large neoplastic cells, often accompanied by geographic necrosis. (**B**) Syncytial variant with sheets of large cells, mimicking large cell non-Hodgkin lymphoma. (**C**) Suppuration (*left upper field*) can be present. (**D**) Fibrohistiocytic variant, with many spindly cells but usually few recognizable Reed–Sternberg cells (such as one in the *mid-upper field*).

are scattered within or sometimes also between the lymphoid nodules (220–222). There are few admixed plasma cells and polymorphs.

Lymphocyte-Depleted. The reticular variant refers to cases with numerous Reed–Sternberg cells, while the diffuse fibrosis variant represents hypocellular cases with reticulin fibrosis and rare diagnostic Reed–Sternberg cells (Fig. 61). Lymphocyte-depleted Hodgkin lymphoma diagnosed before the advent of immunohistochemistry often represents grade II nodular sclerosis Hodgkin lymphoma, DLBCL, or anaplastic large cell lymphoma.

Immunohistochemistry. Reed–Sternberg cells are basically ''crippled'' B cells with deficient expression of B-cell immunophenotype and lack of immunoglobulin synthesis. They are typically CD45−, CD30+, CD15+/− (Fig. 62A). They are usually negative for conventional pan-B markers (CD20, CD79a), immunoglobulin, and the immunoglobulin gene octamer site–transactivating factors Oct-2 and BOB.1, while B-cell transcription factor PAX-5 is positive (223,224). However, CD20 can be expressed in a small proportion of cases, often in a heterogeneous pattern, i.e., the Reed–Sternberg cells show a spectrum of intensity of staining from strong to weak to negative (Fig. 62B).

The background reactive lymphocytes are predominantly CD3+ T cells, except nodular lymphocyte–rich classical Hodgkin lymphoma. In the latter, the small lymphocytes that constitute the nodules are mostly CD20+ B cells, and rosettes of CD3+ T cells surround the Reed–Sternberg cells that reside in the nodules (Fig. 63A-C).

Molecular genetic data. With microdissection technique or using tissue samples rich in Reed–Sternberg cells, clonal immunoglobulin gene rearrangements can be demonstrated (225). The variable region of the heavy-chain gene frequently shows hypermutation, supporting derivation from germinal

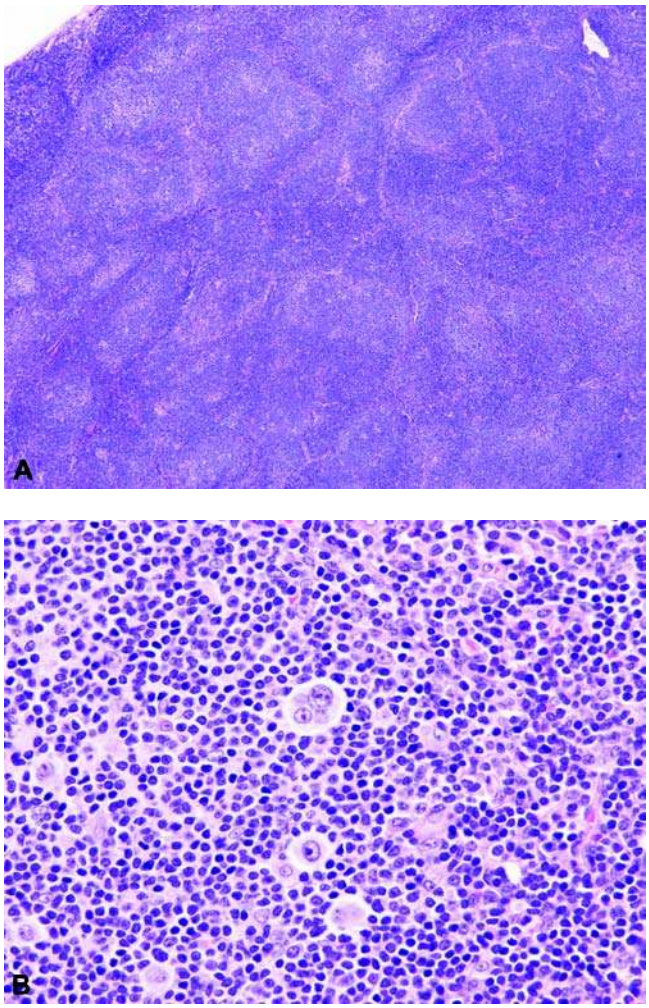

Figure 60 Nodular lymphocyte–rich classical Hodgkin lymphoma. (**A**) There are closely packed large lymphoid nodules. (**B**) The nodules are formed by small lymphocytes interspersed with small numbers of Reed–Sternberg cells or variants. There are few or no plasma cells and eosinophils.

center B cells. Nonetheless, despite presence of immunoglobulin gene rearrangement, immunoglobulin mRNA transcripts are usually absent, probably resulting from functional defects in immunoglobulin gene regulatory elements (225).

About 40% of cases of classical Hodgkin lymphoma are associated with EBV, which can be demonstrated by EBV-LMP1 immunohistochemically or by EBV-encoded early RNA (EBER) by in situ hybridization (226). The association is stronger for the mixed cellularity subtype and cases associated with immunodeficiency (approaching 100%) or from developing countries (~80%). The association with EBV is also stronger at the extremes of age, i.e., children/young adults and old adults.

Differential diagnosis. The range of differential diagnoses depends on the histologic subtype. In cases where Reed–Sternberg cells are relatively few in number (e.g., lymphocyte-rich, mixed cellularity, grade I nodular sclerosis), major distinction is from reactive immunoblastic proliferation, nodular lymphocyte–predominant Hodgkin lymphoma, T-cell/histiocyte-rich large B-cell lymphoma, peripheral T-cell lymphoma (especially angioimmunoblastic lymphoma), and extramedullary hematopoietic tumor (Table 5).

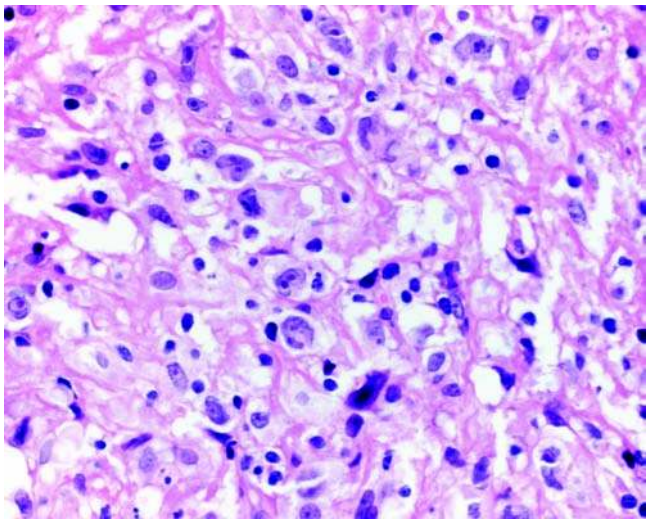

Figure 61 Lymphocyte-depleted classical Hodgkin lymphoma. Reed–Sternberg cells are found in a fibrillary collagenous background.

When Reed–Sternberg cells form large sheets (e.g., syncytial variant of nodular sclerosis, lymphocyte depleted), the differential diagnoses include DLBCL, anaplastic large cell lymphoma, histiocytic sarcoma, and nonhematolymphoid neoplasms, such as carcinoma, germ cell tumor, sarcoma, and melanoma. Cases showing borderline features between classical Hodgkin lymphoma and DLBCL can be given a diagnostic label of ''gray zone lymphoma'' or ''B-cell lymphoma, unclassifiable, with features intermediate between DLBCL and classical Hodgkin lymphoma.''

Treatment and prognosis. Patients with classical Hodgkin lymphoma are treated with chemotherapy, radiotherapy, or a combination of both. The prognosis is good, with >80% of patients cured of the disease (227). Stage remains the most important prognostic factor.

Nodular Lymphocyte–Predominant Hodgkin Lymphoma

Introduction. Nodular lymphocyte–predominant Hodgkin lymphoma is a rare B-cell neoplasm in which the large neoplastic B cells constitute only a minor population, and are scattered within nodules of reactive small B cells. This entity is clinically and biologically distinct from classical Hodgkin lymphoma (228).

Clinical features. The patients are usually children to middle-aged adults, with marked male predominance. Most patients present with solitary enlarged lymph node in the cervical, axillary, or inguinal region (stage I/II disease). Repeated local relapses

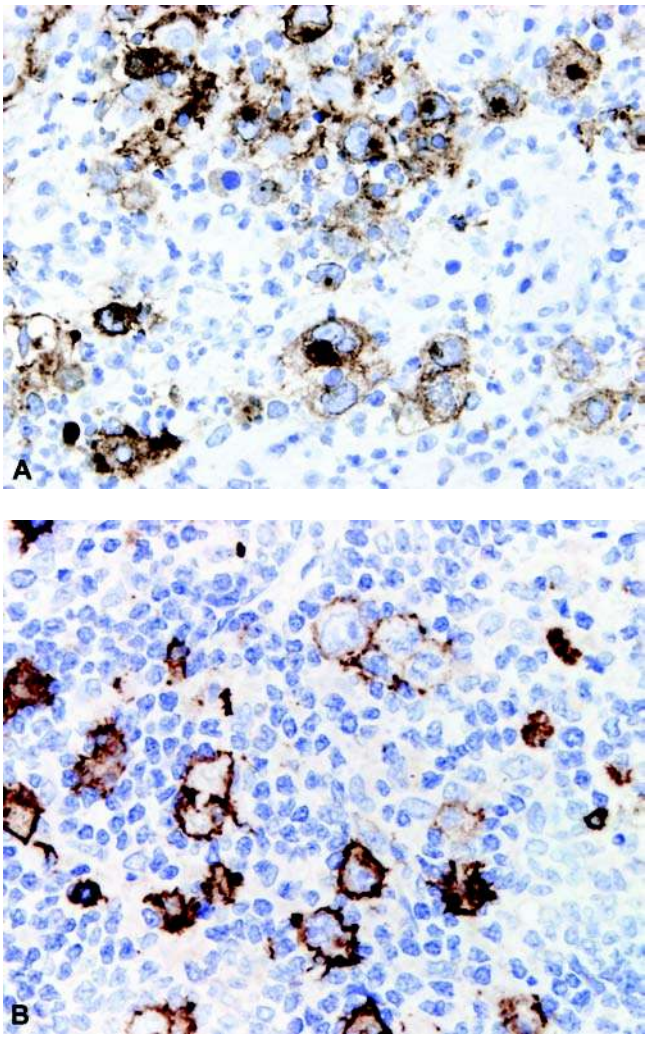

Figure 62 Classical Hodgkin lymphoma, immunohistochemistry. (**A**) The neoplastic (Reed–Sternberg) cells show cell membrane and Golgi staining for CD30. (**B**) Some cases can show immunoreactivity for CD20, often with a range of intensity of staining (instead of uniform staining as commonly observed in diffuse large B-cell lymphoma).

or relapses in another nodal site are common (20–30%), and may be delayed for many years (229–235).

Pathology. The lymph node architecture is effaced by crowded or well-separated, large, dark-staining nodules composed predominantly of small lymphocytes, which sometimes are sprinkled with solitary epithelioid histiocytes (Fig. 64A). There are typically few or no eosinophils and plasma cells. Rarely, sclerotic bands can be present.

The large neoplastic cells (lymphocytic and histiocytic cells or L&H cells) are found mostly within the nodules, although they are commonly also present between the nodules (Fig. 64B). They have been nicknamed ''popcorn cells'' because of the characteristic lobulation of the nuclei with multiple deep notches. The chromatin is fine, and there are multiple small

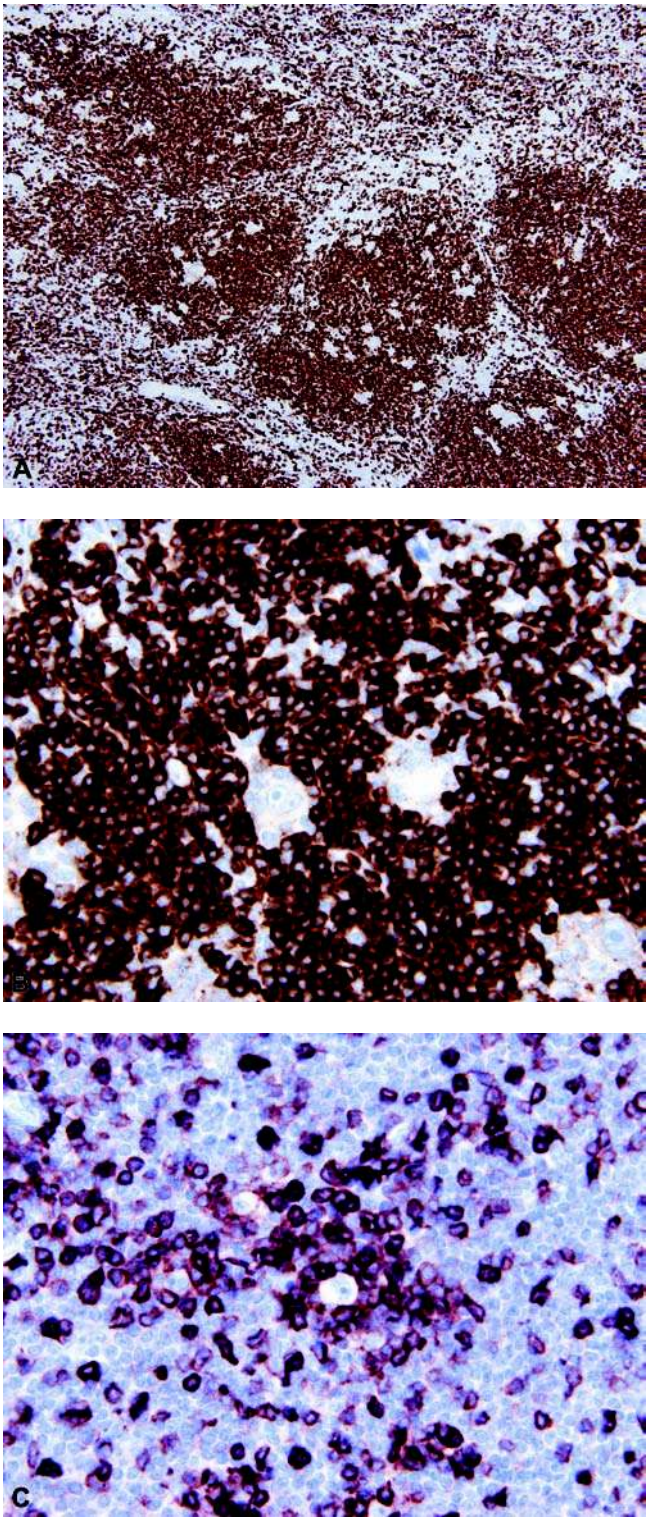

Figure 63 Nodular lymphocyte–rich classical Hodgkin lymphoma, immunohistochemistry. (**A**) The nodules, which are typically rich in CD20+ small lymphoid cells, are punctuated by multiple ''holes.'' (**B**) Higher magnification shows that the ''holes'' are inhabited by Reed–Sternberg cells rosetted by CD20-negative small lymphoid cells. (**C**) CD3 highlights the rosetting small T cells that surround the Reed–Sternberg cells.

Table 5 Differential Diagnosis for Classical Hodgkin Lymphoma

Entity	Distinguishing features
Reactive immunoblastic proliferations (including infectious mononucleosis)	• Reed Sternberg-like cells, if present, are scanty • Too many activated large lymphoid cells (immunoblasts) in the background for a diagnosis of Hodgkin lymphoma • The activated lymphoid cells show transition to plasmablasts and plasma cells • The large cells consist of a mixture of CD20+ B cells and CD3+ T cells
Mature T-cell lymphoma, especially angioimmunoblastic T-cell lymphoma	• The small and medium-sized lymphoid cells in the background also show nuclear atypia • The large cells as well as the small and medium-sized cells are CD3+ (Caveat: There can be scattered EBV+ reactive large B cells resembling Reed–Sternberg cells) • Aberrant T-cell phenotype may be present, e.g., loss of pan-T markers, or abnormal subset phenotype (CD4+CD8+ or CD4−CD8−) • CD45+, CD3+, CD30−/+ • Rearranged TCR genes
Nodular lymphocyte–predominant Hodgkin lymphoma	• Popcorn-like L&H cells within nodules of small lymphocytes • Few plasma cells and eosinophils in the background • Large cells: CD45+, CD20+, CD30−, CD15−, EBV− • Background small lymphocytes: CD20+ in nodules; CD3+ in diffuse areas
T-cell/histiocyte-rich large B-cell lymphoma	• Unlikely to represent classical Hodgkin lymphoma if large cells resemble centroblasts or immunoblasts, with nuclear size less than 2.5 times that of small lymphocytes. For cases with larger cells, distinction from classical Hodgkin lymphoma on morphologic grounds is very difficult • Large cells: CD45+, CD20+, monotypic immunoglobulin+, CD30−/+, CD15− • Oct2, BOB.1: Positive in large cells • EBV rarely positive unless in a setting of immunosuppression
Extramedullary hematopoietic tumor	• Recognizing that the large cells are merely megakaryocytes (factor VIII+), and not Reed–Sternberg cells • Identification of admixed normoblasts

nucleoli. Diagnostic Reed–Sternberg cells are usually but not invariably absent, and are not required for the diagnosis of nodular lymphocyte–predominant Hodgkin lymphoma.

A diffuse component can be present. When this component is extensive, there is association with high-stage disease (stage III/IV) and a higher relapse rate.

Immunohistochemistry. Immunohistochemical studies are mandatory for confirmation of the diagnosis, since reliable distinction from nodular lymphocyte–rich classical Hodgkin lymphoma on pure morphologic grounds cannot be made (236). The highly characteristic immunophenotypic feature of nodular lymphocyte–predominant Hodgkin lymphoma is the presence of nodular aggregates of CD20+ small B cells cavitated by multiple nonstaining spaces in which CD20+ large cells (L&H cells) reside (Fig. 65A). The CD20+ large neoplastic cells stand out so clearly from the background CD20+ small B lymphocytes because they are surrounded by rosettes of nonstaining cells (CD3+ T cells, which often express CD57 and BCL6, and which sometimes appear as medium-sized cells with clear cytoplasm) (Fig. 65B) (237). The internodular zones are rich in CD3+ small T cells. With time, CD3+ small T cells increase within the nodules, accompanied by a reduction in CD20+ small B cells, which may eventually result in a nodule composed of CD20+ L&H cells dispersed among small T cells, with practically no small B cells (Fig. 65C) (238).

The L&H cells express the complete immunophenotypic profile of mature B cells (CD45+, pan-B+) and do not express CD30 and CD15 (Fig. 65B). They are positive for BCL6 and CD40, but not for CD10.

Molecular genetic data. Microdissected L&H cells exhibit clonal functional rearrangements of immunoglobulin genes, which are able to produce immunoglobulin mRNA transcripts. With rare exceptions, there is no association with EBV (239,240).

Transformation to non-Hodgkin lymphoma. A DLBCL supervenes in appropriately 3% to 4% of cases of nodular lymphocyte–predominant Hodgkin lymphoma, either at presentation or subsequently (241–245). It comprises confluent sheets of large cells resembling centroblasts (often multilobated) or immunoblasts. Probably some cases represent genuine non-Hodgkin lymphoma, while some merely represent tumorous overgrowth of L&H cells (246). While some studies suggest that DLBCL arising in nodular lymphocyte–predominant Hodgkin lymphoma is associated with a favorable prognosis, other studies have shown no difference from de novo DLBCL (245,247).

Differential diagnosis. PTGC shows some morphologic similarities to nodular lymphocyte–predominant Hodgkin lymphoma. It differs from the latter in the

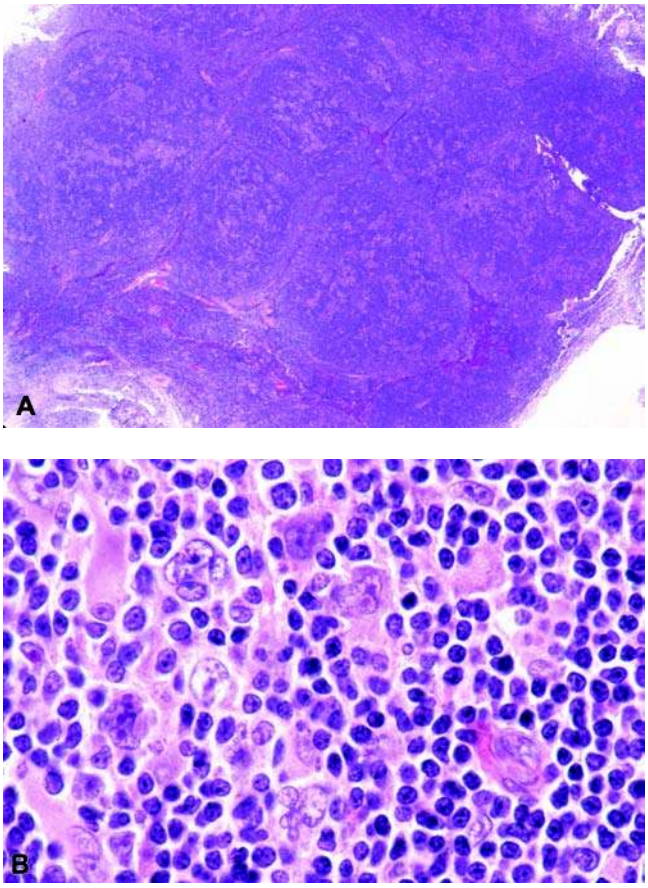

Figure 64 Nodular lymphocyte–predominant Hodgkin lymphoma. (**A**) There are large crowded lymphoid nodules mottled by histiocytes. (**B**) The nodules are formed by small lymphocytes with scattered L&H (popcorn) cells.

following features: (*i*) the abnormal large nodules are scattered among usual reactive follicles, (*ii*) the large nodules are not crowded, (*iii*) absence of L&H cells, and (*iv*) absence of T-cell rosettes around large cells within the nodules (Fig. 66).

There is marked morphologic and immunophenotypic overlap of the diffuse component of nodular lymphocyte–predominant Hodgkin lymphoma with T-cell/histiocyte-rich large B-cell lymphoma. The latter diagnosis should not be made once there is an identifiable (however small) component of nodular lymphocyte–predominant Hodgkin lymphoma, that is, the T-cell-rich diffuse areas are considered the diffuse component of nodular lymphocyte–predominant Hodgkin lymphoma.

Distinction from nodular lymphocyte–rich classical Hodgkin lymphoma is very difficult without recourse to immunohistochemistry. The following features will favor the latter diagnosis: (*i*) many large neoplastic cells fit the morphologic features of diagnostic Reed–Sternberg cells, with prominent

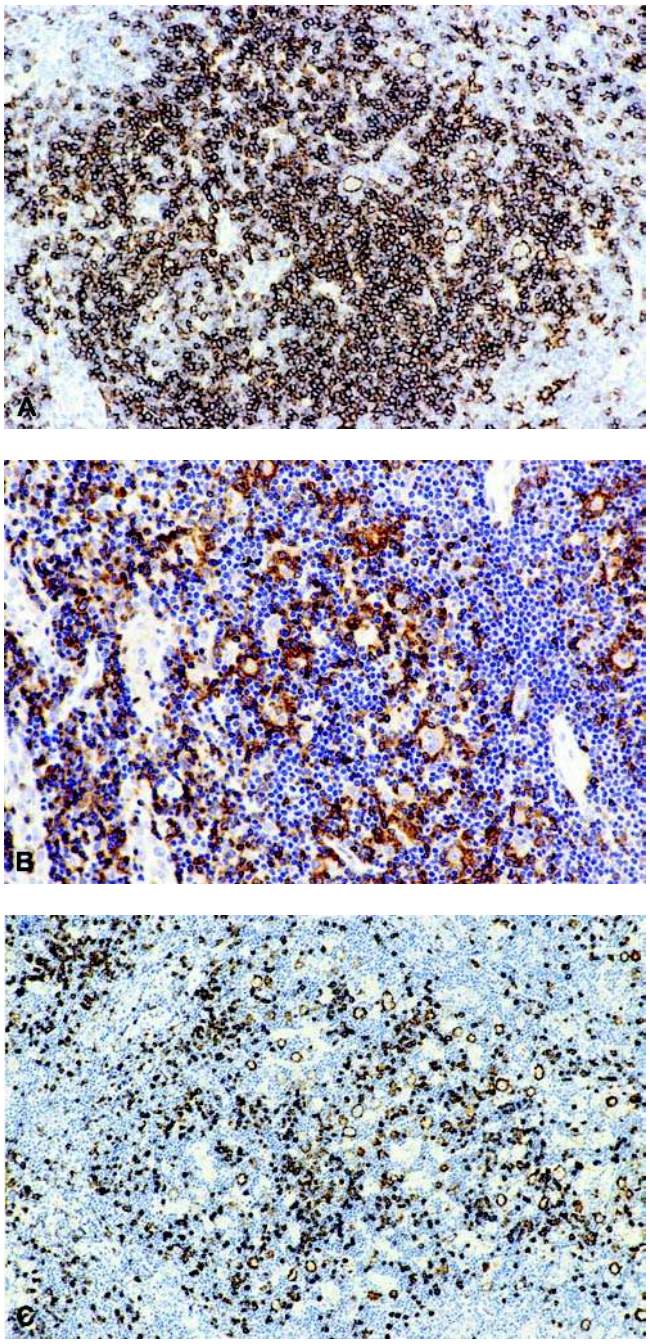

Figure 65 Nodular lymphocyte–predominant Hodgkin lymphoma, immunohistochemistry. (**A**) The nodules are composed of CD20+ small B cells, punctuated by multiple "holes," similar to nodular lymphocyte–rich classical Hodgkin lymphoma, but differ in that the neoplastic (L&H) cells inhabiting the centers of the holes are CD20 positive. These CD20+ large neoplastic cells stand out so well from the background because they are surrounded by a rosette of nonstaining T cells. (**B**) CD3 highlights the rosettes of small T cells that surround the L&H cells, as well as the internodular small lymphoid cells. (**C**) Sometimes the small B cells in the nodules can be replaced by small T cells, such that few CD20+ small lymphocytes remain. However, the nodular grouping of CD20+ L&H cells is still evident.

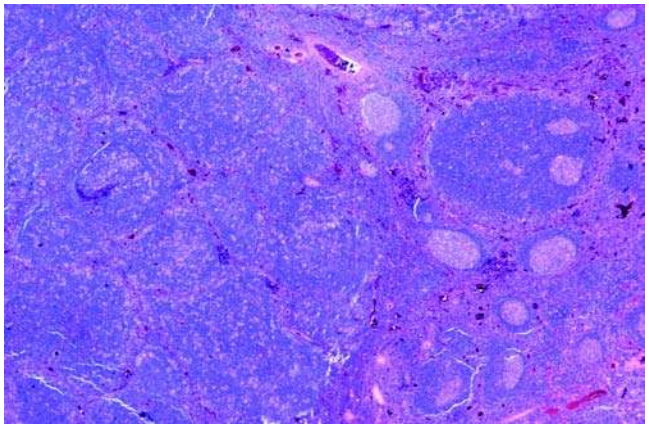

Figure 66 Nodular lymphocyte–predominant Hodgkin lymphoma in association with progressive transformation of germinal centers. The left field depicts the former (with large crowded nodules), and the right field depicts the latter (with occasional large follicles among usual reactive follicles).

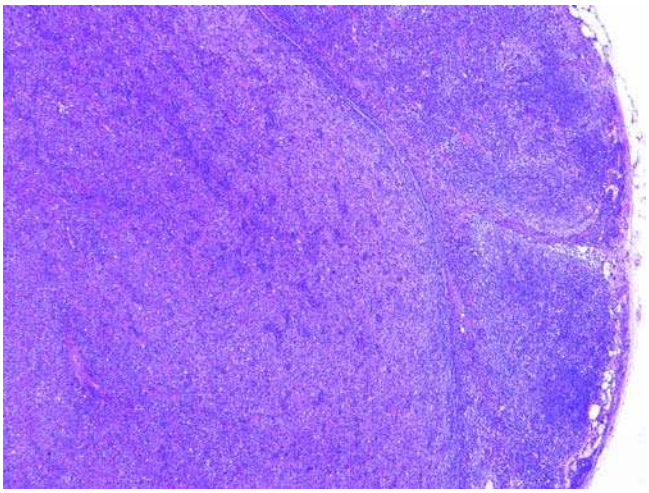

Figure 67 Diffuse large B-cell lymphoma, lymph node. The diffuse infiltrate of lymphoma cells effaces the architecture of the node. In this case, there is still a rim of residual uninvolved nodal parenchyma (*right field*).

nucleoli; (*ii*) the neoplastic cells exhibit a CD30+, CD15+, CD20−/+ immunophenotype; and (*iii*) EBV positivity, if present.

Treatment and prognosis. Patients with early-stage disease have an excellent prognosis, with eight-year disease-specific survival rate of 95%. However, the prognosis for stage IV disease is poor, with eight-year disease-specific survival rate of 41% (248).

The optimal treatment of early-stage nodular lymphocyte–predominant Hodgkin lymphoma is still debated. It appears that surgical excision alone or excision followed by involved field radiation may be adequate. Chemotherapy is required for high-stage disease.

F. Non-Hodgkin Lymphomas

Diffuse Large B-Cell Lymphoma

Introduction. DLBCL is a neoplasm of large B lymphoid cells with nuclear size equal to or exceeding normal macrophage nuclei or more than twice the size of a small lymphocyte (249). Morphological, biological, and clinical studies have subdivided DLBCLs into morphological variants, molecular and immunophenotypical subgroups, and distinct clinicopathologic variants. The term ''DLBCL, not otherwise specified (NOS)'' is applied when the case does not fit the distinct clinicopathologic variants; this remains a biologically heterogeneous category (250).

Clinical features. DLBCL is the most common type of non-Hodgkin lymphoma, accounting for 31% of all cases (210). In populations other than the United States, DLBCL accounts for a even higher percentage (>40%) because of a lower incidence of follicular lymphoma in these populations (251). The median age is 64 years, but any age can be affected (210). There is a slight male predominance (M:F = 1.2:1) (210).

Most patients present with a rapidly growing neck mass (lymph node), but 30% of patients present with extranodal disease and 71% have extranodal involvement during the course of disease (209). About half of the patients have stage I/II disease. One-third has B symptoms such as fever, night sweating, and significant weight loss (209). A minority of cases represent transformation from a preexisting low-grade B-cell lymphoma (such as follicular lymphoma or MALT lymphoma), and these patients may present with sudden increase in size of a long-standing mass.

Pathology. The involved node shows complete or partial effacement of architecture, with diffuse infiltration by large neoplastic lymphoid cells and frequent perinodal extension (Fig. 67). In the head and neck mucosal sites, the diffuse and permeative lymphomatous infiltrate overruns the normal structures, not uncommonly accompanied by necrosis and ulceration. However, the infiltrate can sometimes appear deceptively cohesive, forming a sharp interface with the residual normal tissues, mimicking carcinoma. In parenchymal organs of the head and neck, such as thyroid and salivary gland, the interstitial lymphomatous infiltrate results in wide separation, atrophy, and eventual loss of the glands or follicles.

In DLBCL, the tumor cells are large (nuclear size comparable to or greater than that of a histiocyte nucleus, or more than twice the size of a small lymphocyte). They usually have a centroblastic or immunoblastic morphology (Fig. 68A, B). Centroblasts have round or oval vesicular nuclei, multiple peripherally located nucleoli, and a thin rim of amphophilic cytoplasm; some cases may show multilobation (Fig. 68C). Immunoblasts have round or oval nuclei, a single prominent central nucleolus, and a broader rim of basophilic cytoplasm; some may have plasmacytoid features with eccentric nuclei and paranuclear hof. Cases with >90% immunoblasts are considered

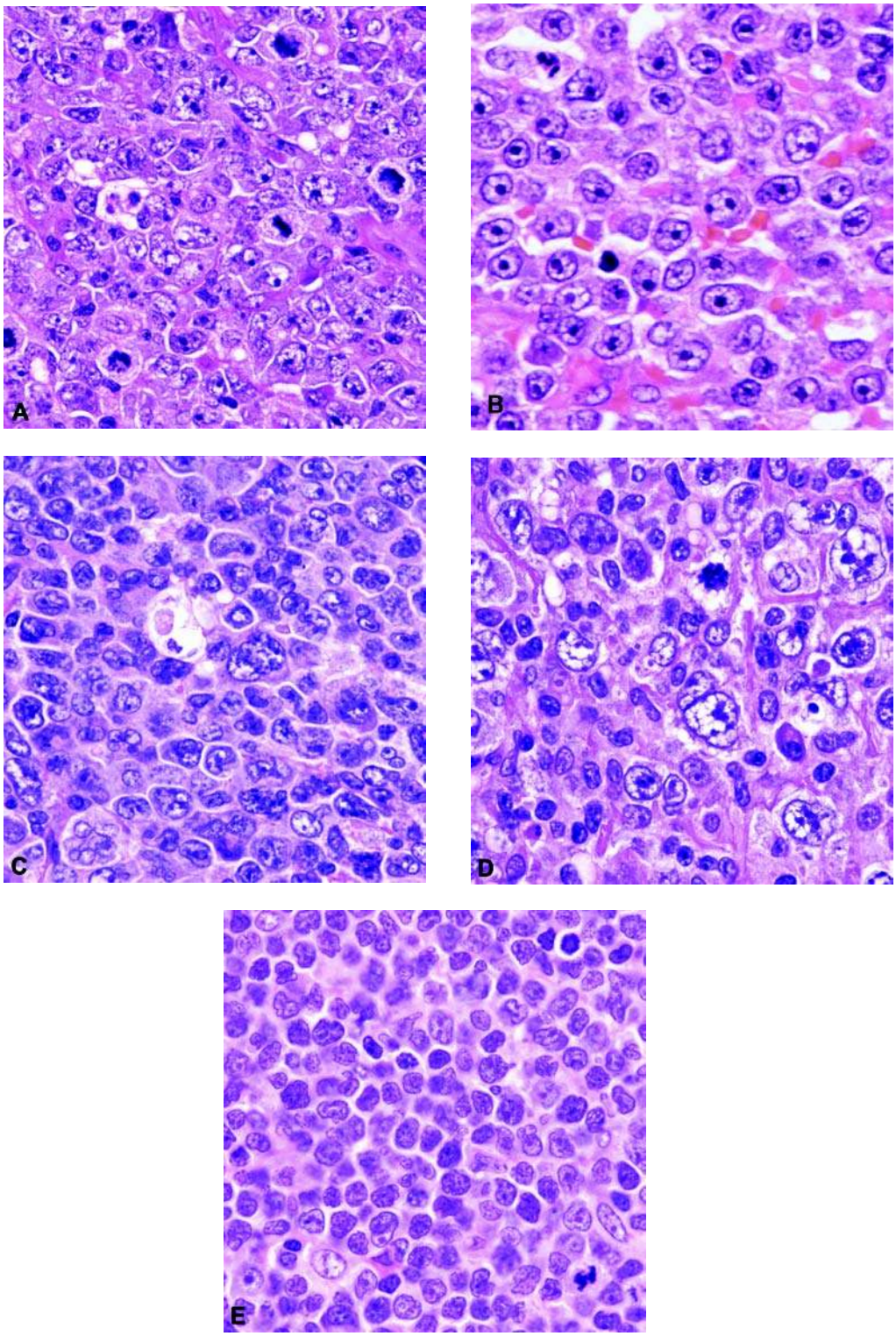

Figure 68 The variable cytologic spectrum of diffuse large B-cell lymphoma. (**A**) Centroblasts with round or irregular nuclei and membrane-bound nucleoli. (**B**) Immunoblasts with round nuclei and centrally located prominent nucleoli. (**C**) Neoplastic cells with frequent nuclear multilobation. (**D**) Anaplastic variant with very large and pleomorphic nuclei. (**E**) Predominantly medium-sized cells.

the immunoblastic variant, while cases with <90% immunoblasts are considered the centroblastic variant (249). However, there are, not uncommonly, cells with intermediate morphologic features, and thus it can be difficult to assign a case to either the centroblastic or immunoblastic category. The anaplastic variant is characterized by bizarre pleomorphic nuclei, multinucleation, abundant cytoplasm, often with cohesive or sinusoidal distribution (Fig. 68D). Nonetheless, categorization of DLBCL-NOS according to the morphologic variants is an optional exercise. Other morphologic variants include DLBCL with myxoid stroma (252), DLBCL with spindle cells (253), DLCBL with signet ring cells (254), DLBCL with clear cells, DLBCL with fibrillary matrix and rosette formation (255,256), DLBCL with crystal-storing histiocytes (257), DLBCL with marked tissue eosinophilia (258), microvillous DLBCL (259), and sinusoidal DLBCL (260). The morphologic variants underscore the protean histologic manifestations of DLBCLs, and the potential of misdiagnosing them for various nonhematolymphoid neoplasms (Fig. 68E).

Immunohistochemistry. DLBCLs express the pan-hematolymphoid marker CD45 and one or more pan-B markers, e.g., CD20, CD22, CD79a, PAX-5 (Fig. 69). Monotypic surface or cytoplasmic immunoglobulin can frequently be demonstrated (IgM > IgG > IgA), and cytoplasmic immunoglobulin is more often found in cases with immunoblastic features. The follicle center cell markers CD10 and BCL6 are expressed in 40% and 60% of cases, respectively (261,262). Some DLBCLs express postgerminal center cell or plasma cell–associated markers such as CD38, VS38, and MUM1, while CD138 is expressed almost exclusively on cases showing morphologic evidence of plasmacytic differentiation, including plasmablastic lymphoma (263,264).

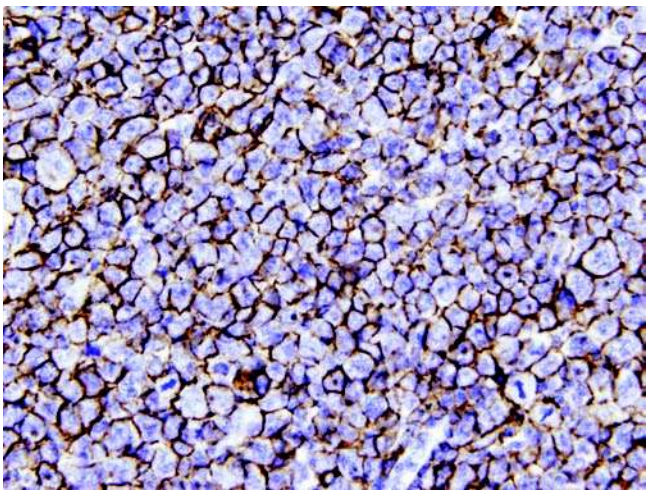

Figure 69 Diffuse large B-cell lymphoma, immunostained for CD20. Note presence of densely packed positive cells, staining with uniform intensity.

About 50% of cases express BCL2 protein (265). A minority of DLBCLs express the activation marker CD30, usually in a heterogeneous pattern (266). CD5 is expressed in approximately 10% of cases (267), and these de novo CD5+ cases have to be distinguished from pleomorphic/blastoid mantle cell lymphoma (cyclin D1+) and Richter transformation from underlying B-chronic lymphocytic leukemia (with CD5+ CD23+ small B lymphoid cells in the background). Ki-67 staining usually shows a high proliferation index (>20%, but often >80%), although some cases may show an index approaching 100% (268).

Molecular genetic data. DLBCLs have rearranged immunoglobulin heavy and light-chain genes, with germ line T-cell receptor genes. The variable region of immunoglobulin heavy-chain gene (*IGH*) is hypermutated, with some cases showing ongoing somatic mutations, indicating a germinal center or postgerminal center stage of differentiation (269).

DLBCL is a heterogeneous disease and the pathogenesis involves at least two different molecular pathways: a transformation pathway and a de novo pathway. (*i*) Approximately 20% of cases of DLBCL show *BCL2* rearrangement due to t(14;18)(q32;q21), a hallmark of follicular lymphoma (270,271). Such cases may have transformed from a known or occult follicular lymphoma, or have evolved to DLBCL without a precursor phase of follicular lymphoma. Additional genetic alterations, such as *P53* mutation, are required for transformation to DLBCL. (*ii*) *BCL6* and perhaps other unidentified genes play an important role in the de novo pathway. *BCL6* (3q27) rearrangement occurs in about 30% of DLBCL (272,273). The most common translocation partner is the *IGH* gene, resulting in t(3;14)(q27;q32).

MYC (8q24) translocation is reported in up to 10% of DLBCLs, more frequently in HIV-infected patients, and in extranodal lymphomas, especially the stomach (274–276). In contrast to Burkitt lymphoma, *MYC* gene translocation is often to a nonimmunoglobulin partner gene, and it often occurs in the context of a complex karyotype. This genetic change is associated with a highly aggressive behavior (277).

Gene expression profiling studies have identified two major groups of DLBCLs, with one expressing genes characteristic of germinal center B cells (GC B-cell-like DLBCL), and one expressing genes normally induced during in vitro activation of peripheral blood B cells (activated B-cell-like DLBCL) (278,279). The former subgroup is associated with a better prognosis (5-year survival 59% vs. 31%) (279).

Distinct clinicopathologic entities of DLBCL. Primary mediastinal (thymic) large B-cell lymphoma is a lymphoma arising in the anterior mediastinum (thymus) and affects mostly young adults with female predominance. The head and neck region is rarely involved, except that some patients occasionally can have simultaneous supraclavicular lymph node involvement. The pathologic features are generally indistinguishable from DLBCL-NOS, although sclerosis, clear cytoplasm, CD30 expression, and CD23 expression are more common. The definitive diagnosis, however, requires clinicopathologic correlation.

T-cell/histiocyte-rich large B-cell lymphoma is characterized by large neoplastic B cells dispersed within a background of small T lymphocytes and histiocytes, with the neoplastic cells accounting for <10% of the cell population (249). By definition, there is no identifiable component of nodular lymphocyte–predominant Hodgkin lymphoma, which if present should lead to reclassification of the case as ''nodular lymphocyte–predominant Hodgkin lymphoma with a diffuse component.'' The large neoplastic B cells usually show definite nuclear atypia, with round, lobated, or irregularly folded nuclei and distinct nucleoli, and can resemble L&H cells or Reed–Sternberg cells (Fig. 70A, B). However, they can also be indistinguishable from reactive immunoblasts, rendering distinction from a reactive process difficult. The large cells should not form dense clusters or sheets. The background small lymphocytes can show small dark round nuclei or mild atypia, with irregular or elongated nuclei. Since most patients have high-stage disease, the overall prognosis is poor.

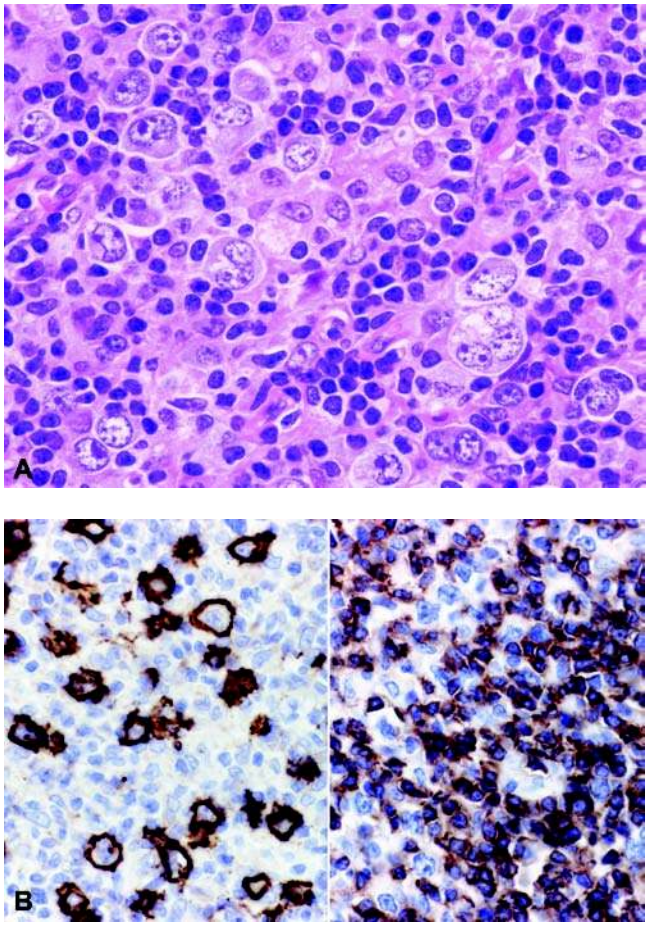

Figure 70 T-cell/histiocyte-rich large B-cell lymphoma. (**A**) Atypical large cells are scattered among small lymphocytes and histiocytes. (**B**) CD20 immunostaining highlights the scattered large neoplastic cells (*left panel*); while CD3 highlights numerous small lymphoid cells in the background (*right panel*).

Intravascular large B-cell lymphoma is characterized by exclusive or predominant localization of the large lymphoma cells within small and medium-sized blood vessels. Head and neck involvement is uncommon, except for occasional cases with presentation in the skin.

ALK+ DLBCL is a rare aggressive variant of DLBCL characterized by monomorphic large immunoblast-like cells that express ALK (280–282). The tumor cells frequently show sinusoidal distribution and may appear cohesive, mimicking metastatic carcinoma. They are often negative for the conventional pan-B markers CD20 and CD79a, suggesting plasmablastic stage of differentiation. Similar to anaplastic large cell lymphoma, they frequently express epithelial membrane antigen (EMA), but in contrast, CD30 expression is rare. The tumor cells commonly express CD138, IgA, and CD4. The ALK expression in ALK+ DLBCL is often cytoplasmic granular and is related to t(2;17)(p23;q23), resulting in fusion of *ALK* gene with *CLTC* gene (283).

Plasmablastic lymphoma is a large B-cell lymphoma with morphologic features resembling immunoblasts but immunophenotypic features of plasma cells (284). This highly aggressive lymphoma was first recognized to occur in the oral cavity of HIV-infected patients (285), but is now recognized to affect other mucosal sites and less commonly lymph nodes, and also patients with no immunodeficiency. The neoplastic cells are large cells with vesicular nuclei, single centrally located prominent nucleolus or multiple peripheral nucleoli, abundant basophilic cytoplasm, and paranuclear hof (Fig. 71). Most cases are monomorphic, particularly for cases located in the upper aerodigestive tract. Some cases can show differentiation into immature plasma cells, particularly for cases involving other extranodal sites and lymph nodes. The immunophenotype is similar to plasma cells and is

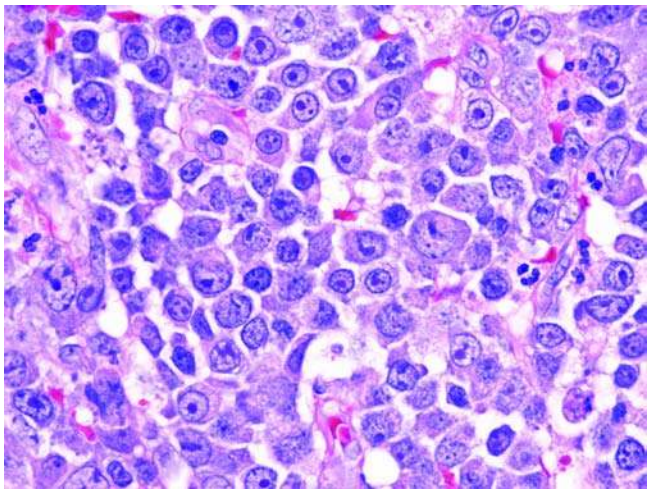

Figure 71 Plasmablastic lymphoma, lymph node. The large neoplastic cells resemble immunoblasts, except that there is a slightly greater amount of amphophilic cytoplasm with recognizable Golgi zone.

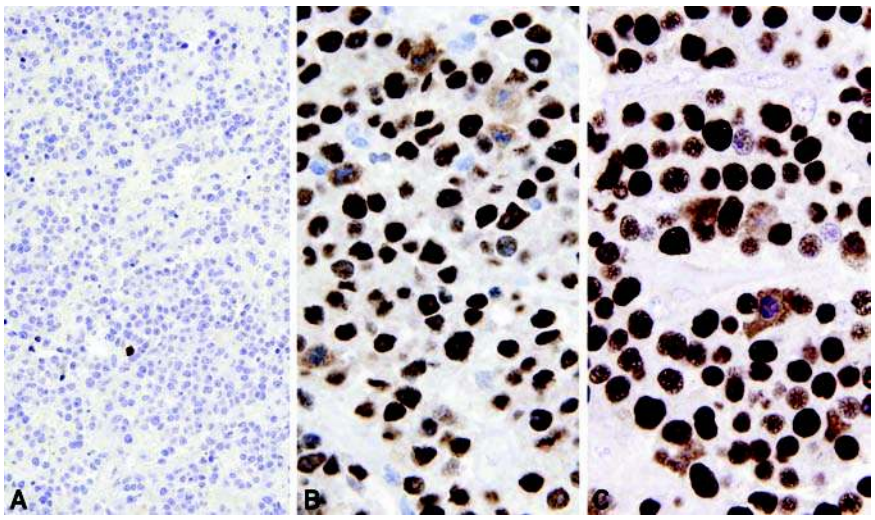

Figure 72 Plasmablastic lymphoma, lymph node. (**A**) Negative immunostaining for CD20. (**B**) Positive nuclear immunostaining for Oct-2. (**C**) This example shows positive labeling for EBER on in situ hybridization.

typically CD45−, CD20−, CD79a+/−, PAX5−, Oct−2+, BOB.1+; the neoplastic cells express plasma cell–associated markers such as CD38, CD138, MUM1, and VS38c, with variable expression of cytoplasmic immunoglobulin (Fig. 72). EBV is positive in 60% to 75% of cases (Fig. 72). It is still an incompletely characterized entity without universal agreement on the minimum diagnostic criteria (285–288). Distinction from anaplastic/plasmablastic plasmacytoma, when there is no known history of multiple myeloma, can be extremely difficult.

Primary cutaneous DLBCL, leg-type is a form DLBCL composed exclusively of large transformed B cells, most commonly arising in the skin of leg and less commonly other cutaneous sites (10–15%) (289). The tumor is moderately aggressive. Histologically, the dermis is diffusely infiltrated by centroblasts and immunoblasts, with no admixed centrocytes. The most common immunophenotype is pan-B+, CD10−, BCL2+, BCL6+, MUM1+, FOXP1+.

DLBCL associated with chronic inflammation occurs in the context of long-standing chronic inflammation and shows association with EBV (290). Most cases involve body cavities or narrow spaces, with the prototype being pyothorax-associated lymphoma, which involves the pleural cavity of patients with long-standing pyothorax. It is extremely rare for this lymphoma type to show head and neck involvement.

EBV-positive DLBCL of the elderly, formerly known as senile EBV-associated lymphoproliferative disorder, occurs in older adults above the age of 50 years (291). The patients have no overt underlying immunodeficiency, but the neoplasm is believed to arise in a background of immunological deterioration that occurs during the aging process (292,293). The patients have a median age of 71 years. Most patients have lymph node involvement, often accompanied by simultaneous extranodal disease (including tonsils), although 20% of patients have extranodal disease alone. The prognosis is poor, with overall 5-year survival of 25% and median survival of 24 months, which are worse than those of conventional DLBCL (294). Histologically, there is a diffuse infiltrate of large lymphoid cells, which may be admixed with variable numbers of small lymphocytes, plasma cells, and histiocytes (Fig. 73). Some lymphoma cells can be large and pleomorphic, resembling Reed–Sternberg cells. Necrosis is common. The lymphoma cells express pan-B markers and are by definition EBV positive.

Primary effusion lymphoma is a DLBCL presenting as serous effusions (most commonly pleural effusion)

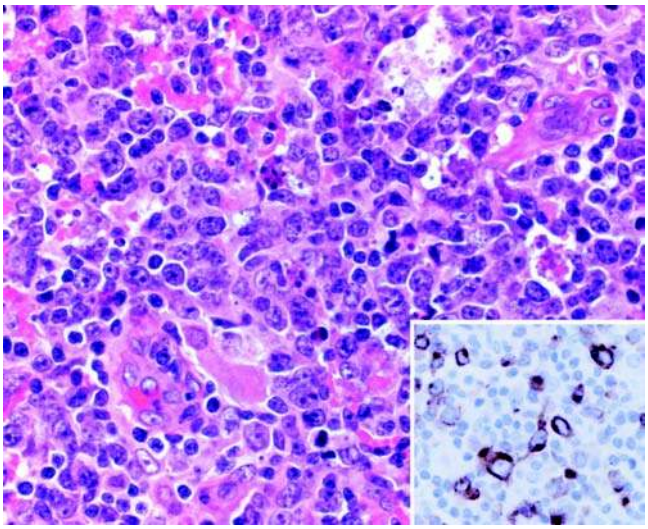

Figure 73 EBV-positive diffuse large B-cell lymphoma of the elderly, lymph node. In this example, the infiltrate is polymorphous, with large lymphoid cells apparently showing maturation toward plasma cells, morphologically similar to polymorphic posttransplant lymphoproliferative disorder. Positive immunostaining for EBV-LMP1 is shown in the inset.

without detectable tumor masses, often in the setting of acquired immunodeficiency syndrome. The neoplastic cells are often very large and show highly pleomorphic appearances. Their immunophenotype corresponds to that of plasmablast, i.e., negative for conventional pan-B markers. There is almost constant association with HHV8 as well as EBV. This lymphoma rarely ever involves the head and neck sites.

Differential diagnosis. The differential diagnoses for DLBCL and their distinguishing features are listed in Table 6. It is most important not to mistake reactive immunoblastic proliferations (such as infectious

Table 6 Differential Diagnosis for Diffuse Large B-Cell Lymphoma

Entity	Distinguishing features
Nonhematolymphoid malignancies	• Usually cohesive growth, while melanoma often shows cellular dehiscence within the cell clusters • Cytoplasm often eosinophilic rather than amphophilic or basophilic • CD45− • Expression of specific immunohistochemical markers (e.g., cytokeratin in carcinoma, S100 protein and HMB45 in melanoma, OCT3/4 and CD117 in seminoma)
Mature T-cell or NK-cell lymphomas	• CD3+, CD20− • CD56+ for NK-cell lymphoma • CD30+ and ALK+ for anaplastic large cell lymphoma, ALK+
Burkitt lymphoma	• More often in children and young adults • Starry-sky pattern • Lymphoma cells: medium sized, monotonous, with ''squaring'' of nuclei and cell borders • BCL2 protein: usually negative • Ki67 index: ~100% • *MYC* gene: rearranged • *BCL2* and *BCL6* genes: not rearranged
Pleomorphic/blastoid variant of mantle cell lymphoma	• Typical areas of mantle cell lymphoma are commonly present in areas • Nuclei often more chromatin rich, with granular quality • Cyclin D1+
Anaplastic plasmacytoma	• May have a history of multiple myeloma • Neoplastic plasma cells of smaller size are frequently present • CD20–, CD138+
Myeloid sarcoma	• More often medium sized, with blastic appearance • May have cytoplasmic eosinophilic granules • May have interspersed eosinophilic myelocytes • Myeloperoxidase+, CD20–
Histiocytic sarcoma	• Tumor cells are often much larger • Cytoplasm usually abundant and eosinophilic, often with fine vacuolation • CD68+, CD163, CD20–
Classical Hodgkin lymphoma: syncytial variant of nodular sclerosis or lymphocyte depleted	• Prominence of eosinophils, if present • CD30+, CD15+/– • CD20– or heterogeneous + • Oct2–, BOB.1– • CD45– • Lack of immunoglobulin light-chain restriction • EBV +/–
Florid reactive immunoblastic proliferation (e.g., infectious mononucleosis)	• At least partial preservation of nodal architecture • Polymorphous background of transformed lymphocytes and plasma cells in addition to immunoblasts and plasmablasts • Large cells usually do not exhibit overt nuclear atypia • Large cells usually comprise a mixture of CD20+ B cells and CD3+ T cells • CD20+ large cells often show a range of staining intensity instead of showing uniform staining intensity • Large lymphoid cells show polytypic immunoglobulin
Kikuchi lymphadenitis	• Patchy karyorrhectic foci containing crescentic histiocytes and activated lymphoid cells • Infiltrate consists of CD68+, MPO+ histiocytes and CD68+, CD123+ plasmacytoid dendritic cells, as well as CD8+ T cells, but very few CD20+ B cells
Extramedullary hematopoietic tumor	• Recognizing that the large cells are merely megakaryocytes (factor VIII+) and not neoplastic cells • Identification of clusters of normoblasts

Table 7 Contrasting Features of T-Cell/Histiocyte-Rich Large B-Cell Lymphoma, Peripheral T-cell Lymphoma, Classical Hodgkin Lymphoma, and Nodular Lymphocyte–Predominant Hodgkin Lymphoma

	Morphology	Immunohistochemistry	Cytogenetic/molecular findings
T-cell/histiocyte-rich large B-cell lymphoma	• Large cells: variable morphology—can resemble centroblast, immunoblast, L&H cell, or Reed–Sternberg cell • Background reactive small lymphocytes may appear mildly activated and show mild atypia • Many admixed inflammatory cells, including histiocytes and sometimes plasma cells and eosinophils	• Large cells: CD20+, CD30−/+, CD15− PAX5+, Oct2+, BOB.1+, EBV− • Small cells: CD3+	• Immunoglobulin genes: clonal rearrangement • T-cell receptor genes: no clonal rearrangement
Peripheral T-cell lymphoma, not otherwise specified	• Continuous range of cell size instead of two distinct cell populations as in classical Hodgkin lymphoma • Cellular atypia is present in cells of all sizes, with frequent nuclear foldings • May have many admixed inflammatory cells such as histiocytes, plasma cells, and eosinophils	• Cells of all sizes: CD3+, CD20−, PAX5−	• T-cell receptor genes: clonal rearrangement • Immunoglobulin genes: no clonal rearrangement
Classical Hodgkin lymphoma	• Large cells: classical Reed–Sternberg cells and variants • Background small lymphocytes usually nonactivated • Few or no immunoblasts in background • Often many admixed inflammatory cells such as histiocytes, plasma cells, and eosinophils	• Large cells: CD30+, CD15+/−, CD20−/+ (heterogeneous staining if positive), PAX5+, Oct2−, BOB.1−, EBV+/− (~40% of cases). • Small cells: CD3+	• Immunoglobulin genes: usually no clonal rearrangement in whole tissue DNA • Microdissected tumor cells show clonal immunoglobulin gene rearrangement
Nodular lymphocyte–predominant Hodgkin lymphoma	• Large cells (popcorn-like L&H cells) found within nodules of nonactivated small lymphocytes • There can be admixed epithelioid histiocytes, but plasma cells and eosinophils are scanty	• Large cells: CD20+, CD30−, CD15−, PAX5+, Oct2+ BOB.1+ • Small cells: CD20+ in nodules, with CD57+ CD3+ cells rosetting around L&H cells; mainly CD3+ in internodular and diffuse areas (Caveat: In some cases, small cells in nodules are mostly CD3+ T cells)	• Immunoglobulin genes: usually no clonal rearrangement in whole tissue DNA • Microdissected tumor cells show clonal immunoglobulin gene rearrangement

mononucleosis) for DLBCL. Whenever a diagnosis of DLBCL is suspected in children and young adults, infectious mononucleosis should be seriously excluded since DLBCL is uncommon in these age groups. For T-cell/histiocyte-rich large B-cell lymphoma, the differential diagnoses include reactive lymphoid hyperplasia, classical Hodgkin lymphoma, nodular lymphocyte–predominant Hodgkin lymphoma, and peripheral T-cell lymphoma (especially angioimmunoblastic T-cell lymphoma) (Table 7).

Treatment and prognosis. DLBCL is an aggressive but potentially curable disease, usually treated by multiagent chemotherapy together with anti-CD20 (Rituximab). The five-year overall survival rate and failure-free survival rate have traditionally been reported as 46% and 41%, respectively (210), but the survival rate has improved by approximately 20% in recent years with addition of Rituximab to the treatment protocol (295–297).

The International Prognostic Index score remains an important prognostic factor. A number of histologic, immunohistochemical, and molecular features have been studied with respect to prognosis. So far, the most consistent poor prognostic indicator is nongerminal center cell phenotype (more accurately assessed by gene expression profiling, but can be predicted by immunohistochemistry) (279,298). BCL2 expression (but not *BCL2* rearrangement) has also been shown to be a poor prognostic indicator, especially in cases with nongerminal center cell phenotype (299,300).

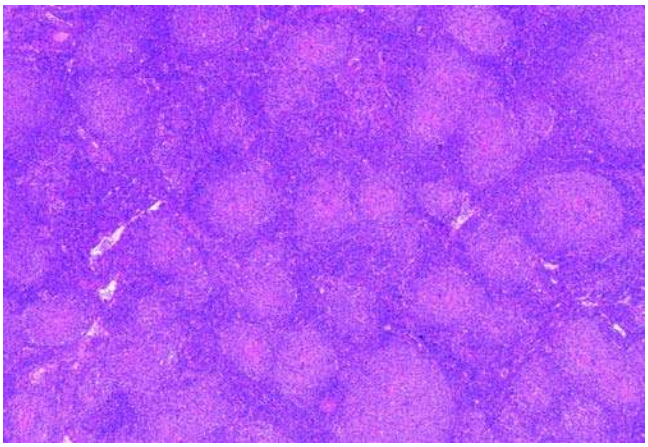

Figure 74 Follicular lymphoma, lymph node. The back-to-back disposition of follicles is a highly diagnostic low-magnification feature of follicular lymphoma.

Follicular Lymphoma

Introduction. Follicular lymphoma is a neoplasm of follicle center B cells in which there is at least focal follicle formation.

Clinical features. Follicular lymphoma is the second most common type of non-Hodgkin lymphomas, accounting for 22% of all cases (210). It is more common in the United States (32%) than mainland Europe (11–18%) and Asia (usually <10%) (212). It is predominantly a disease of adults, with a median age of 59 years (210). The male-to-female ratio is 1:1.4.

Patients frequently present with lymphadenopathy, with two-thirds at stage III/IV at presentation and 28% having B symptoms (209). Spread to extranodal sites is common in the course of the disease.

Pathology. The normal tissue architecture is effaced by neoplastic follicles, which are usually closely packed, ill-defined, and sometimes coalescent (Fig. 74). The follicles frequently lack mantle zone, polarity, and starry-sky pattern (i.e., tingible-body macrophages are scanty or absent) (Fig. 75A, B). They are composed of variable numbers of centrocytes and centroblasts, depending on the histologic grade (see below) (Fig. 76). The centrocytes and centroblasts can resemble their normal counterparts (centrocytes showing angulated or triangular-shaped nuclei and centroblasts showing round vesicular nuclei), or they can show dysplastic features, such as exaggerated elongation of the nuclei, presence of large centrocytes, presence of signet ring cells, and nuclear multilobation of centroblasts.

The narrow interfollicular zone is frequently infiltrated by lymphoma cells, which occur among small lymphocytes (T cells) and high endothelial venules. The interfollicular lymphoma cells are usually small to medium sized and show less irregular foldings and more chromatin condensation compared with the intrafollicular lymphoma cells (Fig. 77) (301).

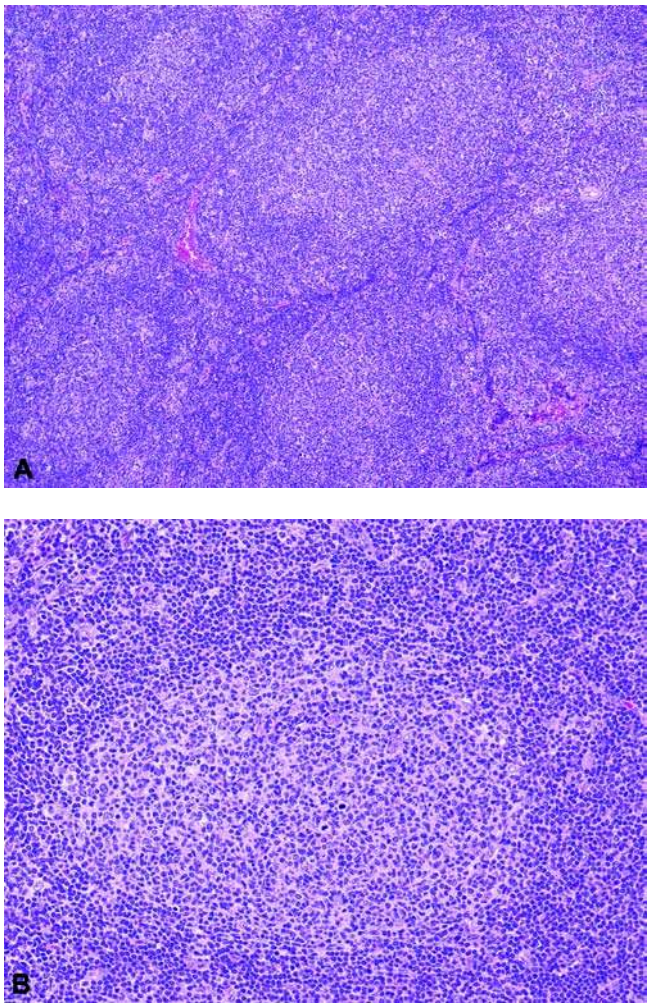

Figure 75 Follicular lymphoma, lymph node. (**A**) The follicles are typically crowded and poorly defined. They lack mantles and polarity. (**B**) The follicle lacks polarity and tingible-body macrophages. The cellular composition is fairly monotonous.

A characteristic feature of follicular lymphoma, although seen in only a proportion of cases, is infiltration of the walls of veins by lymphoma cells (Fig. 78). Sclerosis is not uncommon, particularly in perinodal tissue, inguinal lymph node, mesentery, and retroperitoneum.

There are many morphologic variants of follicular lymphoma: marginal zone differentiation (with parafollicular bands of medium-sized lymphoid cells featuring irregular or kidney-shaped nuclei and a moderate amount of clear cytoplasm); plasmacytic differentiation (predominantly in interfollicular zone but sometimes intrafollicular) (Fig. 79A, B); signet ring cell variant (with cytoplasmic clear vacuole or eosinophilic globule); presence of eosinophilic precipitate; and floral variant (large follicles with tongues of mantle zone lymphocytes extending inward, producing multilobulated germinal centers that resemble flowers with multiple petals); and follicular lymphoma with rosettes.

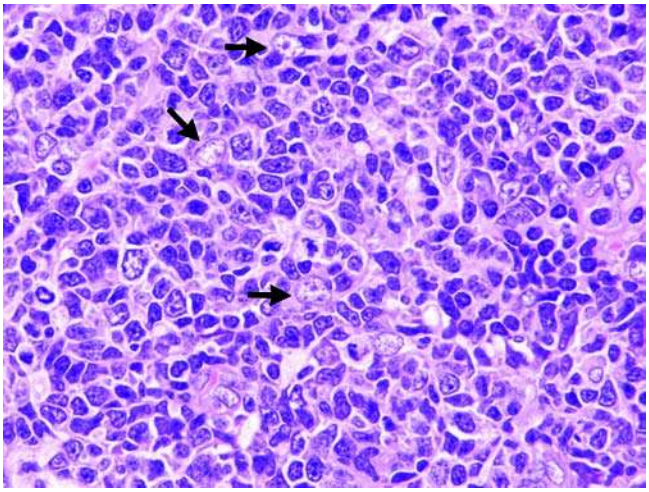

Figure 76 Follicular lymphoma, lymph node. The follicle comprises mostly centrocytes, with some admixed centroblasts with distinct nucleoli. Interspersed follicular dendritic cells can be seen (*arrows*); in contrast to centroblasts, they have indistinct cell borders and thinner nuclear membrane that stain a violaceous color.

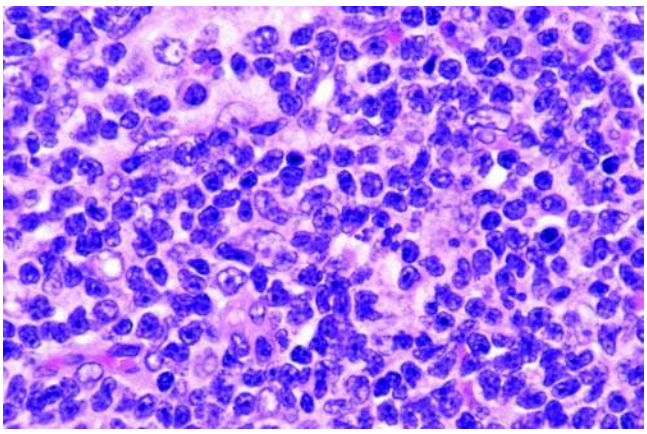

Figure 77 Follicular lymphoma, lymph node, with involved interfollicular zone. Careful inspection of the interfollicular region reveals a significant population of small lymphoid cells with slightly larger nuclei and more open chromatin compared with the admixed small lymphocytes—indicating presence of interfollicular invasion.

Histologic grading and growth pattern. A grade is assigned based on the proportion of centroblasts within the follicles (Fig. 80A–D) (302,303) (Table 8). A count on the number of centroblasts per 40× HPF is calculated based on averaging the counts in ten neoplastic follicles. Follicular dendritic cells should not be mistaken for centroblasts; the former cells differ in having ill-defined cytoplasmic borders, delicate violaceous nuclear membrane, empty nucleoplasm, and

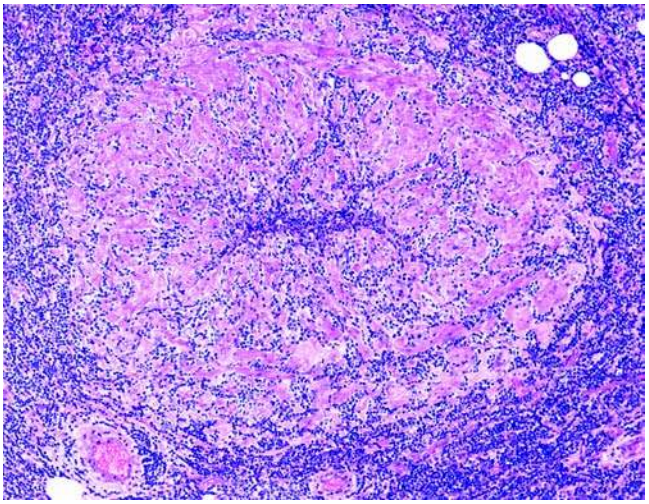

Figure 78 Follicular lymphoma, lymph node. Invasion of the walls of veins is a characteristic, although not invariable, finding in the perinodal tissues.

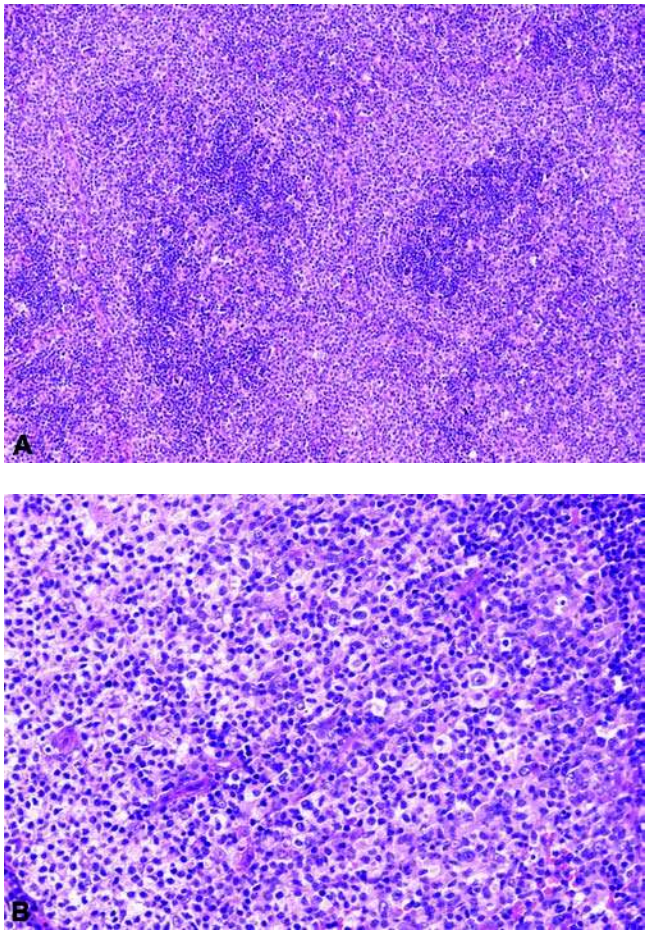

Figure 79 Follicular lymphoma with marginal zone differentiation. (**A**) The abnormal follicles are surrounded by collars of pale-staining cells. (**B**) High magnification shows follicular center cells in the right field and marginal zone cells (resembling monocytoid B cells) in the left field.

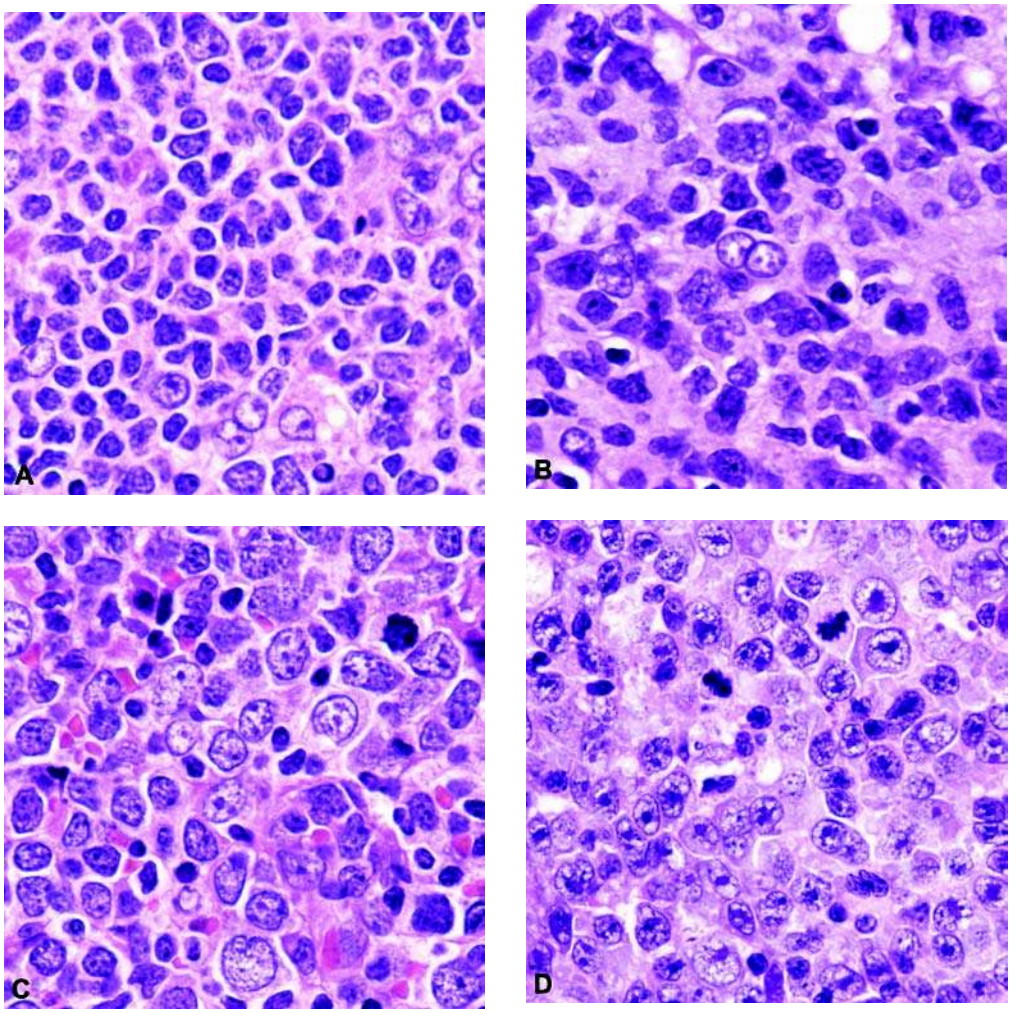

Figure 80 Grading of follicular lymphoma. (**A**) Grade 1. (**B**) Grade 2. A binucleated follicular dendritic cell is seen in the middle of the image. (**C**) Grade 3a. There are still admixed centrocytes. (**D**) Grade 3b.

Table 8 Grading of Follicular Lymphoma

Grade	Definition[a]
1	0–5 Centroblasts per HPF
2	6–15 Centroblasts per HPF
3	>15 Centroblasts per HPF
3a	Centrocytes present
3b	Solid sheets of centroblasts within the neoplastic follicles

[a]Average count from 10 neoplastic follicles
HPF = high-power field, 0.159 mm^2 (18-mm eyepiece)
If using a 20 mm 10× eyepiece (with HPF area of 0.196 mm^2): count 8 HPF and divide by 10, or count 10 HPF and divide by 12.
If using a 22 mm 10× eyepiece (with HPF area of 0.237 mm^2): count 7 HPF and divide by 10, or count 10 HPF and divide by 15.

single small nucleolus (Fig. 76). Admittedly, counting can at times be problematic due to presence of many cells with morphology intermediate between centroblasts and centrocytes.

Some cases of follicular lymphoma have a diffuse component, which is defined as an area of the tissue completely lacking follicles (Fig. 81) (303). It should be noted that a broad interfollicular zone is not considered a diffuse component. If there are uncertainties, immunostaining for CD21 or CD35 can help—identification of foci completely devoid of follicular dendritic cell meshworks supports the presence of a diffuse component. The proportion of follicular area should be estimated and reported, with the pattern further qualified as follicular (>75% follicular area), follicular and diffuse (25–75% follicular area), or focally follicular (<25% follicular area). However, for a grade 3 follicular lymphoma, the presence of any definite diffuse component mandates an additional separate diagnosis of DLBCL. That is, the diagnostic label should be ''follicular lymphoma grade 3 and DLBCL (with estimates of percentage

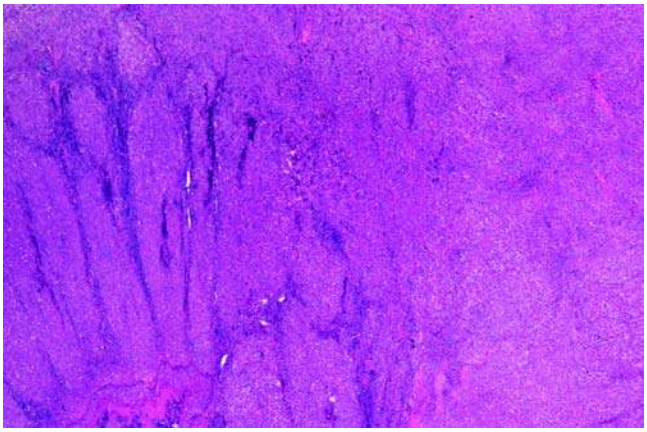

Figure 81 Follicular lymphoma with a diffuse component. The latter is depicted in the right field.

areas occupied by the two components)'' instead of ''follicular grade 3, follicular and diffuse.''

Rare cases with the cytologic composition of grade 1 or 2 follicular lymphoma but a completely diffuse growth pattern are referred to as ''diffuse follicular lymphoma.'' The typical immunophenotype (CD10+, BCL6+) or genotype (*BCL2* rearrangement) must be demonstrated to support this diagnosis versus other small B-cell lymphomas. Nonetheless, if definite neoplastic follicles are identified in other or additional tissue samples, the case will be redesignated as ''follicular lymphoma with diffuse component.''

Immunohistochemistry. The neoplastic cells express pan-B markers and surface immunoglobulin (frequently IgM or IgG) with light-chain restriction. They express the follicle center cell markers CD10 and BCL6. CD5 is negative, and a proportion of cases express CD23. The follicular dendritic cell networks within the neoplastic follicles can be highlighted by markers such as CD21 or CD35.

A notable feature is that neoplastic cells have often invaded into the interfollicular zone. At the immunohistochemical level, this manifests as increased B cells in the interfollicular zone—there are dense clusters and sheets of cells staining for pan-B markers (contrasting with the normal interfollicular zone, which is packed with T cells) (Fig. 82). Furthermore, many interfollicular lymphoid cells stain for the follicle center cell markers CD10 and BCL6, although staining can sometimes be weak or absent due to downregulation of these proteins in the interfollicular lymphoma cells (Fig. 82) (301).

BCL2 protein expression is common, ranging from nearly 100% of grade 1 cases to about 75% of grade 3 cases (Fig. 83A) (304). It is useful in distinguishing follicular hyperplasia from follicular lymphoma: the germinal centers in the former are consistently BCL2 negative (Fig. 83B). However, BCL2 expression is not helpful in excluding other types of lymphomas because many lymphoma types are BCL2 positive.

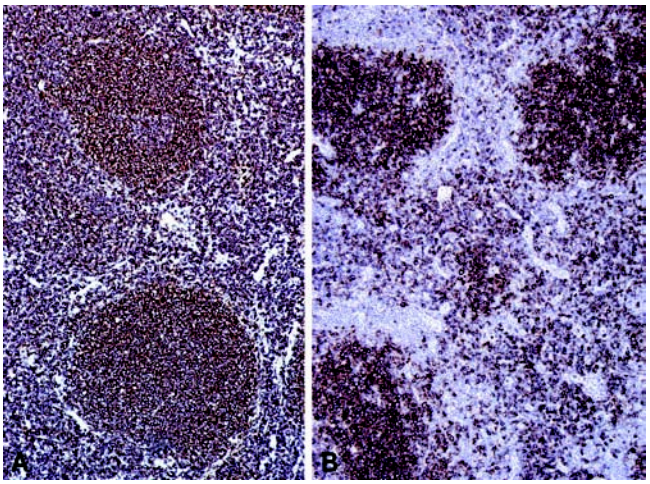

Figure 82 Follicular lymphoma, immunohistochemistry. (**A**) CD20 immunostaining highlights not only the follicles, but also numerous cells in between indicating presence of interfollicular invasion. This is a very useful feature for distinction from reactive follicular hyperplasia. (**B**) The follicles are CD10 positive, and many cells in the interfollicular zone are also positive, also indicating presence of interfollicular invasion. As commonly the case, the interfollicular neoplastic cells show weaker expression of CD10 compared to those located in the follicles.

Molecular genetic data. Follicular lymphomas show rearranged immunoglobulin heavy- and light-chain genes, with germ line T-cell receptor genes. The variable region of *IGH* gene is hypermutated with frequent ongoing somatic mutations, confirming a follicle center cell origin (305). About 80% to 90% of cases harbor t(14;18)(q32;q21), resulting in fusion of *BCL2* gene on chromosome 18 with the *IGH* gene on chromosome 14 (306,307). This translocation can be detected by various methods such as conventional cytogenetics, Southern blotting, polymerase chain reaction, and fluorescence in situ hybridization, with the last technique being most sensitive. It results in the overexpression of BCL2 protein in the cells that constitute the follicles, where BCL2 is not expressed under normal situation. The prevention of apoptosis in the follicles by BCL2 overexpression is believed to be an important pathogenetic step in the development of follicular lymphoma.

For grade 3 follicular lymphomas, recent molecular findings have shown that grade 3a follicular lymphomas are more closely linked to conventional follicular lymphomas, while grade 3b cases are more akin to DLBCL, in which t(14;18) is only implicated in a small proportion of cases (308,309).

Transformation to high-grade lymphoma. About one-third of cases of follicular lymphomas will transform to a high-grade lymphoma (303,310,311), which is associated with a highly aggressive clinical course. The commonest type is DLBCL, but high-grade B-cell lymphoma resembling Burkitt lymphoma or lymphoblastic

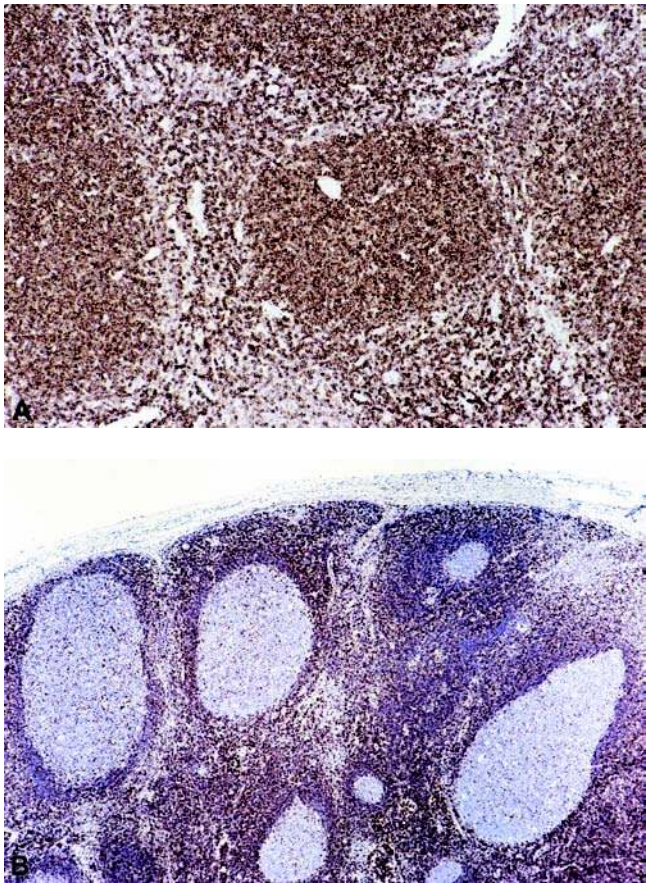

Figure 83 Immunohistochemical staining for BCL2. (**A**) The follicles are commonly BCL2 positive in follicular lymphoma. (**B**) For comparison, the follicles in reactive follicular hyperplasia are negative. The loosely scattered positive cells in the germinal centers are T cells.

lymphoma can also occur (312,313). If the additional genetic alteration mediating the transformation is *MYC* translocation on top of preexisting *BCL2* translocation, the tumor is rapidly lethal.

Differential diagnosis. The main differential diagnosis is reactive follicular hyperplasia, and the distinguishing features are listed in Table 9 (Figs. 84 and 85A, B). Some other types of lymphoma may show a nodular architecture with a true follicular (harboring follicular dendritic cell network) or ''pseudofollicular'' pattern, and the distinguishing features are discussed as follows.

1. Mantle cell lymphoma: Some examples of mantle cell lymphoma show a follicular/nodular growth pattern, mimicking grade 1 follicular lymphoma. There are usually some follicles with small residual germinal centers, indicating a mantle zone growth pattern. Presence of scattered solitary epithelioid histiocytes is also suggestive of mantle cell lymphoma. The lymphoma cells, while showing irregular nuclear foldings, often have a somewhat rounded overall contour, contrasting with the often elongated or triangular nuclear contour of centrocytes in follicular lymphoma. The cells are CD5+, cyclin D1+ and lack follicle center cell markers CD10 and BCL6.
2. Chronic lymphocytic leukemia/small lymphocytic lymphoma (CLL/SLL): The nodules are proliferation centers, which are nonexpansile and consist of prolymphocytes and paraimmunoblasts with round nuclei and single central nucleoli. On immunostaining, there are no or few follicular dendritic cells within these centers. The neoplastic cells are CD5+, CD23+ and are negative for CD10 and BCL6.
3. Nodal or extranodal marginal zone lymphoma: The nodules represent colonization of follicles by neoplastic cells. There are often areas showing other features of marginal zone lymphoma, including reactive follicles, marginal zone growth pattern, plasmacytic component, and lymphoepithelial lesions for extranodal cases. The lymphoma cells are negative for CD10 and BCL6.
4. Nodular lymphocyte–predominant Hodgkin lymphoma: The nodules are composed of small lymphocytes rather than follicle center–type cells, and there are interspersed very large L&H cells.
5. Nodular lymphocyte–rich classical Hodgkin lymphoma: The nodules are composed of small lymphocytes rather than follicle center–type cells, although occasional residual follicle centers can be identified in some nodules. There are interspersed very large Reed–Sternberg cells and variants.

Treatment and prognosis. The five-year overall survival and failure-free survival rates are 72% and 40%, respectively (210), but the outcome has further improved in recent years with the addition of anti-CD20 therapy. The behavior further depends on the grade of the tumor: low-grade (grade 1 and 2) cases are indolent but incurable, while high-grade (grade 3) cases are more aggressive but with a potential for cure (314). Whether the percentage of diffuse area influences the prognosis is controversial (302). Transformation to high-grade lymphoma is associated with a much more aggressive clinical course (310,311).

Distinct subtypes. Several special groups of patients with follicular lymphoma show clinicopathologic distinct from conventional cases of follicular lymphoma.

Pediatric follicular lymphomas are uncommon, but when they do occur, they more frequently involve the tonsils and cervical lymph nodes, have a low clinical stage (stage I or II), and have an excellent prognosis despite a higher proportion of grade 3 tumors (315,316). In contrast to the adult counterpart, the disease is apparently curable. BCL2 expression is uncommon (~30%), and *BCL2* gene is uncommonly rearranged (only 12.5%).

Primary cutaneous follicle center lymphoma usually presents with localized disease, most commonly in the skin of the trunk or the head and neck regions. The prognosis is excellent. BCL2 immunoreactivity and *BCL2* rearrangement occur at a low frequency (317–319).

Table 9 Distinguishing Features Between Reactive Follicular Hyperplasia and Follicular Lymphoma

	Reactive follicular hyperplasia	Follicular lymphoma
Morphology		
Size and shape of follicles	Widely spaced follicles of various sizes	Usually closely packed follicles of similar sizes; follicles are sometimes widely spaced
Mantle zone	Distinct	Usually ill-defined or absent
Polarity	Present, at least in some follicles	Absent
Cellular composition of follicles	Mixture of centrocytes and centroblasts, with the latter predominating	Mixture of centrocytes and centroblasts, with the proportion depending on grade. Centrocyte predominance, if present, is highly suggestive of follicular lymphoma
	Abundant tingible-body macrophages	Tingible-body macrophages are scanty
Cellular composition in interfollicular region	Atypical cells are not seen in the interfollicular region	Atypical cells (often medium-sized, with irregular nuclear foldings) commonly present
Immunohistochemistry		
Pan-B markers	B cells are mainly limited to the follicles, with only scattered B cells in the interfollicular region	Follicles are positive, but interfollicular region is also commonly packed with B cells
Immunoglobulin light chain (often requiring frozen tissue for proper demonstration)	Follicles are polytypic	Follicles and interfollicular B cells are monotypic
CD10 and BCL6 (follicle center cell markers)	Expression limited to the follicles	In addition to the follicles, lymphoid cells in interfollicular region are commonly positive
BCL2 protein	Germinal centers are BCL2 negative	Follicles are frequently BCL2+
Ki67 (proliferative marker)	High proliferative fraction	Proliferative fraction varies with grade, but a low proliferative fraction, if present, is supportive of follicular lymphoma
	Polarity of the follicles can be highlighted with higher number of Ki67+ cells in the dark zone	No polarity highlighted in the follicles
Cytogenetics/molecular finding		
Immunoglobulin gene rearrangement	Polyclonal	Clonal
t(14;18)(q32;q21) with *BCL2* gene rearrangement	Absent	Present (80–90%)

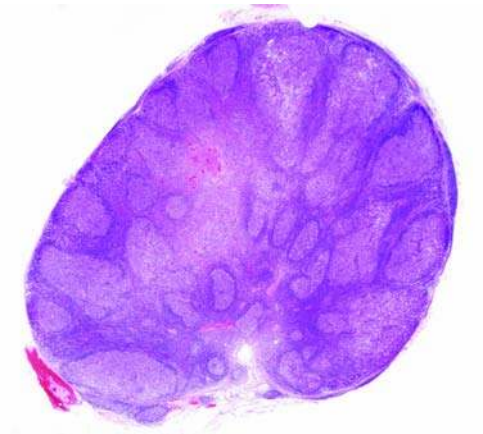

Figure 84 Follicular lymphoma-simulating reactive follicular hyperplasia. The follicles in some cases of follicular lymphoma are not crowded and are still surrounded by intact mantles, resembling reactive follicles. The diagnosis of follicular lymphoma is based on the presence of other diagnostic features such as predominance of centrocytes and presence of interfollicular invasion, and supported by immunostaining.

In situ follicular lymphoma is characterized by the morphology of usual reactive follicular hyperplasia (with or without some follicles exhibiting centrocytes predominance), but with a proportion of germinal centers harboring aggregates of strongly BCL2+ follicle center cells. Some patients have prior or synchronous follicular lymphoma at another site, some develop overt follicular lymphoma on follow-up, while others remain disease-free on follow-up (320).

Mantle Cell Lymphoma

Introduction. Mantle cell lymphoma is a B-cell neoplasm consisting of monomorphous small to medium-sized lymphoid cells with irregular nuclei, which morphologically resemble centrocytes, without neoplastic transformed cells (centroblasts, prolymphocytes, paraimmunoblasts).

Clinical features. Mantle cell lymphoma accounts for 6% of all non-Hodgkin lymphomas (210). Most patients have high-stage disease at presentation (81% stage III/IV). The median age is 63 years, and there is male predominance, with male-to-female ratio of 2.8:1. Most patients present with lymphadenopathy with or without hepatosplenomegaly, and B symptoms are noted in 28% (209). Extranodal

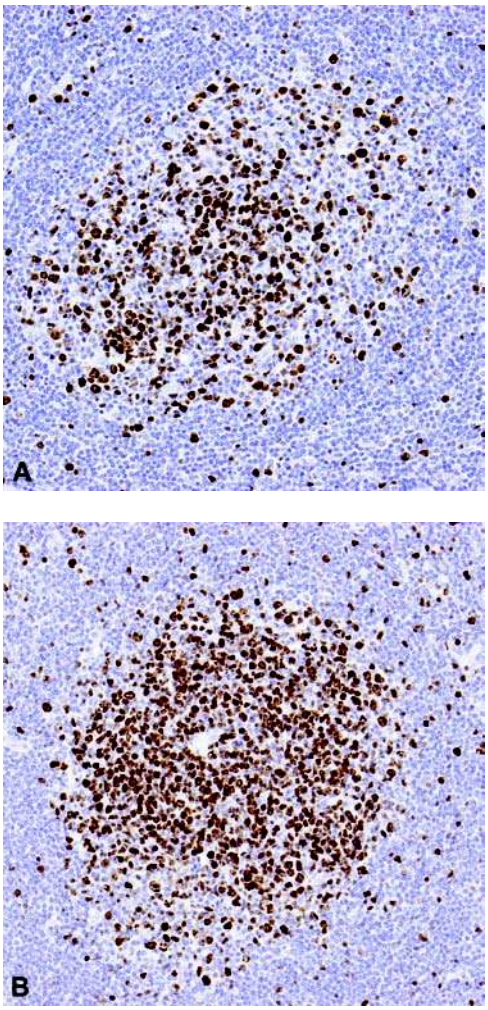

Figure 85 Follicular lymphoma, immunostaining for Ki67. (**A**) Grade 2 follicular lymphoma shows moderate numbers of Ki67+ cells, and the percentage is much lower than that of a reactive follicle. (**B**) Grade 3a follicular lymphoma with numerous Ki67+ cells. The pattern differs from that of reactive follicles in that polarity is not evident (compare with Fig. 6, chap. 16).

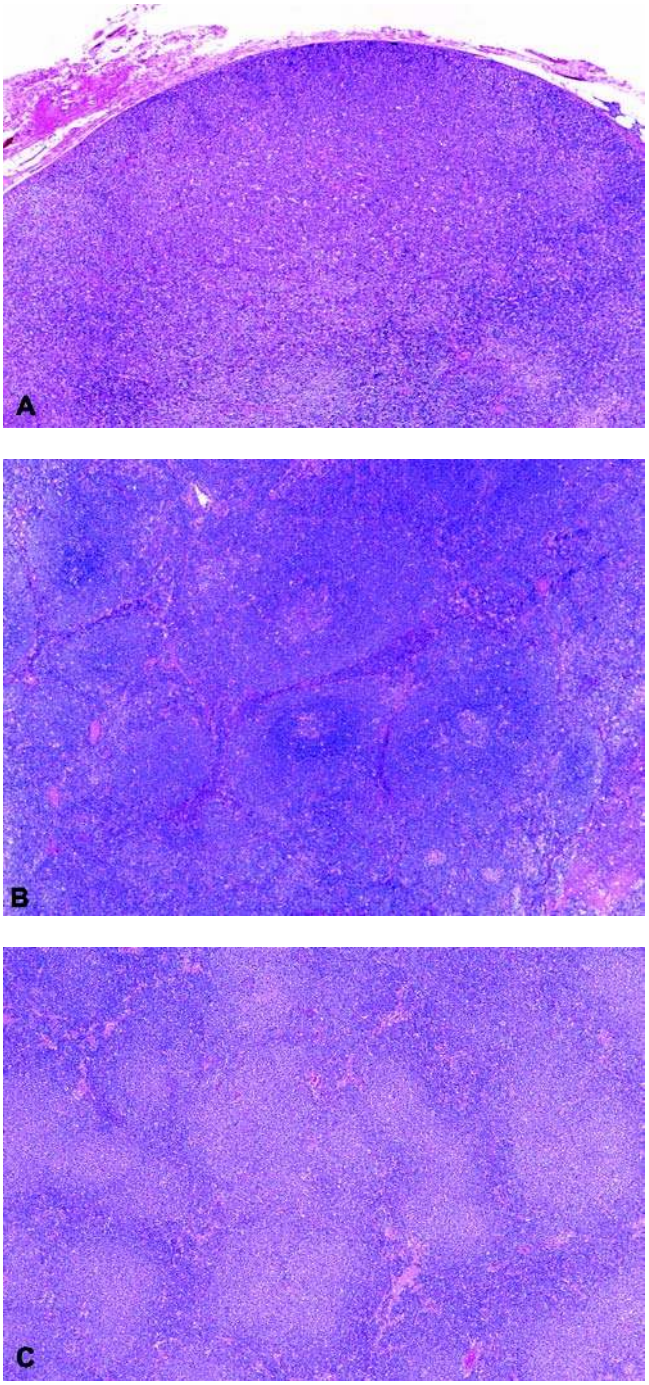

Figure 86 Mantle cell lymphoma. (**A**) Diffuse growth pattern. (**B**) Mantle zone pattern. (**C**) Nodular/follicular growth pattern, mimicking follicular lymphoma.

involvement is frequent and occurs in three-fourths of cases during the course of disease, with marrow and peripheral blood involvement being the commonest findings (321). Waldeyer ring and gastrointestinal tract are involved in 10% of the cases each. Not infrequently, extranodal head and neck disease (e.g., Waldeyer ring, salivary gland, orbit) is the presenting feature (321).

Pathology. The involved lymph node or extranodal site shows effaced architecture, and may show a mantle zone, nodular, or diffuse pattern of involvement (Fig. 86A–C). In the mantle zone pattern, the tumor cells form broad mantles around remnant germinal centers. The nodular pattern may represent a later stage of the mantle zone pattern wherein the reactive follicles have been completely overrun by the tumor cells. Hyalinized small vessels and scattered single epithelioid histiocytes are characteristic features, and when present, provide a strong clue to the diagnosis of mantle cell lymphoma in a small cell lymphoma. In extranodal sites, lymphoepithelial lesions are usually not formed, but when present in the rare cases, MALT lymphoma may be simulated (322).

Cytologically, the tumor infiltrate usually appears monotonous, comprising small to medium-sized cells with mild nuclear irregularities. Nucleoli are generally indistinct, chromatin is fairly dense, and cytoplasm is scanty (Fig. 87A). Occasionally, the tumor cells may have small round nuclei, or may have more abundant clear cytoplasm simulating marginal zone B cells. By definition, neoplastic centroblasts, prolymphocytes, or paraimmunoblasts are not seen. The blastoid variant is characterized by lymphoblast-like nuclei with finely dispersed chromatin and high mitotic rate (commonly at least 20–30/HPF) (Fig. 87B); classical mantle cell lymphoma may sometimes be found in the same, prior, or subsequent biopsy (323). The pleomorphic variant characteristically comprises medium-sized to large cells, often with variation in nuclear size, more open but still granular chromatin and variably distinct nucleoli; this variant is not uncommonly misdiagnosed as DLBCL (Fig. 87C).

Immunohistochemistry. Mantle cell lymphoma expresses pan-B markers, with monotypic surface immunoglobulin (frequently both IgM and IgD). It is commonly CD5+, CD10−, BCL6−, CD23−, and the most characteristic immunohistochemical finding is cyclin D1 expression (Fig. 88) (321,324,325). Although cyclin D1 expression is not absolutely specific, having been reported in hairy cell leukemia, in plasmacytoma, and less commonly in CLL/SLL, it is a sensitive and highly specific marker in the appropriate clinicopathologic setting (324). Recent molecular studies have shown rare cases of mantle cell lymphoma that are cyclin D1 negative, but their clinical, histologic, and genetic profiles are no different from classical mantle cell lymphoma (326). The blastoid variant commonly strongly expresses p53.

Molecular genetic data. Mantle cell lymphomas have rearranged immunoglobulin heavy- and light-chain genes, with germ line T-cell receptor genes. The variable region of *IGH* is usually nonmutated, indicating naïve B-cell stage of differentiation (327,328). The small proportion of cases (20–30%) with hypermutated immunoglobulin gene may represent a distinct subgroup. Nearly all cases of mantle cell lymphoma show fusion of the *CCND1* (cyclin D1) with the *IGH* genes, which results from t(11;14)(q13;q32) or cryptic translocation (329). The detection rate of the gene translocation is usually below 70% by conventional cytogenetics, Southern blot, or polymerase chain reaction, but approaches 100% by fluorescence in situ hybridization.

Differential diagnosis. Various B-cell lymphomas with predominance of small cells enter into the differential diagnosis, such as CLL/SLL, MALT lymphoma, nodal marginal zone lymphoma, and follicular lymphoma. Scattered solitary epithelioid histiocytes and hyalinized venules, if present, would be strongly suggestive of mantle cell lymphoma.

Grade 1 follicular lymphoma can be difficult to distinguish from mantle cell lymphoma with a nodular growth pattern. The latter contains at least some neoplastic centroblasts, and the centrocytes often show greater nuclear irregular foldings and assume triangular or elongated overall nuclear contours (differing from the overall roundish nuclear contours in mantle cell lymphoma) (Fig. 80A, B). Immunophenotyping permits a clear distinction between the two entities, with follicular lymphoma being CD5−, CD10+, BCL6+, cyclin D1− (Fig. 82).

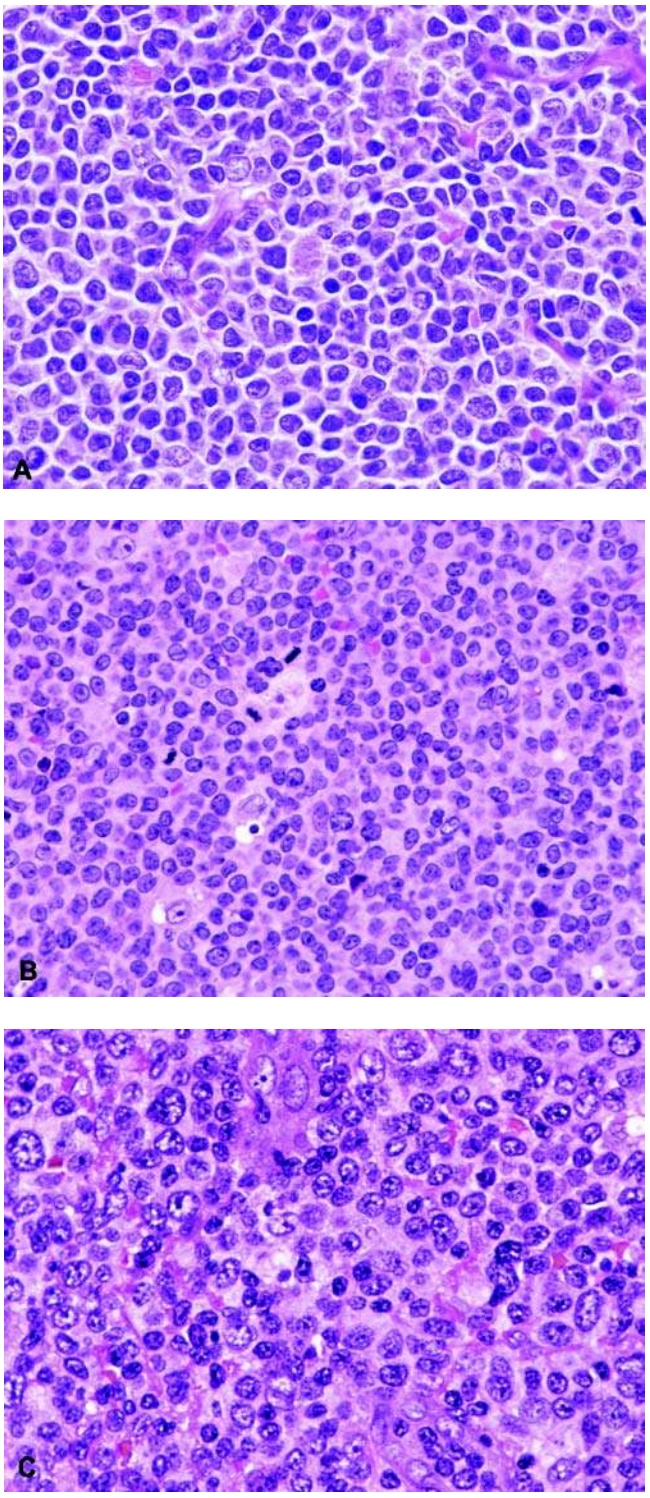

Figure 87 Mantle cell lymphoma. (**A**) Classical cytologic appearance. (**B**) Blastoid variant. (**C**) Pleomorphic variant, which can be difficult to distinguish from large B-cell lymphoma.

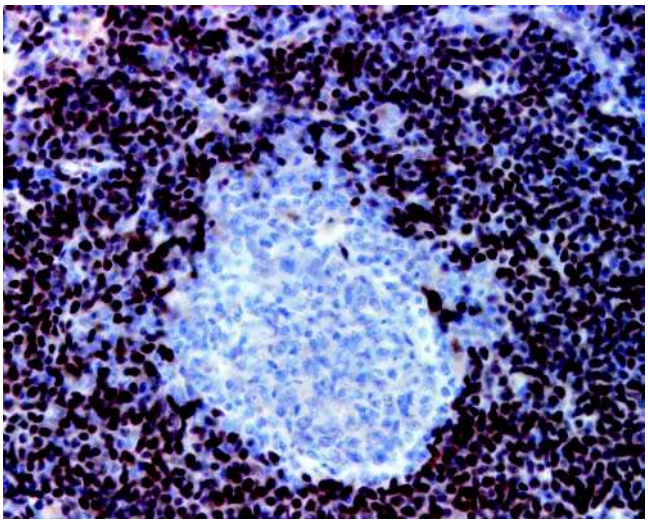

Figure 88 Mantle cell lymphoma, immunostained for cyclin D1. The lymphoma cells show nuclear staining. In this case, a negative residual germinal center is shown in the center.

For CLL/SLL, proliferation centers, which are nonexpansile pale-staining foci within the dark-staining small cell–rich background, are diagnostic when present. Admixed slightly larger cells with distinct nucleoli (prolymphocytes and paraimmunoblasts) is another histologic feature pointing to a diagnosis of CLL/SLL. The tumor cells coexpress CD5 and CD23 and are usually negative for cyclin D1, contrasting with the CD5+, CD23−, cylinD1+ immunophenotype of mantle cell lymphoma.

MALT lymphoma and nodal marginal zone lymphoma frequently show reactive lymphoid follicles, neoplastic cells with marginal zone growth pattern, monotypic plasma cells, and in addition lymphoepithelial lesion for extranodal sites. Rare cases of mantle cell lymphoma can have marginal zone lymphoma-like appearance, especially in extranodal sites; cyclin D1 expression is the main distinguishing feature (330,331).

The pleomorphic variant of mantle cell lymphoma can be difficult to recognize, being commonly misdiagnosed as DLBCL. This diagnosis should be considered for a lymphoma presumptively considered to represent DLBCL but with somewhat more granular chromatin than usual or with CD5 expression. This can be confirmed by extensive and strong immunoreactivity for cyclin D1.

The blastoid variant can be morphologically indistinguishable from B-lymphoblastic leukemia/lymphoma, but can be recognized by (*i*) the older age of the patient; (*ii*) presence of a component of classical mantle cell lymphoma histologically, if present; (*iii*) positivity of cyclin D1; and (*iv*) lack of TdT expression.

Treatment and prognosis. The prognosis is poor, with five-year overall survival and failure-free survival rates of 27% and 11%, respectively (210). The most important prognostic factor remains the International Prognostic Index score. Other significant poor prognostic indicators include high mitotic rate and pleomorphic/blastoid variants (321,332).

Extranodal Marginal Zone Lymphoma of Mucosa-Associated Lymphoid Tissue Type (MALT Lymphoma)

Introduction. Extranodal marginal zone lymphoma of MALT, also known as MALT lymphoma, accounts for 8% of all non-Hodgkin lymphomas (210,333). It is an indolent lymphoma showing architectural and cytologic homology with the normal lymphoid tissues occurring in various mucosal and extranodal sites. Various other head and neck regions can also be involved, most commonly salivary gland, thyroid gland, and ocular adnexa (334).

Clinical features. MALT lymphoma frequently arises in the setting of lymphoid hyperplasia that develops in association with autoimmunity or infection, e.g., Hashimoto thyroiditis in the thyroid, and lymphoepithelial sialadenitis and Sjogren syndrome in the salivary gland.

The patients are usually adults, but children can also be affected, with some associated with HIV infection (335,336). They present with a mass lesion or nonspecific symptoms; some are incidentally found to harbor the lymphoma. Most patients have early stage disease (stage I/II) at presentation. However, there can be synchronous or metachronous involvement of more than one mucosal site, a phenomenon attributed to the homing properties of mucosal lymphocytes.

Pathology. MALT lymphoma shows unifocal or multifocal involvement of the extranodal tissue, often accompanied by some reactive lymphoid follicles. The neoplastic lymphoid infiltrate is usually diffuse, but can be interfollicular or perifollicular (Fig. 89A). It is often heterogeneous, comprising a mixture of cell types, although some cases can exhibit a monomorphic population, especially in the ocular adnexa. The most distinctive cell type is centrocyte-like, being small to medium sized, with slightly folded or elongated angulated nuclei, moderately dense chromatin, inconspicuous nucleoli, and a small amount of pale to clear cytoplasm. Some cells are slightly larger, with abundant clear cytoplasm, resembling monocytoid B cells. Some cells have dark round nuclei, indistinguishable from normal small lymphocytes. There are often isolated admixed large blastic cells resembling centroblasts or immunoblasts. Commonly there are bland-looking or mildly atypical plasma cells that are intimately intermingled with the lymphoid cells or form large clusters. Dutcher bodies (nuclear pseudoinclusions) or crystalline inclusions are sometimes present in these cells. Rarely, amyloid deposits (AL type) can be present.

In MALT lymphoma, lymphoepithelial lesions are frequently formed as a result of invasion and expansion of the epithelial structures by lymphoma cells (Fig. 89B). The lymphoma cells within and around the epithelial structures may assume a centrocyte-like or monocytoid B-cell-like appearance, producing pale

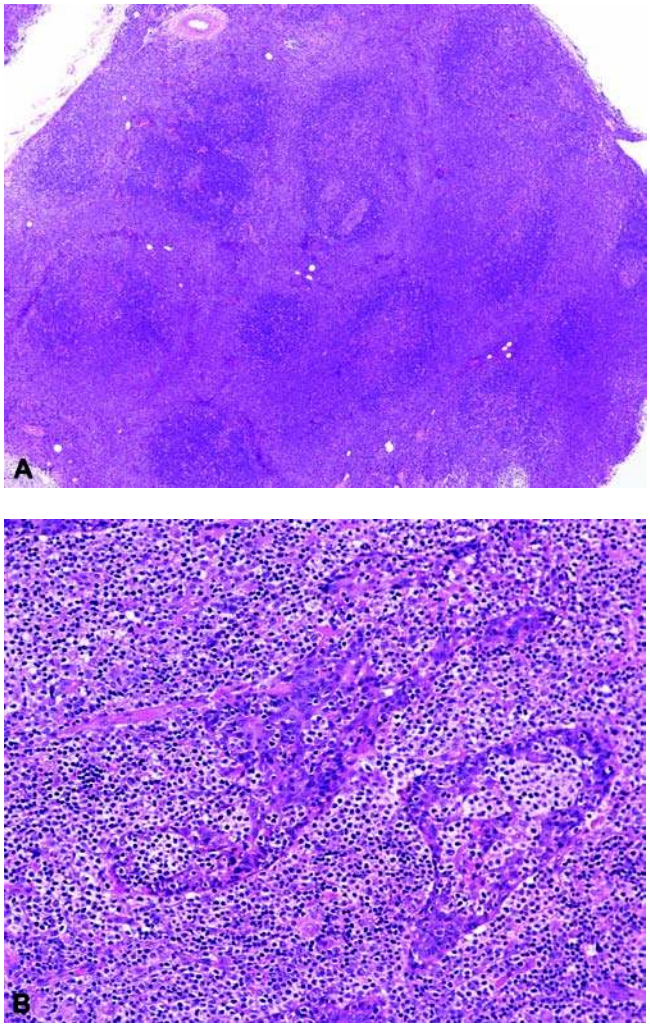

Figure 89 MALT lymphoma. (**A**) Regional lymph node involved by MALT lymphoma. There is perifollicular (marginal zone) growth around reactive follicles. (**B**) MALT lymphoma of parotid gland, showing prominent lymphoepithelial lesions.

collars around the lymphoepithelial lesions, a feature that is often striking in the salivary gland.

In some cases, the preexisting follicles show colonization by lymphoma cells, resulting in vague or discrete abnormal follicular structures mimicking follicular lymphoma. The neoplastic cells that have colonized the follicles may show increased plasma cell differentiation or a more blastic appearance.

The regional lymph nodes are involved by MALT lymphoma in approximately 30% of cases. Early involvement is subtle, being confined to the marginal zones around reactive follicle. Frank involvement is characterized by coalescence of broadened marginal zones, colonization of follicles, and interfollicular invasion, sometimes producing a diffuse pattern (Fig. 89A).

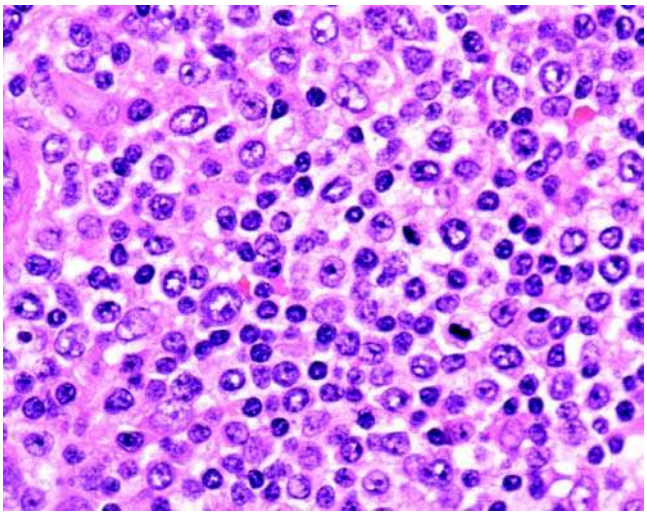

Figure 90 MALT lymphoma with increased large cells, parotid gland. In contrast to a supervening large B-cell lymphoma, the large cells do not form confluent aggregates or sheets.

Large cell transformation in MALT lymphoma. Up to 10% to 30% of cases of MALT lymphoma show transformation to a large B-cell lymphoma. There is general agreement for such a designation (large B-cell lymphoma associated with or arising in MALT lymphoma) when there are compact clusters, confluent aggregates, or sheets of large nucleolated cells (337–339). The appropriate designation when the large cells are singly dispersed within the MALT lymphoma is more problematic. It appears that when there are >5% interspersed large nucleolated cells, a designation ''MALT lymphoma with increased large cells'' is justified because the prognosis is already slightly worsened (Fig. 90) (339–341).

Immunohistochemistry. The lymphoma cells are positive for pan-B markers such as CD20, CD79a, and PAX5, and they express surface immunoglobulin, most frequently IgM, and less commonly IgA or IgG, but almost never IgD. There is immunoglobulin light-chain restriction. Cytoplasmic immunoglobulin light-chain restriction can frequently be identified in the admixed plasma cells, which are monotypic in more than one-third of cases. The tumor cells are negative for CD5, CD10, CD23, BCL6, and cyclin D1, though rare CD5+ cases have been reported (342). Approximately half of the cases show aberrant CD43 expression (343,344).

Molecular genetic data. MALT lymphomas have clonally rearranged immunoglobulin heavy- and light-chain genes and germ line T-cell receptor genes. The variable region of *IGH* is hypermutated, supporting a postgerminal center stage of differentiation (345). Ongoing somatic mutation is observed in some cases raising the possibility of germinal center stage of differentiation (346). However, the absence of a follicle center cell immunophenotype and the

alternative proposals forwarded by other groups favor a postgerminal center stage of differentiation (347,348). There are no rearrangements of the *BCL1*, *BCL2*, and *BCL6* genes.

MALT lymphomas exhibit distinctive chromosomal translocations, including t(11;18)(q21;q21), t(14;18)(q32;q21), t(1;14)(p22;q32), and t(3;14)(q14;q32), involving *API2-MALT1*, *IGH-MALT1*, *IGH-BCL10*, and *FOXP1-IGH* fusion genes, respectively (334,349). The relative incidence of these translocations in MALT lymphoma of different sites is highly variable. For example, *IGH-MALT1* occurs predominantly in MALT lymphoma of the salivary gland, ocular adnexa, skin, and lung, while *FOXP1-IGH* occurs more often in MALT lymphoma of the thyroid and ocular adnexa (50% and 20%, respectively, in one series) than in other sites (349,350). *IGH-BCL10* translocation is very uncommon, and only occurs in rare cases in the lung, intestine, and salivary gland (349). These disparate translocations all produce the effect of constitutive activation of NF- κB, which transactivates genes such as cytokines and growth factors important for cellular activation, proliferation, and survival. Trisomy 3 has also been reported in up to 75% of cases (334,351).

Differential diagnosis. The major differential diagnoses of MALT lymphoma are the reactive lymphoid hyperplasias and chronic inflammatory processes that occur in the various extranodal sites, which will be addressed in detail in the respective sections.

Treatment and prognosis. The tumor usually remains locoregional, and the prognosis is highly favorable. The five-year overall survival according to the Non-Hodgkin Lymphoma Classification Project is 74% (210). The relapse rate is 37%, and the median time to relapse is 47 months (350). The prognosis is worsened when a large cell lymphoma supervenes (338,341,352,353).

Burkitt Lymphoma

Clinical features. Burkitt lymphoma is a highly aggressive B-cell neoplasm, which occurs in three different clinical settings: (*i*) endemic form in central Africa; (*ii*) sporadic form; and (*iii*) immunodeficiency, especially HIV infection (354). The endemic form is consistently associated with EBV, and occurs mostly in children, who present with extranodal disease, most commonly in the jawbone, kidneys, liver, gonads, mesentery and retroperitoneum, and endocrine glands. Lymph node and bone marrow involvement are uncommon. The sporadic form shows variable EBV association, from 15% in developed countries to 80% in developing countries. It affects children and young adults, who present with lymphadenopathy or extranodal disease (most commonly ileocecal region and Waldeyer ring). AIDS-associated Burkitt lymphoma shows association with EBV in 30% of cases. It affects young patients, who present with lymphadenopathy or extranodal disease (most commonly brain, bone marrow, liver, and gastrointestinal tract).

Pathology. There is diffuse infiltration by monotonous medium-sized cells with a starry-sky pattern due to the presence of interspersed tingible-body macrophages. The tumor cells have round or molded nuclei, clumped chromatin, and multiple nucleoli. They have a rim of basophilic cytoplasm, which may contain fine fat vacuoles. Squaring of the cellular contours is often present (Fig. 91). Mitotic figures and apoptotic bodies are typically abundant. Some cases are accompanied by a prominent epithelioid granulomatous reaction, which is associated with EBV positivity, early-stage disease, and favorable prognosis. Plasmacytoid differentiation can sometimes be observed, more commonly seen in the setting of immunodeficiency. Some cases can show greater variation in the size and shape of the nuclei, and bigger but fewer nucleoli—instead of separately labeling them as ''atypical Burkitt lymphoma'' in the 2001 WHO classification, they are simply labeled as ''Burkitt lymphoma'' without further qualifiers in the 2008 WHO classification (355).

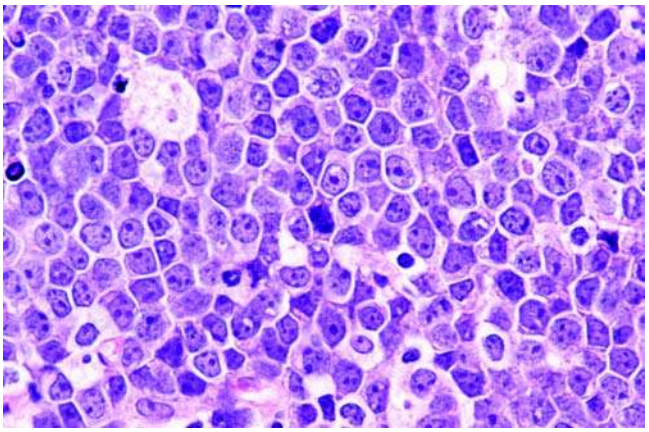

Figure 91 Burkitt lymphoma. Monotonous population of medium-sized cells with ''squaring'' of nuclear and cytoplasmic outlines. Note the presence of fine vacuoles in the amphophilic cytoplasm.

Immunohistochemistry and molecular genetic data. Immunophenotypically, the lymphoma cells express pan-B markers and follicle center cell markers such as CD10 and BCL6. They are usually negative for BCL2, and the proliferation index is nearly 100%. The molecular hallmark of Burkitt lymphoma is fusion of *MYC* gene with an immunoglobulin heavy- or light-chain gene, most commonly resulting from t(8;14)(q24;q32). Although *MYC* translocation can also be seen in some cases of DLBCL or transformed follicular lymphoma, the fusion partner in these lymphoma types is usually a nonimmunoglobulin gene, and this occurs in a setting of complex chromosomal abnormalities. Although gene expression profiling appears to be the best method for defining Burkitt lymphoma (so-called ''molecular Burkitt lymphoma''), this technique is not available in the diagnostic laboratory and has not been fully validated. On encountering cases that pose difficulties in distinction between Burkitt lymphoma and DLBCL, a combination of immunohistochemistry (CD10+, BCL2−, high Ki67) and

fluorescence in situ hybridization (presence of *MYC* rearrangement, and lack of *BCL2* and *BCL6* rearrangement) can help to provide a strong support for the diagnosis of Burkitt lymphoma. Some cases remain unclassifiable or exhibit borderline features, and can be given the diagnostic label of ''B-cell lymphoma, unclassifiable, with features intermediate between DLBCL and Burkitt lymphoma.''

Extramedullary Plasmacytoma

Introduction. Extramedullary plasmacytoma is a tumor-forming plasma cell neoplasm occurring outside the bone, in the absence of clinical history of plasma cell myeloma at presentation. It accounts for up to 4% of all plasma cell neoplasms (356).

Clinical features. About 80% of cases of extramedullary plasmacytoma occur in the upper aerodigestive tract. Most patients are between the fifth and seventh decades of age and show a male-to-female ratio of about 3:1. The commonest involved sites are the nasal cavity and paranasal sinuses (36%), followed by the nasopharynx and oropharynx (15% each) (356). Other head and neck sites of involvement include larynx, cervical lymph node, salivary gland, ear, hypopharynx, trachea, thyroid, and conjunctiva. The patients usually present with a mass lesion or associated symptoms depending on the location of the lesion. By definition, there should be no bony involvement or clinical features of multiple myeloma. However, paraproteinemia, usually of low-titer, can be detected in some patients.

Pathology. The histologic features are similar in the various mucosal sites, with dense sheets of neoplastic plasma cells being observed in the subepithelial stroma (Fig. 92). Well-differentiated tumors comprise mature-looking plasma cells with eccentrically located nuclei with coarse ''clock-face'' chromatin, a moderate amount of amphophilic or basophilic cytoplasm, and paranuclear hof (Fig. 93). The plasma cells can show multinucleation, nuclear atypia (such as larger nuclei, more open chromatin, and irregular nuclear foldings), cytoplasmic globules or crystalline inclusions, and intranuclear inclusions (Dutcher bodies). In poorly differentiated tumors (anaplastic or plasmablastic variant), the large and pleomorphic neoplastic cells may not be readily recognizable as being plasmacytic in nature (Fig. 93). However, usually at least a proportion of cells show coarsely clumped clock-face chromatin, and there are often some admixed immature-looking neoplastic plasma cells. Deposition of AL-type amyloid may be seen in some tumors (Fig. 94).

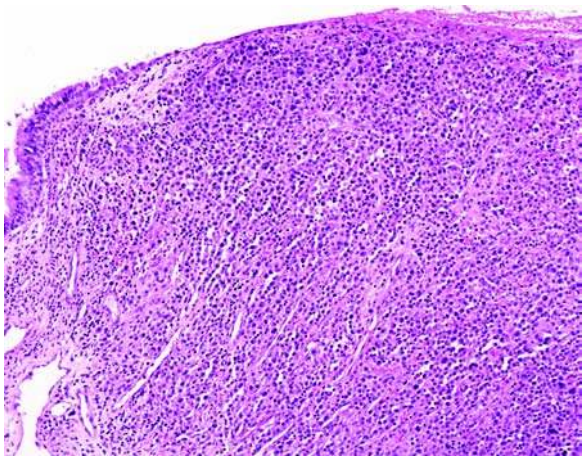

Figure 92 Plasmacytoma of nasopharynx. A diffuse and dense infiltrate of abnormal plasma cells is present, accompanied by focal ulceration of the mucosa (*right field*).

In involved lymph node, thyroid or salivary gland, there is focal or extensive effacement of normal architecture by sheets of plasma cells, which can exhibit a range of atypia as seen in extramedullary plasmacytoma of mucosal sites.

Immunohistochemistry. Plasmacytomas usually express cytoplasmic immunoglobulin, most frequently, IgG (356,357), with monotypic immunoglobulin light chains being demonstrable by immunohistochemistry or in situ hybridization (Fig. 95) (358). They are almost always negative for CD20 and PAX-5, while approximately half of the cases express CD79a (Fig. 96). The B-cell octamer transactivation factors Oct-2 and BOB.1 are commonly positive. The neoplastic cells often express plasma cell–associated markers such as CD38, CD138, MUM1, and VS38c (Fig. 96), but positivity for these markers alone is insufficient to support a diagnosis of plasma cell neoplasm because they can be expressed by nonhematolymphoid tumors.

EMA is commonly expressed, while CD45 is only sometimes positive. About one-third of plasmacytomas express cytokeratin in addition to EMA, resulting in potential misdiagnosis as epithelial tumors (359). Positive staining for CD43 or CD31 in some cases may lead to misinterpretation as T-lineage neoplasm and vascular neoplasm, respectively. Expression of cyclin D1 or CD56 is much more commonly observed in myeloma-related plasmacytoma (33% and 77%, respectively) than extramedullary plasmacytoma (0% and 10%, respectively) (360).

Molecular genetic data. Plasmacytomas show clonal rearrangements of immunoglobulin genes, while T-cell receptor genes are in germ line configuration. EBV is demonstrable in the tumor cells in 15% of cases occurring in the head and neck region (358).

Differential diagnosis. Plasma cell differentiation can occur in some lymphoma types, such as MALT lymphoma, follicular lymphoma, and lymphoplasmacytic lymphoma. The latter lymphomas show in addition a nonplasmacytic neoplastic component, which can best be highlighted by CD20 immunostaining, and there are also characteristic histologic and immunophenotypic features associated with these specific lymphoma types, e.g., CD10 and BCL6 expression in follicular lymphoma. However, distinction between well-differentiated extramedullary plasmacytoma and MALT lymphoma with extensive plasmacytic differentiation can be extremely difficult. In fact, it has been suggested that extramedullary

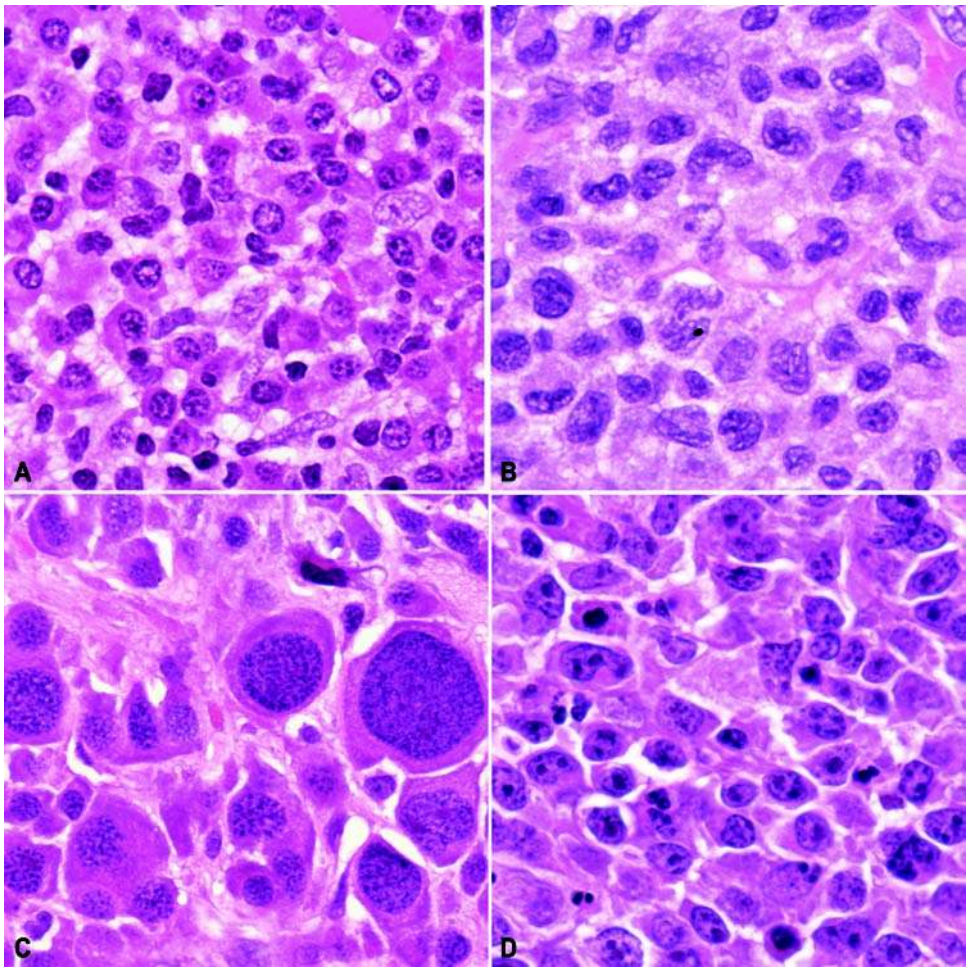

Figure 93 Extramedullary plasmacytoma: cytologic spectrum. (**A**) Readily recognizable plasma cells. (**B**) Cells with irregularly folded to lobated nuclei. (**C**) Cells with marked size variation and coarsely clumped (plasma cell-type) chromatin. (**D**) Plasmablastic cells, difficult to distinguish from large B-cell lymphoma NOS and plasmablastic lymphoma.

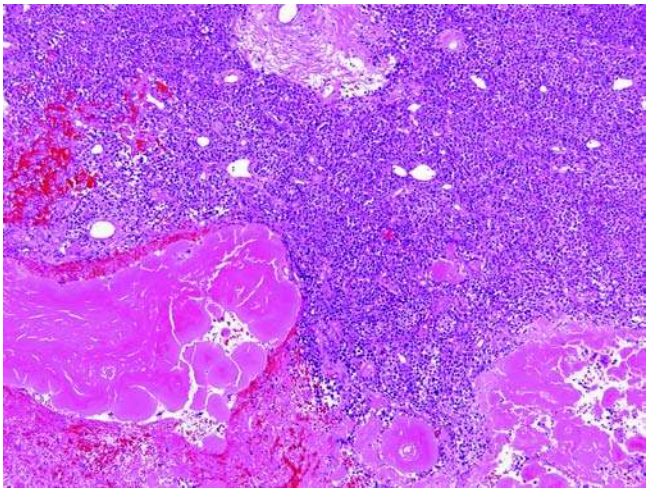

Figure 94 Plasmacytoma of nasal cavity, accompanied by amyloid deposition.

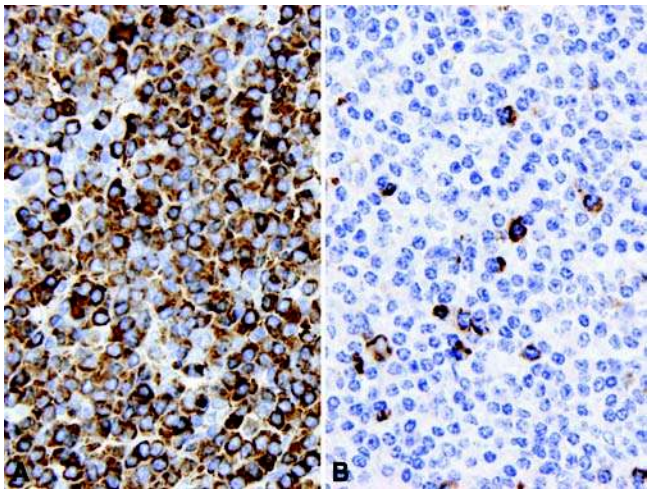

Figure 95 Extramedullary plasmacytoma, immunostained for immunoglobulin. In this example, there is κ light-chain restriction—many κ-positive cells (**A**), and few λ-positive cells (**B**). Note that the λ-positive cells are smaller and represent admixed reactive plasma cells.

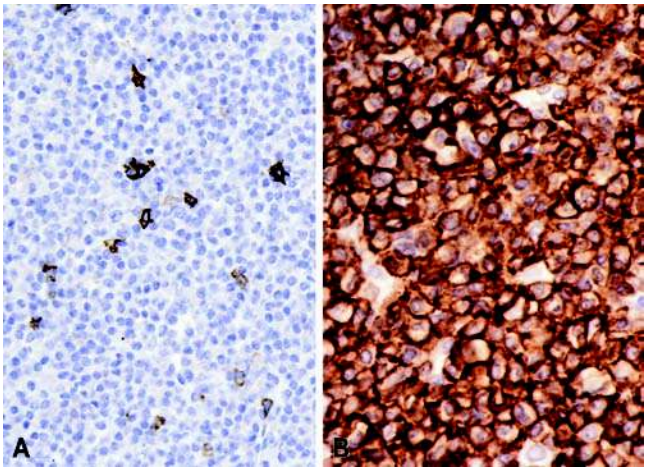

Figure 96 Extramedullary plasmacytoma, immunohistochemistry. (**A**) Negative staining for CD20. (**B**) Positive staining for CD138.

plasmacytoma may represent an extreme form of MALT lymphoma (361), although this concept is not accepted by all (356).

Well-differentiated extramedullary plasmacytoma should be distinguished from reactive conditions with a rich plasma cell component, such as reactive lymphoid hyperplasia (including IgG4-related sclerosing disease), plasma cell–type Castleman disease, Rosai–Dorfman disease, and rhinoscleroma. The plasma cells in these reactive conditions show polytypic immunoglobulin light chains, except for a proportion of cases of plasma cell–type Castleman disease.

Poorly differentiated or anaplastic extramedullary plasmacytoma can mimic large cell lymphoma (such as DLBCL, plasmablastic lymphoma, or anaplastic large cell lymphoma) or nonhematolymphoid malignancies (such as carcinoma, melanoma, germ cell tumor, or sarcoma) (Fig. 92). In contrast to plasmacytoma, DLBCL is commonly CD20+. However, distinction of anaplastic plasmacytoma from plasmablastic lymphoma is still a difficult and contentious issue. The clinical features may need to be considered, e.g., the latter diagnosis is favored if it occurs in the oral cavity of an immunosuppressed host. If a conclusion cannot be reached, a diagnostic label of ''plasmablastic neoplasm, consistent with either anaplastic plasmacytoma or plasmablastic lymphoma'' may have to be given.

Ectopic pituitary adenoma, especially after treatment with bromocriptine, can simulate plasmacytoma cytologically. It can be recognized by the typical fibrovascular septa of neuroendocrine neoplasms, and positive staining for cytokeratin and synaptophysin.

Treatment and prognosis. The treatment of choice is surgery, radiotherapy, or a combination of both. For diseases confined to the upper aerodigestive tract, the outcome is favorable, with recurrence and conversion to multiple myeloma in only 22% and 16%, respectively (356). The median five-year overall survival is 144 to over 300 months; patients receiving combination therapy show better overall survival (356).

Chronic Lymphocytic Leukemia/Small Lymphocytic Lymphoma

Introduction and clinical features. CLL/SLL is an indolent B-cell neoplasm where patients commonly present with incidental marked lymphocytosis. SLL refers to nonleukemic cases where the tissue morphology and immunophenotype are typical of CLL (362). CLL/SLL typically occurs in older subjects. Most patients are incidentally found to have lymphocytosis, lymphadenopathy, or splenomegaly. The lymphadenopathy is often generalized. Bone marrow involvement is common (363). About 40% of patients have B symptoms, which predict a shorter survival. Paraproteinemia is uncommon. The patients are prone to have infection complications, and some may develop autoimmune hemolytic anemia. A small proportion (<5%) of patients develop a supervening DLBCL (Richter syndrome), which may or may not be clonally related to the underlying CLL/SLL. This phenomenon is associated with an aggressive clinical course.

Pathology. In the peripheral blood, the neoplastic cells have the appearance of small lymphocytes, and smudged cells are common. There are also frequently some prolymphocytes, which are slightly larger cells with distinct nucleoli. In involved lymph nodes and extranodal sites, there is a diffuse and dense infiltrate of dark-staining lymphoid cells, which include predominantly small lymphocytes admixed with variable numbers of prolymphocytes (with slightly larger nuclei, more open chromatin, and small distinct central nucleolus) and paraimmunoblasts (medium-sized to large cells with vesicular chromatin and large central nucleolus, and differing from immunoblasts in that the moderate rim of cytoplasm is pale staining rather than amphophilic) (Fig. 97A, B). The most characteristic histologic feature of CLL/SLL, which is found in approximately 80% of cases, is the presence of proliferation centers, which are pale-staining, nonexpansile, rounded to irregular-shaped foci dispersed within the diffuse dark-staining lymphoid infiltrate (Fig. 97A). The proliferation centers represent focal collections of prolymphocytes and paraimmunoblasts.

The neoplastic cells express pan-B markers, but CD20 expression and surface immunoglobulin expression are often weak. These cells characteristically coexpress CD5 and CD23, and cyclin D1 is commonly negative.

Lymphoplasmacytic Lymphoma

Lymphoplasmacytic lymphoma is an indolent B-cell neoplasm showing diffuse proliferation of mature small lymphocytes, plasmacytoid lymphocytes, and plasma cells (364). Intranuclear immunoglobulin inclusions (Dutcher bodies) are characteristic findings. The patients usually have hyperviscosity syndrome due to high serum monoclonal IgM (Waldenström macroglobulinemia). Lymphoplasmacytic lymphoma is a diagnosis by exclusion, i.e., applied only when features of

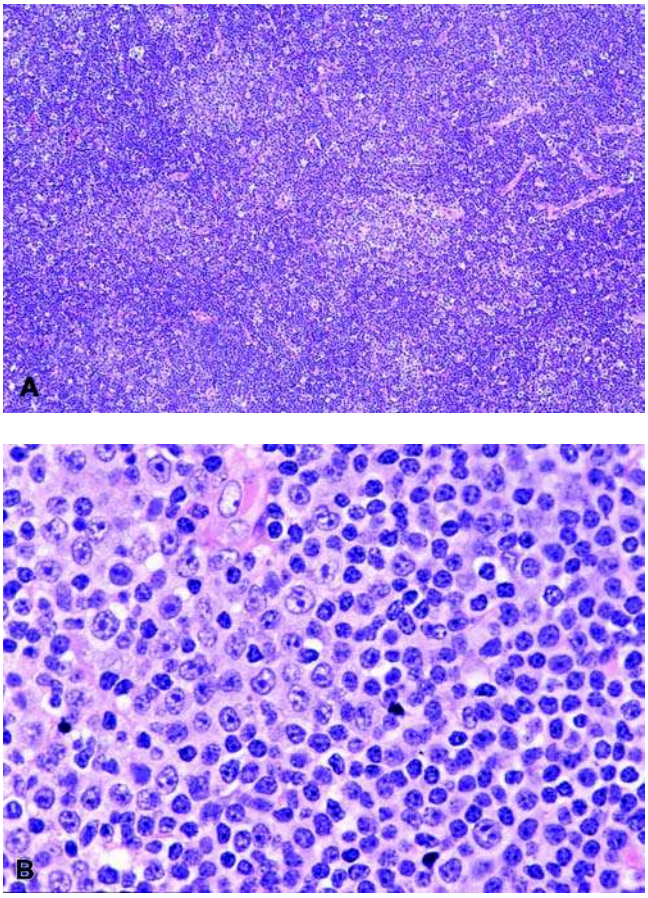

Figure 97 Chronic lymphocytic leukemia/small lymphocytic lymphoma, lymph node. (**A**) There are typically pale-staining proliferation centers within a darkly stained diffuse background. (**B**) The proliferation center (*left field*) comprises predominantly prolymphocytes and paraimmunoblasts, while the background cells (*right field*) are mostly small lymphocytes.

other defined types of lymphoma that may show prominent lymphoplasmacytic differentiation (such as MALT lymphoma and follicular lymphoma) are lacking. Immunophenotypically, the tumor cells express pan-B markers and cytoplasmic immunoglobulin (commonly IgM). Unlike CLL/SLL, they are negative for CD5 and CD23.

Nodal Marginal Zone Lymphoma

Nodal marginal zone lymphoma is a rare, indolent B-cell neoplasm where the lymph nodes are involved by lymphoma cells similar to those seen in MALT lymphoma or splenic marginal zone lymphoma, but without extranodal or splenic disease (365,366). The tumor cells infiltrate the lymph node predominantly in a marginal zone pattern.

B- and T-Lymphoblastic Leukemia/Lymphoma

Introduction and clinical features. Lymphoblastic leukemias/lymphomas are aggressive neoplasms of precursor B or T cells. Cases with predominant leukemic and marrow disease are considered as leukemia (acute lymphoblastic leukemia), while cases with mass lesions (e.g., nodal disease or anterior mediastinal mass) and <25% blasts in the marrow are regarded as lymphoma (367). Those of B-cell phenotype more frequently present as leukemia, while those of T-cell phenotype more often present as lymphoma (e.g., anterior mediastinal mass).

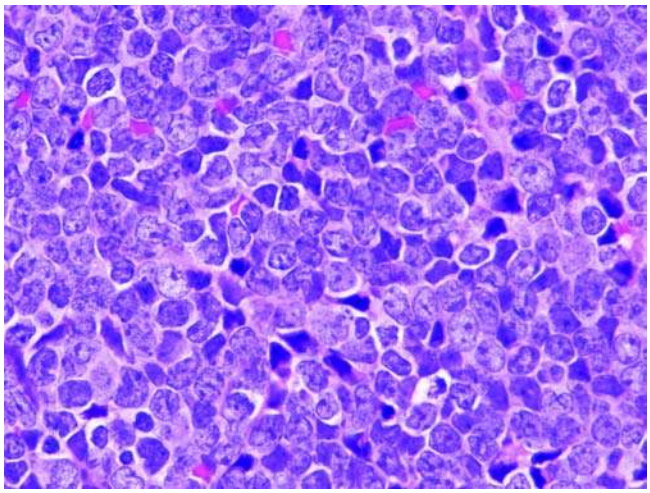

Figure 98 T-lymphoblastic lymphoma, lymph node. Medium-sized cells with round or convoluted nuclei, fine chromatin and scanty cytoplasm.

Lymphoblastic leukemia/lymphoma predominantly occurs in children and young adults. Lymph nodes and various extranodal sites (such as Waldeyer ring) can be involved. The disease is highly aggressive but responds quite well to intensive therapy.

Pathology. Histologically, the lymph node or extranodal tissue shows diffuse infiltration by monotonous medium-sized cells, often with areas exhibiting single-file pattern of infiltration. The lymphoma cells show round or convoluted nuclei, thin nuclear membrane, fine chromatin, indistinct or small nucleoli, and scanty cytoplasm (Fig. 98). Mitotic figures are easy to identify.

The most characteristic immunophenotypic profile is expression of the precursor marker TdT, although rare cases are TdT-negative and require CD99 immunoreactivity to support the precursor nature of the neoplastic cells. Cases of B-cell lineage are often CD20−, and B lineage has to be supported by immunoreactivity for CD19, CD22, CD79a, or PAX-5. For cases of T lineage, there is variable expression of CD2, CD3, CD5, and CD7, with CD7 being most consistently expressed.

Extranodal NK/T-Cell Lymphoma, Nasal-Type

Introduction. Extranodal NK/T-cell lymphoma is a predominantly extranodal lymphoma characterized by vascular damage and destruction, prominent necrosis, cytotoxic immunophenotype, and association

with EBV (368). There is a predilection for the nasal cavity, other parts of the upper aerodigestive tract, and midline facial structures. Most cases of polymorphic reticulosis, malignant midline reticulosis, lethal midline granuloma, and angiocentric immunoproliferative lesion described in the older literature are now classifiable as this lymphoma type.

Clinical features. This lymphoma shows prominent ethnic differences and is more common in Asians and Latin Americans (212,369). There is a very strong etiologic link with EBV (370–372). There is male predominance, with a male-to-female ratio of 3:1, and the median age is 53 years (373). Most patients (80%) have localized disease in the upper aerodigestive tract at presentation (stage IE/IIE) (373,374). Symptoms include nasal obstruction, nasal discharge, epistaxis, facial pain, and facial swelling. Destruction of facial structures is a common finding. Extension to paranasal sinuses, nasopharynx, adjacent bone, and orbit is common (375). Systemic symptoms such as fever, weight loss, and night sweat may be present, and hemophagocytic syndrome with pancytopenia occasionally occurs at presentation, as a terminal event, or at relapse (373). During the course of the disease, the tumor not uncommonly spreads to cervical lymph nodes or other extranodal sites, such as the skin, gastrointestinal tract, liver, and testis.

A proportion of patients present with the disease outside the upper aerodigestive tract. These patients often have high-stage disease, with tumor involving multiple anatomic sites, most commonly the skin, gastrointestinal tract, and testis. Systemic symptoms are not uncommon.

Pathology. The involved mucosa usually shows extensive necrosis and ulceration, with the mucosal glands being separated and destroyed by a diffuse lymphomatous infiltration comprising abnormal lymphoid cells, which can exhibit a range of size from small through medium to large (Figs. 99A, B; 100; and 101). The cell population can be monotonous or mixed. The nuclei often show irregular foldings, but some have round or oval contour. The chromatin is usually granular, but can be vesicular in large cells (Fig. 101). Apoptosis is often a prominent feature even in the absence of necrosis. Cytoplasmic azurophilic granules can be demonstrated by Giemsa stain in touch preparations. In some cases, there is a rich inflammatory component, consisting of small lymphocytes, histiocytes, plasma cells, and eosinophils, masking the lymphoma cells (Fig. 102).

Angiocentricity with angiodestruction is frequently observed, with tumor cells surrounding and infiltrating the vessel walls (Fig. 103). The overlying squamous epithelium may show pseudoepitheliomatous hyperplasia that can mimic well-differentiated squamous cell carcinoma (Fig. 99B).

Immunohistochemistry. The tumor cells most often show an NK-cell immunophenotype, with expression of CD2, cytoplasmic CD3 (CD3ε), and CD56, and lack of expression of surface CD3 (Figs. 104 and 105) (376). These tumors are usually negative for other T-cell markers such as T-cell receptors, CD4, CD5, CD7, and CD8, and they are also negative for other NK-cell markers such as CD16 and CD57 (Fig. 104). CD43 and CD45RO are commonly positive. The lymphoma cells show a cytotoxic phenotype, with expression of TIA1, granzyme B, and perforin (377). FAS (CD95) and FAS ligand (CD95L) expression are frequent, potentially explaining the commonly observed extensive necrosis (378).

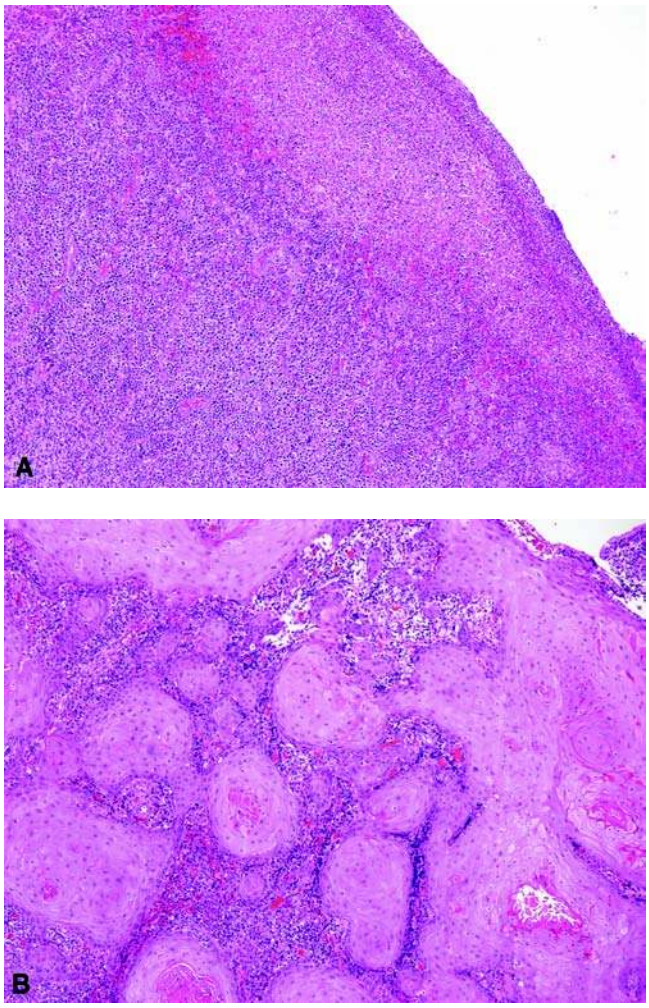

Figure 99 Extranodal NK/T-cell lymphoma of nasal cavity. (**A**) Involved mucosa shows ulceration and necrosis. (**B**) The overlying epithelium can show striking pseudoepitheliomatous hyperplasia, mimicking well-differentiated squamous cell carcinoma.

Some CD56-negative cases with a T-cell immunophenotype have been reported, and they share similar histology, cytotoxic phenotype, and EBV association (379). These cases are still classified as extranodal NK/T-cell lymphoma. However, T-cell lymphomas that lack cytotoxic phenotype and EBV are classified as peripheral T-cell lymphoma NOS.

Molecular genetic data. Cases with NK-cell immunophenotype show germ line T-cell receptors, while the less common cases with T-cell immunophenotype may show rearranged T-cell receptor genes (380). There is consistent association with EBV (370–372), which

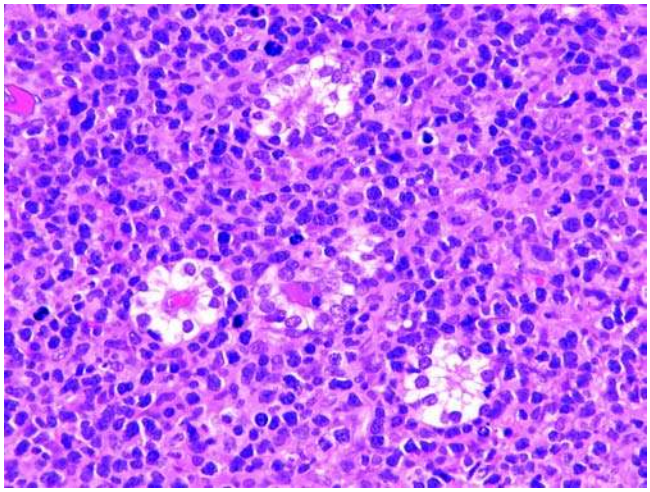

Figure 100 Extranodal NK/T-cell lymphoma of nasal cavity. There is marked interstitial infiltration by lymphoma cells, causing separation and loss of mucosal glands. It is not uncommon for the mucosal glands to undergo clear cell change.

exists in a clonal episomal form (381). The best way to demonstrate EBV is in situ hybridization for EBER, whereby the nuclei of practically all lymphoma cells are labeled (Fig. 106) (371). Immunostaining for EBV latent membrane protein 1 is much less consistent.

Certain cytogenetic abnormalities have been reported, most commonly, isochromosome 1q, isochromosome 6p, partial deletion of 6q, and aberration at 11q (382,383). Comparative genomic hybridization studies and loss of heterozygosity studies have revealed additional findings, and the most frequent abnormalities are del(6)(q21-25), del(17)(p12-p13), del (13)(q14-q34), and gain of 1p32-pter (384–388).

Differential diagnosis. Cases dominated by small cells or accompanied by a heavy inflammatory infiltrate can be difficult to distinguish from benign conditions such as infection, nonspecific reactive lymphoid hyperplasia, and Wegener granulomatosis. Wegener granulomatosis is an immune-mediated disease characterized by serologic positivity for cytoplasmic anti-neutrophilic cytoplasmic antibody, with the antibody directed against proteinase 3 (PR3) (389). The patients present with destructive lesions in the nasal cavity, usually with associated pulmonary and renal abnormalities. Histologic findings include the triad of necrosis, vasculitis, and granulomatosis, although it is unusual to observe all three features in a single biopsy (390). Vasculitis may closely mimic angiocentricity and angiodestruction in extranodal NK/T-cell lymphoma, but the lymphoid cells lack atypia and are negative for CD56 and EBER.

Cases with marked pseudoepitheliomatous hyperplasia may be misdiagnosed as squamous cell carcinoma, if the atypia in the lymphoid cells is overlooked.

For nasal NK/T-cell lymphoma with predominance of large cells, other lymphomas such as DLBCL or even undifferentiated carcinoma may enter into the differential diagnosis, but immunophenotyping should be conclusive. Distinction between peripheral T-cell lymphoma NOS and the CD56-negative nasal NK/T-cell lymphoma is based on the lack of EBER positivity and the absence of cytotoxic phenotype in the former.

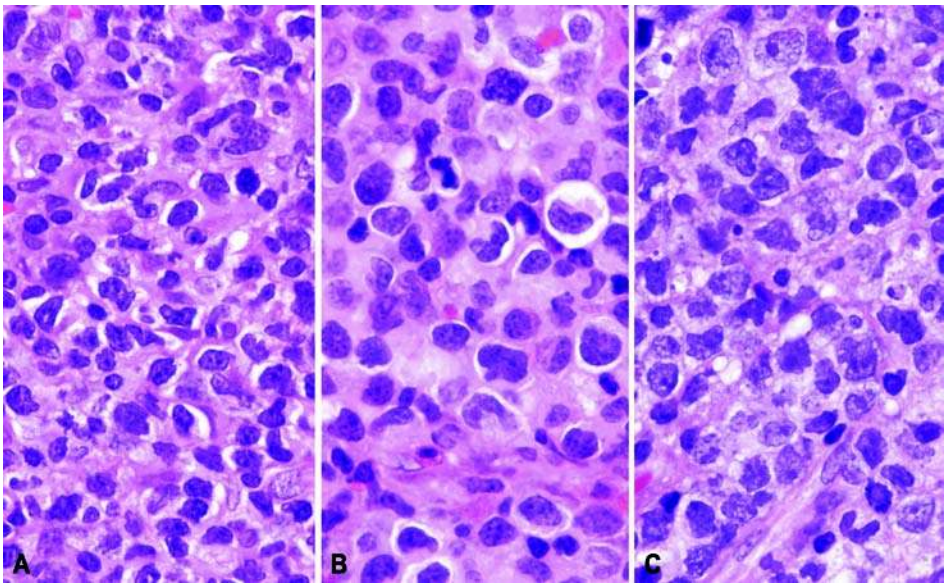

Figure 101 Extranodal NK/T-cell lymphoma of nasal cavity, illustrating the cytologic spectrum. (**A**) Predominantly small to medium-sized cells with irregular nuclear foldings. (**B**) Predominantly medium-sized cells. (**C**) Predominantly large cells. Note presence of admixed apoptotic bodies.

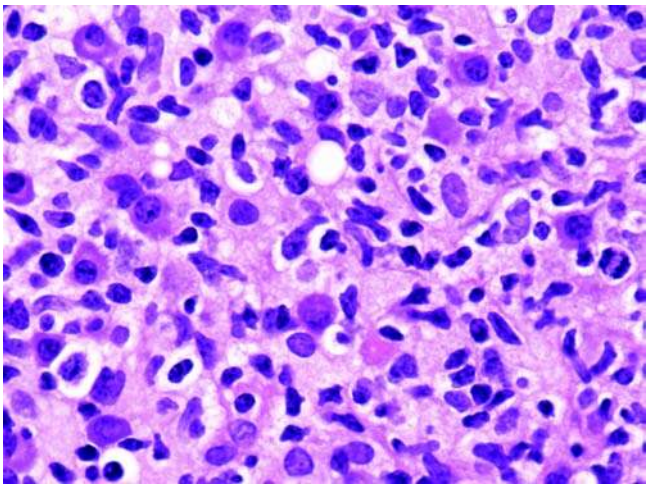

Figure 102 Extranodal NK/T-cell lymphoma of nasal cavity, difficult-to-diagnose case. This case comprises small neoplastic cells with only mild nuclear atypia (compare with the lymphoid cells in the normal nasopharyngeal mucosa in Fig. 12B), and shows many admixed plasma cells.

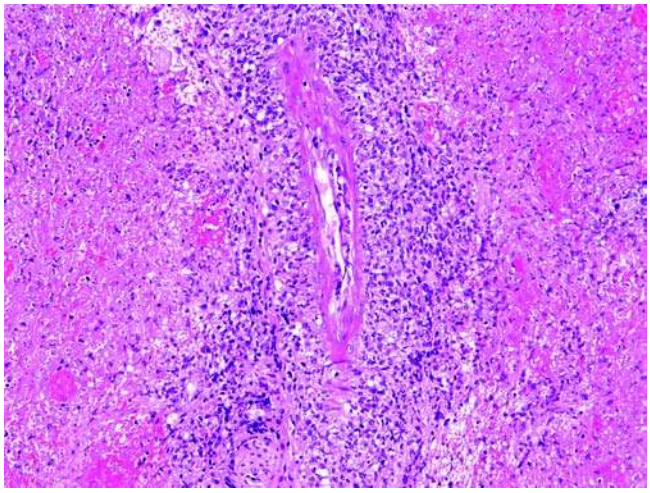

Figure 103 Extranodal NK/T-cell lymphoma of nasal cavity, with angioinvasion and prominent necrosis.

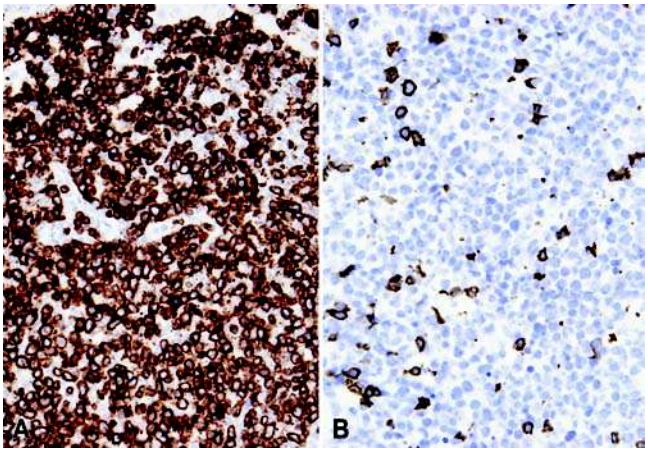

Figure 104 Extranodal NK/T-cell lymphoma of nasal cavity, immunohistochemistry. (**A**) Positive staining for CD3ε. (**B**) Negative staining for CD5.

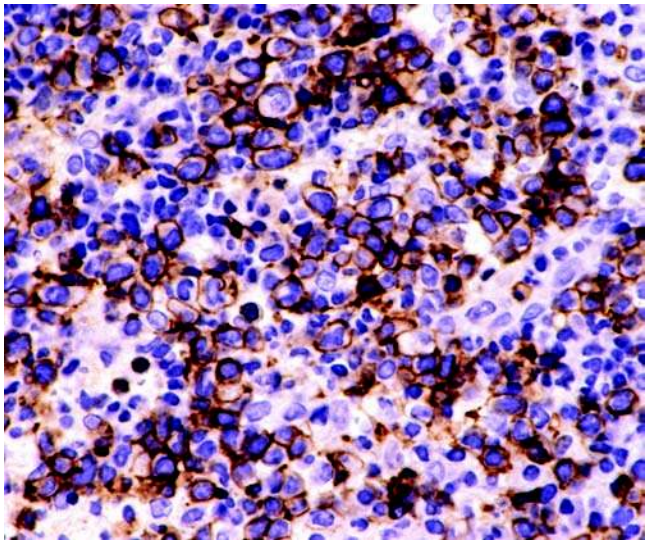

Figure 105 Extranodal NK/T-cell lymphoma of nasal cavity, showing positive immunostaining for CD56.

Other CD56+ tumors may also enter into the differential diagnoses, such as lymphoblastic lymphoma of NK lineage, myeloid sarcoma, plasmacytoma, olfactory neuroblastoma, Ewing sarcoma/primitive neuroepithelial tumor, and rhabdomyosarcoma.

Treatment and prognosis. Upfront radiation therapy and/or multiagent chemotherapy is the treatment of choice for localized disease in the upper aerodigestive tract (373,387,391,392). The overall survival ranges from 30% to 50% (373,387,392–394). In patients achieving complete remission, local relapse occurs in one-third to one half of cases, with frequent systemic failure (392,395). Factors associated with a worse outcome include regional lymph node involvement, advanced stage, poor performance status, B symptoms, bulky disease, local tumor invasion (invasion into bone or skin), high lactate dehydrogenase level, and high International Prognostic Index score (387,391,393,396). There is no conclusive evidence that histologic grading has prognostic significance.

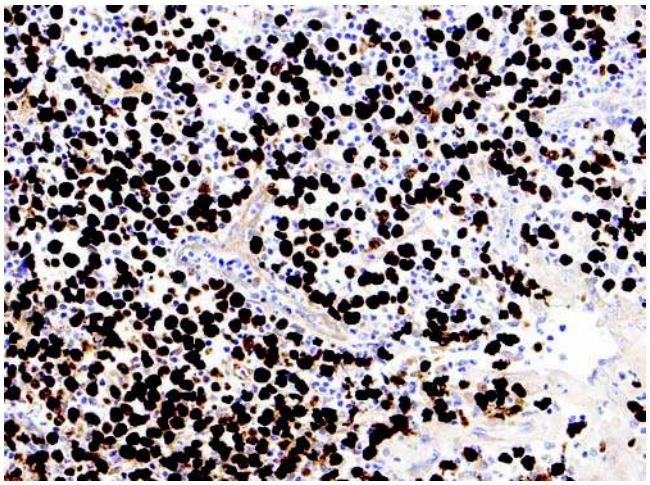

Figure 106 Extranodal NK/T-cell lymphoma of nasal cavity, showing positive labeling of practically all tumor cells on in situ hybridization for EBER.

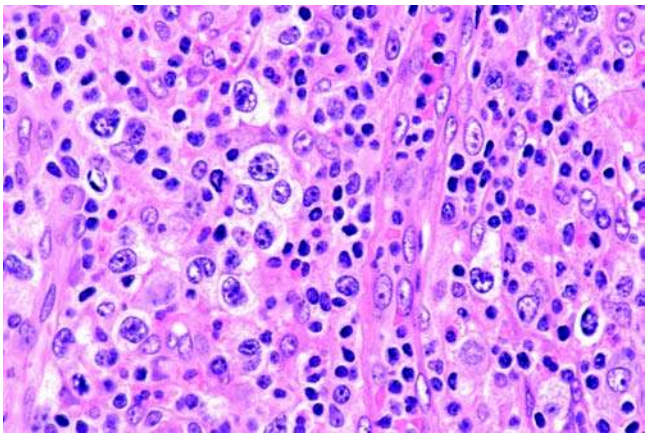

Figure 107 Angioimmunoblastic T-cell lymphoma, lymph node. Typical appearance, with prominent venules, mixture of lymphoid cells usually with round nuclei, clear cells, and admixed eosinophils.

Patients with extranodal NK/T-cell lymphoma of extranasal sites have an even worse prognosis, which may be related to the high-stage disease. Not uncommonly, the lymphoma shows chemotherapy resistance.

Angioimmunoblastic T-Cell Lymphoma

Clinical features. Angioimmunoblastic T-cell lymphoma is a mature T-cell lymphoma of follicular T-helper cells, often presenting with high-stage disease. It usually occurs in the elderly, with slight male predominance. The patients frequently present with generalized lymphadenopathy, hepatosplenomegaly, fever, constitutional symptoms, skin rash, and effusions (397). Polyclonal gammopathy, autoimmune hemolytic anemia, and circulating immune complexes and autoantibodies are common. The patients apparently have impaired-immune functions and are prone to various infections, including opportunistic infections.

The clinical course is variable, ranging from indolent to highly aggressive with resistance to treatment. However, the overall behavior is aggressive. At least half of the deaths are due to complications of infection.

Pathology. The affected lymph node architecture is diffusely effaced, but the subcapsular sinuses are often patent. There are prominent arborizing high endothelial venules. Atypical medium-sized and large lymphoid cells, often with round nuclei and clear cytoplasm, are found among abundant reactive cells such as small lymphocytes, eosinophils, histiocytes, and plasma cells (Fig. 107). There can even be coalescing small clusters of epithelioid histiocytes (Lennert pattern). Some EBV-infected large B cells are frequently present in addition to the neoplastic T cells, and these B cells may be oligoclonal or even monoclonal. In addition to the classical diffuse growth pattern, angioimmunoblastic T-cell lymphoma can uncommonly exhibit the following patterns: (*i*) presence of hyperplastic lymphoid follicles, (*ii*) follicular growth pattern, and (*iii*) perifollicular growth pattern.

Immunohistochemical staining shows that the neoplastic T cells express pan-T markers, CD10, BCL6, CXCL13, and PD-1 (398,399). There is florid proliferation of follicular dendritic cells outside follicles and often surrounding venules, as demonstrated by markers such as CD21 and CD35.

Peripheral T-Cell Lymphoma, Not Otherwise Specified

Clinical features. Peripheral T-cell lymphoma NOS is a ''waste-basket'' category for cases of mature T-cell lymphomas that do not fit the other defined entities (400). It occurs predominantly in older adults, who usually present with systemic disease, in the form of lymphadenopathy (often generalized) and/or extranodal disease. Skin, lung, pleura, liver, spleen, and bone marrow are commonly involved. Constitutional symptoms are common. Peripheral T-cell lymphoma NOS is generally an aggressive; high-stage disease, and high International Prognostic Index is associated with an even worse prognosis.

Pathology. Histologically, there is diffuse infiltration by atypical lymphoid cells of variable sizes, frequently intermixed with reactive inflammatory cells such as histiocytes, eosinophils, and plasma cells (Fig. 108A). Commonly, the lymphoma cells exhibit a continuous spectrum of sizes, although some cases are composed of a monomorphic cellular composition. The nuclei almost always show marked irregular foldings (Fig. 108B, C). Prominent networks of high endothelial venules may be present. Cases with interfollicular growth pattern has been described as T-zone variant, while cases with coalescing small clusters of epithelioid histiocytes have been termed lymphoepithelioid cell

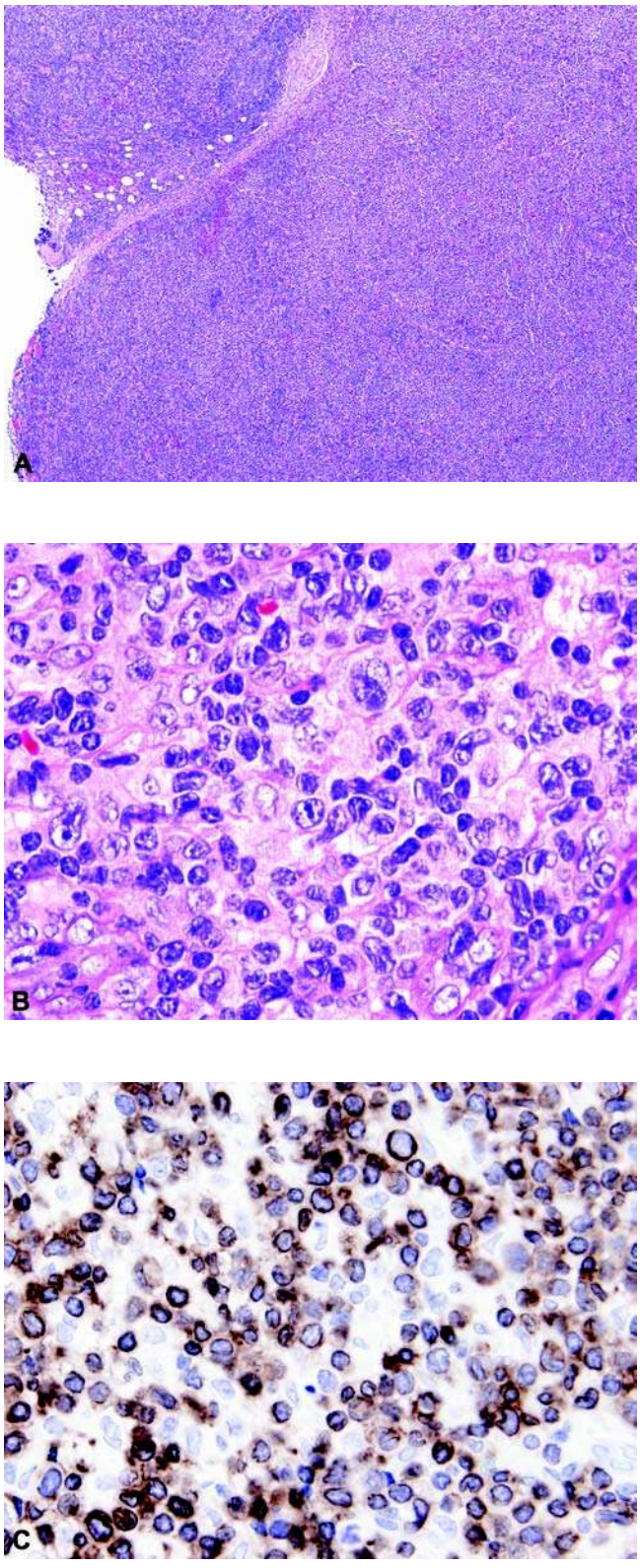

Figure 108 Peripheral T-cell lymphoma, NOS, lymph node. (**A**) Diffuse effacement of nodal architecture. (**B**) Continuous spectrum of small, medium-sized, and large cells, often with irregular nuclear foldings. (**C**) The neoplastic cells show immunoreactivity for CD3ε.

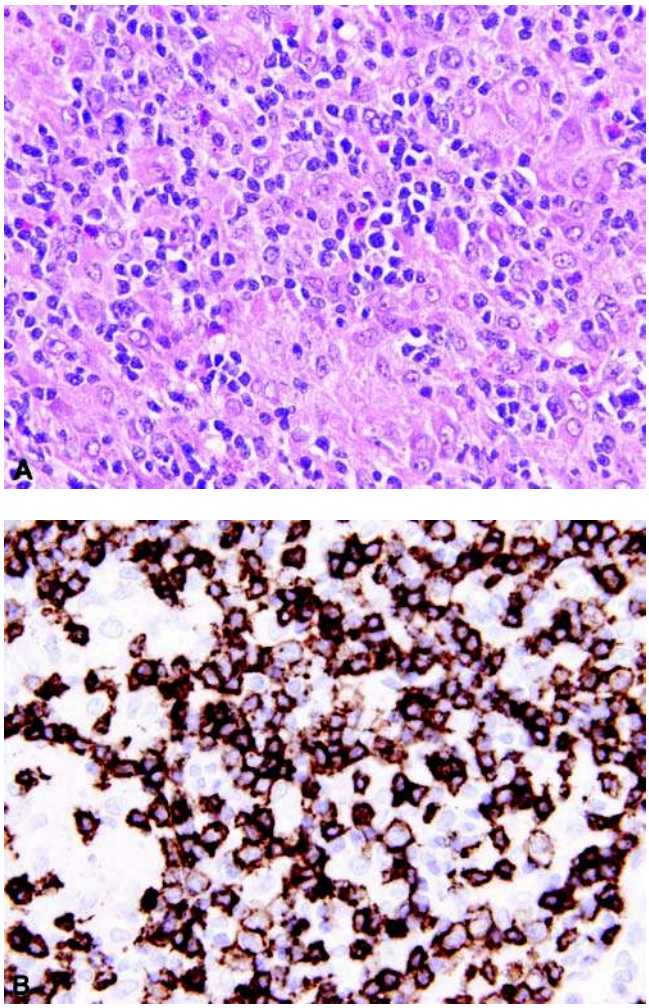

Figure 109 Peripheral T-cell lymphoma, NOS, lymphoepithelioid variant. (**A**) There are admixed small aggregates of epithelioid histiocytes. (**B**) This variant is usually CD8-positive.

variant (or Lennert lymphoma) (Fig. 109A, B). A signet ring cell variant is also recognized.

The tumor cells express pan-T markers (Fig. 108C) and commonly exhibit an aberrant immunophenotype such as loss of certain pan-T antigens. They show rearrangements of T-cell receptor genes.

Anaplastic Large Cell Lymphoma, ALK+

Introduction. ALK+ anaplastic large cell lymphoma is a lymphoma of T- or null-cell lineage with CD30 and ALK expression, characterized by large cells with voluminous cytoplasm, although variants composed of smaller cells are also recognized (Fig. 110A, B) (401). It has to be distinguished from ALK− anaplastic large cell lymphoma (which has a worse prognosis) and primary cutaneous anaplastic large cell lymphoma (which has localized disease that sometimes regresses spontaneously).

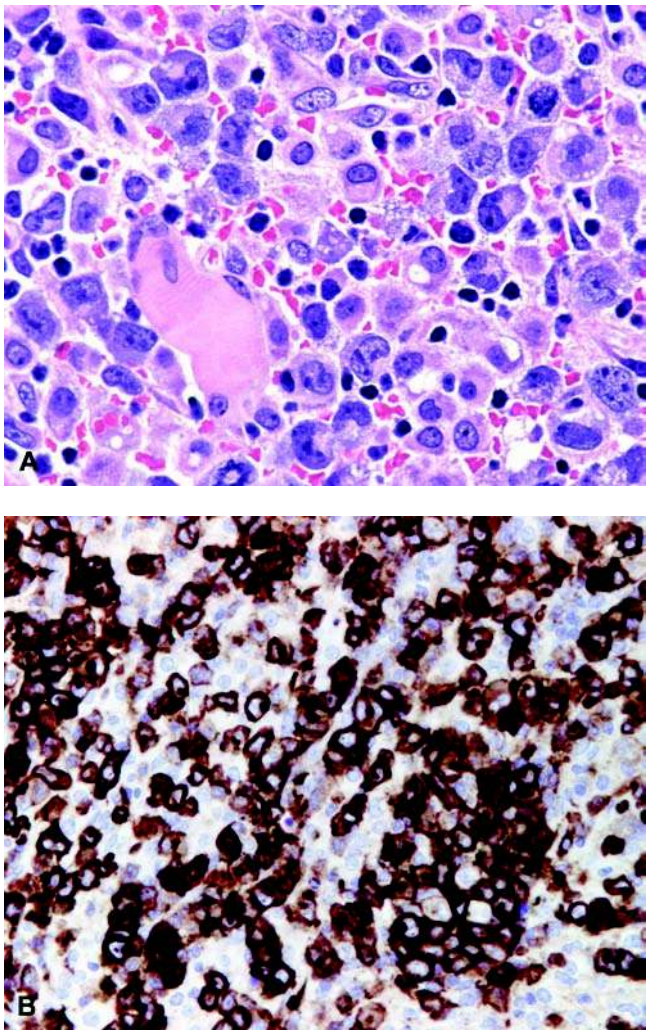

Figure 110 ALK+ anaplastic large cell lymphoma, soft tissue. (**A**) Many hallmark cells with embryo-like nuclei are present. A residual skeletal muscle fiber is seen in the left field. (**B**) Strong positive immunostaining for CD30.

Clinical features. ALK+ anaplastic large cell lymphoma occurs predominantly in young patients, with a median age of 17 to 22 years and male predominance. The clinical presentation is highly variable. Besides lymphadenopathy, presentation in extranodal sites, such as skin, bone, and soft tissue, is not uncommon, usually as part of systemic disease. Systemic symptoms are not uncommon (402). Some patients present with diffuse involvement of the lymphoreticular system with or without hemophagocytic syndrome, simulating malignant histiocytosis.

The tumor is aggressive, but complete remission can often be achieved with multiagent chemotherapy, resulting in a favorable outcome. The overall five-year survival is approximately 80% (402,403). The International Prognostic Index can further stratify patients into different prognostic groups (402).

Pathology. In extranodal sites, the lymphomatous infiltrate is usually diffuse. In lymph nodes, the pattern of infiltration is variable, ranging from subtle interfollicular involvement to predominantly sinusoidal infiltration to diffuse architectural effacement. The lymphoma cells (so-called hallmark cells) are dispersed singly or form clusters and sheets, sometimes with a deceptively cohesive appearance mimicking carcinoma. They are large cells with eccentrically placed, embryo–like or reniform nuclei, multiple small distinct nucleoli, prominent Golgi zone, and abundant amphophilic cytoplasm (Fig. 110A). There can be a variable inflammatory background, which may include small lymphocytes, plasma cells, histiocytes, eosinophils, and neutrophils.

Many morphologic variants are recognized. The *common type is* rich in hallmark cells. There are commonly multinucleated tumor cells with wreath-like nuclei. The *monomorphic variant* comprises medium-sized to large cells that appear monotonous because of uniformity of cell size and shape; some hallmark cells are usually present. The *lymphohistiocytic variant* is characterized by a loose scattering of medium-sized to large immunoblast-like neoplastic cells in a background of small lymphocytes and peculiar histiocytes. The histiocytes are ovoid, with eccentrically placed round nuclei and abundant eosinophilic cytoplasm, with some resemblance to plasma cells. The *small cell variant* is predominated by small lymphoid cells with irregularly folded nuclei and sometimes clear cytoplasm (Fig. 111A). Occasional large cells are often admixed, and they tend to be concentrated around blood vessels. The *mixed cell variant* is similar to the small cell variant except that there are more medium-sized and large cells. The *hypocellular variant* shows a remarkably hypocellular appearance due to the presence of edematous or fibromyxoid stroma (404). The neoplastic cells are mostly small to medium sized, mixed with some large cells (Fig. 111B). Some can appear spindly. The *giant cell variant* is characterized by pleomorphic large bizarre cells and multinucleated tumor cells. The *sarcomatoid variant* comprises plump spindly tumor cells with a storiform growth pattern or a myxoid pattern (Fig. 111C).

Immunohistochemistry. T-lineage markers can be difficult to demonstrate in ALK+ anaplastic large cell lymphoma. CD3 is not always positive, and application of multiple T-cell markers may be required to confirm the T lineage. The most useful ones are CD2, CD4, LAT, CD45RO, and CD43. If all these are negative, the case has to be considered to be of null-cell type. B-lineage markers (including CD20 and PAX5) are negative.

CD30 is expressed in all or most of the neoplastic cells, except the small cell, mixed-cell, and hypocellular variants, in which the small cells are often negative (Figs. 110B and 112). EMA is commonly positive. By definition, ALK is positive, although staining can be negative in the small neoplastic cells, similar to CD30. In most cases, ALK staining is seen in the nuclei and cytoplasm, and this is correlated with the presence of *NPM/ALK* fusion (Fig. 113). In about 15% of cases, the staining is in the cytoplasm or cell membrane only,

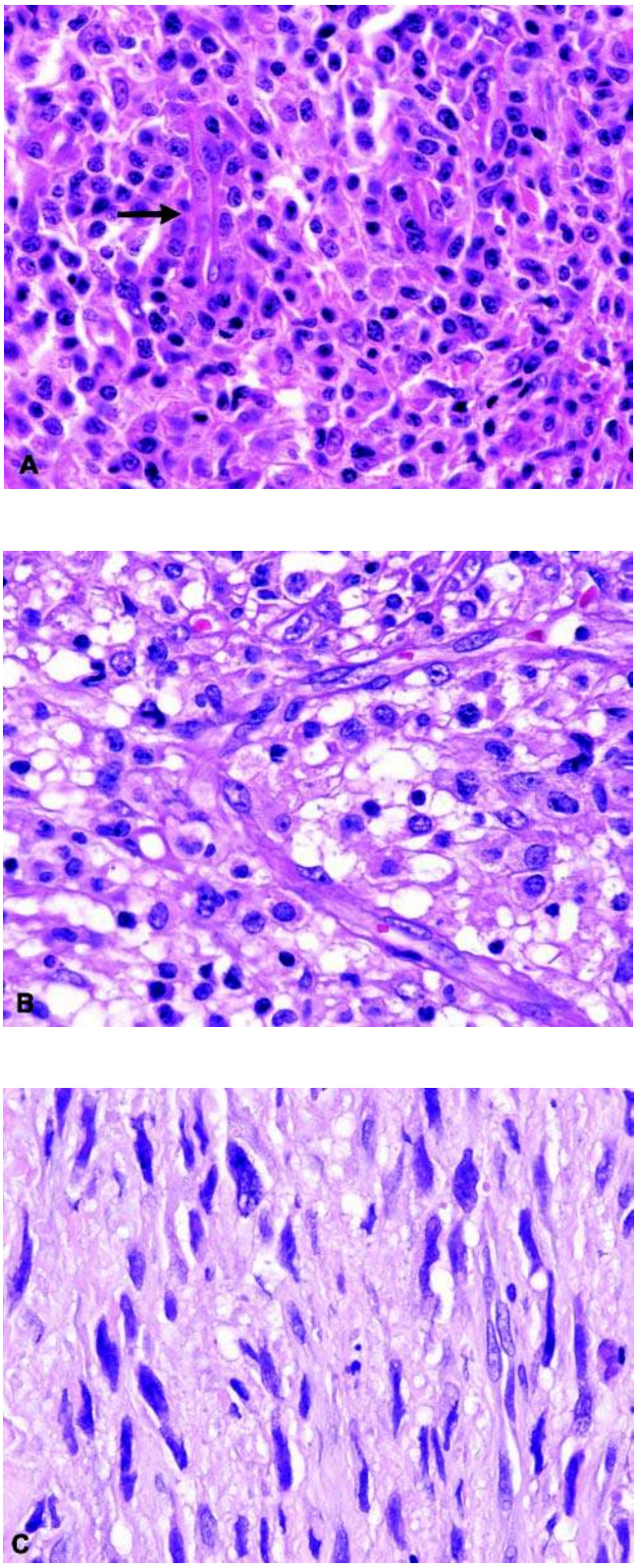

Figure 111 ALK+ anaplastic large cell lymphoma. (**A**) Small cell variant. There is a tendency for the larger cells to aggregate around blood vessels (*arrow*). (**B**) Hypocellular variant. (**C**) Sarcomatoid variant.

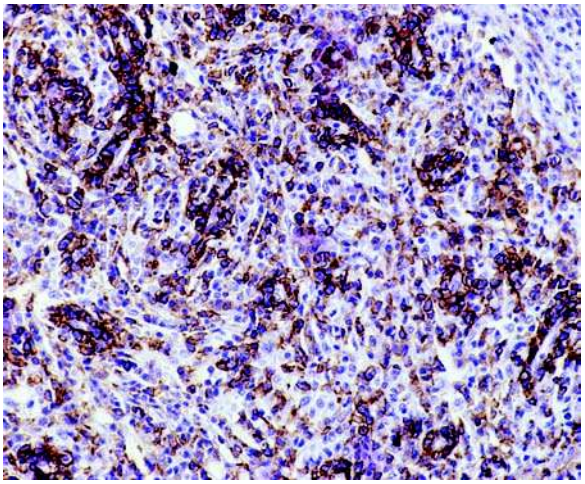

Figure 112 ALK+ anaplastic large cell lymphoma, with positive immunostaining for CD30. Note the cuffing of neoplastic cells around blood vessels, a highly distinctive feature of ALK+ anaplastic large cell lymphoma.

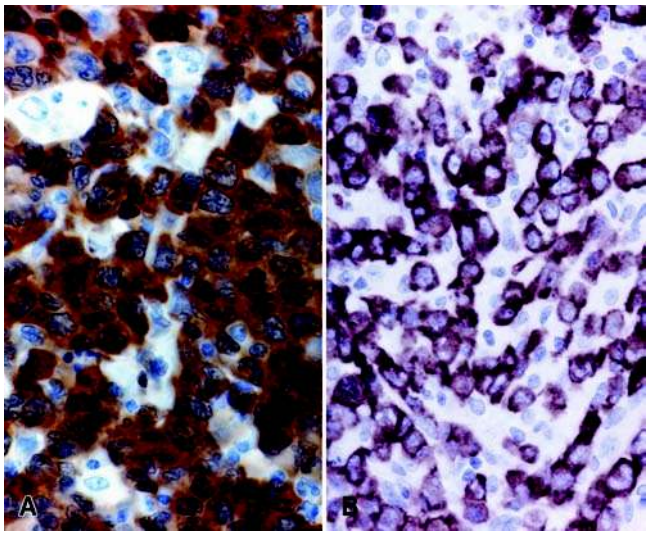

Figure 113 ALK+ anaplastic large cell lymphoma, showing positive immunostaining for AKL. (**A**) Most cases show staining of both nuclei and cytoplasm. (**B**) Some cases show cytoplasmic staining alone.

and this is correlated with *ALK* fusion with a partner gene other than *NPM* (Fig. 113).

Cytotoxic markers clusterin, HLA-DR, and CD25 are commonly positive. Some cases express CD56, which is associated with a worse prognosis.

Molecular genetic data. The T-cell receptor genes are usually clonally rearranged (including the null-cell cases). Most cases show a characteristic genetic

alteration of t(2;5)(p23;q35), which juxtaposes *NPM* (nucleophosmin) gene on 5q35 with *ALK* (anaplastic lymphoma kinase) gene on 2p23. This results in production of a chimeric protein, with the ALK domain being constitutively activated. Other cases show a variant translocation resulting in fusion of *ALK* gene with a housekeeping gene, such as *TPM3* (tropomyosin-III), *TPM4* (tropomyosin-IV), *TFG* (*TRK*-fused gene), *ATIC*, *CLTL* (clathrin), *MSN* (moesin), *CARS*, and *MYH9*. The pattern of ALK immunostaining in these cases depends on the normal distribution of the protein encoded by the partner gene, e.g., cytoplasmic staining with subplasmalemmal accentuation for tropomyosin, cell membrane staining for moesin, and cytoplasmic granular staining for clathrin. Cases showing variant translocation have a prognosis no different from cases exhibiting *NPM/ALK* fusion (405).

Differential diagnosis. Diagnosis of the common type of ALK+ anaplastic large cell lymphoma is usually straightforward, although cases with subtle involvement may be missed as reactive lymphadenopathy. Some cases with cohesive growth pattern can be potentially mistaken for carcinoma.

The small cell, lymphohistiocytic, and hypocellular variants pose significant problems in recognizing their lymphomatous nature, because the neoplastic cells lack significant atypia and are often overshadowed by reactive cellular infiltrate or granulation tissue-like stroma. The following clues should raise a strong suspicion of the diagnosis: (*i*) any unusual-looking, apparently reactive-looking lymph node in children and young adults; (*ii*) presence of cuffs of larger lymphoid cells around blood vessels; or (*iii*) presence of granulation tissue-like fibromyxoid stroma in lymph node, with a rather hypocellular appearance, which is in fact very characteristic of ALK+ anaplastic large cell lymphoma when present.

Anaplastic Large Cell Lymphoma, ALK–

Introduction and clinical features. ALK− anaplastic large cell lymphoma is a primary mature T-cell neoplasm comprising large neoplastic cells with uniform strong expression of CD30, while ALK is negative (406). This term should not be applied for the following situations: (*i*) CD30+ large cell lymphomas that complicate other lymphoma types, such as mycosis fungoides; (*ii*) lymphomas comprising anaplastic large cells but showing clinicopathologic features of other distinctive lymphoma types, such as enteropathy-associated T-cell lymphoma and adult T-cell leukemia/lymphoma; (*iii*) primary cutaneous anaplastic large cell lymphoma; and (*iv*) CD30+ large B-cell lymphoma with anaplastic morphology. There is overlap with examples of peripheral T-cell lymphoma NOS with many CD30+ large cells. The prognosis of ALK− anaplastic large cell lymphoma is similar to or slightly better than that of peripheral T-cell lymphoma NOS (407,408).

This is a disease predominantly of adults with no sex predilection, who present with lymphadenopathy or sometimes extranodal disease. About half of the patients have high-stage disease at presentation (402).

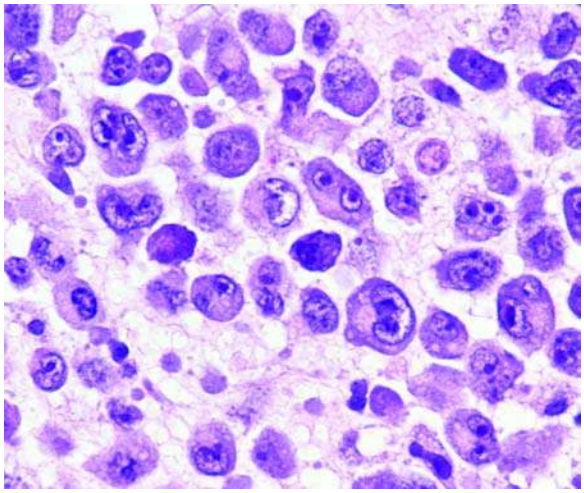

Figure 114 ALK− anaplastic large cell lymphoma. This is morphologically indistinguishable from ALK+ anaplastic large cell lymphoma.

The prognosis is poor, with a five-year failure-free survival of 36% (402,408).

Pathology. The morphologic features are essentially no different from ALK+ anaplastic large cell lymphoma, except that there is no ALK-negative counterpart for the small cell, mixed-cell, lymphohistiocytic, and hypocellular variants (Fig. 114). The neoplastic cells show variable expression of pan-T markers, and a case is considered of null-cell type when all are negative. By definition, there is extensive strong staining for CD30, while ALK is negative. Cytotoxic markers are often positive.

Differential diagnosis. The main differential diagnoses include other large cell lymphomas (including DLBCL of anaplastic type), carcinoma, melanoma, and classical Hodgkin lymphoma. The distinction between ALK− anaplastic large cell lymphoma of null-cell type and tumor cell–rich classical Hodgkin lymphoma can be difficult, because both the entities are characterized by abundant large neoplastic cells with CD30 expression while they lack expression of conventional B (CD20, CD79a) and T (CD2, CD3, CD4, CD8) markers. The latter entity tends to show more frequent coagulative necrosis and eosinophil infiltration, and a diagnosis can be confirmed by positive staining for the B-cell cell transcription factor PAX-5 in the large cells.

Primary Cutaneous CD30+ T-Cell Lymphoproliferative Disorders

Introduction. The spectrum of primary cutaneous CD30+ T-cell lymphoproliferative disorders includes a number of entities with overlapping clinicopathologic features: lymphomatoid papulosis, borderline lesions, and primary cutaneous anaplastic large cell lymphoma. The patients usually present with chronic recurrent skin lesions, which show a tendency to undergo spontaneous regression, with

rates of 100%, 79%, and 24% for the three categories, respectively. Progression to systemic lymphoma occurs in a small proportion of cases (318,409).

These entities share the same immunophenotype: CD30+, pan-T markers+/−, EMA−/+, and cutaneous lymphocyte antigen (HECA-452)+/−. ALK expression is practically always absent.

Lymphomatoid papulosis. The patients are usually young or middle-aged adults, who usually present with crops of papules that regress within three to six weeks. The prognosis is excellent, with five-year disease-specific survival of 100%. However, lymphomas may eventually develop in 5% to 20% of patients (mycosis fungoides, cutaneous anaplastic large cell lymphoma, or Hodgkin lymphoma) (410). Histologically, there is usually a wedge-shaped dermal infiltrate without subcutaneous involvement. Anaplastic large lymphoid cells are typically admixed with numerous small lymphocytes, eosinophils, and neutrophils. Rare lesions are predominated by cells with cerebriform nuclei, and inflammatory cells tend to be sparse in such cases.

Primary cutaneous anaplastic large cell lymphoma. The patients are often in the sixth decade. They usually present with a solitary skin nodule, with or without ulceration. The limbs, head, and buttocks are the most commonly affected sites. The five-year overall survival is 90%, but there is a tendency to relapse (408). Histologically, there are sheets of anaplastic or nonanaplastic large cells, with a variable inflammatory background (Fig. 115A–C). The dermal infiltrate is often diffuse and destructive, and the subcutis may also be involved. There can be epidermal invasion. Rare cases express cytoplasmic ALK protein, which is phosphorylated (activated), in the absence of *ALK* gene translocation (411).

Borderline lesions. These are lesions in which there is a discrepancy between clinical features and histologic features, i.e., difficult to classify either as ''lymphomatoid papulosis'' or ''primary cutaneous anaplastic large cell lymphoma'' (410).

Variant: primary oral CD30+ T-cell lymphoproliferative disorders. There is an oral counterpart of primary cutaneous CD30+ T-cell lymphoproliferative disorders (412,413). The sites of involvement are the gum, buccal mucosa, palate, and tongue. Such lesions tend to regress spontaneously, but recurrences in the oral cavity can occur. The pathologic findings are similar to the cutaneous counterpart, with surface ulceration and infiltration by variable numbers of anaplastic large cells or large lymphoid cells, admixed with many small lymphocytes and eosinophils (Fig. 116A, B).

Mycosis Fungoides

Introduction and clinical features. Mycosis fungoides is an epidermotropic, indolent, mature T-cell lymphoma that presents initially in the skin, with stepwise progression from patches to plaques and tumors. It is the commonest type of primary cutaneous lymphoma (414), affecting adults mostly in the fifth to sixth decades. The skin lesions can occur in any part of the body and are often multiple and extensive.

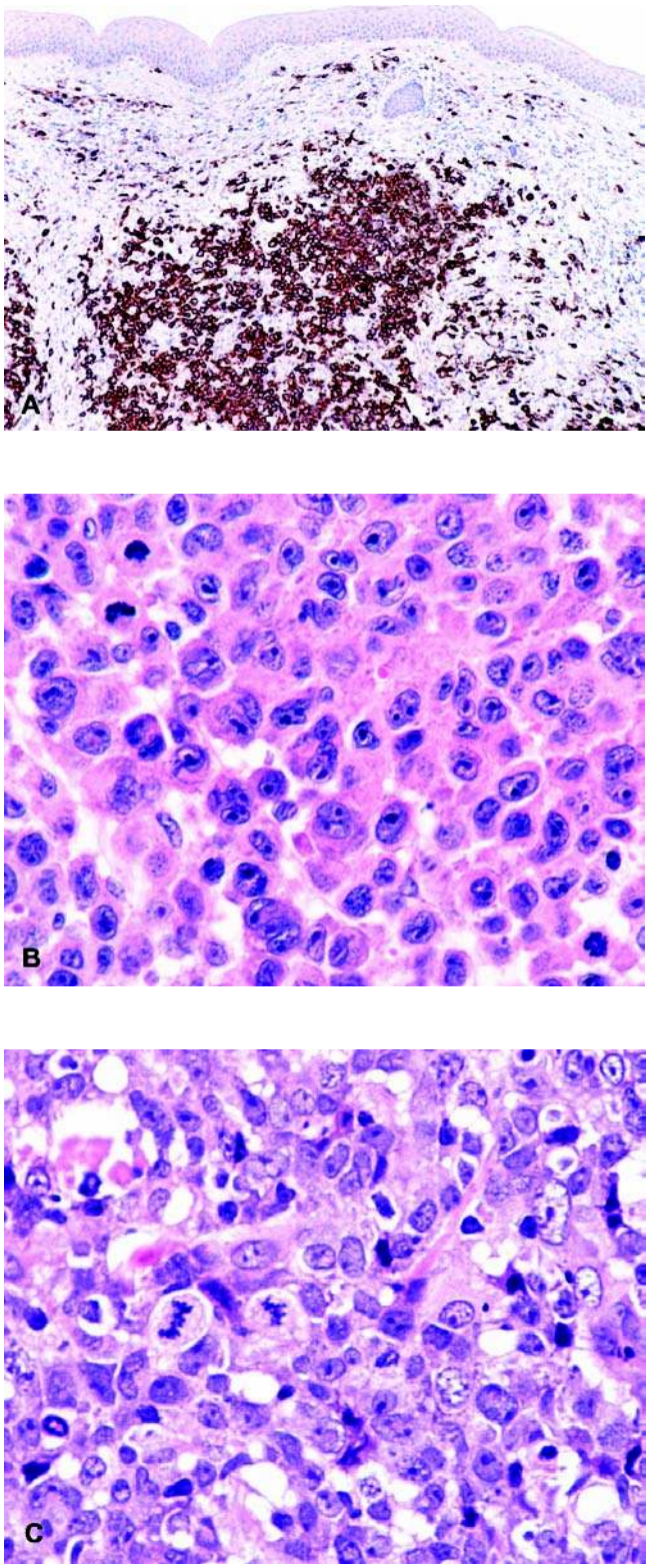

Figure 115 Primary cutaneous anaplastic large cell lymphoma. (**A**) CD30 immunostaining highlights the dense neoplastic infiltrate in the dermis. (**B**) Most cases have an anaplastic cytologic appearance. (**C**) Some cases have a nonanaplastic appearance, resembling peripheral T-cell lymphoma NOS or diffuse large B-cell lymphoma.

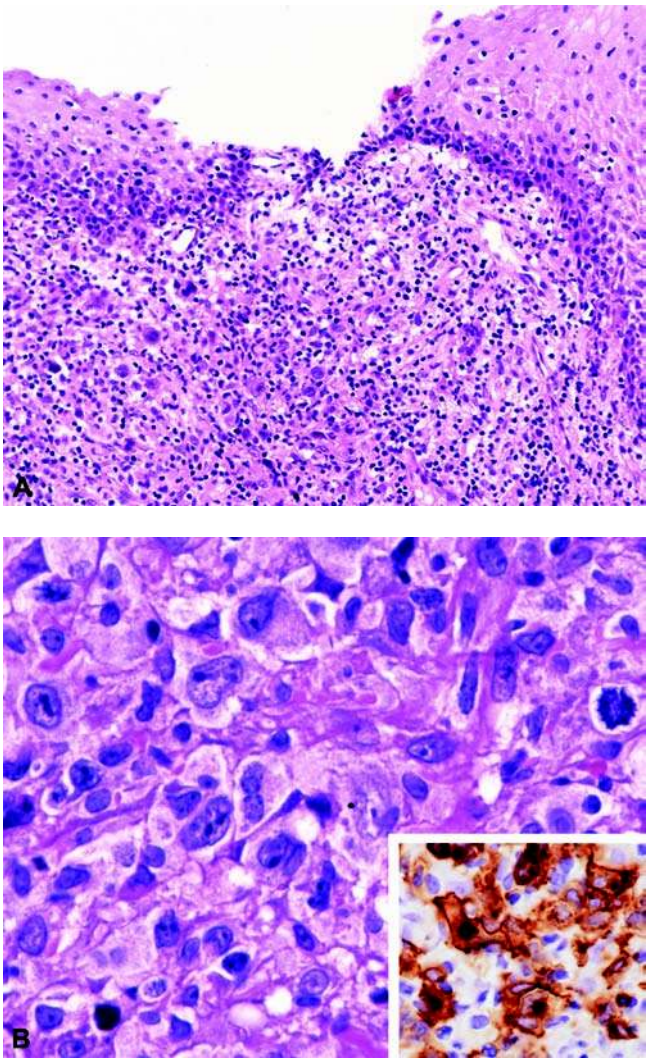

Figure 116 Primary oral CD30+ T-cell lymphoproliferative disorder, tongue. (**A**) The mucosa shows infiltration of large cells. (**B**) The large cells exhibit the cytologic features of anaplastic large cell lymphoma. Positive CD30 immunostaining is shown in the inset.

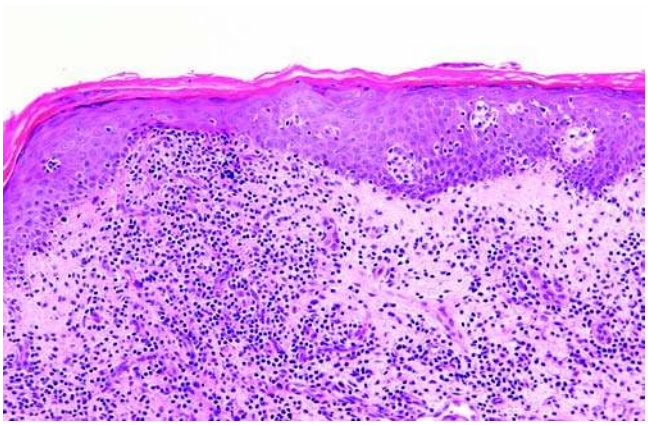

Figure 117 Mycosis fungoides, skin. Small lymphoid cells are seen in the dermis and epidermis. In the epidermis, the lymphoid cells are aligned within the basal layer of the epidermis and accompanied by haloes.

Diseases localized to the skin can be treated by local therapy such as photo(chemo)therapy, topical chemical therapy, or radiotherapy (318). Multiagent chemotherapy is often necessary for cases with lymph node or systemic spread. The outcome depends on the stage and extent of the skin lesions, and the presence of extracutaneous disease. The overall five-year disease-specific survival is 88% (318).

Pathology. The histologic hallmark of mycosis fungoides is the cerebriform small cell with marked nuclear convolutions and epidermotropism. Intraepidermal Pautrier microabscesses are diagnostic but are not always present, especially in the early phases. Characteristic histologic features of the stage are disproportionate epidermotropism, cerebriform cells in epidermis being larger than dermal lymphoid cells, lymphocytes aligned within basal layer of epidermis with no or minimal spongiosis, and haloed lymphocytes within epidermis (Fig. 117). In the plaque stage, there is a band-like subepidermal infiltrate of atypical lymphoid cells, accompanied by epidermal infiltration (Fig. 118A, B). In the tumor stage, there is more extensive dermal infiltration, often with increased proportion of medium-sized and occasionally large cells. Epidermotropism may be lost. Transformation to a large T-cell lymphoma can occur, and is defined by presence of >25% large cells; these cells may be CD30+.

Spread to regional lymph nodes or other organs can occur during tumor progression. Nodal involvement has to be documented by histologic examination, since lymph node enlargement may be due to dermatopathic lymphadenopathy instead.

The lymphoma cells express pan-T markers such as CD3, and they are frequently CD4+ CD8−. Aberrant loss of T-cell markers such as CD2, CD5, or CD7 may occur, assisting the distinction of mycosis fungoides from reactive T-cell infiltrate. The T-cell receptor genes are clonally rearranged.

Sézary Syndrome

Sézary syndrome is a rare variant of cutaneous T-cell lymphoma characterized by generalized erythroderma, lymphadenopathy, and presence of clonal Sézary cells in the peripheral blood. Patients are often over 60 years old, and the disease has a poor prognosis with a median survival of only two to four years (415).

The Sézary cells show marked nuclear convolutions similar to the cells seen in mycosis fungoides. Skin biopsy can show histology similar to that of mycosis fungoides, but can also be nondiagnostic since the number of neoplastic cells can be scanty,

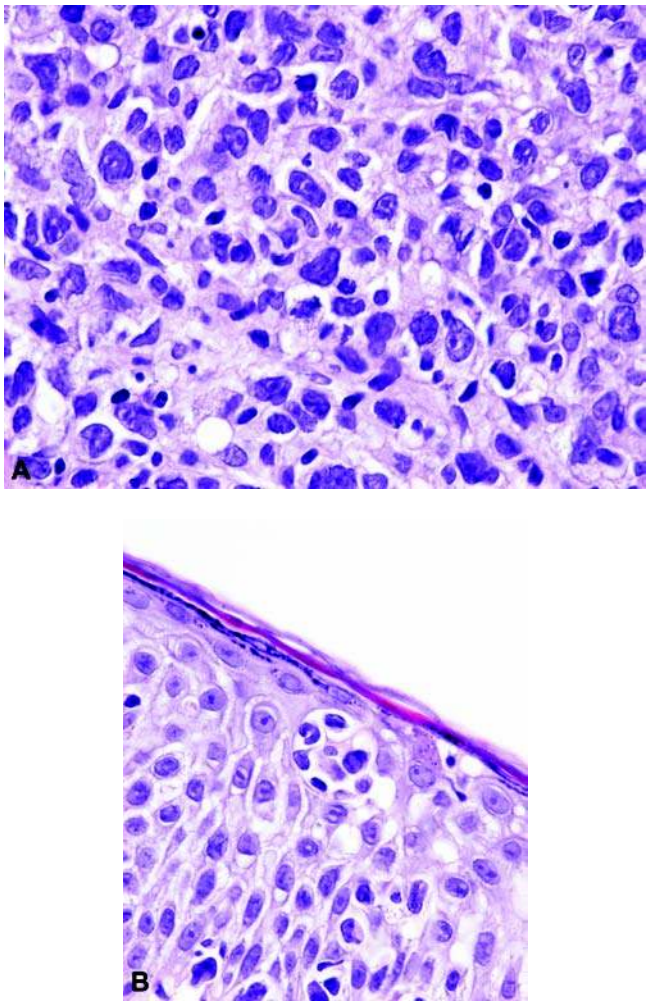

Figure 118 Mycosis fungoides, skin. (**A**) Lymphoma cells show striking cerebriform appearance of the nuclei. (**B**) Pautrier microabscess.

and epidermotropism may be absent. The neoplastic T cells have an immunophenotype similar to that observed in mycosis fungoides, with expression of CD4. There is frequent loss of pan-T antigens, such as CD2, CD3, and CD5. Clonal T-cell receptor gene rearrangements are present.

Subcutaneous Panniculitis-Like T-Cell Lymphoma

Introduction and clinical features. Subcutaneous panniculitis-like T-cell lymphoma is a mature T-cell neoplasm with preferential infiltration of the subcutis by lymphoma cells, often with marked tumor necrosis and karyorrhexis. In contrast to the original definition, cases that express γδ T-cell receptor are excluded and reclassified as ''cutaneous γδ T-cell lymphoma'' (416).

The patients present with solitary or multiple subcutaneous nodules, most commonly on the limbs and trunk, in the absence of other sites of disease. Dissemination to lymph nodes or other organs is uncommon. Hemophagocytic syndrome complicates the disease in 17% of patients. The prognosis is favorable, with a five-year overall survival of 82% (91% and 46% for those without and with hemophagocytic syndrome, respectively).

Pathology. The skin shows lace-like pattern of involvement of the subcutaneous tissue with no or minimal involvement of the dermis (Fig. 119A). The lymphoma cells are often small to medium-sized cells, with mild to moderate cytologic atypia. They characteristically show rimming around individual fat vacuoles (Fig. 119B). There are typically many admixed apoptotic bodies, with interspersed histiocytes having ingested these debris.

The characteristic immunophenotype is CD3+, CD4−, and CD8+ (Fig. 119C). The lymphoma cells express αβ T-cell receptor (detected by antibodies such as βF1), but not γδ T-cell receptor (detected by antibodies such as TCR-δ). There is expression of various cytotoxic markers. CD56 is almost always negative. There is no association with EBV.

Differential diagnosis. The most important differential diagnosis is *cutaneous γδ T-cell lymphoma*, which is associated with a very poor prognosis (5-year overall survival 11%) (416). The characteristic features are (*i*) coexistence of dermal and subcutaneous involvement if the subcutis is involved; and (*ii*) immunophenotype of CD4−, CD8−, TCR-δ+, βF1−, and CD56+.

Subcutaneous panniculitis-like T-cell lymphoma can be distinguished from peripheral T-cell lymphoma NOS with skin involvement by the following features: (*i*) lymphoma infiltrate confined to the subcutis with no or only mild dermal involvement; (*ii*) lymphoma cells often small to medium sized, with admixed apoptotic bodies and macrophages; (*iii*) rimming of individual fat spaces by lymphoma cells; and (*iv*) demonstration of a cytotoxic T-cell phenotype.

Primary Cutaneous CD4+ Small/Medium T-Cell Lymphoma

Primary cutaneous CD4+ small/medium T-cell lymphoma usually presents as a solitary plaque or tumor, most commonly on the face, neck, or upper trunk (417). The prognosis is favorable, with five-year survival of 60% to 80%, and patients with localized skin disease have even more favorable prognosis.

Histologically, the dermis shows nodular or diffuse infiltration by small/medium-sized lymphoid cells with irregular nuclear foldings. There can be up to 30% admixed large cells. Infiltration of the subcutis is common. On immunostaining, the lymphoid cells are CD3+, CD4+, CD8−, CD30−. In cases predominated by small cells, distinction from a reactive T-cell infiltrate can be difficult, and demonstration of T-cell receptor gene rearrangement helps support the diagnosis.

Primary Cutaneous CD8+ Aggressive Epidermotropic Cytotoxic T-Cell Lymphoma

Primary cutaneous CD8+ aggressive epidermotropic cytotoxic T-cell lymphoma usually presents as

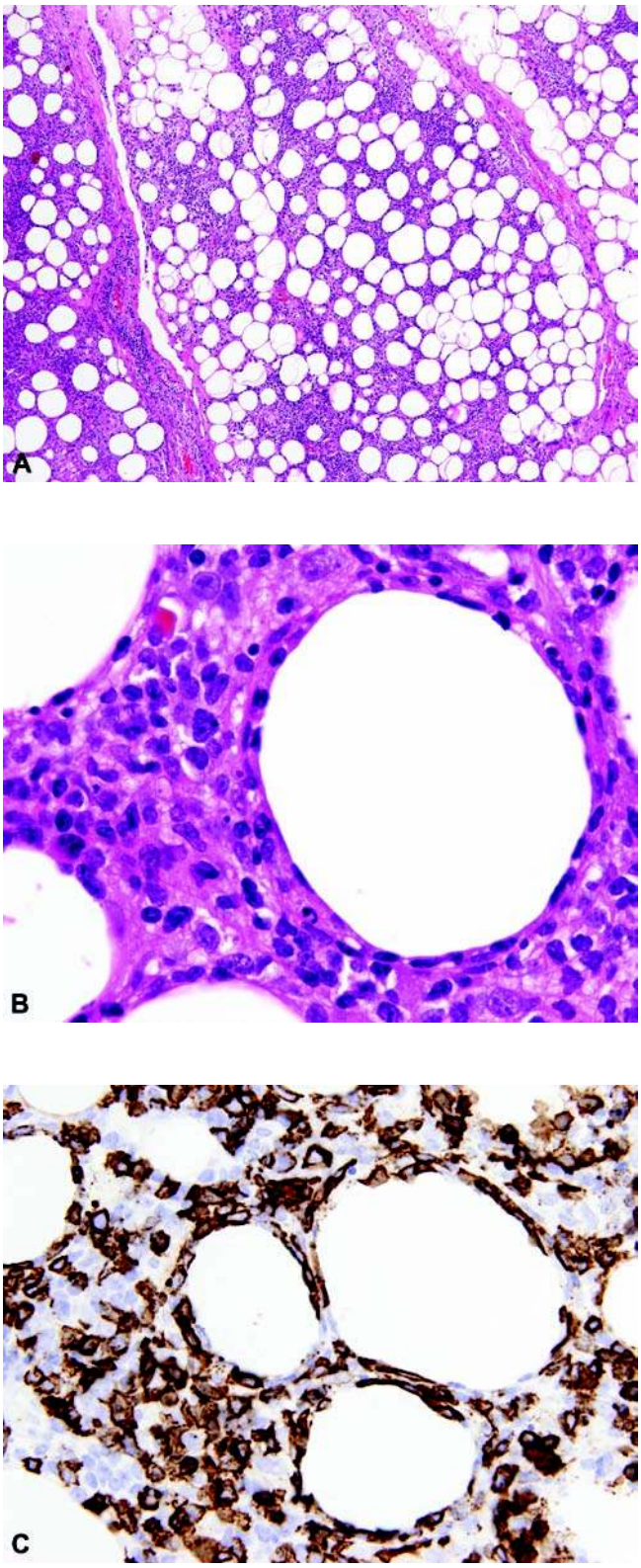

Figure 119 Subcutaneous panniculitis-like T-cell lymphoma. (**A**) Prominent interstitial infiltration of the adipose tissue. (**B**) The lymphoid cells are small to medium sized and have irregularly folded nuclei. There is rimming of cells around fat vacuoles. (**C**) The lymphoma cells show CD8 immunoreactivity.

localized or disseminated eruptive papules, nodules, and tumors with ulceration and necrosis. The tumor may spread to various visceral sites. The prognosis is very poor, with median survival of only 32 months (417).

Histologically, there is a lichenoid band of lymphoid infiltrate with marked epidermotropism. In some cases, there is a deeper nodular infiltrate, with invasion of skin appendages. The lymphoid cells are medium sized to large, often with irregularly folded nuclei. Immunostaining shows an immunophenotype of CD3+, CD4−, CD8+, and cytotoxic marker+. EBV is negative (417).

Hydroa Vacciniforme–Like Lymphoma

Hydroa vacciniforme–like lymphoma is an EBV-positive cutaneous T-cell lymphoma occurring in children and adolescents, and associated with sun sensitivity (418,419). There is a racial predilection for Asians and Native Americans (from Mexico, Central America, and South America). The papulovesicular eruptions appear on sun-exposed areas, including the face and scalp. They often ulcerate and heal with depressed scars. Some patients have recurrent skin lesions over many years, while some progress systemically and are associated with a poor prognosis.

Histologically, the lymphoid infiltrate is located predominantly in the dermis, often with perivascular and periadnexal accentuation. The lymphoid cells are mostly small, with minimal to mild atypia. There can be ulceration. The lymphoid cells are mostly T cells (CD3+) with cytotoxic phenotype, and EBER is positive.

Adult T-Cell Leukemia/Lymphoma

Adult T-cell leukemia/lymphoma is a mature T-cell neoplasm associated with human T-cell lymphotropic virus 1 (420). It is much more common in southern Japan, the Caribbean, and part of central Africa. Several clinical variants have been described (acute, lymphomatous, chronic, and smoldering), and hypercalcemia is commonly observed. Lymph nodes and peripheral blood and skin are commonly involved. ''Flower cells'' with multilobated pleomorphic nuclei are a characteristic finding. The tumor cells express pan-T markers and CD25. Involvement of various head and neck sites can occur as part of systemic disease.

Immunodeficiency-Associated Lymphoproliferative Disorders

The different types of immunodeficiency are: primary immune deficiency, HIV-related, posttransplant, and methotrexate-associaetd. Some of these lesions are indistinguishable from conventional lymphomas seen in nonimmunocompromised patients, except for a much stronger association with EBV, while others exhibit a spectrum of appearances, often with a polymorphous cellular composition. In posttransplant and methotrexate-associated lymphoproliferative disorders, some of the lesions may regress with lowering the intensity of the immunosuppressive therapy (94,421).

Posttransplant lymphoproliferative disorders. There are several major categories of PTLDs, and they are frequently EBV driven (422–424).

1. Early lesions: These occur mostly in children and young patients not previously exposed to EBV, often in the early period after transplantation. They are polyclonal and usually regress spontaneously or with minimal reduction in immunosuppressant. The tonsils and lymph nodes are most commonly involved. Histologically, the tissue architecture is preserved or at least partially preserved, and the proliferated cells do not show atypia. Plasmacytic hyperplasia: mixture of plasma cells and lymphoplasmacytoid cells; germinal centers are hyperplastic, involuted, or absent. Infectious mononucleosis-like lesion: increased immunoblasts, similar to infectious mononucleosis in immunocompetent hosts.
2. Polymorphic PTLDs: These lesions occur in all age groups. Although they are monoclonal, they often regress with reduction in immunosuppression. Nonetheless, some cases do progress despite treatment. The more commonly involved sites are lymph node, lung, gastrointestinal tract, and allograft. In contrast to early lesions, there is tissue destruction with architectural effacement. The infiltrate includes a mixture of small lymphocytes, plasma cells, immunoblasts, and plasmablasts, recapitulating the spectrum of cells seen in B-lymphocyte differentiation (Fig. 120). The immunoblasts may or may not exhibit atypia. Necrosis can be present.
3. Monomorphic PTLDs: These occur in all age groups and are often disseminated at presentation. They are monoclonal, and most cases progress rapidly, although rare cases may regress with reduction in immunosuppression. The more commonly involved sites are lymph node, marrow, and extranodal sites. The morphologic features are indistinguishable from conventional malignant lymphomas and should be categorized accordingly. The commonest types are DLBCL and Burkitt lymphoma. Necrosis is often prominent.
4. Posttransplant Hodgkin lymphoma: These lesions usually develop several years after transplantation. Morphologic and immunophenotypic features are indistinguishable from conventional classical Hodgkin lymphoma, most commonly, mixed-cellularity subtype. The large neoplastic cells are EBV positive.

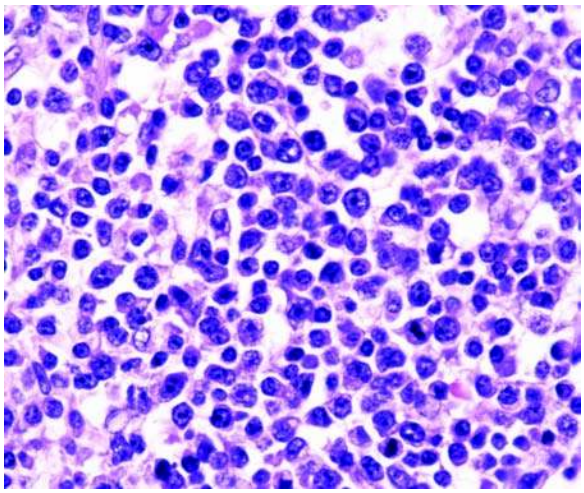

Figure 120 Polymorphic posttransplant lymphoproliferative disorder. There is a spectrum of cells from immunoblasts to plasmablasts and plasma cells.

G. Myeloid, Histiocytic, and Dendritic Cell Tumors

Myeloid Sarcoma

Clinical features. Myeloid sarcoma (granulocytic sarcoma) is a tumorous presentation of acute myeloid leukemia, with mass-forming collections of myeloblasts or immature myeloid cells in extramedullary sites or bone. The tumor may develop before, concurrent or subsequent to the presentation of acute myeloid leukemia, chronic myeloproliferative disorder, or myelodysplastic syndrome. The presence of myeloid sarcoma in the latter two settings indicates blastic transformation to acute myeloid leukemia. Other than bone, commonly involved sites include lymph nodes, skin, and soft tissues (425–427).

Pathology. Histologically, the tumor exhibits a diffuse and dense cellular infiltrate, often with a single-file pattern of permeative infiltration in some areas (Fig. 121A, B). The tumor cells are medium sized, with round to ovoid nuclei, fine chromatin, and a small to moderate amount of eosinophilic cytoplasm (Fig. 122A, B). These blasts may show myeloblastic or monoblastic differentiation, and some maturing forms (promyelocytes and myelocytes) with cytoplasmic granules may be identified (Fig. 122A, C). The blasts show variable expression of myeloperoxidase, CD117, lysozyme, CD68, and CD163, depending on the line of differentiation (Fig. 123). They commonly express CD43. In the absence of expression of other specific pan-T markers (e.g., CD3), myeloid sarcoma should always be excluded for a hematolymphoid neoplasm with a ''CD43+ only'' phenotype.

Myeloid sarcoma is most often misdiagnosed as malignant lymphoma. The most important clues to diagnosis are (*i*) highly permeative growth; (*ii*) blastic appearance of the neoplastic cells; (*iii*) eosinophilic rather than amphophilic cytoplasm; and (*iv*) admixed eosinophilic myelocytes, if present (Fig. 122C).

Histiocytic Sarcoma

Clinical features. Histiocytic sarcoma is malignant proliferation of cells showing morphologic and immunophenotypic features of mature tissue histiocytes (428). Neoplastic proliferations associated with acute monocytic leukemia are excluded. The tumor

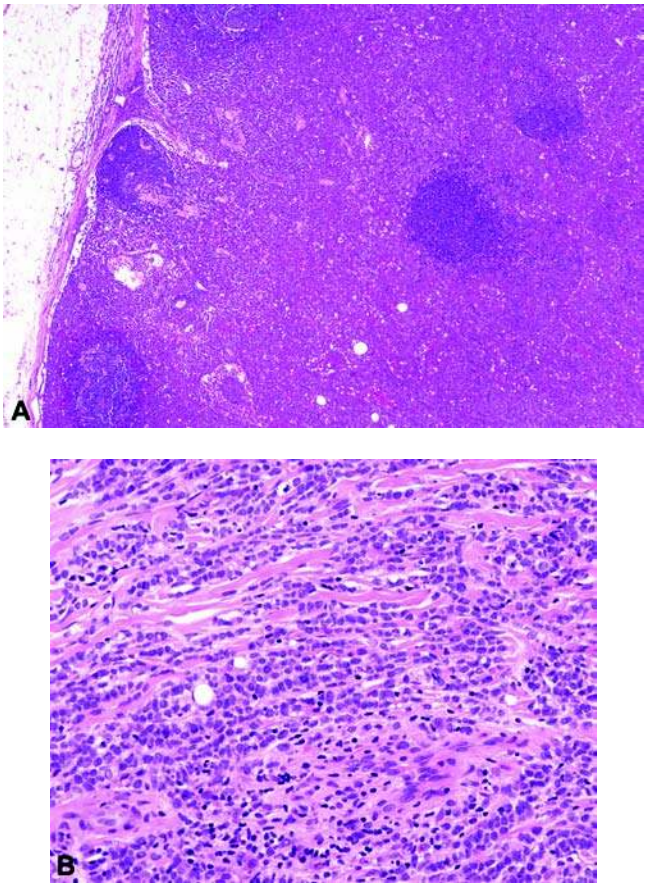

Figure 121 Myeloid sarcoma. (**A**) Diffuse lymph node involvement, with some residual lymphoid follicles. (**B**) Gum involvement. Note the characteristic single-file pattern of infiltration.

may present in lymph node, skin, or other extranodal sites. The tumor is aggressive, with most patients dying of progressive disease.

Pathology. Histologically, the tumor shows a diffuse noncohesive growth of very large pleomorphic cells that may resemble large cell lymphoma but differs from the latter in that the cytoplasm is eosinophilic and abundant and often contains fine vacuoles. The nuclei are eccentrically located, with round, oval, irregular, or grooved contour, and delicate or coarse chromatin, often with small nucleoli (Fig. 124A). Multinucleated forms can be present. It is most uncommon to find phagocytosis in the tumor cells. Some cases are accompanied by a variable inflammatory background, which may include lymphocytes, plasma cells, neutrophils, and eosinophils.

By definition, the tumor cells should be immunoreactive for more than one histiocytic markers, such as CD68, CD163, and lysozyme, and should be negative for Langerhans cell (CD1a, langerin/CD207), follicular dendritic cell (CD21, CD35), and myeloid cell (CD13, CD33, myeloperoxidase) markers (Fig. 124B). There can be heterogeneous staining for S100. Although acute monocytic leukemia with tissue infiltrates shows an

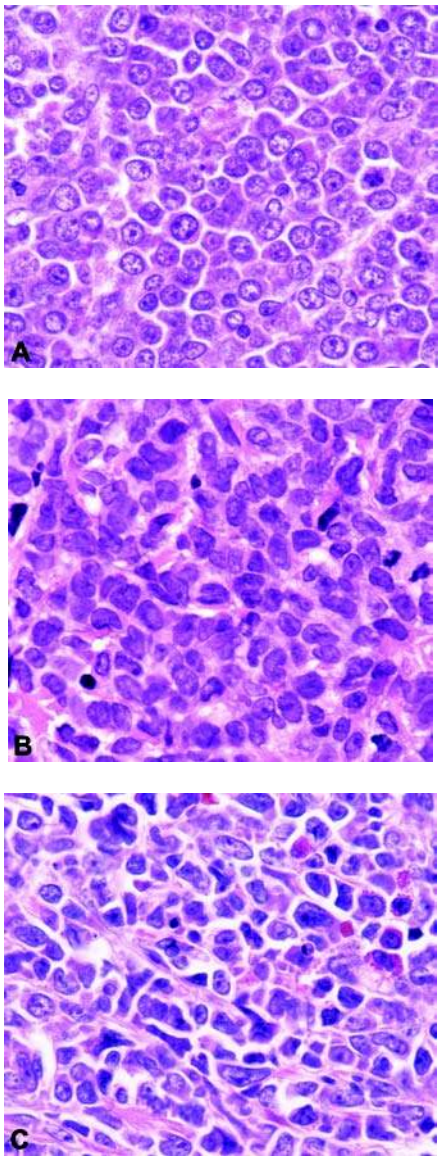

Figure 122 Cytologic spectrum of myeloid sarcoma. (**A**) Medium-sized cells with round nuclei and fine cytoplasmic granules. (**B**) Medium sized with irregular nuclei. The myeloid nature is not evident morphologically. (**C**) Neoplastic cells show cytoplasmic granules, and there are admixed eosinophil myelocytes (*right upper field*), which are helpful pointers to the correct diagnosis.

identical immunophenotype, it can be recognized by the usually monotonous appearance of the infiltrate and the much smaller size of the neoplastic cells.

Langerhans Cell Histiocytosis

Clinical features. Langerhans cell histiocytosis is a neoplastic proliferation of Langerhans cells. Patients are usually children and young adults, with male predominance. Most patients present with unifocal disease (frequently in bone, but may affect lymph node, skin, or lung), and these are usually young

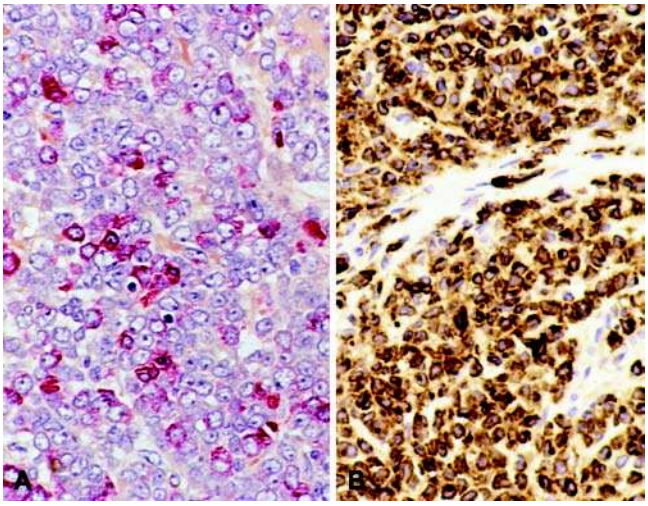

Figure 123 Myeloid sarcoma. (**A**) Positive chloroacetate esterase reaction. (**B**) Positive immunostaining for myeloperoxidase.

adults or older children. Less frequently, patients develop multifocal unisystem disease or multifocal multisystem disease; the former often in young children, and the latter in infants presenting with fever, skin rash, hepatosplenomegaly, lymphadenopathy, pancytopenia, and bone lesions (429).

Treatment options include surgery, radiotherapy, and/or chemotherapy (430). Overall survival of patients with unifocal disease is >95%, but it drops to 75% for those with two organs involved (429).

Pathology. Irrespective of site of involvement, Langerhans cell histiocytosis is characterized by sheets and clusters of Langerhans cells intermixed with eosinophils, reactive lymphocytes, plasma cells, neutrophils, multinucleated giant cells, and some lipid-laden macrophages. The Langerhans cells have ovoid, grooved, and deeply contorted nuclei, thin nuclear membranes, delicate chromatin, and abundant eosinophilic cytoplasm (Fig. 125A). Eosinophils can be abundant, forming abscesses, which are sometimes accompanied by geographic necrosis (Fig. 125B).

In lymph node, there is often predominantly sinusoidal involvement, with variable involvement of the nodal parenchyma (Fig. 125B). Capsular fibrosis and perinodal infiltration are common.

The proliferated cells show the characteristic immunophenotype of Langerhans cells: S100+, CD1a+, and CD207 (langerin)+ (Fig. 126). Ultrastructural study reveals the cytoplasmic Birbeck granules with a tennis racket–like appearance, but this modality of investigation is less important nowadays because the presence of the Birbeck granules can be inferred by positive immunostaining for langerin (CD207).

Langerhans Cell Sarcoma

The term ''Langerhans cell sarcoma'' is applied for a Langerhans cell proliferation with frankly malignant

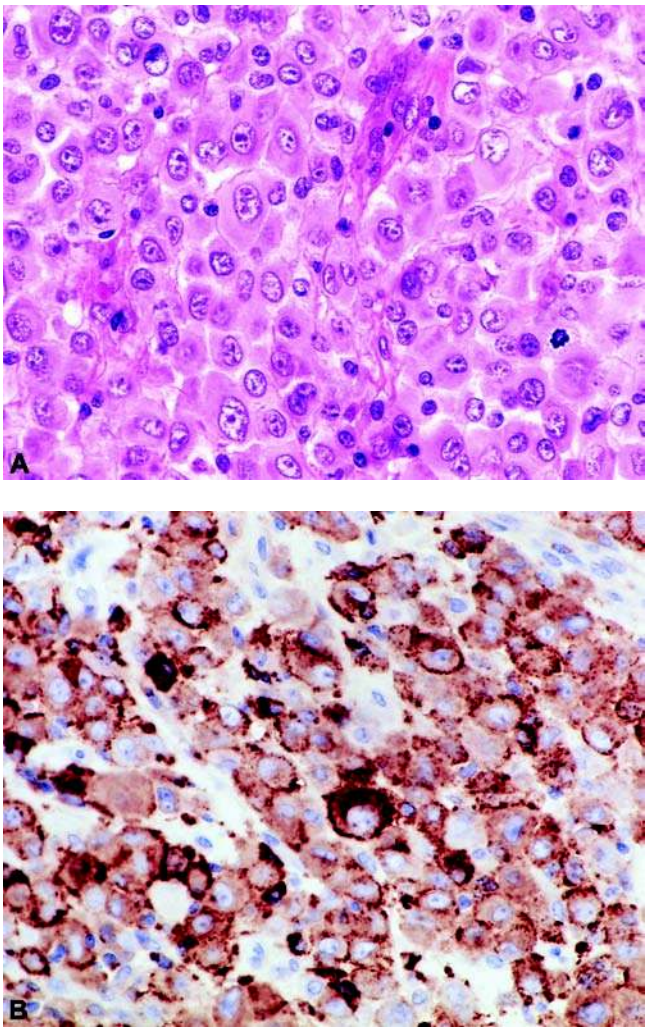

Figure 124 Histiocytic sarcoma, lymph node. (**A**) A diffuse infiltrate of large cells with abundant eosinophilic cytoplasm. (**B**) Positive immunostaining for CD163 confirms the histiocytic nature of the neoplastic cells.

cytologic features (431). Mitotic figures are usually evident. Eosinophils are often absent. The immunophenotype is identical to that of Langerhans cell histiocytosis: S100+, CD1a+, and CD207 (langerin)+.

The patients present with lymphadenopathy or extranodal disease. Compared with Langerhans cell histiocytosis, the patients are older (mean age 40 years), and the disease is more aggressive, with a mortality rate of at least 50% (431).

Follicular Dendritic Cell Sarcoma

Clinical features. Follicular dendritic cell sarcoma is a neoplastic proliferation of spindled to ovoid cells showing morphologic and immunophenotypic features of follicular dendritic cells (432). It occurs predominantly in adults. Half to two-thirds of cases

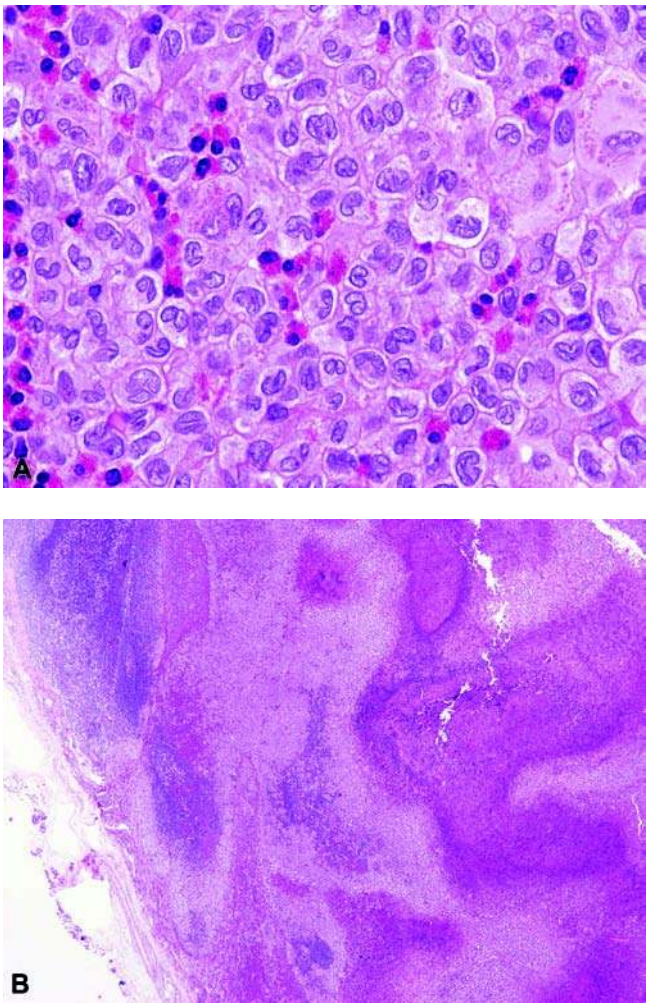

Figure 125 Langerhans cell histiocytosis. (**A**) The lesional cells typically show deeply grooved, coffee bean–like nuclei, thin nuclear membranes, and delicate chromatin. There are almost always admixed eosinophils. (**B**) Involved lymph node shows extensive infiltration by Langerhans cells and eosinophils, accompanied by geographic necrosis.

present with nodal disease, but extranodal presentation in the head and neck region can also occur, such as tonsil, nasopharynx, and oral cavity. A small proportion of cases evolve from an underlying hyaline-vascular-type Castleman disease (129,433).

Follicular dendritic cell sarcomas usually behave as low- to intermediate-grade malignancies, with local recurrence rate of 40% and metastatic rate of at least 28% (431,434,435). Poor prognostic factors include significant cytologic atypia, extensive tumor necrosis, high proliferative index, and large tumor size (434,435).

Pathology. Histologically, the spindle or oval tumor cells are arranged in fascicles, whorls, storiform arrays, vague or discrete nodules, or diffuse sheets (Fig. 127A–C). The tumor cells show variable degrees of cytologic atypia, often with vesicular nuclei, distinct nucleoli, and occasional nuclear pseudoinclusions

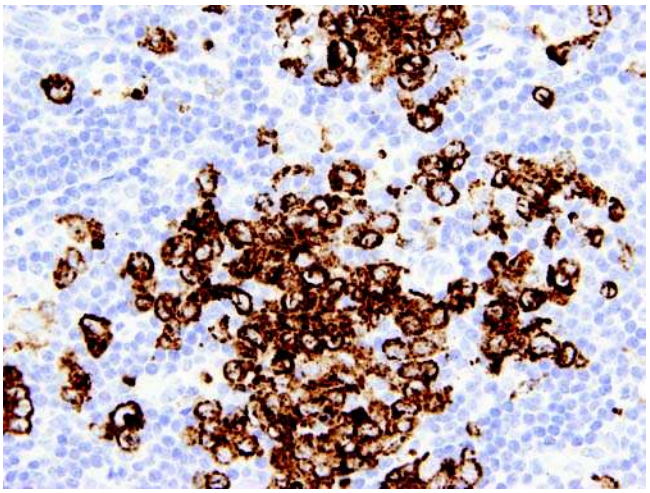

Figure 126 Langerhans cell histiocytosis. Langerin (CD207) immunoreactivity is a key diagnostic feature of this entity.

(Fig. 128). They typically have ill-defined cytoplasmic borders and a moderate amount of eosinophilic cytoplasm (Figs. 128 and 129). The tumor is characteristically sprinkled with small lymphocytes, which can also be accentuated around blood vessels (Figs. 127C and 128). Less common findings include polygonal cells with hyaline cytoplasm, clear cells, myxoid change, neuroendocrine tumor–like vasculature, pseudovascular spaces, perivascular spaces, and admixed osteoclastic giant cells. Rare tumors show broad sclerotic septa delineating jigsaw puzzle–like lobules of tumor, mimicking thymoma.

The diagnosis is confirmed by the positive staining for follicular dendritic cell markers such as CD21, CD23, and CD35, but the staining can be patchy (Fig. 130). Clusterin is often positive. Ultrastructural examination reveals numerous long cytoplasmic processes often connected by desmosomes.

Interdigitating Dendritic Cell Sarcoma

Interdigitating dendritic cell sarcoma is a neoplastic proliferation of spindle to ovoid cells with phenotypic features of interdigitating dendritic cells (436). Most patients are adults, who present with lymphadenopathy or extranodal disease. The tumor is generally aggressive.

In the involved lymph node or extranodal tissue, spindle or oval tumor cells are arranged in a fascicular or storiform pattern. The tumor cells show variable degrees of cytologic atypia. Nuclear grooves can be prominent. There are often admixed small lymphocytes. Some cases are morphologically indistinguishable from follicular dendritic cell sarcoma. Immunophenotypically, the tumor cells are S100+, CD1a−, langerin (CD207)−, CD45+/−, and CD68+/−. Markers for follicular dendritic cells are negative. An important differential diagnosis is malignant melanoma, which is also S100+, but interdigitating dendritic cell sarcoma differs in that delicate dendritic cell

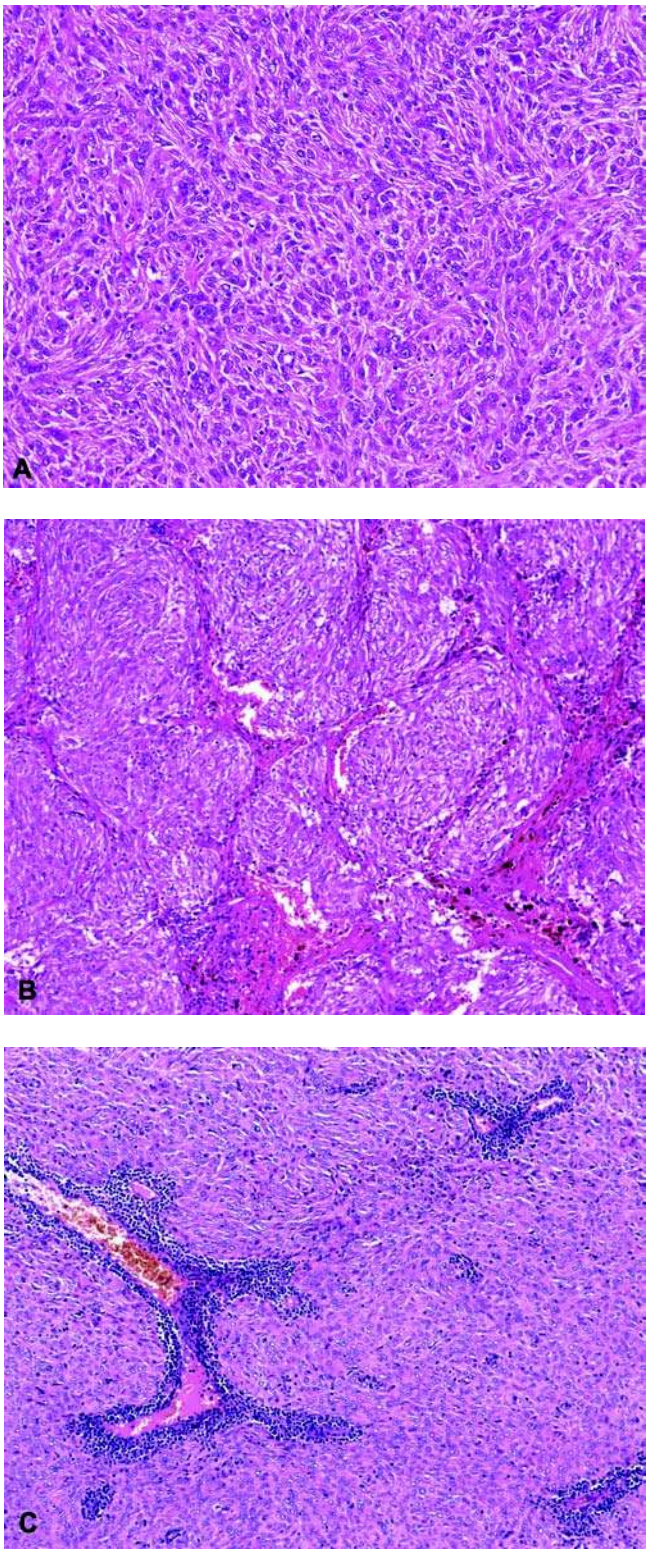

Figure 127 Follicular dendritic cell sarcoma. (**A**) Storiform growth pattern. (**B**) Nodular growth pattern, recapitulating the follicular growth pattern of the normal follicular dendritic cells. (**C**) Diffuse growth pattern. There is also perivascular cuffing of small lymphocytes.

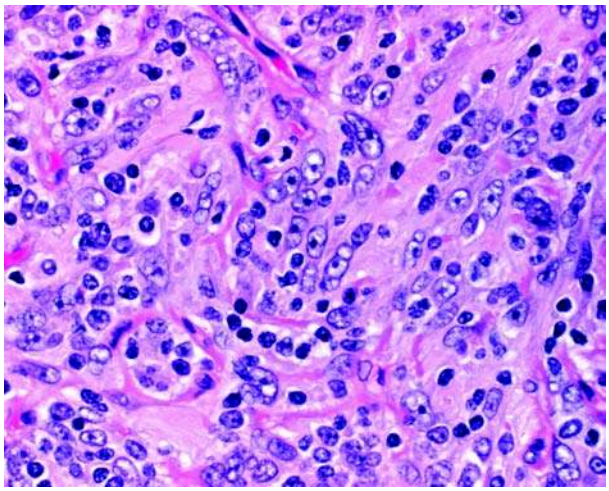

Figure 128 Follicular dendritic cell sarcoma, soft tissue of forehead. The plump spindly tumor cells typically have indistinct cell borders, vesicular nuclei, and distinct nucleoli. There are intermingled small lymphocytes.

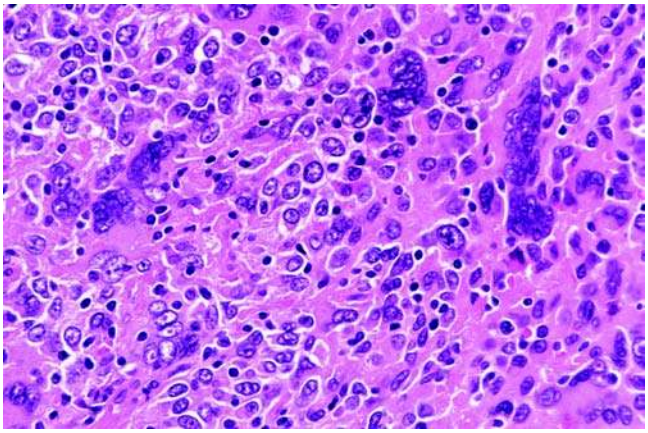

Figure 129 Follicular dendritic cell sarcoma of tonsil. There is a tendency for the tumor cell nuclei to be clustered. Some multinucleated tumor giant cells are also present, reminiscent of polykaryocytes sometimes seen in reactive germinal centers.

processes are highlighted in the S100 immunostain, and the tumor cells are negative for other melanocytic markers such as HMB-45, melan-A, and microphthalmia transcription factor. Ultrastructural examination reveals complex interdigitating cell processes, in the absence of well-formed desmosomes.

Blastic Plasmacytoid Dendritic Cell Neoplasm

Introduction and clinical features. Blastic plasmacytoid dendritic cell neoplasm, also known as CD4+CD56+ hematodermic neoplasm, was previously considered a form of blastic NK-cell lymphoma

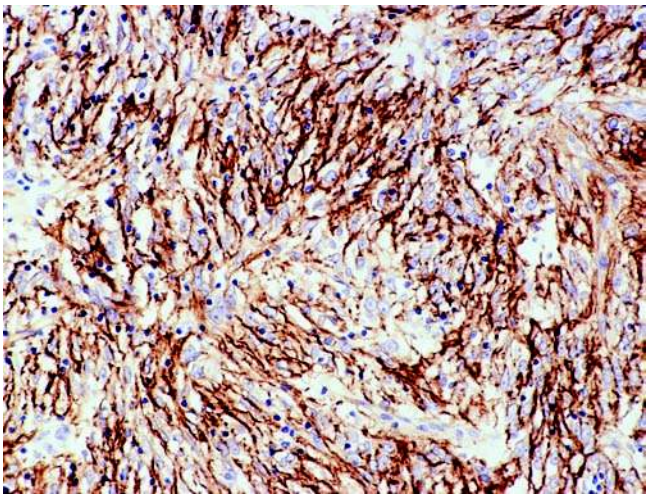

Figure 130 Follicular dendritic cell sarcoma, with positive immunostaining for CD21.

(a misnomer) (437). It is believed to be derived from the precursors of plasmacytoid dendritic cells (437). The tumor occurs mostly in adults, but children can also be affected (438,439). Most patients present with solitary or multiple skin lesions, with or without lymphadenopathy and bone marrow involvement (440,441). Occasional patients have leukemic presentation (439). The tumor is aggressive, with early dissemination and disease relapse despite initial response to therapy. The mean survival is only 12 to 14 months (318).

Pathology. In the skin, the entire dermis, and sometimes the subcutis, shows a diffuse, dense, and monotonous permeative tumor infiltrate, with sparing of the epidermis (Fig. 131A). Lymph node involvement is either total or partial. The neoplastic infiltrate comprises medium-sized cells with round, oval, or folded nuclei, fine chromatin, inconspicuous nucleoli, and a thin rim of pale cytoplasm (Fig. 131B). Mitotic figures are readily found. There is often insinuation of the collagen bundles by tumor cells, producing a single-file pattern. Angioinvasive growth and coagulative necrosis are usually absent.

The typical immunophenotype is CD4+, CD56+, surface CD3−, CD123+, and BDCA-2+ (Fig. 132) (440,442,443). Cytotoxic markers are usually negative. More than half of the cases express TdT (439,444). EBV is negative.

Differential diagnosis. The differential diagnoses are mainly the blastic neoplasms. The neoplastic cells of lymphoblastic lymphoma/leukemia usually have less cytoplasm and express multiple T- or B-lineage markers in addition to TdT, while expression of CD56 is very rare.

Myeloid leukemia/sarcoma usually shows more distinct nucleoli, and the cytoplasm is usually eosinophilic, sometimes with identifiable granules.

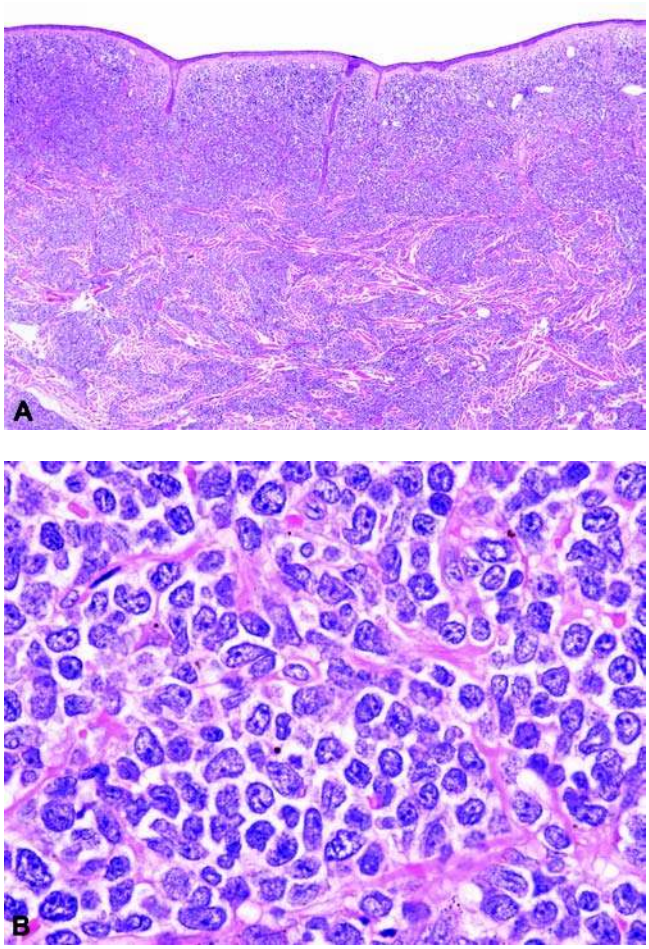

Figure 131 Blastic plasmacytoid dendritic cell neoplasm involving skin. (**A**) There is a diffuse permeative infiltrate in the dermis with no necrosis. (**B**) Neoplastic cells are medium sized, reminiscent of lymphoblastic or myeloid leukemic cells.

Although some cases can express CD56, the diagnosis can be confirmed by immunoreactivity for myeloperoxidase, CD117, and other myeloid markers (such as CD13, CD15, and CD33). Myeloid/NK-cell acute leukemia or myeloid/NK-cell precursor acute leukemia can be distinguished from blastic plasmacytoid dendritic cell neoplasm by the expression of markers of both myeloid cells (such as CD13, CD15, CD33, and, variably, CD34 and myeloperoxidase) and NK cells (CD56 and, variably, CD7), infrequent presentation as skin lesions, and lack of CD4 and CD123 expression (445,446).

Other Rare Dendritic Cell Tumors

Rare types of dendritic cell tumors include the following:

1. Indeterminate dendritic cell tumor: There is frequent cutaneous involvement. The morphology

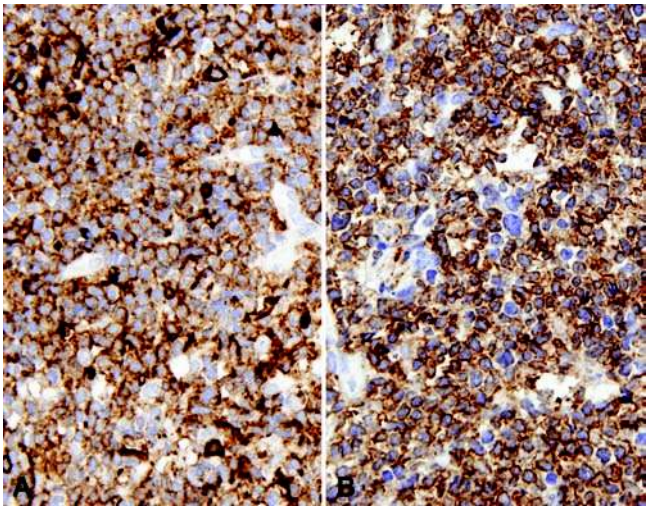

Figure 132 Blastic plasmacytoid dendritic cell neoplasm involving skin, immunohistochemistry. Positive staining for CD4 (**A**) and CD56 (**B**).

simulates Langerhans cell histiocytosis or Langerhans cell sarcoma, but there is no significant eosinophil infiltration. The immunophenotype is identical to Langerhans cell proliferations (S100+, CD1a+), except that langerin (CD207) is negative.
2. Fibroblastic reticular cell tumor: This rare tumor has been recognized in lymph node, spleen, and soft tissue. The morphology resembles follicular dendritic cell sarcoma or interdigitating dendritic cell sarcoma, but there is no expression of immunohistochemical markers characteristic of these tumor types. There is variable immunoreactivity for actin, desmin, cytokeratin, and CD68.
3. Dendritic cell tumor, not otherwise specified: This term is reserved for dendritic cell tumors that defy classification despite extensive workup, or for dendritic cell tumors showing hybrid features.

IV. HEMATOLYMPHOID LESIONS OF LYMPH NODES IN THE HEAD AND NECK REGION

A. Hematolymphoid Neoplasms of Lymph Nodes

The commonest hematolymphoid neoplasms presenting in lymph nodes of the head and neck region are DLBCL, follicular lymphoma, and classical Hodgkin lymphoma. Nonetheless, practically any lymphoma type can involve these lymph nodes, either as the sole finding or as part of systemic disease. Diagnosis and classification are based on clinical findings, morphologic assessment, and immunohistochemical evaluation, and supported by molecular studies where appropriate.

B. Important Reactive or Inflammatory Hematolymphoid Lesions

The practicing pathologists are seeing fewer lymph node excisional biopsies of reactive lymphadenopathies nowadays, mostly as a result of the widespread practice of fine-needle aspiration as the initial investigation for patients presenting with lymphadenopathy. Since the reactive nodes often resolve completely on follow-up, they are rarely excized for histologic examination.

In reactive lymphadenopathies, the majority of cases fall into the category of ''nonspecific reactive hyperplasia.'' Only approximately 20% to 30% of cases conform to specific entities, with the commoner diagnoses being toxoplasmosis, infectious mononucleosis, tuberculosis, and Kikuchi lymphadenitis, but the frequencies of these diagnoses vary greatly in different geographic regions; for example, tuberculosis is more prevalent in developing countries, and Kikuchi lymphadenitis is more prevalent in Oriental people.

C. Diagnostic Considerations

Lymph Node Evaluation

In evaluation of a lymph node, the following questions should be asked:

1. What is the major pattern of change? Pattern assessment can lead to the correct diagnosis or at least a reasonable list of differential diagnoses (Table 10).
2. Do the changes indicate a reactive or malignant process?
3. If reactive, do the changes show features of specific lymphadenopathies?

Is the lymphoid Proliferation Benign or Malignant?

The distinction between a reactive lymphoid proliferation and malignant lymphoma is sometimes straightforward but can at times be very difficult. Good-quality histologic materials are essential. Many mistakes in interpretation are committed because of the suboptimal quality of the histologic sections.

There are no simple rules for making the distinction, and there are always exceptions. As a generalization, a reactive process usually (*i*) shows preserved (albeit distorted sometimes) architecture, typically with preserved sinuses (Fig. 133A); (*ii*) does not form any discrete expansile mass within the node (Figs. 133A and 134); (*iii*) exhibits a mixture of lymphoid cell types (Fig. 133B); and (*iv*) lacks definite cellular atypia, i.e., not deviating from the appearances of the normal and reactive cells (Fig. 133B).

In difficult cases, ancillary studies such as immunohistochemistry can be very helpful. In reactive lymph nodes, CD20 is most helpful for confirming that the immunoarchitecture is preserved—nodular aggregates of CD20+ B cells (lymphoid follicles) in the cortex, with only limited numbers of CD20+ cells (single cells and at most in small aggregates) in the interfollicular zone (Figs. 1B and 3). If there is an increase of CD20+ large cells, the positive cells often exhibit a spectrum of staining intensities, indicating

Table 10 Reactive Lymph Node Patterns and Their Etiologies

Follicular pattern
- Reactive follicular hyperplasia
  - Nonspecific
  - Specific entities (such as toxoplasmosis, syphilis, cytomegalovirus infection, rheumatoid arthritis, plasma cell type of Castleman disease, Kimura disease, IgG4-related lymphadenopathy, reaction to regional tumor)
- Human immunodeficiency virus-associated lymphadenopathy
- Progressive transformation of germinal centers
- Castleman disease, hyaline-vascular type

Mantle zone pattern
- Castleman disease, hyaline-vascular type
- Lymph nodes adjacent to Castleman disease lesion
- Nonspecific mantle zone hyperplasia

Marginal zone pattern
- Marginal zone/monocytoid B-cell hyperplasia, nonspecific
- Specific entities:
  - Toxoplasmosis
  - Human immunodeficiency virus-associated lymphadenopathy
  - Primary EBV infection (some cases)
  - Cytomegalovirus infection
  - Early cat scratch disease

Interfollicular or diffuse increase in large lymphoid cells
- Reactive paracortical hyperplasia, nonspecific (including reaction to tumor in the drainage area)
- Interfollicular Hodgkinoid lymphadenitis
- Viral infection, e.g., EBV (infectious mononucleosis), herpes zoster, herpes simplex, human herpesvirus 6 infection
- Reactive immunoblastic proliferation, e.g., postvaccinial, drug hypersensitivity
- Autoimmune lymphoproliferative syndrome
- Angioimmunoblastic lymphadenopathy
- Kikuchi lymphadenitis
- IgG4-related lymphadenopathy

Sinusoidal expansion
- Sinus histiocytosis (nonspecific or as a reaction to tumor in the draining area)
- Rosai–Dorfman disease (sinus histiocytosis with massive lymphadenopathy)
- Reactive hemophagocytic syndrome
- Histiocytic reaction against foreign materials
- Storage disease, e.g., Gaucher disease, Niemann-Pick disease
- Vascular transformation of sinuses

Necrotizing pattern
- Infarction of lymph node
- Kikuchi lymphadenitis
- Systemic lupus erythematosus
- Kawasaki disease
- Human herpesvirus 6 infection
- Granulomatous lymphadenitis with necrosis (see below)
- Suppurative granulomatous lymphadenitis (see below)
- *Pneumocystis carinii* lymphadenitis

Epithelioid granulomatous reaction[a]
- Tuberculosis and other infections, e.g., brucellosis, fungal infection, Leishmania lymphadenitis
- Sarcoidosis
- Berylliosis
- Crohn disease
- Primary biliary cirrhosis
- Idiopathic
- Granulomatous reaction accompanying tumor, e.g., Hodgkin lymphoma, Burkitt lymphoma, nasopharyngeal carcinoma

Suppurative granulomatous lymphadenitis
- Cat scratch disease
- Lymphogranuloma venereum
- *Yersinia* infection
- Tularemia
- Fungal infection
- Atypical mycobacterial infection
- Chronic granulomatous disease of childhood

Parenchymal histiocytic reaction (other than epithelioid granulomas and suppurative granulomas)
- Dermatopathic lymphadenopathy
- Lepromatous leprosy lymphadenopathy
- *Mycobacterium avium-intracellulare* lymphadenitis/spindle cell pseudotumor
- Toxoplasmosis
- Bacterial lymphadenitis mimicking Lennert lymphoma
- Histiocytic reaction to foreign materials (e.g., silicone, prosthetic material)
- Kikuchi lymphadenitis
- Lupus erythematosus
- Kawasaki disease

Hypocellular appearance or lymphocyte depletion
- Human immunodeficiency virus-associated lymphadenopathy (late phase)
- Reactive hemophagocytic syndrome
- Primary immunodeficiencies
- Angioimmunoblastic lymphadenopathy
- Vascular transformation of sinuses
- Segmental infarction of lymph node
- Proteinaceous lymphadenopathy

Broadening of connective tissue framework
- Perilymphadenitis (various causes)
- Inflammatory pseudotumor of lymph node

[a]Small granulomas are common in syphilitic lymphadenitis and HIV-associated lymphadenopathy, but do not constitute a major feature.

presence of cells at different stages of maturation. Immediately beneath the capsule, there is commonly a thin, continuous band of CD20+ B cells in proximity with the apical regions of the lymphoid follicles. This band extends into the nodal parenchyma alongside the fibrous trabeculae. In an oblique section, this band of B cells may create a false impression of ''sheets of interfollicular B cells'' between follicles in some areas of the node. In reactive lymph nodes, there should be many CD3+ T cells in interfollicular zone. Variable numbers of CD3+ T cells are also found within the germinal centers.

A combination of features have to be considered for supporting a diagnosis of lymphoma. The various features can be grouped under three categories: abnormal architecture, evidence of invasion, and cytologic atypia, which can be evaluated at the morphologic and immunohistochemical levels (Table 11). These criteria can be applied both in lymph nodes and in extranodal sites (Figs. 134–136).

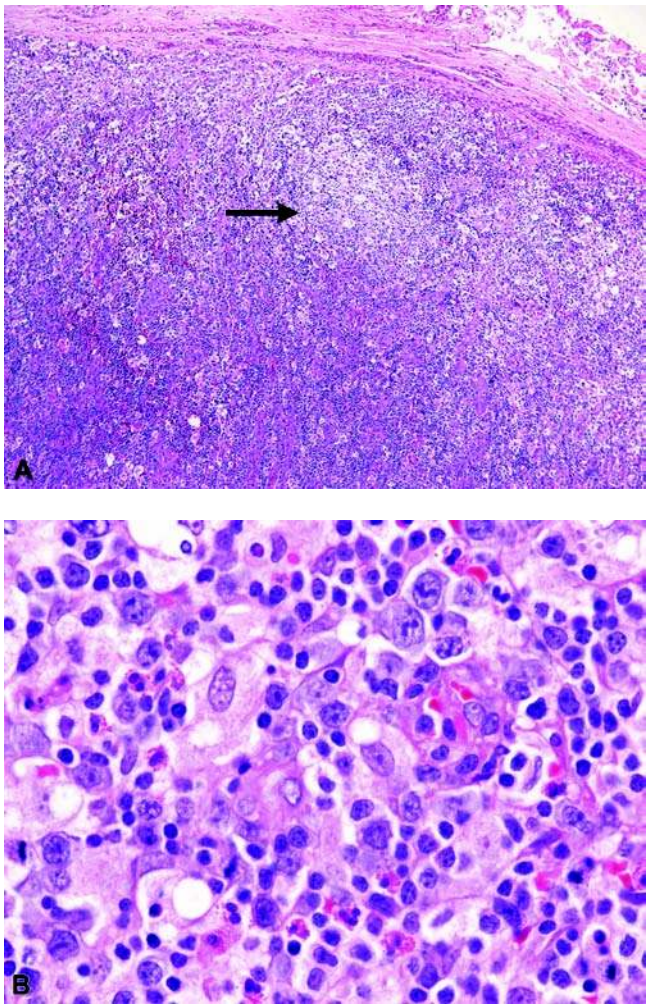

Figure 133 Reactive lymphoid hyperplasia, lymph node. (**A**) The nodal architecture is distorted but not effaced. Residual lymphoid follicles are still seen in the cortex (*arrow*). (**B**) The cellular infiltrate is mixed, and the cells do not exhibit overt nuclear atypia. Eosinophils are prominent in this case (due to hypersensitivity to drugs).

Rendering a Diagnosis of ''Atypical Lymphoid Hyperplasia''

For lymphoid proliferations showing indeterminate features, the term ''atypical lymphoid hyperplasia'' can be applied. This is neither a clinical nor a pathologic entity; it is merely an interim designation for lymphoid proliferations for which the pathologist cannot decide with certainty whether it is benign or malignant. It includes cases of reactive hyperplasia with some features worrisome for lymphoma, and cases of lymphoma with subtle cytologic atypia, subtle nodal involvement, or other unusual features such that the pathologist does not have sufficient confidence to render an outright diagnosis of lymphoma.

The diagnostic term ''atypical lymphoid hyperplasia'' should never be used if a more specific diagnosis can be made. Factors that influence the need to resort to this label include quality of histologic preparations, expertise of the pathologist, and availability of specialized studies to help in further analysis. The patients should be followed up, and repeat biopsy should be performed (immediately or later if there are no more palpable nodes). In repeat biopsies, it is important to reserve materials for culture and special studies.

V. HEMATOLYMPHOID LESIONS OF THE NASAL CAVITY AND PARANASAL SINUSES

A. Hematolymphoid Neoplasms of the Nasal Cavity and Paranasal Sinuses

General Features

Lymphomas account for 14% of all cancers of the nasal cavity and paranasal sinuses, ranking second after squamous cell carcinoma (447). Overall, about 2% of all primary extranodal lymphomas occur in this anatomic region (448), with the two commonest types being extranodal NK/T-cell lymphoma and DLBCL. In the nasal cavity, extranodal NK/T-cell lymphomas are more frequent (50–70%), while in the paranasal sinuses, DLBCLs are more frequent (80%) (Table 12) (373,449–451). The nasal cavity and paranasal sinuses are also predilection sites for extramedullary plasmacytoma, which constitutes 50% of all cases of head and neck extramedullary plasmacytomas.

Other less common lymphoma types of this anatomic location include Burkitt lymphoma (especially in children), follicular lymphoma, MALT lymphoma, mantle cell lymphoma, and peripheral T-cell lymphoma NOS (450). Myeloid sarcoma, Langerhans cell histiocytosis, and histiocytic sarcoma can also rarely involve the nasal cavity or paranasal sinus (431,452–454).

Clinical Features and Behavior

Clinical presentation of lymphoma of the nasal cavity and paranasal sinuses varies and may include nasal obstruction, epistaxis, nasal discharge, facial swelling, and pain. Extranodal NK/T-cell lymphoma sometimes presents as extensive midfacial ulcerative-destructive lesions. The overall survival rate of DLBCL of the nasal cavity and paranasal sinuses is 35% to 60%, which is more favorable compared with extranodal NK/T-cell lymphoma (overall survival 30–50%) (210,373,449,455).

Pathologic Features Related to Anatomic Location

The nasal or paranasal sinus mucosa involved by lymphoma may or may not show ulceration (Figs. 99A and 137A). Less commonly, the epithelium shows squamous metaplasia and florid pseudoepitheliomatous hyperplasia, mimicking well-differentiated squamous cell carcinoma (Fig. 99B). There is usually a diffuse and dense lymphomatous infiltrate, with atrophy and loss of mucosal glands (Fig. 100). There are several histologic features characteristic but not pathognomonic of extranodal NK/T-cell lymphoma: (*i*) extensive ulceration and coagulative necrosis (Fig. 99A); (*ii*) wide separation of

Table 11 Features Supporting a Diagnosis of Lymphoma Over Reactive Lymphoid Hyperplasia

Abnormal architecture
Morphologic
Effacement of architecture
Lymph node—disappearance of sinuses; complete loss of lymphoid follicles in the cortex
Mucosal sites—diffuse lymphoid infiltrate accompanied by loss of mucosal glands (where applicable)
Salivary gland, lacrimal gland, thyroid—diffuse dense infiltrate replacing the parenchyma, with large areas being devoid of acini, ducts or thyroid follicles
Formation of an expansile mass lesion within the lymphoid proliferation
Back-to-back arrangement of lymphoid follicles
Abnormal appearance of lymphoid follicles, e.g., lacking mantles, lacking tingible-body macrophages, monotonous cellular composition
Coalescence of broad marginal zones
Immunohistochemical
Diffuse sheets of CD20+ B cells, in at least one low-power field. (Caveat: Presence of sheets of CD3+ T cells is of no help, since either reactive lymphoid proliferation or T-cell lymphoma can give rise to this pattern.)
Evidence of invasion
Morphologic
Invasion and expansion of epithelial units, forming prominent lymphoepithelial lesions (Caveat: Lymphoepithelium is a normal structure in the Waldeyer ring.)
Permeation of interstitial tissues:
Mucosal sites, salivary gland, lacrimal gland, thyroid – Extensive permeation among epithelial units, accompanied by loss of these specialized units
Extensive permeative infiltration into adipose tissue
Invasion of blood vessel walls
Prominent permeation of fibrous stroma, producing single-file pattern
Tonsil: irregular, infiltrative base
For lymphoid follicular proliferation: atypical lymphoid cells in interfollicular zone
Destruction of the mantles of lymphoid follicles
Colonization of lymphoid follicles
Extensive lymphoid follicles in perinodal tissue
Immunohistochemical
Interfollicular zone packed with sheets of CD20+ B cells
Lymphoid follicular proliferation: interfollicular zone rich in CD10+ lymphoid cells
Lymphoid follicular proliferation: infiltration of vessel wall by CD10+ cells
Cytologic atypia
Morphologic
Presence of significant numbers of cells not normally found in reactive lymphoid tissues. (Caveat: Presence of very rare Reed–Sternberg like cells does not constitute cytologic atypia.)
Very large cells, with nuclear diameter exceeding >3 times that of small lymphocyte, since reactive immunoblasts have nuclear diameter less than 2.5 times that of small lymphocyte
Most cells show marked irregular nuclear foldings (Caveat: The small lymphoid cells in mucosal sites commonly show some degree of irregular nuclear foldings.)
Many cells exhibit granular chromatin pattern
Clear cells, excluding monocytoid B cells. (Caveats: Retraction artifact may simulate cytoplasmic clearing, thus clear cells must be seen among nonclear cells in the same field to be considered genuine. Clear cells may be seen in autoimmune lymphoproliferative syndrome.)
Many unexplained medium-sized cells, excluding monocytoid B cells, marginal zone cells and plasmacytoid dendritic cells. (Caveat: Medium-sized cells are not uncommon in autoimmune lymphoproliferative syndrome.)
Immunohistochemical
Expression of precursor cell marker TdT
Abnormal immunophenotype of B cells
Immunoglobulin light-chain restriction
Aberrant expression of markers not normally expressed or expressed in minority of B cells, such as BCL2 in follicular center cells, CD5, CD43 or cyclin D1
Abnormal immunophenotype of T cells
Abnormal subset marker expression, with exceptions of normal precursor T cells and autoimmune lymphoproliferative syndrome: CD4+ CD8+ (double positive) or CD4− CD8− (double negative)
Loss of pan-T markers, such as CD2, CD3, CD5, CD7
Expression of markers not normally expressed or expressed only in minority of T cells, such as ALK, CD56, γδ T-cell receptor

individual mucosal glands, accompanied by cytoplasmic clearing (Fig. 100); (*iii*) angioinvasion (Fig. 103); and (*iv*) prominent apoptosis(Fig. 101). Nonetheless, they are not invariably present. Immunohistochemical studies are still required to determine the lineage of the lymphoma (Fig. 137B).

B. Important Reactive or Inflammatory Hematolymphoid Lesions

Some infective, inflammatory, or idiopathic conditions producing a significant infiltrate of hematolymphoid cells can affect the nasal cavity and paranasal sinuses.

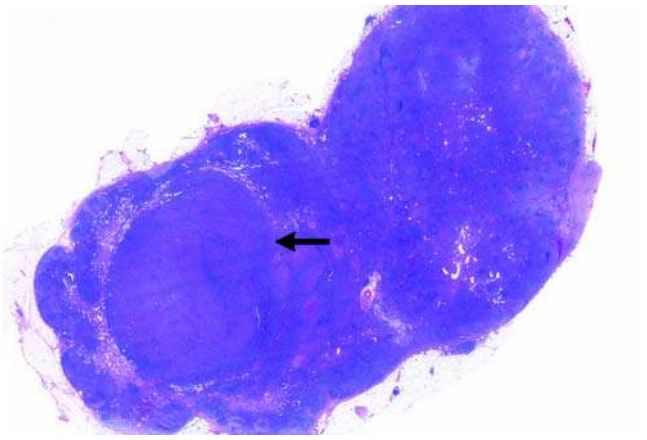

Figure 134 Diffuse large B-cell lymphoma, lymph node. The presence of an expansile nodule (*arrow*) strongly favors a diagnosis of malignancy over reactive lymphoid hyperplasia.

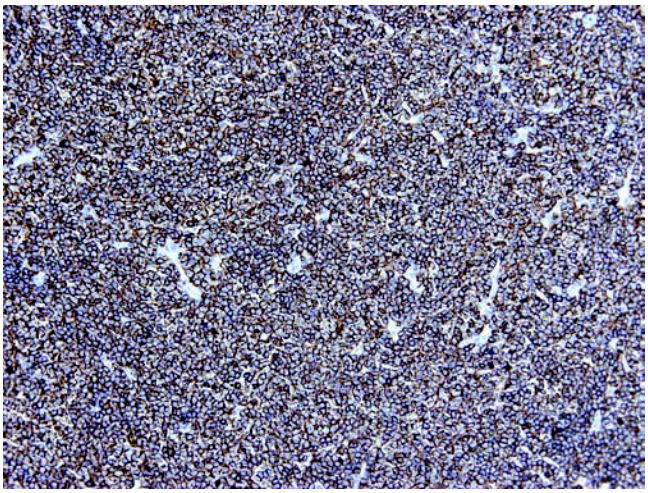

Figure 135 MALT lymphoma of submandibular gland. The presence of diffuse sheets of CD20+ cells strongly favors a diagnosis of lymphoma (B-cell lymphoma) over reactive lymphoid hyperplasia.

Wegener Granulomatosis

Wegener granulomatosis is a systemic vasculitis and necrotizing granulomatosis with predominant involvement of the upper respiratory tract, lungs, and kidneys. The key histologic features in the nasal mucosa include the following:

1. Ulceration
2. Patchy geographic necrosis, often surrounded by palisaded histiocytes and multinucleated giant cells
3. Heavy mixed inflammatory cell infiltrate, including small lymphocytes, plasma cells, eosinophils, and neutrophils (often with microabscess formation)
4. Necrotizing vasculitis involving arterioles, small arteries, and small veins, ranging from acute (patchy fibrinoid necrosis and neutrophil infiltration) to granulomatous (infiltration of histiocytes and multinucleated giant cells)
5. Granulomatosis, in the form of ill-defined aggregates of histiocytes, sometimes with scattered multinucleated giant cells

Rosai–Dorfman Disease

The nasal cavity is a fairly common extranodal site of involvement by Rosai–Dorfman disease (456,457). The characteristic histologic feature is the presence of large aggregates of dark-staining plasma cells alternating with pale-staining areas. Within the latter, closer

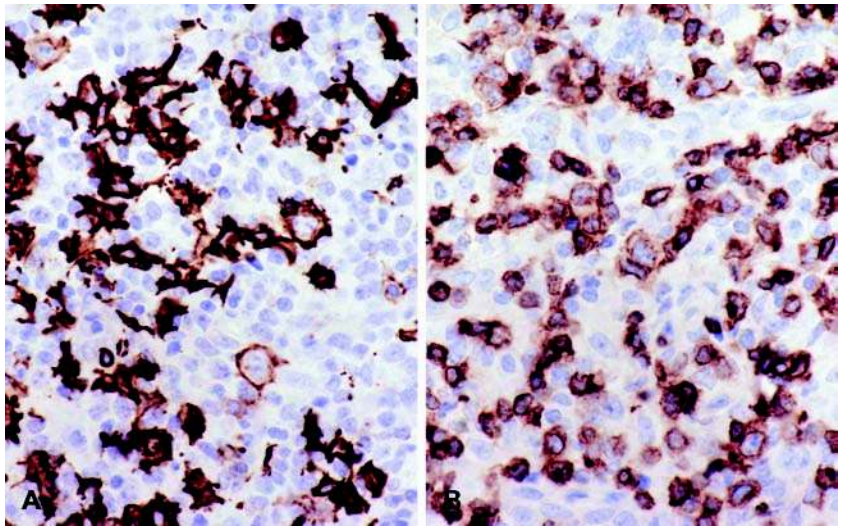

Figure 136 Reactive paracortical hyperplasia of lymph node, immunohistochemistry. (**A**) Immunostaining for CD20 highlights some large cells, with a spectrum of intensity of staining. (**B**) Immunostaining for CD3 also shows up some large cells, indicating that the proliferated lymphoid cells represent a mixture of B and T cells.

Table 12 Most Common Lymphoma Types Occurring in Various Sites

Site	Commonest lymphoma types	Comments
Lymph node	Diffuse large B-cell lymphoma Follicular lymphoma Classical Hodgkin lymphoma	–
Nasal cavity	Extranodal NK/T-cell lymphoma Diffuse large B-cell lymphoma	Extranodal NK/T-cell lymphomas are more prevalent in Orientals, and less common in Caucasians
Paranasal sinuses	Diffuse large B-cell lymphoma[a]	–
Nasopharynx	Diffuse large B-cell lymphoma Extranodal NK/T-cell lymphoma	Primary nasopharyngeal extranodal NK/T-cell lymphoma is less common compared with the nasal cavity
Oral cavity, including tonsils	Diffuse large B-cell lymphoma[a]	–
Salivary gland	MALT lymphoma[a] Diffuse large B-cell lymphoma Follicular lymphoma	Sjogren syndrome is a known predisposing factor Follicular lymphoma probably more commonly originates from intra- or periglandular lymph nodes
Larynx, hypopharynx, trachea	Diffuse large B-cell lymphoma MALT lymphoma	–
Thyroid	Diffuse large B-cell lymphoma MALT lymphoma	Hashimoto thyroiditis is a known predisposing factor
Ocular adnexa	MALT lymphoma[a]	–
Eye	Diffuse large B-cell lymphoma (intraocular lymphoma)	–
Bone	Plasmacytoma Diffuse large B-cell lymphoma	–
Skin	Mycosis fungoides Primary cutaneous CD30+ T-cell lymphoproliferative disorders Primary cutaneous follicle center lymphoma Primary cutaneous MALT lymphoma	*Borrelia burgdorferi* infection has been implicated in MALT lymphomas of the skin in some populations, e.g., Scotland

[a]The lymphoma type accounts for the great majority of lymphomas in the organ site.

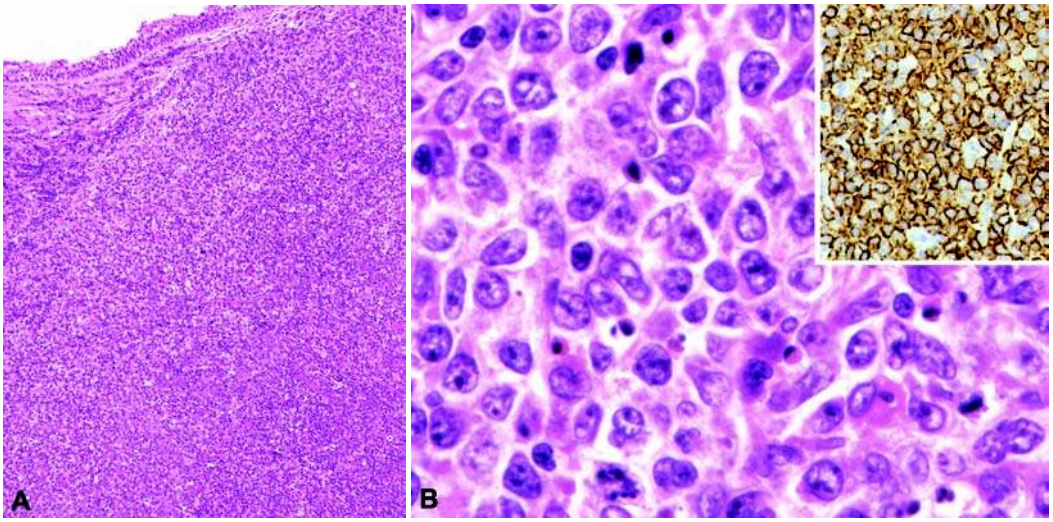

Figure 137 Diffuse large B-cell lymphoma of nasal cavity. (**A**) A diffuse and dense mucosal infiltrate with an intact surface epithelium. (**B**) The cells are large, with round- or irregular-shaped nuclei. Positive CD20 staining is shown in the inset.

scrutiny will reveal the distinctive very large histiocytes with round vesicular nuclei, distinct central nucleoli, and voluminous cytoplasm (Fig. 138A). Sometimes the cell borders are poorly defined, and the cells may appear to merge into a fibrillary background, imparting a neural quality. Emperipolesis can be difficult to appreciate (Fig. 47B). In long-standing lesions, there are secondary changes such as fibrosis

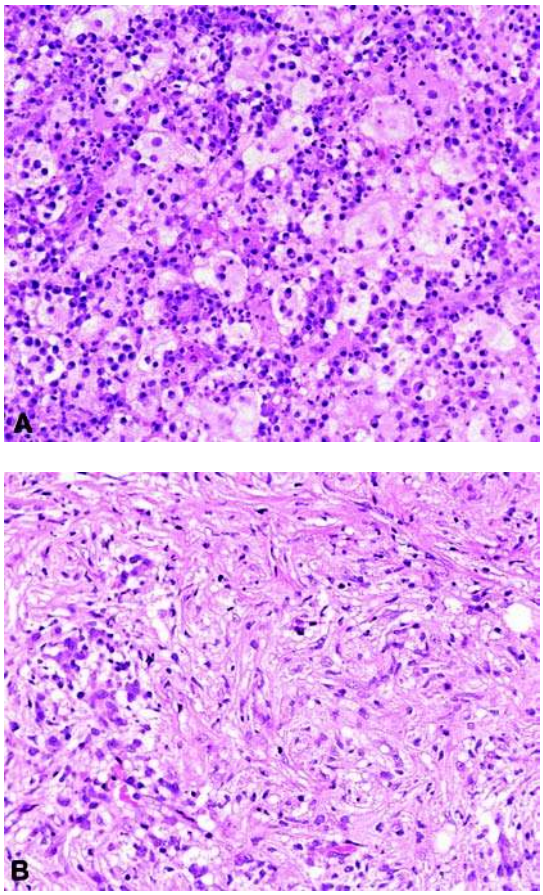

Figure 138 Rosai–Dorfman disease of nasal cavity. (**A**) Bands of pale-staining cells (Rosai–Dorfman histiocytes) typically alternate with bands of dark-staining cells (plasma cells). The histiocytes are very large due to the presence of abundant cytoplasm. (**B**) Focally, the fibrosis and presence of spindly cells in a vague storiform pattern create a fibrohistiocytic tumorlike pattern.

and accumulation of foamy histiocytes, and the diagnostic histiocytes can be sparse. The diagnostic histiocytes can even assume a spindly shape, resembling mesenchymal tumors (Fig. 138B), or show some degree of nuclear atypia, leading to a misdiagnosis of malignancy such as histiocytic sarcoma or large cell lymphoma. Immunostaining for S100 will be diagnostic, highlighting the aggregates of large histiocytes with emperipolesis—the nucleus and cytoplasm of the histiocytes are stained, while the nuclei of the ''phagocytosed'' cells remain unstained (Fig. 47D).

Rhinoscleroma

Rhinoscleroma is a chronic infection caused by *Klebsiella rhinoscleromatis* (a Gram-negative bacillus), involving the nasal cavity and other parts of the upper respiratory tract. It is endemic in Africa and Central America. Biopsy usually shows extensive infiltration by bacteria-containing histiocytes, often with a foamy quality, admixed with many plasma cells. This disease, which requires treatment with antibiotics, has to be distinguished from Rosai–Dorfman disease. It differs from the latter in that the histiocytes are not as large, and the nuclei do not have a round vesicular appearance. The diagnosis of rhinoscleroma can be confirmed by Warthin–Starry stain, wherein the bacilli within the histiocytes can be demonstrated.

Juvenile Xanthogranuloma

Juvenile xanthogranuloma may occasionally present at extracutaneous sites such as the nasal cavity and paranasal sinuses (458,459). The histiocytic proliferation comprises sheets of nondescript ovoid mononuclear cells together with some spindly and foamy cells. Scattered Touton giant cells (multinucleated cells with nuclei arranged in a wreath-like pattern) are readily found. The features may resemble hematolymphoid neoplasms especially Langerhans cell histiocytosis in view of the frequent occurrence in young patients. In contrast to the latter, the lesional cells in juvenile xanthogranuloma are negative for S100, CD1a, and CD207 (langerin), and they express CD68 and factor XIIIa.

Others

Extramedullary hematopoietic tumor presenting as a nasal polyp-like mass has been described in patients with myeloproliferative disorder (165), and inflammatory pseudotumors of the nasal cavity and the paranasal sinuses have also been reported (152).

C. Diagnostic Considerations

The nasal or paranasal sinus mucosa normally does not have a significant component of lymphoid tissue, and thus nonspecific reactive lymphoid hyperplasia as commonly observed in the nasopharynx is rare. If a significant lymphoid infiltrate is seen, it is most often due to lymphoma or an infective process.

The diagnosis of lymphoma is usually straightforward in most cases due to the extensive destructive infiltrate and presence of definite cytologic atypia (Figs. 100, 101, and 137A, B). However, it can be difficult to render a diagnosis of malignancy in some cases of extranodal NK/T-cell lymphoma comprising mostly small lymphoid cells or admixed with many inflammatory cells (Figs. 102 and 139) (368). In such situation, the suspicion for lymphoma is heightened if the mucosa is expanded as evidenced by wide separation of the mucosal glands, invasion and damage of blood vessel walls is present, or necrosis is prominent (Fig. 140). The diagnosis can be confirmed if there are sheets of CD56+ cells or sheets of EBER+ cells, provided that CD3 is also extensively positive (Figs. 105 and 106). If CD3 is negative and only CD56 is positive, a diagnosis of extranodal NK/T-cell lymphoma can be made only if other T-lineage markers (such as CD2) are positive. Otherwise CD56+ nonhematolymphoid tumors such as olfactory neuroblastoma, primitive neuroectodermal tumor and rhabdomyosarcoma should be seriously considered.

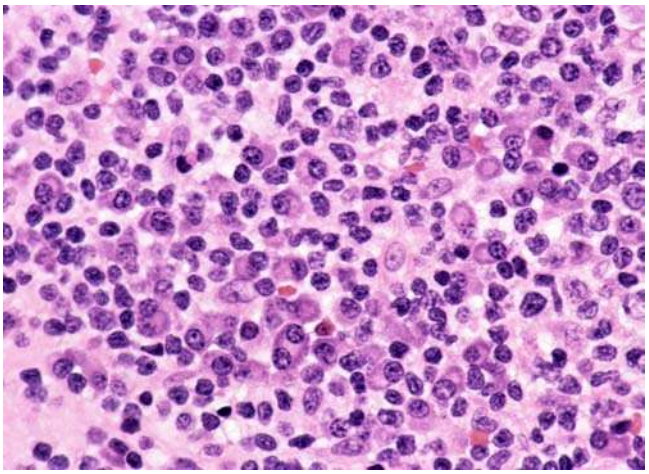

Figure 139 Extranodal NK/T-cell lymphoma of nasal cavity, difficult-to-diagnose case. The neoplastic cells show minimal nuclear atypia, and there are many admixed plasma cells, making it difficult to render a firm diagnosis of lymphoma. Ancillary studies are mandatory for confirming the diagnosis.

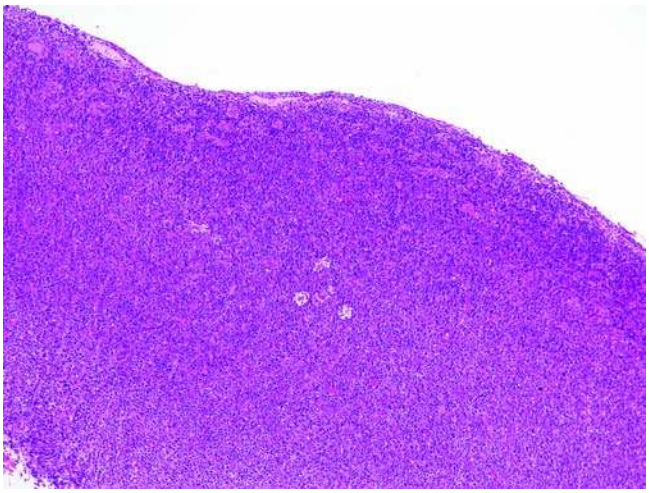

Figure 140 Extranodal NK/T-cell lymphoma of nasal cavity. The extensive lymphoid infiltrate effacing the architecture of the nasal mucosa supports a diagnosis of malignancy. There are few residual mucosal glands.

Wegener granulomatosis and extranodal NK/T-cell lymphoma share many histologic similarities such as ulceration, necrosis, vascular damage, and heavy lymphoid cell infiltration. Features favoring the former diagnosis include presence of serum anti-neutrophil cytoplasmic antibody, lack of definite nuclear atypia in the lymphoid cells, genuine vasculitis instead of infiltration of vessel walls by abnormal lymphoid cells, and presence of few or no CD56+ or EBER+ cells.

Well-differentiated squamous cell carcinoma with keratinization is very rare in the nasal cavity. Before rendering such a diagnosis, the underlying tissue must be scrutinized for the presence of lymphomatous infiltrate since lymphoma can be accompanied by florid pseudoepitheliomatous hyperplasia, simulating squamous cell carcinoma (Fig. 99B).

VI. HEMATOLYMPHOID LESIONS OF THE NASOPHARYNX

A. Hematolymphoid Neoplasms of the Nasopharynx

General Features

Malignant lymphoma is the commonest hematolymphoid lesion of the nasopharynx, and 2.5% of all primary extranodal lymphomas occur in this anatomic region (448). In the literature, nasopharyngeal lymphomas have often been reported together with cases from the nasal cavity or cases in the rest of the Waldeyer ring, rendering it difficult to sort out the features pertinent to nasopharyngeal location (373,460–462). Series reporting primary nasopharyngeal lymphomas alone are very rare (463).

In the West, nearly all cases of primary nasopharyngeal lymphomas are B-cell lymphomas, most frequently DLBCL (460). Other B-cell lymphomas that have been reported include follicular lymphoma, Burkitt lymphoma, mantle cell lymphoma, and MALT lymphoma (373,460,462). The relative incidence of B-cell lymphomas is lower in Asia, accounting for only 50% to 60% of all cases, due to a higher incidence of extranodal NK/T-cell lymphoma and peripheral T-cell lymphomas (373,462). The nasopharynx is also a predilection site for the occurrence of extramedullary plasmacytoma, ranking second after the sinonasal tract in frequency (464).

Rare cases of classical Hodgkin lymphoma can involve the nasopharynx, mostly of mixed cellularity and nodular sclerosis subtypes, and with strong EBV association (465–469).

Other hematolymphoid tumors that can occur in the nasopharynx include myeloid sarcoma (470) and follicular dendritic cell sarcoma (Fig. 141A, B) (433,471). The last entity may develop from an underlying hyaline-vascular Castleman disease (433).

Clinical Features

Patients with nasopharyngeal lymphomas present with epistaxis, nasal obstruction, postnasal drip, hearing loss, otitis media, dysphagia, headache, or neck mass. Associated cervical lymphadenopathy is more often seen in B-cell lymphoma and classical Hodgkin lymphoma than extranodal NK/T-cell lymphoma or peripheral T-cell lymphoma. Most patients (80–90%) have localized disease (stage IE/IIE) at presentation (373,463).

The patients are frequently treated with radiotherapy and/or chemotherapy. The outcome depends on subtype, with extranodal NK/T-cell lymphoma or peripheral T-cell lymphoma being associated with a poorer prognosis compared with B-cell lymphomas or classical Hodgkin lymphoma.

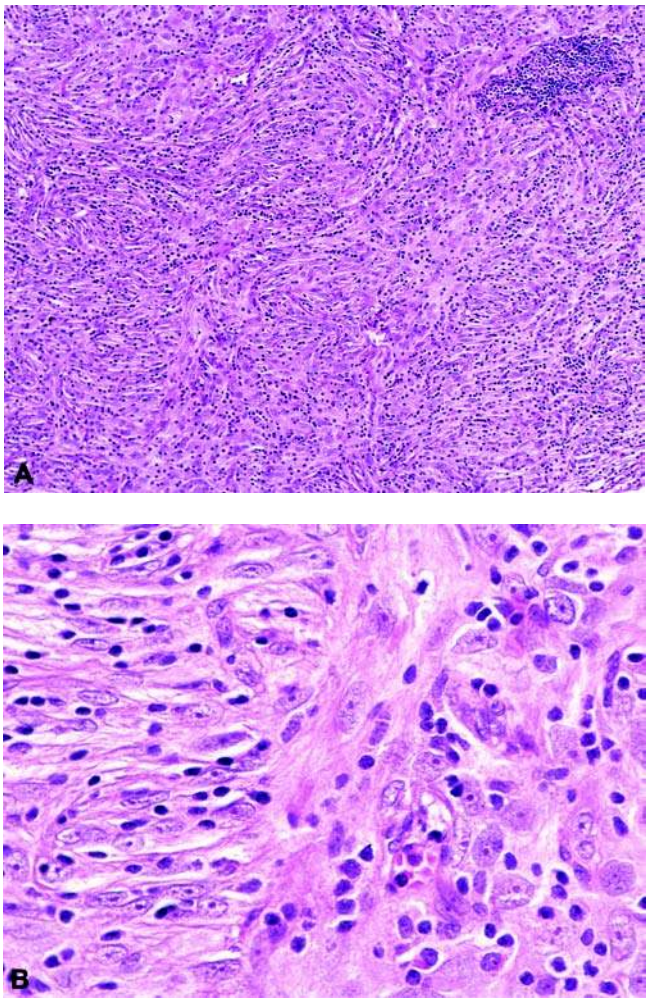

Figure 141 Follicular dendritic cell sarcoma of nasopharynx. (**A**) There is a typical storiform growth of spindly cells, which are intimately admixed with small lymphocytes. (**B**) Higher magnification shows syncytial-appearing tumor cells with oval nuclei and distinct nucleoli.

Pathologic Features Related to Anatomic Location

The nasopharyngeal mucosa involved by lymphoma may or may not show ulceration, but sometimes the metaplastic stratified squamous epithelium can undergo exuberant pseudoepitheliomatous hyperplasia. The stroma is densely infiltrated by lymphoma cells, which may also infiltrate into the surface and crypt epithelium. Like in the nasal cavity, extranodal NK/T-cell lymphoma tends to show coagulative necrosis and angioinvasion, although these features can also be seen in some cases of DLBCL.

B. Important Reactive or Inflammatory Hematolymphoid Lesions

Nonspecific Reactive Lymphoid Hyperplasia

As part of the Waldeyer ring, the lymphoid tissue of the nasopharynx, not uncommonly, undergoes reactive hyperplasia in response to infection, antigenic challenge, or unknown causes. There are two major histologic patterns, both accompanied by an intact surface epithelium. The first pattern is characterized predominantly by an increase and prominence of secondary lymphoid follicles. The interfollicular zone is populated mostly by small lymphocytes, which are admixed with some plasma cells and immunoblasts. The second pattern is characterized by an expanded interfollicular zone or diffuse infiltrate, with aggregates of nonatypical immunoblasts scattered among small lymphocytes (Fig. 14A, B).

Infectious Mononucleosis

Primary EBV infection (infectious mononucleosis) can involve the nasopharynx. There can be ulceration, accompanied by a marked increase in large activated lymphoid cells (immunoblasts), which not uncommonly leads to a misdiagnosis of large cell lymphoma or nasopharyngeal carcinoma. Although the large cells occur in clusters and sheets, they are not monotonous in appearance and lack overt nuclear atypia, but rather show transition to plasmablasts (slightly smaller cells with coarsely clumped chromatin), immature plasma cells, and mature plasma cells. On immunohistochemistry, the large cells show heterogeneous staining for CD20 and CD3, and they show polytypic staining for immunoglobulin. Serologic studies or in situ hybridization for EBV (EBER) can confirm the diagnosis.

IgG4-Related Sclerosing Disease

IgG4-related sclerosing disease can involve the nasopharynx with or without producing symptoms. The main histologic changes are an increase in mature plasma cells in the subepithelial zone, prominence of lymphoid follicles, and increase in interfollicular plasma cells (Fig. 142). Immunostaining for IgG4 and IgG with a ratio of over 40% is confirmatory. Sometimes, a

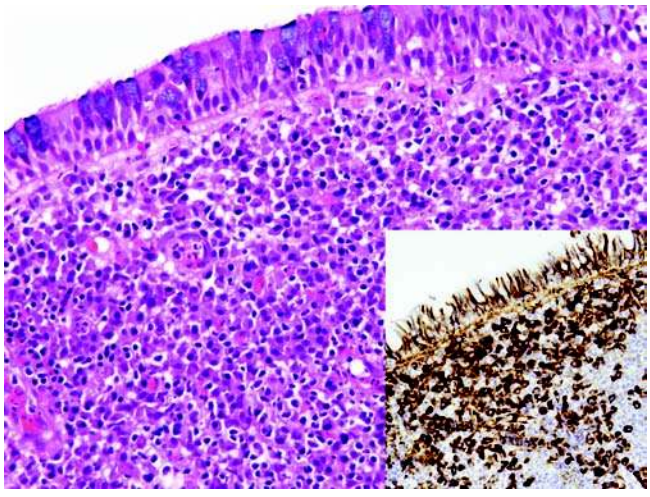

Figure 142 IgG4-related sclerosing disease involving nasopharynx. There is a broadband of plasma cells beneath the epithelium. Many plasma cells show immunostaining for IgG4 (inset).

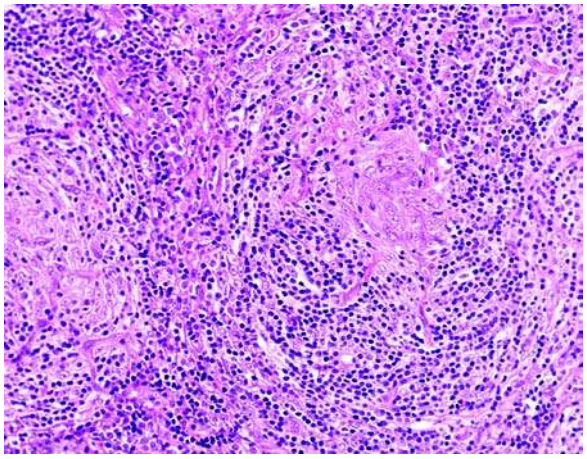

Figure 143 Hyaline-vascular Castleman disease of the nasopharynx.

nasopharyngeal biopsy may provide the first histologic evidence for the diagnosis of IgG4-related sclerosing disease (105).

Others

Other hematolymphoid lesions that have been described in the nasopharynx include hyaline-vascular-type Castleman disease (Fig. 143) (433,472), Rosai–Dorfman disease (144,457), and herpes simplex virus infection (50).

C. Diagnostic Considerations

A nasopharyngeal biopsy showing many large cells will raise the consideration of non-Hodgkin lymphoma (such as DLBCL and extranodal NK/T-cell lymphoma), anaplastic plasmacytoma, nasopharyngeal carcinoma, malignant melanoma, and reactive lymphoid hyperplasia (immunoblastic proliferation). The main features helpful for differential diagnosis are listed in Table 13. In a young patient below the age of 25 years, the possibility of reactive lymphoid hyperplasia (in particular infectious mononucleosis) must be seriously considered and excluded before rendering a diagnosis of malignancy.

Rarely, *herpes simplex virus infection* of the nasopharynx may be associated with necrosis and florid lymphoid cell proliferation, raising the suspicion of extranodal NK/T-cell lymphoma. More confusingly, the lymphoid cells are often CD3+ T cells that may show CD56 expression (50). The identification of the herpes simplex viral inclusions in the epithelial cells and absence of EBV in the lymphoid cells will be diagnostic.

A diagnosis of MALT lymphoma should always be made with great caution on the basis of a nasopharyngeal biopsy alone, since distinction from reactive lymphoid hyperplasia of the nasopharynx is very difficult. In both conditions, there are often reactive follicles and a mixture of cell types with minimal atypia, and lymphoepithelial lesions are present. Thus, a diagnosis of MALT lymphoma can be rendered confidently only when there are diffuse sheets of small B cells associated with light-chain restriction, aberrant immunophenotype (e.g., CD43 coexpression), and/or rearranged immunoglobulin genes.

VII. HEMATOLYMPHOID LESIONS OF THE ORAL CAVITY AND OROPHARYNX

A. Hematolymphoid Neoplasms of the Oral Cavity and Oropharynx

General Features of Lymphomas

The oral cavity and oropharynx include the palate, tongue, floor of mouth, gingiva, buccal mucosa, lips, palatine tonsils, and lingual tonsils. The palatine and lingual tonsils are part of the Waldeyer ring, which normally has a rich lymphoid component and is a site commonly involved by hematolymphoid lesions.

Malignant lymphoma is the most important hematolymphoid disease in this anatomic region, since it is the second most common oral cancer following squamous cell carcinoma, and accounts for 3.5% of all oral malignancies (473). Overall, 13% of all primary extranodal lymphomas arise from this anatomic region (448). The most frequently involved site is the tonsil (about 70%), followed by the palate, gingiva, and tongue (448,473–475).

More than 90% of cases of lymphomas in this anatomic region are B-cell lymphomas, with DLBCL being the commonest, accounting for more than half of all cases (460,475–478). Other B-cell lymphomas include mantle cell lymphoma, follicular lymphoma, MALT lymphoma, and Burkitt lymphoma (460). Pediatric-type follicular lymphoma has a predilection for the

Table 13 Clues to Diagnosis of Infectious Mononucleosis Versus Large Cell Lymphoma

Clinical and morphologic clues
Young age, especially for tonsillar specimens
Architecture not completely effaced
Proliferated large cells do not appear monotonous, and are not overtly atypical in appearance
Features supportive of a reactive process
The large cells exhibit a spectrum of appearances from immunoblasts to plasmablasts, and there is apparent transition to immature and mature plasma cells
CD20 immunostain: many large cells are positive, but with heterogeneous intensities of staining
Immunoglobulin immunostain: the large cells show polytypic staining
CD3 immunostain: some or many large cells are positive
CD4, CD8 and cytotoxic marker immunostains: many T cells are CD8+ cytotoxic cells
In situ hybridization for EBER: a proportion of cells are positive, including some small and large cells
Polymerase chain reaction for immunoglobulin and T-cell receptor gene rearrangements: polyclonal, but sometimes can be oligoclonal

head and neck region, such as the tonsils (316). Extramedullary plasmacytomas can occur in the tonsil, palate, gingiva, pharynx, and tongue (358,360,464,479).

The oral cavity and oropharynx are also common sites for occurrence of immunodeficiency-associated lymphomas. In HIV-associated intraoral lymphomas, most cases are DLBCLs, with 75% of cases being associated with EBV (480,481). It appears that a substantial fraction of such cases represent plasmablastic lymphoma of the oral cavity (285). Rare cases of EBV-associated peripheral T-cell lymphoma have also been reported in this setting (475,482).

Extranodal NK/T-cell lymphoma sometimes involves the palate, tonsil, oropharynx, and the lip, and is more common among Orientals (483,484). Mature T-cell lymphomas including anaplastic large cell lymphoma, lymphoepithelioid/Lennert lymphoma (a peripheral T-cell lymphoma NOS variant), angioimmunoblastic T-cell lymphoma, primary oral CD30+ T-cell lymphoproliferative disorder, and HTLV1-associated adult T-cell leukemia/lymphoma have also been reported (413,475,478,485,486).

Classical Hodgkin lymphomas occasionally involve the Waldeyer ring, especially the palatine tonsils (465,467), and uncommonly the oropharynx, alveolar crest, and gingiva (487–489). Mixed cellularity subtype is the most frequent histologic subtype, often with EBV association (465). Rarely, nodular lymphocyte–predominant Hodgkin lymphoma may affect the palatine and lingual tonsils (465,490).

Clinical Features of Lymphomas

Patients with intraoral lymphomas cover a wide age range, with a median age in the sixth to seventh decades. Burkitt lymphoma occurs more often in children and young adults. Patients with immunodeficiency-associated lymphomas, especially in the setting of posttransplantation or HIV infection, are also usually young.

Common presenting symptoms include ulcer, mass, pain, sensation of fullness of the throat, sore throat, dysphagia, and neck mass. Extranodal NK/T-cell lymphoma tends to produce extensive ulcerations and necrosis. About three-quarters of patients have localized disease (IE/IIE) at presentation. Those with tonsillar lymphoma are prone to develop metachronous or synchronous tumors in the gastrointestinal tract, supporting the homing concept involving different MALT sites (461,491,492).

The treatment options for intraoral lymphomas include radiotherapy and/or chemotherapy. The five-year overall survival for localized disease ranges from 50% to over 80%, depending on histologic subtype (493–497). Poor prognostic factors include high clinical stage, lymphomas of high histologic grade, and T- or NK/T-cell immunophenotype (461,493,495,498,499).

Pathologic Features of Lymphomas Related to Anatomic Location

The surface stratified squamous epithelium of the oral cavity or oropharynx involved by lymphoma can be intact or ulcerated (Fig. 144A, B). The surface epithelium sometimes undergoes striking pseudoepitheliomatous hyperplasia. The stroma shows a dense lymphoid infiltrate, sometimes with coagulative necrosis. The mucosal glands are lost or show wide separation due to interstitial infiltration by lymphoma cells (Fig. 144A). In the tonsils, not only are the normal linearly oriented reactive lymphoid follicles obliterated, there is frequently infiltration beyond the base of the tonsil, resulting in a rugged lower contour (Fig. 145A, B).

The morphologic and immunohistochemical features of the various types of lymphomas have been described in a previous section ''Hematolymphoid Neoplasms of the Head and Neck''(Figs. 146A, B; 147; 148A, B; and 149A, B). Of note, approximately 10% of

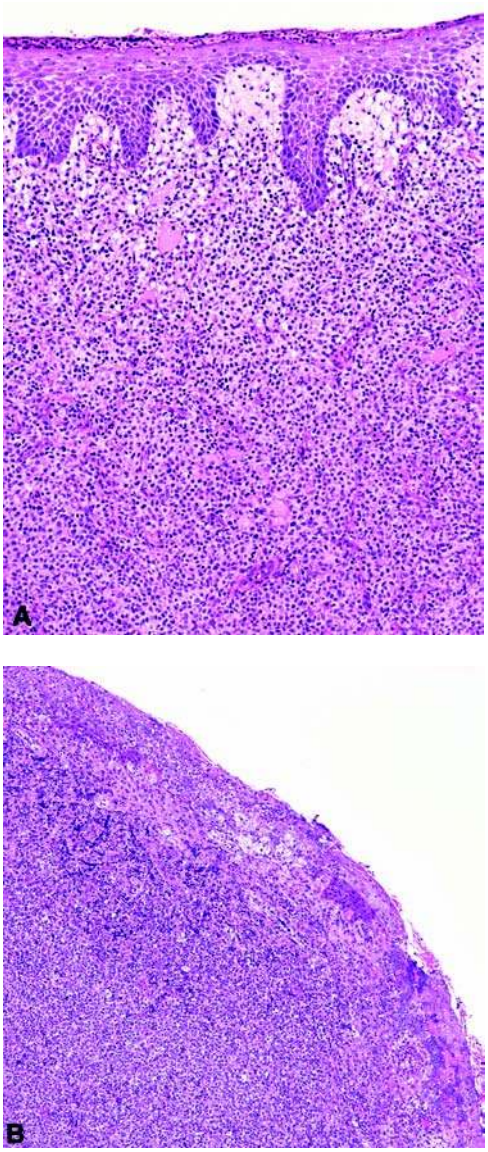

Figure 144 Diffuse large B-cell lymphoma of the oral cavity. (**A**) This lymphoma of the lip is covered by an intact surface epithelium. (**B**) This lymphoma of the tonsil shows mucosal ulceration.

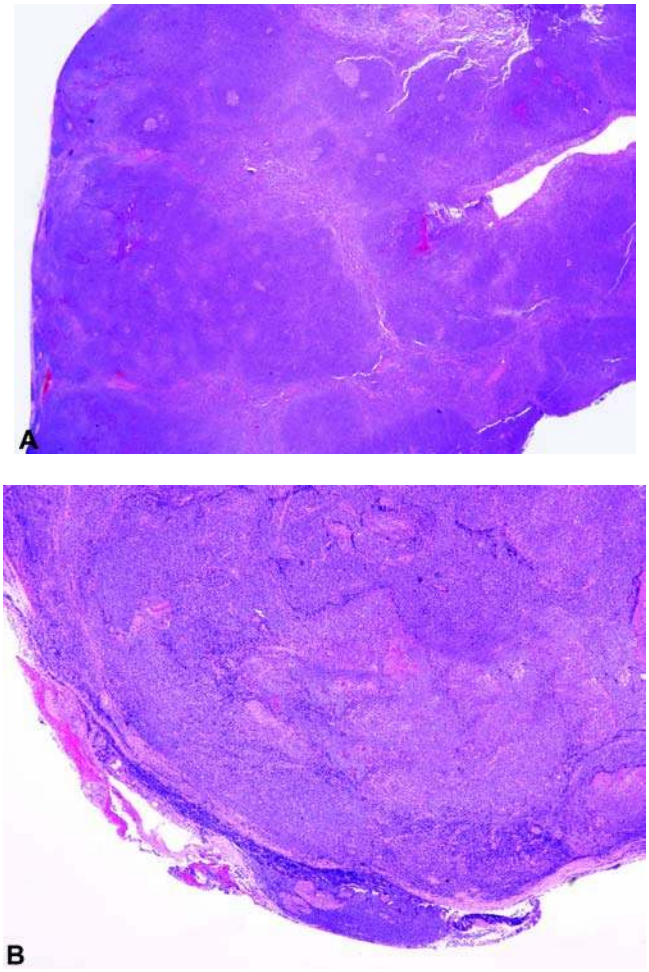

Figure 145 MALT lymphoma of tonsil. (**A**) There is loss of the lymphoid organization of the normal tonsil. Some small reactive follicles are evident. (**B**) The lymphoid infiltrate breaches the normally sharp base of the tonsil.

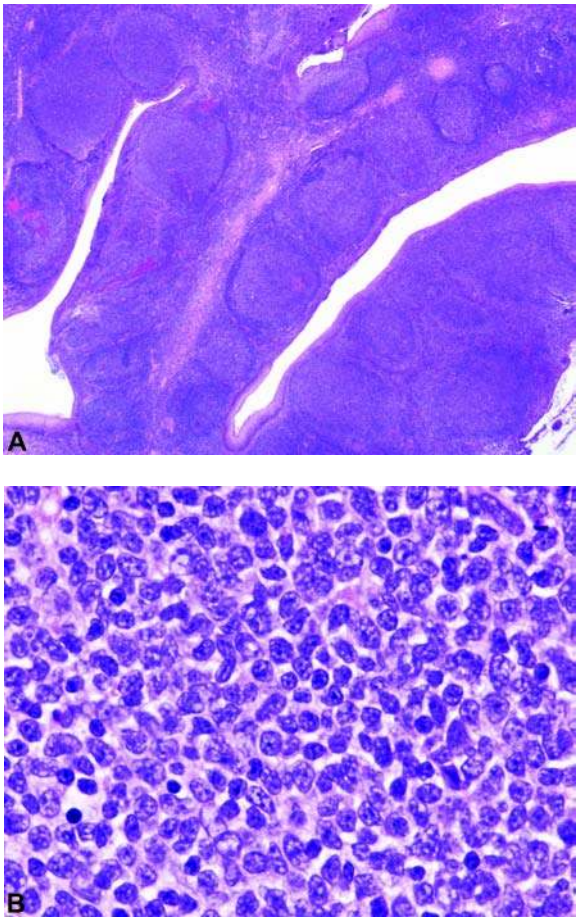

Figure 146 Follicular lymphoma of tonsil. (**A**) The follicles appear abnormal, with crowding and inconspicuous or absent mantles. (**B**) The follicles show predominance of centrocytes and absence of tingible-body macrophages.

cases of tonsillar DLBCL show an unusual feature—presence of focal follicular features in a predominantly diffuse growth, raising the issues of DLBCL with follicular colonization versus follicular lymphoma with large cell transformation (Fig. 150A–C) (500). Since the lymphoma cells lack the immunophenotypic features of germinal center cells, the latter postulation is not favored.

Other Hematolymphoid Neoplasms

About 3.5% of patients with acute myeloid leukemia show diffuse gingival leukemic infiltration, more frequently in cases with monocytic and myelomonocytic differentiation (501). Other than gingival involvement, intraoral myeloid sarcomas have been described in the palate and tonsil (427,453,502,503).

Langerhans cell histiocytosis affects intraoral structures in 10% of patients, mostly as a result of disease of the underlying jawbone, especially the mandible (504).

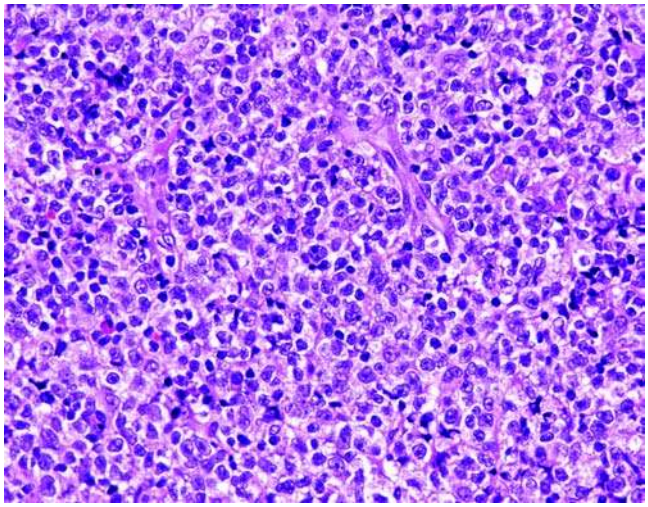

Figure 147 Diffuse large B-cell lymphoma of tonsil.

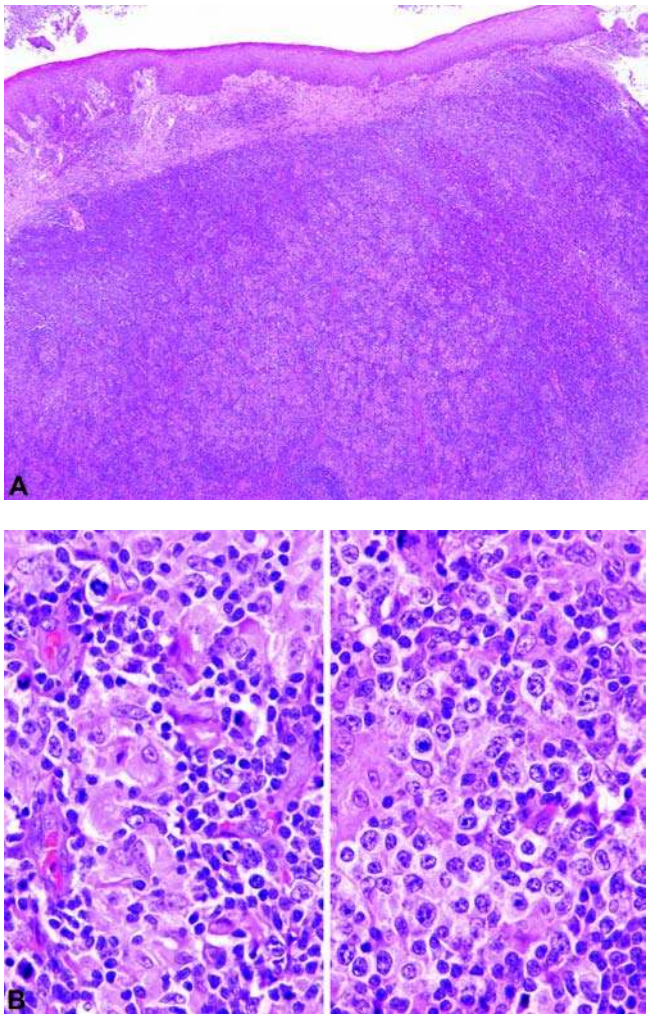

Figure 148 Angioimmunoblastic T-cell lymphoma presenting with tonsillar involvement. (**A**) This example shows coalescing small clusters of epithelioid cells, raising the possibility of Lennert (lymphoepithelioid) lymphoma. (**B**) The cytoarchitectural features are more in keeping with angioimmunoblastic T-cell lymphoma. There is a rich vascularity (*left panel*). Many medium-sized clear cells are present (*right panel*).

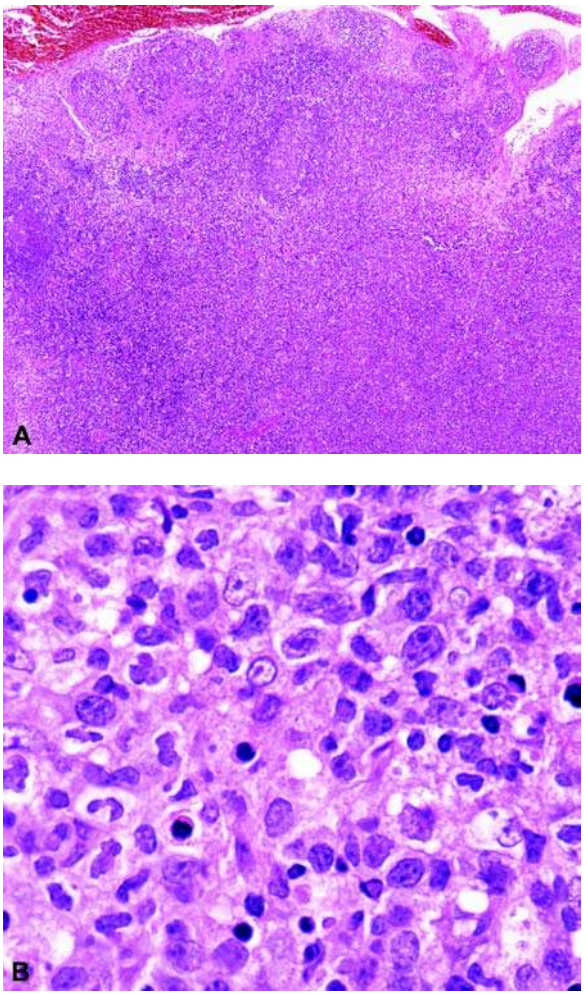

Figure 149 Extranodal NK/T-cell lymphoma of tongue. (**A**) The mucosa shows a dense lymphoid infiltrate, accompanied by surface necrosis and ulceration. (**B**) The infiltrate includes medium-sized and large lymphoid cells with elongated or irregularly folded nuclei.

The gingiva, palate, floor of mouth, buccal mucosa, and the tonsil may also be involved (431,504). Rarely, soft tissue involvement without underlying bony disease may be encountered (505–507).

Follicular dendritic cell sarcomas have been reported in the tonsil, oropharynx, and palate (431,434,435,508,509). Histiocytic sarcoma of the palate has also been described (510).

B. Important Reactive or Inflammatory Hematolymphoid Lesions

Nonspecific Reactive Lymphoid Hyperplasia

Nonspecific reactive lymphoid hyperplasia is the most common pathologic diagnosis in tonsillectomy specimens. In tonsillectomy specimens resected for ''chronic tonsillitis,'' nonspecific reactive follicular hyperplasia is often the only ''abnormality'' that can be detected (Figs. 11A and 13). Since the Waldeyer ring is constantly exposed to antigenic stimulations from the environment, these hyperplastic reactive follicles can be regarded as ''normal'' structures in these locations. In the Waldeyer ring, some of the reactive lymphocytes overlying the lymphoid follicles immediately outside the mantle zone can have a marginal zone B-cell appearance, with nuclear irregularity and moderate amount of clear cytoplasm. These marginal zone B cells often infiltrate into the overlying squamous epithelium, forming lymphoepithelial lesions (Fig. 11C).

Infectious Mononucleosis

Tonsil involved by infectious mononucleosis typically shows ulceration of the surface or at least erosion of

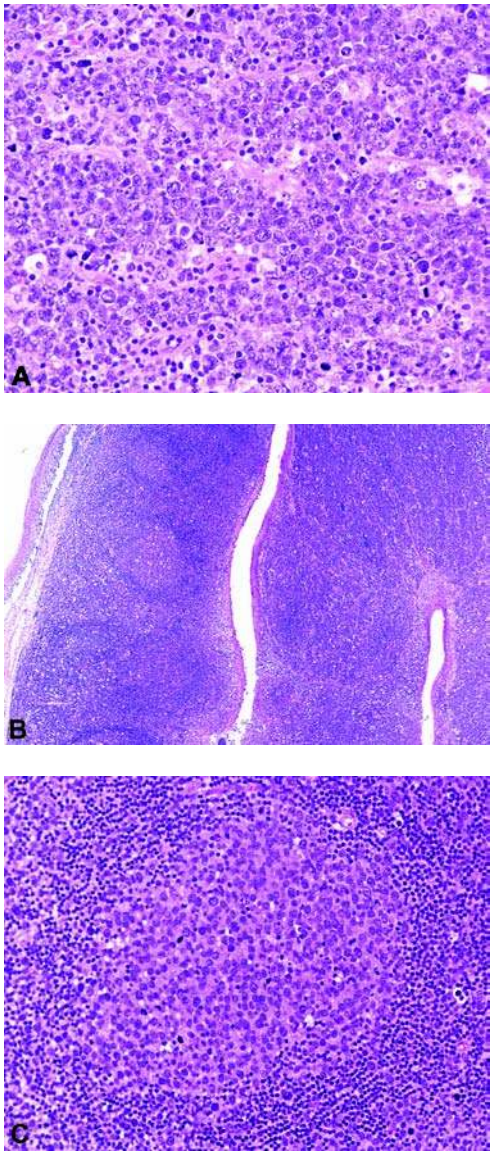

Figure 150 Diffuse large B-cell lymphoma with focal follicular features, tonsil. (**A**) A diagnosis of diffuse large B-cell lymphoma is straightforward. (**B**) Focally, there are ill-defined nodules/follicles (*left field*). (**C**) The nodules/follicles comprise mostly large cells.

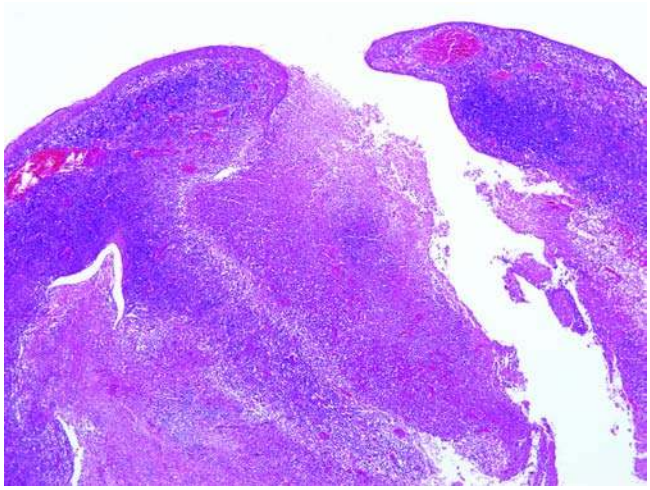

Figure 151 Infectious mononucleosis, tonsil. The mucosa commonly shows patchy ulceration, especially in the crypts.

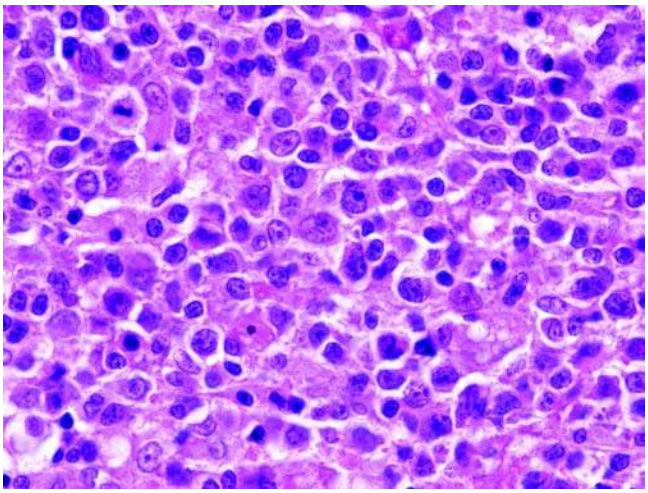

Figure 152 Infectious mononucleosis, tonsil. The lymphoid infiltrate includes an alarming number of large cells, but these cells do not impart an monotonous appearance.

the deep portions of some crypts (Fig. 151). There is a remarkable lymphoid infiltrate including many large cells, and occasional Reed–Sternberg like cells can be scattered singly (Fig. 152). The lymphoid proliferation appears to begin around the base of the crypts. In established lesions, more areas of the tonsillar mucosa are involved, but the architecture is not totally effaced, in that there are almost always some residual lymphoid follicles. Some follicles may exhibit necrosis of the germinal centers. There can be foci of geographic necrosis amid areas of lymphoid cell proliferation. The morphologic features of the lymphoid cells are described in previous sections (''Reactive Hematolymphoid Lesions of the Head and Neck'' and ''Hematolymphoid Lesions of the Nasopharynx'') and in Table 13. Two unnerving features that are practically never seen in other reactive lymphoid hyperplasias but can be seen in some cases of infectious mononucleosis are infiltration of the walls of blood vessels by the lymphoid cells and infiltration beyond the smooth sharp contour of the base of the tonsils (Fig. 153).

The marked increase in large lymphoid cells can easily entice the pathologist to render a wrong diagnosis of lymphoma. This mistake is disastrous, because these young patients will be subjected to unnecessary cytotoxic therapy, which potentially will lead to litigation claims.

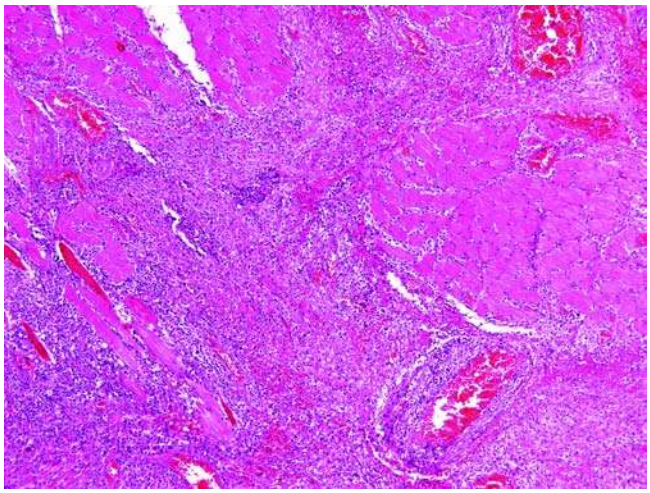

Figure 153 Infectious mononucleosis, tonsil. The lymphoid infiltrate can extend into the adjacent skeletal muscle fibers and can invade the walls of blood vessels. Such "worrisome" features may lead to a misdiagnosis of lymphoma.

Eosinophilic Ulcer

Eosinophilic ulcer, also known as traumatic eosinophilic granuloma or atypical histiocytic granuloma, is a reactive lesion of unknown etiology, most commonly occurring on the tongue. Histologically, It is characterized by a heavy inflammatory infiltrate rich in eosinophils and histiocytes, sometimes with scattered isolated large atypical cells (511–513). In a proportion of cases that show features consistent with eosinophilic ulcer, the large cells are shown to be CD30+ T cells; such cases should be classified as primary oral CD30+ T-cell lymphoproliferative disorder, which tends to undergo spontaneous regression and sometimes local recurrence (412,413,514).

Atypical Marginal Zone Hyperplasia

Atypical marginal zone hyperplasia of the tonsil has been described in children, who remain well without cytotoxic therapy. The lesion cannot be distinguished from MALT lymphoma on morphologic and immunohistochemical grounds. The proliferating marginal zone cells show immunoglobulin light-chain restriction and aberrant CD43 expression, but without clonally rearranged immunoglobulin genes (515).

Indolent T-Lymphoblastic Proliferation

Indolent T-lymphoblastic proliferation is a very rare entity that has been reported to involve the oropharynx, tonsil, and nasopharynx, and practically impossible to distinguish from T-lymphoblastic lymphoma on morphologic and immunohistochemical grounds (516,517). The mucosa shows sheets of lymphoblasts with medium-sized nuclei, fine chromatin, and scanty cytoplasm. These cells express T-lineage markers and the precursor cell marker TdT. In contrast to the T-lymphoblastic lymphoma, these cases do not have clonally rearranged T-cell receptor genes, and the clinical behavior is indolent, with multiple local recurrences over many years but no systemic dissemination, even in the absence of cytotoxic therapy.

Others

Intraoral Rosai–Dorfman disease most commonly involves the palate and tonsils, but can also affect the cheek, tongue, oropharynx, and gingiva (144).

C. Diagnostic Considerations

Beware of an Overdiagnosis of Lymphoma in Young Patients

There are several diagnoses that should be made with utmost caution in oral cavity specimens from children and young adults. If there are uncertainties in diagnosis, it is preferable to further investigate and ''wait and see'' rather than rush to a diagnosis of lymphoma.

1. DLBCL, especially in tonsils—since this tumor is uncommon in young patients, infectious mononucleosis must be seriously excluded (see Table 13 for clues to diagnosis). In infectious mononucleosis, usually only a fraction of the lymphoid cells is EBER positive, and these include small and large cells (Fig. 21C); this contrasts with the usually extensive EBER staining observed in EBV+ DLBCLs. In general, no monoclonal populations are identified in infectious mononucleosis on immunoglobulin and T-cell receptor gene rearrangement analysis (518).
2. MALT lymphoma—the alternative of atypical marginal zone hyperplasia should always be considered.
3. T-lymphoblastic lymphoma—in the absence of other sites of disease, the possibility of indolent T-lymphoblastic proliferation, albeit rare, has to be considered.

Problems in Diagnosis of Large Cell Lymphoma

Large cell lymphomas (such as DLBCLs) of the oral cavity usually pose no problems in diagnosis, but they can assume myriads of unusual appearances mimicking nonhematolymphoid neoplasms. Thus, the possibility of lymphoma should always be considered in the differential diagnosis of any ''poorly differentiated malignant neoplasm,'' except when there is an obvious line of differentiation such as gland formation (adenocarcinoma) or keratinization (squamous cell carcinoma). The neoplastic cells of DLBCL can appear deceptively cohesive, forming a sharp interface with the surrounding tissue, simulating undifferentiated carcinoma (Fig. 154). They can also comprise polygonal clear cells (mimicking clear cell carcinoma), signet ring cells (mimicking signet ring carcinoma), or spindly cells (mimicking sarcoma) (Fig. 155). They can have fibrillary matrix with rosette formation, mimicking primitive neuroectodermal tumor, or myxoid

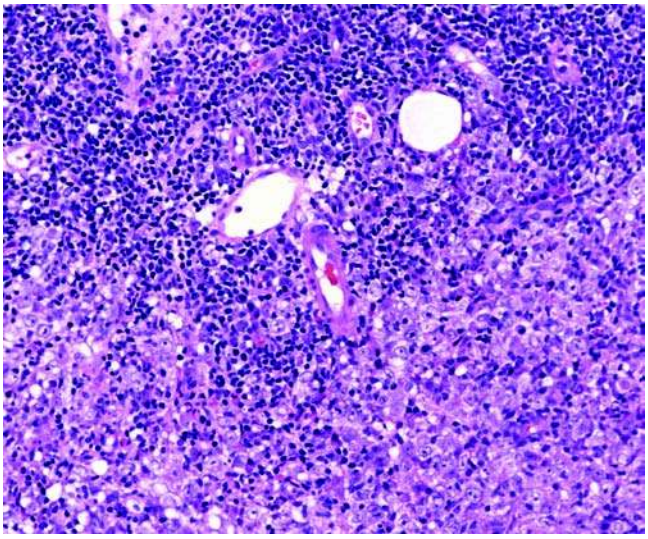

Figure 154 Diffuse large B-cell lymphoma of tonsil with deceptively cohesive growth pattern. Note the sharp interface of the lymphoma (*lower field*) with the residual lymphoid stroma (*upper field*).

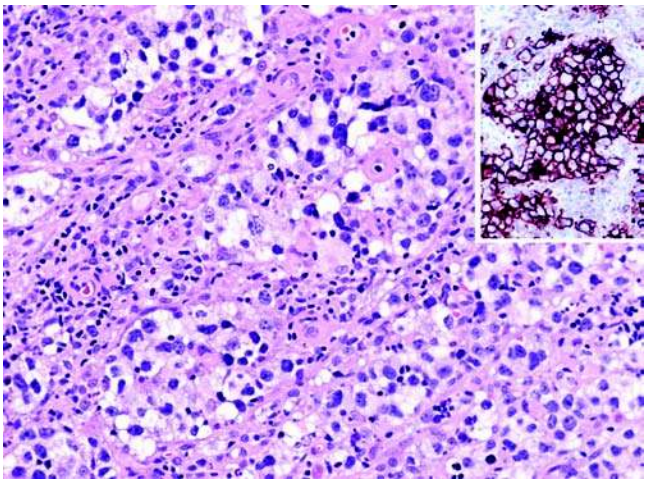

Figure 155 Diffuse large B-cell lymphoma of tonsil. The growth of the neoplastic clear cells in the form of discrete islands strongly mimics clear cell carcinoma. Surprisingly, the neoplasm is positive for CD20 (inset) and negative for cytokeratin, supporting a diagnosis of B-cell lymphoma.

stroma, mimicking various myxoid sarcomas. The diagnosis of lymphoma can be readily confirmed by immunostaining for lymphoid markers, but provided that the possibility of lymphoma has not been lightly dismissed.

On encountering a neoplastic lymphoid proliferation, which is shown to be CD3+, it is prudent to perform further staining for CD30, CD56, cytotoxic markers, and EBV to aid in characterization of the lymphoma. With intense CD30 staining of the large cells, especially in an eosinophil-rich background, primary oral CD30+ T-cell lymphoproliferative disorder has to be considered; it is important to recognize this disease because of the tendency of spontaneous regression and excellent prognosis. Expression of CD56, cytotoxic markers, and EBV is indicative of extranodal NK/T-cell lymphoma, which is a highly aggressive neoplasm.

VIII. HEMATOLYMPHOID LESIONS OF THE SALIVARY GLAND

A. Hematolymphoid Neoplasms of the Salivary Gland

General Features of Lymphomas

Primary malignant lymphomas of the salivary glands account for 5% of all primary extranodal lymphomas (448) and 2% of all salivary gland tumors (519). The parotid gland is the most frequently involved site (75%), followed by the submandibular gland (20%) and the sublingual and minor salivary glands in the oral cavity (5%) (519–521).

By definition, the bulk of the lesion should be in the salivary gland. However, since lymph nodes are normally present within the parotid gland and around the submandibular gland, it is at times impossible to decide whether a tumor is of nodal or salivary gland origin when it extensively involves both the glandular parenchyma and the lymph node. It is difficult to accurately determine the frequency of the various types of *bona fide* primary lymphomas of the salivary glands. From the data of the larger series of the older literature, about half of all cases are follicular lymphomas (519–521). However, many of these cases may represent either nodal primary with infiltration of the salivary gland or MALT lymphoma with follicular colonization. MALT lymphoma represents the most common type of lymphoma that is of true salivary gland origin, accounting for >80% of cases in some recent series (333). About 15% of primary salivary gland lymphomas are DLBCLs, with a proportion of these cases transforming from an underlying low-grade lymphoma. Other lymphomas that can rarely involve the salivary glands include mantle cell lymphoma, follicular lymphoma, SLL/CLL, lymphoplasmacytic lymphoma, Burkitt lymphoma, lymphoblastic leukemia/lymphoma, anaplastic large cell lymphoma, peripheral T-cell lymphoma NOS, extranodal NK/T-cell lymphoma, and Hodgkin lymphoma (classical Hodgkin lymphoma and nodular lymphocyte–predominant Hodgkin lymphoma), but many of these cases represent part of systemic disease (490,522–528).

Of note, malignant lymphoma (including both Hodgkin and non-Hodgkin lymphomas) can rarely develop within the lymphoid stroma of Warthin tumor, with most cases being follicular lymphoma and some being the presenting feature of a more generalized disease (529–531).

Clinical Features of Lymphomas

Most patients with salivary gland lymphoma are in the sixth decade, and multiple glandular involvement (especially bilateral) occurs in 10% of cases (520). The usual clinical presentation is that of a palpable mass, with some patients also experiencing pain and tenderness. Low-grade tumors tend to grow slowly, while rapid enlargement indicates a high-grade malignancy.

Patients with salivary gland MALT lymphoma show a female predominance (532,533). Rare cases may occur in children, with some associated with HIV infection (335,336). On the basis of a recent large series, 91% of cases are of low clinical stage (IE/IIE), with <10% showing bone marrow involvement (532). However, another series reports that one-third of cases show multicentric disease, frequently affecting bilateral parotid glands and ocular adnexa (334). The commonest presenting symptom is a slowly enlarging mass, most frequently in the parotid gland. Patients with Sjogren syndrome may have preexisting enlarged salivary glands; superimposed lymphoma is usually suspected when there is progressive asymmetrical enlargement.

The treatment options for salivary gland MALT lymphoma include local radiotherapy, surgery, and/or chemotherapy. ''Wait and see'' approach may be appropriate in some cases. The prognosis is excellent, with a cause-specific five-year survival of >90% (532,533). Unfavorable prognostic factors include transformation to DLBCL (frequency 12%) and advanced age. Hepatitis C virus infection has been implicated in the pathogenesis of up to 21% of cases in some populations (533). Anecdotal report of regression after anti-viral therapy has also been described in a hepatitis C virus–positive case (534), but the finding has to be confirmed by future studies.

Pathologic Features of Lymphomas Related to Anatomic Location

Salivary gland lymphoma is characterized by a diffuse and dense infiltrate of abnormal lymphoid cells, accompanied by loss and atrophy of salivary acini and ducts. There is frequent infiltration and obliteration of the interlobular fibrous septa (Fig. 156).

The histologic features of salivary gland MALT lymphoma are similar to those occurring elsewhere, such as a lymphoid infiltrate comprising a mixture of cell types, reactive lymphoid follicles, and lymphoepithelial lesions, except that monocytoid B-cell-like clear cells are particularly prominent, and typically form broad cuffs around the lymphoepithelial lesions (Figs. 157 and 158A, B). Rarely, the lymphoepithelial lesions are surrounded by wreaths of epithelioid histiocytes. In some cases, the entrapped ducts undergo cystic dilatation, resulting in a multicystic appearance (Fig. 159). On immunostaining, there are dense sheets of B cells (CD20+), and light-chain restriction can often be demonstrated. The frequencies of *API2-MALT1*, *IGH-MALT1*, *IGH-BCL10*, and *FOXP1-IGH* translocations are 5%, 12%, 3%, and 0%, respectively (334,349,535). Trisomy 3 occurs in 30% to 50% of cases (334,351).

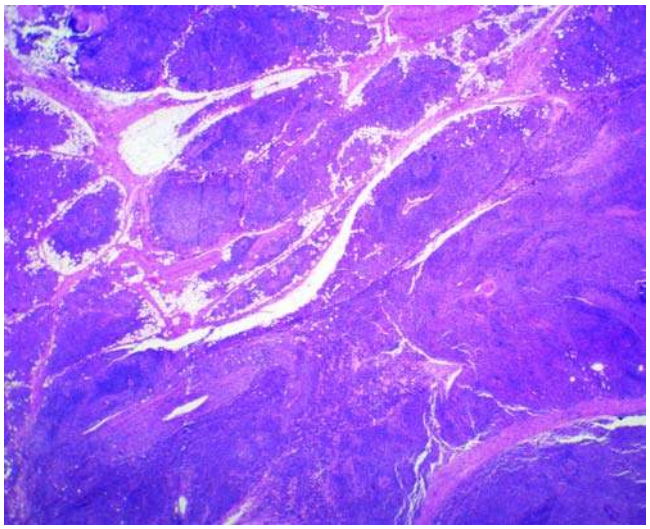

Figure 156 MALT lymphoma of parotid gland. There is extensive lymphoid infiltration, accompanied by obliteration of the lobular septa in areas.

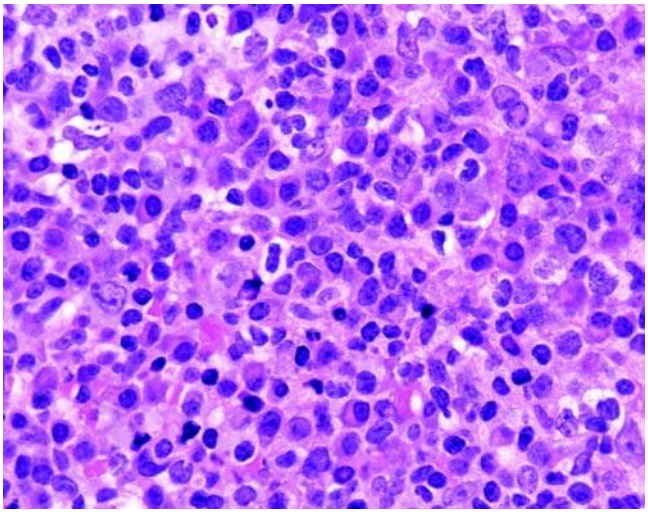

Figure 157 MALT lymphoma of parotid gland. Typically the lymphomatous infiltrate has a mixed appearance, with small lymphoid cells and plasma cells intermingled with occasional large cells.

Other Hematolymphoid Neoplasms

Myeloid sarcoma (427), interdigitating dendritic cell sarcoma (536), Langerhans cell histiocytosis (537), and histiocytic sarcoma (538) have been described in the salivary gland.

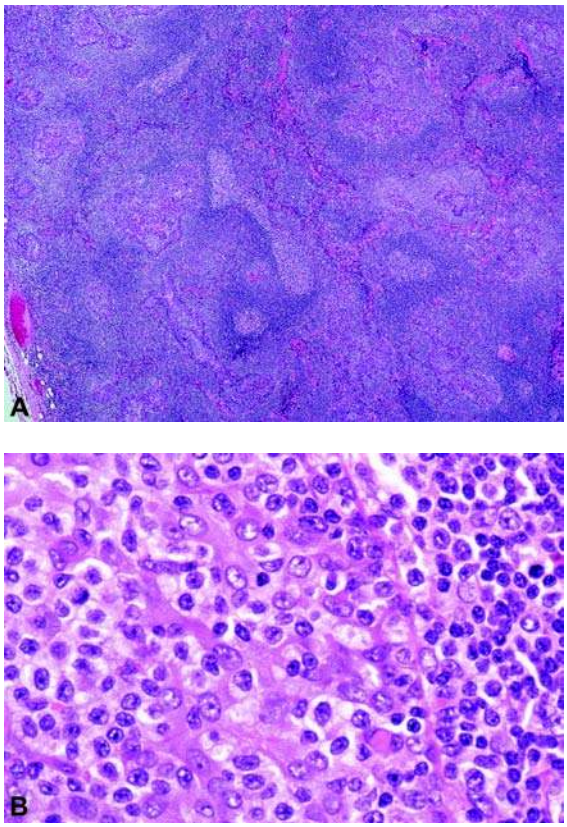

Figure 158 MALT lymphoma of parotid gland. (**A**) Lymphoepithelial lesions are prominent and are surrounded by characteristic pale collars of monocytoid-appearing cells. Reactive lymphoid follicles are also prominent. (**B**) Monocytoid-appearing lymphoid cells infiltrate and expand the epithelial units to form lymphoepithelial lesions.

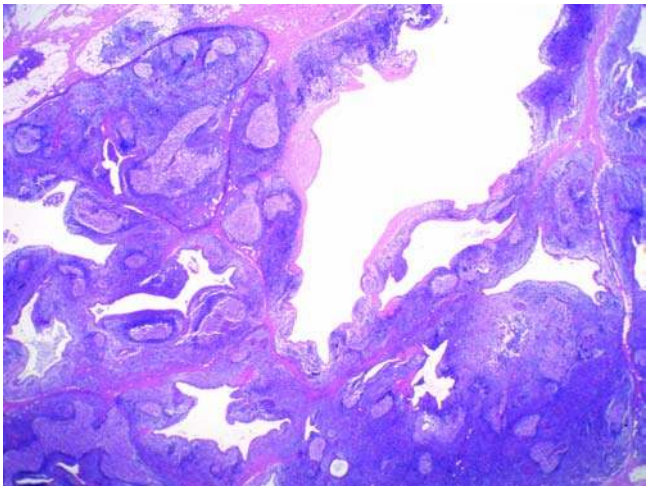

Figure 159 MALT lymphoma of parotid gland. The multicystic appearance results from dilatation of the ducts.

B. Important Reactive or Inflammatory Hematolymphoid Lesions

Lymphoepithelial Sialadenitis

In the salivary gland, lymphoepithelial sialadenitis, formerly known as myoepithelial sialadenitis or benign lymphoepithelial lesion, can occur in patients with or without Sjogren syndrome, an autoimmune disorder characterized by dry eyes and dry mouth resulting from immunologically mediated destruction of the lacrimal and salivary glands (which may or may not show swelling). Most patients are middle-aged females, and systemic symptoms including skin rash and joint pain are common. Serologic study frequently shows elevated levels of autoantibodies SSA and SSB (Ro and La). Patients with Sjogren syndrome have an increased risk (44 times risk, about 10%) of developing lymphoma compared to the general population, and 80% of these lymphomas are MALT lymphomas (99,100,539).

Lymphoepithelial sialadenitis exhibits discrete or ill-defined borders, but the lobular architecture of the salivary gland is preserved (Fig. 160A). The lymphoid infiltrate comprises small lymphocytes and plasma cells with or without germinal center formation. There is loss of acini, but proliferation of the residual ductal epithelium and insinuation of individual lymphocytes into the epithelium result in the characteristic lymphoepithelial lesions (formerly known as ''epimyoepithelial islands''). The lymphoepithelial lesions are round to irregular-shaped solid cellular islands, which may be punctuated by small lumens. The epithelial cells are plump spindly, polygonal to syncytial, and have oval nuclei with fine chromatin. There are typically interspersed hyaline basement membrane–like material (Fig. 160B). On immunostaining, the lymphoid cells in the lymphoepithelial lesions are mostly B cells, while the lymphoid cells in between represent a mixture of B and T cells, with the former being predominant.

It is not uncommon to find clonal immunoglobulin gene rearrangement on molecular studies (540–544). In sequential biopsies, the same clone may persist, but sometimes a different clone emerges with disappearance of the original clone (541–546). Cases with clonal immunoglobulin gene rearrangement do not necessarily progress to overt lymphoma on follow-up.

HIV-Associated Lymphoepithelial Cyst

HIV-associated lymphoepithelial cyst (also known as cystic lymphoid hyperplasia) commonly presents as bilateral parotid swelling, accompanied by cervical lymphadenopathy (70,547). The swellings are slow-growing and painless. Males are more frequently affected. The cyst may represent the first clinical manifestation of HIV infection concurrent with persistent generalized lymphadenopathy syndrome.

The epithelium-lined cysts are variable-sized and often multiple (Fig. 161A). The lymphoid tissue beneath and between the cysts exhibits florid hyperplasia similar to that found in lymph node of

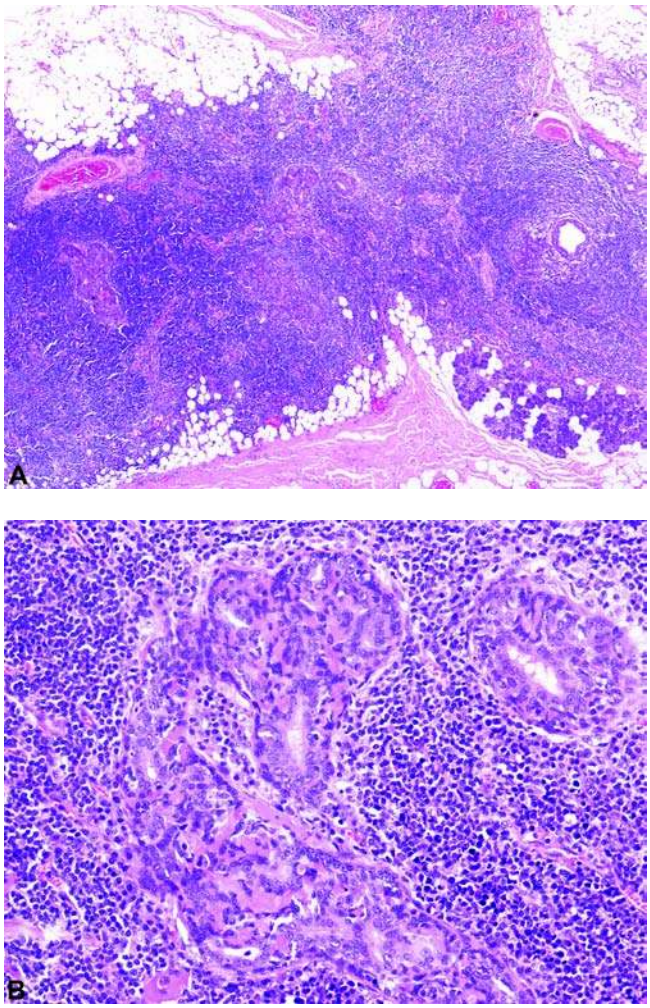

Figure 160 Lymphoepithelial sialadenitis of parotid gland. (**A**) Although there is a dense lymphoid infiltrate, the lobular architecture of the salivary gland is preserved. (**B**) Lymphoepithelial lesions are characteristically present; they differ from those of MALT lymphoma in that there are few or no monocytoid-appearing lymphoid cells, and there are no large aggregates of lymphoid cells within the epithelial units.

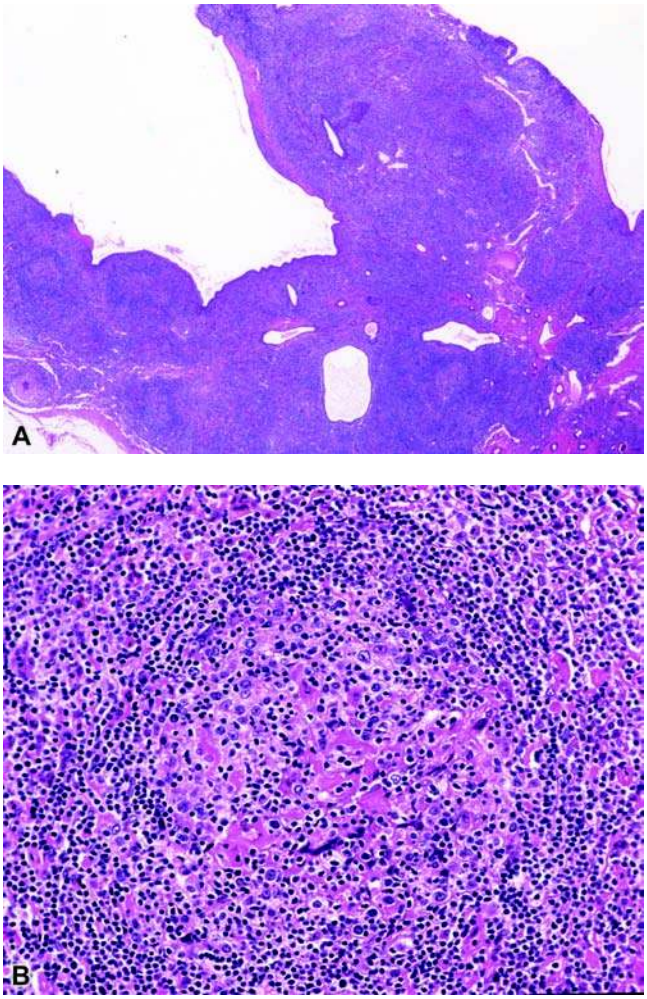

Figure 161 HIV-associated lymphoepithelial cyst. (**A**) Multiple cysts are present among the dense lymphoid infiltrate. (**B**) The lymphoid tissue shows changes similar to those of explosive follicular hyperplasia as seen in lymph nodes of patients with HIV infection.

persistent generalized lymphadenopathy (Fig. 161B). There is explosive follicular hyperplasia, follicle lysis, increased monocytoid B cells, increased vascularity, and plasma cell infiltrate. Multinucleated giant cells are sometimes present (Fig. 26).

Chronic Sclerosing Sialadenitis of Submandibular Gland (Kuttner Tumor) and IgG4-Related Sclerosing Disease of Parotid Gland

Chronic sclerosing sialadenitis of the submandibular gland (Kuttner tumor) is an inflammatory lesion than may clinically or histologically simulate malignancy (548). Patients are usually adults, who present with unilateral or bilateral enlarged and hard submandibular glands. Histologically, the gland shows preserved lobular architecture, thickening of interlobular septa by sclerotic tissue, dense lymphoplasmacytic infiltrate with reactive lymphoid follicle formation, preservation of ducts with periductal fibrosis, and variable loss of acini (Fig. 162A–C). Lymphoepithelial lesions are rare or absent. With time, there is extensive fibrosis and loss of acini, often accompanied by a reduction in the inflammatory infiltrate. Recent studies suggest that most cases belong to the spectrum of IgG4-related sclerosing disease in view of the presence of abundant IgG4+ plasma cells (Fig. 162D) (549). Kuttner tumor is an under-recognized entity and is not uncommonly misdiagnosed as lymphoepithelial sialadenitis; it can be distinguished from the latter by the scarcity or lack of lymphoepithelial lesions and its usually more prominent sclerosis.

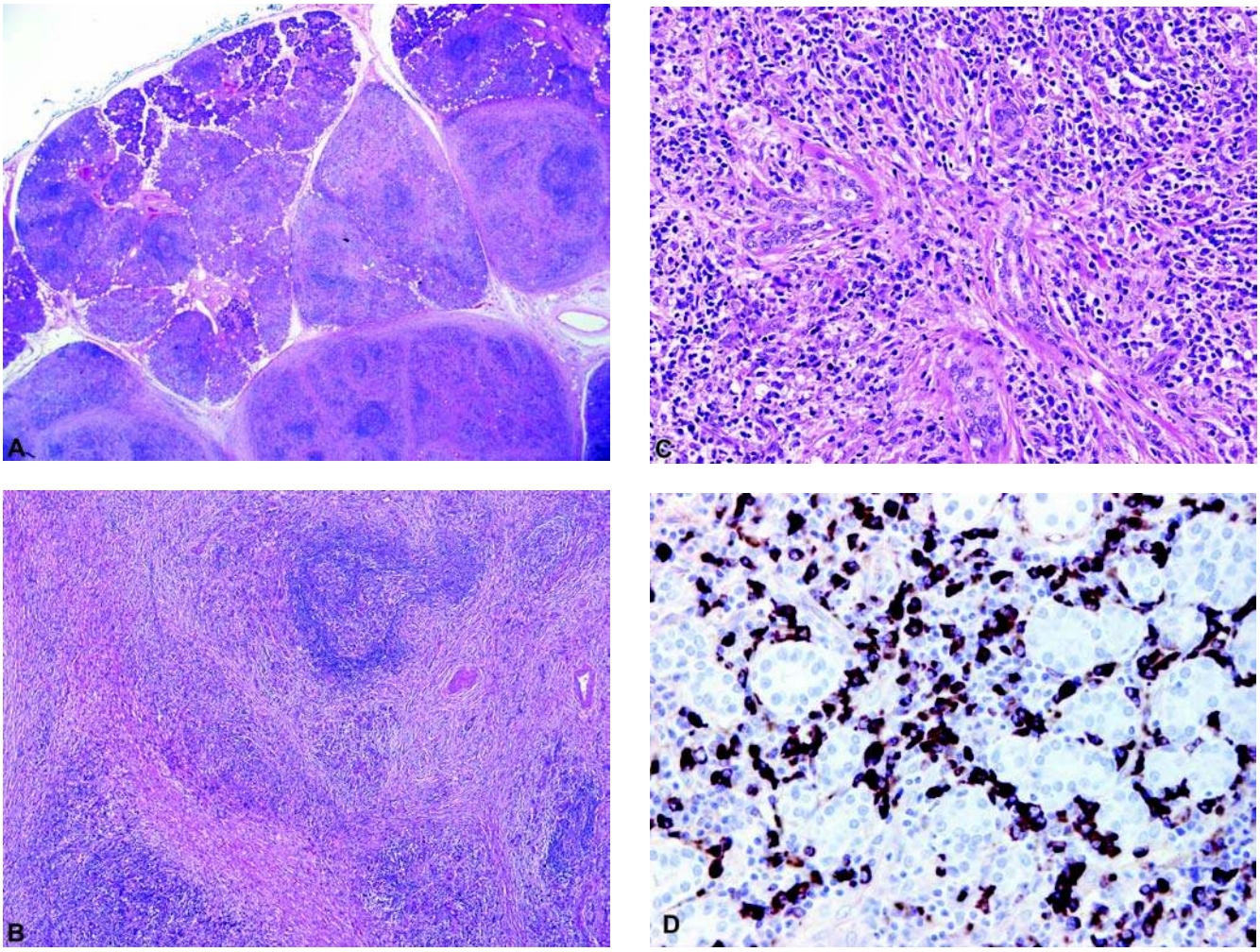

Figure 162 Chronic sclerosing sialadenitis of submandibular gland. (**A**) There is usually subtotal involvement of the gland, and lobular architecture is still preserved. (**B**) The septa show fibrosis, and the lobules show loss of acini and heavy lymphoid infiltrate. Lymphoid follicles are also evident. (**C**) There is a heavy infiltrate of small lymphocytes and plasma cells, accompanied by periductal fibrosis in the residual ducts. (**D**) Many of the plasma cells express IgG4.

The parotid glands can also be affected by IgG4-related sclerosing disease (105). The histologic features are similar to those of Kuttner tumor, except that sclerosis is usually not as striking.

Kimura Disease

Kimura disease commonly involves salivary glands in addition to subcutaneous tissues and lymph nodes of the head and neck (113). This disease is more prevalent in Oriental males, who present with salivary gland swelling. The lesion often persists.

The salivary gland shows heavy inflammatory infiltrate, atrophy and loss of acini, as well as periductal and interlobular sclerosis (Fig. 163A). The inflammatory infiltrate comprises small lymphocytes, plasma cells, and eosinophils in a background rich in high endothelial venules. There are prominent lymphoid follicles, often with germinal center vascularization, necrosis, eosinophil infiltration, or even abscess formation (Fig. 163B, C). In contrast to MALT lymphoma, B cells are limited to the reactive follicles, and there is a heavy eosinophilic infiltrate associated with fibrosis and increased vascularity.

Others

The salivary glands can be involved by Rosai–Dorfman disease and extramedullary hematopoietic tumor (144,457,550).

C. Diagnostic Considerations

The main issue in diagnosis is determining whether a lymphoid cell–rich lesion of the salivary gland represents lymphoepithelial sialadenitis or MALT lymphoma (*de novo* or MALT lymphoma arising in lymphoepithelial sialadenitis). The distinguishing features are listed

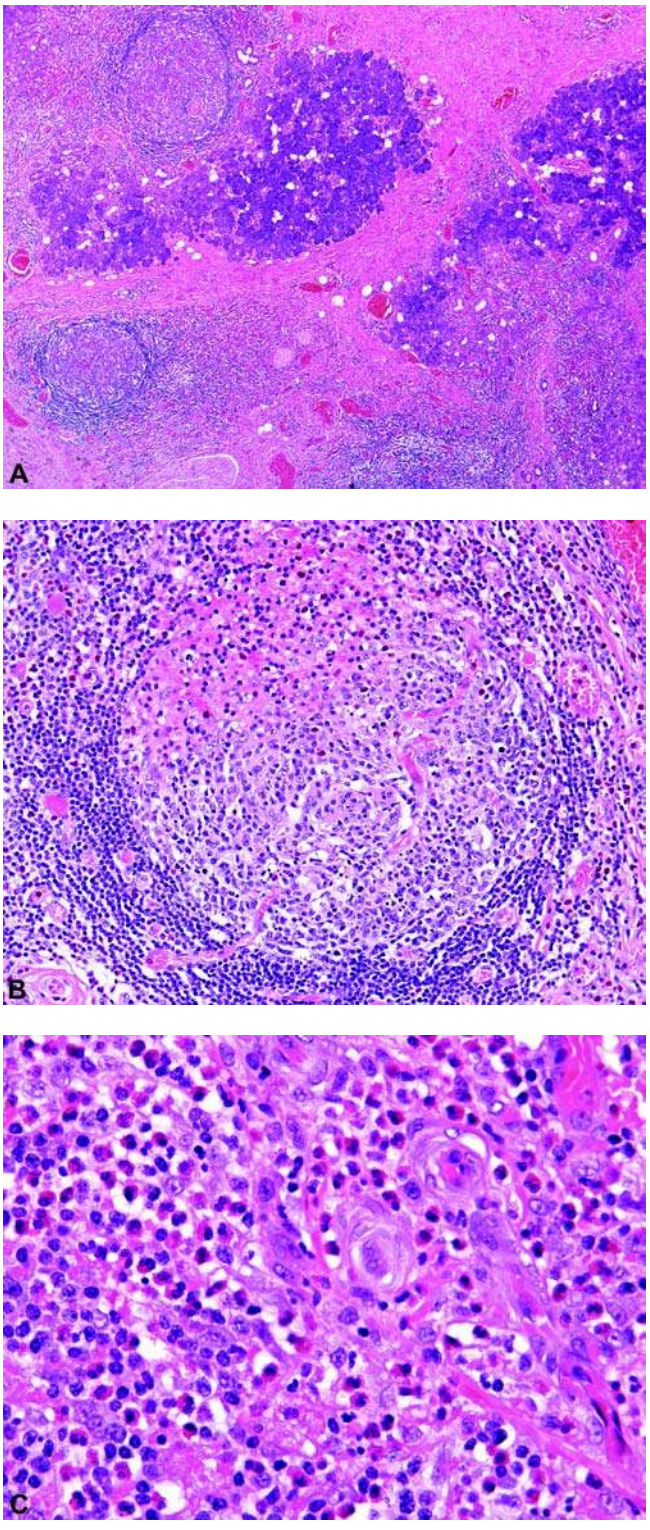

Figure 163 Kimura disease involving parotid gland. (**A**) There is variable patchy involvement, with sclerosis, lymphoid follicle formation, and loss of acini. (**B**) The lymphoid follicles commonly show vascularization, eosinophil infiltration, and necrosis. (**C**) The interfollicular areas show increased venules and infiltration by eosinophils, small lymphocytes, and plasma cells.

in Table 14 (Figs. 164 and 165). The most important feature suggesting a diagnosis of lymphoma is the presence of broad collars of clear cells (monocytoid B cell-like) around the lymphoepithelial lesions; this is considered to be the earliest evidence of a supervening lymphoma in lymphoepithelial sialadenitis (Fig. 165) (551).

IX. HEMATOLYMPHOID LESIONS OF THE LARYNX, HYPOPHARYNX, AND TRACHEA

Primary malignant lymphomas of the larynx, hypopharynx, and trachea are very rare, accounting for only 1% of all primary extranodal lymphomas (448). In contrast, secondary involvement by lymphomas from adjacent structures (such as nose or nasopharynx) is more common, and tumors from the thyroid gland or lymph nodes in the neck and mediastinum may also invade into these anatomic sites.

A. Hematolymphoid Lesions of the Larynx

Patients with primary laryngeal lymphoma frequently present with hoarseness of voice, foreign body sensation in the upper airway, or airway obstruction. Tumor-forming mass is frequently identified on laryngoscopic examination, and rare case with cystic change has been reported (552). Most tumors are B-cell lymphomas, especially of DLBCL and MALT lymphoma (553–557). Extranodal NK/T-cell lymphoma and peripheral T-cell lymphoma NOS have also been described (483,556,558,559). Most primary laryngeal lymphomas are of stage IE/IIE, and treatment options include radiotherapy and/or chemotherapy. The outcome depends on the histologic type, but delayed treatment may result in death due to acute laryngeal obstruction (553). In general, extranodal NK/T-cell lymphoma and peripheral T-cell lymphoma NOS have a worse prognosis compared to B-cell lymphomas (553,555,556,558). A case of laryngeal MALT lymphoma with associated *H. pylori*-related gastric MALT lymphoma has regressed with anti-*H. pylori* treatment, but the role of such treatment has to be carefully assessed by future studies (560).

Extramedullary plasmacytoma (561), myeloid sarcoma (562), Langerhans cell histiocytosis (563), extramedullary hematopoietic tumor (564), inflammatory pseudotumor (153), and Rosai–Dorfman disease (144,457) have been reported to involve the larynx.

B. Hematolymphoid Lesions of the Hypopharynx

Primary hypopharyngeal lymphomas are extremely rare, and patients present with dysphagia or foreign body sensation in the throat. DLBCL, extranodal NK/T-cell lymphoma, and MALT lymphoma have been described (565–567). Extramedullary plasmacytoma and follicular dendritic cell sarcoma have also been reported in the hypopharynx (464,568).

Table 14 Distinguishing Features Between Lymphoepithelial Sialadenitis and MALT Lymphoma Involving Salivary Gland

	Lymphoepithelial sialadenitis	MALT lymphoma
Histology	• Preserved lobular architecture, with "clean" interlobular septa • Lymphoepithelial lesions associated with increased basement membrane-like material; small lymphoid cells within lymphoepithelial lesions occur singly or at most in small clusters; at most a thin rim of monocytoid-appearing lymphoid cells surround lymphoepithelial lesions	• Destroyed lobular architecture with extensive lymphoid infiltrate into interlobular septa and periglandular soft tissue • Broad bands of medium-sized clear lymphoid cells (monocytoid B-cell-like) around and within lymphoepithelial lesions • "Cavitation" of epithelial islands by large clusters of lymphoid cells • Presence of clusters of atypical plasma cells (some cases)
Immunohistochemistry	• Immunoglobulin light chain: polytypic	• Extensive sheets of CD20+ B cells. • Immunoglobulin light chain: monotypic (in frozen sections or in plasmacytic component in paraffin sections) • The neoplastic B cells may show aberrant CD43 expression
Cytogenetic/molecular finding	• Clonally rearranged immunoglobulin genes in >50% of cases. The clone may persist, or may disappear with emergence of a different clone.	• Clonally rearranged immunoglobulin genes • Chromosomal translocations involving *API2-MALT1*, *IGH-MALT1*, or *IGH-BCL10* in a proportion of cases • Trisomy 3 (30%)

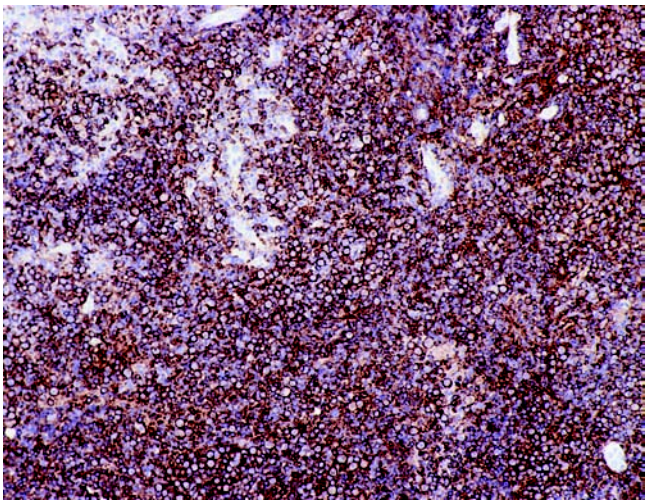

Figure 164 MALT lymphoma of parotid gland, immunostaining for CD20. The extensive diffuse dense population of CD20-positive cells supports a diagnosis of lymphoma.

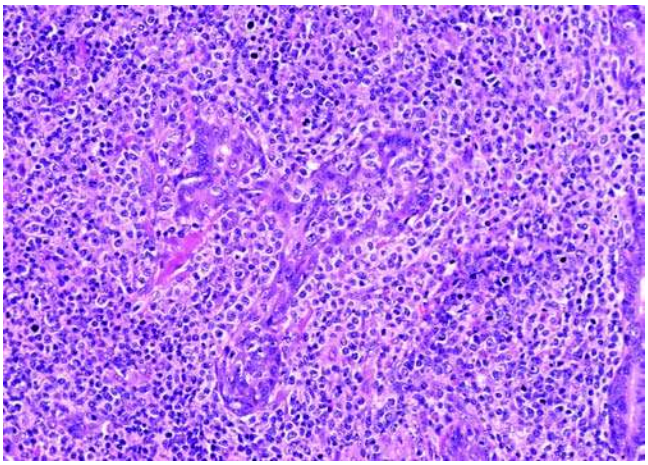

Figure 165 MALT lymphoma of parotid gland. The lymphoepithelial lesions are characteristically surrounded by broad collars of clear or pale cells reminiscent of monocytoid B cells.

C. Hematolymphoid Lesions of the Trachea

Primary tracheal lymphomas are exceptionally rare, and patients present with symptoms of airway obstruction, dyspnea, wheezing, or cough. Most of the reported cases have been MALT lymphoma (569–571). Extramedullary plasmacytoma (572), Langerhans cell histiocytosis (573), inflammatory pseudotumor (574), and Rosai–Dorfman disease (144,457) have been described in the trachea.

X. HEMATOLYMPHOID LESIONS OF THE THYROID

A. Hematolymphoid Neoplasms of the Thyroid

General Features of Lymphoma

Primary thyroid lymphomas are uncommon, accounting for 1% to 5% of all thyroid malignancies (575) and 2.5% of all extranodal lymphomas (448). Patients with Hashimoto thyroiditis have a 67 to 80 times increased risk of developing thyroid lymphoma (576,577). More than 90% of patients with primary thyroid lymphoma

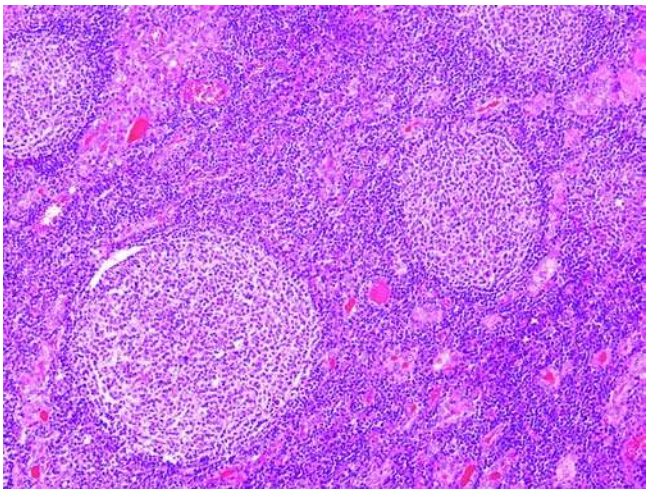

Figure 166 Primary follicular lymphoma of thyroid.

have histologic evidence of autoimmune/Hashimoto thyroiditis (578). The thyroid gland may also be secondarily involved in advanced nodal lymphomas, especially from direct infiltration by tumors originating in cervical lymph nodes.

About 70% of all primary thyroid lymphomas are DLBCLs, and 28% are MALT lymphomas (578). Other types of lymphomas are very uncommon, and include follicular lymphoma, Burkitt or Burkitt-like lymphoma, intravascular large B-cell lymphoma, peripheral T-cell lymphoma, and classical Hodgkin lymphoma (mostly nodular sclerosis subtype) (Fig. 166) (579–581).

Clinical Features of Lymphoma

Most patients with primary thyroid lymphomas are in the sixth to seventh decades, with obvious female predominance (M:F = 1:2–3) (578,580,582). They usually present with a thyroid mass or a goiter, which may be associated with hoarseness of voice, dysphagia, stridor, dyspnea, choking, coughing, or pain (578,583). Some patients with high-grade lymphomas present with rapid onset of a large thyroid mass with extensive infiltration into the surrounding tissues, clinically reminiscent of anaplastic thyroid carcinoma. For patients with underlying Hashimoto thyroiditis, the tumor often arises from an underlying goiter. More than 90% of patients have stage IE/IIE disease at presentation, with stage IE disease accounting for 50% to 60% of cases (578,580,581).

The treatment options for primary thyroid lymphomas include various combinations of surgery, chemotherapy, and/or radiotherapy. Surgery followed by chemotherapy and/or radiotherapy has been advocated by some groups, while chemotherapy and/or radiotherapy alone is favored by others (578,584). It has recently been challenged that the role of surgery may only be limited to stage IE cases of MALT lymphoma (584). The overall five-year survival of primary thyroid lymphomas is 60%, with a five-year disease-specific survival of nearly 80%. The five-year disease-specific survival for MALT lymphoma approaches 100%, while that of DLBCL is around 75% (578). There is no significant difference in outcome between cases of DLBCLs with or without an associated MALT lymphoma component.

Pathologic Features of Lymphomas Related to Anatomic Location

DLBCL of the thyroid often arises *de novo*, but sometimes transforms from an MALT lymphoma. The lymphomatous infiltrate effaces the architecture of the thyroid tissue, with the involved areas often devoid of thyroid follicles (Fig. 167A, B). In the peripheral portion of the tumor, the residual thyroid follicles are often infiltrated by lymphoma cells, which may form aggregates in the follicular lumens (Fig. 167B). The lymphoma cells are large, with round vesicular nuclei, distinct nucleoli, and a moderate amount of amphophilic cytoplasm that may be plasmacytoid (Fig. 167C). They express pan-B markers on immunostaining (Fig. 167D).

The histologic features of *MALT lymphoma* of the thyroid are similar to those occurring in other sites. Reactive lymphoid follicles are often interspersed within the diffuse lymphomatous infiltrate. The lymphoma cells are often heterogeneous, including cells resembling small lymphocytes, centrocytes, or monocytoid B cells (Fig. 168A). Plasma cells are commonly present. There is often remarkable invasion and expansion of the thyroid follicles, resulting in lymphoepithelial lesions and plugging of the follicular lumens by lymphoma cells (Fig. 168B, C). Colonization of the reactive lymphoid follicles can occur and may lead to a misdiagnosis of follicular lymphoma. Among the various distinctive chromosomal translocations of MALT lymphoma, practically only *FOXP1/IGH* fusion is found (in up to half of the cases) (350).

Other Hematolymphoid Neoplasms

Other hematolymphoid lesions that have been reported to affect the thyroid include follicular dendritic cell sarcoma (585), Langerhans cell histiocytosis (586), and plasmacytoma (587). At least some of the reported cases of plasmacytomas probably represent MALT lymphoma with marked plasmacytic differentiation.

When *Langerhans cell histiocytosis* involves the thyroid, it can be the sole lesion or part of disseminated disease. The patients show a wide age range and present as an incidental finding or an enlarged thyroid gland. The prognosis is excellent for disease limited to the thyroid, but poor for disseminated disease. Histologically, involvement of the thyroid can be focal or extensive, and extrathyroidal extension can occur. The Langerhans cells, which are often admixed with eosinophils, infiltrate and destroy the thyroid follicles.

B. Important Reactive or Inflammatory Hematolymphoid Lesions

Hashimoto thyroiditis is the prototype of autoimmune thyroiditis, often causing symmetrical enlargement of

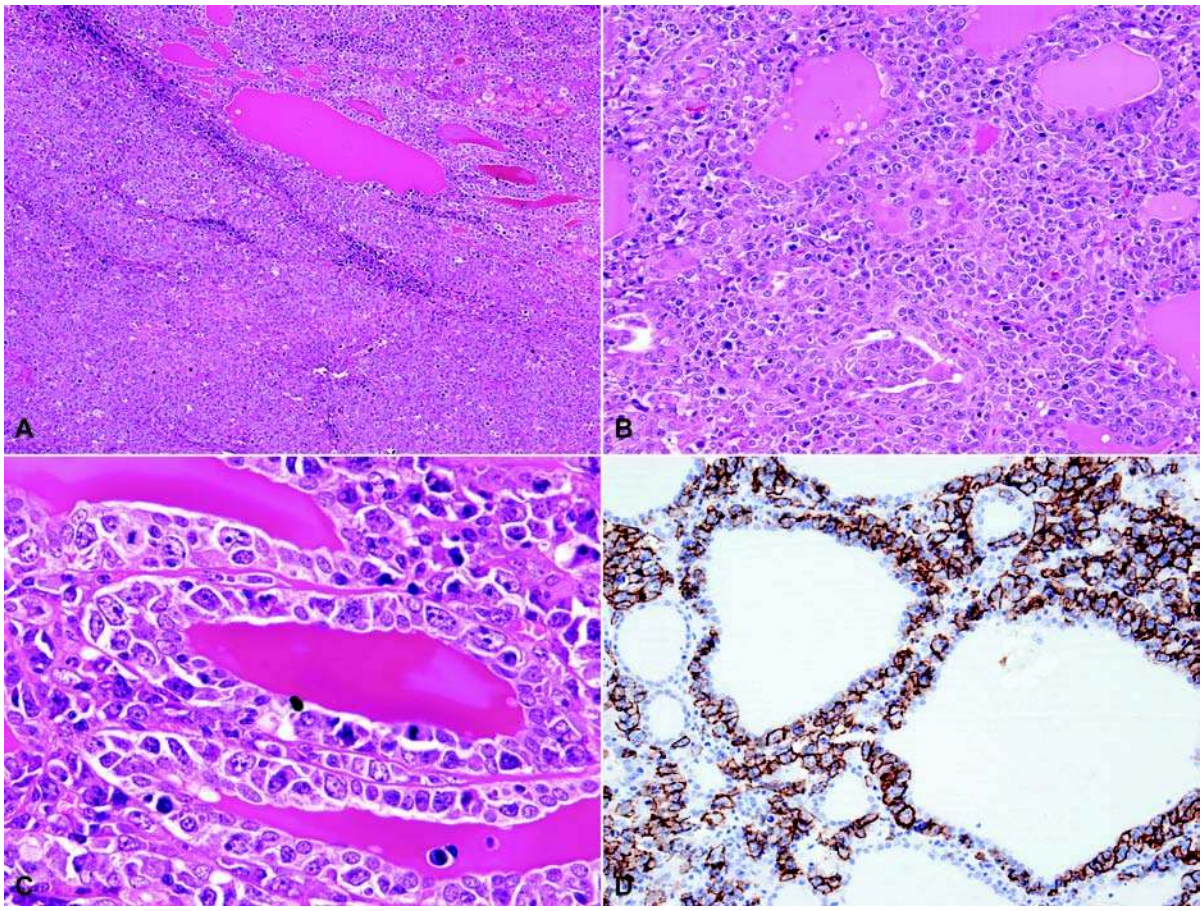

Figure 167 Diffuse large B-cell lymphoma of thyroid. (**A**) Diffuse dense lymphoid infiltration with destruction and loss of thyroid follicles. (**B**) Interstitial infiltration as well as infiltration into the lumens of thyroid follicles. (**C**) Large lymphoma cells replacing the thyroid follicular epithelium. (**D**) CD20 immunostaining highlights the remarkable infiltration of the thyroid follicles.

the thyroid gland and associated with an increase of developing thyroid lymphoma. Histologically, there is moderate infiltration of the interstitium by lymphocytes and plasma cells, often accompanied by scattered reactive lymphoid follicles. There is some loss of thyroid follicles, and the remaining ones are often small and lined by oncocytic epithelial (Hurthle) cells, which commonly have enlarged or pale nuclei and distinct nucleoli. The oncocytic cells show patchy infiltration by small lymphocytes (Fig. 169A, B). When Hashimoto thyroiditis shows florid chronic inflammatory cell infiltrate, it can be difficult to determine if there is superimposed MALT lymphoma.

Rosai–Dorfman disease and inflammatory pseudotumor (plasma cell granuloma) can uncommonly show involvement of the thyroid (144,588).

C. Diagnostic Considerations

The two main issues in diagnosis are as follows:

1. DLBCL versus anaplastic thyroid carcinoma—lack of cellular cohesion and infiltration of the thyroid follicles by large neoplastic cells are histologic features favoring the former diagnosis over the latter (Fig. 167B, C). In contrast, the latter shows cohesive growth and a tendency to permeate and obliterate muscular blood vessels rather than thyroid follicles. The diagnosis can be readily confirmed by immunohistochemistry, with expression of CD45 and pan-B markers by DLBCL.
2. MALT lymphoma versus florid Hashimoto thyroiditis—a dense lymphoid infiltrate with large areas lacking thyroid follicles, broad bands of centrocyte-like cells or clear cells, and prominent lymphoepithelial lesions are histologic features favoring a diagnosis of lymphoma (Fig. 168B, C), which can be further supported by immunohistochemistry to demonstrate sheets of B cells, aberrant coexpression of CD43, or light-chain restriction (Fig. 170). In Hashimoto thyroiditis, the interfollicular lymphocytes are predominantly T cells, and the plasma cells show polytypic immunoglobulin (589). The lymphocytes that infiltrate the thyroid follicles are also mostly T cells (589).

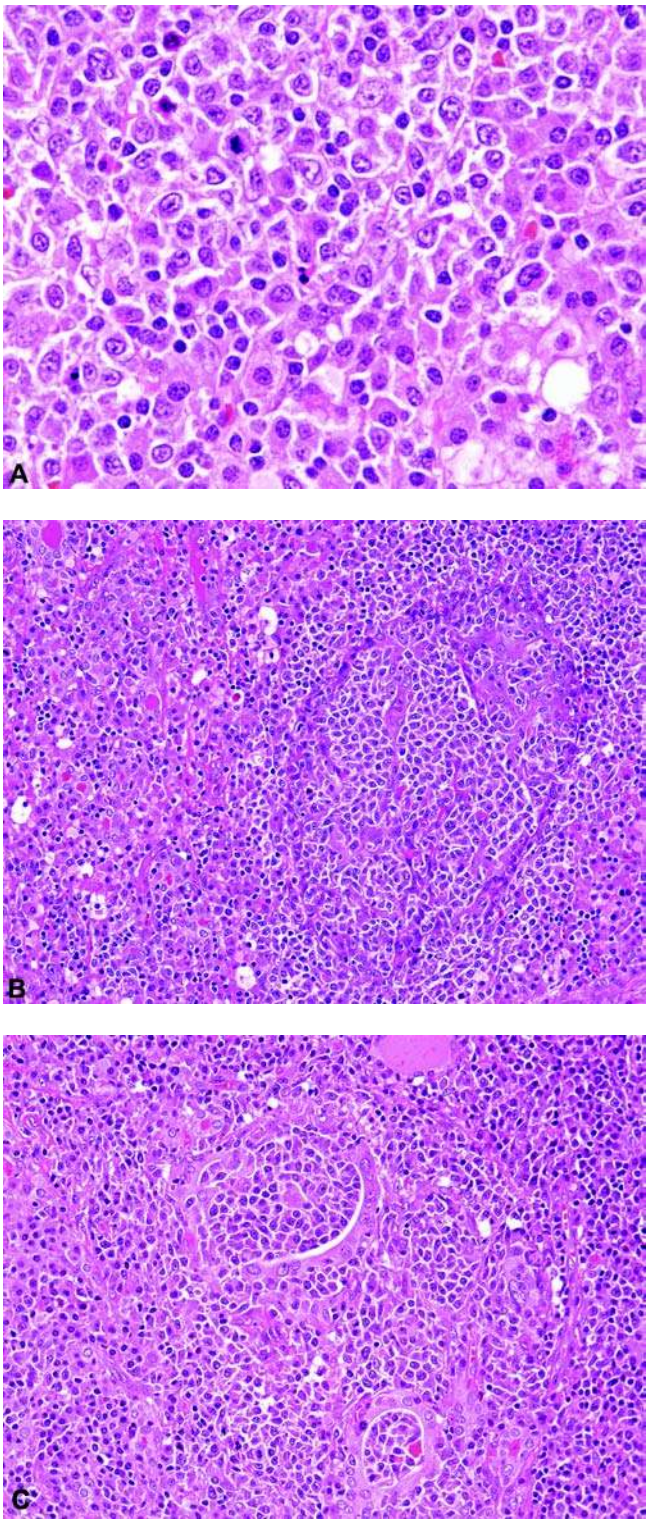

Figure 168 MALT lymphoma of thyroid. (**A**) The infiltrate comprises medium-sized cells and plasma cells. (**B**) A large lymphoepithelial lesion is shown (*right field*). (**C**) Lymphoma cells show a tendency to invade the thyroid follicles and fill up their lumens.

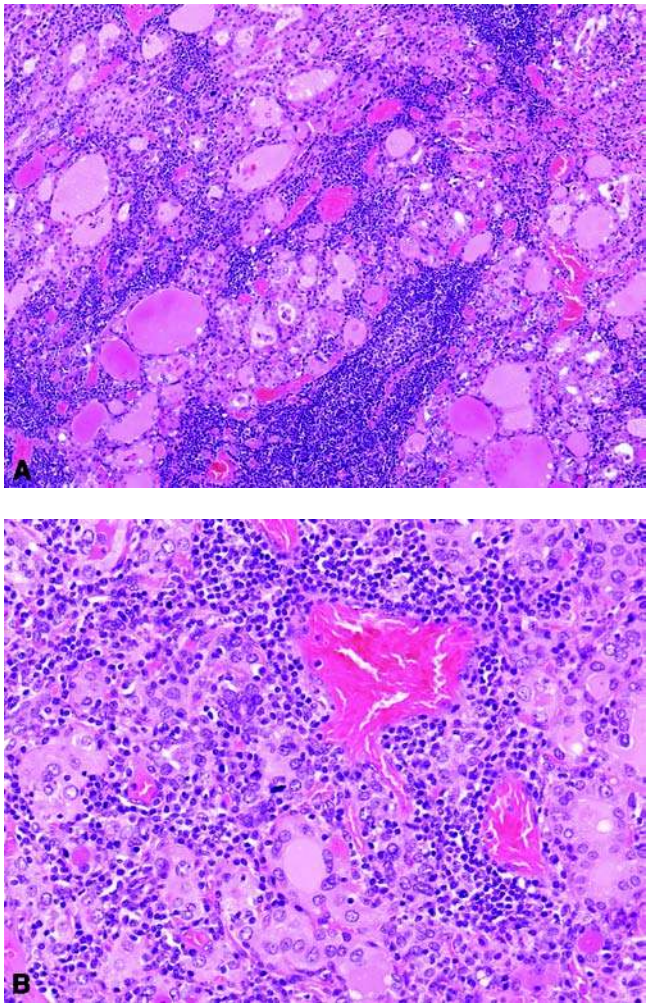

Figure 169 Hashimoto thyroiditis. (**A**) There is interstitial lymphoplasmacytic infiltration. Many thyroid follicles exhibit oncocytic changes. (**B**) It is common to observe scattered enlarged nuclei in the thyroid follicular epithelium.

XI. HEMATOLYMPHOID LESIONS OF THE OCULAR ADNEXA AND EYE

A. Hematolymphoid Neoplasms of Ocular Adnexa and Eye

General Features

The ocular adnexa refers to the tissues around the eye and include eyelid, conjunctiva, lacrimal gland, and the soft tissues of the orbit. Primary malignant lymphoma involving the ocular adnexa is uncommon and accounts for 2% of all extranodal lymphomas (448). About 20% of patients with ocular adnexal lymphomas represent secondary cases with history of lymphoma elsewhere in the body.

MALT lymphoma is the commonest, accounting for 54% to 90% of cases (590–595). A small percentage

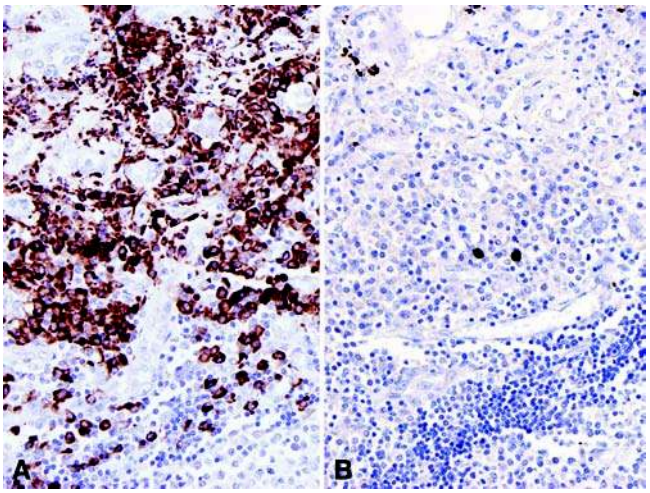

Figure 170 MALT lymphoma of thyroid, in situ hybridization for immunoglobulin mRNA. This example shows clear-cut κ light-chain mRNA restriction (**A**), with few cells expressing λ chain mRNA (**B**), supporting a diagnosis of lymphoma.

of cases apparently complicate IgG4-related sclerosing disease of the lacrimal gland (596,597). Follicular lymphoma accounts for up to 20% of all primary ocular adnexal lymphomas in one series (590), but its relative incidence is lower in other series (593,594), and its absence in two Asian series parallels the geographic difference observed in the incidence of follicular lymphoma in general (591,598). Up to 8% of all primary ocular adnexal lymphomas are DLBCLs, with some representing transformation from underlying low-grade lymphomas such as MALT lymphoma (590).

Other lymphomas that have been reported to involve the ocular adnexa include mantle cell lymphoma, CLL/SLL, B-lymphoblastic lymphoma, Burkitt lymphoma, peripheral T-cell lymphoma, and extranodal NK/T-cell lymphoma (590). Many of these cases represent disseminated disease at presentation or direct infiltration from adjacent organs.

Regarding etiology, only a minority of patients with ocular adnexal lymphoma have underlying autoimmune diseases such as Sjogren syndrome, Hashimoto thyroiditis, myasthenia gravis, Graves disease, or rheumatoid arthritis (590). The association between ocular adnexal MALT lymphoma and Sjogren syndrome is much weaker as compared to the case in salivary glands (590). *Chlamydia psittaci* infection has been reported in up to 80% of cases of ocular adnexal MALT lymphoma in one European series (599), but studies from other countries cannot confirm this association, and geographic difference or methodological biases may explain this discrepancy (592,600,601).

Other hematolymphoid lesions that can rarely affect the ocular adnexa or the eye include myeloid sarcoma (453) and extramedullary plasmacytoma (602).

Clinical Features

Patients with primary ocular adnexal lymphomas show a wide age range, with a mean age of 64 years (590). Presenting symptoms depend on the site of involvement and include a palpable or visible mass, proptosis, ptosis, pain or irritation, diplopia, swelling, tearing, nasolacrimal duct obstruction, redness, change in visual acuity, and glaucoma. Bilateral involvement occurs in about 10% of cases. Most cases are of low clinical stage, with 75% being stage IE (603).

The treatment options for ocular adnexal lymphomas include radiotherapy and/or systemic single-agent or multiagent chemotherapy, depending on the grade and stage of the disease (592,594,603,604). Treatment with antibiotic alone has been reported to result in complete or partial response in about half of all patients with ocular adnexal MALT lymphoma, with or without detectable *C. psittaci* (605,606), but the results cannot be confirmed by another series (607), and thus further long-term studies are necessary to solve this controversy. The prognosis generally depends on lymphoma type. MALT lymphoma has a five-year overall survival of >80%, and the five-year cause-specific survival may reach 100% (592,598,603, 608). Follicular lymphoma and DLBCL have a slightly worse outcome, with five-year lymphoma-related death of 22% and 48%, respectively (594).

Pathologic Features Related to Anatomic Location

The histologic features of ocular adnexal MALT lymphoma are similar to those occurring elsewhere (see sect. ''Hematolymphoid Neoplasms of the Head and Neck'') (Figs. 171A, B; 172A, B; and 173A, B), with the following differences: (*i*) the lymphoid infiltrate often appears monotonous, with predominance of small lymphocytes and plasma cells; cells resembling monocytoid B cells are rare (Fig. 171B); (*ii*) lymphoepithelial lesions are uncommon; they can be infrequent even in the lacrimal gland (Fig. 173A, B); and (*iii*) there are commonly scattered polykaryocytes (Fig. 171B) (595). Among the distinctive chromosomal translocations of MALT lymphomas, practically only *IGH/MALT1* and *FOXP3/IGH* are found (609). Aberrant nuclear expression of BCL10 is found in about 28% of cases, and this phenomenon is suggested to be associated with a shorter failure-free survival (609).

Intraocular Lymphoma

Intraocular lymphoma is a distinctive but very rare form of DLBCL involving primarily the vitreous and retina of the eye, often considered part of the spectrum of primary DLBCL of the central nervous system because many cases have previous, concomitant, or subsequent tumors in the brain (610–613). There is often a delay in diagnosis because the clinical findings mimic those of chronic uveitis.

Patients with intraocular lymphoma are older adults who present with blurred vision or floaters; bilateral disease is common. Slitlamp examination reveals vitreitis that is frequently not responsive to steroid. A correct diagnosis can be made on cytologic

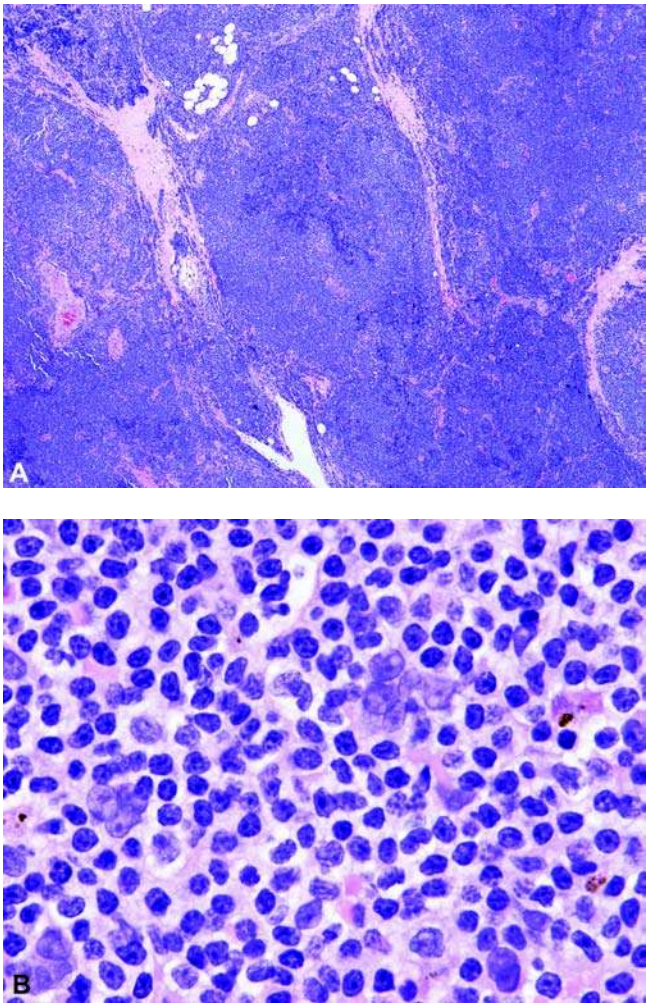

Figure 171 MALT lymphoma of the orbit. (**A**) There is a dense, monotonous lymphoid infiltrate. (**B**) A monotonous population of small lymphoid cells with mild nuclear foldings. There are several interspersed polykaryocytes, a common observation in lymphoid lesions of the ocular adnexa.

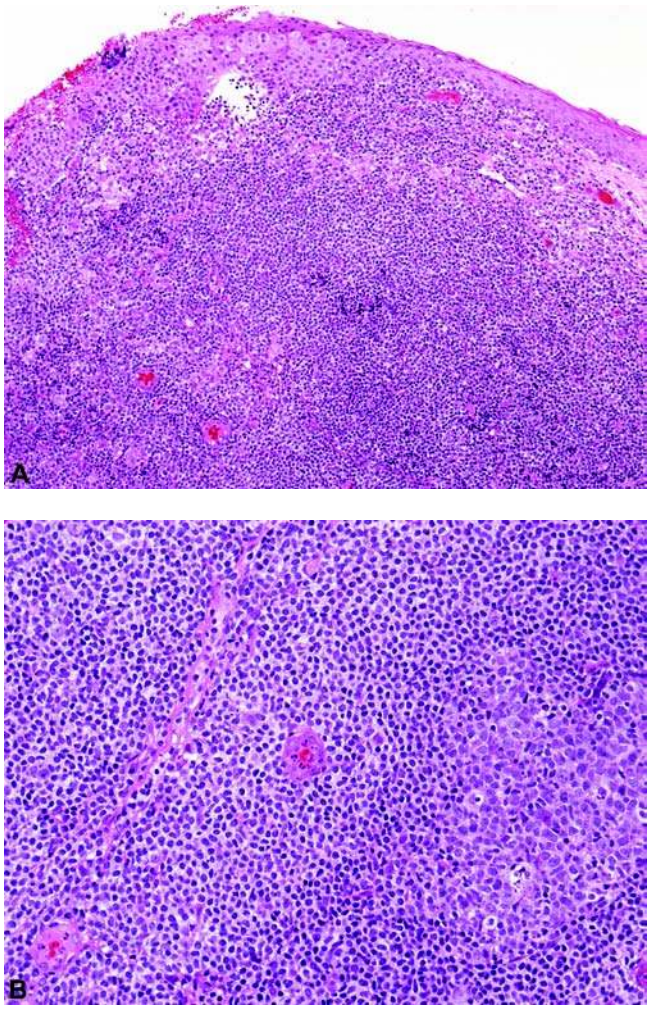

Figure 172 MALT lymphoma of the conjunctiva. (**A**) There is a dense lymphoid infiltrate beneath an intact epithelium. (**B**) This example shows the classical cytoarchitecture of MALT lymphoma, with reactive follicles and a mixture of cell types, including monocytoid-like cells.

examination of the vitrectomy or fine-needle aspiration specimen (614,615). Most cases are DLBCLs, with the large lymphoid cells showing similar cytologic appearance as those found in the nodal counterpart. However, difficulty may arise when there is an associated rich inflammatory component, or when steroid therapy has been given resulting in degeneration of the lymphoma cells. Repeat biopsy may be necessary for a definitive diagnosis. The lymphoma cells express pan-B markers, with immunoglobulin light-chain restriction. For difficult cases, the diagnosis can be confirmed by demonstrating clonal rearrangement of the immunoglobulin genes (616).

The optimal treatment for intraocular lymphoma is yet to be decided, but various combinations of radiotherapy, systemic chemotherapy, and local intravitreous chemotherapy have been employed (617,618). The prognosis is poor, with mortality of nearly 80% (619).

B. Important Reactive or Inflammatory Hematolymphoid Lesions

IgG4-Related Sclerosing Disease of the Ocular Adnexa

Patients with IgG4-related sclerosing disease of the ocular adnexa usually present with lacrimal swelling, which is usually bilateral, and can be accompanied by salivary gland swelling and lymphadenopathy. The predominant site of involvement is the lacrimal gland (IgG4-related chronic sclerosing dacryoadenitis), but the lesion can extend into the orbital soft tissues and entrap optic nerve to cause blindness (105,597). However, the conjunctiva is not involved (597). The serum IgG4 titer is often elevated. The disease ranges from being stable to progressive and may require treatment with surgery, steroid, or radiotherapy. Relapses are not uncommon. In a small proportion of cases, malignant lymphoma, most often MALT lymphoma, can

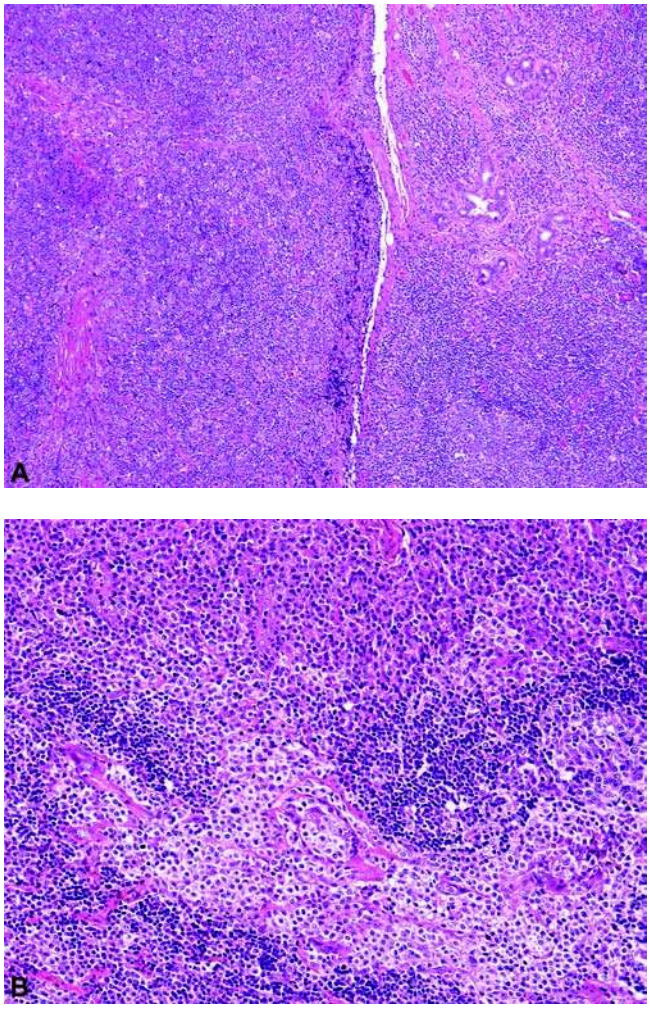

Figure 173 MALT lymphoma of lacrimal gland. (**A**) There is a heavy lymphoid infiltrate replacing the normal architecture. In this example, lymphoepithelial lesions are not found. (**B**) An example with florid lymphoepithelial lesions and monocytoid-like cells, morphologically similar to the salivary gland counterpart.

complicate IgG4-related sclerosing disease of the ocular adnexa (596,597).

The histologic features of the involved lacrimal glands are similar to those of chronic sclerosing sialadenitis of the submandibular gland, with atrophy of acini, heavy lymphoplasmacytic infiltration, lymphoid follicle formation, periductal fibrosis, and stromal sclerosis (Fig. 174A, B). In older lesions, sclerosis can be extensive, accompanied by complete or near-complete loss of the acini and ducts (Fig. 174C). Immunohistochemical demonstration of a significant increase of IgG4+ plasma cells (>50/HPF, with IgG4/IgG ratio >40%) is required to confirm the diagnosis.

Nonspecific Reactive Lymphoid Hyperplasia of the Ocular Adnexa

Nonspecific reactive lymphoid hyperplasia can involve the various anatomic components of the ocular adnexa, such as the conjunctiva, orbital soft tissues,

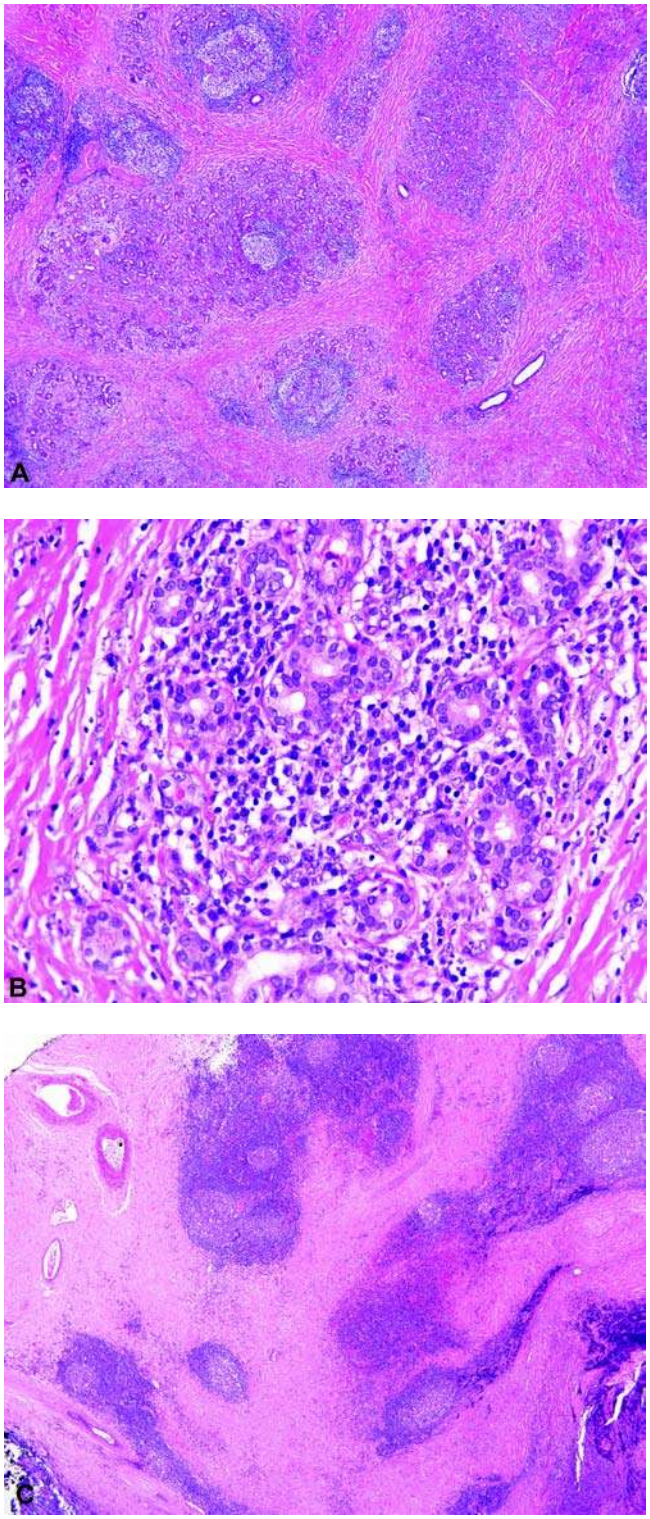

Figure 174 IgG4-related chronic sclerosing dacryoadenitis. (**A**) Septal sclerosis, atrophy of acini, lymphoid follicle formation, and lymphoplasmacytic infiltrates characterize this lesion. (**B**) Many plasma cells are seen among the residual secretory acini and ducts. (**C**) In advanced lesions, there is striking sclerosis with practically complete loss of normal architecture. Only a single residual duct is seen in this image (*left lower field*).

eyelids, and lacrimal gland (595,620). The patients' age, sex, presenting complaints, duration of symptoms, or ophthalmic findings are no different from those with MALT lymphomas involving these sites (620). Histologically, the tissue shows a heavy infiltration of small lymphocytes and plasma cells, often but not invariably accompanied by reactive lymphoid follicles (Fig. 175A–C). In the conjunctiva, the lymphoid cells (B cells) can show infiltration into the conjunctival epithelium (595).

Other Lesions

In patients with Sjogren syndrome, the findings in the lacrimal glands are similar to those in the salivary glands, with lymphoid infiltrate forming reactive lymphoid follicles and lymphoepithelial lesions (621,622). Other benign lesions include inflammatory pseudotumor (623), extramedullary hematopoietic tumor (624), Rosai–Dorfman disease (144,457,625), and Kimura disease (626). The orbital tissues and eye can be involved by Erdheim–Chester disease, a non-Langerhans cell histiocytosis characterized by accumulation of foamy histiocytes and lymphocytes in the involved tissues (627–629).

C. Diagnostic Considerations

The major diagnostic issue is to determine whether a heavy lymphoid infiltrate in the ocular adnexal tissue represents lymphoma or reactive lymphoid hyperplasia (including IgG4-related sclerosing disease). Distinction on morphologic grounds alone is often difficult, except when the infiltrate is very monotonous and extensive or definite cytologic atypia is present (such as centrocyte-like appearance in most cells), when a diagnosis of lymphoma should be favored (Figs. 172B and 173B). Otherwise, immunohistochemical or molecular studies are required to solve the diagnostic dilemma. The major distinguishing features of lymphomas are (*i*) presence of diffuse sheets of CD20+ B cells, especially when there are few admixed CD3+ T cells (Fig. 176A, B); (*ii*) presence of B cells with aberrant immunophenotype (e.g. CD5 or CD43 coexpression); (*iii*) demonstration of immunoglobulin light-chain restriction; (*iv*) presence of clonal immunoglobulin gene rearrangement (620,630,631).

XII. HEMATOLYMPHOID LESIONS OF THE EAR

Lymphomas involving the external ear (pinna) are similar to cutaneous lymphomas involving other parts of the head and neck region. Primary lymphomas in the rest of the ear (external auditory canal, middle ear, or temporal bone) are extremely rare, and reported cases include DLBCL, B-lymphoblastic lymphoma, and peripheral T-cell lymphoma NOS (632–634). Patients may present with pain, hearing loss, and facial nerve palsy, and clinically can mimic mastoiditis. Langerhans cell histiocytosis may also involve the temporal bone and the middle ear in children. A rare

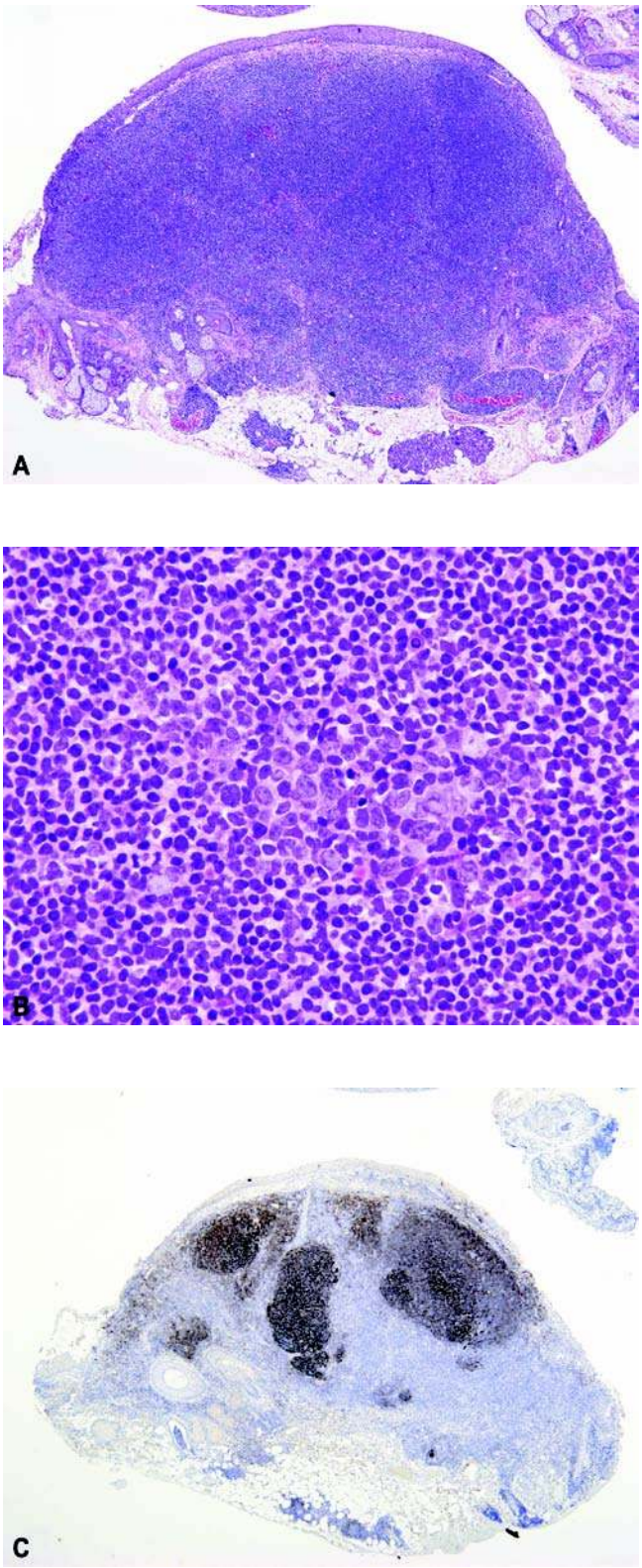

Figure 175 Reactive lymphoid hyperplasia of the caruncle. (**A**) There is a dense, vaguely nodular lymphoid infiltrate. (**B**) Closer inspection reveals the presence of reactive lymphoid follicles. (**C**) CD21 immunostain confirms the presence of a follicular architecture by highlighting the follicular dendritic cell meshworks.

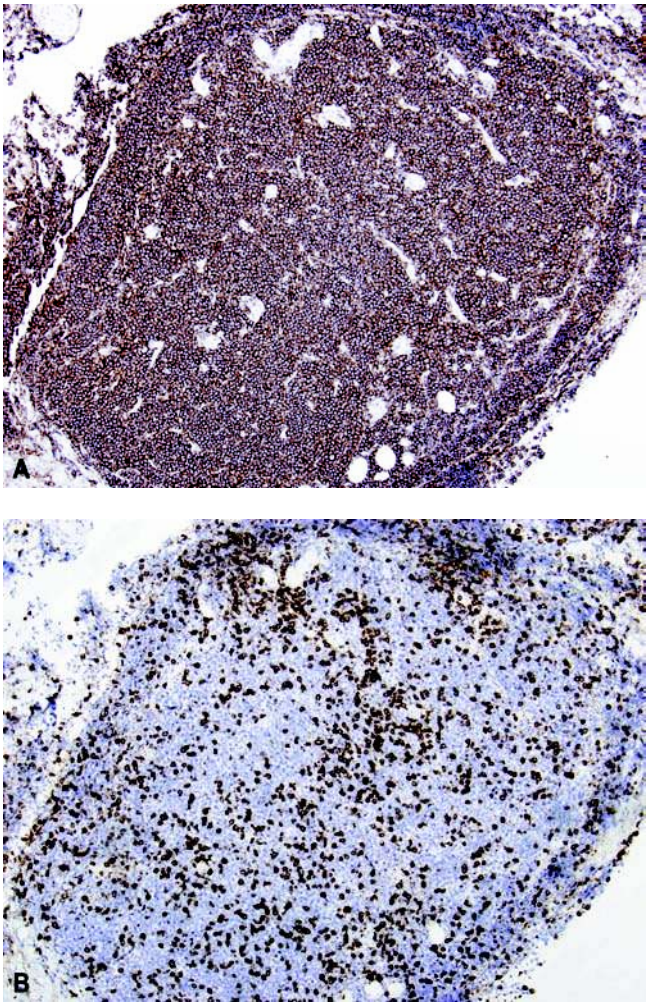

Figure 176 MALT lymphoma of the orbit, immunostaining. (**A**) Sheets of CD20+ cells are present. (**B**) There are few admixed CD3+ T cells. This pattern strongly supports a diagnosis of lymphoma (B-cell lymphoma).

case of Rosai–Dorfman disease of the middle ear has been described (144).

XIII. HEMATOLYMPHOID LESIONS OF BONE

A. Hematolymphoid Neoplasms of Bone

Hematolymphoid neoplasms commonly involve bones, and plasmacytoma is the commonest of all primary malignant bone tumors, accounting for 44% (Table 15) (635). Malignant lymphoma is in the fourth place (8%), following osteosarcoma (20%) and chondrosarcoma (12%).

Plasmacytoma

Plasmacytoma affecting bone can present clinically as part of plasma cell myeloma or less often as isolated solitary bone lesion in the absence of other features of myeloma (solitary plasmacytoma of bone) (636).

Table 15 Relative Frequency of Different Primary Malignant Bone Tumors

Plasmacytoma	44%
Osteosarcoma	20%
Chondrosarcoma	12%
Malignant lymphoma	8%
Ewing sarcoma	6%
Chordoma	4%
Others	6%

Patients are adults with a median age of 68 years. The bone lesions are usually lytic, and the commonly involved bones include vertebrae, ribs, skull, pelvis, femur, clavicle, and scapula.

Plasma cell myeloma is usually incurable with a median survival of 3 to 4 years and 10% survival at 10 years (636,637). Solitary plasmacytoma of bone has a better outcome, with one-third of patients remaining disease-free at 10 years. Two-thirds of patients develop plasma cell myeloma or additional solitary or multiple plasmacytomas.

Histologically, the bony trabeculae and intertrabecular spaces are replaced by solid sheets of neoplastic plasma cells. Well-differentiated tumors comprise cells readily recognizable as plasma cells, but poorly differentiated (anaplastic/plasmablastic) ones closely mimic large cell lymphoma. Immunophenotypically, the tumor cells produce cytoplasmic immunoglobulin (most frequently IgG and less often IgA; very rarely IgD, IgE, or IgM), with light-chain restriction. They are CD20−, PAX5−, CD138+, MUM1+.

Primary Bone Lymphoma

Primary bone lymphomas account for 5% of all primary extranodal lymphomas (448). About 8% of all malignant primary bone tumors are malignant lymphomas, but only about 40% of these cases are considered to be primary in the bone (635). Lymphomas involving the bone more frequently represent secondary spread from disseminated lymphoma or direct infiltration by lymphoma in the adjacent structures (e.g., oral cavity, nasal cavity).

Patients of any age may be affected by primary bone lymphoma, but they are more often adults with a median age in the fifth to sixth decades. The most frequently involved bones are femur and ilium, and multicentric bone involvement occurs in up to 20% of cases (635,638,639). The skull and jawbones are occasionally affected and account for up to 15% in one series (639). About 80% of patients with primary bone lymphomas have stage IE/IIE disease (638), and most patients present with bone pain or swelling. Radiography often reveals an aggressive mixed lytic-sclerotic lesion with ill-defined borders. Patients with primary bone lymphomas are usually treated with radiotherapy and/or chemotherapy. As a group, the five-year overall survival is 59% to 88% (638–640).

More than 90% of cases are DLBCLs, and the tumor cells are similar to those seen in nodal DLBCL, except that nuclear multilobation is a frequent finding

(640,641). Sometimes fibrosis and spindling of lymphoma cells can result in striking mimicry of sarcoma. The diagnosis can be confirmed by expression of pan-B markers such as CD20 and CD79a. Other less common primary bone lymphomas include Burkitt lymphoma (often in the jaws of children from central Africa), B-lymphoblastic lymphoma (more often in children), anaplastic large cell lymphoma, follicular lymphoma, lymphoplasmacytic lymphoma, and classical Hodgkin lymphoma (nodular sclerosis subtype) (638,640,642–644).

Langerhans Cell Histiocytosis of Bone

Langerhans cell histiocytosis accounts for <1% of all bone lesions (645). Patients are usually older children and young adults, with a male predilection. Most patients have unifocal bone disease, but some may have simultaneous involvement of the regional lymph nodes and other sites. The patients present with bone pain and swelling. The skull is the commonest site of involvement (646,647). Temporal bone involvement can result in otitis media, while jawbone involvement can cause teeth loosening. Radiologically, the tumors usually appear as purely lytic lesions with sharp borders. Treatment options include surgery, radiotherapy, and/or chemotherapy (430). Overall survival of patients with unifocal disease is >95% (429).

Histologically, the bone shows destruction and replacement by sheets of Langerhans cells, which are often admixed with numerous eosinophils (Fig. 177). The eosinophils can form abscesses, and necrosis is common (Fig. 177). In older lesions, there are secondary changes such as fibrosis and accumulation of foamy histiocytes, rendering it difficult to identify the Langerhans cells. Positive immunostaining for S100, CD1a, and langerin (CD207) is diagnostic.

Others

Myeloid sarcoma can present as tumefactive lesion in the bone (427); the histologic appearances are similar to the extraosseous counterparts. The jawbones can rarely be involved by systemic mastocytosis (648).

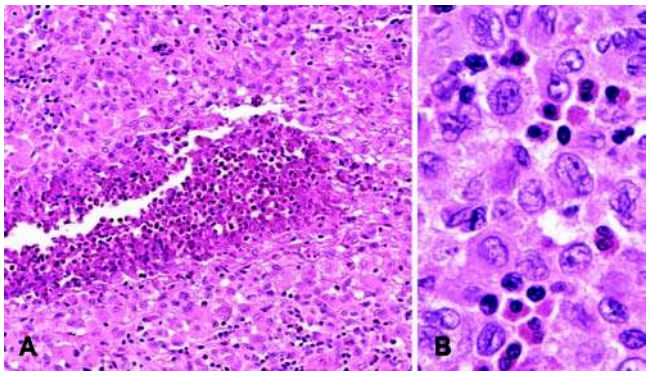

Figure 177 Langerhans cell histiocytosis of bone. (**A**) There is eosinophil abscess formation with necrosis. (**B**) The Langerhans cells show grooved nuclei, and there are admixed eosinophils.

B. Important Reactive or Inflammatory Hematolymphoid Lesions

Rosai–Dorfman disease can rarely occur in bone; in the head and neck sites, temporal bone and pterygoid fossa have been reported to be involved (144,457).

XIV. HEMATOLYMPHOID LESIONS OF SKIN

A. Hematolymphoid Neoplasms of Skin

General Features of Lymphomas

Cutaneous lymphoproliferative disorders range from reactive lymphoid hyperplasia through prelymphomatous disorders to malignant lymphomas (649). Lymphoma involving the skin may represent primary cutaneous disease, or secondary spread from a nodal primary and another extranodal primary site. Primary cutaneous lymphomas are defined as those lymphomas that present in the skin with no evidence of extracutaneous disease at the time of diagnosis (318). They account for 7.5% of all extranodal lymphomas. The classification has long been problematic (448), but the latest WHO-EORTC classification for cutaneous lymphomas (2005) has finally provided an internationally accepted unifying system (Table 16) (211,318). The commonest type is mycosis fungoides and its variants, accounting for nearly half of all cases (318). This is followed by primary cutaneous CD30+ T-cell lymphoproliferative disorders (318). Primary cutaneous B-cell lymphomas account for 23% of cases, with primary cutaneous follicle center lymphoma being the commonest. Extramedullary plasmacytoma and Hodgkin lymphoma have also been reported in the skin. The individual lymphoma types are described in a previous section ''Hematolymphoid Neoplasms of the Head and Neck,'' while additional descriptions are given on certain cutaneous-specific features under this section.

The skin may be secondarily involved by practically any type of lymphomas, such as CLL/SLL and mantle cell lymphoma (650). Cutaneous presentation is an especially common finding in intravascular large B-cell lymphoma and adult T-cell leukemia/lymphoma. The skin is a predilection site for lymphomatoid granulomatosis outside the lung. In children and young adults, lymphoblastic leukemia/lymphoma (especially of B-cell lineage) may present in the skin, frequently in the head and neck region (651).

Primary Cutaneous Follicle Center Lymphoma

Primary cutaneous follicle center lymphoma occurs mostly in middle-aged adults, who present with plaques, nodules or tumors in the trunk or head and neck region (652). The prognosis is excellent (>95% 5-year survival) with regional therapy (radiotherapy) alone. An unusual finding is that this excellent outcome also applies to tumors with a predominant large cleaved cell appearance or with a predominance of centroblasts, that is, cases that may otherwise be classified as DLBCL if it occurs in lymph nodes or other extranodal sites.

Table 16 Classification of Primary Cutaneous Lymphomas, WHO-EORTC (2005) and WHO (2008)

Lymphoma type	Frequency (%)	Clinical behavior
Cutaneous T-cell and NK-cell lymphomas		
Mycosis fungoides	44	Indolent
Mycosis fungoides variants and subtypes		Indolent
Folliculotropic mycosis fungoides	4	
Pagetoid reticulosis	<1	
Granulomatous slack skin	<1	
Sezary syndrome	3	Aggressive
Adult T-cell leukemia/lymphoma	<1	Aggressive
Primary cutaneous CD30+ T-cell lymphoproliferative disorders		Indolent
Primary cutaneous anaplastic large cell lymphoma	8	
Lymphomatoid papulosis	12	
Subcutaneous panniculitis-like T-cell lymphoma	1	Indolent
Extranodal NK/T-cell lymphoma, nasal-type	<1	Aggressive
Primary cutaneous CD8+ aggressive epidermotropic cytotoxic T-cell lymphoma	<1	Aggressive
Primary cutaneous $\gamma\delta$ T-cell lymphoma	<1	Aggressive
Primary cutaneous CD4+ small/medium T-cell lymphoma	2	Indolent
Primary cutaneous peripheral T-cell lymphoma not otherwise specified	2	Aggressive
Hydroa vacciniforme-like lymphoma	<1	Variable
Cutaneous B-cell lymphomas		
Primary cutaneous MALT lymphoma	7	Indolent
Primary cutaneous follicle center lymphoma	11	Indolent
Primary cutaneous diffuse large B-cell lymphoma, leg-type	4	Intermediate
Primary cutaneous intravascular large B-cell lymphoma	<1	Intermediate
Primary cutaneous diffuse large B-cell lymphoma, other	<1	Intermediate

Histologically, there is a dense dermal infiltrate consisting of neoplastic follicle center cells arranged in a follicular, diffuse, or mixed follicular-diffuse pattern (Fig. 178A, B). The tumor cells comprise a mixture of small or large cleaved cells (centrocytes) and large noncleaved cells (centroblasts). Although centroblasts may be abundant, they do not form confluent sheets.

The lymphoma cells express pan-B markers and the follicle center cell marker BCL6. Expression of CD10 is more variable. In contrast to nodal follicular lymphoma, BCL2 is frequently negative. Clonal rearrangements of immunoglobulin genes can be demonstrated, but t(14;18) translocation is rarely found.

Primary Cutaneous DLBCL, Leg-Type

Primary cutaneous DLBCL of leg-type is a disease of the elderly, with a median age of about 70 years (653). Patients present with rapid-growing reddish dome-shaped skin tumors, most commonly on the leg, although the lesions can occur in other sites (including head and neck region) in 10% of cases. The lymphoma is more aggressive than primary cutaneous follicle center lymphoma (even for cases rich in large cells), with a five-year disease-specific survival of 55% (318).

Histologically, there is a diffuse monomorphic infiltrate of medium size or large lymphoid cells

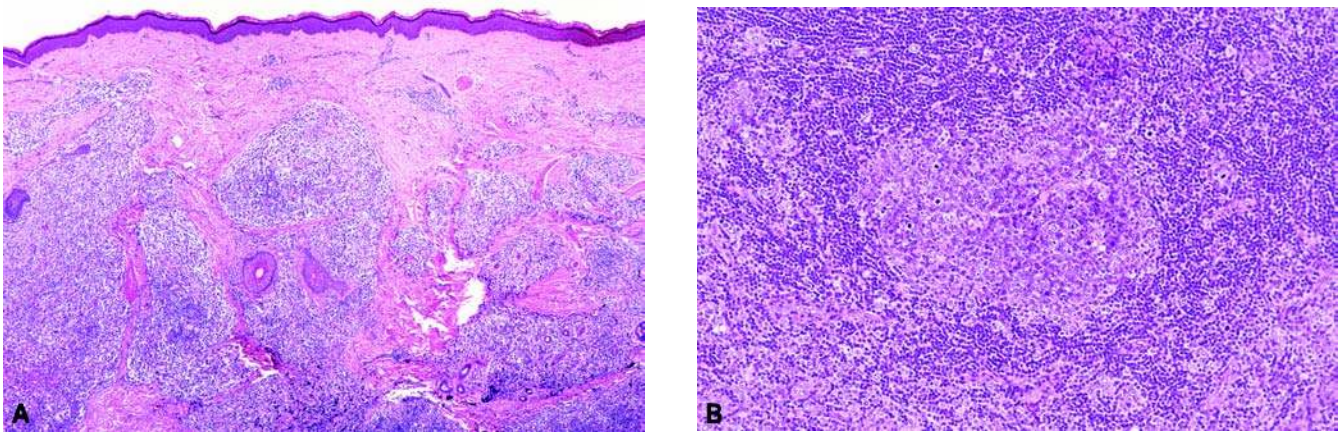

Figure 178 Primary cutaneous follicle center lymphoma. (**A**) A nodular lymphoid infiltrate is present in the dermis. (**B**) Follicles are recognizable.

consisting of centroblasts and immunoblasts. Centrocytes (including large cleaved cells) are not seen, otherwise the tumor will be categorized as primary cutaneous follicle center lymphoma. The tumor cells express pan-B markers and commonly BCL2, BCL6, and MUM1. The BCL2 expression is a clue in the distinction from primary cutaneous follicle center lymphoma, which is commonly BCL2 negative. Primary cutaneous DLBCL of leg-type also has to be distinguished from other cutaneous DLBCLs, such as intravascular large B-cell lymphoma, T-cell/histiocyte-rich large B-cell lymphoma and plasmablastic lymphoma.

Cutaneous Intravascular Large B-Cell Lymphoma

The skin is a common site for presentation of intravascular large B-cell lymphoma. Most patients are older adults, whose skin lesions take the form of tender nodules, livedo-like erythema, linear erythematous streaks, or painful indurated telangiectasia (654). Neurologic symptoms are also common. However, lymphadenopathy, splenomegaly, and circulating lymphoma cells are generally absent. Patients with skin lesions alone have a better prognosis than those with other presentations (3-year survival 56% vs. 22%) (655).

Histologically, the capillaries and venules of the dermis and subcutaneous are dilated and filled with large lymphoma cells, which may be accompanied by fibrin thrombi with or without organization and recanalization (Fig. 179). Occasionally, the lymphoma cells form palisades along the luminal side of the dilated blood vessels, imparting an impression of malignant vascular tumor (angiosarcoma). The diagnosis can be readily confirmed by positive immunostaining for pan-B markers.

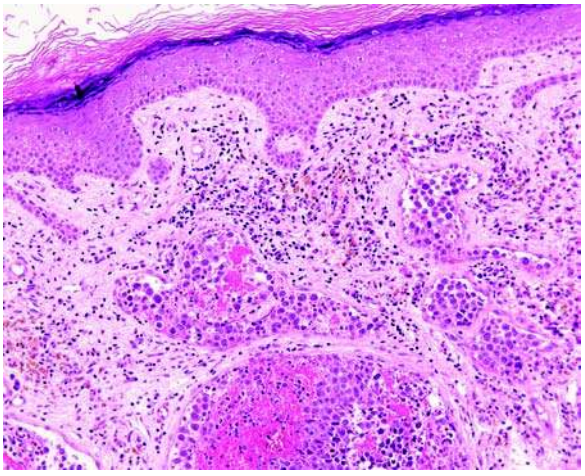

Figure 179 Intravascular large B-cell lymphoma, skin. The dermal blood vessels are distended with large lymphoma cells, sometimes accompanied by thrombus formation.

Primary Cutaneous MALT Lymphoma

Primary cutaneous MALT lymphoma is a disease of adults, frequently over 40 years of age (656). The patients present with violaceous papules, plaques, or nodules, commonly in the upper extremities, followed by head and trunk. In contrast to conventional follicular lymphoma, most patients have localized (stage IE) disease. Some cases from Europe may be associated with *Borrelia burgdorferi* infection (657,658). The prognosis is excellent, with five-year survival of 90% to 100%.

Histologically, there is nodular or diffuse infiltrate of the dermis sparing the epidermis. Reactive germinal centers are frequently present, associated with proliferation of neoplastic marginal zone and centrocyte-like cells together with monotypic plasma cells and scattered larger blastic cells. In contrast to MALT lymphoma of other sites, lymphoepithelial lesions are uncommon.

The neoplastic cells express pan-B markers and show immunoglobulin light-chain restriction (often in the plasma cell component only). Among the distinctive chromosomal translocations of MALT lymphoma, only *IGH/MALT1* and *FOXP1/IGH* are found in a proportion of the cutaneous cases (350,656).

Extranodal NK/T-Cell Lymphoma of the Skin

The skin is a common extranasal site of involvement by extranodal NK/T-cell lymphoma. There is marked racial predilection for Asians, Central Americans, or South Americans. The patients are usually adults, who present with multiple plaques or necrotic nodules, on the trunk, limbs, or head and neck. Some patients have systemic symptoms and/or hemophagocytic syndrome. On staging, many patients are found to have concurrent extracutaneous disease. This lymphoma type is highly aggressive, with a median survival of only 12 months, although rare patients may pursue a more indolent waxing and waning course.

Histologically, the skin shows dermal and subcutaneous involvement. The epidermis is often ulcerated, and there are commonly extensive areas of necrosis in the dermis or subcutis (Fig. 180A). The lymphoma cells range from small to medium-sized to large, and often exhibit irregular nuclear foldings and pale cytoplasm (Fig. 180B). There are often many admixed apoptotic bodies. Angioinvasion is commonly present. Epidermal infiltration can occur in some cases.

The most characteristic phenotype is surface CD3−, cytoplasmic CD3+, CD5−, CD56+, cytotoxic marker+, EBV+ (Fig. 180B). Cases showing predominant subcutaneous involvement have to be distinguished from subcutaneous panniculitis-like T-cell lymphoma; the latter shows no or minimal dermal involvement, and often exhibit a surface CD3+, CD8+, CD56−, EBV− phenotype.

Other Hematolymphoid Neoplasms

Other hematolymphoid neoplasms that can occur in the skin include extramedullary myeloid sarcoma, Langerhans cell histiocytosis (Fig. 181), indeterminate dendritic cell tumor, blastic plasmacytoid dendritic cell neoplasm, and mastocytosis (427,659–663).

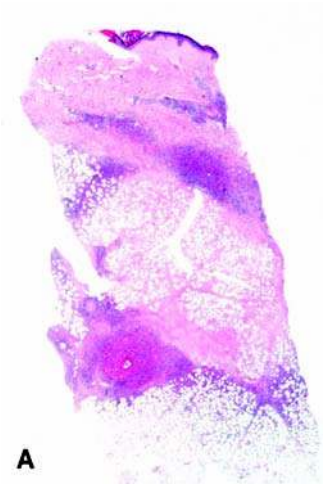

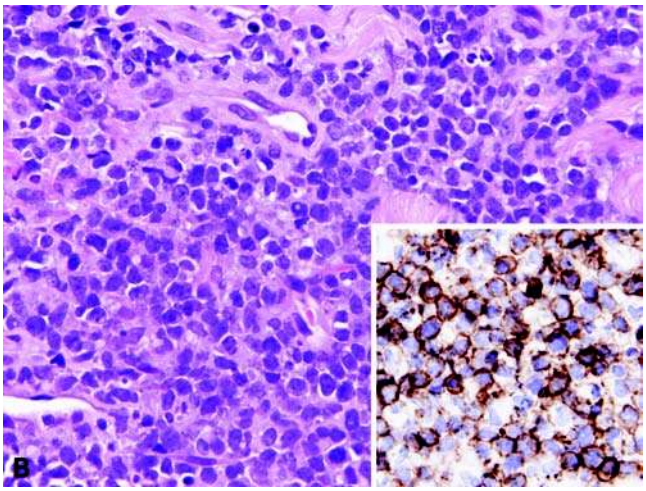

Figure 180 Extranodal NK/T-cell lymphoma of skin. (**A**) There is lymphoid infiltrate in the dermis and subcutis. Two highly characteristic features are: coagulative necrosis in the subcutis and angioinvasion (*left lower field*). (**B**) The lymphoid infiltrate consists mostly of small lymphoid cells with irregular nuclear foldings. These cells are immunoreactive for CD56 (inset).

Mastocytosis is a clonal, neoplastic proliferation of mast cells that accumulate in one or more organ systems (664). The lesions are confined to the skin in cutaneous mastocytosis, while multifocal involvement of bone marrow and at least one extracutaneous organ defines systemic mastocytosis (with about 50% of cases having cutaneous lesions). Cutaneous mastocytosis occurs predominantly in infants and young children, but sometimes also in young adults. The skin lesions take the form of widespread maculopapules, solitary nodule, or diffuse skin thickening. Histologically, there are aggregates of plump spindly or ovoid mast cells in the dermis, often with perivascular and periadnexal accentuation (Fig. 182A). The mast cells have round or oval dark-staining nuclei, and lightly basophilic cytoplasmic granules (Fig. 182B). Granules are sometimes sparse, rendering it difficult to recognize the mastocytic nature of the cells. There are also variable numbers of admixed eosinophils. The lesional cells can be confirmed to be mast cells by staining for chloroacetate esterase or immunostaining for CD117 (cell membrane staining) and mast cell tryptase (Fig. 182C).

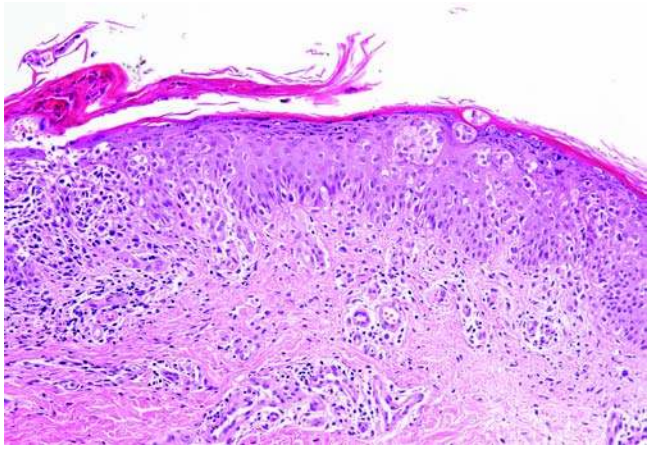

Figure 181 Langerhans cell histiocytosis of skin. There is commonly invasion of the overlying epidermis.

B. Important Reactive or Inflammatory Hematolymphoid Lesions

Cutaneous Pseudolymphoma

The term ''cutaneous pseudolymphoma'' refers to a group of reactive lymphoid proliferations of the skin that morphologically mimic lymphoma. Although many cases are of unknown etiology and can be given a diagnostic label such as ''nonspecific reactive lymphoid hyperplasia'' or ''cutaneous pseudolymphoma, not otherwise specified,'' some cases conform to specific described entities, such as actinic reticuloid, lymphomatoid contact dermatitis, lymphomatoid drug reaction, solitary T-cell pseudolymphoma, lymphocytoma cutis (with some cases being associated with *B. burgdorferi* infection), milker's nodule, arthropod reaction, secondary syphilis, and CD8+ cutaneous infiltrates in HIV patients (665). The diagnosis of these cases requires clinicopathologic correlation, e.g., occupation, drug history, HIV status.

The histologic features are variable, depending on the type of lesion, and include subepidermal band-like infiltrate, nodular infiltrate, and diffuse dense infiltrate in the dermis. Usually the cellular population is mixed, and there are no Pautrier microabscesses as defined by strict criteria. The immunohistochemical profile is also variable. Some cases are predominated by T cells, some by B cells, and some by a mixture of T and B cells. There can even be scattered CD30+ blast cells. Although molecular studies usually reveal polyclonal infiltrates in most cases, monoclonal T- or B-cell populations can be demonstrated in some cases (665).

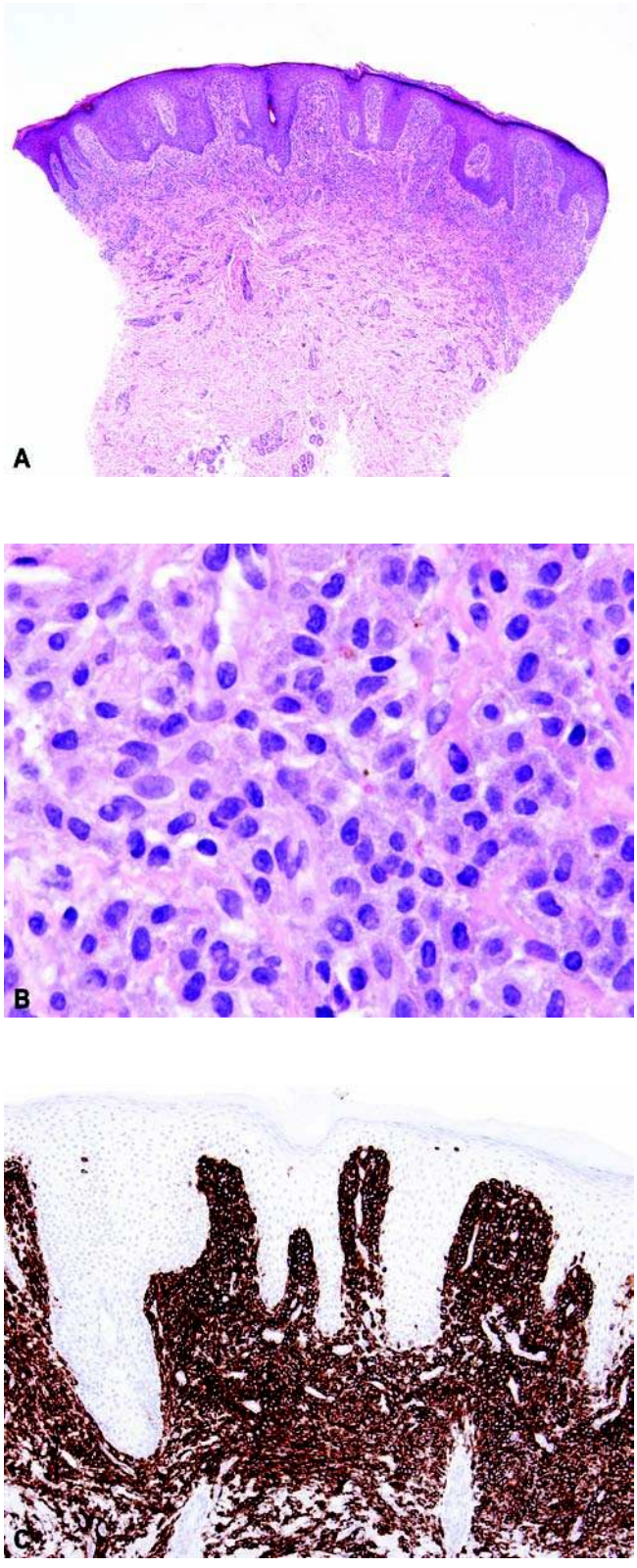

Figure 182 Cutaneous mastocytosis. (**A**) There is a broadband of cellular infiltrate in the upper and mid dermis. (**B**) The cellular infiltrate comprises medium-sized cells with dark round nuclei and fine basophilic cytoplasmic granules. (**C**) The cells can be highlighted by immunostaining for CD117.

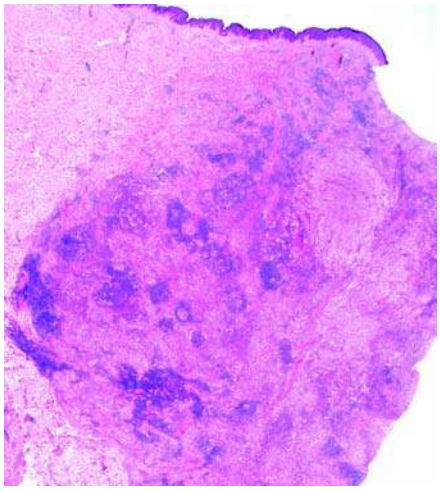

Figure 183 Rosai–Dorfman disease of skin. The infiltrate typically produces alternating dark-staining and light-staining bands.

Cutaneous Rosai–Dorfman Disease

Rosai–Dorfman disease can involve the skin, with or without simultaneous lymph node involvement (144). Clinically, it takes the form of papulonodules, indurated plaques, or tumor mass (666). The limbs are most commonly involved, followed by the trunk and face. The lesions can be treated by excision, but spontaneous remission can occur in some patients.

Histologically, there is often involvement of both the dermis and subcutis. Alternating bands of dark-staining plasma cells and pale-staining foci represent a highly characteristic low-magnification appearance (Figs. 183 and 184A). The distinctive Rosai–Dorfman histiocytes are found in loose aggregates in the latter foci—these are very large cells with round vesicular nuclei, central nucleoli, and voluminous pale cytoplasm (Fig. 184A, B). Some of these cells can have enlarged or hyperchromatic nuclei, mimicking a malignant neoplasm. Emperipolesis can be difficult to appreciate. In long-standing lesions, there can be spindling of the histiocytes, fibrosis, and accumulation of foamy histiocytes, mimicking fibrohistiocytic tumors. In some cases, the subcutaneous involvement is prominent, with numerous plasma cells mixed with lymphocytes, mimicking panniculitis. The diagnosis is easily confirmed by immunostaining for S100 protein.

C. Diagnostic Considerations

Diffuse or Nodular Large Cell Infiltrates

A predominantly large cell infiltrate in the skin usually indicates a neoplastic process. Besides nonhematolymphoid tumors (such as carcinoma, melanoma, and sarcoma), many hematolymphoid neoplasms are associated with a large cell infiltrate, including B-cell lymphomas (such as DLBCL of leg-type or other

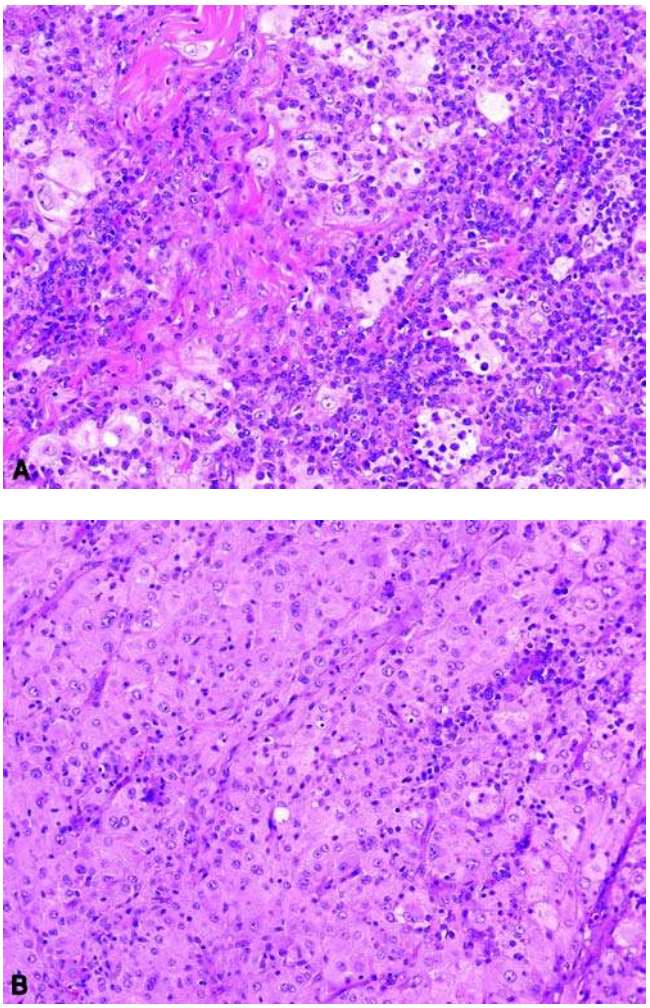

Figure 184 Rosai–Dorfman disease of skin. (**A**) Clusters of pale-staining histiocytes (some with emperipolesis) alternating with bands of plasma cells. (**B**) Sometimes the histiocytes can form broad sheets, raising the differential diagnosis of histiocytic sarcoma.

types, follicle center lymphoma), T- and NK-cell lymphomas (such as anaplastic large cell lymphoma, extranodal NK/T-cell lymphoma, large cell transformation of mycosis fungoides, adult T-cell leukemia/lymphoma, peripheral T-cell lymphoma NOS), and histiocytic sarcoma.

For a large cell neoplasm shown to be of B-lineage, it is important to make a distinction between primary cutaneous follicle center lymphoma and primary cutaneous DLBCL of leg-type, because the former is associated with a much better prognosis. Some cases of cutaneous follicle center lymphoma may comprise many large cells, including large centrocytes and centroblasts, which in lymph nodes and other extranodal sites would otherwise have qualified for a diagnosis of DLBCL. The predilection sites of this lymphoma type are the trunk and head and neck instead of the leg, and histologically there are admixed centrocytes.

For a large cell neoplasm shown to express T-lineage marker, it is most important to perform CD30 immunostain to exclude primary cutaneous anaplastic large cell lymphoma because of its excellent prognosis and tendency to undergo spontaneous regression (Fig. 115A). Of note, the cytologic features of some cases of primary cutaneous anaplastic large cell lymphoma are not necessarily anaplastic but can resemble conventional large cell lymphoma (Fig. 115B, C).

Medium-Sized Cell Infiltrates

Skin showing infiltration by a monotonous population of medium-sized cells is almost always indicative of a neoplastic process. If the cells have a blastic appearance (fine chromatin, with or without distinct nucleolus), the main considerations are (*i*) B- or T-lymphoblastic leukemia/lymphoma, (*ii*) myeloid sarcoma, (*iii*) blastoid variant of mantle cell lymphoma, and (*iii*) blastic plasmacytoid dendritic cell neoplasm. Immunohistochemical studies are required to make a distinction, except that presence of interspersed eosinophilic myelocytes strongly suggests a diagnosis of myeloid sarcoma. If the cells are not blastic, various types of B-cell lymphomas (such as follicle center lymphoma, MALT lymphoma), T- or NK-cell lymphomas (such as CD4+ small/medium-sized T-cell lymphoma, CD8+ aggressive epidermotropic cytotoxic T-cell lymphoma, extranodal NK/T-cell lymphoma, adult T-cell leukemia/lymphoma, subcutaneous panniculitis-like T-cell lymphoma, γδ T-cell lymphoma), Langerhans cell histiocytosis, indeterminate dendritic cell tumor, and mastocytosis have to be considered.

Small Cell or Mixed Cell Infiltrates

Cutaneous lymphoid infiltrates predominated by small cells or showing a mixture of small and large cells are the most difficult, because they can result from either reactive conditions or lymphomas. The clinical, histologic, and immunohistochemical findings have to be taken into consideration in assessment of these lesions. An intimate admixture of B and T cells usually indicates a reactive process. For a B-cell-rich lesion, presence of diffuse sheets of B cells or immunoglobulin light-chain restriction supports a diagnosis of lymphoma. For a T-cell-rich lesion, loss of pan-T antigens such as CD2, CD3, or CD5 strongly suggests a diagnosis of T-cell lymphoma over pseudo-T-cell lymphomas (667). Molecular studies for clonality are also helpful in supporting a diagnosis of lymphoma over cutaneous pseudolymphoma, although the results have to be interpreted with caution because clonal lymphoid populations can occasionally be detected in the latter (665,667).

When there is a *subepidermal band-like infiltrate* of small lymphoid cells (T-cell pattern), mycosis fungoides and a variety of reactive lymphoid proliferations such as actinic reticuloid, lymphomatoid contact dermatitis, lymphomatoid drug reaction, and solitary T-cell pseudolymphoma have to be considered (668). If the lesion is solitary, it is most unlikely to represent

mycosis fungoides. Presence of cells with cerebriform nuclei is of no discriminatory value since these cells can be found in any of these conditions. In reactive lesions, there are usually no significant epidermotropism and definite Pautrier microabscesses. In lymphomatoid contact dermatitis, the commonly found intraepidermal spongiotic vesicles formed predominantly by Langerhans cells should not be mistaken for Pautrier microabscesses (665).

For a *nodular or diffuse dermal infiltrate*, a wide variety of B-cell lymphomas (such as follicle center lymphoma, MALT lymphoma), T- and NK-cell lymphomas (such as extranodal NK/T-cell lymphoma, CD4+ small/medium T-cell lymphoma, γδ T-cell lymphoma, peripheral T-cell lymphoma NOS), and pseudolymphomas (such as lymphocytoma cutis, lymphomatoid drug reaction, arthropod bite reaction) are to be considered. In B-cell-rich pseudolymphomas, there are usually many reactive lymphoid follicles (which are sometimes difficult to appreciate without the help of immunohistochemistry), CD20+ B cells do not form sheets, and immunoglobulin expression is polytypic. In T-cell-rich pseudolymphomas, there is no loss of pan-T antigen, and there are usually many admixed histiocytes and CD8+ T cells (667).

A predominantly *subcutaneous lymphoid infiltrate* enlists differential diagnoses such as subcutaneous panniculitis-like T-cell lymphoma, extranodal NK/T-cell lymphoma, lupus panniculitis, and Rosai–Dorfman disease. The presence of overt cytologic atypia favors a diagnosis of lymphoma, although its absence does not totally rule out this possibility. In general, plasma cells are rare in lymphomas, but prominent in lupus panniculitis and Rosai–Dorfman disease. The distinctive histiocytes are sometimes difficult to identify in the latter entity, and are best visualized by S100 immunostain. Demonstration of characteristic immunophenotypes also helps in diagnosis of lymphomas: CD8+, CD56− cytotoxic T-cell phenotype in subcutaneous panniculitis-like T-cell lymphoma, and CD3+, CD8− CD56+, EBV+ phenotype in extranodal NK/T-cell lymphoma.

REFERENCES

1. Chan JK, Tsang WY. Reactive lymphadenopathies. In: Weiss LM, ed. Pathology of Lymph Nodes. New York: Churchill Livingstone, 1996:81–167.
2. Doglioni C, Dell'Orto P, Zanetti G, et al. Cytokeratin-immunoreactive cells of human lymph nodes and spleen in normal and pathological conditions. An immunocytochemical study. Virchows Arch A Pathol Anat Histopathol 1990; 416:479–490.
3. Sheibani K, Fritz RM, Winberg CD, et al. ''Monocytoid'' cells in reactive follicular hyperplasia with and without multifocal histiocytic reactions: an immunohistochemical study of 21 cases including suspected cases of toxoplasmic lymphadenitis. Am J Clin Pathol 1984; 81:453–458.
4. Stein H, Lennert K, Mason DY, et al. Immature sinus histiocytes. Their identification as a novel B-cell population. Am J Pathol 1984; 117:44–52.
5. Cardoso De Almeida P, Harris NL, Bhan AK. Characterization of immature sinus histiocytes (monocytoid cells) in reactive lymph nodes by use of monoclonal antibodies. Hum Pathol 1984; 15:330–335.
6. Plank L, Hansmann ML, Fischer R. The cytological spectrum of the monocytoid B-cell reaction: recognition of its large cell type. Histopathology 1993; 23:425–431.
7. Kojima M, Nakamura S, Itoh H, et al. Occurrence of monocytoid B-cells in reactive lymph node lesions. Pathol Res Pract 1998; 194:559–565.
8. Sohn CC, Sheibani K, Winberg CD, et al. Monocytoid B lymphocytes: their relation to the patterns of the acquired immunodeficiency syndrome (AIDS) and AIDS-related lymphadenopathy. Hum Pathol 1985; 16:979–985.
9. Anagnostopoulos I, Hummel M, Falini B, et al. Epstein-barr virus infection of monocytoid B-cell proliferates: an early feature of primary viral infection? Am J Surg Pathol 2005; 29:595–601.
10. Gould E, Perez J, Albores-Saavedra J, et al. Signet ring cell sinus histiocytosis. A previously unrecognized histologic condition mimicking metastatic adenocarcinoma in lymph nodes. Am J Clin Pathol 1989; 92:509–512.
11. Osborne BM, Butler JJ, Gresik MV. Progressive transformation of germinal centers: comparison of 23 pediatric patients to the adult population. Mod Pathol 1992; 5:135–140.
12. Ferry JA, Zukerberg LR, Harris NL. Florid progressive transformation of germinal centers. A syndrome affecting young men, without early progression to nodular lymphocyte predominance Hodgkin's disease. Am J Surg Pathol 1992; 16:252–258.
13. Burns BF, Colby TV, Dorfman RF. Differential diagnostic features of nodular L & H Hodgkin's disease, including progressive transformation of germinal centers. Am J Surg Pathol 1984; 8:253–261.
14. Hansmann ML, Fellbaum C, Hui PK, et al. Progressive transformation of germinal centers with and without association to Hodgkin's disease. Am J Clin Pathol 1990; 93:219–226.
15. Osborne BM, Butler JJ. Clinical implications of progressive transformation of germinal centers. Am J Surg Pathol 1984; 8:725–733.
16. Kojima M, Nakamura S, Motoori T, et al. Progressive transformation of germinal centers: a clinicopathological study of 42 Japanese patients. Int J Surg Pathol 2003; 11:101–107.
17. Gould E, Porto R, Albores-Saavedra J, et al. Dermatopathic lymphadenitis. The spectrum and significance of its morphologic features. Arch Pathol Lab Med 1988; 112:1145–1150.
18. Chan JK, Warnke RA, Dorfman R. Vascular transformation of sinuses in lymph nodes. A study of its morphological spectrum and distinction from Kaposi's sarcoma. Am J Surg Pathol 1991; 15:732–743.
19. Cook PD, Czerniak B, Chan JK, et al. Nodular spindle-cell vascular transformation of lymph nodes. A benign process occurring predominantly in retroperitoneal lymph nodes draining carcinomas that can simulate Kaposi's sarcoma or metastatic tumor. Am J Surg Pathol 1995; 19:1010–1020.
20. Norton AJ, Ramsay AD, Isaacson PG. Antigen preservation in infarcted lymphoid tissue. A novel approach to the infarcted lymph node using monoclonal antibodies effective in routinely processed tissues. Am J Surg Pathol 1988; 12:759–767.
21. Maurer R, Schmid U, Davies JD, et al. Lymph-node infarction and malignant lymphoma: a multicentre survey of European, English and American cases. Histopathology 1986; 10:571–588.
22. Cleary KR, Osborne BM, Butler JJ. Lymph node infarction foreshadowing malignant lymphoma. Am J Surg Pathol 1982; 6:435–442.
23. Childs CC, Parham DM, Berard CW. Infectious mononucleosis. The spectrum of morphologic changes simulating

lymphoma in lymph nodes and tonsils. Am J Surg Pathol 1987; 11:122–132.
24. Strickler JG, Fedeli F, Horwitz CA, et al. Infectious mononucleosis in lymphoid tissue. Histopathology, in situ hybridization, and differential diagnosis. Arch Pathol Lab Med 1993; 117:269–278.
25. Segal GH, Kjeldsberg CR, Smith GP, et al. CD30 antigen expression in florid immunoblastic proliferations. A clinicopathologic study of 14 cases. Am J Clin Pathol 1994; 102:292–298.
26. Anagnostopoulos I, Hummel M, Kreschel C, et al. Morphology, immunophenotype, and distribution of latently and/or productively Epstein-Barr virus-infected cells in acute infectious mononucleosis: implications for the interindividual infection route of Epstein-Barr virus. Blood 1995; 85:744–750.
27. Shin SS, Berry GJ, Weiss LM. Infectious mononucleosis. Diagnosis by in situ hybridization in two cases with atypical features. Am J Surg Pathol 1991; 15:625–631.
28. Abbondanzo SL, Sato N, Straus SE, et al. Acute infectious mononucleosis. CD30 (Ki-1) antigen expression and histologic correlations. Am J Clin Pathol 1990; 93:698–702.
29. Reynolds DJ, Banks PM, Gulley ML. New characterization of infectious mononucleosis and a phenotypic comparison with Hodgkin's disease. Am J Pathol 1995; 146:379–388.
30. Niedobitek G, Herbst H, Young LS, et al. Patterns of Epstein-Barr virus infection in non-neoplastic lymphoid tissue. Blood 1992; 79:2520–2526.
31. Strickler JG, Movahed LA, Gajl-Peczalska KJ, et al. Oligoclonal T cell receptor gene rearrangements in blood lymphocytes of patients with acute Epstein-Barr virus-induced infectious mononucleosis. J Clin Invest 1990; 86:1358–1363.
32. Callan MF, Steven N, Krausa P, Large clonal expansions of CD8+ T cells in acute infectious mononucleosis. Nat Med 1996; 2:906–911.
33. Malik UR, Oleksowicz L, Dutcher JP, et al. Atypical clonal T-cell proliferation in infectious mononucleosis. Med Oncol 1996; 13:207–213.
34. Mohrmann RL, Nathwani BN, Brynes RK, et al. Hodgkin's disease occurring in monocytoid B-cell clusters. Am J Clin Pathol 1991; 95:802–808.
35. Rushin JM, Riordan GP, Heaton RB, et al. Cytomegalovirus-infected cells express Leu-M1 antigen. A potential source of diagnostic error. Am J Pathol 1990; 136:989–995.
36. Strickler JG, Manivel JC, Copenhaver CM, et al. Comparison of in situ hybridization and immunohistochemistry for detection of cytomegalovirus and herpes simplex virus. Hum Pathol 1990; 21:443–448.
37. French PD, Birchall MA, Harris JR. Cytomegalovirus ulceration of the oropharynx. J Laryngol Otol 1991; 105:739–742.
38. Yoskovitch A, Cantrell H. Cytomegalovirus infection presenting as chronic sinusitis and nasal polyposis: a case report. Ear Nose Throat J 1998; 77:35–38.
39. Joseph L, Scott MA, Schichman SA, et al. Localized herpes simplex lymphadenitis mimicking large-cell (Richter's) transformation of chronic lymphocytic leukemia/small lymphocytic lymphoma. Am J Hematol 2001; 68:287–291.
40. Pilichowska ME, Smouse JH, Dorfman DM. Concurrent herpes simplex viral lymphadenitis and mantle cell lymphoma: a case report and review of the literature. Arch Pathol Lab Med 2006; 130:536–539.
41. Tamaru J, Mikata A, Horie H, et al. Herpes simplex lymphadenitis. Report of two cases with review of the literature. Am J Surg Pathol 1990; 14:571–577.
42. Audouin J, Le Tourneau A, Aubert JP, et al. Herpes simplex virus lymphadenitis mimicking tumoral relapse in a patient with Hodgkin's disease in remission. Virchows Arch A Pathol Anat Histopathol 1985; 408:313–321.
43. Taxy JB, Tillawi I, Goldman PM. Herpes simplex lymphadenitis. An unusual presentation with necrosis and viral particles. Arch Pathol Lab Med 1985; 109:1043–1044.
44. Howat AJ, Campbell AR, Stewart DJ. Generalized lymphadenopathy due to herpes simplex virus type I. Histopathology 1991; 19:563–564.
45. Epstein JI, Ambinder RF, Kuhajda FP, et al. Localized herpes simplex lymphadenitis. Am J Clin Pathol 1986; 86:444–448.
46. Miliauskas JR, Leong AS. Localized herpes simplex lymphadenitis: report of three cases and review of the literature. Histopathology 1991; 19:355–360.
47. Gaffey MJ, Ben-Ezra JM, Weiss LM. Herpes simplex lymphadenitis. Am J Clin Pathol 1991; 95:709–714.
48. Wat PJ, Strickler JG, Myers JL, et al. Herpes simplex infection causing acute necrotizing tonsillitis. Mayo Clin Proc 1994; 69:269–271.
49. Gonen C, Uner A, Cetinkaya Y, et al. Tonsillar abscess formation due to herpes simplex type-1 in a severely immunocompromised stem cell transplant patient with chronic myeloid leukemia. Transpl Infect Dis 2006; 8:166–170.
50. Taddesse-Heath L, Feldman JI, Fahle GA, et al. Florid CD4+, CD56+ T-Cell infiltrate associated with herpes simplex infection simulating nasal NK-/T-Cell lymphoma. Mod Pathol 2003; 16:166–172.
51. Sumiyoshi Y, Kikuchi M, Ohshima K, et al. A case of human herpesvirus-6 lymphadenitis with infectious mononucleosis-like syndrome. Pathol Int 1995; 45: 947–951.
52. Maric I, Bryant R, Abu-Asab M, et al. Human herpesvirus-6-associated acute lymphadenitis in immunocompetent adults. Mod Pathol 2004; 17:1427–1433.
53. Ioachim HL, Cronin W, Roy M, et al. Persistent lymphadenopathies in people at high risk for HIV infection. Clinicopathologic correlations and long-term follow-up in 79 cases. Am J Clin Pathol 1990; 93:208–218.
54. Chadburn A, Metroka C, Mouradian J. Progressive lymph node histology and its prognostic value in patients with acquired immunodeficiency syndrome and AIDS-related complex. Hum Pathol 1989; 20:579–587.
55. Burns BF, Wood GS, Dorfman RF. The varied histopathology of lymphadenopathy in the homosexual male. Am J Surg Pathol 1985; 9:287–297.
56. Said JW. AIDS-related lymphadenopathies. Semin Diagn Pathol 1988; 5:365–375.
57. Wood GS, Garcia CF, Dorfman RF, et al. The immunohistology of follicle lysis in lymph node biopsies from homosexual men. Blood 1985; 66:1092–1097.
58. Oksenhendler E, Duarte M, Soulier J, Multicentric Castleman's disease in HIV infection: a clinical and pathological study of 20 patients. AIDS 1996; 10:61–67.
59. Soulier J, Grollet L, Oksenhendler E, et al. Kaposi's sarcoma-associated herpesvirus-like DNA sequences in multicentric Castleman's disease. Blood 1995; 86: 1276–1280.
60. Stanley MW, Frizzera G. Diagnostic specificity of histologic features in lymph node biopsy specimens from patients at risk for the acquired immunodeficiency syndrome. Hum Pathol 1986; 17:1231–1239.
61. O'Murchadha MT, Wolf BC, Neiman RS. The histologic features of hyperplastic lymphadenopathy in AIDS-related complex are nonspecific. Am J Surg Pathol 1987; 11:94–99.
62. Biberfeld P, Chayt KJ, Marselle LM, et al. HTLV-III expression in infected lymph nodes and relevance to pathogenesis of lymphadenopathy. Am J Pathol 1986; 125:436–442.

63. Uccini S, Monardo F, Vitolo D, et al. Human immunodeficiency virus (HIV) and Epstein-Barr virus (EBV) antigens and genome in lymph nodes of HIV-positive patients affected by persistent generalized lymphadenopathy (PGL). Am J Clin Pathol 1989; 92:729–735.
64. de Paiva GR, Laurent C, Godel A, et al. Discovery of human immunodeficiency virus infection by immunohistochemistry on lymph node biopsies from patients with unexplained follicular hyperplasia. Am J Surg Pathol 2007; 31:1534–1538.
65. Shibata D, Weiss LM, Nathwani BN, et al. Epstein-Barr virus in benign lymph node biopsies from individuals infected with the human immunodeficiency virus is associated with concurrent or subsequent development of non-Hodgkin's lymphoma. Blood 1991; 77:1527–1533.
66. Shahab I, Osborne BM, Butler JJ. Nasopharyngeal lymphoid tissue masses in patients with human immunodeficiency virus-1. Histologic findings and clinical correlation. Cancer 1994; 74:3083–3088.
67. Wenig BM, Thompson LD, Frankel SS, et al. Lymphoid changes of the nasopharyngeal and palatine tonsils that are indicative of human immunodeficiency virus infection. A clinicopathologic study of 12 cases. Am J Surg Pathol 1996; 20:572–587.
68. Kapadia SB, Wiley CA, Soontornniyomkij V, et al. HIV-associated Waldeyer's ring lymphoid hyperplasias: characterization of multinucleated giant cells and the role of Epstein-Barr virus. Hum Pathol 1999; 30:1383–1388.
69. Dargent JL, Lespagnard L, Kornreich A, et al. HIV-associated multinucleated giant cells in lymphoid tissue of the Waldeyer's ring: a detailed study. Mod Pathol 2000; 13:1293–1299.
70. Maiorano E, Favia G, Viale G. Lymphoepithelial cysts of salivary glands: an immunohistochemical study of HIV-related and HIV-unrelated lesions. Hum Pathol 1998; 29:260–265.
71. Anderson B, Sims K, Regnery R, et al. Detection of Rochalimaea henselae DNA in specimens from cat scratch disease patients by PCR. J Clin Microbiol 1994; 32:942–948.
72. Giladi M, Avidor B, Kletter Y, et al. Cat scratch disease: the rare role of Afipia felis. J Clin Microbiol 1998; 36:2499–2502.
73. Koehler JE, Glaser CA, Tappero JW. Rochalimaea henselae infection. A new zoonosis with the domestic cat as reservoir. JAMA 1994; 271:531–535.
74. Kojima M, Nakamura S, Kurabayashi Y, et al. Suppurative lesions without prominent epithelioid cell response in abscess-forming granulomatous lymphadenitis. Pathol Res Pract 1995; 191:1072–1077.
75. Facchetti F, Agostini C, Chilosi M, et al. Suppurative granulomatous lymphadenitis. Immunohistochemical evidence for a B-cell-associated granuloma. Am J Surg Pathol 1992; 16:955–961.
76. Korbi S, Toccanier MF, Leyvraz G, et al. Use of silver staining (dieterle's stain) in the diagnosis of cat scratch disease. Histopathology 1986; 10:1015–1021.
77. Kudo E, Sakaki A, Sumitomo M, et al. Cat scratch disease. An epidemiological and ultrastructural study of lymphadenitis caused by Warthin-Starry positive bacteria. Virchows Arch A Pathol Anat Histopathol 1988; 412:563–572.
78. Cheuk W, Chan AK, Wong MC, et al. Confirmation of diagnosis of cat scratch disease by immunohistochemistry. Am J Surg Pathol 2006; 30:274–275.
79. Scott MA, McCurley TL, Vnencak-Jones CL, et al. Cat scratch disease: detection of Bartonella henselae DNA in archival biopsies from patients with clinically, serologically, and histologically defined disease. Am J Pathol 1996; 149:2161–2167.
80. Regnery RL, Olson JG, Perkins BA, et al. Serological response to ''Rochalimaea henselae'' antigen in suspected cat-scratch disease. Lancet 1992; 339:1443–1445.
81. Centkowski P, Sawczuk-Chabin J, Prochorec M, et al. Hodgkin's lymphoma and tuberculosis coexistence in cervical lymph nodes. Leuk Lymphoma 2005; 46:471–475.
82. Chen KT. Mycobacterial spindle cell pseudotumor of lymph nodes. Am J Surg Pathol 1992; 16:276–281.
83. Bagla N, Patel MM, Patel RD, et al. Lepromatous lymphadenitis masquerading as lymphoma. Lepr Rev 2005; 76:87–90.
84. Farhi DC, Wells SJ, Siegel RJ. Syphilitic lymphadenopathy. Histology and human immunodeficiency virus status. Am J Clin Pathol 1999; 112:330–334.
85. Tuzuner N, Dogusoy G, Demirkesen C, et al. Value of lymph node biopsy in the diagnosis of acquired toxoplasmosis. J Laryngol Otol 1996; 110:348–352.
86. Lin MH, Kuo TT. Specificity of the histopathological triad for the diagnosis of toxoplasmic lymphadenitis: polymerase chain reaction study. Pathol Int 2001; 51:619–623.
87. Aisner SC, Aisner J, Moravec C, et al. Acquired toxoplasmic lymphadenitis with demonstration of the cyst form. Am J Clin Pathol 1983; 79:125–127.
88. Cohen C, Trapuckd S. Toxoplasma cyst with toxoplasmic lymphadenitis. Hum Pathol 1984; 15:396–397.
89. Weiss LM, Chen YY, Berry GJ, et al. Infrequent detection of Toxoplasma gondii genome in toxoplasmic lymphadenitis: a polymerase chain reaction study. Hum Pathol 1992; 23:154–158.
90. Kenner JR, Aronson NE, Bratthauer GL, et al. Immunohistochemistry to identify Leishmania parasites in fixed tissues. J Cutan Pathol 1999; 26:130–136.
91. Nosanchuk JS, Schnitzer B. Follicular hyperplasia in lymph nodes from patients with rheumatoid arthritis. A clinicopathologic study. Cancer 1969; 24:243–254.
92. Kondratowicz GM, Symmons DP, Bacon PA, et al. Rheumatoid lymphadenopathy: a morphological and immunohistochemical study. J Clin Pathol 1990; 43:106–113.
93. Wong SY, Sewell HF. CD5 positive B cells in peripheral blood and lymph nodes in rheumatoid arthritis. J Clin Pathol 1991; 44:85–86.
94. Harris NL, Swerdlow SH. Methotrexate-associated lmphoproliferative disorders. In: Jaffe ES, Harris NL, Stein H, et al., eds. Pathology and Genetics: Tumours of Haematopoietic and Lymphoid Tissues. World Health Organization Classification of Tumours. Lyon: IARC Press, 2001:270–271.
95. Hoshida Y, Xu JX, Fujita S, et al. Lymphoproliferative Disorders in Rheumatoid Arthritis: Clinicopathological Analysis of 76 Cases in Relation to Methotrexate Medication. J Rheumatol 2007; 34(2):322–331.
96. Hu S, Kuo TT, Hong HS. Lupus lymphadenitis simulating Kikuchi's lymphadenitis in patients with systemic lupus erythematosus: a clinicopathological analysis of six cases and review of the literature. Pathol Int 2003; 53:221–226.
97. Medeiros LJ, Kaynor B, Harris NL. Lupus lymphadenitis: report of a case with immunohistologic studies on frozen sections. Hum Pathol 1989; 20:295–299.
98. Kojima M, Nakamura S, Morishita Y, et al. Reactive follicular hyperplasia in the lymph node lesions from systemic lupus erythematosus patients: a clinicopathological and immunohistological study of 21 cases. Pathol Int 2000; 50:304–312.
99. Kassan SS, Thomas TL, Moutsopoulos HM, et al. Increased risk of lymphoma in sicca syndrome. Ann Intern Med 1978; 89:888–892.
100. Harris NL. Lymphoid proliferations of the salivary glands. Am J Clin Pathol 1999; 111:S94–S103.
101. McCurley TL, Collins RD, Ball E. Nodal and extranodal lymphoproliferative disorders in Sjogren's syndrome: a clinical and immunopathologic study. Hum Pathol 1990; 21:482–492.

102. Ohsawa M, Kanno H, Machii T, et al. Immunoreactivity of neoplastic and non-neoplastic monocytoid B lymphocytes for DBA.44 and other antibodies. J Clin Pathol 1994; 47:928–932.
103. Kamisawa T, Nakajima H, Egawa N, et al. IgG4-related sclerosing disease incorporating sclerosing pancreatitis, cholangitis, sialadenitis and retroperitoneal fibrosis with lymphadenopathy. Pancreatology 2006; 6:132–137.
104. Cheuk W, Yuen HK, Chu SY, et al. Lymphadenopathy of IgG4-related sclerosing disease. Am J Surg Pathol 2008; 32:671–681.
105. Cheuk W, Yuen HK, Chan JK. Chronic sclerosing dacryoadenitis: part of the spectrum of IgG4-related Sclerosing disease? Am J Surg Pathol 2007; 31:643–645.
106. Tsang WY, Chan JK, Ng CS. Kikuchi's lymphadenitis. A morphologic analysis of 75 cases with special reference to unusual features. Am J Surg Pathol 1994; 18:219–231.
107. Kuo TT. Kikuchi's disease (histiocytic necrotizing lymphadenitis). A clinicopathologic study of 79 cases with an analysis of histologic subtypes, immunohistology, and DNA ploidy. Am J Surg Pathol 1995; 19:798–809.
108. Dorfman RF, Berry GJ. Kikuchi's histiocytic necrotizing lymphadenitis: an analysis of 108 cases with emphasis on differential diagnosis. Semin Diagn Pathol 1988; 5:329–345.
109. Sumiyoshi Y, Kikuchi M, Takeshita M, et al. Immunohistologic studies of Kikuchi's disease. Hum Pathol 1993; 24:1114–1119.
110. Felgar RE, Furth EE, Wasik MA, et al. Histiocytic necrotizing lymphadenitis (Kikuchi's disease): in situ end-labeling, immunohistochemical, and serologic evidence supporting cytotoxic lymphocyte-mediated apoptotic cell death. Mod Pathol 1997; 10:231–241.
111. Pileri SA, Facchetti F, Ascani S, et al. Myeloperoxidase expression by histiocytes in Kikuchi's and Kikuchi-like lymphadenopathy. Am J Pathol 2001; 159:915–924.
112. Ishikawa E, Tanaka H, Kakimoto S, et al. A pathological study on eosinophilic lymphfolliculoid granuloma (Kimura's disease). Acta Pathol Jpn 1981; 31:767–781.
113. Chan JK, Hui PK, Ng CS, et al. Epithelioid haemangioma (angiolymphoid hyperplasia with eosinophilia) and Kimura's disease in Chinese. Histopathology 1989; 15:557–574.
114. Li TJ, Chen XM, Wang SZ, et al. Kimura's disease: a clinicopathologic study of 54 Chinese patients. Oral Surg Oral Med Oral Pathol Oral Radiol Endod 1996; 82:549–555.
115. Chen H, Thompson LD, Aguilera NS, et al. Kimura disease: a clinicopathologic study of 21 cases. Am J Surg Pathol 2004; 28:505–513.
116. Newburger JW, Takahashi M, Gerber MA, et al. Diagnosis, treatment, and long-term management of Kawasaki disease: a statement for health professionals from the Committee on Rheumatic Fever, Endocarditis, and Kawasaki Disease, Council on Cardiovascular Disease in the Young, American Heart Association. Pediatrics 2004; 114:1708–1733.
117. Giesker DW, Pastuszak WT, Forouhar FA, et al. Lymph node biopsy for early diagnosis in Kawasaki disease. Am J Surg Pathol 1982; 6:493–501.
118. Keller AR, Hochholzer L, Castleman B. Hyaline-vascular and plasma-cell types of giant lymph node hyperplasia of the mediastinum and other locations. Cancer 1972; 29:670–683.
119. Chen TC, Kuo T. Castleman's disease presenting as a pedunculated nasopharyngeal tumour simulating angiofibroma. Histopathology 1993; 23:485–488.
120. Meyer L, Gibbons D, Ashfaq R, et al. Fine-needle aspiration findings in Castleman's disease. Diagn Cytopathol 1999; 21:57–60.
121. Rivas DM, Saint Blancat P, Marjou F, et al. Intra-orbital Castleman's disease. Clin Neuropathol 2004; 23:91–94.
122. Frizzera G. Castleman's disease and related disorders. Semin Diagn Pathol 1988; 5:346–364.
123. Danon AD, Krishnan J, Frizzera G. Morpho-immunophenotypic diversity of Castleman's disease, hyaline-vascular type: with emphasis on a stroma-rich variant and a new pathogenetic hypothesis. Virchows Arch A Pathol Anat Histopathol 1993; 423:369–382.
124. Martin JM, Bell B, Ruether BA. Giant lymph node hyperplasia (Castleman's disease) of hyaline vascular type. Clinical heterogeneity with immunohistologic uniformity. Am J Clin Pathol 1985; 84:439–446.
125. Carbone A, Manconi R, Volpe R, et al. Immunohistochemical, enzyme histochemical, and immunologic features of giant lymph node hyperplasia of the hyaline-vascular type. Cancer 1986; 58:908–916.
126. Hanson CA, Frizzera G, Patton DF, et al. Clonal rearrangement for immunoglobulin and T-cell receptor genes in systemic Castleman's disease. Association with Epstein-Barr virus. Am J Pathol 1988; 131:84–91.
127. Soulier J, Grollet L, Oksenhendler E, et al. Molecular analysis of clonality in Castleman's disease. Blood 1995; 86:1131–1138.
128. Gerald W, Kostianovsky M, Rosai J. Development of vascular neoplasia in Castleman's disease. Report of seven cases. Am J Surg Pathol 1990; 14:603–614.
129. Chan JK, Tsang WY, Ng CS. Follicular dendritic cell tumor and vascular neoplasm complicating hyaline-vascular Castleman's disease. Am J Surg Pathol 1994; 18:517–525.
130. Madero S, Onate JM, Garzon A. Giant lymph node hyperplasia in an angiolipomatous mediastinal mass. Arch Pathol Lab Med 1986; 110:853–855.
131. Pauwels P, Dal Cin P, Vlasveld LT, et al. A chromosomal abnormality in hyaline vascular Castleman's disease: evidence for clonal proliferation of dysplastic stromal cells. Am J Surg Pathol 2000; 24:882–888.
132. Cokelaere K, Debiec-Rychter M, De Wolf-Peeters C, et al. Hyaline vascular Castleman's disease with HMGIC rearrangement in follicular dendritic cells: molecular evidence of mesenchymal tumorigenesis. Am J Surg Pathol 2002; 26:662–669.
133. Chen WC, Jones D, Ho CL, et al. Cytogenetic anomalies in hyaline vascular Castleman disease: report of two cases with reappraisal of histogenesis. Cancer Genet Cytogenet 2006; 164:110–117.
134. Beck JT, Hsu SM, Wijdenes J, et al. Brief report: alleviation of systemic manifestations of Castleman's disease by monoclonal anti-interleukin-6 antibody. N Engl J Med 1994; 330:602–605.
135. Radaszkiewicz T, Hansmann ML, Lennert K. Monoclonality and polyclonality of plasma cells in Castleman's disease of the plasma cell variant. Histopathology 1989; 14:11–24.
136. Hall PA, Donaghy M, Cotter FE, et al. An immunohistological and genotypic study of the plasma cell form of Castleman's disease. Histopathology 1989; 14:333–346; discussion 429–432.
137. Zarate-Osorno A, Medeiros LJ, Danon AD, et al. Hodgkin's disease with coexistent Castleman-like histologic features. A report of three cases. Arch Pathol Lab Med 1994; 118:270–274.
138. Frizzera G. Multicentric Castleman disease: interleukin-6 syndrome. In: Knowles DM, ed. Neoplastic Hematopathology. Philadelphia: Lippincott Williams & Wilkins, 2001:595–622.
139. Nishimoto N, Sasai M, Shima Y, et al. Improvement in Castleman's disease by humanized anti-interleukin-6 receptor antibody therapy. Blood 2000; 95:56–61.

140. Parravinci C, Corbellino M, Paulli M, et al. Expression of a virus-derived cytokine, KSHV vIL-6, in HIV-seronegative Castleman's disease. Am J Pathol 1997; 151:1517–1522.
141. Dupin N, Diss TL, Kellam P, et al. HHV-8 is associated with a plasmablastic variant of Castleman disease that is linked to HHV-8-positive plasmablastic lymphoma. Blood 2000; 95:1406–1412.
142. Isaacson PG, Campo E, Harris NL. Large B-cell lymphoma arising in HHV8-associated multicentric Castleman disease. In: Swerdlow SH, Campo E, Harris NL, et al., eds. WHO Classification of Tumours of Haematopoietic and Lymphoid Tissues. 4th ed. Lyon: IARC, 2008:258–259.
143. Du MQ, Liu H, Diss TC, et al. Kaposi sarcoma-associated herpesvirus infects monotypic (IgM lambda) but polyclonal naive B cells in Castleman disease and associated lymphoproliferative disorders. Blood 2001; 97:2130–2136.
144. Foucar E, Rosai J, Dorfman R. Sinus histiocytosis with massive lymphadenopathy (Rosai-Dorfman disease): review of the entity. Semin Diagn Pathol 1990; 7:19–73.
145. Maric I, Pittaluga S, Dale JK, et al. Histologic features of sinus histiocytosis with massive lymphadenopathy in patients with autoimmune lymphoproliferative syndrome. Am J Surg Pathol 2005; 29:903–911.
146. Sneller MC, Wang J, Dale JK, et al. Clincal, immunologic, and genetic features of an autoimmune lymphoproliferative syndrome associated with abnormal lymphocyte apoptosis. Blood 1997; 89:1341–1348.
147. Fleisher TA. The autoimmune lymphoproliferative syndrome: an experiment of nature involving lymphocyte apoptosis. Immunol Res 2008; 40:87–92.
148. Worth A, Thrasher AJ, Gaspar HB. Autoimmune lymphoproliferative syndrome: molecular basis of disease and clinical phenotype. Br J Haematol 2006; 133:124–140.
149. Holzelova E, Vonarbourg C, Stolzenberg MC, et al. Autoimmune lymphoproliferative syndrome with somatic Fas mutations. N Engl J Med 2004; 351:1409–1418.
150. Straus SE, Jaffe ES, Puck JM, et al. The development of lymphomas in families with autoimmune lymphoproliferative syndrome with germline Fas mutations and defective lymphocyte apoptosis. Blood 2001; 98:194–200.
151. Lim MS, Straus SE, Dale JK, et al. Pathological findings in human autoimmune lymphoproliferative syndrome. Am J Pathol 1998; 153:1541–1550.
152. Ruaux C, Noret P, Godey B. Inflammatory pseudotumour of the nasal cavity and sinuses. J Laryngol Otol 2001; 115:563–566.
153. Hanna SJ, Blenke E, Sharma R, et al. Laryngeal inflammatory pseudotumour: an unusual cause of airway obstruction. Int J Pediatr Otorhinolaryngol 2005; 69:1253–1255.
154. Williams SB, Foss RD, Ellis GL. Inflammatory pseudotumors of the major salivary glands. Clinicopathologic and immunohistochemical analysis of six cases. Am J Surg Pathol 1992; 16:896–902.
155. Mahr MA, Salomao DR, Garrity JA. Inflammatory orbital pseudotumor with extension beyond the orbit. Am J Ophthalmol 2004; 138:396–400.
156. Chan JK, Cheuk W, Shimizu M. Anaplastic lymphoma kinase expression in inflammatory pseudotumors. Am J Surg Pathol 2001; 25:761–768.
157. Cook JR, Dehner LP, Collins MH, et al. Anaplastic lymphoma kinase (ALK) expression in the inflammatory myofibroblastic tumor: a comparative immunohistochemical study. Am J Surg Pathol 2001; 25:1364–1371.
158. Coffin CM, Patel A, Perkins S, et al. ALK1 and p80 expression and chromosomal rearrangements involving 2p23 in inflammatory myofibroblastic tumor. Mod Pathol 2001; 14:569–576.
159. Moran CA, Suster S, Abbondanzo SL. Inflammatory pseudotumor of lymph nodes: a study of 25 cases with emphasis on morphological heterogeneity. Hum Pathol 1997; 28:332–338.
160. Davis RE, Warnke RA, Dorfman RF. Inflammatory pseudotumor of lymph nodes. Additional observations and evidence for an inflammatory etiology. Am J Surg Pathol 1991; 15:744–756.
161. Kutok JL, Pinkus GS, Dorfman DM, et al. Inflammatory pseudotumor of lymph node and spleen: an entity biologically distinct from inflammatory myofibroblastic tumor. Hum Pathol 2001; 32:1382–1387.
162. Khan A, Milley PS, Spaulding MB, et al. An unusual cause of cervical adenopathy. Extramedullary hematopoiesis. Arch Otolaryngol 1982; 108:523–524.
163. Pless M, Rizzo JF III, Shang J. Orbital apex syndrome: a rare presentation of extramedullary hematopoiesis: case report and review of literature. J Neurooncol 2002; 57:37–40.
164. Applebaum EL, Frankel A. Extramedullary hematopoiesis of the middle ear. Am J Otolaryngol 1989; 10:287–290.
165. Brennan LV, Mayer T, Devitt J. Extramedullary hematopoiesis occurring as a nasal polyp in a man with a myeloproliferative disorder. Ear Nose Throat J 2004; 83:258–259.
166. Barnes EA, Seikaly H, Puttagunta L, et al. Subglottic stenosis secondary to extramedullary hematopoiesis in a patient with postpolycythemia myeloid metaplasia. Head Neck 2000; 22:435–438.
167. Lazzi S, Als C, Mazzucchelli L, et al. Extensive extramedullary hematopoiesis in a thyroid nodule. Mod Pathol 1996; 9:1062–1065.
168. Dagdas S, Ozet G, Alanoglu G, et al. Unusual extramedullary hematopoiesis in a patient receiving granulocyte colony-stimulating factor. Acta Haematol 2006; 116:198–202.
169. Remstein ED, Kurtin PJ, Nascimento AG. Sclerosing extramedullary hematopoietic tumor in chronic myeloproliferative disorders. Am J Surg Pathol 2000; 24:51–55.
170. Abbas AK. Amyloidosis. In: Kumar V, Abbas AK, Fausto N, eds. Robbins and Cotran Pathologic Basis of Disease. 7th ed. Philadelphia: Elsevier Saunders, 2005:258–267.
171. Westermark P, Benson MD, Buxbaum JN, et al. Amyloid: toward terminology clarification. Report from the Nomenclature Committee of the International Society of Amyloidosis. Amyloid 2005; 12:1–4.
172. Picken MM. New insights into systemic amyloidosis: the importance of diagnosis of specific type. Curr Opin Nephrol Hypertens 2007; 16:196–203.
173. Picken MM, Herrera GA. The burden of ''sticky'' amyloid: typing challenges. Arch Pathol Lab Med 2007; 131:850–851.
174. van Rijswijk MH, van Heusden CW. The potassium permanganate method. A reliable method for differentiating amyloid AA from other forms of amyloid in routine laboratory practice. Am J Pathol 1979; 97:43–58.
175. Bardin T, Zingraff J, Shirahama T, et al. Hemodialysis-associated amyloidosis and beta-2 microglobulin. Clinical and immunohistochemical study. Am J Med 1987; 83: 419–424.
176. Kebbel A, Rocken C. Immunohistochemical classification of amyloid in surgical pathology revisited. Am J Surg Pathol 2006; 30:673–683.
177. Satoskar AA, Burdge K, Cowden DJ, et al. Typing of amyloidosis in renal biopsies: diagnostic pitfalls. Arch Pathol Lab Med 2007; 131:917–922.
178. Solomon A, Murphy CL, Westermark P. Unreliability of immunohistochemistry for typing amyloid deposits. Arch Pathol Lab Med 2008; 132:14; author reply 14–15.
179. Kerner MM, Wang MB, Angier G, et al. Amyloidosis of the head and neck. A clinicopathologic study of the UCLA experience, 1955–1991. Arch Otolaryngol Head Neck Surg 1995; 121:778–782.

180. Penner CR, Muller S. Head and neck amyloidosis: a clinicopathologic study of 15 cases. Oral Oncol 2006; 42:421–429.
181. Kimura H, Yamashita S, Ashizawa K, et al. Thyroid dysfunction in patients with amyloid goitre. Clin Endocrinol (Oxf) 1997; 46:769–774.
182. Lewis JE, Olsen KD, Kurtin PJ, et al. Laryngeal amyloidosis: a clinicopathologic and immunohistochemical review. Otolaryngol Head Neck Surg 1992; 106:372–377.
183. Thompson LD, Derringer GA, Wenig BM. Amyloidosis of the larynx: a clinicopathologic study of 11 cases. Mod Pathol 2000; 13:528–535.
184. Timosca G, Gavrilita L. Primary localized amyloidosis of the palate. Oral Surg Oral Med Oral Pathol 1977; 44:76–83.
185. Newland JR, Linke RP, Kleinsasser O, et al. Lymph node enlargement due to amyloid. Virchows Arch A Pathol Anat Histopathol 1983; 399:233–236.
186. Simpson GT II, Strong MS, Skinner M, et al. Localized amyloidosis of the head and neck and upper aerodigestive and lower respiratory tracts. Ann Otol Rhinol Laryngol 1984; 93:374–379.
187. Mufarrij AA, Busaba NY, Zaytoun GM, et al. Primary localized amyloidosis of the nose and paranasal sinuses. A case report with immunohistochemical observations and a review of the literature. Am J Surg Pathol 1990; 14:379–383.
188. Clevens RA, Esclamado RM, DelGaudio JM, et al. Amyloidoma of the neck: case report and review of the literature. Head Neck 1994; 16:191–195.
189. Vavrina J, Muller W, Gebbers JO. Recurrent amyloid tumor of the parotid gland. Eur Arch Otorhinolaryngol 1995; 252:53–56.
190. Lopez Amado M, Lorenzo Patino MJ, Lopez Blanco G, et al. Giant primary amyloidoma of the tonsil. J Laryngol Otol 1996; 110:613–615.
191. Nandapalan V, Jones TM, Morar P, et al. Localized amyloidosis of the parotid gland: a case report and review of the localized amyloidosis of the head and neck. Head Neck 1998; 20:73–78.
192. Patel A, Pambuccian S, Maisel R. Nasopharyngeal amyloidosis. Am J Otolaryngol 2002; 23:308–311.
193. Moon AO, Calamia KT, Walsh JS. Nodular amyloidosis: review and long-term follow-up of 16 cases. Arch Dermatol 2003; 139:1157–1159.
194. Fahrner KS, Black CC, Gosselin BJ. Localized amyloidosis of the tongue: a review. Am J Otolaryngol 2004; 25:186–189.
195. Biewend ML, Menke DM, Calamia KT. The spectrum of localized amyloidosis: a case series of 20 patients and review of the literature. Amyloid 2006; 13:135–142.
196. Leibovitch I, Selva D, Goldberg RA, et al. Periocular and orbital amyloidosis: clinical characteristics, management, and outcome. Ophthalmology 2006; 113:1657–1664.
197. Gheriani H, Tewary R, O'Sullivan TJ. Amyloidosis of the external auditory canal and middle ear: unusual ear tumor. Ear Nose Throat J 2007; 86:92–93, 106.
198. Panda NK, Saravanan K, Purushotaman GP, et al. Localized amyloidosis masquerading as nasopharyngeal tumor: a review. Am J Otolaryngol 2007; 28:208–211.
199. Dedo HH, Izdebski K. Laryngeal amyloidosis in 10 patients. Laryngoscope 2004; 114:1742–1746.
200. Ma L, Bandarchi B, Sasaki C, et al. Primary localized laryngeal amyloidosis: report of 3 cases with long-term follow-up and review of the literature. Arch Pathol Lab Med 2005; 129:215–218.
201. Fukuzawa M, Maejima T, Sano K, et al. Immunohistochemical, electron microscopic, and immunoelectron microscopic features of plasmacytoma of the thyroid with amyloid deposition. Ultrastruct Pathol 1993; 17:681–686.
202. Hidaka H, Ikeda K, Oshima T, et al. A case of extramedullary plasmacytoma arising from the nasal septum. J Laryngol Otol 2000; 114:53–55.
203. Rocken C, Hegenbarth V, Schmitz M, et al. Plasmacytoma of the tonsil with AL amyloidosis: evidence of post-fibrillogenic proteolysis of the fibril protein. Virchows Arch 2000; 436:336–344.
204. Nagasaka T, Lai R, Kuno K, et al. Localized amyloidosis and extramedullary plasmacytoma involving the larynx of a child. Hum Pathol 2001; 32:132–134.
205. Velez D, Hinojar-Gutierrez A, Nam-Cha S, et al. Laryngeal plasmacytoma presenting as amyloid tumour: a case report. Eur Arch Otorhinolaryngol 2007; 264:959–961.
206. Kojima M, Sugihara S, Iijima M, et al. Marginal zone B-cell lymphoma of minor salivary gland representing tumor-forming amyloidosis of the oral cavity. A case report. J Oral Pathol Med 2006; 35:314–316.
207. Sletten K, Westermark P, Natvig JB. Characterization of amyloid fibril proteins from medullary carcinoma of the thyroid. J Exp Med 1976; 143:993–998.
208. Khurana R, Agarwal A, Bajpai VK, et al. Unraveling the amyloid associated with human medullary thyroid carcinoma. Endocrinology 2004; 145:5465–5470.
209. Armitage JO, Weisenburger DD. New approach to classifying non-Hodgkin's lymphomas: clinical features of the major histologic subtypes. Non-Hodgkin's Lymphoma Classification Project. J Clin Oncol 1998; 16:2780–2795.
210. The Non-Hodgkin's Lymphoma Classification Project. A clinical evaluation of the International Lymphoma Study Group classification of non-Hodgkin's lymphoma. Blood 1997; 89:3909–3918.
211. Jaffe ES, Harris NL, Stein H, et al. Introduction and overview of the classification of the lymphoid neoplasms. In: Swerdlow SH, Campo E, Harris NL, et al., eds. WHO Classification of Tumours of Haematopoietic and Lymphoid Tissues. 4th ed. Lyon: IARC, 2008:158–166.
212. Anderson JR, Armitage JO, Weisenburger DD. Epidemiology of the non-Hodgkin's lymphomas: distributions of the major subtypes differ by geographic locations. Non-Hodgkin's Lymphoma Classification Project. Ann Oncol 1998; 9:717–720.
213. Greene FL, Page DL, Fleming ID, et al. AJCC Cancer Staging Handbook. 6th ed. New York: Springer-Verlag, 2002.
214. The International Non-Hodgkin's Lymphoma Prognostic Factors Project. A predictive model for aggressive non-Hodgkin's lymphoma. N Engl J Med 1993; 329:987–994.
215. Hermans J, Krol AD, van Groningen K, et al. International Prognostic Index for aggressive non-Hodgkin's lymphoma is valid for all malignancy grades. Blood 1995; 86: 1460–1463.
216. Stein H, Delsol G, Pileri S, et al. Classical Hodgkin lymphoma. In: Jaffe ES, Harris NL, Stein H, et al., eds. Pathology and Genetics: Tumours of Haematopoietic and Lymphoid Tissues. World Health Organization Classification of Tumours. Lyon: IARC Press, 2001:244–253.
217. Quinones-Avila Mdel P, Gonzalez-Longoria AA, Admirand JH, et al. Hodgkin lymphoma involving Waldeyer ring: a clinicopathologic study of 22 cases. Am J Clin Pathol 2005; 123:651–656.
218. MacLennan KA, Bennett MH, Tu A, et al. Relationship of histopathologic features to survival and relapse in nodular sclerosing Hodgkin's disease. A study of 1659 patients. Cancer 1989; 64:1686–1693.
219. Harris NL, Jaffe ES, Stein H, et al. A revised European-American classification of lymphoid neoplasms: a proposal from the International Lymphoma Study Group. Blood 1994; 84:1361–1392 (see comments).
220. Ashton-Key M, Thorpe PA, Allen JP, et al. Follicular Hodgkin's disease. Am J Surg Pathol 1995; 19:1294–1299.

221. Harris NL. Hodgkin's disease: classification and differential diagnosis. Mod Pathol 1999; 12:159–175.
222. Anagnostopoulos I, Hansmann ML, Franssila K, et al. European Task Force on Lymphoma project on lymphocyte predominance Hodgkin disease: histologic and immunohistologic analysis of submitted cases reveals 2 types of Hodgkin disease with a nodular growth pattern and abundant lymphocytes. Blood 2000; 96:1889–1899.
223. Foss HD, Reusch R, Demel G, et al. Frequent expression of the B-cell-specific activator protein in Reed-Sternberg cells of classical Hodgkin's disease provides further evidence for its B-cell origin. Blood 1999; 94:3108–3113.
224. Stein H, Marafioti T, Foss HD, et al. Down-regulation of BOB.1/OBF.1 and Oct2 in classical Hodgkin disease but not in lymphocyte predominant Hodgkin disease correlates with immunoglobulin transcription. Blood 2001; 97:496–501.
225. Marafioti T, Hummel M, Foss HD, et al. Hodgkin and reed-sternberg cells represent an expansion of a single clone originating from a germinal center B-cell with functional immunoglobulin gene rearrangements but defective immunoglobulin transcription. Blood 2000; 95:1443–1450.
226. Glaser SL, Lin RJ, Stewart SL, et al. Epstein-Barr virus-associated Hodgkin's disease: epidemiologic characteristics in international data. Int J Cancer 1997; 70:375–382.
227. Josting A, Wolf J, Diehl V. Hodgkin disease: prognostic factors and treatment strategies. Curr Opin Oncol 2000; 12:403–411.
228. Stein H, Delsol G, Pileri S, et al. Nodular lymphocyte predominant Hodgkin lymphoma. In: Jaffe ES, Harris NL, Stein H, et al., eds. Pathology and Genetics: Tumours of Haematopoietic and Lymphoid Tissues. World Health Organization Classification of Tumours. Lyon: IARC Press, 2001:240–243.
229. Diehl V, Franklin J, Sextro M, et al. Clinical presentation and treatment of lymphocyte predominance Hodgkin's disease. In: Mauch PM, Armitage JO, Diehl V, et al., eds. Hodgkin's Disease. Philadelphia: Lippincott Williams & Wilkins, 1999:563–582.
230. Diehl V, Sextro M, Franklin J, et al. Clinical presentation, course, and prognostic factors in lymphocyte- predominant Hodgkin's disease and lymphocyte-rich classical Hodgkin's disease: report from the European Task Force on Lymphoma Project on Lymphocyte-Predominant Hodgkin's Disease. J Clin Oncol 1999; 17:776–783).
231. Miettinen M, Franssila KO, Saxen E. Hodgkin's disease, lymphocyte predominance nodualr, increased risk for subsequent non-Hodgkin's lymphomas. Cancer 1983; 51:2293–2300.
232. Hansmann ML, Zwingers T, Boske A, et al. Clinical features of nodular paragranuloma (Hodgkin's disease, lymphocyte predominance type, nodular). J Cancer Res Clin Oncol 1984; 108:321–330.
233. Regula DP Jr., Hoppe RT, Weiss LM. Nodular and diffuse types of lymphocyte predominance Hodgkin's disease. N Engl J Med 1988; 318:214–219.
234. Regula DP Jr., Weiss LM, Warnke RA, et al. Lymphocyte predominance Hodgkin's disease: a reappraisal based upon histological and immunophenotypical findings in relapsing cases. Histopathology 1987; 11:1107–1120.
235. Bodis S, Kraus MD, Pinkus G, et al. Clinical presentation and outcome in lymphocyte-predominant Hodgkin's disease. J Clin Oncol 1997; 15:3060–3066.
236. von Wasielewski R, Werner M, Fischer R, et al. Lymphocyte-predominant Hodgkin's disease. An immunohistochemical analysis of 208 reviewed Hodgkin's disease cases from the German Hodgkin Study Group. Am J Pathol 1997; 150: 793–803.
237. Kraus MD, Haley J. Lymphocyte predominance Hodgkin's disease: the use of bcl-6 and CD57 in diagnosis and differential diagnosis. Am J Surg Pathol 2000; 24:1068–1078.
238. Fan Z, Natkunam Y, Bair E, et al. Characterization of variant patterns of nodular lymphocyte predominant Hodgkin lymphoma with immunohistologic and clinical correlation. Am J Surg Pathol 2003; 27:1346–1356.
239. Chang KC, Khen NT, Jones D, et al. Epstein-Barr virus is associated with all histological subtypes of Hodgkin lymphoma in Vietnamese children with special emphasis on the entity of lymphocyte predominance subtype. Hum Pathol 2005; 36:747–755.
240. Stein H, Diehl V, Marafioti T, et al. The nature of Reed-Sternberg cells, lymphocytic and histiocytic cells and their molecular biology in Hodgkin's disease. In: Mauch PM, Armitage JO, Diehl V, et al., eds. Hodgkin's Disease. Philadelphia: Lippincott Williams & Wilkins, 1999:121–137.
241. Bennett MH, MacLennan KA, Vaughan Hudson G, et al. Non-Hodgkin's lymphoma arising in patients treated for Hodgkin's disease in the BNLI: a 20-year experience. British National Lymphoma Investigation. Ann Oncol 1991; 2(suppl 2):83–92.
242. Hansmann ML, Fellbaum C, Hui PK, et al. Morphological and immunohistochemical investigation of non-Hodgkin's lymphoma combined with Hodgkin's disease. Histopathology 1989; 15:35–48.
243. Sundeen JT, Cossman J, Jaffe ES. Lymphocyte predominant Hodgkin's disease nodular subtype with coexistent ''large cell lymphoma.'' Histological progression or composite malignancy?. Am J Surg Pathol 1988; 12:599–606 (see comments).
244. Jaffe ES, Zarate-Osorno A, Medeiros LJ. The interrelationship of Hodgkin's disease and non-Hodgkin's lymphomas—lessons learned from composite and sequential malignancies. Semin Diagn Pathol 1992; 9:297–303.
245. Huang JZ, Weisenburger DD, Vose JM, et al. Diffuse large B-cell lymphoma arising in nodular lymphocyte predominant Hodgkin lymphoma. A report of 21 cases from the Nebraska Lymphoma Study Group. Leuk Lymphoma 2003; 44:1903–1910.
246. Greiner TC, Gascoyne RD, Anderson ME, et al. Nodular lymphocyte-predominant Hodgkin's disease associated with large- cell lymphoma: analysis of Ig gene rearrangements by V-J polymerase chain reaction. Blood 1996; 88:657–666.
247. Hansmann ML, Stein H, Fellbaum C, et al. Nodular paragranuloma can transform into high-grade malignant lymphoma of B type. Hum Pathol 1989; 20:1169–1175.
248. Diehl V, Sextro M, Franklin J, et al. Clinical presentation, course, and prognostic factors in lymphocyte-predominant Hodgkin's disease and lymphocyte-rich classical Hodgkin's disease: report from the European Task Force on Lymphoma Project on Lymphocyte-Predominant Hodgkin's Disease. J Clin Oncol 1999; 17:776–783.
249. Gatter KC, Warnke RA. Diffuse large B-cell lymphoma. In: Jaffe ES, Harris NL, Stein H, et al., eds. Pathology and Genetics: Tumours of Haematopoietic and Lymphoid Tissues. World Health Organization Classification of Tumours. Lyon: IARC Press, 2001:171–174.
250. Stein H, Warnke RA, Chan WC, et al. Diffuse large B-cell lymphoma, not otherwise specified. In: Swerdlow SH, Campo E, Harris NL, et al., eds. WHO Classification of Tumours of Haematopoietic and Lymphoid Tissues. 4th ed. Lyon: IARC, 2008:233–237.
251. Ko YH, Kim CW, Park CS, et al. REAL classification of malignant lymphomas in the Republic of Korea: incidence of recently recognized entities and changes in clinicopathologic features. Hematolymphoreticular Study Group of the Korean Society of Pathologists. Revised European-American lymphoma. Cancer 1998; 83:806–812.

252. Tse CC, Chan JK, Yuen RW, et al. Malignant lymphoma with myxoid stroma: a new pattern in need of recognition. Histopathology 1991; 18:31–35.
253. Nozawa Y, Wang J, Weiss LM, et al. Diffuse large B-cell lymphoma with spindle cell features. Histopathology 2001; 38:177–178.
254. McCluggage WG, Bharucha H, el-Agnaf M, et al. B cell signet-ring cell lymphoma of bone marrow. J Clin Pathol 1995; 48:275–278.
255. Tsang WY, Chan JK, Tang SK, et al. Large cell lymphoma with fibrillary matrix. Histopathology 1992; 20:80–82.
256. Koo CH, Shin SS, Bracho F, et al. Rosette-forming non-Hodgkin's lymphomas. Histopathology 1996; 29:557–563.
257. Thorson P, Hess JL. Transformation of monocytoid B-cell lymphoma to large cell lymphoma associated with crystal-storing histiocytes. Arch Pathol Lab Med 2000; 124: 460–462.
258. Navarro-Roman L, Medeiros LJ, Kingma DW, et al. Malignant lymphomas of B-cell lineage with marked tissue eosinophilia. A report of five cases. Am J Surg Pathol 1994; 18:347–356.
259. Kinney MC, Glick AD, Stein H, et al. Comparison of anaplastic large cell Ki-1 lymphomas and microvillous lymphomas in their immunologic and ultrastructural features. Am J Surg Pathol 1990; 14:1047–1060.
260. Lai R, Medeiros LJ, Dabbagh L, et al. Sinusoidal CD30-positive large B-cell lymphoma: a morphologic mimic of anaplastic large cell lymphoma. Mod Pathol 2000; 13:223–228.
261. Dogan A, Bagdi E, Munson P, et al. CD10 and BCL-6 expression in paraffin sections of normal lymphoid tissue and B-cell lymphomas. Am J Surg Pathol 2000; 24:846–852.
262. Ree HJ, Yang WI, Kim CW, et al. Coexpression of Bcl-6 and CD10 in diffuse large B-cell lymphomas: significance of Bcl-6 expression patterns in identifying germinal center B-cell lymphoma. Hum Pathol 2001; 32:954–962.
263. Falini B, Fizzotti M, Pucciarini A, et al. A monoclonal antibody (MUM1p) detects expression of the MUM1/IRF4 protein in a subset of germinal center B cells, plasma cells, and activated T cells. Blood 2000; 95:2084–2092.
264. King BE, Chen C, Locker J, et al. Immunophenotypic and genotypic markers of follicular center cell neoplasia in diffuse large B-cell lymphomas. Mod Pathol 2000; 13:1219–1231.
265. Kramer MH, Hermans J, Parker J, et al. Clinical significance of bcl2 and p53 protein expression in diffuse large B-cell lymphoma: a population-based study. J Clin Oncol 1996; 14:2131–2138.
266. Stein H, Mason DY, Gerdes J, et al. The expression of the Hodgkin's disease associated antigen Ki-1 in reactive and neoplastic lymphoid tissue: evidence that Reed-Sternberg cells and histiocytic malignancies are derived from activated lymphoid cells. Blood 1985; 66:848–858.
267. Yamaguchi M, Seto M, Okamoto M, et al. De novo CD5+ diffuse large B-cell lymphoma: a clinicopathologic study of 109 patients. Blood 2002; 99:815–821.
268. Miller TP, Grogan TM, Dahlberg S, et al. Prognostic significance of the Ki-67-associated proliferative antigen in aggressive non-Hodgkin's lymphomas: a prospective Southwest Oncology Group trial. Blood 1994; 83:1460–1466.
269. Lossos IS, Okada CY, Tibshirani R, et al. Molecular analysis of immunoglobulin genes in diffuse large B-cell lymphomas. Blood 2000; 95:1797–1803.
270. Gascoyne RD, Adomat SA, Krajewski S, et al. Prognostic significance of Bcl-2 protein expression and Bcl-2 gene rearrangement in diffuse aggressive non-Hodgkin's lymphoma. Blood 1997; 90:244–251.
271. Hill ME, MacLennan KA, Cunningham DC, et al. Prognostic significance of BCL-2 expression and bcl-2 major breakpoint region rearrangement in diffuse large cell non-Hodgkin's lymphoma: a British National Lymphoma Investigation Study. Blood 1996; 88:1046–1051.
272. Otsuki T, Yano T, Clark HM, et al. Analysis of LAZ3 (BCL-6) status in B-cell non-Hodgkin's lymphomas: results of rearrangement and gene expression studies and a mutational analysis of coding region sequences. Blood 1995; 85:2877–2884.
273. Lo Coco F, Ye BH, Lista F, et al. Rearrangements of the BCL6 gene in diffuse large cell non-Hodgkin's lymphoma. Blood 1994; 83:1757–1759.
274. Kramer MH, Hermans J, Wijburg E, et al. Clinical relevance of BCL2, BCL6, and MYC rearrangements in diffuse large B-cell lymphoma. Blood 1998; 92:3152–3162.
275. Kawasaki C, Ohshim K, Suzumiya J, et al. Rearrangements of bcl-1, bcl-2, bcl-6, and c-myc in diffuse large B-cell lymphomas. Leuk Lymphoma 2001; 42:1099–1106.
276. Ladanyi M, Offit K, Jhanwar SC, et al. MYC rearrangement and translocations involving band 8q24 in diffuse large cell lymphomas. Blood 1991; 77:1057–1063.
277. Hummel M, Bentink S, Berger H, et al. A biologic definition of Burkitt's lymphoma from transcriptional and genomic profiling. N Engl J Med 2006; 354:2419–2430.
278. Alizadeh AA, Eisen MB, Davis RE, et al. Distinct types of diffuse large B-cell lymphoma identified by gene expression profiling. Nature 2000; 403:503–511.
279. Rosenwald A, Wright G, Chan WC, et al. The use of molecular profiling to predict survival after chemotherapy for diffuse large-B-cell lymphoma. N Engl J Med 2002; 346:1937–1947.
280. Delsol G, Lamant L, Mariame B, et al. A new subtype of large B-cell lymphoma expressing the ALK kinase and lacking the 2; 5 translocation. Blood 1997; 89: 1483–1490.
281. Leoncini L, Delsol G, Gascoyne RD, et al. Aggressive B-cell lymphomas: a review based on the workshop of the XI Meeting of the European Association for Haematopathology. Histopathology 2005; 46:241–255.
282. Delsol G, Campo E, Gascoyne R. ALK-positive large B-cell lymphoma. In: Swerdlow SH, Campo E, Harris NL, et al., eds. WHO Classification of Tumours of Haematopoietic and Lymphoid Tissues. 4th ed. Lyon: IARC, 2008:254–255.
283. Gascoyne RD, Lamant L, Martin-Subero JI, et al. ALK-positive diffuse large B-cell lymphoma is associated with Clathrin-ALK rearrangements: report of 6 cases. Blood 2003; 102:2568–2573.
284. Stein H, Harris NL, Campo E. Plasmablastic lymphoma. In: Swerdlow SH, Campo E, Harris NL, et al., eds. WHO Classification of Tumours of Haematopoietic and Lymphoid Tissues. 4th ed. Lyon: IARC, 2008:256–257.
285. Delecluse HJ, Anagnostopoulos I, Dallenbach F, et al. Plasmablastic lymphomas of the oral cavity: a new entity associated with the human immunodeficiency virus infection. Blood 1997; 89:1413–1420.
286. Vega F, Chang CC, Medeiros LJ, et al. Plasmablastic lymphomas and plasmablastic plasma cell myelomas have nearly identical immunophenotypic profiles. Mod Pathol 2005; 18:806–815.
287. Colomo L, Loong F, Rives S, et al. Diffuse large B-cell lymphomas with plasmablastic differentiation represent a heterogeneous group of disease entities. Am J Surg Pathol 2004; 28:736–747.
288. Dong HY, Scadden DT, de Leval L, et al. Plasmablastic lymphoma in HIV-positive patients: an aggressive Epstein-Barr virus-associated extramedullary plasmacytic neoplasm. Am J Surg Pathol 2005; 29:1633–1641.
289. Meijer CJLM, Vergier B, Duncan LM, et al. Primary cutaneous DLBCL, leg type. In: Swerdlow SH, Campo E, Harris NL, et al., eds. WHO Classification of Tumours

of Haematopoietic and Lymphoid Tissues. 4th ed. Lyon: IARC, 2008:242.
290. Chan JKC, Aozasa K, Gaulard P. DLBCL associated with chronic inflammation. In: Swerdlow SH, Campo E, Harris NL, et al., eds. WHO Classification of Tumours of Haematopoietic and Lymphoid Tissues. 4th ed. Lyon: IARC, 2008:245–246.
291. Nakamura S, Jaffe ES, Swerdlow SH. EBV positive diffuse large B-cell lymphoma of the elderly. In: Swerdlow SH, Campo E, Harris NL, et al., eds. WHO Classification of Tumours of Haematopoietic and Lymphoid Tissues. 4th ed. Lyon: IARC, 2008:243–244.
292. Shimoyama Y, Oyama T, Asano N, et al. Senile Epstein-Barr virus-associated B-cell lymphoproliferative disorders: a mini review. J Clin Exp Hematop 2006; 46:1–4.
293. Oyama T, Ichimura K, Suzuki R, et al. Senile EBV+ B-cell lymphoproliferative disorders: a clinicopathologic study of 22 patients. Am J Surg Pathol 2003; 27:16–26.
294. Oyama T, Yamamoto K, Asano N, et al. Age-related EBV-associated B-cell lymphoproliferative disorders constitute a distinct clinicopathologic group: a study of 96 patients. Clin Cancer Res 2007; 13:5124–5132.
295. Sehn LH, Donaldson J, Chhanabhai M, et al. Introduction of combined CHOP plus rituximab therapy dramatically improved outcome of diffuse large B-cell lymphoma in British Columbia. J Clin Oncol 2005; 23:5027–5033.
296. Ngo L, Hee SW, Lim LC, et al. Prognostic factors in patients with diffuse large B cell lymphoma: Before and after the introduction of rituximab. Leuk Lymphoma 2008; 49:462–469.
297. Fu K, Weisenburger DD, Choi WW, et al. Addition of rituximab to standard chemotherapy improves the survival of both the germinal center B-cell-like and non-germinal center B-cell-like subtypes of diffuse large B-cell lymphoma. J Clin Oncol 2008; 26:4587–4594.
298. Hans CP, Weisenburger DD, Greiner TC, et al. Confirmation of the molecular classification of diffuse large B-cell lymphoma by immunohistochemistry using a tissue microarray. Blood 2004; 103:275–282.
299. Barrans SL, Carter I, Owen RG, et al. Germinal center phenotype and bcl-2 expression combined with the International Prognostic Index improves patient risk stratification in diffuse large B-cell lymphoma. Blood 2002; 99:1136–1143.
300. Berglund M, Thunberg U, Amini RM, et al. Evaluation of immunophenotype in diffuse large B-cell lymphoma and its impact on prognosis. Mod Pathol 2005; 18:1113–1120.
301. Dogan A, Du MQ, Aiello A, et al. Follicular lymphomas contain a clonally linked but phenotypically distinct neoplastic B-cell population in the interfollicular zone. Blood 1998; 91:4708–4714.
302. Nathwani BN, Harris NL, Weisenburger D, et al. Follicular lymphoma. In: Jaffe ES, Harris NL, Stein H, et al., eds. Pathology and Genetics: Tumours of Haematopoietic and Lymphoid Tissues. World Health Organization Classification of Tumours. Lyon: IARC Press, 2001:162–167.
303. Harris NL, Swerdlow SH, Jaffe ES, et al. Follicular lymphoma. In: Swerdlow SH, Campo E, Harris NL, et al., eds. WHO Classification of Tumours of Haematopoietic and Lymphoid Tissues. 4th ed. Lyon: IARC, 2008:220–226.
304. Lai R, Arber DA, Chang KL, et al. Frequency of bcl-2 expression in non-Hodgkin's lymphoma: a study of 778 cases with comparison of marginal zone lymphoma and monocytoid B-cell hyperplasia. Mod Pathol 1998; 11:864–869.
305. Ottensmeier CH, Thompsett AR, Zhu D, et al. Analysis of VH genes in follicular and diffuse lymphoma shows ongoing somatic mutation and multiple isotype transcripts in early disease with changes during disease progression. Blood 1998; 91:4292–4299.
306. Tilly H, Rossi A, Stamatoullas A, et al. Prognostic value of chromosomal abnormalities in follicular lymphoma. Blood 1994; 84:1043–1049.
307. Horsman DE, Gascoyne RD, Coupland RW, et al. Comparison of cytogenetic analysis, southern analysis, and polymerase chain reaction for the detection of t(14; 18) in follicular lymphoma. Am J Clin Pathol 1995; 103:472–478.
308. Ott G, Katzenberger T, Lohr A, et al. Cytomorphologic, immunohistochemical, and cytogenetic profiles of follicular lymphoma: 2 types of follicular lymphoma grade 3. Blood 2002; 99:3806–3812.
309. Bosga-Bouwer AG, van den Berg A, Haralambieva E, et al. Molecular, cytogenetic, and immunophenotypic characterization of follicular lymphoma grade 3B; a separate entity or part of the spectrum of diffuse large B-cell lymphoma or follicular lymphoma? Hum Pathol 2006; 37:528–533.
310. Gallagher CJ, Gregory WM, Jones AE, et al. Follicular lymphoma: prognostic factors for response and survival. J Clin Oncol 1986; 4:1470–1480.
311. Oviatt DL, Cousar JB, Collins RD, et al. Malignant lymphomas of follicular center cell origin in humans. V. Incidence, clinical features, and prognostic implications of transformation of small cleaved cell nodular lymphoma. Cancer 1984; 53:1109–1114.
312. Natkunam Y, Warnke RA, Zehnder JL, et al. Blastic/blastoid transformation of follicular lymphoma: immunohistologic and molecular analyses of five cases. Am J Surg Pathol 2000; 24:525–534.
313. Tomita N, Nakamura N, Kanamori H, et al. Atypical Burkitt lymphoma arising from follicular lymphoma: demonstration by polymerase chain reaction following laser capture microdissection and by fluorescence in situ hybridization on paraffin-embedded tissue sections. Am J Surg Pathol 2005; 29:121–124.
314. Martin AR, Weisenburger DD, Chan WC, et al. Prognostic value of cellular proliferation and histologic grade in follicular lymphoma. Blood 1995; 85:3671–3678.
315. Pinto A, Hutchison RE, Grant LH, et al. Follicular lymphomas in pediatric patients. Mod Pathol 1990; 3:308–313.
316. Lorsbach RB, Shay-Seymore D, Moore J, et al. Clinicopathologic analysis of follicular lymphoma occurring in children. Blood 2002; 99:1959–1964.
317. Cerroni L, Volkenandt M, Rieger E, et al. bcl-2 protein expression and correlation with the interchromosomal 14; 18 translocation in cutaneous lymphomas and pseudolymphomas. J Invest Dermatol 1994; 102:231–235.
318. Willemze R, Jaffe ES, Burg G, et al. WHO-EORTC classification for cutaneous lymphomas. Blood 2005; 105:3768–3785.
319. Goodlad JR, Batstone PJ, Hamilton DA, et al. BCL2 gene abnormalities define distinct clinical subsets of follicular lymphoma. Histopathology 2006; 49:229–241.
320. Cong P, Raffeld M, Teruya-Feldstein J, et al. In situ localization of follicular lymphoma: description and analysis by laser capture microdissection. Blood 2002; 99:3376–3382.
321. Argatoff LH, Connors JM, Klasa RJ, et al. Mantle cell lymphoma: a clinicopathologic study of 80 cases. Blood 1997; 89:2067–2078.
322. Fraga M, Lloret E, Sanchez-Verde L, et al. Mucosal mantle cell (centrocytic) lymphomas. Histopathology 1995; 26:413–422.
323. Swerdlow SH, Berger F, Isaacson P, et al. Mantle cell lymphoma. In: Jaffe ES, Harris NL, Stein H, et al., eds. Pathology and Genetics: Tumours of Haematopoietic and Lymphoid Tissues. World Health Organization Classification of Tumours. Lyon: IARC Press, 2001:168–170.
324. Cheuk W, Wong KO, Wong CS, et al. Consistent immunostaining for cyclin D1 can be achieved on a routine

basis using a newly available rabbit monoclonal antibody. Am J Surg Pathol 2004; 28:801–807.
325. Pittaluga S, Wlodarska I, Stul MS, et al. Mantle cell lymphoma: a clinicopathological study of 55 cases. Histopathology 1995; 26:17–24.
326. Fu K, Weisenburger DD, Greiner TC, et al. Cyclin D1-negative mantle cell lymphoma: a clinicopathologic study based on gene expression profiling. Blood 2005; 106:4315–4321.
327. Camacho FI, Algara P, Rodriguez A, et al. Molecular heterogeneity in MCL defined by the use of specific VH genes and the frequency of somatic mutations. Blood 2003; 101:4042–4046.
328. Kienle D, Krober A, Katzenberger T, et al. VH mutation status and VDJ rearrangement structure in mantle cell lymphoma: correlation with genomic aberrations, clinical characteristics, and outcome. Blood 2003; 102:3003–3009.
329. Li JY, Gaillard F, Moreau A, et al. Detection of translocation t(11; 14)(q13; q32) in mantle cell lymphoma by fluorescence in situ hybridization. Am J Pathol 1999; 154:1449–1452.
330. Anagnostopoulos I, Foss HD, Hummel M, et al. Extranodal mantle cell lymphoma mimicking marginal zone cell lymphoma. Histopathology 2001; 39:561–565.
331. Jacobson E, Burke P, Tindle BH. Mantle cell lymphoma disguised as marginal zone lymphoma. Arch Pathol Lab Med 2005; 129:929–932.
332. Norton AJ, Matthews J, Pappa V, et al. Mantle cell lymphoma: natural history defined in a serially biopsied population over a 20-year period. Ann Oncol 1995; 6:249–256.
333. Dunn P, Kuo TT, Shih LY, et al. Primary salivary gland lymphoma: a clinicopathologic study of 23 cases in Taiwan. Acta Haematol 2004; 112:203–208.
334. Raderer M, Wohrer S, Streubel B, et al. Assessment of disease dissemination in gastric compared with extragastric mucosa-associated lymphoid tissue lymphoma using extensive staging: a single-center experience. J Clin Oncol 2006; 24:3136–3141.
335. Taddesse-Heath L, Pittaluga S, Sorbara L, et al. Marginal zone B-cell lymphoma in children and young adults. Am J Surg Pathol 2003; 27:522–531.
336. Joshi VV, Gagnon GA, Chadwick EG, et al. The spectrum of mucosa-associated lymphoid tissue lesions in pediatric patients infected with HIV: A clinicopathologic study of six cases. Am J Clin Pathol 1997; 107:592–600.
337. Chan JK, Ng CS, Isaacson PG. Relationship between high-grade lymphoma and low-grade B-cell mucosa- associated lymphoid tissue lymphoma (MALToma) of the stomach. Am J Pathol 1990; 136:1153–1164.
338. Chan JK. Gastrointestinal lymphomas: an overview with emphasis on new findings and diagnostic problems. Semin Diagn Pathol 1996; 13:260–296.
339. Harris NL, Jaffe ES, Diebold J, et al. World Health Organization Classification of Neoplastic Diseases of the Hematopoietic and Lymphoid Tissues: Report of the Clinical Advisory Committee Meeting-Airlie House, Virginia, November 1997. J Clin Oncol 1999; 17:3835–3849.
340. de Jong D, Boot H, van Heerde P, et al. Histological grading in gastric lymphoma: pretreatment criteria and clinical relevance. Gastroenterology 1997; 112:1466–1474.
341. Nathwani BN, Anderson JR, Armitage JO, et al. Marginal zone B-cell lymphoma: A clinical comparison of nodal and mucosa-associated lymphoid tissue types. J Clin Oncol 1999; 17:2486.
342. Ferry JA, Yang WI, Zukerberg LR, et al. CD5+ extranodal marginal zone B-cell (MALT) lymphoma. A low grade neoplasm with a propensity for bone marrow involvement and relapse. Am J Clin Pathol 1996; 105:31–37.
343. Dorfman DM, Pinkus GS. Utility of immunophenotypic studies in the diagnosis of low-grade lymphoma of mucosa-associated lymphoid tisuse (MALT) and other low-grade non-Hodgkin's lymphomas of extranodal sites. Appl Immunohistochem 1995; 3:160–167.
344. Isaacson PG, Du MQ. Gastrointestinal lymphoma: where morphology meets molecular biology. J Pathol 2005; 205:255–274.
345. Qin Y, Greiner A, Trunk MJ, et al. Somatic hypermutation in low-grade mucosa-associated lymphoid tissue-type B-cell lymphoma. Blood 1995; 86:3528–3534.
346. Bahler DW, Miklos JA, Swerdlow SH. Ongoing Ig gene hypermutation in salivary gland mucosa-associated lymphoid tissue-type lymphomas. Blood 1997; 89:3335–3344.
347. Qin Y, Greiner A, Hallas C, et al. Intraclonal offspring expansion of gastric low-grade MALT-type lymphoma: evidence for the role of antigen-driven high-affinity mutation in lymphomagenesis. Lab Invest 1997; 76:477–485.
348. Du M, Diss TC, Xu C, et al. Ongoing mutation in MALT lymphoma immunoglobulin gene suggests that antigen stimulation plays a role in the clonal expansion. Leukemia 1996; 10:1190–1197.
349. Remstein ED, Dogan A, Einerson RR, et al. The incidence and anatomic site specificity of chromosomal translocations in primary extranodal marginal zone B-cell lymphoma of mucosa-associated lymphoid tissue (MALT lymphoma) in North America. Am J Surg Pathol 2006; 30:1546–1553.
350. Streubel B, Vinatzer U, Lamprecht A, et al. T(3; 14)(p14.1; q32) involving IGH and FOXP1 is a novel recurrent chromosomal aberration in MALT lymphoma. Leukemia 2005; 19:652–658.
351. Wotherspoon AC, Finn TM, Isaacson PG. Trisomy 3 in low-grade B-cell lymphomas of mucosa-associated lymphoid tissue. Blood 1995; 85:2000–2004.
352. Berger F, Felman P, Sonet A, et al. Nonfollicular small B-cell lymphomas: a heterogeneous group of patients with distinct clinical features and outcome. Blood 1994; 83:2829–2835.
353. Cogliatti SB, Schmid U, Schumacher U, et al. Primary B-cell gastric lymphoma: a clinicopathological study of 145 patients. Gastroenterology 1991; 101:1159–1170.
354. Diebold J, Jaffe ES, Raphael M, et al. Burkitt lymphoma. In: Jaffe ES, Harris NL, Stein H, et al., eds. Pathology and Genetics: Tumours of Haematopoietic and Lymphoid Tissues. World Health Organization Classification of Tumours. Lyon: IARC Press, 2001:181–184.
355. Leoncini L, Raphael M, Stein H, et al. Burkitt lymphoma. In: Swerdlow SH, Campo E, Harris NL, et al., eds. WHO Classification of Tumours of Haematopoietic and Lymphoid Tissues. 4th ed. Lyon: IARC, 2008:262–264.
356. Alexiou C, Kau RJ, Dietzfelbinger H, et al. Extramedullary plasmacytoma: tumor occurrence and therapeutic concepts. Cancer 1999; 85:2305–2314.
357. Mock PM, Neal GD, Aufdemorte TB. Immunoperoxidase characterization of extramedullary plasmacytoma of the head and neck. Head Neck Surg 1987; 9:356–361.
358. Aguilera NS, Kapadia SB, Nalesnik MA, et al. Extramedullary plasmacytoma of the head and neck: use of paraffin sections to assess clonality with in situ hybridization, growth fraction, and the presence of Epstein-Barr virus. Mod Pathol 1995; 8:503–508.
359. Wotherspoon AC, Norton AJ, Isaacson PG. Immunoreactive cytokeratins in plasmacytomas. Histopathology 1989; 14:141–150.
360. Kremer M, Ott G, Nathrath M, et al. Primary extramedullary plasmacytoma and multiple myeloma: phenotypic differences revealed by immunohistochemical analysis. J Pathol 2005; 205:92–101.
361. Hussong JW, Perkins SL, Schnitzer B, et al. Extramedullary plasmacytoma. A form of marginal zone cell lymphoma? Am J Clin Pathol 1999; 111:111–116.

362. Muller-Hermelink HK, Catovsky D, Montserrat E, et al. Chronic lymphocytic leukemia/small lymphocytic lymphoma. In: Jaffe ES, Harris NL, Stein H, et al., eds. Pathology and Genetics: Tumours of Haematopoietic and Lymphoid Tissues. World Health Organization Classification of Tumours. Lyon: IARC Press, 2001:127–130.
363. Pangalis GA, Boussiotis VA, Kittas C. Malignant disorders of small lymphocytes. Small lymphocytic lymphoma, lymphoplasmacytic lymphoma, and chronic lymphocytic leukemia: their clinical and laboratory relationship. Am J Clin Pathol 1993; 99:402–408.
364. Berger F, Isaacson PG, Piris MA, et al. Lymphoplasmacytic lymphoma/Waldenstrom macroglobulinemia. In: Jaffe ES, Harris NL, Stein H, et al., eds. Pathology and Genetics: Tumours of Haematopoietic and Lymphoid Tissues. World Health Organization Classification of Tumours. Lyon: IARC Press, 2001:132–134.
365. Isaacson PG, Nathwani BN, Piris MA, et al. Nodal marginal zone B-cell lymphoma. In: Jaffe ES, Harris NL, Stein H, et al., eds. Pathology and Genetics: Tumours of Haematopoietic and Lymphoid Tissues. World Health Organization Classification of Tumours. Lyon: IARC Press, 2001:161.
366. Campo E, Pileri SA, Jaffe ES, et al. Nodal marginal zone lymphoma. In: Swerdlow SH, Campo E, Harris NL, et al., eds. WHO Classification of Tumours of Haematopoietic and Lymphoid Tissues. 4th ed. Lyon: IARC, 2008:218–219.
367. Brunning RD, Borowitz M, Matutes E, et al. Precursor B lymphoblastic leukemia/lymphoblastic lymphoma and Precursor T lymphoblastic leukemia/lymphoblastic lymphoma. In: Jaffe ES, Harris NL, Stein H, et al., eds. Pathology and Genetics: Tumours of Haematopoietic and Lymphoid Tissues. World Health Organization Classification of Tumours. Lyon: IARC Press, 2001:111–117.
368. Chan JKC, Quintanilla-Martinez L, Ferry JA, et al. Extranodal NK/T-cell lymphoma, nasal-type. In: Swerdlow SH, Campo E, Harris NL, et al., eds. WHO Classification of Tumours of Haematopoietic and Lymphoid Tissues. 4th ed. Lyon: IARC, 2008:285–288.
369. Quintanilla-Martinez L, Franklin JL, Guerrero I, et al. Histological and immunophenotypic profile of nasal NK/T cell lymphomas from Peru: high prevalence of p53 overexpression. Hum Pathol 1999; 30:849–855.
370. Arber DA, Weiss LM, Albujar PF, et al. Nasal lymphomas in Peru. High incidence of T-cell immunophenotype and Epstein-Barr virus infection. Am J Surg Pathol 1993; 17:392–399.
371. Chan JK, Yip TT, Tsang WY, et al. Detection of Epstein-Barr viral RNA in malignant lymphomas of the upper aerodigestive tract. Am J Surg Pathol 1994; 18:938–946.
372. Kanavaros P, Lescs MC, Briere J, et al. Nasal T-cell lymphoma: a clinicopathologic entity associated with peculiar phenotype and with Epstein-Barr virus. Blood 1993; 81:2688–2695.
373. Cheung MM, Chan JK, Lau WH, et al. Primary non-Hodgkin's lymphoma of the nose and nasopharynx: clinical features, tumor immunophenotype, and treatment outcome in 113 patients. J Clin Oncol 1998; 16:70–77.
374. Li YX, Coucke PA, Li JY, et al. Primary non-Hodgkin's lymphoma of the nasal cavity: prognostic significance of paranasal extension and the role of radiotherapy and chemotherapy. Cancer 1998; 83:449–456.
375. Ooi GC, Chim CS, Liang R, et al. Nasal T-cell/natural killer cell lymphoma: CT and MR imaging features of a new clinicopathologic entity. AJR Am J Roentgenol 2000; 174:1141–1145.
376. Jaffe ES, Chan JK, Su IJ, et al. Report of the Workshop on Nasal and Related Extranodal Angiocentric T/Natural Killer Cell Lymphomas. Definitions, differential diagnosis, and epidemiology. Am J Surg Pathol 1996; 20:103–111.
377. Ng CS, Lo ST, Chan JK, et al. CD56+ putative natural killer cell lymphomas: production of cytolytic effectors and related proteins mediating tumor cell apoptosis? Hum Pathol 1997; 28:1276–1282.
378. Ng CS, Lo ST, Chan JK. Peripheral T and putative natural killer cell lymphomas commonly coexpress CD95 and CD95 ligand. Hum Pathol 1999; 30:48–53.
379. Chiang AK, Tao Q, Srivastava G, et al. Nasal NK- and T-cell lymphomas share the same type of Epstein-Barr virus latency as nasopharyngeal carcinoma and Hodgkin's disease. Int J Cancer 1996; 68:285–290.
380. Chiang AK, Chan AC, Srivastava G, et al. Nasal T/natural killer (NK)-cell lymphomas are derived from Epstein-Barr virus-infected cytotoxic lymphocytes of both NK- and T-cell lineage. Int J Cancer 1997; 73:332–338.
381. Ho FC, Srivastava G, Loke SL, et al. Presence of Epstein-Barr virus DNA in nasal lymphomas of B and 'T' cell type. Hematol Oncol 1990; 8:271–281.
382. Tien HF, Su IJ, Tang JL, et al. Clonal chromosomal abnormalities as direct evidence for clonality in nasal T/natural killer cell lymphomas. Br J Haematol 1997; 97:621–625.
383. Wong KF, Chan JK, Kwong YL. Identification of del(6)(q21q25) as a recurring chromosomal abnormality in putative NK cell lymphoma/leukaemia. Br J Haematol 1997; 98:922–926.
384. Siu LL, Wong KF, Chan JK, et al. Comparative genomic hybridization analysis of natural killer cell lymphoma/leukemia. Recognition of consistent patterns of genetic alterations. Am J Pathol 1999; 155:1419–1425.
385. Siu LL, Chan V, Chan JK, Consistent patterns of allelic loss in natural killer cell lymphoma. Am J Pathol 2000; 157:1803–1809.
386. Ko YH, Choi KE, Han JH, et al. Comparative genomic hybridization study of nasal-type NK/T-cell lymphoma. Cytometry 2001; 46:85–91.
387. Cheung MM, Chan JK, Wong KF. Natural killer cell neoplasms: a distinctive group of highly aggressive lymphomas/leukemias. Semin Hematol 2003; 40:221–232.
388. Nakashima Y, Tagawa H, Suzuki R, et al. Genome-wide array-based comparative genomic hybridization of natural killer cell lymphoma/leukemia: different genomic alteration patterns of aggressive NK-cell leukemia and extranodal Nk/T-cell lymphoma, nasal type. Genes Chromosomes Cancer 2005; 44:247–255.
389. Bini P, Gabay JE, Teitel A, et al. Antineutrophil cytoplasmic autoantibodies in Wegener's granulomatosis recognize conformational epitope(s) on proteinase 3. J Immunol 1992; 149:1409–1415.
390. Devaney KO, Travis WD, Hoffman G, et al. Interpretation of head and neck biopsies in Wegener's granulomatosis. A pathologic study of 126 biopsies in 70 patients. Am J Surg Pathol 1990; 14:555–564.
391. Chim CS, Ma SY, Au WY, et al. Primary nasal natural killer cell lymphoma: long-term treatment outcome and relationship with the International Prognostic Index. Blood 2004; 103:216–221.
392. Cheung MM, Chan JK, Lau WH, et al. Early stage nasal NK/T-cell lymphoma: clinical outcome, prognostic factors, and the effect of treatment modality. Int J Radiat Oncol Biol Phys 2002; 54:182–190.
393. Lee J, Suh C, Park YH, et al. Extranodal natural killer T-cell lymphoma, nasal-type: a prognostic model from a retrospective multicenter study. J Clin Oncol 2006; 24:612–618.
394. Nakamura S, Katoh E, Koshikawa T, et al. Clinicopathologic study of nasal T/NK-cell lymphoma among the Japanese. Pathol Int 1997; 47:38–53.
395. Kim GE, Cho JH, Yang WI, et al. Angiocentric lymphoma of the head and neck: patterns of systemic failure after radiation treatment. J Clin Oncol 2000; 18:54–63.

396. Kim TM, Park YH, Lee SY, et al. Local tumor invasiveness is more predictive of survival than International Prognostic Index in stage I(E)/II(E) extranodal NK/T-cell lymphoma, nasal type. Blood 2005; 106:3785–3790.
397. Jaffe ES, Ralfkiaer E. Angioimmunoblastic T-cell lymphoma. In: Jaffe ES, Harris NL, Stein H, et al., eds. Pathology and Genetics: Tumours of Haematopoietic and Lymphoid Tissues. World Health Organization Classification of Tumours. Lyon: IARC Press, 2001:225–226.
398. Attygalle A, Al-Jehani R, Diss TC, et al. Neoplastic T cells in angioimmunoblastic T-cell lymphoma express CD10. Blood 2002; 99:627–633.
399. Dupuis J, Boye K, Martin N, et al. Expression of CXCL13 by neoplastic cells in angioimmunoblastic T-cell lymphoma (AITL): a new diagnostic marker providing evidence that AITL derives from follicular helper T cells. Am J Surg Pathol 2006; 30:490–494.
400. Ralfkiaer E, Muller-Hermelink HK, Jaffe ES. Peripheral T-cell lymphoma, unspecified. In: Jaffe ES, Harris NL, Stein H, et al., eds. Pathology and Genetics: Tumours of Haematopoietic and Lymphoid Tissues. World Health Organization Classification of Tumours. Lyon: IARC Press, 2001:227–229.
401. Delsol G, Ralfkiaer E, Stein H, et al. Anaplastic large cell lymphoma. In: Jaffe ES, Harris NL, Stein H, et al., eds. Pathology and Genetics: Tumours of Haematopoietic and Lymphoid Tissues. World Health Organization Classification of Tumours. Lyon: IARC Press, 2001:230–235.
402. Falini B, Pileri S, Zinzani PL, et al. ALK+ lymphoma: clinico-pathological findings and outcome. Blood 1999; 93:2697–2706.
403. Nakamura S, Shiota M, Nakagawa A, et al. Anaplastic large cell lymphoma: a distinct molecular pathologic entity: a reappraisal with special reference to p80(NPM/ALK) expression. Am J Surg Pathol 1997; 21:1420–1432.
404. Cheuk W, Hill RW, Bacchi C, et al. Hypocellular anaplastic large cell lymphoma mimicking inflammatory lesions of lymph nodes. Am J Surg Pathol 2000; 24:1537–1543.
405. Falini B, Pulford K, Pucciarini A, et al. Lymphomas expressing ALK fusion protein(s) other than NPM-ALK. Blood 1999; 94:3509–3515.
406. Mason DY, Harris NL, Delsol G, et al. Anaplastic large cell lymphoma, ALK-negative. In: Swerdlow SH, Campo E, Harris NL, et al., eds. WHO Classification of Tumours of Haematopoietic and Lymphoid Tissues. 4th ed. Lyon: IARC, 2008:317–319.
407. ten Berge RL, de Bruin PC, Oudejans JJ, et al. ALK-negative anaplastic large-cell lymphoma demonstrates similar poor prognosis to peripheral T-cell lymphoma, unspecified. Histopathology 2003; 43:462–469.
408. Savage KJ, Harris NL, Vose JM, et al. ALK- anaplastic large-cell lymphoma is clinically and immunophenotypically different from both ALK+ ALCL and peripheral T-cell lymphoma, not otherwise specified: report from the International Peripheral T-Cell Lymphoma Project. Blood 2008; 111:5496–5504.
409. Paulli M, Berti E, Rosso R, et al. CD30/Ki-1-positive lymphoproliferative disorders of the skin—clinicopathologic correlation and statistical analysis of 86 cases: a multicentric study from the European Organization for Research and Treatment of Cancer Cutaneous Lymphoma Project Group. J Clin Oncol 1995; 13:1343–1354.
410. Kempf W, Willemze R, Jaffe ES, et al. CD30+ T-cell lymphoproliferative disorders. In: LeBoit PE, Burg G, Weedon D, et al., eds. Pathology and Genetics: Skin Tumours. World Health Organization Classification of Tumours. Lyon: IARC Press, 2006:179–181.
411. Kadin ME, Pinkus JL, Pinkus GS, et al. Primary cutaneous ALCL with phosphorylated/activated cytoplasmic ALK and novel phenotype: EMA/MUC1+, cutaneous lymphocyte antigen negative. Am J Surg Pathol 2008; 32:1421–1426.
412. Alobeid B, Pan LX, Milligan L, et al. Eosinophil-rich CD30+ lymphoproliferative disorder of the oral mucosa. A form of ''traumatic eosinophilic granuloma''. Am J Clin Pathol 2004; 121:43–50.
413. Agarwal M, Shenjere P, Blewitt RW, et al. CD30-positive T-cell lymphoproliferative disorder of the oral mucosa—an indolent lesion: report of 4 cases. Int J Surg Pathol 2008; 16:286–290.
414. Burg G, Kempf W, Smoller B, et al. et al. Mycosis fungoides. In: LeBoit PE, Burg G, Weedon D, et al., eds. Pathology and Genetics: Skin Tumours. World Health Organization Classification of Tumours. Lyon: IARC Press, 2006:169–174.
415. Russell-Jones R, Bernengo M, Burg G, et al. Sezary syndrome. In: LeBoit PE, Burg G, Weedon D, et al., eds. Pathology and Genetics: Skin Tumours. World Health Organization Classification of Tumours. Lyon: IARC Press, 2006:175–177.
416. Willemze R, Jansen PM, Cerroni L, et al. Subcutaneous panniculitis-like T-cell lymphoma: definition, classification, and prognostic factors: an EORTC Cutaneous Lymphoma Group Study of 83 cases. Blood 2008; 111:838–845.
417. Ralfkiaer E, Willemze R, Meijer CJLM, et al. Primary cutaneous peripheral T-cell lymphoma, unspecified. In: LeBoit PE, Burg G, Weedon D, et al., eds. Pathology and Genetics: Skin Tumours. World Health Organization Classification of Tumours. Lyon: IARC Press, 2006:184–188.
418. Quintanilla-Martinez L, Kimura H, Jaffe ES. EBV-positive T-cell lymphoproliferative disorders of childhood. In: Swerdlow SH, Campo E, Harris NL, et al., eds. WHO Classification of Tumours of Haematopoietic and Lymphoid Tissues. 4th ed. Lyon: IARC, 2008:278–280.
419. Ohshima K, Kimura H, Yoshino T, et al. Proposed categorization of pathological states of EBV-associated T/natural killer-cell lymphoproliferative disorder (LPD) in children and young adults: overlap with chronic active EBV infection and infantile fulminant EBV T-LPD. Pathol Int 2008; 58:209–217.
420. Kikuchi M, Jaffe ES, Ralfkiaer E. Adult T-cell leukemia/lymphoma. In: Jaffe ES, Harris NL, Stein H, et al., eds. Pathology and Genetics: Tumours of Haematopoietic and Lymphoid Tissues. World Health Organization Classification of Tumours. Lyon: IARC Press, 2001:200–203.
421. Harris NL, Swerdlow SH, Frizzera G, et al. Post-transplant lymphoproliferative disorders. In: Jaffe ES, Harris NL, Stein H, et al., eds. Pathology and Genetics: Tumours of Haematopoietic and Lymphoid Tissues. World Health Organization Classification of Tumours. Lyon: IARC Press, 2001:264–269.
422. Chadburn A, Cesarman E, Knowles DM. Molecular pathology of posttransplantation lymphoproliferative disorders. Semin Diagn Pathol 1997; 14:15–26.
423. Chadburn A, Chen JM, Hsu DT, et al. The morphologic and molecular genetic categories of posttransplantation lymphoproliferative disorders are clinically relevant. Cancer 1998; 82:1978–1987.
424. Wu TT, Swerdlow SH, Locker J, et al. Recurrent Epstein-Barr virus-associated lesions in organ transplant recipients. Hum Pathol 1996; 27:157–164.
425. Brunning RD, Matutes E, Flandrin G, et al. Myeloid sarcoma. In: Jaffe ES, Harris NL, Stein H, et al., eds. Pathology and Genetics: Tumours of Haematopoietic and Lymphoid Tissues. World Health Organization Classification of Tumours. Lyon: IARC Press, 2001:104–105.
426. Chen J, Yanuck RR III, Abbondanzo SL, et al. c-Kit (CD117) reactivity in extramedullary myeloid tumor/

granulocytic sarcoma. Arch Pathol Lab Med 2001; 125:1448–1452.
427. Pileri SA, Ascani S, Cox MC, et al. Myeloid sarcoma: clinico-pathologic, phenotypic and cytogenetic analysis of 92 adult patients. Leukemia 2007; 21:340–350.
428. Weiss LM, Grogan TM, Muller-Hermelink HK, et al. Histiocytic sarcoma. In: Jaffe ES, Harris NL, Stein H, et al., eds. Pathology and Genetics: Tumours of Haematopoietic and Lymphoid Tissues. World Health Organization Classification of Tumours. Lyon: IARC Press, 2001:278–279.
429. Weiss LM, Grogan TM, Muller-Hermelink HK, et al. et al. Langerhans cell histiocytosis. In: Jaffe ES, Harris NL, Stein H, et al., eds. Pathology and Genetics: Tumours of Haematopoietic and Lymphoid Tissues. World Health Organization Classification of Tumours. Lyon: IARC Press, 2001:280–283.
430. Howarth DM, Gilchrist GS, Mullan BP, et al. Langerhans cell histiocytosis: diagnosis, natural history, management, and outcome. Cancer 1999; 85:2278–2290.
431. Pileri SA, Grogan TM, Harris NL, et al. Tumours of histiocytes and accessory dendritic cells: an immunohistochemical approach to classification from the International Lymphoma Study Group based on 61 cases. Histopathology 2002; 41:1–29.
432. Weiss LM, Grogan TM, Muller-Hermelink HK, et al. Follicular dendritic cell sarcoma/tumor. In: Jaffe ES, Harris NL, Stein H, et al., eds. Pathology and Genetics: Tumours of Haematopoietic and Lymphoid Tissues. World Health Organization Classification of Tumours. Lyon: IARC Press, 2001:286–288.
433. Chan AC, Chan KW, Chan JK, et al. Development of follicular dendritic cell sarcoma in hyaline-vascular Castleman's disease of the nasopharynx: tracing its evolution by sequential biopsies. Histopathology 2001; 38:510–518.
434. Chan JK, Fletcher CD, Nayler SJ, et al. Follicular dendritic cell sarcoma. Clinicopathologic analysis of 17 cases suggesting a malignant potential higher than currently recognized. Cancer 1997; 79:294–313.
435. Perez-Ordonez B, Erlandson RA, Rosai J. Follicular dendritic cell tumor: report of 13 additional cases of a distinctive entity. Am J Surg Pathol 1996; 20:944–955.
436. Weiss LM, Grogan TM, Muller-Hermelink HK, et al. Interdigitating dendritic cell sarcoma/tumor. In: Jaffe ES, Harris NL, Stein H, et al., eds. Pathology and Genetics: Tumours of Haematopoietic and Lymphoid Tissues. World Health Organization Classification of Tumours. Lyon: IARC Press, 2001:284–285.
437. Facchetti F, Jones DM, Petrella T. Blastic plasmacytoid dendritic cell neoplasm. In: Swerdlow SH, Campo E, Harris NL, et al., eds. WHO Classification of Tumours of Haematopoietic and Lymphoid Tissues. 4th ed. Lyon: IARC, 2008:145–147.
438. Cong P, Raffeld M, Jaffe E. Blastic NK cell lymphoma/leukemia: a clinicopathological study of 23 cases. Mod Pathol 2001; 14:160A (abstr).
439. Suzuki R, Nakamura S, Suzumiya J, et al. Blastic natural killer cell lymphoma/leukemia (CD56-positive blastic tumor): prognostication and categorization according to anatomic sites of involvement. Cancer 2005; 104:1022–1031.
440. Petrella T, Bagot M, Willemze R, et al. Blastic NK-cell lymphomas (agranular CD4+CD56+ hematodermic neoplasms): a review. Am J Clin Pathol 2005; 123:662–675.
441. Feuillard J, Jacob MC, Valensi F, et al. Clinical and biologic features of CD4(+)CD56(+) malignancies. Blood 2002; 99:1556–1563.
442. Urosevic M, Conrad C, Kamarashev J, et al. CD4+CD56+ hematodermic neoplasms bear a plasmacytoid dendritic cell phenotype. Hum Pathol 2005; 36:1020–1024.
443. Jaye DL, Geigerman CM, Herling M, et al. Expression of the plasmacytoid dendritic cell marker BDCA-2 supports a spectrum of maturation among CD4+ CD56+ hematodermic neoplasms. Mod Pathol 2006; 19:1555–1562.
444. Khoury JD, Medeiros LJ, Manning JT, et al. CD56+ TdT+ blastic natural killer cell tumor of the skin. Cancer 2002; 94:2401–2408.
445. Scott AA, Head DR, Kopecky KJ, et al. HLA-DR-, CD33+, CD56+, CD16- myeloid/natural killer cell acute leukemia: a previously unrecognized form of acute leukemia potentially misdiagnosed as French-American-British acute myeloid leukemia-M3. Blood 1994; 84:244–255.
446. Suzuki R, Yamamoto K, Seto M, et al. CD7+ and CD56+ myeloid/natural killer cell precursor acute leukemia: a distinct hematolymphoid disease entity. Blood 1997; 90:2417–2428.
447. Harbo G, Grau C, Bundgaard T, et al. Cancer of the nasal cavity and paranasal sinuses. A clinico-pathological study of 277 patients. Acta Oncol 1997; 36:45–50.
448. Freeman C, Berg JW, Cutler SJ. Occurrence and prognosis of extranodal lymphomas. Cancer 1972; 29:252–260.
449. Cuadra-Garcia I, Proulx GM, Wu CL, et al. Sinonasal lymphoma: a clinicopathologic analysis of 58 cases from the Massachusetts General Hospital. Am J Surg Pathol 1999; 23:1356–1369.
450. Abbondanzo SL, Wenig BM. Non-Hodgkin's lymphoma of the sinonasal tract. A clinicopathologic and immunophenotypic study of 120 cases. Cancer 1995; 75:1281–1291.
451. Nakamura K, Uehara S, Omagari J, et al. Primary non-Hodgkin lymphoma of the sinonasal cavities: correlation of CT evaluation with clinical outcome. Radiology 1997; 204:431–435.
452. Meis JM, Butler JJ, Osborne BM, et al. Granulocytic sarcoma in nonleukemic patients. Cancer 1986; 58:2697–2709.
453. Roth MJ, Medeiros LJ, Elenitoba-Johnson K, et al. Extramedullary myeloid cell tumors. An immunohistochemical study of 29 cases using routinely fixed and processed paraffin-embedded tissue sections. Arch Pathol Lab Med 1995; 119:790–798.
454. Isago H, Kimura T, Kataura A. A case of Weber-Christian disease accompanied by a nasal symptom (a clinicopathologic case report). J Laryngol Otol 1986; 100:221–227.
455. Logsdon MD, Ha CS, Kavadi VS, et al. Lymphoma of the nasal cavity and paranasal sinuses: improved outcome and altered prognostic factors with combined modality therapy. Cancer 1997; 80:477–488.
456. Foucar E, Rosai J, Dorfman RF. Sinus histiocytosis with massive lymphadenopathy. An analysis of 14 deaths occurring in a patient registry. Cancer 1984; 54:1834–1840.
457. Wenig BM, Abbondanzo SL, Childers EL, et al. Extranodal sinus histiocytosis with massive lymphadenopathy (Rosai-Dorfman disease) of the head and neck. Hum Pathol 1993; 24:483–492.
458. Dehner LP. Juvenile xanthogranulomas in the first two decades of life: a clinicopathologic study of 174 cases with cutaneous and extracutaneous manifestations. Am J Surg Pathol 2003; 27:579–593.
459. Saravanappa N, Rashid AM, Thebe PR, et al. Juvenile xanthogranuloma of the nasal cavity. J Laryngol Otol 2000; 114:460–461.
460. Menarguez J, Mollejo M, Carrion R, et al. Waldeyer ring lymphomas. A clinicopathological study of 79 cases. Histopathology 1994; 24:13–22.
461. Saul SH, Kapadia SB. Primary lymphoma of Waldeyer's ring. Clinicopathologic study of 68 cases. Cancer 1985; 56:157–166.
462. Ye YL, Zhou MH, Lu XY, et al. Nasopharyngeal and nasal malignant lymphoma: a clinicopathological study of 54 cases. Histopathology 1992; 20:511–516 (see comments).

463. Laskar S, Muckaden MA, Bahl G, et al. Primary non-Hodgkin's lymphoma of the nasopharynx: prognostic factors and outcome of 113 Indian patients. Leuk Lymphoma 2006; 47:2132–2139.
464. Kapadia SB, Desai U, Cheng VS. Extramedullary plasmacytoma of the head and neck. A clinicopathologic study of 20 cases. Medicine (Baltimore) 1982; 61:317–329.
465. Kapadia SB, Roman LN, Kingma DW, et al. Hodgkin's disease of Waldeyer's ring. Clinical and histoimmunophenotypic findings and association with Epstein-Barr virus in 16 cases. Am J Surg Pathol 1995; 19:1431–1439.
466. MacNaughton DM, Tewfik TL, Bernstein ML. Hodgkin's disease in the nasopharynx. J Otolaryngol 1990; 19: 282–284.
467. Moghe GM, Borges AM, Soman CS, et al. Hodgkin's disease involving Waldeyer's ring: a study of four cases. Leuk Lymphoma 2001; 41:151–156.
468. Molony NC, Stewart A, Ah-See K, et al. Hodgkin's lymphoma of the nasopharynx. J Laryngol Otol 1998; 112:103–105.
469. O'Reilly BJ, Kershaw JB. Hodgkin's disease of the nasopharynx. J Laryngol Otol 1987; 101:506–507.
470. Traweek ST, Arber DA, Rappaport H, et al. Extramedullary myeloid cell tumors. An immunohistochemical and morphologic study of 28 cases. Am J Surg Pathol 1993; 17:1011–1019.
471. Beham-Schmid C, Beham A, Jakse R, et al. Extranodal follicular dendritic cell tumour of the nasopharynx. Virchows Arch 1998; 432:293–298.
472. Tsai MH, Pai HH, Yen PT, et al. Unusual localization of Castleman's disease: report of the first case in the nasopharynx. Ear Nose Throat J 1997; 76:731–735, 39.
473. Epstein JB, Epstein JD, Le ND, et al. Characteristics of oral and paraoral malignant lymphoma: a population-based review of 361 cases. Oral Surg Oral Med Oral Pathol Oral Radiol Endod 2001; 92:519–525.
474. Takahashi H, Tsuda N, Tezuka F, et al. Primary extranodal non-Hodgkin's lymphoma of the oral region. J Oral Pathol Med 1989; 18:84–91.
475. Leong IT, Fernandes BJ, Mock D. Epstein-Barr virus detection in non-Hodgkin's lymphoma of the oral cavity: an immunocytochemical and in situ hybridization study. Oral Surg Oral Med Oral Pathol Oral Radiol Endod 2001; 92:184–193.
476. Chan JK, Ng CS, Lo ST. Immunohistological characterization of malignant lymphomas of the Waldeyer's ring other than the nasopharynx. Histopathology 1987; 11:885–899.
477. Regezi JA, Zarbo RJ, Stewart JC. Extranodal oral lymphomas: histologic subtypes and immunophenotypes (in routinely processed tissue). Oral Surg Oral Med Oral Pathol 1991; 72:702–708.
478. Takahashi H, Fujita S, Okabe H, et al. Immunophenotypic analysis of extranodal non-Hodgkin's lymphomas in the oral cavity. Pathol Res Pract 1993; 189:300–311.
479. Webb CJ, Makura ZG, Jackson SR, et al. Primary extramedullary plasmacytoma of the tongue base. Case report and review of the literature. ORL J Otorhinolaryngol Relat Spec 2002; 64:278–280.
480. Regezi JA, McMillan A, Dekker N, et al. Apoptosis-associated proteins in oral lymphomas from HIV-positive patients. Oral Surg Oral Med Oral Pathol Oral Radiol Endod 1998; 86:196–202.
481. Gulley ML, Sargeant KP, Grider DJ, et al. Lymphomas of the oral soft tissues are not preferentially associated with latent or replicative Epstein-Barr virus. Oral Surg Oral Med Oral Pathol Oral Radiol Endod 1995; 80:425–431.
482. Thomas JA, Cotter F, Hanby AM, et al. Epstein-Barr virus-related oral T-cell lymphoma associated with human immunodeficiency virus immunosuppression. Blood 1993; 81:3350–3356.
483. Chan JK, Sin VC, Wong KF, et al. Nonnasal lymphoma expressing the natural killer cell marker CD56: a clinicopathologic study of 49 cases of an uncommon aggressive neoplasm. Blood 1997; 89:4501–4513.
484. Tsang WM, Tong AC, Lam KY, et al. Nasal T/NK cell lymphoma: report of 3 cases involving the palate. J Oral Maxillofac Surg 2000; 58:1323–1327.
485. Rosenberg A, Biesma DH, Sie-Go DM, et al. Primary extranodal CD3O-positive T-cell non-Hodgkins lymphoma of the oral mucosa. Report of two cases. Int J Oral Maxillofac Surg 1996; 25:57–59.
486. Tomita Y, Ohsawa M, Mishiro Y, et al. Non-Hodgkin's lymphoma of Waldeyer's ring as a manifestation of lymphoproliferative diseases associated with human T-cell leukemia virus type 1 in southwestern Japan. Mod Pathol 1997; 10:933–938.
487. Aloulou S, Farhat H, Bosq J, et al. Hodgkin's disease primarily involving the oropharynx: case report and review of the literature. Hematol J 2002; 3:164–167.
488. Mathews FR, Appleton SS, Wear DJ. Intraoral Hodgkin's disease. J Oral Maxillofac Surg 1989; 47:502–504.
489. Tanaka J, Yoshida K, Suzuki M, et al. Hodgkin's disease of the maxillary gingiva. A case report. Int J Oral Maxillofac Surg 1992; 21:45–46.
490. Chang KL, Kamel OW, Arber DA, et al. Pathologic features of nodular lymphocyte predominance Hodgkin's disease in extranodal sites. Am J Surg Pathol 1995; 19:1313–1324.
491. Paulsen J, Lennert K. Low-grade B-cell lymphoma of mucosa-associated lymphoid tissue type in Waldeyer's ring. Histopathology 1994; 24:1–11.
492. Ree HJ, Rege VB, Knisley RE, et al. Malignant lymphoma of Waldeyer's ring following gastrointestinal lymphoma. Cancer 1980; 46:1528–1535.
493. Barton JH, Osborne BM, Butler JJ, et al. Non-Hodgkin's lymphoma of the tonsil. A clinicopathologic study of 65 cases. Cancer 1984; 53:86–95.
494. Fujitani T, Takahara T, Hattori H, et al. Radiochemotherapy for non-Hodgkin's lymphoma in palatine tonsil. Cancer 1984; 54:1288–1292.
495. Harabuchi Y, Tsubota H, Ohguro S, et al. Prognostic factors and treatment outcome in non-Hodgkin's lymphoma of Waldeyer's ring. Acta Oncol 1997; 36:413–420.
496. Makepeace AR, Fermont DC, Bennett MH. Non-Hodgkin's lymphoma of the tonsil. Experience of treatment over a 27-year period. J Laryngol Otol 1987; 101:1151–1158.
497. Sunaba K, Shibuya H, Okada N, et al. Radiotherapy for primary localized (stage I and II) non-Hodgkin's lymphoma of the oral cavity. Int J Radiat Oncol Biol Phys 2000; 47:179–183.
498. Shimm DS, Dosoretz DE, Harris NL, et al. Radiation therapy of Waldeyer's ring lymphoma. Cancer 1984; 54:426–431.
499. Wolvius EB, van der Valk P, van der Wal JE, et al. Primary extranodal non-Hodgkin lymphoma of the oral cavity. An analysis of 34 cases. Eur J Cancer B Oral Oncol 1994; 30B:121–125.
500. Ree HJ, Kikuchi M, Lee SS, et al. Focal follicular features in tonsillar diffuse large B-cell lymphomas: follicular lymphoma with diffuse areas or follicular colonization. Hum Pathol 2002; 33:732–740.
501. Dreizen S, McCredie KB, Keating MJ, et al. Malignant gingival and skin ''infiltrates'' in adult leukemia. Oral Surg Oral Med Oral Pathol 1983; 55:572–579.
502. Amin KS, Ehsan A, McGuff HS, et al. Minimally differentiated acute myelogenous leukemia (AML-M0) granulocytic sarcoma presenting in the oral cavity. Oral Oncol 2002; 38:516–519.

503. Ficarra G, Silverman S Jr., Quivey JM, et al. Granulocytic sarcoma (chloroma) of the oral cavity: a case with aleukemic presentation. Oral Surg Oral Med Oral Pathol 1987; 63:709–714.
504. Hartman KS. Histiocytosis X: a review of 114 cases with oral involvement. Oral Surg Oral Med Oral Pathol 1980; 49:38–54.
505. Bottomley WK, Gabriel SA, Corio RL, et al. Histiocytosis X: report of an oral soft tissue lesion without bony involvement. Oral Surg Oral Med Oral Pathol 1987; 63:228–231.
506. Cleveland DB, Goldberg KM, Greenspan JS, et al. Langerhans' cell histiocytosis: report of three cases with unusual oral soft tissue involvement. Oral Surg Oral Med Oral Pathol Oral Radiol Endod 1996; 82:541–548.
507. Milian MA, Bagan JV, Jimenez Y, et al. Langerhans' cell histiocytosis restricted to the oral mucosa. Oral Surg Oral Med Oral Pathol Oral Radiol Endod 2001; 91:76–79.
508. Chan JK, Tsang WY, Ng CS, et al. Follicular dendritic cell tumors of the oral cavity. Am J Surg Pathol 1994; 18:148–157.
509. Satoh K, Hibi G, Yamamoto Y, et al. Follicular dendritic cell tumor in the oro-pharyngeal region: report of a case and a review of the literature. Oral Oncol 2003; 39:415–419.
510. Vos JA, Abbondanzo SL, Barekman CL, et al. Histiocytic sarcoma: a study of five cases including the histiocyte marker CD163. Mod Pathol 2005; 18:693–704.
511. el-Mofty SK, Swanson PE, Wick MR, et al. Eosinophilic ulcer of the oral mucosa. Report of 38 new cases with immunohistochemical observations. Oral Surg Oral Med Oral Pathol 1993; 75:716–722.
512. Elzay RP. Traumatic ulcerative granuloma with stromal eosinophilia (Riga-Fede's disease and traumatic eosinophilic granuloma). Oral Surg Oral Med Oral Pathol 1983; 55:497–506.
513. Eversole LR, Leider AS, Jacobsen PL, et al. Atypical histiocytic granuloma. Light microscopic, ultrastructural, and histochemical findings in an unusual pseudomalignant reactive lesion of the oral cavity. Cancer 1985; 55:1722–1729.
514. Ficarra G, Prignano F, Romagnoli P. Traumatic eosinophilic granuloma of the oral mucosa: a CD30+(Ki-1) lymphoproliferative disorder? Oral Oncol 1997; 33: 375–379.
515. Attygalle AD, Liu H, Shirali S, et al. Atypical marginal zone hyperplasia of mucosa-associated lymphoid tissue: a reactive condition of childhood showing immunoglobulin lambda light-chain restriction. Blood 2004; 104:3343–3348.
516. Strauchen JA. Indolent T-lymphoblastic proliferation: report of a case with an 11-year history and association with myasthenia gravis. Am J Surg Pathol 2001; 25: 411–415.
517. Velankar MM, Nathwani BN, Schlutz MJ, et al. Indolent T-lymphoblastic proliferation: report of a case with a 16-year course without cytotoxic therapy. Am J Surg Pathol 1999; 23:977–981.
518. Plumbley JA, Fan H, Eagan PA, et al. Lymphoid tissues from patients with infectious mononucleosis lack monoclonal B and T cells. J Mol Diagn 2002; 4:37–43.
519. Gleeson MJ, Bennett MH, Cawson RA. Lymphomas of salivary glands. Cancer 1986; 58:699–704.
520. Colby TV, Dorfman RF. Malignant lymphomas involving the salivary glands. Pathol Annu 1979; 14(pt 2):307–324.
521. Hyman GA, Wolff M. Malignant lymphomas of the salivary glands. Review of the literature and report of 33 new cases, including four cases associated with the lymphoepithelial lesion. Am J Clin Pathol 1976; 65:421–438.
522. James M, Norton AJ, Akosa AB. Primary T-cell lymphoma of submandibular salivary gland. Histopathology 1993; 22:83–85.
523. Chan JK, Tsang WY, Hui PK, et al. T- and T/natural killer-cell lymphomas of the salivary gland: a clinicopathologic, immunohistochemical and molecular study of six cases. Hum Pathol 1997; 28:238–245.
524. Hew WS, Carey FA, Kernohan NM, et al. Primary T cell lymphoma of salivary gland: a report of a case and review of the literature. J Clin Pathol 2002; 55:61–63.
525. Schmid U, Helbron D, Lennert K. Primary malignant lymphomas localized in salivary glands. Histopathology 1982; 6:673–687.
526. Baldini L, Guffanti A, Ferrari A, et al. Uncommon clinical presentation of a lymphocytic lymphoma of intermediate differentiation in a patient with systemic sclerosis. Br J Haematol 1994; 86:657–658.
527. Chhieng DC, Cangiarella JF, Cohen JM. Fine-needle aspiration cytology of lymphoproliferative lesions involving the major salivary glands. Am J Clin Pathol 2000; 113: 563–571.
528. Liang R, Loke SL. Non-Hodgkin's lymphomas involving the parotid gland. Clin Oncol (R Coll Radiol) 1991; 3:81–83.
529. Medeiros LJ, Rizzi R, Lardelli P, et al. Malignant lymphoma involving a Warthin's tumor: a case with immunophenotypic and gene rearrangement analysis. Hum Pathol 1990; 21:974–977.
530. Melato M, Falconieri G, Fanin R, et al. Hodgkin's disease occurring in a Warthin's tumor: first case report. Pathol Res Pract 1986; 181:615–620.
531. Saxena A, Memauri B, Hasegawa W. Initial diagnosis of small lymphocytic lymphoma in parotidectomy for Warthin tumour, a rare collision tumour. J Clin Pathol 2005; 58:331–333.
532. Zucca E, Conconi A, Pedrinis E, et al. Nongastric marginal zone B-cell lymphoma of mucosa-associated lymphoid tissue. Blood 2003; 101:2489–2495.
533. Ambrosetti A, Zanotti R, Pattaro C, et al. Most cases of primary salivary mucosa-associated lymphoid tissue lymphoma are associated either with Sjoegren syndrome or hepatitis C virus infection. Br J Haematol 2004; 126:43–49.
534. Svoboda J, Andreadis C, Downs LH, et al. Regression of advanced non-splenic marginal zone lymphoma after treatment of hepatitis C virus infection. Leuk Lymphoma 2005; 46:1365–1368.
535. Borovecki A, Korac P, Ventura RA, et al. MALT1, BCL10 and FOXP1 in salivary gland mucosa-associated lymphoid tissue lymphomas. Pathol Int 2007; 57:47–51.
536. Sharma M, Ahsan F, Ah-See KW, et al. Interdigitating dendritic cell sarcoma of the parotid gland. J Laryngol Otol 2006; 120:244–246.
537. Kojima M, Itoh H, Shimizu K, et al. Incidental Langerhans cell histiocytosis of the parotid gland resembling marginal zone B-cell lymphoma: a case report. J Oral Pathol Med 2006; 35:630–632.
538. Kamel OW, Gocke CD, Kell DL, et al. True histiocytic lymphoma: a study of 12 cases based on current definition. Leuk Lymphoma 1995; 18:81–86.
539. Anaya JM, McGuff HS, Banks PM, et al. Clinicopathological factors relating malignant lymphoma with Sjogren's syndrome. Semin Arthritis Rheum 1996; 25:337–346.
540. Falzon M, Isaacson PG. The natural history of benign lymphoepithelial lesion of the salivary gland in which there is a monoclonal population of B cells. A report of two cases. Am J Surg Pathol 1991; 15:59–65.
541. Fishleder A, Tubbs R, Hesse B, et al. Uniform detection of immunoglobulin-gene rearrangement in benign lymphoepithelial lesions. N Engl J Med 1987; 316:1118–1121.
542. Diss TC, Wotherspoon AC, Speight P, et al. B-cell monoclonality, Epstein Barr virus, and t(14; 18) in myoepithelial sialadenitis and low-grade B-cell MALT lymphoma of the parotid gland. Am J Surg Pathol 1995; 19:531–536.

543. Bahler DW, Swerdlow SH. Clonal salivary gland infiltrates associated with myoepithelial sialadenitis (Sjogren's syndrome) begin as nonmalignant antigen-selected expansions. Blood 1998; 91:1864–1872.
544. Quintana PG, Kapadia SB, Bahler DW, et al. Salivary gland lymphoid infiltrates associated with lymphoepithelial lesions: a clinicopathologic, immunophenotypic, and genotypic study. Hum Pathol 1997; 28:850–861.
545. Hsi ED, Siddiqui J, Schnitzer B, et al. Analysis of immunoglobulin heavy chain gene rearrangement in myoepithelial sialadenitis by polymerase chain reaction. Am J Clin Pathol 1996; 106:498–503.
546. Lasota J, Miettinen MM. Coexistence of different B-cell clones in consecutive lesions of low-grade MALT lymphoma of the salivary gland in Sjogren's disease. Mod Pathol 1997; 10:872–878.
547. d'Agay MF, de Roquancourt A, Peuchmaur M, et al. Cystic benign lymphoepithelial lesion of the salivary glands in HIV-positive patients. Report of two cases with immunohistochemical study. Virchows Arch A Pathol Anat Histopathol 1990; 417:353–356.
548. Chan JK. Kuttner tumor (chronic sclerosing sialadenitis) of the submandibular gland: an underrecognized entity. Adv Anat Pathol 1998; 5:239–251.
549. Kitagawa S, Zen Y, Harada K, et al. Abundant IgG4-positive plasma cell infiltration characterizes chronic sclerosing sialadenitis (Kuttner's tumor). Am J Surg Pathol 2005; 29:783–791.
550. Levine LA, Ansel DG, Murray JP. Agnogenic myeloid metaplasia with a parotid mass. Arch Otolaryngol 1979; 105:205–206.
551. Hyjek E, Smith WJ, Isaacson PG. Primary B-cell lymphoma of salivary glands and its relationship to myoepithelial sialadenitis. Hum Pathol 1988; 19:766–776.
552. Agada FO, Mistry D, Grace AR, et al. Large B-cell non-Hodgkin's lymphoma presenting as a laryngeal cyst. J Laryngol Otol 2005; 119:658–660.
553. Morgan K, MacLennan KA, Narula A, et al. Non-Hodgkin's lymphoma of the larynx (stage IE). Cancer 1989; 64:1123–1127.
554. Diebold J, Audouin J, Viry B, et al. Primary lymphoplasmacytic lymphoma of the larynx: a rare localization of MALT-type lymphoma. Ann Otol Rhinol Laryngol 1990; 99:577–580.
555. Ansell SM, Habermann TM, Hoyer JD, et al. Primary laryngeal lymphoma. Laryngoscope 1997; 107:1502–1506.
556. Kato S, Sakura M, Takooda S, et al. Primary non-Hodgkin's lymphoma of the larynx. J Laryngol Otol 1997; 111: 571–574.
557. Cavalot AL, Preti G, Vione N, et al. Isolated primary non-Hodgkin's malignant lymphoma of the larynx. J Laryngol Otol 2001; 115:324–326.
558. Mok JS, Pak MW, Chan KF, et al. Unusual T- and T/NK-cell non-Hodgkin's lymphoma of the larynx: a diagnostic challenge for clinicians and pathologists. Head Neck 2001; 23:625–628.
559. Marianowski R, Wassef M, Amanou L, et al. Primary T-cell non-Hodgkin lymphoma of the larynx with subsequent cutaneous involvement. Arch Otolaryngol Head Neck Surg 1998; 124:1037–1040.
560. Caletti G, Togliani T, Fusaroli P, et al. Consecutive regression of concurrent laryngeal and gastric MALT lymphoma after anti-Helicobacter pylori therapy. Gastroenterology 2003; 124:537–543.
561. Weissman JL, Myers JN, Kapadia SB. Extramedullary plasmacytoma of the larynx. Am J Otolaryngol 1993; 14:128–131.
562. Vassallo J, Altemani AM, Cardinalli IA, et al. Granulocytic sarcoma of the larynx preceding chronic myeloid leukemia. Pathol Res Pract 1993; 189:1084–1086; discussion 86–89.
563. Duynstee ML, Verwoerd-Verhoef HL, Monnier P, et al. Langerhans cell histiocytosis of the larynx. Int J Pediatr Otorhinolaryngol 2000; 56:65–69.
564. Tzankov A, Krugmann J, Mikuz G. Glottis oedema and interstitial pulmonary disease as a result of extramedullary haemopoiesis in polycythaemia vera rubra causing asphyctic death. J Clin Pathol 2003; 56:79.
565. Stadlmann S, Fend F, Moser P, et al. Epstein-Barr virus-associated extranodal NK/T-cell lymphoma, nasal type of the hypopharynx, in a renal allograft recipient: case report and review of literature. Hum Pathol 2001; 32:1264–1268.
566. Thorp MA, Langman G, Sellars SL. Angiocentric T-cell lymphoma: an extensive lesion involving the posterior tongue, hypopharynx and supraglottis. J Laryngol Otol 1999; 113:263–265.
567. Wenzel C, Dieckmann K, Fiebiger W, et al. CD5 expression in a lymphoma of the mucosa-associated lymphoid tissue (MALT)-type as a marker for early dissemination and aggressive clinical behaviour. Leuk Lymphoma 2001; 42:823–829.
568. Georgalas C, Kanagalingam J, Gallimore A, et al. Follicular dendritic cell sarcoma arising from the hypopharynx. J Laryngol Otol 2004; 118:317–318.
569. Kaplan MA, Pettit CL, Zukerberg LR, et al. Primary lymphoma of the trachea with morphologic and immunophenotypic characteristics of low-grade B-cell lymphoma of mucosa-associated lymphoid tissue. Am J Surg Pathol 1992; 16:71–75.
570. Fidias P, Wright C, Harris NL, et al. Primary tracheal non-Hodgkin's lymphoma. A case report and review of the literature. Cancer 1996; 77:2332–2338.
571. Okubo K, Miyamoto N, Komaki C. Primary mucosa-associated lymphoid tissue (MALT) lymphoma of the trachea: a case of surgical resection and long term survival. Thorax 2005; 60:82–83.
572. Logan PM, Miller RR, Muller NL. Solitary tracheal plasmacytoma: computed tomography and pathological findings. Can Assoc Radiol J 1995; 46:125–126.
573. Fridlender ZG, Glazer M, Amir G, et al. Obstructing tracheal pulmonary Langerhans cell histiocytosis. Chest 2005; 128:1057–1058.
574. Dewar AL, Connett GJ. Inflammatory pseudotumor of the trachea in a ten-month-old infant. Pediatr Pulmonol 1997; 23:307–309.
575. Mack LA, Pasieka JL. An evidence-based approach to the treatment of thyroid lymphoma. World J Surg 2007; 31(5): 978–986.
576. Holm LE, Blomgren H, Lowhagen T. Cancer risks in patients with chronic lymphocytic thyroiditis. N Engl J Med 1985; 312:601–604.
577. Kato I, Tajima K, Suchi T, et al. Chronic thyroiditis as a risk factor of B-cell lymphoma in the thyroid gland. Jpn J Cancer Res 1985; 76:1085–1090.
578. Derringer GA, Thompson LD, Frommelt RA, et al. Malignant lymphoma of the thyroid gland: a clinicopathologic study of 108 cases. Am J Surg Pathol 2000; 24:623–639.
579. Wang SA, Rahemtullah A, Faquin WC, et al. Hodgkin's lymphoma of the thyroid: a clinicopathologic study of five cases and review of the literature. Mod Pathol 2005; 18:1577–1584.
580. Skacel M, Ross CW, Hsi ED. A reassessment of primary thyroid lymphoma: high-grade MALT-type lymphoma as a distinct subtype of diffuse large B-cell lymphoma. Histopathology 2000; 37:10–18.
581. Logue JP, Hale RJ, Stewart AL, et al. Primary malignant lymphoma of the thyroid: a clinicopathological analysis. Int J Radiat Oncol Biol Phys 1992; 22:929–933.

582. Aozasa K, Inoue A, Tajima K, et al. Malignant lymphomas of the thyroid gland. Analysis of 79 patients with emphasis on histologic prognostic factors. Cancer 1986; 58:100–104.
583. Pedersen RK, Pedersen NT. Primary non-Hodgkin's lymphoma of the thyroid gland: a population based study. Histopathology 1996; 28:25–32.
584. Widder S, Pasieka JL. Primary thyroid lymphomas. Curr Treat Options Oncol 2004; 5:307–313.
585. Galati LT, Barnes EL, Myers EN. Dendritic cell sarcoma of the thyroid. Head Neck 1999; 21:273–275.
586. Thompson LD, Wenig BM, Adair CF, et al. Langerhans cell histiocytosis of the thyroid: a series of seven cases and a review of the literature. Mod Pathol 1996; 9:145–149.
587. Aozasa K, Inoue A, Yoshimura H, et al. Plasmacytoma of the thyroid gland. Cancer 1986; 58:105–110.
588. Deniz K, Patiroglu TE, Okten T. Plasma cell granuloma of the thyroid. APMIS 2008; 116:167–172.
589. Hsi ED, Singleton TP, Svoboda SM, et al. Characterization of the lymphoid infiltrate in Hashimoto thyroiditis by immunohistochemistry and polymerase chain reaction for immunoglobulin heavy chain gene rearrangement. Am J Clin Pathol 1998; 110:327–333.
590. Ferry JA, Fung CY, Zukerberg L, et al. Lymphoma of the Ocular Adnexa: A Study of 353 Cases. Am J Surg Pathol 2007; 31:170–184.
591. Cho EY, Han JJ, Ree HJ, et al. Clinicopathologic analysis of ocular adnexal lymphomas: extranodal marginal zone b-cell lymphoma constitutes the vast majority of ocular lymphomas among Koreans and affects younger patients. Am J Hematol 2003; 73:87–96.
592. Rosado MF, Byrne GE Jr., Ding F, et al. et al. Ocular adnexal lymphoma: a clinicopathologic study of a large cohort of patients with no evidence for an association with Chlamydia psittaci. Blood 2006; 107:467–472.
593. Auw-Haedrich C, Coupland SE, Kapp A, et al. Long term outcome of ocular adnexal lymphoma subtyped according to the REAL classification. Revised European and American Lymphoma. Br J Ophthalmol 2001; 85:63–69.
594. Jenkins C, Rose GE, Bunce C, et al. Histological features of ocular adnexal lymphoma (REAL classification) and their association with patient morbidity and survival. Br J Ophthalmol 2000; 84:907–913.
595. Lagoo AS, Haggerty C, Kim Y, et al. Morphologic features of 115 lymphomas of the orbit and ocular adnexa categorized according to the World Health Organization classification: are marginal zone lymphomas in the orbit mucosa-associated lymphoid tissue-type lymphomas? Arch Pathol Lab Med 2008; 132:1405–1416.
596. Cheuk W, Yuen HK, Chan AC, et al. Ocular adnexal lymphoma associated with IgG4+ chronic sclerosing dacryoadenitis: a previously undescribed complication of IgG4-related sclerosing disease. Am J Surg Pathol 2008; 32:1159–1167.
597. Sato Y, Ohshima K, Ichimura K, et al. Ocular adnexal IgG4-related disease has uniform clinicopathology. Pathol Int 2008; 58:465–470.
598. Nakata M, Matsuno Y, Katsumata N, et al. Histology according to the Revised European-American Lymphoma Classification significantly predicts the prognosis of ocular adnexal lymphoma. Leuk Lymphoma 1999; 32:533–543.
599. Ferreri AJ, Guidoboni M, Ponzoni M, et al. Evidence for an association between Chlamydia psittaci and ocular adnexal lymphomas. J Natl Cancer Inst 2004; 96:586–594.
600. Chanudet E, Zhou Y, Bacon CM, et al. Chlamydia psittaci is variably associated with ocular adnexal MALT lymphoma in different geographical regions. J Pathol 2006; 209:344–351.
601. Decaudin D, Dolcetti R, de Cremoux P, et al. Variable association between Chlamydophila psittaci infection and ocular adnexal lymphomas: methodological biases or true geographical variations? Anticancer Drugs 2008; 19: 761–765.
602. Adkins JW, Shields JA, Shields CL, et al. Plasmacytoma of the eye and orbit. Int Ophthalmol 1996; 20:339–343.
603. Fung CY, Tarbell NJ, Lucarelli MJ, et al. Ocular adnexal lymphoma: clinical behavior of distinct World Health Organization classification subtypes. Int J Radiat Oncol Biol Phys 2003; 57:1382–1391.
604. Decaudin D, de Cremoux P, Vincent-Salomon A, et al. Ocular adnexal lymphoma: a review of clinicopathologic features and treatment options. Blood 2006; 108:1451–1460.
605. Ferreri AJ, Ponzoni M, Guidoboni M, et al. Regression of ocular adnexal lymphoma after Chlamydia psittaci-eradicating antibiotic therapy. J Clin Oncol 2005; 23: 5067–5073.
606. Ferreri AJ, Ponzoni M, Guidoboni M, et al. Bacteria-eradicating therapy with doxycycline in ocular adnexal MALT lymphoma: a multicenter prospective trial. J Natl Cancer Inst 2006; 98:1375–1382.
607. Grunberger B, Hauff W, Lukas J, et al. 'Blind' antibiotic treatment targeting Chlamydia is not effective in patients with MALT lymphoma of the ocular adnexa. Ann Oncol 2006; 17:484–487.
608. Uno T, Isobe K, Shikama N, et al. Radiotherapy for extranodal, marginal zone, B-cell lymphoma of mucosa-associated lymphoid tissue originating in the ocular adnexa: a multiinstitutional, retrospective review of 50 patients. Cancer 2003; 98:865–871.
609. Franco R, Camacho FI, Caleo A, et al. Nuclear bcl10 expression characterizes a group of ocular adnexa MALT lymphomas with shorter failure-free survival. Mod Pathol 2006; 19:1055–1067.
610. Peterson K, Gordon KB, Heinemann MH, et al. The clinical spectrum of ocular lymphoma. Cancer 1993; 72:843–849.
611. Akpek EK, Ahmed I, Hochberg FH, et al. Intraocular-central nervous system lymphoma: clinical features, diagnosis, and outcomes. Ophthalmology 1999; 106:1805–1810.
612. Jahnke K, Korfel A, Komm J, et al. Intraocular lymphoma 2000–2005: results of a retrospective multicentre trial. Graefes Arch Clin Exp Ophthalmol 2006; 244:663–669.
613. Choi JY, Kafkala C, Foster CS. Primary intraocular lymphoma: a review. Semin Ophthalmol 2006; 21:125–133.
614. Whitcup SM, de Smet MD, Rubin BI, et al. Intraocular lymphoma. Clinical and histopathologic diagnosis. Ophthalmology 1993; 100:1399–1406.
615. Ljung BM, Char D, Miller TR, et al. Intraocular lymphoma. Cytologic diagnosis and the role of immunologic markers. Acta Cytol 1988; 32:840–847.
616. Baehring JM, Androudi S, Longtine JJ, et al. Analysis of clonal immunoglobulin heavy chain rearrangements in ocular lymphoma. Cancer 2005; 104:591–597.
617. Chan CC, Wallace DJ. Intraocular lymphoma: update on diagnosis and management. Cancer Control 2004; 11:285–295.
618. Kim SK, Chan CC, Wallace DJ. Management of primary intraocular lymphoma. Curr Oncol Rep 2005; 7:74–79.
619. Hoffman PM, McKelvie P, Hall AJ, et al. Intraocular lymphoma: a series of 14 patients with clinicopathological features and treatment outcomes. Eye 2003; 17:513–521.
620. Knowles DM, Jakobiec FA, McNally L, et al. Lymphoid hyperplasia and malignant lymphoma occurring in the ocular adnexa (orbit, conjunctiva, and eyelids): a prospective multiparametric analysis of 108 cases during 1977 to 1987. Hum Pathol 1990; 21:959–973.
621. Xu KP, Katagiri S, Takeuchi T, et al. Biopsy of labial salivary glands and lacrimal glands in the diagnosis of Sjogren's syndrome. J Rheumatol 1996; 23:76–82.
622. Parkin B, Chew JB, White VA, et al. Lymphocytic infiltration and enlargement of the lacrimal glands: a new

subtype of primary Sjogren's syndrome? Ophthalmology 2005; 112:2040–2047.
623. Mottow-Lippa L, Jakobiec FA, Smith M. Idiopathic inflammatory orbital pseudotumor in childhood. II. Results of diagnostic tests and biopsies. Ophthalmology 1981; 88:565–574.
624. Yuen HK, Mahesh L, Tse RK, et al. Orbital sclerosing extramedullary hematopoietic tumor. Arch Ophthalmol 2005; 123:689–691.
625. Yuen HK, Cheuk W, Leung DY, et al. Atypical presentation of Rosai-Dorfman disease in the lacrimal gland mimicking malignancy. Ophthal Plast Reconstr Surg 2006; 22:145–147.
626. Buggage RR, Spraul CW, Wojno TH, et al. Kimura disease of the orbit and ocular adnexa. Surv Ophthalmol 1999; 44:79–91.
627. Biccas Neto L, Zanetti F. [Intraocular involvement in Erdheim-Chester disease–first report in the literature: case report]. Arq Bras Oftalmol 2007; 70:862–867.
628. De Abreu MR, Chung CB, Biswal S, et al. Erdheim-Chester disease: MR imaging, anatomic, and histopathologic correlation of orbital involvement. AJNR Am J Neuroradiol 2004; 25:627–630.
629. Lau WW, Chan E, Chan CW. Orbital involvement in Erdheim-Chester disease. Hong Kong Med J 2007; 13:238–240.
630. Medeiros LJ, Harris NL. Lymphoid infiltrates of the orbit and conjunctiva. A morphologic and immunophenotypic study of 99 cases. Am J Surg Pathol 1989; 13:459–471.
631. Chan JKC. Tumors of the lymphoreticular system. In: Fletcher CDM, ed. Diagnostic Histopathology of Tumors. 3rd ed. London: Churchill Livingstone, 2007:1139–1288.
632. Merkus P, Copper MP, Van Oers MH, et al. Lymphoma in the ear. ORL J Otorhinolaryngol Relat Spec 2000; 62:274–277.
633. Danino J, Joachims HZ, Ben-Arieh Y, et al. T cell lymphoma of the ear presenting as mastoiditis. J Laryngol Otol 1997; 111:852–854.
634. Lang EE, Walsh RM, Leader M. Primary middle-ear lymphoma in a child. J Laryngol Otol 2003; 117:205–207.
635. Unni KK. Dahlin's bone tumors: general aspects and data on 11,087 cases. 5th ed. Philadelphia: Lippincott-Raven, 1996.
636. McKenna RW, Kyle RA, Kuehl WM, et al. Plasma cell neoplasms. In: Swerdlow SH, Campo E, Harris NL, et al., eds. WHO Classification of Tumours of Haematopoietic and Lymphoid Tissues. 4th ed. Lyon: IARC, 2008:200–213.
637. Grogan TM, van Camp B, Kyle RA, et al. Plasma cell neoplasms. In: Jaffe ES, Harris NL, Stein H, et al., eds. Pathology and Genetics: Tumours of Haematopoietic and Lymphoid Tissues. World Health Organization Classification of Tumours. Lyon: IARC Press, 2001:142–156.
638. Beal K, Allen L, Yahalom J. Primary bone lymphoma: treatment results and prognostic factors with long-term follow-up of 82 patients. Cancer 2006; 106:2652–2656.
639. Christie DR, Barton MB, Bryant G, et al. Osteolymphoma (primary bone lymphoma): an Australian review of 70 cases. Australasian Radiation Oncology Lymphoma Group (AROLG). Aust N Z J Med 1999; 29:214–219.
640. Heyning FH, Hogendoorn PC, Kramer MH, et al. Primary non-Hodgkin's lymphoma of bone: a clinicopathological investigation of 60 cases. Leukemia 1999; 13:2094–2098.
641. Pettit CK, Zukerberg LR, Gray MH, et al. Primary lymphoma of bone. A B-cell neoplasm with a high frequency of multilobated cells. Am J Surg Pathol 1990; 14:329–334.
642. Glotzbecker MP, Kersun LS, Choi JK, et al. Primary non-Hodgkin's lymphoma of bone in children. J Bone Joint Surg Am 2006; 88:583–594.
643. Ostrowski ML, Inwards CY, Strickler JG, et al. Osseous Hodgkin disease. Cancer 1999; 85:1166–1178.
644. Nagasaka T, Nakamura S, Medeiros LJ, et al. Anaplastic large cell lymphomas presented as bone lesions: a clinicopathologic study of six cases and review of the literature. Mod Pathol 2000; 13:1143–1149.
645. De Young BR, Unni KK. Langerhans cell histiocytosis. In: Fletcher CDM, Unni KK, Mertens F, eds. Pathology and Genetics: Tumours of Soft Tissue and Bone. World Health Organization Classification of Tumours. Lyon: IARC Press, 2002:345–346.
646. Kilpatrick SE, Wenger DE, Gilchrist GS, et al. Langerhans' cell histiocytosis (histiocytosis X) of bone. A clinicopathologic analysis of 263 pediatric and adult cases. Cancer 1995; 76:2471–2484.
647. Lieberman PH, Jones CR, Steinman RM, et al. Langerhans cell (eosinophilic) granulomatosis. A clinicopathologic study encompassing 50 years. Am J Surg Pathol 1996; 20:519–552.
648. Castling B, Smith AT, Myers B. Involvement of the jaw bones in systemic mastocytosis. Br J Oral Maxillofac Surg 2006; 44:87–88.
649. Burg G, Jaffe ES, Kempf W, et al. Haematolymphoid tumours. In: LeBoit PE, Burg G, Weedon D, et al., eds. Pathology and Genetics: Skin Tumours. World Health Organization Classification of Tumours. Lyon: IARC Press, 2006:165–228.
650. Cerroni L, Zenahlik P, Hofler G, et al. Specific cutaneous infiltrates of B-cell chronic lymphocytic leukemia: a clinicopathologic and prognostic study of 42 patients. Am J Surg Pathol 1996; 20:1000–1010.
651. Chimenti S, Fink-Puches R, Peris K, et al. Cutaneous involvement in lymphoblastic lymphoma. J Cutan Pathol 1999; 26:379–385.
652. Pimpinelli N, Berti E, Burg G, et al. Cutaneous follicle center lymphoma. In: LeBoit PE, Burg G, Weedon D, et al., eds. Pathology and Genetics: Skin Tumours. World Health Organization Classification of Tumours. Lyon: IARC Press, 2006:196–197.
653. Burg G, Jaffe ES, Willemze R, et al. Cutaneous diffuse large B-cell lymphoma. In: LeBoit PE, Burg G, Weedon D, et al., eds. Pathology and Genetics: Skin Tumours. World Health Organization Classification of Tumours. Lyon: IARC Press, 2006:198–199.
654. Kutzner H, Jaffe ES. Intravascular large B-cell lymphoma. In: LeBoit PE, Burg G, Weedon D, et al., eds. Pathology and Genetics: Skin Tumours. World Health Organization Classification of Tumours. Lyon: IARC Press, 2006:200–201.
655. Ferreri AJ, Campo E, Seymour JF, et al., et al. Intravascular lymphoma: clinical presentation, natural history, management and prognostic factors in a series of 38 cases, with special emphasis on the 'cutaneous variant'. Br J Haematol 2004; 127:173–183.
656. Kempf W, Ralfkiaer E, Duncan L, et al., et al. Cutaneous marginal zone B-cell lymphoma. In: LeBoit PE, Burg G, Weedon D, et al., eds. Pathology and Genetics: Skin Tumours. World Health Organization Classification of Tumours. Lyon: IARC Press, 2006:194–195.
657. Goodlad JR, Davidson MM, Hollowood K, et al., et al. Primary cutaneous B-cell lymphoma and Borrelia burgdorferi infection in patients from the Highlands of Scotland. Am J Surg Pathol 2000; 24:1279–1285.
658. Cerroni L, Zochling N, Putz B, et al. Infection by Borrelia burgdorferi and cutaneous B-cell lymphoma. J Cutan Pathol 1997; 24:457–461.
659. Wong KF, Chan JK, Li LP, et al. Primary cutaneous plasmacytoma—report of two cases and review of the literature. Am J Dermatopathol 1994; 16:392–397.
660. Zelger B, Rapini RP, Burgdorf W, et al. Langerhans cell histiocytosis. In: LeBoit PE, Burg G, Weedon D, et al., eds. Pathology and Genetics: Skin Tumours. World Health Organization Classification of Tumours. Lyon: IARC Press, 2006:217–219.

661. Caputo R, Berti E. Indeterminate cell histiocytosis. In: LeBoit PE, Burg G, Weedon D, et al., eds. Pathology and Genetics: Skin Tumours. World Health Organization Classification of Tumours. Lyon: IARC Press, 2006:220.
662. Valent P, Horny HP, Escribano L, et al. Diagnostic criteria and classification of mastocytosis: a consensus proposal. Leuk Res 2001; 25:603–625.
663. Sander CA, Jaffe ES, Flaig MJ, et al. Blastic NK-cell lymphoma. In: LeBoit PE, Burg G, Weedon D, et al., eds. Pathology and Genetics: Skin Tumours. World Health Organization Classification of Tumours. Lyon: IARC Press, 2006:208–209.
664. Horny HP, Metcalfe DD, Bennett JM, et al. Mastocytosis. In: Swerdlow SH, Campo E, Harris NL, et al., eds. WHO Classification of Tumours of Haematopoietic and Lymphoid Tissues. 4th ed. Lyon: IARC, 2008:54–63.
665. Cerroni L, Gatter K, Kerl H. An illustrated guide to skin lymphoma. Oxford: Blackwell Publishing, 2004.
666. Kong YY, Kong JC, Shi DR, et al. Cutaneous Rosai-Dorfman disease: a clinical and histopathologic study of 25 cases in China. Am J Surg Pathol 2007; 31:341–350.
667. Bakels V, van Oostveen JW, van der Putte SC, et al. Immunophenotyping and gene rearrangement analysis provide additional criteria to differentiate between cutaneous T-cell lymphomas and pseudo-T-cell lymphomas. Am J Pathol 1997; 150:1941–1949.
668. Rijlaarsdam U, Willemze R. Cutaneous pseudo-T-cell lymphomas. Semin Diagn Pathol 1991; 8:102–108.

16

Pathology of Neck Dissections

Mario A. Luna
Department of Pathology, The University of Texas, M.D. Anderson Cancer Center, Houston, Texas, U.S.A.

I. INTRODUCTION

The presence of cervical lymph node metastasis at presentation or at initiation of treatment is the main adverse prognostic factor for patients with squamous cell carcinoma (SCC) of the upper aerodigestive tract. Its presence at either of these times reduces the five-year survival rate by approximately 50%, regardless of the primary site of the carcinoma (1). However, clinical and pathologic findings specific to lymph node metastasis provide additional prognostic information related to tumor recurrence and overall survival. Furthermore, accurate pathologic staging of the neck of patients with head and neck cancer is important for providing information and optimizing the treatment plan (2). Pathologic findings in neck dissections are considered definite reference points; therefore, it is essential that both pathologists and clinicians approach the morphologic evidence with rigor, recognizing its limitations as well as its contributions to rational clinical planning (3).

II. LYMPHATIC REGIONS OF THE NECK

Lymphatic tissue in the neck accounts for one-third of all nodal tissue in the entire body. Most cervical lymph nodes are located in the anterior triangle traversing the carotid sheath from the skull base to the thoracic inlet. They can be divided into superficial and deep lymph nodes, and each of these groups can be further divided into lateral and medial lymph nodes.

The superficial medial cervical lymph nodes are distributed around the anterior jugular vein. The superficial lateral cervical lymph nodes are located along the external jugular vein. The deep lateral cervical lymph nodes are arranged in three chains: (*i*) the internal jugular vein chain, (*ii*) the spinal accessory nerve chain, and (*iii*) the supraclavicular lymph node chain. The internal jugular vein lymph nodes and the spinal accessory nerve lymph nodes are divided into upper, middle, and lower nodes. The deep medial cervical group consists of the prelaryngeal, prethyroideal, pretracheal, and paratracheal lymph nodes. However, most head and neck surgeons, radiologists, and oncologists refer to ''nodal levels'' to describe nodal groups involved by disease and encompassed by neck dissections. Figure 1 shows the system for describing the location of lymph nodes in the neck, as recommended in 2002 by the American Academy of Otolaryngology-Head and Neck Surgery and the American Society of Head and Neck Surgery (4). The six cervical lymph node levels are as follows: level I [sublevel IA (submental) and IB (submandibular)]; level II [upper jugular; sublevel IIA (jugulodigastric) and IIB (supraspinal accessory)]; level III (middle jugular); level IV (lower jugular); level V [posterior triangle; sublevel VA (spinal accessory nerve nodes) and VB (transverse cervical and supraclavicular nodes)]; and level VI (anterior group). The anatomic boundaries of these level and sublevels are described in greater detail in other sources (4).

III. CLASSIFICATION OF NECK DISSECTIONS

In 1991, an important new classification system for neck dissections was recommended by The American Academy of Otolaryngology-Head and Neck Surgery and the American Society of Head and Neck Surgery (5). This classification was modified in 2002 to reflect new observations regarding the biologic function of lymph node metastases, further refinements in selective neck dissection (SND) procedures, and the need to redefine the anatomic boundaries used in radiologic studies of the neck (4).

The three most significant changes in the revised classification were (*i*) the way in which various SNDs are described, (*ii*) the use of radiologically depicted anatomic structures to define boundaries between various neck levels and sublevels to accurately designate imaged nodes, and (*iii*) the introduction of sublevels into the classification system, since certain zones have been identified within the six levels that may have biologic significance independent of the large zone in which they lie. These three modifications comprise sublevel IA (submental nodes) and IB (submandibular nodes), sublevel IIA and IIB (together comprising the upper jugular nodes), and sublevel VA (spinal accessory nerve nodes) and VB (transverse cervical and supraclavicular nodes) (4). Each variant is depicted by SND and the use of parentheses to denote the level or sublevel of nodes removed, e.g., SND (I–III).

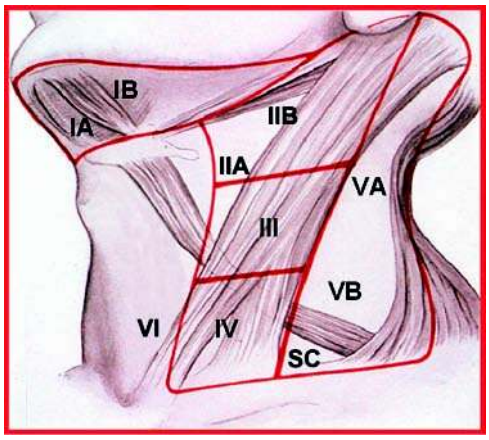

Figure 1 Level and sublevel system of cervical lymph nodes. Level I [sublevels IA (submental) and IB (submandibular)]; level II (upper jugular; sublevels IIA (jugulodigastric) and IIB (supraspinal accessory)); level III (middle jugular); level IV (lower jugular); level V (posterior triangle; sublevels VA (spinal accessory nerve nodes) and VB (transverse cervical and supraclavicular nodes); level VI (anterior group).

Neck dissections are classified primarily on the basis of the lymph node groups that are removed and secondarily on the anatomic structures that may be preserved, such as the spinal accessory nerve, the sternocleidomastoid muscle, and the internal jugular vein.

Neck dissections are divided into four categories: radical, modified radical, selective, and extended radical (Table 1) (4,5).

Radical neck dissection consists of the removal of all five lymph node levels of one side of the neck (levels I–V) and removal of the sternocleidomastoid muscle, the internal jugular vein, and the spinal accessory nerve.

Modified radical neck dissection involves the excision of all lymph nodes routinely removed during radical neck dissection but with preservation of one or more of the nonlymphatic structures (e.g., spinal accessory nerve, internal jugular vein, sternocleidomastoid muscle) routinely removed during a radical neck dissection. The Committee recommends that the structure(s) preserved be specifically identified for record-keeping purposes (e.g., modified radical neck dissection with preservation of the sternocleidomastoid muscle) (5).

Table 1 Categories of Neck Dissections

1991 Categories	2002 Categories
1. Radical	1. Radical
2. Modified radical	2. Modified radical
3. Selective	3. Selective; each variant is depicted by SND; levels or sublevels of removed nodes are shown in parentheses
A. Lateral	
B. Supraomohyoid	
C. Posterolateral	
D. Anterior	
4. Extended radical	4. Extended radical

Source: From Refs. 4, 5.

SND is any type of cervical lymphadenectomy in which one or more of the lymph node groups that are routinely removed in a radical neck dissection are preserved. Determining which lymph node groups to remove is based on the pattern of metastases, which is predictable relative to the location of the primary site of the neoplasm (6). The four subtypes of SNDs are supraomohyoid, posterolateral, lateral, and anterior neck dissection (5). The revised classification no longer includes these terms except in the description of specific lymph node levels. Each variant is depicted by ''SND'' as well as parentheses to denote the levels or sublevels of removed nodes, e.g., SND (I–III), SND (II–IV), or SND (VI) (4).

Extended radical neck dissection includes either lymph node groups or nonlymphatic structures that are not routinely removed in standard radical neck dissection. (Table 2)

IV. GROSS EXAMINATION OF NECK DISSECTION SPECIMENS

Close collaboration between the surgeon and pathologist is essential to extract the maximum information from each dissection. Because the main anatomic and

Table 2 Definition and Terminology of Updated Classification of Neck Dissection

Type of neck dissection removed	lymph node removed	Nonlymphatic structures
1. Radical	I, II, III, IV, V	SCM, IJV, SAN
2. Modified radical	I, II, III, IV, V	Preservation of one or more of the following: SCM, IJV, SAN
3. Selective neck dissection	Preservation of one or more of the following: I, II, III, IV, V Parentheses denote levels or sublevels of nodes removed, e.g., SND (I–IV)	None
4. Extended neck dissection	Resection of one or more or additional lymph node group not encompassed by the RND (e.g., paratracheal)	Resection of one or more nonlymphatic structures not encompassed by the RND (e.g., carotid artery)

Abbreviations: IJV, internal jugular vein; RND, radical neck dissection; SAN, spinal accessory nerve; SCM, sternocleidomastoid muscle; SND, selective neck dissection.
Source: From Ref. 4.

radiologic landmarks are lacking in neck dissection surgical specimens, the surgeon must orient and label the lymph node levels. Ideally, each level and sublevel of lymph nodes should be labeled and submitted to the pathology laboratory in separate containers, one container for each level or sublevel removed (2,4). The pathologist has a choice of two methods for examination of the surgical specimens to assess the lymph nodes (1,2,7). The traditional method relies on identifying lymph nodes by dissection of the received specimen (7). All lymph nodes visible or palpable in each specimen are carefully dissected from the adipose tissue with a rim of perinodal connective tissue or fat. The number of lymph nodes should be noted, and if tumor is present, the size of the metastases (in centimeters) and the presence of extracapsular spread (ECS) also should be noted and recorded. Nodes greater than 2 to 3 cm are bisected along their longest axis plane, and both halves are submitted for microscopic examination. Smaller nodes are submitted in toto. If a group of matted lymph nodes is present, two or three sections through the nodes often are adequate to document the extent of tumor (2,7). Jose et al. proposed a new method for pathologic examination of neck dissections in 2003 (2). Nodes from different levels and sublevels are sent to the laboratory in separately labeled containers and fixed in formalin. Each specimen is cut into 2-mm-thick blocks, embedded in paraffin, sectioned to 6-μm thickness, and stained with hematoxylin and eosin (H&E). Any macroscopically enlarged lymph nodes present are noted and embedded in their entirety. Care must be taken to count those lymph nodes that appear in multiple sections only once. With this method, the lymph node yield obtained is 50.4 nodes per neck dissection, and the average number of microscopic slides generated is 63 (level I–IV dissection). This technique allows pathologic examination of the entire neck specimen rather than only apparent lymph nodes (2).

The following method for pathologic examination of neck dissections is recommended when specimens are submitted to the pathology laboratory as a single surgical specimen rather than in separate containers. It pertains to standard radical neck dissection and needs to be modified for the other subtypes (4). After the surgeon orients the tissue specimen (Fig. 2) and removes the platysma muscle , the first step in a gross examination is to measure the dimensions of the sternocleidomastoid muscle and the internal jugular vein and to describe their involvement by tumor. Next, the pathologist should dissect and divide the submandibular gland, the sternocleidomastoid muscle, and the internal jugular vein and separate the fat-containing nodes into five levels: IA and IB (sublingual and submaxillary), IIA and IIB (upper jugular), III (middle jugular), IV (lower jugular), and VA and VB (posterior triangle). The presence of tumor in soft tissues, submandibular gland, and muscle should be described. The number of lymph nodes (by level) should be noted; if tumor tissue is present, the size of the metastases and the presence of ECS are likewise indicated. Tissue sections of all lymph nodes (separated by levels), the submandibular gland, the sternocleidomastoid muscle, and the internal jugular vein are then submitted for microscopic examination. If the neck dissection is the extended type, sections of all extra lymph node groups and nonlymphatic structures that were removed should also be submitted for microscopic examination (7).

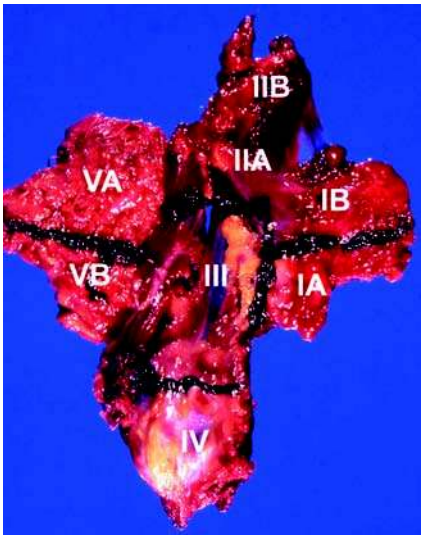

Figure 2 Neck dissection specimen oriented with marked lymph node levels.

A. Radiologic Examination of Neck Dissections

Tissue radiographs are advocated for studies in which very precise localization of lymph nodes is required, but accurate comparison between radiologic images and macroscopic and microscopic pathology is intrinsically difficult. However, the use of specimen radiographs allows the necessary comparisons to be made more accurately. The fixed, pinned-out specimen is immersed in 96% alcohol (which has the same absorption as fat) and placed on top of an X-ray film sealed in a plastic bag. Radiopaque structures, such as the sternocleidomastoid muscle or submandibular gland, should be removed beforehand(8). Radiographs display lymph nodes as small as 1 to 2 mm in diameter and provide both a dissection guide and a permanent record.

B. Gross Examination of Sentinel Lymph Node

The technique for gross examination of the sentinel lymph node (SLN) is based on the premise that metastases to the regional lymph nodes follow an orderly progression. This technique is now used commonly for patients with oropharyngeal SCC. Preoperative localization of the SLN with a radioactive tracer and gamma probe directs the surgeon to the lymphatic basin harboring the SLN. Simultaneous isosulfan blue dye injection may facilitate visualization of the SLN within a group of lymph nodes. A biopsy of

the lymph node or nodes is performed, and specimens are submitted for pathologic examination.

The SLN(s) should be measured, step-sectioned at 150-μm intervals, and submitted in toto. Four adjacent sections are taken from every step, two for H&E and immunohistochemical staining, and two for potential further studies. Negative findings on H&E-stained slides must be re-evaluated by staining the adjacent slide with cytokeratin (9). Positive findings on cytokeratin staining must be confirmed by histomorphologic correlation on the adjacent H&E stain. For SLN findings to be negative, both H&E and cytokeratin staining of all step sections must be negative. For SLN findings to be positive, histomorphologic proof of viable tumor cells on H&E is needed; positive findings on cytokeratin staining alone are not sufficient (9).

V. MICROSCOPIC EXAMINATION

It is important during the microscopic examination of a neck dissection specimen to distinguish lymphoid aggregates from true lymph nodes. Lymph nodes are defined as aggregates of encapsulated lymphoid tissue of any size with a peripheral sinus (Fig. 3).

Microscopic ECS is diagnosed when a tumor extends beyond the lymph node capsule and a desmoplastic stromal response is observed. A soft tissue deposit of carcinoma is identified as metastatic carcinoma in the soft tissues of the neck when no residual lymph node is present, although these soft tissue deposits may represent extralymphatic spread of carcinoma of a totally effaced lymph node (2,3) (Fig. 4).

Established nodal metastases may undergo degenerative changes with accumulation of keratin debris, necrosis, and cystic changes; all these features are more common after radiation therapy (2). Occult primary cancers of the tonsillar fossa and the base of the tongue may present with cystic nodal metastases in the upper jugular region resembling branchial cleft cysts (10) (Fig. 5). A tissue diagnosis of metastatic SCC and its variants in cervical lymph nodes is usually straightforward (Fig. 6). The degree of morphologic differentiation can vary markedly between the primary lesion and its metastasis, the latter tending to be less differentiated (2). A poorly differentiated nonkeratinizing tumor should be distinguished from melanoma, non-Hodgkin lymphomas, or undifferentiated small-cell carcinoma; in these cases, immunohistochemistry is of great help in determining the true nature of the neoplasm (11). Metastatic carcinoma in the neck occasionally coexists with other malignancies, usually thyroid carcinoma, low-grade lymphoma, or chronic lymphocytic leukemia, or with nonneoplastic conditions (12) (see ''Unexpected Lymph Node Pathology in Neck Dissections'' section).

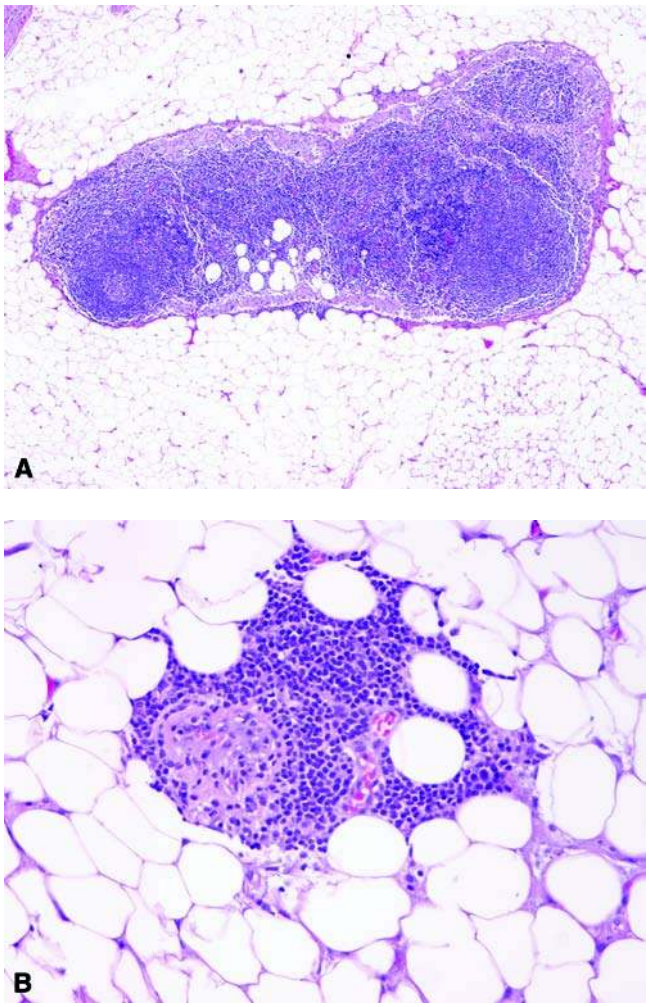

Figure 3 Histologic difference between lymph node and lymphoid aggregate. (**A**) Lymph node with capsule and peripheral sinus. (**B**) Lymphoid aggregate lacking capsule and peripheral sinus.

VI. HISTOLOGIC DETERMINANTS OF PROGNOSIS IN METASTATIC SCC

The aim of microscopic examination of neck dissection specimens from patients with metastatic SCC is to discover the histologic features that are important in predicting patient outcome or in determining whether the patient should be given adjuvant therapy. The seven important parameters consist of (*i*) presence of ECS, (*ii*) presence of soft tissue metastases, (*iii*) invasion of the jugular vein, (*iv*) number of positive lymph nodes, (*v*) presence of metastasis in different levels of lymph nodes, (*vi*) size of the metastasis, and (*vii*) desmoplastic reaction in metastatic tissues (2,4,13–20). However, the relative importance of some of these parameters in predicting recurrent neck disease or survival is still disputed by some authors (21–23).

A. Extracapsular Spread

Of the seven important parameters, ECS has been increasingly identified as the single most important independent indicator of recurrent neck disease and overall survival (13–18). In a study by Johnson et al.

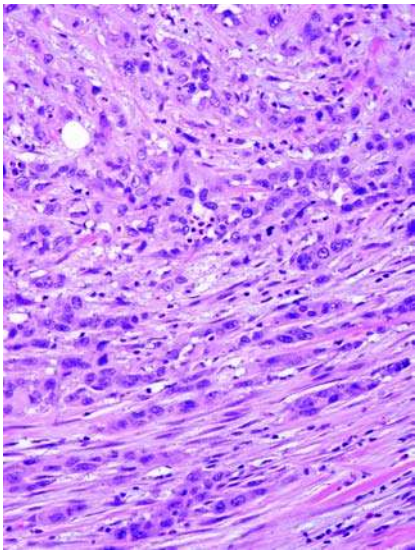

Figure 4 Soft tissue metastasis, which lacks lymph node structures.

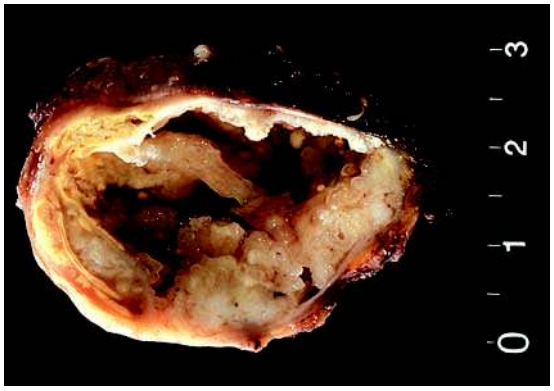

Figure 5 Cystic metastasis from crypt carcinoma of the palatine tonsil.

(18), histopathologic evidence of ECS was associated with a statistically significant reduction in the survival rate. Of patients whose metastases showed evidence of ECS, 39% survived five years, whereas 75% of those without evidence of ECS survived five years. Carter et al. (14) demonstrated a 10-fold difference in the risk of recurrent neck disease among patients with macroscopic or absent ECS; also, patients with ECS had a shorter time to tumor recurrence. Local disease recurred within six months in 42% of patients with ECS and in 18% of patients without ECS, and distant metastases occurred within 18 months in 14% of patients with ECS and in only 4% of patients without ECS. It is important to emphasize, however, that similar results were observed by Woolgar et al. (15) in patients whose tumors showed only microscopic

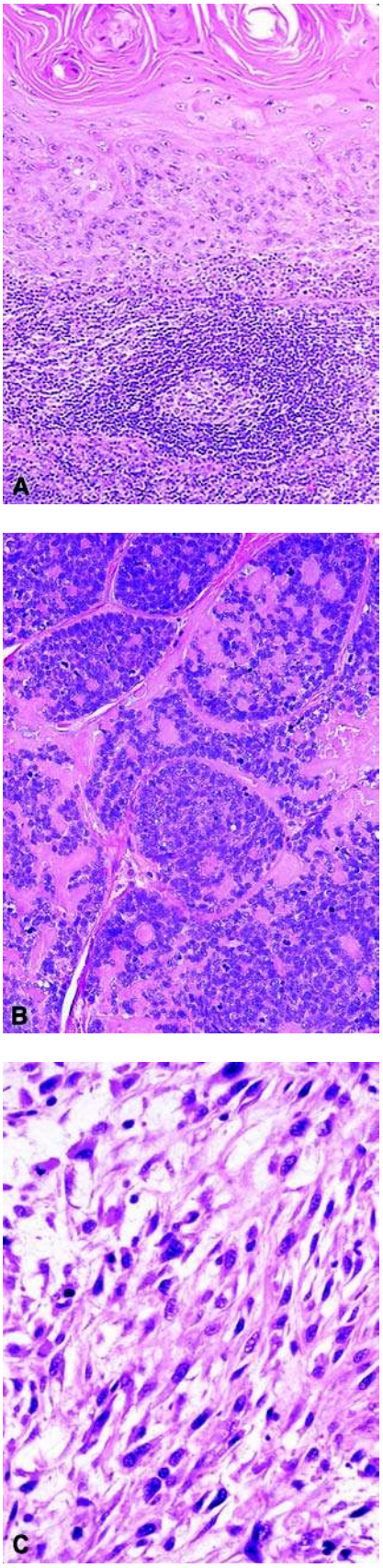

Figure 6 Histologic variants of metastatic squamous cell carcinoma. (**A**) Conventional. (**B**) Basaloid. (**C**) Sarcomatoid carcinoma.

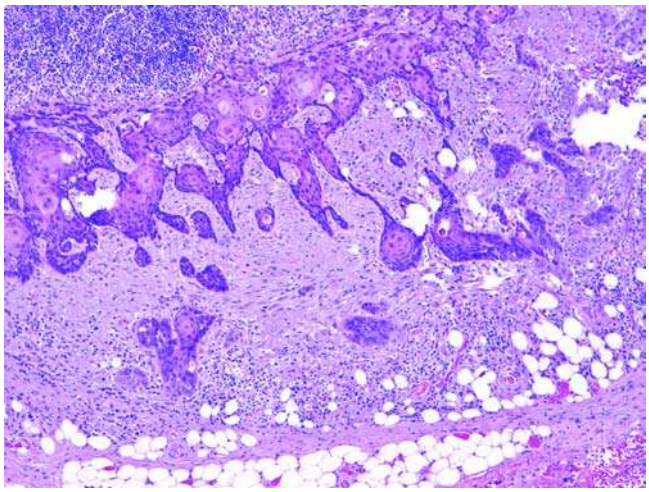

Figure 7 Extracapsular spread of metastatic squamous cell carcinoma, carcinoma infiltrating perinodal adipose tissue.

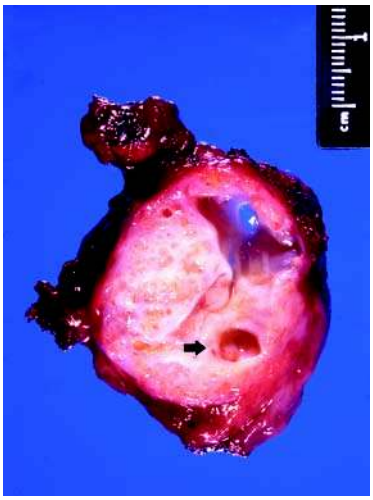

Figure 8 Surgical specimen showing gross metastasis in soft tissue with invasion of jugular vein (*arrow*).

evidence of ECS. Many subsequent investigators have extended and confirmed these observations, and the general features of ECS are broadly consistent in the various published accounts (2,16,17). The prognostic weight of ECS, however, is questioned in a few reports (22,23).

The reported incidence of ECS, in most series, lies between 15% and 30% of dissections. It occurs in irradiated as well as nonirradiated neck dissections. (Fig. 7) There is no consistent association between ECS and the size or degree of differentiation of primary tumor. About 75% of involved nodes larger than 3 cm will show ECS, but extranodal invasion can also be found in about of 20% of small (less than 1 cm) involved nodes (2,14).

B. Soft Tissue Metastases and Jugular Vein Invasion

Neck dissections occasionally contain one or more deposits of metastatic carcinoma in which no associated intact nodal structures can be found (Fig. 4). These deposits are commonly described separately and a recently adopted designation is ''soft tissue metastases'' (2). They are found in approximately 11% to 23% of neck dissections and sometimes are unaccompanied by other typical intranodal metastases (16). Soft tissue metastases can originate from local intralymphatic emboli (24) but most likely represent intranodal metastases of SCC in a totally effaced lymph node (2). Olsen et al. (16) demonstrated that metastases to soft tissues and/or invasion of the jugular vein were associated with a high rate of neck recurrences (84% and 75%, respectively) compared with rates for patients with neither of these two factors (50% and 27%, respectively) (Fig. 8). Similar findings have been observed by other authors (14,24).

C. Level, Number, and Size of Positive Lymph Nodes

The number of involved lymph nodes and the number of involved nodal groups have often been considered to be significant in terms of prognosis; however, the prognostic value of these two factors remains controversial, and the data are contradictory. The level of the involved lymph node (submandibular; upper, middle, and lower jugular; and posterior) is dictated mainly by the location of the primary carcinoma. Involvement of the lower jugular and posterior triangle nodes and noncontiguous or multiple disease sites has been associated with poor prognosis (4,21,25). Stell et al. (25) found strong correlation between node level and survival: a five-year survival of 34% for patients with level I (submandibular) lymph nodes and of only 4% for those with level IV (lower jugular) lymph nodes. In a univariate Cox proportional hazards model analysis for neck disease recurrence performed by Olsen et al. (16), the number of lymph nodes involved (four or more compared with one to three) was associated with an increased risk of local recurrence at two years (51% vs. 79%). However, several authors believe that these two parameters are related to ECS and that they do not represent independent prognostic factors (15,21,26). The size of a lymph node generally is not a useful prognostic factor but does correlate with the presence of histologically proven metastasis. Cachin et al. (26) found that 100% of lymph nodes larger than 5 cm contained metastatic deposits. On the other hand, in the Jose et al. (2) series, one-third of the lymph nodes with metastatic deposits were 3 mm in diameter.

D. Size of Metastases

Micrometastasis is histologically defined as a metastatic focus originating from a lymph node sinus that

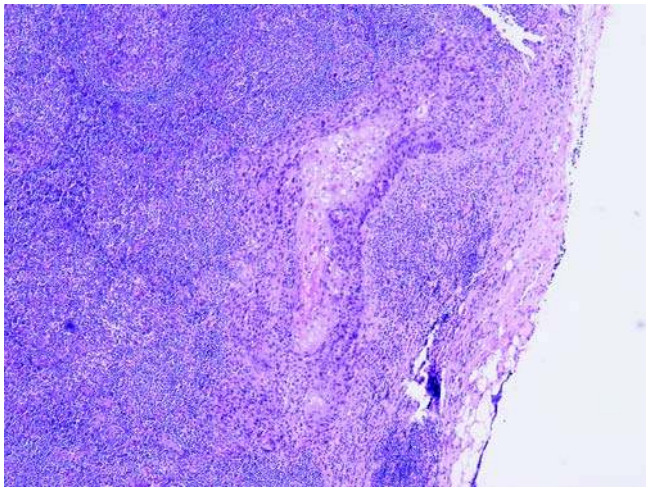

Figure 9 Micrometastasis of squamous cell carcinoma in cervical lymph node.

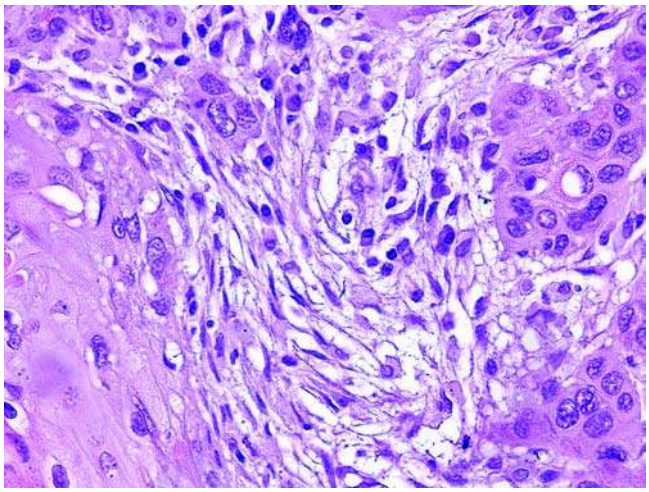

Figure 10 Cervical lymph node metastasis with desmoplastic reaction.

is less than 3 mm in diameter in all histologic section levels and that alters the lymph node architecture only minimally (27,28) (Fig. 9). Approximately 66% to 75% of all micrometastases are located in the area of the subcapsular sinus, where lymphatic fluid flows into the lymph node. Only 25% to 33% of all micrometastases are located in the area of the medullary sinus (27). In rare cases, micrometastases develop from capsular or juxtacapsular lymphatic vessels and then break through the capsule or the wall of the afferent lymphatic vessel (27). Generally, lymph nodes with micrometastases are of normal size, and most patients have only one lymph node affected by micrometastatic spread; however, sometimes two or three metastatic foci can be detected in one lymph node (28). The incidence of micrometastases alone in neck dissections is reportedly between 10% and 20% of all patients with node-positive disease (28), but the data in the literature vary significantly.

How the presence of micrometastases in lymph nodes influences patient prognosis has not yet been clarified for head and neck cancers. Hamakawa et al. (29) observed a correlation; however, their data were collected from a very small patient population. In contrast, Woolgar (28) observed no significant difference between patients with micrometastases and those with no metastases in the lymph nodes. Recently, Woolgar et al. (15) found a correlation between the size of the metastatic lymph node deposits and five-year survival. When the deposits measured less than 3 mm, the survival rate was 80%, compared with 55% when the metastatic deposits were grossly appreciated.

E. Stromal Reactions

In a study by Olsen et al. (16), a desmoplastic stromal pattern was defined as the presence of any fibroblastic proliferation associated with the metastatic tumor, which included the production of a dense collagen matrix (Fig. 10). In this study, a desmoplastic stromal pattern in a lymph node metastasis was associated with a nearly sevenfold increase in the risk of recurrent neck disease. Although desmoplasia seldom occurs in the absence of ECS, among patients with ECS, the presence or absence of desmoplasia significantly affects neck disease recurrence. A finding of desmoplasia as a predictor of neck disease recurrence should be evaluated further in a prospective study (16).

F. Other Histologic Prognostic Factors

There are other histologic factors that have shown varying prognostic merit. For example, intralymphatic emboli and tumor differentiation have been proposed as prognostic indicators (26,30). However, these two are not accepted as independent parameters by most authors (13–23). Clumps of tumor cells within dilated lymphatic vessels are frequently observed in neck dissections (Fig. 11). Strict diagnostic criteria, particularly demonstration of a clear endothelial lining, should be satisfied. Intralymphatic emboli and tumor differentiation usually coexist with intranodal or extranodal disease. Cachin et al. (26) have reported an incidence of approximately 25% and have shown that the presence of intralymphatic emboli is an additional, independent, adverse prognostic factor.

Patients with metastatic SCC in cervical lymph nodes are often treated with surgery and postoperative irradiation with different results, and several authors have noted that patients with metastatic undifferentiated carcinomas (UDCs) or poorly differentiated carcinomas respond better than do patients with metastasis of well- or moderately well-differentiated SCCs. In the Tong et al. (30) series of patients with metastatic SCC of unknown primary, better locoregional control was seen in patients with UDC than in patients with SCC. There was also a significant difference in the five-year disease-specific survival between

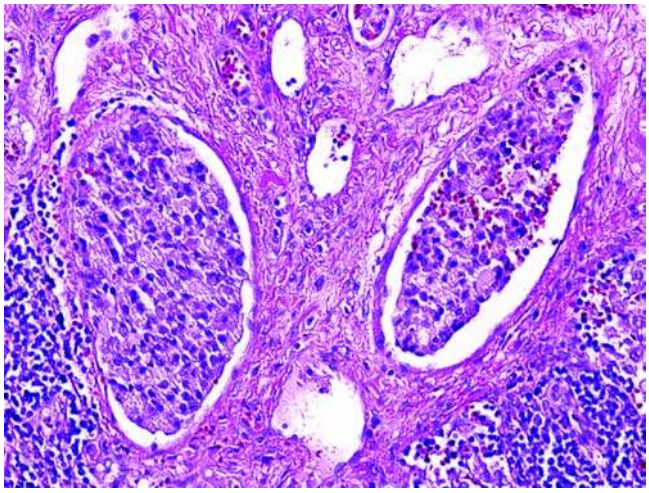

Figure 11 Cervical lymphatic channel with emboli of squamous cell carcinoma.

patients with UDC and SCC: 81% for patients with UDC versus 34% for those with SCC ($p = 0.01$). Similar observations have been made by other authors (31). However, in the Snow et al. (13) series, the opposite was true: poorly differentiated SCC carried a higher risk of recurrence in the neck than did well-differentiated carcinomas; the percentage of patient recurrence at two years after surgery was 34% versus 17% in the latter group.

VII. UNEXPECTED LYMPH NODE PATHOLOGY IN NECK DISSECTIONS

During the pathologic examination of neck dissection specimens, unexpected findings within lymph nodes may be occasionally uncovered (32–34). Such findings may include a second primary tumor, chronic infectious or inflammatory disease, or benign heterotopias, the discovery of which may have implications in terms of management and prognosis. The incidence of these unexpected findings in lymph nodes is between 2% and 5%, depending on the population studied (32–34). There are considerable differences between nodes from nonirradiated and irradiated patients (14). In general, incidentally discovered pathology tends to be indolent in nature, with the underlying SCC remaining the main determinant of patient's prognosis (32–34). However, pathologists and clinicians should always be prepared to recognize and treat an unexpected pathology during neck dissection.

A. Unexpected Second Primary Tumors

Metastatic papillary thyroid carcinoma is the most common incidental malignant tumor found during microscopic examination of neck dissection specimens. In patients with SCC of the head and neck, 0.7% have lymph nodes that harbor metastatic thyroid carcinomas that are clinically occult but histologically malignant (33,35). The true prevalence of metastatic thyroid carcinoma is undoubtedly much higher, since these studies were based on findings of metastatic carcinoma discovered primarily during radical or modified neck dissections, and these dissections usually do not remove lymph nodes from both sides of the neck or from the central neck compartment (level VI), the most common site of drainage for metastatic papillary thyroid carcinoma (4,36).

The incidental finding of a metastatic thyroid cancer does not, itself, point to an ominous primary thyroid carcinoma that demands prompt and aggressive management, particularly when the clinical picture is dominated by some other more harmful head and neck neoplasm, such as melanoma or SCC. Vassilopoulou-Sellin and Weber (37) included cases in their series that were managed with observation alone and remained without clinically apparent thyroid carcinoma for up to four years. In the Ansari-Lari and Westra (33) series of nine patients with incidental metastatic thyroid carcinoma, five patients died of their original tumor, two died of unrelated causes, one was lost to follow-up, and one was free of both malignancies. Clearly, these incidental metastatic implants rarely progress to the point of becoming clinically apparent (32,33,35,37). The second most common incidental malignancies are chronic lymphocytic leukemia and non-Hodgkin lymphomas (32–34). Incidentally discovered low-grade B lymphomas were found in 0.4% of neck dissections (33,34). Infiltration of lymph nodes by chronic lymphocytic leukemia sometimes is discovered during the pathologic examination of neck dissections. The presence of metastatic carcinoma and leukemia in the same lymph node is extremely rare and is rarely documented (34). This is probably because the prognosis in most patients with a low-grade lymphoreticular malignancy discovered during neck dissection for SCC is mainly determined by the SCC.

Incidental intranodal benign salivary gland tumors have rarely been reported in the literature; we are aware of only three cases of Warthin tumor found during the examination of neck dissection specimens (34,38,39). The origin of these tumors is not fully clear; however, most authors believe that they most likely arose from ectopic intranodal salivary gland inclusions (38,39).

B. Granulomatous Lesions

Granulomatous lymphadenitis in neck dissection specimens is not an uncommon incidental finding. Keratin and tuberculous granulomas are the most common, followed by sarcoid and nonspecific granulomas (14,32,34). The diagnosis of tuberculosis lymphadenitis is suggested on the basis of the histomorphology and is confirmed by demonstrating acid-fast bacilli with the help of specials stains.

Keratin granulomas consist histologically of keratin debris, often focally necrotic and calcified, surrounded by multinucleated foreign-body giant cells, histiocytes, lymphocytes, and plasma cells (Fig. 12). They occur in approximately 6% of irradiated neck

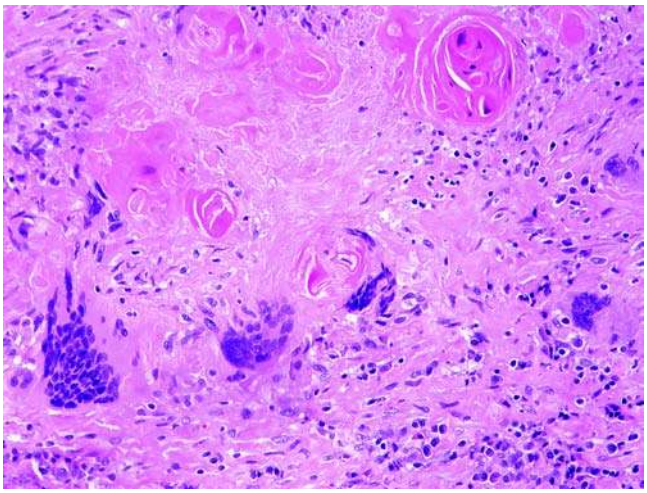

Figure 12 Keratin granuloma showing giant cells, keratin debris, and inflammatory cells.

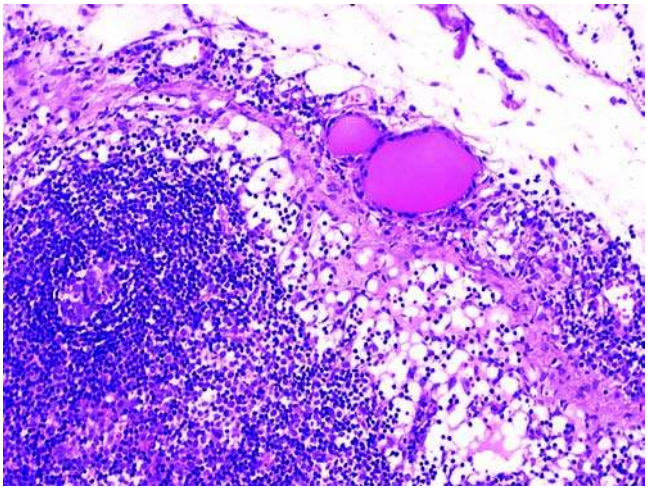

Figure 13 Microscopic picture of benign thyroid follicle inclusions. Note small size and lack of cytoarchitectural features of papillary thyroid carcinoma.

dissections but occasionally can be seen in nonirradiated necks (ratio, 10:1). Keratin granulomas measure up to 5 cm in diameter and may form solid or cystic masses that are sometimes fixed to adjacent structures. Keratin granulomas without intact tumor are almost exclusively confined to irradiated patients who have received a dose greater than 40 Gy, but the time interval before the masses are clinically detected varies from one month to more than a year (14). It is encouraging that no local recurrences have developed in the 11 patients reported by Carter et al. (14).

C. Lymph Node Heterotopias

Thyroid inclusions are the most common incidental heterotopias found in neck dissections. Ansari-Lari and Westra (33) found nine patients (0.8%) harboring ''benign'' thyroid inclusions in 1337 patients who underwent cervical lymph node dissections.

The nature and significance of so-called laterally aberrant tissue has generated considerable debate. Some believe that nodes, no matter how microscopically banal, invariably signify metastatic spread (40). Others believe that nonneoplastic thyroid tissue can be ectopically displaced into lateral neck lymph nodes, and in the absence of cellular atypia, this finding is of no clinical significance whatsoever (41).

Rosai et al. (42) suggested that several criteria may be useful in discriminating metastatic foci from these benign inclusions. Intranodal thyroid tissue may be regarded as possible benign inclusions when (*i*) it is limited to a few small follicles in a single lymph node, (*ii*) it is located in or immediately beneath the nodal capsule, and (*iii*) it does not demonstrate any cytoarchitectural features of papillary thyroid carcinoma (Fig. 13). Fliegelman et al. proposed a diagnostic algorithm that may aid in further work-up and treatment in these unusual cases. (43).

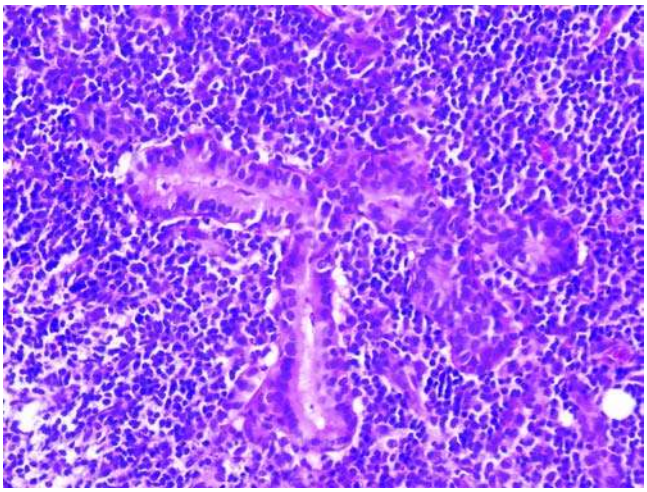

Figure 14 Salivary gland inclusions in cervical lymph node.

Salivary gland and bronchial inclusions are the other benign glandular inclusions found in the cervical lymph nodes during the pathologic examination of neck dissection specimens. Salivary gland inclusions are found more often in the upper cervical lymph nodes, especially around the parotid gland, and consist of normal acini and/or ductal structures (44) (Fig. 14).

Benign nevus cell aggregates have been found in the capsule and in the parenchyma of cervical lymph nodes, especially during neck dissections or during removal of SLNs in patients with melanoma of the head and neck (45,46). This rare finding is more common in the submandibular lymph nodes and should not lead to an erroneous diagnosis of metastatic melanoma (Fig. 15).

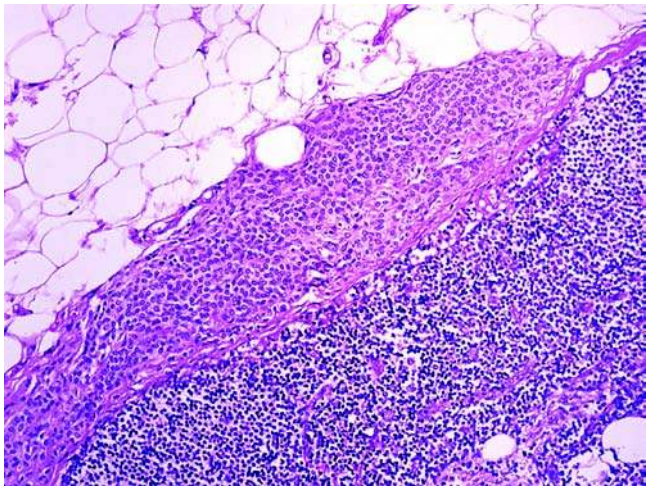

Figure 15 Benign nevus cells in capsule of submandibular lymph node.

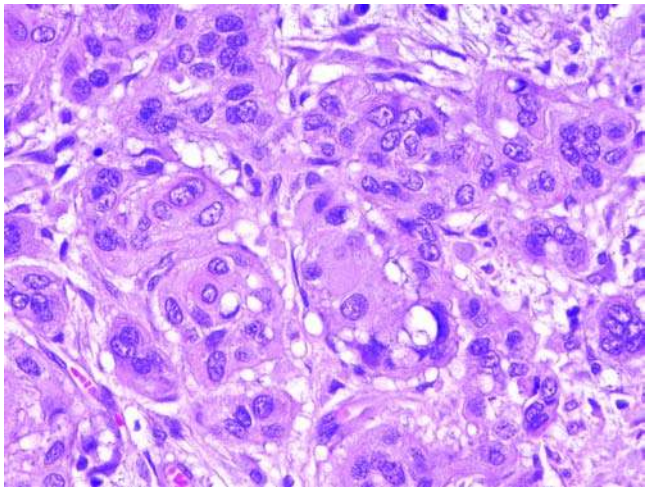

Fig. 17 Metastatic squamous cell carcinoma with radiation effect.

VIII. IRRADIATED NECK DISSECTIONS

Preoperative irradiation, or adjuvant chemotherapy, lead to morphologic alterations of metastatic tumor tissue, which may reflect the desirable effect of tumor regression. This, however, depends on the individual therapeutic response. Several of these effects are predictable. The neck dissection may be more difficult because of the presence of fibrosis, and the eventual yield of lymph nodes is usually less than that in nonirradiated specimens. The number of involved lymph nodes also tends to be smaller and to occur in fewer anatomic groups (Fig. 16). The occurrence of ECS in irradiated and nonirradiated dissections appears to be similar, and it maybe found in small or partly involved nodes (14).

Cytologically, a relative early alteration after irradiation is an increase of abnormal nuclear types, such as micronuclei, double or multiple nuclei, or nuclear buds (47)(Fig. 17). These are already evident in the initial stage of radiotherapy and depend on the radiation dose (48). After chemotherapy, similar alterations can be detected: increased apoptosis is induced, and multiple ultrastructural alterations of the cell nuclei and the cytoplasm become visible. In some cases after chemotherapy, an exaggerated differentiation with hyperkeratinization results (49).

Irradiated nodal metastases are frequently degenerated and necrotic with calcifications forming keratin granulomas (Fig. 12) (see ''Granulomatous Lesions'' section). After degeneration of larger tumor components and the formation of keratin granulomas, viable tumor cells can disappear altogether or coexist with small islands of residual intact tumor (14,48) (Fig. 18). If

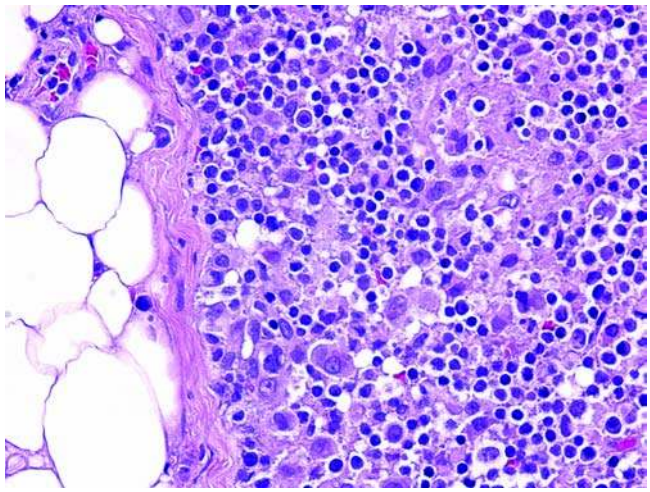

Figure 16 Lymphoid-depleted lymph node after radiotherapy.

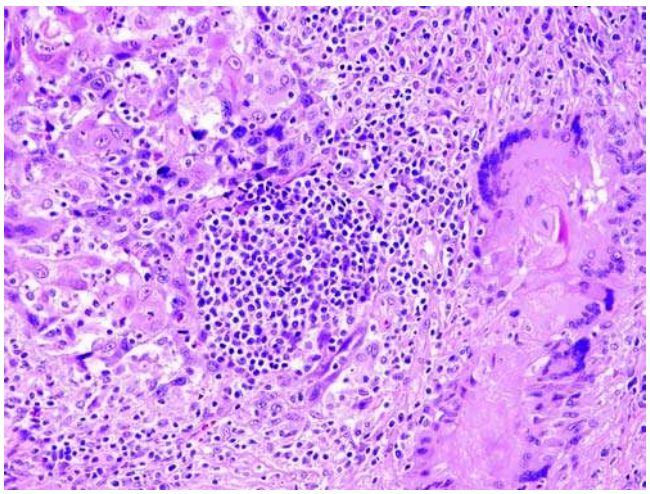

Figure 18 Keratin granuloma with residual metastatic squamous cell carcinoma.

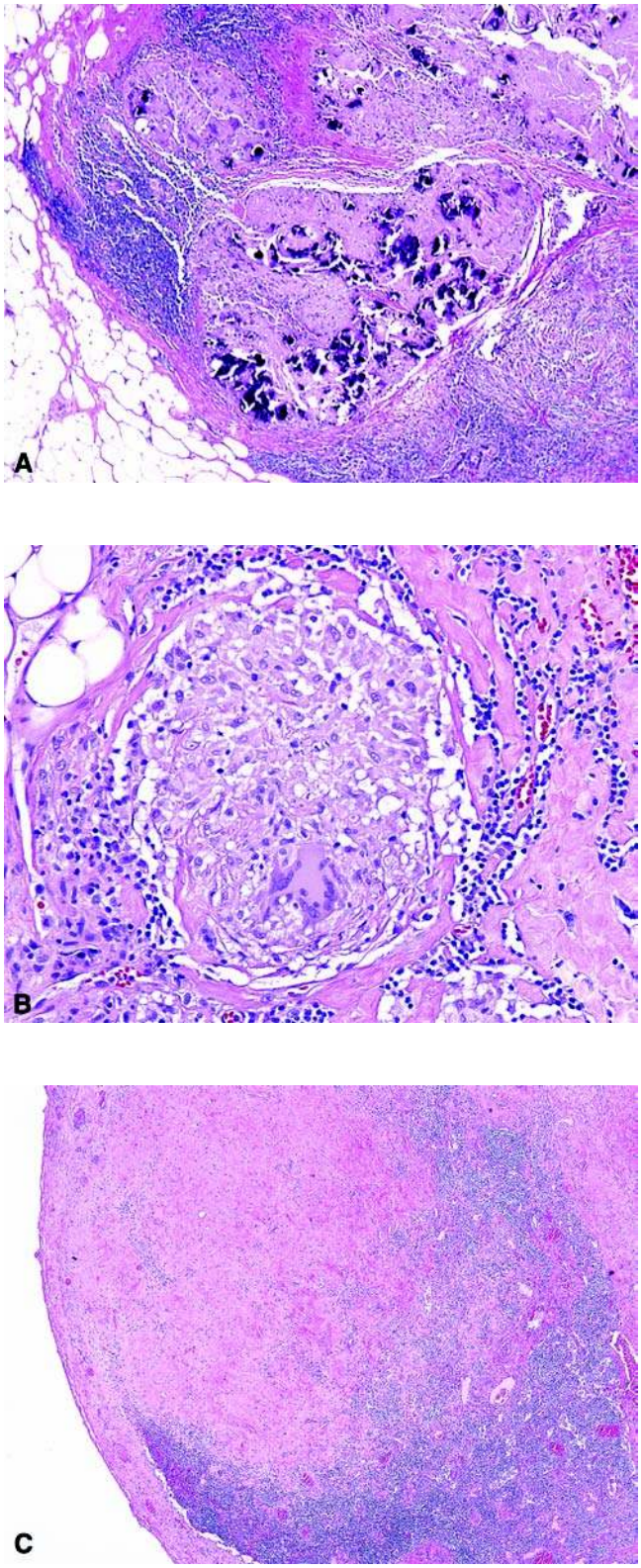

Figure 19 Microscopic evolution of keratin granulomas. (**A**) Granuloma with keratin debris. (**B**) Granuloma with giant cells and histiocytes lacking keratin debris. (**C**) Fibrotic acellular nodule.

the malignant cells disappear completely, the keratin granuloma is replaced by fibrotic acellular nodules (Fig. 19).

IX. NECK DISEASE AND DISTANT METASTASES

Failure to eradicate disease above the clavicles is regarded as the major cause of death in patients who have local or regional advanced SCC of the head and neck (2,50,51). However, with surgery followed by radiation therapy and/or chemotherapy in patients at high risk of local or regional recurrence, a changing pattern of failure is occurring. As fewer patients die of uncontrolled disease above the clavicles, more are exposed to the risk of disseminated carcinoma below the clavicles and to the appearance of second malignancy (50,51). It has been demonstrated that the rate of distant metastases correlates more with the appearance of cervical node metastases than with the T stage of the primary tumor (20). Also, it has been found that the incidence of distant metastases is higher in patients who had ECS, metastases to soft tissue of the neck, and multiple involved lymph nodes (13,16,50,51).

REFERENCES

1. Spiro RH, Alfonso AE, Farrr HW, et al. Cervical node metastasis from epidermoid carcinoma of the oral cavity and oropharynx. A critical assessment of staging. Am J Surg 1974; 128(4):562–567.
2. Jose J, Coatesworth AP, MacLennan K. Cervical metastases un upper aerodigestive tract squamous cell carcinoma: histopathologic analysis and reporting. Head Neck 2003; 25(3):194–197.
3. Carter RL. The pathologist's appraisal of neck dissections. Eur Arch Otorhinolaryngol 1993; 250(8):429–431.
4. Robbins KT, Clayman G, Levine PA, et al. Neck dissection classification update. Revisions, proposed by the American Head and Neck Society and the American Academy of Otolaryngology-Head and Neck Surgery. Arch Otolaryngol Head Neck Surg 2002; 128(6):751–758.
5. Robbins KT, Medina JE, Wolfe GT, et al. Standardizing neck dissection terminology. Arch Otolaryngol Head Neck Surg 1991; 117(7):601–605.
6. Byers RR, Clayman GL, McGill PAC, et al. Selective neck dissection for squamous carcinoma of the upper aerodigestive tract: patterns of regional failure. Head Neck 1999; 21(6):499–505.
7. Gillies EM, Luna MA. Histologic evaluation of neck dissection specimens. Otolaryngol Clin North Am 1998; 31(10): 759–771.
8. Groote AD, Oosterhuis JW, Molenaar WM, et al. Methods in laboratory investigation. Radiographic imaging of lymph nodes in lymph node dissection specimens. Lab Invest 1985; 52(3):326–329.
9. Stoeckli SJ, Pfaltz M, Ross GL, et al. The second international conference on sentinel node biopsy in mucosal head and neck cancer. Ann Surg Oncol 2005; 12(11):919–924.
10. Regauer S, Manhweller S, Anderhuber A, et al. Cystic lymph node metastases of squamous cell carcinoma of Waldeyer's ring. Br J Cancer 1999; 79(9–10):1437–1442.
11. Kauffman O, Fietze E, Dietel M. Immunohistochemical diagnosis in cancer metastasis of unknown primary tumor. Pathologe 2002; 23(3):183–197.

12. Woolgar JA, Scott J, Vaughan ED, et al. Pathological findings in clinically false-negative and false-positive Neck dissections for oral carcinoma. Ann R Coll Surg Engl 1994; 76(4):237–244.
13. Snow GB, Annyas AA, Van Slooten EA, et al. Prognostic factors of neck node metastasis. Clin Otolaryngol 1982; 7(3):185–192.
14. Carter RL, Bliss JM, Soo KC, et al. Radical neck dissections for squamous carcinomas: pathologic findings and their clinical implications with particular reference to transcapsular spread. Int J Radiat Oncol Biol Phys 1987; 13(6):825–832.
15. Woolgar JA, Rogers SN, Lowe D, et al. Cervical lymph node metastasis in oral cancer: the importance of even microscopic extracapsular spread. Oral Oncol 2003; 19(2):130–137.
16. Olsen KD, Caruso M, Foote RL, et al. Primary head and neck cancer. Histopathologic predictors of recurrence after neck dissection in patients with lymph node involvement. Arch Otolaryngol Head Neck Surg 1994; 120(12):1370–1374.
17. Myers JN, Greenberg JS, Mo V, et al. Extracapsular spread. A significant predictor of treatment failures in patients with squamous cell carcinoma of the tongue. Cancer 2001; 92(12):3030–3036.
18. Johnson JT, Myers EN, Bedetti CD, et al. Cervical lymph node metastasis; incidence and implications of extracapsular carcinoma. Arch Otolaryngol 1985; 111(8):534–537.
19. Clark J, Li W, Smith G, et al. Outcome of treatment for advanced cervical metastatic squamous cell carcinoma. Head Neck 2005; 27(2):87–94.
20. Merino OR, Lindberg RD, Fletcher GH. An analysis of distant metastases from squamous cell carcinoma of the upper aerodigestive tracts. Cancer 1977; 40(7):145–151.
21. Schuller DE, McGuirt WF, McCabe BF, et al. The prognostic significance of metastatic cervical lymph nodes. Laryngoscope 1980; 90(4):557–570.
22. Mamelle G, Pampurik J, Luboinski B, et al. Lymph node prognostic factors in head and neck squamous cell carcinoma. Am J Surg 1994; 168(11):494–498.
23. Violaris NS, O'Neil D, Helliwell TR, et al. Soft tissue cervical metastases of squamous carcinoma of the head and neck. Clin Otolaryngol 1994; 19(5):394–399.
24. Toker C. Some observations on the deposition of metastatic carcinoma within cervical lymph nodes. Cancer 1963; 16(3): 364–374.
25. Stell PM, Morton RP, Singh SD. Cervical lymph node metastases. The significance of the level of the lymph node. Clin Oncol 1983; 9(2):101–107.
26. Cachin Y, Sancho-Garnier H, Micheau C, et al. Nodal metastasis from carcinoma of the oropharynx. Otolaryngol Clin North Am 1979; 12(1):145–154.
27. Van de Brekel MWM, van der Waal I, Meijer CJML. The incidence of micrometastasis in Neck dissection specimens obtained from elective neck dissections. Laryngoscope 1996; 106(2):987–991.
28. Woolgar JA. Micrometastasis in oral/oropharyngeal squamous cell carcinoma: incidence, histopathologic features and clinical implications. Br J Oral Maxillofac Surg 1999; 37(3):181–186.
29. Hamakawa H, Takemura K, Sumida T, et al. Histological study of pN upgrading of oral cancer. Virchows Arch 2000; 437(2):116–121.
30. Tong CC, Luk MY, Chow SM, et al. Cervical nodal metastases from occult primary: undifferentiated carcinoma versus squamous cell carcinoma. Head Neck 2002; 24(4):361–369.
31. Jesse RH, Perez CA, Fletcher GH. Cervical lymph node metastases: Unknown primary cancer. Cancer 1973; 31(4): 854–859.
32. Ratcliffe RJ, Soutar DS. Unexpected lymph node pathology in neck dissection for head and neck cancer. Head Neck 1990; 12(5–6):244–246.
33. Ansari-Lari MA, Westra WH. The prevalence and significance of clinically unsuspected neoplasms in cervical lymph nodes. Head Neck 2003; 25(10):841–847.
34. Sheahan P, Hafidh M, Toner M, et al. Unexpected findings in neck dissection for squamous cell carcinoma: incidence and implications. Head Neck 2005; 27(1):28–35.
35. Clark RL, Hickey RC, Butler JJ, et al. Thyroid cancer discovered incidentally during treatment of an unrelated head and neck cancer: review of 16 cases. Ann Surg 1966; 613(6):665–671.
36. Arch-Ferrer J, Velazquez D, Fajardo R, et al. Accuracy of sentinel lymph node in papillary thyroid carcinoma. Surgery 2001; 130(6):907–913.
37. Vassilopoulou-Sellin R, Weber RS. Metastatic thyroid cancer as an incidental finding during neck dissection: significance and management. Head Neck 1992; 14(6):459–463.
38. Demir Y, Aktepe F, Yilmaz MD, et al. Warthin's tumor of a cervical lymph node: an unusual finding. Ann Plast Surg 2002; 48(1):110–111.
39. Cannon CR, Fechner RE. Pathologic quiz case 2: Warthin's tumor arising in a lymph node containing heterotopic salivary gland. Arch Otolaryngol 1985; 111(10):702–703.
40. De Jong SA, Demeter JG, Jarosz H, et al. Primary papillary thyroid carcinoma presenting as cervical lymphadenopathy: the operative approach to the ''lateral aberrant thyroid''. Am Surg 1993; 59(3):172–176.
41. Meyer JS, Steinberg LS. Microscopically benign thyroid follicles in cervical lymph nodes. Serial sections study of lymph node inclusions and entire thyroid gland in 5 cases. Caner 1969; 24(2):302–311.
42. Rosai J, Carcagiu M, DeLellis R. Thyroid tissue in abnormal locations. In: Rosai J, Carcagiu M, DeLellis R. eds. Tumors of the Thyroid Gland. Washington DC: Armed Forces Institute of Pathology, 1990:317–326.
43. Fliegelman L, Genden EM, Brandwein M, et al. Significance and management of thyroid lesions in lymph nodes as an incidental finding during neck dissection. Head Neck 2001; 23(10):885–891.
44. Shinora M, Harada T, Nakamura S, et al. Heterotopic salivary gland tissue in lymph nodes of the cervical region. Int J Oral MaxillofacSurg 1992; 21(3):166–171.
45. Jensen JL, Correll RW. Nevus cell aggregates in submandibular lymph nodes. Oral Surg Oral Med Oral Pathol 1980; 50(6):552–556.
46. Biddle DA, Evans HE, Kemp BL, et al. Intraparenchymal nevus cells aggregates in lymph nodes: a possible diagnostic pitfall with malignant melanoma and carcinoma. Am J Surg Pathol 2003; 27(5):673–681.
47. Rhattathiri NV, Bindu L, Remani P, et al. Radiation induced acute immediate nuclear abnormalities in oral cancer cells: serial cytological evaluation. Acta Cytol 1998; 42(5):1084–1090.
48. Tanner NS, Carr RL, Dalley VM, et al. The irradiated radical Neck dissection in squamous carcinoma; a clinicopathological study. Clin Otolaryngol 1980; 5(4):259–271.
49. Hamakawa H, Bao Y, Takarada M, et al. Histological effect and predictive biomarkers of TTP induction chemotherapy for oral carcinoma. J Oral Pathol Med 1998; 27(2):87–94.
50. Vikran B. Changing patterns of failure in advanced head and neck cancer. Arch Otolaryngol 1984; 110(9):564–565.
51. Known D, Sham J, Choy D. The effect of locoregional control on distant metastatic dissemination in carcinoma of the nasopharynx: An analysis of 1303 patients. Int J Radiat Oncol Biol Phys 1994; 30(5):1029–1030.
52. Ferlito A, Shaha AR, Silver CE, et al. Incidence and sites of distant metastases from head and neck cancer. ORL 2001; 63(4):202–207.

The Occult Primary and Metastases to and from the Head and Neck

Mario A. Luna
Department of Pathology, The University of Texas, M.D. Anderson Cancer Center, Houston, Texas, U.S.A.

I. THE OCCULT PRIMARY AND METASTASES TO CERVICAL NODES

An enlarged cervical lymph node is often the first clinical manifestation of a neoplastic process in the head and neck. Cervical lymph node metastasis is the presenting symptom in 25% of patients with cancer of the oral cavity and oropharynx, 47% of patients with cancer of the nasopharynx, and 23% of patients with thyroid cancer (1,2). In some instances, however, despite a thorough search, a primary tumor cannot be found, and these cases are called carcinoma of unknown primary (CUP). It is difficult to precisely evaluate the frequency of these cervical CUPs relative to the total number of tumors of the upper respiratory and digestive tract. In several large series (Table 1), this frequency varied between 2.6% and 6%, with an average of about 3.7% (3–7).

In the Danish national study, published in 2000 (8), the annual incidence of cervical metastases of squamous cell carcinoma (SCC) from CUP was 0.34/100,000/year and remained stable over the next 20 years (1975 to 1995). In the same period, the number of new head and neck cancers increased, suggesting that the proportion of CUP cases had diminished.

A. Lymphatic Regions of the Neck

According to the anatomical studies of Rouvière (9), the clinical observations of Lindberg (1), and the radiological studies of Som (10) and Som et al. (11), the cervical lymphatic system is organized into three functional units: the Waldeyer's ring, the transitional lymph nodes located between the head and neck, and the cervical lymph nodes in their proper sense.

The Waldeyer's ring consists of the palatine tonsils, lingual tonsil, adenoids, and adjacent submucosal lymphatics. The transitional nodes are arranged in a circular manner at the transition of the head and neck regions and include submental lymph nodes, submandibular lymph nodes, parotid lymph nodes, retroauricular lymph nodes, occipital lymph nodes, retropharyngeal nodes, and sublingual lymph nodes (9).

The cervical lymph nodes can be divided into superficial and deep nodes, and each of these groups is further subdivided into lateral and medial nodes. The deep lateral cervical lymph nodes are arranged in three chains: the internal jugular vein chain, the spinal accessory nerve chain, and the supraclavicular lymph node chain. The internal jugular nodes and the spinal accessory lymph nodes are divided into upper, middle, and lower nodes. The deep medial cervical group consists of the prelaryngeal, prethyroideal, pretracheal, and paratracheal lymph nodes.

The superficial cervical lymph nodes are divided into a lateral group and a medial group. The superficial medial lymph nodes of the neck are distributed around the anterior jugular vein (9). The superficial lateral cervical nodes are located along the external jugular vein. Fig. 1 shows the nodal regions of the neck (12).

B. Clinical Data

According to the data from our institution, these tumors are most frequently diagnosed between the fifth and seventh decade, with an average patient age of 60 years. The patients are predominantly male (4:1), are frequently heavy consumers of alcohol and tobacco, and have tolerated the metastasis for several months before seeking medical attention (13,14). Most adenopathies harboring metastases from an apparently occult primary are single, unilateral, and fixed. Various lymph node groups can be affected, but the most frequently involved are the upper jugular lymph nodes, followed by the midjugular and the supraclavicular nodes (1,13,14). It is possible to have more than one lymph node region involved in a patient. In our experience, 10% of the patients had multiple neck nodes and 9.5% of the patients had bilateral lymph nodes (13).

C. Site of Adenopathy

The lymphatic drainage of the anatomical regions of the head and neck is highly predictable, and the location of the cervical adenopathy may provide a clue to the location of the primary lesion (Fig. 2) (1,12,15). Lindberg (1) reviewed the records of 2044

Table 1 Frequency of CUP

Author (Ref.)	No. of H&N patients	Apparent CUPs (%)
Fried et al. (5)	1900	49 (2.6)
Haas (6)	1818	57 (3.0)
McMahon et al. (3)	571	38 (6.0)
Martin and Morfit (2)	3896	218 (3.0)
Richard and Micheau (7)	5137	57 (3.3)
Vaamonde et al. (4)	648	22 (3.4)

Abbreviations: CUP, cancer of unknown primary; H&N, head and neck.

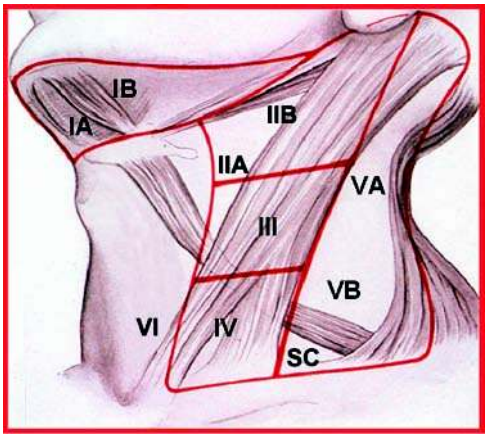

Figure 1 Nodal levels and sublevels. IA, submental; IB, submandibular; IIA, jugulogastric; IB, supraspinal accessory; III, midjugular; IV, lower jugular; V, posterior triangle nodes; VA, spinal accessory nerves nodes; VB, transverse cervical nodes; VI, anterior group; SC supraclavicular.

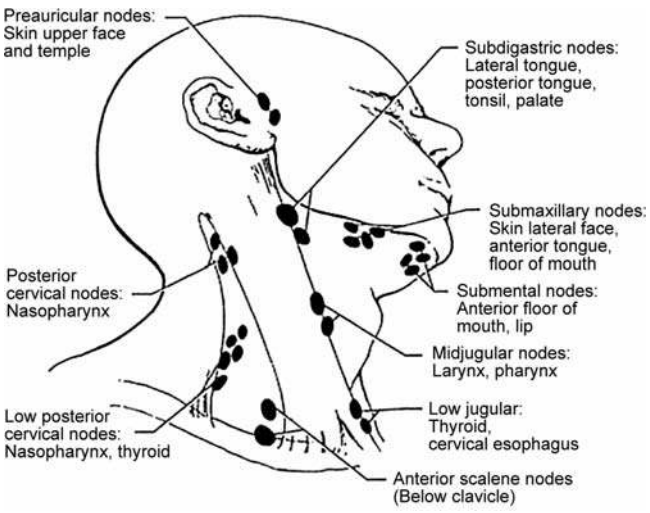

Figure 2 The anatomical location of a cervical lymph node with metastasis can be a clue to the site of the primary cancer.

patients with previously untreated SCC of the head and neck and described the incidence and topographical distribution of lymph node metastases on admission. Metastases in the submental or submandibular nodes usually indicate primary cancer in the skin of the lip, the corner of the mouth, or the lateral aspect of the nose or cheek. A mucosal lesion producing such a node should be metastatic from the anterior floor of the mouth, lower gingiva, or lateral gingival buccal sulcus. The subdigastric (sentinel tonsillar) node, which lies close to the posterior belly of the digastric muscle beneath the angle of the jaw, is the usual metastatic site for a cancer of the middle and posterior third of the tongue, middle and posterior third of the floor of mouth, the faucial arch, or the tonsillar areas. Metastases in nodes lying in the midjugular chain usually are associated with primary cancers in the posterior and lateral pharyngeal wall, pyriform sinus, and supraglottic larynx; thyroid cancer also should be considered. Low jugular nodal metastases usually are associated with thyroid cancer or cancer below the clavicle. Involved nodes lying in the upper posterior triangle are pathognomonic of nasopharyngeal carcinoma until proven otherwise. Metastases in low posterior nodes usually indicate cancer of the nasopharynx or thyroid. Affected nodes in the anterior scalene area just above the clavicle are virtually certain to be metastases from cancer below the clavicle, the most common sites of the primary tumor being the lung, breast, stomach, prostate, and pancreas (16,17). However, this distribution is by no means rigid. Coker et al. (18) found that three patients with lung primaries had metastasis to the upper jugular and submandibular lymph nodes without palpable supraclavicular nodes.

With this in mind, it is important that the surgeon specify accurately the exact location of the lymph node biopsy site. This neglect is especially frustrating in the histopathological evaluation of lymph nodes from the neck, when a surgical pathology request form contains only the information ''neck node.'' If given the precise location of a metastatic tumor within the cervical lymph nodes, as well as adequate clinical information, the pathologist can be very helpful in suggesting possible primary sites for the neoplasm (19).

D. Search for the Primary Lesion

If the search is conducted systematically, the primary cancer can be discovered in 85% to 90% of patients presenting with cervical adenopathy (19). Evaluation protocols have been well outlined by Martin and Morfit (2), Hass (6), Coker et al. (18), and Lowry et al. (20).

The first diagnostic step is obtaining a careful history and making a detailed examination of the skin and mucosa of the head and neck. Information about possible skin cancers that may have been removed in the past should be investigated. A complete otorhinolaryngolical examination should be performed.

If the primary lesion is found, a simple biopsy of that lesion, using any type of biting forceps, is sufficient. However, one should not take a biopsy from a

suspicious lymph node in the neck. In this situation, the surgeon should assume that the node is positive and treat accordingly.

If the foregoing steps do not identify a primary tumor, the first diagnostic procedure after regional physical examination should be a fine-needle aspiration (FNA) biopsy of the suspicious neck mass for cytological investigation (14). A FNA biopsy employed soon after the complete head and neck examination at the time of initial patient visit often can provide a specific diagnosis and guide further investigation. This procedure will also save time and money for the patient (21). In their large series of FNA biopsy specimens from cervical lymph nodes, Eisele et al. (21) and Schwarz et al. (22) have reported excellent results, with false-positive and false-negative rates of less than 1% and 3%, respectively (Fig. 3). A similar experience has been reported by el Hag et al. (23).

If SCC or melanoma is found, there is little need for additional radiographic workup of the gastrointestinal or genitourinary tract. However, if adenocarcinoma is found and thyroid and salivary gland tumors are ruled out, the workup should include investigation of the breast, lungs, and gastrointestinal and genitourinary tracts.

If FNA findings are not diagnostic or are positive for SCC, the patient should receive an examination, under general anesthesia, to include nasopharyngeal examination, direct laryngoscopy, and blind biopsies of the base of the tongue, nasopharynx, tonsillar areas, and pyriform sinus. These areas of the head and neck are the most likely sites of hidden primary cancer, especially if the FNA biopsy has revealed SCC in the lymph node (19).

Only if all these examinations are completed and yield negative results in patients for whom the FNA was not diagnostic, should the surgeon consider histological diagnosis of the adenopathy based on an excision specimen from an intact lymph node. For patients with squamous carcinoma in the lymph node aspirate in whom no primary tumor was found after all these measures, the surgeon can proceed with definitive treatment of the neck.

Ancillary studies include chest X ray and paranasal X-ray films, barium swallows, radioisotopic scans of the thyroid gland, sonography, and computed tomographic (CT) or magnetic resonance imaging (MRI) scan (24). A CT or MRI scan from the nasopharynx to the root of the neck is the single most revealing noninvasive study in the armamentarium (6,17,19). In

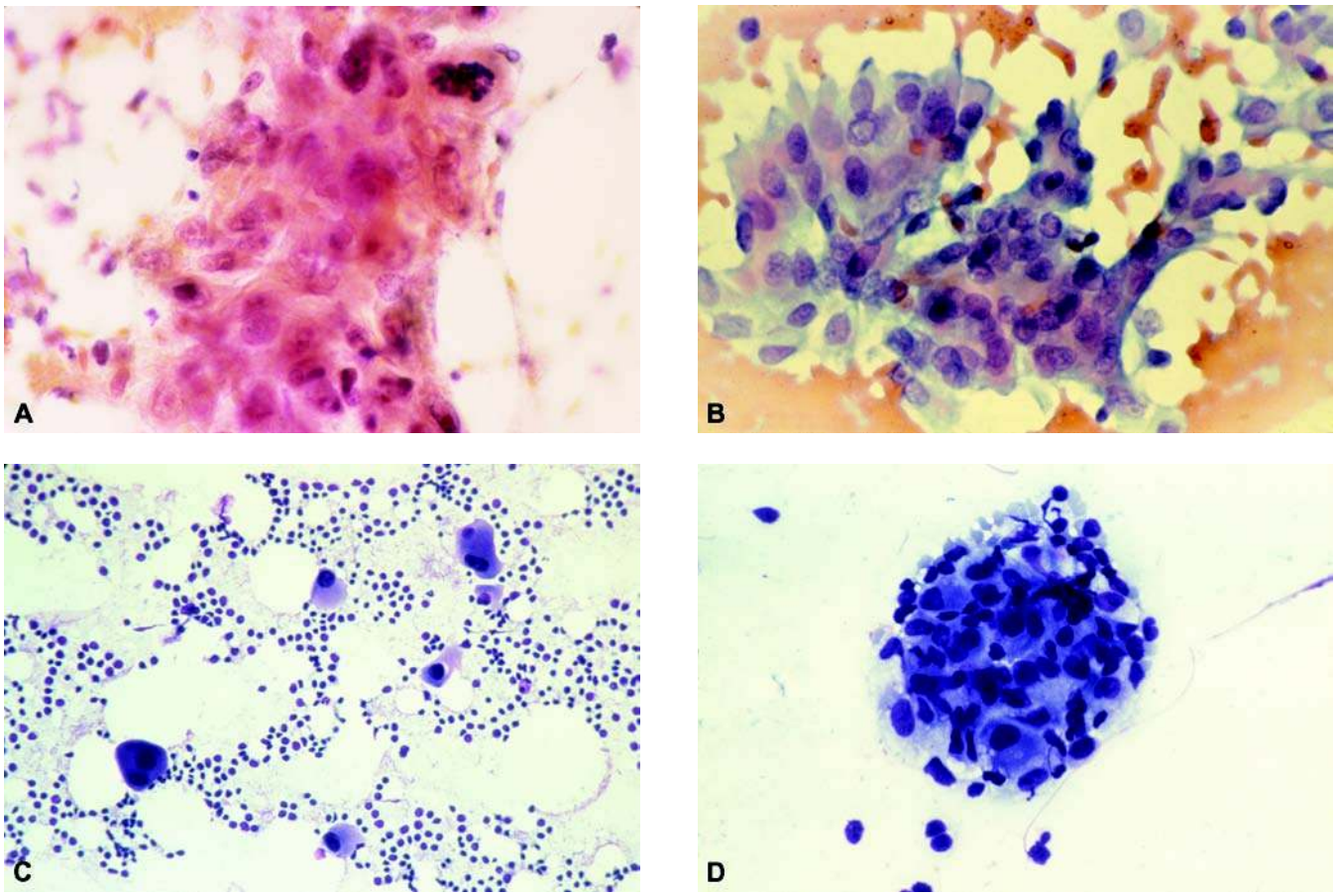

Figure 3 FNA of cervical lymph nodes showing metastasis from (**A**) squamous carcinoma (400×), (**B**) papillary thyroid carcinoma (400×) (**C**) melanoma (300×), (**D**) undifferentiated carcinoma (600×). (Papanicolaou stain).

the case of negative examination with CT and MRI, primary tumor detection with the use of functional imaging modalities, such as positron emission tomography (PET), seems to be a very attractive option. With negative routine clinical examination, CT scan, and MRI, PET allows detection of primary tumors in 5% to 30% of patients (25,26). Higher rates of primary tumor detection are observed in non–head and neck CUP or histological type other than SCC (17). In the series including exclusively SCC head and neck CUP, the detection rate did not exceed 23% (17,25,26).

A serum calcitonin analysis should be performed when there is a thyroid mass (27). After a positive diagnosis of SCC in a cervical lymph node, a test for antibodies to Epstein–Barr virus is helpful. This test includes analysis of antibodies to viral capsid antigen (VCA) and to early antigen, as well as serum immunoglobulin A (IgA) (28,29). When present in high titer, antibodies to VCA of IgA origin appear to have a high degree of specificity in diagnosing nasopharyngeal carcinoma (14,17).

In addition to panendoscopy and imaging for staging, systemic ipsilateral tonsillectomy in the absence of a suspicious lesion is a standard procedure in search of the primary tumor in cervical CUP (30–32), because up to 25% of primary tumors are detected in this site (17,19). The highest rate is observed in the case of involvement of the subdiagastric lymph node group (level IIA), followed by submandibular (level IB) and midjugular nodes (level III) (30). On the other hand, a 10% rate of contralateral spread from occult tonsil lesions seems to justify bilateral tonsillectomy (31,32). In the series of Neider et al. (33), ipsilateral tonsillectomy discovered carcinoma in about 25% of patients, whereas PET detected primary tumors in less than 25% of patients with negative results for routine clinical examination and CT scan and/or MRI (17,33).

E. Lymph Node Biopsy

The histology of the adenopathy can be obtained by FNA biopsy, FNA core biopsy with tissue, and excisional lymph node biopsy. Concerning excisional biopsy, it has long been a dictum that no surgeon should excise a cervical node suspected of being cancerous unless prepared at that time to obtain a frozen section diagnosis and complete the neck cleanout with a radical neck dissection (2,7,13). Such biopsies produce scarring that can complicate future node dissections and may lead to local and possibly distant spread of the tumor (34). McGuirt and McCabe (34) noted a significant increase in wound necrosis, local cervical recurrence, and distant metastases in those patients with premature biopsy compared with those who had biopsy at the time of definitive treatment.

On the other hand, when examining historical controls in patients who had a pretreatment open biopsy, Razack et al. (35) found no difference in neck cancer recurrence or survival between that group and patients undergoing biopsy at the time of definitive treatment. However, distant metastasis was not examined separately. Wang et al. (14) and Robbins et al. (36) did not believe that pretreatment biopsy adversely affects prognosis, provided proper oncological surgical principles and precautions are followed.

The FNA biopsy is a rapid, effective, and safe technique for evaluating a neck mass (21–23). It usually provides a meaningful biopsy specimen without interfering with the ultimate treatment. The needle technique disturbs tissue far less than excision does.

F. Histological Diagnosis

Metastatic squamous carcinoma is by far the most common metastatic tumor to the cervical lymph nodes; 45% to 70% of all metastases of an unknown primary are of this histological type (Table 2). Adenocarcinoma, thyroid carcinoma, melanoma, salivary gland carcinoma, and small-cell carcinoma are the other neoplasms seen in the cervical nodes (2,6,13,16–19). Adenocarcinoma, small-cell carcinoma, and thyroid carcinoma are more common in the supraclavicular and scalene lymph nodes (Fig. 4) (19). Most adenocarcinomas in the upper and middle

Table 2 Histology of Metastases from CUPs

	Location		
Histology	Cervical	Supraclavicular	Total
Squamous carcinoma	153	30	183
Undifferentiated carcinoma	44	25	69
Adenocarcinoma	6	54	60
Thyroid carcinoma	6	5	11
Melanoma	7	0	7
Sarcoma	2	2	4
Salivary gland carcinoma	2	0	2

Source: From Refs. 2, 6, 13, 16–19, 69,72, 73.

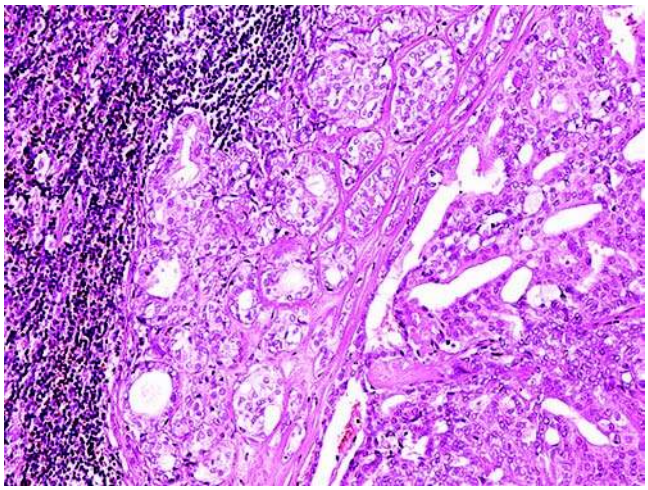

Figure 4 Metastatic adenocarcinoma of unknown origin (H&E 80×).

cervical regions will be metastatic from lesions of the paranasal sinuses, particularly of the ethmoid area.

The morphology of the neoplastic process in the lymph node seldom allows elucidation of the origin of the primary tumor. Only in thyroid (Fig. 5) and prostate carcinoma is the origin of an adenocarcinoma apparent from the histology of the nodal metastases (Fig. 6). The origin of squamous carcinoma is apparent in only two circumstances: in undifferentiated carcinoma of the nasopharyngeal type (Fig. 7), where a nasopharyngeal carcinoma is suggested, and in cystic metastases, which suggest a primary in the palatine tonsil or in Waldeyer's ring (37–39). This type of metastatic cystic squamous carcinoma is often mistaken for a branchial cyst by an unaware pathologist (Figs. 8, 9).

Benign glandular inclusions in cervical lymph nodes should not be mistaken for metastatic adenocarcinoma; heterotopic islands of salivary gland tissue, and benign lymphoepithelial cysts are common in the paraparotid lymph nodes and less frequent in the upper cervical nodes (40). Acinic cell carcinoma, monomorphic adenomas, and mixed tumor arising in ectopic salivary gland tissue have been described in the lymph nodes of the upper and lower neck (Fig. 10) (41). Aggregates of benign nevus cells have been found in the capsule of cervical nodes; although

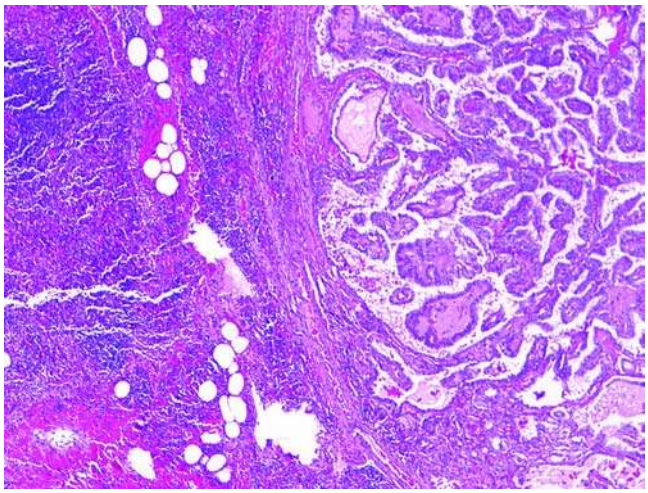

Figure 5 Lymph node showing metastatic papillary carcinoma of the thyroid (H&E 50×).

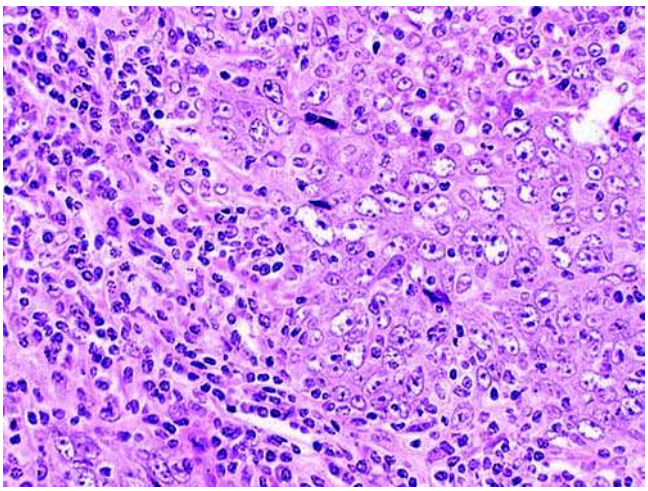

Figure 7 Metastatic undifferentiated nasopharyngeal type of carcinoma (H&E 100×).

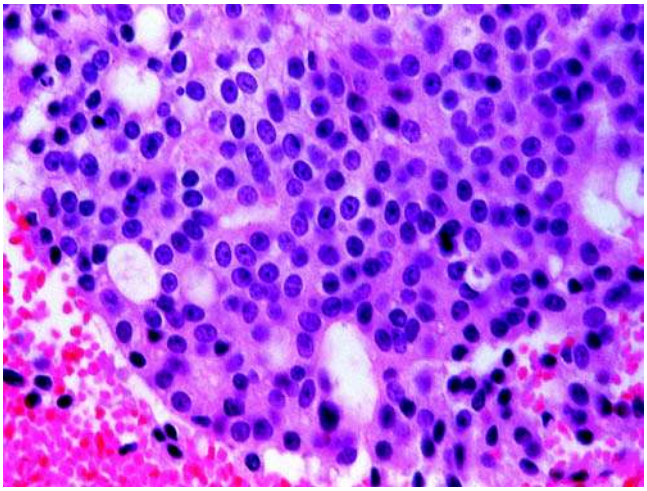

Figure 6 Adenocarcinoma of the prostate in left supraclavicular lymph node (H&E 100×).

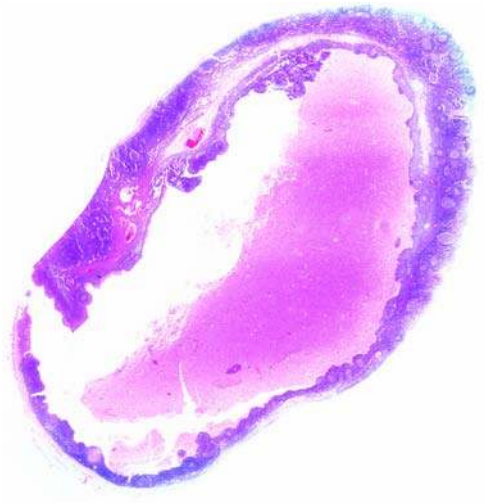

Figure 8 Whole organ section of metastatic cystic squamous carcinoma. (H&E 5×).

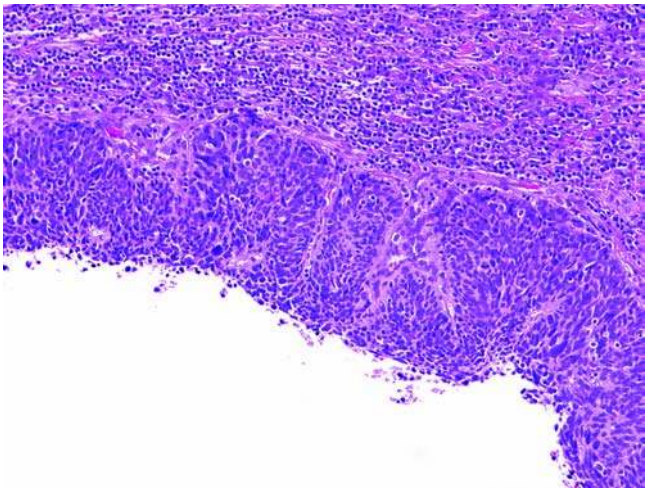

Figure 9 Histology of metastatic cystic squamous carcinoma from palatine tonsil (H&E 50×).

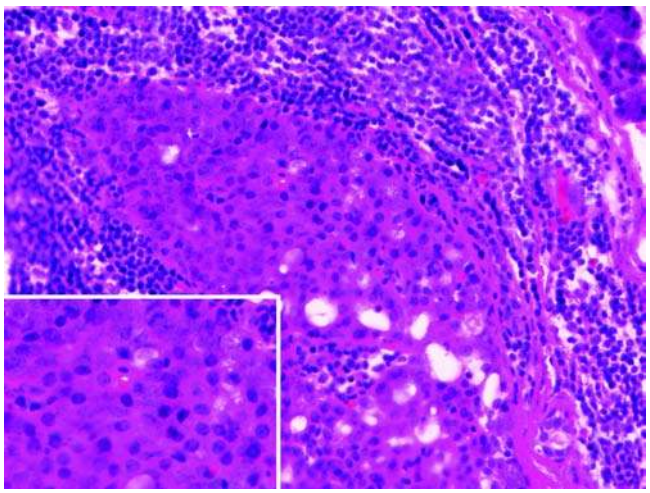

Figure 10 Ectopic acinic cell carcinoma in paraparotid lymph node (H&E 50×).Inset: high power view showing cells with cytoplasmic granules (H&E 200×).

seemingly rare, this extraordinary lesion should be differentiated from metastatic tumor (42,43).

There is still the unresolved problem and the controversies concerning the existence of normal thyroid follicles inside cervical lymph nodes (44,45) (see chap. 16, sect. ''Lymph Node Heterotopias''). It is also true, however, that microscopic deposits of normal thyroid follicles in lymph nodes have not been associated with progressive carcinoma (46). In my experience and in that of other authors, these deposits are always incidental findings discovered during pathological examination of surgically excised tissue for

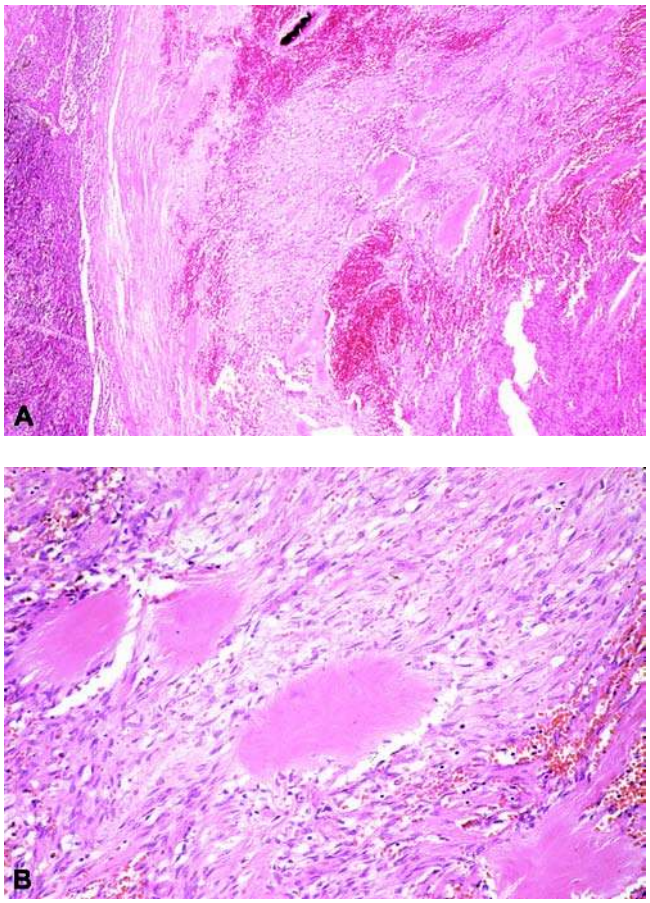

Figure 11 Myofibroblastoma in submandibular lymph node. (**A**) low power (H&E 20×). (**B**) high power (H&E 70×).

another cancer of the head and neck region (44–48). The therapeutic management of these patients has been discussed by Vassilopoulous-Sellin and Weber (47) and Fliegelman et al. (48).

Benign spindle cell neoplasms arising in cervical lymph nodes have been described by Ambrosiani et al. (49) and Alguacil-Garcia (Fig. 11) (50). These benign intranodal myofibroblastomas should be distinguished from metastatic melanoma, sarcoma, or spindle cell malignant neoplasms in lymph nodes presumed to be of reticulum lineage (Fig. 12) (51).

Cervical thymoma and parathyroid cysts are other benign intranodal lesions that should be distinguished from metastatic carcinoma. Cervical thymomas are noteworthy principally for their unusual location, and this feature alone may cause difficulties, not only in clinical management of these tumors but also in the pathological assessment of the excised tissues (52). Parathyroid cyst is another cause of cystic cervical mass. These cysts occur in the anterior cervical triangle (53). FNA biopsy is the principal diagnostic measure, and although it may be curative, persistence or recurrence of the cyst should prompt its surgical removal (54).

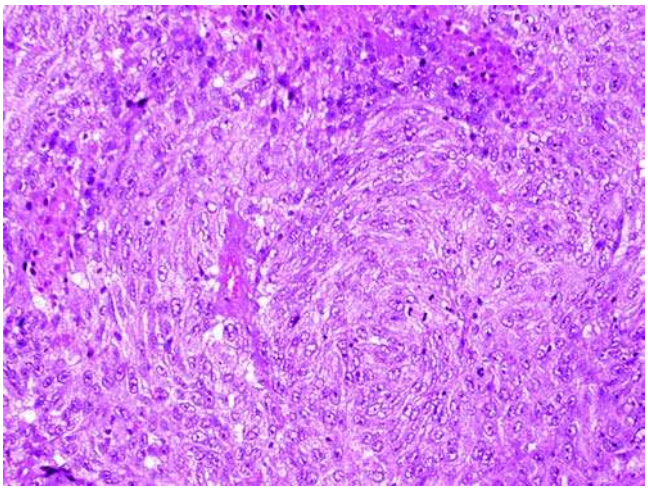

Figure 12 Dendritic cell sarcoma in cervical lymph node (H&E 70×).

II. IMMUNOHISTOCHEMISTRY, ELECTRON MICROSCOPY, AND MOLECULAR STUDIES

In more than 80% of all cases, the diagnosis can be made from tissue sections stained with hematoxylin and eosin, which reliably indicates the presence of SCC. In poorly differentiated or undifferentiated neoplasms, immunohistochemical studies should be used for further classification (55,56). When immunohistochemical staining is inconclusive, demonstration of specific ultrastructural features such as neuroendocrine granules (Fig. 13), melanosomes or premelanosomes (Fig. 13), microvilli or lumens (Fig. 14), desmosomes and/or tonofilaments (Fig. 14) by electron microscopy may contribute to the correct classification (57).

De Young and Wick (58) presented an algorithmic immunohistochemical approach to determining the primary site of metastatic carcinoma of unknown origin using 14 antigens; their experience with this approach yielded a 67% rate of accuracy with regard to the ultimately determined site of origin of metastatic CUPs, a figure similar to that reported by Hunt et al. (59).

Recent molecular studies suggest that cancers originating from different anatomic sites of the upper aerodigestive tract may have different genetic alterations that could allow distinction between different sites of origin within this anatomic region (60). Rodrigo et al. (61) and Huang et al. (62) demonstrated that genetic and chromosomal alterations in head and neck SCC differ by sites within the region. Dacic et al. (63) showed that small-cell neuroendocrine carcinomas display unique profiles of tumor-suppressor gene loss in relationship to the primary site of origin and that a profile of allelic imbalance enables primary site determination for those tumors, despite their similarity in histological appearance.

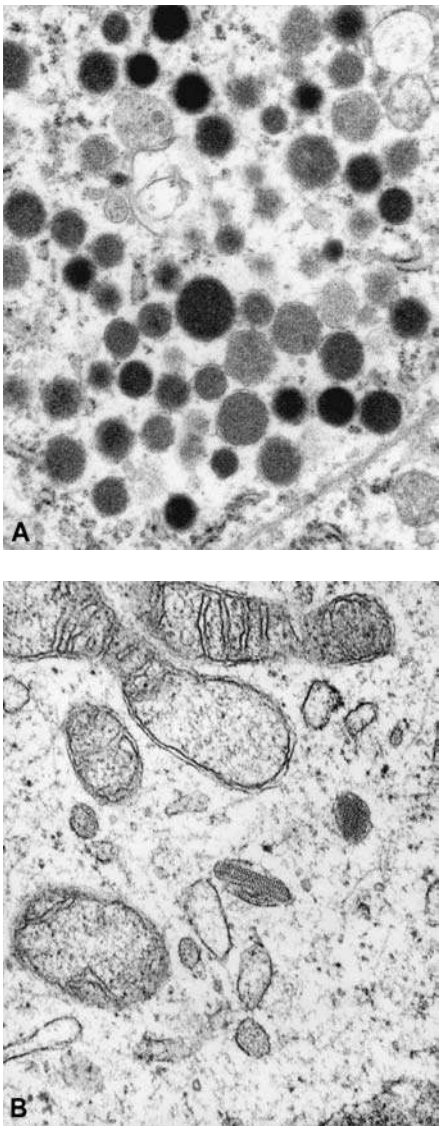

Figure 13 Ultrastructural features of metastatic tumors. (**A**) Merkel cell carcinoma with intracytoplasmic neuroendocrine granules. (**B**) Melanoma showing melanosomes.

With advances in cytogenetic and molecular genetic analyses and increased availability of DNA hybridization and polymerase chain reaction (PCR) facilities, investigations focusing on the identification of specific genetic changes may gain importance, especially with respect to patients with CUP. Several tumor entities that may present clinically as a neck mass, including germ cell tumors, Ewing's sarcoma, synovial sarcoma, alveolar rhabdomyosarcoma, neuroblastoma, neuroepithelial tumors, and non-Hodgkin's lymphomas, can now be identified on the basis of their specific cytogenetic abnormalities (64). In cases of multiple primary SCC not uncommon in the upper aerodigestive tract, the primary tumor, giving rise to the metastatic spread may be verified by

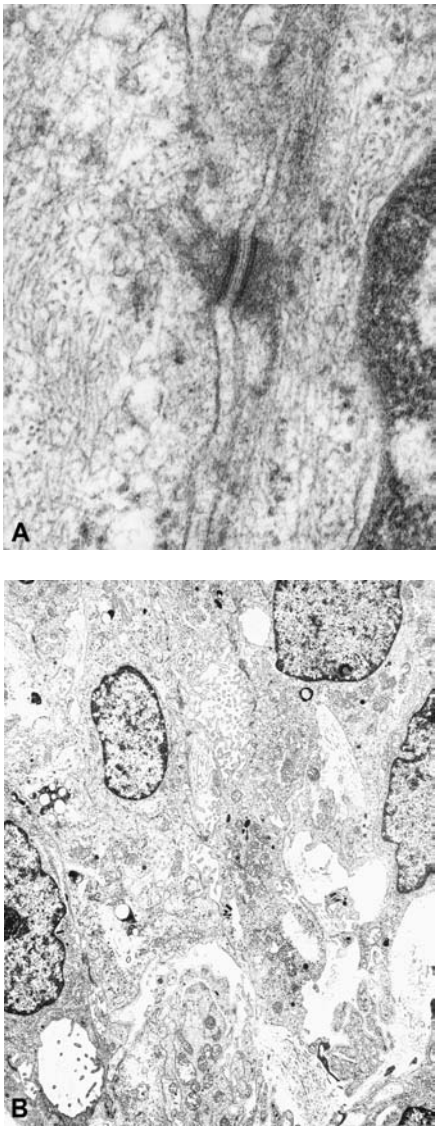

Figure 14 Electron microscopic appearance of metastasis. (**A**) Desmosome and tonofilaments in an epithelial neoplasm. (**B**) Microvilli and lumen diagnostic of adenocarcinoma.

comparing the types of mutations in both primary and metastatic tissues (65).

A. Discovery of the Primary Tumor in Cervical CUPs

A significant number of the occult lesions are not found before treatment or at times during or after conclusion of treatment. Of those found after treatment, most are discovered within three years after initial treatment of the neck lymph nodes (17,19). The success rate of ultimate detection of occult primaries (of various investigators) has varied between 10% and 82.1% (Table 3) (5,6,8,66–71). As might be expected, patients treated with irradiation have shown a significantly lower incidence of detection of occult primaries after treatment (7,13,67). The region of Waldeyer's ring provides nearly 60% of the determined sites of origin of primary carcinomas, originally considered occult, found in patients after treatment of the cervical nodes (Table 4) (2,3,17,19,67–71). The largest number of primary tumors found below the clavicle is in the lungs, followed by the gastrointestinal tract (Table 5) (14,17–19,69,70,72,73).

In those patients in whom the primary tumor is not found, one must postulate that the primary lesion is so small that it is not visible, is in the cervical region, or has regressed spontaneously. The latter consideration is speculative, because spontaneous regression cannot be proved. Although origin of a squamous carcinoma in the wall of a branchiogenic cyst is possible, this entity remains entirely hypothetical (19). Few observers are willing to agree that primary SCC arises in branchiogenic cysts. The most attractive thesis, therefore, is that the primary disease is too small to be detected.

B. Treatment and Results

Although it is now appreciated that distant metastases represent a significant problem in patients with head and neck cancer (74), the control of the primary tumor and regional nodal disease remains critically important (75).

Jesse et al. (13) pointed out that ''radiation therapy and surgical operation are not competing modalities in

Table 3 Discovery of primary tumor in cervical CUPs

Author (Ref.)	Total no. cases	Primary detected (% of total)	Primary found (%)	
			Above clavicle	Below clavicle
Friesland et al. (66)	51	6 (12.2)	100	0
Grau et al. (8)	352	66 (10.0)	60	40
Haas (6)	57	9 (11.3)	100	0
Iganej et al. (67)	106	19 (18.0)	100	0
Issing et al. (68)	167	36 (21.5)	100	0
Koivunen et al. (69)	72	14 (16.0)	71	29
McMahon et al. (3)	38	5 (13.0)	100	0
Munoz et al. (70)	92	76 (82.0)	72	28
Weber et al. (71)	75	33 (44.0)	76	24
Vaamonde et al. (4)	22	10 (23.7)	100	0

Table 4 Location of Primary Head and Neck Carcinomas Originally Considered Occult

Location	Total number
Nasopharynx and oropharynx	31
Tonsil/base of tongue	31
Thyroid	21
Hypopharynx	19
Supraglottis	12
Oral cavity	8
Nose and sinuses	4
Esophagus	3
Miscellaneous head and neck	11
Total	140

Source: From Refs. 2, 13, 17, 19, 67–71.

Table 5 Primary Sites Below Clavicle

Anatomical site	Number of cases
Lung	43
Colon	13
Pancreas	13
Breast	4
Ovary	4
Stomach	4
Prostate	4
Bladder	4
Kidney	3
Adrenal	1
Liver	1
Total	94

Source: From Refs. 14, 17–19, 69, 70, 73.

the treatment of the patients with a cervical node associated with an unknown primary cancer.'' From the clinical presentation of the node or nodes, the treatment team must select the therapy that will give the highest control while providing the patient with an optimal quality of life. Depending on the location of the node, the stage of disease, and the histology, different treatment methods may be selected (66–71).

Depending on patient and tumor characteristics, the reported five-year survival rate ranges from 18% to 48% (8,66,67). The prognostic factors considered important determinants in the prognosis of a patient with cervical node metastasis of unknown origin are (*i*) clinical stage of the neck, (*ii*) presence of extracapsular spread, (*iii*) position of cervical node, (*iv*) histological type of the metastatic neoplasm, (*v*) degree of differentiation in metastatic squamous carcinoma, and (*vi*) desmoplastic lymph node pattern (76–78). The clinical stage of the neck is the single most reliable clinical prognostic indicator, e.g., there is a clear decrease in survival from NX neck (previously excised node, no residual cancer) to N3 neck (unilateral, fixed node or bilateral nodes, fixed or nonfixed). Jesse et al. (13) reported a decrease in the absolute three-year survival rate from 79% to 38% with progression from NX to N3. Similar data for five-year survival are reported by several authors (Table 6) (13,18,66–69). Extracapsular spread of metastatic carcinoma into soft tissues has been identified as the single most important histological prognostic factor in recurrent disease in the neck and in overall survival (77). The location of the largest node is important. Patients with nodes in the supraclavicular area or in the low cervical region are rarely cured by any treatment modality (12,13,78). In the series of Jesse et al. (13), only one patient with supraclavicular node metastasis survived a three-year interval. There were no survivors in a group of eight patients with large, fixed lower cervical nodes. The influence of histological type is evident in that adenocarcinomas, except those of thyroid origin, are associated with few three-year survivals (19). The degree of differentiation in metastatic squamous carcinoma from an occult primary appears to influence survival. A metastatic, well-differentiated squamous carcinoma carries a worse prognosis than a poorly differentiated SCC (5). In a recent study by Olsen et al. (78), a desmoplastic stromal pattern in a lymph node metastasis was associated with a nearly sevenfold increase in the risk of neck disease recurrence.

Table 6 Five-Year Absolute Cure Rate as a Function of Stage and Treatment Modality

Stage	Surgery (%)	Irradiation (%)	Combined (%)
NX	62	75	_
N1	20	_	_
N2	40	_	44
N3	29	30	16

Source: From Ref. 13.

III. BRANCHIOGENIC CARCINOMA

Branchiogenic carcinoma or primary cervical neoplastic cysts are of interest mainly from a historical viewpoint. Few, if any, of the purported examples of this entity fulfill the four criteria that Martin et al. (79) considered necessary to establish the diagnosis. These criteria are as follows: (*i*) the cervical tumor occurs along the line extending from a point just anterior to the tragus, along the anterior border of the sternocleidomastoid muscle, to the clavicle; (*ii*) the histological appearance must be consistent with an origin from tissue known to be present in branchial vestigial; (*iii*) No primary source of the carcinoma should be discovered on at least a five-year follow-up; and (*iv*) there is histological demonstration of cancer arising in the wall of an epithelial-lined cyst situated in the lateral aspect of the neck. They stated that the fourth criterion was the most important in the confirmation of primary branchial cleft carcinoma. According to Thompson and Heffner (37), the lesion can be interpreted as branchiogenic carcinoma only if the cystic lesion is associated with a well-defined sinus tract, with course indicating a branchiogenic developmental anomaly (based on embryological knowledge of the development of the branchial cleft region). The authors did not encounter any such case in their series of 136 cystic neck carcinomas.

The fulfillment of these criteria is practically impossible, and the actual existence of the ''branchiogenic carcinoma'' must remain entirely hypothetical (19). Batsakis and McBurney (80) have estimated that even accepting tentative examples of branchiogenic carcinoma, its incidence would be minuscule (0.3% of

all malignant supraclavicular neoplasms). There is now growing evidence that the majority of cases labeled as branchiogenic carcinomas are actually cervical node metastases with a cystic pattern. The tonsillar region, or more generally the anatomical region of Waldeyer's ring, is notorious for producing cystic solitary metastases that resemble the usual appearance of branchial cysts (37,38). When the primary tumor cannot be found, the hypothesis of CUP with solitary cystic metastasis is most likely (81).

The data on the incidence, etiology, morphological features, and management of true branchiogenic carcinoma are scarce (81). In 1989, Khafif et al. (82) reported on a retrospective review of 67 cases of branchiogenic carcinoma reported in the literature from the time of Martin's report to 1988; these authors found only 12 cases of branchiogenic carcinoma that satisfied all four criteria proposed by Martin et al. (79). In 1999, Hong and associates (83) reported that a review of the English literature identified only 10 cases that completely fulfilled the fourth and most important criterion proposed by Martin et al. (79). The most recent cases published in the literature were made by Girvigian et al. (84) and Katori et al. (85). Further histopathological and clinical studies are warranted to better understand the biology and natural history of cervical cystic malignant lesions. The existence of true branchiogenic carcinoma remains to be verified with new clinical and molecular criteria (81).

IV. EXTRANODAL METASTASES

The identification of extranodal metastases to the head and neck region is often of grave significance for both the patient and physician. The development of such a lesion indicates the failure of ongoing therapy or the recurrence of a neoplasm assumed to have been previously eradicated. Alternatively, extranodal metastases may be the first manifestation of an unsuspected, asymptomatic occult neoplasm.

A. Metastases to Salivary Glands

Parotid and periparotid lymph nodes are a favored site for metastases from malignant tumors of the scalp, temple, ear, and (occasionally) the palate and nasopharynx. The most common metastasizing tumors to the parotid gland are melanoma and squamous carcinoma (86–89). Blood-borne secondary carcinomas rarely occur in the parotid gland. The most common primary sites are the lung and breast (89). Renal cell carcinoma may at times present as a primary clear cell carcinoma of the parotid gland (19). It must be remembered that when there is great difficulty in assigning a given salivary gland neoplasm to a particular category, there is a possibility that it represents a secondary tumor. The submandibular gland is only infrequently the site of either a lymphatic or a hematogenous metastasis (89). The absence of intraglandular lymph nodes is the apparent reason for the rarity of lymphatic metastatic lesions (89,90).

B. Metastatic Tumors to the Oral Regions

Most metastases to the oral region are to the bone. More than 90% of all oral metastatic tumors occur in the bones of the jaws, and of these, nearly 90% are in the mandible (91,92). The tongue is the most common soft tissue site of metastatic involvement (91).

Jaw Metastases

Metastatic involvement of the mandible and maxilla is not uncommon as part of generalized metastasis from carcinoma of the breast, lung, and kidney. However, the true incident of jaw involvement in metastatic disease has not been determined. In 1994, Hirshberg et al. (92) accepted a total of 390 verified cases of metastatic malignancy to the jaws. Metastases to the jaws are more common in female patients and are found most often in the molar region of the mandible. The female predominance is undoubtedly because metastatic carcinoma of the breast accounts for about 30% of all metastases to the mandible (92–94). The average age of such patients is 55 years. The most common symptoms are pain and swelling, but the most significant symptom is anesthesia and paraesthesia of the mandible. The relatively low incidence of metastasis in the maxilla and mandible is associated with the paucity of red bone marrow in the age group in which cancer is most frequent. Most of the metastases occur in patients in their fifth to seventh decades of life.

For women, the most common site of the primary neoplasm is the breast, followed by adrenal glands, colon and rectum, genital organs, and the thyroid. For men, the most common primary sites are lung, prostate, kidney, bone, and adrenal glands.

The primary neoplasms of the adrenal glands were all neuroblastomas. Of particular interest is that 13 of 390 metastases reported by Hirshberg et al. (92) and metastases in two of nine patients reported by McDaniel et al. (93) were from hepatocellular carcinomas, a finding that requires vigilance on the part of the surgical pathologist. In 20% to 30% of the patients with metastasis to the jawbones, jaw metastasis is the first manifestation of a malignant neoplasm. In nine patients seen at our institution who developed symptoms in the jaws before the diagnosis of the primary disease, bronchiogenic carcinoma and thyroid carcinoma were the most common neoplasms showing primary manifestations in the jaws (93).

The prognosis for a patient with metastasis to the jaws is grave; 70% of the patients die within the first year after detection of the metastasis (92–95). The exception to this is metastatic carcinoid and thyroid carcinoma (93).

Metastases to Oral Soft Tissues

Metastases to the soft tissues of the oral region cavity are quite uncommon. Abrams et al. (96), in an analysis of 1000 patients with cancer at autopsy, found only one patient with oral soft tissue metastasis. In a review of the literature of metastases to the soft tissues of the oral cavity, the most common sites of metastasis were

the tongue and gingiva; the lips, buccal mucosa, palate, and tonsil were seldom involved (97). The primary sites of metastases were the lungs, followed by the breasts, skin melanomas, gastrointestinal tract, and liver (98).

A review of 77 cases of lingual metastases has shown that the mobile tongue has a slightly higher incidence of metastases than the base or posterior border (98). The mean age of these patients was 57 years, with a significant 63% male predominance. The lungs, kidneys, and skin were the most common sites of origin of the primary malignant neoplasms, accounting for 60% of all cases of metastases to the tongue. Of greatest interest to oncologists and pathologists is that the tongue was the first presentation of metastases in 61% of all cases of metastases to the tongue; in 13% of cases, it was also the first sign of the primary tumor (98–101).

C. Metastatic Tumors to the Nasal Cavity and Paranasal Sinuses

Metastatic tumors to the paranasal sinuses are infrequent. The maxillary sinus is by far the most common sinus involved; the ethmoid and frontal sinuses are involved in decreasing order. Renal cell carcinoma is by far the most common tumor that metastasizes to the paranasal sinuses (19,102). Carcinoma of the breast is the second most common neoplasm or primary site. The lungs, testes, and thyroid gland follow in decreasing order of frequency (102). Pain and facial deformity are the usual presenting symptoms. Epistaxis is the chief presenting complaint in patients with metastatic renal cell carcinoma to the paranasal sinuses. It has been emphasized that if a highly vascular tumor in the nasal and paranasal sinus is encountered, metastatic renal cell carcinoma must be considered in the differential diagnosis (103,104). It is believed that metastasis from renal cell carcinoma to the nasal and paranasal sinuses occurs by way of the vertebral venous plexus (19).

D. Metastatic Tumors to the Orbit and Eye

The most common signs and symptoms produced by orbital metastases are exophthalmos, pain, decreased vision, periorbital swelling, and visible mass. The breasts and the lungs are the most common primary sites, followed by kidney, prostate, testes, and gastrointestinal tract (105–107). In the Font and Ferry series (107), more than half of the metastatic tumors to the orbit were moderately well-differentiated adenocarcinomas; the others were either undifferentiated or poorly differentiated adenocarcinomas. Only one tumor was classified as SCC. The rarity of SCC metastatic to the orbit should be emphasized. If one encounters such a tumor in the orbit, the possibility of a direct extension from the paranasal sinuses should be given serious consideration. Intraocular metastases are more common than orbital metastases (105). In a review of 227 cases of metastases to the eyes and orbits, Font and Ferry (107) found an eye/orbit ratio of 7:1. Of all intraocular metastases, 50% were from breast carcinoma, with the choroid involved more often than the retina (107,108). Because of the progress of chemotherapeutic medications, the number of patients who manifest choroidal metastases will continue to increase (109).

E. Temporal Bone Metastases

Nelson and Hinojosa (110) and Gloria-Cruz et al. (111) have reviewed the literature on temporal bone metastases and discussed the clinicopathological manifestations. In addition, these authors concluded that temporal bone metastases have been reported with increasing frequency (110,111). The principal sites of origin of these neoplasms are breast, kidney, and lungs. Their spread to the temporal bone is most often by a hematogenous route. An alternate route is by way of cerebrospinal fluid from carcinomatosis of the meninges (112). Hearing loss and facial paralysis are common early signs of temporal bone involvement (113–115).

F. Metastases to the Skin of the Head and Neck

The skin of the head and neck is a favorite site for metastatic carcinoma from remote primary neoplasms (116,117). Breast, lungs, kidney, and gastrointestinal tract are the most common sources of metastases to the skin (116). As pointed out by several authors (116–119), renal cell carcinoma manifests a striking proclivity to affect the skin of the face and scalp. The surgical pathologist must keep in mind that the histological changes in metastatic renal cell carcinoma may simulate the appearance seen in eccrine porosyringoma and in sebaceous gland carcinoma. Recently it has been noticed that metastatic follicular thyroid carcinoma to skin has increased in frequency and often has oncocytic and insular features (120). Immunohistochemistry is a valuable tool to determine the origin of skin metastases, especially when there is no primary history or when this history is unavailable (121).

G. Metastases to the Larynx

Laryngeal metastases are very rare, accounting for 0.09% to 0.40% of all laryngeal tumors (122). Puxeddu et al. (123), in 1997, reviewed 149 cases of secondary laryngeal tumors and reported that primary tumors metastatic to the larynx were, in order of frequency, skin melanoma and kidney, breast, lung, prostate, colon, stomach, and ovarian cancer. Metastatic renal cell carcinoma is unusual, and even more unusual is the occurrence of an isolated laryngeal metastasis revealing itself years after nephrectomy (124).

The pathways of metastatic invasion to the larynx are hematogenous and lymphogenous; therefore, the vast majority of reported laryngeal metastases involve the supraglottic and subglottic larynx, representing 38.2% and 18.4% of secondary laryngeal tumors, respectively (122–125). The reason for this phenomenon is thought to be that these regions have more highly developed lymphatic pathways and

blood circulation than the glottis (122). Hematogenous spread may seed out in the soft tissues and mucosa or may deposit in the laryngeal skeleton. In the former sites, renal cell carcinoma and melanoma are the most common primaries (123,124). Metastases from the breast, lung, and prostate favor the skeleton of the larynx (122). Lymphogenous spread may originate from nearby or distant primaries. Distant primary tumors are well known to spread by lymphatic pathways to the neck (125). The extensive lymphatic network of the subglottis renders this region vulnerable to reticuloendothelial malignancies (122).

V. DISTANT METASTASES FROM SCC OF THE HEAD AND NECK

It is now accepted that distant metastases represent a significant problem in patients with head and neck cancer (126). Before 1941, cancer of the head and neck was usually considered a disease that killed by uncontrollable local tumor, recurrence, or metastatic disease above the clavicle; with the increased local control rate above the clavicle, distant metastases have become a common occurrence. In 1923, Crile (127) reported that only 1% (45 of 4500) of the patients with head and neck cancer had distant metastases at autopsy. Recent series based on clinical data have reported an incidence of 5.3% to 23.7% (126,128), whereas autopsy series reported distant metastases in 30% to 47% of such patients (129,130).

The factors that appear to have bearing on the frequency of distant metastases from SCC of the upper respiratory and digestive tracts are location of the primary cancer, the initial T (especially thickness of the tumors) and N stage of the neoplasm, and the presence or absence of regional control above the clavicle. Patients with advanced nodal disease have a high incidence of distant metastases, particularly in the presence of jugular vein invasion and/or extensive soft tissue disease in the neck (77,78,131).

The occurrence of distant metastases seems to be the result of a complex process that has its origin in the primary tumor in genetically predisposed tumor bearers. This results in the promotion and progression of malignant cell mutations that favor clone expansion and uncontrolled growth due to autocrine growth factors and growth factor receptors (132).

The overall incidence of distant metastases according to the anatomical site of the primary varies from 2.0% for lesions of the lip to 70% for lesions of the nasopharynx (133–136). In the series of Merino et al. (128) and in those more recently reported by several authors (133–136), the incidence correlated with the aggressiveness of the primary lesion, as indicated by the N stage on admission (i.e., 6% of the patients with vocal cord lesions had Nl disease on admission compared with 87% of patients with nasopharyngeal lesions). In the same series, in the oropharyngeal lesions (tonsillar fossa, base of tongue, and pharyngeal wall), the rate of distant metastases was double the rate of the faucial arch neoplasms (15.3% compared with 6.7%).

The incidences of distant metastases are significantly influenced by the T and N stage of the tumors. Probert et al. (137) analyzed 779 patients and reported an overall incidence of distant metastases, both clinical and at autopsy, of 12%. Using random selection and matched pair techniques, they concluded that the most advanced primary tumors (T4) were the most likely to metastasize. However, although the incidence of distant metastases increases as the size of the primary increases (T), the difference is not as striking as it is with the N stage. In the Merino et al. (128) study, the incidence for early N stage (N0 + Nl) was 6.3% versus 24% for late stage (N2 + N3). By comparison, the incidences of distant metastasis were 7.8% for early T stage (Tl + T2) and 14% for late T stage (T3 + T4) in that study. The difference between early and late T and N stages was statistically significant ($p < 0.001$).

The presence and absence of local control above the clavicle seems to be the single most important factor in the incidence of distal metastases (126,128,130,131). Vaidya et al. (131), in 128 autopsies of patients with head and neck SCC, found 40% with distant metastases. At the time of autopsy, however, 95% of the patients with disseminated disease also had local neck involvement. Merino et al. (128) found that the incidence of clinical distant metastases was significantly higher when there was a recurrence above the clavicles (16.7%) than when there was no recurrence (7%, $p = 0.001$).

The lungs, skeletal system, and liver are the organs more often involved at autopsy in distant metastases from head and neck cancers (129,130). In the clinical studies of Calhoun et al. (138) and Kotwall et al. (139), the lungs were involved in 80% of the cases. Next in frequency were the mediastinal lymph nodes, with 34% involvement. The skeletal system, most often the lumbosacral spine and the ribs, was involved in 31% of the patients. Table 7 compares the location of distant metastases first found at autopsy with metastases first detected clinically (128–130,138,139). The location of the first site of distant metastasis is essentially the same, regardless of the site of the primary tumor, with the following exceptions: (*i*) bone is the most common site in nasopharyngeal primaries; (*ii*) liver metastasis is often the first manifestation in tonsillar

Table 7 Sites of Distant Metastases from Head and Neck Squamous Cell Carcinomas

	No. of patients		
Organ	First found clinically	First found at autopsy	Total
Lung	48	41	89
Bone	27	3	30
Liver	9	31	40
Skin	11	2	13
Brain	12	0	12
Adrenal	0	10	10
Heart	0	10	10
Kidney	1	10	11
Mediastinal nodes	1	7	8

Source: From Refs. 129, 137.

fossa carcinoma and the base of the tongue; and (*iii*) mediastinal metastases are more common, being the first manifestation in vocal cord lesions with subglottic extension (128,133–135).

More recently, as technological advances have allowed better combinations of standard therapy, less local-regional disease recurs and patients are living longer, only to die more frequently of subsequent distant metastases or second primary tumors (140,141). Goepfert (142) noted that SCC of the upper aerodigestive tract comprises a heterogeneous group of entities with different biological behaviors. At M. D. Anderson Cancer Center, autopsy reports for the period 1955–1965 were compared with those for the decade beginning in 1973. The findings were as follows: an increase in distant metastases as the cause of death (from 17% to 32%), a drop in the number of deaths from uncontrolled tumors above the clavicle (30% to 15%), a marked reduction of fatal treatment complications (25% to 10%), an increase in unrelated nonmalignant diseases as a cause of death (15% to 28%), and no change in the incidence of second malignancies as the cause of death (14%). Similar observations have been recently made by Vaidya et al. (131), Zender and Petruzzelli (132), and Genden et al. (140).

REFERENCES

1. Lindberg R. Distribution of cervical lymph nodes metastases from squamous cell carcinoma of the upper respiratory and digestive tract. Cancer 1972; 29(6):1446–1449.
2. Martin H, Morfit HM. Cervical lymph node metastasis as the first symptom of cancer. Surg Gynecol Obstet 1944; 78(2):133–159.
3. McMahon J, Hruby G, O'Brien, et al. Neck dissection and ipsilateral radiotherapy in the management of cervical metastatic carcinoma from unknown primary. Aust NZ J Surg 2002; 70(4):263–268.
4. Vaamonde P, Martin C, del Rio Valeiras M, et al. Estudio sobre las metastasis cervicales de primario desconocido. Acta Otorhinolaringol Esp 2002; 53(4):601–606.
5. Fried MP, Diehl WH, Brownson RJ, et al. Cervical metastasis from an unknown primary. Ann Otol Rhinol Laryngol 1975; 84(2):152–157.
6. Haas I. Diagnostic strategies in cervical carcinoma of unknown primary (CUP). Eur Arch Otorhinolaryngol 2002; 259(6):325–333.
7. Richard JM, Micheau C. Malignant cervical adenopathies from carcinomas of unknown origin. Tumori 1977; 63(2): 249–258.
8. Grau C, Johansen J, Jakobsen J, et al. Cervical lymph node metastases from unknown primary tumours. Results from a national survey by the Danish Society for Head and Neck Oncology. Radiother Oncol 2000; 55(2):121–129.
9. Rouvière H. Lymph nodes of the head and neck. In: Anatomy of the Human Lymphatic System. Ann Arbor, MI: Edwards Brothers, 1938:5–28
10. Som PM. Lymph nodes of the neck. Radiology 1987; 165(12):593–600.
11. Som PM, Curtin HD, Mancuso AA. An imaging-based classification for the cervical node designated as an adjuvant to recent clinically based nodal classification. Arch Otolaryngol Head Neck Surg 1999; 125(4):388–396.
12. Robbins KT, Clayman G, Levine P, et al. Neck dissection classification update: Revision proposed by the American Head and Neck Society and the American Academy of Otolaryngology-Head and Neck Surgery. Arch Otolaryngol Head Neck Surg 2002; 128(7):751–758.
13. Jesse RH, Perez CA, Fletcher GH. Cervical lymph node metastasis: Unknown primary cancer. Cancer 1973; 31(4): 854–859.
14. Wang RC, Goepfert H, Barber AE, et al. Unknown primary squamous cell carcinoma metastatic to the neck. Arch Otolaryngol Head Neck Surg 1990; 116(12):1388–1393.
15. Werner AJ, Dunne AA, Myers JN. Functional anatomy of the lymphatic drainage system of the upper aerodigestive tract and its role in metastasis of squamous cell carcinoma. Head Neck 2003; 25(4):322–332.
16. Ellison E, la Puerta P, Martin SE. Supraclavicular masses: results of a series of 309 cases biopsied by fine needle aspiration. Head Neck 1999; 21(3):239–242.
17. Jereczek-Fossa BA, Jassem J, Orechia R. Cervical lymph node metastases of unknown primary. Cancer Treat Rev 2004; 30(2):153–164.
18. Coker DD, Casterline PF, Chambers RG, et al. Metastases to lymph nodes of the head and neck from an unknown primary site. Am J Surg 1977; 134(4):517–522.
19. Batsakis JG. The pathology of head and neck tumors: The occult primary and metastases to the head and neck, Part 10. Head Neck Surg 1981; 3(3):409–423.
20. Lowry LD, Brady LW, Krause CL, et al. Metastatic carcinoma of the neck from an occult primary tumor. In: Snow J, ed. Controversy in Otolaryngology. Philadelphia: WB Saunders, 1980:181.
21. Eisele DW, Sherman ME, Koch WM, et al. Utility of immediate on-site cytopathological procurement and evaluation in fine needle aspiration biopsy of head and neck masses. Laryngoscope 1992; 102(12):1328–1330.
22. Schwarz R, Chan NH, MacFarlane JK. Fine needle aspiration biopsy of head and neck masses. Am J Surg 1990; 159(5):482–485.
23. el Hag IA, Chiedozi LC, al Reyees FA, et al. Fine needle aspiration cytology of head and neck masses. Seven years' experience in a secondary care hospital. Acta Cytol 2003; 47(3):387–392.
24. Ahuja A, Ying M. An overview of neck node sonography. Invest Radiol 2002; 37(6) 333–342.
25. Miller FR, Hussey D, Beeran M, et al. Positron emission tomography in the management of unknown primary head and neck carcinoma. Arch Otolaryngol Head Neck Surg 2005; 131(7):626–629.
26. Gutzeit A, Antoch G, Kuhl H, et al. Unknown primary tumors: detection with dual modality PET/CT—Initial experience. Radiology 2005; 234(1):227–234.
27. Elisei R, Bottici V, Luchetti F, et al. Impact of routine measurement of serum calcitonin on the diagnosis and outcome of medullary thyroid cancer: experience of 10,864 patients with nodular thyroid disorders. J Clin Endocrinol Metab 2004; 89(1):163–168.
28. Kondo S, Horikawa T, Takeshita H, et al. Diagnostic value of serum EBV-DNA quantification and antibody to viral capside antigen in nasopharyngeal carcinoma patients. Cancer Sci 2004; 95(6):508–513.
29. Tsang RK, Vlantis AC, Ho RW, et al. Sensitivity and specificity of Epstein-Barr virus IgA titer in the diagnosis of nasopharyngeal carcinoma: a three-year institution review. Head Neck 2004; 26(7):598–602.
30. Randall D, Johnstone PAS, Foss RD. Tonsillectomy in diagnosis of the unknown primary tumor of the head and neck. Otolaryngol Head Neck Surg 2000; 122(1):52–55.
31. Kazak I, Haisch A, Jovanovic S. Bilateral synchronous tonsillar carcinoma in cervical cancer of unknown primary site (CUPS). Eur Arch Otorhinolaryngol 2003; 260(10): 490–493.

32. Koch WM, Bhatti N, Williams MF, et al. Oncologic rationale for bilateral tonsillectomy in head and neck squamous cell carcinoma of unknown primary source. Otolaryngol Head Neck Surg 2001; 124(3):331–333.
33. Nieder C, Gregoire V, Ang KK. Cervical lymph node metastases from occult squamous cell carcinoma: cut down a tree to get an apple? Int J Radiat Oncol Biol Phys 2001; 50(3):727–733.
34. McGuirt WF, McCabe BF. Significance of node biopsy before definitive treatment of cervical metastatic carcinoma. Laryngoscope 1978; 88(4):594–597.
35. Razack MS, Sako K, Marchetta FC. Influence of initial neck node biopsy on the incidence of recurrence in the neck and survival in patients who subsequently undergo curative resectional surgery. J Surg Oncol 1977; 9(4): 347–352.
36. Robbins KT, Cole R, Marwel J, et al. The violated neck: Cervical node biopsy prior to definitive treatment. Otolaryngol Head Neck Surg 1986; 94(5):605–610.
37. Thompson LDR, Heffner DK. The clinical importance of cystic squamous cell carcinoma in the neck. A study of 136 cases. Cancer 1998; 82(3):944–956.
38. Regauer S, Mannweller S, Anderhuber W, et al. Cystic lymph node metastases of squamous cell carcinoma of Waldeyer's ring origin. Br J Cancer 1999; 79(9–10): 1437–1442.
39. Sheahan P, O'leary G, Lee G, et al. Cystic cervical metastases: Incidence and diagnosis using fine needle aspiration biopsy. Otolaryngol Head Neck Surg 2002; 127(4): 294–298.
40. Shinora M, Harada T, Nakamura S, et al. Heterotopic salivary gland tissue in lymph nodes of the cervical region. Int J Oral Maxillofac Surg 1992; 21(3):166–171.
41. Daniel E, McGuirt WF Sr. Neck mass secondary to heterotopic salivary gland tissue:a 25-years experience Am J otolaryngol 2005; 26(2):96–100.
42. Jensen JL, Correll RW. Nevus cell aggregates in submandibular lymph nodes. Oral Surg Oral Med Oral Pathol 1980; 50(6):552–556.
43. Biddle DA, Evans HE, Kemp BL, et al. Intraparenchymal nevus cells aggregates in lymph nodes: A possible diagnostic pitfall with malignant melanoma and carcinoma. Am J Surg Pathol 2003; 27(5):673–678.
44. DeJong SA, Demetr JG, Jarosz H, et al. Primary papillary thyroid carcinoma presenting as cervical lymphadenopathy: the operative approach to the ''lateral aberrant thyroid.'' Am Surg 1993; 59(3):172–176.
45. Rosai J, Carcagiu M, DeLellis R. Thyroid tissue in abnormal locations. In: Rosai J, Carcagiu M, DeLellis R, eds. Tumors of the Thyroid Gland. Washington, DC: Armed Forces Institute of Pathology, 1990:317–326.
46. Ansari-Lari MA, Westra WH. The prevalence and significance of clinically unsuspected neoplasms in cervical lymph nodes. Head Neck 2003; 25(10):841–847.
47. Vassilopoulous-Sellin R, Weber RS. Metastatic thyroid cancer as an incidental finding during neck dissection: Significance and management. Head Neck 1992; 14(6): 459–463.
48. Fliegelman L, Genden EM, Brandwein M, et al. Significance and management of thyroid lesions in lymph nodes as an incidental finding during neck dissection. Head Neck 2001; 23(10):885–891.
49. Ambrosiani L, Bellone S, Cecchetti G, et al. Lymph node myofibroblastoma: report of a submandibular case with peculiar morphologic and immunohistochemical characteristics. Pathologica 1994; 86(5):541–545.
50. Aguacil-Garcia A. Intranodal myofibroblastoma in submandibular lymph node. A case report. Am J Clin Pathol 1992; 97(1):69–72.
51. Biddle DA, Ro JY, Yoon GS, et al. Extranodal follicular dentritic cell sarcoma of the head and neck region: three new cases, with a review of the literature. Mod Pathol 2002; 15(1):50–58.
52. Mourra N, Duron F, Pare R, et al. Cervical thymoma: a diagnostic pitfall on frozen section. Histopathology 2005; 46(5):583–585.
53. Vicente A, Sastre J, Mollejo M, et al. Parathyroid cysts. Their differential diagnosis from thyroid pathology. A report of two cases. Ann Med Intern 2000; 17(2):84–85.
54. Nozeran S, Duquenenne M, Guyetant S, et al. Diagnosis of parathyroid cysts: value of parathyroid hormone level in puncture fluid. Press Med 2000; 29(17):939–941.
55. Jaffer S, Bleiweiss IJ. Beyond hematoxylin and eosin, the role of immunohistochemistry in surgical pathology. Cancer Invest 2004; 22(3):445–465.
56. Kaufmann O, Fietz E, Dietel M. Immunohistochemical diagnosis in cancer metastasis of unknown origin. Pathologe 2002; 23(3):183–187.
57. Jackson SB, Staurusbauch PH, Finley JL. Desmosomes and microvilli mean a lot: diagnosis of neoplasms of unknown origin using electron microscopy. Ultrastruct Pathol 2003; 27(3):155–161.
58. De Young BR, Wick MR. Immunohistochemical evaluation of metastatic carcinoma of unknown origin: an algorithmic approach. Sem Diagn Pathol 2000; 17(3):184–193.
59. Hunt JI, Tomaszewski JE, Montone T. Prostatic adenocarcinoma metastatic to the head and neck and the workup of an unknown epitheliod neoplasm. Head Neck 2004; 26(2):171–178.
60. Califano J, Westra WH, Koch W, et al. Unknown primary head and neck squamous cell carcinoma: molecular identification of the site of origin. J Natl Cancer Inst 1999; 91(7):599–604.
61. Rodrigo JP, Suarez C, Gonzalez MV, et al. Variability of genetic alterations in different sites of head and neck cancer. Laryngoscope 2001; 111(7):1297–1301.
62. Huang Q, Yu GP, McCormick SA, et al. Genetic differences detected by comparative genomic hybridization in head and neck squamous cell carcinoma from different tumor sites: construction of oncogenetic trees for tumor progression. Gen Chrom Cancer 2002; 34(2):224–233.
63. Dacic S, Finkelstein SD, Baksh FK, et al. Small cell neuroendocrine carcinoma displays unique profiles of tumor-suppressor gene loss in relationship to the primary site formation. Hum Pathol 2002; 33(9):927–932.
64. Ilson DH, Motzer RJ, Rodriguez E, et al. Genetic analysis in the diagnosis of neoplasms of unknown primary site. Semin Oncol 1993; 20(3):229–237.
65. van Oijen MG, Leppers VD, Straat FG, et al. The origin of multiple squamous cell carcinomas in the aerodigestive tract. Cancer 2000; 88(4):884–893.
66. Friesland S, Lind MG, Lundgren J, et al. Outcome of ipsilateral treatment for patients with metastases to neck nodes from unknown origin. Acta Oncol 2001; 40(1):24–28.
67. Iganej S, Kagan R, Anderson P, et al. Metastatic squamous cell carcinoma of the neck from an unknown primary: management options and patterns of relapse. Head Neck 2002; 24(3):236–246.
68. Issing WJ, Taleban B, Tauber S. Diagnosis and management of carcinoma of unknown primary in the head and neck. Eur Arch Otorhinolaryngol 2003; 260(8):436–443.
69. Koivunen P, Laranne J, Virtaniemi J, et al. Cervical metastasis of unknown origin: a series of 72 patients. Acta Otolaryngol 2002; 122(5):569–574.
70. Munoz del Castillo F, Jurado Ramos A, Navarro Ortiz F, et al. Adenopatias metastaticas cervicales sin tumor previo conocido. Estudios iniciados 1996–2001. Anales ORL Iber Amer 2003; 30(5) 489–500.

71. Weber A, Schmoz S, Bootz F. CUP (carcinoma of unknown primary) syndrome in head and neck: clinic, diagnostic, and therapy. Onkologic 2001; 24(1):38–43.
72. Zuur CL, van Velthuysen ML, Schornagel JH, et al. Diagnosis and treatment of isolated neck metastases of adenocarcinoma. Eur J Surg Oncol 2002; 28(2):147–152.
73. Imamura SI, Suzuki H. Head and neck metastases from occult abdominal primary site: a case report and literature review. Acta Otolaryngol 2004; 124(2):147–152.
74. Vikran B. Changing patterns of failure in advanced head and neck cancer. Arch Otolaryngol 1984; 110(9):564–565.
75. Known D, Sham J, Choy D. The effect of locoregional control on distant metastatic dissemination in carcinoma of the nasopharynx: an analysis of 1303 patients. Int J Radiat Oncol Biol Phys 1994; 30(5):1029–1030.
76. Nieder C, Ang KK. Cervical lymph node metastases from occult squamous cell carcinoma. Curr Treat Options Oncol 2002; 3(1):33–40.
77. Woolgar JA, Rogers SN, Lowe D, et al. Cervical lymph node metastasis in oral cancer: the importance of even microscopic extracapsular spread. Oral Oncol 2003; 39(2): 130–137.
78. Olsen KD, Caruso M, Foote RL, et al. Primary head and neck cancer. Histopathologic predictors of recurrence after neck dissection in patients with lymph node involvement. Arch Otolaryngol Head Neck Surg 1994; 120(12): 1370–1374.
79. Martin H, Morfit HM, Enhrlich H. The case for branchiogenic cancer (malignant branchioma) Ann Surg 1950; 132(5):867–887.
80. Batsakis JG, McBurney TA. Metastatic neoplasms to the head and neck. Surg Gynecol Obstet 1971; 133(4):673–677.
81. Jereczek-Fossa BA, Casadio C, Jassem J, et al. Branchiogenic carcinoma: conceptual or true clinico-pathologic entity? Cancer Treat Rev 2005; 31(2):106–114.
82. Khafif RA, Prichep R, Minkowitz S. Primary branchiogenic carcinoma. Head Neck Surg 1989; 11(3–4):153–163.
83. Hong KH, Moon WS, Chung GH. Radiologic appearance of primary branchial cleft carcinoma. J Laryngol Otol 1999; 113(11):1031–1033.
84. Girvigian MR, Rechdouni DK, Zeger GD, et al. Squamous cell carcinoma arising in a second branchial cleft cyst. Am J Clin Oncol 2004; 27(1):96–100.
85. Katori H, Nozawa A, Tsukuda M. Post-operative adjuvant chemoradiotherapy with carboplatin and 5-fluorouracil for primary branchiogenic carcinoma. J Laryngol Otol 2005; 119(6):467–469.
86. Galteland P, Boysen M. Metastasis to the parotid gland. Tidsskr Nor Laegeforen 2001; 121(11):1341–1343.
87. O'Brien CJ. The parotid gland as a metastatic basin for cutaneous cancer. Arch Otolaryngol Head Neck Surg 2005; 131(7):551–556.
88. Hong TS, Kriesel KJ, Hartig GK, et al. Parotid area lymph node metastases from cutaneous squamous cell carcinoma: Implications for diagnosis, treatment, and prognosis. Head Neck 2005; 27(10):851–856.
89. Seifert G, Hennings K, Caselitz J. Metastatic tumors to the parotid and submandibular glands: analysis and differential diagnosis of 108 cases. Pathol Res Pract 1986; 181 (6):684–692.
90. Kunisue H, Mikami Y, Tanaka K, et al. Metastatic papillary thyroid carcinoma of the submandibular gland lymph nodes with extensive squamous metaplasia: report of a case. Surg Today 2003; 33(10):751–754.
91. Van der Waal RI, Buter J, van der Vaal I. Oral metastases: report of 24 cases. Br J Oral Maxillofac Surg 2003; 41(1):3–6.
92. Hirshberg A, Leibovich P, Buchner A. Metastatic tumors to the jawbones: analysis of 390 cases. J Oral Pathol Med 1994; 23(8):337–341.
93. McDaniel RK, Luna MA, Stimson PG. Metastatic tumors in the jaw. Oral Surg 1971; 31(3):380–386.
94. Niedziclska I, Langowska-Adameczyk H, Pajak J, et al. Mandible metastasis of hepatocellular carcinoma. Wiad Lek 2004; 57(7–8):392–394.
95. Kaufmann MG, Perren A, Gratz KW, et al. Condylar metastasis. Review of the literature and report of a case. Mund Kiefer Gesichtschir 2005; 9(5):336–340.
96. Abrams HL, Spiro R, Goldstein N. Metastases in carcinoma: Analysis of 1000 autopsied cases. Cancer 1950; 3(1): 74–85.
97. Hatziotis MC, Constantinidou H, Papanayatou PH. Metastatic tumors of the oral soft tissue. Oral Surg 1973; 36(4): 544–550.
98. Baden E, Duvillard P, Micheau C. Metastatic papillary endometrial carcinoma of the tongue. Case report and review of the literature. Arch Pathol Lab Med 1992; 116(9):965–968.
99. Goel MC, Williams DW, Evans H, et al. Lingual metastasis from renal cell carcinoma management and review of the literature. Urol Int 2003; 71(4):418–421.
100. Terashima T, Matsuzaki T, Kawada I, et al. Tongue metastasis as an initial presentation of a lung cancer. Intern Med 2004; 43(8):727–730.
101. Wang HY, Su CY, Lin JW, et al. Base of the tongue metastatic cancer from hepatocellular carcinoma: a case report. Eur Arch Otorhinolaryngol 2004; 261(10):531–533.
102. Prescher A, Brors D. Metastases to the paranasal sinuses: Case report and review of the literature. Laryngorhinotologie 2001; 80(10):583–594.
103. Ilvan S, Akyildiz EU, Calay Z, et al. Endometrial clear cell carcinoma metastatic to the paranasal sinuses: a case report and review of the literature. Gynecol Oncol 2004; 94(1):232–234.
104. Matsuda H, Tanigaki Y, Yoshida T, et al. A case of metastatic hepatocellular carcinoma in the nasal cavity. Eur Arch Otorhinolaryngol 2006; 263:305–307.
105. Shields JA, Shields CL, Brotman HK, et al. Cancer metastatic to the orbit: The 2000 Robert M Curts Lecture. Ophtal Plast Reconstr Surg 2001; 17(5):346–354.
106. Dieing A, Schultz CO, Schmid P, et al. Orbital metastases in breast cancer: report of two cases and review of the literature. J Cancer Res Clin Oncol 2004; 130(12): 745–748.
107. Font RL, Ferry AP. Carcinoma metastatic to the eye and orbit I. A clinicopathologic study of 227 cases. Arch Ophthalmol 1974; 92(4):276–286.
108. Correa ZM, Burmann TG, Freitas AM, et al. Prevalence of ocular metastasis in patients with known metastatic disease: preliminary results. Arq Bras Oftalmol 2005; 68(2):189–193.
109. Chong JT, Mick A. Choroidal metastasis: case reports and review of the literature. Optometry 2005; 6(5):293–301.
110. Nelson EG, Hinojosa R. Histopathology of metastatic temporal bone tumors. Arch Otolaryngol Head Neck Surg 1991; 117(2):189–193.
111. Gloria-Cruz TI, Schachern PA, Paparella MM, et al. Metastases to temporal bones from primary nonsystemic malignant neoplasms. Arch Otolaryngol Head Neck Surg 2002; 126(2):209–214.
112. Sahin A, Ro JY, Ordonez NG, et al. Temporal bone involvement by prostatic adenocarcinoma: report of two cases and review of the literature. Head Neck 1991; 13(4): 349–353.
113. Miro-Castillo N, Roca-Ribas Serda F, Barnadas-Molins A, et al. Paralisis facial de origin metastatico. Revision de las lesiones metastaticas del hueso temporal. An ORL Iber Amer 2000; 27(3):255–263.

114. Wu Ch, Kaga K, Ohira Y, et al. Histopathology of multiple temporal bone metastasis from pancreatic adenocarcinoma: a case report showing bilateral hearing loss and Bechterew's phenomenon. Otolaryngol Head Neck Surg 2000; 122(4): 613–615.
115. Lan MY, Shiao AS, Li WY. Facial paralysis caused by metastasis of breast carcinoma to the temporal bone. Chin Med Assoc 2004; 67(11):587–590.
116. Schwartz RA. Cutaneous metastatic disease. J Am Acad Dermatol 1995; 33(2 pt 1) (8):161–182.
117. Rosen T. Cutaneous metastases. Med Clin North Am 1980; 64(5):885–900.
118. Lim C, Chan R, Regan W. Renal cell carcinoma with cutaneous metastases. Australas J Dermatol 2005; 46(3): 158–160.
119. Barbagelata Lopez A, Ruibal Moldes M, Blanco Diez A, et al. Cutaneous metastasis of a renal cell carcinoma: case report and review. Arch Esp Urol 2005; 58(3):247–250.
120. Quinn TR, Duncan LM, Zembowicz A, et al. Cutaneous metastases of follicular thyroid carcinoma: a report of four cases and a review of the literature. Am J Dermatopathol 2005; 27(4):306–312.
121. Azoulay S, Adem C, Pelletier FL, et al. Skin metastases from unknown origin: role of immunohistochemistry in the evaluation of cutaneous metastases of carcinoma of unknown origin. Cutan Pathol 2005; 32(8):561–566.
122. El-Naggar AK. Secondary neoplasms. In: Ferlito A, ed. Surgical Pathology of the Laryngeal Neoplasms. London: Chapman & Hall, 1995:465–474.
123. Puxeddu R, Pelagatti CL, Ambu R. Colon adenocarcinoma metastatic to the larynx. Eur Arch Otorhinolaryngol 1997; 254(7):353–355.
124. Dee SL, Eshghi M, Otto CS. Laryngeal metastasis 7 years after radical nephrectomy. Arch Pathol Lab Med 2000; 124(12):1833–1844.
125. Daisuke S, Hideki M, Takafumi Y, et al. A case of metastatic colon adenocarcinoma in the larynx. Acta Oto-Laryngologica 2005; 125(2):220–223.
126. Ferlito A, Shaha AR, Silver CE, et al. Incidence and sites of metastases from head and neck cancer. ORL J Otorhinolaryngol Relat Spec 2001; 63(4):202–207.
127. Crile GW. Carcinoma of the jaws, tongue, cheek, and lips. Surg Gynecol Obstet 1923; 36(2):159–184.
128. Merino OR, Lindberg RD, Fletcher GH. An analysis of distant metastases from squamous cell carcinoma of the upper respiratory and digestive tracts. Cancer 1977; 40(1): 145–151.
129. Zbaren P, Lehmann W. Frequency and sites of distant metastases in head and neck squamous cell carcinoma. An analysis of 101 cases at autopsy. Arch Otolaryngol Head Neck Surg 1987; 113(7):762–764.
130. Nishijima W, Takooda S, Tokita N, et al. Analysis of distant metastases in squamous cell carcinoma of the head and neck and lesions above the clavicle at autopsy. Arch Otolaryngol Head Neck Surg 1993; 119(1):65–68.
131. Vaidya AM, Petruzzelli GJ, Clark J, et al. Patterns of spread in recurrent head and neck squamous cell carcinoma. Otolaryngol Head Neck Surg 2001; 125(4):393–396.
132. Zender CA, Petruzzelli GJ. Why do patients with head and neck squamous cell carcinoma experience distant metastases: Can they be prevented? Curr Opin Otolaryngol Head Neck Surg 2005; 13(2):101–104.
133. Chiesa F, De Paoli F. Distant metastases from nasopharyngeal carcinoma. ORL J Otorhinolaryngol Relat Spec 2001; 63(4):214–216.
134. Spector GJ. Distant metastases from laryngeal and hypopharyngeal cancer. ORL J Otorhinolaryngol Relat Spec 2001; 63(4):224–228.
135. Goodwin WJ. Distant metastases from oropharyngeal carcinoma. ORL J Otorhinolaryngol Relat Spec 2001; 63(4):222–223.
136. Betka J. Distant metastases from lip and oral cavity cancer. ORL J Otorhinolaryngol Relat Spec 2001; 63(4): 217–221.
137. Probert JC, Thompson RW, Bagshaw MA. Patterns of spread of distant metastases in head and neck cancer. Cancer 1974; 33(1):127–133.
138. Calhoun KH, Fulmer P, Weiss R, et al. Distant metastases from head and neck squamous cell carcinoma. Laryngoscope 1994; 104(10):1199–1205.
139. Kotwall C, Sako K, Razack MS, et al. Metastatic patterns in squamous cell cancer of the head and neck. Am J Surg 1987; 154(4):439–442.
140. Genden EM, Ferlito A, Bradley PJ, et al. Neck disease and distant metastases. Oral Oncol 2003; 39(3):207–212.
141. Raghavan U, Quraishi S, Bradley PJ. Multiple primary tumors in patients diagnosed with hypopharyngeal cancer. Otolaryngol Head Neck Surg 2003; 128(3):419–425.
142. Goepfert H. Are we making any progress? Arch Otolaryngol 1984; 110(9):562–563.

18

Cysts and Cyst-like Lesions of the Oral Cavity, Jaws, and Neck

Steven D. Budnick
Emory University School of Medicine, Atlanta, Georgia, U.S.A.

Leon Barnes
Department of Pathology, University of Pittsburgh Medical Center, Presbyterian-University Hospital, Pittsburgh, Pennsylvania, U.S.A.

I. INTRODUCTION

Cysts of the head and neck may occur in soft tissue or bone (Table 1). Many of these lesions are unique to the head and neck because of the specialized anatomy as well as the presence of the odontogenic apparatus. Because many of these cysts have overlapping histologic features, clinical/radiographic correlation is frequently necessary to accurately classify these lesions (Table 1) (Fig. 1).

II. ODONTOGENIC CYSTS

Odontogenic cysts and tumors arise from the structures and remnants associated with tooth development. A brief explanation of tooth development is necessary to understand the origin of these lesions (1).

A. Tooth Development

The initial formation of the tooth begins with a downgrowth of the oral epithelium (dental lamina) into the ectomesenchyme of the jaws. The tooth bud is organized into three parts: the enamel organ, the dental papilla, and the dental follicle (Fig. 2). The cells of the enamel organ give rise to ameloblasts, which produce enamel. The cells of the dental papilla give rise to odontoblasts, which produce dentin (Fig. 3). Mesenchymal cells of the dental papilla form the pulp of the tooth. The dental follicle gives rise to cementoblasts, osteoblasts, and fibroblasts. These cells form the root of the tooth, the alveolar-supporting bone, and the periodontal ligament, which anchors the tooth to the alveolar bone (Fig. 3).

As the crown portion of the tooth nears completion, Hertwig's epithelial root sheath forms. It is responsible for the shape and number of roots and initiates dentin formation in the root. Remnants of Hertwig's root sheath form the rests of Malassez, which are found in the periodontal ligament, while residual foci of the dental lamina, referred to as rests of Serres, are occasionally observed in the gingiva.

B. Developmental Cysts

Primordial Cyst

Etiology and pathogenesis. The term ''primordial cyst'' has been used to denote a cyst that occurs in place of a tooth (1) (Fig. 1D) It has been speculated that primordial cysts are due to cystic degeneration of the enamel organ before calcification takes place. There is disagreement whether primordial cysts exist, some feeling that all primordial cysts represent odontogenic keratocysts (1). Keratocysts will be discussed later in this chapter.

Dentigerous Cyst (Follicular cyst)

Etiology and pathogenesis. The dentigerous cyst is caused by an accumulation of fluid between the follicle of the tooth and crown (1). As with most jaw cysts, hydrostatic and osmotic pressure are responsible for cyst enlargement, as most odontogenic cysts do not exhibit an inherent growth potential.

Clinical features. The dentigerous cyst is always associated with the crown of an impacted tooth (Fig. 1H). It is the most common odontogenic cyst, accounting for approximately 20% of odontogenic cysts (1). Dentigerous cysts rarely affect primary teeth. Mandibular third molars are most commonly affected followed by maxillary third molars, maxillary cuspids, and mandibular premolars (2). They are frequently multiple. Dentigerous cysts are usually asymptomatic but may be symptomatic because of large size or secondary infection. Bone expansion, pain, and swelling are the usual presenting symptoms. Large lesions are uncommon and frequently represent an odontogenic keratocyst or amelobastoma arising from a dentigerous cyst.

Imaging. The dentigerous cyst presents as a well-defined radiolucency around the crown of an impacted tooth (Fig. 4). Occasionally, they may occur lateral to the crown (paradental cyst) (3) or circumferentially around the entire tooth. In some

Table 1 Classification of Cysts and Cystlike Lesions of the Oral Cavity, Jaws, and Neck

I. Odontogenic cysts
  A. Developmental
    1. Primordial cyst
    2. Dentigerous cyst (follicular cyst)
      a. Eruption cyst
    3. Lateral periodontal cyst
      a. Botryoid odontogenic cyst
    4. Glandular odontogenic cyst (sialo-odontogenic cyst)
    5. Odontogenic keratocyst (keratocystic odontogenic tumor)
      a. Nevoid basal cell carcinoma syndrome (Gorlin syndrome)
    6. Gingival cyst
    7. Cysts of the newborn

  B. Inflammatory
    1. Periapical (radicular)
      a. Residual

II. Nonodontogenic cysts
  A. Developmental
    1. Nasopalatine duct cyst (incisive canal cyst)
      a. Cyst of the incisive papilla
    2. Median palatal cyst
    3. Nasolabial cyst
    4. Thyroglossal duct cyst
      a. Thyroglossal duct carcinoma
    5. Branchial cleft cyst (lymphoepithelial)
      a. First branchial
      b. Second branchial
      c. Third branchial
      d. Fourth branchial
      e. Lymphoepithelial cyst of the oral cavity
      f. AIDS-related parotid cyst
      g. Branchial (branchiogenic) carcinoma
    6. Thymic cyst (cervical thymic cyst)
    7. Bronchogenic cyst
    8. Rathke's cyst
    9. Thornwaldt's cyst
    10. Nasopharyngeal cyst
    11. Parathyroid cyst

  B. Nondevelopmental
    1. Mucocele
      a. Salivary duct cyst
    2. Ranula
      a. Simple
      b. Plunging
    3. Mucocele of the paranasal sinuses
      a. Mucous retention cyst and pseudocyst
    4. Dermoid and epidermoid cysts
    5. Oral heterotopic gastrointestinal cyst
    6. Simple bone cyst (traumatic bone cyst)
    7. Stafne defect (Stafne bone cyst)

Abbreviation: AIDS, acquired immune deficiency syndrome.

instances, they may appear multilocular, but multilocular lesions more likely represent an odontogenic tumor or keratocyst. The border of the lesion is usually well defined and may be sclerotic. An enlarged dental follicle may appear similar, radiographically. Occasionally, the tooth may be displaced to the maxillary sinus or the inferior border of the mandible. Resorption of the roots of adjacent teeth may be seen.

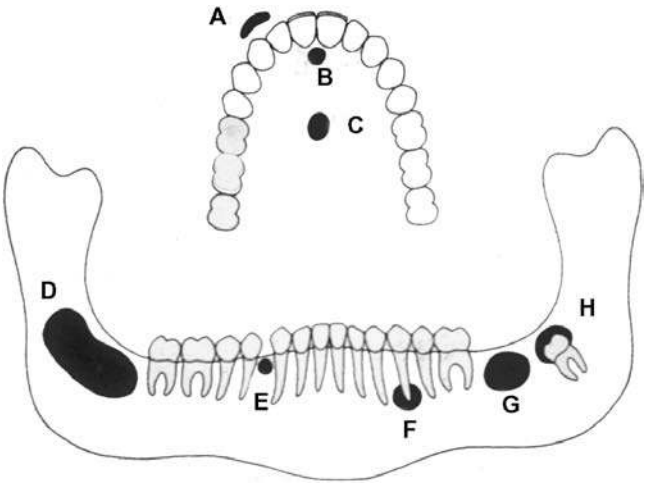

Figure 1 Classification of cysts. (**A**) Nasolabial. (**B**) Nasopalatine. Duct. (**C**) Median palatal. (**D**) Primordial. (**E**) Lateral periodontal. (**F**) Periapical. (**G**) Residual. (**H**) Dentigerous.

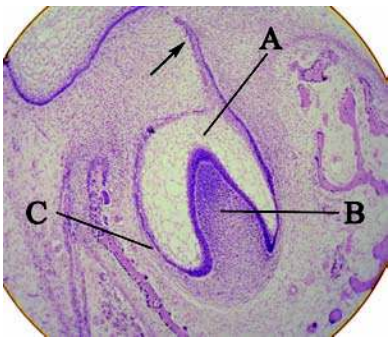

Figure 2 Tooth bud. (**A**) Enamel organ. (**B**). Dental papilla. (**C**) Dental follicle. Note dental lamina (*arrow*). *Source*: Courtesy of Wikipedia, Tooth Development, 2007.

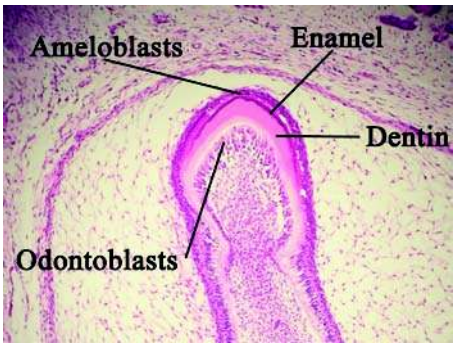

Figure 3 Developing hard tissues of tooth. *Source*: Courtesy of Wikipedia, Tooth Development, 2007.

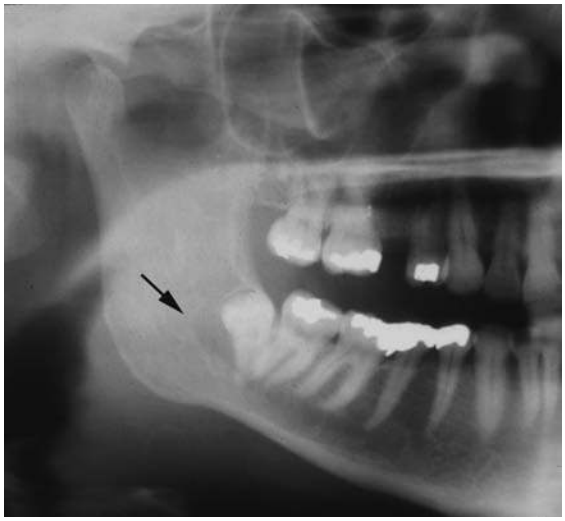

Figure 4 Dentigerous cyst. Radiolucency around the crown of an unerupted mandibular third molar (*arrow*).

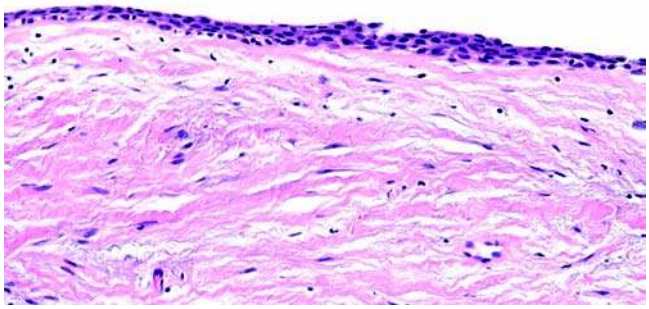

Figure 5 Dentigerous cyst. Stratified squamous epithelial lining. Unless secondarily infected, inflammation is not usually seen.

Pathology. The noninflamed dentigerous cyst is lined by a thin layer of nonkeratinized stratified squamous epithelium (Fig. 5). The cyst wall is composed of myxoid and dense connective tissue, which contains varying amounts of odontogenic epithelium (Fig. 6). If inflamed, the epithelium may be quite hyperplastic. Occasionally, the epithelium may be orthokeratinized, but it does not have the characteristic histologic features of an odontogenic keratocyst. Occasional goblet cells can be seen in the epithelium. Close examination of the epithelial lining is critical to rule out the possibility of ameloblastic transformation. A basaloid appearance to the epithelium and reverse polarity of the basal cells should alert the pathologist to possible transformation (Fig. 7). When these changes are present, recuts should be ordered to rule out an invasive component.

The cyst wall may contain an intense inflammatory infiltrate, and cholesterol clefts are common. These changes are most commonly seen in partially

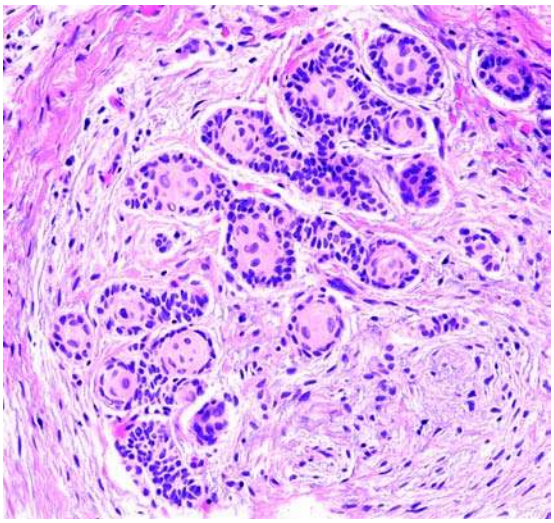

Figure 6 Dentigerous cyst. Proliferative odontogenic epithelium.

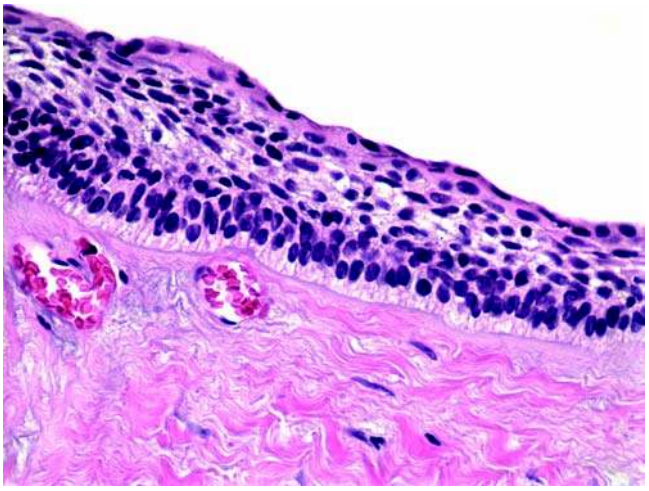

Figure 7 Dentigerous cyst. Ameloblastic change in a dentigerous cyst. Note the prominent reverse polarity of the basal cells.

erupted teeth. Hyperplastic dental follicles are composed of myxoid and dense connective tissue containing varying numbers of odontogenic rests (Fig. 8). No epithelial lining is seen.

The pathologist should be aware of a common pitfall in removal of the teeth before calcification has taken place. The dental papilla of the developing tooth is composed of primitive myxoid connective tissue, which is identical histologically to the odontogenic myxoma (Fig. 9). Clinical and radiographic correlation reveals that a developing tooth has been removed rather than an odontogenic neoplasm.

Intraosseous carcinoma rarely occurs in the lining of odontogenic cysts and usually represents squamous cell carcinoma or mucoepidermoid carcinoma (4,5). Most of these lesions occur in the posterior

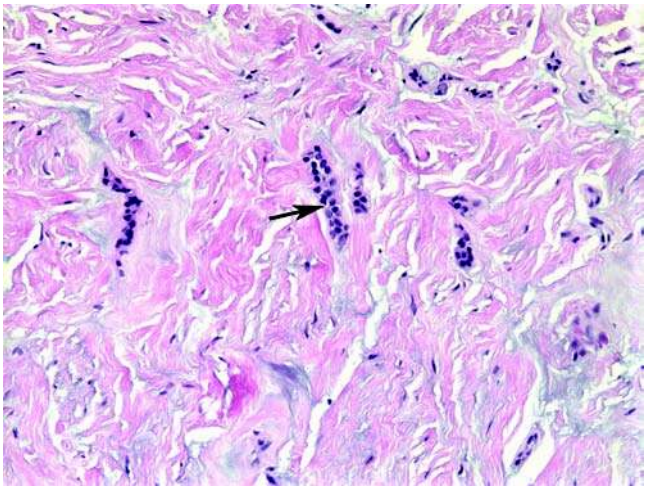

Figure 8 Hyperplastic follicle. Dense connective tissue containing odontogenic rests (*arrow*). No cyst lining is seen.

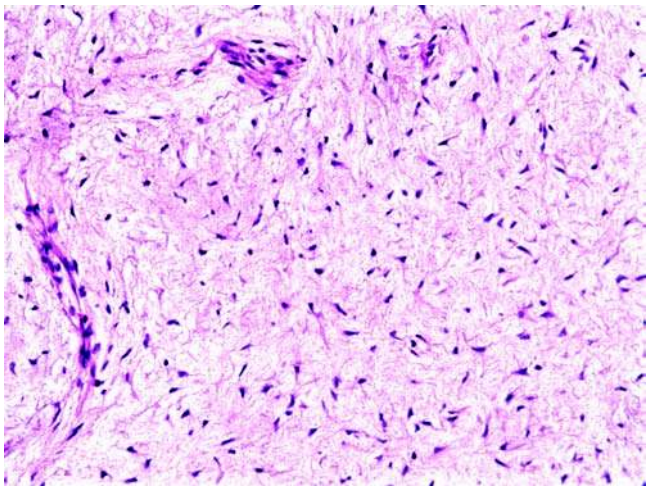

Figure 9 Dental papilla. This developing tooth is often confused with an odontogenic myxoma.

mandible, and the mean age of occurrence is 50 years with a 3:1 male-to-female predominance (6). The most common signs and symptoms are pain and swelling. The two-year survival rate has been reported to be 53% (4). Resection is the treatment of choice.

Treatment and prognosis. For most lesions, enucleation and removal of the tooth is the treatment of choice. Recurrence is rare.

Eruption Cyst (Eruption Hematoma)

Etiology and pathogenesis. The eruption cyst is a soft tissue variant of a dentigerous cyst. It is due to the separation of the dental follicle from the crown of an erupting tooth with subsequent accumulation of fluid or blood (1,2).

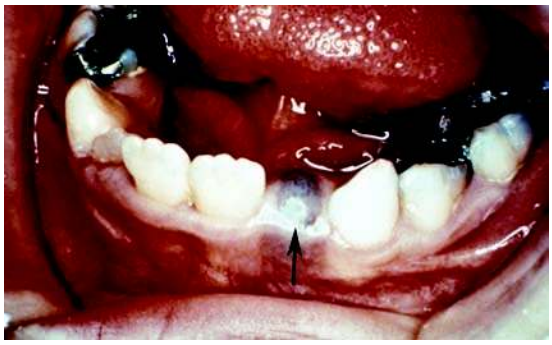

Figure 10 Eruption cyst. Swelling over unerupted first incisor (*arrow*).

Clinical. The cyst appears as a soft swelling over the crown of an erupting tooth (Fig. 10). It is frequently bluish/purple owing to blood that accumulates in the follicular space. It is almost exclusively seen in infants and young children and is commonly associated with the first mandibular molars and incisors (2).

Pathology. The cyst is covered by surface stratified squamous epithelium. The lamina propria contains varying amounts of inflammation. At the base, the roof of the cyst is lined by thin stratified squamous epithelium. Often, no cyst lining is present, and the diagnosis of eruption hematoma should be used.

Treatment and prognosis. The cyst usually resolves spontaneously with the eruption of the associated tooth. In most instances, no surgical intervention is necessary. If the cyst delays the eruption of the tooth, surgical exposure of the roof of the cyst is usually adequate to allow the tooth to erupt.

Lateral Periodontal Cyst

Etiology and pathogenesis. The lateral periodontal cyst is a developmental intraosseous lesion that arises along the lateral aspect or between the roots of vital teeth (Fig. 1E). It develops from rests of the dental lamina.

Clinical. The cysts are usually asymptomatic, and the corresponding teeth are vital. Tooth vitality is important in separating lateral periodontal cysts from laterally located periapical cysts. The cyst is most commonly seen in middle-aged and older individuals. The mandibular premolar-canine region is the most frequent location (1).

Imaging. The lateral periodontal cyst appears as a well-defined radiolucency lying along the side of the root (Fig. 11). It is occasionally multilocular. The border is usually sclerotic, and the lesion rarely exceeds 1 cm. in diameter (2).

Pathology. The lateral periodontal cyst is usually unilocular and is lined by thin stratified squamous epithelium (Fig. 12). The wall is thin and uninflamed. The botryoid odontogenic cyst is a variant of lateral periodontal cyst (3,4). It is multilocular, and the epithelial lining contains nodular collections of glycogen-containing cells (grapelike clusters) (Fig. 13). The wall may contain epithelial rests.

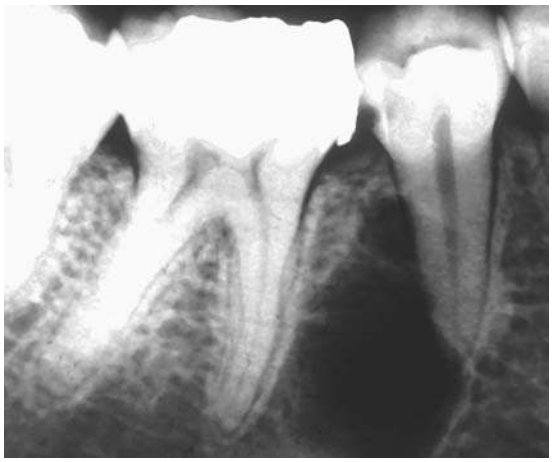

Figure 11 Lateral periodontal cyst. Radiolucency between roots of the premolar and molar.

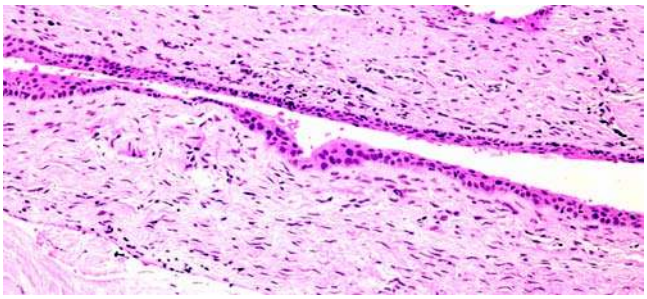

Figure 12 Lateral periodontal cyst. Thin stratified squamous epithelial lining. Note lack of inflammation in wall.

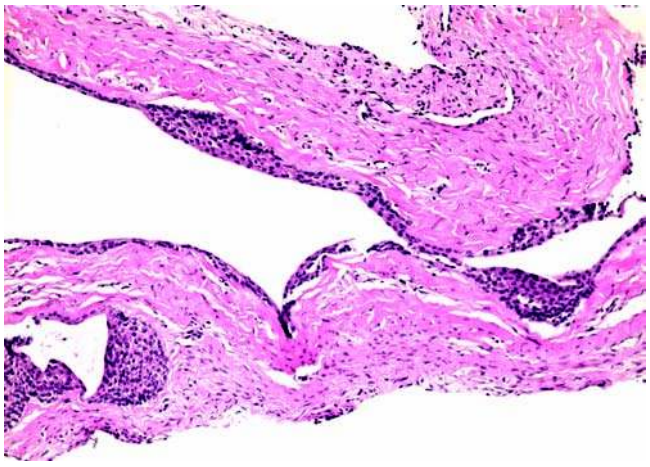

Figure 13 Botryoid odontogenic cyst. Similar stratified squamous epithelial lining to lateral periodontal cyst but exhibiting nodular collections of glycogen containing epithelial cells.

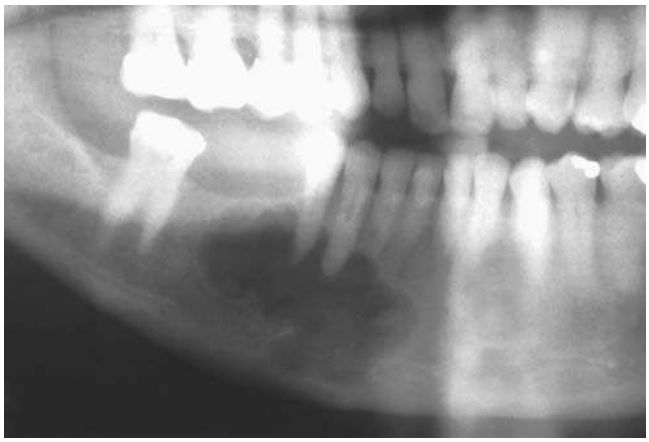

Figure 14 Glandular odontogenic cyst. Multilocular radiolucency of body of the mandible.

It should be noted that odontogenic keratocysts frequently present in a lateral periodontal configuration, but they have a distinctive histologic presentation. They will be discussed in a subsequent section.

Treatment and prognosis. Lateral periodontal cysts have a limited growth potential and rarely recur. Conservative enucleation is the treatment of choice.

Glandular Odontogenic Cyst (Sialo-Odontogenic Cyst)

Etiology and pathogenesis. The glandular odontogenic cyst is thought to be of odontogenic origin. It sometimes exhibits an aggressive clinical course. It shows areas of glandular differentiation, owing to the pluripotentiality of odontogenic epithelium (1–3).

Clinical and imaging. The cyst most frequently occurs in middle age with a slight male preponderance. It is most commonly seen in the mandible with a predilection for the anterior portion of the jaws (1). It presents as either a unilocular or a multilocular radiolucency, often crossing the midline (Fig. 14). The most common clinical presentation is swelling; large lesions may present with paresthesia (1,2).

Pathology. The cyst is primarily lined by stratified squamous epithelium of varying thickness. In areas of glandular differentiation, the cyst lining may be more cuboidal and goblet cells may be prominent (Fig. 15). Pools of mucicarmine positive material may be seen in the epithelium. Spherical nodules, similar to those seen in the botryoid odontogenic cyst, may be present. Consistent with the radiographic findings, the cyst may be multilocular. Significant inflammation is usually not present. Because of the histologic overlap between the glandular odontogenic cyst and low-grade intraosseous mucoepidermoid carcinoma, careful histologic examination, including recuts, is prudent.

Treatment and prognosis. Enucleation is the treatment of choice. The cyst has a recurrence rate of 25% to 35% (3), and some lesions may require conservative resection.

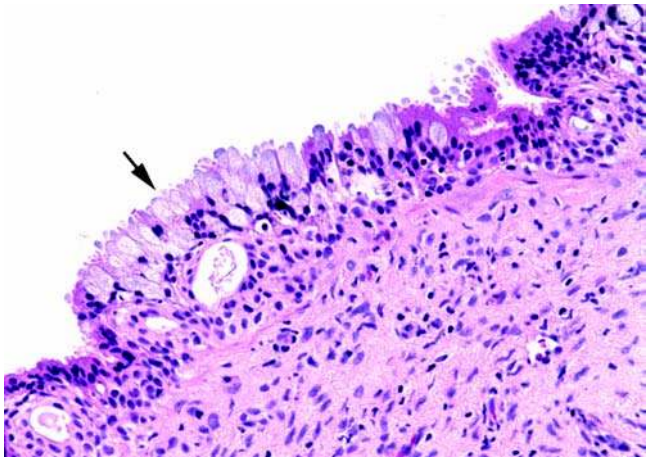

Figure 15 Glandular odontogenic cyst. Prominent goblet cells (*arrow*).

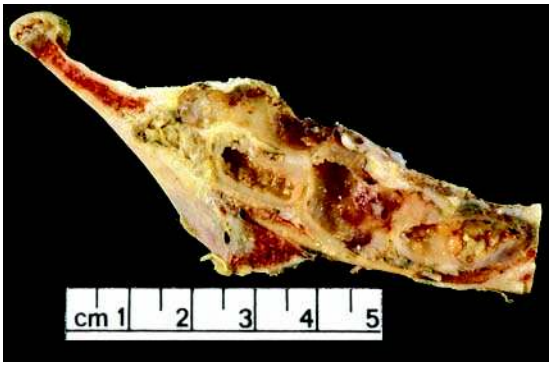

Figure 16 Odontogenic keratocyst. Aggressive multifocal lesion of the mandible. Note anterior/posterior growth with minimal expansion.

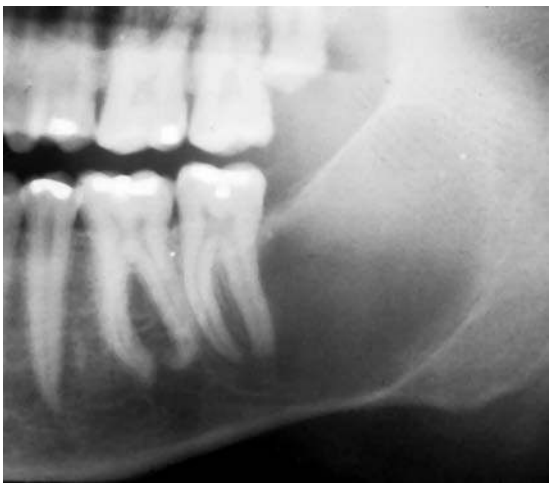

Figure 17 Odontogenic keratocyst. Radiolucency posterior to the mandibular third molar involving the ramus.

Odontogenic Keratocyst (Keratocystic Odontogenic Tumor)

Etiology and pathogenesis. The odontogenic keratocyst arises from the cells of the dental lamina. It has a distinctive clinical and histologic presentation and exhibits a more aggressive and infiltrative growth pattern than the typical odontogenic cyst. The World Health Organization working group has suggested the term ''keratocystic odontogenic tumor'' to more accurately reflect the neoplastic nature of the cyst (1). Recent studies have demonstrated the role of the human homologue of the Drosophila patched gene (PTCH) tumor suppressor gene in odontogenic keratocysts (1,2,3). Somatic mutations of the PTCH gene have been reported in sporadic odontogenic keratocysts as well as those associated with the nevoid basal cell carcinoma syndrome (2,3).

Clinical. Odontogenic keratocysts occur in almost every age group, the mean age being the second and third decades. They make up 3% to 11% of all odontogenic cysts (4,5). The mandible is most commonly involved with a tendency for the posterior mandible and ramus. Small lesions are usually asymptomatic, whereas larger lesions may present with pain, swelling, and secondary infection. Odontogenic keratocysts tend to grow in an anterior/posterior direction and may grow to a large size without significant facial deformity (Fig. 16). The lesions may be multiple, which clinically suggests the possibility of the nevoid basal cell carcinoma syndrome.

Imaging. Odontogenic keratocysts are usually unilocular but may be multilocular (Fig. 17). The borders are well defined and may be sclerotic. The cyst is frequently associated with an unerupted tooth; radiographically they may be indistinguishable from a dentigerous cyst. The lesion may present similar to a lateral periodontal cyst, particularly in the mandibular premolar area. Occasionally, the cyst causes divergence of tooth roots but rarely causes resorption.

Pathology. The odontogenic keratocyst has a distinct histologic appearance (6). The cyst is lined by parakeratinized stratified squamous epithelium, five to seven cells thick (Fig. 18). The lumen may be filled with keratin. Because of the lack of rete ridges, the cyst lining frequently separates from the underlying cyst wall. The parakeratin has a corrugated appearance. The diagnostic feature is a hyperchromatic basal cell layer, which exhibits prominent palisading of the basal cells (Fig. 19). The wall of the cyst is composed of fibrous connective tissue and is usually devoid of inflammation. Secondary inflammatory changes, when present, may alter the typical histologic presentation. Close examination of the entire cyst will exhibit focal areas exhibiting the typical features. ''Daughter cysts'' (Fig. 20) and proliferative odontogenic epithelium (Fig. 21) may be seen in the wall and suggest the possibility of the nevoid basal cell carcinoma syndrome.

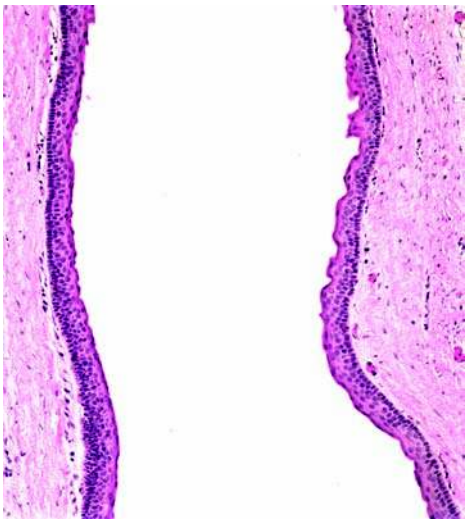

Figure 18 Odontogenic keratocyst. Parakeratinized epithelium five to seven cells thick.

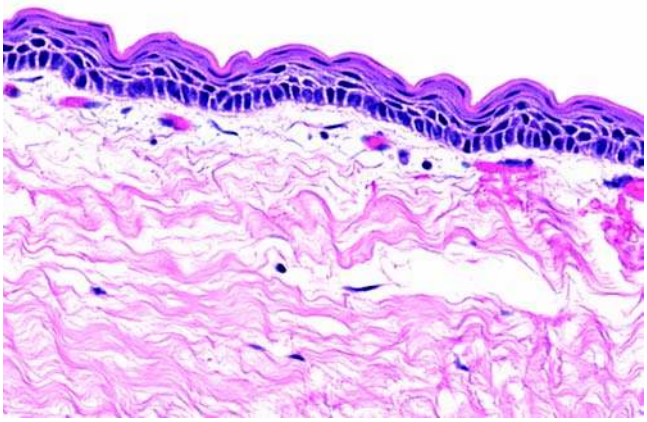

Figure 19 Odontogenic keratocyst. Prominent hyperchromatic palisaded basal cells. This is the diagnostic feature of a keratocyst.

Some odontogenic cysts may demonstrate surface and luminal keratin and be confused with the odontogenic keratocyst (Fig. 22). These cysts do not exhibit the hyperchromatic, palisaded basal cells. These cysts have been termed ''orthokeratinized odontogenic cysts.'' These cysts do not exhibit the aggressive behavior associated with keratocysts.

Treatment and prognosis. The treatment of choice for the odontogenic keratocyst is enucleation and curettage. Because of the thin lining, complete removal in toto is difficult. Removal of surrounding bone and chemical cauterization may be used to eradicate any remnants of the cyst. Odontogenic keratocysts have a propensity to recur with a reported range of 3%–62%. Several reports in large series report

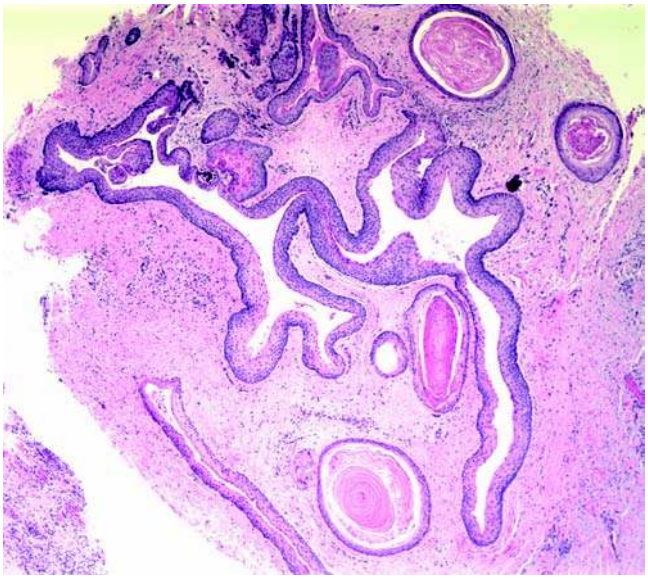

Figure 20 Odontogenic keratocyst. Prominent daughter cyst formation. Daughter cyst formation suggests the possibility of the nevoid basal cell carcinoma syndrome.

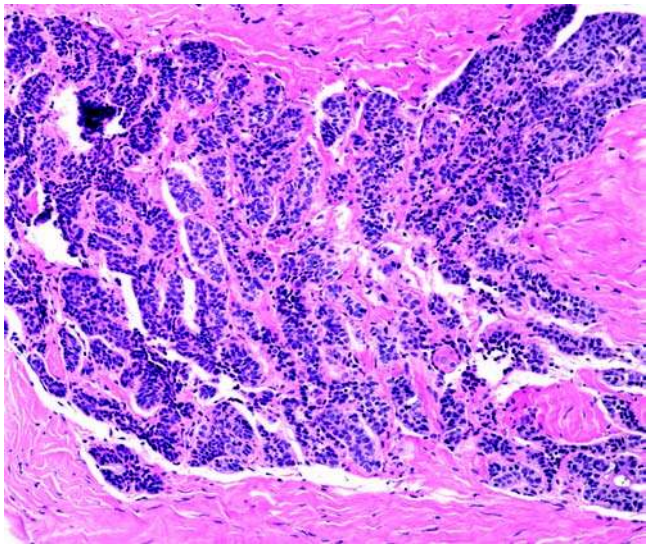

Figure 21 Odontogenic keratocyst. Proliferative odontogenic epithelium.

recurrence rates of approximately 30% (4). A five-year follow-up is recommended, although cysts may recur 10 to 15 years after removal. Patients with multiple odontogenic keratocysts should be evaluated for the nevoid basal call carcinoma syndrome.

Nevoid Basal Cell Carcinoma Syndrome (Gorlin Syndrome)

Etiology and pathogenesis. The nevoid basal cell carcinoma syndrome, also known as Gorlin syndrome, is inherited as an autosomal dominant trait

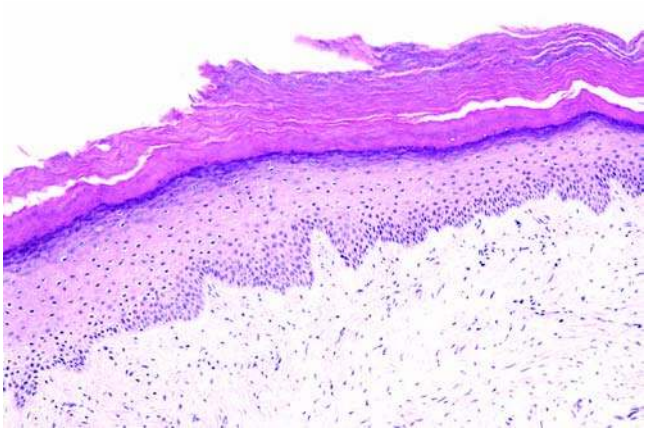

Figure 22 Keratinizing odontogenic cyst. Note orthokeratin and lack of palisaded basal cells.

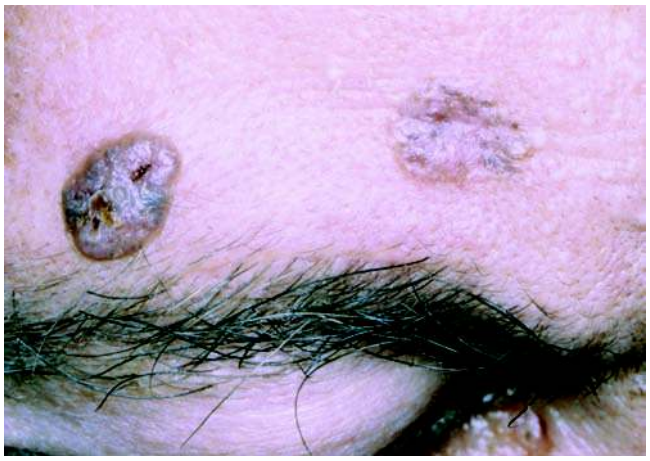

Figure 23 Nevoid basal cell carcinoma syndrome. Multiple basal cell carcinomas.

with variable expressivity. It is linked to chromosome 9q 22.3-q31 and is caused by mutations in the PTCH tumor suppressor gene (1). The prevalence is estimated to be 1:60,000 (2).

Clinical. Many abnormalities have been reported in the syndrome (2,3). Major abnormalities include: odontogenic keratocysts in 74% of patients and basal cell carcinomas in 80% of patients (Fig. 23). Epidermal inclusion cysts, palmar pits (Fig. 24), enlarged head circumference, hypertelorism, and rib abnormalities (bifid rib) occur in greater than 50% of patients. Less common abnormalities include calcified ovarian tumors, pectus excavatum, medulloblastoma, and strabismus. Other abnormalities may also be present.

Imaging. The odontogenic keratocysts are often seen around the crowns of unerupted teeth and appear radiographically similar to dentigerous cysts. Calcification of the falx cerebri is seen in 65% of patients (3).

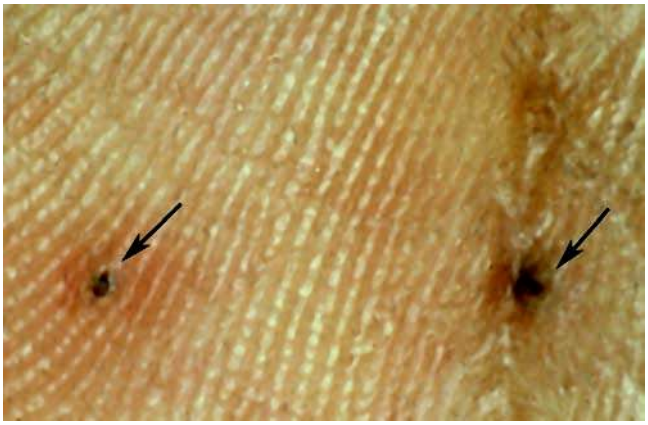

Figure 24 Nevoid basal cell carcinoma syndrome. Palmar pits (*arrows*).

Pathology. The histology of the odontogenic keratocyst was described in the previous section. Although not diagnostic, daughter cysts and proliferative basaloid epithelium may be seen in the wall of the cysts.

Treatment and prognosis. The prognosis of the syndrome usually depends on the number and aggressiveness of basal cell carcinomas. The jaw cysts are treated by enucleation, although in some instances, resection may be necessary. As with all odontogenic keratocysts, recurrence is common.

Gingival Cyst of the Adult

Etiology and pathogenesis. The histogenesis of the gingival cyst of adults is poorly defined. Theories include remnants of the dental lamina (rests of Serres), extensions of the overlying epithelium, and from gingival crevicular epithelium (1,2). The rests of Serres can be seen in normal gingival biopsies, presenting as small collections of epithelial cells exhibiting clear cytoplasm because of the collection of glycogen within the cell.

Clinical. Data pooled from well-documented cases in the literature show that most cases occur in the fifth and sixth decades (1,2). The premolar-canine is the most common site. The lesions present as painless small blue-gray swellings.

Pathology. The epithelial lining of the cyst is composed of flat-to-cuboidal cells one to three cells thick (Fig. 25). Collections of glycogen-rich clear cells may be seen within the lining, similar to those seen in the botryoid odontogenic cyst.

Treatment and prognosis. Simple surgical excision is adequate. Recurrence is uncommon.

Cysts of the Newborn (Epstein's Pearls, Bohn's Nodules)

Etiology and pathogenesis. Gingival cysts of the newborn are thought to develop from remnants of embryonic epithelial rests. Remnants of mucous salivary glands, epithelium present after fusion of the

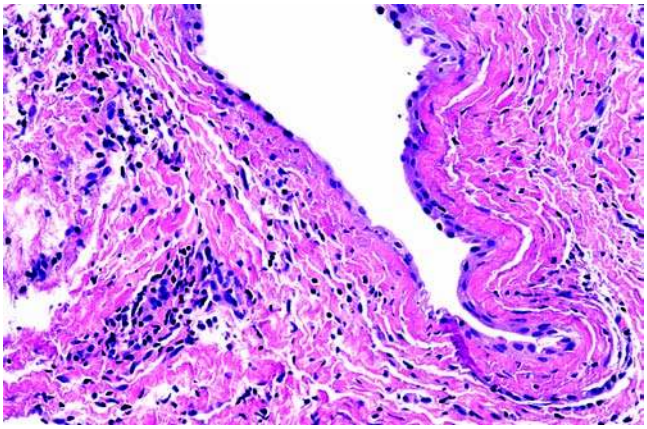

Figure 25 Gingival cyst. Thin epithelial lining one to three cells thick.

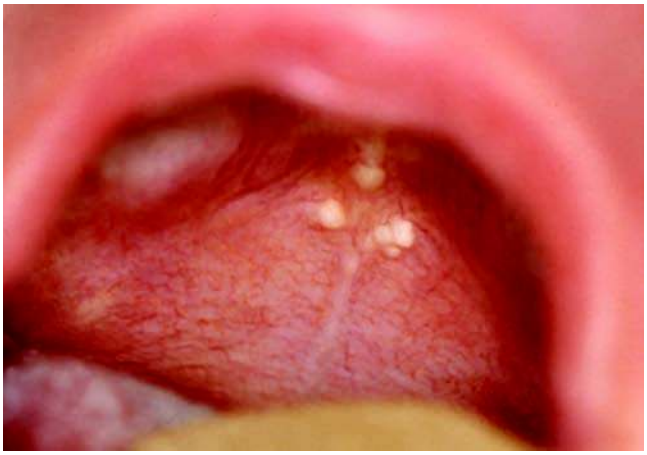

Figure 26 Cysts of the newborn. Small raised white papules of the hard palate.

palatal processes, and rests of the dental lamina likely provide the source for cyst formation. Historically, these cysts were named on the basis of their location; Epstein's pearls on the median raphe of the palate near the junction of the soft palate, Bohn's nodules on the hard palate near the alveolar ridge, and dental lamina cysts on the maxillary alveolar ridge. Practically, these cysts show similar clinical and histologic features and are best termed ''cysts of the newborn'' (1–3).

Clinical features. Cysts of the newborn present as 1- to 3-mm raised firm white or yellow papules (Fig. 26). They are common and have been reported in 65% to 95% of neonates (2,3).

Pathology. The cysts are lined by thin stratified squamous epithelium. The lumen of the cyst is filled with keratin.

Treatment. No treatment is required. They spontaneously resolve a few weeks after birth.

C. Inflammatory Cysts

Periapical Cyst (Radicular Cyst)

Etiology and pathogenesis. Periapical cysts develop from nonvital teeth that have developed necrosis of the pulp. Subsequent inflammation stimulates proliferation of the rests of Malassez contained in the periodontal ligament. In some instances, epithelial-lined cysts develop at the root apex, although lesions may be seen lateral to the tooth, secondary to inflammation from a lateral canal. In many instances, true epithelial-lined cysts do not develop, and this tissue represents inflamed connective tissue. These have been termed ''periapical granuloma.'' These do not represent true granulomas, and the terminology may be confusing. In this author's opinion, when a cyst lining is absent, a descriptive diagnosis (acute and chronic inflammation) more accurately portrays the process.

Clinical. Periapical cysts may be asymptomatic or present with acute symptoms, including pain, swelling, and the formation of fistula. The tooth may be mobile and usually fails to respond to electric pulp testing (1,2).

Imaging. Periapical cysts and periapical inflammation cannot be distinguished radiographically. They both present as radiolucent lesions, usually at the root apex (Fig. 27). Cysts involving a lateral canal (lateral radicular cyst) will be seen between the roots of the teeth. Root resorption may occur. Lesions may become quite large and affect adjacent teeth, causing mobility and root resorption.

Pathology. The cyst is lined by stratified squamous epithelium, which may be hyperplastic (Fig. 28). The cyst wall is composed of fibrous connective tissue and contains variable amounts of acute and chronic

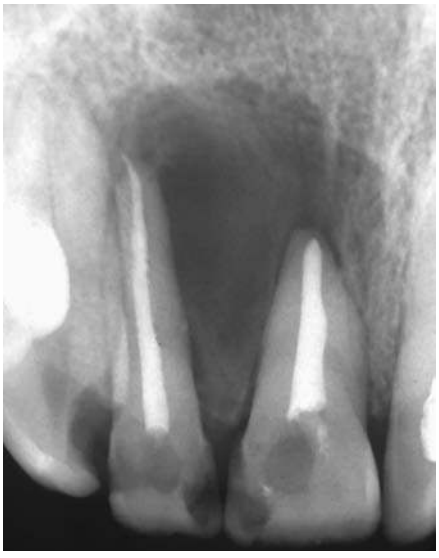

Figure 27 Periapical cyst. Radiolucency at apex of lateral and central incisors. Teeth have been previously treated with root canals with no resolution.

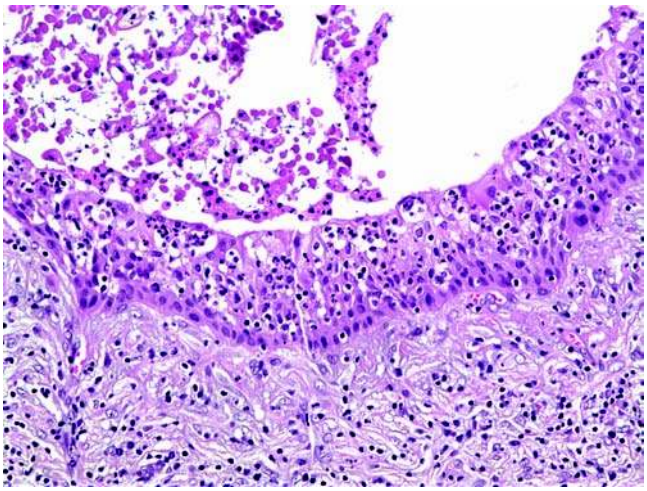

Figure 28 Periapical cyst. Stratified squamous epithelium exhibiting prominent exocytosis. Chronic inflammation is seen in the cyst wall.

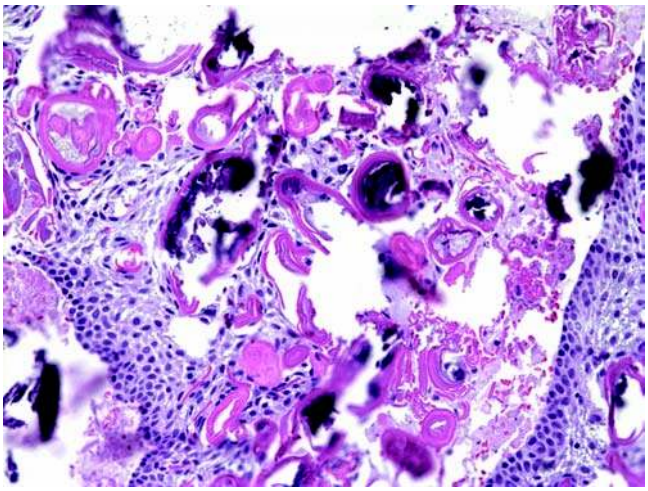

Figure 29 Periapical cyst. Lamellar calcified eosinophilic bodies seen in the epithelium (Rushton bodies).

inflammation. Cholesterol clefts are common. Two unusual histologic features can be seen. Amorphous or lamellar eosinophilic bodies (Rushton bodies) may be seen in the epithelium (Fig. 29). These are thought to be due to single cell necrosis followed by intracellular dystrophic calcification (3). Giant cell hyaline angiopathy presents as small areas of eosinophilic hyaline material surrounded by multinucleated giant cells (Fig. 30). These are thought to be due to fibrin or pooled inflammatory exudates, which undergo fibrosis (4).

Treatment and prognosis. Treatment is designed to remove the source of infection. Extraction of the tooth or endodontic therapy is performed. If the lesion does not resolve after endodontic therapy, surgical

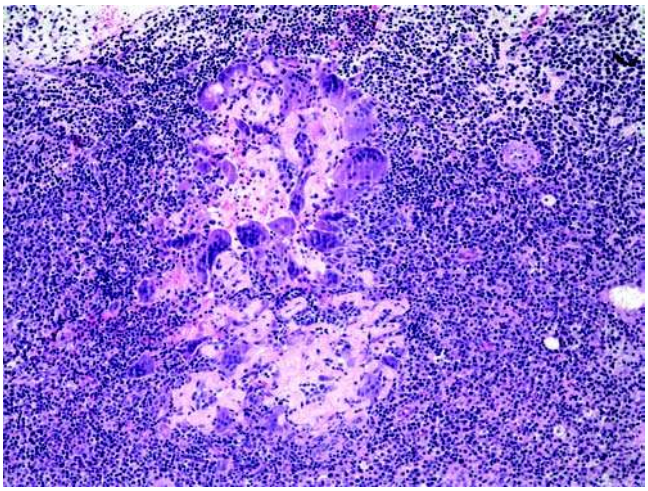

Figure 30 Periapical cyst. Eosinophilic hyaline material surrounded by multinucleated giant cells (giant cell hyaline angiopathy).

removal of the lesion is recommended to aid in resolution and to rule out another pathologic process mimicking a periapical inflammatory lesion. A residual cyst represents a persistent radiolucency after extraction of a tooth. Histologically, it may represent an area of chronic inflammation or have the features of a periapical cyst.

Periapical cysts usually do not recur after appropriate treatment. Occasionally, resolution includes a periapical scar, which may present as a persistent periapical radiolucency.

III. NONODONTOGENIC CYSTS

A. Developmental Cysts

Nasopalatine Duct Cyst (Incisive Canal Cyst)

Pathogenesis. The nasopalatine duct cyst is the most common of the nonodontogenic cysts (1). It arises from the epithelial remnants of the nasopalatine duct, which extends from the lower floor of the nasal cavity to the incisive papilla, which is directly behind the maxillary central incisors. In animals, the nasopalatine duct is thought to deliver phermones from the oral cavity to the vomeronasal organ (2).

Clinical features. The nasopalatine duct cyst may occur at any age but is most common in middle age (1,3). Most lesions are asymptomatic but may present with pain, swelling, and drainage. Care has to be taken not to confuse the nasopalatine duct cyst with periapical cysts because of close association with the roots of the maxillary central incisors (Fig. 1B). Electric pulp testing for tooth vitality as well as clinical examination are necessary to separate the two lesions.

Imaging. The nasopalatine duct cyst presents as a well-defined radiolucent lesion above or between the roots of the maxillary central incisors (Fig. 31).

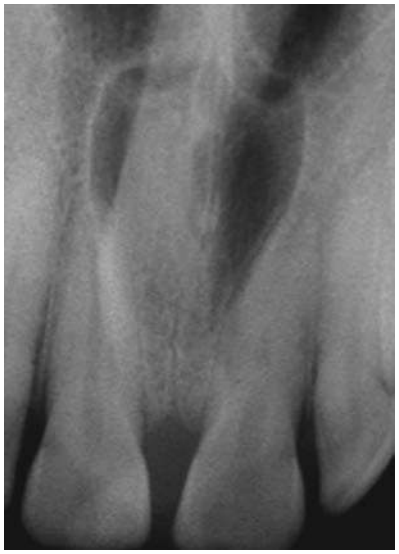

Figure 31 Nasopalatine duct cyst. Radiolucency between the roots of the maxillary central incisors. The nasopalatine duct cyst is easily confused with a radicular cyst radiographically.

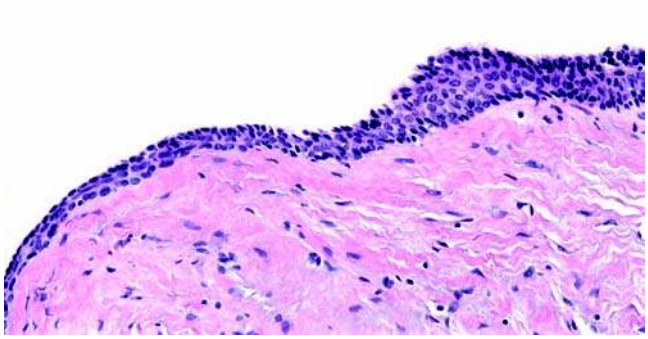

Figure 32 Nasopalatine duct cyst. Cyst lined by both respiratory and stratified squamous epithelium. Note the lack of inflammation.

Occasionally, the incisive foramen is enlarged and may be difficult to separate from a small nasopalatine duct cyst. Most nasopalatine duct cysts exceed 1 cm in size.

Pathology. The cyst is lined by squamous, cuboidal, or respiratory epithelium, either individually or in combination (Fig. 32). The wall of the cyst is composed of fibrous connective tissue and may contain neurovascular bundles, minor salivary glands, cartilage, as well as fat (Fig. 33). Inflammation is variable. A soft tissue variant of the nasopalatine duct cyst exists. It develops from epithelial rests in the incisive foramen. The cyst of the incisive papilla has identical pathology to that of the nasopalatine duct cyst but is found exclusively in soft tissue.

Treatment and prognosis. Enucleation is the treatment of choice. Recurrence is rare (4).

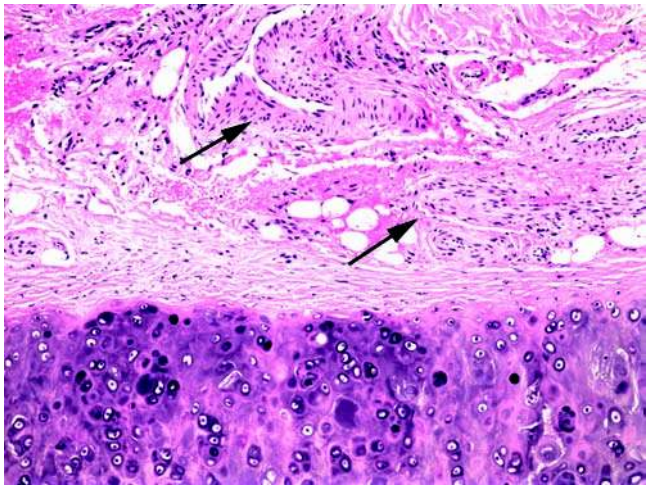

Figure 33 Nasopalatine duct cyst. Large neurovascular bundles (*arrows*) and cartilage. Fat and salivary glands are commonly seen within the wall of the cyst.

Median Palatal Cyst

Etiology and pathogenesis. The median palatal cyst is thought to develop from entrapped epithelium found along the fusion line of lateral palatal shelves (1,2) (Fig. 1C). Depending on location, it may be difficult to distinguish between a medial palatal cyst and a nasopalatine duct cyst.

Clinical. The cyst may be asymptomatic or present as a median palatal swelling posterior to the maxillary central incisor. The cysts frequently exceed 2 cm. Large lesions may cause elevation of the floor of the nose.

Imaging. The cyst presents as an ovoid radiolucency in the midline of the palate (Fig. 34). Anterior palatal lesions may be indistinguishable from nasopalatine duct cysts.

Pathology. The median palatal cyst is usually lined by stratified squamous epithelium (Fig. 35). Unlike the nasopalatine duct cyst, the wall usually does not contain large neurovascular bundles or cartilage. This may help to separate anteriorly located median palatal cysts from nasopalatine duct cysts.

Treatment and prognosis. Surgical excision is the treatment of choice. Recurrence is rare.

Nasolabial Cyst

Etiology and pathogenesis. Nasolabial cyst is a nonodontogenic soft tissue lesion thought to develop from remnants of the nasolacrimal duct. They are located in the soft tissue of the upper lip and lateral aspect of the nose (1,2) (Fig. 1A).

Clinical. The cysts are generally asymptomatic and present as swellings, which frequently elevate the ala of the nose. They are more common in women and are bilateral in 10% of cases (1,2). Pain is unusual unless secondarily infected. Elevation of the inferior turbinate may cause nasal obstruction.

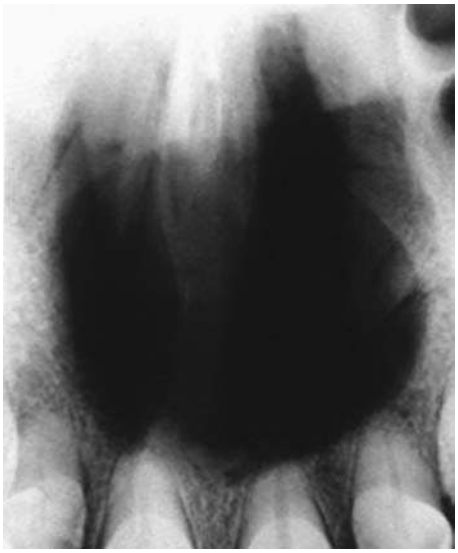

Figure 34 Median palatal cyst. Midline radiolucency of the palate.

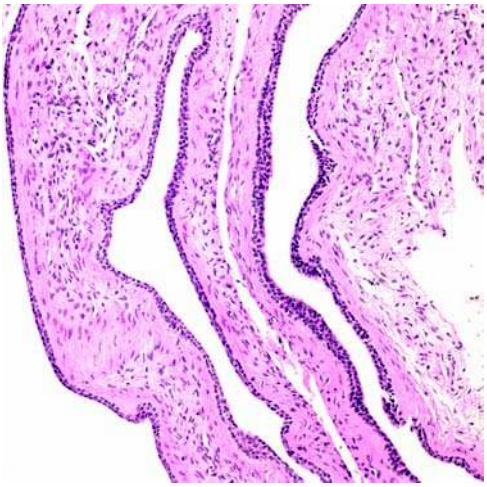

Figure 35 Median palatal cyst. Thin stratified squamous epithelial lining. Respiratory epithelium is usually not present.

Pathology. The cyst is usually lined by pseudostratified columnar, cuboidal, or stratified squamous epithelium or a combination of all types (Fig. 36). Inflammation is usually not present.

Treatment and prognosis. Surgical excision is the treatment of choice (2). Recurrence is rare.

Thyroglossal Duct Cyst

Anatomy and embryology. The thyroid begins to develop during the fourth week of gestation when the embryo is about 2- to 2.5-mm long (1). It originates as a diverticulum from the floor of the pharynx and quickly becomes bilobed as it descends into the neck

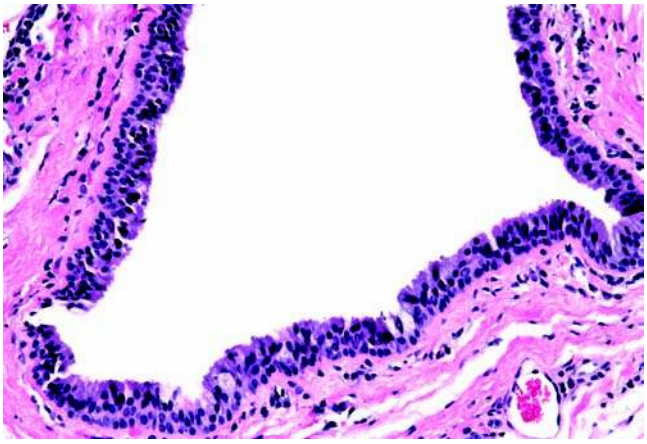

Figure 36 Nasolabial cyst. Pseudostratified columnar epithelial lining with lack of inflammation.

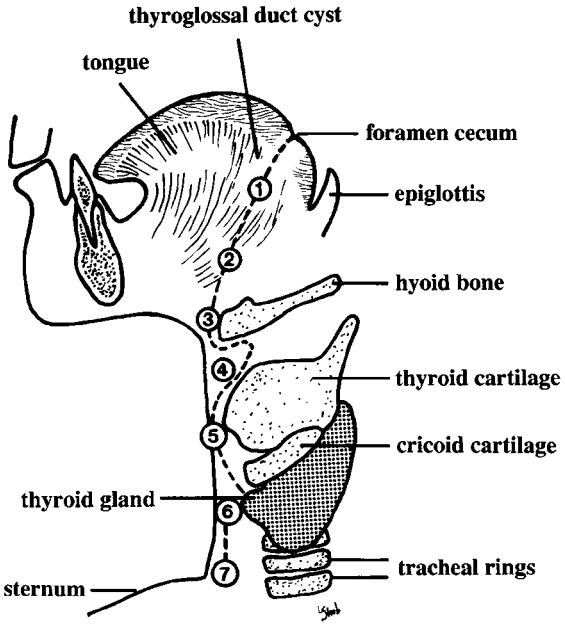

Figure 37 Origin and normal pathway of descent of the thyroid gland from the base of the tongue. Circles indicate potential site of occurrence of thyroglossal duct cysts: (**1**) base of the tongue, (**2**) floor of the mouth, (**3**) at level of hyoid bone, (**4**) subhyoid, (**5**) at level of thyroid cartilage, (**6**) at level of the thyroid gland, and (**7**) sternal area.

(Fig. 37). During migration, the gland remains connected to the floor of the pharynx by means of the thyroglossal duct. The pharyngeal attachment is referred to as the foramen cecum and is located on the dorsal surface of the tongue just posterior to the apex of the V-shaped ridge of the circumvallate papillae. By the sixth or seventh week of development, the duct gradually disappears. If involution fails to take

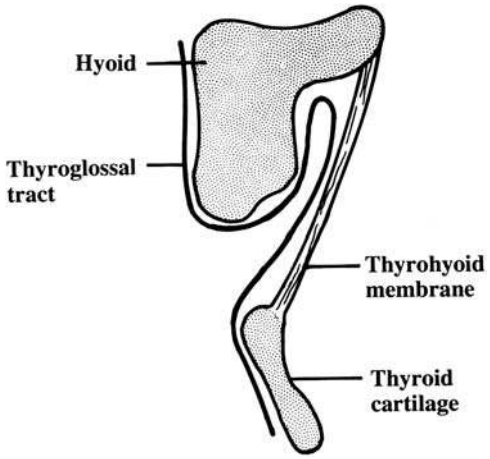

Figure 38 Intimate relation of the thyroglossal tract to the hyoid bone. Note the tract initially lies anterior to the bone, but at the lower border takes a sharp turn to lie on the posterior surface.

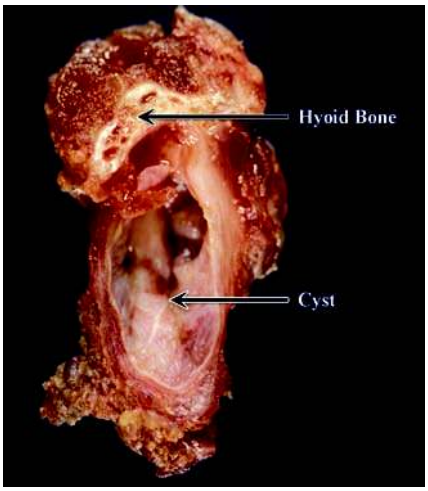

Figure 39 Whole mount of a multilocular thyroglossal duct cyst showing its close relation to the hyoid bone and necessity for removing the central portion of the bone to ensure complete removal of the cyst and its tract.

place, cysts, sinuses, or fistulas may occur anywhere along the pathway of descent (Fig. 37). The only ''normal'' vestigial remnant of the duct is the pyramidal lobe of the thyroid gland, which is seen in about 40% of the population (2).

References are frequently made to the fact that the thyroglossal duct may vary in its relation to the hyoid bone, that is, the duct may be anterior, posterior, or even within the substance of the bone (1,3). Detailed anatomic investigations by Ellis and Van Nostrand however indicate that the duct always develops anterior to the hyoid bone, but during descent it sharply hooks around the anteroinferior border of the hyoid bone to lie in a concavity on its posterior surface before continuing its caudal descent (4) (Fig. 38).

Clinical features. Thyroglossal tract abnormalities have been detected histologically in 7% of adult larynges (4). They are important for three reasons: (*i*) site of recurrent infections, (*ii*) cosmetic deformities, and (*iv*) rare site for carcinoma.

In a review of 1534 cases of thyroglossal duct abnormalities in the literature, Allard observed that, at the time of presentation, 67% of patients had cysts and 33% fistulas (5). In our patient population, sinuses and fistulas, however, have been relatively uncommon. Sixty-five percent of patients are diagnosed between birth and 30 years of age, but in 15% to 30% of cases, patients are older than 50 years before the diagnosis is established (5–8). The male/female ratio is 1:1.

About 75% of all thyroglossal duct cysts (TDCs) present in the midline of the neck either at or just below the level of the hyoid bone (3,5,7) (Figs. 37 and 39). Of the 25% that are suprahyoid, only 2% to 4% arise at the base of the tongue. Some TDCs, however, may present just lateral to the midline, especially if there has been significant inflammation and fibrosis or previous surgery.

Most patients are asymptomatic and seek evaluation for a midline neck mass discovered incidentally by themselves or a family member. The most common manifestations, when symptomatic, are pain, draining sinus or fistula, infection, or dysphagia (9). The cysts arising on the floor of the mouth may cause feeding problems in newborns, whereas those at the base of the tongue have, in rare instances, been responsible for sudden death in infancy (10,11). Despite their close proximity to the larynx, only a few cases have been reported in which the cysts have actually involved this organ (12–14). When it does, the cyst most often extends into the preepiglottic space and masquerades as a supraglottic submucosal mass that may be mistaken for a carcinoma and, especially so, if the cyst happens to erode the thyroid cartilage.

TDCs may fluctuate in size, but more commonly, the history is that of gradual enlargement. Most are usually between 2 and 4 cm in diameter, but a few have even been recorded up to 10 cm (6).

On physical examination, the cysts vary from being soft to firm and characteristically move in a vertical fashion on swallowing or protrusion of the tongue. A cutaneous tract—fistula, with or without drainage, may also be apparent.

Pathology. TDCs, which may be either unilocular or multilocular, are lined by ciliated respiratory or squamous epithelium or, if infection has occurred, by granulation and scar tissue (Figs. 39 and 40). The contents of the cysts are mucoid or pasty or, if there has been significant inflammation, purulent. Fistulas are almost invariably secondary to infection.

In contrast to popular belief, thyroid tissue is not always found in the wall of the cyst. The incidence varies with the diligence in which it is sought, varying in reported cases from a low of 1.5% up to 62% for those that have been thoroughly examined (3,6,7,15–17). Our experience, however, has been of a much higher incidence. Dische and Berg, using radioisotope

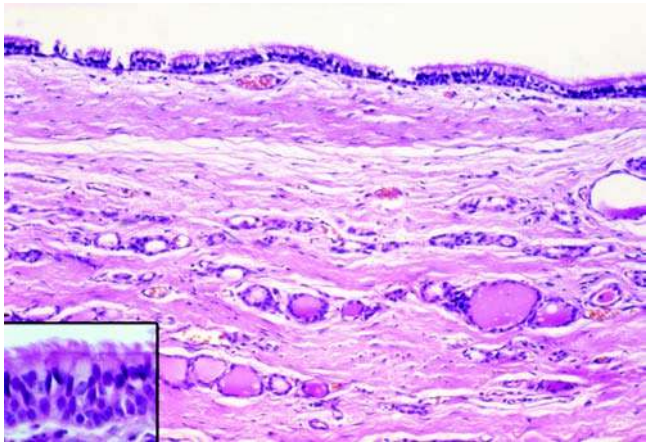

Figure 40 Thyroglossal duct cyst with thyroid follicles in its wall (100×). Ciliated respiratory epithelium lines the cyst (inset, 400×).

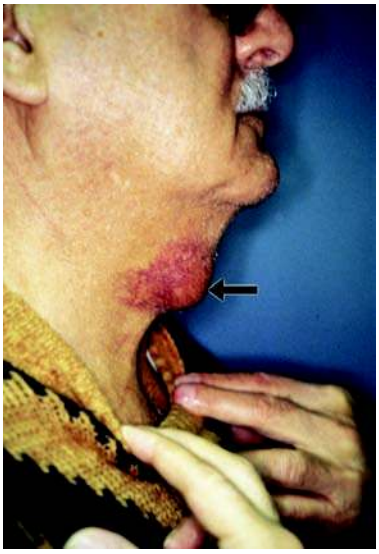

Figure 41 Large clinically obvious thyroglossal duct carcinoma (*arrow*).

scanning, found functioning tissue in one-third of their patients with TDCs (18).

Sade and Rosen have identified mucous glands in 60% of their cases, which they believe are part of the normal anatomy of the thyroglossal tract and not just glands normally found in the base of the tongue (15). Such glands have not been common in our experience. They also indicate that, not infrequently, multiple ducts may extend from the foramen cecum to the hyoid bone; however, the possibility that such a finding may represent branching of a single duct could not be dismissed (15).

Tovi et al. describe a TDC that also contained cartilage (19). The possibility of choristoma, however, could not be completely excluded. Ossified TDCs have also been reported, but are extremely rare (20).

Treatment and prognosis. There is considerable controversy among surgeons as to whether or not patients with presumed TDC should have preoperative thyroid scans to rule out an ectopic thyroid gland (21,22). Because patients with ectopic thyroid glands often do not contain normal additional functional tissue, excision under the mistaken diagnosis of a TDC will render the patient permanently athyroid. Some surgeons, however, are quick to point out that in contrast to TDCs, which occur at or below the level of the hyoid bone, ectopic thyroid glands are found primarily in the base of the tongue and that if the patient has a palpable thyroid gland in the usual location and shows no clinical or laboratory evidence of hypothyroidism, routine preoperative thyroid scans are not indicated.

Once the diagnosis is confirmed, the cyst should be excised by the Sistrunk procedure. This consists of en bloc excision of the entire thyroglossal tract to the foramen cecum as well as removal of the central 1 to 2 cm of the hyoid bone (Fig. 39). If this procedure is employed, the rate of recurrence rarely exceeds 4% to 6% (3,6,23). If the central hyoid bone is not removed, a recurrence rate of 25% or more may be expected (3). Incision and draining of a TDC is not recommended.

According to Bennett et al., factors associated with an increased risk of complications and recurrence include (*i*) occurrence in a patient younger than 10 years, (*ii*) rupture of the cyst at the time of operation, (*iii*) infection, (*iv*) failure to excise the midportion of the hyoid bone and the suprahyoid tract, (*v*) skin involvement, and (*vi*) lobulation of the cyst (9).

Thyroglossal duct carcinoma. Carcinoma arising in a TDC is a rare event, occurring in only about 1% of all TDCs (5) (Fig. 41). They are more common in women by a margin of 1.5:1 to 2:1 and have been described in individuals aged 6 to 84 years (mean 39 years) (24–26).

Approximately 90% of all malignancies complicating TDCs are papillary thyroid carcinomas, 5% squamous carcinomas, and 2% to 3% follicular carcinomas (24–28). Anaplastic thyroid carcinomas are extremely rare, whereas medullary carcinoma has never been recognized (29,30). Benign tumors of the thyroglossal duct, such as the Hurthle cell adenoma described by Tovi et al., are even scarcer than carcinoma (31).

Most thyroglossal duct carcinomas are asymptomatic and are discovered by the pathologist on routine histologic evaluation. Carcinoma, however, should always be suspected when (*i*) there is a sudden increase in size in a preexistent cyst, (*ii*) the cyst is firm to palpation and is immobile, (*iii*) the cyst is associated with one or more enlarged cervical lymph nodes, or (*iv*) there is a history of prior irradiation to the neck. In these instances, a fine-needle aspirate of the cyst may be helpful in confirming the suspicion. There is no relation between the size or duration of the cyst and malignant change (32).

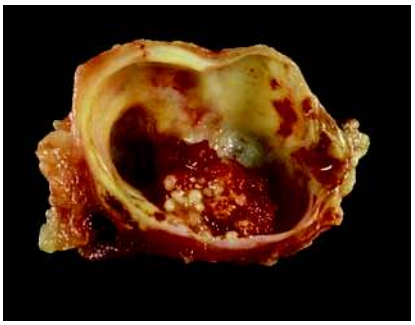

Figure 42 Papillary thyroid carcinoma presenting as a mural nodule in an otherwise typical thyroglossal duct cyst.

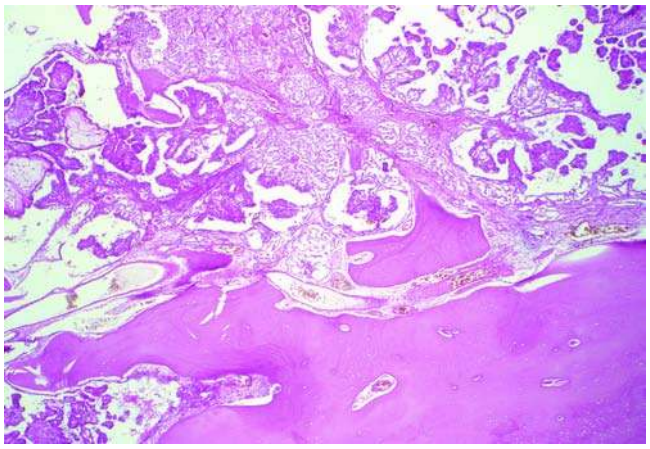

Figure 43 Papillary thyroglossal duct carcinoma invading hyoid bone.

Grossly, the carcinoma may present as a small mural nodule or it may completely fill the cyst (Fig. 42). Invasion of the hyoid bone is common, and in about 20% of cases, there is invasion of tumor through the cyst wall into surrounding soft tissue (Fig. 43). Ten percent to 15% of the carcinomas described thus far have been associated with positive cervical lymph nodes (25,26).

A frequently asked question is, ''How often do patients with thyroglossal duct carcinoma have coexistent carcinoma in their normal thyroid gland?'' The answer is, ''about 10% to 15%'' (25,26).

Because thyroglossal duct carcinomas are usually incidental findings, most are managed initially by the Sistrunk procedure employed in excising ordinary TDC. If the margins are free of tumor and there are no positive cervical lymph nodes, no further treatment is warranted. If the margins or cervical lymph nodes are involved, a wide en bloc excision of the cyst-carcinoma area or lymph node dissection is indicated. The normal thyroid gland should probably also be inspected by scanning technique and, if any abnormality is found, it should be evaluated by fine-needle aspiration and treated accordingly.

Although local recurrences, metastases, and even death have been recorded in a few instances of papillary carcinomas arising in TDCs, it is generally thought that the prognosis of this specific tumor parallels the usual papillary carcinoma of the thyroid gland (25,32,33).

Squamous cell carcinoma, on the other hand, seems to be more aggressive and may warrant more extensive surgery and, possibly, even postoperative irradiation (25,28,34).

Branchial Cysts, Sinuses, and Fistulas

Embryology. The branchial apparatus appears around the fourth week of gestation and gives rise to most of the important structures of the ears, face, oral cavity, and neck (Table 2) (1–5). Anatomically, it consists of a paired series of six arches, five pouches, and five clefts (grooves) (Fig. 44).

The arches are formed as the result of simultaneously apposing ectodermal invagination (clefting or grooving) and endodermal evagination (pouching) (Fig. 44). As the ectoendodermal fronts approximate, the mesoderm is pushed aside, creating a condensation of tissue, referred to as an arch. Each arch, therefore, is separated externally by a cleft (groove) and internally by a pouch. The clefts (ectoderm) and pouches (endoderm) eventually approximate, with little or no intervening mesoderm. If fusion of the two germ layers occurs, the subsequent structure that is formed is referred to as a branchial membrane (Fig. 44). Each arch, in turn, is innervated by a single cranial nerve and has its own blood supply (Table 2).

The arches are numbered 1 to 6, from cranial to caudal, and the clefts and pouches 1 to 5. The corresponding cleft and pouch lie immediately caudal to their numeric arch, that is, the first cleft and pouch lie between the first and second arches, the second cleft and pouch lie between the second and third arches, and so on.

Generally, only the first four arches are apparent externally on the embryo; the fifth and sixth arches are rudimentary or nonexistent (2) (Fig. 45). Likewise, the fifth pouch, also referred to as the ultimobranchial body (*ultimus,* last; *branchia,* gill), and fifth cleft are also usually inapparent (2).

Shortly after the appearance of the branchial apparatus, the second branchial arch (mesoderm) begins to proliferate caudally and eventually overlaps the second, third, and fourth clefts (ectoderm). The caudal extension ultimately fuses with the lateral or external wall of the pharynx, creating an ectodermally lined space, referred to as the cervical sinus of His (Fig. 44). Remnants of the second, third, and fourth clefts that open into this sinus, are termed ''cervical vesicles.'' Eventually, both the sinus and vesicles become obliterated and disappear.

The term ''branchial'' (*branchia*, gill) as applied to the foregoing structures is misleading. Although fish and the human embryo do share many early morphologic features in this area of the body, the clefts and pouches, while in close proximity, do not actually communicate with each other in the form of open gills (1). Accordingly, the adjective ''pharyngeal,''

Table 2 Major Derivatives of the Branchial Apparatus

Location (nerve and blood supply)	Arch (mesoderm)	Cleft (ectoderm)	Pouch (endoderm)
First (Maxillary and mandibular divisions of trigeminal nerve, facial artery)	Mandible, maxilla, body of incus, head and neck of malleus, spheno-mandibular ligament, anterior ligament of malleus, muscles of mastication (temporalis, masseter, pterygoid), anterior belly of digastric muscle, mylohyoid muscle, tensor tympani, tensor palatini, part of pinna of ear, most of anterior two-thirds of tongue	External auditory canal, outer part of tympanic membrane	Middle ear cavity, inner part of tympanic membrane, eustachian tube, mastoid air cells
Second (Facial nerve and lingual branch of external carotid artery)	Long process of incus, handle of malleus, stapes, styloid process, lesser horn and upper body of hyoid, stylohyoid ligament, muscles of facial expression (platysma, auricularis, buccinator, frontalis, occipitalis, orbicularis oculi and oris), posterior belly of digastric muscle, stapedius muscle, part of pinna of ear, possible minor component of anterior two-thirds of tongue	None	Tonsillar fossa, palatine tonsil
Third (Glossopharyngeal nerve and internal carotid artery)	Lower body and greater horn of hyoid, stylopharyngeus muscle, palatopharyngeus muscle, posterior one-third (base) of tongue	None	Inferior parathyroid glands, thymus, pyriform sinus
Fourth (Superior laryngeal branch of vagus nerve and arch of aorta and right subclavian artery)	Levator palatini muscle, cricothyroid muscle, some pharyngeal constrictor muscles, posterior one-third (base) of tongue, contributes to laryngeal cartilages	None	Superior parathyroid glands
Fifth (Recurrent laryngeal branch of vagus nerve and pulmonary arteries)	Contributes to laryngeal cartilages, intrinsic muscles of larynx	None	Ultimobranchial body (C-cells of thyroid)
Sixth (Recurrent laryngeal branch of vagus nerve and pulmonary arteries)	Contributes to laryngeal cartilages, intrinsic muscles of larynx	None	None

Source: From Refs. 1–5.

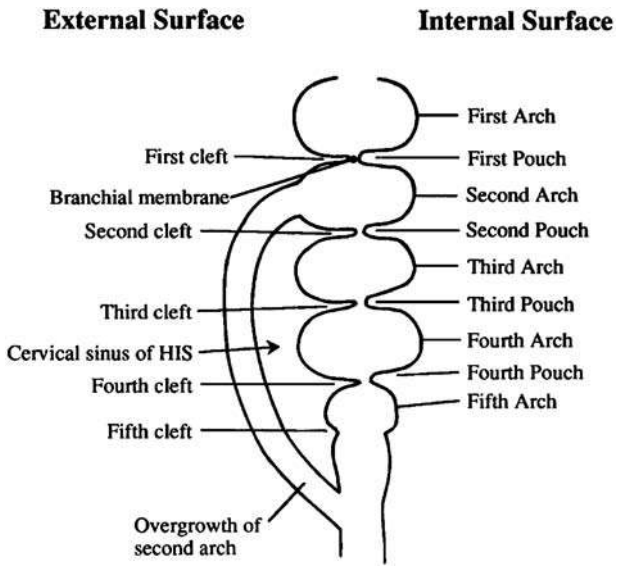

Figure 44 Diagram showing the development and relation of the various branchial clefts, arches, and pouches. Note that second arch eventually overgrows the second, third, and fourth clefts to fuse with the external wall of the pharynx, creating the cervical sinus of His.

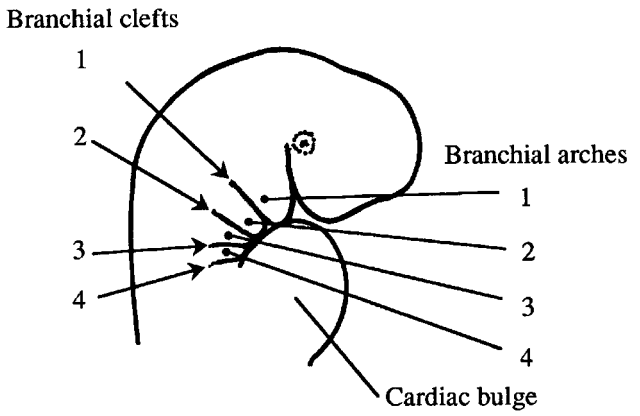

Figure 45 External appearance of the fetus at about five weeks gestation showing relation of the branchial clefts and arches. Generally, only the first four arches and clefts are visible externally.

rather than branchial is more anatomically correct. However, because branchial is so ingrained in the medical literature, it will be used in this text.

Failure of any component of the branchial apparatus to develop or involute results in a variety of abnormalities, the most common of which are cysts,

sinuses, and fistulas. They occur primarily in the neck along the anterior border of the sternocleidomastoid muscle but may also be found in or about the parotid gland, external ear, or auditory canal. The abnormalities are bilateral in 2% to 10% of patients and, on occasion, may be familial, with the mode of inheritance being autosomal dominant with reduced penetrance and variable expressivity (5–8). They generally exist as an isolated phenomenon, but in some instances may be associated with other defects, such as patent ductus arteriosus, tear duct atresia, hearing abnormalities, preauricular pits, accessory tragi, and malformed auricles (6,8).

A discussion of the more common developmental anomalies associated with the various components of the branchial apparatus follows.

Terminology. Some papers dealing with anomalies of the branchial apparatus do not always distinguish between the terms ''sinus'' and ''fistula'' and often use them interchangeably as synonyms.

A *sinus* is a tract that has only one opening, either cutaneous or mucosal. Cutaneous sinus tracts are of branchial cleft (ectodermal) origin, whereas mucosal sinus tracts are of branchial pouch (endodermal) origin.

A *fistula* is a tract that has two openings, cutaneous and mucosal. It results when the branchial membrane or plate, a structure that normally separates the branchial cleft and pouch, ruptures, allowing duct communication between these two structures (Fig. 44).

Generally, branchial cleft sinuses are associated with the first and second branchial apparatus and branchial pouch sinuses with the third and fourth branchial apparatus. Fistulas, in turn, may be associated with the first, second, or third branchial apparatus. A true fistula of the fourth branchial apparatus, although theoretically possible, has allegedly never been described.

A *cyst* is an epithelial-lined structure that may occur independently or in association with a sinus or fistula.

First Branchial Abnormalities. The normal derivatives of the first branchial apparatus are shown in Table 2. Cysts, sinuses, and fistulas of this structure are uncommon and, collectively, account for only 1% to 8% of all branchial defects (5,9–17). They tend to occur in or about the ear, postauricular, preauricular, or infra-auricular; the lobule of the ear; the angle of the jaw; the external auditory canal; and, exceptionally, the middle ear (Fig. 46). Of the first branchial abnormalities reviewed by Olsen et al., 68% were classified as cysts, 16% as sinuses, and 16% as fistulas (12).

They occur preponderantly in females and have been found in all age groups. In general, sinuses and fistulas tend to develop in infants and children, whereas cysts are more common in older age groups. In addition to an occasional fistula or sinus tract, they often masquerade as a parotid tumor or as an otitis with a draining ear (12). Secondary infection may even lead to facial nerve paralysis (18).

Work has classified first branchial disorders into two types (19). Type I are those that embryologically duplicate the cutaneous (membranous) external auditory canal (Fig. 47). Accordingly, they represent an abnormality of the first cleft only and contain only ectodermal components (Table 2). Histologically, they are often confused with ordinary epidermoid cysts, for they are lined solely by keratinized, stratified squamous epithelium, with no adnexal structures (hair follicles, sweat and sebaceous glands) or cartilage (Fig. 48). Characteristically, they are located medial, inferior, or posterior to the concha and pinna. Drainage from the cyst or sinus may occur in any of these sites. The sinus often parallels the external auditory canal and ends in a cul-de-sac at the level of the mesotympanum (Fig. 47). In some instances, parotid tissue may be associated with the tract. The

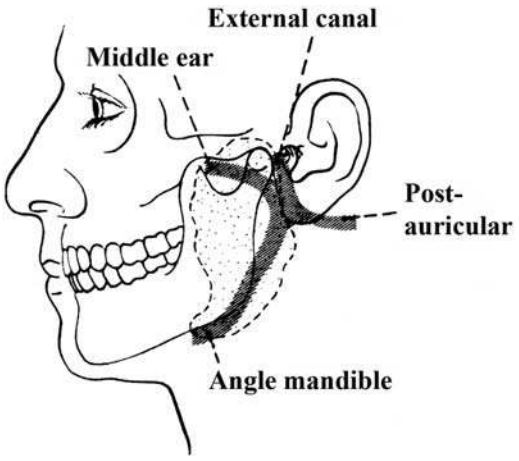

Figure 46 General location of the first branchial anomalies. *Source*: From Ref. 12.

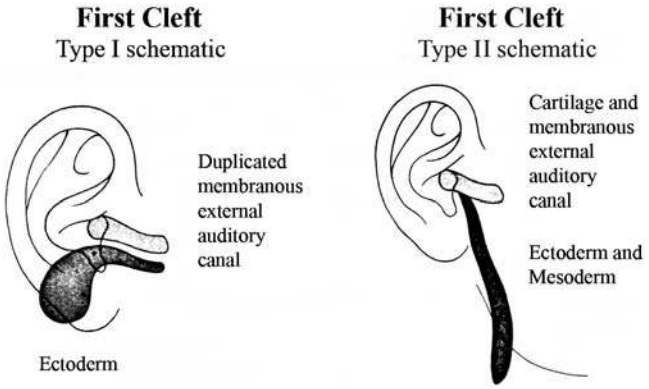

Figure 47 Work's classification of first branchial anomalies. Type I defect is a duplication of the cutaneous (membranous) external auditory canal. The main cystic mass may be anterior or inferior to the ear. Drainage may occur anywhere. A type II defect is an attempt to duplicate both the external auditory canal and pinna. The cyst or sinus may have a stomal opening in the upper neck, external auditory canal, or exceptionally, the middle ear. *Source*: From Ref. 19.

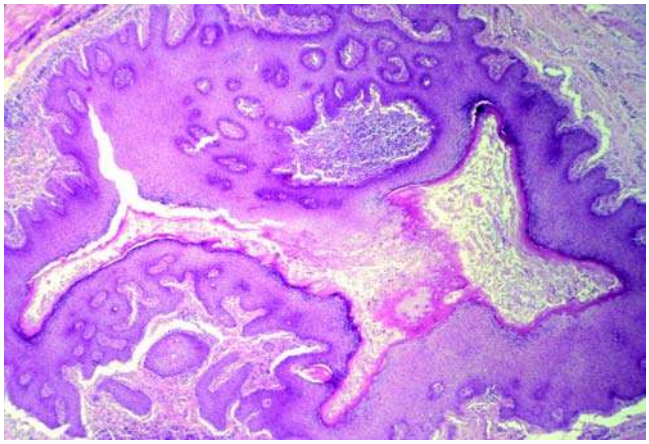

Figure 48 Type I first branchial anomaly: The cyst is lined by squamous epithelium, without adnexal structures and is often regarded as an ordinary epidermoid cyst (30×). Clinical correlation is necessary to establish the correct diagnosis.

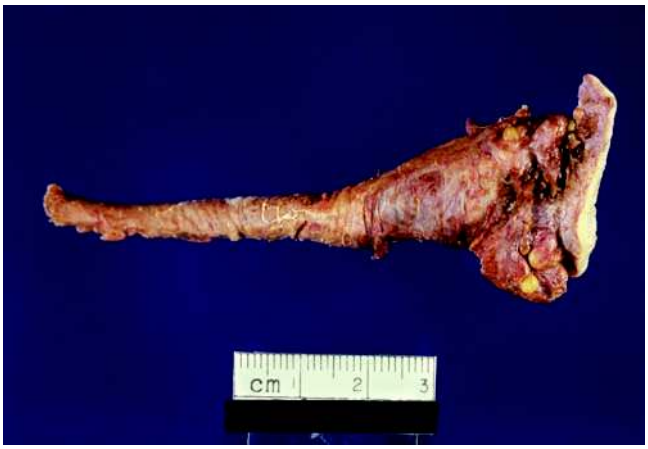

Figure 49 Gross specimen of a type II first branchial anomaly. Note skin on the right and elongated hollow cord of tissue representing a duplication of the external auditory canal.

external auditory canal is generally intact, and hearing is normal.

Type II deformities represent, embryologically, an attempt to duplicate both the external auditory canal and pinna (Figs. 49 and 50). As such, they contain both ectodermal and mesodermal elements derived from the first cleft (ectoderm) and the first and second branchial arches (mesoderm) (Table 2). Therefore, in addition to the skin, they contain cutaneous adnexal structures and cartilage and are often mistaken for dermoids (Fig. 51). Dermoids, however, are more centralized lesions and rarely, if ever, occur as far laterally at first branchial anomalies.

Patients with type II defects usually present with an abscess, sinus or fistula at a point just below the angle of the mandible. The tract extends upward over

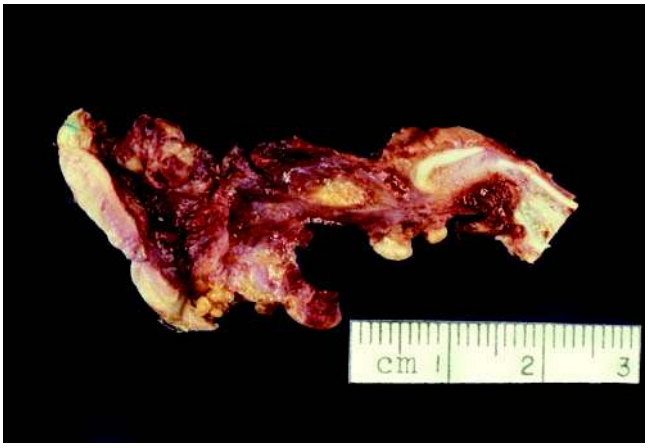

Figure 50 Gross specimen of a type II first branchial anomaly. Skin is on the left and cartilage on the right.

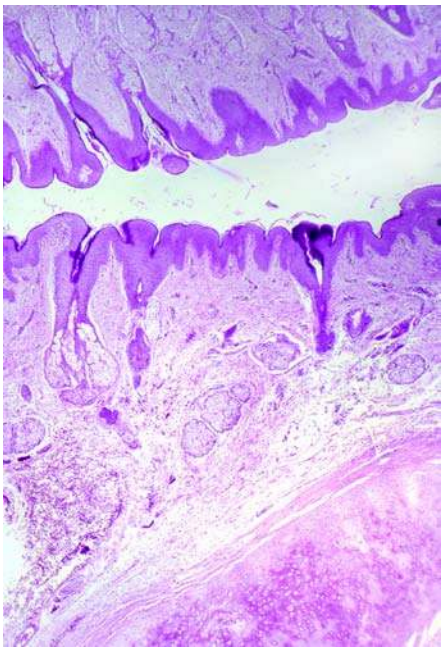

Figure 51 Type II first branchial anomaly. In addition to squamous epithelium, note the presence of skin appendages and cartilage (30×). Compare with Figure 48. Such lesions are often confused with dermoids.

the angle of the mandible through the parotid gland toward the external auditory canal (Fig. 47). The tract may end short of or drain into the external auditory canal, usually along the anteroinferior border near the cartilaginous-bony junction. Communication of the tract with the middle ear is distinctly uncommon (12). Type II defects, therefore, are more intimately associated with the parotid gland than type I defects.

In some instances, because of the clinical findings, location, or histology, a distinction between

type I and type II defects cannot always be made (10,11). Olsen et al. have proposed, therefore, that first branchial abnormalities be classified only as to whether the lesion is a cyst, sinus, or fistula (12).

Complete excision is the only effective form of therapy (20). In some cases, this may necessitate a superficial parotidectomy and removal of part of the external auditory canal. The dissection may be exceptionally difficult and caution must be exercised so that the facial nerve is not injured. Unfortunately, the tract bears no constant relation to the facial nerve; it may pass inferior, superior, lateral, or medial to the nerve or even split the main trunk.

Pathologists must be aware of two issues when dealing with first branchial anomalies. First, in contrast with the ''usual (second)'' branchial cyst, they are rarely, if ever, associated with a prominent lymphoid component, unless significantly inflamed. Second, type I and type II defects are usually mistaken, respectively, for epidermoid cysts and dermoids. Only close clinical and pathologic correlation will establish the correct diagnosis.

Second Branchial Abnormalities. The components derived from the second branchial apparatus are shown in Table 2. Of all branchial disorders, 92% to 99% are associated with this apparatus, probably because of its greater depth and longer persistence (5,10,12,21). Normally, when the phrase ''branchial cyst'' is used without further qualification, one is generally referring to a cyst of second branchial origin.

The histogenesis of second branchial cysts has been the subject of controversy for some time. Most theories center around an origin from salivary gland inclusions into the lymph nodes, the branchial apparatus, or, to a lesser extent, the thymic duct (22).

Bhaskar and Bernier reviewed 468 cysts and concluded that most arose from cystic alterations of parotid inclusions within cervical lymph nodes (23). They based their thesis on the fact that the branchial apparatus normally appears soon after the 26th day of fetal life and disappears between days 32 and 45. Cervical lymph nodes, on the other hand, begin to develop only after the second month of intrauterine life, as aggregates of lymphoblasts, and cannot be recognized as lymph nodes until after the third month. Because of this different temporal sequence, the authors reasoned that it would be highly unlikely that the nodal inclusions were of branchial origin. Instead, they proposed that the inclusions were of parotid derivation because this gland normally begins its development after the 45th day as a loose nonencapsulated anlage, which would allow incorporation of lymph nodes into the definitive gland or allow sequestered parotid tissue to become entrapped in developing lymph nodes. They further found the branchial theory to be unacceptable because (*i*) of the rare finding of similar cysts within the parotid gland that are not of branchial origin; (*ii*) of the failure of this theory to explain the presence of lymphoid tissue in these cysts; (*iii*) branchial cysts, unlike fistulas, are seldom present at birth; and (*iv*) branchial cysts are connected to neither the pharynx nor the skin surface, as are fistulas. From these observations, they concluded that the term ''lymphoepithelial cyst'' would be more appropriate than branchial cyst.

Little and Rickels, however, found the salivary inclusion theory to be untenable on the grounds that cysts described as branchial rarely occur in the parotid area where lymph nodes with salivary inclusions are concentrated (24). Instead, they are found in the upper and midneck, areas that probably contain the greatest concentration of branchial remnants. Because thymic tissue is rarely found in the wall of these cysts, an origin from thymic precursors is deemed unlikely. Moreover, if thymic tissue were identified, the cyst should probably be classified as a cervical thymic cyst (CTC) (25).

Although some lateral cervical cysts that occur either within or adjacent to the parotid gland may develop from salivary inclusions, most authorities still abide by the theory that most of them arise from second branchial inclusions entrapped in cervical lymph nodes during early development. Fistulas, on the other hand, seem to arise when the membrane separating the second cleft and pouch breaks down, creating a complete communication between the pharynx and skin of the neck.

Cysts of the second branchial apparatus are three times more common than sinuses and fistulas (6). They typically occur along the anterior border of the sternocleidomastoid muscle from the hyoid bone to the suprasternal notch, but a few cysts, allegedly derived from the second branchial pouch, have been described even in the lateral wall of the nasopharynx (26–29). There is no gender preference. Most (74%) patients are in the 20–40-year age range at the time of diagnosis. Because less than 3% of cysts present after the age of 50 years, pathologists must be careful in making such a diagnosis in this age group, for a metastatic squamous cell carcinoma in a cervical lymph node with cystic degeneration may masquerade as a branchial cyst.

Fistulas and sinuses are more often found at birth or in early childhood. They are divided into three types: (*i*) external sinuses that have a cutaneous opening but no internal communication with the pharynx; (*ii*) internal sinuses that open into the pharynx but do not have a cutaneous opening; and (*iii*) fistulas with both internal and external orifices (21). About 80% of fistulas and sinuses are of the external type.

The external opening of a sinus or fistula is usually found at the junction of the middle and lower one-third of the sternocleidomastoid muscle along its anterior border. The tract, if complete, typically courses cephalad beneath the platysma and cervical fascia, between the external and internal carotid arteries, over the glossopharyngeal and hypoglossal nerves, beneath the posterior belly of the digastric muscle, to open internally in the region of the tonsil-pharyngeal wall (Fig. 52). The cutaneous orifice often retracts with swallowing. Mucoid secretions can be manually (or spontaneously) expressed, and in some instances, ingested liquids or food particles may pass through the tract. Probing of the tract can produce hoarseness, cough, slowing of the pulse,

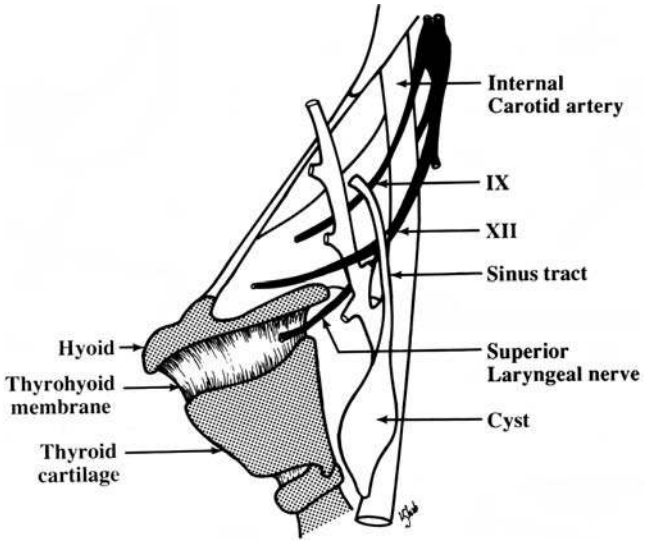

Figure 52 Location and course of a second branchial anomaly. Note that the sinus tract courses over cranial nerves IX and XII and between the internal and external carotid arteries.

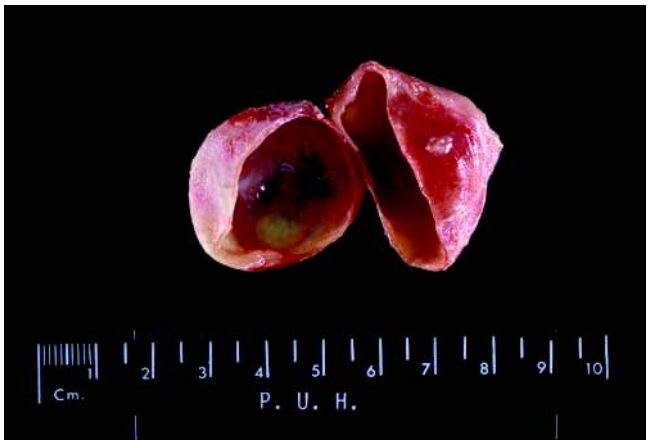

Figure 53 Typical gross specimen of a unilocular second branchial cleft cyst. Note the smooth inner surface devoid of intracystic projections.

pallor, sweating, and faintness. Complete excision may necessitate a tonsillectomy.

Pathologically, second branchial cysts are unilocular, usually between 2 and 6 cm in diameter, and are lined by stratified squamous epithelium (90%), respiratory epithelium (8%), or both (2%) (Figs. 53 and 54). With repeated infections, the wall becomes fibrotic and the epithelium may then be partially replaced by granulation or fibrous tissue. Lymphoid tissue, either nodular or diffuse, occurs in the wall of 97% of the cases and often contains germinal centers and subcapsular and medullary sinuses (23). Exceptionally, one may even find heterotopic salivary tissue in the wall

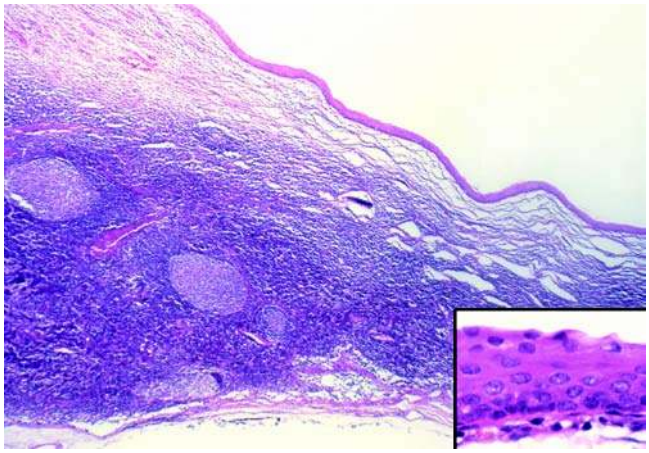

Figure 54 Branchial cleft cyst (derived from second branchial apparatus) contains abundant lymphoid tissue in its wall, often with prominent germinal centers (50×). The cyst is lined by stratified squamous epithelium (inset, 400×).

of the cyst or sinus fistula (30). The cyst contents may be cheesy, mucoid, serous, or, if infected, purulent.

A complete surgical excision of the cyst or sinus fistula is indicated. If there is significant inflammation, surgery may have to be delayed until it is resolved. To identify and ensure complete removal of the sinus or fistula, injection of methylene blue, liquid paraffin, quick-hardening polymers, and the insertion of esophageal bougies, various blunt probes, and the use of balloon embolectomy, all have been tried.

Patients who continue to have persistent branchial remnants with infectious episodes after repeated attempts at surgical excision may benefit from a functional neck dissection (31).

In a review of 274 patients with branchial remnants treated at the Mayo Clinic, the recurrence rate was only 2.7% for cases with no history of surgery or infection, 14% when there was a history of infection, and 21.2% when there had been prior attempts at surgical removal (32).

Third Branchial Abnormalities. The contributions of the third branchial apparatus to normal human development are shown in Table 2. Anomalies of this structure, though extremely rare, should be considered in any patient who presents with recurrent neck abscesses, especially if associated with stridor, or with recurrent episodes of acute suppurative thyroiditis, particularly on the left side (5,6,20,33,34).

If present, a sinus or fistula would open externally along the anterior margin of the lower one-third of the sternocleidomastoid muscle. If complete, the tract should ascend in relation to the carotid sheath, pass superior to the hypoglossal nerve and inferior to the glossopharyngeal nerve, course behind the internal carotid artery, penetrate they thyrohyoid membrane, and open into the pyriform sinus (6,20) (Fig. 55). Cysts may occur anywhere along the tract, but most commonly are found in the anteroinferior cervical triangle or in the region of the laryngeal ventricle (20). The cysts

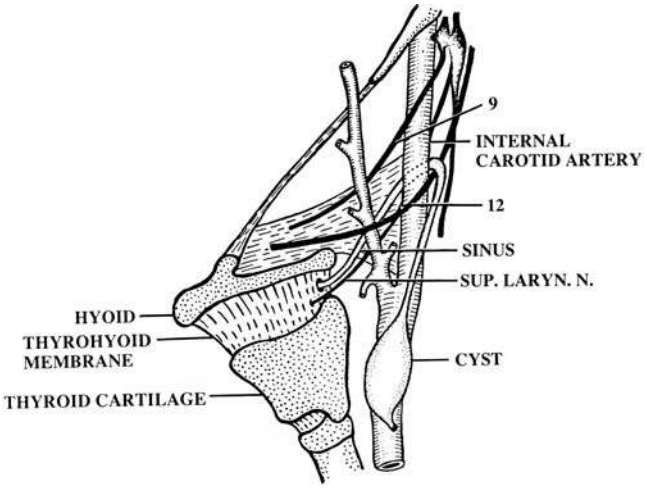

Figure 55 Location and course of a third branchial anomaly. Note the cyst and that the sinus tract courses behind the internal carotid artery between cranial nerves IX and XII and penetrates the thyrohyoid membrane cranially to the superior laryngeal nerve. *Source*: From Ref. 21.

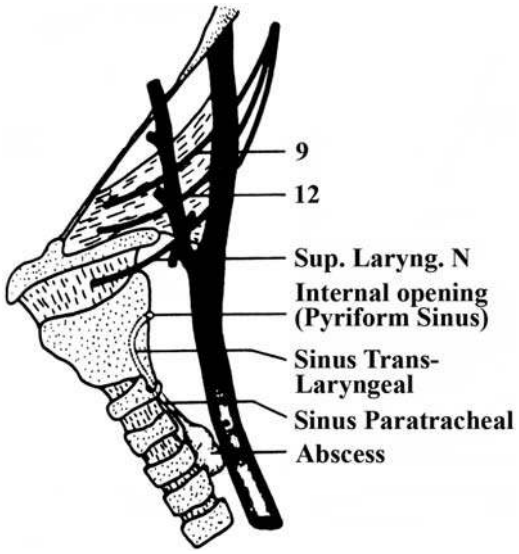

Figure 56 Location and course of a fourth branchial anomaly. Note the abscess and that the sinus tract ascends vertically in the neck, enters the larynx just beneath the thyroid cartilage near the cricothyroid joint, and proceeds caudally to the superior laryngeal nerve to open internally at the apex of the pyriform sinus: compare with Figure 55. *Source*: From Ref. 36.

are lined by stratified squamous or ciliated epithelium and, in some instances, are associated with a dense infiltrate of lymphocytes (33).

Barium swallow, CT scans, and thyroid scan, coupled with direct endoscopic inspection, especially of the pyriform sinus area, are helpful in diagnosis and confirming the extent of the abnormality. Complete surgical excision of the cyst or sinus fistula is mandatory to prevent recurrence and may even require a partial thyroidectomy.

Fourth Branchial Abnormalities. The derivatives of the fourth branchial apparatus are shown in Table 2. Although extremely rare, anomalies of this apparatus are being recognized with increased frequency (5,35–41).

The distinction between abnormalities of the third and fourth branchial apparatus is not possible on the basis of clinical or imaging criteria because both, especially sinuses, originate from the pyriform fossa and have similar clinical manifestations (36). Accordingly, patients with fourth branchial defects typically present with repeated episodes of neck abscesses and acute suppurative unilateral thyroiditis that, almost invariably, involve the left side of the neck. Most patients are symptomatic before 20 years of age (36).

Almost all fourth branchial defects are sinuses. In fact, there is some doubt as to whether or not a true fistula has ever been described. A ''pseudofistula,'' however, may develop after iatrogenic or spontaneous rupture of a cervical abscess associated with a fourth branchial sinus. The usual sinus tract has an internal opening at the apex of the pyriform sinus caudal to the superior laryngeal nerve. It then descends translaryngeally under the thyroid cartilage to emerge beneath the inferior constrictor muscle, exiting the larynx near the cricothyroid joint. It then continues superficial to the recurrent laryngeal nerve and terminates in the paratracheal region or within the thyroid gland (20,36) (Fig. 56).

The distinction between the third and fourth branchial sinuses can be made only by detailed surgical exploration. A third branchial sinus always extends from the pyriform sinus through the thyrohyoid membrane cranial to the superior laryngeal nerve. In contrast, a fourth branchial sinus extends from the pyriform sinus caudal to the superior laryngeal nerve and exits the larynx near the cricothyroid joint (36).

The presence or absence of thymic tissue (a derivative of the third branchial derivative) in the wall of a cyst or sinus cannot be used to distinguish absolutely between a third and fourth branchial defect, because such tissue has also been seen in some instances in fourth branchial abnormalities (36).

The preoperative evaluation and treatment of third and fourth branchial defects are identical (see foregoing discussion under the section ''Third Branchial Abnormalities'').

Lymphoepithelial Cysts of the Oral Cavity (''Branchial Cleft Cysts,'' Tonsillar Cysts, Tonsillar Pseudocysts). Cysts histologically similar to those found in the lateral neck also occur in the oral cavity (Fig. 57). In this site, they are referred to as lymphoepithelial cysts, branchial cleft cysts, tonsillar cysts, or tonsillar pseudocysts. Although in the past they were considered to be derivatives of the first branchial apparatus, most investigators now consider these cysts to arise by one of two mechanisms: obstruction of a crypt of oral lymphoid tissue or cystic change in

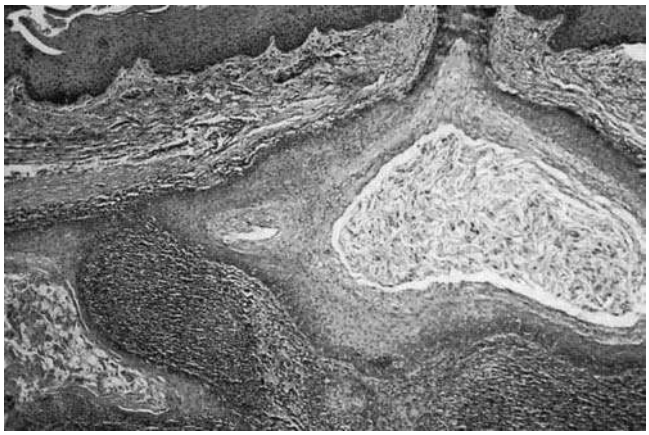

Figure 57 Lymphoepithelial ("branchial cleft") cyst of the oral cavity. The cyst is lined by stratified squamous epithelium, filled with keratin, and partially surrounded by lymphoid tissue (50×).

epithelium entrapped in lymphoid tissue during embryogenesis (6,42).

The cysts present as freely movable yellow or white submucosal masses that are most often found on the floor of the mouth (50% of cases) or on the ventral and posterolateral surfaces of the tongue (37% of cases). They occur in males by a 3:2 ratio (42). In Buchner and Hansen's series of 38 cases, the cysts were all smaller than 1 cm (42). Larger cysts, however, do occur. Most often they are only asymptomatic lesions discovered during routine oral examination, but some may "swell," become painful, or cause a bad taste by spontaneous drainage. Conservative excision is curative.

AIDS-Related Parotid Cysts (Branchial Cleft Cysts, Lymphoepithelial Cysts, Cystic Lymphoepithelial Lesions). Patients with acquired immune deficiency syndrome (AIDS) may have parotid cysts that are often multiple and bilateral and bear, to some extent, a histologic similarity to branchial cysts (43–47). A few patients may even have a Sjogren's-like illness (48).

Branchial Cleft (Branchiogenic) Carcinoma. The development of carcinoma in branchial cleft cysts has been controversial ever since it was first proposed by von Volkman in 1882 (49). In 1950, Martin et al. reviewed 250 alleged branchial cleft carcinomas reported in the literature and accepted only three possible cases, the rest were regarded as metastatic carcinomas (50). They proposed the following criteria for tentative diagnosis of a branchial cleft carcinoma: (*i*) the tumor must have occurred somewhere along a line extending from a point just anterior to the tragus of the ear, downward along the anterior border of the sternocleidomastoid muscle to the clavicle, (*ii*) the histologic appearance of the growth must be consistent with an origin from tissue known to be present in branchial vestiges, (*iii*) the patient must have survived and have been followed by periodic examinations for at least five years without the development of any other lesion that could possibly have been the primary tumor, and (*iv*) most importantly, the histologic demonstration of a cancer developing in a wall of an epithelial-lined cyst situated in the lateral aspect of the neck.

In a study of 22 cases from the Armed Forces Institute of Pathology that were originally thought to be squamous cell carcinoma arising in branchial cysts, a primary tumor was subsequently found in 19 (51). Of the three remaining patients, two were alive at three and six years, respectively, without a proven primary squamous cell carcinoma. The third patient died of an adenocarcinoma of the colon two years later, but no primary squamous cell carcinoma was found during this time. In this study, the average duration from the appearance of the cervical metastasis and the discovery of the primary tumor was two years (51).

It is now apparent that the concept of a carcinoma in a branchial cleft cyst, for all practical purposes, does not exist and that all alleged cases will prove, on thorough evaluation and/or follow-up, to be examples of metastatic squamous cell carcinoma with cystic degeneration (52–58).

Tonsillar carcinomas are notorious for producing cystic lymph node metastases that masquerade as branchial carcinomas. The carcinomas are typically small, arise from the tonsillar crypts (rather than the surface), and metastasize early without producing any significant enlargement of the tonsil (Fig. 58). Most often the metastasis is limited to one lymph node in the upper jugular-digastric region. The carcinoma is usually a nonkeratinizing squamous carcinoma that grows in a ribbonlike pattern with cystic degeneration. Mitoses are frequent and, as observed in normal tonsillar crypt epithelium, lymphocytes can often be seen infiltrating the tumor. In contrast to branchial cleft cysts, which are unilocular with a smooth epithelial lining, cystic lymph node metastasis from a

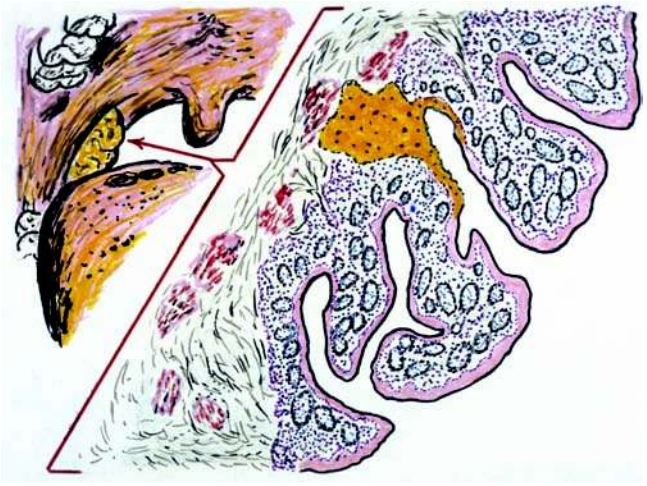

Figure 58 Schematic drawing of a tonsillar crypt carcinoma. Such tumors may metastasize without a visable mucosal abnormality. *Source*: From Ref. 58.

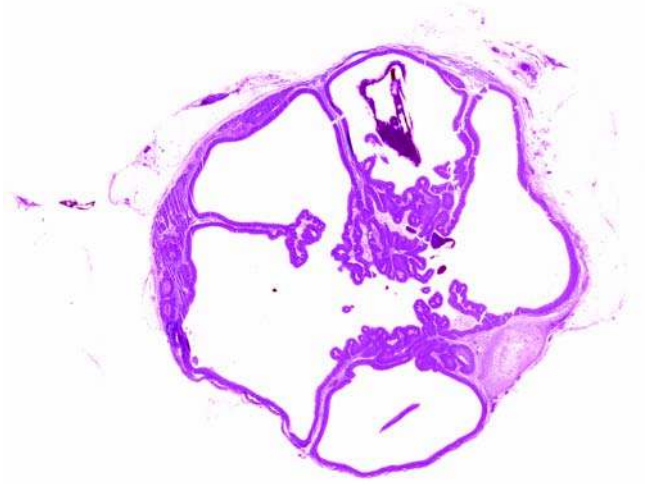

Figure 59 Metastatic nonkeratinizing squamous cell carcinoma in a cervical lymph node that clinically was thought to be a branchial cleft cyst. Note the multilocular (multicystic) appearance and intracystic papillary projections of tumor: compare with Figure 53 (40×).

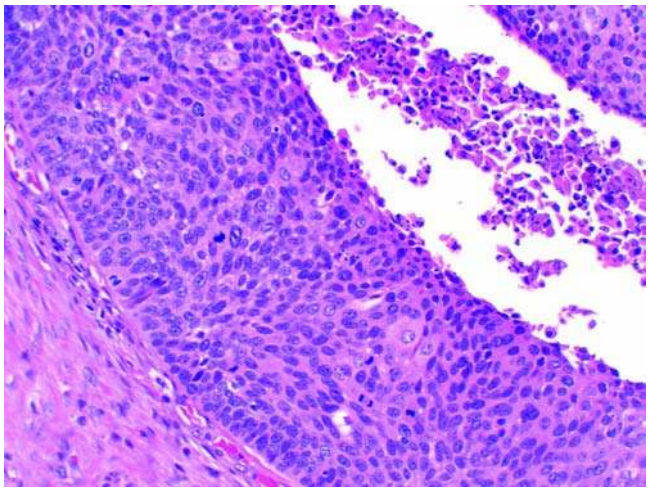

Figure 60 Histologic section of Figure 59. The tumor is a nonkeratinizing squamous cell carcinoma with frequent mitoses. Note the central cystic degeneration (H&E, 200×).

tonsillar primary imitating a branchial cleft cyst is multilocular (multicystic) with frequent intracystic papillary tumor excrescences (Figs. 59 and 60).

Patients who present with cystic metastases with the foregoing morphology and no known primary should have a diagnostic tonsillectomy on the side of the adenopathy. Because these tumors tend to arise in the tonsillar crypts, biopsies are generally too superficial (and distorted) to be useful (Fig. 58). The fact that the tonsil appears clinically normal does not, by any means, rule out a tonsillar carcinoma. Once removed, it is incumbent on the pathologist to totally submit the total tonsil for microscopic evaluation; these tumors are often so small that they can be completely missed on simple gross inspection and random sampling.

Although tonsillar crypt carcinomas are, by far, the most common tumor that can metastasize and masquerade as a branchial cleft carcinoma, tumors from other sites, such as the base of the tongue, nasopharynx, and even papillary carcinoma of the thyroid, may also cause confusion.

Thymic Cyst (CTC)

Embryology. The thymus begins to develop at about the sixth week of gestation and arises primarily from the third branchial pouch (mesoderm), with little, if any, contribution from the fourth pouch (1,2). The third and fourth pouches also give rise, respectively, to the inferior and superior parathyroid glands, which accounts for the presence of parathyroid tissue in the wall of some thymic cysts.

The paired thymic primordia originate in the area of the future pyriform sinuses and descend in the neck along the course of the carotid sheath. However, during descent, the primordia retain their connection to the pharynx by means of two hollow structures, referred to as thymopharyngeal ducts. At seven weeks gestation, the pharyngeal attachments of the ducts are severed, and the lumina are obliterated by epithelial proliferation; as a result, the primordia increase in bulk.

By the eighth week, the paired primordia superficially fuse in the midline of the neck before their final descent into the superior mediastinum. During the third month, the bilobed thymus takes on a lobular pattern, as the thymic epithelium becomes surrounded by mesoderm and accumulates lymphocytes. The thymic epithelium (endoderm) eventually forms the Hassall's corpuscles and then disappears.

Failure of involution or descent of any of the thymic anlagen is responsible for a variety of abnormalities, such as the CTC (Table 3).

Clinical features. Thymic cysts can occur in the neck or mediastinum and may be either congenital or acquired (2–14). In general, those of the neck, the subject of this discussion, are congenital, whereas those of the mediastinum may be either.

Cysts of the neck, herein referred to as CTC, are uncommon. Less than 60 cases were recorded in the world literature in 1977 and fewer than 100 in 1993 (5,13). The distribution between the two sexes has ranged from 1:1 to 2:1 in favor of males. Although rarely present at birth, two-thirds of CTCs manifest during the first decade of life and the remainder in the second and third decades (3).

The cysts can be found anywhere from the angle of the mandible to the sternum, paralleling the sternocleidomastoid muscle and normal descent of the thymus. According to Guba et al., 70% of CTCs are found on the left side of the neck, 23% on the right, and the remainder in the midline (15).

Table 3 Zarbo's Classifications of Developmental Abnormalities of the Thymus

Condition	Definition
Accessory cervical thymus	Solid mass of cervical thymic tissue sequestered from the main gland during descent.
Cervical thymic cyst	Sequestered cervical thymic tissue that has become cystic; a cystic version of accessory cervical thymus.
Undescended cervical thymus	Unilateral solid lobe of thymus that fails to descend into the mediastinum; Differs from accessory cervical thymus in that only one-half of the normally bilobed thymus is present in the mediastinum.
Persistent thymopharyngeal duct cyst	Similar to undescended cervical thymus; however, the thymic duct is cystic and the cervical thymus is solid.
Persistent thymic cord	Cervical prolongation of solid thymic cord, which is continuous with mediastinal thymus. May also be associated with cervical thymic cyst.
Cervical extension of mediastinal thymus	Solid midline thymus at the thoracic inlet owing to incomplete mediastinal descent.
Ectopic thymus	Solid ectopic thymic tissue in abnormal locations (e.g., in the trachea).

Source: From Ref. 2.

Table 4 Comparison of Cervical Thymic and Branchial Cleft Cysts

	Cervical thymic cyst	Branchial cleft cyst
Age	First decade (67%)	Third decade (61%)
Male/female ratio	1:1–2:1	1:1
Location	Anterior cervical triangle	Anterior cervical triangle
Sinus or fistula	No	Common
Swallowing	No effect	May retract if sinus or fistula is present
Valsalva	Transient increase in size	No effect
Chest roentgenogram	Occasionally abnormal	Normal
Histology	Thymic tissue in wall	Lymphoid tissue in wall

About 90% of patients present with a slowly enlarging painless mass that may exhibit a transient increase in size during a Valsalva maneuver. A few (10%), however, may result in dyspnea, hoarseness, dysphagia, or pain. Spontaneous intracystic hemorrhage is rare. In contrast with branchial cysts, CTCs are virtually never associated with sinuses or fistulas. Although a few sporadic reports have described a variety of congenital abnormalities in association with solid cervical masses of thymic tissue, no consistent developmental anomalies have ever been recorded in conjunction with CTCs (16,17).

CTCs may be completely isolated in the neck or be attached by a thin fibrous cord to the mediastinum. They may also be continuous with the intrathoracic thymus by a cord of thymic tissue, or the cyst may also extend into the mediastinum. Accordingly, some patients may have an abnormal chest roentgenogram.

These cysts are virtually never recognized as such, clinically. Most are confused with branchial cysts and, to a lesser extent, with cystic hygromas, laryngoceles, and thyroid lesions. The reader is referred to Table 4 and the excellent paper by May for clinical features useful in differentiating among these conditions (18).

Pathology. The cysts range between 2 and 15 cm and may be either unilocular or multilocular (Fig. 61). They are filled with clear serous fluid or, if hemorrhage has occurred, thick brown material with specks of cholesterol. The cyst walls vary from thick and fibrous to thin and fatty. The inner wall is smooth or trabeculated. The epithelial lining may be cuboidal, columnar, or stratified squamous (Fig. 62). In some areas, the epithelium may be replaced by fibrous or granulation tissue containing cholesterol clefts and multinucleated giant cells. To qualify as a CTC, thymic tissue must be found within the cyst wall; this may require numerous sections.

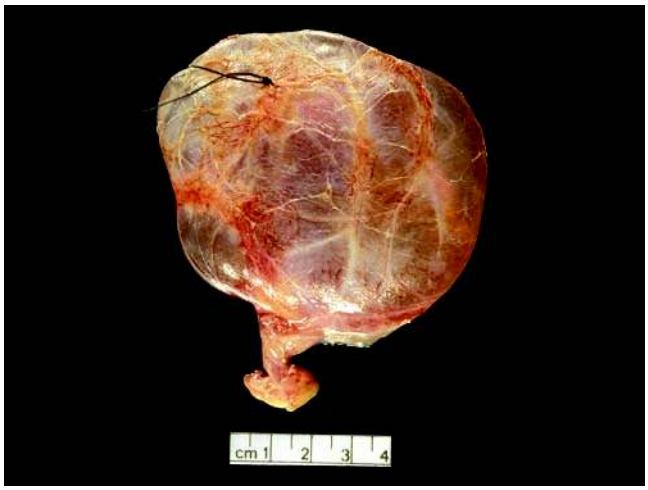

Figure 61 Gross appearance of a cervical thymic cyst.

CTCs have no malignant potential. This is in contrast with mediastinal thymic cysts, in which a few cases have been described that contained incidental mural nodules of thymomas, thymic carcinomas and, on one occasion, even squamous cell carcinoma

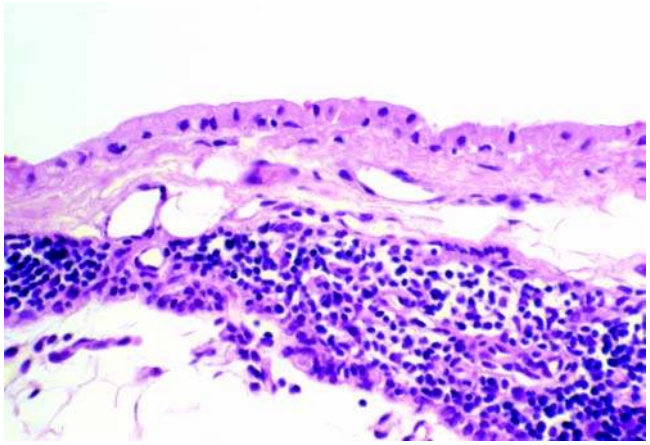

Figure 62 Cervical thymic cyst. The cyst may be lined by cuboidal, columnar, or squamous epithelium. Note the thymic tissue in the wall. Hassal's corpuscles may be apparent in some cysts (H&E, 200×).

(12,19). Pathologists should also be aware that some mediastinal thymomas may undergo cystic degeneration and masquerade as nonneoplastic thymic cysts (20). Likewise, Hodgkin's disease and germinomas of the thymus often appear cystic.

Suster et al. have also described pseudoepitheliomatous hyperplastic changes in multilocular thymic cysts of the mediastinum that may be mistaken for malignancy (21). Such changes, to our knowledge, have not been described thus far in CTC. A few cases of multilocular thymic cysts have also been described in patients infected with the human immunodeficiency virus (HIV), suggesting a possible cause and effect relation (22). No association, however, exists between this virus and the CTC.

Treatment. Simple surgical excision is curative. The cysts are usually easily excised and only exceptionally are adherent to surrounding structures. Local recurrences are practically nonexistent.

Bronchogenic Cysts

Introduction. Bronchogenic (bronchial) cysts are derived from small buds or diverticula that separate from the foregut during formation of the tracheobronchial tree. As such, most are found either in the mediastinum (1–4) or lungs (pulmonary or intrapulmonary) (5,6). A less known fact is that they may occur outside the thoracic cavity, presumably from erratic migration of sequestered primordial cells (7–11). In these instances, they almost invariably present in the skin or subcutaneous tissue in the vicinity of the suprasternal notch or manubrium sterni and, rarely, in the lower anterior neck or shoulder. Cysts in the latter location are referred to as cutaneous bronchogenic cysts (CBC). The following discussion is concerned with only the mediastinal bronchogenic cysts (MBC) and cutaneous variants of these cysts.

Mediastinal bronchogenic cyst. The MBCs constitute 13% of all primary neoplasms and cysts of the mediastinum and 35% to 50% of all developmental cysts of the mediastinum (1,4). They have been described in individuals from birth up to 56 years of age or older (1,2), with an average age reported in three series of 21, 25, and 36 years, respectively (1,4,6). The sex distribution has ranged from 1:1 to 2:1 in favor of males (1,4,12).

The cysts are often asymptomatic in older children and adults and discovered only on routine chest radiographs. In neonates, however, they may produce life-threatening respiratory distress with cough, wheezing, stridor, airway obstruction, and infection (2,12,13).

The MBCs are not always apparent on routine radiologic evaluation and may require additional specialized procedures for diagnosis, such as CT, MRI, barium swallows, and laryngoscopy or bronchoscopy. When visible, they characteristically present as a solitary smooth, noncalcified, round or ovoid cyst in the middle, posterior, or superior mediastinum in close association with the trachea or major bronchi. A few, however, have been described adjacent to or even within the wall of the trachea or esophagus, or attached to the pericardium (3,13). The cysts are typically isolated or sequestered and only exceptionally maintain a patent connection to the tracheobronchial tree. Some, however, may retain a loose, fibrous cord-like attachment to the airway.

The cysts measure up to 15 cm in diameter and, on gross inspection, are thin walled and usually unilocular and, only rarely, multilocular. The contents of the cysts are variable. Some contain serous fluid, whereas others are filled with mucin, serosanguineous fluid, or, if infected, purulent material. The inner walls are smooth, sometimes trabeculated, and lined by ciliated respiratory epithelium. Squamous metaplasia is not uncommon. Mucous (bronchial) glands, cartilage, and smooth muscle are apparent in most, but not all cases (3).

The cysts are usually easily excised by an external approach with few, if any, postoperative complications. With the exception of a rare case associated with congenital deficiency of the pericardium and a few in which the cartilaginous rings of the trachea are absent in the area where the cyst is attached, MBCs are not associated with any significant or consistent development abnormalities (3,4). Although there have been a few reports of adenocarcinoma, squamous cell carcinoma, and even a fibrosarcoma, allegedly arising in pulmonary bronchogenic cysts, malignant change in an MBC has not, to our knowledge, been described (5).

Cutaneous bronchogenic cyst. CBSs present primarily in the skin or subcutaneous tissue in the vicinity of the suprasternal notch or manubrium sterni and, less frequently, in the lower anterior neck or shoulder. About one-third are associated with a sinus tract (9).

They are usually discovered at or soon after birth and appear as asymptomatic nodules that slowly increase in size, or as draining sinuses exuding a mucoid-milky material. They are more common in

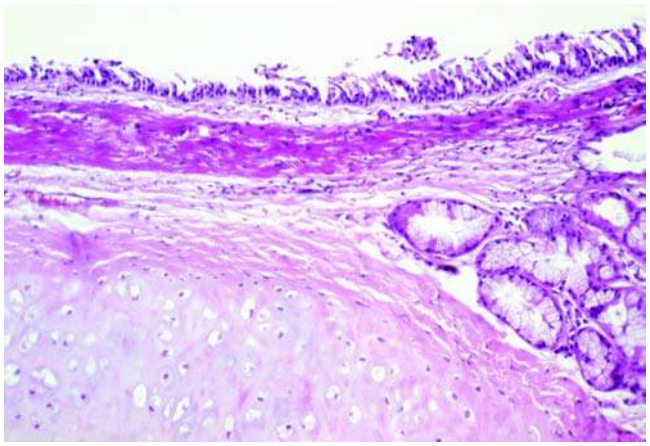

Figure 63 Cutaneous bronchogenic cyst. Observe the respiratory epithelial lining, subepithelial condensation of smooth muscle, mucous glands, and cartilage (100×). The latter component is distinctly uncommon in the cutaneous variant of bronchogenic cysts.

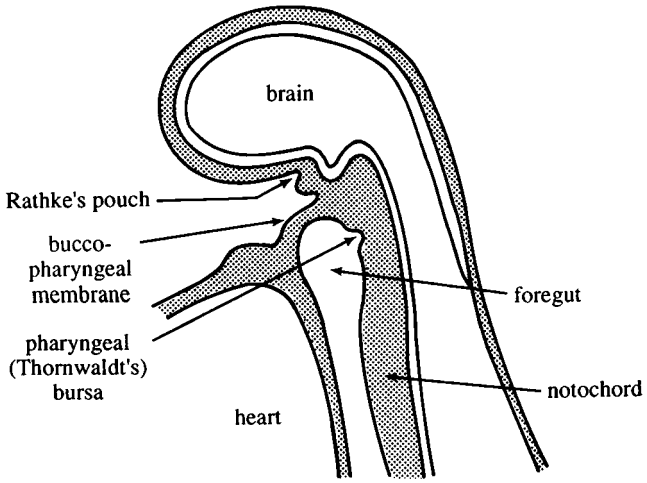

Figure 64 Schematic diagram showing Rathke's pouch originating as a diverticulum from the posterior wall of the primitive oral cavity.

males, in some series, by a margin of 3 to 4:1 (9,14). The cysts range from 0.3 to 6 cm, but may fluctuate in size or, as in the case of Park and Buford, become more conspicuous during the Valsalva maneuver (10). Virtually never recognized as such, clinically, they are often confused with cystic hygromas, epidermoid or sebaceous cysts, thyroglossal duct cysts, branchial cleft cysts, and teratomas or dermoids.

Noninfected cysts are grossly spherical, unilocular, and filled with either a clear serous or a thick, sometimes dark hemorrhagic, mucoid material. The wall is thin and its inner surface smooth or trabeculated. The cyst is lined by ciliated, pseudostratified columnar epithelium, which may be attenuated or thrown into papillary folds (Fig. 63). Although the sinus tract tends to be lined by stratified squamous epithelium, such epithelium rarely forms an integral component of the cyst, unless infected. In the 30 cases studied by Fraga et al., smooth muscle was identified in the wall in 24 and mucoserous glands in 16; however, unlike their intrathoracic counterparts, cartilage was seen in only two cases (9). In eight cases, lymphoid nodules were apparent, but never extensively.

A bronchogenic cyst can be distinguished from a teratoma by the complete absence of tissues other than those that can be explained on the basis of a malformation of the respiratory tract. A dermoid can be excluded by the lack of hair and the relative or absolute absence of squamous epithelium. The presence of smooth muscle, mucoserous glands, and cartilage (should it be found) and the paucity of lymphoid tissue eliminate a branchial cleft cyst. A TDC can be differentiated from a bronchogenic cyst if thyroid follicles are found. Furthermore, a TDC does not contain smooth muscle, and rarely, if ever, cartilage.

Complete surgical excision along with its sinus tract is curative. Similar to mediastinal bronchogenic cysts, CBCs are not associated with any consistent developmental anomalies.

Rathke's Cleft Cyst

Embryology. Rathke's pouch, which ultimately forms the anterior lobe of the pituitary gland, develops around the third week of gestation as an ectodermal outpocketing of the primitive oral cavity immediately superior to the buccopharyngeal membrane (Fig. 64). It subsequently grows toward the infundibulum of the diencephalon, the latter of which forms the posterior lobe of the pituitary gland (1).

By the end of the second month of gestation, the pouch loses its connection with the oral cavity and comes in close contact with the infundibulum (Fig. 65). The cells in the anterior wall of Rathke's pouch increase rapidly in number to form the anterior lobe of the pituitary gland (1). A small extension of this lobe, the pars tuberalis, grows along the stalk of the infundibulum and eventually surrounds it.

The posterior part of Rathke's pouch develops into the pars intermedia. The lumen between the anterior lobe and pars intermedia is gradually obliterated. If the lumen does not close, a cleft (Rathke's cleft) is formed that may ultimately become cystic (Rathke's cyst) (Fig. 65).

Clinical features. Rathke's cleft cysts (RCCs) are usually small, asymptomatic, congenital lesions that can be found incidentally in 13% to 33% of all routine autopsies (2–5). Larger clinically significant cysts, however, do occur, but they are uncommon (6–9). In a review of the literature in 1991, Voelker et al. identified only 155 patients with symptomatic RCCs (10). They represent 2% of all lesions of the sella turcica and occur in a ratio of about 1 RCC for every 93 pituitary adenomas (8,11).

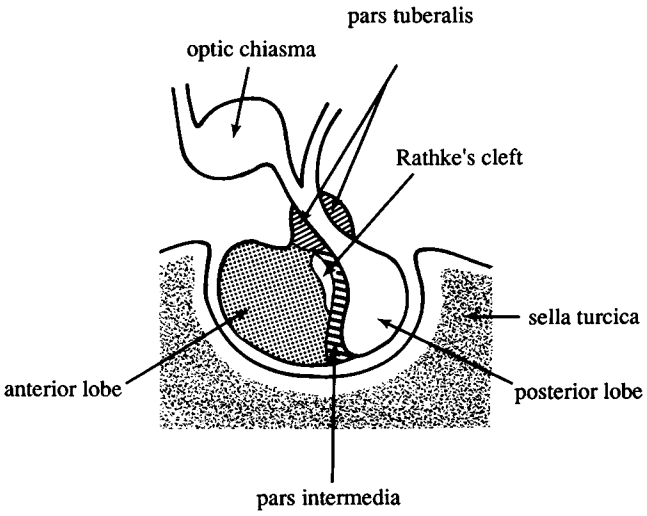

Figure 65 Schematic drawing of the pituitary gland showing the location of Rathke's cleft that, in some instances, becomes cystic and then is referred to as Rathke's cleft cyst.

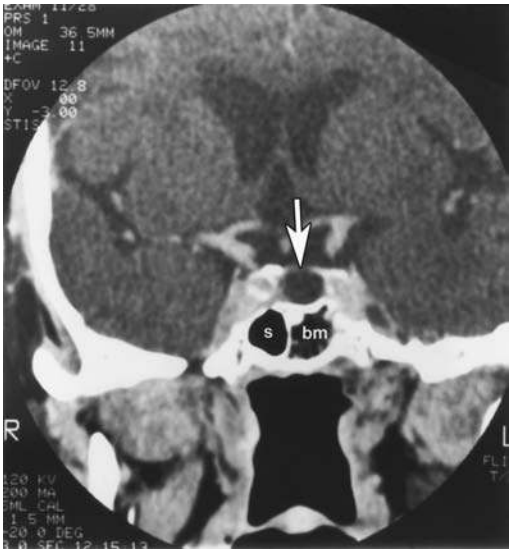

Figure 66 A CT scan of an intrasellar Rathke's cleft cyst (*arrow*). The spaces below the sella turcica represent the sphenoid sinus (s) and bone marrow (bm). *Abbreviation*: CT, computer tomography. *Source*: Courtesy of H. Curtin, formerly of the University of Pittsburgh Medical Center.

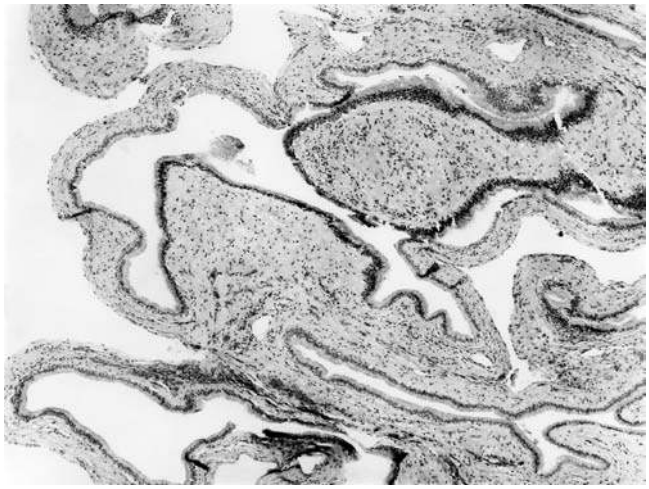

Figure 67 Fragments of a collapsed Rathke's cleft cyst (50×).

Symptomatic RCCs are more common in females by a 2:1 margin and occur in patients averaging 38 years of age (range 6 months–73 years) (10,12). Headaches, visual disturbances, pituitary abnormalities (galactorrhea, amenorrhea, growth retardation, diabetes insipidus), nausea, vomiting, and meningeal irritation are the common signs and symptoms. Some RCCs are also associated with increased levels of serum prolactin (8).

Imaging. Plain skull radiography or sellar tomography will reveal an ''abnormal'' sella turcica in 80% of RCC patients who are symptomatic (10) (Fig. 66). The cysts are characteristically noncalcified with a round or lobulated margin and, on enhanced CT scans, show a homogenous low density, without appreciable contrast enhancement (13,14). Although a rare RCC has been described with calcification, the absence of this mineral deposit is a useful sign that distinguished it from craniopharyngiomas, which are calcified.

On MRI, RCCs have the same intensity as cerebrospinal fluid (13,14). However, depending on the histologic composition of the cyst (i.e., thick mucoid secretions, protein content, and solid components), variations in these typical radiographic appearances may occur.

In a review of 126 RCCs in which the location was known, Voelker et al. noted that in 90 cases (71%) the cysts had both intra- and suprasellar components, 22 (17%) were confined to the sella, 13 (10%) were suprasellar, and 1 (0.08%) was intrasphenoidal (10). Patients with the rare suprasellar RCC will show little, if any, sellar abnormalities on radiographic evaluation.

Pathology. RCCs are virtually never removed intact and, therefore, the sizes of the cysts are usually obtained through imaging studies or by the surgeon's estimate at the time of surgery. In one review of 28 cases, the maximum diameter of the cysts ranged from 3 to 40 mm (average 16 mm) (10).

The cysts are lined by one or more layers of cuboidal-to-columnar cells, with or without cilia and interspersed goblet cells (Figs. 67 and 68). Foci of squamous epithelium are not uncommon.

The epithelial cells, on immunohistochemical staining, are strongly positive for cytokeratin and epithelial membrane antigen and variably positive for carcinoembryonic antigen, S100 protein, vimentin, glial fibrillary acidic protein, and chromogranin (15–17). In addition, sporadic cells may also stain for

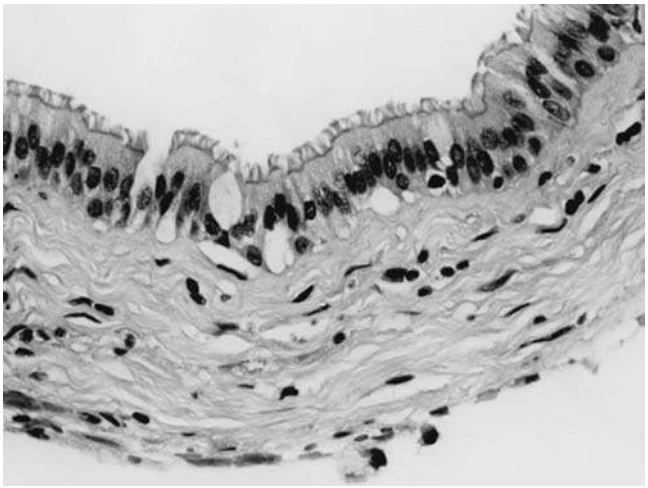

Figure 68 Some areas of the cyst in Figure 67 were lined by a prominent ciliated respritory epithelium (400×).

one or more of the pituitary hormones (prolactin, growth hormone, or other), which should come as no surprise because the cyst and the anterior lobe of the pituitary gland share the same embryological derivation.

Although usually not apparent on imaging, a few cysts may contain small deposits of calcium in their walls as well as cholesterol crystals, xanthomatous cells, and, exceptionally, even amyloid (18,19). Rare examples of RCCs that contain mural nodules of anterior pituitary tissue, consistent with an adenoma, have also been described (11,20,21). Such hybrid lesions have been referred to as ''transitional cell tumors.''

At times it may be difficult to distinguish an RCC from a craniopharyngioma. According to Xin et al., they can be distinguished by immunohistochemistry. The RCC is positive for both cytokeratin 8 and cytokeratin 20, while the craniopharyngioma is typically negative for both (22).

Treatment and prognosis. Simple transphenoidal drainage of the cyst along with partial removal of the cyst wall for diagnosis provides safe and effective therapy (6,7). The recurrence rate with this procedure is only 5% (10). There is no role for radiation therapy.

Thornwaldt's Cyst

Embryology. The notochord appears early in life and functions as a primitive axial skeleton in vertebrates. It lies dorsal to the foregut and extends from the junction of the sphenoid and occipital bones to the tip of the coccyx (Fig. 64).

At about the sixth week of fetal life, the cephalic portion of the notochord begins to involute and, during the process, comes in close contact with the foregut, creating a saclike depression on the posterosuperior nasopharyngeal wall, referred to as the pharyngeal bursa (1–3) (Fig. 64). The cause of the depression may be related to notochordal adhesions, traction bands of the pharyngobasilaris, active growth of the pharyngeal endoderm, or a combination of all three (1).

The pharyngeal-notochordal contact is normally only transient, but it may persist in 7% of the adult population (4). The communication provides a pathway for the ingrowth of pharyngeal respiratory epithelium, creating a potential space that may become walled off, the so-called Thornwaldt's cyst (TWC), and infected (Thornwaldt's disease or syndrome).

TWC lies caudal to the site of origin of RCC. It characteristically occurs on the posterosuperior wall of the nasopharynx, just above the uppermost border of the superior constrictor muscle, and usually extends upward and backward toward the occipital bone, which it sometimes reaches with its apex (1).

Clinical features. TWC (Thronwaldt's bursa, pharyngeal bursa) may be symptomatic or asymptomatic and occurs in any age group. Most, however, are discovered between 15 and 30 years of age, with no sex disposition (3). Symptoms, when infected, include nasopharyngeal drainage, which is often purulent and foul smelling, occipital headaches, soreness or stiffness of the cervical muscles, halitosis, ear fullness, and otalgia (3,5).

It has been suggested that traumatic manipulation of this area during surgery, such as in adenoidectomy, may predispose to infection. Others, however, have found that most patients with TWC have not had previous surgery of the nasopharynx.

On physical examination, indirect nasopharyngoscopy often reveals a firm, smooth, tender or nontender, submucosal mass either in or just off the midline of the posterior pharyngeal wall (3,6,7). The adjacent mucosa is frequently erythmatous and cervical lymph nodes are often enlarged (3,5).

Imaging. With advances in imaging techniques, TWCs are now being identified more frequently as incidental findings in the evaluation of other head and neck conditions. Ford et al., for example, identified four incidental TWCs in a review of 2000 MRI studies of the head and neck over a 16-month interval (8).

If the pharyngeal bursa is unobstructed, air may be seen in the tract, extending from the high posterior midline nasopharynx toward the occipital tubercle (Fig. 69). There may even be a small notch in the occipital bone (7).

On a CT scan, TWC appears as a mass high on the posterior nasopharyngeal wall between the longus capitis muscles (Fig. 70). The cyst may contain low-density fluid, similar to cerebrospinal fluid, and does not enhance after intravenous contrast (7,8). Focal calcification may at times be seen (7).

On MRI, TWC exhibits a high signal intensity on both T1- and T2-weighed images and does not enhance after gadolinium (7–10).

Pathology. TWC is characteristically lined by ciliated respiratory-type epithelium and, if there has been significant infection, metaplastic squamous epithelium.

Differential diagnosis. A TWC may be mistaken for an RCC because the two, at times, exhibit the same histologic features, that is, a cyst lined by ciliated epithelium. The distinction rests on the radiographic

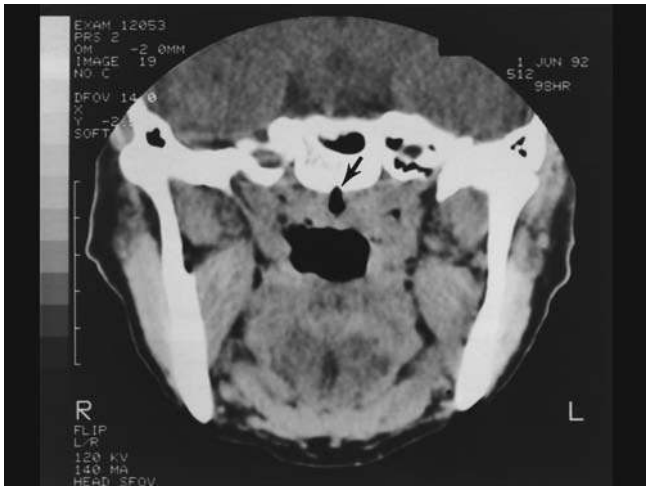

Figure 69 Coronal CT scan demonstrating air in an unobstructed pharyngeal (Thornwaldt's) bursa (*arrow*). The tract extends up to the occipital tubercle where there is a small notch in the bone. *Abbreviation*: CT, computer tomography. *Source*: From Ref. 7.

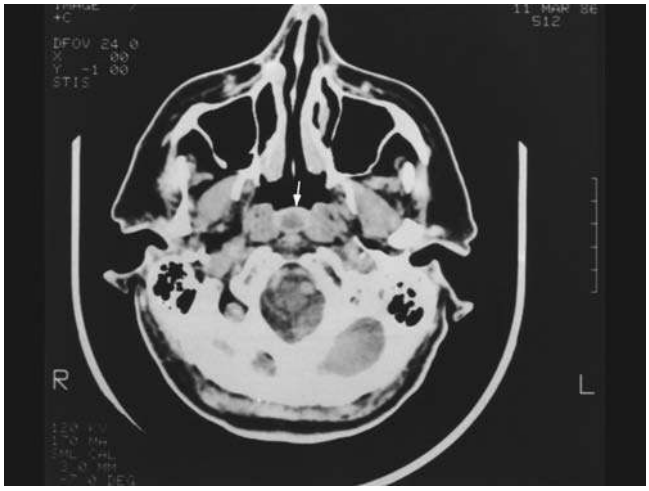

Figure 70 Axial CT scan showing a low-density, well-circumscribed Thornwaldt's cyst (*arrow*) between the longus capitis muscles. *Abbreviation*: CT, computer tomography. *Source*: From Ref. 7.

features. RCCs are located in or in close proximity to the sella turcica, whereas TWCs are found in the high posterior nasopharyngeal wall.

Treatment. Surgical excision or marsupialization is the treatment of choice. Preoperative antibiotics may be necessary if there is significant infection. Incision and drainage are only temporary procedures, for the cyst will almost certainly recur once the drainage site occludes.

Table 5 Classification of Nasopharyngeal Cysts

A. Congenital cyst
1. Midline
   a. Rathke's cleft cyst
   b. Thornwaldt's cyst
   c. Dermoid cyst
2. Lateral
   a. Branchial

B. Acquired cysts
1. Midline
   a. Retention cyst of mucoserous glands
   b. Retention cyst, distended crypt(s) of nasopharyngeal lymphoid tissue (adenoids), or keratin-filled inclusion cyst
2. Lateral
   a. Retention cyst of mucoserous glands
   b. Retention cyst, distended crypt(s) of nasopharyngeal lymphoid tissue (adenoids), or keratin-filled inclusion cyst

Source: From Ref. 1.

Nasopharyngeal Cyst

Cysts of the nasopharynx are uncommon and can be divided into congenital or acquired and midline or lateral (Table 5) (1–6). Dermoid, RCC, and Thornwaldt's cyst are typically midline, whereas branchial cysts are unilateral or, at times, even bilateral. Retention cysts of mucoserous glands and lymphoid crypts may be either.

In 1989, Nicolai reviewed 48 symptomatic nasopharyngeal cysts reported in the literature and observed that 24 were midline and 24 lateral (4). The cysts occurred in all age groups (mean 40 years) and were more common in men by a 3:1 ratio (4).

Nasopharyngeal cysts may be asymptomatic or symptomatic. When symptomatic, the most common complaints are nasal obstruction, hearing abnormalities, headaches, neck pain, snoring, postnasal discharge, halitosis, and stiffness of the muscles of the neck.

Retention cysts are easily diagnosed microscopically (Fig. 71). Congenital cysts, on the other hand, are often difficult to categorize solely on histologic features, for they share a similar ciliated or squamous epithelial lining. Accurate classification depends, in addition, on clinical and radiologic findings.

Effective treatment, regardless of etiology, is surgical excision or marsupialization of the cyst. Each congenital cyst is described in greater detail elsewhere in this chapter.

Parathyroid Cyst

Parathyroid cysts are discussed in chapter 22, ''Pathology of the Parathyroid Glands.''

B. Nondevelopmental Cysts

Mucocele (Mucous Extravasation Phenomenon)

Clinical. The mucocele is a very common lesion, most often occurring on the lower lip (Fig. 72). It is due to rupture of a minor salivary gland duct with

Figure 71 Keratin-filled, squamous-lined cyst involving nasopharyngeal lymphoid tissue (adenoid). Such cysts are sometime referred to as retention cysts, distended crypts of the adenoid, or keratin-filled inclusion cysts (H&E, 50×).

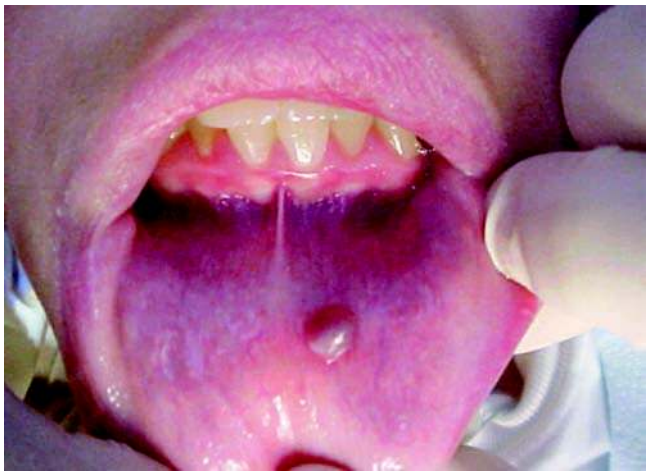

Figure 72 Mucocele. Raised fluctuant lesion of the lower lip.

subsequent spillage of mucin into the surrounding connective tissue (1–3). They present as smooth submucosal nodules, which may manifest as a bluish swelling if located near the surface. The lesion is usually asymptomatic but may rupture and recur. Although the lower lip is the most common location, they may occur on the buccal mucosa, tongue, floor of the mouth, and, less commonly, other areas. Interestingly, they are rare on the upper lip. Lesions of the upper lip presenting clinically as a mucocele more likely represent salivary duct cysts or salivary gland tumors.

Salivary duct cysts are clinically similar to mucoceles but unlike mucoceles they exhibit a true epithelial lining. They may be due to ductal ectasia

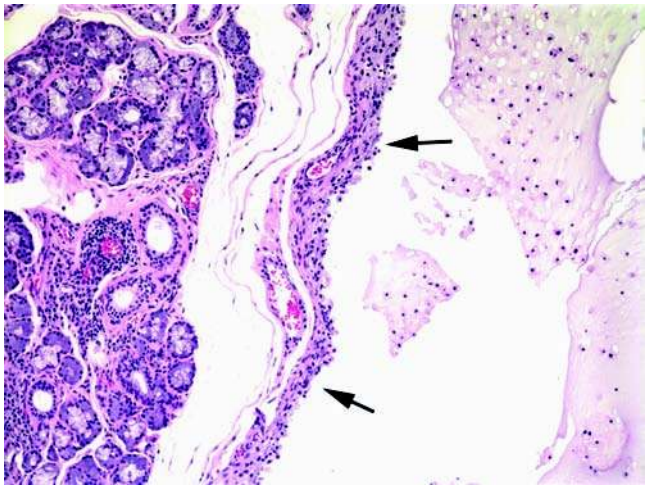

Figure 73 Mucocele. Cyst-like structure containing mucin surrounded by a granulation tissue lining (*arrows*). Minor salivary glands are seen in the wall.

secondary to obstruction. They may involve major and minor salivary glands but are most commonly seen on the lips, floor of mouth, or buccal mucosa (1).

Pathology. Mucoceles are usually surfaced by stratified squamous epithelium, unless secondarily ulcerated. The lamina propria contains extravasated mucin, which is usually surrounded by granulation tissue containing foamy histiocytes (Fig. 73). Minor salivary glands are seen frequently exhibiting chronic sialadenitis. Occasionally, older lesions organize and are composed of granulation and fibrous tissue with very little extravasated mucin. Salivary duct cysts are usually lined by cuboidal and/or stratified squamous epithelium. The lumen is dilated and frequently contains mucin. Occasionally, the lining exhibits oncocytic metaplasia.

Treatment and prognosis. Conservative surgical excision, including surrounding minor salivary glands, is the treatment of choice. If the associated salivary glands are not removed, the lesion may recur.

Ranula

Etiology and pathogenesis. The ranula is a form of mucous extravasation that occurs in the floor of the mouth. It has been divided into simple and plunging forms. The simple ranula is the most common form and is located superior to the mylohyoid muscle. The plunging ranula occurs when the mucous extravasation herniates through the mylohyoid and presents as a swelling in the neck. In most cases, the sublingual gland and duct are involved (1,2).

Clinical features. The simple ranula presents as a blue dome-shaped fluctuant mass in the floor of the mouth (Fig. 74). It can measure several centimeters and elevate the tongue. The plunging ranula presents as a swelling usually in the submandibular space (1,2).

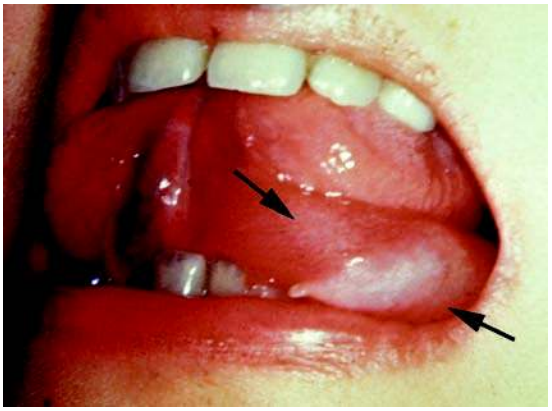

Figure 74 Ranula. Diffuse fluctuant swelling of the floor of mouth (*arrows*).

They may also present with a floor-of-mouth swelling or be independent of an oral lesion.

Pathology. Extravasated mucin with varying amounts of granulation tissue is the typical histologic presentation. Inflammation can be seen, particularly foamy histiocytes.

Treatment and prognosis. Marsupialization is the most common treatment. It involves unroofing the ranula and leaving it open. The cavity can be packed with gauze, which improves the success rate. Removal of the sublingual gland significantly decreases the risk of recurrence in both simple and plunging ranulas (3).

Mucocele of the Paranasal Sinuses

Etiology and pathogenesis. Sinus mucoceles are the result of obstruction of the sinus ostium with subsequent accumulation of mucous secretions in the sinus cavity. Expansion and inflammation may eventually lead to bone erosion and remodeling of the bone (1).

Antral pseudocyst and retention cysts should not be confused with mucoceles (Fig. 75). The pseudocyst is caused by collection of hemorrhage and inflammatory exudate under the sinus mucosa, causing a dome-shaped radiopaque lesion on X-ray (2). Mucous retention cysts are caused by blockage of a salivary gland duct and are seen within the wall of the sinus. Both the pseudocyst and retention cyst are usually asymptomatic and rarely require treatment.

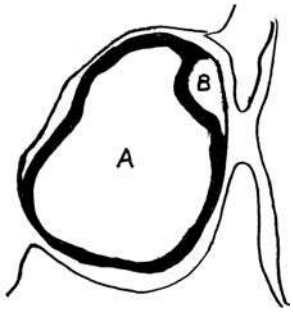

Figure 75 (**A**) Mucocele due to obstruction of ostium with accumulation of mucous in the sinus cavity. (**B**) Antral pseudocyst caused by collection of hemorrhage and exudate between sinus lining and bone.

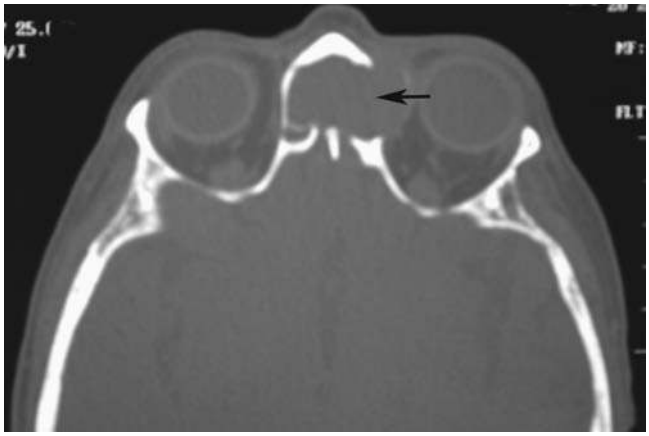

Figure 76 Sinus mucocele. Axial CT exhibiting sinus opacification and bone erosion (*arrow*). *Abbreviation*: CT, computer tomography. *Source*: Courtesy of John DelGaudio, M.D., Emory University, Atlanta, Georgia.

Clinical features. Sinus mucoceles may present with nonspecific symptoms such as headache, nasal obstruction, and swelling. Dramatic symptoms may include facial deformity, proptosis, diplopia, and vision loss. Mucoceles most commonly involve the frontal and ethmoid sinuses with approximately 3% involving the maxillary sinus (1,3). Secondary infection may lead to suppuration (pyocele). Chronic sinusitis and polyps may also be present.

Imaging. Imaging studies show opacification of the sinus, expansion, sinus inflammation, and, in long-standing lesions, bone destruction and remodeling (Fig. 76). CT studies are helpful in delineating the extent of bone destruction.

Pathology. The lining of the mucocele is composed of respiratory epithelium, which may be attenuated due to the pressure of the mucin. Squamous metaplasia may be seen. The wall is frequently fibrotic and contains inflammation. Dystrophic calcifications and reactive bone may also be seen.

Treatment and prognosis. There is increasing evidence that endoscopic management of sinus mucoceles is effective (4,5). Marsupialization and decompression are associated with very low recurrence rates. Follow-up surgery to remove sources of obstruction such as sinus polyps may be necessary.

Dermoid and Epidermoid Cysts

Etiology and pathogenesis. Dermoid cyst is rare in the floor of the mouth. The term ''dermoid cyst'' is frequently used to describe three closely related cysts:

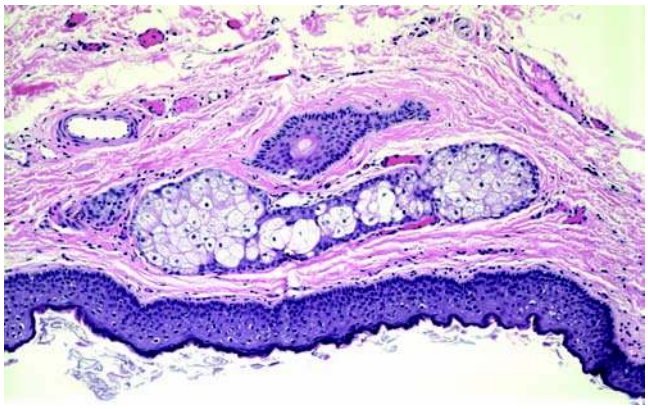

Figure 77 Dermoid cyst. Stratified squamous epithelial lining with skin adnexal structures in wall.

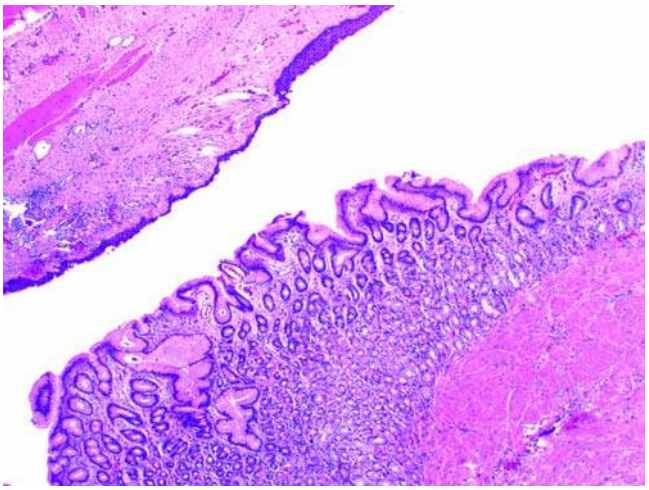

Figure 78 Oral heterotopic gastrointestinal cyst lined by stratified squamous, ciliated columnar, and gastric epithelium.

the dermoid, epidermoid, and cystic teratoma (1). The pathogenesis of these lesions is unknown. The lesions are thought to be congenital (1); theories include an origin from entrapped midline ectodermal tissue from the first and second branchial arches and traumatic implantation in utero of epithelium. Lateral neck lesions are thought to develop from the first pharyngeal pouch or branchial cleft (1). Supporting the congenital theory, the lesion is most frequent in children and young adults and may be present at birth.

Clinical. The cyst is slow growing and painless. It may vary in size from a few millimeters to a large mass. The lesions are usually soft to palpation. Lesions occurring above the geniohyoid muscle cause a sublingual swelling, which may elevate the tongue. Lesions located below the geniohyoid muscle often produce a submental swelling (2). Large lesions may cause difficulty in breathing, eating, and speaking.

Pathology. All dermoids are lined by epithelium. If no skin adnexal structures are present, a diagnosis of epidermoid cyst can be made. If sweat glands, sebaceous glands, or hair follicles are present, a diagnosis of dermoid cyst is appropriate (Fig. 77). A diagnosis of cystic teratoma can be made if representations from all three germinal layers are present (ectoderm, mesoderm, and endoderm). The tissue may include skin appendages, muscle, bone, tooth, and respiratory and gastrointestinal epithelium (1).

Treatment and prognosis. Surgical excision is the method of treatment. If completely excised, they usually do not recur.

Oral Heterotopic Gastrointestinal Cyst

Etiology and pathogenesis. The most commonly held hypothesis is that the cyst is derived from misplaced embryonal remnants during early fetal development (1,2). This process is thought to occur at the four-week embryonic stage when the primitive stomach lies in the neck region.

Clinical. Most cases are seen by two years of age (1). There is a predilection for males. It usually presents as an asymptomatic swelling in the floor of the mouth. Occasionally, difficulty in feeding, swallowing, and respiration have been reported (3).

Pathology. The cyst is lined by gastric or intestinal epithelium (Fig. 78). Stratified squamous or respiratory epithelium may be seen. Smooth muscle and gastric glands may be seen in the wall.

Treatment and prognosis. Surgical excision is the appropriate treatment. Recurrence is rare.

Simple Bone Cyst (Traumatic Bone Cyst)

Etiology and pathogenesis. The etiology of the simple bone cyst is unknown, although some have speculated that idiopathic intramedullary hemorrhage, possibly secondary to trauma, may be one cause (1). Because fibro-osseous lesions may be associated with solitary bone cysts (1–3), some have speculated that degeneration within a fibro-osseous lesion may be an etiology of some of the lesions (1,2).

Clinical. Simple bone cysts of the jaws are common. Although maxillary lesions have been reported (1,2), most cases occur within the mandible. Most lesions are seen in the first two decades of life but have been reported in adults (1,2). They are usually asymptomatic, but occasionally lesions may present as a painless swelling.

Imaging. The lesion usually presents as a well-defined radiolucency, although in some areas the border may be indistinct. In larger lesions, the radiolucency frequently scallops between the roots (Fig. 79). In older individuals, the lesion may be associated with radiopaque areas, which frequently represent fibro-osseous lesions.

Pathology. On exploration, the cavity is essentially empty. A thin band of connective tissue may be seen at the periphery and is usually submitted along

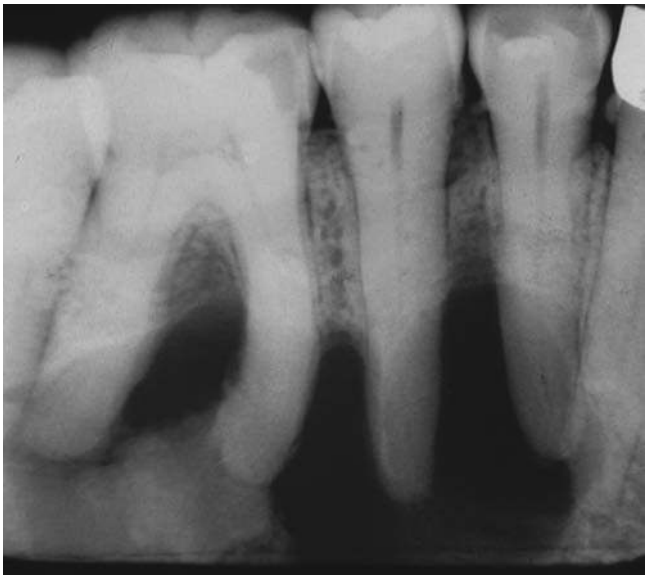

Figure 79 Simple bone cyst. Note scalloping between the teeth.

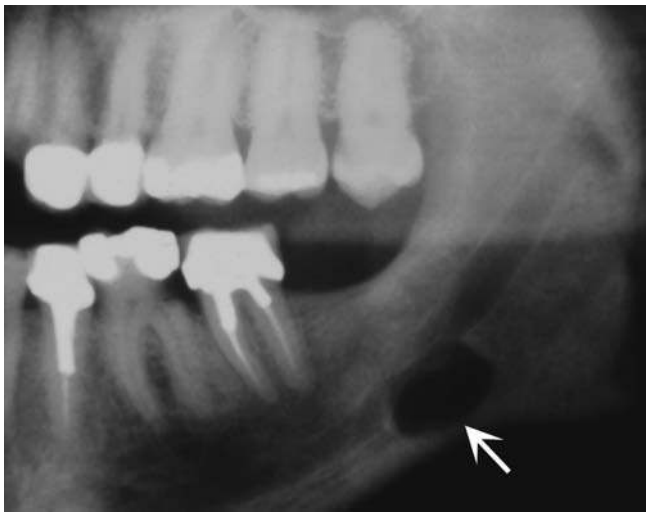

Figure 80 Stafne defect. Well-defined radiolucency at inferior border of the mandible (*arrow*)

with fragments of reactive bone. As previously mentioned, fragments of a fibro-osseous lesion may be present.

Treatment and prognosis. Curettage is the treatment of choice. Most lesions resolve but recurrence has been reported (1,2).

Stafne Defect (Stafne bone cyst)

Etiology and pathogenesis. Stafne defects are concavities seen along the lingual aspect of the posterior mandible. In most cases the defect contains a portion of the submandibular gland (1). Occasional lesions are seen in the anterior mandible, likely related to the sublingual gland.

Clinical and imaging. The lesion is most frequently seen in males (1). Radiographically, the lesion usually presents as a well-defined radiolucency with a sclerotic border (Fig. 80). Most lesions are unilateral. CT scans are helpful in characterizing atypical lesions (2).

Pathology. Although rarely biopsied, the defect usually contains normal salivary gland tissue. Occasional defects may be empty or contain connective tissue and muscle.

Treatment and prognosis. No treatment is necessary. Lesions with an atypical presentation may require biopsy.

REFERENCES

I. ODONTOGENIC CYSTS

1. Barnes L. Surgical Pathology of the Head and Neck, 2nd ed. New York, NY: Marcel Decker Inc., 2001:1439–1440.

A. Developmental Cysts

Primordial Cyst

1. Neville BW, Damm DD, Allen CM, et al. Oral and Maxillofacial Pathology, 2nd ed. Philadelphia, PA: W.B. Saunders Co., 2002:390–393.

Dentigerous Cyst

1. Neville BW, Damm, DD, Allen CM, et al. Oral and Maxillofacial Pathology, 2nd ed. Philadelphia, PA: W.B. Saunders Co., 2002:590–593.
2. Gardner DG. Head and Neck Surgical Pathology, 2nd ed. Lippinicott, Williams and Wilkins, 2001:202–203.
3. Ackermann G, Cohen MA, Altini M. The paradental cyst: a clinico-pathologic study of 50 cases. Oral Surg Oral Med Oral Path 1987; 64:308–312.
4. Eversole LR, Sabes WR, Rovin S. Aggressive growth and neoplastic potential of odontogenic cysts with special reference to central epidermoid and mucoepidermoid carcinomas. Cancer 1975; 35:270–282.
5. Gonzales-Garcia R, Sastre-Perez J, et al. Primary intraosseous carcinoma of the jaws arising in an odontogenic cyst, ameloblastoma and de novo: report of new cases with reconstruction considerations. Oral Surg Oral Med Oral Pathol 2007; 103(2):29–33.
6. Muller S, Waldron CA. Primary intraosseous squamous cell carcinoma. IntJ Oral Maxillofac Surg 1991; 20:362–365.

Eruption Cyst

1. Budnick SD. Handbook of Pediatric Oral Pathology. Year Book Medical Publishers1981:143–144.
2. Bodner L, Goldstein J, Sarnat H. Eruption cysts: a clinical report of 24 new cases. J Clin Pediatr Dent 2004; 28(2):183–186.

Lateral Periodontal Cyst

1. Cohen DA, Neville BW, Damm DD, et al. The lateral periodontal cyst. A report of 37 cases. J Periodontol 1984; 55(4):230–234.
2. Rasmusson LG, Magnusson B, Borrman H. The lateral periodontal cyst. A histopathological and radiographic study of 32 cases. Br J Oral Maxillofac Surg1991; 29(1):54–57.

3. Weathers DR, Waldron CA. Unusual multilocular cysts of the jaws (botryoid odontogenic cyst). Oral Surg 1973; 36:235–241.
4. Ramer M, Valauri D. Multicystic lateral periodontal cyst and botryoid odontogenic cyst. NYSDJ 2005; 71:47–51.

Glandular Odontogenic Cyst (Sialo-Odontogenic Cyst)

1. Koppang HS, Johannessen S, Haugen LK, et al. Glandular odontogenic cyst (sialo-odontogenic cyst): a report of two cases and literature review of 45 previously reported cases. J Oral Pathol Med 1998; 27(9):455–462.
2. Velez I. Glandular odontogenic cyst. Report of two cases and review of the literature. NYSDJ 2006; 72:44–45.
3. Somsak S, Koehler JR, Nasser-Said-Al-Naief. Glandular odontogenic cyst of the anterior maxilla: case report and review of the literature. J Oral Maxillofac Surg 2006; 64(4): 740–745.

Odontogenic Keratocyst

1. Barnes L, Eveson JW, Reichart P, Sidransky D. WHO Classification of Tumors. Head and Neck Tumors. Lyon, France: IARC Press 2005; 306–307.
2. Gu XM, Zhao HS, Sun LS, et al. PTCH mutations in sporadic and Gorlin-syndrome-related odontogenic keratocysts. J Dent Res 2006; 85(9):859–863.
3. Barreto DC, Gomez RS, Bale AE, et al. PTCH gene mutations in odontogenic keratocysts. J Dent Res 2000; 79(6): 1418–1422.
4. Myoung H, Hong SP, Hong SD, et al. Odontogenic keratocyst: review of 256 cases for recurrence and clinicopathologic parameters. Oral Surg Oral Med Oral Pathol 2001; 91(3): 328–333.
5. Brannon RB. The odontogenic keratocyst. A clinicopathologic study of 312 cases. Part I. Clinical features. Oral Surg Oral Med Oral Pathol 1976; 42(1):54–72.
6. Brannon RB. The odontogenic keratocyst. A clinicopathologic study of 312 cases. Part II. Histopathologic features. Oral Surg Oral Med Oral Pathol 1977; 43:233–255.

Nevoid Basal Cell Carcinoma Syndrome

1. Barnes L, Eveson JW, Reichert P, et al. WHO Classification of Tumors. Head and Neck Tumors. Lyon, France: IARC Press, 2005:306–307.
2. Neville BW, Damm DD, Allen CM, et al. Oral and Maxillofacial Pathology, 2nd ed. Philadelphia, PA: W.B. Saunders Co., 2002:598–601.
3. Kimonis VE, Goldstein AM, Pastakia B et al. Clinical manifestations in 105 persons with nevoid basal cell carcinoma syndrome. Am J Med Genet 1997; 69(3):299–308.

Gingival Cyst

1. Bell RC, Chauvin PJ, Tyler MT. Gingival cyst of the adult. J Can Dent Assoc. 1997; 63(7):533–535.
2. Giunta JL Gingival cysts in the adult. J Periodontal 2002; 73(1):827–831.

Cysts of the Newborn (Epstein's Pearls; Bohn's Nodules)

1. Neville BW, Damm DD, Allen CM, et al. Oral and Maxillofacial Pathology, 2nd ed. Philadelphia, PA: W.B. Saunders Co., 2002:601.
2. Kemora K, Kakinoki Y, Nishio K, et al. Cysts of the oral mucosa in newborns: a clinical observation. J UOEH 1983; 5(2):163–168.
3. Cataldo E, Berkman M. Cysts of the oral mucosa in newborns. Am J Dis Child 1968; 116:44–48.

C. Inflammatory Cysts

Periapical Cyst (Radicular Cyst)

1. Neville BW, Damm DD, Allen CM, e al. Oral and Maxillofacial Pathology, 2nd ed. Philadelphia, PA: W.B. Saunders Co., 2002:116–121.
2. Stockdale CR, Chandler NP. The nature of the periapical lesion—a review of 1108 cases. J Dent 1988; 16:123–129.
3. Pesce C, Ferloni M. Apoptosis and Rushton body formation. Histopathology 2002; 40(1):109–111.
4. Chen SY, Fantasia JE, Miller AS. Hyaline bodies in the connective tissue wall of odontogenic cysts. Oral Surg Oral Med Oral Pathol 1981; 10:147–157.

II. NONODONTOGENIC CYSTS

A. Developmental Cysts

Nasopalatine Duct Cyst (Incisive Canal Cyst)

1. Swanson KS, Kaugars GE, Gunsolley JC. Nasopalatine duct cyst: an analysis of 334 cases. J Oral Maxillofac Surg 1991; 49(3):268–271.
2. Jacob S, Zelano BA, Gungor A, et al. Location and gross morphology of the nasopalatine duct cyst in human adults. Arch Otolaryngol Head Neck Surg 2000; 126:741–748.
3. Vasconcelos R, de Aguiar MF, Castro W, et al. Retrospective analysis of 31 cases of nasopalatine duct cyst. Oral Dis 1999; 5(4):325–328.
4. Elliott KA, Franzese CB, Pitman KT. Diagnosis and surgical management of nasopalatine duct cysts. Laryngoscope 2004; 114(8):1336–1340.

Median Palatal Cyst

1. Karacal N, Ambarcoglu O, Kutlu N. Median palatal cyst: report of an unusual entity. Plast Reconstr Surg 2005; 115(4): 1213–1214.
2. Gingell JC, Levy BA, Depaola LG. Median palatine cyst. J Oral Maxillofac Surg 1985; 43:47.

Nasolabial Cyst

1. Choi JH, Cho JH, Kang HJ. Nasolabial cyst: a retrospective analysis of 18 cases. Ear Nose Throat J 2002; 81:94.
2. Yuen HW, Julian CY, Samuel CL. Nasolabial cysts: clinical features, diagnosis and treatment. Br J Oral Maxillofac Surg 2006; 10:1016.

Thyroglossal Duct Cyst

1. Pollock WF, Stevenson EO. Cysts and sinuses of the thyroglossal duct. Am J Surg 1966; 112:225–232.
2. Rosai J, Carcangiu ML, DeLellis RA. Atlas of Tumor Pathology. Tumors of the Thyroid Gland, third series. Washington, DC: Armed Forces Institute of Pathology, 1992:2.
3. Ward GE, Hendrick JW, Chambers RG. Thyroglossal tract abnormalities—cysts and fistulas. Report of 105 cases from the Johns Hopkins Hospital observed during the years 1926-1046. Surg Gynecol Obstet 1949; 89:765–770.
4. Ellis PDM, van Nostrand AWP. The applied anatomy of thyroglossal tract remnants. Laryngoscope 1977; 87:765–770.
5. Allard RHB. The thyroglossal cyst. Head Neck Surg 1982; 5:134–146.
6. Brown PM, Judd ES. Thyroglossal duct cysts and sinuses: results of radical (Sistrunk) operation. Am J Surg 1961; 102:494–501.

7. Ward PH, Strahan RW, Acquarelli M, et al. The many faces of cysts of the thyroglossal duct. Trans Am Acad Ophthalmol Otolaryngol 1970; 74:310–318.
8. Katz AD, Hachigian M. Thyroglossal duct cysts. A thirty-year experience with emphasis on occurrence in older patients. Am J Surg 1988; 155:741–743.
9. Bennett KG, Organ CH Jr., Williams GR. Is the treatment for thyroglossal duct cysts too extensive? Am J Surg 1986; 152:602–605.
10. Dolata J. Thyroglossal duct cyst in the mouth floor: an unusual location. Otolaryngol Head Neck Surg 1994; 110:580–583.
11. Byard RW, Bourne AJ, Silver MM. The association of lingual thyroglossal duct remnants with sudden death in infancy. Int J Pediatr Otorhinolaryngol 1990; 20:107–112.
12. Slotnik D, Som PM, Giebfried J, et al. Thyroglossal duct cysts that mimic laryngeal masses. Laryngoscope 1987; 97:742–745.
13. Cumberworth VL, Bradley PJ. Atypical thyroglossal duct cysts. J Laryngol Otol 1989; 103:700–703.
14. Shaari CM, Ho BT, Som PM, et al. Large thyroglossal duct cyst with laryngeal extension. Head Neck 1994; 16:586–588.
15. Sade J, Rosen G. Thyroglossal cysts and tracts. A histological and histochemical study. Ann Otol Rhinol Laryngol 1968; 77:139–145.
16. LiVolsi VA, Perzin KH, Savetsky L. Carcinoma arising in median ectopic thyroid (including thyroglossal duct tissue). Cancer 1974; 34:1303–1315.
17. El-Silimy OE, Bradly PJ. Thyroglossal tract anomalies. Clin Otolaryngol 1985; 10:329–334.
18. Dische S, Berg AK. An investigation of the thyroglossal tract using the radioisotope scan. Clin Radiol 1963; 14: 298–314.
19. Tovi F, Barki Y, Maor E. Catilage within a thyroglossal duct anomaly. Int J Pediatr Otorhinolaryngol 1988; 15:205–210.
20. Davis JP, Toma AG, Robinson PJ, et al. Ossified thyroglossal cyst—is it of embryological significance? J Laryngol Otol 1994; 108:168–170.
21. Radkowski D, Arnold J, Healey GB, et al. Thyroglossal duct remnants. Preoperative evaluation and management. Arch Otolaryngol Head Neck Surg 1991; 117:1378–1381.
22. Pinczower E, Crockett DM, Atkinson JB, et al. Preoperative thyroid scanning in presumed thyroglossal duct cysts. Arch Otolaryngol head Neck Surg 1992; 118:985–988.
23. Hoffman MA, Schuster SR. Thyroglossal duct remnants in infants and children: reevaluation of histopathology and methods of resection. Ann Otol Rhinol Laryngol 1988; 97:483–486.
24. LiVolsi VA, Perzin KH, Savetsky L. Carcinoma arising in median ectopic thyroid (including thyroglossal duct tissue). Cancer 1974; 34:1303–1315.
25. Renard TH, Choucair RJ, Stevenson ED, et al. Carcinoma of the thyroglossal duct. Surg Gynecol Obstet 1990; 171:305–308.
26. Weiss SD, Orlich CC. Primary papillary carcinoma of a thyroglossal duct cyst: report of a case and review of the literature. Br J Surg 1991; 78:87–89.
27. Lustmann J, Benoliel R, Zeltser R. Squamous cell carcinoma arising in a thyroglossal duct cyst in the tongue. J Oral Maxillofac Surg 1989; 47:81–85.
28. Yanagisawa K, Eisen RN, Sasaki CT. Squamous cell carcinoma arising in a thyroglossal duct cyst. Arch Otolaryngol Head Neck Surg 1992; 118:538–541.
29. Nussbaum M, Buschwald RP, Ribner A, et al. Anaplastic carcinoma arising from median ectopic thyroid (thyroglossal duct remnant). Cancer 1981; 48:2724–2728.
30. Woods RH, Saunders JR, Pearlman S, et al. Anaplastic carcinoma arising in a thyroglossal duct tract. Otolaryngol Head Neck Surg 1993; 109:945–949.
31. Tovi F, Fliss DM, Inbar-Yanai I. Hurthle cell adenoma of the thyroglossal duct. Head Neck Surg 1988; 10:346–349.
32. Joseph TJ, Komorowski RA. Thyroglossal duct carcinoma. Hum Pathol 1975; 6:717–729.
33. LiVolsi VA. Thyroid tissue in unusual sites. In: LiVolsi VA, ed. Surgical Pathology of the Thyroid. Philadelphia, PA: W.B. Saunders Co., 1990:351–363.
34. LaRouere MJ, Drake AF, Baker SR, et al. Evaluation and management of a carcinoma arising in a thyroglossal duct cyst. Am J Otolaryngol 1987; 8:351–355.

Branchial Cysts, Sinuses, and Fistulas

1. Langman J. Digestive tube and its derivatives. In: Medical Embryology. Human Development—Normal and Abnormal, 3rd ed. Baltimore, MD: Williams & Wilkins, 1975:258–281.
2. Wilson DB. Embryonic development of the head and neck: part 2, the branchial region. Head Neck Surg 1979; 2:59–66.
3. Clemente CD. Cytology and embryology. In: Clemente CD, ed. Gray's Anatomy, 30th American ed. Philadelphia, PA: Lea & Febiger, 1985:7–68.
4. Provenza DV, Seibel W. Embryonic development—general and facial. In: Provenza DW, Seibel W, ed. Oral Histology. Inheritance and Development, 2nd ed. Philadelphia, PA: Lea & Febiger, 1986:127–161.
5. Ford GR, Balakrishnan A, Evans JNG, et al. Branchial cleft cyst and pouch anomalies. J Laryngol Otol 1992; 106:137–143.
6. Proctor B, Proctor C. Congenital lesions of the head and neck. Otolaryngol Clin North Am 1970; 3:221–248.
7. Buckingham JM, Lynn HB. Branchial cleft cysts and sinuses in children. Mayo Clin Proc 1974; 49:172–175.
8. Hunter AGW. Inheritance of branchial sinuses and preauricular fistulas. Teratology 1974; 9:225–228.
9. Arnot RS. Defects of the first branchial cleft cysts. S Afr J Surg 1971; 9:93–98.
10. Aronshon RS, Batsakis JG, Rice DH, et al. Anomalies of the first branchial cleft. Arch Otolaryngol 1976; 102:737–740.
11. Belenky WM, Medina JE. First branchial cleft anomalies. Laryngoscope 1988; 90:28–39.
12. Olsen KD, Maragos NE, Weiland LH. First branchial cleft anomalies. Laryngoscope 1980; 90:423–436.
13. Finn DG, Buchalter IH, Sarti E, et al. First branchial cleft cysts: clinical update. Laryngoscope 1987; 97:136–140.
14. Tom LWC, Kenealy JFX, Tosiglieri AJ Jr. First branchial cleft anomalies involving the tympanic membrane and middle ear. Otolaryngol Head Neck Surg 1991; 105:473–477.
15. Violaris NS, Pahor AL. A variation of first branchial cleft anomalies. J Laryngol Otol 1993; 107:625–626.
16. Hickey SA, Scott GA, Traub P. Defects of the first branchial cleft. J Laryngol Otol 1994; 108:240–243.
17. Koltai PJ, Winkelman PE. A first branchial cleft anomaly within the parotid gland. Otolaryngol Head Neck Surg 1980; 88:44–48.
18. Miglets AW. Parotid branchial cleft cyst with facial paralysis. Arch Otolaryngol 1975; 101:637–638.
19. Work WP. Newer concepts of first branchial cleft defects. Laryngoscope 1972; 82:1581–1593.
20. Cunningham MJ. The management of clinical neck masses. Am J Otolaryngol 1992; 13:78–92.
21. Simpson RA. Lateral cervical cysts and fistulas. Laryngoscope 1969; 79:30–59.
22. Golledge J, Ellis H. The aetiology of lateral cervical (branchial) cysts: past and present theories. J Laryngol Otol 1994; 108:653–659.
23. Bhaskar SN, Bernier JL. Histogenesis of branchial cysts. A report of 468 cases. Am J Pathol 1959; 35:407–423.
24. Little JW, Rickles NH. The histogenesis of the branchial cyst. Am J Pathol 1967; 50:533–547.

25. Fahmy S. Cervical thymic cysts: their pathogenesis and relationship to branchial cysts. J Laryngol Otol 1974; 88:47–60.
26. Thaler ER, Tom LWG, Handler SD. Second branchial cleft anomalies presenting as pharyngeal masses. Otolaryngol Head Neck Surg 1993; 109:941–944.
27. Nicolai P, Luzzago F, Maroldi R, et al. Nasopharyngeal cysts. Report of seven cases with review of the literature. Arch Otolaryngol Head Neck Surg 1989; 115:860–864.
28. Shidara K, Uruma T, Yasuoka Y, et al. Two cases of nasopharyngeal branchial cyst. J Laryngol Otol 1993; 107:453–455.
29. Papay FA, Kalucis C, Eliachar I, et al. Nasopharyngeal presentation of second branchial cleft cyst. Otolaryngol Head Neck Surg 1994; 110:232–234.
30. Shvero J, Hadar T, Avidos I, et al. Heterotopic salivary tissue and branchial sinuses. J Laryngol Otol 1986; 100:243–246.
31. Blackwell KE, Calcaterra TC. Functional neck dissection for treatment of recurrent branchial remnants. Arch Otolaryngol Head Neck Surg 1994; 120:417–421.
32. Deane SA, Telander RL. Surgery for thyroglossal duct and branchial cleft anomalies. Am J Surg 1978; 136:348–353.
33. Ostfeld EJ, Wiesel JM, Rabinson S, et al. Parapharyngeal (retrostyloid)—third branchial cleft cyst. J Laryngol Otol 1991; 105:790–792.
34. Har-El G, Sasaki Ct, Prager D, et al. Acute suppurative thyroiditis and the branchial apparatus. Am J Otolaryngol 1991; 12:6–11.
35. Shugar MA, Healey GB. The fourth branchial cleft abnormality. Head Neck Surg 1980; 3:72–75.
36. Ostfeld E, Segal J, Auslander L, et al. Fourth pharyngeal pouch sinus. Laryngoscope 1985; 95:1114–1117.
37. Narcy P, Aumont-Grosskopf C, Bobin S, et al. Fistulae of the fourth endobranchial pouch. Int J Pediatr Otorhinolaryngol 1988; 16:157–165.
38. Godin MS, Kearns DB, Pransky SM, et al. Fourth branchial pouch sinus: principles of diagnosis and management. Laryngoscope 1990; 100:174–178.
39. Takimoto T, Yoshizaki T, Ohoka H, et al. Fourth branchial pouch anomaly. J Laryngol Otol 1991; 104:905–907.
40. Rosenfeld RM, Biller HF. Fourth branchial pouch sinus: diagnosis and treatment. Otolaryngol Head Neck Surg 1991; 105:44–50.
41. Whitworth IH, Suvarna SK, Wight RG, et al. Fourth branchial arch anomaly: a rare incidental finding in an adult. J Laryngol Otol 1993; 107:238–239.
42. Buchner A, Hansen LS. Lymphoepithelial cysts of the oral cavity. Oral Surg Oral Med Oral Pathol 1980; 50:441–449.
43. Smith FB, Rajdeo H, Panesar N, et al. Benign lymphoepithelial lesion of the parotid gland in intravenous drug users. Arch Pathol Lab Med 1988; 112:742–745.
44. Schiodt M. HIV-associated salivary gland disease: a review. Oral Surg Oral Med Oral Pathol 1992; 73:164–167.
45. Mandel L, Reich R. HIV parotid gland lymphoepithelial cysts. Review and case reports. Oral Surg Oral Med Oral Pathol 1992; 74:273–278.
46. Fox PC. Salivary gland involvement in HIV-1 infection. Oral Surg Oral Med Oral Pathol 1992; 73:168–170.
47. Labouyrie E, Merlio JPH, Beylot-Barry M, et al. Human immunodeficiency virus type-1 replication within cystic lymphoepithelial lesion of the salivary gland. Am J Clin Pathol 1993; 100:41–46.
48. Ulirsch RC, Jaffe ES. Sjogren's syndrome-like illness associated with the acquired immunodeficiency syndrome-related complex. Hum Pathol 1987; 18:1063–1068.
49. von Volkman R. Dae tiefe branchiogene Halkacarcinom. Zentralbl Chir 1882; 49:63.
50. Martin H, Morfit HM, Ehrlich H. The case for branchiogenic cancer (malignant branchioma). Ann Surg 1950; 132:867–887.
51. Compagno J, Hyams VJ, Safavian M. Does branchiogenic carcinoma really exist? Arch Pathol Lab Med 1976; 100:311–314.
52. Khafif RA, Prichep R, Minkowitz S. Primary branchiogenic carcinoma. Head Neck 1989; 11:153–163.
53. Micheau C, Cachin Y, Caillou B. Cystic metastases in the neck revealing occult carcinoma of the tonsil. A report of six cases. Cancer 1974; 33:228–233.
54. Micheau C, Klijanienko J, Luboinski B, et al. So-called branchiogenic carcinoma is actually cystic metastases in the neck from a tonsillar primary. Laryngoscope 1990; 100:878–883.
55. Foss RD, Warnock GR, Clark WB, et al. Malignant cyst of the lateral aspect of the neck: branchial cleft carcinoma or metastasis? Oral Surg Oral Med Oral Pathol 1991; 71: 214–217.
56. Wenzel JP, Talbot Jm. Cystic squamous cell carcinoma metastatic to the neck from occult primary. Ann Otol Rhinol Laryngol. 1992; 101:1021–1023.
57. Thompson LDR, Heffner DK. The clinical importance of cystic squamous cell carcinoma in the neck. A study of 136 cases. Cancer 1998; 82:944–956.
58. Barnes L, Johnson JT. Pathological and clinical considerations in the evaluation of major head and neck specimens resected for cancer. In: Sommers SC, Rosen PP, Fechner RE, eds. Part 1. Pathology Annual. Norwalk,CT: Appleton-Century-Crofts, 1986:207.

Thymic Cyst (Cervical Thymic Cyst)

1. Langman J. Pharyngeal gut. In: Langman J, ed. Medical Embryology, 3rd ed. Baltimore, MD: Williams & Wilkins, 1975:260–281.
2. Zarbo RJ, McClatchey KD, Areen RG, et al. Thymopharyngeal duct cyst: a form of cervical thymus. Ann Otol Rhinol Laryngol 1983; 92:284–289.
3. Fahmy S. Cervical thymic cysts: their pathogenesis and relationship to branchial cysts. J Laryngol Otol 1974; 88: 47–60.
4. Speer FD. Thymic cysts. Report of a thymus presenting cysts of three types. Bull NY Med Coll 1938; 1:142–150.
5. Strome M, Eraklis A. Thymic cysts in the neck. Laryngoscope 1977; 87:1645–1649.
6. Raines JM, Rowe LD. Progressive neonatal airway obstruction secondary to cervical thymic cyst. Otolaryngol Head Neck Surg 1981; 89:723–725.
7. Rosevear WH, Singer MI. Symptomatic cervical thymic cyst in a neonate. Otolaryngol Head Neck Surg 1981; 89:738–741.
8. Barat M, Sciubba JJ, Abramson AL. Cervical thymic cyst: case report and review of literature. Laryngoscope 1985; 95:89–91.
9. Lyons TJ, Dickson JAS, Variend S. Cervical thymic cysts. J Pediatr Surg 1989; 24:241–243.
10. Jaramillo D, Perez-Atayde A, Griscom NT. Apparent association between thymic cysts and prior thoracotomy. Radiology 1989; 172:207–209.
11. Shajrawi I, Gertner R, Fradis M, et al. Lateral cervical thymic cyst. Otolaryngol Head Neck Surg 1990; 102:759–761.
12. Suster S, Rosai J. Multilocular thymic cyst: an acquired reactive process. Study of 18 cases. Am J Surg Pathol 1991; 5:388–389.
13. Boyd J, Templer J, Havey A, et al. Persistent thymopharyngeal duct cyst. Otolaryngol Head Neck Surg 1993; 109:135–139.
14. Shenoy PK, David VC. Cervical thymic cyst—a case record. J Laryngol Otol 1993; 107:950–952.
15. Guba AM, Adam AE, Jacques DA, et al. Cervical presentation of thymic cysts. Am J Surg 1978; 136:430–436.

16. Vesterhaus J, Eide SS, Froland B, et al. Maldescent of thymus in a hypoparathyroid infant with pharyngeal pouch syndrome. Acta Paediatr 1975; 64:555–558.
17. Civi I, Kurtay M, Civi S. Bilateral thymus found in association with unilateral cleft lip and palate. Plast Reconstr Surg 1989; 83:143–147.
18. May M. Neck masses in children: diagnosis and treatment. Pediatr Annu 1976; 5:517–535.
19. Leong AS-Y, Brown JH. Malignant transformation in thymic cyst. Am J Surg Pathol 1989; 8:471–475.
20. Suster S, Rosai J. Cystic thymomas. A clinicopathologic study of ten cases. Cancer 1992; 69:92–97.
21. Suster S, Barbuto D, Carlson G, et al. Multilocular thymic cysts with pseudoepitheliomatous hyperplasia. Hum Pathol 1991; 22:455–460.
22. Mishalani SH, Lones MA, Said JW. Multilocular thymic cyst. A novel thymic lesion associated with human immunodeficiency virus infection. Arch Pathol Lab Med 1995; 119:467–470.

Bronchogenic Cysts

1. Abell MR. Mediastinal cysts. Arch Pathol 1956; 61:360–379.
2. Eraklis AJ, Griscom NT, McGovern JB. Bronchogenic cysts of the mediastinum in infancy. N Engl J Med 1969; 281:1150–1155.
3. Maier MC. Bronchogenic cysts of the mediastinum. Ann Surg 1948; 127:476–502.
4. Sayler DC, Sayler DC, Eggleston JC. Benign developmental cysts of the mediastinum. Arch Pathol Lab Med 1977; 101:136–139.
5. Moersch HJ, Clagett OT. Pulmonary cysts. J Thorac Surg 1947; 16:179–194.
6. Rogers LF, Osmer JC. Bronchogenic cyst. A review of 46 cases. Am J Roentgenol Ther Nucl Med 1964; 91:273–283.
7. Constant E, Davis DG, Edminster R. Bronchogenic cyst of the suprasternal area. Plast Reconstr Surg 1973; 52:88–90.
8. Dubois P, Belanger R, Wellington JL. Bronchogenic cyst presenting as a supraclavicular mass. Can J Surg 1981; 24:530–531.
9. Fraga S, Helwig EB, Rosen SH. Bronchogenic cysts in the skin and subcutaneous tissue. Am J Clin Pathol 1971; 56:230–238.
10. Park OK, Buford CH. Bronchogenic cyst of neck and superior mediastinum. Ann Surg 1955; 142:130–133.
11. Seybold WD, Clagett OT. Presternal cyst. Report of a case. J Thorac Surg 1945; 14:217–220.
12. Lazar RH, Younis RT, Bassila MN. Bronchogenic cysts: a cause of stridor in the neonate. Am J Otolaryngol 1991; 12:117–121.
13. Yerman HM, Holinger LD. Bronchogenic cyst with tracheal involvement. Ann Otol Rhinol Laryngol 1990; 99:89–93.
14. Ustundag E, Iseri M, Keskin G, et al. Cervical bronchogenic cysts in head and neck region: review of the literature. J Laryngol Otol 2005; 119:419–423.

Rathke's Cleft Cyst

1. Langman J. In: Medical Embryology, 3rd ed. Baltimore, MD: Williams & Wilkins, 1975:337–363.
2. Gillman T. The incidence of ciliated epithelium and mucous cells in the normal Bantu pituitary. S Afr J Med Sci 1940; 5:30–40.
3. Bayoumi ML. Rathke's cleft and its cysts. Edinb Med J 1948; 55:745–749.
4. Shanklin WM. On the presence of cysts in the human pituitary. Anat Rec 1949; 104:379–407.
5. McGrath P. Cysts of the sellar and pharyngeal hypophysis. Pathology 1971; 3:123–131.
6. Baskin DS, Wilson CB. Transsphenoidal treatment of nonneoplastic intracellular cysts. A report of 38 cases. J Neurosurg 1984; 60:8–13.
7. Midha R, Jay V, Smyth HS. Transsphenoidal management of Rathke's cleft cysts. A clinicopathologic review of 10 cases. Surg Neurol 1991; 35:446–454.
8. Ross DA, Norman D, Wilson CB. Radiologic characteristics and results of surgical management of Rathke's cysts in 43 patients. Neurosurgery 1992; 30:173–179.
9. Sumida M, Uozumi T, Mukadi K, et al. Rathke cleft cysts: correlation of enhanced MR and surgical findings. Am J Neuroradiol 1994; 15:525–532.
10. Voelker JL, Campbell RL, Muller J. Clinical, radiographic, and pathological features of symptomatic Rathke's cleft cysts. J Neurosurg 1991; 74:535–644.
11. Nishio S, Mizuno J, Barrow DL, et al. Pituitary tumors composed of adenohypophysial adenoma and Rathke's cleft cyst elements: a clinicopathologic study. Neurosurgery 1987; 21:371–377.
12. Christophe C, Flamant-Durand J, Hanquinet S, et al. MRI in seven cases of Rathke's cleft cyst in infants and children. Pediatr Radiol 1993; 23:79–82.
13. Kucharczyk W, Peck WW, Kelly WM, et al. Rathke cleft cysts: CT, MR imaging, and pathologic features. Radiology 1987; 165:491–495.
14. Maggio, WW, Cail WS, Brookman JR, et al. Rathke's cleft cyst: computed tomographic and magnetic resonance imaging appearances. Neurosurgery 1987; 21:60–62.
15. Ikeda H, Yoshimoto T, Suzuki J. Immunohistochemical study of Rathke's cleft cyst. Acta Neuropathol 1988; 77:33–38.
16. Inoue T, Matsushima T, Fukui M, et al. Immunohistochemical study of intracranial cysts. Neurosurgery 1988; 23: 576–581.
17. Lach B, Scheithauer BW, Gregor A, et al. Colloid cyst of the third ventricle. A comparative immunohistochemical study of neuroaxis cysts and choroid plexus epithelium. J Neurosurg 1993; 78:101–111.
18. Wolfson AL, Lach B, Benoit BG. Suprasellar xanthomatous Rathke's cleft cyst. Surg Neurol 1992; 38:106–109.
19. Concha S, Hamilton BPN, Millan JC, et al. Symptomatic Rathke's cleft cyst with amyloid stroma. J Neurol Neurosurg Psychiatry 1975; 38:782–786.
20. Kepes JJ. Transitional cell tumor of the pituitary gland developing from a Rathke's cleft cyst. Cancer 1978; 41: 337–343.
21. Yoshyida J, Kobayashi T, Kageyama N, et al. Symptomatic Rathke's cleft cyst. Morphological study with light and electron microscopy and tissue culture. J Neurosurg 1977; 47:451–458.
22. Xin W, Rubin MA, McKeever PE. Differential expression of cytokeratins 8 and 20 distinguishes craniopharyngioma from Rathke cleft cyst. Arch Pathol Lab Med 2002; 126:1174–1178.

Thornwaldt's Cyst

1. Dorrance GM. The so-called bursa pharyngea in man. Its origin, relationship with adjourning nasopharyngeal structures and pathology. Arch Otolaryngol 1931; 13:187–224.
2. Guggenheim P. Cysts of the nasopharynx. Laryngoscope 1967; 77:2147–2168.
3. Miller RH, Sneed WF. Thornwaldt's bursa. Clin Otolaryngol 1985; 10:21–25.
4. Hollender AR. The nasopharynx. A study of 140 autopsy specimens. Laryngoscope 1946; 56:282–304.
5. Boucher RM, Hendrix RA, Guttenplan MD. The diagnosis of Thornwaldt's cyst. Trans Pa Acad Ophthalmol Otolaryngol 1990; 42:1026–1030.

6. Parnes SM. Pathologic quiz case 2. Thornwaldt's cyst. Arch Otolaryngol 1976; 102:254–256.
7. Weissman JL. Thornwaldt's cyst. Am J Otolaryngol 1992; 13:381–385.
8. Ford WJ, Brooks BS, El Gammal T. Thornwaldt cyst: an incidental MR diagnosis. Am J Neuroradiol 1987; 8:922–923.
9. Nofray JF, Rybak LP, Meniroff PM. Magnetic resonance imaging of Thornwaldt's cyst. Ann Otol Rhinol Laryngol 1989; 98:569–570.
10. Shank EC, Burgess LPA, Geyer CA. Thornwaldt's cyst: case report with magnetic resonance imaging (MRI). Otolaryngol Head Neck Surg 1990; 102:169–173.

Nasopharyngeal Cysts

1. Singh KP, Pahor AL. Congenital cyst of nasopharynx. J Laryngol Otol 1977; 91:75–79.
2. Pahor AL. Enterogenic cyst of the nasopharynx. J Laryngol Otol 1980; 94:793–795.
3. Robinson PM. Nasopharyngeal cyst (report of eight cases). J Laryngol Otol 1988; 102:182–183.
4. Nicolai P, Luzzago F, Maroldi R, et al. Nasopharyngeal cysts. Report of seven cases with review of the literature. Arch Otolaryngol Head Neck Surg 1989; 115:860–864.
5. Shidara K, Uruma T, Yasouka Y, et al. Two cases of nasopharyngeal branchial cyst. J Laryngol Otol 1993; 107:453–455.
6. Papy FA, Kalucis C, Eliachar I, et al. Nasopharyngeal presentation of second branchial cleft cyst. Otolaryngol Head Neck Surg 1994; 110:232–234.

B. Nondevelopmental Cysts

Mucocele

1. Neville BW, Damm DD, Allen CM, et al. Oral and Maxillofacial Pathology, 2nd ed. Philadelphia, PA: W.B. Saunders Co. 2002:389–391.
2. Cataldo E, Mosadomi A Mucoceles of the oral mucous membrane. Arch Otolaryngol 1970; 91:360–365.
3. Robinson L, Hjorting-Hansen E. Pathologic changes associated with mucous retention cysts of minor salivary glands. Oral Surg Oral Med Oral Pathol 1964; 18:191–205.

Ranula

1. Zhao YF, Jia Y, Chen XM, et al. Clinical review of 580 ranulas. Oral Surg Oral Med Oral Pathol 2004; 98(3): 281–287.
2. Chidzonga MM, Mahomva L. Ranula: experience with 83 cases in Zimbabwe. J Maxillofac Surg 2007; 65(1):79–82.
3. McGurk M. Management of the ranula. Oral Maxillofac Surg 2007; 65(1):115–116.

Mucocele of the Paranasal Sinuses

1. Natvig K, Larsen TE. Mucocele of the paranasal sinuses: a retrospective clinical and histologic study. J Laryngol Otol 1982; 92:1075–1082.
2. Gardner DG. Pseudocysts and retention cysts of the maxillary sinus. Oral Surg. 1984; 58:561–567.
3. Wolfowitz BL, Solomon A. Mucocoeles of the frontal and ethmoid sinuses. J Laryngol Otol 1972; 86:79–82.
4. Khong JJ, Malhotia R, Selva D, et al. Efficacy of endoscopic sinus surgery for paranasal sinus mucocele including modified endoscopic Lothrop procedure for frontal sinus mucocele. J Laryngol Otol 2004; 118(5):352–356.
5. Har-El G. Endoscopic management of 108 sinus mucoceles. Laryngoscope 2001; 111(12):2131–2134.

Dermoid and Epidermoid Cysts

1. King RC, Smith BR, Burk JL. Dermoid cysts in the floor of the mouth. Review of the literature and case reports. Oral Surg Oral Med Oral Pathol 1994; 78:567–576.
2. Teszler CB, Abu El-Naaj I, Emodi O. Dermoid cysts of the lateral floor of the mouth. A comprehensive anatomo-surgical classification of cysts of the oral floor. J Oral Maxilliofac Surg 2007; 65(2):327–332.

Oral Heterotropic Gastrointestinal Cyst

1. Said-Al Naief N, Fantasia JE, Sciubba JJ, et al. Heterotopic oral gastrointestinal cyst. Report of 2 cases and review of the literature. Oral Surg Oral Med Oral Pathol 1999; 88:80–86.
2. Wetmore RF, Bartlett SP, Papsin B, et al. Heterotopic gastric mucosa of the oral cavity: a rare entity. Int. J. Pediatr Otorhinolaryngol 2002; 66:139–142.
3. Morgan WE, Jones JK, Flaitz CM, et al. Congenital heterotopic gastrointestinal cyst of the oral cavity in a neonate; case report and review of the literature. Int J Pediatr Otorhinolaryngol 1996; 36(1):6977.

Simple Bone Cyst (Traumatic Bone Cyst)

1. Matsumura S, Murakami S, Kakimoto N, et al. Histopathologic and radiographic findings of the simple bone cyst. Oral Surg Oral Med Oral Pathol 1998; 85:619–625.
2. Saito Y, Hoshina Y, Nagamine T, et al. Simple bone cyst. A clinical and histopathologic study of 15 cases. Oral Surg Oral Med Oral Pathol 1992; 74:487–491.
3. Mahomed F, Altini M, Meer S, et al. Cemento-osseous dysplasia with associated simple bone cysts. J Oral Maxillofac Surg 2005; 63(10):1549–1554.

Stafne Defect (Stafne Bone Cyst)

1. Neville BW, Damm DD, Allen CM, et al. Oral and Maxillofacial Pathology, 2nd ed. Philadelphia, PA: W.B. Saunders Co., 2002:23–24.
2. Ariji FN, Fujiwara N, Tabata O, et al. Stafne's bone cavity. Classification based on outline and content determined by computed tomography. Oral Surg Oral Med Oral Pathol 1993; 76(3):375–380.

Index

AAD. *See* Acroangiodermatitis (AAD)
ABC. *See* Aneurysmal bone cyst (ABC)
ABCD. *See* Anterior buccal cortical defect (ABCD)
AC. *See* Atypical carcinoid (AC)
Acanthamoeba keratitis, 1571–1572
Acantholytic actinic keratosis (AK), 1491
Acantholytic squamous cell carcinoma (ALSCC), 159–160
  clinical features, 160
  diagnosis, 160
  etiology, 159–160
  overviews, 159
  pathology, 160
  treatment, 160
Acanthosis, 253
ACC. *See* Adenoid cystic carcinomas (ACC)
Accessory tragi, 425–426
Acinar cells, 20, 27
Acinic cell carcinomas, 29–30, 390, 542–546
Acne keloidolis, 1342
Acoustic neuromas, 454–455, 691–692
Acquired cholesteatomas, 436–437
Acquired encephalocele, 440
Acquired melanosis, 1560–1561
Acquired nonneoplastic lesions, 427–432
  cholesterol granulomas, 430
  inflammatory otic polyps, 431
  malakoplakia, 431–432
  necrotizing malignant external otitis (NEO), 427–428
  otitis media, 428–429
  tympanosclerosis, 429–430
Acroangiodermatitis (AAD), 1522
Actinic cheilitis, 279–280
  clinical features, 279
  defined, 279
  diagnosis, 280
  pathology, 280
  treatment, 280
Actinic keratosis (AK)
  clinical features, 1489–1490
  differential diagnosis, 1490–1491
  histologic features, 1490
  imaging studies, 1490
  immunohistochemical studies, 1490
  treatment and prognosis, 1491
Actinomyces, 1621
Actinomyces spp, 953, 1013
Actinomycoses
  clinical background, 1620–1621
  etiology, 1621
  histopathology, 1621
  treatment, 1621
Acute bacterial rhinosinusitis, 345
Acute bacterial sinusitis, 345
Acute exacerbation of chronic sinusitis (AECS), 1609
Acute myeloid leukemia, 1355
Acute necrotizing ulcerative gingivitis (ANUG), 259
Acute suppurative osteomyelitis
  pathologic features, 958–959
  radiologic features, 958
Acute suppurative sialadenitis, 484–485
Acute thyroiditis, 4, 1391–1392
Acyclovir, 1673
Addison's disease, 1460
Adenocarcinoma, 578–580
  of left supraclavicular lymph node, 1151
Adenocarcinomas
  ceruminal gland, 462–463
  intestinal-type, 383–387
  middle ear, 466–467
  of nasal cavity/paranasal sinuses, classification, 383
  nonintestinal-type, 387–389
Adenoid cystic carcinomas (ACC), 23, 24–25, 76, 168–169, 178, 390, 552–557
Adenoid hyperplasia, 225–226
  pathology, 226
  treatment, 226
Adenoid squamous carcinomas, 313–314
Adenomatoid nodules. *See* Hyperplastic nodules
Adenomatoid odontogenic tumor (AOT)
  AMBN mutation, 1240
  differential diagnosis, 1240
  electron microscopy of, 1239–1240
  imaging, 1236–1237
  immunohistochemistry, 1238–1239
  pathology and pathogenesis, 1238
    patterns of, 1237
  prevalence and incidence, 1235–1236
  treatment and prognosis, 1240
Adenosine triphosphate–binding cassette transporter A1 (ABCAL1), 1730
Adenosquamous carcinomas, 158–159, 312–313
  clinical features, 158
  diagnosis, 159
  etiology, 158
  immunohistochemistry, 159
  overviews, 158
  pathology, 158–159
  treatment, 159
Adipose tissue, 20
Adult onset laryngeal papillomas, 1677
Adult T-cell leukemia/lymphoma, 1072
AFD. *See* Ameloblastic fibrodentinoma (AFD)
AFIP. *See* Armed Forces Institute of Pathology (AFIP)
Afipia felis, 1011
AFOD. *See* Ameloblastic fibro-odontoma (AFOD)
Aggressive osteoblastoma, 970
AIDS, 50
AIDS-related lymphomas, 1667
AIDS-related nasopharyngeal lesions, 1661
AIDS-related parotid cysts (ARPC), 1660–1661
AIDS toxoplasmosis, 1688
AIF. *See* Apoptosis inducing factor (AIF) and apoptotic cell death
AJCC. *See* American Joint Committee on Cancer (AJCC)
AJCC 2002 melanoma staging, 1508
AK. *See* Actinic keratosis (AK)
Albendazole, 1690
Albright's hereditary osteodystrophy, 1460
ALCD. *See* Anterior lingual cortical defect (ALCD)
ALCL. *See* Anaplastic large cell lymphoma (ALCL)
Alcohol, oral cancer, 288
ALHE. *See* Angiolymphoid hyperplasia with eosinophilia (ALHE)
ALK+ anaplastic large cell lymphoma, 1065–1068
  clinical features, 1066
  differential diagnosis, 1068
  immunohistochemistry, 1066–1067
  molecular genetic data, 1067–1068
  pathology, 1066
ALK- anaplastic large cell lymphoma, 1068
ALK+ DLBCL, 1042
ALK gene, 1042
Allergic fungal rhinosinusitis (AFRS), 354–356
  clinical features, 355
  etiology, 355
  pathology, 355–356
  treatment, 356
Allergic fungal sinusitis (eosinophilic mucin rhinosinusitis)
  clinical presentation, 1633
  etiology, 1633
  histopathology, 1633–1634
  treatment, 1634
Allergic granulo matosis and vasculitis (AGV). *See* Churg-Strauss syndrome
Allergic mucus, 354–356
Allergic rhinosinusitis, 343–345
Alopecia, 252
ALSCC. *See* Acantholytic squamous cell carcinoma (ALSCC)
Alternaria, 1640
Alveolar cysts, 1343
Alveolar mucosa, squamous cell carcinomas of, 298–300
Alveolar RMS (ARMS), 869, 872–873
Alveolar soft part sarcoma (ASPS), 901–904, 1363
  in children, 1346
Amalgam tattoo, 204–205
  clinical features, 205
  pathology, 205
  treatment, 205
AMCA. *See* Ameloblastic carcinoma (AMCA)
Ameloblastic carcinoma (AMCA), 1292
  differential diagnosis, 1295
  DNA microarray study, 1295
  etiology of, 1293–1294
  frequency of, 1293
  gender ratio, 1293
  growth rate, 1293
  immunohistochemistry, 1294
  locations of, 1293
  ultrastructure of, 1294
Ameloblastic fibrodentinoma (AFD)
  clinical features, 1247
  immunohistochemistry
    neural tissue markers, 1248
  pathogenesis of, 1247–1248
  treatment and prognosis, 1248
  ultrastructure of, 1248

Ameloblastic fibroma (AMF)
clinical features, 1241–1242
differential diagnosis, 1245–1246
etiology of, 1242–1244
imaging of, 1242
immunohistochemistry, 1244
molecular-genetic data, 1245
treatment and prognosis, 1246–1247
ultrastructure of, 1245
Ameloblastic fibro-odontoma (AFOD)
clinical features, 1248–1249
differential diagnosis, 1252
etiology of, 1249–1250
immunohistochemistry
CK in epithelial component of, 1250
enamel proteins in, 1251
growth factors, 1251
MIB-1 antibody, 1251
nestin and vimentin, 1251
molecular-genetic data, 1252
osteocalcin transcripts and, 1252
radiographs, 1249
treatment and prognosis, 1252
ultrastructure of, 1251–1252
Ameloblastomas, 69
ameloblastin (AMBN) gene mutations in, 1213
amelogenin and, 1213
differential diagnosis, 1214
molecules involved in progression of
angiogenic factors, 1214
cell adhesion molecules, 1213
matrix-degrading proteinases, 1213–1214
osteolytic cytokines, 1214
treatment and prognosis, 1214–1215
tumorigenesis and/or cell differentiation, molecules involved in
apoptosis-related factors, 1212
cell cycle-related factors, 1212
DNA-repair genes, 1211
gene modifications and, 1210–1211
growth factors, 1211–1212
hard tissue-related proteins, 1213
oncogenes, 1210
oncoviruses, 1211
telomerase activity, 1212
tooth development, regulators of, 1213
tumor suppressor genes, 1211
Amelogenin and calcifying odontogenic cyst (COC), 1265
American College of Rheumatology, 253, 652
American Joint Committee on Cancer (AJCC), 863
staging of nasopharyngeal carcinomas, 396
staging of vestibular carcinomas, 373
AMF. *See* Ameloblastic fibroma (AMF)
5-aminolevulinic acid, 1488
Amiodarone drugs, 1386
Amphotericin B, 1631, 1637, 1652
Ampicillin-sulbactam, 1611
Amputation neuroma. *See* Traumatic neuroma
Amyloid, 14
Amyloid goiter, 1391
Amyloidosis, 484, 1027–1029
classification, 1028
clinical features, 1028–1029
pathology, 1029
ANA. *See* Antinuclear antibodies (ANA)
Anaplastic carcinoma, 14–15
clinical features, 1407
molecular genetics, 1408–1409
pathology, 1408
treatment and prognosis, 1409
Anaplastic large cell lymphoma (ALCL), 42–43
ALK+, 1065–1068
ALK-, 1068
ANCA. *See* Antineutrophil cytoplasmic autoantibodies (ANCA)
ANCA titers. *See* Antineutrophil cytoplasmic antibodies (ANCA) titers
Ancillary studies, of lymph nodes, 39–40
cell block, 39
core needle biopsy, 39
FISH studies, 40
flow cytometry, 39–40
PCR studies, 40
Androgen receptor (AR), 31
Aneuploidy, 713
Aneurysmal bone cyst (ABC), 963, 986–987
Angiofibroma
clinical features, 834
differential diagnosis, 836
electron microscopy, 836
imaging, 834–835
immunohistochemistry, 836
molecular-genetic data, 836
pathology, 835–836
treatment and prognosis, 836–837
Angiofibromas, 64
Angioimmunoblastic T-cell lymphoma, 1064
Angiolymphoid hyperplasia with eosinophilia (ALHE)
clinical features, 1528
defined, 1528
differential diagnosis, 1529
electron microscopy, 1529
imaging studies, 1528
immunohistochemistry, 1529
molecular genetics, 1529
pathology, 1528
treatment and prognosis, 1529
Angiomatoid fibrous histiocytoma (AFH). *See* Malignant fibrous histiocytoma
Angiosarcoma, 867–869, 982–983, 1415–1416
Angle recession, 1584
Annexin V activity and apoptotic cells detection, 1212
Anterior buccal cortical defect (ABCD), 963
Anterior lingual cortical defect (ALCD), 963
Anthelmintics, 1690
Anthracosis, 1444
Antibiotics, 260
Anticonvulsants drugs, 260
Antifungal therapy, 257
Antigen, 249
Antimalarial drugs, 254
Antimicrobial therapy, 37
Antineutrophil cytoplasmic antibodies (ANCA) titers, 441
Antineutrophil cytoplasmic antibodies/autoantibodies (ANCA), 649, 650
cytoplasmic (C-ANCA), 650
perinuclear (P-ANCA), 650
Antineutrophil cytoplasmic autoantibodies (ANCA)
in Wegener's granulomatosis, 443–444
Antinuclear antibodies (ANA), 252
Anti-PTH immunohistochemistry, 1434
Antoni type A, 679
Antrochoanal polyps (ACP), 350–351
ANUG. *See* Acute necrotizing ulcerative gingivitis (ANUG)
AOT. *See* Adenomatoid odontogenic tumor (AOT)
APAF-1. *See* Apoptotic protease activating factor-1 (APAF-1) and apoptotic cell death
Aplasia, of salivary glands, 476–477
Aplasia cutis congenital (ACC), 1537
Apocrine hidrocystomas, 1484
Apoptosis inducing factor (AIF) and apoptotic cell death, 1212
Apoptotic protease activating factor-1 (APAF-1) and apoptotic cell death, 1212
AR. *See* Androgen receptor (AR)
Argyrophilic nucleolar organizer regions (AgNORs), 1479
Armed Forces Institute of Pathology (AFIP), 976
ARMS. *See* Alveolar RMS (ARMS)
Arteriovenous hemangioma (arteriovenous malformation)
clinical findings, 776–777
differential diagnosis, 778–779
imaging, 777
immunohistochemistry, 778
pathologic findings, 777–778
prognosis and treatment, 779
Arthralgia, 253
Aspergillosis
acute fulminant invasive, 1630
chronic invasive/chronic granulomatous, 1631–1632
histopathology, 1630–1631
historical background, 1629–1630
serology, 1631
treatment, 1631
Aspergillus flavus, 1630
Aspergillus fumigatus, 354
Aspirin, 968
intolerance, 346–347
ASPS. *See* Alveolar soft part sarcoma (ASPS); Alveolar soft part sarcoma (ASPS)
Asteroid bodies, 1693
Ataxia-telangectasia (AT), 1667
Ataxia-telangiectasia syndrome, 1523
AT-mutated (ATM) gene, 1667
Atrophic rhinosinusitis (ARS), 346
Atypia, 130
Atypical carcinoid (AC), 164–166
clinical features, 164
diagnosis, 165
electron microscopy, 165
immunohistochemistry, 165
pathology, 164
treatment, 165–166
Atypical fibroxanthoma (AFX), 463–464, 1494–1495
clinical features, 1520
differential diagnosis, 1521
electron microscopy, 1521
immunohistochemistry, 1521
molecular genetics, 1521
pathology, 1520–1521
treatment and prognosis, 1521
Atypical keratinocytes, 1489
Atypical lymphoid hyperplasia, 1081
Atypical lymphoreticular cells, 652
Atypical marginal zone hyperplasia, of tonsil, 1093
Atypical teratoid/rhabdoid tumor, 1363
Auditory canal
external. *See* External auditory canal
mlignant neoplasms of, 459–464
Auricular cartilage
of idiopathic cystic chondromalacia, 433–434
Autoimmune diseases, 952
Autoimmune hypoparathyroidism, 1460
Autoimmune lymphoproliferative syndrome, 1024–1025
Autoimmune polyendocrinopathy-candidiasis-ectodermal dystrophy (APECED), 1460

Autoimmune polyglandular syndrome-1, 1460
Autotransplantation, of parathyroid glands, 1462–1463
Azathioprine, 257, 1693
Azithromycin, 1689

Bacillary Angiomatosis (BA)
  clinical presentation, 1628
  culture, PCR, and serological identification, 1628
  differential diagnosis, 1628
  etiology, 1628
  histopathology, 1628
  treatment, 1628
Bacilli Calmette-Guerin (BCG), 1623
Bacterial conjunctivitis, 72
Bacterial meningitis, 654
Bacterial sinusitis
  acute, 1609
  chronic, 1609–1610
Band keratopathy, 1580
Bartonella henselae, 51, 1011
Basal cell adenocarcinoma, 25, 564–567
Basal cell adenoma, 23–24, 34
  clinical features, 522–523
  differential diagnosis, 525
  electron microscopy, 524
  immunohistochemistry, 524–525
  overview, 522
  pathology, 523–524
  treatment, 525–526
Basal cell carcinoma (BCC), 75–76, 459, 1342
  clinical features, 1496
  differential diagnosis, 1498
  eyelids, 1552–1553
  imaging studies, 1496
  immunohistochemistry, 1497–1498
  molecular genetics, 1498
  pathology, 1496–1497
  treatment and prognosis, 1498
Basal cell nevus syndrome, 1342
Basal cell type ameloblastoma, 1206–1207
Basal encephaloceles, 652
Basaloid cells, 23
Basaloid keratinocytes, 1475
Basaloid squamous carcinomas, 309–312, 398. *See also* Squamous cell carcinomas
  differential diagnosis, 311–312
  histologic features, 309–310
  immunohistochemistry, 311
  treatment and prognosis, 310–311
Basaloid squamous cell carcinoma, 62, 155–158
  clinical features, 155
  diagnosis, 157
  electron microscopy, 157
  etiology, 155
  immunohistochemistry, 157
  overviews, 155
  pathology, 155–157
  treatment, 157–158
Basaloid tumors, 25
Basement membrane-associated molecules
  AOT and, 1238
  and CEOT, 1234
Basement membrane zone (BMZ), 246
Basement-type heparan sulfate proteoglycan (HSPG) and solid/multicystic ameloblastoma–central, 1209
Base of tongue, squamous cell carcinomas, 303–305
Basidiobolus, 1638
Basosquamous cell carcinoma (BSCC)
  clinical features, 1498–1499
  differential diagnosis, 1499
  imaging studies, 1499
  immunohistochemistry, 1499
  pathology, 1499
  treatment and prognosis, 1499
B-cell lymphoma
  intravascular large, 1042
  primary mediastinal (thymic) large, 1041–1042
  T-cell/histiocyte-rich large, 1042
B-cells, 39
  lymphoblastic leukemia/lymphoma, 1060
Bcl-2 and inhibitor of apoptosis (IAP) family proteins, modulators of mitochondrial apoptotic pathway, 1212
BCL2 protein expression, follicular lymphoma, 1049
Beckwith-Wiedemann syndrome, 1523
Behcet's disease, 261
Benign epithelial neoplasms
  actinic keratoses (AKs), 1489–1491
  cutaneous lymphadenoma (CL), 1482–1484
  hidrocystomas, 1484–1485
  pilar cysts (PCs), 1477–1478
  pilomatricoma, 1479–1481
  proliferating pilar cyst (PPC), 1478–1479
  sebaceous adenoma, 1488–1489
  sebaceous hyperplasia, 1487–1488
  seborrheic keratoses (SKs), 1475–1477
  syringoma, 1485–1487
  trichilemmomas (TLs), 1481–1482
Benign FHH, 1438
Benign lymphoepithelial lesion (BLEL), 1661
Benign lymphoepithelial tumor, of the skin. *See* Cutaneous lymphadenoma (CL)
Benign mesenchymal tumors
  of external auditory canal, 448–449
Benign mesenchymomas, 895
Benign migratory glossitis, 205–207
  clinical features, 206
  diagnosis, 206
  pathology, 206
  treatment, 207
Benign neoplasms, 1481
  external auditory canal, 447–449
  middle ear and temporal bone, 449–456
Benign odontogenic tumors
  adenomatoid odontogenic tumor, 1235–1240
  ameloblastoma
    desmoplastic ameloblastoma, 1218–1221
    keratoameloblastoma, 1225–1226
    papilliferous keratoameloblastoma, 1226–1228
    solid/multicystic ameloblastoma–central, 1202–1215
    solid/multicystic ameloblastoma–peripheral, 1215–1218
    unicystic ameloblastoma, 1221–1225
  calcifying epithelial odontogenic tumor, 1230–1235
  squamous odontogenic tumor, 1228–1230
Benign thyroid inclusions, in lymph node, 230–231
Benzoylmethylecgonine. *See* Cocaine
Ber-EP4 expression, 1499
Bethanechol chloride, 1691
Bilateral acoustic neuroma. *See* Neurofibromatosis 2
Biopsy
  ABCD, 963
  osteoblastoma, 970
  PLCD, 963
Biphasic synovial sarcoma. *See* Synovial sarcoma
Bipolaris, 1639–1640
Birefringent oxalate crystals, 954
Blastic plasmacytoid dendritic cell neoplasm, 1077–1078
Blastomycosis, 1642, 1648–1651
Blue rubber bleb syndrome, 1523
B- lymphocytes, 952, 953
BMP. *See* Bone morphogenetic protein (BMP), in ameloblastomas
BMZ. *See* Basement membrane zone (BMZ)
Bohn's nodules, 1343. *See also* Oral cavity
Bone, hematolymphoid lesions of, 1108–1109
Bone morphogenetic protein (BMP), in ameloblastomas, 1213
Bone sialoprotein (BSP), in ameloblastomas, 1213
Borrelia burgdorferi, 953, 1692
Botryoid rhabdomyosarcoma, 871
Botulinum toxin, 1485
Bowenoid papulosis, 1676
Bowen's disease. *See* Squamous cell carcinoma (SCC)
BP-antigen, 249
BRAF mutations, 1488, 1510
Branchial cleft anomalies, 426–427
Branchial cleft cyst, 21, 1351–1352
Branchial complexes, 1429
Branchiogenic carcinoma, 1155–1156
BRD4-NUT fusion product, 1730
BRD4 tumors, 1730
BSP. *See* Bone sialoprotein (BSP), in ameloblastomas
Buccal mucosa
  squamous cell carcinomas, 294–295
Buccal nerve, 669
Buccinator muscle, 669
Bullous keratopathy, 1564–1565
Bullous pemphigoid, 248–249
  clinical presentation, 248
  immunology, 249
  immunopathology, 249
  pathology, 248–249
  treatment, 249
Bulls eye, skin lesion, 258, 259
Burkitt's lymphoma, 40–41, 1056–1057, 1355, 1667–1668

Calcification, 1477, 1594
Calcifying cystic odontogenic tumor (CCOT)
  adenomatoid odontogenic tumor-associated, 1268
  ameloblastic fibroma-associated, 1268
  ameloblastic fibro-odontoma-associated, 1268
  clinical features, 1269–1270
  immunohistochemically studies, 1271
  odonto-ameloblastoma-associated, 1269
  odontogenesis stages of, 1270–1271
  odontogenic fibromyxoma-associated, 1269
  odontoma-associated, 1269
  solid/multicystic ameloblastoma–associated, 1267
  treatment and prognosis, 1272
  ultrastructure of, 1271
  unicystic ameloblastoma–associated, 1267–1268
Calcifying epithelial odontogenic tumor (CEOT)
  calcification and, 1233
  clear-cell variant of, 1231–1233
  differential diagnosis, 1235

[Calcifying epithelial odontogenic tumor (CEOT)]
etiology and source, 1232–1233
extraosseous variant of, 1233
immunohistochemistry
CK antibody reaction, 1234
epithelial membrane antigens (EMAs), 1234
proliferation marker Ki-67, 1234
tenascin, 1234
molecular-genetic data, 1235
prevalence and incidence, 1230
radiograms of, 1231–1232
radiolucent–radiopaque type, 1231
treatment and prognosis, 1235
ultrastructural studies, 1234–1235
Calcifying odontogenic cyst (COC), 1262–1263
etiology of, 1263
immunohistochemical studies, 1264
treatment and prognosis, 1267
Calcimimetics, 1456
Calcitonin-producing C cells, 1385
Calcium channel blocking agents, 217–218
Calcium pyrophosphate crystal deposition disease (CPCDD)
pathologic features, 954
radiologic features, 954
Calcium pyrophosphate dihydrate (CPPD), gout, 443
Calcium-sensing receptor (CaSR), 1435
Calcium supplements, 1456
Calretinin and ameloblastic epithelium, 1223
Canalicular adenoma, 24
clinical features, 531
defined, 531
differential diagnosis, 532
immunohistochemistry, 532
pathology, 531–532
treatment, 532
Cancer, 1438
sarcoma staging, AJCC on, 863
Candida albicans, 289
Candida albicans pseudohyphae, 59
Candidiasis, 1645–1646
Canker sores. *See* Recurrent aphthous stomatitis (RAS)
Capillary hemangioma in soft tissues of neck, 1358
Capillary malformations, 1522
Carboxyterminal fragments, 1436
Carcinoembryonic antigen (CEA), 14, 1483
Carcinoma ex pleomorphic adenoma, 583–586
Carcinoma in situ (CIS), 130, 133–135, 269
clinical features, 133
introduction, 133
molecular-genetic data, 134
pathology, 133
treatment, 134–135
Carcinoma of unknown primary (CUP), 1147
frequency, 1148
metastase histology, 1150
Carcinomas. *See also* Granulomas
adenoid squamous, 313–314
adenosquamous, 312–313
exophytic papilloma and, 362–363
inverted papilloma and, 366–368
incidence, 367
molecular biology in HPV-related, 290
neuroendocrine, 322–323
and OSP, 370–371
papillary squamous, 316–318
showing thymus-like differentiation, 1413
[Carcinomas]
spindle cell. *See* Spindle cell carcinomas (SPCC)
squamous cell. *See* Squamous cell carcinomas
staging in nasal vestibule, 373
verrucous. *See* Verrucous carcinomas
Carcinosarcoma, 586–588. *See also* Spindle cell carcinomas (SPCC)
Cardiac myxomas, 1727
Cardiovascular complications, associated with hyperparathyroidism, 1442
Carney complex (CNC), 1726–1727
Carotid body paraganglia (CBPG), 718–721
Cartilaginous lesions, 974
Caseating granulomas, 1012
Caspase-8 apoptosis initiator, role in ameloblastomas, 1212
CaSR gene, 1458
Castleman disease
hyaline-vascular, 1019–1021
localized plasma cell, 1021–1022
multicentric, 1009, 1022–1023
Cataract, 72
B-catenin stabilization, 1481
Cat scratch disease (CSD), 51
clinical features, 1627
etiology, 1627
histopathology, 1627–1628
of lymph node, 1011–1012
serology and PCR, 1628
treatment, 1628
Cavernous hemangiomas, 74, 1596–1597
CBPG. *See* Carotid body paraganglia (CBPG)
CCC. *See* Clear cell carcinoma
C cells tumors
hyperplasia, 1409–1410
medullary thyroid carcinoma, 1410
mixed medullary-follicular carcinoma, 1411
mixed medullary-papillary carcinoma, 1411–1412
CCLE. *See* Chronic cutaneous lupus erythematosus (CCLE)
CCOC. *See* Clear cell odontogenic carcinoma (CCOC)
CCOT. *See* Calcifying cystic odontogenic tumor (CCOT)
CD31, 866, 867
CD34, 866, 867
CD3 and CD4-like moieties, 1435
CD99 immunoreactivity, in ES/PNET, 737
CD3 immunostains, 39
CD20 immunostains, 39
CD44s, inverted papilloma, 368
CE. *See* Congenital epulis (CE)
CEA. *See* Carcinoembroyonic antigen (CEA)
Cefixime, 1618
Cell block, 39
Cellular alterations, in dysplasia, 267
Cellular hemangioma of infancy. *See* Infantile hemangioma (IH)
Cellular neurothekeomas, 694, 695
Cellular PA, 34–35
Cellular schwannomas, 680
CEMBLA. *See* Cementoblastoma (CEMBLA)
Cementoblastoma (CEMBLA)
differential diagnosis, 1290
etiology of, 1289
growth rate, 1288
immunohistochemistry, 1290
prevalence and incidence, 1288
radiographic examination, 1288–1289
treatment and prognosis, 1290
Cemento-osseous dysplasia, 965–966
Cemento-ossifying fibroma, 1279
Central odontogenic fibroma (COF), 1276
differential diagnosis, 1278–1279
etiology of, 1277
histochemical studies, 1278
treatment and prognosis, 1280
ultrastructure of, 1278
CEOT. *See* Calcifying epithelial odontogenic tumor (CEOT)
Cerebrospinal fluid (CSF), 672
leak, 675
rhinorrhea, 675
Ceruminal gland adenocarcinomas, 462–463
Ceruminal gland adenomas, 447
Ceruminal gland neoplasms, 447–448
Ceruminal gland pleomorphic adenomas, 447
Ceruminal glands, 424
Cervical adenopathy location, 1147–1148
Cervical lymphadenitis, 1623
Cervical lymph nodes, 144, 1147, 1148
deep, 1135
levels, 1135
metastasis to, 299–300
superficial, 1135
Cervical thymoma
clinical features, 1724
imaging studies, 1724
pathology, 1724
treatment and prognosis, 1724–1725
CFP-10 (culture filtrate protein 10), 1623
CFS. *See* Chronic fatigue syndrome (CFS)
CFTR. *See* Cystic fibrosis transmembrane conductance regulator (CFTR)
CGH. *See* Comparative genomic hybridization (CGH)
Chalazions, 73, 1553
Charcot-Leyden crystals, 355
Cheilitis glandularis, 490–491
Chemical carcinogens, oral cancer, 286–288
metabolism, 288
Chemodectoma, 717
Chemoreduction, 1594
Chemotherapy, 983
Chemotherapy-induced atypia, 1491
Cherubism, 966–967
Chlamydia, 72
Chlamydial conjunctivitis, 72
Chlorhexidine, 263
Cholesteatomas
acquired, 436–437
congenital, 437–438
Cholesterol granulomas, 30, 357–358
versus congenital cholesteatomas, 438
Chondroblastomas, 69, 978–979
Chondrocalcinosis. *See* Calcium pyrophosphate crystal deposition disease (CPCDD)
Chondrodermatitis nodularis chronicus helicis (CNCH), 432–433
Chondrodermatitis nodularis helicis (CNH)
clinical features, 1534
differential diagnosis, 1535
histologic features, 1534
immunohistochemistry, 1534
treatment and prognosis, 1535
Chondroid metaplasia, 975–976
Chondroma, 976
Chondromatosis, synovial of temporomandibular joint, 435–436
Chondromyxoid fibroma, 978
Chondrosarcoma, 976–978
larynx, 977
law, 977
Chordoid meningioma, 706
Chordoma, 979–981
Choroidal melanoma, 1589
Choroid plexus, 675
Choroquine, 1693

Chromogranin, 67, 1452
Chromosome 22q11 microdeletion syndrome, 1460
Chronic bruxism, 958
Chronic cutaneous lupus erythematosus (CCLE), 252
Chronic diffuse sclerosing osteomyelitis, 960
Chronic fatigue syndrome (CFS), 1666
Chronic granulomatous fungal sinusitis, 1631
Chronic hyperphosphatemia, in children, 963
Chronic invasive fungal sinusitis, 1632
Chronic lymphocytic leukemia/small lymphocytic lymphoma (CLL/SLL), 1059
Chronic sclerosing osteomyelitis, 959–960
Chronic sclerosing sialadenitis, 486–490
  of submandibular gland, 1097–1098
Chronic sinusitis, 345
Chronic suppurative osteomyelitis, 959
Chronic suppurative otitis media (CSOM), 1612
Churg-Strauss syndrome, 650, 657–660, 1610
  clinical features, 658
  criteria for diagnosis, 658
  limited form, 657
  pathology, 658–659
  treatment and prospect, 660
Chvostek's sign, 1460
Cidofovir, 1663
Cigarette smoking, and salivary gland tumors, 506–507
Ciprofloxacin, 1612
Circumferential margin preparation, 98
CIS. *See* Carcinoma in situ (CIS)
Civatte bodies, 260
CK. *See* Cytokeratin (CK)
CK 5/6 expression, 1481
CK 20-positive Merkel cells, 1483
Cladosporium, 1640–1641
Clark level of invasion, 1507
Classical Hodgkin lymphoma, 45
  clinical features, 1032
  differential diagnosis, 1035
  immunohistochemistry, 1034–1035
  lymphocyte-rich, 1033–1034
  molecular genetic data, 1035
  oral cavity and oropharynx, 1089
  pathology, 1032–1034
  treatment and prognosis, 1035
Classic butterfly rash, malar region, 252
Clear cell carcinoma (CCC), 563–564, 1729
Clear cell myoepithelial carcinoma (CMEC), 1729
Clear cell odontogenic carcinoma (CCOC)
  differential diagnosis, 1304
  etiology and pathogenesis, 1302–1303
  gender ratio, 1302
  histochemical and immunohistochemical studies, 1303
  molecular-genetic data, 1304
  prevalence and incidence, 1301
  treatment and prognosis, 1304
  ultrastructural studies, 1303
Clear cells
  change, 31–32
  lesions, 16–17
  meningiomas, 703
  of parathyroid glands, 1432
Clindamycin plus surgical drainage, 1611
Clinical staging system, for rhabdomyosarcoma, 876
CLL/SLL. *See* Chronic lymphocytic leukemia/small lymphocytic lymphoma (CLL/SLL)
Clofaimines, 1691
Clofazimine, 1620, 1627
CMN. *See* Congenital melanocytic nevi (CMN)
CMV. *See* Cytomegalovirus (CMV)
CNB. *See* Core needle biopsy (CNB)
COC. *See* Calcifying odontogenic cyst (COC)
Cocaine
  chronic intranasal inhalation, 663
  clinical features, 663–664
  crack cocaine, 663
  pathology, 664
  treatment and prospect, 664
Coccidioidomycosis, 1646–1648
COF. *See* Central odontogenic fibroma (COF)
CO_2-laser evaporation, 275
Collagen-1α1 gene, 1517, 1519
Collagenous fibroma (desmoplastic fibroblastoma)
  clinical features, 843
  differential diagnosis, 845–846
  electron microscopic findings, 845
  immunohistochemistry, 844–845
  molecular findings, 845
  pathologic findings, 843–844
  prognosis and therapy, 846
  radiologic findings, 843
Colloid cyst, of the thyroid glands, 1457
Colloid nodule. *See* Nodular goiter
Combined small cell neuroendocrine carcinoma, 167
Common cold, 345
Comparative genomic hybridization (CGH), 685
  malignant melanomas, 393
  studies of ITAC, 386
Computed tomography (CT), 1
Condyloma acuminatum, 212–214
  clinical features, 212
  diagnosis, 213
  electron microscopy, 213
  molecular genetic data, 213–214
  overviews, 212
  pathology, 213
  treatment, 214
Condylomas, 1676
Congenital abnormalities, ear, 425–427
Congenital cholesteatomas, 437–438
  versus cholesterol granulomas, 438
Congenital epibulbar melanocytic proliferations, 1560
Congenital epulis. *See* Gingival GCT of newborn
Congenital epulis (CE), 701
Congenital granular cell tumor, 1345
Congenital hemangioendothelioma. *See* Kaposiform hemangioendothelioma
Congenital hemangiopericytoma, 1358
Congenital hereditary lymphedema syndrome, 1523
Congenital herniations, 674
Congenital-infantile fibrosarcoma with spindle cell, 1361
Congenital melanocarcinoma. *See* Melanocytic neuroectodermal tumor of infancy (MNTI)
Congenital pleomorphic adenoma. *See* Salivary gland anlage tumor
Congenital teratoid cyst, 1343
Congo red stain, 14
Conidiobolus, 1638
Conidiobolus coronatus, 1638
Conidiobolus incongruous, 1638
Conjunctiva
  anatomy, 1557
  diseases
    conjunctival intraepithelial neoplasia (CIN), 1558–1559
    limbal dermoid, 1562–1563
    melanoses and melanocytic proliferations, 1559–1562
  specimen handling, 1557–1558
Conjunctival intraepithelial neoplasia (CIN), 1558–1559
Contact granuloma, 111–112
Contact ulcers, 111–112
Conventional chordoma, 980
Conventional osteosarcoma, 972
Convexity meningioma, 703
Cookie-bite appearance, of ASPS, 902
Core needle biopsy (CNB), 39
Cornea
  anatomy, 1563–1564
  biopsy of
    acanthamoeba keratitis, 1571–1572
    pterygium, 1573–1574
    stains for, 1571
  diseases
    bullous keratopathy, 1564–1565
    Fuchs dystrophy, 1566–1567
    graft failure, 1567–1569
    keratoconus, 1569–1570
    pseudophakia, 1565–1566
    stromal dystrophies, 1570–1571
  specimen handling, 1564
Cortex, lymphoid follicles in, 997
Cortical defects of mandible
  anterior buccal cortical defect (ABCD), 963
  anterior lingual cortical defect (ALCD), 963
  posterior buccal cortical defect(PBCD), 963
  posterior lingual cortical defect (PLCD), 962–963
Corticosteroids
  as drug, 1390
  therapy, 1584, 1600, 1693, 1719
Corynebacterium diphtheriae, 346
Cowden syndrome, 1348, 1481
CPCDD. *See* Calcium pyrophosphate crystal deposition disease (CPCDD)
Cranial fasciitis, 966, 1359
Craniopharyngioma
  clinical features, 714
  diagnosis, 716
  overview, 714
  pathology, 715–716
  radiography, 714–715
  somatic genetics, 716
  treatment, 716–717
Craniotomy, 957
Cribriform, 24
Cricoarytenoid joints, 953
Cricothyroid joints, 953
Crohn disease, 228–229
Cryopreservation, of parathyroid tissue, 1462–1463
Cryotherapy, 277
Cryptococcosis, 1642, 1651–1652
Cryptococcus, 1013
CSD. *See* Cat scratch disease (CSD)
CSF. *See* Cerebrospinal fluid (CSF)
CT. *See* Computed tomography (CT)
CT scan
  acute supprative osteomyelitis, 958
  chondroblastomas, 978
  chondromyxoid fibroma, 978
  chondrosarcoma, 977
  chordoma, 980
  chronic suppurative osteomyelitis, 959
  extragnathic osteosarcoma, 972

[CT scan]
hemangioma, 981
ossifying fibroma, 970
osteoblastoma, 969
osteoid osteoma, 968
parosteal osteosarcoma, 973
PLCD, 963
PVNS, 934
relapsing polychondritis, 961
rheumatoid arthritis, 952
CUP. *See* Carcinoma of unknown primary (CUP)
Curvularia, 1640
Cutaneous angiofibroma. *See* Fibrous papules (FP)
Cutaneous intravascular large B-cell lymphoma, 1111
Cutaneous leiomyosarcoma, 877, 879
Cutaneous lymphadenoma (CL)
clinical features, 1482
differential diagnosis, 1483–1484
immunohistochemistry, 1483
molecular genetics, 1483
pathology, 1482–1483
treatment and prognosis, 1484
Cutaneous mastocytosis, 1112, 1113
Cutaneous pseudolymphoma, 1112
Cyclic adenosine monophosphate (cAMP), 688
Cyclin-dependent kinase inhibitor 2A (CDKN2A), 1510
Cyclophasphamide, 1693
Cyclosporine, 217, 257
therapeutic agents, 1344
Cystadenocarcinoma, 568–572
Cystadenoma, 538–540. *See also* Hidrocystomas
Cystic fibrosis, 352–354
clinical features, 353
nasal polyps with, 353
pathology, 353–354
of salivary glands, 478–479
treatment, 354
Cystic fibrosis transmembrane conductance regulator (CFTR), 353
Cystic hygroma-lymphangioma and cystic hygroma colli, 1357
Cystic lesions, 15–16, 21–22
Cystic nests, 1552
Cystogenic type SCC, 1299
histopathology of, 1300
treatment and prognosis, 1301
ultrastructure of, 1301
Cysts, 115–119
ductal, 116
epithelial, 117
oncocytic, 117
saccular, 116
tonsillar, 117
Cytochrome *c* oxidase defects, 1433
Cytokeratin 8, 18, and 19, 1434
Cytokeratin (CK), 31, 983
expression in sinonasal tumors, 379
Cytologic atypia, 1475, 1476
in ASPS, 902
Cytomegalovirus (CMV), 495–497, 1661
in AIDS, 1662
congenital, 1661–1662
epidemiology, 1661
in the head and neck, 1662–1663
histopathology, 1663
infection, 1007–1008
infection in organ transplant recipients, 1662
pathogenesis, 1663
serology, 1663
treatment, 1663
Cytomegalovirus lymphadenitis, 1007–1008
Cytometry, 15

Dalen-Fuchs nodules, 1584
Dapsone, 251, 263, 1627
Debridement, of infected tissues, 1637
Dedifferentiated liposarcoma, 884
Deep lymph nodes
lateral, 1135
medial, 1135
Deep or subcutaneous granuloma annulare (DSGA), 1367
Dendritic cell neoplasm
blastic plasmacytoid, 1077–1078
Dendritic cell sarcoma, 1075–1079
in cervical lymph node, 1153
follicular, 1075–1076
interdigitating, 1076–1077
rare types of, 1078–1079
De novo malignancies, 958
Dental factors, oral cancer, 288–289
Dental lamina cyst, 1343
Dentinogenic ghost cell tumor (DGCT), 1272
β-catenin gene mutation, 1275
etiology of, 1273–1274
histomorphological pattern of, 1275
imunohistochemistry, 1274–1275
treatment and prognosis, 1275
ultrastructure of, 1275
Dentinoid, and COC, 1265
Denture-induced fibrous hyperplasia. *See* Fibrous hyperplasia, denture-induced
Depositional diseases, of joints. *See* Inflammatory diseases, of joints
De Quervain's thyroiditis, 1392
Dermatofibroma (DF), 1482
clinical features, 1515
differential diagnosis, 1517
electron microscopy, 1517
immunohistochemistry, 1516–1517
molecular genetics, 1517
pathology, 1515–1516
treatment and prognosis, 1517
Dermatofibrosarcoma protuberans (DFSP), 687, 697, 880
clinical features, 1518
defined, 1517
differential diagnosis, 1519
electron microscopy, 1519
imaging studies, 1518
immunohistochemistry, 1519
molecular genetics, 1519
pathology, 1518–1519
treatment and prognosis, 1519–1520
Dermatopathic lymphadenopathy, 1005
Dermoid cysts, 73, 957, 1596
in periorbital nodule in infant, 1342–1343
DESAM. *See* Desmoplastic ameloblastoma (DESAM)
Desmin, 903, 904
Desmoglein 1 (DG1), 246
Desmoglein 3 (DG3), 246
Desmoid fibromatosis, 1360
Desmoplastic ameloblastoma (DESAM)
Akt-signaling pathway and MAPKs, role in, 1220
differential diagnosis, 1221
etiology of, 1219
immunohistochemistry, 1219
intraosseous cystic/solid and, 1220
prevalence and incidence, 1218
radiological study, 1218–1219
treatment strategy for, 1221
Wingless type 1 glycoprotein (Wnt1) and SDC-1, 1220–1221
Desmoplastic fibroma, 987–988, 1279
Desmoplastic trichoepithelioma, 1500
Desquamative gingivitis, 249, 255
DFSP. *See* Dermatofibrosarcoma protuberans (DFSP)
DG1. *See* Desmoglein 1 (DG1)
DG3. *See* Desmoglein 3 (DG3)
DGCT. *See* Dentinogenic ghost cell tumor (DGCT)
Diabetic microangiopathy, 1637
Diff-Quik, 1445
Diffuse infiltrative lymphocytosis syndrome (DILS), 1660
Diffuse large B-cell lymphoma (DLBCL), 15, 41–42, 1039–1045. *See also* Large cell lymphoma
with chronic inflammation, 1043
clinical features, 1039
differential diagnosis for, 1044–1045
elderly population with EBV-positive, 1043–1044
immunohistochemistry, 1041
large B-cell lymphoma, 1041–1043
molecular genetic data, 1041
pathology, 1039–1041
primary cutaneous, 1043
primary effusion lymphoma, 1044
of thyroid, 1102
primary cutaneous, leg-type, 1110–1111
of tonsil, 1094
treatment and prognosis., 1045
Diffuse neurofibroma (DNF), 686–687
DiGeorge syndrome, 1387, 1460
Dilantin. *See* Diphenylhydantoin antiepileptic drug
Dilator pupillae smooth muscle fibers, 1586
Diphenylhydantoin antiepileptic drug, 1386
Discoid lupus erythematosus, 1491. *See also* Chronic cutaneous lupus erythematosus (CCLE)
Distant metastases from SCC, 1158–1159
DLBCL. *See* Diffuse large B-cell lymphoma (DLBCL)
Dopamine agonist medications, for pituitary adenomas, 712
Down syndrome, 1342, 1388, 1486
Doxycycline, 1628
DQ stain, 5
Drug-induced gingival hyperplasia. *See* Gingival hyperplasia, drug-induced
DSGA. *See* Deep or subcutaneous granuloma annulare (DSGA)
Ductal cells, 20, 27
Ductal cysts, 116
Ductal eccrine carcinoma. *See* Microcystic adnexal carcinoma (MAC)
Ductal papillomas
intraductal, 535–537
inverted ductal papilloma, 538
sialadenoma papilliferum, 537–538
Dyshormonogenetic goiters, 1391
Dyskeratosis, 130
Dysphagia, 243
Dysplasia, 267
cellular alterations, 267
genetic changes in, 273
malignant transformation, corelation with, 272–273
mild, 269
moderate, 269
severe, 269
with three grades, 269
tissue alterations, 267
WHO classification, 269–270
Dystrophic calcifications, 715, 954–955, 1344

EAF. *See* Eosinophilic angiocentric fibrosis (EAF)
Ear, 953
  external, 423–424
  hematolymphoid lesions of, 1107–1108
  inner, 424–425
  middle, 424
  neoplastic lesions of, 446–467
    benign neoplasms, 447–456
    endolymphatic sac papillary tumor, 457–458
    malignant neoplasms, 459–467
  nonneoplastic lesions, 425–432
    acquired, 427–432
    congenital abnormalities, 425–427
  squamous cell carcinomas, 459–460
EBA. *See* Epidermolysis bullosa acquisita (EBA)
EBV. *See* Epstein-Barr virus (EBV)
EBV nuclear antigens (EBNA), 1665
EBV-positive DLBCL, of elderly, 1043–1044
Eccrine hidrocystomas, 1484
Eccrine poroma, 1476, 1482
ECRS. *See* Eosinophilic chronic rhinosinusitis (ECRS)
ECS. *See* Extracapsular spread
Ectopic acinic cell carcinoma, 1152
Ectopic benign thyroid tissue, in nonlymphoid tissues, 231–232
  clinical features, 231–232
  pathology, 232
  treatment, 232
Ectopic hamartomatous thymoma–branchial anlage mixed tumor
  clinical features, 1725
  differential diagnosis, 1726
  imunohistochemistry, 1726
  pathology, 1725–1726
  treatment and prognosis, 1726
Ectopic lacrimal glands, 74
Ectopic protrusion, 676
Ectopic thyroid, 229–232
  benign thyroid inclusions, in lymph node, 230–231
  benign thyroid tissue, in nonlymphoid tissues, 231–232
  lingual thyroid, 229–230
Edema, 250
EH. *See* Epithelioid hemangioendothelioma (EH)
EKH-6, 1486
Electron microscopy
  of ITAC, 386
  of SCNEC, 381
  of SNUC, 379
ELISA. *See* Enzyme-linked immunosorbent assays (ELISA)
EM. *See* Erythema multiforme (EM)
EMA. *See* Epithelial membrane antigen (EMA)
Embryology
  of external ear, 423
  of inner ear, 424
  of middle ear, 424
Embryonal rhabdomyosarcoma, 1361–1362
Embryonal RMS (ERMS), 869, 870–871
EMC. *See* Epithelialmyoepithelial carcinoma (EMC)
EMC-degrading serine proteinases role in ameloblastomas, 1214
EMMPRIN. *See* Extracellular matrix metalloproteinase inducer (EMMPRIN)
Enamelin and calcifying odontogenic cyst (COC), 1265
Enamel proteins
  in AFOD, 1251
  and AOT, 1238
  CEOT, 1234
Enamelysin and calcifying odontogenic cyst (COC), 1265
Encephalocele, acquired, 440
Encephaloceles, 674
  nasal. *See* Nasal encephalocele
Endemic goiters, 1391
Endodermal sinus tumor, 1365–1366
Endodontic therapy, 959, 960
Endolymphatic sac papillary tumor, 457–458
Endoneurial fibroblasts, 677
Endophytic growth, of the tumor, 1593
Endoscopic sinus surgery, 1609
Endothelial cells, 981, 983
Enneking staging system, for musculoskeletal sarcoma, 863
Entomophthorales
  clinical course, 1637
  epidemiology, 1637
  histopathology, 1637
  serology, 1637
  treatment, 1637
Enucleation
  categorizations for, 1577
  indications, 1577
  phthisis bulbi
    clinical features, 1579
    pathology, 1579–1582
  specimen handling, 1577–1579
  sympathetic ophthalmia, 1583–1586
  traumatic injury, 1582–1583
Enzyme activity, 669
Enzyme-linked immunoabsorbant assay (ELISA), 246, 650
Eosinophilic angiocentric fibrosis (EAF), 359–360
Eosinophilic chronic rhinosinusitis (ECRS), 354–355
Eosinophilic granulomas, 438–439, 989
Eosinophilic ulcer, of tongue, 1093
Eosinophils, 660
Eosin stains, 1445
Ependyma, 675
Epibulbar conjunctival stroma, 1557
Epidermal nevus, congenital and acquired lesions, 1341
Epidermolysis bullosa acquisita (EBA), 243
Epistaxis, 1157
Epithelial atrophy, 253
Epithelial cysts, 117
Epithelial dysplasia, nasal polyps, 350
Epithelial-lined cysts, 1342
Epithelial membrane antigen (EMA), 42–43, 1483
Epithelialmyoepithelial carcinoma (EMC), 31, 561–563
Epithelial-myoepithelial carcinoma (EMEC), 1729
Epithelioid cell sarcomas. *See* Polygonal cell sarcomas
Epithelioid hemangioendothelioma (EH), 61, 863–867, 981–982
Epithelioid hemangioma, 61, 1357
  in dermis and soft tissues of temporal region, 1359
Epithelioid histiocytes, 1584
Epithelioid tumor cells, 864
E-2 promotor-bindingfactor-1(E2F-1) and phosphorylated RB role in ameloblastomas, 1211
Epstein-Barr virus (EBV), 41, 155, 160, 660, 1150, 1483, 1661. *See also* Human papillomavirus (HPV)
  clonal infections, 1665
[Epstein-Barr virus (EBV)]
  disease associated with, 1664
  EBV-lymphoproliferative disorders, 1667–1668
  infectious mononucleosis, 1666–1667
  inverted papilloma, 363
  latent infections, 1664–1665
  nasopharyngeal carcinoma, 1668–1669
  nasopharyngeal carcinomas, 398
  oral hairy leukoplakia, 1669–1670
  overview and pathobiology, 1663–1664
  proteins, 1665–1666
  severe chronic active EBV infection, 1667
  sinonasal NK/T-Cell lymphoma, 1670–1671
  strains of, 1664
  undifferentiated salivary lymphoepithelial carcinoma, 1669
Epstein-Barr virus–encoded RNA (EBER), 398
Epstein's pearls, 1343. *See also* Oral cavity
ER. *See* Estrogen receptor (ER)
ERMS. *See* Embryonal RMS (ERMS)
Erosive lichen planus, 250
Eruptive vellus hair cyst, 1343, 1363
Erythema, 250
Erythema multiforme (EM), 258–261
  clinical presentation, 258–259
  diagnosis, 260–261
  etiology, 260
  pathology, 260
  treatment, 261
Erythromycin, 1628
Erythroplakia, 131, 275–277
  clinical features, 276
  defined, 275
  diagnosis, 277
  pathology, 276–277
  treatment, 277
ESAT-6 (early secretory antigenic target protein 6), 1623
ES/PNET. *See* Ewing's sarcoma and primitive neuroectodermal tumor (ES/PNET)
Estrogen receptor (ER), 31
Eustachian tube, 424
Evan's tumor. *See* Low-grade fibromyxoid sarcoma (LGFMS)
Ewing sarcoma–primitive neuroectodermal tumor (EWS-PNET), 1347
Ewing's sarcoma, 55, 989
Ewing's sarcoma and primitive neuroectodermal tumor (ES/PNET)
  clinical features, 735
  diagnosis, 737–738
  histopathology, 736
  imaging, 735–736
  immunohistochemistry, 736–737
  macroscopy, 736
  overview, 735
  somatic genetics, 737
  treatment, 738
  ultrastructure, 736
EWS-PNET. *See* Ewing sarcoma-primitive neuroectodermal tumor (EWS-PNET)
Excision, 677
Excisional biopsy, hematolymphoid neoplasms, 1031
Exophytic growth, of tumor, 1593
Exophytic papilloma, 362–363
  and carcinomas, 362–363
  HPV incidence in, 363
Exostosis, 967
  external auditory canal, 434–435
Explosive follicular hyperplasia, of lymph node, 1009
Exserohilum, 1639–1640

External auditory canal
benign mesenchymal tumors of, 448–449
benign neoplasms, 447–449
cholesteatomas of, 437
exostosis, 434–435
squamous cell carcinomas of, 460–462
squamous cell carcinomas staging in, 462
External ear, 423–424
mlignant neoplasms of, 459–464
Extracapsular spread (ECS), 1137, 1138–1140
Extracellular matrix metalloproteinase inducer (EMMPRIN), and ameloblastomas, 1214
Extracellular matrix proteins
in AMFs, 1244
and AOT, 1238
Extracranial teratomas, 674
Extragnathic osteosarcoma, 972–973
Extramedullary hematopoietic tumor, 1026–1027
Extramedullary plasmacytoma, 1057–1059
clinical features, 1057
differential diagnosis, 1057–1059
ectopic pituitary adenoma, 1059
immunohistochemistry, 1057
molecular genetic data, 1057
pathology, 1057
treatment and prognosis, 1059
Extranodal marginal zone B-cell lymphoma, 604–607, 1600–1601
Extranodal metastases
head and neck skin, 1157
laryngeal, 1157–1158
metastatic tumors, to eyes, 1157
metastatic tumors, to nasal cavity, 1157
metastatic tumors, to oral regions
jaw metastases, 1156
oral soft tissue metastases, 1156–1157
metastatic tumors, to paranasal sinuses, 1157
salivary glands, 1156
temporal bones, 1157
Extranodal NK/T-cell lymphoma
nasal, 1060–1064
clinical features, 1061
differential diagnosis, 1062–1063
immunohistochemistry, 1061
molecular genetic data, 1061–1062
pathology, 1061
treatment and prognosis, 1063–1064
of oral cavity and oropharynx, 1089
of skin, 1111, 1112
Extranodal sites
head and neck, 1001
HIV-associated lymphoid hyperplasia in head and neck, 1010–1012
reactive lymphoid hyperplasia of, 1001
Extraosseous odontomas, 1253
Extraosseous osteosarcoma, 974
Extravascular proliferation, of atypical endothelial cells, 868
Eye, hematolymphoid lesions of, 1103–1107
clinical features, 1104
diagnostic considerations, 1107
neoplasms, 1103–1105
reactive/inflammatory, 1105–1107
Eyelids
anatomy, 1551
diseases
basal cell carcinoma, 1552–1553
reactive inflammatory processes, 1553–1554
sebaceous neoplasms, 1554–1556
sebaceous tumefactions, 1553
squamous cell carcinoma, 1553
xanthelasma, 1557
specimen handling, 1551–1552
Fabry's syndrome, 1523
Facial bones. *See* Jaw
Factitial rhinosinusitis, 348
Familial hypocalciuric hypercalcemia (FHH), 1436
clinical features, 1457
differential diagnosis, 1458
molecular biology, 1458
pathologic features, 1457
treatment and prognosis, 1458
Familial isolated hyperparathyroidism (FIHP), 1437–1438
Fat stains, 1446
FD. *See* Fibrous dysplasia (FD)
Federation Nationale des Centres de Lutte Contre le Cancer (FNCLCC), France, 862
Fetal development and thyroid gland growth, 1429
Fetal rhabdomyoma, 1361–1362
FGF. *See* Fibroblast growth factors (FGF), in ameloblastoma
FHH. *See* Familial hypocalciuric hypercalcemia (FHH)
Fibrinogen, 257
Fibroblast growth factors (FGF), in ameloblastoma, 1211
Fibroblastic-myofibroblastic tumors, 1358
Fibrodysplasia ossificans progressive (myositis ossificans progressive)
clinical findings, 820–821
differential diagnosis, 821
immunohistochemistry, 821
pathologic findings, 821
prognosis and treatment, 821–822
radiologic imaging, 821
Fibromatosis colli (Torticollis), 1359
clinical features, 828
differential diagnosis, 830
electron microscopy, 830
imaging, 828
immunohistochemistry, 830
molecular findings, 830
pathology, 828
treatment and prognosis, 830
Fibromatosis (desmoid)
clinical findings, 832
differential diagnosis, 833–834
imaging, 832
immunohistochemistry, 833
molecular findings, 833
pathologic findings, 832–833
prognosis and treatment, 834
Fibro-osseous lesions, 68
Fibrosarcoma, 885–892, 988–989
Fibrosis, 1367
in osteoradionecrosis (ORN), 961
Fibrous dysplasia (FD), 960, 964–965
Fibrous hamartoma of infancy
clinical findings, 825
differential diagnosis, 826–828
electron microscopy, 826
imaging, 826
immunohistochemistry, 826
molecular findings, 826
pathologic findings, 826
prognosis and treatment, 828
Fibrous hyperplasia, denture-induced, 218–220
clinical features, 219
pathology, 219
treatment, 220
Fibrous papules (FP)
clinical features, 1513
defined, 1513
differential diagnosis, 1514
[Fibrous papules (FP)]
electron microscopy, 1514
immunohistochemistry, 1514
pathology, 1513
treatment and prognosis, 1514
Fibrous septa, 1487
Fibrous stromal cells, 965
Fibrovascular proliferation, 1579
Fibroxanthoma, atypical, 463–464
FIHH. *See* Familial hypocalciuric hypercalcemia (FHH)
FIHP. *See* Familial isolated hyperparathyroidism (FIHP)
Filaggrin, and COC, 1265
Filobasidiella neoformans, 1651
Fine needle aspiration biopsy (FNAB), 37, 1149
Hodgkin lymphoma, 45–46
Fine-needle aspiration (FNA), 1, 101, 1599
cytology, hematolymphoid neoplasms, 1031
FISH. *See* Fluorescence in situ hybridization (FISH)
FISH studies, 40
Flexner-Wintersteiner rosettes, 78
Floor of the mouth, squamous cell carcinomas, 295–298
Florid interfollicular immunoblastic proliferation, 1355
Flow cytometry, in lymph nodes, 39–40
Fluorescence in situ hybridization (FISH), 728
Fluoroquinolone-resistant gonorrhea, 1618
FLUS. *See* Follicular lesion of undetermined significance (FLUS)
FN. *See* Follicular neoplasm (FN)
FNA. *See* Fine needle aspiration (FNA)
FNAB. *See* Fine needle aspiration biopsy (FNAB)
FNA biopsy. *See* Fine-needle aspiration biopsy (FNAB)
FNCLCC. *See* Federation Nationale des Centres de Lutte Contre le Cancer (FNCLCC), France
Focal epithelial hyperplasia, 211–212. *See also* Heck's disease
Focal lymphocytic thyroiditis, 1389
Focal myositis
clinical features, 797
definition, 796
differential diagnosis, 798
immunohistochemistry, 797–798
laboratory studies, 797
pathology, 797
radiologic imagery, 798
treatment and prognosis, 798
Focal osteoporotic bone marrow defect, 961–962
Follicular carcinoma, 7
Follicular cells, 3, 4
in thyroid gland, 1385
Follicular dendritic cell sarcoma, 1075–1076
Follicular hyperplasia, 1355
Follicular lesion of undetermined significance (FLUS), 9
Follicular lesions, 6–9
Follicular lymphoma, 44–45
clinical features, 1045–1046
differential diagnosis, 1050
histologic grading and growth pattern, 1047–1049
immunohistochemistry, 1049
molecular genetic data, 1049
pathology, 1046
pediatric, 1050
primary cutaneous follicle center lymphoma, 1050
versus reactive follicular hyperplasia, 1051

[Follicular lymphoma]
in situ, 1051
of tonsil, 1090
transformation to high-grade lymphoma, 1049–1050
treatment and prognosis, 1050
Follicular neoplasm (FN), 7
diagnosis, challenges, 7–8
Follicular thyroid tumors
follicular adenomas, 1402
follicular carcinoma, 1402–1404
Follicular variant of papillary carcinoma (FVPC), 7
Folliculosebaceous cystic hamartoma, 1488
Fomivirsen, 1663
Fordyce granules, 201
Foregut duplication cyst, 1348
Foreign body granuloma, 73
Formalin, 10
Foscarnet, 1663
Frontal encephaloceles, 674
Frontofacionasal dysplasia, 674
Frozen-section diagnoses, 95–105
accuracy, 96
contraindications, 97
errors, 96–97
handling tissue sample, 95
indications, 97
intraoperative cytology, 97
overviews, 95
preparation technique, 95–96
regional applications, 97–105
lymph nodes, 100–101
mucosal surfaces, 101
parathyroid gland, 104–105
peripheral nerves, 100
salivary gland, 101–103
surgical margins, 97–100
thyroid gland, 103–104
Frozen section interpretation, of parathyroid, 1444–1446
Fuchs dystrophy, 1566–1567
Fungal conjunctivitis, 72
Fungal infection, 1013
Fungus ball/mycetoma
clinical presentation, 1632
etiology, 1632
histopathology, 1632
PCR techniques, 1632–1633
treatment, 1633
Furstenberg test, 672
Fusarium, 1641
Fusobacterium necrophorum, 1611
FVPC. *See* Follicular variant of papillary carcinoma (FVPC)

Ganciclovir, 1663
Ganglion, 957
GAP. *See* GTPase-activating protein (GAP)
Gardner's syndrome, 967, 1480
GCA. *See* Giant cell angiofibroma (GCA); Giant cell arteritis (GCA)
GCDFP-15. *See* Gross cystic disease fluid protein-15 (GCDFP-15)
GCOC. *See* Ghost cell odontogenic carcinoma (GCOC)
GCOT. *See* Granular cell odontogenic tumor (GCOT)
GCT. *See* Giant cell tumor (GCT); Granular cell tumor (GCT); Granular cell tumor (GCT)
Genetic abnormality, in cystic fibrosis, 353
Genetic linkage analyses, of hereditary PGL, 718
Genetic mutations, in SH3BP2 gene, 966
Germ cell neoplasms, 1364–1365
Germinal centers, progressive transformation of, 1004–1005
Ghost cell glaucoma, 72
Ghost cell odontogenic carcinoma (GCOC), 1212, 1304. *See also* Ameloblastomas
differential diagnosis, 1306
etiology of, 1305
immunohistochemistry, 1306
molecular-genetic data, 1306
prevalence and incidence, 1305
radiographic picture, 1305
treatment and prognosis, 1306
Giant cells, 47
fibroma, 222
lesions, 69
Giant cell angiofibroma (GCA), 1728
Giant cell arteritis (GCA)
angiography and ultrasonography, 1717–1718
clinical features, 1717
differential diagnosis, 1719
laboratory tests, 1718
pathology, 1718–1719
treatment and prognosis, 1719
Giant cell carcinoma (GCC), 161–162
Giant cell granuloma, 984–985
Giant cell-rich malignant fibrous histiocytoma, 889
Giant cell–rich osteosarcomas, 984
Giant cell tumor (GCT), 171–172, 984
Gierke disease, 1392
Gingiva, squamous cell carcinomas of, 298–300
Gingival carcinoma, 300
Gingival fibromatosis
clinical features, 830–831
differential diagnosis, 831–832
electron microscopy, 831
imaging, 831
immunohistochemistry, 831
molecular-genetic data, 831
pathology, 831
treatment and prognosis, 832
Gingival GCT of newborn, 1344
Gingival hyperplasia, drug-induced, 217–218
Glassock–Jackson classification, of glomus tumors, 452
Glaucoma, 1574–1575
Glaukomflecken, 1585
Glial cells missing gene (GCMB), 1435, 1460
Glial heterotopias, 672
Gliosis of the inner retina, 1580
Glomus jugulare. *See* Jugular paraganglioma
Glomus tumors, 717
clinical findings, 793
differential diagnosis, 794–795
electron microscopy, 793
Glassock–Jackson classification, 452
immunohistochemistry, 794
molecular findings, 794
pathologic findings, 793
prognosis and treatment, 795–796
radiologic imaging, 793
Glomus tympanicum. *See* Tympanic paraganglioma
Glottic carcinoma, 139–142
GLUT-1 expression, 1522
GLY382Asp, 1487
Glycosaminoglycans in ODOMYX, 1286
Gnathic osteosarcoma, 971–972
Goiterous thyroids, 1390
Gonorrhea
diagnosis of, 1618
histopathology, 1618
[Gonorrhea]
transmission and epidemiology, 1617–1618
treatment, 1618
Gorham-Stout syndrome, 981
Gorlin–Goltz syndrome, 1344
Gout, 442–443
pathologic features, 953–954
radiologic features, 953
Grading
of follicular lymphoma, 1047–1049
histologic, of sarcoma, 863
of malignant mesenchymal tumors, 862–863
Graft failure, 1567–1569
Graft-*versus*-host disease (GVHD), 258
Gram-negative bacteria, 64
Granular cell ameloblastoma, 1206–1207
Granular cell odontogenic tumor (GCOT), 1214, 1281
clinical features, 1282
differential diagnosis, 1283
histopathology of, 1282
immunohistochemical technique, 1282–1283
surgical removal, 1283
ultrastructure of, 1283
Granular cell tumor (GCT), 54, 60–61, 698–701, 1344
CE, 701
malignant GCT, 700–701
Granulomas. *See also* Carcinomas
cholesterol, 30, 357–358
eosinophilic, 438–439
nasal polyps, 350
Granulomatosis, 438–439
Wegener's. *See* Wegener's granulomatosis
Granulomatous inflammation, 1598
Granulomatous lesions, 73
chalazions, 73
dermoid cyst, 73
foreign body granuloma, 73
sarcoidosis, 73
Wegener's granulomatosis, 73
Whipple's disease, 73
Granulomatous lymphadenitis, 50
Granulomatous thyroiditis, 1390, 1392
Graves' disease, 5–6, 1388–1389, 1484
Gross cystic disease fluid protein-15 (GCDFP-15), 31
Gross-sampling errors, 96
Gross total resection (GTR), 681
Growth factors
and AFOD, 1251
in ODOMYX, 1286
GTPase-activating protein (GAP), 688
GTR. *See* Gross total resection (GTR)
GVHD. *See* Graft-*versus*-host disease (GVHD)

Haemophilus influenza, 953
Haemophilus influenzae, 345
Hairy polyp, 1348–1349
Hairy tongue, 209–210
clinical features, 209
pathology, 210
treatment, 210
Hamartomas, 1348, 1536–1538
respiratory epithelial adenomatoid, 360–361
Hamazaki-Wesenberg inclusions, 1693
Hansen's disease, 1625
Haphazard tangles, of nerve fascicles, 677
Hard palate, squamous cell carcinomas of, 300–301

Hard tissue–related proteins
and AMFs, 1244
AOT, 1238
and CEOT, 1234
Hashimoto's thyroiditis, 4, 1101–1102, 1102, 1103, 1387–1388
Hassal's corpuscles, 1457
Haversian canals, 960, 967
H&E. *See* Hematoxylin and eosin (H&E)
Heck's disease, 1675. *See also* Focal epithelial hyperplasia
Heerfordt's syndrome, 1692
Helicobacter pylori, 261
Hemangiomas, 126–127, 779–780, 981, 1355
in adults, 127
clinical features, 780–782
differential diagnosis, 786–788
imaging, 782
immunohistochemistry, 786
of infancy. *See* Infantile hemangioma (IH)
in infants, 126–127
pathology, 782–786
prognosis and treatment, 788
Hemangiopericytoid vascular pattern
in mesenchymal chondrosarcoma, 896
in monophasic synovial sarcoma, 897
Hemangiopericytomas, 74, 707
Hemangiopericytoma/solitary fibrous tumor
clinical features, 848
differential diagnosis, 849–850
electron microscopy, 849
imaging, 848
immunohistochemistry, 848
molecular findings, 848–849
pathologic findings, 848
prognosis and treatment, 850
Hematolymphoid neoplasms
of bone, 1108–1109
of ear, 1107–1108
of eye, 1103–1107
of head and neck
etiology, 1031
general features, 1029–1031
Hodgkin lymphomas, 1032–1039
myeloid/histiocytic/dendritic cell tumors, 1073–1079
non-Hodgkin lymphomas, 1039–1073
patholgy, 1031
staging, 1031–1032
WHO classification, 1030
of hypopharynx, 1099–1100
of larynx, 1099
of lymph node, 1079–1081
diagnostic considerations, 1079–1081
nasal cavity and paranasal sinuses, 1081–1086
clinical features, 1081
diagnostic considerations, 1085–1086
reactive/inflammatory hematolymphoid lesions, 1082–1085
nasopharynx, 1086–1088
diagnostic considerations, 1088
features of, 1086–1087
reactive/inflammatory hematolymphoid lesions, 1087–1088
of ocular adnexa, 1103–1107
oral cavity and oropharynx, 1088–1094
diagnostic considerations, 1093–1094
features, 1088–1090
reactive/inflammatory hematolymphoid lesions, 1091–1093
of salivary gland, 1094–1099
diagnostic considerations, 1098–1099
features of, 1094–1096
reactive/inflammatory hematolymphoid lesions, 1096–1098
[Hematolymphoid neoplasms]
of skin, 1109–1115
of thyroid, 1100–1103
of trachea, 1100
Hematopoietic tumor, extramedullary, 1026–1027
Hematoxylin, 1445
Hematoxylin and eosin (H&E) stain, 95, 961
Hemidesmosomal proteins, 251
Hemophilus influenza, 429, 1609
Hemorrhagic detachment, of the choroid, 1586
Heparanase, and ameloblastomas, 1214
Hepatocyte growth factor (HGF) role in ameloblastomas, 1211
Hereditary gingival overgrowth, 1344
Her-2 expression, 1485
Herpes simplex virus (HSV), 121, 260, 1008–1009, 1661
clinical course, 1671–1673
epidemiology, 1671
interference with cell-mediated immunity, 1672–1673
treatment, 1673
Herpes simplex virus type I (HSV I), 262
Herpetic whitlow, 1671–1672
Heterophil test, 1666
Heterotopia
of middle ear and mastoid, 427
of neuroglial tissue, 68
of salivary glands, 477–478
HGF. *See* Hepatocyte growth factor (HGF)
HHM. *See* Humoral hypercalcemia of malignancy (HHM)
HHV-8 DNA, 1659–1660
Hidrocystomas
clinical features, 1484
differential diagnosis, 1485
imaging, 1484
immunohistochemistry, 1485
pathology, 1484–1485
treatment and prognosis, 1485
High-grade MEC, 28
Highly active antiretroviral therapy (HAART), 1532, 1657
Histiocytic necrotizing lymphadenitis, 1355. *See also* Kikuchi lymphadenitis
Histiocytic sarcoma, 1073–1074
Histiocytosis, Langerhans cell, 438–439
Histologic frozen-section slide, of surgical margin, 99
Histologic grading, of sarcoma, 863
Histoplasma capsulatum, 1652
Histoplasmosis, 1652–1654, 1691
HIV. *See* Human immunodeficiency virus (HIV)
HIV-associated lymphadenopathy, 1009–1012
lymphocyte depletion in, 1009
HIV-associated lymphoepithelial, of salivary glands, 1096
HIV-associated lymphoid hyperplasia, in head and neck extranodal sites, 1010–1012
HL. *See* Hodgkin's lymphoma (HL)
HLA. *See* Human leukocyte antigens
Hoarseness, as symptom of contact ulcers, 112
Hodgkin lymphomas, 1032–1039, 1354
classical, 1032–1035
nodular lymphocyte–predominant, 1035–1039
versus PTGC, 1005
post transplant, 1073
Hodgkin's disease, 15
Hodgkin's lymphoma (HL), 33, 38
Hordeolum (stye), 1553
Horn cysts, 1476
HPV. *See* Human papilloma virus (HPV)
HRPT2 mutations, 1453, 1457
HSV. *See* Herpes simplex virus (HSV); Herpes simplex virus (HSV)
HSV-1 exposure/infection, 1671
HSV-2 exposure/infection, 1672
HSV I. *See* Herpes simplex virus type I (HSV I)
Human herpesvirus 6 (HHV6) lymphadenitis, 1009
Human immunodeficiency virus (HIV), 38, 1657–1658
clinical categories of, 1657
criteria for infection for adolescents and adults, 1657
epidemiology, 1655
primary infection and latency, 1656–1657
transmission, 1655
treatment, 1658
tropism, 1656
virion and genome, 1655–1656
Human leukocytes antigens (HLA), 122, 649
nasopharyngeal carcinomas, 395
Human milk fat globulin-1 (HMFG1), 1485
Human papilloma virus (HPV), 211, 273
in benign *vs.* dysplastic *vs.* malignant IP, 1681
detection rates
in laryngeal SCC, 1683
in oral cavity SCC, 1683
in oropharyngeal SCC, 1682
diseases, 1675–1684
genome, 1675
incidence
in exophytic papillomas, 363
in oncocytic schneiderian papillomas (OSP), 370
in inverted papaillomas, 1679–1681, 1681
inverted papilloma, 364
life cycle, 1675
molecular biology carcinomas related to, 290
nasopharyngeal carcinomas, 398
nonkeratinizing carcinomas, 376
pathobiology, 1674–1675
subtypes 16 and 18, 1559
transmission, 1673–1674
Humoral hypercalcemia of malignancy (HHM), 1459
Hurthle cell. *See also* Oncocytic neoplasms
lesions, 1441
tumors
adenoma, 1404
carcinomas, 1404–1406
Hyaline cartilage metaplastic, in mesenchymal chondrosarcoma, 896
Hyaline PA, 35–36
Hyaline-vascular Castleman disease, 1019–1021
clinical features, 1019
differential diagnosis, 1021
pathology, 1019–1021
Hyalinization, 703
Hyalinizing trabecular tumor
clinical features, 1400
differential diagnosis, 1401–1402
immunohistochemistry, 1401
microscopic features, 1401
molecular genetics, 1401
pathology of, 1400–1401
treatment and prognosis, 1402
Hyalohyphomycosis, 1641
Hyams grading system, for ONB, 731
Hybrid cysts, 1478
Hybrid tumors, of salivary gland, 596–597
Hydralazine, 252
Hydroa vacciniforme–like lymphoma, 1072

Hydrochloroquine, 1693
Hydroxylysylpyridinoline, urine concentrations, 959
Hyoid bone, 16
Hyperbaric oxygen therapy, 961
Hypercalcemia, non-PTH causes of. *See* Non-PTH-related hypercalcemia
Hyperfunctioning parathyroid glands
  multigland and multifocal disease, 1453–1455
  single-gland disease
    adenoma, 1446–1449
    atypical adenoma, 1449–1450
    carcinoma, 1450
    differential diagnosis and molecular pathology, 1450–1453
Hyperkeratosis, 1677
Hyperorthokeratosis, 253
Hyperparakeratosis, 253
Hyperparathyroidism, 985–986. *See also* Primary hyperparathyroidism; Secondary hyperparathyroidism
Hyperparathyroidism-jaw tumor (HPT-JT) syndrome, 1437–1438
Hyperplasia, 130
  adenoid, 225–226
  atypical, 271
  basal, 271
  fibrous. *See* Fibrous hyperplasia, denture-induced
  gingival. *See* Gingival hyperplasia, drug-induced
  papillary. *See* Inflammatory papillary hyperplasia
  parabasal cell, 271
  squamous, 271
  tonsillar, 222–225
Hyperplastic dental follicles, 1279
Hyperplastic nodules, 5, 7
  diagnosis, challenges, 7–8
Hyperuricemia, 953
Hypervascular follicular hyperplasia, 1009
Hypointense meningiomas, 702
Hypopharynx, hematolymphoid lesions of, 1099–1100
Hypophysis. *See* Pituitary gland

Iatrogenic KS, 1660
ICR. *See* International classification of rhabdomyosarcoma (ICR)
Idiopathic cervical fibrosis
  clinical features, 824
  differential diagnosis, 825
  electron microscopy, 825
  imaging, 824
  immunohistochemistry, 824
  pathology, 824
  treatment and prognosis, 825
Idiopathic cystic chondromalacia, auricular cartilage, 433–434
Idiopathic midline destructive disease (IMDD), 660
Idiopathic orbital inflammation, 73, 1598
IgE antibodies in allergic rhinosinusitis, 344–345
IgG. *See* Immunoglobulin G (IgG)
IgG4-related sclerosing disease, 1014–1015
  of nasopharynx, 1087–1088
  of ocular adnexa, 1105–1106
  of parotid gland, 1097–1098
IHC. *See* Immunohistochemistry (IHC)
IIF. *See* Indirect immunofluorescence
IMDD. *See* Idiopathic midline destructive disease
Immature teratoma, 1365
Immotile cilia syndrome. *See* Primary ciliary dyskinesia (PCD)
Immunoblastic lymphomas, 42
Immunocytochemical stains, 14
Immunocytochemical techniques, 1433
Immunocytochemistry. *See* Cytometry
Immunodeficiency-associated lymphoproliferative disorders, 1072–1073
Immunoglobulin G (IgG), 245, 650
Immunohistochemistry (IHC), 14
  ALK+ anaplastic large cell lymphoma, 1066–1067
  Burkitt lymphoma, 1056–1057
  classical Hodgkin lymphoma, 1034–1035
  of DLBCL, 1041
  extramedullary plasmacytoma, 1057
  extranodal NK/T-cell lymphoma, 1061
  follicular lymphoma, 1049
  of hyaline-vascular Castleman disease, 1021
  intestinal-type adenocarcinomas (ITAC), 386
  of Kikuchi lymphadenitis, 1016
  lymphoepithelial carcinomas (LEC), 382
  malignant melanomas, 393
  MALT lymphoma, 1055
  mantle cell lymphoma, 1053
  nasopharyngeal carcinomas, 398
  nodular lymphocyte–predominant Hodgkin lymphoma, 1037
  nonintestinal-type adenocarcinomass (non-ITAC), 388–389
  nonkeratinizing carcinomas, 377
  papillary adenocarcinomas of nasopharynx, 401
  of Rosai-Dorfman disease, 1024
  sinonasal undifferentiated carcinomas (SNUC), 378–379
  small cell neuroendocrine carcinomas (SCNEC), 381
Immunostains, on synovial sarcoma, 898
Immunosuppressive drugs, 251
Immunosuppressive therapy, 249
Incidental pituitary adenoma, 709
Indirect immunofluorescence (IIF), 650
Indolent T-lymphoblastic proliferation, of oral cavity and oropharynx, 1093
Infantile fibrosarcomas, 885, 886
Infantile hemangioma-hemangioendothelioma, 1355
Infantile hemangioma (IH)
  clinical features, 1525
  defined, 1524
  differential diagnosis, 1526
  imaging studies, 1525
  immunohistochemistry, 1526
  molecular genetics, 1526
  pathology, 1525–1526
  treatment and prognosis, 1526
Infantile myofibroma, 1355
  desmoid and diffuse type, 1360
Infantile systemic hyalinosis, 1344
Infectious arthritis, 953
Infectious mononucleosis, 51, 1007, 1666–1667
  versus large cell lymphoma, 1088
  nasopharynx, 1087
  tonsil, 1091–1092
Infectious rhinosinusitis, 345
Infiltration, fatty, 20
Infiltrative BCC, 1496
Infiltrative fibroblastic disorders, 1344
Inflammatory diseases, of joints, 952–957
  calcium pyrophosphate crystal deposition disease (CPCDD), 954
  dermoid cysts, 957
[Inflammatory diseases, of joints]
  dystrophic calcification, 954–955
  ganglion, 957
  gout, 953–954
  infectious arthritis, 953
  oxalosis, 954
  pigmented villonodular synovitis, 956–957
  rheumatoid arthritis, 952–953
  synovial chondromatosis, 955–956
  synovial cysts, 957
  tumoral calcinosis, 954–955
Inflammatory lesions
  chondrodermatitis nodularis helicis, 1534–1535
  rhinophyma, 1532–1534
  rosacea, 1532–1534
  weathering nodule of the ear, 1535–1536
Inflammatory malignant fibrous histiocytoma, 890
Inflammatory myofibroblastic tumor, 172–173
Inflammatory otic polyps, 431
Inflammatory papillary hyperplasia, 220–221
Inflammatory process, 661
Inflammatory pseudotumor, of lymph node, 1025–1026
Infliximab, 1693
INF-α therapy, 1677
Infundibular cyst, 1342
Inner ear, 424–425
  Meniere disease, 445–446
Insular carcinoma, 14
Insulinlike growths factors (IGFs) expression and stroma of ameloblastomas, 1212
Integrin
  and AOT, 1238
  solid/multicystic ameloblastoma–central, 1209
Interdigitating dendritic cell sarcoma, 1076–1077
Intergroup Rhabdomyosarcoma Study Postsurgical Clinical Grouping System, on RMS staging, 876
Interleukin-1, 958
International Classification Of Rhabdomyosarcoma (ICR), 54
International Prognostic Index (IPI) Scoring System, 1031
International Prognostic Index score, 1032, 1045, 1054, 1063
Intestinal-type adenocarcinomass (ITAC), 383–387
  classification and survival, 384
  clinical features, 383–384
  differential diagnosis, 386–387
  electron microscopy, 386
  etiology, 383
  imaging, 384
  immunohistochemistry, 386
  molecular-genetic data, 386
  Paneth cells in, 386
  pathology, 384–386
  treatment and prognosis, 387
  variants of, 384–385
Intracranial extension, 676
Intracytoplasmic lumen formation, 1486
Intraepithelial alterations, classifications, 267–272
  dysplasia classification, by WHO, 269–270
  Ljubljana classification, 271–272
  squamous intraepithelial neoplasia classification, 270
Intralesional mineralization, 1478
Intralymphatic growth, in ASPS, 902

Intraneural perineurioma, 697
Intraocular conditions, 1576–1586
Intraocular lymphoma, 1104–1105
Intraoperative cytologic evaluations, 1445
Intraoperative parathyroid hormone testing (IOPTH), 1455
Intraosseous basal cell ameloblastoma, 1214
Intraosseous tumors, of salivary gland, 597–598
Intrathyroidal parathyroid glands, 1430
Intravascular large B-cell lymphoma, cutaneous, 1111
Intraventricular meningioma, 703
Intubation granuloma, 111–112
Inverted papilloma, 363–369
  carcinomas and, 366–368
  clinical features, 363–364
  differential diagnosis, 368
  etiology, 364
  imaging, 364
  Krouse staging system for, 369
  pathology, 364–366
  treatment and prognosis, 368–369
Inverting papilloma, 1678
Involucrin and calcifying odontogenic cyst (COC), 1265
Involucrin expression, in TL, 1481
Iodine therapy, 6
Iridocyclectomy, 1587
Iris root, 1587
Iron pigment in thyroid follicular cells, 1393
Irritation fibroma, 221–222
Isoniazid, 252
Isthmus-catagen cyst. *See* Pilar cysts (PCs)
ITAC. *See* Intestinal-type adenocarcinomass (ITAC)
Itraconozole, 1637

Jaw, 68–70
  metastases, 1156
Jeryl Lynn vaccine substrain, 1687
JHF. *See* Juvenile hyaline fibromatosis (JHF)
JNA. *See* Juvenile nasopharyngeal angiofibroma (JNA)
JOC. *See* Juxtaoral organ of Chievitz (JOC)
JOC vs Carcinoma, microscopic features, 671
JTPG. *See* Jugulotympanic paragangliomas (JTPG)
Jugular paraganglioma, 721
Jugulotympanic paragangliomas, 451–454
  classification, 452
Jugulotympanic paragangliomas (JTPG), 721–722
Juvenile hemangioma. *See* Infantile hemangioma (IH)
Juvenile hyaline fibromatosis (JHF), 1344
Juvenile melanoma, 1340
Juvenile nasopharyngeal angiofibroma (JNA), 1360–1361
Juvenile onset laryngeal papillomatosis, 1677
Juvenile xanthogranuloma, nasal cavity, 1085
Juxtaoral organ of Chievitz (JOC)
  clinical features, 669
  diagnosis, 671
  embryology, 669
  histopathology, 670
  immunohistochemistry, 671
  macroscopy, 670
  overview, 669
  physiology, 669
  ultrastructure, 670–671

Kaposiform hemangioendothelioma, 1357–1358
  clinical features, 1527
  defined, 1526–1527
  differential diagnosis, 1527
  electron microscopy, 1527
  imaging studies, 1527
  immunohistochemistry, 1527
  pathology, 1527
  treatment and prognosis, 1527–1528
Kaposi-like infantile hemangioendothelioma. *See* Kaposiform hemangioendothelioma
Kaposi sarcoma (KS), 63, 277, 1659–1660
  clinical features, 1530
  differential diagnosis, 1532
  electron microscopy, 1532
  imaging studies, 1530–1531
  immunohistochemistry, 1531–1532
  molecular genetics, 1532
  pathology, 1531
  treatment and prognosis, 1532
  in vascular transformation of sinuses, 1005–1006
Karyotypes, 727
Kassabach-Merrit syndrome, 1357, 1523
Kawasaki disease, 1018–1019
KCOT. *See* Keratocystic odontogenic tumors (KCOT)
Keloids
  clinical features, 1512
  defined, 1511
  differential diagnosis, 1512–1513
  electron microscopy, 1512
  immunohistochemistry, 1512
  molecular genetics, 1512
  pathology, 1512
  treatment and prognosis, 1513
Kenny–Caffey syndrome, 1460
Keratin-filled clefts, 1678
Keratinization, 715
  in MCE, 28
Keratinized cells, 267
Keratinized papilloma, 123–124
Keratinizing squamous carcinoma, 100
Keratinizing squamous cell carcinomas (KSCC), 285, 290
  pathologic features, 290–292
  variants of, 285
Keratinocyte growth factor (KGF), congenital cholesteatomas, 438
Keratinocytes, in seborrheic keratoses (SK), 1475
Keratinocytic intraepithelial neoplasia (KIN). *See* Actinic keratoses (AKs)
Keratinous cysts of infundibular type, 1342
Keratoacanthoma, 1493–1494
Keratoameloblastoma, 1225–1226
Keratoconus, 1569–1570
Keratocystic odontogenic tumors (KCOT), 1209, 1240
Keratocystoma, 540–542
Keratohyaline granules, 1486
Keratoma. *See* Cholesteatomas, acquired
Keratosis, 129–133
  atypia, 130
  CIS, 130
  clinical features, 131
  dyskeratosis, 130
  erythroplakia, 131
  histology, 129–130
  hyperplasia, 130
  KWD, 131
  KWOD, 131
  leukoplakia, 131
  overviews, 129
  parakeratosis, 130
  treatment, 132–133
Keratosis obturans (KO), congenital cholesteatoma, 438
Keratosis with dysplasia (KWD), 131
Keratosis without dysplasia (KWOD), 131
Keratotic plugging, 253
Kikuchi-Fujimoto disease. *See* Histiocytic necrotizing lymphadenitis; Kikuchi lymphadenitis
Kikuchi histiocytic necrotizing lymphadenitis, 1354
Kikuchi lymphadenitis, 52, 1015–1016
Ki-67 labeling in, 1452
Killian polyps. *See* Antrochoanal polyps (ACP)
Kimura disease, 1016–1018
  clinical features, 1016–1017
  differential diagnosis, 1017–118
  pathology, 1017
  of salivary glands, 1098
KIT mutations, 1510
Klebsiella ozaenae, 346
Klebsiella pneumoniae, 64
Klebsiella rhinoscleromatis, 1085
Klippel-Trenaunay syndrome, 1523
Koch's bacillus, 1621
Koplick's spots, 1685
Krouse staging system, inverted papilloma, 369
KS. *See* Kaposi sarcoma (KS)
Kursteiner's canals, 1431
Kuttner tumor. *See* Chronic sclerosing sialadenitis
Kviem test, 1693
KWD. *See* Keratosis with dysplasia (KWD)
KWOD. *See* Keratosis without dysplasia (KWOD)

Lacrimal gland
  clinical findings, 1599–1600
  extranodal marginal zone B-cell lymphoma, 1600–1601
  lymphoproliferative processes, 1599
Laminin and solid/multicystic ameloblastoma–central, 1208
Langerhans cell histiocytosis (LCH), 438–439, 966, 1074–1075, 1351, 1415
  of bone, 1109
  dermatopathic lymphadenopathy, 1005
  Kimura disease, 1018
  of skin, 1112
Langerhan's cells, 52, 438–439
  and CEOT, 1234
  sarcoma, 1075
Langerhan's histiocytes, 52
Large cell carcinoma, 591–593
Large cell infiltrates, diffuse/nodular diagnosis, of hematolymphoid lesions of skin, 1113–1114
Large cell lymphoma. *See also* Diffuse large B-cell lymphoma (DLBCL)
  anaplastic. *See* Anaplastic large cell lymphoma
  versus infectious mononucleosis, 1088
  problems in diagnosis of, 1093–1094
Laryngeal candidiasis, 1645
Laryngeal carcinoma, 144–145
Laryngeal cartilages invasion, 144
Laryngeal kaposi sarcoma (KS), 1660
Laryngeal leiomyosarcoma, 876
Laryngeal metastases, 1157–1158
Laryngeal papilloma, 1677
Laryngeal paragangliomas (LPG), 723–724
Laryngeal TB, 1622
Laryngoceles, 117–119
Larynx, 953
  hematolymphoid lesions of, 1099

Laser therapy, 277
Latent membrane proteins (LMP), 1664, 1665
Lateral aberrant thyroid tissue, 230
Lateralization of cancer in nasal cavity, 372
LCH. *See* Langerhans cell histiocytosis (LCH); Lobular capillary hemangioma (LCH)
LE. *See* Lupus erythematosus (LE)
LEC. *See* Lymphoepithelial carcinomas (LEC); Lymphoepithelial cysts (LEC)
Leg-type, primary cutaneous DLBCL, 1110–1111
Leiomyomas, 128–129, 1416
  clinical findings, 802–803
  differential diagnosis, 805–806
  electron microscopy, 805
  imaging, 803
  immunohistochemistry, 804
  molecular findings, 804–805
  pathologic findings, 803–804
  prognosis and treatment, 806
Leiomyosarcomas, 58, 876–881
Leishmania, 1013, 1653, 1654
Leishmaniasis, 1013
Lemiere's disease, 1611
Lens
  anatomy, 1575
  cataract, 1575–1576
Lentigo maligna, 1507
  melanoma, 1507–1509
Lepromatous lymphadenitis, 1012
Leprosy
  clinical features, 1625
  culture and PCR identification, 1627
  differential diagnosis, 1627
  head and neck manifestations, 1626
  histopathology, 1626–1627
  immunological considerations, 1625
  Ridley Joplin criteria classification, 1625
  treatment, 1627
LESA. *See* Lymphoepithelial sialadenitis (LESA)
Leser-Trelat, 1477
Lesions
  containing squamous cells, 27–28
  in ocular adnexa, 72–74
Leukoplakia, 59–60, 131, 273–275
  clinical features, 273
  defined, 273
  diagnosis, 274
  pathology, 274
  treatment, 274–275
Levamisole, 263
LGFMS. *See* Low-grade fibromyxoid sarcoma (LGFMS)
Lichenoid drugs, 255–256
Lichen planus, 254–257, 281
  clinical presentation, 254–255
  immunology, 257
  immunopathology, 257
  lichenoid drugs, 255–256
  pathology, 256–257
  treatment, 257
Limbal dermoid, 1562–1563
Limited form of Wegener's granulomatosis (LWG), 654. *See also* Wegener's granulomatosis
Lingual thyroid, 229–230
  clinical features, 230
  pathology, 230
  primordium of thyroid, 1346
  treatment, 230
Lip cancer, 292–294
Lipoadenomas, 1449
Lipoblastoma, 1364
Lipoid proteinosis, 1344
Lipoma, 128
Lipoma, lipoma variants, and reactive lipomatous lesions
  clinical and pathology, 806–812
  differential diagnosis, 812
  immunohistochemistry, 812
  molecular findings, 812
  prognosis and treatment, 812
  radiologic imaging, 812
Lipomatosis, 482
Liposarcomas, 881–885
Lithium, 1438
  and hypercalcemia/hyperparathyroidism, 1458–1459
Ljubljana classification, 269, 271–272
  basal hyperplasia, 271
  malignant lesions, 271
  parabasal cell hyperplasia, 271
  squamous hyperplasia, 271
LMP. *See* Latent membrane proteins (LMP)
LMP-1, nasopharyngeal carcinomas, 400
Lobectomy, 13, 15
Lobular capillary hemangioma, 227–228
  clinical features, 227–228
  diagnosis, 228
  pathology, 228
  treatment, 228
Lobular capillary hemangioma (LCH), 1340
Localized plasma cell Castleman disease, 1021–1022
LOH. *See* Loss of heterozygosity (LOH)
Loss of heterozygosity (LOH), 685
Low-grade fibromyxoid sarcoma (LGFMS), 886, 888
Low grade malignancies *vs.* PA, 36–37
Low-grade MEC, 26
LPG. *See* Laryngeal paragangliomas (LPG)
LPL. *See* Lymphoplasmacytic lymphoma (LPL)
Lupus erythematosus (LE), 252–254, 274
  chronic cutaneous lupus erythematosus, 252
  diagnosis, 253–254
  histopathology, 253
  subacute cutaneous lupus erythematosus, 252–253
  systemic lupus erythematosus, 252
  treatment, 254
Lupus lymphadenitis, 1014
Lupus vulgaris (LV), 1622
LWG. *See* Limited form of Wegener's granulomatosis
Lymphadenomas
  lymphadenoma, 534–535
  sebaceous lymphadenoma, 533–534
Lymphadenopathies, 37, 49–52, 1627
  cat-scratch disease, 51
  dermatopathic, 1005
  granulomatous lymphadenitis, 50
  HIV-associated, 1009–1012
  infectious mononucleosis, 51
  Kikuchi lymphadenitis, 52
  reactive lymphoid hyperplasia, 49–50
  Rosai-Dorfman disease, 51–52
  suppurative lymphadenitis, 50
  toxoplasmosis, 50–51
Lymphangioma, 788, 983–984
  clinical and molecular features, 789
  differential diagnosis, 792
  electron microscopy, 792
  imaging, 789–790
  immunohistochemistry, 792
  pathology, 790–792
  prognosis and treatment, 792–793
Lymphatic malformations (LM), 1522, 1597–1598
Lymph nodes, 37–52, 100–101
  ancillary studies, 39–40
  B-Cell, non-Hodgkin lymphoma, 43–45
  biopsy, 1150
  causes of enlargement of head and neck, 998
  clinical symptoms, 38
  diagnosis, 38–39
  FNA, non-Hodgkin lymphomas, 39
  FNAB, Hodgkin lymphoma, 45–46
  FNAB, non-Hodgkin lymphomas, 40–43
  hematolymphoid neoplasms, 1079–1081
  infarction, 1006
  inflammatory pseudotumor, 1025–1026
  lymphadenopathies, 49–52
  metastatic neoplasms to cervical lymph nodes, FNAB, 46–49
  nonspecific reactive lymphoid hyperplasia, 997–1003
  normal, 997
  patterns and etiology of reactive, 1080
  reactive lymphoid hyperplasia of, 997
Lymphoblastic leukemias/lymphomas, 1060
Lymphoblastic lymphoma, 40
Lymphocyte depletion
  classical Hodgkin lymphoma, 1034
  in fine fibrosis, 1009
Lymphocyte-rich classical Hodgkin lymphoma, 1033–1034
Lymphocytic/histiocytic (L&H) cells, 1005
  nodular lymphocyte–predominant Hodgkin lymphoma, 1037
Lymphocytic thyroiditis, 3
Lymphoepithelial carcinomas (LEC), 33, 160–161, 382–383, 593–595
Lymphoepithelial cysts (LEC), 22, 481–482
Lymphoepithelial lesions, 33
Lymphoepithelial sialadenitis (LESA), 501–505
  of salivary glands, 1096
Lymphoepithelial sialadenitis *versus* MALT lymphoma, 1100
Lymphoepithelial tumor. *See* Cutaneous lymphadenoma (CL)
Lymphoepithelioma, in children, 1355
Lymphoepithelioma-like carcinoma (LE-LC), 1483
Lymphoid cells, 3, 32
Lymphoid hyperplasia, 33
Lymphoid proliferations, 1079–1081
  atypical lymphoid hyperplasia in, 1081
Lymphoid tissues, of Waldeyer ring, 1001
Lymphoma, 15
Lymphoplasmacytic lymphoma (LPL), 43, 1059–1060
Lymphoproliferative disorders, immunodeficiency-associated, 1072–1073
Lymphoproliferative processes, 1599

Macroadenoma, 709
Maffucci syndrome, 1523
Magnet resonance imaging (MRI), 1
MAI. *See* Mycobacterium avium-intracellulare (MAI); *Mycobacterium avium-intracellulare* (MAI)
Mainstay therapy, 976, 983
Major aphthae, 261
Malakoplakia, 431–432
  clinical course, 1690
  etiology, 1690
  histopathology, 1690–1691
  treatment, 1691
Malignant ectomesenchymoma, 1363

Malignant epithelial neoplasms
basal cell carcinoma, 1495–1498
basosquamous cell carcinoma, 1498–1499
merkel cell carcinoma (MCC), 1502–1504
microcystic adnexal carcinoma, 1499–1501
squamous cell carcinoma, 1491–495
trichilemmal carcinoma (TLC), 1501–1502
Malignant extrarenal rhabdoid tumor, 900–901
Malignant fibrous histiocytoma (MFH), 57, 885–892
Malignant GCT, 700–701
Malignant lesions, in nasal cavity sinuses, 64–68
Malignant lymphomas, 32–33, 38
Malignant melanomas, 47–48, 80–81, 170–171, 391–394, 1587
amelanotic, 392
in children, 1341
clinical features, 391–392
differential diagnosis, 393
etiology, 391
immunohistochemistry, 393
molecular-genetic data, 393
oral, 323–326
pathology, 392–393
treatment and prognosis, 393–394
Malignant mesenchymal tumors
ASPS, 901–904
fibrosarcoma, 885–892
grading, 862–863
malignant extrarenal rhabdoid tumor, 900–901
malignant fibrous histiocytoma, 885–892
malignant lipomatous, liposarcomas, 881–885
malignant mesenchymoma, 894–895
malignant skeletal muscle
leiomyosarcomas, 876–881
RMS, 869–876
malignant triton tumor, 892–894
malignant vascular
angiosarcoma, 867–869
epithelioid hemangioendothelioma, 863–867
mesenchymal chondrosarcoma, 895–897
staging, 863
synovial sarcoma, 897–899
Malignant mesenchymoma, 894–895
Malignant neoplasms, 9–15
anaplastic carcinoma, 14–15
of external ear and auditory canal, 459–464
insular carcinoma, 14
lymphoma, 15
medullary carcinoma, 13–14
of middle ear, 465–467
papillary thyroid carcinoma, 9–11
Malignant odontogenic tumors
ameloblastic carcinoma (AMCA), 1292
differential diagnosis, 1295
DNA microarray study, 1295
etiology of, 1293–1294
frequency of, 1293
gender ratio, 1293
growth rate, 1293
immunohistochemistry, 1294
locations of, 1293
ultrastructure of, 1294
metastasizing ameloblastoma (METAM), 1290
age range, 1291
growth rate, 1291
histopathological features of, 1291
immunohistochemistry, 1291–1292
location of, 1291
treatment and prognosis, 1292
secondary (Dedifferentiated) AMCA, 1295
Malignant oral lesions, 61–63
basaloid squamous cell carcinoma, 62
metastatic squamous cell carcinoma, 62–63
nonepithelial tumors, 63
PLGA, 63
salivary gland lesions, 63
squamous cell carcinoma, 61–62
Malignant peripheral nerve sheath tumor (MPNST), 58, 688. *See also* Malignant triton tumor
clinical features, 726
diagnosis, 728
histopathology, 727
imaging, 726–727
immunohistochemistry, 727
macroscopy, 727
overview, 725–726
somatic genetics, 727–728
treatment, 728
ultrastructure, 727
Malignant rhabdoid tumor (MRT), 1363
in floor of mouth, 1364
Malignant round cell neoplasms, 1363
Malignant syringoma. *See* Microcystic adnexal carcinoma (MAC)
Malignant triton tumor, 726, 892–894
Malignant tumors, in ocular adnexa, 75–79
ACC, 76
basal cell carcinomas, 75–76
Merkel cell tumor, 77
metastatic carcinoma, 78–79
orbital teratomas, 77
retinoblastoma, 77–78
sebaceous carcinoma, 76–77
squamous cell carcinoma, 76
MALT. *See* Extranodal marginal zone B-cell lymphoma (MALT)
MALT lymphoma, 33
Manchester clinical diagnostic criteria, for NF2, 690
Mandible, cortical defects. *See* Cortical defects of mandible
Mandibular margin, 99
Mantle cell lymphoma
clinical features, 1051–1052
differential diagnosis, 1053–1054
immunohistochemistry, 1053
molecular genetic data, 1053
pathology, 1052–1053
treatment and prognosis, 105
Mantle cell lymphoma (MCL), 40, 44
Marginal zone lymphoma (MZL), 43
Massachusettes General Hospital, 982
Masson trichrome histochemical stain, 878
Masson vegetant hemangioma. *See* Papillary endothelial hyperplasia
Mastocytosis, cutaneous, 1112, 1113
Mastoid, heterotopias of, 427
Matrix metalloproteinase (MMP), 685
Matrix metalloproteinases (MMP), and ameloblastomas, 1213–1214
Matrix-rich microcirculation architecture, 1587
Maxillary sinuses, squamous cell carcinomas of, 374–376
Mayo Clinic, 96
Mazabraud myxomas, 1728
Mazabraud syndrome, 964, 1727–1728
McCoy cell culture, 72
McCune Albright syndrome, 964
MCL. *See* Mantle cell lymphoma (MCL)
Measles (rubeola), 1685–1687
Mebendazole, 1690
MEC. *See* Mucoepidermoid carcinomas (MEC)
Medial pterygoid muscle, 669
Median rhomboid glossitis, 207–208
clinical features, 207
diagnosis, 208
pathology, 207–208
treatment, 208
Medium-sized cell infiltrates
diagnosis, of hematolymphoid lesions of skin, 1114
Medullary carcinoma, 13–14
Medullary thyroid carcinoma (MTC), 1355, 1356, 1391, 1441, 1451
Medullary thyroid carcinoma (MTC), 685
Meibomian gland, 73
Meige disease, 1523
Melanin, 48
Melanocytic lesions, in ocular adnexa, 79–81
malignant melanoma, 80–81
melanocytoma, 79–80
melanotic neuroectodermal tumor of infancy, 79
Melanocytic neoplasms
melanomas, 1507–1511
spitz nevus, 1504–1507
Melanocytic neuroectodermal tumor of infancy (MNTI)
clinical features, 733
diagnosis, 734
histopathology, 733–734
imaging, 733
immunohistochemistry, 734
macroscopy, 733
overview, 733
somatic genetics, 734
treatment, 734–735
ultrastructure, 734
Melanocytic nevi, cutaneous tumefactions from children
atypical pattern of lentiginous proliferation, 1341
congenital melanocytic nevi (CMN), 1339
giant CMN, 1341
nested and lentiginous junctional component, 1340
neurocytic hamartoma, 1340–1341
risk of a malignancy in, 1340
single cell pattern, 1340
spitz-like features, 1340
Melanocytoma, 79–80
Melanomas
clinical features, 1507–1508
differential diagnosis, 1511
electron microscopy, 1510
imaging studies, 1508
immunohistochemistry, 1510
molecular genetics, 1510
pathology, 1508–1510
staging, 1507
treatment and prognosis, 1511
Melanoses and melanocytic proliferations, 1559–1562
Melanosis, 170
Melanotic ameloblastoma. *See* Melanocytic neuroectodermal tumor of infancy (MNTI)
Melanotic lesions, 170–171
Melanotic neuroectodermal tumor of infancy, 1346
Melanotic neuroectodermal tumor of infancy, 79
Melanotic neuroectodermal tumor of infancy (MNTI), 1346
vimentin and HMB45, 1347
Melanotic progonoma. *See* Melanocytic neuroectodermal tumor of infancy (MNTI)
Mel-CAM glycoprotein and calcifying odontogenic cyst (COC), 1265

Membrane type 1-matrix metalloproteinase (MT1-MMP), and ameloblastomas, 1214
Membranous labyrinth, 424–425
Memorial Sloan-Kettering Cancer Center, 295, 305
MEN. *See* Multiple endocrine neoplasia (MEN); Multiple endocrine neoplasia (MEN)
Meniere disease, inner ear, 445–446
Meningeal sarcoma, 706
Meningioma
  clinical features, 701–702
  diagnosis, 707
  imaging, 702
  immunohistochemistry, 705
  malignant, 704–705
  overview, 701
  pathology, 702–704
  somatic genetics, 705–707
  treatment, 707–708
  WHO classification, 701
Meningioma of the ocular adnexa, 1602
Meningiomas, 75, 455–456
Meningitis, bacterial, 676
Meningoceles, 674
Meningothelial cells, 704
Merkel cell carcinoma (MCC)
  clinical features, 1502
  differential diagnosis, 1503–1504
  electron microscopy, 1503
  immuhistochemistry, 1503
  molecular genetics, 1503
  pathology, 1503
  treatment and prognosis, 1504
Merkel cell tumor, 77
Mesenchymal chondrosarcoma, 895–897
Mesenchymal tumors
  angiosarcoma, 1415–1416
  aytpical fibroxanthoma, 1520–1521
  dermatofibroma, 1515–1517
  dermatofibrosarcoma protuberans, 1517–1520
  fibrous papules (FPs), 1513–1514
  keloids, 1511–1513
  leiomyomas, 1416
  nuchal-type fibroma, 1514–1515
Mesenchymal tumors, benign
  of external auditory canal, 448–449
Metastases, 179
  cervical lymph nodes, 299–300
  clinical features, 179
  nasal cavity/paransal sinuses, 402
  overviews, 179
  prognosis, 179
Metastases , of orbit, 1603
Metastasizing ameloblastoma (METAM), 1290
Metastatic adenocarcinoma, 1150
Metastatic carcinoma, 25, 78–79, 1138
Metastatic cystic squamous carcinoma, 1151, 1152
Metastatic malignancies, 17–18, 31
Metastatic melanoma, 1591
Metastatic neoplasms to cervical lymph nodes, FNAB, 46–49
  malignant melanoma, 47–48
  nasopharyngeal carcinoma, 47
  squamous cell carcinoma, 46–47
  supraclavicular lymph node metastases, 48–49
  thyroid carcinoma, 47
Metastatic neuroblastoma, to skull, 1363
Metastatic papillary carcinoma, of thyroid, 1151
Metastatic squamous cell carcinoma, 62–63
Metastatic thymoma, 1725
Metastatic tumors, to oral regions
  jaw metastases, 1156
  oral soft tissue metastases, 1156–1157
Metastatic tumors to middle ear and temporal bone, 467
Metastatic tumors to thyroid, 1416–1417
Metastatic undifferentiated nasopharyngeal type, of carcinoma, 1151
Methimazole antithyroid drugs, 1386
Methotrexate, 1693
Methylene diphosphonate bone scintigraphy, 961
Metronidozole, 1611
MFH. *See* Malignant fibrous histiocytoma (MFH)
MIB-1 antibody in AFOD, 1251
Microcystic adnexal carcinoma (MAC), 1486–1487
  clinical features, 1499
  differential diagnosis, 1500
  immunohistochemistry, 1500
  molecular genetics, 1500
  pathology, 1499–1500
  treatment and diagnosis, 1500–1501
Microinvasive carcinoma (MIC), 135–136
  clinical features, 136
  overviews, 135–136
  treatment, 136
Microlaryngoscopy with laser excision, 1677
Micronodular BCC, 1496
Microscopic polyangiitis (MPA)
  clinical features, 655
  diagnosis, 655
  pathology, 655
  treatment and prospect, 655–656
Middle ear, 424
  adenocarcinomas, 466–467
  adenomas. *See* Middle ear adenomas
  benign neoplasms of, 449–456
  cholesteatomas of, 436–438
  endolymphatic sac papillary tumor, 457–458
  heterotopias of, 427
  malignant neoplasms of, 465–467
  metastatic tumors, 467
  squamous cell carcinomas, 465–466
Middle ear adenomas, 449–451
  with neuroendocrine differentiation, 450–451
Middle ear squamous cell carcinomas, 465–466
Midfacial destructive diseases, diagnosis of, 664
Midline carcinoma with NUT rearrangement (MCNUTR), 1729–1730
Mild dysplasia, 269
Milial cysts, 1342
Milk alkali syndrome, 1438
Minimally invasive techniques, 1455
Minocycline, 1693
Minocycline ingestion and pigment accumulation in thyroid, 1393
Minor aphthae, 261
Minor aphthous ulcers, 261
Mitomycin-C, 1556
Mitoses, 1480, 1726
Mitotic activity, 1493
Mixed mesoneuroectodermal hamartoma, 1348
MMP. *See* Matrix metalloproteinase (MMP); Mucous membrane pemphigoid (MMP)
MMPs. *See* Matrix metalloproteinases (MMPs) and ameloblastomas
MNTI. *See* Melanotic neuroectodermal tumor of infancy (MNTI)
Moderate dysplasia, 269
Mohs surgery, 1495, 1504, 1510, 1511, 1519
Molecular genetic data
  ALK+ anaplastic large cell lymphoma, 1067–1068
  Burkitt lymphoma, 1056–1057
  classical Hodgkin lymphoma, 1035
  DLBCL, 1041
  extramedullary plasmacytoma, 1057
  extranodal NK/T-cell lymphoma, 1061–1062
  of hyaline-vascular Castleman disease, 1021
  MALT lymphoma, 1055–1056
  mantle cell lymphoma, 1053
  nodular lymphocyte–predominant Hodgkin lymphoma, 1037
Molecular-genetic data
  ITAC, 386
  malignant melanomas, 393
  nasopharyngeal carcinomas, 398–399
Molecular genetic data, follicular lymphoma, 1049
Moll's gland cyst. *See* Hidrocystomas
Molluscum contagiosum, 1684–1685
Monocytoid B cells, 999
Mononucleosis, 1355
Monophasic synovial sarcoma. *See* Synovial sarcoma
Monosodium urate crystals, in gout, 953
Monospot test, 1666
Monostotic fibrous dysplasia, 964–965
MPA. *See* Microscopic polyangiitis
MPNST. *See* Malignant peripheral nerve sheath tumor (MPNST)
MPO. *See* Myeloperoxidase
MRI. *See also* Magnet resonance imaging (MRI)
  acute supprative osteomyelitis, 958
  chondrosarcoma, 977
  chordoma, 980
  chronic suppurative osteomyelitis, 959
  gout, 953
  osteoblastoma, 969
  parosteal osteosarcoma, 973
  PVNS, 956
MRT. *See* Malignant rhabdoid tumor (MRT)
MTC. *See* Medullary thyroid carcinoma (MTC); Medullary thyroid carcinoma (MTC)
MT1-MMP. *See* Membrane type 1-matrix metalloproteinase (MT1-MMP) and ameloblastomas
Mucinous adenocarcinoma, 572
Mucinous carcinoma, 100
Mucoceles, 74, 356–357
Mucoceles, of salivary gland, 480–481
Mucoepidermoid carcinoma, 546–552
Mucoepidermoid carcinoma (MEC), 1352, 1412
Mucoepidermoid carcinomas (MEC), 17, 23, 102, 169, 391
Mucorales
  clinical presentation, 1636
  etiology, 1635–1636
  histopathology, 1636–1637
  serology, 1637
  treatment, 1637
Mucor hyphae, 1637
Mucormycosis, 1637
Mucosa-associated lymphoid tissue (MALT) lymphoma. *See also* Extranodal marginal zone B-cell lymphoma
  clinical features, 1054
  of conjunctiva, 1105
  differential diagnosis, 1056
  immunohistochemistry, 1055
  of lacrimal gland, 1106

[Mucosa-associated lymphoid tissue (MALT)]
large cell transformation in, 1055
lymphoepithelial sialadenitis *versus*, 1100
molecular genetic data, 1055–1056
of orbit, 1105
immunostaining, 1108
pathology, 1054–1555
of salivary glands, 1094–1095
of skin, 1111
of thyroid, 1102, 1103
in situ hybridization for immunoglobulin mRNA, 1104
of tonsil, 1091
treatment and prognosis, 1056
Mucosal neuromas, 692–694
Mucosal surfaces, 101
Mucosal ulcerations, 1657
Mucoserous (salivary) glands, hamartomas, 361
Mucous cell metaplasia, 1207
Mucous membrane pemphigoid (MMP), 243, 249–251
clinical presentation, 249–250
diagnosis, 251
immunology, 251
immunopathology, 250–251
pathology, 250
treatment, 251
Mucous retention cysts, 59
antrochoanal polyp with, 351
Mucus, allergic, 354–356
Mucus-propelling cilia, 351–352
Muir-Torre syndrome, 1488, 1489, 1493, 1553
Multicentric Castleman disease, 1009
clinical features, 1022
pathology, 1023
Multimodality therapy, for ONB, 732
Multinodular goiter, 1390–1391
Multiple endocrine neoplasia, 1437
Multiple endocrine neoplasia (MEN), 1348
Multiple endocrine neoplasia (MEN), 677, 692
Multiple odontomas, 1253
Multiple primary malignancies, 145
Multiple syringomas, 1342
Mumps, 495, 1687
Murine double minute 2 (MDM2) and p14 (ARF) expression in ameloblastomas, 1211
Murk Jansen's chondrodysplasia, 1458
Myalgia, 252
MYC gene translocation, DLBCL, 1041
Mycobacterial cervical lymphadenitis, 1624–1625
Mycobacterial (tuberculous) lymphadenitis, 1012
Mycobacterium avium-intracellulare (MAI), 38
Mycobacterium avium-intracellulare (MAI), 1624
Mycobacterium tuberculosis, 1012
clinical stages, 1621
epidemiology, 1621
in the head and neck, 1622
laryngeal, 1622–1625
mucocutaneous, 1622
primary sinonasal tract, 1622
reactivation, 1621–1622
Mycoplasma pneumoniae, 260
Mycosis fungoides, 1069–1070
Myeloid sarcoma, 1073
of salivary glands, 1095
Myeloperoxidase (MPO), 650
MYH-associated polyposis, 1487
Myoepithelial carcinoma, 580–583
Myoepithelial carcinoma, 36
Myoepithelial cells, 35
Myoepithelioma, 519–522
clinical features, 519
defined, 519
differential diagnosis, 521
immunohistochemistry, 520–521
pathology, 519–520
treatment, 521–522
Myofibroblastoma, 1152
Myofibroma
clinical features, 837
differential diagnosis, 841–842
electron microscopic findings, 840–841
immunohistochemical findings, 840
molecular findings, 840
pathologic findings, 838–840
prognosis and treatment, 842–843
radiologic imaging, 837–838
Myofibromatosis. *See* Infantile myofibroma
Myofibromatosis-myofibroma, 1358
Myogenic neoplasms, 1361
Myosin heavy chain genes (MYH), 1487
Myositis ossificans (MO) circumscripta
clinical findings, 818–819
differential diagnosis, 820
electron microscopy, 820
immunohistochemistry, 820
pathologic findings, 819–820
prognosis and treatment, 820
radiologic imaging, 819
Myospherulosis, 64, 358–359
Myospherulosis, 1643–1644
Myotonic dystrophy, 1480
Myxofibrosarcoma, 886–887, 889
Myxoid liposarcoma, 881, 882
Myxoid liposarcomas, 58–59
Myxoid malignant fibrous histiocytoma. *See* Myxofibrosarcoma
Myxoid neurothekeomas, 695
Myxoid soft tissue sarcomas, 58–59
Myxomas, 1279
external auditory canal, 448–449
MZL. *See* Marginal zone lymphoma (MZL)

NARES. *See* Nonallergic rhinosinusitis with eosinophilia syndrome (NARES)
Nasal biopsy, in ARS, 346
Nasal cavity
extranodal NK/T-cell lymphoma, 1060–1064
hematolymphoid neoplasms, 1081–1086
lateralization of cancer of, 372
metastases to, 402
sinternal anatomy of, 373
squamous cell carcinomas of, 371–374
Nasal cavity sinuses, 63–68
lesions, 64
angiofibromas, 64
myospherulosis, 64
paranasal sinus mucoceles, 64
rhinoscleroma, 64
sinonasal hemangiopericytoma, 64
malignant lesions, 64–68
heterotopia, of neuroglial tissue, 68
nasopharyngeal carcinoma, 64–65
olfactory neuroblastoma, 65–67
paraganglioma, 67–68
sinonasal adenocarcinoma, 67
sinonasal neuroendocrine carcinoma, 67
sinonasal undifferentiated carcinoma, 66–67
Nasal cerebral heterotopia, 1348–1349
Nasal chondromesenchymal hamartoma (NCMH), 974–975, 1351
Nasal encephalocele (NE)
anatomy, 674–675
clinical features, 675
[Nasal encephalocele (NE)]
diagnosis, 675–676
imaging, 675
overview, 674
pathogenesis, 676
pathology, 675
treatment, 676
Nasal glioma (NG), 1348
clinical features, 671–672
diagnosis, 673–674
imaging, 672
overview, 671
pathogenesis, 674
pathology, 672–673
treatment, 674
Nasal heterotopia. *See* Nasal glioma (NG)
Nasal mucosa, 672
Nasal obstruction, rhinosinusitis medicamentosa and, 347
Nasal polyps, 348–350
clinical features, 348
with cystic fibrosis, 353
pathology, 348–350
with squamous metaplasia, 368
treatment, 350
Nasal septum, 953
squamous cell carcinomas, 373–374
Nasal vestibule
squamous cell carcinomas, 372–373
staging of carcinomas, 373
Nasopharyngeal carcinoma (NPC), 47, 64–65, 394–200, 1668–1669
anatomy, 394–395
classification of, 397
clinical features, 395–396
differential diagnosis, 399
Epstein–Barr virus (EBV) genome detection in, 1355
etiology, 395
immunohistochemistry, 398
molecular-genetic data, 398–399
pathology, 396–398
treatment and prognosis, 399–400
undifferentiated nasopharyngeal nonkeratinizing carcinoma, 1357
viral studies, 398
Nasopharynx
carcinomas. *See* Nasopharyngeal carcinomas
hematolymphoid neoplasms, 1086–1088
papillary adenocarcinomas, 400–402
salivary-type neoplasms, 391
National Cancer Institute (NCI), 1
National Institute on Drug Abuse, 663
Natural killer (NK) cells, 262
NBCCS. *See* Nevoid BCC syndrome (NBCCS)
NCI. *See* National Cancer Institute (NCI)
NCMH. *See* Nasal chondromesenchymal hamartoma (NCMH)
NE. *See* Nasal encephalocele (NE)
NEC. *See* Neuroendocrine carcinomas (NEC)
Neck dissections
adjuvant chemotherapy, 1144–1145
extended radical, 1136
gross examination of
radiologic examination, 1137
technique, 1137–1138
microscopic examination, 1138
modified radical, 1136
radical, 1136
selective, 1136
unexpected pathology
granulomatous lesions, 1142
lymph node heterotopias, 1142, 1143
metastatic papillary thyroid carcinoma, 1142

Necrobiosis with palisading mantle of histiocytes, 1367
Necrosis, 1591
Necrotizing external otitis, 427–428
Necrotizing granulomatous lymphadenitis, 1354
Necrotizing granulomatous nodules, 952
Necrotizing sialometaplasia, 491–493
Neisseria gonorrhea, 953
Neonatal hyperparathyroidism, 1458
Neoplasm, in ocular adnexa, 74–75
  cavernous hemangiomas, 74
  hemangiopericytoma, 74
  meningioma, 75
  mucoceles, 74
  pilomatrixoma, 74
  pleomorphic adenoma, 74–75
  schwannoma, 75
Neoplasms
  of bone, hematolymphoid, 1108–1109
  of eye, hematolymphoid, 1103–1105
  of ocular adnexa, hematolymphoid, 1103–1105
  of skin, hematolymphoid, 1109–1112
  of thyroid, hematolymphoid, 1100–1101
Neoplastic cells, 13, 661
Neoplastic diseases, condroid. *See* Neoplastic diseases, osseous
Neoplastic diseases, mesenchymal
  aneurysmal bone cyst, 986–987
  angiosarcoma, 982–983
  desmoplastic fibroma, 987–988
  eosinophilic granuloma, 989
  epithelioid hemangioendothelioma, 981–982
  Ewing's sarcoma, 989
  fibrosarcoma, 988–989
  giant cell granuloma, 984–985
  giant cell tumor, 984
  hemangioma, 981
  hyperparathyroidism, 985–986
  lymphangioma, 983–984
Neoplastic diseases, nonchondroid. *See* Neoplastic diseases, mesenchymal
Neoplastic diseases, nonosseous. *See* Neoplastic diseases, mesenchymal
Neoplastic diseases, osseous
  cartilaginous lesions, 974
  chondroblastomas, 978–979
  chondroid metaplasia, 975–976
  chondroma, 976
  chondromyxoid fibroma, 978
  chondrosarcoma, 976–978
  chordoma, 979–981
  exostosis, 967
  extraosseous osteosarcoma, 974
  nasal chondromesenchymal hamartoma, 974–975
  ossifying fibroma, 970–971
  osteoblastoma, 969–970
  osteochondroma, 968
  osteoid osteoma, 968–969
  osteosarcoma, 971–974
Nephrolithiasis, 1455
Nephrotic syndrome, 252
Nerve sheath myxomas, 694
Nestin antibodies
  AFOD, 1251
  AMF, 1244
  and AOT, 1238
  and ODOMYX, 1286
Neurilemoma, 127–128
Neuroblastoma (NB), 1347, 1355
Neuroendocrine carcinomas (NEC), 322–323, 380. *See also* Primary small cell carcinoma
Neuroendocrine differentiation, middle ear adenomas, 450–451
Neuroendocrine tumors, 162–167
  AC, 164–166
  combined small cell neuroendocrine carcinoma, 167
  overviews, 162
  paraganglioma, 167
  SCNEC, 166–167
  TC, 162–164
Neurofibroma, 63, 127–128, 681–683
Neurofibromatosis 1, 687–689
Neurofibromatosis 2, 689–691
Neurofibromatosis (NF), 676, 1344
Neurofibromatosis type 1 (NF1), 1601
Neurofibrosarcoma. *See* Malignant peripheral nerve sheath tumor (MPNST)
Neurogenic sarcoma. *See* Malignant peripheral nerve sheath tumor (MPNST)
Neurothekeoma, 694–696
Neutrophilic abscesses, 1493–1494
Neutrophilic microabscess, 652, 653
Nevoid BCC syndrome (NBCCS), 1344
Nevus, 170
Nevus sebaceous of Jadassohn (NSJ), 1341–1342
  clinical features, 1536
  differential diagnosis, 1537
  imaging, 1536
  molecular genetics, 1537
  pathology, 1536–1537
  treatment and prognosis, 1537–1538
NF. *See* Neurofibromatosis (NF)
NF-2
  in acoustic neuroma, 454
  in meningiomas, 456
NG. *See* Nasal glioma (NG)
NHL. *See* Non-Hodgkin's lymphoma (NHL)
Nicotiana rustica, 287
Nicotiana tabacum, 287
Nicotinic stomatitis
  clinical features, 208–209, 277–278
  defined, 277
  diagnosis, 278
  pathology, 209, 278
  treatment, 209, 278
NIH diagnostic criteria, for NF1, 687
Nikolsky sign, 250, 259
NK. *See* Natural killer (NK) cells
NK/T-cell lymphomas
  clinical features, 660–661
  immunohistochemistry, 662
  pathology, 661
  treatment and prospect, 662
Nodal and extranodal lymphoma, 63
Nodal marginal zone lymphoma, 1060
Nodular BCC, 1496
Nodular/diffuse dermal infiltrate diagnosis, of hematolymphoid lesions of skin, 1113–1114, 1115
Nodular fasciitis, 54
  in children, 1359
Nodular fasciitis and related lesions including cranial fasciitis, 812
  clinical findings, 813
  differential diagnosis, 813–815
  electron microscopy, 813
  imaging, 813
  immunohistochemistry, 813
  molecular findings, 813
  pathologic findings, 813
  prognosis and treatment, 815
Nodular goiter, 4–5
Nodular KS, 1660
Nodular lymphocyte–predominant Hodgkin lymphomas, 1035–1039
  clinical features, 1036
  differential diagnosis, 1038–1039
  immunohistochemistry, 1037
  molecular genetic data of, 1037
  pathology, 1036–1037
  versus PTGC, 1005
  transformation to non-Hodgkin lymphoma, 1037
  treatment and prognosis, 1039
Nodular melanoma, 1509
Nodular sclerosis, classical Hodgkin lymphoma, 1032–1033
Nodulosis—arthropathy—osteolysis syndrome, 1344
Nonallergic rhinosinusitis with eosinophilia syndrome (NARES), 347
Noncutaneous leiomyosarcoma, 876
Nonepithelial larynx tumors, benign, 126–129
  hemangioma, 126–127
  leiomyoma, 128–129
  lipoma, 128
  neurilemoma, 127–128
  neurofibroma, 127–128
  overviews, 126
Nonepithelial tumors, 63
Non-Hodgkin lymphoma (NHL), 15, 39, 1039–1073, 1354
  adult T-cell leukemia/lymphoma, 1072
  anaplastic large cell lymphoma, 1065–1068
  angioimmunoblastic T-cell lymphoma, 1064
  in B-cell, 43–45
    follicular lymphoma, 44–45
    mantle cell lymphoma, 44
    small lymphocytic lymphoma, 44
  Burkitt lymphoma, 1056–1057
  CLL/SLL, 1059
  DLBCL, 1039–1045
  extramedullary plasmacytoma, 1057–1059
  extranodal NK/T-cell lymphoma, 1060–1064
  FNA, 39
  FNAB, 40–43
    anaplastic large cell lymphoma, 42–43
    Burkitt's lymphoma, 40–41
    diffuse large B-cell lymphoma, 41–42
    immunoblastic lymphomas, 42
    lymphoblastic lymphoma, 40
  follicular lymphoma, 1045–1051
  hydroa vacciniforme-like lymphoma, 1072
  immunodeficiency-associated lymphoproliferative disorders, 1072–1073
  lymphoblastic leukemia/lymphoma, 1060
  lymphoplasmacytic lymphoma, 1059–1060
  MALT lymphoma, 1054–1056
  mantle cell lymphoma, 1051–1054
  mycosis fungoides, 1069–1070
  nodal marginal zone lymphoma, 1060
  peripheral T-cell lymphoma, 1064–1065
  primary cutaneous CD8+ aggressive epidermotropic cytotoxic T-cell lymphoma, 1071–1072
  primary cutaneous CD4+ small/medium T-cell lymphoma, 1071
  primary cutaneous CD30+ T-cell lymphoproliferative disorders, 1068–1069
  Sézary syndrome, 1070–1071
  subcutaneous panniculitis-like T-cell lymphoma, 1071

Noniatrogenic hypoparathyroidism
clinical features, 1460
differential diagnosis, 1460
gene alterations in, 1461
molecular biology, 1461
pathologic features, 1460
treatment and prognosis, 1461
Nonintestinal-type adenocarcinomass (Non-ITAC), 387–389
Nonkeratinizing carcinomas (NKC), 376–377
of nasopharynx, 397
Nonkeratinizing squamous cell carcinomas, 305–308
immunohistochemistry, 307–308
microscopic features, 306–307
Nonkeratinizing undifferentiated carcinomas, 308–309
Nonneoplastic bone diseases
cemento-osseous dysplasia, 965–966
cherubism, 966–967
cortical defects of mandible, 962–963
cranial fasciitis, 966
fibrous dysplasia, 964–965
focal osteoporotic bone marrow defect, 961–962
osteoarthritis, 958
osteomyelitis, 958–960
osteoradionecrosis, 960–961
Paget's disease, 963–964
relapsing polychondritis, 961
Nonneoplastic disease, 3–6
Nonneoplastic joint disease. *See* Nonneoplastic bone disease
Nonneoplastic lesions
acquired. *See* Acquired nonneoplastic lesions
of ear and temporal bone, 425–432
classification, 425
Nonneoplastic salivary gland lesions, 20–21
infiltration, fatty, 20
sialadenitis, 20–21
Non-PTH-related hypercalcemia
clinical features, 1459
differential diagnosis, 1459
molecular biology, 1460
pathologic features, 1459
treatment and diagnosis, 1459–1460
Nonspecific reactive lymphoid hyperplasia
lymph node, 997–1003
nasopharynx, 1087
of ocular adnexa, 1106–1107
of oral cavity and oropharynx, 1091
Nonsteroidal anti-inflammatory drugs, 260
Nonsuppurative osteomyelitis. *See* Chronic sclerosing osteomyelitis
Noonan syndrome, 1523
NSJ. *See* Nevus sebaceous of Jadassohn (NSJ)
Nuchal fibrocartilaginous pseudotumor (NFP), 1728–1729
Nuchal fibroma
clinical features, 846
differential diagnosis, 847
electron microscopy, 847
imaging, 846
immunohistochemistry, 847
pathology, 846–847
treatment and prognosis, 847
Nuchal-type fibroma
clinical features, 1514
differential diagnosis, 1515
imaging studies, 1514
immunohistochemistry, 1514
pathology, 1514
treatment and prognosis, 1515
Nuclear atypia, 7
Nutritional deficiencies, oral cancer, 289
OaCCOT. *See* Odontoma-associated calcifying cystic odontogenic tumor (OaCCOT)
Obstructive sialadenitis, 485–486
Obstructive sleep apnea, 226–227
clinical features, 227
pathology, 227
treatment, 227
Occlusive phlebitis, 1390
Occult primary
to cervical nodes
adenopathy site, 1147–1148
clinical data, 1147
diagnosis, 1150–1152
lymphatic region, of neck, 1147
lymph node biopsy, 1150
primary lesion search, 1148–1150
immunohistochemistry
primary tumor discovery, 1154
treatment, 1154–1155
Ococytoma
clinical features, 530
defined, 530
differential diagnosis, 531
pathology, 530–531
treatment, 531
Octreotide scintigraphy, for PGL, 718
Ocular adnexa, 70–81
diagnosis, 71–72
hematolymphoid lesions of, 1103–1107
clinical features, 1104
diagnostic considerations, 1107
neoplasms, 1103–1105
reactive/inflammatory, 1105–1107
lesions, 72–74
malignant tumors, 75–79
ACC, 76
basal cell carcinomas, 75–76
Merkel cell tumor, 77
metastatic carcinoma, 78–79
orbital teratomas, 77
retinoblastoma, 77–78
sebaceous carcinoma, 76–77
squamous cell carcinoma, 76
melanocytic lesions, 79–81
malignant melanoma, 80–81
melanocytoma, 79–80
melanotic neuroectodermal tumor of infancy, 79
neoplasm, 74–75
orbital cytology, 70
overviews, 70–72
Ocular adnexal lymphoproliferative disorders, 1599
Oculodermal melanocytosis, 1560
ODOMYX. *See* Odontogenic myxoma and myxofibroma (ODOMYX)
Odonto-ameloblastoma
clinical features, 1258–1259
etiology of, 1259
immunohistochemistry, 1260
radiographs, 1259
treatment and prognosis, 1260
Odontogenic cysts, 69–70
Odontogenic fibroma, 1276
Odontogenic ghost cell lesions, 1260–1262
Odontogenic keratocysts, 1344
Odontogenic myxoma, 68–69
Odontogenic myxoma and myxofibroma (ODOMYX), 1283
age range and gender ratio, 1284
differential diagnosis, 1287–1288
etiology of, 1285
HRAS- and *KRAS*-encoded gene products, 1287
immunohistochemistry
CK antibodies, 1286
[Odontogenic myxoma and myxofibroma (ODOMYX)]
[immunohistochemistry]
glycosaminoglycans, 1286
nestin and vimentin antibodies, 1286
molecular-genetic data, 1287
radiographic appearance of, 1284–1285
rate of growth, 1284
treatment and prognosis, 1288
ultrastructure of, 1287
Odontogenic sarcomas
ameloblastic fibrodentino- and fibro-odontosarcoma, 1310–1311
ameloblastic fibrosarcoma, 1307–1310
odontogenic fibrosarcoma, 1311–1312
odontogenic myxosarcoma, 1312–1313
Odontomas
complex and compound odontomas, 1256–1258
complex odontoma (ODTx)
etiology, 1253–1255
imaging of, 1253
prevalence and incidence, 1252–1253
compound odontoma (ODTp)
etiology of, 1256
prevalence and incidents, 1255–1256
radiographs, 1256
odontoma-associated calcifying cystic odontogenic tumor (OaCCOT), 1253
Odynophagia, 243
Oil red O stains, 77
Olfactory neuroblastoma (ONB), 65–66, 65–67, 1363
clinical features, 728–729
diagnosis, 731–732
imaging, 729
immunohistochemistry, 731
overview, 728
pathology, 729–731
versus SNUC, 380
treatment, 731–733
ultrastructure, 731
OLP. *See* Oral lichen planus (OLP)
"On again–off again" symptoms, NARES, 347
ONB. *See* Olfactory neuroblastoma (ONB); Olfactory neuroblastoma (ONB)
ONB vs ES/PNET, 732
ONB vs SNUC, 732
Oncocytic carcinoma, 573–574
Oncocytic cysts, 117
Oncocytic lesions, 168, 482–483
Oncocytic neoplasms, 9
Oncocytic schneiderian papilloma (OSP), 369–371
carcinomas and, 370–371
incidence of HPV in, 370
Oncocytic tumors, 389–390
Oncocytoma, 30
Oncogenic viruses, ora cancer, 288
Onion skinning. *See* Proliferative periostitis
OPG. *See* Orbital paragangliomas (OPG); Osteoprotegerin (OPG) and osteoclastogenesis
Ophthalmoscopy, 78
Optic nerve glioma (juvenile pilocytic astrocytoma), 1601–1602
Optic nerve neoplasms, 1601–1602
Oral cancer. *See also* Squamous cell carcinomas
altered immunity, 289
clinicopathologic consideration, 290
dental factors and chronic inflammation, 288–289
epidemiology/etiology, 385–389
risk factors, 386–389
incidence
in South Asia, 287
in United States, 286
molecular biology/genetics, 289–290

[Oral cancer]
nutritional deficiencies, 289
TNM—staging system for, 291
Oral candidiasis (OC), 1645
Oral cavity, 59–63
anatomy, 285
developmental and/or congenital lesions, 1343
hematolymphoid neoplasms, 1088–1094
malignant oral lesions, 61–63
mucocele of lip and ranulas, 1343
oral lesions, 59–61
overviews, 59
squamous cell carcinomas of, 292–301
Oral hairy leukoplakia, 210–211, 1669–1670
clinical features, 210–211
electron microscopy, 211
pathology, 211
treatment, 211
Oral lesions, ulcerations, 59–61
Oral lichen planus (OLP), 254
Oral malignant melanomas, 323–326
clinical features, 324
pathology, 324–325
treatment and prognosis, 325–326
Oral melanocytic nevi, 203–204
Oral radiation, 59
Oral soft tissue metastases, 1156–1157
Oral squamous cell carcinoma (OSCC), 267
Oral submucous fibrosis (OSF), 278–279
Oral tongue, squamous cell carcinomas, 295–298
Orbit
anatomy, 1595–1596
extramedullary hematopoiesis in, 1027
malformations
dermoid cysts, 1596
inflammation, 1598
lymphatic malformation (lymphangioma), 1597–1598
venous malformation (cavernous hemangioma), 1596–1597
melanomas involving, 1603
metastases to, 1603
specimen handling, 1596
Orbital cytology, 70
Orbital meningiomas, 702
Orbital paragangliomas (OPG), 724
Orbital teratomas, 77
Orbital tumors, 1728
ORN. *See* Osteoradionecrosis (ORN)
Orofacial TB, 1622
Oropharyngeal cancer, TNM—staging system for, 292
Oropharyngeal wall, squamous cell carcinomas, 303
Oropharynx
anatomy, 285
hematolymphoid neoplasms, 1088–1094
squamous cell carcinomas of, 301–305
OSCC. *See* Oral squamous cell carcinoma (OSCC)
OSF. *See* Oral submucous fibrosis (OSF)
Osler-Rendu-Weber syndrome, 1523
Osseous and cartilaginous choristomas
clinical findings, 823
differential diagnosis, 824
imaging, 823
immunohistochemistry, 824
pathologic findings, 823
prognosis and treatment, 822, 824
radiologic imaging, 823
Osseous labyrinth, 425
Osseous metaplasia, of the retinal pigment epithelium (RPE), 1582
Ossifying fibroma, 970–971
Osteitis deformans. *See* Paget's disease
Osteoarthritis, 958
Osteoblastoma, 969–970
Osteoblasts, 959, 965
Osteochondroma, 968
Osteoclasts, 959
Osteoclasts-like giant cells, 979
Osteoid, 972
osteoma, 968–969
Osteoma, 967
Osteomyelitis, 958–960
Osteonecrosis, 958
Osteoprotegerin (OPG) and osteoclastogenesis, 1212
Osteoradionecrosis (ORN)
fibrosis, 961
persistent carcinoma, 961
radiation damages, 960
treatment, 961
wound-healing defect, 961
Osteosarcoma, 57
extragnathic, 972–973
extraosseous, 974
gnathic, 971–972
paget's disease, 963, 974
parosteal, 973
radiation-associated, 974
secondary, 974
syndrome-associated, 974
telangiectatic, 973–974
Otic polyps, inflammatory, 431
Otitis externa, 1611
Otitis media, 428–429, 1611–1612
in children, 958
Otosclerosis, 444–445
Overgrowth syndromes, 1344
Owen, Sir Richard, 1429
Oxalosis
pathologic features, 954
radiologic features, 954
Oxyphil cells, of parathyroid glands, 1432–1433, 1435
Oxyphilic adenomas, 1448
Oxyphil-rich carcinomas, 1450

PA. *See* Pleomorphic adenoma (PA)
PABA. *See* Para-aminobenzoic acid (PABA)
Paget's disease, 963–964
of bone, 445
Palatal cysts, 1343
Palatine tonsils
reactive follicular hyperplasia of, 1001–1003
squamous cell carcinomas, 303–305
Palpation thyroiditis, 1392
PAN. *See* Polyarteritis nodosa
Pancytokeratin, 973
Paneth cells, in intestinal-type adenocarcinomas, 386
Panhypopituitarism, 717
PAP. *See* Prostate acid phosphatase (PAP)
Papanicolaou Society of Cytopathology (PSC), 1
Papanicolaou stain, 5, 33
Papillary adenocarcinomas, nasopharynx, 400–402
clinical features, 400–401
differential diagnosis, 401–402
immunohistochemistry, 401
pathology, 401
treatment and prognosis, 402
Papillary carcinoma, 100
Papillary cystadenocarcinoma (PCA), 29
Papillary dermal fibrosis, 1476
Papillary endothelial hyperplasia, 1357
clinical features, 774
differential diagnosis, 776
immunohistochemistry, 776
pathologic findings, 774–775
prognosis and treatment, 776
ultrastructure, 775
Papillary keratosis. *See* Keratinized papilloma
Papillary squamous carcinomas, 316–318
Papillary squamous cell carcinoma (PSCC), 153–155
Papillary thyroid carcinoma (PTC), 4, 9–11, 1352
clinical features, 1393
differential diagnosis, 1399–1400
immunohistochemical markers, 1399
lipomatous stroma with, 1399
with nodular fasciitis like stroma, 1399
pathology, 1393–1394
RET/PTC rearrangement, genetic alteration in, 1399
treatment and prognosis, 1400
variants of, 11–13, 1395
clear cell, 1399
cribriform-morular, 1398–1399
diffuse sclerosing, 1397
follicular, 1396–1397
oxyphilic (oncocytic/Hurthle cell), 1398
solid, 1397–1398
tall cell, 1397
Warthin-like, 1398
Papilliferous keratoameloblastoma, 1226–1227
Papillomas, 119–124, 215–216, 1676
clinical features, 215
diagnosis, 215–216
keratinized, 123–124
nonkeratinized. *See* Recurrent respiratory papillomatosis (RRP)
pathology, 215
treatment, 216
Papulomatosis, 1675–1677
Para-aminobenzoic acid (PABA), 280
Paracoccidioidomycosis, 1648
Paracortex
lymphoid cells in, 997
reactive paracortical hyperplasia, 999–1000
Paragangliomas (PGL), 67–68, 167
CBPG, 718–721
genetics, 718
imaging, 717–718
immunohistochemistry, 718
JTPG, 721–722
LPG, 723–724
OPG, 724
overview, 717
pathology, 718
SNPG, 724–725
terminology, 717
TPG, 725
VPG, 722–723
Paramyxoviral transcripts, in osteoclasts, 963
Paranasal sinuses. *See also* Nasal cavity sinuses
hematolymphoid neoplasms of, 1081–1086
metastases to, 402
Paranasal sinus mucoceles, 64
Paraneoplastic pemphigus (PNP), 246–248
diagnosis, 248
immunology, 247–248
immunopathology, 247
pathology, 247
Paraneurofibroma. *See* Diffuse neurofibroma (DNF)
Parapharyngeal meningiomas, 702
Parapharyngeal neurofibromas, 682
Parathyroid aspirates, 1441

Parathyroid cysts
clinical features, 1456
differential diagnosis, 1457
molecular biology, 1457
pathologic features, 1456–1457
treatment and prognosis, 1457
Parathyroid embryogenesis, 1429
Parathyroid glands, 19, 104–105
Parathyroid glands, normal
anatomy, 1429–1430
microscopic, 1431–1433
ultrastructural, 1433
distribution of, 1430
embryology, 1429
fat surrounding, 1430
gross appearance, 1430
histochemistry/immunohistochemistry, 1433–1435
molecular biology, 1435
physiology and biochemistry, 1435–1437
receptors, 1435
stroma of, 1431
venous drainage, 1430
weight distribution, 1430
Parathyroid hormone (PTH), 1429. *See also* Primary hyperparathyroidism
action on renal tubular cells, 1436
analytic methods for, 1436–1437
Parathyromatosis, 1454
Parenchyma, 669
Parenchymal cells, 669
Parkes-Weber syndrome, 1523
Parosteal osteosarcoma, 973
PAS. *See* Periodic acid-Schiff (PAS); Periodic acid-Schiff (PAS)
Patched (PTCH) gene underexpression in ameloblastomas, 1213
Patch KS, 1660
Pathogens, in infectious rhinosinusitis, 345
Pathologic examination, in hyperparathyroidism, 1443–1445
Paul-Bunnell IgM test, 1666
PBCD. *See* Posterior buccal cortical defect(PBCD)
PCA. *See* Papillary cystadenocarcinoma (PCA)
PCNA. *See* Proliferating cell nuclear antigen (PCNA)
PCNA L.I. and calcifying odontogenic cyst (COC), 1265
PCR studies, 40
PD-ECGF/TP. *See* Thymidine phosphorylase (PD-ECGF/TP) expression and stroma of ameloblastomas
PDS. *See* Pendred's syndrome (PDS)
Pearly penile papule. *See* Fibrous papules (FPs)
Pemphigoid, 248–250
bullous pemphigoid, 248–249
mucous membrane MMP, 249–251
Pemphigus, 243–248
drug induced, 248
paraneoplastic pemphigus, 246–248
vegetans, 246
vulgaris, 243–246
Pemphigus vegetans, 246
Pemphigus vulgaris (PV), 59, 243–246
clinical presentation, 243–244
immunology, 246
immunopathology, 245–246
overviews, 243
pathology, 244–245
treatment, 246
Pendred's syndrome (PDS), 1391
Penicillins, 1621, 1691
Penicillium marneffei, 1013
Pentoxifyline, 1693
PERAM. *See* Solid/multicystic ameloblastoma-peripheral (PERAM)
Perchlorate antithyroid drugs, 1386
Perineurioma, 696–698
Periodic acid-Schiff (PAS), 60, 253, 670
Peripheral eosinophilia, 658
Peripheral nerves, 100
Peripheral nerve sheath tumors
acoustic neuromas, 691–692
DNF, 686–687
GCT, 698–701
mucosal neuromas, 692–694
neurofibroma, 681–683
neurothekeoma, 694–696
NF1, 687–689
NF2, 689–691
perineurioma, 696–698
PNF, 683–686
schwannoma, 678–681
Peripheral odontogenic fibroma (POF)
differential diagnosis, 1281
immunohistochemistry, 1281
local surgical excision, 1281
pathology, 1280–1281
prevalence and incidence, 1280
ultrastructure of, 1281
Peripheral T-cell lymphoma, 1064–1065
Peritonsillar abscess, 225, 1610
Periungual fibroma. *See* Fibrous papules (FPs)
PET. *See* Positron emission tomography (PET)
PGL. *See* Paragangliomas (PGL)
Phacoanaphylactic endophthalmitis, 73, 1576
Phacolytic cells, 73
Phaeohyphomycosis, 1639
Phakomatous choristoma, 1367–1368
Pharyngeal hypophysis, 708
Pharyngoesophageal diverticulum (PED), 1720–1721
Pharyngoesophageal (Zenker's) diverticulum
clinical features, 1720–1721
pathology, 1719–1720
treatment and prognosis, 1721
Phenylbutazone antithyroid drugs, 1386
Phenytoin, 217
therapeutic agents, 1344
Phosphate-binding agents, 1456
Phospho-retinoblastoma protein (pRb) immunohistochemistry, 1453
Phosphotungstic acid–hematoxylin (PTAH), 1433
Photodynamic therapy, 275, 1488
Phthisical eye, 1583
Phthisis bulbi
clinical features, 1579
pathology, 1579–1582
Pigmented congenital epulis. *See* Melanocytic neuroectodermal tumor of infancy (MNTI)
Pigmented hidrocystomas, 1485
Pigmented villonodular synovitis (PVNS)
immunohistochemistry, 956–57
pathologic features, 956
radiologic features, 956
Pilar cysts (PC), 1342
clinical features, 1477
differential diagnosis, 1478
electron microscopy, 1478
imaging studies, 1477
immunohistochemical studies, 1478
molecular-genetic data, 1478
pathology, 1477–1478
treatment and prognosis, 1478
Pilomatricoma
clinical features, 1480
differential diagnosis, 1481
electron microscopy, 1480
imaging studies, 1480
immunohistochemistry, 1480
molecular genetic data, 1481
pathology, 1480
treatment and prognosis, 1481
Pilomatrixoma, 26, 74
from neck, 1342–1343
Pinna, squamous cell carcinomas of, 460–462
PIOSCC. *See* Primary intraosseous squamous cell carcinoma (PIOSCC)
Piperacillin, 1612
Pituitary adenomas
clinical features, 708–709
diagnosis, 712
imaging, 709–710
incidental, 709
overview, 708
pathogenesis, 714
pathology, 710–712
treatment, 712–713
Pituitary carcinoma, 713
Pituitary gland, 708
Plasmablastic lymphoma, 1042–1042
Plasma cells, 952
Plasmacytoma, 1108
extramedullary, 1057–1059
Platelet-derived growth factor (PDG) expression and stroma of ameloblastomas, 1211–1212
PLCD. *See* Posterior lingual cortical defect (PLCD)
Pleomorphic adenoma (PA), 33–37, 74–75, 168, 389, 511–519, 1722
cellular PA, 34–35
clinical features, 512–513
differential diagnosis, 518–519
hyaline PA, 35–36
immunohistochemistry, 517–518
myoepithelioma, 36
pathology, 513–517
spindle cell lesions, 35
vs. low grade malignancies, 36–37
Pleomorphic cells, 28
Pleomorphic liposarcoma, 884
Pleomorphic RMS, 869, 873
Pleomorphic sarcoma NOS. *See* Storiform pleomorphic malignant fibrous histiocytoma
Pleomorphic sarcomas, 57
Plexiform neurofibroma (PNF), 677, 683–686, 1363
and parotid gland, 1365
Plexiform schwannomas, 680
PLGA. *See* Polymorphous low-grade adenocarcinoma (PLGA)
Plummer-Vinson syndrome (PVS), 175
PMML. *See* Malignant melanomas
Pneumocystis carinii, 430
Pneumocystosis, 1658–1659
Pneumonia, interstitial giant cell pneumonia, 1685
PNF. *See* Plexiform neurofibroma (PNF)
Podoplanin, immunohistochemical stain, 984
POF. *See* Peripheral odontogenic fibroma (POF)
Polyarteritis nodosa (PAN), 655, 656–657
clinical features, 656–657
pathology, 657
treatment and prospect, 657
Polychondritis,relapsing, 440–442
Polyclonal carcinoembryonic antigen (CEA) immunoreactivity, 1386

Polycystic disease, of salivary glands, 478
Polygonal cell sarcomas, 55–56
Polyhydraminios, 1364–1365
Polymethylmethacrylate (PMMA), 1576
Polymicrobial infections, 958
Polymorphous low-grade adenocarcinoma, 557–561
Polymorphous low-grade adenocarcinoma (PLGA), 26, 27, 63
Polyostotic fibrous dyspalsia, 965
Polypoid nasal mass, 672
Pompe disease, 1392
Poorly differentiated carcinoma
  clinical features, 1406
  pathology, 1406
  TP53 and *BRAF* mutations, 1407
  treatment and prognosis, 1407
Positron emission tomography (PET), 1
Postcricoid carcinoma, 176–177
Posterior buccal cortical defect(PBCD), 963
Posterior hypopharyngeal wall carcinoma, 176
Posterior lingual cortical defect (PLCD), 962–963
Postpartum thyroiditis, 1389
Posttransplant lymphoproliferative disorders, 1073, 1667
Postvaccination fatal disseminated infection, 1686
Potassium iodide, 1638
Pouch–derived cysts, 1457
P53 protein
  and AOT, 1238
  p53 mutations in ameloblastomas, 1211
PR. *See* Progesterone receptor (PR)
PR3. *See* Proteinase 3
Prasad's microstaging, mucosal malignant melanomas, 394
Precancerous keratosis. *See* Actinic keratoses (AKs)
Pregnancy, rhinosinusitis during, 347
Primary acquired melanosis, 1561
Primary bone lymphoma, 1108–1109
Primary ciliary dyskinesia (PCD), 351–352
Primary cutaneous CD8+ aggressive epidermotropic cytotoxic T-cell lymphoma, 1071–1072
Primary cutaneous CD4+ small/medium T-cell lymphoma, 1071
Primary cutaneous CD30+ T-cell lymphoproliferative disorders, 1068–1069
Primary cutaneous DLBCL, leg-type, 1110–1111
Primary cutaneous follicle center lymphoma, 1050, 1109–1110
Primary cutaneous MALT lymphoma, 1111
Primary effusion lymphoma, 1044
Primary follicular lymphoma of thyroid, 1101
Primary herpetic stomatitis, 59
Primary hyperparathyroidism
  clinical differential diagnosis, 1438
  clinical presentation, 1438–1439
  definition, 1437
  epidemiology, 1437–1438
  FNA cytology, 1440–1442
  imaging studies, 1439–1440
  preoperative localization, 1439–1442
  selective venous sampling (SVS) for PTH levels, 1440
  treatment and prognosis, 1455–1456
Primary intraosseous squamous cell carcinoma (PIOSCC), 1235, 1297
  frequency, 1298
  histomorphology of, 1298
  immunohistochemistry, 1299
[Primary intraosseous squamous cell carcinoma (PIOSCC)]
  molecular-genetic data, 1299
  radiograms, 1298
  treatment and prognosis, 1299
Primary lymphomas and plasmacytomas, 1414–1415
Primary malignant melanoma of the larynx (PMML). *See* Malignant melanomas
Primary oral CD30+ T-cell lymphoproliferative disorders, 1069
Primary small cell carcinoma, 25–26
Primary systemic amyloidosis, 1391
Priming, 649
Primitive neuroectodermal tumors (PNET), 1503
Procainamide, 252
Progesterone receptor (PR), 31
Progressive transformation of germinal centers (PTGC), 1004–1005
Proliferating cell nuclear antigen (PCNA), 697
Proliferating follicular-cystic neoplasm. *See* Proliferating pilar cyst (PPC)
Proliferating pilar cyst (PPC)
  clinical features, 1478
  differential diagnosis, 1479
  genetic association, 1479
  imaging studies, 1478
  immunohistochemical studies, 1479
  pathology, 1478–1479
  treatment and prognosis, 1479
Proliferating tricholemmal cyst. *See* Proliferating pilar cyst (PPC)
Proliferative myositis, 54
Proliferative myositis/fasciitis and atypical decubital fibroplasia (ischemic fasciitis)
  differential diagnosis, 817–818
  electron microscopy, 817
  immunohistochemistry, 816
  molecular, 817
  pathologic findings, 816
  prognosis and treatment, 818
  radiologic imaging, 815–816
Proliferative periostitis, 960
Proliferative verrucous leukoplakia (PVL), 275
Proptosis, 1596
Propylthiouracil antithyroid drugs, 1386
Prosecretory granules, 1433
Prostate acid phosphatase (PAP), 31
Prostate-specific antigen (PSA), 31
Proteinase 3 (PR3), 650
Proteus syndrome, 1523
Pruritus, 248
Prussak's space, 436
PSA. *See* Prostate-specific antigen (PSA)
Psammoma bodies, 10
PSC. *See* Papanicolaou Society of Cytopathology (PSC)
PSCC. *See* Papillary squamous cell carcinoma (PSCC)
Pseudoallescheriasis, 1637–1638
Pseudoepitheliomatous hyperplasia, 1345
Pseudogout, 442–443. *See also* Calcium pyrophosphate crystal deposition disease (CPCDD)
Pseudohyperparathyroidism
  clinical features, 1460
  differential diagnosis, 1460
  gene alterations in, 1461
  molecular biology, 1461
  pathologic features, 1460
  treatment and prognosis, 1461
Pseudolymphoma, cutaneous, 1112
Pseudomonas aeruginosa, 1609
Pseudophakia, 1565–1566
Pseudovasculitis, 660
Psoralen and ultraviolet light A (PUVA), 257
Pterygium, 1573–1574
PTGC. *See* Progressive transformation of germinal centers (PTGC)
PT stage grouping, 98
Pulmonary cryptococcosis, 1652
Pulsion diverticula, 1720
PUVA. *See* Psoralen and ultraviolet light A (PUVA)
PV. *See* Pemphigus vulgaris (PV)
PVL. *See* Proliferative verrucous leukoplakia (PVL)
PVNS. *See* Pigmented villonodular synovitis (PVNS)
Pyogenic bacterial infections, 1013
Pyogenic granuloma. *See* Lobular capillary hemangioma; Lobular capillary hemangioma (LCH)
Pyriform sinus carcinoma, 175–176
Pyrimethamine, 1689

QPTH. *See* Quick parathyroid hormone (QPTH)
QuantiFERON-TB Gold, 1623
Quick parathyroid hormone (QPTH), 104
Quinidine, 252
Quinolones, 1691

Radiation-associated osteosarcomas, 974
Radiation therapy, 14, 31, 976
Radiography, FD, 964
RANKL. *See* Receptor activator of nuclear factor-kB ligand (RANKL) and osteoclastogenesis
RAS. *See* Recurrent aphthous stomatitis (RAS)
RCC. *See* Renal cell carcinoma (RCC)
Reactive follicular hyperplasia, 997–999
  versus follicular lymphoma, 1051
  monocytoid B cells in, 999
  of palatine tonsils, 1001–1003
Reactive/inflammatory hematolymphoid lesions
  of eyes and ocular adnexa, 1105–1107
  of skin, 1112–1113
  of thyroid, 1101–1102
Reactive lymphoid hyperplasia, 49–50
  of extranodal sites, 1001
  nonspecific, 997–1003
  specific, 1003–1029
  of tonsil, 1002, 1003
Reactive paracortical hyperplasia, 999–1000
Reactive periostitis, BPOP, and turret exostosis
  clinical findings, 818
  differential diagnosis, 818
  immunohistochemistry, 818
  pathologic findings, 818
  prognosis and treatment, 818
  radiologic imaging, 818
Receptor activator of nuclear factor-kB ligand (RANKL) and osteoclastogenesis, 1212
Recurrent aphthous stomatitis (RAS), 261–263
  diagnosis, 262
  etiology, 261
  immunopathology, 262
  pathology, 262
  treatment, 263
Recurrent laryngeal nerve paralysis, 1721
Recurrent parotitis, 494–495

Recurrent respiratory papillomatosis (RRP), 119–123
clinical features, 120
etiology, 119–120
immunohistochemistry, 122
molecular-genetic data, 122
pathology, 121–122
terminology, 119
treatment, 122–123
Reed-Sternberg cells, 44
classical Hodgkin lymphoma, 1032–1035
in cytomegalovirus lymphadenitis, 1008
in infectious mononucleosis, 1007
in Kimura disease, 1018
Regaud type, 1355
Reiter's syndrome, 261
Relapsing polychondritis, 440–442, 961
ANCA titers in, 441
Renal cell carcinoma (RCC), 9, 16, 1459, 1729
Renal cell-like sinonasal adenocarcinoma (RCSA), 1729
Renal disease, 253
Resection margins, 144
Respiratory epithelial adenomatoid hamartomas, 360–361
Retention cyst, 21
Retina
anatomy, 1591
retinoblastoma, 1592–1595
specimen handling, 1592
Retinal anlage tumor. *See* Melanocytic neuroectodermal tumor of infancy (MNTI)
Retinal pigment epithelium (RPE), 1580
Retinoblastoma, 77–78
clinical features, 1592–1593
pathology, 1593–1594
treatment, 1594
Retinoblastoma (RB) tumor suppressor gene in ameloblastomas, 1211
Retinocytoma, 1594
Retinoids, 1678
Retromolar trigone (RMT), squamous cell carcinomas, 301–302
Rhabdoid meningioma, 706
Rhabdomyoblasts, 726
in malignant triton tumor, 893
Rhabdomyoma, 54, 60
clinical features, 798–799
differential diagnosis, 801–802
imaging, 799
immunohistochemistry, 800–801
molecular findings, 801
pathology, 799–800
treatment and prognosis, 802
Rhabdomyomatous mesenchymal hamartoma, 1362
Rhabdomyosarcoma (RMS), 869–876, 1603
nasal polyps, 349–350
Rheumatoid arthritis, 1013–1014
ear, 953
larynx, 953
nasal septum, 953
pathologic features, 952–953
temporomandibular joint, 953
Rhinophyma
clinical features, 1532–1533
defined, 1532
differential diagnosis, 1533
immunohistochemistry, 1533
molecular genetics, 1533
pathology, 1533
treatment and prognosis, 1533–1534
Rhinoscleroma, 64, 1691
clinical features, 1619
clinicopathological stages, 1619
differential diagnosis, 1620
[Rhinoscleroma]
epidemiology, 1618–1619
histopathology, 1619–1620
immunological considerations, 1619
nasal cavity, 1085
treatment, 1620
Rhinosinusitis, 343
in adults, classification, 344
allergic, 343–345
atrophic. *See* Atrophic rhinosinusitis (ARS)
complications, 343–348
factitial, 348
idiopathic, 348
infectious, 345
occupational-environmental, 347
pathology, 343
during pregnancy, 347
signs and symptoms, 344
structural-mechanical, 347
systemic causes, 348
vasomotor, 345–346
Rhinosinusitis medicamentosa, 347
Rhinosporidiosis, 1642–1643
Rhizopus, 1637
Riedel thyroiditis, 1388–1390
Rifampin, 1627
Rituximab, for DLBCL, 1045
RMS. *See* Rhabdomyosarcoma (RMS)
RMT. *See* Retromolar trigone (RMT)
Robinson type lesion, 1484
Romanowsky-type stains, 41
Rosacea
clinical features, 1532–1533
defined, 1532
differential diagnosis, 1533
immunohistochemistry, 1533
molecular genetics, 1533
pathology, 1533
treatment and prognosis, 1533–1534
Rosai-Dorfman disease, 51–52, 439, 1023–1024. *See also* Sinus, histiocytosis with lymphadenopathy
of nasal cavity, 1083–1085
of skin, 1113, 1114
Round cell liposarcoma, 881, 882
Round cell sarcomas, 54–55
Rovamycin, 1689
RRP. *See* Recurrent respiratory papillomatosis (RRP)
Rudimentary lumen formation, 865
Rudimentary meningocele, 1349–1350

Sabin Feldman Dye test, 1688
Saccular cysts, 116
Sac papillary tumor, endolymphatic, 457–458
Saksenea vasoformis, 1638
Salivary duct carcinoma (SDC), 28–29, 574–578
Salivary duct cysts, 481
Salivary gland anlage tumor, 1350
Salivary gland heterotopias, 1352
Bartonella henselae causative organism, 1354
mycobacterial and Bartonella (cat scratch disease) infection, 1353
Salivary gland neoplasm
with besaloid cell, 23–26
adenoid cystic carcinoma, 24–25
basal cell adenocarcinoma, 25
basal cell adenoma, 23–24
pilomatrixoma, 26
primary small cell carcinoma, 25–26
challenges, diagnosis, 22–23
by large cells, 28–32
acinic cell carcinoma, 29–30
clear cell change, 31–32
high-grade MEC, 28
[Salivary gland neoplasm]
[by large cells]
metastatic malignancies, 31
oncocytoma, 30
radiation therapy, 31
salivary duct carcinoma, 28–29
Warthin tumor, 30–31
Salivary glands, 20–37, 101–103
aplasia, 476–477
choristomas, 427
cystic fibrosis, 478–479
cystic lesions, 21–22
cysts
LEC, 481–482
mucoceles, 480–481
salivary duct cysts, 481
functional unit, 475
hematolymphoid neoplasms, 1094–1099
heterotopia, 477–478
HIV-associated lymphoid hyperplasia in, 1010
hyperplasia, 500
infiltrations
amyloidosis, 484
iron deposition, 484
lipomatosis, 482
oncocytic lesions, 482–483
lesions, 63
nonneoplastic salivary gland lesions, 20–21
parotid gland, 475
sebaceous glands, 475, 479–480
sialadenitis. *See* Sialadenitis
submandibular gland, 475–476
tumors. *See* Tumors
Salivary gland tumors, 26–28, 70
lesions containing squamous cells, 27–28
low-grade MEC, 26
in lymphocytes, 32–33
polymorphous low-grade adenocarcinoma, 27
Salivary gland-type neoplasms, 167–170
adenoid cystic carcinoma (ACC), 168–169
mucoepidermoid carcinoma (MEC), 169
oncocytic lesions, 168
overviews, 167–168
pleomorphic adenoma, 168
Salivary-type neoplasms, 389–391
Samter's triad, 346–347
Sarcoid granulomas, 1693
Sarcoidosis, 50, 73, 1354, 1438
causes, 1692–1693
clinical features, 1691–1692
diagnosis, 1693
histopathology, 1693
predispositions, 1691
treatment, 1693
Sarcomas, 52–59, 63
ancillary studies, diagnosis, 53–54
of larynx, 173–174
overviews, 52–53
soft tissue lesions, 54
soft tissue sarcomas, in head and neck region, 54–59
Sarcomatoid carcinoma. *See* Spindlecell carcinomas (SPCC)
Sarcomatoid SCC, 1492
SCC. *See* Squamous cell carcinoma (SCC)
Schistosoma, 1638
Schneiderian mucosa, 1609
Schneiderian papillomas, 361–371
exophytic papillomas, 362–363
frequency of, 362
inverted papilloma. *See* Inverted papilloma
oncocytic schneiderian papilloma (OSP), 369–371
Schopf-Schulz-Passarge syndrome, 1484
Schwann cells, 678

Schwannoma, 75, 678–681, 1363–1365
SCLE. *See* Subacute cutaneous lupus erythematosus (SCLE)
Sclerosing epithelioid fibrosarcoma, 886, 887
Sclerosing mucoepidermoid carcinoma with eosinophilia, 1412
Sclerosing polycystic adenosis, 497–499
Sclerosing sweat duct carcinoma. *See* Microcystic adnexal carcinoma (MAC)
Sclerosing type BCC, 1496
SCNEC. *See* Small cell neuroendocrine carcinomas (SCNEC)
Scrofula, 1623
SDC. *See* Salivary duct carcinoma (SDC)
Sebaceous adenoma (SA), 32, 532–533, 1554
  clinical features, 1488
  differential diagnosis, 1489
  immunohistochemistry, 1489
  molecular genetics, 1489
  pathology, 1488
  treatment and prognosis, 1489
Sebaceous carcinoma, 32, 76–77, 567–568, 1554–1556
Sebaceous differentiation, of salivary glands, 479–480
Sebaceous hyperplasia (SH), 1482
  clinical features, 1487
  differential diagnosis, 1488
  immunohistochemistry, 1487
  molecular genetics, 1487–1488
  pathology, 1487
  treatment and prognosis, 1488
Sebaceous lymphadenocarcinoma, 568
Sebaceous trichofolliculoma, 1488
Seborrheic keratoses (SK)
  associated syndromes, 1477
  clinical features, 1475
  differential diagnosis, 1476–1477
  imaging studies of, 1475
  immunohistochemical studies, 1475
  treatment and prognosis, 1477
Secondary (dedifferentiated) AMCA, 1295
  etiology of, 1296
  histochemical study, 1296
  molecular-genetic data, 1296
  radical surgical resection, 1296
Secondary (dedifferentiated) peripheral (arising in preexisting benign ameloblastoma), 1296
  clinical features, 1297
  differential diagnosis, 1297
  etiology of, 1297
  radiograms, 1297
  treatment and prognosis, 1297
Secondary hyperparathyroidism
  clinical presentation, 1442
  definition, 1442
  epidemiology, 1442
  imaging studies, 1442–1443
  preoperative localization, 1442–1443
  selective venous sampling, 1443
  treatment and prognosis
    standard medical therapy, 1456
    surgical management, 1456
Secondary malignancies, of eyes, 1603
Secondary osteosarcoma, 974
Secretory meningioma, 705
Selective neck dissection (SND), 1135
Senile keratosis. *See* Actinic keratoses (AKs)
Sentinel lymph node (SLN), 101, 1137
Serous otitis media (otitis media with effusion), 1612
Serum calcitonin analysis, 1150
SETTLE. *See* Spindle epithelial tumor with thymus-like differentiation (SETTLE)
Severe chronic active EBV infection, 1667
Severe dysplasia, 269
Sézary syndrome, 1070–1071
Sheathlin and calcifying odontogenic cyst (COC), 1265
Short tau inversion recovery (STIR) sequences, 1518
Sialadenitis, 20–21
  acute suppurative sialadenitis, 484–485
  cheilitis glandularis, 490–491
  chronic, 21, 33
  chronic sclerosing sialadenitis, 486–489
  cytomegalovirus, 495–497
  mumps, 495
  necrotizing sialometaplasia, 491–493
  obstructive sialadenitis, 485–486
  radiation sialadenitis, 489–490
  recurrent parotitis, 494–495
  subacute necrotizing sialadenitis, 493
Sialoadenitis, chronic, 102
Sialoblastoma, 595–596
Sialometaplasia, 102
Sialosis, 20, 499–500
Sincipital encephaloceles, 674
Sinonasal adenocarcinoma, 67
Sinonasal fungal disease
  alternaria, 1640
  aspergillosis, 1629–1632
  bipolaris and exserohilum, 1639–1640
  blastomycosis, 1642
  cladosporium, 1640–1641
  clinicopathological classifications, 1628–1629
  cryptococcosis, 1642
  curvularia, 1640
  fungus ball/mycetoma, 1632–1634
  hyalohyphomycosis, 1641
  mucormycosis and entomophthoromycosis, 1634–1637
  myospherulosis, 1643–1644
  phaeohyphomycosis, 1639
  pseudoallescheriasis, 1637–1638
  rhinosporidiosis, 1642–1643
  sporotrichosis, 1641–1642
Sinonasal hemangiopericytoma, 64
  clinical features, 850
  immunohistochemistry, 850
  molecular findings, 850
  pathology, 850
  treatment and prognosis, 850
Sinonasal leiomyosarcoma, 876
Sinonasal neuroendocrine carcinoma, 67
Sinonasal NK/T-Cell lymphoma, 1670–1671
Sinonasal paragangliomas (SNPG), 724–725
Sinonasal polyposis, 1610
Sinonasal polyps, 674
Sinonasal tumors, cytokeratin expression, 379
Sinonasal undifferentiated carcinoma (SNUC), 731
Sinonasal undifferentiated carcinomas (SNUC), 66–67, 377–380
  histogenesis, 378
Sinuses, 1351
  histiocytosis with lymphadenopathy, 1415
  vascular transformation of, 1005–1006
Sinus histiocytosis, 1000–1001
  with massive lymphadenopathy, 1023–1024
Sinusitis
  acute bacterial, 345
  chronic, 345
Sjögren's syndrome, 32, 1014, 1660
SJS. *See* Stevens–Johnson syndrome (SJS)
Skeletal muscle hemangioma, 1356
Skin
  epidermal and cutaneous adnexal lesions, 1341–1342
[Skin]
  hematolymphoid lesions of, 1109–1115
    diagnostic considerations, 1113–1115
    neoplasms, 1109–1112
    reactive/inflammatory, 1112–1113
  pigmented lesions, 1339–1341
  tag, 1352. *See also* Branchial cleft cyst
Skull meningioma, 703
SLE. *See* Systemic lupus erythematosus (SLE)
SLL. *See* Small lymphocytic lymphoma (SLL)
SLN. *See* Sentinel lymph node (SLN)
Small cell carcinoma, 589–591
Small cell/mixed cell infiltrates
  diagnosis, of hematolymphoid lesions of skin, 1114–1115
Small cell neuroendocrine carcinomas (SCNEC), 166–167, 380–382
  versus SNUC, 380
Small lymphocytic lymphoma (SLL), 33, 44
Smith type lesion, 1484
Smokeless tobacco keratosis, 280–281
  clinical features, 280–281
  defined, 280
  diagnosis, 281
  pathology, 281
  treatment, 281
Smoking, oral cancer, 286–288
SND. *See* Selective neck dissection
SNPG. *See* Sinonasal paragangliomas (SNPG)
SNUC. *See* Sinonasal undifferentiated carcinoma (SNUC); Sinonasal undifferentiated carcinomas (SNUC)
Soft palate, squamous cell carcinomas, 302–303
Soft tissues
  developmental cysts of neck, 1351
  lesions, 54
  lymph node(s), 1353–1355
  metastases, 1140
  neoplasms, 1603
  perineurioma, 697
  tumors and, 1355–1367
    like lesions of, 1367
Soft tissue sarcomas, in head and neck region, 54–59
  Ewing's sarcoma, 55
  leiomyosarcomas, 58
  myxoid soft tissue sarcomas, 58–59
  osteosarcomas, 57
  pleomorphic sarcomas, 57
  polygonal cell sarcomas, 55–56
  round cell sarcomas, 54–55
  spindle cell sarcomas, 58
  synovial sarcomas, 56–57
Soft tissue tumors, of salivary gland, 598–600
  juvenile hemangioma, 600–601
  sialolipoma, 601–603
SOHLs. *See* Squamous odontogenic hamartoid lesions (SOHLs)
Solar elastosis, 1489
Solar keratosis. *See* Actinic keratoses (AKs)
Solid cell nests in thyroid, 1386
Solid/multicystic ameloblastoma–central
  etiology of
    basaloid pattern, 1206–1207
    plexiform growth pattern, 1205
  immunohistochemistry
    basement-type heparan sulfate proteoglycan (HSPG), 1209
    cell proliferation markers, 1209
    CKs and vimentin, 1208
    collagen types, 1208–1209
    extracellular matrix proteins and basement membrane, 1208

[Solid/multicystic ameloblastoma–central]
[immunohistochemistry]
integrin, 1209
laminin, 1208
mitogen-activated protein kinases (MAPKs), roles of, 1209
tenascin, 1208
prevalence and incidence
age range, 1203
frequency of, 1202–1203
location of, 1203
plexiform growth pattern, 1204
radiological appearance and, 1204
Solid/multicystic ameloblastoma–peripheral (PERAM)
CK-19 and Ber-EP4, 1217
differential diagnosis, 1217
gender distribution of, 1215
immunohistochemical studies, 1216–1217
molecular-genetic data, 1217
pathology, 1216
prevalence and incidence, 1215
radiological changes, 1216
treatment and prognosis, 1217–1218
ultrastructure of, 1217
Solid parathyroid adenomas, 19
Somatostatin analogue octreotide, 712
Sonic Hedgehog (SHH) gene underexpression in ameloblastomas, 1213
SOT. *See* Squamous odontogenic tumor (SOT)
South Asia, oral cancer incidence in, 287
SPCC. *See* Spindlecell carcinomas (SPCC)
Sphenoethmoidal, through sphenoethmoid junction, 674
Sphenomaxillary, through sphenoid, 675
Spheno-orbital though superior orbital fissure, 674
Spindle cell carcinomas (SPCC), 146–151, 318–322, 1492
clinical features, 147, 319
diagnosis, 150
etiology, 147
immunohistochemistry, 149–150
molecular genetic data, 150
overviews, 146–147
pathology, 147–149, 319–321
treatment, 150–151
treatment and prognosis, 321–322
Spindle cell lesions, 35
Spindle cell melanoma, 1509–1510
Spindle cell rhabdomyosarcoma, 871–872
Spindle cell sarcomas, 58
Spindle epithelial tumor with thymus-like differentiation (SETTLE), 1412–1413
Spindle-pleomorphic lipoma (SPL), 1728
Spitz nevus
clinical features, 1504
differential diagnosis, 1506
electron microscopy, 1506
immunohistochemistry, 1506
and melanocytic proliferation, 1340
molecular genetics, 1506
pathology, 1504–1506
treatment and prognosis, 1506–1507
Spitzoid melanoma, 1340
Sporothrix, 1638
Sporotrichosis, 1641–1642
S-100 protein, 1286, 1500, 1729
S-100 protein-positive cells, 683
Squamous carcinoma, 21–22
Squamous cell carcinoma (SCC), 588–589, 958, 1147
metastasis determinants
extracapsular spread, 1138–1140
histologic prognostic factors, 1141–1142
micrometastases, 1140–1141
positive lymph nodes, 1140
[Squamous cell carcinoma (SCC)]
[metastasis determinants]
soft tissues, 1140
stromal reactions, 1141
Squamous cell carcinomas (SCC), 46–47, 61–62, 76, 1413–1414, 1476. *See also* Oral cancer
clinical features, 1491
differential diagnosis, 1494–1495
of ear, 459–460
eyelids, 1553
of hypopharynx, 174–177
clinical features, 175–177
etiology, 175
overviews, 174
treatment, 177
keratinizing. *See* Keratinizing squamous cell carcinomas (KSCC)
of larynx, 137–145
glottic carcinoma, 139–142
laryngeal carcinoma, 144–145
molecular genetic data, 145
overviews, 137–139
subglottic carcinoma, 142–143
supraglottic carcinoma, 139
transglottic carcinoma, 143
maxillary sinuses, 374–376
T staging, 375
of middle ear, 465–466
molecular genetics, 1494
nasal cavity, 371–374
of nasopharynx, 397
nonkeratinizing. *See* Nonkeratinizing squamous cell carcinomas
oral cavity, 292–301
buccal mucosa, 294–295
floor of mouth and oral tongue, 295–298
gingiva and alveolar mucosa, 298–300
hard palate, 300–301
lip, 292–294
oropharynx, 301–305
oropharyngeal wall, 303
palatine tonsils and base of tongue, 303–305
retromolar trigone (RMT), 301–302
soft palate and uvula, 302–303
pathology, 1492–1494
of trachea, 178
glottic carcinoma, 139–142
laryngeal carcinoma, 144–145
molecular genetic data, 145
overviews, 137–139
subglottic carcinoma, 142–143
supraglottic carcinoma, 139
transglottic carcinoma, 143
treatment and prognosis, 1495
of upper aerodigestive tract, 1459
variants, 1492–1494
Squamous eddies, 1479
Squamous intraepithelial neoplasia classification, 270
Squamous metaplasia, nasal polyps with, 368
Squamous odontogenic hamartoid lesions (SOHL), 1229
Squamous odontogenic tumor (SOT)
etiology and pathogenesis, 1228–1229
histochemical markers for, 1229
hyperplastic islands, 1229
molecular-genetic data, 1230
prevalence and incidence, 1228
radiograms of, 1228
treatment and prognosis, 1230
Stafne cyst, 962
Stapedial footplate, otosclerosis of, 445
Staphylococcus aureus, 50, 953, 1609
Sternomastoid tumor. *See* Fibromatosis colli
Steroid therapy, 254
Stevens–Johnson syndrome (SJS), 258
Stomal recurrence, 144–145
Storiform pleomorphic malignant fibrous histiocytoma, 886, 888
Stratum fibrosum externum, 672
Stratum fibrosum internum, 670
Stratum nervosum, 670
Streptococcus, 261
Streptococcus pneumoniae, 345, 429, 1392, 1609
Stromal atypia, nasal polyps, 350
Stromal dystrophies, 1570–1571
Stucco keratosis. *See* Seborrheic keratoses (SKs)
Sturge-Weber syndrome, 1523
Subacute cutaneous lupus erythematosus (SCLE), 252–253
Subacute granulomatous thyroiditis, 4
Subacute necrotizing sialadenitis, 493
Subacute sclerosing panencephalitis (SSPE), 1685
Subacute thyroiditis, 1392
Subcutaneous lymphoid infiltrate
diagnosis, of hematolymphoid lesions of skin, 1115
Subcutaneous panniculitis-like T-cell lymphoma, 1071
Subglottic carcinoma, 142–143
Subglottic stenosis, 114
Sulfodiazine, 1689
Sulfonamides, 260
Superficial extending carcinoma (SEC), 136–137
Superficial lymph nodes
lateral, 1135
medial, 1135
Supernumerary parathyroid glands, 1429, 1430
Suppurative granulomas, 1012
Suppurative lymphadenitis, 50
Suprabasal bullae formation, 244
Supraclavicular lymph node metastases, 48–49
Supraglottic carcinoma, 139
Surgical margins, 97–100
Surgical resection, of cancer, 98
Sympathetic ophthalmia, 1583–1586
Synaptophysin, 67
Syndecan-1 (SDC-1) for Wnt induced carcinogenesis, 1213
Syndrome-associated osteosarcoma, 974
Synovectomy, 956
Synovial chondromatosis
pathologic features, 955–956
radiologic features, 955
Synovial chondromatosis of temporomandibular joint, 435–436
Synovial cysts, 957
Synovial sarcomas, 56–57, 897–899, 1360
biphasic, 897
monophasic, 897
Syphilis
congenital, 1615, 1616
differential diagnosis, 1617
epidemiology and historical perspective, 1612–1613
head and neck manifestations, 1613–1614
oral manifestations, 1613
otosyphilis, 1614
primary, 1615–1616
secondary, 1616
serologic identification, 1617
and spirochetes, 1616–1617
tertiary, 1614–1615, 1616
treatment, 1617
Syphilitic (luetic) lymphadenitis, 1012
Syringocystadenoma papilliferum, ceruminal gland, 447–448

Syringomas, 1342
clinical features, 1485–1486
differential diagnosis, 1486–1487
electron microscopic studies, 1486
immunohistochemistry, 1486
molecular genetics, 1486
pathology, 1486
treatment and prognosis, 1487
Systemic lupus erythematosus (SLE), 252

Tachyzoites, 1688
Tamoxifen, 1390
Tangier disease (TD), 1730
Tapered stroma, of the ciliary body, 1587
Tartrateresistant acid phosphatase (TRAP), 557
TC. *See* Typical carcinoid (TC)
T-cell intracellular antigen (TIA)-1, 43
T-cells, 39, 257, 260
lymphoblastic leukemia/lymphoma, 1060
receptor gene, 40
rich B-cell lymphomas, 660
Teflon granulomas, 113–114, 1393
Teflon injections, 976
Teflonoma. *See* Teflon granuloma
Telangectasias, 1533
Telangiectatic osteosarcoma, 973–974
Temporal bone
benign neoplasms of, 449–456
endolymphatic sac papillary tumor, 457–458
metastases, 1157
metastatic tumors, 467
neoplastic lesions of, 446–467
benign neoplasms, 447–456
endolymphatic sac papillary tumor, 457–458
malignant neoplasms, 459–467
nonneoplastic lesions, 425–432
Temporomandibular joint (TMJ), 953
synovial chondromatosis of, 435–436
Tenascin
and calcifying odontogenic cyst (COC), 1265
CEOT, 1234
and DESAM, 1220
solid/multicystic ameloblastoma–central, 1208
Teratocarcinosarcoma, 1366
Teratoma, 1414
Terminal deoxynucleotidyl transferase biotin-dUTP-nick-end labeling (TUNEL) for apoptosis detection, 1212
Tertiary hyperparathyroidism
clinical presentation, 1442
definition, 1442
epidemiology, 1442
imaging studies, 1442–1443
preoperative localization, 1442–1443
selective venous sampling, 1443
treatment and prognosis, 1456
Tetracycline, 263
TGF-β. *See* Transforming growth factor beta (TGF-β) role in ameloblastomas
Thalidomide, 1693
Thiabendazole, 1690
Thiazide diuretics, 1438
Thiocyanate antithyroid drugs, 1386
Thorotrast granulomas
background, 1722–1723
clinical features, 1723
pathology, 1723–1724
treatment and prognosis, 1724
Thorotrast injection, 1723–1724
Thorotrast-related hepatic malignancies, 1724
Thorotrast-related neoplasms, 1723
Thymidine phosphorylase (PD-ECGF/TP) expression and stroma of ameloblastomas, 1211
Thymomas, 1724
Thyroglobulin, 1386
Thyroglossal duct cyst (TGDC), 16, 1351–1352, 1387
Thyroid, hematolymphoid lesions of, 1100–1103
diagnostic considerations, 1102–1103
neoplasms, 1100–1101
reactive/inflammatory, 1101–1102
Thyroid carcinoma, 47
Thyroid cyst fluid, 16
Thyroidectomy, 13, 15, 1429, 1432
Thyroid gland, 103–104
adequasy criteria, 2–3
clear cell lesions, 16–17
clinical implications of, 17
cystic lesions, 15–16
developmental and hereditary abnormalities
aplasia and hypoplasia, 1387
ectopic thyroid tissue, 1387
hereditary abnormalities, 1387
parasitic nodule, 1387
thyroglossal duct cyst, 1387
diagnostic accuracy, 2
diagnostic categories, 1–2
disorders
autoimmune thyroid diseases, 1390
crystals, 1393
goiters, 1390–1391
hypothyroidism, 1392–1393
infections and granulomatous diseases, 1391–1392
levothyroxine therapy, 1390
metabolic diseases, 1392
pigment deposition, 1393
teflon, 1393
drugs effects of, 1386
embryology and development, 1385–1386
follicular lesions, 6–9
invasion, 145
malignant neoplasms, 9–15
metastatic malignancies, 17–18
nonneoplastic disease, 3–6
oncocytic neoplasms, 9
overviews, 1
physiology
thyroid-stimulating hormone (TSH), 1386
thyroxine (T4) and triiodothyronine (T3), hormones, 1386
radiation changes in, 1386–1387
thyroid parenchyma, 1365
thyroid transcription factor-I (TTF-1), 1385
thyrotropin receptor gene, genetic alterations of, 1387
tumors
anaplastic carcinoma, 1407–1409
carcinoma showing thymus-like differentiation, 1413
of C Cells, 1409–1412
follicular thyroid tumors, 1402–1404
hurthle cell tumors, 1404–1406
hyalinizing trabecular tumor, 1400–1402
langerhans cell histiocytosis, 1415
mesenchymal tumors, 1415–1416
mucoepidermoid carcinoma, 1412
papillary thyroid carcinoma (PTC), 1393–1400
poorly differentiated carcinomas, 1406–1407
[Thyroid gland]
[tumors]
primary lymphomas and plasmacytomas, 1414–1415
sclerosing mucoepidermoid carcinoma with eosinophilia, 1412
sinus histiocytosis with massive lymphadenopathy, 1415
smooth muscle tumors, 1416
solitary fibrous tumor, 1415
spindle epithelial tumor with thymus-like differentiation, 1412–1413
squamous cell carcinoma, 1413–1414
teratoma, 1414
Thyroiditis, 3–4
Thyroid nodule, 1
Thyroid parangliomas (TPG), 725
Thyroid transcription factor (TTF)-1, 1503
Thyroid transcription factor-1 (TTF-1), 15
Ticarcillinclavulanate, 1611
Tissue alterations, in dysplasia, 267
Tissue culture, in cranial fasciitis, 966
Tissue eosinophilia, 658
TLA-1. *See* T-cell intracellular antigen (TIA)-1
T- lymphocytes, 952, 953
TMJ. *See* Temporomandibular joint (TMJ)
TNF-related apoptosis-related ligand (TRAIL) 1 and 2, role in ameloblastomas, 1212
TNM classification scheme, 1507–1508
Tobramycin, 1612
Tonsillar cysts, 117
Tonsillar hyperplasia, 222–225, 1610
Tonsillectomy, 1610
Tonsillitis, 222–225, 1610
clinical features, 223
overviews, 222–223
pathology, 223–224
treatment, 224–225
Tophaceous gout, 442–443
Tophus, 953
Topical 5-aminolevulinic acid-mediated photodynamic therapy, 1678
Torg syndrome, 1344
Torus mandibularis, 967
Torus palatinus, 967
Toxic multinodular goiter, 1391
Toxoplasma gondii, 50
Toxoplasmic lymphadenitis, 1012–1013
Toxoplasmosis, 50–51
clinical course, 1687–1688
epidemiology, 1687
histopathology, 1688
IHC, PCR, and serology, 1688–1689
treatment, 1689
TPG. *See* Thyroid parangliomas (TPG)
TP53 gene family in ameloblastomas, 1211
TPO. *See* Tracheopathia osteochondroplastica (TPO)
Trachea, hematolymphoid lesions of, 1100
Tracheopathia osteochondroplastica (TPO), 114–115
TRAIL/Apo2L. *See* Tumor-necrosis-factor-related apoptosis-inducing ligand (TRAIL/Apo2L) expressions and ameloblastomas
Transcription factor deficiency, 1387
Transethmoidal, through cribriform plate, 674
Transforming growth factor beta (TGF-β) role in ameloblastomas, 1211
Transglottic carcinoma, 143
Transillumination, of the eye, 1583
Transsphenoidal, through sphenoid, 675
TRAP. *See* Tartrateresistant acid phosphatase (TRAP)

Traumatic neuroma
  clinical features, 676–677
  diagnosis, 677
  histopathology, 677
  immunohistochemistry, 677
  macroscopy, 677
  overview, 676
  treatment, 677–678
  ultrastructure, 677
Traumatic retinal detachment, 1585
Treponema pallidum, 1012
Trichilemmal carcinoma (TLC), 1479
  clinical features, 1501
  differential diagnosis, 1502
  immunohistochemistry, 1502
  pathology, 1501–1502
  treatment and prognosis, 1502
Trichilemmal cyst. *See* Pilar cysts (PCs)
Trichilemmal keratinization, 1477
Trichilemmomas (TL)
  clinical features, 1481
  differential diagnosis, 1482
  imaging studies, 1481
  immunohistochemistry, 1481–1482
  molecular genetics, 1482
  pathology, 1481
  treatment and prognosis, 1482
Trichinella, 1689
Trichinosis
  clinical course, 1689
  etiology, 1689
  histopathology, 1689–1690
  serology, 1690
  treatment, 1690
Trichloracetic acid treatment, 1487
Trimethoprim sulfamethoxazole, 1691
Trimethoprin-sulfamethoxazole (TS), 655
Trousseau's sign, 1460
Trypanosome, 1654
TS. *See* Trimethoprin-sulfamethoxazole
T-SPOT-TB, 1623
T staging of squamous cell carcinomas
  external auditory canal, 462
  in maxillary sinus, 375
TTF-1. *See* Thyroid transcription factor-I (TTF-1)
Tuberculin skin test, 1623
Tuberculosis and thyroiditis, 1392
Tuberous sclerosis, 1348
Tumefactive fibroinflammatory pseudotumor, 1367
Tumoral calcinosis, 954–955
Tumor necrosis factor α(TNF-α), 655, 958
Tumor-necrosis-factor-related apoptosis-inducing ligand (TRAIL/Apo2L) expressions and ameloblastomas, 1212
Tumor-node-metastasis (TNM) staging, 1495
  malignant melanomas, 394
  for oral cavity cancer, 291
  for oropharyngeal cancer, 292
  of squamous cell carcinomas in external auditory canal, 462
Tumors
  of parapharyngeal space
    anatomy, 1721–1722
    clinical features, 1722
    histology, 1722
    pathology, 1722
    treatment and prognosis, 1722
  of parathyroid glands
    clinical features, 1461–1462
    differential diagnosis, 1462
    pathologic features, 1462
    treatment and prognosis, 1462
  ploidy, 145
  thyroid glands. *See* Thyroid gland, tumors
Tumors, of trachea, 177–178
  adenoid cystic carcinoma, 178
  anatomy, 177–178
  overviews, 177
  squamous cell carcinoma, 178
Tumors, salivary gland
  age distribution, 506
  cigarette smoking and, 506–507
  classifications, 511
  epidemiology, 505–506
  fine-needle aspiration cytology for, 508–509
  frozen section diagnosis, 509
  genetics, 510–511
  imaging procedures of, 507–508
  occupation and, 506
  radiation and, 506
  sex ratio, 506
  site, 506
  viruses and, 506
TUNEL. *See* Terminal deoxynucleotidyl transferase biotin-dUTP-nick-end labeling (TUNEL) for apoptosis detection
Turner syndrome, 1357, 1523
T1-weighted images, 980
T2-weighted images, 980
Tympanic cavity, 424
Tympanic paraganglioma, 721
Tympanosclerosis, 429–430
Typical carcinoid (TC), 162–164
  clinical features, 162–163
  diagnosis, 164
  electron microscopy, 164
  immunohistochemistry, 163–164
  pathology, 163
  treatment, 164
Tyr165Cys, 1487
Tzanck cells, 245, 262

UDCs. *See* Undifferentiated carcinomas
Ulceration, 1478
Ultrasonography, 78
Ultrasound (US), 1, 953
Ultraviolet light (UV), 252
  oral cancer, 288
Ultraviolet (UV) B radiation, 1491
UNAM. *See* Unicystic ameloblastoma (UNAM)
Undifferentiated carcinomas (UDCs), 1141
  nonkeratinizing, 308–309
  of salivary glands, 589
Undifferentiated nasopharyngeal carcinomas (UNPC), 397
  versus SNUC, 380
Unencapsulated parathyroid cells, 1431
Unicystic ameloblastoma (UNAM)
  AgNOR activity, 1224
  differential diagnosis, 1224
  etiology of, 1222–1223
  histological variants of, 1223
  immunohistochemistry, 1223–1224
  molecular-genetic data, 1224
  multilocularity and, 1222
  PCNA and Ki-67 expression, 1224
  prevalence and incidence, 1221–1222
  treatment and prognosis, 1224–1225
  type 1 (intralining) and type 2 (intraluminal), 1225
United States, oral cancer incidence in, 286
UNPC. *See* Undifferentiated nasopharyngeal carcinomas (UNPC)
Upper aerodigestive tract
  nasal cavity and nasopharynx, 1343–1351
  oral cavity and oropharynx, 1343–1348
Urbach-Wiethe syndrome. *See* Lipoid proteinosis
Uremia, 252
US. *See* Ultrasound (US)
UV. *See* Ultraviolet light (UV)
Uveal tract
  anatomy, 1586–1587
  clinical features, 1587–1588
  pathology, 1588–1591
  specimen handling, 1587–1591
UV light–induced SCCs, 1494
Uvula, squamous cell carcinomas, 302–303

Vagal paragangliomas (VPG), 722–723
Varicella Zoster virus (VZV), 1661
Vascular endothelial growth factor (VEGF) role in ameloblastomas, 1214
Vascular malformations
  clinical features, 1522
  differential diagnosis, 1522–1524
  electron microscopy, 1522
  genetics, 1522
  imaging studies, 1522
  immunohistochemistry, 1522
  pathology, 1522
  treatment and prognosis, 1524
Vascular neoplasms, in children, 1355
Vascular proliferations
  angiolymphoid hyperplasia with eosinophilia (ALHE), 1528–1529
  infantile hemangioma (IH), 1524–1526
  kaposiform hemangioendothelioma, 1526–1528
  kaposi sarcoma, 1530–1532
  syndromes associated with, 1523
  vascular malformations, 1521–1524
  vascular tumors, 1524
Vascular transformation of sinuses, 1005–1006
Vasomotor rhinosinusitis, 345–346
VCA. *See* Viral capsid antigen (VCA)
VCNP. *See* Vocal cord nodule and polyp (VCNP)
VEGF. *See* Vascular endothelial growth factor (VEGF)
Venous drainage, of parathyroids, 1430
Venous malformations, 1522
Vernal conjunctivitis, 72
Verruca vulgaris, 214–215, 1476
Verruca vulgaris of larynx (VVL), 124–125
Verruciform xanthoma, 216–217
Verrucous carcinomas, 151–153, 314–316, 1492
  clinical features, 151, 314
  diagnosis, 153
  differential diagnosis, 315–316
  etiology, 151–152
  molecular-genetic data, 152–153
  overviews, 151
  pathology, 152, 315
  treatment, 153
  treatment and prognosis, 316
  and verrucous hyperplasia, 1677–1678
Verrucous hyperplasia (VH), 1678
Versican and calcifying odontogenic cyst (COC), 1265
Vesiculoerosive lesions, 243
Vimentin antibodies
  AFOD, 1251
  and AMF, 1244
  AOT, 1238
  and (ODOMYX), 1286
Viral capsid antigen (VCA), 1150
Viral diseases, 72
Vitamin C, 1691
Vitamin D analogues, 1456

Vitamin D receptor (VDR), 1435
Vitrectomy, 70
Vocal cord nodule and polyp (VCNP), 109–111
  clinical features, 109
  diagnosis, 111
  etiology, 109
  overviews, 109
  pathology, 109–110
  treatment, 111
Vogt-Koyanagi-Harada syndrome (VKH), 1584
Von Hippel–Lindau (VHL) syndrome, 457
Vossius ring, 1586
VPG. *See* Vagal paragangliomas (VPG)
VVL. *See* Verruca vulgaris of larynx (VVL)

Waldeyer's ring, 1147
  normal lymphoid tissues of, 1001
Warthin-Starry stain, 64
Warthin's tumor, 505
  cigarette smoking and, 507
  clinical features, 526
  differential diagnosis, 529–530
  electron microscopy, 529
  etiology, 526–527
  imaging, 526
  immunohistochemistry, 529
  molecular-genetic data, 529
  overview, 526
  pathology, 527–529
  treatment, 530
Warthin tumor, 22, 30–31
Water-clear cells, 1448, 1454
WDLS. *See* Well-differentiated liposarcoma (WDLS)
Weathering nodule of the ear (WNE)
  clinical features, 1535
  differential diagnosis, 1536
  immunohistochemistry, 1536
  pathology, 1535
  treatment and prognosis, 1536
Wegener's granulomatosis (WG), 73, 443–444, 961, 1392, 1610
  clinical features, 650–652
  criteria for diagnosis, 652
  ELK classification, 654
  etiology, 649–650
  limited form of(LWG), 653–654
  nasal cavity, 1083
  pathology, 652–654
  treatment and prospect, 654–655
Well-differentiated liposarcoma (WDLS), 862
''Western'' sinonasal lymphomas, 1670
Wet keratin, 715
WG. *See* Wegener's granulomatosis
Whipple's disease, 73, 1691
White sponge nevus
  clinical features, 201–202
  diagnosis, 203
  molecular and genetic data, 203
  pathology, 202
  treatment, 203
WHO. *See* World Health Organization (WHO)
Wickham's striae, 254
Winkler disease. *See* Chondrodermatitis nodularis chronicus helicis (CNCH)
Wiskott-Aldrich syndrome (WAS), 1667
Wnt signaling pathway in ameloblastomas, 1213
World Health Organization (WHO), 37, 43, 269
  classification
    ossifying fibroma, 970
    osteosarcoma, 972
  dysplasia classification by, 269–270
  histological classification of odontogenic tumors, 1202

Xanthelasma, 1557
Xanthogranuloma, juvenile, 1085
X chromosome-linked IAP (XIAP), and odontogenic epithelial cells, 1212
Xeroderma pigmentosa, 1341
Xeroderma pigmentosum, 76
XIAP. *See* X chromosome-linked IAP (XIAP) and odontogenic epithelial cells
X-linked idiopathic hypoparathyroidism, 1460
X-linked lymphoproliferative syndrome, 1667

Yolk sac carcinoma, 1365

ZEBRA, 1665
Ziehl-Neelsen stain, 1623
Zimmerman tumor. *See* Phakomatous choristoma
Zygomycetes, 1638

about the book...

Surgical Pathology of the Head and Neck, Third Edition is a complete stand-alone reference covering all aspects of head and neck pathology. Providing an interdisciplinary approach to the diagnosis, treatment, and management of head and neck diseases, this source promotes clear communication between pathologists and surgeons. This is the reference of choice for a variety of clinicians, including: oral and general pathologists; oral and maxillofacial, plastic, reconstructive, head and neck, orthopedic, and general surgeons; otolaryngologists; radiologists; and dentists.

Topics covered include:

- incidence
- etiology
- clinical presentation
- pathology
- differential diagnosis
- prognosis for each disorder

With an improved format and design as well as an easy-to-use, quick reference index, the updated and expanded ***Third Edition*** contains more than 1,400 images—200 more full-color images than in previous editions—for optimal illustrations of head and neck lesions.

about the editor...

LEON BARNES is Professor of Pathology and Otolaryngology, Chief of the Division of Head and Neck–Endocrine Pathology and Director of the Head and Neck–Endocrine Pathology Fellowship Program at the University of Pittsburgh Medical Center, and Professor of Oral and Maxillofacial Pathology at the University of Pittsburgh School of Dental Medicine. Dr. Barnes obtained his M.D. degree from the University of Arkansas, Little Rock, Arkansas. He is a founding member of the North American Society of Head and Neck Pathology and has been a frequent honoree on the "Best Doctors in America" list for head and neck pathology. He has contributed numerous peer-reviewed publications, is a co-editor of the most recent World Health Organization "Blue Book" on the Pathology and Genetics of Head and Neck Tumors, and is the editor of the two previous editions of Informa Healthcare's ***Surgical Pathology of the Head and Neck.***

Printed in India

H9164

ISBN 978-1420091649

informa
healthcare
www.informahealthcare.com

52 Vanderbilt Avenue
New York, NY 10017

Telephone House
69-77 Paul Street
London EC2A 4LQ, UK